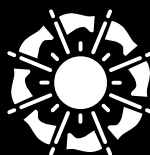


SPIE. PHOTONICS
WEST
BIOS



INTERNATIONAL
YEAR OF LIGHT
2015



2015 TECHNICAL SUMMARIES.

WWW.SPIE.ORG/PW

The Moscone Center
San Francisco, California, USA

Conferences & Courses
7-12 February 2015

Photonics West Exhibition
10-12 February 2015
BIOS EXPO
7-8 February 2015



SPIE. PHOTONICS WEST BIOS

The Moscone Center
San Francisco, California, USA

DATES

Conferences & Courses:
7-12 February 2015

TWO EXHIBITIONS

BiOS EXPO: 7-8 February 2015
Photonics West: 10-12 February 2015

Symposium Chairs



James Fujimoto
Massachusetts Institute of
Technology (USA)



R. Rox Anderson, M.D.
Wellman Center for
Photomedicine, Massachusetts
General Hospital and Harvard
School of Medicine (USA)

Contents

9303A: Photonics in Dermatology and Plastic Surgery	3	9318: Optical Biopsy XIII: Toward Real-Time Spectroscopic Imaging and Diagnosis	228
9303B: Therapeutics and Diagnostics in Urology	11	9319: Optical Tomography and Spectroscopy of Tissue XI	237
9303C: Optical Imaging, Therapeutics, and Advanced Technology in Head and Neck Surgery and Otolaryngology	18	9320: Microfluidics, BioMEMS, and Medical Microsystems XIII	260
9303D: Diagnosis and Treatment of Diseases in the Breast and Reproductive System	26	9321: Optical Interactions with Tissue and Cells XXVI	273
9303E: Diagnostic and Therapeutic Applications of Light in Cardiology	34	9322: Dynamics and Fluctuations in Biomedical Photonics XII	284
9303F: Optics in Bone Surgery and Diagnostics	42	9323: Photons Plus Ultrasound: Imaging and Sensing 2015	295
9304A: Optical Techniques in Pulmonary Medicine II	46	9324: Biophotonics and Immune Responses X	340
9304B: Endoscopic Microscopy X	53	9325: Design and Performance Validation of Phantoms Used in Conjunction with Optical Measurement of Tissue VII	350
9305A: Optical Techniques in Neurosurgery, Brain Imaging, and Neurobiology	64	9326: Energy-based Treatment of Tissue and Assessment VIII	355
9305B: Neurophotonics	72	9327: Optical Elastography and Tissue Biomechanics II	366
9305C: Optogenetics and Optical Control of Cells	87	9328: Imaging, Manipulation, and Analysis of Biomolecules, Cells, and Tissues XIII	377
9306: Lasers in Dentistry XXI	93	9329: Multiphoton Microscopy in the Biomedical Sciences XV	395
9307: Ophthalmic Technologies XXV	99	9330: Three-Dimensional and Multidimensional Microscopy: Image Acquisition and Processing XXII	424
9308: Optical Methods for Tumor Treatment and Detection: Mechanisms and Techniques in Photodynamic Therapy XXIV	118	9331: Single Molecule Spectroscopy and Superresolution Imaging VIII	440
9309: Mechanisms for Low-Light Therapy X	128	9332: Optical Diagnostics and Sensing XV: Toward Point-of-Care Diagnostics	452
9310: Frontiers in Biological Detection: From Nanosensors to Systems	137	9333: Biomedical Applications of Light Scattering IX	463
9311: Molecular-Guided Surgery: Molecules, Devices, and Applications	141	9334: Optical Methods in Developmental Biology III	474
9312: Optical Coherence Tomography and Coherence Domain Optical Methods in Biomedicine XIX	151	9335: Adaptive Optics and Wavefront Control for Biological Systems	483
9313: Advanced Biomedical and Clinical Diagnostic and Surgical Guidance Systems XIII	187	9336: Quantitative Phase Imaging	493
9315: Design and Quality for Biomedical Technologies VIII	203	9337: Nanoscale Imaging, Sensing, and Actuation for Biomedical Applications XII	520
9316: Multimodal Biomedical Imaging X	211	9338: Colloidal Nanoparticles for Biomedical Applications X	526
9317: Optical Fibers and Sensors for Medical Diagnostics and Treatment Applications XV	218	9339: Reporters, Markers, Dyes, Nanoparticles, and Molecular Probes for Biomedical Applications VII	542
		9340: Plasmonics in Biology and Medicine XII	552
		9341: Bioinspired, Biointegrated, Bioengineered Photonic Devices III	561

SPIE is the international society for optics and photonics, a not-for-profit organization founded in 1955 to advance light-based technologies. The Society serves nearly 225,000 constituents from approximately 150 countries, offering conferences, continuing education, books, journals, and a digital library in support of interdisciplinary information exchange, professional growth, and patent precedent. SPIE provided \$3.4 million in support of education and outreach programs in 2014.

Click on the Conference Title
to be sent to that page

Conference 9303A: Photonics in Dermatology and Plastic Surgery

Saturday - Sunday 7-8 February 2015

Part of Proceedings of SPIE Vol. 9303 Photonic Therapeutics and Diagnostics XI

9303-100, Session 1

Differentiating pigmented skin tumors by the tumor-associated melanocytes based on in vivo third harmonic generation microscopy

Wei-Hung Weng M.D., Ming-Rung Tsai, National Taiwan Univ. (Taiwan); Yi-Hua Liao M.D., National Taiwan Univ. Hospital (Taiwan); Chi-Kuang Sun, National Taiwan Univ. (Taiwan)

The morphology and distribution of melanocytes are important in making diagnosis of melanocytic lesions. However, the tumor-associated melanocytes are seldom investigated in non-melanocytic pigmented skin tumors. In our previous study, we successfully took the advantage of the third harmonic generation (THG)-enhanced nature of melanin, and used in vivo multi-harmonic generation microscopy (HGM) to achieve high diagnostic accuracy in non-melanoma pigmented skin tumors. Thus, the unique THG-identified characteristic of melanocytes is now investigated and introduced to differentiate pigmented skin tumors.

In the current study we examined the normal skin tissues and several pigmented skin tumors, including the pathological diagnosis of malignant melanoma, pigmented basal cell carcinoma (BCC), seborrheic keratosis (SK), and melanocytic nevus, by using HGM in vivo and ex vivo. Histopathological correlations of the HGM images were made by comparing with hematoxylin and eosin (H&E) and immunohistochemical (IHC) staining with HMB45 and CD1a which indicated the origin of cell with dendritic processes an melanocyte or a Langerhans cell, respectively. The result showed that the majority of THG-bright cells with dendritic processes were melanocytes that showed differences in their morphology, distribution, size and density between malignant melanoma, pigmented BCC, SK and melanocytic nevus.

Based on the current study, the newly characterized melanocytes identified by THG, which are not able to be identified in traditional histopathological sections, play unique features in various pigmented skin tumors based on our in vivo HGM. This optical diagnostic technique can be beneficially applied to clinical decision and management in the future.

9303-101, Session 1

Assessment of cutaneous melanoma and basal cell carcinoma with photoacoustic imaging

Aedán Breathnach, National Univ. of Ireland, Galway (Ireland); Liz Concannon, Galway Univ. Hospitals (Ireland); Hreesh Molly Subhash, National Univ. of Ireland, Galway (Ireland); Jack Kelly, Galway Univ. Hospitals (Ireland); Martin J. Leahy, National Univ. of Ireland, Galway (Ireland)

Photoacoustic (PA) imaging is a non-invasive imaging modality which combines high optical contrast with high-resolution ultrasonic imaging, and can directly map optical absorption within biological tissue. PA imaging can be used to image pigmented skin lesions due the high absorption of melanin in the visible and near-infrared wavelength range, and hence can be used to determine lesion shape and depth of invasion. In this study we investigate the clinical usefulness of PA imaging in diagnosing and assessing pigmented skin cancers such as cutaneous melanoma and basal cell carcinoma. Pre-operative PA images of patients with suspected cases of either cutaneous melanoma or basal cell carcinoma were taken with the Vevo Lazr® 2100 PA imaging system at several wavelengths. The distribution and maximum

thickness of suspect lesions was determined by imaging at 700nm, and the surrounding vasculature was imaged at 900 nm. Information obtained from the PA images was compared with histological examination of resected surgical specimens.

9303-102, Session 1

In vivo multiphoton microscopy imaging of basal cell carcinoma (*Invited Paper*)

Mihaela Balu, Beckman Laser Institute and Medical Clinic (United States); Christopher B. Zachary M.D., Ronald M. Harris M.D., Univ. of California, Irvine (United States); Tatiana B. Krasieva, Beckman Laser Institute and Medical Clinic (United States); Karsten König, JenLab GmbH (Germany) and Univ. des Saarlandes (Germany); Bruce J. Tromberg, Beckman Laser Institute and Medical Clinic (United States); Kristen M. Kelly M.D., Univ. of California, Irvine (United States)

The standard diagnostic procedure for basal cell carcinoma (BCC), as for other skin cancers, is based on clinical evaluation using dermoscopy and invasive biopsy followed by sample preparation and histopathological examination. An optical imaging technique, which could provide a diagnosis quickly and non-invasively, would benefit both patients and clinicians. We employed a clinical multiphoton microscopy (MPM)-based tomograph (MPTflex, JenLab, Germany) to image in-vivo and non-invasively BCC lesions in 10 patients. We used two-photon excited fluorescence to visualize endogenous fluorophores such as NADH/FAD, keratin, melanin in the epidermal cells and elastin fibers in the dermis. Collagen fibers were imaged by second harmonic generation. The histological subtypes of BCC of the lesions we imaged were superficial, nodular and micronodular. The main histopathological findings were nests of basaloid cells extending into the papillary dermis (superficial BCC) and in the reticular dermis (nodular and micronodular BCC). The main MPM features associated with these lesions were: nests of basaloid cells present in the papillary and upper reticular dermis, elongated cells aligned in the same direction and parallel collagen and elastin bundles surrounding the tumors. Some of the basaloid cell nests showed palisading in the peripheral cell layer. We demonstrate that MPM is capable of imaging in-vivo BCC. These results provide the groundwork for future studies on larger number of patients to assess MPM imaging sensitivity and specificity for in-vivo BCC diagnosis.

9303-103, Session 2

Ultra mobile skin imaging system mapping optical coherence tomography on common-path epiluminescence microscopy

Juan Sancho-Durá, Jose L. Rubio-Guivernau, Eduardo Margallo-Balbas, MedLumics S.L. (Spain); Wolfgang Drexler, Medizinische Univ. Wien (Austria)

Although skin pathologies are the fourth cause of non-fatal disease burden world-wide, dermatological diagnostic tools used in clinical practice have seen limited evolution. Visual inspection supported by skin biopsies and histopathology are the standard of care, in spite of many new non-invasive imaging techniques reported. Epiluminescence microscopy (EM) is among the best adopted modalities, but is only able to provide information

**Conference 9303A:
Photonics in Dermatology and Plastic Surgery**

about tissue surface. Optical Coherence Tomography (OCT) reveals tissue morphology with good resolution and excellent penetration of the skin, but systems have seen limited adoption outside research settings because of shortcomings in workflow integration, reliability, affordability and size.

This work reports a skin imaging system with joint OCT and EM functionality, where the two modalities are physically co-registered in a common-path configuration based on a dichroic mirror. The instrument has been miniaturized by means of a dedicated integrated optical circuit with a footprint of 1.1x19.5mm² that realizes an akinetic axial scan at speeds up to 24kHz. Lateral scanning is based on a low-voltage MEMS scanning mirror and micro-optics. Both subsystems are packaged in a hermetic butterfly module with a volume of 80x27x14mm³, three to four orders of magnitude smaller than comparable state-of-the-art implementations. The complete battery-powered imaging device has a weight of 3kg in a tablet format, enabling point-of-care and ambulatory uses.

This work shows that integration of complementary imaging modalities through suitable miniaturization technology results in clinically valuable instruments that allow patient-centered workflows. This could overcome adoption barriers to new diagnostic methods and improve patient care in dermatology.

9303-104, Session 2

In-vivo quantification of cutaneous melanin concentration and distribution: a comparison of multiphoton microscopy and spatially modulated quantitative spectroscopy *(Invited Paper)*

Rolf B. Saager, Mihaela Balu, Viera Crosignani, Ata Sharif, Anthony J. Durkin, Bruce J. Tromberg, Beckman Laser Institute and Medical Clinic (United States); Kristen M. Kelly M.D., Beckman Laser Institute and Medical Clinic (United States) and Univ. of California, Irvine (United States)

We present a study that employs Multiphoton fluorescence microscopy (MPM) and spatially modulated quantitative spectroscopy (SMoQS) to assess melanin concentration and distribution thickness *in vivo* over the full range of human skin pigmentation (Fitzpatrick skin types I-VI). MPM can be used to visualize *in-vivo* melanin on spatial scales of the order of microns. On the other hand, SMoQS is a quantitative spectroscopic technique that is based on spatial frequency domain methods and can be used to determine tissue chromophores (oxy & deoxy hemoglobin, melanin) over the wavelength range 450 – 970 nm. For this investigation, both MPM and SMoQS were used on 12 patients ranging in age from 23 to 75 years on both dorsal forearm and volar arm, which are generally sun-exposed and non-sun exposed areas, respectively. Using the depth-sectioning capabilities of MPM, we were able to demonstrate that a layered model interpretation of SMoQS data is capable characterizing *in vivo* the average concentration and distribution of melanin to within 15% and tens of microns respectively. The correlation of the data shows an excellent agreement between the two techniques, the R² values being 0.8895 for melanin concentration and 0.8131 for melanin distribution thickness. While SMoQS does not have the ability to match the spatial resolution of microscopy, this study shows that this relatively low cost technology can quantify and segment the effects of melanin in depth within tens of microns.

9303-105, Session 2

Quantitative characterization of traumatic bruises by combined pulsed photothermal radiometry and diffuse reflectance spectroscopy

Luka Vidovic, Matija Milanic, Jožef Stefan Institut (Slovenia); Lise L. Randeberg, Norwegian Univ. of Science and Technology (Norway); Boris Majaron, Jožef Stefan Institut (Slovenia)

The age of traumatic bruises is currently being assessed by visual inspection, which relies on differences in the absorption spectra of intact skin, extravasated hemoglobin, and products of its subsequent biochemical transformations. This approach is subjective and of limited accuracy, because the perceived color of the bruise depends also on the natural skin tone, epidermal and dermal thickness, lighting conditions, etc.

We have recently applied temperature depth profiling by pulsed photothermal radiometry (PPTR) to assessment of hemoglobin dynamics in traumatic bruises *in vivo*. By combining numerical simulations of the laser energy deposition in bruised skin with objective fitting of the predicted and measured PPTR signals we could assess the key structural properties of the affected site as well as key parameters describing the temporal evolution of the bruise (e.g., hemoglobin mass diffusivity and characteristic decomposition time).

In the present study, we supplement the above approach with diffuse reflectance spectroscopy (DRS). In addition to PPTR, we thus perform DRS measurements in visible spectral range and apply diffuse approximation solutions in analysis of the measured spectra. Our combining of two complementary techniques improves the robustness and accuracy of the inverse analysis and provides an additional insight into dynamics of the hemoglobin degradation products (biliverdin, bilirubin).

The obtained results advance our understanding of the bruise evolution process and present an important step toward development of an objective technique for determination of their age in forensic medicine.

9303-106, Session 3

Assessment of venous and arterial occlusion in skin flaps using visible diffuse reflectance spectroscopy and autofluorescence spectroscopy in a rodent model

Caigang Zhu, Shuo Chen, Nanyang Technological Univ. (Singapore); Christopher Hoe-Kong Chui, Bien-Keem Tan, Singapore General Hospital (Singapore); Quan Liu, Nanyang Technological Univ. (Singapore)

Early identification of vascular compromise in reconstructive surgery increases the chance of successful flap salvage. The ability to determine tissue viability is extremely useful when the reconstructive surgeon needs to decide how to inset the flap and whether any tissue must be discarded. Our previous study demonstrated that both visible diffuse reflectance and auto-fluorescence spectroscopy, which yield different sets of biochemical information, have great potential in the early prediction of skin flap failure in a MacFarlane rat dorsal skin flap model. In this report, we further push our technique to detect venous occlusion and arterial occlusion in the same skin flap model. We performed both diffuse reflectance and fluorescence measurements on the skin flap model to identify their value in the assessment of venous occlusion and arterial occlusion. Our preliminary results suggest that visible diffuse reflectance and auto-fluorescence spectroscopy can be potentially used clinically to detect venous occlusion and arterial occlusion and differentiate one from the other.

**Conference 9303A:
Photonics in Dermatology and Plastic Surgery**

9303-107, Session 3

In vivo multimodal optical microscopy for longitudinal tracking of adverse effects following topical steroid treatment

Andrew J. Bower, Univ. of Illinois at Urbana-Champaign (United States); Zane A. Arp, GlaxoSmithKline (United States); Youbo Zhao, Eric J. Chaney, Marina Marjanovic, Stephen A. Boppart M.D., Univ. of Illinois at Urbana-Champaign (United States)

Topical steroids are well known for their anti-inflammatory properties and are often prescribed for treatment of many skin diseases such as eczema and psoriasis. While these treatments are in many cases quite effective, adverse effects including skin thinning and atrophy are common among treated patients. In this study, we investigate the time-lapse progression of these effects in an in vivo mouse model at the cellular level using multimodal optical microscopy. Utilizing a system capable of performing two-photon excitation fluorescence microscopy (TPEF) of nicotinamide adenine dinucleotide (NAD) to visualize the epidermal skin cell layers and second harmonic generation (SHG) microscopy to identify collagen in the dermal region of the skin, allows changes in the skin to be visualized at the cellular level. Fluorescence lifetime imaging microscopy (FLIM) is also utilized to image intracellular NAD levels to obtain molecular information regarding metabolic activity following steroid treatment. In this study, a control group and groups treated with fluticasone propionate (FP) and mometasone furoate (MF) were evaluated longitudinally using multimodal optical microscopy. Prolonged steroid treatment is shown to result in a significant increase in mean fluorescence lifetime of NAD, suggesting a significant increase in metabolic activity. Along with this, alterations to collagen organization and the structural microenvironment are observed. This work demonstrates the ability to noninvasively track the adverse effects of steroid treatment longitudinally at the cellular level in vivo, allowing better insight into the processes of skin atrophy associated with prolonged steroid treatment and could lead to other applications in dermal drug development.

9303-108, Session 3

Visualizing and quantifying melanoma risk factors with coherent anti-Stokes Raman scattering (CARS) and multiphoton microscopy (Invited Paper)

Hequn Wang, Sam Osseiran, Elisabeth Roeder, Vivien Igras, Wellman Ctr. for Photomedicine (United States) and Harvard Medical School (United States); Peter T. C. So, Massachusetts Institute of Technology (United States); David E. Fisher, Conor L. Evans, Wellman Ctr. for Photomedicine (United States) and Harvard Medical School (United States)

Skin cancer is the most common type of cancer in North America, with melanoma representing the vast majority of skin cancer deaths. One in five North Americans will develop skin cancers during their lifetime. Despite routine screening, skin cancers, in particular melanoma, are typically diagnosed in their late stages. Optical techniques, as non-invasive, non-perturbative tools, can provide high-resolution morphological and biochemical analyses of suspect lesions. Coherent anti-Stokes Raman scattering (CARS), with its contrast arising from the vibrations of chemical species, may have an important role to play in the early diagnosis of skin cancer lesions, especially when used as part of a multiphoton microscope (MPM) toolkit. Recent CARS studies have been focused on visualizing and quantifying biomarkers thought to be important to the early stage of melanoma formation. To capture a range of potential chemical markers, a multiphoton system incorporating CARS, two-photon excited fluorescence,

second harmonic generation, and fluorescence lifetime imaging was developed based on a widely tunable Insight light source. Normal and pre-cancerous melanomas of human and murine origin have been imaged using both CARS and MPM, focusing on characterizing lipids, pigments, NADH, FAD, and collagen. Distinct features of the acquired images were extracted, in particular Raman spectral features, which could potentially serve as cancer and pre-cancer biomarkers. Complementary siRNA cell culture studies have additionally identified novel optical signature that may be incorporated in future melanoma imaging efforts.

9303-109, Session 4

Evaluation of the effect of pericytes as treatment for non-healing diabetic wounds using integrated multimodal microscopy

Joanne Li, Andrew J. Bower, Yair Pincus, Marina Marjanovic, Eric J. Chaney, Marni D. Boppart, Stephen A. Boppart M.D., Univ. of Illinois at Urbana-Champaign (United States)

Impaired skin wound healing is a significant co-morbid condition of diabetes, which often results in non-healing diabetic ulcers because of poor peripheral microcirculation and other factors. The objective of this study is to determine the extent to which muscle-derived stem cells, predominantly pericytes, contribute to skin repair in diabetic mice. The effectiveness of regeneration was assessed using a novel integrated multimodal microscopy system, which includes optical coherence tomography/microscopy, two-photon fluorescence imaging, second harmonic generation imaging, and fluorescence lifetime imaging. These imaging modalities, in an integrated platform for spatial and temporal image co-registration, allowed us to monitor the changes in the collagen network, cell dynamics, and metabolic activity of cells in the skin. Fluorescently labeled (DiI)-pericytes were topically applied to the wound bed following punch biopsy, and dynamic imaging demonstrated that the administered cells remained at the edge of the wound bed and projected toward the center with increasing density during the healing process. These results suggest that collagen matrix formation and wound healing in diabetic mice can be improved utilizing these muscle-derived pericytes. Assessment of stem cell therapies using our optical methods can lead to a better understanding of healing mechanisms, and the results can be beneficial to the care and treatment of non-healing wounds in diabetic patients.

9303-110, Session 4

A rapid-drying liquid bandage for the non-invasive transdermal two-dimensional mapping of cutaneous oxygenation (Invited Paper)

Zongxi Li, Conor L. Evans, Massachusetts General Hospital (United States)

Knowledge of tissue oxygenation status is important in the management of burns and skin grafts, as well as in a wide range of skin conditions. Despite the importance of the clinical determination of tissue oxygenation, there is a lack of rapid, user-friendly and quantitative diagnostic tools that allow for non-disruptive, continuous monitoring of oxygen content across large areas of skin and wounds to guide care and therapeutic decisions. In this work, we describe a sensitive, colorimetric, oxygen-sensing paint-on bandage for two-dimensional mapping of tissue oxygenation in skin, burns, and skin grafts. By embedding both an oxygen-sensing porphyrin-dendrimer phosphor and a reference dye in a liquid bandage matrix, we have created a liquid bandage that can be painted onto the skin surface and dries into a thin film that adheres tightly to the skin or wound topology. When captured by a camera-based imaging device, the oxygen-dependent phosphorescence emission of the bandage can be used to quantify and map both the pO₂ and oxygen consumption of the underlying tissue. The system was demonstrated

**Conference 9303A:
Photonics in Dermatology and Plastic Surgery**

in several clinically relevant animal models for the dynamic monitoring of tissue ischemia, burn progression, as well as skin graft integration.

9303-111, Session 4

Microvascular complications associated with injection of cosmetic facelift dermal fillers

Siavash Yousefi, Stanford Univ. (United States) and Univ. of Washington (United States); Mark Prendes M.D., Shu-Hong Chang M.D., Ruikang K. Wang, Univ. of Washington (United States)

Since the FDA clearance of bovine collagen in 1981, injectable dermal fillers have become an increasingly popular procedure of the cosmetic surgery practice to remove skin wrinkles. A variety of permanent, semi-permanent and dissolvable dermal fillers have been introduced to modify the appearance of soft tissue rhytids and contour deformities. Hyaluronic acid (HA) is a hydrophobic polysaccharide that naturally exists in the extracellular matrix of all animal tissues and consists of regularly repeating units of B-acetyl-D-glucosamine and D-glucuronic acid.

With increased use of injectable fillers, growing reports of filler-induced complications have been reported all around the world. Some complications appear immediately after injections (0-2 days) that include under/overcorrection, implant visibility or Tyndall effect, sensitivity to the injected material, and ischemia with or without necrosis. Other complications such as infection, tissue discoloration, inflammation, nodularity, and angioedema may occur in the early post-procedure period (3-14 days). Also long term complications (>14 days) such as persistent erythema, telangiectasia, migration, scarring, and granuloma formation have also been reported formation. Some of these complications are minor and transient, while others may lead to long-term detrimental outcomes.

Although safety studies of dermal fillers have reported that complications from the dermal injections are very rare, different definitions of complication make the assumptions fall apart. The rate of any complication from a filler injection including pain and redness has been reported to occur in up to 5% of patients. More relevant to patients and clinicians is the frequency of severe complications such as infection, granuloma formation, ischemia, and necrosis. The incidence of these severe adverse events is somewhere in the range of 0.04% to 0.001%. Although the chance of such complications is very small, they can be devastating in people who are extremely concerned about their look at first place.

The most devastating complication stemming from cosmetic filler injections is ischemia with subsequent soft tissue necrosis. Filler-induced tissue ischemia has been reported to occur with all types of fillers and in all areas of the face, although it is most commonly seen following glabellar injections. Glabellar necrosis usually happens because the vascular supply to this region is derived from a limited number of larger vessels in the supratrochlear and supraorbital arcades, with less collateral circulation than is present in other areas of the face. Although delayed presentations have been reported, ischemia is typically accompanied with immediate blanching of the tissues adjacent to the site of injection. However, ischemic tissue is not always associated with any pain. Over the subsequent 2-3 days, the skin begins to appear dusky or black. Once this occurs, there is little chance of tissue survival. Ultimately, a necrotic ulcer develops and is often crusted by a black eschar of dead skin.

Methods: To determine the effect of external vascular compression on distal perfusion, we attempted to occlude vessels with subcutaneous hyaluronic acid gel (HAG) bolus injections into the pinna of hairless mice (CrI:SKH1-Hr hr). Following these interventions, OCT angiography was performed serially over one week follow-up. To determine the effect of intravascular HAG injection, we devised and validated a novel method of cannulating the mouse external carotid artery for intra-arterial access to the pinna vasculature. Using this model, we performed intra-arterial HAG injections and completed Laser Speckle and OMAG. Our results were cross-validated with H&E histology of the ear pinna.

Results: Despite large HAG bolus injections directly adjacent to vascular

bundles, we were unable to induce compressive occlusion of the mouse pinna vessels. With intravascular HAG injection, large segments of pinna showed distinct reduction in vascular perfusion along a vascular distribution when they were compared to pre-injection images, most noticeably at the capillary level.

Conclusions: Our novel mouse pinna model combining intravascular access and in vivo microvascular perfusion imaging has furthered our understanding of the mechanism of filler-induced tissue necrosis. Distal capillary perfusion was maintained despite external vascular compression. Intravascular HAG filler injection, however, resulted in large areas of capillary dropout and is the most likely etiology for filler-induced tissue necrosis observed clinically.

9303-112, Session 4

Improvement of the healing process in superficial skin wounds after treatment with EMOLED

Riccardo Cicchi, Istituto Nazionale di Ottica (Italy) and Consiglio Nazionale delle Ricerche (Italy) and European Lab. for Non-linear Spectroscopy (Italy); Francesca P. Rossi, Francesca Tatini, Istituto di Fisica Applicata Nello Carrara (Italy) and Consiglio Nazionale delle Ricerche (Italy); Stefano Bacci, Gaetano De Siena, Univ. degli Studi di Firenze (Italy); Domenico Alfieri, Light4Tech Firenze S.r.l. (Italy); Roberto Pini, Istituto di Fisica Applicata Nello Carrara (Italy) and Consiglio Nazionale delle Ricerche (Italy); Francesco S. Pavone, European Lab. for Non-linear Spectroscopy (Italy) and Univ. degli Studi di Firenze (Italy)

A faster healing process was observed in superficial skin wounds after irradiation with the EMOLED photocoagulator. The instrument consists of a compact handheld photocoagulation device, useful for inducing coagulation in superficial abrasions. In this study, living animals were mechanically abraded in four regions of their back: two regions were left untreated, the other two were treated with EMOLED, healthy skin surrounding the wounds was used as a control. The treatment effect on skin was monitored by visual observations, histopathological analysis, immuno-histochemical analysis, and non-linear microscopic imaging performed 8 days after the treatment, finding no adverse reactions and no thermal damage in both treated areas and surrounding tissues. In addition, a faster healing process, a reduced inflammatory response, a higher collagen content, and a better-recovered skin morphology was evidenced in the treated tissue with respect to the untreated tissue. These morphological features were characterized by means of immuno-histochemical analysis, aimed at imaging fibroblasts and myofibroblasts, and by SHG microscopy, aimed at characterizing collagen organization, demonstrating a fully recovered aspect of dermis as well as a faster neocollagenesis in the treated regions. This study demonstrates that the selective photothermal effect we used for inducing immediate coagulation in superficial wounds is associated to a minimal inflammatory response, which provides reduced recovery times and improved healing process.

9303-113, Session 4

Monitoring wound healing by multiphoton tomography/endoscopy

Karsten König, Univ. des Saarlandes (Germany) and JenLab GmbH (Germany); Martin Weinigel, JenLab GmbH (Germany); Volker Huck, Katharina Zens, Stefan W. Schneider, Ruprecht-Karls-Univ. Heidelberg, Medizinische Fakultät Mannheim (Germany)

**Conference 9303A:
Photonics in Dermatology and Plastic Surgery**

Monitoring wound healing noninvasively with superior 3D resolution is realized by clinical multiphoton tomography without the need of additional contrast agents. The technology behind this investigation is based on nonlinear optical contrast of the multiphoton tomograph MPTflex®.

This flexible clinical imaging system is designed to investigate human skin for dermatological as well as for cosmetic purposes. However imaging chronic wounds with multiphoton tomography is a novel approach to investigate healing processes. Another recent advancement is the application of a miniaturized GRIN-lens to realize more accessibility for more demanding wound conditions with deep cavities. The MPTflex® distinguishes autofluorescence (AF) signals from second harmonic generation (SHG) signals simultaneously. Fluorescence lifetime imaging (FLIM) based on time correlated single photon counting (TCSPC) technology offers additional information on the functional level of the intratissue fluorophores, their binding status, and the contribution of SHG signals in chronic wounds.

Therefore, this technology envisions a deeper understanding of the pathophysiological characteristics of chronic wounds in the near future.

The authors acknowledge financial support within the BMBF project "Woundoptimizer".

9303-114, Session 5

Longitudinal imaging study of vasculature in human burn scars in response to laser treatment using optical coherence tomography

Peijun Gong, Shaghayegh Es'haghian, The Univ. of Western Australia (Australia); Alexandra Murray, Karl-Anton Harms, Royal Perth Hospital (Australia); Suzanne Rea, Brendan F. Kennedy, Fiona M. Wood M.D., David D. Sampson, Robert A. McLaughlin, The Univ. of Western Australia (Australia)

Fractional CO2 laser treatment has shown promise in the treatment of human burn scars. The laser treatment stimulates the wound healing process to reduce scar severity by inducing thermal tissue damage in an array of microscopic treatment zones whilst sparing the surrounding tissue. Assessment of the scar tissue response to the induced thermal injuries is important for the evaluation of treatment efficacy and optimization of treatment strategies. One important feature of pathological scars, such as hypertrophic scars, is a prolific network of blood vessels, usually leading to a red appearance. Laser treatment seeks to occlude some of these vessels through heat-induced tissue coagulation. Our study uses optical coherence tomography (OCT) to assess longitudinal changes in the vasculature of patients in response to laser treatment. Speckle decorrelation was used to automatically identify blood vessels in scans acquired both before and three days after fractional CO2 laser treatment. Care was taken to image the same location in both scans, using physical landmarks on the scar's surface. We were able to obtain a one-to-one correspondence between individual vessels in the scans at both time points, and identified regions in which the vasculature was reduced in response to the laser treatment. This pilot study demonstrates the feasibility of OCT vasculature imaging for longitudinal monitoring of changes in scar vasculature in vivo in response to treatment.

9303-115, Session 5

Non-invasive volumetric imaging of hypertrophic scars in vivo (Invited Paper)

William Lo, Harvard Medical School (United States) and Wellman Ctr. for Photomedicine (United States) and Massachusetts General Hospital (United States); Martin L. Villiger, Harvard Medical School (United States) and Massachusetts General Hospital (United States); Alexander Goldberg, Massachusetts General Hospital (United States)

and Tel Aviv Univ. (Israel); Saiqa Khan, William Austen Jr., Massachusetts General Hospital (United States); Martin Yarmush, Massachusetts General Hospital (United States) and Rutgers Univ. (United States); Brett E. Bouma, Harvard Medical School (United States) and Massachusetts General Hospital (United States) and Wellman Ctr. for Photomedicine (United States)

Hypertrophic scars (HTS), which are frequently seen after traumatic injuries, surgery, or poor wound healing, remain a major clinical challenge due to the limited success of existing therapies. In this study, we investigated the use of polarization-sensitive optical frequency domain imaging (PS-OFDI) for the non-invasive volumetric imaging of an animal model of HTS in vivo. To induce the formation of HTS, a tension device was placed on incisions for 4 to 10 days in rats. Besides structural imaging, PS-OFDI provides additional contrast due to the polarization properties of the tissue, offering insights into the microstructural arrangement of collagen. The HTS regions in all groups consistently demonstrated reduced local birefringence and low depolarization in the dermis. This unique optical signature provides a means to reliably assess the morphology of HTS in vivo. The results were quantitatively compared with histology, showing close correspondence in both the shape and size of the scars. Furthermore, we demonstrated the use of PS-OFDI for studying the evolution of HTS formation by imaging at 1-week intervals for 1 month after device removal. The ability to perform longitudinal, 3-D imaging in vivo provides a powerful means to gain further mechanistic insights into HTS formation and to study the effects of different interventions for scar remodeling.

9303-116, Session 5

Preferential alignment of birefringent tissue measured with polarization sensitive techniques

Jessica C. Ramella-Roman, Florida International Univ. (United States); Pejman Ghassemi, The Catholic Univ. of America (United States)

Assessing collagen alignment is of interest when evaluating a therapeutic strategy and evaluating its outcome in scar management. In this work we introduce a theoretical and experimental methodology for the quantification of collagen and birefringent media alignment based on polarized light transport. The technique relies on the fact that these materials exhibit directional anisotropy. A polarized Monte Carlo model and a spectro-polarimetric imaging system were devised to predict and measure the impact of birefringence on an impinging polarized light beam. Experiments conducted on birefringent phantoms, and biological samples consisting of highly packed parallel birefringent fibers, showed a good agreement with the analytical results.

9303-117, Session 5

Microvascular changes during acne lesion initiation and scarring within human skin is revealed in vivo using optical microangiography

Utku Baran, Yuandong Li, Woo June Choi, Ruikang K. Wang, Univ. of Washington (United States)

Acne is a common skin disease in society and often leads to scarring. Collagen and other tissue damage from the inflammation of acne leads to permanent skin texture changes and fibrosis. Hypertrophic scars consists of dermal collagen fibers, small vasculature, and fibroblasts. In this study we demonstrate the capabilities of swept-source optical coherence tomography (OCT) in detecting in vivo specific features of acne lesion initiation and

**Conference 9303A:
Photonics in Dermatology and Plastic Surgery**

scarring. We apply ultra-high sensitive optical microangiography (UHS-OMAG) technique to evaluate vessel morphology changes corresponding with tissue structure. Thanks to the high sensitivity of UHS-OMAG, we were able to image microvasculature up to capillary level and visualized the deformed vessels around the hypertrophic scar. In contrast to other techniques like histology or microscopy, our technique made it possible to image 3D tissue structure and microvasculature up to 1 mm depth in vivo without the need of exogenous contrast agents in ~10 seconds. The presented results are promising to facilitate clinical trials of treatment and diagnosis of acne lesion initiation and scarring by detecting cutaneous blood flow and structural changes within human skin in vivo.

9303-118, Session Key

Assessing the colors of human skin
(Keynote Presentation)

Nikiforos Kollias, Consultant (United States)

No Abstract Available

9303-119, Session 6

Real-time photoacoustic imaging of grafted artificial dermis in rat burn models

Hideaki Iwazaki, Taiichiro Ida, Yasushi Kawaguchi, Advantest Corp. (Japan); Keiichi Iwaya, Hitoshi Tsuda, Satoko Kawachi, Daizoh Saitoh, Shunichi Sato, National Defense Medical College (Japan)

We developed a real-time photoacoustic (PA) imaging system for burn diagnosis and previously showed the validity of the system for burn depth assessment in the experiments using rat burn models. In this study, we investigated the validity of the system for monitoring adhesion of the grafted artificial dermis. A deep burn of 20 mm diameter was made in the rat dorsal skin by exposing the 20-mm-diameter skin area to water at 98°C for 10 s. The full-thickness wound was resected, to which an artificial dermis composed of an atelocollagen sponge sheet and a silicone film was grafted. For comparison, an artificial dermis was also grafted onto the full-thickness open wound in a rat without burn. We performed PA imaging for the grafted artificial dermis in both models for 9 days after grafting. In the both models, PA signals appeared in the bottom region of the artificial dermis at 3 days post-grafting, and the depth of signal shifted to the shallower region with the elapse of time. The results of the histological analysis showed that PA signals in both models reflected neovascularities in the grafted artificial dermis. However, the amplitudes of the PA signals in the burn model were lower than those in the nonburn model, indicating less efficient neovascularities in the burn model. These results show the usefulness of our PA imaging system not only for burn depth assessment but also for adhesion monitoring of the grafted artificial dermis.

9303-120, Session 6

The importance of illumination in a non-contact photoplethysmography imaging system for burn wound assessment

Weirong Mo, Spectral MD, Inc. (United States); Rachit Mohan, Spectral MD (United States); Weizhi Li, Xu Zhang, Eric Sellke, Wensheng Fan, Michael J. DiMaio, Jeffery E. Thatcher, Spectral MD, Inc. (United States)

We present a new non-contact reflective-mode time-domain photoplethysmogram (PPG) method and a functional prototype system for identifying the presence of dermal burn wounds during a burn

debridement surgery, which aims to provide assistance and tool for debridement surgeries and/or wound triage decisions. We developed an LED array, a tungsten light source, and eventually high-power LED emitters as illumination methods for our PPG imaging device. Initially, using a PPG tissue phantom model we performed regression analysis to identify the relationship between illumination intensity and PPG signal strength. Next, these three different illumination sources were tested in a controlled tissue phantom model and an animal burn model. We found that the low heat and even illumination pattern using high power LED emitters provided a substantial improvement to the collected PPG signal in our animal burn model. These improvements allow the PPG signal from different pixels to be comparable in both time-domain and frequency-domain, simplify the illumination subsystem complexity, and remove the necessity of using high dynamic range cameras. Through the burn model output comparison, such as the blood volume in animal burn data and controlled tissue phantom model, our optical improvements have led to more clinically applicable images to aid in burn debridement surgery.

9303-122, Session 7

The stepwise multi-photon activation fluorescence guided ablation of melanin

Zhenhua Lai, Zetong Gu, Charles A. DiMarzio, Northeastern Univ. (United States)

Previous research has shown that the stepwise multi-photon activation fluorescence (SMPAF) of melanin, activated by a continuous-wave (CW) mode near infrared (NIR) laser, is a low-cost, high-specificity and high-precision method of detecting melanin. We have developed a device utilizing the melanin SMPAF to guide the ablation of melanin with a 975 nm CW laser. This method provides the ability of targeting individual melanin particles with micrometer resolution, and therefore, localized ablation of melanin can be performed without collateral damage. Compared to the traditional selective photothermolysis, which uses nanosecond pulsed lasers for melanin ablation, this method demonstrates higher precision, higher specificity and deeper penetration. Therefore, the SMPAF guided selective ablation of melanin is a promising tool of removing melanin for both medical and cosmetic purposes.

9303-123, Session 7

Controlled laser delivery into biological tissue via thin-film optical tunneling and refraction *(Invited Paper)*

Paul J. D. Whiteside, Benjamin S. Goldschmidt, Randy D. Curry, Univ. of Missouri-Columbia (United States); John A. Viator, Duquesne Univ. (United States)

Due to the often extreme energies employed, contemporary methods of laser delivery utilized in clinical dermatology allow for a dangerous amount of high-intensity laser light to reflect off a multitude of surfaces, including the patient's own skin. Such techniques consistently represent a clear and present threat to both patients and practitioners alike. The intention of this work was therefore to develop a technique that mitigates this problem by coupling the light directly into the tissue via physical contact with an optical waveguide. In this manner, planar waveguides clad in silver with thin-film active areas were used to illuminate agar tissue phantoms with nanosecond-pulsed laser light at 532 nm. The light then either refracted or optically tunneled through the active area, photoacoustically generating ultrasonic waves within the phantom, whose peak-to-peak intensity directly correlated to the internal reflection angle of the beam. Consequently, angular spectra for energy delivery were recorded for sub-wavelength silver and titanium films of variable thickness. Optimal energy delivery was achieved for internal reflection angles ranging from 43 to 50 degrees, depending on the active area and thin film geometries, with titanium films consistently delivering more energy across the entire angular spectrum,

**Conference 9303A:
Photonics in Dermatology and Plastic Surgery**

due to its relatively high refractive index. The technique demonstrated herein therefore not only represents a viable method of energy delivery for biological tissue while minimizing the possibility for stray light, but also demonstrates the possibility for utilizing thin films of high refractive index metals to redirect light out of an optical waveguide.

on the illuminated pixels. Results will be presented showing how these quantified measurements of roughness can be linked with more qualitative perceptions of skin quality (dryness) and how improvements can be tracked over time through the use of skin care products and potentially pharmaceuticals.

9303-124, Session 7

Study on fractional CO₂ laser-assisted drug delivery with optical coherence tomography

Ting-Yen Tsai, Chang Gung Univ. (Taiwan); FengYu Preston Chang, Yi-Cheng Lee, Meng-Tsan Tsai, Chang Gung Univ. (Taiwan); Chih-Hsung Yang M.D., Chang Gung Memorial Hospital (Taiwan)

Laser photothermal therapy is an effective method for skin resurfacing. Delivering drug into nail is essential for the topical therapy of nail diseases, e.g. nail fungal infection. A variety of physical methods or chemical enhancers have been tested to increase drug permeation into the intact nail plate. Therefore, in this study, we propose to use optical coherence tomography (OCT), to investigate the effect of laser exposure on the nail with three-dimensional imaging. Clinically it is difficult to evaluate the effect of laser exposure noninvasively since the parameters including the penetration depth and the beam diameter cannot be obtained immediately. In our experiments, the nails after fractional laser exposures were scanned with our SS-OCT system. The quantitative results from OCT images including the penetration depth and ablative area are analyzed and also compared with the histology results. In addition to observe the results after fractional laser exposures with OCT, we use OCT to evaluate the water diffusion through laser ablative channels based on estimating speckle variance of OCT signal. The results showed that OCT can be effective to monitor the photothermal effect induced by fractional CO₂ laser and to evaluate the water or drug diffusion from the microthermal zone to the nail bed.

9303-125, Session 7

Quantification of skin quality through speckle analysis

John M. Girkin, Durham Univ. (United Kingdom); Kim-Kristin K. Buttenschoen, Durham Univ. (United Kingdom) and Lein Applied Diagnostics (United Kingdom); Amrit Lotay, Durham Univ. (United Kingdom)

The outer textural surface of skin plays an important role both in the diagnosis of many clinical conditions but also in relation to aging and the acceptance of many consumer products. Whilst considerable resource has been applied to skin in terms of cancer diagnosis the actual surface finish of the tissue has been frequently overlooked. Indeed even in cancer diagnosis the surface of a lesion may provide clinically significant information in terms of diagnosis and disease progression. Commercial products as diverse as soap, laundry cleaners, diapers and skin care creams all interact with the skin and thus a method of quantifying any effect they may have on the surface finish is important to the development of such products.

The pattern of light that is seen when a low power laser is scattered off any non-smooth surface is well known as a grainy speckle and the structure of the speckle contains significant information about the surface and local sub-surface of the material. With recent increases in computing power it has become possible to quantify this pattern of light to provide physical information about the surface rapidly.

The speckle pattern back scattered to a camera was recorded and the pattern subsequently analyzed using a computer based co-variance method

9303-126, Session 7

Laser technology and propranolol in the treatment of complex infantile hemangiomas

Ivan A. Abushkin, South Ural State Medical Univ. (Russian Federation); Olga A. Sudeikina M.D., Lipetsk Oblast Children's Hospital (Russian Federation) and South Ural State Medical Univ. (Russian Federation); Anna Denis, Olga Romanova, Igor S. Vasilyev M.D., Veniamin O. Lapin, South Ural State Medical Univ. (Russian Federation); Alexander V. Lappa, Chelyabinsk State Univ. (Russian Federation); Valeriy A. Privalov M.D., South Ural State Medical Univ. (Russian Federation)

We have presented here two minimally invasive laser technology for the treatment of complicated infantile hemangiomas. Preferentially localized hemangiomas had a face. All hemangiomas were located in the skin and under the skin. We have developed a technology of contactless and interstitial 0.97 - micron laser thermotherapy infantile hemangiomas. These technologies have been highly effective. However, the defect was necessity of general anesthesia and the risk of scarring. Since 2011, in the treatment of complicated hemangiomas started using propranolol. Nevertheless, with a strong blood supply infantile hemangiomas effectiveness of propranolol was insufficient. The combined use of propranolol with laser thermotherapy significantly increased the effectiveness of the treatment of infantile hemangiomas, smoothed disadvantages of each of these methods. Propranolol dose was reduced, reduced the frequency of sessions of laser thermotherapy and intensity of the laser irradiation on the hemangioma. There was thus reduced effect on the cardiovascular system of the patient and the risk of general anesthesia and scar development. These processing techniques have been applied in more than 2000 patients with good results.

9303-127, Session Psun

Co-registration of optical microangiography and multiphoton microscopy for tracking dynamic wound healing

Wan Qin, Yuandong Li, Ruikang K. Wang, Univ. of Washington (United States)

Wound healing is a complex and dynamic process of replacing devitalized and missing cellular structures and tissue layers. The classic model of wound healing is divided into four sequential phases including hemostasis, inflammation, proliferation, and remodeling. Upon injury to the skin, a set of complex biochemical events take place in a closely orchestrated cascade to repair the damage. Conventional techniques for studying wound healing are mainly based on analyzing histological samples, which could not track the dynamic healing mechanism. Some in vivo imaging techniques, such as magnetic resonance imaging and computed tomography, have been applied to this field but with limited applicability due to their insufficient spatial and temporal resolutions. Here we report the use of a novel multi-modality optical imaging approach for concurrently observing multiple functional processes of wound healing in vivo. We employed optical microangiography (OMAG) to record large-scale microvascular and lymphatic networks around the wound to study angiogenesis and lymphangiogenesis during the wound healing. The microvascular images were also used to guide the subsequent

**Conference 9303A:
Photonics in Dermatology and Plastic Surgery**

imaging with two-photon excited fluorescence (TPEF) microscopy and second harmonic generation (SHG) microscopy as a map. The TPEF imaging provided detailed microvasculature information in response to the wound and linked the SHG imaging to the microvasculature map created with OMAG. SHG imaging enabled tracking the collagen deposition and remodeling. The proposed method was validated with a 30-day monitoring of a biopsy punch wound on a mouse ear. This multi-modality imaging approach has great potential to provide novel insight towards understanding the mechanism of wound healing and thus developing more effective therapeutics.

Conference 9303B: Therapeutics and Diagnostics in Urology

Saturday 7 -7 February 2015

Part of Proceedings of SPIE Vol. 9303 Photonic Therapeutics and Diagnostics XI

9303-200, Session 9

Discrimination of healthy and cancer cells of the bladder by metabolic state, based on autofluorescence

Scott Palmer, Karina Litvinova, Univ. of Dundee (United Kingdom); Edik U. Rafailov, Aston Univ. (United Kingdom); Ghulam Nabi, Univ. of Dundee (United Kingdom)

Bladder cancer is among the most common cancers worldwide (4th in men). It is responsible for high patient morbidity and displays rapid recurrence and progression. Lack of sensitivity of gold standard techniques (white light cystoscopy, voided urine cytology) means many early treatable cases are missed. The result is a large number of advanced cases of bladder cancer which require extensive treatment and monitoring. For this reason, bladder cancer is the single most expensive cancer to treat on a per patient basis. In recent years, autofluorescence spectroscopy has begun to shed light into disease research. Of particular interest in cancer research are the fluorescent metabolic cofactors NADH and FAD. Early in tumour development, cancer cells often undergo a metabolic shift (the Warburg effect) resulting in increased NADH. The ratio of NADH to FAD ("redox ratio") can therefore be used as an indicator of the metabolic status of cells. Redox ratio measurements have been used to differentiate between healthy and cancer breast cells and to monitor cellular responses to therapies. Here, we have demonstrated, using healthy and bladder cancer cell lines, a statistically significant difference in the redox ratio of bladder cancer cells, indicative of a metabolic shift. To do this we customised a standard flow cytometer to excite and record fluorescence specifically from NADH and FAD, along with a method for automatically calculating the redox ratio of individual cells within large populations. These results could inform the design of novel probes and screening systems for the early detection of bladder cancer.

9303-201, Session 9

Near infrared spectroscopy evaluation of bladder function: the impact of skin pigmentation on detection of physiologic change during voiding

Babak Shadgan M.D., The Univ. of British Columbia (Canada); Lynn Stothers M.D., The Univ. of British Columbia (Canada); Behnam Molavi, BC Children's Hospital (Canada); Sharif Mutabazi, Ronald Mukisa, Cure Medical Centre (Uganda); Andrew Macnab, Univ of British Columbia (Canada) and Cure Medical Clinic, (Uganda)

Background:

Prior research indicates the epidermal pigment layer of human skin (Melanin) has a significant absorption coefficient in the near infra-red (NIR) region; hence attenuation of light in vivo is a potential confounder for NIR spectroscopy (NIRS). A NIRS method developed for transcutaneous evaluation of bladder function is being investigated as a means of improving the burden of bladder disease in sub-Saharan Africa. This required development of a wireless NIRS device suitable for use as a screening tool in patients with pigmented skin where the NIR light emitted would penetrate through the epidermal pigment layer and return in sufficient quantity to provide effective monitoring.

Methods:

Two healthy subjects, one with fair skin and one with pigmented skin, were monitored as they voided voluntarily using the prototype transcutaneous

NIRS device positioned over the bladder. The device was a self-contained wireless unit with light emitting diodes (wavelengths 760/850 nanometers) and interoptode distance 4cm. The raw optical data was transmitted to a laptop where graphs of chromophore change were generated with proprietary software and compared between the subjects and with prior data from asymptomatic subjects.

Results:

Serial monitoring was successful in both subjects. Voiding volumes varied between 150 and 420 cc. In each subject the patterns of chromophore change were similar and matched the physiologic increase in total and oxygenated hemoglobin recognized to occur in normal bladder contraction.

Conclusions:

Skin pigmentation does not compromise the ability of transcutaneous NIRS to interrogate physiologic change in the bladder during bladder contraction in healthy subjects.

9303-202, Session 9

Method for improving photodynamic diagnosis and surgery of bladder tumours using cystoscopes

Lars R. Lindvold, Technical Univ. of Denmark (Denmark); Gregers G. Hermann, Frederiksberg Hospital (Denmark)

At Photonics West 2013 we presented a paper (8565-41) on how to remove unwanted green fluorescence from urine during Photodynamic Diagnostics (PDD) of tumours in the bladder using cystoscopy. This paper was based on spectroscopic observations of urine and the photosensitiser Protoporphyrin IX (PpIX).

A high power LED based light source (525 nm) has been made in our laboratory according to the findings presented in paper 8565-41. This light source is tailored to match most commercially available rigid cystoscopes. A suitable spectral filter and adapter, for the eyepiece of the cystoscope, has been made which allows the urologist to observe both red fluorescence from tumours and autofluorescence from healthy tissue at the same time.

In this paper we will present our findings from a series of test on patients in the operating room (OR) based on the tailor-made LED light source. The purpose of this test is to demonstrate that PDD can be performed on bladder tumours in the OR using the tailor-made high power LED light source using a rigid cystoscope. The paper also addresses the issue of photobleaching of the photosensitiser with respect to the excitation wavelength. Spectro fluorometrical measurements showing the improvement in photosensitiser lifetime and hence extended observation time for the urologist will be presented.

9303-203, Session 9

A novel excitation-emission wavelength model to facilitate the diagnosis of urinary bladder diseases

Ilya E. Rafailov, Scott Palmer, Karina Litvinova, Univ. of Dundee (United Kingdom); Victor Dremine, Andrey V. Dunaev, State Univ. Educational Scientific Production Complex (Russian Federation); Ghulam Nabi, Univ. of Dundee (United Kingdom)

Diseases of urinary bladder are a common healthcare problem world

Conference 9303B: Therapeutics and Diagnostics in Urology

over. Diagnostic precision and predicting response to treatment are major issues. This study aims to create an optical cross-sectional model of a bladder, capable of visually representing the passage of photons through the tissue layers. Fresh pig bladders were dissected into 2cm² sections and subjected to spectrophotometric analysis. The absorption, transmission and reflectance data, along with the dimensions of the analysed sections and complimentary literature data were used in the creation of a “generic” cross-section optical property model simulating the passage of thousands of photons through the tissue at different wavelengths. Fluorescence spectra of diagnostically relevant biomarkers excited by the UV and blue wavelengths were modelled on the basis of the Monte-Carlo method. Further to this, fluorescence data gathered by the MLNDS system LAKK-M from pig bladders was applied to the model for a specific representation of the photon passage through the tissues. The ultimate goal of this study is to employ this model to simulate the effects of different laser wavelength and energy inputs to bladder tissue and to determine the effectiveness of potential photonics based devices for the diagnosis of bladder pathologies. The model will aid in observing differences between healthy and pathological bladder tissues registered by photonics based devices.

9303-204, Session 10

In-vivo laser induced urethral stricture animal model for investigating the potential of LDR-brachytherapy

Ronald Sroka, Laser-Forschungslabor (Germany); Katja Lellig, Markus Bader, Christian G. Stief, Ludwig-Maximilians-Univ. Hospital München (Germany); Patrick Weidlich, Klinikum Traunstein AG (Germany); Walter Assmann, Ludwig-Maximilians-Univ. München (Germany); Ricarda Becker, Laser-Forschungslabor (Germany); Wael Khoder, Ludwig-Maximilians-Univ. München (Germany)

Purpose: Treatment of urethral strictures is a major challenge in urology. For investigation of different treatment methods an animal model was developed by reproducible induction of urethral strictures in rabbits to mimic the human clinical situation. By means of this model the potential of endoluminal LDR brachytherapy using β -irradiation as prophylaxis of recurrent urethral strictures investigated.

Material and Methods: A circumferential urethral stricture was induced by energy deposition using laser light application (wavelength $\lambda=1470$ nm, 10 W, 10 s, applied energy 100 J) in the posterior urethra of anaesthetized New Zealand White male rabbits. The radial light emitting fibre was introduced by means of a children resectoscope (14F). The grade of urethral stricture was evaluated in 18 rabbits using videourethroscopy and urethrography at day 28 after stricture induction.

An innovative catheter was developed based on a β -irradiation emitting foil containing ³²P, which was wrapped around the application system. Two main groups (each n=18) were separated. The “internal urethrotomy group” received after 28 days of stricture induction immediately after surgical urethrotomy of the stricture the radioactive catheter for one week in a randomized, controlled and blinded manner. There were 3 subgroups with 6 animals each receiving 0 Gy, 15 Gy and 30 Gy. In contrast animals from the “De Nuovo group” received directly after the stricture induction (day 0) the radioactive catheter also for the duration of one week divided into the same dose subgroups. In order to determine the radiation tolerance of the urethral mucosa, additional animals without any stricture induction received a radioactive catheter applying a total dose of 30 Gy (n=2) and 15 Gy (n=1). Cystourethrography and endoscopic examination of urethra were performed on all operation days for monitoring treatment progress. Based on these investigation a classification of the stricture size was performed and documented for correlation. At further 28 days after catheter removal the animals were euthanized and the urethra tissue was harvested. Histological examination of tissue with assessment of radiation damage, fibrotic and inflammatory changes were performed. After debinding histological findings were correlated with the applied dose.

Results: All animals developed a stricture, while 15/18 (83,3%) showed a

significant, high grade stricture with more than 90% lumen narrowing. Histopathological examination including evaluation of urethral inflammation, fibrosis and collagen content were investigated in additional 6 rabbits confirming the former findings. No rabbits died prematurely during the study.

The experiments showed that the procedure of the application of radioactive catheter was safe without any problems in contamination and protection handling. The combination of internal urethrotomy and LDR-brachytherapy results in a stricture free rate of 66.7% in the 15-Gy group, compared with only 33.3% among animals from the 0- and 30-Gy groups. Furthermore histological classification of inflammation and fibrosis of 0 Gy and 15 Gy showed similar extent.

Conclusion: This new method of laser induced urethral stricture was very efficient and showed a high reproducibility, thus being useful for studying stenosis treatments. The experiments showed that application of local β -irradiation by means of radioactive catheters modulated the stenosis development. This kind of LDR-brachytherapy shows potential for prophylaxis of urethral stricture. As this was an animal pilot experiment a clinical dose response study is needed.

9303-205, Session 10

Optical diagnosis of urinary tract infection

Babak Shadgan M.D., Mark Nigro, Andrew J. Macnab M.D., Lynn Stothers M.D., The Univ. of British Columbia (Canada); A. M. Kajbafzadeh, Tehran Univ. of Medical Sciences (Iran, Islamic Republic of)

Background: Lower urinary tract infection (LUTI) is a common and important urological condition that requires early diagnosis and treatment. Diagnosis is based on history and clinical symptoms confirmed by positive urine culture, which although feasible for the general population, it is not readily applicable in young children and individuals with neurogenic bladder where a reliable history and changes in sensation are lacking.

Objectives: To determine if monitoring bladder oxygenation level, using a transcutaneous near-infrared spectroscopy (NIRS) system allows detection of the presence or absence of LUTI in children.

Design, setting and participants: A convenience sample of children referred to a pediatric urology clinic with an acute LUTI, and a matched control group, were studied. Diagnosis was confirmed by history, physical examination, laboratory investigations. Participants had transcutaneous measurement of an absolute measure of tissue oxygen saturation (TSI%) in their bladder wall, and a quadriceps muscle control site, using a spatially-resolved wireless NIRS device. Average measures of bladder wall TSI% (B.TSI%) and quadriceps TSI% (Q.TSI%) and their differences (TSI.diff) were calculated and compared between those with LUTI and controls by performing a two-way ANOVA.

Results: Forty-eight patients met the inclusion criteria (24 LUTI and 24 controls). Comparing LUTI to controls B.TSI% and TSI.diff values were significantly higher in the LUTI group ($p < 0.0001$), while Q.TSI% values were not significantly different.

Conclusions: NIRS optical monitoring of an absolute measure of bladder wall oxygenation may offer a means of screening for LUTI where history and/or clinical signs are not available or adequate.

9303-206, Session 10

Label-free serial optical coherence tomography for visualizing development of unilateral ureteral obstruction

Sungbea Ban, Songye Baek, Junwon Lee, Sunwoo Jung, Eunjung Min, Andrey Vavilin, Woonggyu Jung, Ulsan National Institute of Science and Technology (Korea, Republic of)

**Conference 9303B:
Therapeutics and Diagnostics in Urology**

One of chronic kidney diseases, Unilateral Ureter Obstruction (UO), is the gradual process of renal tubulo-interstitial fibrosis by increasing the production of intercellular matrix and aberrant blood vessel fibrosis. It brings about severe loss in renal function over a period of time. Thus far, the principal method to investigate whether the damage in microcirculation occurred has been mainly proceeded by biological analytic technique.

However, there has been no optimal imaging tool to quantify the blood vessel network as well as morphology of intrarenal structure. For this reason, we developed the serial sectioning Optical Coherence Tomography which offers high resolution, cross-sectional tissue structure similar to histology, non-invasively. Since OCT uses the back scattering signal from tissue, it does not require the labeling technique. Not only OCT delivers contrast to blood vessel network, but also microstructure in kidney. Our system is based on the spectral domain OCT at 1310 nm central wavelength having 70 nm full width half maximum. In order to evaluate the performance of the developed system, we imaged renal structure, and reconstructed 3D blood vessel architecture. Acquired OCT images were compared to other imaging modalities such as histology, confocal microscopy, MRI, and CT. Our results shows stronger visualization of vessel arrangement which cannot be provided from existing imaging tool mentioned above. Through this experiment, it is expected that our imaging system would be used as a versatile tool for implication and quantification of renal disease pathology.

9303-207, Session 11

Kidney stone ablation times and peak saline temperatures during Holmium:YAG and Thulium fiber laser lithotripsy, in vitro, in a ureteral model

Luke A. Hardy, Christopher R. Wilson, The Univ. of North Carolina at Charlotte (United States); Pierce B. Irby M.D., Carolinas Medical Ctr. (United States); Nathaniel M. Fried, The Univ. of North Carolina at Charlotte (United States)

Introduction: Laser lithotripsy using clinical Holmium:YAG and experimental Thulium fiber lasers (TFL) was studied.

Methods: A 6-mm-inner-diameter tube with sieve and micro-thermocouples was used as a ureteral model for measuring stone ablation times and saline temperatures during Holmium:YAG and TFL lithotripsy. The Holmium laser (wavelength=2120 nm) was operated with typical parameters of 600 mJ, 350 microseconds, 6 Hz, and 270-micrometer-core optical fiber. The TFL (wavelength=1908 nm) was operated with 35 mJ, 500 microseconds, 500 Hz, and 100-micrometer-core fiber. Urinary stones (60% calcium oxalate monohydrate/40% calcium phosphate), of uniform mass and diameter (4-5 mm) taken from a single patient, were laser irradiated with fibers through a flexible ureteroscope and under saline irrigation. Total laser irradiation and procedure times were recorded once all stone fragments passed through a 1.5-mm sieve.

Results: Holmium laser irradiation and operation times measured 167±41 s and 207±50 s, respectively (n=12 stones, initial mass of 59±4 mg). TFL irradiation and operation times measured 23±4 s and 60±22 s, respectively (n=12 stones, initial mass of 66±10 mg). Peak saline irrigation temperatures reached 26 oC and 48 oC, for Holmium and TFL. Temperature was highly dependent on laser duty cycle for TFL.

Conclusions: The TFL rapidly fragmented kidney stones due in part to its high pulse rate, high average power, and observation of reduced stone repulsion, and may provide an alternative to conventional Holmium:YAG laser for lithotripsy. To avoid thermal buildup, TFL lithotripsy should be performed in short bursts with pulse rates below 500 Hz and/or increased saline irrigation rates.

9303-208, Session 11

Study of fiber-tip damage mechanism during Ho:YAG laser lithotripsy by high-speed camera and the Schlieren method

Jian J. Zhang, American Medical Systems (United States)

Fiber-tip degradation, damage, or burn back is a common problem during the ureteroscopic laser lithotripsy procedure to treat urolithiasis. Fiber-tip burn back results in reduced transmission of laser energy, which greatly reduces the efficiency of stone comminution. In some cases, the fiber-tip degradation is so severe that the damaged fiber-tip will absorb most of the laser energy, which can cause the tip portion to be overheated and melt the cladding or jacket layers of the fiber. Though it is known that the higher the energy density (which is the ratio of the laser energy fluence over the cross section area of the fiber core), the faster the fiber-tip degradation, the damage mechanism of the fiber-tip is still unclear. In this study, fiber-tip degradation was investigated by visualization of shockwave, cavitation/bubble dynamics, and calculus debris ejection with a high-speed camera and the Schlieren method. A commercialized, pulsed Ho:YAG laser at 2.12 um, 273/365/550-um core fibers, and calculus phantoms (Plaster of Paris, 10?10?10 mm cube) were utilized to mimic the laser lithotripsy procedure. Laser energy induced shockwave, cavitation/bubble dynamics, and stone debris ejection were recorded by a high-speed camera with a frame rate of 10,000 to 300,000 fps. The results suggested that using a high-speed camera and the Schlieren method to visualize the shockwave provided valuable information about time-dependent acoustic energy propagation and its interaction with cavitation and calculus. Detailed investigation on acoustic energy beam shaping by fiber-tip modification and interaction between shockwave, cavitation/bubble dynamics, and calculus debris ejection will be conducted as a future study.

9303-209, Session 11

Innovative techniques for partial nephrectomy: comparison of clinical outcome

Wael Khoder, Ludwig-Maximilians-Univ. München (Germany); Armin J. Becker, Christian G. Stief, Matthias Trottmann, Ludwig-Maximilians-Univ. Hospital München (Germany); Ronald Sroka, Laser-Forschungslabor (Germany)

Purpose: Evaluation of innovative techniques that could facilitate the technique and outcomes of the laparoscopic partial nephrectomy (LPN) for small renal tumours in a prospective study.

Patients and methods: In a prospective non-randomised study beginning at 2007, patients suffering from peripherally located renal tumours were candidates for nephron-sparing surgery (n=12 open partial nephrectomy (OPN), n=12 LPN). Cryoablation of renal tumours was followed in the same session by open (n=5 C-OPN) and laparoscopic (n=18 C-LPN) partial nephrectomy. Renal tumours were excised with laser (n=18 laser-assisted-LPN (L-LPN), n=7 L-OPN). Sonosurg (Ultraschall scissor) was used in S-LPN in 30 cases. Perioperative and follow-up parameters were estimated. All results were compared.

Results: Mean age for C-OPN was 74 years (69-83) with mean blood loss 140ml (50-200); for C-LPN: 65 years (47-80) with 100ml (50-750). All procedures were completed successfully without conversions (C-LPN), transfusions or intra-operative complications. Compared to OPN/LPN, C-OPN and C-LPN were associated with a longer operative time (P<0.05) and a comparable postoperative hospital stay. Histopathology showed cytologic changes suggesting fresh coagulative necrosis, glomerular vascular congestion and interstitial haemorrhages (acute cryo-effects). One patient (C-LPN) developed a pararenal abscess necessitating puncture after 7weeks. The follow-up (9-42months) was uneventful.

Conference 9303B: Therapeutics and Diagnostics in Urology

Mean age for laser assisted technique was 59 years. Mean operative time was 120 minutes (100-180) vs. 135 (85-255) vs. 100.6 (50-160) for L-LPN vs. LPN vs. OPN, respectively. Median estimated blood loss was 175 ml (50-600) vs. 250 (50-700) vs. 470 (100-900) for L-LPN vs. LPN vs. OPN, respectively. There were no reported perioperative complications/conversions. There were no positive margins. Histological evaluations were not compromised in any L-LPN-case.

Mean age of sonosurg assisted S-LPN was 63 years with mean operative time 145 minutes (90-180min) and median blood loss of 180ml (50-900ml). There were no reported perioperative complications.

Conclusions: The current experience shows that all used techniques are reproducible and efficient. Beside reduction of renal ischemia, L-LPN and C-LPN offered lower blood loss, good haemostasis and minimal parenchyma damage. Surgical and oncological outcomes are comparable to the standardised techniques of LPN and OPN without increasing procedure morbidity or compromising surgical and oncological outcomes.

9303-210, Session 11

In-vivo, percutaneous, optical biopsy of renal masses using optical coherence tomography

Abel Swaan, Peter G. Wagstaff, Henricus J. C. M. Sterenberg, Jean J. de la Rosette, M. Pilar Laguna Pes, Otto M. Van Delden, Ton G. Van Leeuwen, Daniel M. de Bruin, Dirk J. Faber, Academisch Medisch Centrum (Netherlands)

Optical Coherence Tomography (OCT) is based on the backscattering of near infrared light and provides real time images (~10µm spatial resolution, 2mm tissue penetration). OCT systems with a rotating fiber based probe are now commercially available. The outer diameter of 0.9 mm allows for insertion through needles and scopes. Within the OCT images, the loss of signal as function of penetration depth, the attenuation coefficient, is calculated. The attenuation coefficient is a tissue specific property, providing a quantitative parameter for tissue differentiation.

Until recently, renal mass treatment decisions have been made primarily on the basis of age, comorbidity and gross imaging characteristics. However, these parameters and diagnostic methods lack the finesse to truly detect the malignant potential of a renal mass. A successful core biopsy or fine needle aspiration provides objective tumor differentiation with both sensitivity and specificity in the range of 95-100%. However, a non-diagnostic rate of 10-20% overall, and even up to 30% in small renal masses is to be expected, impairing clinical practicality.

We aim to develop OCT into an optical biopsy, providing real-time imaging combined with on-the-spot tumor differentiation by means of the attenuation coefficient. The detailed step-by-step approach for percutaneous OCT of renal masses and the results of the first measurements will be presented at the conference.

Acknowledgements

This study was funded by Dutch Technology Foundation (STW) grant numbers iMIT-PROSPECT 12707, ZonMW and the Cure for Cancer Foundation.

9303-214, Session PSat

Quantitative diagnosis of bladder cancer by morphometric analysis of H&E images

Binlin Wu, Weill Cornell Medical College (United States); Samantha V. Nebylitsa, Bronx High School of Science (United States); Sushmita Mukherjee, Manu Jain, Weill Cornell Medical College (United States)

In clinical practice, histopathological analysis of biopsied tissue is the main method for bladder cancer diagnosis and prognosis. The diagnosis is performed by a pathologist based on the morphological features in the image of a hematoxylin and eosin (H&E) stained tissue sample. This manuscript proposes algorithms to perform morphometric analysis on the H&E images, quantify the features in the images, and discriminate bladder cancers with different grades, i.e. high grade and low grade. The nuclei are separated from the background and other types of cells such as red blood cells (RBCs) using image segmentation either by thresholding on individual channels of the RGB images, or color deconvolution with all channels combined since different colors are shown in different cells and structures. A mask of nuclei is generated for each image. The features of the nuclei in the mask image including area size, shape, orientation, and their spatial distributions are measured. K-nearest-neighbor (KNN) algorithm is used to quantify local clustering of certain nuclei that carry common properties such as large area, elongated shape and/or well organized patterns. The global distribution of the features is measured using histogram of the KNN distances. A linear discriminant analysis (LDA) is used to classify the high grade and low grade bladder cancers with high sensitivity and specificity. This study shows the proposed approach can potentially help expedite pathological diagnosis by triaging potentially suspicious biopsies.

9303-215, Session PSat

Optical and electrical stimulation of the rat prostate cavernous nerves: priming and fatigue studies

Ghalla S. Kaouk, William C. Perkins, The Univ. of North Carolina at Charlotte (United States); Gwen A. Lagoda, Arthur L. Burnett M.D., The Johns Hopkins Hospital (United States); Nathaniel M. Fried, The Univ. of North Carolina at Charlotte (United States)

Introduction: Optical nerve stimulation (ONS) is being explored as an alternative to electrical nerve stimulation (ENS) for use as an intra-operative diagnostic method for identification and preservation of cavernous nerves (CN's) during prostate cancer surgery. Continuous-wave, infrared irradiation of CN's produces an intracavernous pressure (ICP) response in rats. Nerve priming and fatigue studies were performed to further characterize CN's and provide insight into ONS mechanisms. ENS studies were conducted for comparison.

Methods: ENS was performed with standard parameters (4 V, 5 ms, 16 Hz) for fatigue studies, but incrementally increasing/decreasing voltage (0.1-4.0 V) for priming studies. For ONS priming studies, a 1455-nm diode laser coupled to fiber optic probe delivered a 1-mm-diameter laser spot on CN's, and laser power was escalated (15-60 mW) for 15 s, until a strong ICP response was observed, and then power was de-escalated. Fatigue studies were performed at constant laser power (ONS) or voltage (ENS) for 10 min. A total of 19 rats were studied.

Results: Stimulation threshold was ~20% higher during initial escalating laser power steps (6.4 W/cm²) than in subsequently de-escalating laser power steps (5.1 W/cm²), demonstrating nerve priming. No evidence of nerve priming during ENS was observed. For fatigue studies, ONS of CN's showed peak ICP response at ~90 s, followed by a gradual decay in ICP, while ENS maintained a strong, but cyclical ICP.

Conclusions: Nerve priming may allow repetitive ONS of CN's at lower and safer laser power. Nerve fatigue studies revealed different ICP response curves for ONS and ENS.

**Conference 9303B:
Therapeutics and Diagnostics in Urology**

9303-216, Session PSat

Infrared laser sealing of porcine tissues: preliminary in vivo studies

Christopher M. Cilip, Thomas C. Hutchens, The Univ. of North Carolina at Charlotte (United States); Duane E. Kerr, Cassandra Latimer, Covidien (United States); Sarah B. Rosenbury, Nicholas C. Giglio, Gino R. Schweinsberger, William C. Perkins, Christopher R. Wilson, The Univ. of North Carolina at Charlotte (United States); Arlen K. Ward, William H. Nau Jr., Covidien (United States); Nathaniel M. Fried, The Univ. of North Carolina at Charlotte (United States)

Introduction: Energy-based, electrosurgical and ultrasonic devices currently provide rapid surgical hemostasis, but may create undesirably large collateral zones of thermal damage and tissue necrosis. We are exploring infrared lasers as an alternative. Previously, a 1470-nm infrared laser sealed and cut ex vivo porcine renal arteries of 1-8 mm in 2 s, yielding burst pressures > 1200 mmHg (compared to normal systolic blood pressure of 120 mmHg) and thermal coagulation zones < 3 mm (including the seal). This preliminary study describes in vivo testing of a laser probe in a porcine model.

Methods: A prototype, fiber optic based handheld probe with vessel/tissue clamping mechanism was tested on blood vessels < 6 mm diameter using incident 1470-nm laser power of 35 W for 1-5 s. The probe was evaluated for hemostasis after sealing isolated and bundled vasculature of abdomen and hind leg, as well as liver and lung parenchyma. Sealed vessel samples were collected for histological analysis of lateral thermal damage.

Results: Hemostasis was achieved in 57 of 73 seals (78%). The probe consistently sealed vasculature in small bowel mesentery, mesometrium, and gastro splenic and epiploic regions. Seal performance was less consistent on hind leg vasculature including saphenous arteries and bundles and femoral and iliac arteries. Collagen denaturation averaged 1.6 mm in 8 samples excised for histologic examination.

Conclusions: A handheld laser probe sealed porcine vessels in vivo. With further improvements in probe design and laser parameter optimization, lasers may provide an alternative to radiofrequency and ultrasonic vessel sealing devices.

9303-217, Session PSat

Thulium fiber laser damage to Nitinol stone baskets

Christopher R. Wilson, Luke A. Hardy, The Univ. of North Carolina at Charlotte (United States); Pierce B. Irby M.D., Carolinas Medical Ctr. (United States); Nathaniel M. Fried, The Univ. of North Carolina at Charlotte (United States)

Introduction: Nitinol stone baskets are commonly used during clinical Holmium:YAG laser lithotripsy procedures for stone stabilization and retrieval. However, baskets are susceptible to laser-induced damage when the fiber tip is in contact with or in close proximity to basket wires. This study characterizes stone basket damage from an alternative, experimental, Thulium fiber laser (TFL) lithotripter.

Methods: The TFL (wavelength=1908 nm) was operated at 35 mJ, 500 microseconds, 50-500 Hz, and with a 100-micrometer-core silica optical fiber. Nitinol wires from 1.9-Fr clinical stone baskets were tested with the laser fiber oriented perpendicular to the wire. Damage was graded as a function of pulse rate, number of pulses, and working distance. A 0-5 scale was used for evaluation, representing no damage (0%), discoloration, partial cuts (25, 50, 75%), and complete cut (100%), respectively. Five samples were tested for each parameter set.

Results: Nitinol basket wire damage decreased as working distance

increased and was non-existent > 1.0 mm from basket wires. In contact mode, a total of 500 pulses delivered at pulse rates > 200 Hz (or less than 2.5 s) was sufficient to cut wires.

Conclusions: TFL-induced damage to stone basket wires was observed during contact mode and at distances < 1.0 mm. By comparison, the Holmium laser has been reported to damage basket wires at working distances up to ~ 4 mm. Improvement in fiber tip centering during TFL lithotripsy, potentially through use of integrated fiber / stone basket devices, may further reduce probability of nitinol basket damage.

9303-218, Session PSat

Photoacoustic imaging guided laser treatment for superficial bladder carcinoma: feasibility study

Van Phuc Nguyen, Pukyong National Univ. (Korea, Republic of) and Interdisciplinary Program of Marine-Bio, Electrical & Mechanical Engineering (Korea, Republic of); JungHwan Oh, Hyun Wook Kang, Pukyong National Univ. (Korea, Republic of) and Ctr. for Marine-Integrated Biomedical Technology (Korea, Republic of)

Photoacoustic imaging (PAI) is a novel technology providing a high contrast and non-invasive method of visualizing tumor depth in bladder cancer. The objective of this study was to investigate the efficiency of laser treatment for eliminating superficial cancer cells in bladder and noninvasively monitor the thermally treated lesions with PAI. An 80-W 532-nm laser system was implemented to induce thermal necrosis in five fresh canine bladders with superficial tumor in vitro. Then, the thermal treated lesions was detected by PAI system at various wavelengths. In addition, the injection of indocyanine green (ICG) into bladder tumor was utilized to enhance PAI image contrast. Simultaneously, the bladder tumor was superficially ablated with laser beam under the guidance of photoacoustic images. The tip of fiber was held between 0.25 mm to 0.75 mm distance from the tumor while laser was activated. Temperature rise of tissue under treatment was between 40 to 60 oC to induce cellular death. Complete tumor removal was accomplished for all treatments with the treatment time of 50 to 60 s. The treated volume was estimated around 65 mm³. PA imaging results showed that bladder tumors were clearly visualized after injection of ICG. In addition, the PA signal of bladder tumor was enhanced by approximately five times in compared with normal tissues. The current study implies that the integration of PAI and laser therapy can be an effective means of identifying the precise location of tumor and can be a promising and emerging method for monitoring laser thermal treatment for solid tumors.

9303-219, Session PSat

Transurethral application of optical cylindrical diffuser for urethrostenosis treatment

Hyun Shin, Pukyong National Univ. (Korea, Republic of); Trung Hau Nguyen, Ctr. of Marine-Interated Biomedical Technology, Pukyong National Univ. (Korea, Republic of); HyunWook Kang, Pukyong National Univ. (Korea, Republic of)

Urethrostenosis is a narrowing of urethra caused by injury or disease, resulting in urethritis with pain during urination and inability to fully empty the bladder. The development of more effective and long-lasting techniques for urethrostenosis treatments has focused on removing infection and acquiring a urethral canal. The purpose of this study was to validate efficacy and safety of optical diffuser as a potential treatment for removing infection in urethra without any injury to normal tissue. An optical diffuser was developed to achieve the uniform light distribution by micro-machining

**Conference 9303B:
Therapeutics and Diagnostics in Urology**

the surface of an optical fiber using focused CO₂ laser light at 10 W. Spatial distributions of light, temperature, and energy were measured in order to show beam propagation from diffuser. Bovine liver tissue was used as a tissue model for in vitro testing to observe coagulated depth as a function of fabrication angle, irradiation time, and power. In addition, canine urethra tissue was used for ex vivo testing to explore the effect of irradiation time and power on the degree of tissue coagulation. Light distribution area presented up to 24.4 % percent difference from expected distribution for the uniform radial light distribution. Thermal image and power measurement demonstrated rather lopsided-elliptical distribution of laser light possibly due to shallower fabrication depth (~30 μm). Tissue testing presented no dependence of coagulation depth on fabrication angles. Longer irradiation time and higher power facilitated coagulation process in tissue. The application of optical cylindrical diffuser can be a feasible method to treat urethrostenosis in a safe and efficacious manner by removing infections without any injury to normal tissue.

9303-220, Session PSat

Photoactive dye-enhanced tissue ablation for endoscopic laser prostatectomy

Minwoo Ahn, Van Phuc Nguyen, Trung Hau Nguyen, Pukyong National Univ. (Korea, Republic of); JungHwan Oh, Pukyong National Univ. (Korea, Republic of) and Interdisciplinary Program of Marine-Bio, Electrical & Mechanical Engineering, Pukyong National Univ. (Korea, Republic of) and Ctr. for Marine-Integrated Biomedical Technology (BK21 Plus), Pukyong National Univ. (Korea, Republic of); Hyun Wook Kang, Pukyong National Univ. (Korea, Republic of) and Interdisciplinary Program of Marine-Bio, Electrical & Mechanical Engineering, Pukyong National Univ. (Korea, Republic of) and Ctr. for Marine-Integrated Biomedical Technology, Pukyong National Univ. (Korea, Republic of)

Laser light has been widely used as a surgical tool to treat benign prostate hyperplasia with high laser power. The purpose of this study was to validate the feasibility of photoactive dye injection to enhance light absorption and eventually to facilitate tissue ablation with low laser power. The experiment was implemented on chicken breast due to minimal optical absorption. Amaranth (AR), black dye (BD), hemoglobin powder (HP), and endoscopic marker (EM), were selected and tested in vitro with a customized 532-nm laser system with radiant exposure ranging from 0.9 to 3.9 J/cm². Light absorbance and ablation threshold were measured with UV-VIS spectrometer and Probit analysis, respectively, and compared to feature the function of the injected dyes. Ablation performance with dye-injection was evaluated in light of radiant exposure, dye concentration, and number of injection. Higher light absorption by injected dyes led to lower ablation threshold as well as more efficient tissue removal in the order of AR, BD, HP, and EM. Regardless of the injected dyes, ablation efficiency principally increased with input parameter. Among the dyes, AR created the highest ablation rate of 44.2±0.2 μm/pulse due to higher absorbance and lower ablation threshold. Preliminary tests on canine prostate with a hydraulic injection system demonstrated that 80 W with dye injection yielded comparable ablation efficiency to 120 W with no injection, indicating 33 % reduced laser power with almost equivalent performance. In-depth comprehension on photoactive dye-enhanced tissue ablation can help accomplish efficient and safe laser treatment for BPH with low power application.

9303-211, Session 12

Probed-based confocal laser endomicroscopy (pCLE): a new life cell imaging technique to evaluate sperm-oviduct interaction

Sabine Koelle, Univ. College Dublin (Ireland); Irene Alba-Alejandre, Univ. Medical Ctr. of Obstetrics and Gynaecology, Ludwig-Maximilians-Univ. München (Germany); Regina Leeb, Ludwig-Maximilians-Univ. München (Germany); Ronald Sroka, Herbert Stepp, LIFE Ctr., Klinikum Grosshadern, Ludwig-Maximilians-Univ. München (Germany); Bernhard Liedl, Clinics for Surgery, Munich-Bogenhausen (Ghana); Kate Dulohery, Univ. College Dublin (Ireland); Christian G. Stief, Ludwig-Maximilians-Univ. München (Germany); Matthias Trottmann, Univ. München (Germany)

Introduction and objective: For successful pregnancy, the functional integrity of the sperm-oviduct interaction is essential. According to estimates, up to 30% of idiopathic infertility might be caused by alterations of the oviduct which negatively impact sperm-oviduct interaction. Therefore the aim of our study was to evaluate the use of probe-based confocal laser endomicroscopy (pCLE), which is routinely used for in vivo investigations in gastroenterology and pulmonology, for the in vivo evaluation of gameto-maternal interaction on a cellular level and in real-time.

Material and Methods: Sperm-oviduct interaction was analysed in a) 7 transsexual females, b) 2 transsexual patients who had had intercourse 2.5 days before surgery and c) 9 premenopausal women undergoing hysterectomy. Ampulla and isthmus with and without co-incubation with a) native and b) frozen thawed spermatozoa were examined by using the Cellvizio® (Mauna Kea Technologies, France) pCLE system. Confocal microprobe ProFlex™ S1500 (diameter 1.5 mm, lateral resolution 3.3 μm) and microprobe Ultra Mini O (diameter 2.6 mm, lateral resolution 1.4 μm) were compared. Fluorescent labelling was performed by incubation with either 0.001% fluorescein isothiocyanate (FITC), 5% cresyl violet solution (CV), 0.001% TO-PRO®-3 Iodide (T3) and 0.04 % acriflavine (AF). pCLE imaging was correlated to images obtained by confocal laser microscopy, light microscopy and scanning electron microscopy (SEM).

Results: pCLE allows visualization of the formation of the sperm reservoir in real-time and on a cellular level. Only spermatozoa with an intact plasma membrane are able to bind and to stay viable. After attachment to the cilia of the oviductal epithelial cells the spermatozoa stay motile. Application of hormones such as testosterone results in distinct dedifferentiation of the oviductal cells and in the accumulation of mucus which impair sperm binding.

Conclusions: Our studies for the first time allow to visualize sperm-oviduct interaction on a cellular level and in real-time. By using pCLE in combination with fertiloscopy in vivo imaging of the physiology and pathology of the oviductal microarchitecture as well as oviduct-sperm interaction on a microscopic level might be a valuable tool for opening up new therapeutic concepts for successful treatment of idiopathic infertility.

**Conference 9303B:
Therapeutics and Diagnostics in Urology**

9303-212, Session 12

Intravital two-photon microscopy of the aging kidney

Hengchang Guo, Univ. of Maryland, College Park (United States); Peter M. Andrews, Erik Anderson M.D., Georgetown Univ. Medical Ctr. (United States); Tikina Smith, Yu Chen, Univ. of Maryland, College Park (United States)

Chronic Kidney Disease (CKD) is a growing problem among the aging population. In this study, we used the advantages of two-photon fluorescence microscopy (TPM) to evaluate pathological changes in a living rat model of the aging kidney.

With the advantages of high resolution and deep penetration imaging, TPM is unique in its ability to provide valuable insights into the tubular and glomerular pathology of a living kidney. It is important to image these changes in the living kidney because of well known confounding artifacts associated with the preservation (i.e., fixation) of the kidney. TPM revealed atrophy, and necrosis of some tubules leading to interstitial fibrosis and dilation and hyaline casts in other tubules. Glomerular permeability and flow of glomerular filtrate through the uriniferous tubules were evaluated by intravenous infusion of fluorophore-labeled dextrans. The TPM studied kidneys were preserved by vascular perfusion fixation for comparison with convention light microscopy.

The procedures of TPM imaging revealed that tubular atrophy/necrosis, tubular dilation, hyaline cast and interstitial fibrosis are common in the 12-month-old male Munich-Wistar rat strain. These changes become progressively more severe over the next 4-6 months (i.e., 16-18 month old group). Glomerulosclerosis was characterized by slower than normal glomerular permeability, shrinkage of the glomerular tuft and atrophied capillary loops. In addition, we noted selected permeability across the glomerular wall of some sclerotic glomeruli, supporting the concept of "blow-out" sites proposed to be responsible for proteinuria. Tubular dilation was so severe in the 16-18 month old group, that cysts of dilated tubules covered the surfaces of these kidneys. The 16-18 month old rats showed a significant rise in serum creatinine levels, polyuria and significant declines in body weight.

Together, the foregoing observations provide unique insights into the progression of end-stage renal function in the aging kidney.

9303-213, Session 12

Investigation of the potential of optical coherence tomography (OCT) as a non-invasive diagnostic tool in reproductive medicine

Matthias Trottmann, Regina Leeb, Ludwig-Maximilians-Univ. Hospital München (Germany); Christian Homann, Daniel Doering, Julia Kuznetsova, Laser-Forschungslabor (Germany); Sven Reese, Institute of Veterinary Anatomy, Histology and Embryology, Ludwig-Maximilians-Univ. München (Germany); Christian G. Stief, Ludwig-Maximilians-Univ. Hospital München (Germany); Sabine Koelle, Univ. College Dublin (Ireland); Ronald Sroka, Laser-Forschungslabor (Germany)

Introduction and objective: In Europe, nearly every sixth couple in the reproductive age is involuntarily childless. In about 30%, both male and female reveal fertility problems. In about 10% of infertile men, azoospermia is the underlying cause. As conventional therapeutic options are limited, surgical testicular sperm extraction (TESE) is necessary to obtain sperms for assisted reproductive techniques. Regarding the females, up to 30% of all idiopathic infertilities are due to alterations of the uterine tube. So far,

no imaging technique, which does not require any labelling, is available to evaluate the male and female genital tract at a microscopic level under in vivo conditions. Thus, the aim of this study was to investigate the potential of optical coherence tomography (OCT) as a non-invasive diagnostic tool in gynaecology and andrology.

Material and Methods: Tissues samples from the bovine testis, epididymis, vas deferens, ovary, oviduct (ampulla and isthmus) and uterus were obtained immediately after slaughter (14 cows aged 3 to 8 years and 14 bulls aged 3 to 6 years; breeds: Holstein-Friesian, and Deutsches Fleckvieh). Imaging was done by using the US Food and Drug Administration (FDA) approved probe-based Niris Imaging System (Imalux, Cleveland, Ohio, USA) and the Telesto 1325 nm OCT System and Ganymede 930 nm OCT System (Thorlabs Inc., Dachau, Germany). All images obtained were compared to histological images after paraffin embedding and H&E staining.

Results: OCT imaging visualized the microarchitecture of the testis, epididymis, spermatic duct and the ovary, oviduct and uterus. Using the Thorlabs systems a axial resolution of approx. 5µm and lateral resolution of 8-15µm could be achieved. Different optical tissue volumes could be visualized, which depends on the optical penetration depth of the wavelength of the system used. While the tissue volume observed by probe based Imalux-OCT is similar to the used Thorlabs systems, the optical resolution is reduced. By means of the microscopic OCT-system differentiation of testicular tissue structures like content and diameter of seminiferous tubules and the epididymal duct was possible. Structures of the female oviduct, like the primary, secondary and tertiary folds including the typical epithelium consisting of secretory and ciliated cells were identified. Ampulla and isthmus were clearly differentiated by the height of the folds and the thickness of the smooth muscle layer. Imaging was successful both from the outside wall and from the inner lumen. After experience with microscopic OCT-structure identification such structures could also be identified by means of probe based OCT.

Conclusions: Technical improvement of probe-based OCT up to a high-resolution level of nowadays-available OCT microscopic systems could open up new ways of in vivo imaging in the reproductive tract. Potential applications could be an OCT-guided testicular biopsy for improving sperm retrieval or microscopic evaluation of the oviduct by OCT-assisted fertiloscopy. The latter would provide a valuable tool to facilitate the decision of which type of assisted reproductive techniques might be preferred.

Conference 9303C: Optical Imaging, Therapeutics, and Advanced Technology in Head and Neck Surgery and Otolaryngology

Saturday - Sunday 7-8 February 2015

Part of Proceedings of SPIE Vol. 9303 Photonic Therapeutics and Diagnostics XI

9303-301, Session 1

Quantitative measurement of tympanic membrane compliance in normal and diseased patients

Ryan L. Shelton, Guillermo L. Monroy, Ryan M. Nolan, Univ. of Illinois at Urbana-Champaign (United States); Michael A. Novak M.D., Malcolm C. Hill M.D., Carle Foundation Hospital (United States); Stephen A. Boppart M.D., Univ. of Illinois at Urbana-Champaign (United States)

Otoscopy is used routinely by primary care physicians and ear specialists to assess the health of the middle ear by examining the surface of the tympanic membrane (TM). Users evaluate subjective visual markers of the TM such as coloration, opacity, and position (distension/retraction). With this information, they attempt to evaluate the middle ear, which cannot be directly observed. Pneumatic otoscopy adds the ability to change the pressure of the sealed ear canal during a standard otoscopy exam. The canal is sealed using a special speculum tip and the middle ear pressure is modulated using an insufflation bulb connected to a pneumatic port on the otoscope. This allows the user to evaluate the mobility of the TM, which correlates to middle ear pressure and eardrum stiffness, characteristics of middle ear disease.

We have previously shown a proof-of-concept imaging system that provides the user with the ability to measure displacements of the TM on the order of 10 microns. The system used low-coherence interferometry (LCI), an optical depth profiling technique, to measure thickness and displacement of the membrane. Expanding upon this initial work, we have characterized the ability of the imaging system to measure changes in middle ear pressure in phantoms. Additionally, we have directly compared our technique with standard pneumatic otoscopy in vivo in both control and diseased patients. A prototype optical coherence tomography (OCT) handheld imaging system capable of pneumatic measurements was also built and characterized. Performance of the OCT vs. LCI implementations for pneumatic measurements are evaluated and discussed.

9303-302, Session 1

A compact structured light based otoscope for three dimensional imaging of the tympanic membrane

Anshuman J. Das, Massachusetts Institute of Technology (United States); Julio C. Estrada-Rico, Ctr. de Investigaciones en Óptica, A.C. (Mexico); Zhifei Ge, Sara Dolcetti, Deborah L Chen, MIT (United States); Ramesh Raskar, MIT Media Lab. (United States)

Several factors lead to positive or negative pressure in the middle ear causing the tympanic membrane to bulge or retract. Typically a positive pressure results due to effusion in cases of acute otitis media whereas negative pressure may occur due to a weak tympanic membrane or incomplete opening of the eustachian tube. In either case, a bulge or retraction is often not detected by visual examination and leads to misdiagnosis. We have designed and developed an otoscope that is capable of carrying out visual examination and can simultaneously image the curvature of the tympanic membrane. This device uses structured light illumination with phase shifting algorithms to detect the surface of

the tympanic membrane. Illumination is carried out using a high definition portable projector and the imaging is done by a high resolution camera equipped with a magnifying telephoto lens. As a result depth features in the order of 20 microns can be distinguished with our device. The form factor of the device is similar to that of a conventional otoscope making it compact and portable as compared to holographic or optical coherence tomography techniques. The operation of the device does not require any additional training and hence can be seamlessly adopted by clinical practitioners.

9303-303, Session 1

Initial results of an OCT vibration measuring otoscope

Tracy C. Petrie, Anh T. Nguyen-Huynh, Steven L. Jacques, Alfred L. Nuttall, Oregon Health & Science Univ. (United States)

We present the initial results of an otoscope device that includes an optical coherence tomography capability for measuring the vibration of the ossicles behind an intact tympanic membrane. The device includes a directed sound source to stimulate the vibration response of the middle ear at precise frequencies and uses a microphone to monitor the sound pressure level. This work follows on from previous research using phase-sensitive OCT (PS-OCT) to detect sub-nanometer vibrations in fresh human cadaver ears. We have replaced the earlier spectral-domain OCT system with a swept-source OCT system offering a longer imaging range. We will present results obtained from both phantoms and humans.

9303-323, Session 1

Middle ear full-range vibrometry with Fourier-domain phase sensitive optical coherence tomography

Hrebesh Molly Subhash, National Univ. of Ireland, Galway (Ireland)

As a non invasive depth resolved optical imaging technology, optical coherence tomography become a well established clinical imaging tool in many areas including ophthalmology, dermatology and cardiology. Recently, there is an increasing interest in the development of OCT for functional and structural imaging of middle ear structures in the field of otology. We have recently successfully demonstrated the feasibility of a phase sensitive Fourier domain OCT (ps-FD OCT) for both structural and vibrational imaging of the intact tympanic membrane and the ossicular chain on a human cadaver model. The ps FD OCT has the potential to provide localized depth resolved detection of quantitative vibration amplitude of middle ear structures for the diagnosis of conductive hearing loss. However one of the main drawback of conventional ps FD OCT is the complex conjugate artifact, which restricts the utilization of the available imaging range to only one-half. In order to resolve this issue, we propose a full-range ps FD OCT base vibrometer for imaging both structural and functional imaging of the middle ear structures. We demonstrates the feasibility of the proposed system for imaging the temporal bone of an ex vivo mouse.

**Conference 9303C: Optical Imaging, Therapeutics, and Advanced Technology in
 Head and Neck Surgery and Otolaryngology**

9303-326, Session 1

**Light-based contact hearing device:
 maximum equivalent pressure output and
 gain before feedback**

 Sunil Puria, Rodney Perkins, EarLens Corp. (United States);
 Peter Santa Maria, Stanford Univ. (United States)

The EarLens system is a non-surgical investigational hearing device consisting of two components: a tympanic contact actuator (TCA), which is a light-activated balanced-armature transducer that drives the middle ear through direct contact with the umbo; and a behind-the-ear unit (BTE) that encodes amplified sound into pulses of light that are emitted via a light source in the ear canal to wirelessly drive and power the TCA. In comparison to conventional acoustic hearing aids, this approach is designed to provide higher levels of output and functional gain over a broad frequency range; and has a significantly higher maximum gain before feedback (GBF).

The maximum equivalent pressure output (MEPO) of the TCA provides an important guideline for setting BTE light output levels and fitting of the device to a subject's hearing profile. MEPO varies across subjects, and is in part a function of the distance between the light source and TCA. It was designed to exceed 100 dB SPL at many frequencies. Because MEPO could not be measured in subjects, and given that no suitable artificial middle ear model exists for testing the system, we performed our measurements on fresh human cadaver temporal-bone specimens.

To calculate MEPO and GBF, we measured ear-canal pressure (PEC) within 2–3 mm of the eardrum, using a probe-tube microphone; and stapes velocity (VST), using a Polytec HLV-1000 laser Doppler vibrometer; for: 1) the baseline case of sound-driven stimulation (unaided), and 2) light-driven cases using a BTE and custom-shaped TCA.

The baseline sound-driven measurements (e.g., around 0.1 (mm/s)/Pa near 1 kHz) are consistent with previous reports (Rosowski et al., 2007). The overall average MEPO (N=4) varies from 117 to 127 dB SPL in the 0.7 to 10 kHz range, with the peak occurring at 7.6 kHz. Below 0.7 kHz, it varies from 83 to 117 dB SPL. In terms of the average GBF, a broad minimum of about 10 dB occurs in the 1–4 kHz range. Above about 4 kHz, it rises and the overall average reaches 42 dB at 7.6 kHz. Above this, a sharp decline in GBF occurs at around 11 kHz. From 0.2 to 1 kHz, GBF decreases linearly from about 40 dB as the frequency increases.

In summary, the direct-contact photonic hearing device provides high output and high gain margins, which may offer a feasible way of providing broad-spectrum amplification appropriate to treat listeners with mild-to-severe hearing impairment.

9303-305, Session 2

**Label-free imaging of in vivo cochlear
 blood flow using functional optical
 coherence tomography**

 Ruikang K. Wang, Univ. of Washington (United States);
 Alfred L. Nuttall, Oregon Health & Science Univ. (United States)

Studying the inner ear microvascular dynamics is extremely important to understand the cochlear function and to further advance the diagnosis, prevention and treatment of many otologic disorders. However, there is currently no effective imaging tool available that is able to access the blood flow within the intact cochlea. In this paper, we report the use of an ultrahigh sensitive optical micro angiography (UHS-OMAG) imaging system to image 3D microvascular perfusion within the intact cochlea in living mice. The UHS-OMAG image system used in this study is based on spectral domain optical coherence tomography, which uses a broadband light source centered at 1300nm with an imaging rate of 92,000 A-scans per second, capable of acquiring high-resolution B scans at 300 frames/sec. The technique is sensitive enough to image very slow blood flow velocities, such

as those found in capillary networks. The 3D imaging acquisition time for a whole cochlea is ~4.1 sec. We demonstrate that volumetric reconstruction of microvascular flow obtained by UHS-OMAG provides a comprehensive perfusion map of several regions of the cochlea, including the otic capsule, the stria vascularis of the apical and middle turns and the radiating arterioles that emanate from the modiolus.

9303-306, Session 2

**In vivo vibratory response of the organ of
 Corti in the apex of the mouse cochlea**

 Audrey K. Ellerbee, Hee Yoon Lee, Patrick D. Raphael, John
 S. Oghalai M.D., Stanford Univ. (United States); Brian E.
 Applegate, Texas A&M Univ. (United States)

Sound-induced vibrations of the organ of Corti (OC) stimulate transduction via sensory hair cells, which transmit the information to the auditory nerve. To measure these sub-nanometer vibrations, most in vivo studies of cochlear mechanics have opened the cochlea, placed a reflective glass bead on the undersurface of the OC (the basilar membrane, BM), and then measured sound-evoked movements of the bead using a laser Doppler vibrometer (LDV). However, the OC is a non-rigid structure with multiple layers of cells and extracellular matrix, each with different mechanical properties. In addition, the outer hair cells produce force to amplify the traveling wave, a process termed cochlear amplification. Cochlear amplification develops within the complex, interlocking, three-dimensional structure of the OC, which likely does not vibrate as a rigid body. We used a new technique called volumetric optical coherence tomography vibrometry (VOCTV) to obtain depth-resolved displacement measurements of the OC with sensitivity and speed comparable to LDV. Traveling wave propagation within the cochlea of living mice could be measured over a 3D volume of tissue by non-invasively imaging through the bony shell that surrounds the cochlea. We report the first in vivo displacement measurements of the tectorial membrane – the structure that directly stimulates the hair cell stereociliary bundles to transduce sound – and compare its vibratory response to that of its commonly-measured counterpart, the BM. The larger non-linearities associated with cochlear amplification demonstrated by the tectorial membrane compared with the BM experimentally explain discrepancies between afferent auditory nerve and basilar membrane response patterns.

9303-307, Session 2

**Two dimensional vibrations of the organ
 of Corti measured using phase sensitive
 Fourier domain optical coherence
 tomography**

 Sripriya Ramamoorthy, Yuan Zhang, Tracy C. Petrie,
 Oregon Health & Science Univ. (United States); Anders
 Fridberger, Linköping Univ. (Sweden); Tianying Ren,
 Oregon Health & Science Univ. (United States); Ruikang
 K. Wang, Univ. of Washington (United States); Steven L.
 Jacques, Alfred L. Nuttall, Oregon Health & Science Univ.
 (United States)

The sound-induced vibrations of the organ of Corti are hypothesized to have components in two directions, both axial and radial. The vibrations of the basilar membrane are expected to be primarily axial. However, according to the above hypothesis, a structure within the organ of Corti called the 'tectorial membrane' resonates radially and this resonance occurs at a frequency half-octave below the best frequency at a given tonotopic (longitudinal) location. This theory has important consequences for hearing, but it has not been tested in vivo. In this study, we measure the in vivo apical-turn vibrations of the guinea pig organ of Corti in both axial and radial directions using phase-sensitive Fourier domain optical coherence

**Conference 9303C: Optical Imaging, Therapeutics, and Advanced Technology in
Head and Neck Surgery and Otolaryngology**

tomography. The guinea pig apical turn has best frequencies around 100 – 500 Hz which are relevant for human speech. Preliminary data from this study will be presented in this report.

9303-309, Session 2

The optimal low level laser therapy (LLLT) dosage to treat noise-induced hearing loss (NIHL) in rats

Chung-Ku Rhee M.D., Dankook Univ. Hospital (Korea, Republic of); Kevin Song, Univ. of Illinois at Champaign-Urbana (United States); So Young Chang, Dankook Univ. Hospital (Korea, Republic of); Jae Yun Jung, Dankook Univ. (Korea, Republic of); Phil-Sang Chung M.D., Dankook Univ. Hospital (Korea, Republic of); Myung-Whan Suh M.D., Seoul National Univ. (Korea, Republic of)

Aim: The LLLT was found to recover NIHL and ototoxicity induced hearing loss in rats but the optimal LLLT laser dosage to treat NIHL needs to be determined. The aim of this study was to find the optimal laser dosage to recover a NIHL with transcanal-LLLT.

Methods: Bilateral ears of rats were exposed to noise (narrow band noise, 120 dB, 16 kHz, 6 h). Left ears of the rats were irradiated with transcanal-LLLT (830 nm) of 50, 100, 150, 200, 250, 300 mW for 60 minutes per day for 12 days, starting 1 day post induction of NIHL. Right ears were not irradiated and used as control ears. The hearing levels were measured at each frequency of 8, 12, and 32 kHz before and 1, 3, 8, and 12 days post noise exposure. The differences of hearing levels between left treated ear and right controlled ear at each frequency of different laser dosages (50 – 300 mW) were compared to see the most effective laser dosages to treat NIHL. The ear drums of 50, 100, 250, and 300 mW laser irradiated ears were examined using endoscope daily.

Results: Hearing levels were most improved by 100 and 150 mW, slightly improve by 200 mW, not improved by 50 and 250 mW, and became worse by 300 mW. Endoscopic examinations of the laser treated ear drums showed hyperemic changes only by 100 – 250 mW and hyperemic edema and burn damages by 300 mW.

Conclusion: The results of this study suggest that most optimal laser dosage to treat NIHL with transcanal-LLLT was 100 to 150 dB for 12 days and it was not effective by 50, 250, and 300 mW. Ear drums remained intact by 50 – 250 mW, but showed edema and burn damage by 300 mW.

9303-324, Session 2

Comparison of temporal properties of auditory single units in response to cochlear infrared laser stimulation recorded with multi-channel and single tungsten electrodes

Xiaodong Tan, Northwestern State Univ. (United States); Hunter K. Young, Northwestern Univ. (United States); Agnella I. Matic, Consultant (United States); Nan Xia, Claus-Peter Richter, Northwestern Univ. (United States)

Infrared Neural Stimulation (INS) is potentially beneficial to auditory prosthesis for its selective activation of spiral ganglion neurons (SGNs). This selective activation in cochlea could be relayed to the central nucleus of inferior colliculus (ICC) where a tonotopic organization is deployed in layers, with low frequencies more superficial and high frequencies deeper. The selective activation profile of INS is well represented by multi-channel electrode (MCE). To characterize single unit properties in response to INS, however, single tungsten electrode (STE) might be better to get

recordings with higher signal-to-noise ratio. In this study, we compared the temporal properties of ICC single units recorded with MCE and STE, to lay the groundwork for the characterization of single auditory neurons in response to INS. Neural activities recorded by 16-channel electrodes covered a frequency range of about 2.25 octaves in ICC of guinea pigs. The activation range of INS in ICC recorded with 16-channel electrode was about 0.9 octave, slightly wider than that of STE (0.6 octave). The temporal properties of single units showed higher limiting rate and shorter latency in MCE recordings than those in STE recordings. However, when the preset amplitude threshold for multi-channel electrode was raised up to 2 times over the noise level, the temporal properties of the single units became similar to those in STE recordings. Undistinguishable neural activities from multiple sources in MCE recordings could be responsible for the response property difference between MCE and STE. Thus, caution should be taken in single unit recordings with MCE.

This project has been funded by the NIDCD, R01 DC011855, and by Lockheed Martin Aculight.

9303-325, Session 2

A family of fiber-optic based pressure sensors for intracochlear measurements

Elizabeth Olson, Columbia Univ. (United States); Hideko Heidi Nakajima, Harvard Medical School (United States)

Fiber-optic pressure transducers were developed in 1995 for measurements of intracochlear pressure. The first generation sensors, designed for measurements near the cochlear partition in rodent, were 145 um in diameter, which was then reduced to 125 um. A further reduction to 80 um was achieved by adapting the light source (from LED to SLED) and fiber type (from multi-mode to single-mode). A dual pressure+voltage sensor was constructed by adhering a 28um diameter isonel-insulated platinum wire to a 125 um diameter sensor. For use in human temporal bone, the diameter was increased to 225 um, which simplified construction.

In rodent, these sensors have been used to map the intracochlear pressure field and, in concert with motion measurements, to determine the mechanical impedance of the cochlear partition and the input impedance of the cochlea. They have been used to explore middle ear transmission, distortion product generation and transmission, and the electro-mechanics of cochlear amplification.

In fresh human cadaveric preparations, the sensors have been used to measure the intracochlear pressure near the oval and round windows in order to determine the input pressure drive to the cochlea. Pressure drive was found for various types of stimulation (air conduction, bone conduction, round window prosthetic) and in various disease states (ossicular fixation, canal dehiscence). Simultaneous velocity measurements allowed for the quantification of inner ear mechanical impedances, and informed our understanding of how these impedances affect the efficacy of the different stimulation modalities.

9303-329, Session 2

Characterization of the mouse organ of Corti cytoarchitecture using a stick representation

Joris A. Soons, Stanford Univ. (United States) and Univ. Antwerpen (Belgium); Anthony Ricci, Stanford Univ. School of Medicine (United States); Charles R. Steele, Stanford Univ. (United States); Sunil Puria, Stanford Univ. (United States) and Stanford Univ. School of Medicine (United States)

The cells in the organ of Corti are highly organized. Their precise 3D micro-structure is not known and hypothesized to be important to understand

**Conference 9303C: Optical Imaging, Therapeutics, and Advanced Technology in
Head and Neck Surgery and Otolaryngology**

cochlear function. Here we combine the imaging capabilities of two-photon microscopy with the autofluorescent cell membranes of the genetically modified mTmG mouse to provide quantitative data on the mouse organ of Corti cytoarchitecture. This combination allows us to perform in situ imaging on freshly excised tissue without subjecting the tissue to potential distortions due to fixation, staining, physical slicing, or micro-dissection procedures.

9303-310, Session 3

Monte Carlo modeling of light propagation in the human head for applications in sinus imaging

Albert E. Cerussi, Beckman Laser Institute and Medical Clinic (United States); Nikhil Mishra, Northwood High School (United States) and Beckman Laser Institute and Medical Clinic (United States); Joon You, Praxis BioSciences, Inc. (United States); Naveen Bhandarkar M.D., Univ. of California, Irvine School of Medicine (United States); Brian J. F. Wong M.D., Beckman Laser Institute and Medical Clinic (United States)

Sinus blockages are a common reason for physician visits, affecting 1 out of 7 in the United States. Over 20 million cases of acute bacterial sinusitis become chronic and require medical treatment. Diagnosis in the primary care setting is challenging because symptom criteria (via detailed clinical history) plus objective imaging (CT or endoscopy) is recommended. Unfortunately, neither option is routinely available in primary care. Our previous work demonstrated that low-cost near infrared (NIR) transillumination instruments produced signals that correlated with the bulk findings of sinus opacity measured by CT. We have upgraded the technology, but questions remain such as finding the optimal arrangement of light sources, measuring the influence of specific anatomical structures, and determining detection limits. In order to address these questions, we have modeled diffusive NIR light propagation inside the adult human head using a mesh-based Monte Carlo algorithm (MMCLab) applied to a mesh constructed from CT anatomical images. This model simulated the general performance of the imager. In this application the sinus itself, which normally is a void region (e.g., non-scattering), is the region of interest instead of an obstacle to other contrast mechanisms. We report preliminary simulations and compare them with clinical measurements.

9303-311, Session 3

Future aspects of cellular and molecular research in clinical voice treatment

Mette K. Pedersen, Sanila Mahmood, The Medical Ctr. (Denmark)

Focus is upon our clinical experience in a prospective cohort study on cure of dystonia where the mode of treatment was fexofenadine tablets and local budesonide inhaler in the larynx, and in a randomized controlled trial of lifestyle change related to acid provocation of food and habits in laryngopharyngeal reflux (LPR). The advanced high-speed films is one new tool, another being optical coherence tomography (OCT), which should be used in the future in randomized controlled trials.

We are focusing on OCT of the swallowing process in the oesophagus and larynx as well as the vocal fold function. It can be shown on OCT how the layer of the vocal folds develop, possibly corresponding to hormonal and paediatric development. The arytenoid area in the larynx should also be focused upon with OCT in pathology. The thyroid function is related to voice and the swallowing function, both hormonally and pathoanatomically. We know too little about voice and thyroid hormones in an updated way as well as the outer anatomic supporting muscular structure of the larynx, related to thyroid immune degeneration and cysts. Also, here OCT analyses might

be of value.

References

1. Pedersen M, Eeg M, (2012) Does treatment of the laryngeal mucosa reduce dystonic symptoms? A prospective clinical cohort study of mannose binding lectin and other immunological parameters with diagnostic use of phonatory function studies, European Archives of Otorhinolaryngology, May 2012, Vol 269, issue 5, pp 1477-1482
2. Pedersen M, Eeg M (2012) Laryngopharyngeal Reflux – A Randomized Clinical Controlled Trial, Otolaryngology, OMICS publishing group. S1:004. doi: 10.4172/2161-119X.S1-004
3. Pedersen M (2008). Normal Development of Voice in Children. ISBN: 978-3-540-69358-1

9303-312, Session 3

Swept-source anatomical optical coherence tomography for quantitative upper airway geometry to inform computational fluid dynamics

Amy L. Oldenburg, Kushal C. Wijesundara, Julia Kimbell, The Univ. of North Carolina at Chapel Hill (United States); Nicusor V. Iftimia, Physical Sciences Inc. (United States); Carlton Zdanski, The Univ. of North Carolina at Chapel Hill (United States)

We report our recent progress on a portable, swept-source anatomical optical coherence tomography (aOCT) system that is delivered via a commercial pediatric laryngoscope. The fiber-optic delivery system employs a ball-lens design that maintains a sufficiently small diameter to slide into the 1.05 mm bore of the laryngoscope. aOCT images were collected within 3D airway phantoms and pig airways ex vivo. A custom, automated segmentation routine was developed to segment the aOCT data to provide airway geometries. These airway surfaces were then imported into Mimics™, where computational meshes of the airway lumen using unstructured tetrahedral elements were created. Then, computational fluid dynamics (CFD) was performed by simulating steady-state laminar airflow. Flow streamlines, airway wall pressure, and wall shear rate were computed using Fluent™. The accuracy of the aOCT-derived airway geometry and subsequent CFD was compared against that of matched CT images. Comparing the two imaging methods, CT required ~1.5 hour scan time at a 50 um isotropic voxel size, while aOCT required <1 minute scan time at a 25 um radial x 50-200 um longitudinal & azimuthal resolution, respectively. In phantoms, we found that the segmented cross-sectional area (CSA) varied by 2.2% from the true geometry, which is yet limited by systematic error that may yield further improvement. In pig airways, we found that CFD results by aOCT closely resembled those obtained by CT. This has importance for quantitative bronchoscopy in children suffering from obstructive upper airway disorders, where accurate geometry enables CFD to estimate the total airflow resistance.

9303-313, Session 3

Localization of biogel injection in scar tissue enabled by ultrafast laser ablation: model for treatment of vocal fold scar

Murat Yildirim, Adela Ben-Yakar, The Univ. of Texas at Austin (United States); Steven M. Zeitels M.D., James B. Kobler, Sandeep Karajanagi, Massachusetts General Hospital (United States)

Background and Objective: Vocal fold scarring is a predominant cause of voice disorders yet lacks a reliable treatment. The injection of biomaterials to restore mechanical functionality of the vocal folds is a promising

Conference 9303C: Optical Imaging, Therapeutics, and Advanced Technology in Head and Neck Surgery and Otolaryngology

treatment. However, direct injection into the scarred vocal fold tissue is difficult. Here, we characterize injection and localization of biogels inside sub-epithelial voids created by ultrafast pulses within scarred cheek pouch samples. The ultrafast fiber laser based technique that we used can create sub-epithelial planar voids with image assistance, providing space for the injected material to fill.

Materials and Methods: To create planar voids, high intensity, picosecond pulses were tightly focused in the superficial lamina propria of control and scarred cheek pouches. Multimodal, nonlinear imaging was performed with the same laser at low intensities, to characterize the dimensions of the voids. A mixture of Rhodamine and Polyethylene Glycol was injected into the voids under a fluorescent stereoscope and visualized to monitor the localization of the biogels.

Results: We have successfully demonstrated localization of the biomaterial into the ablated sub-epithelial voids of different sizes ranging from 1-10 mm² in a scarred pouch. The presence of sub-epithelial voids provides a space for the biomaterial, which greatly reduced back-flow at the injection site and resulted in a lasting localization of the injected biomaterial.

Conclusions: Ultrafast laser ablation assisted biomaterial injection can enable the surgeons to improve the localization of injected biomaterials for the treatment of vocal fold scarring.

9303-314, Session 3

Tracheal stenosis treatment with balloon catheter-based diffuser

Trung Hau Nguyen, Hyeon Shin, Junghwan Oh, Hyun Wook Kang, Pukyong National Univ. (Korea, Republic of)

Photothermal therapy with conventional fibers often demonstrates poor application due to limited direction of light propagation especially in treating tubular structures such as trachea, urethra, and vascular tissue. In this study, we demonstrated the development of a novel balloon catheter-based diffusing optical device to photothermally treat tracheal stenosis and to ensure sufficient airway passage. A 400 μ m fiber was micro-machined to diffuse the incident laser light in a radial direction. Spatial light distribution of the diffuser was visibly characterized with HeNe light (632.8 nm). Infrared thermography evaluated temperature development around the diffuser in response to near-IR light (980 nm, 1 W). A visible wavelength laser (532 nm, 30 W) combined with the balloon catheter-based diffuser was used to thermally coagulate rabbit tracheal tissue structure at various irradiation times. The prototype diffuser demonstrated almost uniform distribution of the light, which corresponded to gradual increase up to 85 degree in temperature gradient along the fiber. In vitro tissue experiments presented that the extent of coagulative necrosis increased up to 5 mm with irradiation time and applied laser power. H&E-stained specimens confirmed that the density in the mucosal layer was over 15% lower than that in control (i.e. no treatment), implying feasible thermal denaturation merely confined in the stenosis area without peripheral injury to tracheal cartilage. Photocoagulation also induced approximately 25 % increase in tracheal airway area, compared to control (stenosis trachea with no treatment). By providing direct delivery of diffuse light to target tissue along with minimal photothermal damage to adjacent tissue, the proposed catheter-based diffuser can be a feasible therapeutic device to treat tracheal stenosis.

9303-327, Session 3

Improving anatomical accuracy of 3D models of the upper airway by incorporating magnetic tracking with optical coherence tomography in the awake patient

Brian T. Lemieux, Erica Su, Max Wiedmann, Brian J. F. Wong M.D., Beckman Laser Institute and Medical Clinic

(United States) and Univ. of California, Irvine (United States)

No Abstract Available

9303-328, Session 3

Measurement of ciliary beat frequency using high speed fourier domain Doppler optical coherence tomography

Brian T. Lemieux, Joseph C. Jing, Zhongping Chen, Brian J. F. Wong M.D., Beckman Laser Institute and Medical Clinic (United States) and Univ. of California, Irvine (United States)

No Abstract Available

9303-331, Session 3

Vertical cavity surface emission laser based optical coherence tomography and optical Doppler tomography of the vocal folds

Giriraj K. Sharma M.D., Joseph C. Jing, Zhongping Chen, Brian J. F. Wong M.D., Beckman Laser Institute and Medical Clinic (United States)

Benign or malignant processes of the larynx often disrupt the interface between adjacent mucosal layers of the vocal cord (VC). Change in VC vibration parameters during phonation is a potential sequela of VC lesions. In vivo, minimally-invasive measurement of VC vibration parameters may ultimately provide information on the effect of VC lesions on mucosa and submucosa microanatomy. We used a swept-source vertical cavity surface emission laser (VCSEL) optical coherence tomography (OCT) and optical Doppler tomography (ODT) system to acquire high-resolution cross-sectional images of the VC and to measure VC vibrational parameters in ex vivo swine models. A VCSEL source allows for an increased imaging range as compared with other swept-source OCT techniques.

9303-316, Session 4

Rapid in vivo wide-field OCT imaging in the oral cavity

Anthony Lee M.D., Lucas Cahill, Kelly Y. P. Liu, Catherine F. Poh D.D.S., Calum E. MacAulay, The BC Cancer Agency Research Ctr. (Canada); Samson Ng D.D.S., The Univ. of British Columbia (Canada); Pierre M. Lane, The BC Cancer Agency Research Ctr. (Canada)

Oral cancer continues to be a global health problem with over 300,000 estimated new cases worldwide in 2012. Image-guided techniques may be able to play an important role in clinical practice by 1) facilitating accurate diagnosis through biopsy site selection in large lesions; and 2) delineating subclinical tumour boundaries prior to surgery. The latter has the potential to significantly improve the management of oral cancer by reducing disease recurrence. To be practically useful for these clinical applications, a rapid imaging system with a large field of view (FOV) is essential.

We present a swept-source Optical Coherence Tomography (OCT) instrument capable of wide-field imaging in the oral cavity. This instrument uses a hand-held side-looking fiber-optic rotary pullback catheter to cover two dimensional tissue imaging fields greater than 2.5 mm wide by 40mm

Conference 9303C: Optical Imaging, Therapeutics, and Advanced Technology in Head and Neck Surgery and Otolaryngology

in length in a single acquisition. This field of view (FOV) is at least an order of magnitude greater than OCT systems previously demonstrated in the oral cavity. The rotary probe spins at 100 Hz with pullback speeds up to 15 mm/s allowing imaging of the entire FOV in seconds. Two catheter holders have been made to allow imaging in most locations of the oral cavity where oral cancer is prevalent. We present our initial imaging results using this system in vivo in patients.

9303-317, Session 4

Full-field OCT for fast diagnostic of head and neck cancer

Frederic De Leeuw, Odile Casiraghi, Aïcha Ben Lakhdar, Muriel Abbaci, Corinne Laplace-Builhé, Institut Gustave Roussy (France)

Full-Field OCT (FFOCT) produces optical slices of tissue using white light interferometry providing in-depth 2D images, with an isotropic resolution around 1 micrometer. These optical biopsy images are similar to those obtained with conventional histological procedures, but without tissue preparation and within few minutes. This technology could be useful when diagnosing a lesion or at the time of its surgical management.

Here we evaluate the clinical value of FFOCT imaging in the management of patients with Head and Neck cancers by assessing the accuracy of the diagnosis done on FFOCT images from resected specimen.

In a previous step, FFOCT images from Head and Neck samples were first compared to the gold standard (conventional histology). An image atlas dedicated to the training of pathologists was built and diagnosis criteria were identified.

Here, we perform a morphological correlative study: both healthy and cancerous samples from patients who undergo Head and Neck surgery of oral cavity, pharynx, and larynx were imaged. Images were interpreted in a random way by two pathologists and the FFOCT based diagnostics were compared with HES slides (gold standard) of the same samples.

The statistical analysis of our study is still underway, but our results already show that FFOCT images allow pathologists to make differential diagnosis and that FFOCT provides a quick assessment of tissue architecture at microscopic level that could guide surgeons for tumor margin delineation during intraoperative procedure. In the CAREIOCA project context, we evaluate soon an endoscopic version of the current FFOCT used in this study

9303-318, Session 4

Development of a supraglottic and subglottic tumor model and multimodal imaging of endobronchial ultrasound and optical coherence tomography

Sung Won Kim, Kosin Univ., College of Medicine (Korea, Republic of); Sang-Seok Hwang, Yugyeong Chae, Jaechul Jung, Pukyong National Univ. (Korea, Republic of) and Ctr. for Marine-Integrated Biomedical Technology (Korea, Republic of); Chulho Oak, Kosin Univ., College of Medicine (Korea, Republic of) and Innovative Biomedical Technology Research Ctr. (Korea, Republic of); Yeh-Chan Ahn, Pukyong National Univ. (Korea, Republic of) and Ctr. for Marine-Integrated Biomedical Technology (Korea, Republic of) and Innovative Biomedical Technology Research Ctr. (Korea, Republic of)

Cancers in aerodynamic tract affect adjacent tracheal wall and cartilage around glottic area with the most rapid increasing incidence rate. Assessment of preoperative invasion by aerodynamic tract cancers is

important for the selection of the best treatment. Multimodal imaging of these cancers using endobronchial ultrasound (EBUS) and optical coherence tomography (OCT) is a promising complementary approach in diagnosis and monitoring of cancers. This study was performed to visualize the submucosal tumor in aerodynamic tract using OCT and EBUS according to the depth of invasion and to develop a fusion image in assessment of supraglottic and subglottic tumor invasion in a rabbit model. We injected VX2 tumor cells by percutaneously under bronchoscopic guidance. The tumor growth was found within 2 weeks in supraglottic area, subglottic area, respectively. EBUS revealed tumor invasion and cartilage structure and OCT showed mucosal invasion. This is the first investigation using OCT and EBUS to assess aerodynamic tract cancer. The multimodal imaging has a potential to become a valuable tool for the assessment of aerodynamic tract cancer.

9303-319, Session 5

The feasibility of photothermal treatment using locally injected nanoshell-loaded macrophage around tumor in animal model

Seung-Kuk Baek M.D., Korea Univ. College of Medicine (Korea, Republic of); Taeseok D. Yang, KAIST (Korea, Republic of); Wonshik Choi, Jungho Moon, Jae-Seung Lee, Jang Ho Joo, Korea Univ. (Korea, Republic of); Min-Goo Lee M.D., Korea Univ. College of Medicine (Korea, Republic of); Byoungjae Kim, Kyung Min Choi, Hong Soon Yim, Korea Univ. (Korea, Republic of); Jung Joo Lee, Heejin Kim, Dong Wook Lee, LivsMed Inc. (Korea, Republic of); Min Woo Park M.D., Kwang-Yoon Jung M.D., Korea Univ. College of Medicine (Korea, Republic of)

Various methods to increase the target-specificity of nanoshells (NS) have been studied. Among them, one is the use of macrophage as cellular vector for nanoshells. The aim of the present study is to evaluate viability and mobility of NS-loaded macrophage in vivo situation and to prove the ability of macrophage to invade into tumor. The animal model was made of the nude mouse injected with FRO anaplastic cancer cells and then the nanoshells-loaded macrophages were injected around the tumor on the mouse. The peritumoral-injected macrophages penetrated into tumor at 48 hours after injection of them. The viability and mobility of them was not different irrespective of the presence of nanoshells. Furthermore, the amount of nanoshells efficient to make photothermal effect may be transferred by macrophage and the thermally induced death of cancer cells were induced by using NIR laser light at irradiation of 1W for 2 minutes. NS-loaded macrophage functioned as a cellular vector and photothermal effect of NS was effective to kill cancer cells in vivo situation.

9303-320, Session 5

Combined concurrent photodynamic and gold nanoshell loaded macrophage-mediated photothermal therapies: an in vitro study on squamous cell head and neck carcinoma

Henry Hirschberg M.D., Anthony Trinidad, Catherine E. Christie M.D., Beckman Laser Institute and Medical Clinic (United States); Qian Peng M.D., DNR (Norway); Young J Kwon, Depts. of Chemical Engineering / Material Science, Dept. of Pharmaceutical Sciences, University of (United States); Steen J. Madsen III, Univ. of Nevada, Las Vegas (United States)

Conference 9303C: Optical Imaging, Therapeutics, and Advanced Technology in Head and Neck Surgery and Otolaryngology

Treatment modalities, such as hyperthermia and photodynamic therapy (PDT) have been used in the treatment of a variety of head and neck squamous cell carcinoma (HNSCC), either alone or as an adjuvant therapy. Macrophages loaded with gold nanoshells, that convert near infrared light to heat, can be used as transport vectors for photothermal hyperthermia of tumors. The purpose of this study was to investigate the effects of combined macrophage mediated photothermal therapy (PTT) and PDT on HNSCC cells.

Gold nanoshell loaded rat macrophages either alone or combined with human FaDu squamous cells in hybrid monolayers were subjected to PTT, PDT, or a simultaneous combination of the two light treatments. Therapies were given concurrently employing two laser light sources of 670nm (PDT) and 810nm (PTT) respectively. AIPcS2a mediated PDT at a fluence level of 0.25J/cm² and PTT at 14 W/cm² irradiance had little effect on cell viability, when given separately, with a FaDu/Ma (ratio 2:1) hybrid monolayers. In contrast, combined treatment reduced the cell viability to less than 40% at these same laser power settings. The results of this study provide proof of concept for the use of macrophages as a delivery vector of AuNS for photothermal enhancement of the effects of PDT on squamous cell carcinoma. A significant synergy was demonstrated with combined PDT and PTT compared to each modality applied separately.

9303-321, Session 5

LLLT on anaplastic thyroid cancer

Yun-Hee Rhee, Jeon-Hwan Moon, Dankook Univ. (Korea, Republic of); Jin-Chul Ahn M.D., Phil-Sang Chung M.D., Dankook Univ. Hospital (Korea, Republic of)

Low-level laser therapy (LLLT) is a non-thermal phototherapy used in several medical applications, including wound healing, reduction of pain and amelioration of oral mucositis. Nevertheless, the effects of LLLT upon cancer or dysplastic cells have been so far poorly studied. Here we report that the effects of laser irradiation on anaplastic thyroid cancer cells leads to hyperplasia. 650nm of laser diode was performed with different time interval (0, 15, 30, 60J/cm², 25mW) on anaplastic thyroid cancer cell line FRO in vivo. FRO was orthotopically injected into thyroid gland of nude mice and the irradiation was performed with same method described previously. After irradiation, the xenograft evaluation was followed for one month. The thyroid tissues from sacrificed mice were underwent to H&E staining and immunohistochemical staining with HIF-1 β , Akt, TGF- β 1. We found the aggressive proliferation of FRO on thyroid gland with dose dependent. In case of 60 J/cm² of energy density, the necrotic bodies were found in a center of thyroid. The phosphorylation of HIF-1 β and Akt was detected in thyroid gland which explained the survival signaling of anaplastic cancer cell was turned on in thyroid gland. Furthermore, TGF- β 1 expression was decreased after irradiation. In this study, we demonstrated that insufficient energy density irradiation occurred the decreasing of TGF- β 1 which corresponding to the phosphorylation of Akt/HIF-1 β . This aggressive proliferation resulted to hypoxic condition of tissue for angiogenesis. We suggest that LLLT may influence to cancer aggressiveness associated with a decrease in TGF- β 1 and increase in Akt/HIF-1 β .

9303-300, Session PSun

Wide-field diagonal scanning 3D OCT probe for in vivo human tympanic membrane

Kibeom Park, Nam Hyun Cho, Kyungpook National Univ. (Korea, Republic of); Jeong Hun Jang, Kyungpook National Univ., College of Medicine (Korea, Republic of); Jeehyun Kim, Kyungpook National Univ. (Korea, Republic of)

This paper reports the development of a wide-field OCT (Optical Coherence

Tomography) probe adapting diagonal scanning scheme for 3-D in vivo imaging of tympanic membrane in human. The probe consists of relay lens to enhance the lateral scanning range up to 7 mm. Motion artifact occurring with the handheld probe could be dramatically decreased owing to the diagonal scan that crosses the center of the sample through the entire 3D scans. Each 2D OCT images acquired by the diagonal scanning implemented a 3D image in a small number of samples. In order to demonstrate the usefulness and performance of the developed system with the handheld probe, in vivo tympanic membrane of human and animal are imaged in real time.

9303-304, Session PSun

The color mapping of a tympanic membrane in vivo using Doppler OCT

Deokmin Jeon, Nam Hyun Cho, Kibeom Park, Kanghae Kim, Jihyeon Kim, Kyungpook National Univ. (Korea, Republic of)

Color Map of the tympanic membrane is made by Doppler effect of the back scattering beam from a middle ear oscillating of the animals in vivo by Speaker making Sine Wave about 0.1kHz-10kHz using Doppler Optical Coherence Tomography(Doppler OCT) and Kasai's algorithm is used for Autocorrelation Method.

This system offers real time image of 2-dimension color map about depth axis and X-Galvanometer Scanner. 3-dimension color map can be made by Y-Galvanometer Scanner from many 2D images. Then, this shows the vibration of the surface of the tympanic membrane to color map and it can make a diagnosis easily about the vibration of tympanic membrane like a hearing loss. It can demodulate to sine wave via 3D signal processing for an analysis.

9303-308, Session PSun

3D-OCT imaging for endolymphatic hydrops models evaluation of surgical method

Nam Hyun Cho, Kyungpook National Univ. (Korea, Republic of); Woonggyu Jung, Ulsan National Institute of Science and Technology (Korea, Republic of); Jeong Hun Jang, Kyungpook National Univ., College of Medicine (Korea, Republic of); Jeehyun Kim, Kyungpook National Univ. (Korea, Republic of)

OCT, an emerging noninvasive imaging modality, has been applied to better visualize the internal structure of the cochlea. The decalcification of the cochlear bony wall using ethylenediamine tetra-acetic acid (EDTA) has been applied. We could clearly visualize internal structures of the cochlea and identify endolymphatic hydrops (EH) and 3D image was reconstructed. Guinea pig (Slc: Hartley strain, 5weeks, 180g) was used in this study. Hearing level was estimated using ABR was measured (System 3, Tucker-Davis Technologies, USA) at 1 week and 2 weeks postoperatively. The image of cochlea was acquired by OCT and the structural change of whole cochlea was evaluated by 3D reconstruction. The structural and functional changes of EH were identified by OCT image and ABR, respectively. Conclusion: By decalcifying the bony wall of the cochlea, we could clearly and widely visualize the internal structures of pathological cochleae. These findings indicate that imaging the decalcified cochlea by using OCT would be of great value when examining cochlear pathology, especially EH, prior to or without histological examinations. These findings indicate that observing the decalcified cochlea by using OCT would be of great value when examining cochlear pathology, especially EH, prior to or without histological examinations.

9303-330, Session PSun

Comparing methods for enhancement of ALA-induced PpIX in skin: Contrasting ALA penetration enhancement, heme cycle enhancement and iron chelation

Ana Luisa Ribeiro de Souza, Thayer School of Engineering at Dartmouth (United States) and CAPES Foundation (Brazil); Kimberley S. Samkoe, Thayer School of Engineering at Dartmouth (United States) and Geisel School of Medicine at Dartmouth (United States); Stephen Chad Kanick, Jason R. Gunn, Thayer School of Engineering at Dartmouth (United States); Edward V. Maytin M.D., Cleveland Clinic Lerner Research Institute (United States); Tayyaba Hasan, Wellman Ctr. for Photomedicine (United States); Clovis Augusto Ribeiro, UNESP (Brazil); Brian W. Pogue, Thayer School of Engineering at Dartmouth (United States) and Geisel School of Medicine at Dartmouth (United States) and Wellman Ctr. for Photomedicine (United States)

Several approaches have been examined to enhance PDT effect from ALA-induced protoporphyrin IX, which target different parts of the PpIX production limitation, going from i) ALA transcutaneous delivery through ii) PpIX production cycle in the heme synthesis pathway, through to iii) preservation of PpIX by removal of iron to limit heme production. It is not obvious which of these three key factors truly limit PpIX-mediated PDT in skin cancers. For the first issue, development of drug delivery systems such as liposomes, microemulsions and cubic phase liquid crystalline systems providing an increase in the penetration of ALA could help if this delivery is the limiting factor in production, especially at deeper depth lesions. This approach was systematically examined through co-delivery of Levulan and liquid crystal delivery. Usage of iron chelator (deferoxamine) and differentiation therapy (Vitamin D) were also used to examine the effects. Optical measurements of PpIX fluorescence were acquired to verify which provided maximal production advantage. It was expected that the relative enhancement advantages seen in normal skin would not be seen in thicker skin lesions, and results to date would agree with this hypothesis. This is likely because the limitations to PpIX production vary considerably between normal skin and thicker cancer lesions. Individual study of a variety of lesions in terms of penetration, production, and heme escape is likely needed.

Conference 9303D: Diagnosis and Treatment of Diseases in the Breast and Reproductive System

Saturday 7 February 2015

Part of Proceedings of SPIE Vol. 9303 Photonic Therapeutics and Diagnostics XI

9303-400, Session 1

Imaging the tumor/stromal boundary

(Invited Paper)

Patricia Keely, Kevin W. Eliceiri, Univ. of Wisconsin-Madison (United States)

Tumors exist in the context of a microenvironment composed of the extracellular matrix, various stromal cells, blood vessels, and numerous biochemical signals. Using multiphoton and intravital imaging, we have found that collagen fibers surrounding tumors become aligned and reoriented perpendicular to the tumor boundary, creating adhesion highways on which cells invade out from the tumor. The local collagen microenvironment moreover recruits immune cells, and alters the metabolism of tumor cells, both imaged in situ using unique fluorescent lifetime signatures of the endogenous fluorophores, FAD and NADH.

9303-401, Session 1

Polarimetry for organizational analysis of collagen in breast cancer

Adam Gribble, I. Alex Vitkin, Univ. of Toronto (Canada)

One of the largest risk factors for developing breast cancer is a high breast density, characterized by increased amounts of connective tissue, such as collagen. Most techniques to diagnose breast cancer focus on epithelial cells. However, the tissue extracellular matrix (ECM) plays an important role in maintaining normal cell behavior, and improper interactions between epithelial cells and the ECM can promote tumorigenesis. Thus understanding ECM interactions in the breast is of great importance, and may have use as diagnostic tool.

Our collaborators at the University of Wisconsin have shown, using two-photon microscopy combined with second harmonic generation, that collagen undergoes organizational changes early in breast cancer, through to metastasis. These different structural arrangements can be classified as Tumor Associated Collagen Signatures.

A promising method to investigate the structural alignment of biological tissues is with Mueller matrix polarimetry, a type of polarized light imaging. Mueller matrix polarimetry has the advantages of greater penetration depth and a larger field of view than second harmonic generation. Here we present a direct comparison between the two techniques, illustrating the ability of polarimetry to distinguish between different regions of collagen organization in ex-vivo mouse mammary glands. Effects of collagen density on ECM organization and breast tumor progression are being studied using collagen-dense mouse models. This represents the first step towards a polarimetry platform for optical analysis of breast cancer, with possibilities for diagnosis, staging, surgical guidance and treatment monitoring.

9303-402, Session 1

Quantitative changes in collagen subtypes during breast cancer progression by multivariate analysis of Raman and second harmonic generation microscopy

Sixian You, Yuan Liu, Haohua Tu, Eric J. Chaney, Marina Marjanovic, Stephen A. Boppart M.D., Univ. of Illinois at Urbana-Champaign (United States)

Evidence for the interaction between collagen subtypes and progression of breast tumors is rapidly growing. However, it is difficult to quantify changes in collagen subtype composition without special sample processing such as picro-sirius staining or immunofluorescence, thus making its application for noninvasive study or in vivo diagnosis challenging. In this study, we quantified the longitudinal changes in collagen composition and architecture during breast cancer progression using fresh rat mammary tissue from a carcinogen-induced tumor model, and developed a robust classifier for the diagnosis of early stage breast cancer. More than 10,000 Raman spectra were obtained ex vivo from 72 tissue sites from 24 rats, including 14 tumor sites, 25 surrounding tumor sites, and 33 normal tissue sites, using a confocal Raman microscope. Statistical analysis of these Raman spectra showed that there are significant alterations in collagen subtype deposition not only at the tumor site but also in the adjacent mammary tissue that was labeled as benign by pathologists. In addition to these biochemical changes, complementary structural information was provided by SHG microscopy. We found that abnormal up-regulation of certain collagen subtypes were usually accompanied by more heterogeneous fiber distribution by comparing the results from these two modalities. In addition, a multivariate analysis algorithm was used to generate the classification models. The algorithm was tested by K-fold cross-validation (K=5), yielding a positive predictive value, negative predictive value, sensitivity, and specificity of 94.8%, 99.5%, 97.1%, and 99.1%, respectively, for the diagnosis of breast cancer.

9303-403, Session 1

Monitoring nanostructural ECM changes by mammary fibroblasts using polarization-sensitive optical coherence tomography to image diffusing gold nanorods

Richard L. Blackmon, Patricia Carabas-Hernandez, Melissa A. Troester, The Univ. of North Carolina at Chapel Hill (United States); Joseph B. Tracy, Wei-Chen Wu, North Carolina State Univ. (United States); Amy L. Oldenburg, The Univ. of North Carolina at Chapel Hill (United States)

Cancer-associated stromal fibroblasts are known to play a role in remodeling the extracellular matrix (ECM) during mammary tumorigenesis. PS-OCT enables longitudinal monitoring of 3D mammary tissues cultures within a microenvironment that recapitulates many in vivo features. 3D mammary tissue cultures are prepared from collagen:Matrigel seeded with reduction mammoplasty fibroblasts (RMFs). PEG-coated gold nanorods (GNRs) of 83 x 22 nm, which do not exhibit cellular uptake, are topically added as diffusive probes of the ECM nanostructure. The GNR diffusion rate is quantified from the speckle fluctuation rate in the orthogonal linear polarization states of the PS-OCT signal. In molecular fluids, we have shown that PS-OCT of diffusive GNRs enables spatially resolving fluid viscosity. In polymer solutions, we find that GNRs, which are smaller than traditional microrheology probes, are only weakly-constrained by the polymeric medium; thus, they remain highly diffusive and amenable for topical addition, while their diffusion rate is sensitive to changes in the polymer correlation length. In biopolymeric ECM, we hypothesize that during remodeling of the ECM by RMFs, the fibers become strained and more concentrated, restricting the diffusion rate of GNR probes. Our experiments confirm that by increasing the RMF seed density and incubation time, the translational diffusion rate of GNRs is slowed by up to 70%, which we attribute to the increased deposition of collagen by the proliferating RMFs. This minimally invasive technique for 3D cultures that recapitulate the tumor microenvironment is a crucial step toward the direct observation of nanostructural ECM changes that govern tumorigenesis.

Conference 9303D: Diagnosis and Treatment of Diseases in the Breast and Reproductive System

9303-404, Session 1

Optical coherence micro-elastography on excised breast cancer specimens: comparison with optical coherence tomography and histology

Brendan F. Kennedy, Robert A. McLaughlin, Kelsey M. Kennedy, Lixin Chin, Philip Wijesinghe, Alan Tien, The Univ. of Western Australia (Australia); Bruce Latham, PathWest (Australia); Christobel M. Saunders, David D. Sampson, The Univ. of Western Australia (Australia)

A key issue during breast-conserving surgery is ensuring complete removal of the tumor. Intraoperative microscopic examination of tumor margins is available using techniques such as frozen section analysis and imprint cytology, but these techniques are time-consuming and have not proven effective in reducing the number of repeat surgeries. Optical coherence tomography (OCT) has potential for rapid, intraoperative imaging of margins, but tissue contrast based on optical backscattering is often insufficient for differentiating malignant and normal tissues. Optical coherence micro-elastography (OCME) is an emerging technique that provides micro-scale images (micro-elastograms) of tissue local strain (the spatial derivative of displacement), using phase-sensitive OCT to measure the displacement of tissue under a compressive load. As the mechanical properties of breast tumor are distinct from those of healthy breast tissue, OCME may be capable of delineating tumor margins intraoperatively.

We have developed a portable, phase-sensitive compression OCME system to assess tissue freshly excised from breast cancer patients. We have imaged 50 specimens from 20 patients with this system, obtaining matching H&E histology in each case. Our results demonstrate changes in micro-scale mechanical properties in the presence of infiltrating malignant cells. In addition, the structural disruptions caused by invasive cancer in stromal tissue give rise to a characteristic texture in elastograms. We present representative results from a number of patients, demonstrating the ability of OCME to visualize these changes. In many instances, OCME is able to visualize features present in histology that are not visible in the corresponding OCT.

9303-405, Session 1

Multiphoton microscopy for the characterization and treatment of malignant breast lesions

Alex J. Walsh, Rebecca S. Cook, Melinda E. Sanders M.D., Carlos L. Arteaga, Melissa C. Skala, Vanderbilt Univ. (United States)

Multiphoton microscopy techniques, including fluorescence lifetime imaging and second harmonic generation imaging, are uniquely advantageous for the characterization of breast cancers. In this study, we used two-photon fluorescence microscopy of NADH and FAD to probe the basal cellular metabolism of bulk breast tumor specimens as well as murine models and tumor-derived organoids. NADH and FAD are endogenous fluorophores and function as metabolic co-enzymes during cellular metabolism. Additionally, we used collagen second harmonic generation to image and analyze the collagen extracellular matrix of murine xenografts and bulk breast cancer samples. NADH and FAD were excited at the two-photon wavelengths of 750 nm and 890 nm, respectively and collagen SHG was illuminated at 890 nm. Customized filters separated NADH, FAD, and collagen emission. We found significant increases in metabolism endpoints, due to estrogen receptor expression and HER2 overexpression ($p < 0.05$) in immortalized cells and organoids. Furthermore, we detected significant decreases in the metabolism of responsive organoids when treated with anti-cancer drugs ($p < 0.05$). This provides a novel platform for testing individual patient drug response in a high-throughput manner. Additionally, multiphoton

microscopy technologies provide comprehensive, quantifiable images both of cellular metabolism and extracellular matrix for improved drug discovery studies.

9303-406, Session 2

Imaging and modeling the extracellular matrix in ovarian cancer (Invited Paper)

Paul J. Campagnola, Karissa B. Tilbury, Kirby Campbell, Visar Ajeti, Kevin W. Eliceiri, Manish Patankar, Univ. of Wisconsin-Madison (United States)

A profound remodeling of the extracellular matrix (ECM) occurs in human ovarian cancer. We show that Second Harmonic Generation (SHG) imaging microscopy can quantify changes in the architecture in normal and malignant ovaries. We compared the collagen organization using forward-backward (F/B) directional and polarization anisotropy measurements, which are reflective of the fibril and fiber assembly respectively. We found that the stromal collagen in high grade serous tumors is extensively remodeled in the form of new collagen synthesis. We have also used these metrics to compare the collagen structure in normal tissue, benign tumors, and lowgrade tumors and found intermediate behavior between normal and high grade disease. We further investigate the role of the ECM in ovarian cancer by fabricating biomimetic models to investigate operative cell-matrix interactions in invasion/metastasis. For this purpose we use multiphoton excited (MPE) polymerization as this technique can create scaffolds with complex, 3D submicron morphology directly from ECM proteins. Our stromal scaffold designs are derived directly from "blueprints" based on SHG images. The models are seeded with different cancer cell lines and this allows decoupling of the roles of cell characteristics (metastatic potential) and ECM structure and composition (normal vs cancer) on adhesion/migration dynamics. We found the malignant stroma structure promotes enhanced migration and cytoskeletal alignment. These models cannot be synthesized by other conventional fabrication methods and we suggest the MPE image-based fabrication method will enable a variety of studies in cancer biology. We further suggest the integrated approach of imaging and modeling has great translational utility.

9303-407, Session 2

Characterization of cervical remodeling during pregnancy using in vivo Raman spectroscopy

Christine M. O'Brien, Vanderbilt Univ. (United States); Elizabeth Vargis, Utah State Univ. (United States); Chris Slaughter, Kelly A. Bennett, Jeff Reese, Anita Mahadevan-Jansen, Vanderbilt Univ. (United States)

In vivo Raman spectroscopy is an inelastic scattering technique that can be used to investigate the biochemical makeup of tissue longitudinally and without damage. Our group has applied this method to the problem of understanding preterm birth. Globally, fifteen million babies are born preterm each year. Preterm births affect 1 in 8 pregnancies in the US. For this study, Raman spectroscopy will be used to investigate the cervix, an organ that provides mechanical stability and acts as a barrier to infection. Cervical remodeling is a process that includes a biochemical cascade of changes that ultimately result in the thinning and dilation of the cervix for passage of a fetus. This remodeling process is dynamic and driven by biochemical changes that we will measure using Raman spectroscopy in vivo- over the course of pregnancy. Thirty pregnant patients receiving prenatal care at Vanderbilt University Medical Center and were expected to have normal pregnancies were recruited and measured throughout pregnancy. Results were analyzed using generalized estimating equations, an extension of general linear models that account for repeated measures. Preliminary findings revealed decreasing intensity in Amide bands throughout pregnancy, likely due to extracellular matrix degradation. Biochemicals

Conference 9303D: Diagnosis and Treatment of Diseases in the Breast and Reproductive System

that will be further analyzed include fibrillar collagens, hyaluronan, sulfated glycosaminoglycans, and water, all of which are important in the cervical remodeling process. This method has high potential to unveil molecular dynamics essential for cervical remodeling and may eventually improve patient care by providing a biochemical tool that can detect premature remodeling during pregnancy.

9303-408, Session 2

In vivo angle-resolved low coherence interferometry for detection of cervical dysplasia

Tyler K. Drake, Derek Ho, Duke Univ. (United States); Loris Hwang, Univ. of California, San Francisco, School of Medicine (United States); Adam Wax, Duke Univ. (United States)

Angle-resolved low coherence interferometry (a/LCI) is an optical biopsy technique used to measure the average size and optical density of cell nuclei in epithelial tissue to determine tissue health. The angular distribution of elastically scattered light from cell nuclei and other small scatterers in the target tissue is collected and compared to Mie Theory. a/LCI obtains depth-resolved measurements without the use of exogenous contrast agents, with submicron accuracy.

a/LCI has been successful in identifying dysplasia in human and animal epithelial tissues via depth resolved nuclear morphology measurements. In a pilot study conducted at Duke University Medical Center, a/LCI was able to identify cervical dysplasia in ex vivo tissue (n= 23) with a sensitivity of 100% and specificity of 90%. Further, it was discovered that by integrating a/LCI data across scattering angle, producing depth scans (A-scans), endocervical and ectocervical epithelium could be differentiated from one another.

We will report on the adaptation of our a/LCI probe for in vivo cervical studies. We will report on our in vivo pilot study at University of California, San Francisco which is aimed to define the nuclear morphology structure of cervical tissue with 30 participants. A custom handheld fiber optic probe will be built to interface with the cervix. Co-registered a/LCI data points will be compared with pathological assessment performed by UCSF Pathology to determine sensitivity and specificity of a/LCI in detecting cervical dysplasia.

9303-409, Session 2

Photodynamic therapy as a new approach in vulvovaginal candidiasis in murine model

Maria E. Santi M.D., Rubia G. Lopes, Renato A. Prates, Aline Sousa, Luis R. Ferreira, UNINOVE (Brazil); Adjaci U. Fernandes, UNICASTELO (Brazil); Sandra K. Bussadori, Alessandro M. Deana, UNINOVE (Brazil)

Vulvovaginal candidiasis is the second most common cause of vaginal infections and it affects 75% of women at least once during lifetime. Furthermore, recurrent vulvovaginal candidosis still represents a challenge in gynecological practice, since patients take long antifungal periods and frequently fall in new episode only after treatment. Photodynamic Therapy (PDT) has been used to treat localized infection such as fungal vaginosis. PDT is the association of photosensitizer and a low-intensity light source to generate massive amounts of reactive oxygen species (ROS) and it is able to inactivate microbial cells. The aim of this study was to investigate the efficiency of photodynamic therapy against yeast cells in mice. For this proposes, we used two different photosensitizers: methylene blue (MB) and a special designed protoporphirin (PpNeTNI). Female BALB-c mice were infected with *Candida albicans* ATCC 90028. Five days latter, PDT was applied with two different light sources, intravaginal and transabdominal,

according to the photosensitizer requirement. Vaginal washes were performed and cultivated on Agar Saboraud dextrose plates for microbial quantification. Euthanasia was performed to histological study of treatment effects. PDT was able to decrease microbial content with MB and PpNetNI ($p < 0.001$). The results of this study demonstrate that PDT may be a viable alternative treatment for vaginal candidiasis.

9303-410, Session 3

Preclinical monitoring of breast and prostate chemotherapy response with spatial frequency domain imaging

Darren M. Roblyer, Syeda Tabassum, Raef Istfan, Yanyu Zhao, Junjie Wu, David J. Waxman, Boston Univ. (United States)

In vivo optical detection of early chemotherapy induced changes would serve as a powerful means to confirm successful drug delivery and treatment efficacy for patients undergoing cancer treatment. In order to explore these rapid and early metabolic changes in a controlled preclinical setting, we are utilizing Spatial Frequency Domain Imaging (SFDI) to track treatment response in prostate and breast tumor models. SFDI is a non-contact near-infrared diffuse optical imaging technique for quantitative and wide-field characterization of tissue absorption and scattering properties. These parameters can then be used for mapping tumor metabolic markers, e.g., oxy- and deoxyhemoglobin, lipid and water. We present here some of the first work using SFDI for monitoring preclinical chemotherapy response in the first hours and days of treatments. To do so, we first evaluated the feasibility of preclinical animal measurements with SFDI and determined optimal measurements parameters including the choice of spatial frequencies, height correction and smoothing algorithms, and the tumor optical contrast for different tumor types and implantation sites. Additionally we determined the precision of optical property extraction from repeated measurements to be within 5%. Over the next several months we will track tumor growth and chemotherapy response to cytotoxic and anti-angiogenic, with a special emphasis on measurements in the hours-to-days after injection timescale. We will investigate correlations between tissue optical parameters and tissue-level biomarkers of acute immune response, vascular health, and tumor metabolism. This work will help to establish SFDI as a new tool for evaluating chemotherapy response for current and emerging cancer drugs.

9303-411, Session 3

Diffuse optical quantification of early hemodynamic changes by chemotherapy on breast cancer xenografts & its implication for therapeutic prediction in clinic

Regine Choe, Ashley R. Proctor, Ki Won Jung, Russell R. Adams, Hyun Jin Kim, Songfeng Han, Emmanuel K. Manno, Daniel K. Byun, Kelley S. Madden, Edward B. Brown III, Univ. of Rochester (United States); Parisa Farzam, Turgut Durduran, ICFO - Institut de Ciències Fotòniques (Spain)

Especially for non-responders, early prediction of cancer therapeutic efficacy is important to avoid unnecessary side effects and improve survival rate by switching to alternative therapies without losing time. Several clinical studies have demonstrated that diffuse optical methods have potential to predict neoadjuvant chemotherapeutic efficacy in breast cancer. However, most studies did not have enough subject numbers to take advantage of full potential of diffuse optics: oxygen metabolism and multi-parametric analysis. We have combined a diffuse correlation spectroscopy and a

Conference 9303D: Diagnosis and Treatment of Diseases in the Breast and Reproductive System

diffuse optical spectroscopy to simultaneously measure blood flow, total hemoglobin concentration, blood oxygen saturation, and tissue scattering of in vivo breast cancer xenografts, with the aim to develop a multi-parametric prediction model based on full access to hemodynamic and metabolic information. BALB/c mice with 4T1, murine breast cancer, xenografts in the mammary fatpad were measured at seven time points with diffuse optics: before, 1, 3, 5, 7, 9, and 11 days after injection of either treatment drug or saline. Typical chemotherapeutic drugs for breast cancer treatment such as doxorubicin, cyclophosphamide, and paclitaxel were investigated for their early hemodynamic/metabolic effects. Preliminary results showed that cyclophosphamide induced clear hemodynamic changes between treatment and control group starting from day 3, whereas doxorubicin and paclitaxel did not for single dose applications. The combination of doxorubicin and cyclophosphamide, close to clinical practice, is being investigated. Based on these results, prediction model based on longitudinal statistical method will be developed and its implication to clinical translation will be discussed.

9303-412, Session 3

Early identification of non-responding locally advanced breast tumors receiving neoadjuvant chemotherapy

Boudewijn E. Schaafsma M.D., Leiden Univ. Medical Ctr. (Netherlands); Martijn Van de Giessen, Leiden Univ. Medical Ctr. (Netherlands) and Technische Univ. Delft (Netherlands); Ayoub Charehbili M.D., Vincent T. H. B. M. Smit M.D., Judith R. Kroep M.D., Leiden Univ. Medical Ctr. (Netherlands); Boudewijn P. F. Lelieveldt M.D., Leiden Univ. Medical Ctr. (Netherlands) and Technische Univ. Delft (Netherlands); Gerrit-Jan Liefers M.D., Leiden Univ. Medical Ctr. (Netherlands); Alan Chan, Leiden Univ. Medical Ctr. (Netherlands) and Percuros B.V. (Netherlands); Clemens W. G. M. Lowik, Jouke Dijkstra, Cornelis J. H. Van de Velde M.D., Martin N. J. M. Wasser M.D., Alexander L. Vahrmeijer M.D., Leiden Univ. Medical Ctr. (Netherlands)

Diffuse optical spectroscopy (DOS) has the potential to enable monitoring of tumor response during the early stages of chemotherapy treatment. This study aims to assess the feasibility of time-domain DOS for monitoring treatment response in HER2-negative breast cancer patients receiving neoadjuvant chemotherapy, particularly after the first therapy cycle. We also compared DOS to tumor response assessment by dynamic contrast enhanced MRI (DCE-MRI) halfway therapy and before surgery.

Patients received neoadjuvant chemotherapy in 6 cycles of 3 weeks. In addition to standard treatment monitoring by DCE-MRI, DOS scans were acquired after the first, third and last cycle of chemotherapy. The predictive value of DOS and DCE-MRI compared to pathological response were assessed.

18 out of 22 patients had a partial or complete tumor response at pathologic examination as a result of neoadjuvant chemotherapy, whereas 4 patients were non-responders. Already after the first chemotherapy cycle a significant difference between responders and non-responders was found using DOS (HbO₂ 86%±25 vs. 136%±25, P=.023). The significant differences between groups of responders and non-responders continued during treatment (halfway treatment, HbO₂ 68%±22 vs 110%±10, P=.010). No significant difference in DCE-MRI for pathological responders and non-responders was found halfway treatment (P=.100).

DOS provided a more accurate response prediction (area under curve (AUC)=0.92, 0.96, 0.87 after 1, 3 and 6 therapy cycles) compared to DCE-MRI (AUC=0.78 and 0.52 after 3 and 6 cycles). This makes DOS a promising modality for (early) treatment monitoring of neoadjuvant chemotherapy and clinical decision making.

9303-413, Session 3

Photoacoustic spectroscopy based evaluation of breast cancer condition

Mallika Priya, Biophysics Unit, School Of Life Sciences, Manipal Univ. (India); Subhas Chandra, Bola Sadashiva Sadashiva S. Rao, School Of Life Sciences, Manipal Univ. (India); Satadru Ray, Prashanth Shetty, Stanley Mathew, Kasturba Medical Collage, Manipal Univ. (India); Krishna Kishore Mahato, School Of Life Sciences, Manipal Univ. (India)

Photoacoustic spectroscopy, a hybrid of optics and acoustics has been gaining popularity in the biomedical field very fast. The main aim in the present study was to apply this technique to detect and distinguish breast tumor tissues from normal and hence develop a tool for clinical applications. There were 224 photoacoustic spectra recorded from 28 normal and 28 breast tumor tissues using PZT detector at 281nm pulsed laser excitations from Nd-YAG laser pumped frequency doubled dye laser system. The recorded time domain photoacoustic spectra were fast Fourier transformed into frequency domain patterns in the frequency region 0-1250kHz and from each pattern, 7 features (mean, median, mode, variance, standard deviation, area under the curve & spectral residual after fitting with 10th degree polynomial) were extracted using MATLAB algorithms. These features were then tested for their significance between normal and malignant conditions using Student T-test and two of them (variance, std. deviation) showing significant variation were selected for further discrimination analysis using supervised quadratic discriminate analysis (QDA). In QDA, 60 spectra from each of the normal and malignant were used for making the respective calibration sets and the remaining 52 spectra from each were used for the validation. The performance of the analysis tested for the frequency region 406.25 - 625.31 kHz, showed specificity and sensitivity values of 100% and 88.46% respectively suggesting possible application of the technique in breast tumor detection.

9303-414, Session 3

Intraoperative breast cancer margin assessment by a hand-held microsecond scale vibrational spectroscopy pen

ChienSheng Liao, Pu Wang, Ping Wang, Robert A. Oglesbee, Ji-Xin Cheng, Purdue Univ. (United States)

Surgical resection is considered as the most effective procedure in treating human breast cancer. However, incomplete excision of cancerous tissue results in metastasis or recurrence of tumor. Conventionally histology examines the excised tissue post-surgery, but the high re-operation rate of 20-40 % demands for a sensitive intraoperative tool assessing tumor margin. Currently cytological examination and frozen section are time consuming. Ultrasound and radio frequency spectroscopy improve the procedure time but lack of sensitivity. Raman spectroscopy provides high chemical sensitivity but the long acquisition time limits its application. Here we develop microsecond scale vibrational spectroscopy by modulation multiplexed stimulated Raman scattering. We modulate each color of a broadband femtosecond pump beam with a distinct frequency by scanning the dispersed pump beam on a spatial pattern. Through the stimulated Raman scattering process, the vibrational spectrum of the sample is coded in the narrowband Stokes beam, and then decoded by Fourier transform analysis of detected photons. This technique enables fast spectroscopy imaging of human breast cancer tissue with a 60 ps pixel dwell time, covering 0.5 x 0.5 mm with sub-micron resolution. By multivariate curve resolution analysis, protein to lipid ratio which is an indicator of tumor margin was determined pixel-by-pixel. Therefore tumor margin can be identified based on chemical composition. We further built a prototype of a hand-held spectroscopy pen which enables spectral acquisition in 60 ps from a 30 x 30 μm² focused spot. With the high chemical sensitivity,

Conference 9303D: Diagnosis and Treatment of Diseases in the Breast and Reproductive System

our spectroscopy pen provides a real-time composition analysis for intraoperative margin assessment.

9303-420, Session PSat

Measurement of the optical redox ratio in breast cancer cell lines with a microplate reader

Taylor M. Cannon, Amy T. Shah, Melissa C. Skala, Alex J. Walsh, Vanderbilt Univ. (United States)

There is a need for accurate, high-throughput, functional measures to gauge the efficacy of potential drugs. Cellular metabolism is an early marker of drug response in cells, and therefore provides an attractive platform for high-throughput drug testing. NADH and FAD are autofluorescent cellular metabolic coenzymes that can be non-invasively monitored using optical techniques. Relative rates of glycolysis and oxidative phosphorylation in a cell are conveniently quantified by the redox ratio, defined as the autofluorescence intensity of NADH divided by that of FAD. However, current methods for redox ratio quantification are time intensive and low-throughput, which limits the number of samples that can be practically tested for drug screening. Alternatively, microplate readers are high-throughput instruments that can measure NADH and FAD autofluorescence intensities for hundreds of wells in minutes.

This study tests the sensitivity of a plate reader in differentiating between breast cancer cell lines of differing receptor status, and monitors cellular response to a HER2 inhibitor, trastuzumab. The BT474 (HER2+/ER+) cell line consistently exhibited the highest redox ratio, followed by the SKBr3 (HER2+/ER-), MCF7 (HER2-/ER+), and MDA-MB-231 (HER2-/ER-) cell lines; all redox ratios were significantly distinct ($p < 0.05$, rank-sum test). Following treatment with trastuzumab, the redox ratios of the HER2-positive cell lines decreased ($p < 0.001$), whereas the redox ratios of the HER2-negative cell lines were unaffected. The findings indicate that plate readers are capable of identifying subtle differences in redox ratio between cell lines, and changes produced by treatment, thus demonstrating increases in throughput to accelerate drug discovery.

9303-421, Session PSat

Cervical confocal endoscope for in vivo cellular resolution biopsy target selection

Colin L. Schlosser, The BC Cancer Agency Research Ctr. (Canada); Fahime Sheikhzadeh, The BC Cancer Agency Research Ctr. (Canada) and UBC (Canada); Calum E. MacAulay, The BC Cancer Agency Research Ctr. (Canada); Michele Follen M.D., Brookdale Univ. Hospital and Medical Ctr. (United States); Martial Guillaud, Pierre M. Lane, The BC Cancer Agency Research Ctr. (Canada)

When the number of biopsy sites is limited, accurate diagnosis of disease relies on selecting samples from the most pathological areas of the tissue. However, it can be difficult to establish which tissue is most at risk of malignant transformation, and if the biopsy results fail to confirm the clinical impression or the results of other diagnostic tests, the clinician is faced with a difficult dilemma. In tissues which permit endoscopic access, in-vivo confocal microscopy is a promising solution to this problem, reducing uncertainty by offering immediate evaluation of cellular-level tissue morphology at many sites rapidly and the subsequent selection of the most appropriate biopsy targets.

We present a handheld fibre-based confocal endoscope designed to image the cervix in a clinical setting. The endoscope's low profile, simple, and robust optical assembly are made possible by employing a chromatically corrected miniature refractive GRIN lens element combination, while closed-loop actuation of the fibre-lens spacing using a linear piezo positioner allows for accurate and repeatable focusing of the device within

the stringent spatial constraints. The system uses a 457-nm laser diode where the reflected excitation is blocked by a 475-nm long-pass filter, thus allowing detection of the fluorescence emitted by a topically applied acriflavine hydrochloride contrast agent.

By giving the clinician a real-time (15 [fps]), cellular-level (a targeted axial and lateral resolution of $\sim 15[\mu\text{m}]$ and $\sim 1[\mu\text{m}]$ respectively) view of the cervix tissue over a $240[\mu\text{m}]$ field, the device permits biopsy selection based on relevant cellular features, such as nuclear size, nucleus to nucleus spacing and an inferred N/C ratio, which in turn provide greater confidence in their results.

9303-422, Session PSat

Longitudinal in vivo transcutaneous observation of Raman signals from breast cancer during chemotherapy in small animal model

Myeongsu Seong, Gwangju Institute of Science and Technology (Korea, Republic of); NoSung Myoung, Advanced Photonics Research Institute (Korea, Republic of); Sang-Youp Yim, Jae G. Kim, Gwangju Institute of Science and Technology (Korea, Republic of)

Mammography, the gold standard of breast cancer screening and monitoring treatment efficacy, has the disadvantage of being harmful, painful, and providing only morphological information. These drawbacks have arisen a critical need for new methods to diagnose or monitor breast cancer treatment. In this study, we hypothesized that the change of biochemical composition in the tumor occurs earlier than morphological changes during treatment.

4 Fisher 344 female rats bearing 13762 MAT B-III breast cancer were used to test our hypothesis. To minimize autofluorescence and deep penetration, fiber-optic Raman spectroscopy with 785-nm laser was employed. We acquired Raman signals from 3 triangular points around the nipple, before and after breast cancer cell inoculation. Differential Raman spectra were acquired by subtracting Raman spectra of the contralateral normal breast from those of the breast tumor. In addition, a principal component (PC) analysis of baseline and breast tumor was performed.

The differential Raman spectra between breast tumor and contralateral normal breast did not show a strong correlation in either tumor progression or regression after chemotherapy. A biplot of 2-PCs also did not show a clear classification between baseline (before breast cancer cell inoculation) and the breast tumor.

The results did not satisfy our hypothesis and we reason that it may be due to the inappropriate design of our current probe, mostly interrogating superficial layer of tissue. Thus, we will employ spatially-offset Raman spectroscopy, which has a few millimeter separation between excitation fiber and collection fiber, so that we can acquire more Raman signals from the breast tumor and suppress the Raman signals from skin.

9303-423, Session PSat

Predictive potential of photoacoustic spectroscopy in breast tumor detection based on xenograft serum profiles

Mallika Priya, Biophysics Unit, School Of Life Sciences, Manipal Univ. (India); Bola Sadashiva S. Rao, Subhas Chandra, School Of Life Sciences, Manipal Univ. (India); Satadru Ray, Kasturba Medical Collage, Manipal Univ. (India); Krishna Kishore Mahato, School Of Life Sciences, Manipal Univ. (India)

Breast cancer is the second most common cancer all over the world.

Conference 9303D: Diagnosis and Treatment of Diseases in the Breast and Reproductive System

Heterogeneity in breast cancer makes it a difficult task to detect with the existing serum markers at an early stage. With an aim to detect the disease early at the pre-malignant level, MCF-7 cells xenografts were developed using female nude mice and blood serum were extracted on days 0th, 10th, 15th & 20th post tumor cells injection (N=12 for each time point). Photoacoustic spectra were recorded on the serum samples at 281nm pulsed laser excitations. A total of 144 time domain spectra were recorded from 48 serum samples belonging to 4 different time points. These spectra were then converted into frequency domain (0-1250kHz) using MATLAB algorithms. Subsequently, seven features (mean, median, mode, variance, standard deviation, area under the curve & spectral residuals after 10th degree polynomial fit) were extracted from them and used for PCA. Further, using the first three Principal components (PCs) of the data, Linear Discriminate Analysis has been carried out. The performance of the analysis showed 82.64% accuracy in predicting various time points under study. Further, frequency-region wise analysis was also performed on the data and found 95 - 203.13 kHz region most suitable for the discrimination among the 4 time points. The analysis provided a clear discrimination in most of the spectral features under study suggesting that the photoacoustic technique has the potential to be a diagnostic tool for early detection of breast tumor development.

9303-424, Session PSat

An opto-electronic joint detection system based on DSP aiming at early cervical cancer screening

Weiya Wang, Mengyu Jia, School of Precision Instrument and Optoelectronics Engineering, Tianjin Univ. (China); Feng Gao, School of Precision Instrument and Optoelectronics Engineering, Tianjin Univ. (China) and Tianjin Key Lab. of Biomedical Detecting Techniques and Instruments (China); Lihong Yang, Pengpeng Qu, Tianjin Central Hospital of Gynecology Obstetrics (China); Changping Zou M.D., Univ. of Connecticut Health Ctr. (United States); Pengxi Liu, School of Precision Instrument and Optoelectronics Engineering, Tianjin Univ. (China); Huijuan Zhao, School of Precision Instrument and Optoelectronics Engineering, Tianjin Univ. (China) and Tianjin Key Lab. of Biomedical Detecting Techniques and Instruments (China)

The cervical cancer screening at a pre-cancer stage is beneficial to reduce the mortality of women. A system based on opto-electronic joint detection has been developed to satisfy the need for improving the cervical cancer screening efficiency. The photoelectrode placed at the tip of the handheld probe is used to stimulate the cervical tissue and detect the response of tissue to the stimulation. In this system, three electrodes alternately discharge and three light emitting diodes in different wavelengths (NIR940nm R660nm, G530nm) alternately irradiate. Then the optical and electrical parameters-- relative reflectance and voltage attenuation constant can be obtained by optical and electrical detection, respectively. Using these parameters, the classification algorithm based on Support Vector Machine (SVM) discriminates abnormal cervical tissue from normal. We use particle swarm optimization to optimize two key parameters of SVM, i.e. nuclear factor and cost factor. The clinical data were collected on 313 people to build a clinical database of tissue response under optical and electrical stimulation by comparing with the gold standard of histopathologic examination. The classification result shows that the opto-electronic joint detection has higher total coincidence rate than that using only optical detection or electrical detection. The sensitivity, specificity and total coincidence rate are increased with fixed testing set but increased training set. The average total coincidence rate of the system can reach 85.1% compared with the histopathologic examination. The system is small in size and simple operation, so it is of important significance to early cervical cancer screening, especially to that in underdeveloped countries.

9303-425, Session PSat

Time-domain hemoglobin diffuse optical tomography of breast: a pilot study

Wenjuan Ma, Shuping Zhang, Tianjin Medical Univ., Cancer Institute and Hospital, Tianjin (China) and National Clinical Research Ctr. of Cancer (China) and Key Lab. of Cancer Prevention and Therapy (China); Limin Zhang, Tianjin Univ. (China)

The objective of this study was to primary certify the validity of a time-domain diffuse optical tomography system for breast tumor diagnosis. A time-domain diffuse optical tomography system is proposed based on the multi-channel time-correlated single-photon counting technique. Aligning 32 coaxial fibers around the tissue surface equally; the system scans objects in a parallel-beam mode analogous to X-ray CT so that the time-resolved projections at different incident positions can be obtained. By applying the relevant iteration reconstruction algorithm, promising images have been produced from measurements on one patient. Reconstructed images correctly disclose the mass location and various of contrast mechanisms (oxy-hemoglobin, deoxy-hemoglobin, total hemoglobin and blood oxygen saturation), but the reconstructed images disclose the poor spatial resolution and mass size larger than the ultrasound and magnetic resonance imaging. The results primary indicate this system works reliably, and we need to measure more cases to assess the feasibility of using this system to distinguish between benign and malignant cases?

9303-426, Session PSat

Full-field optical coherence tomography (FFOCT) for evaluation of endometrial cancer

Alexis Bruhat, Univ. of Pittsburgh (United States); Marais Combrinck, PathWest Lab. Medicine WA (Australia); Eugénie Dalimier, Fabrice Harms, LLTech SAS (France); Jeffrey L. Fine, Univ. of Pittsburgh (United States)

Full-field optical coherence tomography (FFOCT) offers direct, nondestructive tissue images that resemble brightfield photomicrographs, which may lead to clinical applications based on existing diagnostic expertise without extensive re-training. Axial and transverse resolution (about 1 micron each) compare favorably with whole slide image microscopy. Pursuing intra-operative clinical applications, we examined endometrial cancer depth-of-invasion assessment. This preliminary report emphasizes the technical aspects of our study.

More than forty samples were imaged with FFOCT, then were examined by microscopy for gold-standard histopathology correlation. FFOCT required much less time than conventional histology (e.g., 30 minutes versus 8-10 hours). Endometrium showed good contrast between glands, stroma, and myometrium, therefore FFOCT was generally consistent with histological diagnosis. In addition to single-slice FFOCT images, we captured sets of 3 virtual slices to simulate conventional microscopy workflow; this may improve diagnostic accuracy. Other enhanced image processing techniques were explored, to optimize contrast for specific applications (i.e. analogous to CT image "windows", LUT table manipulation, high pass image filter).

Our preliminary analysis indicates there is potential application of FFOCT for intraoperative assessment of endometrial cancer. Following comparison of our 3-slice image capture and enhanced image processing the next step will be a larger review of images with more subject pathologists. Such data may then justify prospective clinical studies. It is hoped that FFOCT will revolutionize pathology practice by slashing turn-around time and permitting potential in vivo diagnosis. FFOCT is therefore a very exciting technology for digital pathology.

**Conference 9303D: Diagnosis and Treatment of
Diseases in the Breast and Reproductive System**

9303-415, Session 4

Quantitative optical imaging of cilia-driven fluid flow: a new area of research in reproductive health? (Invited Paper)

Michael A. Choma M.D., Yale School of Medicine (United States)

Motile cilia are cellular organelles that generate directional fluid flows across many different mucosal surfaces in the human body. Recently, there has been growing interest in using optical methods to quantify cilia-driven fluid flow. While most of this work has focused on the respiratory system, many of the methods and animal models have potential in studying cilia-driven fluid flow in the fallopian tubes. I will discuss our research in cilia-driven fluid flow and its potential to better understand female reproductive health.

9303-416, Session 4

Optical imaging of breast cancer metabolic signatures in 3D acini using co-registered CARS and FLIM microscopy

Jue Hou, Eric O. Potma, Elliot L. Botvinick, Chung-Ho Sun, Beckman Laser Institute and Medical Clinic, Univ. of California, Irvine (United States); Enrico Gratton, Beckman Laser Institute, Univ. of California, Irvine (United States); Bruce J. Tromberg, Beckman Laser Institute and Medical Clinic, Univ. of California, Irvine (United States)

We present a novel approach to study tissue engineered 3D breast cancer model with nonlinear optical imaging. Coherent anti-Stokes Raman scattering (CARS) microscopy is utilized to map out the lipid distribution. Two photon excitation fluorescence (TPEF) and fluorescence lifetime microscopy (FLIM) are used to assess cellular glucose metabolism. Both the NADH/FAD intensity ratio and NADH fluorescence lifetime are collected to evaluate the metabolic rate. T47D, MB231 and primary mammary epithelial cells are suspended in the matrigel/collagen mixtures and plated onto separate imaging dishes. Their morphological patterns and metabolic status are dynamically monitored for 16 days. Different morphological features and metabolic signatures are observed. The normal cells form the mammary gland functional unit (acini) with polarized structure and hollowed center. In comparison, the T47D cancer cells turn into solid spheroids and become growth arrested after 7 days. MB231 metastatic tumor cells do not form any structures but spread throughout extracellular matrix. Compared to normal cells, both tumor cell lines show higher NADH/FAD ratio and shorter fluorescence lifetime which correspond to higher glycolytic rate where T47D is the highest. Moreover, the cellular glycolytic rate shifts from low to high starting from exterior to interior in this polarized structure. Such metabolic rate gradient is possibly related to the cell's fate. CARS images are reconstructed into 3D sets at the same time period. The lipid concentration demonstrated a negative correlation with tumor malignancy. However, the total amount of lipid during the acini formation initially decreases followed by an increase for all three cell lines.

9303-417, Session 4

Optical diagnosis of mammary ductal carcinoma using advanced optical technology

Yan Wu, Fujian Normal Univ. (China); Fangmeng Fu, Yuane Lian, The Affiliated Union Hospital, Fujian Medical Univ. (China); Yuting Nie, Shuangmu Zhuo, Fujian Normal Univ. (China); Chuan Wang, The Affiliated Union Hospital, Fujian

Medical Univ. (China); Jianxin Chen, Fujian Normal Univ. (China)

Mammary ductal carcinoma is the most common type of breast cancer in women. Clinical diagnostic methods include mammography, ultrasound, and magnetic resonance. X-ray mammography is the most effective screening technique but has high false positive rate in women under 50. Magnetic resonance imaging (MRI) and ultrasound are used in addition to X-ray mammography, but have limitations such as high cost, low throughput, limited specificity (MRI), and low sensitivity (ultrasound). Multiphoton microscopy (MPM) has become a potentially attractive optical technique to bridge the current gap in clinical utility, which relies on nonlinear optical processes such as two-photon excited fluorescence (TPEF) and second harmonic generation (SHG). In this paper, MPM was used to image normal and ductal cancerous breast tissue. It was found that the epithelial cells lining the lumen of the duct generated high TPEF signals, while the basement membranes of the duct generated high SHG signals. TPEF images showed that malignant epithelial cells confined to the ductal system in ductal carcinoma in situ (DCIS) but infiltrated into the surrounding stroma in invasive ductal carcinoma (IDC). SHG images revealed that the basement membrane maintained well in DCIS and disappeared in IDC. By combining TPEF/SHG signals, MPM can differentiate mammary ductal carcinoma (DCIS and IDC) from normal breast tissue comparable to histology. These findings indicate that, with integration of MPM into the transdermal biopsy needle, it has the potential to make a real-time histological diagnosis of mammary ductal carcinoma in vivo.

9303-418, Session 4

Evaluation of breast glandular proliferations with full-field optical coherence tomography

Ana Tereza Nadan, Institut Curie (France); Eugénie Dalimier, LLTech SAS (France); Vincent Servois, Institut Curie (France); Fabrice Harms, LLTech SAS (France); Brigitte Sigal-Zafrani, Institut Curie (France)

Full-field optical coherence tomography (FFOCT) is a real-time and non-invasive method of obtaining images of unprocessed biological tissues at ultrahigh resolution (1µm in all 3 directions). This study aimed to investigate the potential of FFOCT as a diagnostic complementary tool, in particular for the evaluation of breast glandular proliferations in breast biopsies.

Sixty specimens from forty-two patients who had breast lesion assessed by biopsy or surgical resection were collected. They were imaged with FFOCT after fixation and before routine histology. Two blinded pathologists analyzed the images to classify them in two categories: atypical glandular proliferation (AGP) and non-atypical glandular proliferation (NAGP). The results were compared with histological diagnosis. Furthermore, image quality was compared with different tissue fixation procedures (AFA, formalin, no fixation but preservation in RPMI medium).

Normal breast architecture (adipocytes, fibrous stroma, lobules, ducts and blood vessels) were readily identified with FFOCT. On the glandular proliferation assessment, the sensitivity was 90% and the specificity 69%. It was found that in tissues fixed with formalin and AFA, the contrast of the fibrous stroma was attenuated as compared to the stroma visualized on fresh tissues preserved in RPMI. With the AFA preparation, another effect was the enhancement of the nuclei contrast, which appeared hyper-reflective with AFA, instead of hypo-reflective in fresh or formalin-fixed tissues.

FFOCT evaluation of breast glandular proliferations is feasible and concordant with histological diagnosis. With further pathologist experience and possible image enhancement or post-processing, it could become an attractive tool for the rapid evaluation of breast biopsies.

9303-419, Session 4

**Differentiating cancerous from normal
breast tissue by redox imaging**

He N. Xu, Julia C. Tchou, Min Feng, Univ. of Pennsylvania (United States); Huaqing Zhao, Temple Univ. (United States); Lin Z. Li, Univ. of Pennsylvania (United States)

Abnormal metabolism can be a hallmark of cancer occurring early before detectable histological changes and may serve as an early detection biomarker. The current gold standard to establish breast cancer (BC) diagnosis is histological examination of biopsy. Previously we have found that pre-cancer and cancer tissues in animal models displayed abnormal mitochondrial redox state. Our technique of quantitatively measuring the mitochondrial redox state may be implemented as an early detection tool for BC and may provide prognostic value. We therefore in this present study, investigated the feasibility of quantifying the redox state of tumor samples from 16 BC patients. Tumor tissue aliquots were collected from both normal and cancerous tissue from the affected cancer-bearing breasts of 16 female patients (5 TNBC, 9 ER+, 2 ER+/Her2+) shortly after surgical resection. All specimens were snap-frozen with liquid nitrogen and scanned with the Chance redox scanner, i.e., the 3D cryogenic NADH/oxidized flavoprotein (Fp) fluorescence imager. Our preliminary results showed that both Fp (including FAD) and NADH contents in the cancerous tissues roughly tripled those in the normal tissues ($p < 0.05$); and the redox ratio $Fp/(NADH+Fp)$ was about 27% higher in the cancerous tissues than in the normal ones ($p < 0.05$). Our findings suggest that the redox state could differentiate between cancer and non-cancer breast tissues in human patients and this novel redox scanning procedure may assist in tissue diagnosis in freshly procured biopsy samples prior to tissue fixation. We are in the process of evaluating the prognostic value of the redox imaging indices for BC.

Conference 9303E: Diagnostic and Therapeutic Applications of Light in Cardiology

Saturday - Sunday 7-8 February 2015

Part of Proceedings of SPIE Vol. 9303 Photonic Therapeutics and Diagnostics XI

9303-500, Session 1

Ideal flushing agents for integrated optical acoustic imaging system

Jiawen Li, Hataka Minami, Univ. of California, Irvine (United States); Dilbahar Mohar, Univ. of California, Irvine School of Medicine (United States); Teng Ma, Koping Kirk Shung, Qifa Zhou, The Univ. of Southern California (United States); Pranav M. Patel, Univ. of California, Irvine School of Medicine (United States); Zhongping Chen, Univ. of California, Irvine (United States)

Great progress has been made in developing a fully-integrated IVUS OCT system and catheter. However, to our knowledge, no research has been performed to find ideal flushing agents that work for both OCT and US. Blood is a high-scattering source for OCT signals. Either blood occlusion or continuous flushing is needed for intravascular OCT imaging. Although there is no need for any flushing agents in US imaging, some OCT flushing agent may hinder the transmission of US signals when using IVUS and OCT functions simultaneously. Thus, it is critical to identify flushing agents that match the dual nature of IVUS-OCT imaging. This research will also benefit acoustic-optics (AO), photoacoustic (PA) imaging and spectroscopy, acoustic radiation force optical electrograph (ARF-OCE) and other imaging techniques that simultaneously use light and ultrasound.

X-ray contrast agents are usually used for intravascular imaging to clear blood for OCT. But the use of contrast agents may lead to renal function disorder. Some patients may also encounter life-threatening reactions, such as cardiotoxic effects and seizures. Thus, apart from testing the commonly-used contrast agent in our experiments, we selected three other solutions Perfluorocarbon, Mannitol and Dextran as flushing agents to test for their image-enhancing effects and toxicities. Quantitative testing of the effects of Mannitol, Dextran and Iohexol was later performed. Both optical and acoustic attenuation coefficients of each flushing agent were measured and compared. The effect of each flushing agent was also tested on rabbits in vivo.

9303-501, Session 1

Ca²⁺ sensitive photoacoustic imaging in vitro

Nicholas P. Dana, R. Andrew Fowler, Laura Geuss, Alicia Allen, Laura J. Suggs, Stanislav Y. Emelianov, The Univ. of Texas at Austin (United States)

Quantitative measurement of calcium ion (Ca²⁺) concentration can yield valuable clinical information, such as in cardiac arrhythmia diagnosis or pharmacotherapeutic efficacy assessment. Unfortunately, due to strong optical scattering in tissue, depth-resolved, dynamic measurement of Ca²⁺ concentration, remains difficult using optical-sensing techniques. In this study we investigate the potential for photoacoustic (PA) imaging, in concert Arsenazo III (AszIII), a Ca²⁺ sensitive dye, to visualize Ca²⁺ concentration in vitro. Reference spectra standards were generated by measuring UV-Vis absorbance while varying both Ca²⁺ and AszIII concentration. AszIII and Ca²⁺ phantoms, with various concentrations, were then imaged using photoacoustics and that data was then validated against reference spectra. AszIII dye was also encapsulated in cationic liposomes to enhance the cellular uptake of the AszIII dye. Liposomal stability was validated using both UV-Vis and PA imaging. A myocardial cell line (HL-1), capable of spontaneous contraction, was used as an in vitro cell model. Finally, media containing liposomes with AszIII, as well as dye free and

liposome free control media, were used to incubate HL-1 cells, which were later imaged using photoacoustics. PA measurement of Ca²⁺ from phantom studies agreed well with UV-Vis reference spectra using a ratiometric multi-wavelength approach - which is robust to changes in fluence - to estimate Ca²⁺ concentration. Furthermore, initial cell studies indicate that Ca²⁺ PA imaging using AszIII may be able to assess dynamic cytosolic changes in Ca²⁺ concentration. These results suggest that Ca²⁺ sensitive PA imaging may be a valuable tool to visualize Ca²⁺ changes with high spatiotemporal resolution.

9303-502, Session 1

Dual modality catheter for real-Time IVUS/IVPA imaging of atherosclerotic plaques

Andrei B. Karpouk, Donald VanderLaan, Douglas E. Yeager, Stanislav Y. Emelianov, The Univ. of Texas at Austin (United States)

Detection of atherosclerotic plaques developed within arterial walls and differentiation of rupture-prone plaques has recently been demonstrated using different designs of imaging catheter prototypes capable of combined intravascular ultrasound (IVUS) and intravascular photoacoustic (IVPA) imaging. While both ex vivo and in vivo results have been reported, clinical translation of the technique requires real-time, 30 or more frames/second, IVUS/IVPA imaging using safe, flexible and miniature catheters. We present a prototype of a real-time IVUS/IVPA imaging system and a 1-mm diameter integrated IVUS/IVPA catheter that comprises an optical fiber-based light delivery system and an ultrasound transducer aligned to ensure best overlap between ultrasound and light beams. To enable total internal reflection at a distal end, the optical fiber with core diameter of 300 μ m was polished at 32.5 degree in respect to its longitudinal axis and sealed by a gas-trapping cap. The transducer with center frequency of 40 MHz was. Both co-axial cable and optical fiber were located inside the 0.6 mm diameter hollow torque drive cable to allow for catheter rotation. The proximal end of the catheter was optically coupled with a laser source and electronically connected to the ultrasound pulser/receiver. The catheter was mechanically rotated by the motor. The real-time imaging system further comprised a high pulse repetition frequency (up to 10 kHz) laser and processing unit. IVUS and IVPA signals were acquired in real-time and images were reconstructed from 256 A-lines. The results suggest that the developed catheter design is suitable for real-time IVUS/IVPA imaging.

9303-503, Session 1

Intravascular laser speckle imaging of coronary plaque mechanical properties using an omni-directional viewing catheter

Jing Wang, Wellman Ctr. for Photomedicine, Harvard Medical School and Massachusetts General Hospital (United States); Masaki Hosoda, Canon USA, Inc. (United States); Diane M. Tshikudi, Wellman Ctr. for Photomedicine, Harvard Medical School and Massachusetts General Hospital (United States); Seemantini K. Nadkarni, Wellman Ctr for Photomedicine, Harvard Medical School and Massachusetts General Hospital (United States)

Intracoronary laser speckle imaging (ILSI) has demonstrated its capability to evaluate the mechanical properties of coronary plaques intimately related with the risk of plaque rupture. In ILSI, the speckle decorrelation

Conference 9303E: Diagnostic and Therapeutic Applications of Light in Cardiology

time constant, defined as the exponential decay rate of the speckle intensity autocorrelation function, provides an index of viscoelasticity that is closely related with plaque mechanical properties and composition. The diagnostic capability of our previous side-viewing ILSI catheter is limited since it can only recover the viscoelastic properties of the coronary wall at discrete locations along the artery. Here we discuss the utility of a next-generation ILSI catheter that enables omni-directional viewing to quantify arterial mechanical properties over the entire coronary circumference simultaneously during pull-back. The performance of the catheter is tested using a polyacrylamide coronary phantom with mechanical moduli that vary in both circumferential and longitudinal directions. Cylindrical distributions of the speckle time constants at different circumferential and longitudinal locations along the phantom show a strong correspondence with the mechanical moduli measured via standard rheometry. Furthermore, ILSI is conducted in human cadaveric hearts to quantify cylindrical maps of the viscoelasticity differences over the circumference and length of coronary segments. A comparison of ILSI maps with Histopathology cross-sections exhibit distinct differences between the time constant distributions of the necrotic core plaques and those of normal and fibrous coronary plaques. These studies highlight the capability for omni-directional assessment of coronary artery viscoelastic properties using ILSI to obtain key mechanical metrics for identifying high-risk plaques.

9303-504, Session 1

Assessment of fibrinolytic activity using Optical Thromboelastography (OTEG) for cardiovascular applications

Markandey M. Tripathi, Massachusetts General Hospital (United States) and Harvard Medical School (United States); Diane M. Tshikudi, Massachusetts General Hospital (United States); Zeinab Hajjarian Kashany, Seemantini K. Nadkarni, Massachusetts General Hospital (United States) and Harvard Medical School (United States)

Fibrinolysis is an essential component of hemostatic cascade that regulates the breakdown of a blood clot to enable wound healing. Abnormalities in the fibrinolysis pathway may cause hyperfibrinolysis which is associated with the increased risk of life-threatening bleeding particularly following cardiac surgery. Early assessment of fibrinolytic activity in these patients can enable timely administration of fibrinolysis inhibitors that can significantly improve patient recovery. Optical thromboelastography (OTEG), a novel technique to assess blood coagulation status, has the potential to quantify fibrinolysis in real-time at point-of-care. The goal of the current study is to test the accuracy of OTEG in quantifying fibrinolysis in blood sample. Fibrinolysis is activated in a blood sample by adding varying concentrations of tissue plasminogen activator (tPA), a known fibrinolysis activator. The blood sample is illuminated by laser light and the speckle intensity autocorrelation curve is measured to derive changes in clot viscoelastic modulus during coagulation. From the OTEG trace, the coagulation parameters, clotting time (R), clot progression time (K), maximum clot strength (MA), and clot lysis (LY%) are derived. In this study, increasing dosage of tPA (1:5 μ M/ml) cause dose-dependent MA reduction and increased LY% in OTEG measurements. For instance, the addition of 5 μ M/ml of tPA altered the MA from, 49 to 31 and increased LY% from 2.4% to 96.8%. OTEG measurements also show a strong correlation with standard-reference Thromboelastography (TEG) measurements ($R=0.73$, $p<0.05$). These results demonstrate that OTEG can accurately evaluate fibrinolysis and has the potential for real-time assessment of fibrinolytic activity in patients following cardiac surgery.

9303-505, Session 2

Ultrahigh speed integrated intravascular ultrasound and optical coherence tomography imaging system and catheter

Jiawen Li, Univ. of California, Irvine (United States); Teng Ma, The Univ. of Southern California (United States); Youmin He, Univ. of California, Irvine (United States); Koping Kirk Shung, Qifa Zhou, The Univ. of Southern California (United States); Zhongping Chen, Univ. of California, Irvine (United States)

Fully combined intravascular ultrasound optical coherence tomography (IVUS-OCT) has raised great interest of physicians due to successful in vivo demonstrations. However, its translation into clinical practice is still hindered by the big gap between IVUS and OCT imaging speed. 1900 frames per minute is the fastest speed which has ever been reported by using a commercial IVUS system, while commercial OCT systems usually perform at 6000 frames per minute.

Here, we attempted to challenge the limited speed of IVUS. With a modified design of the imaging system and a stronger mechanical design for the catheter (than our previous published one), we succeeded in acquiring integrated IVUS-OCT imaging at 2500 frames per second, 400 A-lines per frame. The rotation was generated by an external motor and transferred to the integrated probe by a timing belt. The rotation and pullback system were enclosed in an aluminum box and tested for electrical safety. A slip ring holder (with wire protection and electromagnetic shielding) was designed to secure the slip ring at the proximal end of catheter and connected the holder close to the bracket supporting the fiber rotary joint. A 50 kHz swept source laser and a 200 MHz pulser receiver was used for OCT and US sub-system, respectively. OCT and IVUS signals were acquired by two channels from the same digitizer. The A-line trigger of the laser was used to synchronize the digitizer and pulser. A pre-trigger was used for the IVUS channel.

9303-506, Session 2

Time-resolved fluorescence spectroscopy and ultrasound backscatter microscopy for non-destructive evaluation of vascular grafts

Hussain Fatakdawala, Leigh G. Griffiths, Sterling Humphrey, Laura Marcu, Univ. of California, Davis (United States)

Quantitative and qualitative evaluation of structure and composition are important in monitoring development of engineered vascular tissue both in-vitro and in-vivo. Destructive techniques are an obstacle for performing time-lapse analyses from a single sample or animal. This study aims to demonstrate the ability of time-resolved fluorescence spectroscopy (TRFS) and ultrasound backscatter microscopy (UBM), as non-destructive and synergistic techniques, for compositional and morphological analysis of tissue grafts respectively. We report imaging results from ex-vivo carotid arteries from 3 pigs (porcine carotid arteriotomy model). UBM images and integrated back-scatter coefficients (IBC) demonstrated the ability to visualize and quantify post implantation changes in vascular graft biomaterials, such as loss of the external elastic lamina and intimal/medial thickening over the grafted region as well as graft integration with the surrounding tissue. IBC values were found to be higher for grafted areas (-7.31 \pm 4.11 dB) due to increased collagen content compared to normal tissue areas (-12.19 \pm 5.18 dB). TRFS results show significant changes in spectra, average lifetime and fluorescence-decay parameters owing to changes in collagen, elastin and cellular content between normal and grafted tissue regions. Average lifetime values over 370-410 nm band were higher for grafted tissue regions (6.18 \pm 0.10 ns) when compared to normal regions (5.82 \pm 0.40 ns). Second order Laguerre coefficients that describe

Conference 9303E: Diagnostic and Therapeutic Applications of Light in Cardiology

fluorescence decay dynamics also showed contrast between normal and grafted regions with values at -0.056 ± 0.027 and -0.027 ± 0.020 respectively over 410-515 nm band. These results lay foundation for the application of a bimodal catheter-based technique for in-vivo evaluation of vascular grafts using TRFS and UBM.

9303-507, Session 2

Second-generation optical coherence tomography and near-infrared spectroscopy for simultaneous microstructural and compositional imaging of coronary artery

Ali M. Fard, Harvard Medical School (United States); Daryl Chulho Hyun, Robert R. Carruth, Joseph A. Gardecki, Hao Wang, Giovanni Jacopo J. Ughi, Guillermo J. Tearney M.D., Massachusetts General Hospital (United States)

Coronary artery disease (CAD), comprising the build up of atherosclerotic plaques in artery walls, is a progressive disease that can lead to thrombosis and acute myocardial infarction. Owing to its superior resolution, optical coherence tomography (OCT) provides microscopic images of coronary walls, facilitating CAD treatment decisions based on detailed morphology. However, OCT does not directly identify chemical contents that are crucial for accurate diagnosis of atherosclerosis. It is therefore desirable to obtain OCT images in combination with compositional information.

Here we report on an intravascular imaging technology that uniquely integrates OCT and near-infrared spectroscopy (NIRS) into one imaging device. This imaging system uses a near-infrared wavelength-swept (1250-1350nm) light source to perform high-resolution (10-12 μ m axial resolution) imaging and spectroscopy at 100,000 A-scans/s. The imaging catheter illuminates the tissue through a single-mode fiber and collects the back-scattered OCT light, while a multimode fiber collects the NIRS light, 1.5-mm from the illumination location. A dual-channel fiber rotary junction enables simultaneous acquisition of OCT-NIRS images by use of an optical combiner to combine OCT and NIRS signals into a double-clad fiber (DCF). Subsequently, a custom-made DCF coupler and a time-domain balanced detection scheme are employed to extract and detect the NIRS signal.

Previously, we incorporated the optical combiner within the catheter. Because the inclusion of this combiner increases the complexity and cost, we have now developed a different strategy that incorporates the optical combiner within the rotary junction. Furthermore, we have developed a special interchangeable connector for the catheter that contains two optical ports. Using this new catheter, we found that the optical performance (<0.1 -dB insertion loss) was comparable to that of the previous design, while improving the imaging speed up to 100-frames/s. To conclude, the new design for the OCT-NIRS catheter and rotary junction provides improved performance to our prior OCT-NIRS catheter that incorporated and integrated optical combiner. Other advantages of this new device include shorter rigid length that will facilitate pullback and reduced catheter cost that will improve potential for in-vivo studies.

9303-508, Session 2

Integrated optical coherence tomography and ultrasound imaging system towards intravascular diagnosis

Jian Ren, Milen Shishkov, Martin L. Villiger, Brett E. Bouma, Wellman Ctr. for Photomedicine (United States)

Intravascular imaging is an important method to diagnose lesions inside blood vessels. In particular, the morphology of specific physiological structures, such as the thin fibrous cap and the necrotic core of an atheromatous plaque, offers insight into a deeper understanding of diseases

like atherosclerosis. Moreover, in a clinical practice, patients with acute coronary syndrome might benefit significantly from an accurate and timely intravascular imaging examination, which provides the information that physicians can rely on to make clinical decision within the critical treatment window. Two modalities are currently available for high fidelity intravascular imaging: optical coherence tomography (OCT) and intravascular ultrasound (IVUS). While ultrasonic images have a penetration depth deeper than 5 mm enabling visualization of vessel wall, OCT images do have a resolution around 10 microns that can resolve fine structures, such as the thin fibrous cap, very well. At the same time, the limitation of both methods, namely lower resolution of ultrasound images and shallower penetration of OCT, makes the integration of the two modalities a synergic combination. Previous works have demonstrated the capability of such dual-modality imaging systems. Hybrid catheters with both optical and ultrasonic sensors were fabricated to conduct imaging studies on both ex vivo human cadaver and in vivo animal samples. Aiming to eventually bring this dual-modality imaging apparatus into clinical setting, we have developed a prototype system, which includes a hybrid rotary joint that, unlike the previous works, decouples the electrical slip ring from the catheter. Because of the high cost of the slip ring, this technology allows for disposable catheters. We have also reduced the size of the catheters (OD=0.56 mm) so that they can fit into a 2.7 Fr sheath. The speed of the current system is increased to 52KHz for OCT and 36KHz for ultrasound. Further improvement and more imaging studies are ongoing.

9303-509, Session 3

Automated myocardial characterization using optical coherence tomography

Yu Gan, Columbia Univ. (United States); David Tsay, Columbia Univ. Medical Ctr. (United States); Syed A. Bin Amir, Columbia Univ. (United States); Charles C. Marboe, Columbia Univ. Medical Ctr. (United States); Christine P. Hendon, Columbia Univ. (United States)

The ability to distinguish diseased myocardial tissue from normal tissue is very important for early detection and therapeutic management of patients with cardiovascular disease. We present a machine learning method to automatically classify multiple tissue types within cardiac tissue from OCT images.

To facilitate an accurate classification, B-scans from OCT volumes were segmented based on intensity. Sixteen features, including optical properties, images statistics with high moments, and texture analysis on texture feature code method, were extracted for each segmented area. We formulated a probabilistic model of relevance vector machine (RVM) to classify tissue types. To validate the accuracy of our algorithm, whole human hearts (n=9) were obtained from the National Disease Research Interchange Tissue Bank within 48 hours of donor death. Tissue samples were taken from the right/left atrium, right/left ventricular free wall, and right/left ventricular septum. A total of 132 segmented areas were obtained from 68 OCT images, and were categorized into fibrotic tissue, adipose tissue, normal myocardium, and normal endothelium by comparing against their histology. The algorithm was tested by randomizing a subset of images as training data and using the rest of images as testing data.

We perform ANOVA and accept difference at $P < 0.05$. Experiments show that certain features, such as intensity and attenuations, are significantly different among four tissue types. The results demonstrate the four tissue types can be classified with an accuracy of over 85% within a short runtime, which can potentially enhance the OCT based diagnosis and treatment of cardiovascular diseases.

**Conference 9303E: Diagnostic and Therapeutic
Applications of Light in Cardiology**

9303-510, Session 3

Towards mapping the human Purkinje fiber network using high-resolution OCT

Xinwen Yao, Christine P. Hendon, Columbia Univ. (United States)

Morphological research has implicated that the Purkinje fiber network plays an important role in the genesis of ventricular arrhythmias. While most of the commercial OCT systems at 1300 nm have an axial resolution of 5 to 10 micrometer, we have observed that is not sufficient to visualize the fine structures in the subendocardium. We designed and developed a spectral domain optical coherence tomography (SDOCT) system that can achieve a superior resolution as well as a long imaging depth in tissue, making it capable for mapping out the Purkinje fiber network in the subendocardium.

The spectrometer of the SDOCT system is customized to accommodate a bandwidth of 180 nm centered at 800 nm, corresponding to an axial resolution of 1.3 micrometer and an imaging depth of 1.4 mm in tissue. The focusing optics was optimized for the fringe visibility on the imaging plane. We have tested the system using multiplexed SLD at 850 nm with a 3-dB bandwidth of 74 nm. The nonlinear dispersion is compensated numerically and the 6-dB falloff range is measured to be 0.75 mm. Moreover, we have acquired images of right ventricular septum tissues from swine hearts and human hearts. The imaging depth was 0.5 ± 0.05 mm from 5 different samples.

In the future, we will incorporate the state-of-art supercontinuum (SC) light source that matches our designed spectrometer bandwidth, optimize the visibility of the spectrometer, and obtain high resolution maps of the Purkinje fiber network in human heart samples *ex vivo*.

9303-511, Session 3

The direct interplay between collagen turnover and cardiac arrhythmogenesis in an intact animal heart: A new multimodal-imaging platform using SS PS-OCT and fluorescent optical mapping systems

Jong Jin Kim, Korean Electrotechnology Research Institute (Korea, Republic of); Beop-Min Kim, Min-Gyu Hyeon, Korea Univ. (Korea, Republic of)

Introduction: Collagen accumulation in myocardium upon pathological stimuli is known to provide a substrate for cardiac arrhythmia. The direct interplay between the collagen deposition and cardiac arrhythmogenesis in an intact animal heart however has not been fully elucidated. We developed a multimodal optical system, which enables us to map the degree of collagen turnover and local conduction slowing simultaneously in diseased hearts.

Methods and Results: Polarization-sensitive optical coherence tomography system utilizing a swept source (SS PS-OCT) has been built to detect collagen density in isolated animal hearts. SCMOs camera-based fluorescent optical mapping (FOM) system was combined to the SS PS-OCT. A Langendorff's perfused rat hearts were stained with voltage sensitive dye (Di-4 ANEPPS). After excitation with a 488nm LED, emission signals (650 ± 40 nm) from a heart were focused on the SCMOs. SS PS-OCT signals (>1300 nm) from the same field of view were separated from FOM signals and focused on a photodetector. SS PS-OCT signals were converted to collagen contents and local conduction velocity (CV) was calculated throughout the heart. Regional correlation coefficient between local CV and collagen density was calculated with R-squared. Burst stimulation was applied to induce arrhythmia. Once arrhythmia was induced, the sites of arrhythmia foci were spatially correlated with regional distribution of measured collagen density. We observed tight spatial correlation between collagen distribution and local CV. Intriguingly, arrhythmia foci were anchored at the sites with high collagen density. The simultaneous optical

measurement of collagen density and electrical activity can provide a great insight about the mechanisms underlying cardiac arrhythmia.

9303-512, Session 3

Near-infrared spectroscopic device for lesion depth assessment in myocardial tissue

Rajinder P. Singh-Moon, Christine P. Hendon, Columbia Univ. (United States)

Successful lesion formation is a key factor contributing to the effectiveness of radiofrequency ablation (RFA) treatment of cardiac arrhythmias. RFA-induced necrotic tissues undergo distinguishing structural and biochemical composition changes that may be revealed in tissue optical parameters. Near-infrared spectroscopy (NIRS) has been widely used for the recovery of optical properties in biological tissues. We present a NIRS-integrated catheter capable of extracting optical properties and apply it to determine extent of RFA treatment on myocardial tissue.

A modified Beers law was used to model the dependence of reflectance on tissue optical properties based on Monte Carlo simulations. A source-detector separation of 3.5 mm was selected to allow for direct sampling of the zone of resistive heating. A Levenberg-Marquardt routine was used to invert measurements of diffuse reflectance to yield absorption and reduced scattering coefficients. Validation experiments were done in phantoms with known optical properties. Samples (n=36) from four swine hearts were subject to varying degrees of RFA treatment. Extracted optical properties were then compared as a function of lesion depth determined by triphenyl tetrazolium chloride staining.

Reduced scattering and absorption was significantly greater in both superficial and deep lesions as compared to normal myocardium values ($p < 0.01$). While reduced scattering was comparable, absorption in deeper lesions were consistently greater than superficial lesions ($p < 0.05$). Furthermore, measurements in whole blood revealed substantial changes in signal intensity when the catheter makes contact with tissue. These results suggest that the proposed device could be used to help guide therapeutic interventions by contact and successful lesion verification.

9303-513, Session 3

Imaging myocardial fiber architecture of the mouse heart using Stokes vector analysis from fiber-based polarization-sensitive optical frequency domain imaging

Sun-Joo Jang, Taejin Park, Paul Shin, Wang-Yuhl Oh, KAIST (Korea, Republic of)

Objectives: Understanding myocardial fiber architecture would provide the linkage between myocardial structure and pathophysiology of various heart diseases. We sought to analyze the myocardial fiber orientation by fiber-based polarization-sensitive optical frequency domain imaging (PS-OFDI) in a normal or infarcted mouse heart.

Methods: We used fiber-based PS-OFDI using polarization modulator. The effect of fiber-based optical components on determination of the principal axis of the sample was corrected on the Poincare sphere by imaging linearly polarized rubber phantom. The polarization mode dispersion was also compensated with spectral binning method. The myocardial fiber orientation was presented as the angle of the linearly polarized principal axis of the sample. We developed automatic algorithm for the depth-resolved images of fiber orientation and presented the results as arrow images and color-coded tractography according to the angle of the principal axis orientation. The results from normal or infarcted (4 weeks after coronary artery ligation) mouse hearts were compared.

Conference 9303E: Diagnostic and Therapeutic Applications of Light in Cardiology

Results: The normal left ventricular myocardium showed regular pattern of myocardial fiber orientation. The depth-resolved images in normal myocardium revealed helical fiber architecture. The irregular fiber orientation of the infarcted myocardium was well visualized by our automatic color-coded tractography.

Conclusion: We demonstrated the tractography of myocardial fiber orientation using Stokes-vector analysis from fiber-based PS-OFDI. The infarcted myocardium showed irregular myocardial fiber orientation whereas the normal myocardial fibers showed regular directionality.

9303-514, Session 4

Three-dimensional analysis of stent malapposition and lack of coverage by intravascular optical coherence tomography

Giovanni Jacopo J. Ughi, Tom Adriaenssens, Dries Decock, Walter Desmet, Jan D'Hooge, Katholieke Univ. Leuven (Belgium)

The use of intravascular optical coherence tomography (IVOCT) has provided new insights into the incidence and clinical implications of stent strut malapposition as well as to the incidence of uncovered struts in a stented segment. Due to the lack of an automated process, clinical and preclinical IVOCT studies typically only report the amount (e.g., percentage) of malapposed and uncovered struts, lacking detailed information on their spatial distribution (i.e. whether they accumulate in groups or are more homogeneously distributed along the entire stented segment).

Our group has developed and validated a robust algorithm for the automated analysis of stent strut apposition and coverage in coronary arteries. In this study we present the further development of an algorithm capable of automatically classifying malapposed/uncovered stent struts as 'isolated' or 'clustered', i.e. belonging to a 'cluster of malapposed/uncovered struts'. This allows to automatically quantify the spatial distribution of such struts and automatically visualize clusters of malapposed/uncovered struts in a 3D fashion.

The algorithm was then applied to a set of clinical IVOCT pullbacks acquired immediately after DES implantation (n=64) and at 9 months follow-up (n=55). We demonstrated that the proposed algorithm facilitates the quantification of strut apposition and coverage in combination with comprehensive information about spatial strut distribution in an automated way. Given that the occurrence of malapposed and uncovered struts has been linked to an increased risk of acute and late thrombotic events, this implies that the proposed new algorithm may be used for the optimization of PCI (e.g., reducing the degree and extent of cluster of malapposed struts) as well as for stent implantation follow-up and therapies (e.g., extend antiplatelet therapy in case of significant clusters of uncovered stent struts).

9303-515, Session 4

Optical coherence tomography tissue type (OC3T) imaging: attenuation index for plaque diagnosis

Muthukaruppan Gnanadesigan, Erasmus MC (Netherlands); Takeyoshi Kameyama, Erasmus MC (Netherlands) and Tohoku Univ. (Japan); Antonius F. W. van der Steen, Karen Witberg, Jurgen M. A. Ligthart, Antonis Karanasos, Nienke Ditzhuijzen, Evelyn Regar M.D., Gijs van Soest, Erasmus MC (Netherlands)

Detection of coronary vulnerable plaques is important for early diagnosis and better therapy of ischemic heart disease. No single modality is able at present to detect vulnerable plaques with sufficient accuracy. We are developing optical coherence tomography (OCT) attenuation imaging as

tissue characterization method. To investigate the ability of atherosclerotic tissue characterization in vivo, we are conducting the Optical Coherence Tomography Tissue Type (OC3T) study: a prospective single-center validation study of 62 patients, comparing OCT-derived optical attenuation to near-infrared reflection spectroscopy and intravascular ultrasound (NIRS/IVUS; Infraredx TVC).

We analyze the OCT data (C7XR, St Jude Medical) to create color coded maps of optical attenuation. To facilitate the comparison with NIRS/IVUS, we transform the pullback attenuation data in a longitudinal/en-face display by sampling a user specified depth window from the lumen border and match them longitudinally and circumferentially based on major side branches. To compare with LCBI (Lipid Core Burden Index) of the chemogram, we also compute a Plaque Attenuation Index (PAI) which is the ratio of the high-attenuation pixels to the total number of pixels. In each pullback we selected a 4 mm plaque area in the chemogram with the highest LCBI and compared the PAI calculated for the same area from the OCT attenuation data.

LCBI and PAI, in general for all lipid plaques, have modest correlation (R=0.45). When categorizing lipid-rich plaques according to cap thickness based on OCT, there is no difference in LCBI between thin (<65 μm) and thick cap fibroatheroma. The mean PAI for thick-cap plaques is 263 while for thin cap fibroatheroma it is 355 (p = 0.014).

9303-516, Session 4

Measuring collagen with intravascular polarization sensitive OCT

Martin L. Villiger, Ellen Z. Zhang, Wellman Ctr. for Photomedicine, Massachusetts General Hospital and Harvard Medical School (United States); Wang-Yuhl Oh, KAIST (Korea, Republic of); Gijs van Soest, Heleen M. M. van Beusekom, Evelyn Regar M.D., Thorax Ctr., Erasmus MC (Netherlands); Benjamin J. Vakoc, Wellman Ctr. for Photomedicine, Massachusetts General Hospital (United States) and Harvard Medical School (United States); Seemantini K. Nadkarni, Wellman Ctr for Photomedicine, Massachusetts General Hospital (United States) and Harvard Medical School (United States); Brett E. Bouma, Wellman Ctr. for Photomedicine, Massachusetts General Hospital (United States) and Harvard Medical School (United States)

Polarization sensitive optical coherence tomography (PS-OCT) has shown promise as an intracoronary imaging modality for the characterization of atherosclerotic plaques. In addition to the structural intensity signal, PS-OCT provides a measure of tissue birefringence and depolarization. In order to investigate the dependence of the PS-OCT parameters on the quantity and the microstructural arrangement of intimal collagen, we have performed a detailed correlation study with histology of cadaveric human hearts. We established a set of 100 independent PS-OCT and histological cross-sections of various plaques types. Histological sections were imaged with second harmonic generation microscopy, or stained with hematoxylin and eosin, trichrome and picrosirius red (PSR) and observed under normal or cross-polarized light. PSR is specific for collagen and intensifies the intrinsic birefringence of collagen. Further, it provides an additional color hue that is indicative of the fibril thickness. The alignment of collagen fibrils with the optical beam also impacts the measured amount of birefringence, both for PS-OCT and the histological cross-sections. We correlate the measured PS-OCT parameters with morphometric image analysis of the histology in matching octants of the segmented intimal layers, in order to quantify the ability of PS-OCT to assess the intimal collagen content. Mediated by collagen, PS-OCT could offer valuable insight into the mechanical integrity of atherosclerotic plaques and the collagenolytic effect of inflammation. This offers interesting avenues to assist the development of novel drugs that target inflammation and the possibility to improve the patient management in the catheterization laboratory by personalizing the medication.

**Conference 9303E: Diagnostic and Therapeutic
Applications of Light in Cardiology**

9303-517, Session 4

Heartbeat OCT enables comprehensive visualization of coronary interventions

Tianshi Wang, Erasmus MC (Netherlands); Tom Pfeiffer, Ludwig-Maximilians-Univ. München (Germany); Evelyn Regar M.D., Erasmus MC (Netherlands); Wolfgang Wieser, Ludwig-Maximilians-Univ. München (Germany); Heleen M. M. van Beusekom, Charles T. Lancee, Geert Springeling, Ilona Peters, Antonius F. W. van der Steen, Erasmus MC (Netherlands); Robert A. Huber, Univ. zu Lübeck (Germany); Gijs van Soest, Erasmus MC (Netherlands)

Intravascular optical coherence tomography (IV-OCT) has generated a wealth of data that has deepened our understanding of coronary artery disease and catheter-based interventions. However, IV-OCT images are affected by issues such as cardiac motion artifacts and undersampling. Heartbeat OCT, a new generation of IV-OCT, has an imaging speed that is 25 times higher than commercial systems. A sampling pitch that is smaller than the imaging beam width provides faithful longitudinal and 3D renderings of the entire artery. We will present Heartbeat OCT imaging of coronary interventions in vitro and in vivo, showing the benefits of fully sampled data in a comparison with conventional IV-OCT.

9303-518, Session 5

Automatic visualization of dual-modality intravascular optical coherence tomography (OCT) and near-infrared fluorescence (NIRF) images for assessing vessel wall microstructure and quantitative molecular imaging

Giovanni Jacopo J. Ughi, Wellman Ctr. for Photomedicine (United States); Tetsuya Hara, Eric A. Osborn, Johan Verjans, Hao Wang, Harvard Medical School, Massachusetts General Hospital (United States); Ali M. Fard, Adam Mauskampf, Wellman Ctr. for Photomedicine (United States); Farouc A. Jaffer M.D., Harvard Medical School, Massachusetts General Hospital (United States); Guillermo J. Tearney M.D., Wellman Ctr. for Photomedicine (United States)

Intravascular optical coherence tomography (OCT) is a high-resolution catheter based imaging technique for the in vivo assessment of coronary artery microstructure and intracoronary stents. Near-infrared fluorescence (NIRF) imaging is an emerging powerful method for the molecular and functional imaging of coronary arteries. Our group recently demonstrated that dual-modality OCT-NIRF has the potential to improve the assessment of atherosclerosis.

One of the current challenges with NIRF imaging is that the signal intensity attenuates as a function of the distance of the imaging catheter to the vessel wall. While the NIRF signal can be corrected for distance based on the OCT-defined catheter position, manual processing and calibration of NIRF data (200+ images per acquisition) is unfeasible for on-line OCT-NIRF image visualization and cumbersome for the processing of data acquired in large studies.

In order to address this challenge, we developed an algorithm that automatically segments the vessel wall in OCT images and subsequently calibrates the corresponding NIRF signal intensity. This method was validated by comparing automatic to manual segmentation (gold standard) results in n=300 OCT-NIRF images acquired from 10 different New Zealand White Rabbit aortas. Subsequently, we compared 2D NIRF calibrated vessel maps (n=20) to fluorescence microscopy (FM) and fluorescence reflectance

imaging (FRI), the gold standard for the assessment of vessel fluorescence.

A high Dice similarity coefficient was found between automatic and manual segmentation (0.97 ± 0.02) together with an average individual A-line error of 26 μm . In addition, the comparison to FM and FRI demonstrated a very robust match between the two modalities. These results suggest that our algorithm for fully-automated generation of quantitative NIRF signal and visualization of dual modality OCT-NIRF images is accurate. This algorithm will be an important step for the practical application and the clinical translation of dual-modality OCT-NIRF intravascular imaging.

9303-519, Session 5

Preclinical validation of dual-modality optical coherence tomography (OCT) and near-infrared fluorescence (NIRF) molecular imaging for the in vivo assessment of atherosclerosis and current treatments

Giovanni Jacopo J. Ughi, Wellman Ctr. for Photomedicine (United States); Eric A. Osborn, Tetsuya Hara, Harvard Medical School, Massachusetts General Hospital (United States); Johan Verjans, Harvard Medical School, Massachusetts General Hospital (United States); Iwata Hiroshi, Hao Wang, Brigham and Women's Hospital, Harvard Medical School (United States); Ali M. Fard, Wellman Ctr. for Photomedicine (United States); Adam Mauskampf, Harvard Medical School, Massachusetts General Hospital (United States); Masanori Aikawa, Brigham and Women's Hospital, Harvard Medical School (United States); Farouc A. Jaffer M.D., Harvard Medical School, Massachusetts General Hospital (United States); Guillermo J. Tearney M.D., Wellman Ctr. for Photomedicine (United States)

Multimodality optical coherence tomography (OCT) and near infrared fluorescence (NIRF) molecular imaging enable the simultaneous acquisition of microstructural and molecular information associated with coronary atherosclerosis. We have developed an intravascular OCT-NIRF imaging system comprising state-of-the-art OCT and NIRF imaging combined at a custom-fabricated dual-modality rotary junction and then coupled into a 2.6F double-clad fiber catheter.

In order to validate the OCT-NIRF technology, we conducted serial imaging of atherosclerosis in a total of n=15 New Zealand White Rabbit (NZWR) aorta atheroma following balloon injury and hyperlipidemia. Prosense VM110 (n=8) or indocyanine green (ICG, n=7), were injected i.v. in the animals: VM110 is a quenched molecular beacon that generates fluorescence after cleavage by active cathepsin proteolytic enzymes; ICG is postulated to enter plaques through dysfunctional endothelium, being phagocytosed by macrophages and binding to extracellular lipid.

In addition, we conducted studies of bare-metal (BMS) and drug-eluting (DES) stent implanted in rabbits. The stent injury process was imaged in vivo (n=31 NZWR aortas), using a Cy7 NIRF-conjugated fibrin-targeted peptide or Prosense VM110 to demonstrate that NIRF may serve for the study of stent healing and inflammation. Finally, feasibility studies in atherosclerotic swine coronary arteries and swine coronary stent model (n=6 animals) in vivo were performed.

Our results demonstrate that OCT-NIRF can monitor atherosclerotic plaque progression over time and that this image modality has the capability of accurately detecting stent inflammation in vivo and subsequently monitoring progressive vessel wall healing following stent implantation. Furthermore, the findings of this study demonstrate the efficacy, utility and safety of dual modality OCT-NIRF imaging in animals in vivo, meriting the future investigation in clinical patients.

**Conference 9303E: Diagnostic and Therapeutic
Applications of Light in Cardiology**

9303-520, Session 5

Intravascular structural/molecular imaging in-vivo using a clinically available ICG with high-speed OCT/NIRF hybrid system

Han Saem Cho, KAIST (Korea, Republic of); Min Woo Lee, Hanyang Univ. (Korea, Republic of); Sunki Lee, Korea Univ., Guro Hospital (Korea, Republic of); Sunwon Kim, Joon Woo Song, Korea Univ., Guro Hospital (Korea, Republic of); Kyunghun Kim, Tae Shik Kim, Sun-Joo Jang, KAIST (Korea, Republic of); Hyeong Soo Nam, Hanyang Univ. (Korea, Republic of); Kyeongsoon Park, Korea Basic Science Institute (Korea, Republic of); Sukyoung Ryu, KAIST (Korea, Republic of); Jin Won Kim, KAIST (Korea, Republic of) and Korea Univ., Guro Hospital (Korea, Republic of); Hongki Yoo, Hanyang Univ. (Korea, Republic of); Wang-Yuhl Oh, KAIST (Korea, Republic of)

Atherosclerotic plaque rupture is regarded as a leading cause of acute myocardial infarction (AMI). In the progress of atherosclerosis, coronary arteries become narrower and atherosclerotic plaque constituents are changed. A probability of plaque rupture depends not only on degree of stenosis but also coronary plaque composition. Therefore, it is crucial to analyze coronary arteries morphologically and compositionally.

Optical coherence tomography (OCT) can show a high-resolution morphology of coronary arteries but has a limitation to resolve the constituents in atherosclerotic plaques precisely. Recently, near-infrared fluorescence (NIRF) imaging has been highlighted because it can analyze the composition of atherosclerotic plaques. However, it cannot provide morphological information of coronary arteries.

To overcome these limitations of the two imaging modalities, we demonstrate fully-integrated high-speed OCT-NIRF intravascular imaging system. For NIRF imaging, we used a clinically-available (the Food and Drug Administration-approved) NIRF-emitting indocyanine green (ICG). It is a marker of high-risk (lipid-rich inflamed) plaques because it has a tendency to bind to lipoproteins. To integrate two imaging modalities, we developed an integrated fiber-optic rotary junction and an integrated catheter. In order to verify our imaging system, we did intravascular imaging in animal models of atherosclerosis in vivo. We acquired OCT-NIRF fusion images from a 45 mm long coronary-sized vessel in 2.5 second with a 200 μ m longitudinal pitch.

9303-521, Session 5

Multimodal imaging approaches for macrophage-rich plaque in vivo with a mannose receptor targeting probe

Min Woo Lee, Hanyang Univ. (Korea, Republic of); Han Saem Cho, Jiheun Ryu, KAIST (Korea, Republic of); Jae Joong Lee, Ji Bak Kim, Korea Univ., Guro Hospital (Korea, Republic of); Kyeongsoon Park, Chuncheon Ctr., Korea Basic Science Institute (Korea, Republic of); Joon Woo Song, Korea Univ., Guro Hospital (Korea, Republic of); Hyeong Soo Nam, Hanyang Univ. (Korea, Republic of); Dae-Gab Gweon, Wang-Yuhl Oh, KAIST (Korea, Republic of); Jin Won Kim, Korea Univ., Guro Hospital (Korea, Republic of); Hongki Yoo, Hanyang Univ. (Korea, Republic of)

Macrophage-rich inflammatory plaques, which are prone to rupture, are highly associated with acute coronary events. In this study, we newly developed an optical molecular imaging probe targeting macrophage

mannose receptor (MMR) with near-infrared fluorescence (NIRF) emitting cyanine (Cy) dyes to identify vulnerable plaques. We also developed two imaging systems that visualize fluorescent signals as well as microstructures of plaques in vivo: a multi-channel confocal fluorescent microscope and an integrated optical coherence tomography (OCT)/NIRF catheter system. First, the MMR targeting NIRF probe was evaluated in carotid artery of apoE knock-out mice using the customized multi-channel intravital confocal fluorescent microscope. Real-time imaging capability of the intravital microscope enabled in vivo imaging of the carotid plaque. High-resolution fluorescence imaging after injection of MMR probe showed plaque-specific high signal in carotid arteries in apoE mice fed a high cholesterol diet. In a following study using a rabbit model of atherosclerosis, we performed in vivo multi-modal intravascular imaging in coronary-sized vessels of atherosclerotic rabbits using the integrated OCT/NIRF catheter. An integrated rotary junction and a catheter based on a double-clad fiber enabled simultaneous imaging of vessel microstructure and molecular information from MMR-Cy probe with a high-speed rotation of 100rps and a pullback rate of 20mm/s. Macrophage-rich plaques identified by OCT images showed strong NIRF signal from the MMR-Cy probe. These novel multimodal imaging approaches could have the potential to identify high-risk macrophage-rich plaque prone to rupture.

9303-522, Session 6

Identifying the molecular source of near-infrared excited autofluorescence in lipid-rich atherosclerotic plaques

Hao Wang, Joseph A. Gardecki, Jie Zhao, Brijesh Bhayana, Wellman Ctr. for Photomedicine (United States); James R. Stone, Massachusetts General Hospital, Harvard Medical School (United States); Giovanni Jacopo J. Ughi, Wellman Ctr. for Photomedicine (United States); Guillermo J. Tearney M.D., Wellman Ctr. for Photomedicine (United States) and Massachusetts General Hospital, Harvard Medical School (United States) and Harvard-MIT Health Sciences and Technology (United States)

Cardiovascular disease is the leading cause of death in the United States and other industrialized nations. Identification of lipid-rich necrotic core plaques that are prone to rupture is a clinically important area undergoing intensive research. Previously, we have demonstrated strong correlation between near infrared autofluorescence intensity and plaque pathology. However, the molecular origin(s) of the NIRAF signal and how it relates to our current understanding of atherosclerotic plaque progression is not known.

In order to determine the molecular origin of the NIRAF signal, fresh frozen thin sections from 50 human cadaver aorta plaques were measured by NIRAF microspectroscopy at 633nm excitation. Histopathology of these plaques showed that the primary location of NIRAF source is within the necrotic core region of fibroatheromas, but can also be occasionally seen within calcific lesions that were previously necrotic cores. In addition, immunohistochemistry demonstrated a strong correlation between NIRAF and MMP-2 staining, a marker of inflammatory activity. Using confocal autofluorescence microscopy overlaid with phase microscopy, we validated NIRAF microspectroscopy measurements and further observed elevated fluorescence within plaque locations that contained degraded proteins. To investigate fluorescence from protein degradation products, different degradation products that have previously been found in necrotic core were synthesized and subsequently measured by fluorescence spectroscopy.

Our results 1) confirm that the NIRAF signal originates predominantly from necrotic cores, 2) the NIRAF signal is found in areas of high inflammatory activity, and 3) protein oxidation products may contribute to NIRAF in necrotic core regions and extracellular lipid pool. These results suggest that NIRAF may originate from byproducts of oxidative stress in plaques, thereby providing a unique signal for the understanding and diagnosis of coronary atherosclerosis.

**Conference 9303E: Diagnostic and Therapeutic
Applications of Light in Cardiology**

9303-523, Session 6

In-vivo validation of fluorescence lifetime imaging (FLIm) of coronary arteries in swine

Julien Bec, Dinglong M. Ma, Diego R. Yankelevich, Dimitris S. Gorpas, William T. Ferrier D.V.M., Jeffrey Southard M.D., Laura Marcu, Univ. of California, Davis (United States)

We report a scanning imaging system that enables high speed multispectral fluorescence lifetime imaging (FLIm) of coronary arteries. This system combines a custom low profile (3 Fr) imaging catheter using a 200 μm core side viewing UV-grade silica fiber optic, an acquisition system able to measure fluorescence decays over four spectral bands at 20 kHz and a fast data analysis and display module. In vivo use of the system has been optimized, with particular emphasis on clearing blood from the optical pathway. A short acquisition time (5 seconds for a 20 mm long coronary segment) enabled data acquisition during a bolus saline solution injection through the 7 Fr catheter guide. The injection parameters were precisely controlled using a power injector and optimized to provide good image quality while limiting the bolus injection duration and volume (12 cc/s, 80 cc total volume). The ability of the system to acquire data in vivo was validated in healthy swine by imaging different sections of the left anterior descending (LAD) coronary. A stent coated with fluorescent markers was placed in the LAD and imaged, demonstrating the ability of the system to discriminate in vivo different fluorescent features and structures from the vessel background fluorescence using spectral and lifetime information. Intensity en face images over the four bands of the instrument were available within seconds whereas lifetime images were computed in 2 minutes, providing efficient feedback during the procedure. This successful demonstration of FLIm in coronaries enables future study of atherosclerotic cardiovascular diseases.

9303-524, Session 6

Atherosclerotic plaque detection by confocal Brillouin and Raman microscopies

Vladislav V. Yakovlev, Texas A&M Univ. (United States)

Atherosclerosis, the development of intraluminal plaques, is the fundamental pathology of cardiovascular disease, which remains the leading cause of morbidity and mortality worldwide. Biomechanical in nature, plaque rupture occurs when the mechanical properties of the plaque, related to the geometry and viscoelastic properties, are compromised, resulting in intraluminal thrombosis and reduction of coronary blood flow. During the progression of atherosclerosis, from endothelial dysfunction to plaque rupture, the durability of the plaque and thereby the risk to rupture is largely dependent on the arterial chemical and mechanical properties. Therefore, in this study, we describe the first simultaneous application of confocal Brillouin and Raman microscopy to samples of ex vivo arterial tissue, in order to provide a noninvasive, high specificity approach to determine a relationship between the biochemical and mechanical properties of atherosclerotic tissue. Raman and Brillouin data were taken at selected, equidistant points along the lumen of samples of Watanabe Heritable Hyperlipidaemic (WHHL) rabbit aortas and the results were compared with histopathology. This technique opens the route to improve current models of atherosclerosis and potentially in vivo real time diagnostics, as well as extending the use of simultaneous biochemical and mechanical mapping for multiple biomedical and bioengineering applications.

9303-525, Session PSun

Automatic classification of atherosclerotic plaque in intravascular optical coherence tomography images

Hyeong Soo Nam, Hanyang Univ. (Korea, Republic of); Sun-Joo Jang, KAIST (Korea, Republic of); Jin Won Kim, Korea Univ. Medical Ctr. (Korea, Republic of); Wang-Yuhl Oh, KAIST (Korea, Republic of); Hongki Yoo, Hanyang Univ. (Korea, Republic of)

Atherosclerotic plaques are classified into 3 main types: lipid-rich, calcified and fibrotic. Detailed identification of atherosclerotic plaque may accelerate understanding of atherosclerosis pathology and development of optimized therapy. Intravascular optical coherence tomography (IV-OCT) is able to visualize microscopic features of each plaque types from arterial segments due to its high spatial resolution. However, it is often ambiguous to distinguish plaque types in IV-OCT images, which use only intensity information. Thus, robust and accurate classification methods for characterizing atherosclerotic plaque types are required. Herein, we present an automatic depth-resolved classification method for distinguishing 3 main plaque types and thrombus. We developed the classification algorithm based on a linear discriminant analysis. Mainly, spectroscopic information was used for classification. Depth-resolved spectrograms were acquired from the short-time Fourier transform of an axial interference signal. After image preprocessing, we derived features for the automatic classification by calculating depth-by-depth absorption spectra from the spectrograms. Principal component analysis was used to extract the classification features from the depth-by-depth absorption spectra. Also, other features, including mean intensity, were extracted from the spectra. An ex-vivo phantom study was conducted to identify the spectra of each plaque type. The classification results, which were presented as color-coded probability map for easily interpretable visualization, showed a high true-prediction rate. Also, the automatic classification algorithm was developed as graphical user interface for user-friendly usage. This method would offer a new opportunity for better understanding of atherosclerosis pathology.

9303-526, Session PSun

Angioscopic image-enhanced observation of atherosclerotic plaque phantom by near-infrared multispectral imaging at wavelengths around 1200 nm

Katsunori Ishii, Ryo Nagao, Daichi Matsui, Kunio Awazu, Osaka Univ. (Japan)

Spectroscopic techniques have been researched for intravascular diagnostic imaging of atherosclerotic plaque. Near infrared (NIR) light efficiently penetrates of biological tissues, and the NIR region contains the characteristic absorption range of lipid-rich plaques. In addition, NIR spectroscopy may enable lipid-rich plaques to be imaged in the presence of blood because the NIR absorption by blood is low. The objective of this study is to observe atherosclerotic plaque using a near-infrared (NIR) multispectral angioscopic imaging. Atherosclerotic phantom and the environment were prepared using a biological tissue model and bovine fat. For the study, we developed an NIR multispectral angioscopic imaging system with a halogen light, mercury-cadmium-telluride camera, band-pass filters and an image fiber. Apparent spectral absorbance was obtained at three wavelengths, 1150, 1200 and 1300 nm. Data were obtained in saline to simulate an angioscopic environment for the phantom. Multispectral images of the phantom were constructed using a spectral angle mapper algorithm. As a result, the lipid area, which was difficult to observe in a visible image, could be clearly observed in a multispectral image. Our results show that image-enhanced observation of atherosclerotic plaque by NIR multispectral imaging at wavelengths around 1200 nm is a promising angioscopic technique with the potential to identify lipid-rich plaques.

Conference 9303F: Optics in Bone Surgery and Diagnostics

Saturday 7 -7 February 2015

Part of Proceedings of SPIE Vol. 9303 Photonic Therapeutics and Diagnostics XI

9303-600, Session 1

Depth feedback-controlled hard tissue ablation with one-micron industrial fiber laser (*Invited Paper*)

Chenman Yin, Yang Ji, Christopher M. Galbraith, Queen's Univ. (Canada); Paul J. L. Webster, Laser Depth Dynamics Inc. (Canada); James M. Fraser, Queen's Univ. (Canada)

Laser ablation has found success in various industrial and medical applications due to its high transverse precision as well as the wide range of workable materials. However, it has been a long-standing challenge to identify how deep the laser beam has milled into the material. Especially for surgical applications, there is a need for high speed laser cutting with depth control. High-power long-pulse ablation produces stochastic dynamics, but bears the potential to achieve high speed ablation compared to ultrafast lasers. We have demonstrated micron-precision cutting in bone with closed-loop feedback control enabled by a diagnostic tool called in-line coherent imaging (ICI). ICI utilizes similar imaging principles as optical coherence tomography, where the imaging optical path is combined with the machining laser beam along the sample arm of a Michelson-type interferometer. Our ICI system possesses >80dB sensitivity, dynamic range of 60dB, and imaging speed up to 312kHz. This opens a window to probe the light matter interaction dynamics on microsecond time scales. Recently, an interesting carbon-absorption-mediated laser ablation regime has been found in cortical bone where "self-cleaning" ablation was achieved with easily-delivered 1?m industrial laser. This source is in contrast to standard medical lasers that exploit water absorption at 3?m or 10?m but are difficult to deliver. With in-situ depth feedback control capability of ICI, user-defined complicated 3D structures were created on bone surface where little carbonization remains after the process. Furthermore, we have optimized the ablation conditions for both speed and cleanliness and we explore the ablation mechanism at 1?m.

9303-601, Session 1

Changes in chemical composition of bone matrix in ovariectomized (OVX) rats detected by Raman spectroscopy and multivariate analysis

Yusuke Oshima, Tadahiro Iimura D.D.S., Takashi Saitou, Takeshi Imamura M.D., Ehime Univ. (Japan)

Osteoporosis is a major bone disease that connotes the risk of fragility fractures resulting from alterations to bone quantity and/or quality to mechanical competence. Bone strength arises from both bone quantity and quality. Assessment of bone quality and bone quantity is important for prediction of fracture risk. In spite of the two factors contribute to maintain the bone strength, only one factor, bone mineral density is used to determine the bone strength in the current diagnosis of osteoporosis. On the other hand, there is no practical method to measure chemical composition of bone tissue including hydroxyapatite and collagen non-invasively. Raman spectroscopy is a powerful technique to analyze chemical composition and material properties of bone matrix non-invasively. Here we demonstrated Raman spectroscopic analysis of the bone matrix in osteoporosis model rat. Ovariectomized (OVX) rat was made and the decalcified sections of tibias were analyzed by a Raman microscope. In the results, Raman bands of typical collagen appeared in the obtained spectra. Although the typical mineral bands at 960 cm⁻¹ (Phosphate) was absent due to decalcified processing, we found that Raman peak intensities of

amide I and C-C stretching bands were significantly different between OVX and sham-operated specimens. These differences on the Raman spectra were statistically compared by multivariate analyses, principal component analysis (PCA) and liner discrimination analysis (LDA). Our analyses suggest that amide I and C-C stretching bands can be related to stability of bone matrix which reflects bone quality.

9303-602, Session 1

Raman spectrum to evaluate the bone-ligament interface

Yang Wu, Fudan Univ. (China); Michael B. Fenn, Larry L. Hench, Florida Institute of Technology (United States)

Injuries to the Anterior Cruciate Ligament (ACL) and rotator cuff tendon (RCT) are common in physically active and elderly individuals. The development of an artificial prosthesis for repair/reconstruction of ACL and RCT injuries is of increasing interest due to the need for viable tissue and reduced surgically-related co-morbidity. An optimal prosthesis design is still elusive, therefore an improved understanding of the bone-soft tissue interface is necessary. We use Raman spectral mapping for analysis, at the micron level, of the chemical composition and corresponding structure of the bone-soft tissue interface. Raman spectroscopic mapping was performed using a Raman spectrometer with a 785nm laser coupled to a microscope. ACLs and RCTs were extracted from three skeletally mature fresh-frozen rabbits. Both line-mapping and 3-D Raman mapping procedures were performed on the ACL and RCT bone insertion sites (spatial resolution of 1-2.5?m). A Direct Classical Least Squares (DCLS) model was created from reference spectra derived from pure bone and soft-tissue components, and spectral maps collected at multiple sites from RCT and ACL specimens. The gradient of the mineral composition was significantly steeper in RCT compared to ACL based on the line map ($p=0.0032, <0.05$). Raman 3D maps showed that the ligament/tendon and bone interface was not smooth, and that the tide mark of the RCT showed more coarseness compared to the ACL. These findings, along with additional image analysis findings, can provide the important details of the complex microstructural-functional relationship to allow for biomimetic recapitulation for enhanced prosthesis design of synthetic ligament and tendons.

9303-604, Session 1

Tissue level material composition and mechanical properties in Brlt/+ mouse model of osteogenesis imperfecta after sclerostin antibody treatment

William R. Lloyd III, Benjamin P. Sinder, Joseph Salemi, Univ. of Michigan (United States); Michael S. Ominsky, Amgen Inc. (United States); Joan C. Marini, National Institutes of Health (United States); Michelle S. Caird, Michael D. Morris, Univ. of Michigan (United States); Kenneth M. Kozloff, Univ. of Michigan (United States)

Osteogenesis imperfecta (OI) is a collagen-related genetic disorder which causes brittle bones. Antiresorptive bisphosphonate treatment increases bone mass in the axial skeleton of OI patients. However, it has limited effects at reducing long bone fracture rate. Sclerostin antibody (Scl-Ab), a new therapy in clinical trials to treat osteoporosis, stimulates bone formation and may have the potential to reduce long bone fracture rates in OI. Scl-Ab has been investigated as an anabolic therapy for OI in a Brlt/+ mouse model of

**Conference 9303F:
Optics in Bone Surgery and Diagnostics**

moderately severe Type IV OI. While Scl-Ab increases long bone mass in the Brl/+ mouse, it is unclear whether material properties and composition changes also occur. Here, we studied wild type and Brl/+ young (3 week) and adult (6 month) male mice with and without Scl-Ab treatment. Scl-Ab treatment was administered over 5 weeks (25mg/kg, 2x/week). Raman microspectroscopy and nanoindentation investigated compositional and mechanical bone property changes with and without treatment. Fluorescent labels (calcein and alizarin) were given at 4 time points encompassing the entire treatment period to enable bone measurements of a specific tissue age. Differences between wild type and Brl/+ groups included variations in the mineral and matrix lattices, particularly the phosphate v1, carbonate v1, and the v(CC) proline and hydroxyproline stretch vibrations. Results of Raman spectroscopy corresponded to nanoindentation findings indicating that old bone (near midcortex) is stiffer (higher elastic modulus) than new bone. We will compare and contrast mineral to matrix and carbonate to phosphate ratios in young and adult mice with and without treatment.

9303-608, Session 1

Photonic monitoring of chitosan nanostructured alginate microcapsule for drug release

D. Roy Mahapatra, Deepak Kumar Khajuria, Indian Institute of Science (India)

Bisphosphonates are currently the most important class of inhibitors of osteoclast-mediated bone resorption and are widely used in the treatment of osteoporosis. Bisphosphonate (risedronate) suffers from very poor oral bioavailability (1–2%) in humans due to the low absorption in gastrointestinal tract. A novel carrier using chitosan nanoparticles entrapped into alginate microcapsules is proposed to overcome this. Photonic tagging is done while performing in-vitro tests on microfluidic assays simulating the gastro-intestinal cellular conditions. Alginate gelation is used to form microcapsules that protect drug molecules against the gastric environment. In addition, alginate microcapsules possess a bio-adhesive property that allows them to stick to the intestinal mucosa and thus increase drug residence time. In order to solve the drug diffusion problem, chitosan which is a natural nontoxic biocompatible and biodegradable polysaccharide with good mucoadhesive properties, is used in the gelation in the form of nanoparticles. It carries positive charge and can weakly bind with negatively charged surfaces (e.g. mucus) to prolong retention time and improve the bioavailability. The synthesized microcapsules are characterized by optical and electron microscopy. The kinetic properties of the microcapsules are controlled via temperature, additional coating or cross-linking process. Stability of the formulation is studied via photonic imaging of the nanostructures in simulated gastric and intestinal fluid conditions, with the percentage of drug remaining in the alginate microcapsules being more than 90% after 24 hours of incubation. Quantitative correlation is established in terms of diffusion rate of drug formulation and fluorescence signals.

9303-609, Session 1

The use of optical coherence tomography in maxillofacial surgery (Invited Paper)

Mohammed Al-Obaidi, Rahul Tandon D.D.S., Paul Tiwana, Univ. of Texas SW Medical Ctr. (United States) and Parkland Memorial Hospital (United States)

The ever-evolving medical field continues to trend toward less invasive approaches in the diagnosis and treatment of pathological conditions. Basic science research has allowed for improved technologies that are translated to the clinical sciences. Similarly, advancements in imaging modalities continue to improve as their applications become more varied. As such, surgeons and pathologists are able to depend on smaller samples for tissue diagnosis of pathological disease, where once large sections of tissue were

needed. Optical coherence tomography (OCT), a high-resolution imaging technique, has been used extensively in different medical fields, improving diagnostic yield. Its use in dental fields, particularly in oral & maxillofacial surgery, remains limited. In this talk we will assess the use of OCT for improving soft and hard tissue analysis and diagnosis, particularly for its applications in the field of oral & maxillofacial surgery.

9303-603, Session 2

Photoacoustic imaging: a potential new platform for assessment of bone health (Invited Paper)

Xueding Wang, Ting Feng, Jie Yuan, Kenneth M. Kozloff, Cheri Deng, Univ. of Michigan Medical School (United States)

Osteoporosis, a major public health threat with significant physical, psychosocial, and financial consequences, is expected to increase in association with worldwide aging of the population. The goal of this research is to develop a safe and effective diagnostic platform, based on the emerging photoacoustic technologies, for comprehensive assessment of bone density and bone quality, the two main features determining bone health. We propose to develop a quantitative photoacoustic (QPA) platform integrating two techniques, thermal photoacoustic (TPA) measurement and photoacoustic spectral analysis (PASA), for bone characterization. TPA measurement exploits the dependence of photoacoustic signal on the chemical constituents in tissues, and enables quantitative measurement of bone mineral density (BMD). PASA characterizes micron size physical features in tissues, and has shown promise for objective assessment of bone microarchitecture (BMA). This integrated QPA platform can assess both bone mass and microstructure simultaneously without involving invasive biopsy or ionizing radiation. Unlike conventional ultrasound technologies, the QPA technology is based on highly sensitive optical contrast, and is conducted in a reflection mode, facilitating assessment of not only peripheral sites but also central sites, such as spine which is one of the main areas at risk from osteoporotic fractures. Moreover, the good resolution of photoacoustic imaging allows the spatial distributions of BMD and BMA to be presented for evaluating the local variation of these properties within the same bone, e.g. cortical vs. trabecular, or diaphyseal vs. metaphyseal. Considering that QPA is non-ionizing, non-invasive, and has sufficient imaging depths, it holds unique advantages for clinical translation.

9303-610, Session 2

Photoacoustic and ultrasound characterization of bone composition (Invited Paper)

Bahman Lashkari, Univ. of Toronto (Canada); Lifeng Yang, Univ. of Toronto (Canada) and Univ. of Electronic Science and Technology of China (China); Joel W. Y. Tan, Univ. of Toronto (Canada); Andreas Mandelis, Univ. of Toronto (Canada) and Univ. of Electronic Science and Technology of China (China)

This study examines the sensitivity and specificity of backscattered ultrasound (US) and backscattering photoacoustic (PA) signals for bone composition variation assessment. We examine the sensitivity of both US and PA to density variation in cortical and trabecular layers (separately). Similar to our previous studies, measurements were performed on bone samples before and after mild demineralization and decollagenization at the exact same points. The sensitivity of US and PA to demineralization of bone can easily and accurately be assessed by employing well-established micro-computed tomography (μCT). The evaluation of changes in collagen content of bone required destructive methods, nevertheless the volume changes can

**Conference 9303F:
Optics in Bone Surgery and Diagnostics**

be compared with presented modalities. Results show that combining both modalities can enhance the sensitivity and specificity of diagnostic tool.

9303-611, Session 2

Imaging microfractures and other abnormalities of bone using a supercontinuum laser source with wavelengths in the four NIR optical windows

Laura A. Sordillo, Peter P. Sordillo M.D., Yury Budansky, The City College of New York (United States); Philippe Leproux, XLIM UMR CNRS (France); Robert R. Alfano, The City College of New York (United States)

Many areas of the body such as the tibia have minimal tissue thickness overlying bone. Near-infrared (NIR) optical windows may be used to image more deeply to reveal abnormalities hidden beneath tissue. We report on the use of a compact Leukos supercontinuum laser source (model STM-2000-IR) with wavelengths in the four NIR optical windows (from 650 nm to 950 nm, 1,100 nm to 1,350 nm, 1,600 to 1,870, and 2,100 nm to 2,300 nm, respectively) and between 200 - 500 microwatt/nm power, with InGaAs (Goodrich Sensors Inc. SU320-1.7RT) and InSb detectors (Teledyne Technologies) to image microfractures and abnormalities of bone.

9303-605, Session 3

Reinforcement of osteogenesis with nanofabricated hydroxyapatite and GelMA nanocomposite

Vladislav V. Yakovlev, Texas A&M Univ. (United States)

Every year in the United States approximately 1.5 million people are suffering from weak bones and bone fractures. Current treatment solutions include surgeries, grafting process etc; however it does not show any osteoconductive action which is the most important characteristic of a biomaterial. Hence, the main objective of this project is to develop a novel nanocomposite comprising of Hydroxyapatite (HAP) nanospheres (~40nm) and gelatin methacrylate (GelMA) to promote bone regeneration without any osteoinductive factors. Hydroxyapatite (HAP) is a natural occurring mineral form of calcium apatite and constitutes more than 60% of the natural bone. HAP has been an interesting nanoparticle for the past 20 years as it has been used in medicine and dentistry, mainly in the form of a biomaterial. Modern implants like bone conduction implants are coated with hydroxyapatite, promoting osteointegration. With proper alignment, HAP nanospheres could possibly lead to 3D scaffold that could serve as a scaffold for regenerative medicine. Here, we hypothesize that addition of HAP nanospheres to the polymer matrix elevates the physical and chemical properties of the nanocomposite matrix and induce osteogenic differentiation without using any growth factors. To validate our hypothesis that chemical properties of nanocomposite get enhanced, Raman spectroscopy was performed. Raman analysis has been a popular method for molecular identification of material as it easily examines and provides an insight into orientation of HAP nanoparticles and GelMA polymer in nanocomposite, and does not involve any damage to the sample. In addition to this, Brillouin spectroscopy was implemented. Elastic modulus obtained from Brillouin spectroscopy further strengthens our hypothesis that there is an increase in mechanical strength of our nanocomposite.

9303-606, Session 3

Probing microscopic mechanical properties of hard tissues with Brillouin spectroscopy

Vladislav V. Yakovlev, Zhaokai Meng, Texas A&M Univ. (United States)

Mechanical properties of hard tissues plays an important role in understanding its underlying biological structures, as well as promoting the quality of artificial bone replacement materials. However, the existing mechanical tests are destructive, and usually require a considerable amount of bones. To the contrary, Brillouin spectroscopy (BS) provides an alternative and non-invasive approach for probing the local sound speed within a small volume. Moreover, recent advances in background-free Brillouin spectroscopy enable investigators to imaging not only transparent samples, but also turbid ones. In this sense, the microscopic bone elasticity (associated with local sound speed) could be characterized using BS.

The Brillouin spectra were obtained by a background free VIPA (virtually imaged phased array) spectrometer described in the previous report [1]. As a reference, the Raman spectra were also acquired for each pixel.

1. Meng, Z., Traverso, A. J., & Yakovlev, V. V., Optics express, 2014, 22(5), 5410-5416.

9303-607, Session 3

Bone tissue heterogeneity is associated with fracture toughness: a polarization Raman spectroscopy study

Alexander J. Makowski, Vanderbilt Univ. (United States) and U.S. Dept. of Veterans Affairs (United States); Mathilde Granke, Sasidhar Uppuganti, Anita Mahadevan-Jansen, Vanderbilt Univ. (United States); Jeffrey S. Nyman, Vanderbilt Univ. (United States) and U.S. Dept. of Veterans Affairs (United States)

Polarization Raman Spectroscopy has been used to demonstrate microstructural features and collagen fiber orientation in human and mouse bone, concurrently measuring both organization and composition; however, it is unclear as to what extent these measurements explain the mechanical quality of bone. In a cohort of age and gender matched cadaveric cortical bone samples (23-101 yo), we show homogeneity of both composition and structure are associated with the age related decrease in fracture toughness. 64 samples were machined into uniform specimens and notched for mechanical fracture toughness testing and polished for Raman Spectroscopy. Fingerprint region spectra were acquired on wet bone prior to mechanical testing by sampling nine different microstructural features spaced in a 750x750 μm grid in the region of intended crack propagation. After ASTM E1820 single edge notched beam fracture toughness tests, the sample was dried in ethanol and the osteonal-interstitial border of one osteon was samples in a 32x32 grid of 2μm2 pixels for two orthogonal orientations relative to the long bone axis. Standard peak ratios from the 9 separate microstructures show heterogeneity between structures but do not sufficiently explain fracture toughness; however, peak ratios from mapping highlight both lamellar contrast (?1Phos/Amidel) and osteon-interstitial contrast (?1Phos/Proline). Combining registered orthogonal maps allowed for multivariate analysis of underlying biochemical signatures. Image entropy and homogeneity metrics of single principal components significantly explain resistance to crack initiation and propagation. Ultimately, a combination of polarization content and multivariate Raman signatures allowed for the association of microstructure tissue heterogeneity with fracture resistance.

Conference 9303F:
Optics in Bone Surgery and Diagnostics

9303-612, Session 3

Novel, near-infrared spectroscopic, label-free, techniques to assess bone abnormalities such as Paget's disease, osteoporosis and bone fractures (*Invited Paper*)

Diana C. Sordillo, Laura A. Sordillo, Lingyan Shi, Yury Budansky, Peter P. Sordillo M.D., Robert R. Alfano, The City College of New York (United States)

Recently, several novel, NIR, label-free, techniques have been developed to assess Paget's disease, osteoporosis and abnormalities such as microfractures. We have designed a Bone Optical Analyzer (BOA) which utilizes the first NIR window to image bone and to measure changes in Hb and HbO₂. Two-photon (2P) microscopy with 800 nm excitation was used to acquire images of the periosteum of bone and to allow us to obtain spatial frequency spectra (based on emission of collagen). Longer NIR wavelengths (1,100 nm-1,350 nm, 1,600 nm-1,870 nm, 2,100 nm-2,300 nm) can be used to image more deeply through tissue and reveal bone microfractures.

9303-613, Session 3

Thermoacoustic imaging of finger joints and bones: a feasibility study

Lin Huang, Weizhi Qi, Dan Wu, Jian Rong, Dakui Lai, Univ. of Electronic Science and Technology of China (China); Huabei Jiang, Univ. of Florida (United States) and Univ. of Electronic Science and Technology of China (China)

No Abstract Available

Conference 9304A: Optical Techniques in Pulmonary Medicine II

Saturday - Sunday 7-8 February 2015

Part of Proceedings of SPIE Vol. 9304 Endoscopic Microscopy X; and Optical Techniques in Pulmonary Medicine II

9304-100, Session 1

Optical imaging, microscale physiology, and pediatric respiratory disease (*Invited Paper*)

Michael A. Choma M.D., Yale School of Medicine (United States)

Respiratory diseases are major causes of pediatric morbidity and mortality. These diseases are incompletely understood, which is a barrier to improving clinical care. Optical imaging technologies are enabling the study of new microscale physiological mechanisms that may improve the understanding, diagnosis, and treatment of pediatric respiratory diseases. These physiological mechanisms include complex alveolar dynamics and cilia-driven fluid flow. By using new optical imaging to better understand physiology that is inaccessible to traditional imaging modalities, there are new opportunities to improve the care of common (e.g. asthma) and rare (e.g. cystic fibrosis) pediatric respiratory diseases.

9304-101, Session 1

Quantification of transverse, sub-500 $\mu\text{m/s}$ cilia-driven fluid flow using dynamic light scattering OCT

Brendan K. Huang, Yale Univ. (United States); Mustafa K. Khokha M.D., Yale School of Medicine (United States); Michael A. Choma M.D., Yale Univ. (United States) and Yale School of Medicine (United States)

Quantification of cilia-driven fluid flow is important in the study of diseases of mucociliary clearance, but measurement of flow velocities presents unique challenges. Ciliary flow is primarily transverse to the optical axis, making standard Doppler methods inadequate. The flow is not oriented along an anatomical surface, as is blood in vessels, necessitating the need for measurement of both directionality and fluid speed. Lastly, ciliary flow can be slow, typically in the sub-500 $\mu\text{m/s}$ regime. Dynamic light scattering (DLS)-based OCT methods, which involve the statistical analysis and modeling of the time-varying interferometric OCT signal, recently have been applied to measuring total fluid flow speed in blood vessels. These measurements are limited in that they (a) typically involve flows greater than 500 $\mu\text{m/s}$ and (b) recover total flow speed and not directional velocity. Here, we demonstrate our novel DLS acquisition protocol for recovering directional measurements of transverse flow velocities in quantifying biological cilia-driven fluid flow in *Xenopus laevis*, an important animal model in ciliary biology. Our approach enables directional velocity measurement by adding a variable scan bias that isolates fluid flow along the scan direction. Furthermore, we demonstrate that by imparting a variable scan bias, our measurements are independent of the diffusivity of the underlying particles, allowing us to measure the velocities of polydisperse solutions. Using our technique, we show measurement of two-component, cilia-driven fluid flow profiles in ciliated *Xenopus laevis* embryos.

9304-102, Session 1

Dual-modality μOCT and fluorescence imaging of the CF airway

Tim N. Ford, Kengyeh K. Chu, Wellman Ctr. for Photomedicine (United States); Susan E. Birket, The Univ. of Alabama at Birmingham (United States); Diana Mojahed, Wellman Ctr. for Photomedicine (United States) and Tufts Univ. (United States); Steven M. Rowe, The Univ. of Alabama at Birmingham (United States) and Cystic Fibrosis Research Ctr. (United States); Guillermo J. Tearney M.D., Wellman Ctr. for Photomedicine (United States) and Massachusetts General Hospital (United States) and Harvard-MIT, Div. of Health Sciences and Technology (United States)

Cystic fibrosis (CF) airway disease is characterized by impaired mucociliary clearance and chronic bacterial infection and inflammation. The genetic cause of CF disease is linked to mutations of the cystic fibrosis transmembrane conductance regulator (CFTR), but the mechanism of progression from defective ion transport to advanced lung disease is not well understood. Distinctive features of the CF airway include functional microanatomical defects such as depleted airway surface liquid (ASL) and periciliary layer (PCL) depths, reduced mucociliary transport (MCT), and slow ciliary beat frequency (CBF), as well as biochemical aspects such as impaired salt and pH homeostasis which modulate mucus production, hydration and bacterial killing. Causative relationships between these physical and biochemical parameters during disease progression are unclear due to lack of quantitative tools suitable for in situ studies.

We present the latest developments of a dual-modality micro-optical coherence tomography (μOCT) and fluorescence system for simultaneous study of depth-resolved airway microanatomy, mechanical properties of ciliary motion and mucus transport, and local biochemistry in situ. Biochemistry is probed using the pH-sensitive fluorescent dye BCECF. Intensity modulation and steering of the excitation beams allow fluorescence recovery after photobleaching (FRAP) experiments to probe both diffusion and mucus flow. This improved system allows longitudinal in situ study of CF and non-CF cell and tissue culture, and will be a useful tool for elucidating causative relationships between microanatomical and biochemical parameters during the pathogenesis and treatment of CF airway disease.

9304-103, Session 2

Investigating exogenous modulators of mucociliary clearance: effect of temperature and hyperoxia on cilia-driven flow velocity

Ute A. Gamm, Brendan K. Huang, Mansoor Syed, Vineet Bhandari, Michael A. Choma M.D., Yale School of Medicine (United States)

Premature infants are at high risk for respiratory diseases due to an underdeveloped respiratory system that is very susceptible to infection and inflammation. One critical aspect of respiratory health is the state of the ciliated respiratory epithelium that lines the trachea and bronchi. The ciliated epithelium is responsible for trapping and removing pathogens

**Conference 9304A:
Optical Techniques in Pulmonary Medicine II**

and pollutants from the lungs and an impairment of ciliary functionality can lead to recurring respiratory infections and subsequent lung damage. The impact of medical interventions such as hyperoxia and the effect of drugs on the developing ciliated epithelium are incompletely understood. Our research aims to close this critical knowledge gap by investigating modulators of ciliary functionality in the animal models frog embryo and mouse. We are using optical coherence tomography (OCT) to visualize ciliary fluid flow and quantify flow velocities through particle tracking velocimetry (PTV). Chemical modulators of ciliary flow are serotonin and para-cholorphenylalanine (PCPA). Serotonin is an endogeneous activator of ciliary beating and PCPA is known to deplete serotonin from the cells. This depletion, in turn, decreases ciliary movement. We were able to quantify the change in cilia driven fluid flow with PTV-OCT after administration of PCPA and to recover ciliary flow by incubating the embryos with serotonin rescue. We also investigated the effect of temperature on the cilia-driven fluid flow in 10 ex vivo adolescent mice trachea. Our data suggest an effect of temperature on the speed of ciliary fluid-flow that showed a maximum at body temperature with a decrease at lower and higher temperatures (n=10). We are currently testing the influence of hyperoxia on ciliary functionality by exposing live mice to hyperoxia for 21 h (until now n=6) and 65 h (until now n=6) before harvesting the trachea.

9304-104, Session 2

Micro-optical coherence tomography flow mapping of regenerating respiratory epithelium

Kengyeh K. Chu, Vladimir Vinarsky, Jayaraj Rajagopal, Guillermo J. Tearney M.D., Massachusetts General Hospital (United States)

Cilia are hair-like organelles that beat in coordinated fashion many times per second to convey mucus out of mammalian airways, and mucociliary clearance is an important defense mechanism, clearing debris and bacteria away from the lungs. Ciliated cells can be lost as a result of physical injury, chemical insult, or infection, and are repopulated by differentiation of basal stem cells. Because of the similarity of cilia across mammalian species, small animals such as mice would be appropriate models for the study of regeneration, though limited by the difficulty of quantitatively assessing ciliary function in vivo. Recently developed culturing techniques in our laboratories have enabled the establishment of a murine trachea explant injury model to facilitate imaging access to the ciliated epithelium as regeneration occurs.

We have characterized the murine trachea in vitro regeneration model using micro-optical coherence tomography (μ OCT), a high-speed, high-resolution form of OCT with 1- μ m axial and 2- μ m lateral resolution. We have previously demonstrated using μ OCT that the explants regenerated ciliated epithelia within 14 days after chemical injury by sulfur dioxide, and that the epithelia not only regain their capacity for transport, but also retain their original particulate transport directions, suggesting an underlying mechanism for ciliary axis memory, possibly in the relatively undamaged basal cell layer. However, in more severely damaged samples, where new basal cells must migrate to fill a gap, transport direction is chaotic and difficult to characterize with μ OCT B-scans which are limited to a single direction.

We now present a new technique for measurement of flow fields with arbitrary direction. The μ OCT beam is scanned circularly, rather than linearly, to produce B-scans of cylindrical shape. The direction of transport is determined by the scan position at which maximal measured velocity of tracer microspheres occurs. The circular scan geometry thus allows flow direction to be mapped across an explant, and correlated with measurements of planar cell polarity proteins such as VANGL1 to provide a method for probing the mechanism of ciliary direction.

9304-105, Session 2

Sensing mucus hydration via diffusion of gold nanorods using polarization-sensitive optical coherence tomography

Richard L. Blackmon, David B. Hill, Brian Button, The Univ. of North Carolina at Chapel Hill (United States); Joseph B. Tracy, Wei-Chen Wu, North Carolina State Univ. (United States); Amy L. Oldenburg, The Univ. of North Carolina at Chapel Hill (United States)

Muco-ciliary clearance is necessary in combating airborne pathogens and hydrating epithelial cells. However, diseases like cystic fibrosis and COPD inhibit this natural flow, resulting in chronic lung infection. Optical coherence tomography (OCT) provides excellent visualization of the lung epithelium and can be used to quantify mucus flow and monitor changes in ciliary beat frequency. Mucus concentration (% solids) is also an important indicator of health, as mucus dehydration commonly occurs in disease and acts to inhibit clearance. As such, we have demonstrated an OCT-based method to distinguish mucus % solids over the range from healthy to disease-like in actively transporting in vitro human bronchi-epithelial (hBE) models. This method is based upon quantifying the diffusion rate of topically applied PEG-coated gold nanorods (GNRs) of (83 X 22 nm) that are weakly-constrained by mucus polymers. GNR diffusion is measured via OCT-based polarized dynamic light scattering, which provides a rapid (<0.5 s) and minimally-invasive method of measuring mucus % solids. Previously this technique was limited to \approx 3.5% solids due to slowing of the transitional diffusion of GNRs. However, the optical anisotropy of GNRs also allows for measurement of the faster rotational diffusion fluctuations, as we have previously shown for Newtonian fluids. Here we will demonstrate that measuring both the rotational and translational diffusion rates of GNRs in mucus provides an expanded measurement capability, up to 5% solids. This may further expand the capabilities of this technique particularly for diseased patients and applications in monitoring mucus-thinning therapies.

9304-106, Session 2

Fluorescence recovery after photobleaching (FRAP) implementation in micro-optical coherence tomography rheology

Diana Mojahed, Massachusetts General Hospital (United States) and Tufts Univ. (United States); Kengyeh K. Chu, Tim N. Ford, Massachusetts General Hospital (United States); Susan E. Birket, The Univ. of Alabama at Birmingham School of Medicine (United States); Courtney Fernandez, Steven M. Rowe, The Univ. of Alabama at Birmingham (United States); Guillermo J. Tearney M.D., Massachusetts General Hospital (United States)

Cystic fibrosis (CF) is an autosomal recessive genetic disorder that diminishes mucus clearance in the airways, resulting in life threatening infections. While it is thought that mutations in the cystic fibrosis transmembrane conductance regulator (CFTR) gene result in an ionic imbalance in mucus that affects its viscosity, the relationship between altered mucus viscosity and the function of the mucociliary clearance apparatus is not well understood.

Micro-optical coherence tomography (μ OCT) is a high-resolution imaging modality that has been previously demonstrated to provide detailed information about the functional microscopic parameters of the airway, such as airway surface liquid (ASL) and periciliary liquid layer (PCL) depth, ciliary beat frequency (CBF), and rate of mucociliary transport (MCT). In order to study the relationship between mucus mechanical properties and these parameters, we have developed an apparatus that simultaneously

**Conference 9304A:
Optical Techniques in Pulmonary Medicine II**

conducts μ OCT imaging and measures co-localized mucus viscosity using fluorescence recovery after photobleaching (FRAP). A 488-nm laser beam is co-aligned with the μ OCT beam, and an avalanche photodiode collects fluorescent output. An inline switch is used to interrupt the scanning mirror drive signal to stop the beam and begin photobleaching, and upon restoration of the linear scan, the fluorescent profile of the dye evolves and reveals the diffusion properties of the mucus.

Simultaneous μ OCT/FRAP of a fluorescein-dyed 5% dextran-500 solution confirmed an increased time constant of recovery (1.32 ± 0.04 sec) compared to water (1.14 ± 0.03 sec, $p < 0.001$) based on the curve-fitting confidence interval for the time constant. The FRAP capability now adds an additional mechanism for measuring localized fluid properties within the structural context of μ OCT and will be useful for investigating the link between mucus viscosity and mucociliary clearance in CF.

9304-107, Session 3

Optical and acoustic imaging in lung cancer: current status and opportunities
(Invited Paper)

Septimiu D. Murgu M.D., The Univ. of Chicago (United States)

Lung cancer is the leading cause of cancer mortality. Screening patient populations at risk with computed tomography improves survival. Optimal management of lung cancer includes proper assessment of the intrathoracic lymph nodes for accurate tumor staging. Diagnosis and staging can be performed using minimally invasive methods. Navigation bronchoscopy is used for diagnosis of peripheral lung cancer. Endobronchial ultrasound-guided transbronchial needle aspiration allows evaluation of mediastinal lymph node metastasis. Optical imaging can complement current technologies by improving the visualization of microstructures in the airways, peripheral nodules and lymph nodes, thus accurately assessing the extent and depth of airway tumor, confirming intralesional location of biopsy tools, and allowing sampling of areas relevant for diagnosis and molecular testing.

9304-108, Session 3

In vivo polarization sensitive OCT imaging of human airways

Anthony Lee M.D., Lucas Cahill, Hamid Pahlevaninezhad, Alexander J. Ritchie M.D., Wei Zhang M.D., Tawimas Shaipanich M.D., Calum E. MacAulay, Stephen Lam M.D., Pierre M. Lane, The BC Cancer Agency Research Ctr. (Canada)

Structural optical coherence tomography imaging has shown promise as a useful modality for imaging and quantification of airway morphology. Functional OCT imaging extensions such as Doppler OCT have also allowed vascular imaging in the lung. Further differentiation of lung tissues such as fibrosis and airway smooth muscle (ASM) could greatly help in the diagnosis and management of lung diseases. For example, identification of fibrosis may allow more accurate identification of tumour area for biopsy while quantification of ASM may allow monitoring of therapeutic treatments for asthma. Polarization sensitive OCT (PSOCT) can image fibrotic tissue and ASM owing to their innate birefringence. In vivo PSOCT imaging of airways requires an implementation of this technique using fiber-optic probes.

We present a novel endoscopic fiber based swept source PSOCT system for in vivo lung imaging. This PSOCT implementation uses only passive optical components and requires no calibration while adding minimal additional cost to a standard structural OCT imaging system. Endoscopic access through the instrument channel of a standard bronchoscope is accomplished using a 1.5 mm diameter fiber-optic rotary pullback probe that images at frame rates up to 100 Hz with pullback speeds up to 15 mm/s.

We present our initial PSOCT imaging results using this system in vivo in patients.

9304-109, Session 3

Co-registered autofluorescence Doppler optical coherence tomography versus endoscopic ultrasound imaging for peripheral lung cancers

Wei Zhang M.D., The BC Cancer Agency Research Ctr. (Canada); Alexander J. Ritchie M.D., The BC Cancer Agency Research Ctr (Canada); Hamid Pahlevaninezhad, The BC Cancer Agency Research Ctr. (Canada); Anthony Lee M.D., The BC Cancer Agency Research Ctr (Canada); Geoffrey Hohert, Lucas Cahill, Tawimas Shaipanich M.D., Calum E. MacAulay, Stephen Lam M.D., Pierre M. Lane, The BC Cancer Agency Research Ctr. (Canada)

Diagnosis of peripheral lung nodules is challenging because they are rarely visualized endobronchially. Imaging techniques such as endobronchial ultrasound (EBUS) are employed to improve tumor localization. The current EBUS probe provides limited nodule characterization and its diameter of 1.4 mm restricts access to small peripheral airways. We report a novel co-registered Autofluorescence Doppler Optical Coherence Tomography (AF/DOCT) system with a 0.9 mm probe diameter to characterize peripheral lung nodules prior to biopsy in vivo.

Method: Patients referred for evaluation of lung cancer underwent bronchoscopy with standard EBUS examination and with the novel AF/DOCT system. The lesion of interest was first identified with EBUS and then imaged with the AF/DOCT system. Control AF/DOCT images were also obtained from a radiologically normal airway. The abnormal area was biopsied. Pathology specimens were reviewed against the matching AF/DOCT images by a panel comprised of a pathologist, respirologists and AF/DOCT experts.

Results: Nine patients with biopsy proven lung cancer underwent examination with AF/DOCT. A positive diagnosis of cancer was achieved at bronchoscopy in eight cases. The majority of the cancers were adenocarcinoma. There was good visual agreement between the AF/DOCT image and histopathology features. Doppler identified vessels prior to biopsy. The procedure was well tolerated and there were no complications.

Conclusion: In this pilot study, AF/DOCT obtained high quality images of peripheral pulmonary nodules. The present study supports the safety and feasibility of AF/DOCT for the evaluation of lung cancer. The addition of Doppler information may improve biopsy site selection and reduce bleeding.

9304-110, Session 3

Endotracheal tube biofilm formation from adult intensive care patients quantified using 3-D optical coherence tomography

Andrew E. Heidari, OCT Medical Imaging Inc.. (United States); Kimberly K. Truong M.D., Univ. of California, Irvine (United States); Samer Moghaddam M.D., Univ. of California, Irvine Medical Ctr. (United States); Li-Dek Chou, Sari B. Mahoni, Beckman Laser Institute and Medical Clinic, Univ. of California, Irvine (United States); Carl Genberg, N8 Medical (United States); Matthew Brenner M.D., Beckman Laser Institute and Medical Clinic, Univ. of California, Irvine (United States)

Hospitalized patients in intensive care units often require mechanical

**Conference 9304A:
Optical Techniques in Pulmonary Medicine II**

ventilation via endotracheal tube intubation. Endotracheal tube occlusion due to accumulated secretions and bacterial biofilm has been a clinical challenge, necessitating urgent re-establishment of a patent airway. In addition to intraluminal volume loss, the formation of biofilm on the inner surface of endotracheal tubes has been implicated in the development of ventilator-associated pneumonia. Previous studies have suggested that the dislodgement of bacterial biofilm aggregates into the distal airway may serve as a nidus for infection and onset of pneumonia. Bacterial biofilm is defined as an aggregate of bacteria that are embedded within a self-produced matrix of extracellular polymeric substance, in which aggregates of cells adhere to each other and to a surface.

3-D swept source optical coherence tomography (SS-OCT) has the ability to accurately detect formation of biofilm in endotracheal tubes obtained from prior mechanically ventilated patients. The detection of biofilm, its rate of progression and its association with ventilator-associated pneumonia has not been conducted. Therefore, we utilize a rapid acquisition swept source laser 3-D-optical coherence tomography system to investigate morphological changes of biofilm formation and its progression, thickness, and characteristics in endotracheal tubes. Endotracheal tubes are collected at the time of extubation from adult intensive care patients. A flexible fiber optic SS-OCT probe was inserted through the endotracheal tubes and pulled back to image the distal internal lumen of endotracheal tubes and its biofilm. The images were obtained at baseline (never been used endotracheal tubes) and from endotracheal tubes that have been used for a varying amount of time (preliminary minimum duration: 5 hours, maximum duration: 22 days, median duration: 5 days). Scanning electron microscopy will then be used to confirm biofilm material and bacteria. SS-OCT was able to detect increased thickness of biofilm in endotracheal tubes within hours of intubation time. SS-OCT is also capable of quantifying and characterizing progressive changes in biofilm formation in previously intubated endotracheal tubes. 3D SS-OCT may provide a method for more accurate determination of biofilm progression and its associated risk of endotracheal tube occlusion and ventilator-associated pneumonia.

9304-111, Session 4

In vivo co-registered Doppler optical coherence tomography and autofluorescence imaging of human airway

Hamid Pahlevaninezhad, Anthony Lee M.D., Stephen Lam M.D., Geoffrey Hohert, Lucas Cahill, Tawimas Shaipanich M.D., Alexander J. Ritchie M.D., Wei Zhang M.D., Calum E. MacAulay, Pierre M. Lane, The BC Cancer Agency Research Ctr. (Canada)

Doppler optical coherence tomography (DOCT) is a powerful technique for imaging sub-surface tissue morphology and vascularity. AF imaging of endogenous tissue fluorophores provides valuable information about the biochemical composition and metabolic state of the tissue. By co-registering DOCT with AF, the structure and function of tissue structures can be defined more accurately for diagnosis, biopsy guidance, and studying the response to therapy. For example, a combined AF and DOCT imaging system could quantify the fraction of AF loss due to collagen remodeling in the stroma by removing the epithelial attenuation effects. In this work, we present a power-efficient fiber-based imaging system capable of co-registered AF and DOCT imaging. The system employs a custom fiber optic rotary joint (FORJ) with an embedded dichroic mirror to efficiently combine the OCT and AF pathways. A custom 900 μm diameter catheter consisting of a rotating double-clad fiber (DCF) and lens assembly inside a stationary plastic tube was fabricated to allow AF and DOCT imaging of central and peripheral airways in vivo. We demonstrate the performance of the co-registered AF and DOCT imaging system in vivo in normal and abnormal airways in patients undergoing bronchoscopy for suspected lung cancer.

9304-112, Session 4

Optical coherence tomography airway morphology measurements differ between lung lobes in subjects with chronic obstructive pulmonary disease

Miranda Kirby, The Univ. of British Columbia (Canada) and The James Hogg iCAPTURE Ctr. for Cardiovascular and Pulmonary Research, St. Paul's Hospital (Canada); Keishi Ohtani M.D., Anthony Lee M.D., Calum E. MacAulay, Pierre M. Lane, Stephen Lam M.D., The BC Cancer Agency Research Ctr. (Canada); Harvey O. Coxson, The James Hogg iCAPTURE Ctr. for Cardiovascular and Pulmonary Research, St. Paul's Hospital (Canada)

Rationale: Differences in airway wall dimensions among the lobes have been demonstrated using computed tomography (CT). However, CT resolution limits evaluation of the small airways. Optical coherence tomography (OCT) is a technique capable of evaluating small bronchioles with resolution approaching histology. Our objective was to determine whether there are differences for small airway measurements between the lobes, and to determine whether each individual lobe is representative of overall pulmonary function.

Methods: Ninety six current or ex-smokers underwent OCT, CT, and spirometry for measurement of the forced expiratory volume in 1sec (FEV1). OCT was performed in the right lower lobe (RLL, RB8 or RB9) or the left lower lobe (LLL, LB8 or LB9). The OCT percentage of the airway that is wall (wall area percent, WA%) was generated using ImageJ software (NIH, USA). For CT, the relative area of the CT density histogram with attenuation values ≤ -950 HU (RA950) and the total lung volume (TLC) were also calculated.

Results: There were no significant differences between subjects in the RLL (n=77) and LLL (n=19) group with respect to age (p=0.29), sex (p=0.61), smoking status (p=0.79), FEV1 (p=0.36), RA950 (p=0.99) or TLC (p=0.47). However, significant greater WA% (p=0.04) was found in the LLL than the RLL. Airway wall measurements were significantly correlated with FEV1 for the LLL (WA%: r=-0.66, p=0.002) but not for the RLL (WA%: r=-0.20, p=0.08).

Conclusions: These data suggest that there are differences in OCT-derived airway morphology measurements and relationships with overall pulmonary function between the lower lobes.

9304-113, Session 4

Flow-through integrating cavity for analysis of exhaled breath

Joel N. Bixler, Vladislav V. Yakovlev, Texas A&M Univ. (United States)

Raman spectroscopy is a powerful technique that can be used to obtain detailed chemical information about a system without the need for chemical markers. It has been widely used for a variety of applications such as cancer diagnosis and material characterization. However, Raman scattering is a highly inefficient process, where one in 10¹¹ scattered photons carry the needed information. Several methods have been developed to enhance this inherently weak effect, including surface enhanced Raman scattering and coherent anti-Stokes Raman scattering. These techniques suffer from drawbacks limiting their commercial use, such as the need for spatial localization of target molecules to a 'hot spot', or the need for complex laser systems.

We have previously developed an integrating cavity capable of offering significant enhancement to any linear optical technique, such as fluorescence emission or Raman scattering (1). Such cavities have been used for the ultrasensitive detection of contaminants in water and air, where contamination was detected down to femtomolar levels, and can also be

**Conference 9304A:
Optical Techniques in Pulmonary Medicine II**

applied to analyzing the chemistry of exhaled breath.

In our presentation, we will describe a modified integrating cavity that can be used for breath analysis, the experimental setup needed, and present preliminary data showing the great potential of this device for optical analysis and diagnostics in pulmonary medicine of conditions such as asthma, chronic obstructive pulmonary disease, and lung cancer.

References:

1. J. N. Bixler, et. al, "Ultrasensitive detection of waste products in water using fluorescence emission cavity-enhanced spectroscopy," Proceedings of the National Academy of Sciences 111(20), 7208-7211 (2014)

9304-114, Session 4

Flexible optical coherence tomography needle for bronchoscopic biopsy

Yan Wang, Milen Shishkov, Lida P. Hariri M.D., David C. Adams, Alyssa J. Miller, Brett E. Bouma, Michael Lanuti, Melissa J. Suter, Massachusetts General Hospital (United States)

Lung cancer has been leading cause of cancer related deaths in US. Early diagnosis of lung cancer is critical for an increased patient survival rate. Macroscopic imaging techniques such as CT and bronchoscopy do not have the required specificity to diagnose malignancy. Currently, diagnosis of malignancy can only be accomplished with excisional biopsy. Trans-thoracic and surgical approaches carry higher intrinsic risk of complications, and low-risk bronchoscopy techniques have low diagnostic yields. We previously demonstrated a flexible and removable optical coherence tomography needle catheter for guiding and confirming the needle placement within the target lesion prior to biopsy. However, the clinical utility of this flexible needle probe has been hindered by two issues: the drive shaft results in non-uniform rotary distortion (NURD), and shearing of the protective outer sheath of the catheter by the biopsy needle potentially resulting in damage to the optics and deposition of debris in lung. We have designed a new catheter to overcome these issues. The catheter consists of a double-layer torque coil to reduce NURD and a metal sleeve with optical window to avoid damage of the sheath by the needle. In addition, current available clinical transbronchial aspiration needles (TBNA) either have no channel for passing the OCT probe or are not long enough to reach peripheral regions of the lung. We have developed a customized peripheral TBNA needle with a working channel that is compatible with our OCT probe for imaging and facilitates the collection of tissue specimens for histology. The efficacy of the new flexible catheter and the TBNA was assessed by imaging guided needle biopsy of artificial pulmonary nodules embedded in swine lung.

9304-115, Session 5

High-speed imaging of in-vivo mice trachea with fourier domain optical coherence microscopy

Hinnerk Schulz-Hildebrandt, Mario Pieper, Peter König, Gereon Hüttmann, Univ. zu Lübeck (Germany)

Malfunction of the clearing function of the lung is associated with different diseases like primary ciliary dysknesia and cystic fibrosis.

Our optical coherence microscopy (OCM) setup consists of a broadband supercontinuum light source and a customized 300 nm high-speed spectrometer, which allows us to image at up to 200000 A-Scans per second with an axial resolution of 2 μm in air and a lateral resolution in the focal plane of 0.7 μm with high high sensitivity.

We present images taken from airway tissue of in vivo mice at subcellular resolution. We quantify the thickness of the mucus-layer by imaging from outside through the trachea wall. Besides looking at morphological structures, we imaged physiological functions like the ciliary beating

frequency and the change of the thickness of the liquid layer after vaporization of phosphate buffered saline (PBS).

9304-116, Session 5

Multimodal optical coherence tomography and fluorescence spectroscopy MEMS probe to assess inflammation in acute lung injury

Lida P. Hariri M.D., Massachusetts General Hospital (United States); Liane Bernstein, Ecole Polytechnique de Montréal (Canada); David C. Adams, Massachusetts General Hospital (United States); Wendy-Julie Madore, Ecole Polytechnique de Montréal (Canada); Alyssa J. Miller, Yan Wang, Massachusetts General Hospital (United States); Mathias Strupler, Étienne De Montigny, Kathy Beaudette, Nicolas Godbout, Caroline Boudoux, Ecole Polytechnique de Montréal (Canada); Melissa J. Suter, Massachusetts General Hospital (United States)

Inflammation plays a critical role in many disease processes in the lung, including infectious etiologies, acute lung injury, asthma, and carcinomas. Optical coherence tomography (OCT) is capable of assessing tissue microstructural changes with high resolution, but cannot reliably detect inflammation in tissues due to lack of sufficient contrast and resolution. Fluorescence spectroscopy (FS) provides a strong complement to OCT and can assess functional inflammatory activity when coupled with protease-activated fluorophores. In this study, we develop a dual OCT-FS MEMS probe to simultaneously assess tissue microarchitecture and inflammatory activity using a protease-activated fluorescent agent. The OCT-FS probe uses a double clad fiber, where the core guides OCT and fluorescence excitation light to the tissue. A double clad fiber coupler separates the OCT signal returning in the single-mode core from the fluorescence light captured by the inner cladding. A MEMS mirror at the distal end of the probe allows for three dimensional tissue scanning. We utilized the dual OCT-FS probe to assess airway injury in rabbits treated with topical lipopolysaccharide (LPS), which causes a well-characterized, rapid inflammatory response in the lungs. The OCT-FS MEMS probe obtained simultaneous, co-registered imaging of the injured rabbit airway, visualizing both microarchitectural distortions and protease activity from inflammatory infiltrates during lung injury. The combination of the structural information provided by OCT and functional inflammatory activity provided by FS offers a powerful tool for assessing and studying the role of inflammation in pulmonary disease.

9304-117, Session 5

Does low level light therapy reduce inflammation and tissue damage from ventilator induced lung injury?

Alyssa J. Miller, Margit V. Szabari M.D., Lida P. Hariri M.D., Michael R. Hamblin, Guido Musch M.D., Melissa J. Suter, Massachusetts General Hospital (United States)

Background: Mechanical ventilation has been shown to exacerbate existing lung injury and cause injury in otherwise healthy lungs. Over-stretching of the lungs by mechanical ventilation can damage alveoli, initiating an organ-wide inflammatory response that can progress to severe, life-threatening illness. Low level light therapy (LLLT) can reduce inflammation and speed wound healing from a variety of injuries. We tested whether LLLT could reduce pulmonary inflammation and morphological damage from injurious mechanical ventilation in mice.

Methods: Mice were divided into 4 groups: protective ventilation (6 hours, VT=9 ml/kg, FR 140/min, 50% FiO2, 2.5 cmH20 positive end expiratory

**Conference 9304A:
Optical Techniques in Pulmonary Medicine II**

pressure [PEEP]) with or without LLLT, and injurious ventilation (3 hours, VT=25-30 ml/kg, FR 50/min, 50% FiO₂, 0 cmH₂O PEEP), followed by 3 hours of protective ventilation with or without LLLT. 10 J/cm² energy was delivered to the lungs during the first hour of ventilation using an 810nm LED system. Lung mechanics were monitored throughout the procedure. After sacrifice, bronchoalveolar lavage was performed and inflammatory cells counted. Lungs were removed en-bloc and fixed for histological analysis.

Results: We successfully developed a ventilator induced lung injury (VILI) model in mice and performed a pilot study to assess the effect of LLLT on VILI. Preliminary results suggest mice that received LLLT had decreased levels of inflammatory cells in the BAL and histology.

Conclusions: We hypothesize that LLLT can effectively reduce lung damage and inflammation from VILI. This therapy could easily be translated into clinical practice, and has potential to improve outcomes in patients requiring mechanical ventilation.

9304-118, Session 5

Validation and exploration of airway smooth muscle distributions as visualized with PS-OCT

David C. Adams, Alyssa J. Miller, Lida P. Hariri, Yan Wang, Andrew D. Luster, Benjamin D. Medoff, Massachusetts General Hospital (United States)

Present understanding of the pathophysiological mechanisms of asthma has been severely limited by the lack of an imaging modality capable of assessing airway conditions of asthma patients in vivo. Of particular interest is the role that airway smooth muscle (ASM) plays in the development of asthma and asthma related symptoms. With standard Optical Coherence Tomography (OCT), imaging ASM is often not possible due to poor structural contrast between the muscle and surrounding tissues. A potential solution to this problem is to utilize additional optical contrast factors intrinsic to the tissue, such as birefringence. Due to its highly ordered structure, ASM is strongly birefringent. Previously, we demonstrated that Polarization Sensitive OCT (PS-OCT) has the potential to be used to visualize ASM as well as easily segment it from the surrounding (weakly) birefringent tissue by exploiting a property which allows it to discriminate the orientation of birefringent fibers. In this work we use a catheter-based approach to demonstrate the ability of PS-OCT to image ASM in segments of porcine and canine airways, over a range of airway sizes. By carefully matching the PS-OCT data with histology and assessing the ASM segments in both, we show excellent correlation indicating strong potential for PS-OCT to be used as a diagnostic and therapeutic guidance tool for the assessment of ASM in asthma. Additionally, we present in vivo data taken in the airways of human subjects, thereby demonstrating the immediate clinical translatability of this technology.

9304-119, Session 6

In vivo optical coherence tomography imaging of airway and alveolar dynamics during bronchial challenge test

Chulho Oak, Kosin Univ., College of Medicine (Korea, Republic of) and Innovative Biomedical Technology Research Ctr. (Korea, Republic of); Sang-Seok Hwang, Yugyeong Chae, Pukyong National Univ. (Korea, Republic of) and Ctr. for Marine-Integrated Biomedical Technology (Korea, Republic of); Eun-Kee Park, Kosin Univ., College of Medicine (Korea, Republic of) and Innovative Biomedical Technology Research Ctr. (Korea, Republic of); Yeh-Chan Ahn, Pukyong National Univ. (Korea, Republic of) and

Ctr. for Marine-Integrated Biomedical Technology (Korea, Republic of) and Innovative Biomedical Technology Research Ctr. (Korea, Republic of)

The asthmatic patients have airway hyper responsiveness, which induces bronchoconstriction resulting in ventilation defect. Bronchial challenge test is useful to demonstrate airway hyper responsiveness with airway constriction. Anatomical optical coherence tomography has been used to image airway hyper responsiveness with aid of endoscopic probe. Recently, thoracic window was reported through which one can have direct visualization of alveolar structure. In this study, we imaged the change of in vivo right main bronchus and alveolar structure during bronchial challenge test using spectral-domain optical coherence tomography and correlated to airway resistance. An intubated rabbit sequentially inhaled normal saline, metacholine (2, 5 µg/ml). The airway resistance were measured by mechanical ventilation and airway structures were monitored by OCT. We demonstrated early decrease in the size of right main bronchus and alveoli in accordance with increased airway resistance after metacholin inhalation. To our knowledge, this is the first report for real-time airway dynamics including right main bronchus and alveoli during bronchial challenge test.

9304-120, Session 6

Electromagnetic optical coherence tomography guided needle biopsy of lung nodules

Yan Wang, Milen Shishkov, Massachusetts General Hospital (United States); Kirby G. Vosburgh, Brigham and Women's Hospital (United States); Lida P. Hariri M.D., David C. Adams, Alyssa J. Miller, Massachusetts General Hospital (United States); Raúl San-Jose Estépar, Brigham and Women's Hospital (United States); Michael Lanuti, Brett E. Bouma, Melissa J. Suter, Massachusetts General Hospital (United States)

Early diagnosis of lung cancer is critical for an increased patient survival rate. Currently, diagnosis of malignancy can only be accomplished with excisional biopsy. Low-risk bronchoscopy techniques for retrieving biopsy tissues are hampered by low diagnostic yields, and trans-thoracic and surgical approaches carry higher intrinsic risk of complications. Our previous studies demonstrated that OCT can assess pulmonary pathology relevant to lung cancer. In this study, we developed a multimodality imaging platform to assess solitary pulmonary nodules (SPNs) and guide bronchoscopic biopsy. We utilized CT scan and electromagnetic (EM) sensor to provide spatial guidance to SPNs like a GPS, and OCT for microscopic volumetric imaging. An EM sensor and OCT optic fiber probe were incorporated into a single catheter. A flexible bronchoscope compatible peripheral lung biopsy needle was custom made to provide a working channel for EM-OCT catheter, which facilitates both imaging and specimen collection during the procedure. The proximal handle of the catheter is connected to a customized hybrid electric-optic rotary junction enabling spinning both the EM sensor and optic fiber probe. High resolution CT scan of swine lungs with artificial SPNs (aSPNs) was processed to generate a virtual volume. The EM sensor was used to macroscopically guide the catheter and biopsy needle to the spatial locations of aSPNs, and OCT images were obtained to microscopically assess the tissue and confirm needle placement within the aSPN. Needle aspirates of the aSPNs were collected for validation.

9304-121, Session 6

Measuring the force of contraction of airway smooth muscle with PS-OCT

David C. Adams, Lida P. Hariri, Alyssa J. Miller, Yan Wang, Melissa J. Suter, Massachusetts General Hospital (United States)

Conference 9304A: Optical Techniques in Pulmonary Medicine II

The ability to observe airway dynamics is fundamental to forming a complete understanding of pulmonary diseases such as asthma. We have previously demonstrated that Optical Coherence Tomography (OCT) can be used to observe structural changes in the airway during bronchoconstriction, but standard OCT lacks the contrast to discriminate airway smooth muscle (ASM) bands- ASM being responsible for generating the force that drives airway constriction- from the surrounding tissue. Since ASM in general exhibits a greater degree of birefringence than the surrounding tissue, a potential solution to this problem lies in the implementation of polarization sensitivity (PS) to the OCT system. By modifying the OCT system so that it is sensitive to the birefringence of tissue under inspection, we can visualize the ASM with much greater clarity and definition. In this presentation we show that the force of contraction can be indirectly measured by an associated increase in the birefringence signal of the ASM. We validate this approach by attaching segments of swine trachea to an isometric force transducer and stimulating contraction, while simultaneously measuring the exerted force and imaging the segment with PS-OCT. We do this for the case of an intact tracheal segment, as well as for an excised, isolated strip of smooth muscle. We further demonstrate the applicability of this technique by performing full volumetric scans of swine bronchioles pre- and post- contraction.

9304-122, Session PSun

Development of a micro structured reflective sensor for the wrist-worn pulse oximeter

Chang-Sheng Chu, Shuang-Chao Chung, Yeh Wen Lee, Chih-Chun Fan, Yu-Tang Li, Jyh-Chern Chen, Taiwan Biophotonic Corp. (Taiwan)

We present the development of a micro structured reflective pulse oximetry sensor for measuring the pulse rate and blood oxygen saturation at low perfusion sites, such as wrist skin. This new design will help to address the need of a wrist-worn pulse oximeter to perform regular monitoring for patients with chronic obstructive pulmonary disease. Current pulse oximeters generally require the patient to be clamped onto a fingertip of earlobe with a transmittance sensor. A better wrist-worn device would rely on a reflective sensor attached to the wrist and allows patients to be measured pulse rate and blood oxygen saturation without hindering their normal activities. However, the wrist site has a much lower blood perfusion in comparison to other anatomical locations such as the fingertip or earlobe. It is very difficult to receive enough signals from the wrist because the light needed to create the signal must be reflected or backscattered from the skin. In this study, the micro structured reflective sensor consists of two LEDs, one photodiode and one micro structured optical element. This micro structured optical element is designed to modulate photon propagation in the skin tissue so that the intensity of reflected or backscattered lights detected by the photodiode is therefore enhanced. Experimental studies have shown that the signal-to-noise ratio of the reflective sensor is thereby enhanced approximately 10 times by the micro structured optical element. A prototype of wrist-worn pulse oximetry device was made and tested with medical-grade accuracy.

Conference 9304B: Endoscopic Microscopy X

Sunday - Monday 8-9 February 2015

Part of Proceedings of SPIE Vol. 9304 Endoscopic Microscopy X; and Optical Techniques in Pulmonary Medicine II

9304-200, Session 1

Imaging self-luminous objects with a single optical fiber (*Invited Paper*)

Jerome Mertz, Roman Barankov, Boston Univ. (United States)

Optical imaging devices have become ubiquitous in our society, and a trend toward their miniaturization has been inexorable. In addition to facilitating portability, miniaturization can enable imaging of targets that are difficult to access. For example, in the biomedical field, miniaturized endoscopes can provide microscopic images of subsurface structures within tissue. Such imaging is generally based on the use of miniaturized lenses, though for extreme miniaturization lensless strategies may be required. One such strategy involves imaging through a single, bare optical fiber by treating it as deterministic mode scrambler. This strategy requires laser illumination and is highly sensitive to fiber bending. We demonstrate an alternative strategy that enables the imaging of self-luminous (i.e. incoherent) objects with high throughput independent of pixel number. Our technique is insensitive to fiber bending, contains no moving parts, and is amenable to extreme miniaturization.

9304-201, Session 2

In vivo laser-based imaging of the human fallopian tube for future cancer detection

Eric J. Seibel, Charles D. Melville, Richard S. Johnston, Yuanzheng Gong, Kathy Agnew, Seine Chiang, Elizabeth M. Swisher, Univ. of Washington (United States)

Inherited mutations in BRCA1 and BRCA2 lead to 20-50% lifetime risk of ovarian, tubal, or peritoneal carcinoma. Clinical recommendations for women with these genetic mutations include the prophylactic removal of ovaries and fallopian tubes by age 40 after child-bearing. Recent findings suggest that many presumed ovarian or peritoneal carcinomas arise in fallopian tube epithelium. Although survival rate is >90% when ovarian cancer is detected early (Stage_I), 70% of women have advanced disease (Stage_III/IV) at presentation when survival is less than 20%. Over the years, effective early detection of ovarian cancer has remained elusive, possibly because screening techniques have mistakenly focused on the ovary as origin of ovarian carcinoma. Unlike ovaries, the fallopian tubes are amenable to direct visual imaging without invasive surgery, using access through the cervix. To develop future screening protocols, we investigated using our 1.2-mm diameter, forward-viewing, scanning fiber endoscope (SFE) to image luminal surfaces of the fallopian tube before laparoscopic surgical removal. Three anesthetized human subjects participated in our protocol development which eventually led to 70-80% of the length of fallopian tubes being imaged in scanning reflectance, using red (632nm), green (532nm), and blue (442nm) laser light. A hysteroscope with saline uterine distention was used to locate the tubal ostia. To facilitate passage of the SFE through the interstitial portion of the fallopian tube, an introducer catheter was inserted 1-cm through each ostia. During insertion, saline was flushed to reduce friction and provide clearer viewing. This is likely the first high-resolution intraluminal visualization of fallopian tubes.

9304-202, Session 2

Near infrared probe-based confocal laser endomicroscopy for in vivo diagnostic of peritoneal carcinomatosis

Muriel Abbaci, Peggy Dartigues, Ranya Soufan, Frederic De Leeuw, Corinne Laplace-Builhé, Institut Gustave Roussy (France)

Peritoneal carcinomatosis is metastatic stage aggravating digestive, gynecological or bladder cancer dissemination and the preoperative evaluation of lesions remains difficult. There is therefore a need for minimal invasive innovative techniques to establish a precise preoperative assessment of cancer peritoneal cavity. Probe-based confocal laser endomicroscopy (pCLE) provides dynamic images of the microarchitecture of tissues during an endoscopy. The PERSEE project proposes new developments in robotics and pCLE for the exploration of the peritoneal cavity during laparoscopy.

Two fluorescent dyes, Patent blue V and Indocyanine green have been evaluated on human ex vivo samples to improve the contrast of pCLE images. For a future implementation in clinical study, two topically staining protocols operable in vivo have been validated on 70 specimens from 25 patients with a peritoneal carcinomatosis. The specimens were then imaged by pCLE with an optical probe designed for the application. A histomorphological correlative study was performed on 350 pCLE images and 70 standard histological preparations. All images were interpreted in a random way by two pathologists.

Differential histological diagnosis such as normal peritoneum or pseudomyxoma can be done on pCLE images. The statistical analysis of the correlative study is underway. These dyes already approved for human use are interesting for pCLE imaging because some micromorphological criteria look like to conventional histology and are readable by pathologist. Thus pCLE images using these two new dyes do not require a specific semiology unlike that is described in the literature, for pCLE associated with fluorescein for in vivo imaging of pancreatic cysts.

9304-203, Session 2

Laparoscopic volume holographic system for in vivo: simultaneous multi-section imaging of ovary

Jennifer K. Barton, Isela D. Howlett, Michael Gordon, Photini S. Rice, Kenneth D. Hatch M.D., Raymond K. Kostuk, The Univ. of Arizona (United States)

A laparoscopic volume holographic imaging system (VHIS) was created for minimally-invasive imaging of the ovary. VHIS systems enable simultaneous multiple-depth-section epireflectance imaging through the use of a multiplexed volume hologram, inexpensive light emitting diode source, and moderately-priced camera. Our design incorporates these elements into a compact handle. Light is relayed to and from the ovary through a 3 mm diameter, 27 cm long probe. The probe optics include three 2.7 mm diameter gradient index (GRIN) optical elements, including a coupling lens, relay lens, and imaging lens. The distal end of the GRIN probe is protected by a 3 mm diameter BK7 window. The window provides protection and necessary separation between the GRIN lens and the tissue. The proximal end of the probe contains a negative lens used as a field flattener and backscatter reducer. The probe is mounted to the handle with a threaded retainer and can be removed for sterilization between patients. Simple software is used to acquire images or videos.

The laparoscopic system has lateral and axial resolutions of approximately 4 and 22 μm , and simultaneous imaging from two depths. An ex vivo study of surgical biopsy tissue from 28 patients shows the ability to distinguish normal from cancerous tissue either visually or through quantitative image analysis (e.g. significant differences in high to low ratio spatial frequency). An in vivo study is ongoing to determine if similar results are obtained in a surgical setting.

9304-204, Session 2

A six-color four-laser mobile platform for multi-spectral fluorescence imaging endoscopy

John F. Black, Glanvanta, Inc. (United States); Tyler Tate, Molly Keenan, Elizabeth J. Swan, Urs Utzinger, Jennifer K. Barton, The Univ. of Arizona (United States)

The properties of multi-spectral fluorescence imaging using deep-UV-illumination have recently been explored using a fiber-coupled thermal source at 280 nm. The resulting images show a remarkable level of contrast thought to result from the signal being overwhelmingly generated in the uppermost few cell layers of tissue, making this approach valuable for the study of diseases that originate in the endothelial tissues of the body. With a view to extending the technique with new wavelengths, and improving beam quality for efficient small core fiber coupling we have developed a mobile self-contained tunable solid-state laser source of deep UV light. An alexandrite laser, lasing at around 750 nm is frequency doubled to produce 375 nm and then tripled to produce 250 nm light. An optical deck added to the system allows other laser sources to be incorporated into the UV beam-line and a lens system has been designed to couple these sources into a single delivery fiber with core diameters down to 50 microns. Our system incorporates five wavelengths [250 nm, 375 nm, 442 nm (HeCd), 543 nm (HeNe) and 638 nm (diode laser)] as the illumination source for a small diameter falposcope designed for the study of the distal Fallopian tube origins of high grade serous ovarian cancer. The tunability of alexandrite offers the potential to generate other wavelengths in the 720–800, 360–400 and 240–265 nm ranges, plus other non-linear optical conversion techniques taking advantage of the high peak powers of the laser.

9304-205, Session 2

Demonstration and performance of SERS enabled scanning fiber endoscope

Liang Lim, Patrick Z. McVeigh, Santa Borel, Brian C. Wilson, Princess Margaret Cancer Ctr., Univ. Health Network (Canada)

We are reporting a surface enhanced Raman scattering (SERS) enabled scanning fiber endoscope (SFE). The SFE system was based on a previously reported ultrathin flexible endoscope that is capable of high resolution (>600 lines) large field of view color imaging at video rate, and which has been used in human imaging trials in the gastrointestinal system as well as preclinical fluorescence imaging in mice. The modified SERS SFE system makes use of an ultranarrow tunable filter to select individual Raman lines for bandpass imaging at video rate, or can provide full spectral collection at a subset of points within the endoscope's field of view. The spectroscopic imaging system operates in the NIR (785nm excitation) to minimize tissue background signals and does not interfere with the endoscope's standard RGB imaging mode. We have characterized the SERS SFE system's sensitivity and response to known concentrations of commercially-available SERS nanoparticles, and determined the optimum operating settings (spectral resolution, image resolution, integration time, frame rate) suitable for clinically relevant imaging conditions. We have validated the SERS SFE system's performance using both tissue mimicking phantoms and present preliminary limit-of-detection studies using a relevant animal model. Finally, we compared the performance of SERS SFE system with our recently

reported widefield SERS imaging system. By limiting the Raman detection to specific Raman spectral bands, our widefield SERS system was able to multiplex up to 4 SERS nanoparticles while acquiring in vivo images in <10 s.

9304-206, Session 2

Simultaneous fingerprint and high-wavenumber Raman endoscopy for in vivo diagnosis of colorectal precancer

Mads Sylvest Bergholt, Kan Lin, Jianfeng Wang, Wei Zheng, National Univ. of Singapore (Singapore); Hongzhi Xu, Jian-lin Ren, Institute of Digestive Disease, Zhongshan Hospital (China); Khek Yu Ho, Yong Loo Lin School of Medicine (Singapore); Supriya Srivastava, Yong Loo Lin School of Medicine (Singapore) and National Univ. of Singapore (Singapore); Ming Teh, Khay Guan Yeoh, Yong Loo Lin School of Medicine (Singapore); Zhiwei Huang, National Univ. of Singapore (Singapore)

Adenoma represents a precursor to colorectal cancer. Differential diagnosis between adenoma and benign hyperplastic polyps remains an unambiguous challenge. Raman spectroscopy is a vibrational spectroscopic technique sensitive to the changes of biomolecular structures and compositions occurring in tissue. We have developed a simultaneous fingerprint (FP) and high-wavenumber (HW) Raman endoscopy technique for in vivo Raman tissue diagnosis (optical biopsy) in the colorectum.

We recruited 5 colorectal patients for in vivo FP/HW measurements (n=119 spectra) during colorectal endoscopy. Partial least squares - discriminant analysis (PLS-DA) was used to assess the spectral differences and clustering among hyperplastic polyps and adenoma.

High quality in vivo FP/HW Raman spectra can be acquired and processed in real-time within 0.5 sec during clinical endoscopic examinations. Significant differences in Raman spectra between hyperplastic polyps and adenoma are observed reflecting the pathological transformation associated with gastric carcinogenesis (i.e., protein, DNA, lipids and water composition and structures). The FP/HW Raman endoscopic technique developed could differentiate adenoma from hyperplastic polyps with sensitivity of 80.3% (49/61) and specificity of 84.5% (49/58) and provide new insights into the molecular features of the colorectum.

This study shows that FP/HW Raman endoscopy has great potential as a screening tool for in vivo diagnosis of precancer during colorectal endoscopy.

9304-207, Session 3

Real-time high-resolution fiber bundle-based two-photon endomicroscope

Jiyi Cheng, Yina Chang, Shih-Chi Chen, The Chinese Univ. of Hong Kong (Hong Kong, China)

In this work, we present a new fiber bundle-based endomicroscope that can provide real-time two-photon imaging with submicron resolution. Fiber bundle based endomicroscope has been widely used for its compact size and ease of setup from a standard laser scanning microscope, but its resolution is limited by the interstitial spacing among individual fibers. State-of-the-art fiber bundles are typically 1 – 3 mm in diameter containing up to 100,000 fibers with approximately 3 μm center-to-center spacing. According to the sampling theory, the highest possible spatial frequency that may be resolved is $1/(2 \times \text{distance between fibers})$. As such, the best lateral resolution that may be achieved with preceding technology is a few microns. Detailed structures and information in the gaps are lost. To tackle this problem and obtain high resolution images, we integrate a micro-scanner that can rapidly scan the distal end of the fiber bundle in the x and y directions by $\pm 1.5 \mu\text{m}$. The distal end scanning as well as the

image acquisition and processing are synchronized in real time. Two fast algorithms to control the scanning and image reconstruction are developed for real time imaging processing. As a result, lost information from the fiber interspatial spacing can be regained to increase the optical resolution to $\sim 0.8 \mu\text{m}$. The hardware design (including the actuation mechanism and integration of the micro-positioner with the fiber bundle and objective lens) and control strategy (with or without feedback from the micro-scanner) will be presented with detailed discussion.

9304-209, Session 3

High-speed, quasi-simultaneous white light and line-scan confocal fluorescence endomicroscopy through a single fibre bundle

Michael R. Hughes, Guang-Zhong Yang, Imperial College London (United Kingdom)

The aim of endomicroscopy is to acquire images with clinically relevant contrast. To this end, several approaches have been explored, including single and multi-channel fluorescence microscopy, reflection-mode microscopy and white light endocytoscopy. A confocal fluorescence endomicroscope using imaging bundles is available commercially (Mauna Kea Technologies), and clinical prototypes of white light endocytoscopes are also in use (Olympus). However, to-date there has been little work on combining these modalities into a single, compact instrument.

We have recently demonstrated that imaging bundle based white light endocytoscopy is practical when using a separate multimode illumination fibre to eradicate the problem of back reflections. We also reported proof-of-concept experiments showing that the same bundle can be used with confocal fluorescence endomicroscopy. However, images from the two channels were acquired alternately to prevent cross-talk and so the low net frame rate (5 Hz) led to significant motion artefacts, making image fusion difficult.

We demonstrate in this work a combined instrument that acquires alternate white light and confocal fluorescence endomicroscopic images with a combined frame rate of 30 Hz. The confocal channel uses line rather than point confocal scanning to achieve short frame acquisition times while maintaining a good degree of optical sectioning, albeit with a significant tail at larger defocuses. A high speed line-scan CCD camera with a 70 kHz line-rate allows a 600 line image frame to be acquired in as little as 8 ms. Depending on the desired integration time for the white light images, the inter-channel temporal delay can therefore be brought down to a few ms. Both channels are also amenable to image expansion by mosaicking, offering the prospect of dual-mode, large-area tissue characterisation.

9304-210, Session 3

Electromagnetic tracking of handheld high-resolution microendoscopy probes to assist with real-time video mosaicking

Khushi K. Vyas, Michael R. Hughes, Guang-Zhong Yang, Imperial College London (United Kingdom)

Fiber-bundle based high-resolution microendoscopy (HRME), a combination of microscopy and endoscopy techniques, has emerged as an inexpensive, in vivo cellular-level imaging modality to detect malignancies in various clinical studies. A limitation of such an imaging system however is that its field-of-view (FOV), defined by the size of the fiber bundle, is less than 1mm^2 . With such a small FOV it is difficult to associate individual image frames with the larger scale anatomical structure. Video-sequence mosaicking algorithms have been proposed as a solution for increasing the image FOV by stitching together the HRME images while still maintaining microscopic-level resolution. Whereas significant research has focused on image processing and mosaicking algorithms, there has been less work on localization of the

probe to assist with building high quality mosaics over large areas of tissue.

In this paper we propose the use of electromagnetic (EM) navigation to assist with large-area mosaicking of hand-held HRME probes. Six degree-of-freedom (DOF) EM sensors are used to track in real-time the position and orientation of the tip of the imaging probe during free-hand scanning. We present a proof-of-principle system for EM-video data co-calibration and registration and then describe a two-step image registration algorithm that assists mosaic reconstruction. Preliminary experimental investigations are carried out on phantoms and ex vivo porcine tissue for free-hand scanning on planar and non-planar surfaces. The results demonstrate that the proposed methodology significantly improves the quality and accuracy of reconstructed mosaics compared to reconstructions based only on conventional pair-wise image registration and in principle can be applied to other optical biopsy techniques such as confocal endomicroscopy.

9304-211, Session 4

Integrated OCT-US catheter for detection of cancer in gastrointestinal tract

Jiawen Li, Univ. of California, Irvine (United States); Teng Ma, Thomas M. Cummins, Koping Kirk Shung, Jacques Van Dam, Qifa Zhou, The Univ. of Southern California (United States); Zhongping Chen, Univ. of California, Irvine (United States)

Gastrointestinal tract cancer, the most common type of cancer, has a very low survival rate, especially for pancreatic cancer (five year survival rate of 5%) and bile duct cancer (five year survival rate of 12%). Here we propose to use an integrated OCT-US catheter for cancer detection. OCT is targeted for detailed information, such as dysplasia and neoplasia, for early detection of tumors. US is used for staging tumors, according to the size of the primary tumor and whether it has invaded lymph nodes and other parts of the body.

Considering the lumen size of the GI tract, an OCT system with a long image range ($> 10\text{mm}$) and a US imaging system with a center frequency at 40MHz (penetration depth $> 5\text{mm}$) were used. The OCT probe is also designed for long range imaging. The focal length is 5mm for GRIN-lens-based probe and up to 4mm for ball-lens-based probe. The side-view OCT and US probes were sealed inside one probe cap piece and one torque coil and became an integrated probe. It was then inserted into a catheter sheath which fits in the channel of an ERCP endoscope and is able to be navigated smoothly into the bile duct by the elevator of the ERCP endoscope.

We have imaged 5 healthy and 2 diseased bile ducts. In the OCT image, disorganized layer structure and heterogeneous regions demonstrated the existence of tumor. Micro-calcification can be observed inside the bile duct wall in the corresponding US image.

9304-212, Session 4

Ultrahigh speed endoscopic optical coherence tomography for structural and angiographic imaging

Osman O. Ahsen, Hsiang-Chieh Lee, Kaicheng Liang, Michael G. Giacomelli, Zhao Wang, Massachusetts Institute of Technology (United States); Benjamin M. Potsaid, Massachusetts Institute of Technology (United States) and Thorlabs Inc. (United States); Marisa Figueiredo, Qin Huang, VA Boston Healthcare System (United States); Alex E. Cable, Thorlabs, Inc. (United States); Vijaysekhar Jayaraman, Praevium Research, Inc. (United States); Hiroshi Mashimo M.D., VA Boston Healthcare System (United States); James G. Fujimoto, Massachusetts Institute of Technology (United States)

Several endoscopic imaging techniques such as magnification endoscopy, narrowband imaging (NBI) and chromoendoscopy have been developed to enhance visualization of GI pathology, but can have limited sensitivity and specificity. Endoscopic Optical Coherence Tomography (OCT) performs volumetric imaging with near-microscopic resolution, however, with commercial endoscopic OCT systems visualization is mainly limited to cross-sectional imaging planes owing to limitations in imaging speed and the image distortions due to proximal scanning. Furthermore, scanning instabilities make OCT angiography (OCTA) methods difficult. We have recently demonstrated an ultrahigh speed endoscopic OCT system with a distal scanning micromotor catheter. The imaging catheter has 3.2 mm diameter and can be introduced through a 3.7 mm accessory channel of the endoscope. This system operates at a 600 kHz axial scan rate using swept source OCT with a vertical cavity surface emitting laser (VCSEL) at 1.3 μm wavelength. The micromotor catheter scans at 400 Hz rotation frequency, which provides sufficient sampling and scanning precision to enable visualization of three dimensional structure as well as intensity decorrelation based OCTA with high resolution and contrast. We discuss imaging artifacts related to nonuniform rotational distortion (NURD) that are present due to micromotor instability and demonstrate a computationally efficient fiducial marker based algorithm to correct its detrimental effects on structural and angiographic images. We also present a cross sectional survey of upper and lower GI pathology from patients undergoing surveillance endoscopy and colonoscopy at the Veterans Affairs Boston Healthcare System (VABHS).

9304-213, Session 4

Endoscopic full-field optical coherence tomography for in vivo and in situ head and neck cancer assessment with a rigid probe

Emilie Benoit à La Guillaume, Fabrice Harms, Franck Martins, LLTech SAS (France); A. Claude Boccara, Institut Langevin (France)

In cancer screening, early cellular changes often occurring in the deep part of the epithelium remain inaccessible to traditional endoscopic techniques. Doctors are thus forced to perform a biopsy, whose diagnosis will be known only once the surgical procedure is finished. Consequently, there is a major interest in providing the surgeon with a minimally invasive tool able to image tissue abnormalities in depth at the microscopic level and adapted to intraoperative procedures.

We present here a rigid endoscope based on Full-Field Optical Coherence Tomography (FFOCT) equipped with a 5-mm diameter probe of length 20 cm. This endoscope provides "en face" images of the tissue microstructures located 20 μm after the surface in contact, with a high transverse resolution of 2.5 μm . The FFOCT technique is implemented through a tandem interferometer configuration under incoherent illumination composed of a Fabry-Perot processing interferometer external to the probe and a common-path imaging interferometer at distal end of the probe. The path modulation required to extract the OCT signal and the imaging depth within the sample are controlled via the processing interferometer which relaxes the design constraints on the probe and allows in situ measurement. A large field of view of 1 mm² is transmitted to the camera through gradient index lenses.

Promising images were recorded on breast tissue and rat brain ex vivo. A pre-clinical study including researchers and pathologists of Institut Gustave Roussy (France) will soon start on Head & Neck cancer biopsies and in vivo tests are planned on a medium animal model.

9304-214, Session 4

Tethered capsule endomicroscopy for comprehensive imaging of the human small intestine

Michalina J. Gora, Amna R. Soomro, Weina Lu, Robert W. Carruth, Mireille Rosenberg, Norman S. Nishioka M.D., Wellman Ctr. for Photomedicine (United States); Alessio Fasano M.D., Massachusetts General Hospital (United States); Guillermo J. Tearney M.D., Wellman Ctr. for Photomedicine (United States)

The diagnosis of celiac disease in duodenum is based on histologic findings from endoscopic biopsies, which requires patient sedation and is limited by sampling error. We have developed a new technology, tethered capsule endomicroscopy (TCE) that uses infrared light beam scanned circumferentially at 20 frames/s to collect cross-sectional optical coherence tomography (OCT) images of the GI tract. After overnight fast, unsedated subjects swallowed the TCE device (11mm x 25mm capsule attached to the 2m-long flexible tether). Following the capsule's passage through the pylorus using subject positioning and natural emptying of the stomach, slack in the tether was removed to prevent coiling. After the capsule descended 20 cm through duodenum, it was slowly retracted at a constant velocity to the pylorus. This procedure was repeated twice before the capsule was removed via the mouth.

So far 4 healthy volunteers and subjects with celiac disease have been enrolled in the TCE duodenum imaging study. Successful imaging of the small intestine was achieved in 3/4 (75%) of cases. In the three successful cases, the capsule entered the duodenum in 90, 30 and 15 min. In one case, the capsule was unable to pass through the pylorus. For all successful imaging cases, the duodenum constricted around the capsule, enabling circumferential imaging of the entire intestinal surface, including both sides of the circular folds. OCT image quality was excellent, with little effect from bile and other debris.

These preliminary results in humans suggest that TCE can provide high-resolution images of the microscopic structure of the whole duodenum without sedation. TCE may therefore become a powerful, minimally invasive imaging tool for aiding in the diagnosis of celiac disease.

9304-215, Session 4

Endoscopic polarization sensitive optical coherence tomography with completely fiber based passive optical components

Lucas Cahill, Anthony Lee M.D., Hamid Pahlevaninezhad, Catherine F. Poh D.D.S., The BC Cancer Agency Research Ctr. (Canada); Samson Ng D.D.S., UBC Dentistry (Canada); Calum E. MacAulay, Pierre M. Lane, The BC Cancer Agency Research Ctr. (Canada)

Polarization Sensitive Optical Coherence Tomography (PSOCT) is a functional extension of Optical Coherence Tomography (OCT) that is sensitive to well-structured, birefringent tissue such as scars, smooth muscle and cartilage. PSOCT has been used for a number of different clinical applications including in ophthalmology for segmentation of different structure boundaries such as the retinal pigment epithelium, in intracoronary imaging to detect fibrotic plaques and in human knee joints during surgery to help differentiate osteoarthritic tissue from normal tissue. Fiber-optic OCT catheters are desired for endoscopic use and for accessing difficult-to-reach body sites. Previously demonstrated fiber-optic PSOCT implementations are complex and rely on additional active instrumentation such as polarization modulators.

We present a novel completely fiber based swept source PSOCT system using a fiber-optic rotary pullback catheter. This PSOCT implementation

uses only passive optical components and requires no calibration while adding minimal additional cost to a standard structural OCT imaging system. Due to its complete fiber construction, the system can be made compact and robust, while the fiber-optic catheter allows access to most endoscopic imaging sites. The 1.5mm diameter endoscopic probe can capture 100 frames per second at pullback speeds up to 15 mm/s allowing rapid traversal of large imaging fields. We validate the PS-OCT system with known birefringent tissues and demonstrate its in vivo PS-OCT imaging of human oral scar tissue.

9304-216, Session 5

Ultrahigh speed swept source OCT forward viewing endomicroscopy

Kaicheng Liang, Osman O. Ahsen, Zhao Wang, Hsiang-Chieh Lee, Michael G. Giacomelli, Massachusetts Institute of Technology (United States); Benjamin M. Potsaid, Massachusetts Institute of Technology (United States) and Thorlabs Inc. (United States); Vijaysekhar Jayaraman, Praevium Research, Inc. (United States); Tsung-Han Tsai, Massachusetts Institute of Technology (United States); Wenxuan Liang, Johns Hopkins Univ. (United States); Alex E. Cable, Thorlabs, Inc. (United States); Hiroshi Mashimo M.D., VA Boston Healthcare System (United States); Xingde Li, Johns Hopkins Univ. (United States); James G. Fujimoto, Massachusetts Institute of Technology (United States)

Optical coherence tomography (OCT) can perform three dimensional imaging of tissue architecture. The majority of endoscopic OCT imaging studies to date used proximally actuated torque cable pullback/rotation for beam scanning. These probes can cover large areas, but have limited scanning speeds and can introduce imaging artifacts due to nonuniform rotation and pullback. Forward-viewing probe technology using a piezoelectric actuator and scanning fiber has the scanning mechanism at the distal end of the probe, resulting in precise 2-dimensional scanning required for microscopic resolution. We have developed a forward viewing endomicroscopy probe for use with an ultrahigh speed swept source OCT system with a vertical cavity surface emitting laser (VCSEL) at 600 kHz axial scan rate. The probe has 3.3mm outer diameter and <20mm rigid length, which is compatible with the accessory port of a dual channel gastroscope or colonoscope. The probe uses a cylindrical piezoelectric actuator to scan a fiber in resonance with a spiral pattern. The scanning fiber deflection is >1mm at 2kHz resonance and 30V driving amplitude, which is within IEC safety limits. The probe is designed to operate with different optical magnifications, ranging from high magnification (1mm field) with 6um spot size and tissue in contact, to low magnification (5mm field) with 30um spot size and 10mm working distance. The probe can be electrically zoomed by adjusting the deflection of the scanning fiber. Clinical studies are beginning and we expect to present OCT endoscopic imaging data for upper and lower GI pathologies by the time of the conference.

9304-217, Session 5

Tethered capsule OCT endomicroscopy with image guided biopsy for technology validation

Amna R. Soomro, Michalina J. Gora, William Puricelli, Mireille Rosenberg, Norman S. Nishioka, Guillermo J. Tearney M.D., Massachusetts General Hospital (United States)

The current standard of care for Barrett's Esophagus (BE) management

is endoscopic surveillance with random biopsy - an invasive procedure requiring sedation and having a high probability of sampling error. We developed a new technology termed tethered capsule endomicroscopy (TCE) that captures microscopic OCT images (20 fps) of the entire esophagus without sedation. In addition to its diagnostic capabilities, this device can potentially be used to guide biopsy by identifying regions of interest (ROI) on the OCT images, and then applying endoscopically visible superficial laser cautery marks. Following marking, the capsule is withdrawn and the marked tissue removed by standard endoscopic biopsy. Here, we describe our initial clinical experience with TCE-guided biopsy. Unsedated patients swallowed an 11x25 mm capsule device. With the capsule in the esophagus, up to 4 ROI were marked in each patient. Laser cautery was applied through the capsule using 400mW of 1450nm laser irradiation. Different laser parameters, such as exposure time (2-second vs. 1-second) and marking patterns (dots vs. lines) were tested.

To date, 8 subjects with BE diagnosis have been enrolled. A total of 95% (18/19) marks were localized and biopsied during subsequent endoscopy procedures. There was a high degree of correspondence between intent to mark OCT ROI diagnoses and histopathologic diagnoses of the marked regions (accuracy 94%; CI: 73-99%). Though the accuracy was high, significant motion artifacts interfered in some of the 2-second marks. Decreasing exposure time to 1-second, improved the marking precision, but at the cost of endoscopic visibility. Our results demonstrate that TCE guided biopsy is a safe and well-tolerated technique. Further optimization of the laser power and exposure parameters of the laser-marking platform will improve the precision of TCE guided biopsy, making it a viable option for surveillance in BE patients.

9304-218, Session 5

Polarization sensitive OCT imaging with needle probes

Martin L. Villiger, Wellman Ctr. for Photomedicine (United States) and Massachusetts General Hospital (United States) and Harvard Medical School (United States); Dirk Lorensen, The Univ. of Western Australia (Australia); Brett E. Bouma, Wellman Ctr. for Photomedicine (United States) and Massachusetts Institute of Technology (United States) and Harvard Medical School (United States); Robert A. McLaughlin, David D. Sampson, The Univ. of Western Australia (Australia)

The integration of miniaturized, side-viewing optical coherence tomography (OCT) fiber probes into hypodermic needles has enabled in-situ imaging of tissue locations beyond the reach of conventional OCT. Whilst needle-based imaging using the structural OCT intensity signal has shown promise in a number of applications, tissue differentiation could be further improved by exploiting functional extensions such as polarization-sensitive (PS) OCT. Needle-based PS-OCT has particular utility in cancer imaging. In breast cancer, for example, areas of malignancy often appear similar to stromal tissue under standard OCT due to comparable optical backscatter. However, the high birefringence of stromal collagen allows PS-OCT to provide additional contrast from areas of malignancy.

Here, we present the first demonstration of PS-OCT with needle probes, using a state-of-the-art fiber-based swept-source OCT system with polarization diversity detection. We use two orthogonal input polarization states, delayed with respect to each other to encode their respective signals at different depths in the reconstructed tomogram. With the Mueller matrix formalism, both a measure of tissue birefringence and tissue depolarization is reconstructed, independent of fiber motion and the precise polarization states incident on the sample. We will discuss the required calibration procedure and present the characterization of this needle-based PS-OCT instrument with validation measurements of phantoms and ex-vivo tissues. The additional polarimetric image data could significantly improve the diagnostic potential of needle-based OCT in birefringent or depolarizing tissues.

9304-219, Session 6

Spectrally dispersed illumination spectral imaging

Dvir Yelin, Yair Bar Ilan, Technion-Israel Institute of Technology (Israel)

Measuring the spectrum emitted from each point on a specimen could provide useful information on its chemical and structural composition. The main challenge of spectral imaging, however, is the acquisition, in a timely manner, of the large three-dimensional data sets that may comprise high-resolution spectra within high-pixel-count images. Moreover, in most biomedical applications the light intensity that a given sample could tolerate is strictly limited, which often results in low signal-to-noise ratios or, alternatively, impractically long imaging times. Here, we present a method for efficient, high signal-to-noise ratio spectral imaging termed spectrally dispersed illumination spectral imaging (SDISI). By using a diffraction grating and a cylindrical lens for illumination, and a monochromatic camera for detection, we capture wavelength-dependent reflections from each location on a sample as it slowly scanned along a single axis. The reflection spectral cube that was assembled from the continuously acquired digital images contained high number of resolvable point in both spatial and spectral dimensions. The system was studied and calibrated using spectral imaging of a scattering resolution target and a color test chart, and its potential for biomedical applications was demonstrated by imaging the finger of a human volunteer. By illuminating a large area and detecting spectrally encoded reflectance from an entire sample plane, SDISI could be efficiently conducted at low irradiance levels and without the need for a rapid two-dimensional scanning. Compared to traditional point- and line-scanning techniques, SDISI exhibit orders-of-magnitude advantage in SNR and is capable of high spectral and spatial resolutions.

9304-220, Session 6

Comprehensive confocal microscopy of human esophagus in vivo using an SECM endoscopic probe

DongKyun Kang, Robert W. Carruth, Minkyu Kim, Tao Wu, Simon C. Schlachter, Nima Tabatabaei, Amna R. Soomro, Mireille Rosenberg, Norman S. Nishioka M.D., Guillermo J. Tearney M.D., Massachusetts General Hospital (United States)

Spectrally encoded confocal microscopy (SECM) is a form of confocal microscopy that uses a broadband light source and a diffraction grating to acquire line images of the tissue without using any beam scanning devices. SECM can achieve an imaging speed that is an order of magnitude faster than those of conventional confocal microscopy technologies. The high imaging speed of SECM, in conjunction with an endoscopic imaging device that can rapidly scan a large area of an internal organ, can uniquely enable comprehensive confocal microscopy of the entire organ. In this paper, we present results from a preliminary study of imaging human esophagus in vivo with an SECM endoscopic probe. Patients undergoing upper gastrointestinal endoscopy were enrolled in this study. Each patient was examined with video endoscopy first, and the distal esophagus was then sprayed with 2.5 % acetic acid to increase the nuclear contrast. An SECM endoscopic probe (outer diameter = 7 mm; lateral resolution = 2 μ m; axial resolution = 17 μ m) was placed to the gastroesophageal junction (GEJ) over a guide wire. A large segment (length = 5 - 10 cm) of the tissue around the GEJ was rapidly imaged (imaging time = 2 - 4 min). SECM images clearly revealed characteristic cellular features: SECM images of normal esophagus visualized squamous cell nuclei and papillae; stomach images showed columnar cell nuclei on cardia glands; and SECM images of Barrett's esophagus (BE) exhibited glandular structure. Results from this preliminary study suggest that SECM can be utilized to comprehensively image the entire distal esophagus and improve the diagnoses of various esophageal diseases, including BE and its more progressed forms.

9304-221, Session 6

Large-area imaging of breast tissues with spectrally encoded confocal microscopy (SECM)

Elena F. Brachtel, Barbara L. Smith, Guillermo J. Tearney M.D., DongKyun Kang, Massachusetts General Hospital (United States)

Spectrally encoded confocal microscopy (SECM) is a reflectance confocal microscopy technology that can image a very large area (10 mm by 10 mm) of the tissue at microscopic resolution (1 μ m) within a short procedural time (15 seconds). SECM can be used to image the margins of the entire surgical specimens during breast-conserving lumpectomy and determine presence and locations of any residual tumors. The surgeon can then use this margin status information to conduct additional re-excisions and achieve more thorough removal of the tumor during the initial lumpectomy procedure. We have conducted a preliminary study of imaging breast tissues with SECM to determine diagnostic accuracy of SECM in detecting breast cancers. Discarded breast specimens (N=46) from lumpectomy or mastectomy procedures were used in this study. 5% acetic acid was topically sprayed on the breast specimen to increase the nuclear contrast. Each specimen was first imaged with SECM over a large area (4 mm x 2 mm to 14 mm x 6 mm) and then prepared as hematoxylin and eosin (H&E)-stained histology slides. 186 matching pairs of SECM and histologic images (each image size = 500 μ m x 500 μ m) were generated based on morphologic similarities. Comparative analysis of SECM and histologic images showed that SECM images can visualize key cellular features associated various breast tissue types: normal breast tissues showed benign ducts and lobules with nuclear details; low-grade invasive carcinoma showed small glands invading the stroma; and high-grade invasive carcinoma showed pleomorphic tumor cells with little stroma. These results suggest that SECM has the potential to accurately detect breast cancers from surgical specimens during lumpectomy.

9304-222, Session 6

Confocal microscopy of the esophagus using a tethered capsule endomicroscopy device enables the visualization of individual eosinophils in eosinophilic esophagitis patients

Nima Tabatabaei, DongKyun Kang, Weina Lu, Tao Wu, Minkyu Kim, Robert W. Carruth, Amna R. Soomro, Elena G. Quijano, Mireille Rosenberg, Jenny S. Sauk, Paul E. Hesterberg, Norman S. Nishioka M.D., Qian Yuan, John J. Garber, Aubrey J. Katz M.D., Guillermo J. Tearney M.D., Massachusetts General Hospital (United States)

Eosinophilic esophagitis (EoE), an esophageal disease caused by food allergy, is characterized by presence of eosinophils in the esophageal mucosa. Endoscopic biopsy is currently used to diagnose and follow the progression of EoE, where random biopsies are taken and histologically analyzed to count the number of eosinophils. Endoscopic biopsy is a costly and burdensome procedure because it requires patient sedation. The expense and inconvenience of endoscopy is particularly problematic for EoE patients who may need many of these procedures during the course of the disease. Spectrally encoded confocal microscopy (SECM), a high-speed reflectance confocal microscopy technology, has previously been shown to be capable of imaging individual eosinophils in freshly biopsied esophageal tissues. Our lab has developed a tethered SECM capsule (diameter = 7 mm; length = 30 mm) that can be swallowed by unsedated patients. Once swallowed, the device acquires large area confocal microscopy images of the esophageal wall as it traverses the esophagus. In this paper, we present results from our first clinical study using the tethered SECM endomicroscopy

capsule. A total of 8 healthy human subjects and 5 EoE patients have been enrolled in this study to date. The SECM capsule was swallowed by each untested subject, allowed to pass to the stomach via peristalsis, and then was manually pulled back up through the esophagus using the tether. SECM images were continuously recorded while the capsule travelled between the gastroesophageal junction and the proximal esophagus for a total of 4 passes. The average imaging time was 12 minutes per patient. There were no complications of the procedure. SECM images acquired from EoE patients showed abundant eosinophils as highly scattering cells in squamous epithelium, while SECM images from healthy subjects did not exhibit these highly scattering cells. Results from this study suggest that the SECM capsule has the potential to become a less-invasive, cost-effective tool for diagnosing EoE and monitoring the response of this disease to therapy.

9304-223, Session 6

Spectral imaging using forward-viewing spectrally encoded endoscopy

Adel Zeidan, Dvir Yelin, Technion-Israel Institute of Technology (Israel)

Utilizing spatial wavelength encoding, spectrally encoded endoscopy (SEE) promises miniature, small diameter endoscopic probes that allow easy access to hard-to-reach locations within the body. Using spectral dispersion also allows color and spectral imaging that could distinguish between different tissue types based on their unique spectral signature, and provide useful information on the tissue chemical and structural composition. Contrary to previous SEE miniature probes with side-viewing angles, we have recently presented a novel forward-viewing SEE probe that has been shown suitable for imaging within small-diameter ducts. High-quality imaging was demonstrated using a 1 mm diameter probe, including a wide field of view, a large number of resolvable points and low speckle contrast. In this work, we use the forward-viewing probe to demonstrate effective color and spectral imaging of targets that mimic the cylindrical geometries of the inner surfaces of narrow vessels. Using a separate illumination channel of incoherent broadband light in the visible range, the probe is capable of acquiring color and spectral imaging as it rotates around its axis and advances through the cylindrical duct. Potential applications of this method include early detection of malignancies within narrow ducts and detection of various blood vessel wall pathologies.

9304-224, Session 6

Mega-pixel imaging through a 350- μ m-diameter spectrally encoded endoscopy (SEE) probe

DongKyun Kang, Massachusetts General Hospital (United States); Mitsuhiro Ikuta, Canon USA, Inc. (United States); Daryl Chulho Hyun, Massachusetts General Hospital (United States); Ramses V. Martinez, George M. Whitesides, Harvard Univ. (United States); Guillermo J. Tearney M.D., Massachusetts General Hospital (United States)

Spectrally encoded endoscopy (SEE) is an endoscopic imaging technology that can acquire high-definition images of the tissue through a sub-mm probe. Previously, we demonstrated real-time acquisition of tissue images with approximately 400 by 400 effective pixels through a 500- μ m-diameter SEE probe. Although this number of effective pixels is larger than that of a fiber bundle with a similar diameter, 10,000 pixels for a 500- μ m-diameter fiber bundle, further increase of the number of effective pixels will expand the clinical utility of the SEE technology. In this paper, we describe a new SEE probe with a diameter of 350 μ m that can acquire 1 Mpixels per image. The new SEE probe significantly increased the number of effective pixels by using a diffraction grating with a high groove density (2000

lpmm) and a large spectral bandwidth (415 – 820 nm). This combination of the groove density and bandwidth resulted in a field angle of 77° and 500 resolvable points, which generated 1000 effective pixels. The diffraction grating was custom designed to achieve high diffraction efficiency for the given spectral bandwidth, and photo nanoimprint lithography was used to fabricate miniature gratings at distal end of the SEE probe optics. The SEE probe was scanned back and forth by a galvo scanner over an angular range of 70° at a rate of 10 Hz. Each spectrally encoded line was sampled by 1000 pixels and 1000 spectrally encoded lines were acquired for each image, which produced 1 Mpixels per image. SEE images of mouse embryos *ex vivo* clearly visualized characteristic anatomic features, including eyes, tails, paws, and claws. This new probe now makes it possible to conduct high-quality endoscopic imaging in a device with a diameter of less than 350 μ m, which will open up opportunities for outpatient endoscopy in a wide array of medical fields including orthopedics, otolaryngology, and neurology.

9304-225, Session 7

Dual-modal optical imaging microendoscope for ovarian cancer detection

Molly Keenan, Tyler Tate, Elizabeth J. Swan, The Univ. of Arizona (United States); John F. Black, Glannaventa, Inc. (United States); Urs Utzinger, Jennifer K. Barton, The Univ. of Arizona (United States)

We have combined optical coherence tomography (OCT) and multispectral fluorescence imaging (MFI) into a 0.7mm outer diameter steerable endoscope to image the Fallopian tubes and ovaries. This endoscope can be introduced to the Fallopian tubes transvaginally, creating a minimally invasive screening method for high risk women. We have previously shown that multispectral imaging utilizing the endogenous fluorescence of tissue can improve lesion contrast in *ex vivo* samples. In addition, OCT can identify structural differences between normal, benign cysts and adenocarcinoma in human ovary surgical samples. The OCT subsystem consists of an 890nm SDOCT engine coupled to a side-viewing 125 μ m fiber to achieve 6 μ m lateral x 4 μ m axial resolution. The MFI illumination system consists of five wavelengths (255, 370, 442, 543, and 638nm) from four lasers coupled into a 100 μ m core diameter multimode fiber. The two UV wavelengths are provided by a custom built Alexandrite laser. Reflected and fluorescence emission light from the tissue is imaged into a 3000 element fiber bundle using a custom designed 3 element objective. The 300 μ m diameter lenses provide a 70° full FOV over a working distance of 3 to 10mm. The distal tip of the falposcope combines the fiber bundle, objective, MFI illumination fiber, OCT fiber and two small pull wires in an inner ferrule. An outer sheath protects the assembly and provides flexibility and biocompatibility. Optical screening of the ovary through a natural orifice appears to be feasible.

9304-226, Session 7

Improved chromatical and field correction of high-NA GRIN-based endomicroscopic imaging systems for new biophotonic applications

Gregor Matz, Bernhard Messerschmidt, Grintech GmbH (Germany); Herbert Gross, Friedrich-Schiller-Univ. Jena (Germany)

GRIN microobjectives have been widely used in non-linear, linear confocal and fluorescence endomicroscopic imaging applications, especially in brain and cancer research. High numerical apertures of up to 0.8 and submicron resolution are achieved by combining GRIN lenses with a single refractive plano-convex micro-lens while keeping the diameter of the mounted objective to less than 1.4 mm. However, off-axis aberrations limited the usable field of view to about 200 μ m and the missing colour correction

made the successful application to CARS and linear confocal fluorescent modalities difficult.

Here, we present new optical design approaches to increase the field of view significantly and to correct chromatic aberration which open up new in-vivo endomicroscope applications and make the use of GRIN optics more attractive in brain and cancer research and in clinical diagnostics. The optical designs are evaluated by confocal resolution experiments and wavefront aberration measurements.

9304-227, Session 7

In-vivo multispectral fluorescence imaging of murine colonic dysplasia with scanning fiber endoscopy

Arlene Smith, Asha Pant, Bishnu P. Joshi, Emily F. Rabinsky, Juan Zhou, Xiyu Duan, Univ. of Michigan (United States); Chenying Yang, Eric J. Seibel, Univ. of Washington (United States); Thomas D. Wang M.D., Univ. of Michigan (United States)

Conventional clinical endoscopes use white light to detect architectural change in pre-malignant lesions in colonic mucosa. Gastrointestinal cancers can be heterogeneous and can express multiple cell surface targets that can potentially be imaged during endoscopic investigation.

The scanning fiber endoscope (SFE) is an ultrathin, flexible instrument, which has been developed for wide area multi-spectral fluorescence imaging. Excitation at 424nm, 488nm and 642nm is delivered into a single, spiral-scanning fiber, and fluorescence is collected by a ring of multimode optical fibers positioned around the edge of the probe. The forward-viewing system provides high resolution, color fluorescence images in three channels simultaneously and optional grayscale reflectance.

In this study, three fluorescently-labeled peptides were used as molecular probes and delivered topically into the colon of a CPC;Apc mouse model of spontaneous dysplasia. The excitation peaks of each of the selected fluorescent dyes – 7-diethylaminocoumarin-3-carboxylic acid (DEAC), fluorescein isothiocyanate (FITC) and cyanine5.5 NHS ester (Cy5.5). Each peptide was administered topically in the colon of normal and CPC;Apc mice and excited using the SFE probe. The target-to-background ratio was measured for each peptide excitation channel separately. The system was also operated in multi-channel mode, with specific binding of two and three peptides imaged simultaneously. The target-to-background ratio was measured for this case and compared to the single channel results. Furthermore, the presence of inter-channel crosstalk was investigated and quantified.

These results demonstrate the potential of this multispectral instrument to visualize multiple imaging targets concurrently to address molecular heterogeneity for the early detection of colorectal cancer.

9304-228, Session 7

Towards the development of an ultracompact optically sectioning endoscope with no distal optics

Youngchan Kim, Sean Warren, Imperial College London (United Kingdom); James M. Stone, James Roper, Jonathan C. Knight, Univ. of Bath (United Kingdom); Mark Neil, Carl Paterson, Christopher W. Dunsby, Paul M. W. French, Imperial College London (United Kingdom)

The development of techniques to control the phase profile of light wave emerging from distorting media [e.g. 1,2,3] prompted us to explore the development of ultracompact laser scanning endoscopes without distal optics to focus or steer the illuminating radiation. We demonstrated this

approach using a spatial light modulator (SLM) to control the phase of light propagating in the cores of a coherent fibre-optic bundle (FOB) and demonstrated distal scanning and focussing of a laser beam with no optical or mechanical components at the distal end of the fibre optic bundle [4]. Subsequently this has been combined with rapid proximal scanning and extended to demonstrate multiphoton excitation [5]. In parallel several groups have applied this approach to transmit images through a single multimode fibre, utilising the higher order modes to convey the image information [e.g. 6]. While this approach is compact and elegant, it has been limited in the number of image pixels achieved and the inherent dispersion of optical pathlengths of the higher order modes seems to preclude the use of femtosecond pulses for multiphoton imaging. The latter issue also presents challenges for the FOB approach but we show that this can be overcome by designing a custom FOB with appropriate V parameters that minimise path length dispersion between cores [7]. We also present the first results implementing our approach with polarisation-maintaining FOB and the first demonstration of real-time measurement of the phase of every core of the FOB and adaptive correction with an update rate of 180 Hz.

1. I. M. Vellekoop, & A. P. Mosk, *Opt. Lett.* 32, 2309-2311 (2007).
2. S. Popoff et al, *Nat. Commun.* 1, 1-5 (2010).
3. O. Katz et al, *Nat. Photon.* 5, 372 (2011).
4. A. J. Thompson et al, *Opt. Lett.* 36, 1707 (2011).
5. E. Andresen et al, *Opt Express* 21, 20713 (2013).
6. T. Cizmar & K. Dholakia, *Nat. Commun.* 3, 1027 (2012).
7. J. Roper et al. *CLEO, Structured Fibres and Structured Light, CTu3K* (2013)

9304-229, Session 8

Clinical experience with a confocal microlaparoscope for ovarian cancer detection

Andrew R. Rouse, Matthew D. Risi, Setsuko K. Chambers, Kenneth D. Hatch M.D., Wenxin Zheng, Arthur F. Gmitro, The Univ. of Arizona (United States)

Our group has developed and previously reported on a confocal microlaparoscope that allows real-time, high-resolution in vivo imaging of ovarian epithelium. In this work, we describe the successes and challenges faced in using this instrument in a clinical setting, both during laparoscopic and open surgical procedures. We also present results from a 45 patient clinical study that tested the performance of the instrumentation for the detection of ovarian cancer. Participants were recruited from patients scheduled for laparoscopic or open oophorectomy at the University of Arizona Medical Center. Ovaries were typically stained with acridine orange and imaged with the confocal microlaparoscope. Five observers were trained on a small subset of the images and then asked to rate the remaining images on a 6 point scale, ranging from “definitely not cancer” to “definitely cancer”. Receiver operator characteristic curves were generated by using these scores and histopathological diagnosis of the tissue samples as the gold standard. The average area under these curves was 0.88 with an average standard error of 0.02. The performance difference between images obtained in vivo and those obtained with ex vivo tissue was not statistically significant. These results demonstrate the diagnostic potential of the confocal microlaparoscope for the detection of ovarian cancer in vivo.

9304-230, Session 8

Aberration correction of gradient index lens based combined two-photon microscopy and optical coherence tomography

Taejun Wang, Won Hyuk Jang, Pohang Univ. of Science and Technology (Korea, Republic of); Junggho Moon,

Conference 9304B: Endoscopic Microscopy X

Eunsung Seo, Korea Univ. (Korea, Republic of); Gyungseok Oh, Gwangju Institute of Science and Technology (Korea, Republic of); Young Eun Kim, G-One Ahn, Pohang Univ. of Science and Technology (Korea, Republic of); Euiheon Chung, Gwangju Institute of Science and Technology (Korea, Republic of); Wonshik Choi, Korea Univ. (Korea, Republic of); Seung-Jae Myung, Asan Medical Ctr. (Korea, Republic of); Ki Hean Kim, Pohang Univ. of Science and Technology (Korea, Republic of)

Previously, a gradient index (GRIN) lens based combined two-photon microscopy (TPM) and optical coherence tomography (OCT) was developed for endoscopic imaging of the mouse colon. Several layers composing mouse colon were revealed in cross-sectional OCT image with rapid screening on large regions, and specific sections which needed cellular imaging were localized. About these localized positions, TPM was performed to image glandular structures with or without fluorescent markers. The GRIN lens probe consisted of GRIN lenses and a reflecting 45° prism at its distal end for side-viewing. It was attached in front of an objective lens-based typical microscopic system. Although this probe enabled endoscopic imaging, TPM images had poor qualities due to aberration of the GRIN lens probe and individual cells were hardly resolved. So, it is necessary to compensate this aberration for an endoscopic imaging with better contrast. In recent years, various wave-front sensing and shaping methods have been developed to correct severe aberrations and have been applied to endoscopic imaging through image-distorting media. The common underlying principle of such recent methods is the characterization of the image distortion by the measurement of the medium's input-output response in the form of a transmission matrix. Recently, this transmission matrix was measured by using the interference of waves originating from different pixels of the liquid crystal type of spatial light modulator (LC-SLM) or digital micromirror device (DMD) for high-speed wave-front shaping. We will attempt to correct aberration in the GRIN lens probe by using one of those methods for high-resolution cellular imaging.

9304-231, Session 8

Two-photon endoscope with no distal optics

Hervé Rigneault, Esben R. Andresen, Institut Fresnel (France); Géraud Bouwmans, Univ. des Sciences et Technologies de Lille (France); Serge Monneret, Institut Fresnel (France)

We report a step toward scanning two-photon endomicroscopy without distal optics. We have been developing a lensless point scanning endoscope where the size of the endoscope distal probe is reduced to the fundamental limit—the 360 microns diameter of the endoscope fiber itself. Following in the footsteps of coherent laser beam combining, the focusing of the beam at the distal end of a fiber bundle is achieved by imposing a parabolic phase profile across the bundle exit face with the aid of a two-dimensional spatial light modulator (SLM). We used a bundle of single mode fiber (SMF) cores specifically designed for the purpose which exhibits extremely low cross-talk between the individual cores. This bundle is also designed with an outer air ring such that the stack of SMFs acts as an inner multimode cladding that can efficiently collect the back-scattered two-photon signal. We demonstrate first video-rate transverse scanning of the focal spot by using scan mirrors before the SLM [1]. Second, we extend lensless endoscopy based on bundles of SMFs to pulsed lasers and true endoscopic operation (with proximal signal collection) and demonstrate TPEF endoscopic imaging of a test sample of rhodamine 6G (Rh6G) crystals as well as tissue samples [2]. We believe that our setup can contribute to the further miniaturization of endoscope probes without sacrificing image speed, or quality. Our designed point scanning endoscope is in principle compatible with other nonlinear imaging schemes such as second and third harmonic generation where SMF are required to deliver a short and intense pulse to the sample.

[1] E. R. Andresen, G. Bouwmans, S. Monneret, and H. Rigneault, 'Toward endoscopes with no distal optics: video-rate scanning microscopy through a fiber bundle', *Optics Letters* 38, 609-611 (2013)

[2] E. Andresen, G. Bouwmans, S. Monneret, H. Rigneault, "Two-photon lensless endoscope", *Opt. Expr.* 21, 20713-20721 (2013)

9304-232, Session 8

Low cost and compact nonlinear (SHG/TPE) laser scanning endoscope for biomedical application

Jia Yun Liu, Singapore Institute of Manufacturing Technology (Singapore); Ken Choong Lim, Singapore Institute of Manufacturing Technology (Singapore) and Nanyang Technological University (Singapore); Hao Li, Hon Luen Seck, Xia Yu, Shawwei Kok, Ying Zhang, Singapore Institute of Manufacturing Technology (Singapore)

A low cost and compact nonlinear laser scanning endoscope apparatus consist of second harmonic generation and two-photon fluorescence imaging capability is developed. By the using low cost and compact fiber laser source instead of Ti:sapphire laser source, the system cost and dimension can be significantly reduced by at least 60% and 80% respectively. To enable using fiber laser source with low cost but low power and relative poor beam quality for SHG/TPE imaging, a high throughput optical system including precision GVD dispersion compensation module, miniaturized fiber scanner probe, high efficient emission collection and photon detection module is developed. High signal to noise ratio TPE/SHG images from liver tissue, liver surface membrane, skin surface, bone marrow, and retina RPE are obtained. The performances of developed system including spatial resolution, scanner non-linearity, optical dispersion, laser beam divergence, optical power delivery and emission collection efficiency as well as their effect on image quality are evaluated and discussed.

9304-233, Session 9

MEMS-based handheld multiphoton endomicroscope for in vivo imaging

Xiyu Duan, Haijun Li, Zhen Qiu, Bishnu P. Joshi, Asha Pant, Katsuo Kurabayashi, Kenn R. Oldham, Thomas D. Wang M.D., Univ. of Michigan (United States)

Colorectal cancer is a leading cause of cancer-related deaths in the United States, despite the widespread availability of colonoscopy. By using cancer targeting molecular probes and high resolution imaging, it is possible to capture the molecular changes in the colon in the early stage of cancer. Multiphoton microscopy is a powerful tool to perform high resolution imaging of biological tissues, with properties including minimal photo damage and deep penetration. With recent development in miniature actuators and micro optics, it is now possible to miniaturize the bulky tabletop microscope into an endoscope. We aim to develop a MEMS-based handheld multiphoton endomicroscope that reveals binding of a FITC-labeled peptide to colonic dysplasia in mice in vivo. The distal end of the endoscope has an outer diameter of 3.4 mm and a length of 30 mm. Femtosecond laser pulses with center wavelength of 780 nm are delivered through a photonic crystal fiber into the handheld instrument. A 2D resonant MEMS mirror is used to scan the laser pulses in a Lissajous pattern at 5 frames/s with 400 x 400 pixels. Fluorescence images are collected with a lateral and axial resolution of 1 and 8 μm, respectively, over a field-of-view of 250 μm x 250 μm. By using a FITC labeled peptide that targets colon cancer, we demonstrate in vivo imaging of colonic dysplasia in mice with histology-like imaging performance. In vivo imaging results show that this instrument can be used to visualize specific peptide binding to dysplasia in the mouse colon, which can potentially be used for early detection and staging of colon cancer.

9304-234, Session 9

Forward-viewing MEMS fiber scanner for endomicroscopic applications

Yeong-Hyeon Seo, Hyeon-Cheol Park, Kyungmin Hwang, Ki-Hun Jeong, KAIST (Korea, Republic of)

Optical endomicroscopy holds great promise for clinical applications such as optical biopsy or image guided surgery. Forward-viewing imaging can provide same viewing direction as conventional endoscope through the accessory channel, so that it is more suitable for endomicroscopic applications. Resonant fiber scanners using PZT tube actuator are widely used for forward-viewing imaging because of its merits, such as, simple, compact and robust packaging. Nevertheless, it has limits for miniaturization and high price.

We report a novel two dimensional forward-viewing MEMS fiber scanner for endomicroscope. The MEMS fiber scanner consists with hot arm structures, and a single mode optical fiber which is directly mounted on hot arm structure. Thermal expansion of hot arm structure induced by Joule heating makes lateral scanning, while bent cantilever of hot arm structure induced by fixed end fiber makes vertical actuation. Asymmetric structure of scanner separates resonance frequencies of fiber with x, y direction without additional structure, and the proposed MEMS fiber scanner successfully demonstrates lissajous pattern within 40V.

The proposed MEMS fiber scanner was fabricated by using deep reactive ion etching (DRIE) process on a heavily doped 6 inch silicon SOI wafer with good electrical conductivity, and its physical dimensions are smaller than conventional quadratic PZT tube.

A spectral-domain OCT system was combined with the MEMS fiber scanner, and this MEMS fiber scanner can provide a new direction for compact forward-viewing endomicroscopic applications.

9304-235, Session PMon

Multi-camera synchronization core implemented on USB3 based FPGA platform

Ricardo M. Sousa, Univ. da Madeira (Portugal); Martin Wány, Pedro Santos, AWAIBA Lda. (Portugal); Morgado Dias, Univ. da Madeira (Portugal)

Based on Awaiba's NanEye CMOS image sensor family and an FPGA platform with USB3 interface, the aim of this paper is to demonstrate a novel technique to perfectly synchronize up to 8 individual self-timed cameras. Minimal form factor self-timed camera modules of 1 mm x 1 mm or smaller do not generally allow external synchronization. However, for stereo vision or 3D reconstruction with multiple cameras as well as for applications requiring pulsed illumination it is required to synchronize multiple cameras. In this work, the challenge to synchronize multiple self-timed cameras with only 4 wire interface has been solved by adaptively regulating the power supply for each of the cameras to synchronize they're frame rate and frame phase. To that effect, a control core was created to constantly monitor the operating frequency of each camera by measuring the line period in each frame based on a well-defined sampling signal. The frequency is adjusted by varying the voltage level applied to the sensor based on the error between the measured line period and the desired line period. To ensure phase synchronization between frames of multiple cameras, a Master-Slave interface was implemented. A single camera is defined as the Master entity, with its operating frequency being controlled directly through a PC based interface. The remaining cameras are setup in Slave mode and are interfaced directly with the Master camera control module. This enables the remaining cameras to monitor its line and frame period and adjust their own to achieve phase and frequency synchronization.

The control core was tested in a laboratory environment with up to 4 cameras. Results indicate it is able to maintain perfect synchronization in changing ambient temperatures. Tests show that even in the presence

of temperature gradients of 60 °C between cameras, phase and frequency synchronization is still maintained. The temperature range (tested from -2 °C to 60 °C) is only limited by the self-imposed voltage limits to the camera supply. Furthermore, the average phase error between frames was measured to be 3.77 μs. Taking into account that the nominal frame rate of a NanEye camera is 44 fps this means the average error is approximately 0.017%. The control module has also shown it is independent from cable length and NanEye camera version. The result of this work will allow the realization of smaller than 3mm diameter 3D stereo vision and 3D meteorology equipment in medical endoscopic context, such as endoscopic surgical robotic or micro invasive surgery.

9304-236, Session PMon

Stray light mitigation in a novel endoscope for fallopian tubes

Elizabeth J. Swan, Tyler Tate, Molly Keenan, The Univ. of Arizona (United States); John F. Black, Glannaventa, Inc. (United States); Urs Utzinger, Jennifer K. Barton, The Univ. of Arizona (United States)

Stray light in an endoscope largely contributes to whether a signal can be resolved or not. This FRED analysis used a novel endoscope for the fallopian tubes to show how common endoscope elements cause stray light contamination, and to offer suggestions on how to mitigate it. Standard and advanced optical raytracing was performed. Raytrace reports determined which ray paths caused the highest power and irradiance distributions at the back of the imaging fiber's lenses. This revealed that the cover plate introduced the most stray light. The imaging lenses and variable stop reflectivity had a negligible impact on the signal. To compensate, the source NA was adjusted to 0.35 and 0.25 to keep the stray light within the same order of magnitude and an order of magnitude lower than the desired signal respectively. There was a single specular reflection off of the cover plate surface closest to the tissue. This illumination reflected back into the imaging fiber without first scattering off the tissue, which resulted in high power at the back of the imaging lenses. The specular light appeared brighter at wider fields of view and saturated the desired signal at the edge of the imaging fiber. Since changing the design of the optics is not favorable, future FRED analysis will use finer iterations to find the optimal source numerical aperture. That way, the system will have maximum illumination to image the tissue, with minimal stray light degrading the desired signal.

9304-237, Session PMon

Endoscopic imaging probe for high-resolution optical coherence tomography

Jun Young Kim, Hyeong Soo Nam, Min Woo Lee, Hanyang Univ. (Korea, Republic of); Seung-Il Jang, Se-Hun Kwon, Pusan National Univ. (Korea, Republic of); Hongki Yoo, Hanyang Univ. (Korea, Republic of)

Optical coherence tomography (OCT) acquires three-dimensional microstructure of biological samples. In general, it has ~10μm resolution in both axial and transverse directions, which is not enough to visualize individual cells and sub-cellular structures. High-resolution OCT with an improved spatial resolution up to 1μm enables clear visualization of cellular and sub-cellular features of biological samples. To investigate internal organ in vivo using the high-resolution OCT, an endoscopic probe that achieves high resolution is vital. Therefore, we have developed a high-resolution endoscopic probe using a gradient-index (GRIN) lens and a high-resolution OCT system, using a broadband supercontinuum laser with a center wavelength of 830nm and a bandwidth of 280nm. The imaging probe has an outer diameter of 1.0mm and a length of 9.5mm. In order to increase the imaging range, we applied apodization technique on the surface of the GRIN lens. Simulation analysis shows that the designed probe has a spot radius

of 2.08 μm . To validate the performance of the developed high resolution OCT endoscopic imaging system, we acquired images of phantoms made of micro-beads with 1 μm -diameter. Experimental results showed the extended depth of focus with high spatial resolution. These results indicate that our high resolution OCT imaging probe system might be useful for various pre-clinical and clinical in vivo studies.

9304-238, Session PMon

Development of a new laparoscopic system for detection of gastric cancer using fluorescent clip emitting near-infrared light

Shunko A. Inada, Nagoya Univ. (Japan); Shingo Fuchi, Aoyama Gakuin Univ. (Japan); Kensaku Mori, Nagoya Univ. (Japan); Junichi Hasegawa, Chukyo Univ. (Japan); Kazunari Misawa M.D., Hayao Nakanishi, Aichi Cancer Ctr. (Japan)

Recently, laparoscopic surgery is performed for the treatment of gastric cancer because of several benefits such as low-burden, low-invasiveness and high efficacy which is equivalent to the open surgery. For identify location of the tumor intraperitoneally for extirpation of the gastric cancer, charcoal ink is injected around the primary tumor. However, during laparoscopic operation, it is sometimes difficult to estimate exact location of the primary tumor, because the injected charcoal ink diffusely spread to the area distant from the primary tumor in the stomach which results in the resection of the stomach with the wide margin. To overcome this problem, we noticed the near-infrared wavelength of 1000nm band which have high biological transmission. In this study, we developed a fluorescent clip which was realized with glass phosphor (Yb³⁺, Nd³⁺ doped to Bi₂O₃-B₂O₃ based glasses. λ_p : 976 nm, FWHM: 100 nm, size: 2x1x3 mm) and the laparoscopic fluorescent detection system for clip-derived near-infrared light. To evaluate clinical performance of a fluorescent clip and the laparoscopic detection system, we used resected stomach (thickness: 13 mm) from the patients. Fluorescent clip was fixed on the gastric mucosa, and an excitation light (λ : 808 nm) was irradiated from outside of stomach for detection of fluorescence through stomach wall. As a result, fluorescent emission from the clip was successfully detected.

These results suggest that the fluorescent clip in combination with laparoscopic detection system is very useful method to identify the exact location of the primary gastric cancer.

Conference 9305A: Optical Techniques in Neurosurgery, Brain Imaging, and Neurobiology

Saturday - Sunday 7-8 February 2015

Part of Proceedings of SPIE Vol. 9305 Optical Techniques in Neurosurgery, Neurophotonics, and Optogenetics II

9305-100, Session 1

Micro-optical coherence tomography of ependymal cilia

Kengyeh K. Chu, Massachusetts General Hospital (United States); Timothy W. Vogel, Cincinnati Children's Hospital Medical Ctr. (United States); Robert W. Carruth, Guillermo J. Tearney M.D., Massachusetts General Hospital (United States)

The fluid-filled ventricles of the brain are lined with a ciliated epithelium known as the ependyma. Though ependymal cilia unquestionably interact with and transport cerebral spinal fluid (CSF), their role in the regulation of CSF hydrodynamics and the prevention of hydrocephalus remains unknown. Primary defects of cilia are associated with but not universally correlated with hydrocephalus, which implies a function for ependymal cilia in regulation of CSF flow and pressure, but the lack of hydrocephalus in some patients with highly immotile cilia underscores our lack of understanding of their importance. Existing imaging methods available for ependymal cilia either require fixation (electron microscopy and histology) extraction of thin samples for video microscopy.

We have previously developed 1- μ m resolution micro-optical coherence tomography (μ OCT), which we have utilized extensively for the quantification of ciliary function in airway epithelia. μ OCT directly visualizes cilia and produces co-localized measures of their function, including ciliary beat frequency (CBF) and the velocity of resultant transport. We now demonstrate the application of μ OCT imaging to ependymal cilia in mouse models. High-speed (80 fps) 1- μ m resolution μ OCT images were obtained from mouse ventricular cilia, immediately following sacrifice. We conducted initial experiments to test whether or not μ OCT could distinguish changes in ependymal ciliary function as a function of physiologically relevant parameters including pH and pressure ($n=1$ per independent variable). Our results showed that ependymal CBF increased slightly after application of a small amount of pH 10 buffer (16.2 ± 0.5 Hz baseline, 17.4 ± 1.4 Hz after 8 minutes, $p < 0.05$) and dropped after application of 4 cmH₂O elevated static pressure (18.0 ± 5.6 Hz baseline, 7.7 ± 1.0 Hz high pressure, $p < 0.05$). These initial results suggest that μ OCT may be capable of measuring parameters that can help in the understanding of the role of ependymal cilia, due to its unique ability to quantify ciliary function in situ.

9305-101, Session 1

Integration of optical coherence tomography with tissue clearing for deep brain imaging

Sunwoo Jung, Junwon Lee, Eunjung Min, Woonggyu Jung, Ulsan National Institute of Science and Technology (Korea, Republic of)

Modern optical imaging modalities allow us to visualize brain structure at microscopic scale. However, deep brain imaging still remained challenging due to light scattering in turbid tissues. To solve this problem, tissue clearing has been developed as one of the pioneering techniques. Optical imaging technique with tissue clearing extends the depth of light penetration by reducing the scattering property. Even though tissue clearing opens up the possibility of the deep brain imaging, there is still room to be improved. In particular, there is few research paper investigating the combination between optical coherence tomography (OCT) and tissue clearing for volumetric brain visualization. Hence, we present a novel 3D brain imaging technique integrated by OCT and tissue clearing. Because OCT performs

label-free, non-invasive and cross-sectional imaging from intact biological sample with spatial resolution of 10 μ m and penetration depth up to 2mm, OCT enables us to reduce the complex procedure. In our study, we uses spectral domain OCT centered at 1310 nm and ClearT solution which reduces the scattering by closing the gap of refractive indices. Since OCT image contrast is based on light scattering, optimal degree of clearing has to be determined. For the optimal condition, we monitor the change of OCT depth profile and volume in the basis of solution concentration. Moreover, we measure the tendency of light attenuation in the cleared brain to investigate interaction light with tissue clearing. These results demonstrate that integration of the tissue clearing and OCT could be useful tool for deep brain imaging

9305-102, Session 1

Quantitative biochemical investigation of various neuropathologies using high-resolution spectral CARS microscopy

Kelvin W. C. Poon, Craig Brideau, Univ. of Calgary (Canada); Geert J. Schenk, Roel Klaver, Vrije Univ. Medical Ctr. (Netherlands); Antoine M. Klausner, Jean H. Kawasoe, Univ. of Calgary (Canada); Jeroen J. Geurts, Vrije Univ. Medical Ctr. (Netherlands); Peter K. Stys, Univ. of Calgary (Canada)

Non-linear vibrational spectroscopic modalities such as Coherent anti-Stokes Raman Scattering (CARS) have been recognized as an increasingly unique tool in neuroscience as a label-free microscopic technique used to probe the intrinsic molecular biochemistry of neurological diseases, without the reliance on exogenous labelling. While largely succeeding as a high-resolution imaging method, only recently has the rich, molecular vibrational information inherent to the technique been capitalized upon. Broadband, spectrally-resolved CARS (sCARS) has the ability to not only provide images of high spatial resolution but also simultaneous per-pixel spectral data containing complete vibrational spectral information. Complex demyelinating diseases such as multiple sclerosis (MS) are perfectly suited to investigation using sCARS, whose strength lies in lipid imaging. A comprehensive study was carried out on all aspects of the disease including oligodendrocyte precursor maturation cell culture models, lesion formation and remyelination in animal models of multiple sclerosis (experimental autoimmune encephalomyelitis/cuprizone), through to studies on human MS pathological samples, where sCARS was used to analyse the 'normal-appearing' white matter (NAWM) adjacent to lesions. These NAWM regions were shown to reveal abnormalities despite morphological classifications indicating otherwise. Fundamental myelin and axon biology of the peripheral and central nervous system will be also be shown in unprecedented detail using ex-vivo and in-vivo preparations in transgenic mouse models. Finally, examples of sCARS in application to glioblastoma and spinal cord contusion injuries in mouse models will be demonstrated. Spectral data were analyzed using a unique non-linear algorithm, which allows quantification and classification through gated parameters and displayed through bivariate histograms.

9305-103, Session 1

Coaxial cavity injected OCT and fiber laser ablation system for real-time monitoring of ablative processes

Jamil Jivraj, Yize Huang, Ronnie Wong, Yi Lu, Barry Vuong,

Conference 9305A: Optical Techniques in Neurosurgery, Brain Imaging, and Neurobiology

Joel Ramjst, Xijia J. Gu, Victor X. D. Yang M.D., Ryerson Univ. (Canada)

Real-time monitoring and control of laser ablation of tissue can be of significant use in medical applications. Specifically for surgery, highly controlled removal for hard tissue during laser ablation is necessary to guarantee reduced or no collateral soft tissue damage. Optical coherence tomography (OCT) proves to be an ideal imaging modality for this purpose because of its fast acquisition speed and microscopic scale of visualization. As well, given the wavelength-discrimination properties inherent in OCT, the ablation process can be easily monitored in real-time without being affected by backscatter and glare of the ablation laser light.

Previous designs of incorporating the two systems involve coaxially combining the OCT light with the ablation laser light using a dichroic mirror just before the objective stage. The use of this structure involves bulky free-space optics (dichroic mirror) and lossy free-space transport of the combined resulting beam. We present a design overcomes these limitations. The design of the system involves the high-powered fiber laser being built directly into the sample arm of the OCT system. Since the OCT system and fiber laser system both use unique wavelengths (1310nm for OCT and 1064nm for ablation), the OCT laser light and subsequent backscatter pass relatively unaffected through the fiber laser. Initial results are presented showing monitoring of the ablation process of various materials (wood, bone) at single point in real time using m-mode imaging.

9305-104, Session 1

Cellular resolution imaging of healthy and pathological human brain tissue at 800nm and 1300nm with SD-OCT

Kostadinka Bizheva, Mojtaba Hajialamdari, Univ. of Waterloo (Canada); Sandrine de Ribaupierre, The Univ. of Western Ontario (Canada)

Approximately 2800 Canadians are diagnosed with a primary brain tumour each year and 1850 die from them. Of those diagnosed, 40% are glioblastoma multiforme, a particularly aggressive form of primary brain tumour, with median survival times of 14-16 months. For most brain tumours, the extent of surgical resection is extremely important, changes the prognosis radically and extends the event free survival. However, most infiltrative tumours are not recognizable under a surgical microscope from normal brain tissue, and therefore when the main tumour has been removed, the surgeon has currently no indication whether there is microscopic tumour left in place or not. In this project, two novel, research grade SD-OCT systems operating at 800nm and 1300nm were used to image healthy human brain tissue, and samples from a variety of brain tumors, to determine if tumors can be distinguished from healthy brain tissue in OCT tomograms. The 800nm SD-OCT provides 0.95 μ m axial and ~2 μ m lateral resolution and penetration depth of ~500 μ m in brain tissue. The 1300nm SD-OCT system provides 2 μ m axial and ~3 μ m lateral resolution and penetration depth > 1000 μ m in brain tissue. The high spatial resolution offered by the SD-OCT systems allowed for visualization of morphological features such as neuronal nuclei, myelinated fibers and CNS vasculature. The OCT tomograms were compared to histological cross-sections of the imaged brain tissue samples. Further development of fiberoptic imaging probes would permit the use of the high resolution OCT technology intra-operatively for in-vivo imaging of surgical beds of brain tumors.

9305-105, Session 2

Cadaveric in-situ testing of optical coherence tomography system based skull base surgery guidance

Cuiru Sun, Ryerson Univ. (Canada); Osaama H. Khan, Sunnybrook Health Sciences Ctr. (Canada); Peter Siegler,

Jamil Jivraj, Ronnie Wong, Barry Vuong, Ryerson Univ. (Canada); Victor X. D. Yang M.D., Ryerson Univ. (Canada) and Sunnybrook Health Sciences Ctr. (Canada) and Univ. of Toronto (Canada)

Optical Coherence Tomography (OCT) has extensive potential for producing clinical impact in the field of neurological diseases. A neurosurgical OCT hand-held forward viewing probe in Bayonet shape has been developed. In this study, we test the feasibility of integrating this imaging probe with modern navigation technology for guidance and monitoring of skull base surgery. Cadaver heads were used to simulate relevant surgical approaches for treatment of sellar, parasellar and skull base pathology. A high-resolution 3D CT scan was performed on the cadaver head to provide baseline data for navigation. The cadaver head was mounted on existing 3- or 4-point fixation systems. Tracking markers were attached to the OCT probe and the surgeon-probe-OCT interface was calibrated. 2D OCT images were shown in real time together with the optical tracking images to the surgeon during surgery. The intraoperative video and multimodality imaging data set, consisting of real time OCT images, OCT probe location registered to neurosurgical navigation were assessed. The integration of intraoperative OCT imaging with navigation technology provides the surgeon with updated image information, which is important to deal with tissue shifts and deformations during surgery. Preliminary results demonstrate that the clinical neurosurgical navigation system can provide the hand held OCT probe gross anatomical localization. The near-histological imaging resolution of intraoperative OCT can improve the identification of microstructural/morphology differences. The OCT imaging data, combined with the neurosurgical navigation tracking has the potential to improve image interpretation, precision and accuracy of the therapeutic procedure.

9305-106, Session 2

Characterizing the significance of multiple enzyme-bound formulations of NADH and their role in cerebral metabolism using 2-Photon fluorescence lifetime microscopy

Mohammad A. Yaseen, Sava Sakad?ic, Buyin Fu, Weicheng Wu, David A. Boas, Massachusetts General Hospital (United States)

Although fluorescence lifetime microscopy (FLIM) of the intrinsic fluorophore NADH is a potentially powerful tool for investigating subtle changes in metabolic activity with high resolution, the technique requires further characterization and validation. Using FLIM, the time-resolved profile of NADH autofluorescence can be separated into distinct components, or species, with distinct lifetimes. These species reportedly represent different enzyme-bound formulations of NADH; however, the roles of these species in energy metabolism remain poorly understood. Here we explore the significance of these NADH species for characterizing cerebral metabolism in vivo. Using time-correlated single photon counting (TCSPC) equipment incorporated in a custom-built multimodal imaging system, we collected 2-photon based measurements of NADH FLIM in vivo from the cerebral cortices of rats before and after local administration of chemical modulators of glycolysis, the Krebs' cycle, or oxidative phosphorylation. Multi-exponential fits for NADH fluorescence lifetimes reveal that manipulations of the Krebs' cycle and oxidative phosphorylation induce notable changes in the NADH intensity and the relative proportions of NADH species. Metabolic manipulations with greater physiological relevance will also be tested for comparison. The relative proportions of NADH species could yield more comprehensive information than NADH intensity measurements, potentially indicating inhibition of different metabolic pathways. NADH FLIM measurements could ultimately lead to a deeper understanding of cerebral energetics and its pathology-related alterations. Such knowledge will aid development of therapeutic strategies for neurodegenerative diseases such as Alzheimer's Disease, Parkinson's disease, and stroke.

**Conference 9305A: Optical Techniques in
Neurosurgery, Brain Imaging, and Neurobiology**

9305-107, Session 2

**Birefringence based assessment of
neuritic plaques in Alzheimer's disease by
polarization sensitive OCT**

 Bernhard Baumann, Adelheid Wöhrer, Christian
Mitter, Erich Götzinger, Gabor G. Kovacs, Christoph K.
Hitzenberger, Medizinische Univ. Wien (Austria)

Alzheimer's disease (AD) is the most common form of dementia. AD is hallmarked by degeneration of neurons in the brain preceded by the formation of intracellular neurofibrillary tangles and the formation of extracellular senile plaques composed of amyloid-beta (A β). A β plaques are birefringent due to the parallel arrangement of amyloid fibrils. Polarization sensitive optical coherence tomography (PS-OCT) enables 3D structural imaging with micrometer scale resolution based on tissue reflectivity plus additional contrast based on tissue polarization properties such as birefringence or depolarization. Here, we present PS-OCT for imaging neuritic A β plaques based on their birefringent properties. A spectral domain PS-OCT system operating at 840 nm and based on polarization-maintaining fiber optics was used in a scanning confocal microscopy configuration. Unstained tissue blocks as well as thin, deparaffinized histological sections of formalin-fixed, post-mortem tissue from advanced-stage AD patients were imaged. For correlation with histomorphology, Congo red stained sections of corresponding tissue blocks were investigated. Two- and three-dimensional PS-OCT images of reflectivity, phase retardation and optic axis orientation were computed. Cortical grey matter appeared polarization preserving, whereas neuritic plaques exhibited increased retardation. These results showcase the ability of PS-OCT to assess neuritic plaques in AD based on their intrinsic birefringent properties.

9305-108, Session 2

**Spinal cord deformation due to nozzle
gas flow effects using optical coherence
tomography**

 Ronnie Wong, Jamil Jivraj, Barry Vuong, Joel Ramjist,
Cuiru Sun, Yize Huang, Victor X. D. Yang M.D., Ryerson
Univ. (Canada)

Gas assisted laser machining of materials is a common practice in the manufacturing industry. The use of inert gases reduces the likelihood of flare-ups when cutting flammable material and also assists in blowing away debris from the ablated region. Even though this method is well established in manufacturing and processing of hard materials, this is not the case in the context of neurosurgery. Laser cutting of osseous tissue can benefit from gas-assist. The goal is to cut through osseous tissue without damaging the underlying neural tissue. A large exit pressure could cause a destructive mechanical deformation to the dura and spinal cord tissue.

In this study we acquire volumetric flow rates and exit pressures through a gas nozzle on the dura and spinal cord regions. Gas flow effects are imaged using optical coherence tomography (OCT) to determine acceptable thresholds of deformation. Computational fluid dynamics was simulated to verify the pressure and deformation measurements made by OCT. A comparison is given on the effects of gas flow over the spinal cord, with and without dura.

9305-109, Session 3

**Introduction to the sessions on photonics
in the neurosurgical OR and beyond**

 Henry Hirschberg M.D., Beckman Laser Institute and
Medical Clinic (United States)

Opportunities for lasers and optical techniques in neurosurgery exist both in the OR and as post operative treatment. Some of the unmet needs in treatment of brain tumors could be covered by new strategies employing photonics. This introductory talk will try to put the papers presented in this session in a clinical perspective. Emphasis will be placed on operative as well as post operative modalities aimed at sterilizing the surgical resection cavity to avoid tumor recurrence.

9305-110, Session 3

**Macrophage mediated PCI enhanced gene-
directed enzyme pro-drug therapy**

 Catherine E. Christie M.D., Genesis Zamora, Beckman
Laser Institute and Medical Clinic (United States); Kristian
Berg, The Norwegian Radium Hospital (Norway); Steen J.
Madsen, Univ. of Nevada, Las Vegas (United States); Henry
Hirschberg M.D., Beckman Laser Institute and Medical
Clinic (United States)

Photochemical internalization (PCI) is a photodynamic therapy-based approach for improving the delivery of macromolecules and genes into the cell cytosol. Prodrug activating gene therapy (suicide gene therapy) employing the transduction of the E. coli cytosine deaminase (CD) gene into tumor cells, is a promising method. Expression of this gene within the target cell produces an enzyme that converts the nontoxic prodrug, 5-FC, to the toxic metabolite, 5-fluorouracil (5-FU). 5-FC may be particularly suitable for brain tumors, because it can readily cross the blood-brain barrier (BBB). In addition the bystander effect, where activated drug is exported from the transfected cancer cells into the tumor microenvironment, plays an important role by inhibiting growth of adjacent tumor cells.

Tumor-associated macrophages are frequently found in and around glioblastomas. Monocytes or macrophages (Ma) loaded with anti cancer agents could therefore be used to target tumors via local synthesis of chemo attractive factors.

The basic concept of the experiments reported here is ; 1)PCI enhanced transfection of the CD gene into Ma, 2) Infiltration of the Ma into tumors, 3) Application of 5-FC which will be converted into 5-FU in the Ma 4) 5-FU is exported from the Ma, inhibiting the growth of the adjacent tumor cells via the bystander effect.

All studies were conducted in vitro using hybrid multitumor/Ma spheroids using rat F98 glioma cells and rat and murine macrophages . The introduction of subpopulations of CD transfected cells into the F98 tumor spheroids inhibited the growth of the spheroids in the presence but not the absence of 5-FC.

9305-111, Session 3

**Interstitial photodynamic therapy and
glioblastoma: light fractionation study on
preclinical model: preliminary results**

 Henri-Arthur Leroy, Lille Univ. Hospital (France) and
INSERM U 703 "ONCO THAI" (France); Maximilien
Vermandel, INSERM (France); Marie-Charlotte Tetard,
DEPARTMENT OF NEUROSURGERY, LILLE UNIVERSITY
HOSPITAL (France) and INSERM U 703 (France); Jean-
Paul Lejeune M.D., Univ. des Sciences et Technologies de
Lille (France); Serge R. Mordon, INSERM (France); Nicolas
Reyns M.D., Lille Univ. Hospital (France) and INSERM
(France)

Background

Glioblastoma is a high-grade cerebral tumor with local recurrence and poor

Conference 9305A: Optical Techniques in Neurosurgery, Brain Imaging, and Neurobiology

outcome. Photodynamic therapy (PDT) is a local treatment based on the light activation of a photosensitizer (PS) in the presence of oxygen to form cytotoxic species. Fractionation of light delivery may enhance treatment efficiency restoring tissue oxygenation.

Objective

To evaluate the increased efficiency of light fractionation and to determine a radio-histological correlation using diffusion and perfusion MRI sequences.

Materials and Methods

Forty "Nude" rats were grafted with human U87 cells into the right putamen. After PS precursor intake (5-ALA), an optic fiber was introduced into the tumor. The rats were randomized in three groups, first one without illumination, second one with monofractionated illumination with a pause of 150 seconds after 20% of power delivered and the third one with multifractionated light. Treatment effects were assessed with early MRI. The animals were finally sacrificed to perform brain histology.

Results

On MRI, we observed a central tumor necrosis, more important with multifractionated PDT. Diffusion was elevated in the middle of the tumor in treated animals, especially in multifractionated group. Regarding perfusion, it decreased around the treatment site, more markedly in multifractionated group. Histology confirmed our MRI observations, with a more extensive necrosis and a rarified angiogenic network in the treatment area after multifractionated PDT. However, we observed neovascularization in the peripheral ring after multifractionated PDT.

Conclusion

The multifractionated interstitial PDT induced more tumoral necrosis with an inner antiangiogenic effect. Diffusion and perfusion were able to predict the histological lesions.

9305-112, Session 3

Efficacy of combined photothermal therapy and chemotherapeutic drugs

Steen J. Madsen, En-Chung Shih, Univ. of Nevada, Las Vegas (United States); Henry Hirschberg M.D., Beckman Laser Institute and Medical Clinic, Univ. of California, Irvine (United States)

Hyperthermia has been shown to enhance the effects of chemotherapeutic agents in a wide variety of cancers. The purpose of this study was to investigate the combined effects of a number of commonly used chemotherapeutic drugs (bleomycin, doxorubicin and cisplatin) with photothermal therapy (PTT)-induced hyperthermia. PTT was accomplished via near infra-red (NIR) irradiation of gold-silica nanoshells (AuNS).

All studies were conducted in vitro using a human head and neck squamous cell carcinoma line (FaDu). Rat alveolar macrophages (Ma) were used to deliver the AuNS. Ma were incubated with AuNS for 24 h. Thereafter, 1000 AuNS-loaded Ma (MaNS) were combined with 2000 FaDu cells in each well of a 48 well plate and the plate was placed in an incubator for 12 h. Thereafter, the chemotherapy drug was added to the wells and the plate was placed in an incubator for 24 h. Immediately following incubation, the plate was placed in another incubator in order to maintain physiological conditions during NIR laser irradiation. Each well was irradiated with an 810 nm diode laser coupled to an optical fiber (3 mm beam dia.; 7 W cm⁻² irradiance; 5 min. irradiation time). Controls consisted of drug-only, PTT-only Ma-only and MaNS-only groups. In all cases, cells were incubated for five days following treatment and then subjected to a colorimetric cell proliferation assay (MTS) to determine treatment efficacy.

A synergistic effect was observed for the combination of PTT and cisplatin while additive effects were found for PTT + bleomycin and PTT + doxorubicin.

9305-113, Session 3

Femtosecond laser-induced attachment of single neurons

Nir Katchinskiy, Indrani Dutta, Helly R. Goetz, Roseline Godbout, Abdulhakem Y. Elezzabi, Univ. of Alberta (Canada)

Neuronal injury may cause an irreversible damage to the cellular, organ and organism's function. There are multiple etiologies for neuronal injury including trauma, infection, inflammation, immune mediated disorders, toxins and hereditary conditions. It is of paramount importance to have a precise mean to selectively connect specific axons to neuron cell body. Such scientific tool will open up doorways to new research frontiers in neurology, cell biology, biochemistry, and electrophysiology. Connecting neurons, before or right after injury, enables the preservation of the viability of the neural network and thus allowing complex pathophysiological processes, such as neurogenesis, Wallerian degeneration, segmental demyelination, and axonal degeneration to be further understood. To date, experimental work on spinal cord injury repair has been carried out with only partial success. Here, we present a technique for neuron connection, using femtosecond laser pulses, while maintaining cellular viability. This technique is an effective neuronal connection tools as it allows to select single cells for isolation, connection, and cutting. The technique is also shown to be universal and applicable to multiple cell types and their media. Selected neurons for connection were identified, isolated and brought into contact using an optical tweezer such that the protruding axon of one neuron touches another neuron's soma. Then, femtosecond laser pulses were delivered to the axon and cell soma connection point in order to induce an attachment. To validate that a connection was achieved, one of the neurons was moved using optical tweezer, and it was inspected that all neurons followed a corresponding path.

9305-115, Session 4

A neurosurgical guidance spectroscopic probe system for combined single-point detection of intrinsic fluorescence, diffuse reflectance and inelastic scattering

Jeanne Mercier, Ecole Polytechnique de Montréal (Canada); Michael Jermyn, Ecole Polytechnique de Montréal (Canada) and Brain Tumour Research Ctr., Montreal Neurological Institute and Hospital, McGill Univ. (Canada); Kelvin Mok, Brain Tumour Research Ctr., Montreal Neurological Institute and Hospital, McGill Univ. (Canada); Joannie Desroches, McGill Univ. (Canada); Cedric Lemieux-Leduc, Karl St-Arnaud, Julien Pichette, Ecole Polytechnique de Montréal (Canada); Marie-Christine Guiot, McGill Univ. (Canada); Kevin Petrecca, Brain Tumor Research Ctr., Montreal Neurological Institute and Hospital, McGill Univ. (Canada); Frédéric Leblond, Ecole Polytechnique de Montréal (Canada)

Our previous in humans work has demonstrated that single-point Raman spectroscopy can detect brain cancer invasions for grade 2 to 4 gliomas with accuracy, sensitivity, and specificity all greater than 90%. We are now investigating the combination of Raman spectroscopy with the optical contrast from intrinsic fluorescence and diffuse reflectance to further improve the intraoperative detection of cancer cells, especially in invasive areas beyond what magnetic resonance imaging can detect. Invasion occurs as a gradient of cancer cells extending from the main cancer mass into the normal tissue, and is the main cause of glioma recurrences. By minimizing the volume of the residual tumour during surgery, and by preserving as much normal brain as possible, our system could significantly improve the

Conference 9305A: Optical Techniques in Neurosurgery, Brain Imaging, and Neurobiology

progression-free and overall survival of patients.

A trimodal fiber optics hand-held probe system was developed and a detailed evaluation is presented in terms of calibration procedure, detection sensitivity and quantification of intrinsic tissue fluorescence. Fluorescence and diffuse reflectance spectra are detected by collecting the re-emitted light following brain tissue excitation with 365 nm, 405 nm and 455 nm light-emitting diodes, and a broadband light, respectively. Also, the results of a preliminary study in humans assessing the added diagnostic value of intrinsic fluorescence and diffuse reflectance with Raman spectroscopy are presented. Tissue classification differentiating between normal, low density cancer invasion, and dense cancer is achieved using a machine learning algorithm based on histopathology analysis of samples collected at the surgical cavity location where the measurements are made.

9305-116, Session 4

Characterization of a sub-diffuse optical spectroscopy system to guide brain needle biopsies

Andreanne Goyette, Julien Pichette, Marie-Andrée Tremblay, Audrey Laurence, Ecole Polytechnique de Montréal (Canada); Michael Jermyn, McGill Univ. (Canada); Wendy-Julie Madore, Mathias Strupler, Caroline Boudoux, Ecole Polytechnique de Montréal (Canada); Brian C. Wilson, Ontario Cancer Institute (Canada); Frédéric Leblond, Ecole Polytechnique de Montréal (Canada)

Brain needle biopsies are performed to sample tissues in order to get more pathological information about a lesion (e.g. brain tumor) than what is available with conventional imaging systems. The decision about the best course of treatment for the patient, possibly including surgical resection, is guided by these results. One of the main risks associated with the standard of care procedure is hemorrhaging due to clipping blood vessels during tissue extraction. Moreover, misdiagnosis can occur when the sample is collected in an area not representative of the pathology. To address these issues, we present an innovative device integrating a sub-diffuse optical tomography technique to detect blood vessels and a spectroscopic technique detecting aminolevulinic acid induced protoporphyrin IX fluorescence, thus mitigating biopsies related risks and improving the diagnostic yield.

This integrated optical spectroscopy system uses diffuse reflectance signals to perform a 360-degree reconstruction of the tissue adjacent to the biopsy needle. This reconstruction is based on the optical contrast associated with hemoglobin light absorption, hence allowing for localization of blood vessels. A detailed sensitivity analysis of the imaging system is presented using liquid phantoms with optical properties similar to those of normal brain. The sensitivity is evaluated in terms of the ability to detect and image blood vessels distributions with a range of sizes, optical contrasts and relative positions with respect to the probe. Furthermore, a comparison of the experimental data with Monte Carlo based light transport simulations is presented allowing to assess the overall performance and reliability of the system.

9305-118, Session 4

Video rate high definition near infra red (NIR) Intra-operative imaging of brain tumors using BLZ-100

Pramod V. Butte, Adam Mamelak M.D., David S. Kittle, Cedars-Sinai Medical Ctr. (United States); Stacey Hansen, Julie Novak, Blaze Bioscience, Inc. (United States); Keith L. Black M.D., Cedars-Sinai Medical Ctr. (United States)

There has been great enthusiasm regarding the use of fluorescent agents

bound to a tumor targeting moiety such as antibody or a peptide to identify specific tumors. Developing instrumentation which can detect far smaller amounts of fluorescent dye to aid the surgeon to detect and identify these tumors intra-operatively has seen much interest in recent years. Current NIR imaging systems are designed to image blood vessels using high concentrations of a common dye, indocyanine green (ICG). Latest developments in tumor markers attached with NIR dyes require newer, more sensitive imaging systems with high resolution in order to guide surgical resection. We have built a clinical, fluorescence image-guided surgery system (SIRIS: Synchronized InfraRed Imaging System) aimed at overcoming the limitations of current systems. SIRIS is a basic, single sensor solution which uses alternate excitation and illumination, capable of capturing both visible (RGB) and NIR fluorescence images and displaying them as a full HD resolution video at 60 frames per sec. We present our data on the performance of the imaging system as a surgical guidance tool for tumor resection. In this report we detail the use of SIRIS to image induced brain tumors in mice and spontaneous tumors in canines tagged with Chlorotoxin conjugated ICG dye (BLZ-100, Blaze Bioscience Inc.).

9305-119, Session 4

Real-time, quantitative fluorescence imaging using single snapshot optical properties imaging for neurosurgical guidance

Pablo A. Valdes Quevedo, Brigham and Women's Hospital (United States); Joseph Angelo, Sylvain Gioux, Beth Israel Deaconess Medical Ctr. (United States)

Extent of tumor resection (EOR) is a key guiding principle in tumor surgery. Fluorescence imaging has been used as a surgical adjunct in neurosurgery and oncologic surgery to improve EOR. Current fluorescence image guided surgery provides subjective, raw assessments of tissue fluorescence which do not account for the heterogeneous attenuation effects of tissue optical properties on fluorescence excitation and emission, thus making it a non-quantitative technique and potentially providing inaccurate assessments of fluorescent tumor biomarkers. Recently, quantitative fluorescence techniques using point probe systems in neurosurgery have shown a significant increase in diagnostic performance by providing objective assessments of the tissue fluorescence using a tissue attenuating algorithm and data collection scheme for estimation of the intrinsic or quantitative fluorescence in tissue. In this work we present a novel imaging system, technique and algorithm that performs real time quantitative fluorescence imaging for surgical guidance using Single Snapshot Optical Properties (SSOP) imaging. We performed phantom studies to validate the quantitative capabilities of the technique and in vivo animal experiments to demonstrate its intraoperative feasibility. Maps of tissue optical properties were acquired in real time using SSOP and used to calculate the quantitative fluorescence. Overall, this work introduces a novel real-time quantitative fluorescence imaging method capable of being used intraoperatively for neurosurgical guidance.

9305-120, Session 5

Simultaneous imaging of near-infrared diffuse reflectance and blood flow for a rat stroke model: pathophysiology analysis using light scattering signals

Satoko Kawauchi, Shunichi Sato, National Defense Medical College (Japan); Izumi Nishidate, Tokyo Univ. of Agriculture and Technology (Japan); Hiroshi Nawashiro, Tokorozawa Central Hospital (Japan); Toshiya Takemura, National Defense Medical College (Japan)

**Conference 9305A: Optical Techniques in
Neurosurgery, Brain Imaging, and Neurobiology**

To understand the pathophysiology of ischemic stroke, in vivo imaging of brain tissue viability and the related spreading depolarization is crucial. For this purpose, light-scattering signal, which is sensitive to cellular/subcellular structural integrity, is a potential indicator. We previously performed near-infrared (NIR) diffuse reflectance imaging for a rat stroke model and observed increased light scattering in and around the ischemic region, which was attributable to progression of infarction. Wave-like scattering changes observed around the ischemic region reflected peri-infarct depolarizations (PIDs), which could be coupled with metabolic disturbance. However, the implications of the scattering signal changes were not fully understood. In this study, we performed simultaneous imaging of NIR diffuse reflectance and blood flow based on laser speckle contrast for a rat middle cerebral artery (MCA) occlusion model. After occluding the left MCA, NIR reflectance (scattering signal) increased around the rim of the region that showed a decreased blood flow (BF), where PIDs occurred with a local BF decrease. The local BF decrease can be associated with vasoconstriction due to the PIDs, which may cause morphological alteration in the cells due to metabolic disturbance, resulting in the scattering increase. In the outside of the region showing the decreased BF, on the other hand, we observed a large BF increase, which would be associated with collateral circulation. However, there was no clear increase in the scattering due to the increased number of blood cells. These findings indicate the usefulness of light scattering signals for detailed observation of the pathophysiology of ischemic stroke.

Manabu Sato, Yamagata Univ. (Japan)

Diffuse reflectance spectroscopy using fiber optic probe is one of most promising technique for evaluating optical properties of biological tissue. We investigated a new method determining the reduced scattering coefficients μ_s' , the absorption coefficients μ_a , and tissue oxygen saturation StO_2 of in vivo brain tissue using single reflectance fiber probe with two source-collector geometries. In the present study, we performed in vivo recordings of diffuse reflectance spectra and the electrophysiological signals for exposed brain of rats during normoxia, hypoxia, and anoxia. The time courses of μ_a in the range from 500 to 584 nm and StO_2 indicated the hemodynamic change in cerebral cortex. Time courses of μ_s' are well correlated with those of μ_a in the range from 530 to 570 nm, which also reflect the scattering by red blood cells. On the other hand, a fast decrease in μ_s' at 800 nm were observed after the respiratory arrest and it synchronized with the negative deflection of the extracellular DC potential so-called anoxic depolarization. It is said that the DC shift coincident with a rise in extracellular potassium and can evoke cell deformation generated by water movement between intracellular and extracellular compartments, and hence the light scattering by tissue. Therefore, the increase in μ_s' at 800 nm after the respiratory arrest is indicative of changes in light scattering by tissue. The results in this study indicate potential of the method to evaluate the pathophysiological conditions and loss of tissue viability in brain tissue.

9305-121, Session 5

Hemodynamic and morphologic responses in mouse brain during acute focal head injury by multispectral structured illumination

David Abookasis, Boris Volkov, Ariel Univ. (Israel); Marlon S. Mathews M.D., Univ. of California, Irvine Medical Ctr. (United States)

Multispectral imaging has received significant attention in recent years in medicine as it integrate spectroscopy and imaging analysis to acquire both spatial and spectral information from a sample under test at the same time. In the present study, a multispectral setup based on projection of structured illumination at several near-infrared wavelengths and at different spatial frequencies is applied to quantitatively assess brain function before, during, and after the onset of focal traumatic brain injury in intact mouse brain (n=5). For the production of head injury, we used the weight drop method where weight cylindrical metallic rod falling along a metal tube striking the mouse's head. Structured light was projected onto the scalp surface and diffuse reflected light was recorded by a CCD camera positioned perpendicular to the mouse head. Following data analysis, we were able to concurrently show a series of hemodynamic and morphologic changes over time including higher deoxyhemoglobin, reduction in oxygen saturation, cell swelling, etc., in comparison with baseline measurements. Overall, our results demonstrates the capability of multispectral imaging based structured illumination to detect and map brain tissue optical and physiological properties occurring during brain injury in a simple noninvasive and noncontact manner.

9305-122, Session 5

In vivo estimation of light scattering and absorption properties of rat brain using single reflectance fiber probe during anoxic depolarization

Izumi Nishidate, Keiichiro Yoshida, Tokyo Univ. of Agriculture and Technology (Japan); Satoko Kawauchi, Shunichi Sato, National Defense Medical College (Japan);

9305-123, Session 5

FNIRS-based evaluation of cortical plasticity in children with cerebral palsy undergoing constraint-induced movement therapy

Jianwei Cao, Bilal Khan, Nathan Hervey, Fenghua Tian, The Univ. of Texas at Arlington (United States); Mauricio R. Delgado, Nancy J. Clegg, Linsley Smith, Dahlia Reid, Kirsten Tulchin-Francis, Angela Shierk, Texas Scottish Rite Hospital for Children (United States); Laura Shagman, Duncan MacFarlane, The Univ. of Texas at Dallas (United States); Hanli Liu, George Alexandrakis, The Univ. of Texas at Arlington (United States)

Functional near-infrared spectroscopy (fNIRS) was demonstrated to evaluate sensorimotor cortex plasticity induced in children with hemiplegic cerebral palsy (CP) that underwent constraint-induced movement therapy (CIMT). FNIRS imaging measurements were done in six children with CP (10.4 ± 1.6 years old) by performing a finger-tapping task before, immediately after, and six months after therapy. Measurements were also performed on five age-matched healthy controls (11.0 ± 0.0 years old) at the same time points. Spatial metrics of activation (laterality index and activation area), temporal ones (time-to-peak over duration) and resting-state functional connectivity were tested as potential fNIRS-based biomarkers for assessing the effects of therapy. A shift in the laterality index from ipsilateral/bilateral to contralateral hemisphere, increased total activation area in the injured brain hemisphere and decreased overall connectivity strength between sensorimotor centers immediately after therapy resembled measurements on healthy controls, but relapsed at six months post-therapy. Interestingly, in contrast to all other fNIRS metrics tested, the ratio of activation time-to-peak over activation duration for all sensorimotor centers during finger tapping displayed significant improvements after therapy that persisted six months later. Taken together, these results indicate that although the local temporal hemodynamic response of each sensorimotor center sustained longer term normalization, the interaction between sensorimotor centers only normalized in the short term, but then relapsed. Also, the measured fNIRS-based metrics reflecting changes in sensorimotor network normalization with time had consistent trends with corresponding clinical assessment scores for these subjects.

**Conference 9305A: Optical Techniques in
Neurosurgery, Brain Imaging, and Neurobiology**

9305-124, Session 5

Study of gender-related effects of prefrontal cortex connectivity by using functional optical tomography

Chun-Jung Huang, Chia-Wei Sun, Jung-Chih Chen, Ching-Cheng Chuang, National Chiao Tung Univ. (Taiwan)

The prefrontal cortex (PFC) is thought to play an important role in "higher" brain functions such as personality and emotion that may associated with several gender-related mental disorders. In this study, the gender effects of functional connectivity, cortical lateralization and significantly differences in the PFC were investigated by using resting-state functional optical tomography (fOT) measurement. A total of forty subjects including twenty healthy male and twenty healthy female adults were recruited for this study. In the results, the hemoglobin responses are higher in the male group. Additionally, male group exhibited the stronger connectivity in the PFC regions. In the result of lateralization, leftward dominant was observed in the male group but bilateral dominance in the female group. Finally, the 11 channels of the inferior PFC regions (corresponding to the region of Brodmann area 45) are significant different with spectrum analysis. Our findings suggest that the resting-state fOT method can provide high potential to apply to clinical neuroscience for several gender-related mental disorders diagnosis.

9305-125, Session 5

Assessment of brain functional connectivity by implementing graph theory analysis to atlas-guided diffuse optical tomography

Lin Li, The Univ. of Texas at Arlington (United States); Mary Cazzell, Cook Children's Medical Ctr. (United States); Hanli Liu, The Univ. of Texas at Arlington (United States)

Evidence has accumulated that functional networks throughout the brain are necessary, in particular for higher-level, cognitive functions such as memory, language, attention, and decision-making. Also, many studies have been recently reported to investigate the complex brain networks using graph theory. However, currently no or few report is found to apply graph theory analysis (GTA) to diffuse optical tomography. In this study, we provided a technical strategy that can bridge this gap. First, we segmented functional regions in the brain and obtained respective regions of interest (ROIs) within atlas-guided functional diffuse optical tomography (fDOT). Second, we collected temporal sequence information from fDOT measurement for each ROI and their cross-correlation matrix between each pair of ROIs. Third, we performed GTA and obtained a set of GTA-derived metrics to characterize the complex brain networks. More specifically, with this analysis strategy, we investigated the resting state functional connectivity by monitoring the voxel-wised brain networks in 20 healthy adults (age from 25 to 80 years). Results revealed a significantly different brain network pattern between two age groups (young adults: from 25 to 40 years, elder adults: from 65 to 80 years), which is consistent with a previous study.

9305-114, Session 6

Optomechanical design of a miniaturized intraoperative fluorescence-guided surgical resection camera system

David S. Kittle, Adam Mamelak M.D., Cedars-Sinai Medical Ctr. (United States); Julie Novak, Stacey Hansen, Blaze Bioscience, Inc. (United States); Keith L. Black M.D.,

Pramod V. Butte, Cedars-Sinai Medical Ctr. (United States)

Current NIR imaging systems are designed to image vasculature using high concentrations of a common dye, indocyanine green (ICG). Recent developments in tumor markers conjugated with NIR dyes require newer, more sensitive imaging systems with high resolution in order to guide surgical resection. We report the opto-mechanical design and performance of a clinical, fluorescence image-guided surgery system (SIRIS: Synchronized InfraRed Imaging System) aimed at overcoming the limitations of current systems. The device is designed for wide field, real-time imaging (at 60fps combined NIR+visible display). The imaging system design utilizes a dual light source consisting of visible light and NIR excitation (785nm). The illumination component was designed to adhere with class 1M safety standards. The light is delivered via two separate optical fibers (1mm, 0.22 NA) to a 80 square centimeter surgical field at <0.5mW/cm² for white light and 4.10mW/cm² for the laser excitation with a working distance of 350mm. The unique optomechanical design of the imaging system allows the use of a single camera to capture both visible and NIR fluorescence with high efficiency. The imaging camera (44x30x30mm) uses a sensor (CMOSIS CMV2000, 340 fps, full HD) modified for high sensitivity in both NIR and visible spectrums. We will present our performance data with serial dilutions of ICG along with a newly developed tumor dye (BLZ-100, ICG conjugated peptide). We will demonstrate the sensitivity of the system to detect picomolar concentrations allowing for visualization of submicron sources of fluorescence during surgical resection.

9305-126, Session 6

Evaluation of hemodynamics changes during interventional stent placement using Doppler optical coherence tomography

Barry Vuong, Helen Genis, Joel Ramjist, Jamil Jivraj, Ronnie Wong, Cuiru Sun, Victor X. D. Yang M.D., Ryerson Univ. (Canada)

Carotid atherosclerosis is a critical medical concern that can lead to ischemic stroke. Local hemodynamic patterns have also been associated with the development of atherosclerosis, particularly in regions with disturbed flow patterns such as bifurcations. Traditionally, this disease was treated using carotid endarterectomy, however recently there is an increasing performance of carotid artery stenting due to its minimally invasive nature. It is well known that this interventional technique creates changes in vasculature geometry and hemodynamic patterns due to the interaction of stent struts with arterial lumen, and is associated with complications such as restenosis. Currently, there is no standard imaging technique to evaluate regional hemodynamic patterns found in stented vessels.

Doppler optical coherence tomography (DOCT) provides an opportunity to identify in vivo hemodynamic changes in vasculature using high-resolution imaging. In this study, blood profiles were examined at the bifurcation junction in the internal carotid artery (ICA) in a porcine model following stent deployment. Doppler imaging was further conducted using pulsatile flow in a phantom model, and then compared to computational fluid dynamics (CFD) simulation of a virtual bifurcation to assist with the interpretation of in vivo results.

9305-127, Session 6

Patient specific intracranial aneurysm flow phantom imaging with optical coherence tomography

Barry Vuong, Helen Genis, Joel Ramjist, Jamil Jivraj, Ronnie Wong, Raphael Jakubovic, Ryerson Univ. (Canada); Julia Keith M.D., Sunnybrook Health Sciences

**Conference 9305A: Optical Techniques in
Neurosurgery, Brain Imaging, and Neurobiology**

Ctr. (Canada); Rasmus Kiehl M.D., Univ. Health Network (Canada); Victor X. D. Yang M.D., Ryerson Univ. (Canada)

The most common cause for spontaneous subarachnoid hemorrhage (SAH) is the rupture of an intracranial aneurysm. The factors that attribute to this catastrophic event remain uncertain. The formation, growth and rupture of the intracranial aneurysm could be due to congenital diseases, hypertension, or atherosclerotic disease, which affect the extracellular matrix of the artery wall. In order for the body to compensate, vascular remodelling occurs resulting in hemodynamic changes in the artery wall. Recirculation zones in mature intracranial aneurysm often results in formation of thrombosis in the stagnate regions. Doppler optical coherence tomography (DOCT) has the potential to provide high resolution and high velocity dynamic range of in vivo velocity measurements in the blood vessel of the intracranial aneurysm.

In this study we acquire 3D angiography and extracted the geometry of the patient's artery. Using the volumetric rendering, the patient specific intracranial aneurysm flow phantoms were constructed. Pulsatile flow was coupled to the phantom and DOCT images were acquired. Computational fluid dynamics of the patient specific aneurysm was virtually simulated to verify the DOCT measurements. A stented treatment of the intracranial aneurysm was also recreated in the phantom model. We compare the pre-surgical and post surgical blood flow changes through DOCT.

9305-128, Session 6

Label free, real time visualization of tissue histology at subcellular resolution: a study of primary versus secondary human brain cancer tissues

Carmen Kut, Wenxuan Liang, Gunnstein Hall, Kaisorn Chaichana M.D., Alfredo Quinones-Hinojosa M.D., Xingde Li, The Johns Hopkins Hospital (United States)

Surgery is the primary treatment of brain cancer. Since both complete tumor resection and healthy tissue sparing are paramount in brain tumor surgery, accurate tumor margin identification becomes particularly critical. This study aims to determine if multiphoton microscopy can be used to detect cancer versus non-cancer in real time without the need for staining. **METHODS:** Freshly resected human brain cancer tissues from 8 patients (5 glioma, 3 lung cancer metastases to the brain) were imaged *ex vivo* and label-free with a homebuilt multiphoton microscope with a 780nm excitation wavelength. FAD, NADH and SHG signals were obtained. After imaging, all tissues were processed for histological validation and correlations. **RESULTS:** Label-free multiphoton imaging exhibited clear morphological differences among non-cancer white matter and gray matter, primary brain cancer and secondary brain cancer tissues at subcellular resolution. Our results demonstrated characteristic cancer-specific features including 1) increased angiogenesis and hyperplastic blood vessels in low grade and high grade glioma; 2) fibrovascular core and mucinous tissues in non-small cell lung adenocarcinoma; 3) pleomorphic giant cells in poorly differentiated non-small-cell lung adenocarcinoma; and 4) densely populated oat cells in small cell lung carcinoma. In summary, our results suggest the excellent potential of real-time, label-free multiphoton fluorescence imaging in providing high-resolution histologic information for cancer versus non-cancer regions in the brain, thus confirming the extent of cancer resection during surgery. A systematic study is underway for the intra-operative, *in vivo* detection of cancer versus non-cancer in the brain in mammalian models.

9305-117, Session 7

Accuracy of image-guided surgical navigation using NIR optical tracking

Raphael Jakubovic, Hamza Farooq, Joseph Alarcon, Ryerson Univ. (Canada); Victor X. D. Yang M.D., Ryerson Univ. (Canada) and Div. of Neurosurgery, Sunnybrook

Health Sciences Ctr. (Canada)

Spinal surgery is particularly challenging for surgeons, requiring a high level of expertise and precision without being able to see beyond the surface of the bone. Accurate insertion of pedicle screws is critical considering perforation of the pedicle can result in profound clinical consequences including nerve root, vertebral artery spinal cord injury, neurological deficits, chronic pain, and/or failed back syndrome.

Various navigation systems have been designed to guide pedicle screw fixation. Computed tomography (CT)-based image guided navigation systems increase the accuracy of screw placement allowing for 3-dimensional visualization of the spinal anatomy. Current localization techniques require extensive preparation and introduce spatial variations. Use of near infrared (NIR) optical tracking allows for real-time navigation of the surgery by utilizing the deep photon penetration of light, greatly enhancing the surgeon's ability to visualize beyond the surface of the bone. While the incidence of pedicle screw perforation and complications have been significantly reduced with the introduction of modern navigational technologies, some error exists. Several parameters have been suggested including fiducial localization and registration error, target registration error, and angular deviation. However, many of these techniques quantify error using the pre-operative CT and an intra-operative screenshot without assessing the true screw trajectory.

In this study we quantified *in-vivo* error by comparing the true screw trajectory to the intra-operative trajectory. Pre- and post- operative CT as well as intra-operative screenshots were obtained for a cohort of patients undergoing spinal surgery. We quantified entry point error and angular deviation in the axial and sagittal planes.

9305-129, Session PSun

3D surgical microscope based on optical coherence tomography for microsurgery on the brain

Youjin Ahn, Sungwon Shin, Ulsan National Institute of Science and Technology (Korea, Republic of); Pil Un Kim, Oz-tec Co., Ltd. (Korea, Republic of); Hwakyoung Shin, Pusan National Univ. (Korea, Republic of); Jeehyun Kim, Kyungpook National Univ. (Korea, Republic of); Woonggyu Jung, Ulsan National Institute of Science and Technology (Korea, Republic of)

In the past decade, surgical microscope has been used as indispensable tool to observe the micro-structure in the brain surgery. Conventional surgical microscope provides high resolution tissue morphology from the top view, but visualizes only surface structure in narrow field of view. Thus, the operation to find uncertain structure underneath the surface is very challenged under the microscope, which often leads to medical malpractice. In particular, microsurgery on the brain has more challenges compared to other organs, because it deals with the complicated biological components such as vascular and nervous structure.

Here, we suggested advanced optical imaging tool for microsurgery on the brain. Our system is based on OCT (Optical Coherence Tomography) which provides high-resolution cross-sectional image in real-time, non-invasively. This system is made up of four major modular parts: (1) surgical microscope, (2) surface recording system, (3) OCT image acquisition unit, and (4) beam projection module. The 3D surgical OCT system simultaneously acquired OCT image and microscopic view by sharing the same optical path. The main function of integrated beam projector is to duplicate OCT image through the eyepieces which avoid surgeons to look at the monitoring screen while operation.

To evaluate the imaging capability of the system, we used our device in microsurgical resection of brain tumor and intracranial hematoma in mouse model. Through our research, it is believed that advanced microscope is promising tool for intraoperative brain imaging as well as contributes to accurate microsurgical operation in future.

Conference 9305B: Neurophotonics

Monday - Tuesday 9-10 February 2015

Part of Proceedings of SPIE Vol. 9305 Optical Techniques in Neurosurgery, Neurophotonics, and Optogenetics II

9305-200, Session 1

Optical inhibition for rapid and reversible block of axonal sub-populations (*Invited Paper*)

Emilie H. Lothet, Yves T. Wang, Niloy Bhadra, Kevin L. Kilgore, Case Western Reserve Univ. (United States); E. Duco Jansen, Vanderbilt Univ. (United States); Hillel J. Chiel, Michael W. Jenkins, Case Western Reserve Univ. (United States)

Treatments for chronic pain using drugs or surgery lack real-time control. Kilohertz high frequency alternating current to block neurons is a new alternative, and we previously demonstrated that the significant onset response could be abolished with optical inhibition. Here, we show that optical inhibition alone can block all or subpopulations of unmyelinated axons.

Suction electrodes were placed for stimulation and recording on each end of an unmyelinated pleural-abdominal nerve from *Aplysia californica*, with a 600- μm optical fiber in between, delivering 200 Hz 200- μs pulses. Block was repeatably established with no detectable change in nerve function afterwards. At threshold for optical inhibition, small slow fibers were blocked more quickly than large fast fibers, after which all fibers were blocked. Small slow fibers could also be stably blocked without affecting large fast fibers. Additionally, at 4% duty cycle, block threshold was not significantly different between 25 and 800 Hz. At 2 Hz, the optical inhibition threshold increased, and block could be established in approximately 30 ms. Furthermore, raising bath temperature reduced the power needed for optical inhibition. At higher bath temperatures, block could be induced without optical input. These results suggest that the mechanism of optical inhibition may be due to increases in temperature.

Optical inhibition provides rapid neural block and enables small slow fibers to be blocked first, contrary to the order produced by electrical block. Since sensory neurons are smaller than motor neurons, this may provide a treatment for chronic pain without affecting motor control.

9305-201, Session 1

Mapping neuronal microcircuits with super-resolution localization microscopy: challenges and our recent progresses (*Invited Paper*)

Zhen-Li Huang, Shaoqun Zeng, Yina Wang, Zhe Hu, Lingxi Zhao, Yue Du, Britton Chance Ctr. for Biomedical Photonics (China)

Fluorescence microscopy has become an important tool in various fields of neuroscience. However, it is not sufficient to use conventional fluorescence microscopy to characterize the ultrastructure of several core signaling compartments of neurons and neuronal circuits—presynaptic active zones, postsynaptic densities and dendritic spines. On the other hand, with the advent and rapid development of super-resolution microscopy and fluorescence probes, it is now possible to investigate the capabilities of super-resolution microscopy in neuroscience. Here we introduce the potentials and limitations of mapping neuronal microcircuits with a major super-resolution microscopy technique called super-resolution localization microscopy. We then present our recent studies in super-resolution localization microscopy imaging of brain tissues, with a special emphasize on the labeling strategy.

9305-202, Session 1

Visualization and neuronal cell targeting during electrophysiological recordings facilitated by quantum dots

Lauren D Field, US Naval Research Laboratory (United States); Bertalan K. Andrásfalvy, Hungarian Academy of Sciences (Hungary); Gregorio L. Galíñanes, Daniel Huber, Univ. de Genève (Switzerland); Mladen Barbic, Janelia Farm Research Campus (United States); John J. Macklin, Howard Hughes Medical Institute (United States) and Janelia Farm Research Campus (United States); Kimihiro Susumu, James B. Delehanty III, Alan L. Huston, U.S. Naval Research Lab. (United States); Judit K. Makara, Hungarian Academy of Sciences (Hungary); Igor L. Medintz, U.S. Naval Research Lab. (United States)

The simultaneous visualization, identification and targeting of neurons during patch clamp-mediated electrophysiological recordings is a basic technique in neuroscience, yet it is often complicated by the inability to visualize the pipette tip, particularly in deep brain tissue. Here we demonstrate a novel approach in which fluorescent quantum dot probes are used to coat pipettes prior to their use. The strong two-photon absorption cross sections of the quantum dots afford robust contrast at significantly deeper penetration depths than current methods allow. We demonstrate the utility of this technique in multiple recording formats both in vitro and in vivo where imaging of the pipettes is achieved at remarkable depths (up to 800 microns). Notably, minimal perturbation of cellular physiology is observed over the hours-long time course of neuronal recordings. We discuss our results within the context of the role that quantum dot nanoprobe may play in understanding neuronal cell physiology.

9305-203, Session 1

Abnormal hemodynamic response to forepaw stimulation in rat brain after cocaine injection

Wei Chen, Kicheon Park, Jeonghun Choi, Peng Liu, Yingtian Pan, Congwu Du, Stony Brook Univ. (United States)

Simultaneous measurement of hemodynamics is of great importance to evaluate the brain functional changes induced by brain diseases such as drug addiction. Previously, we developed a multimodal-imaging platform (OFI) which combined laser speckle contrast imaging with multi-wavelength imaging to simultaneously characterize the changes in cerebral blood flow (CBF), oxygenated- and deoxygenated- hemoglobin (HbO and HbR) from animal brain. Recently, we improved our OFI system that enables detection of hemodynamic changes in response to electrical forepaw-stimulation to study the potential brain activity changes by cocaine. The improvement includes 1) high sensitivity to detect the cortical response to single electrical forepaw-stimulation; 2) high temporal resolution (i.e., 16Hz/channel) to resolve time-sensitive variations in drug-delivery study; 3) high spatial resolution to separate the stimulation-evoked hemodynamic changes in vascular compartments from those in tissue. The system was validated by imaging the hemodynamic responses to the forepaw-stimulations in the somatosensory cortex of cocaine-treated rats. The stimulations and acquisitions were conducted every 2 minutes till 40 minutes in total (i.e., 10 minutes before and 30 minutes after cocaine challenge). Our results show that the HbO response decreased first (at -4 minutes) followed by the

decrease of HbR response (at -6 minutes) after cocaine administration, and both were not fully recovered during the recording period. Interestingly, while CBF correspondingly decreased at 4 minutes, it partially recovered by 18 minutes after cocaine administration. The results indicate the inhomogeneity of cocaine's effects on vasculature and tissue metabolism, thus demonstrating the unique capability of optical imaging for brain functional studies.

9305-204, Session 1

Optical inhibition in a cardiac developmental model

Yves T. Wang, Andrew M. Rollins, Michael W. Jenkins, Case Western Reserve Univ. (United States)

Controlled alteration of heart rate in tiny embryonic hearts is difficult, but is necessary to study the effects of cardiac functional abnormalities on embryonic development. Previously, we demonstrated that optical stimulation could be applied to achieve 1:1 pacing of quail embryonic hearts at a variety of stages, both in in vivo shell-less cultures and in ex vivo excised hearts. Here, we demonstrate that optical inhibition can also be used in developing hearts.

This study was conducted in excised hearts from 2-day quail embryos and intact 2-day quail embryos in a shell-less culture. Pulses of infrared light were produced by a multi-mode laser at 1878 nm with a fiber core diameter of 600 μm or a single-mode laser at 1465 nm with a 12- μm spot. Various laser locations, frequencies, and duty cycles were tested.

We found that inhibition could be achieved with spatial selectivity with the heart recovering after the applied block. Initiation of action potentials could be stopped when the atrium was illuminated, producing cardiac arrest. Propagation of action potentials could be interrupted when the ventricle was illuminated, producing heart block. Additionally, we determined that diffuse heating of the heart by the pulsed laser light also produced cardiac arrest, supporting an absolute temperature mechanism of conduction block.

Optical inhibition provides a way to interrupt the normal beating of the tiny embryonic heart and can be potentially used to enable imaging of a still heart or combined with optical stimulation to produce various abnormal cardiac activation patterns.

9305-205, Session 2

High-resolution and high-throughput brain connection imaging with chemical activation of GFP fluorescence (*Invited Paper*)

Hanqing Xiong, Xiaohua Lv, Anan Li, Hui Gong, Huazhong Univ. of Science and Technology (China); Qingming Luo, Huazhong Univ. of Science & Technology (China); Shaoqun Zeng, Britton Chance Ctr. for Biomedical Photonics (China) and Huazhong Univ. of Science and Technology (China)

In a cellular phone, the information flow is present in real functional connections. Similarly, in our brains, information is transmitted within and between neural circuits through functional neuronal connections based on axonal projections. Revealing the axonal projection of a single neuron is essential to understand the brain functions, in terms of health and disease. The axon is less than 1 μm in diameter, whereas its projection length may exceed 1 cm. Consequently, tracing a single axon within the centimeter range in three dimensions (3D) is challenging. Here we propose a new optical imaging method to obtain high-resolution brain images with high-throughput, and demonstrated using a thyl-YFP H mouse brain as an example. This method provides a new starting point to image large scale fluorescence-labeled specimen in resin embedding manner.

9305-206, Session 2

GRIN lens based confocal system for deep brain calcium imaging (*Invited Paper*)

Qingchun Guo, Britton Chance Ctr. for Biomedical Photonics, Wuhan National Lab. for Optoelectronics (China) and MoE Key Lab. for Biomedical Photonics, Huazhong Univ. of Science and Technology (China); Qian Liu, Britton Chance Ctr. for Biomedical Photonics (China) and MoE Key Lab. for Biomedical Photonics, Huazhong Univ. of Science and Technology (China); Minmin Luo, National Institute of Biological Sciences (China) and Tsinghua Univ. (China); Ling Fu, Britton Chance Ctr. for Biomedical Photonics (China) and MoE Key Lab. for Biomedical Photonics, Huazhong Univ. of Science and Technology (China)

Neural network activity is accompanied with dynamic transients of calcium ion concentration, which is visible for us by using calcium sensitive dyes or probes. Two-photon microscopy is a quite useful method to detect calcium signal of the superficial brain area of anesthetized or head fixed animals with perfect resolution and contrast. For deep brain calcium signal detection, optical fiber based approaches are usually used, and can be easily constructed for free moving animals. By using a single multi-mode fiber (MMF), calcium signal of a cluster of neurons could be detected with high temporal resolution. To detect the calcium signal of deep brain area with single cell resolution, we developed a laser scanning confocal microscope based on gradient index lens (GRIN lens). By using a resonant scanner for fast axis scan, frame rate of this system can reach 15 frames per second with 512 \times 512 pixels in each frame. This is important to catch the dynamic process of calcium signal transients, and to reduce photo bleaching in long term observation. A 500 μm diameter GRIN lens can be easily implanted into a mouse brain with little injury, which will provide us a perfect 200 μm diameter field of view of the deep region with single cell resolution. The pinhole before the PMT detector can exclude most of the out-of-focus background fluorescence to improve the contrast of the result. This imaging system will be suitable for researches in deep brain area with a good temporal and spatial resolution.

9305-207, Session 2

Laser-acupuncture for autism spectrum disorder a randomized sham controlled trial

Shahzad Anwar M.D., Anwar Shah Trust for Cerebral Palsy & Paralysis (Pakistan)

OBJECTIVES: To evaluate the efficacy, safety, and compliance of laser-acupuncture in children with autism spectrum disorder (ASD). **DESIGN:** Randomized, sham controlled, single blind trial, with blinded evaluation and statistical analysis of results. **SUBJECTS AND INTERVENTIONS:** Children with ASD were randomly separated into two groups one receiving laser-acupuncture (LA) group (n=60) and the other sham laser-acupuncture (SLA) group (n=56) matched by age and severity of autism. The LA group received laser-acupuncture for selected acupoints while the SLA group received sham laser-acupuncture to sham acupoints. A total of 24 LA and SLA sessions over 12 weeks were given. Primary outcome measures included Functional Independence Measure for Children (WeeFIM), Pediatric Evaluation of Disability Inventory (PEDI), Leiter International Performance Scale- Revised (Leiter-R), and Clinical Global Impression- Improvement (CGI-I) scale. Secondary outcome measures consisted of Aberrant Behavior Checklist (ABC), Ritvo-Freeman Real Life Scale (RFRLS), Reynell Developmental Language Scale (RDLS), and a Standardized Parental Report. Data were analyzed by the Mann-Whitney test. **RESULTS:** There were significant improvements in the language comprehension domain of

WeeFIM ($p=0.02$), self-care caregiver assistant domain of PEDI ($p=0.028$), and CGI-I ($p=0.003$) in the LA group compared to the SLA group. As for the parental report, the LA group also showed significantly better social initiation ($p=0.01$), receptive language ($p=0.006$), motor skills ($p=0.034$), coordination ($p=0.07$), and attention span ($p=0.003$). All children with ASD adapted to laser-acupuncture easily. Mild side effects of irritability during laser-acupuncture were observed. **CONCLUSION:** A twelve-week (24 sessions) course of laser-acupuncture is useful to improve specific functions in children with ASD, especially for language comprehension and self-care ability.

9305-208, Session 2

A new versatile clearing method for brain imaging

Irene Costantini, Antonino Paolo Di Giovanna, Anna Letizia Allegra Mascaro, Ludovico Silvestri, European Lab. for Non-linear Spectroscopy, Univ. degli Studi di Firenze (Italy); Marie Caroline Müllenbroich, European Laboratory for Non-linear Spectroscopy, University of Florence (Italy); Leonardo Sacconi, National Institute of Optics, Consiglio Nazionale delle Ricerche (Italy) and European Lab. for Non-linear Spectroscopy, Univ. degli Studi di Firenze (Italy); Francesco S. Pavone, European Lab. for Non-linear Spectroscopy, Univ. degli Studi di Firenze (Italy) and National Institute of Optics, Consiglio Nazionale delle Ricerche (Italy) and Univ. degli Studi di Firenze (Italy)

Light scattering inside biological tissue is a limitation for large volumes imaging with microscopic resolution. Based on refractive index matching, different approaches have been developed to reduce scattering in fixed tissue. High refractive index organic solvents and water-based optical clearing agents, such as Sca/e, SeeDB and CUBIC have been used for optical clearing of entire mouse brain. Although these methods guarantee high transparency and preservation of the fluorescence, though present other non-negligible limitations. Tissue transformation by CLARITY allows high transparency, whole brain immunolabelling and structural and molecular preservation. This method however requires a highly expensive refractive index matching solution limiting practical applicability to large volumes.

In this work we investigate the effectiveness of a water-soluble clearing agent, the 2,2'-thiodiethanol (TDE) to clear mouse and human brain. TDE does not quench the fluorescence signal, is compatible with immunostaining and does not introduce any deformation at sub-cellular level. The not viscous nature of the TDE make it a suitable agent to perform brain slicing during serial two-photon (STP) tomography. In fact, by improving penetration depth it reduces tissue slicing, decreasing the acquisition time and cutting artefacts. TDE can also be used as a refractive index medium for CLARITY. The potential of this method has been explored by imaging blocks of dysplastic human brain transformed with CLARITY, immunostained and cleared with the TDE. This clearing approach significantly expands the application of single and two-photon imaging, providing a new useful method for quantitative morphological analysis of structure in mouse and human brain.

9305-209, Session 3

Volumetric optical coherence tomography of ex vivo mouse brain (Invited Paper)

Woonggyu Jung, Ulsan National Institute of Science and Technology (Korea, Republic of)

Advanced optical imaging techniques developed over the last decade have enabled neuroscientists to better understand how brain works. High sensitivity, high spatial resolution and non-invasive imaging methods

have now become indispensable tools for probing brain functions and dysfunctions at the level of cultured neurons or brain slices. However, acquiring high-resolution brain anatomy over a whole brain remains a difficult challenge due to the effect of light scattering, which limits the penetration depth and lateral resolution. Recently, various optical imaging methods have been introduced to create volumetric neuro-anatomy data of ex vivo mouse brains using physical tissue sectioning or optical clearing. Even though these new approaches present the distinguished whole-brain architecture in various scales, they are still not suitable for use in statistical studies with multiple brains. They typically require long data acquisition period, exorbitant image processing effort and sometimes sophisticated sample preparation such as exogenous labeling of specific neurons or over-expressing genes for imaging contrast.

Optical coherence tomography (OCT) is a potential technique to build volumetric anatomy of mouse brains due to its simplicity, efficiency, robustness, and high-throughput capabilities. OCT is a high-speed, label-free, and deep tissue imaging method and has widely been used in clinical applications for in vivo observation. Despite its inherent advantages, limited efforts have been applied in using OCT for whole brain imaging. This presentation covers the latest work of volumetric mouse brain imaging using OCT. Specifically, the talk will highlight the correlation study to conventional brain imaging techniques as well as tissue clearing.

9305-210, Session 3

In vivo live imaging reveal organization of dendritic golgi outposts

Wei Zhou, Britton Chance Ctr. for Biomedical Photonics, HUST (China)

Golgi complexes (Golgi) are important in the development and function of neurons. Not only are Golgi present in the neuronal soma, they also exist in the dendrites as Golgi outposts. However, it is unclear about structure and function of dendritic golgi outposts. *Drosophila* larvae, which have a transparent epidermis, provide an opportunity to get high-resolution images by confocal microscopy. In vivo imaging for whole animal put a neuron into an intact neuronal circuit; it allow us to study the structure and function of Golgi. Here we show in *Drosophila* that, unlike somal Golgi, the biochemically distinct cis, medial, and trans compartments of Golgi are often disconnected in dendrites in vivo. The Golgi structural protein GM130 is responsible for connecting distinct Golgi compartments in soma and dendritic branch points, and the specific distribution of GM130 determines the compartmental organization of dendritic Golgi in dendritic shafts. We further show that compartmental organization regulates the role of Golgi in centrosomal microtubule growth in dendrites and in dendritic branching. Our study provides insights into the structure and function of dendritic Golgi outposts as well as the regulation of compartmental organization of Golgi in general.

9305-211, Session 3

Hemodynamic low-frequency oscillation reflects resting-state neuronal activity in rodent brain

Wei Chen, Peng Liu, James Li, Yingtian Pan, Congwu Du, Stony Brook Univ. (United States)

Brain functional connectivity is mapped using spontaneous low-frequency oscillations (LFOs) in blood-oxygen-level-dependent (BOLD) signals using fMRI. However, the source of spontaneous BOLD oscillations remains elusive. Specifically the regional hemodynamic LFOs coupling to neuronal activity in the resting-state of brain is rarely examined directly. Here we present an instantaneous-frequency (IF) based method to detect the regional LFOs of cerebral blood flow (CBF) along with the local field potential (LFP) changes of neurons at the resting animal to study neurovascular coupling. CBF and LFP were simultaneously acquired using laser Doppler flowmetry (LDF)

and electroencephalography in the rat's somatosensory cortex with high temporal resolution (i.e., 20 Hz for CBF and 2 kHz for LDF, respectively). Instead of performing fast Fourier transform, a peak-detection algorithm was used to define the LFP activities and CBF spontaneous oscillations in the time domain and the time lapses were used to calculate the IFs of hemodynamic (i.e., CBF) oscillations and neuronal (i.e., LFP) activities. Our results showed that the CBF mostly oscillated at ~ 0.1 Hz with a full-half-bandwidth of {0.08Hz, 0.15Hz}. In addition, the maximal frequency of LFP firings was also approximately at 0.1 Hz, which corresponded to the frequency of CBF oscillation. Interestingly, the CBF followed a linear pass increase along with the LFP activity up to 0.15 Hz ($r=0.93$), and both signals then decreased rapidly as a function of activity frequency. This indicates the spontaneous hemodynamic LFOs were associated with neuronal activities, thus confirming that the hemodynamic oscillation is of neuronal origin.

9305-213, Session 3

Resting-state functional connectivity accessed by spontaneous optical neural, hemodynamic and metabolic signals

Jinling Lu, Britton Chance Ctr. for Biomedical Photonics (China); Bin Li, Qin Huang, Qin Huang, Dong Wen, Sheng Gui, Britton Chance Ctr for Biomedical Photonics (China); Pengcheng Li, Britton Chance Ctr. for Biomedical Photonics (China)

Resting-state functional connectivity (RSFC) of spontaneous hemodynamic fluctuations is widely used to investigate large-scale functional brain networks. Spontaneous electrophysiological signals such as electroencephalograph (EEG), local field potential (LFP), were investigated to understand the neural basis of RSFC in previous studies. However, because of the limited spatial resolution of the recorded electrophysiological signals, there is still a lack of the direct comparison between the spatial pattern of functional connectivity based on high resolution neural activity signal and that based on hemodynamic signals to understand the underlying neural mechanisms of RSFC. Moreover, it is necessary to investigate whether the RSFC based on low-frequency fluctuations of hemodynamic signal can remain to reflect the functional brain networks during those conditions that neurovascular uncoupling may occur. Here we reported the RSFC measured by optical imaging of voltage-sensitive dyes, which could provide a high spatial resolution, within the motor, somatosensory and visual cortexes of mice. Although it is found that RSFC of neural activity of slow cortical potentials (0.1-4 Hz) had a similar spatial pattern of correlation as that of spontaneous hemodynamic signals, the RSFC of neural activity between bilateral cortexes was significant asymmetry, which can also be observed in the functional activation pattern evoked by the sensory stimulations. Furthermore, the coupling between RSFC of slow cortical potentials and that of hemodynamic signals was attenuated by increasing anesthetic levels, and RSFC of hemodynamic signals became discrete in the sensorimotor cortex during deep anesthesia. Our results disclose the RSFC of neural activity with a high spatial resolution and suggest that spontaneous hemodynamic signals are coupled with slow cortical potentials at resting state. The comparison between RSFC of neural activity and that of hemodynamic signals indicates that the slow cortical potentials may have a better localization of RSFC networks than spontaneous hemodynamic signals, especially under deep anesthesia.

9305-214, Session 4

Ultra-high-resolution optical coherence microscopy for nondestructive evaluation of neuronal changes in organotypic brain cultures

Chao Zhou, Lehigh Univ. (United States)

Three-dimensional organotypic brain cultures have been used as effective models for studying different neurological diseases including epilepsy. High-throughput, non-destructive techniques are essential for rapid assessment of disease-related processes such as progressive cell death. In this study, an ultrahigh-resolution optical coherence microscopy (UHR-OCM) system with ~1.5- μm axial resolution and ~2.3- μm transverse resolution was developed to evaluate seizure-induced neuronal injury in organotypic rat hippocampal cultures. The capability of UHR-OCM to visualize cells in neural tissue was confirmed by comparison of UHR-OCM images with confocal immunostained images of the same cultures. In order to evaluate the progression of neuronal injury, UHR-OCM images were obtained from cultures on 7, 14, 21 and 28 days-in-vitro (DIVs). In comparison to DIV 7, statistically significant reductions in 3D cell count and culture thickness from UHR-OCM images were observed on subsequent time points. In cultures treated with kynurenic acid (KYNA), significantly less reduction in cell count and culture thickness was observed compared to control specimens. These results demonstrate the capability of UHR-OCM to perform rapid, label-free, and non-destructive evaluation of neuronal death in organotypic hippocampal cultures. UHR-OCM, in combination with 3D organotypic brain cultures, can potentially prove to be a promising tool for high throughput screening of drugs targeting various brain disorders.

9305-215, Session 4

Enhancing motor performance improvement by personalizing non-invasive cortical stimulation with concurrent functional near-infrared spectroscopy and multi-modal motor measurements (*Invited Paper*)

Bilal Khan, The Univ. of Texas at Arlington (United States); Timea Hodics, The Univ. of Texas Southwestern Medical Ctr. at Dallas (United States); Nathan Hervey, George V. Kondraske, The Univ. of Texas at Arlington (United States); Ann M. Stowe, The Univ. of Texas Southwestern Medical Ctr. at Dallas (United States); George Alexandrakis, The Univ. of Texas at Arlington (United States)

Transcranial direct current stimulation (tDCS) is a non-invasive cortical stimulation technique that can facilitate task-specific plasticity that can improve motor performance. Current tDCS interventions uniformly apply a chosen electrode montage to a subject population without personalizing electrode placement for optimal motor gains. We propose a novel perturbation tDCS (ptDCS) paradigm for determining a personalized electrode montage in which tDCS intervention yields maximal motor performance improvements during stimulation. PtDCS was applied to ten healthy adults and five stroke patients with upper hemiparesis as they performed an isometric wrist flexion task with their non-dominant arm. Simultaneous recordings of torque applied to a stationary handle, muscle activity by electromyography (EMG), and cortical activity by functional near-infrared spectroscopy (fNIRS) during ptDCS helped interpret how cortical activity perturbations by any given electrode montage related to changes in muscle activity and task performance quantified by a Reaction Time (RT) X Error product. PtDCS enabled quantifying the effect on task performance of 20 different electrode pair montages placed over the sensorimotor cortex. Interestingly, the electrode montage maximizing performance in all healthy adults did not match any of the ones being explored in current literature as a means of improving the motor performance of stroke patients. Furthermore, the optimal montage was found to be different in each stroke patient and the resulting motor gains were very significant during stimulation. This study supports the notion that task-specific ptDCS optimization can lend itself to personalizing the rehabilitation of patients with brain injury.

9305-216, Session 4

A portable fNIRS system with eight channels

Juanning Si, Ruirui Zhao, Yujin Zhang, Nianming Zuo, Xin Zhang, Tianzi Jiang, Chinese Academy of Sciences (China)

Abundant study on the hemodynamic response of a brain have brought quite a few advances in technologies of measuring it. The most benefitted is the functional near infrared spectroscopy (fNIRS). There were not only algorithms proposed to process fNIRS signals, but also devices designed for a variety of applications. Because portable fNIRS systems were more advantageous to measure responses than other modalities, several kinds of portable fNIRS systems have been reported. However, they all required a computer to involve to process or display signals. The extra computer increases a cost of a fNIRS system without doubt. What's more noticeable is the space required to locate the computer even for a portable system. It will discount the portability of the fNIRS system. So we designed a self-contained eight channel fNIRS system, which didn't demand a computer to receive data and display data. Instead, the system is centered by an ARM core CPU, which takes charge in organizing data and displaying data on a touch screen.

The system have four sources and four detectors. Each source can emit two near infrared light, 690nm and 830nm. In order to decrease cross talk both between the two lights and between sources, all near infrared light is encoded by distinct frequencies. Because of the frequency-multiplexing technique, we can demodulate two channels for a signal of a detector. The system consists of eight channels to detect hemodynamic responses. Finally, the ARM-core architecture accompanying with touch screen makes the system measure brain activity independently.

9305-229, Session PMon

Studying neural circuitry plasticity of prefrontal cortex during depression occurrence and following medicine treatment in mice model in vivo

Tonghui Xu, Huazhong Univ. of Science and Technology (China)

Stressful life events in modern society predispose more and more susceptible individuals to a variety of psychiatric conditions, especially depression. The study of pathogenesis and therapy of the depression arouses great public concern. Altered functional activity and morphological alterations within neural circuitry of medial prefrontal cortex (mPFC) is thought to be important for mediating depression: acute stress induces a transient, physiological weakening of PFC network connections, and chronic stress has robust effects on the branching patterns of neural circuitry in mPFC. However, little is known about the neural substrates that underlie functional deficits of neural circuitry in depression. Moreover, the effectiveness of medication such as fluoxetine and estrogen for depression is still questionable so far. To investigate the process of prefrontal cortical dendritic morphology being changed in depression before and after fluoxetine and estrogen treatment, we repeatedly image the same apical dendrites of layer V pyramidal neurons marked by the transgenic expression of yellow fluorescent protein (YFP-H line) in mPFC in vivo during depression occurrence and following medicine treatment using transcranial two-photon microscopy. Our preliminary result has shown obvious change of prefrontal cortical dendritic morphology in depression mice model. Classic electrophysiological recording method and calcium imaging assay in vivo will also be used to study the functional changes.

9305-230, Session PMon

Experimental studies with selected light sources for NIRS of brain tissue: quantifying tissue chromophore concentration

Teemu S. Myllylä, Univ. of Oulu (Finland); Vesa O. Korhonen, Vesa Kiviniemi, Oulu Univ. Hospital (Finland); Valery V. Tuchin, N.G. Chernyshevsky Saratov State Univ. (Russian Federation) and Univ. of Oulu (Finland)

Near-infrared spectroscopy (NIRS) based techniques are utilised in quantifying changes of chromophore concentrations in tissue. Particularly, non-invasive in vivo measurements of tissue oxygenation in the cerebral cortex are of interest. The measurement method is based on illuminating tissue and measuring the back-scattered light at wavelengths of interest. Tissue illumination can be realised using different techniques and various light sources. Commonly, lasers and laser diodes (LD) are utilised, but also high-power light emitting diodes (HPLED) are becoming more common. At the moment, a wide range of available narrow-band light sources exists, covering basically the entire spectrum of interest in brain tissue NIRS measurements.

In this paper, in the centre of our interest are LDs and HPLEDs, because of their affordability, efficiency in terms of radiant flux versus size and easiness to adopt in in vivo medical applications. We compare characteristics of LDs and HPLEDs at specific wavelengths and their suitability for in vivo quantifying of different tissue chromophore concentration, particularly in cerebral blood flow (CBF). A special focus is on shape and width of the wavelength bands of interest, generated by the LDs and HPLEDs. Moreover, we experimentally study such effects as, spectroscopy cross talk, separability and signal-to-noise ratio (SNR) when quantifying tissue chromophore concentration. Chromophores of our interest are cytochrome C, haemoglobin and water. Various LDs and HPLEDs, producing narrow-band wavelengths in the range from 500 nm to 1000 nm are tested.

9305-231, Session PMon

Automated extraction of mouse brain contour by using resampling-based variational model

Jing Li, Tingwei Quan, Shiwei Li, Hang Zhou, Qingming Luo, Hui Gong, Shaoqun Zeng, Wuhan National Lab. for Optoelectronics (China)

Digital reconstruction of brain morphology essential for imaging registration and data visualization requires extracting the brain contour. Recent progress in molecular labeling and microscopy imaging system makes high-throughput acquisition of sequence images from mouse brain imaging become a reality and provides a base for extracting the brain contour. However, the traditional shape detection methods, such as active contour and level set based methods etc., experience the difficulty, mostly originated from the fact that the signal inside and outside the brain edge is not uniform and furthermore the contrast is low in some case. Here, we translated extracting the mouse brain contour into successively reconstructing the boundary of each cross-sectional brain, and adopt the strategy that the current reconstruction is achieved by solving a variational model on the resampling region whose center curve is the last reconstructed boundary, continues to do this for the next construction until all cross-sectional brain boundaries can be reconstructed. The variational model used to current reconstruction can control the direction of boundary element due to resampling way, meantime, contains the information of previous construction. This containing is based on a slow change in the two adjacent cross-sectional boundaries. So, compared with other shape detection methods, our method significantly increases the accuracy in extracting of mouse brain contour, and the average value of recall and precision are

about 98% by contrast with the manual results. In addition, our method only analyzed the resampling rejoin (local) instead of the whole dataset and is very effective, and can extract a brain contour (5000 cross-sectional images) within 6 hours.

9305-232, Session PMon

Cerebral functional connectivity and vasomotion: phenomena and separability

Jonathan Bumstead, Adam Q. Bauer, Joseph P. Culver, Washington Univ. in St. Louis (United States)

Resting-state functional connectivity (RSFC) is a neuroimaging technique used to identify brain networks. At the basis of RSFC is the analysis of hemodynamic oscillations less than 0.08 Hz. In addition to RSFC studies, numerous studies in vascular physiology have focused on another spontaneous low frequency hemodynamic oscillation (LFHO), known as vasomotion. Vasomotion is a rhythmic oscillation of vascular tone that is independent of neural activity and generally reported at ~ 0.1 Hz. As RSFC becomes an increasingly popular neuroimaging technique, it is essential to clarify how vasomotion effects RSFC analysis.

We analyzed fluctuations of oxy-hemoglobin (HbO₂) over the majority of resting mouse cortex using functional connectivity optical intrinsic signal imaging (fcOIS). Twenty mice were anesthetized with ketamine-xylazine and imaged for 20 minutes. To determine if a mouse had vasomotion, the fast Fourier transform of HbO₂ traces was analyzed. A distinctive peak between 0.1 and 0.3 Hz in the HbO₂ spectra indicated vasomotion of variable intensity across the group of 20 mice. Resting-state brain networks were then identified by band-pass filtering HbO₂ traces between 0.009 – 0.08 Hz and conducting seed-based correlation analysis. Regardless of the presence of vasomotion, the correlation maps generated by our analysis revealed similar resting-state brain networks in all mice. These results demonstrate that vasomotion can easily be detected in the spectra of HbO₂ traces measured with fcOIS, and that RSFC and vasomotion can be separated by applying an appropriate band-pass filter.

9305-233, Session PMon

Mapping the neural circuit with an automated high-throughput high-resolution imaging system

Tao Yang, Wuhan National Lab. for Optoelectronics (China)

Mapping the neural circuit and obtaining long-range connectivity is essential for understanding the brain function. Recent years, combined with biological technique, some excellent fluorescence microscopic imaging systems can be used to obtain these important information within the brain. However, it is inefficiency when 3D structure needs to be reconstructed over millimeters with a resolution sufficient to identify thin axons. As imaging a mouse brain needs ten days now, it will be intolerable to image the whole human brain which is much bigger than mouse brain.

Here we demonstrate an automated high-throughput imaging system combined with serial sectioning. Industrial surface detection technology is improved to image the neuron structure. Line-illumination and non-stop stage-scanning methods are used to achieve high imaging speed. Just imaging several strips can cover the whole tissue surface. We use time delay integration method to solve the low signal-noise-ratio problem that is caused by short pixel-dwell time at high imaging speed. Embedded in resin, the tissues can be cut off using the diamond knife, range from 200nm to 5 μ m. The total time for imaging one mouse brain, cutting 2000 times and each cutting thickness is 5 μ m, is less than 2 days. And the voxel resolution 0.6 μ m \times 0.6 μ m \times 5 μ m is sufficient to trace the axons. This will help scientists accelerate the brain research by automatically obtaining 3D datasets to reconstruct the neuronal circuits.

9305-234, Session PMon

Spatio-temporal coherence in cortical calcium transients in mice

Patrick W. Wright, Adam Q. Bauer, Joseph P. Culver, Washington Univ. in St. Louis (United States)

Functional connectivity (FC) describes the functional relationships within brain networks. FC patterns of low frequency (0.009-0.08Hz) spontaneous brain activity can be quantified through analysis of spatio-temporal correlations in time series brain imaging data. Brain dynamics are commonly recorded using imaging contrasts that depend on changes in local concentrations of hemoglobin, such as functional MRI or optical intrinsic signal (fcOIS) imaging. However, hemodynamic fluctuations are a relatively indirect report of brain function; they are driven by electrical and metabolic activity through neurovascular coupling. Here we extend FC imaging beyond hemodynamic contrasts to calcium transients, which should be temporally distinct due to their dependence on synaptic potential-dependent calcium concentration changes. Transgenic mice expressing a fluorescent calcium indicator (GCaMP3) driven by the Emx1 promoter in glutamatergic neurons and glia in the cortex were created using Cre-lox recombination and imaged transcranially with sequential LED illumination (to acquire both GCaMP3 fluorescence and OIS). Following electrical hindpaw stimulation, GCaMP3 provided an evoked response time course that was sensitive to high frequency (>3Hz) stimulus presentations, whereas the OIS hemoglobin traces followed the stereotypical hemodynamic response function independent of pulse frequency. Furthermore, bilateral FC maps created using eight canonical seeds remained intact in higher frequency bands (>=5.5Hz) relative to OIS maps. Using Ca²⁺ as a target for functional neuroimaging has provided evidence that organized temporal coherence in cortical activity across the brain exists for ion dynamics as well as hemodynamics. This combined Ca²⁺ and hemoglobin mapping will be useful in understanding the effects of neurodegeneration on functional connections.

9305-235, Session PMon

Improvement of the background optical property reconstruction of the two-layered slab sample based on a region-stepwise-reconstruction method

Ming Liu, Tianjin Univ. (China); Zhuanping Qin, Tianjin University of Technology and Education (China); Mengyu Jia, Huijuan Zhao, Feng Gao, Tianjin Univ. (China)

Two-layered slab is a rational simplified sample to the near-infrared functional brain imaging using diffuse optical tomography (DOT). The quality of reconstructed images is substantially affected by the accuracy of the background optical properties. In this paper, region stepwise reconstruction method is proposed for reconstructing the background optical properties of the two-layered slab sample with the known geometric information based on continuous wave (CW) DOT. The optical properties of the top and bottom layers are respectively reconstructed utilizing the different source-detector-separation groups according to the depth of maximum brain sensitivity of the source-detector-separation. We demonstrate the feasibility of the proposed method and investigate the application range of the source-detector-separation groups by the numerical simulations. The numerical simulation results indicate the proposed method can effectively reconstruct the background optical properties of two-layered slab sample. The relative reconstruction errors are less than 10% when the thickness of the top layer is approximate 10mm. The reconstruction of target caused by brain activation is investigated with the reconstructed optical properties as well. The effective reconstruction depth of the region-of-interest (ROI) is more than that of conventional simultaneous reconstruction method; and the quantitiveness ratio of the ROI is about 80% which is higher than that of the conventional method.

9305-236, Session PMon

Cell-based optical assay for amyloid β -induced neuronal cell dysfunction using femtosecond-pulsed laser

Seunghee Lee, Jonghee Yoon, Chulhee Choi, KAIST (Korea, Republic of)

Amyloid β -protein ($A\beta$) is known as a key molecule related to the pathogenesis of Alzheimer's disease (AD). Gradual increase of $A\beta_{42}/A\beta_{40}$ ratio triggers a process called amyloid cascade which cause severe and permanent impairment in synaptic function. Over time, the event disrupts essential roles of mitochondria including Ca^{2+} homeostasis and reactive oxygen species (ROS) regulation, and eventually leads to neuronal cell death. However, there have been no method that can analyze and discriminate neurons in pathologic conditions quantitatively. Here we suggest a cell-based optical assay to investigate the function of neurons in AD using femtosecond-pulsed laser. We observed that laser stimulation on primary rat hippocampal neurons for a few microseconds induced intracellular Ca^{2+} level increases or intracellular ROS production in neuronal cell death depending on delivered energy. Although $A\beta$ treatment alone had little effect on neuronal morphologies and networks in a few hours, $A\beta$ -treated neurons showed delayed laser-induced Ca^{2+} increase pattern and were more vulnerable to laser-induced cell death compared to normal neurons. Our results collectively indicate that femtosecond laser stimulation can be a useful tool to study AD pathologies. We anticipate this optical method enables study in early progression of neuronal impairments and quantitative evaluation of drug effects on neurons in neurodegenerative diseases including AD and Parkinson's disease in a preclinical study.

9305-237, Session PMon

NeuroGPS 2, dense and brain-wide reconstruction of single-neuron trees

Tingwei Quan, Hang Zhou, Shiwei Li, Jing Li, Qingming Luo, Hui Gong, Shaoqun Zeng, Wuhan National Lab. for Optoelectronics (China)

Digital reconstruction of neuronal morphology, including shape reconstruction of somas, neuronal processes and spines from microscopic imaging datasets, plays a key role in drawing neuronal circuits and investigating how information is integrated and processed in neuronal circuits. Automated dense and large-scale reconstruction of single-neuron tree, as the central problem in digitizing neuronal morphology, still remains a challenge. The challenge is mainly originated from many densely distributed neurons that are imaged and thus cause many spurious spatial connections among neuronal processes. Aiming at this challenge, Inspired by that the human-being examines a suspicious fiber connection by using the comprehensive related information (intensity, shape, orientation etc.) at different spatial scales, rather than simply using the local image intensity, we develop a co-operative and progressive image analysis technique to realize single-neuron tree reconstruction from the image stack of dense neuronal networks. In this model, some statistical information from neuronal morphology has been applied in the related signals of which the scale ranges from the micrometer level to the millimeter level to identify spurious reconstructed connections. This work has been incorporated into our previous software NeuroGPS, called NeuroGPS 2. The results show that this technique can reconstruct single-neuron tree with about 80% of recall and precision from the dense dataset not solved by the recently proposed methods. In addition, we design an effective algorithm for the fusion of reconstructed results of different data blocks. Combined with this fusion algorithm, we can achieve brain-wide reconstruction of single neuron trees.

9305-238, Session PMon

NeuroGPS, automated localization of neurons at the brain-wide scale

Hang Zhou, Wuhan National Lab. for Optoelectronics (China); Tingwei Quan, Wuhan National Lab. for Optoelectronics (China) and School of Mathematics and Economics, Hubei Univ. of Education (China); Shiwei Li, Jing Li, Qingming Luo, Hui Gong, Shaoqun Zeng, Wuhan National Lab. for Optoelectronics (China)

Localization of neurons, as the first step in digitizing neuronal morphology, has been widely researched. In spite of significant advance in localization methods, automated brain-wide localization of neurons experiences difficulties. The main difficulty for this is that the brain-wide scale localization requires analyzing hundreds of GB or TB size of imaging datasets usually including plentiful signals that severely disturb the localization results. Aiming at this difficulty, for eliminating the interference of these disturbed signals on soma localization, we design the procedure containing the following main steps. Firstly, we reconstruct the shapes of some disturbed signals and somas by using sphere-based variational model. Secondly, we extract the features of the reconstructed shapes such as average radius, the ratio of the longest radius and shortest radius, the cross section that is centered at the center point of the reconstructed shape and has the smallest area. The difference between the shape features of somas and the disturbed signals is obvious. Thirdly, by using support vector learning, we build a decision rule for distinguishing the somas from the disturbed signals. Finally, we use the decision rule for the analysis of the whole-brain scale datasets. We call this procedure shape-feedback to localization. This procedure can boost the accuracy of our previous localization method based on L1 minimization model. We integrate this procedure into our software NeuroGPS, and by using NeuroGPS brain-wide localization of neurons can be accurately achieved within 60 hours.

9305-239, Session PMon

Polarization-sensitive optical coherence tomography for cross-sectional imaging of neural activity

Yi-Jou Yeh, Adam J. Black, Univ. of Minnesota, Twin Cities (United States); David Landowne, Univ. of Miami (United States); Taner Akkin, Univ. of Minnesota, Twin Cities (United States)

Optical imaging of neural activity has been actively investigated over the recent decades. Light scattering, birefringence, fluorescence and structural changes can be optically detected during action potential propagation. Optical coherence tomography (OCT) allows for depth-resolved monitoring of the tissue function with high resolution and sensitivity. OCT has been shown to measure intrinsic light scattering changes during neural activity in various preparations, including the abdominal ganglion of sea slug, squid nerve, rat retina and chicken retina.

In this work, we built a functional polarization-sensitive optical coherence tomography cross-sectional scanner to detect neural activity using a voltage-sensitive dye as a contrast-enhancing potentiometric probe. Squid (*Loligo pealeii*, Marine Biological Laboratory, Woods Hole, MA) were dissected to obtain the giant axon and the surrounding small nerve fibers. The nerve was stained with an oxonol voltage-sensitive dye (NK3630, 0.25mg/mL in seawater with 1% DMSO, 20 minutes). Transient changes in backscattered light intensity in main and cross-polarized channels and the phase signals were simultaneously detected in optical cross-sections during action potential propagation. Intensity changes associated with action potentials were seen in stained nerves. Phase changes were observed in both stained and unstained nerves. This functional imaging technology provides high-resolution, depth-resolved assessment of neural activity in

cross-sectional images. This could be expanded to record function in a three-dimensional volume by employing an additional scanner.

9305-240, Session PMon

Temporal synchrony within functional brain networks during state transitions

Adam Q. Bauer, Annie R. Bice, Patrick W. Wright, Matthew D. Reisman, Grant Baxter, Ben J. Palanca, Joseph P. Culver, Washington Univ. School of Medicine in St. Louis (United States)

Resting-state functional magnetic resonance imaging studies have shown spatiotemporal correlations in spontaneous activity between functionally-related brain networks. Recent human studies have investigated the significance of intrinsic brain activity to explain altered states of consciousness. Extensive reduction of neural activity by anesthetics is evidenced by burst-suppression (using EEG) that may increase mortality risk for critically-ill patients, but the corresponding features of network topology during anesthetic transition remain unclear. Several distinct spontaneous coherent networks persist in anesthetized primates (1.25% isoflurane) but investigation in small rodents have been sparse. We asked whether coherent networks persist during electrocortical silence and if they represent a fundamental and intrinsic property of functional brain organization. In order to understand the underlying mechanisms of neural activity in the brain under deep anesthesia, we imaged spontaneous activity in the mouse brain using functional connectivity (fc) optical intrinsic signal imaging as awake-behaving mice transitioned through increasing levels of isoflurane anesthesia (0-2%). We quantified the extent of motor movement, spectral content in concurrently-recorded EEG, and the presence/absence of electrical burst-suppression. Over the course of anesthetic transition we observe a progressive, regional reduction in the magnitude and coherence of spontaneous activity over the cortex. While deep anesthesia was found to ablate fc globally over the brain, activity in some networks (e.g., somatosensory) persisted longer than others with increasing anesthesia. Results from measuring fc under state transitions could shed light on the functional significance of intrinsic brain activity, and the role of fc as a correlate of anesthetic depth.

9305-242, Session PMon

Photoacoustic imaging for transvascular drug delivery to the rat brain

Ryota Watanabe, Keio Univ. (Japan); Shunichi Sato, National Defense Medical College Research Institute (Japan); Yasuyuki Tsunoi, Keio Univ. (Japan); Satoko Kawauchi, Toshiya Takemura, National Defense Medical College Research Institute (Japan); Mitsuhiro Terakawa, Keio Univ. (Japan)

Transvascular drug delivery to the brain is difficult due to the blood-brain barrier (BBB). Thus, various methods for safely opening the BBB have been investigated, for which real-time imaging both for the blood vessels and distribution of a drug is needed. Photoacoustic (PA) imaging method, which enables depth-resolved visualization of chromophores in tissue, would be useful for this purpose. In this study, we performed in vivo PA imaging of the blood vessels and distribution of a drug in the rat brain by using an originally developed compact PA imaging system with fiber-based illumination.

As a test drug, Evans blue (EB) was used. An absorption peak of EB is located at ~610 nm, but 670 nm was used for imaging of EB to reduce the absorption by hemoglobin. To visualize blood vessels, 532 nm was used. We first used a local injection model to examine imaging characteristics of the system. After a cranial window was made, a 0.5-microliters solution of 1% EB was injected into the brain at a depth of 1 mm and PA imaging was

performed at 532 nm and 670 nm. We clearly visualized blood vessels with diameters larger than 50 micrometers in the depth range up to 2 mm and distribution of EB in the depth range from 1 to 1.3 mm. We then applied the method to visualize distribution of EB that was transvascularly delivered to the brain by using photomechanical waves (PMWs), showing spatiotemporal characteristics of EB that was extravasated by the effect of PMWs.

9305-243, Session PMon

Optical imaging of new protein synthesis in live neurons and brain tissues by stimulated Raman scattering microscopy

Lu Wei, Wei Min, Columbia Univ. (United States)

Synthesis of new proteins is a pivotal process in nervous systems. Most notably, long-lasting neuronal plasticity, such as those underlying learning and memory, require active proteins synthesis in a space- and time-dependent manner. Therefore, direct visualization of newly synthesized proteins in neurons will be indispensable to unraveling spatial-temporal characteristics of neuronal plasticity. However, sensitive imaging of global protein synthesis in live neurons with subcellular resolution is challenging despite the extensive efforts of autoradiography, fluorescence and mass spectrometry. Herein we report a novel optical imaging technique to visualize protein synthesis activities in neuronal systems by coupling the stimulated Raman scattering (SRS) microscopy with metabolic incorporation of deuterium-labeled amino acids. SRS microscopy, a nonlinear vibrational imaging technique, offers distinctive advantages such as Raman amplification, bond-selectivity, background-free and biocompatibility, whereas the introduction of deuterium as an exogenous contrast is minimally perturbative. Thus SRS imaging of deuterium-labeled new proteins is highly sensitive, specific, and biocompatible. We applied our technique to live primary neurons and organotypic brain tissues. In vitro neurons, our technique has successfully imaged newly synthesized proteins in both soma and fine structures (i.e., dendritic spines). In ex vivo brain tissues, a spatially defined subpopulation of neurons with active protein synthesis has been identified in the hippocampus region. Hence, SRS microscopy coupling with stable isotope incorporation will be a valuable tool for studying the complex spatial and temporal dynamics of protein synthesis activities in neuronal systems. Wei L, Yu Y, Shen Y, Wang MC, Min W. PNAS 110, 11226 (2013).

9305-244, Session PMon

Automated sparse reconstruction of single-neuron tree at the brain-wide scale

Shiwei Li, Wuhan National Lab. for Optoelectronics (China); Tingwei Quan, Wuhan National Lab. for Optoelectronics (China) and School of Mathematics and Economics (China); Hang Zhou, Jing Li, Qingming Luo, Hui Gong, Shaoqun Zeng, Wuhan National Lab. for Optoelectronics (China)

Progress in molecular labeling and imaging techniques allows for the whole-brain scale imaging of several neurons at submicron spatial resolution. The imaging signals of these neurons are extremely sparsely distributed in the datasets with the size of hundreds of GBs or TBs. In this case, fast digital reconstruction of these neurons used for high throughput quantifying analysis still experiences difficulties. For example, self-automated reconstruction usually process multi-level resolution datasets that can be generated from the original dataset with tremendous time-consuming (analyzing 1TB size of dataset costs about 7 days). The most of the automated reconstructed methods require analysis of the whole-brain scale datasets which includes massive invalid signals and thus the time-consuming of the reconstruction is still substantial. Here, we developed a method based on a combination of identification method of neuronal branching and tracing method of neuronal processes. Briefly, we

use constrained principal curve to trace a neuronal process. After finishing this tracing, from the traced points, the neuronal branching points can be identified. For each identified branching point, starting at its position, the tracing of neuronal process continues to be carried out. Repeat this procedure until there are no identified branching points. This procedure only uses the local information for reconstruction and thus is very effective. In addition, this procedure is superior to the conventional methods such as Open-snake and NeuroStudio in dealing with the weak signal. We demonstrate that this method can reconstruct the single-neuron trees at the whole-brain scale within several hours.

9305-245, Session PMon

Multichannel fiber-based diffuse reflectance spectroscopy for the rat brain exposed to a laser-induced shock wave: comparison between ipsi- and contralateral hemispheres

Mai Miyaki, Tokyo Univ. of Agriculture and Technology (Japan); Satoko Kawauchi, Div. of Biomedical Information Sciences, National Defense Medical College Research Institute (Japan); Wataru Okuda, Tokyo Univ. of Agriculture and Technology (Japan); Hiroshi Nawashiro, Div. of Neurosurgery, Tokorozawa Central Hospital (Japan); Toshiya Takemura, Shunichi Sato, Div. of Biomedical Information Sciences, National Defense Medical College Research Institute (Japan); Izumi Nishidate, Tokyo Univ. of Agriculture and Technology (Japan)

Due to considerable increase in the terrorism using explosive devices, blast-induced traumatic brain injury (bTBI) attracts worldwide attention. However, little is known about the pathological conditions and mechanism of bTBI. In our previous study, we found that cortical spreading depolarization (CSD) occurred in the hemisphere exposed a laser-induced shock wave (LISW), which was followed by long-lasting hypoxemia-oligemia. However, there was no information on the events occurred in the contralateral hemisphere. In this study, we performed multichannel fiber-based diffuse reflectance spectroscopy for the rat brain exposed to an LISW and compared the results obtained for the ipsilateral hemisphere with those obtained for the contralateral hemisphere. A pair of optical fibers was put both on the exposed right parietal bone and left parietal bone; white light was delivered to the brain through source fibers and diffuse reflectance signals were collected through detection fibers. An LISW was applied to the region near the fiber pair on the left hemisphere (ipsilateral hemisphere). By analyzing reflectance signals, we evaluated occurrence of CSD, blood volume and oxygen saturation for both hemispheres. In the ipsilateral hemispheres of all 6 rats examined, we observed occurrence of CSD and long-lasting hypoxemia-oligemia, as observed in our previous study. In the contralateral hemispheres, on the other hand, occurrence of CSD was not observed in all 6 rats. However, we observed oligemia in all the 6 rats and hypoxemia in 2 of these 6 rats, suggesting a mechanism to cause hypoxemia-oligemia in the contralateral hemisphere, which is not directly associated with CSD.

9305-246, Session PMon

Optimized optical clearing method for imaging central nervous system

Tingting Yu, Yisong Qi, Hui Gong, Qingming Luo, Dan Zhu, Britton Chance Ctr. for Biomedical Photonics (China)

The development of various optical clearing methods provides a great potential for imaging entire central nervous system by combining with labelling and microscopic imaging techniques. The 3DISCO can make mouse brain and spinal cord very transparent, which enables to obtain

three-dimensional reconstruction of neuronal networks in the with light sheet fluorescence microscopy. However, the general limitations of antibody penetration make immune-labelling of tissue block difficult. In contrast, the CLARITY can achieve multiple rounds molecular phenotyping to get structural and molecular information by transforming the intact mouse brain into optically transparent and macromolecule-permeable through hydrogel-tissue fusion and electrophoretic tissue clearing. However, it needs to be proved whether it is effective for mouse adult spinal cord. Actually, the differences of structures and compositions between the two tissues indicate that some brain optical clearing method is not suitable for spinal cord completely. In this study, we developed several optimal methods to enhance the transparency of brain and spinal cord and accelerate the clearing speed without influence on the fluorescence in Thy1-GFP-M transgenic mouse and immune-labelling. The optimized optical clearing method makes it suitable for imaging the whole central nervous system, including the mouse brain and non-sectioned adult spinal cord.

9305-247, Session PMon

Activity analysis and characterization of tissue-engineered 3D neural networks

Erez Shor, Anat Marom, Technion-Israel Institute of Technology (Israel); Sanjeev K. Mahto, Technion-Israel Institute of Technology (Israel) and Indian Institute Of Technology(BHU) (India); Shulamit Levenberg, Shy Shoham, Technion-Israel Institute of Technology (Israel)

Planar neural networks and interfaces serve as versatile in vitro models of central nervous system (CNS) physiology but do not fully model the complex behavior of three dimensional (3D) neural networks. Furthermore, tissue engineering applications require physical constructs which are 3D by nature. In this study we use neurophotonics tools to characterize the activity of 3D rat cortical neural cultures as they develop on different types of scaffolds.

To image network activity across multiple planes of the 3D scaffold with single cell resolution and high frame rate, we used a new microscopy system and culture chambers for extended-duration imaging of GCaMP6m calcium signals. The system couples wide field fluorescence microscopy with a piezoelectric device that sequentially shifts the focal plane to multiple z-planes, whose images are later processed using nearest-neighbor deconvolution. This optical system is used to probe activity in tissue-engineered 3D neural 'optoneets' embedded in Matrigel as well as a neural transplant based on neurons seeded on PLLA/PLGA scaffolds. Our results using this method provide a detailed characterization of the networks' activity patterns as the network matures and goes through different stages of development. In addition, we examined pharmacological effects on the activity of the network using a microfluidic device capable of site-specific delivery of drugs.

9305-248, Session PMon

Simultaneous optical measurement of electrical activity on cortical surface and hemodynamic changes in subcortical area during deep brain stimulation

Hyuna Song, Sedef Erdogan, Young-kyu Kim, Beop-Min Kim, Jong J. Kim, Korea Univ. (Korea, Republic of)

Introduction: Deep Brain Stimulation (DBS) has been widely used to treat brain malfunction such as Parkinson's disease or other psychiatric disorders. Despite its extensive applications in the clinical setting, the clear mechanism through which DBS leads to neuronal recovery remains incompletely understood.

Methods: A new multimodal imaging system, which is composed of sCMOS-

based fluorescent optical mapping and near-infrared spectroscopy (NIRS) systems, was recently developed. A microelectrode for DBS was inserted at the targeted sites such as the anterior nucleus of thalamus (ANT) or subthalamic nucleus (STN) in a rodent brain. The brain was topically stained with voltage sensitive dye. Upon varying stimulation parameters, simultaneous optical measurement of electrical activities on the motor cortex and hemodynamic changes in deep brain was performed.

Results: The spatial distribution of neuronal activation in motor cortex was tightly associated with the parameters of DBS. The interplay between DBS and neuronal activation was investigated by analyzing functional connectivity of cortical response and electrophysiology recording of deep brain. Spatial correlation coefficient between DBS and local activation mapping of cortical area revealed that the DBS effect is highly related to particular pathways of motor loops. In sum, our results show that optical imaging of electrical activities and hemodynamics can provide insight into cortico-thalamic connectivity and neural networks in deep brain.

Conclusion: The newly built multimodal optical imaging can be used as a reliable platform to investigate the therapeutic effect of DBS in clinical practice.

9305-249, Session PMon

Rapid 3D mapping of whole mouse brain in high resolution using SI-fMOST

Dongli Xu, Bihe Hu, Hui Gong, Qingming Luo, Britton Chance Ctr. for Biomedical Photonics, Huazhong Univ. of Science and Technology (China)

Mapping the mammalian brain in high resolution is one of the key challenges in neuroscience study, and it requires one to obtain sub-micron dendritic arbor morphology and axonal pathways on a centimeter scale. However, existing whole-brain imaging protocols generally consume weeks to mapping the whole mouse brain, and lack co-localized reference to locate the neuron. Here, we present a full-automated imaging technology for fast mapping of whole mouse brain in high resolution, named SI-fMOST (structured illumination fluorescence micro-optical sectioning tomography), which combines multi-color fluorescence structured illumination microscopy and ultramicrotome sectioning of resin-embedded tissue. Instead of conventional point-scanning optical sectioning method, widefield imaging based structured illumination microscopy is employed to increase the imaging through-put and generate optical sections. In addition, to reduce the background fluorescence in the thick sample and improve the signal noise ratio of SI-fMOST optical section, a whole-brain Sudan black staining method is introduced in the tissue preparation protocol. To provide a co-localized cytoarchitectonic reference, we also develop a real-time nuclear counterstain method for whole brain sample, which permit staining and imaging the cell nuclei on the tissue surface simultaneously. SI-fMOST enables simultaneous visualization of neural structural information and co-localized cytoarchitectonic reference of a mouse brain, and the entire process (including tissue preparation, counterstain and imaging) takes 10 days to complete. We acquired a two-channel whole-brain dataset of a 60 days-old Thy—GFP-M mouse. Based on the cytoarchitectonic reference, neuronal reconstruction in the barrel cortex is showed. The results demonstrate SI-fMOST a promising tool for whole-brain mapping.

9305-250, Session PMon

System aberration correction in a light sheet microscope compatible with clearing solutions

M. Caroline Müllenbroich, European Lab. for Non-linear Spectroscopy (Italy) and Univ. degli Studi di Firenze (Italy); Ludovico Silvestri, European Lab. for Non-Linear Spectroscopy, Univ. degli Studi di Firenze (Italy); Leonardo

Sacconi, European Lab. for Non-Linear Spectroscopy, Univ. degli Studi di Firenze (Italy) and National Institute of Optics (Italy); Francesco S. Pavone, European Lab. for Non-Linear Spectroscopy, Univ. degli Studi di Firenze (Italy) and National Institute of Optics (Italy) and International Ctr. for Computational Neurophotonics (Italy)

One of the most promising applications of light sheet microscopy is the reconstruction of macroscopic biological specimens with microscopic resolution without physical sectioning. To this aim, light sheet microscopy is combined with clearing protocols based on refractive index matching, which render the tissue transparent. Recently objectives suitable for light sheet microscopy have become commercially available which have been designed for use with clearing solutions and typically also feature a correction collar for the compensation of a certain amount of spherical aberration. However, a complete correction of system induced aberrations requires the ability to also correct for residual spherical aberration and higher order aberrations introduced by the sample mount and slight misalignment of the optical system. The province of adaptive optics is to compensate for aberrations introduced by the optical system and the sample under investigation and restore diffraction limited imaging where possible. Here we investigate the possibility of correcting for aberrations by introducing a deformable membrane mirror into the detection path of a light sheet microscope. The shape of the deformable membrane mirror has been determined in a wavefront sensorless fashion through a random search algorithm optimisation. The improvement in image quality due to system aberration correction is demonstrated using fluorescent beads and murine brain which has been optically cleared using the CLARITY protocol. Increasing the fluorescent yield through aberration correction allows for higher quality imaging, shortened acquisition times and additionally to reduce the incident laser power which decreases the risk of photobleaching.

9305-251, Session PMon

Optical coherence tomography for non-contact detection of action potentials in functionally stimulated Limulus nerve

M. Shahidul Islam, Thorlabs, Inc. (United States); Md. Rezuhanul Haque, Christian M. Oh, Univ. of California, Riverside (United States); Yan Wang, Massachusetts General Hospital (United States); Md. Monirul Hasan, B. Hyle Park, Univ. of California, Riverside (United States)

The exquisite phase-sensitivity of optical coherence tomography has been demonstrated to be sufficient to detect the nanometer-scale changes in axonal thickness known to accompany action potential propagation. Previously published analyses rely heavily on identification of the upper and lower surfaces of large nerves, such as the squid giant axon, and involve subtraction of the phases from only these two points in depth. We have developed a novel analysis that utilizes short term correlations of phase differences over small depth ranges to improve detection of transient axon thickness changes associated with action potential propagation in smaller nerves. This method removes the requirement for identification of the upper and lower surfaces of a nerve, and improves the overall robustness of detection. In this study, we demonstrate this new analysis in ex vivo Limulus (horseshoe crab) optic nerve. These optically detected thickness changes are temporally correlated with the propagating electrical signal recorded in electrophysiology. The optic nerve was functionally stimulated through visual stimulus to the eye. No averaging over multiple trials was required, indicating the capability of single-shot detection of nerve impulses.

9305-252, Session PMon

The evaluation of cerebral autoregulation in patients with obstructive sleep apnea syndrome with near-infrared spectroscopy

Zhongxing Zhang, Marco Laures, Maja Schneider, Gordana Hügli, Ming Qi, Ramin Khatami, Clinic Barmelweid (Switzerland)

In obstructive sleep apnea (OSA) respiratory events lead to disturbed oxygenation with profound systemic hemodynamic consequences, whereas the ability of cerebral autoregulation to cope with these systemic hemodynamic changes remains essentially unknown. The comparisons between cerebral and peripheral (i.e., as a 'control') hemodynamics during respiratory events like apnea/hypopnea with/without consecutive limb movements (LMs) may provide a novel methodology to solve this issue. Therefore, 8 OSA patients underwent all-night-video-polysomnography combined with cerebral near-infrared spectroscopy (NIRS). Apnea/hypopnea was sub-divided into those with and without LMs. Correlations of degree of desaturation in peripheral oxygen saturation (SpO₂) measured with pulse oximetry and cerebral HbO₂ (cHbO₂) measured with NIRS were tested (Pearson correlation, $p < 0.05$). Correlations between desaturation in SpO₂ and cHbO₂ for all respiratory events were found in 4 patients who were older and had higher apnea/hypopnea index (AHI), indicating autoregulation cannot cope with the systemic desaturation induced by apnea/hypopnea events. For respiratory events with LMs, correlation existed in none patient whereas in 5 subjects correlations were found for apnea/hypopnea without LMs. Our results suggest that the influence of cerebral autoregulation on hemodynamics to cope with systemic desaturation following OSA event seems to vary depending on individual patient and the type of respiratory events. Apnea/hypopnea with LMs following an obstructive airflow limitation might improve the capacity of cerebral autoregulation to stabilize cerebral HbO₂. Patients who are older and with higher AHI values may have weaker capacity of cerebral autoregulation to compensate the deficit of oxygen supply induced by respiratory events.

9305-253, Session PMon

Decreased optical attenuation detected during cerebral edema in vivo with optical coherence tomography

Carissa L. R. Rodriguez, Jenny I. Szu, Melissa M. Eberle, Mike S. Hsu, Devin K. Binder M.D., B. Hyle Park, Univ. of California, Riverside (United States)

Cerebral edema, an increase in brain water content, can be caused by a number of conditions and injuries to the brain and often contributes to poor prognosis. Early detection and continuous monitoring are important for management and treatment of the condition. In this study, we examine the ability of optical coherence tomography (OCT) to detect changes in the optical properties of the brain tissue during cerebral edema.

A water intoxication mouse model of cerebral edema was imaged with a spectral-domain OCT setup centered at 1300 nm. The mouse was first anesthetized and prepared with a thinned-skull cortical window, which provided increased imaging depth while preserving the physiological condition of the brain. After 20 minutes of baseline recording, an intraperitoneal injection of water was given to induce edema and imaging continued for 1 hour.

Analysis of the depth-resolved attenuation coefficient showed that the average attenuation coefficient in the cerebral cortex decreased over time as edema progressed. The attenuation values began to decrease within minutes of inducing edema and the percent change of the average attenuation coefficient after 1 hour was 8%. Analysis of local regions within the brain showed the same trend, consistent with this global edema model. These results demonstrate the ability of OCT to detect cerebral edema based on a change in the attenuation coefficient and highlight the potential of OCT for high-resolution 3D imaging of cerebral edema progression.

9305-254, Session PMon

Spatially and temporally registered optical coherence tomography and fluorescence microscopy for enhanced detection of neural activity

Md. Rezuanul Haque, Univ. of California, Riverside (United States); M. Shahidul Islam, Thorlabs, Inc. (United States); Christian M. Oh, Michael C. Oliveira, Sang S. Lee, Michael E. Adams, B. Hyle Park, Univ. of California, Riverside (United States)

Optical coherence tomography (OCT) is a minimally-invasive technology capable of rapid two- and three-dimensional imaging of 2-3mm of subsurface tissue structure with micrometer resolution. However, while OCT excels at acquisition of structural information, it lacks chemical specificity. Fluorescence microscopy (FM), on the other hand, provides biochemical, metabolism and molecular information of the tissue. In this study, a combined OCT and FM system has been developed to acquire both structural and functional information of the biological sample. The OCT and FM systems have been spatially and temporally registered in order to acquire information of the dynamics of structural and functional change of the tissue over time. The fluorescence response of GCaMP-labeled bursicon and kinin cells in CNS of *Drosophila* larvae in response to presentation of ecdysis triggering hormone (ETH) has been well-characterized. Simultaneous OCT and FM images were acquired prior to and after ETH presentation. We demonstrate the use of OCT to detect intrinsic optical changes in active kinin and bursicon cells by correlated time-dependent changes in OCT to fluorescence measurements. The results suggest that OCT can be used as a functional tool for neural activity detection in a label free manner.

9305-255, Session PMon

Altered prefrontal connectivity in post-traumatic stress disorder: A functional near infrared spectroscopy study with graph theoretical analysis

Fenghua Tian, Alexa Smith-Osborne, Amarnath S. Yennu, Li Zeng, The Univ. of Texas at Arlington (United States); Carol S. North, The Univ. of Texas Southwestern Medical Ctr. at Dallas (United States); Hanli Liu, The Univ. of Texas at Arlington (United States)

The human brain is a complex network that is organized structurally and functionally to support efficient segregation and integration of information processing. Examination of the patterns of human brain connectivity facilitates researchers and clinicians to better understand neurological processes of human behaviors as well as to comprehend mechanisms of neurological diseases. Graph theoretical analysis (GTA) is a powerful mathematical framework that analyzes the topological properties of the brain networks and provides valuable insights into the configuration and efficiency of the connectivity.

In the past a few years, we have measured the prefrontal activities in 17 veterans diagnosed with PTSD as well as in age- and gender- matched controls during a digit-span task, by using a high-performance fNIRS system. The present study applied GTA to analyze the task-driven brain connectivity and networks in this cohort. In summary, both control and PTSD groups showed small-world networks during the task. However, veterans with PTSD had significantly decreased global efficiency and significantly increased path length, without and with normalization. The PTSD group also had decreased regional nodal efficiency and a reduced number of hubs in the right hemisphere. These results demonstrated the feasibility and sensitivity of fNIRS to detect and quantify the altered properties of brain connectivity and networks associated with PTSD.

9305-256, Session PMon

Miniature device for chronic, label-free multi-modal optical imaging of cortical hemodynamics in rats

Raanan Gad, Iliya Sigal, Dene Ringuette, Univ. of Toronto (Canada); Margaret Koletar, Bojana Stefanovic, Sunnybrook Research Institute (Canada); Ofer Levi, Univ. of Toronto (Canada)

We report on a novel miniature head-mounted imaging system for simultaneous optical recording of brain blood flow and changes in brain blood oxygenation in a rat. Measurements of blood flow speed are accomplished using Laser Speckle Contrast Imaging (LSCI) technique, while changes in blood oxygenation are measured via Intrinsic Optical Signal Imaging (IOSI) technique. A single multi-wavelength (wavelength = 680, 795, 850 nm) package of vertical cavity surface emitting lasers (VCSELs) is used as the sole brain illumination source. VCSELs enable rapid toggling between wavelengths, and between high-coherence and low-coherence modes, necessary for LSCI and IOSI, respectively. The combination of a miniature light source and a small 10-bit CCD camera sensor lead to a sub-20g device mass. The miniature imaging system, including the lens, camera, and illumination lasers, is packaged as a module, and is mounted on a chronic implanted observation window that is surgically placed in the skull, allowing for repeated measurements and removal of the imaging system from the rat's head after the imaging session. The imaging system allows for a 2mm-diameter field of view and a resolution of 6 micrometers. It will allow neurophysiologists to correlate standard behavioural assays to neurovascular response in animal models, and thus enrich their understanding of neurovascular coupling dynamics of brain disorders and diseases such as stroke and epilepsy.

9305-258, Session PMon

Near-infrared spectroscopy assessment of divided visual attention task-invoked cerebral hemodynamics during prolonged true driving

Ting Li, Yue Zhao, Yunlong Sun, Yuan Gao, Yu Su, Univ. of Electronic Science and Technology of China (China); Yiyi Hetian, Min Chen, Univ. of Electronic Science and Technology of China (China)

Driver fatigue is one of the leading causes of traffic accidents. It is imperative to develop a technique to monitor fatigue of drivers in real situation. Near-infrared spectroscopy (fNIRS) is now capable of measuring brain functional activity noninvasively in terms of hemodynamic responses sensitively, which shed a light to us that it may be possible to detect fatigue-specified brain functional activity signal. We developed a sensitive, portable and absolute-measure fNIRS, and utilized it to monitor cerebral hemodynamics on car drivers during prolonged true driving. A odd-ball protocol was employed to trigger the drivers' visual divided attention, which is a critical function in safe driving. We found that oxyhemoglobin concentration and blood volume in prefrontal lobe dramatically increased with driving duration (stand for fatigue degree; 2-10 hours), while deoxyhemoglobin concentration increased to the top at 4 hours then decreased slowly. The behavior performance showed clear decrement only after 6 hours. Our study showed the strong potential of fNIRS combined with divided visual attention protocol in driving fatigue degree monitoring. Our findings indicated the fNIRS-measured hemodynamic parameters were more sensitive than behavior performance evaluation.

9305-218, Session 5

Low frequency hemodynamic and calcium oscillations in brain reflect neuronal activity: evidence from optical imaging (Invited Paper)

Congwu Du, Yingtain Pan, Stony Brook Univ. (United States)

Spontaneous low-frequency oscillations (LFOs) of BOLD in brain constitute the basis for mapping resting functional connectivity with fMRI. However the origin for these LFOs is not well understood. Using optical imaging we provide evidences to show that LFOs in calcium have similar frequencies as deoxyhemoglobin LFOs. In addition, the hemodynamic slow oscillations correlate with spontaneous neuronal firing frequency, thus indicating the neuronal basis underlying resting state fMRI

9305-219, Session 5

Stroke in newborns: important but poor understood problem, new experimental model, priority for optical diagnostics, mechanisms (Invited Paper)

Oxana V. Semyachkina-Glushkovskaya, Vladislav Lichagov, Olga A. Bibikova, Sergey S. Sindeev, Ekaterina Zinchenko, Artem Gekaluyk, Maria V. Ulanova, N.G. Chernyshevsky Saratov State Univ. (Russian Federation); Zhang Yang, Huazhong Univ. of Science and Technology, Wuhan National Lab. for Optoelectronics (China); Qin Huang, Huazhong Univ. of Science and Technology (China); Pengcheng Li, Huazhong Univ. of Science and Technology, Wuhan National Lab. for Optoelectronics (China); Dan Zhu, Huazhong Univ. of Science and Technology (China); Valery V. Tuchin, N.G. Chernyshevsky Saratov State Univ. (Russian Federation); Qingming Luo, Huazhong Univ. of Science and Technology, Wuhan National Lab. for Optoelectronics (China)

Hemorrhagic stroke (HS) in newborns is an important but understudied problem. The incidence of HS is typically asymptomatic and cannot be effectively detected by standard diagnostic methods. The lack of effective diagnostic technologies for early determination and criteria of HS risk in newborns explains the high rate of neonatal death and less optimistic neurologic prognosis in infants after HS. Currently, there are no proven strategies for the medical management of childhood stroke. Recommendations and treatment guidelines have largely been extrapolated from adult data.

A small number of animal studies have examined the mechanisms of HS in neonatal period. There is no experimental model that mimics the clinical situation. We developed the new original model of HS in newborn rats and mice using harmful effects of infrasound on the brain. The results of MRI and histological analysis of the brain tissue of newborn rodents showed multiple HS in the cortex 24 hours after noise stress. The results of LSCI and DOCT recording of rCBF in newborn rodents demonstrated that development of HS is associated with hyperperfusion and hyperemia of brain tissue that is closely correlated with histological data. Imminofluorescent and immunoblot analysis showed that pathological changes in CBF is accompanied by high expression of Sur1 receptors and beta2-adrenoreceptors as well as by decrease permeability of brain blood barrier.

These findings can be useful for better understanding mechanisms of HS in newborns and also for the further study of sensitive markers of predictability of HS in newborns.

Supported by grant ? 14-15-00128

9305-220, Session 5

Tools for high resolution optical imaging of neuronal, glial, vascular, and metabolic activity for neuroscience studies in vivo *(Invited Paper)*

Anna Devor, Univ. of California, San Diego (United States)

What is the first association that comes to your mind when you hear “fiber optics”? Connecting one side of the Atlantic Ocean to the other or high-definition TV? For sure, it would not be manipulation of neuronal firing ... unless you are a neuroscientist. While neuroscience has relied on optics to power discovery from the beginning of times, brain imaging remains an exotic application in the mainstream optics and photonics. Arguably the most significant breakthroughs in neuroscience have been powered by advancements in optical technology, from the discovery of synaptic junctions by the father of modern neuroscience Ramón y Cajal in 1880s, to the contemporary advances in cell- and system-level neuroscience through utilization of 2-photon microscopy, optogenetics, and superresolution microscopy. In this talk, we will consider the current state-of-the-art of a number of key microscopy technologies that now power high-resolution mechanistic in vivo neuroscience studies and review example applications from our work where the use of these novel technologies has been instrumental for biological discoveries. These endpoint biological insights are a product of long-term multidisciplinary collaboration enabling application-driven comprehensive technological developments.

9305-221, Session 5

Non-invasive whole brain monitoring of multiple hemodynamic parameters and fast calcium dynamics using five-dimensional optoacoustic tomography *(Invited Paper)*

Sven Gottschalk, Gali Sela, Antonella Lauri, Xosé Luis Deán-Ben, Helmholtz Zentrum München GmbH (Germany); Thomas Felix Fehm, Moritz Kneipp, Helmholtz Zentrum München GmbH (Germany) and Technische Univ. München (Germany); Shy Shoham, Technion-Israel Institute of Technology (Israel); Gil Geger Westmeyer, Daniel Razansky, Helmholtz Zentrum München GmbH (Germany) and Technische Univ. München (Germany)

Currently available functional neuroimaging techniques are not adequate for real-time monitoring of multiple hemodynamic parameters or of fast neuronal activation events across entire brains. We present a five-dimensional optoacoustic imaging system for non-invasive whole-brain monitoring of cerebral hemodynamics and neuronal activation. By means of fast wavelength tuning and instantaneous acquisition of volumetric datasets, the system can render three-dimensional images of spectrally resolved tissue chromophores and markers of neuronal activity in real time, thus offering an imaging performance that is unparalleled among current neuroimaging modalities. We demonstrate noninvasive high-resolution imaging of cerebral hemodynamics, blood oxygenation, and of fast calcium dynamics in brains of living mice and zebrafish at various developmental stages.

9305-222, Session 5

Simultaneous measurement of cerebral and muscle tissue parameters during cardiac arrest and cardiopulmonary resuscitation

Vladislav Toronov, Ryerson Univ. (Canada); Andrew Ramadeen, Univ. of Toronto (Canada)

Cardiac arrest is an extreme condition in which tissue damage may occur due to the severe lack of perfusion. Continuous, real-time monitoring of tissue viability parameters (especially cerebral tissue) is important for assessing the quality of resuscitation both during and after the arrest. We performed comprehensive time-resolved measurements of various parameters in a porcine model of cardiac arrest. We used our hyperspectral near-infrared spectroscopy (hNIRS) system to measure cerebral and muscle concentrations of oxy- and deoxyhemoglobin, and changes in the cytochrome c oxidase redox state. In addition, we used invasive sensors to measure aortic pressure, carotid blood flow, and femoral blood flow. Cerebral hNIRS was performed both non-invasively and on cerebral dura matter through a burr hole in the skull. We have carefully analyzed our hNIRS measurements to compare invasive and non-invasive cerebral hNIRS results with other measured parameters. Our conclusion is that hNIRS can be translated to clinical trials in cardiac arrest patients.

9305-223, Session 5

Dual-wavelength polarization-sensitive optical coherence tomography for dye contrast detection of neural activity

Yi-Jou Yeh, Adam J. Black, Hui Wang, Univ. of Minnesota, Twin Cities (United States); David Landowne, Univ. of Miami (United States); Taner Akkin, Univ. of Minnesota, Twin Cities (United States)

The use of light to detect functional neural activity has been studied for decades. Optical coherence tomography (OCT) has been used for depth-resolved measurements of backscattered light intensity and phase changes for the detection of neural action potentials. In this work, we have designed and constructed a dual-wavelength polarization-sensitive spectral-domain optical coherence tomography (PS-SDOCT) apparatus for functional neural activity studies with voltage-sensitive dyes. Backscattered light intensity changes of the main and cross-polarization channels were recorded simultaneously for two wavelength bands at 690 nm and 840 nm. Phase signals due to structural changes in the nerve sample were analyzed. Using photodetectors, the system also records the transmission-mode light intensity changes during action potential propagation.

The giant axon and surrounding small nerve fibers were dissected from squid (*Loligo pealeii*, Marine Biological Laboratory, Woods Hole, MA), and stained for 20 minutes with a voltage-sensitive dye (1mg/mL in seawater with 1% DMSO). Of all the dyes we tested, NK3630 and IR144 demonstrated the most prominent signal changes. The nerve stained with NK3630 showed a decrease in transmission of 690 nm light during action potential arrival to the measurement site, which is consistent with results reported in literature. A semi-automatic detection and signal processing algorithms were developed for faster and better analysis, respectively. This optical measurement scheme extracts functional spectroscopic features with contrast-enhancing voltage-sensitive dye. Although this study reports results from a depth profile (M-mode imaging), function in cross-sectional slices may be attained by employing a fast and stable scanner together with high-speed cameras.

9305-259, Session 6

Nanoparticle-assisted-multiphoton microscopy for in vivo brain imaging of mice

Jun Qian, Zhejiang Univ. (China)

Neuro/brain study has attracted much attention during past few years, and many optical methods have been utilized in order to obtain accurate and complete neural information inside the brain. Relying on simultaneous absorption of two or more near-infrared photons by a fluorophore, multiphoton microscopy can achieve deep tissue penetration and efficient light detection noninvasively, which makes it very suitable for thick-tissue and in vivo bioimaging. Nanoparticles possess many unique optical and chemical properties, such as anti-photobleaching, large multiphoton absorption cross-section, and high stability in biological environment, which facilitates their applications in long-term multiphoton microscopy as contrast agents. In this paper, we will introduce several typical nanoparticles (e.g. organic dye doped polymer nanoparticles and gold nanorods) with high multiphoton fluorescence efficiency. We further applied them in two- and three-photon in vivo functional brain imaging of mice, such as brain-microglia imaging, 3D architecture reconstruction of brain blood vessel, and blood velocity measurement.

9305-260, Session 6

Biological imaging in the second near infrared window

Hongjie Dai, Stanford Univ. (United States)

I will present our recent work on fluorescence imaging in the second near-infrared 1000-1700 nm (NIR-II) window. Since 2009, our group has shown NIR-II imaging as a novel in vivo biomedical imaging modality for imaging at up to 4-5 mm tissue depth with sub-10 micron spatial resolution, using a wide range of fluorescent agents including carbon nanotubes, Ag₂S quantum dots, donor-acceptor conjugated polymers and small organic molecules emitting in 1000-1700nm range [Welscher, Nature Nano, 2009; PNAS 2011; Hong, Nature Medicine, 2012] (Ag₂S quantum dots: Hong, Angew Chemie, 2012). I will show ultrafast fluorescence imaging to reveal the blood flow pattern within a single cardiac-cycle of a mouse (Hong, Nature Comm., 2014), and through-skull imaging of the brain of a mouse without craniotomy (Hong, Nature Photonics, 2014). Through these work, our group has shown the advantage of NIR-II imaging over traditional NIR imaging due to much reduced photon scattering of long wavelength light by tissues and ultra-low indigenous background of biological systems in this long wavelength range. The NIR-II imaging modality is capable of video-rate imaging with dynamic contrast, can quantitate blood flows in both normal and ischemic vessels with the capability of high temporal and spatial resolution (micron scale) and deep-tissue penetration up to ~ 5 mm depth (compared to ~ 0.25 mm depth for traditional NIR imaging). These could lead to new opportunities in biology and medicine.

9305-261, Session 6

In-vivo photoacoustic imaging of 3D neural activity of rat brain

Lun-De Liao, Nitish V. Thakor, Bin Liu, National Univ. of Singapore (Singapore)

Optical recording techniques provide powerful tools for neurobiologists and cardiac physiologists to measure the electrical activity of large populations of cells over time and space either through a microscope or in bulk suspension. Hemicyanine (Styryl dyes), one general class of dye chromophores, has emerged as a good foundation for voltage-sensitive dyes (VSDs), due to their electrochromism property. The operation

mechanism of VSDs involves the differential interaction of the electric field in the membrane with the ground and excited states of the dye. Several important hemicyanine dyes were produced over the years, for instance, di-4-ANEPPS, di-8-ANEPPS. As the electrochromic mechanism is a direct interaction of the electric field with the dye, it does not require any movement of the dye molecule, which provides rapid absorbance and fluorescence responses to membrane potentials.

To further our understanding in neurovascular functions of deep brain by increasing the penetration depth of the imaging, voltage-sensitive photoacoustic dyes (VS-PAD) is highly desirable, which is expected to probe the level of neuronal activations and corresponding hemodynamic changes simultaneously in deeper brain region via the current fPAM technique. In this regard, we have developed several tetraphenylethylene (TPE) functionalized VS-PAD by taking advantages of free rotation of the phenylene rings to generation strong photoacoustic signals. The designed dyes are also sensitive to voltage changes of neural membrane. Upon neuron activation, the VS-PAD will gather closely to the activated location, and the level of local aggregation should be in proportion to the potential changes of neural membrane.

9305-262, Session 6

Serial opto-electrocorticography Investigating functional recovery in brain connectivity after rat cerebral infarction

Hsin-Yi Lai, Chang Gung Memorial Hospital (Taiwan) and Chang Gung Univ. (Taiwan); Li-Wei Kuo, National Health Research Institutes (Taiwan); Ching-Rao Chang, Chao-Ting Wang, National Yang-Ming Univ. (Taiwan); Lun-De Liao, National Univ. of Singapore (Singapore); You-Yin Chen, National Yang-Ming Univ. (Taiwan)

Previous studies have shown that whisker stimulation in rats, if initiated within 2 h of middle cerebral artery (MCA) occlusion, can protect the brain by reducing the size of brain ischemia and decreasing neurological deficits. However, the protection mechanism induced by tactile stimulation remains unclear. We proposed, in the present study, that the location of tactile stimulation determines the magnitude of protection effect. Specifically, the protection effect peaks when the ischemic area covers the homologous region corresponding to the location of tactile stimulation. To this end, we employed the photothrombotic ischemia (PTI) model targeted the forelimb region of primary somatosensory cortex (S1FL) in 15 male Sprague Dawley rats (300-350g). The animals were divided into three groups: the forelimb stimulation, hindlimb stimulation, and control (no tactile stimulation) groups. The tactile stimulation was delivered to the forepaw for 40 s with a monophasic constant current of 2-mA, a pulse width of 0.2 ms, and frequency of 3 Hz. Rats were evaluated by laser speckle contrast imaging (LSCI) and electrocorticography (ECoG) at several times points to monitor the effect on cortical hemodynamics and functional connectivity, respectively. The forelimb, hindlimb and control groups showed 0%, 30% and 40% reduction of blood flow induced by PTI, respectively, indicating the protection effect is mediated by the maintenance of blood supply to the ischemic site. Functional connectivity analysis showed that forelimb stimulation induced a slight increase of inter-hemisphere coherence, while hindlimb stimulation induced a decrease of inter-hemisphere coherence. The control group showed a 60% decrease of inter-hemisphere coherence. Finally, the infarct volume measured by 2,3,5-triphenyltetrazolium chloride (TTC) staining, an indicator of cellular respiration, showed a significantly smaller affected volume in the forelimb stimulation group (7.30±0.22 mm³) and no significant difference in hindlimb stimulation group (16.38±2.18 mm³) compared with control group (16.96±2.72 mm³). The results demonstrate that the hemodynamic effect that mediates brain protection is location specific and that the inter-hemisphere coherence highly correlates with the infarct volume and blood flow. This suggests that increased neuronal activity during stroke evolution can mitigate the effects of brain ischemia.

9305-225, Session 8

Connectomics: from terabytes of pixels to intuitive brain networks

Hong-Wei Dong, The Univ. of Southern California (United States)

With the impetus of generating the mammalian connectome, connectivity data is being collected at an unprecedented rate, which will continue to accelerate over the next decade as the recent BRAIN Initiative gathers momentum. Converting these enormously abundant connectivity data, essentially tens and hundreds of terabytes of raw imaging data, into comprehensible knowledge will provide the foundation upon which hypotheses regarding the functional assignments of neural networks can be posed and more accurately tested. I will report the recent progress of our NIH-funded Mouse Connectome Project (www.MouseConnectome.org), elaborating on our general strategy of data production, collection, and informatics development. In particular, I will focus on how our informatics tools are used to accurately and efficiently analyze the large-scale connectivity data in a high-throughput fashion, how to graphically reconstruct pathways for generating connectivity maps, and how these eventually enable us to assemble global neural networks. These assembled networks provide the structural basis for understanding how information is encoded and processed by specific neural circuits and how neural coding and processing lead to perception, emotion, cognition and behavior.

9305-226, Session 8

Whole brain optical imaging (*Invited Paper*)

Ludovico Silvestri, Anna Letizia Allegra Mascaro, National Institute of Optics (INO-CNR) (Italy) and European Lab for Non-linear Spectroscopy (Italy); Irene Costantini, European Lab for Non-linear Spectroscopy (Italy); Leonardo Sacconi, National Institute of Optics (INO-CNR) (Italy) and European Lab for Non-linear Spectroscopy (Italy); Francesco S Pavone, European Lab for Non-linear Spectroscopy (Italy)

Nowadays, there are several imaging techniques offering a complementary approach to visualize intact neural networks on large areas. Each of those offers a different strategy and furnish complementary information on the role of neural components.

We will describe different approaches enabling to move from single neuron details to whole brain imaging, connecting short range structural information to long range one. In particular, some examples of correlative microscopies, combining linear and non linear techniques will also be described.

9305-227, Session 8

Mapping functional corticostriatal and thalamostriatal excitatory synapses on striatal spiny projection neurons

Jun Ding, Yu-Wei Wu, Stanford School of Medicine (United States)

One of the most remarkable features of neural circuit is highly convergent and divergent synaptic connection established between pre- and postsynaptic neurons. Postsynaptic neuron receives convergent synaptic inputs from molecularly and anatomically distinctive presynaptic inputs. How different excitatory synaptic inputs form functional synapses onto a single postsynaptic neuron remains fundamental question in neuroscience.

In the striatum, spiny projection neurons (SPNs) receive convergent inputs from various parts of cortex and thalamus. The majority of excitatory inputs are from M1 motor cortex and S1 somatosensory cortex, as well as centrolateral (CL) and centralmedial and parafascicular (CM/Pf) nucleus of thalamus. Here, we investigated anatomical and physiological differences between functional corticostriatal and thalamostriatal synapses formed on postsynaptic SPNs using combined optogenetics and 2-photon laser scanning microscopy calcium imaging. We found that functional corticostriatal and thalamostriatal synapses are uniquely distributed throughout the dendritic tree. Activation of convergent inputs with discrete spatial distributions may result in very distinct forms of dendritic integration, and ultimately, different SPN spiking output.

9305-228, Session 8

Advances in visualizing a mouse brain-wide networks at single-neuron resolution (*Invited Paper*)

Qingming Luo, Britton Chance Ctr. for Biomedical Photonics (China)

We obtained a three-dimensional (3D) structural data set of a Golgi-stained whole mouse brain at the neurite level with our developed Micro-Optical Sectioning Tomography (MOST) system, which directly demonstrates the whole-brain structural connectivity at the neurite level in a standard format. Based on MOST, we developed several prototypes and protocols for fluorescence imaging with long-range axon tracing and 3D cellular and vascular imaging. In this presentation, I will update the recent progresses of visualizing mouse brain-wide networks at single-neuron resolution and discuss the technological challenges in 3D high-resolution optical imaging configuration, neuron/blood vessel labeling and sample preparation, and massive data processing and visualization.

Conference 9305C: Optogenetics and Optical Control of Cells

Saturday - Sunday 7-8 February 2015

Part of Proceedings of SPIE Vol. 9305 Optical Techniques in Neurosurgery, Neurophotonics, and Optogenetics II

9305-300, Session 1

Implantable, wireless optoelectronic systems for optogenetics (*Keynote Presentation*)

John A. Rogers, Univ. of Illinois at Urbana-Champaign (United States)

No Abstract Available

9305-301, Session 1

Demonstration of a setup for chronic optogenetic stimulation and recording across cortical areas in non-human primates

Azadeh Yazdan-Shahmorad, Camilo Diaz-Botia, Timothy Hanson, Univ. of California, San Francisco (United States); Peter Ledochowitsch, UCSF/UCB Joint Graduate Group in Bioengineering (United States); Michel M. Maharabiz, Univ. of California, Berkeley (United States); Philip N. Sabes, Univ. of California, San Francisco (United States)

Although several studies have shown the feasibility of using optogenetics in non-human primates (NHP), reliable large-scale chronic interfaces have not yet been reported for such studies in NHP. Here we introduce a chronic setup that combines optogenetics with transparent artificial dura (AD) and high-density micro-electrocorticography (mECOG).

To obtain expression across large areas of cortex, we infused AAV5-CamKIIa-C1V1-EYFP viral vector using a novel infusion technique based on convection-enhanced delivery in primary somatosensory (S1) and motor (M1) cortices. By epifluorescent imaging through AD we were able to confirm high levels of expression covering about 110 mm² of S1 and M1. We then incorporated a 192-channel mECOG array spanning 192 mm² into the AD for simultaneous electrophysiological recording during optical stimulation. The array consists of Pt-Au-Pt metal traces embedded in ~10 μm Parylene C insulator. The parylene is sufficiently transparent to allow minimally attenuated optical access for optogenetic stimulation. The array was chronically implanted over the opsin-expressing areas in M1 and S1 for the span of several weeks. Optical stimulation was delivered via a fiber optic placed on the surface of the AD. With this setup, we were able to record reliable evoked activity following light stimulation at several locations and across days.

These results show the feasibility of a chronic interface for combined large-scale optogenetic stimulation and cortical recordings, with stability across several weeks. This interface is a powerful tool to study neural circuits and connectivity across cortical circuits and during behavioral experiments.

9305-302, Session 1

Visible Array Waveguide Gratings for Applications of Optical Neural Probes

Eran Segev, Trevor M. Fowler, Andrei Faraon, Michael L. Roukes, California Institute of Technology (United States)

Computation and information processing in the brain, including perception, learning, and behavior arise from the coordinated activation of large assemblies of neurons distributed across the brain. Current methods for studying these assemblies lack the required ability to deliver precise, dense, and specific stimulation patterns across deep brain circuits, with high spatial and temporal resolution.

We developed ultra-compact multi-channel implantable neural probes for deep brain opto-genetic stimulation. To insure a compact design, each stimulation point is addressed using laser light at a specific wavelength. The routing to each stimulation point is done via Wavelength-Division-Multiplexing/Demultiplexing, implemented with Array Waveguide Gratings (AWGs). The devices are fabricated in a silicon nitride layer deposited on an oxidized SOI wafer. The modulation of each spectral channel is done off-chip thus minimizing any unnecessary dissipation and heat generation on the probe.

We demonstrate AWGs working in the visible spectrum, with spectra centered around wavelengths in the red (673nm) and blue (473nm) having a bandwidth of 1nm/channel, and total footprints of less than 220x170 μm² and 150x110 μm² respectively. As a proof of concept, these AWGs are used to drive up-to 9 highly dense illumination points fabricated on a single neural probe shank. The scalability of this technology ensures that tens to hundreds of independent stimulation points can be fabricated on each probe at will. This approach is completely compatible with semiconductor foundry mass-production processes and about 100 probes can be fabricated on a single 4" wafer.

9305-303, Session 1

Automated laser tracking and optogenetic manipulation system for multiple freely moving *Drosophila* adults (*Invited Paper*)

Yen-Yin Lin, Ming-Chin Wu, Po-Yen Hsiao, Li-An Chu, Chih-Wei Hsu, Chien-Chung Fu, Ann-Shyn Chiang, National Tsing Hua Univ. (Taiwan)

Social behavior investigation plays an important role in neuroscience because animal behaviors reflect the internal neuron activities. In this talk, we present an automated laser tracking and optogenetic manipulation system (ALTOMS) for studying social behaviors in freely moving fruit flies (*Drosophila melanogaster*), because several light-activated protein channels were recently developed for mimicking a real stimulus in behavior assays. ALTOMS comprises an intelligent central control module for real-time fly behavior analysis (~40 fps) and a laser scanning module for targeting three lasers at 473 nm, 593.5 nm and 1064 nm in wavelength independently on any specified body parts of two freely moving *Drosophila* adults. ALTOMS also can control the behavior arena's temperature by near-infrared illuminator. By using ALTOMS to monitor and compute the location, orientation, wing posture, and relative distance between two flies in real-time and using high-intensity laser irradiation as an aversive stimulus, this laser tracking system can be used for a new operant conditioning assay in which a courting male quickly learns and forms a long-lasting memory to stay away from a freely moving virgin female. With the equipped lasers, channelrhodopsin-2 and/or halorhodopsin expressed in selected neurons can be triggered on the basis of interactive behaviors between two flies. Temperature sensitive genetic tools also can be manipulated by equipped near-infrared illuminator. Given its capacity for optogenetic manipulation to acutely and independently turn on/off selective neural activity, ALTOMS offers opportunities to systematically map brain circuits that orchestrate specific *Drosophila* behaviors.

**Conference 9305C:
Optogenetics and Optical Control of Cells**

9305-304, Session 1

Laser-induced perturbation into molecular dynamics localized in neuronal cell

Chie Hosokawa, National Institute of Advanced Industrial Science and Technology (Japan); Naoko Takeda, National Institute of Advanced Industrial Science and Technology (Japan) and Kwansei Gakuin Univ. (Japan); Suguru N. Kudoh, Kwansei Gakuin Univ. (Japan); Takahisa Taguchi, National Institute of Advanced Industrial Science and Technology (Japan)

Neurons in brain systems communicate through synaptic connections and form a complex network. The molecular dynamics including neurotransmitter receptors and a variety of scaffolding and signaling proteins at synaptic terminals are essential for synaptic plasticity and subsequent modulation of cellular functions in a living neuronal network. In order to realize artificial control of neuronal activity without any drugs and genes, we demonstrate laser-induced perturbation into molecular dynamics in living neurons. The optical trapping and assembling dynamics of synaptic vesicles or neural cell adhesion molecules (NCAMs) at plasma membrane in hippocampal neurons was evaluated by fluorescence imaging and fluorescence correlation spectroscopy (FCS). When a 1064-nm laser beam was focused on the synaptic vesicles labeled with a fluorescent dye FM1-43 in a neuronal cell, the fluorescence intensity gradually increased with the laser irradiation time, suggesting that synaptic vesicles were optically trapped and assembled at the focus. Moreover, we applied laser-induced perturbation to NCAMs labeled with quantum dots (Q-dots) in neurons. The NCAM whose diameter is ~10 nm labeled with a few tens of nm-sized Q-dot can be trapped slightly easily as compared to trapping of the single molecule. After focusing a trapping laser on NCAMs labeled with Q-dots in a neuronal cell, the fluorescence intensity of Q-dots increased at the focal spot. The assembling dynamics of NCAMs in an optical trap was revealed by FCS that the particle motion of Q-dots attached to NCAM was constrained at the laser focus due to optical trapping force. Our method has a potential to achieve the realization of optical control of synaptic transmission in living neuronal network.

9305-305, Session 1

Fabrication of multipoint light emitting optical fibers for optogenetics

Leonardo Sileo, Istituto Italiano di Tecnologia (Italy); Marco Pisanello, Massimo De Vittorio, Istituto Italiano di Tecnologia (Italy) and Univ. del Salento (Italy); Ferruccio Pisanello, Istituto Italiano di Tecnologia (Italy)

Although genetic techniques allow targeting well-defined neuronal sub-populations with light-sensitive proteins, controlled delivery of light at specific and/or multiple locations of the brain still represents a challenge. Indeed, most in vivo optogenetic experiments are performed with a single optical fiber, whose illumination is limited to a fixed volume of the brain.

We describe the fabrication and the in vivo implementation of a new and minimally invasive optogenetic device [F. Pisanello et al., *Neuron* 82, 1245 (2014)] that allows dynamic and selective stimulation of multiple brain regions through a single, thin and sharp fiber optic. It is composed by a tapered optical fiber whose tapered region is covered with gold to avoid uncontrolled leakage of light. Along the 1mm-long taper, Focused Ion Beam milling is used to open micrometer-sized windows, through which light is allowed to out-couple. Each window can be selectively activated by changing the light-coupling angle θ at the distal end of the fiber, thus injecting different modal subsets into the fiber. When the injected modal subset reaches the taper, it undergoes to a modal manipulation process that allows window-selective emission: low order modes (low θ) are emitted by windows close to the taper tip, while high order modes (high θ) are out-coupled at distal windows.

The ability to address optical excitation to different parts of the brain along the length of the fiber was tested in the brain of head-restrained awake mice, showing the suitability of this device for layer-selective control of neural activity in mouse motor cortex.

9305-307, Session 2

Optical tools for mapping and engineering the brain (Keynote Presentation)

Edward S. Boyden, MIT Media Lab. (United States)

No Abstract Available

9305-308, Session 2

In vivo all-optical interrogation of neurons in mice using optogenetics and calcium imaging with two-photon fluorescence microscopy

James R. Mester, Sunnybrook Research Institute (Canada) and Univ. of Toronto (Canada); Margaret Koletar, Sunnybrook Research Institute (Canada); John G. Sled, Univ. of Toronto (Canada) and Toronto Ctr. for Phenogenomics (Canada); Bojana Stefanovic, Sunnybrook Research Institute (Canada) and Univ. of Toronto (Canada)

Combined optical stimulation and recording of individual neurons in vivo has recently been made possible by the development of red-shifted genetically-encoded calcium indicators (GECIs) such as RCaMP. This is due to reduced spectral overlap in the two-photon (2P) excitation cross-sections of Channelrhodopsin-2 (ChR2) and RCaMP. All-optical interrogation of individually-stimulated neurons in deep cortical layers becomes possible using simultaneous 2P excitation and 2P imaging in mice co-expressing ChR2 and RCaMP. In this work, expression has been driven via co-transfection of adeno-associated viruses (AAV) containing ChR2 (AAV1. hSyn.ChR2(H134R)-eYFP.WPRE.hGH, UPenn vector core) or RCaMP (AAV1. Syn.RCaMP1h.WPRE.SV40, UPenn vector core). Injections of AAVs were performed 2-3 weeks prior to imaging sessions to allow for viral expression to occur. With ChR2 and RCaMP expressing in excitatory pyramidal neurons of the primary somatosensory cortex in C57/BL6 mice equipped with a closed cranial window, optical interrogation of single cells was done through simultaneous illumination at wavelengths of 920 nm for ChR2 stimulation and 1020 nm for RCaMP fluorescence imaging. Illumination power did not exceed 20 mW to avoid tissue damage, while still providing sufficient light for ChR2 activation and RCaMP imaging. Dual wavelength illumination is performed with two Ti:sapphire lasers (Mai Tai DeepSee, Spectra Physics) attached to a commercial 2P microscope (FV1000, Olympus). We have contrasted the relative SNR and spatiotemporal features of RCaMP fluorescence resulting from LED-driven versus 2P ChR2 stimulation as to evaluate the advantages and disadvantages of simultaneous, spatially-resolved photoactivation and fluorescence imaging when compared to conventional ChR2 photoactivation and recording techniques.

9305-309, Session 2

Near-infrared (NIR) optogenetics using up-conversion system

Shoko Hososhima, Graduate School of Life Sciences, Tohoku Univ. (Japan) and JST, CREST (Japan) and Research Fellow of Japan Society for the Promotion of Science (Japan); Hideya Yuasa, Graduate School of Bioscience and Biotechnology, Tokyo Institute of

**Conference 9305C:
Optogenetics and Optical Control of Cells**

Technology (Japan); Toru Ishizuka, Hiromu Yawo, Graduate School of Life Sciences, Tohoku Univ. (Japan) and JST, CREST (Japan)

Non-invasive remote control technologies designed to manipulate neural functions are long-awaited for the comprehensive and quantitative understanding of neuronal network in the brain as well as for the therapy of neurological disorders. Recently the neuronal activity is enabled to be optically manipulated using biological photo-reactive molecules such as channelrhodopsin-2 (ChR2). However, ChR2 and its relatives are mostly reactive to visible light which does not effectively penetrate through biological tissues. In contrast, near-infrared (NIR) light (650–1450 nm) penetrates deep into the tissues because biological systems are almost transparent to light within this so-called 'imaging window'. Here we used lanthanide nanoparticles (LNPs), which composed of rare-earth elements, as luminous bodies to activate channelrhodopsins (ChRs) since they absorb low-energy NIR light to emit high-energy visible light (up-conversion). Neuron-glioma-hybrid ND-7/23 cells were cultured with LiYF₄(Yb/Er 20/2) particles (peak emission, 543 nm) and transfected to express CIV1 (peak absorbance, 539 nm), a chimera of ChR1 and VChR1. Two days later, photocurrents were measured under whole-cell patch clamp at -60 mV in response to NIR laser light (976 nm). The amplitude of photocurrent was dependent on the laser power and reached the maximal level as same as that evoked by LED light (peak, 490–520 nm; 0.33 mWmm⁻²) or filtered Hg lamp (530–550 nm; 1.6 mWmm⁻²). It is suggested that the green luminescent light emitted from LNPs effectively activated CIV1 to generate photocurrent. This system would be applied to activate neurons deep in the brain non-invasively with the optimization of LNPs, acceptor photo-reactive biomolecules and optics.

9305-310, Session 2

Normalization through local excitation and inhibition in macaque primary visual cortex (*Invited Paper*)

Jonathan J. Nassi, The Salk Institute for Biological Studies (United States)

Normalization has been proposed as a canonical cortical computation operating across a wide range of sensory modalities, brain areas and species. Its defining property is that the excitability of a neuron is inversely proportional to the overall activity level of the network. In primary visual cortex (V1) this can account for a wide range of non-linear response properties, including the sigmoidal shape of the contrast response function and cross-orientation suppression. One of the key components of normalization is a broadly-tuned, divisive input signal that scales with stimulus contrast. The underlying circuitry of this so-called "normalization pool" remains poorly understood. Here, we measured the causal effects of locally-generated excitation and inhibition on spontaneous and visually-evoked responses in V1 of alert, fixating macaque monkeys. Optogenetic depolarization of excitatory neurons produced both facilitation and suppression of spontaneous activity, consistent with the interpretation that optogenetic stimulation activated the normalization circuit, causing both increased excitatory drive as well as indirect divisive inhibition. Increased recruitment of both excitation and inhibition with stimulation intensity produced non-linear response properties similar to those typically observed with increased luminance contrast. Accordingly, we hypothesized that simultaneous visual and optogenetic stimulation should interact as predicted by a normalization model. According to the model, optogenetic stimulation added excitatory drive and divisive suppression to the visual contrast response function. The ratio of optogenetic induced excitation and inhibition was assumed to vary across the population and scaled with both stimulation intensity and contrast. As predicted by the model, simultaneous visual and optogenetic stimulation produced sub-additive responses that were well characterized by a weighted sum of the individual responses. The weights depended strongly on the relative intensity of visual and optogenetic stimulation, ranging from near-equal averaging to winner-take-all. We observed a range of effects of optogenetic stimulation on the visual

contrast response functions, all of which were well accounted for by the model. These results suggest that optogenetic depolarization of excitatory neurons activates the neural elements that mediate normalization in the primate cortex.

9305-311, Session 2

Bringing the light to high throughput screening: use of optogenetic tools for the development of recombinant cellular assays

Viviana Agus, Alberto Di Silvio, Jean Francois Rolland, Anna Mondini, Sara Tremolada, Katharina Montag, Lia Scarabottolo, Loredana Redaelli, Stefan Lohmer, AXXAM S.p.A. (Italy)

Recently the use of optogenetics technologies has encountered numerous and widespread applications in the manipulation of cellular processes.

The use of genetically encoded light-controlled proteins has been successfully validated in complex biological system, such as iPSC cells, intact tissues or animal behavior, providing a very convenient method to interrogate, dissect and understand many cellular mechanisms, with high specificity and temporal precision.

All the advantages of the use of light-controlled actuators, such as genetic targeting to specific cell types or cell compartments, reversible stimulation, avoidance of chemical perturbation, mimicking of native electric activities, might be very useful if transferred to the early stage of the drug discovery process. The possibility to set up Screening Assays using such an optical modulation would indeed represent a very powerful technology, which helps in the identification of modulators of therapeutically relevant targets in the early steps of drug discovery processes.

Our aim was to validate and test the performance of different light-gated actuators and different sensors in the generation of novel cellular recombinant assays, in order to prove their robustness and adaptability to early drug discovery assays and eventually also to HTS instrumentation.

We successfully generated a recombinant cell line where the activity of a voltage-gated calcium channel is modulated by the use of Channelrhodopsin 2, and the activity of state-dependent blockers is well detected. We also successfully tested the performance of different Channelrhodopsin mutants to modulate ion channel targets, and of genetically encoded voltage sensors recently disclosed, such as ArcLight.

In our presentation, we will describe all the results obtained based on the generation of recombinant cellular assays, showing the performance of different optogenetics tools in a miniaturized format and their compatibility with the most used HTS fluorescence readers.

9305-312, Session 2

Photonic crystal fiber supercontinuum sources for optogenetics

Eugene D. Ark, Univ. of Illinois at Urbana-Champaign (United States); Kush Paul, Haohua Tu, Youbo Zhao, Beckman Institute for Advanced Science and Technology (United States); Stephen A. Boppart, Beckman Institute for Advanced Science and Technology (United States) and Univ. of Illinois at Urbana-Champaign (United States)

The rapid development of novel opsins and fluorescent indicators has introduced a large palette of biochemical probes for optogenetic stimulation and cellular imaging. The spectral sensitivities of these molecules cover the full wavelength range of visible light. However, two-photon interactions frequently necessitate the use of high-power sources with narrow bandwidth outputs. Although tunable sources, such as the titanium-

**Conference 9305C:
Optogenetics and Optical Control of Cells**

sapphire laser, provide some degree of flexibility, researchers are typically restricted to those molecules whose responses are evoked from within small, discrete wavelength ranges. Because of the often prohibitive cost and space constraints associated with utilizing multiple laser sources on a single optical table, we sought an alternative source for use in conjunction with these new probes.

Recent advances in optical fiber technologies include photonic crystal fibers capable of generating coherent, stable supercontinua. This fiber-based supercontinuum generation exhibits an output light that possesses a wide range of wavelengths with uniform spatial profile at powers suitable for two-photon interactions with optically-responsive molecules in tissue. Furthermore, this broadband light, which can span 800 - 1300 nm, covers the majority of the near-infrared "optical window" of biological tissues for which depth of penetration is greatest. We demonstrate the use of a photonic crystal fiber pumped by a Ytterbium laser as a broadband femtosecond pulsed source for two-photon optogenetics and imaging, along with whole-cell patch clamp recordings of cells expressing ChR2 and two-photon images of various tissues. Our results also suggest that these supercontinuum sources hold potential for experiments involving simultaneous use of multiple optically-sensitive molecular probes.

9305-313, Session 2

Optically controlled delivery of actin-staining molecules and opsin-encoding plasmids into mammalian cells

Kamal Dhakal, Samarendra K. Mohanty, The Univ. of Texas at Arlington (United States)

Visualization, activation, and detection of the cell(s) and their activity require delivery of exogenous impermeable molecules and targeted expression of genes encoding labeling proteins, ion-channels and voltage indicators. While genes can be delivered by viral vector to cells, delivery of other impermeable molecules into the cytoplasm of targeted cells requires microinjection by mechanical needle or microelectrodes, which pose significant challenge to the viability of the neurons. The virus-based gene transfer method is prone to cause unexpected inflammatory responses, immunological reactions, and limit the size of plasmid that can be packaged for delivery. Further, for understanding of the functioning of cellular circuitry, it will be useful to localize the expression of the targeted molecules not only in specific cell types, but to specific neurons in restricted spatial regions. We recently demonstrated use of ultrafast NIR laser microbeam for spatially-localized transfection of retina explant with Thy1-ChR2-YFP-plasmids. Here, we report use of the ultrafast NIR laser beam for delivery of ReaChR-encoding genes and impermeable actin-staining molecules into targeted HEK cells and cortical neurons.

9305-314, Session 3

Engineering proteins for visualization and control of signaling networks in vivo
(Keynote Presentation)

Klaus Hahn, The Univ. of North Carolina at Chapel Hill (United States)

Cell motility requires the orchestration of many dynamic cellular systems, which can only be fully understood through quantitation of protein activity in living cells and animals. This talk will describe new tools to visualize and manipulate signaling in vivo, using Rho family GTPase networks and cell motility as test beds. Multiplexed imaging of biosensors and computational image analysis will be used to examine the coordination of GTPases. The role of specific protein activation events regulating coordination will be probed using engineered allosteric switches and different methods to control the dynamics of protein activity with light. New technologies will include methods to direct activated kinases to specific targets, broadly

applicable methods to control sequestration of proteins at intracellular membranes with light, and improvements in biosensor design for applications in animals.

9305-315, Session 3

Broad spectral excitation of ReaChR-sensitized cells

Subrata Batabyal, Sarmishtha Satpathy, Kamal Dhakal, Young-tae Kim, The Univ. of Texas at Arlington (United States); John Y. Lin, Univ. of California, San Diego (United States); Samarendra K. Mohanty, The Univ. of Texas at Arlington (United States)

In addition to higher resolution, optogenetics has several advantages over electrical stimulation such as cellular specificity and non-invasiveness. However, till now narrow-band light has been used for optogenetic excitation. Here, we report use of broad spectral excitation for optogenetic stimulation of ReaChR-sensitized cells. We observed robust ReaChR excitation with broad-band light offering higher photocurrents compared to spectrally-filtered narrow-band light. The rise in photocurrent due to increase in intensity of broad-band light is found to be higher than that due to narrow-band light. Further, the broad-band excitation of ReaChR led to faster ion-channel kinetics in contrast to spectrally-filtered light.

9305-316, Session 3

Spatio-angular light control in microscopes using micro mirror arrays

Florian Ruckerl, Institut Pasteur, Imagopole, Plateforme d'Imagerie Dynamique (PFID) (France); Jörg Heber, Dirk Berndt, Michael Wagner, Fraunhofer-Institut für Photonische Mikrosysteme (Germany); Spencer L. Shorte, Institut Pasteur, Imagopole, Plateforme d'Imagerie Dynamique (PFID) (France)

We combine a microscopy setup with two micromirror arrays (MMA), which allow not only to spatially restrict the shape of the light across the field of view, but also to control the direction of the incident light. In order to achieve this, one MMA is imaged in the focal plane and used as a black and white (or greyscale) mask, while the second MMA is imaged in the backfocal plane for angular control. Overall, the setup allows selective illumination of subcellular regions enabling the precise, localized activation of optogenetic probes and enables to minimize illumination of out-of-focus objects.

9305-317, Session 3

Using optogenetics to map the spatial organization of local circuits
(Invited Paper)

George J. Augustine, Duke-NUS Graduate Medical School (Singapore)

No Abstract Available

**Conference 9305C:
 Optogenetics and Optical Control of Cells**

9305-318, Session 3

Highly compact MEMS-based optrodes with integrated light sources (*Invited Paper*)

Patrick Ruther, Michael Schwaerzle, Christian Gossler, Ulrich T. Schwarz, Oliver Paul, Univ. of Freiburg (Germany)

Over the past decade, the controlled modification of neural activity of specific types of neurons in well-defined brain regions by optical stimuli has emerged as one of the most appealing experimental approaches in neuroscience. Besides the development of optically sensitive biomolecules and their expression in neurons, miniaturized micro-optical tools, so-called optrodes, enabling simultaneous tissue illumination and electrical recording of neural signals have fuelled a rapidly-growing research topic in biomedical engineering.

The lecture will review the state of the art in optrode technologies from glass fibers combined with simple wire electrodes and silicon-based probe arrays to three-dimensional probe arrangements combined with sophisticated illumination setups implementing waveguide arrays. This will be contrasted by recent developments of our research teams aiming at the direct integration of bare laser diode (LD) chips and light emitting diodes (LEDs) on silicon probe shafts, MEMS-based housings as well as flexible polymer-based substrates. While the silicon shafts comprise polymer waveguides combined with LD chips flip-chip-bonded onto the probe base, thin film LEDs are wafer bonded onto silicon shafts and polymer substrates using an innovative laser lift-off process. Alternatively, LED chips are combined with MEMS housings, short glass fibers, and highly flexible polyimide ribbon cables. The three systems have in common that a larger number of light sources is integrated in the probe, thereby enabling the direct electrical control of the optrodes without mechanical perturbation by external glass fibers. The systems are designed for basic research and being applied in optical cochlear implants.

9305-319, Session 3

Metal coated chemically etched fiber probe for single cell culture

Kozo Taguchi, Ritsumeikan Univ. (Japan)

A wide variety of naturally occurring bacteria cannot be isolated by classical microbiological methods. The principal procedures for obtaining pure cultures of bacterial strains have not been much improved since Robert Koch introduced the agar plating technique more than 100 years ago. Ashkin et al. proposed the optical trapping of dielectric particles by a single-beam gradient force trap for the first time. This laser beam trapping method is considered to be useful for manipulation of biological object because of noninvasive technology.

We have already developed an optical trapping system with a chemically etched fiber probe. A transparent micro object can be trapped and manipulated by the laser beam from optical fiber. This system is simpler and more flexible than conventional optical tweezers. However, these fiber optical tweezers cannot form a Three-Dimensional optical trap by using just single one optical fiber due to the weakly focused laser beam. Furthermore, optical tweezers cannot discriminate between live and dead cells.

Therefore, in this paper, dielectrophoresis tweezers using metal coated chemically etched fiber was proposed for cell manipulation and isolation. We proposed a simple and low cost dielectrophoretic device for picking out and relocating single target cells. The device consists of a single metal coated chemically etched fiber and an AC signal generator. It does not require microfabrication technologies or sophisticated electronics. From experimental results, it was found that our proposed dielectrophoretic manipulator could discriminate between live and dead cells. We also could see the cell reproduction of yeast cells trapped using our proposed dielectrophoresis tweezers.

9305-320, Session 3

Polarimetric detection of cellular activation by optogenetic excitation

Sarmishtha Satpathy, Subrata Batabyal, Young-tae Kim, Samarendra K. Mohanty, The Univ. of Texas at Arlington (United States)

Current methods for detection of cellular activation such as multielectrode array and optical functional imaging either have very poor resolution or are invasive in nature. Here, we report use of polarized light for wide-field detection of optogenetically-stimulated activity in HEK cells and cortical neurons. During depolarization of cells, the activation of sodium channels induces a reorientation of the peptide bonds in membrane, thus altering the polarization of scattered light within sub-ms time scale. Thus, no exogenous labeling is required and cellular activity can be detected with high spatial and temporal resolution by wide-field, polarimetric imaging. The large-scale and long-term recording of activities by polarimetric imaging at high temporal and spatial resolution during optical modulation will allow analysis of complex cellular network activities under broad set of conditions.

9305-321, Session 4

Playing the piano with neural circuits: simultaneous 3D all-optical imaging and activation of neurons in vivo (*Keynote Presentation*)

Rafael Yuste M.D., Columbia Univ. (United States)

I will review the efforts of our group developing optical methods to perform two-photon imaging and photostimulation of neuronal populations using spatial light modulators, PSF engineering and a variety of optical, optogenetic and optochemical sensors. These techniques have single cell resolution and enable online "piano" experiments on populations of neurons, such as detecting spatiotemporal patterns of neuronal activity in primary visual cortex from awake behaving mice and optically interfering with them.

9305-322, Session 4

Experimental systems for optogenetic control of protein activity with photodissociable fluorescent proteins

Xin Zhou, Michael Lin, Stanford Univ. (United States)

We describe a previously unknown feature of a variant of the photochromic green fluorescent protein (FP) Dronpa - the ability to undergo light-dependent dissociation and association, and use it to control protein activities with light. We propose a Fluorescent Light-inducible Proteins (FLiPs) design in which Dronpa domains are fused to both termini of an enzyme domain. In the dark, the Dronpa domains tetramerize and cage the protein, but light induces Dronpa dissociation and activates the protein. This method enabled optical control over guanine nucleotide exchange factor and protease domains with temporal and spatial resolution, and we are currently generalizing it to other protein families including kinase and DNA nuclease. We further simplified the system by designing and engineering the heterodimerizing and homodimerizing Dronpa domains. The heterodimer enables us to develop Dronpa-based translocation system and the homodimers largely improve the protein folding as well as the caging efficiency. We also used molecular dynamics (MD) simulations to illustrate the mechanism of protein caging with Dronpa domains. Our findings expand the applications of FPs from exclusively sensing functions to also encompass optogenetic control.

Conference 9305C:
Optogenetics and Optical Control of Cells

9305-323, Session 4

Multi-opsin construct for effective stimulation of cells by broad-band light

Gregory M. Cervenka, Subrata Batabyal, Kamal Dhakal, Young-tae Kim, Samarendra K. Mohanty, The Univ. of Texas at Arlington (United States)

Currently, use of optogenetic sensitization of retinal cells combined with activation/inhibition has potential as alternative to retinal implantations that would have required electrodes inside every single neuron for high visual resolution. However, clinical translation of optogenetic activation for restoration of vision suffers from the drawback that narrow spectral sensitivity of opsin requires active stimulation by blue laser or LED having intensity much higher than ambient light. In order to allow ambient-light based stimulation paradigm, here we report development of multi-opsin construct that has broad spectral excitability in the entire visible spectrum. The cells sensitized with multi-opsin construct shows order of magnitude higher excitability with white light as compared to that using only the narrow-band light components. The use of multi-opsin construct will allow higher sensitivity of the opsin-sensitized higher-order neurons in degenerated retina to ambient white light, and therefore, significantly lower activation-threshold in contrast to conventional approach of intense, narrow band light based active-stimulation.

9305-324, Session 4

Distributed optogenetic interfacing with retinas, optonets and brains: photonics and potential applications (*Invited Paper*)

Shy Shoham, Technion-Israel Institute of Technology (Israel)

No Abstract Available

9305-325, Session 4

All-optical control of construction, manipulation, modulation and detection of neural circuit and activities

Samarendra K. Mohanty, The Univ. of Texas at Arlington (United States)

No Abstract Available

Conference 9306: Lasers in Dentistry XXI

Sunday 8 February 2015

Part of Proceedings of SPIE Vol. 9306 Lasers in Dentistry XXI

9306-1, Session 1

Evaluation of three different laser modalities for periodontal therapy

Neha Yadav, Arundeeep K. Lamba, Farrukh Faraz, Shruti Tandon, Maulana Azad Institute of Dental Sciences (India)

Periodontal therapy aims at removal of supra- and subgingival deposits from the root surface to decrease bacterial load and stop disease progression. Although, plaque biofilm and calculus removal by scaling and root planing (SRP) is a critical part of periodontal therapy, complete removal is not always possible especially in inaccessible sites such as deeper pockets and furcation areas. The purpose of the study was to evaluate the adjunctive effect of antimicrobial photodynamic therapy (aPDT), Diode Laser and Er,Cr:YSGG Laser in treatment of patients with chronic periodontitis. Following scaling and root planing, re-evaluation was done after 4-6 weeks and clinical parameters recorded. Patients with the presence of at least 2 non adjacent teeth with probing depth ≥ 6 mm, and bleeding on probing were included. Forty (40) subjects with chronic periodontitis, divided into 4 groups were recruited and treated using either SRP+aPDT, SRP+diode laser, SRP+Er,Cr:YSGG-Laser or SRP alone. Clinical indices recorded were Plaque Index (PI), modified sulcular bleeding index (mSBI), pocket probing depth (PD), clinical attachment level (CAL). Patients were recalled after 1 month and 3 months, for evaluation of clinical parameters. All modalities yielded significant improvement in clinical parameters. There was greater reduction in probing-depth, gain in attachment with aPDT followed by Diode and Er,Cr:YSGG-Laser.

9306-2, Session 1

Short pulse mid-infrared radiation removal of tooth tissue

Tatjana Dostálová M.D., Charles Univ. in Prague (Czech Republic); Helena Jelínková, Jan Sulc, Michal Nemeč, Czech Technical Univ. in Prague (Czech Republic)

The main goal was an investigation of powerful Er:YSGG radiation (wavelength 2.79 μm) interaction with ivory. As source of radiation, the free-running/Q-switched Er:YSGG laser was used. This laser generates 250 us/100 ns long pulses (FWHM) with the pulse energy of 123 mJ/41 mJ, respectively, repetition rate 1 Hz. The slice of ivory with the thickness of 1.3 mm was utilized as an interaction tissue. The lens with the focal length 85 mm was used for concentration of the radiation on interacting material. The ablation rate was checked for case of both above mentioned regimes as well as for the cases of without and with water cooling of interacting material. It was found that for long pulse with the energy density of 176 J/cm² the slice was perforated for 15 pulses and the corresponding ablation rate was 0.033 mm³/J (without water spray). In the case of 100 ns pulses with the energy density of 46 J/cm² the slice was not perforated even for 1000 pulses without water spray. With the water film the slice was perforated after 160 pulses and the ablation rate was 0.012 mm³/J.

9306-3, Session 1

Investigations of the damage mechanisms during ultrashort pulse laser ablation of dental tissue

Matthias Domke, FH Vorarlberg (Austria); Sebastian Wick, Hochschule für Angewandte Wissenschaften München (Germany); Maike Wahler, LIFE-Zentrum, Klinikum der

Univ. München (Germany); Stephan Rapp, Hochschule für Angewandte Wissenschaften München (Germany); Julia Kuznetsova, Christian Homann, LIFE-Zentrum, Klinikum der Univ. München (Germany); Heinz P. Huber, Munich Univ. of Applied Sciences (Germany); Ronald Sroka, LIFE-Zentrum, Klinikum der Univ. München (Germany)

Several investigations of dental tissue ablation with ultrashort pulses usually suggest that these lasers enable precise and selective material removal and reduce the formation of micro cracks and thermal effects in contrast to ns-pulses. In this study, we present two damage mechanisms occurring during ultrashort pulse ablation of dentin using a 400 fs-laser at wavelength of 1040 nm and investigate their driving mechanisms.

First, it was found that nano cracks appear around the craters after single pulse ablation. These cracks are directed to the crater and cross the dentinal tubules. Transient investigation of the single pulse ablation process by pump-probe microscopy suggest that the driving mechanism could be a pressure wave that is released after stress confinement.

Second, squared holes were ablated using scan speeds between 0.5 mm/s and 2.0 m/s and fluences up to 4.5 J/cm². It was found that deep cracks appear at the edges of the squared holes, if the pulse overlap is above 85%. In contrast, the fluence has only a minor impact on the crack formation. The crack propagation was investigated in the depth using x-ray micro tomography and optical coherence tomography. It was found that these cracks appear in the depth down to the dental pulp. These findings suggest that fast scanning of the laser beam is the key for damage free processing using ultrashort pulse lasers. Then, ablation rates of about 2,5 – 3,5 mm³/min/W can be achieved in dentine with pulse durations of 400 fs.

9306-4, Session 1

Investigations on the potential of a low power diode pumped Er:YAG laser system for oral surgery

Karl Stock, Florian Hausladen, Raimund Hibst, Univ. Ulm (Germany)

Flashlamp pumped Er:YAG-lasers are used in clinical practice for dental applications successfully. As an alternative, several diode pumped Er:YAG laser systems (Pantec Engineering AG) become available, with mean laser power of 2W, 15W, and 30W.

The aim of the presented study is to investigate the potential of the 2W Er:YAG laser system for oral surgery.

At first an appropriate experimental set-up was realized with a beam delivery and both, a focusing unit for non contact tissue cutting and a fiber tip for tissue cutting in contact mode. In order to produce reproducible cuts, the samples (porcine gingiva) were moved by a computer controlled translation stage. On the fresh samples cutting depth and quality were determined by light microscopy. Afterwards histological sections were prepared and microscopically analyzed regarding cutting depth and the thermal damage zone.

The experiments show, that low laser power $\leq 2\text{W}$ is sufficient to perform efficient oral soft tissue cutting with cut depth up to 2mm (sample movement 2mm/s). The width of the thermal damage zone (about 50 μm to 300 μm) can be controlled by the irradiation parameters. In general, thermal injury is more pronounced using fiber tips in contact mode compared to the focused laser beam.

In conclusion the results reveal that even the low power diode pumped Er:YAG laser is an appropriate tool for oral surgery.

9306-5, Session 1
810 nm, 980 nm, 1470 nm and 1950 nm diode laser comparison: a preliminary ex vivo study on oral soft tissues

Carlo Fornaini M.D., Elisabetta Merigo, Michele Sozzi, Annamaria Cucinotta, Paolo Vescovi, Stefano Selleri, Univ. degli Studi di Parma (Italy)

The introduction of diode lasers in dentistry has several advantages, mainly due to their reduced size, reduced cost and optical fibers beam delivery. Nowadays the two main wavelengths used for soft tissue treatments in dental field are 810 and 980 nm.

The aim of this study was to compare soft tissues ablation effectiveness of four wavelengths: 810, 980, 1470 and 1950 nm.

Several samples of veal tongue were exposed to the four wavelengths, at different fluences. The internal temperature of the exposed samples has been monitored with a thermocouple during the experiment. The excision quality has been characterized by means of an optical microscope. Tissue damages and the cut regularity have been evaluated on the base of established criteria.

The lowest superficial thermal increases were recorded for 1950 nm laser with values of 8.4 and 11.9 °C for respectively 2 W and 4 W emitted power.

Best quality and speed of incision were obtained by the same wavelength with total incision time of 2 minutes and 59 seconds for 2 W and 1 minute and 32 seconds for 4 W.

By evaluating epithelial, stromal and vascular damages for all the used wavelengths, the best result, in terms of "tissue respect", have been obtained for 1470 and 1950 nm exposures.

From the obtained results 1470 and 1950 nm wavelengths showed to be the best performer among those used in this "ex vivo" study, probably due to their higher affinity to water.

9306-6, Session 2
A novel laser-based method for controlled crystallization in dental prosthesis materials

Peter Cam, Beat Neuenschwander, Patrick Schwaller, Benjamin Köhli, Berner Fachhochschule Technik und Informatik (Switzerland); Beat Lüscher, Florian Senn, Fachhochschule NordWestschweiz (Switzerland); Alain Kounga, Christoph Appert, Institut Straumann AG (Switzerland)

Glass-ceramic materials are increasingly becoming the material of choice in the field of dental prosthetics, as they can feature both high strength and very good aesthetics. It is believed that their color and microstructure and mechanical properties can be tuned such as to achieve a lifelike performance. In order to reach that ultimate a controlled arrangement of amorphous and crystalline phases in the material is required. A phase transition from amorphous to crystalline is achieved by a heat treatment at defined temperature levels. The traditional approach is to perform the heat treatment in a furnace. This, however only allows a homogeneous degree of crystallization over the whole volume of material.

Here a novel approach using a local heat treatment by laser irradiation is presented. To investigate the potential of this approach the crystallization process of SiO₂-Li₂O-Al₂O₃-based material has been studied. For the experiments a continuous-wave laser (808nm wavelength) and pulsed nanosecond lasers (1064nm wavelength) have been used.

Our results show the feasibility of gradual and partial crystallization of the base material using continuous laser irradiation. A dental prosthesis machined from the glassy state can be effectively treated with laser

irradiation and crystallized within a confined region of a few millimeters starting from the body surface. Very good aesthetics and good mechanical stability have been achieved. The findings obtained with the continuous wave laser will be compared with the results from crystallization experiments using pulsed nanosecond lasers of 1064nm wavelength and a few hundreds nanoseconds pulse width. The use of laser pulses should allow more accuracy of the controlled crystallization.

9306-7, Session 2
Dental composite polymerization: a three different sources comparison

Michele Sozzi, Carlo Fornaini M.D., Giuseppe Lagori, Elisabetta Merigo, Annamaria Cucinotta, Paolo Vescovi, Stefano Selleri, Univ. degli Studi di Parma (Italy)

The introduction of photo-activators, with absorption spectra in the violet region, in composite resins raised interest in the use of 405 nm diode lasers for polymerization.

The purpose of this research is the evaluation of resins polymerization by means of violet diode laser compared to traditional lamps. Two different resins have been used for the experiments: Filtek Supreme XT flow (3M ESPE) and Tetric Evo flow (Ivoclar Vivadent). The photo-activator used is Camphoroquinone, alone, or in combination with Lucirin TPO. The resins have been cured with an halogen lamp (Heliolux DXL, Ivoclar Vivadent), a broadband LED curing light (Valo Ultradent) and a 405 nm laser (Euphoton). The measure of cure depth, of the volumetric shrinkage, and the conversion degree (DC%) of the double bond during the curing process have been evaluated.

A composite layer of 3 mm was cured in Filtek Supreme resin (Camphoroquinone activator), lower if compared to the use of the other two light sources. Tests on Tetric Evo (Camphoroquinone + Lucirin) didn't show any improvement of the use of laser compared to the halogen lamp and the broadband LED. By measuring the volumetric shrinkage the laser induced the lower change with both the composites. In terms of DC% the lower performance was obtained with the laser.

Considering that the polymerization process strongly depends on the kind of composite used the effectiveness of 405 nm laser proved to be lower than halogen lamps and broadband LEDs.

9306-8, Session 2
All-ceramic crown removal with an Er:YAG laser: a proof-of-principle laboratory study

Peter Rechmann, Natalie C. H. Buu, Beate M. T. Rechmann, Frederick C. Finzen, Univ. of California, San Francisco (United States)

Background and Objectives

The removal of all-ceramic crowns is a time consuming and destructive procedure in the dental office. Little research has been done in alternative removal techniques for all-ceramic crowns. The first objective of this laboratory proof-of-principle study was to evaluate whether with regards to absorption and transmission characteristics of bonding cements and ceramics, all-ceramic crowns can be removed from natural teeth using an Erbium laser.

The second objective was to evaluate whether Ivoclar Vivadent all-ceramic crowns can be efficiently removed from natural teeth without damage to the underlying tooth structure using an Erbium laser.

Study Design/Materials and Methods

The Fourier-Transform-Infrared-Spectroscopy (FTIR) was used on flat ceramic sample (leucite glass-ceramic, Lithium-disilicate, Zirconium-oxide) to assess infrared laser wavelength transmission.

FTIR spectra for four bonding cements (Variolink Veneer, VariolinkII,

Multilink Automix, SpeedCEM; Ivoclar Vivadent, Liechtenstein) were obtained.

The Er:YAG laser energy transmission (wavelength 2,940nm, 1,100µm diameter fiber tip, 10Hz repetition-rate, pulse-duration 100µs at 126mJ/pulse to 400µs at 590mJ/pulse; Syneron, Yokneam, Israel) through different ceramic thicknesses was measured. Ablation thresholds for bonding cements were determined.

Molars were prepared to receive all-ceramic crowns. The all-ceramic crowns were bonded with Ivoclar Multilink Automix. The time for Er:YAG laser debonding of each crown was measured.

Results

Ceramics did not show characteristic water absorption bands in the FTIR, bonding cements showed a broad H₂O/OH absorption band. Some cements exhibited a distinct absorption peak at the Er:YAG laser wavelength. Depending on the ceramic thickness, Empress-Esthetic, E.max-CAD and E.max-ZirCAD transmitted between 5 and 60% of the incident Er:YAG energy.

9306-9, Session 2

Photodynamic therapy: a synergy between light and colors

Elisabetta Merigo, Michele Sozzi, Tecla Ciociola, Stefania Conti, Carlo Fornaini M.D., Stefano Selleri, Paolo Vescovi, Annamaria Cucinotta, Univ. degli Studi di Parma (Italy)

In this work we investigated the application of different laser wavelengths in combination with different photosensitizing dyes, to bacterial cultures, in liquid or solid mean.

Two types of Streptococcus mutans cultures have been used for the experiments, in agar and saline solution.

Three different laser wavelengths have been applied to the bacterial cultures together with a photosensitizing dye: 650 nm on cultures stained with Toluidine Blue, 450 nm on cultures stained with Curcumin, and KTP laser (532 nm) on cultures stained with Erythrosine. The dye choice has been made considering the color affinity with the used wavelength. Tests without dyes have also been performed.

Experimental results show that with the blue laser a bacterial inhibition growth of 40.77% has been obtained in a saline solution, while the combination with Curcumin increased the inhibition to 99.1%, for a fluence of 30 J/cm². No inhibition has been observed using the red laser in saline solution without dye, while the combination with Toluidine Blue resulted in a 100% inhibition for 20 and 30 J/cm² fluences. An inhibition growth of 16.26% has been obtained with the use of KTP laser in saline solution, without dye. A complete inhibition was possible with the use of Erythrosine. Results for solid cultures confirmed the inhibition growth rates of liquid cultures, by measuring the quantification of inhibition growth area.

From the obtained results it is possible to observe that the combination of laser wavelength with a particular photosensitizing dye can dramatically increase the bacterial growth.

9306-10, Session 3

Chromatic dispersive confocal technology for intra-oral scanning: first in-vitro results

Thomas P. Ertl, Dentsply Intl. (Germany); Michael Zint, Annelene Konz, Institut für Lasertechnologien in der Medizin und Messtechnik (Germany); Edgar Brauer, Institut für Lasertechnologien in der Medizin und Messtechnik (Germany); Heiner Hörhold, Degudent GmbH (Germany); Raimund Hibst, Institut für Lasertechnologien in der Medizin und Messtechnik (Germany)

Intra-oral scanning requires an optical scan technology producing reliable surface information from volume scattering objects as teeth and soft tissue. Confocal technology is known to work well with volume scattering objects, but so far all systems used in dentistry had mechanically moving parts, limiting the possible frame rate and long term reliability of the IO-scanner.

To achieve good scanning precision especially in interproximal areas and at the preparation margin of teeth the chromatic confocal lens system was designed with a tele-centric ray path. The system provides video-like capture of 3D data frames with 20 – 30 fps, which are combined to a full data set by best fit algorithms.

Plaster models, plaster models equipped with extracted teeth and pig jaws representing various clinical situations were used for in-vitro scanning tests.

Results:

Compared to µCT data an average error of 18 – 30 µm was achieved for a single tooth scan area and less than 40 to 60 µm error measured over the restoration + the neighbor teeth and pontic areas up to 7 units. Mean error for a full jaw is within 100 – 140 µm. The length error for a 3 – 4 unit bridge situation from contact point to contact point is below 100 µm and excellent interproximal surface coverage and prep margin clarity was achieved.

9306-11, Session 3

Real time imaging of in vivo caries and gingivitis

Mari-Alina I. Timoshchuk, Amanda Sams, Jeremy S. Ridge, Leonard Y. Nelson, Eric J. Seibel, Univ. of Washington (United States)

An ultrathin scanning fiber endoscope, originally developed for cancer diagnosis, was used in a case study to locate caries formation and gingivitis. The imaging system incorporated software mitigation of background autofluorescence. In conventional fluorescence imaging, varying autofluorescence along a tooth surface can mask low level porphyrin signals. Laser-induced autofluorescence signals of dental tissue excited using a 405-nm laser typically produce fluorescence over a wavelength range extending from 440-nm to 750-nm. Anaerobic bacterial metabolism produces various porphyrin species (eg. protoporphyrin IX) that are located in carious enamel, dentin, gingivitis sites, and plaque. In our case study, these porphyrin deposits remained as long as one day after prophylaxis. Imaging the tooth surface using 405-nm excitation and subtracting the natural autofluorescence enhances the image contrast of low-level porphyrin deposits, which would otherwise be masked by the high background AF. In a case study, healthy tissues as well as sites of early and advanced caries formations were scanned for visual and quantitative signs of red fluorescence associated with porphyrin species using a background mitigation algorithm. Healthy gums and gingivitis sites after prophylaxis were also scanned. Initial findings show increasing amplitudes of red fluorescence as caries progresses from early to late stages. Sites of gingivitis also displayed red fluorescence similar to that found in carious dental tissue. The use of real-time background mitigation of natural dental AF can enhance the detection of low porphyrin concentrations that are indicators of early stage caries formation.

9306-12, Session 3

Analysis of eroded bovine teeth through laser speckle imaging

Nelson H. Koshiji, Sandra K. Bussadori, Carolina C. Bortoletto, Marcelo T. Oliveira, Renato A. Prates, Alessandro M. Deana, UNINOVE (Brazil)

In this work we investigate the use of laser speckle imaging in order to detect artificially induced non-carious incipient lesion in a bovine tooth model. 32 samples of bovine incisors were divided in four groups with different acid etching protocol. After analyzing the spackle images of

the eroded samples in the spatial domain, the speckle patterns obtained demonstrated a good correlation with the acid etching duration, which is associated with mineral and hardness loss from the enamel, therefore it was possible not only to detect, but also to quantify incipient shifts in the microstructure of the tooth surface and the erosion progression itself. Besides detection, this work also demonstrates, for the first time to our knowledge, a non-destructive method for quantification of the mineral loss due to the erosion progression. To the best of our knowledge, this is the first study to demonstrate the correlation between speckle patterns and lesion progression.

9306-13, Session 3

All-optical photoacoustic imaging and detection of early-stage dental caries

Ashwin Sampathkumar, Riverside Research Institute (United States); David A. Hughes, Univ. of the West of Scotland (United Kingdom); Chris Longbottom, Dental Innovation and Translational Ctr., King's College London (United Kingdom); Katherine Kirk, Univ. of the West of Scotland (United Kingdom)

Dental caries remain as one of the most common oral diseases in the world. Current detection methods suffer from poor sensitivity and specificity at the earliest (and reversible) stages of the disease because of the small size (< 100 microns) of early-stage lesions. We have developed a fine-resolution (480 nm), ultra-broadband (1 GHz), all-optical photoacoustic imaging (AOPAI) system to image and detect early stages of tooth decay. This AOPAI system provides a non-contact, non-invasive and non-ionizing means of detecting early-stage dental caries. Ex-vivo teeth exhibiting early-stage, white-spot lesions were imaged using all-optical photoacoustic imaging. Experimental scans targeted each early-stage lesion and a reference healthy enamel region. Photoacoustic (PA) signals were generated in the tooth using a 532-nm pulsed laser and the light-induced broadband ultrasound signal was detected at the surface of the tooth with an optical path-stabilized Michelson interferometer operating at 532 nm. The measured time-domain signal was spatially resolved and back-projected to form 2D and 3D maps of the lesion using k-wave reconstruction methods. Experimental data collected from areas of healthy and diseased enamel indicate that the lesion generated a larger PA response compared to healthy enamel. 3D PA reconstruction of the diseased tooth also indicated a sub-surface lesion, at a depth of 0.6 mm in addition to the surface lesion. These results suggest that our AOPAI system is well suited for rapid clinical assessment of early-stage dental caries. An overview of the AOPAI system, fine-resolution PA and histology results of diseased and healthy teeth will be presented.

9306-14, Session 4

In-vitro near-infrared imaging of natural secondary caries

Jacob Simon, Michal Staninec, Seth Lucas, Cynthia L. Darling, Robert Lee, Roger Pelzner, Grant Tsuji, Daniel Fried, Univ. of California, San Francisco (United States)

No Abstract Available

9306-15, Session 4

Assessing near-IR reflectance image-guided removal of natural occlusal caries lesions using PS-OCT

Kenneth H. Chan, Henry Tom, Cynthia L. Darling, Daniel Fried, Univ. of California, San Francisco (United States)

No Abstract Available

9306-16, Session 4

Assessment of the remineralization of artificial lesions via dehydration with near-IR reflectance imaging

Robert Lee, Cynthia L. Darling, Daniel Fried, Univ. of California, San Francisco (United States)

No Abstract Available

9306-17, Session PSun

Observation of the pulp horn by swept source optical coherence tomography and cone beam computed tomography

Yoshiko Iino D.D.S., Toshihiko Yoshioka D.D.S., Takahiro Hanada D.D.S., Arata Ebihara D.D.S., Tokyo Medical and Dental Univ. (Japan); Mitsuhiro Sunakawa D.D.S., Tokyo Medical and Dental Univ. (Japan); Yasunori Sumi D.D.S., National Ctr. for Geriatrics and Gerontology (Japan); Hideaki Suda, Tokyo Medical and Dental Univ. (Japan)

Introduction:

Cone Beam Computed Tomography (CBCT) is an ionizing radiation technique useful for dental diagnosis, while Swept Source Optical Coherence Tomography (SS-OCT) has been introduced recently as a nondestructive, real time, high resolution and no ionizing radiation imaging technique using low-coherence interferometry.

Aim:

The purpose of this study was to evaluate the ability of SS-OCT to detect the pulp horn (PH) in comparison with that of CBCT.

Materials & Methods:

Ten extracted human mandibular molars were used. After horizontally removing a half of the tooth crown, the distance from the cut dentin surface to PH was measured by micro-focus CT (SL) as a gold standard, by CBCT (CL) and by SS-OCT (OL). In the SS-OCT group, only when PH was observed beneath the overlying dentin, the distance from the cut dentin surface to PH was recorded. If the pulp was exposed, it was defined as pulp exposure (PE). The results obtained by the three methods were statistically analyzed by Spearman's rank correlation coefficient ($P < 0.01$).

Results:

SS-OCT detected the presence of PH when the distance from the cut dentin surface to PH determined by SL was 2.33 mm or less. Strong correlations of the measured values were found between SL and CL ($r = 0.87$), SL and OL ($r = 0.96$), and CL and OL ($r = 0.86$).

Conclusion:

The results showed that SS-OCT images were well correlated with CBCT images, suggesting that SS-OCT can be a useful tool for the detection of PH.

9306-18, Session PSun

Apices of maxillary premolars observed by swept source optical coherence tomography

Arata Ebihara D.D.S., Yoshiko Iino D.D.S., Toshihiko Yoshioka D.D.S., Takahiro Hanada D.D.S., Mitsuhiro Sunakawa D.D.S., Tokyo Medical and Dental Univ. (Japan); Yasunori Sumi D.D.S., National Ctr. for Geriatrics and Gerontology (Japan); Hideaki Suda D.D.S., Tokyo Medical and Dental Univ. (Japan)

Introduction

Apicoectomy is performed for the management of apical periodontitis when orthograde root canal treatment is not effective or unable. Prior to the surgery, cone beam computed tomography (CBCT) examination is often performed to evaluate the lesion, adjacent tissues and the other structures. In the surgery, the root apex is resected, and the resected surface is usually observed under a dental operating microscope (DOM). It is difficult, however, to evaluate the fine subsurface structures of the root by CBCT and/or DOM, while a new diagnostic system, swept source optical coherence tomography (SS-OCT), has been developed to observe fine subsurface anatomical structures.

Aim

The aim of this study was to observe resected apical root canals of human maxillary premolars by SS-OCT in comparison with CBCT and DOM.

Materials & Methods

Six extracted human maxillary premolars were used. After micro CT and CBCT scanning of the root, 1 mm of the apex was cut perpendicular to the long axis of the tooth. Each resected surface was treated with EDTA, irrigated with saline solution, and stained with methylene blue dye. The resected surface was observed under DOM and SS-OCT. The number of root canals was counted and statistically evaluated.

Results

As to the accuracy rate for the detection of root canals, there were no significant differences among CBCT, DOM and SS-OCT ($p > 0.05$, McNemar test).

Conclusion

Since SS-OCT can be easily used during surgery, it would be a useful tool for the observation of resected apical root canals in real time.

9306-19, Session PSun

Photowhiting of human dentine under 405nm irradiation

Natalia I. Kazadaeva, Leonid E. Dolotov, Alexander B. Pravdin, N.G. Chernyshevsky Saratov State Univ. (Russian Federation); Gregory B. Altshuler, Ilya V. Yaroslavsky, Cynosure, Inc. (United States); Valery V. Tuchin, N.G. Chernyshevsky Saratov State Univ. (Russian Federation)

In early work we performed the experiments on direct photowhiting of human tooth without the employment of oxidizing agents. In this paper we study, in order to optimize the process of whitening with the reduction of procedure duration in mind, a dependence of photowhiting efficacy on the chemical conditions of the process. The strength of whitening was assessed by two independent methods: i. from the spectra of effective optical density obtained from dentine autofluorescence; ii. from the Lab chromatic components of digital images. We have shown that the process of photowhiting under 405nm irradiation is oxygen-dependent, and the increase of ambient pH decreases whitening efficacy. Addition of extra amount of oxygen (by bubbling) reduces bleaching time at the setting stage and allows us to get the desired bleaching level in the shorter term. Increase

of ambient pH decreases bleaching rate not only at the setting stage of photowhiting but at the final stage as well.

9306-20, Session PSun

Biostimulation effect of low level laser on healing proces after third molars surgery based on biochemical markers in saliva

Veronika Kroulikova, Tatjana Dostálová M.D., Petra Hlinakova, Stepan Podzimek, Charles Univ. in Prague (Czech Republic)

Third molar extractions in general anesthesia have become a standard procedure in dentistry. There is an effort to shorten healing time and decrease the number of complications as well as increase comfort after the treatment. Low-level lasers are known for their analgesic, anti-inflammatory and stimulatory effect. The aim of study is to evaluate the effect of low level laser after surgery in general anesthesia, which reduced the patient's discomfort mainly pain and to monitor process of biostimulation. The 79 patients of Department of Stomatology, 2nd Medical Faculty, Charles University and Faculty Hospital Motol participated on our study. Diagnosis was third molar retention. The diode low level laser radiation with wavelength 808 nm, output power 270 mW, probe aperture of 6,4 cm² and energy of 15 J/cm² was applied. Control group was treated using placebo - red light. The exposition time was 11 second immediately after the suture, than every day for following 4 days. For objectification of effect of laser biostimulation immunological tests - the objective markers of healing - sIgA and lysozyme in non-stimulated saliva of patients - was used. The sIgA decreases after laser application from 544.36 mg/l to 323.68 mg/l and in control group from 602.12 mg/l to 425.62 mg/l. Level of lysozyme decreases 52.897mg/l to 3.366 mg/l after laser biostimulation, from 297.11mg/l to 109.05 mg/l after placebo effect. The results were significant. The study confirmed low level laser healing effect which was not in direct connection with pain.

9306-21, Session PSun

Selective removal of demineralized enamel using a CO2 laser coupled with near-IR reflectance imaging

Henry Tom, Kenneth H. Chan, Cynthia L. Darling, Daniel Fried, Univ. of California, San Francisco (United States)

No Abstract Available

9306-22, Session PSun

Use of near-IR transillumination for guiding the selective removal of occlusal caries lesions with a 9.3-µm CO2 laser

Leon Chung, Henry Tom, Kenneth H. Chan, Jacob Simon, Robert Lee, Daniel Fried, Cynthia L. Darling, Univ. of California, San Francisco (United States)

No Abstract Available

9306-23, Session PSun

Selective removal of dental caries with a diode-pumped Er:YAG laser operating at high pulse repetition rates

Jingru Yan, Kenneth H. Chan, Henry Tom, Jacob Simon, Cynthia L. Darling, Daniel Fried, Univ. of California, San Francisco (United States)

No Abstract Available

9306-24, Session PSun

Automated detection of dentinal lesions in optical coherence tomography

Hobin J. Kang, Univ. of the Pacific (United States); Cynthia L. Darling, Daniel Fried, Univ. of California, San Francisco (United States)

No Abstract Available

9306-25, Session PSun

Selective photothermolysis of periodontal pathogens

David M. Harris, Bio-Medical Consultants, Inc. (United States); Lou Reinisch, Farmingdale State College (United States); Steven L. Jacques, Oregon Health & Science Univ. (United States); Richard P. Darveau, Univ. of Washington (United States)

We have developed a computational model [1] of the optical and time-dependent thermal properties of periodontal tissues including periodontal pathogens. With this model we have simulated the surgical procedure: Laser Sulcular Debridement. Movies of the simulations will be presented.

Absorption and scattering coefficients of *Porphyromonas gingivalis* (Pg), *Prevotella intermedia* (Pi), *Prevotella nigrescens* (Pn) and *Tanarella forsythia* (Tf) were calculated from diffuse reflection spectroscopy measurements from 500-1100 nm of bacteria suspended in microspheres. Virtual bacterial colonies are placed at different depths in the model to define the "kill zones" given various dental laser parameters (wavelength, peak power, pulse duration, scan rate, etc.).

Accumulated background heat from multiple passes increases the depth of the kill zone. The pulsed-Nd:YAG achieves a 2-3 mm deep kill zone for Pg and Pi in soft tissue without surface damage (selective photoantiseptis) which is significantly deeper than achieved by the gated-diode or pulsed-Er:YAG dental lasers.

[1] L. Reinisch, G.C. Garrett, M. Courey, A Simplified Laser Treatment Planning System: Proof of Concept, *Laser Surg. Med.* 45:679-685 (2013).

Conference 9307: Ophthalmic Technologies XXV

Saturday - Sunday 7-8 February 2015

Part of Proceedings of SPIE Vol. 9307 Ophthalmic Technologies XXV

9307-1, Session 1

OCT angiography-based graphing protocol for imaging and characterization of the rat inner retinal vascular network

Conor Leahy, Harsha Radhakrishnan, Vivek J. Srinivasan, Univ. of California, Davis (United States)

Normal functioning of the retina is dependent upon a sufficient supply of oxygen and other nutrients, as well as the removal of waste, by a network of blood vessels. The metabolic needs of the inner retina are supported largely by the inner retinal vasculature. Characterizing baseline vascular architecture is important to understand how energy delivery is coupled to metabolic needs. Optical imaging methods offer the opportunity to quantitatively assess vasculature non-invasively and in vivo.

In this work, we provide a characterization of the topology and distribution of vascular patterns in the rodent inner retina, based on optical coherence tomography (OCT) imaging protocols, including angiography and Doppler. 3D image processing techniques are applied to the angiographic data in order to obtain an accurate mapping of the blood vessels. A vectorized representation of the vasculature is then produced by deriving connectivity information from the segmented vascular map. We use an analogy of a resistive network to infer a spatial model of flow for the inner retinal vasculature.

We anticipate that accurate biophysical models, when informed by independent in vivo measurements of flow and metabolism, will ultimately aid in delineating the principles of inner retinal vascularization, metabolism, and neurovascular control. These data will advance our understanding of the relationship between flow, metabolism, and neuronal activity elsewhere in the central nervous system, and constitute a baseline to characterize changes in numerous retinal diseases.

9307-2, Session 1

High-resolution retinal imaging: enhancement techniques

Mircea Mujat, Ankit H. Patel, Nicusor V. Iftimia, Physical Sciences Inc. (United States); James D. Akula, Anne B. Fulton M.D., Boston Children's Hospital (United States) and Harvard Medical School (United States); R. Daniel Ferguson, Physical Sciences Inc. (United States)

Adaptive optics has recently achieved success in a range of applications in ophthalmology. It's being used as a tool to understand the structural and functional aspects of vision, the complex retinal circuitry, and its dissolution during the progression of disease. In all applications, the building blocks of retinal microstructures such as cone photoreceptors, rods, RPE cells, blood cells, and microvasculature need to be identified, counted, and mapped properly. Multiple images are acquired at the same location and are registered. They can be averaged to improve the SNR or analyzed for temporal dynamics. For small patches image registration is relatively easy using simple cross-correlations, though, as the image size increases more sophisticated image registration techniques are needed. Strip-based stack registration has been developed based on the assumption that deformations along the strip are relatively negligible. However, if the deformation along the strip is comparable to the cone size, strip-based registration will actually blur out the cones. We have recently applied non-rigid image registration that significantly improves the quality of the processed images both in mapping cones and rods and in blood flow analysis in dark-field imaging. By using local grid deformations non-rigid registration accounts for stretching and compression in different directions in different parts of the images. In addition, high-speed imaging (130 fps) provides additional benefits as

compared to regular SLO imaging (26 fps). Individual blood cells can be traced as they move along capillaries and their dynamics can be analyzed. We present a detailed discussion of these new features.

9307-3, Session 1

Automatic segmentation of fluid and retinal layers on OCT images with severe diabetic macular edema using kernel regression-based classification

Stephanie J. Chiu, Michael J. Allingham, Priyatham S. Mettu, Scott W. Cousins, Joseph A. Izatt, Sina Farsiu, Duke Univ. (United States)

In recent years, optical coherence tomography (OCT) imaging has prompted groups to correlate OCT retinal morphology with diabetic macular edema (DME) and vision outcomes. Despite the development of numerous algorithms for OCT retinal layer segmentation, most DME studies unfortunately still require manual or semi-automatic image evaluation. This is because most automated algorithms were designed based on assumptions of high image quality or minimal pathologic disturbance of retinal layers. We therefore developed a fully automatic algorithm to identify fluid and eight retinal layer boundaries on real-world OCT images of eyes with DME. Two phases were involved in the development of this algorithm: 1) we developed a kernel regression-based classification method to generate pilot estimates of fluid and retinal layer positions, and 2) we used these classification estimates as a guide to more accurately segment the layer boundaries using our GTDP framework. To validate our algorithm, we compared our fully automatic segmentation to expert manual segmentation on clinical images with higher levels of noise and severe DME pathology. While improvement of the quantitative results is part of our ongoing work, current results show significant improvements over popular classic graph-based layer segmentation algorithms. To the best of our knowledge, this is the first fully-automated, multi-layer segmentation method which has been applied to real-world images containing severe DME. Accurate identification of DME imaging biomarkers is extremely important, as it facilitates the stratification of patients based on disease mechanisms. This will ultimately enable physicians to provide personalized therapies to patients for improved vision outcomes.

9307-4, Session 1

Fully automated detection of retinal diseases from optical coherence tomography images

Pratul P. Srinivasan, Duke Univ. (United States); Leo A. Kim, Schepens Eye Research Institute (United States) and Harvard Univ. (United States); Priyatham S. Mettu, Scott W. Cousins, Duke Univ. (United States); Grant M. Comer, Kellogg Eye Ctr., Univ. of Michigan (United States); Joseph A. Izatt, Duke Univ. (United States) and Duke Univ. Medical Ctr. (United States); Sina Farsiu, Duke Univ. Medical Ctr. (United States) and Duke Univ. (United States)

Automated analysis of OCT images is an active field of research to speed up the diagnostic process and enable the remote identification of ophthalmic diseases. Despite recent advances, automated layer segmentation methods often fail to deal with diseases which manifest severe deformation of retinal layers. To deal with significantly diseased eyes, few algorithms have been developed for the automatic detection of ocular diseases with less emphasis

on the direct comparison of retinal layer thicknesses. Previous attempts to address this problem were limited in that they either only attempted to perform binary classification to differentiate between normal eyes and eyes with a specific disease, or they required manual input to select a single good-quality OCT image per volume, which best manifests the disease imaging biomarkers. In this work, we propose a method that does not rely on the segmentation of inner retinal layers and is applicable to clinical grade OCT images (as opposed to experimental grade images attained through long imaging sessions). We utilize an easy to implement classification method based on Histogram of Oriented Gradients descriptors and support vector machines for images enhanced by freely available online sparsity based denoising methods. In our preliminary cross validation results, our algorithm achieved perfect sensitivity and high specificity in the detection of dry age-related macular degeneration and diabetic macular edema despite utilizing images captured with different scanning protocols, which is often the case in the real clinical practice. This fully automated technique is a potentially valuable tool for remote diagnosis applications.

9307-5, Session 2

Novel microscope-integrated stereoscopic display for intrasurgical optical coherence tomography

Liangbo Shen, Oscar Carrasco-Zevallos, Brenton Keller, Christian Viehland, Gar Waterman, Duke Univ. (United States); Philip Desouza, Paul Hahn M.D., Anthony N. Kuo M.D., Duke Univ. Medical Ctr. (United States); Cynthia A. Toth M.D., Duke Univ. Medical Ctr. (United States) and Duke Univ. (United States); Joseph A. Izatt, Duke Univ. (United States) and Duke Univ. Medical Ctr. (United States)

The first generation of intrasurgical optical coherence tomography (OCT) systems displayed OCT data onto a separate computer monitor, requiring surgeons to look away from the surgical microscope. In order to provide real-time OCT feedback without requiring surgeons to look away during surgeries, recent prototype research and commercial intrasurgical OCT systems have integrated heads-up display (HUD) systems into the surgical microscopes to allow the surgeons to access the OCT data and the surgical field through the oculars concurrently. However, all current intrasurgical OCT systems with a HUD are only capable of imaging through one ocular limiting the surgeon's depth perception of OCT volumes. Stereoscopy is an effective technology to dramatically increase depth perception by presenting an image from slightly different angles to each eye. Conventional stereoscopic HUD use a pair of micro displays which require bulky optics. Several new approaches for HUDs are reported to use only one micro display at the expense of image brightness or increased footprint. Therefore, these techniques for HUD are not suitable to be integrated into microscopes. We have developed a novel stereoscopic HUD with one micro display and only three optical elements for our microscope-integrated OCT system. Simultaneous stereoscopic views of OCT volumes are computed in real time by GPU-enabled OCT system software. We present, to our knowledge, the first microscope integrated stereoscopic HUD used for intrasurgical OCT and a novel optical design for stereoscopic viewing devices.

9307-6, Session 2

Automated real-time instrument tracking for microscope-integrated intraoperative OCT imaging of ophthalmic surgical maneuvers

Mohamed T. El-Haddad, Justis P. Ehlers, Sunil K. Srivastava, Yuankai K. Tao, The Cleveland Clinic (United States)

Optical coherence tomography (OCT) allows high-resolution imaging

of tissue microstructure and is the gold-standard for clinical ophthalmic diagnostics. Recent development of microscope-integrated intraoperative OCT (iOCT) systems has allowed cross-sectional imaging of surgical dynamics, but limitations in real-time visualization of instrument-tissue interactions remain the critical barrier for iOCT-guided ophthalmic surgery. Spatial compounding has been previously presented as a method for acquiring, processing, and visualizing cross-sectional iOCT images of surgical maneuvers. However, spatial compounding trades-off temporal resolution and FOV, which generally limits video-rate visualization to small regions at the tip of surgical instruments. To overcome these limitations, we present methods for automated dynamic surgical instrument tracking iOCT. B-scans are obtained along and orthogonal to the instrument axis and centered at the instrument tip at all times to allow cross-sectional visualization of ophthalmic surgical maneuvers for intraoperative guidance. Surgical instrument tracking has been previously demonstrated using different imaging modalities, including an OCT-integrated scanning probe. However, the latter uses large feature points, which are impractical in a surgical setting. Here, we describe automated stereo-vision instrument tracking, which achieves <250 μm accuracy, using tracking feature points that are easily integrated with ophthalmic surgical instruments. The instrument tracking system was integrated with an iOCT system to provide video-rate instrument tip tracked cross-sectional B-scan imaging during ophthalmic surgical maneuvers, allowing visualization of tissue-instrument interactions and providing feedback on positioning, depth of penetration, and tissue compression in cadaveric porcine eyes. Real-time instrument tracked cross-sectional imaging can potentially help guide clinical decision-making during ophthalmic surgery.

9307-7, Session 2

Image-guided modified deep anterior lamellar keratoplasty (DALK) corneal transplant using intraoperative optical coherence tomography

Yuankai K. Tao, The Cleveland Clinic (United States); Michael LaBarbera, Cleveland Clinic Lerner College of Medicine of Case Western Reserve University (United States); Justis P. Ehlers, Sunil K. Srivastava, William J. Dupps Jr., The Cleveland Clinic (United States)

Deep anterior lamellar keratoplasty (DALK) is an alternative to full-thickness corneal transplant and has advantages including the absence of allograft rejection; shortened duration of topical corticosteroid treatment and reduced associated risk of glaucoma, cataract, or infection; and enables use of grafts with poor endothelial quality. DALK begins by performing a trephination of approximately 80% stromal thickness, as measured by pachymetry. After removal of the anterior stroma, a needle is inserted into the residual stroma to inject air or viscoelastic to dissect Descemet's membrane. These procedures are inherently difficult and intraoperative rates of Descemet's membrane perforation between 4-39% have been reported. Optical coherence tomography (OCT) provides high-resolution images of tissue microstructures in the cornea, including Descemet's membrane, and allows quantitation of corneal layer thicknesses. Here, we use cross-sectional intraoperative OCT (iOCT) measurements of corneal thickness during surgery and a novel micrometer-adjustable biopsy punch to precision-cut the stroma down to Descemet's membrane. Our prototype cutting tool allows us to establish a dissection plane at the corneal endothelium interface, mitigates variability in cut-depths as a result of tremor, reduces procedure complexity, and reduces complication rates. iOCT-guided modified DALK procedures were performed on 47 cadaveric porcine eyes by non-experts and achieved a perforation rate of ~5% with a mean corneal dissection time <18 minutes. The procedure was also successfully performed on a human donor eye without perforation. Our data shows the potential for iOCT-guided precision anterior segment surgery without variability as a result of tremor and improvements to standard clinical care.

9307-8, Session 2
Swept-source microscope integrated optical coherence tomography for real-time 3D imaging of ophthalmic human surgery

Oscar Carrasco-Zevallos, Brenton Keller, Christian Viehland, Liangbo Shen, Gar Waterman, Philip Desouza, Paul Hahn M.D., Anthony N. Kuo M.D., Cynthia A. Toth M.D., Joseph A. Izatt, Duke Univ. (United States)

Ophthalmic surgery is performed with a stereoscopic surgical microscope that provides a wide field, en face view of the surgical field and limited depth perception. Surgeons often rely on indirect cues for depth information, which may be insufficient for precise depth localization of tissue-tool interfaces. Optical coherence tomography (OCT) enables micron-scale tomographic imaging of posterior and anterior segments of the human eye and can provide direct axial visualization of ophthalmic surgical procedures. However, current research and commercial intraoperative OCT imaging system prototypes are limited to cross-sectional B-scans for real time imaging; volumetric images are restricted to 3-5 seconds acquisition times and cannot be rendered in real-time. Surgical manipulations are performed in a 3D surgical field; therefore, cross-sectional images only capture a limited amount of information about the surgical manipulations. We report on the development of Swept-Source MIOCT (SS-MIOCT) system for fast volumetric in vivo imaging of anterior segment and vitreoretinal surgical procedures. We have merged our previously published MIOCT sample arm scanner with a custom swept-source OCT engine and implemented GPU-based custom software for real-time acquisition, processing, and rendering of volumetric images. With SS-MIOCT, volumetric images of anterior segment and retinal human surgeries were acquired. 4D OCT data acquisition enabled volumetric recording of epiretinal membrane (ERM) peels in retinal surgery and 3D monitoring of cataract surgery to demonstrate the utility of fast volumetric OCT imaging towards image guided ophthalmic surgery.

9307-9, Session 2
Design and evaluation of an intraocular B-scan OCT-guided 36-gauge needle tip

Jin H. Shen, Karen M. Joos M.D., Vanderbilt Univ. (United States)

Optical coherence tomography imaging is widely used in ophthalmology clinics for diagnosing retinal disorders. External microscope-mounted OCT operating room systems have imaged retinal changes immediately following surgical manipulations. However, the goal is to image critical surgical maneuvers in real time. External microscope-mounted OCT systems have limitations with problems tracking constantly moving intraocular surgical instruments, and formation of absolute shadows by the metallic surgical instruments upon the underlying tissues of interest. An intraocular OCT-imaging probe was developed to resolve these problems. A disposable 25-gauge probe tip extended beyond the handpiece, with a 36-gauge needle welded to a disposable tip with its end extending an additional 3.5 mm. A sealed 0.35 mm diameter GRIN lens protected the fiber scanner and focused the scanning beam at a 3 to 4 mm distance. The OCT engine was a very high-resolution spectral-domain optical coherence tomography (SDOCT) system (840 nm, BiopTigen, Inc. Durham, NC) which produced 2000 A-scan lines per B-scan image at a frequency of 5 Hz with the fiber optic oscillations matched to this frequency. Real-time imaging of the needle tip as it touched the porcine ex vivo retinal surface, perforated the retina, and injected saline under the neurosensory retina to form a retinal detachment was performed. A B-scan OCT-needle was capable of real-time performance and imaging of sub-retinal injection to form a discreet retinal detachment without requiring the aid of a surgical microscope. In the same manner as an intraocular endoscope, the OCT probe will bypass corneal and lenticular opacities for improved imaging.

9307-10, Session 2
Power-controlled temperature guided retinal photocoagulation

Alexander Baade, Wadim Schwarzer, Medizinisches Laserzentrum Lübeck GmbH (Germany); Stefan Koinzer, Univ. Schleswig-Holstein (Germany); Kerstin Schlott, Medizinisches Laserzentrum Lübeck GmbH (Germany); Ralf Brinkmann, Medizinisches Laserzentrum Lübeck GmbH (Germany) and Institute of Biomedical Optics, Lübeck (Germany)

Retinal photocoagulation is an established treatment for various diseases. The temperature development during a treatment can be monitored using the photoacoustic effect by applying short laser pulses in addition to the treatment laser light. The laser pulses induce thermoelastic pressure waves with temperature dependent amplitude that can be detected at the cornea.

We present a power switched temperature feedback technique to create homogeneous lesions reproducibly in a fixed time in order to facilitate automated pattern coagulation. This is achieved by monitoring the tissue response to the treatment radiation optoacoustically and thereby determining the appropriate laser power to reach a predefined temperature Taim. The method was tested on rabbits in vivo for an irradiation time of 150 ms for each the probe and treatment irradiation and an aim RPE peak temperature Taim of 65 °C.

The resulting mean temperature was found to be 67 °C with a standard deviation of 4.2 °C. The achieved lesion diameters 1 h after the treatment were of homogeneous appearance with a mean diameter of 149 µm with a standard deviation of 17 µm.

9307-11, Session Key
Implementation of fs cataract surgery in the clinic, needs for further technology? (Keynote Presentation)

Nagy Zoltán, Semmelweis Univ. (Hungary)

No Abstract Available

9307-12, Session 3
Model-based solution for remotely scanned in-vivo mouse retinal imaging

Adi Schejter, Technion-Israel Institute of Technology (Israel); Nairouz Farah, Technion-Israel Institute of Technology (Israel) and Bar-Ilan Univ. (Israel); Shy Shoham, Technion-Israel Institute of Technology (Israel)

Non-invasive fluorescence fundus imaging is an important tool for in-vivo small animal retinal imaging in a wide array of translational vision applications, including the tracking of fluorescently tagged cells and blood vessels over time, as well as functional fluorescence imaging where calcium probes are used for monitoring retinal neuronal activity; these various applications require systems capable of imaging fine retinal structures in-vivo.

In this study we use an intuitive paraxial optical model-based approach to analyze the requirements from an in vivo mouse retinal imaging system. Using these design criteria, we built a system based on a two-photon laser scanning microscope and 10x water immersion objective lens which yields fundus images of optically sectioned, well-resolved fluorescent microstructures down to the cellular scale. The imaging is depth-scanned using an electronically tunable lens (ETL) integrated into the optical path.

Our solution is found to provide major advantages in comparison to wide field imaging systems based on low NA objectives, and to allow long-term repeated imaging, in a simple, widely accessible design. Furthermore, the use of wavelengths which are not visible to the mouse for fluorescent excitation (near-infrared) could potentially also enable artifact-free functional imaging of neuronal retinal activity in response to natural or artificial-optogenetic visual stimuli in the visible spectrum.

9307-13, Session 3

Morphological and functional changes in the rat retina measured with a combined OCT+ERG system during acute ocular pressure elevation

Bingyao Tan, Akshay Gurdita, Kirsten Carter, Vivian Choh, Univ. of Waterloo (Canada); Karen M. Joos M.D., Vanderbilt Univ. (United States); Kostadinka Bizheva, Univ. of Waterloo (Canada)

Glaucoma is a chronic disease, characterised by progressive degeneration of the optic nerve resulting in loss of retinal ganglion cells (RGCs) and eventually blindness. In this study we used a combined, research-grade, high-resolution OCT+ERG system in an acutely elevated IOP rat model of glaucoma. Results from our study indicate that acutely elevated IOP to 35 mmHg causes transient changes in the functional response of the retina to a flash stimulus (single white light flash of 7 ms duration and 3.73 cd.s/m² brightness, illuminating -5mm² of the retinal surface). The elevated IOP caused a transient increase in the amplitudes of the ERG a- and b-waves as compared to the a- and b-waves magnitudes of ERG recordings acquired during baseline and post IOP elevation. Morphological OCT 3D scans of the retina reveal backward bowing of the optic nerve head during elevated IOP, though no significant changes in the NFL + RGC layers and IPL thicknesses. Histological evaluation of the treated retinas revealed no significant cellular changes as compared to the control eye retinas.

9307-14, Session 3

In vivo functional optical coherence tomography of fast intrinsic optical signals in frog retina

Qiuxiang Zhang, Rongwen Lu, Benquan Wang, Xincheng Yao, The Univ. of Alabama at Birmingham (United States)

The purpose of this study was to identify signal sources of fast intrinsic optical signals (IOSs) in the retina and investigate their spatial and temporal characteristics correlated with retinal stimulation. IOS imaging promises a new method for high spatiotemporal resolution assessment of retinal function. The IOS reflects near infrared light intensity changes in the stimulus activated retina. Using a rapid line-scan confocal imager, we have previously demonstrated in vivo IOS imaging of frog retinas. However, due to limited axial resolution of the confocal system, it has been challenging to accurately verify the IOS signal sources within multiple layers of the retina. By providing unprecedented resolution to differentiate individual retinal layers, optical coherence tomography (OCT) promises excellent capability to characterize the sources of fast IOSs. A custom designed spectral-domain OCT system, configured with retinal stimulator and fundus monitoring, was developed. The OCT provided isotropic resolution (3 μm x 3 μm x 3 μm) in three dimensions, with frame rate up to 500 Hz. Fast IOSs were consistently recorded with mixed polarities (decreasing or increasing light intensities). The fast IOSs occurred within 4 ms after the stimulus delivery, and were predominately observed at the photoreceptor outer segment. We speculated that the fast IOSs might correlate with early phototransduction process of retinal photoreceptors. The OCT ability to compare functional IOS signals at sub-cellular resolution will facilitate in-depth understanding of the visual system, and can also provide a noninvasive approach for improved detection and treatment evaluation of eye diseases.

9307-15, Session 3

Reflective afocal adaptive optics scanning laser ophthalmoscope for high resolution in vivo mouse retinal imaging: visualization of retinal micro-vasculature

Robert J. Zawadzki, Pengfei Zhang, Azhar Zam, Ravi S. Jonnal, Sang Hyuck Lee, Univ. of California, Davis (United States); Dae Yu Kim, Beckman Laser Institute-Korea (Korea, Republic of) and Dankook Univ. (Korea, Republic of); John S. Werner, Edward N. Pugh Jr., Univ. of California, Davis (United States)

We present a reflective afocal AO-SLO retinal imaging system designed for high resolution in vivo retinal imaging in mice. The optical performance of this instrument is compared to other state-of-the-art AO based mouse retinal imaging systems. To simplify the animal alignment and handling we have used hard contact lens (0 Dpt) mounted in the pupil plane of the system. The feasibility of new AO instrumentation for visualizing retinal microvasculature was tested and compared to images acquired on the same animal with phase variance (pv-) OCT based vasculature imaging. Additionally, images of the retinal structures acquired with "standard resolution" (non AO) SLO and our new AO-SLO system will be presented. Additional applications of the new instrumentation will be discussed as well.

9307-16, Session 3

Multispectral scanning laser ophthalmoscopy combined with optical coherence tomography for simultaneous in vivo mouse retinal imaging

Pengfei Zhang, Azhar Zam, Univ. of California, Davis (United States); Yifan Jian, Simon Fraser Univ. (Canada); Xinlei O. Wang, Marie E. Burns, Univ. of California, Davis (United States); Marinko V. Sarunic, Simon Fraser Univ. (Canada); Edward N. Pugh Jr., Robert J. Zawadzki, Univ. of California, Davis (United States)

A multispectral (two fluorescent channels and one reflection channel) SLO system which captures independent GFP and mCherry fluorescence and back scattered intensity imaging in three independent channels, was integrated with an Fd-OCT system.

A supercontinuum laser (Fianium, SC 400) is used as the light source for SLO sub-system. A dual-band bandpass filter (Semrock, FF01-482/563) was placed in the laser beam to restrict the light source light to two spectral bands that provide GFP and mCherry excitation. By choosing corresponding dichroic mirror (Semrock, Di01-R488/561) and filters (Semrock, FF01-525/45 and FF01-609-54), the emitted light from these two proteins was collected by 2 PMTs (Hamamatsu, H7422-40). Reflected light signal was acquired by another PMT (Hamamatsu, H7422-20). Our custom high acquisition speed Fourier-domain OCT (Fd-OCT) system broadband light source (Superlum, broadlighter 890) and CMOS camera (Basler, Sprint sPL4096-140km) operates at speeds up to 125,000 A-scan/s) was introduced by the second dichroic mirror (Semrock, FF705-di01), and used to acquire retinal B-scans and volumetric data sets.

The GFP (green color) and mCherry (red color) channels share the same light delivery path, and therefore these signals are co-registered spatially and temporarily on the retina. Thus, they can be directly combined together, without need for additional co-registration. The OCT B-scan provides the layer information of the retina, and also can be generated as 3D volume display. The combined system collects complimentary information from the sample simultaneously, simplifying data registration and analysis. Several more examples and details of these systems will be presented and discussed in the future.

9307-17, Session 3

In vivo tracking of microglial turnover and vascular integrity in a mouse model of bone marrow transplantation with a multi-color scanning laser ophthalmoscope

Clemens Alt, Judith M. Runnels, Luke J. Mortensen, Walid Zaher, Charles P. Lin, Wellman Ctr. for Photomedicine (United States)

Bone marrow transplantation (BMT) following exposure to gamma irradiation is a routine clinical treatment of hematologic malignancies. Malignant cells in the bone marrow are the intended targets, but healthy hematopoietic cells are also ablated and injuries to other tissues, including the central nervous system (CNS), have been reported. Here, we examine radiation effects in the retina, in particular 1) on microglial cells, the resident immune sentinels of the CNS, 2) on bone marrow derived cells (BMDCs) that may be recruited in case of injury and 3) on the integrity of the blood retinal barrier.

A multi-color scanning laser ophthalmoscope (SLO) was developed that enables simultaneous tracking of distinctly fluorescently labeled cell populations. Two-color chimeric mice were generated by lethal irradiation of heterozygous CX3CR1-GFP mice that express GFP in microglial cells, followed by BMT from universal DsRed donor mice. Resident microglia (GFP+) and BMDCs (DsRed+) were quantified by serial *in vivo* imaging for 10 weeks after irradiation. Fluorescein angiography assess vascular integrity in wild-type mice. We tested, if anti-inflammatory therapy (dexamethasone) can protect retinal structure from radiation damage.

Ionizing radiation resulted in loss of 75% of the resident retinal microglia population. Delayed BMDC infiltration resulted in a transient depletion of the total immune cell number in the retina. Dexamethasone treatment reduced microglial turnover and preserved vascular integrity.

Exposure to ionizing radiation causes turnover of retinal microglia, accompanied by long-term low-grade inflammation. Suppression of the inflammatory response protects resident microglia and vascular structure from radiation-induced damage.

9307-18, Session 4

Investigation of corneal collagen crosslinking using polarization-sensitive optical coherence tomography

Myeong Jin Ju, Shuo Tang, The Univ. of British Columbia (Canada)

Corneal collagen cross-linking (CXL) is standard treatment method for slowing down or stopping the progression of keratoconus. In this study, Jones-matrix-based optical coherence tomography (Jones matrix OCT), one of the sub-type of polarization sensitive OCT, was employed for investigating morphological change in corneal stroma after the CXL treatment. Fresh bovine eye was enucleated and measured within a few hours postmortem. As following the standard CXL treatment, riboflavin solution was instilled into the cornea after its epithelium was removed. After instilling the solution, the cornea was irradiated with UV-A light over 30 min. During and after the CXL treatment, series of measurements were taken with Jones matrix OCT. From the measurement results, temporal and spatial structure alterations were observed from scattering and phase retardation contrast images. Especially, noticeable stromal structure changes were detected from scattering contrast image during the mid-phase of the treatment and also after the treatment. These change were also appeared in the phase retardation image with more high and homogeneous values. In addition, decrease of the stromal thickness was observed and quantitatively analyzed with robust corneal segmentation algorithm. The analysis results showed that the stromal thickness was sharply decreased after the treatment while it was more slowly decreased during the treatment.

In contrast, the structure appearing after starting the treatment was kept increasing rapidly during the treatment and moderately after the treatment. As a result, it was demonstrated that proposed method has potential for monitoring and determining CXL treatment effect.

9307-19, Session 4

Evaluation of filtering blebs using polarization-sensitive optical coherence tomography

Masahiro Yamanari, Tomey Corp. (Japan); Satoru Tsuda, Tohoku Univ. School of Medicine (Japan); Taiki Kokubun, Tohoku Univ. School of Medicine (Japan) and Iwaki Kyoritsu Hospital (Japan); Yuji Tanaka, Yukihiro Shiga, Yu Yokoyama, Morin Ryu, Shiho Kunimatsu-Sanuki, Hidetoshi Takahashi, Kazuichi Maruyama, Hiroshi Kunikata, Toru Nakazawa, Tohoku Univ. School of Medicine (Japan)

Functioning of the filtering bleb after trabeculectomy is known to decrease because of fibrosis in subconjunctival tissue. Although conventional OCT is useful to measure a volume of the cleft and to visualize closed pathway of the aqueous outflow in the bleb, fibrosis of the tissue cannot be detected directly. Previous studies of imaging the anterior eye segment using polarization-sensitive OCT (PS-OCT) showed a potential of birefringence imaging for detecting fibrous tissue and scar tissue. In this presentation, we demonstrate our prototype PS-OCT and its application for evaluation of the filtering blebs. A functioning filtering bleb that had intraocular pressure (IOP) of 10 mmHg showed no significant birefringence in the bleb wall. In contrast, a nonfunctioning bleb that had IOP of 36 mmHg showed birefringent scar tissue over the cleft, and it encapsulated the cleft in volumetric images. Another nonfunctioning bleb that had IOP of 22 mmHg showed birefringent scar tissue in a part of the bleb wall. The scar tissue of the eye was removed by reconstructive surgery, and the IOP was decreased to be 4 mmHg. In local retardation images, it was confirmed that the birefringent scar tissue was successfully removed. The removed scar tissue was sectioned, stained with Elastica-Masson stain and observed by microscopy and polarization microscopy. It was found that the scar tissue contained collagen and elastic fibers, and only the collagen fiber showed birefringence. PS-OCT may be useful for follow-up of trabeculectomy and planning of reconstructive surgery of the bleb.

9307-20, Session 4

Non-invasive birefringence imaging of anterior eye by PS-OCT: application for glaucoma filtration surgery evaluation

Deepa K. Kasaragod, Shinichi Fukuda, Sujin Hoshi, Tetsuro Oshika, Yoshiaki Yasuno, Univ. of Tsukuba (Japan)

One of the treatments of glaucoma is lowering intraocular pressure (IOP) by filtration surgery (trabeculectomy). However, the filtration known treatment structure created by the surgery (filtering bleb) is difficult to be maintained for a long term. Because natural wound healing process destroys the structure and its functionality. In this study, we monitor the scarring of the filtering bleb by using polarization sensitive OCT (PS-OCT). The fibrosis at the filtering bleb is quantitatively assessed by monitoring its birefringence. The quantitative birefringence of the bleb is obtained by using local Jones matrix analysis and Bayesian maximum likelihood estimator. An automatic algorithm was developed to assess the functionality of the filtering blebs. This algorithm provides a score associated with the fibrosis of each bleb (fibrosis score). The utility of the method is evaluated by a pilot clinical study involving 12 cases and 10 normal controls. The fibrosis score was utilized to distinguish functioning and malfunctioning blebs. The area under receiver operating characteristic curve (AROC) of this classification was

found to be 0.81. This study shows the presented method is useful for the automatic evaluation of the functionality of filtering blebs.

9307-21, Session 4

Analysis of retardation and birefringence along retinal nerve fiber bundles by polarization sensitive OCT

Mitsuro Sugita, Medizinische Univ. Wien (Austria) and Canon Inc. (Japan); Stefan Zotter, Michael Pircher, Bernhard Baumann, Clemens Vass M.D., Christoph K. Hitzenberger, Medizinische Univ. Wien (Austria)

Polarimetric analysis of the retinal nerve fiber layer (RNFL) is widely used for glaucoma diagnostics. Deviations of the RNFL retardation pattern from normal are indications for glaucoma. Recent studies in animal models have indicated that the birefringence (retardation per unit depth) decreases in experimental glaucoma before the onset of measurable RNFL thinning. Therefore, birefringence of the RNFL is an interesting parameter for early glaucoma diagnostics.

The measurement of birefringence requires a depth-resolved measurement of retardation which can be provided by polarization sensitive OCT (PS-OCT). We have developed an improved PS-OCT system with an integrated retinal tracker that provides high-quality, motion-artifact free 3D images of the human retina. Intensity, retardation, and optic axis orientation data are acquired simultaneously at a speed of 70 k A-scans/s.

In this work, we explore a new scheme of retardation and birefringence analysis of the RNFL: After recording a 3D PS-OCT data set, we trace the individual nerve fiber bundles, starting from the optic nerve head (ONH), and plot RNFL retardation, thickness, and birefringence as measured along the course of the fiber bundle. In a healthy eye, retardation and thickness of the RNFL decrease along the length of the fiber bundles with distance from the ONH, while the birefringence stays rather constant. Our hypothesis is that structural damage caused to the ganglion cell axons in early stages of glaucoma will alter this pattern of constant birefringence along a fiber bundle, providing insight into the location of the damage and possibly into the associated patho-mechanisms of glaucoma.

9307-22, Session 4

Polarimetric imaging of retinal disease by polarization sensitive SLO

Masahiro Miura, Tokyo Medical Univ. Ibaraki Medical Ctr. (Japan) and Tokyo Medical Univ. (Japan); Ann E. Elsner, School of Optometry, Indiana Univ. (United States); Takuya Iwasaki, Tokyo Medical Univ. Ibaraki Medical Ctr. (Japan); Hiroshi Goto, Tokyo Medical Univ. (Japan)

Polarimetry imaging is used to evaluate different features of the macular disease. Polarimetry images were recorded using a commercially- available polarization-sensitive scanning laser ophthalmoscope at 780 nm (PS-SLO, GDx-N). From data sets of PS-SLO, we computed average reflectance image, depolarized light images, and ratio-depolarized light images. The average reflectance image is the grand mean of all input polarization states. The depolarized light image is the minimum of crossed channel. The ratio-depolarized light image is a ratio between the average reflectance image and depolarized light image, and was used to compensate for variation of brightness. Each polarimetry image is compared with the autofluorescence image at 800 nm (NIR-AF) and autofluorescence image at 500 nm (SW-AF). We evaluated four eyes with geographic atrophy in age related macular degeneration, one eye with retinal pigment epithelium hyperplasia, and two eyes with chronic central serous chorioretinopathy. Polarization analysis could selectively emphasize different features of the retina. Findings in ratio depolarized light image had similarities and differences with NIR-AF images.

Area of hyper-AF in NIR-AF images showed high intensity areas in the ratio depolarized light image, representing melanin accumulation. Areas of hypo-AF in NIR-AF images showed low intensity areas in the ratio depolarized light images, representing melanin loss. Drusen were high-intensity areas in the ratio depolarized light image, but NIR-AF images was insensitive to the presence of drusen. Unlike NIR-AF images, SW-AF images showed completely different features from the ratio depolarized images. Polarization sensitive imaging is an effective tool as a non-invasive assessment of macular disease.

9307-23, Session 4

Fiber-based Jones-matrix polarization-sensitive OCT of the human retina

Boy Braaf, Vrije Univ. Amsterdam (Netherlands) and Rotterdam Ophthalmic Institute (Netherlands); Koenraad A. Vermeer, Rotterdam Ophthalmic Institute (Netherlands); Mattijs de Groot, Vrije Univ. Amsterdam (Netherlands) and Rotterdam Ophthalmic Institute (Netherlands); Kari V. Vienola, Rotterdam Ophthalmic Institute (Netherlands); Johannes F. de Boer, Vrije Univ. Amsterdam (Netherlands) and Rotterdam Ophthalmic Institute (Netherlands)

In polarization-sensitive optical coherence tomography (PS OCT) the use of single-mode fibers (SMFs) can cause wavenumber dependent polarization distortions. This problem is addressed by a novel Jones matrix analysis method that spectrally analyses the sample polarization state to correct the polarization distortions induced by the system hardware. The method was implemented on an SMF-based PS-OCT setup that uses a 1- μm 100 kHz swept-source and a passive polarization-delay unit. The en face intensity, double-pass phase retardation and relative optic axis orientation were determined for the retina of a healthy volunteer and a glaucoma patient. The retinal structures were visualized by the intensity maps and showed several structures such as the optic nerve head (ONH) and several large blood vessels. The birefringent fibrous structures of the retina were visualized by the phase retardation and showed a significant reduction around the ONH for the glaucoma patient due to glaucoma-induced retinal nerve fiber loss. The angular orientation of the fibrous structures within the retina were visualized by their relative optic axis orientation in Poincaré orientation and showed the radial orientations of the Henle's fibers around the fovea and the retinal nerve fibers around the ONH. This confirmed that the novel Jones matrix method corrected hardware induced polarization distortions and allowed the determination of the polarization properties of the retina. The measurement of the retinal polarization properties is potentially interesting for the early detection and monitoring of pathological changes in neurodegenerative diseases such as glaucoma.

9307-24, Session 4

Local birefringence imaging of posterior eye by multi-functional Jones matrix optical coherence tomography

Satoshi Sugiyama, Univ. of Tsukuba (Japan) and Tomey Corp. (Japan); Young-Joo Hong, Deepa K. Kasaragod, Shuichi Makita, Univ. of Tsukuba (Japan); Masahiro Miura, Tokyo Medical Univ. (Japan); Yasushi Ikuno M.D., Osaka Univ. (Japan); Yoshiaki Yasuno, Univ. of Tsukuba (Japan)

A simultaneous local birefringence and Doppler imaging of posterior eye is performed by a multi-functional Jones matrix OCT (MF-OCT). The polarization information of a tissue is obtained by a local birefringence analysis, not by a conventional phase-retardation imaging. The local birefringence imaging does not rely on a strong implicit assumption utilized in phase retardation imaging, i.e., the net tissue from the surface

to a point of measurement should be a linear polarization component. Since this assumption is not satisfied for other tissues than a nerve fiber layer, the conventional phase retardation imaging does not provide correct birefringence information of a sample. The local birefringence imaging uses only a weak assumption of polarization linearity, and it can stand for eye tissue.

Local birefringence imaging has not been applied to true clinical imaging because of two major problems. The first problem is the inherent low signal-to-noise ratio of birefringence image. It is resolved by developing Bayesian maximum likelihood estimator. The second issue is the complexity of the optical system and its large system size. This is resolved by refactoring the entire hardware to reduce the foot print.

Several cases including normal and pathologic cases are presented in the conference. The local birefringence image shows more rational understanding of the posterior tissues and pathologies than a phase retardation image. Local birefringence image showed tissue difference such as fibrosis, myopic conus, lamina cribrosa, and vessel wall. The imaging was done with a newly developed MF-OCT prototype which can be operated in clinical site.

9307-25, Session 5

The first prototype of chromatic pupillometer for objective perimetry in retinal degeneration patients

Ygal Rotenstreich, Ron Chibel, Sheba Medical Ctr. (Israel) and Tel Aviv Univ. (Israel); Soad Haj Yahia, Sheba Medical Ctr. (Israel); Anat Achiron M.D., Wolfson Medical Ctr. (Israel); Mohamad Mahajna, Michael Belkin, Ifat Sher, Sheba Medical Ctr. (Israel) and Tel Aviv Univ. (Israel)

PURPOSE: We recently demonstrated the feasibility of quantifying pupil responses (PR) to multifocal chromatic light stimuli for objectively assessing visual field (VF). Here we assessed the first prototype of chromatic multifocal pupillometer device with 76 LEDs of 18 degree visual field and a smaller spot size aimed of achieving better perimetric resolution.

METHODS: A computerized infrared pupillometer was used to record PR to short- and long-wavelength stimuli (peak 485 nm and 620 nm, respectively) presented by 76 LEDs, 1.8mm spot size, at light intensities of 10-1000 cd/m² at different points of the 30 degree VF. PR latency, amplitude, constriction velocity and redilation velocity were measured in 9 retinitis pigmentosa (RP) patients and 17 normal aged-matched controls.

RESULTS: RP patients demonstrated statistically significant reduced pupil contraction amplitude and velocity in majority of perimetric locations under testing conditions that emphasized rod contribution (short-wavelength stimuli at 200 cd-s/m², p<0.05). By contrast, the amplitude and constriction velocity of pupillary responses under testing conditions that emphasized cone cell contribution (long-wavelength stimuli at 1000 cd-s/m²) were not significant different between the groups in majority of perimetric locations, particularly in central locations. Minimal pupil contraction amplitude and velocity were recorded in areas that were non-detected by chromatic Goldmann.

CONCLUSIONS: This study demonstrates the feasibility of using pupillometer-based chromatic perimetry for objective assessment of VF defects and demonstrate defects in rods or cones preferentially according to the light stimuli.

9307-26, Session 5

Fast optical measurement of intraocular straylight

Harilaos Ginis, Univ. de Murcia (Spain); Onurcan Sahin, Institute of Vision & Optics, Univ. of Crete (Greece); Pablo

Artal, Univ. de Murcia (Spain)

Light scattering in the human eye can deteriorate image quality and limit visual performance especially at the presence of a glare source. Optical measurement of straylight in the human eye is a challenging task where issues related to various inherent artifacts must be addressed. We report on a novel instrument based on the principle of double-pass optical integration that has been adapted for fast measurements suitable for a clinical setting. The instrument utilizes a light source formed by an array of green light emitting diodes that is projected onto the ocular fundus. The source has two concentric parts, a disk (field angle 0-3 degrees) and an annulus (3 - 8 degrees) that are modulated at different frequencies. A silicon photomultiplier receives the light reflected from the central part of the fundus and the Fourier transform of the signal reveals the contribution of each part of the source. Their relative amplitude is used to quantify light scattering by means of the straylight parameter. The instrument was initially validated using known diffusers. Straylight in a cohort of cataract patients (N=39) was measured. The optically measured straylight parameter was correlated to the clinical cataract grade as well to the psychophysically estimated value. The measurement method, utilizing rotational symmetry and coding field angles with different frequencies eliminates the need for a high-performance camera and allows fast measurements. This approach can be further advanced with multiple wavelengths and field angles to perform other measurements such as that of the macular pigment density.

9307-27, Session 5

Clinical trials of interference-based extended depth of focus intra ocular lens design

Zeev Zalevsky, Bar-Ilan Univ. (Israel); Ido Raveh, Ofer Limon, Shai Ben Yaish, Karen Lahav-Yacouel, Ravid Doron, Alex Zlotnik, Xceed Imaging Ltd. (Israel)

The extended depth of focus solution presented in this paper produces continuously focused vision over the full required range that in regular eye is covered by accommodation of 3.00D (from near range of 33cm and up to infinity). All this is obtained with static element with high energetic efficiency and without any need of applying force by the muscles of the eye. The solution is based upon addition of special annular like engraved profile on the surface of the lens. The engraving has depth of less than 1 micron. This profile generates extended depth of focus (EDOF) by fulfilling proper interference conditions within a focus channel starting before and ending after the original focal plane of the lens. The engraved profile does not contain any high spatial frequencies and therefore it is relatively easy and cheap for fabrication and its diffraction effects and chromatic dispersion are small whereas the energetic efficiency is high, as no energy is diverted into diffraction orders away from the central order of interest as in the case of diffractive optical elements. We present clinical trial involving IOL design implementing the above mentioned EDOF solution. The clinical results of the EDOF IOL show significant improvement in all near and intermediate distances without decreasing the distance VA. With respect to the distance corrected VA only, the average improvement for 40 cm is 3 lines and 3 letters. The performance are compared to Restor 3 and showed better results for all distances, especially in the 65 cm tested distance, where the proposed EDOF solution excelled the Restor 3 by one line and one letter in average.

9307-28, Session 5

Photovoltaic restoration of sight with high visual acuity in rats with retinal degeneration

Daniel V. Palanker, Georges Goetz, Henri Lorach, Stanford Univ. (United States); Yossi Mandel M.D., Bar-Ilan Univ.

(Israel); Richard Smith, Univ. of California, Santa Cruz (United States); David Boinagrov, Xin Lei, Theodore I. Kamins, James S. Harris Jr., Stanford Univ. (United States); Alexander Sher, Univ. of California, Santa Cruz (United States); Keith Mathieson, Univ. of Strathclyde (United Kingdom)

Patients with retinal degeneration lose sight due to gradual demise of photoreceptors. Electrical stimulation of the surviving retinal neurons provides an alternative route for delivery of visual information. Subretinal photovoltaic arrays with hexagonal 70 μ m pixels were used to convert pulsed near-IR light (880-915nm) into pulsed current to stimulate the nearby inner retinal neurons. Network mediated responses of the retinal ganglion cells (RGCs) could be modulated by pulse width (1-20ms) and peak irradiance (0.5-10 mW/mm²). Similarly to normal vision, retinal response to prosthetic stimulation exhibits flicker fusion at high frequencies, adaptation to static images and non-linear spatial summation. Spatial resolution was assessed in-vitro and in-vivo using rapidly pulsed illumination (20-40Hz) of alternating gratings with variable stripe width. In-vitro, average size of the electrical receptive fields in normal retina was 248 \pm 59 μ m – similar to their visible light RF size: 249 \pm 44 μ m. RGCs responded to grating stripes down to 67 μ m using photovoltaic stimulation in degenerate rat retina, and 28 μ m with visible light in normal retina. In-vivo, visual acuity in normally-sighted controls was 29 μ m/stripe, vs. 64 μ m/stripe in rats with subretinal photovoltaic arrays, corresponding to 20/250 acuity in human eye. With the enhanced acuity provided by eye movements and perceptual learning in human patients, visual acuity might cross the 20/200 threshold of legal blindness. Ease of implantation and tiling of these wireless arrays to cover a large visual field, combined with their high resolution opens the door to highly functional restoration of sight.

9307-29, Session 6

Confidence weighted retinal flow visualization in Doppler optical coherence tomography

Maximilian G. Graefe, Leah S. Wilk, Vrije Univ. Amsterdam (Netherlands) and Rotterdam Ophthalmic Institute (Netherlands); Boy Braaf, Vrije Univ. Amsterdam (Netherlands); Jan H. de Jong, Rotterdam Ophthalmic Institute (Netherlands); Jelena Novosel, Rotterdam Ophthalmic Institute (Netherlands) and Technische Univ. Delft (Netherlands); Koenraad A. Vermeer, Rotterdam Ophthalmic Institute (Netherlands); Johannes F. de Boer, Vrije Univ. Amsterdam (Netherlands)

Doppler Optical frequency domain imaging (OFDI) is a promising technique to investigate retinal vascular pathology. An inter-B-scan Doppler OFDI setup was earlier developed in our group, to measure and visualize retinal and choroidal blood flow. In order to reduce artifacts and improve the sensitivity in visualizing flow, adaptive data processing is needed to extract the contribution of real flow from the measured (noisy) signal. We present a novel approach for this purpose that evaluates the reliability of the flow and weights every voxel with its flow probability based on estimated phase noise levels. First, the phase noise was decomposed into two error sources: shot noise and noise caused by revisitation errors. The latter describes the noise which is caused by the displacement of the illumination spot in between the B-scans that are used for the inter-B-scan Doppler OFDI comparison. A flow probability was assigned as a weighting factor to each voxel using the estimated noise levels for both error sources. We investigated the behavior of our novel processing approach on data taken in patients with Age-Related Macular Degeneration. We found that the contrast for small vessels, which mainly can be found in the fovea of the human eye, becomes higher. Furthermore, artifacts, especially caused by revisitation errors, were reduced and thus gave a better visualization of the vasculature. In conclusion, our novel Doppler OFDI processing approach gives a promising improvement

for the evaluation of vascular pathology in patients, which might lead to better clinical diagnostics.

9307-30, Session 6

Evaluation of the effect of acutely elevated IOP on retinal capillary bed and total retinal blood flow

Zhongwei Zhi, Univ. of Washington (United States); William Cepurna, John C. Morrison, Elaine Johnson, Casey Eye Institute (United States); Ruikang K. Wang, Univ. of Washington (United States)

Elevated intraocular pressure (IOP) is the best defined glaucoma risk factor and controlling IOP is the mainstay of glaucoma therapy. Reduction of ocular blood flow caused by increased IOP may contribute to the glaucoma progression. The capability to visualize detailed capillary network and quantify the total retinal blood flow would be a big advance for better evaluation of the effect of elevated IOP on the retina and ONH function. In this study, we performed a comprehensive evaluation of the effect of acutely elevated IOP on the retinal capillary bed and total retinal blood flow (RBF) in anesthetized rats using Optical microangiography (OMAG)/OCT. An OMAG/OCT system which provides depth-resolved microvasculature of rodent retina with real capillary sensitivity and resolution was developed. The effect of elevated IOP on microvasculature within the nerve fiber layer/ganglion cell layer (NFL/GCL), inner plexiform layer (IPL) and outer plexiform layer (OPL) were observed respectively. OPL capillary vessel density and total RBF change versus IOP increase and perfusion pressure decrease were quantified. Our results indicate that the both total RBF and capillary beds was not affected to lower levels of IOP elevation (< 30 mmHg), which may be a manifestation of vascular autoregulation. Interestingly, the capillary bed responds slower to the IOP elevation than total RBF. This may be due to autoregulation of the capillary bed response to increasing IOP. Alternatively, capillary density change as revealed by OCT angiography may not adequately reflect the responses of capillary blood flow to changing IOP.

9307-31, Session 6

Ultrahigh speed swept source OCT angiography for in vivo imaging of retinal and choriocapillaris vasculature in patients with diabetes mellitus

Eric M. Moul, WooJhon Choi, Massachusetts Institute of Technology (United States); Mehreen Adhi M.D., Nadia K. Waheed, Tufts Medical Ctr. (United States) and New England Eye Ctr. (United States); Vijaysekhar Jayaraman, Praevium Research, Inc. (United States); ByungKun Lee, Massachusetts Institute of Technology (United States); Benjamin M. Potsaid, Thorlabs, Inc. (United States); Talisa De Carlo, Tufts Medical Ctr. (United States) and New England Eye Ctr. (United States); Alex E. Cable, Thorlabs, Inc. (United States); Jay S. Duker, New England Eye Ctr. (United States) and Tufts Medical Ctr. (United States); James G. Fujimoto, Massachusetts Institute of Technology (United States)

In vivo visualization of retinal and choriocapillaris vasculature is important for understanding the pathophysiology of retinal diseases, including diabetic retinopathy. In this study, a 400kHz A-scan rate vertical cavity surface emitting laser (VCSEL) swept light source centered at 1 μ m was used to perform in vivo intensity decorrelation optical coherence tomography

(OCT) angiography imaging of retinal and choriocapillaris vasculature in patients with diabetes mellitus and various states of diabetic retinopathy. En face OCT angiograms of the retinal and choriocapillaris vasculature were visualized by acquiring volumetric OCT angiograms. Two different field sizes, 6mm²6mm and 5mm²5mm, were used. The microvasculature of 53 diabetes mellitus patients with no apparent diabetic retinopathy (30 subjects), with nonproliferative diabetic retinopathy (16 subjects) and with proliferative diabetic retinopathy (7 subjects) were characterized.

9307-32, Session 6

Dual beam wide field OCT angiography at 400 kHz using angular compounding

Laurin Ginner, Cedric Blatter, Daniel Fechtig, Ursula Schmidt-Erfurth, Medizinische Univ. Wien (Austria); Martin Gröschl, Technische Univ. Wien (Austria); Rainer A. Leitgeb, Medizinische Univ. Wien (Austria)

Optical Coherence Tomography (OCT) Angiography has the potential to provide vascular contrast in a depth resolved manner, with high resolution, and in particular without the need of dye administration. Dual beam Doppler OCT on the other hand allows for reliable angle independent assessment of blood flow within retinal vessels, via illumination from two distinct well-defined directions. The blood flow itself is an important parameter to estimate tissue health and oxygen supply. The combination of both offers therefore important biomarkers for disease diagnosis that are currently not available. We demonstrate the intrinsic advantage of dual beam OCT using angular compounding for improving the contrast of angiographies by co-registration and summation of both channels. In addition we employ a commercially available swept source laser using two interleaved sources, each operating at 100kHz, and together achieving 200kHz. Further spectral splitting allows achieving 400kHz, and thereby improving the covered field of view to 16deg.

9307-33, Session 6

Investigation of age-related macular degeneration using optical microangiography

Qinqin Zhang, Yanping Huang, Univ. of Washington (United States); Utkarsh Sharma, Carl Zeiss Meditec, Inc. (United States); Mariana R. Thorell, Univ. of Miami Miller School of Medicine (United States); Ruikang K. Wang, Univ. of Washington (United States); Lin An, Mary Durbin, Michal Laron, Carl Zeiss Meditec, Inc. (United States); Philip J. Rosenfeld, Univ. of Miami Miller School of Medicine (United States)

To detect and enhance the features of different stages of age-related macular degeneration (AMD) using optical microangiography (OMAG). Twenty AMD patients were recruited, including early stage AMD, geographic atrophy (GA), neovascular AMD and polypoidal choroidal vasculopathy (PCV). After minimizing the bulk tissue motion by 2D cross-correlation method, OMAG algorithm based on intensity differentiation was used to extract the blood flow. The 3D angiography was segmented into 4 layers to give better demonstration, including superficial retinal (GCL+IPL) layer, deep retinal (INL+OPL) layer, neovascular layer, and choroid layer. The en-face maximum projection was used to obtain 2-dimensional angiograms of different layers coded with different colors. Flow and structure images were combined for cross-sectional view. En-face OMAG images of AMD patients showed good agreement with fluorescein angiography (FA). OMAG images gave more distinct vascular network visualization for the cases that were less affected by subretinal hemorrhage. The small drusen was observed in the early stage AMD patient. For GA patient, the abnormality of RPE

layer could be delineated; choriocapillaries and large choroidal vessel were detected and observed by OMAG angiograms. Feeding and draining vessels were visualized in the OMAG angiograms from neovascular AMD and PCV patients. The CNV regions were demarcated compared with FA images, which were obscured by the leakage in the late phase. OMAG provides depth-resolved information and detailed vascular images of AMD patients.

9307-34, Session 7

Concept for image-guided vitreo-retinal fs-laser surgery: adaptive optics and optical coherence tomography for laser beam shaping and positioning

Ben Matthias, Laser Zentrum Hannover e.V. (Germany); Dorothee Brockmann, Medizinische Hochschule Hannover (Germany); Anja Hansen, Konstanze Horke, Gesche Knoop, Timo Gewohn, Miroslav Zabic, Alexander Krüger, Tammo Ripken, Laser Zentrum Hannover e.V. (Germany)

Fs-lasers are well established in ophthalmic surgery as high precision tools for corneal flap cutting during laser in situ keratomileusis (LASIK) and increasingly utilized for cutting the crystalline lens, e.g. in assisting cataract surgery. For addressing eye structures beyond the cornea, an intraoperative depth resolved imaging is crucial to the safety and success of the surgical procedure due to interindividual anatomical disparities. Extending the field of application even deeper to the posterior eye segment, individual eye aberrations play an important role and surgery with fs-laser is impaired by focus degradation. Our demonstrated concept for image-guided vitreo-retinal fs-laser surgery combines adaptive optics (AO) for spatial beam shaping and optical coherence tomography (OCT) for focus positioning guidance. The laboratory setup comprises an adaptive optics assisted 800 nm fs-laser system and is extended by a Fourier domain optical coherence tomography system. Phantom structures are targeted, which mimic tractional epiretinal membranes in front of excised porcine retina within an eye model. AO and OCT are set up to share the same scanning and focusing optics. A Hartmann-Shack sensor is employed for aberration measurement and a deformable mirror for aberration correction. By means of adaptive optics the threshold energy for laser induced optical breakdown is lowered and cutting precision is increased. 3D OCT imaging of typical ocular tissue structures is achieved with sufficient resolution and the images can be used for orientation of the fs-laser beam. We present targeted dissection of the phantom structures and its evaluation with regard to retinal safety.

9307-35, Session 7

A computational approach to high-resolution imaging of the living human retina without hardware adaptive optics

Nathan D. Shemonski, Univ. of Illinois at Urbana-Champaign (United States); Steven G. Adie, Univ. of Illinois at Urbana-Champaign (United States) and Cornell Univ. (United States); Yuan-Zhi Liu, Fredrick A. South, Paul S. Carney, Stephen A. Boppart, Univ. of Illinois at Urbana-Champaign (United States)

We demonstrate high-resolution imaging of the living human retina by computationally correcting high-order ocular aberrations. These corrections are performed post-acquisition and without the need for a deformable mirror or wavefront sensor that are commonly employed in hardware adaptive optics (HAO) systems. With the introduction of HAO to ophthalmic imaging, high-resolution near diffraction-limited imaging of the living human retina has become possible. The combination of a deformable mirror, wavefront sensor, and supporting hardware/software, though, can more than double the cost of the underlying imaging

modality, in addition to significantly increasing the system complexity and sensitivity to misalignment. Optical coherence tomography (OCT) allows 3-D imaging in addition to naturally providing the complex optical field of backscattered light. This is unlike a scanning laser ophthalmoscope which measures only the intensity of the backscattered light. Previously, our group has demonstrated the utility of a technique called computational adaptive optics (CAO) which utilizes the complex field measured with OCT to computationally correct for optical aberrations in a manner similar to HAO. Until now, CAO has been applied to ex vivo imaging and in vivo skin imaging. We demonstrate, for the first time, in vivo imaging of the retinal nerve fiber layer and cone photoreceptors using CAO. Additional practical considerations such as the choice of imaging modality, imaging speed, and stability will also be discussed.

9307-36, Session 7

Novel dark field detection methods in adaptive optics imaging of the inner retina

R. Daniel Ferguson, Mircea Mujat, Ankit H. Patel, Nicusor V. Iftimia, Physical Sciences Inc. (United States); James D. Akula, Anne B. Fulton, Boston Children's Hospital (United States) and Harvard Medical School (United States)

Cellular resolution retinal is becoming a valuable tool for clinicians in diagnosis of many eye diseases. Physical Sciences Inc (PSI) has developed advanced multimodal AO retinal imaging technology, including high-resolution confocal AO-SLO/SD-OCT platforms, and a compact AO-LSO/OCT (line-scanning ophthalmoscope) system designed for cone photoreceptor density mapping. Recently, much progress has been made with the addition of dark field imaging modalities. A number of related techniques can be exploited for imaging of the inner retina where the layers and structures (e.g. vessels, RGCs) are substantially transparent. We have developed novel modalities with existing AOSLO/OCT system for high resolution, high-frame-rate dark-field capillary micro-flowmetry. Strip imaging sub-frame rates to >300fps have been tested enabling direct video velocimetry and visualization of local flow pulsatility, zero flow and flow reversal. PSI's new time-domain integration (TDI) line-camera approach to AO-LSO imaging retains inner retinal image phase information using oblique back-illumination geometry with spatially flexible dark field illumination control, enabling unique imaging approaches analogous to phase-contrast or phase-gradient microscopy. By displacing the illumination line onto photoreceptors below the layers where the AO-LSO imager is focused, oblique back-illumination methods produce phase contrast images of weak phase objects in the inner retina. Vessels, capillaries and flow can be seen in the image in the images presented. In conclusion, dark field imaging and related modalities can be far more widely exploited for new functional imaging capabilities. New AOSLO and AO-LSO techniques are complementary and together may yield a more comprehensive picture of retinal structure, especially in the inner retina. .

9307-37, Session 7

Imaging modal content of cone photoreceptors using adaptive optics optical coherence tomography

Zhuolin Liu, Omer P. Kocaoglu, Timothy L. Turner, Donald T. Miller, Indiana Univ. (United States)

It has been long established that photoreceptors capture light based on the principles of optical waveguiding. Yet after decades of experimental and theoretical investigations considerable uncertainty remains even for the most basic prediction of whether photoreceptors support more than a single waveguide mode. Such predictions are of much interest for human vision as modes define visual performance at the cone level and may be perturbed early in the disease process, thus a potentially sensitive biomarker of photoreceptor health. To test for modal behavior of cones, we

take advantage of adaptive-optics optical coherence tomography to resolve the reflectance profiles "inside" the inner and outer segments (IS, OS) of cone photoreceptors in human subjects. Mode content is examined for a range of cone diameters by imaging cones at different retinal eccentricities. Critical to the method is accurate axial registration and layer segmentation to extract reflections at the IS/OS junction and posterior tip of outer segments. Cone modal content is quantified using second moment analysis and average/variance maps. Both qualitative observations and quantitative analyzes indicate waveguiding properties of cone IS and OS depend on the diameter of the segments. At the examined wavelength of 785nm, cone IS supports a single mode near the fovea (<3°) and multiple modes further away (>5°). A fraction-of-a-micron change in cone size distinguishes performance between single and multi-mode, and reflects the sensitivity of the modes to extremely small changes. In contrast, no evidence of multiple modes was found in the cone outer segment regardless of retinal location.

9307-38, Session 7

Adaptive optics optical coherence tomography at 1 MHz

Omer P. Kocaoglu, Timothy L. Turner, Zhuolin Liu, Donald T. Miller, Indiana Univ. (United States)

Image acquisition speed of optical coherence tomography (OCT) remains a fundamental barrier that limits its scientific and clinical utility. Here we demonstrate a novel multi-camera adaptive optics (AO-)OCT system for ophthalmologic use that operates at 1 million A-lines/s at a wavelength of 790 nm. Central to the spectral-domain design is a novel detection channel based on four high-speed custom spectrometers that receive light sequentially from a cascade of three custom optical switches. Absence of moving parts in the switches enabled ultra-fast (50ns) and precise switching with low insertion loss (< 0.22 dB). This manner of control makes use of all available light in the detection channel and avoids camera dead-time, both critical for imaging at high speeds. In combination with AO, additional benefit in signal-to-noise accrues from the larger numerical aperture, which collects up to 10x more of the retinal reflection compared to OCT alone. We validated system performance by: calibrating the timing pattern that controls the spectrometers, optical switches and galvo-scanners; optically measuring the switch assembly performance via four high-speed point detectors connected to the switch ports; measuring system sensitivity; and finally acquiring volume images of the living human retina. System sensitivity was 90 to 96 dB, depending on the speed and camera configuration. We demonstrate the performance of our MHz AO-OCT system to capture detailed images of retinal nerve fiber bundles and photoreceptors with fine spatial sampling (1 μm/pixel) across 1.3°x1.3° and 3.6°x3.6° fields of view. This is the fastest system we know of based on SD-OCT technology.

9307-39, Session 8

Optical characterization of vitreous structure in health and disease

Ashwin Sampathkumar, Riverside Research Institute (United States); Jerry Sebag M.D., VMR Institute (United States); Jeffrey A. Ketterling, Riverside Research Institute (United States)

Patients with myopic vitreopathy and posterior vitreous detachment see floaters, which can significantly degrade contrast sensitivity. In comparison, asteroid hyalosis (AH) is characterized by spherical white asteroid bodies (ABs) that move with vitreous displacement during eye movements, but that typically do not interfere with vision. We hypothesize that the distinguishing feature of myopic vitreopathy and age-related vitreous opacification from AH is an irregular surface on the floaters in comparison to the smooth surface of ABs. A finite-element model was developed to characterize the static and dynamic light-scattering fields of vitreous opacities in myopia, aging, and AH. Vitreous opacities were modeled under different lighting

conditions as spherical, cylindrical, spiral, or conical in shape with random perturbations added to their surfaces to vary light scattering properties and to model disturbances in vision from simple diffraction rings to more-complex patterns. Small (1-ml) samples of ex vivo human vitreous were placed in a custom spectrophotometer, and the static light scattering of the sample was measured in the spectral range of 400-1100 nm with a resolution of 0.3 nm. Simulation results were compared to experimental data to characterize vitreous opacities quantitatively and to distinguish between structures that significantly impact vision, such as those due to myopic vitreopathy and aging, from those that have little impact, like ABs. The ability to determine the structural significance of vitreous opacification would be very useful in selecting patients for surgical treatment as well as evaluating the efficacy of experimental non-surgical therapies for floaters.

9307-40, Session 8

Determining the optomechanical properties of accommodating gel for lens refilling surgery using finite element analysis and numerical ray-tracing

Hooman Mohammad Pour, The Univ. of New South Wales (Australia)

A requisite step in the design of polymer gel to replace the natural contents of the presbyopic human crystalline lens is to determine the equivalent isotropic mechanical and material properties of the gel that yields the same optical response as the natural lens with its gradient properties. This process is compounded by the interplay between the mechanical and optical gradient. In order to quantify the equivalent isotropic properties of the lens, both gradients need to be considered. In this paper, numerical ray-tracing and finite element method (FEM) are implemented to investigate the effects of varying the isotropic elasticity and refractive index on the accommodative response of the lens; in particular, its accommodative amplitude. Our results show that the accommodative amplitude can be mathematically expressed as a function of gel refractive index and Young's modulus of elasticity.

9307-41, Session 8

Assessing age-related changes of biomechanical properties of crystalline lens in rabbit eyes using a co-focused ultrasound and optical coherence elastography system

Chen Wu, Zhaolong Han, Shang Wang, Jiasong Li, Manmohan Singh, Chih Hao Liu, Univ. of Houston (United States); Salavat R. Aglyamov, Stanislav Y. Emelianov, The Univ. of Texas at Austin (United States); Fabrice Manns, Bascom Palmer Eye Institute (United States) and Univ. of Miami (United States); Kirill V. Larin, Univ. of Houston (United States) and Baylor College of Medicine (United States)

In this study, we utilize a confocal ultrasound and phase-sensitive optical coherence elastography (OCE) system to assess age-related changes in biomechanical properties of the crystalline lens in intact rabbit eyes in situ. Low-amplitude elastic deformations, induced on the surface of the lens by localized acoustic radiation force, were measured using phase-sensitive OCT. The results demonstrate that the displacements induced in young rabbit lenses are significantly larger than those in the mature lenses. Temporal analyses of the surface displacement are also demonstrated significant difference between young and old lenses, indicating that the stiffness of lens increases with the age. These results demonstrate possibility of OCE for completely noninvasive analysis and quantification of lens biomechanical

properties, which could be used in many clinical and basic science applications such as surgeries and studies on lens physiology and function.

9307-42, Session 8

Near-infrared radiation damage mechanism in the lens

Per G. Söderberg, Uppsala Univ. (Sweden)

No Abstract Available

9307-43, Session 8

Three dimensional mapping of the cornea elasticity using optical coherence elastography

Manmohan Singh, Jiasong Li, Shang Wang, Srilatha Vantipalli, Michael D. Twa, Univ. of Houston (United States); Kirill V. Larin, Univ. of Houston (United States) and Baylor College of Medicine (United States)

We demonstrate a novel method for noncontact noninvasive elastic wave velocity measurement in three dimensions using phase-stabilized swept source optical coherence elastography (PhS-SSOCE). A focused air-pulse delivery system induces an elastic wave, which is then captured by the PhS-SSOCE system. By calculating the velocity in all radial directions and depths from the origin of the induced elastic wave, we are able to create a volumetric map of elasticity from the elastic wave velocity of the sample. Due to the high spatial sensitivity of PhS-SSOCE, the induced deformation amplitude can be sub-micron, thus preserving the structure and function of the delicate corneal tissue. The results show that this noncontact noninvasive method for elasticity measurement can provide a volumetric mapping of elasticity and differentiate between untreated and UV induced collagen crosslinked corneas. As expected, the elastic wave velocity is significantly higher in the crosslinked cornea as compared to the untreated cornea.

9307-44, Session 8

Quantitative assessment of corneal biomechanical properties using optical coherence elastography and a lamb-frequency model

Zhaolong Han, Jiasong Li, Manmohan Singh, Shang Wang, Srilatha Vantipalli, Chen Wu, Chih Hao Liu, Rita Idugboe, Thomas T. C. Hsu, Michael D. Twa, Kirill V. Larin, Univ. of Houston (United States)

We demonstrate a noninvasive method for quantitative assessment of the biomechanical properties of normal porcine corneas using optical coherence elastography (OCE). A focused air-pulse was applied to induce an elastic wave in the cornea. Phase velocities of the elastic wave were extracted by spectral analysis using the fast Fourier transform. Experiments were performed on 2% agar phantoms (n=3), and the Young's moduli were assessed by the cylindrical lamb-frequency equation (LFE), which was validated using a uniaxial mechanical compressional test. This method was then applied to porcine corneas (n=3), in which the fluid-solid effect was considered. The Young's moduli of the corneas were measured to be ~85 kPa with a viscosity ~3.0 Pa·s. These data demonstrate that the combination of OCE and LFE is a promising noninvasive method for assessing the corneal biomechanical properties and may be potentially useful in vivo in clinical studies.

9307-45, Session 9

New asymmetric optical model of the human eye for the design of wide-field imaging instruments

James M. Polans, Ryan P. McNabb, Duke Univ. (United States); Bart Jaeken, Pablo Artal, Univ. de Murcia (Spain); Joseph A. Izatt, Duke Univ. (United States)

We describe an asymmetric optical model of the human eye with a tilted and decentered crystalline lens that reproduces experimentally measured wavefront data. To our knowledge, this is the first model to portray accurately the optical aberrations across a wide field of view (80°) within anatomical constraints. We compare our proposed schematic eye to previously published models as well as experimentally measured Shack-Hartmann wavefront data. Our model agrees better with the measured data both comprehensively and for both low-order and high-order Zernike terms. Our model especially excels at replicating the aberrations of the retinal periphery. Additionally, we outline a robust reverse eye building technique that is able to predict anatomical trends beyond those defined explicitly in the optimization routine. Using the measured aberration profile as a function of field angle, a realistic tilt and decentration of the crystalline lens arose as a natural product of the design process. Finally, we present a preliminary example of how to use this new eye model to design ophthalmic imaging systems that preemptively correct the aberrations of the average human eye over a wide visual field. The proposed eye model shows great promise towards the design of wide-field imaging instrumentation, including OCT, SLO, fluorescence imaging and fundus photography, as well as the study of the peripheral optics of the human eye.

9307-46, Session 9

Comparison of optical coherence tomography cup-to-disc ratio measurements with an optic nerve head-retina phantom

Daniel X. Hammer, Jigesh Baxi, William R. Calhoun III, U.S. Food and Drug Administration (United States); Chieh-Li Chen, Hiroshi Ishikawa M.D., Joel S. Schuman M.D., Gadi Wollstein M.D., UPMC Eye Ctr. (United States); Anant Agrawal, U.S. Food and Drug Administration (United States)

Glaucoma detection and progression monitoring are performed with clinical optical coherence tomography (OCT) devices using metrics including nerve fiber layer (NFL) thickness and cup-to-disc ratio (CDR). In order to understand and quantify CDR measurement differences across instruments, we constructed three optic nerve head (ONH) phantoms. The phantoms are fabricated with two components: ONH and peripapillary regions. The peripapillary region is constructed with techniques similar to those previously developed for a retina-simulating phantom - including layer-by-layer spin coat deposition of polydimethylsiloxane (PDMS) with embedded nanoparticles designed to match the thickness and reflectivity of 12 retinal layers. For the ONH phantom, layer deposition was designed to more closely match the peripapillary region. The ONH region was constructed by femtosecond laser etching a homogenous scattering substrate. Three ONH phantoms were made to model healthy, moderate, and advanced glaucomatous eyes. The phantoms were imaged with three clinical OCT instruments as well as a custom-built OCT system. Generally accepted definitions of the disc and cup boundaries are Bruch's membrane termination and the cup margin 150 μm above this point. The three clinical devices used different segmentation algorithms to locate these points, which led to inter-device variability. We describe the causes of variability as well as the suitability of the ONH phantom to explore systemic and algorithmic differences. The results can be used when patients are imaged

across platforms, which may be important in tracking disease progression. Quantified models can also eventually be used to separate patient and instrument variability, leading to better normative and disease databases.

9307-47, Session 9

Real-time calibration-free C-scan images of the eye fundus using master slave swept source optical coherence tomography

Adrian Bradu, Konstantin Kapinchev, Fred Barnes, Univ. of Kent (United Kingdom); David F. Garway-Heath, Ranjan Rajendram, Pearse Keane, NIHR Biomedical Research Ctr., Moorfields Eye Hospital (United Kingdom); Adrian G. Podoleanu, Univ. of Kent (United Kingdom)

Recently, we introduced a novel Optical Coherence Tomography (OCT) method, termed as Master Slave OCT (MS-OCT). This uses principles of spectral domain interferometry in two stages. MS-OCT operates like a time domain OCT, selecting signal from a selected depth only while scanning the laser beam across the eye. Time domain OCT allows real time production of an en-face image, although relatively slowly. As a major advance, the Master Slave method allows the collection of a signal from any number of depths, as required by the user. By the end of the acquired frame ($T_a = 1.6$ s) being scanned, using our computing capacity, 4 simultaneous 200x200 pixel en-face images can be created in about $T = 0.8$ s. Taking advantage of the parallel processing allowed by the MS method, implemented on graphic cards, the MS-OCT allows the production of a larger number of en-face images with no time penalty. Typically we can display 40 en-face images in about $T_d = 0.3$ s. We demonstrate images obtained with a swept source at 100 kHz (which determines the acquisition time T_a) equipped with Master Slave electronics. Other faster swept source engines can be used with no difference in terms of T_d . With 40 images (or more), volumes can be created for 3D display, using en-face images, as opposed to the current technology where volumes are created using cross section OCT images.

9307-48, Session 9

Automatic optimization high-speed high-resolution OCT retinal imaging at 1 μm

Eunice Michelle C. Cua, Yifan Jian, Xiyun Liu, Simon Fraser Univ. (Canada); Stefano Bonora, IFN-CNR LUXOR Lab. (Italy); Robert J. Zawadzki, Univ. of California, Davis (United States); Paul J. Mackenzie, The Univ. of British Columbia (Canada); Marinko V. Sarunic, Simon Fraser Univ. (Canada)

High-resolution retinal imaging is important in providing visualization of various retinal structures to aid vision researchers in better understanding the pathogenesis of diseases causing blindness. In glaucoma, for example, studies on non-human primates have indicated that morphological changes in the lamina cribrosa may precede the degeneration of retinal ganglion cell axons in the nerve fiber layer. Similarly, changes in the density of the photoreceptor mosaic are associated with functional vision loss and retinal dystrophy.

Current commercial OCT systems that operate at ~ 830 nm do not have sufficient depth of penetration and resolution to resolve the photoreceptor layer, or to image the deeper structures in the optic nerve head (ONH), such as the lamina cribrosa. OCT systems with an operating wavelength centered at $\sim 1\mu\text{m}$ provide increased penetration into the choroid and ONH. Furthermore, the conventional OCT systems are unable to resolve detailed structures, such as the laminar pores or photoreceptor mosaic, due to uncorrected optical aberrations within the eye. Traditional adaptive optics systems depend on the addition of a deformable mirror and/or wavefront sensor which greatly complicates the setup.

In this report, we describe a novel, auto-focus, high-speed SS-OCT imaging system that can clearly visualize microstructures within the retina and ONH. We optimized resolution in the desired depth region by adding a variable-focus lens to our setup that provided automated focus adjustment. Real-time processing and display of the volumetric data (cross-sectional scans and en face depth planes) during the imaging session was performed using our open-source GPU code.

9307-49, Session 9

1050nm handheld optical frequency domain imaging system for pediatric retinoblastoma patients

Oleg Nadiarnykh, Vrije Univ. Amsterdam (Netherlands);
Annette C. Moll, Vrije Univ. Medical Ctr. (Netherlands);
Johannes F. de Boer, Vrije Univ. Amsterdam (Netherlands)

We demonstrate a novel optical coherence tomography (OCT) system with a handheld probe specifically developed and validated for complementary clinical imaging of retinoblastoma tumors in pediatric patients. Retinoblastoma is a malignant tumor of the retina, where treatment approaches aim at vision preservation while risking tumor (re)growth, regions near the macula and optic nerve being the most critical. Currently, the patients at risk are monitored monthly under general anesthesia due to limitations of the existing real-time diagnostic tools. The cross-sectional depth profiles and improved axial and lateral resolution of interference-based OCT imaging answer the pressing need for detection of vital tumor tissue concurrent with local treatment. Our system uses 1050nm wavelength for deeper penetration into the choroid layers of retina. The prototype is designed and validated for children in supine position under general anesthesia, where ergonomically designed handheld probe is connected to fiber-based optical setup via umbilical cord. The system conforms to clinical safety requirements, including fully isolated low-voltage electric circuit. Focusing with mechanically tunable lens accommodates for the wide range of optical parameters of the eye that change rapidly in infancy. Imaging is performed at 101.6dB sensitivity with the 10 μ m lateral resolution varying with focusing. The implemented Doppler imaging mode probes blood flow in microvasculature.

We discuss nuances of design, performance limitations, and results of the ongoing clinical study, including newly developed OCT diagnostic criteria, correlation with the previously used approaches, and follow-up images obtained from the patients monitored after local and systemic treatments.

9307-50, Session 9

Ultra-compact switchable SLO/OCT handheld probe design

Francesco LaRocca, Derek Nankivil, Theodore B. DuBose,
Sina Farsiu, Joseph A. Izatt, Duke Univ. (United States)

Handheld scanning laser ophthalmoscope (SLO) and optical coherence tomography (OCT) systems facilitate imaging of young children and subjects with less stable fixation. More compact and lightweight probes allow for better portability and increased comfort for the operator of the handheld probe. We describe a very compact, novel SLO and OCT handheld probe design. A single 2D microelectromechanical systems (MEMS) scanner and a custom optical design using a converging beam prior to the scanner permitted significant reduction in the system size. Our design utilized a combination of commercial and custom optics that were optimized in Zemax to achieve near diffraction-limited resolution of 8 μ m over a 7 $^\circ$ field of view. The handheld probe has a form factor of 7 x 6 x 2.5 cm and a weight of only 94 g, which is over an order of magnitude lighter than prior SLO-OCT handheld probes. Images were acquired from a normal subject with an incident power on the eye under the ANSI limit. With this device, which is the world's lightest and smallest SLO-OCT system, we were able to

visualize parafoveal cone photoreceptors and nerve fiber bundles without the use of adaptive optics.

9307-51, Session PSun

Developing a flammability test system for sunglasses: results

Renan Magri, Liliane Ventura, Univ. de São Paulo (Brazil)

Sunglasses popularity has increased tremendously. Just in Brazil, the number of units sold overtakes 10.5 million a year. This fact has further led to the need of certifying sunglasses accordingly to the standard NBR 15111 to protect consumers from damages and secondary hazards caused by sunglasses use. The ongoing need comes at the expense that none certification institution in Brazil performs all tests procedures required by the NBR 15111. This manuscript presents the development of a flammability test system for sunglasses and the assessments results. The equipment for testing flammability developed is made of an electrical furnace with a thermocouple and electronic system that maintains the temperature in 650 $^\circ$ C. This furnace heats a steel rod used for testing flammability. A steel cable connected to a linear actuator drives the rod. The main control system is based on an ARM Cortex M0 microcontroller and we developed a PC interface in LabView to acquire data and store it. The equipment built also has a control panel with a push button, status LEDs and temperature indicator. We performed flammability tests in 45 sunglasses: 45 lenses and 45 frames using the equipment described. None of the samples ignited or continued to glow when the test has finished, however, all polycarbonate samples were melted in the contact region with the steel rod. All samples complied with the NBR 15111. The proof argues that the polycarbonate is extremely resistant to ignition. Moreover, another study concluded that the material is flame-resistant and self-extinguishing.

9307-52, Session PSun

Deep stroma investigation by confocal microscopy

Francesca P. Rossi, Francesca Tatini, Roberto Pini,
Consiglio Nazionale delle Ricerche (Italy); Paola Valente,
Nuovo Ospedale Santo Stefano (Italy); Roberta Ardia, Univ.
degli Studi di Roma "Tor Vergata" (Italy); Luca Buzzonetti,
Nuovo Ospedale Santo Stefano (Italy); Annalisa Canovetti,
Alex Malandrini, Ivo Lenzetti, Luca Menabuoni M.D., Univ.
degli Studi di Roma "Tor Vergata" (Italy)

Laser assisted keratoplasty is nowadays largely used to perform minimally invasive surgery and partial thickness keratoplasty. The use of the femtosecond laser enables to perform a customized surgery, solving the specific problem of the single patient, designing new graft profiles and partial thickness keratoplasty (PTK). The common characteristics of the PTKs and that make them eligible respect to the standard penetrating keratoplasty, are: the preservation of eyeball integrity, a reduced risk of graft rejection, a controlled postoperative astigmatism. On the other hand, the optimal surgical results after these PTKs are related to a correct comprehension of the deep stroma layers morphology, that can help in the identification of the correct cleavage plane during surgeries. In the last years some studies were published, giving new insights about the posterior stroma morphology in adult subjects. In this work we present a study performed on two groups of tissues: one group is from 20 adult subjects aged 59 \pm 18 y.o., and the other group is from 15 young subjects, aged 12 \pm 5 y.o.. The samples were from tissues not suitable for transplant in patients. The analysis of the deep stroma was performed by confocal microscopy and Transmission Electron Microscopy (TEM). The preliminary results of this analysis show the main differences in between young and adult tissues, enabling to improve the knowledge of the morphology and of the biomechanical properties of human cornea, in order to improve the surgical results in partial thickness keratoplasty.

9307-53, Session PSun

Equivalence between solar irradiance and simulators in solarization tests of sunglasses

Mauro Masili, Homero Schiabel, Liliane Ventura, Univ. de São Paulo (Brazil)

The present literature establishes safe limits on the exposure of the eyes to ultraviolet radiation (UVR). Ultraviolet radiation upon the eyes is related to many ocular pathologies. Regarding UV protection for ocular media, the resistance-to-irradiance test of many national standards requires irradiating the lenses for 50 continuous hours with a 450 W solar simulator, providing a correspondingly evaluation of the exposure to the Sun. The main concern of this test is to establish a reliable correspondence between the solar irradiation and the simulator lamp considering that solar irradiation depends on geographical coordinates, time of year and atmospheric conditions. Our calculation indicates that this stress test is ineffective in that present form. Suggestions for the revision of the parameters of these tests are offered to establish safe limits appropriate to the UV irradiance.

9307-54, Session PSun

Progress on the self-service kiosk for testing the UV protection on sunglasses: polynomial and neural network approximation for calculating light transmittance

Liliane Ventura, Marcio M. Makiyama Mello, Univ. de São Paulo (Brazil)

A method using different light sources and sensors has already been used to approximate weighting functions to calculate light transmittance in sunglasses. Although it made possible to build a self service kiosk to inform users about the UV protection of their sunglasses, each transmittance test is still dependent of its components. Methodology using polynomial approximation and artificial neural network has been tested which provides the possibility for using fixed light source and sensor for all light transmittance tests. Spectrophotometry was performed in 45 lenses of sunglasses for general use, and their respective transmittance (visible, traffic light), used as samples for testing the methodologies. The tests included a white LED as light source and a RGB sensor, and electronic for control and signal acquisition. Bland - Altman analysis tool was used to calculate the agreement between the method and the transmittances calculated in the spectrophotometer. Both methods, polynomial and neural had an approximation within the deviation limit required by sunglasses standards. The system with the polynomial regression presented lower deviations than artificial neural networks. Many meters in the market do not calculate accurately the transmittance measurements required for the sunglasses, and none calculates in the same equipment all light transmittances. The methodology was applied only for the visible light, while UV and infrared spectrum are being tested. The current methodology proved to be more efficient than previous methodologies that we have been working with in all of the other kiosk's versions.

9307-55, Session PSun

Single-photon time-gated fluorescence lifetime microscope for in vivo corneal imaging

Susana F. Silva, IBILI, Univ. de Coimbra (Portugal); Ana Batista, IBILI, Univ. de Coimbra (Portugal) and Univ. des

Saarlandes (Germany); Maria João Quadrado, IBILI, Univ. de Coimbra (Portugal) and Ctr. Hospitalar e Univ. de Coimbra (Portugal); António Miguel Morgado, Univ. de Coimbra (Portugal) and IBILI (Portugal)

Corneal metabolic imaging may provide the clinicians a method for diagnosing corneal cells dysfunction prior to its pathologic expression. Changes in metabolism can be monitored noninvasively through the assessment of the relative amounts of free and protein-bound components of the metabolic co-factor flavin adenine dinucleotide (FAD), present in cells mitochondria. As FAD fluorescence decay shows short and long lifetime component, corresponding respectively, to its protein-bound and free state, fluorescence lifetime imaging microscopy (FLIM) can be used to monitor corneal cells metabolism.

Here we describe a single-photon fluorescence lifetime microscope for in vivo corneal imaging. The instrument is a whole field microscope based on the Time-Gated imaging technique. Single-photon fluorescence excitation is provided by a picosecond diode laser with emission at 440 nm, a wavelength suitable for exciting FAD. Fluorescence detection and imaging is achieved by an ultrafast time-gated intensified CCD camera operating with time-gates down to 200 ps.

Optical sectioning is obtained using the structured illumination technique based on a computer-controlled digital micromirror device (DMD). The DMD, a micro-electro-mechanical system (MEMS) made up of 684x608 switchable mirrors, is used to produce the fringe patterns required by the Fourier-based image reconstruction process of structured illumination.

We present data on the instrument performance as well as images acquired with normal human corneas, unsuitable for transplantation, and human diseased corneas, both obtained from the Department of Ophthalmology of Coimbra's University Hospital. In vivo imaging performance is assessed using Wistar rats.

9307-56, Session PSun

Real-time processing and visualization of volumetric adaptive optics optical coherence tomography images

Timothy L. Turner, Indiana Univ. (United States); Jeffrey E. Kriske Jr., Brandon A. Shafer, Indiana Univ.-Purdue Univ. Indianapolis (United States); Omer P. Kocaoglu, Zhuolin Liu, Indiana Univ. (United States); John J. Lee, Indiana Univ.-Purdue Univ. Indianapolis (United States); Donald T. Miller, Indiana Univ. (United States)

As adaptive optics optical coherence tomography (AO-OCT) datasets become larger in size and acquired at ever higher rates, sequentially processed data handling, processing and visualization methods inevitably give rise to computational bottle-necks. To address this problem we have developed highly efficient parallel computing methods and streamlined data management approaches to visualize large AO-OCT data-streams (e.g., -1.5 Gigabytes/s), which require intensive computations to generate, register, and display images and mine the data. The required computational bandwidth is well beyond that of high-end computer workstations. Using CUDA with C++, we exploit data-level parallelism, e.g., single instruction multiple data architectures, realized with general-purpose computation on a graphics processing unit (GPGPU) and extend early demonstrations of parallel processing devices for OCT. Data is grouped and processed in units of entire B-scans for organizational purposes and meaningful visualization of real-time feedback onscreen. To maintain GPGPU parallelism with minimal latency we utilize a multi-threaded approach on the host PC to separate acquisition tasks from processing and control tasks, ensuring temporary blocking on one task does not block the others. At 240 A-lines/B-scan and 240 B-scans/volume our non-GPGPU software visualized rudimentarily-processed images at 3 volumes/second. Our previous offline algorithm fully processed the same dataset at 0.004 volumes/second. Current GPGPU-based algorithm achieves visualization of fully processed real-time

AO-OCT images at 6 volumes/second, representing a 1700x speedup. This technology is suitable for further development to include 3D registration and data mining, all at real-time rates and amenable for scientific and clinical AO-OCT examination of the retina.

9307-57, Session PSun

Dynamic biometric response of the accommodative plant measured with OCT

Marco Ruggeri, Ophthalmic Biophysics Ctr., Bascom Palmer Eye Institute (United States); Victor M. Hernandez, Siobhan Williams, Carolina De Freitas, Ophthalmic Biophysics Ctr., Bascom Palmer Eye Institute (United States) and Univ. of Miami (United States) and Univ. of Miami Miller School of Medicine (United States); Florence A. Cabot, Ophthalmic Biophysics Ctr., Bascom Palmer Eye Institute (United States) and Univ. of Miami Miller School of Medicine (United States); Fabrice Manns, Ophthalmic Biophysics Ctr., Bascom Palmer Eye Institute (United States) and Univ. of Miami (United States) and Univ. of Miami Miller School of Medicine (United States); Jean-Marie Parel, Ophthalmic Biophysics Ctr., Bascom Palmer Eye Institute (United States) and Univ. of Miami (United States) and VisionCRC (Australia)

A complete understanding of the mechanics of the accommodative apparatus, including the crystalline lens, the suspensory ligaments and the ciliary muscle, is necessary to successfully design methods for restoring accommodation. The structural changes and movements of the crystalline lens and the ciliary muscle have been independently quantified using MRI, ultrasound, Scheimpflug imaging, PCI and OCT, in function of static accommodative amplitudes. Quantifying the dynamic accommodative response to a step stimulus is also important to enable a complete assessment of accommodative function. Dynamics of accommodation have been mainly quantified in terms of optical refraction and intraocular distances. We recently developed a dual-wavelength OCT system with high speed for simultaneous imaging of the crystalline lens and the ciliary muscle dynamics during accommodation. In the current study, the system was used to sequentially acquire OCT images of the accommodative plant over time while an accommodation stimulus stepping from distance to near was provided to the subject. The OCT time sequence was processed to segment the anterior segment surfaces and the ciliary muscle contour. After the segmented boundaries were corrected for distortion, the time courses of the crystalline lens thickness and axial shift and the area of the ciliary muscle were extracted. Preliminary results suggest that the ciliary muscle area has similar time course of the crystalline lens axial shift and thickness without significant delay. A shift of the centroid of the ciliary muscle toward the crystalline lens equator was also measured during accommodation.

9307-58, Session PSun

Dynamic refraction and biometry of the anterior segment during accommodation

Victor M. Hernandez, Bascom Palmer Eye Institute (United States) and Univ. of Miami (United States); Marco Ruggeri, Florence A. Cabot, Bascom Palmer Eye Institute (United States); Arthur Ho, Bascom Palmer Eye Institute (United States) and Brien Holden Vision Institute (Australia) and The Univ. of New South Wales (Australia); Fabrice Manns, Bascom Palmer Eye Institute (United States) and Univ. of Miami (United States); Jean-Marie Parel, Bascom Palmer Eye Institute (United States) and Brien Holden Vision

Institute (Australia)

Presbyopia, the loss of near visual ability with age, is a growing concern for the aging world population. There are a number of surgical and optical techniques currently available which are meant to return near visual function to the patient. These solutions often times come with trade-offs, such as reduced spatial acuity and poor night vision, and address the symptom of presbyopia without restoring a natural dynamic visual range. A lens refilling surgical procedure called Phaco Ersatz, is under development which will restore a dynamic visual range.

Currently, a routinely used method of testing near visual ability is the push-up technique. The subject views a target that is moved closer to their face and they are asked to notify the administrator of the exam when the target is no longer in focus. This is a subjective method of determining near visual function and is not a reliable method of verifying the results of current and future presbyopia correction techniques. The purpose of this project is to design and evaluate a system that will, for the first time, allow for objective assessment of accommodation in real time. The device combines a Hartmann-Shack based autorefractor to measure the accommodation amplitude, an extended-depth SD-OCT to measure the change in shape of the crystalline lens, a trans-scleral SD-OCT to measure the ciliary muscle, and an accommodation stimulus.

9307-60, Session PSun

En-face imaging of the ellipsoid zone in the retina from optical coherence tomography B-scans

Tim Holmes, Sean Larkin, Lickenbrock Technologies, LLC (United States); Markie Downing, Karl Csaky, Retina Foundation of the Southwest (United States)

It is generally believed that photoreceptor integrity is related to the ellipsoid zone appearance in optical coherence tomography (OCT) B-scans. Algorithms and software were developed for viewing and analyzing the ellipsoid zone. The software performs the following: (a), automated ellipsoid zone isolation in the B-scans, (b), en-face view of the ellipsoid-zone reflectance, (c), alignment and overlay of (b) onto reflectance images of the retina, and (d), alignment and overlay of (c) with microperimetry sensitivity points. Dataset groups were compared from normal and dry age related macular degeneration (DAMD) subjects. Scalar measurements for correlation against condition included the mean and standard deviation of the ellipsoid-zone's reflectance. The image-processing techniques for automatically finding the ellipsoid zone are based upon a calculation of optical flow which tracks the edges of laminated structures across an image. Statistical significance (e.g, P-value = 10⁻⁵) was shown in T-tests of these measurements with the population pools separated as normal and DAMD subjects. A display of en-face ellipsoid-zone reflectance shows a clear and recognizable difference between any of the normal and DAMD subjects in that they show generally uniform and nonuniform reflectance, respectively, over the region near the macula. Regions surrounding points of low microperimetry sensitivity have nonregular and lower levels of ellipsoid-zone reflectance nearby. These findings support the idea that the photoreceptor integrity could be affecting both the ellipsoid-zone reflectance and the sensitivity measurements.

9307-61, Session PSun

High power visible diode laser for the treatment of eye diseases by laser coagulation

Arne Heinrich, Clemens Hagen, Maximilian Harlander, Bernhard Nussbaumer, Pantec Engineering AG (Liechtenstein)

We present a high power green diode laser enabling the low-cost treatment of eye diseases including the two leading causes of blindness in the USA: Diabetic retinopathy and age-related macular degeneration. The need for treatment is constantly growing, due to the demographic trend, the increasing average life expectancy and medical care demand in developing countries. To fulfil this increasing need it becomes capital providing the medical market with a simple, reliable and price competitive technology. The treatment, laser coagulation, relies on the high absorption of eye melanin and hemoglobin in the green wavelength range and requires the exposure of the eye to green laser radiation. Radiation usually obtained via second harmonic generation (SHG) of a Nd:YAG laser, an expensive, fragile, inefficient and large system. Our approach is to replace Nd:YAG laser by a tapered laser diode (TLD), which can produce several watts of output power in a beam with high spatial and spectral brightness. Unfortunately laser diodes in general can just produce high power laser light in the infrared, but the TLD's beam properties allow for direct SHG. Our laser system, FAMgreen, consists of a TLD, a beam shaping based on the proprietary fast axis matching (FAM) scheme and a proprietary multipass SHG stage to produce the required power in the green. To conclude FAMgreen is highly price competitive, superior in robustness, size and flexibility over existing Nd:YAG lasers and allows the low-cost treatment of eye diseases by laser coagulation.

9307-62, Session PSun

Two-photon autofluorescence lifetime and SHG imaging of healthy and diseased human corneas

Ana Batista, IBILI, Univ. de Coimbra (Portugal) and Univ. des Saarlandes (Germany); Hans Georg Breunig, Univ. des Saarlandes (Germany) and JenLab GmbH (Germany); Aisada Uchugonova, Berthold Seitz M.D., Univ. des Saarlandes (Germany); António Miguel Morgado, IBILI, Univ. de Coimbra (Portugal); Karsten König, Univ. des Saarlandes (Germany) and JenLab GmbH (Germany)

The cornea is the outermost structure of the human eye. It is a transparent tissue responsible for two-thirds of the total reflective power of the eye. Its function can be drastically affected by several degenerations and dystrophies, which manifest initially through anomalies in cornea's structural organization and in cells metabolic activity. In this study, we propose to assess these anomalies by two-photon autofluorescence lifetime imaging of metabolic co-factors NADH and flavins, as well as by second harmonic generation (SHG) imaging of collagen fibrils.

Autofluorescence lifetime and SHG imaging were performed using a laser-scanning microscope with a broadband sub-15fs NIR laser and a 16-channel PMT detector for signal collection. This setup allows simultaneous excitation of metabolic co-factors and to spectrally resolve them based on their fluorescence spectra. Normal human corneas, unsuitable for transplantation, were obtained from the Lions Cornea Bank Saar-Lor-Lux. Corneas exhibiting dystrophies, keratitis, and keratoconus were obtained from the University Hospital of Saarland following keratoplasty.

We are able to differentiate between healthy and diseased human corneas, as well as between different diseases. Based on NADH and flavins' autofluorescence signals, changes within epithelial cells' morphology were observed. Furthermore, fluorescence lifetime analysis showed changes in cell metabolism, while SHG imaging revealed an altered structural organization of the stroma.

In the future, we intend to correlate the metabolic and structural changes with degenerations and dystrophies progression. This can be a step forward in achieving early diagnosis.

9307-63, Session PSun

Axial resolution enhancement of FD-OCT by parametric spectral analysis for ocular imaging

Xinyu Liu, Xiaojun Yu, Dongyao Cui, Linbo Liu, Nanyang Technological Univ. (Singapore)

It is known that the axial resolution of an OCT system is determined by the coherence length of the detecting light. Here we present a method to break this limit employing modern spectral estimation techniques. In FDOCT, the depth information is encoded in compounding sinusoidal modulation on interfering spectrum of two coherent beams often configured as a Michelson interferometer, one backscattered from the sample and the other reflected from a reference mirror. To decode the depth information, the power spectral density (PSD) of the interfering spectrum is calculated digitally as the profile of one A-scan. Conventionally, Fourier Transform (FT) is used to retrieve the depth profile which provides reasonable results. However, in terms of spectral analysis of a signal series, the approach based on FT, known as the periodogram, has inherent limitations such as frequency resolution and spectral leakage, appearing as low axial resolution and large sidelobes degrading OCT A-scan's Point Spread Function (PSF). In this work, we apply modified covariance estimation based on Autoregressive (AR) model to replace FT-based method. Resolution enhancement is shown by resolving microstructures such as endothelial cells and Descemet's membrane of a rat cornea which cannot be resolved by the existing technique. Also we found that under the same source spectral width, the axial resolution using this method is further limited by the SNR and unbalanced dispersion between detection and reference arms.

9307-64, Session PSun

Implementation of a capsular bag model to enable sufficient lens stabilization within a mechanical eye model

Natascha Bayer, Elisabet Rank, Lukas Traxler, Fachhochschule Technikum Wien (Austria); Erik Beckert, Fraunhofer-Institut für Angewandte Optik und Feinmechanik (Germany); Andreas Drauschke, Fachhochschule Technikum Wien (Austria)

Cataract still remains the leading cause of blindness affecting 20 million people worldwide. To restore the patient's vision the natural lens is removed and replaced by an intraocular lens (IOL). In modern cataract surgery the posterior capsular bag is maintained to prevent inflammation and to enable stabilization of the implant. Refractive changes following cataract surgery are attributable to lens misalignments occurring due to postoperative shifts and tilts of the artificial lens. Mechanical eye models allow a preoperative investigation of the impact of such misalignments and are crucial to improve the quality of the patient's sense of sight. Furthermore the success of sophisticated IOLs that correct high order aberrations is depending on a critical evaluation of the lens' position.

A new type of an IOL holder is designed and implemented into a preexisting mechanical eye model. A physiological representation of the capsular bag is realized with an integrated film element to guarantee lens stabilization and centering. The positioning sensitivity of the IOL is evaluated by performing shifts and tilts in reference to the optical axis. The modulation transfer function is used to measure the optical quality at each position. Lens stability tests within the holder itself are performed by determining the modulation transfer function before and after measurement sequence. Mechanical stability and reproducible measurement results are guaranteed with the novel capsular bag model that allows a precise interpretation of postoperative lens misalignments. The integrated film element offers additional stabilization during measurement routine without damaging the haptics or deteriorating the optical performance.

9307-65, Session PSun

Cornea based imaging via its tactile spatial stimulation

Zeev Zalevsky, Yevgeny Beiderman, Bar-Ilan Univ. (Israel);
Ygal Rotenstreich, Michael Belkin, Goldschleger Eye
Research Institute (Israel)

The possibility of alleviating blindness is one of the most challenging tasks that researchers, particularly from the fields of neuroscience and nanotechnology currently face. The recent technological advances in those fields led to the development of the concept of artificial retina in which a light sensitive device is implanted in the eye in order to directly stimulate the retinal cells. However, such solutions beside of being very invasive have significant limitations in respect of allowing high resolution imaging over a long period of time. The cornea is the most densely innervated body tissue. The nerves density of the corneal epithelium is 300 to 600 times larger than that of regular skin. Most of these nerves are sensory producing touch, thermal and chemical sensations, mostly manifested as pain. These nerves are mostly derived from the ophthalmic division of the trigeminal nerve and serve to protect the eye, preserve the integrity of the ocular surface by being the afferent arm of the blink reflex and ensure the optical characteristics of the eye, by being instrumental in the stimulation of tear production. The anatomy of the corneal nerves has been studied before. However, there is no data regarding the two points discrimination threshold of the human cornea. Following our former research we proposed to mount a camera and after proper encoding to transmit the visual information to special contact lens that will perform tactile stimulation of the cornea and therefore will allow "seeing" with the eyes but not via the retinal photo receptors that are connected to the visual cortex but rather through the tactile sensors of the cornea. In a way it is similar to "Braille" reading that is done not via the finger tips but rather via the tactile sensation of the cornea. This technology can potentially be a non-invasive sensory substitution allowing blind people to perceive images.

The purpose of this study is to show for the first time ever that the tactile sense of the cornea has spatial discrimination capability and thus it can be used to transmit spatial information. Corneal tactile stimulation can thus be potentially considered for use as vision substitute for blind people by teaching them to associate the tactile spatial feeling of the stimulation to real spatial shapes and images. All these features we show in this paper in preliminary human trials.

9307-66, Session PSun

In-vivo human corneal nerve imaging using Fourier-domain OCT

Jun Geun Shin, Byeong Ha Lee, Tae Joong Eom, Gwangju
Institute of Science and Technology (Korea, Republic of);
Ho Sik Hwang, Chuncheon Sacred Heart Hospital (Korea,
Republic of)

We have imaged the human corneal nerve bundles by using real-time Fourier-domain OCT (FD-OCT). In general, corneal nerves contribute to the maintenance of healthy ocular surface owing to their trophic influences on the corneal epithelium. However, corneal nerves are routinely injured due to refractive surgical procedures, corneal diseases, and cataract surgery also. This damage causes chronic neurotropic defects and dry eye. The corneal nerves has been successfully imaged by using a FD-OCT system based on a swept laser of a 50 kHz sweeping rate and 1.31 μ m center wavelength. We acquired 4096 samples in each A-scan and the acquired 3D volume image size was 700 \times 500 \times 500 voxels. The area covering the sclera, limbus, and cornea was scanned by using the FD-OCT system, which produced the in-vivo tomograms of corneal nerve bundles. The scan range was 5 mm (left to right, B-scan (500 A-scans)) 5 mm (top to bottom, C-scan (500 B-scans)). The regions of iris, corneal epithelium and endothelium were clipped out from the 3D data due to their high signal intensities compared with the stromal region where the nerve bundle is located. Due to the vibration of the

subject caused by heartbeat or unconscious movement, image of corneal nerve bundle possibly be distorted in 3D rendering. In this study, the every A-scan images were realigned to have a flattened air-surface boundary. With this effort, we could align corneal nerve bundle to have relative same depth and successfully get the 3D image showing the branched and threadlike corneal nerve bundles.

9307-67, Session PSun

Preliminary studies for the diagnosis and treatment of ocular surface squamous neoplasia

Yugyeong Chae, Sang-Seok Hwang, Jaechul Jung,
Pukyong National Univ. (Korea, Republic of); Sang-
Won Lee, Korea Research Institute of Standards and
Science (Korea, Republic of); Sang Joon Lee, Chulho
Oak, Kosin Univ. College of Medicine (Korea, Republic
of) and Innovative Biomedical Technology Research Ctr.
(Korea, Republic of); Rangarirai Masanganise, Univ. of
Zimbabwe (Zimbabwe); Yeh-Chan Ahn, Pukyong National
Univ. (Korea, Republic of) and Ctr. for Marine-Integrated
Biomedical Technology (Korea, Republic of) and
Innovative Biomedical Technology Research Ctr. (Korea,
Republic of)

The incidence rate of ocular surface squamous neoplasia (OSSN) increases rapidly in the working aged people of 20 to 50 with AIDS in Africa where prevalence rate of AIDS exceeds 30%. In the case of OSSN of the southeast Africa, the rate of progress is quite faster than other place. For this reason, operable cases are not much and, in most cases, exenteration is performed. It causes increment of medical expenses and degradation of quality of life with psychological problem. In a large percentage of cases, patients miss the right time to receive surgery. It leads to mortality growth, reduction of labor force and orphan problem. Therefore OSSN is becoming a serious social and economic issue in Africa. However, basic research concerning OSSN has been limited due to the lack of an ocular tumor animal model and the implementation difficulties on the animal model with diagnostic and treatment tools for human. In this study, we developed a reproducible animal model of subconjunctival squamous carcinoma in moderate-sized immunocompetent rabbits with VX2 carcinoma cells under optical coherence tomography (OCT) and slit lamp guidance. In addition, we verified the effect of NIR diode laser photodynamic therapy using intravenous Indocyanine Green (ICG). Furthermore, we confirm the possibility of OCT as an early diagnostic modality for OSSN patients in Zimbabwe.

9307-68, Session PSun

A new polarization randomness parameter for quantitative pigmented tissue imaging using polarization-sensitive optical coherence tomography

Shuichi Makita, Young-Joo Hong, Univ. of Tsukuba (Japan);
Masahiro Miura, Tokyo Medical Univ. (Japan); Yoshiaki
Yasuno, Univ. of Tsukuba (Japan)

Polarization-sensitive optical coherence tomography (PS-OCT) enables depth-resolved imaging of polarization properties of biological tissues. Recently, contrasting pigmented tissue in the retina, such as retinal pigmented epithelium (RPE) demonstrated. That is based-on polarization change due to multiple scattering is random, and the measurement of randomness of polarization states of backscattered lights will represents the degree of multiple scattering.

However, the system noise affect the measurement of polarization state randomness. Although it can be used as a contrast agent, quantity of randomness parameter will strongly depends on signal-to-noise ratio (SNR). This SNR-dependency makes quantitative evaluation of polarization randomness difficult.

In this study, we propose a modified parameter for degree of polarization uniformity (DOPU) measurement. The new parameter is designed to be less sensitive to system noise. The noise error corrected Stokes parameters derived from the PS-OCT signal model with additive noise. The noise-error-corrected DOPU is defined from the spatial averaged noise-corrected Stokes vectors.

The imaging and quantitative performance was analyzed with in vivo human retinal imaging using Jones-matrix optical coherence tomography where the wavelength swept laser has the central wavelength of 1060 nm with 100 nm bandwidth. Both of two input polarization lights are used for polarization randomness calculation.

The imaging contrast of the RPE is higher than previous methods. The quantitative evaluation with different SNR shows less sensitivity to noise of the new parameter has been shown. The new parameter will be suitable for stable interpreting and quantitatively investigating pigmented tissues.

9307-69, Session PSun

A novel platform for minimally invasive delivery of cellular therapy as a thin layer across the subretina for treatment of retinal degeneration

Ygal Rotenstreich, Adi Tzameret, Sapir E. Kalish, Michael Belkin, Tel Aviv Univ. (Israel) and Sheba Medical Ctr. (Israel); Amilia Meir, Avraham J. Treves, Arnon Nagler, Sheba Medical Ctr. (Israel); Ifat Sher, Sheba Medical Ctr. (Israel) and Tel Aviv Univ. (Israel)

Purpose: Incurable retinal degenerations affect millions worldwide. Stem cell transplantation rescued visual functions in animal models of retinal degeneration. In those studies cells were transplanted in subretinal “blebs”, limited number of cells could be injected and photoreceptor rescue was restricted to areas in proximity to the injection sites. We developed a minimally-invasive surgical platform for drug and cell delivery in a thin layer across the subretina and extravascular spaces of the choroid.

Methods: A novel system comprised of a syringe with a flexible needle and an adjustable pin was developed. Human bone marrow mesenchymal stem cells (hBM-MSCs) were transplanted in eyes of RCS rats and NZW rabbits through a longitudinal triangular scleral incision. No immunosuppressants were used. Retinal function was determined by electroretinogram analysis and retinal structure was determined by histological analysis and OCT.

Results: Transplanted cells were identified as a thin layer across the subretina and extravascular spaces of the choroid. In RCS rats, cell transplantation delayed photoreceptor degeneration across the entire retina and significantly enhanced retinal functions. No changes in retinal functions were recorded in rabbits following transplantation. No retinal detachment or choroidal hemorrhages were observed.

Conclusions: This novel platform opens a new avenue for drug and cell delivery, placing the transplanted cells in close proximity to the damaged RPE and retina as a thin layer, across the subretina and thereby slowing down cell death and photoreceptor degeneration, without retinal detachment or choroidal hemorrhage.

This new transplantation system may increase the therapeutic effect of other cell-based therapies and therapeutic agents. This study is expected to directly lead to phase I clinical trials for autologous hBM-MSCs transplantation in retinal degeneration patients.

9307-70, Session PSun

High precision laser sclerostomy

Wojciech S. Góra, Artur Ulrich, Heriot-Watt Univ. (United Kingdom); Lisa McIntosh, Univ. of Strathclyde (United Kingdom); Richard M. Carter, Heriot-Watt Univ. (United Kingdom); Clive G. Wilson, Univ. of Strathclyde (United Kingdom); Baljean Dhillon, The Univ. of Edinburgh (United Kingdom); Duncan P. Hand, Jonathan D. Shephard, Heriot-Watt Univ. (United Kingdom)

Ultrafast lasers offer a possibility of removing soft ophthalmic tissue without introducing collateral damage to the ablation site or the surrounding tissue. The potential for using ultrashort pico- and femtosecond pulse lasers for modification of ophthalmic tissue has been reported elsewhere and has resulted in the introduction of new, minimally invasive, procedures into clinical practice.

Our research aims to define the most efficient parameters to allow for the modification of scleral tissue without introducing collateral damage. Our experiments were carried out on hydrated porcine sclera in vitro. Porcine sclera, which has similar collagen organization, histology and water content (~70%) to human tissue was used.

Supporting this work we present a 2D finite element blow-off model which employs a one-step heating process. It is assumed that the incident laser radiation that is not reflected is absorbed according in the tissue to the Beer-Lambert law and transformed into heat energy.

The experimental setup uses an industrial picosecond laser (TRUMPF TruMicro 5x50) with 5.9 ps pulses at 1030 nm, with pulse energies up to 125 ?J and a focused spot diameter of 35 ?m. Use of a beam steering scan head allows flexibility in designing complicated scanning patterns.

In this study we have demonstrated that picosecond pulses are capable of removing scleral tissue without introducing any major thermal damage which offers a possible route for minimally invasive sclerostomy. In assessing this we have tested several different scanning patterns including single line ablation, square and circular cavity removal.

9307-71, Session PSun

Characterization of rat model of acute anterior uveitis using optical coherence tomography angiography

Woo June Choi, Kathryn L. Pepple, Zhongwei Zhi, Ruikang K. Wang, Univ. of Washington (United States)

Uveitis, or ocular inflammation, is a cause of severe visual impairment. Rodent models of uveitis are powerful tools used to investigate the pathological mechanisms of ocular inflammation and to study the efficacy of new therapies prior to human testing. In this paper, we report the utility of spectral-domain optical coherence tomography (SD-OCT) angiography in characterizing the inflammatory changes induced in the anterior segment of a rat model of uveitis. Acute anterior uveitis was induced in Lewis rats by intravitreal injection of a killed mycobacterial extract. A second group of rats received a concurrent periocular injection of steroids to model a treatment effect. OCT imaging was performed prior to inflammation induction on day 0 (baseline), and 2 days post-injection (peak inflammation). Baseline and inflamed images were compared. OCT angiography identified swelling of the cornea, inflammatory cells in the anterior and posterior chambers, a fibrinous papillary membrane, and dilation of iris vessels in the inflamed eyes when compared to baseline images. Steroid treatment was shown to prevent the changes associated with inflammation. This is a novel application of anterior OCT imaging in animal models of uveitis, and provides a high resolution, in vivo assay for detecting and quantifying ocular inflammation and the response to new therapies.

9307-72, Session PSun

Comparison of confocal microscopy and two-photon microscopy in studying fungal keratitis

Jun Ho Lee, Seunghun Lee, Pohang Univ. of Science and Technology (Korea, Republic of); Jin Hyoung Park, Myoung Joon Kim, Asan Medical Ctr. (Korea, Republic of); Ki Hean Kim, Pohang Univ. of Science and Technology (Korea, Republic of)

Fungal keratitis is one of major and severe eye disease, its early diagnosis is important in order to treat the proper ocular medicine. However, current diagnosis method has limitation to initial diagnosis because it spends a lot of time. Confocal reflectance microscopy (CRM) is one of promising technique to solve this problem, it commonly used to detect pathogen in pre-clinical study. And two-photon microscopy (TPM) is based on auto-fluorescence and Second harmonic generation signal (SHG) from cell and collagen in cornea, it is another modality to diagnostic infectious keratitis model. In this study, we applied these two modalities to the imaging of rabbit fungal keratitis model ex-vivo, and compared their performance to understand fungal keratitis model. For comparison the performance of two-modalities, fungal keratitis rabbit cornea were used.

In case of fungal keratitis rabbit cornea sample, CRM visualized filament shaped fungi in surface of inflammation region of cornea. And we imaged same section of same rabbit cornea with TPM. In TPM, filament shaped fungi in same region was also imaged and visualized additional information, such as stromal collagen lamellae under inflamed region of cornea. However, fluorescence signal of filament-shaped fungi is weaker than surroundings immune cells and collagen lamellae. In CRM, we could find out fungal pathogen in inflamed cornea but immune response could not visualize good contrast. In TPM, we could not distinguish fungal pathogen clearly, but we could obtain additional information of immune response in good contrast, such as immune cells and distribution of collagen lamellae.

9307-73, Session PSun

Dual three-dimensional spectral-domain OCT with interlaced detection for simultaneous imaging of the whole eye

Hyung-Jin Kim, Korea Univ. (Korea, Republic of); Pil Un Kim, Oz-tec Co., Ltd. (Korea, Republic of); Hyun-Woo Jeong, Johns Hopkins Univ. (United States); Min-Gyu Hyeon, Korea Univ. (Korea, Republic of); Jeehyun Kim, Kyungpook National Univ. (Korea, Republic of); Beop-Min Kim, Korea Univ. (Korea, Republic of)

A dual-mode spectral domain optical coherence tomography (SD-OCT) system utilizing single spectrometer for whole eye imaging was recently developed. A previous version of spectrometer in our lab was modified in order to extend imaging depth up to 9.5 mm. The dual SD-OCT system uses two orthogonally polarized lights from one SLD source. One is focused on the anterior segment for imaging from the cornea to the posterior surface of the crystalline lens. The other is incident on the retina via the crystalline lens. In the detector arm, single spectrometer combined with an ultrafast optical switch was used for interlaced detection. Newly built software was applied to three-dimensional whole eye imaging. The new dual-mode SD-OCT platform allows simultaneous imaging acquisition of both the anterior segment and retina. In addition, we applied an off-pivot complex conjugate removal technique to double the imaging depth, which is essential for entire anterior segment imaging. Taken together, we obtained images of the anterior segment and the retina with high axial resolution. Since Dual-mode image acquisition generated too bulky data set, GPU based processing was performed, which facilitates real-time display of two-dimensional cross-sectional images as well as fast acquisition of three-dimensional volumetric

images. In conclusion, the novel dual-mode SD-OCT platform can hold great promise for ophthalmologic diagnostics from a retina to a cornea in clinical practice.

9307-74, Session PSun

Biomechanical properties of corneas as a function of IOP and CXL assessed using optical coherence elastography

Jiasong Li, Manmohan Singh, Srilatha Vantipalli, Zhaolong Han, Kirill V. Larin, Michael D. Twa, Univ. of Houston (United States)

Structural properties of the cornea determine the shape and visual acuity of the eye. Keratoconus, a structural degeneration of the cornea, is often treated with UV-induced collagen cross-linking (CXL) to increase tissue resistance to further deformation and degeneration. Optimal treatments require individual customization and considerations of preexisting structural properties as well as the (dynamic) effects induced by CXL treatment. Therefore, there is a great demand for a technique capable of noninvasively measure tissue biomechanical properties. In this study, phase-stabilized swept source optical coherence elastography (PhS-SSOCE) was used to investigate the effects of UV-induced CXL in porcine eyes. Low-amplitude ($\sim 10 \mu\text{m}$) elastic waves were induced by a focused air-pulse. Wave velocity was measured over a $\sim 6\text{mm}$ line across the apex of the corneas. In addition, the relaxation rate of the surface deformation was measured at the apex of the corneas. Wave velocity and relaxation rate were compared in corneas before and after CXL, as well as at changing intraocular pressures (IOP). The wave velocity and relaxation rate were greater at higher IOPs and after the CXL treatment and is consistent with the increased tissue stiffness, which agrees with our previous studies. These results demonstrate that the combination of the PhS-SSOCE and a focused air pulse is capable of measuring low amplitude tissue deformation and assessing corneal stiffness.

9307-75, Session PSun

Multimodal nonlinear imaging of the eye

Oliver Stachs, Univ. Rostock (Germany); Tobias Ehmke, Franck Emmanuel Gounou, Friedrich-Schiller-Univ. Jena (Germany); Stephan Reiss, Univ. Rostock (Germany); Alexander Heisterkamp, Leibniz Univ. Hannover (Germany) and Excellence cluster REBIRTH (Germany)

Nonlinear imaging enables contrasted representation of biological tissue with a high resolution. The specific tissue answer strongly depends on the nonlinear susceptibilities which are present in the tissue. Thus, detected signals as two-photon fluorescence, second and third harmonic signals as well as signals based on wave mixing processes involving different incident frequencies are generated tissue specifically. Especially the well-defined compartments of eye provide structures which can be visualized by those signals. Lens, cornea, iris and chamber angle can be imaged based on two-photon autofluorescence. The collagenous structure present in the stromal region of the cornea provides strong second harmonic signals. Furthermore, non-resonant four-wave mixing can be used for imaging parts of the lens and the sclera. Overall, this observation method may help to decipher the causes of diseases and disease related changes in the eye using a label free way of imaging. Furthermore, these label free imaging modalities are powerful in combination with disease specific animal models.

Conference 9308: Optical Methods for Tumor Treatment and Detection: Mechanisms and Techniques in Photodynamic Therapy XXIV

Saturday - Sunday 7-8 February 2015

Part of Proceedings of SPIE Vol. 9308 Optical Methods for Tumor Treatment and Detection: Mechanisms and Techniques in Photodynamic Therapy XXIV

9308-1, Session 1

A strategy for enhancing PDT efficacy *(Invited Paper)*

David H. Kessel, Neha Aggarwal, Bonnie F. Sloane, Wayne State Univ. School of Medicine (United States)

A low level of lysosomal photodamage, resulting in death of <10% of cells markedly potentiated photokilling by subsequent mitochondrial photodamage. This effect appears to involve a pro-apoptotic signal that could be inhibited by cysteine protease antagonists, calcium chelation, or by ATG5 or ATG7 knockdowns. The effect appears to involve release of lysosomal proteases that can trigger some additional cellular response that results in promotion of apoptosis. One candidate is the calpain-dependent cleavage of ATG5 to yield a pro-apoptotic fragment, but there is clearly more to the story since protease inhibition and calcium chelation do not completely reverse the effect observed.

9308-2, Session 1

Exploiting PDT effects in the design of mechanism-based combination treatments *(Invited Paper)*

Tayyaba Hasan, Huang-Chiao Huang, Imran Rizvi, Srivalleesha Mallidi, Massachusetts General Hospital (United States); Ashish Kalra, Jonathan Fitzgerald, Merrimack Pharmaceuticals, Inc. (United States)

It is becoming increasingly clear that the complexity of cancer biology requires well-thought out, mechanistically sound combinations to address the problem of multiple and often compensatory pathways involved in cancer development and progression. Toward this end, we have been developing mechanism and image guided, PDT-based combination treatments. The goal of the current study is to demonstrate such a combination in orthotopic models of pancreatic cancer with PDT and a recently reported chemotherapeutic agent MM-398 (liposomal irinotecan, Merrimack Pharmaceuticals Inc.). Results from initial studies and mechanistic basis of the observed synergism along with clinical translation potential will be discussed.

9308-3, Session 1

Targeting cellular and microenvironmental determinants of tumor heterogeneity for PDT-based combinations *(Invited Paper)*

Imran Rizvi, Brigham and Women's Hospital (United States) and Massachusetts General Hospital (United States) and Harvard Medical School (United States); Emma Briars, Nan Xu, Heather Gudejko, Sriram R. Anbil, Shazia Khan, Massachusetts General Hospital (United States); Gwendolyn M. Cramer, Jonathan P. Celli, Univ. of Massachusetts Boston (United States); Tayyaba Hasan, Massachusetts General Hospital (United States)

The biological characteristics and treatment response of cancers is influenced by an array of factors including epithelial-mesenchymal (EMT) status and communication with stromal partners, which play deterministic roles in the fate of disseminated tumors. EMT is a process by which epithelial cells trade specialized function and proliferative capabilities for a migratory and invasive phenotype that is characteristic of mesenchymal cells, and is associated with increased metastatic potential and resistance in many tumors, including ovarian cancer. A range of cues in the tumor microenvironment can cause increased EMT including flow-induced shear stress, hypoxia, as well as molecular signaling via, for example, the TGF- β /Smad3 pathways. Among other heterotypic signaling partners, tumor endothelial cells are emerging as dynamic regulators of metastatic progression and mediators of treatment susceptibility. Establishing the influence of these and other microenvironmental cues on the molecular and morphological characteristics of the resultant disease is critical to designing photodynamic therapy (PDT)-based combinations. A particular emphasis on developing strategies that use PDT to target or regionally prime resistant and stubborn tumor populations may be essential to overcoming key barriers to management with traditional agents while minimizing toxicity. Characterizing key features of this target population and identifying the optimal combination schedule and selection of agents requires an array of research tools including bioengineered in vitro 3D platforms that integrate key microenvironmental cues. Current findings on the impact of EMT status and communication with tumor endothelial cells on the susceptibility of ovarian cancer cultures to PDT and conventional therapies will be presented.

9308-4, Session 2

Chemoresistant glioblastoma stem-like cells respond to photodynamic therapy

Bryan Q. Spring, Harvard Medical School (United States); Kohei Watanabe, Canon, Inc. (United States); Tatsuyuki Matsudaira, Health Sciences & Technology, Harvard-MIT (United States); Hiroaki Wakimoto, Massachusetts General Hospital (United States); Srivalleesha Mallidi, Harvard Medical School (United States); Tayyaba Hasan, Harvard Medical School (United States) and Massachusetts General Hospital (United States)

Glioblastoma stem cells (GSCs) isolated from patients with newly diagnosed disease are potent tumor initiators that express biomarkers associated with stem cells. These stem-like cells are thought to drive treatment resistance and tumor recurrence. Preclinical models suggest that the GSC subpopulation becomes enriched and re-populates the tumor milieu following conventional therapies. This talk will discuss the use of photodynamic therapy to overcome treatment resistance in a preclinical model of human GSC neurosphere cell cultures.

9308-5, Session 2

Carbonic Anhydrase-9 (CAIX) expression as a marker to predict response of aminolevulinic acid based photodynamic therapy

Srivalleesha Mallidi, Imran Rizvi, Zhiming Mai, Harvard

**Conference 9308: Optical Methods for Tumor Treatment and Detection:
Mechanisms and Techniques in Photodynamic Therapy XXIV**

Medical School (United States); Jonathan P. Celli, Univ. of Massachusetts Boston (United States); Tayyaba Hasan, Harvard Medical School (United States)

Hypoxia-regulated carbonic anhydrase-9 (CAIX) is a transmembrane protein belonging to the family of zinc metalloenzymes and its expression has been shown to correlate with poor tumor vascularization and resistance to chemo and radiation therapy by several researchers. It is a known fact that photodynamic therapy (PDT) causes hypoxic environments in the tumor due to the photochemical reaction between the photosensitizer (PS) and ground state oxygen to generate cytotoxic reactive oxygen species. Therefore we hypothesized that CAIX expression, a marker of hypoxia in the tumor, could be used for treatment prediction. Specifically, we treated a group squamous cell carcinoma (A431 cells) subcutaneous tumors using aminolevulinic acid (170 mg/kg) and 635 nm light dose (20 J/cm²). Post therapy, the tumor volume and weight were monitored upto a week and the tumors were extracted post euthanasia to evaluate CAIX expression. Treatment responders that showed decrease in tumor volume had high expression of CAIX while the non-responders that had increase in tumor volume post therapy showcased low CAIX expression. These changes in CAIX expression based on treatment response are indicative of hypoxic environments created at the time of PDT. Our future studies will involve evaluating the expression of CAIX in tumors that have initially showed response to therapy but regrew after a few days.

9308-6, Session 2
An analytical expression for light fluence rate distribution in semi-infinite medium

Joseph A. Spano, Timothy C. Zhu, Michele M. Kim, Univ. of Pennsylvania School of Medicine (United States)

The goal of this study was to determine an analytical expression for the light fluence rate in a turbid medium in a semi-infinite condition as function of depth, radius of the circular beam and its optical properties, i.e., the coefficients of absorption and reduced scattering (μ_a and μ_s'). The light fluence rate for a pencil-beam was calculated using a Monte Carlo simulation, both inside and outside of the tissue medium. In addition, diffuse reflectance as a function of radius and exit angles was obtained for the pencil-beam. An equation for diffuse reflectance based on μ_a , μ_s' , and the indices of refraction of the two materials was calculated. The MC simulation results for the pencil-beam were then integrated volumetrically in the radial direction to obtain the light fluence rate on the central-axis for a series of circular incident photon fields with various radius (1 - 8 cm) using the reciprocity theory. The light fluence rate for different radius for a range of optical properties were fitted to: fluence rate = $k \cdot e^{(\mu_{eff} \cdot z)}$, where z is the depth below the medium-tissue interface (medium = air or water), k is the backscatter coefficient, and μ_{eff} is the effective attenuation coefficient. We were able to obtain analytical equations for k and μ_{eff} as a function of tissue optical properties and beam radius, with an accuracy of 2.5% that are accurate where the diffusion theory fails. The medium index of refraction effect above the tissue is also studied.

9308-7, Session 3
**Estimating Verteporfin delivery and light treatment planning for pancreas PDT
(Invited Paper)**

Brian W. Pogue, Scott C. Davis, Kimberley S. Samkoe, Jonathan T. Elliott, Jason Gunn, Thayer School of Engineering at Dartmouth (United States); Stephen Pereira, Univ. College London Hospital (United Kingdom); Tayyaba Hasan, Harvard Medical School (United States)

PDT with verteporfin is a complex dosimetry challenge, given the combined

vascular and cellular targeting of the drug, and the light delivery at 690nm needing careful treatment planning for maximum efficacy. Estimation of the drug delivery can be done by perfusion imaging studies, as shown in both rodent and rabbit models, yet interestingly the clinical data suggests that perfusion is inversely related to treatment outcome. This latter conclusion indicates that treatment delivery is currently limited by light attenuation, where the blood perfusion is actually simply attenuating the light delivery. This implies there is ample drug delivery to cause the treatment effect, and so is a secondary or less important consideration. The data for designing the ideal treatment delivery will be reviewed and the proposed pathway forward in clinical work will be outlined.

9308-8, Session 3
Real-time treatment light dose guidance of Pleural PDT: an update

Timothy C. Zhu, Michele M. Kim, The Univ. of Pennsylvania Health System (United States); Steven L. Jacques, Oregon Health & Science Univ. (United States); Rozhin Penjweini, Andreea Dimofte, Jarod C. Finlay, Charles B. Simone M.D., The Univ. of Pennsylvania Health System (United States); Keith A. Cengel, Univ. of Pennsylvania School of Medicine (United States); Joseph S. Friedberg, Div. of Thoracic Surgery, Penn Presbyterian Medical Ctr. (United States)

No Abstract Available

9308-9, Session 3
In vivo outcome study of BPD-mediated PDT using the macroscopic singlet oxygen model

Michele M. Kim, Timothy C. Zhu, Univ. of Pennsylvania School of Medicine (United States)

Macroscopic modeling of the apparent reacted singlet oxygen concentration ($[^1O_2]_{rx}$) for use with photodynamic therapy (PDT) has been developed and studied for benzoporphyrin derivative monoacid ring A (BPD), a common photosensitizer. The four photophysical parameters (τ , ϕ , γ , λ) and threshold singlet oxygen dose have been investigated and determined using the RIF model of murine fibrosarcomas and interstitial treatment delivery. These parameters are examined and verified further by monitoring tumor growth post-PDT. BPD was administered at 1 mg/kg, and mice were treated 3 hours later with fluence rates greater than 75 mW/cm and total fluences greater than 135 J/cm. The sensitizer concentrations and optical properties were characterized for each mouse using a custom contact probe to measure fluorescence and absorption. Changes in tumor volume were tracked following treatment and compared using dose metrics including total light dose, PDT dose, and reacted singlet oxygen. Furthermore, photosensitizer photobleaching was quantified to use as a second check for the model. Correlation between outcomes and various dose metrics indicate that reacted singlet oxygen serves as a good dosimetric quantity for predicting PDT outcome.

9308-10, Session 3
New insights into treatment resistance through microvesicular traffic and its role in PDT

Akilan Palanisami, Emma Briars, Thais Santos, Tayyaba Hasan, Massachusetts General Hospital (United States)

Conference 9308: Optical Methods for Tumor Treatment and Detection: Mechanisms and Techniques in Photodynamic Therapy XXIV

Extracellular microvesicles (MV) are increasingly recognized as important mediators of intercellular communication. Cancer cells in particular have been shown to manipulate the local environment to their benefit via the MV-mediated transfer of epidermal growth factor receptor (EGFR). This talk examines the effects of PDT on MV-mediated EGFR transfer and the associated survival benefit to the recipient cells.

9308-11, Session 4

Measuring and modulating tumor hemodynamics during PDT

Malavika Chandra, Wesley B. Baker, Joann Miller, Arjun G. Yodh, Theresa M. Busch, Univ. of Pennsylvania (United States)

Heterogeneities in vascularization and perfusion contribute to instabilities in tumor hemodynamics, and pre-existing and treatment-created variability in tumor hemodynamic properties are present both spatially and temporally, with consequences to therapy response. During the delivery of PDT, tumor blood flow is affected by the illumination parameters. This effect provides an opportunity to optimize PDT while illumination is in progress, as long as relevant information about tumor hemodynamics is collectable in real time. In preclinical studies, we have tested an interactive hemodynamic-monitoring-system that utilizes diffuse correlation spectroscopy to measure PDT-induced changes in blood flow and then automatically adjusts illumination fluence rate when flow reductions exceed a pre-determined threshold. Real time monitoring of blood flow was achieved using Labview software, and based on the flow reduction values, the software automatically adjusted the fluence rate by increasing the attenuation in a digital attenuator that was placed in-line with the optical delivery fiber. Murine RIF tumors were treated with Photofrin-PDT (135 J/cm²) at 75 or 25 mW/cm², or with adjustable illumination. Adjustable illumination involved initiating illumination at 75 mW/cm², followed by decreases to 50, 25, and 10 mW/cm² each time that flow reduction values exceeded 10%/min (measured as a moving average over 3.5 minutes). Among animals that were treated by adjustable illumination, three experienced drops in fluence rate to 50 mW/cm², while two each experienced drops to 25 and 10 mW/cm². Importantly, adjustable PDT produced the greatest extent of vascular damage, assessed as a 1 h post-PDT reduction in blood flow by 46% (relative to baseline values), compared to 22% and 4% reductions at 25 and 75 mW/cm², respectively.

9308-12, Session 4

EtNBS PLGA nanoparticle and integrin-targeted, PEG-enhanced photosensitizer constructs for lysosome-mediated cell death

Hsin- I Hung, Wellman Ctr. for Photomedicine, Harvard Medical School, Massachusetts General Hospital (United States); Oliver Klein, Wellman Ctr. for Photomedicine, Harvard Medical School, Massachusetts General Hospital (United States); Hushan Yuan, Lee Josephson, Massachusetts General Hospital (United States); Conor L. Evans, Wellman Ctr. for Photomedicine, Harvard Medical School, Massachusetts General Hospital (United States)

The uptake of photosensitizers by tumors is limited by delivery barriers, such as a lack of perfusion or the adherence to the extracellular matrix or fibrous capsules, leading to subcurative therapy in many instances. Approaches to improve photosensitizer accumulation in tumors, such as the use of highly cationic agents, can cause different problems such as dark toxicity. Furthermore, even when photosensitizers reach their intended destination, effects of the local environment can reduce cytotoxic

potential. To overcome these problems, we pursued two approaches: encapsulation of EtNBS in nanoparticle delivery vectors as well as the creation of agents exploiting "PEG-photosensitizer shielding," where a photosensitizer is covalently linked to a modular peptide backbone coupled to a polyethylene glycol (PEG) polymer PLGA-nanoparticle bound EtNBS was found to have significantly reduced dark toxicity while retaining the same level of efficacy as free EtNBS. Release of EtNBS from the nanoparticle is through to occur through a light-generated radical-mediated process. Importantly, EtNBS nanoparticle formulations were found to be equally effective in both normoxic and hypoxic environments. EtNBS, when coupled to a PEG-peptide construct featuring a cyclic cell-targeting peptide, was found to have high cellular uptake and good photodynamic activity. When delivered to large 3D in vitro tumor models, this construct had remarkably high diffusivity and readily penetrated tumor spheroids many hundreds of microns in diameter. The EtNBS-PEGylated construct also had no measurable cytotoxicity, making it safe for future systemic administration. Current experiments are focusing on investigating the use of these constructs for use in vivo in animal studies.

9308-13, Session 4

Towards PDT with genetically encoded photosensitizer KillerRed: a comparison of continuous and pulsed laser regimes in 3D and animal tumor models

Marina V. Shirmanova, Nizhny Novgorod State Medical Academy (Russian Federation) and N.I. Lobachevsky State Univ. of Nizhni Novgorod (Russian Federation); Daria S. Kusnetzova, Nizhny Novgorod State Medical Academy (Russian Federation); Diana V. Yuzhakova, Nizhny Novgorod State Medical Academy (Russian Federation) and N.I. Lobachevsky State Univ. of Nizhni Novgorod (Russian Federation); Vladislav A. Kamensky, Ilya V. Turchin, Institute of Applied Physics (Russian Federation); Ludmila B. Snopova M.D., Nizhny Novgorod State Medical Academy (Russian Federation); Varvara V. Dudenkova, N.I. Lobachevsky State Univ. of Nizhni Novgorod (Russian Federation); Sergey A. Lukyanov, Shemyakin-Ovchinnikov Institute of Bioorganic Chemistry (Russian Federation) and Nizhny Novgorod State Medical Academy (Russian Federation); Elena V. Zagaynova M.D., Nizhny Novgorod State Medical Academy (Russian Federation)

Strong phototoxicity of red fluorescent protein KillerRed allow to consider it as a potential genetically encoded photosensitizer for photodynamic therapy (PDT) of cancer. The advantages of KillerRed over chemical photosensitizers are expression in tumor cells transduced with appropriate gene, direct cell killing through precise damage of desirable cell compartment, no side-effects associated with nonspecific drug distribution. Earlier the ability of KillerRed to affect cell division and induce cell death was demonstrated in cancer cell lines in vitro and HeLa tumor xenografts in vivo. However, further development of this approach for PDT requires an optimization of the treatment mode. In this study a comparison of continuous (593 nm) and pulsed laser (584 nm, 10 Hz, 18 ns) regimes was performed to achieve a sufficient antitumor effect. The research was implemented on HeLa and CT26 tumor spheroids and subcutaneous mouse tumors CT26 expressing KillerRed in fusion with histone H2B. The results showed that pulse regime provided stronger photobleaching of KillerRed without temperature increase. PDT at 160 ??????, 200 ?????? caused preferentially apoptotic cell death in tumor spheroids treated with pulse laser, and necrosis when treated with continuous irradiation. PDT with continuous laser was ineffective against CT26 tumors in mice, while pulse regime induced pronounced histopathological changes and tumor growth inhibition. Therefore, pulsed laser treatment was found to be more effective for PDT with genetically encoded photosensitizer KillerRed.

**Conference 9308: Optical Methods for Tumor Treatment and Detection:
Mechanisms and Techniques in Photodynamic Therapy XXIV**

9308-14, Session 5

NIH and NCI grant-related changes during fiscal years 2014 and 2015 (Invited Paper)

Rosemary S. Wong, National Cancer Institute (United States)

The 2014 fiscal year continues to be challenging for all federal agencies despite the Congressional strategies proposed to address the U.S. budget deficit. The Bipartisan Budget Act of 2013 passed by the House and Senate in December 2013 approved a two-year spending bill cancelling the proposed sequester cuts (i.e., 4-5% NIH/NCI budget reductions) required in 2014 and 2015, but extending the sequestration period through 2023. What impact this passage will have on the final 2014 NIH/NCI appropriations for 2014 and subsequent number of NIH/NCI grants funded in 2014 remains to be seen.

The overall success rate and funding paylines for NIH/NCI applications in all areas of research besides the Photodynamic Therapy research field will be provided for the past few years. Information on new initiatives and funding opportunities including Dr. Varmus' Provocative Question initiative during the past two years will also be discussed.

The new NIH grant-related policy changes implemented in 2014 and those proposed for 2015 will be highlighted. These changes could impact the grant application and award process for applicants and their academic institutions. Information on various NIH resources available for grant applicants and their institutions will also be provided.

The 2015 budget is currently being discussed by Congress with the hopes of a passage before the October 1, 2014 new fiscal year start date. If not, then a Continuing Resolution will be needed to keep the government operational and hopefully without delaying the funding of on-going and new NIH extramural biomedical research.

9308-15, Session 6

To be announced - Wang (Invited Paper)

Kenneth K. Wang M.D., Mayo Clinic (United States)

No Abstract Available

9308-16, Session 6

To be announced - Cengal (Invited Paper)

No Abstract Available

9308-17, Session 6

Clinical potential for vitamin D as a neoadjuvant for photodynamic therapy of nonmelanoma skin cancer (Invited Paper)

Edward V. Maytin M.D., Sanjay Anand, Kishore Rollakanti, Cleveland Clinic Lerner Research Institute (United States)

Nonmelanoma skin cancer (NMSC), comprising basal cell carcinoma (BCC) and squamous cell carcinoma (SCC), is the most common form of human cancer worldwide. Effective therapies include surgical excision, cryotherapy, and ionizing radiation, but all of these cause scarring. ALA-based PDT is a non-scarring modality used routinely for NMSC in Europe but not in the USA, primarily due to lingering uncertainties about efficacy. We have identified three agents (methotrexate, 5-fluorouracil, and vitamin D) that can be used as neoadjuvants, i.e., can be given as a pretreatment prior to ALA-PDT, to improve the efficacy of tumor killing in mouse models of NMSC. Vitamin D (Vit D; calcitriol) is the most recent neoadjuvant on this list. In this presentation we make the case that Vit D may be superior to

the other agents to improve results of ALA-PDT skin cancer treatment. Topically, calcitriol is available as a pharmaceutical grade cream or ointment (FDA-approved for psoriasis), and works well for boosting ALA-PDT tumor treatment in mouse models. For deep tumors not reachable by a topical route, calcitriol can be given systemically and is very effective, but carries a risk of causing hypercalcemia as a side effect. To circumvent this risk, we have conducted experiments with the natural dietary form of Vit D (cholecalciferol), and shown that this improves ALA-PDT efficacy almost to the same extent as calcitriol. Because cholecalciferol does not increase serum calcium levels, this represents a potentially extremely safe approach. Data in mouse models of BCC and SCC will be presented.

9308-18, Session 6

Enabling technology for photodynamic therapy in global health settings: battery-powered irradiation and smartphone-based imaging for ALA-PDT (Invited Paper)

Joshua Hempstead, Dustin P. Jones, Gwendolyn M. Cramer, Univ. of Massachusetts Boston (United States); Srivaleesha Mallidi, Imran Rizvi, Zhiming Mai, Massachusetts General Hospital (United States); Abdelali Ziouche, Univ. Paris 13 (France); Stephen Arnason, Univ. of Massachusetts Boston (United States); Tayyaba Hasan, Massachusetts General Hospital (United States); Jonathan P. Celli, Univ. of Massachusetts Boston (United States)

A lack of access to effective cancer therapeutics in resource-limited settings is widely implicated in global cancer health disparities. Photodynamic therapy (PDT) is a light-based treatment modality shown to be safe and effective in the clinic. Motivated by the fact that PDT wavelength/irradiance requirements can be met with battery-powered LED sources we assess here low-cost enabling technology to extend clinical benefit of PDT to regions with little or no access to electricity or medical infrastructure. We demonstrate the efficacy of a device based on 635nm high-output LED powered by three AA disposable alkaline batteries in A431 squamous carcinoma cells, in vitro and in a murine xenograft, following photosensitization via aminolevulinic acid (ALA) to induced accumulation of protoporphyrin IX (PpIX). We characterized the device performance, including battery drain and voltage stability over relevant PDT dose parameters. Further motivated by the capacity of PDT photosensitizers to serve simultaneously as tumor-selective fluorescence contrast agents, we demonstrate the capability of a consumer smartphone coupled with an assembly of 405nm LEDs and a PpIX emission filter to image PpIX fluorescence. Collectively this work suggests the feasibility of introducing a low-cost platform for image-guided ALA-PDT in resource-limited settings.

9308-19, Session 7

Use of cylindrical diffusing fibers as detectors for interstitial tissue spectroscopy

Timothy M. Baran, Thomas H. Foster, Univ. of Rochester Medical Ctr. (United States)

Interstitial photodynamic therapy (iPDT) describes the use of implanted optical fibers for delivery of treatment light to large volumes that can be located deep within the body. Since sensitive healthy structures are often located nearby, this requires careful treatment planning that is dependent on tissue optical properties. Determination of these values usually involves the insertion of additional fibers into the target volume, or the use of flat-cleaved optical fibers as both treatment sources and detectors. The insertion of additional fibers is undesirable, and cylindrical diffusers have been shown to offer superior treatment characteristics compared to flat-cleaved fibers.

Conference 9308: Optical Methods for Tumor Treatment and Detection: Mechanisms and Techniques in Photodynamic Therapy XXIV

Using cylindrical diffusers as detectors for spectroscopic measurement is therefore highly attractive.

We describe the determination of the detection profile for multiple types of cylindrical diffusers. This detection profile is shown to be dependent on the diffuser construction. For diffusers with a constant scatterer concentration and distal mirror, the detection profile is localized to the proximal end of the diffusing region. For diffusers with a variable scattering concentration along their length and no distal mirror, the detection profile is shown to be more uniform along the diffusing region.

We also present preliminary results showing the recovery of optical properties using arrays of cylindrical diffusing fibers as sources and detectors. The accuracy of these results is comparable to those obtained with other methods of optical property recovery. This would allow for the determination of optical properties using implanted treatment fibers, allowing for real-time updates of iPDT treatment plans.

9308-20, Session 7

Effects of verteporfin-mediated photodynamic therapy on endothelial cells

Daniel Kraus, Bin Chen, Univ. of the Sciences in Philadelphia (United States)

Photodynamic therapy (PDT) is a treatment modality in which cytotoxic reactive oxygen species are generated from oxygen and other biological molecules when a photosensitizer is activated by light. PDT has been approved for the treatment of diseases typically involving over stimulated cell proliferation such as cancers and age-related macular degeneration (AMD) due to its effectiveness in cell killing with manageable normal tissue complications. Endothelial cells form the lining between the blood and vasculature, where they are ideally positioned for exposure to high concentration of photosensitizer in an optimally oxygenated environment. As such, endothelial cells are important targets of PDT, especially vascular targeted PDT. Vascular targeted PDT using photosensitizer verteporfin has been used for the treatment of AMD in clinic and is under investigation for cancer treatment.

In this study, we characterized the effects of verteporfin-PDT on SVEC mouse endothelial cells and determined its underlying cell death mechanisms. After incubation with verteporfin, SVEC cells had a rapid cellular uptake of verteporfin. Verteporfin was primarily localized in mitochondria and endoplasmic reticulum (ER) in SVEC cells. Light treatment of photosensitized SVEC cells induced a rapid onset of cell apoptosis. In addition to significant structural damages to mitochondria and ER, verteporfin-PDT caused substantial degradation of ER signaling molecules, suggesting ER stress. Interestingly, our data indicate that PDT with verteporfin inhibited autophagy as well. All these results demonstrate that verteporfin-PDT triggered SVEC cell apoptosis by both mitochondrial and ER stress pathways. Results from this study may lead to novel therapeutic approaches to enhance PDT outcome.

9308-21, Session 7

Block copolymers encapsulated poly (aryl benzyl ether) dendrimer silicon (IV) phthalocyanine for in vivo and in vitro photodynamic efficacy of choroidal neovascularization

Xiongwei Wang, Kuizhi Chen, Fujian Normal Univ (China); Zheng Huang, Yiru Peng, Fujian Normal Univ. (China)

In this paper, we developed a novel series of silicon phthalocyanines containing four poly (aryl benzyl ether) dendritic substituents with terminal carboxylic acid functionalities. The dendritic substitutions with a large number of hydrophilic surface groups not only enhance the solubility

of these phthalocyanines in water, but also prevent their molecular aggregation to some extent, resulting in superior photophysical properties. On the other hand, we developed a block copolymers mPEG-PLGA and evaluated its potential in delivering dendrimer phthalocyanine. The photodynamic therapy effect of nanoparticles on human umbilical vein endothelial cells (HUVEC), human retinal pigment epithelium (RPE) cells and the experimental CNV in the Brown-Norway (BN) rat eyes were evaluated.

9308-22, Session 8

Assessment of singlet oxygen generated by 1268nm infrared laser irradiation

Scott Palmer, Ilya E. Rafailov, Karina Litvinova, Univ. of Dundee (United Kingdom); Sergei G. Sokolovski, Edik U. Rafailov, Aston Univ. (United Kingdom); Ghulam Nabi, Univ. of Dundee (United Kingdom)

Photodynamic Therapy (PDT) is a common therapy used to treat many cancers (ranging from skin to bladder). This technique relies on the excitation of specific dyes (photosensitisers) and subsequent energy transfer to molecular oxygen to form toxic singlet states. Unfortunately, this is often hampered by low tissue penetration of photosensitisers and is associated with significant cost and patient lay-up time. Recent years in PDT research are marked by the emergence of new photosensitisers (PSs) and new approaches, including so called "light oxygen effect", wherein 1268nm laser pulses induce transitions of molecular oxygen to singlet oxygen without the need of PSs. This technique has gained interest as a means to kill cancer without the expensive and time consuming application of dyes, with the long wavelength of light allowing deeper tissue penetration than currently afforded using red lasers (660nm). Early demonstrations (Anquez, F., et al., 2012, Sokolovski S.G, et al., 2013) of cancer cell killing using 1268nm irradiation suggested immense potential for therapeutic applications. However, in order to progress this technique, it is essential to characterise and quantify singlet oxygen generated under different irradiation doses and in conditions close to in vivo. To detect singlet oxygen we utilised its oxidation effect on the organic molecule Anthracene (ADPA). We used diminishing absorption and fluorescence of ADPA as a measure of singlet oxygen generation within solutions under various 1268nm laser irradiation conditions. We then used this data to inform the optimisation of regimes for cancer cell killing and evaluated the effects of these regimes on the "5637" bladder cancer cell line.

9308-23, Session 8

In-vivo outcome study of HPPH mediated PDT using singlet oxygen explicit dosimetry (SOED)

Rozhin Penjweini, Michele M. Kim, Timothy C. Zhu, Univ. of Pennsylvania (United States)

Type II photodynamic therapy (PDT) is based on the use of photochemical reactions mediated through an interaction between a tumor-selective photosensitizer, photoexcitation with a specific wavelength of light, and production of reactive singlet oxygen. However, the medical application of this technique has been limited due to inaccurate PDT dosimetric methods. The goal of this study is to examine the relationship between outcome (in terms of tumor growth rate) and calculated reacted singlet oxygen concentration ($[1O_2]_{rx}$) after HPPH-mediated PDT to compare with other PDT dose matrix, such as PDT dose and total light fluence. Mice with RIF tumors were treated under a variety of light fluence and fluence rate conditions. Explicit measurements of photosensitizer drug concentration and tissue optical properties via fluorescence and absorption measurement with a contact probe before and after PDT were taken to then quantify total light fluence, PDT dose, and $[1O_2]_{rx}$ based on a macroscopic model of singlet oxygen. In addition, photosensitizer photobleaching were measured during PDT as a second check of the model. Changes in tumor volume were

**Conference 9308: Optical Methods for Tumor Treatment and Detection:
Mechanisms and Techniques in Photodynamic Therapy XXIV**

tracked following treatment and compared to the three calculated dose metrics. The correlations between total light fluence, PDT dose, reacted [102]rx and tumor growth demonstrate that [102]rx serves as a better dosimetric quantity for predicting treatment outcome and a clinically relevant tumor growth endpoint.

9308-24, Session 8
Monte Carlo fluence simulation for prospective evaluation of interstitial photodynamic therapy treatment plans

Jeffrey Cassidy, Vaughn Betz, Univ. of Toronto (Canada);
Lothar D. Lilge, Univ. of Toronto (Canada) and Princess
Margaret Cancer Ctr. (Canada)

Photodynamic therapy (PDT) delivers a localized cytotoxic dose that is a function of tissue oxygen availability, photosensitive drug concentration, and light fluence. Providing safe and effective PDT requires an understanding of all three elements and the physiological response to the radicals generated. Interstitial PDT (IPDT) for solid tumours poses particular challenges due to complex organ geometries and the associated limitations for diffusion theory based fluence rate prediction, in addition to restricted access for light delivery and dose monitoring.

As a first step towards enabling a complete prospective IPDT treatment-planning platform, we demonstrate use of our previously developed FullMonte tetrahedral Monte Carlo simulation engine for modeling of the interstitial fluence field due to percutaneous insertion of extended light sources. The goal is to enable a complete treatment planning and monitoring workflow analogous to that used in ionizing radiation therapy, including plan evaluation through dose-volume histograms and algorithmic treatment plan optimization.

FullMonte is to our knowledge the fastest open-source tetrahedral MC light propagation software. Using custom hardware acceleration, we achieve 4x faster computing with 67x better power efficiency compared to the software. Ongoing work will improve the performance advantage to 16x, enabling algorithmic plan optimization in reasonable time.

Using FullMonte, we demonstrate significant new plan-evaluation capabilities including fluence field visualization, generation of organ dose-volume histograms, and rendering of isofluence surfaces for representative head-and-neck and bladder cancer meshes from real patients. We also discuss the advantages of MC simulations for dose-volume histogram generation and the need for online personalized fluence-rate monitoring.

9308-25, Session 8
Fluorescence time course imaging of healthy and diseased skin for PpIX metabolic maps used in topical PDT and its correlation to the skin and lesions structures

Olena Kulyk, Univ. of St. Andrews (United Kingdom);
James Ferguson, Sally Ibbotson, Harry Moseley, Ronan M.
Valentine, Ninewells Hospital and Medical School, Univ. of
Dundee (United Kingdom); Ifor D. W. Samuel, Univ. of St.
Andrews (United Kingdom)

Topical Photodynamic therapy (PDT) is an effective treatment for superficial non-melanoma skin cancers (NMSC) and dysplasia with excellent cosmetic outcome. During the treatment light activates a photosensitizer (PpIX), metabolised from a pro-drug in a cream (5-Aminolaevulinic Acid (ALA), Ameluz and Methyl Aminolevulinic Acid (MAL), Metvix®). Molecular oxygen, light, and PpIX, induces oxidative stress, inflammation and cell death. The concentration of PpIX, is an important treatment parameter and can be

measured by detecting its fluorescence.

In this study fluorescence images of healthy and diseased skin, actinic keratosis (AK) and basal cell carcinoma (BCC) have been gathered to better understand uptake and metabolism of the topical pro-drug to PpIX and response to PDT. Fluorescence images are taken using a customised camera every 10 minutes during a three-hour application of pro-drug in healthy volunteers and patients and images are analysed in Matlab. Preliminary results show metabolic maps of PpIX in healthy volunteers and patients, and provide the information about the metabolism rates of PpIX in different individuals. The correlation of the fluorescence distribution in the skin and lesion structures is discussed. We anticipate that these data will improve our knowledge relating to the optimal time to commence irradiation during PDT. In future we will investigate whether the recurrence or persistence of BCC and AK is associated with fluorescence distribution. This will improve our understanding of PDT outcomes and assist with optimisation of treatment regimes.

9308-26, Session 9
Topical calcitriol prior to photodynamic therapy enhances treatment efficacy in non-melanoma skin cancer mouse models

Kishore Reddy Rollakanti, The Cleveland Clinic (United States) and Cleveland State Univ. (United States); Sanjay Anand, Edward V. Maytin M.D., The Cleveland Clinic (United States)

Non-melanoma skin cancers (NMSCs) such as basal cell carcinoma (BCC) and squamous cell carcinoma (SCC) are the most common form of human cancer worldwide, and their incidence is increasing. Photodynamic therapy (PDT), mediated by topically applied aminolevulinic acid (ALA) and subsequent exposure to light (either a laser or a noncoherent source), is being increasingly used for the treatment of dermatological disorders, including BCC and SCC. However, therapeutic responses of NMSCs to ALA-PDT are currently not superior to standard therapies, although the latter have undesirable side effects including scarring. In this study, we report that preconditioning of skin tumors with calcitriol (active form of Vitamin D; Vit D) prior to ALA-PDT, significantly improves the treatment outcome. In BCC and UVB-induced SCC mouse models, we identified an increase in tumor-specific accumulation of ALA induced photosensitizer (protoporphyrin IX, PpIX) due to Vit D preconditioning, of up to 4-fold in vivo. In addition, increased expression of differentiation (218 ± 21.2 fold) and proliferation (38 ± 4.0 fold) markers were identified in BCC tumors, all leading to increased tumor destruction (12 ± 2.3 fold) with the combination approach, as compared to ALA-PDT alone. Histomorphological changes identified using hematoxylin and eosin staining, and results of TUNEL staining, together documented a beneficial effect of Vit D pretreatment upon tumor cell death. We conclude that this new combination approach with Vit D and ALA-PDT has great potential to achieve complete remission of NMSC tumors, with excellent cosmetic results and an overall beneficial impact upon patient care.

9308-27, Session 9
Crystalline organic nanoparticles for diagnosis and PDT

Rudolf W. Steiner, Jasmin Breymayer, Angelika C. Rueck, Univ. Ulm (Germany); Victor B. Loschenov, Anastatsia Ryabova, A. M. Prokhorov General Physics Institute (Russian Federation)

Abstract. The crystalline structure of Aluminium Phthalocyanine (AlPc) and other organic photosensitizers used in photodynamic therapy (PDT) can be described as stacked planar molecules [1]. In pure water there is no fluorescence observed after excitation because of quenching effects. Nanoparticles (nAlPc) prepared of AlPc and injected intravenously into

Conference 9308: Optical Methods for Tumor Treatment and Detection: Mechanisms and Techniques in Photodynamic Therapy XXIV

mice revealed a strong fluorescence but only in inflamed tissue regions. Due to the special tissue environment single molecules are dissolved from the nanoparticles and can act as sensitizers in diagnostic and therapeutic PDT. This effect will highly improve selectivity and specificity of the photodynamic diagnostic and therapy.

Materials and Methods

Crystalline AIPc raw material was fragmented to nanoparticles (NP) with a hydrodynamic size of 150nm by ultrasound. The size distribution was measured by dynamic light scattering and the samples have been provided by Biospec, Moscow. The flat molecules are stacked together with quenching of the fluorescence. Under certain conditions, AIPc molecules will dissolve from the NP being fluorescent and an active photosensitizer. In inflamed tissue (skin transplants on mice), after incubation with AIPcNP, a strong fluorescence appears, whereas in not inflamed skin transplants no fluorescence can be observed [2]. In vitro cell experiments have been performed to study the mechanism and the special conditions for the dissolution of the molecules from the nanoparticles.

Results

From experiments with different cell lines it turned out that mainly macrophages are the target cells where free molecules are dissolved from the nanoparticles after incorporation into the cell. This happens in normal and also stimulated macrophages. To simulate an inflammation model, a mixture of different skin cell lines (HaCaT) and mouse fibroblast cells (L929) in combination with J774A.1 cells and also human macrophages were used. After 24 hours of incubation with AIPcNP, regions of interest (ROI) of homogeneous and identical cells were marked. The fluorescence intensity of the ROIs was taken as measure of the amount of dissolved monomeric AIPc. The results demonstrated that the fluorescence in macrophages was dominant compared to the relative low fluorescence in the other cell types.

Besides fluorescence measurements, the co-localisation of hAIPc was studied in the nucleus (DAPI), in the mitochondria (Rhodamin 123) and in the lysosomes with LysoTracker® using a laser scanning microscope (LSM 710, C Zeiss).

Fluorescence lifetime measurements showed a biphasic exponential behaviour, a composition of molecules detaching from the nanoparticles and of free AIPc molecules.

Further studies are planned to learn more about the microenvironment or molecules responsible for the dissolution of free molecules from the AIPc nanoparticles and the role of bacteria.

References

1. D. Wöhrle, G. Schnurpfeil, S. Makarov and O. Suvorova, Chem. Unserer Zeit, 2012, 46, 12-46.
2. S.Y. Vasilchenko, A.I. Volkova, A.V. Ryabova, V.B. Loschenov, V.I. Konov, A.A. Mamedov, S.G. Kuzmin and E.A. Lukyanets, Journal of Biophotonics, 2010, 3(5-6), 336-346.

9308-28, Session 9

Low fluence thresholds for photodynamic therapy

Brad A. Hartl, Univ. of California, Davis (United States); Henry Hirschberg M.D., Univ. of California, Irvine (United States); Laura Marcu, Simon R. Cherry, Univ. of California, Davis (United States)

Photodynamic therapy (PDT) is a treatment method that has been shown effective for a wide variety of diseases. Presently, the translation of PDT to the clinical setting has mostly been limited to superficial diseases where traditional light delivery with lasers and LEDs is noninvasive. In order to overcome this limitation and allow PDT to be clinically implemented for a wider range of diseases, a variety of mechanisms have been proposed to noninvasively deliver light to deep tissues. These include nanosensitizers, long-lived phosphorescent nanoparticles, upconverting nanoparticles and radionuclides for Cerenkov luminescence among others. With respect to traditional clinical light sources, these methods produce light at shorter

and often more effective wavelengths, but at much lower intensities. This work evaluates the minimum amount of light required by these methods to produce a meaningful PDT effect in the in vitro setting under representative low fluence and wavelength conditions. To perform these experiments, a novel LED illumination system for multi-well plate studies, capable of rapidly generating fluence dose-response curves from a single plate, was developed and characterized. With the use of this setup the low fluence thresholds were found to be around 260 mJ/cm² using the more clinically relevant photosensitizer aminolevulinic acid and 17 mJ/cm² for the more efficient photosensitizer TPPS2a. These values can be used as approximate low fluence thresholds to serve as guidance when developing noninvasive deep light sources.

9308-29, Session 9

An empirical approach to estimate near-infra-red photon propagation and optically induced drug release in brain tissues

Akshay Prabhu Verleker, Purdue Univ. School of Health Sciences (United States); Qianqian Fang, Martinos Ctr. for Biomedical Imaging, Harvard Medical School (United States); Mi-Ran Choi, Susan Clare, Feinberg School of Medicine, Northwestern Univ. (United States); Keith M. Stantz, Purdue Univ. School of Health Sciences (United States)

Purpose: The purpose of this study is to develop an alternate empirical approach to estimate near-infra-red (NIR) photon propagation and quantify optically induced drug release in brain metastasis, without relying on computationally expensive Monte Carlo techniques (gold standard).

Introduction: Targeted drug delivery with optically induced drug release is a non-invasive means to treat cancers and metastasis. This study is part of a larger project to treat brain metastasis by delivering lapatinib-drug-nanocomplexes and activating NIR-induced drug release. The empirical model was developed using a weighted approach to estimate photon scattering in tissues and calibrated using a GPU based 3D Monte Carlo. The empirical model was developed and tested against Monte Carlo in optical brain phantoms for pencil beams (width 1mm) and broad beams (width 10mm).

Materials and Methods: The empirical algorithm was tested against the Monte Carlo for different albedos along with diffusion equation and in simulated brain phantoms resembling white-matter ($\mu_s=8.25\text{mm}^{-1}$, $\mu_a=0.005\text{mm}^{-1}$) and gray-matter ($\mu_s=2.45\text{mm}^{-1}$, $\mu_a=0.035\text{mm}^{-1}$) at wavelength 800nm. The goodness of fit between the two models was determined using coefficient of determination (R-squared analysis).

Results: Preliminary results show the Empirical algorithm matches Monte Carlo simulated fluence over a wide range of albedo (0.7 to 0.99), while the diffusion equation fails for lower albedo. The photon fluence generated by empirical code matched the Monte Carlo in homogeneous phantoms (R²=0.99). While GPU based Monte Carlo achieved 300X acceleration compared to earlier CPU based models, the empirical code is 700X faster than the Monte Carlo for a typical super-Gaussian laser beam.

9308-33, Session PSun

Photoinduced electron transfer between the dendritic zinc phthalocyanines and anthraquinone

Kuizhi Chen, Fujian Normal Univ. (China); Junri Wen, Jiangsheng Liu, Zhenzhen Chen, Sujuan Pan, Zheng Huang, Yiru Peng, Fujian Normal Univ (China)

A novel series of zinc(II) phthalocyanines carrying four poly (aryl benzyl

**Conference 9308: Optical Methods for Tumor Treatment and Detection:
 Mechanisms and Techniques in Photodynamic Therapy XXIV**

ether) dendritic substituents with phenyl ketone terminal functionalities (Gn-DPcZn (Gn=n-generation dendimer, n=1-2)) have been synthesized. The fluorescence of two dendritic phthalocyanines was quenched by addition of anthraquinone. The quenching rate constant (k_q) was $1.0 \times 10^{11} \text{ M}^{-1} \text{ s}^{-1}$. This data indicated that simultaneous presence of intermolecular static and dynamic component in the fluorescence quenching for Gn-DPcZn-anthraquinone system. The Stern-Volmer constant (K_{sv}) of Gn-DPcZn was decreased and increased with the generation.

9308-34, Session PSun

Macroscopic singlet oxygen model incorporating photobleaching as input parameter

Michele M. Kim, Jarod C. Finlay, Timothy C. Zhu, Univ. of Pennsylvania School of Medicine (United States)

The macroscopic singlet oxygen model for photodynamic therapy (PDT) has been used extensively to calculate the apparent reacted singlet oxygen concentration for various photosensitizers. The four photophysical parameters (τ , ϕ , σ , σ_0) and threshold singlet oxygen dose can be found for various drugs and drug-light intervals using a fitting algorithm. The input parameters for this model included the fluence, photosensitizer concentration, optical properties, and necrosis radius. An additional input variable was implemented in this study. Photobleaching was measured by using the pre-PDT and post-PDT sensitizer concentrations. Using the RIF model of murine fibrosarcoma, mice were treated with a linear source with fluence rates from 12-150 mW/cm and total fluences from 24-135 J/cm. The two main drugs investigated were benzoporphyrin derivative monoacid ring A (BPD) and HPPH (2-[1-hexyloxyethyl]-2-devinyl pyropheophorbide-a). Previously stated photophysical parameters were fine-tuned and verified using photobleaching as the additional fitting parameter. Furthermore, photobleaching could be used as an indicator of the robustness of the model for the particular mouse experiment by comparing the experimental and model-calculated photobleaching ratio.

9308-38, Session PSun

Silica coated magnetic nanoparticles for photodynamic therapy

Rajesh V. Kanawade, Institute of Photonic Technologies, Friedrich-Alexander-Univ. Erlangen-Nürnberg (Germany) and Erlangen Graduate School in Advanced Optical Technologies (Germany); Lucas Kreiss, Institute of Photonic Technologies, Friedrich-Alexander-Univ. Erlangen-Nürnberg (Germany); Stephanie Fanselow, Institute of Particle Technology, Friedrich-Alexander-Univ. Erlangen-Nürnberg (Germany); Florian Klämpfl, Institute of Photonic Technologies, Friedrich-Alexander-Univ. Erlangen-Nürnberg (Germany); Peukert Wolfgang, Institute of Particle Technology, Friedrich-Alexander-Univ. Erlangen-Nürnberg (Germany); Stephan Roth, Bayerisches Laserzentrum GmbH, Konrad-Zuse-Straße 2-6, 91052 Erlangen, Germany (Germany); Michael Schmidt, Institute of Photonic Technologies, Friedrich-Alexander-Univ. Erlangen-Nürnberg (Germany) and Erlangen Graduate School in Advanced Optical Technologies (Germany)

Our research interest is to produce photosensitizer-conjugated magnetic nanoparticles and test its clinical applicability for photodynamic therapy (cancer treatment). In this study, silica material is selected as a photosensitizer because the literature reports that silica nanoparticles are capable of generating singlet oxygen under laser irradiation. The

average core diameter of the Fe₃O₄ nanoparticles used in this study is around 100 nm. Different thicknesses of the silica shell are investigated. Photophysical properties of these nanoparticles such as absorption and scattering coefficient are investigated. These photophysical properties are measured before and after laser irradiation. Photocatalytic activity of the photofunctional magnetic nanoparticles is evaluated by photosensitized oxidation reaction of silica in D₂O under laser irradiation. The clinical applicability of the photodynamic therapy is tested on oxygenated hemoglobin solution by monitoring singlet oxygen after laser irradiation. The obtained results from hemoglobin mixed with the silica coated Fe₃O₄ nanoparticles conclude that after each laser irradiation the oxygen content decreases. The decreasing oxygen peaks of the absorbance at 540 nm and 574 nm show the transformation of the oxygen from the oxygenated to the de-oxygenated state and it confirms that the photosensitizer generates singlet oxygen by consuming oxygen. The decreasing fluorescence spectrums after each irradiation time indicate that the photosensitizers are activated by the laser. Preliminary studies conclude that the photosensitizer-conjugated magnetic nanoparticles can be a good option to improve the current noninvasive methods of cancer treatment.

9308-39, Session PSun

PAMAM modified PpIX generations in experimental photodynamic therapy induce antitumoral effect on stomach cancer cells

Tugba Kiris, Necmi M. Burgucu, Tugba Sagir, Mehmet Senel, Sevim Isik, Fatih Univ. (Turkey); Gamze Bölükbaşı Ates, Bogaziçi Univ. (Turkey); Hasim Özgür Tabakoglu, Fatih Univ. (Turkey)

In this study, effect of a novel LED-based light source developed for 96-well-plates cell culture applications, was tried on AGS stomach cancer cell line, in combination with Poly(amido amine) (PAMAM) modified - porphyrin molecule. For each 4 generation of modified PpIX molecule 5 different concentrations tried. According to results PAMAM molecule doesn't have any photosensitizer property also didn't show any toxic effect even if higher concentrations. Morphology and real time monitoring analysis results hold up each other and confirmed that, PpIX molecules with and without modified high concentrations (>100 μM) caused cell death via toxicity this reason optimal concentration for PAMAM modified PpIX should be between 25 - 50 μM concentration .

9308-30, Session PMon

A brief history of PDT

David H. Kessel, Wayne State Univ. School of Medicine (United States)

Progress in PDT

9308-31, Session PMon

Comparison of optical properties determined by interstitial and surface contact probes in phantoms

Andreea Dimofte, Jarod C. Finlay, Timothy C. Zhu, The Univ. of Pennsylvania Health System (United States)

Knowing the optical properties of the tissue to be treated with PDT is an important factor in the treatment outcome. Determination of optical properties (absorption (μ_a) and scattering (μ_s) coefficients) is important when it comes to accurate calculation of fluence rate in and around tissue

Conference 9308: Optical Methods for Tumor Treatment and Detection: Mechanisms and Techniques in Photodynamic Therapy XXIV

area. In this study we compared two ways of determining the optical properties in liquid phantoms with known optical properties, made of black India ink (absorption), Intralipid (scattering) and water. One method (interstitial) uses two parallel catheters, placed 5mm apart. In one of the catheters a 2 mm long linear diffusing light source is placed while in the second catheter, a calibrated isotropic detector is placed. The detector is scanned along the length of the light source containing catheter. The second method (surface probe) uses an in-house built probe that has a light source with 10 detector fibers that are illuminated by a tungsten lamp (Avalight, Avantes, Inc.). A CCD-based spectrograph (InSpectrum, Roper Scientific) was coupled to the detector fibers and recorded the spectrum for each fiber. Measurements are done by pushing a button that triggers data collection, once the probe is placed on the phantom surface. The two methods were compared to determine the agreement between the two as a mean to determine tissue optical properties. Future work will include determination of optical properties in preclinical and clinical settings.

9308-32, Session PMon

Early photosensitizer uptake kinetics predict optimum drug-light interval for photodynamic

Lagnojita Sinha, Illinois Institute of Technology (United States); Jonathan T. Elliott, Thayer School of Engineering at Dartmouth (United States); Tayyaba Hasan, Wellman Ctr. for Photomedicine, Massachusetts General Hospital (United States); Brian W. Pogue, Kimberley S. Samkoe, Thayer School of Engineering at Dartmouth (United States); Kenneth M. Tichauer, Illinois Institute of Technology (United States)

Photodynamic therapy (PDT) has shown promising results in targeted treatment of cancerous cells by developing localized toxicity with the help of light induced generation of reactive molecular species. The efficacy of this therapy depends on the product of the intensity of light dose and the concentration of photosensitizer (PS) in the region of interest (ROI). On account of this, the dynamic and variable nature of PS delivery and retention that can depend on many physiological factors known to be heterogeneous within and amongst tumors (e.g., blood flow, blood volume, vascular permeability, and lymph drainage rate) presents a major challenge in the determination of an appropriate drug-light interval when the concentration of PS molecule will be at its maximum in the ROI. In this paper a predictive algorithm is developed, which takes into consideration the variability and dynamic nature of PS distribution in the body on a region-by-region basis and gives an estimate of the optimum time when its concentration will be maximum in the ROI. The advantage of the algorithm lies in the fact that it predicts the time in advance as it takes only a sample of initial data points (-12 min) as input. The optimum time calculated using the algorithm estimated a maximum dose time that was only $3.7 \pm 2.7\%$ under the true maximum dose compared to a mean dose error of $76 \pm 21\%$ if a 3 h optimal light deliver time was assumed.

9308-35, Session PMon

Characterization of rare-earth-doped nanophosphors for photodynamic therapy excited by clinical ionizing radiation beams

Arash Darafsheh, The Univ. of Pennsylvania Health System (United States); Taejong Paik, Stan Najmr, Univ. of Pennsylvania (United States); Michael Tenuto, The Univ. of Pennsylvania Health System (United States); Christopher B. Murray, Univ. of Pennsylvania (United States); Joseph

S. Friedberg, Jarod C. Finlay, The Univ. of Pennsylvania Health System (United States)

Nanoparticle phosphors with emission tunability and high surface area that facilitates attachment with targeting reagents are promising in situ light source candidates for molecular imaging or exciting a photosensitizer for combined radiation and photodynamic therapies. In this work, optical properties of terbium (Tb³⁺)- and europium (Eu³⁺)-doped nanophosphors with various host compounds irradiated by electron and photon beams generated by using a medical linear accelerator were investigated for their potential as optical probes. The emission spectra of nanophosphors embedded in tissue-mimicking phantoms were collected by an optical fiber connected to a CCD-coupled spectrograph while the samples were irradiated by a medical linear accelerator with electron beams of energies 6-20 MeV or X-ray beams of energies of 6 and 15 MV. We characterized the cathodoluminescence and X-ray luminescence of such nanophosphors as a function of the beam type and energy and observed dose dependency of the luminescence signal. We also evaluated the excitation of a porphyrin-based photosensitizer with absorbance features that match the luminescence spectra of these nanophosphors when irradiated.

9308-36, Session PMon

In vivo suppression of solid Ehrlich cancer via chlorophyllin derivative mediated PDT: an albino mouse tumor model

Iman E. Gomaa, Hend O. Saraya, The German Univ. in Cairo (Egypt); Maha Zekri, Cairo Univ. (Egypt); Mahmoud H. Abdelkader, The German Univ. in Cairo (Egypt)

In this study, copper chlorophyllin derivative was used for PDT mediated therapy in Ehrlich tumor mouse model. Six groups of animals comprising 5 animals per group were subcutaneously transplanted with 10⁶ cells Ehrlich tumor cells. A single dose of 200 µg/gm body

weight chlorophyllin derivative was administered by intravenous (IV) or intratumoral (IT) routes. Mice were exposed to monochromatic red laser of 630 nm for 1 hour, and tumor regression post treatment was followed up for 3 consecutive months. Several Biochemical, histological and molecular tests were performed in order to evaluate the efficacy, safety and investigate the molecular mechanisms of chlorophyllin derivative mediated PDT. Animals belonging to both IV-PDT and IT-PDT groups showed significant decrease in tumor size at 72 hours post-treatment. Tumors at the IV-PDT group disappeared totally within a week with no recurrence over three months follow up period. In the IT-PDT, the decrease in tumor size at the first week was followed by a slight increase but without regaining the original tumor size. Histological examination of tumor tissues at 24 hours post treatment demonstrated restoring the normal muscle tissue architecture in animals belonging to the IV-PDT group, and the biochemical assays indicated normal liver functions. The immunohistochemical analysis for caspase-3, and the quantitative PCR results of caspases-8 and 9 proved the presence of extrinsic apoptotic pathway via PDT mediated tumor therapy. In conclusion IV-PDT mediated solid tumor therapy proved better tumor cure rate than the IT-PDT, with no tumor recurrence over three months follow up period.

9308-37, Session PMon

Photodynamic therapy using hemagglutinating virus of Japan envelope (HVJ-E): a novel therapeutic approach for the treatment of hormone antagonistic prostate cancer

Mizuho Inai, Masaya Yamauchi, Norihiro Honda, Hisanao Hazama, Osaka Univ. (Japan); Shoji Tachikawa, Gakushuin Univ., Tokyo Institute of Technology (Japan); Hiroyuki

**Conference 9308: Optical Methods for Tumor Treatment and Detection:
Mechanisms and Techniques in Photodynamic Therapy XXIV**

Nakamura, Tokyo Institute of Technology (Japan); Tomoki Nishida, Hidehiro Yasuda, Osaka University (Japan); Yasufumi Kaneda, Kunio Awazu, Osaka Univ. (Japan)

Traditional treatment options for prostate cancer include surgery, chemotherapy, and radiation therapy, yet these methods are insufficient to cure metastatic and advanced drug-resistant prostate cancer. Thus, as a form of complementary treatment, we have focused on photodynamic therapy (PDT) with a novel photosensitizer, using UV-inactivated viral vector, called hemagglutinating virus of Japan envelope (HVJ-E). HVJ-E is a highly efficient non-viral drug-delivering vector, which can also initiate host immune response against cancer. In our study, we have exploited such unique characteristics of HVJ-E to establish a novel photosensitizing agent, named porphyrus envelope (PE), by inserting lipidated protoporphyrin IX (PpIX lipid) via centrifugation. To evaluate the photodynamic efficiency of PE for hormone antagonistic prostate cancer cells (PC-3), subcellular localization of PE derived PpIX lipid was compared using confocal laser scanning fluorescence microscopy to those of exogenous PpIX lipid and PpIX induced from exogenous administered precursor of 5-aminolevulinic acid (5-ALA). As a result, all drug types exhibited similar fluorescence distributions of PpIX, indicating their localization in mitochondria. Next, to evaluate the efficacy of PE - PDT, light was irradiated to PC-3 cells treated with PE, PpIX lipid and 5-ALA, using a laser diode at the wavelength of 405 nm and the power density of 100mW/cm^2 for 60 seconds. The results revealed the 200-fold and 28.6×10^3 -fold increase in therapeutic efficacy when compared to those of PDT using PpIX lipid and 5-ALA induced PpIX, respectively. Our findings suggest how PE can enhance the therapeutic efficacy of PDT.

Conference 9309: Mechanisms for Low-Light Therapy X

Saturday - Sunday 7 -8 February 2015

Part of Proceedings of SPIE Vol. 9309 Mechanisms for Low-Light Therapy X

9309-1, Session 1

Low level light therapy: the path forward (Invited Paper)

Michael R. Hamblin, Wellman Ctr. for Photomedicine
(United States)

Low level laser (light) therapy (LLLT) also known as photobiomodulation has been practiced for almost fifty years, and hundreds of positive clinical trials and thousands of laboratory studies have been published. Despite these impressive accomplishments LLLT has still not reached the stage of acceptance by mainstream medicine. The reasons for this are many and various including scientists claiming a lack of mechanism, and no agreement on dosimetry and parameters, physicians claiming there is a lack of large clinical trials / systematic reviews, hospital and insurance administrators cannot agree on reimbursement, and marketing hype / misinformation from industry. To overcome these objections we need better guidelines with standardized protocols and consistent parameters. Studies should be published in higher impact scientific and medical journals. Companies should avoid false promises and deceptive marketing, and physicians should receive a clearly defined return on investment with insurance reimbursement.

9309-2, Session 1

The roadmap for LLLT to become a mainstream medical procedure (Invited Paper)

James D. Carroll, THOR Photomedicine Ltd. (United
Kingdom)

The path from "bench to bedside" is fraught with challenges for all new medical devices. LLLT/PBM is one of the most exciting technologies on the medical horizon, it solves several significant unmet medical needs at relatively low cost and has no apparent side effects, yet it shows no immediate signs of significant commercial success. Why is this? The normal medical device barriers in the USA include FDA clearance, reimbursement, standard care guidelines and opinion leader support. Many LLLT devices have achieved FDA clearance but not reimbursement, standard care guidelines or opinion leader support. The roadmap for LLLT/PBM to get from "bench to bedside" also needs to take into account normal market acceptance phases as illustrated by the "technology adoption life cycle" and the "Gartner Hype-Cycle". The LLLT/PBM industry hinders its own progress by producing products that do not perform to claimed specification, researchers misreport report beam and dose parameters and there are a myriad of radiometric terms that doctors and therapists are not familiar with.

9309-3, Session 1

Clinical translation with low light therapies: current barriers and new frontiers (Invited Paper)

Praveen Arany, National Institute of Dental and
Craniofacial Research (United States)

The popular use of light based technologies in health care is expanding rapidly to encompass conventional imaging, surgery and ablative modalities. The field of therapeutic low power applications has been dodged with lack of clinical robustness and consistency. The major obstacles for more mainstream use of these treatment modalities appear to be a lack of

our understanding of its biological tissue responses. This has prevented development of rigorous clinical treatment protocols. This presentation will attempt to highlight our current understanding of the molecular pathways invoked by laser treatments and outline a clinical dosing regimen we are using in our lab. Data from ongoing studies will be presented that specifically emphasize utility of key device parameters and biological assays that could aid in future development of safe and effective low power light treatment regimens.

This research was supported by the Intramural Research Program of the NIH, NIDCR.

9309-4, Session 1

Beam profile measurements for dental phototherapy: the effect of distance, wavelength and tissue thickness

William M. Palin, Mohammed A. Hadis, Michael R. Milward,
The Univ. of Birmingham (United Kingdom); James D.
Carroll, THOR Photomedicine Ltd. (United Kingdom); Paul
R. Cooper, The Univ. of Birmingham (United Kingdom)

Background: The removal of bacterial contamination from infected teeth and the promotion of natural dental tissue repair processes may obviate the need for further restorative procedures. Light delivery for bacterial disinfection (UV/blue) and photobiomodulation (near-IR) requires specific, concentrated and controllable local irradiance and dose. Dental targets for light involve dentine, which scatters, absorbs and reflects light, reducing local irradiance. This study compared the effectiveness of LEDs (400-900nm) and lasers (660nm and 810nm; THOR Photomedicine Ltd, UK) to penetrate dentine.

Methods: Caries-free wisdom teeth were sectioned through the pulp-chamber by either cutting perpendicular to the crown, the buccal aspect or obliquely. Wet-polishing to 1, 2 or 3mm thicknesses exposed the dentine on opposing surfaces. The beam profile of the LEDs/lasers were measured through dentine specimens (n=5; SP620, Ophir, Spiricon) to obtain beam width following optical calibration, and spatial irradiance distribution following photodiode power calibration (PD300, Ophir, Spiricon).

Results: Results demonstrated significant differences of wavelengths (light penetration was optimized above 600nm $p < 0.05$) and orientation, (crown-sectioned specimens exhibited lower light attenuation). The beam area increased significantly ($P < 0.05$) with increasing specimen thickness/distance (albeit with decreased irradiance) for lasers but not for LEDs. There was a noticeable shift in beam position for all light sources in buccal and oblique specimens.

Conclusion: Dentine tubule orientation may alter the direction of light through tissue bulk. Optimal light penetration and distribution through dentine at specific distance is best achieved with, flat-top beams that cover the whole tooth, and are best projected vertically through the crown.

9309-5, Session 2

The effect of UV-Vis to near-infrared light on the biological response of human dental pulp cells

Mohammed A. Hadis, Paul R. Cooper, Michael R. Milward,
The Univ. of Birmingham (United Kingdom); Patricia
Gorecki, Univ. of Birmingham (United Kingdom); Edward
Tarte, James Churm, William M. Palin, The Univ. of
Birmingham (United Kingdom)

Background: The application of light irradiation in dentistry may be used for low level laser/light therapy (LLLT or photobiomodulation) or bacterial disinfection of tissues. Photobiomodulation of dental tissues may reduce pain and inflammation and promote natural healing and tooth repair processes using specific wavelength and doses (product of irradiance and exposure time). The purpose of this study was to investigate the biological response of dental pulp cells (DPCs) following irradiation at specific wavelength, irradiance and exposure times.

Methods: Human DPCs were isolated and cultured in phenol-red-free ?-MEM/10%-FCS. DPCs at passages 2-4 were seeded (150µL; 25,000 cell/ml) in black 96-microwell plates with transparent bases. 24h after seeding, cultures were irradiated using a bespoke LED array consisting of 60 LEDs (3.5mW/cm²) of wavelengths from 400nm-900nm (10 wavelengths, n= 6) for time intervals of up-to 120s. Metabolic and mitochondrial activity was assessed via a modified MTT assay. Statistical differences were identified by using Two-way analysis of variance and post-hoc Tukey tests (P=0.05).

Results: The biological responses were significantly dependent upon both wavelength and exposure time (P<0.05). At relatively short wavelength irradiances (400nm and 475nm), a significant reduction in mitochondrial activity was measured (P<0.05), whereas longer wavelength irradiances (625, 660 and 800nm) increased mitochondrial activity (P<0.05) in DPCs. Mitochondrial activity were increased and reached a plateau at 60-90s exposures.

Conclusions: The biological responses of human DPCs were both wavelength and exposure-time dependent. The optimisation of these irradiation parameters will be key to the successful application of LLLT in dentistry.

9309-6, Session 2

Impact of blue LED irradiation on proliferation and gene expression of cultured human keratinocytes

Anja Becker, Carsten Sticht, Harsh Dweep, Ruprecht-Karls- Univ. Heidelberg (Germany); Frank A. van Abeelen, Philips Research (Netherlands); Norbert Gretz, Ruprecht-Karls- Univ. Heidelberg (Germany); Gerrit Oversluizen, Philips Research Nederland B.V. (Netherlands)

Blue light is known for its anti-microbial, anti-proliferative and anti-inflammatory effects. Furthermore, it is already used for the treatment of neonatal jaundice, actinic keratosis, basal cell carcinoma and acne. However, little is known about the exact mechanisms of action on gene expression level.

The aim of this study was to assess the impact of blue LED irradiation on the proliferation and gene expression on immortalized human keratinocytes (HaCat) in vitro. Furthermore its safety was assessed.

XTT-tests revealed a decrease in cell proliferation of blue light irradiated cells depending on the duration of light irradiation. Moreover, gene expression analysis exhibited deregulated genes already 3 hours after blue light irradiation. 24 hours after blue light irradiation the effects seemed to be even more pronounced. The oxidative stress response was significantly increased, pointing to increased ROS production due to blue light, as well as steroid hormone biosynthesis. Downregulated pathways or biological processes were connected to anti-inflammatory response and cell cycle arrest.

Interestingly, also the melanoma pathway contained significantly downregulated genes 24 hours after blue light irradiation, which stands in accordance to literature that blue light can also inhibit proliferation in cancer cells. First tests with melanoma cells showed a decrease in cell proliferation after blue light irradiation with even higher effects compared to human keratinocytes. In conclusion, blue light irradiation might open avenues to new therapeutic regimens; at least blue light seems to have no effect that benefits cancer growth or formation.

9309-7, Session 2

Controversial effects of low level laser irradiation on the proliferation of human osteoblasts

Gamze Bölükbaşı Ates, Bogaziçi Üniv. (Turkey); Ayse Ak, Erzincan Univ. (Turkey); Bora Garipcan, Sahru Yüksel, Murat Gülsoy, Bogaziçi Üniv. (Turkey)

Low level laser irradiation (LLLI) is the application of red or near infrared lasers irradiating between 600-1100 nm with an output power of 1-500 mW. Several studies indicate that LLLI modulates cellular mechanisms and leads to enhanced cell proliferation.

Although the biological mechanisms are not fully understood, it is known that the effects depend on several parameters such as wavelength, irradiation duration, energy level, beam type and energy density.

The aim of this study is to investigate the effect of low level laser irradiation at varying energy densities with two different wavelengths (635 nm and 809 nm) on the proliferation of human osteoblasts in vitro .

The cells are seeded on 96 well plates (10000cells/well) and after 24 h incubation cells are irradiated at energy densities 0.5 J/cm², 1 J/cm² and 2 J/cm². Cell viability test is applied after 24h, 48h and 72h in order to examine early and late effects of laser irradiation on osteoblast proliferation.

635 nm light irradiation did not appear to have significant effect on the proliferation of osteoblasts as compared to the control. On the other hand, 809 nm irradiation at the same energy densities caused significant (p < 0.01) biostimulating effect on the osteoblast cell cultures at 24 h and 48 h.

In conclusion, irradiation with both wavelengths did not cause any cytotoxic effects. 809 nm light irradiation can promote proliferation of human osteoblasts in vitro. On the other hand, 635 nm light irradiation does not seem to have any proliferating effect. As a result, LLLI applied using different wavelengths on the same cell type may lead to different biological effects.

9309-8, Session 2

Biomodulatory effects of laser irradiation on dental pulp cells in vitro

Michael R. Milward, Mohammed A. Hadis, Paul R. Cooper, The Univ. of Birmingham (United Kingdom); Patricia Gorecki, Univ. of Birmingham (United Kingdom); James D. Carroll, THOR Photomedicine Ltd. (United Kingdom); William M. Palin, The Univ. of Birmingham (United Kingdom)

Background and Aim: Low level laser/light therapy (LLLT) or photobiomodulation is a biophysical approach that can be used to reduce pain, inflammation and modulate tissue healing and repair. However its application has yet to be fully realised for dental disease treatment. The aim of this study was to assess the modulation of dental pulp cell (DPC) responses using two LLLT lasers with wavelengths of 660nm and 810nm.

Materials and Methods: Human DPCs were isolated and cultured in phenol-red-free ?-MEM/10%-FCS. Central wells of transparent-based black 96-microplates were seeded with DPCs (passages 2-4; 150µL; 25,000 cell/ml) At 24h, cultures were irradiated using a Thor Photomedicine LLLT device (THORlabs, UK) at 660nm (13, 6 or 3s to give 10, 5 and 2J/cm²) or 810nm (5, 2 or 1s to give 20, 10 and 5J/cm²). Metabolic and mitochondrial activity was assessed via a modified MTT assay 24h following irradiation. Statistical differences were identified using analysis of variance and post-hoc Tukey tests (P=0.05) compared with non-irradiated controls.

Results: Significantly higher MTT activity was obtained for both lasers (P<0.05) compared to control for the high and intermediate radiant exposures (5-20J/cm²). The MTT response significantly decreased (P<0.05) at lower radiant exposures with no statistical difference from control.

Conclusion: Although both therapeutic lasers effectively modulated biological activity in DPCs, enhanced parameters were apparent in terms of dose. These parameters should be further optimised to identify the most effective therapeutic conditions.

9309-9, Session 3

Low level light in combination with metabolic modulators for effective therapy *(Invited Paper)*

Mei X. Wu M.D., Ting T. Dong, Harvard Medical School (United States)

Hypoxia occurs at the injured site of the brain following traumatic brain injury (TBI) owing to vascular damage. Persistent hypoxia is often linked to secondary brain damage and poor outcomes, since efficient ATP production at mitochondrial respiratory chain relies on oxygen and is essential for repairing the damaged tissue. We found high levels of glycolysis, reduced ATP generation, and increased ROS formation, prone to apoptosis in hypoxic neurons, strikingly, all of which could be significantly reversed by low level laser therapy (LLLT). The effect of LLLT was furthered by a combination with metabolic substrates like pyruvate or lactate both in vivo and in vitro. When injured brain was exposed to LLL, along with intraperitoneal injection of pyruvate, the mice could perform memory and learning activities normally at the end of treatment, whereas LLL or pyruvate-treated or untreated control mice displayed either partial or severe deficiency in these cognitive functions. Consistent with this, combined LLLT and pyruvate greatly prevented secondary brain damage and completely protected the hippocampus tissue, while TBI-caused cortical damage progressed into the hippocampus region in the controls. Likewise, a combination of LLLT with CoQ10, a natural diet supplement, greatly accelerated wound healing in diabetic mice as compared with LLLT or CoQ10-treated or untreated mice. These data clearly suggest that a combination of LLLT and energy metabolic modulators can additively or synergistically enhance the therapeutic effect of LLL in energy-producing insufficient tissues.

9309-10, Session 3

Different treatment paradigms of 830 nm photobiomodulation are retinoprotective in a rodent model of retinitis pigmentosa *(Invited Paper)*

Janis T. Eells, Heather Schmitt, Univ. of Wisconsin-Milwaukee (United States); Phyllis Summerfelt, Medical College of Wisconsin (United States); Adam Dubis, Univ. College London (United Kingdom); Joseph Carroll, Medical College of Wisconsin (United States); Sandeep Gopalakrishnan, Univ. of Wisconsin-Milwaukee (United States)

Previous studies in our laboratory have shown that 830 nm photobiomodulation (PBM) protects against retinal dysfunction and photoreceptor cell death in the P23H rat model of retinitis pigmentosa when administered early in the course of the disease. The present study determined if 830nm PBM would continue to protect against retinal dysfunction and photoreceptor cell death as the animals matured. P23H rats were treated once per day with 830 nm light (180 s; 25 mW/cm²; 4.5 J/cm²) using a light-emitting diode array (QDI, Barneveld WI) from [1] postnatal day p10 to p25, [2] p10 to p40 or [3] p20 to p40. Retinal function was assessed by measuring photoreceptor function with electroretinography (ERG), and retinal morphology was determined by using spectral domain optical coherence tomography (SD-OCT). 830nm PBM preserved retinal function and retinal morphology in 830 nm light-treated animals in comparison to the sham-treated group in each treatment protocol. ERG

responses were greater in 830 nm light-treated P23H rats compared to sham-treated P23H rats. SD-OCT imaging showed that 830nm PBM also preserved the structural integrity of the retina in each treatment protocol. Our findings confirm that the retinoprotective effects of 830 PBM observed early in the course of retinal degeneration in the P23H rat persist as the animals mature. Based on our findings and on other studies documenting the neuroprotective actions of PBM in experimental and clinical studies, we propose that photobiomodulation is an innovative, non-invasive therapeutic approach for the treatment of retinal degenerative disease.

9309-11, Session 3

Transcranial low-level laser therapy increases memory, learning, neuroprogenitor cells, BDNF and synaptogenesis in mice with traumatic brain injury *(Invited Paper)*

Michael R. Hamblin, Fatma Vatansever M.D., Weijun Xuan, Liyi Huang, Wellman Ctr. for Photomedicine (United States)

Background and Motivation: Increasing concern is evident over the epidemic of traumatic brain injury in both civilian and military medicine, and the lack of approved treatments. Transcranial low level laser therapy (tLLLT) is a new approach in which near infrared laser is delivered to the head, penetrates the scalp and skull to reach the brain.

Objective: To explore whether tLLLT at 810-nm improves memory and learning in mice with controlled cortical impact traumatic brain injury. To investigate the mechanism of action by immunofluorescence studies in sections from brains of mice sacrificed at different times.

Results: Mice with TBI treated with 1 or 3 daily laser applications performed better on Morris Water Maze test at 28 days. Laser treated mice had increased BrdU incorporation into NeuN positive cells in the dentate gyrus and subventricular zone indicating formation of neuroprogenitor cells at 7 days and less at 28 days. Markers of neuron migration (DCX and Tuj1) were also increased, as was the neurotrophin, brain derived neurotrophic factor (BDNF) at 7 days. Markers of synaptogenesis (formation of new connections between existing neurons) were increased in the perilesional cortex at 28 days.

Conclusion: tLLLT is proposed to be able to induce the brain to repair itself after injury. However its ability to induce neurogenesis and synaptogenesis suggests that tLLLT may have much wider applications to neurodegenerative and psychiatric disorders.

9309-12, Session 3

Optical properties of mice skin for optical therapy relevant wavelengths: influence of gender and pigmentation

Caetano Padias Sabino, Ctr. for Lasers and Applications, Institute for Nuclear and Energetic Research-CNEN/SP (Brazil); Alessandro M. Deana, Daniela F. Silva, Cristiane M. França, Biophotonics Post Graduation Program, Univ. Nove de Julho (Brazil); Tania M. Yoshimura, Martha S. Ribeiro, Ctr. for Lasers and Applications, Institute for Nuclear and Energetic Research-CNEN/SP (Brazil)

Red and near-infrared light have been widely employed in optical therapies. Skin is the most common optical barrier in non-invasive techniques and in many cases it is the target tissue itself. Consequently, to optimize the outcomes brought by light-based therapies, the optical properties of skin tissue must be very well elucidated. In the present study, we evaluated the dorsal skin optical properties of albino (BALB/c) and pigmented (C57BL/6)

Conference 9309: Mechanisms for Low-Light Therapy X

mice using the Kubelka-Munk photon transport model. We evaluated samples from male and female young mice of both strains. Analysis was performed for wavelengths at 630, 660, 780, 810 and 905 nm due to their prevalent use in optical therapies, such as low-level light (or laser) and photodynamic therapies. Spectrophotometric measurements of diffuse transmittance and reflectance were performed using a single integrating sphere coupled to a proper spectrophotometer. Statistical analysis was made by two-way ANOVA, with Tukey as post-test and Levene and Shapiro-Wilks as pre-tests. Statistical significance was considered when $p < 0.05$. Our results show only a slight transmittance increment ($< 10\%$) as wavelengths are increased from 630 to 905 nm, and no statistical significance was observed. Albino male mice present reduced transmittance levels for all wavelengths. The organization and abundance of skin composing tissues significantly influence its scattering optical properties although absorption remains constant. We conclude that factors such as subcutaneous adiposity and connective tissue structure can have statistically significant influence on mice skin optical properties and these factors have relevant variations among different gender and strains.

9309-13, Session 3
Effect of photon energy in collagen generation by interstitial low level laser stimulation

Eunkwon Jun, Yonsei Univ. (Korea, Republic of); Myungjin Ha, Sangyeob Lee, Edalat Radfar, Jihoon Park, Yonsei Univ. (Korea, Republic of); Byungjo Jung, Yonsei Univ. (Korea, Republic of)

Although the mechanism of low level laser therapy (LLLT) is unclear, many studies demonstrated the positive clinical performance of LLLT for skin rejuvenation. An increase in dermal collagen plays an important role in skin rejuvenation and wound healing. This study aims to investigate collagen formation after a minimally invasive laser needle system (MILNS). Rabbits were divided into three groups: animals that applied MILNS (wavelength 660nm; power 20mW; energy density 8J), animals that applied MILNS (wavelength 660nm; power 20mW; energy density 10J) and animals not treated with MILNS. MILNS was just applied once to the backside of rabbits. Collagen formation was evaluated every 24 hours by ultrasound skin scanner during one week. Results show that MILNS groups (8J and 10J) have more collagen density than control.

9309-29, Session PSat
Effect of low power laser on wound healing and blood sugar in diabetic rats

Hadi Morshedi, Ali Safary III, Namatoola Gheibi D.D.S., Qazvin Univ. of Medical Sciences (Iran, Islamic Republic of)

Methods: 36 male rats weighing of 200 to 250 g were divided into 4 groups including 9 animals in each group. Groups I and II were considered as two control groups. Group I is the control group without skin wound (normal control) and the II group with skin wound (sham operated) that treated by laser. Group III was considered as diabetic with skin wound. Also that IV group was treated by low power laser with a wavelength of 632.8 nm and a power of 5 mW. Induction of diabetes was carried out by injection of 65mg/Kg of streptozotocin (STZ). One week after injection of STZ the blood sugar of diabetic animals were measured and the blood sugar concentration up to 300mg/dl considered as diabetic. The wounded animals were anesthetized with ketamine and xylazine and in sterile conditions a round wound with the size of 3cm² induced by cutting the thickness of the epidermis and dermis. In the time scales of 4, 7 and 10 days after surgery, the wound area was measured to calculation of wound healing. Blood sugar levels and urine hydroxyproline were measured by colorimetric method.

Finding: The calculation of the percentage of wound healing in the 7th day

of treatment in both second group (Laser normal animals) and forth group (diabetic laser) obtained significant with $p < 0.05$ and $p < 0.01$ respectively, in comparison with the control group. On the 10th day, the mention two groups show significant difference with $p < 0.05$ in compared with control group and the significant change of 3th group with the control group was $P < 0.01$. The measuring of glucose concentration between diabetic groups including control diabetic (group III) and laser-treated diabetic group (IV), in three time courses of treatment were obtained significant with ($P < 0.001$), ($P < 0.001$) and I ($P < 0.001$), respectively. Hydroxyproline assay and histological examination results are consistent with the healing effects of the laser.

Conclusion: The laser treatment in the wavelength of 632.8nm and 5 mW power and energy of 4 J/cm² in both normal and diabetic wound healing showed significant effect on blood sugar levels and wound healing in time dependent manner. Laser healing effects emphasized with both histological and biochemical studies or hydroxyproline concentration in the treated groups were confirmed

9309-30, Session PSat
Non-invasive optical monitoring of blood flow with a single-tau software correlator

Detian Wang, Univ. of Pennsylvania (United States) and Institute of Fluid Physics (China); Wesley B. Baker, Univ. of Pennsylvania (United States); Zhe Li, Univ. of Pennsylvania (United States) and Tianjin Univ. (China); Ashwin B. Parthasarathy, Univ. of Pennsylvania (United States); David R. Busch, Univ. of Pennsylvania (United States) and Children's Hospital of Philadelphia (United States); Steven Schenkel, Kenneth Abramson, Arjun G. Yodh, Univ. of Pennsylvania (United States)

Low-level light therapy (LLLT) is a relatively new non-invasive technology. It has been used for wound healing, pain relief, treatment of inflammation and swelling, and recently, it has been explored for treatment of stroke and traumatic brain injury. Despite the popularity of LLLT devices, however, widespread use has arguably been limited by uncertainty about the physical/physiological mechanisms that underly the therapy. In this study, we take steps to characterize responses to LLLT. Specifically, we utilize quantitative diffuse optical spectroscopy (DOS) and diffuse correlation spectroscopy (DCS) to measure the LLLT effects on blood volume, blood oxygenation, and blood flow in head and muscle tissue of healthy subjects. To our knowledge, this study is the first application of DCS to directly measure microvascular tissue blood flow following LLLT; i.e., previous studies have indirectly probed flow (e.g., with continuous wave DOS), and have probed flow in superficial tissues (e.g., laser Doppler) and large blood vessels (e.g., Doppler ultrasound). Our analysis separates the hemodynamic response of superficial (skin) from deeper tissues, potentially permitting assessment of LLLT affects for deep tissue stimulation. Recruitment for this study is ongoing. While the results are preliminary and cannot lead to definitive conclusions, we believe that this research will help establish a roadmap for quantitative assessment of LLLT therapeutic strategies.

9309-31, Session PSat
Low level light promotes the proliferation and differentiation of bone marrow derived mesenchymal stem cells

Jin-Chul Ahn, Yun-Hee Rhee, Sun-Hyang Choi, Dae Yu Kim, Phil-Sang Chung M.D., Dankook Univ. (Korea, Republic of)

Low-level light irradiation (LLLI) reported to stimulate the proliferation or differentiation of a variety of cell types. However, very little is known about the effect of light therapy on stem cells. The aim of the present study was to

evaluate the effect of LLLI on the molecular physiological change of human bone marrow derived stem cells (hBMSC) by wavelength (470, 630, 660, 740 and 850, 50mW). The laser diode was performed with different time interval (0, 7.5, 15, 30J/cm², 50mW) on hBMSC. To determine the molecular physiological changes of cellular level of hBMSC, the clonogenic assay, ATP assay, reactive oxygen species (ROS) detection, mitochondria membrane potential (MMP?) staining and calcium efflux assay were assessed after irradiation.

There was a difference between with and without irradiation on hBMSCs. An energy density of over 30 J/cm² improved the cell proliferation in comparison to the control group. Among these irradiated group, 630 and 660nm were significantly increased the cell proliferation. The cellular level of ATP and calcium influx was increased with energy dose-dependent in all LLLI groups. Meanwhile, ROS and MMP? were also increased after irradiation except 470nm. It can be concluded that LLLI using infrared light and an energy density over 30 J/cm² has a positive stimulatory effect on the proliferation or differentiation of hBMSCs. Our results suggest that LLLI may influence to the mitochondrial membrane potential activity through ATP synthesis and increased cell metabolism which leads to cell proliferation and differentiation.

9309-32, Session PSat

Regulation of hypoxia-increased osteoclast formation by low level laser therapy

Man-Seok Bang, Graduate School, Dankook Univ. (Korea, Republic of); Chung-Hun Oh, School of Dentistry, Dankook Univ. (Korea, Republic of)

The cells were seeded at a density of 5 × 10³ cells / well in 96-well or 15 × 10⁴ cells / well in 6well plates and cultured in osteoclast differentiation medium of ?-MEM supplemented with 10 % FBS and 50 ng / ml receptor activator of nuclear factor-?B ligand (RANKL) for 3 days. Gas mixture containing 5 % CO₂ and 20, 11, 8, 5, or 2% O₂ (balanced with N₂) was then flushed through the inlet at a flow rate of 10 - 15 cc / min until culture was terminated. LED light source irradiation was performed for at 2 m W/cm². Cell viability was evaluated by MTT assay. The number of osteoclasts and total TRAP activity was estimated by TRAP staining and TRAP solution assay, respectively. Total RNAs isolated using TRIzol (Invitrogen) were cDNA synthesis with iScript™ cDNA synthesis kit (Bio-rad) according to the manufacturer's protocol. The SYBR Green based real-time PCR was performed on a StepONE Plus real-time PCR system (Applied Biosystems, Foster city, USA).

9309-33, Session PSat

Effectiveness of antimicrobial photodynamic therapy on staphylococcus aureus using phenothiazinium dye with red laser

Juliana S. C. Monteiro, Univ. Estadual de Feira de Santana (Brazil) and Univ. Federal da Bahia (Brazil); Susana Carla P. S. de Oliveira D.D.S., Gustavo M. Pires-Santos, Fernando José P. Sampaio D.D.S., Maria de Fátima M. Gesteira D.D.S., Luiz Guilherme P. Soares, Antônio Luiz B. Pinheiro D.D.S., Univ. Federal da Bahia (Brazil)

The objective of this study was to evaluate the bactericidal effect of Antimicrobial Photodynamic Therapy using phenothiazinium dye a concentrations of 12.5 ?g/mL irradiated with the red laser at doses of 12J/cm² on strain of Staphylococcus aureus (ATCC 23529) in vitro. Test groups: Negative control and bacterial suspensions were irradiated with laser energy 12J/cm² in the absence of photosensitizer; bacterial suspensions were irradiated with laser in the presence 12.5?g/mL of photosensitizer and finally

bacterial suspensions only in the presence of phenothiazinium dye. Effect of Antimicrobial Photodynamic Therapy in which there was a percentage inhibition of 81%.

9309-34, Session PSat

Prospective study of luminous radiation associated technology photosensitive compounds for treatment of diseases

Gustavo M. Pires-Santos, Fernando José P. Sampaio D.D.S., Susana Carla P. S. de Oliveira D.D.S., Univ. Federal da Bahia (Brazil); Juliana S. C. Monteiro D.D.S., Univ. Estadual de Feira de Santana (Brazil); Maria de Fátima M. Gesteira D.D.S., Luiz Guilherme P. Soares, Paulo Fernando de Almeida, Antônio Luiz B. Pinheiro D.D.S., Univ. Federal da Bahia (Brazil)

In order to assess the advancement of technologies that use light sources photosensitive molecules that activate this prospective study has listed patents, electronic banking 'Spacenet Patent Search', which used codes descriptors: 'A61K41', 'A61N5/06'. 326 documents were analyzed. However, the peak deposit occurred between 90 and 2000. These documents have descriptors related to the porphyrin family of molecules, whose absorption peak is in the blue range. Current studies seek new photosensitizers, this may change the incidence of the use of blue light or UV main wavelengths used, thus helping in the development of a new stage of development of this technology.

9309-35, Session PSat

Evaluation of the efficacy of photodynamic antimicrobial therapy using a phenothiazine compound and LED (red-orange) on the interface: macrophage vs S. aureus

Fernando José P. Sampaio D.D.S., Susana Carla P. S. de Oliveira D.D.S., Univ. Federal da Bahia (Brazil); Juliana S. C. Monteiro, Univ. Federal da Bahia (Brazil) and Univ. Estadual de Feira de Santana (Brazil); Gustavo M. Pires-Santos, Maria de Fátima M. Gesteira D.D.S., Luiz Guilherme P. Soares, Paulo Fernando de Almeida, Antônio Luiz B. Pinheiro D.D.S., Univ. Federal da Bahia (Brazil)

Is possible to kill bacteria with a light source after the microorganisms have been sensitized. The aim of this study was to evaluate the phagocytic function of macrophages J774 against S. aureus in the presence and absence of PDT with phenothiazine compound (12.5?g/mL) and LED red-orange. Experimental groups: Control Group (L-F-), Phenothiazine group (L-F+) Laser group (L+F-), Group Photodynamic therapy (L+F+). This study demonstrated that therapy is able to increase about twice the phagocytic ability of macrophages, however the bactericidal capacity of these cells did not show a substantial improvement, probably because the oxidative burst was little intense.

9309-36, Session PSat

Evaluation of laser photobiomodulation on bone defect in the femur of osteoporotic rats: a Raman spectral study

Luiz Guilherme P. Soares, Joubert Mateus S. Aciole, Univ. Federal da Bahia (Brazil); Landulfo Silveira Jr., Camilo Castelo Branco Univ. (Brazil); Antônio Luiz B. Pinheiro D.D.S., Univ. Federal da Bahia (Brazil)

Phototherapies have shown positive effects on bone tissue. The aim of this study was to assess through Raman spectroscopy, the efficacy of laser phototherapy on the bone repair process of osteoporotic rats. Thirty rats were divided into 4 groups then subdivided in subgroups (15 and 30 days). After the osteoporosis induction time (60 days), bone defect with 2mm was created. Irradiation protocol was applied every 48 hours during 15 days. Statistical analysis (ANOVA, Student-T test) of the data for hydroxiapatite have shown significant difference between groups ($p \leq 0.001$). It was concluded that the Laser phototherapy increased deposition of HA.

9309-14, Session 4

To evaluate the safety and efficiency of low level laser therapy (LLLT) in treating decubitus ulcers: a review

Ambereen Ahmed M.D., A&M AssortedTherapy.LLC (United States)

Inflammation is the body's normal physiological response to injury. The normal inflammatory response maintains homeostasis and allows for tissue healing. Chronic inflammation leads to all sorts of organ dysfunctions. Pressure ulcers from immobile patients usually results in prolonged periods of hospitalization. Although low level laser therapy (LLLT) for acceleration in wound healing has been experimented before, there were many unanswered questions such as the underlying mechanisms and the specific wave forms, timing of stimulation and consistency that would result in optimal effect.

PubMed, Medline, Science Direct, and Google Scholar were searched for relevant articles comparing safety and efficacy of LLLT as an adjunct to chronic wound management in immobile and debilitated patients.

The review assessed the effectiveness and feasibility of incorporating LLLT for chronic wound healing such as decubitus ulcers. LLLT had been used effectively with a good safety profile for a wide range of chronic wounds including decubitus ulcers.

9309-15, Session 4

Tri-wave laser therapy for spinal cord injury, neuropathic pain management, and restoration of motor function

Mark D. Chariff, Therapeutic Laser Applications, LLC (United States); Peter Olszak, GO Advanced Laser Systems (United States)

A novel laser therapy device using three combined beams with wavelengths 532 nm, 808 nm, and 1064 nm has been demonstrated in clinical trials. Primarily, therapeutic lasers have used wavelengths in the ranges of 632 nm through 1064 nm, where the optical density is below 5 OD, to achieve pain relief and tissue regeneration. Conventional wisdom in the low level therapeutic laser field would argue against the using wavelengths in the region of 532 nm, where the optical density is 8 OD, due to poor penetration; however, the author's clinical observations dispute this notion. It is hypothesized that the combination of wavelengths work in synergy.

The 532 nm light is absorbed by chromophores such as oxyhemoglobin, deoxyhemoglobin, and cytochrome c oxidase providing energy to accelerate the healing process. The 808 nm light is known to result in Nitric Oxide production thereby reducing inflammation and oxidative stress. All three laser wavelengths likely contribute to pain relief by inhibiting nerve conduction; however, the 1064 nm has the deepest penetration. Through the use of this device over the past 10 years on patients with a variety of acute and chronic neuro-musculoskeletal disorders, the author has observed that a large portion of these individuals experienced rapid relief from their presenting conditions. Additionally, the phenomena of a tingling sensation was observed in a majority of patients when the area of presumed greatest inflammation was irradiated. This phenomenon was observed in patients with visceral and musculoskeletal conditions, as well as in patients with spinal cord injuries. Patient testimonials as well as thermal images have been collected to document the results of the laser therapy. These clinical trials test the effectiveness of laser therapy in spinal cord stimulation and demonstrate the ability of laser therapy to rapidly alleviate pain from both acute and chronic conditions. Additionally, studies performed at the University of Miami Project to Cure Paralysis indicate that this device has the potential for treating a number of spinal cord syndromes, including, but not limited to paralysis and neuropathic pain.

9309-16, Session 4

Currently available methods for control and assessment of wave technologies in complex treatment of oncology patients with lung cancer

Lena Sheiko M.D., FBGU Rostov Research Institute of Oncology, Rostov-on-Don (Russian Federation)

Background: Patient with lung cancer applying the adjuvant therapy using effects of noncoherent monochromatic optic irradiation of red spectrum by blood photomodification aimed at stimulation of non specific resistance in complex treatment related with the attempt of minimization of chemotherapy and radiation toxic actions.

Methods: The γ -parameter, characterizing the quantitative ratio of one- and two-coil nucleic acids in blood lymphocytes, has been chosen as a prognostic criteria for control and assessment of adjuvant therapy.

Results: It is shown that when γ -parameter has low values (0.067 ± 0.001 ru.) the possible impairment in state of patients and the fall in antitumor of non specific resistance have taken place during the course of the complex treatment. And with the high values of γ -parameter (2.09 ± 0.71 ru.) the patient's status improved and negative changes, side effects of toxic actions were never observed. Moreover the stimulation of spontaneous and mitogen-induced lymphocytes proliferation, enhancement of expression of T- and NK-cells membrane receptors has been indicated. With the growing of the level of non specific resistance and of clinical effect the value of γ -parameter was increased (from 1,12 to 2.37 ru).

Conclusions: Thus, with the help of γ -parameter one can get the information about the patient's status, and this may be used as integral index, as signal test to define the level of non specific antitumor resistance and may be used also as a prognostic criteria for control and assessment of wave technologies in the complex treatment for lung cancer patient.

9309-17, Session 4

Comparison of clinical effectiveness of laser acupuncture and amitrytyline in diabetic peripheral neuropathy (DPN) a sham controlled randomized clinical trial

Shahzad Anwar M.D., Iffat Anwar Medical Complex (Pakistan)

Objective: To assess the effect of laser acupuncture in patients suffering from painful diabetic neuropathy and its comparison with standard of care.

Results: A total of 164 subjects were included in the study who were subdivided into three groups labeled as A, B and C for laser therapy treatment, amitriptyline treatment and controls respectively. The mean age of subjects was 51.54±10.46 in Group A, 49.38±10.56 in Group B and 51.70±11.43 in Group C. The difference of mean ages in all study groups was statistically insignificant (p-value= 0.469). The average pain score in patients who received laser therapy was 5.95±0.91 before treatment, whereas after treatment it was 4.31±0.98. The mean pain score in subjects having Amitriptyline before starting the treatment was 6.87±0.71 and after treatment, it was 6.23±0.98. The mean score for daily life activities in subjects who received laser therapy was 9.56±2.37 before treatment, while after treatment it was 7.56±1.54. The average score for daily life activities in patients having Amitriptyline before starting the treatment was 9.05±1.93 and after treatment, it was 8.11±1.71. Average depression and anxiety score in patients receiving laser therapy was 9.29±2.28 before treatment, whereas after treatment it was found to be 7.42±1.91. Similarly, the mean depression and anxiety score in patients of Amitriptyline group before starting the treatment was 9.38±2.21 and after treatment, it was 8.38±2.14.

Conclusion: The mean score in our study reveals that laser therapy shows better outcomes in improvement of pain relief, depression, anxiety and daily life activities compared to amitriptyline in patients of diabetic neuropathy.

9309-18, Session 4

Assessment of LED (I 850 ± 10 nm) phototherapy in the inflammatory process of rat's TMJ induced by carrageenan

Isabele C. V. de Castro, Cristiane B. Rosa, Carolina M. Carvalho, Luiz Guilherme P. Soares, Maria Cristina T. Cangussu D.D.S., Jean N. dos Santos, Antônio Luiz B. Pinheiro D.D.S., Univ. Federal da Bahia (Brazil)

Temporomandibular disorders are commonly found in the population and usually involve inflammatory processes. Previous studies have shown the effectiveness of LED (Light emitting diodes) phototherapy in inflammatory process. The aim of this study was to assess through histological analysis the effectiveness LED on the inflammation of the temporomandibular joint of rats induced by carrageenan. Based on the data obtained and the authors' own experience, LED phototherapy resulted in a reduction of inflammatory infiltrate in the temporomandibular joint of rat.

9309-19, Session 4

LED phototherapy on midpalatal suture after rapid maxilla expansion: a Raman spectroscopic study

Cristiane B. Rosa, Fernando Antonio L. Habib, Telma M. de Araújo, Jean N. dos Santos, Univ. Federal da Bahia (Brazil); Artur Felipe S. Barbosa M.D., Univ. Federal da Bahia (Brazil) and Univ. Federal de Pernambuco (Brazil); Isabele C. V. de Castro, Luiz Guilherme P. Soares, Antônio Luiz B. Pinheiro D.D.S., Univ. Federal da Bahia (Brazil)

A quick bone formation following maxillary expansion would reduce treatment time and LED light may accelerate bone deposition. This work aimed to analyze the effect of LED phototherapy on bone formation on the midpalatal suture after maxillary expansion in rats. The effect of the treatment was assessed by Raman spectroscopy. Near infrared Raman spectroscopic analyzes demonstrated that LED irradiation increased the deposition of hydroxiapatite in the midpalatal suture after expansion and that LED light contributes for the acceleration of bone formation in the midpalatal suture after expansion procedure.

9309-20, Session 5

Low-level laser therapy renders mice neutrophils more efficient when rechallenged with the pathogenic fungus *paracoccidioides brasiliensis*

Eva Burger, Giulia M. A. C. Bani, Ana Carolina S. C. Mendes, Maisa R. P. L. Brigagão, Gersika B. Santos, Luiz Cosme C. Malaquias, Jorge K. Chavasco, Univ. Federal de Alfenas (Brazil); Liana M. Verinaud, Univ. Estadual de Campinas (Brazil); Felipe F. Sperandio, Univ. Federal de Alfenas (Brazil)

The host defense against fungi counts with the active participation of the innate immunity; consonantly, neutrophils (PMN) play a central role in the fungal infection paracoccidioidomycosis (PCM). The treatment for PCM includes the use of antifungals directed against its fungal agent: *Paracoccidioides brasiliensis* (Pb). Nevertheless, drug administration needs to be highly prolonged to be efficient, also presenting many side effects and often resistance. Thus, we aimed to utilize low-level laser therapy (LLLT) to render PMN more activated against a first in vivo and second in vitro exposure to Pb. LLLT (wavelength of 780 nm; power of 50 mW; energy density of 12.5 J/cm²; 90 seconds per point and 112.5 J of total energy) was applied in vivo on alternate days as two points on hind paws of Swiss mice inoculated in subcutaneous air pouches with a virulent strain of Pb or Zymosan (Z); the aim was to reach the bone marrow of femur with LLLT; unirradiated animals were used as controls. After 10 days of infection we obtained a highly pure PMN population, which was subsequently cultured in the presence of Pb for trials of protein production, evaluation of mitochondrial activity, reactive oxygen species production (ROS) and quantification of viable fungi growth. In vivo LLLT rendered PMN more active metabolically, leading to higher fungicidal activity against Pb, probably due to increased production of ROS and independently of primary or secondary exposure to the fungus. The kinetic behavior of protein production was crescent for unirradiated mice and decrescent for LLLT-treated animals.

9309-21, Session 5

Evaluation of the efficacy of photodynamic antimicrobial therapy using a phenothiazine compound and Laser (I=660nm) on the interface: macrophage vs *S. aureus*

Susana Carla P. S. de Oliveira, Univ. Federal da Bahia (Brazil); Juliana S. C. Monteiro D.D.S., Univ. Estadual de Feira de Santana (Brazil) and Univ. Federal da Bahia (Brazil); Gustavo M. Pires-Santos, Fernando José P. Sampaio D.D.S., Maria de Fátima M. Gesteira D.D.S., Luiz Guilherme P. Soares, Antônio Luiz B. Pinheiro D.D.S., Univ. Federal da Bahia (Brazil)

Photodynamic inactivation has been proposed as an alternative treatment for localized bacterial infections. The aim of this study was to evaluate the phagocytic function of macrophages J774 against *S. aureus* in the presence and absence of PDT with phenothiazine compound (12.5?g/mL) and low level laser (?=660nm, 12 J/cm²). Experimental groups: Group (L-F-), Phenothiazine group (L-F+) Laser group (L+F-), Group Photodynamic therapy (L+F+) Control, we evaluated the following conditions in triplicate. With this study it was demonstrated that the therapy is able to increase the phagocytic ability of macrophages as well as improved bactericidal capacity, probably by allowing a more intense oxidative burst.

9309-22, Session 5

Enhancement of monoclonal antibody production in CHO cells by exposure to He-Ne laser radiation

Rana A. Ghaleb, Medical College, Babylon Univ. (Iraq)

This study tested the effectiveness of laser biostimulation in small-scale cultures in vitro. We investigated the response of recombinant CHO cells, which are used for the production of monoclonal antibody, to low level laser radiation. The cells were irradiated using a 632.8 nm He-Ne laser in a continuous wave mode at different energy doses. We incubated the irradiated cells in small batch cultures and assessed their proliferation and productivity at various time intervals. Compared to untreated cells, the irradiated cells showed a significant increase in antibody production. Moreover, the results showed that laser irradiation did not affect viability and slightly enhanced proliferation rate.

9309-28, Session 5

Brief review on the effect of low-power laser irradiation on neutrophils with emphasis on emerging fungal infections

Felipe F. Sperandio, Giulia M. A. C. Bani, Ana Carolina S. C. Mendes, Maisa R. P. L. Brigagão, Gersika B. Santos, Luiz Cosme C. Malaquias, Jorge K. Chavasco, UNIFAL (Brazil); Liana M. Verinaud, Univ. Estadual de Campinas (Brazil); Eva Burger, UNIFAL (Brazil)

Polymorphonuclear neutrophils (PMN) participate in an active way within the innate immunity developed after the fungal infection paracoccidioidomycosis (PCM). Nevertheless, the sole participation of neutrophils is not sufficient to eradicate PCM's pathogenic fungus: *Paracoccidioides brasiliensis* (Pb). In that way, we aimed to develop a treatment capable of stimulating PMN to the site of injury through low-level laser therapy (LLLT). The methodology consisted of using a low-power laser device (50 mW of power; wavelength of 780 nm; energy density of 12.5 J/cm²; 90 seconds per point and 112.5 J of total energy) applied in vivo as two points on each hind paw of mice on alternate days focusing the bone marrow of femur, in mice either infected with the highly virulent Pb isolate or inoculated with Zymosan (Z) in subcutaneous air pouches; the control groups were infected with Pb or inoculated with Z but did not receive LLLT. Then, PMN isolated from the air pouches were analyzed after 10 days of infection or inoculation and the absolute number of PMN cells, cell viability, protein production (BCA), ability to produce reactive oxygen species (ROS) and fungicidal capacity by quantification of colony forming units (CFU) were assessed. LLLT increased the production of ROS, total proteins and PMN's fungicidal activity in both Pb and Z groups. Interestingly, LLLT decreased the total number of PMN in animals infected with Pb, but not in animals inoculated with Z. LLLT activated PMN and increased their fungicidal activity, what suggests this treatment as a complementary therapy for PCM.

9309-23, Session 6

Far red/near infrared light-induced cardioprotection under normal and diabetic conditions

Agnes Keszler, Shelley Baumgardt, Christopher Hwe, Martin Bienengraeber, Medical College of Wisconsin (United States)

Far red/near infrared light (NIR) is beneficial against cardiac ischemia and reperfusion injury (I/R), although the exact underlying mechanism is

unknown. Previously we established that NIR enhanced the cardioprotection of nitrite in rabbit heart. Furthermore, we observed that the nitrosyl myoglobin (MbNO) level in ischemic tissue decreased upon irradiation of the dissected heart. Our hypothesis was that protection against I/R is dependent on nitric oxide (NO)-release from heme-proteins, and remains present during diabetes. When mice were subjected to I/R with no NIR (control) or NIR (660 nm) during the beginning of reperfusion NIR reduced infarct size dose dependently. Similarly, the isolated (Langendorff) heart model resulted in sustained left ventricular diastolic pressure after I/R upon NIR (660 nm) treatment. NIR-induced protection was preserved in a diabetic mouse model (db/db) and during acute hyperglycemia. NIR liberated NO from nitrosyl hemoglobin (HbNO) and MbNO as well as from HbNO isolated from the blood of diabetic animals. In the Langendorff model, with application of a nitrosylated form of a hemoglobin-based oxygen carrier as NO donor NIR induced an increase in NADH level, suggesting a mild inhibition of mitochondrial respiration by NO during reperfusion. Taken together, NIR applied during reperfusion protects the myocardium against I/R in a NO-dependent and mitochondrion-targeted manner. This unique mechanism is conserved under diabetic conditions where other protective strategies fail.

9309-24, Session 6

Low power laser irradiation stimulates cell proliferation via proliferating cell nuclear antigen and Ki-67 expression during tissue repair

Vijendra Prabhu, Manipal Institute of Technology, Manipal Univ. (India) and Biophysics Unit, School of Life Sciences, Manipal Univ. (India); Bola Sadashiva Satish Rao, Krishna Kishore Mahato, School of Life Sciences, Manipal Univ. (India)

Low power laser irradiation (LPLI) is becoming an increasingly popular and fast growing therapeutic modality in dermatology to treat various ailments without any reported side effects. In the present study an attempt was made to investigate the proliferative potential of red laser light during tissue repair in Swiss albino mice. To this end, full thickness excisional wounds of diameter 15 mm created on mice were exposed to single dose of Helium-Neon laser (632.8 nm; 7 mW; 4.02 mWcm⁻²; Linear polarization) at 2 Jcm⁻² and 10 Jcm⁻² along with un-illuminated controls. The granulation tissues from all the respective experimental groups were harvested on day 10 post-wounding following euthanization. Subsequently, tissue regeneration potential of these laser doses under study were evaluated by monitoring proliferating cell nuclear antigen and Ki-67 following the laser treatment and comparing it with the un-illuminated controls. The percentages of Ki-67 or PCNA positive cells were determined by counting positive nuclei (Ki-67/PCNA) and total nuclei in five random fields per tissue sections. Animal wounds treated with single exposure of the 2 Jcm⁻² indicated significant elevation in PCNA (P<0.01) and Ki-67 (P<0.05) compared to un-illuminated control and P<0.01 compared to 10 Jcm⁻² expression as compared to other tested experimental groups as evidenced by the microscopy results in the study. In summary, the findings of the present study have clearly demonstrated the regulation of cell proliferation by LPLI via PCNA and Ki-67 expression during tissue regeneration.

9309-26, Session 6

Biostimulative effects of 809 nm diode laser on cutaneous skin wounds

Hakan Solmaz, Murat Gülsoy, Yekta Ülgen, Bogaziçi Üniv. (Turkey)

The use of low-level laser therapy (LLLT) for therapeutic purposes in medicine has become widespread recently. There are many studies in

Conference 9309: Mechanisms for Low-Light Therapy X

literature supporting the idea of therapeutic effects of laser irradiation on biological tissues. The aim of this study is to investigate the biostimulative effect of 809nm infrared laser irradiation on the healing process of cutaneous incisional skin wounds.

3-4 months old male Wistar Albino rats weighing 350 to 400 gr were used throughout this study. Low-level laser therapy was applied through local irradiation of 809nm infrared laser on open skin incisional wounds of 1 cm length. Each animal had six identical incisions on their right and left dorsal region symmetrical to each other. The wounds were separated into three groups of control, 1 J/cm² and 3 J/cm² of laser irradiation. Two of these six wounds were kept as control group and did not receive any laser application. Rest of the incisions was irradiated with continuous diode laser of 809nm in wavelength and 20mW power output. Two of them were subjected to laser irradiation of 1 J/cm² and the other two were subjected to laser light with energy density of 3 J/cm². Biostimulative effects of irradiation were studied by means of tensile strength tests and histological examinations. Wounded skin samples were morphologically examined and removed for mechanical and histological examinations at days 3, 5 and 7 following the laser applications. Three of the six fragments of skin incisions including a portion of peripheral healthy tissue from each animal were subjected to mechanical tests by means of a universal tensile test machine, whereas the other three samples were embedded in paraffin and stained with hematoxylin and eosin for histological examinations.

Tensile strength test results and histological examinations show that tissue repair following laser irradiation of 809nm has been accelerated in terms of tissue morphology, strength and cellular content. These results seem to be consistent with the results of many researches previously published in literature and support the idea that LLLT has therapeutic effect on wound healing process.

9309-27, Session 6

Effects of laser pulsing parameters on cell viability

Karl Engel, National Institute of Health (United States);
Praveen Arany, National Institute of Dental and
Craniofacial Research (United States)

No Abstract Available

Conference 9310: Frontiers in Biological Detection: From Nanosensors to Systems

Saturday 7 February 2015

Part of Proceedings of SPIE Vol. 9310 Frontiers in Biological Detection: From Nanosensors to Systems VII

9310-3, Session 1

Photonic crystal microring resonators for label-free DNA sensing

Stanley M. Lo, Shuren Hu, Yiorgos Kostoulas, Sharon M. Weiss, Philippe M. Fauchet, Vanderbilt Univ. (United States)

We report label-free DNA sensing using a highly dispersive photonic crystal microring resonator (PhCR).

While traditional ring resonators have been demonstrated as highly effective biosensors due to their competitive sensitivity and compatibility with standard CMOS processing, their ultimate detection sensitivity is limited by relatively poor light-matter interaction with target molecules on the ring surface. PhCRs have the same advantages as traditional rings for chemical and biological sensing, but they allow improved light-matter interaction with target molecules. A fraction of the optical field in the ring is located inside the air holes where molecules can bind. The PhCR used in this work has a photonic bandgap near 1555nm. At the resonances within the slow-light regime, a loaded quality factor of ~3200 was measured. The largest estimated group index was ~50 near the band edge.

We previously reported the PhCR as a refractive index sensor with a detection sensitivity of ~170nm/RIU by exposing it to different analytes that changed the dielectric environment. In this work, we benchmark the performance of the PhCR as a label-free DNA biosensor. Traditional conjugation techniques were used to functionalize the PhCR. All molecular additions were verified by transmission measurements that showed the expected spectral changes of the resonances after each step of molecular attachment. Exposure of the functionalized PhCR to 10⁷M target PNA gave rise to a large resonance redshift of ~1.7nm. This result demonstrates a 2-fold improvement over traditional ring resonators tested under similar conditions.

9310-4, Session 1

Optical waveguide biosensor based on cascaded Mach-Zehnder interferometer and ring resonator with Vernier effect

Xianxin Jiang, Longhua Tang, Jinyan Song, Mingyu Li, Jian-Jun He, Zhejiang Univ. (China)

Optical waveguide biosensors based on silicon-on-insulator (SOI) have been extensively investigated owing to its various advantages and many potential applications. In this article, we demonstrate a novel highly sensitive biosensor based on cascaded Mach-Zehnder interferometer (MZI) and ring resonator with the Vernier effect using wavelength interrogation. The sensor consists of a MZI cascaded with a ring resonator, in which the MZI is used for sensing while the ring resonator acts as a reference. The MZI has periodic transmission peaks which are determined by the phase difference between the sensing arm and the reference arm. The cascading with a ring resonator results in a series of transmission peaks with a periodic envelope function. A change of the refractive index in the sensing arm of the MZI causes a shift of its peaks, which is then translated into a much larger shift of the envelope function due to the Vernier effect. The sensor response was first investigated using NaCl solutions of varying concentrations. The experimental results show that the sensitivity reached 1960nm/RIU and 22700nm/RIU for sensors based on MZI alone and cascaded MZI-ring with Vernier effect, respectively. A biosensing application was demonstrated by monitoring the interaction between goat and antigoat immunoglobulin G (IgG) pairs. The measured results show that 1ng/ml IgG resulted in 60pm and 1.1nm wavelength shift for sensors based on MZI alone and MZI-ring, respectively.

Besides, theoretical analysis show that this sensor can be designed to achieve completely temperature insensitive. This integrated high sensitivity biosensor has great potential for medical diagnostic applications.

9310-5, Session 1

An optical biosensor for detection of pathogen biomarkers of Shiga toxin-producing Escherichia coli in ground beef samples

Loreen R. Lamoureux, The Univ. of New Mexico, Ctr. for Biomedical Engineering (United States) and Los Alamos National Lab., Physical Chemistry and Applied Spectroscopy (United States) and The New Mexico Consortium (United States); Afsheen Banisadr, Los Alamos National Lab., Physical Chemistry and Applied Spectroscopy (United States); Peter Adams, Los Alamos National Lab., Ctr. for Integrated Nanotechnology (United States); Zachary R. Stromberg, Univ. of Nebraska-Lincoln, Ctr. for Veterinary Medicine and Biomedical Sciences (United States); Steven W. Graves, The Univ. of New Mexico, Ctr. for Biomedical Engineering (United States); Rodney Moxley, Univ. of Nebraska-Lincoln, Ctr. for Veterinary Medicine and Biomedical Sciences (United States); Gabriel Montañó, Los Alamos National Lab., Ctr. for Integrated Nanotechnology (United States); Harshini Mukundan, Los Alamos National Lab., Physical Chemistry and Applied Spectroscopy (United States) and The New Mexico Consortium (United States)

Shiga Toxin-producing Escherichia coli (STEC) pose a serious threat to human health through the consumption of contaminated food products, particularly beef and produce. Early detection in the food chain, and discrimination from other non-pathogenic Escherichia coli (E. coli), is critical to preventing human outbreaks, and meeting current agricultural screening standards. These pathogens often present in low concentrations in contaminated samples, making discriminatory detection difficult without the use of costly, time-consuming methods (e.g. culture). Using multiple signal transduction schemes (including novel optical methods designed for amphiphiles), specific recognition ligands, and a waveguide-based optical biosensor developed at Los Alamos National Laboratory, we have developed ultrasensitive detection methods for lipopolysaccharides (LPS), and protein biomarkers (Shiga toxin) of STEC in complex samples (e.g. beef lysates). Waveguides functionalized with phospholipid bilayers were used to pull down amphiphilic LPS, using methods (membrane insertion) developed by our team. The assay format exploits the amphiphilic biochemistry of lipoglycans, and allows for rapid, sensitive detection with a single fluorescent reporter. We have used a combination of biophysical methods (atomic force and fluorescence microscopy) to characterize the interaction of amphiphiles with lipid bilayers, to efficiently design these assays. Sandwich immunoassays were used for detection of protein toxins. Biomarkers were spiked into homogenated ground beef samples in physiologically relevant concentrations to determine performance and limit of detection in relevant applications. Future work will focus on the development of discriminatory ligands for STEC serotypes and using quantum dots as the fluorescence reporter, to enable multiplex screening of biomarkers.

**Conference 9310: Frontiers in Biological Detection:
 From Nanosensors to Systems**

9310-6, Session 2

Sensitivity enhancement in optofluidic devices using total internal reflection

Fei Du, Eric J. Mahoney, Huan-Hsuan Hsu, Ponnambalam R. Selvaganapathy, Qiyin Fang M.D., McMaster Univ. (Canada)

The emergence of optofluidic devices in the past few years provides unique advantages by combining microfluidics with optical detection in the same platform to achieve miniaturization, integration and automation. However, miniaturization and complexity in the fabrication process also lead to weak optical signal, mostly due to small sample volumes. We developed a total internal reflection assisted (TIRA) optical platform for sensitivity enhancement in optofluidics sensors for environmental and clinical applications. A fluorescence based dissolved oxygen sensor was fabricated using a Ru(dpp)₃²⁺ fluorescence film on which oxygen can cause a quenching effect, in conjunction with a PDMS channel membrane and glass slide substrate. Excitation light is confined within the glass slide by total internal reflection to produce multiple sensing sites. Experimental results show that optical sensitivity can be increased up to 9 times in TIRA sensors. It is also observed that both sensitivity and linearity can be increased 4 times by reducing the thickness of fluorescence film. These results suggest the potential of TIRA scheme as a sensing and characterizing platform for optofluidic devices in environmental and point-of-care diagnostic applications.

9310-7, Session 2

Examining small molecule - HIV RNA interactions using arrayed imaging reflectometry

Wanaruk Chaimayo, Benjamin L. Miller, Univ. of Rochester Medical Ctr. (United States)

Human Immunodeficiency Virus (HIV) has been the subject of intense research for more than three decades due to causing a currently incurable disease (Acquired Immunodeficiency Syndrome: AIDS). In the pursuit of a medical treatment, RNA-targeted small molecules are emerging as promising targets. In order to understand the binding kinetics of small molecules and HIV RNA, association (k_a) and dissociation (k_d) kinetic constants must be obtained, ideally for large numbers of sequences to assess selectivity. We have developed Aqueous Array Imaged Reflectometry (Aq-AIR) to address this challenge. Using a simple light interference phenomenon, Aq-AIR provides real-time high-throughput multiplex capabilities to sense binding of analytes to surface-immobilized targets in a label-free microarray format. We will discuss the use of Aq-AIR in the specific context of small molecules able to bind RNA sequences derived from the HIV virus.

9310-8, Session 2

A novel antibody immobilization strategy for optical biosensors

Mark A. Lifson, Univ. of Rochester Medical Ctr. (United States); Jared A. Carter, Adarza BioSystems, Inc. (United States); Benjamin L. Miller, Univ. of Rochester Medical Ctr. (United States)

Arrayed Imaging Reflectometry (AIR) is a highly sensitive label-free biosensor which can be used to detect hundreds of antigens on a single substrate. The signal monitored with AIR is the light intensity of an angled beam reflected off of a flat substrate which is composed of a protein-reactive film on a thermally grown silicon oxide layer. If the angle, wavelength, and polarization of the incident light beam is fixed, a near-zero

reflectance condition can be obtained by adjusting the thickness of the thermally grown oxide. In a typical AIR biosensing experiment, antibodies are printed (using a piezo-driven microarrayer) on top of the oxide layer to create a minimum reflectance condition. If the substrate is exposed to a complex solution (such as serum), the patterned antibodies bind to their specific targets increasing the effective spot thickness, which perturbs the anti-reflective condition and causes a measurable signal increase. One of the main considerations with AIR is evaluating and controlling the bioactivity and efficiency of antibody immobilization after printing, since these factors significantly affect the dynamic range and limit of detection. In this work, we present a novel antibody immobilization strategy which shows significant improvement when compared with conventionally prepared substrates. This method can be generalized to work with other microarray technology formats, including those that are not label-free.

9310-16, Session 2

Label-free single molecule detection using microtoroid optical resonators

Judith Su, California Institute of Technology (United States)

Label-free single molecule detection has been a long standing goal of bioengineers and physicists. The main obstacle to detecting single molecules, however, is decreasing the noise level of the measurements such that a single molecule can be distinguished from background. We have used laser frequency locking in combination with balanced detection and data processing techniques to improve the signal-to-noise ratio of microtoroid optical resonators and report the detection of a wide range of nanoscale objects ranging from nanoparticles with radii from 100 to 2.5 nm, to exosomes, ribosomes, and single protein molecules (mouse immunoglobulin G and human interleukin-2). We further extend the exosome results towards creating a minimally invasive tumor biopsy assay. Our results, covering several orders of magnitude of particle radius (100 nm to 2 nm), agree with the 'reactive' model prediction for the frequency shift of the resonator upon particle binding. We anticipate that our results will enable many applications, including more sensitive medical diagnostics and fundamental studies of single receptor-ligand and protein-protein interactions in real time.

9310-9, Session 3

Cost-effective, high enhancing SERS substrates based on imprinted nanoporous gold (*Invited Paper*)

Sharon M. Weiss, Vanderbilt Univ. (United States)

An easy-to-fabricate, uniform, and sensitive SERS-active substrate that combines the self-organized and highly interacting nanoscale morphology of nanoporous gold (NPG) with the advantages of reproducibly nanopatterned periodic structures will be discussed. A straightforward process is utilized to stamp two-dimensional grating patterns in NPG films. Both localized surface plasmons and propagating surface plasmons contribute to the SERS signal enhancement. Uniform SERS substrates without hot spots are demonstrated with enhancements near 10^8 compared to non-enhancing substrates. The design, fabrication, and characterization of the patterned NPG SERS substrates will be reported along with progress toward specific chemical functionalization and incorporation as flexible substrates.

**Conference 9310: Frontiers in Biological Detection:
From Nanosensors to Systems**

9310-10, Session 3

Plasmonic nanoparticle interaction with cell membrane for diagnostic applications

Sumana Das, Akshata Arikady, Ramakrishna Vasireddi, Krishna Harika, Manish Konnur, Gopalkrishna M. Hegde, D. Roy Mahapatra, Indian Institute of Science (India)

The science and technology of optical fiber is a subject intense research, driven in part by the development of new types of fibers that incorporate interior microchannels and optofluidic interaction, sensing and manipulation. Pulsed laser microbeams offer significant advantages for non-contact manipulation of cells, for example to lysis of cells as well as transient cell membrane transport. In such integrated optofluidics, one can achieve high throughput and shorter detection time. Exposure of the cell to laser micro-beam in a plasmonic nanoparticle integrated microfluidics channel is studied. Details and results are discussed in the present paper. A light path is coupled in a microfluidic channel where the light transmission at specific wavelength monitors spectral peak due to DNA released through lysis of cells. Plasmonically induced lysis results obtained by using this quantification technique is compared with that from laboratory standard lysis and cell expression assay. Specificity of DNA peaks are achieved by creating binding sites on the light transmission path. The binding sites employs nano-structures, first for incubation with a complementary ssDNA and then for binding of target DNA. DNA binding yield obtained in situ within the optofluidic channel is compared with standard test results from fluorimeter, UV-Visible spectrophotometer and qPCR. Further, the plasmonic transport characteristics due to certain optical modes of the fiber waveguides with plasmonic nanoparticle functionalization are analyzed. Effect of plasmonic nanoparticle core-shell structures on the cell expression and DNA release efficiency are investigated.

9310-13, Session 3

Smartphone fluorescence spectroscopy

Hojoeng Yu, Yafang Tan, Brian T. Cunningham, Univ. of Illinois at Urbana-Champaign (United States)

We demonstrated that the internal camera of a smartphone, combined with a set of optical components for providing wavelength dispersion, and a compact, inexpensive green laser pointer, serves the function of a highly sensitive fluorescence spectrometer. By packaging the optical components in the form of a custom cradle that easily interfaces with the smartphone, the system serves as a portable tool for performing fluorescence assays for point-of-use diagnostics applications. We demonstrated operation of the system in the context of a molecular beacon FRET assay for detection of a specific miRNA sequence with 1.3 pM limits of detection (LOD), and that the assay was specific against detection of a miRNA sequence that differed from the target sequence by only one base. The demonstrated approach is applicable to any liquid-based assay using a light-emitting reporter, such as fluorescence, quantum dots, chemiluminescence, and phosphorescence. Because the approach measures the spectral output of the assay, it enables separation of light components such as scattering of the excitation source, donor emission, and acceptor emission. The smartphone-based fluorimeter reported in this work outperforms the laboratory fluorimeter because we utilize a laser light source that more efficiently excites the Cy3 tag than the Xe lamp within the fluorimeter. Our results show the mobile system is capable of providing sensitivity that is sufficient for many applications.

9310-14, Session 3

Non-invasive, label free biophotonic sensing with sensitized glass

Gin Jose, Tarun Kakkar, Toney T. Fernandez, Matthew Murray, Jayakrishnan Chandrappan, Ramzi Ajjan, Sikha

Saha, Billy D. Richards, Animesh Jha, David P. Steenson, Peter J. Grant, Univ. of Leeds (United Kingdom)

We present a novel non-invasive biosensor technology that relies on the fluorescence and random lasing properties of a photonic chip that interacts with blood and interstitial fluid through skin. The technology which has huge potential for continuous monitoring of biomolecules and metabolites is currently being applied for non-invasive glucose monitoring device development with the formation. The photonic chip consists of surface modified glass with fluorescent rare earth ions fabricated by a new femtosecond laser based plasma implantation technology. Our measurement principle is based on the variation of photoluminescence lifetime of the photonic chip via macroscopic electromagnetic interactions with molecules to be detected and quantified.

Early stage product development through a pilot clinical study involving cohort of twelve Type 1 diabetes subjects has undertaken and it provided direct real-time measurement of optical response giving high signal to noise sensitivity for glucose. Our results shows excellent correlation (>92%) with blood glucose concentration measured using finger stick meter. We also compared our results with commercial CGMs which rely on measurement of glucose in the interstitial fluid. Diligent control of blood glucose is highly essential for Type 1 diabetes patients and self-monitoring of blood glucose (SMBG) levels is currently carried out by invasive finger stick method and our technology offers a viable non-invasive alternative. The concept proven for glucose is also investigated for other biomarkers so as to build a comprehensive non-invasive sensor platform suitable for mobile platforms and for point of care application in the longer term.

9310-2, Session 4

Laser cross-linking protein captures for living cells on a biochip

Chih-Lang Lin, Central Taiwan Univ. of Science and Technology (Taiwan); Che-Kuan Lin, Yi-Jui Liu, Feng Chia Univ. (Taiwan); Hai-Wen Chen, Chung-Han Chiang, Chuen-Fu Lin, Shyang-Guang Wang, Central Taiwan Univ. of Science and Technology (Taiwan); Patrice L. Baldeck, Ctr. National de la Recherche Scientifique (France)

We report on bio-sensing pads to capture living cells, which are fabricated on bio-chips by cross-linking proteins/antibodies using laser induced photochemistry. The bio-sensing pads are fabricated by a commercial photo-induced 3D-microfabrication machine (Teem Photonics Inc.) with a passively Q-switched Nd-YAG microchip laser of 532 nm wavelength. The dimension of the pad is 20?20?2 ?m3. First, we demonstrated the negative (E. coli BL21) and positive (S. aureus ATCC 25923) detection tests with GFP-AcmA' protein sensing pad. AcmA' protein is known to specifically bond to peptidoglycan that makes the thick outside layer of Gram-positive bacteria. The experiment results show only Gram-positive bacteria were bound on GFP-AcmA' pad after minutes of incubation and phosphate buffered saline rinsing. No binding was observed by Gram-negative bacteria, and with reference pad made of neutral bovine serum albumin (BSA). Second, A-type red blood cells (RBCs) were chosen as the model cell to demonstrate the blood typing feasibility of the anti-A pad in microchannel. The A-type RBCs were captured only by the anti-A pad, but not the reference pad made of BSA. The detections were readily done by optical microscopy observation. The biological functions of protein/antibody with the laser induced photochemistry were verified. This study provides a new platform for simple and direct detection of living cells that could be potentially used in point-of-care settings.

**Conference 9310: Frontiers in Biological Detection:
 From Nanosensors to Systems**

9310-12, Session 4

Magnetic modulation biosensing for rapid and sensitive detection of cardiac troponin I

Schakked O. Halperin, Paul Olivo, MagBiosense LLC (United States); Amos Danielli, Bar-Ilan Univ. (Israel)

Rapid and highly sensitive detection of proteins is crucial in many application. For example, each year, over 5.5 million people visit Emergency Departments across the U.S. with chest pain suggestive of heart attack. The American Heart Association recommends measurement of cardiac Troponin I (cTnI) levels for heart attack diagnosis. Current assays have relatively low sensitivity, which limits their ability to detect elevated cTnI levels at early times after the onset of symptoms. New assays achieve high sensitivity, but are performed in a central laboratory, and time is lost in transport, processing, and measurement, which nullify the clinical advantages of a high sensitivity assay. Here, we present a novel platform to measure low concentrations of cTnI that can be applied to a point-of-care device. This system, termed Magnetic Modulation Biosensing, uniquely combines magnetic- and fluorescent-labeling of cTnI. We use a two-site 'sandwich' assay, which consists of streptavidin-coated paramagnetic beads bound to biotinylated cTnI antibodies that attach to cTnI in serum. The cTnI is also coupled to fluorescently labeled cTnI antibodies. An alternating magnetic field gradient condenses the magnetic beads to a small volume to increase the fluorescent signal. The beads are set in periodic motion in and out of an orthogonal laser beam, enabling the differentiation of background fluorescence from the oscillating cTnI-bound fluorescent signal. The modulation eliminates the need for washing steps, making the assay simpler, particularly useful for point-of-care applications. This system has successfully distinguished between varying concentrations of cTnI in serum.

9310-15, Session 4

Quantifying DNA and proteins using laser-induced thermophoresis

Li-Hsien Yu, Chih-Hsuan Wang, National Cheng Kung Univ. (Taiwan); Yih-Fan Chen, National Yang-Ming Univ. (Taiwan)

The study utilized thermophoresis, the directed motion of molecules in a temperature gradient to quantify DNA and proteins for point-of-care applications. Because the direction and speed of thermophoretic motion is dependent on the size, charge, and conformation of the molecules, the binding between molecules can induce changes in their thermophoretic motion. To quantify biomolecules using thermophoresis, we mixed fluorescently-labeled capture probes with the samples and then used an infrared laser to create a temperature gradient in the solution. By adding a small fraction of polymers to the buffer solution, we accumulated the fluorescent probes in the hotter regions using the thermophoretic effects during laser irradiation. The thermophoretic motion of the fluorescent probes significantly changed as the target molecules bind to the specially designed capture probes. Consequently, the level of thermophoretic accumulation, determined by the spatial distribution of fluorescent probes, could be used to quantify molecules. This method could function well even when the buffer contained 10% serum, which suggested that the detection was resistant to the interferences from the molecules in serum.

The thermophoresis-based detection method developed in this study only requires a laser and an epi-fluorescence microscope during the detection. Unlike many other commonly seen biosensing methods, quantifying molecules using thermophoresis does not need any channels or pumps for washing away unbound molecules during the detection process. In addition, the detection does not rely on any micro- or nanofabricated chips. In short, this thermophoresis-based biosensing method can be a simple, robust, and sensitive method for quantifying proteins and DNA.

Conference 9311: Molecular-Guided Surgery: Molecules, Devices, and Applications

Saturday - Sunday 7-8 February 2015

Part of Proceedings of SPIE Vol. 9311 Molecular-Guided Surgery: Molecules, Devices, and Applications

9311-1, Session 1

What endogenous contrast is accessible from diffuse spectroscopic signals in tissues? (*Invited Paper*)

Albert E. Cerussi, Beckman Laser Institute and Medical Clinic (United States)

Quantifying contrast that distinguishes between disease and normal tissue states is an important goal for molecular imaging. Exogenous contrast agents can be engineered to create contrast for specific biological mechanisms. Optical absorbers and fluorophores, for example, can be attached to targeting agents to add specificity and sensitivity to molecular imaging.

However, the magnitude and spectral shape of endogenous contrast can limit the effectiveness of the exogenous contrast agents. Tissue scattering not only degrades image quality, but also affects quantitative reliability. Endogenous absorbers reduce both emission and excitation light and distort the detected emission spectrum. If the endogenous tissue optical properties are known, then the localization and characterization of the exogenous agent will be better quantified. For this reason, it is important to characterize these endogenous optical properties, typically the absorption and scattering, at all wavelengths of interest.

The endogenous tissue optical properties also serve as contrast mechanisms in their own right. For example, within the near infrared spectral region important molecules such as hemoglobin, water and lipids have value as biomarkers for disease and response to therapy.

In this paper we will explore the array of endogenous signals that have been measured in tissues with diffuse optical technologies (i.e., intense multiple scattering). We will provide a survey of efforts in the biomedical optics field, especially from our own work at the Beckman Laser Institute, to quantify endogenous contrast. Particular attention will be given to the absorption and scattering contributions to these important endogenous signals.

9311-2, Session 1

Multimodal imaging strategies for early cancer diagnostics (*Invited Paper*)

Tomasz S. Tkaczyk, Rice Univ. (United States)

Monitoring and diagnostics of many cancers like oral, cervical or esophageal adenocarcinomas often require multimodal approach to perform successful diagnostics. Both morphological imaging and spectral assessment are important tools used in these applications. When, used separately, either method cannot easily achieve both high sensitivity and specificity. On the other hand if combined and working in tandem they can significantly improve the diagnostic performance. Therefore this paper focuses on analysis of multimodal approaches/instrumentation for early in vivo cancer detection. Two groups of devices will be discussed: (1) miniature-integrated imaging microscopes (endomicroscopes) to provide morphological content and (2) multi and hyperspectral high speed systems to obtain bio-chemical signatures of the tissue. Practical aspects of multi-modal system integration, fabrication and data processing will be discussed together with the design consideration to balance field of view and resolution of individual sub-systems. Number of imaging results will be presented including (for morphological assessment): contact imaging, confocal, structure illumination, and multi-photon imaging and (in area of spectral detection) narrow band imaging (NBI), image mapping spectrometry IMS, array snapshot systems.

9311-3, Session 1

Non-uniqueness and diagnostic relevance of multispectral measurements of the total diffuse reflectance from biological tissues

Pilar Beatriz García-Allende, Technische Univ. München (Germany) and Helmholtz Zentrum München GmbH (Germany); Karin Radrich, Technische Univ. München (Germany) and Helmholtz Zentrum München GmbH (Germany); Panagiotis Symvoulidis, Helmholtz Zentrum München GmbH (Germany) and Technische Univ. München (Germany); Jürgen Glatz, Maximilian W. Koch, Technische Univ. München (Germany) and Helmholtz Zentrum München GmbH (Germany); Jorge Ripoll, Univ. Carlos III de Madrid (Spain); Vasilis Ntziachristos, Technische Univ. München (Germany) and Helmholtz Zentrum München GmbH (Germany)

Multispectral reflectance imaging of tissue is continuously gaining diagnostic and therapeutic importance in clinical and preclinical procedures. Because of the skin being openly accessible and really suitable to be imaged with optical systems, numerous examples are found in dermatology, but advantage of the capabilities of multispectral imaging has been widely demonstrated also in endoscopic exploration and retina inspection. In spite of this acceptance, the physical formulation behind these measurements is not fully understood, and image interpretation commonly relies on data-driven pattern recognition algorithms for the automation of the diagnosis. Herein, we investigate the physical formulation of reflectance measurements provided by epi-illumination and detection camera-based systems based on a recently proposed analytical model accounting for an exponentially decaying source and encompassing an absorption-dependent coefficient in the formulation of the diffusion coefficient. We first state a condition on non-uniqueness by analytically demonstrating that simultaneous unique recovery of the chromophore concentrations and the wavelength-independent parameters describing the spectral variation of scattering properties according to the Mie formula cannot be achieved. Secondly, we discuss that in spite of the demonstrated scale invariance of multispectral measurements on the quotient of the chromophore concentrations and the scattering amplitude, the scattering power and the oxygen saturation, both having stand-alone diagnostic value can still be recovered.

9311-4, Session 1

Multispectral reflectance enhancement for breast cancer visualization in the operating room

Gaspar Fernandez-Barreras, Eusebio Real, Univ. de Cantabria (Spain); Ashley M. Laughney, Cancer Biology and Genetics Program, Memorial Sloan-Kettering Cancer Ctr. (United States); Venkataramanan Krishnaswamy, Keith D. Paulsen, Thayer School of Engineering at Dartmouth (United States); José Miguel López-Higuera, Univ. de Cantabria (Spain); Brian W. Pogue, Thayer School of Engineering at Dartmouth (United States); Olga M. Conde, Univ. de Cantabria (Spain)

A color enhancement method to optimize the visualization of breast

**Conference 9311: Molecular-Guided Surgery:
Molecules, Devices, and Applications**

tumors in cancer pathology is proposed. Light scattering measurements are minimally invasive, and allow the estimation of tissue morphology and composition to guide the surgeon in resection surgeries. The usability of scatter and absorption signatures acquired with a microsampling reflectance spectral imaging system was improved employing an empirical approximation to the Mie theory to estimate the scattering power on a per-pixel basis. The proposed methodology generates a new image with blended color and diagnostic purposes coming from the emphasis or highlighting of specific wavelengths or features. These features can be the specific absorbent tissue components (oxygenated and deoxygenated hemoglobin, etc.), additional parameters as scattering power or amplitude or even the combination of both. The goal is to obtain an improved and inherent tissue contrast working only with the local reflectance of tissue. To this aim, it is provided a visual interpretation of what is considered non-malignant (normal epithelia and stroma, benign epithelia and stroma, inflammation), malignant (DCIS, IDC, ILC) and adipose tissue. Consequently, a fast visualization map of the intracavity area can be offered to the surgeon providing relevant diagnostic information. No labeling or extrinsic indicators are required for proposed methodology and therefore the possibility of transferring absorption and scattering features simultaneously into visualization, fusing their effects into a single image, can guide surgeons efficiently.

9311-5, Session 1
Label-free multimodal multiphoton imaging by adaptively shaping fiber supercontinuum pulses

Yuan Liu, Haohua Tu, Eric J. Chaney, Sixian You, Stephen A. Boppart M.D., Univ. of Illinois at Urbana-Champaign (United States)

Multiphoton imaging provides three-dimensional high-resolution imaging with deeper penetration and reduced photodamage, and has been established as a powerful technology in biomedicine. The most attractive aspect of multiphoton imaging is the wealth of molecular contrast it can generate from various modalities. Coherent anti-Stokes Raman/stimulated Raman scattering (CARS/SRS) probes molecular vibration, two-/three-photon fluorescence (2PF/3PF) visualizes intrinsic fluorophores, and second/third harmonic generation (SHG/THG) maps non-centrosymmetric media and heterogeneity. Combining multiple modalities realizes imaging of complementary endogenous biomolecules and therefore is highly desirable for biomedical diagnostics. However, integration and further translation of these techniques, particularly for image-guided surgical applications, are not trivial due to the complexity of the laser(s) and imaging systems, and requirements for multiple modalities need to be met, and often compromised. A potential solution is a fiber-based ultrafast source to simplify the bulky lasers, and a pulse processing device to arbitrarily tailor the illumination pulses for multiple modalities. We demonstrate an integrated multimodal multiphoton imaging platform using fiber supercontinuum and pulse shaping. The high-quality fiber supercontinuum is generated in a highly nonlinear all-normal-dispersion fiber, achieving a spectrum spanning the optical biological window with high coherence, high power, and long-term stability. Adaptive pulse shaping of the supercontinuum pulses enables high-performance CARS/2PF/SHG/3PF/THG imaging of normal/cancerous human breast tissue, as well as the longitudinal molecular/structural changes during mammary tumor formation in a carcinogen-induced rat tumor model. This multimodal multiphoton imaging platform offers improved simplicity and expanded versatility, and the results show a promising path for the translation of multiphoton imaging to surgical applications.

9311-6, Session 1
Imaging of live cancer cells using molecular imaging needles

Loretta Scolaro, Louisa A. Ho, Dirk Lorensen, The Univ. of Western Australia (Australia); Elizabeth Thomas, St. John of God Hospital (Australia); David D. Sampson, Rebecca O. Fuller, Robert A. McLaughlin, The Univ. of Western Australia (Australia)

Molecular imaging (MI) needles, which combine single-cell sensitivity 2D fluorescence with 3D optical coherence tomography imaging, show wide promise for imaging disease. Here we present a step towards this by demonstrating, for the first time, MI needles imaging live cells.

The MI needle probe consists of a length of double-clad fiber (DCF), with the inner core guiding an OCT signal and delivering fluorescence excitation light, while the inner cladding collects the returning fluorescence. The imaging end is terminated by lengths of graded-index fiber and coreless silica fiber to focus and redirect the light beam perpendicular to the probe. This is encased in a hypodermic needle (outer diameter 640 microns), enabling it to be inserted deep within tissue. The proximal end is connected to both a 1300 nm OCT scanner and a fluorescence imaging system via a DCF coupler. Rotating the needle during insertion, a 3D OCT data volume and a radial fluorescence image are simultaneously acquired.

Strains of live human breast cancer cells (MCF-7 and MDA-231) were cultured on glass slides at a concentration of 4×10^5 cells/ml. To label the cells, we synthesized a fluorescent biomarker, using an analogue of the chemotherapeutic drug, Tamoxifen, and linking it to a BODIPY fluorophore. Results showed MI needles were able to distinguish fluorescence from individual cells. While the fluorescence image provided greater localization of cells in cell cultures than OCT, the OCT provided a 3D structural image which complements the 2D fluorescence projection image.

9311-7, Session 2
Quantitative wide-field fluorescence imaging in neurosurgery (*Invited Paper*)

Keith D. Paulsen, Thayer School of Engineering at Dartmouth (United States) and Geisel School of Medicine (United States) and Norris Cotton Cancer Ctr. (United States); Pablo A. Valdes Quevedo M.D., Brigham and Women's Hospital (United States) and Harvard Medical School (United States); Frédéric Leblond, Ecole Polytechnique de Montréal (Canada); Brian C. Wilson, Ontario Cancer Institute (Canada); Brian W. Pogue, Thayer School of Engineering at Dartmouth (United States) and Geisel School of Medicine (United States) and Norris Cotton Cancer Ctr (United States); David W. Roberts M.D., Dartmouth Hitchcock Medical Ctr. (United States) and Geisel School of Medicine (United States) and Norris Cotton Cancer Ctr. (United States)

Coresistered image-based neuro-navigation has a considerable track record of success in guiding open cranial surgery to the extent that most modern procedures routinely apply the enabling technology. Over the last decade, intraoperative fluorescence has emerged as a new way of guiding resection decisions by providing the surgeon with visual cues directly in the surgical field. Indeed, the visual signal from 5 aminolevulinic acid (ALA)-induced protoporphyrin IX (PpIX) fluorescence as a marker of high grade glial tumors is striking. Its advantages over white-light resection on progression free survival have been documented, and its impact on overall survival has also been suggested in patients with high grade glioma, even though lower grade disease has failed to fluoresce visually in the vast majority of studies. Recent results suggest more diagnostic information, beyond the visually

**Conference 9311: Molecular-Guided Surgery:
Molecules, Devices, and Applications**

evident fluorescence, is available from PpIX as an intraoperative biomarker of tumor, if the concentration of the fluorophore can be determined. In an on-going, multi-disciplinary, multi-institutional collaboration, we have been developing, evaluating and clinically translating optical measurement and imaging technology to sense quantitatively fluorophore concentrations in vivo during surgery. This presentation will summarize our latest findings, and in doing so, will make the case that quantitative wide-field fluorescence imaging is not only possible, but also essential for maximizing the surgical (and ultimately clinical outcome) benefits of guiding neurosurgery, at least with ALA-induced PpIX as an intraoperative biomarker of brain tumor.

9311-8, Session 2

Rigid endoscopic polarimetric wide-field imaging (*Invited Paper*)

Ji Qi, Mohan Singh, Anne Pigula, Neil T. Clancy, Daniel S. Elson, Imperial College London (United Kingdom)

Tissue polarimetry can provide additional information in terms of the polarisation properties such as depolarisation, diattenuation and retardance, which are sensitive to morphological, structural and compositional changes. These parameters can be extracted from Mueller matrices that fully characterise the polarisation response of a medium. The imaging of Mueller matrices has already shown potential in detecting cancerous tissue changes, although there have been few reports of endoscopic approaches in a wide-field imaging modality.

This talk reviews recent designs for rigid endoscopic narrow-band 3 ? 3 and 4 ? 4 Mueller matrix polarimetric imaging, as well as a new design that uses a stereo endoscope to record parallel and crossed polarization images under dual polarization illumination at video rate. The aim in each implementation is to adapt and modify conventional surgical hardware by adapting the polarization generator and analyser to allow all of the required polarisation states to be conveniently and rapidly cycled. Initial results consisting of test targets, ex vivo tissues and in vivo porcine abdominal organs show that these systems can distinguish superficial tissue structures based on their different polarisation properties, particularly vasculature and disruption to connective tissues.

9311-9, Session 2

Quantitative molecular receptor imaging is facilitated by arterial input function acquisition combined with kinetic modeling

Jonathan T. Elliott, Dartmouth College (United States); Kenneth M. Tichauer, Illinois Institute of Technology (United States); Scott C. Davis, Kimberley S. Samkoe, Jason R. Gunn, Dartmouth College (United States); David W. Roberts M.D., Dartmouth Hitchcock Medical Ctr. (United States); Keith D. Paulsen, Brian W. Pogue, Dartmouth College (United States)

Fluorescence guided surgery (FGS) designed to provide tissue contrast based on molecular cell-surface receptor expression, can be implemented to guide surgical resection. Simpler single-timepoint imaging approaches borrowed from preclinical research are being replaced by more sophisticated PET and SPECT-derived kinetic models. Combining these with widefield fluorescence imaging of targeted fluorophores, FGS can provide quantitative concentration images and hopefully improve sensitivity and specificity. Here we present an arterial input function (AIF) method to quantify binding potential in vivo, using a short acquisition time and a targeted/untargeted tracer pair with markedly different pharmacokinetics. These two innovations (AIF and dual-tracer imaging with different pharmacokinetics) are two factors which are particularly relevant to clinical

use. To test the approach, athymic mice (n = 5) were inoculated with human glioblastoma multiforme cells (U251; 10⁷ cells) and tumors were imaged using IRDye800 (LI-COR Biosciences) conjugated to anti-EGFR affibody (ABY029, Affibody Ab), a tracer undergoing preclinical testing for future GMP-based investigational use, and an untargeted IRDye800 (LI-COR) conjugated to negative control affibody. Extended Kety modeling was used to calculate kinetic parameters, including specific binding and non-specific retention. Binding potential for tumor was 0.98 ± 0.28 compared with 0.90 ± 0.20 calculated from ex vivo data in another group of mice. These were measured despite a 100-fold difference in fast pharmacokinetic clearance rate (-0.014/min for targeted vs. -1.4/min for untargeted), and only 20 minutes of imaging. AIF-driven techniques borrowed from nuclear medicine will dramatically improve in vivo fluorescence molecular imaging, especially as applied in FGS.

9311-10, Session 2

Quantitative fluorescence imaging enabled by spatial frequency domain imaging in the sub-diffusive regime for image-guided glioma resection

Mira Sibai, Univ. of Toronto (Canada) and Princess Margaret Cancer Ctr., Universal Health Network (Canada); Israel Veilleux, Princess Margaret Cancer Ctr., Universal Health Network (Canada); Michael Jermyn, Guillaume Sheehy, Audrey Laurence, Frédéric Leblond, Ecole Polytechnique de Montréal (Canada); Brian C. Wilson, Univ. of Toronto (Canada) and Princess Margaret Hospital, Univ. Health Network (Canada)

Intraoperative fluorescence guidance enables maximum safe resection of glioblastomas by providing surgeons with real-time tumor optical contrast. Specifically, 5-aminolevulinic acid (ALA)-induced Protoporphyrin IX (PpIX) fluorescence guided resection can improve surgical outcomes by better defining tumor margins and identifying satellite tumor foci. However, visual assessment of PpIX fluorescence is subjective and limited by the distorting effects of light attenuation and background tissue autofluorescence. We have previously shown, using a point fluorescence-reflectance fiber-optic probe, that non-invasive measurement of the absolute PpIX concentration, [PpIX], further improves sensitivity and specificity leading to the demonstration that the technique can also detect low-grade gliomas as well as otherwise undetectable residual tumor cells.

Here, we extend this approach to wide-field quantitative fluorescence imaging (qFI) by implementing Spatial Frequency Domain Imaging (SFDI) to recover the tissue optical absorption and transport scattering coefficients across the field of view. We report on the performance of this approach to determine [PpIX] in tissue-simulating phantoms with optical properties in both the fully diffusive (i.e. scatter-dominated) and sub-diffusive (low transport albedo) regimes. The use of high-frequency SFDI in the quantitative fluorescence light transport model is also evaluated. SFDI-enabled qFI is then demonstrated on optically-thick tissue slices ex vivo from intracranial glioma-tumor bearing rats after ALA administration, as a well-controlled intermediate stage towards evaluating the performance of the system in vivo. The estimated [PpIX] values are compared to those obtained from the point contact probe to determine the limits of accuracy of the wide-field technique

9311-11, Session 2

Tumor implantation model for rapid testing of lymphatic dye uptake from paw to node in small animals

Alisha V. DSouza, Jonathan T. Elliott, Jason R. Gunn,

**Conference 9311: Molecular-Guided Surgery:
Molecules, Devices, and Applications**

Thayer School of Engineering at Dartmouth (United States); Richard J. Barth M.D., Kimberley S. Samkoe, Geisel School of Medicine (United States); Kenneth M. Tichauer, Illinois Institute of Technology (United States); Brian W. Pogue, Thayer School of Engineering at Dartmouth (United States)

Surgical resection followed by pathological testing of lymph nodes is most commonly used to stage metastatic spread of cancer. Morbidity and complexity involved in a secondary surgery calls for staging techniques that are less invasive. While visible blue dyes are commonly used in locating sentinel lymph nodes, since they follow tumor-draining lymphatic vessels, they do not provide a metric to evaluate presence of cancer. An area of active research is to use fluorescent dyes to assess tumor burden of sentinel and secondary lymph nodes within and outside a surgical environment.

The goal of this work was to successfully use fluorescence properties of a clinically relevant blue dye, specifically methylene blue – used in the sentinel lymph node procedure – to quantitatively segregate tumor bearing from normal lymph nodes, using a planar fluorescence imaging system (Pearl Impulse, LI-COR Biosciences, Lincoln, NE). A direct-injection based tumor model was employed in 11 athymic rats (6 control animals), where luciferase-gene expressing-breast cancer cells were injected into axillary lymph nodes. Tumor presence in nodes was confirmed by bioluminescence imaging before and after fluorescence imaging. Lymphatic uptake from the injection site (intradermal on forepaw) to lymph nodes was imaged at frame rates of approximately 2per/minute. Large variability was observed within each cohort; however, when lymph vessel input fluorescence was used to account for heterogeneities in nodal uptake, heterogeneity in nodal fluorescence resulting from differences in delivery could be corrected. Following this correction, a significant difference ($p < 0.05$) was observed between normal and tumor bearing nodes owing to the differences in lymph system flow rate, owing to tumor-cell disruption of flow through the nodes.

9311-12, Session 2
Development of a spectrally-resolved near-infrared fluorescence imaging system based on a wavelength-swept laser

Jaedu Cho, Tiffany C. Kwong, Farouk Nouizi, Univ. of California, Irvine (United States); Chang-Seok Kim, Pusan National Univ. (Korea, Republic of); Gultekin Gulsen, Univ. of California, Irvine (United States)

Near-infrared fluorescence imaging (NIRF) is a very suitable tool for molecular-guided surgery that visualize distribution of molecular probes targeting specific diseases. Most of the current NIRF systems reveals only gray scale fluorescence intensity maps using a single wavelength light source, such that the spectral information of fluorescence emission is ignored during image processing. Liquid crystal based variable bandpass filters might be used at the detection site to achieve hyperspectral imaging but this method is a very expensive one. In this work, we propose a novel method for spectrally-resolved NIRF based on a wavelength-swept laser. The wavelength-swept laser is based on a fiber-optic extended cavity, a semiconductor optical amplifier, and a grating-based wavelength selector. It is centered at 800 nm with a swept-bandwidth of 40 nm. The measured laser output power at the center wavelength is 14 mW. This wavelength-swept laser is designed to excite indocyanine green (ICG), the only approved near-infrared fluorescence imaging agent for clinical applications by the U.S. Food and Drug Administration. Variations in the wavelength-dependent excitation cross section of the different fluorescent biomarkers gives rise to wavelength-dependent fluorescence intensity. This in turn, results in additional contrast between different biomarkers or the same biomarkers in different biological environment. In addition, we also investigate a robust spectrum decomposition method using the spectrum centroid and the spectrum flatness obtained from the wavelength-dependent fluorescence intensity measurement. In this work, we demonstrate spectrally-resolved NIRF images using tissue mimicking gelatin phantoms and ICG in different environments with the wavelength-swept laser based NIRF system.

9311-13, Session 3
Fluorescence image-guided surgery: from benchtop to bedside (Invited Paper)

Siavash Yazdanfar, Victoria E. Cotero, Tiberiu M. Siclovan, Dmitry V. Dylov, Cristina A. Tan Hehir, GE Global Research (United States)

Fluorescence image guided surgery (FIGS) improves intraoperative visualization of critical structures, with applications spanning neurology, cardiology and oncology. Over the last decade, FIGS has seen tremendous growth, with new contrast agents and instruments systematically advancing from benchtop to bedside. Clinical translation of FIGS requires the development of targeted contrast agents, coupled with instrumentation for intraoperative imaging. Our group has recently focused on the unmet clinical need to prevent iatrogenic nerve damage, a major cause of post-surgical morbidity, pain, and loss of function. This presentation will give an overview of our ongoing efforts to bring FIGS into the clinic, with particular emphasis on minimally invasive nerve sparing surgery.

9311-14, Session 3
Molecular-guided endoscopic mucosal resection of early neoplasia in Barrett's esophagus (Invited Paper)

Thomas D. Wang M.D., Univ. of Michigan (United States)

Endoscopic mucosal resection is a minimally-invasive therapy for early neoplasia in Barrett's esophagus. Clear identification of tumor margins in vivo is challenged by flat morphology and patchy distribution. We demonstrate a molecular-guided approach for performing resection on wide-field endoscopy with a fluorescently-labeled peptide-based imaging agent. We use registered fluorescence and reflectance to form ratio-based images that correct for differences in distance and geometry over the field-of-view to quantify intensities. The threshold that maximized variance between high and low intensities was used to form binary images. The contours around these regions were used to segment disease and guide therapy.

9311-15, Session 3
Light-weight, concomitant color and NIR fluorescence imaging system for molecular-guided minimal invasive interventions

Maximilian W. Koch, Technische Univ. München (Germany) and Helmholtz Zentrum München GmbH (Germany); Pilar Beatriz Garcia Allende, Vasilis Ntziachristos, Technische Univ. München (Germany)

Fluorescence molecular imaging methods have emerged as a promising alternative to aid clinical decision making in surgical oncology. Their advantage over visual and tactile inspection is that they provide functional and molecular information, and allow biomarker-based disease delineation and demarcation.

Targeted fluorescence imaging for intra-operative guidance needs to fulfill several requirements, particularly sufficient frame rate, resolution and a high sensitivity. In the case of minimally invasive interventions, light-weight and compactness are also demanded to make hand held or robotic force-resilient operation feasible. However, requirements for compact sizes and low weight inherently contradict demands on sensitivity, resolution and frame rate.

An imaging system that provides sufficient ergonomics while maintaining

Conference 9311: Molecular-Guided Surgery: Molecules, Devices, and Applications

highest fluorescence imaging performance is presented here. The system is based on an earlier presented concurrent video-rate color and NIR fluorescence laparoscopic system, adopted in a way that the fluorescence signal is relayed by a coherent fiber bundle to the highly sensitive EMCCD. The weight reduction of the laparoscope by uncoupling heavy components by a flexible link makes hand held or robotic operation feasible while sensitivity and resolution is maintained by combining of the spatial and temporal information from both, fluorescence and reflectance channels.

The proposed system supports the optimization of the fluorescence sensitivity by motion compensation. We show the feasibility to execute the proposed algorithms at low-latencies in video-rate using a GPU accelerated implementation. Furthermore we compare the proposed system and method against two reference designs, discuss applications and conclude on advantages and limitations.

9311-16, Session 3

Augmented microscopy with near infrared fluorescence detection

Jeff Watson, Nikolay Martirosyan, Jesse Skoch M.D., Michael Lemole Jr., Rein Anton M.D., Marek Romanowski, The Univ. of Arizona (United States)

Near-infrared (NIR) fluorescence has become a frequently used intraoperative technique for image-guided surgical interventions. In procedures such as cerebral angiography, surgeons use the optical surgical microscope for the color view of surgical field, and then switch to an electronic display for the NIR fluorescence images. However, the lack of stereoscopic, real-time, and on-site coregistration adds time and uncertainty to image-guided surgical procedures. To address these limitations, we developed the augmented microscope, whereby the electronically processed NIR fluorescence image is overlaid with the anatomical optical image in real-time within the optical path of the microscope. In vitro, the augmented microscope can detect and display indocyanine green (ICG) concentrations down to 94.5 nM, overlaid with the anatomical color image. We prepared polyacrylamide tissue phantoms with embedded polystyrene beads, yielding scattering properties similar to brain matter. In this model, 6.05 μ M solution of ICG was detectable up to depths of 2 mm. ICG angiography was then performed in anesthetized rats. A dynamic process of ICG distribution in the vascular system overlaid with anatomical color images was observed and recorded. In summary, the augmented microscope demonstrates superior NIR fluorescence detection with real-time coregistration displayed within the ocular of the stereomicroscope. In comparison to other techniques, the augmented microscope retains full stereoscopic vision and optical controls including magnification and focus, camera capture, and multiuser access. Augmented microscopy may find application in surgeries where the use of traditional microscopes can be enhanced by contrast agents and image guided delivery of therapeutics, including oncology, neurosurgery, and ophthalmology.

9311-17, Session 3

The combination design for open and endoscopic surgery using fluorescence molecular imaging technology

Yamin Mao, Institute of Automation (China); Shixin Jiang, Beijing Jiaotong Univ. (China); Jinzuo Ye, Institute of Automation (China); Yu An, Beijing Jiaotong Univ. (China); Chongwei Chi, Xin Yang, Jie Tian, Institute of Automation (China)

In clinical surgery, it is still a challenge to objectively determine tumor margins. With the development of medical imaging technology, fluorescence molecular imaging (FMI) method can provide intraoperative tumor margin information. For the aspect of clinical applications, surgical

navigation system plays an important role for precise tumor margin detection. However, limitation of detection depth exists in the FMI method. For clinical application aims, convenient switch from macro superficial detection to micro deep tissue detection is needed. In this study, we combined advantages of both open surgery and endoscopic imaging system with FMI technology. Our system shows great potential in the application of various tumor precision dissections.

There were two charge coupled device cameras (CCD) equipped in our system, one was used to collect near infrared (NIR) fluorescence images (ProEM 1024B Excelon EMCCD, Princeton Instrument, USA) with a fluorescence filter (wavelength 810nm-870nm), the other was used to collect white-light images (ace 2040-25gc, Basler, Germany) with a visible light filter (wavelength 400nm-650nm). Two cameras acquired images in the same region via a dual-channel connection part (DC2, Photometrics, USA). We used laser (MW-SGX-785, Changchun Lei Shi Optoelectronic Technology Co., Ltd., China) and halogen (KL2500LCD, SCHOTT, Germany) to provide light source. Furthermore, we used a C mount lens (Pentax TV LENS 12.5mm, f/1.4) for macro fluorescence imaging and endoscope lens (1F6C5X1, OLYMPUS, Japan) for deep tissue detection in the corner. For clinical applications, surgeons can flexible change lens on their demands.

Indocyanine green (ICG) experiments were performed to confirm the feasibility of fluorescence detection of our system. The 4mg ICG powder was dissolved in 1ml of phosphate buffer synonymous (PBS) solution. 100 μ l ICG solutions were added to the 96-well plate with a pipette. The serial ICG samples were prepared by 2 times the concentration gradient dilution with PBS ranging from 4mg/ml to 1.22 \times 10⁻⁴ mg/ml with a volume of 50 μ l. Then, the ICG signal was photographed in the detection area with our system. When the system connected with endoscope lens, the minimum quantity of ICG detected by our system was 3 μ g. For aspect of C mount lens, the sensitivity of ICG detection with our system was 48 μ g. The ICG experiments proved that it was feasible to detect fluorescence images with both lens and endoscopic lens which has higher sensitivity. Finally, we hope our system could supply a solution for various image-guided surgery applications during surgery.

9311-18, Session 4

Activatable fluorescence probes appropriate for assisting surgical and endoscopic procedures (*Invited Paper*)

Hisataka Kobayashi, National Cancer Institute (United States)

A unique aspect of optical imaging is that fluorescence probes can be designed to be activatable, i.e. only "turned on" under certain conditions. These probes can be designed to emit signal only after binding a target tissue, thus, dramatically improving the target-to-background ratio leading to increased sensitivity and specificity. There are two basic types of activatable fluorescence probes; 1) enzymatically activatable probes, which exist in the quenched state until activated by enzymatic cleavage, and 2) target-cell specific activatable probes, which are quenched until activated in targeted cells by lysosomal processing that follows cell binding and subsequent internalization. Designing probes based on their photochemical (e.g. activation strategy), pharmacological (e.g. biodistribution), and biological (e.g. target specificity) properties has allowed the rational design and synthesis of target-cell specific activatable fluorescence imaging probes which can be conjugated to a wide variety of targeting molecules. Given the wide range of photochemical mechanisms and properties, target-cell specific activatable probes possess considerable flexibility and can be adapted to real world needs for clinical practices. Herein, we summarize rational designs of activatable imaging probes by introducing practical preclinical and translational examples and demonstrate their potential clinical use.

**Conference 9311: Molecular-Guided Surgery:
Molecules, Devices, and Applications**

9311-19, Session 4

Clinical trials in near infrared fluorescence imaging with IRDye 800CW (Invited Paper)

Daniel R. Draney, LI-COR Biosciences (United States)

A monofunctional, heptamethine dye, IRDye® 800CW, is being manufactured under GMP conditions for use in human clinical trials. When attached to a suitable targeting agent and paired with an appropriate camera system, the dye allows Near Infrared (NIR) fluorescence imaging of tumor tissue during surgery. The talk will describe the properties of the dye and give an overview of current and planned clinical trials in Europe and the USA. The dye is available in both the NHS ester and carboxylate forms for conjugation to targeting molecules. A GMP toxicology study of the dye was described in a previous publication.

9311-20, Session 4

Improving fluorescent contrast for image-guided surgery (Invited Paper)

Summer L. Gibbs, Oregon Health & Science Univ. (United States)

Fluorescence image-guided surgery has the potential to significantly improve outcome for a variety of interventions, as it would provide surgeons with disease and tissue specific guidance. However, optimized tissue and disease specific contrast agents are of paramount importance. Substantial preclinical effort has been focused on the development of molecular imaging agents, but the hurdle to clinical translation has not often been overcome and few fluorophores are available for clinical use. My laboratory is focused on development of both tissue and disease specific fluorophores with current work on contrast for nerve tissue and pancreatic cancer. Although agents have already been developed for nerve tissue and various cancers, the main focus has been on systemically administered agents that will partition from the blood into the tissues of interest. Systemic administration often proves difficult to optimize for targeted agents and creates a significant barrier to clinical translation. To alleviate this difficulty, my lab is working on the development of agents for local and ex vivo administration facilitating rapid clinical translation. Specifically my laboratory is working on the development of fluorophores and delivery protocols to enable local administration during nerve-sparing prostatectomy where systemic administration would create excessive background in the innervated organ. We are also working on the development of molecularly targeted contrast agents for intraoperative margin assessment of pancreatic cancer in the operating room. Through this work we anticipate demonstrating the utility and feasibility of clinical translation of site-specific fluorophores for image-guided surgery.

9311-21, Session 4

Novel near-infrared imaging agents targeting prostate cancer

Xinning Wang, Brian Q. Tsui, Gopolakrishnan Ramamurthy, Case Western Reserve Univ. (United States); Warren D. W. Heston, The Cleveland Clinic (United States); James P. Basilion, Case Western Reserve Univ. (United States)

Prostate cancer is the most common noncutaneous malignancy affecting men in North America. Abundantly expressed in prostate cancer, prostate specific membrane antigen (PSMA) is an ideal target for the detection of prostate cancer. The purpose of this study was to develop PSMA-targeted near infrared optical imaging probes for the intraoperative visualization of prostate cancer. We synthesized a high affinity PSMA ligand (PSMA-1) with a low molecular weight, and further labeled it with IRDye800 or Cy5.5. PSMA-1 (IC50=2.30nM), PSMA-1-IR800 (IC50=1.57nM), and PSMA-

1-Cy5.5 (IC50=2.07nM) all showed better binding affinity) than the parent ligand Cys-CO-Glu (IC50=9.93nM). In vitro cellular uptake experiments demonstrated selective uptake of PSMA-1-IR800 and PSMA-1-Cy5.5 in PSMA-positive PC3pip cells but not in PSMA-negative PC3flu cells. In vivo experiments, both PSMA-1-IRDye800 and PSMA-1-Cy5.5 showed excellent binding selectivity to PC3pip tumors (both orthotopic and heterotopic implantations) with more than a 10-fold differential between PC3pip and PC3flu tumors. Interestingly, the two probes showed distinctively different pharmacokinetic behaviors. The amount of PSMA-1-IR800 reached its highest levels in PC3pip tumors at 4 hours post injection, clearing in 24-120 hours; however, it took PSMA-1-Cy5.5 24 hours to reach its highest amount in PC3pip tumors, and the amount remained virtually unchanged 5 days after administration. In summary, our data suggested that our PSMA-NIR probes have the ability to effectively distinguish among PSMA-expressing tumors, non-PSMA expressing tumors and other tissues. They have the potential to help in the diagnosis of prostate cancer. More importantly, they may also have the potential to aid standard prostatectomies.

9311-22, Session 4

Improved tumor identification using dual tracer molecular imaging in fluorescence guided brain surgery

Xiaochun Xu, Veronica Torres, Illinois Institute of Technology (United States); David Straus, Rush Univ. Medical Ctr. (United States); Eric M Brey, Illinois Institute of Technology (United States); Richard W. Byrne, Rush Univ. Medical Ctr. (United States); Kenneth M. Tichauer, Illinois Institute of Technology (United States)

Molecular imaging guided brain tumor resection is an emerging approach to distinguish the tumor from normal brain tissue that aims to leverage the up-regulation of specific cell-surface receptors, regarded as a sign of tumor presence. However, the relationship between imaging reporter uptake and targeted receptor concentrations is not necessarily correlated, particularly with respect to brain imaging, where variability in the level of blood-brain barrier disruption can substantially affect the identification of cancerous tissue. Dual-reporter methodologies, which use signal from an untargeted tracer to normalize the targeted tracer signal on a region-by-region basis, are capable of converting the complex signal information into receptor binding potential (BP), a parameter linearly correlated to receptor concentration. A dual-reporter method was explored in theoretical models and evaluated in a single time point in vivo mouse glioma study. Athymic mice were inoculated orthotopically with red fluorescence protein gene transfected U251 human glioma cells. At two weeks post-inoculation, 1 nmole each of an epidermal growth factor receptor (EGFR, a receptor over-expressed in many tumor cells) targeted tracer [anti-EGFR antibody (Abcam) conjugated with fluorescent Cy5 (GE Healthcare)] and an untargeted tracer [Fitc (Thermo Scientific)], were injected systemically. At 2 h post-inject, the brains were snap frozen, sliced and analyzed on a confocal microscope (Zeiss Axiovert 200M). Initial results demonstrate that tumor contrast-to-noise ratio was amplified by >6 times using the dual-tracer map of BP compared to single targeted tracer fluorescence alone. Using this method, BP can be plotted during surgery to help surgeon accurately evaluate the tumor margin.

9311-23, Session 5

Fluorescence molecular imaging heads for the clinics: benefits and pitfalls (Invited Paper)

Vasilis Ntziachristos, Technische Univ. München (Germany) and Helmholtz Zentrum (Germany)

The talk presents progress with clinical fluorescence molecular imaging

Conference 9311: Molecular-Guided Surgery: Molecules, Devices, and Applications

addressing aspects of agent clinical translation and camera accuracy. The importance of understanding camera performance to validate results coming from clinical trials is outlined. Developments in fluorescence endoscopy imaging are presented. Finally, the potential to use optoacoustic imaging to bring synergy to the clinical examination is discussed.

9311-24, Session 5

The current state of clinical translation of optical imaging agents (*Invited Paper*)

Jonathan M. Sorger, Intuitive Surgical, Inc. (United States)

The development of molecular imaging agents over the past few decades has been frustrating for those in academia as well as industry. While examples of FDA-approved optical and nuclear imaging agents do exist, the numerous compounds produced by academia coupled with investors' reticence to invest in a field with no great precedents for success has led to stagnation on the translational front. Historical perspective and current efforts at development will be reviewed.

9311-25, Session 5

A miniaturized imaging system for optical guided surgery of head and neck cancer

Ihab Atallah, CHU Grenoble (France); Clément Milet, maxime Henry, INSERM (France); Paul Dorval, Pascal Gayet, Philippe Rizo, Fluoptics (France); Emile Reyt, CHU Grenoble (France); Véronique Josserand, Amandine Hurbin, INSERM (France); Christian A. Righini, CHU Grenoble (France); Jean-Luc Coll, INSERM (France)

We developed an optimized animal model for orthotopic HNSCC with prolonged survival which allows efficacy and survival studies of novel medical or surgical treatments like near-infrared (NIR) optical imaging guided surgery. We used an original surgical technique for mice intraoral implantation of tumor fragments obtained from subcutaneous tumors of human HNSCC cell line. Resection of orthotopic tumors were performed 30 days after implantation without or with the aid of FluoStick™, a miniaturized clinical grade NIR optical imaging device adapted for mouth surgery, after systemic administration of Angiostamp™, a RGD-based probe that targets $\alpha_3\beta_3$ integrin expressed by solid tumors. Histological and immunohistochemical analyses were performed. All mice developed orthotopic tumors that could be left in situ for 30 days without any interference with mice well-being. In addition, all mice survived after tumor resection. NIR optical imaging guided surgery increased recurrence-free survival rate by 50% in our model through the detection of fluorescent cancer residues as small as 185 μm that could remain unidentified if resection was performed exclusively under visual guidance. This orthotopic model of human HNSCC allows efficacy, toxicity, and survival studies of novel medical or surgical treatments for HNSCC. This is currently, to our knowledge, the one that is closest to clinical practice. We also proved that NIR optical imaging guided surgery improves the quality of HNSCC resection in our model with a consequent positive impact on recurrence-free survival rate. This preclinical stage is essential before testing NIR optical imaging guided surgery in human HNSCC.

9311-26, Session 5

Ex-vivo tissue classification of cell surface receptor concentrations using kinetic modeling

Lagnojita Sinha, Illinois Institute of Technology (United States); Yu Wang, Stony Brook Univ. (United States) and

Univ. of Washington (United States); Cynthia S. Yang, Illinois Institute of Technology (United States); Altaz Khan, Jonathan T. C. Liu, Stony Brook Univ. (United States) and Univ. of Washington (United States); Kenneth M. Tichauer, Illinois Institute of Technology (United States)

One of the major challenges in the complete resection of cancer is the difficulty of distinctly classifying tumor and healthy tissue. This paper investigates the capability of competing kinetic modeling approaches for identifying different tissue types based on differential cell-surface receptor expressions. These approaches require fresh resected tissues to be stained with a mixture of two probes: one targeted to a cancer specific cell-surface receptor, and another left "untargeted" to account for nonspecific retention of the targeted agent, with subsequent repeated rinsing and imaging of the probe concentrations. Analysis of the results were carried out in simulations and in animal experiments for the cancer target, epidermal growth factor receptor (EGFR), a cell surface receptor overexpressed by many cancers. In the animal experiments, subcutaneous xenografts of human glioma (U251; moderate EGFR) and human epidermoid (A431; high EGFR) tumors, grown in six athymic mice, were excised and stained with EGFR targeted surface-enhanced Raman scattering (SERS NP) and untargeted SERS NP pair. The salient finding in this study was that significant non-specific retention was observed for the EGFR targeted probe [anti-EGFR antibody labeled with a surface-enhanced Raman scattering (SERS) nanoparticle], but could be corrected for by the equivalent non-specific retention of the untargeted probe (isotype control antibody labeled with a different SERS nanoparticle). Once this non-specific binding was accounted for, the kinetic model was able to predict the expected differences in EGFR concentration among different tissue types: healthy, U251, and A431 in accordance with an ex vivo flow cytometry analysis, successfully classifying different tissue types.

9311-27, Session 5

Small animal imaging platform for quantitative short wave infrared emitting contrast agents

Philip Hu, Marco Mingozzi, Laura M. Higgins, Vidya Ganapathy, Margot Zevon, Rutgers, The State Univ. of New Jersey (United States); Richard E Riman, Rutgers State Univ of New Jersey (United States); Charles M. Roth, Prabhav V. Moghe, Mark C. Pierce, Rutgers, The State Univ. of New Jersey (United States)

We report the design, calibration, and testing of a pre-clinical imaging system for capturing wide-field images of mice administered with short-wave infrared (SWIR) emitting contrast agents. Molecularly-targeted optical reporters including quantum dots, carbon nanotubes, and rare-earth doped nanocomposites may be advantageous over visible and near-infrared emitters due to reduced scattering in tissue, allowing for imaging of deeper targets. While VIS / NIR agents can be evaluated and optimized on commercially available small animal imagers equipped with silicon based sensors, SWIR-emitting agents require systems using alternative detectors with sensitivity in the 1-2 micron wavelength region.

Here, we use a collimated 980 nm laser beam, 8 mm in diameter, to excite rare-earth-doped nanocomposites administered via tail vein or intratumoral injection in a mouse model. Fluorescence in the 1550 nm wavelength region from these NaYF₄:Er,Yb materials is detected by a 640 x 512 pixel InGaAs area camera. Multiple individual images are captured as the excitation beam is raster scanned over a 12 cm x 6 cm area. Automated image reconstruction is performed in software to generate a composite fluorescence image of the entire animal. Background adjustment and intensity non-uniformity corrections are applied in software based on one-time calibration images. The final SWIR fluorescence image is overlaid onto a standard white-light image for registration of contrast agent uptake with respect to anatomical features. This platform is expected to accelerate pre-clinical evaluation and testing of new SWIR-emitting optical contrast agents in a range of disease-specific applications.

**Conference 9311: Molecular-Guided Surgery:
Molecules, Devices, and Applications**

9311-28, Session 6

Image guided surgery using near infrared fluorescent light: from bench to bedside
(Invited Paper)

 Leonora S Boogerd M.D., Henricus J Handgraaf M.D.,
Cornelis J van de Velde M.D., Alexander L. Vahrmeijer M.D.,
Leiden Univ. Medical Ctr. (Netherlands)

Despite many improvements in pre-operative imaging modalities, the surgeon still has to rely on visual inspection and palpation to determine what structures should be resected. As a consequence, it is not uncommon that the resection margins are not tumor free. Due to its relatively high tissue penetration, near-infrared (NIR) fluorescent light has the potential to visualize structures that need to be resected (e.g. tumors, lymph nodes) and structures that need to be spared (e.g. nerves, ureters, bile ducts). Our group has utilized various imaging systems including the Mini-FLARE™ to perform first-in-human clinical trials in a variety of human surgeries, with clinically available NIR fluorescent contrast agents (methylene blue and indocyanine green). To date, we have performed NIRF guided surgery in over 500 patients in more than 25 approved clinical trials. Trials were focused on NIR fluorescent sentinel lymph node mapping, where a tracer is injected around the tumor to detect the first draining lymph node for evaluation of lymph node metastases. Other trials were focused on tumor identification, including breast tumors and colorectal liver metastases. Moreover, trials to identify structures that need to be spared were performed (ureters and bile ducts). We will review the key results from these studies and from recent pre-clinical and clinical studies using tumor targeted contrast agents, discuss the advantages and limitations of the technology, and suggest various imaging system and contrast agent parameters that could be optimized in future trials. Moreover, a clear roadmap for clinical translation of targeted probes will be presented.

9311-29, Session 6

Sentinel lymph node detection in breast cancer patients using surgical navigation system based on fluorescence molecular imaging technology *(Invited Paper)*

Chongwei Chi, Institute of Automation (China); Deqiang Kou, The General Surgery Ctr., People's Liberation Army General Hospital (China); Jinzuo Ye, Yamin Mao, Institute of Automation (China); Jingdan Qiu, Jiandong Wang, The General Surgery Ctr., People's Liberation Army General Hospital (China); Xin Yang, Institute of Automation, China (China); Jie Tian, Institute of Automation (China)

Introduction: Precision and personalization treatments are expected to be effective methods for early stage cancer studies. Breast cancer is a major threat to women's health and sentinel lymph node biopsy (SLNB) is an effective method to realize precision and personalized treatment for axillary lymph node (ALN) negative patients. In this study, we developed a surgical navigation system (SNS) based on optical molecular imaging technology for the precise detection of the sentinel lymph node (SLN) in breast cancer patients. This approach helps surgeons in precise positioning during surgery.

Methods: The SNS was mainly based on the technology of optical molecular imaging. A novel optical path has been designed in our hardware system and a feature-matching algorithm has been devised to achieve rapid fluorescence and color image registration fusion. Ten *in vivo* studies of SLN detection in rabbits using indocyanine green (ICG) and blue dye were executed for system evaluation and 8 breast cancer patients accepted the combination method for therapy.

Results: The detection rate of the combination method was 100% and an average of 2.6 SLNs was found in all patients. Our results showed that

the method of using SNS to detect SLN has the potential to promote its application.

Conclusion: The advantage of this system is the real-time tracing of lymph flow in a one-step procedure. The results demonstrated the feasibility of the system for providing accurate location and reliable treatment for surgeons. Our approach delivers valuable information and facilitates more detailed exploration for image-guided surgery research.

9311-30, Session 6

Clinical applications of fluorescence imaging for enhancing safety and therapeutic efficacy of hepatobiliary and pancreatic surgery

Takeaki Ishizawa M.D., The Univ. of Tokyo (Japan) and Cancer Institute Ariake Hospital, Japanese Foundation for Cancer Research (Japan); Yasuteru Urano, Mako Kamiya, Akinori Miyata, Suguru Yamashita M.D., The Univ. of Tokyo (Japan); Yosuke Inoue, Junichi Arita, Yu Takahashi, Akio Saiura, Cancer Institute Ariake Hospital, Japanese Foundation for Cancer Research (Japan); Norihiro Kokudo M.D., The Univ. of Tokyo (Japan)

Background: Recently, fluorescence imaging using indocyanine green (ICG) has been applied to intraoperative visualization of the bile ducts (fluorescence cholangiography) and hepatic malignancies. A chymotrypsin-activated fluorescence probe is newly developed for identification of pancreatic leak during pancreatic resection.

Methods and Results: 1) Fluorescence cholangiography: Fluorescence images of the extrahepatic bile ducts can be obtained by intrabiliary injection of ICG solution (0.025 mg/mL) or preoperative intravenous injection of ICG (2.5 mg). The latter technique is beginning to be used widely for confirmation of the bile duct anatomy during laparoscopic cholecystectomy. 2) Identification of hepatic malignancies: Intraoperative fluorescence imaging enables identification of small tumors on liver surfaces during open and laparoscopic hepatectomy, through visualization of ICG retained in hepatocellular carcinoma tissues and in non-cancerous hepatic parenchyma around liver metastasis, following preoperative intravenous injection at a dose of 0.5 mg/kg for liver function test. Photoacoustic imaging has the potential to visualize the intrahepatic distribution of ICG in and around cancerous tissues on intraoperative ultrasound images. 3) Visualization of pancreatic leak: In a swine model, fluorescence imaging following spraying the chymotrypsin-activated probe (glutaryl-phenylalanine hydroxymethyl rhodamine green with added trypsin) enables visualization of pancreatic juice leaking from the pancreatic stump. A preclinical animal study is being conducted to confirm safety in spraying the chymotrypsin probe in the patient's abdominal cavity.

Conclusions: *In vivo* fluorescence imaging is helpful for surgeons to identify biological structures in real time during surgery, enhancing safety and efficacy of surgical treatments for hepatobiliary and pancreatic diseases.

9311-31, Session 6

Intraoperative imaging of tumors with indo-cyanine green fluorescence with an endoscope

Ashwin B. Parthasarathy, Sang Hoon Chong, Univ. of Pennsylvania (United States); Frank A. Moscatelli, Swarthmore College (United States); Sunil Singhal, Hospital of the Univ. of Pennsylvania (United States); Arjun G. Yodh, Univ. of Pennsylvania (United States)

Conference 9311: Molecular-Guided Surgery: Molecules, Devices, and Applications

Surgery is the most effective treatment strategy for solid tumors. Intraoperative imaging of tumors helps detect tumor margins and establish the most appropriate surgical margins. Endoscopic surgery is a standard of care procedure for the resection of tumors, and is applicable for a wide range of solid tumors. While several imaging methodologies can be used for intraoperative imaging, optical imaging is promising for clinical application because it can detect microscopic disease, is minimally invasive, is inexpensive, does not require advance training for surgeons and can provide real-time images. Fluorescence from an injected contrast agent (Indo-cyanine green, ICG) has been effectively used for the identification of tumors in humans. In this study, we adapt a commercially available endoscope for intraoperative imaging of solid tumors. Our instrument utilizes light from a near-infrared 785nm laser to illuminate the surgical field of view and two CCD cameras for imaging the reflected fluorescence as well as the background tissue. We show that our instrument can simultaneously image fluorescence from the tumor as well as the background tissue. We characterize our instrument in tissue simulating phantoms, with tumor simulating 'targets'. We also present images from a pilot in vivo study. ICG was systematically injected into cancer patients, and the endoscope system was used to image the surgical site before, during and after surgery.

9311-32, Session 6

Quantitative assessment of the potential for Cerenkov luminescence imaging guided oncologic surgery

Justin S. Klein, Gregory S. Mitchell, Simon R. Cherry, Univ. of California, Davis (United States)

Radioguided surgery uses a radiotracer and a radiation-detecting wand which is coarsely swept over the surgical site to locate the tumor. Minimal spatial information is provided by this technique, making it challenging to distinguish tumor from background. Cerenkov luminescence (CL) is an optical signal produced by many radiotracers and can be imaged, potentially providing enhanced tumor demarcation and improved surgical outcomes.

To assess potential advantages of CL-guided surgery, Monte Carlo was used to model the generation and transport of all radiation (beta particle, gamma rays, optical) emitted by fluorine-18 from a tumor in a surgical geometry. 18F-fluorodeoxyglucose, a widely used radiotracer that has high uptake in many tumors was simulated with a 3:1 tumor to background ratio at depths ranging from 0.001 to 10 mm in tissue.

The maximum depth at which the contrast-to-noise ratio is sufficient to distinguish the tumor from surrounding tissue was determined. For a scenario with a typical radiotracer concentration of 5 MBq/kg tissue, a 5 mm tumor and 1 second integration time, beta particle detection is most sensitive at depths <0.3 mm. CL is most sensitive at depths between 0.3 mm and 2 mm, depending on tissue type. At depths >2 mm gamma detection is most sensitive. For smaller tumors (<2 mm), CL is more sensitive than gamma detection over a wider depth range owing to the penetrating gamma background.

Cerenkov luminescence imaging is a promising modality for radioguided surgery, and may offer superior sensitivity when tumors are small and depths a few mm.

9311-33, Session PSun

A miniature wearable optical imaging system for guiding surgeries

Christopher Mela, Carrie Patterson, Yang Liu, The Univ. of Akron (United States)

Surgical medicine faces many great challenges due to the difficulty in capturing and presenting intraoperative imaging data. To date, the intraoperative ultrasound scanner has been used as the clinical modality of choice for many surgical applications. However, ultrasound suffers

from a small field of view and low signal to noise ratio. Furthermore, the requirement of surface contact makes ultrasound difficult to apply in many cases. Other intraoperative modalities include intraoperative MRI and CT. MRI and CT do not offer real time imaging capacity, and they can be costly. To overcome these problems, we developed a new compact wearable imaging system that can provide disease information in real time based on optical signatures. The large field of view and the ability to interrogate the functional status of tissues are highly desirable, and could potentially complement existing clinical modalities for guiding surgeries. The data is presented in the wearable display in real time, which can be potentially integrated with clinical workflow with ease. We have characterized the new system and conducted the proof-of-concept studies ex vivo. Our preliminary data has shown that it is a promising candidate for guiding various surgical operations.

9311-34, Session PSun

Fluorescently labeled small molecules for pancreatic adenocarcinoma surgical margin assessment in the operating room

Dianmu Zhang, Emily Schultz, Summer L. Gibbs, Oregon Health & Science Univ. (United States)

With a 5-year survival rate of just over 5%, pancreatic adenocarcinoma (PDAC) remains one of the most lethal cancers. The only curative therapy for PDAC is surgery where success rate is directly related to margin status, and incomplete resections are considered palliative at best. Unfortunately, complete surgical resection with negative margins is a difficult task and 15-85% of patients are left with residual disease. Fluorescence imaging has the potential to improve intraoperative margin assessment, but targeted contrast for PDAC does not exist. In the current work, fluorescent derivatives of the epidermal growth factor receptor (EGFR) tyrosine kinase inhibitors (TKIs) Erlotinib and its analog PD153035 were synthesized for ex vivo margin characterization on resected pancreas tissue. EGFR binding affinity was assessed for the small molecule fluorophore conjugates with varied fluorophore position around the EGFR TKIs as well as by adding varied length chemical spacers to Erlotinib and PD153035 prior to fluorophore conjugation. In vitro competitive binding assays were performed to determine the uptake of the modified small molecules in comparison to unmodified Erlotinib and PD153035. Although assessment of margin status ex vivo will enable rapid translation to the clinic, non-specific tissue uptake confounds cancer-specific fluorescence. To differentiate between EGFR cancer specific uptake and non-specific tissue uptake, spectrally distinct fluorescent derivatives were synthesized with and without the fluorophore conjugated at the protein-binding site, enabling ratiometric imaging. The specificity of the small molecule fluorophores to differentiate normal pancreas from PDAC were assessed using resected pancreas tissue from Whipple procedures.

9311-35, Session PSun

Local administration of nerve-specific fluorophores to guide nerve-sparing radical prostatectomy

Kayla M. Hackman, Brandon Lei, Oregon Health & Science Univ. (United States); Adam Alani, Oregon State Univ. (United States); Summer L. Gibbs, Oregon Health & Science Univ. (United States)

Prostate cancer cure is the primary goal of radical prostatectomy, however preserving the nerve structures responsible for continence and potency are vital for maintained quality of life. Although the first paper on the nerve-sparing surgical technique was published over 30 years ago, nerve damage following radical prostatectomy continues to plague surgical treatment and is reported in some form in up to 60% of patients one to two

Conference 9311: Molecular-Guided Surgery: Molecules, Devices, and Applications

years post surgery. Surprisingly, no method exists to enhance direct nerve visualization in the surgical suite, and nerve detection is completed through a combination of palpation and visualization when possible. Importantly, a few classes of fluorescent small molecules have recently been demonstrated to have nerve specificity following systemic administration including the distyrylbenzenes (DSB), certain oxazines (oxazine 4 perchlorate), and particular cyanines (3,3'-diethylthiatricarbocyanine iodine). However, the prostate is a highly innervated organ, where direct labeling of the cavernous nerve and neurovascular bundle (NVB) would provide significantly improved imaging contrast by comparison to systemically labeling all nerve structures in the gland. In the current work, a local administration procedure was optimized for application of each class of nerve-specific fluorophores during nerve-sparing prostatectomy. Micelle encapsulation was utilized to deliver these lipophilic fluorophores topically and through installation in the isolated tissue pedicle. Tissue washing procedures were optimized to enhance nerve signal to background ratio in rodent nerve models. These promising results will be translated to swine prostate models enabling imaging of the cavernous nerve and NVB using the optimized local administration procedure.

9311-36, Session PSun

Activity and pharmacokinetics testing of anti-EGFR Affibody linked to IRDye 800CW maleimide

Jason R. Gunn, Thayer School of Engineering at Dartmouth (United States); Brian W. Pogue, Thayer School of Engineering at Dartmouth (United States); Alisha V. Dsouza, Johnathan T. Elliott, Thayer School of Engineering at Dartmouth (United States); Kimberley S. Samkoe, Dartmouth Hitchcock Medical Ctr. (United States); Keith D. Paulsen, Thayer School of Engineering at Dartmouth (United States); Daniel R. Draney, LI-COR Biosciences (United States); Joachim Feldwisch, Affibody AB (Sweden)

A new production of anti-EGFR Affibody molecules was produced through peptide synthesis, and bound to IRDye 800CW through maleimide reaction. The completed test batch of this molecule, named ABY-029, was tested for solubility, affinity to human and rat EGFR, as well as evaluation of the in vivo pharmacokinetics. ABY-029 appeared soluble in DMSO and water, with less solubility in methanol. The binding efficiency was consistent with commercially available Affibody molecule. The pharmacokinetics were examined through whole body fluorescent imaging of mice injected IV, with continuous imaging for up to 1 hour of the carotid artery and internal organs. The plasma clearance lifetime was on the order of a few hours, while the tumor uptake appeared to saturate after about 1 hour of imaging. The primary clearance organs appeared to be both liver and kidney.

9311-37, Session PSun

Fiber optic quantification of dual-fluorophores to provide both tissue and vascular contrast during resection of brain tumors

Jaime Bravo, Stephen C. Kanick, Thayer School of Engineering at Dartmouth (United States); Pablo A. Valdes Quevedo M.D., Brigham and Women's Hospital (United States); David W. Roberts M.D., Dartmouth Hitchcock Medical Ctr. (United States); Keith D. Paulsen, Thayer School of Engineering at Dartmouth (United States)

Fluorescence-guided neurosurgery is a technique that utilizes targeted

fluorescent molecules to distinguish between normal and cancerous tissue. One fluorophore of interest is protoporphyrin IX (PpIX), which is known to accumulate in high-grade gliomas in high enough concentrations for visual detection under blue light. However, interpretation of fluorescence emission is complicated because remission intensity is dependent on PpIX concentration and attenuation due to background absorption and scattering properties of the tissue. Recent work in this field has led to the development of fiberoptic probe techniques that return quantitative PpIX fluorescence in localized tissue volumes, which are independent of the distortive effects of absorption and scattering; this approach has shown increased diagnostic sensitivity in vivo. The current study aims to develop a more-generalized correction algorithm that is applicable not only for PpIX (i.e. where absorption >> scattering at the excitation wavelength), but for light transport characteristics where scatter dominates, as in the 500-800 nm region. This algorithm is applied to the measurement of fluorescein, a marker commonly used to visualize vasculature within tissue. This study will present quantitative measurements of fluorescein in tissue simulating phantoms composed of Intralipid and whole blood to mimic a range of background optical properties commonly found in tissue [$\mu_a = 0-60 \text{ cm}^{-1}$, $\mu_s = 10-50 \text{ cm}^{-1}$]. These results motivate the use of quantitative optical spectroscopy to sample dual-fluorophores within a localized tissue volume. Ongoing translation of this approach may provide increased diagnostic sensitivity to tumors by providing markers of both cellular metabolism (PpIX) and vascular distribution (fluorescein).

9311-43, Session PSun

Radiometric configuration parameters to consider in quantitative clinical fluorescence imaging measurements

Maritoni Litorja, Aaron Urbas, National Institute of Standards and Technology (United States)

The quantitative determination of the fluorescent light detected by a clinical imager is generally understood to be correlated to the amount of fluorescent substance being measured. There are many contributors to the light measurement uncertainty namely the instrumentation, the scene being viewed, the sample being investigated and the model used to analyze the data. This is a challenging field radiometric measurement since the imager is moveable, but keeping a radiometric calibration is feasible if aperture sizes, sample-detector distance and optic axis are tracked during its clinical use. Here we discuss the effects of radiometric configuration as a contributor to the measurement uncertainty and the possible use of a standard reference material as intrascene calibrator to facilitate reproducible fluorescence measurements across instruments.

Conference 9312: Optical Coherence Tomography and Coherence Domain Optical Methods in Biomedicine XIX

Monday - Wednesday 9-11 February 2015

Part of Proceedings of SPIE Vol. 9312 Optical Coherence Tomography and Coherence Domain Optical Methods in Biomedicine XIX

9312-85, Session PSun

Lighting, edge, and depth enhanced ray casting for real-time volumetric visualization of intraoperative ophthalmic OCT

Christian Viehland, Oscar Carrasco-Zevallos, Brenton Keller, Derek Nankivil, Joseph A. Izatt, Duke Univ. (United States)

Optical coherence tomography allows rapid imaging of the human retina and cornea providing dynamic axial visualization of surgical maneuvers. Current research and commercial intrasurgical OCT prototypes are limited to acquiring B-scans in real time. We have developed a swept-source OCT based intrasurgical OCT which is capable of real time volumetric intrasurgical imaging. Current-generation GPU enhanced rendering software based on simple ray casting results in volume visualizations with sub-optimal depth perception of volumetric features. Post processed rendering using commercial software provide much clearer volume visualization, but cannot be used interactively during surgery. We report on the development of an enhanced, real time, integrated volumetric rendering engine for OCT data. We incorporate high performance volumetric median and Gaussian filtering, boundary and feature enhancement, depth encoding, and lighting into a ray casting volume rendering model. We developed a CUDA implementation of this enhanced ray casting model that can generate real time dynamic renders that mimic the quality of those produced in commercial post-processing software. We demonstrate this improved model on data from tissue phantom and live human surgeries showing improved depth perception and visualization of volumetric features.

9312-86, Session PSun

Simultaneous optical coherence tomography and lipofuscin autofluorescence imaging of the retina with a single broadband light source at 480nm

Minshan Jiang, Tan Liu, Xiaojing Liu, Shuliang Jiao, Florida International Univ. (United States)

We accomplished simultaneous spectral domain optical coherence tomography (SD-OCT) and auto-fluorescence (AF) microscopy with a single broadband light source centered at 480 nm for imaging the retina in vivo. The two imaging modalities share the same probing light, which was scanned and delivered to the retina with the same optics used in conventional OCT. The light reflected from the retina was detected by an interferometer in the spectral-domain for OCT imaging. In the same time, the AF signal generated from fluorophores in the retina was separated from the reflected light, filtered by a long-pass filter, and then detected with a photomultiplier tube (PMT). With a bandwidth of 20 nm the visible light OCT achieved a calibrated depth resolution of 5.8 nm in air. Since the two imaging modalities are provided by the same group of photons, the images are intrinsically registered. The wavelength was selected to provide both structural OCT imaging and molecular contrast for lipofuscin imaging. Lipofuscin is one of the major pigments in the retinal pigment epithelium (RPE) cells, the accumulation of which is a hallmark of aging of the retina. By imaging the same rat retina in vivo at different ages we have successfully tested the system on monitoring the accumulation of lipofuscin with aging.

The experimental results showed that our system can be a potentially powerful tool in clinical study of age-related degenerative retinal diseases.

9312-87, Session PSun

Dual-band spectral-domain OCT at 480nm and 830 nm for in vivo imaging the spectral contrasts of the retinal nerve fiber layer

Minshan Jiang, Tan Liu, Xiaojing Liu, Shuliang Jiao, Florida International Univ. (United States)

Studies using a rat model of glaucoma have shown that the optical reflectance of the damaged RNFL at short wavelength (<500nm) is reduced much more than that at longer wavelength, which provides spectral contrast for imaging the earliest damage to the RNFL. To image the spectral contrast we built a dual-band SD-OCT centered at 830nm (NIR) and 480nm (VIS). The light source for the NIR OCT is a SLD. The light source for the VIS OCT is a supercontinuum laser. The calibrated depth resolutions of the NIR-OCT and VIS-OCT systems are 6.0 μ m and 5.8 μ m in the air, respectively. The system was applied to imaging the rat retina in vivo. As the VIS-OCT and NIR-OCT images were acquired simultaneously, the two images are spatially registered. By segmenting the boundaries of the RNFL layer manually in both the VIS and NIR OCT images and summing the signals from the RNFL, the ratio of the light reflected from the RNFL of the two bands can be calculated. We applied the system in imaging a rat model of glaucoma. Compared to the control eyes, the treated eyes have a lower VIS to NIR RNFL reflection ratio, which is consistent with previous ex vivo studies. These preliminary results demonstrated that the dual-band OCT system is feasible for imaging the spectral contrast of the RNFL.

9312-88, Session PSun

Enhancing the visualization of human retina vascular networks by GPU accelerated speckle variance OCT and graph cut retinal layer segmentation

Jing Xu, Kevin S. K. Wong, Vincent Wong, Sieun Lee, Eunice Michelle C. Cua, Yifan Jian, Marinko V. Sarunic, Simon Fraser Univ. (Canada)

We report on a GPU-accelerated 2D Graph Cut (GC) segmentation approach to delineate the layers in human retinal volumetric OCT data. In addition to measuring retinal thickness, this algorithm was applied on datasets acquired for speckle variance Optical Coherence Tomography (svOCT) in order to enhance the real-time visualization of the retinal vascular networks. The svOCT is a valuable asset in clinical ophthalmic diagnosis, providing not only structural volumetric information such as retinal thickness, but also the functional information of the retina such as blood flow. The addition of automated segmentation can restrict the results to the relevant region of interest, making the results more suitable for clinical analysis. However, the Graph Cut segmentation algorithm is a computationally expensive task that is commonly implemented in post-processing. In order to mitigate this bottleneck such that the entire processing pipeline (FD-OCT, motion correction, segmentation, and speckle variance) is executed in a similar amount of time as the acquisition of a single volume (a few seconds), we implemented a GPU-accelerated GC segmentation algorithm using the CUDA NPP library. This approach was implemented to segment the

Conference 9312: Optical Coherence Tomography and Coherence Domain Optical Methods in Biomedicine XIX

inner limiting membrane and the Bruch's membrane/retinal pigmented epithelium layers of the human retina, and was capable of doing so even with large motion artifacts. In this report, we compare the results generated by our 2D GPU GC implementation with previously reported results using 3D GC segmentation algorithm implemented in Matlab. Furthermore, we demonstrate the 2D GPU GC application for enhancing real-time visualization of the human retinal vascular networks.

9312-89, Session PSun

Progress on developing wavefront sensorless adaptive optics optical coherence tomography for in vivo retinal imaging in mice

Azhar Zam, Pengfei Zhang, Univ. of California, Davis (United States); Yifan Jian, Marinko V. Sarunic, Simon Fraser Univ. (Canada); Stefano Bonora, CNR-Istituto di Fotonica e Nanotecnologie (Italy); Edward N. Pugh Jr., Robert J. Zawadzki, Univ. of California, Davis (United States)

Most AO systems require the use of a wavefront sensor to measure wavefront error. However, this generates several constraints that restrict the imaging system design. In an effort to overcome these limitations, as previously reported, we are developing a WSAO-OCT system for in vivo imaging of the mouse retinas. The elimination of the wavefront sensor allows the application of refractive optics that greatly simplifies the system design and alignment. Our previous designs implemented a refraction-cancelling contact lens which allowed easy control of the focus, but limited the usable pupil size and imaging Field of View (FOV) of the instrument. The novel implementation of a WSAO OCT system presented here builds the previous work, but further simplifies the optical design, including elimination of long focal length scanning optics and optical conjugation of vertical and horizontal scanners. This modification provides a large FOV for retinal screening (25 degree VA), while permitting an area of interest to be selected for "zoomed-in", high resolution aberration-corrected imaging. Additionally in the present system no refraction-canceling contact lens is used, and defocus (axial focus position) is controlled by collimation of the OCT sample arm entrance beam.

9312-90, Session PSun

A wide angle low coherence interferometry based eye length optometer

Alexander Meadway, John T. Seigwart, The Univ. of Alabama at Birmingham (United States); Christine F. Wildsoet, Univ. of California, Berkeley (United States); Thomas T. Norton, Yuhua Zhang, The Univ. of Alabama at Birmingham (United States)

Interest in eye growth regulation has burgeoned with the rise in myopia prevalence world-wide. Eye length and eye shape are fundamental metrics for related research, although current in-vivo measurement techniques are generally uni-dimensional, limited to the optical axis of the eye. We describe a high resolution, time domain low coherence interferometry based optometer for measuring the eye length of small mammals over a 2 dimensional field. The system is based upon a Michelson interferometer. It uses a superluminescent diode as a source. The light from the source is split into the sample arm and the reference arm. The sample arm is further split into two paths by a polarisation beam splitter; one focuses the light on the cornea and the other focuses the light on the retina. This method has a high efficiency of detection for reflections from both surfaces. The reference arm contains a custom high speed linear motor with 25 mm stroke and equipped

with a precision displacement encoder. Light reflected from the cornea and the retina are combined with the reference beam and low coherence interferograms are generated. Two galvo scanners are employed to deflect the light to different angles so that the eye length over a field of view of 20° x 20° can be measured. The system has a theoretical resolution of 4.5 μm and the motor provides accurate movement, allowing for precise and repeatable measurement of coherence peak positions. Example scans from a living tree shrew are presented.

9312-91, Session PSun

Fourier domain optical coherence tomography artifact and speckle reduction with autoregressive (AR) spectral estimation without a loss of resolution

Evgenia Bousi, Costas Pitris, Univ. of Cyprus (Cyprus)

Fourier Domain (FD) Optical Coherence Tomography (OCT) interferograms require a Fourier transformation in order to be converted to A-Scans representing the backscattering intensity from the different depths of the tissue microstructure. Most often, this transformation is performed using a discrete Fourier transform, i.e. the well-known Fast Fourier Transform (FFT). However, there are many alternatives for performing the necessary spectral conversion. Autoregressive (AR) spectral estimation techniques are one such example. The parametric nature of AR techniques offers several advantages, compared to the commonly-used FFT, including faster convergence and less susceptibility to noise. They can also be adjusted to represent more or less of the signal's detail depending on the order of the autoregression. These features make them uniquely suited for processing the FD OCT data. The advantages of the proposed methodology are illustrated on in vivo skin imaging data and the resolution is verified on single back-reflections from a glass surface. AR spectral estimation can be used to convert the interferograms to A-Scans while at the same time reducing the artifacts caused by high intensity back-reflections (~20 dB reduction) and diminishing the speckle (~12 dB reduction) all without the degradation in the resolution associated with other techniques.

9312-92, Session PSun

Generic frequency-domain method for ultrafast and robust characterization of optical attenuation from OCT images

Wu Yuan, Johns Hopkins Univ. (United States); Carmen Kut, The Johns Hopkins Hospital (United States); Wenxuan Liang, Xingde Li, Johns Hopkins Univ. (United States)

We developed a new frequency-domain algorithm with high computational efficiency and accuracy to enable ultrafast characterization of optical attenuation from OCT images. Real-time attenuation imaging has been demonstrated for both phantom and brain tumor tissues with a 1300 nm sweep-source OCT (SS-OCT) system. Combined with a GPU implementation, this algorithm can be applied to real-time high-speed OCT attenuation imaging with a processing speed over 1,500 k A-scans/sec.

9312-93, Session PSun

CloudOCT: An online data- and code-sharing platform to accelerate research progress

Kristen L. Lurie, Behram F. T. Mistree, Audrey K. Ellerbee, Stanford Univ. (United States)

Conference 9312: Optical Coherence Tomography and Coherence Domain Optical Methods in Biomedicine XIX

In light of the broad success and maturity of OCT technology, we believe the OCT research community and the constituents it serves would benefit greatly from a strong practice of sharing. Informed by our own experiences and discussions with colleagues, we have developed CloudOCT, a new web-based platform to facilitate sharing of code and data. One unique aspect of this platform, compared to those developed by other communities, is the strong notion of privacy and ownership of code and data that we have incorporated into it. These facets are extremely important given the time investment required to develop code or acquire data and potential concerns about sharing them due to the publish-or-perish environment of academic research, the need to exercise caution when using medical data constrained by HIPAA and IRB regulations, and recent changes to U.S. patent law even amongst growing entrepreneurial interest within universities. Deployed on Amazon's commodity cloud infrastructure, CloudOCT has been tested with up to 10 simultaneous users and architected to both handle failure and scale to many more users. A beta version of the site for a limited number of users (~25) and full public release will be announced soon. We believe that CloudOCT can play a central role in accelerating research progress in OCT, increasing the ability to benchmark software and algorithms, providing access to broader datasets to better generalize methodologies, and improving the ability to collaborate across research groups.

9312-94, Session PSun

Lateral resolution enhancement via imbricated spectral domain optical coherence tomography in a maximum-a-posterior reconstruction framework

Ameneh Boroomand, Mohammad Javad Shafiee, Alexander Wong, Kostadinka Bizheva, Univ. of Waterloo (Canada)

The lateral resolution of a Spectral Domain Optical Coherence Tomography (SD-OCT) image is limited by the focusing properties of the imaging optics of OCT system, the wavelength range which SD-OCT system operates at, spherical and chromatic aberrations induced by the imaging optics and the optical properties of the imaged object, and in the special case of in-vivo retinal imaging by the optics of the eye. This limitation often results in challenges with resolving fine details and structures of the imaged sample outside of the Depth-Of-Focus (DOF) range. Here, we propose a novel technique for generating Laterally Resolved OCT (LR-OCT) images using OCT measurements acquired with intentional imbrications. We design our proposed method within a Maximum A Posteriori (MAP) reconstruction framework which takes advantage of a Stochastic Fully Connected Conditional Random Field (SFCRF) model to compensate for the artifacts and noise when reconstructing a LR-OCT image from imbricated OCT measurement. The proposed lateral resolution enhancement method was tested on synthetic OCT measurement as well as human cornea SD-OCT image to evaluate the usefulness of the proposed approach in lateral resolution enhancement. Experimental results show that applying this method noticeably improved the sharpness of morphological features in the OCT image and in lateral direction, thus demonstrating better delineation of fine dot shape details in the synthetic OCT test as well as better delineation of the keratocyte cells in human corneal OCT test.

9312-95, Session PSun

Axial resolution improvement in spectral domain optical coherence tomography using a depth-adaptive maximum-a-posterior framework

Ameneh Boroomand, Bingyao Tan, Alexander Wong, Kostadinka Bizheva, Univ. of Waterloo (Canada)

The axial resolution of Spectral Domain Optical Coherence Tomography

(SD-OCT) images degrades with scanning depth due to limited pixel number and pixel size of the camera, aberrations in the spectrometer optics and wavelength dependent scattering and absorption in the imaged object. Here we propose a novel algorithm which compensates for the blurring effect of the depth-dependent axial Point Spread Function (PSF) on SD-OCT images. We designed the proposed method in a Maximum A Posteriori (MAP) reconstruction framework which takes advantage of a Stochastic Fully Connected Conditional Random Field (SFCRF) model. The aim is to compensate for the depth-dependent axial blur in SD-OCT images and simultaneously suppress the speckle noise which is inherent to all OCT images. Applying the proposed depth-dependent axial resolution enhancement technique to an OCT image of cucumber considerably improved the axial resolution of the image especially at higher imaging depths and allowed for better visualization of cellular membrane and nuclei. Comparing the result of our proposed method with the conventional Lucy-Richardson deconvolution algorithm clearly demonstrates the efficiency of our proposed technique in better visualization and preservation of fine details and structures of the imaged sample as well as better speckle noise suppression. This illustrates the potential power of our proposed technique as a suitable replacement for the hardware approaches which are often very costly and complicated.

9312-96, Session PSun

Signal simulation and signal processing for multiple reference optical coherence tomography

Kai Neuhaus, Hrebesh Molly Subhash, Roshan I. Dsouza, National Univ. of Ireland, Galway (Ireland); Josh Hogan, Carol J. Wilson, Compact Imaging, Inc. (United States); Martin J. Leahy, National Univ. of Ireland, Galway (Ireland)

The new approach of multiple reference optical coherence tomography (MR-OCT) enhances the capabilities of ordinary time domain OCT (TD-OCT) by adding a partial mirror into the reference arm of the interferometer. The partial mirror causes multiple reflections in the reference arm and introduces a path delay for each additional reflection (or order) thereby increasing the total depth scanning range. The virtual scanning range of each order also increases which increases the frequencies of the resulting interference signals of each of the orders. The resultant signal is a sum of all partial interference signals, which is detected by the photo detector. After digitizing, the signal is digitally filtered to separate the different signals. To improve the filter design and filter processing, the MR-OCT signal is simulated and the results of the simulation data are compared with measured data.

9312-97, Session PSun

The drivers of the OCT market growth in healthcare applications

Clémentine Bouyé, Benoît d'Humières, TEMATYS (France)

The development of Optical Coherence Tomography (OCT) systems started in the 1990's. The technology early found its application in Ophthalmology. At the beginning of the 2000's, the OCT market started to grow quickly with a CAGR between 15 and 20 %. Today more than 75% of the OCT market comes from the ophthalmic sector. However the growth of the ophthalmology OCT market has been slowing down for the last years. In this article, we present the results of our prospective study on the drivers of the OCT market growth in the coming years, based on bibliographical research and interviews with key players.

In parallel of being used for ophthalmology, OCT has been developed and tested in new medical domains like cardiology, dermatology, gastroenterology, etc. OCT addresses key societal challenges such as the diagnosis of coronary artery diseases or skin cancer. There is a strong demand for fast, high-resolution and in vivo imaging tools in these fields.

Conference 9312: Optical Coherence Tomography and Coherence Domain Optical Methods in Biomedicine XIX

That is why, in the last 5 years, R&D efforts have been made to improve the performance and the compactness of OCT components and sub-systems. Advances in integrated photonics will enable the miniaturization of components and sub-systems and thus open Point-of-Care applications. Moreover the developments of new functionalities of OCT systems are undertaken to reach more complex diagnosis. OCT will no longer be a simple imaging device, it is on the verge of becoming a quantitative measurement tool.

Our study shows that the emergence of new applications along with the improvements of components performance and the progress of functional OCT will drive the OCT market growth in the coming years.

9312-98, Session PSun

Optical coherence photoacoustic microscopy (OC-PAM) for in vivo multimodal retinal imaging

Xiaojing Liu, Tan Liu, Shuliang Jiao, Florida International Univ. (United States)

We developed an optical coherence photoacoustic microscopy (OC-PAM) system using a single pulsed broadband light source with a center wavelength of 810 nm and a FWHM bandwidth of 26 nm. OC-PAM can accomplish simultaneous multimodal OCT and PAM imaging with a single light source, thus can image simultaneously the scattering and absorption contrasts. Generated from the same group of photons the OCT and PAM images are intrinsically registered. The output of the light source was coupled into a 2x2 optical fiber coupler, which formed a fiber-based interferometer for OCT imaging. The light was split into the sample and reference arms. The output light from the sample arm was collimated, scanned by a galvanometer scanner, and delivered to the eye through a couple of lenses and mirrors. The combined reflected light from the sample and the reference arms was detected by a spectrometer to accomplish the OCT function. In the meantime an ultrasonic transducer was used to detect the photoacoustic signals generated from the absorbed photons to accomplish the PAM function. To test the capabilities of the system on multimodal ophthalmic imaging we imaged the retina of pigmented rats. The OCT images revealed the retinal structures with quality similar to conventional OCT while the PAM images revealed the distribution of absorbers in the retina. Since the absorption of hemoglobin is relatively weak at around 810 nm, the NIR PAM signals are mainly from melanin in the retinal pigment epithelium (RPE) cells, thus provide melanin specific imaging of the retina.

9312-99, Session PSun

Spectroscopy by joint spectral and time domain optical coherence tomography

Maciej Szkulmowski, Szymon Tamborski, Maciej Wojtkowski, Nicolaus Copernicus Univ. (Poland)

We present the methodology for spectroscopic examination of absorbing media being the combination of Spectral Optical Coherence Tomography and Fourier Transform Spectroscopy. The method bases on the joint Spectral and Time OCT computational scheme and simplifies data analysis procedure as compared to the mostly used windowing-based Spectroscopic OCT methods. The proposed experimental setup is self-calibrating in terms of wavelength-pixel assignment. The performance of the method in measuring absorption spectrum was checked with the use of the reflecting phantom filled with the absorbing agent (indocyanine green). The results show quantitative accordance with the controlled exact results provided by the reference method.

9312-100, Session PSun

Tissue classification of lupus nephritis using OCT and OCE

Kirill V. Larin, Chih Hao Liu, Manmohan Singh, Jiasong Li, Chen Wu, Rita Idugboe, Yong Du, Chandra Mohan, Michael D. Twa, Univ. of Houston (United States)

Lupus nephritis caused by systemic lupus erythematosus (SLE) is considered as a high morbidity and mortality renal disease. Currently, diagnosis of nephritic tissue is based on ultrasound and CT image-guided tissue biopsy. However, compared with ultrasound and CT imaging, optical coherence tomography (OCT) provides superior image resolution (micron scale) than ultrasound and no ionizing radiation as in CT. In addition to the structural information, elasticity information from tissues can also be retrieved by optical coherence tomography based elastography (OCE). In this study, we propose a novel application of OCT combined with OCE for nephritic tissue classification utilizing the sample optical and elastic properties. The optical coherence tomography signal slope and speckle variance and Young's modulus estimated from the elastic wave velocity are used for tissue classification. Using these three metrics, the results show good clustering, which show that combining OCT image analysis with OCE is a promising method for nephritis diagnosis. In the future, we intend to use a larger sample size and include the more elasticity parameters for better classification.

9312-101, Session PSun

Photothermal full field OCT for exogenous and endogenous contrast detection

Amir Nahas, Mariana Varna, Emmanuel Fort, Charles-Edouard Leroux, Emmanuel Bossy, A. Claude Boccara, Institut Langevin (France)

OCT by using a sensitive interferometric detection is able to detect very small changes of the optical path in the sample arm. In this study we have used a Full Field OCT (FFOCT) setup coupled to various heating (ranging from infrared to UV) and probing sources of different wavelengths in order to induce a small temperature variation of the probed volume through the Photothermal effect (absorption and heat relaxation). Using heat diffusion equations with various sources geometries we have been able to model the time dependence of the signal that is function of the source-probe distance and of the volume distribution of the absorbing centers. We have shown that the time evolution of the Full Field OCT images after step heating induced by Photothermal effects in tissue are able to reveal weakly absorbing zones as well as to localize them by taking advantage of the time dependence of the signal following the heating illumination. Exogenous contrast (gold particles) and endogenous ones (DNA) effects will be shown as well as the 3D character of heat diffusion in tissue. We believe that through such studies a 3D absorption mapping will complement the usual morphologic FFOCT images keeping the micron scale resolution in 3D that characterizes this technique.

9312-102, Session PSun

Optical coherence elastography (OCE) as a method for identifying benign and malignant prostate biopsies

Chunhui Li, Guangying Guan, Yuting Ling, Stephen Lang, Univ. of Dundee (United Kingdom); Ruikang K. Wang, Univ. of Dundee (United Kingdom) and Univ. of Washington (United States); Zhihong Huang, Ghulam Nabi, Univ. of

**Conference 9312: Optical Coherence Tomography and
Coherence Domain Optical Methods in Biomedicine XIX**

Dundee (United Kingdom)

Prostate cancer is the most frequently diagnosed malignancy in men. Digital rectal examination (DRE) - a known clinical tool based on alteration in the mechanical properties of tissues due to cancer has traditionally been used for screening prostate cancer. Essentially, DRE estimates relative stiffness of cancerous and normal prostate tissue. Such as measurement provides insight into detection and progression of disease. Suspected men with abnormal DRE are offered further diagnostic test to confirm diagnosis. Current diagnostic approach using grey scale ultrasound guided biopsies has multiple limitations including inability to differentiate aggressive from indolent prostate cancers. This proposal addresses the challenge by evaluating the role of three dimensional (3D) quantitative optical coherence elastography (OCE) in the detection and differentiation of aggressive from indolent cancers. OCE has several inherent advantages such as micron-scale resolution, millimetre-scale penetration depth and non-destructive imaging and has huge clinical potential. The OCE method potentially offers a novel approach for diagnosis and characterization of PCa by providing high resolution image to identify the location and volume as well as quantitatively evaluating elasticity of the cancerous tissue. This approach provides a new and easy to deploy, elastography-based paradigm, that not only can distinguish prostate cancer from normal/benign conditions, but also can predict the aggressiveness of PCa quantitatively.

9312-103, Session PSun

**A comparison study on capillary vessel
imaging with optical micro-angiography
and two-photon microscopy**

Wan Qin, Utku Baran, Yuandong Li, Univ. of Washington (United States); Hequn Wang, Wellman Ctr. for Photomedicine (United States); Wenbo Wang, Haishan Zeng, The BC Cancer Agency Research Ctr. (Canada); Ruikang K. Wang, Univ. of Washington (United States)

Vasculature is an integral and essential part of human body and plays a significant role in maintaining the healthy state of living tissue. Blood vessels are also heavily involved in a variety of health-related conditions. Vasculature network has been previously studied mainly using conventional histological analysis, which is highly invasive and may not well represent the morphology under living environment. Some noninvasive techniques, such as laser Doppler imaging (LDI), laser Doppler flowmetry (LDF), ultrasound imaging, and MRI have been used to study changes in blood flow in many physiological states. However, due to the limited spatial resolution, these techniques are incapable of imaging small capillary vessels. Optical micro-angiography (OMAG) is a variation of optical coherence tomography (OCT), proposed for 3D information of vasculature. It has been extensively utilized to study 3D tissue vasculature in vivo as well as quantitatively analyze blood flow down to the capillary level. However, the lateral resolution of OMAG is just comparable to the diameter of typical capillary vessels (5-10 μm). Consequently, some concerns were raised as (1) whether the capillaries seen by OMAG are accurate; (2) if yes, whether OMAG is reliable for quantitative analysis of vascular structures close to or even smaller than its imaging resolution. In this study, we compare in vivo vasculature images of mouse brain acquired with OMAG and two-photon microscopy (TPM), which is capable of depth-resolved high-resolution ($\sim 1 \mu\text{m}$) imaging of biological tissue structures. To the best of our knowledge, this is the first time that validation of OMAG vasculature imaging is performed using TPM.

9312-104, Session PSun

**Observation of Au nanoring distribution
during cancer cell uptake with
spectroscopic optical coherence
tomography**

Ting-Ta Chi, Ming-Jyun Li, Yi-Chou Tu, Shih-Yang Chen, Chih-Ken Chu, Che-Kuan Chu, Yu-Wei Chang, Yean-Woei Kiang, Chih-Chung Yang, National Taiwan Univ. (Taiwan)

Because of the interferometry imaging nature of optical coherence tomography (OCT) and the strong coherent scattering characteristics of localized surface plasmon (LSP) resonance on a metal nanoparticle (NP), OCT scanning is an effective approach for mapping the distribution of metal NP in a bio-tissue or bio-solution. In this study, we build a spectral-domain OCT system with a light source of $\sim 200 \text{ nm}$ in spectral width to achieve the depth and lateral resolutions of ~ 2 and < 4 microns in air, respectively. This OCT system is used for scanning two kinds of human oral cancer cells (SCC4 and SAS) with applied Au nanorings (NRIs). The LSP resonance behavior of the Au NRIs, which results in strong scattering of the Au NRIs for OCT imaging, is well controlled such that the long- and short-wavelength halves of the OCT source spectrum have different LSP resonance strengths. Based on this spectral distribution, the spectroscopic operation of the OCT system can lead to the different imaging intensities of the Au NRI distribution in the cell solution between the long- and short-wavelength images. OCT scans are performed at four stages of cell solution, including those before the application of Au NRIs, after the application of Au NRIs, after the washout of the Au NRIs not adsorbed or internalized by the cells, and after the etching of the Au NRIs not internalized by the cells. From the OCT images, particularly the differences between the long- and short-wavelength images in the spectroscopic operation, one can identify the adsorbed and internalized Au NRIs by the cells.

9312-105, Session PSun

**Dynamic photothermal optical coherence
tomography in a blood vessel with Au
nanorings: A phantom study**

Ting-Ta Chi, Yi-Chou Tu, Ming-Jyun Li, Shih-Yang Chen, Chih-Ken Chu, Yu-Wei Chang, Che-Kuan Chu, Yean-Woei Kiang, Chih-Chung Yang, National Taiwan Univ. (Taiwan)

The technique of photothermal optical coherence tomography (PT-OCT) has been developed based on the enhanced absorption of localized surface plasmon (LSP) resonance of an Au nanoparticle (NP), including Au nanorod, nanoshell, and nanoring (NRI). In PT-OCT operation, the spectral intensity of the measured phase data in an M-mode scan is usually defined as the photothermal signal intensity. Although PT-OCT has been demonstrated with Au NPs in static phantoms and bio-tissues, the PT-OCT technique in a vessel with a flowing medium, such as in a blood vessel, has not been investigated yet. A PT-OCT technique is useful for monitoring the Au NP concentration in a blood vessel that is important when bio-conjugated Au NPs are delivered for photothermal therapy. In this paper, a swept-source OCT system is used to scan a flowing phantom medium in a capillary tube for simulating a blood vessel and observe the photothermal effect induced by the mixed Au NRIs and modulated laser illumination. The heating of the flowing medium leads to the periodical generation and annihilation of air bubbles with a period of about 6 sec. With the periodical illumination of modulated laser, the bubbles expand and shrink periodically, resulting in the vibrations of the flowing medium and capillary tube wall. The vibration reaches a resonance condition, under which the OCT photothermal signal has a maximum level. The resonance frequency of laser modulation depends on the flowing medium content and is independent of flow speed.

**Conference 9312: Optical Coherence Tomography and
Coherence Domain Optical Methods in Biomedicine XIX**

9312-106, Session PSun

**Optical coherence tomography imaging of
tibialis anterior muscle for early diagnosis
of sarcopenia in a rat model**

Yugyeong Chae, Pukyong National Univ. (Korea, Republic of) and Ctr. for Marine-Integrated Biomedical Technology, Pukyong National Univ. (Korea, Republic of); Young-Sik Kim, Research Institute of Radiation Science and Technology, Pukyong National Univ. (Korea, Republic of); Sang Hoon Kang, Jeong-Eun Park, Pukyong National Univ. (Korea, Republic of); Eun-Kee Park, Kosin Univ. (Korea, Republic of) and Innovative Biomedical Technology Research Ctr. (Korea, Republic of); Byeong-Hwan Jeon, School of Sports and Health, Kyungsoo Univ. (Korea, Republic of); Yeh-Chan Ahn, Pukyong National Univ. (Korea, Republic of) and Innovative Biomedical Technology Research Ctr. (Korea, Republic of) and Ctr. for Marine-Integrated Biomedical Technology, Pukyong National Univ. (Korea, Republic of)

Sarcopenia is caused by several known factors including senility, malignancy, neuronal degeneration drug and sepsis. In the case of sarcopenia with aging process, muscle mass has been declined by 0.5 to 1% per year for people aged 40 and 50 yrs. Early diagnosis and understanding of the mechanism of sarcopenia are important to prevent muscle loss along with aging process. However, it is difficult due to the lack of the suitable imaging modality to observe the change of muscle structure. Histology is the gold standard to confirm the morphological structure, but it need to excision of muscle tissue. The other imaging modality such as computed tomography, ultrasound, and magnetic resonance imaging have the advantage of in vivo imaging modalities and have been used to imaging muscle. But computed tomography caused a tissue ionization that restricts routine checks due to safety precautions. Ultrasound has a low spatial resolution that is not enough to figure out individual muscle fibers. Magnetic resonance imaging needs too high medical expense to be used for muscle diagnosis. In this reason, optical coherence tomography could be great solution as diagnostic modality for sarcopenia.

We developed surgically denervated and streptozotocin induced diabetes rat models to cause a rapid atrophy in the tibialis anterior (TA), and imaged its structural changes using optical coherence tomography (OCT) and histology during 8 weeks. In addition, biomarker analysis was also conducted with tumor necrosis factor (TNF-?) and interleukin-6.

9312-108, Session PSun

**Nano-particle doped hydroxyapatite
material evaluation using Spectroscopic
Polarization Sensitive Optical Coherence
Tomography**

Paulina Strakowska, Michal Trojanowski, Gdansk Univ. of Technology (Poland); Mateusz Gardas, Garocin Labs. (Poland); Maciej J. Glowacki, Maciej Kraszewski, Marcin R. Strakowski, Gdansk Univ. of Technology (Poland)

Bio-ceramics such as hydroxyapatite (HAp) are widely used materials in medical applications especially as an interface between implants and living tissues. There are many ways of creating structures from HAp like electrochemical assisted deposition, biomimetic, electrophoresis, pulsed laser deposition or zol-gel processing. Our research is based on analyzing the parameters of the zol-gel method for creating thin layers of HAp. In order to achieve this, we propose to use Optical Coherence Tomography (OCT) for non-destructive and non-invasive evaluation. Our system works in

the IR spectrum, which is helpful due to the wide range of nanocomposites being opaque in the VIS range. In order to use our method we need to measure two samples, one which is a reference HAp solution and second: a similar HAp solution with nanoparticles introduced inside. We use silver nanoparticles below 300 nm. The aim of this research is to analyze the concentration, dispersion and orientation of nanodopants in the bio-ceramic matrix. Furthermore, the quality of the HAp coating and deposition process repetition have been monitored. For this purpose the polarization sensitive OCT with additional spectroscopic analysis is being investigated. Despite the other methods, which are suitable for nanocomposite materials evaluation, the OCT with additional features seems to be one of the few which belong to the NDE/NDT group. Here we are presenting the OCT system for evaluation of the HAp with nano-particles, as well as HAp manufacturing process. A brief discussion on the usefulness of OCT for bio-ceramics materials examination is also being presented.

9312-109, Session PSun

**Volumetric Mouse Brain Imaging with
Optical Coherence Tomography**

Junwon Lee, Eunjung Min, Sunwoo Jung, Andrey Vavilin, Sungwon Shin, Ulsan National Institute of Science and Technology (Korea, Republic of); Jeehyun Kim, Kyungpook National Univ. (Korea, Republic of); Woonggyu Jung, Ulsan National Institute of Science and Technology (Korea, Republic of)

Light microscopy has been an essential method to discover unprecedented anatomy and physiology of brain. However, volumetric mouse brain imaging has been challenged due to light scattering in turbid media. Recently, several methods utilizing sectioning techniques have been developed to overcome the aforementioned limitation. Among these methods, serial two-photon tomography begins a new approach to visualize volumetric nature of mouse brain with two-photon microscopy. This method performs serial block-face imaging that is repeatedly sectioning the top of a mounted specimen and imaging the remaining specimen block by means of deep tissue imaging. Thus, it eliminates tissue damages originating from histological processing, and reduces the burden of aligning individual images. Additionally, its deep tissue imaging allows to obtain series of undisturbed optical sections. With its advance, the field of views of light microscopy is no longer limitation to explore entire brain of animal models. Despite the success of the serial block-face imaging, it has been applied only to fluorescence microscopy. Thus, there are still more opportunities for further improvements by introducing label-free imaging.

Here, we present a novel imaging method that enables label-free volumetric imaging of mouse brain. This method uses the system of optical coherence tomography with serial block-face imaging. Because OCT performs deep tissue imaging of microscopic structures based on light scattering, we expected that OCT would reduce the high density of tissue sectioning and the need of handling fluorescence labels. We evaluated this method by imaging and reconstructing several mouse brains and segmenting their gross structures of interest.

9312-110, Session PSun

**Application of optical coherence
tomography attenuation imaging for
quantification of optical properties in
medulloblastoma**

Barry Vuong, Patryk Skowron, Ryerson Univ. (Canada); Tim-Rasmus Kiehl M.D., Univ. Health Network (Canada); Matthew J. Kyan, Ryerson Univ. (Canada); Livia Garzia, The Hospital for Sick Children (SickKids) (Canada); Helen Genis, Cuiru Sun, Ryerson Univ. (Canada); Michael Taylor

**Conference 9312: Optical Coherence Tomography and
Coherence Domain Optical Methods in Biomedicine XIX**

M.D., The Hospital for Sick Children (SickKids) (Canada);
Victor X. D. Yang M.D., Ryerson Univ. (Canada)

Medulloblastoma is a highly malignant pediatric brain. A significant challenge in the treatment of the disease is the potential for reoccurrence, as well as long-term neurological impairment of the child. One potential solution is to provide a high resolution imaging tool that distinctly visualizes regions of tumor for the surgeons. We present a method that quantifies the optical attenuation coefficient of normal and medulloblastoma in mice. Visualization of key structures in normal tissue were more easily defined in the optical coherence tomography optical attenuation. As a result this method provides additional information to surgeons during tumor resection.

9312-111, Session PSun

**Line-Scan Spectral-Domain OCT for
Ultrahigh-Speed In-Vivo Imaging of
Chicken Embryo**

Kalpesh Mehta, Zaineb Al-Qazwini, Nanguang Chen,
National Univ. of Singapore (Singapore)

Optical coherence tomography (OCT) is a widely used structural imaging method in various clinical applications. The image acquisition speed of OCT is limited by the beam scanner, and currently the fastest OCT system can acquire an A-line in less than one microsecond. In conventional OCT systems configured for cross-sectional imaging, A-lines are recorded sequentially when the weakly focused sample beam is shifted to scan along the transverse direction. While a galvanometer is usually employed as the scanning device, the typical resonant frequency of high-end galvanometers is few kilohertz. It is therefore very challenging for existing OCT techniques to go beyond 20 thousand frames per second. Recently a line scan implementation of OCT was proposed. With the line scan it is possible to acquire a B-Scan in a single exposure using a 2-D camera. This improves the scanning speed significantly.

In this work, we have implemented ultrafast line-scan OCT that features illumination of the sample with a light sheet and collection of the interferometric signal in parallel by the use of ultrafast two-dimensional image sensor. A single exposure at the image sensor results in a spectrum array, a two-dimensional function of transverse displacement and optical wavelength. One-dimensional Fourier Transform is then applied to the spectrum array along the wavelength dimension to generate a full frame cross-sectional image. Using this setup, we present ultrahigh speed in-vivo imaging of chicken embryo.

9312-112, Session PSun

**Nondestructive germination speed analysis
of Capsicum annum seeds under distinct
chemical conditions using high-resolution
swept source OCT**

Ruchire E. Henry Wijesinghe, Nam Hyun Cho, Kibeom Park,
Muhammad Faizan Shirazi, Upeksha Muhandiram, Sa-Youl
Ghim, Hee-Young Jung, Jeehyun Kim, Kyungpook National
Univ. (Korea, Republic of)

Conventional imaging methods such as destructive biological or serological methods in the agricultural industry and biotechnology have less potential to provide informative cross-sectional depth images at high resolution. The existing imaging methods frequently detect only the top surface of biological samples due to less depth penetration. In this study, we verified a novel non-destructive application to investigate the germination speed and the internal anatomical variations of Capsicum annum seeds which were kept under distinct chemical conditions. The cross-sectional images were acquired using 1310 nm SS-OCT system for ten consecutive days.

The seeds were germinated under three different chemical environments such as sterile distilled water (SDW), Butandiol 0.05 mm and Hexadecene 0.001 mm. The external room temperature and the light conditions were constantly maintained during the 10 days. The observed SS-OCT images showed a rapid and a significant internal anatomical variations of seeds which were treated under Hexadecene 0.001 mm compared to SDW and Butandiol 0.05 mm. A histology experiment was performed simultaneously to identify the external anatomical variations and it could be notified that the root length as well as the weight of the Hexadecene 0.001 mm sample was increased rapidly compared to other samples. Our results indicate that 1310 nm SS-OCT shows a potential as a tool to reveal the internal anatomical structural changes according to the germination speed caused by various chemical environments.

9312-113, Session PSun

**Motion analysis and removal in intensity
variation based OCT microangiography**

Xuan Liu, Mitchell Kirby, Feng Zhao, Michigan
Technological Univ. (United States)

In this work, we investigated how bulk motion degrades optical coherence tomography (OCT) microangiography. We demonstrated theoretically and experimentally that the spatial average of OCT microangiography signal (interframe variation of structural OCT signal) had an explicit functional dependency on bulk motion. Our result suggested bulk motion resulted in an increased background that is identical for different spatial locations in microangiography image. Based on our motion analysis, we proposed to reduce transient bulk motion induced artifact in OCT microangiography through adaptive thresholding. Motion artifact reduced microangiography was demonstrated in a 1.3µm spectral domain OCT system. We implemented signal processing using graphic processing unit for real-time imaging and conducted in vivo microvasculature imaging on human skin. Our results clearly show that the adaptive thresholding method is highly effective in motion artifact removal.

9312-114, Session PSun

**Enhanced delineation of degradation in
aortic walls through OCT**

Eusebio Real, Univ. de Cantabria (Spain); José Fernando
Val-Bernal, Univ. Hospital Marques de Valdecilla (Spain)
and Univ. de Cantabria (Spain); José M. Revuelta, Univ. de
Cantabria (Spain); Alejandro Pontón, Marta Calvo, Marta
Mayorga, Univ. Hospital Marques de Valdecilla (Spain);
José Miguel López-Higuera, Olga M. Conde, Univ. de
Cantabria (Spain)

Degradation of the wall of human ascending thoracic aorta has been assessed through Optical Coherence Tomography (OCT). OCT images of the media layer of the aortic wall exhibit micro-structure degradation in case of diseased aortas from aneurysmal vessels or in aortas prone to aortic dissections. The degeneration in vessel walls appears as low-reflectivity areas due to the invasive appearance of acidic polysaccharides and mucopolysaccharides within a typical ordered microstructure of parallel lamellae of smooth muscle cell, elastin and collagen fibers. An OCT indicator of wall degradation can be generated upon the spatial quantification of the extension of degraded areas in a similar way as conventional histopathology. This proposed OCT marker offers a real-time clinical insight of the vessel status to help cardiovascular surgeons in vessel repair interventions. However, the delineation of degraded areas on the B-scan image from OCT is sometimes difficult due to presence of speckle noise, variable SNR conditions on the measurement process, etc. Degraded areas could be outlined by basic thresholding techniques taking advantage of disorders evidences in B-scan images, but this delineation is not always optimum and requires complex additional processing stages. This work proposes an

**Conference 9312: Optical Coherence Tomography and
Coherence Domain Optical Methods in Biomedicine XIX**

optimized delineation of degraded spots in vessel walls, robust to noisy environments, based on the analysis of the second order variation of image intensity to determine the type of local structure. Results improve the delineation of wall anomalies providing a deeper physiological perception of the vessel conditions. Achievements could be also transferred to other clinical scenarios: carotid arteries, aorto-iliac or ilio-femoral sections, intracranial, etc.

9312-115, Session PSun

Usefulness of optical coherence tomography to demonstrate the healing phase of achilles tendon rupture on rats

Young-Sik Kim, Research Institute of Radiation Science and Technology, Pukyong National Univ. (Korea, Republic of); Yugyeong Chae, Pukyong National Univ. (Korea, Republic of) and Ctr. for Marine-Integrated Biomedical Technology, Pukyong National Univ. (Korea, Republic of); Jong-Kyoung Choi, Kosin Univ. (Korea, Republic of); Eun-Keel Park, Kosin Univ. (Korea, Republic of) and Innovative Biomedical Technology Research Ctr. (Korea, Republic of); Dong-Kyu Kim, Kosin Univ. (Korea, Republic of); Yeh-Chan Ahn, Pukyong National Univ. (Korea, Republic of) and Ctr. for Marine-Integrated Biomedical Technology (Korea, Republic of) and Innovative Biomedical Technology Research Ctr. (Korea, Republic of)

Optical coherence tomography (OCT) that based on backscattering of near infra-red light from tissue is a non-invasive and high resolution technique comparing with US and MRI for microscopic investigation of tissue. We thought that OCT method could be a tool for monitoring the healing process of tendon. In this study, we attempted to evaluate tendon injury and recovery by using OCT through rat model that has received the Achilles tendon(AT) injury. We made two groups to observe a variety of healing phase. One rat group was cut AT with neurectomy of sciatic nerves, and the other group was cut without neurectomy. The Achilles tendon was enucleated and fixed by formalin on 1st week and 2nd week. OCT was applied to image detailed structure of ruptured AT on 1st week and 2nd week. There were swellings on both groups on 1st week. And on 2nd week, on gross finding and histopathological findings, the denervated rat showed a remodeling phase of healing and the non denervated rat showed an early proliferative phase. On OCT image the denervated rat showed almost healed state and the non-denervated rat showed a large defect lesion that was a scaffolding tissue. We evaluated OCT to investigate structures of injured AT in the most suitable rat model. We were able to evaluate the organization of micro-living tissue. OCT is beneficial to make a treatment plan, especially the timing and intensity of rehabilitation.

9312-116, Session PSun

Precise measurement of instantaneous volume of eccrine sweat gland in mental sweating by optical coherence tomography

Masato Ohmi, Yoshihiko Sugawa, Akihiro Fukuda, Osaka Univ. (Japan)

We have demonstrated the dynamic OCT for in vivo observation of physiological functions of small organs such as eccrine sweat glands and peripheral vessels under the human skin surface. In particular, we discussed in detail mental sweating where mental or physical stress was applied to a volunteer to accelerate excess sweating. When a sound stress was used, we found internal mental sweating without ejection of excess sweat to the skin

surface, which was used for evaluation of activity of the sympathetic nerve. By use of the swept-source OCT (SS-OCT), we demonstrate the dynamic OCT possible for a few tens of eccrine sweat glands. In the experiment, the dynamic analysis of mental sweating for sound stimulus of sweat glands is performed by the time-sequential piled-up en-face OCT images. This method utilizes the summation of the reflection light intensity of the sweat gland in the OCT images. Therefore, the quantitative evaluation of mental sweating is not feasible.

In this paper, we propose a method for extraction of the target eccrine sweat gland by use of the connected component extraction process and the adaptive threshold method, where the en-face OCT images are constructed by the SS-OCT. Furthermore, we demonstrate precise measurement of instantaneous volume of the sweat gland in response to the external stimulus. The dynamic change of instantaneous volume of eccrine sweat gland in mental sweating is performed by this method during the period of 300 sec with the frame intervals of 3.23 sec.

9312-1, Session 1

Full volumetric video rate OCT of the posterior eye with 255x255x450 voxels at 20.8 volumes/s

Jan Philip Kolb, Univ. zu Lübeck (Germany) and Ludwig-Maximilians-Univ. München (Germany); Thomas Klein, Wolfgang Wieser, Wolfgang Draxinger, Ludwig-Maximilians-Univ. München (Germany); Robert A. Huber, Univ. zu Lübeck (Germany)

Full volumetric high speed OCT imaging of the retina at 20.8 volumes per second (V/s) is presented. Each volume consists of 255x255 A-scans over 20°x20° with 450 samples per depth scan. The system is based on a 1060nm Fourier domain mode locked (FDML) laser with 1.6MHz line rate. Scanning along the fast axis is performed with a 2691Hz resonant galvo operated in bidirectional scanning mode, while a standard galvo scanner is used for the slow axis. The performance is analyzed with respect to various potential applications, like intraoperative OCT.

9312-2, Session 1

High-speed numerically refocused retinal imaging with line-field parallel swept source imaging at 0.6 MHz

Daniel Fechtig, Abhishek Kumar, Laurin Ginner, Wolfgang Drexler, Rainer A. Leitgeb, Medizinische Univ. Wien (Austria)

We demonstrate in vivo retinal imaging with Line-field parallel swept source imaging (LPSI), a 3D imaging modality employing off-axis configuration of the reference arm. An angle between reference and sample field creates a modulation of the detected cross correlation signal across the line sensor, which leads to a separation of the respective interference terms in spatial frequency space. Band-limiting the spatial frequency content of the imaged object structure to one half of the full frequency space allows removing the complex conjugate artifact and the DC term for full-range imaging. This allows reducing the number of spectral sampling points resulting in increased imaging speed, which is important for in-vivo retinal imaging. Retinal imaging was performed with 600 kHz equivalent A-scan rate and a sensitivity of 93 dB. A full volume is acquired in only 0.83s. The lateral FOV on the retina is approx. 2.5mm along the line focus and 1.5mm in scanning direction. What's more, the intrinsic phase stability of the parallel imaging scheme allows for application of numerical refocusing to recover the spatial resolution in out-of-focus regions. We applied an algorithm based on Fresnel wave propagation, where the original interferometric phase data is multiplied by a phase factor correcting for defocus. We show images of human retina around the fovea before and after applying digital refocusing.

Conference 9312: Optical Coherence Tomography and Coherence Domain Optical Methods in Biomedicine XIX

To the best of our knowledge, LPSI is competitive with respective point scanning modalities in terms of speed, penetration depth, sensitivity and resolution.

9312-3, Session 1

First in human swept-source ophthalmic intrasurgical OCT with real time 3D visualization

Brenton Keller, Oscar Carrasco-Zevallos, Christian Viehland, Liangbo Shen, Gar Waterman, Duke Univ. (United States); Philip Desouza, Paul Hahn M.D., Duke Univ. Medical Ctr. (United States); Anthony N. Kuo M.D., Duke Univ. School of Medicine (United States); Cynthia A. Toth M.D., Duke Univ. Medical Ctr. (United States); Joseph A. Izatt, Duke Univ. (United States)

Vitreoretinal and anterior segment surgeries are performed with a stereoscopic surgical microscope, which provides an en face view of the surgical field with limited depth perception. Therefore, surgeons often rely on indirect cues for depth localization of tissue-tool interfaces. Many ophthalmic surgical procedures, such as corneal dissections and external limiting membrane peeling, necessitate precise axial manipulation of tissue. Currently, intraoperative optical coherence tomography (OCT) systems employ real time B-scans to provide surgeons with precise depth information of the surgical field. However, cross-sectional images provide limited information about the 3D surgical field. Furthermore, these systems require 3-5 seconds to acquire volumes and these volumes cannot be rendered in real time. Volumetric imaging, in addition to cross-sectional B-scans, may be necessary for true OCT image-guided ophthalmic surgery. We report on the development and first human surgical use of a swept-source microscope integrated OCT system (SS-MIOCT) for fast volumetric in vivo imaging. We merged our previously published MIOCT scanner with a custom swept-source OCT engine and implemented GPU-based custom software. The GPU-based software allowed for real time acquisition, processing, single layer segmentation, and rendering of volumetric images. We demonstrate the utility of fast volumetric OCT imaging towards image guided ophthalmic surgery by using SS-MIOCT to acquire volumetric images of cataract removal and epiretinal membrane peels in human surgery.

9312-4, Session 1

Intraoperative optical coherence tomography using an optimized reflective optical relay, real-time heads-up display, and semitransparent surgical instrumentation

Yuankai K. Tao, Mohamed T. El-Haddad, Sunil K. Srivastava, Daniel Feiler, The Cleveland Clinic (United States); Amanda I. Noonan, Andrew M. Rollins, Case Western Reserve Univ. (United States); Justis P. Ehlers, The Cleveland Clinic (United States)

Ophthalmic surgical maneuvers are currently limited by the ability of surgeons to visualize and manipulate semitransparent tissue layers as thin as tens of microns. OCT allows non-invasive, high-resolution in vivo imaging of tissue microstructure and has become the gold-standard for clinical diagnostics, tracking disease progression, and treatment planning in ophthalmology. Application of OCT immediately before and during ophthalmic surgery has demonstrated the utility of image-guided clinical decision-making by allowing contrast-free visualization of transparent tissue structures otherwise indistinguishable on conventional widefield microscopy/ophthalmoscopy. Microscope-integrated intraoperative OCT

(iOCT) allows imaging during retinal and corneal procedures to visualize epiretinal membrane, macular hole, retinal detachment, vitreomacular traction, and lamellar keratoplasty. Here, we describe several iterative advances in iOCT technology, including a novel iOCT system, real-time heads-up display (HUD) feedback, visualization of intraoperative maneuvers, and OCT-compatible surgical instrumentation. Simulated surgical maneuvers were performed on freshly enucleated porcine eyes. Subretinal space cannulation with injection was performed and imaged using spatial compounding. The optical properties of six semitransparent materials were quantified using OCT to identify ophthalmic surgical instrument substrates with optimal attenuation coefficient and scattering density. OCT-compatible polycarbonate surgical instrument prototypes were machined to accommodate a 23-gauge valved trocar cannula for simulated vitreoretinal surgery, including corneal needles, surgical picks, and retinal forceps. Densely sampled volumetric scans and sparsely sampled spatial compounding scans were used to visualize static and dynamic tissue instrument interactions. This study demonstrated subsequent integrative advances that may be critical to the widespread assimilation of this technology into every day surgical practice.

9312-5, Session 1

Imaging of retinal vessels using adaptive optics assisted SLO/OCT

Michael Pircher, Matthias Reichenmacher, Franz Felberer, Richard Haindl, Bernhard Baumann, Christoph K. Hitzenberger, Medizinische Univ. Wien (Austria)

Our previously developed adaptive optics (AO) scanning laser ophthalmoscope (SLO)/ optical coherence tomography (OCT) instrument has been adapted to image retinal vessels. The system records SLO and OCT images simultaneously with a pixel to pixel correspondence which allows a direct comparison between those imaging modalities. Different field of views ranging from 1°x1° up to 4°x4° are supported by the instrument. One key factor is the implemented active axial eye tracking for the OCT channel which allows time resolved measurements of retinal blood flow with cellular resolution.

9312-6, Session 1

Ultrahigh speed swept source OCT angiography for imaging retinal and choriocapillaris vasculature in patients with age-related macular degeneration

WooJhon Choi, Massachusetts Institute of Technology (United States); Eric M. Moul, Harvard-MIT Health Sciences and Technology (United States); Nadia K. Waheed, Mehreen Adhi M.D., New England Eye Ctr., Tufts Medical Ctr. (United States); Benjamin M. Potsaid, Advanced Imaging Group, Thorlabs, Inc. (United States); ByungKun Lee, Massachusetts Institute of Technology (United States); Vijaysekhar Jayaraman, Praevium Research, Inc. (United States); Talisa De Carlo, New England Eye Ctr., Tufts Medical Ctr. (United States); Alex E. Cable, Advanced Imaging Group, Thorlabs, Inc. (United States); Jay S. Duker M.D., New England Eye Ctr., Tufts Medical Ctr. (United States); James G. Fujimoto, Massachusetts Institute of Technology (United States)

Age-related macular degeneration (AMD) is a leading cause of vision loss or impairment in developed countries. Although the current clinical practice for monitoring AMD depends primarily on assessing structural information, choroidal blood circulation is believed to be an important marker in AMD.

Conference 9312: Optical Coherence Tomography and Coherence Domain Optical Methods in Biomedicine XIX

In this study we assess the potential of using ultrahigh speed swept source OCT angiography to visualize the microvascular changes in the retina and choriocapillaris in patients with AMD. A cross sectional, observational study was performed in 35 normal volunteers and 41 AMD patients (7 patients had GA, 15 patients had exudative AMD and 26 patients had dry AMD without GA in at least one eye). The retinal microvasculature and choriocapillaris were characterized using an ultrahigh speed, swept source OCT prototype with a vertical cavity surface emitting laser (VCSEL) light source centered at 1 μ m with a 400kHz A-scan rate. Two different field sizes, 6mm \times 6mm and 3mm \times 3mm, were used.

9312-7, Session 2

Simplified wavelength-swept lasers for high performance optical frequency domain imaging (OFDI)

Changsu Jun, Wellman Ctr. for Photomedicine (United States) and Harvard Medical School (United States); Martin L. Villiger, Wellman Ctr. for Photomedicine, Massachusetts General Hospital (United States); Wang-Yuhl Oh, KAIST (Korea, Republic of); Brett E. Bouma, Wellman Ctr. for Photomedicine (United States)

Novel wavelength-swept light source technologies have enabled high performance optical frequency domain imaging (OFDI). However, they are typically costly and hard to customize and many require access to proprietary materials or devices. We demonstrate alternative designs with simple configurations at low cost that provide robust operation without polarization control, all while providing high performance. Specifically, we demonstrate a short-length ring laser that can be built by fusion-splicing three readily available components including a Fabry-Perot (F-P) tunable filter. We also describe an external cavity laser that is based on a low-cost micro-electromechanical system (MEMS) scanning mirror. We demonstrate 100-300 kHz operation with 120-150 nm sweep range and 50-100 mW of average output power at 1.3 μ m. High quality imaging was verified for all configurations.

9312-8, Session 2

Stability and performance of a 1.5 MHz electronically controlled self-starting 1310 nm FDML laser

Wolfgang Wieser, Thomas Klein, Wolfgang Draxinger, Ludwig-Maximilians-Univ. München (Germany); Robert A. Huber, Univ. zu Lübeck (Germany)

We present an electronically controlled and self-starting FDML laser with a sweep rate of 1.5 MHz (375 kHz fundamental, 4x buffered). The laser operates over a sweep range of 115 nm centered at 1315 nm and provides an average output power of >80 mW. We characterize the laser performance, roll-off, coherence length and especially investigate the wavelength and phase stability of the laser output under changing environmental conditions. The high output power allows imaging with a sensitivity of 108 dB at 1.5 MHz.

9312-9, Session 2

200 kHz 1310nm and 400 kHz 1060nm swept lasers for optical coherence tomography

Brian D. Goldberg, Walid Atia, Mark Kuznetsov, Bart C.

Johnson, Vaibhav Mathur, Ranko Galeb, Peter Whitney, AXSUN Technologies Inc. (United States)

We have developed a new laser cavity architecture capable of operating over a wide range of tuning rates and sweep bandwidths with multi-centimeter coherence lengths. The new laser architecture fits entirely within a standard 14-pin butterfly package without the need for an external fiber stub as in our previous published designs. We present recent advances with A-line rates up to 200kHz at 1310nm and 400kHz at 1060nm for use in OCT. In addition we present long depth imaging capability with coherence lengths in excess of 30mm for 100kHz-140nm, and 45mm for 50kHz-110nm tuning bandwidth at 1310nm with clean PSFs better than -55dB.

9312-10, Session 2

A flexible wavelength tuning of active mode locking fiber laser for SS-OCT

Hwi Don Lee, Myung Yung Jeong, Chang-Seok Kim, Pusan National Univ. (Korea, Republic of); Jun Geun Shin, Byeong Ha Lee, Tae Joong Eom, Gwangju Institute of Science and Technology (Korea, Republic of)

We demonstrate a flexible wavelength tuning of active mode locking (AML) fiber laser in the various wavelength region such as 800 nm, 1310nm and 1550 nm. In this all-electric AML wavelength (wavenumber) tuning mechanism, the conventional wavelength selection filter is eliminated, and instead a suitable programmed electric modulation signal is applied directly to the gain medium. Therefore, the flexible wavelength (wavenumber) tuning such as dual- and triple wavelength switching, wavelength-spacing tuning, and wavelength (wavenumber) sweeping can be demonstrated. Especially, for swept-source optical coherence tomography (ss-OCT), the linearly wavenumber sweeping signal has been applied to overcome nonlinearity in wavenumber domain. We have obtained in-vivo OCT imaging without any wavenumber space resampling process. We successfully demonstrate a linearly wavenumber-swept AML fiber laser with 26.5 mW of output power for obtaining in-vivo OCT images at a sweep rate of 100 kHz.

9312-11, Session 2

Optimal operational conditions for supercontinuum-based ultrahigh-resolution endoscopic OCT imaging

Wu Yuan, Jessica Mavadia-Shukla, Jiefeng Xi, Wenxuan Liang, Xiaoyun Yu, Shaoyong Yu, Xingde Li, Johns Hopkins Univ. (United States)

We investigated the optimal operational conditions for utilizing a broadband supercontinuum (SC) source in a portable 800 nm spectral-domain endoscopic OCT (SD-OCT) system to enable high-resolution, high-sensitivity, and high-speed imaging in vivo. An SC source with a 3-dB bandwidth of ~246 nm was employed to obtain an axial resolution of ~2.7 μ m (in air) and an optimal detection sensitivity of ~-107 dB with an imaging speed up to 35 frames/sec. The performance of the SD-OCT endoscopy system with this SC source was demonstrated by imaging guinea pig esophagus in vivo, achieving image quality comparable to that acquired with a 7-fs Ti:Sapphire laser.

**Conference 9312: Optical Coherence Tomography and
Coherence Domain Optical Methods in Biomedicine XIX**

9312-12, Session 2

Miniaturized optical coherence tomography system based on silicon photonics

Juan Sancho-Durá, Kirill E. Zinoviev, Juan Lloret-Soler, Jose L. Rubio-Guivernau, Eduardo Margallo-Balbás, MedLumics S.L. (Spain); Wolfgang Drexler, Medizinische Univ. Wien (Austria)

This work describes the smallest OCT engine to date, with a footprint of 30cm³ and a weight under 150g. Fully encapsulated within a 40-pin butterfly package, the engine includes an axial scanner implemented on a silicon photonic circuit, which is capable of imaging at speeds up to 24KAscan/s and of sensitivities up to 93dB, a low-voltage MEMS-based lateral scanner providing 12mm of linear scan, as well as photo-detection and amplification electronics. The only required external components are standard SLED module (<2cm³) and custom electronics (< 60cm²) which control the engine and read-out and process signals to create the images.

9312-13, Session 3

Assessing airway smooth muscle with orientation-calibrated PS-OCT

David C. Adams, Lida P. Hariri M.D., Alyssa J. Miller, Yan Wang, Andrew D. Luster, Benjamin D. Medoff, Melissa J. Suter, Massachusetts General Hospital (United States)

Present understanding of the pathophysiological mechanisms of asthma has been severely limited by the lack of an imaging modality capable of assessing airway conditions of asthma patients in vivo. Of particular interest is the role that airway smooth muscle (ASM) plays in the development of asthma and asthma related symptoms. In this work we demonstrate how Polarization Sensitive Optical Coherence Tomography (PS-OCT) can be used to visualize and assess ASM. Using both bench-top and catheter-based approaches, we demonstrate the ability of PS-OCT to image ASM in segments of porcine airways, over a range of airway sizes. The quality of these results is bolstered by novel processing methods developed specifically for this application, chief among which is an approach for obtaining information about the optic axis of the sample by using the catheter sheath as a calibration reference. With this technique we are able to separate out the circumferential component of birefringence in the sample, corresponding to the orientation of ASM in the airway. Using this and other processing techniques we are better able to isolate and accurately depict ASM bands in the airway, allowing for calculation of ASM burdens and precise correlation with histology. Excellent correlation of this data provides evidence that PS-OCT offers enormous potential for imaging and assessing ASM. Finally, we present in vivo data taken in the airways of human volunteers, thereby demonstrating the potential applicability of this technology to human patients.

9312-14, Session 3

Endoscopic polarization sensitive optical frequency domain imaging for in vivo lung imaging

Fabio Feroldi, Jianan Li, Mattijs de Groot, Vrije Univ. Amsterdam (Netherlands); Joop de Langen, Johannes M. A. Daniels, Katrien Grunberg, Tom Gani Sutedja M.D., Vrije Univ. Medical Ctr. (Netherlands); Johannes F. de Boer, Vrije Univ. Amsterdam (Netherlands)

Lung cancer is the fourth most occurring type of cancer in Europe and

high resolution imaging of the superficial tissue layers of the bronchi in the human lung is therefore of high importance. Optical frequency domain imaging (OFDI) is a high resolution optical interferometric imaging technique for cross-sectional imaging of tissues. A high speed fiber-based polarization-sensitive OFDI system is presented for endoscopic imaging of the bronchi with a catheter that features distal scanning through the implementation of a micromotor at its end. The OFDI system used two depth-multiplexed orthogonal polarization states that simultaneously illuminated the tissue and polarization-sensitive detection to determine the tissue birefringence. The OFDI system performance was evaluated with special attention to the chromatic dispersion (CD) and polarization mode dispersion (PMD). A significant amount of CD was found, which could be compensated numerically, while a negligible amount of PMD was observed. Ex vivo OFDI imaging was performed on a caprine lung for which the results were highly correlated with the histology of the same specimen. In addition, OFDI imaging on an in vivo goat lung demonstrated similar results and proved the in vivo applicability of our instrument. Polarization sensitive OFDI on ex vivo human lungs showed promising results and clearly distinguished cartilage from other tissue types through birefringence imaging. These results are promising for future in vivo human lung imaging to fully proof the potential of polarization sensitive OFDI for the in vivo diagnosis of lung cancer.

9312-15, Session 3

Endoscopic and ophthalmic swept source polarization sensitive OCT

Zhao Wang, Hsiang-Chieh Lee, Osman O. Ahsen, ByungKun Lee, WooJhon Choi, Massachusetts Institute of Technology (United States); Benjamin Potsaid, Massachusetts Institute of Technology (United States) and Thorlabs Inc. (United States); Vijaysekhar Jayaraman, Praevium Research, Inc. (United States); Alex E. Cable, Thorlabs, Inc. (United States); Kaicheng Liang, James G. Fujimoto, Massachusetts Institute of Technology (United States)

Polarization sensitive OCT (PS-OCT) is an important functional extension of conventional OCT and can assess depth-resolved birefringence of tissue. Clinical translation of PS-OCT has been limited partially due to the high complexity of existing PS-OCT systems. We present simplified all-fiber swept source PS-OCT designs that can be used for both ophthalmic imaging and catheter-based endoscopic imaging. Two time multiplexed incident polarization states were generated using a polarization maintaining fiber and signals were detected using fiber polarization beam splitters. Jones matrix analysis was employed to extract tissue birefringence information. A simplified post-processing algorithm was developed for speckle noise reduction relaxing the demand for phase stability. We demonstrate ophthalmic PS-OCT imaging with an extended imaging range by electronically doubling the k-clock from a commercially available short cavity laser. For endoscopic imaging, we demonstrate ultrahigh speed PS-OCT with a MEMS-tunable vertical cavity surface emitting laser (VCSEL) and a high speed micromotor imaging catheter. We applied the PS-OCT systems both for in vivo retinal imaging and for guiding endoscopic radio-frequency ablation therapy for treating dysplastic Barrett's esophagus. The proposed PS-OCT designs require minimal alignment which greatly simplify system implementation and maintenance, and can be easily translated to clinical applications.

9312-16, Session 3

In vivo micro-OCT of airway cilia

Kengyeh K. Chu, Massachusetts General Hospital (United States); Carolin I. Unglert, Massachusetts General Hospital (United States) and Massachusetts Institute of Technology

Conference 9312: Optical Coherence Tomography and Coherence Domain Optical Methods in Biomedicine XIX

(United States); Tim N. Ford, Robert W. Carruth, Kanwarpal Singh, Massachusetts General Hospital (United States); Susan E. Birket, George M. Solomon, Steven M. Rowe, The Univ. of Alabama at Birmingham (United States); Guillermo J. Tearney M.D., Massachusetts General Hospital (United States)

Cystic fibrosis (CF) is an autosomal recessive genetic disease that causes life-threatening respiratory dysfunction, associated with increased incidence of infection, elevated mucus viscosity, and delayed mucociliary clearance of the lung. However, the pathogenesis and progression of CF lung disease is poorly understood, particularly in its earliest stages. The development of effective therapeutics is severely hampered by the lack of understanding of the causal relationships between the observed airway impairments.

We have previously employed 1- μ m resolution Micro-Coherence Tomography (μ OCT) as a benchtop tool for ex vivo interrogation of CF model piglets, extracting quantitative metrics of mucociliary function such as the depths of the airway surface liquid (ASL) and periciliary layer (PCL), ciliary beat frequency (CBF), and the velocity of mucociliary transport (MCT). To translate these quantitative capabilities to in vivo settings, we have developed an endoscopic μ OCT airway probe. The probe has a 4 mm outer diameter and utilizes a piezoelectric scanning mechanism to produce a 400 μ m field of view at 40 fps, while preserving the annular beam geometry and resolution of the benchtop system to directly visualize cilia and mucus transport. In the present work, we demonstrate imaging results from this probe in adult swine airways in vivo, including mechanical and algorithmic methods for image stabilization and quantitation of epithelial function. The ability to image and quantify airway function in vivo allows direct interrogation of CF pathogenesis, expanding on ex vivo and in vitro findings, and leading to an improved understanding of the disease and the ability to monitor treatment response.

9312-17, Session 3

OCT imaging of the upper airway using a VCSEL source

Joseph C. Jing, Univ. of California, Irvine (United States); Li-dek Chou, Giriraj K. Sharma M.D., Beckman Laser Institute and Medical Clinic (United States); Brian J. F. Wong M.D., Zhongping Chen, Univ. of California, Irvine (United States)

We developed a high speed OCT system utilizing a VCSEL source for imaging of the human upper airway. An external MZI with delay of 96 mm was built to generate a linear K-clock. The system is capable of an imaging range of 20 mm at an imaging rate of 100 frames per second. An integrated OCT imaging probe featuring a rotational micromotor and magnetic positioning tracker was developed to accurately reconstruct 3D models from the OCT images. Real time image processing was achieved utilizing dual commercial graphics processing units. Imaging was performed in awake adult and pediatric subjects in clinic as well as in neonatal patients to image airway obstructions.

9312-18, Session 3

Ultra-thin OCT endoscopy probe without focusing optics

Jangbeom Lee, Kookmin Univ. (Korea, Republic of); Yugyeong Chae, Yeh-Chan Ahn, Pukyong National Univ. (Korea, Republic of); Sucbei Moon, Kookmin Univ. (Korea, Republic of)

In this talk, we introduce a miniaturized fiber-based endoscopy probe for optical coherence tomography (OCT) which is made of a series of fused

optical fibers instead of the conventional scheme based on an objective lens. The large-core fiber with a core diameter of 30 microns was utilized for the probe while a standard single-mode fiber of core diameter 8.2 microns mainly delivered the OCT signal light to the probe. Those fibers were spliced with bridge fibers of intermediate core sizes to form a stepwise taper structure for an enhanced coupling efficiency. The final light at the exit of the large-core fiber had a large beam diameter to be radiated with a wide depth of focus for a sufficient OCT imaging depth. By our probe, an acceptable imaging depth of 1 mm was obtained with a lateral resolution better than 40 microns throughout the imaging range. Due to the simple structure, our fiber-based probe could be fabricated in a thin bare fiber form with an outer diameter of 85 microns. The compactness and mechanical flexibility provided better accessibility to internal organs by truly minimally invasive manners. In vivo and ex vivo sample imaging results will also be presented in the talk.

9312-19, Session 3

A combined swept source optical coherence tomography and fluorescence lifetime imaging system for morphological and biochemical investigations of atherosclerosis

Sebina Shrestha, Brian E. Applegate, Javier A. Jo, Texas A&M Univ. (United States); Brial L. Walton, Siquin Zhaorigetu, The Texas Heart Institute (United States); Xi Chen, Jesung Park, Jesus Rico-Jimenez, Michael J. Serafino, Texas A&M Univ. (United States)

Previously, we developed a multimodal system combining Optical Coherence Tomography (OCT) and Fluorescence Lifetime Imaging (FLIM) to generate co-registered morphological and biochemical artery images with the objective of improving the characterization of atherosclerotic plaques. Unfortunately, many molecules/receptors in the artery that are responsible for various stages of atherosclerosis are not fluorescent. A straightforward technique to image these molecules is to tag them with a dye and characterize the emission. We have integrated a 532nm pulsed laser into the system and interleaved it with the pulses from the 355nm laser. These interleaved pulses probe exogenous and endogenous fluorescence respectively, and provide the respective FLIM images simultaneously. Likewise, we have replaced the Fourier Domain Michelson interferometry based OCT (centered at 830nm) in the prior OCT-FLIM system with a Mach-Zehnder based Swept source OCT (SSOCT) system. The wavelength-swept source in the SSOCT has a sweep rate of 50 kHz, tuning bandwidth of 120nm being centered at 1310nm and a coherence length of 6mm in air. Hence, the OCT system now provides deeper volumetric images. Preliminary testing of this system was conducted on Watanabe Rabbit aorta, which was non-specifically tagged with antibody conjugated with Alexa532 ex-vivo. Results demonstrate that it can successfully render an OCT image and map the exogenous emission without disturbing endogenous emission acquisition. Our goal is to tag one or more specific molecules and use the system to gain a comprehensive understanding of the state of atherosclerosis based on the tissue morphology, biochemistry and molecular functionality.

9312-20, Session 3

Portable, ultrahigh-resolution, distal end scanning endoscopic SD-OCT system at 800 nm

Jessica Mavadia-Shukla, Wu Yuan, Jiefeng Xi, Xingde Li, Johns Hopkins Univ. (United States)

We present the first portable, ultrahigh resolution, distal end scanning SD-OCT endoscope system operating at a central wavelength of ~850nm.

Conference 9312: Optical Coherence Tomography and Coherence Domain Optical Methods in Biomedicine XIX

The endoscopic system consists of a portable supercontinuum (SC) light source, broadband spectrometer and distal end scanning endoscope. The use of a compact, turn-key, SC light source was able to provide a 3dB bandwidth of ~160nm with a near Gaussian shape, allowing us to achieve an axial resolution of 2.8 μ m endoscopically. The endoscope performed circumferential scanning via a miniature 1.5 mm diameter motor. We then demonstrate the capability of our endoscope through intraluminal imaging of ex vivo rabbit esophagus and ex vivo rat colon.

9312-21, Session 4

Handheld, rapidly switchable, full depth anterior/posterior swept source ophthalmic optical coherence tomography using coherence revival

Derek Nankivil, Gar Waterman, Brenton Keller, Christian Viehland, Duke Univ. (United States); Anthony N. Kuo M.D., Duke Univ. School of Medicine (United States) and Duke Univ. (United States); Joseph A. Izatt, Duke Univ. (United States)

A swept source optical coherence tomography system that uses coherence revival to image both the anterior and posterior segments with a single handheld MEMS-based optical probe was designed. The use of coherence revival enabled full-depth imaging of the anterior segment by resolving the complex conjugate artifact as well as imaging at either depth without adjustment of the reference delay. Both systems share a common objective and each optical path was optimized for its respective application using a GRIN lens eye model with dispersion to match that from literature. The system has a working distance of 26.1 mm and a measured axial resolution of 7 μ m (in air). In posterior segment mode, the system design has a lateral resolution of 9 μ m (in tissue), a 20° field-of-view (FOV), and a 3.7 mm depth range (z6dB = 4.6 mm). In anterior segment mode, the system design has a lateral resolution of 24 μ m, a depth-of-focus of 3.6 mm, an 11.2 mm square FOV, and a depth range of 7.4 mm (z6dB = 9.5 mm). In addition, the probe includes a wide-field IR LED illuminated iris imaging system to simplify alignment. A bi-stable solenoid actuated fold mirror assembly was used to switch between anterior and posterior segment measurement modes, and a miniature motorized translation stage was used to adjust the objective position to correct for patient refraction up to \pm 8D. The entire probe weighs less than 1.2 lbs with a form factor of 8 x 3? x 3? in. Healthy volunteers were imaged.

9312-22, Session 4

3D spectral imaging system for anterior chamber metrology

Trevor B. Anderson, Armin Segref, Grant Frisken, Steven Frisken, Cylite Pty Ltd. (Australia)

Accurate metrology of the anterior chamber of the eye is useful for a number of diagnostic and clinical applications. In particular, accurate corneal topography and corneal thickness data is desirable for fitting contact lenses, screening for diseases and monitoring corneal changes. Anterior OCT systems can be used to measure anterior chamber surfaces, however accurate curvature measurements for single point scanning systems are known to be very sensitive to patient movement. To overcome this problem we have developed a parallel 3D spectral metrology system that captures simultaneous A-scans on a 2D lateral grid. This approach enables estimates of the elevation and curvature of anterior and posterior corneal surfaces that are robust to sample movement. Furthermore, multiple simultaneous surface measurements greatly improve the ability to register consecutive frames and enable aggregate measurements over a finer lateral grid. A key element of our approach has been to exploit standard low cost optical components including lenslets arrays and a 2D sensor to provide a path towards low

cost implementation. We demonstrate a first prototype based on a 6 Mpixel sensor using a 250 μ m pitch lenslet array with 300 sample beams to achieve an RMS elevation accuracy of 1.0 μ m with 95 dB sensitivity and a 4 mm range. Initial tests on Porcine eyes, model eyes and calibration spheres demonstrate the validity of the concept. With the next iteration of designs we expect to be able to achieve over 1000 simultaneous A-scans with 7.5 mm range and in excess of 50 frames per second.

9312-23, Session 4

Modal analysis of sound-induced corneal vibration by phase-sensitive optical coherence tomography

Imran B. Akca, Ernest W. Chang, Wellman Ctr. for Photomedicine, Massachusetts General Hospital (United States) and Harvard Medical School (United States); Sabine Kling, Consejo Superior de Investigaciones Científicas (Spain); Giuliano Scarcelli, Wellman Ctr. for Photomedicine, Massachusetts General Hospital (United States) and Harvard Medical School (United States); Susana Marcos, Consejo Superior de Investigaciones Científicas (Spain); Seok-Hyun Yun, Wellman Ctr. for Photomedicine, Massachusetts General Hospital (United States) and Harvard Medical School (United States)

The mechanical integrity of the cornea is essential to its physiological function. Measurement of the mechanical integrity is useful in various applications ranging from biomechanics-based diagnosis of progressive keratoconus and monitoring collagen crosslinking to the measurement of intraocular pressure. There have been considerable efforts to develop noninvasive, sensitive methods to measure corneal biomechanics in the clinic. Here, we introduce a novel technique to analyze corneal vibrations that are excited by acoustic sound and detected by phase-sensitive optical coherence tomography (OCT). It is a modified scheme of dynamic OCT capable of producing snapshots of periodic tissue motion by employing motion-triggered laser scanning. A speaker generating monotone signals is used to excite acoustic vibration in the cornea, and the frequency is scanned for a modal analysis. The magnitude of corneal deformation is in the order of μ m or less which reduces discomfort to patients and probes the cornea in a nearly linear-elasticity regime. The experimental results were compared, in good agreement, with analytic membrane theory and finite element method simulation. Corneal vibrography revealed well-defined vibrational resonance modes of the cornea in the bovine eye ex vivo. We also measured the effect of UV-induced cross-linking on corneal vibrational modes, showing the potential of this technique for clinical applications. The resonance spectra showed remarkable changes by UV-induced collagen cross-linking of the cornea.

9312-24, Session 4

Off-axis full-field optical coherence tomography for in-vivo retinal imaging

Hendrik Spahr, Institut für Biomedizinische Optik, Univ. zu Lübeck (Germany); Dierck Hillmann, Thorlabs GmbH (Germany); Carola Hain, Helge M. Sudkamp, Gesa L. Franke, Gereon Hüttmann, Institut für Biomedizinische Optik, Univ. zu Lübeck (Germany)

Imaging speed and sensitivity of optical coherence tomography (OCT) systems is limited by the maximum permissible exposure (MPE). Especially retinal imaging is limited by the radiant flux, which can be brought into the eye. Full-field swept-source OCT (FF-SS-OCT) increases the MPE by an areal illumination and a highly parallelized image acquisition. However, it suffers from additional artifacts caused by autocorrelation of sample or

Conference 9312: Optical Coherence Tomography and Coherence Domain Optical Methods in Biomedicine XIX

reference light. Introducing an angle between sample and reference light, similar to off-axis holography, enables full-range imaging and filtering of DC and autocorrelation artifacts. We evaluate off-axis FF-SS-OCT for in-vivo imaging of the human retina. Images acquired at more than 60 MHz (on-axis) and 15 MHz (off-axis) A-scan rate are presented. The off-axis detection results in a significant sensitivity gain at the cost of a reduced numerical aperture and a reduced A-scan rate. Image quality and sensitivity are evaluated quantitatively and compared to scanning OCT data.

9312-25, Session 4

Velocity vector field reconstruction in retinal vessels via dual-beam bidirectional Doppler optical coherence tomography

Gerold Aschinger, Medizinische Univ. Wien (Austria) and Technische Univ. Wien (Austria); Leopold Schmetterer, Medizinische Univ. Wien (Austria); Veronika Doblhoff-Dier, Medizinische Univ. Wien (Austria) and Technische Univ. Wien (Austria); Rainer A. Leitgeb, René M. Werkmeister, Medizinische Univ. Wien (Austria)

We present a novel approach to reconstruct the blood flow velocity vector field in retinal vessels from dual-beam bidirectional Doppler optical coherence tomography measurements. For a better comprehension of measured phase profiles, several flow situations were simulated, taking the known dual-beam measurement geometry into account. Hence, we were able to find the vector field parameters that determine the measured phase profiles. This allowed us to develop an algorithm to reconstruct the velocity vector field from measured phase data. Subsequently, measurements were performed at a straight vessel section and at a venous convergence and the measured phase data were analyzed by means of the new method. The reconstructed flow velocity vector field for the straight vessel section yielded a parabolic flow. However, the reconstructed vector field for the venous convergence deviated from a parabolic profile. Both of the reconstructed velocity vector fields were in very good agreement with the simulations performed for the given vessel geometry; this confirmed that the proposed algorithm allows prediction of the velocity vector field. Furthermore, the approach is sensitive to directional changes of the flow velocity as small as $<1^\circ$, and thereby provides insight into the flow characteristics of the non-Newtonian fluid blood in microvessels.

9312-26, Session 4

Pupil tracking optical coherence tomography for precise control of pupil entry position

Oscar Carrasco-Zevallos, Derek Nankivil, Brenton Keller, Liangbo Shen, Duke Univ. (United States); Bhavna J. Antony, Brandon J. Lujan, Univ. of California, Berkeley (United States); Joseph A. Izatt, Duke Univ. (United States)

Conventional OCT retinal imaging systems employ a telescope to image the beam scanning pivot onto the pupil plane of the patient. To maximize collection efficiency of back-scattered light and to minimize aberrations and vignetting, the scanning beam should optimally rotate through the central cornea and the scan pivot should be imaged at the center of the ocular pupil. Moreover, specific retinal features, such as the cone photoreceptors and Henle's Fiber Layer (HFL), exhibit back-reflected intensity dependence on pupil entry position. Commercial OCT systems employ an IR pupil camera to allow alignment of the OCT beam onto the patient's eye and to vary pupil entry position. However, such systems are still vulnerable to lateral patient motion and depend upon active involvement of the photographer to obtain and maintain alignment. In this work, we describe an automated method for controlling the lateral pupil entry position of retinal OCT by utilizing

automated pupil tracking in conjunction with a 2D fast steering mirror placed conjugate to the retinal plane. Pupil tracking OCT prevents lateral motion artifacts and vignetting from obscuring the desired pupil entry location. Furthermore, we employ GPU-based real-time RPE segmentation for quantifying apparent retinal tilt of the OCT B-scans as a function of pupil entry position. We demonstrate direct HFL visualization by varying the pupil entry position eccentrically. In future work, our system may facilitate OCT studies concerning directional sensitivity of retinal structures by automated control of the pupil entry position.

9312-27, Session 4

Detection of retinal degeneration in an animal model using two dimensional angle-resolved low coherence interferometry combined with optical coherence tomography

Sanghoon Kim, Stephanie Heflin, Derek Ho, Sina Farsiu, Vadim Y. Arshavsky, William J. Brown, Adam Wax, Duke Univ. (United States)

Angle-resolved low coherence interferometry (a/LCI) is a light scattering technique that combines the sub-cellular sensitivity of light scattering with the depth resolution of optical coherence tomography (OCT). Using a/LCI, depth dependent cellular structural information such as nuclear size and shape can be determined with sub-wavelength precision and accuracy by analyzing the variation in the angular dependence of scattered light. In addition, tissue morphology such as cell nuclei spacing can be accessed via analysis of long range correlation due to coherent scattering. a/LCI has already shown promising results in the potential detection of neoplasia in vivo in the esophageal epithelium of Barrett's esophagus patients. Recently, we developed a 2D a/LCI system which has the capability of detecting the entire scattering field in two dimensions to provide more detailed information about the scattering structures. The preliminary data demonstrates that there are changes in the structural organization of photoreceptors in an animal model of retinal degeneration that can be quantitatively evaluated using this 2D a/LCI system. Here, we apply the technology to directly measure and characterize the structural changes within intact mouse eyes ex vivo. An OCT scanner is integrated into the 2D a/LCI system to allow for the direct comparison of a/LCI measurements and OCT images on the same tissue sample. Using this combined modality, quantitative biomarkers are presented which could be used to predict the onset and progression of neurodegenerative ocular pathologies. The potential for future clinical application can be evaluated through measurements in a well characterized animal model of progressive retinal degeneration.

9312-28, Session 4

High resolution polarization sensitive OCT for ocular imaging in rodents

Stanislava Fialová, Sabine Rauscher, Marion Gröger, Christoph K. Hitzenberger, Michael Pircher, Bernhard Baumann, Medizinische Univ. Wien (Austria)

A new high-resolution polarization sensitive optical coherence tomography system was developed for imaging rodent retina. Various light-tissue interactions such as birefringence and depolarization can change the polarization state of light. In the eye, there are several tissues that have these properties, for example retinal pigment epithelium (depolarization) and sclera (birefringence). These layers play key roles in diseases like age-related macular degeneration or glaucoma. Animal models are an important component for understanding disease pathogenesis. The gold standard for the evaluation of preclinical experiments is histology, which is an invasive and terminal procedure. Since OCT is non-invasive, it has the potential to be

Conference 9312: Optical Coherence Tomography and Coherence Domain Optical Methods in Biomedicine XIX

an alternative to histology with the benefit of long-term study of the disease progression in the same animal. In this study, a superluminescent diode with spectrum width 100 nm and mean wavelength 840 nm is used as a light source in order to enable high axial resolution. Spectrometers are custom built to enable high imaging speed that allows acquiring 3D data sets with 1024x200x1536 voxels in 3.44 s. From the acquired data, images displaying phase retardation induced by birefringence and orientation of birefringent axis were calculated. In first measurements, we were able to identify the RPE-choroid complex (depolarization effect) and the sclera (strong birefringence) in the retina of Long-Evans and Sprague-Dawley rats. Our preliminary results demonstrate the feasibility of the system for high speed/resolution imaging of the rodent retina. This is useful for longitudinal studies of disease models of retinal disease in rats and mice.

9312-13, Session PMon

Assessment of setting behavior of biocements using intensity correlation based multiple reference optical coherence tomography

Roshan I. Dsouza, Hrebesh Molly Subhash, Kai Neuhaus, National Univ. of Ireland, Galway (Ireland); Josh Hogan, Carol J. Wilson, Compact Imaging, Inc. (United States); Martin J. Leahy, National Univ. of Ireland, Galway (Ireland)

Biocement has a pivotal place in the domain of synthetic biomaterials. Over the past decade, there have been various cementation products available in the field of dentistry and orthopedics. To date, biocement has been used for various medical applications such as restorative filling materials, cement-retained restorations in dentistry, and knee and hip replacements. The curing kinetics and setting behavior of these products has been a key area of research. This is because the biocements used in the restorative applications can undergo volumetric shrinkage during the curing process, which can create a number of unwanted outcomes including marginal gaps, pain and damage to the restoration site. Dynamic light scattering and laser speckle imaging are well-established nondestructive testing (NDT) methods adapted for monitoring curing kinetics. However, these techniques are limited by their superficial imaging capability and cannot provide depth resolved information about the curing process. In this work, the depth resolved monitoring of curing kinetics of biocement is demonstrated using a novel, low cost NDT technology called multiple reference optical coherence tomography (MR-OCT) in conjunction with an intensity-based correlation mapping (CM) method. CM is an alternative, robust way to detect dynamic scatterers. The CM method uses a 2-dimensional correlation algorithm on the intensity images to separate dynamic from static scatterers. We believe our approach will demonstrate an enhanced quality assessment of biocements. To the best of our knowledge, this is the first demonstration using the CM method for the quantification of setting time.

9312-118, Session PMon

Low cost, high resolution optical coherence tomography utilizing a narrowband laser diode

Kentaro Osawa, Naoko Senda, Hiroyuki Minemura, Koichi Watanabe, Hitachi, Ltd. (Japan); Jun Hato, Daisuke Tomita, Hitachi-LG Data Storage, Inc. (Japan)

We developed a low cost, high resolution optical coherence tomography (OCT) system utilizing a narrowband laser diode (LD). To achieve high axial resolution, we constructed a free-space interferometer including a phase-diversity detection system and a high numerical aperture (NA) objective. In a conventional OCT system using a broadband light source such as a superluminescent light emitting diode (SLD) or a swept source laser (SSL), axial resolution is inversely proportional to the bandwidth of the light

source, and is typically around 10 μ m. Although the higher axial resolution less than a few microns is required for cellular-level imaging of biological tissues, it is difficult to realize broader bandwidth with a SLD or a SSL. On the other hand, with our approach, a broadband light source is unnecessary because the axial resolution is not determined by the bandwidth of the light source, but by the center wavelength and the NA of objective. Therefore, we utilized the narrowband LD which is generally used in an optical pick-up for compact disc because of its low price and high output power (up to 125 mW in continuous wave operation). The axial and lateral resolution of our OCT system was about 2.6 μ m and 1 μ m in the air, respectively. The tomographic imaging of the biological tissue (human oral mucosal epithelial cell sheet) was demonstrated, and the results showed that our OCT system enabled the evaluation of the thickness of cell sheet and visualization of cell nuclei due to the high axial resolution.

9312-119, Session PMon

Akinetic swept source with adjustable coherence length for SS-OCT

Radu F. Stancu, David A. Jackson, Adrian G. Podoleanu, Univ. of Kent (United Kingdom)

An electronically controlled optical swept source at 1550 nm using mode locking in a dispersive ring cavity is described. Active mode-locking was achieved by directly modulating the current of a semiconductor optical amplifier (SOA) used as a gain medium. In the static regime, parameters such as linewidth, tuning bandwidth and contrast were measured, while the axial range was determined dynamically. Two types of fiber, dispersion compensation and single mode, are employed in the laser ring cavity. It is demonstrated that the relative lengths of the two types of fiber have little effect on the linewidth, while more control on the linewidth is obtained via the frequency of the signal driving the SOA. Linewidths less than 60 pm and over 1 nm were measured in the static regime while driving the SOA at 50 – 500 MHz. The narrowest linewidths were achieved when the proportion of dispersion compensation fiber in the cavity is 80-90% of the total length. The optical source is developed to respond to the demands of OCT applications in general as well as address the need for low cost tunable lasers for configurations where a large tuning bandwidths and long coherence length might not be necessary.

9312-120, Session PMon

The mid-infrared swept-laser: life beyond OCT?

Stephen J. Matcher, David T. D. Childs, Richard A. Hogg, Dmitry G. Revin, Ihtesham U. Rehman, John W. Cockburn, The Univ. of Sheffield (United Kingdom)

Near-infrared external cavity lasers with high tuning rates ("swept lasers") have come to dominate the field of near-infrared low-coherence imaging of biological tissues. Compared with time-domain OCT, swept-source OCT a) replaces slow mechanical scanning of a bulky reference mirror with much faster tuning of a laser cavity filter element and b) provides a $\frac{1}{N}$ (N being the number of axial pixels per A-scan) speed advantage with no loss of SNR.

We will argue that this striking speed advantage has not yet been fully exploited within biophotonics but will next make its effects felt in the mid-infrared. This transformation is likely to be driven by recent advances in external cavity quantum cascade lasers, which are the mid-IR counterpart to the OCT swept-source. These mid-IR sources are rapidly emerging in the area of infrared spectroscopy. By noting a direct analogy between time-domain OCT and FTIR spectroscopy we show analytically and via simulations that the mid-IR swept laser can acquire an infrared spectrum $\frac{1}{N}$ faster than an FTIR instrument, using identical detected flux levels and identical receiver noise.

A prototype external cavity mid-IR swept laser is demonstrated, offering a comparatively low sweep rate of 400 Hz over 60 cm^{-1} with 2 cm^{-1}

Conference 9312: Optical Coherence Tomography and Coherence Domain Optical Methods in Biomedicine XIX

linewidth, but which provides evidence that sweep rates of over a 100 kHz should be readily achievable simply by speeding up the cavity tuning element.

Translating the knowledge and experience gained in near-IR OCT into mid-IR source development may result in sources offering significant benefits in certain spectroscopic applications.

9312-121, Session PMon

Phase evolution and instantaneous linewidth of a Fourier Domain Mode Locked laser

Bryan Kelleher, Svetlana Slepneva, Ben O'Shaughnessy, David Goulding, Tyndall National Institute (Ireland); Andrei G. Vladimirov, Weierstrass-Institut für Angewandte Analysis und Stochastik (Germany); Stephen P. Hegarty, Tyndall National Institute (Ireland); Guillaume Huyet, Tyndall National Institute (Ireland) and National Research Univ. of Information Technologies, Mechanics and Optics (Russian Federation)

Conventional swept laser sources can have cavity lengths of several meters that act to limit the sweep rate while maintaining efficient lasing. By incorporating a long optical delay so that the cavity round-trip time matches the tuning period of the filter, a swept source laser can be made to operate in the so-called Fourier Domain Mode Locked regime. This is characterized by high efficiency and more coherent lasing due to the fact that a whole sweep is stored in the cavity and the lasing does not have to continually restart from amplified spontaneous emission. A sweep-direction asymmetry is well-known for these sources and is manifest in both intensity and in phase. We show that the asymmetry has a fundamental origin and we also identify the underlying physical mechanisms for both the forward sweep and the backward sweep. In one direction the output undergoes a process similar to mode-hopping. The instantaneous linewidth is very narrow when the operation is on one of the stable modes but it is punctuated by large, discontinuous phase fluctuations during the transitions from one mode to another, rendering poor image formation. In the other direction, the intensity undergoes chaotic fluctuations for the entire duration and the linewidth is relatively broad throughout. However, importantly, the phase evolution is continuous and so, the chaotic behaviour may be beneficial for applications. Detailed experimental analyses using novel interferometric phase measurements are supported and guided by a numerical model.

9312-122, Session PMon

Tunable semiconductor laser at 1025-1095 nm range for OCT applications with an extended imaging depth

Mikhail V. Shramenko, Alexander Chamorovskiy, Superlum (Ireland); Hong Chou Lyu, Nicolaus Copernicus Univ. (Poland); Andrei Lobintsov, Superlum (Ireland); Karol Karnowski, Nicolaus Copernicus Univ. (Poland); Sergei D. Yakubovich, Moscow State Technical Univ. of Radioengineering, Electronics and Automation (Russian Federation) and Superlum (Ireland); Maciej Wojtkowski, Nicolaus Copernicus Univ. (Poland)

We demonstrate a tunable semiconductor laser for the 1025-1095 nm range for OCT applications with an extended imaging depth. The laser is based on the novel thin double quantum well InGaAs broadband semiconductor optical amplifier (SOA) and a PM fiber ring cavity. Laser was comprised of an acousto-optic tunable filter (AOTF) with a quasi-collinear interaction of optical and acoustic waves. Mode-hop-free tuning with up to 70 nm

range and tuning speeds from 2 nm/s up to 10000 nm/s are demonstrated. Measured instantaneous linewidth was in the range of 0.06-0.08 nm, side-mode suppression was around 50 dB and polarization extinction ratio was more than 18 dB. Output optical power in single mode fiber exceeded 20 mW. Laser provides the following operation modes: CW operation at any wavelength within the tuning range; linear wavelength sweeps over the full tuning range with an adjustable sweep speed; switching between any two wavelengths within the tuning range with an adjustable repetition frequency. Applications of the developed swept laser for OCT imaging are discussed. Narrow linewidth and high output power allows the extended OCT imaging depth. The tunable laser was used in a swept source OCT system for an imaging of a contact lens. Contact lens sample was immersed in a 0.5% intra-lipid solution within 2 mm thick glass cube. The interference fringe signal was acquired by 1MS/s sampling rate and 6912 points per A-scan were acquired. System enables cross-section imaging with more than 5 mm depth.

9312-123, Session PMon

Dynamics, instantaneous linewidth and device optimization for a short cavity swept-source OCT laser

Bryan Kelleher, Svetlana Slepneva, Ben O'Shaughnessy, Tyndall National Institute (Ireland); Hong Chou Lyu, Nicolaus Copernicus Univ. (Poland); Thomas P. Butler, David Goulding, Stephen P. Hegarty, Tyndall National Institute (Ireland); Andrei G. Vladimirov, Weierstrass-Institut für Angewandte Analysis und Stochastik (Germany); Karol Karnowski, Maciej Wojtkowski, Nicolaus Copernicus Univ. (Poland); Guillaume Huyet, Tyndall National Institute (Ireland) and National Research Univ. of Information Technologies, Mechanics and Optics (Russian Federation)

We analyze the dynamical behavior of a short cavity OCT swept-source laser experimentally and theoretically. Experimental measurements are carried out using a fast digital oscilloscope allowing detailed analyses of both the temporal evolution of the intensity and frequency. As is common with swept-source devices, the output displays a sweep direction asymmetry. When the tuning rate is low, discrete mode-hopping between continuous wave lasing outputs is observed both in the forward and backward components of the sweep. These continuous wave solutions are separated by transient pulse packets. As the sweep speed is increased these transients eventually merge allowing non-linear wave-mixing to generate novel outputs. For the forward sweep a sliding frequency mode-locking is obtained in the form of a periodic pulse train. For the backward sweep the same physical mechanism gives rise to a chaotic pulse train. The asymmetry is a consequence of the non-zero phase amplitude coupling obtained with semiconductor material. A delay differential equation model reproduces the dynamics extremely well and allows insights towards device optimization. Simple arguments lead to estimations of both the minimum and maximum sweep speeds for the sliding mode-locking regime. Increasing the filter width one can increase the maximum sweep speed but only at the cost of an increased instantaneous linewidth and so the accrued benefits for OCT applications must be carefully weighed against each other. A novel experimental interferometric technique allows for time-resolved measurements of the phase and instantaneous linewidth. The linewidth is shown to be dominated by deterministic rather than stochastic effects.

**Conference 9312: Optical Coherence Tomography and
Coherence Domain Optical Methods in Biomedicine XIX**

9312-124, Session PMon

**Supercontinuum noise in low coherence
interferometry systems**

 William J. Brown, Sanghoon Kim, Adam Wax, Duke Univ.
(United States)

As low coherence interferometry (LCI) has expanded from white light interferometry to optical coherence tomography (OCT), the need for broadband light sources with high spectral density has increased. Supercontinuum sources meet these needs except for the excess noise generated by pulse to pulse variation. We present the noise characterization of two supercontinuum sources using two low coherence interferometry imaging systems. The first is an ms²/LCI system from our lab and the second is a commercial OCT system. The two supercontinuum sources are an SC-450-4 from Fianium and a SuperK Extreme Low Noise from NKT Photonics.

With the ms²/LCI system the increase in OSNR is measured as a function of averaging time. Relative intensity noise dictates that measurements be made across a-scans or within a-scans with background subtraction. The OSNR increases with averaging up to acquisition times of 20 to 50 seconds and then decreases. In the OCT system noise levels are measured as a function of integration time and then Scotch™ tape phantoms are imaged. Relative contrast in the images is used to compare performance. The NKT supercontinuum shows better relative contrast than the Fianium, but not as good as a superluminescent diode. Noise effects can be mitigated with enhanced depth imaging (EDI) which moves the image to lower noise areas.

Supercontinuum light sources are now viable options for low coherence interferometry systems. The combination of high power and broad bandwidth provide functionality unavailable in other light source. Use of imaging techniques such as EDI can improve imaging metrics.

9312-125, Session PMon

**Simple and inexpensive long range swept
source for optical coherence tomography
applications**

 Bastian Braeuer, Norman Lippok, Stuart G. Murdoch,
Frédérique Vanholsbeeck, The Univ. of Auckland (New
Zealand)

Optical coherence tomography (OCT) is a 3D real time imaging technique based on white light interferometry. In swept source OCT (SS-OCT), a fast wavelength swept source is used and the spectral fringes are detected using a photodiode. Good imaging conditions require a long coherence length source (ie narrow instantaneous line width) at a suitable wavelength between 800 nm and 1300nm with an optical power in the tens of mW.

The coherence length is an important property of the setup. It determines, along with the sample absorption and scattering properties, the imaging depth. Commercially available sources have typical coherence lengths of 12mm and more recent sources have now reached coherence lengths of 20mm in air.

New advances in light sources and electronics have enabled the possibility to develop swept source laser with coherence length of 4 cm and more. The drawbacks of these light sources are the instability and expensive components which make them not yet commercially available. Moreover, these new systems operate mainly at 1500nm, a wavelength not ideally suited for OCT imaging of biological samples because of the high water absorption. In this paper we report a fast, inexpensive, stable and simple way to build a swept source using a fast spinning polygonal mirror and multiple quantum well chips in a Littman-Metcalf design cavity with a coherence length of 14mm, a 60nm bandwidth and an output power of 20mW at central wavelength of 1310nm. The advantage of our laser scheme is that almost any central wavelength can be implemented by changing the gain chip. A swept source at 800nm with a bandwidth of 35nm and a coherence length of 14mm has been demonstrated.

9312-126, Session PMon

**Compact OCT system designed for
portability and easy clinical deployment**

 Nate J. Kemp, Brian D. Goldberg, Bob Jenner, Noble
Larson, Bart C. Johnson, AXSUN Technologies Inc. (United
States)

The construction of today's clinical OCT systems typically consists of a tabletop or upright cart-based instrument. Substantial physical dimensions, along with high hardware costs, confines OCT to the specialist's office or hospital setting. Availability in primary care practices, urgent care and outpatient settings, and the developing world could dramatically enhance OCT's impact on patient care, especially for screening applications.

We demonstrate a portable OCT engine that facilitates a potential paradigm shift in clinical workflows and costs. The fundamental SS-OCT system components, including a MEMs-based swept laser, fiber interferometer, adjustable reference delay line, dual balanced photoreceivers, and dual-channel high-speed digitizer, are packaged in a compact 5.5"x7"x2" volume.

The engine provides on-board OCT image generation, JPEG compression, and real-time streaming over Gigabit Ethernet. This use of ubiquitous consumer technologies offers unprecedented ease of integration with inexpensive mobile computing platforms such as laptops, tablets, and smartphones. A generic sample arm interface facilitates connection to x-y galvanometers, rotational & pullback motors, or other application-specific scanners.

Results are presented from the portable integrated OCT engine operating with a 100kHz A-line rate, 1310nm center wavelength, 110nm sweep bandwidth, and >5mm ranging depth. A 100mm-long helical scan is generated in 2 seconds via a 0.8mm-diameter catheter probe. A probe interface module incorporates the catheter's optical-mechanical connection with a 12000 RPM rotational motor and optical rotary joint in an integrated multi-functional connector.

OCT can now participate in the rapid convergence toward cost-effective, handheld, and digitally interconnected healthcare devices.

9312-127, Session PMon

**Dual parametric compounding approach
for speckle reduction in OCT**

 Jan Philip Kolb, Univ. zu Lübeck (Germany) and Ludwig-
Maximilians-Univ. München (Germany); Philipp Schwarz,
Thomas Klein, Wolfgang Wieser, Ludwig-Maximilians-Univ.
München (Germany); Robert A. Huber, Univ. zu Lübeck
(Germany)

OCT as a coherent imaging technique inherently suffers from speckle. We present a new dual parametric compounding approach to reduce speckle. The approach is to acquire several OCT volumes with different numerical apertures (NAs). Then in post processing, a first spatial compounding step is performed by averaging of adjacent B-frames. In a second step data from the different volume is averaged. Retinal imaging data comparing this idea with standard spatial compounding is presented and analyzed and necessary parameters such as the required variation of the NA and number of different NAs are discussed

9312-128, Session PMon

**A comparison of OCT techniques for blood
velocimetry**

 Conrad W. Merkle, Univ. of California, Davis (United
States); Aaron C. Chan, The Univ. of Hong Kong (Hong

Conference 9312: Optical Coherence Tomography and Coherence Domain Optical Methods in Biomedicine XIX

Kong, China) and Univ. of California, Davis (United States); Vivek J. Srinivasan, Univ. of California, Davis (United States)

Doppler techniques have been used with Optical Coherence Tomography (OCT) for years to measure blood flow in vivo. While the general robustness and simplicity of Doppler measurements have led to its success and widespread use, there are certain conditions such as low flow rates or flow perpendicular to the beam axis where Doppler may not be the best method for measuring velocity. Two additional methods that have been developed to address some of the shortcomings of Doppler measurements are a decorrelation method and a red blood cell (RBC) tracking method. These methods are tested and cross-validated by measuring velocity profiles across intralipid and blood flow phantoms. Despite showing very promising results in an intralipid flow phantom, decorrelation methods did not generate accurate velocity measurements at large depths in a blood flow phantom. With this in mind, decorrelation based methods could be useful in small vessels and capillaries where Doppler signals are low. RBC tracking appears to be an accurate method for measuring RBC velocity across deep vessels and is most accurate for slower flow rates and low hematocrits. RBC tracking has potential applications for measuring low flow rates normally obscured by noise in the Doppler signal. Doppler remains the most robust and simplest velocity estimator of the three techniques described here. It is largely unaffected by multiple-scattering effects present in OCT scans of blood and has excellent range. When Doppler shifts are too small to quantify, decorrelation or RBC tracking methods may provide more accurate speed measurements.

9312-129, Session PMon

Master-slave optical coherence tomography for parallel processing, calibration free and dispersion tolerance operation

Adrian Bradu, Univ. of Kent (United Kingdom); Konstantin Kapinchev, Fred Barnes, Univ of Kent (United Kingdom); Adrian G. Podoleanu, Univ. of Kent (United Kingdom)

We present the Master Slave (MS) interferometry method that we published in the intervening time from the last conference. In this communication, we additionally demonstrate an important feature of the MS method, that of tolerance to dispersion. MS interferometry produces the interference of a selected point in depth based on principles of spectral domain (SD) interferometry, but without the need of a Fast Fourier transformation (FFT). The method can be used to directly produce en-face optical coherence tomography (OCT) images but also as a tool to accurately measure distances in low coherence interferometry for sensing applications. In the MS-OCT method, cross-correlation is applied to both methods of SD-OCT, spectrometer based (Sp) or swept source (SS)-OCT. The channelled spectrum provided by an OCT system is correlated with the signal produced by reading a stored mask. Several such masks can be used simultaneously. The masks operate as adaptive filters. Each mask (filter) determines recognition in the measured channelled spectrum delivered by the interferometer, of the pattern corresponding to each optical path difference to be "recognized". The method presents net advantages in comparison with the classical method of producing axial reflectivity profiles by FFT: no need for resampling of data, possibility to tailor the trade-off between depth resolution and sensitivity. Here, using a swept source, the MS method is used to obtain axial reflectivity profiles, which are compared to the axial profiles obtained by calibration of data and FFT. The tolerance to dispersion of the MS method was assumed in [1] but not demonstrated. Here, measurements are performed to demonstrate its axial resolution independence on dispersion. More will be presented in the conference, in terms of its radical difference from the conventional FFT based SD-OCT, in terms of parallelization, feature which allows direct production of an en-face OCT image, and not only.

9312-130, Session PMon

Balanced spectral domain optical coherence tomography with single camera and a time delay fiber

Min-Gyu Hyeon, Hyung-Jin Kim, Beop-Min Kim, Korea Univ. (Korea, Republic of); Tae Joong Eom, Advanced Photonics Research Institute (Korea, Republic of)

We propose a spectral domain optical coherence tomography (SD-OCT) system using a single detection scheme for balanced detection. The method using two different spectrometers with two cameras has been utilized in fiber-based SD-OCT studies to acquire two spectra having π phase difference simultaneously. We applied an optical switch and a fiber bundle for the proposed balanced SD-OCT with single camera. The optical switch plays a role as transmitting the two spectra to a spectrometer by turns. The optical fiber bundle was applied as time buffering to measure the two interference fringes without concerning unwanted phase difference. The length of the time delay fiber was confined by the camera line rate. The TTL signals for the camera triggering and the optical switching are 76 kHz and 38 kHz, respectively. When the optical switch is on, one of the two spectra are propagated to the single camera and the other one travels to the time delay fiber. When the optical switch is off, the light circled inside the time delay fiber finally is transmitted to the single camera. Thus, two measured fringe spectra had the opposed phase was generated at same time. If the time delay fiber is not used in the proposed balanced SD-OCT system, the signal-to-noise ratio decreases due to balancing two interference signals created at different time. To probe proposed scheme, we demonstrated the balanced SD-OCT, measured the fringe signals, and compared the point spectral functions, respectively. The signal noise ratios showed approximately 4.04 dB difference between with- and without the time delay fiber.

9312-131, Session PMon

Advances in high resolution holoscopy

Gesa L. Franke, Institut für Biomedizinische Optik, Univ. zu Lübeck (Germany); Dierck Hillmann, Thorlabs GmbH (Germany); Sabrina Lohmann, Institut für Biomedizinische Optik, Univ. zu Lübeck (Germany); Christian Winter, Jörn Wollenzin, Thorlabs GmbH (Germany); Hinnerk Schulz-Hildebrandt, Institut für Biomedizinische Optik, Univ. zu Lübeck (Germany); Gereon Hüttmann, Institut für Biomedizinische Optik, Univ. zu Lübeck (Germany) and Medizinisches Laserzentrum Lübeck GmbH (Germany)

Holoscopy is a new imaging approach, which combines techniques of digital holography and full-field swept-source optical coherence tomography and thereby overcomes limitations of conventional imaging. The interference pattern of the light scattered by a sample with a reference wave is recorded digitally at multiple wavelengths and numerical processing of the data provides a 3D image of the sample with diffraction limited lateral resolution over the whole measurement depth. This benefit increases at high lateral resolution since the focal depth of conventional imaging methods gets significantly smaller with higher numerical apertures. Correct and complete sampling of the interference signal is crucial to avoid image artifacts. We present a setup for high resolution imaging that holds the sampling requirements. Furthermore we present a new approach for a broadband tunable light source consisting of a supercontinuum source and a tunable filter to enable imaging at high lateral and axial resolutions.

**Conference 9312: Optical Coherence Tomography and
Coherence Domain Optical Methods in Biomedicine XIX**

9312-132, Session PMon

Wavelength to pixel calibration for FdOCT

Maciej Szkulmowski, Szymon Tamborski, Maciej Wojtkowski, Nicolaus Copernicus Univ. (Poland)

We show that in Fourier domain Optical Coherence Tomography (FdOCT) it is possible to determine the wavelength of light for each point of the detected spectrum using any measurable physical quantity that has linear dependency on wavenumber. The presented approach is robust as the actual values of the measured quantity have no importance for the algorithm. As example we calibrate a SOCT spectrometer using Doppler frequency induced in time-dependent spectral fringes by a mirror moving in one of the arm of the interferometer. The results of calibration are validated using narrow spectral lines generated by optical parametric oscillator.

9312-133, Session PMon

Real time FPGA resampling for swept source OCT

Bart C. Johnson, Noble Larson, Brian D. Goldberg, Mark Kuznetsov, AXSUN Technologies Inc. (United States)

Real-time swept source OCT data is most often sampled using a specially cut hardware k-clock. We present a system that mathematically resamples data within an FPGA-based data acquisition board based on data sampled from a wide free spectral range reference interferometer. The FPGA can then multiply up the reference clock rate to achieve greater imaging depth. The Nyquist fold-over depth can thus be programmed from a standard reference to an arbitrary depth, much as PLL frequency synthesizer can produce many frequencies from a standard stable reference. This system is also capable of real-time performance.

We present point-spread data and images that were resampled by this method, using a 100 nm sweep from a 1060 nm, 100 kHz swept source. An 81.5 GHz reference interferometer was multiplied 3.81 times to achieve a 3.5 mm Nyquist depth. We achieved shot noise limited sensitivity and transform limited point spread widths. As implemented, there are sideband artifacts from the linear interpolation step. Simulations show that a switch to a band-limited interpolation algorithm will eliminate this problem.

We believe this FPGA-based approach to resampling will enable new real-time imaging and phase-sensitive applications. It will allow both more standardization of hardware and more flexibility of application.

9312-135, Session PMon

2 μ m axial resolution, fiber-optic SD-OCT operating at \sim 1300 nm for cellular resolution imaging of biological tissue

Kostadinka Bizheva, Univ. of Waterloo (Canada)

Development of fiberoptic based SD-OCT systems operating in the 1300 nm spectral region and capable of providing micrometer scale axial resolution in biological tissue is particularly challenging due to the large spectral bandwidth that has to be transmitted through the optical and fiberoptic components of the imaging system with minimal spectral and power losses. Furthermore, the large spectral bandwidth requires cameras with larger number of pixels to achieve a decent scanning range. Here we present a novel fiberoptic SD-OCT light source (NKT), a custom filter to select the necessary spectral bandwidth and a novel 146 kHz, 2046 pixel CCD (Sensors Unlimited). All optical and fiberoptic components of the system were specifically selected to sustain a spectral bandwidth $>$ 260 nm centered at \sim 1250 nm and to provide 2.9 μ m axial resolution in free space, corresponding to 2.1 μ m in biological tissue ($n = 1.38$). The axial resolution of the system was tested by imaging a pellicle with physical thickness of \sim 2 μ m, as well as healthy human skin (fingertip). SNR $>$ 90dB was measured

at \sim 100 μ m depth with 5 mW optical power out of the imaging probe and at the full speed of the CCD camera. The SNR drop off over the scanning range of \sim 1.3 mm was \sim 15 dB. The overall low SNR is a combination of significant optical power loss in the current imaging probe and laser noise and can be improved on by redesigning the imaging probe and filtering of the images.

9312-136, Session PMon

Sub-micrometer axial resolution, fiber-optic SD-OCT operating at \sim 800 nm for cellular resolution imaging of biological tissue

Mojtaba Hajialamdari, Michal Vymyslicky, Kostadinka Bizheva, Univ. of Waterloo (Canada)

Development of fiberoptic based SD-OCT systems operating in the 800 nm spectral region and capable of providing sub-micrometer axial resolution in biological tissue is particularly challenging due to the large spectral bandwidth that has to be transmitted through the optical and fiberoptic components of the imaging system and the strong dispersion of light both in glass and biological tissue. Here we present a novel fiberoptic SD-OCT designed to operate at 785 nm central wavelength and to provide 1.3 μ m axial resolution in free space, corresponding to 0.95 μ m in biological tissue ($n = 1.38$). The system utilizes a commercial supercontinuum light source (NKT), a custom filter to select the necessary spectral bandwidth and a 34 kHz CCD. All optical and fiberoptic components of the system were specifically selected to sustain a spectral bandwidth $>$ 260 nm centered at \sim 785 nm. An imaging probe was designed using commercially available broadband achromat lenses to allow for \sim 2 μ m lateral resolution in biological tissue. The axial resolution of the system was tested by imaging a pellicle with physical thickness of \sim 2 μ m. Images of cucumber and human skin demonstrate the ability of the novel SD-OCT to image individual cells and sub-cellular organelles in biological tissue.

9312-137, Session PMon

A comparison of techniques for full 3D field deformation tracking with optical coherence tomography

Sam P. Richardson, Amir HajiRassouliha, Matthew Parker, Norman Lippok, Frédérique Vanholsbeeck, Martyn Nash, Andrew Taberner, Poul F. Nielsen, The Univ. of Auckland (New Zealand)

We present an optical coherence tomography based diagnostic tool that uses phase sensitivity to accurately map full 3D deformation fields in tissue. This capability facilitates the characterization of meso scale tissue properties, such as the mechanical response of a tissue. Polarization sensitivity enables determination of collagen alignment; this can be applied clinically to the detection of skin cancers, which have high prevalence around the world and especially in New Zealand. The initial stages of this study are concerned with determining the most suitable tracking algorithms and determining the accuracy of the deformation and strain mapping. We compare both phase based cross correlation techniques and volumetric digital image correlation techniques. The system comprises of a swept source laser (Axsun Technologies Inc) which emits a beam with an output power of 18 mW, a centre wavelength of $\lambda = 1310$ nm and a bandwidth of $\Delta\lambda = 100$ nm. This gives an axial resolution of 10 μ m in air. The stacking of sequential B-Scans across the volume provides a detailed map of how the tissue structure changes through the deformation process.

The comparison of the two techniques showed that VDIC yielded higher accuracy in images with a high noise component. VDIC enables tracking of deformation using multiple images in the same data set. These techniques reduce error in estimates of deformation compared to phase based cross correlation.

**Conference 9312: Optical Coherence Tomography and
Coherence Domain Optical Methods in Biomedicine XIX**

9312-138, Session PMon

**Enhance resolution on OCT profilometry
measurements using harmonic artifacts**

Marcus Paulo Raele, Lucas De Pretto, Anderson Z. de Freitas, Instituto de Pesquisas Energéticas e Nucleares (Brazil)

The measurement of profiles or simply, profilometry is crucial in many fields of knowledge aiming inspection, quality control and evaluation. There are several approaches able to provide this information. Some of the most broadly used systems are based on interferometry, cantilevers, confocal microscopy and scanning electron microscopy.

White light interferometry, based on low coherence interferometry (LCI), is widely considered the gold standard when looking to profilometry due to its high precision and contactless measurements. Optical Coherence Tomography or simply OCT, also LCI based, is already available in many laboratories around the world, however, being a system improved to perform tomographic images of biological samples, it cannot perform profilometry as good as other white light systems.

When measuring samples with high reflectivity using OCT frequency domain systems, detrimental features on OCT signal appear as a replication of the original structure in various depths on the resulting image, called harmonics.

A previous effort made by our group has showed the potential to access better axial resolution and accuracy results on profile measurements analyzing higher harmonics present on the processed image (post Fourier transform). Resolution improvement by a factor of two was achieved using a step height standard of 2 microns.

In this work a more practical approach was made, analyzing high reflectivity samples with a variety of different features, such as roughness, angles and depths, in order to demonstrate the advantages of this approach as a low cost way to have better visualization of reliefs below the system axial resolution.

9312-139, Session PMon

**One-micron resolution optical coherence
tomography (OCT) in vivo for cellular level
imaging**

Dongyao Cui, Xinyu Liu, Xiaojun Yu, Ding Sun, Yuemei Luo, Jun Gu, Perry Ping Shum, Linbo Liu, Nanyang Technological Univ. (Singapore); Jing Zhang, Nanyang Technological Univ (Singapore)

In order to resolve the microstructures of biological tissues better and obtain cellular/subcellular level resolution in real-time images, research has been focused on 1-micron optical coherence tomography (OCT) technologies for in vivo applications. As most cells have sizes of around few microns, a 1-micron resolution is desirable for clinical and medical applications. The resolution of current OCT imaging systems is limited by the emission bandwidth of individual light sources.

To solve this problem, we developed a spectral domain OCT system combining two NIR, CW light sources of different spectral range. Its resolving power is validated by visualizing the cellular structures of zebra fish larvae in vivo. An NIR extended illumination from 755-1100 nm is achieved. The axial resolution is 1.27 μm in air, corresponding to 0.93 μm in tissue ($n=1.36$), which is the highest axial resolution using NIR, CW laser sources up to date to the best of our knowledge. In vivo imaging is conducted to demonstrate the resolving power of proposed one-micron resolution OCT system. The top and bottom surfaces of individual disk-like red blood cell is reliably visualized, as well as flat, spindle shaped endothelial cells lining along the luminal surface of the blood vessel wall. This study provides a clinically viable solution for cellular and subcellular level OCT imaging system which is also very competitive in cost and sensitivity.

9312-140, Session PMon

**Large area full field optical coherence
tomography based on swept source for
morphological investigation of samples**

Muhammad Faizan Shirazi, Nam Hyun Cho, Kibeom Park, Ruchire E. Henry Wijesinghe, Jeehyun Kim, Kyungpook National Univ. (Korea, Republic of)

Swept source based full field optical coherence tomography (SSFFOCT) has advantage to provide enface images corresponding to the respective wavelengths without any mechanical movement. FFOCT system has good axial and transverse resolution to investigate surface morphology of samples. In this system, swept source based on solid state broad band laser and acousto optic tunable filter is designed to have free space link cavity. The advantage of this swept source is high power, broad tuning range and large penetration depth. This free space swept source is integrated with FFOCT system to obtain depth information of samples without any mechanical scanning. Using this system, different biological and industrial samples are analyzed to detect morphological information of samples nondestructively. The topography and tomography results verified the accuracy and effectiveness of system with high resolution and fast acquisition speed. For real time investigation of samples graphics processing unit (GPU) is utilized to increase the processing speed.

9312-141, Session PMon

**Alternative optical design form for optical
coherence tomography probes**

Daniel Staloff, Klaus Hartkorn, Corning Incorporated (United States)

Many fiber based probes used in Optical Coherence Tomography (OCT) are comprised of a spacer, GRIN lens, and a microprism. This design has the benefit of being relatively simple given the need for only three optical components. However, because of constraints to the probe working distance and spot size, the spacer, and GRIN lens will have tight tolerances for component length. These tight tolerances are a detriment to high volume manufacturing. In this paper we present a monolithic, single component design form which is more robust for high volume manufacturing.

9312-142, Session PMon

**Quantitative measurement of tissue
birefringence by single mode fiber based
PS-OCT with a single input polarization
state using Muller matrix**

Zhenyang Ding, Chia-Pin Liang, Qinggong Tang, Yu Chen, Univ. of Maryland, College Park (United States)

We present a simple but effective method to measure phase retardance of tissue by single mode fiber (SMF) based polarization sensitive optical coherence tomography (PS-OCT) with a single input polarization state. By analysis the Muller matrix of SMF system and sample, we theoretically verify that SMF-based PS-OCT system can measure the phase retardance reliably when the phase retardance in SMF system is integer multiple π ?. To make the phase retardance in SMF system is integer multiple π , we use a quarter wave plate (QWP) to calibrate the SMF system. We adjust polarization controller on the sample arm to make the output stokes vector of the front and back surfaces of the QWP are $[0, 0, 1]T$ and $[0, 0, -1]T$, respectively. Based on the proposed method, we experimentally test the ability of measuring phase retardance using a Berek polarization compensator. The measurement errors of phase retardance are greatly reduced by QWP calibration. We also present the phase retardance imaging of human nails

Conference 9312: Optical Coherence Tomography and Coherence Domain Optical Methods in Biomedicine XIX

and pig muscle tissues. Distinct layered patterns of tissues caused by birefringence can be detected. Although only phase retardance can be obtained by this method, in many applications such as cancer detection, dentistry, retina diagnosis, among others, phase retardance could be sufficient for disease characterization.

9312-143, Session PMon

Single shot single mode fiber based polarization sensitive optical coherence tomography

Bastian Braeuer, Norman Lippok, Frédérique Vanholsbeek, The Univ. of Auckland (New Zealand)

In polarization sensitive optical coherence tomography (PS-OCT), the birefringence properties of the sample are measured by detecting the interferometric signal using two balanced photo detectors. In standard PS-OCT configurations the two orthogonal polarization states are separated after the sample and reference arm signals have interfered. Furthermore an electro optic modulator (EOM) has to be used to continuously modulate the intensity of the laser to have different orthogonal polarization states incident on the sample. Here, we present an improved method for PS-OCT enabling the measurement of backscattered intensity and birefringence without the need for an electro-optic modulator (EOM) or polarization maintaining fibers. Intensity and birefringence measurement are recorded in the conventional way by scanning the beam in a fast transversal way. However, in our setup the sample arm signal is directly separated in two orthogonal polarization states at the sample and there are two reference arms. The two arms enable us the possibility of adjusting the path length independently from each other.

Furthermore by splitting the polarization states before they interfere we can use single mode fibers in the entire setup enabling us to have more freedom in adjusting the polarization in the fibers with polarization controllers.

Proof of concept measurements was done using chicken breast and human fingers. The accuracy of the method is proven by measuring well defined polarization states using a Berek compensator adjusted for different retardance at different angles. Our system allows for direct and accurate single shot measurement of the retardance without the use of an EOM or PM fibers. Accuracy was determined by calculating the set retardation angles at the Berek compensator by measuring the ratio of the two intensities of the polarization states. Measurements in the range of 0 to 180 degrees in 10 degrees increments were performed. Those measurements were repeated five times and a maximum mean standard deviation of +/- 0.8 degrees was calculated.

9312-144, Session PMon

Coherent signal composition in signal multiplexed polarization sensitive Optical Coherence Tomography

Jianan Li, Johannes F. de Boer, Vrije Univ. Amsterdam (Netherlands)

We present an analysis of the structural image information acquired with polarization sensitive Optical Coherence Tomography (PS-OCT). In PS-OCT a total of four channels of data are acquired; two orthogonal polarization state components for each of two incident polarization states by which the sample is interrogated. Up to recently, the structural information of the sample was obtained by incoherent summation of these four channels. Here we developed a coherent composition method based on the SU(2) properties of the detected 2*2 field matrices. We derive an expression for the image intensity based on the determinant of the complex field matrix. With a fiber based passive delay Polarization Sensitive Optical Frequency Domain Imaging (PS-OFDI) setup we demonstrate that, if the four detection channels maintain phase correlation, the Signal to Noise ratio

of the structural information can be improved by 2.3 dB by constructively composing the signal while leaving the noise canceling out. We compare the method with the conventional intensity sum method and argue that the SU(2) shape of Jones Matrices is key to understanding the coherent composition and the SNR improvement. The effect is evaluated by assessing both the measured OCT A-line profile and an image of a biological sample. We also discuss a global phase of the Jones matrix in signal multiplexed PS-OCT.

9312-145, Session PMon

Polarization Sensitive Spectroscopic Optical Coherence Tomography for multimodal imaging

Marcin R. Strakowski, Maciej Kraszewski, Paulina Strakowska, Michal Trojanowski, Gdansk Univ. of Technology (Poland)

Optical coherence tomography (OCT) is a non-invasive method for 3D and cross-sectional imaging of biological and non-biological objects. The OCT measurements are provided in non-contact and absolutely safe way for the tested sample. Nowadays, the OCT is widely applied in medical diagnosis especially in ophthalmology, as well as dermatology, oncology and many more. Despite of great progress in OCT measurements there are still a vast number of issues like tissue recognition or imaging contrast enhancement that have not been solved yet. Here we are going to present the polarization sensitive spectroscopic OCT system (PS-SOCT). The PS-SOCT combines the polarization sensitive analysis with time-frequency analysis. Unlike standard polarization sensitive OCT the PS-SOCT delivers spectral information about measured quantities e.g. tested object birefringence changes over the light spectra. This solution overcomes the limits of polarization sensitive analysis applied in standard PS-OCT. Based on spectral data obtained from PS-SOCT the exact value of birefringence can be calculated even for the objects that provide higher order of retardation. In this contribution the benefits of using the combination of time-frequency and polarization sensitive analysis are being expressed. Moreover, the PS-SOCT system features, as well as OCT measurement examples are presented. For this purpose, the OCT measurements have been taken for the artificial skin phantoms with collagen.

9312-146, Session PMon

Tooth structure analysis by using Jones-matrix optical coherence tomography

Cheng-Han Huang, Ching-Cheng Chuang, Chia-Wei Sun, National Chiao Tung Univ. (Taiwan)

Optical coherence tomography (OCT) has been developed as a high potential noninvasive imaging tool for oral diagnose. Oral diseases are strongly associated with systemic health such as oral cancer, periodontitis, oral mucosal infection, mouth ulcers, crack tooth syndrome, pulpitis and dental caries. However, caries and periodontitis are the major and common diseases in the oral cavity. In this study, a Jones matrix optical coherence tomography (JM-OCT) system that provides the polarization sensitive image was used for calculus, caries, and crack detection. The original OCT intensity image was compared with the polarization sensitive image of JM-OCT. We demonstrated that the JM-OCT imaging system provide structural information with polarization effects for dental calculus quantification. The direction of the structure of calculus is different in normal teeth structures. Therefore, the JM-OCT image can specifically characterize the structures based on the calculus. This optical method, using JM-OCT, provides a useful method for quantify tooth calculus.

**Conference 9312: Optical Coherence Tomography and
Coherence Domain Optical Methods in Biomedicine XIX**

9312-29, Session 5

Heartbeat OCT: motion-free three-dimensional in vivo coronary artery microscopy

Tianshi Wang, Thoraxcenter, Erasmus MC (Netherlands); Tom Pfeiffer, Ludwig-Maximilians-Univ. München (Germany); Evelyn Regar M.D., Thoraxcenter, Erasmus MC (Netherlands); Wolfgang Wieser, Ludwig-Maximilians-Univ. München (Germany); Heleen M. M. van Beusekom, Charles T. Lancée, Geert Springeling, Ilona Peters, Thoraxcenter, Erasmus MC (Netherlands); Antonius F. W. van der Steen, Thoraxcenter, Erasmus MC (Netherlands) and Shenzhen Institute of Advanced Technology (China) and Technische Univ. Delft (Netherlands); Robert A. Huber, Ludwig-Maximilians-Univ. München (Germany); Gijs van Soest, Thoraxcenter, Erasmus MC (Netherlands)

Intravascular optical coherence tomography (IV-OCT) has entered clinical interventional cardiology practice, providing high-resolution imaging of the artery wall, pathology of atherosclerosis, and coronary interventions. The quality of transverse cross sectional images and longitudinal sections through the data is vastly different, however. Cardiac motion artifacts, non-uniform rotational distortion and undersampling strongly affect the usability and interpretation of three-dimensional (3D) visualization, and thereby limit the impact of IV-OCT on clinical decisions and intervention guidance. Here we report Heartbeat OCT, an in vivo system provides faithfully rendered vessel wall architecture and accurate volume measurements by speeding up the image acquisition by a factor > 20. Using a motorized catheter and a Fourier Domain Mode Locked laser, we achieved IV-OCT imaging up to 5600 frames per second (fps) in vitro and 4000 fps in vivo, deployed at a 100 mm/s pullback velocity. Heartbeat OCT enables acquisition of a uniformly sampled data set within one cardiac cycle to restore 3D IV-OCT image fidelity.

9312-30, Session 5

First-in-human dual-modality optical coherence tomography (OCT) and near-infrared autofluorescence (NIRAF) molecular imaging of coronary arteries

Giovanni Jacopo J. Ughi, Hao Wang, Wellman Ctr. for Photomedicine (United States); Eric Osborne, Harvard Medical School (United States) and Massachusetts General Hospital (United States); Joseph Gardeki, Michalina J. Gora, Ali M. Fard, Ehsan Hamidi, Paulino Vacas-Jacques, Wellman Ctr. for Photomedicine (United States); Farouc A. Jaffer M.D., Harvard Medical School (United States) and Massachusetts General Hospital (United States); Guillermo J. Tearney M.D., Wellman Ctr. for Photomedicine (United States)

Combination of intravascular optical coherence tomography (OCT) with near-infrared fluorescence (NIRF) enables the simultaneous acquisition of complementary data that places quantitative molecular information in the context of co-localized microscopic structure.

We developed a dual-modality intravascular imaging system comprising state-of-the-art OCT and NIRF imaging combined at a custom-fabricated dual-modality rotary junction and then coupled into a 2.6F double-clad fiber catheter, capable of focusing and collecting OCT and NIRF light at the same time from the same locations on the artery wall.

The developed OCT-NIRF system acquires data at a speed of 100,000

A-lines/second (e.g., 200 images/second) with a pullback speed up to 40 mm/sec. OCT has an axial resolution of 10-15 μm and NIRF a resolution of 100 μm .

In an ex vivo study, we have recently discovered that Near-infrared Autofluorescence (NIRAF) signal is elevated in necrotic cores (Fig. 1 and Figure 2) and that the NIRAF signal is found in areas of high inflammatory activity; this signal may therefore provide key diagnostic information that is critical for the identification of plaques at risk for necrotic core rupture in vivo.

Finally, we completed the clinical translation of this technology by performing the first-in-human dual-modality OCT-NIRAF studies. We performed 3-coronary studies (imaging both the culprit and non-culprit segments) in multiple patients undergoing percutaneous coronary intervention (PCI) at Massachusetts General Hospital. Results showed that the developed system reliably detects NIRAF molecular signature of atherosclerotic plaques in vivo. Moreover, acquired OCT images presented the same image quality of single-modality (commercial available) OCT systems.

We believe that this new intravascular imaging technique may improve our ability to study human atherosclerosis and our diagnostic capabilities for important clinical problems such as the identification of high-risk intracoronary plaques and stent failures.

9312-31, Session 5

Multimodality intravascular endoscope for diagnosis of vulnerable plaques

Shanshan Liang, Beckman Laser Institute and Medical Clinic (United States); Teng Ma, The Univ. of Southern California (United States); Joseph Jing, Beckman Laser Institute and Medical Clinic (United States); Xiang Li, The Univ. of Southern California (United States); Jiawen Li, Beckman Laser Institute and Medical Clinic (United States); Qifa Zhou, K. Kirk Shung, The Univ. of Southern California (United States); Jun Zhang, Zhongping Chen, Beckman Laser Institute and Medical Clinic (United States)

In this paper, optical coherence tomography (OCT), fluorescence intensity imaging and intravascular ultrasound imaging techniques were combined together. An integrated system and a tri-modality endoscope were designed and fabricated. The combined system is capable of acquiring OCT, ultrasound and fluorescence data simultaneously and displaying images in real time. The intravascular probe for the integrated system was fabricated based on a single element ultrasound transducer and a dual modality OCT and fluorescence combined optical probe. Images from ex-vivo rabbit aortas have demonstrated the tri-modality system's capability to obtain high resolution OCT cross sectional images, deep penetration depth ultrasound structural images, and a specific molecular fluorescence. By utilizing this multimodality intravascular probe we are able to obtain more detailed information from different types of plaques simultaneously. In vitro images showed that this integrated system would be an efficient tool for atherosclerosis diagnosis.

9312-32, Session 5

Ultrahigh speed endoscopic structural and angiographic OCT imaging

Hsiang-Chieh Lee, Osman O. Ahsen, Kaicheng Liang, Michael G. Giacomelli, Zhao Wang, Massachusetts Institute of Technology (United States); Benjamin M. Potsaid, Massachusetts Institute of Technology (United States) and Thorlabs Inc. (United States); Vijaysekhar Jayaraman, Praevium Research, Inc. (United States); Marisa Figueiredo,

Conference 9312: Optical Coherence Tomography and Coherence Domain Optical Methods in Biomedicine XIX

Qin Huang, VA Boston Healthcare System (United States) and Harvard Medical School (United States); Alex E. Cable, Thorlabs, Inc. (United States); Hiroshi Mashimo M.D., VA Boston Healthcare System (United States) and Harvard Medical School (United States); James G. Fujimoto, Massachusetts Institute of Technology (United States)

We demonstrate ultrahigh speed endoscopic OCT in patients with upper and lower GI pathologies. Swept source OCT imaging was performed with a VCSEL light source and micromotor imaging probe. The micromotor probe avoids the need for a distal fiber rotary joint and can achieve higher rotation speed with minimum rotation instability compared with probes using torque cables. The high imaging speed and stable beam scanning enables OCT angiography to visualize three-dimensional vasculature without exogenous dyes. The VCSEL operates at 1.3 μ m wavelength supports an imaging speed of 600,000 A-scans per second and 8 μ m axial resolution in tissue. The micromotor imaging probe operates at 400 frames per second with minimum rotation instability and has 15 μ m lateral resolution. The micromotor catheter was 3.2 mm in diameter and could be introduced through the 3.7 mm accessory port of a dual channel gastroscope or colonoscope. A computationally efficient fiducial marker based algorithm was applied to correct residual nonuniform rotation distortion from the micromotor, improving the quality of structural and angiographic images. Endoscopic OCT angiography was performed on the distortion-corrected 3D-OCT dataset by measuring the intensity decorrelation between consecutive frames. A cross sectional survey of upper and lower GI pathologies is presented from patients undergoing surveillance endoscopy and colonoscopy at the Veterans Affairs Boston Healthcare Systems (VABHS). Patients with Barrett's esophagus (BE), dysplasia, and inflammatory bowel disease were imaged.

9312-33, Session 5

Clinical experience with tethered capsule OCT endomicroscopy for screening for Barrett's esophagus

Michalina J. Gora, Amna R. Soomro, Robert W. Carruth, Weina Lu, Mireille Rosenberg, Wellman Ctr. for Photomedicine (United States); Norman S. Nishioka M.D., Wellman Ctr. for Photomedicine (United States) and Massachusetts General Hospital (United States); Guillermo J. Tearney M.D., Wellman Ctr. for Photomedicine (United States)

Endoscopic examination of the upper gastrointestinal tract is costly, inconvenient, and typically requires that the patient be sedated. Furthermore, endoscopy only provides macroscopic information and, as a result, biopsies must be excised in order to obtain a microscopic tissue diagnosis.

We have developed a swallowable tethered capsule OCT endomicroscopy (TCE) device that acquires microscopic of the whole human esophagus in a short and comfortable procedure that does not require sedation or endoscopy assistance. After the 11x 25 mm capsule has been swallowed, cross-sectional images of the esophageal wall circumference are displayed in real time (20 frames/second) as the capsule traverses the esophagus.

Here we report results obtained in a clinical study using the TCE device, focused on safety and feasibility of TCE for screening for Barrett's esophagus (BE). We have performed 40 procedures in 33 subjects. A total of 18 procedures were conducted in presumed normal volunteers and 22 were performed in patients with a known diagnosis of BE. The average duration of the procedure was 5 min +/- 1.7 min. 88% of subjects successfully swallowed the capsule without difficulty. There were no significant complications of TCE administration. Preliminary analysis of the OCT data demonstrated a sensitivity of 88% (95% CI: 0.73-1.04) and specificity of 81% (95% CI: 0.62-1.00) for differentiating between presumed normal volunteers and patients with BE.

Results obtained in this clinical study indicate that capsule endomicroscopy procedure is safe and provides diagnostically relevant OCT images of the human esophagus. Since the device can be disinfected and reused many times, it has the potential to be utilized by a large number patients for BE screening in a cost-effective manner.

9312-34, Session 5

Endoscopic system for high-efficiency autofluorescence imaging and co-registered Doppler optical coherence tomography

Hamid Pahlevaninezhad, Anthony Lee M.D., Stephen Lam M.D., Geoffrey Hohert, Lucas Cahill, Tawimas Shaipanich, Alexander J. Ritchie M.D., Wei Zhang M.D., Calum E. MacAulay, Pierre M. Lane, The BC Cancer Agency Research Ctr. (Canada)

In this work, we present a power-efficient, fiber-based endoscopic imaging system capable of co-registered autofluorescence imaging and Doppler optical coherence tomography (AF/DOCT). The system employs a custom fiber optic rotary joint (FORJ) with an embedded dichroic mirror to efficiently combine the OCT and AF pathways. This three-port FORJ setup has a throughput of more than 83% for collected AF emission, more efficient compared to previously reported fiber-based methods. A custom 900 μ m diameter catheter consisting of a rotating lens assembly, double-clad fiber (DCF), and torque cable inside a stationary plastic tube was fabricated to allow endoscopic AF/DOCT imaging of cylindrical structures such as airways in vivo. The lateral resolutions were measured to be [16 μ m, 24 μ m] and [82 μ m, 88 μ m] for OCT and AF imaging, respectively. In the OCT subsystem, a 50.4 kHz wavelength-swept laser source (20 mW output power; 1310 nm \pm 50 nm wavelength range) drives a fiber-based Mach-Zehnder interferometer and a balanced photo-detector detects the interference. In the AF imaging subsystem, the AF excitation source (445 nm wavelength) is coupled to the FORJ dichroic mirror using free-space optics to provide about 7 mW optical power to the sample and a PMT detector module detects the collected AF emission. We demonstrate the performance of the system in co-registered AF/DOCT imaging of peripheral airways in vivo. By co-registering DOCT with AF, the structure and function of tissue structures can be defined more accurately for diagnosis, biopsy guidance, and studying the response to therapy. Providing biochemical information about tissue co-localized with structural information, this system could find several diagnostic applications in lung and other organs.

9312-35, Session 6

Measurement of multiple-capillary RBC flux in the retina with optical coherence tomography

Zhongwei Zhi, Ruikang K. Wang, Univ. of Washington (United States)

Abnormal ocular blood flow was shown to be related to many ocular diseases such as age-related macular degeneration, diabetic retinopathy, and glaucoma. Capillary RBC flux, i.e. the number of RBC flow through the capillary per unit time, is an important capillary flow parameter. Current techniques i.e. fluorescence labeling method for flux measurement usually requires dye injection. In this work, we propose to utilize optical coherence tomography (OCT) imaging technique to achieve noninvasive and label-free measurement of RBC flux within multiple capillary of retina. A fast speed spectral-domain OCT imaging system at 820nm with a line scan rate of 240 kHz was developed to image mouse retina. By acquiring repeated B-scans at an ultrafast 720 fps frame rate, we were able to detect the fluctuating OCT signal intensity caused by the passage of single RBC through the capillary. RBC flux within single capillary was obtained by

**Conference 9312: Optical Coherence Tomography and
Coherence Domain Optical Methods in Biomedicine XIX**

counting the number of peaks in the OCT intensity profile after applying a Gaussian filtering algorithm. Multiple capillaries in the cross-sectional were isolated and their flux was measured automatically with this algorithm. The developed technique was applied to measure the RBC flux of capillaries within retina of BTBR ob/ob mice, which is a diabetic model, as well as its wild type (WT) controls. The results indicate that the ob/ob mice retina have a lower average RBC flux than WT mice, which may provide a way for early diagnosis of Diabetic retinopathy.

9312-36, Session 6

**Total retinal blood flow measurement
by 3-beam Doppler optical coherence
tomography**

Richard Haindl, Wolfgang Trasischker, Bernhard Baumann, Michael Pircher, Christoph K. Hitzemberger, Medizinische Univ. Wien (Austria) and Medical Imaging Cluster (Austria)

An improved 3-beam Doppler optical coherence tomograph was developed. The transversal resolution at the sample is increased by use of a custom made three facet prism telescope. In addition the system utilizes a two axis gimbal less MEMS mirror to reduce off pivot beam movement at the eye's pupil, enabling circular scan patterns.

The system comprises three individual superluminescent diode sources operated at a central wavelength of 840 nm, with a spectral bandwidth of 50 nm. The outgoing collimated beams are aligned in parallel to each other, resembling a triangle geometry with the beams set to the corners of the triangle. The beams share a mutual bulk optic sample and reference arm, while the detection unit consists of three identical spectrometers. For measurements, the beams are focused on a common focus spot, providing sample illumination from three non-coplanar directions. This enables the reconstruction of the absolute flow and velocity vector of moving scatterers, without the need of prior knowledge on the vessel geometry.

We show the systems functionality for in vitro circular scanning, measuring the absolute velocity vector and flow on a bifurcation flow phantom. Furthermore in vivo circular scanning is performed around the optic nerve head to demonstrate total retinal blood flow measurement.

Absolute flow and vector orientation show good agreement with the expected values for in vitro measurements. For in vivo measurement the calculated vessel geometry corresponds well with the actual geometry. Furthermore total arterial and venous blood flow shows good agreement, demonstrating the applicability of the system.

9312-37, Session 6

**Wavefront sensorless adaptive optics
optical coherence tomography for in vivo
imaging of human photoreceptors**

Yifan Jian, Kevin S. K. Wong, Eunice Michelle C. Cua, Jing Xu, Simon Fraser Univ. (Canada); Stefano Bonora, CNR-Istituto di Fotonica e Nanotecnologie (Italy); Robert J. Zawadzki, Univ. of California, Davis (United States); Marinko V. Sarunic, Simon Fraser Univ. (Canada)

The use of adaptive optics (AO) in large numerical aperture (NA) optical systems is essential for in vivo high-resolution retinal imaging. In conventional AO systems, the ocular aberrations are first measured/detected using a wavefront sensor (WFS) and then corrected by modifying the shape of an adaptive component such as a deformable mirror. Despite great success in implementing the WFS based AO correction there are several factors that might limit its performance due to non-common path errors, wavefront spot centroiding errors, wavefront reconstruction errors, lack of well-defined reference plane and back-reflections from the optical elements in the system. Wavefront sensorless adaptive optics optical coherence

tomography (WSAO-OCT) is a novel technique for in vivo high-resolution imaging that bypasses the challenges encountered with sensor-based designs. This technique replaces the wavefront sensor with an image-driven optimization algorithm by leveraging our ultrahigh speed GPU processing software. After eliminating the wavefront sensor, we were able to pursue a lens-based optical design that would otherwise introduce deleterious back-reflections for wavefront sensing. This lens-based approach is especially advantageous for developing a compact and robust adaptive optics system suitable for a clinical high-resolution retinal imaging. We describe our novel WSAO-OCT system for imaging the human photoreceptors in vivo and present results acquired at several retinal eccentricities along the superior meridian.

9312-38, Session 6

**Fiber-based polarization-sensitive OCT of
the human retina with correction of system
polarization distortions**

Boy Braaf, Vrije Univ. Amsterdam (Netherlands) and Rotterdam Ophthalmic Institute (Netherlands); Koenraad A. Vermeer, Rotterdam Ophthalmic Institute (Netherlands); Mattijs de Groot, Vrije Univ. Amsterdam (Netherlands) and Rotterdam Ophthalmic Institute (Netherlands); Kari V. Vienola, Rotterdam Ophthalmic Institute (Netherlands); Johannes F. de Boer, Vrije Univ. Amsterdam (Netherlands) and Rotterdam Ophthalmic Institute (Netherlands)

In polarization-sensitive optical coherence tomography (PS OCT) the use of single-mode fibers (SMFs) can cause wavenumber dependent polarization distortions. This problem is addressed by a novel Jones matrix analysis method that spectrally analyses the sample polarization state to correct the polarization distortions induced by the system hardware. The method was implemented on an SMF-based PS-OCT setup that uses a 1- μ m 100 kHz swept-source and a passive polarization-delay unit. The double-pass phase retardation, diattenuation and relative optic axis orientation were determined for the retina of a healthy subject. At the retinal surface the correction decreased the average phase retardation from 0.20 ± 0.19 rad to 0.14 ± 0.11 rad, while the median diattenuation reduced from 0.09 (IQR: 0.04 - 0.17) to 0.06 (IQR: 0.03 - 0.12). After correction the relative optic axis orientation showed the expected radial distribution of Henle's fiber layer in the inner/outer segments layer. The en face visualization of the retinal polarization properties showed strong phase retardation for the nerve fiber bundles leaving the optic nerve head (ONH). Around the fovea a donut of increased retardation was observed caused by Henle's fiber layer. The relative optic axis orientation clearly visualized the orientation of the nerve fibers leaving the ONH in all radial directions, while the radial extension of the Henle fibers was clearly observed in the fovea. The novel Jones matrix method reduced noise and corrected erroneous offsets on the measured polarization parameters. The increased accuracy of tissue polarization measurements is potentially interesting for the early detection and monitoring of pathological changes in neurodegenerative diseases such as glaucoma.

9312-39, Session 6

**Polarization mode dispersion correction
for optically buffered Jones matrix
based multi-functional optical coherence
tomography**

Young-Joo Hong, Shuichi Makita, Yoshiaki Yasuno, Univ. of Tsukuba (Japan)

The polarization mode dispersion (PMD) degrades the performance of Jones matrix based polarization-sensitive and multi-functional OCT (JM-OCT). This

Conference 9312: Optical Coherence Tomography and Coherence Domain Optical Methods in Biomedicine XIX

paper aims at presenting a method to correct the effect of PMD in optically buffered JM-OCT.

The PMD appearance in optically buffered JM-OCT was modeled. A 45° oriented linear polarizer was utilized in passive polarization delay unit and polarization diversity detection unit. The two linear polarizers unified the different PMD influence of the four entries of the measured Jones matrix, and the four entries of Jones matrix become to be modulated consistently by the envelope and the phase of the identical modulation function. Hence the phase relation among four elements of Jones matrix was maintained. However, the different PMD amount between buffered and non-buffered gives different modulation, and it induces different point spread function (PSF) and dispersion characteristics. The different PSF of buffered and non-buffered A-lines degrades OCT intensity image.

The PMD difference was compensated by reshaping the differently modulated interference fringe envelope and separate chromatic dispersion compensation for buffered and non-buffered A-lines. The envelope modulation of OCT signal is corrected by a fringe analysis based method. Because the spectral interference signals are stochastic, the ensemble root-mean-square of the interference fringe among A-lines gives us an envelope of the fringe modulation. And each spectrum was demodulated with inverse of the estimated fringe modulation.

Based on the PMD corrected OCT intensity imaging, structure, vasculature, birefringence and retinal pigment epithelium discriminable MF-OCT images were obtained with 200 kHz A-line rate.

9312-40, Session 6

Polarization-sensitive swept-source optical coherence tomography for imaging of the anterior eye segment

Masahiro Yamanari, Tomey Corp. (Japan); Satoru Tsuda, Tohoku Univ. School of Medicine (Japan); Taiki Kokubun, Tohoku Univ. School of Medicine (Japan) and Iwaki Kyoritsu Hospital (Japan); Yuji Tanaka, Yukihiro Shiga, Yu Yokoyama, Morin Ryu, Shiho Kunitatsu-Sanuki, Hidetoshi Takahashi, Kazuichi Maruyama, Hiroshi Kunikata, Toru Nakazawa, Tohoku Univ. School of Medicine (Japan)

PS-OCT has been developed for visualization of birefringent tissues in various applications. Despite increased attention, it has not been extensively used in clinics compared to standard OCT. Its primary reason is that more technical improvements are required to break a barrier of usefulness for non-experts in both meanings of the system and applications. Here, we demonstrate our prototype PS-OCT designed for imaging of the anterior eye segment, which has been in operation at a clinic. The system can measure Jones matrices of the sample with depth-encoding of two orthogonal incident polarizations and polarization-sensitive detection. Optical clock is generated using a quadrature modulator and a logical XOR circuit to double the clock frequency, enabling an axial measurement range of 15.28 mm for standard OCT imaging or 6.68 mm for depth-encoded PS-OCT imaging. Since our method applies the phase shift optically, it enables robust phase shifting that is independent of sweep nonlinearity of the light source. Systematic artifacts in measured Jones matrices caused by axial subpixel displacement between the depth-encoded signals are numerically compensated using signals at the surface of the sample. This processing effectively reduces polarimetric speckle noise. Local retardation images show improved visualization of conjunctiva, sclera, and scar tissue. In particular, scarred region in subconjunctival bleb wall is clearly distinguished from non-scarred region, suggesting that local retardation images are useful for follow-up of trabeculectomy and planning of reconstructive surgery of the bleb.

9312-41, Session 7

Wide dynamic range high-speed three-dimensional quantitative microangiographic OCT

Taejin Park, Sun-Joo Jang, KAIST (Korea, Republic of); Benjamin J. Vakoc, Massachusetts General Hospital (United States); Wang-Yuhl Oh, KAIST (Korea, Republic of)

Objectives: Measuring blood flow velocity in living tissue potentially provides critical information for studying tissue viability and functionality. We have built a high-speed quantitative microangiographic optical coherence tomography (OCT) visualizing three-dimensional (3D) map of blood flow over a broad range of flow velocities.

Methods: A frequency-multiplexed dual-beam scanned with a pre-programmed waveform that automatically performs multiple flow measurements with different time intervals provides wide dynamic range in blood flow speed imaging. By utilizing combination of single-beam and dual-beam imaging schemes, short time intervals are acquired from dual beam scans and long time intervals are acquired from single-beam inter-frame (inter B-scan) scans, respectively.

Results: We have demonstrated 3D quantitative microangiographic imaging of the mouse dorsal skinfold chamber with a velocity range of 0.011 mm/s to 2.44 mm/s over a large volume of 6mm (X: 512 lines) x 4mm (Y: 342 lines) x 4mm (Z) in 57s. Arterioles, venules and capillaries were clearly distinguished to each other.

Conclusion: We have demonstrated a wide dynamic range high-speed quantitative microangiographic OCT system that provides 3D blood flow imaging over a large volume.

9312-42, Session 7

Single-shot axial and transverse flow measurements using intensity-based dynamic light scattering in optical coherence tomography

Néstor Uribe-Patarroyo, Yoon Jinoh Jung, Brett E. Bouma, Wellman Ctr. for Photomedicine (United States)

Flow measurements have attracted interest in a diverse range of clinical applications, including retinal blood-flow measurements in ophthalmology, tumor angiogenesis and lymphangiogenesis for determining the viability of cancer treatments, the assessment of stenoses in cardiology, the study of cerebral pathophysiology, among many others. Optical coherence tomography (OCT) is an imaging modality that provides high-resolution imaging and moderate penetration depths, and is commonly used in biomedical and clinical applications due to its combination of optical sectioning, axial resolution and high-speed imaging. Dynamic light scattering- (DLS-) OCT analyzes the time autocorrelation function of the complex OCT signal to determine the dynamics of the scatterers that produce the OCT signal. The use of the phase information allows DLS-OCT to determine both the diffusion, axial and the transverse components of the motion of the scatterers in the three-dimensional OCT tomogram, but requires stringent phase stability in the acquisition system which limits its implementation in fast swept-source OCT systems. In this work, we present a new technique that allows the determination of the same information acquired in DLS-OCT (namely, diffusion, axial and transversal components of motion) based solely on the intensity of the OCT signal, without the need of repeated measurements. This novel technique could open new applications to DLS-OCT where the sample dynamics require faster acquisition times, a situation in which frequency-domain OCT excels, without being impacted by its phase instability.

**Conference 9312: Optical Coherence Tomography and
 Coherence Domain Optical Methods in Biomedicine XIX**

9312-43, Session 7

Ultrasensitive quantification of 3D cerebral capillary blood flow network dynamics

Jiang You, Kicheon Park, Congwu Du, Yingtian Pan, Stony Brook Univ. (United States)

Quantitative imaging of heterogeneous cerebral blood flow velocity (CBFv) is of great important for studying neuronal activity as well as its regulation to CBF. Even though two-photon microscopy (TPM) is widely used for quantifying red blood cell velocity (vRBC), its limited field of view (FOV) only allows to measure vRBC in very few capillaries rather than the capillary networks and veins/arteries of different calibers. Optical Doppler tomography (ODT), on the other hand, enables imaging of the heterogeneous CBFv network over a large FOV. However, the poor sensitivity of ODT prevents it from detecting slow capillary flows. Here, we report a new method, contrast-enhanced ODT with intralipid that dramatically enhances ODT sensitivity by alleviating vRBC underestimation resulting from the long latency between flowing RBCs (low hematocrit $\approx 20\%$) in capillaries. To quantify the efficacy, we compared the fill factor (FF), defined as pixel # of occupied by capillary flows / pixel # of the entire region of interest (ROI), before and after intralipid injection. Results show a dramatic increase (230%) of FF (i.e., capillary flow detectability). In addition, we demonstrate that contrast-enhanced ODT allow to uncover the ischemic CBFv (including capillary network) on a mouse sensorimotor cortex undergoing chronic cocaine exposures. As intralipid is widely used for parenteral nutrition, this contrast method has translational potential for clinical applications.

9312-44, Session 7

Oxygenation mapping with visible wavelength spectroscopic OCT

Shau Poh Chong, Conrad W. Merkle, Harsha Radhakrishnan, Conor Leahy, Vivek J. Srinivasan, Univ. of California, Davis (United States)

Oxygen metabolism is an important parameter in the brain, in which cerebral blood flow (CBF), cerebral blood volume (CBV) and cerebral metabolic rate of oxygen consumption (CMRO₂) are tightly regulated, albeit by mechanisms that remain poorly understood. Thus, novel and improved imaging methods to quantify oxygen consumption in vivo could help to unravel the mechanisms of neurovascular and neurometabolic coupling in healthy brain, as well as in diseases such as stroke and cancer.

In this work, we present a high-speed, ultrahigh axial resolution spectral/Fourier domain OCT system in the visible wavelength range using a supercontinuum light source that performs angiography, oximetry, and speed assessment in individual vessels of mouse brain in vivo. We present a strategy for performing spatial mapping of hemoglobin oxygen saturation in the en face plane based on estimating vascular absorbance spectra with ≈ 20 micron resolution. We describe approaches for mitigating confounds associated with scattering and noise. Visible light OCT allows more precise oxygenation mapping mainly due to the much higher absorption relative to scattering at visible wavelengths. By comparison, at infrared wavelengths, scattering dominates relative to absorption and oxygenation mapping is more challenging.

From the calibrated OCT angiogram data, we extract depth-resolved absorbance spectra of blood by short-time Fourier Transform (STFT) analysis, which are then used to determine the oxygen saturation by fitting using a modified Beer-Lambert Law. Lastly, we demonstrate in vivo quantitative oxygenation mapping of vasculature in the mouse brain through a thinned-skull during normoxia and mild hypoxia.

9312-45, Session 7

Optical microangiography reveals collateral blood perfusion dynamics in mouse cerebral cortex after focal stroke

Utku Baran, Yuandong Li, Ruikang K. Wang, Univ. of Washington (United States)

Changes in blood perfusion in highly interconnected pial arterioles provide important insights about the vascular response to ischemic regions in brain. Arteriolo-arteriolar anastomosis (AAA) forms boundary zones between major cerebral arteries where hemodynamic compensation occurs through penetrating arterioles during ischemia. AAA's role in regulating blood perfusion through penetrating arterioles is yet to be discovered. We apply ultra-high sensitive optical microangiography (UHS-OMAG) and Doppler optical microangiography (DOMAG) techniques to evaluate vessel diameter and red blood cell (RBC) velocity changes in large number of pial and penetrating arterioles in relation with arteriolo-arteriolar anastomosis after focal stroke. Thanks to high sensitivity of UHS-OMAG, we were able to image pial microvasculature up to capillary level through a cranial window (9 mm²), and DOMAG provided clear image of penetrating arterioles up to 500 μ m depth. In contrast to two-photon laser-scanning microscopy, our technique made it possible to image a larger number of vessels in a short imaging time without the need of exogenous contrast agents during time-sensitive MCAO experiment, thus providing the ability to compare various regions in the stroke penumbra in the parietal cortex with and without AAA existence. Results showed that penetrating arterioles close to a strong AAA connection dilate whereas penetrating arterioles constrict significantly in weaker AAA regions. These results suggest that AAA plays a major role in active regulation of the pial arterioles, and weaker AAA connections lead to poor blood perfusion to penumbra through penetrating arterioles.

9312-46, Session 7

Doppler optical coherence tomography imaging reveals the blood flow profile of the adult rodent cortex during ischemia stroke

Jiang Zhu, Gangjun Liu, Yongzhao Du, Beckman Laser Institute and Medical Clinic (United States); Aneeka M. Hancock, Melissa F. Davis, Ron D. Frostig, Univ. of California, Irvine (United States); Zhongping Chen, Beckman Laser Institute and Medical Clinic (United States)

Stroke is the 4th leading cause of death and the leading cause of long-term disability in the U.S. Almost 90% of reported strokes are due to ischemia. Finding and clarifying the mechanism for the reduction or prevention of injury due to ischemia could drastically decrease the impact of this disease. Combining Doppler principle with optical coherence tomography (OCT), Doppler OCT uses the intrinsic optical signals backscattered by the moving blood cells inside blood vessels as the contrast. Here, we show the use of Doppler OCT for the determination of the blood flow profile in terms of direction and velocity following permanent middle cerebral artery occlusion (pMCAO). The flow direction can be obtained from the sign of the phase change measured by phase-resolved Doppler OCT, and flow velocity is proportional to the value calculated by intensity-based Doppler variance until the flow velocity becomes saturated. A reduction of the flow velocity was found in major MCA branches immediately after pMCAO. After 24 hrs of pMCAO, the flow speed in the major larger MCA branches significantly decreased in comparison to the baseline values. In the capillaries with relative slow flow speed, a blood flow velocity increment can be seen in the reperfusion map after 24 hours of pMCAO.

**Conference 9312: Optical Coherence Tomography and
Coherence Domain Optical Methods in Biomedicine XIX**

9312-47, Session 7

In vivo microvascular imaging of human oral and nasal cavities using swept-source optical coherence tomography with a single forward/side viewing probe

Woo June Choi, Ruikang K. Wang, Univ. of Washington (United States)

We report three-dimensional (3D) imaging of microcirculation within human cavity tissues in vivo using a high-speed swept-source optical coherence tomography (SS-OCT) at 1300 nm with a modified probe interface. Volumetric structural OCT images of the inner tissues of oral and nasal cavities are acquired with a field of view of 2 mm × 2 mm. Two types of disposable and detachable probe attachments are devised and applied to the port of the imaging probe of OCT system, enabling forward and side imaging scans for selective and easy access to specific cavity tissue sites. Blood perfusion is mapped with OCT-based microangiography from 3D structural OCT images, in which a novel vessel extraction algorithm is used to decouple dynamic light scattering signals, due to moving blood cells, from the background scattering signals due to static tissue elements. Characteristic tissue anatomy and microvessel architectures of various cavity tissue regions of a healthy human volunteer are identified with the 3D OCT images and the corresponding 3D vascular perfusion maps at a level approaching capillary resolution. The initial finding suggests that the proposed method may be engineered into a promising tool for evaluating and monitoring tissue microcirculation and its alteration within a wide-range of cavity tissues in the patients with various pathological conditions.

9312-48, Session 7

Improved contrast for OCT angiography using speckle variance with angular compounding

Laurin Ginner, Daniel Fehdig, Cedric Blatter, Medizinische Univ. Wien (Austria); Martin Gröschl, Technische Univ. Wien (Austria); Rainer A. Leitgeb, Medizinische Univ. Wien (Austria)

We propose a new approach for improving the contrast of optical angiography by using angular compounding. The latter uses the fact that illuminating a sample from different angles results in distinct speckle patterns, that are averaged on summation of both channels. We employ dual beam OCT and demonstrate the dramatic gain in contrast of parafoveal microvasculature in-vivo over 8 deg and for microvasculature in the optic nerve head region over 16deg. The swept source OCT system operates at 400kHz A-scan rate. The vascular contrast is achieved via speckle variance technique. The axial projections from motion contrast volumes are co-registered and then averaged, resulting in speckle reduction and contrast enhancement. The system is capable of both angle independent quantitative flow assessment and high contrast optical angiography.

9312-49, Session 8

High-resolution mapping of Young's modulus using optical coherence micro-elastography and a compliant stress sensor

Kelsey M. Kennedy, Robert A. McLaughlin, David D. Sampson, Brendan F. Kennedy, The Univ. of Western Australia (Australia)

Compression optical coherence elastography (OCE) has potential to differentiate healthy and diseased tissue within a sample but is currently

limited to relative mechanical contrast based on strain. We use a novel stress sensor to provide the first quantitative elastograms in compression OCE. The sensor consists of a compliant silicone layer with well-characterized stress-strain behavior. Phase-sensitive measurements of strain in the silicone layer are used to estimate the two-dimensional stress distribution at the sample surface, which is combined with three-dimensional measurements of local axial strain in the sample to estimate the local Young's modulus. These quantitative elastograms expand the capabilities of compression OCE for inter-sample comparison and longitudinal studies of the micro-scale mechanical properties of tissue. We demonstrate the technique in freshly excised human lymph node tissue, highlighting metastasis based on an elevated Young's modulus.

9312-50, Session 8

Volumetric optical coherence tomography: vibrometry for in vivo measurement of traveling waves in the mouse inner ear with picometer sensitivity

Hee Yoon Lee, Patrick D. Raphael, Stanford Univ. (United States); Jesung Park, Texas A&M Univ. (United States); Audrey K. Ellerbee, John S. Oghalai M.D., Stanford Univ. (United States); Brian E. Applegate, Texas A&M Univ. (United States)

Our best understanding of the mechanical function of the cochlea is derived from complex mathematical models designed to account for the experimental observations of cochlear structure and vibratory response. Unfortunately, experimental measurements of the vibratory response in the soft tissues of the living mammalian cochlea are confounded by the mass of dense bone encapsulating the organ. The predominant approach is to create a hole in the bone exposing the soft tissues and enabling measurements via laser Doppler vibrometry (LDV) at the surface of the basilar membrane. However, this procedure can potentially change the mechanical properties of the cochlea and often results in damage to the soft tissues leading to unreliable results. We have recently overcome this issue by using phase-sensitive OCT (PhOCT) which enables imaging through the intact bone of the mouse cochlea. PhOCT can generate detailed morphological images resolving the substructures of the entire organ of Corti. At each spatial point, the vibratory response can be measured with picometer sensitivity generating very large datasets. Manipulating and processing this large dataset was extremely time consuming. Nevertheless the ability to quantitatively measure the evolution of the vibration in time and space could yield new understandings of cochlear function. Motivated by this potential we set out to develop high-speed processing algorithms and imaging speed improvements to our system that would enable 3D vibrometry. We will discuss the details of the system development and show the first in vivo measurements of a sound evoked wave traveling up the organ of Corti.

9312-51, Session 8

High speed imaging of remotely induced shear waves using phase-sensitive optical coherence tomography

Shaozhen Song, Nhan Minh Le, Zhihong Huang, Univ. of Dundee (United Kingdom); Ruikang K. Wang, Univ. of Washington (United States)

Shear wave imaging (SWI) is the foundation of shear wave elasticity imaging (SWEI), which is a quantitative approach to assess tissue structures and pathological status. Compared to other approaches of elasticity imaging, the induced strain in SWEI can be highly localized, giving high spatial resolution of elasticity map. In order to achieve a shorter excitation

Conference 9312: Optical Coherence Tomography and Coherence Domain Optical Methods in Biomedicine XIX

wave length for enhancing elastography resolution, it places stricter requirement on the temporal resolution requirements of SWI device. Here we introduced two approaches to remotely induce high frequency shear waves within tissue samples: ultrasound acoustic radiation force impulse (ARFI), and high energy nanosecond pulsed laser. The maximum frequency of pulsed laser induced shear waves in tissue-mimicking phantoms can go up to 25 kHz, which is not possible to be captured and tracked by other SWI modalities. We use a custom-built SWI-OCT system to visualize and capture the nanometer scale shear waves, achieving a spatial resolution up to 15 μm and frame rate of 92 kHz. The dynamic wave propagation data was then used for the reconstruction of localized wave velocity and elasticity. This study demonstrates the non-contact shear wave generation with pulsed laser source, and ultra-fast, high-resolution sectional acoustical wave tracking with remarkable sensitivity, promising a future clinical application for a high-resolution quantitative mapping of elasticity in vivo, non-contact and real time in OCT-accessible tissue, especially in ocular tissues.

9312-52, Session 8

In-plane bidirectional micro-displacement measurement using correlation coefficients of OCT signals

Kazuhiro Kurokawa, Shuichi Makita, Young-Joo Hong, Yoshiaki Yasuno, Univ. of Tsukuba (Japan)

Optical coherence tomography (OCT) has been utilized to measure micro-displacements of a biological specimen in order to characterize the biomechanical property and monitor the tissue micro-displacement induced by laser coagulation.

In this study, we propose a method to measure in-plane bidirectional displacement using correlation coefficients of OCT signals. The method is able to visualize rigid-body in-plane displacements with a presence of out-of-plane displacements.

In order to confirm its applicability, the method is used for the observation of the thermal changes of an ex vivo porcine retina during laser irradiation. The spatially resolved displacements are calculated from the reference OCT B-scan which is taken before the laser irradiation, and the target OCT B-scan which is taken during and after the laser irradiation.

The result successfully shows the bidirectional displacements of the retinal tissue due to the laser irradiation. The results indicate that the retinal tissue at inner retinal layer is radially expanded from the irradiation site of the retinal pigment epithelium (RPE) complex. On the other hand, the RPE and its posterior tissue was displaced downward and presented large out-of-plane displacement. However, it would not be real displacements but rather the alterations of tissue micro-structure, because the large out-of-plane displacement did not decrease long after the laser irradiation.

In conclusion, we developed a method to measure in-plane bidirectional displacement with the presence of the out-of-plane displacement, and the method successfully visualized the thermal change of an ex vivo porcine retina during laser irradiation.

9312-53, Session 8

Simultaneous measurement of flow and diffusion using optical coherence tomography

Nicolas Weiss, Ton G. van Leeuwen, Academisch Medisch Centrum (Netherlands); Jeroen Kalkman, Technische Univ. Delft (Netherlands)

Modern experiments to study mass transport phenomena in complex rheological systems such as microfluidics, polymer solutions, biofilms, blood microcirculation, and blood demand spatially and time resolved probing of concentration fields, pressure gradients, velocity profiles, wall

shear stress, and diffusion coefficients. Optical coherence tomography (OCT) is an imaging technique in which low coherence interferometry is used to produce depth resolved complex-valued backscatter profiles of (biological) samples up to a few milliliters deep. Several studies have shown the potential of OCT to measure sample dynamics, such as, axial flow, lateral flow, and particle diffusion.

We present measurements of the path-length resolved OCT signal and its correlation function for the simultaneous measurement of flow and diffusion. Based on our model of the path-length resolved autocorrelation function we obtained accurate results by fitting the model to the measured data with no free/unknown parameters. The model is validated by measuring the lateral flow velocity and the diffusion coefficient locally in a colloidal suspension. We show that sample morphology, flow velocities, and diffusion coefficients are all determined simultaneously with high spatiotemporal resolution. Furthermore, we show the regimes where the flow velocity and the diffusion coefficient can be reliably estimated. We anticipate that the presented method will improve the quantification of complex dynamical rheological processes, such as blood flow in the microvasculature.

9312-54, Session 8

Localization and visualization of depth-resolved changes in attenuation coefficient during focal seizure propagation with optical coherence tomography

Melissa M. Eberle, Mike S. Hsu, Carissa L. R. Rodriguez, Jenny I. Szu, Michael C. Oliveira, Devin K. Binder, B. Hyle Park, Univ. of California, Riverside (United States)

High resolution and minimally invasive optical imaging techniques have been vital in visualizing the functionality of the brain in vivo. Scattering is the dominant source of light attenuation in biological tissue, making a reflective imaging technique ideal for studying changes in the optical properties of cortical tissue. Optical coherence tomography (OCT) is a label-free, high-resolution, minimally-invasive, reflective imaging technique, capable of producing depth-resolved, cross-sectional, three-dimensional (3D) volumes and has shown to be a promising method for in vivo imaging in highly scattering tissues such as the cerebral cortex. The objective of this study was to fully utilize the spatiotemporal resolution of OCT in order to localize the changes in the optical properties of murine cerebral cortex during seizure progression in vivo. To achieve this, we used a recently published method for determining per-pixel depth-resolved tissue attenuation coefficients. We then applied a confidence interval statistical analysis method to localize and quantify regions with significant changes in attenuation coefficient volumes during the progression of a focal seizure model induced with 4-aminopyridine (4-AP). From our analyses, we were able to visualize depth-dependent increases and decreases in attenuation during seizures as well as track focal seizure propagation with high spatiotemporal resolution. To compare the electrical and optical temporal evolution, we included implanted electrodes for EEG analysis in our 4-AP model. The results from this study demonstrate the potential utility of OCT as a label-free, minimally-invasive tool to study brain function with high spatiotemporal resolution.

9312-55, Session 8

Real time photothermal OCT of fluorophores in tissue

Jason M. Tucker-Schwartz, Maryse Lapierre-Landry, Melissa C. Skala, Vanderbilt Univ. (United States)

Current methods for acquiring and analyzing photothermal OCT (PTOCT) images (i.e. digital lock-in) require lengthy scan times, massive data burden, and time-consuming offline signal analysis. To address these practical concerns, we have incorporated optical lock-in techniques to perform real

Conference 9312: Optical Coherence Tomography and Coherence Domain Optical Methods in Biomedicine XIX

time PTOCT (rtPTOCT) imaging. In addition, we demonstrate the sensitivity of rtPTOCT to the FDA approved fluorophore indocyanine green (ICG), a clinically used dye with well-established functionalization chemistry. Scattering phantoms containing ICG were imaged, and the rtPTOCT signal was characterized with respect to modulation frequency and ICG concentration, then directly compared to PTOCT. In addition, a piece of chicken tissue was imaged before and after direct injection of ICG (10 µg/ml). The rtPTOCT signal scaled predictably according to theory, with a linear increase due to increased ICG concentration ($r^2 = 0.99$), and a nonlinear decrease with faster modulation frequencies. In addition, rtPTOCT identified a significant increase in signal over controls due to ICG concentrations as low as 1 µg/ml (10 repeated images, $p < 0.05$). When imaging the same phantom, comparisons revealed similar mean contrast to noise ratio (CNR) between digital lock-in PTOCT (5.7 ± 2.0) and rtPTOCT (6.0 ± 2.9). However, rtPTOCT imaged the same region 16.7 times faster, required a 1000 fold decrease in digital data collection, and allowed for real time analysis. Finally, rtPTOCT identified spatially confined increases in signal after injection of ICG into chicken tissue. The development of rtPTOCT for imaging near infrared fluorophores could have broad implications in studies of drug discovery, drug delivery, molecular imaging, and biological studies of pathogenesis.

9312-56, Session 8

In vivo photothermal optical coherence tomography for non-invasive endogenous absorption agent imaging

Shuichi Makita, Young-Joo Hong, Yoshiaki Yasuno, Univ. of Tsukuba (Japan)

Optical coherence tomography (OCT) is tomographic imaging of biological tissues and visualize its cross-sectional micro-structure with backscattering contrast. Its clinical value has been proven in several applications such as ophthalmology and cardiology. In addition to structural information given by the backscattering, the optical absorption will also provide yet another powerful contrast.

Optical absorbers in biological tissues, such as hemoglobin and melanin, exhibits important roles. Photothermal OCT has been emerged to contrast absorbers through measuring the local displacement due to photothermal effect. However, only demonstrations with exogenous agents are presented for cross-sectional imaging.

In this study, photothermal OCT for in vivo absorption contrast imaging is developed. A swept-source OCT system is used with a wavelength swept laser at 1310 nm with a scanning rate and range of 47 kHz and of 100 nm, respectively. Photocurrents from balanced photoreceivers are sampled by a high-speed digitizer by using k-clock from the source to sample optical spectrum in k-linear domain. The sensitivity of 110 dB is achieved. At the sample arm, the OCT probe beam and an excitation laser are combined by a dielectric mirror. The fiber-coupled laser diode of 406 nm wavelength is used for excitation.

The absorption coefficients of endogenous absorption agents are usually smaller than those of exogenous agents. Hence, the higher sensitivity is required. Spatio-temporal modulation of thermal excitation and demultiplexing of it is used to enhance the sensitivity to photothermal effect. In vivo human skin imaging of endogenous absorption agent was demonstrated.

9312-57, Session 9

Three-dimensional in vivo motion correction for high-resolution computed optical interferometric tomography

Nathan D. Shemonski, Shawn S. Ahn, Yuan-Zhi Liu, Fredrick A. South, Paul S. Carney, Stephen A. Boppart, Univ. of Illinois at Urbana-Champaign (United States)

Over the years, many computed optical interferometric techniques have been developed to perform high-resolution volumetric tomography. By utilizing the phase and amplitude information provided with interferometric detection, post-acquisition corrections for defocus and optical aberrations can be performed. The introduction of the phase, though, can dramatically increase the sensitivity to motion (most prominently along the optical axis). Here, we present the combination of two algorithms which, together, can correct for motion in all three dimensions with enough accuracy for defocus and aberration correction in computed optical interferometric tomography. The first algorithm utilizes phase differences within the acquired data to correct for motion along the optical axis. The second algorithm utilizes the addition of a speckle tracking system using temporally and spatially coherent illumination to measure motion orthogonal to the optical axis. The use of coherent illumination allows for high-contrast speckle patterns even when imaging apparently uniform samples or when highly aberrated beams cannot be avoided.

9312-58, Session 9

Anisotropic aberration correction in Fourier domain OCT using region of interest based digital adaptive optics

Abhishek Kumar, Tschackad Kamali, René Platzter, Angelika Unterhuber, Wolfgang Drexler, Rainer A. Leitgeb, Medizinische Univ. Wien (Austria)

For the first time to our knowledge, we demonstrate the numerical correction of spatially variant aberration in scanning Fourier domain (FD) OCT/OCM using region of interest (ROI) based digital adaptive optics (DAO). Using this technique, we show that diffraction limited performance can be achieved over an extended imaging depth beyond the depth of focus (DOF) for a high imaging NA of 0.6. We show the proof of principle using an iron oxide phantom sample. We also demonstrate the capability of this method by correcting anisotropic aberrations in an invitro mouse adipose tissue layer at a distance of 108 microns ($\sim 33x$ Rayleigh range) from the focal plane, thus achieving an unprecedented DOF improvement of about 17x at NA of 0.6.

9312-59, Session 9

Polarization-sensitive interferometric synthetic aperture microscopy

Fredrick A. South, Nathan D. Shemonski, Yuan-Zhi Liu, Yang Xu, Paul S. Carney, Stephen A. Boppart M.D., Univ. of Illinois at Urbana-Champaign (United States)

Interferometric synthetic aperture microscopy (ISAM) is a solution to the coherent microscopy inverse problem that enables computational 3D defocus correction. We demonstrate the extension of ISAM to polarization sensitive imaging, termed polarization-sensitive interferometric synthetic aperture microscopy (PS-ISAM). This technique is the first functionalization of the ISAM method, and it provides improved depth-of-field for polarization-sensitive imaging. We demonstrate the technique using a swept-source polarization sensitive optical coherence tomography (PS-OCT) system to image a scattering phantom. Phase stability of the system is measured and shown to be within the ISAM operating limits. After PS-ISAM processing, the defocus artifacts seen in the PS-OCT images are no longer present in the refocused PS ISAM images. This technique provides uniform resolution throughout depth and enables volumetric polarization sensitive imaging at increased numerical aperture (NA) and imaging depth. PS-ISAM will prove valuable for high-resolution volumetric imaging of birefringent materials and biological tissues of interest.

**Conference 9312: Optical Coherence Tomography and
Coherence Domain Optical Methods in Biomedicine XIX**

9312-60, Session 9

Analysis of beam shaping in optical coherence tomography in the presence of sample-induced aberrations and scattering

Andrea Curatolo, Dirk Lorenser, Peter R. T. Munro, Parvathy Sreekumar, C. Christian Singe, The Univ. of Western Australia (Australia)

Beam shaping has been employed in optical coherence tomography (OCT) for two main purposes: to extend the depth-of-focus (DOF), and, to overcome the fundamental limit imposed on imaging depth by sample induced aberration and scattering. Whilst static beam shaping can preserve resolution over larger DOFs, it does so at the expense of a reduced maximum SNR, since power is redistributed in both the transverse and axial planes. A thorough analysis of the use of extended DOF beams in OCT, and their self-reconstructing properties, should consider how these benefits and shortcomings in free-space or in sparse and low-scattering samples translate to the case of imaging through sample-induced aberration and scattering arising when imaging through dense turbid tissue. We propose such an analysis based on OCT point-spread function (PSF). We present both simulated and experimental results of imaging through aberrating layers, using Gaussian, pupil-filtered Gaussian and Bessel-like beams, each with lateral resolution of 2.6 μ m. The aberrating layers are 150 μ m thick and comprise mono-dispersions of spherical scatterers of varying diameters, resulting in OCT signal attenuation of -10 dB. We demonstrate that the higher the scattering anisotropy of the mono-dispersions, the higher the on-axis contribution of correlated scattering, and therefore the lower the image quality regardless of the beam type used. Furthermore, power redistribution along the optical axis makes the extended DOF beams more susceptible than the focal region of Gaussian beams to sample-induced aberration and scattering. However, extended DOF beams could be beneficial in regions outside of the equivalent Gaussian focus.

9312-61, Session 9

Numerical aberration correction in optical coherence tomography and holoscopy by optimization of image quality

Dierck Hillmann, Thorlabs GmbH (Germany); Hendrik Spahr, Univ. zu Lübeck (Germany); Gesa L. Franke, Carola Hain, Hinnerk Schulz-Hildebrandt, Sabrina Lohmann, Helge M. Sudkamp, Institut für Biomedizinische Optik, Univ. zu Lübeck (Germany); Gereon Hüttmann, Institut für Biomedizinische Optik, Univ. zu Lübeck (Germany) and Medizinisches Laserzentrum Lübeck GmbH (Germany)

Imaging quality and imaging depth of optical coherence tomography (OCT) are reduced by defocus and aberrations that are introduced by the imaging optics or by the sample itself. While adaptive optics is able to increase the imaging quality significantly, it is expensive and can be very involved. In addition, imaging is still limited to the Rayleigh length. We demonstrate a simple numerical approach that corrects the OCT images for aberrations and defocus. The correction is achieved by convolution of the complex en-face images with a complex phase function. The phase function is obtained by blind minimization of aberrations in the images based on an optimization algorithm (covariance matrix adaptation evolution strategy) with a suitable sharpness metric to quantify image quality. The chosen optimization algorithm works well for global optimization and noisy optimization targets and the sharpness metric shows good performance even for images of scattering structures subjected to speckle noise. Effects are shown for three-dimensional scanning Fourier-domain and full-field swept-source OCT data. Significant improvements in imaging quality could be achieved correcting aberrations and defocus over several Rayleigh lengths.

9312-62, Session 9

Demonstration of depth resolved wavefront sensing using a swept-source coherence-gated Shack-Hartmann wavefront sensor

Jingyu Wang, Adrian G. Podoleanu, Univ. of Kent (United Kingdom)

In this report we demonstrate results of measuring wavefront aberrations from different depths in a fabricated phantom using a coherence-gated Shack-Hartman wavefront sensing technique (CG-SH/WFS). The SH/WFS is equipped with a Mach-Zehnder interferometer and the coherence gating operates on principles of swept source (SS) interferometry. The CG-SH/WFS is able to differentiate wavefront signals from different depths separated by a depth resolution of 7.1 micron. The CG-SH/WFS delivers a similar SH spot pattern as that provided by a conventional SH/WFS. Due to the coherence gate, the sensor is capable of eliminating stray reflections. Hereby we present the results of measuring depth-resolved wavefront aberrations. The method is robust and all depth-resolved aberrations are recorded simultaneously without any mechanical movement. This technique has the potential of providing better correction in adaptive optics assisted ophthalmology imaging and in nonlinear microscopy.

9312-63, Session 10

OCT imaging with dynamic focus using active ultrahigh speed acousto-optic tunable lens

Ireneusz Grulkowski, Krzysztof Szulzycki, Maciej Wojtkowski, Nicolaus Copernicus Univ. (Poland)

Light delivery and collection systems play an important role in the imaging systems. The development of novel techniques of improved performance drives new applications. Several methods have been implemented to optimize the performance of axial imaging including: mechanical movement of the sample with respect to the objective lens (and vice versa), multi-beam scanning, non-diffractive beams, adaptive focus, variable focus (based on the electro-optical, electromechanical, thermo-optical or acousto-mechanical effects) etc. The aim of this study was to demonstrate application of high-speed acousto-optic tunable lens in OCT imaging. The operation of the designed acousto-optic cell was characterized theoretically and experimentally. Dynamic focusing was simulated using beam propagation method and Fourier optics. This technology was later implemented in high-resolution Fourier-domain OCT system. The impact of acousto-optic dynamic focusing on the OCT performance was assessed, and finally microscopic OCT imaging with dynamic focusing with MHz-range speed was performed. The results of OCT imaging demonstrate the ability of tunable acousto-optic lens to improve photon collection efficiency and enhance OCT image quality. Imaging with active optical elements can be also helpful in long depth range OCT imaging.

9312-64, Session 10

Simultaneous optical coherence tomography and fluorescence imaging utilizing a single illumination source

Ryan P. McNabb, Tomas Blanco, Howard M. Bomze, Henry C. Tseng, Daniel R. Saban, Duke Univ. School of Medicine (United States); Joseph A. Izatt, Duke Univ. (United States) and Duke Univ. School of Medicine (United States); Anthony N. Kuo M.D., Duke Univ. School of Medicine

**Conference 9312: Optical Coherence Tomography and
Coherence Domain Optical Methods in Biomedicine XIX**

(United States)

Standard approaches for imaging the temporal course of ocular disease typically require large cohorts of individual animals sacrificed to represent specific time points during disease development. In contrast, in vivo imaging permits true longitudinal studies of the disease process in the same animal over time. Two examples of in vivo ophthalmic imaging techniques are fluorescence imaging and optical coherence tomography (OCT). These two modalities provide different yet complementary types of information – cellular versus structural data – about the disease process. In this abstract, we describe the novel development of a truly simultaneous OCT and fluorescence imaging system sharing identical fields of view and utilizing only a single light source for illumination of both modalities. This allows both modalities to be acquired simultaneously, and the benefits of both techniques are realized without incurring increased costs in variability and time as would occur when the modalities are used separately. We show the capabilities of this system by imaging a progression of samples that exhibit both scattering and fluorescence: starting with resolution targets, progressing to ex vivo thy1-YFP mouse retinal and corneal tissue, and culminating with an in vivo longitudinal time course of a CX3CR1-GFP ocular allergy mouse model. This imaging system has the potential to be a powerful tool for scientists to non-destructively acquire in vivo imaging of both gross (OCT) and cellular (fluorescence) structures.

9312-65, Session 10

Fast volumetric imaging with subcellular resolution by Fourier domain optical coherence microscopy with numerical refocusing

Hinnerk Schulz-Hildebrandt, Gereon Hüttmann, Helge M. Sudkamp, Mario Pieper, Peter König, Gesa L. Franke, Univ. zu Lübeck (Germany); Dierck Hillmann, Thorlabs GmbH (Germany); Sabrina Lohmann, Univ. zu Lübeck (Germany)

We present an optical coherence microscopy setup using a supercontinuum light source and a 400 nm broadband spectrometer. Utilizing an objective with a numerical aperture of 0.8, we achieve a lateral resolution below 0.6 μm and an axial resolution of 1 μm in air. We present measurements of dynamic processes like cilia motion and mucus transport of tissue with subcellular resolution taken at an A-scan rate of more than 200,000 Hz.

The FD-OCT gating gives an exponential signal fall-off with depth, whereas the suppression by the confocal gating is only polynomial. Therefore, even with a depth resolution comparable to the Rayleigh length, multiple en-face planes can be imaged in parallel. The high radiant flux on the sample, which is possible due to the supercontinuum source, enables parallel imaging over tens of Rayleigh lengths. However outside the focal plane lateral resolution is considerably decreased. We demonstrate that an optimization algorithm is able to restore the image information, which is distorted by defocus and aberrations.

9312-66, Session 10

Imaging capabilities with the use of spatiotemporal optical coherence (STOC) control method

Maciej Nowakowski, Dawid Borycki, Blazej Ruszczycki, Maciej Wojtkowski, Nicolaus Copernicus Univ. (Poland)

We present a novel method of spatiotemporal optical coherence (STOC) imaging, in which the effective coherence properties of the optical field are adjusted by modulating phase of the spectral degree of coherence. Our method involves modulating the phase of the spectral degree of coherence (?), which is achieved by tailoring the optical field in object arm of the interferometer by a dynamic complex spatial filter (CSF). The CSF with a

complex transmission function is implemented using spatial light modulator (SLM), which produce phase masks with desired phase distribution. The subsequent phase masks are loaded to the SLM for the predetermined time period, which is synchronized with their acquisition and therefore, the detected light intensity at the exit of the interferometer has the desired statistical properties, corresponding to the properties of desirable secondary light source. In particular, we show that the Michelson's visibility $C = (I_{\text{max}} - I_{\text{min}}) / (I_{\text{max}} + I_{\text{min}})$ can be controlled across the interference pattern; it may be tuned from 1 to 0 (interferometric fringes washout). Our work shows preliminary experimental demonstration of scattering localization using coherence-only properties of light. Our experimental results show an improvement of spatial resolution when the STOC method is incorporated in imaging process. This is a proof of concept that the dynamic change of the phase mask (and the same the modulation of the phase of the spectral degree of coherence (?)) can provide information needed to localize the secondary source of detected light (due to scattering or reflection) and the same to be used for imaging.

9312-67, Session 10

Common-path OCT with 0.5mm forward-viewing probe

Xiaoyong Fu, Yves T. Wang, Michael W. Jenkins, Andrew M. Rollins, Case Western Reserve Univ. (United States)

Advances in miniaturized endoscopy probes for optical coherence tomography (OCT) are important to continue to make OCT endoscopy a useful tool for minimally invasive medical diagnosis, as the accessibility of some internal organs is limited by the size of the probe. We are investigating potential clinical applications like OCT imaging of the interior heart wall for radio-frequency ablation (RFA) monitoring, and OCT imaging of the renal pelvis for cancer staging. Both of these applications require OCT probes no larger than 1mm in diameter. Our previously demonstrated cone-scanning, forward viewing probes are too big, so there is a need to design and fabricate smaller scanning forward-viewing probes. We demonstrate a simple 0.5mm flexible cone-scanning forward-viewing OCT probe by splicing a 200 μm section of core-less fiber and a 150 μm section of gradient-index (GRIN) fiber to the end of a single mode (SM) fiber. The probe is designed for common-path OCT imaging and the back-reflection of the GRIN fiber/air interface is used as the reference signal. A 6.8dB signal-to-noise ratio (SNR) improvement is achieved with a 2 degree polished probe tip compared with a flat polished probe tip. A correlation algorithm is used to correct image distortion caused by the non-uniform rotation of the thin probe. Human skin is imaged to demonstrate the usability of this very thin forward-viewing probe. We will use this ultra-thin forward viewing probe for in vivo research, such as inserting it into the working channel of a flexible ureteroscope for renal pelvis monitoring and combining with an RFA probe for RFA procedure monitoring, and the results will be presented.

9312-68, Session 10

Single-shot speckle noise reduction using interleaved optical coherence tomography

Lian Duan, Hee Yoon Lee, Gary C. F. Lee, Tahereh Marvdashti, Jennifer T. Smith, Audrey K. Ellerbee, Stanford Univ. (United States)

Speckle noise is an inherent characteristic of optical coherence tomography (OCT) images associated with its nature as a coherent imaging technique. Although some speckle carries important signal information, it mostly degrades both lateral and axial resolution and blurs boundaries in OCT images. Methods of speckle noise restraint can be implemented by processed filtering of a single image or averaging images with different speckle patterns. Besides the computational expense, filtering methods are usually unable to distinguish real structures with scales close to the pixel size, and the problem with many compounding methods is that they often

**Conference 9312: Optical Coherence Tomography and
Coherence Domain Optical Methods in Biomedicine XIX**

require multiple measurements to generate a single A-scan, resulting in a reduced imaging speed.

Interleaved OCT (iOCT) is a technique capable of acquiring multiple resolvable A-lines simultaneously via spectral encoding. By proper design of the sample arm we can apply multiple illumination conditions to each the A-line and implement single-shot speckle reduction by intensity averaging of signals from different illumination channels.

In this work, two speckle noise reduction strategies are developed: 1) Spatial compounding is achieved by distributing resolvable A-lines onto a short line perpendicular to lateral scanning direction on the sample; 2) Resolvable A-lines that illuminate the same point from different incident angles permit angular compounding. We evaluate the speckle reduction efficiency of these methods compared to that of repeated scanning of the same location. Experimental results show that both spatial and angular compounding offer better speckle reduction efficiency than repeated scanning.

9312-69, Session 11

OCT imaging to determine whether ethanol-induced congenital heart defects arise through impact on cardiac neural crest cells

Lindsay M. Peterson, Pei Ma, Ganga Karunamuni, Shi Gu, Yves T. Wang, Michiko Watanabe, Michael W. Jenkins, Andrew M. Rollins, Case Western Reserve Univ. (United States)

Fetal alcohol syndrome commonly results in neurological and craniofacial defects, however as high as 54% of live-born children with this syndrome also possess cardiac abnormalities. Neural crest cells have been shown to be influenced by alcohol exposure and a subset of these cells named cardiac neural crest cells (CNCCs) play a vital role in the development of the heart. Alterations to the proliferation or migration of these cells have been shown to cause conotruncal congenital heart defects (CHDs) in syndromes such as CHARGE and DiGeorge. Here we attempt to better understand the role CNCCs play in ethanol-induced congenital heart defects (CHDs) by monitoring perturbed quail embryos at two stages of development. Cohorts of control, ethanol-exposed, and CNCC-ablated embryos were cultured and imaged with OCT at HH stage 19, while the heart is looping, and HH stage 34, after the heart has formed four chambers. At HH stage 19, the treated groups displayed abnormal gross body phenotypes, increased percentage of retrograde blood flow, abnormal pulsed Doppler trace patterns, and abnormal cardiac cushion formation. Once the embryos reached HH stage 34, perturbed groups displayed reduced volume and abnormal orientation of atrioventricular valve leaflets as well as reduced size and abnormal patterning of the great vessels, including the absence of some great vessels. The similarities in the types of structural and functional abnormalities in both ethanol-exposed and CNCC-ablated embryos suggest that CNCCs may play a role in our observed ethanol-induced CHDs.

9312-70, Session 11

Probing myocardium biomechanics using quantitative optical coherence elastography

Shang Wang, Baylor College of Medicine (United States) and Univ. of Houston (United States); Andrew L. Lopez III, Yuka Morikawa, Ge Tao, Baylor College of Medicine (United States); Jiasong Li, Univ. of Houston (United States); Irina V. Larina, Baylor College of Medicine (United States); James F. Martin, Baylor College of Medicine (United States) and The Texas Heart Institute (United States); Kirill V. Larin, Univ. of Houston (United States) and Baylor

College of Medicine (United States)

Nondestructive characterization of the myocardium biomechanics is of great importance to assist the studies in engineering and regeneration of cardiac muscle tissue. In this paper, we present a quantitative optical coherence elastographic method for noncontact assessment of the myocardium elasticity. The method is based on shear wave imaging optical coherence tomography (SWI-OCT), where a focused air-puff system is used to induce localized tissue deformation through a low-pressure short-duration air stream and a phase-sensitive OCT system is utilized to monitor the propagation of the induced tissue displacement with nano-scale sensitivity. The 1-D scanning of M-mode OCT imaging and the application of optical phase retrieval and mapping techniques enable the reconstruction and visualization of the 2-D depth-resolved shear wave propagation in tissue with ultra-high frame rate. The wave group velocity is quantified through the cross-correlation of the tissue temporal deformation profiles at all measurement locations and also the linear fit of the correlation data plotted in the domain of time delay versus wave propagation distance. The feasibility of this method in quantitative elasticity measurement is demonstrated on tissue-mimicking phantoms with the estimated Young's modulus compared with uniaxial compression tests. We also performed pilot experiments on ex vivo mouse cardiac muscle tissues with normal and genetically altered cardiomyocytes. Our results indicate this noncontact quantitative optical coherence elastographic method can be a useful tool for the cardiac muscle research and studies.

9312-71, Session 11

Evaluation of the functional role of a circadian gene, cryptochrome, on Drosophila heart development using ultrahigh resolution optical coherence microscopy

Aneesh Alex, Lehigh Univ. (United States); Airong Li, Genetics and Aging Research Unit, Harvard Medical School (United States); Xianxu Zeng, Zhan Zhang, Third Affiliated Hospital of Zhengzhou Univ. (China); Rudolph E. Tanzi, Genetics and Aging Research Unit, Harvard Medical School (United States); Chao Zhou, Lehigh Univ. (United States)

We present a longitudinal study analyzing the structural and functional changes of the Drosophila heart in the same specimen throughout its post-embryonic lifecycle using an ultrahigh resolution optical coherence microscopy (OCM) system. The OCM system was capable of acquiring M-mode images at a frame rate of 128 Hz, and provided axial and transverse resolutions of 1.5 μm and 3.9 μm , respectively. The Drosophila heart exhibited major structural and functional alterations during its development lifecycle. Notably, a conical chamber was formed de novo and the heart became two segments shorter by eliminating the posterior heart region during metamorphosis. Heart rate (HR) reduced significantly as the specimen entered the pupa stage and stopped beating completely during most of pupa day 2. The heart restarted to beat during pupa day 3 and HR increased to reach its maximum at the adult stage. In addition to HR, heartbeat duty cycle also showed significant variations during the Drosophila lifecycle. To identify whether a circadian gene, Cryptochrome (dCry), affects the heart development in Drosophila, we silenced dCry in Drosophila heart and quantitatively determined the functional effect of dCry on heart development. Silencing of dCry resulted in slower heart rate, reduced heartbeat duty cycle, smaller heart chamber size and pupa lethality. Our results provided novel evidence that the circadian gene, dCry, played a critical role in heart morphogenesis and function. Thus, this longitudinal study in Drosophila demonstrates OCM as a promising tool for evaluating genes associated with cardiac development and to understand the underlying functional mechanisms.

**Conference 9312: Optical Coherence Tomography and
Coherence Domain Optical Methods in Biomedicine XIX**

9312-72, Session 11

Monitoring the vascular response to biomaterials with speckle variance OCT

Kristin M. Poole, Devin R. McCormack, Christopher E. Nelson, Craig L. Duvall, Melissa C. Skala, Vanderbilt Univ. (United States)

The use of biomaterials to deliver therapeutics that promote vascularization and ameliorate oxidative stress is of interest for many disease applications including peripheral arterial disease (PAD). Diabetic patients are especially susceptible to PAD due to chronic inflammation and increased reactive oxygen species (ROS) production. Preclinical studies in the diabetic mouse hind limb ischemia (HLI) model of PAD have shown that the impaired vascular response can be improved by reducing oxidative stress, indicating that delivery of antioxidant therapeutics has significant potential for treatment of chronic inflammatory diseases like diabetic PAD. In this work, we validated the use of speckle variance optical coherence tomography (OCT) and hyperspectral imaging for detecting quantitative differences in the vascular response to HLI using two mouse strains with differing ischemic recovery. We established quantitative metrics for this model, and applied the non-invasive, quantitative imaging methods to evaluate the response to a novel ROS-responsive, antioxidant/anti-inflammatory therapy for diabetic PAD. Quantitative analysis of speckle variance OCT revealed significant increases in vessel diameter, area density, and length fraction in FVB mice in comparison to Balb/c mice which are known to have poor recovery. In our evaluation of the therapeutic treatment, diabetic mice receiving therapy demonstrated enhanced recovery in measurements of hemoglobin oxygen saturation (hyperspectral imaging) and vascular morphology parameters (OCT). These results demonstrate the utility of our optical imaging approach for evaluating the vascular response to biomaterials in preclinical studies, and the potential for ROS-responsive microspheres as a "smart" vehicle for on-demand drug release for treatment of chronic inflammatory diseases.

9312-73, Session 11

Local depolarization in polarization sensitive optical coherence tomography

Norman Lippok, Martin L. Villiger, Brett E. Bouma, Wellman Ctr. for Photomedicine, Massachusetts General Hospital (United States) and Harvard Medical School (United States)

Polarization sensitive optical coherence tomography (PS-OCT) measures the sample Jones matrix as a function of depth. Conventional reconstructions retrieve sample retardation and diattenuation, either as cumulative measurements in respect to the sample surface, or as a local expression, by comparing the polarization states over a short differential depth. Such local, or differential tissue polarimetry has attracted increased interest to provide more intuitive measures of polarization properties, especially for tissues with a layered architecture. In this work we use spatial averaging to generate experimental measurements of general Mueller matrices. In order to reconstruct the local, depth-dependent tissue properties, we apply the differential Mueller matrix formalism and extract several local depolarization parameters in addition to local retardation and diattenuation for various samples. This local polarimetry provides additional insight into tissue optical properties and might prove useful in the disease diagnosis and characterization.

9312-74, Session 11

Molecular imaging needles combining OCT with fluorescence for identification of cell-specific antibodies in deep tissue

Loretta Scolaro, Dirk Lorensen, Anne Kramer, George C. Yeoh, David D. Sampson, Robert A. McLaughlin, The Univ. of Western Australia (Australia)

Molecular imaging (MI) needles are miniaturized optical imaging probes that combine single-cell sensitivity molecular (fluorescence) imaging with structural imaging (optical coherence tomography, OCT). For the first time, we demonstrate the capability of these probes to acquire dual-modality images of antibody-labelled tissue in whole mouse livers

The probe is based on a double-clad fiber (DCF) design to carry both the OCT signal and fluorescence signal, and is encased in a hypodermic needle (outer diameter 640 microns), which facilitates imaging deep within solid tissue. The MI needle was measured to have an OCT FWHM lateral resolution of 7 microns at a distance of 300 microns, and a sensitivity of 100dB. For fluorescence detection, the MI needle was able to detect 5nM fluorescein diluted in saline at pH 9.5. Using an asymmetric DCF coupler, it was interfaced to a 1310nm swept-source OCT system and a fluorescence imaging system.

To assess imaging in whole organs, livers were dissected from two mice. In the first, epithelial cells lining the common bile duct were labelled with an epithelial cell adhesion molecule antibody (EpCAM) conjugated with the fluorophore Alexa Fluor 488. In a second liver, endothelial cells were labelled with FITC-conjugated albumin. An MI needle was inserted into each whole liver, and acquired a co-registered 3D OCT data set and a 2D radial fluorescence projection image.

Results showed fluorescently-labelled epithelial and endothelial cells, respectively, at a depth of > 10mm. The 3D OCT data was found to help facilitate interpretation of the 2D radial fluorescence projection image.

9312-75, Session 11

Correlation between polarization sensitive optical coherence tomography and second harmonic generation microscopy in skin

Hoan Viet Le, Seunghun Lee, Bumju Kim, Yeoreum Yoon, Ki Hean Kim, Pohang Univ. of Science and Technology (Korea, Republic of)

In the field of optical imaging, polarization sensitive optical coherence tomography (PS-OCT) and second harmonic generation (SHG) microscopy are two promising tools for visualizing skin dermis layer structures. Our purpose is to examine the correlation between skin images from PS OCT and SHG microscopy. We imaged rat skin samples by both SHG microscopy and PS-OCT and conducted qualitative and quantitative analysis on these images. Collagen orientation index was extracted from power plot of SHG images Fast Fourier Transform while birefringence property was characterized by slope of the phase retardation plot of PS OCT images. For PS OCT images, we saw that the transition from black to white region in rat back skin images is slower and less even than in rat leg skin images. SHG images showed the collagen in dermis layer of rat leg skin with higher organization than of rat back skin. The correlation was confirmed by data from quantitative analysis: rat leg skin which has a significantly higher slope in the phase retardation plot has a higher values of collagen orientation index. We imaged various rat skin samples to get statistical correlation coefficient. The statistical result showed a linear correlation between phase retardation slope and collagen orientation index. This is an interesting relationship between birefringence, a microscopic property and collagen organization, a bulk property of skin dermis layer, it may be useful in the further studies of skin diseases or burn.

**Conference 9312: Optical Coherence Tomography and
Coherence Domain Optical Methods in Biomedicine XIX**

9312-76, Session 11

Analysis of multidimensional scanning dynamic light scattering-based optical coherence tomography for diffusion-independent, sub-500 $\mu\text{m/s}$ in vivo transverse velocimetry

Brendan K. Huang, Kevin C. Zhou, Yale Univ. (United States); Mustafa K. Khokha, Hemant D. Tagare, Yale School of Medicine (United States); Michael A. Choma M.D., Yale Univ. (United States) and Yale School of Medicine (United States)

Quantification of flow transverse to the optical axis is important for many problems in medicine, including studying mucociliary flow. Unlike standard Doppler velocimetry, which is insensitive to transverse flow, the OCT-based dynamic light scattering (DLS) signal is sensitive to transverse motion of scatterers. We recently showed that by introducing a scan bias to our DLS-OCT protocol, we could overcome one limitation of standard DLS-OCT and resolve both directionality and speed of flow. The introduction of the scan bias, however, adds a new dimension of data processing. Here, we present a framework for analyzing higher dimensional DLS-OCT data. Using this analysis, we show that our method has the additional advantage of being insensitive to solution dispersity, in contrast to standard DLS. Finally, we demonstrate sub-500 $\mu\text{m/s}$ transverse velocimetry in the *Xenopus laevis* animal model system of ciliary flow.

9312-77, Session 12

Real-time, label-free optical property mapping for detecting glioma invasion with SSOCT for potential guidance of surgical intervention

Carmen Kut, Jiefeng Xi, Kaisorn Chaichana M.D., Jordina Rincon-Torroella, Fausto Rodriguez, Elliot McVeigh, Alfredo Quinones-Hinojosa M.D., Xingde Li, The Johns Hopkins Hospital (United States)

Glioblastoma (GBM) is the most common and most aggressive primary brain cancer in adults, with a median survival of 14 months. Surgery is the first-line therapy for GBM and the extent of resection is the most important factor in delaying cancer recurrence and prolonging survival for GBM patients. Thus, there is a critical need for a technology that can provide real-time, intra-operative guidance in brain tumor detection. Compared to other explored surgical guidance technologies, OCT offers an excellent balance between imaging resolution and volume and is label free. In addition, quantitative analysis of OCT images can also generate color-coded optical property maps, which enable direct visualization of tumor versus non-tumor and thus provide guidance during surgery. In this study, we have systematically characterized the optical properties of brain tumor versus non-tumor tissues in 32 patients with excellent sensitivity and specificity. We have also developed a GPU accelerated method to process and display optical properties in real-time within 1-2 seconds for volumetric tissue samples. To our knowledge, this is the first study to achieve real-time imaging and optical property mapping capabilities in differentiating brain cancer from non-cancer tissues; the significant speed-up will greatly increase the translational and practical potential of bringing the OCT technology into the neurosurgical operating room. The intraoperative use of OCT may facilitate safe, extensive resection of infiltrative brain cancers and may lead to safer surgeries with improved outcomes.

9312-78, Session 12

Light scattering from myelinated axons in optical coherence microscopy imaging of the cerebral cortex

Dawid Borycki, Univ. of California, Davis (United States) and Nicolaus Copernicus Univ. (Poland); Conor Leahy, Vivek J. Srinivasan, Univ. of California, Davis (United States)

In this study we report on the capabilities and limitations of the Optical Coherence Microscopy (OCM) employed for imaging of myelinated axons. Cortical myelination plays an important role in the workings of the neural circuits since it speeds up the propagation of nerve impulses between synapses. Successful transmission of neural signals through axons is required for many cognitive, sensory and motor functions. Thus, noninvasive in vivo and ex vivo techniques for cortical myelination imaging may help in both performing tractography of the normal brain and in characterizing demyelination in diseases.

However, myelinated axons exhibit orientation-dependent backscattering characteristics. Therefore, only the backscattering from myelinated axons in the en face plane can be clearly visualized by distinguishing them from the background signal. For tractography applications, it is desirable to image all myelin orientations. Accordingly, to enhance the contrast of other orientations of myelin fibers it is necessary to understand light scattering from those structures.

To this end we have developed theoretical model, which incorporates the generalized Lorenz-Mie theory of the arbitrary beam scattering from multilayered, concentric, infinite cylinders. In our framework the set of linear equations for field expansion coefficients (Mie coefficients) is represented in a matrix form, while the incident electromagnetic field is described using the beam-shape distributions.

Furthermore, we present results of the far-field angular distribution of the plane wave and Gaussian beam scattered from two-layered concentric cylinder, which model the myelinated axon. We compare the model results with OCM imaging of myelinated axons in cortical tissue.

9312-79, Session 12

Three-dimensional ultrastructure study of cervical collagen fibers using optical coherence tomography

Yu Gan, Wang Yao, Kristin M. Myers, Joy Y. Vink, Ronald J. Wapner, Christine P. Hendon, Columbia Univ. (United States)

The ultrastructure of collagen fiber bundle is an important determination of cervix as it functions as a mechanical barrier for delivery. We develop an image processing tool to investigate the ultrastructure of cervix using optical coherence tomography (OCT).

We first increase the field of view (FOV) through a registration method to view the whole axial slice of cervix. We pair multiple OCT volumes using shift invariant features and globally estimate the offsets between volumes on en face plane and at depth. We employ an error auto-correction procedure to eliminate the highly erroneous pair-wise estimation. We use a gain compensation and multiband blending method to smooth the overlapped space between adjacent volumes. Then, we apply a gradient based fiber orientation algorithm to measure directionality map of collagen fiber bundles for OCT images that are parallel to surface. Given that the collagen fiber bundles shows dispersion in cervical samples, we analyze the dispersion of directionality map at different locations of cervix. We obtain representative samples from patients using an Institutional Review Board (IRB) approved protocol at the Columbia University Medical Center. We acquired at least 40 OCT volumes from each cervix, for non-pregnant and pregnant samples. We stitch the volumes and perform dispersion analysis

Conference 9312: Optical Coherence Tomography and Coherence Domain Optical Methods in Biomedicine XIX

on each sample.

Experimental results show that we have the capability to enlarge the volume by stitching and visualizing multiple OCT volumes. Dispersion analysis confirms statistical difference in ultrastructure between pregnant and non-pregnant samples. Ultrastructure in enlarged FOV of OCT imaging sets will facilitate mechanical tests of cervix.

9312-80, Session 12

Long-range memory in OCT fluctuations reveals stromal-epithelial interactions in 3D co-culture

Amy L. Oldenburg, Thomas Gilliss, Oluwafemi S. Alabi, Russell M. Taylor II, Melissa A. Troester, The Univ. of North Carolina at Chapel Hill (United States)

A richness of functional information is available from time-dependent (speckle fluctuation) properties of tissues. While speckle fluctuation models have been well-developed for particle flow and diffusion in OCT, little is known about the shape of the power spectra arising from intracellular motions in living tissues. We find that the power spectrum of intracellular motility in vitro appears to be well-described by an inverse power law, and is distinct from the Lorentzian distribution expected for diffusion. Interestingly, the inverse power law (also known as $1/f$ noise) is scale-invariant and arises in systems with long-range memory.

Here we demonstrate the relevance of the exponent, alpha, of inverse power law scaling in 3D breast tissue models. 3D tissues are important in cancer research due to microenvironmental effects that are not recapitulated in 2D. We measured alpha from the speckle fluctuation spectra of normal and pre-malignant mammary epithelial cells in 3D co-culture with stromal fibroblasts. We observed larger alpha from cells on the shell of the spheroid compared to the core, and larger alpha value of cells within the core in response to increasing density of stromal fibroblasts. This suggests that the biophysical evidence of stromal-epithelial interactions can be directly observed in 3D co-cultures in real-time and non-invasively using only endogenous contrast signals available in OCT. The relevance of the inverse power law in this study implicates biophysical processes with scale invariance and long-range memory. Thus, this type of model could lead to new methods to disambiguate biophysical processes with long-range memory.

9312-81, Session 12

Differentiation of morphotic elements in the human blood using optical coherence tomography with microfluidic setup

Pawel Ossowski, Nicolaus Copernicus Univ. (Poland) and AM2M LLC-LP (Poland); Anna Raiter, Anna Szkulmowska, AM2M LLC-LP (Poland); Maciej Wojtkowski, Nicolaus Copernicus Univ. (Poland) and AM2M LLC-LP (Poland)

We demonstrate a novel label-free method allowing optical detection and differentiation of moving micro objects, such as blood cells using amplitude and phase information from OCT signals applying dedicated microfluidic device. In this study we use standard Fd-OCT/OCM system with broadband light source (axial resolution: $3\ \mu\text{m}$ in tissue and lateral resolution $4\text{-}8\ \mu\text{m}$) and microfluidic sample setup. The microfluidic device consists of microchannels embedded in scattering medium (polymer mixed with TiO_2). Sample scanning is not performed during M-scan measurements since the flow inside the microchannel is forced by a syringe pump. The novel part of this method is that the optical identification is based on optical signal coming from optically uniform scattering media localized beneath the flowing/moving objects and not from the objects itself. This signal reveals as an enhancement in speckle pattern on intensity images and non-zero phase change on phase images. Statistical parameters of such signals depend

on the features of the object, like its size, shape, internal structure, etc. In order to demonstrate the effectiveness and reliability of proposed method, we performed an experiment to differentiate erythrocytes and leukocytes. Obtained OCT cross-sectional images present signal enhancement from blood cells (modulation signals) in the scattering base, both on intensity and phase-change images. This modulation signals, corresponding to erythrocytes and leukocytes, are significantly different and could be easily distinguished qualitatively. Statistical parameters used for the analysis also represent satisfactory separation to distinguish between different kinds of cells. Above-mentioned results of differentiation are presented in this submission.

9312-82, Session 12

Optical coherence tomography of discrete random media

Dirk J. Faber, Mitra Almasian, Nienke Bosschaart, Ton G. van Leeuwen, Academisch Medisch Centrum (Netherlands)

Changes in cellular ultrastructure during disease development lead to measurable differences in light scattering. To understand measured optical properties in terms of sample organization, we derive an expression for the OCT signal obtained from Discrete Random Media which is determined by (a) the scattering properties of individual particles and (b) the interference of their scattered fields as expressed by the Structure factor (the Fourier transform of the pair correlation function, i.e. the probability density function for particle separations). We regard this as an essential stepstone to quantitatively link OCT derived optical properties to pathology reports of suspected lesions.

9312-83, Session 12

Image quality assessment in speckle variance optical coherence angiography

Andrea Lozzi, Anant Agrawal, Noah Greenbaum, Erkinay Abliz, Cristin G. Welle, Daniel X. Hammer, U.S. Food and Drug Administration (United States)

Optical coherence angiography (OCA) is a variant of optical coherence tomography (OCT) used to visualize vasculature. This technique is able to detect inter-B-scan intensity (speckle) or phase changes that arise from moving particles (erythrocytes). To quantify flow velocity (mm/s) it requires temporal sampling of the particle-beam interaction. In order to achieve high image quality in OCA, optical and algorithmic parameters need to be adjusted depending on the application and flow range. The experimental and algorithmic parameter space can be large and typically requires trade-offs to achieve optimum performance. The goal in general is to maximize image quality, and several quantitative metrics has been established for reflectance OCT. Image quality metrics and a comprehensive exploration of parameter space for speckle variance OCA has not been fully investigated. We used a 1300-nm spectrometer-based OCT system to image the capillary network in mouse primary motor cortex. We varied optical and algorithmic parameters, including spot size, B-scan difference mode, gate length (number of B-scans), and correlation width (flow algorithm parameter), and compared image quality in a region of capillaries in terms of Michelson contrast and signal-to-noise ratio. For the B-scan difference mode, the image contrast for mean absolute difference was ~ 1.2 times better than for traditional variance (standard deviation) for 100 average B-scans. This resulted in a more contiguous capillary network with lower background noise. Better quantification of speckle variance OCA image quality will enable investigators to make better informed design decisions to achieve optimal visualization of vasculature and detection of flow velocities.

9312-84, Session 12

**In-vivo visualization of skin inflammation
by optical coherence tomography and
two-photon microscopy**Bumju Kim, Seong Hun Lee, Ki Hean Kim, Pohang Univ. of
Science and Technology (Korea, Republic of)

Inflammation is one of defensive mechanism of biological tissue. It includes heat, swelling, blood vessel dilation, immune cell migration and other symptom. It is hard to image such as complex biological response with only one imaging system. We used optical coherence tomography (OCT) and two-photon microscopy (TPM) for imaging the inflammation response of the mouse ear. These two imaging modalities provide complementary information since each system based on different physical phenomenon: structural and physiological information by OCT, and molecular and cellular information by TPM. Inflammation was induced by spreading lipopolysaccharide (LPS) on the mouse ear pinna and were imaged longitudinally. From this inflammation model, we could visualized thickening of the ear caused due to swelling by intensity OCT, vessel dilation by angiographic OCT in a few millimeter field of view. Capillary dilation and the migration of immune cells were visualized by autofluorescence based TPM at the sub cellular resolution in a few hundred micrometer field of view. These results showed that combination of OCT and TPM provided various information about inflammation process within tissues in vivo.

Conference 9313: Advanced Biomedical and Clinical Diagnostic and Surgical Guidance Systems XIII

Sunday - Tuesday 8-10 February 2015

Part of Proceedings of SPIE Vol. 9313 Advanced Biomedical and Clinical Diagnostic and Surgical Guidance Systems XIII

9313-1, Session 1

Human thyroid imaging using optical coherence tomography

Sarah J. Erickson-Bhatt, Ryan M. Nolan, Fredrick A. South, Nathan D. Shemonski, Adeel Ahmad, Eric J. Chaney, Marina Marjanovic, Univ. of Illinois at Urbana-Champaign (United States); Andrew J. Cittadine, Adam M. Zysk, Diagnostic Photonics, Inc. (United States); Daniel T. McCormick, AdvancedMEMS (United States); Jeffrey Putney, Donald Darga, Diagnostic Photonics, Inc. (United States); Steven G. Adie, Univ. of Illinois Urbana-Champaign (United States); Paul S. Carney, Univ. of Illinois at Urbana-Champaign (United States); John Brockenbrough M.D., Zheng G. Liu M.D., Kelly Cunningham M.D., Carle Foundation Hospital (United States); Stephen A. Boppart M.D., Univ. of Illinois at Urbana-Champaign (United States)

The thyroid gland (located at the front of the neck) is responsible for secreting hormones which influence metabolism, growth and development, and body temperature. Thyroid cancer is the most common cancer of the endocrine system, and the National Cancer Institute predicts 62,980 new cases of thyroid cancer and 1,890 deaths in the U.S. in 2014. Imaging methods for thyroid diagnostics include ultrasound, magnetic resonance imaging (MRI), computed tomography (CT), nuclear scintigraphy, and fine needle aspiration (FNA) followed by light microscopy. These methods are typically used to diagnose "suspicious" thyroid nodules which could be indicative of cancer. However, there are several challenges during thyroid surgery that indicate the need for intraoperative imaging tools. Those challenges include distinguishing benign adenoma from carcinoma, assessing the state of metastatic spread of cancer beyond the thyroid, and examining lymph nodes, the most common route of metastasis and recurrence. Optical coherence tomography (OCT), the optical analogue to ultrasound imaging, has demonstrated the ability to distinguish normal, benign, and malignant thyroid tissue with micron-scale resolution. Our group has developed a novel portable intraoperative OCT system with a handheld surgical probe, and previously demonstrated in vivo imaging within the tumor cavity during breast cancer surgery. OCT images of over 100 ex vivo human thyroid specimens (including normal, benign, and malignant tissues) from more than 25 patients have been collected, and optical biomarkers for specific tissue types have been identified. These biomarkers are subsequently being used to identify tissue types during intraoperative OCT imaging using our portable OCT system.

9313-2, Session 1

Real-time intraoperative auto-fluorescence imaging for parathyroid detection

Melanie A. McWade, Vanderbilt Univ. (United States); James T. Broome, St. Thomas Hospital (United States); Carmen C. Solorzano, Anita Mahadevan-Jansen, Vanderbilt Univ. (United States)

The inability to accurately localize the parathyroid glands is a significant cause of unfavorable surgical outcomes during endocrine surgery. Trauma or accidental removal of normal parathyroid glands can damage serum calcium regulation. Current imaging methods are restricted by their inability to detect healthy glands or provide intraoperative information. Feasibility

of intraoperative parathyroid detection has been previously shown using fluorescence spectroscopy because the parathyroid emits a near-infrared (NIR) auto-fluorescence signal of higher intensity than the thyroid and surrounding neck tissue. We have furthered this technology by developing an imaging system for parathyroid detection that provides non-contact, real-time, spatial imaging of the entire surgical field. In a clinical study, an endoscope camera adapted for use in the NIR was used for imaging on patients undergoing parathyroidectomy or thyroidectomy. Results show a robust, consistent NIR auto-fluorescence signal emitted from the parathyroid gland can be detected with fluorescence imaging with 100% accuracy regardless of disease state. Fluorescence images consistently showed 2.4 - 8.5 times higher emission intensity from the parathyroid than surrounding tissue. This intraoperative tool for parathyroid detection does not require administration of exogenous contrast agents, thereby reducing procedure time and eliminating potential toxicity risks.

9313-3, Session 1

Performance comparison of different compact NIR fluorescent imaging systems with goggle display for intraoperative image-guidance

Shengkui Gao, Suman B. Mondal, Washington Univ. in St. Louis (United States); Nan Zhu, Rongguang Liang, College of Optical Sciences, The Univ. of Arizona (United States); Samuel Achilefu, Washington Univ. School of Medicine in St. Louis (United States); Viktor Gruev, Washington Univ. in St. Louis (United States)

Near-infrared (NIR) fluorescent imaging modality for image guided surgery has witnessed tremendous progress in the last few years due to the emergence of both NIR molecular markers and NIR-visible spectrum imaging systems. These imaging systems have been successfully used in the operating room setting, assisting the surgeons in accurate visualization of tumor tissue from healthy tissue. Several commercial NIR fluorescent imaging systems (NFIS) have been developed for human trials and clinical research. However, most existing NFIS have complex opto-electronic setup and large footprint, which make them impractical for surgical use due to the limited space in the operating room. A compact NFIS coupled with goggle display can greatly facilitate intraoperative use and can offer hand-free feature and direct hand-eye coordination of the surgeon. In this paper, we present performance comparison of three compact NFIS prototypes that we developed for intraoperative guidance: dual miniature lenses camera with LED tracker, three lenses camera with stereoscopic view and miniature dichroic NIR-visible camera. Their performance is evaluated according to sensitivity regarding different ICG concentrations, accuracy of image overlay between NIR and visible channels, compactness and practicability in intraoperative use. According to the comparison results, our prototypes establish better or equal performance than current available NFIS in sensitivity, accuracy and compactness, which suggest great potentials of using these NFIS to improve user experience and surgical outcomes in intraoperative use.

**Conference 9313: Advanced Biomedical and
Clinical Diagnostic and Surgical Guidance Systems XIII**

9313-4, Session 1

**Real-time fluorescence-guided tumor
visualization for intraoperative surgical
resection**

David S. Kittle, Adam Mamelak M.D., Cedars-Sinai Medical Ctr. (United States); Julie Novak, Stacey Hansen, Blaze Bioscience, Inc. (United States); Keith L. Black M.D., Pramod V. Butte, Cedars-Sinai Medical Ctr. (United States)

There has been immense excitement regarding the use of targeted fluorescent agents bound to an antibody, peptide, or nanobody, enabling visualization of tumors intra-operatively to aid near-complete resection. Consequently, developing instrumentation for this purpose has seen much enthusiasm over the past few years. We report on a simple, single camera solution using strobed excitation and illumination, enabling novel advanced imaging processing opportunities. The system captures both visible reflectance and NIR fluorescence at 300 fps while displaying full HD resolution video at 60 fps, with ambient light background subtraction, high-dynamic range sequences, fluorescent image overlay, noise cancellation, and autofocus analysis. The system is capable of operating with minimal user intervention, however the user can choose between many different modes of operation such as visible only, visible with NIR, NIR fluorescence only and a special high contrast mode depending on sensitivity level and ambient background lighting conditions. We will demonstrate that our algorithm is capable of displaying the video of the surgical field with less than 60ms latency even though the high frame-rate of the camera requires enormous processing of data (>850 MB/s). Continuous recording at 30 or 60 fps in full HD resolution for up to several hours is user selectable along with still capture at any time during the operation via foot pedal. We have built an intra-operative imaging system using a single RGB camera capable of capturing both visible and NIR fluorescence, using efficient image processing enabling capture of full HD resolution at 300 fps and display 60 fps.

9313-5, Session 2

**In-vivo tumor bed assessment after soft
tissue sarcoma excision using Raman and
fluorescence spectroscopy**

John Quan M. Nguyen, Vanderbilt Univ. (United States); Zain S. Gowani, Vanderbilt Univ. Medical Ctr. (United States) and Vanderbilt Medical Scholars Program (United States); Maggie E. O'Connor, Vanderbilt Univ. (United States); The-Quyen Nguyen, Northwestern Univ. (United States); Ginger E. Holt, Vanderbilt Univ. Medical Ctr. (United States); Anita Mahadevan-Jansen, Vanderbilt Univ. (United States)

Soft Tissue Sarcomas (STS) are a heterogeneous group of malignant tumors that arise from mesenchymal tissues. The current mainstay of treatment is to completely excise the tumor within a margin of normal tissue so that malignant cells no longer remain within the tumor bed, as the presence of residuals has been associated with local recurrence and reduced patient survival rates. Margin status is a central prognostic factor for curative treatment and is currently done using post-operative frozen section biopsies. However, this method is time consuming and suffers from sampling error. Here, we will demonstrate that near-infrared autofluorescence imaging combined with Raman spectroscopy can provide differential diagnosis of STS and normal tissues with high sensitivity and specificity. Both Raman and fluorescence spectra were acquired in-vivo from human patients undergoing STS resection at the Vanderbilt University Medical Center. This combination provides a rapid, non-invasive, and non-destructive surgical guidance tool that can be intraoperatively used to identify suspicious margins for immediate re-excision.

9313-6, Session 2

**Smart surgical tools: real-time time-
resolved fluorescence spectroscopy
integration with surgical tools for intra-
operative tumor detection**

Pramod V. Butte, Cedars-Sinai Medical Ctr. (United States); Fartash Vasefi, Cedars-Sinai Medical Ctr (United States); David S. Kittle, Cedars-Sinai Medical Ctr. (United States); Chirag Patil M.D., Cedars-Sinai Medical Ctr (United States); Ray Chu M.D., Keith L. Black M.D., Cedars-Sinai Medical Ctr. (United States)

Time resolved fluorescence spectroscopy (TRFS) has demonstrated potential in characterizing brain tumors. In order to translate from bench to bed-side, integration of this technology in existing surgical tools is necessary. We have built novel prototype instrumentation with integration of the optical fiber in the surgical devices for real-time data capture and analysis. The instrument uses a 355 nm laser to excite the tissue and record the demuxed (6 distinct color bands between 360-700 nm) fluorescence using a MCP-PMT (80 ps rise time). The data is digitized at 7 GSamples/s and analyzed using laguerre deconvolution with a lifetime accuracy of <50 ps in real-time. The optical fiber with very low auto-fluorescence has been integrated with a Roton sucker used in neurosurgery. The TRFS system is currently undergoing clinical trials to record data from patients undergoing brain surgery. The pathology of the tissue scanned with TRFS is then confirmed with a biopsy and H&E staining. We will present our system characteristics along with preliminary intra-operative data recorded from human patients and our experience of using a real-time TRFS integrated with a surgical instrument. Integration with Roton sucker has allowed a seamless data collection without extending the surgical procedure time. The TRFS system is able to differentiate the tumorous tissue from normal brain tissue using their fluorescence decay responses in six spectral channels. This work presents an example of integrating a fiber optic probe into a surgical suction instrument for intra-operative tissue assessment capability transforming current instrumentation to a new smart surgical tool.

9313-7, Session 2

**High spatial frequency structured light
imaging for intraoperative breast tumor
margin assessment**

David M McClatchy III, Venkataramanan Krishnaswamy, Stephen C. Kanick, Jonathan T. Elliott, Thayer School of Engineering at Dartmouth (United States); Wendy A. Wells M.D., Richard J. Barth M.D., Dartmouth Hitchcock Medical Ctr. (United States); Keith D. Paulsen, Brian W. Pogue, Thayer School of Engineering at Dartmouth (United States)

A new superficial wide-field imaging technique is presented, which utilizes high spatial frequency structured illumination to constrain the light sampling volume to a sub-diffuse regime. In this transport regime, the effects of absorption are drastically reduced and the sensitivity to local scattering from ultrastructural alterations is increased. Absorption independence is validated with multiple experiments including a bovine blood-intralipid solution matrix and avian tissue with superficial bovine blood. The resulting structured light demodulated images show a complete insensitivity to the blood over Hb concentrations of 0 - 240 μ M. Increased sensitivity to ultrastructural changes is demonstrated by imaging avian tissue with controlled morphological alterations including formalin-induced crosslinking. This imaging technique is currently being translated towards intraoperative assessment of breast tumor margins because of its ability to capture an entire lumpectomy margin in a single field of view, insensitivity

Conference 9313: Advanced Biomedical and Clinical Diagnostic and Surgical Guidance Systems XIII

to confounding surface blood present on lumpectomies, and its inherent scatter signal without the need of any model inversion. Further, a new lumpectomy marking system is introduced that allows for both the surgeon to mark the lumpectomy during excision and optical assessment of the specimen after the margins have been marked. Structured light images acquired intraoperatively of all margins of lumpectomy specimens are presented to show feasibility of clinical translation. Immediate future work will focus on developing a multi-spectral system.

9313-8, Session 2

Molecular imaging for the detection of kidney tumor margins

Shona D. Stewart, Patrick J. Treado, Heather Kirschner, Jeffrey Horn, ChemImage Corp. (United States); Amonu Opong, Jeffrey K. Cohen M.D., Allegheny General Hospital (United States)

More than 1.6 million people in the United States are expected to be diagnosed with cancer in 2014; approximately 585,000 people are expected to die of cancer. Local recurrence of disease is a critical problem which can often result from incomplete tumor excision during initial surgery. Between 20% and 30% of patients who undergo surgery require reoperation because of incomplete excision. Currently, tumor margins are identified post-surgery through histological evaluation of the tissue biopsy. As such, one in four patients who undergo tumor resection surgery will require re-operation in order to fully excise the malignant tissue.

We are currently developing an intraoperative device for detecting tumor margins in real-time. Molecular Imaging (MI) exploits liquid crystal tunable filter technology and combines digital imaging with molecular spectroscopy to provide information-rich hyperspectral images of biological materials without the use of reagents. MI of human kidneys in the visible and near infrared (Vis/NIR) regions has differentiated, with high performance, tumor from non-tumor. In a preliminary study of 13 whole kidneys removed during surgery, tumor and non-tumor spectra extracted from Vis/NIR molecular images were used to generate a PLS-DA model for detecting kidney tumors. The performance of this model was 83% sensitivity and 89% specificity.

Hyperspectral imaging is a high resolution technique for developing analytical methodologies. In order to adapt MI to real-time speeds for intraoperative use, the conventional MI technology must be modified. Our product development strategy for MI tumor margin detection exploits the concepts of compressive sensing and dual polarization.

9313-9, Session 3

A 360 degree view endoscope using miniaturized panomorph optics for 3-D colon mapping

Qiyin Fang M.D., McMaster Univ. (Canada); Simon Thibault, Univ. Laval (Canada); Samir Sahli, McMaster Univ. (Canada); Pierre Desaulniers, Univ. Laval (Canada); Brendan Kaas, Ian Phillips, McMaster Univ. (Canada); Patrice Roulet, ImmerVision (Canada); Jocelyn Parent, ImmerVision (Canada); Hu Zhang, ImmerVision (Canada); David Armstrong, Frances Tse, Shawn Petrik, McMaster Univ. (Canada)

Cancer of the gastrointestinal tract is the second most common cause of cancer death. Studies have shown early diagnosis and intervention could significantly improve their prognosis. Routine, wide viewing angle gastrointestinal endoscopy is invaluable for the identification, diagnosis and treatment of inflammatory, pre-neoplastic and neoplastic lesions in the upper and lower gastrointestinal tract. Instead of current 2-dimensional videos, a 3-dimension view of the colon is invaluable for clinical review,

localization of lesions requiring repeated monitoring, and training. Current wide angle endoscopes are optimized for forward viewing that is not suitable for generation of 3-D view of the colon wall.

Using the patented panomorph technology, we developed a custom designed colonoscope optimal for the 360 degree acquisition of the colon. Allowing an increase the resolution on the periphery of the field of view, this miniaturized panomorph optics (less than 4.0mm) was combined with an electronics imager, and image processing components to override the limitation of colonoscopy. A fast image processing algorithm is also developed and implemented to convert the panoramic images into a cylindrical 3-D view or a 2-D map of the colon wall. The performance of the endoscopy instrumentation is characterized in terms of resolution, field of view, and image quality at different angles. The image processing algorithm is validated in a colon phantom.

9313-10, Session 3

Technique for real-time tissue diagnosis based on multi-spectral time-resolved fluorescence spectroscopy

Dinglong M. Ma, Julien Bec, Dimitris S. Gorpas, Diego R. Yankelevich, Laura Marcu, Univ. of California, Davis (United States)

We report a novel technique for continuous acquisition, processing and display of fluorescence lifetimes enabling real-time tissue diagnosis through a single handheld/biopsy fiber-optic probe. A robust multi-spectral time-resolved fluorescence spectroscopy data acquisition method was developed to address the dynamic changes of fluorescence intensity typically encountered in clinical application. A fast algorithm was implemented in the system software, providing up to 15 Hz continuous lifetime display. Potential applications of this technique, including biopsy guidance, and surgical margins delineation were demonstrated in proof-of-concept experiments. Current results showed accurate display of fluorescence lifetimes and discrimination of fluorescence markers and tissue types in real-time.

9313-11, Session 3

In-situ photopolymerization and monitoring device for controlled shaping of tissue fillers, replacements, and implants

Andreas Schmocker, Azadeh Khoushabi, Dominique Pioletti, Pierre-Etienne Bourban, Christophe Moser, Ecole Polytechnique Fédérale de Lausanne (Switzerland)

Photopolymerization is a common tool to harden materials initially in a liquid state. A surgeon can directly trigger the solidification of a dental implant or a bone or tissue filler. Traditionally, photopolymerization has been used mainly in dentistry. Over the last decade advances in material development including a wide range of biocompatible gel- and cement-systems open up a new avenue for in-situ photopolymerization.

However, at the device level, adapted surgical and endoscopic probes haven't yet been invented. We present a miniaturized light probe where a photoactive material can be 1) mixed, pressurized and injected 2) photopolymerized or photoactivated and 3) monitored during the chemical reaction. The device enables surgeries to be conducted through a hole smaller than 1 mm in diameter.

Beside basic injection mechanics, the tool consists of an optical fiber guiding the light required for photopolymerization and for chemical analysis. Combining photorheology and fluorescence spectroscopy, the current state of the photopolymerization is inferred and monitored in real time. Biocompatible and highly tunable Poly-Ethylene-Glycol (PEG) hydrogels were used as injected material.

Conference 9313: Advanced Biomedical and Clinical Diagnostic and Surgical Guidance Systems XIII

The device was tested on a model for intervertebral disc replacement. Gels were successfully implanted into a bovine caudal model and mechanically tested in-vitro during two weeks. The photopolymerized gel was evaluated at the tissue level (adherence and mechanical properties of the implant), at the cellular level (biocompatibility and cytotoxicity) and ergonomic level (sterilization procedure and feasibility study). Furthermore, the gels were applied to an aneurism model where an aneurism cavity could be filled with gel.

9313-12, Session 3

Imaging spinal structures with polarization-sensitive optical coherence tomography

Zhenyang Ding, Chia-Pin Liang, Univ. of Maryland, College Park (United States); Qinggong Tang, Univ of Maryland, College Park (United States); Kyle Wu, Anthony Sandler, Sheikh Zayed Institute for Pediatric Surgical Innovation, Children's National Medical Ctr. (United States); Yu Chen, Univ. of Maryland, College Park (United States)

We investigate polarization-sensitive optical coherence tomography (PS-OCT) for its possible use in spine interventional procedures (such as epidural anesthesia) as a means of providing real-time guidance information. PS-OCT enables depth-resolved mapping of sample polarization information, which is particularly useful when the nano-scale organization of tissues that are difficult to be observed in the intensity images of a regular optical coherence tomography (OCT). Using a commercially-available PS-OCT system (PSOCT1300, Thorlabs Inc.), we obtain both intensity and polarization contrast images of in-vivo spinal structures such as subcutaneous fat, supraspinous ligament, interspinous ligament, dura, and spinal cord in a piglet model. We also compare the in-vivo results with ex-vivo imaging of corresponding spinal structures. From the polarization contrast images, we found that subcutaneous fat and ligamentum flavum do not have strong birefringence, but supraspinous ligament and interspinous ligament have strong birefringence. In the intensity image, there are subtle differences between these tissues. Therefore, the polarization information can provide more structural characteristics for guidance in spine interventional procedures. With further development, PS-OCT can be interfaced with a needle imaging device for reducing complications from spinal injection procedures. In addition, we also show characteristic birefringence patterns exhibited by neural structures in the polarization contrast images of spinal cord in-vivo, which may be useful in assessing and diagnosing the extent of nerve injury in the future interventional procedures.

9313-13, Session 3

Tissue identification during Pneumoperitoneum in laparoscopy

Yin Chang, Chi-Yang Tzang, National Yang-Ming Univ. (Taiwan)

Pneumoperitoneum is the beginning procedure of laparoscopy to enlarge the abdominal cavity in order to allow the surgical instruments to insert for surgical purpose. However, the insertion of Veress needle is a blind fashion that could cause blood vessels or visceral injury without attention and results in undetectable internal bleeding. Seriously it may cause a life-threatening complication. We have developed a method that can monitor the tissue reflective spectrum, which can be used for tissue discrimination, in real time during the puncture of the Veress needle. The system includes a modified Veress needle which contains an optical bundle, a light spectrum analyzing and control unit. The results in vitro study using porcine tissue showed that the correlation coefficient (r) of the reflective spectrum can be 0.79-0.95 for the wavelength range of 350-1000 nm and 0.85-0.98 for the wavelength range of 350-650 nm in the same tissue of various sites

which were obtained from different days. An alternative way for tissue discrimination is achieved through a decision making tree according to the characteristics of tissue spectrum. For single blind test the success rate is nearly 98%.

9313-14, Session 4

Pump-probe imaging of pigmented cutaneous melanoma gives insight into lesions' metastatic potential

Francisco E. Robles, Warren S. Warren, Duke Univ. (United States)

One the most important aspect of diagnosis and staging cutaneous melanoma is identifying patients with metastatic disease in order to initiate appropriate treatments. Non-invasive melanomas, for instance, are readily treatable by excision followed by 'watchful waiting,' whereas metastatic melanomas require a significantly more aggressive strategy. Note that survival rates fall from 98% for non-invasive melanomas to 16% for metastatic disease.

Sentinel lymph node biopsy (SLNB) has been found to be very instrumental in identifying metastatic disease, but the procedure has non-negligible risks including infection, seroma, lymphatic fistula, hematoma, and neuropraxia. Thus it is crucial to identify features in primary lesions that determine which patients will truly benefit from SLNBs. Unfortunately, available biomarkers have poor specificity (<12.5%), meaning many patients undergo this procedure unnecessarily. Further, the vast majority of patients with thin melanomas (which make 65% of all cases) are not recommended for a SLNB, yet 15% die of metastatic disease. This clearly represents an unmet clinical need.

Here, we utilize pump-probe microscopy to identify metastatic and non-metastatic melanocytic melanomas by imaging thin, unstained biopsy slides from primary tumors and comparing the results to SLNB (N = 34, 12 metastatic). This nonlinear imaging technique provides chemical information of endogenous melanin pigments by probing their electronic excited state dynamics, with subcellular resolution. We find that melanin chemistry and structure are promising surrogate biomarkers for metastatic disease with good sensitivity (85%) and specificity (83%). A detailed description of the experimental method, data processing, and statistical procedure will be presented.

9313-15, Session 4

High-area-throughput automated gigapixel imaging of whole prostate tumor resection surfaces using structured illumination microscopy

J. Quincy Brown, Tyler Schlichenmeyer, Mei Wang, Tulane Univ. (United States); Hillary Z. Kimbrell, Tulane Univ., School of Medicine (United States); David Tulman, Carola Wenk, Tulane Univ. (United States); Benjamin R. Lee, Tulane Univ., School of Medicine (United States)

Uncorrected positive surgical margins affect 11-38% of radical prostatectomy patients regardless of tumor stage, and over 50% of patients with the most advanced tumors. However, the large surface area of the removed prostate (100-500 cm²) renders traditional intra-operative pathology techniques, such as frozen section analysis, ineffective due to the inability to accurately sample the involved area of the margin for histopathology processing. To that end, we are developing a comprehensive strategy towards a clinically-translatable microscopic specimen scanner, which could be used to provide pathologists with gigapixel mosaics of the entire ex vivo resection surface in intra-operative timeframes, and aid in detection of residual tumor in time to correct the surgery. To achieve the required imaging speed, we have

**Conference 9313: Advanced Biomedical and
Clinical Diagnostic and Surgical Guidance Systems XIII**

developed video-rate structured illumination microscopy (VR-SIM), which, by rejecting out-of-focus light, can acquire high-contrast images of thick fluorescently-stained tissue surfaces at 33 frames/sec (2048 x 2048 pixels/frame). Combined with a rapidly automated stage, we have achieved area-throughput rates of 4.4 cm²/min at 1.3 micron lateral resolution. To obviate the need to cut or compress the tissue, we have developed rapid structured-light-assisted autofocus algorithms, which allows automatic tracking of the tissue surface topography within the objective working distance. Finally, to enable fast and facile analysis of the large, high-information-content gigapixel images, we have adapted web-based multi-resolution visualization tools compatible with clinical workflows. In this paper we will present our overall technical and clinical strategy, and will present the most up to date results of our ongoing IRB-approved study for imaging entire prostatectomy specimens.

9313-16, Session 4

**Compact handheld multispectral
fluorescence lifetime imaging (FLIM)
system for in vivo imaging of the oral
mucosa**

Shuna Cheng, Rodrigo Cuenca, Bilal H. Malik, Joey M. Jabbour, Texas A&M Univ. (United States); Yi-Shing Lisa Cheng D.D.S., John Wright D.D.S., Texas A&M Health Science Ctr. (United States); Rock Rickel, Brian E. Applegate, Kristen C. Maitland, Javier A. Jo, Texas A&M Univ. (United States)

A compact handheld system for simultaneous multispectral FLIM imaging based on a MEMS scanner and small diameter (6.25 mm) lenses is presented. The handheld endoscope consists of a compact enclosure (10 X 5 X 3 cm³ in volume) with a rigid probe (0.8 cm diameter, 12 cm length). The customized enclosure holds the MEMS scanner and allows slightly angle adjustment for a dichroic mirror placed at 45° angle to the incoming excitation beam. The rigid probe includes four achromatic lenses (f = 30mm). The first two lenses form a relay system to extend the length of the probe. The most distal lens works as an objective to focus the light onto the sample. An additional lens is placed in the intermediate image plane of the relay system to serve as a field lens which increases the FOV from ~3.6 mm to ~5 mm. The system lateral resolution is ~100 μm measured by imaging an USAF target. The time-resolved fluorescence emission is spectrally divided in three emission bands and multiplexed in time following a strategy previously reported. Thus, for a single excitation pulse, multiple decays corresponding to different spectral bands can be recorded using a single detector. The multispectral fluorescence signal is detected by an MCP-PMT and digitized at 6.25 GS/s. Real-time image processing is accomplished by embedding FLIM deconvolution within the imaging instrumentation. A pixel acquisition and processing of 10 kHz is demonstrated. The system is validated by imaging standard fluorescent dyes, oral biopsy ex vivo and human oral mucosa in vivo.

9313-17, Session 4

**A broadband confocal Raman endoscopy
for in vivo diagnosis of intestinal
metaplasia in the stomach**

Kan Lin, Mads Sylvest Bergholt, Jianfeng Wang, Wei Zheng, National Univ. of Singapore (Singapore); Hongzhi Xu, Institute of Digestive Disease, Zhongshan Hospital (China); Zhiwei Huang, National Univ. of Singapore (Singapore)

We report a novel simultaneous fingerprint (FP) and high-wavenumber (HW) fiber-optic confocal Raman spectroscopy for in vivo diagnosis of

intestinal metaplasia (IM) in the stomach under wide-field endoscopic imaging. The FP/HW Raman endoscopy technique was performed on 39 gastric patients and differentiate IM from normal tissues with sensitivity of 88.7% (102/115) and specificity of 82.6% (76/92). This study shows the great potential of the FP/HW Raman endoscopic technique developed for early diagnosis of non-neoplastic gastric disease in vivo during routine endoscopic examination.

9313-18, Session 4

**An Advanced Design of Non-radioactive
Image Capturing and Management System
for Applications in Non-invasive Skin
Disorder Diagnosis**

Carol Y. B. Liu, Hong Kong Productivity Council (Hong Kong, China); Kany ZHOU, Bryan SO, Derek LOUIE, Hong Kong Productivity Council (Hong Kong, China); David C. K. Luk M.D., United Christian Hospital (Hong Kong, China)

Due to the increasing incidences of malignant melanoma, there is a rising demand for assistive technologies for its early diagnosis and improving the survival rate. The commonly used visual screening method is with limited accuracy as the early phase of melanoma shares many clinical features with an atypical nevus, while conventional dermoscopes are not user-friendly in terms of setup time and operations. Therefore, the development of an intelligent and handy system to assist the accurate screening and long-term monitoring of melanocytic skin lesions is crucial for early diagnosis and prevention of melanoma. In this paper, an advanced design of non-invasive and non-radioactive dermoscopy system was reported. Computer-aided simulations were conducted for optimizing the optical design and uniform illumination distribution. Functional prototype and the software system were further developed, which could enable image capturing at 10x amplified and general modes, convenient data transmission, analysis of dermoscopic features (e.g., asymmetry, border irregularity, color, diameter and dermoscopic structure) for assisting the early detection of melanoma, extract patient information (e.g. code, lesion location) and integrate with dermoscopic images, thus further support long term monitoring of diagnostic analysis results.

A clinical trial study was further conducted on 185 Chinese children (0-18 years old). The results showed that for all subjects, skin conditions diagnosed based on the developed system accurately confirmed the diagnoses by conventional clinical procedures. Besides, clinical analysis on dermoscopic features and a potential standard approach by the developed system to support identifying specific melanocytic patterns for dermoscopic examination in Chinese children were also reported.

9313-19, Session 5

**Characterization of oral cancer with
multispectral fluorescence lifetime
imaging in the hamster model of oral
carcinogenesis in vivo**

Bilal H. Malik, Joohyung Lee, Shuna Cheng, Rodrigo Cuenca, Joey M. Jabbour, Texas A&M Univ. (United States); Yi-Shing Lisa Cheng D.D.S., John Wright D.D.S., Texas A&M Univ., Baylor College of Dentistry (United States); Beena Ahmed, Texas A&M Univ. (Qatar); Kristen C. Maitland, Javier A. Jo, Texas A&M Univ. (United States)

Oral cancer is a significant global healthcare problem with relatively high morbidity and mortality rates. Current standard of care in early detection of oral cancer includes comprehensive oral examination for screening of potentially malignant disorders. A number of commercially offered optical

**Conference 9313: Advanced Biomedical and
Clinical Diagnostic and Surgical Guidance Systems XIII**

imaging approaches are available as adjunctive tools for detection of oral cancer; however, the literature suggests that most of these modalities lack specificity and, therefore, fail to improve the detection of oral carcinomas over conventional oral examination techniques. To this end, we present the potential of multispectral fluorescence lifetime imaging (FLIM) toward objective characterization of oral cancer in the hamster cheek pouch model of oral carcinogenesis *in vivo*. Our FLIM system utilized a 355 nm excitation source for excitation of multiple endogenous fluorophores and provided en face maps of the tissue autofluorescence intensity and different temporal dynamics at three emission bands, simultaneously, with a field of view of 16 x 16 mm² and lateral resolution of 62.5 μm. The results demonstrate that quantitative differences in between low-risk and high-risk oral lesions can be resolved with FLIM. We analyzed over twenty FLIM features using statistical analysis and sequential feature selection, and methodically selected a subset of features which were able to distinguish between low-risk and high-risk oral lesions with detection rate of 92 %. We will also discuss the challenges and limitations associated with the current embodiment of our FLIM system toward detection of oral cancer, and provide a potential scheme to circumvent these limitations.

9313-20, Session 5

Multispectral fluorescence imaging of human ovarian and fallopian tube tissue for early stage cancer detection

Tyler Tate, Brenda Baggett, Jennifer M. Watson, Gabriel V. Orsinger, Molly Keenan, Kenneth D. Hatch M.D., Setsuko K. Chambers, The Univ. of Arizona (United States); John F. Black, Glannaventa Inc. (United States); Jennifer K. Barton, Urs Utzinger, The Univ. of Arizona (United States)

With early detection, five year survival rates for ovarian cancer are over 90%, yet no effective early screening method exists. Emerging consensus suggests that perhaps over 50% of the most lethal form of the disease, high grade serous ovarian cancer, originates in the Fallopian tube. Cancer changes molecular concentrations of various endogenous fluorophores. Using specific excitation wavelengths and emissions bands on a Multispectral Fluorescence Imaging (MFI) system, spatial and spectral data over a wide field of view can be collected from endogenous fluorophores. Wavelength specific reflectance images provide additional information to normalize for tissue geometry and blood absorption. Ratiometric combination of the images creates high contrast between neighboring normal and abnormal tissue. Twenty-six women undergoing oophorectomy or debulking surgery consented the use of surgical discard tissue samples for MFI imaging. Forty-nine pieces of ovarian tissue and thirty-two pieces of fallopian tube tissue were collected and imaged with excitation wavelengths between 280 nm and 550 nm. After imaging, each tissue sample was fixed, sectioned and H&E stained for pathological evaluation. Comparison of mean intensity values between normal, benign, and cancerous tissue demonstrate a general trend of increased fluorescence of benign tissue and decreased fluorescence of cancerous tissue when compared to normal tissue. Using the changes in fluorescent intensity of the component images, ratiometric images are created to enhance contrast between normal and abnormal tissue. The enhanced contrast images provide improved diagnostic capabilities. Adaption of the system for *in vivo* Fallopian tube and ovary endoscopic imaging will be discussed.

9313-21, Session 5

Light reflectance spectroscopy for prostate cancer identification: cost-effective tool for intraoperative positive margin detection

Xinlong Wang, Li Zeng, The Univ. of Texas at Arlington

(United States); Monica Morgan, Payal Kapur, Jeffrey A. Cadeddu, Claus R. Roehrborn, The Univ. of Texas Southwestern Medical Ctr. at Dallas (United States); Hanli Liu, The Univ. of Texas at Arlington (United States)

Accurate detection of positive surgical margin (PSM) on prostate capsule is critical for post-operative patient care. In this study, we investigated the feasibility of using a cost-effective optical system, Light Reflectance Spectroscopy (LRS), to detect PSM on capsules using 17 *ex vivo* human prostate specimens. The measurements were taken within 1-1.5 hour after its removal from the patient. An optical model and Mie theory were used to process the LRS data; a feature selection algorithm and logistic model were utilized for prostate cancer identification and classification, with overall percent of 85% for sensitivity, specificity, accuracy and receiver operating characteristic curves.

9313-22, Session 5

Detection of colorectal cancer in blood serum using Raman molecular imaging

Patrick J. Treado, ChemImage Corp. (United States); Bergein F. Overholt M.D., Gastrointestinal Associates, P.C. (United States); Shona D. Stewart, Aaron Smith, Heather Kirschner, Chris Post, ChemImage Corp. (United States)

Colorectal cancer (CRC) is the third most common cancer in men and women in the United States. Raman Molecular Imaging (RMI) is an effective technique to evaluate human tissue, cells and bodily fluids, including blood serum for disease diagnosis. ChemImage Corporation, in collaboration with clinicians, has been engaged in development of an *in vitro* diagnostic Raman assay focused on CRC detection. The Raman Assay for Colorectal Cancer (RACC) exploits the high specificity of Raman imaging to distinguish diseased from normal dried blood serum droplets without additional reagents. Pilot Study results from testing of more than 250 biobank patient samples have demonstrated that RACC discriminates between CRC and clinical background with sensitivity and specificity approaching 90% or greater. Further testing also indicates that RACC distinguishes between CRC and other types of cancer including breast, lung, ovarian and prostate. Importantly, pilot studies conducted to date suggest that RACC is sensitive to early stage CRC and the presence of polyps, including advanced adenomas. For RACC to be commercialized as a cost effective tool to screen patients for pre-cancerous polyps and CRC, it will need high throughput capability. To this end, a high throughput instrument is being developed and validated by comparing data collected with low throughput Raman instrumentation.

9313-23, Session 6

Fluorescence lifetime imaging to differentiate bound from unbound ICG-CRGD both *in vitro* and *in vivo*

Paulien L. Stegehuis, Martin C. Boonstra, Leiden Univ. Medical Ctr. (Netherlands); Karien E. de Rooij, Percuro BV (Netherlands) and Leiden Univ. Medical Ctr. (Netherlands); François E. Powolny, Riccardo Sinisi, Ecole Polytechnique Fédérale de Lausanne (Switzerland); Harald Homulle, Technische Univ. Delft (Netherlands); Claudio E. Bruschini, Ecole Polytechnique Fédérale de Lausanne (Switzerland); Edoardo Charbon, Technische Univ. Delft (Netherlands) and École Polytechnique Fédérale de Lausanne (Switzerland); Cornelis JH van de Velde, Leiden University Medical Center (Netherlands); Boudewijn P. F. Lelieveldt M.D., Leiden Univ. Medical Ctr. (Netherlands)

**Conference 9313: Advanced Biomedical and
Clinical Diagnostic and Surgical Guidance Systems XIII**

and Technische Univ. Delft (Netherlands); Alexander L. Vahrmeijer M.D., Jouke Dijkstra, Leiden Univ. Medical Ctr. (Netherlands); Martijn van de Giessen, Leiden Univ. Medical Ctr. (Netherlands) and Technische Univ. Delft (Netherlands)

Excision of the whole tumor is crucial, but remains difficult for many tumor types. Fluorescence lifetime imaging could be helpful intraoperative to differentiate normal from tumor tissue. In this study we investigated the difference in fluorescence lifetime imaging of indocyanine green coupled to cyclic RGD free in solution/serum or bound to integrins e.g. in tumors. The U87-MG glioblastoma cell line, expressing high integrin levels, was cultured to use in vitro and to induce 4 subcutaneous tumors in a-thymic mice (n=4). Lifetimes of bound and unbound probe were measured with an experimental time-domain single-photon avalanche diode array (time resolution <100ps). In vivo measurements were taken 30-60 minutes after intravenous injection, and after 24 hours.

The in vitro lifetime of the fluorophores was similar at different concentrations (20, 50 and 100 μ M) and showed a statistically significant higher lifetime (p<0.001) of bound probe compared to unbound probe. In vivo, lifetimes of the fluorophores in tumors were significantly higher (p<0.001) than at the control site (tail) at 30-60 minutes after probe injection. Lifetimes after 24 hours confirmed tumor-specific binding (also validated by fluorescence intensity images).

Based on the difference in lifetime imaging, it can be concluded that it is feasible to separate between bound and unbound probes in vivo.

9313-24, Session 6

Real-time endoscopic optical properties imaging using single snapshot of optical properties (SSOP) imaging

Joseph P. Angelo Jr., Boston Univ. (United States); Martijn van de Giessen, Leiden Univ. Medical Ctr. (Netherlands); Sylvain Gioux, Beth Israel Deaconess Medical Ctr. (United States)

Minimally invasive surgeries are approaching 50% of all interventional procedures in the US allowing faster and safer procedures along with faster patient recovery. However, working through an endoscope reduces the surgeon's ability to assess tissue viability from a lack of sight and touch. It is therefore necessary to develop new tools allowing surgeons to objectively assess the surgical field intraoperatively during minimally invasive procedures.

Endogenous imaging has the potential to provide physiologically-relevant information to healthcare professionals during screening or interventional procedures. Our lab has recently developed an imaging method called Single Snapshot of Optical Properties (SSOP) that enables video-rate optical properties acquisition. Because this method is working in real-time, it is insensitive to movement artifacts and allows to image tissues within the constraints of endoscopy.

In this study, light from a laser diode at 670nm was collimated and shined onto a transmissive spatial modulator to create patterns of light and coupled into one channel of a stereo endoscope. Diffuse reflectance was collected through the second channel and imaged onto a CCD camera. Optical property maps were obtained using tissue simulating phantoms and in vivo samples. All samples were validated against standard wide-field SFDI acquisition and processing.

The results show good agreement (within 5%) for endoscopic SSOP versus wide-field SFDI in both phantom and in vivo samples. However, SSOP acquisition allows for video-rate sampling, limited only by the exposure time of image capture. These results show promise for an objective endoscopic tissue viability assessment tool being achievable in a clinical setting.

9313-25, Session 6

Analysis of feature stability for laser-based determination of tissue thickness

Floris Ernst, Achim Schweikard, Patrick Stüber, Ralf Bruder, Benjamin Wagner, Tobias Wissel, Univ. zu Lübeck (Germany)

For stereotactic radiotherapy of lesions in the brain, accurate localisation of the cranial bone is mandatory. Using our previously presented system based on laser triangulation and determination of additional tissue features, accurate determination of the skull's position is possible without typically used X-ray imaging.

To determine the applicability of our machine learning-based method to clinical settings, we have collected long-term scans of five subjects to analyse the feature stability over time.

Our results show that the noise of the tissue features is low enough to allow discrimination of tissue thicknesses of 0.5mm.

9313-26, Session 6

Label-free IgG/anti-IgG biosensing based on long period fiber gratings: a comprehensive feasibility study

Francesco Baldini, Francesco Chiavaioli, Cosimo Trono, Ambra Giannetti, Istituto di Fisica Applicata Nello Carrara, IFAC-CNR (Italy); Palas Biswas, CSIR-CGCR, Central Glass and Ceramic Research Institute (India); Sara Tombelli, Istituto di Fisica Applicata Nello Carrara (Italy); Somnath Bandyopadhyay, Sunirmal Jana, Susanta Bera, Aparajita Mallick, CSIR-CGCR, Central Glass and Ceramic Research Institute (India)

Long period fiber gratings (LPGs) have been proposed as label-free biosensors for a few years. A biochemical interaction occurring along the grating region can be evaluated as a refractive index (RI) change, which modifies the transmission spectrum of the fiber. This is an emergent, effective and alternative choice with respect to other label-free optical platforms, such as surface plasmon resonance, interferometric and in-fiber configurations, and resonating structures. Various types of LPG (standard, turn-around point, coated) were manufactured for increasing the RI sensitivity of these sensors. After the functionalization of the fiber surface using Eudragit L100 copolymer, a label-free IgG/anti-IgG bioassay was realized for analyzing the antigen/antibody interaction following the same model assay. A comprehensive feasibility study was carried out among the different LPGs in order to assess and compare the biosensor performance, highlighting the advantages and the disadvantages of each type. Experimental results proved an improvement in the RI sensitivity and in the biosensor performance in the case of both turn-around point and coated LPGs, with values of detection limit lower than 70 ng mL⁻¹ (460 pM). This was also confirmed using complex matrixes made up of human serum.

9313-27, Session 7

Thermal Imaging: (re)discovering the potentials for diagnostics and treatment evaluation in the clinical procedures (review)

Rudolf M. Verdaasdonk, John H. Klaessens, Albert J. van der Veen, Vrije Univ. Medical Ctr. (Netherlands)

Although thermo camera's have been around for decades, they were too

Conference 9313: Advanced Biomedical and Clinical Diagnostic and Surgical Guidance Systems XIII

cumbersome to be accepted for routine clinical applications. Nowadays, thermo camera's have become small and practical without special cooling systems and calibration procedures and have a high image and temperature resolution (<0.1 K). Some clinical applications have been re-invented and new applications are being developed. Thermal imaging can be useful to image physiological processes, perfusion, inflammation, friction and breathing. Temperature changes can be induced or provoked to observe dynamic changes to differentiate between healthy and abnormal responses. In the VU university medical center many specialism's have become interested in the potential of thermo imaging and various feasibility studies have started:

Cardiology: prediction of spasm of artery in arm before cardiac catheterisation.

Urology: cause of impotence after radical prostatectomy

Anesthesiology: effectiveness of anesthetic block and pain treatment, non contact monitoring of vital functions

Plastic surgery: perfusion quality of skin flap for breast reconstruction, effectiveness of cryotherapy of hypertrophic scars, burn wound skin transplantation

Dermatology: objective and sensitive imaging of allergic reactions, laser treatments

The thermo camera could easily be used in the clinic with approval of ethical committee since there is no contact with the patient so risks are minimal. Clinician appreciate the technology and are more 'image minded'. Either the thermo imaging helps to improve an treatment or can become a new diagnostics tool. Still there is a longer way for acceptance and becoming the new golden standard. Besides the many potentials in the hospital, thermo camera's should become standard equipment in the office of general practitioners.

9313-28, Session 7

A high-speed OCT needle probe for rapid volumetric scanning

Bryden C. Quirk, Rodney W. Kirk, David D. Sampson, Robert A. McLaughlin, The Univ. of Western Australia (Australia)

OCT needle probes consist of miniaturised focusing optics encased within a hypodermic needle. The needle may be inserted into tissue, enabling OCT images to be acquired deep within tissue. Previous needle probes have been limited to slow acquisition speeds, with volumetric C-scans typically taking minutes to acquire, which is problematic for in vivo scenarios. In this work, we present a high-speed needle probe able to acquire a 180-degree volumetric dataset (half-cylinder) in 2.5 seconds.

The probe consists of an inner needle which can be translated back and forth at high speed, and a larger enclosing needle with an elongated slit window (length 1.5mm). The focusing optics of the inner needle consists of lengths of no-core and gradient-index fiber spliced to the end of a section of single-mode fiber. This is terminated with angle-polished no-core fibre to redirect the light beam, and encased within a glass capillary to maintain a glass-air interface and achieve total internal reflection. Fusing the capillary directly to the imaging window of the inner needle minimized parasitic back-reflections, achieving a sensitivity of 110dB. The inner needle was encased within the larger enclosing needle and connected to two piezoelectric parallel bimorph actuators, capable of translating back and forth with a stroke of 1mm, acquiring B-scans along the needle axis at a rate of 140Hz. The dual-needle assembly was integrated into a handheld probe and rotated using a servomotor through a half volume in 2.5 seconds. We demonstrate the use of this probe on phantoms and ex vivo tissues.

9313-29, Session 7

Development and verification of a novel device for dental intra-oral 3D scanning using chromatic confocal technology

Michael Zint, Karl Stock, ILM, Univ. Ulm (Germany); Rainer Graser, Cubert GmbH (Germany); Edgar Brauer, ILM, Univ. Ulm (Germany); Jan Heyninck, Joris Vanbiervliet, Stefaan Dhondt, Pieter De Ceuninck, Dentsply International (Belgium); Thomas P. Ertl, Dentsply International (Germany); Raimund Hibst, ILM, Univ. Ulm (Germany)

The use of optical intra-oral scanners in dentistry is on the rise. Many IO-scanners use optical techniques which require powder to scan bulk scattering or glossy materials like human teeth. Confocal imaging can solve this problem, but usually requires either moving mechanical parts for a z-scan (monochromatic) or means for lateral positioning of the probe or specimen (single point chromatic confocal). Both approaches above are disadvantageous regarding scanning speed, accuracy and reliability.

The presented work describes the development and verification of a novel optical, powder-free IO-scanner based on chromatic confocal technology combined with a multifocal approach. This allows miniaturizing of the device and provides increased scan speed by a factor of 1000. The optical design comprises of a telecentric hyperchromatic lens providing an 11mm lateral object height with 11mm chromatic focal shift, and a detection system for analyzing 1000 data points in parallel. A single picture of the device delivers 3D data within a volume of more than 1cm³ with full depth resolution.

Results:

The average height deviation on a flat ceramic is $17\mu\text{m}\pm 9\mu\text{m}$, whereas the average point wise reproducibility is $4\mu\text{m}\pm 1\mu\text{m}$. The average distance deviation between reference spheres is $43\mu\text{m}\pm 18\mu\text{m}$ (30mm to 50mm distance) and the average diameter deviation on 4mm ceramic spheres is $31\mu\text{m}\pm 18\mu\text{m}$. The device allows precise and fast video-like intra-oral capturing of human teeth and tissue with 30fps at an accuracy which meets the clinical relevant requirements.

9313-30, Session 7

Needle tip tissue identification: Raman spectroscopy for epidural space

Jeon Woong Kang, Massachusetts Institute of Technology (United States); Thomas A. Anderson, Massachusetts General Hospital (United States); Ramachandra R. Dasari, Peter T. C. So, Massachusetts Institute of Technology (United States)

Many medical procedures use a blind, or semi-blind, approach for needle tip placement. These procedures include epidural catheter placement, laparoscopic surgery trocar placement, tissue biopsies, joint injection, lumbar puncture, and fluid collection aspiration. Complications related to these procedures can be serious and are commonly a result of needle tip misplacement. There is a tremendous need for devices which allows identification of tissues at the tip of needles in vivo. Each year, 2.4 million epidural catheters are placed for labor and delivery. An equal number are placed for postoperative acute pain control annually as well. There is a high rate of obesity in surgical patients and this population is associated with a greater number of epidural blockade complications. The failure rate for epidural catheter analgesia is 12-13% due to the failure to accurately locate the epidural space.

Multi-modal spectroscopy using Raman spectroscopy, diffuse reflectance spectroscopy, and intrinsic fluorescence spectroscopy can measure biochemical and morphological information about tissues non-destructively. MMS has previously been shown to differentiate between cancerous and normal tissues and to enable identification of atherosclerotic plaques. We

Conference 9313: Advanced Biomedical and Clinical Diagnostic and Surgical Guidance Systems XIII

have shown that Raman spectroscopy can differentiate the tissues overlying the epidural space (skin, fat, muscle, supra-/intra-spinous ligament, ligamentum flavum) and those beyond it (epidural fat, dura mater, spinal cord) in an ex vivo animal model. Target area (ligamentum flavum) was clearly distinguished from surrounding tissue layers. We have also shown that RS can differentiate tissues of the abdominal wall and abdomen (skin, fat, muscle, liver, spleen, pancreas, kidney) in the same model.

9313-31, Session 8

Optical heterogeneous bioassay for the detection of suPAR as prognostic biomarker for inflammatory diseases

Francesco Baldini, Sara Tombelli, Barbara Adinolfi, Francesco Chiavaioli, Ambra Giannetti, Cosimo Trono, Istituto di Fisica Applicata Nello Carrara, IFAC-CNR (Italy); Romeo Bernini, Immacolata A. Grimaldi, Gianluca Persichetti, Genni Testa, IREA-CNR, Institute for Electromagnetic Sensing of the Environment (Italy); Jesper Eugen-Olsen, Clinical Research Ctr., Hvidovre Hospital (Denmark) and Virogates A/S (Denmark)

Soluble urokinase plasminogen activator receptor (suPAR) was recently proposed as a very effective inflammatory marker, potentially capable of acting also as a prognostic biomarker, with a clinical range of interest between 0.4 µg and 70 µg/L in plasma. In the proposed heterogeneous assay, capture and detection antibodies are a rat anti-human and a biotinylated mouse anti-human suPAR antibody, respectively. Optical detection was achieved by a successive exposure of the biotinylated sandwich to streptavidin labelled with ATTO647N. The heterogeneous assay was implemented on a multichannel PMMA optical biochip, potentially capable of the simultaneous detection of more than one analyte. Capture antibody was immobilized on the PMMA surface of the microfluidic channel and the protocol followed the following steps: i) surface blocking with Prionex, ii) incubation with suPAR or PBS, iii) incubation with biotinylated suPAR detection Ab and iv) incubation with streptavidin-ATTO647N. Promising preliminary results were obtained with this protocol. Ad-hoc optical configuration was adopted in order to isolate completely the photodetector from any influence of the source light, which can create unwanted background effects.

9313-32, Session 8

Direct ultrasound to video registration using photoacoustic markers from a single image pose

Alexis Cheng, Xiaoyu Guo, Johns Hopkins Univ. (United States); Michael A. Choti M.D., The Univ. of Texas Southwestern Medical Ctr. at Dallas (United States); Jin U. Kang, Russell H. Taylor, Emad M. Boctor, Johns Hopkins Univ. (United States)

Fusion of video and other imaging modalities is common in modern surgical scenarios to provide surgeons with additional information. Doing so requires the use of interventional guidance equipment and surgical navigation systems to register the tools and devices used in surgery with each other. In this work, we focus explicitly on registering ultrasound with a stereocamera system using photoacoustic markers. Previous work has shown that photoacoustic markers can be used to register three-dimensional ultrasound with video resulting in target registration errors lower than the current available systems. Photoacoustic markers are non-collinear laser spots projected onto some surface. They can be simultaneously visualized by a stereocamera system and in an ultrasound volume because of the photoacoustic effect. This work replaces the three-dimensional ultrasound

volume with images from a single ultrasound image pose.

While an ultrasound volume provides more information than an ultrasound image, it has its disadvantages such as higher cost and slower acquisition rate. However, in general, it is difficult to register two-dimensional with three-dimensional spatial data. We propose the use of photoacoustic markers viewed by a convex array ultrasound transducer. Each photoacoustic marker's wavefront provides information on its elevational position, resulting in three-dimensional spatial data. This development enhances this method's practicality as convex array transducers are more common in surgical practice than three-dimensional transducers. This work is demonstrated in simulation and on a synthetic phantom. The resulting target registration error for this experiment was 2.47mm and the standard deviations was 1.29mm, which is comparable to current available systems.

9313-33, Session 8

Shifted excitation Raman difference spectroscopy using a dual-wavelength DBR diode laser at 785 nm

Martin Maiwald, Bernd Eppich, Jörg Fricke, Arnim Ginolas, Franck Bugge, Andreas Klehr, Bernd Sumpf, Götz Erbert, Günther Tränkle, Ferdinand-Braun-Institut (Germany)

For several years portable Raman spectroscopy becomes more and more important as in situ sensor techniques such as food safety, detection of explosives, and point of care diagnostic. However, measurements of real-world samples have additional challenges. Sources of interference such as fluorescence or ambient light can complicate the analysis of unknown substances. Here, shifted excitation Raman difference spectroscopy (SERDS) has been proven as a simple and powerful technique to separate Raman signals from disturbing background signals.

In this contribution, the application of SERDS using a dual-wavelength Y-branch distributed Bragg reflector (DBR) diode laser at 785 nm will be presented. First, the design of the light source will be shown. After this, electro-optical and spectral properties will be discussed with respect to the requirements for SERDS. An optical power of 140 mW is achieved at a heatsink temperature of 25°C in cw-operation mode for the two wavelengths at 784.5 nm and 785.1 nm. Raman experiments are carried out using selected samples. Different test scenarios demonstrate the suitability of the dual-wavelength diode laser for SERDS.

Moreover, the above described dual-wavelength excitation light source is integrated into a master oscillator power amplifier (MOPA) diode laser system. This laser system reaches optical powers larger than 750 mW while the spectral properties of the dual-wavelength laser remain unchanged. The higher output power enables short SERDS measurement times and large excitation spot sizes to realize rapid monitoring of spatial heterogeneous samples such as meat in the food industry or human skin in clinical diagnostic.

9313-34, Session 8

Real-time quantitative lifetime unmixing of fluorophore mixtures using time resolved fluorescence spectroscopy

Fartash Vasefi, David S. Kittle, Keith L. Black M.D., Pramod V. Butte, Cedars-Sinai Medical Ctr. (United States)

We present the performance of time resolved fluorescence spectroscopy (TRFS) system for unmixing the lifetime decays of fluorophore mixtures in real-time. Unmixing of lifetime decays allows the estimation of relative concentrations of fluorophores in the dye mixtures.

The TRFS system uses a 355nm laser pulse (400ps, 5 µJ/pulse) to excite the mixture, a custom demuxer to split the spectral channels into 6 discrete wavelength bands from 360nm to 700 nm, a custom fiber

**Conference 9313: Advanced Biomedical and
 Clinical Diagnostic and Surgical Guidance Systems XIII**

delay unit to delay individual color bands before being combined onto the photomultiplier tube (MCP-PMT, 80 ps rise time), a MCP-PMT to detect fluorescence and a digitizer to sample the fluorescence lifetime measurements. The fluorescence decay was estimated at each color band using laguerre deconvolution for both single and double fluorophore mixtures. Four dyes individually and in mixture were studied using TRFS (Rose Bengal, Rhodamine B, K4-503 and K4-204, SETA Biomedicals). The fluorescence decay was further studied with bi-exponential curve fitting to the laguerre kernels.

The TRFS system is able to estimate fluorescence lifetimes with very high accuracy (~ 50 ps) even at low SNR (<20% of PMT signal at the highest gain). We also demonstrate the ability of TRFS system to accurately resolve the relative concentrations of the fluorophores in the mixtures. The results showed that the system can resolve a concentration difference down to 10%.

The TRFS system is able to detect fluorescence lifetime with 50 ps accuracy and resolve the relative concentrations of fluorescent dyes in a mixture.

9313-44, Session 8
A surgical microscope combining real-time surface reconstruction and spectroscopic fluorescence imaging with a light transport model to quantify visible and near-infrared fluorescent molecular markers

Leticia M. Angulo-Rodríguez, Ecole Polytechnique de Montréal (Canada); Michael Jermyn, Ecole Polytechnique de Montréal (Canada) and Montreal Neurological Institute and Hospital (Canada); Kolbein Kolste, Thayer School of Engineering at Dartmouth (United States); Pablo A. Valdes Quevedo, Geisel School of Medicine, Dartmouth College (United States); Julien Pichette, Guillaume Sheehy, Yoann Gosselin, Ecole Polytechnique de Montréal (Canada); Mira Sibai, Princess Margaret Cancer Ctr., Univ. of Toronto (Canada); Kelvin Mok, Kevin Petrecca, Montreal Neurological Hospital and Institute (Canada); David W. Roberts M.D., Dartmouth Hitchcock Medical Ctr. (Canada); Keith D. Paulsen, Thayer School of Engineering at Dartmouth (United States); Brian C. Wilson, Princess Margaret Cancer Ctr., Univ. of Toronto (Canada); Frédéric Leblond, Ecole Polytechnique de Montréal (Canada)

The development, regulatory approval and clinical adoption of fluorescent molecular markers to guide surgical interventions are challenging. However, there is also a need for the development of optical systems that can provide standardized quantitative images that are highly sensitive and specific to molecular targets. We present an imaging system in which the optical components are seamlessly integrated into a commercial neurosurgical microscope. The system integrates: (1) A broad-beam excitation system with wavelengths between 390 and 635nm; (2) A spatially-modulated digital light projector that projects patterns of varying spatial frequencies and orientations on the surgical cavity, (3) a dual-camera system connected through a coherent bundle to the microscope that can provide structural detection of wide-field hyper-spectral reflectance and fluorescence images.

The quantification of visible and near infrared (NIR) fluorophores requires novel techniques to be applied pixel-by-pixel in order to account for (i) the geometry of the surface, (ii) the optical properties of the tissue, (iii) the variable sampling depth of light that depend on the fluorophore excitation and emission wavelengths. Using the visible/NIR molecule protoporphyrin IX, we present a quantitative reconstruction technique to quantify visible markers (within the first millimeter of the tissue surface) and tomographically quantify NIR markers (potentially located at larger depths). The technique has been developed for fluorescence-guided brain cancer surgery but it can be applied to other organs when coupled with the right molecular marker(s).

9313-45, Session PSun
Fluorescence detection of lymph node metastasis using 5-aminolevulinic acid in human colorectal cancer

Yoshinori Harada, Takeo Minamikawa, Hisataka Matsuo, Yoshihisa Yamaoka, Ping Dai, Tetsuro Takamatsu, Kyoto Prefectural Univ. of Medicine (Japan)

Lymph node examination is requisite for determining treatment course of colorectal cancer patients. In this study, we sought to demonstrate fluorescence detection of lymph node (LN) metastasis using 5-aminolevulinic acid (ALA) in human colorectal cancer. A total of 87 LNs excised from 17 surgically treated CRC patients were subjected to analysis. After oral administration of 5-ALA prior to operations, fluorescence spectral images of half-cut LNs were acquired. Spectral unmixing was applied to decrease the overlay of collagen autofluorescence on 5-ALA-induced protoporphyrin IX (PpIX) fluorescence in the LNs. No obvious adverse effect was observed in this study. Spectral unmixed fluorescence signal of PpIX was seen without apparent overlay of collagen autofluorescence in metastatic LNs. The spectral unmixed fluorescence intensity of PpIX in metastatic LNs was 10.2-fold larger than that in nonmetastatic LNs. The receiver-operating-characteristic analysis showed that the area under the curve was calculated as 0.95. The results demonstrated the potential of 5-ALA-induced PpIX fluorescence treated by spectral unmixing for detecting LN metastases in CRC patients, suggesting that this rapid method is applicable to gross evaluation of excised LN specimens in pathology laboratories.

Reference: Int J Mol Sci 2013;14:23140-23152.

9313-46, Session PSun
Label-free evaluation of myocardial infarction by spontaneous Raman spectroscopy

Takeo Minamikawa, Yoshinori Harada, Tetsuro Takamatsu, Kyoto Prefectural Univ. of Medicine (Japan)

Myocardial infarction (MI) following ischemia is a major cause of mortality worldwide. The determination of surgical treatment of MI is based on myocardial viability, which is the potential to recover functions of myocardium. Magnetic resonance imaging and myocardial scintigraphy are generally used for the evaluation of myocardial viability before cardiac surgery. Since there is lack of direct evaluation method of myocardial viability, surgeons should make decision of surgical procedure during surgery only based on preoperative evaluation. An intraoperative estimation method of myocardial viability is therefore deeply desired to obtain better outcome of cardiac surgery. In this study, we propose a label-free and direct evaluation technique of MI by using spontaneous Raman spectroscopy. Firstly, we evaluated normal hearts and those with fresh and old MI of Wistar rats. A multivariate spectral analysis, partial least squares regression analysis, enables us to evaluate MI and its repair process on the basis of molecular constituents without staining. Secondly, we applied our proposed method to human patients undergoing surgical ventricular restoration. The Raman spectroscopy with the multivariate spectral analysis clearly visualized residual intact myocardium and infarcted region of MI of the patients. These results suggest the potential of the Raman spectroscopic observation for noninvasive and label-free estimation of myocardial viability, and we expect that this method could become a key technique for cardiac surgery.

**Conference 9313: Advanced Biomedical and
Clinical Diagnostic and Surgical Guidance Systems XIII**

9313-47, Session PSun

**Principal component analysis of
indocyanine green fluorescence dynamics
for diagnosis of vascular diseases**

 Jihye Seo, Yuri An, Jungsul Lee, Chulhee Choi, KAIST
(Korea, Republic of)

Indocyanine green (ICG), a near-infrared fluorophore, has been used in visualization of vascular structure and non-invasive diagnosis of vascular disease. Although many imaging techniques have been developed, there are still limitations in diagnosis of vascular diseases. We have recently developed a minimally invasive diagnostics system based on ICG fluorescence imaging for sensitive detection of vascular insufficiency. In this study, we used principal component analysis (PCA) to examine ICG spatiotemporal profile and to obtain pathophysiological information from ICG dynamics. Here we demonstrated that principal components of ICG dynamics in both feet showed significant differences between normal control and diabetic patients with vascular complications. We extracted the PCA time courses of the first three components and found distinct pattern in diabetic patient. We propose that PCA of ICG dynamics reveal better classification performance compared to fluorescence intensity analysis. We anticipate that specific feature of spatiotemporal ICG dynamics can be useful in diagnosis of various vascular diseases.

9313-48, Session PSun

**New diagnostic and therapeutic systems
for total management of neonatal
hyperbilirubinemia using laser diodes,
LEDs and OLEDs**

Mostafa Hamza, Mansoura Univ. (Egypt); Mohammed H. sayed El-Ahl, Military Medical Academy (Egypt); Ahmad Mohmmad Hamza, National Research Ctr. (Egypt); Aya M. Hamza, Yahya Mohammad Hamza, Tabarak Children's Hospital (Egypt)

Globally, neonatal jaundice is a major cause of newborn death and disability. The burden of brain injury due to jaundice remains a well-recognized threat in many countries in the world. It is important to detect jaundice in its early stages to prevent kernicterus in newborn infants. When jaundice is properly diagnosed, severe elevation of serum bilirubin can be prevented and effectively treated, preventing brain injury. However the accuracy and precision of the results obtained from conventional bilirubin meters have undesirable variability. In this paper the authors introduce the theory, design and operating principles of new non-invasive transcutaneous bilirubin sensors. The sensors are implemented using laser diodes and LEDs. The operation principle of these novel compact and low-cost bilirubin sensors is primarily based on the absorption characteristics of bilirubin in the visible region of the spectrum. Accurate measurement of bilirubin concentration is a major determination in the clinical management of neonatal hyperbilirubinemia. The management includes using blue laser diodes, or LEDs and organic LEDs (OLEDs) for efficient phototherapy of jaundice. Non-invasive transcutaneous bilirubinometry using these novel sensors was used in our clinics and hospitals for accurate and timely identification of neonates at risk of hyperbilirubinemia in addition to efficient phototherapy.

9313-49, Session PSun

**Towards characterization of ductal
carcinoma in situ using optical coherence
tomography**

Syed A. Bin Amir, Yu Gan, Fatih L. Balci, Hanina Hibshoosh,

 Sheldon Feldman, Christine P. Hendon, Columbia Univ.
(United States)

Early detection of Ductal Carcinoma in Situ (DCIS) is integral in reducing the risk of cancer recurrence in breast tissue. Optical Coherence Tomography (OCT) is capable of producing cross-sectional images of breast tissue with high resolution and identifying key tissue morphology. We present a classification model to detect DCIS within OCT images of human breast tissue samples ex-vivo implemented using machine learning.

Multiple parameters were extracted based on intensity and texture. These include optical parameters such as local entropy, texture parameters acquired from gray-level co-occurrence matrices (GLCM), and texture code numbers (TCN). The Molecular Pathology department in Columbia University Medical Center provided eleven breast tissue samples of various sizes from mastectomy and breast reduction procedures, and histology staining was performed every millimeter throughout the tissue following image acquisition. The histology sections were used to distinguish between fibrous, adipose, DCIS, and lesions in the OCT B-scans.

Adipose tissue with DCIS exhibited greater GLCM and TCN homogeneity and lower intensity and texture entropy with p-values less than 0.05 compared to normal adipose tissue, due to the presence of enlarged, highly backscattering nuclei. A Support Vector Machine (SVM) classifier with 53% training data produced an overall accuracy of 79% in tissue classification, with a sensitivity of 90% in distinguishing adipose tissue containing DCIS from other tissue types. Initial results indicate that this model can be used to detect breast carcinoma and expanded to other machine learning methods to classify DCIS from healthy adipose tissue, and detect the presence of DCIS along tumor margins.

9313-50, Session PSun

**A study on the quantitative evaluation of
skin barrier function**

Tomomi Maruyama, Yasuhiro KABETANI, Michiko Kido, Kenji Yamada, Hieyong Jeong, Osaka Univ. Graduate School of Medicine (Japan); Yuko Ohno, Osaka Univ. Graduate School of Medicine (Japan); Hirotoishi OIKAZE, Yohei TAKECHI, Tomotaka FURUTA, Shoichi ISHII, Panasonic Corporation (Japan); Haruna KATAYAMA, Osaka Univ. Graduate School of Medicine (Japan); Hieyong Jeong, Yuko Ohno, Osaka Univ. (Japan)

We propose a quantitative evaluation method of skin barrier function using the system with coherency of near-infrared light. There are a lot of skin problems such as itching, irritation and so on. It has been recognized skin problems are caused by impairment of skin barrier function, which prevents damage from various external stimuli and loss of water. To evaluate skin barrier function, it is common strategy that they observe skin surface. On the other hand, it is necessary to observe inner structure of skin for evaluating skin condition. In this study, we evaluate changes of stratum corneum structure which is important for evaluating skin barrier function by comparing water-penetrated skin with normal skin using a system with coherency of near-infrared light. Proposed method can obtain in vivo 3D images of inner structure of body tissue, which is non-invasive and non-destructive measuring method. Compared with Optical Coherence Tomography (OCT), it has the advantages of high-resolution imaging. Using our system to evaluate inner structure, we get 3D images of water-penetrated skin and normal skin. Then, we can observe increase of signal intensity in an x-z plane of water-penetrated skin compared with normal skin, it follows that we evaluate the penetration of water. In conclusion, we discuss relationship between changes of inner structure by water penetration and changes of amount of moisture in stratum corneum, pH and transepidermal water loss (TEWL). In addition, we evaluate difference of arm sites such as palm and forearm.

**Conference 9313: Advanced Biomedical and
Clinical Diagnostic and Surgical Guidance Systems XIII**

9313-51, Session PSun

Optical characteristics of prostate tissues and the key chromophores and fluorophores within tissues related to carcinogenesis

Kenneth J. Zhou, Stony Brook Univ. (United States); Jun Chen, Department of Cardiology, Tianjin Medical University General Hospital (China)

Tissues are an impressive complex creation comprised of a vast of assortment of molecules, structures and functional units. Despite this overwhelming complexity, we may still discuss average optical properties as long as we realize the limitations involved. There are five independent macroscopic parameters that are believed to characterize light propagation in tissue: the index of refraction (n), the absorption coefficient (μ_a), the scattering coefficient (μ_s), and the scattering anisotropy (g). This paper summarizes the Optical characteristics of tissue of prostate tissues *ex vivo* and the key fluorophores related to carcinogenesis.

The absorption coefficient (μ_a) describes the effectiveness of light absorbed by certain chromophore. The key spectra fingerprints of water were introduced to distinguish different water contents in normal and cancerous prostate tissues. Fluorescence occurs when a molecule, atom or nanostructure relaxes to its ground state after being electrically excited. There are three fluorescence parameters of interest we may concern in tissue optics: the fluorescence lifetime (τ), the fluorescence quantum yield (Φ) and the fluorescence emission peak (λ_{max}). The key wavelengths which can be used for cancer detection were reviewed. Scattering of light occurs in media which contains fluctuations in the refractive index n . Tissue ultrastructure extends from membranes to membrane aggregates to collagen fibers to nuclei to cells, which may be an alternative way to detect cancer in tissues.

9313-52, Session PSun

Surgical Doppler OCT microscope using augmented reality

Kanghae Kim, Nam Hyun Cho, Kibeom Park, Deokmin Jeon, Jeehyun Kim, Kyungpook National Univ. (Korea, Republic of)

We developed surgical doppler optical coherence tomography (Doppler OCT) microscope using augmented reality. In this technic we used a common optical path for surgical microscope and doppler OCT, thus we obtained the surgical microscope, OCT and doppler OCT images simultaneously. This system was used to study microstructures of a mouse's middle ear. From the obtained results, we expect this system would serve a wide-range of OCT applications.

9313-53, Session PSun

Gastrointestinal tract volume measurement method using a compound eye type endoscope

Kayo Yoshimoto, Osaka City Univ. (Japan); Kenji Yamada, Kenji Watabe, Michiko Kido, Osaka Univ. (Japan); Toshiaki Nagakura, Osaka Electro-Communication Univ. (Japan); Hideya Takahashi, Osaka City Univ. (Japan); Tsutomu Nishida, Hideki Iijima, Masahiko Tsujii, Tetsuo Takehara, Yuko Ohno, Osaka Univ. (Japan)

We propose an intestine volume measurement method using a compound

eye type endoscope. This method aims at assessment of the gastrointestinal function.

Gastrointestinal diseases are mainly based on morphological abnormalities. However, gastrointestinal symptoms are sometimes apparent without visible abnormalities. Such diseases are called functional gastrointestinal disorder, for example, functional dyspepsia, and irritable bowel syndrome. For the diagnosis of the gastrointestinal tract, both aspects of organic and functional assessment is important. While endoscopic diagnosis is essential for assessment of organic abnormalities, three-dimensional information is required for assessment of the functional abnormalities. Thus, we proposed the three dimensional endoscope system using compound eye.

In this study, we forces on the volume of intestine tract. The quantitative assessment of intestine motility is determined by the volume change of the intestine tract. The compliance and capacity of the tract can be calculated from pressure and volume. These parameters also evaluate intestine motility. So the volume measurement is important for assessing the motility. In our system, we use a compound eye type endoscope system to obtain three-dimensional information of the tract. The volume can calculate by integrating the slice data of the intestine tract shape using the obtained three-dimensional information. First, we evaluate the proposed method by known-shape tube. Then, we confirm that the proposed method can be measure the tract volume using *in vivo* experimental data.

Our system can assess the wall of gastrointestinal tract directly in a three-dimensional manner. Our system can be used for examination of gastric morphological and functional abnormalities.

9313-54, Session PSun

The gender differences of extremities microcirculation: far-infrared illumination test

Wei-Long Kao, Chia-Wei Sun, Ching-Cheng Chuang, National Chiao Tung Univ. (Taiwan)

In recent year, many studies have shown that microcirculation can directly respond to disease-related symptoms. However, capacity of microcirculation would vary because of gender differences. Far Infrared Therapy Unit emits broadband far-infrared (FIR) to stimulate irradiated region changing microcirculation. Near-infrared spectroscopy (NIRS) is a noninvasive technique to monitor tissue oxygenation status. In this research, we use FIR irradiating lower arm of subjects and NIRS monitoring the changing of microcirculation. In conclusion, our experimental results indicate the obvious difference of oxygenation status between men and women groups during FIR illumination.

9313-55, Session PSun

Detection of paroxysmal migraine without aura by using near-infrared spectroscopy

Chao-Che Lee, Chia-Wei Sun, Ching-Cheng Chuang, National Chiao Tung Univ. (Taiwan); Wei-Ta Chen, Taipei Veterans General Hospital (Taiwan) and National Yang-Ming Univ. (Taiwan)

Migraine is a neurological disorder characterized by recurrent moderate to severe headaches. It usually leads the patients to disability. In definition, the headache days per month less than fifteen days called paroxysmal migraine. Paroxysmal migraine can be divided migraine with and without aura. In this study, we used near-infrared spectroscopy (NIRS) system to detect the changes of oxyhemoglobin (HbO₂) and deoxyhemoglobin (Hb) in prefrontal cortex of healthy people and patients with paroxysmal migraine without aura under breath holding test. The correlation between the changes of hemoglobin in prefrontal cortex and neurological disorder characterized by headaches is demonstrated in this paper.

**Conference 9313: Advanced Biomedical and
Clinical Diagnostic and Surgical Guidance Systems XIII**

9313-56, Session PSun

**Monitoring anticoagulation status using
optical thromboelastography (OTEG)**

 Diane M. Tshikudi, Markandey M. Tripathi, Zeinab Hajjarian
Kashany, Seemantini K. Nadkarni, Massachusetts General
Hospital (United States)

Defective blood coagulation resulting from excessive procoagulant activity often leads to thrombotic disorders such as stroke and pulmonary thromboembolism. A variety of injectable and oral anticoagulant drugs are prescribed for short or long-term therapy to prevent or treat life-threatening thrombosis. However, due to bleeding complication often associated with anticoagulant therapy, routine monitoring and accurate dosing of anticoagulant therapy is imperative. We have developed Optical thromboelastography (OTEG), a non-contact approach that utilizes a drop of whole blood to measure blood coagulation status in patients. Here, we demonstrate the capability of OTEG for rapidly monitoring and dosing anticoagulation in patients. OTEG monitors coagulation status by assessing changes in blood viscosity from temporal intensity fluctuations of laser speckle patterns during clotting. In OTEG a blood drop is illuminated with coherent light and the blood viscosity is measured from the speckle intensity autocorrelation curve, $g_2(t)$. The metrics, reaction time (R), clotting time (R+k), clot progression (K) and maximum clot stiffness (MA) are then extracted. The aim of the current study was to evaluate the accuracy of OTEG in assessing the anticoagulant status of common anticoagulants, heparin and argatroban. A dose-dependent prolongation of R and R+k was observed in anticoagulated blood, which closely corresponded with standard-reference Thromboelastography (TEG) ($r^2 > 0.95$, $P > 0.01$ for all cases). In both OTEG and TEG, MA was unaffected by heparin or argatroban. In conclusion, OTEG can accurately monitor anticoagulation treatment and is potentially a powerful tool for routine anticoagulation monitoring in patients at the point-of-care or in the home setting.

9313-57, Session PSun

**Changes of absorption and reduced
scattering coefficients during vessel
occlusion test: time-resolved diffuse
optical signal study**

 Chen-Wun Ciou, Ching-Cheng Chuang, National Chiao
Tung Univ. (Taiwan); Chung-Ming Chen, National Taiwan
Univ. (Taiwan); Chia-Wei Sun, National Chiao Tung Univ.
(Taiwan)

We present the experimental results of in-vivo oxygenation dynamic monitoring based on a time-resolved diffuse optical imaging (TRDOI) system. The TRDOI was performed with picosecond diode lasers (dual-wavelength near-infrared source) and a fast-gated single-photon avalanche diode (SPAD) that coupled to a time-correlated single-photon counting electronics. Venous and arterial occlusion is the index of microcirculation. We investigated the changes of absorption and reduced scattering coefficients in venous and arterial occlusion of arm from the mean time of flight and the variance of the measured distribution of times of flight (DToF). Our result indicates the differences of change of optical properties with venous and arterial occlusion. Change of optical properties with occlusion help us to comprehend microcirculation in clinical diagnosis.

9313-58, Session PSun

**Forensic application of Raman
spectroscopy for blood age analysis**

Kiana Jansen, Univ. School of Nashville (United States);

 Maggie E. O'Connor, Vanderbilt Univ. (United States);
Maurice C. Aalders, Academisch Medisch Centrum
(Netherlands); Isaac J. Pence, Anita Mahadevan-Jansen,
Vanderbilt Univ. (United States)

Blood is a key component of many crime scenes and can provide valuable information about those involved. A major limitation in forensics is a lack of non-destructive techniques that can provide accurate information to form a timeline. Using optical techniques to evaluate blood has been shown to provide insight about when a crime has occurred. Current research includes the use of diffuse reflectance spectroscopy to determine the age of a bloodstain; however, measurements lose accuracy as a bloodstain ages. We propose Raman spectroscopy for this application. Previous work on Raman spectroscopy for biological fluids in forensics has differentiated between blood and other bodily fluids as well as determined if the blood was from a human or animal. However, no work has been reported about the potential of Raman spectroscopic techniques to non-destructively determine the age of a bloodstain. Here we report our investigation of changes in the Raman spectra of blood as a function of time. Raman spectra were acquired using a commercial Raman microscope and custom sample slide for precise time course measurements. Spectra were then characterized for differences between the signals over time. These findings form the basis of a model that will enable accurate prediction of bloodstain age using Raman spectroscopy. Development of these optical techniques for crime scene analysis has the potential to aid in the formation of a realistic timeline and evaluate alibis without the presence of a victim's body.

9313-35, Session 9

**Characterization of a hybrid diffuse
correlation spectroscopy and time-
resolved near-infrared spectroscopy
system for real-time monitoring of cerebral
blood flow and oxygenation**

 Kyle Verdecchia, Mamadou Diop, Lawson Health Research
Institute (Canada) and Western Univ. (Canada); Albert
Lee, Western Univ. (Canada); Keith St. Lawrence, Lawson
Health Research Institute (Canada) and Western Univ.
(Canada)

The combination of near-infrared spectroscopy (NIRS) with diffuse correlation spectroscopy (DCS) offers the ability to provide real-time monitoring of cerebral oxygenation, blood flow and oxygen consumption. However, measuring these parameters accurately requires depth sensitive techniques that can remove the effects of signal contamination from extracerebral tissues. Towards this goal, we developed and characterized a hybrid DCS/time-resolved (TR)-NIRS system. Both systems acquire data at three source-detector distances (SDD: 7, 20 and 30 mm) to provide depth sensitivity. The TR-NIRS system uses three pulsed lasers (760, 810, and 830 nm) to quantify tissue optical properties, and DCS uses one continuous-wave, long coherence length (>5 m) laser (785 nm) for blood flow monitoring. The stability of the TR-NIRS system was characterized by continuously measuring the instrument response function (IRF) for four hours, and a warm-up period of two hours was required to reduce the coefficient of variation of the extracted optical properties to < 2%. The error in the optical properties was <10% at SSDs of 20 and 30 mm; however, the error at 7-mm was greater due to the effects of the IRF. The number of DCS detectors at each SDD and the minimum count-rate (20 kHz per detector resulting in <10% uncertainty in the extracted blood flow index) were optimized using a homogenous phantom. The depth sensitivity was assessed using a two-layer phantom; the flow rate in the bottom layer was altered to mimic cerebral blood flow.

**Conference 9313: Advanced Biomedical and
Clinical Diagnostic and Surgical Guidance Systems XIII**

9313-36, Session 9

Handheld MEMS based swept-source optical coherence tomography for microvascular anastomosis in murine model

Yong Huang, Johns Hopkins Univ. (United States); Georg J. Furtmuller, Johns Hopkins Univ., School of Medicine (United States); Dedi Tong, Johns Hopkins Univ., School of Medicine (United States) and Beijing Jishuitan Hospital (China); Shan Zhu, Johns Hopkins Univ., School of Medicine (United States) and Peking Union Medical College Hospital (China); W. P. Andrew Lee M.D., Gerald Brandacher M.D., Johns Hopkins Univ., School of Medicine (United States); Jin U. Kang, Johns Hopkins Univ. (United States)

A miniature handheld optical coherence tomography (OCT) probe built and evaluated for real time intraoperative vascular patency evaluation in the setting of super-microsurgical vessel anastomosis. A handheld Fourier domain Doppler optical coherence tomography is based on a 1.3- μm central wavelength swept source. A compact handheld probe was built using a 2.4-mm diameter microelectromechanical systems (MEMS) scanning mirror, additionally a 12.7-mm diameter lens system was designed and combined with the MEMS mirror to keep the probe slim to achieve optimal functionality as a handheld system. With an adjustable lateral image field of view up to 1.5 mm by 1.5 mm, high-resolution simultaneous structural and flow imaging of the blood vessels were successfully acquired for mouse after orthotopic hind limb transplantation using a non-suture cuff technique and mouse after femoral artery anastomosis using a suture technique. The axial and lateral resolution of the probe is 12.6 μm in air and 17.5 μm respectively. The probe exhibited a sensitivity of 84 dB and sensitivity roll-off of 5.7 dB/mm over an imaging range of 5mm. Real-time simultaneous structure and Doppler imaging at a frame rate of 36 Hz for an image size of 1000(lateral) x 512(axial) pixels using a 50,000 A-lines per second swept source was achieved. Quantitative vessel lumen patency, lumen narrowing and thrombosis analysis were performed based on acquired structure and Doppler images.

9313-37, Session 9

Non-contact continuous-wave diffuse optical tomographic system to capture vascular dynamics in the foot

Jennifer W. Hoi, Hyun-Keol Kim, Alessandro Marone, Michael A. Khalil, Columbia Univ. (United States); Gautam Shrikhande M.D., New York-Presbyterian Hospital (United States) and Columbia Univ. (United States); Andreas H. Hielscher, Columbia Univ. (United States)

Dynamic optical tomographic imaging has shown promise in diagnosing and monitoring peripheral arterial disease (PAD), which affects 8 to 12 million in the United States. PAD is the narrowing of the arteries that supply blood to the lower extremities. Prolonged reduced blood flow to the foot leads to ulcers and gangrene, which makes placement of optical fibers for contact-based optical tomography systems difficult and cumbersome. Since many diabetic PAD patients have foot wounds, a non-contact interface is highly desirable. We present a novel non-contact dynamic continuous-wave optical tomographic imaging system that images the vasculature in the foot for evaluating PAD. The system images at up to 1Hz by delivering 2 wavelengths of light to the top of the foot at up to 20 source positions through collimated source fibers. Transmitted light is collected with an electron multiplying charge couple device (EMCCD) camera. We demonstrate that the system can resolve absorbers at various locations in a phantom study

and show the system's first clinical 3D images of total hemoglobin changes in the foot during venous occlusion at the thigh. Our initial results indicate that this system is effective in capturing the vascular dynamics within the foot and can be used to diagnose and monitor treatment of PAD in diabetic patients. Results of our ongoing clinical study will be presented.

9313-38, Session 9

Highly portable and clinic-friendly instrument for monitoring peripheral perfusion in a point of care setting

Sean M. White, Bruce Yang, Tyler B. Rice, Laser Associated Sciences (United States)

Peripheral perfusion is highly dynamic and is reflective of a wide variety of clinical conditions. For example, hypovolemic shock, peripheral vascular disease, and sleep apnea all induce significant changes in peripheral blood flow, and the ability to quantify the dynamics of these changes may aid in earlier diagnosis or improved treatment outcomes.

We therefore developed a clinic-friendly clip-on probe for use in measuring peripheral perfusion. Our probe is compact, measures perfusion in real time with a sampling rate of 260 Hz, and is simple enough to be operated by a minimally-trained technician. The probe employs laser speckle imaging in a transmission geometry, rather than a traditional reflection geometry, allowing perfusion measurements from large tissue thicknesses (>1 cm). As such, it is the first device capable of performing perfusion measurements from the entire microvascular system of a finger or toe. Our device is additionally capable of detecting pulse waveform dynamics that cannot be observed using conventional laser speckle imaging systems or laser Doppler.

We have demonstrated the clinical utility of our probe by measuring peripheral perfusion in a porcine model of hemorrhage. We found that the onset of hemorrhage was significantly correlated to a decrease in peripheral perfusion and that peripheral perfusion measurements using our probe are capable of detecting hemorrhagic shock earlier than continuous blood oxygen saturation and cardiac output measurements.

9313-39, Session 9

Noninvasive submilligram level quantification of in vivo blood components with slitless high-sensitivity spectrometer and noncooled NIR detector

Ryosuke Kuribayashi, Hiromitsu Furukawa, National Institute of Advanced Industrial Science and Technology (Japan)

A portable low-cost non-invasive monitor for intravascular blood components such as glucose, lipid, and protein, has been extensively studied for several decades. However, optical blood monitor, one of the most promising method, has not yet been put into practical use except for the pulse oximeter, mainly due to the insufficient accuracy for quantification.

In this paper, we report non-invasive real-time transmission-type measurement of cardiac-pulsating blood components using a newly-developed highly sensitive and stable Fourier-transform spectrometer with no slits and no moving mechanical parts. The slit-less structure enables us to capture light signals from a wider area of a subject than a conventional spectrometer, while maintaining irradiation power density and spectral resolution.

As a result, we demonstrate that cardiac-pulsation amplitude can be extracted from 4.0-level optical density (OD) spectra of a fingertip, with an OD resolution of less than 0.0005 OD units and a spectral resolution of less than several tens of nanometers, even when using a low-cost "non-cooled" near-infrared linear sensor.

**Conference 9313: Advanced Biomedical and
Clinical Diagnostic and Surgical Guidance Systems XIII**

Furthermore, from a simple least-squares-based analysis of the extracted spectrum over 1,000 - 1,400 nm, the average amounts of three components in pulsating blood, i.e., water, oxyhemoglobin, and lipids/proteins corresponding to the peak at 1,200 nm, are deduced to be 2.2 +/- 0.1, 1.2 +/- 0.1, and 0.6 +/- 0.1 mg/cm², respectively, for the passing volume of a probe light beam through a fingertip. The results indicate the capacity of the spectrometer for low-cost portable use in daily healthcare or point-of-care testing, as well as in high-end analytic research.

9313-40, Session 10

In vivo performance comparison study of wide-field oxygenation imaging methods

Martijn van de Giessen, Leiden Univ. Medical Ctr. (Netherlands) and Technische Univ. Delft (Netherlands); Joseph P. Angelo Jr., Boston Univ. (United States) and Beth Israel Deaconess Medical Ctr. (United States); Christina Vargas M.D., Beth Israel Deaconess Medical Ctr. (United States); Sylvain Gioux, Harvard Medical School (United States) and Beth Israel Deaconess Medical Ctr. (United States)

Wide-field imaging of oxygenation saturation of biological tissue has many promising clinical applications. Examples are viability assessment of burn wounds or skin flaps (in reconstructive surgery), colon resection planning, wound healing, anastomosis and perfusion imaging after dottering.

In near-infrared (NIR), below 900nm, the dominant sources of absorption are oxyhemoglobin and deoxyhemoglobin, making this an ideal window for imaging. However, wide-field oxygenation saturation imaging remains challenging because the reflected intensity does not only depend on absorption, but also on tissue dependent scattering. To cope with scattering, several models have been proposed that differ in assumptions and robustness.

We studied the robustness and accuracy of five families of models: ignoring scattering, assuming a constant pathlength, diffuse reflectance with constant scattering, photon random walk with constant scattering and diffuse reflectance with measured absorption and scattering. The sensitivity to parameter errors, such as constant scattering, and to calibration errors was studied using longitudinal in-vivo data of skin flaps with venous and arterial occlusions. Surface-profile corrected spatial frequency domain imaging was taken as ground truth.

We found that models ignoring scattering were robust to calibration errors, but too inaccurate for tissue viability assessment. Models assuming constant path length were more robust to calibration errors than models with constant scattering. Accuracies were similar, but the constant scattering assumption pathlengths/scattering hampers accurate longitudinal saturation estimates in burn wounds and healing tissue with time-dependent scattering changes. Estimating both scattering and absorption was most sensitive calibration errors, but delivered both the most accurate results and widest clinical applicability.

9313-41, Session 10

Clinical evaluation of blood coagulation status in patients using optical thromboelastography (OTEG)

Markandey M. Tripathi, Massachusetts General Hospital (United States) and Harvard Medical School (United States); Diane M. Tshikudi, Massachusetts General Hospital (United States); Zeinab Hajjarian Kashany, Elizabeth M. Van Cott, Seemantini K. Nadkarni, Massachusetts General Hospital (United States) and Harvard Medical School (United States)

Bleeding and thrombotic disorders account for increased in-hospital mortality in injured, surgical and critically ill patients. The early assessment of coagulation defects at point-of-care is therefore critical in improving clinical outcome. Here we conduct a clinical study in 150 patients to evaluate Optical Thromboelastography (OTEG), a novel technique to measure blood coagulation status, and demonstrate its diagnostic efficacy in detecting coagulation defects in patients. In OTEG, temporal laser speckle intensity fluctuations from a drop of clotting blood are measured using a CMOS camera. During blood coagulation, the formation of a fibrin-platelet clot regulates Brownian displacements of intrinsic light scattering centers, altering the rate of speckle intensity fluctuations. To quantify coagulation status, the speckle intensity autocorrelation function is measured, the mean square displacement of scattering particles is extracted, and viscoelastic modulus (G), during coagulation is measured via the generalized Stokes-Einstein relation. By quantifying time-resolved changes in G, the coagulation parameters, reaction time (R), clot progression time (K), and maximum clot strength (MA) are derived. In this study, the above coagulation parameters were measured using OTEG and compared with standard mechanical Thromboelastography (TEG). Our results showed a strong correlation between OTEG and TEG measurements for all parameters: R-time (R=0.80, p<0.001), clotting time (R=0.76, p<0.001), and MA (R=0.56, p<0.001). In addition, OTEG achieved a diagnostic sensitivity of 100% and specificity of 90% in detecting coagulation defects in patients. These results demonstrate the potential of OTEG to be utilized for evaluating real-time blood coagulation status in patients and detecting coagulation defects at the point-of-care.

9313-42, Session 10

Study on migraine signal of prefrontal cortex with gender difference based on NIRS method

Chen Yu Lin, National Chiao Tung Univ. (Taiwan); Chia-Wei Sun, Biomedical Optical Imaging Lab., National Chiao Tung Univ. (Taiwan); Ching Cheng Chuang, National Chiao Tung Univ. (Taiwan)

Migraine is a complex chronic neurological disorder in which the interictal changes in neuronal excitability and vascular reactivity in the cerebral cortex were detected.

The disorder is more prevalent in women than in men, and the response in women could be stronger than in men. In this study, we measure a group of women and men with and without migraine by breathe holding task with near infrared spectroscopy. Measurements of the relative changes in concentration of deoxy-hemoglobin and oxy-hemoglobin are performed on subjects during fast normal breathing of two minutes and three breath holdings of 15 seconds interleaved with 45 seconds of normal breathing. The result of our study suggest that breathe holding effect on cerebral hemodynamic of subject with migraine and without migraine could be due to different vascular reactivity to blood oxygen content.

9313-43, Session 10

Noninvasive diagnosis and continuous monitoring of thrombosis in clinics by near-infrared spectroscopy

Ting Li, Yunglong Sun, Univ. of Electronic Science and Technology of China (China); Xiao Chen, Univ of Electronic Science and Technology of China (China); Yue Zhao, Univ. of Electronic Science and Technology of China (China); Rongrong Ren, Department of Anesthesiology and Surgical Intensive Care Unit, Xinhua Hospital (China); Mushuang Liu, Univ of Electronic Science and Technology

**Conference 9313: Advanced Biomedical and
Clinical Diagnostic and Surgical Guidance Systems XIII**

of China (China)

Thrombosis became one of the most severe disease hazard to human health, and its incidence rate grows increasingly higher throughout the world. The conventional diagnosis and monitoring of thrombosis mainly relied on the invasive techniques, e.g., digital subtraction angiography and blood sample analysis, and expensive and ionizing techniques, e.g., magnetic resonance angiography. And those techniques can not measure continuously. Here we reported our preliminary exploration of using near-infrared spectroscopy (NIRS) in clinical monitoring of thrombosis. 5 healthy subjects and 3 thrombosis patients at similar age participated the NIRS measurements of tissue oxygen saturation (StO₂) on 6 particular parts of legs. We repeated StO₂ measurement at the same specified time each day after thrombolytic therapy, and terminated till the patients were cured and left hospital. We found that: (1) StO₂ kept lower than 83% in thrombosis patients and higher than 92% in healthy people ($p < 0.001$); (2) StO₂ kept increasing in the thrombosis leg but decreasing in healthy leg for the patients after thrombolytic therapy, and coincidentally, StO₂ acted consistent just when the patients were cured and left. Our study successfully extended the application of NIRS in noninvasive, continuous, and low-cost monitoring of thrombosis in clinics. Our findings showed the powerful potential of StO₂ by NIRS in diagnosis and therapeutic effect evaluation of thrombosis.

Conference 9315: Design and Quality for Biomedical Technologies VIII

Saturday - Sunday 7-8 February 2015

Part of Proceedings of SPIE Vol. 9315 Design and Quality for Biomedical Technologies VIII

9315-1, Session 1

Design and phantom-based validation of a bimodal ultrasound-photoacoustic imaging system for spectral detection of optical biomarkers

William C. Vogt, Congxian Jia, Keith A. Wear, Brian S. Garra, T. Joshua Pfefer, U.S. Food and Drug Administration (United States)

The construction of photoacoustic tomography (PAT) systems that combine tunable laser sources and ultrasound systems for bimodal imaging and spectroscopic applications such as oximetry presents novel challenges to the biophotonics researcher. We address some of the design issues, including system synchronization, cross-platform integration, and image reconstruction algorithms, and present techniques for device performance validation. Our system comprises a pulsed Nd:YAG laser-pumped optical parametric oscillator for near-infrared tunability and a research-grade ultrasound acquisition system compatible with multiple clinical transducers to enable wide variation in operating parameters. Considerations such as pulse energy variability, ultrasound transducer properties, and spectral energy compensation, and their impact on measurements are presented. Spectral imaging was performed on tissue-simulating phantoms made of a custom polyvinyl chloride (PVC) plastisol gel designed to mimic both the optical properties (absorption, scattering) and acoustic properties (sound velocity, attenuation) of human breast tissue. Phantoms contained fluid channels at various depths which were injected with either organic dye or gold nanorod solutions as absorptive targets. Spectral analysis of these solutions was performed for channel depths from 0.5 to 3 cm and at radiant exposures up to the ANSI maximum permissible exposure. Recovered photoacoustic spectra are compared with absorption spectra measured using spectrophotometry. Results provide insightful characterization of the influence of factors that impact the quality of spectroscopic measurements and reconstructed images in ultrasound-PAT systems.

9315-2, Session 1

Oximetry system performance assessment with POM phantoms incorporating hemoglobin calibration standards and customized saturation levels

Hyounguk Jang, Karam Singh, Univ. of Maryland, College Park (United States); T. Joshua Pfefer, U.S. Food and Drug Administration (United States); Yu Chen, Univ. of Maryland, College Park (United States)

Evaluation of biophotonic systems for detection of hemoglobin (Hb) content and oxygenation, such as those based on near-infrared spectroscopy (NIRS), have often involved tissue-simulating phantoms incorporating artificial dyes or flow systems. We have developed and evaluated a simple test method based on cuvette inserts in solid turbid phantoms for measuring commercially-available Hb oximetry standards and custom-formulated oxy/deoxy-Hb solutions. This study involved characterization of polyaxymethylene (POM) absorption and scattering properties over visible and NIR wavelengths using two approaches: (a) inverse-adding-doubling based on measurements with a spectrophotometer and integrating sphere; and (b) a fiberoptic-probe-based NIRS system. The stability of POM optical properties over time was also evaluated. We fabricated POM phantoms into

which a standard quartz cuvette or a custom fabricated POM cuvette could be inserted. Cuvettes were filled with commercially-available Hb calibration standards as well as custom Hb solutions at various saturation levels, using yeast for deoxygenation. Measurements were performed in POM phantoms with superficial layers of varying thicknesses to evaluate the effect of source-detector separation on saturation measurement accuracy. Optical property results for POM indicated low absorption and a level of scattering towards the high end of the biologically relevant range. Minimal difference in results was seen for the two cuvette types. Overall, our preliminary results indicate that the POM-Hb phantom approach may be suitable for benchtop assessment of device quality, and thus may facilitate preclinical development as well as comparison, recalibration and quality control testing for a variety of biophotonic devices.

9315-4, Session 2

Shack-Hartmann sensor based optical quality testing of whole slide imaging systems for digital pathology

S. Mojtaba Shakeri, Technische Univ. Delft (Netherlands); Bas Hulsken, Philips Digital Pathology (Netherlands); Lucas J. van Vliet, Sjoerd Stallinga, Technische Univ. Delft (Netherlands)

Digital pathology is based on digital images of tissues of ~15 mm² size and resolution of ~0.25 μm/pixel. These are generated by Whole Slide Scanners (WSS) which sweep the slide lane by lane (~1mm wide) and stitch the lanes into the final high resolution image. It is important in assembly and maintenance to test and monitor the optical quality of the WSS. Such optical quality tests can be implemented by analysing through-focus images of custom test targets for measuring the Modulation Transfer Function (MTF) and subsequently extracting the different primary aberration coefficients [S.M. Shakeri et al., manuscript in preparation]. This MTF-based method needs validation using direct aberration measurements.

Here we present the results of Shack-Hartmann wavefront sensor based aberration measurements and compare it to MTF-based results. A small pinhole in the glass slide with cover slip is used as a point source, and the line scan camera of the WSS is replaced by the Shack-Hartmann sensor and attached collimating lens for the duration of the experiment. Moving the pinhole in the field-of-view of the objective lens provides a full-field map of the different aberrations. In the presentation we will show the comparison of these full-field aberration maps to the MTF-based aberration test for two different objective lens-tube lens assemblies. In addition, we present an analysis of the full-field aberration maps [R. Tessieres, MSc Thesis, 2003] for revealing different misalignments such as decentre and tilt of optical components for a configuration with intentional misalignment.

9315-5, Session 2

A dynamic opto-physiological model to effectively interpret retinal microvascular circulation

Harnani Hassan, Sijung Hu, Vincent Dwyer, Loughborough Univ. (United Kingdom)

The demand of non-invasive ocular disease diagnosis and assessment is rapidly growing due to increase of age related eye diseases worldwide. To meet the requirement of cost-effective screening, there is an indeed in-depth understanding of optical properties for ocular tissue. The complexity

**Conference 9315:
Design and Quality for Biomedical Technologies VIII**

nature of retinal tissue caused both absorption and scattering became essential as it is not only for optical driven clinical treatment purpose, but also for non-invasive, painless and non-radiation diagnosis. The research aims to investigate an effective biomedical engineering approach to allow process region of interests (ROIs) in eyes thus to reveal relevant diseases. A dynamic opto-physiological model (OPM) representing retinal microvascular circulation system and underlying a diffusion approximation to solve radiative transport theorem (RTT) has been developed to interpret patho-physiological phenomena. OPM will be applied in available imaging photoplethysmography (iPPG). The non-invasive iPPG system will be able to extract PPG signals from a series of two dimensional matrix images during screening process to monitor blood perfusion and oxygen saturation (SpO₂) distributions. Thus, a variation of microvascular circulation on retinal tissue region can be clearly mapped for an effectively clinical screening. The robustness, miniaturization and artefact reduction capability of developed OPM to discriminate oxygenation levels in retina will offer a new insight to access retinal patho-physiological status.

Keywords: region of interests (ROIs); opto-physiological (OPM); retinal microvascular circulation, blood perfusion; radiative transport theorem (RTT); imaging photoplethysmography (iPPG); oxygen saturation (SpO₂); patho-physiological change.

9315-6, Session 2

Quantitative light scattering of single sub-micron particles for flow cytometry standardization

Frank Coumans, Edwin van der Pol, Anita N. Böing, Academic Medical Ctr., Amsterdam (Netherlands); Guus Sturk, Rienk Nieuwland, Academic Medical Ctr. Amsterdam (Netherlands); Ton G. van Leeuwen, Academic Medical Ctr., Amsterdam (Netherlands)

Background: Blood contains platelet microparticles (PMP) with a diameter of 50-2000 nm. The PMP concentration is a potential biomarker for thrombosis and can be determined by flow cytometry. However, since flow cytometers differ in sensitivity, reliable determination of the PMP concentration requires standardization of the detected size range. The current standard, based on calibration with polystyrene beads, resulted in a coefficient of variation (CV) of 91% of the PMP concentration. This poor reproducibility is attributed to the variety of optical configurations in flow cytometers and the refractive index mismatch between PMP (1.40) and polystyrene (1.61).

Method: A well-defined polystyrene beads mixture and a PMP standard were measured on 63 flow cytometers in 32 laboratories worldwide. The instrument-specific relationship between particle size, refractive index, and scatter was obtained by describing the data from the beads mixture with Mie theory. The relationship was used to set a PMP size gate, taking into account the refractive index of PMP.

Results: Preliminary data show that the CV of the PMP concentration has improved to 70%. The size detection limit of instruments of the same model can differ more than two-fold and the current 500-900 nm polystyrene bead standard gates PMP of 800-2200 nm. Final results from the 32 sites are expected in September 2014.

Conclusions: Applying Mie theory to standardize the size range detected by flow cytometry improves the reproducibility of the PMP concentration with 21% compared to the current standard. Our method allows inclusion of conventional and novel flow cytometer designs.

9315-7, Session 2

Standardized cell samples for midIR technology development

Jürgen Schneckeburger, Lena Kastl, Christina E. Rommel,

Björn Kemper, Westfälische Wilhelms-Univ. Münster (Germany)

The application of midIR spectroscopy towards human cell and tissue samples is impaired by the need for technical solutions and lacking sample standards for technology development. We here present the standardization of stable test samples for the development and testing of novel optical components for skin surface analysis.

We have selected cell lines representing major cellular skin constituents (NIH-3T3 fibroblasts, HaCaT keratinocytes). In addition, two skin cancer cell types (A-375, SK-MEL-28 cells) were analyzed. Cells were seeded on CaF₂ or BaF₂ substrates and measured dried and under aqueous medium as well as fixated and unfixated over a period of 44 days. Several independent cell preparations were analyzed with an FTIR spectrometer in the wave number range from 1000 - 4000 cm⁻¹. The obtained data demonstrate that fixed and dehydrated cells on CaF₂ can be stored in pure ethanol for several weeks without significant losses in quality of the spectral properties.

The established protocol of cell seeding on CaF₂ substrates, chemical fixation, dehydration, storage under ethanol and air-drying is suitable for the production of reliable and reproducible midIR standards. The retrieved spectra demonstrate that fixed cells on CaF₂ can be prepared reproducibly; with stable midIR spectral properties over several weeks and properties mimicking unfixed cells. Moreover, the fixated samples show clear differences in cell type specific spectra that can be identified by principle component analysis.

In summary, the standardized cell culture samples on CaF₂ substrates are suitable for the development of midIR devices and the optimization of the specific midIR spectra.

9315-8, Session 2

Calibration of NIRS-measured hemodynamics with best-matched hemoglobin extinction coefficients and group statics on human-blood-model data

Ting Li, Yue Zhao, Univ. of Electronic Science and Technology of China (China); Yunlong Sun, Kai Li, Wenjie Li, Chi Zhang, Junpeng Liu, Univ of Electronic Science and Technology of China (China)

Near-infrared spectroscopy has been extensively developed for in-vivo measurements of tissue vascular oxygenation, breast tumor detection, and functional brain imaging, by groups of physicists, biomedical engineers, and mathematicians. To quantify concentrations of oxyhemoglobin, deoxyhemoglobin, and total hemoglobin (hemodynamics), extinction coefficients of hemoglobin (?) have to be employed. However, it is still controversial what? values should be used and relatively what calibration should be done in NIRS quantification to achieve the highest precision, although that the differences in?values among published data resulted in ~20% variation in quantification of hemoglobin concentration is reported based a single human blood test. We collected 12 blood sample from 12 healthy people, and with each blood sample performed blood tissue model experiments. 4 teams of published extinction value widely used in NIRS fields were employed respectively in our quantification. Calibrations based least square analysis and regression between real and estimated hemodynamics for 12 subjects were performed with each team of ?values respectively. We found that: Moaveni's?values contributed to highest accuracy; Regression method produced quite effective calibration, and when it combined with Morie's?values, the calibration reduced the std/mean of estimation by two orders of magnitude. Thus Moaveni's?values are most recommended to use in NIRS quantification, especially with our calibration matrix based on regression analysis with a group of subjects' blood sample.

**Conference 9315:
Design and Quality for Biomedical Technologies VIII**

9315-9, Session 3

Photoacoustic tomography: ultrasonically beating optical diffusion and diffraction
(Keynote Presentation)

Lihong V. Wang, Washington Univ. in St. Louis (United States)

No Abstract Available

9315-10, Session 4

Bridging the gap in colonoscopy with optical and engineering solutions *(Invited Paper)*

Bhaskar Banerjee, The Univ. of Arizona (United States)

Colonoscopy is the preferred procedure for the detection, biopsy and removal of neoplastic lesions of the colon. It is estimated that about 14 million colonoscopies will have been performed in the US in 2014. The number of patients undergoing colonoscopy worldwide is also increasing, however, the procedure is far from perfect and recent studies have questioned its impact on colon cancer prevention, particularly in the proximal colon. Whereas standard endoscopes are designed to provide a view of a cylindrical lumen, the colon is not a simple hollow tube, but a tortuous organ with many folds that can prevent polyps from being seen. Poor color contrast of some flat lesions also make detection more difficult. A number of techniques have been developed to increase the surface area of the colon viewed, from accessories that can be used with existing colonoscopes to new endoscopy systems. Methods to improve lesion contrast are also being developed. The ideal device should not only maximize the surface of the colon viewed and improve lesion contrast to aid detection, but should do so inexpensively and without increasing the complexity and duration of the procedure. Healthcare reform will soon require endoscopists to report the quality of their procedures, as measured by individual rates of adenoma detection. Therefore the need to develop new devices that improve lesion detection is profound, but for any product to be clinically assimilated, it needs to be easy to use and affordable.

9315-11, Session 4

All plastic fluorescence image guided goggle system

Nan Zhu, The Univ. of Arizona (United States); Shengkui Gao, Suman B. Mondal, Samuel Achilefu, Viktor Gruev, Washington Univ. in St. Louis (United Kingdom); Rongguang Liang, The Univ. of Arizona (United States)

9315-12, Session 4

Optical design of a dual-view endoscope

Rajender Katkam, Bhaskar Banerjee, Rongguang Liang, The Univ. of Arizona (United States)

No Abstract Available

9315-3, Session 5

Standardizing flow cytometric assays in long-term population-based studies
(Invited Paper)

Susanne Melzer, Jozsef Bocsi, Univ. Leipzig, Pediatric Cardiology, Heart Ctr. Leipzig GmbH (Germany); Attila Tarnok, Univ. Leipzig (Germany) and Univ. Leipzig, Pediatric Cardiology, Heart Ctr. Leipzig GmbH (Germany)

Long-term flow cytometric (FCM) studies require a strict quality management. Quality checks should particularly control for instrument fluctuations, variations in sample-preparation and data analysis that are a substantial source of error and may hamper the sensitive measurement of biological variation.

We analyzed more than 1500 blood samples of a population-based study over a period of four years using FCM. In short, a ten-color 13 antibody FCM was used to quantify leukocyte subpopulations by characterizing their surface antigen expression pattern [1]. The comparability of all data was assured by the following quality measures: Laser alignment was daily checked using FlowCheck Pro to assure stable half-peak coefficient of variation values for all fluorescences over the years. Rainbow beads were used to normalize the mean fluorescent intensity (MFI) variations over time. The day-to-day MFI variations were less than +/-4.0% for most antibodies. Titration experiments were performed, the antibody cocktail stability tested, and the intra-assay variance of the sample-preparation was checked. Data analysis was performed by sequential manual gating. The reliability of gating was checked by analyzing identical samples by three readers as well as by analyzing the same samples by the same reader with a time-lag of 3 months between the readings. Inter-reader and intra-reader accordance were $R^2=0.993$ to 0.999 and $R^2=0.99$, respectively. For the reliable detection of biological variation and the control of variation in instrument performance and analysis, the presented multi-step quality measures for long-term and longitudinal analyses is of universal use.

1 OMIP-023; DOI: cyto.a.22505

9315-13, Session 5

Spatial frequency domain imaging (SFDI): evolution of a translational system *(Invited Paper)*

Amaan Mazhar, Pierre Khoury, Steve Saggese, Modulated Imaging, Inc. (United States); Anthony J. Durkin, Univ. of California, Irvine (United States); David Cuccia, Modulated Imaging, Inc. (United States)

Quantitative assessment of tissue structure and function is one of the most challenging problems in biomedical imaging. To this end, we have been developing a robust and user-friendly platform system based on Spatial Frequency Domain Imaging (SFDI) capable of rapid wide-field mapping of optical properties and chromophores in tissue. We will present: 1) Design and fabrication of a clinic-ready hardware platform with increased field-of-view (20cm x 15cm), spectral multiplexing (11 wavelengths), improved stability (<0.5% drift/hr) and enhanced ease of use (cart-mounted instrumentation); 2) Development of research-friendly software with automated analysis and refined tissue-specific algorithms; 3) Development of internal and external verification and validation procedures in phantoms; 4) In-vivo evaluation to establish benchmarks of performance and sensitivity for quantitative hemoglobin parameter recovery and correlation to histological benchmarks. Development of this system has enabled pre-clinical and clinical research in applications such as wound healing, burn assessment, and reconstructive surgery.

**Conference 9315:
Design and Quality for Biomedical Technologies VIII**

9315-14, Session 5

Multifocal confocal spectral microscope

Shaun Pacheco, Rongguang Liang, The Univ. of Arizona (United States)

No Abstract Available

9315-15, Session 5

Application of maximum-likelihood estimation in optical coherence tomography for nanometer-class thickness estimation

Jinxin Huang, Univ. of Rochester (United States); Qun Yuan, Nanjing Univ. of Science and Technology (China); Patrice Tankam, Univ. of Rochester (United States); Eric W. Clarkson, Matthew A. Kupinski, The Univ. of Arizona (United States); Holly B. Hindman, James V. Aquavella, Jannick P. Rolland, Univ. of Rochester (United States)

In biophotonics imaging, one important and quantitative task is layer-thickness estimation. In this study, we investigate the approach of combining optical coherence tomography and a maximum-likelihood (ML) estimator for layer thickness estimation in the context of tear film imaging. The motivation of this study is to extend our understanding of tear film dynamics, which is the prerequisite to advance the management of Dry Eye Disease, through the simultaneous estimation of the thickness of the tear film lipid and aqueous layers. The estimator takes into account the different statistical processes associated with the imaging chain. We theoretically investigated the impact of key system parameters, such as the axial point spread functions (PSF) and various sources of noise on measurement uncertainty. Simulations show that an OCT system with a 1 micron axial PSF (FWHM) allows unbiased estimates down to nanometers with nanometer precision. In implementation, we built a customized Fourier domain OCT system that operates in the 600 to 1000 nm spectral window and achieves 0.95 micron axial PSF in corneal tissue. We then validated the theoretical framework with physical phantoms made of custom optical coatings, with layer thicknesses from tens of nanometers to microns. Results demonstrate unbiased nanometer-class thickness estimates in three different physical phantoms.

9315-16, Session 5

A high-throughput automated confocal imaging system for three-dimensional examination of neuronal regeneration of C. elegans post-injury axons

Ki Hyun Kim, Evan Hegarty, Sertan K. Gokce, Adela Ben-Yakar, The Univ. of Texas at Austin (United States)

We present a high-throughput automated confocal imaging system for three-dimensional examination of neuronal regeneration of C. elegans post-injury axons. The examination of neuronal regeneration of C. elegans imposes two challenges: (1) the autofluorescent signal from the surroundings of the axon dominates the axon's fluorescent signal, (2) the worm's orientation interferes with the imaging of the axon. Hence we developed the automated confocal imaging system consisting of the high-speed confocal microscope, which addresses the former challenge, and the microfluidic device with the multiple trapping channels, which solves the latter. Our high-speed confocal microscope is capable of imaging a 350 μm x 50 μm field-of-view (FOV) at 30 frames-per-second (FPS) using a 40X oil immersion objective and a 670 μm x 50 μm FOV at 40 FPS using

a 20X water dipping objective. Our confocal microscope can control its FOV continuously to match the different sizes of C. elegans at different ages. Our microfluidic device has 24 worm trapping channels which are designed to trap C. elegans in the preferable orientation for axon imaging. Our automated imaging system works as follows: (a) worms are loaded inside the microfluidic device, (b) the locations of target axons are identified by wide-field fluorescent imaging, and (c) the target axons are imaged by the high-speed confocal microscope. Imaging of all the worms inside the microfluidic device takes less than thirty minutes. Our automated imaging system will speed up the collection of a large number of samples for neuro-regenerative studies using C. elegans.

9315-17, Session 6

FPGA-based real-time multiplexed fluorescence lifetime imaging by Fourier multiplexed FLIM (Invited Paper)

Ming Zhao, Yu Li, Leilei Peng, College of Optical Sciences, The Univ. of Arizona (United States)

We describe a low-cost fast fluorescence lifetime microscopy method that simultaneously produces processed multi-channel lifetime images in real time. The method solves two major challenges in applying FLIM to biomedical studies: First, multi-channel lifetime imaging in parallel; second, real-time lifetime calculation.

Parallel multi-channel lifetime imaging could allow tracking of multiple biological processes in living biological samples, however it is very difficult to realize with existing FLIM methods. We achieve parallel multi-channel lifetime imaging through the principle of Fourier multiplexing. Multi-wavelength excitation sources are modulated by a Fourier transform interferometer into frequency sweeping intensity modulations. Modulation frequencies are inversely proportional to wavelengths, which allow parallel fluorescence lifetime measurements at multiple excitation and emission wavelength combinations [1].

Real-time fluorescence lifetime calculations are needed for live readout of biological processes. We developed a fast non-iterative lifetime data analysis method that consists of simple arithmetic computations and is implemented in FPGA. The method has equivalent performance compared to iterative non-linear fitting. FPGA implementation of the method allows calculation of fluorescence lifetime results at multiple Ex-Em channels in real-time.

The system is compatible with confocal microscopy for imaging multiple biological processes in live cells through time-lapse multiplexed FLIM. It is also combined with scanning laser optical tomography to probe multiple biochemical conditions in live embryos in 3D.

Reference:

[1] M. Zhao, Y. Li and L. Peng, Opt. Express, 22:10221.

9315-18, Session 6

Effective duty cycle of galvanometer-based scanners: impact on OCT imaging

Virgil-Florin Duma, Aurel Vlaicu Univ. of Arad (Romania) and West Univ. of Timisoara (Romania) and Polytechnics Univ. of Timisoara (Romania); Patrice Tankam, Jinxin Huang, Jannick P. Rolland, The Institute of Optics, Univ. of Rochester (United States)

We study experimentally the scanning functions of galvanometer-based scanners (GSs) in order to optimize them for biomedical imaging in general, and for Optical Coherence Tomography (OCT) in particular. The main scanning parameters of the scanning process are taken into account: theoretical duty cycle (of the input signal of the GS), scan frequency (fs) and scan amplitude (μm). Triangular to sawtooth scanning regimes are thus considered. We demonstrate that when increasing the scan frequency

**Conference 9315:
Design and Quality for Biomedical Technologies VIII**

and amplitude, the scanning function (i.e., the angular position of the galvomirror) is not able to follow anymore the input signal. Furthermore, as the theoretical duty cycle is increased, the result is unexpected: the effective duty cycle actually decreases – for high f_s and φ_m . A saturation of the device therefore occurs. The practical limits of this phenomenon are discussed. GS users are thus provided with a multi-parameter analysis that allows them for optimizing their scanning regimes and to avoid pushing the devices to their limit – when that actually results in decreasing the quality of the images obtained, by example in OCT. Gabor Domain Optical Coherence Microscopy (GD-OCM) images are made to show effects of this phenomenon. Selected references: [1] Duma, V.-F., Lee, K.-S., Meemon, P., and Rolland, J. P., “Experimental investigations of the scanning functions of galvanometer-based scanners with applications in OCT,” *Appl. Opt.* 50(29), 5735-5749 (2011). [2] Duma, V.-F., “Optimal scanning function of a galvanometer scanner for an increased duty cycle,” *Opt. Engineering* 49(10), 103001 (2010).

9315-19, Session 6

Optimization of whispering gallery mode sensor design for applications in biosensing

Tess Reynolds, Alexandre François, Matthew R. Henderson, The Univ. of Adelaide (Australia); Stephen J. Nicholls, South Australian Health & Medical Research Institute (SAHMRI) (Australia); Tanya M. Monro, The Univ. of Adelaide (Australia)

Whispering gallery modes (WGM) have been extensively studied, both theoretically and experimentally, for applications in biosensing due to their ability to conduct highly selective, sensitive and label-free detection of molecules. The majority of the work previously conducted has focused on using only a handful of resonator materials. Silica and polystyrene are most commonly utilized with other materials remaining largely unexplored. Investigating other resonator materials provides an opportunity to extend the WGM platform and may assist in creating specialized biosensing devices. Key characteristics such as the quality factor and sensitivity of the resonator, along with considerations of the final application contribute to the final determination of the optimal WGM sensor design. This work looks to predict and investigate the combinations of resonator material and size, along with excitation and coupling scheme to provide guidelines to assist in the decision making when undertaking refractive index biosensing exploiting WGMs.

9315-20, Session 6

Optimal selection of cut-on wavelength in soliton self-frequency shift for nonlinear optical microscopy

Ke Wang, Ping Qiu, Shenzhen Univ. (China)

Soliton self-frequency shift (SSFS) has become an enabling tool for reaching the highest nonlinear optical imaging depth in mouse brain *in vivo*, offering new methodology for neuroscience research in deep brain. Imaging deeper requires an increase in excitation energy in soliton, and minimizing extra energy deposition. Since the soliton spectrally overlaps with the residual dramatically, how to properly filter it out is the key to getting as much nonlinear signal as possible and minimizing tissue photodamage due to extra energy deposition. In this paper we propose maximizing the ratio between multiphoton signal and the n th power of the excitation pulse energy as a criterion for optimal spectral filtering in SSFS, when the soliton shows dramatic overlapping with the residual. This optimization is based on most efficient signal generation and entirely depends on physical quantities that can be easily measured experimentally. Its application to MPM may reduce tissue damage, while maintaining high signal levels for efficient deep penetration, benefiting neuroscience research especially for the deep brain.

9315-21, Session 6

A new engineering approach to reveal correlation of physiological change and spontaneous expression from video images

Fenglei Yang, Shanghai Univ. (China); Sijung Hu, Loughborough Univ. (United Kingdom); Xiaoyun Ma, Shanghai Univ. (China); Harnani Hassan, Loughborough Univ. (United Kingdom); Dongqing Wei, Shanghai Jiao Tong Univ. (China)

Spontaneous expression is associated with physiological states, i.e., heart rate, respiration, oxygen saturation (SpO₂%), and heart rate variability (HRV). There have been yet not sufficient efforts to explore correlation of physiological change and spontaneous expression. This study aims to research how spontaneous expression is associated with physiological changes with an approved protocol or through the videos provided from Denver Intensity of Spontaneous Facial Action Database. Not like a posed expression, motion artefact in spontaneous expression is one of evitable challenges to be overcome. To obtain physiological signs from region of interests (ROIs), a new engineering approach is being developed with an artefact-reduction method in consolidation of an active appearance model, planar motion compensation with opto-physiological mode based imaging photoplethysmography (iPPG). Also, a statistical association spaces is being applied to interpret the correlation of spontaneous expressions and physiological states including their probability distributions by means of Gaussian Mixture Model. The present work is revealing a new avenue to study association of spontaneous expressions and physiological states with its prospect of applications on effective physiological and psychological assessment.

Keywords: spontaneous expression, region of interest (ROI), physiological states, imaging photoplethysmography (iPPG), Gaussian Mixture Model, physiological and psychological assessment

9315-22, Session 7

From astronomy and telecommunications to biomedicine (*Invited Paper*)

Bradford B. Behr, Tornado Spectral Systems (United States); Scott A. Baker, Yusuf Bismilla, Andrew T. Cenko, Brandon DesRoches, Tornado Spectral Systems (Canada); Arsen R. Hajian, Tornado Spectral Systems (United States); Jeffrey T. Meade, Tornado Spectral Systems (Canada); Arthur Nitkowski, Kyle J. Preston, Tornado Spectral Systems (United States); Bradley S. Schmidt, Tornado Spectral Systems (Canada); Nicolás Sherwood-Droz, Tornado Spectral Systems (United States); Jared Slaa, Tornado Spectral Systems (Canada)

Photonics is an inherently interdisciplinary endeavor, as technologies and techniques invented or developed in one scientific field are often found to be applicable to other fields or disciplines. We present two case studies in which optical spectroscopy technologies originating from stellar astrophysics and optical telecommunications multiplexing have been successfully adapted for biomedical applications. The first case involves a design concept called the High Throughput Virtual Slit, or HTVS, which provides high spectral resolution without the throughput inefficiency typically associated with a narrow spectrometer slit. HTVS-enhanced spectrometers have been found to significantly improve the sensitivity and speed of fiber-fed Raman analysis systems, and the method is now being adapted for hyperspectral imaging for medical and biological sensing. The second example of technology transfer into biomedicine centers on integrated optics, in which optical waveguides are fabricated

**Conference 9315:
Design and Quality for Biomedical Technologies VIII**

on silicon substrates in a substantially similar fashion as integrated circuits in computer chips. We describe an architecture referred to as OCTANE which implements a small and robust "spectrometer-on-a-chip" which is optimized for optical coherence tomography (OCT). OCTANE-based OCT systems deliver three-dimensional imaging resolution at the micron scale with greater stability and lower cost than equivalent conventional OCT approaches. Both HTVS and OCTANE enable higher precision and improved reliability under environmental conditions that are typically found in a clinical or laboratory setting.

9315-23, Session 7

Enhancement of absorption and resistance of motion utilizing a multi-channel opto-electronic sensor to effectively monitor physiological signs during sport exercise

Abdullah Alzahrani, Sijung Hu, Vicente Azorin-Peris, Laura Barrett, Dale Eslinger, Loughborough Univ. (United Kingdom); Matthew Hayes, Cambridge Consultants Ltd. (United Kingdom); Shafique Akbare, Univ. Paris-Sud (France); Jerome Achart, Sylvain Kuoch, Université Paris-sud (France)

This study presents an effective engineering approach to continuously monitor human vital signs, an area of growth given the aging population and the need for personalised healthcare. The aim of this research is to determine how to capture critical sport physiological parameters efficiently through a well contracted electronic design and robust a multi-channel opto-electronics together with real-time, noise reduction and wireless communication functionality. Multiplexed wavelength illumination sources with a novel electronic design have been introduced with a MEMS 3-axis accelerometer in order to enhance the pulsatile absorption, compensate for motion artefact and increase the signal to noise ratio. The results show significant improvement on the measurement of dynamic change of tissue optical amplitude, as well as the waveforms of pulsate signals are more resistive and stable against motion artefacts. An approved protocol with a variety of activity modes and a well-controlled experimental setup are being implemented in Loughborough University, a global leader in sport science. The results of sport physiological effects are being extracted from the datasets of physical movements including sitting, standing, waking, running and cycling. The results demonstrate that the goal of the high performance wearable multi-channel opto-electronics is viable and feasible.

9315-24, Session 7

Ultrasensitive detection allows for singlet oxygen phosphorescence detection, an important prerequisite for photodynamic therapy

Uwe Ortman, Christian Litwinski, Manoel Veiga, Sebastian Tannert, Felix Koberling, Volker Buschmann, Matthias Patting, Marcus Sackrow, Michael Wahl, Rainer Erdmann, PicoQuant GmbH (Germany); Peter Kapusta, J. Heyrovsk? Institute of Physical Chemistry of the ASCR, v.v.i. (Czech Republic); Christian Wolf, Humberto Rodriguez-Alvarez, PVcomB, Helmholtz-Zentrum Berlin für Materialien und Energie GmbH (Germany)

Detection sensitivity from the ultraviolet to the near infrared spectral region is a key parameter to meet today's demand for handling smallest analyte amounts and short measurement times in the optical evaluation of miscellaneous samples. The introduction of single photon counting based data acquisition has proven to yield a major sensitivity increase

and very high dynamic range – it is the ideal method for measuring weak luminescence.

We present the hardware and handling optimization of a state of the art spectrometer for steady-state and time-resolved fluorescence measurements. The high sensitivity of the spectrometer was shown by measurements of popular fluorescent dyes as well as the Raman spectrum of water under well defined and reproducible conditions. The achieved sensitivity allows us to quantify singlet oxygen generation and to characterize the singlet oxygen phosphorescence decay, a prerequisite when studying photosensitisers like porphyrins and phthalocyanines used for example in photodynamic therapy (PDT). Moreover with the help of an integrating sphere fluorescence quantum yields of low fluorescent samples like Ru(bpy)₃ in water can be determined very precisely.

The fibre connection of the spectrometer to a time-resolved fluorescence microscope (MicroTime100/200) was also realized. The combination of the advantages of both setups makes it e.g. possible to perform 2D-lifetime imaging with a freely tunable detection window for low luminescent samples even far into the near infrared region. The measurements with such a combination give not only the spectral and lifetime information of a luminescent sample but also the spatial information which is especially important for heterogeneous samples.

9315-25, Session 7

Separation of Cerenkov radiation in irradiated optical fibers by optical spectroscopy

Arash Darafsheh, Haoyang Liu, The Univ. of Pennsylvania Health System (United States); Rongxiao Zhang, Stephen C. Kanick, Brian W. Pogue, Dartmouth College (United States); Timothy C. Zhu, Jarod C. Finlay, The Univ. of Pennsylvania Health System (United States)

Accurate dose assessment is crucial in radiation therapy quality assurance. Fiber optic dosimetry using scintillating materials is a promising choice for radiation therapy dose assessment. However, the main problem with fiber optic dosimetry is that the signal received by the detector through the fiber is contaminated with Cerenkov radiation, which may not be directly proportional to dose. In this work, we demonstrate a generic spectroscopic method for separation of Cerenkov radiation from the recorded signal based on the assumption that the latter is a linear superposition of two basis spectra: Cerenkov radiation and characteristic luminescence of the scintillating medium. Experimentally, we evaluated our method by using phosphor-based and scintillator fiber microprobes irradiated by electron and photon beams generated by a clinical linear accelerator. We showed that our method is generic and works well for various phosphor as well as scintillating materials. By introducing different levels of random noise to the recorded spectra, we found that our method is very robust to noise. Our Monte Carlo simulations of the Cerenkov radiation generated in the fiber are in good agreement with the experimental results.

9315-26, Session 7

Evaluation of the optical interference in a combined measurement system used for assessment of tissue blood flow

Zahra Abdollahi, Panicos Kyriacou, Justin Phillips, City Univ. London (United Kingdom)

This study was performed to evaluate optical interference between PPG and LDF in a combined system. This dual-wavelength pulse oximetry system combined with laser Doppler was developed for the assessment of perfusion. Red and infrared PPG and Doppler signals were recorded from a healthy volunteer in three studies at different measurement sites

**Conference 9315:
Design and Quality for Biomedical Technologies VIII**

to investigate the interference between PPG and laser Doppler flowmetry (LDF). This preliminary evaluation study showed that good quality PPG and LDF signals could be acquired using the new combined probe. From the all results of this experiment it was found that the PPG is not greatly affected by LDF; in the worst case the change in AC amplitude when the LDF system is switched on was less than 8%. Results from this trial study showed that by increasing the distance between the LDF and the photodiode, the effect of optical interference from LDF on both red and infrared PPG signals decreased. Also it was found that R PPG is proportionally more affected by LDF light than IR PPG. The results also show that the effect on reported LDF flux from the PPG light sources is more marked. In the worst case the change in LDF flux amplitude when the PPG system is switched on was less just over 14.7%. Like the PPG amplitudes, it was found that increasing the distance between the LDF and the photodiode had the effect of reducing the optical interference from PPG light sources on the LDF flux values.

9315-30, Session PSun

A novel optical biopsy probe design combining elastic scattering spectroscopy and optical coherence tomography

Abel Swaan, Paul R. Bloemen, Anouk L. Post, Xu Zhang, Daniel M. de Bruin, M. Pilar Laguna Pes, Henricus J. C. M. Sterenberg, Dirk J. Faber, Jean J. de la Rosette, Ton G. van Leeuwen, Academisch Medisch Centrum (Netherlands)

Prostate cancer is usually diagnosed by transrectal ultrasound guided biopsies. Unfortunately, this has a low sensitivity and the tendency to underestimate. As a result, patients undergo multiple series of biopsies; 10-20 are taken in a single series and follow-up series can be necessary.

Guiding biopsies with real time information on location and possible grading of suspected lesions could reduce the amount of biopsies and increase diagnostic accuracy. Optical Coherence Tomography (OCT) and Elastic Scattering Spectroscopy (ESS) offer structural, physiological and biochemical information of tissue *in vivo*.

We will develop a needle based probe that integrates OCT and ESS. However, some challenges need to be addressed. First, ESS and OCT operate at different wavelengths (300-1000 vs. 1290-1350 nm) and employs multimode and single mode fiber. Second, most ESS-probes are stationary and forward-looking, whereas the design of our approach performs a rotating side-firing pullback.

To overcome these challenges, we designed a GRIN lens and prism based side-fire aperture in the fiber tip that support both ESS and OCT. The fibers from the OCT and ESS are coupled into a double clad fiber (DCF) by a double clad fiber coupler (DCFC). In the Fiber Optic Rotary Joint (FORJ), the static DCF and the rotary DCF are coupled using two GRIN lenses. To test the feasibility of this design, we simulated ray propagation in the probe using Zemax with promising results. Based on this, we are going to realize the first prototype from which preliminary results will be shown at the conference.

Acknowledgements

This study was funded by Dutch Technology Foundation (STW) grant numbers iMIT-PROSPECT 12707.

9315-31, Session PSun

A simple analysis of extinction spectra of cancerous and normal prostate tissues in near infrared range using a size discrete particle distribution and Mie scattering model

Kenneth J. Zhou, Stony Brook Univ. (United States); Jun Chen, Tianjin Medical Univ. General Hospital (China)

The extinction spectra and optical coefficients of human cancerous and normal prostate tissues were investigated in the spectral range of 750 nm - 860 nm. The scattering coefficient (μ_{s}) was determined from the extinction measurements on thin prostate tissue and Beer's law. The absorption coefficient (μ_{a}) and the reduced scattering coefficient (μ_{s}') were extracted from integrate sphere intensity measurements on prostate tissue of which the thickness is in the multiple scattering range. The anisotropy factor (g) was calculated using the extracted values of μ_{s} and μ_{s}' . A micro-optical model of soft biological tissue was introduced to simulate the numerical computation of the absolute magnitudes of its scattering coefficients from the refractive index and a particle distribution function based on the Mie theory. A key assumption of the model is that the refractive index variations caused by microscopic tissue elements can be treated as particles with sizes distributed according to a skewed log-normal distribution function. The particle distribution and mean particle size of the two types of tissues were then calculated. Results show that the mean diameter of the particle size of cancerous tissue is larger than that of the cancerous tissue, which is responsible for larger reduced scattering coefficient of normal tissue in comparison with cancerous tissue. The results can be explained the change of tissue during prostate cancer evolution defined by Gleason Grade. The difference of the particles distribution and optical coefficients of cancerous and normal prostate tissues may present a potential criterion for prostate cancer detection.

9315-32, Session PSun

Blood flow measurement by 320 multi-detectors CT: A phantom study

Jun Chen, Xuefang Yu, Department of Cardiology, Tianjin Medical University General Hospital (China); Shaopeng Xu, Tianjin Medical Univ. General Hospital (China); Kenneth J. Zhou, Stony Brook Univ. (United States)

A 320 row detector X-ray computed tomography (CT) was used to evaluate the feasibility of measuring the myocardial blood flow with reduced radiation. Coronary artery was simulated with a pipeline of 4 mm diameter and connected with the simulated aorta. The simulated aorta was connected with a container with 1500ml saline. The CT scan acquired the three dimensional imaging of the simulated aorta by injecting contrast agent into the container with a speed of 20ml/s to get the linear changing concentration of contrast agent. A pumping syringe linked to the simulated aorta at downward will withdraw the contrast agent solution with a speed of 25ml/s while another pumping syringe at downward simulated coronary artery will withdraw with a speed of 1 ml/s, 2 ml/s, 3 ml/s, 4 ml/s, 5 ml/s respectively. CT scans started after 1 second of injection of the contrast agent. CT images were processed as follows: the second CT scan images with contrast agents subtract first CT scan images without contrast agents. The calculated increased CT value of simulated heart and the changes of CT value of the aorta were used to calculate the total inflow of myocardial blood flow. The simulated CT myocardial blood flows were calculated as: 0.94 ml/s, 2.09 ml/s, 2.74 ml/s, 4.18 ml/s, 4.86 ml/s. By compared with the known flow rate, the correlation coefficient was achieved to be 0.994 and r^2 is 0.97, indicating that the method of measuring the myocardial blood flow by two scans should be feasible.

9315-33, Session PSun

Quantitative assessment of myocardial perfusion by first-pass technique: animal study

Jun Chen, Department of Cardiology, Tianjin Medical University General Hospital (China); Zhang Zhang, Xuefang Yu, Tianjin Medical Univ. General Hospital (China); Kenneth J. Zhou, Stony Brook Univ. (United States)

**Conference 9315:
Design and Quality for Biomedical Technologies VIII**

Objective: To evaluate the quantitative assessment method of myocardial perfusion using 320 row CT.

Methods: a total 5 swines were enrolled in this study. Stenoses were made with balloon by interventional procedures. In the hyperemia condition, Fractional Flow Rate (FFR) was measured by pressure wire and myocardial perfusion flow was measured with colored microspheres technique. CT was scanned twice in first-pass phase.

Results: A total of 11 different degrees of stenoses were made. The measured FFR, Myocardial perfusion blood flow, the minimum ratio of CT value and the minimum ratio of perfusion are obtained as 0.72 ± 0.17 , 1.5 ± 0.8 ml/min/g, 0.82 ± 0.17 and 0.47 ± 0.13 , respectively. Regression and receiver operating characteristic (ROC) analysis are used to evaluate the accuracy of the CT results. When FFR is regarded as the gold standard, the $r^2 = 0.74$ and 0.91 while $AUC = 0.75$ and 0.86 in the minimum ratio of CT value and the minimum ratio of perfusion respectively. When we regard myocardial perfusion flow measured by colored microspheres as the gold standard, the correlation coefficient are obtained as $r^2 = 0.81$ and 0.94 for the minimum ratio of CT value and the minimum ratio of perfusion, respectively, while the Areas Under the Curve (AUC) is 0.75 and 0.91 .

Conclusion: The maximum perfusion ratio is better than the minimum ratio of CT value and it may be used as an indicator of myocardial ischemia.

9315-34, Session PSun

Characteristics of photo-acoustic probe having light source inner the ultrasound transducer

Yong-Jae Lee, Eun-Ju Jeong, Hyun-Woo Song, Chang-Geun Ahn, Hyung-Wook Noh, Electronics and Telecommunications Research Institute (Korea, Republic of); Min Yong Jeon, Chungnam National Univ. (Korea, Republic of); Susung Lee, ALPINION Medical Systems (Korea, Republic of); Bong Kyu Kim, Electronics and Telecommunications Research Institute (Korea, Republic of); Hee-Won Kim, ALPINION Medical Systems (Korea, Republic of)

Recently the Photo-acoustic probe structure has been developed by several research group to connect the light source at ultrasound transducer because PA probe system is similar to the conventional ultrasound system. They simply add a light source outside the ultrasound transducer. These probes would be inconvenient to use for a diagnosis because of the larger size. Most of them have an oblique light illumination to an acoustic beam; therefore they have a standard dark-zone illumination and reduced sensitivity. In recent, an illumination structure directly to the interest region was introduced for overcoming the limitation, in which the optical connector axis is perpendicular to the ultrasound array axis. we propose the photo-acoustic probe, in which the optical connector axis and ultrasound receiver axis are parallel and light source is positioned inside the ultrasound transducer. This study examine the characteristics of the proposed photo-acoustic probe.

We made a hole of 1 mm thickness used as the optical path in the middle of the inner transducer. The end of the hole connected to the optical fiber is blocked with an acrylic for impedance matching to free space. In addition, intensity of the light coming out of the probe is sufficient to get the photo-acoustic image. The experimental result is the photo-acoustic image obtained by simple experiment using a fluorescent substance.

This work was supported by Industrial strategic technology development program, 10042581 funded by the Ministry of Trade, Industry & Energy (MOTIE) in Korea

Conference 9316: Multimodal Biomedical Imaging X

Saturday 7 February 2015

Part of Proceedings of SPIE Vol. 9316 Multimodal Biomedical Imaging X

9316-1, Session 1

Mammogram incorporated diffuse optical imaging with transmission and reflection parallel scanning

Jhao-Ming Yu, Liang-Yu Chen, National Central Univ. (Taiwan); Min-Cheng Pan, Tungnan Univ. (Taiwan); Shen-Yih Sun, Chia-Cheng Chou, Taoyuan General Hospital (Taiwan); Min-Chun Pan, National Central Univ. (Taiwan)

In this presentation, we demonstrate a working prototype of an optical breast imaging system using parallel-paddle architecture with dual-direction scanning, of which the designed module can be incorporated with a mammographic system for the acquisition of optical transmission and reflection information in both directions of up-down and down-up. This scanning module is handled through compressing breast tissue with using two parallel paddles like used in mammography, and moving two XY translation stages above and beneath, respectively, the compression paddles. In the study compared with before, the optical scanning module was modified to enable the collection of reflection NIR data for enhancing reconstructed optical-property images. Additionally, the scanning module enables to move with a designated pitch to accommodate varied breast size for acquiring adequate data to reconstruct the images. Currently, both the direct current and modulated near infrared illumination modules are used for experimentation. The feasibility of proposed transmission and reflection parallel scanning will be presented by the test of designated phantoms and preliminary clinical trial for breast screening.

For a dual-modality imaging scheme, suspected regions are first circled from a mammogram, and the plane in the sagittal view including that suspected region is to be optically scanned for subsequent image reconstruction. Three types of initial guess are investigated to locate the depth of tumors. The proposed computation scheme is validated by using designated phantoms including various size, contrast and location of inclusions to background, and also a phantom made of fat, lean meat and bone.

9316-2, Session 1

Dense motion analysis and segmentation of ultrasound images

Ryo Yokoyama, Kota Aoki, Hiroshi Nagahashi, Tokyo Institute of Technology (Japan)

We propose a dense motion analysis and segmentation method for ultrasound images, which utilizes both tracker and detector. Our motion analysis can be achieved by tracking a lot of lattice points. These points are connected by multiple spring-models based on a simple assumption that the positional relationship among them is almost invariable. Even if a point may have large tracking error due to speckle disappearance, the spring-model can correct the error from its neighboring points that have small tracking errors. Furthermore, each spring-model grasps the motion independently and the flexibility increases, and then, high density in motions analysis is achieved by integrating their results. Our detector learns texture information around the lattice points, to detect them by their likelihood tests and correct the tracking errors of the lattice points. We only use the detection results that have high confidence values, and hence, the false corrections of the tracking errors are decreased drastically. We evaluated our method using a sequence of artificial ultrasound images. To evaluate the tracking performance, we used average and maximum errors. Both errors represent the tracking performance of global motion and that of local motion respectively. The average and maximum errors of our method achieved the best performance in the conventional methods. In the last frame of the ultrasound images, the tracking result of our method showed

that the positional relationship among the lattice points is best ordered in the comparative methods. This means that our method also achieved a long-term accurate motion analysis.

9316-3, Session 1

Tomographic fluorescence reconstruction by a spectral projected gradient pursuit method

Jinzuo Ye, Institute of Automation (China); Yu An, Beijing Jiaotong Univ. (China); Yamin Mao, Institute of Automation, Chinese Academy of Sciences (China); Shixin Jiang, The Department of Biomedical Engineering, School of Computer and Information Technology (China); Xin Yang, Institute of Automation, Chinese Academy of Sciences (China); Chongwei Chi, Jie Tian, Institute of Automation (China)

In vivo fluorescence molecular imaging (FMI) has played an increasingly important role in biomedical research of pre-clinical area. Fluorescence molecular tomography (FMT) further upgrades the two-dimensional FMI optical information to three-dimensional fluorescent source distribution, which can greatly facilitate applications in related studies. However, FMT presents a challenging inverse problem which is quite ill-posed and ill-conditioned. Continuous efforts to develop more practical and efficient methods for FMT reconstruction are still needed. In this paper, a fast and robust method based on spectral projected gradient pursuit (SPGP) has been proposed for FMT reconstruction. The proposed method was based on the directional pursuit framework. A mathematical strategy named the nonmonotone line search was associated with the SPGP method, which guaranteed the global convergence. In addition, the Barzilai-Borwein step length was utilized to build the optimal step length of the SPGP method, which only required little computational work and could greatly speed up the convergence of this gradient method. To evaluate the performance of the proposed method, several heterogeneous simulation experiments including multisource cases as well as comparative analyses have been conducted. The results demonstrated that, the proposed method was able to achieve satisfactory source localization with a bias less than 1 mm; the computational efficiency of the method was one order of magnitude faster than the conjugate gradient method with the L2 norm; and the SPGP method was robust to the different regularization parameters. All the results demonstrated the potential for practical FMT application with the SPGP method.

9316-4, Session 1

Clinical implementation of L-curve based reconstruction in MRI guided optical tomography

Yan Zhao, Michael A. Mastanduno, Shudong Jiang, Fadi El-Ghoussein, Thayer School of Engineering at Dartmouth (United States); Jiang Gui, Dartmouth College (United States); Brian W. Pogue, Keith D. Paulsen, Thayer School of Engineering at Dartmouth (United States)

A hybrid frequency domain (FD)-continuous wave (CW) MRI/NIRS system was validated in a clinical trial involving patients with at least ACR 4 radiologic findings in Xi'an, China. In this study, Non-linear iterative reconstructions of MRI-Guided Near-infrared spectroscopic (NIRS) images are recovered using an L-curve based algorithm, and applied to clinical trial

data, to optimize recovery which maximizes the difference between the malignant and benign lesions. Comparison of recovery with NIRS amplitude-only data versus NIRS amplitude & phase at 100 MHz, shows that more differentiation is feasible with just the former smaller data set. (p -value=0.01 & AUC=0.81, versus p -value=0.01 & AUC=0.79, respectively in terms of HbT). Through a combination of both biomarkers, total hemoglobin and tissue optical index, the AUC for differentiating malignant from benign patients increased from 82.9% (fixed regulation=0.1) to 94.4% (Optimum method). In addition to the optimization of the image reconstruction algorithm, a systematic optimization of the system hardware design has been conducted as well. We are able to get less than 3% variation in tumor contrast to the surrounding normal tissue, by reducing the number of FD detectors from 16 to 6, showing the potential of reducing the FD detectors. Furthermore, a lookup table of the scattering properties has been made by averaging four MRI-identified breast density groups. By using this look-up table for the patient with the noisy phase data, similar AUCs and p -values are achieved for differentiating the malignant from benign patients.

9316-5, Session 2

Double clad fiber devices for combined optical coherence tomography and laser tissue coagulation

Kathy Beaudette, Ecole Polytechnique de Montréal (Canada); Martin L. Villiger, Harvard Medical School and Massachusetts General Hospital (United States); Mathias Strupler, Ecole Polytechnique de Montréal (Canada); Milen Shishkov, Jian Ren, Harvard Medical School and Massachusetts General Hospital (United States); Wendy-Julie Madore, Nicolas Godbout, Ecole Polytechnique de Montréal (Canada); Brett E. Bouma, Harvard Medical School and Massachusetts General Hospital (United States); Caroline Boudoux, Ecole Polytechnique de Montréal (Canada)

Optical coherence tomography (OCT) used in combination with a mechanism to mark select regions of interest could efficiently guide biopsy and, therefore, reduce false-negatives. Double clad fibers (DCFs) could enable simultaneous OCT – through the single-mode core – and coagulation of tissue by laser marking – through the multimode inner cladding – in a co-localized manner. Such a system would allow the use of a multimode marking source, an increased beam spot size as well as lower power density travelling through the endoscope. To efficiently combine both signals within the DCF, a DCF coupler optimized to inject the marking laser within the inner cladding was developed. This prototype, built using a fusion-tapering technique, allows transmission of the core signal (1260-1380nm) with more than -90% and greater than 65% coupling of the marking laser light through the inner cladding ($\lambda = 1436\text{nm}$). We also investigated possible OCT image degradation mechanisms due to crosstalk between both channels of the DCF. It was found that those artifacts reach a maximum of 15dB above the noise floor, which can be mitigated by optimizing fiber splices. Imaging of a scattering sample confirmed that the system provides sufficient dynamic range (-40-60dB) for in vivo imaging. An endoscopic system, including a rotary junction and a multimodal probe, is currently under development to allow circumferential imaging in the context of Barrett's esophagus. This combined endoscopic system will enable real-time image-guided laser marking and could further be readily adapted to real-time image-guided laser thermal therapy.

9316-6, Session 2

Illumination-compensated non-contact imaging photoplethysmography via dual-mode temporally-coded illumination

Robert Amelard, Christian Scharfenberger, Alexander Wong, David A. Clausi, Univ. of Waterloo (Canada)

Non-contact camera-based imaging photoplethysmography (iPPG) is useful for measuring heart rate in conditions where contact devices are problematic due to issues such as sanitation, comfort, or mobility. Existing iPPG methods analyse the reflectance of either active or passive (ambient) illumination. Many active iPPG methods assume the incident ambient light is negligible to the active illumination, resulting in high power requirements, while many passive iPPG methods assume near-constant ambient conditions. These assumptions can only be achieved in environments with controlled illumination and thus greatly constrain the use of such devices. To increase the number of possible applications of iPPG devices, we propose a dual-mode active iPPG system that is robust to changes in ambient illumination. Our system uses a temporally-coded illumination sequence that is synchronized with the camera to measure reflectance data from both active and ambient illumination for determining heart rate. By subtracting the ambient contribution from the reflectance data, the remaining reflectance data can be attributed to the controlled illuminant. Our device comprises a camera and an LED illuminant ($\lambda = 530\text{nm}$) controlled by a microcontroller. The microcontroller drives the temporal code via synchronizing the frame captures and illumination time. By simulating changes in ambient light conditions, experimental results show our device is able to assess heart rate accurately in challenging lighting conditions. By varying the temporal code, we demonstrate the trade-off between camera frame rate and ambient light compensation for optimal blood pulse detection.

9316-7, Session 2

Multi-modal contrast of tissue anatomy enables correlative biomarker imaging

Karl E. Garsha, Franklin Ventura, Gary Pestano, Michael Otter, Dea Nagy, Ventana Medical Systems, Inc. (United States); Ray B Nagle, University of Arizona (United States); Esteban Roberts, Michael Barnes, Ventana Medical Systems, Inc. (United States)

The interest of personalized medicine is to develop therapeutics that target specific molecular mechanisms of diseases such as cancer. The ability to evaluate distribution, expression level, and genotype for multiplexed biomarkers, in the context of anatomic pathology, provides important information for advancing the science of personalized medicine.

Classical cancer diagnostic methods are based on direct inspection of tissue morphology on prepared slides using light-absorbing contrast agents. The contrast provided by classical stains is familiar, and permits the physician to devote her efforts to interpreting anatomical and morphological features relevant to pathology determination. However, such contrast agents are not well suited to measurement of multiplexed molecular information.

Sophisticated analytical imaging techniques are being developed that promise to greatly increase the information content related to specific molecular reporters. Such reporters and imaging modalities typically do not produce contrast in the structural and anatomic context of the surrounding tissue, making it difficult to reconcile molecular information with morphological context.

We report a solution that enables visualization of the tissue morphology on sections prepared for analytical biomarker imaging. Our approach combines multiple modes of optical contrast and of image capture to enable visualization of tissue architecture in addition to analytical measurement of biomarkers in anatomic areas of interest. Digitization of tissue morphology permits physician selection of relevant regions for further interrogation

using a hyperspectral fluorescence imaging approach. The system enables practical correlative analysis of molecular changes within areas of anatomic pathology.

9316-8, Session 2

Multimodality and image guided interventional devices (*Invited Paper*)

Martin B. van der Mark, Philips Research Nederland B.V. (Netherlands)

Image guided interventions and therapy with smart minimally invasive devices can improve diagnostic value, shorten clinical procedures and hence can lead to better patient outcome at reduced cost. Application data from combined ultrasound and optical tissue spectroscopy as well as real-time 3-D tracking of catheters using optical shape sensing technology co registered with x-ray images will be shown.

9316-9, Session 2

High-resolution motion-compensated imaging photoplethysmography for remote heart rate monitoring

Audrey Chung, Xiao Yu Wang, Robert Amelard, Christian Scharfenberger, Joanne Leong, Alexander Wong, David A. Clausi, Univ. of Waterloo (Canada)

We present a novel non-contact photoplethysmographic (PPG) imaging system based on high-resolution video recordings of ambient reflectance of human bodies that compensates for body motion and takes advantage of skin erythema fluctuations to improve measurement reliability for the purpose of remote heart rate monitoring. Multiple measurement locations for recording the ambient reflectance are automatically identified on an individual, and the motion for each location is determined over time via measurement location tracking. Based on the determined motion information, motion-compensated reflectance measurements at different wavelengths for each measurement location can be acquired, thus providing more reliable measurements of the same location on the human over time. The reflectance measurements from different locations at the different wavelengths are then used jointly to determine skin erythema fluctuations over time, resulting in the capture of PPG signals with a higher signal-to-noise ratio than can be achieved by individual measurements. To test the efficacy of the proposed system, a set of experiments involving human motion in a front-facing position were performed under natural ambient light. The experimental results demonstrated that the proposed system can achieve noticeably improved average accuracy in heart rate measurement when compared to previously proposed non-contact PPG imaging systems.

9316-10, Session 2

Non-contact monitoring of vital signs independent of light conditions and skin tone: system validation and first clinical results

John H. Klaessens, Rudolf M. Verdaasdonk, Albert J. van der Veen, Jordi Penedo, Joost de Jong, Frank A. M. van den Dungen, Vrije Univ. Medical Ctr. (Netherlands)

The heart rate can be derived from the small variation in skin tone during the heart cycle using ordinary cameras and even smart phones apps. The respiration rate can be derived from minuscule motion. However, it will not work in dark environments or for dark skin tones. For reliable clinical use, non-contact monitoring (photoplethysmography) was improved for

both day and night use and for all skin types using near infrared (NIR) illumination and thermography in view of monitoring neonates.

The video stream from a NIR camera was analyzed by defining a region of interest on the skin, calculating the mean pixel value and performing a Fourier transformation using a band-pass filter revealing the main frequency component representing the heart rate. A clinical pulse oximeter was used as reference. From temperature variations near the nostrils imaged with a thermo camera the respiration rate was derived.

In a population of 20 volunteers equally divided along the Fitzpatrick skin tone scale (1-6), the heart rate could be derived for all skin tones within 3% accuracy compared to the pulse oximeter using NIR illumination. However, the HR could only be derived in 45% of dark skin tones using white light illumination. In a preliminary clinical study with 10 neonates the HR was accurate within 3%.

Using NIR light, non-contact monitoring of heart and respiration rate is possible, independent of light conditions and skin tone and has potential for many applications e.g. baby monitoring, patients in MRI. Other vital parameters like oxygenation can be added. The technique has to be developed into a real time application and validated in clinical studies.

9316-11, Session 2

Dual multispectral and 3D structured light laparoscope

Neil T. Clancy, Imperial College London (United Kingdom); Jianyu Lin, Shobhit Arya, Danail Stoyanov, George B. Hanna, Daniel S. Elson, Imperial College London (United Kingdom)

Intraoperative feedback on tissue function, such as blood volume and oxygen saturation would be useful to the surgeon in cases where current clinical practice relies on subjective measures, such as identification of ischaemic bowel or tissue viability during anastomosis formation. Also, tissue surface profiling may be used to detect and identify certain pathologies, as well as diagnosing aspects of tissue health such as gut motility.

In this paper a dual modality laparoscopic system is presented that combines multispectral reflectance and 3D surface imaging. White light illumination from a xenon source is detected by a laparoscope-mounted fast filter wheel camera to assemble a multispectral image (MSI) cube. Surface shape is then calculated using a spectrally-encoded structured light (SL) pattern detected by the same camera and triangulated using an active stereo technique.

Images of porcine small bowel were acquired during open surgery. Using a linear model of tissue reflectance blood volume was calculated at each spatial pixel across the bowel wall and mesentery. SL features were segmented and identified using multilayer thresholding and the colour vector of each spot. Using the 3D geometry defined by the camera coordinate system the multispectral data could be overlaid onto the surface mesh.

Dual MSI and SL imaging has the potential to provide augmented views to the surgeon supplying diagnostic information related to blood supply health and organ function. Future work on this system will include filter optimisation to reduce noise in tissue optical property measurement, and minimise spot identification errors in the SL pattern.

9316-12, Session 3

Correlative super-resolution fluorescence microscopy combined with optical coherence tomography

Sungho Kim, Gyeongtae Kim, Sanghee Shim, Sungchul Bae, Ulsan National Institute of Science and Technology (Korea, Republic of)

Conference 9316: Multimodal Biomedical Imaging X

Recent development of super-resolution fluorescence imaging technique such as stochastic optical reconstruction microscopy (STORM) and photoactivated localization microscope (PALM) brings us beyond the diffraction limit. It allows numerous opportunities in biology because vast amount of formerly obscured molecular structures, due to lack of spatial resolution, now can be directly observed. A drawback of fluorescence imaging, however, is that it lacks complete structural information. For this reason, we have developed a super-resolution multimodal imaging system based on STORM and full-field optical coherence tomography (FF-OCT). FF-OCT is a type of interferometry systems based on a broadband light source and a bulk Michelson interferometer, which provides label-free and non-invasive visualization of biological samples. The integration between the two systems is simple because both systems use a wide-field illumination scheme and a conventional microscope. This combined imaging system gives us both functional information at a molecular level (~20nm) and structural information at the sub-cellular level (~1 μ m). For thick samples such as tissue slices, while FF-OCT is readily capable of imaging the 3D architecture, STORM suffer from aberrations and high background fluorescence that substantially degrade the resolution. In order to correct the aberrations in thick tissues, we employed an adaptive optics system in the detection path of the STORM microscope. We use our multimodal system to obtain images on brain tissue samples with structural and functional information.

9316-13, Session 3

Multimodal non-invasive optical imaging methods for structure and functional assay of nociceptive pain model in *Drosophila melanogaster*

Chiao-Ying Lin, Chii-Wann Lin, Jyh-Horng Chen, National Taiwan Univ. (Taiwan)

Many studies have described ultraviolet damage to organisms in the *Drosophila melanogaster* model also cause "sunburn" effect, leading to hemocyte and epidermal in their development will have a problem. In this study, we used the multimodality imaging to investigate globe to local image the *Drosophila* larvae after UV irradiation damage in vivo. Combined with multimodality nociceptive image assay method, provided a non-invasive observation of *Drosophila* larvae after UV light to stimulate the micro to macro approach to research, hoping this analysis of future studies in *Drosophila* or other organisms to assess and understand the harm felt by after UV stimulation, in addition to damage to the skin, may also affect the superficial muscle tissue.

9316-14, Session 3

Detection of oral precancer with fluorescence lifetime imaging and reflectance confocal microscopy

Bilal H. Malik, Shuna Cheng, Joey M. Jabbour, Rodrigo Cuenca, Texas A&M Univ. (United States); Yi-Shing Lisa Cheng D.D.S., Texas A&M Univ., Baylor College of Dentistry (United States); John Wright, Texas A&M Univ.; Baylor College of Dentistry (United States); Javier A. Jo, Kristen C. Maitland, Texas A&M Univ. (United States)

Current clinical guidelines for detection of oral cancer include visual and tactile examination of the oral cavity. The actual evaluation of risk usually requires tissue biopsy, the location of which is increasingly critical to identify. Therefore, development of adjunctive screening aids that can help the clinician identify the most accurate sites of precancerous lesions is of great importance and can potentially increase the diagnostic yield of the overall screening process. We have developed a multi-modal, multi-scale

imaging system that combines macroscopic fluorescence lifetime imaging (FLIM) with high resolution reflectance confocal microscopy (RCM) for detection of oral precancer. The FLIM module uses a 355 nm wavelength excitation to probe the biochemical changes in endogenous biomarkers of carcinogenesis at three emission bands, with a lateral resolution of 100 μ m and field-of-view (FOV) of 10 x 10 mm². The RCM module utilizes a source at wavelength of 810 nm and provides sub-cellular resolution, optically sectioned images through the depth of the oral epithelium, with variable lateral and axial resolution of 1-2 and 4-14 μ m, and FOV of 625 μ m. We present the results from clinical application of the imaging system ex vivo, which shows that both quantitative and qualitative differences between clinically normal, benign, and precancerous lesions can be resolved with FLIM/RCM imaging. The results demonstrate that an integrated imaging approach based on macroscopic FLIM to rapidly evaluate a large suspicious area followed by microscopic RCM to provide tissue morphology at high resolution can potentially serve as a screening tool for detection of oral precancer.

9316-15, Session 3

Integrated ultrasound and optical coherence tomography (OCT) endoscope for enhanced endoscopic diagnosis of bile duct cancer (cholangiocarcinoma)

Teng Ma, The Univ. of Southern California (United States) and NIH Resource Ctr. on Medical Ultrasonic Transducer Technology (United States); Jiawen Li, Univ. of California, Irvine (United States) and Beckman Laser Institute and Medical Clinic (United States); Thomas M. Cummins, The Univ. of Southern California (United States) and NIH Resource Ctr. on Medical Ultrasonic Transducer Technology (United States); Jacques Van Dam, The Univ. of Southern California (United States); Koping Kirk Shung, The Univ. of Southern California (United States) and NIH Resource Ctr. on Medical Ultrasonic Transducer Technology (United States); Zhongping Chen, Univ. of California, Irvine (United States) and Beckman Laser Institute and Medical Clinic (United States); Qifa Zhou, The Univ. of Southern California (United States) and NIH Resource Ctr. on Medical Ultrasonic Transducer Technology (United States)

Cholangiocarcinoma (CCA) of the bile duct, an example of an epithelial cancer of the digestive system, is the second most common primary hepatic malignancy in the United States. The five-year relative survival rate for people diagnosed with early stage CCA is about 30%. However, only about 20% of CCA is detected early. The conventional gold standard for diagnosing CCA is to advance a tiny catheter-based brush into the bile duct to scrape the surface of duct wall in the hopes of capturing malignant cells for cytological analysis. This crude approach damages the tissue wall, is time-consuming and suffers from the poor accuracy of 50%. Since early detection is the only effective treatment of CCA, a much better diagnostic technology is urgently needed. Our solution is a multi-modality imaging catheter with an integrated needle biopsy sampling mechanism to provide real-time image guidance for needle biopsy of the epithelial tissue of the bile duct, which can be also implemented on other gastrointestinal tract cancer diagnoses. The hallmark of bile duct cancer is disorganization and proliferation of epithelium. The basis of our imaging technology is OCT, a high-resolution imaging system has 10 μ m resolving power to detect alteration of cellular structure, and high frequency ultrasound, which is capable of providing high resolution imaging in depth up to 4-5mm. In vitro imaging of several healthy and diseased human bile duct samples has demonstrate such multi-modality imaging system's translational potential to allow comprehensive visualization of bile duct tissue and improve the early diagnosis of CCA.

9316-16, Session 3
Multimodal dual-clad fiber MEMS probe for simultaneous OCT and fluorescence imaging of inflammation in the lung

Liane Bernstein, Ecole Polytechnique de Montréal (Canada); Lida P. Hariri, Massachusetts General Hospital (United States); Wendy-Julie Madore, Ecole Polytechnique de Montréal (Canada); David C. Adams, Massachusetts General Hospital (United States); Mathias Strupler, Étienne De Montigny, Kathy Beaudette, Ecole Polytechnique de Montréal (Canada); Yan Wang, Massachusetts General Hospital (United States); Nicolas Godbout, Ecole Polytechnique de Montréal (Canada); Melissa J. Suter, Massachusetts General Hospital (United States); Caroline Boudoux, Ecole Polytechnique de Montréal (Canada)

The ability to assess tissue microstructure is vital for obtaining diagnoses and treating diseases effectively. Recently, optical coherence tomography (OCT) has been used to obtain high-resolution architectural information of airways. However, OCT does not have sufficient contrast and resolution (~10 μm) to distinguish inflammation from adjacent tissues, which is an important indicator in many types of disease including asthma, cancer, infection, and acute injury. Fluorescence microscopy allows the noninvasive assessment of protease-activated airway inflammation. We present a multimodality OCT and fluorescence probe to combine the in-depth structural imaging of OCT with the inflammation-resolving power of fluorescence. A 750 nm laser for fluorescence excitation was coupled into single-mode fiber (SMF) at the output of our swept-source OCT system with a custom-made wavelength-division multiplexer. The SMF was spliced to a dual-clad fiber (DCF), which was attached to a MEMS scanner to allow acquisition of OCT volumes. Fluorescence light was collected in the inner cladding of the DCF and extracted into a multimode fiber with >70% efficiency using a state-of-the-art dual-clad fiber coupler. The OCT signal was collected in the core of the DCF and was transmitted with >90% efficiency through the system. We conducted a preclinical study in rabbits with Prosense 750 FAST using the developed multimodal probe to obtain co-registered fluorescence and OCT images of a lipopolysaccharide-induced airway injury model. We believe that the molecular and microstructural information obtained with our dual-modality imaging system will be instrumental in the assessment and basic understanding of inflammatory lung diseases.

9316-17, Session 3
Multifunctional highly dispersible PEGylated Eu³⁺-doped CaMoO₄@Au-nanorods core/shell nanoparticles for fluorescence imaging, surface-enhanced Raman spectroscopy (SERS) detection, and photo-thermal therapy (PTT) applications of human lung cancer cells

Qifei Li, Abdul K. Parchur, Anhong Zhou, Utah State Univ. (United States)

We synthesized multifunctional highly dispersible Eu³⁺-doped CaMoO₄@Au-nanorods (GNR) core/shell nanoparticles (NPs) for fluorescence imaging, SERS detection and PTT applications in human lung cancer cells A549. Surface of CaMoO₄ nanoparticles (core) are modified with HS-PEG-COOH and GNR (10 nm x 30 nm, Surface Plasmon Resonance (SPR) ~780 nm) were conjugated on the surface of the core. The size of core is found to be ~15 nm. Electric dipole of transition of Eu³⁺ ion (5D₀?7F₂) shows strong luminescence around ~615 nm on excitation at 464 nm. The GNR component serves both as a SERS-active and PTT substrates. By conjugating with a

Raman reporter molecule, 4-mercaptobenzoic acid (MBA), it generates SERS signals. By selecting the SERS peak at 1070 cm⁻¹ (characteristic peak for MBA) for Raman mapping, it confirmed the distribution of these NPs on single A549 cells. Meantime, the temperature of CaMoO₄:Eu@GNR NPs suspension in medium is found to be rapidly generated under 808 nm near-infrared (NIR) laser irradiation. This photo-thermal effect of PEGylated CaMoO₄:Eu@GNR NPs on A549 cells was investigated for in vitro cancer cells therapy experiment. Upon irradiation at 808 nm laser, the treated A549 cells were obviously damaged, effectively suppressing A549 cells viability. Fluorescence microscopy images indicated that these particles mainly distributed around cellular cytoplasm. Our results show the multifunctionalities of CaMoO₄:Eu@GNR NPs and their potential applications in imaging, detection, and thermal treatment of cancer cells.

9316-18, Session 4
Development of a multi-scale and multi-modality imaging system to characterize tumors and their microenvironment in vivo

Valérie Rouffiac, Institut Gustave Roussy (France) and Imagerie par Résonance Magnétique Médicale et Multi-Modalités, CNRS, Univ. Paris-Sud, (France); Karine Ser-Leroux, Emilie Dugon, Institut Gustave Roussy (France); Ingrid Leguerney, Imagerie par Résonance Magnétique Médicale et Multi-Modalités, CNRS, Univ. Paris-Sud, (France) and Institut Gustave Roussy (France); Melanie Polrot, Institut Gustave Roussy (France); Sandra Robin, Imagerie par Résonance Magnétique Médicale et Multi-Modalités, CNRS, Univ. Paris-Sud, (France) and Institut Gustave Roussy (France); Sophie Salome-Desnoulez, Institut Gustave Roussy (France); Jean-Christophe Ginefri, Catherine Sebrie, Imagerie par Résonance Magnétique Médicale et Multi-Modalités, CNRS, Univ. Paris-Sud, (France); Corinne Laplace-Builhé, Institut Gustave Roussy (France) and Imagerie par Résonance Magnétique Médicale et Multi-Modalités, CNRS, Univ. Paris-Sud, (France)

In vivo high-resolution imaging of tumor development is possible through dorsal skinfold chamber implantable on mice model. However, current intravital imaging systems are weakly tolerated along time by mice and do not allow multimodality imaging. Our project aims to develop a new chamber for: 1- long-term micro/macrosopic visualization of tumor (vascular and cellular compartments) and tissue microenvironment; and 2- multimodality imaging (photonic, MRI and sonography).

Our new experimental device was patented in March 2014 and was primarily assessed on 60 mouse engrafted with 4T1-Luc tumor cell line, and validated in confocal and multiphoton imaging after staining the mice vasculature using Dextran 155kDa-TRITC or Dextran 2000kDa-FITC. Simultaneously, a universal stage was designed for optimal removal of respiratory and cardiac artifacts during microscopy assays. Experimental results from optical, ultrasound (B-mode and pulse subtraction mode) and MRI imaging (anatomic sequences) showed that our patented design, unlike commercial devices, improves longitudinal monitoring over several weeks (45 days on average against 12 for the commercial chamber) and allows a better characterization of the early and late tissue alterations due to tumor development. We also demonstrated the compatibility for multimodality imaging and the increase of mice survival was by a factor of 3.75, with our new skinfold chamber.

Current developments include: 1- defining new procedures for multi-labelling of cells and tissue (screening of fluorescent molecules and imaging protocols); 2- developing ultrasound and MRI imaging procedures with specific probes; 3- correlating optical/ultrasound/MRI data for a complete mapping of tumor development and microenvironment.

9316-19, Session 4

Co-registration of Ultrasound and Frequency-Domain Photoacoustic Radar Images and Image Improvement for tumor detection

Edem Dovlo, Bahman Lashkari, Univ. of Toronto (Canada);
Sung soo Sean Choi, University of Toronto (Canada);
Andreas Mandelis, Univ. of Toronto (Canada)

This paper explores leveraging the merits of ultrasound and cross-correlation (radar) frequency-domain (FD) photoacoustic imaging for accurate tumor detection. Achieving photoacoustic (PA) imaging functionality on a commercial Ultrasound (US) instrument could accelerate clinical acceptance and use. Commercial US imagers possess sophisticated software for rapid image acquisition that could also dramatically speed-up PA imaging. To improve FD photoacoustic radar imaging parameters such as signal-to-noise ratio (SNR), contrast and spatial resolution, the image generated from the amplitude of the cross-correlation between detected and input signals is filtered by the phase of the correlation signal.

Experimental results presented show enhancements in SNR, contrast and spatial resolution via this method. In the experiments, a Laser Light Solutions (LLS) diode laser illuminates the sample from above, and a standard commercial 64-element, 3MHz Ultrasonix phased array transducer detects the PA signals generated. Obtaining both US and PA images, and by extension their co-registration, is simplified since the same transducer is employed for both modalities. The sample and transducer are fully-submerged in water for acoustic coupling. Signal processing is performed using Lab View, Matlab software and data acquisition system (NI PXIe-1065).

Results for a sample made of a small piece of a 2mm diameter graphite rod attached at the end of a glass rod, as well as a tumor-infected mouse clearly indicate the location of the absorber and improvements in contrast and spatial resolution when the phase filter is applied. Images are amplified (scaled and squared) to further reduce absorber spread and artifacts in the image.

9316-20, Session 4

Multi-modality imaging using a handheld gamma camera and MRI for tumor localization

Cheryl Dika, Cubresa Inc. (Canada); Dianne Georgian-Smith M.D., Brigham and Women's Hospital (United States)

Purpose:

The purpose of this study is to test pre-clinically a new MR-compatible hand held gamma camera using a tissue phantom and known targets to determine the camera's sensitivity at various radioactive doses and differences in distance from source-target to camera.

Materials and Methods

The MR-compatible Gamma Camera's (Cubresa) field of view is 14x14mm, dimensions of 30x23x105mm and weight of 140g. A 3T (Siemens Verio) magnet, 4 Channel Breast Coil with grid localization (Noras), attachment arm and image overlaying software (Cubresa) were used. The MRI images were obtained: 3D Flash Sagittal, Axial and Coronal sequences and slice thickness of 0.8mm. Breast tissue was simulated using a 12x24cm roast.

The cobalt point sources were 2mm: $1\mu\text{Ci}$, $6.5\mu\text{Ci}$, $25\mu\text{Ci}$ at 1, 6 and 10 cm respectively from the gamma camera.

The coil and tissue remained in position on the MR table throughout. The gamma camera location was based on the location of the sources in the MR images.

Results:

The effect of source to camera distance was verified by imaging the tissue from both the lateral and medial views. The time required for gamma

imaging each source was predetermined to be adequate at 2 minutes.

Conclusion:

This study shows that this gamma camera can be paired with MRI to potentially add functionality and specificity to the marked sensitivity of MRI.

Since the tissue has not been moved through this process, the next step in theory could be to biopsy the source or lesion based on the information gathered from the MR and gamma images.

9316-21, Session 4

Photo-magnetic imaging: high resolution optical imaging modality

Alex T. Luk, Gultekin Gulsen, Farouk Nouzi, Univ. of California, Irvine (United States)

Photo-Magnetic Imaging (PMI) is a true multi-modality imaging technique for non-invasive, high resolution optical omography imaging. It combines Magnetic Resonance Imaging and Diffuse Optical Tomography to provide a quantitative optical absorption maps at MRI spatial resolution. First, proton resonance frequency shift method is used to acquire a high resolution temperature elevation map induced by laser illumination. Afterwards this temperature map is converted into high resolution optical absorption map using a finite element based PMI forward and inverse solver by modeling photon migration and heat diffusion in tissue. We have utilized 3Tesla human and 7 Tesla animal imaging MR systems to demonstrate the feasibility of multi-wavelength PMI for different applications. Mainly, 785nm, 808nm and 850nm wavelength lasers have been used to resolve the spatial distribution for different tissue chromophores and exogenous contrast agents such as indocyanine green (ICG) and gold nano particles. We will summarize PMI results obtained by using fisher rats bearing R3220 AC breast cancer tumor models. Besides measuring tumor heterogeneity with high resolution based on tissue intrinsic contrast, we have performed Dynamic Contrast Enhanced PMI to verify the pharmacokinetics of indocyanine green (ICG) in tumor after tail-vein injection. Finally, multi-wavelength PMI measurements have been also acquired to visualize accumulation of gold nanoparticles in tumor 24 hours after injection. Encouraged by these results, our near-future aim is developing a clinical PMI breast imaging interface for breast cancer.

9316-22, Session 4

Microscopic x-ray luminescence computed tomography

Wei Zhang, Dianwen Zhu, Kun Zhang, Changqing Li, Univ. of California, Merced (United States)

X-ray luminescence computed tomography (XLCT) was emerged as a new hybrid imaging modality, in which the x-rays are used to excite phosphors emitting optical photons to be measured for imaging. In this paper, we reported a microscopic x-ray luminescence computed tomography (microXLCT) with a spatial resolution up to hundreds of micrometers for deep targets. We use a superfine x-ray pencil beam to scan the phosphor targets. The superfine x-ray pencil beam is generated by a small collimator mounted in front of a powerful x-ray tube (93212, Oxford Instrument). A CT detector is used to image the x-ray beam. We have generated an x-ray beam with a diameter of 150 micrometers with a collimator of 100 micrometers in diameter. The emitted optical photons on the top surface of phantom are reflected by a mirror and acquired by an electron multiplier charge-coupled device (EMCC) camera (C9100-13). The microXLCT imaging system is built inside an x-ray shielding and light tight cabinet. The EMCCD camera is placed in a lead box. All the imaging components are controlled by a Labview program. The optical photon propagation is modeled with the diffusion equation solved by the finite element method. We have applied different regularization methods including L2 and L1 in the microXLCT reconstruction algorithms. We have also used a mask approach to further improve the spatial resolution of microXLCT. Numerical simulations and phantom experiments are used to validate the microXLCT imaging system.

9316-23, Session PSun

Non-contact assessment of melanin distribution via multispectral temporal illumination coding

Robert Amelard, Christian Scharfenberger, Alexander Wong, David A. Clausi, Univ. of Waterloo (Canada)

Melanin is a pigment that is highly absorptive in the UV and visible electromagnetic spectra. It is responsible for perceived skin tone, and protects against harmful UV effects. Abnormal melanin distribution is often an indicator for melanoma. We propose a novel approach for non-contact melanin distribution via multispectral temporal illumination coding to estimate the 2D melanin distribution based on its absorptive characteristics. In the proposed system, a novel multispectral, cross-polarized, temporally-coded illumination sequence is synchronized with a camera to measure reflectance under both multispectral and ambient illumination. This allows us to eliminate the ambient illumination contribution from the acquired reflectance measurements, and also to determine the melanin distribution in an observed region based on the spectral properties of melanin using the Beer-Lambert law. Using this information, melanin distribution maps can be generated for objective, quantitative assessment of skin type of individuals. We show that individuals with different skin types can be differentiated using this model, and that the melanin distribution map correctly identifies areas with high melanin densities (e.g., nevi).

9316-24, Session PSun

Acquisition of priori tissue optical structure based on non-rigid image registration

Wenbo Wan, Tianjin Univ. (China); Jiao Li, Tianjin Univ. (China) and Tianjin Key Lab. of Biomedical Detecting Techniques and Instruments (China); Lingling Liu, Yihan Wang, Yan Zhang, Tianjin Univ. (China); Feng Gao, Tianjin Univ. (China) and Tianjin Key Lab. of Biomedical Detecting Techniques and Instruments (China)

Region-labeling diffuse optical tomography (DOT), which is based on the assumption that different anatomical regions have their respective sets of homogenous optical parameters distribution, is of benefit to improve the ill-posedness of the inverse problem in the corresponding process. The priori tissue optical structure should be acquired with the assistance of anatomical imaging methods such as X-ray computed tomography(XCT) which could not provide high definition images of soft tissues including different optical characteristic regions. Thus, we present a non-rigid image registration method to obtain anatomical structure of interest regions using XCT image of the standard organism with known structures of anatomical regions. By elastically aligning the standard image to the target one, structure of anatomical regions, especially soft tissues, in the target organism can be calculated during image registration. Combining the known optical parameters of each organ to the calculated structure of anatomical regions, optical structure of the target organism can be obtained as the priori information for DOT image reconstruction. With the application in the mice model, the proposed method is demonstrated to be effective.

9316-25, Session PSun

Photoacoustic tomography guided diffuse optical tomography for small-animal model

Yihan Wang, Tianjin Univ. (China); Feng Gao, Tianjin Univ. (China) and Tianjin Key Lab. of Biomedical Detecting Techniques and Instruments (China); Wenbo Wan, Yan Zhang, Tianjin Univ. (China); Jiao Li, Tianjin Univ. (China) and Tianjin Key Lab. of Biomedical Detecting Techniques and Instruments (China)

Diffuse optical tomography (DOT) is a biomedical imaging technology for noninvasive visualization of spatial variation about the optical properties of tissue, which can be applied to in vivo small-animal disease model. However, traditional DOT suffers low spatial resolution due to tissue scattering. To overcome this intrinsic shortcoming, multi-modal approaches that incorporate DOT with other imaging techniques have been intensively investigated, where a priori information provided by the other modalities is normally used to reasonably regularize the inverse problem of DOT. Nevertheless, these approaches usually consider the anatomical structure, which is different from the optical structure. Photoacoustic tomography (PAT) is an emerging imaging modality that is particularly useful for visualizing light-absorbing structures embedded in soft tissue with higher spatial resolution compared with pure optical imaging. Thus, we present a PAT-guided DOT approach, to obtain the location a priori information of optical structure provided by PAT first, and then guide DOT to reconstruct the optical parameters quantitatively. The results of reconstruction of phantom experiments demonstrate both quantification and spatial resolution of DOT could be highly improved by the regularization of feasible-region information provided by PAT.

9316-26, Session PSun

Solid-state parallel acquisition system for NIR imaging within the MR

Fadi El-Ghoussein, Thayer School of Engineering at Dartmouth (United States)

Magnetic Resonance Imaging (MRI)-guided near-infrared spectroscopic tomography (NIRST) for breast imaging has shown to improve the specificity of MRI images in characterizing breast lesions. In our present MRI-NIR system, 16 fiber bundles with a diameter of 12 mm are used for imaging 1 cm of the breast length from chest wall towards the nipple. In order to improve the sensitivity of NIRST data to the MRI-derived region of interest and substantially increase breast coverage, a 64-channel prototype MRI-NIR system has been developed. In this new system, 64 photodiodes that are in direct contact with the breast tissue inside the MRI are used for collecting the diffused light. The output currents of the photodiodes are tethered to amplifier circuitry located outside the MRI room through a 10 m electrical cable where each photodiode is connected to a programmable-gain (PGA) low-noise transimpedance amplifier. The PGA functionality is implemented by using a relay and two different feedback resistors for each photodiode in order to maximize the dynamic range of the system. Another PGA is also used on the data acquisition (DAQ) card in order to ensure that the maximum resolution of the analog-to-digital converter is used. Compared to our exciting system, the new system enables increased breast coverage at a very low cost (less than \$60/channel) and offers 108 (160dB) dynamic range with sensitivity down to 1 pW.

Conference 9317: Optical Fibers and Sensors for Medical Diagnostics and Treatment Applications XV

Saturday - Sunday 7-8 February 2015

Part of Proceedings of SPIE Vol. 9317 Optical Fibers and Sensors for Medical Diagnostics and Treatment Applications XV

9317-1, Session 1

In-vivo assessment of ultra-structural alterations as an early event in cancer progression: implications for cancer screening

Adam Eshein, Andrew J. Radosevich, Nikhil N. Mutyal, The-Guyen Nguyen, Wenli Wu, Bradley Gould, Northwestern Univ. (United States); Hemant K. Roy, Boston Medical Ctr. (United States); Vadim Backman, Northwestern Univ. (United States)

In order to further reduce cancer mortality, there remains a need for screening methods that are both sensitive to early lesions and minimally invasive to the patient. One solution is to detect the ultra-structural (i.e., sub-diffractive) changes occurring in the earliest stages of cancer as part of field carcinogenesis. In field carcinogenesis, ultra-structural alterations spread diffusively throughout an organ creating a fertile "field" for cancerous lesions to develop. The implications of field carcinogenesis are two-fold: Cancer risk can be assessed through analysis of easily accessible surrogate tissue sites and at a very early time point. To quantify such ultra-structural changes, our group invented an optical sensing technique known as low-coherence enhanced backscattering spectroscopy (LEBS). To translate LEBS into the clinic, our group developed a fiber-optic based LEBS probe to target the ultra-structural alterations occurring in field carcinogenesis in-vivo. In clinical studies of three different cancer types, we assessed the cancer risk of more than 800 patients by analysis of easily accessible tissue sites (rectum for colorectal cancer, duodenum for pancreatic cancer, and the cheek for lung cancer). We had excellent diagnostic performance in all three studies and found a consistent increase in the slope of scattering spectrum indicating a change in the mass-density correlation function. These results imply that although different cancers progress along different genetic pathways, ultra-structural alterations appear to be the common denominator of early cancer progression.

9317-2, Session 1

Compact Raman needle probe with fine needle aspiration biopsy for solid tissues

Jianfeng Wang, Wei Zheng, Zhiwei Huang, National Univ. of Singapore (Singapore)

Raman spectroscopy represents a label-free vibrational spectroscopic technique for studying the biochemical and biomolecular composition of human body. Raman probe is a key component to facilitate the in vivo diagnosis by using Raman spectroscopy. Most of the current fiber-optic Raman probes are made of silica fibers, showing intensive Raman peaks of their own and interfering the weak tissue Raman signals. Even bifurcated multiple fiber bundles are currently available for fiber-optic Raman probe design; they might be too bulky to be used in solid tissue diagnosis, i.e., lymphatic system. The aim of the current study was to investigate a compact Raman needle probe design intended to be integrated into a device that can also take biopsies of solid tissues for cytological assessment, enabling concurrent Raman spectroscopic interrogation and fine needle aspiration (FNA) biopsy with a single needle penetration. We describe the Monte Carlo simulation results to optimize the compact Raman needle probe design. Also described is the fabrication of the Raman needle probe and its assembly with the biopsy device. Example Raman spectra of various solid tissues are shown.

9317-3, Session 1

Photoacoustic spectroscopy of gas phase biomarker in simulated exhale breath and liquid phase biomarker on biological sample surface

Hanh N. D. Le, Johns Hopkins Univ. (United States); Do-Hyun Kim, U.S. Food and Drug Administration (United States)

Numerous metabolic disorders and human diseases cause changes in gas concentration in exhaled human breath and liquid phase biomarkers in body fluids. For example, the presence of the volatile biomarkers acetone, ammonia and methane have been shown to indicate lung cancer, asthma and intestinal problems, while increases in glucose levels in bodily fluids may be a sign of diabetes. Due to its high sensitivity, photoacoustic spectroscopy presents a noninvasive, real-time method for measuring biomarkers in both liquid and gas phase samples. In this study, a photoacoustic detector integrated with Fourier-transform infrared spectroscopy was used to measure biomarkers in gas and liquid samples independently. Simulated exhaled breath samples were created by mixing varying concentrations of the biomarkers acetone, ammonia and ethane with normally present exhaled gases. For liquid phase detection, optical signatures of artificial tears and urine with different chemical component concentrations were collected. The results of these measurements demonstrate the potential of photoacoustic spectroscopy to serve as a useful tool for biomarker detection in multiple types of human biological samples.

9317-4, Session 1

Transferability of antibody pairs from ELISA to fiber optic-surface plasmon resonance for infliximab detection

Thomas Van Stappen, Jiadi Lu, Katholieke Univ. Leuven (Belgium); Maarten Bloemen, KU Leuven (Belgium); Nick Geukens, Dragana Spasic, Filip Delpport, Katholieke Univ. Leuven (Belgium); Thierry Verbiest, KU Leuven (Belgium); Jeroen Lammertyn, Ann Gils, Katholieke Univ. Leuven (Belgium)

Tumor necrosis factor (TNF)-alpha is a pleiotropic cytokine up-regulated in inflammatory bowel disease, rheumatoid arthritis and psoriasis. The introduction of anti-TNF drugs such as infliximab has revolutionized the treatment of these diseases. Recently, therapeutic drug monitoring (TDM) of infliximab has been introduced in clinical decision making to increase cost-efficiency. Nowadays, TDM is performed using either radio-immunoassays, homogeneous mobility shift assays or ELISA. Unfortunately, these assays do not allow for in situ treatment optimization, because of the required sample transportation to centralized laboratories and the subsequent assay execution time. In this perspective, we evaluated the potential of fiber optic-surface plasmon resonance (FO-SPR).

From a panel of 55 in-house developed and characterized monoclonal anti-infliximab antibodies, 22 antibody combinations were selected through pairwise sandwich ELISA for testing on the FO-SPR platform. In our "dip-in/dip-out" FO-SPR setup, primary antibody was coupled to the fiber and dipped into spiked infliximab solutions. Next, the signal was amplified using gold nanoparticles functionalized with secondary antibody and the wavelength shift was determined, revealing a good transferability from

Conference 9317: Optical Fibers and Sensors for Medical Diagnostics and Treatment Applications XV

ELISA to FO-SPR. Dose-response curves of one selected antibody pair revealed a sensitivity in the pM range. Furthermore, the introduction of a plate shaker reduced the individual sample analysis time to less than 30 minutes.

In conclusion, antibody pairs can be easily transferred from ELISA to FO-SPR, with a sensitivity within a pharmacological relevant range. The speed of the assay as well as its potential for miniaturization makes FO-SPR a highly promising platform for on-site infliximab monitoring.

9317-5, Session 1

Fast depth-sensitive fluorescence measurements in turbid media using fiber rings

Yi Hong Ong, Quan Liu, Nanyang Technological Univ. (Singapore)

Autofluorescence spectroscopy in the ultraviolet/visible spectrum offers a non-invasive and effective approach for the detection of various epithelial cancers and precancers. However, achieving high depth sensitivity to a specific subsurface region in human epithelial tissue is a great challenge as photons will be quickly scattered when entering a tissue that is a diffusively scattering medium. Furthermore, the dominance of fluorescence signals from overlying layers greatly reduces the contrast of fluorescence signals originated from the subsurface region of interest, thus limiting the diagnostic performance of this technique.

In this study, we demonstrated a fast depth-sensitive fluorescence measurements method in a two-layered epithelial tissue phantom using a cone shell configuration implemented by an axicon lens and a fiber assembly including five rings of collection fibers. Each collection fiber ring, located at a different radial distance away from the center, corresponds to a different targeted depth in the tissue phantom for which fluorescence measurements from all rings showed a larger range of sensitivities to the top and bottom layers compared to the previously reported cone shell configuration[1]. Furthermore, multiple fluorescence spectra corresponding to a range of successive targeted depths can be obtained simultaneously, which shortened data acquisition dramatically. The setup is also unique as it does not involve any mechanical moving components and maintains a fixed probe-sample distance for depth sensitive optical measurements. This setup therefore would be preferred in a clinical setting.

Reference:

1. Y. H. Ong and Q. Liu, Opt. Lett. 38(15), 2647-2649 (2013)

9317-6, Session 2

Long period grating biosensors (Keynote Presentation)

Wojtek Bock, Univ. du Québec en Outaouais (Canada)

No Abstract Available

9317-7, Session 3

Automated long-term tracking of freely moving animal and functional brain imaging based on fiber-optic microscopy

Jaepyeong Cha, Gyeong Woo Cheon, Jin U. Kang, Johns Hopkins Univ. (United States)

Deciphering the relationships between brain activity and animal behavior is a key challenge for neuroscience. Over the last decade, enormous efforts have been channelized towards comprehensive sampling of cellular

activities within the brain during specific animal behaviors, but these efforts have been impeded by the limited access of bench-top microscopes to the freely moving animals. However, recent developments in fiber-optic technology have enabled brain imaging in freely moving animals. Optical fiber's small diameter, flexibility and long probe length allow easy access to the brain of small animals via guiding cannula while maintaining high-resolution imaging.

In this work, we introduce a long-term tracking platform for studying unconstrained rodent behaviors and imaging brain activities for either short or extended periods of time. Our platform incorporates a motion tracking NIR camera to observe animal behaviors for 24 hours and a fiber-bundle based fluorescence microscope. All the functions including triggering laser and recording videos/images are synchronized and integrated in the developed software. Automated analysis allows quantification of all behaviors and their brain activities over extended periods of time. Therefore, our platform can be used to build a profile of the brain activities in different behavioral states. Our platform is also well suited for longitudinal studies, where migrating cells within the brain are studied over long periods. The database of all animal behaviors throughout the day and night will be a powerful tool for interrogation of the brain activities. It will further advance our understanding of the functional interactions between cellular networks and animal behaviors.

9317-8, Session 3

In-vivo concentration ratio estimation of two fluorescent probes for early detection of Alzheimer's disease

Osnat Harbater, Israel Gannot, Tel Aviv Univ. (Israel)

In-vivo measurement of the concentrations of biological compounds using fluorescence is one of the challenging biophotonic fields. These measurements are useful in diagnostic and treatment monitoring applications that use fluorescent probes which may bond to specific proteins and drugs. In some cases the relative concentration of two compounds is a sufficient biological indicator. For instance, it has been shown that the ratio between Amyloid-Beta and tau protein in the Cerebrospinal fluid (CSF) may predict the development of Alzheimer's disease (AD) several years before current diagnosis. We have previously suggested a system that could measure the concentration ratio of these two proteins in-vivo without the need to collect CSF samples. This system uses a miniature needle with an optical fiber which is coupled to a laser source and a detector. The fiber excites fluorescent probes which were injected and bond to the proteins in the CSF, and collects the fluorescence emission. Using the fluorescence intensity ratio, the concentration ratio between the proteins is estimated, and AD may be diagnosed.

In this work we present the results of an in-vivo trial performed on mice. Miniature tubes containing two fluorescent probes in several concentration ratios were inserted into the mice in two locations: subcutaneously, and deeper in the abdomen. The fluorescent probes were excited and the fluorescence intensity was measured. The concentration ratios were extracted from the fluorescence intensities using a simple calibration curve. The extracted ratios are compared to the true ratios and the system's accuracy is estimated.

9317-9, Session 3

Farfield intensity profiles of HPLC fiber-optic flow cells in the UV-VIS region

Jan Werner, Technische Hochschule Mittelhessen (Germany); Mathias Belz, World Precision Instruments (United States); Karl-Friedrich Klein, Technische Hochschule Mittelhessen (Germany)

High Pressure Liquid Chromatography (HPLC) is one of the most used

Conference 9317: Optical Fibers and Sensors for Medical Diagnostics and Treatment Applications XV

detection techniques in analytical chemistry. With the trend to smaller sample sizes and faster analysis techniques, light transfer in UV-VIS absorbance flow cells becomes very critical and more often, waveguide based sample cells are used.

Such flow cells behave optically like an optical fiber. Especially the interface between core and cladding influence the optical key parameters, i.e. transmission and numerical aperture. In this work we introduce an experimental setup to determine the far-field intensity profiles of flow cells at different wavelengths; in addition to the visible part of the light spectrum, the focus will be the UV-region below 320 nm.

9317-10, Session 4

MIR chalcogenide fiber and devices *(Invited Paper)*

Francois Chenard, Oseas Alvarez, Hassan Moawad, IRflex Corp. (United States)

Chalcogenide glass fibers are very stable, durable, and insensible to moisture. IRflex manufactures arsenic trisulfide (As₂S₃) and arsenic triselenide (As₂Se₃) fiber for applications in chemical sensing, military and medical applications. The sulfide-based fiber transmits well in the 1.5-6 micron wavelength range as the selenide-based fiber transmits in the 2-9.5 micron range. The optical loss of the chalcogenide fiber depends on the content of impurities and structural defects. Preparation of high-purity chalcogenide glass requires ultra-low content of impurities. IRflex works intensively of the purification of the initial elements (arsenic, sulfur, selenium) and glass synthesis methods to remove impurities content. Impurities are manifested by corresponding absorption bands in the fiber transmission: hydrogen in the form of S-H (4.01 micron), Se-H (4.57 micron), OH groups (2.92 micron), and CO₂ (4.33 micron). Also the presence of inclusions of submicron size (carbon, SiO₂) leads to additional optical loss due to absorption and scattering. Mechanical strength and laser induced damage threshold (LIDT) are also very sensitive to the presence of inclusions. Laser ultramicroscopy is used to determine the size and concentration of the inclusions. Fiber draw techniques have been developed to produce high-quality chalcogenide fiber: fiber diameter control ±1 micron, core/cladding concentricity error <2 micron. Our results demonstrate the feasibility to produce commercial chalcogenide fiber with low-loss (<0.1dB/meter) and high tensile strength (>30 kpsi). High-power laser transmission of 8 MW/cm² CW in singlemode fiber was limited by the available laser power.

9317-11, Session 4

Multicore optical fiber grating array fabrication for medical sensing applications

Paul S. Westbrook, Kenneth S. Feder, Tristan Kremp, Thierry F. Taunay, Eric M. Monberg, Debra A. Simoff, Gabe S. Puc, Roy M. Ortiz, OFS Fitel LLC (United States)

As optical fiber sensors have become accepted in more industrial and medical applications, there has been increased interest in high performance fiber grating arrays that enable next generation sensing modalities such as shape sensing. In optical fiber shape sensing light scattering from one or more cores of a fiber is used to reconstruct the shape and position of the optical fiber. Inclusion of shape sensing fibers in next generation medical devices holds the promise for improved outcomes in various surgical procedures. The many requirements for such sensors include, low cost, high volume, compact size, speed and accuracy over lengths in excess of a meter, and have led to interest in continuous multicore fiber grating arrays as a potential solution.

In this work we describe a flexible and scalable fiber grating array fabrication platform to address all of these requirements. Our system

employs a reel to reel fiber handling system and inscribes gratings using a UV excimer laser. Our multicore fiber has a UV transparent coating that allows for rapid single pulse inscription of gratings in all cores without the requirements of stripping the coating, thus retaining high mechanical strength over the grating array. Precision positioning of the fiber allows for quasi continuous gratings over lengths from a few cm to more than 10m. The system allows for a large range of spectral characteristics, including uniform period with sub nm widths over many meters, to chirped gratings that reflect light over more than 20nm near 1550nm.

9317-12, Session 4

Fiber spectroscopy for biomedical diagnostics in-vivo

Viacheslav Artyushenko, art photonics GmbH (Germany)

A review of fiber spectroscopy probes and systems will cover main range of methods - starting from fluorescence control of cells vitality and diffused scattering reflection of tissue to Mid IR absorption and Raman scattering spectroscopy used for molecular tissue analysis. The most promising fiber solutions for cancer screening and tumor margin diagnostics will be compared, starting from research spectroscopy systems used in a broad 0.3-16µm-range to fiber sensing already used in clinics. Possible advantages of a multispectral tissue analysis will be discussed to yield more sensitive, more specific and precise diagnostics in-vivo for reduced cost and dimensions of fiber sensors.

Various fiber spectroscopy systems used in 0.3-16µm range will be presented with focus on their fiber probe design: fluorescence probes used in endoscopy/ laparoscopy; Diffused Reflection Scattering probes, ATR-fiber probes for FTIR-spectrometers and Raman spectroscopy probes.

While the most of fiber spectroscopy diagnostic systems using absorption/transmission, reflection, fluorescence and Raman-spectroscopy are limited to silica fiber transmission from 180nm to 2.4µm, - the newest IR-glass fibers, Polycrystalline PIR-fibers and Hollow Waveguides cover the Mid IR-range up to 16µm, i.e. the most informative "finger-print" region describing content of various organic molecules in tissue or bio-liquids. Same time IR-absorption and Raman scattering spectroscopy are complimentary techniques in molecular analysis - that's why they are specially compared in use for cancer diagnostics, including their combination, together with the other multispectral methods.

9317-13, Session 4

All-optical power and data transfer in catheters using an efficient LED

Anneke van Dusschoten, Philips Research Europe (Netherlands); Martin Pekar, Philips Research Europe (Netherlands) and Thoraxcenter, Erasmus MC (Netherlands); Martin B. van der Mark, Philips Research Europe (Netherlands)

Diagnostic value of minimally invasive medical devices can be improved by putting electronic functionality at the tip. This requires wires for signal transfer and electric power, but at the same time the device should remain slim, flexible and affordable. The thin electrical wires used presently have fragile interconnects and compromise bandwidth as well as RF and MRI compatibility. We improve on this by using a single optical fiber and GaN LED for photovoltaic power delivery at 2.3 V as well as data communication. We find that the simultaneous transfer of high power and data by a single LED can be achieved via Photo-Induced Electro Luminescence (PIEL), but only in case the LED has a high bidirectional conversion efficiency (>0.3). PIEL is the effect of forward current through the LED as a consequence of open-loop voltage build-up. We deal with further challenges that arise. Firstly, due to limited space, the photovoltaic device should be small (< 1 mm²) and hence must convert energy efficiently at high power density (~1W/mm²) because conversion losses may lead to tissue heating. Secondly,

Conference 9317: Optical Fibers and Sensors for Medical Diagnostics and Treatment Applications XV

these medical devices are disposables and thus costs should be kept low by a high level of integration. As demonstrator we have built a catheter with monolithically integrated ASIC and pressure sensitive MEMS that translates pressures around 1 bar to a frequency modulated signal around 1 MHz. The device is powered from a 405 nm laser via an optical fiber coupled to a high-power LED that is used simultaneously as a photovoltaic source and as a light source for signal transfer.

9317-14, Session 4

Improved deep UV fiber for medical and spectroscopy applications

John H. Shannon, Valery K. Khalilov, Richard J. Timmerman, Dale Geshell, Polymicro Technologies (United States)

An effort to demonstrate long term transmission stability in a high -OH synthetic fused silica step index multimode optical fiber optimized for Deep-UV operation, designated as FDP, was successfully completed at Polymicro Technologies. The development achieved significant improvement in long term stability for the 214 and 265nm absorption bands typically associated with solarization affects in fused silica. The improvements were applied to fiber core sizes from 67 to 100 μ m, a common size range for bundle applications used in medical and spectroscopy. Results of UV degradation measurements for the fiber with minimum 70 hour exposures are presented along with a description of the test protocols.

9317-15, Session 4

Noninvasive continuous blood pressure monitoring

Armen R. Poghosyan, Vahram Mouradian, Levon Hovhannisyan, Sensogram Technologies Inc. (United States)

We are presenting a novel photoplethysmographic (PPG) optical sensor and device with ambient optical, electrical and electromagnetic noises cancellation, thus allowing only the useful optical signals to be received by the health monitoring device. We are also disclosing a new processing technique for canceling the ambient noises contributed by optical, electrical and electromagnetic artifacts in the measured PPG signals. Such a device and method allow the enhancement of the performance of the PPG sensors compared to conventional apparatus and methods. The presented sensor and methodology have been integrated into a prototype device for noninvasive, continuous, wearable, remote and mobile monitoring of blood pressure and other human vital signs, such as heart rate, oxygen saturation, respiration rate, etc. This small device allows the user to read, store, process and transmit all the measurements made using the PPG optical sensor and the electronic unit to a remote location.

9317-16, Session 5

Investigation of silver-only and silver/TOPAS coated hollow glass waveguides for visible and NIR laser delivery

Jeffrey E. Melzer, James A. Harrington, Rutgers, The State Univ. of New Jersey (United States)

Hollow Glass Waveguides (HGWs) present a viable option for the low-loss transmission of radiation over a broad range spanning from visible to far-infrared wavelengths. Cyclic Olefin Copolymer (COC), a commercially available polymer known as TOPAS, is chosen for this study due to its exceptionally low absorption losses throughout the spectrum, particularly

in the visible and near-infrared (NIR) regions. While silver-coated HGWs are capable of transmitting visible and NIR radiation with low losses, theory predicts that the addition of a uniform dielectric thin film of quarter-wavelength thickness will reduce these losses for both straight and bent configurations, while additionally providing a potentially more desirable modal output for laser applications. In this paper, the procedures for the deposition of the silver and subsequent COC films are outlined. Spectroscopy is used to obtain the thickness of the polymer film. The theoretical attenuation losses of the silver and silver / COC HGWs are explored and experimental values are obtained using various visible and IR lasers. Moreover, the modal output of the silver and silver / COC HGWs is qualitatively compared. The possibility of use of these silver / COC HGWs at mid- and far-IR wavelengths is discussed.

9317-17, Session 5

Improvement of transmission properties for a rugged polymer-coated silver hollow fiber

Katsumasa Iwai, Hiroyuki Takaku, Sendai National College of Technology (Japan); Mitsunobu Miyagi, Tohoku Institute of Technology (Japan); Yi-Wei Shi, School of Information Science and Engineering, Fudan Univ. (China); Yuji Matsuura, Graduate School of Engineering, Tohoku Univ. (Japan)

A rugged hollow fiber is fabricated by liquid-phase coating technique. A silica glass capillary is used as the substrate and vitreous film is firstly coated on the inner surface of the capillary to protect the glass tube from moisture. This protective coating keeps the thin-wall glass tube away from damage due to the following silver plating process. The additional transmission loss by the roughness of a protective film is controlled by limiting the part which forms a protective film. The whole length of 0.7-mm-bore hollow fiber was 1 m and the length of the rugged part which formed the protective film was 30 cm. Transmission properties of the rugged polymer-coated silver hollow fibers for the Er:YAG laser delivery have been improved.

9317-18, Session 5

Quantitative study of surface contaminant and the monitoring of bacterial persistence on medical device surfaces using hyperspectral imaging.

Hanh N. D. Le, Johns Hopkins Univ. (United States); Victoria M. Hitchins, U.S. Food and Drug Administration (United States); Moon S. Kim, U.S. Dept. of Agriculture (United States); Jeeseong C. Hwang, National Institute of Standards and Technology (United States); Jin U. Kang, Johns Hopkins Univ. (United States); Do-Hyun Kim, U.S. Food and Drug Administration (United States)

Medical device surface contamination from biological or chemical substances is difficult to detect using optical techniques due to thin coverage and background distortion. To evaluate surface contamination quantitatively and determine the clean portion of a medical device, we propose the Mapped Average Principal component Score (MAPS) method. This method is an adaptation of conventional principal component analysis and data binning to produce a measure of fractional contaminant coverage. The MAPS concept was proven by analyzing samples composed of various medical device materials and textures that were contaminated with thin bacterial films, and compared with other statistical spectral analysis techniques including Spectral Angle Mapper (SAM). MAPS is also used to monitor the shear stress of the bacterial thin film under different

**Conference 9317: Optical Fibers and Sensors for
Medical Diagnostics and Treatment Applications XV**

angle alignment, and thus provides the bacterial adherence on certain medical devices. *Pseudomonas aeruginosa* biofilms were grown on glass, polycarbonate, polytetrafluoroethylene and stainless steel surfaces, all of which are commonly used in medical devices. The influence of material surface texture on bacterial morphology was also studied using a gradient of stainless steel textures, from smooth polished to coarse scratched surfaces. The results of this study promote the ability to differentiate clean and contaminated medical surfaces with high sensitivity and low cost using MAPS.

9317-19, Session 5

Fiber-based polarimetric stress sensor for measuring the Young's modulus of biomaterials

Mark C. Harrison, Andrea M. Armani, The Univ. of Southern California (United States)

Polarimetric optical fiber-based stress and pressure sensors have proven to be a robust tool for measuring and detecting changes in the Young's modulus (E) of materials in response to external stimuli, including the real-time monitoring of the structural integrity of bridges and buildings. These sensors typically work by using a pair of polarizers before and after the sensing region of the fiber, and high sensitivity or precision is achieved by using fiber coils or long lengths of fiber ($L > 10\text{m}$) embedded in the material. The ability to perform similar measurements in natural and in engineered biomaterials could provide significant insights and enable research advancement and preventative healthcare. However, in order for this approach to be successful, it is necessary to reduce the length of fiber needed, which requires a significant improvement in sensitivity. As the first step in this path, we have developed a new route for performing these measurements. By generalizing and expanding established theoretical analyses for these types of sensors, we have developed a predictive theoretical model. Additionally, by replacing the conventional free space components and polarization filters with a polarimeter, we have constructed a sensor system with higher sensitivity and which is semi-portable. In initial experiments, a series of polydimethylsiloxane (PDMS) samples with several base:curing agent ratios ranging from 5:1 up to 30:1 were prepared with embedded polarization-maintaining optical fibers. By simultaneously producing stress-strain curves using a load frame and monitoring the polarization change of light traveling through the samples, we verified the accuracy of our theoretical model.

9317-20, Session 5

Low cost fiber optic sensing of sugar solution

Esakkimuthuraju Murugan, Anurag Reddy Patlolla, Badrinath Vadakkapattu Canthadai, Vidya Jyothi Institute of Technology (India); Vengal Rao Pachava, National Institute of Technology, Warangal (India)

The demand for highly sensitive and reliable sensors to assess the refractive index of liquid get many applications in chemical and biomedical areas. Indeed, the physical parameters such as concentration, pressure and density, etc., can be found using the refractive index of liquid. In contrast to the conventional refractometer for measurement, optical fiber sensor has several advantages like remote sensing, small in size, low cost, immune to EMI etc.,. In this paper we have discussed determination of refractive index of sugar solution using optical fiber. An intensity modulated low cost plastic fiber optic Refractive index sensor has been designed for the study. The sensor is based on principle of change in angle of reflected light caused by refractive index change of the medium surrounding the fiber. The experimental results obtained for the sugar solution of different refractive indices prove that the fiber optic sensor is capable of measuring the refractive indices as well as the concentrations.

9317-42, Session 5

Optical coherent tomography (OCT) in laser tissue bonding of incisions in the cornea

Yishai Porat, David Varsano, Irina S. Barequet, Meira Neudorfer, Tel Aviv Univ. (Israel); Mordechai Rosner M.D., Sheba Medical Ctr. (Israel); Abraham Katzir, Tel Aviv Univ. (Israel)

Laser tissue bonding could be used as an alternative to sutures or glues, as it offers several desirable attributes for various types of operations, such as water-tight closure, non-contact application, reduced scarring, and faster healing. One area in which this technology may be highly beneficial is the closure of corneal incisions, which today require significant surgical skill, the incisions heal very slowly and the surgical procedure often produces weak bonds. We carried CO₂ laser welding experiments on bovine eyes, *in vitro*. We heated the incision, spot by spot, where each spot was heated to a bonding temperature T_B for exposure time t_B . Typically $T_B = 60\text{--}65\text{C}$ and $t_B = 10\text{sec}$. In this study we aimed to broaden our understanding of corneal tissues reactions to laser heating, in the regime relevant to laser bonding procedures. For this purpose we used Optical Coherence Tomography (OCT) which is capable of producing depth images of the cornea, without the need to perform a histological analysis. This imaging allowed the quantitative analysis of the tissue response with respect to the heating profile, using a statistical approach, along with advanced morphological tools. A computer simulation was generated to model the laser tissue interaction in the experiment, providing deeper insight into the theoretical aspects of the procedure, and a rough estimate of the expected results. A specialized image processing algorithm was developed to handle the OCT data. In addition, selected samples were sent to histological assessment, to confirm the processed OCT results and draw conclusions on the strengths and weaknesses of each method.

We also studied the bond strength, as a function of the heating profile, using the same system settings. This made it possible to tie our results with the actual medical application. In our experiments, and in all previous ones, when a spot on the cornea was heated to temperature T_B for time t_B a lesion was formed. We observed that the depth D of the lesion was the most effective measure in estimating the extent of the heating effect on the tissue. D increased linearly as a function of t_B , or as a function of T_B , within the boundaries of the experiment. The change in opacity detected in the OCT images was found to correspond well with the loss of the organization seen in the histological sections. However, more severe changes to the structure, such as vacuolated coagulation and charring, were not detected in the OCT images. The bond strength experiment showed that there was an optimal temperature, at which the yield peaked, and that a linkage could be made between the bond strength and the lesion depth, through their respective linear responses.

In addition to the scientific contribution of this research, these conclusions open the way for possible advanced applications which are very promising. One example is the live 3D imaging of the incision, displaying the structural transformation of the tissue into the depth of the cut. Another potential application is a fiber-optic implementation of the OCT which can measure the depth of the reaction at the point of application, even in endoscopic operations, and act as a feedback mechanism indicating when the required bonding effect has been achieved.

9317-21, Session 6

Controlled single cell destruction using optical fibers

Hao Wang, Anna Pyayt, Univ. of South Florida (United States)

We present experimental study describing controlled single cell destruction using optical fibers. It requires use of a new optically sensitive magnetic

**Conference 9317: Optical Fibers and Sensors for
Medical Diagnostics and Treatment Applications XV**

material that can be delivered to a needed location using external magnets. Then light can be delivered using optical fiber, and cell can be destroyed at precise location. This process is visualized under microscope using Trypan Blue solution.

9317-22, Session 6

Biconically tapered fiber optic sensor with ultrahigh sensitivity for biosensing applications

Ertan Salik, Martin Sanchez, California State Polytechnic Univ., Pomona (United States); Ragip Pala, California Institute of Technology (United States); Adrian Ortiz, Victor Herrera, Christian Garrido, California State Polytechnic Univ., Pomona (United States)

Biconically tapered fiber sensors (BTOF) are refractive index (RI) sensors that are simple to fabricate yet very sensitive. A BTOF is a modal Mach Zehnder interferometer. When a single-mode fiber is tapered, the two modes of the tapered region that have the largest overlap with the single mode of the untapered fiber are HE₁₁ and HE₁₂ modes. We studied the dependence of sensitivity on the profile of a taper and the wavelength of light used, and experimentally demonstrated tapered fiber optic refractive index (RI) sensors with sensitivities > 11000 nm/RIU, which is an order of magnitude higher than the previously published results. We measured higher sensitivity at longer wavelengths. In order to theoretically calculate the sensitivity, we measured the profile of the taper waist as a function of position along the taper using scanning electron microscopy. Based on our theoretical analysis, we predict that tapered fiber RI sensors with sensitivities exceeding 50000 nm/RIU can be developed. We attribute the enhanced sensitivity mainly to the nonlinear variation of the difference in mode propagation constants with wavelength near the cut-off of the HE₁₂ mode. Such ultrahigh sensitivity combined with low cost and simplicity for tapered fiber RI sensors makes them good candidates for numerous label-free sensing applications in medical diagnosis, food safety, environmental monitoring, and biodefense. To demonstrate the enhanced sensitivity for biological sensing, we performed experiments using immunoglobulin-G (IgG) and anti-IgG binding experiments, where the sensor surface was functionalized with IgG and tested against anti-IgG of varying concentrations.

9317-23, Session 6

SMART micro-scissors based precise incision

Hyuncheol Park, Chaebeom Yeo, Cheol Song, Daegu Gyeongbuk Institute of Science & Technology (Korea, Republic of)

Microsurgeons require hand tremor reduction and stable manipulation of the tool tip during microsurgery. We develop the OCT sensor guided SMART micro-scissors and demonstrate improved compensation of the scissors tip position and incision performance. Compared to freehand incision, it demonstrates enhanced incision performance on dry phantoms with hand tremor suppression. The result of proof-of-concept study may support surgical performance during microsurgery.

9317-24, Session 6

Mode division multiplexing and mode excitation/detection in multimode optical fibers (*Invited Paper*)

Giovanni Milione, City College of New York (United States)

Mode division multiplexing (MDM) is a burgeoning method in optical fiber communication where spatial modes are used as additional information channels carrying independent signals over a multimode optical fiber communication link. MDM has great potential to increase the information capacity of optical fiber communication systems beyond fundamental Shannon information capacity limits. In this work, I will give an overview of our recent work on MDM using various bases of modes such as LP modes, orbital angular momentum modes, and vector modes. Particular attention will be given to novel methods of mode excitation and detection using liquid crystal spatial light modulators, liquid crystal q-plates, and an orbital angular momentum mode "sorter."

9317-25, Session 6

Phosphor-based fiber optic microprobes for ionizing beam radiation dosimetry

Arash Darafsheh, The Univ. of Pennsylvania Health System (United States); Taejong Paik, Stan Najmr, Michael Tenuto, Christopher B. Murray, Univ. of Pennsylvania (United States); Joseph S. Friedberg, Jarod C. Finlay, The Univ. of Pennsylvania Health System (United States)

Fiber optic probes in conjunction with scintillating materials are promising candidates for radiation therapy. The total optical signal transmitted by the fiber to the detector, however, has unwanted components in addition to the useful scintillator's signal. The main problem with fiber optic probes is these unwanted signals that are primarily the β erenkov radiation generated in the irradiated portion of the fiber. In this work, as a proof-of-concept, we design, fabricate, and characterize a fiber probe composed of terbium-based phosphors for ionizing radiation dosimetry. Fiber optic probes consisting of a thin layer of terbium-based phosphors covering the tip embedded in tissue-mimicking phantoms were irradiated with electron and photon beams produced by a medical linear accelerator. Optical spectra of irradiated tips were taken using a fiber spectrometer. By using a singular value decomposition method, the luminescence signal from the phosphors is spectrally separated from the β erenkov radiation generated in the fiber. At each beam energy, the resultant decomposed spectra corresponding to emission from the phosphors were considered as an indicator of absorbed dose in order to obtain a percent depth dose curve. The measured depth dose curves using our fiber probes are in agreement with measurements performed by an electron diode and ion chamber, indicating the feasibility of using such fiber probes for electron or photon beam dosimetry.

9317-26, Session 7

UV-fibers: two decades of improvements in medical and sensing applications (*Keynote Presentation*)

Karl-Friedrich Klein, Technische Hochschule Mittelhessen (Germany); Valery K. Khalilov, Polymicro Technologies, A Subsidiary of Molex Inc. (United States)

For applications below 250 nm, silica-based UV-fibers with high-OH undoped core and fluorine-doped cladding have been used for more than 30 years. However, the life-time or time of operation in fiber-optic based systems was often limited by the generation of optically active defects in this wavelength region. Additionally, damages with pulsed lasers were

**Conference 9317: Optical Fibers and Sensors for
Medical Diagnostics and Treatment Applications XV**

observed at wavelengths below 380 nm.

Over the past two decades, UV-properties such as basic transmission and induced losses have been continuously improved in UV-fibers with a focus on deuterium-lamp usage. These improvements were achieved by preform modifications, fiber drawing and fiber processing. Although high-OH fibers seemed most favorable, also low-OH fibers were optimized as wide range fibers for the deep UV to NIR region up to 2000 nm wavelength. The steps of improvement will be discussed in detail.

Inexpensive compact high power laser and LED light sources for fluorescence applications have put stringed requirements on fiber performances in the UV region below 400 nm. too. As a result, laser-induced UV-damage caused by two-photon absorption was studied and the performance of different UV fibers compared.

Parallel to the fiber improvements, testing equipment and testing methodology were developed and implemented to control quality and reproducibility of the various fiber generations. This has led to standard tests for optical degradation of UV-fibers and has recently been adopted by the German standardization (DIN) group.

In addition to fluorescence analyses, several novel UV applications, such as fiber-optic thin-layer chromatography, liquid and gas spectroscopy and other analytical instrumentation will be discussed, only to name a few. Current work on these fiber-optic laser systems for analytical applications with light power levels up to 10 mW will be presented. Finally, an outlook on further possibilities and applications will be given,

9317-27, Session 8

Design and fabrication of disposable plasmonic fiber probes for biosensing

Carmelo Fallauto, Andrea Braglia, Alberto Vallan, Guido Perrone, Politecnico di Torino (Italy); Vasile A. Popescu, Nicolae N. Puscas IV, Univ. Politehnica of Bucharest (Romania)

Surface plasmon resonance based fiber sensors are particularly attractive for the detection of bio-chemicals in clinical applications because they combine high sensitivity with the advantages of optical fibers, such as reduced invasive impact, absence of electrocution risk and simplified insertion into the patient body through catheters. Today their use is still mainly confined to lab demonstrators, but in view of a wider diffusion it is necessary to devise a transducer head (i.e. the disposable part) geometry easy to fabricate and simple to connect to the interrogating system. The realization of a typical probe requires depositing a suitable sequence of metal layers onto the fiber core, followed by functionalizations specific for the molecules to be sensed. The paper analyzes different technological solutions, both with simulations and experiments, to realize cost effective probes, such as: i) use of large core and high numerical aperture fibers - with and without tapering to reduce the core in the sensing region - to simplify mating and therefore to avoid expensive connectors; ii) use of dual-core fiber cables to avoid couplers; iii) use of a simplified layer deposition process that does not require turning the fiber and thus allows speeding up the fabrication process, although it implies a reduction in the effective interaction length and, moreover, a non-uniform layer thickness in the radial direction. The sensor characteristics (e.g. spectral resolution, loss spectra, FWHM notch peak, amplitude sensitivity, etc.) are compared with standard probes made by fully coated optical fibers or with recently proposed high performance fiber sensors in which an inner gold layer is replaced with a GaP reflector layer.

9317-28, Session 8

Active depth-locking handheld micro-injector based on common-path swept source optical coherence tomography

Gyeong Woo Cheon, Yong Huang, Jin U. Kang, Johns Hopkins Univ. (United States)

In this work, we built and studied a freehand motion-compensated micro-injector with an intuitive control system that allows the injecting needle tip to lock the desired depth during the injection with several micron order accuracy. One of the essential requirements for a successful microsurgery is a surgeon's accurate and precise tool tip manipulation. However, it is nearly impossible to perform micron-scale-precision tasks in freehand microsurgery even for highly-experienced surgeons. One of the main reasons is hand tremor which exists mainly in the 6-12Hz frequency domain with several hundred micrometer of amplitude. So far, there have been different attempts to compensate for such motion problems. Our research group has been pursuing an axial motion compensation approach that utilizes an optical coherence tomography (OCT) a distal sensor. Specifically, common path OCT (CP-OCT) was chosen for a distal sensor due to its advantageous characteristics: simple structure, dispersion free, and polarization free. To achieve this goal, we developed a control algorithm to advance the concept of motion control from passive motion compensation to overcome hand tremor to active surgical tool guidance for highly precise injection-depth-targeting. Through 60-insertions test, depth targeting with high accuracy on the order of several microns is demonstrated with high repeatability. The potential effectiveness of precise drug delivery is also demonstrated in fluorescein dye injection test.

9317-29, Session 8

Fiber-optic direct Raman imaging system based on a hollow-core fiber bundle

Satomi Inoue, Graduate School of Biomedical Engineering, Tohoku Univ. (Japan); Takashi Katagiri, Graduate School of Engineering, Tohoku Univ. (Japan); Yuji Matsuura, Graduate School of Biomedical Engineering, Tohoku Univ. (Japan)

A Raman imaging system which combined a hollow fiber bundle and a direct imaging technique was constructed for high-speed fiber-optic Raman imaging. The hollow fiber bundle is fabricated by depositing a silver thin film on the inner surface of pre-drawn glass capillary bundle. It performs as a fiber optic probe guiding Raman image with high signal to noise ratio simply by being aligned at the focal plane of a microscope because it has little light scattering in the air core. The field of view on the sample is uniformly irradiated by the excitation laser light via the probe. The back-scattered image is collected by the probe and captured directly by an image sensor. A tunable bandpass filter is formed by stacking pairs of thin film tunable filters with a small angle between them to obtain a target Raman band with high spectral resolution. This direct imaging system enables flexible and high-speed Raman imaging of biological tissues by sacrificing spatial resolution and/or spectral information.

9317-30, Session 9

All-fiber probe for laser-induced thermotherapy with integrated temperature measurement capabilities

Yu Liu, Wei Chen, Hao Yu, R. Gassino, Andrea Braglia, Massimo Olivero, Alberto Vallan, Guido Perrone, Politecnico di Torino (Italy)

The paper presents our recent results towards the development of a

Conference 9317: Optical Fibers and Sensors for Medical Diagnostics and Treatment Applications XV

miniaturized all fiber probe for laser induced thermal ablation of tumor cells. According to medical literature, the controlled necrosis of cells requires to induce a temperature of about 60 °C for few seconds; this can be obtained for instance with a laser beam at about 1 μm, a wavelength that ensures a sufficient penetration and at which many high power sources are available. Optimal results, however, demand the accurate balancing between laser power and exposure time, and this, in turn, requires the accurate control of the temperature. Indeed, while a lower temperature could not be efficient or could require longer exposures to kill the malignant cells, a higher temperature induces unwanted carbonization of the tissue. Nevertheless, the exact temperature obtained during irradiation is not easy to predict a priori because it is strongly dependent on the tissue composition. To overcome this limitation we have developed a probe that takes advantage of a dual cladding fiber structure for integrating a low thermal inertia fiber Bragg grating (FBG) temperature sensor with the delivery of a NIR high power ablating beam and of a low power visible aiming beam. This has been obtained by realizing a suitable fused fiber combiner for merging the ablating and the aiming beams with the signal that feeds the temperature sensor. Similar technology has been used also for the probe end-cap. Then, since the temperature may rise during the thermal treatment quite abruptly, a fast FBG interrogation system (time response of about 20ms/10%) has been implemented.

9317-31, Session 9

Nonlinearly fiber-converted coherent source with broad spectral coverage for multiphoton imaging

Haohua Tu, Yuan Liu, Youbo Zhao, Stephen A. Boppart M.D., Univ. of Illinois at Urbana-Champaign (United States)

The last decade has witnessed an increased application of femtosecond solid-state lasers in biophotonics. Representative techniques include label-free multiphoton microscopy and endoscopy that visualize endogenous biomolecules, photodynamic therapy by in situ nonlinear photon conversion, and femtosecond-pulse-assisted microsurgery. However, ultrafast solid-state lasers are often bulky and alignment-sensitive, restricting these systems and techniques to dedicated optical laboratories. To translate these techniques to the clinic, there is a critical need to replace the solid-state lasers with portable, low-maintenance, and environmentally-stable fiber lasers. Unfortunately, conventional ultrafast fiber lasers have narrow gain bandwidth, so that the emission is limited to a few discrete wavelengths of rare earth dopants, such as ~1040 nm (Yb), ~1550 nm (Er), and ~2000 nm (Tm).

To address this key limitation, we developed a configurable fiber-laser-like source employing a series of wavelength-conversion microstructured (or circular) silica fibers, the dispersion properties of which are special for the femtosecond pump pulses of the source. The Er: fiber laser was chosen as the pump to target the 370-830 nm and 2000-3500 nm regions through fiber Cherenkov radiation, and the 1200-2000 nm region through coherent supercontinuum generation. Also, the Yb: fiber laser was chosen as the pump to target the 780-1320 nm region through coherent supercontinuum generation. In this way, compressed near-transform-limited sub-25 fs pulses with a central wavelength anywhere within 450-3000 nm can be generated with a peak-power of >10 kW. Compared to various solid-state lasers, the generated supercontinuum across 780-1320 nm has demonstrated similar or better performance for multiphoton imaging of unstained biological tissues.

9317-32, Session 9

Suspended core photonic crystal Fibers fluorescence sensor platform for nucleic acid detection

Alessandro Candiani, Michele Sozzi, Alessandro Tonelli, Annamaria Cucinotta, Roberto Corradini, Stefano Selleri,

Univ. degli Studi di Parma (Italy)

Suspended Core Photonic Crystal Fibers (SC-PCFs) have been widely researched in the last ten years, due to their unique manufacturing technology: the capillaries running along their length constitute a powerful microfluidic platform that can be exploited for performing selective sensing experiments. Moreover, the small cross area section together with the high overlap factor of the evanescent field make SC-PCFs a versatile photonic element for chemical and biological sensing applications.

In the present work a SC fiber fluorescence sensor platform for nucleic acid detection has been investigated. Genomic RNA of viruses of clinical interest has been labeled with an opportune fluorophore and then it has been infiltrate into the fiber microchannels. A blue LED at λ=490 nm, coupled into the fiber core, has been used as the excitation source exploiting the evanescent field that travels along the fiber channels. The fluorescence emission has been then recollecting in the fiber core and read using a 520 nm optical filter and an Optical Spectrum Analyzer (OSA). The main aim of this work was to perform a nucleic acid analysis without any functionalization of the fiber surface. The optical system has been characterized with standard solutions and tested with clinical samples.

9317-33, Session 9

Wireless implantable microscopy using oblique back-illumination

Tim N. Ford, Kengyeh K. Chu, Tao Wu, Robert W. Carruth, Daryl Chulho Hyun, Weina Lu, MGH Wellman Ctr. for Photomedicine (United States); Guillermo J. Tearney M.D., MGH Wellman Ctr. for Photomedicine (United States) and MGH Pathology (United States) and Harvard-MIT Div. of Health Science and Technology (United States)

Human disease originates and develops in the body as cellular abnormalities but a lack of tools for long-term visualization and monitoring of these cellular processes in vivo limits our ability for monitoring and treatment. An untethered imaging device capable of continuously monitoring cells in situ could transform the way we diagnose, study, treat, and prevent conditions in the fields of cancer, transplant immunology, cardiopulmonary medicine, and more.

We present a miniature wireless implantable imaging device for long-term monitoring of cellular processes in an awake and freely moving animal. The wireless implantable microscope (WIM) is self-contained in a biocompatible package, is battery powered, and transmits image data wirelessly to an extracorporeal receiver using a 2.4 GHz radiofrequency (RF) transmitter. The WIM imaging platform was demonstrated using oblique back-illumination microscopy, a new form of light microscopy for lateral phase-gradient imaging of cells in thick, scattering tissues. Cellular and microarchitectural monitoring can be achieved through time lapse imaging of a constant field of view in an awake and freely moving animal over a period of days or weeks.

Many technical challenges are addressed in this work, including building a high-performance miniature optical system, mechanical placement and assembly, electrical control and signal transmission, biocompatibility and surgical implantation, and signal recovery, storage and processing. These results demonstrate proof-of-concept of the WIM platform and open the door to a revolutionary new method of high-performance, untethered monitoring of cellular and physiological processes.

9317-34, Session 9

Peripheral circulation detection by using portable near-infrared spectroscopy: the study of temperature effect

Chun-Jung Huang, BOIL (Taiwan) and National Chiao Tung

**Conference 9317: Optical Fibers and Sensors for
Medical Diagnostics and Treatment Applications XV**

Univ. (Taiwan); Ching-Cheng Chuang, BOIL (Taiwan); Chia-Wei Sun, National Chiao Tung Univ. (Taiwan) and BOIL (Taiwan)

Peripheral blood circulation presents in the small vasculature embedded within tissue and it deals with the circulation of blood from the heart to arteries, veins and capillaries. The Peripheral blood circulation could response the physiological condition of human. In this study, we measure the change of oxygenation status and the vein image of human peripheral blood circulation in different temperature and different pressure. The near-infrared diffuse photon penetrates deeper tissue and reveals the information of peripheral blood circulation. The optical assessment shows an interpretation of tissue microcirculation change with oxygenation dynamics.

9317-35, Session 10

**Simultaneous Electroencephalography /
Near-infrared Spectroscopy measurement
on prefrontal cortex with WCST task**

Dai-Chen Lu, Chia-Wei Sun, Ching-Cheng Chuang, National Chiao Tung Univ. (Taiwan)

Near-infrared spectroscopy (NIRS) is a noninvasive neuroimaging tool for measuring evoked functional changes of brain oxygenation. Electroencephalography (EEG) coherence can be used to evaluate the functionality of cortical connections and to obtain information of regional cortical activity. Coregistration of EEG-NIRS is a dual-modality technique that was used to detect the changes in both electrical and local hemodynamic activities of human brain. The coregistration is useful to avoid misleading interpretation of NIRS, especially in the diagnosis of neurological disorders. In this research, we investigate an approach to the analysis of enhance accuracy of NIRS by EEG for physiological activities in mental focus task. Based on the Wisconsin Card Sorting Test (WCST) as subjects mental focus task, we find the EEG and NIRS signals has different trends for normal subjects. These information can help us to understand brain activation status. Furthermore, we can determine subject's degree of mental concentration. The result implies information of neurological status and it might be used for the clinical diagnosis of neurological disorders.

9317-36, Session 10

**Correction method of bending loss in
the hollow optical fiber for endoscopic
submucosal dissection using carbon
dioxide laser**

Daisuke Kusakari, Hisanao Hazama, Graduate School of Engineering, Osaka Univ. (Japan); Kunio Awazu, Graduate School of Engineering, Osaka Univ. (Japan) and Graduate School of Frontier Bioscience, Osaka Univ. (Japan) and The Ctr. for Advanced Medical Engineering and Informatics, Osaka Univ. (Japan)

Endoscopic submucosal dissection using carbon dioxide laser is a promising treatment of early digestive cancer because it can avoid the risk of perforation. Although a hollow optical fiber transmitting mid-infrared light has been used, it was observed that the irradiation effect was influenced by bending a gastrointestinal endoscope due to the change in transmittance by the bending loss. Therefore, we quantitatively evaluated the change in the irradiation effect by bending the hollow optical fiber in the endoscope and proposed a correction method to stabilize the irradiation effect. First, the relationships between the irradiated laser energy density and the incision depth for porcine stomach were measured by bending the head of the endoscope. Next, the relationships between the bending angle of the head of the endoscope and the temperature rise of the hollow optical fiber in

the head of the endoscope were measured during the laser irradiation. As a result, the laser energy density and the incision depth decreased as the bending angle increased, and linear correlation between the laser energy density and the incision depth was observed. It was found that the bending angle can be estimated by the ratio of the setting laser power to time derivative of the temporal profile of the temperature of the hollow optical fiber. In conclusion, it is suggested that the correction of the laser energy density and stabilization of the incision capability is possible by measuring the temporal profile of the temperature of the hollow optical fiber.

9317-37, Session 10

**Wide dynamic range sensing in photonic
crystal microcavity biosensors**

Chun-Ju Yang, Yi Zou, The Univ. of Texas at Austin (United States); Naimei Tang, Omega Optics, Inc. (United States); Hai Yan, The Univ. of Texas at Austin (United States); Swapnajit Chakravarty, Omega Optics, Inc. (United States); Ray T. Chen, The Univ. of Texas at Austin (United States) and Omega Optics, Inc. (United States)

In several applications in biosensing, particularly in drug discovery and therapeutic drug monitoring, it is essential to have sensors that can register concentrations of analytes over a wide dynamic range of at least five orders of magnitude. Recently, numerous optical devices have been investigated for label free detectors. Among all the label free detectors and optical devices, photonic crystal (PC) has provided the unique characteristics with slow light effect which enhance the interaction between traveling light the analyte. The slow light effect in PC sensors has been investigated by our group in numerous applications. However, each PC microcavity sensor in a triangular lattice PC, that we have demonstrated have a dynamic range of approximately 4 orders of magnitude, with the linear region of the S-shaped concentration versus wavelength shift curve being linear over just 3 orders of magnitude. Integrated optics however provides the unique ability to multiplex sensors on the same chip that can be measured simultaneously at the same time with the same sample due to the miniature dimensions of the sensors. In this paper, we experimentally demonstrate a novel design for achieving wide dynamic detection range whereby multimode interference (MMI) devices are multiplexed with photonic crystal microcavities of different geometries, each covering a different concentration range and thereby achieving a wide dynamic range of 7-8 orders of magnitude.

9317-38, Session 10

**Distributed fibre optic surface plasmon
resonance sensors**

Mohamad Daa Baiad, Raman Kashyap, Ecole Polytechnique de Montréal (Canada)

An experimental multichannel optical fiber surface Plasmon resonance (SPR) sensor scheme excited by a gold and silicon-coated fiber with a tilted fiber Bragg grating (TFBG) is presented. The device detects the SPR signature in the transmitted spectrum, allowing easy comparison between the channels which have different TFBG tilt angle and operating wavelength. Different fibers have been used and each one shows a unique refractive index operating range. The channels are coated with 2 nm chromium, 35 nm gold and 10 nm silicon. The thickness of the high-index dielectric layer of silicon layer is used to tune the SPR refractive index operating range to a desired value. Comparison between different layer thicknesses is provided. Also, the silicon layer has been used to improve the sensitivity of the system compared to previous techniques [1-2]. The polarization state of each channel based on the TFBG orientation can be used to turn each SPR channel on or off as required. Experimental results predict a shift in the central SPR resonance wavelength due to the shift of the SPR resonance angle [3]. This system provides an improvement in the refractive index operating range from 1.32 to 1.44 RIU which is the largest reported range so

Conference 9317: Optical Fibers and Sensors for Medical Diagnostics and Treatment Applications XV

far of such a sensor to our knowledge, and a maximum improved sensitivity of about 900?nm/RIU. The flexibility and the improved ease of use of the proposed scheme can be adapted to many SPR-TFBG based sensors applications.

References:

- [1] M. Baiad, M. Gagné, W. Madore, E. De Montigny, N. Godbout, C. Boudoux, and R. Kashyap, "Surface plasmon resonance sensor interrogation with a double-clad fiber coupler and cladding modes excited by a tilted fiber Bragg grating," *Opt. Lett.* 38, 4911-4914 (2013).
- [2] Y. Shevchenko, C. Chen, M. Dakka, and J. Albert, "Polarization-selective grating excitation of plasmons in cylindrical optical fibers," *Opt. Lett.* 35, 637-639 (2010).
- [3] P. Bhatia and B. Gupta, "Surface-plasmon-resonance-based fiber-optic refractive index sensor: sensitivity enhancement," *Appl. Opt.* 50, 2032-2036 (2011).

9317-39, Session PSun

All optical phase stepping for optical imaging with nonlinearity in specialty fiber

Eun-Seo Choi, Seung Suk Lee, Joo Ha Kim, Chosun Univ. (Korea, Republic of); Bok Hyeon Kim, Tae Joong Eom, Advanced Photonics Research Institute (Korea, Republic of)

Refractive index variation in rare-earth doped specialty fiber can be possible through resonantly enhanced optical nonlinearity. The quantity of the variation under low-power optical pumping is enough to induce 2- π phase shift. By using this nonlinear effect in the specialty fiber, optical imaging system utilizing phase shift can perform imaging without mechanically controlled phase stepping for bucket process. The pump-induced refractive index from the specialty fiber in reference arm of interferometer can produce optical delay depending on applied optical pumping power. At low optical power under few hundred mW, optical delay corresponding to 2- π can be yield in the reference arm. Since operating wavelength window around of 1310 nm is far from the resonantly enhanced nonlinearity regime, the dispersion due to the refractive index change under optical pumping is not significant across the window. Contrast to the conventional mechanical phase stepping method, optically actuated phase stepping with the specialty optical fiber can prevent electrical feedback process for mechanical hysteresis without high voltage controllable electronics. The pumping power for phase shift could be reduced further depending on doping material property and fabrication process optimization. Therefore, thermally induced refractive index during operation could be prevented and more detailed control at lower pumping power is to be appreciated. The proposed method is suggested with demonstrating full range imaging in optical coherence tomography. Extended imaging range under optical phase stepping is to be presented. The proposed method could be applied for detailed control of phase shift-based interferometry.

9317-40, Session PSun

Hand-held micro-forceps incorporating a motor-derived grasping on an OCT sensor-guided SMART surgical tool platform

Phillip Lee, Gyeong Woo Cheon, Johns Hopkins Univ. (United States); Peter L. Gehlbach, Johns Hopkins School of Medicine (United States); Jin U. Kang, Johns Hopkins Univ. (United States)

We designed and built a handheld micro-forceps with a motor-driven closing and opening of the forceps that built upon a OCT sensor guided SMART surgical tool platform. The tool is designed to stabilize the grasping process, minimizing errors from human tremor, and to grasp the targeting

layer at an exact fixed depth. The device consists of small linear actuator modules with integrated driver and closed-loop control, allowing a slim design. This enables the device to be conveniently hand held during surgeries. The SMART micro-forceps utilizes two motors, one for opening and closing the forceps tips and the other for controlling the depth of the grasping area. The system's grasping parts are positioned in the needle shaft. The tips of the micro-forceps open and close according to the relative motion between these grasping parts and the needle shaft. One motor, which is located at the rear end of the shaft, induces this relative motion and it controls the opening of forceps tips. This motor is connected to a force sensor that detects the degree of squeezing force of a surgeon. This information is then used to control the degree of forceps tip opening. Another feature of the SMART micro-forceps is the ability to measure the distance between forceps tips and targeting surface using OCT sensor. This distance is used in the other motor, also located at the most rear end of the shaft, to precisely position the forceps tips from the target, thereby eliminating risks and errors from human tremor. Therefore, this OCT sensor-guided approach in the SMART micro-forceps is expected to facilitate surgical procedures to be more accurate, efficient and safe.

9317-41, Session PSun

Real-time 3D reconstruction of catheter shape using FBGs based sensors

Francois Parent, Ecole Polytechnique de Montréal (Canada)

During vascular interventions using devices such as catheters, 3D real-time visualization of catheters may be of clinical value for the localization within heart chambers. This is typically performed using fluoroscopic imaging with contrast agent. However, these systems only provide images in two dimensions and it remains challenging to obtain a precise 3D representation with a sequence of images. The procedure time can become very long and exposure to this type of radiation can be harmful for patients. Here, we propose a new alternative using several fiber Bragg gratings (FBG) based sensors to reconstruct the three-dimensional shape of catheters. Based on a similar model [1] adapted to our case, an $n+1$ -th order polynomial approximation fitting the number of sensors integrated within the catheter, is used to monitor the position and shape of the entire catheter in real-time. Assuming that the curvature of the catheter is constant at the base and at the tip, the coefficients of the polynomial can be determined using a reconstruction algorithm. We present preliminary results demonstrating the promising aspects of this approach. The problems and limitations will also be discussed, such as the dependencies of the FBGs with respect to body temperature fluctuations along the catheters.

[1] Seifabadi, Reza., "Teleoperated MRI-Guided Prostate Needle Placement", Thesis submitted to the Department of Mechanical and Material Engineering, Queen's University, Chapter 6, 2013.

Conference 9318: Optical Biopsy XIII: Toward Real-Time Spectroscopic Imaging and Diagnosis

Tuesday - Wednesday 10-11 February 2015

Part of Proceedings of SPIE Vol. 9318 Optical Biopsy XIII: Toward Real-Time Spectroscopic Imaging and Diagnosis

9318-1, Session 1

Non-contact optical imaging of healing and non-healing diabetic foot ulcers

Anuradha Godavarty, Yamini Khandavilli, YoungJin Jung, Florida International Univ. (United States); Someshwara Rao, Dr.Somesh Diabetic Foot Clinic (India)

Diabetic foot ulcer is the most devastating complication of diabetes that is still un-recognized. The treatment costs of these ulcers are very high to eventually save the leg/foot from amputation. To date, clinicians employ visual inspection of the wound site during its standard 4-week of healing process via monitoring of surface granulation. There is a need to develop on-site, low-cost imaging tools that can monitor the wound healing process periodically during the standard 4- week treatment process. A novel ultra-portable near-infrared optical scanner (NIROS) has been developed at the Optical Imaging Laboratory that can perform non-contact 2D area imaging of the wound site. Non-contact optical imaging studies were carried on diabetic subjects with foot ulcers (at Somesh Diabetic Foot Clinic, India) that were of healing and non-healing nature. A 710 nm LED source and a compact NIR sensitive CCD camera system were employed during non-contact imaging of the diabetic foot in order to obtain the near-infrared absorption images. From these preliminary studies it was observed that the non-healing wounds had a greater absorption contrast with respect to the normal site, unlike in the healing wounds. The reconstructed absorption coefficient and NIR images from venous occlusion studies around the wound site are currently extracted from the real-time dynamic NIR images. Demonstrating the ability of NIROS to differentiate healing vs. non-healing wounds in diabetic subjects can potentially impact early intervention in the treatment of diabetic foot ulcers.

9318-2, Session 1

Exhaled breath analysis with quantum cascade laser spectroscopy

Adonis Reyes Reyes, Technische Univ. Delft (Netherlands); Esther van Mastriigt M.D., Marielle W. Pijnenburg M.D., Johan C. de Jongste M.D., Erasmus MC, Sophia Children's Hospital (Netherlands); H. Paul Urbach, Nandini Bhattacharya, Technische Univ. Delft (Netherlands)

We present our latest results on exhaled human breath analysis using a novel non-invasive mid-infrared quantum cascade laser (QCL) spectrometer. We have investigated the concentration changes in exhaled acetone in type 1 diabetes. Our results show the feasibility to use our technique as a diagnosis tool for ketosis and diabetic ketoacidosis. We are also using this system to identify new potential biomarkers to diagnose and monitor respiratory diseases such as asthma and cystic fibrosis. All this is possible thanks to the broadband coverage of our device (7.9 - 12 microns), which allows to determine the concentration of molecular species with overlapping absorption signatures. Specifically, we have detected ppmv and ppbv concentrations of acetone, ethanol and freon in the presence of 2-5% water and 15% CO₂ concentrations.

The setup is based on direct absorption spectroscopy and therefore no sample pre-processing is required. It uses state-of-the-art quantum cascade lasers and Mercury Cadmium Telluride (MCT) detectors operating at room temperature. Its 54.36 meters multipass cell ensures a noise equivalent absorption sensitivity of 2.99710⁻⁷cm⁻¹Hz^{-1/2}, ideal to detect sub-ppmv molecular concentrations.

The results show how our setup can help in identifying new disease biomarkers. In the future this will greatly benefit the development of new non-invasive diagnosis and monitoring devices based on the analysis of exhaled human breath.

9318-3, Session 1

High histologic grade and increased relative content of tryptophan in breast cancer using ratios from fingerprint fluorescence spectral peaks

Laura A. Sordillo, Peter P. Sordillo M.D., Yury Budansky, Yang Pu, Robert R. Alfano, The City College of New York (United States)

Histologic grade is a proven, but underappreciated, measure of breast cancer aggressiveness. Despite its importance, it has historically not been included as one of the criteria for staging of this cancer. We investigate the correlation between tumor histologic grade and changes in relative tryptophan levels from the spectral profiles of 17 patients with breast carcinoma. Emission intensity spectra of key organic biomolecules such as tryptophan, NADH and collagen in the tissue were acquired using the conventional LS-50 spectrometer and a novel ratiometer unit (S3-LED). The relative intensities or ratios (R) of emission intensity peaks at 340 nm, 440 nm and 460 nm from malignant tissue samples (R1=I₃₄₀/I₄₄₀ and R2=I₃₄₀/I₄₆₀) and from paired normal tissue samples (R3=I₃₄₀/I₄₄₀ and R4= I₃₄₀/I₄₆₀) were calculated. Tumor characteristics were assessed from cancerous ratios (R1, R2) over normal samples ratios (R3, R4) to give R5=R1/R3 and R6=R2/R4. We report increased relative tryptophan levels in breast cancer ratios R5 and R6 correlates strongly with high grade but not with number of lymph node metastases, estrogen receptor, progesterone receptor or Her-2-Neu receptor status. As histologic grade is becoming recognized as an increasingly important measure of prognosis for patients with breast carcinoma, the measurement of increased relative tryptophan content may also be useful in the assessment of these cancers.

9318-4, Session 2

Photoacoustic biopsy: a feasibility study (Invited Paper)

Guan Xu, Scott Tomlins, Javed Siddiqui, Mandy Davis, Lakshmi P. Kunju, John Wei, Xueding Wang, Univ. of Michigan Medical School (United States)

Ultrasound (US) guided biopsy is the standard procedure for evaluating the presence of prostate cancer. US biopsies are not targeted and randomly sample broad areas of the prostate, which can either miss cancer or undersample aggressive cancer. Aggressive cancer is defined by high Gleason score. The Gleason scoring system is an architectural assessment of tumor grade that is highly prognostic and performed by pathologists on biopsy tissue. The Gleason patterns, per se the clustering patterns of the cancer cells, can be visualized by staining the cancer cells with optical contrast enhancing nanoparticles (NPs). This research investigates the feasibility of evaluating the NP stained Gleason patterns by photoacoustic (PA) measurements. As a preliminary study, we scanned sliced prostate tissue with Hematoxylin and Eosin Staining. The sliced samples were covered by US coupling gels. Laser energy of 6 mJ per square centimeter was delivered to the sample surface. A needle hydrophone was used to

Conference 9318: Optical Biopsy XIII: Toward Real-Time Spectroscopic Imaging and Diagnosis

acquire the PA signals. A total of 3 normal and 3 cancerous samples were scanned along four different directions (0, 45, 90 and 180 degrees) around the samples. The PA signals were characterized by the method of PA spectrum analysis (PASA). In PASA, the power spectrum of PA signals is approximated by a linear model and the microstructures of the examined tissue are quantified by the parameters of the linear model, including slope, intercept and midband-fit. Statistical analysis of the PASA parameters representing the microstructure in the sample specimens has shown that this approach is capable of differentiating cancerous tissues from normal ones by identifying the Gleason patterns of cancer cells.

9318-5, Session 2

Raman spectroscopy complements optical coherent tomography in tissue classification and cancer detection

Ji Qi, Narendran Sudheendran, Chih Hao Liu, Univ. of Houston (United States); Gregg Santos, Univ of Houston (United States); Eric D Young, Alexander Lazar, Dina Lev, Raphael Pollock, The University of Texas MD Anderson Cancer Center (United States); Kirill V. Larin, Wei-Chuan Shih, Univ. of Houston (United States)

Optical coherence tomography (OCT) provides significant advantages of high-resolution (approaching the histopathology level) real-time imaging of tissues without use of contrast agents. Based on these advantages, the microstructural features of tumors can be visualized and detected intra-operatively. However, it is still not clinically accepted for tumor margin delineation due to poor specificity and accuracy. In contrast, Raman spectroscopy (RS) can obtain tissue information at the molecular level, but does not provide real-time imaging capability. Therefore, combining OCT and RS could provide synergy. To this end, we present a tissue analysis and classification method using both the slope of OCT intensity signal versus depth and the principle components from the RS spectrum as the indicators for tissue characterization. Our pilot experiments were performed on mouse kidneys, livers, and small intestines. The prediction accuracy with five-fold cross validation of the method has been evaluated by support vector machine method. The results demonstrate that RS can effectively improve tissue classification compared to OCT alone. Next, we demonstrate that the boundary between myxoid liposarcoma and normal fat which is easily identifiable both Raman and OCT. In cases where structural images are indistinguishable, for example, in normal fat and well differentiated liposarcoma (WDLs) or gastrointestinal sarcoma tumor (GIST) and Myxoma, distinct molecular spectra have been obtained. The results suggest RS can effectively complement OCT to tumor boundary demarcation with high specificity.

REFERENCES:

1. Peter Liu, Ji Qi, Wei-Chuan Shih, and Kirill Larin, "Improvement of tissue analysis and classification using Optical Coherence Tomography combined with Raman spectroscopy," *Journal of Innovative Optical Health Sciences* 2014.
2. Narendran Sudheendran*, Ji Qi*, Eric D. Young, Alexander J. Lazar, Dina C. Lev, Raphael E. Pollock, Kirill V. Larin, Wei-Chuan Shih**, "High throughput Raman spectral imaging complements optical coherence tomography for tumor boundary detection," *Laser Physics Letters* 2014 (Accepted).

9318-6, Session 2

Tissue classification and diagnostics using a fiber probe for combined Raman and fluorescence spectroscopy

Riccardo Cicchi, Istituto Nazionale di Ottica (Italy) and European Lab. for Non-linear Spectroscopy (Italy); Suresh

Anand, European Lab. for Non-linear Spectroscopy (Italy); Alfonso Crisci, Univ. degli Studi di Firenze (Italy); Flavio Giordano, Azienda Ospedaliera Univ. Anna Meyer (Italy); Susanna Rossari M.D., Vincenzo De Giorgi, Vincenza Maio, Daniela Massi, Gabriella Nesi, Anna Maria Buccoliero, Marco Carini, Univ. degli Studi di Firenze (Italy); Renzo Guerrini, "Anna Meyer" Pediatric Hospital (Italy); Nicola Pimpinelli, Univ. degli Studi di Firenze (Italy); Francesco S. Pavone, European Lab. for Non-linear Spectroscopy (Italy) and Univ. degli Studi di Firenze (Italy)

Two different optical fiber probes for combined Raman and fluorescence spectroscopic measurements were designed, developed and used for tissue diagnostics. Two visible laser diodes were used for fluorescence spectroscopy, whereas a laser diode emitting in the NIR was used for Raman spectroscopy. The two probes were based on fiber bundles with a central multimode optical fiber, used for delivering light to the tissue, and 24 surrounding optical fibers for signal collection. Both fluorescence and Raman spectra were acquired using the same detection unit, based on a cooled CCD camera, connected to a spectrograph. The two probes were successfully employed for diagnostic purposes on various tissues in a good agreement with common routine histology. This study included skin, brain and bladder tissues and in particular the classification of: malignant melanoma against melanocytic lesions and healthy skin; urothelial carcinoma against healthy bladder mucosa; brain tumor against dysplastic brain tissue. The diagnostic capabilities were determined using a cross-validation method with a leave-one-out approach, finding very high sensitivity and specificity for all the examined tissues. The obtained results demonstrated that the multimodal approach is crucial for improving diagnostic capabilities. The system presented here can improve diagnostic capabilities on a broad range of tissues and has the potential of being used for endoscopic inspections in the near future.

9318-7, Session 2

Targeted detection and risk stratification of breast lesions using spectroscopy-based characterization of microcalcifications

Ishan Barman, Johns Hopkins Univ. (United States); R. Sathyavathi, Anushree Saha, Case Western Reserve Univ., School of Medicine (United States); Ramachandra R. Dasari, Massachusetts Institute of Technology (United States); Maryann Fitzmaurice, Case Western Reserve Univ., School of Medicine (United States)

Integration of optical spectroscopy, analytical chemistry and pattern recognition methods are driving the development of biophotonic systems that have the capacity to elucidate latent information of a diverse array of pathophysiological conditions. This talk will focus on our pursuit of a combination of optical modalities for the real time characterization of breast cancer lesions at the patient bedside. Given the inability of existing techniques to accurately diagnose benign and malignant lesions, we have proposed a spectroscopy-based real-time guidance mechanism for biopsy procedures. Subjective assessments are replaced, in this paradigm, by spectroscopy-based quantitative recognition permitting high throughput, observer-invariant diagnosis. In this talk, we report the first application of Raman spectroscopy for determining the nature of breast lesion (pathological grade of disease) via characterization of the associated calcified cluster (microcalcifications) at stereotactic biopsy. Using a diagnostic algorithm developed from the contributions of the chemical-morphological model constituents, the composite Raman information acquired from the freshly excised tissue cores was translated to provide quantitative measures of the chemical makeup of the lesion. Our results show even using a fiber-probe for bulk tissue spectroscopy (which considerably increases the overall sampling volume to microcalcification ratio), one can reliably determine the higher carbonate intercalation in

**Conference 9318: Optical Biopsy XIII:
Toward Real-Time Spectroscopic Imaging and Diagnosis**

hydroxyapatite lattice of type II microcalcifications associated with benign breast lesions (such as fibrocystic change and fibroadenoma) as opposed to in situ and invasive carcinomas. Our findings outline the feasibility of using calcium carbonate, a little studied constituent of breast microcalcifications, as a diagnostic and potentially a prognostic marker in breast pathology.

9318-8, Session 3

Time resolved fluorescence spectroscopy using a single fiber probe for fluorescence lifetime assessment in real-time

Fartash Vasefi, David S. Kittle, Keith L. Black M.D., Pramod V. Butte, Cedars-Sinai Medical Ctr. (United States)

Time resolved fluorescence spectroscopy (TRFS) has the potential to identify tumors intra-operatively. Most TRFS systems use a fiber bundle with separate excitation and collection fibers. A single fiber utilizes the same fiber for excitation and collection of fluorescence. Transitioning from a fiber bundle to a single optical fiber probe will allow integration of TRFS with smart surgical tools. However, the excitation laser causes interference from auto-fluorescence of the fiber getting mixed with the weak fluorescence signal from the target. This can be minimized by utilizing a fiber with low auto-fluorescence and quantifying the auto-fluorescence of the fiber against the fluorescence from the biological tissues. We present the auto-fluorescence data from commercially available high (hydroxyl groups) OH fibers at different core sizes (e.g. FDP and FVP-UVMI, Polymicro) and compare it with fluorescence from intrinsic biological fluorophores such as Collagen I-IV, FAD, NADH, Riboflavin, and Pyridoxine in PBS.

The excitation light from the laser (355nm, 400ps, 5 uJ/pulse) is delivered to the fluorophores and collected using a single fiber. This fiber is coupled to a custom demuxer to split the spectral channels into 6 discrete wavelength bands from 360nm to 700 nm and a custom fiber delay unit then delays the output of each spectral band before being combined onto the photomultiplier tube (MCP-PMT, 80 ps rise time), and a digitizer to transfer the fluorescence lifetime measurements to a computer.

We will demonstrate the effect of fiber auto-fluorescence on the biological fluorescence and present a method to correct the interference of fiber auto-fluorescence.

9318-9, Session 3

Fluorescence lifetime spectroscopy for breast cancer margins assessment (*Invited Paper*)

Dimitris S. Gorpas, Hussain Fatakdawala, Yanhong Zhang, Richard Bold, Laura Marcu, Univ. of California, Davis (United States)

During breast conserving surgery (BCS), which is the preferred approach to treat most early stage breast cancers, the surgeon attempts to excise the tumor volume, surrounded by thin margin of normal tissue. The intra-operative assessment of cancerous areas is a challenging procedure, with the surgeon usually relying on visual or tactile guidance. This study evaluates whether time-resolved fluorescence spectroscopy (TRFS) presents the potential to address this problem. Point TRFS measurements were obtained from 19 fresh tissue slices (7 patients) and parameters that characterize the transient signals were quantified via constrained least squares deconvolution scheme. Fibrotic tissue (FT, n=69), adipose tissue (AT, n=76), and invasive ductal carcinoma (IDC, n=27) were identified in histology and univariate statistical analysis, followed by multi-comparison test, was applied to the corresponding lifetime data. Significant differentiation between the three tissue types exists at 390 nm and 500 nm bands. The average lifetime is 3.25 ± 0.73 ns for AT, 4.34 ± 0.73 ns for FT and 4.77 ± 0.38 ns for IDC ($p < 0.01$) at 390 nm. Due to the smaller contribution of collagen in AT the average lifetime value is different from FT and IDC.

Additionally, although intensity measurements do not show difference between FT and IDC, lifetime can distinguish them. Similarly, in 500 nm these values are 7.15 ± 1.1 ns, 5.45 ± 0.97 ns and 4.43 ± 0.81 ns correspondingly ($p < 0.01$) and this contrast is due to differentiation in retinol or flavins relative concentration, mostly contributing to AT. Results demonstrate the potential of TRFS to intra-operatively characterize BCS breast excised tissue in real-time and assess tumor margins.

9318-10, Session 3

Implementing multi-biomarker optical biopsy using fluorescence microendoscopy

Akilan Palanisami, Bryan Q. Spring, Tayyaba Hasan, Massachusetts General Hospital (United States)

High content imaging of multiple biomarkers and tumor cell types in situ using minimally invasive approaches is highly desired for studying dynamic molecular treatment responses and basic cancer biology. Here we present a system that integrates fluorescence microendoscopy, molecular probes, and hyperspectral detection with an 850 micron fiber bundle to accomplish multi-molecular optical biopsy. As proof of concept we unmix fluorescent microspheres with overlapping spectra. This talk will highlight key challenges and solutions for implementing such a system.

9318-11, Session 3

Intraoperative detection of glioma invasion beyond MRI enhancement with Raman spectroscopy in humans

Michael Jermyn, Kelvin Mok, McGill Univ. (Canada); Jeanne Mercier, Ecole Polytechnique de Montréal (Canada); Joannie Desroches, McGill Univ. (Canada); Julien Pichette, Karl Saint-Arnaud, Ecole Polytechnique de Montréal (Canada); Marie-Christine Guiot, Kevin Petrecca, McGill Univ. (Canada); Frédéric Leblond, Ecole Polytechnique de Montréal (Canada)

Cancer tissue is frequently impossible to distinguish from normal brain during surgery. Gliomas are a class of brain cancer which invade into the normal brain. If left unresected, these invasive cancer cells are the source of glioma recurrence. Moreover, these invasion areas do not show up on standard-of-care pre-operative Magnetic Resonance Imaging (MRI). This inability to fully visualize invasive brain cancers results in subtotal surgical resections, negatively impacting patient survival. To address this issue, we have demonstrated the efficacy of single-point in vivo Raman spectroscopy using a contact hand-held fiber optic probe for rapid detection of cancer invasion in 8 patients with low and high grade gliomas. Using a supervised machine learning algorithm to analyze the Raman spectra obtained in vivo, we were able to distinguish normal brain from the presence of cancer cells with sensitivity and specificity greater than 90%. Moreover, by correlating these results with pre-operative MRI we demonstrate the ability to detect low density cancer invasion up to 1.5cm beyond the cancer extent visible using MRI. This represents the potential for significant improvements in progression-free and overall patient survival, by identifying previously undetectable residual cancer cell populations and preventing the resection of normal brain tissue. While the importance of maximizing the volume of tumor resection is important for all grades of gliomas, the impact for low grade gliomas can be dramatic because surgery can even be curative. This convenient technology can rapidly classify cancer invasion in real-time, making it ideal for intraoperative use in brain tumor resection.

**Conference 9318: Optical Biopsy XIII:
Toward Real-Time Spectroscopic Imaging and Diagnosis**

9318-12, Session 4

MUSE: deep UV excitation microscopy for imaging of exogenous fluorophores in tissue with applications in histology and pathology (*Invited Paper*)

Farzad Fereidouni, Ananya Datta Mitra, Univ. of California, Davis (United States); Stavros G. Demos, Lawrence Livermore National Lab. (United States); Richard M. Levenson M.D., Univ. of California, Davis (United States)

Microscopy with UV-sectioning excitation (MUSE) described here is a variation of widefield microscopy that can provide intrinsic optical sectioning performance with freshly excised tissue samples. Deep UV illumination of biological specimens will penetrate only a few microns into the surface of a specimen and can be used to excite many fluorophores simultaneously. The sectioning property of the UV light (as opposed to more conventional illumination in the visible range) obviates the need for additional physical or alternative optical (e.g., confocal) methods for generating acceptable axial resolution.

This method has previously been reported for the detection of endogenous fluorescent molecules in intact preclinical and human tissues for functional and structural characterization. Here we demonstrate the utilization of deep UV excitation (comprising various wavelength bands between 210 and 270 nm) of tissues stained with exogenous fluorophores that provide higher contrast from tissue by selectively labeling specific or general structures. By employing a tunable laser system, UV transitions of fluorophores are employed for excitation, and their visible emission is collected. We demonstrate that this method can be a fast and reliable approach for imaging tissue specimens and may prove to be a good alternative to conventional, time-consuming, histopathology procedures.

9318-13, Session 4

Vessel contrast enhancement in hyperspectral images

Asgeir Bjørgan, Martin Denstedt, Matija Milanic, Lukasz A. Paluchowski, Lise L. Randeberg, Norwegian Univ. of Science and Technology (Norway)

Imaging of vessel structures can be useful for investigation of endothelial function, angiogenesis and hyper-vascularization. The vessel structures imaged in mesoscopic, wide field, hyperspectral images of tissue are frequently challenging to visualize and monitor. The pure vessel signal from deeper vessels is in this case obscured by scattering and absorption from other chromophores. These factors make vessels structures appear unclear and diffuse even in wavelength bands with optimal, natural contrast. To be able to elucidate and interpret hyperspectral vessel images accurately, it is essential to combine statistical, numerical and more physics informed models.

In this study, processing techniques for enhancement of vessel contrast in hyperspectral images of human tissue were investigated. In vivo hyperspectral images collected from human skin and other tissue using two hyperspectral cameras (Hyspex VNIR-1600, Hyspex SWIR-320-me) were processed. Wavelet

processing was used to enhance the contrast between larger vessels and other tissue. In addition, an inverse diffusion model was used to estimate vessel depth, dermal blood content and hemoglobin oxygenation. The vessel contrast enhanced images were run through further enhancement using a multi-scale vesselness filter. The tested methods were found suitable for real-time processing using GPU and CPU parallelization. The presented methods were compared to band ratio metrics and statistical methods such as PCA.

The results show that vessel structures in hyperspectral images can be enhanced and characterized using wavelet techniques, diffusion modeling and filtering.

9318-14, Session 4

Experimental evaluation of a hyperspectral imager for near-infrared fluorescent contrast agent studies

Siri Luthman, Univ. of Cambridge (United Kingdom); Sarah E. Bohndiek, Univ. of Cambridge (United Kingdom) and Cancer Research UK Cambridge Institute (United Kingdom) and CRUK & EPSRC Cancer Imaging Ctr. in Cambridge and Manchester (United Kingdom)

Hyperspectral imagers (HSI) have the potential to combine morphological and spectral information to provide detailed information for high sensitivity readout in biological and medical applications. As HSI provide simultaneous detection in several spectral bands, the technology has significant potential for use in real-time multiplexed contrast agent studies. Examples include tumor detection in intraoperative and endoscopic imaging, as well as histopathology. A multiplexed readout from multiple pathological targets, including cell surface receptors overexpressed in cancer cells, could improve both sensitivity and specificity of tumor identification.

This work evaluates the capability of a commercial, compact and low cost near-infrared hyperspectral imager with 70 spectral bands between 600-900nm for multiplexed fluorescent contrast agent studies. A platform for wide-field reflectance imaging of fluorophore binding to excised tissue sections, with fluorophore specific LED excitation, has been developed. The hyperspectral imaging performance of the platform has been evaluated, including sensor calibration, wavelength band response and spectral response non-uniformity. The applicability of the imaging platform has been demonstrated using a dilution series of Alexa Fluor 594 and Alexa Fluor 647, indicating that a fluorophore concentration of less than a nanomole can be detected. Initial results also show that the HSI can also clearly resolve the emission spectra of the two fluorophores in mixtures of concentrations across several orders of magnitude, indicating high dynamic range performance. These results provide the first demonstration of HSI methods in a multiplexed wide-field fluorescent contrast agent study and yield promising results for the future integration of HSI in clinical applications.

9318-15, Session 4

Fast spectral imaging with reconfigurable spectral bands

Sarfraz Baig, Hui Lu, Guomin Jiang, Michael R. Wang, Univ. of Miami (United States)

Spectral imaging is a technique that acquires 3-D image data cube consisting 2-D spatial image and 1-D spectral information. The added spectral information with fine resolution to the spatial images offers the ability in identifying spectrally unique objects through filtering and processing discrimination with imaging backgrounds. Conventional spectral imaging techniques such as spectral scanning and pushbroom scanning are very slow making them only suitable for imaging stationary or slow moving objects. The tunable filter techniques like acousto-optic tunable filters and liquid-crystal tunable filters suffer from limited acceptance windows and the presence of spectral side lobes. The reported computed-tomography imaging technique is fast in snap-shot image acquisition but is slow in computing spectral image recovery.

Practical spectral imaging applications require dynamic spectral band selection and real-time spectral image acquisition and display. To avoid acquiring a huge number of spectral images due to fine spectral resolution, a spectral zooming concept was introduced earlier by us. The reported moving slit for Fourier transform spectral image acquisition has potential for high speed spectral imaging, but has not yet demonstrated the needed real-time operation. The translational slit movement at higher speed may result in un-tolerable system transverse vibration and related imaging blurring. Herein, we introduce the technique of dual-mirror scanning for fast spectral image acquisition with the slit width used for spectral resolution selection.

**Conference 9318: Optical Biopsy XIII:
Toward Real-Time Spectroscopic Imaging and Diagnosis**

The dual-mirror scanning can minimize optical system aberration yet is extremely fast. The spectral imaging has been used to image the fundus of a rat eye showing desirable performance.

9318-16, Session 4

Discrimination of premalignant conditions of oral cancer using Raman spectroscopy of urinary metabolites

Brindha Elumalai, Ramu Rajasekaran, Prakasarao Aruna, Anna Univ. Chennai (India); Dornadula Koteeswaran, Meenakshi Ammal Dental College & Hospital (India); Singaravelu Ganesan, Anna Univ. Chennai (India)

Oral cancers are considered to be one of the most commonly occurring malignancy worldwide. Over 70% of the cases report to the doctor only in advanced stages of the disease, resulting in poor survival rates. Hence it is necessary to detect the disease at the earliest which may increase the five year survival rate up to 90%. Among various optical spectroscopic techniques, Raman spectroscopy has been emerged as a tool in identifying several diseased conditions, including oral cancers. Around 30 - 80% of the malignancies of the oral cavity arise from premalignant lesions. Hence, understanding the molecular/spectral differences at the premalignant stage may help in identifying the cancer at the earliest and increase patient's survival rate. Among various bio-fluids such as blood, urine and saliva, urine is considered as one of the diagnostically potential bio-fluids, as it has many metabolites. The distribution and the physiochemical properties of the urinary metabolites may vary due to the changes associated with the pathologic conditions. The present study is aimed to characterize the urine of 70 healthy subjects and 51 pre-malignant patients using Raman spectroscopy under 785 nm excitation, to know the molecular/spectral differences between healthy subjects and premalignant conditions of oral malignancy. Principal component analysis based Linear discriminant analysis were also made to find the statistical significance and the present technique yields the sensitivity and specificity of 86.3% and 92.9% with an overall accuracy of 90.9% in the discrimination of premalignant conditions from healthy subjects urine.

9318-34, Session 4

Application of two photon microscope in quantification of blood-brain barrier solute permeability increased by focused ultrasound sonication

Lingyan Shi, Paolo Palacio-Mancheno, Joseph Badami, Da W. Shin, Mn Zeng, Luis Cardoso, Raymond Tu, Bingmei Fu, The City College of New York (United States)

Two Photon Microscopy was applied to quantify the change of Blood-Brain Barrier (BBB) permeability to macromolecular at antibody level, which was induced by focused ultrasound sonication (FUS) together with microbubbles in microvessels. This method provides an accurate in vivo assessment for the transient BBB permeability under FUS.

9318-17, Session PTues

Brain NIR transmission windows for deeper imaging

Lingyan Shi, Laura A. Sordillo, Robert R. Alfano, The City College of New York (United States)

Near-infrared (NIR) region allows for deep penetration and minimal

absorption for 1Photon and 2 Photon imaging through high scattering tissue media. NIR light has conventionally been used through the first NIR optical tissue window with wavelengths from 650 nm to 950 nm. Longer NIR wavelengths have been overlooked a lack of NIR-CCD detectors. The transmission lengths Lt second NIR spectral window from 1,100 nm to 1,350 nm, third window spectral window from 1,600 nm to 1,870 nm and fourth optical window centered at 2,200nm were measure in Brain tissue. Optical attenuation measurements from thin slices of rat brain tissue were obtained in the spectral range from 400 nm to 2,500 nm. Due to a reduction in scattering (blurring light) and minimal absorption, longer attenuation length should give clearer images.

9318-26, Session PTues

Optical Biopsy - a new armamentarium to detect disease using light

Yang Pu, Robert R. Alfano, The City College of New York (United States)

Optical spectroscopy has been considered a promising technique for cancer detection for thirty years because of its advantages over the conventional diagnostic methods of no tissue removal, minimal invasiveness, less time consumption and reproducibility since it's first use in 1984 by Alfano.

Human tissue is mainly composed of extracellular matrix of collagen fiber, proteins, fat, water, and epithelial cells. Tissues contain a number of key fingerprint native endogenous fluorophore molecules: tryptophan, collagen, elastin, reduced nicotinamide adenine dinucleotide (NADH), flavin adenine dinucleotide (FAD) and porohyrins. It is well known that abnormalities in metabolic activity precede the onset of a lot of diseases: carcinoma, diabetes mellitus, atherosclerosis, Alzheimer, and Parkinson's disease, etc. Conceivably the biochemical or morphologic changes that cause the spectra variations would appear earlier than the histological aberration. Therefore, "optical biopsy" holds a great promise as clinical tool for diagnosing early stage of carcinomas and other deceases by combining with available technology (e.g. fibers spectroscopic radiometer, fiber-optic endomicroscope and nasopharyngoscope) for in vivo use.

In this paper, a systematic studies of distinguishing cancerous prostate tissues and/or cells from normal prostate tissues and/or cells by native optical differences such as fluorescence, stokes shift, scattering, Raman, and time-resolved spectroscopy will be reviewed. The underlying physical and biological basis for these optical approaches will be discussed with examples. Many research works may not be covered here due to page limit. The idea is to present some of the salient works to show the usefulness and methods of Optical Biopsy for cancer detection.

9318-27, Session PTues

Nonnegative constraint analysis of key fluorophores within human breast cancer using native fluorescence spectroscopy excited by selective wavelength of 300 nm

Yang Pu, The City College of New York (United States); Laura A. Sordillo, City College of New York (United States); Robert R. Alfano, The City College of New York (United States)

Native fluorescence spectroscopy offers an important role in cancer discrimination. It is widely acknowledged that the emission spectrum of tissue is a superposition of spectra of various salient fluorophores. However, the components quantification is essentially an ill-posed problem.

To address this problem, the native fluorescence spectra of human cancerous and normal breast tissues excited by selected wavelength of 300 nm are used to investigate the key fluorophores tryptophan and NADH. The basis spectra of these key fluorophores' contribution to the tissue emission

Conference 9318: Optical Biopsy XIII: Toward Real-Time Spectroscopic Imaging and Diagnosis

spectra are obtained by Principal component analysis (PCA). The emission spectra of human cancerous and normal tissue samples are projected onto the fluorophore spectral subspace. Since previous studies indicate that tryptophan and NADH are key-fluorophores related with tumor evolution, it is essential to obtain their information from tissue fluorescence but discard the redundancy. To evaluate the efficacy of for cancer detection, a support vector machine (SVM) classifier is trained in the subspace to evaluate the sensitivity, and specificity. This research demonstrates that the native fluorescence spectroscopy measurements are effective to detect changes of fluorophores' compositions in tissues due to the development of cancer.

9318-28, Session PTues

Validation of hierarchical cluster analysis for identification of bacterial species using 42 bacterial isolates

Meron Y. Ghebremedhin, Shubha Yesupriya, Nicole J. Crane, Naval Medical Research Ctr. (United States); Janos Luka, Naval Medical Research Center (United States)

Recent studies have demonstrated the potential advantages of the use of Raman spectroscopy in the biomedical field due to its rapidity and noninvasive nature. We are particularly interested in using Raman spectroscopy to classify bacterial isolates. In this study, Raman spectroscopy is applied as a method for differentiating between bacteria on the genus level. We create models for identifying 28 bacterial samples using spectra collected with a 785 nm laser excitation Raman spectroscopic system. In order to investigate the groupings of these samples, partial least squares discriminant analysis (PLS-DA) and hierarchical cluster analysis (HCA) was implemented using MATLAB. Multiple PLS-DA models and HCA methods were examined and included criteria like Ward's method, nearest neighbor and average paired distance. In addition, cluster analyses of the isolates were performed using various data types consisting of, biochemical tests, gene sequence alignment, high resolution melt (HRM) analysis and antimicrobial susceptibility tests of minimum inhibitory concentration (MIC) and degree of antimicrobial resistance (SIR). In order to evaluate the ability of these models to correctly classify bacterial isolates using solely Raman spectroscopic data, a set of 14 validation samples were tested on the PLS-DA models and consequently the HCA models. We also performed cluster analysis of the DNA sequences, MICs/SIRs, HRM and biochemistries of all 42 bacterial samples for the purpose of comparison. The initial PLS-DA model classified our Raman spectra data with an overall average of 81.6% at the gram, and genus taxonomic levels. Our ultimate goal is to produce a model that can detect the presence and identity of bacteria in clinical infections. This study clearly demonstrates that the discrimination of bacterial species using Raman spectroscopic data and hierarchical cluster analysis is possible and has the potential to be a powerful point-of-care tool in clinical settings.

9318-29, Session PTues

Tryptophan as biomarker to detect gastrointestinal tract cancer using non-negative biochemical analysis of native fluorescence and Stokes shift spectroscopy

Leana Wang, New York Univ. (United States); Yan Zhou M.D., The General Hospital of the Air Force, PLA (China); Cheng-Hui Liu, The City College of New York (United States); Lixin Zhou M.D., Beijing Cancer Hospital (China); Yong He, Beijing Normal Univ. (China); Yang Pu, Thien-An Nguyen, Robert R. Alfano, The City College of New York (United States)

Optical biopsy (OB) has been found to be a promising diagnostic method.

This report is application of OB method to find out the fingerprints for discrimination of cancerous tissue from normal tissue.

Optical biopsy (OB) has been found to be a promising diagnostic method. This report is application of OB method to find out the fingerprints for discrimination of cancerous tissue from normal tissue.

The native fluorescence and Stokes shift (SS) spectra of twenty-one human colorectal (colon, rectum) and gastric tissues obtained from nine patients were studied in vitro using three selected excitation wavelengths. Each pair of cancerous and normal colorectal and gastric tissue samples were taken from same patient. One hundred and forty-one spectra were analyzed.

The emission spectra of key fluorophores including tryptophan, collagen, elastin, reduced nicotinamide adenine dinucleotide hydrate (NADH), mitochondrial NADH and FAD were identified from the measured fluorescence and SS spectra of colorectal and gastric tissues. Three distinct biomarkers of tryptophan, collagen and NADH were used to differentiate cancerous tissues from the normal tissues. The spectral profiles of tryptophan exhibit in sharp peak in cancerous tissues under 300 nm excitation as compared with normal tissues. This sharp and enhanced feature of tryptophan is also presented in SS spectrum with a $\Delta\lambda = 40$ nm for cancerous tissues. The reduced contribution from collagen and broadening spectral profiles of NADH and mitochondrial NADH were also observed in cancerous tissues under excitation 320 nm and 340 nm.

The preliminary analysis of fluorescence spectra of cancerous and normal tissues by non-negative basic biochemical component analysis model (BBCA) reveals that the content changes of these key components exhibited by the native fluorescence spectroscopy can be used to classify cancer and normal tissues.

9318-30, Session PTues

A comparison study of different excitation wavelengths to determine the relative content of key biomolecules in breast cancer and breast normal tissue

Laura A. Sordillo, Peter P. Sordillo M.D., Yury Budansky, Yang Pu, Robert R. Alfano, The City College of New York (United States)

In this study, fluorescence profiles from breast cancer and breast normal tissue samples with excitation wavelengths at 280 nm and 340 nm were obtained using the conventional LS-50 Perkin-Elmer spectrometer and a novel S3-LED ratiometer unit. Information on optical spectral emission fingerprints of key native organic biomolecules in tissue such as tryptophan, NADH and collagen were acquired from emission intensity peaks at 340 nm, 440 nm and 460 nm. Ratios from these intensity peaks, using single excitation wavelength at 280 nm and conventional methods, were calculated from malignant tissue samples ($R1 = I_{exc280, em340} / I_{exc280, em440}$ and $R2 = I_{exc280, em340} / I_{exc280, em460}$) and normal tissue samples ($R3 = I_{exc280, em340} / I_{exc280, em440}$ and $R4 = I_{exc280, em340} / I_{exc280, em460}$). Extent of increase from the emission intensity peak at 340 nm was measured from the ratios of cancerous ratios ($R1, R2$) over normal ratios ($R3, R4$) to give $R5$ and $R6$. These results were compared with the ratios from cancerous tissue samples ($Ra = I_{exc280, em340} / I_{exc340, em440}$ and $Rb = I_{exc280, em340} / I_{exc340, em460}$) and normal tissue samples ($Rc = I_{exc280, em340} / I_{exc340, em440}$ and $Rd = I_{exc280, em340} / I_{exc340, em460}$) using dual excitation wavelengths at 280 nm and 340 nm. Fluorescence ratios from normal and malignant cancerous tissues from different breast cancer patients, demonstrated by increased in $R5$ and $R6$ and by increased in $R5$ and $R6$ correlate strongly with increased tryptophan levels regardless of excitation emission intensity similar correlations with tumor characteristics were obtained with both methods. This suggests that dual excitation wavelengths may be as effective as single excitation wavelength in calculating the relative content of biomolecules in tissue.

**Conference 9318: Optical Biopsy XIII:
Toward Real-Time Spectroscopic Imaging and Diagnosis**

9318-31, Session PTues

Real-time Raman sensing without spectrometer

Dinesh Kumar, Ulsan National Institute of Science and Technology (Korea, Republic of); Young Heon Kim, Ulsan National Institute of Science and Technology (Korea, Republic of); Timothy K. Yang, Ulsan National Institute of Science and Technology (Korea, Republic of) and Ctr. for Soft and Living Matter, Institute of Basic Science (Korea, Republic of); Sungho Kim, Ulsan National Institute of Science and Technology (Korea, Republic of); Sung Chul Bae, Ulsan National Institute of Science and Technology (Korea, Republic of) and Ctr. for Soft and Living Matter, Institute of Basic Science (Korea, Republic of); Min Ju Kim, Pohang Univ. of Science and Technology (Korea, Republic of)

Raman spectroscopy has been a powerful tool in various fields of science and technology ranging from analytical chemistry to biomedical imaging. In spite of unique features, Raman spectroscopy has also some limitations. Among them are 1) weak Raman signal compared to strong fluorescence and 2) relatively complicated setup with expensive and bulky spectrometer. In order to increase the sensitivity of Raman technique, many clever attempts have been made and some of them were very successful including CARS, SRS, and so on. However, these still requires expensive and more complicated setup. In this work, we have attempted to build a real-time compact Raman sensor without spectrometer. Conventional spectrometer was replaced with a narrow-band optical filter and alternatively modulated two lasers with slightly different wavelengths. At one laser, Raman signal from a target molecule was transmitted through the optical filter. At the other laser, this signal was blocked by the optical filter and could not be detected by photon detector. The alternative modulation of two lasers will modulate the Raman signal from a target molecule at the same modulation frequency. This modulated weak Raman signal was amplified by a lock-in amplifier. The advantages of this setup includes compactness, low cost, real-time monitoring, and so on. We have tested the sensitivity of this setup and we found that it doesn't have enough sensitivity to detect single molecule-level, but it is still good enough to monitor the change of major chemical composition in the sample.

9318-32, Session PTues

Resonant Raman spectra of grades of human brain glioma tumors reveal the content of tryptophan

Yan Zhou M.D., The General Hospital of the Air Force, PLA (China); Cheng-Hui Liu, IUSL, The City College of New York (United States); Lixin Zhou M.D., Beijing Cancer Hospital (China); Ke Zhu, Yulong Liu, Institute of Physics (China); Lin Zhang, The City College of New York (United States); Susie Boydston-White, The City College of New York (United States) and Borough of Manhattan Community College (United States); Gangge Cheng M.D., The General Hospital of the Air Force, PLA (China); Das Bidyut, Fairfield Univ. (United States); Yang Pu, Robert R. Alfano, The City College of New York (United States)

Researchers have indicated that heterocyclic amino acid tryptophan plays a key factor during the metabolic process in the human brain gliomas. This report indicates that tryptophan is produced in human gliomas and it is involved in tumor progression. L-tryptophan catabolism and its metabolites may completely block the immune function. This report is to present the

relative contents of tryptophan (W) in various grades of glioma tumors by Resonance Raman (RR) spectroscopy method.

RR spectra of normal brain tissues and grade III and IV malignant glioma tumors and lower grade I and II gliomas were observed by confocal micro Raman spectrometer with excitation wavelength of 532nm. Fifteen glioma tumors samples including three astrocytomas, which were obtained from thirteen patients, forty three RR spectra were analyzed.

This study results: (1). The RR spectra characteristic molecular peaks of normal brain tissue arise at 1157cm⁻¹ and 1521cm⁻¹ which proposed arising from carotene. (2). The RR spectra of key fingerprints of tryptophan for main vibrational modes at 1588cm⁻¹, 1554cm⁻¹, 1357cm⁻¹, 1007cm⁻¹ and 753cm⁻¹ were observed. (3). Tryptophan contribution was accumulated in gliomas from grade I to IV gliomas was investigated. The special calculation for peak intensity of mode at 1588 cm⁻¹ in grade IV malignant gliomas were enhanced by resonance and reached the maximum 27 times higher than in grade I glioma. (4). the results proved that tryptophan content increased during its catabolism pathway in gliomas by optical spectroscopy method. RR fingerprints of tryptophan can be used to detect brain glioma tumors in different grades.

9318-33, Session PTues

Automation of a dispersive Raman spectrometer using LabVIEW aiming in vivo diagnosis of skin cancer

Landulfo Silveira Jr., Giovanni Schettino, Camilo Castelo Branco Univ. (Brazil); Ailson N. Campos, Instituto de Aeronáutica e Espaço (Brazil); Renato A. Zângaro M.D., Marcos T. Pacheco, Univ. Camilo Castelo Branco (Brazil); Carlos A. Pasqualucci M.D., Faculdade de Medicina, Univ. de São Paulo (Brazil)

The development of optical techniques for minimally or non-invasive diagnosis of human tumors, and consequent discrimination between malignant, benign and normal tissues, can lead to rapid tumor diagnosis in situ with high sensitivity and specificity. Integrated optical systems that perform automated collection of spectra and provide diagnostic information in vivo in real time is a challenge for modern medicine. This work aimed to automate the spectra collection of a dispersive Raman spectrometer for use in in vivo experiments of skin cancer diagnosis. The routine of data collection, storage, pre-processing and processing of spectral data was developed within the Scientific Imaging Toolkit (Roper Scientific) under the computational environment LabVIEW (National Instruments), which has virtual instruments to control the excitation parameters (laser power), spectrometer (exposure time, number of accumulations), pre-processing signals (cosmic rays filtering, removal of fluorescence background and normalization) and spectral analysis (spectral models based on PCA and tissue biochemistry) in real time. The "RamanLife" routine allowed the use of the Raman spectrometer in procedures for skin tumors removal, with the estimation of the relative amount of basal compounds that constitute the biological tissues, such as lipids, phospholipids, proteins, amino acids, nucleic acids among others, is obtained during the collection of spectra. This provided reliable diagnostic information useful to differentiate between neoplastic, benign and normal tissues, offering the possibility of routine use in clinical diagnosis and in supporting histopathological evaluation for neoplastic skin lesions in vivo in real-time, avoiding unnecessary incisional biopsies and thus enabling assessments in large population groups.

9318-35, Session PTues

Q plate 4F phase mask microscopy for edge enhancement in life science media

Richard Gozali, Thien-An Nguyen, Robert R. Alfano, The City College of New York (United States)

**Conference 9318: Optical Biopsy XIII:
Toward Real-Time Spectroscopic Imaging and Diagnosis**

Orbital Angular Momentum beams with $L = 1$? from Q-plates are used to enhance images of biological cells and letters at the Fourier plane in a 4F lens system. The process of producing a beam with OAM from the Q-plate alters the spatial frequencies in a way enhancing the edges of the image. This work demonstrates that components within cell structure in bright field can be imaged to improve the quality of microscopic images.

9318-18, Session 5

Biophotonics of skin: method for correction of deep Raman spectra distorted by elastic scattering

Blandine Roig, Anne Koenig, François Perraut, CEA-LETI (France); Olivier Piot, MéDIAN Biophotonique et Technologies pour la Santé, Univ. de Reims Champagne-Ardenne (France); Cyril Gobinet, Michel Manfait, MéDIAN Biophotonique et Technologies pour la Santé, Univ. de Reims Champagne-Ardenne (France); Jean-Marc Dinten, CEA-LETI (France)

Confocal Raman microspectroscopy allows in-depth molecular and conformational characterization of biological tissues non-invasively. Unfortunately, spectral distortions occur due to elastic scattering. Our objective is to correct the attenuation of in-depth Raman peaks intensity by considering this phenomenon, enabling thus quantitative diagnosis.

In this purpose, we developed PDMS phantoms mimicking skin optical properties. An optical system based on a fibers bundle has been previously developed for in vivo skin characterization with Diffuse Reflectance Spectroscopy (DRS). Used on our phantoms, this technique allows checking their optical properties: the targeted ones were retrieved.

Raman microspectroscopy was performed using a commercial confocal microscope. Depth profiles were constructed from integrated intensity of some specific PDMS Raman vibrations. Acquired on monolayer phantoms, they display a decline which is increasing with the scattering coefficient. Furthermore, when acquiring Raman spectra on multilayered phantoms, the signal attenuation through each single layer is directly dependent on its own scattering property. Therefore, determining the optical properties of any biological sample, obtained with DRS for example, is crucial to correct properly Raman depth profiles.

A model, inspired from S.L. Jacques's expression for Confocal Reflectance Microscopy and modified at some points, is proposed and tested to fit the depth profiles obtained on the phantoms as function of the reduced scattering coefficient.

Consequently, once the optical properties of a biological sample are known, the intensity of deep Raman spectra distorted by elastic scattering can be corrected with our reliable model, permitting thus to consider quantitative studies for purposes of characterization or diagnosis.

9318-19, Session 5

Noise removal of Raman spectra with extremely low signal to noise ratio

Shuo Chen, Xiaoqian Lin, Clement Yuen, Nanyang Technological Univ. (Singapore); Saraswathi Padmanabhan, Roger W. Beuerman, Singapore Eye Research Institute (Singapore); Quan Liu, Nanyang Technological Univ. (Singapore)

Raman spectroscopy is a powerful non-destructive technique for qualitatively and quantitatively characterizing materials. However, noise often obscures interesting Raman peaks due to the inherently weak Raman signal, especially in biological samples. In this study, we develop a method based on spectral reconstruction to recover Raman spectra with low signal-

to-noise ratio (SNR). The synthesis of narrow-band measurements from low-SNR Raman spectra eliminates the effect of noise by integrating the Raman signal along the wavenumber dimension, which is followed by spectral reconstruction based on Wiener estimation to recover the Raman spectrum with high spectral resolution. A total of 25 agar phantoms and 20 bacteria samples were measured to validate our method. Four commonly used de-noising methods in Raman spectroscopy, i.e. Savitzky-Golay algorithm, finite impulse response filtration, wavelet transform and factor analysis, were also evaluated on the same set of data in addition to the proposed method for comparison. The proposed method showed the superior accuracy in the recovery of Raman spectra from measurements with extremely low SNR, compared with the four commonly used de-noising methods.

9318-20, Session 5

Inhibition of cellular respiration with a femtosecond laser via impulsive stimulated Raman scattering

Chieh Han Lu, Kung Hsuan Lin, Academia Sinica (Taiwan); Kong Thon Tsen, Arizona State Univ. (United States); Yung Shu Kuan, Institute of Biological Chemistry, Academia Sinica (Taiwan)

Visible femtosecond laser is shown to be capable of selectively inactivating a wide spectrum of microorganisms through Impulsive Stimulated Raman Scattering (ISRS) process. However, the mechanism of how femtosecond laser affects the viability of bacteria is still elusive. In this study, the inhibition of aerobic cellular respiration of Escherichia coli (E. coli) induced by low power visible femtosecond laser has been studied. Our results showed that a brief femtosecond laser treatment was capable to induce a reduction of 75% of the glucose dependent respiratory rate by maneuvering a laser which has $\lambda = 415$ nm and a pulse width of 100 fs. Moreover, enzymatic assays indicated that respiratory enzymes involving in the E. coli electron transport chain exhibited divergent susceptibility after laser irradiation. This interruption of cellular respiration after a short irradiation is presumed to be a dominant effect on the early stage of bacteria inactivation. Also, our work demonstrates that by using a low power visible femtosecond laser, the cellular metabolism can be interrupted by shining laser pulses onto living bacteria. These finding may shed a light on the developing of new technique in the study of respiratory metabolism of living microorganism.

9318-21, Session 6

Image enhancement of surface micro-structure on mucosa for polarimetric endoscopy (Invited Paper)

Katsuhiko Kanamori, Panasonic Corp. (Japan)

It is important to observe the surface micro-structure on the mucosa with an endoscope. However, it is difficult to observe the micro-structure under the ordinary white light due to its translucent optical characteristics. Therefore an invasive method such as spraying blue indigocarmine fluid from the tip is used to make visible the structure. The objective of this study is to develop a novel technique that can observe the micro-structure of mucosa clearly using non-invasive imaging.

The subtracted polarization technique using the polarized lighting and polarized imaging is newly applied for this objective.

Two pairs of parallel and crossed nicol polarimetric images captured under two different linearly polarized lightings, and an averaged subtracted polarization image (AVSPI) is used with a subsequent image processing to enhance the micro-structure. This capturing method has a great advantage to deal with the strong anisotropy of object surface unevenness and to compensate the image degradation due to the simple subtraction under the different two lightings and two optical and sensor characteristics.

**Conference 9318: Optical Biopsy XIII:
Toward Real-Time Spectroscopic Imaging and Diagnosis**

First experiments are executed using the manual experiment setting with ring-type lighting, two rotating polarizers and color camera. Next, an online rigid-type polarimetric endoscope system using a polarized ring-shaped LED and a special three-CCD color polarimetric camera is developed.

Image enhancement experiments using a gastric mucosa of porcine were executed, and pseudo indigocarmine sprayed images were created. These images are better than the result from the conventional color intensity imaging, and this work suggests the effectiveness of polarimetric endoscope for close inspection of mucosa surface.

9318-22, Session 6

Propagation of Laguerre-Gaussian beams in turbid-tissue like scattering medium

Alexander Doronin, Igor V. Meglinski, Univ. of Otago (New Zealand); Robert R. Alfano, The City College of New York (United States)

Presently, there is a growing interest in the Laguerre-Gaussian (LG) donut light, known also as twisted photons, for light-matter interaction. LG beams carry orbital angular momentum of light and the potential of its use in probing and imaging of turbid tissue-like scattering media is of particular interest. We report on the computational studies in which the polarized LG donut beams with different orbital angular momenta are propagating through turbid-tissue like scattering medium. The propagation dynamics of LG beams are analyzed and discussed. Classic phenomena, such as an optical memory effect in scattering media and the orbital angular momentum flip, are clearly observed for the LG beams of different orbital angular momenta backscattered by the media. The results obtained for LG beams are presented in comparison with the results for Gaussian beams propagating in the scattering media of same optical properties.

9318-23, Session 6

Role of helicity reversal in the state of polarization of scattered circularly polarized light

Callum M. Macdonald, Alexander Doronin, Univ. of Otago (New Zealand); Stephen L. Jacques, Oregon Health & Science Univ. (United States); Igor V. Meglinski, Univ. of Otago (New Zealand)

We explore the polarization memory of circularly polarized light scattering within a medium consisting of spherical scattering particles, and attempt to relate the particle sizes to the average state of polarization after an arbitrary number of scattering events. We assess the helicity survival, and demonstrate the contribution to the measured degree of polarization. The proposed model shows excellent agreement with lab measurements conducted using polystyrene micro-spheres, and offers flexibility in applying to many different media and source-detector configurations.

9318-24, Session 6

Classification of normal and precancerous cervical tissues using nonlinear maximum representation and discrimination features (NMRDF) on polarized reflectance data

Seema Devi, Asima Pradhan, Indian Institute of Technology Kanpur (India); Asha Agarwal, Kiran Pandey, Ganesh Shanker Vidhyarthi Memorial Medical College (India)

Reflectance spectroscopy contains information of scatterers and absorbers present inside biological tissues and has been successfully used to diagnose disease. Success of any diagnostic tool depends upon the potential of statistical algorithm to extract appropriate diagnostic features from the measured optical data. In our recent study, we have used the potential of the classification algorithm, Nonlinear Maximum Representation and Discrimination Features (NMRDF) to extract the important diagnostic features from reflectance spectra of normal and dysplastic human cervical tissue. This NMRDF algorithm uses the higher order correlation information in the input data, which is helpful to represent the asymmetrically distributed data and provides the close form solution of the nonlinear transform for maximum discrimination. We have recorded unpolarized, co and cross-polarized reflectance spectra from 350nm to 650nm, illuminating the tissue epithelium with white light source. A total of 98 samples were divided into training and validation data sets. The input parameters were optimized using training data sets to extract the appropriate nonlinear features from the input reflectance spectra. These extracted nonlinear features are used as input for nearest mean classifier to calculate the sensitivity and specificity for both training as well for validation data sets. We have observed that co-polarized components provide maximum sensitivity and specificity compared to cross-polarized components and unpolarized data. This is expected since co-polarized light provides subsurface information while cross-polarized and unpolarized data mask the vital epithelial information through high diffuse scattering.

9318-25, Session 6

Compact supercontinuum sources for biomedical applications (Invited Paper)

Philippe Leproux, XLIM Institut de Recherche (France) and Leukos (France); Vincent Couderc, Claire Lefort, XLIM Institut de Recherche (France)

This talk will review recent developments and demonstrations of compact white-light supercontinuum laser sources. These sources are of high interest for a huge spectrum of applications. In particular, some promising results in the biomedical field will be introduced. These results relate especially to optical coherence tomography (OCT), coherent anti-Stokes Raman scattering (CARS) microspectroscopy and flow cytometry. They were obtained on different biological samples at different scales (cell, microorganism, tissue and organ). All these results suggest interesting prospects regarding the use of compact supercontinuum sources intended for combining several modalities of cell imaging, counting and sorting.

Conference 9319: Optical Tomography and Spectroscopy of Tissue XI

Monday - Wednesday 9-11 February 2015

Part of Proceedings of SPIE Vol. 9319 Optical Tomography and Spectroscopy of Tissue XI

9319-1, Session 1

A MD-NIR interactance based wireless sensing platform for the measurement of a subcutaneous fat thickness: a pilot study

Minseok Lee, Kyoung Su Park, Seung-ha Lee, Sehwan Kim, Dankook Univ. (Korea, Republic of)

This paper presents a new approach for the estimation of a subcutaneous fat thickness, called multi-distance near infrared (MD-NIR) interactance by a wireless sensing platform. MD-NIR interactance is a safe, affordable, noninvasive solution and based on the fundamentals of light absorption, reflection, and near-infrared spectroscopy. In order to measure at several distances at the same time, two light sources with different wavelengths are located at one end of a line followed by eight photo diodes. Two different wavelengths are selected to measure the thickness of fat, one is the pure fat absorption band and the other is the low fat absorption band. Bluetooth Low Energy are adopted as their primary communication protocol as a wireless communication. The Bluetooth Low Energy (BLE) subset incorporates many compelling features in terms of energy efficiency, more flexible topologies, and direct smart mobile interoperability. The measured data from the MD-NIR interactance sensors is wirelessly transmitted to a laptop to be analyzed. The feasibility of the approach and wireless platform is demonstrated using the ex-vivo subcutaneous pig fat layer and the fat-mimicking phantoms. The results confirm the feasibility that our proposed MD-NIR interactance based technique can estimate a subcutaneous fat thickness and also has the potential to provide beneficial measurement for the thickness of subcutaneous fat as well as the difference before and after medical surgery (ex. Liposuction), treatment, exercises and massage.

9319-2, Session 1

Spectral changes in subcutaneous fat with weight loss measured by diffuse optical spectroscopy

Goutham Ganesan, Ylenia Santoro, Robert V. Warren, Anais Leproux, Enrico Gratton, Shaista Malik M.D., Pietro R. Galassetti, Bruce J. Tromberg, Univ. of California, Irvine (United States)

Recent advances in physiology have highlighted the critical role played by adipose tissue (AT) in the development of metabolic and vascular diseases. It is now recognized that changes in AT metabolism and/or structure can alter physiology generally. Subcutaneous AT, given its location and relative homogeneity, is amenable to interrogation by near infrared (NIR) (650-1000 nm) diffuse optical techniques in reflectance mode. We hypothesized that diffuse optical spectroscopy (DOS) could be used to characterize spectral changes in AT absorption in response to changes in metabolic phenotype. We measured AT in 10 adults (4 F) enrolled in a calorie-restriction (CR) based weight loss program at baseline, and following six weeks of CR. DOS is a noninvasive technique that is based on white-light steady-state (SS) measurements and the acquisition of frequency-domain (FD) data at several wavelengths to obtain biochemical information on hemoglobin, bulk lipids and water concentration by NIR tissue absorption and scattering. In order to characterize subtle absorption changes happening during the CR regime, we used a self-referencing differential spectroscopy (SRDS) method. This technique exploits the presence or absence of a spectral absorption signature originated by changes in metabolic phenotype. Preliminary results showed consistent subject-specific spectral absorption signatures in various locations within subjects. The SRDS revealed significant peaks in the wavelength ranges corresponding to lipids and deoxyhemoglobin, indicating

a possible metabolic shift happening early in the course of CR-driven weight loss. Future studies will include measurements at longer time intervals, as well as analysis of a non-dieting control group.

9319-3, Session 1

Non-invasive response monitoring of lymphoma patients treated with chemotherapy, immunotherapy and radiation therapy using diffuse optics

So Hyun Chung, Julien Menko, Univ. of Pennsylvania (United States); Jakub Svoboda M.D., Stephen J. Schuster M.D., Sunita Nasta M.D., John Plastaras M.D., Hospital of the Univ. of Pennsylvania (United States); David R. Busch, The Children's Hospital of Philadelphia (United States); Jennifer M. Lynch, Sarah Grundy, Steven Schenkel, Univ. of Pennsylvania (United States); Madeline E. Winters, The Children's Hospital of Philadelphia (United States); Jerry D. Glickson, Hospital of the Univ. of Pennsylvania (United States); Arjun G. Yodh, Univ. of Pennsylvania (United States)

For the first time, using diffuse optics, we have monitored responses of lymphoma to various therapies. We employed two different diffuse optical spectroscopy (DOS) systems and a diffuse correlation spectroscopy (DCS). Total 17 lymphoma patients and 11 healthy volunteers were measured. The healthy volunteer measurements provided fluctuations of normal tissue values. The kinds of lymphoma tumors measured were mostly non-Hodgkin's lymphoma (N=16) and a few of Hodgkin's lymphoma (N=3) (one patient had two types of lymphoma and two had relapses). Body location wise, measured lymphoma tumors were in the neck (N=11), axilla (N=2), groin (N=4) and chest (N=1). Measurements were performed at pre-treatment, 24-hour post 1st infusion and after every cycle of treatment. For control values, contra-lateral normal side and/or bicep muscles were measured during every measurement. The source-detector separation for DOS was 2.2 cm and DCS was 1, 1.9 and 2.8 cm. Among the cases analyzed, responses to immunotherapy appeared as decrease in oxy- and deoxy-hemoglobin, water, blood flow and relative metabolic rate, and increase in lipid and tissue oxygenation. Responses to radiation therapy were similar except that decrease of oxy-hemoglobin was not apparent. Early responses to immunotherapy demonstrated flare like phenomena: increase in oxy- and deoxy-hemoglobin. This effect was not observed in radiation therapy responders. We successfully predicted a relapse of a radiation therapy patient by showing increase of oxy- and total-hemoglobin concentrations near the end of therapy. Although data analysis is ongoing, these preliminary results suggest successful application of diffuse optics to lymphoma treatment response monitoring.

9319-4, Session 1

Multi-spectral wide field imaging technique for monitoring treatment outcomes in Kaposi Sarcoma and Cushing Syndrome (Invited Paper)

Amir Gandjbakhche, National Institutes of Health (United States)

No Abstract Available

Conference 9319:
Optical Tomography and Spectroscopy of Tissue XI

9319-5, Session 2

Fast computational subject-specific models for real-time diffuse optical imaging of the human brain (*Invited Paper*)

Hamid Dehghani, Xue Wu, The Univ. of Birmingham (United Kingdom); Adam T. Eggebrecht, Silvina L. Ferradal, Joseph P. Culver, Washington Univ. School of Medicine in St. Louis (United States)

Image recovery in Diffuse Optical Tomography (DOT) often relies on the use of model-based reconstruction algorithms, which in the case of a complex volume and large data-set is computationally expensive. In the case of human brain imaging, investigators often rely on models that are a weak approximation of the volume being imaged. We will present results from our NIRFAST toolbox that demonstrates the use of atlas-based modeling that can provide an accurate predictions of light propagation in the volume, which in turn can be used for image reconstruction. Furthermore, we will present novel computational techniques to calculate the image mapping matrix (often referred to as Jacobian or sensitivity matrix) for a full adult head and over 3000 source/detector pairs in minutes. We will present data to demonstrate that for the first time, it is possible to recover functional parameters from full head measurements, real-time, on a subject-specific model that is derived from atlas-based registration methods.

9319-6, Session 2

Atlas-based high-density diffuse optical tomography for imaging the whole human cortex

Xue Wu, The Univ. of Birmingham (United Kingdom); Adam T. Eggebrecht, Washington Univ. School of Medicine in St. Louis (United States); Silvina L. Ferradal, Joseph P. Culver, Washington Univ. School of Medicine in St. Louis (United States) and Washington Univ. in St. Louis (United States); Hamid Dehghani, The Univ. of Birmingham (United Kingdom)

Diffuse optical tomography (DOT) for brain imaging has the potential to be an alternative human brain mapping technique when MRI imaging is not applicable. It recovers tissue chromophore concentrations of brain tissue through measures of light transmission to monitor for example the resting-state brain dynamics. This imaging technique relies on simulation of the light propagation which can be generated based on a subject-specific model. There has been some study on using rigid atlas models as alternatives for model based DOT when subject-specific anatomical data is not available; but there is still a lack of detailed analysis between geometrical accuracy and internal light propagation in tissue for atlas-based DOT. This work is focused on High-Density DOT (HD-DOT) of the whole cortex based on atlas models from 11 different rigid registration algorithms across 24 subjects, and the results are evaluated in 19 areas of the human head. The correlation between geometrical surface error and internal light propagation errors is strong in most area but varies in different regions from $R^2 = 0.75$ in the region around top of the head to $R^2 = 0.98$ in the region around the temples. In the 11 registration methods, basic-4-landmark registration with 4mm average surface error and 50% average internal light propagation errors is shown to be the least accurate registration method whereas full-head landmark with non-iterative point to point with 1.5mm average surface error and 32% average internal light propagation error is shown to be the most accurate registration method for atlas-based DOT.

9319-7, Session 2

Evidence of ventricular contamination of the optical signal in preterm neonates with post hemorrhagic ventricle dilation

Jessica Kishimoto, Mamadou Diop, Lawson Health Research Institute (Canada) and Western Univ. (Canada); Peter McLachlan, Western Univ. (Canada) and Lawson Health Research Institute (Canada); David S. C. Lee, London Health Sciences Ctr. (Canada); Sandrine de Ribaupierre, Western Univ. (Canada); Keith St. Lawrence, Lawson Health Research Institute (Canada) and Western Univ. (Canada)

Ventriculomegaly, dilation of the cerebral ventricles, commonly occurs in preterm neonates. This disease can be either congenital in nature, or due to a bleed into the ventricles early in life, known as intraventricular hemorrhage (IVH). Ventriculomegaly can lead to life-long sequelae such as cerebral palsy and epilepsy if progressive ventricular dilation (PVD) develops. There is currently no means of accurately predicting PVD, and the timing of interventions, such as ventricular tapping to remove cerebrospinal fluid (CSF), are not optimal as clinical signs of elevated intracranial pressure are known to lack sensitivity and may delay interventions. NIRS can provide clinicians with more direct measures of brain function, specifically decreases in oxygen saturation or cerebral blood flow, and these may provide a better indication of when an intervention should occur. However, the accuracy of NIRS may be affected by signal contamination from enlarged ventricles, especially if there are blood breakdown products (bbp) in the CSF following IVH. In this study, continuous-wave, broadband NIRS spectra along with ultrasound images were acquired from 35 neonates diagnosed with IVH and/or PVD, and 6 with normal-sized ventricles. Spectra were also acquired from CSF samples obtained during ventricular tapping to investigate the presence of bbp. Compared to normal-sized ventricles, the spectra from PVD/IVH patients exhibited signal changes at 970 and 770 nm likely due to increased water and bbp signals from the enlarged ventricles. These findings explain associated problems with NIRS in IVH patients and highlight the added value of broadband NIRS to resolve the additional chromophores.

9319-8, Session 2

Imaging brain function in children with Autism Spectrum Disorder with diffuse optical tomography

Adam T. Eggebrecht, John R. Pruett Jr., Bradley L. Schlaggar, Steven E. Petersen, John N. Constantino, Joseph P. Culver, Washington Univ. School of Medicine in St. Louis (United States)

Autism Spectrum Disorder (ASD) is a common and currently incurable neurodevelopmental disorder defined by impaired social interactions, altered language function, and repetitive behaviors. ASD affects an estimated 1% of children, and engenders enormous personal, social, and economic costs. Investigating the neuroscience of ASD in childhood is vital because early behavioral and educational interventions starting at 18-24 months of age have been shown to improve outcomes. Neuroimaging studies using functional magnetic resonance imaging (fMRI) have identified specific brain regions whose responses to biological motion perception stimuli are correlated with behavioral metrics of ASD; these responses are potential interventional outcome measures. However, current neuroimaging methods (e.g., fMRI) are limited in ASD due to the constrained imaging environment. Our lab has been developing diffuse optical tomography (DOT) methods that overcome ergonomic limitations of fMRI and image brain function with a wearable cap. The wearability of DOT will allow a fuller assessment of brain function in severely affected children with ASD, exceedingly challenging to study with MRI methods. We present here a

**Conference 9319:
 Optical Tomography and Spectroscopy of Tissue XI**

feasibility study imaging with our high density DOT system school-aged typically developing children (TDC) and sex/age/IQ-matched children with autism (ASD). Both groups of children are able to tolerate imaging for over 30 minutes, and exhibit acceptable raw data quality, and maps of functional brain activity in response to simple language tasks like hearing words and verb generation. Group-matched brain responses of biological motion perception and resting state networks will also be presented.

9319-9, Session 2

Mapping brain function at the bedside during acute stroke recovery using High-Density DOT

Karla M. Bergonzi, Washington Univ. in St. Louis (United States); Adam T. Eggebrecht, Washington Univ. School of Medicine in St. Louis (United States); Andrew Fishell, Jin-Moo Lee, Joseph P. Culver, Washington Univ. in St. Louis (United States)

Stroke is the fourth leading cause of death in the US, and is the leading cause of adult disability. Throughout the acute and sub-acute phases of stroke recovery, early detection of neurological deterioration is essential and close neurological monitoring is critical. Bedside functional neuroimaging has tremendous potential as a diagnostic and prognostic tool to improve critical care. Our lab has developed a portable and wearable high-density diffuse optical tomography (DOT) system which can perform bedside imaging of sensory and motor areas in the occipital, parietal, auditory, and frontal cortices. The imaging cap provides efficient coupling of fiber optics to the scalp by allowing the fiber tips to extend from the inside of the cap by approximately 1mm to comb through the hair. The cap can be fit onto a subject in approximately 10 minutes with a comfort level to allow for over an hour of imaging. Herein we evaluated functional connectivity (fc) DOT imaging as a potential lesion indicator. Concurrent with fcDOT imaging we acquired NIHSS (NIH Stroke Scale) evaluations as a behavioral metric of stroke-induced functional deficit. To compare stroke subjects to healthy subjects we calculated a similarity fcDOT metrics, which compares how similar fc-maps of a single subject are to a healthy population average. In select regions, the similarity metric showed a strong correlation to NIHSS. Building on these results, fcDOT has the potential to serve as a continuous longitudinal surrogate to behavioral exams and to help inform clinical decisions in the initial hours of stroke recovery.

9319-10, Session 3

An optimized near-infrared spectral tomography system for real-time imaging of breast tumor responses during the process of neoadjuvant chemotherapy infusion

Yan Zhao, Fadi El-Ghoussein, Thayer School of Engineering at Dartmouth (United States); Ziqi Zhang, Boston Univ. (United States); Brian W. Pogue, Keith D. Paulsen, Shudong Jiang, Thayer School of Engineering at Dartmouth (United States)

A portable hybrid frequency domain (FD)-continuous wave (CW) Near-Infrared spectroscopy NIRS system has been developed for quantifying changes in total hemoglobin, oxygen saturation and water content in the breast during neoadjuvant chemotherapy. During the imaging sessions, the subject is seated in a reclining position and the breast is surrounded uniformly by an interface of 16 bifurcated fiber bundles. The other 32 ends of these 16 fiber bundles are uniformly connected to a circulating plate of source and detectors. One pair of the two ends is coupled individually to FD and CW light sources while the other ends of pairs of 15 bifurcated fibers

are coupled to PMT and PD detectors, respectively. 12 laser diodes, in the wavelength range of 650-1000 nm, have been divided to two groups, and each group contains 3 CW and 3 FD lasers. For each group, FD and CW data at six wavelengths has been acquired simultaneously by digital lock-in detection. The two groups of laser diodes illuminate the breast sequentially, and the total imaging time for acquiring data from 12 wavelengths for one tomographic plane is less than 1 minute. For validating the imaging stability of the reclining position, a normal subject was imaged. The estimated total hemoglobin, oxygen saturation and water values are 23 uM, 75% and 70%, respectively. These values are in excellent agreement with the data obtained when this subject was positioned prone on an exam table. The study of integrating this system into the workflow of clinical oncology practice is ongoing.

9319-11, Session 3

Dynamic optical tomography for monitoring tumor response in breast cancer patients receiving neoadjuvant chemotherapy

Jacqueline E. Gunther, Emerson Lim, Hyun-Keol Kim, Molly L. Flexman, Lukas Zweck, Columbia Univ. (United States); Susan Refice, Melinda Brown, Herbert Irving Comprehensive Cancer Ctr. (United States); Kevin Kalinsky, Dawn L. Hershman, Columbia Univ. (United States) and Herbert Irving Comprehensive Cancer Ctr. (United States); Andreas H. Hieslcher, Columbia Univ. (United States)

Neoadjuvant chemotherapy (NACT) is widely used for patients with locally advance breast cancer to shrink the size of the tumor and allow for breast conserving surgery. Additionally, a positive response to treatment has been corresponded with higher survival rate. However, patients do not always respond to NACT. We are currently performing a clinical trial that uses dynamic diffuse optical tomography (DDOT) to observe tumor progression throughout NACT. The purpose of the monitoring study is to determine early within the treatment whether the patient will respond to the therapy or not. Therefore, more personalized treatments could be developed to optimize the patient outcome of those who do not respond.

Our DDOT system is capable of 3D imaging of both breasts simultaneously. Each subject receives twelve cycles of paclitaxel every week followed by four cycles of doxorubicin and cyclophosphamide given every other week. Subjects are imaged at 6 time points throughout their treatment: baseline, two weeks, four weeks, before switching chemotherapy agents, two weeks after switching, and before surgery. Patients hold their breath for about 30 seconds during imaging to observe the hemodynamic effects in the breast.

Preliminary results of the first 23 subjects reveal that the hemoglobin washout rate after the breath hold at week 2 is significantly slower for patients who do not receive a pathological complete response (pCR) compared to those who did (p=0.039). Additionally, subjects that had no response to treatment had higher 15-sec post-breath hold %[Hb] values compared to patients that had pCR or partial response (p=0.045).

9319-12, Session 3

Value of diffuse optical imaging in prediction of response after the start of single-agent bevacizumab followed by neoadjuvant chemotherapy for breast cancer patients

Shiget Ueda, Toshiaki Saeki, Hideki Takeuchi, Saitama Medical Univ. (Japan)

Purpose: Diffuse optical spectroscopic imaging (DOSI) has been described

**Conference 9319:
Optical Tomography and Spectroscopy of Tissue XI**

as a method to assess tumor vascularity and oxygenation by measuring tissue hemoglobin concentration. This technology is expected to develop a noninvasive hemodynamic biomarker for predicting of tumor response for an anti-angiogenic drug.

Methods: Breast imaging system using TRS20 (Hamamatsu K.K., Japan) was established in our institute. Nine patients with advanced or metastatic breast cancer were treated with single-agent bevacizumab (5mg/kg) followed by addition of weekly paclitaxel (80mg/m²) to bevacizumab. DOSI was performed baseline and days 1, 3, and 6 after the first infusion of bevacizumab alone and then days 1 and 6 after starting paclitaxel, measuring tumor total hemoglobin concentration (tHb) and oxygen saturation (StO₂). To assess clinical response, MRI, FDG-PET, and FMISO-PET scans were administered at baseline and after 2 cycles of the regimen.

Results: Nine patients were dichotomized as responders (n = 6) and non-responders (n = 3) according to clinical response. Both groups resulted in significant attenuation of tumor mean tHb as early as day 1 after therapy initiation, but the individual response appeared different. Non-responders had relatively lower baseline mean StO₂ level compared with responders and did not improve mean StO₂ after infusion of bevacizumab alone and during addition of paclitaxel to it.

Conclusion: Non-responders had unique feature of StO₂ change at very early point after use of single-agent bevacizumab.

9319-13, Session 3

Tumor vascular reactivity as a marker to predict tumor response to chemotherapy

Songhyun Lee, Myeongsu Seong, Hyeryun Jeong, Jae G. Kim, Gwangju Institute of Science and Technology (Korea, Republic of)

Breast cancer is one of the most common cancers for females. Its treatment efficacy is visualized by monitoring tumor volume changes after treatment using mammography, ultrasound imaging, computed tomography, or magnetic resonance imaging. It can take up to 3 to 4 weeks to observe the treatment effectiveness via anatomical size changes using the aforementioned imaging tools. Therefore, the development of a new method to predict the early outcome of chemotherapy is desired in order to reduce unnecessary treatments and to provide a guide for personalized treatment. In this study, we used a near-infrared spectroscopy (NIRS), along with inhalational gas interventions to observe breast cancer treatment efficacy in rats bearing 13762 MAT B-III breast tumors. We took daily measurements of tumor vascular reactivity by means of changes of oxy-hemoglobin concentration when hypoxic gas condition is altered to a hyperoxic gas condition during tumor growth and chemotherapy. The results showed that the vascular reactivity is well correlated with tumor progression and regression during chemotherapy. In addition, we performed double exponential fitting to the changes of oxy-hemoglobin during gas intervention to find two amplitude values which corresponds to well perfused and poorly perfused region, respectively. All the results indicate the possibility to predict tumor response to chemotherapy earlier than tumor volume changes by way of vascular reactivity monitoring. Our work demonstrates that NIRS has great potential as a monitoring tool for breast cancer treatment efficacy.

9319-14, Session 3

Diffuse optical tomography measured macroscopic physiological and metabolic parameters correlate with microscopic proliferation and vessel area breastcancer biomarkers.

So Hyun Chung, Univ. of Pennsylvania (United States); Michael D. Feldman M.D., The Univ. of Pennsylvania Health

System (United States); Regine Choe, Univ. of Rochester (United States); Daniel Martinez, The Children's Hospital of Philadelphia (United States); Helen Kim, Mary E. Putt, Univ. of Pennsylvania (United States); David R. Busch, The Children's Hospital of Philadelphia (United States); Brian Czerniecki M.D., Julia C. Tchou M.D., Mitchell D. Schnell M.D., Mark A. Rosen M.D., Hospital of the Univ. of Pennsylvania (United States); Angela DeMichele M.D., The Univ. of Pennsylvania Health System (United States); Arjun G. Yodh, Univ. of Pennsylvania (United States)

The goal of this study is to understand how measured optical parameters can complement pathological biomarker information utilized by clinicians for decisions on treatment strategy. In this study on 36 breast cancer cases, we investigate the correlations between macroscopic DOT physiological parameters and microscopic histopathological biomarkers in malignant tumors, i.e., the Ki67 proliferation marker, the CD34 stained vascular properties marker, nuclear morphology, and others. The tumor-to-normal relative ratio of Ki67-positive nuclei is observed to be positively correlated with DOT-measured relative tissue blood oxygen saturation (Correlation: 0.89, p-value: 0.001). Lower tumor-to-normal deoxy-hemoglobin concentration (p-value: 0.01) and lower mammary metabolic rate of oxygen (Correlation=-1, p-value: 0.017) is associated with higher expression level of Ki67-positive nuclei. Further, we find that CD34 stained mean vessel area in tumor is positively correlated with tumor-to-normal total- and oxy-hemoglobin concentrations (Correlation: 0.67, p-value: 0.002 and Correlation: 0.63, p-value: 0.005, respectively). Finally, we observe that cell nuclei tend to exhibit a more elongated shape in the less oxygenated environments, as determined by diffuse optical parameters; this trend was most apparent in a subset of triple-negative cancers. Collectively, our data is consistent with the notion that increased blood is supplied to the more proliferative cancers, but that less conversion of oxy- to deoxy-hemoglobin occurs in these cancers. Overall, the observations corroborate expectations that macroscopic measurement of breast cancer physiology using DOT can reveal microscopic pathological properties of breast cancer and hold potential to complement pathological biomarker information.

9319-15, Session 3

Predicting hormonal therapy response in breast cancer using diffuse optical spectroscopic imaging (DOSI): ongoing clinical study

Thomas D. O'Sullivan, Anais Leproux, Kyle Cutler, George P. Philipopoulos, Alice M. Police, Freddie Combs, Univ. of California, Irvine (United States); Dorota Wisner, Univ. of California, San Francisco (United States); Albert E. Cerussi, Min-Ying Su, Bruce J. Tromberg, Univ. of California, Irvine (United States)

Recent studies have demonstrated that hormonal therapies are more effective at reducing breast cancer risk in women who exhibit >10% reduction in breast density compared to women who had little or no density change, suggesting that breast density is a predictor of tamoxifen effectiveness. The goal of this multi-site prospective study is to validate that diffuse optical spectroscopic imaging (DOSI) can measure the change in breast density caused by hormonal chemotherapy treatments such as tamoxifen.

The primary aim is to determine whether the change in the DOSI measurement of water correlates with the change in the MRI measurement of breast density after 18 months of treatment in the contralateral normal breast of subjects receiving tamoxifen. Pre-menopausal subjects receiving tamoxifen and age-matched controls are being enrolled and measured with DOSI and non-contrast MRI before, and 6, 12 and 18 months after beginning tamoxifen. Out of the target accrual of 36, 11 subjects have been enrolled to

**Conference 9319:
Optical Tomography and Spectroscopy of Tissue XI**

date at the University of California, Irvine and San Francisco.

To enable the study, we developed a whole-breast imaging technique to co-register the 3D breast MRI with the DOSI data. The entire breast is scanned by a handheld probe in a pre-determined grid pattern, which is delineated by multi-modality fiducial markers. The markers provide MRI contrast and allow us to wrap the 2D optical data on the individual 3D MRI contour of the breast. This technique allows us to co-register and evaluate subsurface sources of optical contrast of dense fibroglandular tissue. Preliminary study data will also be presented.

9319-16, Session 4

Multi-modal dynamic breast compression imaging using diffuse optical tomography and x-ray digital breast tomosynthesis (DBT)

Bin Deng, Bernhard Zimmermann, Qianqian Fang, David A. Boas, Massachusetts General Hospital (United States) and Athinoula A. Martinos Ctr. for Biomedical Imaging (United States); Jayne A. Cormier, Daniel B. Kopans, Mansi A. Saksena, Massachusetts General Hospital (United States); Stefan A. Carp, Massachusetts General Hospital (United States) and Athinoula A. Martinos Ctr. for Biomedical Imaging (United States)

While stand-alone optical tomography systems have demonstrated sensitivity to breast cancer, integration of structural prior information has been shown to offer substantial increases in optical contrast and resolution. Taking into account the eventual path to large-scale clinical implementation, we believe the best multi-modal approach is the integration of optical imaging with x-ray mammography (and its recent development, 3D digital breast tomosynthesis (DBT)). To this end, we have recently completed our second generation optical-DBT imaging system with the ability to conduct dynamic optical imaging studies as well as obtain simultaneous co-registered DBT images in conjunction with a Hologic Selenia Dimensions FDA-approved breast DBT scanner. We used a hybrid design that combines a dense 96 source, 32 detector 8Hz continuous-wave imager with a 24 source, 20 detector, 0.2 Hz frequency domain imager. Both systems use 690 and 830 nm laser diode sources. Here, we present preliminary dynamic imaging results on both healthy volunteers and breast cancer patients during fractional and full mammographic compression. We have previously shown that malignant tumors have a distinctive differential behavior vs. the surround normal tissue during compression and that this differential behavior fades away in tumor responding to chemotherapy. As a continuation of this work, we describe the multi-modal compression imaging protocol and summarize our efforts to establish an optimal compression procedure that has the highest sensitivity to the presence of breast lesions.

9319-17, Session 4

Malignant and normal breast tissues present different vascular responses to paced breathing measured by diffuse optical spectroscopy

Anais Leproux, Michael T. Ghijssen, Amanda F. Durkin, Albert E. Cerussi, Bruce J. Tromberg, Beckman Laser Institute and Medical Clinic (United States)

Diffuse optical spectroscopy (DOS) is a non-invasive technique that employs near-infrared (NIR) light to measure functional information several centimeters below the tissue surface. We used DOS to measure hemodynamic differences between healthy and malignant breast tissues

induced by paced breathing. We hypothesize that these changes are the result of an impedance mismatch between the arterial and venous networks in the tumor compared with normal tissue due to the abnormal vascular supply and oxygen consumption of malignant tumors.

DOS data was collected using the PocketNIRS CW instrument (DynaSense Inc., Hamamatsu, Japan) sampling at 30Hz with 3 NIR wavelengths (735, 810 and 850nm). Two NIR probes collected data simultaneously on both breasts of 4 breast cancer patients during paced breathing (up to 7 breathing frequencies ranging from 0.1 to 0.25 Hz). Five similar measurements were obtained in control subjects.

The changes in the relative amplitude and phase of oxyhemoglobin and deoxyhemoglobin oscillations derived from these paced breathing measurements were characterized.

The oxyhemoglobin and deoxyhemoglobin oscillations showed phase differences between areolar (high metabolism) and breast tissue (lower metabolism). We also observed reduced amplitude in deoxyhemoglobin oscillations in tumor compared to normal breast tissue. The amplitude ratio of deoxyhemoglobin to oxyhemoglobin depended upon the breathing frequency in malignant tissues but not in normal tissues. Our data illustrates different vascularity in tumors compared to normal breast tissues. This preliminary study shows the feasibility of characterizing malignant tissues from non-invasive measurement of dynamic vascular changes using DOS.

9319-18, Session 4

Optical mammography instrument for broadband spectroscopy (600-1,000nm), 2D imaging with fine spatial sampling (2mm²2mm), and depth sensitivity

Nishanth Krishnamurthy, Pamela G. Anderson, Jana M. Kainerstorfer, Angelo Sassaroli, Sergio Fantini, Tufts Univ. (United States)

Diffuse optical mammography uses near-infrared light to map breast tissue composition and structure based on measurements of optical absorption and scattering properties. Of particular interest are the tissue concentrations of oxy-hemoglobin, deoxy-hemoglobin, water, and lipids, which carry structural, metabolic, and vascular information relating to the presence of cancer. We have recently developed a new instrument for optical mammography that enhances the spectral and imaging capabilities of the system currently deployed in the clinic for patient measurements. The light source is a 250 W quartz-tungsten-halogen lamp (Oriel-6334NS, Newport) that achieves a temporal stability of emission to within <1%/min and provides continuous spectral coverage from the visible to near-infrared range. A cooled, charged-coupled device (CCD) (PIXIS400, Princeton Instruments) with high quantum-efficiency in the near-infrared (35% at 1,000 nm) allows for spectral collection from 600-1,000 nm. This wavelength range enhances sensitivity to water and lipids. A new motorized stage (Xslide, Velmex) decreases the scan time to 1-2 min per breast in a parallel-plane geometry (tandem raster-scan of illumination and collection optical fibers on opposite sides of a gently compressed breast). Its enhanced stability also reduces the intensity-noise due to scanning to <2.5%. Furthermore, the new instrument implements a new depth sensitivity capability by using multiple off-axis detection optical fibers realized by a four-legged collection optical fiber that is spatially multiplexed onto the CCD chip. We present initial results on tissue-like phantoms and healthy subjects to characterize the performance of our new instrument and to demonstrate its applicability to human subjects.

9319-19, Session 4

Diffuse optical imaging of the breast using structured-light

Jessica Kwong, Farouk Nouizi, Jaedu Cho, Jie Zheng, Yifan

**Conference 9319:
Optical Tomography and Spectroscopy of Tissue XI**

Li, Jeon-Hor Chen, Min-Ying Su, Gultekin Gulsen, Univ. of California, Irvine (United States)

Diffuse optical imaging of the breast using structured-light would allow for rapid, wide-field acquisition of measurements at multiple near infrared wavelengths for spectroscopy. To test the feasibility of structured-light illumination and detection, simulations were performed based on numerical breast phantoms generated from MRI-based segmentations of the fibroglandular tissue within the breast. MR slices of the breast were used to build the mesh geometry in COMSOL. The optical properties of the fibroglandular and adipose tissue were assigned based on their respective water, lipid and hemoglobin content. With the breast mesh, photon diffusion was simulated with an illuminated pattern and measurements were calculated with an integration of a detection pattern at five near infrared wavelengths within the water, lipid and hemoglobin absorption spectrum. Combinations of 12 distinct patterns, consisting of stripes and checkerboards, for illumination and detection allows for 144 point measurements to be obtained. Using these synthetic measurements, a 3D reconstruction of the breast was performed with a Tikhonov minimization. The reconstructed chromophore maps were then compared to the original MR images of the breast. Additionally, an experimental set-up using digital micromirror devices was built and agar phantoms with multiple inclusions were used to test the feasibility of the system. Our near-future aim is to translate this system into the clinical setting. Diffuse optical imaging of the breast with structured-light would provide a quick screening tool for breast cancer while also providing important functional information based on hemoglobin concentration.

9319-20, Session 4

Quantitative oximetry with broadband optical mammography: clinical results

Pamela G. Anderson, Jana M. Kainerstorfer, Nishanth Krishnamurthy, Tufts Univ. (United States); Marc J. Homer, Tufts Medical Ctr. (United States); Angelo Sassaroli, Tufts Univ. (United States); Roger A. Graham, Tufts Medical Ctr. (United States); Sergio Fantini, Tufts Univ. (United States)

We present results on quantitative oximetry of breast cancer using a broadband (650-850 nm), continuous-wave optical mammography instrument. Our system operates in parallel plate geometry, where the breast is scanned on a plane and the transmitted intensity is collected every 2 mm in the x and y directions. We have implemented a diffusion based, homogeneous model to process the optical data and create 2D maps of deoxy- and oxy-hemoglobin, lipid and water concentrations. Twenty-six breast cancer patients have been imaged and we have found the tumor to have increased concentrations of total hemoglobin ($+2.3 \pm 0.4\%$) and water ($+7 \pm 1\%$ v/v) along with a decreased lipid content ($-8 \pm 2\%$ v/v) with respect to the background tissue. Contrary to other findings in the NIRS field, we report hemoglobin saturation to be significantly lower within the tumor region when compared to the background tissue (average decrease of $5 \pm 1\%$). Hemoglobin saturation (SO₂) provides information about the metabolic state of the tissue. Microenvironment studies have found decreased tissue oxygenation (measured by oxygen partial pressure in tissue, pO₂) in tumors, which is due to an increased metabolic demand along with heterogeneous distribution of tortuous angiogenic blood vessels within the tumor. We report our measurement technique and discuss the possible impact that the microenvironment of a tumor may have on the diffuse NIRS measurements.

9319-62, Session PMon

Diffuse correlation spectroscopy (DCS) and diffuse optical spectroscopy (DOS) measurements of blood flow changes from arm cuff ischemia: a comparison study

Zhe Li, Univ. of Pennsylvania (United States) and Tianjin Univ. (China); Steven Schenkel, Wesley B. Baker, Univ. of Pennsylvania (United States); Detian Wang, The Univ. of Pennsylvania (United States) and Institute of Fluid Physics (China); Ashwin B. Parthasarathy, Arjun G. Yodh, Univ. of Pennsylvania (United States)

Quantification of absolute blood flow (BF) in skeletal muscle is important for applications in exercise and sports medicine. Diffuse optical methods including diffuse optical spectroscopy (DOS) and diffuse correlation spectroscopy (DCS) have gained popularity for this application, since they are noninvasive, portable, relatively inexpensive, and can be real-time. DOS can be utilized to derive absolute blood flow using the venous occlusion technique; the rate of increase in concentration of total hemoglobin due to a venous occlusion derives an indirect and one-time estimate of blood flow. Contrastingly, DCS is a new but well validated technology that directly quantifies blood flow continuously. DCS was hence employed to validate changes in blood flow derived using DOS/venous-occlusion, due to a static forearm exercise (3 minutes handgrip of 10 lbs). DCS monitored blood flow changes continuously during the entire experiment, while the DOS/venous-occlusion method was used to estimate absolute blood flow before and during static exercise. The change in blood flow measured by DCS was then compared with the change of absolute blood flow measured by DOS/venous-occlusion. Preliminary results (n=1) from this ongoing study are presented here. During static exercise, DOS/venous-occlusion measured a 55.8% increase in blood flow, which was confirmed by DCS derived increase in blood flow of 55.4%. To the best of our knowledge, this is the first independent validation of the DOS/venous-occlusion method to measure blood flow. Measurements from more subjects will be used to further validate and confirm agreement between the two techniques.

9319-63, Session PMon

In vivo experimental validation for a featured-data time-domain diffuse fluorescence tomography based on the radiative transfer equation

Yan Zhang, Limin Zhang, Tianjin Univ. (China); Huijuan Zhao, Feng Gao, Tianjin Univ. (China) and Tianjin Key Lab. of Biomedical Detecting Techniques and Instruments (China); Jiao Li, Tianjin Univ. (China)

Diffuse fluorescence tomography (DFT) could be applied to in-vivo visualize interior cellular and molecular events for small-animal disease model through quantitatively recovering biodistributions of specific molecular probes. In DFT, when the source-detector separation is less than 5 mean-free-path lengths and where biological tissue has a void-like region, as in the situations of small animal imaging, diffuse approximation of radiative transfer equation (RTE) used as the forward models is unsuited to the situations. Therefore, we present a RTE-based featured-data scheme for time-domain DFT, which combines the discrete solid-angle-element method and the finite element method to obtain numerical solutions of the Laplace-transformed time-domain RTE. The scheme is validated by in-vivo small-animal experiments using a CT-analogous time-domain DFT system, and the reconstructed results are compared to the ones of DE-based scheme.

**Conference 9319:
Optical Tomography and Spectroscopy of Tissue XI**

9319-64, Session PMon

Optimisation of acquisition time in bioluminescence imaging

Shelley L. Taylor, Suzannah Mason, Sophie Grinton, The Univ. of Birmingham (United Kingdom); Mark Cobbold, School of Immunity and Infection, Medical School, University of Birmingham (United Kingdom); Iain B. Styles, The Univ. of Birmingham (United Kingdom); Hamid Dehghani, The Univ. of Birmingham (United Kingdom) and School of Computer Science, Univ. of Birmingham (United Kingdom)

Multispectral imaging data acquisition is highly dependent on system performance and appropriate characterisation. Specifically, data quality and acquisition time depends on the spectral filter used during signal measurement, both in terms of the transmission percentage and bandwidth. Minimising the imaging time is vital when performing pre-clinical imaging as the time which the animals are under anaesthetic is minimised, whilst maximising imaging throughput.

When performing tomographic reconstructions using bioluminescence data, specifically using model-based algorithms, only single narrow width detection wavelengths are considered in the calculation. Reconstruction models do not account for the type of filters used, specifically the range of wavelengths which contribute to the measurement data. This leads to a model-data mismatch which is largely ignored.

This work demonstrates how collecting multi-spectral data using filters of different bandwidths and transmission percentages affects the signal quality, image acquisition time and tomographic source recovery, using both simulated and experimental data. Modification of an existing reconstruction model to account for the filter properties will be presented to demonstrate its effectiveness in quantitative bioluminescence tomography.

9319-65, Session PMon

Development of a multispectral diffuse optical tomography system for earlier diagnosis of rheumatoid arthritis

HaoYang Wu, Hamid Dehghani, The Univ. of Birmingham (United Kingdom); Andrew Filer, The Univ. of Birmingham (United Kingdom) and School of Immunity and Infection (United Kingdom); Iain B. Styles, The Univ. of Birmingham (United Kingdom)

Rheumatoid Arthritis (RA) is a persistent autoimmune disease causing impairment of hand joints. Early stage of progression of the disease is known to change the appearance of the fluid in joint space. Diffusion Optical Tomography is an imaging technique whereby the diffused trans-illuminated light of a region of interest is measured and used to determine spatial distribution of optical properties, based on the 3D finite element model of the region and physical model of light in media. Reconstructed absorption and scattering at a single wavelength has been shown to have a high sensitivity and specificity that associates with changes of RA disease. To further improve the current techniques, we are developing a non-contact multispectral optical imaging system.

Our system is an efficient CW domain system that consists a lens-coupled CCD camera and a filter wheel and optical fibres-coupled halogen light and two mini projectors for surface topology capture. We are able to provide an accurate 3D finite element model (FEM) of a hand based on the digital fringe projection profilometry using projectors and the camera. The system can also achieve raster source scanning and simultaneous spectral measurements of trans-illumination of the light transmitted at the surface of hand. By incorporating spectral information and model based image recovery, our system has a potential to improve achievable sensitivity and

specificity in detecting RA. Spectral constraint reconstruction also improves extraction of tissue oxygenation and hypoxia maps, which provide an important biomarker for early RA disease.

9319-66, Session PMon

High resolution 3D fluorescence tomography using ballistic photon

Jie Zheng, Farouk Nouizi, Jessica Kwong, Gultekin Gulsen, JohnTu & Thomas Yuen Ctr. for Functional Onco-Imaging (United States) and Univ. of California, Irvine (United States)

We are developing a ballistic-photon based approach for improving the spatial resolution of fluorescence tomography using time-domain measurements. This approach uses early photon information contained in measured time-of-flight distributions originating from fluorescence emission. The time point spread functions (TPSF) from both excitation light and emission light are acquired with gated single photon Avalanche detector (SPAD) and time-correlated single photon counting after a short laser pulse. To determine the ballistic photons for reconstruction, the lifetime of the fluorophore and the time gate from the excitation profiles will be used for calibration, and then the time gate of the fluorescence profile can be defined by a simple time convolution. By mimicking first generation CT data acquisition, the source-detector pair will translate across and also rotate around the subject. The measurement from each source-detector position will be reshaped into a histogram that can be used by a simple back-projection algorithm in order to reconstruct high resolution fluorescence images. Finally, from these 2D sectioning slides, a 3D inclusion can be reconstructed accurately. To validate the approach, simulation of light transport is performed for biological tissue-like media with embedded fluorescent inclusion by solving the diffusion equation with Finite Element Method using COMSOL Multiphysics simulation. The reconstruction results from simulation studies confirms that this approach drastically improves the spatial resolution of fluorescence tomography. Moreover, all the results have shown the feasibility of this technique for high resolution small animal imaging up to several centimeters.

9319-67, Session PMon

High-resolution fluorescence molecular tomography in the second near-infrared window

Kan Wang, Xiaoquan Yang, Yong Deng, Hui Gong, Qingming Luo, Huazhong Univ. of Science and Technology (China)

Fluorescence molecular tomography (FMT) is a non-invasive in-vivo imaging technique which can get the localization and quantification information of fluorescence. Light with the wavelengths in the near-infrared (NIR) window from 650 nm to 950 nm has been conventionally chosen for fluorescence molecular tomography (FMT). However, the spatial resolution is very limited in the NIR window. In this study, we introduce longer NIR wavelengths from 1100 nm to 1350 nm, also known as the second NIR window (NIR-II), to FMT. Light in NIR-II have a reduced scattering coefficient and similar absorption coefficient for biological tissues. We acquired the singular-value intensity at the wavelength from NIR to NIR-II, in a simulated phantom. We found that the singular-value intensity will be higher in the NIR-II, which suggests that it may reduce the ill-posedness of inverse problem in FMT. A FMT system combining InGaAs camera and CCD camera for simultaneous imaging in NIR-II and NIR is constructed. The Ag2S quantum dots and DiR are used as fluorophore for NIR-II and NIR, respectively. The phantom studies demonstrated that the resolution and image quality in NIR-II are better than that in NIR. Although the performance of InGaAs camera we used is much lower than that of CCD camera, and the quantum efficiency of the Ag2S is much worse than that of DiR. The superiority of FMT in NIR-II is still obvious.

**Conference 9319:
Optical Tomography and Spectroscopy of Tissue XI**

9319-68, Session PMon

Analysis for nonlinear inversion technique developed to estimate depth-distribution of absorption by spatially resolved backscattering measurement

Kazuhiro Nishida, Hokkaido Univ. (Japan); Takeshi Namita, Kyoto Univ. Graduate School of Medicine (Japan); Yuji Kato, Koichi Shimizu, Hokkaido Univ. (Japan)

We have proposed a new nonlinear inversion technique to estimate the distribution of the absorption coefficient (μ_a) in the depth direction of a turbid medium by spatially resolved backscattering measurement. With this technique, we can obtain cross-sectional image of μ_a as deep as the backscattered light traveled even when the transmitted light through the medium cannot be detected.

In this technique, the depth distribution of absorption coefficient is determined by iterative calculation using the spatial path-length distribution (SPD) as a function of source-detector distance. In this calculation, the variance of path-length of many photons in each layer is also required. The SPD and the variance of path-length are obtained by Monte Carlo simulation using a known reduced scattering coefficient (μ_s'). Therefore, we need to know the μ_s' of the turbid medium beforehand. We have shown in computer simulation that this technique works well when the μ_s' is the typical values of mammalian body tissue, or 1.0 /mm.

In this study, the accuracy of the μ_a estimation was analyzed and its dependence on the μ_s' was clarified quantitatively in various situations expected in practice. 10% deviations in μ_s' resulted in about 30% error in μ_a estimation, in average. This suggested that the measurement or the appropriate estimation of μ_s' is required to utilize the proposed technique effectively. Through this analysis, the effectiveness and the limitation of the newly proposed technique were clarified, and the problems to be solved were identified.

9319-69, Session PMon

Imaging of tissue using a NIR supercontinuum laser light source with wavelengths in the second and third NIR optical windows

Laura A. Sordillo, Lukas Lindwasser, Yury Budansky, The City College of New York (United States); Philippe Leproux, Faculte des Sciences et Techniques (France); Robert R. Alfano, The City College of New York (United States)

Supercontinuum light at wavelengths in the second (1,100 nm to 1,350 nm) and third (1,600 nm to 1,870 nm) NIR optical windows can be used to penetrate more deeply into tissue media. Images can be blurred due to photon scattering and can be distorted due to absorption by biomolecules in tissue such as collagen and elastin, lipids, hemoglobin or deoxyhemoglobin. Penetration depths of light through turbid media are determined by scattering and absorption (Beer-Lambert's intensity law) properties of photons in tissue. At longer wavelengths, image quality is increased due to the inverse wavelength power dependence ($1/\lambda^n$ where $n \geq 1$) and minimal water absorption. We report on the use of a NIR supercontinuum laser light source utilizing wavelengths in the second and third NIR optical windows to image tissue. The supercontinuum laser, Leukos model STM-2000-IR with spectral range from 700 nm to 2,400 nm and between 200-500 microwatt/nm power at the second and third NIR windows, provides an intense light source with a greater number of outgoing photons compared to a halogen lamp light source. With the supercontinuum laser and IR- CCD InGaAs camera detector (Goodrich Sensors Inc. high response camera SU320KTSW-1.7RT with spectral

response between 900 nm and 1,700 nm highlighting the second and third optical windows), images of tissue at various thicknesses overlying 1 mm thick black wires were obtained. The supercontinuum laser with wavelengths from the second and third NIR optical windows can improve penetration depths through tissue and may suggest a better method from imaging abnormalities hidden beneath tissue.

9319-70, Session PMon

Broadband characterization of tissue simulating phantoms using a supercontinuum laser in a scanning diffuse optical spectroscopy instrument

Albert E. Cerussi, Beckman Laser Institute and Medical Clinic (United States); Kevin Conde, Corona de Mar High School (United States) and Beckman Laser Institute and Medical Clinic (United States); Jesse H. Lam, Beckman Laser Institute and Medical Clinic (United States); Vaibhav Verma, Beckman High School (United States) and Beckman Laser Institute and Medical Clinic (United States)

Near Infrared (NIR) optical spectroscopy and imaging technologies are increasingly applied to clinical and pre-clinical applications due to their strong functional sensitivity. These technologies often rely upon calibrations to remove system artifacts. The most common calibration method is to measure a tissue-simulating phantom with known optical properties (absorption and reduced scattering) to remove temporal and/or spatial artifacts from the measured data. While this method can be effective under certain conditions, there is no universal agreement on how to measure calibration phantom optical properties. An independent method for measuring calibration phantom broadband optical spectra is desired, especially without calibration with known optical properties.

We have developed a broadband instrument that recovers the absolute optical properties of phantoms from 620 to 1050 nm. The instrument scans a supercontinuum laser beam across the phantom surface and collects light via a spectrometer-coupled optical fiber. A Monte Carlo algorithm was used to fit the reflectance as a function of source-detector separation and recover absorption and scattering spectra. The only calibration required is a measurement of the laser spot positions on the phantom surface. Spectral constraints were used to create a robust fitting procedure. We demonstrate that the algorithm is capable of recovering accurate absolute scattering and absorption spectra, with better than 10% accuracy using simulated Monte Carlo data. We demonstrate experimental repeatability by measuring the same phantom multiple times and recover spectra with <10% precision across the entire NIR region. We demonstrated experimental accuracy by comparing results with a discrete wavelength frequency-domain instrument calibrated without phantoms.

9319-71, Session PMon

Characterizing infantile hemangiomas with a near-infrared spectroscopic handheld wireless device

Christopher J. Fong, Jennifer W. Hoi, Hyun-Keol Kim, Gerald Behr, Lauren Geller, Nina Antonov, Molly L. Flexman, Maria Garzon, Andreas H. Hielscher, Columbia Univ. (United States)

Infantile hemangiomas (IH) are common vascular growths that occur in 5-10% of neonates and have the potential to cause disfiguring and even life-threatening complications. Currently, no objective tool exist to monitor either progression or treatment of IH. To address this unmet clinical need, we have developed a handheld wireless device (HWD) that uses diffuse

**Conference 9319:
Optical Tomography and Spectroscopy of Tissue XI**

optical spectroscopy for the assessment of IH. The system employs 2 wavelengths ($\lambda=780\text{nm}$, 805nm , 850nm , and 905nm) and 6 source-detector pairs with distances between 0.6 and 20 mm. Placed on the skin surface, backreflection data is obtained and a multispectral evolution algorithm is used to determine total hemoglobin concentration and tissue oxygen saturation. First results of an ongoing pilot study involving 13 patients (average enrollment age = 25 months) suggest that an increase in hypoxic stress over time can lead to the proliferation of IH. Involving IH lesions showed an increase in tissue oxygen saturation as well as a decrease in total hemoglobin.

9319-72, Session PMon

Whole-body temperature modulated fluorescence tomography for small animals

Farouk Nouzi, Tiffany C. Kwong, Jaedu Cho, Univ. of California, Irvine (United States); Uma Sampathkumaran, Yue Zhu, Maksudul M. Alam, InnoSense LLC (United States); Gultekin Gulsen, Univ. of California, Irvine (United States)

Conventional Fluorescence tomography provides us quantitative distribution of fluorescent agents within thick biological tissues. However, the reconstruction of these fluorescence maps is challenging due to the highly scattering nature of these mediums. Previously, we introduced a method termed "Temperature-Modulated Fluorescence Tomography (TM-FT)" that generates fluorescence images at focused ultrasound spatial resolution. The principle of this method is based on scanning the medium with a focused ultrasound (HIFU) while conventional fluorescence tomography measurements are acquired. A sudden temperature increase is observed at the focal spot of the HIFU ($\approx 1\text{ mm}$) positioned up to 6 cm deep in the tissue. The increase in temperature due to the HIFU scanning produces an increase of the emitted fluorescence signal only when temperature sensitive fluorescent agents (ThermoDots) are present within the focal spot of the HIFU. Thus, an accurate map of the distribution of the ThermoDots is generated and used as a-priori to produce high spatial resolution fluorescence maps with high quantitative accuracy in deep tissue using a dedicated image reconstruction algorithm. The major disadvantage of our method was the long data acquisition time using a step and shoot mode. In this contribution, we present a new fast scanning method that drastically reduces the data acquisition time. By continuously scanning the ultrasound beam over a 50 mm by 25 mm field-of-view covering the whole-body of a small animal, we achieved high-resolution fluorescence imaging of the whole sample in less than 30 minutes, which is critical for in-vivo application of our novel TM-FT technique.

9319-73, Session PMon

Monitoring the effect of strength training on muscle structure and metabolism with diffuse optical spectroscopy

Robert V. Warren, Goutham Ganesan, Joshua Cotter, Pietro R. Galassetti, Bruce J. Tromberg, Univ. of California, Irvine (United States)

Diffuse optical spectroscopy (DOS) allows researchers to non-invasively characterize the optical properties of biological tissue. In this study, we used DOS to measure absorption and scattering coefficients at various locations across the human gastrocnemius before and after several strength training regimens. Using measured absorption coefficients, we were able to quantify absolute concentrations of absorbers within the biological tissue. In particular, in this study we quantified oxy- and deoxy-hemoglobin, water, and lipid. Five male subjects were trained for five weeks, where each leg was trained with one of three exercise protocols: low-intensity ($n=3$), high-intensity ($n=4$), and low-intensity with blood flow restriction ($n=3$). A

grid of measurements were taken on each calf, with each grid consisting of 6 rows and 8 columns. Concentrations of absorbers were averaged over all 48 measurements on each leg. The largest changes after training were seen in concentrations of oxy-hemoglobin ($[\text{HbO}_2]$). The low-intensity, high-intensity, and low-intensity training regimens resulted in a 19%, 28%, and 23% increase in $[\text{HbO}_2]$, respectively. Images were created for each grid and color scales were used to depict the quantity of each absorber from each location in the calf. The two heads of the gastrocnemius were easily identified in each image, demonstrating the ability of the DOS technology to sense the heterogeneous structure of the calf. More subjects are being studied in the interim to determine if changes in the concentration of each absorber are isolated to specific areas of the calf.

9319-74, Session PMon

Implementation of 3D prostrate ring-scanning mechanism for NIR diffuse optical imaging phantom validation

Jhao-Ming Yu, Liang-Yu Chen, National Central Univ. (Taiwan); Min-Cheng Pan, Tungnan Univ. (Taiwan); Ya-Fen Hsu, Landseed Hospital, Taiwan (Taiwan); Min-Chun Pan, National Central Univ. (Taiwan)

Diffuse optical imaging (DOI) providing functional information of tissues has drawn great attention for the last two decades. Near infrared (NIR) DOI systems composed of scanning bench, opt-electrical measurement module, system control, and data processing and image reconstruction schemes are developed for the screening and diagnosis of breast tumors. Mostly, the scanning bench belonging to fixed source-and-detector configuration limits computed image resolution to an extent. To cope with the issue, we propose, design and implement a 3D prostrate ring-scanning equipment for NIR DOI with flexible combinations of illumination and detection, and with the function of radial, circular and vertical movement without hard compression of breast tissue like the imaging system using or incorporating with X-ray mammographic bench. Especially, a rotation-sliding-and-moving mechanism was designed for the guidance of source- and detection-channel movement. Following the previous justification for synthesized image reconstruction, in the paper the validation using varied phantoms is further conducted and 3D image reconstruction for their absorption and scattering coefficients is illustrated through the computation of our inhouse coded schemes. The source and detection NIR data are acquired to reconstruct the 3D images through the operation of scanning bench in the movement of vertical, radial and circular directions. Rather than the fixed configuration, the addressed screening/diagnosing equipment has the flexibility for optical-channel expansion with a compromise among construction cost, operation time, and spatial resolution of reconstructed absorption and scattering images.

9319-75, Session PMon

Measuring the functional response of lower back muscles using diffuse optical spectroscopy

Gerard D. Tran, Goutham Ganesan, Mijin Choi, Beckman Laser Institute and Medical Clinic (United States); Todd May, Camp Pendleton (United States); Albert E. Cerussi, Beckman Laser Institute and Medical Clinic (United States)

Lower back pain is a leading cause of disability and remains a common reason for medical consultations. Muscle tissues are heated to increase blood flow with techniques such as therapeutic ultrasound in order to promote healing. Therapeutic ultrasound is commonly employed in order to assist in physical therapy. The effects of therapeutic ultrasound, both thermal and non-thermal, are hard to evaluate due to technology and operator variances and a lack of physiological feedback. Despite widespread

**Conference 9319:
Optical Tomography and Spectroscopy of Tissue XI**

use, there is a surprising lack of evidence for measuring blood flow increases below the skin surface. We present the use of diffuse optical spectroscopy (DOS) to monitor the metabolic changes induced in the lower back by therapeutic ultrasound. In this pilot study, we mapped the back muscles of eight healthy subjects with time-resolved DOS spectroscopy in order to establish a range of expected optical absorption and scattering values. We then used broadband DOS to measure the responses of lower back muscles to heating treatments from a handheld therapeutic ultrasound unit. We observed significant increases in tissue oxyhemoglobin concentration after 10 to 15 minutes of heating with therapeutic ultrasound. We are currently looking at how the hemodynamics of the tissue changes with treatment time in order to characterize the local metabolic effects of therapeutic ultrasound. This preliminary data may serve as a basis for future studies that will investigate tissue responses to therapies in order to enhance treatment effectiveness and promote recovery.

9319-76, Session PMon

Robustness of diffuse optical spectroscopy and imaging (DOSI) system by observing reproducibility of near-infrared absorption and scattering spectra

Mijin Choi, Albert E. Cerussi, Soroush M. Zarandi, Beckman Laser Institute and Medical Clinic (United States)

Diffuse Optical Spectroscopic Imaging (DOSI) is a non-invasive technology that quantified the subsurface compositions and states of hemoglobin, water and lipids. Our DOSI instrument combines frequency-domain and broadband steady-state spectroscopy methods to separate scattering from absorption across the entire near-infrared band (650 to 1000nm). DOSI is undergoing standardization for use in multi-center clinical trials designed to track changes in breast tumor physiology in response to neoadjuvant chemotherapy. Previously we have shown that DOSI technology, with a handheld probe used in the same spirit as conventional ultrasound, is capable of measuring homogeneous tissue-simulating phantoms with a high degree of repeatability across multiple instruments, operators and measurement sites. However, the reproducibility of the imaging capabilities of DOSI technology has not been well characterized. We have tested the imaging precision of the DOSI handheld probe by performing repeat measurements of different tumor-simulating phantoms. The phantoms have an absorbing mass in the center to at different depths below the surface designed to simulate different degrees of contrast between tumor and normal tissues. Phantoms were measured with a 60 x 60 mm grid (10mm spacing) using the DOSI handheld probe. The absorption spectra of “normal” and “tumor” regions of the phantom were extracted in similar fashion to the procedure used in clinical measurements. The absorption and scattering spectra from five imaging sessions overlapped with average of six percent variation over the entire NIR bandwidth. Our data shows that the day-to-day imaging variation is significantly smaller than the typical contrast changes observed in tumors that respond to neoadjuvant chemotherapy.

9319-77, Session PMon

A reduced-space basis function neural network method for diffuse optical tomography

Hyun-Keol Kim, Jacqueline E. Gunther, Jennifer W. Hoi, Andreas H. Hielscher, Columbia Univ. (United States)

Over decades diffuse optical tomographic imaging has seen considerable progress and been widely used as a viable tool to probe biological tissue since it provides a three dimensional distribution of physiologically important parameters such as oxy-hemoglobin (HbO₂) and deoxy-hemoglobin (Hb) in tissue. However, there is still room for improvements.

For example, traditional voxel based image reconstruction methods still suffer from being highly susceptible to random noises, initial guesses, and regularization parameters, which often misleads visual inspection and/or creates difficulties for accurate interpretation of reconstructed images. To overcome these drawbacks of traditional methods, we propose here a reduced space image reconstruction method that makes use of basis function neural network (BFNN) within the framework of PDE-constrained algorithm. This method reduces the solution space using global (or local) basis functions together with the separation of variable technique, and finds the optimal solution through the neural network learning. Basis functions essentially improve the ill-posed nature of the original inverse problem, having the same effect as regularizing the solution space. The proposed method was evaluated on various basis functions in terms of accuracy and speed using numerical simulations and experimental data of breast and foot. The results show that the BFNN method is more robust to both random noise and initial guess, and is also faster than the traditional voxel-based reconstruction method.

9319-78, Session PMon

Optimization of optode assignment in a combined continuous wave and frequency domain tomographic optical breast imaging system

Bernhard Zimmermann, Massachusetts General Hospital (United States) and Athinoula A. Martinos Ctr. for Biomedical Imaging (United States) and Massachusetts Institute of Technology (United States); Matthias C. Hofmann, Massachusetts General Hospital (United States) and Athinoula A. Martinos Ctr. for Biomedical Imaging (United States); Stefan A. Carp, David A. Boas, Qianqian Fang, Massachusetts General Hospital (United States) and Athinoula A. Martinos Ctr. for Biomedical Imaging (United States)

Our second generation tomographic optical breast imaging system consists of two distinct sub-systems, a continuous wave (CW-NIRS) and a frequency domain near-infrared spectroscopy (FD-NIRS) system with 24 sources and 20 detectors, and 96 sources and 32 detectors respectively. To obtain the maximum amount of information per measurement, the sources and detectors of each sub-system have to be assigned optimally to the 120 source and 54 detector optodes of our breast probe.

An exhaustive search over all solutions is not possible due to the prohibitively large number of combinations. Therefore, we decided to use a crowdsourcing strategy to find the optimal assignment. A website was set up to allow lab members to submit their choices of optode assignments, and a competition was started where the best solution would win a prize. Scoring was based on the slope of the singular spectrum of the Jacobian matrix, a measure of the ill-posedness of the system. Participants had access to the scoring function, so it was also possible for them to create custom optimization algorithms besides just manually picking solutions.

Nine participants submitted over 1000 probe designs. The best result was achieved by using a genetic algorithm. The algorithm starts with a random distribution, then generates 100 children by random permutation of a pair of optodes. The 10 best out of the 100 are then used as the seed for the next generation. This algorithm finds solutions with scores that approach the absolute upper bound and are significantly higher than manually found solutions.

**Conference 9319:
Optical Tomography and Spectroscopy of Tissue XI**

9319-79, Session PMon

Comparison of linear reconstruction technique for diffuse optical tomography in in-vitro experiment

Tanju Mercan, Hüseyin Özgür Kazancı, Murat Canpolat, Akdeniz Üniv. (Turkey)

Previously, David Boas et al worked simulation experiment in diffuse optical tomography (DOT). In the simulations, they compared the linear reconstruction techniques. In our works, we also compare the linear reconstruction techniques such as SIRT, truncated SVD, and CG using the data obtained in-vitro experiments. In DOT system we use 808 nm laser source. There are 49 source fibers and 49 detector fibers on the prob. All the source and detector fibers of the probe are located on a 10x10 grid. Fibers on the prob were designed like chess board shape. There are 22 different source-detector neighborhoods. The smallest distance between the first neighborhood is 3 mm, and the largest is 36.1 mm. Penetration of the light in the breast phantoms change with the distance between the source-detector pairs. The breast phantoms were prepared using 1% Intralipid with reduced scattering (μ_s) 10 cm⁻¹ and indocyanine green (ICG) with an absorption coefficient (μ_a) of 0.04 cm⁻¹, respectively. An inclusion made up using 1% Intralipid and ICG, with μ_s and μ_a of 10 cm⁻¹ and 0.16 cm⁻¹, respectively. We prepared inclusions with different sizes and put different depth. The weight matrix were obtained using Monte Carlo simulations and from Rytov approximation of the diffusion equation. After the calibration of the data acquired, perturbation data were obtained using direct subtraction. In comparing the SIRT, truncated SVD, and CG methods we choose manually from L-curve corner without information of the true solution for number of iterations for CG or singular values for Truncated SVD. On the other hands, after comparing the true solution, we can chose the best solution for SIRT.

9319-80, Session PMon

Diffuse optical tomography system design and reconstruction of tail fat of sheep as a breast phantom

Murat Canpolat, Hüseyin Özgür Kazancı, Tanju Mercan, Akdeniz Üniv. (Turkey)

A continuous wave reflectance diffuse optical tomography (rDOT) system with an optical fiber probe, including 49 sources and 49 detectors has been developed and tested using breast tissue phantoms with an inclusion. All the source and detector fibers are located on 10 x 10 grids with dimensions of 28 mm x 28 mm. In total, there are 22 different source-detector distances on the probe. Data acquired from a breast phantom made of a tail fat and spleen of a sheep. The tail fat was in dimensions of 5x5x5 cm. After acquiring data from the tail fat, a small piece of the spleen in spherical shape with a diameter of 6 mm was placed inside the tail fat as an inclusion. The spleen was 1 cm far from the surface of the tail fat where the optical probe laced to acquire the data. The measurements perturbation data were obtained in two different ways. In the first way, perturbation data was obtained by subtraction of the measurements from the tail fat without and with the spleen. In the second, the perturbation data were obtained only from the measurement of the tail fat with a spleen by subtracting measurement of each source-detector pair from the average taken over the all source-detector pairs with the same separation. The both perturbation data were used for the reconstruction of the breast phantom using linear reconstruction algorithms; SIRT, CG and TSVD. Obtained tomographic images were similar to each other. The biggest difference was the reconstruction times; it was two seconds for CG and 15 minutes SIRT.

9319-81, Session PMon

Vertical-cavity surface-emitting lasers (VCSELs) sources for frequency domain photon migration

Thomas D. O'Sullivan, Keun-Sik No, Alex Matlock, Brian Hill, Albert E. Cerussi, Bruce J. Tromberg, Univ. of California, Irvine (United States)

Frequency-domain photon migration (FDPM) is a technique used to measure optical absorption and scattering of turbid media. FDPM-derived absorption properties can be used for noninvasive, quantitative assessment of tissue hemodynamics, which is useful in a number of clinical applications. To separate absorption and scattering effects, the amplitude and phase of intensity-modulated laser light is measured after propagation through tissue. Clinical FDPM systems typically require sources with at least 10mW fiber-coupled optical power (650-1000nm) modulated at >100MHz. VCSELs have not been historically applied to FDPM techniques because of perceived low output power. However, modern, commercially-available uncooled continuous-wave VCSELs output up to several hundred mW depending on wavelength (650-1100nm+) and >10W in a 2D array format. VCSELs can be easily intensity modulated at frequencies relevant for optical property (OP) recovery, while their small size and simple packaging enables new applications in tissue optics.

We show that single VCSELs and VCSEL arrays provide sufficient output power and bandwidth for OP recovery in phantom and human experiments. To compare measured OPs between standard laser diodes and VCSELs, we measured solid silicone-based phantoms simulating a range of tissue OPs at a source-detection separation of 10mm. Over the three phantoms measured, OPs at similar wavelengths agreed, on average, within 3%. We also demonstrate a unique, compact optical probe that was enabled by VCSEL technology. About the size of a deck of cards, the probe contains a tri-color VCSEL package, an avalanche photodiode, and the DC/RF electronics necessary to individually address the source channels—all controlled by an FDPM instrument module.

9319-82, Session PMon

Potential role of ultrasound-guided diffuse optical tomography in diagnosis of malignant and benign breast lesions

Quing Zhu, Univ. of Connecticut (United States); Andrew Ricci Jr., Hartford Hospital (United States); Poornima Hegde, Mark Kane M.D., Univ. of Connecticut Health Ctr. (United States); Edward Cronin, Hartford Hospital (United States); Yan Xu, B. Tavakoli, Univ. of Connecticut (United States); Susan Tannenbaum M.D., Univ. of Connecticut Health Ctr. (United States)

We report ultrasound-guided diffuse optical tomography (US-DOT) results of consecutive 287 patients of 296 lesions studied. The purpose of the study was to validate the earlier results that US-DOT has a great potential to distinguish cancers from benign lesions of the breast. Patients who underwent US-guided biopsy were imaged with a hand-held probe consisting of a co-registered US transducer and a DOT imager. The lesion location provided by co-registered US was used to guide optical imaging. Light absorption maps were reconstructed at four optical wavelengths of 740, 780, 808, 830 nm and total hemoglobin (tHb), oxygenated and deoxygenated hemoglobin (oxyHb, deoxyHb) were computed from the absorption maps. There were 1 in situ carcinoma (Tis), 36 T1 carcinomas, 20 T2-T4 carcinomas, and 239 benign lesions. The mean maximum and mean average tHb, oxyHb, deoxyHb of the Tis-T1 group were 87.84 and 61.76 mol/L, 62.85 and 44.35 mol/L, 33.31 and 23.52 mol/L, and the values of the T2-T4 group were 84.90 and 58.19 mol/L, 57.15 and 39.01 mol/L, 34.43 and 24.07 mol/L, respectively. The mean maximum and mean average of

**Conference 9319:
Optical Tomography and Spectroscopy of Tissue XI**

the benign group were 54.72 and 37.75 mol/L, 38.38 and 26.75 mol/L, 25.48 and 17.82 mol/L, respectively. Both maximum and average tHb, oxyHb and deoxyHb levels were statistically significantly higher in the malignant groups than the benign group ($P < 0.001$, $P < 0.001$, $P < 0.01$). The tumor tHb level correlates with tumor grade and moderately correlates with tumor HER2 status which indicate that tHb is a robust measure of tumor aggressiveness.

9319-83, Session PMon

The effect and correction of reference heterogeneity in diffuse optical tomography

Hamed Vavadi, Chen Xu, Quing Zhu, Univ. of Connecticut (United States)

Near infrared (NIR) diffuse optical tomography has demonstrated great potential in the initial diagnosis of tumor and in the assessment of tumor vasculature response to neoadjuvant chemotherapy. To reconstruct the absorption map of a breast lesion, perturbation is needed which is the normalized difference between the measurements of lesion-side breast and contralateral reference breast. However, the heterogeneity on the reference breast can produce unwanted perturbation which will result in distortion of the reconstructed target absorption map. In this report, a filtering method is introduced to overcome the reference heterogeneity. This method corrects affected source-detector measurements obtained from the reference side by using averages of unaffected measurements. As a result, the filtered perturbation has decreased the effect of heterogeneity on the reconstructed absorption maps. To evaluate the performance of this filtering method, we have compared the reconstructed results with and without the filtering algorithm using simulated heterogeneous reference with heterogeneous absorbers ranging from 0.05 to 0.20 cm⁻¹ and heterogeneous scatters ranging from 10 to 20 cm⁻¹. The results show that the algorithm can improve the maximum reconstructed target value up to 99% of the value without reference heterogeneity. In the worst case of high absorption heterogeneity in reference side, the maximum reconstructed value was around 30.85% of the true absorption without filtering correction and was improved to 60.4% of the true absorption value which is 95% of the reconstructed value when using the homogeneous reference. A similar improvement is observed in several clinical examples. More clinical data will be quantitatively analyzed.

9319-84, Session PMon

Development of a robust and fast calibration procedure for diffuse optical tomography

Chen Xu, Hai Li, Guangqian Yuan, Hamed Vavadi, Quing Zhu, Univ. of Connecticut (United States)

Near infrared (NIR) diffuse optical tomography has demonstrated great potential in the initial diagnosis of tumor and the assessment of tumor vasculature response to neoadjuvant chemotherapy. A fast and robust data processing is critical to move this technique from lab research to bench-side application. Our lab developed frequency-domain diffuse optical tomography system for clinical applications. So far, we still collect data at hospital and do the data processing off-line. In this paper, a robust calibration procedure and fast processing program were developed to overcome this limitation. Because each detection channel had its own electronic delay, the calibration procedure measured amplitude linearity and phase linearity of each channel, and formed a look-up table. The experimental measurements were corrected by the table and the fitting accuracy improved by 45.8%. To further improve the processing speed, the data collection and processing program were converted to C++ from matlab program. The overall processing speed was improved by two times. We expect the new processing program can move diffuse optical tomography one step close to bench-side clinical applications.

9319-85, Session PMon

Cognitive control of muscle assessed using simultaneous diffuse optical spectroscopy and electrophysiology

Joshua Tromberg, Univ. of California, Irvine (United States)

No Abstract Available

9319-21, Session 5

Functional connectivity in the mouse brain using diffuse optical tomography

Matthew D. Reisman, Adam Q. Bauer, Joseph P. Culver, Washington Univ. in St. Louis (United States)

The study of correlated spontaneous neural and hemodynamic activity in functionally related brain regions using functional connectivity magnetic resonance imaging (fcMRI) has recently allowed comprehensive mapping of distributed brain networks in humans. Similar fcMRI studies in mice are elusive due to the difficulty in achieving high resolution and signal-to-noise in the small volume of the mouse brain. Instead, optical intrinsic signal (OIS) techniques, which use a simple diffuse reflectance imaging geometry, have provided most of the observations of functional connectivity in the mouse brain. While effective and efficient, fcOIS methods require removal of the scalp tissue and are limited to the superficial cortical tissues. Here we extend diffuse optical tomography techniques, using structured light illumination, to map functional connectivity in mice. Using a single CCD camera and a digital micromirror device to produce structured illumination source patterns, we performed diffuse optical tomography consisting of ~10⁶ source detector pair measurements with 0.15mm spacing at a speed of ~10Hz. This system increases the spatial sampling by >10x compared to existing human functional neuroimaging DOT systems, and increases the speed by >10x over previous CCD-based mouse DOT. Phantom studies comparing OIS to DOT demonstrate the expected increase in depth sensitivity and capability of depth sectioning of DOT. In principle, this new DOT-based mouse neuroimaging technique will enable maps of functional connectivity throughout an increased coverage of both cortical and subcortical brain regions.

9319-22, Session 5

Coherent hemodynamics spectroscopy: a new tool to measure cerebral autoregulation in the microcirculation (Invited Paper)

Jana M. Kainerstorfer, Angelo Sassaroli, Kristen Tgavalekos, Sergio Fantini, Tufts Univ. (United States)

Near-Infrared Spectroscopy can measure cerebral concentrations of oxy- and deoxy-hemoglobin, which are determined by cerebral blood volume (CBV), cerebral blood flow (CBF), and metabolic rate of oxygen (CMRO₂). We have recently introduced a time-dependent hemodynamic model, which, in conjunction with induced changes in the systemic mean arterial blood pressure (MAP), led to a technique that we have named Coherent Hemodynamics Spectroscopy (CHS). Such MAP perturbations can be induced by cyclic thigh cuff occlusions at a set of sequentially controlled frequencies. The phase and amplitude of the induced cerebral hemodynamic oscillations are quantified by the novel hemodynamic model in terms of physiological and vascular parameters such as the blood transit times in the microvasculature, the autoregulation cutoff frequency, and the microvascular blood volume. In a clinical study in the dialysis unit, we found longer capillary transit times, i.e. a reduced cerebral blood flow, in hemodialysis patients compared to healthy controls. Here we present our recent advances

**Conference 9319:
Optical Tomography and Spectroscopy of Tissue XI**

in CHS, where systemic MAP changes are induced in a single transient that still contains the frequency information of sequential cyclic perturbations, thereby reducing the measurement time significantly. This method is based on the fast deflation of two pneumatic cuffs around the subject's thighs after they have been kept inflated for 2 min at a pressure of 200 mmHg. Using this approach, we have verified the enhanced cerebral autoregulation associated with hypocapnia, as achieved by hyperventilation, in eleven healthy subjects. Our results indicate that CHS can yield quantitative information about cerebral autoregulation in the microvasculature.

9319-23, Session 5

Cerebral hemodynamic effects of hypoxia-ischemia and hypothermia

Erin M. Buckley, Massachusetts General Hospital (United States); Shyama Patel, Weill Cornell Medical College (United States); Benjamin Miller, Massachusetts General Hospital (United States); Patricia E. Grant M.D., Boston Children's Hospital (United States); Maria Angela Franceschini, Massachusetts General Hospital (United States); Susan Vannucci, Weill Cornell Medical College (United States)

Neonatal hypoxic-ischemic (HI) encephalopathy can cause devastating motor, cognitive, and behavioral disabilities. Currently, therapeutic hypothermia (TH) is the only available treatment with proven efficacy. TH acts partially by decreasing cerebral metabolism, thus preserving energy stores. Since successful TH treatment following HI is associated with decreased cerebral metabolism and cerebral blood flow (CBF), it is important to assess these parameters at the bedside. We employ diffuse correlation spectroscopy (DCS) to describe the evolution of CBF following HI with or without TH in the immature rat.

HI was induced in N=48 P11 rat pups by unilateral carotid artery occlusion followed by 70 minutes hypoxia (8% oxygen). Following HI, pups recovered under 4-hours of mild hypothermia (HI-TH, N=24) or under normothermia (HI, N=24). CBF measurements were made in each hemisphere in un-anesthetized rats at baseline, 0, 1, 2, 3, 4, 5, 24, and 48 hours post-HI. One week later, animals were sacrificed to assess brain injury; TH was neuro-protective ($p = 0.019$).

Immediately after HI, contralateral CBF was elevated. By two hours post-HI, CBF significantly dropped in the HI-TH group and remained depressed for the duration of TH; however CBF in the HI group was not significantly decreased. By 24 hours, CBF in HI pups was significantly elevated, whereas CBF in HI-TH pups returned to baseline levels.

Future work will investigate the relationship between CBF changes and subsequent cerebral damage. We will identify CBF trajectories associated with the best outcomes, first in rats and then in human neonates.

9319-24, Session 5

Multimodal assessment of cerebrovascular disturbances during extracorporeal support

Fenghua Tian, The Univ. of Texas at Arlington (United States); Lakshmi Raman, Children's Medical Ctr. Dallas (United States); Hanli Liu, The Univ. of Texas at Arlington (United States)

Extracorporeal membrane oxygenation (ECMO) is a form of advanced cardio-respiratory support provided to critically ill patients with severe respiratory and/or cardiovascular failure. It is typically used as a rescue therapy for many life-threatening, reversible conditions such as severe shock states, severe respiratory failure, congenital heart disease and neonates

with persistent pulmonary hypertension. ECMO therapy is associated with significant mortality and morbidity, which are attributed to a number of pre-ECMO and ECMO-related factors such as severe hypoxia, hypercarbia, hypertension and cannulation of great blood vessels.

The present study aims to assess the cerebrovascular disturbances during extracorporeal support and its potential role for developing cerebral injuries. Specifically, a multimodal setup is used to monitor the mean arterial pressure along an arterial line, cerebral blood flow with transcranial Doppler (TCD), and cerebral oxygenation with near-infrared spectroscopy (NIRS). The severity of cerebrovascular disturbances during ECMO is assessed by delineating the relationship of the cerebral blood flow/oxygenation with the changes in arterial blood pressure, which is then correlated with the patient's short-term treatment outcome.

Currently there is no reliable bedside tool available to evaluate the cerebrovascular impairments during ECMO other than head ultrasounds conducted in the neonatal age group. Diagnostic imaging such as CT scans are often too challenging for these patients. A multimodal approach to identify the cerebrovascular impairments during ECMO may hold potential to enable optimal modification of ECMO factors and early interventional trials to improve the treatment outcome.

9319-25, Session 5

Rapid event-related fNIRS to study prefrontal hemodynamic responses during associative recognition

Amarnath S. Yennu, James D. Schaeffer, Kellen C. Gandy, Fenghua Tian, Heekyeong Park, Hanli Liu, The Univ. of Texas at Arlington (United States)

Over the past two decades, fNIRS with blocked experimental designs were commonly used in investigation of brain functions. Although rapid event-related designs are widely used in fMRI in cognitive studies, its applicability to fNIRS has not been extensively examined. A rapid event-related design provides better experimental flexibility and more realistic experimental conditions for investigating human cognition. In this study, therefore, we explored rapid event-related fNIRS to investigate prefrontal activity during associative-recognition. The fNIRS experiments were performed on 22 healthy volunteers. Each participant performed 4 runs of study-test sessions. During each study-test session, participants studied lists of word pairs that were later presented as intact (same pair) or rearranged (different pair) along with new word pairs during a memory test (retrieval) session. Each event was presented rapidly (~4s) without inter-trial-interval. In order to investigate associative memory, oxy-hemoglobin (HbO) responses during correct associative-recognition were compared to responses during incorrect associative-recognition toward intact test pairs (studied pairing). HbO responses during associative-recognition were also compared to responses during associative-encoding. The general linear model was used on fNIRS data to quantify prefrontal increases and/or decreases in HbO. During retrieval, significant increases ($p < 0.05$) in HbO were observed in dorsolateral (DL) and ventrolateral prefrontal cortex (PFC) for successful associative-recognition. When comparing retrieval to encoding, significant increases ($p < 0.05$) in HbO were also observed in DLPFC. The current fNIRS results are consistent with previous fMRI findings; therefore, the present study validates the versatile use of fNIRS with a rapid event-related design for investigation of complex cognitive processes.

9319-26, Session 5

Functional near-infrared spectroscopy for adaptive human-computer interfaces

Beste F. Yuksel, Tufts Univ. (United States); Evan M. Peck, Bucknell Univ. (United States) and Tufts Univ. (United States); Daniel Afergan, Samuel W. Hincks, Tomoki Shibata, Jana M. Kainerstorfer, Kristen Tgavalekos, Angelo Sassaroli,

**Conference 9319:
Optical Tomography and Spectroscopy of Tissue XI**

Sergio Fantini, Robert J. K. Jacob, Tufts Univ. (United States)

We present a brain-computer interface system that collects functional near-infrared spectroscopy (fNIRS) data on the user's prefrontal cortex. The measurement protocol includes an initial calibration on each user followed by real-time fNIRS data collection during user's tasks to guide adaptive human-computer interfaces. The calibration, or training, phase is based on established cognitive tasks (n-back paradigms) that induce controlled high or low working-memory workloads. During training, we compare time series of change in light intensity to a baseline period for each of the 16 measurement channels (2 optical detectors x 4 sources x 2 wavelengths). fNIRS data is filtered for heart rate and respiration using third-degree polynomial and low-pass elliptical filters. We use the mean and slope for the 30-second period of every n-back trial. These two features are calculated for each of the 16 channels which results in 32 features per trial. Features for each trial are fed into the machine learning library LIBSVM which builds a model that can classify subsequent fNIRS data into high and low cognitive workload categories with associated probability estimates. These classifications and respective probability estimates are used for real-time adaptation based on users' cognitive workload. We present an example application of our system where users' cognitive workload is used to add and remove unmanned aerial vehicles in a simulation. Results showed that users' errors were reduced by 35% compared to a baseline condition. We demonstrate that our system can use fNIRS to assist users by adapting tasks in real-time based on their cognitive workload.

9319-27, Session 6

Fluorescent lifetime imaging of deep seated fluorophore

Ilya V. Turchin, Institute of Applied Physics (Russian Federation); Alexander V. Khilov, Institute of Applied Physics (Russian Federation); Ilya I. Fiks, Vladimir I. Plehanov, Mikhail Y. Kirillin, Institute of Applied Physics (Russian Federation)

Fluorescence lifetime imaging is extremely important for a number of biological studies and can be performed in microscopic studies using pulsed picosecond lasers for a fluorescence excitation and either time-correlated photon counters or cameras with a gating time of 200 picoseconds or less for the registration of fluorescence decay kinetics. However, it is necessary to take into account light scattering in biological tissues blurring both the excitation pulse and the fluorescence response. This phenomenon is essential for in vivo studies. This blurring leads to differences between the measured and initial lifetimes of a fluorescent agent.

This effect was studied using the Monte-Carlo simulation. Fluorescence response from a deep seated fluorophore is obtained by convolution of the excitation pulse propagating to a certain depth (position of the fluorophore), initial fluorescence decay kinetics and emission light propagating from the fluorophore to the tissue surface. We have found that the difference between the lifetime estimated by the blurred fluorescence kinetics and the initial lifetime is only several dozen picoseconds for depths up to 2 cm for long-lived fluorophores (with lifetimes of several nanoseconds). However, this difference is very significant for fluorophores with lifetimes of several hundred picoseconds and amounts up to 50%. We also investigated the dependence of measured lifetime on optical parameters of a turbid medium (absorption coefficient and scattering coefficient), the depth of fluorescent agent in a turbid medium and the distance between a light source and a detector. Also, we performed model experiments which proved the results of the numerical modeling.

9319-28, Session 6

Fluorescence molecular imaging system with a novel mouse surface extraction method and a rotary scanning scheme

Yue Zhao, Dianwen Zhu, Rehemai Baikejiang, Changqing Li, Univ. of California, Merced (United States)

We developed a new Fluorescence Molecular Tomography (FMT) imaging system with a novel mouse surface geometry extraction method and a rotary scanning scheme. Phase shifting method is adopted to reconstruct the mouse surface by utilization of a projector and a camera, following with DigiWarp method to warp a finite element mesh of a standard digital mouse to measured mouse surface. We built the FMT system based on rotary scanning, in which a line pattern laser excites the fluorescence molecules inside the mouse. Numerical simulations and phantom experiments are used to evaluate the performance of the FMT imaging system.

9319-29, Session 6

Accelerating spatially non-uniform update for sparse target recovery in fluorescence molecular tomography by ordered subsets and momentum methods

Dianwen Zhu, Changqing Li, Univ. of California, Merced (United States)

Fluorescence molecular tomography (FMT) is a significant preclinical imaging modality that has been actively studied in the past two decades. However, it remains a challenging task to obtain fast and accurate reconstruction of fluorescent probe distribution in small animals due to the ill-posed nature of the inverse problem, noisy measurements, and the large computational burden. We have recently studied a non-uniform multiplicative updating algorithm, and obtained some further speed gain with the ordered subsets (OS) method. However, increasing the number of OS leads to larger approximation errors and the speed gain from larger number of OS is limited. In this paper, we propose to further enhance the convergence speed by incorporating the first order momentum method that uses previous iterations to achieve a quadratic convergence rate. Using cubic phantom experiment, we showed that the proposed method indeed leads to a much faster convergence.

9319-30, Session 6

Multiplexed fluorescence tomography with spectral and temporal data: intrinsic regularization with nonnegative least squares (Invited Paper)

Vivian E. Pera, Dana H. Brooks, Mark J. Niedre, Northeastern Univ. (United States)

Fluorescence molecular tomography has become an important tool in preclinical biomedical imaging. However, the inability to perform high-throughput imaging of multiple fluorescent targets in bulk tissue remains a limitation. Specifically, the narrow (~200 nm wide) near-infrared "diagnostic window" and relatively broad emission spectra of common organic fluorophores make accurate identification ("demixing") challenging. Moreover, light experiences a "red-shift" as it propagates through tissue due to non-linear attenuation by hemoglobin that further complicates spectral demixing. Recent work in our group suggests that joint measurement of spectral and temporal fluorophore data can enable robust demixing and localization of four concurrent fluorophores. To this end, we have developed a novel time-domain hyperspectral tomographic instrument capable of

**Conference 9319:
Optical Tomography and Spectroscopy of Tissue XI**

acquiring time-resolved fluorescence data with 16 spectral channels in the 650-850 nm range.

Here we present a novel demixing strategy for this data, which uses a suitable "library" of fluorophore signatures (measured or modeled) to compute a nonnegative least-squares (NNLS) estimate of each fluorophore component. We find that NNLS succeeds even when the library is rank-deficient, thereby eliminating the dependence on a regularization parameter. Moreover, the standard Matlab implementation of NNLS has converged quickly in all our tests to date, allowing us to demix 648 measurements in about five minutes. In our simulations, we have simultaneously demixed four fluorophores (Alexafluor 680, 700, 750, and 790) in a 25 mm diameter cross-sectional area with an error of less than 3% per fluorophore. Further study of the impact of model mismatch is underway, along with in vitro experimental testing.

9319-31, Session 7

Fast full angle fluorescence molecular tomography system based on rotating mirrors

Daifa Wang, Jin He, Yubo Fan, Deyu Li, BeiHang Univ. (China)

Fluorescence molecular tomography (FMT) in the near-infrared region is becoming a powerful modality for mapping the three-dimensional quantitative distributions of fluorochromes in live small animals. Because of the scattered light propagation inside turbid tissue media, the image reconstruction in FMT is highly ill-posed and has limited spatial resolution. High density sampling is considered an effective approach to handle this challenge, where dense illumination and detection are performed at different views over full angle. However, most current prototype systems with full angle of view need rotating the animals or the illumination/detection modules. The former make the experiment procedure complex and has the risk of internal organ movement during animal rotation; the latter needs a large and complex rotational gantry to mount all the light source, optical lens, and detection modules such as sensor-cooled camera, making the design complicated. Some other systems also use conical mirror to acquire full angle view while avoiding rotation, which however has limited camera sensor-chip utilization efficiency. In this article, a full angle FMT system is proposed, where full angle acquisition is achieved by mounting one reflection mirror for illumination and triple reflection mirrors for detection on a rotational gantry. Two dimensional galvanometer mirrors are used for fast scanning of illumination points. Since the mirrors are compact in size and light in weight, the rotational gantry is rather simple to implement and can run at fast speed. By using the rotating mirrors, the system has high camera sensor-chip utilization efficiency at each angle view and doesn't have to rotate animal, light source, and camera. The effectiveness and fast imaging capacity of the proposed system were verified by phantom and in-vivo experiments.

9319-32, Session 7

Multispectral time-resolved diffuse fluorescence tomography

Ying Mu, Mark J. Niedre, Northeastern Univ. (United States)

Diffuse fluorescence tomography is an increasingly important tool in biomedical research. Multiplexed imaging of fluorescent targets would in principle allow simultaneous visualization of the activity of multiple genes and molecular markers in whole animals. However, the relatively narrow "optical window" in the near-infrared range, combined with the broad emission spectra of organic fluorophores means that multiplexed imaging is challenging. Combined use of fluorescence lifetime and spectral data has been proposed to allow accurate demixing and imaging of 4 or more fluorescent targets simultaneously. Accordingly, we developed an instrument for multi-wavelength, time-resolved fluorescence lifetime

tomography. In this presentation, we describe this instrument and image processing algorithms, and demonstrate its application in tissue-simulating optical phantoms in vitro.

We used an ultra-fast near-infrared pulsed laser to illuminate the sample. Fluorescent light emitted from the sample surface was detected by a set of 3 fiber optodes, each of which was coupled to a time-resolved spectrometer. Each was capable of time-resolved single photon counting (TCPSC) on 16 spectral channels simultaneously between 650-858 nm with 13 nm spectral and 12 ps temporal resolution (PML-16-C, Becker&Hickl). The sample and detectors were mounted on independently rotatable motorized gantries, so that spectral and lifetime data could be obtained over a 360o scan. We tested the performance of the instrument with custom made tissue simulating optical phantoms with multiple inclusions. We validated the ability to de-mix and tomographically reconstruct the position of up to 4 fluorophores. We anticipate this instrument will have application in many areas of pre-clinical research.

9319-33, Session 7

Excitation light leakage suppression using temperature sensitive fluorescent agents

Farouk Nouizi, Tiffany C. Kwong, Jessica Kwong, Jaedu Cho, Yu-wen Chan, Univ. of California, Irvine (United States); Uma Sampathkumaran, Yue Zhu, Maksudul M. Alam, InnoSense LLC (United States); Gultekin Gulsen, Univ. of California, Irvine (United States)

In addition to being non invasive, non ionizing and using low cost instrumentation, fluorescence tomography (FT) is an imaging technique that can provide the 3D distribution of fluorescent agents within thick tissue. However, highly scattering nature of the tissue makes the reconstruction of these fluorescence maps a very challenging process. In fact, its low spatial resolution delayed translation of the FT to the clinical arena. This is mainly due to the underdetermined and ill-posed nature of FT image reconstruction algorithms. Another key factor affecting the quality of the FT images is the contamination of the measurements by the excitation light leakage through the rejection filters. In this study, we present a new method to eliminate excitation light leakage based on the use of a temperature sensitive fluorescence agents termed "ThermoDots". The fluorescence emission of ThermoDots vary within a 4oC temperature range. Indeed, at the low bound of this range, the quantum yield of ThermoDots is quasi-null. A measurement at this temperature would reveal the excitation light leakage. Afterwards, a second measurement is acquired by increasing the temperature of the medium by 4oC, which is composed of the fluorescence signal in addition to the excitation leakage. A simple subtraction of the two sets of data allows us to correct our measurements yielding to a better image quality and quantification accuracy. Our experimental results using this technique confirmed its potential for in-vivo small animal imaging use.

9319-34, Session 7

Targeting tumor hypoxia: third generation 2-nitroimidazole ICG conjugate

Feifei Zhou, Saeid Zanganeh, Innus Mohammad, Akram Abuteen, Michael B. Smith, Quing Zhu, Univ. of Connecticut (United States)

Tumor hypoxia is associated with the rapid proliferation and growth of malignant tumors. Targeting tumor hypoxia is significant in predicting tumor response to anti-cancer treatments. The 2-nitroimidazole and indocyanine green (ICG) conjugate using piperazine linker (2-nitro-ICG-p) was reported by us to improve tumor hypoxia targeting as compared with the first generation 2-nitroimidazole ICG conjugate using ethanolamine linker. Based on the hypothesis that molecules with more planar and rigid structures have a higher fluorescence yield as they could release less absorbed

**Conference 9319:
Optical Tomography and Spectroscopy of Tissue XI**

energy through molecular vibration or collision, we have developed a third generation 2-nitroimidazole ICG conjugate, named hypoxia-targeted rigid dye. The targeted rigid dye was initially prepared as non-targeted rigid dye from ICG bis-carboxylic acid but with two carbons less in the polyene linker and then it was coupled to 2-nitroimidazole with piperazine linker to synthesize the hypoxia targeted rigid dye. The spectrum measurements show that its absorption/emission wavelengths, 655/670 nm, have shifted ~100 nm from the second generation hypoxia dye of 755/790 nm. Its fluorescence quantum yield was measured to be ~0.2 which is about 3-4 times higher than that of the second generation hypoxia dye of 0.066. In vivo experiments were conducted with mouse tumor model using IVIS[®] Lumina II Imaging System. The targeted rigid dye showed more than twice fluorescence intensity in tumor 2 hours post retro-orbital injection as compared with the second generation hypoxia dye. These initial results suggest that the targeted rigid dye may significantly improve in vivo tumor hypoxia targeting.

9319-35, Session 8

Real-time acquisition of tissue optical properties and surface profile using 3D-SSOP

Martijn Van de Giessen, Leiden Univ. Medical Ctr. (Netherlands) and Technische Univ. Delft (Netherlands); Joseph Angelo, Boston Univ. (United States) and Beth Israel Deaconess Medical Ctr. (United States); Christina Vargas M.D., Beth Israel Deaconess Medical Ctr. (United States); Sylvain Gioux, Beth Israel Deaconess Medical Ctr. (United States) and Harvard Medical School (United States)

Spatial frequency domain imaging (SFDI) enables wide-field acquisition of both the scattering and absorption properties of biomedical tissue. A typical surface profile-corrected SFDI acquisition requires minimum number of 9 images: 6 images for estimating optical properties (2 frequencies, 3 phases) and 3 images for estimating the surface profile (3 phases). This hampers real-time imaging and thereby surgical image guidance applications, e.g. oxygenation imaging.

We propose 3D-Single Snapshot Optical Property imaging (3D-SSOP) to simultaneously acquire optical properties and surface profile. To this end a pattern is projected that is both sensitive to optical properties at two spatial frequencies (0 mm⁻¹ (DC) and 0.2 mm⁻¹ (AC)) and height sensitive. We present an efficient processing strategy for extraction of the two spatial frequency components and a profilometry phase. Height corrected absorption and reduced scattering coefficient maps are then derived from the AC and DC components.

The accuracy and precision of 3D-SSOP was compared to profile-corrected SFDI by imaging phantoms and in-vivo samples, in particular hands and porcine skin flaps. All acquisitions were at 670nm illumination, projected through a digital micromirror device.

Estimates of optical property maps were unbiased when compared to SFDI, with a precision in the order of 5% on smoothly varying surfaces. Near edges more severe artifacts arose due to implicit spatial averaging over edges when estimating AC, DC and height profile. Processing time for extracting AC, DC and height took 0.14 s/frame with a non-optimized MATLAB implementation. Real-time imaging was demonstrated in in-vivo movie acquisitions.

9319-36, Session 8

Portable integrated frequency domain and continuous wave real-time diffuse optical spectroscopy and imaging

Soroush M. Zarandi, Beckman Laser Institute and Medical Clinic (United States); Siavash Sedighzadeh Yazdi, Univ. of California, Irvine (United States); Thomas D. O'Sullivan, Brian Hill, Beckman Laser Institute and Medical Clinic (United States); Michael Green, Univ. of California, Irvine (United States); Albert E. Cerussi, Bruce J. Tromberg, Beckman Laser Institute and Medical Clinic (United States)

In this work, we present a portable (10cm×5.5cm×3.25cm) high speed integrated frequency-domain and continuous wave (CW) system for spectroscopic imaging in diffuse media. This system measures four tissue chromophore concentrations (water, lipid, deoxygenated and oxygenated hemoglobin) at eight near-infrared wavelengths ranging from 660nm to 980nm, in real-time. The frequency domain (FD) module measures the phase and amplitude of diffusing light from 50-250 MHz with an operating speed of 2Hz while the CW module operates at 80Hz. The FD component provides quantitative information by separating scattering from absorption using the acquired phase and amplitude data. The CW component expands spectral bandwidth and improves acquisition speed by measuring only amplitude changes. The CW system has 110 dB dynamic range, enabling measurements in tissue with a source-detector spacing up to 4.5cm. The CW module frequency-encodes wavelengths for parallel illumination resulting in rapid data acquisition. It is also less sensitive to background noise from ambient light by utilizing low-frequency modulation and a narrow bandpass filter on the source and detector sides, respectively. The standalone FD module can be utilized in applications where scattering coefficients are required from every measurement and only deoxygenated and oxygenated hemoglobin concentrations are desired. In combined mode, concurrent FD and CW measurements are available where information about water and lipid contents is also necessary. In media with constant scattering, a single FD measurement can be used as a baseline and the CW module can be used for subsequent measurements to extract the absolute chromophore absorption coefficients. Finally, if only relative changes in tissue content, (e.g., oxygen saturation) are desired, the instrument can operate in standalone CW mode. We will demonstrate the performance of this combined system using a tissue-simulating (Breast tissue) phantom with an embedded inclusion (tumor) located at 1 cm beneath the surface.

9319-37, Session 8

Determining scattering anisotropy by combining single fiber reflectance spectroscopy and optical coherence tomography

Anouk L. Post, Xu Zhang, Nienke Bosschaart, Abel Swaan, Ton G. van Leeuwen, Henricus J. C. M. Sterenberg, Dirk J. Faber, Academisch Medisch Centrum, Univ. van Amsterdam (Netherlands)

Both Optical Coherence Tomography (OCT) and Single Fiber Reflectance Spectroscopy (SFR) can be used to determine various optical properties of tissue. However, scattering anisotropy is a property neither single technique can reliably determine. The scattering anisotropy parameterizes the scattering phase function (the angular distribution of scattered light) which is intimately associated with the cellular organization and ultrastructure of tissue. Since these physical parameters change during e.g. carcinogenesis and development; quantification of the scattering anisotropy may allow for improved non-invasive, in vivo discrimination between healthy and diseased tissue. By combining OCT and SFR in a single measurement this determination may become feasible. To this end, we are currently

**Conference 9319:
 Optical Tomography and Spectroscopy of Tissue XI**

developing a combined OCT and SFR probe.

With OCT the scattering coefficient can be extracted by fitting the OCT signal as a function of depth to a widely used model for the signal as a function of the attenuation coefficient (Faber et al, Optics Express 12(19), 2004). With SFR the reduced scattering coefficient can be calculated from a measured reflectance spectrum (Kanick et al., Optics Letter 36(15), 2011). Consequently, from SFR and OCT measurements at the same wavelengths, the μ_s' - wavelength dependent - scattering anisotropy (g) can be calculated using $\mu_s' = \mu_s * (1-g)$.

We have performed OCT measurements at 600 and 800 nm for different dilutions of Intralipid-20% to determine their scattering coefficients. For similar solutions we will also measure the reflectance spectra with SFR and present our results at the conference.

9319-38, Session 8

A compact, multi-wavelength, and high frequency response light source for diffuse optical spectroscopy and imaging

Kyoung Su Park, Minseok Lee, Phil-Sang Chung M.D., Sehwan Kim, Dankook Univ. (Korea, Republic of)

The diffuse optical spectroscopic technique can characterize turbid media such as tissue in terms of absorption coefficient (μ_a) and reduced scattering coefficient (μ_s'), which can offer a variety of information for the physiological processes associated with disease or therapy. The fiber optics-based approaches to measure tissue optical properties have employed multi-wavelengths to cover the near-infrared (NIR) spectral range. This is because wavelength-dependent absorption is helpful in quantifying the concentration of biologically important chromophores. In addition, the light source for diffuse optical spectroscopic measurements can be performed with continuous-wave broadband or radio-frequency intensity modulated sources. In order to satisfy the requirement of the light source for the diffuse optical spectroscopic technique, in this paper, we propose a single fiber-based multi-wavelength light source with high frequency bandwidth. It is for the measurement of the tissue optical properties from diffuse optical spectroscopy and imaging. The developed light source is equipped with six laser diodes, 658, 690, 705, 785, 830, and 850nm and one multi-mode step index optical fiber with 400 μ m diameter core. We conduct the simulations to figure out design parameters and also confirm the feasibility of the light source. The evaluation results present that the coupling efficiency of the fabricated light source is 80-85% and the frequency response of S21 mode is to 3.38GHz at 3-dB bandwidth. The developed light source has the potential to provide beneficial future development of fast measurement and compact systems for non-or minimal-invasive medical monitoring and diagnostics.

9319-39, Session 8

A diffuse optical probe for the evaluation of subsurface tissue composition and metabolism during minimally invasive surgery

Jesse H. Lam, Hossein Yazdi, Soroush M. Mirzaei Zarandi, Beckman Laser Institute and Medical Clinic (United States); Zhamshid Okhunov, Univ. of California, Irvine (United States); Jue Hou, Beckman Laser Institute and Medical Clinic (United States); Michael del Junco, Jaime Landman, Univ. of California, Irvine (United States); Bruce J. Tromberg, Albert E. Cerussi, Beckman Laser Institute and Medical Clinic (United States)

Subsurface tissue viability and composition are important to measure during surgery, but cannot be quantified with the unaided eye. Diffuse

optical spectroscopy (DOS) can extract chromophore concentrations and states by quantifying near-infrared absorption and scattering spectra with combined frequency domain and broadband steady-state components. Diffuse correlation spectroscopy (DCS) recovers blood flow information by measurement of the coherence loss of a single mode light source due to red blood cell motion. By combining these two well-established optical techniques into a sub 12 mm diameter probe designed to fit inside a standard laparoscopic trocar, the concentrations of water, lipid, and oxygenated & deoxygenated hemoglobin as well as flow can be obtained during laparoscopy. We have tested the technology in vivo using a live porcine model, showing metabolic changes between live and excised tissue as well as flow dynamics during renal occlusion and release. Macroscopically-measured water and lipid concentrations obtained by DOS were compared with Raman microscopy with a high level of agreement. Continued development of the combined DOSDCS probe may allow surgeons to intraoperatively evaluate sub surface content to characterize tissue types. Furthermore, the probe may also be used as a metabolic sensor by combining oxygenation information from DOS and blood flow information from DCS to determine tissue ischemia states.

9319-40, Session 8

Multispectral spatial frequency domain imaging for three-dimensional reconstruction of tissue hemoglobin content in vivo

Robert H. Wilson, Kyle P. Nadeau, Michael T. Ghijsen, Bernard Choi, Anthony J. Durkin, Bruce J. Tromberg, Univ. of California, Irvine (United States)

A key challenge in biomedical optics is the accurate reconstruction of spatially-varying tissue optical properties. Wide-field imaging techniques, such as spatial frequency domain imaging (SFDI), can offer a potential solution to this problem by providing quantitatively accurate spatial maps of tissue absorption and scattering coefficients. Here, we extend this wide-field imaging method into three dimensions by employing a combination of multi-spectral imaging (using wavelengths extending from the visible to the near-infrared) and SFDI to generate three-dimensional (x,y,z) maps of tissue absorption properties in vivo. The two-dimensional wide-field multispectral and SFDI data are input into optical tomography algorithms that employ Rytov approximation and Monte Carlo methods to reconstruct tissue hemoglobin concentration and oxygenation in three dimensions. By localizing the hemoglobin concentration in three dimensions, the tomography algorithm can prevent partial-volume effects from significantly reducing the magnitude of the extracted hemoglobin concentration. Using SFDI and multispectral data in tandem allows for a more quantitatively accurate 3D reconstruction of tissue hemoglobin content, as SFDI provides better depth localization and the multispectral data provides a more accurate estimate of the magnitude of the hemoglobin concentration. The technique is verified by acquiring images of a human wrist and reconstructing a three-dimensional map of the total hemoglobin concentration and oxygenation within a large vein ~2 mm beneath the surface of the wrist.

9319-41, Session 9

Comparison of linear and nonlinear models for coherent hemodynamics spectroscopy

Angelo Sassaroli, Jana M. Kainerstorfer, Sergio Fantini, Tufts Univ. (United States)

Recently we have proposed a new hemodynamic model and a novel method for retrieving physiological information from optical measurements with near infrared spectroscopy (NIRS), namely, Coherent Hemodynamic Spectroscopy (CHS). CHS is based on inducing periodic hemodynamic oscillations in the brain or in other organs (either by paced breathing, cyclic

**Conference 9319:
Optical Tomography and Spectroscopy of Tissue XI**

high cuff occlusion, tilting bed etc.) and by measuring the relationships between the oscillations of oxy- (O), deoxy- (D) and total hemoglobin (T) concentrations in the target organ. The hemodynamic model assumes that the capillary and the venous compartments act as a linear systems (more specifically as low pass filters) with the changes of blood flow, and oxygen consumption as inputs and the spatially averaged change in oxygenation in the capillary and venous compartments as outputs. In this study we were motivated to understand to what extent a linear time invariant model could be used when the changes of blood flow are larger than 10% (as it is reported in the literature during brain activation). For this purpose we are proposing an original exact solution for the relationship between blood flow changes and hemoglobin saturation changes that can be used potentially for any arbitrary temporal trend of the blood flow. We provide a semi-analytical solution of the nonlinear problem when the induced oscillations are sinusoidal (as assumed in CHS) and compare the results with those of the linear model.

9319-42, Session 9

Boundary conditions independent diffuse correlation spectroscopy

Mamadou Diop, Keith St. Lawrence, Lawson Health Research Institute (Canada)

The diffusive nature of light propagation in strongly scattering media has led to the development of analytical models that enabled the extension of dynamic light scattering (DLS) techniques to optically opaque media. A major breakthrough was the finding that the field auto-correlation function that characterizes the dynamics of the light scatters is a solution to the diffusion equation. This has led to the development of diffuse correlation spectroscopy (DCS), also known as diffuse wave spectroscopy (DWS), which provides a theoretical framework that enables the interpretation of DLS measurements in diffuse media. However, solving the diffusion equation requires taking into account the boundary conditions which can be very difficult and even impossible in many cases.

We present a DCS (DWS) approach that is independent of the boundary conditions. The method is similar to the approaches developed by Yodh et al. (Phys. Rev. B, 1990) and Popescu and Dogariu (Appl. Opt., 2001) but in contrast to them, our technique does not require any gating or scanning of the optical pathlengths in the medium which makes it very fast (few ms). First, a robust deconvolution algorithm was used to extract the true probability distribution function (PDF) of the photons' pathlengths from time-resolved measurements. The PDF was then used to fit the measured field auto-correlation function to obtain the effective diffusion coefficient of the light scatters. The validity of this approach was tested with simulations and tissue mimicking phantoms, and subsequently applied to measure perfusion changes in brain and joints.

9319-43, Session 9

A non-stochastic iterative computational method to model light propagation in turbid media

Thomas J. McIntyre, Roger Zemp, Univ. of Alberta (Canada)

Monte Carlo models are widely used to model light transport in turbid media, however their results implicitly contain stochastic variations. These fluctuations are not ideal, especially for inverse problems where Jacobian matrix errors can lead to large uncertainties upon matrix inversion. Yet Monte Carlo approaches are more computationally favorable than solving the full Radiative Transport Equation. Here, a non-stochastic computational method of estimating fluence distributions in turbid media is proposed, which we call the Non-Stochastic Propagation by Iterative Radiance Evaluation Method (NSPIRE). Rather than using stochastic means to determine a random walk for each photon packet, the scattering and

propagation of light from each pixel to all other pixels in a grid are modelled simultaneously. The number of iterations of our algorithm is equal to or greater than the mean number of scattering events of a photon packet. For locally homogenous anisotropic turbid media, the matrices used to represent scattering and propagation are shown to be Toeplitz, which leads to computational simplification via convolution operators. To evaluate the accuracy of the algorithm, 2D simulations were done and compared against Monte Carlo models for the cases of an isotropic point source and a pencil beam incident on a semi-infinite turbid medium. The model was shown to have a mean percent error of less than 2%. The algorithm represents a new paradigm in radiative transport modelling and may offer a non-stochastic alternative to modeling light transport in anisotropic scattering medium for applications where the diffusion approximation is insufficient.

9319-44, Session 9

Modified Beer-Lambert law for blood flow

Wesley B. Baker, Ashwin B. Parthasarathy, Univ. of Pennsylvania (United States); David R. Busch, Univ. of Pennsylvania (United States) and The Children's Hospital of Philadelphia (United States); Rickson C. Mesquita, Univ. Estadual de Campinas (Brazil); Joel H. Greenberg, Arjun G. Yodh, Univ. of Pennsylvania (United States)

The modified Beer-Lambert law is among the most widely used approaches for analysis of near-infrared spectroscopy (NIRS) reflectance signals for measurements of tissue blood volume and oxygenation. Briefly, the modified Beer-Lambert paradigm is a scheme to derive changes in tissue optical properties based on continuous-wave (CW) diffuse optical intensity measurements. In its simplest form, the scheme relates differential changes in light transmission (in any geometry) to differential changes in tissue absorption. Here we extend this paradigm to the measurement of tissue blood flow by diffuse correlation spectroscopy (DCS). In the new approach, differential changes of the intensity temporal auto-correlation function at a single delay-time are related to differential changes in blood flow. The key theoretical results for measurement of blood flow changes in any tissue geometry are derived, and we demonstrate the new method to monitor cerebral blood flow in a pig under conditions wherein the semi-infinite geometry approximation is fairly good. Specifically, the drug dinitrophenol was injected in the pig to induce a gradual 200% increase in cerebral blood flow, as measured with MRI velocity flow mapping and by DCS. The modified Beer-Lambert law for flow accurately recovered these flow changes using only a single delay-time in the intensity auto-correlation function curve. The scheme offers increased DCS measurement speed of blood flow. Further, the same techniques using the modified Beer-Lambert law to filter out superficial tissue effects in NIRS measurements of deep tissues can be applied to the DCS modified Beer-Lambert law for blood flow monitoring of deep tissues.

9319-45, Session 9

Analytical model for sub-diffusive light reflection and the application to spatial frequency-domain imaging

Michael Reilly, Min Xu, Fairfield Univ. (United States)

There have been numerous developments in empirical models for light reflectance at a close source-detector separation recently. Such models are critical for fiber-based spectroscopy of tissue and gain extra importance for spatial frequency-domain imaging. Unfortunately, currently there is still not an analytical model which is able to describe sub-diffusive light reflectance when the source-detector separation is less than one single scattering length (~100 micro in tissue) where the details of the phase function of light scattering play a significant role.

In this presentation, we report here an analytical model describing light reflectance at an arbitrary source-detector separation covering both sub-

**Conference 9319:
Optical Tomography and Spectroscopy of Tissue XI**

diffusive and diffusion regimes for forward-peaked scattering media such as biological tissue. The model incorporates the small-angle scattering approximation (SAA) to radiative transfer for sub-diffusive light reflectance at a source-detector separation less than one single scattering length where the details of the phase function of light scattering dominate. The performance of the model is verified by Monte Carlo simulations. We also present the application of this analytical model in spatial frequency-domain imaging, in particular, when the spatial frequency is pushed below the reduced scattering coefficient.

9319-46, Session 9

3D parameter reconstruction in hyperspectral diffuse optical tomography

Arvind Krishna Saibaba, Nishanth Krishnamurthy, Pamela G. Anderson, Jana M. Kainerstorfer, Angelo Sassaroli, Eric L. Miller, Sergio Fantini, Misha E. Kilmer, Tufts Univ. (United States)

The imaging of chromophore concentration using Diffuse Optical Tomography (DOT) data is a highly ill-posed inverse problem. New technology developed in our group allows for the collection of hyperspectral data, which can substantially improve our ability to stably, recover chromophore information. However, such data sets introduce a significant computational burden as the reconstruction algorithms require the solution of thousands of large-scale linear systems obtained by discretizing the PDEs in complex 3D geometries. In this paper we develop and demonstrate a novel recycling-based Krylov subspace approach for the solution of these systems that exploits fundamental physical and geometric structure in the underlying problem. We demonstrate the utility of the method in the context of an inversion algorithm in which we linearize the parameter-to-observation map using the Born approximation and employ a level-set scheme to recover the medium properties under a piecewise constant assumption. In terms of forward model performance, our results demonstrate a 40% reduction in the number of iterations. By exploiting redundancies in information content across wavelengths, we demonstrate a 80% reduction in numerical rank of the measurement operator. We will demonstrate the resulting computational gains and validity of our approach by comparison on experimental data.

9319-47, Session 10

Characterization of hemodynamics and oxygenation in the renal cortex of rats

Dirk Grosenick, Heidrun Wabnitz, Rainer Macdonald, Physikalisch-Technische Bundesanstalt (Germany); Thoralf Niendorf, Max-Delbrück-Ctr. für Molekulare Medizin Berlin-Buch (Germany); Kathleen Cantow, Bert Flemming, Charité Universitätsmedizin Berlin (Germany); Karen Arakelyan, Max-Delbrück-Ctr. für Molekulare Medizin Berlin-Buch (Germany); Erdmann Seeliger, Charité Universitätsmedizin Berlin (Germany)

We have performed a pre-clinical study on 13 rats to investigate the potential of near-infrared spectroscopy for quantification of hemoglobin concentration and oxygen saturation of hemoglobin in the renal cortex of small animals. A fiber optic probe with source-detector separations between 2 mm and 8 mm was used to record spatially-resolved diffuse reflectance at three near-infrared wavelengths from the surface of the exposed kidney. Measurements were combined with laser-Doppler fluxmetry and a fluorescence quenching technique for quantification of tissue oxygen tension by employing a fiber optic probe inserted into the renal cortex. Hemoglobin concentration and oxygen saturation of hemoglobin were derived by a Monte Carlo model of photon propagation and by calibration of diffuse reflectance data using a phantom with known optical properties. We

applied our methods to investigate temporal changes during several types of interventions. For short occlusions of the renal artery or vein the decrease or increase in the cortical hemoglobin concentration per tissue volume could be quantified. Furthermore, the temporal behavior of oxygen saturation of hemoglobin and tissue oxygen tension in the kidney was found to be different. In a second group of interventions the mixture of the inspired gas was changed to induce hyperoxic, hypoxic and hypercapnic conditions which resulted in an increase, a decrease, or unaltered oxygen saturation. As expected, changes in hemoglobin concentration were much smaller during these interventions compared to the occlusions. Our results show the benefit of combining NIRS and invasive methods to better understand the physiology of the kidney.

9319-48, Session 10

Quantification of joint inflammation in rheumatoid arthritis by time-resolved diffuse optical spectroscopy and tracer kinetic modeling

Seva Ioussoufovitch, Laura B. Morrison, Keith St. Lawrence, Ting-Yim Lee, Mamadou Diop, Lawson Health Research Institute (Canada)

Rheumatoid arthritis (RA) is a chronic inflammatory disease affecting about 1% of the population. The disease is associated with reduced quality of life, depression and progressive joint damage. Although most symptoms of the disease can be efficiently reduced with current treatment strategies, progressive joint damage remains a major issue in the management of RA. Since inflammation is recognized as the main cause of progressive joint damage, eliminating joint inflammation is a major focus of RA treatment.

Current methods of monitoring joint inflammation during RA treatment are either not sensitive enough to measure low levels of inflammation or unpractical for routine clinical use. Diffuse optical spectroscopy (DOS) has been long recognized as an ideal candidate for monitoring disease activity in RA; however its clinical implementation has been hampered by a lack of quantification. The few DOS applications to RA have been limited to qualitative assessment of joint optical properties or uptake of fluorescence dye, and did not attempt to convert the measurements into quantitative physiological parameters. To provide clinically relevant data, DOS measurements need to be converted into quantitative physiological parameters that can be easily interpreted by the clinical team. We propose a method based on tracer kinetics modeling that can convert time-resolved DOS measurements into clinically relevant physiological parameters for rapid and reliable assessment of joint inflammation. Preliminary results obtained from two subjects (rabbit model of RA) show increased blood flow (20 to 60 ml/100g/min) and deoxy-hemoglobin (40 to 56 μM) in inflamed joints while oxy-hemoglobin decreases (80 to 20 μM).

9319-49, Session 10

A novel bioluminescence tomography guided system for preclinical radiation research

Bin Zhang, Ken Kang-Hsin Wang, Sohrab Eslami, Iulian I. Iordachita, Johns Hopkins Univ. (United States); Michael S. Patterson, McMaster Univ. (Canada); John Wong, Johns Hopkins Univ. (United States)

Using the existing cone beam computed tomography (CBCT) system on board the small animal radiation research platform (SARRP), localization of low contrast soft tissue targets remains challenging. A dual-use (on-board SARRP and offline) bioluminescence tomography (BLT) system has been developed to provide high sensitivity soft tissue guidance for preclinical radiation studies.

**Conference 9319:
Optical Tomography and Spectroscopy of Tissue XI**

The BLT system comprises a motorized camera-filter-mirror assembly with a light-tight enclosure. A 3-mirror system was adopted to reflect the bioluminescence emitted from the subject to the CCD camera. The CBCT and diffuse optical tomography provide the anatomical information for mesh generation and optical properties, respectively. To increase the reconstruction accuracy, the bioluminescence was acquired at multiple-wavelengths. The center of mass (CoM) of the reconstructed result was calculated for radiation-guidance. Gafchromic films were used to verify the targeting accuracy by comparing the CBCT- and BLT-guided results. For the phantom and in vivo experiments, where a 1mm by 2mm self-illuminated source was imbedded, the on-board BLT guidance can recover the CoM with 1mm accuracy. A systematic study of the targeting uncertainty will be conducted to provide an appropriate radiation margin. The targeting uncertainty using the on-board SARRP and offline configuration will also be evaluated. In vivo experiments with realistic tumor models will be performed to assess the system performance.

The integrated CBCT/BLT system provides a compelling solution to guide focal irradiation for soft tissue targets. The dual-use system is expected to extend the application of optical tomography for radiation studies.

9319-50, Session 10

A non-contact system for three dimensional blood flow imaging in mouse leg using diffuse correlation tomography

Songfeng Han, Univ. of Rochester (United States); Johannes Johansson, Miguel A. Mireles, ICFO - Institut de Ciències Fotòniques (Spain); Ashley R. Proctor, Univ. of Rochester (United States); Turgut Durduran, ICFO - Institut de Ciències Fotòniques (Spain); Regine Choe, Univ. of Rochester (United States)

Microvascular function is one of the important parameters for monitoring bone healing. Micro-computed tomography, widely used preclinical method for vascularization quantification, requires sacrifice of mice, not allowing longitudinal monitoring from the same subject. Diffuse correlation techniques are sensitive to microvascular blood flow in tissues several millimeters to centimeter deep without contrast agent injection. While diffuse correlation spectroscopy has been utilized to monitor average blood flow in brain, breast, and brain, diffuse correlation tomography (DCT) has limited literature in rat brain.

Here, we report a non-contact system for imaging 3D blood flow in mouse leg using remission DCT. A probe was designed to yield 2 - 10 mm range source-detector separations, providing penetration depth up to 5 mm below skin. A dual-axis galvo was integrated into the non-contact lens system to scan the probe over a 15x15 mm region.

For DCT reconstruction, finite element method based forward solver was developed to solve correlation diffusion equation. An objective function in Rytov formulation was constructed to minimize the difference between measured data and forward-solver-calculated correlation function. To update spatial blood flow distribution, Jacobian matrix with Tikhonov regularization was inverted using a singular value decomposition.

New DCT scheme was tested with a liquid phantom where a 2 mm diameter tube simulating mouse femur with different flow speed was placed in the intralipid solution. In vivo measurements on a mouse leg were performed to demonstrate the DCT capability of deep tissue blood flow imaging. Preliminary results from DCT reconstructions will be presented with discussion of challenges.

9319-51, Session 10

Diffuse correlation and optical spectroscopies for the monitoring and detection of spinal cord ischemia

Angela S. D'souza, Stony Brook Univ. (United States); Rickson C. Mesquita, Univ. of Pennsylvania (United States) and Univ. Estadual de Campinas (Brazil); Thomas Bilfinger, Robert Galler, Stony Brook Univ. Medical Ctr. (United States); Arjun G. Yodh, Univ. of Pennsylvania (United States); Thomas Floyd, Stony Brook Univ. (United States)

BACKGROUND: Spinal cord ischemia can occur during thoracic and spinal surgeries, and after spinal trauma. Current methods to detect ischemia, based upon evoked potential monitoring, are indirect, non-specific, and temporally insensitive. Previously, we reported the accuracy and precision of an optical monitor we developed, based on Diffuse Correlation (DCS) and Optical Spectroscopies, in detection of spinal cord blood flow and oxygenation in a sheep model. Here we report preliminary results after aortic occlusion and spinal cord crush injury, and comparison with evoked potential monitoring techniques.

METHODS: Testing was carried out in twenty-six Dorsett sheep. Sensitivity in detecting spinal cord blood flow and oxygenation changes during aortic occlusion and spinal cord crush injury was assessed. DCS measurement accuracy was determined via comparison to microsphere measurements. Upon aortic occlusion, the time taken by DCS to detect loss of blood flow was compared to time taken by motor and somatosensory evoked potentials to loose signal amplitude.

RESULTS: The device immediately detected fall in blood flow ($\approx 100 \pm 37\%$, $n=32$) and oxygenation ($\approx 17 \pm 13\%$, $n=11$) associated with intra-aortic occlusion. Balloon inflation onto the spinal cord resulted in an immediate decrease in blood flow ($-100 \pm 50\%$, $n=10$), which recovered as soon as the balloon was released. The device is accurate in detecting spinal cord blood flow changes in comparison with microspheres ($R^2=0.49$, $p<0.01$) and immediately detected loss of blood flow (9 seconds) upon aortic occlusion compared to evoked potentials (≈ 16 minutes).

CONCLUSIONS: The fiber-optic probe is capable of continuously measuring spinal cord blood flow and oxygenation preoperatively, intraoperatively, and postoperatively.

9319-52, Session 11

In vivo time-resolved multidistance near infra-red spectroscopy of adult heads: time shift tolerance of measured reflectance to suppress the coupling between absorption and reduced scattering coefficients

Tadatoshi Tanifuji, Daisuke Sakai, Kitami Institute of Technology (Japan)

Absorption and reduced scattering coefficients (μ_a and μ_s') of adult heads were noninvasively determined by multidistance time-resolved reflectance measurements. The finite difference time domain analysis was used to calculate time-resolved reflectance from realistic adult head models composed of four layers (i.e. scalp, skull, gray matter and white matter) with subarachnoid spaces and brain grooves filled with a non-scattering cerebrospinal fluid. In vivo time-resolved reflectances of human heads were measured by a system composed of a time-correlated single photon counter and diode lasers operating at 680 nm and 780 nm. By minimizing the objective functions that compare theoretical and experimental time-resolved reflectances, μ_a and μ_s' of brain were determined. Time shift tolerances of measured reflectance, which is important to improve the accuracies of retrieved optical parameters by suppressing the coupling between absorption and reduced scattering coefficients, are studied using

**Conference 9319:
 Optical Tomography and Spectroscopy of Tissue XI**

the multidistance system with source detector separations (d) of 20 mm, 30 mm, and 40 mm. Detector reading consists of 980 time points, which are equally spaced by $\Delta t = 4.07$ ps. μ_{ya} and μ_{ys} of the four layers were estimated by introducing the same fixed time shift for measured reflectance at all d . The results show that time shift tolerance of measured reflectance for reducing deviations of μ_{ya} and μ_{ys} to less than 10% from the values obtained by optimum time shifts is more than $20.35 (= 5\Delta t)$ ps at both wavelengths. The tolerance is enough for conventional time-resolved measurement systems, which shows time-resolved methods are promising to improve depth sensitivity in cerebral hemodynamics.

9319-53, Session 11

Dynamic image reconstruction in time-resolved diffuse optical tomography

Samuel Powell, Robert J. Cooper, Jeremy Hebden, Simon R. Arridge, Univ. College London (United Kingdom)

Time-resolved diffuse optical tomography presents an opportunity to quantify the haemodynamic responses to functional and pathological events over the whole neonatal head.

A conventional approach to time resolved imaging involves the measurement of the time of flight of individual photons between multiple optical source and detector positions. Each source is used serially, and acquisition continues until the noise in the data is reduced to a level which permits image reconstruction. This process can take many minutes, over which time the transient physiological responses of interest are averaged out.

We take two approaches to increasing the acquisition rate; i) a traditional data 'frame' consisting of the temporal point spread functions of all source detector pairs is split to consider each source at a time, and, ii) the acquisition time for each source detector pair is significantly reduced. This results in noisier measurements, each of which probes only a small part of the full region to be imaged.

To permit the dynamic reconstruction of the full volume using such data requires additional spatio-temporal constraints to be applied to the image reconstruction procedure. In this work we explore the use of a variational form extended Kalman filter which incorporates assumptions regarding the dynamic evolution of the optical parameters of interest. We begin by justifying our choice of temporally-derived measurement types, before describing the algorithm and some of the computational challenges in its implementation. We then present results of dynamic phantom experiments performed with UCL's second generation time-resolved imaging system, MONSTIR II.

9319-54, Session 11

Towards next generation time-domain diffuse optics devices (*Invited Paper*)

Alberto Dalla Mora, Davide Contini, Politecnico di Milano (Italy); Simon R. Arridge, Univ. College London (United Kingdom); Fabrizio Martelli, Univ. degli Studi di Firenze (Italy); Alberto Tosi, Gianluca Boso, Politecnico di Milano (Italy); Andrea Farina, Consiglio Nazionale delle Ricerche (Italy); Turgut Durduran, ICFO - Institut de Ciències Fotòniques (Spain); Edoardo Martinenghi, Alessandro Torricelli, Antonio Pifferi, Politecnico di Milano (Italy)

Diffuse Optics is growing in terms of applications ranging from e.g. oximetry, to mammography, molecular imaging, quality assessment of food and pharmaceuticals, wood optics, physics of random media. Time-Domain (TD) approaches, although appealing in terms of quantitation and depth sensibility, are presently limited to large fibre-based systems, with limited number of source-detector pairs. We present a miniaturised TD

source-detector probe embedding integrated laser sources and single-photon detectors. Some electronics are still external (e.g. power supply, pulse generators, timing electronics), yet full integration on-board using already proven technologies is feasible. The novel devices were successfully validated both on homogeneous and heterogeneous phantoms as well as in vivo on a motor task brain activation exercise, showing performances comparable to large state-of-the-art TD rack-based systems. With an investigation based on simulations we provide numerical evidence that the possibility to stack many TD compact source-detector pairs in a dense, null source-detector distance arrangement could yield on the brain cortex about 1 decade higher contrast as compared to a continuous wave (CW) approach. Further, a 3-fold increase in the maximum depth (down to 6 cm) is estimated, opening accessibility to new organs such as the lung or the heart. Finally, these new technologies show the way towards compact and wearable TD probes with orders of magnitude reduction in size and cost, for a widespread use of TD devices in real life.

9319-55, Session 11

Diffuse optical tomography by using time-resolved single pixel camera

Cosimo D'Andrea, Politecnico di Milano (Italy) and Istituto Italiano di Tecnologia (Italy); Andrea Farina, CNR-Istituto di Fotonica e Nanotecnologie (Italy); Martina Lepore, Laura Di Sieno, Alberto Dalla Mora, Politecnico di Milano (Italy); Nicolas Ducros, Institut National des Sciences Appliquées de Lyon (France); Antonio Pifferi, Gianluca Valentini, Politecnico di Milano (Italy); Simon R. Arridge, Univ. College London (United Kingdom)

In order to increase the Spatial resolution of Diffuse Optical Tomography (DOT) and Fluorescence Molecular Tomography (FMT) a dense raster scanning of the point light source and highly parallel detection (e.g. CCD) are generally adopted. This leads to a huge data set which poses severe limits to the acquisition time and computational tomographic inversion processes. The problem is further complicated when a multidimensional data set is needed, such as temporal and spectral (excitation and detection) information. The highly scattering behavior of biological tissue leads to a low bandwidth of the information spatial distribution and hence the sampling can be preferably carried out in the spatial frequency space. This has led, in the recent years, to the development of structured light based approaches. The low bandwidth can be further exploited on the detection side by adopting compressive sampling schemes. This leads to a significant reduction of the data set while preserving the information content, especially if the compression of both the source and detector space can be carried out at the acquisition level. In this work, a time-resolved single pixel camera scheme combined with structured light method is presented and experimentally validated on phantoms measurements. In particular the use of a single detector combined with Digital Micromirror Device (DMD) and Time Correlated Single Photon Counting (TCSPC) allows to acquire the time-resolved images of the diffuse light exiting the sample. Results will be correlated with the more relevant parameters such as acquisition/computational times, number of adopted patterns.

9319-56, Session 12

Optical tomography using a random diffuser and digital phase conjugation

Yuta Goto, Atsushi Okamoto, Atsushi Shibukawa, Akihisa Tomita, Hokkaido Univ. (Japan); Kunihiro Sato, Hokkai-Gakuen Univ. (Japan)

We propose a new technology for tomographic imaging based on beam diffusion and wavefront reconstruction through digital phase conjugation in a computer. The principle of this technology is highly unique and completely

**Conference 9319:
Optical Tomography and Spectroscopy of Tissue XI**

different from that of well-known optical coherence tomography (OCT) because it does not utilize the coherence property of light. In our method, during the encryption step before the optical measurement, the diffused wavefront is obtained by passing an incident plane wave through a virtual diffuser in a computer. Then, the resultant wavefront is displayed on a spatial light modulator, and irradiated to a biological tissue. The reflection wavefront from the biological tissue is detected by a phase detector. During the decryption step, the detected wavefront is reconstructed through digital phase conjugation in the computer. This method enables the extraction of signal components from the target layer at the specific depth and the elimination of noise components from non-target layers, which are spatially spread due to the diffuser. In addition, this technology relies on image-based processing, thus enabling image-wise measurement without the need for mechanical scanning. Furthermore, this method can yield considerably higher resolution than the conventional methods for OCT. Specifically the depth resolution of this method depends on focus depth of an objective lens and it is smaller than $1\mu\text{m}$ when using the objective lens with NA of 0.8. In our experiment, the depth resolution of smaller than $5\mu\text{m}$ was obtained when using the objective lens with NA of 0.42. In addition, extraction of the information from a specific specimen among several specimens arranged along optical axis was achieved.

9319-57, Session 12

Long-term validation of a multi-wavelength frequency-domain diffuse optical spectroscopy instrument

Thomas D. O'Sullivan, Keun-Sik No, Alex Matlock, Amanda F. Durkin, Brian Hill, Anais Leproux, Albert E. Cerussi, Bruce J. Tromberg, Univ. of California, Irvine (United States)

Frequency domain photon migration provides non-invasive measurements of tissue hemoglobin concentrations and oxygenation states. When combined with broadband continuous-wave near-infrared spectroscopy, the technique becomes a powerful quantitative analysis tool to assess tissue concentrations of water, lipid, cytochromes, and other chromophores with near-infrared absorption signatures. We have designed a miniature diffuse optical spectroscopy instrument that is built on a custom, board-based FDPM module that has four intensity-modulated (50-500MHz) laser diodes (660, 690, 785, and 830nm) and a selectable detector channel to either an internal, fiber-coupled avalanche photodiode (APD) detector or an external tissue-contact APD for recovery of deeper tissue signals.

We have designed, replicated, and internationally distributed 7 of these miniature diffuse optical spectroscopy instruments that are approximately the size of a desktop computer. An optical probe and computer are all that are needed to acquire data, and multiple units can be networked for multi-channel acquisition. We have tested this design in a series of tissue-simulating phantoms and compared them with our established devices that are being tested in a national clinical trial. We will present over two 2 years of instrument performance, including precision, reproducibility, and clinical data that validates its utility - especially in breast oncology.

9319-58, Session 12

Utilizing an open-microcavity optoacoustic sensor for spectroscopic determination of methemoglobin concentration

Ralph W. Peterson, The Univ. of Texas at San Antonio (United States); Kavya Kadugodinandareddy, Vinitha Karunakaran, Casey Whitney, The University of Texas at San Antonio (United States); Amber N. Miller, The Univ. of Texas at San Antonio (United States); Jian Ling, Southwest Research Institute (United States); Jing Yong Ye, The Univ. of Texas at San Antonio (United States)

We present a non-destructive photoacoustic spectroscopy method utilizing a unique open-microcavity optoacoustic sensor to measure the concentration ratio of Methemoglobin (MetHb) in an optically scattering medium. Elevated levels of MetHb, present for example in the blood disorder Methemoglobinemia, cannot be detected by conventional pulse oximetry, and may result in inaccurate arterial oxygen saturation measurements. Samples with different ratios of Oxygenated Hemoglobin (HbO₂), Deoxygenated Hemoglobin (HHb), and MetHb were obtained and mixed with latex beads having a diameter of 300 nm to present an optical scattering effect. A sample chamber containing 1 μL of each sample was positioned directly underneath our patented optoacoustic sensor. Different from a piezoelectric transducer, our optoacoustic sensor allows an excitation laser beam from an OPO laser to pass through it and be absorbed by the sample to produce a photoacoustic signal. The cavity layer of the optoacoustic sensor was exposed directly to the resulting ultrasound signal, which caused an intensity modulation of a HeNe laser that was used to monitor the resonance condition of the sensor. The probe laser beam was total internally reflected off of the sensor and detected with a fiber-coupled APD detector. Three wavelengths at 500 nm, 554 nm, and 578 nm were chosen from our excitation laser due to the absorption peaks of HHb, HbO₂, and MetHb at these wavelengths, respectively. Using established values of the molar extinction coefficients of HbO₂, HHb, and MetHb a set of three simultaneous equations can be solved to accurately determine the concentration ratio of MetHb.

9319-59, Session 12

Real time mapping and tracking of optical properties in deep tissue

Kyle Cutler, Zachary DeStefano, Soroush M. Zarandi, Thomas D. O'Sullivan, Albert E. Cerussi, Gopi Meenakshisundaram, Aditi Majumder, Univ. of California, Irvine (United States); Seung-ha Lee, Dankook Univ. (Korea, Democratic Peoples Republic of); Bruce J. Tromberg, Univ. of California, Irvine (United States)

The measurement of optical properties in deep tissue is playing an increasingly important role in the areas of medical diagnostics and patient monitoring. Two areas that are important to the clinical translation of these type of measurements are tracking and visualization the properties in real time. Previous attempts to track the motion of measurement probes on a surface have been done with electromagnetic fields as well using multiple cameras with markers. Our group has designed a solution to this problem by using a combination of 3D surface geometry, optical flow sensors, and an integrated motion unit. The combination of this data allows for recording and visualizing of optical properties tissues under a surface.

The motion tracking system is currently integrated into a handheld imaging probe that measures optical properties using modulated NIR light. In preliminary tests, the imaging probe was tested on a flat optical phantom with known properties and the 2D spatial distribution of these properties was recovered. We have a process to scan the surface being measured, import it into the 3D visualization software and track where on the surface optical properties measurements are collected. We hope to expand to other handheld imaging probes so they may benefit from this real time mapping and tracking of optical properties. This research was supported in part by NIH Grants P41EB015890 and R01CA142989 and the Arnold and Mabel Beckman Foundation.

9319-60, Session 12

Real-time multispectral spatial frequency domain imaging using binary patterns and a frequency encoded source

Kyle P. Nadeau, Michael T. Ghijsen, Anthony J. Durkin,

**Conference 9319:
 Optical Tomography and Spectroscopy of Tissue XI**

Bruce J. Tromberg, Beckman Laser Institute and Medical Clinic (United States)

Multispectral imaging with structured light allows for the quantification of chromophores beneath the tissue surface. A modality of this type, known as spatial frequency domain imaging (SFDI), typically employs single frequency sinusoidal patterns for light source modulation. Conventional SFDI requires three projections per wavelength per spatial frequency, which limits data acquisition speed. The requirement for multiple projections per spatial frequency can be obviated by increasing the complexity of the spatially modulated light. We have devised a new spatial frequency synthesis approach, which employs illumination using custom patterns having multiple spatial frequency components. We have applied this synthesis approach to binary, square wave patterns. Since these patterns have only two unique values (off and on), they can be projected more rapidly than single frequency sinusoids, which require grayscale values. We have adapted this approach to a real-time SFDI platform using a high speed digital micromirror device (DMD) to generate binary patterns, having a refresh rate faster than the camera exposure time. The light source consists of a temporally-modulated multispectral LED module. Each LED wavelength is modulated at a different temporal frequency, and spectral components are separated by analyzing the frequency spectrum detected at each pixel. Our results demonstrate the ability of our multi-frequency spatial frequency synthesis approach to obtain reflectance and optical property values with accuracy and precision comparable to those obtained using conventional SFDI. We have used our real-time SFDI platform to image an in vivo arm pressure-cuff occlusion model, and obtained tissue oxygen saturation maps at video rates.

9319-61, Session 12

Imaging metabolic oxygen consumption using coherent single snapshot optical properties (cSSOP)

Michael T. Ghijssen, Univ. of California, Irvine (United States); Kyle P. Nadeau, Bernard Choi, Anthony J. Durkin, Beckman Laser Institute and Medical Clinic (United States); Sylvain Gioux, Beth Israel Deaconess Medical Ctr. (United States); Bruce J. Tromberg, Beckman Laser Institute and Medical Clinic (United States)

Aberrations in tissue metabolism are present in multiple disease states including peripheral artery disease and cancer. Important diagnostic and prognostic information can be gained from imaging the metabolic rate of oxygen consumption in these tissues. Spatial frequency domain imaging (SFDI) is a noncontact wide-field modality that can quantitatively determine concentrations of oxyhemoglobin and deoxyhemoglobin. Laser speckle imaging (LSI) is a related technique that can estimate blood-flow. SFDI with a coherent source (cSFDI) can measure intrinsically coregistered absorption, scattering, and scatter-corrected speckle contrast, providing a noninvasive means of measuring the tissue oxygen consumption. Previously, demodulation techniques in SFDI have limited data acquisition speed. Single Snapshot Optical Properties (SSOP) is a novel form of SFDI that reconstructs optical properties using a single frame of data by extracting AC and DC content simultaneously, reducing acquisition time by a factor of six. This same method can be applied to cSFDI where single captured images are processed to reconstruct both the optical properties and speckle contrast. In this work we perform dynamic coherent SSOP (cSSOP) imaging using 670 and 808 nm long coherence length sources spatially modulated at 0.2 mm⁻¹ with a frame rate of 25 Hz. We report real-time chromophore and speckle flow index (SFI) reconstruction of the forearm in a subject undergoing cuff-occlusion. We combine this information toward a quantitative measure of oxygen consumption.

Conference 9320: Microfluidics, BioMEMS, and Medical Microsystems XIII

Saturday - Monday 7-9 February 2015

Part of Proceedings of SPIE Vol. 9320 Microfluidics, BioMEMS, and Medical Microsystems XIII

9320-1, Session 1

Materials selection and manufacturing of thermoplastic elastomer microfluidics (Invited Paper)

Dan Sameoto, Abdul Wasay, Univ. of Alberta (Canada)

Thermoplastic elastomers (TPEs) are a class of material that is seeing increasing application in the fields of microfluidics and BioMEMS. Unlike the more commonly used polydimethylsiloxane (PDMS) elastomers, these TPEs can be processed very quickly (mold times less than 30 seconds), can be easily welded to other thermoplastic materials, and have a wide range of mechanical properties, from soft and tacky to a hard rubber consistency. While PDMS, and in particular Sylgard 184, has been extensively characterized in the literature, there are few design guidelines for micromanufacturing with thermoplastic elastomers with respect to material choice, molding methods and compatible processes. We have developed a new soft-lithographic molding technology that directly compression molds these thermoplastics into the appropriate geometries for microfluidic applications. With appropriate material choice, sub-100 nm replication fidelity can be achieved. Issues such as material outgassing during molding, surface quality and bondability are investigated for a select number of thermoplastic elastomers from different commercial suppliers. A new reversible bonding methodology, feasible with the use of relatively soft thermoplastics, is also characterized to demonstrate the unique options available when thermoplastics may be highly structured or even molded with interlocked features. In comparison to PDMS bonding strategies, the techniques demonstrated here are easily integrated with rigid thermoplastics, like polystyrene and polypropylene, commonly used in macroscale applications like cell culturing and polymerase chain reaction. As a result, the path to commercialization of thermoplastic elastomer microfluidics may be shortened by virtue of being compatible with large-scale manufacturing technologies including hot-embossing and injection molding.

9320-2, Session 1

Rapid prototyping of microfluidic channels in nitrocellulose using laser-direct-write patterning

Peijun J. W. He, Ioannis N. Katis, Robert W. Eason, Collin L. Sones, Univ. of Southampton (United Kingdom)

The demand for low-cost alternatives to conventional point-of-care (POC) diagnostic tools has led to significant developments in the field of microfluidics in porous paper. Several approaches have already been reported for fabricating fluidic devices in such materials, which include photolithography, inkjet printing, printing of wax, plasma oxidation, laser-cutting, and shaping. Nitrocellulose is a particularly important material that is routinely used in lateral-flow type medical diagnostic tests used in POC environments.

Here, we report the patterning of microfluidic structures in porous nitrocellulose through a simple laser-direct-write (LDW) procedure, which relies on light-induced photo-polymerisation of a photopolymer previously impregnated in the nitrocellulose membranes. During the subsequent development step, the un-polymerised photopolymer is removed, while the polymerized structures remain. These resulting hydrophobic structures extend throughout the thickness of the nitrocellulose and form the barrier-walls of the interconnected hydrophilic fluidic patterns they demarcate. Analysis showed that these structures can contain and guide the flow of liquids without any leakage, and hence this technique can be used to

produce an array of microfluidic devices for many applications such as clinical diagnostics and analytical chemistry. Our results show that the smallest dimensions that can be achieved for hydrophobic barrier-walls and microfluidic channels using this method are ~ 60 μm and ~ 100 μm respectively, both of which are the smallest values reported so far for fabrication of nitrocellulose-based microfluidic devices. In addition, the process steps for this LDW process are compatible for roll-to-roll processing, which would lead to device production on a commercial-scale.

9320-3, Session 1

Rapid prototyping of glass microfluidic chips

Frederik Kotz, Karlsruher Institut für Technologie (Germany); Klaus Plewa, Werner Bauer, Thomas Hanemann, Ansgar Waldbaur, Karlsruhe Institute of Technology (Germany); Elisabeth Wilhelm, Christiane Neumann, Bastian E. Rapp, Karlsruher Institut für Technologie (Germany)

Most microfluidic prototypes used in research are usually made either by polydimethylsiloxane (PDMS) soft lithography or stereolithography (STL) of commercially available photopolymers. However, when microreactors with high chemical and temperature resistance are needed glass is still the material of choice. Unfortunately glass structuring is usually done by masking or photo structuring of glass substrates and subsequently wet chemically etching with hydrofluoric acid (HF) solutions. The usage of the extremely hazardous substance HF is a major drawback of this structuring process.

We have previously developed a maskless projection lithography system based on a digital mirror device (DMD). In recent works we have already reported the suitability of this system to structure photoresists and to create grayscale protein bitmaps. In this work we suggest a new method to create transparent and leakproof microfluidic chips. Therefore we dispersed silica powder of different sizes in acrylic mixtures of hydroxyethylmethacrylate (HEMA), butandioldiacrylate (BDDA) and an appropriate initiator. Structuring of microfluidic chips can then be done by molding or STL. After thermal or photopolymerisation the components are debindered by pyrolysis and sintered in an oven at atmospheric conditions. The used acrylic mixture allows the dispersion of high silica powder concentrations (up to 50 vol. %) which are required for high quality sintered parts.

9320-4, Session 1

Protein assay structured on paper by using lithography

Elisabeth Wilhelm, Tobias M. Nargang, Wala Al Bitar, Björn Waterkotte, Bastian E. Rapp, Karlsruher Institut für Technologie (Germany)

There are two main problems that have to be addressed during the manufacturing of a robust paper based microfluidic devices. The first one is to create the hydrophobic barrier. The second challenge is the creation of the sensitive layer for the assay.

In mass production wax often applied to create hydrophobic barriers. However wax tends to break when the paper is bended. An alternative to wax is usage of silanes such as dimethoxydimethylsilane (DMDMS). However, thermally initiated silanization techniques are time consuming. Commonly used methods for structuring sensitive layers are often not

**Conference 9320:
Microfluidics, BioMEMS, and Medical Microsystems XIII**

applicable to proteins, because these tend to lose their immunological activity during immobilization.

We propose a method in which we create the hydrophobic layer by using UV-light based silanization by mixing DMDMS with a photo acid generator and bidistilled water. With this method we can reduce the fabrication time for creating hydrophobic barrier from 90 minutes to 5 minutes. A light-based approach that allows easy creation of a sensitive protein layer is also demonstrated. Therefore immobilization of fluorescein-5-biotin on Whatman 1 filter paper is carried out by means of photobleaching with visible light using a maskless projection lithography system. The light-based structuring allows fast immobilization of defined amounts of proteins as well as the formation of protein gradients. The immunological activity, which is not influenced by the low energy light applied, was illustrated by biotin/streptavidin-Cy3 interaction.

Through the combination of DMDMS-based structuring and photobleaching it is possible to quickly create paper-based protein assay in less than 90 minutes.

9320-5, Session 1

Direct-write laser techniques for the manufacture of multiplexed paper-based diagnostic sensors

Ioannis N. Katis, Peijun J. W. He, Robert W. Eason, Collin L. Sones, Optoelectronics Research Ctr., Univ. of Southampton (United Kingdom)

The ever-present need for affordable and reliable devices for health monitoring has led to a significant growth over the past few years in the development and applications of paper-based point-of-care diagnostics that operate with minimal reagent volumes, are portable and need no special training or equipment for their use.

We present here our work on the fabrication of multiplexed paper-based diagnostic sensors for the detection of glucose and bovine serum albumin (BSA) using lasers-based methods. Our use of lasers for the fabrication of the devices is justified by the versatility, speed of production, and cost, all of which are of critical importance for mass-market applications. A laser direct-write process, Laser-Induced Forward Transfer (LIFT), was used to print the reagents and biological molecules on paper substrates that facilitate the sensing of the specific analytes. A second laser-based process was also implemented to create hydrophobic walls and barriers in paper and membrane substrates, which define the wells and channels that can guide biological and chemical solutions through the paper devices. A pulsed KrF excimer laser operating at 248 nm was used for LIFT and a continuous wave laser at 405 nm was used for patterning of the paper. The small dimensions of the structures produced (~100 μm) and the precise and low-volume (nl) deposition of materials by these processes enable the miniaturisation of these devices ensuring the minimal use of reagents. We have quantified the speed and cost of our laser-based methods and believe they can be up-scaled for mass production.

9320-6, Session 2

Silicon photonics biosensing: different packaging platforms and application possibilities (*Invited Paper*)

C. Arce, E. Hallynck, Sam Werquin, Jan-Willem F. I. B. Hoste, Daan Martens, Peter Bienstman, Univ. Gent (Belgium)

Silicon photonics is an attractive platform for biosensors and lab-on-a-chip systems. First, it benefits from a high refractive index contrast permitting very compact sensors of which many can be incorporated on a single chip, enabling multiplexed sensing. Second, silicon-on-insulator photonic

chips can be made with CMOS-compatible process steps, allowing for a strong reduction of the chip cost by high-volume fabrication. By using ring resonators with high quality factors that have very narrow resonance peaks, very small spectral shifts can be detected.

In this talk, we will discuss a number of different novel microfluidic contexts in which these devices can be operated: at the facet of an optical fibre, integrated in the bottom of a reaction tube or inside a digital microfluidic platform. Also, we will discuss point-of-care applications, as well as a configuration which allow one to measure conformational changes of biomolecules in a 2D array of sensors.

9320-7, Session 2

An scalable engineering approach to improve performance of a miniaturized optical detection system for in vitro point-of-care testing

Hannah R. Robbins, Sijung Hu, Changqing Liu, Loughborough Univ. (United Kingdom)

The demand of rapid screening technologies, to be used outside of a traditional healthcare setting, has been vastly expanding. This is requiring a new engineering platform for faster and cost effective techniques to be easily adopted through forward-thinking manufacturing procedures, i.e., advanced miniaturisation and heterogeneous integration of high performance microfluidics based point-of-care testing (POCT) systems. Although there has been a considerable amount of research into POCT systems, there exist tremendous challengers and bottlenecks in the design and manufacturing in order to reach a clinical acceptability in robustness and cost effectiveness, as well as smart microsystems for homecare. The project aims to research how to enable scalable production of such complex systems through 1) advanced miniaturisation of a physical layout and opto-electronic component allocation through an optimal design; and 2) heterogeneous integration of multiplexed fluorescence detection (MFD) for in vitro POCT. Understanding multi-physical principles for MFD system is essential by means of Comsol software - to provide a clear guideline for manufacturing a functional prototype. Verification is being arranged through an experimental testing with a series of dilutions of fluorescence dye, i.e. Cy5. Iterative procedures will be engaged until satisfaction of the detection limit and repeatability is met as proposed. The research creates a new avenue of rapid screening POCT manufacturing solutions with a particular view on high performance and multi-functional detection systems not only in POCT, but also life sciences and environmental applications.

9320-8, Session 2

Comparison of roll-to-roll replication approaches for microfluidic and optical functions in lab-on-a-chip diagnostic devices

Christian Brecher, Fraunhofer-Institut für Produktionstechnologie (Germany) and Lab. for Machine Tools and Production Engineering (WZL) (Germany); Christian Wenzel, Thomas Bastuck, Christoph Baum, Fraunhofer-Institut für Produktionstechnologie (Germany)

Economically advantageous microfabrication technologies for lab-on-a-chip diagnostic devices substituting commonly used glass etching or injection molding processes are one of the key enablers for the emerging market of microfluidic devices. On-site detection in fields of life sciences, point of care diagnostics and environmental analysis require compact, disposable and highly functionalized systems. Roll-to-roll production as a high volume process has become the emerging fabrication technology for integrated, complex high technology products within recent years (e.g. fuel cells).

**Conference 9320:
Microfluidics, BioMEMS, and Medical Microsystems XIII**

Differently functionalized polymer films enable researchers creating a new generation of lab-on-a-chip devices by combining electronic, microfluidic and optical functions in multilayer architecture.

For replication of microfluidic and optical functions via roll-to-roll production process competitive approaches are available. One is to imprint fluidic channels and optical structures of micro- or nanometer scale from embossing rollers into UV curable lacquers on polymer substrates. Depending on dimension, shape and quantity of those structures there are alternative manufacturing technologies for the embossing roller. Ultra-precise diamond turning, electroforming or casting polymer materials are used either for direct structuring or manufacturing of roller sleeves. Mastering methods are selected by application according to replication quality required, structure complexity and cost effectiveness. Criteria for the replication quality are surface roughness and contour accuracy. Structure complexity is evaluated by shapes producible (e.g. linear, circular) and aspect ratio. Costs for the mastering process and structure lifetime have crucial influence on the cost effectiveness.

The alternative replication approaches are introduced and analyzed corresponding to the criteria presented. Advantages and drawbacks of each technology are discussed and exemplary applications are given.

9320-9, Session 2

Environmental sensing with optical fiber sensors processed with focused ion beam and atomic layer deposition

Jaime Viegas, Ricardo Janeiro, Raquel Flores, Ammar Alqahtani, Marcus V. S. Dahlem, Masdar Institute of Science & Technology (United Arab Emirates)

We report an optical fiber chemical sensor based on a focused ion beam processed optical fiber. The demonstrated sensor is based on a cavity formed onto a standard 1550 nm single-mode fiber by either chemical etching, focused ion beam milling (FIB) or femtosecond laser ablation, on which side channels are drilled by either ion beam milling or femtosecond laser irradiation. The encapsulation of the cavity is achieved by optimized fusion splicing onto a standard single or multimode fiber. The empty cavity can be used as semi-curved Fabry-Pèrot resonator for gas or liquid sensing. Increased reflectivity of the formed cavity mirrors can be achieved with atomic layer deposition (ALD) of alternating metal oxides. For chemical selective optical sensors, we demonstrate the same FIB-formed cavity concept, but filled with different materials, such as polydimethylsiloxane (PDMS), poly(methyl methacrylate) (PMMA) which show selective swelling when immersed in different solvents. Finally, a reducing agent sensor based on a FIB formed cavity partially sealed by fusion splicing and coated with a thin ZnO layer by ALD is presented and the results discussed. Sensor interrogation is achieved with spectral or multi-channel intensity measurements.

9320-10, Session 3

Photo-patterned free-standing hydrogel microarrays for massively parallel protein analysis (Invited Paper)

Todd A. Duncombe, Amy E. Herr, Univ. of California, Berkeley, Bioengineering (United States)

Microfluidic technologies have largely been realized within enclosed microchannels. While powerful, a principle limitation of closed-channel microfluidics is the difficulty for sample extraction and downstream processing. To address this limitation and expand the utility of microfluidic analytical separation tools, we developed an open-channel hydrogel architecture for rapid protein analysis. Designed for compatibility with slab-gel polyacrylamide gel electrophoresis (PAGE) reagents and instruments, we detail the development of free-standing polyacrylamide

gel (fsPAG) microstructures supporting electrophoretic performance rivaling that of microfluidic platforms. Owing to its open architecture – the platform can be easily interfaced with automated robotic controllers and downstream processing (e.g., sample spotters, immunological probing, mass spectroscopy). The fsPAG devices are directly photopatterned atop of and covalently attached to planar polymer or glass surfaces. Due to the fast < 1 hr design-prototype-test cycle – significantly faster than mold based fabrication techniques – rapid prototyping devices with fsPAG microstructures provides researchers a powerful tool for developing custom analytical assays. Leveraging the rapid prototyping benefits – we up-scale from a unit separation to an array of 96 concurrent fsPAGE assays in 10 min run time driven by one electrode pair. The fsPAGE platform is uniquely well-suited for massively parallelized proteomics, a major unrealized goal from bioanalytical technology.

9320-11, Session 3

Modelling defect tolerance sensitivity to microfluidic channel periodic post parameters

Mahyar Mehran, Bonnie L. Gray, Glenn H. Chapman, Simon Fraser Univ. (Canada)

Previously we explored the benefits of using microfluidic channels and chambers that utilize a “cathedral-ceiling” design through the development of a semi-automated technique that combines rule-base defect placement system and Monte Carlo method for modeling the fluid dynamics and blockage formation based on the likelihood of blockages forming in areas of high particle traffic and low flow. Earlier results indicated that cathedral channels that are supported by an array of 10 by 10 periodic posts with the same size as the channels have six times higher lifetime expectancy compared to arrays of 10 parallel channels through the provision of multiple paths during localized blockage formation. In this paper we have continued our investigations by considering the defect tolerance sensitivity to parameters such as the number and size of the posts and channels. Having the same number of posts in the channel and same starting position for the first 10 blockages, we shrunk the size of the posts to 65% of the original size so that the channels are now twice the size of the posts. Iterating models as before, we observe that in the first iteration 80% of the blockages are formed in the same locations and as we proceed this number decays but still produces similar overall flow and pressure patterns. In addition we are also starting simulations based on longer microfluidic channels supported by arrays 10 by 20 periodic posts to explore the microfluidic behaviors under similar modeling conditions and to further prepare for our experimental verification.

9320-12, Session 3

A novel reciprocating micropump based on Lorentz force

Alinaghi Salari, Univ. of Calgary (Canada); Abbas Hakimsima, Sharif Energy Research Institute (Iran, Islamic Republic of); Mohammad Behshad Shafii, Sharif Univ. of Technology (Iran, Islamic Republic of)

Lorentz force is the pumping basis of many electromagnetic micropumps used in lab-on-a-chip. In this paper a novel reciprocating single-chamber micropump is proposed, in which the actuation technique is based on Lorentz force acting on an array of microelectrodes attached on a membrane surface. An alternative current is applied through the microelectrodes in the presence of a magnetic field. The resultant force causes the membrane to oscillate and pushes the fluid to flow through microchannel using a ball-valve. The pump chamber (3 mm depth) was fabricated on a 5mm thick Polymethylmethacrylate (PMMA) substrate using laser engraving technique. The chamber was covered by a 200 μm thick hyper-elastic latex rubber diaphragm. Two miniature permanent magnets

**Conference 9320:
 Microfluidics, BioMEMS, and Medical Microsystems XIII**

capable of providing magnetic field of 0.09 T at the center of the diaphragm were mounted on each side of the chamber. Square wave electric current with low-frequencies in the range of 5-8 Hz was generated using a function generator. Cylindrical copper microelectrodes (250 μ m diameter and 10 mm length) were attached side-by-side on top surface of the diaphragm. Thin loosely attached wires were used as connectors to energize the electrodes. Due to large displacement length of the diaphragm (~3 mm) a high efficiency (~80%) ball valve (2 mm diameter stainless steel ball on a 4 mm diameter ball seat) was used in the pump outlet. The micropump exhibits a flow rate as high as 490 μ l/s and pressure up to 1.5 kPa showing that the pump is categorized among high-flow-rate mechanical micropumps reported to date.

9320-13, Session 3

A light-activated optopiezoelectric thin-film actuator for microfluidic applications

Hsin-Hu Wang, Chih-Kung Lee, Yu-Hsiang Hsu, National Taiwan Univ. (Taiwan)

In this paper, we present a photoconductor-coupled piezoelectric thin-film for serving as a light-activated actuator for integrating with a microfluidic device. This optopiezoelectric thin-film combines the unique characteristic of both photoconductive material (titanium oxide phthalocyanine: TiOPc) and piezoelectric polyvinylidene fluoride (PVDF). The photoconductive material serves as one of the electrodes of the piezoelectric thin-film that can be spatially and temporally activated by illuminating with a visible light source. The PVDF thin-film provides mechanical forces that can introduce bending deformation for pumping and valving applications in a microfluidic device. Using this design, different locations of an optopiezoelectric thin film can be optically switched on and off with a programmable light mask. Thus, multiple areas of different locations can be activated on a PVDF thin-film.

By using this concept and integrating into a microfluidic device, multiple pumps and valves could be operated independently by using one driving voltage source and a programmed mask. This new type of microfluidic actuator can bypass the fundamental limitations of a multi-functioned microfluidic device, where multiple pumps and valves are usually needed. Traditional methods usually need to connect a considerable amount of pressurized pipes or driving voltage sources to control each pump and valve independently. With the newly developed optopiezoelectric actuator, complex operations of a large scale microfluidic device could be largely simplified and be scaled up very easily. Both finite element simulations and experimental verifications will be detailed to demonstrate the feasibility of this optopiezoelectric thin-film actuator.

9320-14, Session 4

Micro and nano sensors on a rotating disc
(Invited Paper)

Anja Boisen, Technical Univ. of Denmark (Denmark)

The optics and mechanics from a DVD player can be used to realize compact and sensitive sensor systems. By rotating a disc with integrated microfluidic channels it is possible to manipulate liquid samples such as blood – performing crucial operations like separation and mixing. We integrate sensors such as cantilevers, nanoparticles and resonating strings with centrifugal microfluidics. The sensors are read out by a DVD pick-up head which can perform transmission/absorption measurements and which can detect nm deflections. Also, electrodes are integrated on a disc platform, facilitating electrochemical measurements.

In cantilever-based sensing, micrometer sized cantilevers are functionalized on one side with probe molecules. As target analytes bind to the probe molecules the cantilever deflects due to changes in surface stress. This deflection is typically in the nm range and normally only a few cantilevers can be read-out simultaneously. Using a rotating disc system hundreds of cantilevers can be read-out in one second. We will demonstrate how

this approach can be used for detection of biomarkers and explosives. Hollow cantilevers will be briefly discussed as a new way of performing IR spectroscopy on pl amount of sample. Vibrating micrometer sized strings can be used for efficient and sensitive mass detection and for chemical analysis of single nanoparticles. We will show examples from drug characterization and illustrate how the strings can be read-out using blue-ray optics. Finally, we will show how agglutination based assays can be handled and read-out using the disc platform – here targeting biomarkers.

9320-15, Session 4

Particle trajectory in microfluidic channels determined by spatially modulated fluorescence emission

Joerg Martini, Bowen Cheng, Malte F. Huck, Peter Kiesel, Michael I. Recht, Doron Kletter, Palo Alto Research Center, Inc. (United States)

We demonstrate three-dimensional (3D) observation of particle trajectories in microfluidic channels utilizing spatially modulated fluorescence emission. Spatial transmission masks are used to convert the light of continuously fluorescing and linearly moving particles into a time dependent intensity signal. We use this spatial encoding method to measure 3D particle flow trajectories along a 1.2mm long flow path in 125 μ m wide and 25 μ m deep microfluidic channels. The mask pattern, speed of the particle, and its relative position to the mask affect the particle's time dependent signal. For a given mask, particle speed and trajectory can be simultaneously determined by the time dependent intensity measurements that are recorded by a single pixel detector. For periodic mask features, the speed of the particle – typically on the order of 1 m/s - can for example be calculated from a Fourier transform of the particle signature. Triangular mask features reveal the lateral particle position through a duty cycle analysis of fluorescence signals with a standard deviation of < 4 μ m. Particle depth measurements can be performed with periodic masks that have been created with a superimposed fine structure. The relative contribution of course and fine structure to two discrete peaks in the Fourier spectrum of a particle signature, allows for a depth determination with a standard deviation of < 2 μ m. The developed techniques can be used for particle control in microfluidic sorting, filtering and enrichment applications.

9320-16, Session 4

Fluid flow optimization of an AC electrothermal micropump consisting of two opposing rows of microelectrodes for biofluidic applications

Alinaghi Salari, Colin Dalton, Univ. of Calgary (Canada)

Electrokinetics has many applications in a wide range of areas, such as lab-on-a-chip and biomedical microdevices. The electrothermal effect has been used for biofluid delivery systems since it has high pumping efficiency for high conductive liquids (>0.1 S/m) compared to other electrokinetic techniques such as electroosmosis. AC electrothermal (ACET) micropumps are based on the temperature gradient caused by Joule heating or an external heat source, which generates permittivity and conductivity gradients in the bulk of the liquid. When the liquid is subjected to an electric field, the ACET force is created. Electrode geometry significantly affects the electric field distribution, which can yield stronger ACET forces. Previously electrode dimension optimization has been performed for a single-row coplanar asymmetric configuration in order to obtain maximum ACET velocities. In this paper we expand the optimization procedure to other governing physical parameters in a two-row microelectrode array configuration consisting of microelectrodes placed on the top and bottom of a microchannel. The studied parameters are the electrodes' vertical asymmetry, actuation voltage asymmetry, distance between electrode

**Conference 9320:
Microfluidics, BioMEMS, and Medical Microsystems XIII**

rows and the substrates' thickness. Electrode dimensions remain constant during the study (120 μm wide and 20 μm thin electrodes, 20 μm gap). The optimization is performed using finite element analysis software for one pair of microelectrodes on each row with periodic boundary conditions. The simulation data is then compared with experimental data for a combination of the aforementioned parameters. The results show that these parameters can dramatically affect the ACET flow and need to be considered among controlling parameters.

9320-17, Session 4

Laser direct writing 3D structures for microfluidic channels: flow meter and mixer

Chih-Lang Lin, Central Taiwan Univ. of Science and Technology (Taiwan); Yi-Hsiung Lee, Jiun-Yi Yang, Po-Yu Chen, Yi-Jui Liu, Feng Chia Univ. (Taiwan); Patrice L. Baldeck, Ctr. National de la Recherche Scientifique (France)

This study introduces a direct reading flow meter and a three-dimensional (3D) passive mixer fabricated by laser direct writing for microfluidic channel applications. The flow meter consists of a rod-spring, a 3D frame and an indicator, installed inside a microfluidic channel. The whole size of the flow meter is about 23 μm (z) \times 31 μm \times 20 μm (x-y). The width and the depth of main channel separately are 80 μm and 25 μm . The indicator is deflected by the flowing fluid while restrained by the spring (square section: 0.63 μm \times 1.2 μm) to establish an equilibrium indication according to the flow rate. The measurement is readily carried out by optical microscopy observation. The 3D passive mixer with screw shape is designed to disturb the laminar flow in three dimensions to enhance the mixing efficiency. The whole size of the screw is about 50 μm \times 30 μm \times 45 μm . The width and the depth of main channel separately are 50 μm and 45 μm . The simulation results indicate that the screw provides 3D streamlines in the microchannel. The parameters of thread pitch, the screw length, and the blade number were evaluated for an optimal design of high efficient mixing. Eventually, a three-blade screw was fabricated in-line within the microchannel for demonstration. Thanks to the laser direct writing technology, this study performs the ingenious applications of 3D structures for microchannels.

9320-18, Session 5

Deformation cytometry: mechanical phenotyping for label free detection of cellular disease states (Invited Paper)

Eric D. Diebold, Jonathan Lin, Dino Di Carlo, Univ. of California, Los Angeles (United States)

Label-free, rapid detection of cellular abnormality and disease is a long-sought goal of clinical diagnostics. While biochemical markers are commonly used to improve the sensitivity and specificity of diagnostic techniques, label-free biophysical markers have seen only limited adoption in clinical and research applications. One biophysical marker, cellular deformation under mechanical stress, is an intrinsic cellular property that can be used to classify populations at the single-cell level. Using a microfluidic extensional flow, we perform high throughput cellular deformation measurements on thousands of cells per second, using a high-speed camera and digital image processing to characterize multiple biophysical parameters of each cell as they deform. These multiparameter measurements ultimately compose a mechanical phenotype, enabling high dimensional mechanical classification of cells in a high throughput manner. Here, we present new technological advances to extract these measurements, using phase contrast microscopy to expand our biophysical parameter feature set, and light scattering to improve the capture efficiency of the technique.

9320-19, Session 5

DNA separation and fluorescent detection in an optofluidic chip with sub-base-pair resolution

Markus Pollnau, Manfred Hammer, Chaitanya Dongre, Hugo J. W. M. Hoekstra, Univ. Twente (Netherlands)

DNA sequencing in a lab-on-a-chip aims at providing cheap, high-speed analysis of low reagent volumes to, e.g., identify genomic deletions or insertions associated with genetic illnesses. Detecting single base-pair insertions/deletions from DNA fragments in the diagnostically relevant range of 150-1000 base-pairs requires a sizing accuracy of $S < 10^{-3}$. Here we demonstrate $S = 4 \times 10^{-4}$.

A microfluidic chip was post-processed by femtosecond-laser writing of an optical waveguide. 12 blue-labeled and 23 red-labeled DNA fragments were separated in size by capillary electrophoresis, each set excited by either of two lasers power-modulated at different frequencies, their fluorescence detected by a photomultiplier, and blue/red signals distinguished by Fourier analysis. Different calibration strategies were tested: a) use either set of DNA molecules as reference to calibrate the set-up and identify the base-pair sizes of the other set in the same flow experiment, thereby eliminating variations in temperature, wall-coating and sieving-gel conditions, and actuation voltages; b) use the same molecular set as reference and sample with the same fluorescence label, flown in consecutive experiments; c) perform cross-experiments based on different molecular sets with different labels, flown in consecutive experiments.

From the results we conclude: Applying quadratic instead of linear fit functions improves the calibration accuracy. Blue-labeled molecules are separated with higher accuracy. The influence of dye label is higher than fluctuations between two experiments. Choosing a single, suitable dye label combined with reference calibration and sample investigation in consecutive experiments results in $S = 4 \times 10^{-4}$, enabling detection of single base-pair insertion/deletion in a lab-on-a-chip.

9320-20, Session 5

Monolithically integrated microfluidic nanoporous gold disk (NPGD) surface-enhanced Raman scattering (SERS) sensor for rapid and label-free biomolecular detection

Ming Li, Fusheng Zhao, Jianbo Zeng, Univ. of Houston (United States); Gregg Santos, Univ of Houston (United States); Wei-Chuan Shih, Univ. of Houston (United States)

We present a novel microfluidic surface-enhanced Raman scattering (SERS) sensor for rapid and label-free biomolecular detection. Our sensor design mitigates a common limiting factor in microfluidic SERS sensors that utilize integrated nanostructures: low-efficiency transport of biomolecules to nanostructured surface which adversely impacts sensitivity. Our strategy is to increase the total usable nanostructured surface area, which provides more adsorption sites for biomolecules. Specifically, nanoporous gold disk (NPGD) array, a highly effective SERS substrate, has been monolithically integrated inside a microfluidic chip. Individual NPGD is known to feature an order of magnitude larger surface area than its projected disk area. The increased surface area arises from nanoscale pores and ligaments 3-dimensionally distributed in the NPGD, which manifest themselves as high-density SERS hot-spots. High-density NPGD arrays further guarantee large coverage of these hot-spots on the microchannel floor. The SERS-active NPGD arrays enable highly-reproducible SERS measurements with relative intensity variations from 8% to -8%. R6G solutions in the concentrations ranging from 1 μM to 1 mM have been detected and quantitatively evaluated, and the performance of the sensor in continuous-flow condition has been assessed. Moreover, the sensor's capabilities have

**Conference 9320:
Microfluidics, BioMEMS, and Medical Microsystems XIII**

been studied by detecting and identifying a neurotransmitter (DA), and a physiological metabolite (urea), and the results show lower detection limit compared to best results from most recent work using integrated nanostructured surface inside microchannels. We expect that the sensor would be applicable for detecting, identifying and quantifying molecules for some point-of-care applications, i.e. urine screening.

REFERENCES:

Ming Li, Fusheng Zhao, Jianbo Zeng, Ji Qi, Jing Lu, and Wei-Chuan Shih, "Microfluidic surface-enhanced Raman scattering (SERS) sensor with monolithically integrated nanoporous gold disk (NPGD) arrays for rapid and label-free biomolecular detection," *Journal of Biomedical Optics* 2014 (Accepted).

9320-21, Session 5

Optical detection of clot contractility in a 'wound-in-a-chip' device

Nikita Taparia, Lucas H. Ting, Annie O. Smith, Nathan J. Sniadecki, Univ. of Washington (United States)

Platelets activate, aggregate, and contract into a strong clot in response to a vascular wound site. Any platelet dysfunction can cause excessive bleeding. Currently, clinicians use thrombelastography to help determine the clot contractility and the correct transfusion protocol but this technique requires at least thirty minutes, which is too long for a trauma setting. Recently, our lab developed a 'wound-in-a-chip' device. This device contains force sensors, which includes a rigid block to activate the platelets through pathological shear rates and a micropost to measure the force generation. Typically, an expensive fluorescence microscope with a high magnification oil lens tracks the deflections. However, the small field of view limits the throughput and in general, it is not ideal for a clinical setting. Thus, we have designed a compact, cheap fluorescent microscope capable of tracking submicron deflections for rapid diagnosis of platelet dysfunction. This microscope uses a CMOS sensor and a reversed webcam lens, which enables a field of view similar to a 10x objective but with a resolution better than a 20x objective. A light emitting diode and condenser illuminate the sample with focused light. For fluorescence detection, TRITC filters were used to excite and capture the Dil stained microposts. With this new system, we have measured the clot contractile forces of many blood donors within five minutes in comparison to a normal microscope. In conclusion, we have created a rapid diagnostic tool to identify platelet dysfunction in trauma and surgical settings.

9320-22, Session 6

New generation of neural prosthetic ECoG arrays using glassy carbon-based micromachined microelectrodes (Invited Paper)

Sam Kassegne, San Diego State Univ. (United States)

In this talk, we report on our recently demonstrated glassy carbon-based array of microelectrodes on a flexible substrate for applications in neural sensing and simulations. The microelectrodes are made of pyrolyzed carbon derived from polymer pre-cursor using GC-MEMS (Glassy Carbon MEMS) process and are capable of interrogating a wider area. The ensuing 'microelectrode array fabric' could be used for both implantable as well as wearable applications. We report on the electrical, electrochemical, mechanical stiffness and hardness tunability of patternable glassy carbon (GC) microelectrode probe structures for potential applications in the broader areas of bio-electrical signal recording and stimulation. The glassy carbon microelectrodes have excellent electrochemical stability in ionic solutions and excellent response to chemical surface treatments for surface property modifications. In addition, lithographically patternable GC material offers a unique tailorability functionality that enables fabrication

of electrodes with a range of mechanical, electrical, and electrochemical properties that closely match the behavior of soft tissues. The pyrolysis conditions (maximum temperature, duration of pyrolysis, and ramp rate) that drive this flexibility, could be varied to enable useful tailorable properties such as: (i) tailorable mechanical stiffness that is softer than silicon shanks or metals, offering a much better stiffness-matching with soft tissues, (ii) tailorable electrical impedance characteristics for better impedance-matching with tissues, and (iii) tailorable electrochemical property useful for optimized electrical stimulation and recording.

The talk will also demonstrate that GC carbon electrodes could have higher electro-kinetics at their surface with high charge injection capacity as compared to conventional metal probes, low impedance, and modulus in the range of 25-55 GPa. Therefore, we believe that these results reported here could help make GC-MEMS microelectrodes, probes of choice for bio-signal sensing and stimulation applications, particularly for β -ECoG and ECG systems.

9320-23, Session 6

Beyond isolated cells: microfluidic transport of large tissue for pancreatic cancer diagnosis

Ronnie Das, Rachel G. Murphy, Eric J. Seibel, Univ. of Washington (United States)

For cancer diagnoses, core biopsies (CBs) obtained from patients using coring needles (CNs) are traditionally visualized and assessed on microscope slides by pathologists after samples are processed and sectioned. A fundamental gain in optical information (i.e., diagnosis/staging) may be achieved when whole, unsectioned CBs (L=5-20, D=0.5-2.0mm) are analyzed in 3D. This approach preserves CBs for traditional pathology and maximizes the diagnostic potential of patient samples. To bridge CNs/CBs with imaging, our group developed a microfluidic device that performs biospecimen preparation on unsectioned CBs for pathology. The ultimate goal is an automated and rapid point-of-care system that aids pathologists by processing tissue for advanced 3D imaging platforms. An inherent, but essential device feature is the microfluidic transport of CBs, which has not been previously investigated. Early experiments demonstrated proof-of-concept: pancreas CBs (D=0.3-2.0mm) of set lengths were transported in straight/curved microchannels, but dimensional tolerance and flow rates were variable, and preservation of CB integrity was uncontrolled. A second study used metal cylinder substitutes (L=10, D=1mm) in microchannels to understand the transport mechanism. However, CBs are imperfectly shaped, rough, porous and viscoelastic. In this study, fresh/formalin-fixed porcine and human pancreas CBs were deposited into our device through a custom interface using clinical CNs. CB integrity (i.e., sample viability) may be assessed at every stage using an optomechanical metric: physical breaks were determined when specimen intensity profile data deviated beyond $\chi_{avg}+2\sigma$. Flow rates for human CBs were determined for several CNs, and microfluidic transport of fresh and formalin-fixed CBs was analyzed.

9320-24, Session 6

Influence of direct laser written three-dimensional topographies on osteoblast-like cells

Judith K. Hohmann, Research Ctr. OPTIMAS, Technische Univ. Kaiserslautern (Germany); Georg von Freymann, Research Ctr. OPTIMAS, Technische Univ. Kaiserslautern (Germany) and Fraunhofer-Institut für Physikalische Messtechnik (Germany)

With society growing older, implants are often necessary to preserve mobility and health-related quality of life. In up to eight percent dental implants fail, usually because of deficit osseointegration or insufficient

**Conference 9320:
Microfluidics, BioMEMS, and Medical Microsystems XIII**

adaptation of soft tissue, which is unpleasant and painful.

Many approaches to improve dental implant acceptance deal with chemical and/or physical surface treatment (e.g. acid-etching, sand-blasting) leading to randomly shaped surface topographies, making it difficult to understand how topographies influence biological cells.

We aim at understanding the physical influence of 3D topographic features on osteoblast-like cells. We fabricate well-defined three-dimensional templates by direct laser writing and subsequent coating with titanium dioxide via atomic layer deposition. This allows us to provide biocompatible substrates with nearly arbitrary micro structures. Simultaneously, we are able to systematically vary geometric parameters.

We report on how these geometric parameters influence viability parameters of osteoblast-like cells. We observe a significantly higher proliferation (up to 170 %) on particular topographies compared to unstructured surfaces. Additionally, an influence of structural parameters on the morphology and focal adhesion contacts of osteoblast-like cells is obtained and differentiation is verified via alkaline phosphatase staining. Our results might lead to novel dental implant surfaces which promote osseointegration.

9320-25, Session 6

A microfabricated, microfluidic biomems device to model human brain aneurysms: the aneurysm-on-a-chip

Lisa M. Reece, Jian-Wei Khor, Raviraj V. Thakur, Steven T. Wereley, James F. Leary, Purdue Univ. (United States)

An "organ-on-a-chip" microfluidic BioMEMS device was designed, constructed and tested to model human brain aneurysms which are difficult to detect and to study in vivo. Brain aneurysms are not only a major problem in the general population but are particularly a problem in soldiers experiencing explosive penetrating brain injuries on the battle field. In these studies, we constructed a microfluidic BioMEMS device, the Aneurysm-on-a-Chip™, that models three different types of aneurysms. Velocity, pressure, and wall shear stresses aid in the pathogenesis and growth of aneurysms, and it is known that shear force mechanisms effecting human cell wound closure in vivo are elusive. To aid in the study of these vascular lesions, the proposed design is an in vitro system to obtain preliminary data to analyze the fluid flow patterns of an "aneurysm" in an effort to better understand the fluid dynamics inside these defects for the ultimate repair across the aneurysm neck. The Aneurysm-on-a-Chip™ apparatus is designed to track particles/cells when it is coupled to a PIV software package. The fluid flow is visualized using standard microscopy techniques and movies are taken and analyzed. Particle image velocimetry (PIV) measurements of microparticles and cells flowing through the device were made and computational fluid dynamics (CFD) analyses were performed on paired images taken from fluid flow movies. Wall shear stress and fluid flow velocities were calculated from the resultant images. This human Aneurysm-on-a-Chip™ model will allow for rapid testing of new strategies for early detection and more effective treatment of aneurysms.

9320-41, Session PSun

Fabrication of 3D microenvironments to study MCF-7 cell growth

Oriana Avila, Adriano J. G. Otuka, Instituto de Física de São Carlos, Univ. de São Paulo (Brazil); Laura M. de Freitas, Univ. Estadual Paulista "Júlio de Mesquita Filho" (Brazil); Vinicius Tribuzi, Instituto de Física de São Carlos, Univ. de São Paulo (Brazil); Carla R. Fontana, Cleber R. Mendonça, Univ. Estadual Paulista "Júlio de Mesquita Filho" (Brazil)

The study of cellular growth in specially designed microenvironments can

help to understand the fundamental mechanisms of cell development. In this work we used two-photon absorption polymerization to fabricate three-dimensional microenvironments, composed of circular or square cross-sections pillars, with distinct spacing. These microenvironments were used to evaluate the development of Michigan Cancer Foundation-7 (MCF-7) cells, labeled with green fluorescent protein (GFP).

The microstructures were produced using a Ti:sapphire laser oscillator (790 nm, 100 fs pulses, 82 MHz). The laser beam is focused by microscope objective into an acrylic resin containing a photoinitiator. A pair of scanning mirrors moves the laser beam in the x-y direction, while the sample's axial (z) position is controlled by a motorized stage. Upon completion of polymerization, the sample is immersed in ethanol to wash away the unsolidified resin.

Once the fabricated microenvironments provided favorable conditions for cell development, the influence of microenvironments' geometrical features on cells growth was analyzed by transmission and fluorescence microscopies. Our results indicate that the cell density decreases as the distance between structures in the environment is increased. Additionally, cell growth shows slightly better results for the microenvironments composed of circular cross-section structures. Thus, such results reveal that the proper design of microenvironments' geometrical features can be used to control the cell density in microenvironments, with implications in tissue engineering and microbiology studies.

Authors acknowledge Prof. E. M Espreafico group, from the Faculdade de Medicina de Ribeirão Preto - USP, for the supplying the cell line used in this study.

9320-42, Session PSun

A novel AC electrothermal micropump for biofluid transport using parallel interdigitated microelectrode array

Alinaghi Salari, Colin Dalton, Univ. of Calgary (Canada)

Electrokinetic micropumps have been widely used in lab-on-a-chip devices. The AC electrothermal (ACET) effect is highly efficient for biofluidic micropumping, but is unable to generate high flow rates. Attempts to increase ACET flows, such as applying a wide range of actuation voltage, using asymmetric microelectrode array and using 3D microelectrodes have been reported. In this paper a novel idea of employing two arrays of coplanar asymmetric microelectrodes placed on the top and bottom of a microchannel is explored. One pair of microelectrodes is simulated using COMSOL Multiphysics software. Experiments were then conducted for two microelectrode rows fabricated on 1mm thick glass using photolithography. Soft lithography was employed for fabrication of an 800µm deep fluidic channel. The micropump output shows the flow rate can be increased by up to 105% compared to other ACET single-row microelectrode devices which have the same electrode dimensions. Moreover, the substrate material can dramatically affect the pumping efficiency of the ACET micropump. ACET flow variation for different substrate materials such as PDMS, silicon, and glass are also reported. It is shown that if the fluidic microchannel depth (FMD) is chosen to be deep enough, and glass substrates are used, then the pumping efficiency increases. Also, in lower FMDs (<250 µm) one peak velocity profile, similar to conventional ACET, is observed. In higher FMDs, the flow velocity obtains a two-peak semi-flat profile, which is similar to AC electroosmosis flows. This new ACET pumping design can be utilized for any lab-on-a-chip application specifically in biofluid delivery systems.

9320-43, Session PSun

A bioMEMS device for the study of mechanical properties of cells

Joseph M. Sanders, Logan Butt, Ashley N. Clark, James K. Williams, Michael R. Padgen, SUNY College of Nanoscale Science and Engineering (United States); Patricia Keely,

**Conference 9320:
Microfluidics, BioMEMS, and Medical Microsystems XIII**

Univ. of Wisconsin-Madison (United States); John S. Condeelis, Albert Einstein College of Medicine (United States); Julio Aguirre-Ghiso, Icahn School of Medicine at Mount Sinai (United States); James Castracane, SUNY College of Nanoscale Science and Engineering (United States)

The tumor microenvironment is a complex system which is not fully understood. New technologies are needed to provide a better understanding of the role of the tumor microenvironment in promoting metastasis. The Nano Intravital Device, or NANIVID, has been developed as an optically transparent, implantable tool to study the tumor microenvironment. Two etched glass substrates are sealed using a thin polymer membrane to create a reservoir with a single outlet. This reservoir is loaded with a custom hydrogel blend that contains selected factors for delivery to the tumor microenvironment. When the device is implanted in the tumor, the hydrogel swells and releases these entrapped molecules, forming a sustained concentration gradient. The NANIVID has previously been successful in manipulating the tumor microenvironment both in vitro as well as in vivo.

As metastatic cells intravasate, it has been shown that some are able to do so unscathed and reach their new location, while others are cleaved during the process. There is clearly a correlation between cell migration and the mechanical properties of these cells. In conjunction with the NANIVID technology, which is utilized to create a chemotactic gradient of epidermal growth factor, atomic force microscopy will be used to monitor the mechanical properties of mTln3 rat mammary cells as they move in a directed manner. Scanning confocal laser microscopy will also be used to monitor movement of the cells over time. These experiments will shed light on the mechanical changes in metastatic cells as they migrate towards a gradient similar to that encountered during the extravasation process.

9320-44, Session PSun

A novel organic diode design using only PCBM as an active polymer layer

Haleh Shahbazbegian, Jasbir N. Patel, Bozena Kaminska, Simon Fraser Univ. (Canada)

Polymer electronic devices especially transistors and diodes attracted researchers recently. The conventional fabrication technologies require high precision clean-room equipment. Such facilities require high set-up and operational cost. Additionally, integrating conventional diode is difficult in a polymer based fully flexible systems. Using organic devices can solve these limitations.

Most of the studies for polymer diode are based on using a charge donor (such as poly (3,4-ethylenedioxythiophene) polystyrene sulfonate (PEDOT:PSS)) and a charge acceptor (such as poly[2-methoxy-5-(2-ethylhexyloxy)-1,4-phenylenevinylene] (MEH-PPV), or a blend of poly(3-hexylthiophene) (P3HT) and phenyl-C61-butyric acid methyl ester (PCBM)). P3HT requires Nitrogen atmosphere for processing and it is light sensitive. Hence, P3HT based polymer diode lacks repeatability.

To further simplify the polymer diode design and fabrication, a polymer diode using only PCBM as an active layer is proposed here. The proposed polymer stack uses PEDOT: PSS and PCBM for the polymer diode. The subsequent experiment further simplifies the design by using only PCBM. The proposed designs do not use any other polymers (such as MEH-PPV, PQT-12, P3HT) to reduce cost and increase simplicity of the diode design.

Commercially available Indium-tin Oxide (ITO) coated PET substrate is coated with PEDOT: PSS and PCBM for the first design. For the improved design, only PCBM layer is spun on the ITO coated substrate. Finally, an Aluminum electrode is chosen as the cathode.

The Keithley 2400 source meter and NI LabView interface is used to measure current-voltage characteristics. The breakdown voltage for both diode designs is 0.7 V with very high repeatability.

9320-45, Session PSun

Microfluidics diffusive gradient monitored by time-lapse images of microbial cells

Aline F. Oliveira, Carlos L. Cesar, UNICAMP (Brazil); Reinaldo G. Bastos, UFSCAR (Brazil); Lucimara G. de La Torre, UNICAMP (Brazil)

The objective of this paper is to show the applicability of the microfluidics concentration gradients diffusive for the development of industrial bioprocesses monitored by time lapse images. We used this microfluidic device to evaluate the behavior of free *Saccharomyces cerevisiae* ATCC 7754 cells, in the range up to 40 g/L glucose in YPD medium, against different concentrations of limiting substrate (glucose) and determine the favorable conditions and kinetic parameters for microbial growth. The diffusive gradient and cell growth happens in the bottom level of our device, while linear flow of solutions with different concentrations happen at the top level, with access to the bottom level through small holes. The system operated at 30 °C and flow rate of 15 μ L/min in anaerobic environment. Microorganism behavior was monitored for 10 h with a Zeiss LSM 780 confocal microscope automatically capturing an image every 30 min, used to determine the range with larger number of cells in each microchannel. We observed microbial growth in the range of 23 g/L and 30 g/L of glucose and obtained the microbial growth curve and the specific growth rates of yeast in microfluidic system as $(\mu_x) 0.24 \pm 0.080$ 1/h. The use of time lapse images made it possible to evaluate the behavior cells inside the microfluidic device. Our results show that this technique can be applied to determine ideal profiles for microbial growth, with kinetic parameters similar to batch fermentation, with fast assays and results for optimization of bioprocesses.

9320-46, Session PSun

Novel polymer microfluidic optics for quantum cascade lasers in the mid-infrared

Sheng Wu, California Institute of Technology (United States)

Current materials and structures for optofluidics are mainly designed for UV-Visible-Near Infrared (250nm to 3micron), and they have poor transmission for Mid-Infrared (MIR) wavelength ranging from 3 micron to over 10microns. Also, fluids like water and oil have even poorer transmission in the MIR, requiring very thin optical depth to be probed, thus limiting the sensitivity of the optofluidic system.

We show that thin wall (~10 microns) polymer tubings with ID less than 200 microns could be utilized for MIR optofluidic applications. Because of the superior beam quality and brightness for QCLs, the beam could be focused into cross section less than 100 micron inside the polymer inside diameter structure, and realize optical path from under 20microns to over 100 microns. Micro water droplet in oil flow on-column detection of much less than nanograms of chemicals with quantum cascade lasers (QCLs) are demonstrated. Enrichment of chemical by polymer and response time issues will be discussed. Also, thin wall polymer and QCLs enables Whispering Gallery mode coupling and the potential enhancement in evanescent wave detection is explored.

Applications of such microfluidic for MIR including chemical specific chemical/biological sensors [1] and LC-IR [2] hyphenated detection will be discussed.

References

[1] J. Giammarco, et.al. Towards universal enrichment nanocoating for IR-ATR waveguides. *Chemical Communications* 2011, 47, 9104.

[2] T. F. Beskers, et.al. High performance liquid chromatography with mid-infrared detection based on a broadly tunable quantum cascade laser. *Analyst* 2014, 139, 2057.

**Conference 9320:
Microfluidics, BioMEMS, and Medical Microsystems XIII**

9320-47, Session PSun

Vibration effect on cross-flow and co-flow focusing mechanisms for microbubble generation

Alinaghi Salari, Colin Dalton, Univ. of Calgary (Canada)

Microbubbles are widely used in many industries such as water treatment, drug coating, and ultrasonic contrast agents. Cross-flow focusing and co-flow focusing are considered basic mechanisms used for microbubble generation. If gas is used as the central flow and liquid as the side flows, microbubbles can be generated. Typically, to achieve micron-sized bubbles requires structure dimensions in the same order of magnitude of the desired bubble sizes. In this paper we report a method of applying an external vibration to a cross-flow and co-flow focusing structure, which allows for smaller bubbles to be generated. The orifice dimension was 700-400 μm , and the channel width was 800 μm . Deionized water mixed with surfactant was used as side flows, and atmospheric air as the central flow. Linear vibration was exerted on the microchannel structure in the direction of central flow. A 2D structure was simulated using finite element software, and the resultant data were compared to experimental data taken from flow focusing structures with the same orifice dimensions fabricated in Polymethylmethacrylate (PMMA). The results show that in a co-flow focusing structure, the bubble generation regime depends on flow ratio (Q_a/Q_w) and vibration parameter (Amp/Freq), while in cross-flow focusing, the side flow rate does not have a significant effect on the regime. For both structures, decreasing the flow ratio can increase the chance of bubble generation. Briefly, applying a low-cost linear vibration to the conventional co-flow focusing structure can be used as an accurate controlling technique for increasing the chance of microbubble generation.

9320-48, Session PSun

High efficient biofluid micromixing using ultra-fast AC electrothermal flow

Alinaghi Salari, Colin Dalton, Univ. of Calgary (Canada)

Electrokinetics have been widely used in lab-on-a-chip devices for fluid manipulation applications. AC electrothermal (ACET) effect is a highly efficient technique for biofluids ($\sigma > 0.1 \text{ S/m}$) active micromixing, which can be used in chemical, biological, and medical analysis systems. In this paper, a novel idea of employing microelectrode arrays placed on side-walls of a fluidic microchannel for increasing the mixing efficiency of biofluids is numerically investigated. It was reported that coplanar asymmetric microelectrode arrays are capable of creating ACET vortices in the bulk of a high conductive electrolyte solution. Two electrode arrays can be placed on the side walls of a microchannel, each of which has a different role, one pumps the biofluid while the other mixes it. Two different actuation patterns were applied to the electrodes. One pair of microelectrodes was simulated and the simulation procedure was then verified by conducting experiments for ACET flow measurement in a similar geometry. Microelectrode arrays were fabricated on 1mm thick glass substrates using photolithography. A 800 μm thick fluidic microchannel was fabricated by soft lithography of Polydimethylsiloxane (PDMS). The results showed that such a technique can dramatically increase the mixing of the solution while pumping is taking place. The mechanism was capable of efficiently mixing biofluid solutions (resultant concentration ratio of up to 80%) in a short time ($< 3 \text{ min}$) and short distance ($< 600 \mu\text{m}$) for a 300-300 μm^2 fluidic microchannel cross section area. Medical analysis such as heterogeneous immunoassays can be potential applications of such micromixing technique.

9320-49, Session PSun

Cellular temperature monitoring using dielectrophoretic impedance measurement

Kozo Taguchi, Ryo Kido, Ritsumeikan Univ. (Japan)

In the field of food and beverage production, it is very important to measure and control the metabolic heat of cells. Various studies have been searching for new methods on how to measure the cellular temperature. Because of cellular temperature measurement facilitates more productive and guarantees high quality in the food and beverage industries. Furthermore, measuring the cellular temperature is demanded in the area of biology and medicine because cellular functions are concerned with cellular temperature. Conventional research is to use small thermocouple and thermal susceptibility fluorescent material for cellular temperature monitoring. However, these methods are complex.

In this research, we suggest a new method for cellular temperature measurement to use dielectrophoresis (DEP). DEP can sort between viable and non-viable cells by their differences of the dielectric constant under a non-uniform electric field. In general, a micro electrode of DEP is fabricated by photolithography or laser ablation and so on. These methods are costly and need many processes. Therefore, we have already suggested a simplified fabrication method of Au DEP chip. Cellular temperature measurement using DEP chip fabricated by our proposed method can be more quickly, easier, and little damage to the cell.

From experimental results, it was found that the impedance between the electrodes with trapped cell had a thermal property. The cellular temperature could be measured by observing the change in shunt voltage. In the future, we want to measure a single cellular temperature with isolation by optical tweezers.

9320-36, Session 7

Extraction and fractionation of RNA and DNA from single cells using selective lysing and isotachopheresis (Invited Paper)

Hirofumi Shintaku, Kyoto Univ. (Japan) and Stanford Univ. (United States); Juan G. Santiago, Stanford Univ. (United States)

Single cell analyses of RNA and DNA are crucial to understanding the heterogeneity of cell populations. The number tools and approaches to analyze single cells are expanding, but sequence specific measurements of nucleic acids have typically been limited to studies of either DNA or RNA, and not both. This analysis still remains a challenge as RNA and DNA have very similar physical and biochemical properties, and cross-contamination with each other may introduce false positive results. We here present an electrokinetic technique that creates the opportunity to fractionate and deliver RNA and DNA to independent downstream analyses. Our technique uses an on-chip system that enables selective lysing of cytoplasmic membrane, extraction of RNA (away from DNA and nucleus), focusing, absolute quantification of cytoplasmic RNA mass. The absolute RNA mass quantification is performed using fluorescence observation without enzymatic amplification in less than 5 min. The cell nucleus is left intact and the relative DNA amount in the nucleus can be measured. The nucleus is available for fractionation to a separate output reservoir. We demonstrate the technique using single mouse B lymphocyte cells, for which we extracted an average of 14.1 pg total cytoplasmic RNA per cell. We also demonstrate correlation analysis between the absolute amount of RNA and relative amount of DNA, showing heterogeneity associated with cell cycle.

**Conference 9320:
Microfluidics, BioMEMS, and Medical Microsystems XIII**

9320-37, Session 7

Fluorescence cross-correlation spectroscopy for time dependent flows: a numerical investigation

Nicolo' G Ceffa, Univ degli Studi di Milano-Bicocca (Italy); Paolo Pozzi, Univ. degli Studi di Milano-Bicocca (Italy); Margaux Bouzin, Univ. degli Studi di Milano Bicocca (Italy); Cassia A. Marquezin, Instituto Federal de Goiás (Brazil); Laura Sironi, Laura D'Alfonso, Maddalena Collini, Giuseppe Chirico, Univ. degli Studi di Milano-Bicocca (Italy)

Hemodynamics in complex micro-vasculature must be characterized at micrometer and millisecond resolution to provide relevant morphogenetic details together with flow speeds. We aim at developing fluorescence cross-correlation image methods to follow in time blood flows. We have previously investigated Zebrafish hemodynamics with holographic microscopy [1] and EM-CCD based microscopes [2]. The analysis of the Cross-Correlation Function (CCF) of signals coming from pixels at a distance $|R|$ provided the flow speed and direction. The extension of these experiments to more complex systems with high branching of capillaries and/or inverted flows needs a theoretical investigation that we present here.

We focused first on straight capillaries and harmonic flows with speeds $V_{min} < V < V_{max}$. The Fluorescence CCF shows multiple peaks at lag times that do not correspond directly the maximum and minimum flow speeds. The general analytical expression of the CCF is given, the position of its maxima are discussed by means of geometrical considerations and numerical analysis and an experimental validation is presented.

The second discussed case is the flow in the branches of a y-shaped junction in a microcapillary. By simply modeling the branching in laminar flow (low Reynold numbers) and assuming a smooth transition of speeds along the branch we derive a simple treatment of the CCF to provide estimates of the flow speed in the two branches. Preliminary experimental validation of these numerical simulations to in-vitro experiments in microcapillaries are also discussed.

[1] Gandolfi, Pozzi et al. Front. Cell. Neurosci. doi: 10.3389/fncel.2014.00092

[2] Pozzi, Sironi et al. J. Biomed. Optics, 19(6), 067007, 2014.

9320-38, Session 7

Microfluidic system for the identification of bacterial pathogens causing urinary tract infections

Holger Becker, Nadine Hlawatsch, microfluidic ChipShop GmbH (Germany); Tommy Haraldsson, Wouter van der Wijngaart, KTH Royal Institute of Technology (Sweden); Anders Lind, Q-Linea AB (Sweden); Surbi Malhotra-Kumar, Agata Turlej-Rogacka, Herman Goossens, Univ. Antwerpen (Belgium)

Urinary tract infections (UTIs) are among the most common bacterial infections and pose a significant healthcare burden. The growing trend in antibiotic resistance makes it mandatory to develop diagnostic kits which allow not only the determination of a pathogen but also the antibiotic resistances. We have developed a microfluidic cartridge which takes a direct urine sample, extracts the DNA, performs an amplification using batch-PCR and flows the sample over a microarray which is printed into a microchannel for fluorescence detection. The cartridge is injection-molded out of COP and contains a set of two-component injection-molded rotary valves to switch between input and to isolate the PCR chamber during thermocycling. The hybridization probes were spotted directly onto a functionalized section of the outlet microchannel. We have been able to successfully perform PCR of E.coli in urine in this chip and perform a fluorescence detection of PCR

products. An upgraded design of the cartridge contains the buffers and reagents in blisters stored on the chip.

9320-39, Session 7

Simultaneous detection of mycophenolic acid and tacrolimus with a thirteen channel optical biochip

Francesco Baldini, Ambra Giannetti, Sara Tombelli, Cosimo Trono, Istituto di Fisica Applicata Nello Carrara, IFAC-CNR (Italy); Giampiero Porro, Datamed S.r.L. (Italy); Clemens Kremer, Holger Becker, microfluidic ChipShop GmbH (Germany)

The measurement of immunosuppressants is essential in transplanted patient in order to avoid the rejection of the transplanted organ. The correct administration window is very narrow and changes from patient to patient. Clinical practice is based on the periodical administration of a combination of two or more immunosuppressants combined with measurement of the drug concentration in plasma before its next administration with the purpose to avoid overdosing.

Heterogeneous competitive immunoassays for the detection of mycophenolic acid and tacrolimus were implemented on a thirteen microchannel PMMA chip. Derivatives of tacrolimus and mycophenolic acid were immobilised on different microchannels of the chip and the conditions of the bioassays were optimised. The optical biochip was interrogated with an optical platform based on fluorescence anisotropy, previously developed by IFAC and Datamed.

For tacrolimus a limit of detection of 0.11 ng/mL, a limit of quantification of 0.57 ng/mL and a coefficient of variation of 25% were achieved. For mycophenolic acid preliminary experiments indicated a good sensitivity down to ng/mL concentrations.

In both cases particular attention was paid to the regeneration of the chip in order to perform more than one assay on each channel.

9320-40, Session 7

Capture of CD4 cell with the circular microfluidic device functionalized by glutaraldehyde

Yeu-Farn Shih, Nien-Tsu Huang, Chih-Kung Lee, National Taiwan Univ. (Taiwan)

About one-third of world's population has been infected by Tuberculosis and it is expected that three hundred billion people will get infected in the next decade and ninety million will become ill and around thirty million will die from this disease. In general, mycobacterium tuberculosis can cause active disease in approximately 5-10% of those who suffer from latently tuberculosis and the chance of getting ill is the highest within a year. Today, in spite of detecting the tuberculosis through stimulating CD4 cells to produce interferon- γ in the whole blood, it is hard to confirm if interferon- γ is produced by CD4 cells. It is also difficult to count the CD4 cells. In this paper, a functionalized polydimethylsiloxane (PDMS) device with dextran was designed and fabricated to capture CD4 cells in order to make final detection more accurate and more sensitive.

The oxidized dextran was adopted as a linker to facilitate the antibody-cell interaction. A microfluidics subsystem based on opto-piezoelectronic technology was also integrated to create the microfluidic system. To enhance the capture efficiency, we designed a geometric PDMS structure with lots of pillars placed regularly in it. With Comsol as the simulation tool, we modified the gap between the pillars, pillars' dimension and the position to make the streamline's distribution uniform so as to increase the chance of having the cells collide with pillars and be caught by the antibody. Detailed

**Conference 9320:
Microfluidics, BioMEMS, and Medical Microsystems XIII**

design, simulation and experimental results, improved design identified, etc. were all be presented in detail.

9320-26, Session 8

High-pressure microfluidics (*Invited Paper*)

Klas Hjort, Uppsala Univ. (Sweden)

In green chemistry and bioprocesses, extraction, synthesis and analyses often excel at high densities and temperatures. This is accessible through high pressures. Capillary chemistry has been used since long but, just like in low-pressure applications, there are several potential advantages in using microfluidic platforms, e.g., planar isothermal set-ups, large local variations in geometries, dense form factors, small dead volumes and precisely positioned microstructures for control of reactions, catalysis, mixing and separation. From a review of the state-of-art and frontiers of high pressure microfluidics, the focus will be on different solutions demonstrated for microfluidic handling at high pressures.

9320-27, Session 8

BIOFOS: micro-ring resonator-based biophotonic system for food analysis

Ioanna Zergioti, Christos Kouloumentas, Maria Massaouti, Hercules Avramopoulos, National Technical Univ. of Athens (Greece); Henk Leeuwis, René G. Heideman, Eric Schreuder, Lionix BV (Netherlands); Siegfried Graf, Helmut F. Knapp, Ctr. Suisse d'Electronique et de Microtechnique SA, CSEM (Switzerland); Lise Barthelmebs, Thierry Noguier, Univ. de Perpignan Via Domitia, UPVD (France); George Tsekenis, Biomedical Research Foundation, Academy of Athens (Greece); Maria Patitsa, Biomedical Research Foundation, Academy of Athens, BRFAA (Greece); Anke Trilling, Luc Scheres, Surfex BV (Netherlands); Maarten Smulders, Han T. Zuilhof, Wageningen Univ. (Netherlands); Gerard J. T. Heesink, Saxion Univ. of Applied Sciences (Netherlands); Agusti Romero, IRTA (Spain); Layla Fernandez, COVAP (Spain)

BIOFOS* aims to develop a simple, fast, low-cost, sensitive, portable and reliable, screening tool for in-situ detection of food contaminations in nuts, olive oil and milk and also for the quantitative detection of lactose in milk. In this aspect, BIOFOS combines the most promising concepts from the photonic, biological, nanochemical and fluidic parts of Lab-on-a-Chip (LoC) systems, aiming to achieve low sensitivity and high specificity, excellent reliability and compactness. Current methodologies for detection of food contamination based on heavy analytical tools cannot guarantee a safe and stable food supply. The need for screening tools that will be still reliable but simple, fast, low-cost, sensitive and portable for in-situ application is thus urgent. BIOFOS aims to address this need through a high-added value, reusable biosensor system based on optical interference and lab-on-a-chip (LoC) technology.

BIOFOS relies on the ultra-low loss TriPLeX photonic platform in order to integrate, on a single chip (4x5 mm²), 8 micro-ring resonators, a VCSEL and Si photodiodes, and achieve a record detection limit in the change of the refractive index of 5•10⁻⁸ RIU.

Targeting to a reusable and compact device, BIOFOS relies on the use of aptameric sequences as bio-recognition elements of the sensor, where advanced surface functionalization techniques are used for their immobilization while new microfluidic structures will be introduced for the sample pre-treatment and the regeneration processes. Results on the design and fabrication of the photonic structures and immobilization and regeneration of the aptamers will be discussed in this conference.

*BIOFOS is an EU collaborative project FP7/ICT/2013/10

9320-28, Session 8

Integrated microfluidic system with automatic sampling for permanent molecular and antigen-based detection of CBRNE-related pathogens

Holger Becker, Sebastian Schattschneider, Richard Klemm, Nadine Hlawatsch, Claudia Gärtner, microfluidic ChipShop GmbH (Germany)

The continuous monitoring of the environment for lethal pathogens is a central task in the field of biothreat detection. Typical scenarios involve air-sampling in locations such as public transport systems or large public events and a subsequent analysis of the samples by a portable instrument. Lab-on-a-chip technologies are one of the promising technological candidates for such a system. We have developed an integrated microfluidic system with automatic sampling for permanent molecular and antigen-based detection of CBRNE-related pathogens such as *F. tularensis*, *B. anthracis* or *Y. pestis*. It consists of an air sampler which also concentrates the sample using solvent evaporation. The sampler is coupled to microfluidic cartridge the size of a SBS titerplate. The chip contains a two-pronged analysis strategy, on the one hand an immunological track using antibodies immobilized on a frit to capture antigens on the cell membranes of the respective pathogen and a subsequent photometric detection (darkening of the frits), on the other hand a molecular biology approach using continuous-flow PCR with a fluorescence end-point detection. The cartridge contains two-component molded rotary valve to allow active fluid control and switching between channels. The accompanying instrument contains all elements for fluidic and valve actuation, thermal control, as well as the two detection modalities. Reagents are stored in dedicated reagent packs which are connected directly to the cartridge. With this system, we have been able to demonstrate the detection of a variety of pathogen species.

9320-29, Session 8

High-throughput microfluidic line scan imaging for cytological characterization

Joshua A. Hutcheson, Amy J. Powless, Aneeka A. Majid, Adair Claycomb, Ingrid Fritsch, Kartik Balachandran, Timothy J. Muldoon, Univ. of Arkansas (United States)

Imaging cells in a microfluidic chamber with an area scan camera is difficult due to motion blur and data loss; this is consequent of frame read times causing discontinuity of data acquisition as cells move at relatively high speeds through the chamber. We have developed a method to continuously acquire high-resolution images of cells in motion through a microfluidics chamber using a high-speed line scan camera. The sensor acquires images in a line-by-line fashion in order to image moving objects without motion blur. The optical setup comprises an epi-illuminated microscope with a 40X oil immersion, 1.4 NA objective and a 150 mm tube lens focused on a microfluidic channel. Samples containing suspended cells fluorescently stained with 0.01% (w/v) proflavine in saline are introduced into the microfluidics chamber via a syringe pump; illumination is provided by a blue LED (455 nm). Images were taken of samples at the focal plane using an ELiIXA+ 8k/4k monochrome line-scan camera at a line rate of up to 40 kHz. The system's line rate and fluid velocity are tightly controlled to reduce image distortion and are validated using fluorescent microspheres. Image acquisition was controlled via MATLAB's Image Acquisition toolbox. Data sets comprise discrete images of every detectable cell which may be subsequently mined for morphological statistics and definable features by a custom texture analysis algorithm. This high-throughput screening method, comparable to cell counting by flow cytometry, provided efficient examination including counting, classification, and differentiation of saliva, blood, and cultured human cancer cells.

**Conference 9320:
Microfluidics, BioMEMS, and Medical Microsystems XIII**

9320-30, Session 8

Three-dimensional optofluidic device for isolating microbes

Anusha Keloth, Lynn Paterson, Gerard H. Markx, Ajoy K. Kar, Heriot-Watt Univ. (United Kingdom)

Marine microorganisms present an almost untapped resource with huge potential for biotechnological applications, including the production of new antibiotics. One of the main reasons for the low rate of identification is the lack of efficient methods for isolating microorganisms and growing them under laboratory conditions. Conventional approaches for direct isolation of single cells put high demands on the skill of the operator and are also highly labour intensive. An alternative technique involves the fabrication of novel Lab On a Chip (LOC) devices that can be used to enable sorting, growth, maintenance and assay of microbial cells. We demonstrate the fabrication and design of an optofluidic device, capable of isolating marine bacterial cells. The technique of direct femtosecond laser writing combined with selective etching is used to fabricate optofluidic devices in fused silica. The unique three-dimensional capability of femtosecond laser writing is utilized to integrate intricate microfluidic channels and waveguides within the same substrate. The main microfluidic channel in the device constitutes the path of the sample. Waveguides and additional microfluidic channels are fabricated on either side, at right angles to the main channel, to facilitate single cell isolation. A 980nm CW laser source, coupled to the waveguide, is used to exert radiation pressure on the particle to be isolated. As a first demonstration, device functionality is validated using fluorescent microbeads. The minimum power at which the fluorescent beads can be pushed to the side channel is measured for different flow rates of the particles.

9320-31, Session 9

Optofluidic technologies for mobile and global health (*Invited Paper*)

David Erickson, Cornell Univ. (United States)

Smartphones and other mobile technologies will be transformative to the deployment of molecular diagnostics both domestically and worldwide. In this talk, I will review the existing commercial and technical roadblocks to the deployment molecular diagnostics to the consumer market and how they can be fundamentally altered by taking advantage of the now ubiquitous installed base of smartphones. I will discuss two technologies in this talk. The first is our KS-Detect system which is a solar-powered PCR system currently targeted towards the diagnosis of Kaposi's sarcoma in sub-Saharan Africa. The second is our NutriPhone technology which is designed to detect micronutrient and vitamin deficiencies both in individuals and populations. In addition to covering the basic engineering science advancements that led to the development of these technologies, I will also discuss our strategies for deployment and commercialization.

9320-32, Session 9

Realization of integral 3-dimensional image using fabricated tunable liquid lens array

Muyoung Lee, Junoh Kim, Cheoljoong Kim, Jin Su Lee, Yonghyub Won, KAIST (Korea, Republic of)

Recently, electrowetting has been widely studied for various optical applications such as optical switch, sensor, prism, and display. In this study, we develop vari-focal liquid lens array using electrowetting principle to construct integral 3-dimensional imaging. The electrowetting principle that changes the surface tension by varying electrical potential difference has several advantages to realize active optical device such as fast response

time, low electrical consumption, and no mechanical moving parts. Two immiscible liquids that are water and oil are used for forming lens. By applying a voltage to the water, the focal length of the lens could be tuned as changing contact angle of water. The fabricated electrowetting vari-focal liquid lens array has 1mm diameter spherical lens shape that has 1.1mm distance between each lens. The number of lenses on the panel is 33x33 and fill-factor is 64.9%. The focal length of the lens array is simultaneously tuned from -130 to 120 diopters depending on the applied voltage. The fabricated lens array is implemented to integral 3-dimensional imaging that is promising autostereoscopic 3D display technology. 3D object is reconstructed by fabricated liquid lens array with 33x33 elemental images that are generated by 3D max tools when liquid lens array is tuned as convex state. From vari-focal liquid lens array implemented integral imaging system, we expect that depth enhanced integral imaging can be realized in the near future.

9320-33, Session 9

Ultralow-loss waveguide crossings for the integration of microfluidics and optical waveguide sensors

Zheng Wang, Hai Yan, The Univ. of Texas at Austin (United States); Zongxing Wang, Omega Optics, Inc. (United States); Yi Zou, Chun-Ju Yang, The Univ. of Texas at Austin (United States); Swapnajit Chakravarty, Harish Subbaraman, Naimei Tang, Xiaochuan Xu, Omega Optics, Inc. (United States); Ray T. Chen, The Univ. of Texas at Austin (United States)

Integrating photonic waveguide sensors with microfluidics is promising in achieving high-sensitivity and cost-effective biological and chemical sensing applications. One challenge in the integration is that an air gap would exist between the microfluidic channel and the photonic waveguide when the micro-channel and the waveguide intersect. The air gap creates a path for the fluid to leak out of the micro-channel. Potential solutions, such as oxide deposition followed by surface planarization, would introduce additional fabrication steps and thus are not cost-effective. Here we propose a reliable and efficient approach for making closed microfluidic channels on a waveguide sensing chip. The technique we use is adding waveguide crossings, i.e., perpendicularly intersecting waveguides, to block the etched trenches and prevent the fluid from leaking through the air gap. The waveguide crossings offer a smooth interface for microfluidic channel bonding while bring negligible additional propagation loss (0.024 dB/crossing based on simulation). They are also fabrication friendly since they can be patterned and fabricated in the same step with waveguides. We experimentally integrated microfluidic channels with photonic crystal (PC) microcavity sensor chips on silicon-on-insulator substrate and demonstrated leak-free sensing measurement with waveguide crossings. The microfluidic channel was made from PDMS and pressure bonded to the silicon chip. The tested flow rates varied from 0.2 μ L/min to 200 μ L/min. Strong resonances from the PC cavity were observed from the transmission spectra. The spectra also show that the waveguide crossings did not induce any significant additional loss or affect the resonances.

9320-34, Session 9

Femtosecond laser fabricated optofluidic device to mechanically discriminate between cells

Rebeca Martinez Vazquez, CNR-Istituto di Fotonica e Nanotecnologie (Italy); Giovanni Nava, Tie Yang, Univ. degli Studi di Pavia (Italy); Manuela Vegliione, Istituto di Genetica Molecolare, CNR (Italy); Paolo Minzioni, Univ. degli Studi di Pavia (Italy); Francesca Bragheri, CNR-

**Conference 9320:
 Microfluidics, BioMEMS, and Medical Microsystems XIII**

Istituto di Fotonica e Nanotecnologie (Italy); Ilaria Chiodi, Maira Di Tano, Chiara Mondello, Istituto di Genetica Molecolare, CNR (Italy); Ilaria Cristiani, Univ. degli Studi di Pavia (Italy); Roberto Osellame, CNR-Istituto di Fotonica e Nanotecnologie (Italy)

In recent years, considerable effort has been devoted to the development of integrated and low-cost optofluidic devices able to study single cells properties. Such devices usually rely on microfluidic circuits that guarantee a controlled flow of the cells while optical radiation is often exploited to probe or manipulate the cells under test. Among the different microfabrication technologies, femtosecond laser micromachining is ideally suited for this purpose as it provides the integration of both microfluidic and optical functions on the same glass chip leading to monolithic, perfectly aligned, robust and portable optofluidic devices. Diseased cells such as cancer cells are known to have different deformability compared to their healthy counterparts. Such difference can also be used to distinguish between metastatic and non-metastatic cancer cells. An effective approach to quantify cell mechanical characteristics in-vitro is to force them through micro-fluidic constrictions. We have fabricated and demonstrated a multipurpose optofluidic chip that integrates sorting of single cells by optical forces and a deformability assay based on a passage through a constriction. This device allows us to distinguish between non-metastatic and metastatic cancer cells with a fast and reliable method, depending on the fluidic pressure needed to force cells through the constriction. Comparison with well-assessed optical stretching measurements demonstrates the high sensitivity of this approach, notwithstanding its inherent simplicity. Further validation of the devices is provided with different cell lines and by investigating the effect of specific drugs on tumorigenic and metastatic cells.

9320-35, Session 9

Nanoplasmonic microparticles: enhanced sensitivity for high-throughput bioassay

Zhengtuo Zhao, Di Hu, Gargi Ghosh, Joe F. Lo, Univ. of Michigan-Dearborn (United States)

Advances in medical diagnostics and personalized therapy require sensitive and rapid measurement of minute amounts of proteins in body fluids. Standard ELISA is difficult to multiplex and involves lengthy protocols. Here we propose a novel nanoplasmonic-enhanced microdroplet to enable multiplexed detection of protein biomarkers in high-throughput microfluidics. Our technique incorporate gold nanoparticle encapsulation, trapping, and flow perfusion on a single device. Convergence of enhanced optical detection with efficient microfluidics brings about an innovation in high-throughput bioassays, a key enabling technology in numerous personalized medicine applications.

In the device, the two phase flows of mineral oil and UV-curable PEG gel (1 mg/ml photoinitiator, 8% PEGDA 20k) met at a cross-section where a series of 500 μ m droplets were generated. These droplets were trapped by designed pockets away from shear flows in the channels. Occupied pocket redirects subsequent flow down the serpentine to the next trapper pocket, where the shorter trapper flow path allow droplet to flow in. After trapping, exposure to 365 nm UV intensity activated the hydrogel crosslinking, hardening droplets to allow aqueous phase interactions.

To demonstrate trapped microdroplet's utility for high-throughput assay, we flowed in fluorescein and 250 kDa FITC-dextran for a 50 minute incubation and then measured their washing by PBS flow. To quantify the enhanced reporter fluorescence, microparticles with bare GNP and GNP conjugated with matching fluorescent probe were compared. Using these enhanced microparticles, microfluidic bioassays of VEGF were conducted, with improved probe intensity signal to noise and reduced assay time.

Conference 9321: Optical Interactions with Tissue and Cells XXVI

Sunday - Tuesday 8-10 February 2015

Part of Proceedings of SPIE Vol. 9321 Optical Interactions with Tissue and Cells XXVI

9321-1, Session 1

Laser-induced formation of micro-pores in the tissues for cartilage repair and treatment of glaucoma

Emil N. Sobol, Olga I. Baum, Institute on Laser and Information Technologies (Russian Federation); Alexander Shnirelman, Concordia Univ. (Canada); Valerii Vinokour, Argonne National Lab. (United States)

One of the reasons of arthritis and other diseases of cartilage is poor aqueous transport to the cells due to the blocking of natural pores in the intracellular matrix which hinders cell feeding, breathing and functioning. Uveoscleral outflow is a natural mechanism of intraocular pressure normalization. Acceleration of water transport via formation of micro-pores promotes cartilage regeneration in spine discs and joints. Pores in sclera are a candidate pathway for aqueous transport in glaucomatous eyes. Depending on tissue localization and function, there is an optimal size of the pores for effective water transport. Here we show that controllable formation of pores in cartilaginous and sclera tissues can be achieved as a result of the laser-induced stress relaxation in the biopolymers. We develop the theoretical model (based on the solution of non-linear thermo-mechanical problem without common assumptions of the smallness of deformations) which can describe dynamics of pore formation in the tissue and predict pore size and spatial distribution. The theoretical predictions are verified with experimental data obtained for laser-induced structural alterations in cartilage and sclera tissues by the means of optical and Atomic Force Microscopy, and also using non-destructive techniques of light scattering measurements and optoacoustic microscopy. Our results demonstrate how to optimize laser setting to promote controllable formation of pores in cartilage and sclera towards development of the novel approaches for treatment of arthritis and glaucoma.

9321-2, Session 1

Femtosecond laser collagen cross-linking without traditional photosensitizers

Nicola G. Celi, Michael D. Yu, Sinisa Vukelic, Columbia Univ. (United States)

Collagen cross-linking in cornea has the capability of enhancing its mechanical properties and thereby providing an alternative treatment for eye diseases such as keratoconus. Currently, riboflavin assisted UVA light irradiation is a method of choice for cross-link induction in eyes. However, ultrafast pulsed laser interactions may be a powerful alternative enabling in-depth treatment while simultaneously diminishing harmful side effects such as, keratocyte apoptosis. In this study, femtosecond laser is utilized for treatment of bovine cornea slices. It is hypothesized that non-linear absorption of femtosecond laser pulses plays a major role in the maturation of immature cross-links and the promotion of their growth. Targeted irradiation with tightly focused laser pulses allows for the absence of a photosensitizing agent. A parametric study was conducted to determine laser parameters under which the irradiation will not damage the tissue while inducing the desired cross-links. Raman spectroscopy was utilized to study subtle changes in the chemical composition of treated slices. The effects of treatment are analyzed by observing shifts in Amide I and Amide III bands, which suggest deformation of the collagen structure in cornea due to presence of newly formed cross-links.

9321-3, Session 2

Evaluation of different laser systems for decolonization of bacteria under transparent nanocrystalline yttria-stabilized-zirconia cranial implants

Yasaman Damestani, Yasuhiro Kodera, Javier E. Garay, Guillermo Aguilar, Univ. of California, Riverside (United States)

Infection is the leading cause for failure and removal of implants. Staphylococci account for the majority of infections, both on temporarily and permanently cranial implants. Transparent nanocrystalline Yttria-Stabilized-Zirconia (nc-YSZ) cranial implants provide a unique possibility to optically treat the infected tissue under the implant non-invasively and chronically on-demand without the need for removal of the implant. Staphylococcus aureus bacteria were grown on Trypticase Soy Broth and used to inoculate agar plates. nc-YSZ implants were placed on the agar plate and irradiated with 1064 or 810 nm laser wavelengths with energy density ranging from 0 (control) to 50 J/cm² and power output ranging from 1 to 3 W. During the experiment, the temperatures of nc-YSZ surface and implant-tissue interface were recorded using an infrared thermal camera and thermocouples, respectively. The laser generated acoustic shockwave was recorded using a high-speed camera. Counting the bacteria colony forming units quantitatively indicated the efficacy of laser with specific parameters. The results suggest that the reduction in the bacteria colony-forming units may be due to either plasma formation and, therefore, a laser generated shockwave or local temperature increase or both. In either case, the results show that both lasers have the ability to generate a stress wave sufficiently powerful to eliminate the bacteria under nc-YSZ without adverse effect to the underlying host structure as long as appropriate parameters are used. Thus, using nc-YSZ as a cranial implant allows for non-invasive, chronic treatment of the bacteria layer that might form under the cranial implant.

9321-4, Session 3

Hemifusion of cells using femtosecond laser pulses

Nir Katchinskiy, Roseline Godbout, Helly R. Goez, Abdulhakem Y. Elezzabi, Univ. of Alberta (Canada)

Surgically attaching single cells can potentially provide a platform for creation of engineered tissue and cell cultures. This technology can also be used for improving surgical methods that require extreme precision. The first demonstration of laser-induced cell-cell hemifusion using femtosecond laser pulses is reported in this article. It has been demonstrated that in order to perform hemifusion of single cells, sub-10 femtosecond laser pulses, with 800nm central wavelength can be used. It was shown that attachment of cells was performed without the induction of full cell fusion, with attachment efficiency of 95%, and while preserving the cells' viability. Cell-cell hemifusion was achieved by delivery of femtosecond laser pulses trains lasting 15 ms each. It is postulated that laser-induced ionization process led to an ultrafast, reversible, destabilization of the phospholipid layer of the cellular membranes. It was shown that during hemifusion, the inner cell membrane molecules remained intact and the cells' cytoplasm remained isolated from the surrounding medium. A strong physical attachment between the cells was obtained due to the bonding of the membranes' ionized phospholipid molecules and the formation of a joint cellular membrane at the connection point.

9321-5, Session 4

Investigation of the formation mechanism and morphology of the features created in the interior of cornea by femtosecond laser pulses

Yizang Guo, Sinisa Vukelic, Columbia Univ. (United States)

Laser assisted corneal surgeries often rely on the nonlinear absorption effect of ultrafast lasers to induce features in the interior of the cornea without affecting the surface. In particular, corneal flap formation in femtosecond assisted Laser-Assisted in situ Keratomileusis (LASIK) is based on the bubble creation. This study focuses on the interaction between the tissue and the femtosecond laser. Interior of cornea is treated with tightly focused femtosecond laser pulses. Due to the nature of the process, heating of the tissue within and around the focal volume is practically instantaneous. The affected region is subject to thermoelastic stress that arises with the steep temperature elevation. To predict the size of the region subject to the morphological changes due to the laser treatment, the strain field is calculated assuming viscoelastic properties of cornea. Cavitation bubble initiation and expansion process, which acts as precursor to the stress induced tissue trauma, is taken into account as well. Theoretical findings are compared against experimental results. High-speed camera is utilized to assess the laser treatment process, showing the temporal development of the cavitation bubbles. After the laser treatment, the strain distribution in the cornea is measured using an inflation system. The results obtained in this study facilitate a better understanding of the effects of femtosecond laser assisted corneal surgeries and help in choosing optimal laser parameters.

9321-6, Session 4

Role of molecular photodissociation in ultrafast laser surgery

Jenny Wang, Stanford Univ. (United States); Georg Schuele, Abbott Medical Optics (United States); Philip Huie, Daniel V. Palanker, Stanford Univ. (United States)

Transparent ocular tissues such as cornea and crystalline lens can be precisely ablated or dissected using ultrafast ultraviolet, visible, and infrared lasers. In refractive surgery, corneal ablation by 193 nm excimer laser is driven by explosive vaporization of the sub-micrometer surface layer of tissue. In refractive or cataract surgery, cutting of the cornea, lens and lens capsule is typically produced by dielectric breakdown in the focus of a short-pulse laser. Ionized matter absorbs light, resulting in overheating and explosive vaporization of the interstitial water, which mechanically ruptures the surrounding tissue. Here, we report that tissue can also be disrupted below the threshold of bubble appearance using 400 nm femtosecond pulses with minimal mechanical defects.

Gel electrophoresis and Liquid Chromatography/Mass Spectrometry demonstrated photodissociation of proteins and polypeptides by 400 nm femtosecond pulses both below and above the cavitation bubble threshold. Unlike the 193 nm ArF laser, where photodissociation was a single-photon event, longer wavelength lasers (UV and Visible) induced molecular breakdown only with a tightly focused beam, indicating the multiphoton nature of such interactions. Negligible protein dissociation was observed with 800 nm femtosecond lasers even above the threshold of dielectric breakdown. Scanning electron microscopy of the cut edges in porcine lens capsule demonstrated that plasma-mediated cutting results in the formation of grooves. Below the cavitation bubble threshold, however, precise cutting was still possible with 400 nm femtosecond pulses, likely due to molecular photodissociation of structural proteins. Resulting edges of the cut were remarkably smooth indicating the non-explosive nature of this mechanism.

9321-7, Session 5

Temperature Dependence of Melanosome Microcavitation Thresholds Produced by Single Nanosecond Laser Pulses

Morgan S. Schmidt, Paul K. Kennedy, Air Force Research Lab. (United States); Gary D. Noojin, TASC, Inc. (United States); Robert J. Thomas, Benjamin A. Rockwell, Air Force Research Lab. (United States)

In the field of laser bioeffects, the type of cellular damage induced during ocular exposure depends on the laser wavelength and exposure duration. Furthermore, high temperatures and pressures can be obtained around laser-irradiated melanosomes, which are pigments of the retinal pigment epithelium (RPE) layer. In the nanosecond to microsecond regime, melanosome microcavitation leads to spatially confined mechanical damage to the surrounding tissue. A better understanding of the particle surface temperature required for cavitation is necessary to determine the damage mechanisms. This research focused on the threshold for microcavitation as a function of temperature around absorbing melanosomes. Modeling efforts were also implemented in order to estimate absorption coefficients and validate experimental data for bubble formation around melanosomes.

Melanosomes were irradiated using a Nd:YAG coupled with an OPO (1000 – 1500 nm) as well as a q-switched Nd:YAG (532 nm). Time-resolved microscopy was accomplished by varying the delay between the irradiation beam and an illumination beam allowing stroboscopic imaging of microcavitation events. Thresholds for microcavitation of single bovine retinal melanosomes were determined as a function of temperature using single nanosecond laser pulses at 532 nm as well as the NIR (1000 – 1500 nm) wavelength regime. Results indicated a decrease in fluence threshold for single pulses with increasing sample temperature. The nucleation temperature was extrapolated through the linear relationship between the temperature increases on the particle surface per radiant exposure. Melanosome absorption coefficients were calculated from temperature and threshold data using the model of Brinkmann.

9321-8, Session 5

Two-wavelength approach for control of coagulation depth during laser tissue soldering

Martin M. Wehner, Mirko Aden, Nina Toedter, Beate Rosenkranz, Fraunhofer-Institut für Lasertechnik (Germany)

Laser soldering of a protein solution is considered for the fixation of wound dressings. During thermal denaturation of the protein solution (solder) the morphology of the solder layer changes and light scattering increases. This results in a reduction of the optical penetration depth and could lead to insufficient bonding to the tissue. In our approach we are employing two laser sources with different wavelengths to control the optical penetration depth during coagulation.

Experiments are carried out on a 3-layer model consisting of a membrane, albumin solder and a soft tissue phantom. The absorption coefficient μ_a , scattering coefficient μ_s and anisotropy factor g are determined by spectrometric measurements numerical analysis both in the native and the coagulated state. Beam propagation for 980 nm and 1540 nm laser radiation is simulated based on the Monte Carlo model. The beginning of the coagulation process is characterized by a clear solder layer, but the final state is strongly scattering. The resulting optical penetration depth was calculated and compared with the coagulated volume of the soft tissue phantom.

The simulated optical penetration depth varied between 4 mm in the native state and 1 mm in the coagulated state. The simulation is in reasonable agreement with the experimental observation of coagulation depths. The

**Conference 9321:
 Optical Interactions with Tissue and Cells XXVI**

coagulation depth can be varied experimentally between 1.5 mm to 3.5 mm by changing the irradiation parameters. Changing laser wavelength during coagulation leads to a concept for minimizing heat input while maintaining a strong bond between the solder layer and the tissue phantom.

9321-9, Session 6

Porcine cadaver iris model for iris heating during corneal surgery with a femtosecond laser

Hui Sun, Zhongwei Fan, Jiang Wang, Ying Yan, Academy of Opto-Electronics (China); Tibor Juhasz, Ronald M. Kurtz, Univ. of California, Irvine (United States)

Purpose: Multiple femtosecond lasers have now been cleared for use for ophthalmic surgery, including for creation of corneal flaps in LASIK surgery. Preliminary study indicated that during typical surgical use, laser energy may pass beyond the cornea with potential effects on the iris. As a model for laser exposure of the iris during femtosecond corneal surgery, we simulated the temperature rise in porcine cadaver iris during direct illumination by the femtosecond laser. Additionally, ex-vivo iris heating due to femtosecond laser irradiation was measured with an infrared thermal camera (Fluke corp. Everett, WA) as a validation of the simulation.

Methods: A computer simulation was developed using Comsol Multiphysics to calculate the temperature rise in the iris during femtosecond laser corneal surgery. Porcine irises excised from thirty eyes were irradiated with iFS Advanced Femtosecond Laser and the temperature rise was measured with an infrared thermal camera.

Results: Temperature increases up to 2.45 °C (corresponding to 2 J laser pulse energy and 24 second illumination) were observed in the porcine cadaver iris from the simulation with little variation in temperature profiles compared with specimens for the same laser energy illumination in ex-vivo experiment.

Conclusions: Our studies suggest that the magnitude of iris heating that occurs during routine femtosecond laser corneal surgery with normal clinical parameters is well beneath the threshold for iris damage. The simulation predictions are in agreement with thermal measurements providing a level of experimental validation.

9321-10, Session 6

Improvement of thermal effects to rabbit atherosclerotic aortas by macro pulse irradiation of a quantum cascade laser in the 5.7 μm wavelength range

Keisuke Hashimura, Katsunori Ishii, Kunio Awazu, Osaka Univ. (Japan)

Atherosclerotic plaques mainly consist of cholesteryl esters. Cholesteryl esters have an absorption peak at the wavelength of 5.75 μm originated from C=O stretching vibration mode of ester bond. Our group achieved making cutting difference between atherosclerotic lesions and normal vessels using a quantum cascade laser (QCL) in the 5.7 μm wavelength range. QCLs are relatively new types of semiconductor lasers that can emit mid-infrared range. They are sufficiently compact and have recently achieved their high-power emission. However, large thermal damage was observed because the QCL worked as a quasi-continuous wave laser due to its short pulse interval. To realize less-invasive ablation by the QCL, reducing thermal effects to normal vessels is needed. In this study, we tried improving the thermal effects by changing pulse structure. First, irradiation effects to rabbit atherosclerotic aortas by macro pulse irradiation (irradiation of pulses at intervals) and conventional continuous pulse irradiation were compared. The macro pulse width and the macro pulse interval were set to 0.54 and 12 ms, respectively, because the thermal relaxation time of rabbit

normal and atherosclerotic aortas in the oscillation wavelength of the QCL was 0.54-12 ms. As a result, ablation depth became longer and coagulation width became shorter by the macro pulse irradiation. In addition, cutting difference between rabbit normal and atherosclerotic aortas was observed by macro pulse irradiation. Therefore, the macro pulse irradiation achieved the improvement of thermal effects by the QCL in the 5.7 μm wavelength range. The QCL has the potential of realizing less-invasive laser an-gioplasty.

9321-11, Session 6

Brillouin spectroscopy characterizes microscopic viscoelasticity associated with skin injury

Zhaokai Meng, Vladislav V. Yakovlev, Texas A&M Univ. (United States)

The viscoelasticity of skin is an important indicator of its healthy condition. Monitoring the mechanical properties is usually invasive and destructive. To the contrary, Brillouin spectroscopy (BS) provides an alternative and non-invasive approach for probing the local sound speed within a small volume. Moreover, recent advances in background-free Brillouin spectroscopy enable investigators to imaging not only transparent samples, but also turbid ones. In this sense, the microscopic skin elasticity (associated with local sound speed) could be characterized using BS.

In this study, we employed various skin samples, including chicken skin purchased from local grocery markets. To induce injuries with different degrees, we burned the chicken skins with high power laser, as well as treating them using corrosive liquids. The Brillouin spectra were obtained by a background free VIPA (virtually imaged phased array) spectrometer described in the previous report [1]. In order to acquire 2-dimensional images, we employed a scanning procedure. As a reference, the Raman spectra were also acquired for each pixel.

Reference:

1. Meng, Z., Traverso, A. J., & Yakovlev, V. V., Optics express, 2014, 22(5), 5410-5416.

9321-12, Session 6

Modeling tissue heating under tunable near IR radiation

Joel N. Bixler, Brett H. Hokr, Texas A&M Univ. (United States); Aaron F. Hoffman, Fort Hays State Univ. (United States); Michael L. Denton, TASC, Inc. (United States); Benjamin A. Rockwell, Air Force Research Lab. (United States); Vladislav V. Yakovlev, Texas A&M Univ. (United States); Robert J. Thomas, Air Force Research Lab. (United States)

Nonlinear microscopic techniques such as multi-photon fluorescence microscopy have allowed for non-invasive, high-resolution, deep-tissue imaging. These techniques utilize the rejection of stray signal as well as NIR sources to enhance penetration depth. Many multi-photon studies utilize 800 nm excitation radiation due to the wide availability of titanium-doped sapphire imaging systems, as well as the availability of commercial two-photon dyes that absorb in this range. As high-powered, short-pulse optical parametric oscillators (OPOs) and optical parametric amplifiers (OPAs) become more common in research laboratories, researchers are afforded more flexibility in the excitation wavelength used for deep-tissue imaging.

One limiting factor, with respect to the depth at which images can be obtained, is how much radiation can safely be delivered to the sample. Thermal damage along the entire optical path must be considered for evaluating safe exposure, and this measure can also provide researchers with a means to optimize the wavelength selection for deep-tissue imaging applications.

**Conference 9321:
Optical Interactions with Tissue and Cells XXVI**

In our presentation, we will discuss the results of simulations of tissue heating using a custom Monte Carlo model which can be used to simulate optical radiation thermal interactions with a multi-layer tissue model, and provides simulations of the temperature response of tissue and analysis of damage resulting for the thermal response. We examine the thermal response of tissue from wavelengths ranging from 700 nm to 1600 nm in both collimated and various focusing geometries and present damage thresholds based on these results.

9321-13, Session 7

Optical properties and laser dose-mortality curves for anopheles stephensi mosquitoes

Matthew D. Keller, David Leahy, Emma Mullen, Bryan J. Norton, Eric Johanson, Maclen Marvit, Artyom Makagon, Intellectual Ventures Lab. (United States)

The Photonic Fence is a system designed to detect malaria-transmitting mosquitoes in an active region and to apply lethal doses of laser light to them. For both tracking and dosing systems, determining the optical properties of key *Anopheles stephensi* body segments would provide useful information for the choice of lasers. Despite the challenges presented by mosquitoes' size and geometry, reasonable estimates of the optical properties of cuticles and wings were obtained from 250-1100 nm. Absorption properties were dominated by the characteristic shape of melanin, and reduced scattering coefficients were similar in magnitude and shape to those of many mammalian tissues. Experiments were then conducted to identify laser dosing conditions required to kill or disable female *A. stephensi* mosquitoes as a function of several parameters, including laser wavelength, power, pulse duration, and spot size. Mortality and disablement relative to handled, but un-dosed controls were assessed 24 hours after dosing, according to WHO guidelines on insect mortality assays. Logistic regression of mortality data as a function of fluence was used to identify the LD50 and LD90 points for each dose-response curve. Using 2-6 mm spot diameters and 25 ms pulses, blue (445 nm) and green (532 nm) wavelengths had 3-4 times lower LD90 fluence values than near infrared (980 and 1064 nm) wavelengths. As the power increased and pulse duration decreased, the LD90 values declined (though with diminishing returns), as did visible vs NIR lethal threshold differences. Most importantly, both wavelength regions offer modestly priced, commercially available options for the dosing laser.

9321-14, Session 7

The photothermal effects of 1940nm thulium fiber laser on brain tissue: in vivo dosimetry study

Burcu Tunç Çamlıbel, Murat Gülsoy, Bogaziçi Üniv. (Turkey)

Background and Objective: Different types of lasers and other energy sources like electrocoagulation and radiofrequency have been used and investigated for decades in neurosurgery, in order to cut, vaporize/ablate and coagulate the tissue with minimal thermal damage to the surrounding healthy tissue. The coagulation of the tissue can be an unwanted result of continuous wave laser application in some medical cases, especially in neurosurgical applications. In this study, it is aimed to find the appropriate laser parameters in order to perform highest ablation efficiency with minimum collateral damage, which is calculated as the ratio of ablation zone diameter to the total thermally altered zone diameter. **Study Design/ Materials and Methods:** Healthy male Wistar rats, 3-4 months old, weighing 220-260 g were used. Rats were placed in the stereotaxic instrument after anesthesia. The skin was retracted and holes were drilled in the skull. Bilateral lesions were created with 1940-nm thulium fiber laser. During lasing temperature of the tissue was also monitored. Thermal effects of the laser were quantified in terms of ablation (thermally removed tissue), severe

and mild coagulation (irreversible thermal damage) and reversible thermal damage areas. The ablation and coagulation diameters were measured under light microscope after CFV staining. **Results:** The relationship between laser parameters, temperature increase and ablation (removal of tissue) efficiency was determined. **Conclusion:** It has been shown that 1940-nm thulium fiber laser can be used in neurosurgery, with proper laser power and exposure time. And also the temperature increase in the tissue is a good indicator about the quality of the lesion.

9321-15, Session 7

Evidence of thermal additivity during short laser pulses in an in vitro retinal model

Michael L. Denton, TASC, Inc. (United States); Amanda J. Tijerina, Conceptual MindWorks, Inc. (United States); Gary D. Noojin, John M. Rickman, TASC, Inc. (United States); Cherry C. Castellanos, Air Force Research Lab. (United States); Phillip N. Dyer, TASC, Inc. (United States); Benjamin A. Rockwell, Robert J. Thomas, Air Force Research Lab. (United States)

Laser damage thresholds were determined for exposure to 2.5-ms 532-nm pulses in an established in vitro retinal model. Single and multiple pulses (10, 100, 1000) were delivered to the cultured cells at three different pulse repetition frequency (PRF) values, and overt damage (membrane breach) was scored 1 hr post laser exposure. Trends in the damage data within and across the PRF range identified significant thermal additivity as PRF was increased, as evidenced by drastically reduced threshold values (< 40% of single pulse value). Microthermography data that were collected in real time during each exposure also provided evidence of thermal additivity between successive laser pulses. Temperature rise and decay profiles from microthermography data from continuous wave laser exposures were used in computational predictions of damage thresholds of the repetitive-pulse exposures.

9321-16, Session 7

Computational model of heterogeneous heating in melanin

Jason M. Kellicker, Gregory J. Kowalski, Charles A. DiMarzio, Northeastern Univ. (United States)

Previous research has relied on a spherical or ellipsoidal model of melanin particles with a smooth surface for Mie scattering analysis, FDTD analysis of a theta line-scanning confocal microscope, and FDTD analysis of light scattering from cells. Modeling melanin without taking into consideration the heterogeneous surface morphology yields results that underestimate the strongest signals or over-estimate their spatial extent. Melanin particles often present as an aggregate of smaller melanin pigment granules and have a heterogeneous surface morphology. When irradiated with light within the absorption spectrum of melanin, these heterogeneities produce measurable concentrations of the field that result in temperature gradients or multi-photon excited fluorescence from thermal effects that are not seen with spherical or ellipsoidal modeling of melanin. The heterogeneities, presented in this research as bumps on the surface of the melanin particle, act to concentrate the field, similar to the field enhancement of a lightning rod, and produce a larger temperature increase in localized areas. This, in return, produces effects similar to that seen in three-photon excitation and the suspected photothermal response. This research demonstrates the heterogeneous heating that occurs in melanin through application of a rigorous optical, thermal and mechanical computational analysis while providing good agreement with results obtained from previous laboratory experiments.

**Conference 9321:
Optical Interactions with Tissue and Cells XXVI**

9321-32, Session PMon

Study optical properties of biological tissue in the presence of microbubbles

Homa Assadi, Vincent Lee, Raffi Karshafian, Ryerson Univ. (Canada); Alexandre Douplik, Ryerson Univ. (Canada) and Erlangen Graduate School in Advanced Optical Technologies (Germany)

Optical contrast agents introduce distinct property to induce detectable changes in native tissue properties [1]. In ultrasound imaging, microbubbles (MBs) – a gas-core shell-encapsulated agent – are used clinically as contrast agents. The working hypothesis of this study is that microbubbles can be employed as an intravascular contrast agent in optical imaging systems. Microbubbles can produce refractive index mismatches which makes it distinguish from surrounding media. In this work, the interaction of collimated light and microbubbles in a biological phantom solution was investigated. Biological medium was comprised of intralipid and human blood which was constructed to cover the range of soft tissue optical property. The effect of microbubbles on the optical properties such as reduced scattering and absorption coefficients was considered. Diffuse reflectance (DR) and total transmittance (TT) of a biological phantom solution were measured using spectroscopic integrating sphere system in the absence and presence of Definity® microbubbles. The optical properties were computed using the inverse adding doubling (IAD) software. The presence of microbubbles increased DR and decreased TT of the phantom. In the presence of MB's (2.5% volume concentration), the reflectance of the phantom increased by 25% in optical window. There is no absorption event and only scattering happened after light-microbubbles interactions. The reduced scattering coefficient increased significantly (30%) indicating potential use MBs as optical contrast agents. In conclusion, reflectance of a media can be enhanced by adding microbubbles to increase scattering properties and detect more light getting back to the surface of tissue.

9321-33, Session PMon

DNA fragmentation and nuclear phenotype in tendons exposed to low-intensity infrared laser

Flavia de Paoli, Larissa Ramos Cerqueira, Univ. Federal de Juiz de Fora (Brazil); Mayara Martins Ramos, Centro Univ. Serra dos Órgãos (Brazil); Vera M. Campos, Univ. do Estado do Rio de Janeiro (Brazil); Samara C. Ferreira-Machado, Univ. Federal Fluminense (Brazil); Mauro Geller, Centro Univ. Serra dos Órgãos (Brazil); Adenilson Souza da Fonseca, Univ. do Estado do Rio de Janeiro (Brazil) and Centro Univ. Serra dos Órgãos (Brazil)

Clinical protocols are recommended in device guidelines outlined for treating many diseases on empirical basis. However, effects of low-intensity infrared lasers at fluences used in clinical protocols on DNA are controversial. Excitation of endogenous chromophores in tissues and free radicals generation could be described as a consequence of laser used. DNA lesions induced by free radicals cause changes in DNA structure, chromatin organization, ploidy degrees and cell death. In this work, we investigated whether low-intensity infrared laser therapy could alter the fibroblasts nuclei characteristics and induce DNA fragmentation. Tendons of Wistar rats were exposed to low-intensity infrared laser (830 nm), at different fluences (1, 5 and 10 J/cm²), in continuous wave (power output of 10mW, power density of 79.6 mW/cm²). Different frequencies were analyzed for the higher fluence (10 J/cm²), at pulsed emission mode (2.5, 250 and 2500 Hz), with the laser source at surface of skin. Geometric, densitometric and textural parameters obtained for Feulgen-stained nuclei by image analysis were used to define nuclear phenotypes. Significant differences were observed on the nuclear phenotype of tendons after exposure to laser, as well as, high cell death percentages was observed for all fluences and frequencies analyzed here,

exception 1 J/cm² fluence. Our results indicate that low-intensity infrared laser can alter geometric, densitometric and textural parameters in tendon fibroblasts nuclei. Laser can also induce DNA fragmentation, chromatin lost and consequently cell death, using fluences, frequencies and emission modes took out from clinical protocols.

9321-34, Session PMon

Effects of formalin fixation on tissue optical properties of in vitro brain samples

Suresh Anand, European Lab. for Non-linear Spectroscopy (Italy); Riccardo Cicchi, Istituto Nazionale di Ottica, CNR (Italy) and European Lab. for Non-Linear Spectroscopy (Italy) and Univ. degli Studi di Firenze (Italy); Fabrizio Martelli, Univ. degli Studi di Firenze (Italy); Flavio Giordano, Azienda Ospedaliera Univ. Anna Meyer (Italy); Anna Maria Buccoliero, Renzo Guerrini, Univ. degli Studi di Firenze (Italy); Francesco S. Pavone, European Lab. for Non-linear Spectroscopy (Italy) and Istituto Nazionale di Ottica, CNR (Italy) and Univ. degli Studi di Firenze (Italy)

Application of light spectroscopy based techniques for the detection of cancers have emerged as a promising technology for tumor diagnostics. In vivo or freshly excised samples are normally used for point spectroscopic studies. However, constraints imposed upon measurements by ethical issues, sample availability and deterioration in vivo or studies on fresh samples could be limited. There has been a few studies reported on the application of formalin fixed samples with good discrimination capability. Usually formalin fixation in tissues is performed to prevent degradation of tissues after surgical resection. Fixing tissues in formalin prevents cell death by forming cross-linkages with proteins. Previous investigations have revealed that washing tissues fixed in formalin using phosphate buffered saline is known to reduce the effects of formalin during spectroscopic measurements. But this could not be the case with reflectance measurements. Hemoglobin is a principal absorbing medium in biological tissues in the visible range. Formalin fixation causes hemoglobin to seep out from red blood cells. Also, there could be alterations in the refractive index of tissues when fixed in formalin. In this study, we propose to investigate the changes in tissue optical properties between freshly excised and formalin fixed brain tissues. The results indicate a complete change in the spectral profile in the visible range where hemoglobin has its maximum absorption peaks. The characteristic bands of oxy-hemoglobin at 540, 580 nm and de-oxyhemoglobin at 555 nm disappear in the case of samples fixed in formalin. In addition, an increased spectral intensity was observed for the wavelengths greater than 650 nm where scattering phenomena are presumed to dominate. In addition, the variation in tissue optical properties between fresh and formalin fixed samples would be discussed apart.

9321-35, Session PMon

Dynamics of water-mediated hard dental tissue ablation with Ho:YAG laser visualized by high speed photography

Zhenlin Zhan, Chuanguo Chen, Xuwei Li, Fujian Normal Univ. (China)

External water plays an important role in the laser ablation of hard dental tissue. At first, the external water spray was only thought as a cooling agent to reduce the thermal damage on the surrounding normal tissues. Then it is assumed that supplying water externally also serves to increase ablation efficiency, alter surface morphology and enhance bond strength to restorative materials. However, the interaction mechanism between water, laser light and dental tissues is not clearly understood and is somewhat controversial so far. In this study, the dynamic process of water-mediated

**Conference 9321:
Optical Interactions with Tissue and Cells XXVI**

hard dental tissue ablation induced by Ho:YAG laser was monitored by high-speed camera. The wavelength of pulsed Ho:YAG laser is 2.08 μm , and pulse repetition rate is 3 Hz. The laser energy ranged from 300 to 2000 mJ. The frame rate of high-speed camera used in the experiment was 50525 fps. Based on the observation by high-speed camera, the dynamic process of vapor channel formation and water-mediated ablation induced by Ho:YAG laser was evaluated. The pulsation period, the maximum length and width of vapor channel as a function of laser energy were attained. On this basis, the influence of external water on dental tissue ablation was discussed.

9321-36, Session PMon

Photobiostimulation on chondrocytes proliferation in different concentration of fetal bovine serum under low-level laser irradiation

Liqin Zheng, Fujian Normal Univ. (China)

Low-level laser irradiation has been used to modulate cell proliferation in many cell types. The aim of this study was to evaluate the influence of low-level laser irradiation (LLLI) on the proliferation of chondrocytes cultured in different concentration of fetal bovine serum (FBS) using 658 nm, 785 nm and 830 nm diode laser. The chondrocytes were isolated from the cartilage sample of 8-week-old healthy Sprague Dawley rats and the first passage of chondrocytes were used in this study. All cells were seeded into 96-well microplates with 3000 cells per well for experiment. The time of laser irradiation was 68 seconds per well and the laser power was tunable in this study. After 24 hours serum starvation, the role of energy density (10-60 mJ·cm⁻²) on cell proliferation following near-infrared laser irradiation for 2 days was investigated to find out the best laser fluence. Then the time-dependent responses of cell proliferation after different wavelength LLLI and the effect of LLLI on the proliferation of chondrocytes cultured with FBS at 0%, 2%, 5% and 10% were also evaluated. The results assessed by MTT assay showed that there was no or little photobiostimulation on the proliferation of chondrocytes cultured with 10% FBS; the cell proliferation at 0%, 2% or 5% FBS was more or less modulated by LLLI, and the maximum proliferation promotion was at 2% FBS.

9321-37, Session PMon

Assessment of ultra-high resolution optical coherence tomography for monitoring tissue effects caused by laser photocoagulation of ex-vivo porcine retina

Patrick Steiner, Univ. Bern (Switzerland); Volker Enzmann, Sebastian Wolf, Inselspital Bern (Switzerland); Anke Bossen, Christoph Meier, Berner Fachhochschule Technik und Informatik (Switzerland); Raphael Sznitman, ARTORG Center, University of Bern (Switzerland) and Department of Ophthalmology, Inselspital (Switzerland)

In the last decades, retinal laser photocoagulation has been established as a successful treatment for a variety of retinal diseases. However, laser photocoagulation shows the drawback of employing high energy lasers which are capable of physically destroying the neuronal retina. Monitoring of the caused tissue effects is therefore crucial for reliable therapy. We assess the use of ultra-high resolution optical coherence tomography (OCT) to represent tissue changes caused by photothermal interaction during laser application.

Laser lesions were placed on porcine retina ex-vivo using a 577 nm laser and an irradiation time of 10 ms. Applied energies varied from 0.7 to 20 mJ equivalent to laser powers between 70 mW and 2 W and lesions were examined using a proprietary OCT system with an axial resolution of 1.78 μm . To link optical and biological changes in the tissue, histological sections

from the same samples were prepared to provide an overview of the biological tissue effects. OCT scans included volume scans before and after irradiation, as well as time lapse scans (Mscan) of the lesions. The data was evaluated using an experimental software framework designed to quantify and classify the extent of the lesions by segmenting and analyzing the RPE and adjacent layers.

In a pilot study, the proposed method featured OCT lesion visibility thresholds 40-50 mW (17% reduction) lower than for visual inspection. With the ultra-high resolution OCT, 42% of ophthalmoscopically invisible lesions could be detected and lesions that were under- or overexposed could be distinguished using the Mscan software framework.

9321-38, Session PMon

Optical cryoimaging of rat kidney and the effective role of chromosome 13 in salt-induced hypertension

Fahimeh Salehpour, Mahsa Ranji, Univ. of Wisconsin-Milwaukee (United States); Allen W. Cowley Jr., Chun Yang, Theresa Kurth, Medical College of Wisconsin (United States)

It is known that oxidative stress plays a causal role in the progression of salt-induced hypertension, especially in the kidney. To determine the effect of salt-induced hypertension, Dahl salt-induced (SS) rats with P67phox gene knocked out were used (SSP67phox^{-/-}). In this study, we showed that this genetic manipulation affects the metabolism and oxidative stress in the outer renal medulla of the SS rat. Mitochondrial metabolic coenzymes NADH and FAD, which are autofluorescent, are the primary electron carriers in oxidative phosphorylation. It has been shown that the ratio of these fluorophores, (NADH/FAD), called the mitochondrial redox ratio (RR), is a marker of the oxidation state of tissue. We used cryoimaging to quantify oxidative stress due to expression of P67phox. A total of two groups of rats (SS and SSP67phox^{-/-}) were fed on a high salt diet (4% NaCl). After 21 days animals were sacrificed and their kidneys extracted for cryo imaging. For this study, slice thickness in z direction was chosen at 30 μm , which resulted in 400 slices per rat kidney. Mitochondrial redox ratio results demonstrated a 46% decrease in the mean histogram of RR in kidneys from a SS rat (1.001 \pm 0.079; n=4) compared to a SSP67phox^{-/-} rat (1.458 \pm 0.114). We conclude that expression of p67phox reduces redox ratio due to mitochondrial dysfunction that can be quantified by cryo imaging.

9321-39, Session PMon

Low-intensity infrared laser effects on zymosan-induced articular inflammatory response

Lúcia Mara Januário dos Anjos, Univ. Federal de Juiz de Fora (Brazil); Adenilson Souza da Fonseca, Univ. do Estado do Rio de Janeiro (Brazil); Jacy Gameiro, Flávia de Paoli, Univ. Federal de Juiz de Fora (Brazil)

Low-level therapy laser is a phototherapy treatment that involves the application of low power light in the red or infrared wavelengths in various diseases such as arthritis. Even though this treatment has been used to treat several clinical conditions, the mechanisms and cells responses are still incompletely understood. In this work, we investigated whether low-intensity infrared laser therapy, recommended in device guidelines, could cause DNA damage and consequently cell death in cartilage cells after zymosan-induced articular inflammatory process. Inflammatory process was induced in C57BL/6 mouse by intra-articular injection of zymosan into rear tibio-tarsal joints. Thirty animals were divided in five groups: (I) control, (II) laser, (III) zymosan-induced, (IV) zymosan-induced + laser and (V) dexamethasone. Laser exposure was performed 5 h, 24h, 48h and 72h after zymosan administration with low-intensity infrared laser (830 nm),

**Conference 9321:
Optical Interactions with Tissue and Cells XXVI**

power 10 mW, fluence 3.0 J/cm² at continuous mode emission. Twenty-four hours after last irradiation, the animals were sacrificed and the right joints fixed and demineralized. Morphological analysis was observed by hematoxylin and eosin stain, pro-apoptotic (caspase-6) was analyzed by immunocytochemistry and DNA fragmentation was performed by TUNEL assay in articular cartilage cells. Inflammatory process was observed in connective tissue near to articular cartilage, in IV and V groups, indicating zymosan effect. This process was decreased in both groups after laser treatment and dexamethasone, respectively. Although groups III and IV presented higher caspase-6 and DNA fragmentation percentages, statistical differences were not observed when compared to groups I and II. Our results suggest that therapies based on low-intensity infrared lasers could reduce inflammatory process and could not cause DNA fragmentation and consequently cell death in articular cartilage cells after zymosan-induced inflammatory process.

9321-40, Session PMon

Adipose tissue ablation efficiency measurement for mid-infrared laser-assisted lipolysis

Bongkyun Kim, Jin-Chul Ahn, Phil-Sang Chung, Dankook Univ. (Korea, Republic of)

Laser assisted lipolysis is a widely accepted method for removal of fatty tissue. The studies on laser-assisted lipolysis have drawn considerable interest and played an important role in many clinical applications such as micro-cannula liposuction and body contouring. The efficiency of laser lipolysis is substantially affected by several parameters such as, optical fluence rate, wavelength of the laser source and the optical properties of target tissue. Mid-infrared laser sources are quite attractive, since they provide superior optical absorption properties in adipose tissue. In this study, ablation of porcine adipose tissue using a fiber delivered mid-infrared laser have been investigated and quantified by measuring the mass of tissue removed as a function of incident laser radiant energy. Our study was conducted using custom built mid-infrared laser module which utilizes periodically poled nonlinear crystal. Wavelength and radiant exposure dependent tissue ablation efficiency will be demonstrated, and the potential medical applications of the proposed laser will be discussed.

9321-41, Session PMon

Optical characterization of pancreatic normal and tumor tissues with double integrating sphere system

Tugba Kiris, Saadet Akbulut, Aysenur Kiris, Fatih Univ. (Turkey); Zuhail Guçin, Bezmialem Foundation Univ. (Turkey); Oguzhan Karatepe, Medipol Univ. Hospital (Turkey); Burcu Tunç Çamlıbel, Boğaziçi Üniv. (Turkey); Hasim Özgür Tabakoglu, Fatih Univ. (Turkey)

In order to use light to develop minimally invasive, fast and accurate diagnostic/therapeutic methods in medicine the first step is to examine how the light propagates, scatters and transmitted through matter. So as to find out appropriate wavelengths and dosages for new methods, it is required to correctly determine the optical properties of tissues. Aim of this study is to measure the optical properties of both tumor and healthy ex-vivo pancreatic tissue samples. Results will be compared to observe how cancerous and noncancerous tissues respond to different wavelengths. By doing so, it will be tried to estimate pathological results without using histological staining methods and to develop new methods and techniques for pathologic assessments in order to help surgeons and pathologists during surgical operations.

In this study, double-integrating-sphere system was used. Absorption and reduced scattering coefficients of healthy and cancerous pancreatic tissues

has been determined within the range of 450-650 nm. 6 surgery specimen obtained via whipple procedure at Bezmialem Medicine Faculty Hospital have been examined. Ex-vivo tissues were kept in isotonic solution at 4°C and examined in 24h. Circular teflon fabric separator used for to fix tissue between slides.

Two-tailed and paired student t-test showed the significant differences at 550nm and 630nm wavelength for absorption coefficients. It could be interpreted as that, at 550nm and 630 nm wavelengths, healthy and cancerous pancreas tissues have showed significantly different absorption coefficients because of the pancreas tissue's structure and optical properties.

9321-17, Session 8

Cytotoxicity change with albumin binding of Talaporfin sodium in extracellular photosensitization reaction on cardiomyocyte

Emiyu Ogawa, Sayaka Motohashi, Tsunenori Arai, Graduate School, Keio Univ. (Japan)

We studied the myocardial cell necrosis measuring cell lethality with various albumin concentrations against oxidative stress by extracellular photosensitization reaction using talaporfin sodium. We have proposed to induce the photosensitization reaction in interstitial space of myocardium with short drug-light interval to realize the immediate cell damage by myocardial cell membrane for tachyarrhythmia treatment. To understand the effect of the particular extracellular photosensitization reaction in interstitial space, we measured the myocardial cell lethality 2 hours after the photosensitization reaction by WST assay varying the talaporfin sodium concentration, radiant exposure, and wide albumin concentration of 0-15 mg/ml. The cell lethality was decreased with albumin concentration increasing over 85 % in binding ratio between talaporfin sodium and albumin. The cell lethality didn't change between 0-85% in binding ratio between talaporfin sodium and albumin. The calculated deposited energy to the talaporfin sodium solution was nearly constant of 8.43±1.63 J/well in average varying albumin concentration. We think the cell killing effect by the extracellular photosensitization reaction has a threshold between 85-100% in binding ratio between talaporfin sodium and albumin in the case of the talaporfin sodium concentration of 40 µg/ml and radiant exposure of 0-40 J/cm².

9321-18, Session 8

Photoinduced conformational changes to porphyrin-bound albumin reduces albumin binding to Osteonectin

Sarah C. Rozinek, The Univ. of Texas at San Antonio (United States) and Air Force Research Lab. (United States); Robert J. Thomas, Air Force Research Lab. (United States); Lorenzo Brancaleon, The Univ. of Texas at San Antonio (United States)

Much work has shown light-induced structural changes to proteins are possible. For instance, we have previously shown that, small secondary and tertiary structural changes occur to albumin when it is bound (non-covalently) to meso-tetrakis(4-sulfonatophenyl)porphyrin (TSPP) and irradiated with a low intensity laser. Further study of this light-induced protein modification could advance the understanding of albumin's structure/function relationship. Then, this structural modification technique might be implemented to deactivate unwanted protein functions or even to bestow non-native protein properties. A necessary step toward this goal is to determine if and how protein function is affected once its structure is modified. The current study aims to explore the light-induced conformational change to TSPP-bound albumin by testing its ability to bind the biologically relevant albumin receptor, Osteonectin. In this

**Conference 9321:
Optical Interactions with Tissue and Cells XXVI**

Affinity-Depletion experiment, Osteonectin has been covalently attached to magnetic beads, forming an affinity column. TSPP-albumin will non-covalently bind the column, and we predict that the light-induced change to albumin will cause a reduction in binding to Osteonectin. This loss of binding ability would mean a deactivation of albumin's natural cellular functions.

9321-19, Session 8

Evaluation of cell killing effect by PDT with different beam profiles to investigate efficient therapeutic condition

Hitomi Yabe, Hisanao Hazama, Norihiro Honda, Osaka Univ. (Japan); Takuya Ishii, Katsushi Inoue, Masahiro Ishizuka, Tohru Tanaka, SBI Pharmaceuticals Co., Ltd. (Japan); Kunio Awazu, Osaka Univ. (Japan)

It is well known that photodynamic therapy (PDT) effects depend on irradiation energy density, drug concentrations, and the amount of reactive oxygen species (ROS) generation. The permissible ranges of irradiation energy and the amount of ROS to obtain sufficient cell killing effect have never been clarified. In this study, the permissible range of energy density in PDT was investigated in vitro experiments and theoretical calculations.

An optical set up to obtain a graded intensity profile was constructed using a laser diode with a wavelength of 635 nm. Then, in vitro PDT experiments were performed for a mouse mammary carcinoma cell line EMT6 mouse blast tumor adhesive cells. 5-aminolevulinic acid was administered at a concentration of 250 μM , and laser irradiation time was 200 s. After that, each nucleus of dead cells was stained by fluorescence dye for counting the cell survival rate. As a result, the cell survival rate decreased to 1/e at the laser power density within 11.30 J/cm^2 . On the other hand, the concentration of ROS was calculated at each power density by the theoretical equation of ROS generation taking account of photobleaching of the photosensitizer. As a result, the range of concentration of ROS which reduce the cell survival rate to 1/e was $10^2 \mu\text{M}$.

9321-20, Session 8

Origins of intracellular calcium mobilization evoked by infrared laser stimulation

Cory A. Olsovsky, Texas A&M Univ. (United States); Gleb P. Tolstykh, General Dynamics Information Technology (United States); Bennett L. Ibey, Hope T. Beier, Air Force Research Lab. (United States)

Delivery of pulsed IR laser energy has been shown to stimulate action potentials in neurons. The mechanism for this stimulation is not completely understood. Certain hypotheses suggest the rise in temperature from IR exposure could activate temperature- or pressure-sensitive channels, or create pores in the membrane. Studies using intensity-based Ca^{2+} -responsive dyes show changes in Ca^{2+} levels after various IR stimulation parameters; however, determination of the origin of this signal proved difficult. An influx of larger, typically plasma-membrane-impermeant ions has been demonstrated, which suggests that Ca^{2+} may originate from the external solution. However, activation of intracellular signaling pathways, possibly indicating a more complex role of Ca^{2+} , has also been shown. By using Fura-2 and a high-speed ratiometric imaging system that rapidly alternates the excitation wavelengths, we quantify the Ca^{2+} mobilization in terms of influx from the external solution and efflux from intracellular organelles. CHO-K1 cells, which lack voltage-gated Ca^{2+} channels, and NG-108 neuroblastoma cells, which do not produce action potentials in an early undifferentiated state, are used, in conjunction with pharmaceutical agents, to determine the origin of the Ca^{2+} signals and investigate the role these mechanisms may play in IR neural stimulation. This study attempts to progress fundamental understanding of IR stimulation of neurons.

9321-21, Session 8

Raman spectroscopy for the exploration of lipid peroxidation from electromagnetic exposure

Maria A. Troyanova-Wood, Texas A&M Univ. (United States); Gary L. Thompson, Oak Ridge Institute for Science & Education (United States); Bennett L. Ibey, Hope T. Beier, Air Force Research Lab. (United States)

Lipid peroxidation has been shown to alter the function of the cell membrane, including increased membrane permeability, and the products of lipid oxidation are also shown to be a part of some crucial biological functions, such as cell signaling. Electromagnetic exposure from pulsed electric fields has been shown to induce changes in membrane fluidity and permeability. These exposures have also been shown to initiate plasma membrane derived intracellular pathways, suggesting the stimulus is acting on the membrane directly. Additionally, it has been shown that short electric pulses initiate generation of reactive oxygen species (ROS) that may lead to free radical-initiated oxidation of membrane lipids. Therefore, it is important to obtain a deeper understanding of possible pathways and products of lipid oxidation from these exposures. We use Raman spectroscopy, a powerful technique that provides chemically-specific contrast and allows for differentiation between chemical species, to evaluate lipid peroxidation within a phospholipid bilayer membrane. Oxidation of lipid solutions consisting of DOPC and DPPC, was initiated by the application of hydrogen peroxide and nanosecond electric pulses. Bulk Raman spectra were obtained to determine whether oxidation induced by either stimulus caused a quantifiable spectral change. Understanding whether the electric field plays a direct role in oxidation of the lipids, thus activating cellular signaling pathways, is critical to understanding the cell response.

9321-22, Session 8

Time response of electrical conduction block in novel cardiomyocyte wire by extra-cellular photosensitization reaction at various irradiances

Mariko Kurotsu, Emiyu Ogawa, Graduate School, Keio Univ. (Japan); Tsunenori Arai, Keio Univ. (Japan)

We studied time response of electrical conduction (EC) block in a novel cardiomyocyte wire by extra-cellular photosensitization reaction (EPR) at various irradiances. This EC block using the EPR has been studied to develop a non-thermal arrhythmia therapeutic methodology. Despite the EC block in acute phase is needed to judge therapeutic endpoint in clinical arrhythmia therapy, time response of the EC block by the EPR in acute phase hasn't been studied. We measured the time to EC block occurrence by the EPR with intra-cellular Ca^{2+} concentration change using Fluo-4 AM fluorescence measurement by a confocal laser microscope system. The pattern cultivation cover glass with 10 mm² which had 60 μm width cultivation areas with 300 μm separations was used to form the cardiomyocyte wires. Rat cardiomyocyte with 10.8×10^5 cells was disseminated to the cover glasses installed in a 35 mm² dish. After 3 days from the dissemination, the EPR was operated to the cardiomyocyte wires for 10 min varying 3-120 mW/cm² in 663 nm laser irradiances with 20 $\mu\text{g/ml}$ talaporfin sodium. An irradiation area was approximately 60x340 μm^2 on each wires. Cross correlation functions (CCF) in measured fluorescence images in every 10 s were calculated across the irradiation area. The time to EC block occurrence was defined as the time of the max difference between adjacent CCFs. By decreasing irradiances in 30-6 mW/cm², the time to EC block occurrence became longer from 294 to 434 s. In 30-120 mW/cm², the time to EC block occurrence was nearly constant in 300 s.

**Conference 9321:
Optical Interactions with Tissue and Cells XXVI**

9321-23, Session 8

Terahertz spectroscopy and detection of brain tumor in rat fresh-tissue samples

Sayuri Yamaguchi, Canon Inc. (Japan); Yasuko Fukushi, Hamamatsu Univ. School of Medicine (Japan); Oichi Kubota, Takeaki Itsuji, Canon Inc. (Japan); Seiji Yamamoto, Hamamatsu Univ. School of Medicine (Japan); Toshihiko Ouchi, Canon Inc. (Japan)

Terahertz (THz) spectroscopy and imaging of biomedical samples is expected to be one of the important applications in the THz field. Identification and localization of the tumor tissue, imaging of other biological samples, analysis of DNA, etc., have been demonstrated in the past. THz time-domain spectroscopy (TDS) is useful to obtain refractive index in broadband. However, THz-TDS spectra of fresh-tissue samples are sensitive to measurement procedures including sample-preparation, and a unified measurement protocol is required. Therefore, in this work, we establish such protocol for measurements of fresh-tissue THz spectra and demonstrate reliable detection of brain tumor of rats.

We use a reflection-type THz-TDS system to measure the refractive-index spectra of the samples mounted on top of a quartz plate. The tissue samples have been measured right after cutting to suppress sample denaturalization during storing. Special care has been taken numerically in THz data processing to eliminate parasitic reflections and reduce noise. The error level in our refractive-index measurements was as low as 0.02 in the frequency range 0.8-1.5 THz. Refractive index in the tumor and normal regions were monotonically decreased similar to water and 0.02 higher in the tumor regions in the frequency range. The spectral data suggests that the tumor regions have higher water content. With the help of additional hematoxylin-eosin stained images, we find that the cell density is also responsible for the observed spectral features. A set of samples from five rats show consistent results. Our results suggest that reliable tumor detection in fresh tissue without pretreatment is possible with THz spectroscopic measurements. THz spectroscopy has potential to become a method of real-time in-vivo diagnostics.

9321-24, Session 8

Investigation of the effects of low- and high-power 2.52 THz radiation on human keratinocytes

Cesario Z. Cerna, General Dynamics Advanced Information Systems (United States); David P. Elam, Consortium Research Fellows Program (United States); Mark A. Sloan, General Dynamics Advanced Information Systems (United States); Ibey L. Bennet, Air Force Research Lab. (United States); Ibtissam Echchgadda, General Dynamics Advanced Information Systems (United States)

Terahertz (THz) imaging and sensing technologies are being used at international airports for security screening purposes and at major medical centers for cancer and burn diagnosis. The emergence of THz-based applications has directly resulted in an increased interest regarding the biological effects associated with this frequency range. In this study, we investigated the cellular response of human keratinocytes exposed to low- and high- power 2.52 THz radiation. During exposures, we maintained the cells under controlled standard tissue culture conditions using our recently developed THz exposure system, which integrated a modified, industry grade, cell culture incubator to an optically pumped molecular gas THz source. We used a custom spectrum analyzer to evaluate the frequency-power spectrum, and a pyroelectric array and calorimeter to characterize the absolute power, width, and intensity profile of the THz beam. We monitored THz power as DC voltage-logged values (LabVIEW™ IV log) during all THz exposures. To determine the heating profiles during THz

exposure, we measured temperature changes in the unexposed (control sham) and THz-exposed cells using thermocouples. We then used these values to set the thermally-matched bulk-heating controls. We examined cellular viability of control cells and THz-exposed cells 4 hours post-exposure using MTT colorimetric assays. We evaluated the cellular response to low- and high-power THz radiation relative to controls using messenger RNA (mRNA) microarrays and bioinformatics analysis. Our data provide a global comparison of genetic changes induced in cells exposed to low- and high-power 2.52 THz radiation.

9321-25, Session 8

Effects of different terahertz frequencies on gene expression in human keratinocytes

Ibtissam Echchgadda, Cesario Z. Cerna, Mark A. Sloan, General Dynamics Advanced Information Systems (United States); David P. Elam, Consortium Research Fellows Program (United States); Bennet L. Ibey, Air Force Research Lab. (United States)

In recent years, a surge in the development of many terahertz (THz) sensing and imaging technologies occurred leading to increased use in military and civil operations. Therefore, understanding the biological effects associated with exposures to this radiation is becoming increasingly important. Previous studies have speculated that cells exposed to different frequencies of THz radiation may exhibit differential responses. However, empirical studies to confirm such differences have not been performed. The question of whether cells exposed to different THz frequencies exhibited specific biological responses remains unclear. In this study, we exposed human keratinocytes to a THz laser tuned to several different THz frequencies using our recently developed THz exposure system. This system consists of an optically pumped molecular gas THz laser source coupled to a modified cell culture incubator permitting THz radiation exposures under controlled standard tissue culture conditions. For all frequencies, we matched the THz exposure duration and irradiance. During THz exposure, we monitored the power as DC voltage-logged values (LabVIEW™ IV log). To determine the temperature changes by THz exposure, we collected temperature readings from the unexposed and THz-exposed cells using thermocouples. We assessed cellular viability after exposure using MTT colorimetric assays. We compared the changes in gene expression profiles using messenger RNA (mRNA) microarrays, and we identified the THz-induced signaling pathways for each frequency using bioinformatics. Our data provide valuable new insights that give a comparative picture of the genes and intracellular signaling pathways triggered in cells exposed to THz radiation at different frequencies.

9321-26, Session 9

Optical clearing of the mouse brain and light attenuation quantitation

Angela M. d'Esposito, Daniil I. Nikitichev, Simon Walker-Samuel, Adrien E. Desjardins, Mark F. Lythgoe, Univ. College London (United Kingdom)

Biological tissue can be made optically transparent by reducing light scattering in order to image molecular information in 3D. However the extent of clearing is limited by the clearing technique. We have developed a method to assess the quality of clearing in mouse brain and have assessed three different clearing approaches (BABB, pBABB, CLARITY).

2mm thick sagittal brain slices (n=24) from perfused mice were optically cleared with the three examined techniques.

Transmission spectra of the brains were acquired with a custom made system. Light source is coupled to an optic fibre to illuminate the sample. The spectra, acquired by a spectrometer, were measured in three regions (region 1: olfactory bulb, region 2: pons, region 3: cerebellum). 100 spectra

**Conference 9321:
Optical Interactions with Tissue and Cells XXVI**

were taken under the same conditions and averaged using Matlab.

The optical clearing level varies within the brain, depending on structure and composition of each area. The samples cleared with pBABB and BABB resulted in lower absorption peaks (pBABB: 0.7, BABB: 0.68, CLARITY: 1.38) when compared to CLARITY. The latter presented a maximum of absorption at higher wavelengths.

The slices were then imaged with Optical Projection Tomography to study light attenuation in the whole brain section with three different channels.

This work shows a novel way to quantify efficiency of optical clearing protocols, which is essential to evaluate imaging data. Furthermore, assessing the transparency of a cleared tissue is important when imaging with systems like Optical Projection Tomography, since reduced light scattering can lead to higher spatial resolution and better contrast.

9321-27, Session 9

Simulation and measurement of transcranial near infrared light penetration

Lan Yue, The Univ. of Southern California (United States); Manuel Monge, California Institute of Technology (United States); Mehmet H. Ozgur, The Univ. of Southern California (United States); Kevin Murphy, University of Southern California (United States); Stan Louie, Carol Miller, The Univ. of Southern California (United States); Azita Emami, California Institute of Technology (United States); Mark S. Humayun, The Univ. of Southern California (United States)

We are studying the transmission of LED array-emitted near-infrared (NIR) light through human tissues. Herein, we simulated and measured transcranial NIR penetration in highly scattering human head tissues. Using finite element analysis, we first simulated photon diffusion in a multilayered 3D human head model that consists of scalp, skull, modified cerebral spinal fluid, gray matter and white matter. The optical properties of each layer, namely scattering and absorption coefficient, correspond to the 900-1000 nm NIR range. The geometry of the model is minimally modified from the IEEE standard and the LED array, represented by 0.4 cm diameter illumination spots with inter-unit distances of 1-3 cm, interface with the scalp. Simulation results show that 500 mW output power of single LED emitters generate a photon flux of 10^{15} - 10^{14} cm⁻²s⁻¹ 3cm deep in a human head. Further, our results show that photon distribution does not present much variation at similar brain depth but attenuates rapidly as the depth increases, suggesting that due to strong scattering effects of the tissues, discrete spatial arrangements of LED emitters in an array has the potential to create quasi-uniform illumination field at similar brain depths. Measurements on cadaveric human head tissues excised from occipital, parietal, frontal and temporal regions show that illumination with a high-power 850 nm LED emitter (500 mW) rendered a photon flux that closely follows simulation results. In addition, prolonged illumination of LED emitted NIR showed minimal thermal effects on the brain. We'd like to thank WMKeck Foundation for the financial support.

9321-28, Session 9

Comparison of Monte Carlo ray optics method and Lorenz-Mie theory for study of scattering of a focused laser beam in Zebrafish brain

Itia A. Favre-Bulle, The Univ. of Queensland (Australia)

Optogenetics methods use light to manipulate neural activity with high precision in genetically or functionally defined neurons. Larval Zebrafish are widely used in optogenetics studies as they are easily grown, are a convenient size, and relatively transparent. As neurons of Zebrafish are about 5µm in size, it is essential to be able to control light precisely

to manipulate the activity of one, and only one, neuron. Spatial light modulators are a widely used and convenient tool to control and shape light beams and thus manipulate neural activity in three dimensions. However, scattering in the brain tissue can significantly limit imaging, and can also trigger unwanted activity in surrounding neurons.

Ideally, we would focus the beam so that we can excite a single neuron. However, we observe that the beam is considerably broadened by scattering in the brain tissue, with the width of the beam increasing with depth. Noticeable differences can be seen from high to low neuron density regions.

Modelling of the scattering of the beam in the Zebrafish tissue is a challenging task since a large volume of tissue must be included in the calculation. Approximate calculations have been performed with Monte Carlo ray tracing method and full-wave calculation in the single-scattering approximation. Both methods will be presented.

9321-29, Session 9

Calculating optical properties of specific structure inside tissue using transmission electron microscopy (TEM)

Wenli Wu, Andrew J. Radosevich, The-Quyen Nguyen, Scott T. Young, Yue Li, Adam Eshein, Graham Spicer, Northwestern Univ. (United States); Hemant K. Roy, Boston Univ. (United States); Vadim Backman, Northwestern Univ. (United States)

Typically, the methods to measure optical properties of biological tissues only account for a bulk measurement of the whole tissue. However, tissue is composed of a wide range of structures (e.g., cells, stroma, bloods vessels, etc) that contain many optically distinct features within. The bulk measurement is only the accumulative optical properties of all of these specific structures. It is therefore difficult to determine which part of the tissue actually contributes to the optical property changes. This is especially problematic in studying field carcinogenesis, where the structural changes are at a subcellular scale. While, due to the fact that the scattering events that occur in tissue are weak, we can use the Born approximation. Under this assumption, the spatial refractive index auto-correlation function ($B_n(rd)$) is the primary physical characteristic of structural properties of tissue from which light scattering is determined. Given a measurement of $B_n(rd)$ from Transmission Electron Microscopy (TEM) image of cells, we can extract the optical properties like anisotropy factor (g) or scattering coefficient (μ_s) from the random density distribution of a specific structure analytically. In this work, we first obtain high resolution mass density map of the specific structures we are interested in inside the cells from TEM. From that density map we can extract $B_n(rd)$ by using the Gladstone-Dale relation and Fourier's Transforms. Next, we derive the optical properties of the structures from the autocorrelation function based on Born approximation. Finally, we apply this technique to a study of cell nuclei in field carcinogenesis.

9321-30, Session 9

Measurement of the absorption coefficient of biological materials using integrating cavity ring-down spectroscopy

Joel N. Bixler, Michael T. Cone, John D. Mason, Eleonora Figueroa, Brett H. Hokr, Texas A&M Univ. (United States); Jeffrey C. Wagle, Benjamin A. Rockwell, Air Force Research Lab. (United States); Vladislav V. Yakovlev, Edward S. Fry, Texas A&M Univ. (United States)

An accurate knowledge of optical absorption coefficients for cells and their constituents is critical to the continued progression of biomedical procedures and modeling. However, the large scattering cross section associated with many biological materials presents a significant

**Conference 9321:
 Optical Interactions with Tissue and Cells XXVI**

complication in accurately determining the optical properties of biological compounds through transmission-style experiments. Transmission-style experiments measure the attenuation coefficient by comparing the intensity of a light source before and after it passes through a desired medium. For highly scattering media, the light lost through scattering contributes significantly towards the attenuation coefficient.

Using Integrating Ring-Down Spectroscopy (ICRDS), we are able to directly measure the absorption coefficient of any highly scattering media even in the presence of larger scattering cross sections and small absorptions. In traditional cavity ring-down spectroscopy (CRDS), a temporally short pulse is injected into a traditional two mirror cavity. By itself, the pulse naturally decays due to losses at the mirrors. However, in the presence of an absorber, the pulse will decay even faster depending on the strength of the absorption coefficient. While CRDS is plagued with the scattering problems of transmission-style experiments, ICRDS has managed to overcome these obstacles. By replacing the two mirrors with a fully-enclosed cylindrical cavity made from a new diffuse reflecting material, high-purity fumed silica, an isotropic field of illumination is created eliminating scattering losses in ring-down measurements. Our presentation discusses the technique in great deal and discusses experimental results using retinal pigment epithelium cells.

9321-31, Session 9

Use of extended source model to predict spatially resolved diffuse reflectance close to the source for semi-infinite medium

Pankaj Singh, Prabodh Kumar Pandey, Asima Pradhan,
 Indian Institute of Technology Kanpur (India)

Under the assumption of high scattering and weak absorbing media, diffusion approximation holds in the radiative transport equation to model propagation of light but it is valid deep inside the medium. To study subsurface phenomenon, we need to implement accurate boundary conditions. Diffuse reflectance close to the source, majorly depends on the source model inside the medium and boundary conditions. Partial current boundary condition plays a big role for exponentially decaying source model inside the medium. Farrell and Patterson (1992) had implemented only an extrapolated boundary condition and an isotropic point source model inside the medium at one scattering length to find the analytical form of diffuse reflectance at different distances from source. This model, however, provides accurate diffuse reflectance at a distance more than 10 mean free paths. A. Kienle and Patterson(1997) implemented both partial current and extrapolated boundary conditions applying isotropic point source model inside the medium at one scattering mean free path from the surface. Their analytical results are matching to Monte-Carlo and experimental results close to one mean free path from source. We have implemented partial current boundary condition and extrapolated boundary condition with exponentially decaying isotropic source model instead of point source model. Our model predicts diffuse reflectance close to the source at distance less than one mean free path more accurately than the other methods. We have validated our predicted spatially resolved diffuse reflectance results with Monte-Carlo simulation (mcml) programmed by Wang et al. Validation of this result with experiment is in the progress.

Conference 9322: Dynamics and Fluctuations in Biomedical Photonics XII

Saturday - Sunday 7-8 February 2015

Part of Proceedings of SPIE Vol. 9322 Dynamics and Fluctuations in Biomedical Photonics XII

9322-1, Session 1

Multi-modal imaging approach for functional quantitative visualization of acute vascular reaction (*Invited Paper*)

Vyacheslav Kalchenko, Yuri Kuznetsov, Weizmann Institute of Science (Israel); Igor V. Meglinski, Univ. of Otago (New Zealand); Alon Harmelin, Weizmann Institute of Science (Israel)

We present a multi-modal imaging approach and the results of functional quantitative imaging. We demonstrate the acute vascular reaction in response to topical application to the skin of optical clearing agents and an irritant. The common optical clearing agents we used were water solutions of glycerol and dimethyl sulfoxide (DMSO). Methyl salicylate was used as an irritant. The reaction of the vascular network consisted of variation in blood micro-flows and increased vascular permeability. Laser speckle imaging was used to demonstrate blood micro-flows and vascular permeability was assessed by fluorescent microscopy utilizing a high molecular weight fluorescent marker. Our study demonstrates, to our knowledge for the first time, both quantitatively and in real time that in contrast to topical application of irritants to the skin, optical clearing agents do not elicit a significant acute vascular reaction. The proposed imaging approach is expected to be useful for routine functional screening of the cutaneous vascular response induced by irritants, allergens, chemical agents and other new materials used in the pharmaceutical industry.

9322-2, Session 1

Nematic liquid crystal spatial light modulator for mimicking laser speckle contrast imaging

Mitchell Kirby, Kosar Khaksari, Sean J. Kirkpatrick, Michigan Technological Univ. (United States)

Laser speckle contrast imaging (LSCI) is a non- or minimally- invasive modality for observing relative blood flow or perfusion. Recently, there has been an effort to use LSCI for truly quantitative blood flow measurements. However, this effort has been hampered not only by real theoretical issues, but also by challenges associated with numerous experimental parameters that can potentially impact the calculated contrast values. In this work, we present our efforts at using a nematic liquid crystal, phase-only, spatial light modulator (SLM) to mimic LSCI experiments with precisely controlled experimental parameters. This approach permits the rapid experimental investigation of numerous factors including: The effects of different flow models of LSCI contrast values; the effect of multiple decorrelations times in the same depth of field; the effects of 'static' scatterers; and the effects of camera settings relative to speckle decorrelation times, just to name a few. We have found that an SLM is a useful tool for the experimental investigation of LSCI that eliminates many of the experimental variables associated with typical flow model experiments or in vivo experimentation. LSCI experiments with SLMs are a useful intermediary between computer simulations and physical flow models.

9322-3, Session 1

Alternative contrast mechanisms in optical coherence tomography: speckle temporal synchronization effects

Valentin Demidov, I. Alex Vitkin, Univ. of Toronto (Canada)

Optical coherence tomography (OCT) is an emerging non-invasive imaging modality for visualizing subsurface tissue microstructure in-vivo at resolutions approaching histology and blood flow details at the microcirculation level. The obtained OCT images exhibit grainy patterns called speckles which are produced by interference of coherent waves scattered by object features that are smaller than the OCT spatial resolution. While adding to noise, speckle characteristics are also known to contain useful information related to tissue type, cellularity, response to therapy and other quantities of interest that are not directly visible nor spatially resolved on the images. In the current report, we consider an alternative OCT contrast mechanism based on the analysis of speckle temporal synchronization. We show that the changes in speckle intensities with time carry information that can be used to differentiate tissue types and provide a source of additional contrast for in-vivo tissue imaging. The developed technique is demonstrated in-vivo, using the tumour model of mammary carcinoma grown within the mouse dorsal skin-fold window chambers.

9322-4, Session 1

Compact, transmission-based speckle sensor for clinical assessment of peripheral blood circulation and vascular tone

Tyler B. Rice, Laser Associated Sciences, LLC (United States) and Beckman Laser Institute (United States); Sean M. White, Bruce Yang, Laser Associated Sciences, LLC (United States); Pietro R. Galassetti, Univ. of California (United States)

Blood circulation speed and vascular tone in peripheral tissues are of high clinical relevance. Some important conditions that affect the microcirculation are hypovolemic and septic shock, peripheral vascular disease, endothelial dysfunction, and sleep apnea. Hundreds of millions of individuals worldwide suffer from one or more of these conditions.

In order better to diagnose and monitor diseases that affect peripheral circulation, we developed a novel, clinic-friendly instrument for assessing blood flow speed in the microvasculature. The instrument is designed as a clip-on form factor similar to a familiar pulse-oximeter, and can be used on a finger or toe. The technology is based on transmission laser speckle contrast analysis, as opposed to reflection, which allows for the entire microvascular system to be probed in tissue up to 1cm thick. By utilizing transmitted speckle fluctuations, we are able to see a high quality signal that shows peripheral flow waveforms with a level of detail and sensitivity not achievable in conventional speckle or laser Doppler systems.

To demonstrate the utility of our probe to measure peripheral blood flow and tone, several experiments were performed that affect the vascular tone in a known manner in healthy individuals. These include normal respiration, deep inspiratory gasps to induce sympathetic nerve response vasoconstriction, flow mediated vasodilation, exercise induced vasodilation, and others. These experiments show that our device can determine respiration rate and vascular tone with a high degree of sensitivity and specificity.

**Conference 9322:
Dynamics and Fluctuations in Biomedical Photonics XII**

9322-5, Session 1

Bayesian analysis of the OCT-based dynamic light scattering signal for improved directional velocimetry

Kevin C. Zhou, Brendan K. Huang, Michael A. Choma, Yale Univ. (United States)

We demonstrated that a Bayesian framework enables improved precision in cross-sectional velocimetry using dynamic light scattering (DLS)-based OCT. In addition, we demonstrated that precision can be maintained using fewer repeated measures compared to a more typical maximum likelihood approach. Our results are important for several different biomedical applications (e.g. cilia-driven fluid flow, blood flow). Since Doppler signals are sensitive only to axial motions, DLS-OCT is an attractive approach to lateral/transverse velocimetry because it analyzes the rate of signal decorrelation within the point-spread function, which is directly related to total flow speed. Since DLS-OCT models use more parameters than traditional Doppler OCT does, dependencies among the parameters can complicate parameter fitting and velocity estimation. We analyzed DLS-OCT data using Bayesian statistics, specifically Markov chain Monte Carlo (MCMC), which (a) incorporates prior information about the parameter values, (b) estimates uncertainties in parameter values and (c) reveals dependencies among the parameters. We imaged a calibrated flow phantom and reconstructed the lateral parabolic flow profile using our novel variable-scan bias procedure, which uses multiple scan velocities to eliminate the directional ambiguity inherent to DLS. We demonstrate quantitatively that prior information in a Bayesian MCMC framework can reduce parameter dependencies, offer improvements in flow velocity estimation, and allow for fewer repeated measures. Such a framework should be a useful tool for analyzing complex models in general.

9322-8, Session 1

Full-field interferometric confocal microscopy for the phase-sensitive quantification of axial and lateral/transverse motion

Ikbal Sencan, Brendan K. Huang, Brandon Redding, Hui Cao, Michael A. Choma, Yale Univ. (United States)

We present initial results in full-field interferometric confocal microscopy for the highly parallelized acquisition of phase-sensitive and Doppler bandwidth measures of axial and lateral/transverse sample motion. Our full-field system is illuminated by partially coherent light that is generated by passing a standard HeNe laser through a newly commercially-available high-speed diffuser with a 300 Hz oscillation rate (Optotune). Confocal microscopy is an important modality for high resolution biomedical imaging. Parallelization of confocal microscopy without physical pinholes can be realized using full-field interferometry with sources that have partial spatial coherence. In this implementation, the interferometric signal is confocal in nature. Our recent work with sources that have partial spatial coherence while maintaining high power per spatial mode (e.g. random lasers, vertical-cavity surface-emitting laser [VCSEL] arrays) demonstrated the feasibility of using these sources in non-interferometric and interferometric imaging. Here, we show our initial feasibility data in (a) using a fast diffuser to reduce the spatial coherence of single-mode HeNe laser emission in a full-field interferometric confocal imaging system and (b) using the complex-valued interferometric signal from such a system to generate phase-sensitive measures of sample motion. The complex interferometric signal is retrieved using off-axis interferometry and Hilbert transform-type analysis. We demonstrate that (a) interferometric phase scales as expected with linear increases in axial displacement of an object and (b) Doppler bandwidth increases as the rate of lateral translation of a scattering object increases.

9322-52, Session 1

3D reconstruction of live mammalian embryo vasculature using sparsity-integrated speckle anomaly detection and speckle variance OCT

Prathamesh Kulkarni, Nicolas Rey-Villamizar, Amine Merouane, Narendran Sudheendran, Univ. of Houston (United States); Shang Wang, Monica D. Garcia, Irina V. Larina, Baylor College of Medicine (United States); Badrinath Roysam, Univ. of Houston (United States); Kirill V. Larin, Univ. of Houston (United States) and Baylor College of Medicine (United States)

To study the longitudinal development of vascular networks in developing mouse embryos using optical coherence tomography (OCT), it becomes imperative to develop algorithms to perform robust reconstructions of 3D network of blood vessels. Previous algorithms such as Doppler OCT, phase variance (PV) or speckle variance (SV) have been shown to detect blood vessels, however, there are numerous challenges which are encountered by these algorithms such as presence of vessel structures at multiple spatial scales, thin blood vessels with weak flow, and artifacts resulting from bulk tissue motion (BTM). To overcome these challenges, a robust and scalable reconstruction algorithm is introduced in this paper, which is based on anomaly detection and parametric dictionary based sparse representation of blood vessels from structural OCT data, referred to as the SSAD algorithm. Both SV and SSAD algorithms were implemented on 3D OCT structural data. By establishing confocal images as a baseline, it was demonstrated that SSAD algorithm enables detection of blood vessels, which are weakly detected or completely missed by SV algorithm. Finally, quantitative measurements of vessel reconstruction indicate an overall higher quality of vessel reconstruction with the proposed method.

9322-9, Session 2

Tracing red blood cells in human capillary automatically by third harmonic generation microscopy

Guan-Liang Lin, Chien-Ming Lee, Yuan-Ta Shih, Ming-Rung Tsai, Chi-Kuang Sun, National Taiwan Univ. (Taiwan)

In vivo blood flow velocity measurement is an important issue in hemodynamic. There are two ways to measure the blood flow velocity, which can be classified by tracing red blood cells or artificial tracer particles to evaluate blood flow speed in the vessel. Tracing artificial articles requires more preparations, as the injection is indispensable while special care should be taken for avoiding the artificial particles affecting organs. Moreover, the usage of artificial tracer particles is not suitable with some situations, like studies in very early developmental stages or longitudinal studies. Compared to artificial tracer particles, red blood cells in creatures are naturally-present particles which can be used without the limitation of artificial tracer particles. Our previous studies indicate that the hemoglobin in red blood cells provides strong contrasts for optical third harmonic generation, so that red blood cell can be easily in vivo visualized directly by using harmonic generation microscopy with a strong enhancement. In this presentation, we present our design of a computer vision algorithm to separate and trace individual red blood cell from virtual slice movies, so as to enable the blood flow velocity measurement. In addition, the pathways of red blood cells are counted to reconstruct the vascular edge, so that the vessel and the blood flow could be visualized by the computer vision algorithm. With the combination of image post-processing algorithm, we believe that harmonic generation microscopy can provide a non-invasive method of blood flow measurements, and simultaneously obtain virtual anatomical tissue slices as distinct as histopathological biopsy sections.

**Conference 9322:
Dynamics and Fluctuations in Biomedical Photonics XII**

9322-10, Session 2

RBC aggregation based system for long-term photoplethysmography (PPG): new prospects for PPG applications (*Invited Paper*)

Leonid D. Shvartsman, The Hebrew Univ. of Jerusalem (Israel); Boris Tverskoy, Oxirate, Inc. (United States)

We present a novel system for long-term continuous PPG monitoring, and physical model for PPG analysis. The system is based on the ideology of light scattering modulated by the process of RBC aggregation - disaggregation. The system developed in OXIRATE works in reflection geometry and is motion-artifact stable. The sensor is tiny, it has small energy consumption and can be placed nearly everywhere on the body surface. The system is completely mobile phone compatible. These technical features allow overnight comfortable PPG monitoring that was performed and analyzed. We can define various sleep stages on the basis of different time-behavior of PPG signal. This behavior is very reproducible both in time and in frequency domain. This behavior can be explained on the basis of simple physical model. The results of analysis are compared with other existing methods such as EEG, ECG overnight studies, etc. Our system of PPG monitoring has considerable prospect also for extreme PPG studies, such as diving and flying.

9322-11, Session 2

Quantitative assessment of the elasticity change in hyaline cartilage during optical clearing using optical coherence elastography

Chih Hao Liu, Rita Idugboe, Jiasong Li, Manmohan Singh, Zhaolong Han, Wu Chen, Shang Wang, Thomas Hsu, Valery P. Zakharov, Emil N. Sobol, Valery V. Tuchin, Michael D. Twa, Kirill V. Larin, Univ. of Houston (United States)

Elasticity is one of the most important properties that characterizing hyaline cartilage health and structural integrity. Tissue optical clearing is an emerging technique for dynamic modification of tissue optical properties that can be used for a number of applications ranging from imaging to functional diagnostics. However, so far, how the elastic property of tissues varies during optical clearing remains an open question. In this paper, we report the first study on using optical coherence elastography (OCE) to quantitatively monitor the elasticity change of the hyaline cartilage during the optical clearing using glucose. An OCE system that combines a focused air-puff device and phase sensitive swept-source OCT is employed to imaging the elastic wave propagation in the hyaline cartilage over time, and the velocity of the elastic wave was used to quantify the Young's modulus of the tissue. Different glucose concentrations, including 20%, 30%, 40%, 50% and 60% are utilized to assess tissue biomechanical properties during diffusion processes. During the OCE measurement, 0.9% saline solution is applied first to the hyaline cartilage as the control, and then the glucose solution is used to clear the sample, and finally the clearing process is reversed through the use of the same saline solution. As the results, we found that the stiffness of the hyaline cartilage increases during the optical clearing of the tissue. In addition, the elastic property of cartilage sample is reversible based on the diffusion status of the water inside the tissue. The measurement of the mechanical properties is verified using uniaxial compression test. This study might be potentially useful for the early detection of osteoarthritis disease.

9322-51, Session 2

Characterizing the micro structural and kinetics of fast changing samples by simultaneous polarization measurements

Ran Liao, Honghui He, Nan Zeng, Hui Ma, Graduate School at Shenzhen, Tsinghua Univ. (China)

Taking accurate measurements of the state of polarization (SOP) is the key for the success of polarization sensitive techniques which can provide rich information on the microstructure of complex scattering media, such as biological tissues. For static or slow varying samples, SOP measurements can be achieved by time-sequential recoding of different polarization components controlled by rotating polarizers and wave plates or temporal modulation devices such as photoelastic modulator or liquid crystal variable retarders. When the sample is moving or changing its status quickly, polarization components recoded at different time may correspond to different SOPs, which can lead to significant errors in the final results. Simultaneous polarization measurements are necessary for probing such dynamic samples. In this paper, we test different simultaneous polarization techniques for both single point sensing and 2D imaging. Using the simultaneously recorded polarization components, we are able to mimic time sequential polarization schemes and examine in details how the measured SOPs are affected by the time delays in the time-sequential measurements for fast varying samples. The results demonstrate that such time delay results in a systematic deviation of the mean values and an increase in the statistical errors of the measured SOPs. It is also demonstrated that the simultaneously recorded polarization components reveals additional information on the orientation of fibrous scatterers as well as their translation and rotation dynamics.

9322-12, Session 3

Analysis of the penetration of nanoparticles into the hair follicles by laser scanning microscopy (*Invited Paper*)

Juergen M. Lademann, Charité Universitätsmedizin Berlin (Germany)

Since it was demonstrated a few decades ago that nanoparticles are capable of penetrating efficiently through the blood-brain barrier, the use of nanoparticles for drug delivery through the skin has become a topic of intense research. In general, there are two penetration pathways for the topically applied substances to pass through the cutaneous barrier; the intercellular and the follicular one. While the intercellular penetration is investigated using diffusion cells, the analysis of the follicular penetration requires spatially resolved methods, e.g., laser scanning microscopy.

In the present contribution the penetration of various nanoparticles of ≥ 40 nm in size is described; the investigations were performed both in vivo and in vitro using laser scanning microscopy. The findings have shown that nanoparticles of diameters exceeding 40 nm do not pass through the intact cutaneous barrier. Although they penetrate into the hair follicles and are stored there for maximally 10 days, they are excreted onto the skin surface again through the moving hair and the sebum flow.

Nanoparticles will be seen in a new light if they are loaded with drugs, delivered into the hair follicles and subsequently release their drug load close to the target structures via an external trigger signal.

**Conference 9322:
Dynamics and Fluctuations in Biomedical Photonics XII**

9322-13, Session 3

Effect of speckle decorrelation on the application of optical phase conjugation (OPC) in biological tissue

Haowen Ruan, Mooseok Jang, California Institute of Technology (United States); Euiheon Chung, Gwangju Institute of Science and Technology (Korea, Republic of); Ivo M. Vellekoop, Univ. Twente (Netherlands); Benjamin Judkewitz, Charité Universitätsmedizin Berlin (Germany) and California Institute of Technology (United States); Changhuei Yang, California Institute of Technology (United States)

Optically scattering property of biological tissues poses a big challenge to light focusing deep inside the tissue. Optical Phase Conjugation (OPC) technique is one of the techniques that allows light to focus deep inside the tissue. This technique first records the phase of the scattered light from the tissue and then creates the phase-conjugated light which then travels back to the origin of the scattered light due to time reversal symmetry. However, in living tissue, another challenge comes out as the scatterers are highly dynamic compared to the OPC processing time. This results in the degradation of time reversal symmetry and consequently the decay of reconstructed light intensity. Here, we characterized the reconstructed light intensity decay through theoretical analysis and experiment and found that it agrees with the optical speckle correlation – a conventional measurement of scatterer motion. We then investigated the decorrelation characteristic time (half-life time) of a 1.5-mm-thick dorsal skin flap of a living mouse and found that it ranges from 50 ms to 2 s depending on the level of immobilization. Importantly, the reconstructed light was able to be observed after half-life time of the speckle correlation as large number of controllable optical modes enables high reconstructed light intensity. The study suggests the possibility of applying OPC technique to biological tissue in vivo. It also demonstrates that the working regime of OPC in terms of timing is possible to be extended to a regime where OPC processing speed is lower than speckle decorrelation time.

9322-14, Session 3

Monitoring of interaction of low frequency electric field with biological tissues upon optical clearing with optical coherence tomography

Adrian F. Peña Delgado, Alexander Doronin, Univ. of Otago (New Zealand); Valery V. Tuchin, N.G. Chernyshevsky Saratov State Univ. (Russian Federation); Igor V. Meglinski, Univ. of Otago (New Zealand)

The influence of low frequency electric field, applied to soft biological tissues ex vivo at normal conditions and upon the topical application of optical clearing agents, has been studied by optical coherence tomography (OCT).

The electro-kinetic response of tissues has been observed and quantitatively evaluated by the double correlation OCT approach utilizing consistent application of an adaptive Wiener filtering and Fourier domain correlation algorithm. The results show that fluctuations, induced by the electric field, within the biological tissues are exponentially increased in time. We demonstrate that in comparison to impedance measurements and mapping of temperature profile at the surface of tissue samples, the double correlation OCT approach is much more sensitive to observation the changes associated with the tissues' electro-kinetic response. We also found that topical application of optical clearing agent reduces the tissues' electro-kinetic response and is cooling the tissue, reducing for a few degrees the temperature induced by the electric current. We anticipate

that double correlation OCT approach can find a new application in bio-electrical impedance analysis and monitoring of the electric properties of biological tissues, including the resistivity of high water content tissues and its variations.

9322-15, Session 3

Application of new optical coherence elastography to monitor the mineralization processing in bone tissue engineering constructs

Guangying Guan, Shaozhen Song, Zhihong Huang, Univ. of Dundee (United Kingdom); Ying Yang, Keele Univ. (United Kingdom)

Generation of functional tissue in vitro through tissue engineering technique is a promising direction to repair and replace malfunctioned organ and tissue in the modern medicine for various diseases which could not be treated well by conventional therapy. Similar to the embryo development, the generation of tissue in vitro is a highly dynamic processing. Obtaining the feedback of the processing real time is highly demanded. In this study, a new methodology has been explored aiming to monitor the morphological and mechanical property alteration of bone tissue engineering constructs simultaneously. Optical coherence elastography (OCE) equipped with an LDS V201 permanent magnet shaker to provide a vibration signal, has been used for the real time and non-destructive monitoring. A phantom construct system has been used to optimize the measurement conditions in which agar hydrogel with concentration from 0, 0.75 to 2% with/without hydroxyapatite particles have been injected to 3D porous poly (lactic acid) scaffolds to simulate the collagenous extracellular matrix (ECM) and mineralized ECM. The structural and elastography images of the constructs have clearly demonstrated the linear relation with the increased mechanical property versus the increase of agar concentration within the pores of the scaffolds. The MG63 bone cells seeded in the scaffolds and cultured for 4 weeks have been monitored by the established protocol exhibiting the increased mechanical strength in the pore wall where the mineralized ECM was assumed to be formed. This study confirms that OCE-ARF could become a valuable tool in regenerative medicine to assess the biological events in response to external stimulation.

9322-16, Session 3

Towards non-invasive 3D hepatotoxicity assays with optical coherence phase microscopy

Leonard Nelson, Andreas Koulovasilopoulos, Philipp Treskes, The Univ. of Edinburgh (United Kingdom); Peter C Hayes, College of Medicine and Veterinary Medicine, University of Edinburgh (United Kingdom); John Plevris, Pierre O. Bagnaninchi, The Univ. of Edinburgh (United Kingdom)

Three-dimensional tissue-engineered models are increasingly recognised as more physiologically-relevant than standard 2D cell culture for pre-clinical drug toxicity testing. However, many types of conventional toxicity assays are incompatible with dense 3D tissues. This study investigated the use of optical coherence phase microscopy (OCPM) as a novel approach to assess cell death in 3D tissue culture.

For 3D spheroid formation Human hepatic C3A cells were encapsulated in 50% Matrigel™ and cultured in 100% MEME/10%FBS in 96-well plates. After spheroid formation the 3D liver constructs were exposed to 0-40mM acetaminophen on culture day 8. Paracetamol hepatotoxicity [0-40mM] in 3D cultures was evaluated using PrestoBlue, lactate release as cytotoxicity markers.

An inverted OCPM in common path configuration was developed with a Callisto OCT engine (Thorlabs), centred at 930nm and a custom scanning head. Intensity data were used to perform in-depth microstructural imaging. In addition, phase fluctuations were measured by collecting several successive B scans at the same location, and statistics on the first time derivative of the phase, i.e. time fluctuations, were analysed over the acquisition time interval to retrieve overall cell viability. OCPM intensity (cell cluster size) and phase fluctuation statistics were directly compared with biochemical assays. Prestoblue and lactate cytotoxicity metabolic activity/viability markers showed similar dose-response trends to 2D cultures.

In this study, we investigated optical coherence phase tomography to assess cell death in a 3d liver model after exposure to a prototypical hepatotoxin, acetaminophen. We showed that OCPM has the potential to assess noninvasively drug toxicity in 3D tissue models.

9322-17, Session 3

S-transform based approach for probing refractive index fluctuations in connective tissues for precancer detection

Sabyasachi Mukhopadhyay, Indian Institute of Science Education and Research Kolkata (India); Asima Pradhan, Indian Institute of Technology Kanpur (India); Nirmalya Ghosh, Prasanta K. Panigrahi, Indian Institute of Science Education and Research Kolkata (India)

S-transform based approach is well-suited for phase synchrony analysis of a wide class of signals. Here, S-transform is used for finding phase synchrony of refractive index variations in the epithelium among different grades of human cervical cancerous tissues. It is known that this method provides the better time-frequency resolution than other transforms like short time Fourier transform (STFT) and wavelets. As a result, it can extract out more hidden informations about the refractive index fluctuations of the medium which is quite useful for analyzing the morphological structures of Differential Interference Contrast (DIC) images of epithelium regions. It is clearly observed that the phase synchronization is more prominent between the pairs of grade-I and grade-III and grade II and grade-III tissues. Interestingly this synchronization is not observed between grade-I and grade-II tissues, indicating strong phase fluctuations between these two grades. This in-phase and out of phase information may reveal how the dynamics of the refractive index fluctuation varies among different grades. Our DIC imaging and S-transform based analysis confirm the ability to diagnose and detect the early stage of pre-cancer in cervical tissues.

9322-18, Session 3

Photothermal light harvesting and light-gated molecular release by nanoporous gold disks (Invited Paper)

Greggy M. Santos, Univ. of Houston (United States); Fusheng Zhao, Jianbo Zeng, Univ of Houston (United States); Wei-Chuan Shih, Univ. of Houston (United States)

Photothermal heating has been an effective mechanism for harvesting light energy by plasmonic resonance. Photothermally generated hyperthermia can alter cell behavior, change cell microenvironment, and promote or suppress cell growth. In the past, colloidal nanoparticles such as gold nanospheres, nanoshells, nanorods, and nanocages have been developed for various applications. Here, we show that nanoporous gold disks (NPGDs) with 400 nm diameter, 75 nm thickness, and 13 nm pores exhibit large specific surface area and effective photothermal light harvesting capability. Another potential application is demonstrated by light-gated, multi-step molecular release of pre-adsorbed R6G fluorescent dye on arrayed NPGDs. Through the use of time-resolved temperature mapping, the spatial and temporal characteristics of photothermal heating in NPGD arrays is

successfully demonstrated for both aqueous and air ambient environments. By applying a thermodynamic model to our experimental data, we determined the photothermal conversion efficiency at 56% for NPGD arrays. As a potential application, light-gated, multi-stage release of pre-adsorbed R6G dye molecules from NPGD arrays has been demonstrated. The results establish the foundation that NPGDs can be employed for photothermal light harvesting and light-gated molecular release.

Greggy M. Santos, Fusheng Zhao, Jianbo Zeng, and Wei-Chuan Shih, "Characterization of nanoporous gold disks for photothermal light harvesting and light-gated molecular release," *Nanoscale* 6(11), 5718-5724, 2014.

9322-19, Session 4

Investigation of diseases through red blood cells' shape using photoacoustic response technique

Deblina Biswas, Abhijeet Gorey, Indian Institute of Technology Indore (India); George C. K. Chen, BC Photonics Technological Co. (Canada); Norman Sharma, Choitram Hospital and Research Ctr. (India); Srivathsan Vasudevan, Indian Institute of Technology Indore (India)

Photoacoustic (PA) imaging is a non-invasive real-time technique, widely applied to many biomedical imaging studies in the recent years. While most of these studies have been focussed on obtaining an image after reconstruction, various features of time domain signal (e.g. amplitude, width, rise and relaxation time) would provide very high sensitivity in detecting morphological changes in cells during a biological study. Different haematological disorders (e.g., sickle cell anemia, thalassemia) exhibit significant morphological cellular changes. In this context, this study explores the possibility of utilizing the developed photoacoustic response technique to apply onto blood samples. Results of our preliminary study demonstrate that there is a significant change in signal amplitude due to change in concentration of the blood. Thus it shows the sensitivity of the developed photoacoustic technique towards red blood cell count (related to haematological disease like anemia). Subsequently, morphological changes in RBC (i.e. swollen and shrunk compared to normal RBC) induced by hypotonic and hypertonic solutions respectively were also experimented. The result shows a distinct change in PA signal amplitude. This would serve as a diagnostic signature for many future studies on cellular morphological disorders.

9322-20, Session 4

Correlation mapping microscopy

James McGrath, Sergey A. Alexandrov, National Univ. of Ireland, Galway (Ireland); Martin J. Leahy, National Univ. of Ireland, Galway (Ireland) and Royal College of Surgeons (Ireland)

The microcirculation plays an important role in health. Structural and functional changes in the microcirculation have been associated with various pathological conditions including Raynaud's disease. To facilitate regular assessment of the microcirculation in-vivo, non-invasive imaging techniques such as nailfold capillaroscopy are required in clinics. However, depth ambiguity is a limitation of these modalities. It is becoming more known that 2D biology does not translate to the real 3D situation and that imaging techniques which can support depth-resolved 2D imaging and 3D image reconstruction are required. Recently a correlation mapping technique has been applied to Optical Coherence Tomography (OCT) which extends the capabilities of OCT to microcirculation morphology imaging. This technique, known as cmOCT has been shown to extract parameters such as capillary density and vessel diameter which are key clinical markers associated with early changes in microvascular diseases. However, OCT has limited spatial

**Conference 9322:
Dynamics and Fluctuations in Biomedical Photonics XII**

resolution in both the transverse and depth directions. Here, we extend this correlation mapping technique to other microscopy modalities, including confocal microscopy and take advantage of the higher spatial resolution offered by these modalities. The technique is achieved as a processing step on microscopy images and does not require any modification or addition to the microscope hardware. Results are presented which show that this correlation mapping microscopy technique can extend the capabilities of conventional microscopy to enable mapping of vascular networks in-vivo with high spatial resolution in both the transverse and depth directions.

9322-21, Session 4

Parametric imaging of viscoelastic creep deformation in soft tissue using compression optical coherence elastography

Philip Wijesinghe, Robert A. McLaughlin, David D. Sampson, Brendan F. Kennedy, The Univ. of Western Australia (Australia)

Diseases such as breast cancer and conditions such as fibrosis and edema modify the viscoelastic properties of soft tissue. Imaging viscoelastic properties on the microscopic scale could provide information on such diseases and conditions that may aid in clinical assessment. Imaging of viscoelastic properties has been investigated in ultrasound and MRI elastography, but has received little attention using optical methods.

We demonstrate the capacity of optical coherence elastography (OCE) to image the viscoelasticity of soft tissue. Viscoelastic creep deformation is induced by placing the sample under a constant compressive load and the time-varying deformation is measured using phase-sensitive optical coherence tomography. From a series of co-located B-scans we estimate the local strain rates as a function of time, and fit these to a parametric, constitutive model of viscoelastic creep. We implement a fitting algorithm that employs strain-rate based weighting to optimize the accuracy of the parametric fit. We estimate local viscoelastic strain, ϵ_1 , and time constant, τ , and, for the first time, present these graphically as dual-parameter visco-elastograms. We demonstrate good repeatability of our technique on six silicone tissue-simulating phantoms of varying viscoelasticity, reporting viscoelastic strains in the range of 4×10^{-5} to 3×10^{-3} and time constants in the range of 3.6 to 11.6 s. We present images of murine tissue featuring contrast between muscle fascia and surrounding muscle fibers in gastrocnemius muscle, and between peritoneal epithelial layer, extraperitoneal fat and transverse abdominal muscle. Our results demonstrate the capability of OCE to parameterize viscoelastic creep of soft tissue.

9322-22, Session 4

In vivo imaging of microvascular changes within inflammatory human skin induced by tape stripping and mosquito saliva using optical microangiography

Utku Baran, Woo June Choi, Ruikang K. Wang, Univ. of Washington (United States)

Vasculature response is a hallmark for most inflammatory skin disorders. Tape stripping on human skin induces mechanical disruptions of the epidermal barrier that lead to minor skin inflammation which leads to changes in microvasculature. On the other hand, when mosquitoes probe the skin for blood feeding, they inject saliva in dermal tissue. Mosquito saliva is known to exert various biological activities, such as dermal mast cell degranulation, leading to fluid extravasation and neutrophil influx. This inflammatory response remain longer than the tape stripping case. In this study we demonstrate the capabilities of swept-source optical

coherence tomography (OCT) in detecting in vivo microvascular response of inflammatory human skin. Optical microangiography (OMAG), noninvasive volumetric microvasculature in vivo imaging method, has been used to track the vascular responses after tape stripping and mosquito bite. Vessel density has been quantified and used to correlate with the degree of skin irritation. The proved capability of OMAG technique in visualizing the microvasculature network under inflamed skin condition can play an important role in clinical trials of treatment and diagnosis of inflammatory skin disorders as well as studying mosquito bite's perception by the immune system and its role in parasite transmission.

9322-23, Session 5

Full skin quantitative optical coherence elastography achieved by combining vibration and surface acoustic wave methods

Chunhui Li, Guangying Guan, Zhihong Huang, Ghulam Nabi, Univ. of Dundee (United Kingdom)

By combining with the phase sensitive optical coherence tomography (PhS-OCT), vibration and surface acoustic wave (SAW) methods have been reported to provide elastography of skin tissue respectively. However, neither of these two methods can provide the elastography in full skin depth in current systems. This paper presents a feasibility study on an optical coherence elastography method which combines both vibration and SAW in order to give the quantitative mechanical properties of skin tissue with full depth range, including epidermis, dermis and subcutaneous fat. Experiments are carried out on layered tissue mimicking phantoms and in vivo human forearm and palm skin. A ring actuator generates vibration while a line actuator were used to excited SAWs. A PhS-OCT system is employed to provide the ultrahigh sensitive measurement of the generated waves. The experimental results demonstrate that by the combination of vibration and SAW method the full skin bulk mechanical properties can be quantitatively measured and further the elastography can be obtained with a sensing depth from -0mm to -4mm. This method is promising to apply in clinics where the quantitative elasticity of localized skin diseases is needed to aid the diagnosis and treatment.

9322-24, Session 5

Optical clearing kinetic of deep-tissue imaging enhancement mediated by upconversion phosphors

Alexey P. Popov, Univ. of Oulu (Finland); Eugeny V. Khaydukov, Institute on Laser and Information Technologies (Russian Federation); Alexander V. Bykov, Univ. of Oulu (Finland); Semchishen A. Vladimir, Institute on Laser and Information Technologies (Russian Federation); Artashes V. Karmenyan, National Yang-Ming Univ. (Taiwan); Valery V. Tuchin, Univ. of Oulu (Finland) and N.G. Chernyshevsky Saratov State Univ. (Russian Federation) and Institute of Precise Mechanics and Control (Russian Federation)

Diagnostic imaging faces limitations due to intrinsic scattering and absorption properties of biological tissues.

The near-infrared spectral range in the so-called "diagnostic window" (650-1100 nm) is beneficial to offset these drawbacks. Contrast enhancement of tissue-embedded inhomogeneities (e.g. tumors) can be performed by administration of contrast agents such as fluorophores. However, utilizing the same spectral window for both fluorophore excitation and detection is not trivial.

**Conference 9322:
 Dynamics and Fluctuations in Biomedical Photonics XII**

In this paper, we use novel Tm-doped upconversion phosphors overcoming the mentioned challenges (excitation wavelength: 980 nm, detection wavelength: 800 nm) and glycerol as an optical clearing agent to enhance imaging from under 6-mm-thick porcine muscle tissue samples. We show that improvement of luminescent label visualization is caused by transforming of the diffuse label-emitted light into the direct component. This results in

5-fold increase in visibility (ratio of the sum and difference of the maximal and minimal intensity) of the label and 20-fold increase in maximal signal intensity thus making the combination of the phosphors and optical clearing promising for precise detection of tissue-embedded labelled inhomogeneities. Besides imaging ability, the method is also useful for estimation of the diffusion coefficient of glycerol in the tissue when using sub-millimeter-thick samples.

9322-25, Session 5

Tissue optical clearing window for microvessel and blood flow imaging
(Invited Paper)

Dan Zhu, Huazhong Univ. of Science and Technology (China)

The tissue optical clearing (TOC) technique could significantly improve the biomedical optical imaging depth, but most current investigations are limited to in vitro studies. For in vivo applications, the TOC method must provide a rapid treatment process, sufficient transparency, and safety for animals, which makes it more difficult. Recently developed innovative optical clearing methods for in vivo use show great potential for enhancing the contrast and resolution of laser speckle contrast imaging (LSCI) for blood flow monitoring. This paper gives an overview of recent progress in the use of TOC for vascular visualization with LSCI. First, the principle of TOC-induced improvement of LSCI and a quantitative analysis method for evaluating the improvement are described briefly. Second, the paper introduces transparent windows, including various skin windows and a cranial window, that permit LSCI to monitor dermal or cortical blood flow, respectively, with high resolution and contrast. Third, preliminary investigations of the safety of TOC demonstrate that the transparent skin window is switchable, which enables LSCI to repeatedly image blood flow. Future work should focus on developing a highly effective, safe method and extending its applications.

9322-26, Session 6

Bedside optical imaging for personal health monitoring
(Invited Paper)

Bruce J. Tromberg, Beckman Laser Institute and Medical Clinic (United States)

No Abstract Available

9322-29, Session 6

The role of camera and illumination choices in absolute blood velocity measurements
(Invited Paper)

Jessica C. Ramella-Roman, Stephen Winhoven, Florida International Univ. (United States)

Non-invasive measurements of blood velocity at the capillary level are of interest for many clinical applications. Recently we presented a new method for the quantitative estimation of blood flow velocity, based on the use of the Radon transform. The technique was based on narrow band illumination

at 525 nm and tracking of non-uniform distribution of red blood cells within the vessel, rather than the individual blood cells themselves. Here we present a complete error analysis of this useful technique, highlighting the role of camera and illumination choices. Finally we propose in-vivo examples on retinal flow imaging and compare the results obtained with this technique to the one proposed by a commercial system.

9322-30, Session 7

Dynamic in-vivo optical imaging and microscopy of the living brain
(Invited Paper)

Elizabeth M. Hillman, Columbia Univ. (United States)

No Abstract Available

9322-31, Session 7

Effects of combined scattering and absorption coefficients on laser speckle contrast imaging values

Kosar Khaksari, Sean J. Kirkpatrick, Michigan Technological Univ. (United States)

Laser Speckle contrast imaging (LSCI) is a non-invasive or minimally invasive method for visualizing blood flow and perfusion in biological tissues. In LSCI the motion of scattering particles results in a reduction in global and regional speckle contrast. A variety of parameters can affect the calculated contrast values in LSCI techniques, including the optical properties of the fluid and surrounding tissue. In typical LSCI where the motion of blood is of interests, optical properties are influenced by hematocrit. In this work we considered the combined effects of both the scattering and absorption coefficients on LSCI measurements on a flow phantom. Fluid phantoms consisting of various concentrations of neutrally buoyant 10 micron microspheres and india ink mixed with DI water were formulated to mimic the optical properties of whole blood with various levels of hematocrit. In these flow studies, it was found that an increase in scattering and/or absorption led to a decrease in contrast values when all other experimental parameters were held constant. The observed reduction in contrast due to optical property changes could easily be confused with a contrast reduction due to increased flow velocity. These results suggest that optical properties need to be considered when using LSCI to make flow estimates.

9322-33, Session 7

Investigation of the red blood cells flux change during hypercapnia in the rat brain with optical coherence tomography

Baoqiang Li, Ecole Polytechnique de Montréal (Canada); Jonghwan Lee, David A. Boas, Massachusetts General Hospital/Harvard Medical School (United States); Frédéric Lesage, Ecole Polytechnique de Montréal (Canada)

Introduction: It was previously reported that spectral-domain optical coherence tomography (SD-OCT) could capture individual red blood cell (RBC) passages at multiple capillaries; thus, provide a means to quantify the RBCs flow and monitor the hemodynamic in the brain. Objective: As an extended study, the objective was to quantify RBCs flow in the capillary networks of rat brains, and analyze the hemodynamic and RBCs flux change under normocapnia and hypercapnia. Method: The measurements were acquired using a commercial but customer optimized SD-OCT system. Experiments: The following experimental procedure was approved by

**Conference 9322:
 Dynamics and Fluctuations in Biomedical Photonics XII**

the ethics committee of Massachusetts General Hospital. A total of eight rats were imaged. They were anesthetized with the mixture of isoflurane and oxygen, following craniotomy on the somatosensory cortex of brain. For each rat, an angiogram was formed using the differential imaging protocol described previously; and then, multiple B-scans were acquired to simultaneously monitor the RBCs flow of multiple capillaries over minutes. The results suggest no global correlation of RBCs flux change for different capillaries at all depths with response to hypercapnia. However, the flux change of capillaries located deeper in the brain saw larger changes under hypercapnia. Discussion & conclusion: In this study, SD-OCT was applied to monitor the RBCs flux in the rat brain. Although the current acquisition frequency limits RBC passage counting, especially for high flux, we observed that capillaries at different depths had distinguishable behaviors while responding to hypercapnia, which suggests further investigation in the mechanisms of the capillary networks response to changing physiological conditions.

9322-34, Session 7

Depth resolved perfusion measurements using multi-distance diffuse correlation spectroscopy in conjunction with a Monte Carlo realistic multi-layer correlation transport model

Stefan A. Carp, Erin M. Buckley, Massachusetts General Hospital (United States); Daniel S. Yang, Woodbridge High School (United States); David A. Boas, Suk-Tak Chen, Karleyton C. Evans, Juliette J. Selb, Massachusetts General Hospital (United States)

Cerebral blood flow (CBF) is a sensitive marker of brain physiological state and is significantly impacted by many pathological changes. Further, by combining CBF with the oxygen extraction fraction (OEF) derived from near infrared spectroscopy (NIRS) measurements, the cerebral metabolic rate of oxygen (CMRO₂) can be computed, a valuable biomarker of brain health. CBF (and hence CMRO₂) changes can be estimated from combined NIRS measurements together with Diffuse Correlation Spectroscopy, as DCS offers a way to directly estimate CBF, and the combination of DCS and NIRS measurements can offer more robust CMRO₂ quantification. However, both techniques employ diffusely reflected light that has traveled mostly through extracerebral tissues. Attempts to increase cerebral sensitivity of the DCS measurements have been reported, either by limiting the data analysis to the shorter correlation times that are more sensitive to deeper propagating photons or using two or multi-layer theoretical models based on the correlation diffusion equation. However, none of the reports so far have employed either simultaneous fitting to multi-distance measurements, or Monte Carlo modeling of correlation transport. In this paper, we report a Monte Carlo (MC) based multi-layer DCS model and we summarize the performance of multi-distance simulated DCS measurements in distinguishing between scalp/skull and cerebral perfusion changes. Further, we present a method for estimating superficial thickness from experimental data by varying the assumed thickness with the goal of minimizing the fit residuals between the MC based model and actual data.

9322-50, Session 7

Detecting brain cancer at the cellular level

Anna N. Yaroslavsky, Xin Feng, Univ. of Massachusetts Lowell (United States); Yulian Ramirez, Univ. of Massachusetts Medical School (United States); Ying-Ying Huang, Massachusetts General Hospital (United States); Alonzo Ross, Univ. of Massachusetts Medical School (United States); Michael R. Hamblin, Massachusetts General Hospital (United States)

Identifying single cancer cells is one of the greatest challenges in oncology. The goal of this work was to investigate if by monitoring fluorescence polarization of MB we could quantitatively discriminate brain cancer cells from normal. Fluorescence polarization is sensitive to the changes in biochemical and biophysical properties of the fluorophore environment. Cancer cells have higher cell division rate as compared to normal cells, which may leads to differences in cell membrane fluidity, intracellular viscosity, as well as dye localization and binding within the cells. In this study, we used multimodal confocal microscopy to image and quantify MB stained live human glioblastoma cells and astrocytes. The cell lines investigated included: U87MG, U118MG, U251MG, primary 5075 glioblastoma cells and primary human normal astrocytes. Confocal reflectance, fluorescence and fluorescence polarization images were acquired, intracellular dye localization sites were determined and fluorescence polarization values were calculated for both cancer and normal cells. We have found that fluorescence polarization of cancer cells is significantly higher than that of normal cells for all cell lines investigated. Our results indicate that detection of changes in fluorescence polarization may allow for discrimination of cancer cells reliably and rapidly. Quantitative fluorescence polarization imaging shows promise for the detecting of brain cancer at the single cell level.

9322-6, Session PSun

Measurement of total velocity components of particle flow with optical coherence tomography

Hongxian Zhou, Northeastern Univ. at Qinhuangdao (China); Zhenhe Ma, Northeastern University (China); Yi Wang, Northeastern Univ. at Qinhuangdao (China)

We present a new model for describing the light back-scattered from flowing particles by introducing an amplitude modulation function. When passing through the probe beam, moving particles modulate the back-scattered light, and encode a transit time that is inversely proportional to the transverse component of flow velocity into the amplitude modulation function. We extract the distribution of the transit time from time-varying laser speckle images and map the flow velocities of particle flow. The proposed model is experimentally verified using polystyrene particle suspension flow.

9322-27, Session PSun

Quantitative analyses of spectral measurement error based on Monte-Carlo simulation

Jingying Jiang, Congcong Ma, Qi Zhang, Junsheng Lu, Tianjin Univ. (China); Kexin Xu, Tianjin Univ. (China) and State Key Lab. of Precision Measuring Technology and Instruments (China)

The spectral measurement error is controlled by the resolution and the sensitivity of the spectroscopic instrument and the instability of involved environment. In this talk, the spectral measurement error is analyzed quantitatively by using the Monte Carlo simulation. Take the floating reference point for example, in the process of the measurement, the measuring position and the theoretical position has a deviation due to various influence factors. In order to define the error caused by the positioning accuracy of the measuring device, Monte Carlo simulation has been carried out with the wavelength of the source at 1311nm, the concentration of Intralipid solution at 2%, the number of 10⁹ photons and the sampling interval of the ring at 1?m. The results indicate that the Monte Carlo simulation can be used to quantitatively analyze the spectral measurement error caused by the positioning inaccuracy.

**Conference 9322:
Dynamics and Fluctuations in Biomedical Photonics XII**

9322-28, Session PSun

SIFT-based error compensation for ear feature matching and recognition system

Jingying Jiang, Qi Zhang, Congcong Ma, Junsheng Lu, Kexin Xu, Tianjin Univ. (China)

The established Ear feature matching and recognition system, based on Scale Invariant Feature Transform (SIFT) image matching algorithm, can realize the human ear feature matching and detect the displacement of the human ear so as to reproduce the human ear position and posture. However, due to the influence of image acquisition equipment performance and lighting conditions, too dark or too bright background could bring the locally underexposed or overexposed image. This could result in the loss of some image details so as to make it impossible to identify the image and reduce the recognition rate. In this talk, the application of image gray level normalization processing can reduce the sensitivity of imaging to light intensity, accordingly, greatly improve the recognition rate of human ears. Furthermore, it has been found that even if the object is stationary, the image matching results still could have certain fluctuation changes, which should be caused by the system error. In order to reduce the error, the Background-based Compensation Model (BCM) has been established by studying differences of the system error caused by the working environment changes. The results show that, BCM can be used to compensate the system errors of ear recognition matching and further improve the matching accuracy of human ear.

9322-32, Session PSun

THz-generation in semiconductor superlattice in the external tilted magnetic field

Vladimir V Makarov, Vladimir A Maksimenko, Research and Educational Center "Nonlinear Dynamics of Complex Systems", Saratov State Technical Uni (Russian Federation) and Saratov State University (Russian Federation); Anton O Selskii, Research and Educational Center "Nonlinear Dynamics of Complex Systems", Saratov State Technical Uni (Russian Federation); Alexey N. Pavlov, N.G. Chernyshevsky Saratov State Univ. (Russian Federation) and Saratov State Technical Univ. (Russian Federation); Marina V Khramova, Saratov State University (Russian Federation); Alexey A. Koronovskii, N.G. Chernyshevsky Saratov State Univ. (Russian Federation) and Saratov State Technical Univ. (Russian Federation); Alexander E. Hramov, Saratov State Technical Univ. (Russian Federation) and N.G. Chernyshevsky Saratov State Univ. (Russian Federation)

Electroencephalographic methods are widely used for monitoring electrical brain activity and for diagnosing pathological dynamics related, e.g., with epilepsy. The electroencephalogram contains information about mean electrical fields of synaptically interconnected neuronal ensembles that are located in the vicinity of the recording electrode. This signal has a complex time-frequency organization and comprises a wide variety of rhythmic components, whose frequencies represent important quantities of the functional activity of different neuronal structures. In this report neuronal oscillatory pattern recognition based on two approaches for time-frequency analysis of electroencephalograms (EEGs) is discussed, namely, the continuous wavelet transform (CWT) and the empirical mode decomposition (EMD). Possibilities and limitations of both these techniques are considered. A combined approach using wavelets and empirical modes is proposed that demonstrates a high efficiency for automatic pattern detection and outperforms recognition methods with a separated application of CWT or EMD.

9322-35, Session PSun

Age-dependent seizures of absence epilepsy and sleep spindles dynamics in WAG/Rij rats

Vadim V. Grubov, N.G. Chernyshevsky Saratov State Univ. (Russian Federation) and Saratov State Technical Univ. (Russian Federation); Evgenia Sitnikova, Institute of Higher Nervous Activity and Neurophysiology (Russian Federation) and N.G. Chernyshevsky Saratov State Univ. (Russian Federation); Alexey N. Pavlov, Marina V. Khramova, Alexey A. Koronovskii, N.G. Chernyshevsky Saratov State Univ. (Russian Federation) and Saratov State Technical Univ. (Russian Federation); Alexander E. Hramov, N.G. Chernyshevsky Saratov State Univ. (Russian Federation)

The risk of neurological diseases increases with age. In WAG/Rij rat model of absence epilepsy, the incidence of epileptic spike-wave discharges is known to be elevated with age. Considering close relationship between epileptic spike-wave discharges and physiologic sleep spindles, it was assumed that age-dependent increase of epileptic activity may affect time-frequency characteristics of sleep spindles. In order to examine this hypothesis, electroencephalograms (EEG) were recorded in WAG/Rij rats successively at the ages 5, 7, and 9 months. Spike-wave discharges and sleep spindles were detected in frontal EEG channel. Sleep spindles were identified automatically using wavelet-based algorithm. Instantaneous (localized in time) frequency of sleep spindles was determined using continuous wavelet transform of EEG signal, and intraspindle frequency dynamics were further examined. It was found that in 5-months-old rats epileptic activity has not fully developed (preclinical stage) and sleep spindles demonstrated an increase of instantaneous frequency from beginning to the end. At the age of 7 and 9 months, when animals developed matured and longer epileptic discharges (symptomatic stage), their sleep spindles did not display changes of intrinsic frequency. The present data suggest that age-dependent increase of epileptic activity in WAG/Rij rats affects intrinsic dynamics of sleep spindle frequency.

9322-36, Session PSun

Analysis of structural patterns in the brain with the complex network approach

Vladimir A. Maksimenko, Vladimir V. Makarov, N.G. Chernyshevsky Saratov State Univ. (Russian Federation) and Saratov State Technical Univ. (Russian Federation); Alexander A. Kharchenko, Saratov State University (Russian Federation) and Research and Educational Center "Nonlinear Dynamics of Complex Systems", Saratov State Technical Uni (Russian Federation); Alexey N. Pavlov, Marina V. Khramova, Alexey A. Koronovskii, N.G. Chernyshevsky Saratov State Univ. (Russian Federation) and Saratov State Technical Univ. (Russian Federation); Alexander E. Hramov, Saratov State Technical Univ. (Russian Federation) and N.G. Chernyshevsky Saratov State Univ. (Russian Federation)

This work is devoted to the analysis of structural features of neural ensembles by means of network approach. At first we considered the model of the complex network with the adaptive links, in which the synchronous dynamics of oscillators leads to the appearance of clusters of strongly coupled elements and shown that the structural changes strongly affect the summary signal, produced by all oscillators. We demonstrated the strong possibility of the analysis of the cluster formation in the network via the

**Conference 9322:
Dynamics and Fluctuations in Biomedical Photonics XII**

consideration of its summary signal. Further we use the proposed method to analyze the experimental data present itself EGG signal and observe the strong correlation between synchronous patterns in EEG and structural patterns in complex adaptive network.

9322-37, Session PSun

Cerebral venous dynamics in newborn mice with intracranial hemorrhage studied using wavelets

Alexey N. Pavlov, N.G. Chernyshevsky Saratov State Univ. (Russian Federation) and Saratov State Technical Univ. (Russian Federation); Oxana V. Semyachkina-Glushkovskaya, Olga A. Bibikova, Sergey S. Sincdeev, Vladislav V. Lychagov, N.G. Chernyshevsky Saratov State Univ. (Russian Federation); Qin Huang, Dan Zhu, Pengcheng Li, Huazhong University of Science and Technology (China); Valery V Tuchin, N.G. Chernyshevsky Saratov State Univ. (Russian Federation); Qingming Luo, Huazhong University of Science and Technology (China)

Intracranial hemorrhage (ICH) is related to the main problems of neonatal intensive care. Pathologies of cerebral venous blood flow (CVBF) are critical for the development of ICH. At present, there is no clear answer about the mechanisms responsible for the development of ICH in newborns. According to the current studies, an important role in this process is associated with the activation of the adrenorelated vasorelaxation. In order to obtain more information about the discussed mechanisms, we study in this work cerebrovascular dynamics in newborn animals based on the laser speckle contrast imaging being the noninvasive experimental technique that provides monitoring of the blood flow, and the multiresolution analysis based on the wavelet transform for data processing. We discuss abilities of the multiresolution analysis for revealing stress-induced changes in vessels dynamics associated with different physiological control mechanisms. Based on this mathematical approach we found that the stress-induced intracranial hemorrhages are accompanied by changes in the sagittal vein dynamics caused by sympathetic components of variability of cerebrovascular blood flow. The obtained results show that a high activation of the adrenergic-related vasodilatory responses to severe stress in newborn animals may be one of the important mechanisms underlying the development of ICH.

9322-38, Session PSun

In vivo imaging of embryonic chick heart using optical coherence tomography

Siyu Ma, Clemson Univ. (United States); Richard L. Goodwin, Univ. of South Carolina (United States); Roger R. Markwald, Thomas K. Borg, Medical Univ. of South Carolina (United States); Raymond B. Runyan, The Univ. of Arizona (United States); Bruce Z. Gao, Clemson Univ. (United States)

Heart valve malformation is a common congenital heart defect, which is speculated to relate to improper gene expression caused by endothelial cilia mediated response to shear-stress alterations; these alterations may result in the failure of transition from endothelial cell to mesenchymal cell (EMT) and ultimately lead to remodeling of heart morphology. Current methods, such as immunohistochemistry and in situ hybridization (ISH), for studying how shear-stress changes regulate EMT are postmortem. To visualize the procedure in real time so as to obtain direct evidence of shear stress induced improper gene expression, a noninvasive imaging technique capable of penetrating layers of the heart wall and imaging coupling of blood flow and heart-wall movement with high resolution is required. In this paper, we presented an optical coherence tomography

(OCT) system that incorporated photonic crystal fiber (PCF) to increase the imaging resolution via expanding the bandwidth of incident light and the streak-mode-scanning mechanism to increase the imaging speed via 2D spectrum recording. This OCT enabled high resolution (~3 μ m in tissue) in vivo imaging of outflow tract of an embryonic chick heart, one of the two locations where EMT took place. With altered shear stress by venous clip, the transition process of endocardial cells were observed and compared with that under normal shear stress. The real time data was later verified by ISH of activin receptor-like kinase, an endocardial activation indicator. This application demonstrates the potential of OCT for further studies of how the interactions of genetic and environmental factors affect embryonic heart remodeling.

9322-39, Session PSun

Molecular effective coverage surface area of optical clearing agents for predicting optical clearing potential

Wei Feng, Ning Ma, Dan Zhu, Huazhong Univ. of Science and Technology (China)

Tissue optical clearing technique shows a great potential for improving optical imaging performance to obtain tissue structural and functional information. How to screen efficient optical clearing agents is still a hot topic. Experimental methods are very common, but too time-consuming and blindless. The molecular dynamic simulation, as a simple theoretical approach, has been used to predict the optical clearing potential of agents by analyzing the hydrogen bonds, hydrogen bridges and hydrogen bridges type forming between the agents and collagen. However, the methods suffer from some problem, especially, for analyzing those cyclic molecules. In this study, a molecular effective coverage surface area based on the molecular dynamic simulation was proposed to predict the potential of optical clearing agents. Two typical cyclic molecules, fructose, glucose and two chain molecules, sorbitol, xylitol were analyzed by calculating their molecular effective coverage surface area, numbers of hydrogen bonds and hydrogen bridges, and types of hydrogen bridge, respectively. In order to evaluate the exact of different analysis methods, in vitro skin samples optical clearing efficacy were measured after 25 min immersing in the solutions, fructose, glucose, sorbitol and xylitol at concentration of 3.5 M using 1951 USAF resolution test target. The experimental results show accordance totally with prediction of molecular effective coverage surface area. Comparing molecular effective coverage surface area with other parameters, the molecular effective coverage surface area has a better performance in predicting optical clearing potential of agents.

9322-40, Session PSun

Combination of infrared thermography and reflectance spectroscopy for classification of hair follicle sub-stage

Yue Guan, Jianru Wang, Caihua Liu, Dan Zhu, Huazhong Univ. of Science and Technology (China)

Hair follicles enjoy continual cycle of anagen, catagen and telogen all life which not only provide a unique opportunity to study the physiological mechanism of organ regeneration, but also benefit to guide the treatment of organ repair in regenerative medicine. Usually, the histological examination as a gold standard has been applied to determine the stage of hair follicle cycle, but noninvasive classification of hair cycle stage in vivo remains unsolved. In this study, the thermal infrared imager was applied to measure the temperature change of mouse dorsal skin with hair follicle cycle, and the change of diffuse reflectance was monitored by the optical fiber spectrometer. Histological examination was used to verify the hair follicle stages. The results indicated that the skin temperature increased at the beginning of anagen. After having stayed a high value for several days, the temperature began to drop. The skin diffuse reflectance decreased during

**Conference 9322:
 Dynamics and Fluctuations in Biomedical Photonics XII**

the whole anagen. When the hair follicle entered into catagen stage, the diffuse reflectance increased; while the temperature continued to drop, and then began to rise gradually. During the telogen, both of the temperature and the diffuse reflectance increased, and then to relative platform. Both methods can only distinguish the stage of the hair follicle cycle rather than sub-stages. In contrast, the combination method can evaluate the hair follicle sub-stages. This study will be useful for the therapeutic investigations on hair regeneration.

9322-41, Session PSun

High-resolution label-free optical lymphangiography

Wan Qin, Utku Baran, Zhongwei Zhi, Ruikang K. Wang,
 Univ. of Washington (United States)

Lymphatic system, as a part of the circulatory system, is complementary to the cardiovascular system. The lymphatic system aids the immune system in removing and destroying waste, debris, dead blood cells, pathogens, toxins, and cancer cells. It also absorbs fats and fat-soluble vitamins from the digestive system and delivers these nutrients to tissue and cells. Visualization of lymphatic vessels plays an important role in understanding the lymphangiogenesis in development and human diseases such as lymphedema, lymphadenopathy, cancer, and various infections. Presently, few tools (e.g. computed tomography, X-Ray, and magnetic resonance imaging) are available for imaging the lymphatics, and most of them require exogenous contrast agents. The applicability of these techniques is limited due to the difficulty of contrast agent uptake and their potential side effects. Optical microangiography (OMAG) is a variation of optical coherence tomography (OCT) that was proposed for label-free noninvasive 3D imaging of vasculature. It has also been applied to lymphatic imaging without the need of contrast agents. However, the spatial resolution of OMAG (6-12 μm) is insufficient to resolve lymphatic capillaries. In this study, we adapted the concept of optical coherence microscopy (OCM) to the OMAG setup. Ultrahigh-resolution microstructure images were captured with a high NA scanning Gaussian beam. The Hessian filter-based automatic segmentation algorithm was employed to separate the lymphatic vessels from the microstructure images based on the fact that lymph is transparent and lymphatic vessels appear as dark hollow vessel-like regions in structural cross sections. Mechanical vertical scan with a translation stage was used to compensate the loss of imaging depth due to the shorter length of focal depth resulted from the high NA of the scanning beam. The *in vivo* imaging results demonstrated that our high-resolution optical lymphangiography was able to resolve tiny lymphatic capillaries and could be a valuable tool for diagnostic and therapeutic studies of lymphatics-related disease.

9322-42, Session PSun

Imaging patients with glaucoma using spectral-domain optical coherence tomography and optical microangiography

Kris Auyeung, Kelsey Auyeung, Castilleja School (United States); Rei Kono, Univ. of Washington (United States); Chieh-Li Chen, Qinqin Zhang, University of Washington (United States); Ruikang K. Wang, Univ. of Washington (United States)

In ophthalmology, a reliable means of diagnosing glaucoma in its early stages is still an open issue. Past efforts, including forays into fluorescent angiography (FA) and early optical coherence tomography (OCT) systems, to develop a potential biomarker for the disease have been explored. However, this development has been hindered by the inability of the current techniques to provide useful depth and microvasculature information of the optic nerve head (ONH), which have been debated as possible hallmarks of glaucoma progression. We reasoned that a system incorporating spectral-domain OCT (SD-OCT) and optical microangiography (OMAG),

could allow an effective, non-invasive methodology to evaluate effects on microvasculature by glaucoma. SD-OCT follows the principle of light reflection and interference to produce detailed cross-sectional and 3D images of the eye. OMAG produces imaging contrasts via endogenous light scattering from moving particles, allowing for 3D image productions of dynamic blood perfusion at capillary-level resolution. Images from normal and glaucomatous patients were obtained using an OCT system (850nm wavelength) for blood flow and structural images, allowing for comparisons. Preliminary results from blood flow and vessel density analysis revealed loss of microvasculature and reduced blood perfusion around the ONH and within the lamina cribrosa in glaucomatous cases as compared to normal ones. This is most likely due to high intraocular pressure in many glaucoma patients, which significantly reduces retinal blood flow and supply of oxygen, resulting in capillary dropouts. We conclude that SD-OCT and OMAG may provide promise and viability for glaucoma screening.

Conference 9323: Photons Plus Ultrasound: Imaging and Sensing 2015

Sunday - Tuesday 8-10 February 2015

Part of Proceedings of SPIE Vol. 9323 Photons Plus Ultrasound: Imaging and Sensing 2015

9323-1, Session 1

Monitoring cerebral venous blood oxygenation in neonates with a medical-grade optoacoustic system

Rinat O. Esenaliev, Irene Y. Petrov, Rafael A. Fonseca, Yuriy Petrov, Karon E. Wynne, Donald S. Prough, Andrey Petrov, C. Joan Richardson, The Univ. of Texas Medical Branch (United States)

Premature, very-low-birth-weight (VLBW; ≤ 1500 g) and low-birth-weight (LBW; 1500-2499 g) infants are at increased risk for severe neurological disability. 25-50% of the 63,000 VLBW infants born annually in the USA have major long-term cognitive or neurobehavioral deficits in which cerebral hypoxia plays an important role. At present, no technology is capable of noninvasive, accurate monitoring of cerebral oxygenation in newborns. We proposed to use an optoacoustic technique for noninvasive cerebral hypoxia monitoring by probing the superior sagittal sinus (SSS). Recently, we developed and built a medical grade, multi-wavelength, near-infrared optoacoustic system suitable for neonatal applications. We designed and built an adjustable patient interface for neonates with VLBW, LBW, and normal weight (NBW) that provides single or continuous measurements of the SSS blood oxygenation. We performed clinical tests of the system in 12 VLBW, LBW, and NBW infants admitted to the neonatal intensive care unit. The system was capable of detecting SSS signals through the open anterior and posterior fontanelles and through the skull and allowed for monitoring of the SSS blood oxygenation. The software developed by our group provided real-time, absolute measurements and display of the SSS blood oxygenation. The averaged SSS blood oxygenation ranged from 59% to 77% in hemodynamically stable preterm infants. Optoacoustic monitoring of the SSS blood oxygenation provides valuable information because adequate cerebral oxygenation would suggest that no therapy was necessary; conversely, evidence of cerebral hypoxia would prompt therapy to increase cerebral blood flow.

9323-2, Session 1

Wavelength optimization for in vivo multispectral photoacoustic tomography of hemoglobin oxygenation in ovarian cancer: clinical studies

Hassan S. Salehi, Hai Li, Patrick D. Kumavor, Quing Zhu, Univ. of Connecticut (United States)

Most of the cancer types in the ovary are detected when the cancer has already metastasized to the peritoneum and other organs because there is no adequate technology to detect early stage ovarian cancers. Thus, ovarian cancer has the highest mortality rate of all gynecologic cancers. Therefore, it is significant to improve the current diagnostic techniques and consequently increase the survival rate in patients. In this regard, we have developed a co-registered photoacoustic/ultrasound system and imaging probe for noninvasive transvaginal examination of the ovaries. Recently, we obtained IRB approval for human subject studies at the University of Connecticut Health Center (UCHC). Based on available wavelength range of the tunable laser source, four sets of optical wavelengths were investigated to image hemoglobin oxygen saturation (sO₂). Each wavelength set contained four wavelengths between 710nm up to 840nm. The criteria for the optimal wavelength selection were condition numbers of the molar extinction coefficient matrices of the oxygenated hemoglobin (HbO₂) and deoxygenated hemoglobin (Hb), and their optical absorption spectrum.

These wavelength sets were first tested on the mouse model to map the spatial distribution of hemoglobin oxygenation (sO₂) using in vivo photoacoustic measurements. In clinical studies, the optimal wavelength set was successfully used to image human ovaries in vivo and noninvasively. We found that the image quality and monitoring tumor vasculature and oxygenation depend strongly on measurement wavelengths.

9323-3, Session 1

Deep melanoma in vivo imaging by a handheld photoacoustic microscope

Yong Zhou, Wenxin Xing, Konstantin I. Maslov, Washington Univ. in St. Louis (United States); Lynn A. Cornelius, Washington Univ. School of Medicine in St. Louis (United States); Lihong V. Wang, Washington Univ. in St. Louis (United States)

Because of the high and increasing incident rate of melanoma, there is an imperative demand for its accurate diagnosis, prognosis, and treatment. Previously, we reported that cutaneous pigmented lesions, melanoma, and the surrounding vasculature could be successfully detected by using dual-wavelength PAM. In that study, light was transmitted through the whole melanoma, resulting in high attenuation, with only very few photons reaching the base of the melanoma (the true tumor depth). In the end, PA signals were very strong from the surface of the tumor but very weak from the deepest portion. In this report, we present a novel handheld photoacoustic microscope (PAM) to detect melanoma and determine tumor depth in nude mice in vivo. A new light delivery mechanism is introduced to improve light penetration. By allowing light to bypass the center of the tumor, more photons reach the inferior depth of the melanoma. We first theoretically demonstrate that the signal-to-noise ratio of the melanoma at the bottom boundary is 1660 times larger with the new light illumination mechanism. Then we show that melanomas with thicknesses ranging from 0.7 mm to 4.1 mm can be successfully detected in the phantom experiments. At last, we show that melanoma as thick as 3.7 mm can be detected in the in vivo experiment. With its deep melanoma imaging ability and handheld design, this system is ready for testing in clinical melanoma diagnosis, prognosis, and surgical planning for patients at the bedside.

9323-4, Session 1

Real-time dual modality ultrasound/photoacoustic in-vivo imaging with a portable system

Pim J. van den Berg, Khalid Daoudi, Univ. Twente (Netherlands); Hein J. Bernelot Moens, Hospital Group Twente (Netherlands); Peter J. Brands, Esaote Europe B.V. (Netherlands); Wiendelt Steenbergen, Univ. Twente (Netherlands)

Among advantages that have enabled ultrasound-imaging to become a clinical standard imaging technique are its ease of access within hospitals, its cost-effectiveness and the possibility to perform real-time imaging for several clinical applications. The lack of such characteristics prevents Photoacoustics (PA) to find a definite place in the hospital. Achieving a merger between Ultrasound (US) and PA functionality in a portable and cost-effective approach, with real time imaging, will facilitate the widespread clinical use of photoacoustic imaging.

Real-time ultrasound/photoacoustic in-vivo imaging will be demonstrated

**Conference 9323: Photons Plus Ultrasound:
Imaging and Sensing 2015**

using such a portable and cost-effective imager. This dual-modality imager features a pulsed diode laser integrated into a hand-held ultrasound probe, forgoing an expensive Q-switched laser and optical fiber coupling. The 800-nm-wavelength diode laser can produce 0.6 mJ pulses after the probe aperture in a 20 mm × 4 mm rectangular beam and a corresponding 1.5 mJ/cm² fluence. The laser can be fired with this fluence at 210 Hz, limited by the Maximum Permissible Exposure.

In-vivo imaging that will be demonstrated will include finger-joint imaging for future early detection of inflammation in rheumatoid diseases. New photoacoustic techniques that might increase the sensitivity of the detection of inflammation, such as PA Doppler, will also be discussed.

9323-5, Session 1
Investigation of deep clinical OA imaging of large blood vessels in the neck, abdomen and limbs

Michael Jaeger, Martin Frenz, Univ. Bern (Switzerland)

The combination of optoacoustic (OA) imaging and classical ultrasound (US), with the irradiation optics integrated into the acoustic transducer in an epi-style handheld probe, is promising as a real-time multimodal clinical imaging system. Although theoretically feasible, the several centimetres OA imaging depth theoretically predicted still remain a clinical challenge. Reasons are that long averaging times (seconds) are required to sufficiently reduce system noise, which however make compensation of tissue motion mandatory to achieve deep imaging. In addition, systematic clutter limits imaging depth even above the noise limit. Such clutter can be reduced by deformation-compensated averaging (DCA), a technique that involves active tissue deformation and continuous averaging of motion-compensated OA images.

We have implemented motion compensation based on US speckle tracking on our combined OA and US research system. In comparison to a previous study of DCA in clinical imaging, we have optimised our system to allow both lateral and axial motion compensation, and a tracking framerate of up to 200 Hz in order to facilitate motion tracking of pulsating vessels such as the aorta over the duration of several heart cycles. As a consequence, this system allows successful averaging in regions containing large vessels, and thus the investigation of the limits of deep clinical OA imaging in the neck, abdomen, and limbs, in human volunteer studies.

9323-6, Session 1
Optoacoustic monitoring of real-time lesion formation during radiofrequency catheter ablation

Genny A. Pang, Erwin Bay, Xosé Luis Deán-Ben, Daniel Razansky, Helmholtz Zentrum München GmbH (Germany)

Radiofrequency ablation (RFA) is commonly used to treat certain cardiac arrhythmias; however, there are currently still a non-negligible number of ineffective procedures that require repeat treatment to be successful. The effectiveness of the ablation treatments can be improved if real-time lesion monitoring and guidance become available. Laser-based diagnostics can provide the desired feedback, and optoacoustic imaging is especially ideal for this because it can deliver both high spectrally-enriched (functional) contrast and deep tissue penetration. We demonstrate, for the first time, application of an optoacoustic monitoring technique to capture real-time three-dimensional formation of RFA-generated lesions with high contrast. Radiofrequency catheter ablation on freshly-excised porcine ventricular myocardial tissue was optoacoustically monitored by means of pulsed-laser illumination in the near-infrared spectrum. The images resulting from tomographic reconstructions capture the three-dimensional formation of the lesion with high contrast and spatial resolution, captured at a rate of 10 Hz. The size and geometry of the lesion was shown to be in excellent agreement

with the histological examinations, indicating accurate imaging of the lesion size. The wavelength dependence of the optoacoustic contrast between highly coagulated and unablated tissue in the near infrared was also measured by using multispectral excitation in the wavelength range 740 nm to 860 nm. Overall, this work demonstrates that optoacoustic monitoring has the potential for providing critical feedback on lesion position and size that can significantly impact the outcome of clinical radiofrequency ablation procedures.

9323-7, Session 1
Recent advances in clinical application of photoacoustic flow cytometry for detection of circulating tumor cells and clots in vivo and ex vivo

Vladimir P. Zharov, Yulian Menyayev, Mazen A. Juratli, Mustafa Sarimollaoglu, Dmitry A. Nedosekin, Ekaterina I. Galanzha, James Y. Suen, Laura F. Hutchins, Univ. of Arkansas for Medical Sciences (United States)

The examination of a total blood volume in vivo could provide potentially detection one CTC in a whole human blood volume. This could reach an ultimate CTC detection limit of 1 CTC in 5 liter of blood that is approximately three orders of magnitude better than the sensitivity threshold of existing CTC assays. We developed the clinical prototype for in vivo photoacoustic (PA) flow cytometry (PAFC) of CTCs, which provides the assessment of 1-3 liter of blood during 30-60 minutes. The principle of PAFC is based on the irradiation of a hand blood vessel with near-infrared high pulse repetition laser and detection of laser-induced acoustic waves from single CTC with ultrasound transducer attached to skin. In this report we present first clinical results with focus on detection of CTCs in melanoma patients. The advantages of in vivo PAFC were validated through comparison with the results of existing ex vivo/in vitro tests including in vitro PAFC and immunohistochemical staining with antibody cocktails. In vivo PAFC method revealed a larger (3-5-fold) number of CTC-associated PA signals in whole blood, compared to other assays. This suggests that new approach is more accurate and rapid (≤ 1 hour) than conventional time-consuming (many hours) CTC assays requiring multiple processing and measuring steps (e.g., enrichment, separation, labeling, or washings) that result in substantial loss of CTCs. In addition, PA clinical prototype demonstrated the capability to label-free simultaneous monitoring of melanoma CTCs and cancer-associated clots.

9323-14, Session 1
Clinical study of ex vivo photoacoustic imaging in endoscopic mucosal resection tissues

Liang Lim, Princess Margaret Cancer Ctr., Univ. Health Network (Canada); Catherine J. Streutker, Norman E. Marcon, Maria Cirocco, Vladimir V. Iakovlev, St. Michael's Hospital (Canada); Ralph DaCosta, Ontario Cancer Institute (Canada); F. Stuart Foster, Sunnybrook Health Sciences Ctr. (Canada); Brian C. Wilson, Princess Margaret Cancer Ctr., Univ. Health Network (Canada)

Accurate endoscopic detection and dysplasia in patients with Barrett's esophagus (BE) remains a major unmet clinical need. Current diagnosis use multiple biopsies under endoscopic image guidance, where up to 99% of the tissue remains unsampled, leading to significant risk of missing dysplasia.

We conducted an ex vivo clinical trial using photoacoustic imaging (PAI) in patients undergoing endoscopic mucosal resection (EMR) with known high-grade dysplasia for the purpose of characterizing the esophageal

**Conference 9323: Photons Plus Ultrasound:
Imaging and Sensing 2015**

microvascular pattern, with the long-term goal of performing endoscopic PAI for dysplasia detection and therapeutic guidance. EMR tissues taken immediately from the patient were mounted on an agar layer and covered with ultrasound gel. Digital photography guided the placement of the PAI transducer, which operated at 40 MHz and scanned the luminal side of the specimen in 14 mm wide strips at 680, 750, 824, 850 and 970 nm. Acoustic images were simultaneously acquired. Tissues were then sliced and fixed in formalin for histopathology, including CD31/D2-40 staining. Ongoing analysis includes co-registration and correlation between the intrinsic PAI features and the histological images.

Preliminary PAI+ultrasound images have demonstrated the technical feasibility of this approach and point to the potential of PAI to reveal the microvascular pattern within the EMR specimens. There are several technical factors to be considered in rigorous interpretation of the PAI characteristics, including the loss of blood from the ex vivo specimens and the limited depth penetration of the PA signal.

9323-9, Session 2
Photoacoustic imaging of single circulating melanoma cells in vivo

Lidai Wang, Junjie Yao, Ruiying Zhang, Guo Li, Washington Univ. in St. Louis (United States); Jun Zou, Texas A&M Univ. (United States); Lihong V. Wang, Washington Univ. in St. Louis (United States)

Melanoma, one of the most common types of skin cancer, has a high mortality rate, mainly due to a high propensity for tumor metastasis. The presence of circulating tumor cells (CTCs) is a potential predictor for metastasis. Label-free imaging of single circulating melanoma cells in vivo would provide rich information on tumor progress. Here we present photoacoustic microscopy of single melanoma cells in living animals. We used a fast-scanning optical-resolution photoacoustic microscope to image the microvasculature in mouse ears. The imaging system has sub-cellular spatial resolution and works in reflection mode. A fast-scanning mirror allows the system to acquire four volumetric images per second over 1?1 mm². A 500 kHz pulsed laser was used to image blood and CTCs with two optical wavelengths (532 nm and 1064 nm). Single flowing melanoma cells were observed in both capillaries and trunk vessels. These high-resolution images allow us to quantify the cell size, counts, circulating time, and flow speeds. This technique enables direct imaging of cancer cells shedding from either a primary tumor or its metastases, which addresses an urgent clinical need.

9323-10, Session 2
Optimizing the optical wavelength for the photoacoustic imaging of inflammatory arthritis

Janggun Jo, Univ of Michigan Medical School (United States); Guan Xu, Univ. of Michigan Medical School (United States); Jack Hu, Sheeja Francis, Univ. of Michigan (United States); April L Marquardt, Univ of Michigan Medical School (United States); Jie Yuan, Nanjing Univ. (China); Gandikota Girish, Xueding Wang, Univ. of Michigan Medical School (United States)

The identification of neoangiogenesis, or hemoglobin content increase, in finger joints by photoacoustic (PA) imaging, as an approach for the diagnosis of inflammatory arthritis, has been extensively investigated during the past years. One of the challenges in visualizing the inflammation in finger joints based on the endogenous contrast is that the PA signals from hemoglobin have to compete with the strong signals from the joint bones as a result of the high optical absorption of by their calcium content. To enhance the contrast of hemoglobin over that of the bone, shorter

wavelengths in the visible region are preferred which, however, lead to decreased penetration depth of light in tissue. The optimal illumination wavelength has thereby been searched considering the balance between the contrast and depth of PA imaging. To best mimic the scenario of acute inflammatory arthritis in human peripheral joints, we injected 1 ml of fresh human blood into the Metacarpophalangeal (MCP) joints of a cadaver hand. The PA images were acquired by a CL15-7 ultrasound (US) array driven by a real time PA and US dual-modality system built on Verasonics platform. The illumination source is a tunable dye laser pumped by an Nd:YAG laser with a 10 Hz repetition rate. With an optical density of 5 mJ per square centimeter at the skin of the finger, 10-15 mm imaging depth has been achieved, which is sufficient to accommodate the detection of inflammation in human MCP and proximal interphalangeal joints. The experiment result suggests that illumination at 580 nm has the potential to produce the best imaging performance.

9323-11, Session 2
Quantifying bone thickness, light transmission, and contrast interrelationships in transcranial photoacoustic imaging

Muyinatu A. Lediju Bell, Anastasia K. Ostrowski, Johns Hopkins Univ. (United States); Ke Li, Johns Hopkins Univ (United States); Peter Kaanzides, Johns Hopkins Univ. (United States); Emad M. Boctor, Johns Hopkins Outpatient Ctr. (United States)

We previously introduced photoacoustic imaging to identify blood vessels hidden by bone and thereby eliminate the deadly risk of carotid artery injury during transsphenoidal, endonasal surgeries. An optical fiber would be attached to the surgical drill, while a transcranial probe is placed on the temporal region of the skull for reception of the photoacoustic signals. The drill could be operated by a robot to remove sphenoid bone in the nasal cavity for access to and resection of pituitary tumors. The purpose of this study was to quantify the relationship between optical penetration and photoacoustic image quality as the sphenoid bone is drilled. A frontal bone from a human cadaver skull was cut into seven 3 cm x 3 cm chips and sanded to thicknesses ranging 1-4 mm, which coincides with the thickness of the sphenoid bone. These skull specimens were individually placed in the optical path of a cylindrical photoacoustic target that mimicked a blood vessel, as the wavelength was varied between 700-940 nm. Optical energy and vessel contrast was determined as a function of bone thickness and laser wavelength. The optical energy and contrast loss, measured as a ratio of these properties before and after bone placement, decreased by 55-82% and 57-85%, respectively, as thickness increased (mean of all wavelengths) and decreased by less than 5% as the wavelength was increased. The mean contrast, CNR, and SNR was decreased by 0.88 dB, 1.97, and 7.93, respectively, when comparing images acquired with the 4 mm bone to those acquired with the 1 mm bone. We are investigating whether these image quality metrics could be used as an input to the robotic system to determine the thickness of bone that remains to be drilled.

9323-12, Session 2
Developing a clinically translatable light-enhanced transesophageal echocardiography system for monitoring mixed venous oxygen saturation in vivo

Li Li, Balachundhar Subramaniam, Harvard Medical School (United States); Brett Simon, Beth Israel Deaconess Medical Ctr. (United States); Guillermo J. Tearney, Harvard Medical School (United States) and Wellman Ctr. for

**Conference 9323: Photons Plus Ultrasound:
Imaging and Sensing 2015**

Photomedicine (United States)

Mixed venous oxygen saturation (SvO₂), measured from pulmonary arteries, is a gold-standard dynamic indicator of the global oxygen sufficiency in the cardiopulmonary circulation. A low SvO₂ (< 60%) strongly suggests the onset of life-threatening circulatory shock. Goal-oriented hemodynamic therapy, targeted at restoring SvO₂ back to the normal level, could improve the outcomes of critically ill patients. Traditionally, SvO₂ is measured by pulmonary artery catheters (PAC). However, the intravascular insertion of PAC is an invasive procedure that is associated with a 10% complication rate.

We have proposed that light-enhanced transesophageal echocardiography (leTEE), integrating transesophageal echocardiography with photoacoustic oximetry, could enable noninvasive monitoring of SvO₂. Previously using a bench-top photoacoustic system, our ex-vivo studies on en-bloc tissue models demonstrated that leTEE could accurately measure SvO₂. Here, we will further introduce a clinically translatable leTEE system for in-vivo validation of the technology. The oximetric esophageal probe includes a flexible fiber bundle and has an outer diameter smaller than 15 mm, which will make it tolerable for most patients. Using this device, ultrasonic and photoacoustic images of cardiac anatomy are acquired at 10 frames per second and displayed in real time to guide the deployment of the probe. SvO₂ is calculated on-line and updated every 200 milliseconds. In addition to describing the device, we will report the performance of the clinical prototype evaluated in ongoing studies in living swine.

9323-13, Session 2

High-resolution multispectral photoacoustic tomography of human lymph nodes based on multiple sources of intrinsic contrast

James A. Guggenheim, Thomas J. Allen, Univ. College London (United Kingdom); Andrew Plumb, Univ. College London (United Kingdom) and Univ. College London Hospitals NHS Foundation Trust (United Kingdom); Edward Z. Zhang, Univ. College London (United Kingdom); Manuel Rodriguez-Justo, Shonit Punwani, Univ. College London (United Kingdom) and Univ. College London Hospitals NHS Foundation Trust (United Kingdom); Paul C. Beard, Univ. College London (United Kingdom)

Lymph nodes are a common site of metastases in cancers, and determining whether or not cancer has spread to lymph nodes has a vital role in disease staging, prognosis and treatment planning. This often requires surgical removal of nodes for histopathological assessment. Owing to the invasiveness of this, the risk of complications such as bleeding, infection or lymphedema, there is tremendous motivation for monitoring lymph nodes in vivo. It is proposed that photoacoustic tomography (PAT) can be used clinically for this purpose and 3D, multispectral PAT images of whole human nodes are presented.

Images demonstrate multiple sources of contrast arising from intrinsic chromophores including lipids in the fatty layer encapsulating the node and haemoglobin in vasculature. The lipid layer provides a structural reference permitting assessment of node morphology and furthermore the intactness of the boundary. This has clinical relevance as extranodal spread may influence subsequent treatment. Vasculature is observed with high contrast providing further structural information, certain vessel-types being characteristic of certain locations within nodes. Furthermore, vessel patterns are perturbed by disease, for example due to neoangiogenesis in the early stages of cancer. Together the multiple sources of contrast are complimentary and build a comprehensive data set.

Images are obtained using a Fabry-Perot-sensor-based PAT system permitting high resolution images spanning the full depth of multiple nodes. Magnetic resonance imaging, ultrasound and histopathology are used for validation. This work suggests PAT may have a significant role as a non-invasive diagnostic tool for the clinical assessment of metastatic cancer and lymphoid malignancies.

9323-126, Session 2

Photoacoustic (PA) tomography of a fluorescent contrast agent and genetically expressed proteins using excited state lifetime modulation

Julia Märk, Hakan Dortay, Franz-Josef Schmitt, Technische Univ. Berlin (Germany); Jan G. Laufer, Technische Univ. Berlin (Germany) and Charité - Universitätsmedizin Berlin (Germany)

Pump-probe excitation can be used to induce stimulated emission in fluorophores and thus modulate the excited state lifetime. By varying the time delay between the pump and probe pulses, the thermalized energy, and hence PA signal amplitude, can be varied in a controlled manner. Since this effect is not observed in endogenous tissue chromophores, the location of the fluorophore can be obtained using PA difference imaging. By exploiting the differences in the absorption and emission spectra of fluorophores, multiplexed detection and visualisation can be achieved. Furthermore, by plotting the amplitude of the difference signal as a function of the pump-probe time delay, differences in the excited state (fluorescence) lifetime can be detected. This may provide an additional contrast mechanism not only for multiplexed fluorophore detection but also for probing environmental conditions, such as the local pH, or for detecting Förster resonance energy transfer (FRET). In this study, the potential for making such measurements is explored. PA difference signals are measured in a cuvette in solutions of a fluorescent dye (Atto680) and genetically expressed fluorescent proteins (mOrange, mPapaya, iRFP) at visible and near-infrared pump-probe wavelengths, and for different pump-probe time delays. The excited state lifetime of Atto680 is varied using water and methanol as solvents. PA tomography of differences in excited state lifetime of the dye and iRFP solutions is investigated in tissue phantom experiments where difference images are acquired as a function of time delay. To evaluate the potential for detecting FRET, measurements are made in cuvettes and tissue phantoms using fluorophore solutions with different acceptor dye concentrations.

9323-15, Session 3

Photoacoustic imaging with internal illumination

Li Lin, Jun Xia, Terence T. W. Wong, Ruiying Zhang, Lihong V. Wang, Washington Univ. in St. Louis (United States)

We demonstrate, for the first time, in vivo photoacoustic imaging of rats, by means of internal light delivery. In biological tissue, low frequency acoustic signals (1-10 MHz) suffer much less attenuation and scattering than photons, so delivering more light into the tissue is the key to increase photoacoustic imaging depth.

With fiber illumination via the rat's mouth, we delivered light directly into the bottom of the brain, much more than what can be delivered by external illumination. The study was performed using a photoacoustic computed tomography (PACT) system equipped with a 512-element full-ring transducer array, providing a full two-dimensional view aperture. Using internal illumination, the PACT system gave cross sectional photoacoustic images from the palate to the middle brain of live rats (about 80 g).

We also imaged the rat's kidney, by delivering light from the colon. The experiment was performed on large rats of around 300 g weight. We acquired images using a photoacoustic macroscopy (PAMac) system, which employed a 10 MHz spherically focused ultrasonic transducer. The internal illumination provided much clearer kidney vascular images than external illumination. Thus, internal illumination can potentially be used for photoacoustic imaging of internal organs near cavities.

**Conference 9323: Photons Plus Ultrasound:
 Imaging and Sensing 2015**

9323-16, Session 3

**Retrospective respiration-gated
 whole-body photoacoustic computed
 tomography of mice**

Jun Xia, Wanyi Chen, Konstantin I. Maslov, Mark A. Anastasio, Lihong V. Wang, Washington Univ. in St. Louis (United States)

Photoacoustic tomography is an emerging technique that has great potential for preclinical whole-body imaging. To date, most whole-body photoacoustic tomography systems require multiple laser shots to generate one cross-sectional image, yielding a frame rate of less than 1 Hz. Because a mouse breathes at up to 3 Hz, without proper gating mechanisms, acquired images are susceptible to motion artifacts. Here, we introduce, for the first time to our knowledge, retrospective respiratory gating for whole-body photoacoustic computed tomography. This new method involves simultaneous capturing of the animal's respiratory waveform during photoacoustic data acquisition. The recorded photoacoustic signals are sorted and clustered according to the respiratory phase, and an image of the animal at each respiratory phase is reconstructed subsequently from the corresponding cluster. The new method was tested in a ring-shaped confocal photoacoustic computed tomography system with a hardware-limited frame rate of 0.625 Hz. After respiratory gating, we observed sharper vascular and anatomical images at different positions of the animal body. The entire breathing cycle could also be visualized at 20 frames per cycle.

9323-17, Session 3

**Isotropic-resolution linear-array-based
 photoacoustic computed tomography
 through inverse radon transformation**

Guo Li, Jun Xia, Lei Li, Lidai Wang, Lihong V. Wang, Washington Univ. in St. Louis (United States)

Linear transducer arrays are readily available for ultrasonic detection in photoacoustic computed tomography. They offer low cost, hand-held convenience, and conventional ultrasonic imaging. However, the elevational resolution of linear transducer arrays, which is usually determined by the weak focus of the cylindrical acoustic lens, is about one order of magnitude worse than the in-plane axial and lateral spatial resolutions. Therefore, conventional linear scanning along the elevational direction cannot provide high-quality three-dimensional photoacoustic images due to the anisotropic spatial resolutions. Here we propose an innovative method to achieve isotropic resolutions for three-dimensional photoacoustic images through combined linear and rotational scanning. In each scan step, we first elevationally scan the linear transducer array, then we rotate the linear transducer array along its center in small steps, and scan again until 180 degrees have been covered. To reconstruct isotropic three-dimensional images from the multiple-directional scanning dataset, we use the standard inverse Radon transformation originating from X-ray CT. We acquired a three-dimensional microsphere phantom image through the inverse Radon transformation method and compared it with a single-elevation-scan three-dimensional image. The comparison shows that our method improves the elevational resolution by up to one order of magnitude, approaching the in-plane lateral-direction resolution. In vivo mouse images were also acquired.

9323-18, Session 3

**Evaluation of MultiSpectral Optoacoustic
 Tomography (MSOT) performance in
 phantoms and in vivo**

James Joseph, Univ. of Cambridge (United Kingdom); Kaisar Dauyey, Univ. of Cambridge (United Kingdom) and Nazarbayev Univ. (Kazakhstan); Fiona J. E. Morgan, Univ. of Cambridge (United Kingdom); Sarah E. Bohndiek, Univ. of Cambridge (United Kingdom) and Cancer Research UK Cambridge Institute (United Kingdom) and CRUK & EPSRC Cancer Imaging Ctr. in Cambridge and Manchester (United Kingdom)

The therapeutic response of a range of human cancers is determined by the extent of drug delivery and the degree of tumor cell hypoxia. High resolution imaging of the tumor vascular network and blood oxygenation could therefore yield significant prognostic insight in a clinical setting.

MultiSpectral Optoacoustic Tomography (MSOT) combines the high contrast of optical imaging with the spatial resolution and penetration depth of ultrasound, using the photoacoustic effect. MSOT is exquisitely sensitive to the proportion of oxy- and deoxyhemoglobin in the vasculature, enabling direct visualization of blood oxygenation. This modality has shown promise in a range of biomedical applications, including cancer imaging.

To understand the modulation of hemoglobin concentration and oxygenation that can be sensitively detected within tumors, knowledge of MSOT signal stability and reproducibility is vital. Here, we developed a simplified cell phantom to enable such measurements to be performed in vitro and established a small animal imaging protocol to minimise baseline variability in vivo.

Our simplified cell phantom incorporates cells expressing a near infrared fluorescent reporter protein (iRFP) together with a stable uniform absorber as contrast sources. Stability and reproducibility measures from a wide range of cell densities (between 10³ - 10⁸ cells) were compared to the readout from the uniform absorber, to decouple system variation from photobleaching and cell viability. Parameters that could modulate the in vivo MSOT signal from hemoglobin include body temperature, anesthetic concentration and inhaled gas composition. The effect of these parameters on the MSOT signal from living subjects will be presented.

9323-19, Session 3

**In vivo label-free imaging of mouse
 femoral nerve by multispectral
 photoacoustic tomography**

Rui Li, Evan Phillips, Pu Wang, Craig J. Goergen, Ji-Xin Cheng, Purdue Univ. (United States)

Iatrogenic damage to peripheral nerves is a leading cause of morbidity attributed to surgical procedures. Unintentional surgical damage to nerves is mainly due to poor visualization of tissues of interest relative to adjacent structures. Multispectral photoacoustic tomography can provide chemical information with specificity and ultrasonic spatial resolution with centimeter imaging depth, making it a potential tool for noninvasive neural imaging. To implement this label-free imaging approach of peripheral nerves, we built a multispectral photoacoustic tomography platform that integrates a small animal ultrasound imaging system. A customized optical parametric oscillator, pumped by the second harmonic of a Nd:YAG laser, was used as the light excitation source. Using a tissue-mimicking polyvinyl alcohol (PVA) phantom, we demonstrated penetration depth up to 2.7 centimeter while attaining a 75 μ m axial resolution. We further performed ex vivo and in vivo imaging of the femoral nerve in a nude mouse. Through multivariate curve resolution (MCR) analysis of spectroscopic images ranging from 1100 nm to 1250 nm, we can discriminate femoral nerve from femoral artery and

**Conference 9323: Photons Plus Ultrasound:
Imaging and Sensing 2015**

generate chemical maps of their spatial distributions. This study has great clinical potentials, and will open the opportunity of label-free imaging of peripheral nerves with high specificity.

9323-20, Session 3

Label free ultrasound-guided spectroscopic photoacoustic imaging of lymph node micrometastases

Geoffrey P. Luke, The Univ. of Texas at Austin (United States) and The Univ. of Texas M.D. Anderson Cancer Ctr. (United States); Stanislav Y. Emelianov, The Univ. of Texas at Austin (United States) and The Univ. of Texas M.D. Anderson Cancer Ctr. (United States)

Once a primary tumor is detected, accurate determination of its spread is critical for formulating a treatment strategy. Many types of tumors metastasize to the regional lymph nodes en route to distant organs. In order to detect these metastatic foci, the current standard of care is to perform a sentinel lymph node biopsy. The procedure, however, is hampered by high rates of morbidity and nontrivial false negative rates. To address this, we have developed a new lymph node imaging technique, ultrasound-guided spectroscopic photoacoustic imaging, to noninvasively detect micrometastases in lymph nodes. We evaluated the technique on a metastatic mouse model of oral cancer. Three-dimensional ultrasound and spectroscopic photoacoustic imaging was performed in the region containing the cervical lymph nodes (the site of metastasis) using a Vevo LAZR imaging system. A linear least squares spectral unmixing algorithm was used to measure the blood oxygenation throughout the lymph nodes. In total, 31 lymph nodes in 17 mice were imaged. Metastatic murine lymph nodes (N = 7) exhibited a statistically significant ($p = .0021$) lower blood oxygen saturation (60.5%) than healthy nodes (67.2%). This technique allowed for the detection of metastatic foci as small as $2.6 \times 10^{-3} \text{ mm}^3$. This enables sensitive detection of small metastatic deposits without the use of ionizing radiation or exogenous contrast agents. These initial results could pave the way for clinical photoacoustic imaging and reduce the overall morbidity associated with the sentinel lymph node biopsy procedure.

9323-21, Session 3

Label-free structural photoacoustic tomography of intact mouse brain

Lei Li, Jun Xia, Guo Li, Alejandro Garcia-Urbe, Lihong V. Wang, Washington Univ. in St. Louis (United States)

Capitalizing on endogenous hemoglobin contrast, photoacoustic computed tomography (PACT), a deep-tissue high-resolution imaging modality, has drawn increasing interest in neuro-imaging. However, most existing studies are limited to functional imaging of the cortical surface. While deep-brain structural imaging has been briefly explored, origin of the structural contrast is still unclear.

Here, we explicitly studied the limiting factors of deep mouse brain PACT imaging. We found that the skull distorted the acoustic signal, and that blood absorption suppressed the structural contrast from other chromophores, such as cytochromes. After successfully mitigating the two effects, we show that PACT can provide high-resolution label-free structural imaging of the entire mouse brain. With $100 \mu\text{m}$ in-plane resolution, we can clearly identify major structures of the brain, and the image quality is comparable to that of magnetic resonance microscopy. Spectral PACT studies indicate that structural contrasts mainly originate from cytochrome and lipid, and that the wavelength range from 520 nm to 620 nm would be the proper band for brain structural imaging. We also experimentally proved the viability of imaging both cortex vessel anatomy and deep brain structures at the same time. The feasibility of imaging the structures of the brain in vivo is also discussed. Our results demonstrate that PACT is a promising modality for both structural and functional brain imaging.

9323-22, Session 4

Three-dimensional laser optoacoustic and laser ultrasound imaging system for biomedical research (LOUIS-3DM)

Sergey A. Ermilov, Richard Su, Tanmayi Oruganti, TomoWave Laboratories, Inc. (United States); Kun Wang, Fatima Anis, Mark A. Anastasio, Washington Univ. in St. Louis (United States); Alexander A. Oraevsky, TomoWave Laboratories, Inc. (United States)

We present an improved prototype of 3D imaging system that combines optoacoustic (photoacoustic) tomography (OAT) and laser ultrasound tomography (LUT) to obtain coregistered maps of tissue optical absorption and speed of sound (SoS) in live mice. The tomographic scans are performed by a 360 degree rotation of a mouse with respect to an arc-shaped array of wide band ultrasonic transducers. A Q-switched laser system is used to establish optoacoustic illumination pattern appropriate for deep tissue imaging with a tunable (730-840 nm) output wavelengths operated at 10 Hz pulse repetition rate. The reconstructed 3D optoacoustic images provide information valuable for preclinical cancer research, angiography, mapping blood oxygenation, monitoring thermal therapy and biodistribution of optoacoustic contrast agents. The LUT unit creates maps of SoS, which provide additional diagnostic dimension and could be employed by an OAT algorithm for compensation of aberrations in optoacoustic wavefield. LUT is performed in multiple slices orthogonal to the axis o rotation of the animal. A single hemispherical broadband laser ultrasound emitter is used with the optoacoustic array of receivers rotated 90 degrees for planar imaging of SoS distributions reconstructed from the time-of-flight (ToF) data. Laser generated ultrasound has advantages of clean non-reverberating broadband pulses, ideal for ToF detection and ultrasound spectral analysis. The performance of the system is evaluated through multi-wavelength OAT co-registered with the SoS imaging of tissue simulating phantoms and live mice. We also discuss design and advanced imaging features available in commercial version of LOUIS-3DM.

9323-23, Session 4

Multimodal imaging of cancer tissues in liver samples and of vascular structure on rat brain using acousto-optical imaging

Kevin Contreras, Jean-Baptiste Laudereau, Institut Langevin (France); Vincent Servois, Pascale Mariani, Institut Curie (France); Alexander A. Grabar, Uzhgorod National Univ. (Ukraine); Ivan Cohen, Univ. Pierre et Marie Curie (France); Mikael Tanter, Jean-Luc Gennisson, François Ramaz, Institut Langevin (France)

Due to the complexity of cancer tissues, no single imaging modality is sufficient to obtain all of the desired information. Contrast-enhanced techniques and multimodality imaging are expected to offer new advantages.

Currently, several techniques are widely used for preclinical and clinical cancer imaging, such as computed tomography, single-photon emission computed tomography, positron emission tomography, magnetic resonance imaging, ultrasound and optical techniques. In this context, ultrasound and optical techniques share many common features. These two imaging techniques are complementary. In this paper, we report a multimodal imaging system based on the principle of ultrasound tagged photons where the acousto-optical signal is detected using the self-adaptive wave front holography implemented with a Te-doped Sn₂P₂S₆ photorefractive crystal at

a near-infrared wavelength of 780 nm. We present a detailed analysis oriented to improve the specificity and sensibility for the detection of

Conference 9323: Photons Plus Ultrasound: Imaging and Sensing 2015

tumors and to image the vascular structure at a rat brain. Firstly, we have analyzed some ex-vivo liver samples containing tumors. These tumors are concerned to the uveal melanoma, where the optical contrast can give us more information about the concentration of melanin. Secondly, we have imaged the vascular structure inside ex-vivo rat brain. This structure is put in evidence with the injection of ink. Our preliminary experimental results are encouraging. The acousto-optical imaging as multimodal technique has a great potential for biomedical applications but it is yet necessary to reduce time processing for example, which shall allow us to apply it to in vivo biological tissues. Finally, we will detail some aspects about a novel reflection configuration for acousto-optical imaging.

9323-24, Session 4

Ultrasound-aided multi-parametric transcranial photoacoustic microscopy of the mouse brain

Bo Ning, Adam J. Dixon, James Bonaffini, Matthew J. Kennedy, Rui Cao, Univ. of Virginia (United States); Ruimin Chen, Qifa Zhou, Koping Kirk Shung, The Univ. of Southern California (United States); John A. Hossack, Song Hu, Univ. of Virginia (United States)

The brain, which represents only 2% of the human weight, accounts for more than 20% of the total oxygen consumption at the resting state. Disruption of cerebral oxygen metabolism plays a key role in the progression of multiple life-threatening brain disorders. Thus, in vivo quantification of the cerebral metabolic rate of oxygen (CMRO₂) in preclinical models is crucial for understanding brain dysfunctions and formulating new therapeutic strategies. However, none of existing optical microscopy techniques can provide quantitative measurements of regional CMRO₂ in the brain.

To break this technical bottleneck, we have developed a combined ultrasound and photoacoustic microscope (PAM) for multi-parametric brain imaging through the intact mouse skull. Specifically, the surface contour of mouse skull is ultrasonically extracted and interpolated. With the guidance of the contour map, three-dimensional (3D)-scanning PAM dynamically focuses on the underlying cortical vasculature and concurrently quantifies three parameters prerequisite for regional CMRO₂ calculation—including the total concentration of hemoglobin (CHb), the oxygen saturation of hemoglobin (sO₂), and cerebral blood flow (CBF)—at the microscopic level. Fusing the 3D ultrasonic and optical images allows us to separate the skull and cortical vessels for deriving the oxygen extraction fraction (OEF) in the cortex of interest by $OEF = \frac{(s_a O_2 - s_v O_2)}{(s_a O_2)}$. Upon the quantification of all four prerequisite parameters, we can derive microscopic CMRO₂ by $(1.39 \cdot C_{Hb} \cdot s_a O_2 \cdot OEF \cdot CBF) / 100$, where $s_a O_2$ is the arterial sO₂.

This innovation fills a major technical gap and is expected to provide major new insights into the pathogenic mechanisms of a broad spectrum of neurovascular disorders, in particular ischemic stroke.

9323-25, Session 4

In vivo photoacoustic / optical coherence tomography imaging: human skin pathologies and their relation to subcutaneous vascular abnormalities

Behrooz Zabihian, Jessika Weingast, Mengyang Liu, Boris Hermann, Medizinische Univ. Wien (Austria); Edward Z. Zhang, Paul C. Beard, Univ. College London (United Kingdom); Hubert Pehamberger, Wolfgang Drexler, Medizinische Univ. Wien (Austria)

Multimodal biomedical imaging devices are increasingly emerging in

clinical applications. Their advantage is the complementary information for better diagnosis. Photoacoustic tomography (PAT), as an imaging modality based on absorption of light is a good counterpart to optical coherence tomography (OCT) whose contrast is mainly due to scattering of light. The supplemental information can provide comprehensive tissue characterization to better understand the underlying causes and conditions of diseases such as skin diseases, providing valuable information for clinicians. OCT can characterize and identify the morphological changes of the skin. On the other hand PAT reveals the vascular structure in the tissue, supplying blood and nutritious to it. We use a Fabry-Pérot interferometer (FPI) to detect the ultrasound (US) signal for PAT and effectively resolve features up to 7 mm in depth. In the OCT part we utilize a swept source laser with the central wavelength of 1060nm and the bandwidth of 100 nm. Since the FPI is transparent for this wavelength region, we obtain auto-coregistered 3D images of both modalities. In this study we imaged several patients and here we present auto-coregistered 3D fused PAT/OCT images of in vivo human skin with various skin pathologies. It was aimed to investigate their relation to the subcutaneous vascular abnormalities such as aneurysms. The results from healthy subjects are also provided to be compared against the pathologies.

9323-26, Session 4

Dual modality investigation of bone pathologies using quantitative ultrasound and photoacoustics

Idan Steinberg, Tel Aviv Univ. (Israel); Israel Gannot, Tel Aviv Univ. (Israel) and Johns Hopkins Univ. (United States); Avishay Eyal, Tel Aviv Univ. (Israel)

Osteoporosis is widespread, has a catastrophic impact on patients lives and overwhelming related healthcare costs. In recent works, we have investigated a multi-spectral, frequency domain photoacoustic method for the evaluation of bone pathologies. Such a system has great advantages over pure ultrasonic or optical methods as provides both molecular information from the bone absorption spectrum and bone mechanical status from the characteristics of the ultrasound propagation. These characteristics include both the Speed of Sound (SOS) and Broadband Ultrasonic Attenuation (BUA). To test the method's quantitative predictions, we have constructed a combined ultrasound and photoacoustic setup. This work presents the dual modality system, and compares between the methods via bone samples in-vitro.

The experimental setup is based on a portable triple laser-diode system (650nm, 760nm and 1064nm). These were all coupled to the same fiber through an optical switch and delivered to a lamb bone to excite acoustic signals in a distal location along the bone. In addition a single element ultrasonic transducer was used to generate US coupled into the bone shaft. The excitation position was sampled in a few points along the bone while the acoustic phase and amplitude is measured proximally by a second transducer. A chelating agent (EDTA) was used to mimic the osteoporotic process. The effect of such process on both PA and US signals was investigated.

The comparison of these two modalities will be presented and discussed. The differences between the two modalities are shown to provide valuable insight into the bone structure and functional status.

9323-27, Session 4

Real-time sono-photoacoustic imaging of gold nanoemulsions

Bastien Arnal, Chen-Wei Wei, Camilo Perez, Thu-Mai Nguyen, Michael Lombardo, Univ. of Washington (United States); Ivan M. Pelivanov, Univ. of Washington (United States) and Moscow State Univ. (Russian Federation); Lilo

**Conference 9323: Photons Plus Ultrasound:
Imaging and Sensing 2015**

D. Pozzo, Matthew O'Donnell, Univ. of Washington (United States)

Phase transition contrast agents were first introduced in ultrasound (US) in the form of perfluorocarbon droplets. When their size is reduced to the nanoscale, surface tension dominates their stability and high pressure is required to vaporize them using long US emissions at high frequencies. Our group recently showed that nanoemulsion beads (100-300 nm) coated with gold nanospheres could be used as non-linear contrast agents. Beads can be vaporized with light only, inducing stronger photoacoustic signals by increasing thermal expansion. A photoacoustic cavitation threshold study (US: 1.2 MHz, Laser 750 nm & 10-ns pulse) shows that the vaporization thresholds of NEB-GNS can be greatly reduced using simultaneous light and US excitations. The resulting signal is driven only by the pressure amplitude from a fluence of 2.4 mJ/cm². At diagnostic exposures, it is possible to capture very high signals from the vaporized beads at concentrations reduced to 10 pM with absorption smaller than 0.01 cm⁻¹. A real-time imaging mode selectively isolating vaporization signals was implemented on a Verasonics system. A linear US probe (L74, 3 MHz) launched short US bursts before light was emitted from the laser. Vaporization of NEB-GNS resulted in a persistent 50-dB signal enhancement compared to a dye with the same absorption. Specific vaporization signals were retrieved in phantom experiments with US scatterers. This technique, called sono-photoacoustics, has great potential for targeted molecular imaging and therapy using compact nanoprobe with potentially high-penetrability into tissue.

9323-28, Session 4

**Cyclic magnetomotive photoacoustic/
ultrasound imaging**

Bastien Arnal, Chen-Wei Wei, Thu-Mai Nguyen, Junwei Li, Univ. of Washington (United States); Ivan M. Pelivanov, Univ. of Washington (United States) and Moscow State Univ. (United States); Xiaohu Gao, Matthew O'Donnell, Univ. of Washington (United States)

The robustness of magnetomotive photoacoustic/ultrasound imaging is greatly reduced when background physiologic motion is present, such as cardiac-induced motion and respiration. Cyclic magnetomotive imaging with narrowband coded excitation was proposed to differentiate targeted objects moving coherently with the excitation from background static signals and signals moving incoherently. Results show that magnetic-nanoparticle-targeted cells injected subcutaneously on the back of a mouse were successfully differentiated from the background, with less than 20 μm coherent magnetic induced displacements isolated from millimetric background breathing motion. This demonstrates the motion robustness of this technique for highly sensitive and specific diagnosis.

9323-29, Session 4

**Photoacoustic and optical coherence
tomography whole-body imaging of chick
embryos at multiple normal developmental
stages**

Mengyang Liu, Barbara Maurer, Boris Hermann, Behrooz Zabihian, Medizinische Univ. Wien (Austria); Michelle Sandrian, Univ. of Pittsburgh (United States); Angelika Unterhuber, Bernhard Baumann, Medizinische Univ. Wien (Austria); Edward Z. Zhang, Paul C. Beard, Univ. College London (United Kingdom); Wolfgang J. Weninger, Wolfgang Drexler, Medizinische Univ. Wien (Austria)

Being an animal model for a variety of biomedical studies for decades, chick

embryos play a vital role in our understanding of many physiological as well as pathological processes. To better utilize this animal model in studies of vasculature related phenomena, whole-body imaging of chick embryos is under high demand. However, current imaging modalities such as magnetic resonance microscopy, high resolution episcopic microscopy or light sheet microscopy all show their limitations for imaging the chick embryo in toto, making them only suitable in post-mortem studies. In our work, we explored the application of our dual modality photoacoustic and optical coherence tomography system in the whole-body imaging of chick embryos at three different normal development stages. The deep penetration depth achieved by photoacoustic tomography revealed the general vasculature while the fine resolution of optical coherence tomography provided delicate morphological structures. Comparison between the 3D reconstructed dual modality images acquired from three different development stages showed a clear indication of the cardiac and visual organ development, as well as the limb and trunk changes, which were confirmed by high resolution episcopic microscopy. Co-registered 3D volumes of photoacoustic and optical coherence tomography proved that this dual modality optical imaging system is a powerful tool for chick embryo imaging applications. With some improvements, it can also permit longitudinal monitoring of the same chick embryo, providing vital information for developmental biology studies using this animal model.

9323-30, Session 4

**Real-time system for intravascular
ultrasound and photoacoustic imaging**

Donald VanderLaan, Andrei B. Karpouk, Douglas E. Yeager, Stanislav Y. Emelianov, The Univ. of Texas at Austin (United States)

To identify anatomical, compositional and cellular/molecular properties of atherosclerotic plaques, combined intravascular ultrasound (IVUS) and intravascular photoacoustic (IVPA) imaging has been introduced and investigated. Clinical translation of this multi-modal imaging technology requires real-time operation. We present development and implementation of a real-time IVUS/IVPA system and integrated IVUS/IVPA catheter. Our system addresses several technical and fundamental challenges of real-time IVUS/IVPA imaging: combined catheter; high data throughput and computational complexity requisite for real-time visualization; synchronization with appropriate high pulse-repetition-frequency lasers; and intricate mechanical assembly for transmission of high-bandwidth RF signals across the rotating frame while maintaining a central path for laser-light delivery. The PXIe platform was chosen to implement system control and synchronization, data acquisition, signal/image processing and display, along with user interface. Custom software ran on an embedded PXIe controller, synchronized all hardware, and pipelined the image generation process from acquisition through final rendering. A Panametrics 5910PR was employed for pulse-echo IVUS, while receiving PA transients interleaved between US echoes. Baseband digitization occurs at 200 MSamples/s with 12 bit sample depth. A hollow electrical rotary joint, brushless servo motor, and 8192-line encoder permitted indefinite and smooth IVUS/IVPA catheter rotation with an uninterrupted return path for receiving ultrasound echoes. IVUS/IVPA imaging was tested using a DPSS Nd:YAG laser capable of up to 10 kHz pulse repetition rate. Preliminary results using test phantoms and vessel models confirmed operation of IVUS/IVPA imaging system at 30 frames per second using a custom-made dual-modality IVUS/IVPA catheter.

9323-91, Session PSun

**Development of photoacoustic imaging
technology overlaid on ultrasound imaging
and its clinical application**

Miya Ishihara, National Defense Medical College (Japan); Kazuhiro Tsujita, FUJIFILM Corp. (Japan); Akio Horiguchi, National Defense Medical College (Japan); Kaku Irisawa,

**Conference 9323: Photons Plus Ultrasound:
Imaging and Sensing 2015**

FUJIFILM Corp. (Japan); Tomohiro Komatsu, National Defense Medical College (Japan); Makoto Ayaori, Tokorozawa Heart Ctr. (Japan); Takeshi Hirasawa, National Defense Medical College (Japan); Tadashi Kasamatsu, Kazuhiro Hirota, FUJIFILM Corp. (Japan); Hitoshi Tsuda, Katsunori Ikekawa, Tomohiko Asano, National Defense Medical College (Japan)

Optical and ultrasound imagings have the advantage of fast and easy access. To make the best use of the advantage, we developed two types of hand-held photoacoustic probes integrated with a clinical ultrasound array system to provide co-registered photoacoustic and ultrasound images. A conventional linear array ultrasound probe combined with optical illumination enabled to visualize vessels with diameters as small as 300 μ m at depths within a few centimeters in experiments with a phantom and inguinal region in a rabbit. A transrectal ultrasound (TRUS) type of photoacoustic probe had almost as same field-of-view (FOV) as the ultrasound.

In order to demonstrate the clinical feasibility of the technique, we designed and conducted clinical research trials of urology and vascular medicine with the approval of the medical human ethics committee of the National Defense Medical College. We successfully acquired high dynamic range images of the vascular network ranging from capillaries to landmark artery in periprostatic tissues. In particular, the photoacoustic images of the periprostatic tissues in all resected specimens showed substantial signals especially strong on the posterolateral surface of the prostate. In the pathology image double-stained with anti-CD34 and anti-S-100 antibodies, periprostatic microvessels was nearly co-localized with nerve fibers and their distribution was consistent with the photoacoustic image. Consequently, the photoacoustic image was useful to visualize the neurovascular bundle (NVB). The intraoperative identification of the NVB under co-registered photoacoustic and ultrasound images was easier than that under TRUS alone.

9323-92, Session PSun

Integrating sphere-based photoacoustic setup for simultaneous absorption coefficient and Grüneisen parameter measurements of biomedical liquids

Yolanda Villanueva, Erwin Hondebrink, Wilma Petersen, Wiendelt Steenbergen, Univ. Twente (Netherlands)

Knowing both absorption coefficient μ_a and Grüneisen parameter G of target absorbers is an important step in realizing quantitative photoacoustic imaging of biological tissues. We have developed a method for simultaneously measuring μ_a and G of absorbing liquids. The absorber is mounted inside two integrating spheres using a soft transparent tube with inner diameter of 0.58mm. One end of the tube is inserted through a small hole in the port plug of one sphere while the other end is inserted through that of the other sphere. The absorber is injected into one end of the tube and flows towards the other end so that the same absorber is simultaneously mounted in the two sphere setup. One sphere is used for optical measurements using a continuous wave light source. Light is made directly incident on the sphere wall and multiple reflections homogeneously illuminate the absorber inside the tube. A spectrometer is used to measure the escaping light. The optical output signal is used to determine the μ_a of the absorber. On the other hand, pulsed light is delivered to the second sphere. The subsequently generated photoacoustic signal is detected by a transducer connected to the sphere wall. The voltage-peak-to-peak amplitude of the detected photoacoustic signal is used to determine the G of the absorbing sample in the tube. We will present measurements on various biomedically relevant media such as blood and contrast agents.

9323-93, Session PSun

Optical absorbance measurements and photoacoustic evaluation of freeze-thawed polyvinyl-alcohol vessel phantoms

Mustafa U. Arabul, Technische Univ. Eindhoven (Netherlands); Maarten Heres, Eindhoven University of Technology (Netherlands); Marcel C. M. Rutten, Frans N. van de Vosse, Richard G. P. Lopata, Technische Univ. Eindhoven (Netherlands)

Multispectral photoacoustic (MPA) imaging is a promising tool for the diagnosis of atherosclerotic carotids. Exciting the different constituents of a plaque with different wavelengths may provide morphological information to evaluate plaque vulnerability. Preclinical validation of in vivo photoacoustic (PA) imaging requires a comprehensive phantom study. Polyvinyl alcohol (PVA) phantoms are already used for ultrasound purposes.

In this study, the design of optically realistic vessel phantoms for photoacoustics was examined by characterizing their optical properties for different dye concentrations and mechanical properties, and comparing these to PA measurements.

Four different concentrations of Indian ink and molecular dye were added to a 13 wt% PVA and 0.86 wt% orgasol mixture. Next, the homogeneously mixed gels were subjected to five freeze-thaw cycles to increase the stiffness of vessel phantoms ($r_{inner} = 2.5$ mm, $r_{outer} = 4$ mm). For each cycle, the optical absorbance was measured between 400 nm – 990 nm using a plate reader. Additionally, photoacoustic responses of each vessel phantom at 808 nm were tested with a novel, hand-held, integrated PA probe (Esaote).

Measurements show that the PA signal intensity increases with the optical absorber concentration (0.3 to 0.9) in close agreement with the absorbance measurements. The freeze - thaw process has no significant effect on PA intensity. Although the total attenuation of optical energy increases after each freeze-thaw cycle, it is primarily due to the increase in the scattering coefficient. In future work, the complexity of these phantoms will be increased to examine the feasibility of distinguishing different constituents with MPA imaging.

9323-95, Session PSun

Hybrid ultrahigh resolution optical coherence / photoacoustic microscopy

Boris Hermann, Mengyang Liu, Wolfgang Drexler, Medizinische Univ. Wien (Austria)

We present an ultrahigh resolution dual modality optical resolution photoacoustic microscopy (OR-PAM) and spectral domain optical coherence tomography (SD-OCT) system. The ultrahigh sub-micron lateral resolution is provided by the high numerical aperture of the objective lens used while the ultrahigh axial resolution is provided by the broadband OCT laser that covers 110 nm with a central wavelength of 830 nm. The synchronized simultaneous acquisition for the two modalities is achieved using a 40 MHz FPGAs. 2D-scanning is realized by two orthogonal translation stages (PI, 400 nm resolution).

The transversal resolution of the system is 0.5 μ m, the axial resolutions are 30 μ m (PAM) and 3 μ m (OCT), respectively. The values have been determined experimentally using nanospheres (diameter 10-200 nm).

For a demonstration of the imaging capability we present images from thin slices of chick embryo vasculature, as well as excised tissue samples.

**Conference 9323: Photons Plus Ultrasound:
Imaging and Sensing 2015**

9323-96, Session PSun

High frame rate photoacoustic computed tomography using coded excitation

Masataka Azuma, Kyoto Univ. (Japan); Haichong K. Zhang, Johns Hopkins Univ. (United States) and Kyoto Univ. Graduate School of Medicine (Japan); Kengo Kondo, Kyoto Univ. (Japan); Takeshi Namita, Kyoto Univ. Graduate School of Medicine (Japan); Makoto Yamakawa, Kyoto Univ. (Japan); Tsuyoshi Shiina, Kyoto Univ. Graduate School of Medicine (Japan)

Photoacoustic Computed Tomography (PACT) records signals from a wide range of angles to achieve uniform, high-resolution images. A high-power laser is generally used for PACT, but the long acquisition time with a single probe is a problem due to the low pulse-repetition frequency (PRF). For PACT, this degrades image resolution and contrast because it is hard to scan with a small step interval. Moreover, in vivo measurement requires a fast image acquisition system to avoid motion artifacts. The problem can be resolved by using a high PRF laser, which provides only weak energy. Averaging measured signals many times can mitigate the low signal-to-noise issue, but the PRF is restricted by the acoustic time-of-flight, so this is a new source of measurement time increase. Here, we present the coded-excitation approach, which we previously proposed for linear scan (BIOS2013), to speed up the PACT frame rate. Coded excitation irradiates temporally encoded pulses and enhances the signal amplitude through decoding. The PRF is thus not restricted to acoustic time-of-flight, and consequently acquisition time can be shortened by increasing PRF and the SNR increases for the same measurement time. To validate the proposed idea, we conducted experiments using a high PRF laser with a revolving motor and compared the performance of coded excitation to that of averaging. Results showed that the contamination of a signal acquired from different angles was negligible, and the scanning pitch was remarkably improved because the start point of decoding can be set in any code in the periodic sequence.

9323-97, Session PSun

Multispectral photoacoustic microscopy based on an optical-acoustic objective

Rui Cao, Joseph P. Kilroy, Bo Ning, Tianxiong Wang, John A. Hossack, Song Hu, Univ. of Virginia (United States)

Photoacoustic microscopy (PAM) fills the long-standing gap in high-resolution imaging of optical absorption contrast in vivo. To date, label-free PAM of endogenous contrasts from DNA/RNA, hemoglobin, melanin, water, lipid, and glucose has been individually demonstrated. Combining the multiple intrinsic absorption contrasts would provide major new insights into the pathogenic mechanisms of a broad spectrum of vascular and metabolic disorders at the cellular level. However, multispectral PAM over a broad spectral range, from ultraviolet to near infrared, is complicated by the chromatic aberration of the optics.

To address this unmet technical challenge, we have developed a novel multispectral PAM system, where two technical innovations are introduced to circumvent the optical aberration. Specifically, a reflective microscope objective with zero chromatic aberration is employed to achieve near-identical spatial resolution over a broadband spectral range. Moreover, a homemade ultrasonic transducer is attached to the reflective objective for convenient confocal alignment of optical excitation and acoustic detection, which avoids the optical aberration and acoustic loss induced by the otherwise needed optical-acoustic beam combiner. With a high-repetition-rate wavelength-tunable optical-parametric-oscillator laser, we have demonstrated multispectral PAM over an unprecedented ultrabroad spectral range of 210–1400 nm. A constant spatial resolution of ~3 μm is quantified experimentally. Capitalizing on the ultrabroad spectral range and constant spatial resolution, we have achieved concurrent PAM of cell nucleus (DNA/

RNA contrast at 270 nm), vascular anatomy and blood oxygenation (oxy- and deoxy-hemoglobin contrasts at 532 and 559 nm), and sebaceous gland (lipid contrast at 1260 nm).

9323-98, Session PSun

Fast calibration of speed-of-sound using temperature prior in whole-body small animal optoacoustic imaging

Subhamoy Mandal, Technische Univ. München (Germany) and Helmholtz Zentrum München GmbH (Germany); Elena Nasonova, iThera Medical GmbH (Germany); Xosé Luis Deán-Ben, Helmholtz Zentrum München GmbH (Germany); Daniel Razansky, Technische Univ. München (Germany) and Helmholtz Zentrum München GmbH (Germany)

Accurate calibration of reconstruction parameters is essential for optimizing the resolution and contrast as well as associated quality measures of optoacoustic tomographic images. Commonly, a constant value of the SoS in biological tissues is generally assumed for tomographic reconstructions. However, spatial variations of the speed of sound (SoS), attenuation and other acoustic properties of the propagation medium affect the collected optoacoustic signals and therefore must be correctly accounted for in the reconstruction procedure. In this paper, several hybrid focus functions are described that present higher sensitivity and success rate in determining the best matching SoS compared to state-of-the-art approaches. The hybrid autofocusing measures incorporate key improvisation, viz. edge detection or diffusion, which not only enhance the focusing performance but also makes them more suitable for reconstructing realistic tomographic images acquired from small animals. An a-priori determined SoS in water is used as an initial guess for a fast calibration of the SoS in the reconstruction. Continuous monitoring of temperature is shown to significantly increase the convergence speed of the methods. Experimental results obtained with small animals in vivo showcase the convenience of using autofocusing-based calibration of SoS for automatic image quality enhancement.

9323-99, Session PSun

Technique development for photoacoustic imaging guided interventions

Qian Cheng, Tongji Univ. (China) and Univ. of Michigan (United States); Haonan Zhang, Tongji Univ. (China) and Univ. of Michigan (United States); Jie Yuan, Nanjing Univ. (China); Ting Feng, Nanjing Univ. (China) and Univ. of Michigan Medical School (United States); Guan Xu, Univ. of Michigan Medical School (United States); Xueding Wang, Univ. of Michigan Medical School (United States) and Tongji Univ. (China)

Ultrasound (US) is currently the gold standard technology for guiding needle biopsy and other interventions. The drawbacks of US guided needle biopsy, besides limited sensitivity and specificity, also include poor visualization of needle, which is especially a problem when the acoustic window is limited while the echo signals from the needle or other intervention apparatus are out of the receive range of the probe. In our research, by using an optical fiber-based probe, the feasibility to achieve photoacoustic in vivo biopsy has been investigated. In comparison with optical spectroscopy based needle biopsy, the photoacoustic biopsy may cover larger areas of tissue and, more importantly, could evaluate histological microstructures in tissues. Moreover, with optical fibers integrated into the biopsy needle, the trajectory and position of the needle could be visualized clearly in B-scan US by picking up the photoacoustic signal generated at the fiber tip. Using this compound guiding technique, the problem of poor needle visualization faced by conventional US can be

**Conference 9323: Photons Plus Ultrasound:
Imaging and Sensing 2015**

solved. Our initial experiments on tissues and phantoms have demonstrated the better performance of this compound needle guidance technique. On the US B-scan mode, the needle disappeared when the angle between the needle and the probe surface was larger than 30°. On the compound guiding mode where the photoacoustic signals from the optical fiber were monitored in US, the needle could be visualized without any problem even when the angle between the needle and the probe surface was larger than 75°.

9323-100, Session PSun

Texture generation in compressional photoacoustic elastography

Julian W. Schmid, Univ. Wien (Austria) and Medizinische Univ. Wien (Austria); Thomas Widlak, Univ. Wien (Austria); Behrooz Zabihian, Medizinische Univ. Wien (Austria); Thomas Glatz, Univ. Wien (Austria); Mengyang Liu, Wolfgang Drexler, Medizinische Univ. Wien (Austria); Otmar Scherzer, Univ. Wien (Austria) and Radon Institute of Computational and Applied Mathematics (Austria)

Elastography is a coupled imaging technique that visualizes the elastic properties of tissue. In experiments this is realized by applying a mechanical force and measuring the resulting displacement. Common imaging modalities used for elastography are ultrasound, optical coherence tomography and magnetic resonance imaging, while photoacoustics has not been used as a stand-alone elastography modality but in conjunction with ultrasound elastography. The reason that photoacoustics is not used in single mode elastography is the weak speckle, which complicates the use of tracking and optical flow algorithms. However, while conventional ultrasound only uses a single frequency, photoacoustics operates with a broad frequency spectrum. We are therefore able to generate texture by using only a frequency band limited part of the recorded data, which after inversion reveals speckle.

In this work we apply a well defined static compression to a phantom, laterally and axially. Pre- and post compression data are recorded via a Fabry-Pérot interferometer planar sensor setup. Non-uniform-fast-Fourier reconstructions are applied for imaging. The displacement vector fields, between pre and post compressed data are then computationally determined via optical flow and block-matching algorithms from truncated, band limited measurement data. While the implementation of texture generation during post processing reduces image quality overall, it turns out that it improves the detection of moving patterns and is therefore better suited for elastography.

9323-101, Session PSun

Early detection of melanoma with the combined use of acoustic microscopy, infrared reflectance and Raman spectroscopy

Georgios T. Karagiannis, Univ. of Thessaly (Greece) and Ormylia Foundation (Greece); Giannis Grivas, Anastasia Tjigotzidou, Aristotle Univ. of Thessaloniki (Greece); Georgios K. Apostolidis, Ifigeneia Grigoriadou, ORMYLIA Art Diagnosis Ctr. (Greece); Ioanna Dori, Argyrios Doumas, Kyriaki-Nefeli Poulatsidou, Aristotle University of Thessaloniki (Greece); Stefan Wesarg, Fraunhofer-Institut für Graphische Datenverarbeitung (Germany); Panagiotis Georgoulas, Univ. of Thessaly (Greece)

Melanoma cancer has not only rapidly increased, but also is fatal due to fast metastasis. Thus, early detection is deemed crucial. The objective of

the current study is to detect melanoma as early as possible combining acoustic microscopy, infrared (IR) and Raman spectroscopies. Acoustic microscopy provides with information about the 3D structure, whereas, both spectroscopic modalities give qualitative insight of biochemical changes occurring as melanoma evolves.

Firstly, propagation of ultrasonic and electromagnetic waves in skin and melanoma simulated structures were performed in order to efficiently set up the final devices.

Secondly, with the aforementioned modalities synthetic and grape extract melanin injected in depth of the order of hundreds of μm were scanned. Concerning the acoustic microscopy, both cases were scanned with central operating frequencies of 110MHz and 175MHz resulting to the tomographic imaging of the simulated tumor while with the spectroscopic modalities, IR and Raman the differences among spectra of clear and melanin injected cases were identified in depth of the skin.

Thirdly, highly invasive SK-MEL-28 skin melanoma cells were used to cultivate real melanoma in immunocompromised NOD/SCID mice. On the cultivated tumors acoustic microscopy and spectroscopy were applied.

The growing of the tumor within three weeks was displayed using acoustic microscopy. Moreover, at the same time, the changes of the infrared and Raman spectra were observed and studied between the healthy skin and the melanoma infected one. The most significant changes between the healthy skin and the melanoma area were observed in the range of 900-1800 cm^{-1} and 350-2000 cm^{-1} respectively.

9323-102, Session PSun

Longitudinal multi-wavelength photoacoustic imaging of MCF-7 xenograft tumors with inducible tyrosinase expression

Robert J. Paproski, Univ. of Alberta (Canada); Andrew Heinmiller, VisualSonics Inc. (Canada); Roger J. Zemp, Univ. of Alberta (Canada)

We have previously shown that the tyrosinase (TYR) gene, involved in melanin production, can be used as a reporter gene for photoacoustic imaging. In the current study, we developed MCF-7 breast cancer xenograft tumors in mice which have inducible expression of TYR by adding doxycycline to animal drinking water. Induction of TYR expression caused visibly dark tumors. Tumors were imaged with a VisualSonics Vevo LAZR system (21 MHz transducer) before and 1 week after administration of 1 mg/mL doxycycline drinking water. Ultrasound/photoacoustic data were overlaid and estimated relative melanin and oxygen saturation levels were determined. A new constrained least squares algorithm ensured positivity of concentrations and physiological oxygen saturation levels. Only tumors containing the TYR gene demonstrated significantly increased photoacoustic signal within the tumor and only after doxycycline administration. At 680 nm, contrast ratios for melanin levels between +/- TYR tumors were ~7 while unmixing the photoacoustic signals using images from multiple wavelengths (680, 700, 750, 800, 850, 900, and 950 nm) allowed relative estimated melanin contrast ratios of ~40 between +/- TYR tumors. Estimations of cells and photoacoustic signal per voxel suggest that mere tens of TYR-expressing cells could be visualized with our system. Animals were euthanized, exsanguinated, and imaged again which verified that the photoacoustic signal in the tumors was primarily due to melanin and not blood. Melanin derived photoacoustic signal variability within tumors matched that of the visible melanin patterns in the excised tumors, suggesting that photoacoustic imaging of TYR is a powerful tool for imaging gene expression.

**Conference 9323: Photons Plus Ultrasound:
Imaging and Sensing 2015**

9323-103, Session PSun

Comparing blanket illumination vs scanned-mosaicing imaging schemes for wide-area photoacoustic tomography

Quinn Barber, Tyler Harrison, Roger J. Zemp, Univ. of Alberta (Canada)

Photoacoustic tomography of the breast has previously been demonstrated using powerful lasers with widefield illumination. We hypothesized that spot-scanned illuminations would prove advantageous over blanket illumination because locally higher fluence could be achieved. For each illumination, a locally high-SNR image patch is reconstructed then mosaicked with image patches from other illuminations. In a given area, a single pulse with fluence Φ may produce sufficient SNR (say SNR_{min}) at a given depth, whereas averaging with initial diffused fluence Φ/N (where N is the illumination area divided by the initial beam footprint) would require N^2 laser shots to attain SNR_{min} , because averaging N^2 times would be required to attain an SNR improvement of N . This is in contrast to the scanned beam approach, which would use N rather than N^2 laser shots to attain the minimum acceptable SNR. Of course, this simple argument requires some modification in practice because as spot size is decreased, the fluence area coverage will be more limited at significant depths. A Monte Carlo simulation as a function of beam-spot size is performed to quantify this trade-off. We experimentally test both blanket illumination and the scanned-mosaicing scheme using a 256-element ring array with 8-cm diameter and 5MHz center frequency. Signals from the ring-array are read-out using a Verasonics ultrasound platform with programmable time-gain compensation. Breast-mimicking phantoms are imaged to experimentally compare imaging performance. Besides SNR advantages, the scanned-mosaicing approach offers more robustness to motion artifacts because it mitigates averaging during tissue motion.

9323-104, Session PSun

Tissue type characterization using photoacoustic power spectrum, a feasibility study

Behnoosh Tavakoli, Seth Goldstein, Jin U. Kang, Johns Hopkins Univ. (United States); Michael A. Choti, The Univ. of Texas Southwestern Medical Ctr. at Dallas (United States); Emad M. Boctor, Johns Hopkins Outpatient Ctr. (United States)

The development of techniques capable of non-invasive characterization of tissue can significantly improve diagnostic and therapeutic interventions. In this study we investigated the feasibility of a noninvasive method based on a photoacoustic (PA) approach for characterizing biological tissues. The power spectrum of photoacoustic signal induced by a pulsed laser light from tissue was analyzed and features were extracted to study their correlation with tissue biomechanical properties. The measurement was performed in the transmission mode with a wideband hydrophone while a tunable Q-switched Nd:YAG pulsed laser was used for illumination. For a controlled study, tissue mimicking gelatin phantoms with different densities and same optical absorptions were used as targets. The correlation between gelatin concentration of such phantoms and their mechanical properties were validated independently with a dynamic machine analyzer. It was shown that PA spectrums were shifted towards higher frequencies by increasing gelatin concentration. In order to quantify this effect, signal energy in two intervals of low and high frequency ranges were calculated. Gelatin concentration was correlated with PA energy in high frequency range with $R^2=0.91$. Subsequently, PA signals generated from freshly resected human thyroid specimens were measured and analyzed similarly. We found that malignant thyroid tissue contain approximately 1.5 times lower energy in the high frequency range in comparison to normal thyroid tissue ($p<0.01$). This ratio increased with increasing illumination wavelength

from 700 nm to 900nm. In summary, this study demonstrated the feasibility of using photoacoustic technique for characterizing tissue based on these biomechanical changes.

9323-105, Session PSun

Hybrid optoacoustic and ultrasound imaging in three dimensions and real time by optical excitation of a passive element

Thomas F. Fehm, Technische Univ. München (Germany); Xosé Luis Deán-Ben, Helmholtz Zentrum München GmbH (Germany); Daniel Razansky, Technische Univ. München (Germany)

Pulse-echo ultrasound and optoacoustic imaging possess very different yet highly complementary advantages of mechanical and optical contrast in living tissues. Integration of pulse-echo ultrasound with optoacoustic imaging may therefore significantly enhance the potential range of clinical applications. Nonetheless, efficient integration of these modalities remains challenging owing to the fundamental differences in the underlying physical contrast, optimal signal acquisition and image reconstruction approaches. We report on a new method for hybrid three-dimensional optoacoustic and pulse-echo ultrasound imaging based on passive generation of ultrasound with a spherical optical absorber, thus avoiding the hardware complexity of active ultrasound generation. The proposed approach allows for acquisition of complete hybrid datasets with a single laser interrogation pulse, resulting in simultaneous rendering of ultrasound and optoacoustic images at a rate of 10 volumetric frames per second. Real time image rendering for both modalities is enabled by using parallel GPU-based implementation of the reconstruction algorithms. Performance is first characterized in tubing phantoms followed by in-vivo measurements in healthy human volunteers, confirming general clinical applicability of the method.

9323-106, Session PSun

Needle visualization using photoacoustic effect

Hyun Jae Kang, Xiaoyu Guo, Alexis Cheng, Michael A. Choti, Emad M. Boctor, Johns Hopkins Univ. (United States)

Medical ultrasound (US) imaging is frequently used for interventional tool tracking in the operation room since it provides real-time data visualization, is mobile, and is harmless for the patient and the operator. Moreover, needle visualization and localization are very important for the safety and success of needle biopsy surgery or thermal ablation surgery. However, the exact localization of a needle-tip is difficult to achieve because the needle usually generates noise artifacts such as refraction and shadowing on the brightness mode (B-mode) image. To overcome this limitation, we propose a novel needle visualization using the photoacoustic (PA) effect to enhance needle-tip tracking.

In this research, an optical fiber and laser source are used to generate acoustic waves inside a needle with the PA effect. The PA phenomenon converts light energy to acoustic waves through optical absorption, localized thermal excitation, and localized pressure transient of a target material. Contrary to piezoelectric materials, this method does not require high driving voltage to generate acoustic pulses. Acoustic waves generated at the needle surface with the emission of laser from the optical fiber. They travel along the needle and some amount of acoustic energy leaks into the surrounding material. The leakage of acoustic waves is captured by a conventional US transducer and US channel data collection system. US beamforming and envelope detection algorithms are applied to the collected channel data to generate a PA image. The needle-tip can be visualized more clearly in this PA image than a general US B-mode image.

**Conference 9323: Photons Plus Ultrasound:
Imaging and Sensing 2015**

9323-107, Session P Sun

A micromachined silicon parallel acoustic delay line (PADL) array for real-time photoacoustic tomography (PAT)

Young Y. Cho, Cheng-Chung Chang, Texas A&M Univ. (United States); Lihong V. Wang, Washington Univ. in St. Louis (United States); Jun Zou, Texas A&M Univ. (United States)

To achieve real-time photoacoustic tomography (PAT), massive transducer arrays and data acquisition (DAQ) electronics are needed to receive the PA signals simultaneously, which results in complex and high-cost ultrasound receiver systems. To address this issue, we have developed a new PA data acquisition approach using acoustic time delay. Optical fibers were used as parallel acoustic delay lines (PADLs) to create different time delays in multiple channels of PA signals. This makes the PA signals reach a single-element transducer at different times. As a result, they can be properly received by single-channel DAQ electronics. However, due to their small diameter and fragility, using optical fiber as acoustic delay lines poses a number of challenges in the design, construction and packaging of the PADLs, thereby limiting their performances and use in real imaging applications.

In this paper, we report the development of new silicon PADLs, which are directly made from silicon wafers using advanced micromachining technologies. The silicon PADLs have very low acoustic attenuation and distortion. A linear array of 16 silicon PADLs were assembled into a handheld package with one common input port and one common output port. To demonstrate its real-time PAT capability, the silicon PADL array (with its output port interfaced with a single-element transducer) was used to receive 16 channels of PA signals simultaneously from a tissue-mimicking optical phantom sample. The reconstructed PA image matches well with the imaging target. Therefore, the silicon PADL array can provide a 16^x reduction in the ultrasound DAQ channels for real-time PAT.

9323-108, Session P Sun

Photoacoustic imaging with rotational compounding for improved signal detection

Alexander Forbrich, Univ. of Alberta (Canada) and FujiFilms VisualSonics Inc. (Canada); Andrew Heinmiller, FujiFilms VisualSonics Inc. (Canada); Jithin Jose, FujiFilms VisualSonics Inc. (Netherlands); Andrew Needles, Desmond Hirson, FujiFilms VisualSonics Inc. (Canada)

Photoacoustic imaging is a rapidly evolving field that combines the high depth-to-resolution ratio afforded by acoustic imaging with optical-based contrast. Due to the strong absorbance and unique absorption spectrum of hemoglobin, photoacoustic imaging has proven useful for non-invasively visualizing the vascular network and evaluating physiologically important properties including local blood oxygen saturation and consumption, in vivo. Unfortunately, many ultrasound transducers are sensitive to a very limited angular range and preferentially detect signals from structures lying perpendicular to the axis of the transducer. Several techniques have been explored to overcome this limitation including by using ring arrays as detectors and by using a tomographic approach to reconstruct the images.

We present a unique imaging scheme that combines a linear array transducer with a rotational stage which provides 180 degree rotation and a lateral scanning stage which enables three dimensional imaging. Motor controls are fully integrated into the ultrasound system (Vevo[®] LAZR, VisualSonics) enabling image acquisition at various angular positions. The collected images are combined to form a rotational compounded image. We characterize the signal-to-noise ratio (SNR) and resolution using phantom studies. In vivo imaging studies were conducted on the hindlimb of mice

and various organs, including the kidney and brain, to further assess image quality. For a scan covering 100 degrees with 10 degrees step size, we found that the SNR increased by ~3 fold. Furthermore, sidelobe and reverberation artifacts were substantially reduced. With this technique, blood vessels could be visualized that could not be detected in a single image.

9323-109, Session P Sun

New potentials in design and driving of acousto-optic scanners used in two-photon microscopes

Pál A. Maák, Budapest Univ. of Technology and Economics (Hungary); Gergely Katona, Femtonics Ltd. (Hungary); Gergely Szalay, Institute of Experimental Medicine (Hungary); Máté Veress, Femtonics Ltd. (Hungary); Balazs J. Rózsa, Institute of Experimental Medicine (Hungary)

The true 3D scanning possibilities revealed by acousto-optic scanning and focusing revolutionized the field of scanning laser microscopy. We have built custom acousto-optic scanners for two-photon microscopes to investigate biological samples in vitro and in vivo. Detailed computational modeling of the acousto-optic effect and the microscope optical system allows continuous improvement of the microscope parameters.

We report here modeling and experimental results that demonstrate that the scanning speed can be increased by special drive sequences applied to the acousto-optic devices. These contain specially engineered frequency chirps adapted to the optical relay between the deflectors. Moreover, modeling also shows that special 3D trajectories can be also programmed without considerable change in the excitation spot distribution thus maintaining optical resolution. This needs to apply special acoustic frequency chirps. In this way the measurement speed can be at least ten times bigger than that of the raster scanning, where the pixel dwell time is determined by the acoustic velocity. We present optical design considerations used to also correct optical aberrations by programming the appropriate driving functions.

We also present new design aspects of acousto-optic deflectors that allow more homogeneous optical aperture and optical wavelength tunability without mechanical movement and loss in angular range. These include new crystallographic orientations, application of multiple transducers and new electric matching methods of the transducers. Wavelength tunable systems allow the use of several fluorescent dyes or genetically encoded fluorescent proteins. The proper design of these devices helps to minimize material dispersion, optical complexity and total equipment costs.

9323-110, Session P Sun

Label-free optical-resolution photoacoustic endomicroscopy in vivo

Joon-Mo Yang, Chiye Li, Washington Univ. in St. Louis (United States); Ruimin Chen, The Univ. of Southern California (United States); Bin Rao, Junjie Yao, Amos Danielli, Konstantin I. Maslov, Washington Univ. in St. Louis (United States); Qifa Zhou, Koping Kirk Shung, The Univ. of Southern California (United States); Lihong V. Wang, Washington Univ. in St. Louis (United States)

Intravital microscopy techniques have become increasingly important in biomedical research because they can provide unique microscopic views of various biological or disease development processes, such as tumor growth, in situ. In recent years, several groups working in biomedical photoacoustics have pursued the development of optical-resolution photoacoustic endomicroscopy (OR-PAE) systems. However, all the reported image demonstrations are limited to phantoms or are ex vivo because the imaging probes were not fully encapsulated. In this study, we developed

**Conference 9323: Photons Plus Ultrasound:
Imaging and Sensing 2015**

the first fully-encapsulated OR-PAE system that enables visualization of internal organs with a much finer resolution than conventional acoustic-resolution photoacoustic endoscopy (AR-PAE) systems in vivo. We utilized the previous scanning mirror and micromotor-based built-in scanning mechanism for stable mechanical scanning and also applied the same ultrasonic ring transducer-based confocal optical-illumination and acoustic-detection mechanism for more efficient photoacoustic signal detection. However, by employing gradient index (GRIN) lens-based optical focusing, we significantly improved the transverse resolution to as fine as $\sim 10 \mu\text{m}$, which is about a ten-fold improvement in spatial resolution over conventional AR-PAE systems, at an optical working distance of 6.5 mm and an acoustic working distance of 4.3 mm. We quantified the imaging performance of this OR-PAE system and acquired the first in vivo imaging data from a rat colon. In this presentation, we introduce our OR-PAE system and discuss its future application directions.

9323-111, Session PSun

Quantitative assessment of photoacoustic tomography systems integrating clinical ultrasound transducers using novel tissue-simulating phantoms

William C. Vogt, Congxian Jia, Keith A. Wear, Brian S. Garra, T. Joshua Pfefer, U.S. Food and Drug Administration (United States)

Photoacoustic Tomography (PAT) systems based on commercial ultrasound instruments have the benefit of dual-modality imaging, which increases their appeal from a clinical standpoint. However, factors that influence PAT system performance have not been thoroughly investigated and standardized test methods have not been established for image quality evaluation. To address these issues we have adapted phantom-based approaches from ultrasound imaging standards and implemented them to assess a PAT system developed for vascular imaging. Our system comprises a tunable near-infrared pulsed laser and a commercial ultrasound system, including three interchangeable linear array clinical ultrasound transducers with varying acoustic bandwidths and geometries. Phantoms consisted of a customized PVC plastisol gel that accurately simulates both optical and acoustic properties of breast tissue. One phantom incorporates a sub-resolution filament array suitable for bimodal ultrasound-photoacoustic imaging, while another contains an array of hemoglobin-filled cylindrical inclusions at various depths. Key performance characteristics were evaluated, including spatial resolution, signal uniformity, field of view, signal-to-noise ratio, and penetration depth. These characteristics were evaluated over wavelengths of 700-900 nm and radiant exposures up to ANSI safety limits. Effects of transducer properties on imaging performance were evaluated. Axial and lateral resolution ranged from 0.33-0.52 mm and 0.75-0.97 mm, respectively, and penetration depths from 1.0-2.5 cm were achieved. Phantom test results are compared to measurements of hemoglobin-filled tubes embedded in chicken breast. These results demonstrate variation in PAT system performance based on clinical transducer selection, as well as the utility of realistic phantom-based test methods in performing benchtop evaluations of system performance.

9323-112, Session PSun

Three-dimensional photoacoustic and ultrasonic endoscopic imaging of a rabbit esophagus

Joon-Mo Yang, Christopher P. Favazza, Junjie Yao, Washington Univ. in St. Louis (United States); Ruimin Chen, Qifa Zhou, Koping Kirk Shung, The Univ. of Southern California (United States); Lihong V. Wang, Washington Univ. in St. Louis (United States)

The seamless addition of photoacoustic endoscopy to conventional endoscopic ultrasound will improve diagnosis of gastrointestinal tract diseases. In this study, using a 3.8-mm diameter dual-mode photoacoustic and ultrasonic endoscopic probe, we performed ex vivo imaging of an intact rabbit esophagus and correlated the acquired images with histology to investigate photoacoustic and ultrasonic image features of the esophageal wall and its neighboring region without the effects of motion artifacts. With the full resolving power of the endoscopic device, we acquired the first in situ three-dimensional vasculature map of the esophagus and mediastinum, along with coregistered tissue density information (at present, to the best of our knowledge, no other reported photoacoustic endoscopic systems are capable of volumetric intra-luminal imaging in situ). Blood vessels with apparent diameters as small as $\sim 190 \mu\text{m}$ were photoacoustically resolved without the aid of any contrast agent. More importantly, with the dual-modal photoacoustic and ultrasonic imaging capability of the system, we were able to better identify and characterize the detailed anatomic structures of the esophageal lumen, such as the mucosal and submucosal layers in the esophageal wall. We believe these results indicate photoacoustic endoscopy's strong clinical potential for imaging vasculatures important to esophagectomy procedures and esophageal diseases, such as Barrett's esophagus. In this presentation, we will talk about the clinical potential of this dual-modal endoscopic technique and discuss directions for future technology development toward use in clinical settings.

9323-113, Session PSun

Analysis of current ultrasound: optical tomography systems in an epi-illumination mode

Joseph L. Hollmann, Charles A. DiMarzio, Northeastern Univ. (United States)

The ability to focus light in most tissue degrades quickly with depth due to high optical scattering. Researchers have investigated using both ultrasound (US) and light synergistically to overcome this difficulty. The US beam modulates diffuse light propagating through its waist. Spatial information may be obtained by isolating the modulated signal.

However, a small fraction of the optical power is modulated by the US beam. Detecting the signal requires isolating the modulated and rejecting the unmodulated light. Several systems have been demonstrated experimentally in a transmissive geometry. Detection of US modulated diffusive light is difficult to achieve in an epi or reflective geometry and presents a substantial hurdle for the technology's adoption for clinical applications.

This paper will utilize a recently developed Green's function for US-modulated diffuse light to analyze the performance of existing experimental systems to evaluate their suitability for a reflective geometry. The paper will also determine the maximum theoretical imaging depth for these experimental system in both transmissive and epi geometries.

9323-114, Session PSun

Wide-field two-dimensional multifocal optical-resolution photoacoustic computed microscopy

Jun Xia, Guo Li, Lidai Wang, Mohammadreza Nasirivanaki, Konstantin I. Maslov, John Engelbach, Joel R. Garbow, Lihong V. Wang, Washington Univ. in St. Louis (United States)

Optical-resolution photoacoustic microscopy (OR-PAM) is an emerging technique that directly images optical absorption in tissue at high spatial resolution. To date, the majority of OR-PAM systems are based on single focused optical excitation and ultrasonic detection, limiting the wide-field imaging speed. While one-dimensional multifocal OR-PAM (1D-MFOR-PAM) has been developed, the potential of microlens and transducer

**Conference 9323: Photons Plus Ultrasound:
Imaging and Sensing 2015**

arrays has not been fully realized. Here, we present the development of two-dimensional multifocal optical-resolution photoacoustic computed microscopy (2D-MFOR-PACM), using a 2D microlens array and a full-ring ultrasonic transducer array. The $10 \times 10 \text{ mm}^2$ microlens array generates 1800 optical foci within the focal plane of the 512-element transducer array, and raster scanning the microlens array yields optical-resolution photoacoustic images. The system has improved the in-plane resolution of a full-ring transducer array from $\geq 100 \mu\text{m}$ to $29 \mu\text{m}$ and achieved an imaging time of 36 seconds over a $10 \times 10 \text{ mm}^2$ field of view. In comparison, the 1D-MFOR-PAM would take more than 4 minutes to image over the same field of view. The imaging capability of the system was demonstrated on phantoms and animals both ex vivo and in vivo.

9323-115, Session PSun

Photoacoustic measurement of targeted cellular delivery of gold nanoparticles

Wei Qian, IMRA America, Inc. (United States); Chao Tian, Zhixing Xie, Xia S. Shao, Xueding Wang, Univ. of Michigan (United States)

Gold nanoparticles have been an attractive choice for contrast enhancing agent for photoacoustic imaging due to their high optical absorption cross-section, which leads to four to six orders of magnitude stronger absorption compared to conventional fluorescent markers. Over the past decade, it is an area of intense research of using gold nanoparticles conjugated with certain targeting ligands specific for cell surface receptors in the photoacoustic imaging to develop a very sensitive technique for many biomedical applications, for example, the early detection of cancer cells and visualizing cellular processes at the molecular level. However, the dependence of the photoacoustic signal from cells after being incubated with this kind of gold nanoparticles on density of cell targeting ligands bound to the surface of individual nanoparticles has not been characterized yet. In this presentation, we investigated such dependence by using RGD peptidated-conjugated gold nanoparticles and human prostate carcinoma DU145 cell line. In our experiment, a series of samples of DU 145 cells were prepared via the overnight incubation of these cells in cell culture medium containing equal concentration of RGD-peptide conjugated gold nanoparticles only differing in the density of RGD peptide immobilized onto individual nanoparticles. Photoacoustic measurements of these cells revealed that the photoacoustic signal approached the maximum at the certain density of RGD peptide bound onto nanoparticles and then decreased as we continued to increase surface density of RGD peptide. This observation is very significant to the design and preparation of Au nanoparticles as photoacoustic imaging contrast agents with the maximum performance.

9323-31, Session 5

In vivo intravascular photoacoustic imaging of atherosclerotic arteries in Ossabaw swine

Pu Wang, Purdue Univ. (United States); Teng Ma, The Univ. of Southern California (United States); Shanshan Liang, Beckman Laser Institute and Medical Clinic (United States); Mikhail Slipchenko, Spectral Energies, LLC (United States); Jie Hui, Purdue Univ. (United States); Rebecca Bruning, Indiana Univ. (United States); Sukesh Roy, Spectral Energies, LLC (United States); Michael Sturek, Indiana Univ.-Purdue Univ. Indianapolis (United States); Qifa Zhou, The Univ. of Southern California (United States); Zhongping Chen, Beckman Laser Institute and Medical Clinic (United States); Ji-Xin Cheng, Purdue Univ. (United States)

Vulnerable atherosclerotic plaques possess a high risk of rupture and thrombosis, which accounts for the majority of fatal cardiovascular events. Current medical imaging technologies are not able to accurately assess plaque stability due to various limitations, including the lack of chemical selectivity. Without chemical selectivity, the ability to accurately monitor disease progression and the efficacy of therapeutic interventions is limited. Photoacoustic imaging using the intrinsic contrast from harmonic vibration of C-H bonds allows selective mapping of lipids deposition inside the arterial wall. However, there is no existing photoacoustic imaging system that can perform high-speed in vivo selective chemical imaging of lipid deposition within the arterial wall. We herein demonstrate a high-speed photoacoustic imaging system based on a KGW-based Raman laser with 1 KHz repetition rate with 1730 nm excitation wavelength. This system allows the imaging of an atherosclerotic artery at speed of 4 frames per second, 2 order of magnitude faster than the current available systems.

9323-32, Session 5

Toward minimally invasive optical-resolution photoacoustic endomicroscopy with a fluid-filled capillary

Olivier Simandoux, Institut Langevin (France); Nicolino Stasio, Ecole Polytechnique Fédérale de Lausanne (Switzerland); Jérôme Gateau, Lab. Kastler-Brossel, CNRS (France) and Institut Langevin (France); Jean-Pierre Huguinard, Jphopto (France); Christophe Moser, Demetri Psaltis, Ecole Polytechnique Fédérale de Lausanne (Switzerland); Emmanuel Bossy, Institut Langevin (France)

Optical-resolution photoacoustic endomicroscopy (OR-PAE) goes beyond the limited penetration depth and large footprint of conventional optical-resolution photoacoustic microscope (OR-PAM). In current OR-PAE devices, bundles of single-mode fibers are used to focus light and the generated photoacoustic waves are detected after propagation back through tissue (therefore with a limited imaging depth for high frequency photoacoustic waves). In this work, we introduce the use of a fluid-filled silica capillary as a minimal footprint device to both guide the illumination pulse into the tissue and guide the photoacoustic waves outside the tissue. As a proof-of-principle, we first demonstrate that high-frequency photoacoustic signals generated by raster-scanning a focused pulsed nanosecond beam through a microscope objective can be guided by the capillary to form an optical-resolution photoacoustic image through the tissue. Specifically, an optical-resolution photoacoustic image of a $30 \mu\text{m}$ diameter absorbing nylon thread was obtained by guiding the acoustic waves in a 30 mm long capillary ($150 \mu\text{m}$ inner diameter, $330 \mu\text{m}$ outer diameter) through a 3cm thick pork fat layer. The transmission loss through the capillary was -20 dB, much lower than the measured -120 dB acoustic attenuation through the fat layer around 20 MHz. Second, we demonstrate that both light and ultrasound can be respectively injected and detected through the same proximal tip of the capillary. By use of digital-phase conjugation through multi-mode optical waveguide, as introduced for OR-PAM in [Papadopoulos et al, APL 102(21), 2013], the proposed capillary has the potential to provide optical-resolution photoacoustic sensing with a passive distal tip inserted in the tissue.

9323-33, Session 5

Catheter-based photoacoustic endoscope for use in the instrument channel of a clinical video endoscope

Joon-Mo Yang, Chiye Li, Washington Univ. in St. Louis (United States); Ruimin Chen, Qifa Zhou, Koping Kirk Shung, The Univ. of Southern California (United States); Lihong V. Wang, Washington Univ. in St. Louis (United States)

**Conference 9323: Photons Plus Ultrasound:
 Imaging and Sensing 2015**

We have developed a fully-sheathed, flexible shaft-based, mechanical scanning photoacoustic endoscopy (PAE) system for imaging the human gastrointestinal tract via the instrument channel of a clinical video endoscope [Yang et al., Journal of Biomedical Optics 19(6), 066001 (2014)]. Building such a catheter endoscope is an important step in advancing biomedical photoacoustics into clinical settings. In this study, by applying a single element ultrasonic transducer and flexible shaft-based proximal actuation mechanism, which is commonly utilized in many clinical endoscopic ultrasound imaging miniprobes, we successfully created a catheter-based photoacoustic endoscope with a 3.2 mm diameter and ~2.5 m long flexible section. Also, by using a mechanical drive for scanning mirror rotation at the proximal part of the imaging probe, we greatly reduced the rigid distal section length of the imaging probe, to ~16 mm, about two times shorter than in previous micromotor-based endoscopic probes. We deliver laser pulses through a rotating optical fiber coaxially placed inside the flexible shaft, and transmit electric signals from an ultrasonic transducer through a static signal wire that is affixed on the outer surface of a plastic sheath. To the best of our knowledge, this is the first PAE system that has been fully encapsulated in a plastic catheter and sufficiently miniaturized to be usable for endoscopic imaging via the 3.7-mm diameter instrument channel of a standard clinical video endoscope. In this talk, we present our experimental results that demonstrate the intra-instrument channel workability and in vivo animal imaging capability of the new PAE system, and we discuss future technology development directions.

9323-34, Session 5
**Laser-scanning optical resolution
 photoacoustic microscopy using a Fabry
 Perot fibre optic sensor**

Thomas J. Allen, Edward Z. Zhang, Paul C. Beard, Univ.
 College London (United Kingdom)

The frame rate limitations of mechanically scanned optical resolution photoacoustic microscopy (ORPAM) can be overcome by optically scanning a focused excitation beam using an x-y galvanometer scanner and detecting the photoacoustic signals with a single stationary planar detector offset from the scan area. Such a method allows for high frame rates to be obtained (a few seconds for an image of 400X400 pixels). So far this method has been implemented using a relatively large planar PZT detector but this has several drawbacks; (1) it is not optimal for detecting the spherical waves produced by a focused excitation beam and (2) its directional response restricts the imaging field of view (FOV).

An alternative would be to use a small diameter (<100µm) detector, which would provide a much less directional response allowing for a large FOV to be obtained and minimise spatial averaging of the incident acoustic wave. Such a detector could also be placed in close proximity to the imaged area, reducing the path length the acoustic wave has to travel and therefore mitigating the attenuating effects of the inverse square law. However it is challenging to achieve sufficiently high sensitivity with sub-100µm element sizes using piezoelectric receivers since detection sensitivity scales with active area. Fabry-Perot based fibre optic ultrasound sensors do not suffer from this limitation and can provide very high detection sensitivity (NEP<10Pa over a 25 MHz measurement bandwidth) with an optically defined element size as small as 10µm. This suggests they have the potential to outperform piezoelectric detectors for Laser-Scanning Optical Resolution Photoacoustic Microscopy (LS-ORPAM). To investigate this, a Fabry Perot fibre optic ultrasound sensor was combined with a LS-ORPAM system. In a first instance, a phantom study was undertaken to evaluate the imaging system. Then to demonstrate the full potential of the imaging system, the microvasculature of a mouse ear was imaged.

9323-35, Session 5
**Amplitude-masked photoacoustic
 wavefront shaping and application in
 flowmetry**

Jinyang Liang, Jian Wei Tay, Ashton S. Hemphill, Lihong V.
 Wang, Washington Univ. in St. Louis (United States)

Photoacoustic flowmetry (PAF) is a non-invasive measurement technique that has been demonstrated to be useful for single-cell sensing. In PAF, photoacoustic (PA) signals, which are generated upon the absorption of pulsed laser light, are used. To resolve single cells, PAF requires high spatial resolution, which is commonly achieved using optical focusing. However, at depths beyond one optical transport mean free path (in the diffusive regime), light propagating in optically scattering media becomes diffused, making direct focusing impossible. This diffusion confines the operational depth of PAF to ~1 mm in soft tissue. Optical diffusion also reduces the amount of light arriving at the region of interest, reducing the detection signal-to-noise ratio (SNR).

In this paper, we report on a proof-of-principle demonstration showing that PA-based wavefront shaping can be used to extend the operational depth of PAF into the diffusive regime. Specifically, we used a digital micromirror device (DMD) for binary-amplitude masking to enhance light focusing in the presence of scattering. Here, the transmission modes that contributed constructively to the fluence at the optical focus were first identified and then selectively illuminated. By controlling 1024 independent DMD segments, the fluence at the optical focus was enhanced by 14 times. This fluence increase gave a corresponding increase in measurement SNR, allowing single particle flow speeds to be measured in scattering media. This technique can potentially extend the operational depth of PAF to the diffusive regime in tissue.

9323-36, Session 5
**Frequency response optimised fiber
 optic photoacoustic imaging probes for
 endoscopic applications**

Edward Z. Zhang, Sunish J. Mathews, Adrien E. Desjardins,
 Paul C. Beard, Univ. College London (United Kingdom)

Miniature photoacoustic probes are required for a number of important clinical applications in which the target tissue can only be accessed by introducing an endoscopic probe percutaneously or through a natural orifice. Among these applications are the assessment of cancers in the prostate and the guidance of interventional procedures such as needle biopsies. The design of a photoacoustic probe for endoscopic applications poses several challenges using conventional piezoelectric based receivers. These include the question of how to integrate the delivery optical fibre with the ultrasound receiver to avoid obscuring the excitation laser pulses, obtaining the necessary level of miniaturisation and achieving low unit cost for single use applications. To address these challenges, a range of miniature all-optical laser micromachined photoacoustic probes which employ a transparent Fabry Perot ultrasound sensor at the tip of an optical fibre have been developed. This approach offers unprecedented levels of miniaturisation with probe diameters as small as 100µm, inexpensive fabrication using vacuum deposition and laser processing techniques and the potential to be combined with other imaging modalities such as OCT and pulse-echo ultrasound. Two types of probe have been developed. A forward viewing probe for guiding interventional procedures such as needle biopsies and a sideviewing imaging probe for visualising the interior of hollow anatomical structures such as the urinary or biliary tracts. Both probes provide sub-kPa noise equivalent pressures and an acoustic bandwidth extending to 50MHz and have been evaluated using a variety of tissue phantoms and ex vivo tissues. Furthermore, measures have been taken to optimise the acoustic frequency of fibre optic FP sensor probes, which result in significant reduction in temporal signal distortions commonly associated with needle hydrophones due to diffraction, ringing etc. The

**Conference 9323: Photons Plus Ultrasound:
Imaging and Sensing 2015**

unprecedented levels of miniaturisation and performance that this approach offers the prospect of opening up a new class of minimally invasive photoacoustic applications not available to existing methods.

9323-37, Session 5

Orthogonal Fabry-Pérot sensor array system for minimal artifact photoacoustic tomography

Robert J. Ellwood, Edward Z. Zhang, Paul C. Beard, Benjamin T. Cox, Univ. College London (United Kingdom)

Photoacoustic images of exquisite quality have been obtained using planar Fabry-Pérot (FP) ultrasound sensor arrays, due to their ability to detect with high sensitivity over small element sizes (10s μm). However, their planar geometry – chosen for ease of manufacture and interrogation – gives rise to limited-view artifacts in the images, and prevents exact reconstruction. In this work, the use of a novel V-shaped sensor configuration to overcome this limitation and provide near artifact-free, full-view imaging of unprecedented image quality, is described. The two planar FP sensors, mounted orthogonally, were addressed using a galvanometer-based optical interrogation system and aligned using a novel mechanical linkage. As there are no exact, one-step, reconstruction algorithms for this open-surface measurement configuration, images were reconstructed iteratively by computing the successive terms of a Neumann series using numerical time reversal. Each time reversed iteration was implemented using a computationally efficient k-space acoustic propagation code, k-Wave. Three-dimensional photoacoustic images of phantoms, including black ribbons and ink-filled tubes, and ex vivo images of the mouse brain and abdominal organs, will be presented to demonstrate the superior quality of the images over those obtained using a single planar array. The nature of this sensor configuration, in particular the open measuring platform, makes it ideal for high resolution, high quality, whole body preclinical imaging.

9323-38, Session 6

Mitigation of the effect of inaccurate ultrasonic transducer responses on image reconstruction in photoacoustic computed tomography

Mark A. Anastasio, Qiwei Sheng, Kun Wang, Lihong V. Wang, Washington Univ. in St. Louis (United States)

Photoacoustic computed tomography (PACT) is an emerging computed imaging modality that exploits optical contrast and ultrasonic detection principles to form images of the absorbed optical energy density within tissue. When the imaging system employs conventional piezoelectric ultrasonic transducers, the photoacoustic (PA) signals are convolved with the transducers' acousto-electric impulse responses (EIRs) before being sampled and recorded. If unaccounted for, this will result in a modulation of the spatial frequency components of the reconstructed image. In principle, the effect of the EIRs on the measured PA signals can be removed via deconvolution; images can be reconstructed subsequently by application of a reconstruction method that assumes an idealized EIR. Alternatively, the EIR can be incorporated into a discrete imaging model to compensate for its effect implicitly during reconstruction. In either case, image quality can be limited by noise and other errors in the assumed EIRs. In this work, a joint optimization approach to PACT image reconstruction is proposed for mitigating errors in reconstructed images that are caused by use of an inaccurate EIR. The method exploits the separable nature of the imaging model and seeks to refine the measured EIR during the process of reconstructing the sought after absorbed optical energy density. When an array of transducers is employed that is characterized by a collection of EIRs, the reconstruction method will determine a single effective EIR. Computer-simulation and experimental studies are conducted to illustrate the effectiveness of the proposed scheme.

9323-39, Session 6

Image reconstruction of multi-channel photoacoustic and laser-ultrasound data using reverse time migration

Jami L. Johnson, The Univ. of Auckland (New Zealand); Jeffrey Shragge, The Univ. of Western Australia (Australia); Kasper van Wijk, The Univ. of Auckland (New Zealand)

The unique physics of photoacoustic imaging has motivated many new approaches to image reconstruction. However, complications such as limited view geometries, acoustic heterogeneity, and detector limitations remain challenges for accurate reconstruction. We propose a new reconstruction algorithm for photoacoustic and laser-ultrasound imaging based on reverse time migration (RTM), a depth imaging algorithm originally developed for seismology. RTM inherently handles strong velocity heterogeneity and complex propagation paths. Successful RTM results in enhanced signal-to-noise, accurately located structures, and minimal artifacts. Laser-ultrasound begins with a source wavefield generated at the surface that propagates through the sample. Acoustic scatterers in the propagation path give rise to a scattered wavefield, which travels to the surface and is recorded by an acoustic detector. To reconstruct the laser-ultrasound image, a synthetic source function is forward propagated and cross-correlated with the recorded (scattered) wavefield to image the scatterers at the correct location. Conversely, photoacoustic waves are generated by chromophores within the sample and propagate "one-way" to the detection surface. Therefore, we utilize the velocity model validated by the laser-ultrasound reconstruction to accurately reconstruct the photoacoustic image with RTM. This approach is first validated with simulations, where inclusions behave both as a photoacoustic source and an acoustic scatterer. Subsequently, we demonstrate the capabilities of RTM with tissue phantom experiments using an all-optical, multi-channel acquisition geometry.

9323-40, Session 6

Accelerated iterative image reconstruction in three-dimensional photoacoustic tomography

Fatima Anis, Yang Lou, Kun Wang, Washington Univ. in St. Louis (United States); Richard Su, Tanmayi Oruganti, André Conjusteau, Sergey A. Ermilov, Alexander A. Oraevsky, TomoWave Laboratories, Inc. (United States); Mark A. Anastasio, Washington Univ. in St. Louis (United States)

Photoacoustic tomography (OAT), also known as photoacoustic computed tomography, has found many biomedical applications. Because they can model complicated imaging physics, compensate for imperfect data acquisition systems, and exploit prior information regarding the object, iterative image reconstruction algorithms, in general, produce higher quality images than do analytical image reconstruction algorithms. However, three-dimensional (3D) iterative image reconstruction is computationally burdensome. Even with graphics processing unit (GPU)-accelerated implementations, to our knowledge, it still takes at least five hours to reconstruct the 3D volume of a whole-body mouse. This computational burden greatly hinders the application of advanced image reconstruction algorithms to applications with a large field-of-view (FOV), such as breast imaging.

In this study, an improved GPU-based implementation of a numerical imaging model and its adjoint have been developed for use with general gradient-based iterative image reconstruction algorithms. Particularly, two types of computation-reduced discretization methods are employed; a parallel fast Fourier transform (FFT) algorithm is employed to accelerate the calculation of the temporal convolution with ultrasonic transducer responses; and a volume-reduction method is proposed to reduce the

**Conference 9323: Photons Plus Ultrasound:
 Imaging and Sensing 2015**

computation for applications with irregular FOV. Both computer-simulation and experimental studies are conducted to investigate the efficiency and accuracy of the proposed implementation. The results suggest that the proposed implementation is more than five times faster than previous implementations. Using the proposed implementation, a 3D whole-body mouse image can be reconstructed in less than one hour. The developed algorithm is also evaluated for 3D OAT breast imaging with sub millimeter resolution.

9323-41, Session 6

Frequency analysis of the photoacoustic signal generated by coronary atherosclerotic plaque

Min Wu, Verya Daeichin, Erasmus MC (Netherlands); Antonius F. W. van der Steen, Erasmus MC (Netherlands) and Interuniversity Cardiology Institute of The Netherlands (Netherlands) and Delft Univ. of Technology (Netherlands); Gijs van Soest, Erasmus MC (Netherlands)

The identification of vulnerable atherosclerotic plaques in the coronary artery is emerging as an important tool for guiding percutaneous coronary interventions, and may enable preventive treatment of such plaques in the future. The structure and composition of the plaque are significant determinants of its vulnerability. Spectroscopic photoacoustic (sPA) imaging can visualize the atherosclerotic plaque composition on the basis of the optical absorption contrast. It is an established fact that the frequency range of the PA signal is correlated with the structural tissue properties. As PA signals can be weak, it is important to match the transducer sensitivity to the signal frequency content for in-vivo imaging. In this ex vivo study on human coronary arteries, we combined sPA imaging and analysis of frequency component of its PA signals. Utilizing a broadband PVDF transducer (-3 dB one-way bandwidth of 10-35 MHz) with a 1mm needle hydrophone (calibrated for 0.25-20 MHz) in the setup, we covered a large frequency range (0.25-35 MHz) for receiving the PA signal. sPA imaging was performed at wavelengths ranging from 1125 to 1275 nm with a step of 2 nm, allowing discrimination between plaque lipids and adventitial tissue. Guided by the sPA imaging, frequency content of the PA signal from the plaque lipids was quantified. Our data shows that more than 80% of the PA energy of the coronary plaque lipids lies in the frequency band below 10 MHz. This frequency information can guide the choice of the transducer element used for PA catheter fabrication as well.

9323-42, Session 6

Multispectral photoacoustic decomposition with localized regularization for detecting targeted contrast agent

Behnoosh Tavakoli, Ying Chen, Xiaoyu Guo, Hyun Jae Kang, Johns Hopkins Univ. (United States); Martin Pomper, The Johns Hopkins Hospital (United States); Emad M. Boctor, Johns Hopkins Outpatient Ctr. (United States)

Targeted contrast agents can improve sensitivity of imaging systems for cancer detection and monitoring the treatment. In order to accurately detect contrast agent concentration from photoacoustic images, we developed a decomposition algorithm to separate photoacoustic absorption spectrum into components from individual absorbers. In this study, we evaluated novel prostate-specific membrane antigen (PSMA) targeted agents for photoacoustic imaging. The agents YC-39 and YC-27 were synthesized through conjugating PSMA-targeting urea with two optical dyes, ICG and IRDye800CW, respectively. In our preliminary PA study, dyes were injected in a thin wall plastic tube embedded in an agar gel phantom. The tube

was illuminated with pulsed laser light using a tunable Q-switch ND-YAG laser. PA signal along with the B-mode ultrasound images were detected with a linear ultrasound probe in orthogonal mode. PA spectrum of each dye at 1 to 50 μM concentrations were estimated using the maximum PA signal extracted from images which were obtained at different illumination wavelengths. The peak wavelengths for YC-39 and YC-27 occurred at approximately 790 nm and 780 nm respectively while YC-39 showed generally higher PA signal at the same concentrations. Subsequently, we used nonnegative linear least square optimization method along with localized regularization to solve the spectral unmixing. The algorithm was tested by imaging mixture of those dyes. The concentration was estimated with less than 20% error for the mixture composed of 50 μM of each dye albeit the small separation between dyes spectrum.

9323-43, Session 6

Tracking photoacoustic signal by clinical ultrasound systems using inverse beamforming method

Xiaoyu Guo, Hyun Jae Kang, Alexis Cheng, Ralph Etienne-Cummings, Emad M. Boctor, Johns Hopkins Univ. (United States)

In recent years photoacoustic (PA) tracking technologies have been investigated for medical applications. As a combination of optical and ultrasonic (US) technique, laser beams are delivered with the surgical tools, the generated PA signal can be used for localization in the US domain. However, one of problems preventing it from clinical applications is the requirement of customized US systems. To localize the PA signal source, pre-beamforming data directly acquired from each probe element is required. In most clinical US systems, hardware beamformers are implemented to process the raw data, so users only have access to the beamformer output. The beamformer is designed for B-mode imaging, which has a different image formation than the PA imaging. In this work, we focus explicitly on the method to convert the clinical US system beamformer output back to the pre-beamforming data for photoacoustic applications. A system independent inverse-beamforming method has been proposed. In this approach, PA light source is synchronized with an US system operating in the conventional B-mode, the transmission is turned off. An inverse-beamforming program receives the data from the US system, convert it back to the pre-beamforming data, and localize the signal source positions. Pre-beamforming data directly collected by a DAQ system is used as the ground truth. Localization errors are measured by comparing the corresponding signal center in the DAQ and the inverse-beamformed images. The results proved that inversed-beamforming is capable to reconstruct the pre-beamforming data for the PA tracking application with a signal source localization error less than 7 μm .

9323-44, Session 6

Photoacoustic reconstruction using beamformed RF data: a synthetic aperture imaging approach

Haichong K. Zhang, Xiaoyu Guo, Hyun Jae Kang, Emad M. Boctor, Johns Hopkins Univ. (United States)

Photoacoustic (PA) imaging is becoming an important tool for various clinical and pre-clinical applications. Acquiring pre-beamformed channel ultrasound data is essential to reconstruct PA images. Accessing these pre-beamformed channel data requires custom hardware to allow parallel beam-forming, and is available for only few research ultrasound platforms. However, post-beamformed radio frequency (RF) data is readily available in real-time and in several clinical and research ultrasound platforms. To broaden the impact of clinical PA imaging, our goal is to devise new PA reconstruction approach based on these post-beamformed RF data. In this paper, we propose to generate PA image by using a single receive focus

**Conference 9323: Photons Plus Ultrasound:
Imaging and Sensing 2015**

beamformed RF data. These beamformed RF data are considered as pre-beamformed input data to a synthetic aperture beamforming algorithm, where the focal point per received RF line is a virtual element. To validate this approach, a set of channel data was used as ground truth, and receive-beamformed RF data with a single focal point were generated from this channel data. Proposed beamforming algorithm was applied afterwards, and full width at half maximum (FWHM) of a reconstructed point source was examined. As a result, our proposed method showed a consistent performance producing FWHM of 1.14 mm, 0.86 mm, and 0.79 mm, for receive aperture elements of 17, 33, and 65, respectively. At the same time, the channel data were beamformed using conventional delay and sum with dynamic focusing for comparison, and FWHM of 1.11 mm was measured.

9323-45, Session 7

Photoacoustic tomography using a single xenon flash lamp

Terence T. W. Wong, Yong Zhou, Alejandro Garcia-Uribe, Lei Li, Konstantin I. Maslov, Lihong V. Wang, Washington Univ. in St. Louis (United States)

Lasers have been especially useful for photoacoustic imaging/spectroscopy. Lasers offer high power, high spatial and temporal coherency, and highly collimated, short pulsed illumination. However, they are not cheap or easily maintained, hampering their application in clinical systems.

As a possible alternative to lasers, here we explore using a single xenon flash lamp as the illumination source for photoacoustic tomography. In photoacoustic tomography, the key factors in choosing an illumination source are energy and temporal pulse width. A high energy produces strong enough acoustic wave for detection, and a short temporal pulse width provides high image resolution. Thus, the xenon flash lamp, a high power and micro-second pulsed lamp, is a good fit for photoacoustic tomography. We demonstrate that by using a single xenon flash lamp, we can image different biologically related phantoms, e.g., a breast phantom, which consists of a phantom embedded in a homogenous background made by mixing 50% lard, 2.5% agar and 47.5% water to mimic the fatty tissue of a human breast. With this safe illumination, xenon flash lamps can thus potentially be used for in vivo human breast cancer study. Note that multiple lamps can also be employed to increase the signal-to-noise ratio or the imaging field-of-view.

9323-46, Session 7

Multimodal Raman-photoacoustic imaging for detection and multiplex biomarker assessment of magnetically-trapped circulating tumor cells with single-cell detection capabilities

Wei Shi, Robert J. Paproski, Roger J. Zemp, Univ. of Alberta (Canada)

Detection of circulating tumor cells (CTCs) is challenging due to low concentration in blood. Also specificity of CTC detection is critical to avoid false detection. In our previous studies, we developed a Raman imaging system employing both surface-enhanced-Raman-scattering nanoparticles (SERS NPs) for SERS detection of CTCs and magnetic NPs for enrichment of pre-labelled CTCs. Using two types of NPs could potentially improve the specificity of CTC detection. Additionally free nanoparticles will not be detected with this approach since only CTCs targeted with both SERS and magnetic NPs will be trapped and detected.

We presently demonstrate that single CTCs can be detected in whole blood using our Raman and magnetic approach. We target NPs to folate receptor and other cell-surface antigens both in cell growth media and in whole blood without pre-targeting. Not only can we detect single cells,

but we can profile tumor cell phenotypes by using multiplexed targeting of SERS NPs which can be spectrally unmixed with effectively no crosstalk. Multi-modality Raman-photoacoustic imaging provides capabilities to image blood vessel structures in vivo and to identify nanoparticle labelled CTCs.

SERS NPs with 60 nm gold core and a layer of SERS reporter encapsulated inside a 30 nm silica are used for generating multiplexing SERS signals, while MNPs with 500 nm maghemite core are used for magnetic enrichment of CTCs. Both nanoparticles are functionalized with thiol groups which enable easy conjugation of NPs to maleimide-folate-PEG and maleimide-PEG for further targeting to folate receptors of CTCs. Antibody labelling permits targeting other cell-surface receptors as well. In our multimodality imaging system, SERS imaging subsystem is based on a Raman spectrometer with an EMCCD. The minimum detectable SERS NP concentration is ~ 1 pM and the maximum imaging depth in tissue mimic system is ~ 2.5 mm. We demonstrate that this sensitivity is sufficient for detecting single CTCs. The photoacoustic imaging subsystem uses a 50 MHz ultrasound transducer and a 10 Hz Q-switch laser with ~ 50 - μ m lateral spatial resolution.

In our studies, rat blood is first mixed with high folate receptor expression HeLa cells. SERS NPs and MNPs are then added and the mixed fluid flows inside tygon tubing pumped by a syringe pump. A cone magnet is used to exert strong magnet filed gradient at the optical focus and ultrasonic focus of SERS and photoacoustic imaging subsystems. Co-registered imaging demonstrate the system can be used for trapping and detecting native targeted CTCs, and provide structural information of vasculature as well. We further demonstrate the ability to differentiate cell types using spectrally unmixed Raman signatures from multiplex-targeted CTCs.

We anticipate that the ability to trap and detect single CTCs and to profile their phenotype could have considerable potential in ex vivo and in vivo studies of metastasis.

9323-48, Session 7

Ultra-sensitive plano-convex optical microresonator detectors for deep tissue photoacoustic imaging

James A. Guggenheim, Jing Li, Edward Z. Zhang, Paul C. Beard, Univ. College London (United Kingdom)

Currently, most photoacoustic scanners employ piezoelectric detectors. However, piezoelectric detectors suffer from two key limitations. First, they are optically opaque which inhibits backward mode operation. Second, it can be difficult to achieve adequate detection sensitivity with element sizes that are small enough to provide a near-omnidirectional response as required by most tomographic image reconstruction algorithms. For example, element sizes on a scale of a few tens of microns are required for an omnidirectional response at MHz frequencies. Planar Fabry-Perot (FP) ultrasound sensing etalons can overcome both of these limitations and have proved extremely effective for superficial (<1 cm) imaging applications. To achieve small element sizes (<100 μ m), the etalon is illuminated with a focused laser beam. However, this has the disadvantage that beam walk-off due to the divergence of the beam fundamentally limits the etalon finesse and thus sensitivity - in essence, the problem is one of insufficient optical confinement. To overcome this issue, a novel planoconvex FP sensor has been developed featuring an array of ink-jet printed micro-domes, whose curvatures match the interrogation laser wavefront. This affords significantly better confinement of the beam, and therefore higher finesse and sensitivity. In addition, the flexibility of the fabrication method used permits tailoring the sensor thickness and thus its acoustic bandwidth to match the required imaging penetration depth. To illustrate this, a range of sensor arrays with bandwidths ranging from 3MHz to 20MHz have been fabricated and characterised in terms of their noise equivalent pressure (NEP), frequency response, directivity and effective acoustic element size. Unprecedentedly high sensitivity has been achieved. For example, for a 250 μ m thick planoconvex sensor with a -3dB bandwidth of 5MHz, the NEP was 4 Pa. This NEP is comparable to that provided by mm scale piezoelectric detectors used for breast imaging applications but with broader bandwidth, more uniform frequency response characteristics and an order-of-magnitude

**Conference 9323: Photons Plus Ultrasound:
Imaging and Sensing 2015**

smaller element size. This new approach offers the prospect of bringing the advantages of optical ultrasound detection to clinical breast imaging and other deep tissue photoacoustic imaging applications previously the preserve of piezoelectric based detection schemes.

9323-49, Session 7

Assessment of bone mineral density via thermal photoacoustic measurement

Ting Feng, Nanjing Univ. (China); Kenneth M. Kozloff, Univ. of Michigan Medical School (United States); Cheri Deng, Univ. of Michigan (United States); Jie Yuan, Sidan Du, Nanjing Univ. (China); Xueding Wang, Univ. of Michigan Medical School (United States)

Development of safe and effective technologies for screening, early diagnosis, and sensitive therapeutic monitoring is critically important for prevention and management of osteoporosis. Photoacoustic (PA) imaging, as a functional and chemical imaging technology, may allow sensitive and objective evaluation of osteoporosis and responses to therapies by monitoring molecular and biochemical markers of bone turnover. In this work, a new technique named thermal photoacoustic (TPA) measurement has been studied, and its potential application in assessment of bone health has been explored. Unlike conventional PA techniques, TPA is targeting the change in PA signal intensity as a function of the sample temperature, i.e. the temperature dependent Grüneisen parameter which is closely associated with the chemical properties in the sample. We found that PA signal intensities from organic tissues rose obviously when the temperature increases; while the signals from non-organic mineral has little change with the temperature. Based on this, quantified TPA measurement has potential for objective assessment of bone mineral density (BMD) and loss as a result of osteoporosis. In an experiment on three groups of rat tibia bones with different BMD, PA measurement from each bone was conducted over a temperature range from 37 °C to 44 °C. The trend of PA intensity change vs. temperature, i.e. the TPA slope, was then quantified for each bone. The experiment result shows that osteoporosis samples have higher TPA slope which can be used to distinguish the disease bone specimens from the normal ones. PA findings are confirmed by the gold standard microCT.

9323-50, Session 7

Imaging and sensing based on dual-pulse nonlinear photoacoustic contrast: a preliminary study on fatty liver

Chao Tian, Univ. of Michigan Health System (United States); Zhixing Xie, Univ. of Michigan Medical School (United States); Mario Fabiilli, Univ. of Michigan Health System (United States); Xueding Wang, Univ. of Michigan Medical School (United States)

The feasibility of photoacoustic (PA) imaging presenting a new contrast based on the dual-pulse nonlinear PA effect in biological tissues has been investigated. When the first laser pulse is illuminated on a sample, an instant temperature rise due to the local optical energy deposition is induced which will affect the PA signal amplitude from the second laser pulse that is fired quickly after the first one. The difference in PA signal intensity from the second pulse with and without the firing of the first pulse will then be a function of several parameters, including the pulse energies and the wavelengths of the 1st and the 2nd pulses, the tissue optical absorption coefficients at the two wavelengths, and the delay between the two pulses. Unlike classic PA imaging techniques which mostly target the mapping of optical absorption in biological samples, the new contrast from the dual-pulse excitation process can reflect the temperature dependent Grüneisen parameter which is closely associated with the chemical contents in the tissue. As an example, the thermal photoacoustic characteristics of water-

rich tissues and lipid-rich tissues are highly different due to their difference in temperature dependent Grüneisen parameters. Based on this difference, dual-pulse nonlinear photoacoustic contrast could be used to diagnosis of a variety of diseases, such as non-alcoholic fatty liver disease. Our preliminary experiments on phantoms and rat liver models have demonstrated that the new contrast can effectively distinguish samples with different lipid contents, and holds potential for diagnosis and grading of fatty liver.

9323-51, Session 7

Photoacoustic-guided optical wavefront shaping in scattering media with improved performances

Thomas Chaigne, Jérôme Gateau, Ori Katz, Institut Langevin (France) and Lab. Kastler-Brossel, CNRS (France); Emmanuel Bossy, Institut Langevin (France); Sylvain Gigan, Lab. Kastler-Brossel, CNRS (France) and Institut Langevin (France)

In biological tissue, light scattering limits the penetration depth of most optical imaging techniques to a few hundred micrometers. In the last few years, wavefront shaping appeared as a powerful tool to compensate light scattering and focus light in deep tissue. However it requires a feedback signal that monitors the light intensity on the target. In most practical scenarios, one cannot directly place a photodetector at the target position. Photoacoustic imaging has been investigated to provide such a feedback and to perform controlled focusing deep inside scattering media. We recently demonstrated light focusing using photoacoustic feedback from an ultrasound array and a transmission-matrix approach [Chaigne et al, Opt. Letters 39(9), 2014; Chaigne et al, Nat. Photonics 8, 2014]. The first challenge to apply this technique in practical situation is the millisecond decorrelation time in tissue. The second challenge is the mismatch between the acoustic resolution (tens of micrometers) and the speckle grain size inside tissue (fractions of micrometers): the modulation of the photoacoustic feedback signal vanishes when too many speckle grains are contained within one acoustic resolution cell. We report on the use of improved instrumentation to address these issues. We use a 200Hz repetition rate laser, which is able to almost follow the decorrelation of the scattering sample. We also use a Spatial Light Modulator with both high-resolution and high damage threshold, in order to benefit from a large number of input modes and increased SNR.

9323-52, Session 7

Forward-viewing multi-element photoacoustic probe for 3D endoscopy

Rehman Ansari, Edward Z. Zhang, Adrien E. Desjardins, Paul C. Beard, Univ. College London (United Kingdom)

There is considerable interest in the development of photoacoustic endoscopy probes (PAE) for the clinical assessment of pathologies such as those in the gastrointestinal (GI) tract. However, most previous PAE probes integrate mechanical scanners and piezoelectric transducers at the distal end which can be technically complex, expensive and pose challenges in achieving the necessary level of miniaturisation. We present a novel all-optical multi-element forward-viewing endoscopic probe operating in tomography mode that has the potential to overcome these limitations. It comprises a transparent Fabry-Pérot ultrasound sensor deposited at the tip of a flexible, coherent fibre-optic bundle. The distal end of the probe is fitted with relay optics that deliver interrogation light to different locations on the Fabry-Pérot sensor. In this way, the sensor acts as a 2D array of ultrasound detectors at the tip of the bundle. The pulsed excitation laser beam is full-field coupled into the fibre bundle at the proximal end and uniformly illuminates the tissue at the tip. In order to record the photoacoustic waves arriving at the probe tip, the proximal end of the fibre bundle is optically scanned in 2D with a CW wavelength-tunable interrogation laser beam

**Conference 9323: Photons Plus Ultrasound:
Imaging and Sensing 2015**

thereby interrogating different spatial points on the sensor. A time-reversal image reconstruction algorithm was used to reconstruct a 3D image from the detected signals. Miniature 3D imaging probes with a range of outer diameters ranging from 3 mm to 10 mm were constructed and evaluated using tissue phantoms and ex vivo tissues. This new approach to PAE offers several advantages over previous distal-end scanning probes. These include a high degree of miniaturisation, no moving parts at the distal end and simple and inexpensive fabrication with the potential to realise disposable probes for clinical imaging of the GI tract.

9323-53, Session 7

Lifetime-weighted photoacoustic imaging

Roger J. Zemp, Alexander Forbrich, Peng Shao, Wei Shi,
Univ. of Alberta (Canada)

It has previously been shown that photoacoustic imaging can interrogate lifetimes of exogenous agents by a sequence of pulses with varying pump-probe delay intervals. Rather than attempt to unmix molecules based on their composite lifetime profile, we introduce a technique called lifetime weighted imaging (LWI), which preferentially weights signals from chromophores with long lifetimes (including exogenous contrast agents such as Methylene Blue and porphyrins with microsecond-scale lifetimes) while nulling chromophores with short lifetimes (including hemoglobin with ps-scale lifetimes). A probe beam is used to interrogate samples with or without a pump beam. By subtracting probe-beam photoacoustic signals with pump- from those without a pump excitation, we effectively eliminate probe signals from chromophores with short lifetimes while preserving excited-state photoacoustic signals from long-lifetimes. This difference signal will be weighted by a decaying exponential function of the pump-probe delay divided by the exogenous agent lifetime. Pulsed or modulated CW lasers at 660-680nm (near an absorption peak of our agents) were used as a pump excitation source. A pulsed probe beam at ~810nm was used to image exogenous agents (including methylene blue and porphyrin-lipid nanoparticles) while rejecting signals from blood. Furthermore, oxygen-dependent lifetimes of the porphyrin-based nanoparticles is demonstrated. LWI could be used for photodynamic therapy dosimetry guidance, oxygen sensing, or other molecular imaging applications.

9323-54, Session 7

**Simplified axial sectioning in
photoacoustic microscopy via transient
absorption**

Scott P. Mattison, Brian E. Applegate, Texas A&M Univ.
(United States)

Photoacoustic microscopy (PAM) is a hybrid imaging modality that combines optical illumination with ultrasonic detection to achieve absorption contrast imaging of chromophores. Optical resolution PAM achieves high lateral-resolution through tight focusing of excitation light; however the axial resolution is typically defined by the bandwidth of the ultrasonic transducer used for detection. As a result, PAM images have highly asymmetric point-spread functions with submicron lateral resolution and axial resolution typically limited to tens of microns. We have previously reported on a resonant multiphoton approach to PAM called transient absorption ultrasonic microscopy (TAUM), which enables axial resolution defined by the optical excitation. By frequency encoding the photoacoustic signal at the overlap of a pump and a probe beam, TAUM enables photoacoustic imaging with subcellular resolution on par with other multiphoton microscopy techniques. Here, we report on an innovation that enables TAUM imaging with a much less sophisticated optical system than previously reported. If we allow the time delay between the pump and probe to collapse to zero, the pump and probe optical paths can be combined. An amplitude modulator in the single beam path is sufficient to encode the TAUM signal at the second harmonic of the modulation frequency. The resulting system is essentially a standard optical resolution

PAM system that incorporates an amplitude modulator and utilizes a Fourier post processing algorithm to provide axial resolution defined by the optical diffraction limit.

9323-55, Session 7

**In vivo optical-resolution photoacoustic
remote sensing microscopy**

Parsin Haji Reza, Roger J. Zemp, Univ. of Alberta (Canada)

In most photoacoustic and ultrasound imaging systems piezoelectric transducers have been employed, in which an ultrasound coupling medium such as water or ultrasound gel is required. However for many applications such as burn diagnostics, surgery, wound healing and many endoscopic procedures physical contact, coupling, or immersion is undesirable or impractical. We propose a novel new imaging technology which we call photoacoustic remote sensing (PARS). A pulsed fiber laser in visible range is focused to produce micron-scale focal spots to generate photoacoustic signals. The acoustic signatures are interrogated using a long-coherence length (100 kHz linewidth and tunable wavelength of 1530-1570nm) probe beam co-focused with the excitation spot. Michelson interferometry and common path interferometry are used in order to remotely record the large local initial pressures from chromophores. Because signals are optically sensed locally where the photoacoustic signals are generated very high signal-to-noise ratio imaging is achieved. PARS images of carbon fiber networks with ~7µm diameter and in vivo chicken embryo capillaries network is shown. Our PARS microscopy system offers optical lateral resolution but is depth-limited to a transport mean-free path similar to optical-resolution photoacoustic microscopy. Phantom studies indicate ~5 µm resolution. Unlike previous non-contact photoacoustic imaging systems, the PARS is capable of in vivo imaging and offers optical resolution. PARS microscopy exhibited significantly higher signal-to-noise when compared to OR-PAM using piezoelectric transducers in phantom studies. We anticipate PARS with its confocal lateral resolution will make an impact on photoacoustic imaging approaches.

9323-56, Session 7

**Multi-frequency intravascular imaging
probe for ultrasound and frequency
domain photoacoustic imaging**

Robin F. Castelino, Univ. of Toronto (Canada) and
Sunnybrook Health Sciences Ctr. (Canada); Hyunggyun
Lee, Sunnybrook Research Institute (Canada); F. Stuart
Foster, Univ. of Toronto (Canada) and Sunnybrook Health
Sciences Ctr. (Canada)

Intravascular photoacoustic (IVPA) imaging has potential to characterize lipid-rich structures based on optical absorption contrast of tissues. Previously, we have demonstrated IVPA imaging with a continuous wave laser diode using the frequency domain photoacoustics approach, denoted FD-IVPA. A challenge to this technique, especially in intravascular applications, is to amplitude modulate light at high frequencies sensitive to the bandwidth (BW) of the detector. In this study, we develop a novel multi-frequency intravascular imaging prototype capable of simultaneous IVUS and FD-IVPA imaging. The probe consists of two back-to-back transducers viewing outward at 180 degrees with independent signal electrodes, sharing a common backing layer. The IVUS transducer has an active area of 0.5mm by 0.5mm and centered at 40MHz (35% BW). The active area of the FD-IVPA transducer is 1mm by 1mm, centred at 22MHz (60% BW) and co-aligned with a 400µm fiber delivering 1.5W over an amplitude modulated linear chirp from 16-25MHz. An agar vessel phantom with thin absorbing graphite rods was used showing an 14dB increase in PA signal of the targets when compared to the surrounding.

9323-57, Session 7

Broadband ultrasonic sensor array via optical frequency domain reflectometry

Haniel Gabai, Idan Steinberg, Avishay Eyal, Tel Aviv Univ. (Israel)

Distributed and broadband ultrasound detection has an enormous potential in biomedical imaging, since it has the ability to provide non-destructive, high resolution and functional imaging in deep tissues. Currently, the detection of ultrasonic fields is primarily implemented by piezoelectric detectors.

Despite their tremendous success in the field of ultrasound detection, piezoelectric detectors suffer from several inherent limitations; Detection sensitivity is determined by the size of the detector, hence, in cases where small detectors are needed, performing high quality measurements may become a challenging task. In addition, piezoelectric detectors are prone to electromagnetic disturbances and may not be effective in electromagnetically noisy environments. Arrays of piezoelectric elements require parallel hardware for amplification, conditioning and digitizing which can be costly and complex.

In this work, we introduce a fiber optic system which can overcome these inherent limitations of piezoelectric detectors. The proposed system is based on a recently developed optical frequency domain reflectometry (OFDR) design. It is advantageous in comparison to the traditional piezoelectric sensor arrays mainly in the following aspects. The sensing elements and their connecting cables are optical fibers which are practically immune to electromagnetic interference. The entire sensing array is multiplexed in the frequency domain and is connected to a single digitizing circuit. In addition the sensor array can be interrogated at very high rates.

The proposed method was demonstrated by multiplexing four ultrasonic sensors (bandwidth of ~5MHz each) using 1X4 fiber coupler. The sensing fibers were interrogated at kHz rates enabling real time measurement of dynamic processes.

9323-58, Session 7

Optoacoustic imaging in five dimensions

Xosé Luis Deán-Ben, Sven Gottschalk, Thomas F. Fehm, Daniel Razansky, Helmholtz Zentrum München GmbH (Germany)

Here we report on development of a handheld optoacoustic imaging system capable of acquiring volumetric optoacoustic data in real time. The system is based on simultaneous acquisition of optoacoustic signals from 512 different tomographic projections by means of a spherical matrix array. Thereby, volumetric reconstructions can be done at high frame rate, only limited by the pulse repetition rate of the laser. The developed tomographic approach presents important advantages over previously reported systems that use scanning for attaining volumetric optoacoustic data. First, dynamic processes, such as the biodistribution of molecular probes, can be monitored in the entire volume of interest. Second, out-of-plane and motion artifacts that could degrade the image quality when imaging living specimen can be avoided. Finally, real-time 3D performance can obviously save time required for experimental and clinical observations. Finally, the feasibility of optoacoustic imaging in five dimensions, i.e. real time acquisition of volumetric datasets at multiple wavelengths, is reported. In this way, volumetric images of spectrally resolved chromophores are rendered in real time, thus offering an unparalleled imaging performance among the current bio-imaging modalities. This performance is subsequently showcased by video-rate visualization of *in vivo* biodistribution of contrast agents in mouse brain and handheld visualization of blood oxygenation in deep human vessels. The newly discovered capacities open new prospects for translating the optoacoustic technology into highly performing imaging modality for biomedical research and clinical practice with multiple applications envisioned, from cardiovascular and cancer diagnostics to neuroimaging and ophthalmology.

9323-59, Session 7

Three-dimensional multispectral hand-held optoacoustic imaging with microsecond-level delayed laser pulses

Xosé Luis Deán-Ben, Erwin Bay, Daniel Razansky, Helmholtz Zentrum München GmbH (Germany)

Three-dimensional hand-held optoacoustic imaging comes with important advantages that prompt the clinical translation of this modality, with applications envisioned in cardiovascular and peripheral vascular disease, disorders of the lymphatic system, breast cancer, arthritis or inflammation. Of particular importance is the multispectral acquisition of data by exciting the tissue at several wavelengths, which enables functional imaging applications. However, multispectral imaging of entire three-dimensional regions is significantly challenged by motion artefacts in concurrent acquisitions at different wavelengths. A method based on acquisition of volumetric datasets having a microsecond-level delay between pulses at different wavelengths is described in this work. This method can avoid image artefacts imposed by a scanning velocity greater than 2 m/s, thus, does not only facilitate imaging influenced by respiratory, cardiac or other intrinsic fast movements in living tissues, but can achieve artifact-free imaging in the presence of more significant motion, e.g. abrupt displacements during handheld-mode operation in a clinical environment.

9323-60, Session 7

A real-time ultrasonic field mapping system using a Fabry Perot single pixel camera for 3D photoacoustic imaging

Nam Trung Huynh, Edward Z. Zhang, Marta Betcke, Simon R. Arridge, Paul C. Beard, Benjamin T. Cox, Univ. College London (United Kingdom)

Broadband ultrasound sensor arrays for photoacoustic imaging and ultrasonic field mapping are typically limited either in terms of the number of array elements, by the need for sequential point scanning, or by the sampling rate. Here, a novel coherent-light single pixel camera, working within a compressive sensing framework, was used to interrogate a Fabry-Perot (FP) polymer film ultrasound sensor. FP sensor arrays have been shown to provide exquisite photoacoustic images. However, their interrogation using single point raster scanning leads to slow data acquisition times, and parallel detection using CCD or CMOS camera suffers from very slow sampling rates. Here, a digital micromirror device (DMD) was used to pattern widebeam light reflected from the sensor before it was collected into a single photodiode. By choosing an appropriate set of patterns, such as scrambled Hadamard, this pattern-based approach enables compressed sensing to be used. This means that if the field is sparse in some basis, it is only necessary to measure with a fraction of the total number of scrambled Hadamard patterns in order to be able to recover the full data set, facilitating rapid data collection. In addition, since a full 3D photoacoustic image can be reconstructed from the signals recorded by a single photodiode, this approach offers dramatically lower cost and technical complexity than a conventional array of ultrasound detectors. Results of both dynamic real-time ultrasound field mapping at up to 160Hz frame rate (32x32 pixels, using 12.5% of the complete set of patterns), and photoacoustic imaging of several phantoms will be shown. These preliminary results show that this completely new approach to ultrasound array measurements can dramatically increase data acquisition speed offering the prospect of achieving real-time 3D photoacoustic imaging at modest cost.

**Conference 9323: Photons Plus Ultrasound:
 Imaging and Sensing 2015**

9323-117, Session PMon

**Realistic photoacoustic image simulations
 of collections of solid spheres using linear
 array transducer**

Subhajit Karmakar, The Univ. of Burdwan (India); Eno Hysi, Michael C. Koliou, Ryerson Univ. (Canada); Ratan K. Saha, Saha Institute of Nuclear Physics (India)

A theoretical framework for photoacoustic (PA) image simulation of collection of fluid spheres using single element focused transducer has recently been developed. This particle-based approach has given considerable insight into the source of PA signals and has extensively been applied in probing red blood cell morphologies. Extending to more clinically-relevant transducers and absorber geometries would aid in testing new image reconstruction and processing algorithms aimed at improving sensitivity of PA imaging.

Numerical phantoms containing polystyrene beads were constructed using a Monte Carlo based method which randomly placed particles within the field of view of a 40 MHz, 256-element transducer. The particles were chosen to correspond to two different ultrasonic scatterer regimes, Rayleigh (1.8 μm) and Faran (7.4 μm). Illumination of each phantom was uniform and delay-and-sum beamforming was implemented to generate PA images using a 64-element sub-aperture. The frequency-domain and envelope statistics of PA radio-frequency lines were used to characterize the phantoms as well as examine the applicability of these ultrasound-derived techniques for PA tissue characterization.

The midband fit of the Faran phantom was 30 dB higher compared to the Rayleigh phantom while the generalized gamma scale parameter was 31x greater. The simulated results are in qualitative agreement with published experimental results on these same phantoms. Such simulation results suggest that the particle-based approach of PA simulations could be used in practice to simulate PA images of samples comprising discrete absorbers with regular shapes. This methodology has the potential to be applied to samples of irregular, non-uniform geometries.

9323-118, Session PMon

**Synergistic image reconstruction for
 hybrid ultrasound and photoacoustic
 computed tomography**

Thomas P. Matthews, Kun Wang, Lihong V. Wang, Mark A. Anastasio, Washington Univ. in St. Louis (United States)

Conventional PACT image reconstruction methods assume that the object and surrounding medium are described by a constant speed-of-sound (SOS) value. In order to accurately recover fine structures, SOS heterogeneities should be quantified and compensated for during PACT reconstruction. To address this problem, several groups have proposed hybrid systems that combine PACT with ultrasound computed tomography (USCT). In such systems, a SOS map is reconstructed first via USCT. Consequently, this SOS map is employed to inform the PACT reconstruction method. Additionally, the SOS map can provide structural information regarding tissue, which is complementary to the functional information from the PACT image.

We propose a paradigm shift in the way that images are reconstructed in hybrid PACT-USCT imaging. Inspired by our observation that information about the SOS distribution is encoded in PACT measurements, we propose to jointly reconstruct the absorbed optical energy density and SOS distributions from a combined set of USCT and PACT measurements, thereby reducing the two reconstruction problems into one. This innovative approach has several advantages over conventional approaches in which PACT and USCT images are reconstructed independently: (1) Variations in the SOS will automatically be accounted for, optimizing PACT image quality; (2) The reconstructed PACT and USCT images will possess minimal systematic artifacts because errors in the imaging models will be optimally balanced during the joint reconstruction; (3) Due to the exploitation of

information regarding the SOS distribution in the full-view PACT data, our approach will permit high-resolution reconstruction of the SOS distribution from sparse array data.

9323-119, Session PMon

**Full-wave iterative image reconstruction
 in transcranial photoacoustic computed
 tomography of the brain**

Kenji Mitsuhashi, Lihong V. Wang, Mark A. Anastasio, Washington Univ. in St. Louis (United States)

Photoacoustic computed tomography (PACT) holds great promise in transcranial brain imaging. However, the strong reflection, scattering, attenuation, and mode-conversion of photoacoustic waves in the skull pose serious challenges to establishing the method. The lack of an appropriate model of solid media in conventional PACT imaging models, which are based on the canonical scalar wave equation, causes a significant model mismatch in the presence of the skull and thus results in deteriorated reconstructed images. The goal of this study was to develop an image reconstruction algorithm that accurately models the skull and thereby ameliorates the quality of reconstructed images. The propagation of photoacoustic waves through the skull was modeled by a viscoelastic stress tensor wave equation, which was subsequently discretized by use of a staggered grid fourth-order finite difference time-domain (FDTD) method. The matched adjoint of the FDTD-based wave propagation operator was derived for implementing a backprojection operator. By use of this forward and backprojection operator pair, an iterative image reconstruction algorithm that seeks to minimize a total variation (TV)-regularized penalized least squares (PLS) cost function was implemented. Systematic computer simulations were conducted to demonstrate the effectiveness of the algorithm for use in a realistic three-dimensional PACT brain imaging system. The results suggest that the proposed algorithm can successfully reconstruct images from transcranially-measured pressure data and readily be translated to clinical PACT brain imaging applications.

9323-120, Session PMon

**Photoacoustic imaging of small organic
 molecule-based photoacoustic probe in
 subcutaneous tumor using P(VDF-TrFE)
 acoustic sensor**

Takeshi Hirasawa, Shinpei Okawa, National Defense Medical College (Japan); Mako Kamiya, Yasuteru Urano, The Univ. of Tokyo (Japan); Miya Ishihara, National Defense Medical College (Japan)

A photoacoustic (PA) molecular imaging using small organic molecule-based probes is discussed. Intrinsic photon absorbers such as hemoglobin are present as strong backgrounds. Thus, the methods to discriminate the probe signals from the backgrounds are required.

We have been using acoustic sensors made of P(VDF-TrFE) films, focusing on the broadband frequency spectra of PA signals. In this research, we developed a broadband acoustic sensor with uniform sensitivity in a frequency range of 0.5 – 20 MHz to acquire the probe signals with various frequencies. A multispectral PA imaging (MS-PAI) technique was used to discriminate the probe signals based on absorption spectra of the probes. The probes which were synthesized by our group were rhodamines and silicon-rhodamines whose absorption maximum appear at 495, 530, 645 nm, respectively. The probe discrimination capabilities of MS-PAI using the P(VDF-TrFE) sensor was evaluated, and then it was compared with that of a commercially available PZT sensor with central frequency of 20 MHz.

MS-PAIs of subcutaneous tumors of mice injected with the probes were performed. The probe discrimination capabilities were obtained from

**Conference 9323: Photons Plus Ultrasound:
 Imaging and Sensing 2015**

the relation of the probes concentrations and the intensities of the probe signals.

As results, the probe with absorption maximum at 645 nm was discriminated at highest discrimination capabilities. MS-PAI using the PZT sensor demonstrated lower discrimination capabilities to the probe at low concentration which produces low frequency signals, because the sensitivity decreases at low frequency.

The P(VDF-TrFE) sensor is advantageous because the probe discrimination capabilities are less affected by the probe signal frequencies.

9323-121, Session PMon
Photoacoustic imaging using NIR two-photon excitation for ultrasonic wave generation

Ben E. Urban Jr., Univ. of North Texas (United States)

We generated ultrasonic waves using two-photon (TP) excitation from a NIR femtosecond pulsed laser source. The expected quadratic relation of the generated ultrasonic waves and photoluminescence (PL) signal intensity to the laser fluence was experimentally verified using Rhodamine B fluorescent dye. A temporal pulse delay experiment was conducted to further verify the nonlinear relation. Attenuation of the nonlinear PA and PL signal intensity was compared by imaging a quartz capillary tube containing Rhodamine B in highly scattering media. Two dimensional nonlinear PA and PL cross-sectional images were compared at different scattering increments. Experimental results show the lower attenuation of the nonlinear PA signal, expressing the advantage of TP-PA imaging in highly scattering media. Finally, we stacked multiple two dimensional cross-sectional images, taken at 10 micrometer axial increments, to create a three dimensional image of the phantom in highly scattering media using TP-PA. Our results show the increase resolution of TP-PA over PA microscopy and lower attenuation as compared to TP-PL microscopy.

9323-122, Session PMon
In vivo dual modality cystography: photoacoustic and fluorescence imaging using indocyanine green

Sungjo Park, Jae-Won Song, Kyungpook National Univ. (Korea, Republic of); Jeesu Kim, Mansik Jeon, Chulhong Kim, Pohang Univ. of Science and Technology (Korea, Republic of)

Conventional cystography uses radio-opaque materials (X-ray contrast agent), but this method uses harmful ionizing radiation and are not sensitive. In this study, we demonstrate nonionizing and noninvasive photoacoustic (PA) and fluorescence (FL) cystography imaging using indocyanine green (ICG) in vivo. ICG has both optical absorption and fluorescence properties within a near-infrared spectrum (from 700 to 900 nm) where light can penetrate deeper. More importantly, ICG is approved by the Food and Drug Administration (FDA) and has been widely used in clinical applications. Using a custom-made PA and FL imaging systems, we have successfully imaged a rat's bladder filled with ICG. After transurethral injection of ICG through a catheter, the rat's bladders were photoacoustically and fluorescently visualized. The PA and FL amplitude was enhanced by approximately 1300 and 270 %, respectively. A deeply (i.e., beyond 1 cm) positioned bladder below the skin surface was clearly visible in the PA and FL image using a laser pulse energy of less than 2 mJ/cm² (1/15 of the safety limit). Then the in vivo imaging results have been validated through the ex vivo studies. Our results suggest that dual modal cystography imaging can provide a nonionizing and noninvasive for bladder mapping

9323-123, Session PMon
Quantitative photoacoustic tomography: estimating chromophore concentrations using a radiance Monte Carlo model

Roman Hochuli, Simon R. Arridge, Paul C. Beard, Benjamin T. Cox, Univ. College London (United Kingdom)

Estimating chromophore concentrations is one of the most challenging unsolved problems in photoacoustic imaging, and one that is of great importance in a broad range of clinical and pre-clinical applications. A promising approach is based on iteratively minimising the error between the data and a simulation. Previously, finite element (FE) implementations of the optical diffusion equation (DA) or the radiative transport equation (RTE) have been used as forward models in such iterative inversion schemes. However, the DA tends to be inaccurate in modelling the fluence near the source and the RTE has domain-scaling limitations due to excessive memory demands. Given the increased power and accessibility of parallel computing platforms, highly parallel algorithms such as Monte Carlo (MC) models are highly attractive. In this study, we present a novel MC code that, unlike traditional codes, computes spatially- and angularly-dependent radiance. Previously, MC simulation of the radiance was not possible due to the excessive memory requirements of discretising the domain both spatially and angularly; however, here, computational efficiency is maximised through angular discretisation in Fourier- and Legendre-bases, which affords compact storage of radiance fields and fast computation of functional gradients via an adjoint method. We demonstrate the computational benefits of spectral basis to perform angular discretisation relative to traditional discretisation techniques, and validate the 2D radiance MC (2D-RMC) model against a FE-RTE simulation. Finally, the 2D-RMC model is used to simulate the forward and adjoint radiance to compute functional gradients in an iterative inversion scheme used to estimate the absorption and scattering coefficients in simulated data. As MC can be straightforwardly implemented in 3D, this opens up a new computationally tractable route to high-resolution quantitative photoacoustic imaging.

9323-124, Session PMon
Multi-color high-resolution fluorescence imaging in deep tissue

Baohong Yuan, Bingbing Cheng, Ming-Yuan Wei, The Univ. of Texas at Arlington (United States); Venugopal Bandi, Univ. of North Texas (United States); Yanbo Pei, Yi Hong, Kytai T. Nguyen, The Univ. of Texas at Arlington (United States); Francis D'Souza, Univ. of North Texas (United States)

In biomedical optical imaging field, tissue with a depth of centimeters is usually considered deep tissue. Many unique tissue micro-events occur at such a depth, such as microcirculation, tumor micro-metastasis, etc. Therefore, it is highly desirable to noninvasively, clearly and simultaneously image multiple micro-events in deep tissue. This is because it not only provides details about tissue's structural, functional, and molecular information but also enables to investigate the interaction or cross-talk among multiple types of molecules or targets that are involved in the tissue micro-events. Unfortunately, current biomedical optical imaging techniques are limited either in penetration depth (microscopy) or spatial resolution (diffuse light based imaging) as a result of strong light scattering in deep tissue. To overcome this limitation, we developed a multi-color ultrasound-switchable fluorescence (USF) imaging technique whereby ultrasound was used to switch on/off the emission of multiple near infrared (NIR) fluorophores. We synthesized and characterized unique NIR USF contrast agents. The excellent switching properties of these agents, combined with the sensitive USF imaging system developed in this study, enabled us to simultaneously image multiple fluorescent targets in deep tissue with high spatial resolution.

**Conference 9323: Photons Plus Ultrasound:
Imaging and Sensing 2015**

9323-125, Session PMon

Experimental validation of a theoretical model of dual wavelength photoacoustic (PA) pump-probe excitation in fluorophores

Julia Märk, Christoph Theiss, Franz-Josef Schmitt, Jan G. Laufer, Technische Univ. Berlin (Germany)

Fluorophores, such as exogenous dyes and genetically expressed proteins, exhibit radiative relaxation with long excited state lifetimes. This can be exploited for PA detection based on dual wavelength excitation using pump and probe wavelengths that coincide with the absorption and emission spectra, respectively. While the pump pulse raises the fluorophore to a long-lived excited state, simultaneous illumination with the probe pulse reduces the excited state lifetime due to stimulated emission (SE). This causes the fluorophore to undergo an increased number of excitation-relaxation cycles during the excitation pulse, which changes the thermalized energy, and hence PA signal amplitude, compared to single wavelength illumination. By introducing a time delay between pump and probe pulses, the change in the PA amplitude can be modulated. Since this effect is not observed in endogenous chromophores, it provides a contrast mechanism for the detection of fluorophores via PA difference imaging. In this study, a theoretical model of the PA signal generation in fluorophores was developed and experimentally validated. The model is based on a system of coupled rate equations and describes the spatial and temporal changes in the population of the molecular energy levels as a function of pump-probe energy, excitation and SE wavelengths, and concentration. This allows the prediction of the thermalized energy distribution, and hence the time-resolved PA signal amplitude. The model was validated on cuvette measurements in solutions of Rhodamine 6G, a well-known laser dye, and was used to predict the conditions required for the optimal detection of fluorescent labels in typical biological settings.

9323-128, Session PMon

Optical-resolution photoacoustic microscopy of the metabolic rate of oxygen in a mouse renal tumor model

Chenghung Yeh, Washington Univ. in St. Louis (United States); Song Hu, Univ. of Virginia (United States); Jinyang Liang, Lei Li, Brian T. Soetikno, Washington Univ. in St. Louis (United States); Zhi-Hong Lu, Rebecca E. Sohn, Washington Univ. School of Medicine in St. Louis (United States); Konstantin I. Maslov, Washington Univ. in St. Louis (United States); Jeffrey M. Arbeit, Washington Univ. School of Medicine in St. Louis (United States); Lihong V. Wang, Washington Univ. in St. Louis (United States)

The mammalian target of rapamycin (mTOR) has been a key factor in cell-signaling pathways regulated in human cancer metabolism and growth. Measurement of the metabolic rate of oxygen (MRO2) is a useful indicator to tumor oxygen metabolism. MRO2 is also an important parameter of cell functionality, associated with the product of blood flow flux and arteriovenous oxygenation difference. Although our understanding of tumor metabolism has advanced tremendously, we lack a tool to noninvasively and longitudinally quantify MRO2 in tumors.

Here, we present noninvasive, label-free, longitudinal optical-resolution photoacoustic microscopy (L-ORPAM) to quantify blood flow flux, oxygen saturation (sO2), and thereby MRO2 for a renal tumor model in the same mouse over weeks to months. Experiments showed that sO2 difference between the artery and vein within the tumor region decreased greatly due to the arteriovenous shunting effect during tumor growth. In contrast, the blood flow flux increased over 4 times compared to the baseline. Moreover, hypermetabolism was exhibited by a 3-fold increase in MRO2 during natural

growth. After mTOR inhibitor treatment, the blood flow flux and MRO2 were reduced by 76% and 72%, respectively, with respect to pre-treatment. This result suggests that L-ORPAM is a promising tool for the studies of metabolism in tumor and other diseases.

9323-129, Session PMon

Speed of sound and acoustic attenuation of compounds affected during optoacoustic monitoring of thermal therapies measured in the temperature range from 5°C to 60°C

Tanmayi Oruganti, Elena V. Petrova, Alexander A. Oraevsky, Sergey A. Ermilov, TomoWave Laboratories, Inc. (United States)

Optoacoustic (photoacoustic) imaging is being adopted for monitoring tissue temperature during hypothermic and hyperthermic cancer treatments. The technique's accuracy benefits from the knowledge of speed of sound (SoS) and acoustic attenuation (AcA) as they change with temperature in biological tissues, blood, and acoustic lens of an ultrasound probe. In these studies we measured SoS and spectral AcA of different ex vivo tissues and blood components (plasma and erythrocyte concentrates) in the temperature range from 5°C to 60°C. We used the technique based on measurements of time-delay and spectral amplitude of pressure pulses generated by wideband planar acoustic waves propagating through the interrogated medium. Water was used as a reference medium with known acoustic properties. In order to validate our experimental technique, we measured the temperature dependence of SoS and AcA for aqueous NaCl solution of known concentration and obtained the results in agreement with published data. Similar to NaCl solution and pure water, SoS in blood and plasma was monotonously increasing with temperature. However, SoS of erythrocyte concentrates displayed abnormalities at temperatures above 45°C, suggesting potential effects from hemoglobin denaturation and/or hemolysis of erythrocytes. On the contrary to aqueous solutions, the SoS in polyvinyl-chloride (plastisol) – a material frequently used for mimicking optical and acoustic properties of tissues – decreased with temperature. We also measured SoS and AcA in silicon material of an acoustic lens and did not observe any temperature-related changes in them.

9323-131, Session PMon

Real-time interleaved ultrasound/photoacoustic imaging for interventional procedure guidance

Chen-Wei Wei, Thu-Mai Nguyen, Jinjun Xia, Bastien Arnal, Univ. of Washington (United States); Ivan M. Pelivanov, Univ. of Washington (United States) and International Laser Center (Russian Federation); Matthew O'Donnell, Univ. of Washington (United States)

Ultrasound-guided photoacoustic imaging has shown its potential in many clinical applications including vascular visualization, detection of nanoprobe sensing molecular profiles, and guidance for interventional procedures. However, bulky and costly lasers are usually required to provide sufficient pulse energies for deep imaging. The low pulse repetition rate also obstructs the advancement of an integrated real-time ultrasound/photoacoustic system. With a compact and low-cost laser operating at a kHz repetition rate, we aim to integrate photoacoustics into a commercial ultrasound machine utilizing an interleaved scanning approach, with imaging depth up to a few centimeters and frame rates > 30 Hz ready for clinical translation. Multiple photoacoustic sub-frames are formed by scanning laser firings covering a large scan region with a rotating galvo mirror, and then combined to a final frame. Ultrasound pulse-echo beams are interleaved

**Conference 9323: Photons Plus Ultrasound:
 Imaging and Sensing 2015**

between laser firings/PA receives. The approach was implemented with a diode-pumped laser (TECH-1053 Specific, Laser-Export Co. Ltd., Moscow, Russia), a commercial ultrasound scanner (Vantage, Verasonics, Redmond, WA), and a linear array transducer (AT8L12-5 50 mm, Broadsound, Taiwan). The insertion of an 18-gauge needle into a piece of chicken tissue and the injection of absorptive agent into the tissue were imaged, with an integrated ultrasound/photoacoustic frame rate of 30 Hz, covering a 2.8 cm \times 2.8 cm imaging plane. Given this real-time image rate and high contrast (> 35 dB at more than 1-cm depth in the photoacoustic image), we have demonstrated that this approach is potentially attractive for clinical needle guidance.

9323-132, Session PMon

Noninvasive photoacoustic microscopy of methemoglobin in vivo

Yong Zhou, Min Tang, Ruiying Zhang, Lihong V. Wang, Washington Univ. in St. Louis (United States)

Due to the various causes of methemoglobinemia and its potential to be confused with other diseases, in vivo measurements of both the average percentage and the distribution of methemoglobin have significant applications in clinics. Existing techniques such as pulse oximetry, arterial blood gas analysis, and co-oximetry are either unreliable or unable to image the distribution of methemoglobin. In this work, we used photoacoustic microscopy (PAM) to quantify the average percentage and the distribution of methemoglobin both in vitro and in vivo. Three wavelengths (610 nm, 620 nm, and 630 nm) were selected to measure methemoglobin percentage in blood mixtures based on the absorption spectra of methemoglobin, deoxyhemoglobin, and oxyhemoglobin. The methemoglobin percentages calculated from the PA signals fitted well to the measurements with a spectrophotometer. Then we mapped the methemoglobin distributions in several blood-vessel-mimicking tubes. Average percentages calculated for the five samples also fitted well to the results from the spectrophotometer. Finally, we demonstrated the ability of PAM to map and quantify methemoglobin in vivo using a mouse model. Methemoglobin was induced in the mouse with intravenous injection of sodium nitrite, and the methemoglobin level was monitored by PAM system during the induction and self-recovery period. The result was in accordance with published researches on induction of methemoglobin in mice. Our project showed that PAM can quantitatively measure methemoglobin distribution in vivo.

9323-133, Session PMon

Optimal illumination design investigation for partially illuminated optoacoustic breast tomography

Yang Lou, Washington Univ. in St. Louis (United States); Vyacheslav V. Nadvoretzkiy, TomoWave Laboratories, Inc. (United States); Kun Wang, Washington Univ. in St. Louis (United States); Sergey Emilov, Alexander A. Oraevsky, TomoWave Laboratories, Inc. (United States); Mark A. Anastasio, Washington Univ. in St. Louis (United States)

Optoacoustic tomography (OAT) holds great potential for breast imaging for its ability to provide functional information based on hemoglobin contrast. The design of an OAT breast imager involves a trade-off between the light delivery and acoustic detection strategy. Namely, it is typically difficult to have full-view acoustic detection while simultaneously delivering light in a uniform way. Our team has recently constructed an OAT breast imager in which an ultrasonic arc array and light delivery system are simultaneously rotated around the breast, causing the light distribution within the breast varying with tomographic view angle. Applying conventional OAT reconstruction methods, which requires light distribution to be fixed, will generate artifacts in this rotating-partial-illumination case, which can further impair cancer detection. This work investigates optimal light illumination

design in terms of resolution and SNR for partially illuminated OAT systems. We first studied the effect of non-fixed light distribution on two typical OAT reconstruction methods: delay-and-sum method and an iterative method minimizing a penalized least square cost function, based on which various illumination schemes are proposed. The optical absorption map for each illumination design is generated using Monte Carlo simulation with realistic optical properties. Simulations of forward and reconstruction processes are done while incorporating transducer directivity and electrical response to better simulate experimental procedure. The optimal illumination design is chosen after quantitatively comparing different figures of merits from the reconstructed images for all illumination designs.

9323-134, Session PMon

Laser diode-based, multi-wavelength optoacoustic system for monitoring, imaging, and sensing

Rinat O. Esenaliev, Yuriy Y. Petrov, Irene Y. Petrov, Donald S. Prough, Andrey Petrov, The Univ. of Texas Medical Branch (United States)

Many applications of optoacoustic monitoring, imaging, and sensing (in particular, clinical applications) require a multi-wavelength pulsed laser source that is compact and light-weight, while providing sufficient pulse energy and repetition rate. Obtaining adequate resolution, contrast, and sensitivity requires stress-confined irradiation conditions, which in practice means that pulse duration should not exceed ~ 150 ns. We developed and built a high-power, multi-wavelength, fiber-coupled laser diode system for optoacoustic monitoring, imaging, and sensing. The system operates in the near infrared spectral range and generates nanosecond pulses with high (~ 1 kHz) repetition rate. The system was tested in human subjects and provided optoacoustic signals from important blood vessels such as the radial artery, internal jugular vein, superior sagittal sinus, and peripheral veins. The high energy of the pulses emitted from the optoacoustic probe enabled measurements with a high signal-to-noise ratio.

9323-135, Session PMon

Noninvasive, optoacoustic detection and characterization of intra- and extracranial hematomas and cerebral hypoxia

Rinat O. Esenaliev, Andrey Petrov, Donald S. Prough, Yuriy Y. Petrov, Irene Y. Petrov, The Univ. of Texas Medical Branch (United States); Vasantha Asokan, Adaeze Agbor, Claudia S. Robertson, Baylor College of Medicine (United States)

Early diagnosis of intracranial hematomas is necessary to improve outcome in patients with traumatic brain injury (TBI). CT and MRI can diagnose intracranial hematomas, but cannot be used until the patient arrives at a major healthcare facility, resulting in delayed diagnosis. Near infrared spectroscopy may suggest the presence of unilateral intracranial hematomas, but provides minimal information on hematoma type and location due to limitations associated with strong light scattering. We have used optoacoustics (which combines high endogenous optical contrast with the resolution of ultrasound) to diagnose hematomas and monitor cerebral oxygenation. We performed animal and clinical studies on detection and characterization of hematomas and on monitoring cerebral hypoxia by probing the superior sagittal sinus (SSS). Recently, we built a medical grade, multi-wavelength, OPO-based optoacoustic system tunable in the near infrared spectral range. We developed a new patient interface for measurements in the presence of dense hair and used it in patients with TBI. The optoacoustic system was capable of detecting intra- and extracranial hematomas and provided valuable information on the hematomas' location and oxygenation. SSS blood oxygenation was measured as well with the new interface. The obtained results indicate that the optoacoustic system

**Conference 9323: Photons Plus Ultrasound:
 Imaging and Sensing 2015**

can be used with the new interface for early detection and characterization of hematomas in TBI patients, as well as for cerebral venous blood oxygenation monitoring through hair.

9323-136, Session PMon

Multi-depth photoacoustic microscopy with a focus tunable lens

Kiri Lee, Tae Joong Eom, Euiheon Chung, Gwangju Institute of Science and Technology (Korea, Republic of)

Optical-resolution photoacoustic microscopy (OR-PAM) has been studied to improve its imaging resolution and speed. However the use of high numerical aperture (NA) objective lens confines the field of view or the imaging range of OR-PAM. In order to obtain images at different layers, one needs to change either the sample position or the focusing position by mechanical scanning. This mechanical movement of the sample or the objective lens limits the scanning speed and precision. It could cause the risk of contact damage between the sample and objective lens. In this study, we propose a multi-depth PAM with a focus tunable lens. We electrically adjusted the focal length in the depth direction of the sample, and extended the imaging range up to 2.8 mm with the objective lens (10x, NA 0.3). The proposed approach can increase scanning speed and avoid step motor induced distortions during PA signal acquisitions without mechanical scanning in the depth direction. To investigate the performance of the multi-depth PAM system, we scanned a black human hair and the dorsal skin of a living nude mouse (BALB/c Nude). The moving stages scanned the sample in the x-y plane with a stage moving speed of 1 mm/sec, the response time of the tunable lens was 4.5 msec, respectively. The measured PA signals were amplified by a low noise amplifier and filtered unwanted high frequency noise by a low pass filter with 55 MHz cutoff frequency. The volumetric rendering of black hair and vasculature of the nude mouse are presented.

9323-137, Session PMon

Hybrid photoacoustic-ultrasound transmission tomography for imaging and 2D spatio-temporal monitoring of temperature in photothermal therapy

Khalid Daoudi, Peter van Es, Srirang Manohar, Wiendelt Steenbergen, Univ. Twente (Netherlands)

Thermal therapy is a method aspiring to locally destroy malignant tissues without affecting surrounding environment. To ensure efficacy of the thermal therapy in destroying tumors while sparing normal tissue, it is crucial to monitor the temperature both spatially and temporally, while also imaging the region of interest to identify location and extent of the lesion. In this work, we use an approach based on speed of sound (SOS) tomography in a photoacoustic (CT) imager, to image and monitor spatio-temporal evolution of temperature. In our method called 'passive element' enriched PA CT, in a conventional PA imager, we placed passive absorbers with a small cross-section in the laser light path that illuminates the object under PA examination. These "passive elements" create laser induced ultrasound which propagates through the object allowing ultrasound transmission CT to be performed. Simultaneously, a large fraction of the incident light that does not interact with the finite number of passive elements, illuminates the object permitting conventional PA CT. From the SOS tomograms, we derive two-dimensional temperature maps estimated from the relationship between the temperature and SOS of water. Proof-of-principle is demonstrated in a tissue-mimicking Agar-based test object embedded with sodium alginate beads carrying different concentration of gold nanospheres, with the imaging system modified to include a 532 nm continuous wave (CW) laser for the photothermal experiments. The experimental results were supported by simulations involving Monte Carlo

modeling of light propagation and the heat diffusion equation to estimate the spatial temperature distribution.

9323-138, Session PMon

Multi-view optical resolution photoacoustic microscopy

Liren Zhu, Lei Li, Liang S. Gao, Lihong V. Wang, Washington Univ. in St. Louis (United States)

Conventional optical-resolution photoacoustic microscopes (OR-PAM) focus light within the acoustic focal zone, providing a lateral resolution down to submicron level. However, optical focusing cannot provide adequate axial resolution in most practical cases. OR-PAM relies on time-of-flight detection of acoustic signals to provide axial resolution. The acoustically determined axial resolution is usually around tens of microns, an order of magnitude worse than the lateral resolution. This relatively poor axial resolution limits OR-PAM's application in imaging translucent small animals because such biological objects typically have fine features in all three dimensions.

To overcome this limitation, herein we present multi-view OR-PAM (MV-OR-PAM) by imaging an object from multiple view angles and merging the data through multi-view deconvolution. Compared to previous methods, our technique enables a longer working distance and a higher imaging speed. By using multi-view OR-PAM, we have achieved a 3D isotropic optical resolution of 4.7 microns, a 9-fold improvement over an acoustically determined value. In addition, we also demonstrated the resolution improvement and information completeness of multi-view OR-PAM in imaging a zebrafish.

Unlike previously proposed methods, MV-OR-PAM does not sacrifice the system's working distance, imaging depth, or imaging speed. This technique should open up new areas of investigation in photoacoustic microscopy, especially in imaging translucent small animals, such as zebrafish and *Drosophila*.

9323-139, Session PMon

Microbubble enhanced photoacoustic tomography

Lidai Wang, Guo Li, Lihong V. Wang, Washington Univ. in St. Louis (United States)

To date, most photoacoustic imaging modalities have been limited to detection of directly emitted ultrasonic waves generated by optical absorption. To enhance imaging capabilities, we explore a new approach in photoacoustics, generating and detecting scattered ultrasonic waves. We use microbubbles to generate or enhance photoacoustic scattering in blood. The microbubbles have very different acoustic impedance with their surrounding media and thus can strongly scatter photoacoustic waves. The detection of the scattered photoacoustic waves brings at least two advantages. First, the scattered photoacoustic waves do not show as strong spatial correlation as that of the directly emitted ones, so they propagate in all directions, rather than only normal to the absorber boundaries. This solves the limited view problem in many photoacoustic imaging modalities. Second, like speckles in pulse-echoed ultrasonic imaging, the scattered photoacoustic signal generates speckles in homogeneous or nearly homogeneous absorbing media, which allows blood flow imaging by tracking the motions of the speckles. To demonstrate these advantages, we imaged whole blood mixed with clinical-dose microbubbles (~1 μm in diameter), using an acoustic-resolution linear photoacoustic computed tomography system. Results clearly show the improved view angle by visualizing vertical blood vessels, as well as the capability to measure blood flow.

**Conference 9323: Photons Plus Ultrasound:
Imaging and Sensing 2015**

9323-140, Session PMon

Assessing carotid atherosclerosis by fiber-optic multispectral photoacoustic tomography

Jie Hui, Rui Li, Pu Wang, Evan Phillips, Purdue Univ. (United States); Rebecca Bruning, Indiana Univ. School of Medicine (United States); ChienSheng Liao, Purdue Univ. (United States); Michael Sturek, Indiana Univ. School of Medicine (United States); Craig J. Goergen, Ji-Xin Cheng, Purdue Univ. (United States)

Atherosclerotic plaque at the carotid bifurcation is the underlying cause of the majority of ischemic strokes. Noninvasive imaging and quantification of the compositional changes preceding gross anatomic changes within the arterial wall is essential for diagnosis of disease. Current imaging modalities are limited to detection of flow-limiting lesions. Here, we demonstrate a fiber-based multispectral photoacoustic tomography (PAT) system for excitation of lipids and external acoustic detection of the generated ultrasound. Using sequential ultrasound imaging of ex vivo preparations we achieved ~2 cm imaging depth and chemical selectivity for assessment of arterial plaques in Ossabaw Swine. A multivariate curve resolution alternating least squares (MCR-ALS) analysis method was applied to resolve the major chemical components, including intravascular lipid, intramuscular fat, and blood. These results show the promise of detecting carotid plaque in vivo through esophageal fiber-optic excitation of lipids and external acoustic detection of the generated ultrasound.

9323-141, Session PMon

Multimodal non-contact photoacoustic and OCT imaging with galvanometer scanning

Thomas Berer, Armin Hochreiner, Elisabeth Leiss-Holzinger, Johannes Bauer-Marschallinger, Andreas Buchsbaum, RECENDT GmbH (Austria)

We present multimodal non-contact photoacoustic and OCT imaging using a galvanometer scanner. Optical Coherence Tomography (OCT) is a fast and non-contact imaging method and allows to acquire depth resolved images of subsurface features in turbid media. In photoacoustic imaging (PAI) ultrasonic waves, generated by thermoelastic expansion, are usually acquired using piezoelectric ultrasonic transducers which require acoustic coupling with a specimen. To make full use of the remote nature of OCT, a combination of OCT and PAI should ideally not rely on any physical contact to a specimen. As alternative to contacting transducers in PAI, non-contact photoacoustic imaging techniques have been employed.

In this work photoacoustic signals are acquired without contact on the surface of a specimen using a Mach-Zehnder interferometer. The interferometer is realized in a fiber-optic network using a fiber laser at 1550 nm as source. In the same fiber-optic network a spectral-domain OCT system is realized, using a broadband light source at 1300 nm. Light from the fiber laser and the OCT source are multiplexed into the same fiber and the same objective is used for both imaging modalities. Light reflected from specimens is demultiplexed and guided to the respective imaging systems. To allow fast non-contact photoacoustic and OCT imaging the detection spot is scanned across the specimens' surface using a galvanometer scanner. Imaging is demonstrated on tissue mimicking phantoms and biological samples. As the same fiber network and same optical components are used for photoacoustic and OCT imaging the obtained images are co-registered intrinsically.

9323-142, Session PMon

Photoacoustic projection imaging using a 64-channel fiber optic detector array

Johannes Bauer-Marschallinger, Karoline Felbermayer, Klaus-Dieter Bouchal, Istvan A. Veres, Hubert Grün, Peter Burgholzer, Thomas Berer, RECENDT GmbH (Austria)

We present photoacoustic projection imaging with a 64-channel integrating line detector array. Integrating line detectors (ILDs) average the pressure over cylindrical surfaces. For imaging the line detectors are arranged parallel to each other on a cylindrical surface surrounding a specimen. Thereby, the three-dimensional imaging problem is reduced to a two-dimensional problem. After acquisition of a dataset of pressure signals, a two-dimensional photoacoustic projection image is reconstructed. If three-dimensional imaging is required, the specimen is rotated relatively to the ILDs to acquire projection images from different angles. A three-dimensional image can then be generated from the two-dimensional projection images by using the inverse Radon transform.

The 64 channel line detector array is realized using optical fibers being part of interferometers. The sensing parts of these interferometers consist of graded-index polymer-optical fibers (POFs), which exhibit better sensitivity than standard glass-optical fibers. Ultrasonic waves striking the POFs change the phase of light in the fiber-core due to the strain-optic effect and the pressure signals are demodulated using high-bandwidth balanced photo-detectors. The interferometers are operated in quantum-noise limit. A low-bandwidth laser at 1550 nm is used as source and the quadrature points of the interferometers are stabilized using electro-optical phase-shifter and analogue controllers. In the setup 16 channels are read out in parallel; fiber optic switches are used to multiplex the 64 ILDs to these 16 channels. This configuration allows close to real-time photoacoustic projecting imaging. Photoacoustic projection imaging is experimentally demonstrated on tissue mimicking phantoms and biological samples.

9323-143, Session PMon

A tunable MOPA laser for real-time optical resolution photoacoustic microscopy

Mohammad S. Mahmud, Alexander Forbrich, Wei Shi, Roger J. Zemp, Univ. of Alberta (Canada)

We demonstrate the use of a tunable MOPA laser system for OR-PAM for the first time. This unique laser is capable of tuning the repetition rate (0.1-120MHz), the wavelength (1030-1080nm), the pulse-width (100ps-5ns) and power (up to 1.1W). It is also capable of programmable dithering and synchronization with other laser systems to within -ps jitter. To apply it to OR-PAM we take advantage of frequency doubling to convert IR light into green light. For doubling, a periodically poled magnesium doped lithium niobate (MgO:LiNbO3) crystal was chosen. Wavelength tuning was accomplished by tuning the output wavelength of the MOPA then tuning the temperature of the MgO: LiNbO3 crystal to generate tunable visible light. We demonstrate the use of the system for phantom and in vivo imaging.

9323-144, Session PMon

Dual modality of non-contact photoacoustic tomography and fluorescence imaging using double cladding fiber

Jonghyun Eom, Seong Jun Park, Ju Wan Kim, Soongho Park, Byeong Ha Lee, Gwangju Institute of Science and Technology (Korea, Republic of)

**Conference 9323: Photons Plus Ultrasound:
Imaging and Sensing 2015**

We present a fiber-based dual-modal imaging system that combines non-contact photoacoustic tomography (NPAT) and fluorescence imaging (FI) by using double cladding fiber (DCF) to simultaneously provide PA image and fluorescence image. The NPAT system utilizing an all-fiber heterodyne interferometer measures the photoacoustic signal at the sample surface without physical contact. The probe consists of a specially fabricated DCF coupler and a lensed fiber so as to acquire the NPAT and the FI with the same probe. The DCF has a core and two claddings, inner and outer, concentrically structured, which allows two light-guiding channels via the core and the inner cladding. Through the core of DCF, the interrogating light for the PA detection signal is delivered to the sample, and the light reflected at the sample is collected by the same core of DCF. While, the excited fluorescence light is collected separately via the inner cladding of the DCF and directed to a photodetector with a DCF coupler. The lensed fiber of the DCF probe is compactly fabricated to focus the interferometer light and increases the collecting efficiency of the fluorescence signal at the same time. To demonstrate the feasibility of the proposed dual modal system, we have conducted a phantom experiment using a tissue mimicking phantom which contained a couple tubes filled with fluorescein solution and black ink, respectively. Because the proposed imaging system is implanted with all fiber-optic configurations, it has the potential for minimally invasive and improved diagnosis and guided treatment of diseases.

9323-145, Session PMon

Comparative experiments of photoacoustic system using laser light source and LED array light source

Toshitaka Agano, Naoto Sato, Hitoshi Nakatsuka, XTrillion, Inc. (Japan); Kazuo Kitagawa, Takamitsu Hanaoka, Koji Morisono, Yusuke Shigeta, Funai Electric Co., Ltd. (Japan)

We have successfully measured photoacoustic signal by near infrared light emitting diodes (NIR-LED) array that has very small power, approx. 1/1500 of light amount compare with Nd:YAG laser coupled to an optical parametric oscillator (Nd:YAG-OPO) light. In order to achieve high output power, we drove NIR-LED array with unusual amount of electric current. The experiment results showed that the photoacoustic signal strength was about 1/40 of the laser, which suggests NIR-LED array has good photoacoustic reception efficiency versus the ultrasound transducer bandwidth. Moreover, by using high-speed cycle pulse, NIR-LED array photoacoustic system may be able to achieve high-speed-imaging which cannot be obtained by the solid-state laser. NIR-LED system can be a game changer for photoacoustic imaging.

9323-146, Session PMon

Light and ultrasound reflecting off-axis parabolic mirror for photoacoustic endoscopy

Zhonglie Piao, Beckman Laser Institute and Medical Clinic (United States) and Pusan National Univ. (Korea, Republic of); Teng Ma, The Univ. of Southern California (United States); Joseph C. Jing, Jiawen Li, Shanshan Liang, Jun Zhang, Beckman Laser Institute and Medical Clinic (United States); Qifa Zhou, Koping Kirk Shung, The Univ. of Southern California (United States); Chang-Seok Kim, Pusan National Univ. (Korea, Republic of); Zhongping Chen, Beckman Laser Institute and Medical Clinic (United States)

Photoacoustic endoscopy (PAE) becomes a useful tool for internal organ imaging because of its optical absorption-based contrast with high spatial resolution and imaging depth. Therefore, optimization of optical illumination

and acoustic detection are needed to achieve ultimate detection sensitivity. In this work, we will present a new miniaturized side-view PAE with a scanning off-axis parabolic (OAP) mirror that can coaxially focus and reflect laser illumination and acoustic waves. The distal section is encapsulated by a thin-walled plastic tube, composed of a waterproof micromotor, a diamond turned OAP mirror, a 40 MHz single element ring transducer and a multimode fiber. The outer diameter and length of the distal section are 2.4 mm and 30 mm respectively, which could be further reduced. The scanning OAP mirror enables a higher than 1200 rpm rotation speed with a larger than 300° angle of view in spite of the angle being slightly blocked by the power wire. The pulsed laser is guided through a standard 0.22 NA multimode fiber and is reflected at a right angle by the OAP mirror on to the tissue which induces a photoacoustic signal. Due to the parabolic machined metal surface of the OAP mirror, the diverged laser beam can be re-focused; meanwhile, the higher acoustic numerical aperture enhances the lateral resolution and detecting sensitivity of the endoscopy, and also reduces the laser energy needed to generate the photoacoustic signal. The imaging ability of this endoscopy was evaluated with a low repetition rate laser in phantom experiments. The lateral and axial resolutions were measured at 100 μ m and 40 μ m, respectively. In the future, a high repetition rate laser will be equipped for animal imaging experiments.

9323-147, Session PMon

Attempts to increase penetration of photoacoustic system using led array light source

Toshitaka Agano, Naoto Sato, Hitoshi Nakatsuka, XTrillion, Inc. (Japan); Kazuo Kitagawa, Takamitsu Hanaoka, Koji Morisono, Yusuke Shigeta, Funai Electric Co., Ltd. (Japan)

When we consider the needle visualization in the field of point of care by utilizing the photoacoustic imaging system, and using the conventional solid state laser light source, the issue arises such as device size and not a green system due to the high power consumption. Therefore, we aimed at an environmental friendly and compact system with low power consumption by using a near infrared LED (NIR-LED) array light source.

Because the intensity of NIR-LED light is weak compared to the solid-state laser, the photoacoustic signal is also weak. However, by averaging photoacoustic signals with multiple pulse, we have improved S/N of the photoacoustic signal. As a result, we have achieved penetration depth of 30mm.

9323-148, Session PMon

A compact and cost-efficient photoacoustic microscopy system with a pulsed laser diode excitation

Tianheng Wang, Sreyankar Nandy, Hassan S. Salehi, Patrick D. Kumavor, Quing Zhu, Univ. of Connecticut (United States)

Photoacoustic microscopy (PAM) is capable of mapping microvasculature networks in biological tissue and has demonstrated great potential for biomedical applications. However, the clinical application of the PAM system is limited due to the use of bulky and expensive pulsed laser sources. In this paper, a compact and low-cost optical-resolution PAM system with a pulsed laser diode excitation has been introduced. The lateral resolution of this PAM system was estimated to be 7 μ m by imaging a carbon fiber. The phantoms made of polyethylene tubes filled with blood and a mouse ear were imaged to demonstrate the feasibility of this PAM system for imaging biological tissues.

9323-149, Session PMon

Fast optical-resolution photoacoustic microscopy using 2-axis MEMS scanner

Jin Young Kim, Changho Lee, Kyungjin Park, Geunbae Lim, Chulhong Kim, Pohang Univ. of Science and Technology (Korea, Republic of)

Optical-resolution photoacoustic microscopy (OR-PAM) is a novel microscopic tool to provide in vivo optically sensitive images in biomedical researches. This distinctive technique guarantees that medical searching goes successfully in a deeper region beyond one optical transport mean free path, where other pure optical microscopy modalities cannot reach. Typically, the real-time imaging capability is vital to identify specific diseases. To achieve a fast imaging speed and wide scanning range, herein we introduce a 2-axis MEMS scanner made through soft lithography using Polydimethylsiloxane (PDMS) for a flexible scanner structure. The small size and simple operation of the 2-axis MEMS scanner can greatly reduce the complexity of the OR-PAM system as well. By pairing with electromagnetic force, this flexible frame results in a wide scanning range (i.e., 11 × 11 mm² along the x and y axes, respectively) with a high speed (i.e., 25 frames of B-scan per second). The size of the fabricated MEMS scanner is 15 × 15 × 15 mm³ along x, y, and z axes, respectively, and the scanning ability in water makes the MEMS scanner possible to reflect both ultrasound and laser beam, simultaneously. Confocally aligned laser and resultant photoacoustic waves were scanned by the torsional vibration of the scanner along to the x and y axes. The OR-PAM system equipped with the 2-axis MEMS scanner has a lateral resolution of 3.6 μm. We have successfully obtained in vivo PA images of vasculatures in an entire mouse ear.

9323-150, Session PMon

Quantitative ultrasound modulated optical tomography: sensitivity functions, uniqueness, and image reconstruction

Samuel Powell, Simon R. Arridge, Terence S. Leung, Univ. College London (United Kingdom)

Ultrasound modulated optical tomography (UOT) is an imaging modality which uses the spatially localised acoustically driven modulation of coherent light as a probe of the structure and optical properties of biological tissues.

There are two principal challenges facing this technique; i) the coherent detection of the small modulated flux against the large unmodulated background, and, ii) relating the measured data to an image of the parameters of interest.

In this work we approach the latter problem, common to all hybrid imaging modalities. We begin by presenting an overview of different approaches to modelling the forward problem in UOT. After considering the computational viability and experimental applicability of each of the methods we proceed to pose the inverse problem in the context of a diffusion-style formulation.

As part of our exposition we analyse the form of the sensitivity functions which arise in this imaging modality. We consider the problem of uniqueness in UOT, making comparisons with the same problem in photoacoustic tomography, and demonstrate methods by which multiple parameters (optical absorption and scattering) can be uniquely and simultaneously be recovered.

Using the demonstrated techniques, we close this work by performing a simulated recovery of the optical parameters in a three-dimensional domain by employing a computationally efficient, adjoint-assisted, gradient based technique.

9323-151, Session PMon

Model-based inversion for frequency domain optoacoustic tomography

Stephan Kellnberger, Pouyan Mohajerani, Hong Yang, Vasilis Ntziachristos, Helmholtz Zentrum München GmbH (Germany)

Optoacoustic imaging is typically implemented in the time domain employing pulsed nanosecond lasers. Alternatively, optoacoustic imaging can also be implemented in the frequency domain using continuous wave lasers. In frequency domain, imaging is performed by raster scanning a focused transducer over the sample or by applying the chirp technique to resolve the depth of absorbers. Here, we present a model-based image reconstruction approach for frequency domain optoacoustic tomography using complex acoustic signals. We show simulation results and demonstrate the ability to reconstruct images of optical absorption from amplitude and phase measurements at multiple discrete frequencies.

9323-152, Session PMon

Narrowband second harmonic thermoacoustic signals from solid and soft tissues

Stephan Kellnberger, Murad Omar, Helmholtz Zentrum München GmbH (Germany); George Sergiadis, Helmholtz Zentrum München GmbH (Germany); Vasilis Ntziachristos, Helmholtz Zentrum München GmbH (Germany)

Tissue exposure to short sub-microsecond pulses generates broadband acoustic signals. Corresponding thermoacoustic signals have been used to perform thermoacoustic imaging, showing radiofrequency (RF) absorption in tissue with spatial resolutions in the order of 100 μm to few millimeter. We recently introduced near-field thermoacoustic tomography which enables efficient signal coupling and ultrashort excitation to obtain high resolution thermoacoustic images. Here we investigate acoustic responses of tissue exposed to continuous wave radiofrequency sources. We experimentally interrogate mechanical responses of tissue at RF frequencies below 10 MHz, showing thermoacoustic signal generation at the double frequency of the RF excitation.

9323-153, Session PMon

Photoacoustic perfusion measurements: a comparison with power Doppler in phantoms

Maarten Heres, Ümit Arabul, Benjamin Tchang, Frans N. Van de Vosse, Marcel C. M. Rutten, Richard G. P. Lopata, Technische Univ. Eindhoven (Netherlands)

Ultrasound-based measurements using Doppler, contrast, and more recently photoacoustics (PA) have emerged as techniques for tissue perfusion measurements. In this study, the feasibility of perfusion measurements with a fully integrated, hand-held, photoacoustic probe was investigated and compared to Power Doppler (PD).

Three cylindrical polyvinyl alcohol phantoms were made (diameter = 15 mm) containing 100, 200 and 400 parallel polysulfone tubes (diameter = 0.2 mm), resulting in a perfused cross-sectional area of 1.8, 3.6 and 7.1% respectively. Each phantom was perfused with porcine blood (15 mL/min). Cross-sectional PA images (λ = 808nm, frame rate = 10Hz) and PD images (PRF = 750Hz) were acquired with a MyLab One and MyLab 70 scanner (Esaote, NL), respectively. Data were averaged over 70 frames. The average PA signal intensity was calculated in a region-of-interest of 4 by 6 mm. The

**Conference 9323: Photons Plus Ultrasound:
Imaging and Sensing 2015**

percentage of colored PD pixels was measured in the entire phantom.

The average signal intensity of the PA images increased linearly ($R^2 = 0.99$) with perfusion density, being $0.54 (\pm 0.01)$, $0.56 (\pm 0.01)$, $0.58 (\pm 0.01)$ with an average background signal of 0.53 in the three phantoms, respectively. For PD, the percentage of colored pixels in the phantom area ($1.6\% (\pm 0.1\%)$, $3.8\% (\pm 0.3\%)$, $10.9\% (\pm 0.3\%)$) also increased linearly ($R^2 = 0.99$). These preliminary results show that PA imaging with an integrated probe can detect an increase in perfused area and is not inferior to PD. In the future, in vivo measurements will be explored, although validation will be more complex.

9323-154, Session PMon

The influence of cellular uptake on the photostability and photoacoustic conversion efficiency of gold nanorods

Lucia Cavigli, Fulvio Ratto, Francesca Tatini, Paolo Matteini, Alberto Cini, Istituto di Fisica Applicata Nello Carrara (Italy); Ilaria Giovannelli, Dipartimento di Fisica e Astronomia, Università di Firenze (Italy); Marella de Angelis, Francesca P. Rossi, Istituto di Fisica Applicata Nello Carrara (Italy); Sonia Centi, Univ. degli Studi di Firenze (Italy); Roberto Pini, Istituto di Fisica Applicata Nello Carrara (Italy)

Because of their intense optical absorbance in the near-infrared (NIR) window and their chemical versatility, Gold Nanorods (GNRs) are attractive for a range of biomedical applications, such as the photothermal ablation or photoacoustic (PA) imaging of cancer.

In order to exploit the potential of GNRs for biomedical applications, we focus on their interaction with biological systems and in particular on the effect of a cellular environment on their performances of photoacoustic conversion. When GNRs are irradiated with nanosecond laser pulses in resonance with their plasmon oscillations at around 800 nm, such as those in use for photoacoustic microscopy or tomography, their overheating tends to trigger processes of reshaping or fragmentation, which result into dramatic optical modifications. These issues may become even more relevant when GNRs are internalized by cells, since their accumulation into intracellular vesicles may exacerbate their overheating.

In this contribution, we investigate how the cellular uptake influences the stability and PA conversion efficiency of GNRs taken up by macrophages and then embedded in biomimetic scaffolds. PEGylated GNRs with a cationic profile were internalized by J774a.1 macrophages and then these cells were dispersed into chitosan films. The stability and PA conversion efficiency under NIR pulsed irradiation at different laser fluences were investigated and revealed the occurrence of subtle modifications that may be interpreted in the light of the configuration dictated by the cellular physiology.

We expect that these results will be of importance for many biomedical applications involving plasmonic nanoparticles, such as PA imaging and microsurgery.

9323-155, Session PMon

Detecting inflammation and fibrosis in bowel wall with photoacoustic imaging in a Crohn's disease animal model

Guan Xu, Laura Johnson, Univ. of Michigan Medical School (United States); Jack Hu, Univ. of Michigan (United States); Jonathan R. Dillman, Peter D. R. Higgins, Xueding Wang, Univ. of Michigan Medical School (United States)

Crohn's disease is an autoimmune disease affecting 1.2 million people in the

United States. This condition may cause obstructing intestinal narrowings (strictures) due to inflammation, fibrosis (deposition of collagen), or a combination of both. Presently, there is no diagnostic method (e.g., CT or MRI) that allows accurate detection of bowel wall fibrosis, especially when inflammation is also present. Utilizing the unique positive optical absorption contrast of collagen over other chemical components in bowel wall at 1370 nm, this study investigated the feasibility of non-invasively characterizing intestinal strictures using photoacoustic (PA) imaging. Using an established Crohn's disease rodent model, pure inflammatory distal colonic strictures were created in 10 animals, while mixed inflammatory and fibrotic strictures were created in 9 animals. To quantitatively understand the differences in the amounts of bowel wall collagen between the animal groups, bowel wall samples from each individual rat were scanned by an ultrasound and PA parallel real-time imaging system with an L7-4 array. Each of the bowel samples was flattened and cut into a circular shape with 12.5 mm diameter. An OPO laser pumped by a 532nm Nd:YAG laser was used to generate laser pulse at 1370 nm with 8 ns pulse width and 10 Hz repetition rate. Optical power density of 7 mJ per square centimeter was delivered to the surface of the samples. The total PA signal magnitudes within the tissue regions were quantified. Statistical analysis has shown a significant difference between the PA measurements from purely inflammatory and mixed inflammatory-fibrotic strictures.

9323-156, Session PMon

Image registration for limited-view photoacoustic imaging using two linear array transducers

Weihang Shu, The Univ. of British Columbia (Canada); Min Ai, Univ of British Columbia (Canada); Tim E. Salcudean, Robert N. Rohling, Purang Abolmaesumi, Shuo Tang, The Univ. of British Columbia (Canada)

Imaging complicated structures with photoacoustic (PA) modality when the field of view is limited can result in serious imaging artifacts. Limited view reconstruction can also lead to missing structures. One approach to solving this problem is to use different reconstruction algorithms, such as iterative or de-convolution reconstruction. Another approach is to design specific transducer structures, such as hemi-spherical transducer arrays for breast cancer detection. However, most existing PA imaging techniques require either full-view complete projection data collection or complex computational procedure. These requirements are not only time-consuming but also unsuitable for many clinical applications, since most clinical imaging is constrained to limited reconstruction angles. In this paper, we present a method of using two commercial linear array transducers at different orientations to increase the view angle and thus improve the reconstruction of PA imaging. The method involves a two-step process. First, conventional ultrasound is applied to calibrate the relative position of these two linear transducers. Second, two PA images are obtained by a simple back projection algorithm and these images are registered using the information from the ultrasound calibration. The final registered image contains more detailed structures without the requirements of a specialized transducer or long processing time. Experimental results show that this method has the potential to provide good imaging visualization using linear array transducers.

9323-61, Session 8

High-frequency photoacoustic imaging of erythrocyte aggregation and oxygen saturation: probing hemodynamic relations under pulsatile blood flow

Tae-Hoon Bok, Eno Hysi, Michael C. Kolios, Ryerson Univ. (Canada)

**Conference 9323: Photons Plus Ultrasound:
Imaging and Sensing 2015**

Blood flow ensures the oxygenation of tissues through erythrocyte-mediated gas exchange. During low-shear rate pathologies such as deep vein thrombosis, erythrocytes become hyper-aggregated. Erythrocyte aggregation (EA) is known to alter blood viscosity affecting vascular resistance and tissue perfusion. Hence, a non-invasive assessment of EA and oxygen saturation (sO₂) could provide a new biomarker for circulatory disorders affected by blood viscosity and oxygen transport.

In this paper, high-frequency photoacoustic (PA) imaging is proposed to simultaneously evaluate EA and sO₂. Pulsatile flow (30-360 bpm) was generated by flowing human whole blood within a 2-mm-diameter vessel phantom. PA images were acquired using the Vevo LAZR PA imaging system equipped with a 40-MHz-linear-array probe, and sO₂ was calculated using 750/850 nm illumination.

The PA amplitude (PAA) and vessel diameter (VD) cyclically varied at intervals of the beat rate, for both optical wavelengths. The maximum PAA varied 0.41 to 0.46 a.u. (arbitrary unit) at 850 nm/60 bpm, and 0.33 to 0.38 a.u. at 750 nm/90 bpm. However, the cyclic variations of PAA and VD were out of phase. Such a relationship is expected since it is well documented that when VD decreases during diastole, the radial shear rate decreases resulting in enhanced EA and increased PAA. Cyclic variations in sO₂ (maximally 59 to 67% at 30 bpm) were observed at all beat rates. This suggested that the temporal variation in sO₂ can be correlated to the presence of EA under pulsatile blood flow, since it has been reported that oxygen release is inhibited by EA.

9323-62, Session 8
A noninvasive single wavelength monitoring of blood oxygen saturation utilizing both photoacoustics absorption and light scattering

Qiwen Peng, Fei Gao, Xiaohua Feng, Yuanjin Zheng, Nanyang Technological Univ. (Singapore)

Blood oxygen saturation (SO₂) reflects the oxygenation level in blood transport and tissue. Previous studies have shown the capability of non-invasive quantitative measurements of SO₂ by multi-wavelength photoacoustic (PA) spectroscopy for diagnosis of brain, tumor hemodynamics and other pathophysiological phenomena. However, those multi-wavelength methods require a tunable laser or multiple lasers which are relatively expensive and bulky for field measurement environment and applications. Besides, the operation of multiple wavelengths, calibration procedures and data processing gets system complicated, which reduces the feasibility and flexibility for continuous real-time monitoring. Here we report a newly proposed method by combining PA and scattered light signals wherein imposing a hypothesis that scattering intensity is linear to the concentrations of oxygenated hemoglobin and deoxygenated hemoglobin weighed by blood scattering coefficients. A rigorous theoretical relationship between PA and scattering signals is thus established, making it possible that SO₂ can be measured with only one excitation wavelength. To verify the theory basis, both dual-ink phantoms and fresh porcine blood sample have been employed in the experiments. The phantom experiment is able to quantify the concentration of mixed red-green ink that is in precise agreement with pre-set values. The in vitro experiment with fresh porcine blood was conducted and the results of the proposed single-wavelength method achieved high accuracy of 1% - 4% errors. These demonstrated that the proposed single-wavelength SO₂ detection is able to provide non-invasive, accurate measurement of blood oxygenation, and herein create potential for applying it to real clinical applications with low cost and high flexibility.

9323-63, Session 8
Evaluation of Gleason scores by photoacoustic spectral analysis

Guan Xu, Scott Tomlins, Javed Siddiqui, Mandy Davis, Lakshmi P. Kunju, John Wei, Xueding Wang, Univ. of Michigan Medical School (United States)

Ultrasound (US) guided biopsy is the standard procedure for evaluating the presence of prostate cancer. US biopsies are not targeted and randomly sample broad areas of the prostate, which can either miss cancer or undersample aggressive cancer. Aggressive cancers are defined by high Gleason scores. The Gleason scoring system is an architectural assessment of tumor grade that is highly prognostic and performed by pathologists on biopsy tissue. The Gleason patterns, per se the clustering patterns of the cancer cells, can be visualized by cancer targeting, optical contrast enhancing nanoparticles (NPs). In this work, the possibility of identifying cancerous areas by using photoacoustic (PA) techniques for improved US biopsy is investigated. By illuminating the prostate tissue with a side-firing fiber integrated to the biopsy needle and receiving the PA signals with a hydrophone, the Gleason patterns visualized by the NPs could potentially be evaluated in vivo without the need to harvest tissue. The newly developed method of PA spectral analysis (PASA) characterizes the power spectrum of PA signals with a linear model and quantifies the microstructures in tissue with slope, intercept and midband-fit of the linear model. As a preliminary study, we scanned sliced human prostate tissues with Hematoxylin and Eosin staining. A total of 3 normal and 3 cancerous samples were scanned, each along four different directions (0, 45, 90 and 180 degrees) around the sample. Statistical analysis of the PASA parameters has shown that this approach has high sensitivity in identifying the heterogeneous Gleason patterns in cancerous prostate tissues.

9323-64, Session 8
Quantitative photoacoustic assessment of ex-vivo lymph nodes of colorectal cancer patients

Ashwin Sampathkumar, Riverside Research Institute (United States); Emi Saegusa-Beercroft, Univ. of Hawai'i (United States); Jonathan Mamou, Riverside Research Institute (United States); Parag V. Chitnis, George Mason Univ. (United States); Junji Machi, Univ. of Hawai'i at Manoa (United States) and Kuakini Medical Ctr. (United States); Ernest J. Feleppa, Riverside Research Institute (United States)

Colorectal cancer ranks third as a cause of cancer death in the United States. Staging of tumors and selection of appropriate treatment requires histological examination of multiple dissected nodes per patient, so that a staggering number of nodes require histopathological examination, and the finite resources of pathology facilities create a severe processing bottleneck. In this work, we assess the feasibility of using quantitative photoacoustics (QPA) to alleviate this bottleneck and overcome the resulting under sampling in node assessments. QPA is emerging as a new hybrid modality that assesses tissue properties and classifies tissue type based on multiple estimates derived from spectrum analysis of photoacoustic (PA) radiofrequency (RF) data and from statistical analysis of envelope-signal data derived from the RF signals. Our study seeks to use QPA to distinguish cancerous from non-cancerous regions of dissected lymph nodes. Dissected lymph nodes were placed in a water bath and PA signals were generated using a wavelength-tunable (680-950 nm) laser. A 26-MHz, f-2 transducer was used to sense the PA signals. We will present an overview of our experimental setup; provide a statistical analysis of multi-wavelength classification parameters (mid-band fit, slope, intercept) obtained from the PA signal spectrum generated in the lymph nodes; and compare QPA performance with our established quantitative ultrasound (QUS) techniques

**Conference 9323: Photons Plus Ultrasound:
Imaging and Sensing 2015**

in distinguishing metastatic from non-cancerous tissue in dissected lymph nodes. QPA-QUS methods offer a novel general means of tissue typing and evaluation in a broad range of disease-assessment applications.

9323-65, Session 8

Cardiac function and perfusion dynamics measured on a beat-by-beat basis in the live mouse using ultra-fast 4D optoacoustic imaging

Steven J. Ford, Xosé Luis Deán-Ben, Helmholtz Zentrum München GmbH (Germany); Daniel Razansky, Helmholtz Zentrum München GmbH (Germany) and Technische Univ. München (Germany)

The fast heart rate (~7 Hz) of the mouse makes cardiac imaging and functional analysis difficult when studying mouse models of cardiovascular disease, and cannot be done truly in real-time and 3D using established imaging modalities. Optoacoustic imaging, on the other hand, provides ultra-fast imaging at up to 50 volumetric frames per second, allowing for acquisition of several frames per mouse cardiac cycle. In this study, we combined a recently-developed 3D optoacoustic imaging array with novel analytical techniques to assess cardiac function and perfusion dynamics of the mouse heart at high, 4D spatiotemporal resolution. In brief, the heart of an anesthetized mouse was imaged over a series of multiple volumetric frames; in another experiment, an intravenous bolus of indocyanine green (ICG) was injected and its distribution was subsequently imaged in the heart. Unique temporal features of the cardiac cycle and ICG distribution profiles were used to segment the heart from background and to assess cardiac function. The 3D nature of the experimental data allowed for determination of cardiac volumes at ~7-8 frames per mouse cardiac cycle, providing important cardiac function parameters (e.g. stroke volume, ejection fraction) on a beat-by-beat basis, which has been previously unachieved by any other cardiac imaging modality. Furthermore, ICG distribution dynamics allowed for the determination of pulmonary transit time and thus additional quantitative measures of cardiovascular function. This work demonstrates the potential for optoacoustic cardiac imaging and is expected to have a major contribution toward future preclinical studies of animal models of cardiovascular health and disease.

9323-66, Session 8

Estimating blood oxygenation from photoacoustic images

Roman Hochuli, Paul C. Beard, Benjamin T. Cox, Univ. College London (United Kingdom)

Blood oxygenation (sO_2) is a key indicator of tissue function and pathology, and photoacoustic imaging offers the promise of high-resolution 3D images of sO_2 in vivo. Clearly, it is important to know how accurately this can be achieved. Direct estimation of sO_2 from photoacoustic images is complicated by the fact that images are not proportional to the absorption coefficient, but its product with the unknown, spatially- and wavelength-dependent light fluence. It is sometimes assumed that the fluence is constant with wavelength, meaning sO_2 can be recovered via a straightforward linear inversion, which is not true in general. In this study, we use two numerical phantoms – a blood-filled tube in a scattering background, and a realistic phantom of vascularised tissue – and a Monte Carlo model of light transport to examine when this assumption is accurate. Using image without acoustic reconstruction artefacts, it is shown that sO_2 cannot be accurately estimated in the tube phantom when wavelengths are blindly chosen; however, selecting wavelengths where the absorption coefficient is both low and of similar magnitude allows more accurate sO_2 estimation. A simple exponential correction for light attenuation can reduce the variance of estimates but does not improve the accuracy. These results

are extended to the tissue-realistic phantom, demonstrating that sO_2 can be estimated to within $\pm 2\%$, but only to a depth of 2mm, and only using a pair of wavelengths where the absorption coefficient of blood is low and undergoes minimal change between wavelengths. There seems, therefore, to be an inherent trade-off between lack of accuracy due to changes in fluence between wavelengths, and lack of accuracy due to low SNR. We conclude that a linear inversion is only useful in practice in microscopy mode or at shallow depths in tomography mode.

9323-67, Session 8

Towards quantitative photoacoustic spectroscopy by measuring fluence variations using acousto-optic modulation

Altaf Hussain, Jacob W. Staley, Erwin Hondebrink, Wilma Petersen, Wiendelt Steenbergen, Univ. Twente (Netherlands)

Photoacoustic imaging (PAI) has emerged as a promising biomedical optical imaging modality with applications ranging from microscopy to deep tissue imaging such breast cancer detection and small animal imaging. Photoacoustic spectroscopy (PAS) has enabled deep tissue high resolution functional imaging with capability to distinguish between different intrinsic/extrinsic chromophores because of their distinct absorption spectra. A challenge is to render the technique quantitative, because PA signals depend not only on local absorption coefficient but also on unknown local fluence, which varies with the illumination wavelength. The variation in local fluence is a result of the wavelength dependent optical properties of the biological tissue. Formerly, we have shown that by combining acousto-optics (AO) modulation with the PA measurements it is possible to compensate PA signals for fluence variations. Now, based on the combination of AO modulation with PA we demonstrate compensation of wavelength dependent local fluence variations in PAS by measuring relative absorption coefficient of given chromophores at various wavelengths in tomographic settings, which shows agreement with photospectrometric measurements. Further, we quantify the pre-set oxygen saturation levels of blood at different depths in turbid inhomogeneous media using the combination of AO and PA at two wavelengths and without the use of a priori knowledge of the medium properties. Our method can further be used for spectral un-mixing of PA images for identification of different chromophores presence in PA image and is a step closer to absolute absorption coefficient imaging.

9323-68, Session 8

Influence of the light propagation models on a linearized photoacoustic image reconstruction of the light absorption coefficient

Shinpei Okawa, Takeshi Hirasawa, Toshihiro Kushibiki, Miya Ishihara, National Defense Medical College (Japan)

Quantification of the optical properties of the tissues and blood vessels by noninvasive photoacoustic (PA) imaging provides useful information for screening and early diagnosis of diseases. A linearized 2D image reconstruction of the absorption coefficient of the photon absorber from the photoacoustic (PA) signals is discussed. The linearized 2D image reconstruction algorithm is based on PA wave equation and the photon diffusion equation (PDE). The reconstructed image is affected by the light propagation in the measured object. The quantitative capability and the quality of the image reconstructed by the method are investigated for the light propagations based on the radiative transfer equation and the PDE. The numerical simulation with the 3D Monte Carlo (MC) simulation and that with the finite element calculation of the PDE were carried out. The phantom experiment was also conducted. In the phantom experiment, the

**Conference 9323: Photons Plus Ultrasound:
Imaging and Sensing 2015**

PA signals were obtained by a PA probe which coaxially had an optical fiber for illumination and the ring shaped P(VDF-TrFE) ultrasound transducer. The measured object was made of Intralipid and Indocyanine green. In the numerical simulations, it was shown that the linearized image reconstruction method recovered the absorption coefficients with alleviating the dependency of the PA amplitude on the depth of the photon absorber. The linearized image reconstruction method worked effectively under the light propagation calculated by 3D-MC simulation, although the linearized image reconstruction employed 2D-PDE. The phantom experiments validated the result of the numerical simulations.

9323-69, Session 9

Universal temperature-dependent normalized optoacoustic response of blood

Elena V. Petrova, Anton Liopo, Alexander A. Oraevsky, Sergey A. Ermilov, TomoWave Laboratories, Inc. (United States)

We revealed and interpreted the universal temperature-dependent optoacoustic (photoacoustic) response (ThOR) in blood; the normalized ThOR is invariant with respect to hematocrit at the hemoglobin's isosbestic point. The unique compartmentalization of hemoglobin, the primary absorbing agent at 805 nm, inside red blood cells (RBCs) causes the effect. The phenomenon is explicated in terms of the Gruneisen parameter dependence on temperature and the nil optoacoustic response achieved at the temperature of maximum density (T₀). Similar to electrolytes, hemoglobin solutions exhibit linear concentration function of the temperature T₀. When this function is extrapolated to the average hemoglobin concentration inside erythrocytes, the temperature T₀ was found to be consistent with that measured in whole and diluted blood. Low variability of hemoglobin concentration inside RBCs results in small sample-to-sample variation of the blood ThOR. The normalization of optoacoustic image intensity at certain temperature makes calibration curve independent from both laser fluence and optical absorbance of blood allowing temperature measurements in any vascularized tissue and blood vessels. The universal behavior of ThOR in blood has high potential for non-invasive optoacoustic temperature monitoring.

9323-70, Session 9

Probing the in vivo changes in oxygen saturation with photoacoustic imaging as a non-invasive means of assessing treatment progression

Eno Hysi, Ryerson Univ. (Canada); Jonathan P. May, The Univ. of British Columbia (Canada); Lauren Wirtzfeld, Ryerson Univ. (Canada); Elijus Undzys, Ontario Institute for Cancer Research (Canada); Shyh-Dar Li, The Univ. of British Columbia (Canada); Michael C. Kolios, Ryerson Univ. (Canada)

Tumor vascularity is a critical component dictating the degree of malignancy and efficacy of cancer therapies. Often the target of therapies, vasculature is either disrupted to starve the tumor of nutrients, or normalized to improve drug delivery. We hypothesize that photoacoustic imaging, particularly oxygen saturation (sO₂) distributions, will be sensitive to treatment-induced, structural/functional changes in tumor vasculature and can be predictors of treatment efficacy.

EMT-6 (mouse mammary carcinoma) tumors were grown into the footpads of Balb/c mice and were treated with doxorubicin (DOX), either as systemic-free-drug (n=7) or by localized delivery through a thermosensitive-liposome formulation (HaT-DOX, n=12). Saline (n=12) was used as a

control group and footpads of these 3 groups were heated to 42C for 1h while 7 mice were kept unheated/untreated. VevoLAZR (VisualSonics) was used to acquire 3D-coregistered, ultrasound/photoacoustic images (40MHz/750/850nm/80µm-apart) pre-treatment and 30min/2h/5h/24h/7d post-treatment. Anatomical-segmentation of tumors was performed using ultrasound in order to map the oxygen distribution using histograms of sO₂ values.

The mode of sO₂ histograms was computed for all time-points. Within 30min post-treatment, HaT-DOX/DOX-treated animals' mode dropped 17%, and was sustained for >5h. By 24h, oxygenation had approached pre-treatment levels and by 7d, it was 24% and 10% higher than pre-treatment values of HaT-DOX and DOX, respectively. In comparison, the saline and unheated/untreated animals' sO₂ mode did not significantly change within 24h, but increased by 20% 7d post-treatment. Given the number of animals imaged, assessing the in vivo whole-tumor oxygenation changes through histogram-based approaches shows great potential as a predictive marker of treatment progression.

9323-71, Session 9

Tissue oxygen monitoring by photoacoustic lifetime imaging (PALI) and its application to image-guided photodynamic therapy (PDT)

Qi Shao, Ekaterina Morgounova, Shai Ashkenazi, Univ. of Minnesota, Twin Cities (United States)

The oxygen partial pressure (pO₂), which results from the balance between oxygen delivery and its consumption, is a key component of the physiological state of a tissue. Images of oxygen distribution can provide essential information for identifying hypoxic tissue and optimizing cancer treatment. Previously, we have reported a non-invasive in vivo imaging modality based on photoacoustic lifetime. The technique maps the excited triplet state of oxygen-sensitive dye, thus reflects the spatial and temporal distribution of tissue oxygen. We have applied PALI on tumor on small animals to identify hypoxia area. We also showed that PALI can monitor changes of tissue oxygen, in an acute ischemia and breathing modulation model.

Here we present our work on developing a treatment/imaging modality (PDT-PALI) that integrates PDT and a combined ultrasound/photoacoustic imaging system. The system provides real-time feedback of three essential parameters namely: tissue oxygen, light penetration in tumor location, and distribution of photosensitizer. Tissue oxygen imaging is performed by applying PALI, which relies on photoacoustic probing of oxygen-dependent, excitation lifetime of Methylene Blue (MB) photosensitizer. Lifetime information can also be used to generate image showing the distribution of photosensitizer. The level and penetration depth of PDT illumination can be deduced from photoacoustic imaging at the same wavelength. All images will be combined with ultrasound B-mode images for anatomical reference.

We expect that PDT efficacy can be improved by applying PALI imaging feedback in real-time to determine, and individually optimize, O₂-enriched gas breathing parameters and PDT light-dose during treatment.

9323-72, Session 9

Real-time needle guidance with photoacoustic and laser-generated ultrasound probes

Richard Colchester, Edward Z. Zhang, Charles A. Mosse, Daniil I. Nikitichev, Univ. College London (United Kingdom); Simeon West, Univ. College Hospital (United Kingdom); Paul C. Beard, Ioannis Papakonstantinou, Adrien E. Desjardins, Univ. College London (United Kingdom)

**Conference 9323: Photons Plus Ultrasound:
Imaging and Sensing 2015**

Detection of vascular structures is of critical importance during many needle-based minimally invasive procedures. For instance, in interventional pain management procedures that involve injections in the vicinity of nerves, unintentional injections into arteries can lead to strokes or cardiotoxicity. Reliable detection with current external imaging systems remains elusive. Optical generation and reception of ultrasound allow for depth-resolved detection of vascular structures, and they can be performed with miniature probes positioned within needles used in clinical practice. The probes in this study included separate optical fibers for generating and receiving ultrasound. Ultrasound generation was performed with the photoacoustic effect, using pulsed excitation light. Two ultrasound generation mechanisms were explored, which provided complementary contrast mechanisms. In the first, excitation light was provided to tissue at the vicinity of the needle tip, and ultrasound waves were generated upon absorption. In the second, ultrasound was generated at an optically absorbing coating on the distal end face of an optical fiber, and ultrasound waves reflected by tissue were received. Ultrasound reception was performed with an optical fiber sensor with a high-finesse Fabry-Pérot cavity. The sensor data was displayed with a real-time interface. The performance of the probes was measured using needle insertions toward absorbing targets in phantoms and biological tissue. Methods for integrating the probes within 21-gauge needle cannulas, including the use of 3D printing, are discussed. The results indicate that the probes can detect vascular structures in advance of the needle tips.

9323-73, Session 9
A novel approach to delineating bone interfaces and joint spaces in photoacoustic tomography of the finger

Samir Biswas, Peter van Es, Univ. Twente (Netherlands); Hein J. Bernelot Moens, Hospital Group Twente (Netherlands); Wiendelt Steenbergen, Srirang Manohar, Univ. Twente (Netherlands)

Photoacoustic (PA) tomography of the finger has potential in the diagnosis and monitoring of inflammatory diseases such as rheumatoid arthritis. The method depicts the vasculature with high detail and may be able to visualize the inflamed synovial membrane with its changed vascularity. However, PA images of the finger are often challenging to interpret in the absence of structural information especially regarding joint-gap position, where the synovial membrane encapsulates the joint. Further, the presence of bone results in strong reflection artifacts by scattering of PA epidermal signals. In this work we developed a novel method to provide information regarding joint spaces by visualizing the bone surface in the finger, using these reflection artifacts. The skin surface in the PA image is thought to represent multiple ultrasound emitters and the bone surface the reflecting interface. A backprojection algorithm was modified to reconstruct cross-sectional US reflection images from epidermal PA signals undergoing single scattering off bone. The approach involves first obtaining the travel time between the US probe and the epidermis perpendicular to it. This segment is removed from the original time trace and the remaining part of the signal used for backprojection, as if locations on the epidermis are US pulsers/receivers. We have been successful in estimating the size and shape of bone mimicking objects in a finger phantom, and in the index finger of a volunteer. Our method assists in fast and easy interpretation of PA images and can be applied to identify the interphalangeal joint gaps for applications in rheumatology.

9323-74, Session 9
Use of multi-wavelength photoacoustic imaging to distinguish HIFU ablation lesions

Joshua P. Gray, The Univ. of Texas M.D. Anderson Cancer Ctr. (United States) and Univ. of Texas Graduate School of

Biomedical Sciences at Houston (United States); Nicholas P. Dana, The Univ. of Texas at Austin (United States); Florian Maier, Oguzhan Ege, The Univ. of Texas M.D. Anderson Cancer Ctr. (United States); Trevor Mitcham, Jason Stafford, The Univ. of Texas M.D. Anderson Cancer Ctr. (United States) and Univ. of Texas Graduate School of Biomedical Sciences at Houston (United States); Stanislav Y. Emelianov, The Univ. of Texas M.D. Anderson Cancer Ctr. (United States) and The Univ. of Texas at Austin (United States); Richard Bouchard, The Univ. of Texas M.D. Anderson Cancer Ctr. (United States) and Univ. of Texas Graduate School of Biomedical Sciences at Houston (United States)

High-intensity focused ultrasound (HIFU) thermal ablation therapies can provide non-invasive treatment to a wide variety of tissues while minimizing damage to non-targeted regions. In this study, we demonstrate the feasibility of using photoacoustic (PA) imaging to characterize HIFU tissue damage. At ablative temperatures, hemoglobin denatures and becomes oxidized resulting in a modified absorption spectrum in the near-infrared region. This change in the absorption spectra of hemoglobin allows multi-wavelength PA imaging to distinguish between areas of ablated and non-ablated tissue. Thus, PA imaging could provide more direct (i.e., assesses treatment endpoint) image guidance with greater spatiotemporal resolution and at a lower cost than magnetic resonance temperature imaging, the gold standard for clinical thermography. Imaging samples were acquired from fresh porcine cardiac and liver tissue, embedded into agar phantoms, and ablated using a LabFUS 2.5-MHz, small-animal HIFU system (Image Guided Therapy Inc., Paris, France). Following HIFU ablation, combined ultrasound and multi-wavelength PA imaging in the NIR spectrum (680-970 nm) was performed using a Vevo LAZR imaging system (FUJIFILM VisualSonics Inc., Toronto, Canada). Tissue slices were then stained using triphenyl tetrazolium chloride (TTC), a redox stain that identifies metabolically active tissue. The observed PA spectra were then correlated to reference spectra to generate a tissue characterization map identifying ablated and non-ablated regions and validated with co-registered gross pathology images of the stained tissue sections. Multi-wavelength PA imaging was able to successfully distinguish adjacent ablated and non-ablated regions in tissue samples and was able to successfully predict lesion boundaries to sub-millimeter precision.

9323-75, Session 10
Spatially Fourier-encoded photoacoustic microscopy using a digital micromirror device

Jinyang Liang, Liang S. Gao, Chiye Li, Lihong V. Wang, Washington Univ. in St. Louis (United States)

In optical-resolution photoacoustic microscopy (OR-PAM), the photoacoustic (PA) signal amplitude depends on both the optical absorption coefficient of the target and the local light fluence. A common way to achieve high specific optical absorption (J/m^3) is to increase the local light fluence. For biological samples, however, the maximum light fluence is usually restricted by the ANSI safety standard for in vivo experiments. As the resultant PA signal is always mingled with the random noise, the low PA signal-to-noise ratio (SNR) translates into a low contrast-to-noise ratio (CNR), limiting the visibility of features and the accuracy of functional imaging.

Here, we present a spatially Fourier-encoded PAM (SFE-PAM) system using a digital micromirror device (DMD). The DMD works as an optical multiplexing encoder to produce time-domain discrete Fourier modulation patterns for each individual spatial element. The spatial optical absorption distribution is recovered by decoding a series of Fourier-encoded PA measurements. Compared to raster scanning with the same number of measurements, the SFE-PAM system enables more energy-efficient

**Conference 9323: Photons Plus Ultrasound:
Imaging and Sensing 2015**

delivery of laser illumination. In addition, this system possesses the Fellgett advantage, in terms of PA SNR, in the Fourier-decoded PA A-lines. We first imaged a chromium target of the letters "WU" to demonstrate spatial Fourier-encoding in PAM, then applied SFE-PAM to two biological samples. The enhanced SNR benefited PA images by increasing the image CNR and target identifiability. The SFE-PAM system is an attractive tool for accurate PA measurement of biological targets with low optical absorption coefficients or low damage thresholds.

9323-76, Session 10
High-speed photoacoustic microscopy of epilepsy in the mouse brain

Pengfei Hai, Junjie Yao, Lihong V. Wang, Washington Univ. in St. Louis (United States)

The study of the neurovascular coupling and hemodynamic responses during epilepsy is of great significance for understanding and treating this disease. Current functional brain imaging modalities lack either high spatial resolution or temporal resolution for imaging complex localized transient brain activities during epileptic seizures. Here, we demonstrate the feasibility of imaging epilepsy in the mouse brain with a high-speed photoacoustic microscope (PAM). Epilepsy, induced by focal injection of 4-aminopyridine (4-AP) in the mouse cortex, was imaged by the PAM with both high spatial ($\sim 5 \mu\text{m}$) and high temporal ($\sim 0.5 \text{ Hz}$) resolutions, and validated by simultaneously recorded electroencephalogram (EEG) signals during epileptic seizures. The high-speed PAM was able to monitor the spatiotemporal propagation of epileptiform seizures based on optical absorption contrast. By cross-correlation, the propagation speeds of epileptic waves were estimated. Changes in blood vessel diameter were also investigated. Vessel dilations in response to epileptic seizures were observed, and the dilation decreased with the distance to the injection site of 4-AP. The results demonstrated that high-speed PAM can be a useful tool for imaging epileptic seizures, and may have potential applications in drug delivery and epilepsy surgeries.

9323-77, Session 10
Retrieving small features in reflection-mode raster-scan photoacoustic microscopy using multi-frequency reconstruction

Murad Omar, Dominik Soliman, Technische Univ. München (Germany) and Helmholtz Zentrum München GmbH (Germany); Jerome Gateau, Institut Langevin (France); Vasilis Ntziachristos, Technische Univ. München (Germany) and Helmholtz Zentrum München GmbH (Germany)

We developed a reflection-mode raster-scan photoacoustic microscopy system for imaging of mesoscopic scale biological samples; this means samples which are larger than what optical microscopy can efficiently image, but still smaller than where tomographic methods become relevant, what we call the mesoscopic gap. This gap contains several interesting applications; imaging of model organisms, such as zebrafish, imaging of tumor development, and imaging of skin diseases. The implementation of the system is based on a custom-made ultrasonic detector, which enables coupling of light from the same side as the detector, enabling reflection-mode operation. The detector has a wide bandwidth of 20 MHz, i.e. a bandwidth covering multiple scales. To optimally use this bandwidth, we implemented multi-frequency reconstruction, where the detection bandwidth is divided into smaller sub-bands, each sub-band is processed separately, and at the end all the sub-bands are recombined. This reconstruction scheme improves the resolution of the system, and enhances the visibility of small structures. System characterization shows that the system achieves a resolution of $4 \mu\text{m}$ axially, and $18 \mu\text{m}$ laterally, at penetration depths reaching up to 5 mm. After characterization, we showcased the system performance in imaging a zebrafish ex-vivo, and an

excised mouse ear. From the zebrafish image, features such as the lateral line, the intestines, the eyes, and the melanocytes are seen, on the mouse ear image, the vessels network is seen, where both large vessels, and small microvasculature are seen, the microvasculature only appears after applying the multi-frequency reconstruction.

9323-78, Session 10
Photo-imprint super-resolution photoacoustic microscopy

Junjie Yao, Lidai Wang, Chiye Li, Chi Zhang, Lihong V. Wang, Washington Univ. in St. Louis (United States)

Super-resolution optical microscopy allows the imaging of cellular and subcellular structures with resolution finer than the diffraction limit. Here, combining the absorption-based photoacoustic effect and intensity-dependent photobleaching effect, we demonstrate a simple method for super-resolution photoacoustic imaging of both fluorescent and non-fluorescent samples. Our method is based on a double-excitation process, where the first excitation pulse partially and inhomogeneously bleaches the molecules in the diffraction-limited excitation volume, thus biasing the signal contributions from a second excitation pulse striking the same region. The differential signal between the two excitations preserves the signal contribution mostly from the center of the excitation volume, and dramatically improves the lateral resolution. Moreover, due to the nonlinear nature of the signal, our method offers inherent optical sectioning capability, which is lacking in conventional photoacoustic microscopy. By scanning the excitation beam, we performed three-dimensional sub-diffraction imaging of varied fluorescent and non-fluorescent species. A lateral resolution of 80 nm and an axial resolution of 370 nm have been demonstrated, which are the highest resolutions achieved so far in photoacoustic imaging. As any molecules have absorption, this technique has the potential to enable label-free super-resolution imaging, and can be transferred to other optical imaging modalities or combined with other super-resolution methods.

9323-79, Session 10
Photoacoustic and quantitative phase cell imaging using a low-profile low-cost ultrasonic detector

Adi Sheinfeld, Will J. Eldridge, Carl Herickhoff, Adam Wax, Duke Univ. (United States)

Photoacoustic microscopy (PAM) has been developed for a variety of imaging applications at the cellular and subcellular level. However, most PAM systems are based on relatively bulky ultrasonic transducers to provide the large bandwidth required when exciting with short laser pulses. Such transducers require engineering of cumbersome systems to provide confocal excitation and detection and avoid beam blocking by the transducer. Ring transducers suggested to overcome this limitation have often been custom-made and expensive.

We suggest a PAM system based on sinusoidal modulation of the excitation beam and a narrow-band detection that utilizes a low profile and extremely low cost piezo-ceramic ring. High quality images of cancer cells tagged with gold nanoparticles (GNPs) were obtained with the proposed system without damaging the cells. The GNPs were functionalized with anti-epidermal growth factor receptor (EGFR) for specific binding to cancer cells. In addition, the use of a ring transducer enabled the simple addition of a co-registered quantitative phase image (QPI) based on off-axis holography. QPI provided high resolution imaging of the cellular structures while PAM provided EGFR molecular contrast. The PAM excitation and the QPI detection could also be combined to generate photothermal imaging of the GNPs with optical lock-in detection. A comparison of the photothermal and photoacoustic images is discussed. This dual-modality microscopy method can potentially be implemented in a compact and low cost probe and be used for cellular imaging as well as other applications.

9323-80, Session 10

Margin analysis of breast specimens using photoacoustic microscopy

Ruiying Zhang, Terence T. W. Wong, Chi Zhang, Tao Ju, Deborah V. Novack, Rebecca L. Aft, Lihong V. Wang, Washington Univ. in St. Louis (United States)

Re-excision surgeries for breast cancer are a burden to patients physically and psychologically. Moreover, they increase healthcare costs and can delay recommended adjuvant treatment. During breast conserving surgery, photoacoustic microscopy can potentially be used for the intraoperative assessment of breast cancer tissue via intrinsic optical contrast in the ultraviolet (UV) wavelength range. Fresh tissue from the surgery was imaged by a reflection-mode photoacoustic microscopy system at 266 nm. The time-resolved photoacoustic signals were detected by a 42 MHz ultrasonic transducer, and a 2D maximum amplitude image of the specimen was obtained through raster scan. The strong optical absorption of cell nuclei in the UV range provided excellent contrast for the breast cancer margin analysis. Based on the nuclear features, the breast tissue margin was evaluated and classified. Such intraoperative margin analysis with photoacoustic imaging can potentially eliminate the needs for a second surgical procedure for margin control, leading to more efficient treatment for cancer patients.

9323-81, Session 11

Screening circulating tumor cells and microemboli using optical and photoacoustic microscopy

Jason R. Cook, Chun-Hsien Wu, The Univ. of Texas at Austin (United States); Konstantin V. Sokolov, The Univ. of Texas M.D. Anderson Cancer Ctr. (United States) and The Univ. of Texas at Austin (United States); Stanislav Y. Emelianov, The Univ. of Texas at Austin (United States)

Approximately 90% of all cancer related deaths occur in patients with metastases in distant tissues. Although not the only metastatic pathway, the circulatory system can transport disseminated tumor cells to any point in the body. Factors including diagnosis, prognosis, treatment planning, and treatment monitoring can be assessed by screening for cancer cells in the blood. Currently, numerous investigators and companies have been developing techniques focused on the detection of circulating tumor cells (CTCs). Although merit can be attributed to these approaches, none can reliably differentiate individual cells from microemboli. Circulating tumor microemboli (CTMs) have a higher metastatic potential because of their larger size and enhanced viability. Here, we describe a new technique centered on combined photoacoustic and optical microscopy to detect and enumerate both CTCs and CTMs. Our technique first labels CTCs/CTMs in whole blood with a molecularly-specific combined magnetic and plasmonic nanocluster. The labeled cells are enriched from the whole blood using a gentle immunomagnetic capture method. The captured cells are then imaged using PA microscopy to identify CTCs/CTMs and optical microscopy to visualize cell boundaries. The results of the combined imaging are used to discern and enumerate both CTCs and CTMs. We tested the feasibility of our screening technique using whole human blood samples spiked with A431 squamous cell carcinoma. Excellent sensitivity discerning labeled cancer cells from leukocytes was demonstrated using PA microscopy. By combining the PA image with bright-field optical microscopy, we were able to enumerate both CTCs and CTMs, and characterize the size of the CTMs.

9323-82, Session 11

Nanosecond dynamics of laser-induced vaporization from polymeric microcapsules studied using an ultrafast optical camera

Guillaume Lajoinie, Erik Gelderblom, Univ. Twente (Netherlands); Ceciel Chlon, Marcel Böhmer, Philips Research Nederland B.V. (Netherlands); Wiendelt Steenbergen, Univ. Twente (Netherlands); Nico de Jong, Erasmus MC (Netherlands); Srirang Manohar, Michel Versluis, Univ. Twente (Netherlands)

There is considerable interest in contrast agents for photoacoustic imaging. Recently a new class of agents based on laser triggered phase-change or thermal cavitation has been introduced. Typically these comprise a fluid whose vaporization is triggered beyond its boiling point by strong light absorption by means of optical absorbers localized in the liquid, here in the wall of a capsule. The localized heat deposition and phase conversion produces cavitation that emits acoustic responses more intense than those from conventional contrast agents. While this approach shows great potential in diagnostic and therapeutic applications, the precise physical mechanisms associated with vaporization have not been clarified. This is primarily due to the sub-microsecond timescale of the vapor bubble dynamics. Here we study single micron-sized polymeric capsules with the optical absorber embedded in the shell using an ultrafast optical camera – the Brandaris 128 – , together with sensitive acoustic detection. Pulsed laser excitation leads to controlled vapor bubble formation and collapse and a simple physical model captures the observed radial dynamics and resulting acoustic pressures. Remarkably, CW laser excitation results in sustained oscillations, which we explain by a sequence of vaporization/condensation cycles, a result of the movement of absorbing microcapsule fragments in and out of the laser beam. A model incorporating rapid thermal diffusion from the polymer shell into the oil core and surrounding water revealed the physical mechanisms behind the onset of vaporization. Excellent agreement was observed between the modeled dynamics of the water-vapor interface and the experiments.

9323-83, Session 11

Triggered vaporization of gold nanodroplets for enhanced photothermal therapy

Shu-Wei Liu, Wei-Wen Liu, Pai-Chi Li, National Taiwan Univ. (Taiwan)

Acoustic droplet vaporization has been proposed for sonoporation. In this study, we hypothesize that, by using gold nanodroplets (AuNDs), vaporization can be triggered with external application of laser irradiation. In addition, the vaporization assisted sonoporation can enhance delivery of gold nanoparticles (AuNPs) into the cells, thus potentially enhancing effects of plasmonic photothermal therapy. To test our hypothesis, in vitro and in vivo studies were conducted. The delivery efficiency of AuNDs was also compared to that of AuNPs encapsulated in ultrasound microbubbles (AuMBs). The inertial cavitation dose (ICD), optical density (OD) value of AuNPs, and temperature rise were all measured under the applications of ultrasound only, laser only, and both ultrasound and laser. Results show that the cavitation effects and microbubble destruction were the highest with both ultrasound and laser being applied. In addition, destruction ratio of AuNDs was around 45%, compared to 35% microbubble destruction of AuMBs. Likewise, the OD value of AuNDs is 1.5 times higher than that of AuMBs under the same conditions, indicating that cavitation resulting from microbubble destruction did have the capability to assist the delivery of AuNPs into the cells. After the delivery, laser heating resulted in cell death. The cell viability with AuNDs was 40% in the in vitro studies. In vivo experiments also demonstrate the tumor treatment effects. Synergistic effects were also evident when combining laser with ultrasound.

**Conference 9323: Photons Plus Ultrasound:
Imaging and Sensing 2015**

9323-84, Session 11

Photothermal stimuli-responsive nanoamplifier as a dynamic photoacoustic contrast agent

Soon Joon Yoon, Yun-Sheng Chen, Stanislav Y. Emelianov, The Univ. of Texas at Austin (United States)

We present metal-hydrogel nanocomposites consisting of CuS nanospheres encapsulated within photothermal stimuli-responsive poly-N-isopropylacrylamide (PNIPAM) nanogel carriers as a dynamic contrast agent for photoacoustic imaging. We synthesized the PNIPAM-CuS nanoclusters with the overall size of 700 nm in diameter at room temperature. These nanocomposites shrink to 350 nm when temperature rises above their lower critical solution temperature (LCST). More than five times higher photoacoustic signal enhancement was observed from a tissue-mimicking phantom containing PNIPAM-CuS nanoamplifiers when temperature exceeded the LCST (32°C). We investigated the PNIPAM-CuS nanoamplifiers in ex-vivo mouse imaging experiments where the mixture of PNIPAM-CuS nanocomposites and matrigel was implanted into the flank of a Nu/Nu mouse. As a control, the individual CuS nanospheres were injected adjacent to the PNIPAM-CuS nanocomposites for photoacoustic signal comparison. During the photoacoustic imaging at 1064 nm, a continuous wave Nd:YAG laser operating at 1064 nm was periodically turned on and off for heating the area where the nanoparticles were located. The photoacoustic signal from the region injected with the PNIPAM-CuS nanocomposites was much stronger compared to that of the individual CuS nanospheres. In addition, the dynamically changing (i.e., blinking) photoacoustic signals were monitored in real-time as the photoacoustic signal from the PNIPAM-CuS nanocomposites region closely followed the periodic CW laser on-off cycles. Consequently, photoacoustic images with high contrast-to-noise ratio were produced. The results indicate that the PNIPAM-CuS nanocomposites, irradiated by an external trigger signal, can be optically modulated and act as dynamic photoacoustic contrast agent for molecular imaging and an image-guided drug delivery and controlled release.

9323-85, Session 11

Non-invasive photoacoustic imaging of the intestine with organic naphthalocyanines nanoparticles

Mansik Jeon, Pohang Univ. of Science and Technology (Korea, Republic of); Yumiao Zhang, Jonathan Lovell, Univ. at Buffalo (United States); Chulhong Kim, Pohang Univ. of Science and Technology (Korea, Republic of)

Presently, there is a need for safer and improved approaches for non-invasive imaging of the gastrointestinal (GI) tract. Many of diseases are localized to particular sections of the intestine, but can be difficult to diagnose, given the internal, winding and extensive length of the GI tract. In this study, we have photoacoustically imaged the GI tract of small animals in vivo using a novel organic nanoformulated naphthalocyanines, which is called nanonaps that can withstand the harsh conditions of the stomach and intestines. We used two types of combined photoacoustic (PA) and ultrasound (US) systems. The first one was a custom-made volumetric reflection-mode PAT system using a single element ultrasound transducer with raster scanning, whereas the other one was a commercial Vevo LAZR (VisualSonics) US/PA imaging system for real-time imaging with 21 MHz transducer frequency. The movement of nanonaps in the digestive system was photoacoustically monitored after gavage of nanonaps in female BALB/c mice. The progression of nanonaps through the intestine was clearly observed, as well as detailed anatomical features. Negligible background signal was detected, enabling clear resolution of intestinal features and individual small bowel diverticula were distinguishable. Depth encoding of the small intestine revealed the spatial information about nanonaps in the intestine. We have successfully imaged the GI tract and shown the utility of

nanonaps as a contrast agent for PA imaging. GI imaging using nanonaps and real-time PA/US imaging enabled high resolution, low-background, real-time mapping of intestinal anatomy and function.

9323-86, Session 11

Blinking perfluorocarbon nanoparticles for background-free optically activated ultrasound and photoacoustic imaging

Alexander Hannah, Geoffrey P. Luke, Stanislav Y. Emelianov, The Univ. of Texas at Austin (United States)

Medical ultrasound imaging commonly utilizes injectable microbubble contrast agents to highlight regions of interest and improve its diagnostic capabilities. Additionally, photoacoustic imaging agents on the nanometer scale are used to enhance image contrast. We have developed an optically activated dual contrast nanoagent for ultrasound and photoacoustic imaging, a liquid perfluorohexane nanodroplet encased in a surfactant shell and encapsulating a near infrared optical absorber. This droplet vaporizes in response to a pulsed laser, providing a photoacoustic signal, which is stronger than from thermal expansion of the photoabsorber. The droplet also induces phase-change ultrasound contrast, and immediately recondenses due to its high boiling point relative to body temperature. By imaging the droplets using high frame rate ultrasound, we capture this rapid phase-change "blinking" behavior. Due to the known repetition rate of the pulsed laser and hence nanodroplet vaporization, an autocorrelation algorithm of the differential ultrasound intensity can be used to discern the nanodroplets from the surrounding tissue and provide a background-free map of the particles. Phantom studies were conducted to optimize the particle formulation and image processing. The nanodroplets were then injected into a murine model, and the lymph node was imaged in vivo. The contrast-to-noise ratio of the in vivo processed image is 37 dB, compared to 5.3 dB using conventional B-mode imaging. These nanodroplets combined with the imaging technique substantially improve image contrast and identify the location of the injected particles.

9323-87, Session 11

Effects of silica coating and interfacial thermal resistances on the photoacoustic generation by a gold nanosphere

Florian Poisson, Amaury Prost, Olivier Simandoux, Anisia Popescu, Jérôme Gateau, Emmanuel Bossy, Institut Langevin (France)

Photoacoustic imaging provides a unique and high optical-absorption contrast in biological tissue. To selectively map anatomical or physiological feature, one alternative to endogenous absorption is to use contrast agents. Gold nanoparticles have emerged as excellent candidates because they are biocompatible, readily functionalizable, and have a particularly high effective absorption cross section. The photoacoustic signal generation from these particles is however not yet fully understood and can be affected by their surrounding environment. In particular several recent experimental studies have shown that adding a layer of silica on the particles tends to enhance the generated photoacoustic signal. To better understand the photoacoustic generation in the case of a gold nanoparticle, we model and solve both the thermal and thermo-elastic problems in the case of a gold nanosphere. Specifically, we study the influence of a variable-sized silica coating and of the interfacial thermal resistances between the different materials (gold, silica, water). The thermal problem is first solved either analytically (using the Laplace transform) or by use of a finite-difference time-domain approach. For the simplest cases where both analytical and FDTD solutions are available, the results were in perfect agreement, validating the FDTD approach that could then be applied to more complex situations. The spatio-temporal temperature field was then used as a source term in a thermo-elastic model solved by a FDTD approach to compute

**Conference 9323: Photons Plus Ultrasound:
Imaging and Sensing 2015**

the photoacoustic signals. We report quantitative estimates of how the temperature fields and the photoacoustic signals are significantly affected by the interfacial thermal resistances and the silica coating.

9323-88, Session 11

Validating tyrosinase homologue MelA as a photoacoustic reporter gene for imaging escherichia coli

Robert J. Paproski, Yan Li, Quinn Barber, John D. Lewis, Robert E. Campbell, Roger J. Zemp, Univ. of Alberta (Canada)

Antibiotic drug resistance is a major worldwide issue. Development of new therapies against pathogenic bacteria requires appropriate research tools for replicating and characterizing the infection. Previously fluorescence and bioluminescence modalities have been used to image infectious burden in animal models but scattering significantly limits imaging depth and resolution. We hypothesize that photoacoustic imaging, which has improved depth-to-resolution ratio, could be useful for visualizing MelA expressing bacteria since MelA is a bacterial tyrosinase homologue involved in melanin production which provides strong photoacoustic signal. *E. coli* were transformed with the pTrc plasmid containing the MelA gene and MelA was induced with isopropyl β-D-1-thiogalactopyranoside, causing visibly black bacteria in liquid culture. Phosphate buffered saline (PBS), MelA expressing bacteria (at different dilutions in PBS), and chicken embryo blood were injected in plastic tubes which were imaged using a VisualSonics Vevo LAZR system. Photoacoustic imaging at 5 different wavelengths (700, 750, 800, 850 and 900nm) enabled spectral de-mixing to distinguish melanin signals from blood. The signal to noise ratio of 9x diluted MelA bacteria was 55, suggesting that ~20 bacteria cells could be detected with our system. When MelA bacteria were injected as a 100 μL bolus into a chicken embryo, photoacoustic signals from deoxy- and oxy- hemoglobin as well as MelA bacteria could be separated and overlaid on an ultrasound image, allowing visualization of the bacterial location. We show for the first time that photoacoustic imaging may be a useful tool for visualizing bacterial infections and further work incorporating photoacoustic reporters into infectious bacterial strains is warranted.

9323-89, Session 11

Optimal parameters for non-linear photoacoustic generation from gold nanospheres in the thermoelastic regime

Amaury Prost, Olivier Simandoux, Institut Langevin (France); Jérôme Gateau, Institut Langevin (France) and Lab. Kastler-Brossel (France); Emmanuel Bossy, Florian Poisson, Institut Langevin (France)

Gold nanoparticles have emerged as excellent contrast agents for photoacoustic imaging, in particular because they have large absorption cross sections. When gold nanoparticles are illuminated by nanosecond pulsed light, very high temperature rises can occur at the immediate vicinity of the particle. In particular, nano-bubbles may be formed for sufficiently high temperature rises, leading to a non-linear relationship between the photoacoustic emission and the laser fluence. However, one also expects a lower range of laser fluence for which the temperature rise remains high enough to induce a nonlinear relationship in the thermoelastic regime without phase transition. This effect has been theoretically studied for idealized point-absorbers more than ten years ago [Calasso, Craig and Diebold, PRL 86(16), 2001], and is based on the temperature-dependence of the thermal expansion coefficient. In this work, we study theoretically the non-linear photoacoustic generation by a finite-size gold nanosphere, by taking into account the full thermal conduction problem and the thermo-elastic generation within the sphere and its aqueous environment. A

modified photoacoustic equation with a temperature-dependent thermal expansion coefficient is introduced, as a correction to the conventional textbook equation used so far. Quantitative predictions are obtained by numerically solving the governing equations (by use of finite-difference time-domain computations). Specifically, we show that there is an optimal sphere diameter to maximize the photoacoustic non-linearity. We also demonstrate the weight of the non-linearities depends on the ultrasound frequency band. The nonlinearity is also shown to affect the photoacoustic generation as a function of the equilibrium temperature in water.

9323-90, Session 11

In vitro characterization of a lifetime-based activatable photoacoustic probe

Ekaterina Morgounova, Sadie M. Johnson, Qi Shao, Benjamin J. Hackel, Michael Wilson, Shai Ashkenazi, Univ. of Minnesota, Twin Cities (United States)

Activatable photoacoustic probes hold great promise for in vivo imaging of enzyme activity as they exhibit high contrast and high selectivity at depths similar to that of ultrasound imaging. Here we report the synthesis and testing of a MMP-2 specific peptide probe capable of changing its transient photoacoustic lifetime from short to long after activation. The intact probe comprises an enzyme-specific cleavable sequence conjugated to a pair of methylene blue (MB) molecules that tend to aggregate in dimers, resulting in static quenching. Upon cleavage, the MB molecules diffuse away and recover their intrinsic excited-state lifetime of more than 2 μs. We demonstrated using a pump-probe photoacoustic imaging approach and flash-photolysis that the cleaved probe exhibits a transient signal with lifetime comparable to that of MB monomers, whereas no lifetime was detected for the uncleaved probe. This could allow for detection of the cleaved probe in the presence of high levels of intact probe as well as short transients due to endogenous tissue absorbers, thereby providing high contrast and low background noise. Finally, we have compared peptide sequences of varying length and structure using absorption spectrometry in order to select the probe best suited for our imaging needs. Preliminary results suggest that both factors could potentially have an impact on dimerization efficiency and the cleavage rate of the peptide. However all probes provided a high degree of dimerization and efficient separation after cleavage, indicating that a lifetime-based activatable peptide can be constructed for in vivo applications using a two-wavelength imaging approach.

9323-157, Session PTue

Advanced laser systems for photoacoustic imaging

Marc Klosner, Light Age, Inc. (United States); Ashwin Sampathkumar, Riverside Research Institute (United States); Gary Chan, Chunbai Wu, Donald F. Heller, Light Age, Inc. (United States)

We describe the ongoing development of laser systems for advanced photoacoustic imaging (PAI). We discuss the characteristics of these laser systems and their particular benefits for soft tissue imaging and next-generation mammography. We provide an overview of the laser performance and compare this with other laser systems that have been used for early-stage development of PAI. These advanced systems feature higher-pulse-energy output at clinically relevant repetition rates, as well as a novel wavelength-cycling output pulse format. Wavelength cycling provides pulse sequences for which the output repeatedly alternates between two wavelengths that provide differential imaging. This capability improves co-registration of captured differential images. We present imaging results of porcine blood phantoms obtained with a commercial ultrasound detector system and a wavelength-cycling laser source providing 500 mJ/pulse at 755 and 797 nm, operating at 25 Hz. The results include photoacoustic

**Conference 9323: Photons Plus Ultrasound:
Imaging and Sensing 2015**

images and oxygen saturation maps of tubular structures ranging from 25–100 microns, mimicking blood vessels in biological tissue. We discuss the application of these systems to the contrast-enhanced detection of various tissue types and tumors.

9323-158, Session PTue

**Evaluating the distensibility of
microvessels by photoacoustic microscopy**

Cheng Wang, Univ. of Shanghai for Science and Technology (China); Guan Xu, Univ. of Michigan Medical School (United States); Qian Cheng, Tongji Univ. (China); Xueding Wang, Univ. of Michigan Medical School (United States)

Stiffness of arteries, especially small arteries, is an important marker for many diseases and a good parameter to evaluate the risks of many cardiovascular problems. In this research, we proposed a new method for measurement of local arterial distensibility by using acoustic resolution photoacoustic microscopy (AR-PAM) technology, taking advantages from its excellent sensitivity and high spatial resolution in imaging micro-vessels in deep tissue. An AR-PAM system involving a 50 MHz focused transducer and an array of optical fibers forming a dark-field light illumination was developed. The system has obtained axial resolution up to 25 μm and lateral resolution up to 50 μm in the 500- μm focal zone of the transducer, and can present detailed morphology of a small vessel accurately without need to involve any contrast agent. B-scan images of vessels are obtained through raster scan of the probe along the cross-section of the vessels with a step size of 15 μm . The preliminary experiment on well-controlled gel phantoms demonstrates the feasibility of this method in evaluating the stiffness of small vessels. When working in the linear elastic range of a vessel, quantifying the initial and the distended diameters of the vessel before and after pressure change facilitates objective assessment of vessel distensibility. This PAM based technology holds potential for the study of a broad range of peripheral vascular diseases.

9323-159, Session PTue

**Phantom studies with gold nanorods as
contrast agents for photoacoustic imaging:
novel and old approaches**

Cinzia Avigo, Nicole Di Lascio, Consiglio Nazionale delle Ricerche (Italy); Paolo Armanetti, Univ. di Pisa (Italy); Francesco Stea, Consiglio Nazionale delle Ricerche (Italy); Lucia Cavigli, Fulvio Ratto, Roberto Pini, Istituto di Fisica Applicata Nello Carrara (Italy); Sandro Meucci, Marco Cecchini, Scuola Normale Superiore (Italy) and Lab. NEST, CNR (Italy); Claudia Kusmic, Francesco Faita, Istituto di Fisiologia Clinica (Italy); Luca Menichetti, Istituto di Fisiologia Clinica (Italy) and Fondazione Toscana G. Monasterio, CNR (Italy)

Photoacoustic imaging is emerging as a bioimaging technique. The development of contrast agents extend the potential towards novel application. The design of stable phantoms is needed to achieve a semi-quantitative evaluation of the performance of contrast agents. The aim of this study was to investigate the PA signal generated from gold nanorods loaded in custom made phantoms.

VevoLAZR (VisualSonics Inc., Toronto) was used with custom made agar phantom, with 5 parallel polyethylene tubes with 0.6mm internal and 0.99mm external diameter, and an innovative PDMS microfluidic phantom, with six parallel channels with sizes from 50 μm to 500 μm , loaded with synthesized PEGilated-GNRs(53nm length and 11nm axial diameter, plasmon

resonance at 840nm). Commercially available gold nanorods (NPZ) by Nanopartz Inc.(Loveland CO) were employed as standard material.

The absorption spectra acquired with the PA system and the spectrophotometer were compared. The reproducibility and stability of the PA signal were evaluated at different dilutions. The dynamic variation of the PA signal was evaluated as function of the number and of the characteristics of the GNRs(aspect ratio, absorbance, Au content). The SNR and the PA spatial resolution were measured across the range of concentrations studied.

The agar and PDMS phantoms demonstrated suitable for the characterization of PA contrast agents. The precise (μm resolution) and controlled geometry of the PDMS phantom allows to estimate the PA spatial resolution and the minimum number of detectable nanoparticles. The phantoms selected allowed to characterize the GNRs and to compare the results to those of commercial NPZ.

9323-160, Session PTue

**Evaluation of accumulation kinetics of
gold nanorods in excretory organs**

Nicole Di Lascio, Cinzia Avigo, Istituto di Fisiologia Clinica (Italy); Paolo Armanetti, Univ. di Pisa (Italy); Francesco Stea, Consiglio Nazionale delle Ricerche (Italy); Lucia Cavigli, Fulvio Ratto, Roberto Pini, Istituto di Fisica Applicata Nello Carrara (Italy); Claudia Kusmic, Istituto di Fisiologia Clinica (Italy); Luca Menichetti, Istituto di Fisiologia Clinica (Italy) and Fondazione Toscana G. Monasterio, CNR (Italy); Francesco Faita, Istituto di Fisiologia Clinica (Italy)

Gold nanorods (GNRs) offer a tunable optical absorption in the near infra-red wavelength region due to their plasmon resonance, which results in strong photoacoustic (PA) signal and make them suitable as contrast agent by means of PA imaging. The aim of this study was to examine the performance of synthesized PEGilated-GNRs as contrast agent for in vivo PA imaging and to evaluate their accumulation and distribution real time.

A bolus of 200 μL of synthesized PEGilated-GNRs (53nm length and 11nm axial diameter, plasmon resonance at 840nm, 1mM gold concentration) solution was injected intravenously into mice and detected using Vevo LAZR system (VisualSonics Inc., Toronto). The accumulation of GNRs in the spleen, kidney and liver was studied by means of the amplitude dynamic variation of the PA signal during time. GNRs contrast was clearly distinguished from endogenous background by means of the nanoparticle spectroscopic specificity.

Our results suggest that PA imaging could allow an efficient and non invasive tool for in vivo detection of GNRs content and for the assessment of the kinetic parameters in target organs. The coregistration of γ -ultrasound and PA imaging is crucial for the real time evaluation of the GNRs distribution in different organs and could open new possibilities, with the use of power doppler and color coppler modality, for flow and vascular density image fusion.

9323-161, Session PTue

**Label-free photoacoustic detection of
macrophages**

Ruiying Zhang, Lidai Wang, Chi Zhang, Lihong V. Wang, Washington Univ. in St. Louis (United States)

Macrophages are involved in the removal of cellular debris and play key roles in host defense. In this study, we used a transmission-mode photoacoustic system to measure the optical absorption spectrum of macrophages every 5 nm from 405 nm to 610 nm. The calibrated absorption spectrum of macrophages indicated an increasing optical absorption

**Conference 9323: Photons Plus Ultrasound:
Imaging and Sensing 2015**

coefficient with shorter wavelengths within the measured wavelength range. Photoacoustic signals of macrophages on a glass slide were detected by a 50 MHz ultrasonic transducer. A 2D label-free image of macrophages was acquired by raster scanning the sample stage at the optimized wavelength based on the measured spectrum. Moreover, flowing macrophages suspended in a silicone tube filled with phosphate buffered saline solution could be clearly detected in M-mode at a 1 kHz laser repetition rate. Based on the measured spectrum and intrinsic optical contrast, macrophages can be potentially identified spectrally by PA in diseased tissues or in lymphatic fluid. The label-free PA detection of macrophages can be a valuable tool for the analysis of the cell components in vivo and the study of macrophage-related diseases, such as cancer, atherosclerosis, and myocardial infarction.

9323-164, Session PTue

A theoretical model for photoacoustic spectral analysis

Guan Xu, Univ. of Michigan Medical School (United States); J. Brian Fowlkes, Univ. of Michigan Medical School (United States); Xiaojun Liu, Chao Tao, Nanjing Univ. (China); Xueding Wang, Univ. of Michigan Medical School (United States)

Photoacoustic spectrum analysis (PASA), i.e. systematically analyzing the power spectrum of photoacoustic (PA) radio-frequency signals, has demonstrated the capability of characterizing the histological microstructures in biological tissues. The purpose of this study is to theoretically validate the method of PASA. The analytical solution to the power spectrum of PA signals generated by identical microspheres following discrete uniform random distribution in space was derived. The power spectrum was decomposed into several independent factors, of which the explicit analytical expressions were individually derived. The analytical expressions in combination allow the quantification of the power spectrum profiles and the PASA parameters. The simulation and experiment validation of analytical solution include: 1) the power spectrum profile of a single microsphere with a diameter of 300 μm ; and 2) the PASA parameters of the PA signals generated by randomly distributed microspheres of diameters of 100, 200, 300, 400 and 500 μm , and at concentrations of 30, 60, 120, 240, 480 per 1.53 cubic centimeter in the observation range of [0.5, 13 MHz]. The single microsphere experiment confirmed our hypothesis that the periodical fluctuations of the PA signal power spectrum can be used to quantify the dimension of the microsphere. The multiple microsphere experiment validated that the PASA could quantify the dimensions and concentrations of the optical absorbers. In addition, slope, in comparison with other PASA parameters, is more robust as it is less affected by the uncertainties brought in by the optical illumination.

9323-165, Session PTue

Photoacoustic physio-chemical analysis and its implementation in deep tissue with a catheter setup

Guan Xu, Univ. of Michigan Medical School (United States); Zhuoxian Meng, Jiandie Lin, Univ. of Michigan (United States); Qian Cheng, Tongji Univ. (China); Xueding Wang, Univ. of Michigan Medical School (United States)

Most pathological conditions involve both microstructural and chemical changes in tissues. Due to its unique multi-physics nature, the emerging photoacoustic (PA) technology can, for the first time, present information regarding both microscopic morphology and chemical contents in a biological sample simultaneously in a non-invasive manner. A 2 dimensional (2D) physio-chemical spectrogram (PCS) can be generated by 1) performing PA measurements of a tissue over a broad optical spectrum covering the absorption peaks of specifically relevant chemical components in the tissue,

2) transforming the signals into the frequency domain, and 3) arranging the frequency domain power spectra side-by-side in the order of the optical wavelengths. This PCS derived from photoacoustic measurements presents the "optical signature" and the "ultrasound (US) signature" simultaneously in a 2D map, containing very rich pathological information. The analysis of such PCS, or namely PA physio-chemical analysis (PAPCA) enables simultaneous quantification of not only the relative concentrations but also the spatial distributions (or microfeatures) of a variety of chemical components in biological tissues. Through the study on both ex vivo and in situ mouse liver models, we have examined the feasibility of PAPCA in characterizing liver conditions including steatosis and fibrosis during the progression of non-alcoholic fatty liver disease. To resolve the challenge associated with limited PA imaging depth, we have also explored the possibility to achieve deep tissue characterization through a miniaturized probe that can be delivered through a catheter. The initial study on this setup has shown satisfactory accuracy in differentiating steatotic livers from normal ones.

9323-167, Session PTue

3D optoacoustic mesoscopy with a 24MHz translate-rotate scanner

Andrei Chekkoury, Helmholtz Zentrum München GmbH (Germany) and Technische Univ. München (Germany); Jerome Gateau, Institut Langevin (France); Vasilis Ntziachristos, Helmholtz Zentrum München GmbH (Germany) and Technische Univ. München (Germany)

Optoacoustic mesoscopy aims at imaging small organisms and entire organs at depths that go beyond typical microscopy methods and with a sub-100 μm resolution, to retrieve anatomical, functional and molecular information. To obtain volumetric optoacoustic images of samples sized up to 9x9x9 mm³, we designed a novel translate-rotate tomographic geometry for a 24MHz linear ultrasound detector array (128 elements, 7.5mm focal distance). By translating the array across and around the sample, we extended the receiving aperture along the focusing direction of the array and took advantage of the large aperture in the other direction. Optical excitation was performed using a nanosecond pulsed laser, delivering <10ns duration pulses at 760nm with a repetition rate of 10Hz. The large aperture resulting from the novel geometry improved both resolution and spatial fidelity over a simple translation of the array. Imaging 10 μm microspheres dispersed in a turbid agar phantom, we demonstrate a high spatial resolution: 30 μm in two dimensions and 100 μm in the third one. The biological capabilities of the current implementation were showcased on a freshly excised, intact mouse kidney. The complex 3D architecture of the kidney vasculature was reconstructed, and matched against anatomical pictures taken during the subsequent sectioning of the organ. At least five orders of vessel branching, from the renal vein to interlobular vessels, were resolved. The developed system shows an unprecedented combination of imaged volume, angular detection aperture, and high 3D resolution and is therefore expected to be of great interest for biological study at mesoscopic scale.

9323-168, Session PTue

Ultra-wideband three-dimensional optoacoustic tomography

Andrei Chekkoury, Helmholtz Zentrum München GmbH (Germany) and Technische Univ. München (Germany); Jérôme Gateau, Institut Langevin (France); Vasilis Ntziachristos, Helmholtz Zentrum München GmbH (Germany) and Technische Univ. München (Germany)

In optoacoustics, absorbing structures excited with short laser pulses generate broadband ultrasound waves, whose frequency content depends

**Conference 9323: Photons Plus Ultrasound:
Imaging and Sensing 2015**

on their size, shape, and orientation with regards to the detector. Thus, the center frequency and bandwidth of a given detector define the range of structure sizes it is able to resolve, and usually act as a band-pass filter. Therefore, detectors with different frequency bandwidths record different subsets of information in complex biological sample. To retrieve the information from an ultra wideband, we investigated here the operation of successive scanning of a sample with two ultrasound arrays featuring center frequencies of 6MHz and 24MHz, respectively.

We employed a novel translate-rotate scanning geometry that takes advantage of the high sensitivity and parallel acquisition capabilities of linear arrays to provide high-resolution 3D images. A volumetric optoacoustic system that could incorporate both linear ultrasound arrays to record datasets from the same sample was implemented. By combining the detection bandwidth of the 6MHz transducer (100kHz - 12MHz) with the 24MHz transducer (2MHz-40MHz), the system recorded a broad spectrum of frequencies.

We demonstrated the biological imaging capabilities of this novel implementation on freshly excised murine organs (spleen, liver and kidneys). 3D images were reconstructed for each band, and we developed advanced visualization techniques to overlay all the information together. Structures ranging from entire organs to microvasculature were reconstructed and we found that each frequency band provide complementary information allowing to obtain a more complete picture of the spatial optical absorption in the samples.

9323-169, Session PTue

Photoacoustic spectrum analysis for bone microstructure characterization

Ting Feng, Nanjing Univ. (China); Kenneth M. Kozloff, Univ. of Michigan Medical School (United States); Cheri Deng, Univ. of Michigan (United States); Jie Yuan, Sidan Du, Nanjing Univ. (China); Xueding Wang, Univ. of Michigan Medical School (United States)

Osteoporosis is a progressive bone disease that is characterized by a decrease in bone mass and deterioration in microarchitecture. This study investigates the feasibility of characterizing bone microstructure by analyzing the frequency spectrum of the photoacoustic signals from the bone. Modeling and numerical simulation of photoacoustic signals and their frequency-domain analysis were performed on trabecular bones with different mineral densities. The resulting quasi-linear photoacoustic spectra were fit by linear regression, from which spectral parameters including slope, midband fit and intercept can be quantified. The modeling demonstrates that, at an optical wavelength of 685 nm, bone specimens with lower mineral densities have higher slope, higher midband fit, and higher intercept. Preliminary experiment on osteoporosis rat tibia bones with different mineral contents has also been conducted, and the results were validated by the gold standard microCT. The findings from the experiment are in good agreement with the modeling, both demonstrating that the frequency-domain analysis of photoacoustic signals can provide objective assessment of bone microstructure and deterioration. Considering that photoacoustic measurement is non-ionizing, non-invasive, and has sufficient penetration in both calcified and non-calcified tissues, this new technology holds unique advantages for clinical translation. Moreover, unlike conventional transmission ultrasound techniques, the photoacoustic technique evaluates bone based on highly sensitive optical contrast, and is conducted in a reflection mode, facilitating the assessment of not only peripheral sites, such as heel and wrist, but also central sites, such as spine which is one of the main areas at risk from osteoporotic fractures.

9323-170, Session PTue

Quantification of absolute blood oxygen saturation with photoacoustic imaging

Aedán Breathnach, Hrebesh Molly Subhash, Martin J. Leahy, National Univ. of Ireland, Galway (Ireland)

Photoacoustic (PA) imaging refers to a non-invasive hybrid imaging modality which has broad applications in diagnostic medicine, cancer detection, and therapy monitoring. By detecting acoustic waves generated through the PA effect, PA imaging can directly measure specific optical absorption, which is the product of the tissue-intrinsic optical absorption coefficient and the local optical fluence. Therefore, quantitative PA imaging, such as quantification of blood oxygen saturation (sO₂), requires knowledge of the local optical fluence, which can only be estimated with sophisticated modelling techniques or through invasive measurements. By calculating the ratio of PA pressure amplitudes at several wavelengths, an expression for absolute blood oxygen saturation can be derived. By using the fact that sO₂ is uniform (~97% in resting conditions in humans) throughout the arterial tree, and indeed can be measured anywhere (e.g. the finger), we can calculate relative fluence values in any artery within the field of view by imaging at several wavelengths. An interpolation can be done to calculate relative fluence in nearby veins, which are distinguished from arteries using colour Doppler ultrasound on the Vevo Lazr® 2100 imaging system. The new method was validated with both in vivo and phantom experiments.

9323-171, Session PTue

Soft tissue imaging using a high voxel rate quantum-memory-based acousto-optic technique

Luke R. Taylor, Alexander Doronin, Igor V. Meglinski, Jevon J. Longdell, Univ. of Otago (New Zealand)

We present recent results on the use of a quantum memory based acousto-optic technique for non-invasive, deep tissue, high voxel rate imaging of biological samples. The interaction between an acoustic and an optical pulse leads to sideband modulation on the carrier, and information on the common volume can be obtained provided one can selectively detect the highly scattered and subtly frequency shifted light. Using a pair of atomic frequency combs (AFC) as a highly frequency selective filter (better than 1 part in 10⁸) we are easily able to discriminate between ultrasound tagged and carrier photons (up to ca. 50dB). The absorbed and frequency shifted signal is recovered as a photon echo (with 10-20% efficiency) delayed in time by the reciprocal of the comb tooth spacing (6.6μs). The technique is based on optical pumping alone, without need for additional fields, in cryogenic Pr³⁺:Y₂SiO₅.

We demonstrate 3D imaging at depth in highly scattering media, with voxel acquisition rates in excess of 10kHz. We present results on both the technical process and images of artificial media with inhomogeneous scattering properties. Given the nature of the technique, we consider it particularly suited for, amongst others, the determination of basal cell carcinoma boundaries, early cancer detection, or more generally, the detection of subtle changes in optical (scattering) properties an imaged tissue, such as diffusion of a substance through the skin.

9323-172, Session PTue

Surgical microscopy system using multimodal imaging system and augmented reality

Changho Lee, Donghyun Lee, Pohang Univ. of Science and Technology (Korea, Republic of); Jeehyun Kim, Kyungpook National Univ. (Korea, Republic of); Chulhong Kim, Pohang Univ. of Science and Technology (Korea, Republic of)

We have developed a virtual intraoperative surgical multimodal imaging (VIS-MI) system by combining photoacoustic microscopy (PAM), optical coherence tomography (OCT) and conventional surgical microscopy to provide simultaneous complementary biological information, such as vascular networks, tissue microstructures and magnified surface, to surgeons in real-time. By sharing the common optical path in the PAM, OCT and optical microscopy system, we can simultaneously acquire the co-registered PAM, OCT and microscope images. Moreover, by utilizing a mini-sized beam projector, two-dimensional depth-sensitive B-mode PAM and OCT images are back-projected onto the microscope view plane as augmented reality. Therefore, both the conventional microscopic and 2D cross-sectional PAM and OCT images are displayed on the plane via ocular lenses in the microscope. In this approach, additional image display monitor is not required, which can be significantly convenient to the surgeons without moving their sights during the surgeries. To demonstrate the performance of our VIS-MI system, we have successfully monitored needle intervention in phantoms. Furthermore, we have successfully guided needle insertion into mice skins *in vivo* by visualizing surrounding blood vessels as well as micro-structures from the PA-OCT images and the magnified skin surfaces from the conventional microscopic images simultaneously.

9323-173, Session PTue

Two-photon photoacoustic microscopy using image subtraction with two different pulse excitations

Yoshihisa Yamaoka, Yoshinori Harada, Kyoto Prefectural Univ. of Medicine (Japan); Masaaki Sakakura, Kyoto Univ. (Japan); Takeo Minamikawa, Kyoto Prefectural Univ. of Medicine (Japan); Shigeru Nishino, Seiji Maehara, Shujiro Hamano, Terasaki Electric Co., Ltd. (Japan); Hideo Tanaka, Tetsuro Takamatsu, Kyoto Prefectural Univ. of Medicine (Japan)

To improve the depth resolution in photoacoustic microscopy, we have proposed two-photon photoacoustic microscopy (TP-PAM). However, since the probability of two-photon absorption is lower than that of one-photon absorption, the improvement of the selectivity of two-photon photoacoustic signals is required. Detailed investigation of photoacoustic signals generated by ultrashort optical pulses in the range of femtosecond and picosecond (250 fs - 7 ps) showed that the intensity of the one-photon photoacoustic signal was independent of the pulse duration while the pulse energy was kept constant. On the other hand, the intensity of the two-photon photoacoustic signal depended on the pulse duration while the pulse energy was kept constant.

In this report, based on our findings, we proposed an image subtraction method using two excitation pulses with different pulse durations in TP-PAM. The subtraction of images for longer-pulse excitation from those for shorter-pulse excitation extracts two-photon photoacoustic images effectively. The obtained image using the subtraction method improved the contrast of the cross-sectional image of silicone hollow filled with the mixture of one-photon and two-photon absorption solutions. Two-photon photoacoustic microscopy with the subtraction method will provide new insights in detailed investigation of deep structures in biological tissues.

9323-174, Session PTue

A self-monitored theranostic platform based on nanoparticle hyperthermia therapy and alternating magnetic field induced thermoacoustic imaging

Xiaohua Feng, Fei Gao, Yuanjin Zheng, Nanyang Technological Univ. (Singapore)

Recently, low frequency radio frequencies had been advocated for thermoacoustic imaging to exploit their inherent deeper penetrations. However, despite of some theoretical explorations in thermoacoustic process of magnetic nanoparticles under alternating magnetic field (AMF), experimental demonstrations are rare. AMF induced thermoacoustic imaging of magnetic nanoparticles is particularly appealing since the system setup is inherently compatible with nanoparticle hyperthermia therapy. More importantly, owing to the capacity of thermoacoustics for accurate temperature measurement, the integration of AMF induced thermoacoustic imaging into nanoparticle hyperthermia therapy will potentially enable a theranostic platform with imaging guidance and temperature monitoring capabilities. We present herein first experimentally the AMF induced thermoacoustic process of magnetic nanoparticles and then investigate furthermore its utilization in temperature monitoring for the nanoparticle hyperthermia. To demonstrate the concept of an integrated theranostic system with minimal overhead, a single coil with an added ferrite core to enhance the delivered magnetic field is used for both the hyperthermia heating and thermoacoustic imaging by interleaving the two processes in time domain. In the thermoacoustic imaging mode, the power is set at the amplifier's maximum value whereas to avoid excess heating of the coil in hyperthermia-mode, the power is switched to a lower value and the coil is further cooled by static water. Phantom imaging results of the magnetic nanoparticles and the temperature monitoring with sub-degree accuracy during hyperthermia process by interleaved thermoacoustic sequence are demonstrated. These proof-of-concept experiments showcase the potential to integrate thermoacoustic imaging with nanoparticle hyperthermia system and identify some of the challenges therein.

9323-175, Session PTue

Dynamic ultrasound modulated optical tomography by self-referenced photorefractive holography

Jean-Baptiste Laudereau, Institut Langevin (France); Emilie Benoit à La Guillaume, LLTech SAS (France); Fabrice Devaux, FEMTO-ST (France); Umberto Bortolozzo, Institut Non Linéaire de Nice Sophia Antipolis (France); Alexander A. Grabar, Uzhgorod National Univ. (Ukraine); Jean-Pierre Huignard, Jphopto (France); Stefania Residori, Institut Non Linéaire de Nice Sophia Antipolis (France); François Ramaz, Institut Langevin (France)

Biological tissues are very strong light-scattering media. As a consequence, current medical imaging devices do not allow optical imaging of thick samples. Acousto-optic imaging is a light-ultrasound coupling technique that uses the sidebands created by acousto-optic effect to map the local light intensity within the medium. Thanks to the ballistic propagation of ultrasound in biological tissues, it accesses optical contrast with a millimeter resolution. However, acousto-optic signal is weak and presents a speckle pattern. Consequently, classical detection schemes based on interferometry with plane wave references lead to poor SNR. We developed a system based on Sn₂P₂S₆ photorefractive wavefront adaptive holography that allows to measure acousto-optic signal on a photodiode with a SNR theoretically 10⁴ times higher. However, reference beam fanning through photorefractive crystals adds a strong coherent background noise that decreases this SNR. Because the complex illumination pattern of the speckled signal has grains

**Conference 9323: Photons Plus Ultrasound:
Imaging and Sensing 2015**

size of the order of the Debye length in our crystals, it is possible to remove the reference beam and use the setup in a self-referenced configuration. Shining the crystal with a random wavefront will engrave a random and complex hologram that will act as a correlator in order to measure the speckle blurring that goes along with the generation of tagged photons, as described by F. Devaux et al. (*Opt. Express*, 22(9), 2014 May). As this blurring is proportional to the number of generated tagged photons, it is thus possible to obtain acousto-optic image in a self-referenced configuration at 800 nm within the optical therapeutic window.

9323-176, Session PTue

Integrated system for photomechanical drug delivery and photoacoustic imaging of pharmacokinetics

Yasuyuki Tsunoi, Keio Univ. (Japan); Shunichi Sato, National Defense Medical College (Japan); Ryota Watanabe, Keio Univ. (Japan); Satoko Kawauchi, Yoshihiro Miyagawa, Daisuke Mizokami, Nobuaki Tanaka, Koji Araki, Akihiro Shiotani, Toshiya Takemura, National Defense Medical College (Japan); Mitsuhiro Terakawa, Keio Univ. (Japan)

For safe and efficient pharmacological treatment, a drug must be distributed appropriately in the diseased tissue, for which a method for drug delivery and its monitoring are needed. We found that photomechanical waves (PMWs) are useful for targeted transvascular drug delivery, while photoacoustic (PA) imaging is valid to monitor distribution of a drug in tissue. Since nanosecond laser pulses are used both for PMW-based drug delivery and PA imaging, these two functions can be integrated. In this study, we developed a theranostic system for drug delivery and its monitoring. The probe consists of three main components: obliquely arranged quadruple optical fibers for transmission of nanosecond laser pulses, an ultrasound sensor with an acoustic lens for PA signal detection and a holder for the fibers and sensor. Performance characteristics of the system were investigated for the rat skin *in vivo*. A solution of Evans blue (EB) was intravenously injected to the rat. We put a black rubber target on the dorsal skin, on which the probe described above was placed. We first transmitted high-energy laser pulses (Nd:YAG laser; 532 nm; 6 ns; 13 mJ) through the fibers to hit the target for generation of PMWs, causing extravasation. The target was removed, and then we transmitted low-energy laser pulses (OPO; 610 nm; 9 ns; 0.1 mJ) through the fibers for PA imaging of EB in the tissue. We observed spatiotemporal change in the distribution of EB that was delivered by PMWs in the tissue, indicating the usefulness of our system.

9323-177, Session PTue

Photoacoustic tomography of the human finger: towards the assessment of inflammatory joint diseases

Peter van Es, Samir Biswas, Univ. Twente (Netherlands); Hein J. Bernelot Moens, Hospital Group Twente (Netherlands); Wiendelt Steenbergen, Srirang Manohar, Univ. Twente (Netherlands)

Inflammatory arthritis is often manifested in finger joints. The growth of new or withdrawal of old blood vessels can be a sensitive marker for these diseases. Photoacoustic (PA) imaging has great potential in this respect since it allows the sensitive and highly resolved visualization of blood. We systematically investigated PA imaging of finger vasculature in healthy volunteers using a newly developed PA tomographic system. The PA slice images at multiple wavelengths in the near-infrared were correlated with power Doppler ultrasound as a reference. We present the PA results which

show an unprecedented high detail of the vasculature over a length of several cm in the finger. Vessels with diameters ranging between 100 μm and 1.5 mm are visible along with details of the skin, including the epidermis and the subpapillary plexus. Results from functional studies involving the PA responses of the phalangeal vasculature to externally applied triggers such as application of a pressure cuff in the upper arm and temperature changes in the bath are also presented. The effect of skin color on the results, including presence of artefacts due to reflection of skin signals on underlying bone, are also shown. The focus of all the studies is at the proximal and distal interphalangeal joints, and in the context of ultimately visualizing the inflamed synovial membrane in patients. This work is important in laying the foundation for detailed research into PA imaging of the phalangeal vasculature in patients suffering from rheumatoid arthritis.

9323-178, Session PTue

Dual color photoacoustic mapping of sentinel lymph nodes *in vivo* using organic nanoformulated naphthalocyanines

Jeesu Kim, Changho Lee, Mansik Jeon, Pohang Univ. of Science and Technology (Korea, Republic of); Yumiao Zhang, Jonathan Lovell, Univ. at Buffalo (United States); Chulhong Kim, Pohang Univ. of Science and Technology (Korea, Republic of)

Delineating and examining sentinel lymph nodes (SLNs) and lymphatic systems are significantly important to provide the accurate status of cancer metastasis in clinical practice. Recently, photoacoustic imaging (PA) with help of external contrast agents has shown great potentials on these clinical objectives in humans. Here, we have successfully acquired dual color PA SLN images of small animals *in vivo* using recently developed organic nanoparticles, nanoformulated naphthalocyanines (referred to as nanonaps). We have used two types of nanonaps that have their own significant optical absorption peaks at 707 and 860 nm. We have independently injected each type nanonap at the left forepaw of a healthy Sprague-Dawley rat and acquired PA images of lymphatic vessels and SLNs *in vivo* using our custom-built PA imaging system. Further, we have simultaneously acquired *in vivo* dual color PA images of SLNs by separately injecting each colored nanonap into each side of the axillary region in one animal. The lymphatic vessels and SLNs were clearly visible, and their spectral characteristics followed that of each nanonap. After *in vivo* imaging, we extracted SLNs from each axillar and confirmed their accumulation in the SLNs *ex vivo*. Dual color PA imaging can potentially be useful for clinical SLN mapping.

9323-179, Session PTue

Denosing framework for multispectral optoacoustic imaging based on a combined wavelet-Karhunen-Loève representation

Stratis Tzoumas, Amir Rozenenthal, Christian Lutzweiler, Daniel Razansky, Vasilis Ntziachristos, Helmholtz Zentrum München GmbH (Germany)

One of the major challenges in dynamic multispectral optoacoustic (photoacoustic) tomography and microscopy is the relatively low signal-to-noise ratio which often requires repetitive signal acquisition and averaging, thus limiting imaging rate. In this paper, a spatio-spectral denoising method is developed for multispectral optoacoustic imaging which prevents the need for signal averaging in time, but rather exploits the implicit sparsity of multispectral optoacoustic signals both in space as well as in spectrum. Noise suppression is achieved by applying thresholding on a combined wavelet-Karhunen-Loève representation in which multispectral optoacoustic signals appear particularly sparse. The method is based

**Conference 9323: Photons Plus Ultrasound:
Imaging and Sensing 2015**

on the inherent characteristics of multispectral photoacoustic signals of tissues, offering promise for general application in different incarnations of multispectral photoacoustic tomography and microscopy. The performance of the proposed method is demonstrated on simulations and experimental images of animals acquired in vivo, for two common additive noise sources: time-varying parasitic signals and white Gaussian noise. In both cases, the proposed method shows significant improvement in image quality as compared to previously considered denoising strategies that do not exploit the available multispectral information. Overall the presented methodology bears promise for expediting image acquisition in cases of electronic noise interference.

9323-180, Session PTue

**Multiscale, multiwavelength, and
multiplane whole body photoacoustic
image of small animals in vivo**

Jeesu Kim, Mansik Jeon, Mingu Jeon, Chulhong Kim,
Pohang Univ. of Science and Technology (Korea, Republic
of)

We have successfully developed a novel multiscale and multiwavelength photoacoustic (PA) imaging system. We have successfully acquired multiscale PA images of small animals in vivo using ultrasound transducers of two different center frequencies (i.e., 5 vs 40 MHz) in a single imaging platform. The PA image acquired with the low-frequency ultrasound transducer shows vasculatures of small animals up to ~10 mm deep and the axial resolution is ~150 μ m. That obtained with the high-frequency ultrasound transducer shows vasculatures up to ~3 mm and the axial resolution is ~50 μ m. Further, we have enlarged the scanning range of the system to show the whole body imaging capability. We have successfully acquired the whole body PA images of small animals in vivo at four different planes (i.e., left sagittal, right sagittal, ventral, and dorsal). In addition, we have tuned four different wavelengths of optical excitation laser (i.e., 532, 700, 850, and 1064 nm). At each imaging plane and wavelength, the internal organs (e.g. spleen, intestine, etc.) and major blood vessels (e.g., carotid artery, mammalian vessels, etc.) of small animals are clearly identifiable. We have verified the spectral optical absorption responses of the internal structures at each wavelength of the PA image. After in vivo imaging, we have validated the position of each organ in the PA images by comparing with invasively acquired photographs. The developed multiscale and multiwavelength PA imaging system would be a principal imaging modality for small animal studies.

9323-181, Session PTue

**High repetition nanosecond Ti:sapphire
laser for photoacoustic microscopy**

Timothy K. Yang, Ulsan National Institute of Science and
Technology (Korea, Republic of) and Institute of Basic
Science Ctr. for Soft and Living Matter (Korea, Republic
of); Min Ju Kim, Ulsan National Institute of Science and
Technology (Korea, Republic of); Chulhong Kim, Pohang
Univ. of Science and Technology (Korea, Republic of);
Sungchul Bae, Ulsan National Institute of Science and
Technology (Korea, Republic of) and Institute of Basic
Science Ctr. for Soft and Living Matter (Korea, Republic of)

High resolution optical imaging technologies, such as optical coherence tomography or multiphoton microscopy has given us an opportunity to do in vivo imaging noninvasively. However, due to the high laser scattering, these optical imaging techniques were prohibited from obtaining high resolution in the diffusive regime. Photoacoustic microscopy (PAM) can overcome this soft depth limit and maintain high resolution at the

same time. In the past, PAM was limited to using an Nd:YAG laser, which requires an optical parametric oscillator (OPO) to obtain wavelengths selectively other than the second harmonic. However, OPO is unstable and cumbersome to control. We replaced the Nd:YAG laser and the OPO with a nanosecond pulsed Ti:Sapphire laser to give PAM more flexibility in the speed and the input wavelength while reducing the footprint of our system. This also increased our stability by removing OPO. Using a Ti:Sapphire laser allowed us to increase the repetition rate to 100-500 kHz. Normally, micro-lasers with this repetition rate will suffer from a significant decrease in pulse energy, but we were able to maintain stable pulses with a few hundreds nJ. Also, a well-known advantage of a Ti:Sapphire laser is its tunability from 650 to 1100 nm. For our PAM application, we used a range from 700 to 900 nm to obtain significant functional images. This added flexibility can help acquire functional images such as the angiogenesis process with better contrast. Here, we present a nanosecond Ti:Sapphire laser designated for PAM applications with increased contrast imaging.

Conference 9324: Biophotonics and Immune Responses X

Monday - Tuesday 9-10 February 2015

Part of Proceedings of SPIE Vol. 9324 Biophotonics and Immune Responses X

9324-1, Session 1

The pendulum of laser-tissue interactions swings between diagnostics and therapeutic/surgical techniques: a historical perspective (*Invited Paper*)

Steven L. Jacques, Oregon Health & Science Univ. (United States)

About 35 years ago, photomedicine was dominated by a variety of therapies and surgical techniques using lasers and conventional light sources. People irradiated tissues with lasers for photothermal and photomechanical effects, or exposed tissues for photochemical effects, then looked at the histology to learn what happened. About 25 years ago, the understanding of light transport and tissue optical properties improved sharply, coinciding with a wave of new optical devices/detectors/imagers and the adoption of math from the communications industry. The consequence of this convergence of understanding, devices and math was an explosion of diagnostic and imaging methods, which have become quite mature today. Now, the pendulum is swinging back toward laser/light interactions with cells and tissues as translational applications in medicine and biology are sought. The valuable tools developed over the last 30 years are now being applied to monitor the processes of photobiology and photomedicine.

9324-2, Session 1

Development of a novel cancer treatment from bench top to bedside (*Invited Paper*)

Tomas Hode, Lu Alleruzzo, Joseph Raker, Samuel Lam, Peter Jenkins, Immunophotonics, Inc. (United States); Robert E. Nordquist, Wound Healing of Oklahoma, Inc. (United States); Wei R. Chen, Univ. of Central Oklahoma (United States)

A novel therapy, inCVAX, for late-stage, metastatic solid cancers is currently under development by Immunophotonics, Inc, a biotech company. inCVAX combines phototherapy and immunotherapy to induce systemic anti-tumor immune responses in the hosts. With the efforts of scientists, engineers, physicians, and entrepreneurs, inCVAX has been developed from a simple concept to a promising clinical tool during the past 20 years. This talk will review the progress of the scientific development, pre-clinical and clinical studies that lead to the current status - international clinical trials for breast cancer. The obstacles overcome in the past, the milestones achieved, and the challenges lay ahead the research and business teams will be discussed. Overall, our team is extremely optimistic that inCVAX holds great promises for late-stage cancers patients who face severely limited options.

9324-3, Session 1

Photodynamic therapy (*Invited Paper*)

Tayyaba Hasan, Massachusetts General Hospital (United States)

One of the well-known applications of Laser-Tissue Interactions is Photodynamic Therapy (PDT). PDT is an approach where light activatable molecules called photosensitizers are located in target tissue and excited typically generally red light. It relies on the strategy that exogenous molecules can be localized in targets of interest and controlled

photochemistry and detection can be developed. PDT is approved in many countries of the world for several cancer and non- cancer applications. As with other therapies, the biological processes associated with PDT can be complex and may elicit molecular responses that can be exploited to enrich our arsenal of cancer treatments with novel combinatorial constructs. Often this requires the development of new delivery systems incorporating chemistry and nanotechnology. The presentation will discuss the current state of PDT and future directions.

9324-4, Session 1

Stimulation of anti-tumor immune response after photodynamic therapy for cancer (*Invited Paper*)

Michael R. Hamblin, Wellman Ctr. for Photomedicine (United States)

Photodynamic therapy (PDT) has been used as a cancer therapy for forty years but has not yet advanced to a mainstream cancer treatment. Although PDT has been shown to be an efficient photochemical way to destroy local tumors by a combination of non-toxic dyes and harmless visible light, it is its additional effects in mediating the stimulation of the host immune system that gives PDT a great potential to become more widely used. Although the stimulation of tumor-specific cytotoxic T-cells that can destroy distant tumor deposits after PDT has been reported in some animal models, it remains the exception rather than the rule. This realization has prompted several investigators to test various combination approaches that could potentiate the immune recognition of tumor antigens that have been released after PDT. Some of these combination approaches use immunostimulants including various microbial preparations that activate Toll-like receptors and other receptors for pathogen associated molecular patterns. Other approaches use cytokines and growth factors whether directly administered or genetically encoded. A promising approach targets regulatory T-cells. We believe that by understanding the methods employed by tumors to evade immune response and neutralizing them, more precise ways of potentiating PDT-induced immunity can be devised.

9324-5, Session 1

Clinical experience with laser immunotherapy (LIT) (*Invited Paper*)

Mark F. Naylor, Dermatology Associates of San Antonio (United States); Gabriela L. Ferrel, Hospital Nacional Edgardo Rebagliati Martins (Peru); Xiaosong Li, The First Affiliated Hospital of Chinese PLA General Hospital (China); Tomas Hode, Immunophotonics, Inc. (United States); Robert E. Nordquist, Wound Healing of Oklahoma, Inc. (United States); Wei R. Chen, Univ. of Central Oklahoma (United States)

We began studying laser immunotherapy (LIT) as a clinical tool in 2004. A phase I trial in 11 stage III and stage IV melanoma patients showed that LIT was an effective palliative treatment for local skin involvement (8 out of 11 patients demonstrated complete local clearance of tumor). Complete systemic responses also occurred (6 out of 11 patients). However, tumor relapse was the rule, although most patients remained responsive to re-treatment. Stage III and early stage IV patients were the most responsive, and those with greater tumor burden, less so. A phase I study in advanced breast cancer among patients expected to die within 12 months who had

**Conference 9324:
Biophotonics and Immune Responses X**

exhausted all other options yielded an objective response rate of LIT 62.5%. Four years later, 2 out of 8 evaluable patients were long-term survivors with durable complete responses, 1 out of 8 is alive with stable disease and 1 other lived 3 years before succumbing to the tumor. Laser immunotherapy is a general approach to tumor therapy which does not depend on specific mechanisms unique to the target tumor type such as tumor-specific growth factor pathway mutations. Since all tumors are susceptible to immune attack, it will probably work in many if not most tumor types. Chemotherapy unresponsive tumors will probably be first on the list of candidate tumors for laser treatment. Immunotherapy is currently leading to breakthroughs in tumor treatment. LIT represents an important advance which can synergistically leverage the effectiveness of other immunotherapies.

* Contact author

9324-6, Session 2

Activity of glycosylated chitosan and other adjuvants to PDT vaccines (*Invited Paper*)

Mladen Korbek, Judit Banath, BC Cancer Agency (Canada); Wei R. Chen, Univ. of Central Oklahoma (United States)

Therapeutic cancer vaccines generated by photodynamic therapy (PDT) represent a prominent tool in tumor immunotherapy. They are prepared by treating autologous tumor tissue or cells by PDT and then injecting this material or their lysates into tumor hosts. Although PDT vaccines are very efficient in eliciting immune response against treated tumors mediated by cytotoxic T cells, it is becoming clear that a number of factors can influence the final clinical outcome. Protocols incorporating approaches for positive modulation of these factors can increase substantially therapeutic efficacy of PDT vaccines. For instance, interventions blocking the activity of immunoregulatory populations (Tregs and myeloid-derived suppressor cells) have proven beneficial when combined with PDT vaccine treatment. Encouraging results were also obtained with glycosylated chitosan (GC), a novel immunoadjuvant prepared by attaching galactose molecules to linear polysaccharide structure of chitosan. GC was already shown to improve tumor curative effect of classical PDT, while in preliminary clinical trials where it was combined with laser phototherapy it was shown to induce immune reaction against both treated primary tumors and untreated distant metastases. A single tumor-localized GC injection (0.1 ml per mouse) given immediately after PDT vaccine treatment of mice bearing squamous cell carcinomas SCCVII caused a marked retardation of growth progression of these tumors when compared to the effect of PDT vaccine alone. Our ongoing experiments are devoted to uncovering elements of PDT vaccine-elicited immune response that are stimulated by GC treatment.

9324-7, Session 2

Development of photodynamic therapy regimens that control primary tumor growth and inhibit secondary disease (*Invited Paper*)

Sandra O. Gollnick, Roswell Park Cancer Institute (United States)

Effective therapy for advanced cancer often requires treatment of both primary tumors and systemic disease that may not be apparent at initial diagnosis. Numerous studies have shown that stimulation of the host immune system can result in the generation of anti-tumor immune responses capable of controlling metastatic tumor growth. Thus there is interest in the development of combination therapies that both control primary tumor growth and stimulate anti-tumor immunity for control of metastatic disease and subsequent tumor growth. Photodynamic therapy (PDT) is an FDA approved anti-cancer modality that has been shown to enhance anti-tumor immunity. Augmentation of anti-tumor immunity by

PDT is regimen dependent and PDT regimens that enhance anti-tumor immunity have been defined. Unfortunately these regimens have limited ability to control primary tumor growth. Therefore a two-step combination therapy was devised in which a tumor controlling PDT regimen was combined with an immune enhancing PDT regimen. To determine whether the two-step combination therapy enhanced anti-tumor immunity resistance to subsequent tumor challenge and T cell activation and function was measured. The ability to control distant disease was also determined. The results showed that the novel combination therapy stimulated anti-tumor immunity while retaining the ability to inhibit primary tumor growth of both murine colon (Colon26-HA) and mammary (4T1) carcinomas. The combination therapy resulted in enhanced tumor specific T cell activation and controlled metastatic tumor growth. These results suggest that PDT may be an effective adjuvant for therapies that fail to stimulate the host anti-tumor immune response.

9324-8, Session 2

Non-ablative fractional laser in conjunction with microneedle arrays for improved cutaneous vaccination (*Invited Paper*)

Mei X. Wu, Ji Wang, Bo Li, Harvard Medical School (United States)

Skin is much more potent than the muscle for vaccination, but it is not a common immunization route in the clinics to date, in part, owing to extreme sensitivity of skin to vaccine/adjuvant-evoked inflammation and difficulty of administration. Vaccine/adjuvant-provoked local reactogenicity includes erythema, swelling, ulceration that can persist for weeks and potentially breach skin integrity, risking infections. We found that treatment of the inoculation site with a FDA-approved, handheld, non-ablative fractional laser (NAFL) resulted in active recruitment of plasmacytoid dendritic cells (pDCs) but suppression of skin irritation-stimulating cytokines and mediators. Consequently, NAFL not only augments adaptive immunity but also importantly, reduces unwanted skin reactions significantly. When NAFL was combined with biodegradable microneedle (MN) arrays, little skin irritation was observed at the inoculation site, in sharp contrast to conventional intradermal vaccination that often causes severe lesion and permanent scars in the skin. Animals that were immunized by a MN array patch inserted into a NAFL-treated site developed robust immune responses, and were fully protected from influenza viral challenge. In contrast, only moderate immune responses and partial protection were attained in mice receiving the patch alone. NAFL as a standalone immune stimulator doesn't affect the loading capacity and fabrication process of biodegradable MN array patches, which are the major obstacles for embedding conventional adjuvants into the patch. NAFL in conjunction with biodegradable MN array patches represents a novel strategy for skin irritation-free, convenient, and effective vaccinations.

9324-9, Session 2

ALA-PDT mediated DC vaccine for skin squamous cell carcinoma (*Invited Paper*)

Jie Ji, Xiuli Wang, Zhixia Fan, Shanghai Dermatology Hospital (China); Wei R. Chen, Univ. of Central Oklahoma (United States); Haiyan Zhang, Shanghai Dermatology Hospital (China); Hongwei Wang, Huadong Hospital (China); Lei Shi, Shanghai Skin Diseases and STD Hospital (China)

With recent advances in dendritic cell (DC) research, DC-based vaccine has become a promising immunotherapy for cancers. However, most vaccines mediated by DC so far have only achieved limited success in cancer treatment. Photodynamic therapy (PDT), an established cancer therapy, can cause immunogenic apoptosis to induce an effective antitumor

**Conference 9324:
Biophotonics and Immune Responses X**

immune response. In this study, we developed a DC-based cancer vaccine using ALA-PDT-treated PECA (skin squamous cell carcinoma) cells. The maturation of DCs induced by PDT-treated apoptotic PECA cells was studied using electron microscopy, FACS and ELISA. The anti-tumor immunity of the ALA-PDT DC vaccine was tested in mice. We observed the maturation of DCs could be potentiated by ALA-PDT treated PECA tumor cells, including morphology maturation (enlargement of dendrites and increase of cytoplasm), phenotypic maturation (upregulation of surface expression of MHC-II, DC80, and CD86), and functional maturation (enhanced capability to secrete INF- γ and IL-12 and to induce T cell proliferation). Most interestingly, we found that PDT induced apoptotic tumor cells are more capable in potentiating maturation of DCs than PDT treated or freeze/thaw treated necrotic tumor cells, particularly using a light dose of 0.5J/cm² with a ALA concentration of 0.5mM. ALA-PDT DC vaccine provided protection against skin squamous cell carcinoma in mice, far stronger than that of DC vaccine obtained from freeze/thaw of tumor cells. Our results indicate that in addition to its therapeutic role in cancer treatment, ALA-PDT can also be an effective method for DC-based cancer vaccine.

9324-10, Session 3

Melanoma patients treated with laser immunotherapy (LIT) and T-cell stimulators (ipilimumab)

Mark F. Naylor, Dermatology Associates of San Antonio (United States); Tomas Hode, Immunophotonics, Inc. (United States); Robert E. Nordquist, Wound Healing of Oklahoma, Inc. (United States); Wei R. Chen, Univ. of Central Oklahoma (United States)

Immunotherapy has been a breakthrough treatment technology for a number of difficult to treat tumors, particularly melanoma, the prototypical chemotherapy-resistant tumor against which many new T-cell stimulating drugs were first tried. T-cell stimulating drugs such as ipilimumab require the presence of CD8⁺ anti-tumor T-cells for their action. T-cell stimulating drugs like ipilimumab should work better if the patient has prior treatments to increase the number and quality of anti-tumor T-cells. Laser immunotherapy (LIT) is thought to work by stimulating adaptive immunity, so pre-treatment with LIT should make drugs such as ipilimumab more effective. We have recently treated three stage IV melanoma patients with combinations of LIT and ipilimumab. Two patients were treated with LIT followed weeks to a few months later with one or more courses of ipilimumab. One patient was treated first with two courses of ipilimumab, and a few months later, with LIT. The two patients who received LIT followed by ipilimumab in the correct sequence had a significant anti-tumor response and are still alive two years after treatment. The patient who received ipilimumab followed by LIT died a few months after LIT treatment. While anecdotal, the responses seen in these three patients tend to support the hypothesis that LIT increases the number and quality of anti-tumor T-cells so that ipilimumab and other T-cell stimulating drugs work better when given after preparatory LIT treatment.

* Contact author

9324-11, Session 3

Translation of immunophotonic cancer therapy: from mouse to human to cat

Richard M. Levenson, Univ. of California, Davis (United States); Tomas Hode, Immunophotonics, Inc. (United States)

Acanthomatous ameloblastoma is an aggressive, locally invasive tumor arising in the gingiva that can progress rapidly, invade and destroy bone. Local control is imperative. However, if the lesion involves the upper jaw, surgical excision may not be possible, and other therapies have not

been fully evaluated. The primary author's cat (Gabriella) developed this tumor, with gingival masses around teeth in the upper jaw and evidence of widespread bony destruction of the hard palate, documented by CAT scan. Treatment using the protocol developed by Immunophotonics, Inc. was initiated; this involved laser irradiation plus local infiltration of a polysaccharide-based adjuvant with the intent to induce systemic anti-cancer immunity. One treatment session was performed in a veterinary clinic in Arkansas, and two follow-up sessions were performed at the small animal hospital at the UC Davis veterinary school. Side effects were generally limited except for an episode of local thermal injury from the laser at the last session, leading to an antibiotic-responsive infection. No other therapy for the neoplastic process was provided. As of this writing, at 2.5 years after first treatment and 2 years, 8 months after presentation, Gabriella is well, with no evidence of disease. This successful outcome has led to plans to conduct a clinical trial of this immunotherapy approach for treatment of cancer in companion animals at UC Davis Veterinary School.

9324-12, Session 3

Thermal cytotoxic effects of laser immunotherapy assisted with cyclophosphamide

Cody F. Bahavar, Wei R. Chen, Joseph T. Acquaviva III, Feifan Zhou, Sheyla Rabei, Aamr Hasanjee, Univ. of Central Oklahoma (United States); Roman F. Wolf, The Univ. of Oklahoma Health Sciences Ctr. (United States)

Laser Immunotherapy (LIT) is a modality for late-stage, metastatic cancers incorporating laser irradiation and immunological stimulation to generate an antitumor immunity. Recent clinical trials have shown that LIT can successfully treat patients with late-stage breast cancer and melanoma. Cyclophosphamide (CY) is a chemotherapeutic drug that suppresses regulatory T cells when used at low doses. In this study tumor-bearing rats were treated with LIT using an 805-nm laser with multiple power densities and low-dose cyclophosphamide. Glycated chitosan (GC) was used as an immunoadjuvant, administered after interstitial laser irradiation. Under the same laser density, an irradiation duration of 10 minutes resulted in a significantly higher animal survival rate than that of 5 minutes. Different irradiation powers were selected in this study. Our preliminary results could help determine the effects of thermal effects in laser immunotherapy in addition to low-dose CY and GC on the survival of the tumor-bearing rats.

9324-13, Session 4

Visualization of fluorescent model antigen-elicited specific immune response in vivo (Invited Paper)

Zhihong Zhang, Huazhong Univ. of Science and Technology (China)

Intravital optical imaging provided a useful approach for clarifying how, when, and where the immune cells involved in tumor immunity. Model antigens have been widely used to simplify the investigation of complicated anti-tumor immune response. However, the classical model antigens (e.g., OVA) cannot be directly detected without fluorescent labeling. Thus, it's necessary to develop a visualized model antigen system based on fluorescent protein itself for the intravital imaging of tumor immunity. Fluorescent protein KatushkaS158A displayed perfect optical characters and was quite suitable for optical imaging in vivo. The data indicated that it elicited both cellular and humoral immune response in the immunized C57BL/6 mice, resulting in the attenuation of the tumorigenesis of KatushkaS158A-expressing melanoma cells (K-B16) in vivo. To visualize the specific anti-tumor immune response in tumor microenvironment, EGFP-transgenic C57BL/6 mice were immunized twice with IFA-emulsified KatushkaS158A on Day 14 and Day 7 before the implantation of K-B16 cells

**Conference 9324:
Biophotonics and Immune Responses X**

into the dorsal skin-fold window chambers. The intravital imaging data indicated that strong and specific immune response against K-B16 cells was occurred in the KatushkaS158A-immunized mice at 2 days after the implantation of K-B16 cells, which swarms of EGFP+ immunocytes rushed toward the tumor cells with significantly higher motility and retained in the middle of the tumor area with high density. These responsive immunocytes eliminated K-B16 cells and blocked the growth of melanoma cells in vivo. Thus, KatushkaS158A protein was not only acted as a fluorescent marker for tumor imaging, but also used as a model antigen to elicit specific tumor immune response in C57BL/6 mice.

9324-14, Session 4
In vivo imaging of dynamic change of multiple immune cells in tumor microenvironment during immunotherapy

Shuhong Qi, Zhihong Zhang, Huazhong Univ. of Science and Technology (China)

The immunotherapy has been proven as the most efficient treatment for melanoma patients, could lead to objective tumor regression in more than 50% of patients. Cyclophosphamide (CY) is a conventional Chemotherapy drug for cancer and recent studies suggest that before adoptive T cells therapy, low dose of CY is able to deplete Tregs and increase the antitumor immune responses. Although this combined treatment is effective, the underlying mechanism of CY increased the antitumor activity of adoptive T cell is still not well understood. In our study, we used skin windows chamber model to dynamically image three different immune cells in situ in tumor microenvironment after CY treatment combined adoptive T cells therapy for murine Melanoma. We in vivo observed exogenous adoptive T cells and endogenous tumor infiltrating lymphocytes (TILs) migration and movement in the tumor microenvironment. Furthermore, we also observed that the dynamic change of Tregs and DCs in tumor microenvironment. Results show that significantly enhanced tumor suppression was observed in the combined treatment group compared with control groups. After CY treatment, the number of Tregs was significant decreased in tumor microenvironment compared to untreated groups. Furthermore, the TILs infiltrated into tumor areas were significantly increased in the combined treatment group and the intratumoral migration remained active. We conclude that by in vivo imaging, we confirmed that CY treatment could deplete Tregs in murine melanoma microenvironment to break the "Immunosuppressive Ring" around the solid tumor, increase the number of TILs and DCs infiltration into tumor areas.

9324-15, Session 5
Noninvasive and label-free detection of circulating melanoma cells by in vivo photoacoustic flow cytometry (Invited Paper)

Xunbin Wei, Shanghai Jiao Tong Univ. (China)

Melanoma, a malignant tumor of melanocytes, is the most serious type of skin cancer in the world. It accounts for about 80% of deaths of all skin cancer. For cancer detection, circulating tumor cells (CTCs) serve as a marker for metastasis development, cancer recurrence, and therapeutic efficacy. Melanoma tumor cells have high content of melanin, which has high light absorption and can serve as endogenous biomarker for CTC detection without labeling. Here, we have developed an in vivo photoacoustic flow cytometry (PAFC) to monitor circulating melanoma cancer by counting CTCs of melanoma tumor bearing mice in vivo. To test in vivo PAFC's capability of detecting melanoma cancer, we have constructed a melanoma tumor model by subcutaneous inoculation of highly metastatic murine melanoma cancer cells. The in vivo flow cytometry (IVFC) has shown a great potential for detecting circulating tumor cells quantitatively in the blood stream. Compared with fluorescence-based in vivo flow cytometry

(IVFC), PAFC technique can be used for in vivo, label-free, and noninvasive detection of circulating tumor cells (CTCs).

9324-16, Session 5
Ultrafast photoswitching of fluorescent proteins for tracking of single circulating cells in vivo (Invited Paper)

Ekaterina I. Galanzha, Dmitry A. Nedosekin, Univ. of Arkansas for Medical Sciences (United States); Vladislav V. Verkhusha, Albert Einstein College of Medicine of Yeshiva Univ. (United States); Vladimir P. Zharov, Univ. of Arkansas for Medical Sciences (United States)

Circulating normal and abnormal cells plays the crucial roles in many organism functions including immunity and disease spreading (e.g., cancer, sepsis). A big challenge, however, is tracking single circulating cells and determining their health-hazard status within a highly heterogeneous blood environment. Here we introduce the new generation of in vivo flow cytometry, called photoswitchable flow cytometry (PFC), for noninvasive single cell analysis in vivo that integrates photolabelling of controlled number of cells directly in the bloodstream and tracking them within the whole organism. The concept of PFC is based on ultrafast switching of photoswitchable fluorescent proteins (PSFPs) that change their fluorescent color (e.g., from green to red for Dendra2 PFPs) in response to light. We focused our study on circulating tumor cells (CTCs) as unique biomarkers of deadly cancer metastasis. In tumor-bearing mice, PFC enabled the capability for studying recirculation, migration, and distribution of CTCs during metastasis progression. For the first time, we monitored real-time dynamics of CTCs released from primary tumor and discovered the capability of CTCs to colonize existing metastasis (reseeding phenomenon). We also demonstrated the capability of PFC to identify dormant cells, and image CTCs colonizing a primary tumor (self-seeding). Integration of genetically encoded PSFPs, fast photoswitching, flow cytometry, and imaging makes in vivo single cell analysis in the circulation feasible to provide the insights into the behavior of CTCs and potentially immune-related cells which may inspire advanced strategies for disease therapeutics.

9324-17, Session 5
Imaging tuberculosis cytosolic translocation with two-photon fluorescence resonance energy transfer microscopy

Yassel Acosta, Qi Zhang, Hugues Ouelett, Jianjun Sun, Chunqiang Li, The Univ. of Texas at El Paso (United States)

It is estimated that one-third of the world population is latently infected by Mycobacterium tuberculosis. The transition from latency to active tuberculosis requires Mtb to penetrate phagosomal membrane and translocate to the cytosol of the host macrophage, termed as "cytosolic translocation". We use Mycobacterium marinum as a surrogate model organism to study the mechanisms of mycobacterial cytosolic translocation. Mouse macrophages were infected with wild-type or mutant strains of M. marinum and M. smegmatis (non-infectious). By using two-photon fluorescence resonance energy transfer (FRET) microscopy, we demonstrate the capability to monitor mycobacterial infection of mouse macrophages through a β -lactamase-based FRET assay. Macrophages were loaded with CCF-4, a FRET-based fluorescent substrate that allows to discriminate phagosomal location from host cytosol by a change of the FRET signal. Samples were imaged after 48 and 96 hours of infection. Individual host cells were segmented using CellProfiler and the mean intensity was quantified for each cell in the blue and green fluorescent channels. The ratio of blue/green was calculated as an indication of the presence of bacteria in the phagosome or cytosol. Higher fluorescent ratios have been obtained

**Conference 9324:
Biophotonics and Immune Responses X**

for *M. marinum* after 48 and 96 hours of infection, indicating its ability to gain access to the cytosol of macrophages. The use of sensitive cytoplasmic FRET reporter CCF-4 combined with our two photon laser scanning fluorescence microscope provides quantitative analysis of phagosomal rupture and cytosolic entry of cellular pathogens.

9324-18, Session 5

Quantitative characterization of neutrophil chemotaxis using micro-optical coherence tomography

Kengyeh K. Chu, Mark E. Kusek, Lael Yonker, Massachusetts General Hospital (United States); Jin-hyeob Ryu, Massachusetts General Hospital (United States) and The Univ. of Tokyo (Japan); Bryan P. Hurley, Guillermo J. Tearney, Massachusetts General Hospital (United States)

Neutrophils are immune cells that detect and migrate towards chemical attractants (chemotaxis), which may be released by cells at the site of an infection. Neutrophils are known to be able to migrate across epithelial boundaries in an active process that requires the epithelium to allow neutrophil passage without compromising its function as a barrier. In some cases, as in many inflammatory disorders, excessive neutrophil migration can cause damage to epithelium itself. The signaling pathways and mechanisms that facilitate trans-epithelial migration are not fully characterized.

In this abstract, we report the utilization of high-resolution micro-optical coherence tomography (μ OCT) to image neutrophil migration across epithelial monolayers in vitro. A chemoattractant or infectious agent is applied apical side of inverted monolayer, and human neutrophils are placed in the basolateral compartment. The 2- μ m lateral resolution and 1- μ m axial resolution of μ OCT allow visualization of individual neutrophils as they undergo chemotactic migration. We have previously described the use of μ OCT for deriving quantitative metrics of migration volume in a variety of monolayer types and using several chemoattractants. We now describe variations in chemotaxis as a function of neutrophil treatments that are hypothesized to alter migration behavior. Neutrophils treated with antibodies that interfere with the CD18 receptor, a known facilitator of trans-epithelial migration, are models for leukocyte adhesion deficiency. Anti-CD18 neutrophils exhibited reduced migration across T84 intestinal epithelium on a standard 24-well transwell filter (4.4 ± 0.7 for anti-CD18, 10.6 ± 3.2 for control in 104 neutrophil units, $p < 0.05$) after two hours as measured by myeloperoxidase (MPO) activity. μ OCT time-lapse imaging also indicates a decrease in migration volume in an initial experiment ($n=1$), but also reveals that anti-CD18 treated neutrophils remain more adherent to the apical epithelial surface after migration (98% of migrated neutrophils remain attached for anti-CD18 at 2 hours, 76% for positive control antibody IgG1, and 72% for negative control).

These results suggest that μ OCT may become a unique research tool for direct observation of abnormal neutrophils, which may allow researchers to uncover new patterns and mechanisms of migration alteration in cells from patients with inflammatory diseases.

9324-19, Session 5

Evaluation of the effect of recombinant murine interleukin-12 on skin regeneration and bone marrow-derived cell trafficking

Joanne Li, Andrew J. Bower, Univ. of Illinois at Urbana-Champaign (United States); Vladimir Vainstein, Zoya Gluzman-Poltorak, Neumedicines Inc. (United States); Eric J. Chaney, Marina Marjanovic, Univ. of Illinois at Urbana-Champaign (United States); Lena A. Basile, Neumedicines

Inc. (United States); Stephen A. Boppart, Univ. of Illinois at Urbana-Champaign (United States)

Interleukin-12 (IL-12) is a heterodimeric cytokine known for its role in immunity, and it has been shown to have an essential role in the interaction between the innate and adaptive arms of the immune system by regulating inflammatory responses and innate resistance to infection. Previous studies have demonstrated that IL-12 can provide potent mitigation of radiation injury, which leads to significant increases in survival. In this study, we examined the effect of IL-12 on cellular dynamics and metabolic activities in wound healing to further understand the role of IL-12. To investigate these cellular dynamics and metabolic changes, we utilized a novel multimodal integrated optical coherence and multiphoton microscopy system, which includes optical coherence tomography/microscopy, two-photon fluorescence imaging, second harmonic generation imaging, and fluorescence lifetime imaging. These imaging modalities in an integrated platform for spatial and temporal image co-registration allowed us to monitor the changes in the collagen network and metabolic activity of cells in the skin. Results showed that the wounded animals that received the IL-12 injection experienced an earlier response and a significantly higher level of cellular metabolic activity compared to the wounded animals that received placebo. In addition, we also observed that the collagen reformation fluctuated less in the IL-12 treated animal, which could suggest better controlled wounding healing. These results can lead to a better understanding of the effect and the response mechanism of IL-12 in both wound healing and acute radiation syndrome.

9324-29, Session PMon

Treating cutaneous squamous cell carcinoma using ALA PLGA nanoparticles-mediated PDT in a mouse model

Jie Ji, Xiaojie Wang, Xiuli Wang, Lei Shi, Shanghai Dermatology Hospital (China); Hongwei Wang, Huadong Hospital, Fudan Univ. (China)

Background: Squamous cell carcinoma (SCC) is a common skin cancer and its treatment is still difficult. The aim of this study was to evaluate the efficacy of nanoparticle (NP)-assisted ALA delivery for topical photodynamic therapy (PDT) of cutaneous SCC.

Methods: UV-induced cutaneous SCCs were established in a mouse model. ALA loaded PLGA NPs were prepared and characterized. The kinetics of ALA PLGA NPs-induced PpIX fluorescence in SCCs and the therapeutic efficacy of ALA NP-mediated PDT were examined.

Results: PLGA NPs could enhance PpIX production in SCC. ALA PLGA NPs mediated topical PDT was more effective than free ALA of the same concentration in treating cutaneous SCC.

Conclusion: ALA PLGA NPs PDT provides a promising therapeutic strategy for treating cutaneous SCC.

9324-30, Session PMon

Temperature simulation of photothermal therapy in different size of tumors

Zhifang Li, Hui Li, Fujian Normal Univ. (China); Wei R. Chen, Univ. of Central Oklahoma (United States)

Interstitial laser immunotherapy (ILIT) has already shown significant clinical success for late-stage melanoma and breast cancer patients. Photothermal interaction is an integral part of ILIT. Appropriate thermal interaction is still crucial in order to achieve a long-term, systemic effect for cancer treatment. Hence, ILIT requires inquiring temperature distribution in tumor. We propose the method combining Monte Carlo (MC) with finite element method (FEM) to simulate the temperature in tumor with dimensions of 0.5cm -2cm in diameter. Our model is based on calculations describing the

**Conference 9324:
Biophotonics and Immune Responses X**

light distribution using the MC method. The temperature rises using the bioheat equation. The results show optimization of laser parameters and nanoparticle in tumor for ILIT.

9324-31, Session PMon

Immunosuppressive effects of 365nm ultraviolet irradiation in human neutrophils in vitro

Leiting Pan, Nankai Univ. (China)

Ultraviolet (UV) light has an important influence on human health. Especially, ultraviolet blood irradiation was used to treat many nonspecific diseases in clinics. As the first line of host defense, neutrophils play a significant role in many inflammatory processes. In the present work, human neutrophils were exposed to long-wave UV light (365 nm) to study the effects of long-wave UV irradiation on physiological functions of neutrophils in vitro. Cells were acquired from the peripheral blood of healthy individuals by step-density gradient centrifugation over Histopaque 1077 and 1119 solutions at 500g for 10 min. In addition, a novel irradiation method for treating neutrophils by 365 nm UV light at the single-cell level was developed based on the inverted fluorescence microscope. Cells were irradiated by the 365 nm UV light at about 91 J/cm². It was found that 365 nm UV irradiation significantly blocked FMLP-induced calcium mobilization, migration, production of reactive oxygen species and phagocytosis in neutrophils in vitro, suggesting the immunosuppressive effects of 365 nm UV irradiation in human neutrophils. We believe that these results might be helpful for the clinical application of UV light.

9324-32, Session PMon

The action of NIR (808nm) laser radiation and gold nanorods labeled with IgA and IgG human antibodies on methicillin-resistant and methicillin sensitive strains of staphylococcus aureus

Elena S. Tuchina, Pavel O. Petrov, Kristina V. Kozina, N.G. Chernyshevsky Saratov State Univ. (Russian Federation); Fulvio Ratto, Istituto di Fisica Applicata Nello Carrara (Italy); Sonia Centi, Univ. degli Studi di Firenze (Italy); Roberto Pini, Istituto di Fisica Applicata Nello Carrara (Italy); Valery V. Tuchin, N.G. Chernyshevsky Saratov State Univ. (Russian Federation)

We investigate the action of near infrared laser irradiation on two *S. aureus* strains (methicillin-sensitive and methicillin-resistant) treated with conjugates of gold nanorods and IgA or IgG antibodies. Microbial cells expressing protein A are targeted using suspensions of gold nanorods (concentration of 0.4 mM Au) that are PEGylated and conjugated with antibodies through their Fc-fragments. Light is delivered from a NIR laser (808 nm, 100 mW/cm²) in the CW mode with exposures of 5, 10, 15 and 30 min. We show that the combination of NIR light and gold nanorods with IgG effectively suppresses the growth of bacterial populations. After 30 min irradiation, we report a 97% reduction in the number of methicillin-resistant *S. aureus* colony forming units.

9324-33, Session PMon

In vitro and in vivo antitumor efficacy of berberine-nanostructured lipid carriers against H22 tumor

Zhiping Wang, Guangdong Pharmaceutical Univ. (China); Junbiao Wu, Guangzhou Univ. of Chinese Medicine (China); Tongsheng Chen, South China Normal Univ. (China); Qun Zhou, Huazhong Univ. of Science and Technology (China); Yifei Wang, Jinan Univ. (China)

Hepatocarcinoma, a malignant cancer, threaten human life badly. It is a current issue to seek the effective natural remedy from plant to treat cancer due to the resistance of the advanced hepatocarcinoma to chemotherapy. Berberine (Ber), an isoquinoline derivative alkaloid, has a wide range of pharmacological properties and is considered to have anti-hepatocarcinoma effects. However its low oral bioavailability restricts its wide application. In this report, Ber loaded nanostructured lipid carriers (Ber-NLC) was prepared by hot melting and then high pressure homogenization technique. Both in vitro and in vivo anti-hepatocarcinoma effects of Ber-NLC relative to efficacy of bulk Ber were evaluated. The particle size and zeta potential of Ber-NLC were 166.1 ± 0.8 nm and 21.59 ± 0.81 mV, respectively. CCK-8 assay showed that Ber-NLC effectively inhibited the proliferation of H22 cells, and the corresponding IC50 values were 6.3 µg/ml (18.3 µg/ml of bulk Ber). In vivo studies also showed higher antitumor efficacy, and inhibition rates was 68.3 % (41.4 % of bulk Ber) at 100 mg/kg intragastric administration in the H22 solid tumor bearing mice. These results suggest that the delivery of Ber-NLC is a promising approach for treating tumors.

9324-34, Session PMon

Photo-nano-therapy for bactericidal using graphene oxide

Jie Wu, Jin Chao Gao M.D., Xian Pei Chen, Yu Jia Xie, Beijing Normal Univ. (China)

Graphene oxide are attracted more attention because of the universal property, and rapidly applied in biomedical field, such as drug carriers, imaging or therapy. Graphene oxide has been considered biocompatible with a broad variety of eukaryotic cells. Here, we show that, graphene oxide kill Gram-positive and -negative bacteria rapidly and efficiently, with light irradiation. We investigated the efficacy of graphene oxide on bactericidal activation, the antibacterial activity of graphene oxide is concentration dependent, and strongly enhanced by light irradiation. Our results describe the discovery of a property of partially graphene oxide as a potent antibacterial agent.

9324-35, Session PMon

Fluorescent and metabolic imaging of an Octa-RGD probe for detecting binding affinity in xenograft tumor bearing mice

Shuang Sha, Qiaoya Lin, Anle Wang, Zhihong Zhang, Britton Chance Ctr. for Biomedical Photonics (China)

Assessing binding affinity of a peptide for targeting cancer cells is important for clinical diagnostic. The traditional methods for assessment are expensive and indirect. So developing a convenient and effective method is urgent. Recently, we developed an endogenous octavalent fluorescent probe- Octa-RGD based on the tetrameric katushkaS158A, one red fluorescent protein, and linked with RGD peptide, which has the ability to screen the surface integrin receptor in the tumor cells. We validated the targeting of Octo-RGD sensor both in vitro and in vivo by using integrin receptor positive and negative cells, respectively. Then we used this sensor to screen a variety

**Conference 9324:
Biophotonics and Immune Responses X**

of tumor cells, and differentiated their binding affinities by using the fluorescence of the probe. Among these cells, HT1080 cells, the positive cells we used had the highest red fluorescence intensity, while the B16 cells had the lowest corresponded with their receptor expression. Moreover, the probe was taken up into cells via lysosomal pathway. More importantly, we found that the distribution of sensor in positive tumors (HT1080 cells) are correlated with the tumor metabolism with the ratio of endogenous reduced nicotinamide adenine dinucleotide (NADH)/oxidized flavoproteins (Fp), while the negative tumors (B16 cells) not.

9324-36, Session PMon

Tumor redox metabolism correlation with the expression level of red fluorescent protein

Shuang Sha, Anle Wang, Qiaoya Lin, Zhihong Zhang, Britton Chance Ctr. for Biomedical Photonics (China)

The redox metabolism is variable and complicated with the progress of tumor development. Whether the tumor redox state will affect the exogenous gene expression or not are still not clear now. To investigate the relationship between tumor endogenous redox state and the exogenous gene expression level, a far red fluorescent protein katushkaS158A was used to monitor tumor cells proliferation and as a exogenous protein expression in tumors. NADH (nicotinamide adenine dinucleotide) and Fp (flavin adenine dinucleotide) are two important coenzymes in the mitochondria respiratory chain, which can be used as a standard representation for redox metabolism state. Three subcutaneous tumor models (melanoma, human pancreatic carcinoma and nasopharyngeal carcinoma) were used to observe their redox state and gene expression by our home-made redox scanner. The results showed that the distribution of katushkaS158A fluorescent protein expression in the inner tumor regions are heterogeneous, and the fluorescent intensity expression of katushkaS158A and the fluorescent intensities of NADH are highly correlated. In addition, we also found the linear coefficient in three tumors are different, the value is ($R^2 = 0.831$ and $R^2 = 0.938$) in melanoma, ($R^2 = 0.569$ and $R^2 = 0.758$) in human pancreatic carcinoma and ($R^2 = 0.6$) in nasopharyngeal carcinoma, respectively. From these results, we concluded that the exogenous protein expression of katushkaS158A in tumor had some relationship with the tumor redox state of NADH.

9324-37, Session PMon

Assessment of antiretroviral drug metabolism within optically treated cell populations

Thulile Khanyile, Council for Scientific and Industrial Research (South Africa) and Univ. of the Witwatersrand (South Africa); Patience Mthunzi, Council for Scientific and Industrial Research (South Africa)

Drug metabolism is the biochemical breakdown of pharmaceutical products by mammalian cells. In living systems, the time it takes for drug metabolism usually indicates the rate and efficiency of the pharmacological action of that drug [1]. Antiretroviral (ARV) drugs slow down the progression of human immunodeficiency virus type-1 (HIV-1) infection to acquired immunodeficiency syndrome (AIDS) by blocking/interfering with specific parts of the viral life cycle [2]. ARVs are grouped into four categories according to their mechanism of action, namely entry inhibitors (EI, e.g. maraviroc), reverse transcriptase inhibitors (nucleoside reverse transcriptase inhibitors (NRTI, e.g. tenofovir) and non-nucleoside reverse transcriptase inhibitors (NNRTI, e.g. efavirenz)), integrase inhibitors (INs, e.g. raltegravir) and protease inhibitors (PI, e.g. ritonavir) [2]. In our research we assessed the metabolism of tenofovir, nevirapine and efavirenz by optically treated T2M-bl cells. Basically, the drugs were delivered via photo-translocation

from a home-built optical setup. A subtype C HIV-1 envelope-pseudovirus (ZM53) was utilized to evaluate the effects of ARV photo-translocation on viral replication. Following this, a HIV-1 inhibition assay was used to measure the success of ARV drug photo-translocation.

The photo-translocation of tenofovir and nevirapine resulted in an enhanced level of ZM53 env-pseudotyped viral inhibition. However, no detectable change in viral inhibition was observed in the photo-translocation of efavirenz which was efficiently metabolised by T2M-bl cells regardless of the presence or absence of laser assistance. We show for the first time that laser technology is an efficient targeted drug delivery system. The study also highlights that the manner in which cells metabolise drugs should be considered during drug administration.

References

- [1] SUN, H. & SCOTT, D.O. (2010) Structure-based drug metabolism predictions for drug design. *Chemical Biology & Drug Design*, 75, 3-17.
[2] WARNKE, D., BARRETO, J. & TEMESGEN, Z. (2007) Antiretroviral drugs. *J Clin Pharmacol*, 47, 1570-9.

9324-38, Session PMon

Improving the signal analysis for in vivo photoacoustic flow cytometry

Xunbin Wei, Shanghai Jiao Tong Univ. (China)

Circulating tumor cells (CTCs) serve as a marker for metastasis development, cancer recurrence, and therapeutic efficacy. Melanoma tumor cells have high content of melanin, which has high light absorption and can serve as endogenous biomarker for CTC detection without labeling. Here, we have developed an in vivo photoacoustic flow cytometry (PAFC) to monitor circulating melanoma cancer by counting CTCs of melanoma tumor bearing mice in vivo. Various means have been utilized to improve the signal analysis for in vivo photoacoustic flow cytometry.

9324-39, Session PMon

Effects of laser immunotherapy for the treatment of metastatic tumor cells

Cody F. Bahavar, Aamr Hasanjee, Feifan Zhou, Univ. of Central Oklahoma (United States); Rebaz A. Ahmed, Kurdistan Institution for Strategic Study and Scientific Research (Iraq); Sheyla Rabei, Univ. of Central Oklahoma (United States); Hong Liu, The Univ. of Oklahoma (United States); Wei R. Chen, Univ. of Central Oklahoma (United States)

Laser Immunotherapy (LIT) is an innovative modality for treating late-stage, metastatic cancers. The two main components of LIT are laser irradiation and immunological stimulation. LIT has shown success in treating patients with late-stage breast cancer and melanoma; however, research is still being conducted to help understand its mechanism and to optimize the treatment protocols. In this study, 4T1 cancer cells were irradiated in vitro by lasers in the near infrared region, specifically with wavelengths of 805-nm and 980-nm, with different laser parameters including power density and irradiation duration. Photothermal effects were observed in vitro after the laser irradiation, particularly as functions of laser parameters. Single-walled carbon nanotubes (SWNTs) were used to enhance the absorption of the 980-nm laser when irradiating the tumor cells. Significant enhancement of thermal cytotoxicity to tumor cells was achieved with the laser-SWNT combination. The results of this study could provide a deeper understanding of the thermal effect of LIT as well as its mechanism. Furthermore, these results can be used to obtain optimal laser parameters for pre-clinical and clinical studies in the treatment of cancers.

**Conference 9324:
Biophotonics and Immune Responses X**

9324-40, Session PMon

In vivo efficacy studies of immunologically modified carbon nanotubes and phototherapy against rat tumors

Joseph T. Acquaviva III, Cody F. Bahavar, Aamr Hasanjee, Fefian Zhou, Univ. of Central Oklahoma (United States); Roman F. Wolf, Eric W. Howard, The Univ. of Oklahoma Health Sciences Ctr. (United States); Wei R. Chen, Univ. of Central Oklahoma (United States)

While cancer treatments have increased in efficacy in the past 100 years, cancer is still one of the leading causes of death around the world. In particular, metastases and cancer re-occurrences are primary reasons for cancer deaths. Previously, an innovative cancer treatment, laser immunotherapy, has induced effective immunological anti-tumor responses in patients with late-stage, metastatic cancers. Recently, nanotechnology has become increasingly used in biomedical applications. In particular, single-walled carbon nanotubes (SWNTs) have a high absorption peak in the near-infrared region and are capable of crossing the cellular membrane. However, SWNTs alone are not capable of inducing a systemic anti-tumor response, or successfully treating cancer re-occurrences. To this end, a biocompatible immunoadjuvant, glycated chitosan (GC), was developed. By conjugating SWNTs with GC, a novel immunologically modified carbon nanotube (SWNT-GC) was created for the treatment of metastatic cancers. SWNT-GC was injected into the primary tumor in rats and laser light was administered for 10 minutes or 5 minutes at wavelength of 980 nm with a power density of 1.0 W/cm². After treatment, the sizes of the primary and metastatic tumors were measured. Laser+SWNT-GC for 10 minutes proved to be more effective at causing regression of primary and metastatic tumors; it produced a higher survival rate, 50% n=10, compared to Laser+SWNT-GC for 5 minutes, 0% n=8. Furthermore, 120 days after successful treatment the surviving rats were re-challenged with ten times the original concentration of cancer cells. Only one of the five rats had a cancer re-occurrence; however, the tumor size has decreased in volume over time and eventually disappeared, demonstrating the long-term memory of the treated rats. This novel nanotechnology-based laser immunotherapy could lead to an effective therapy for metastatic cancers.

9324-41, Session PMon

The combination of radiotherapy and immunotherapy using glycated chitosan as an immunological stimulant

Chun-Yuan Chang, National Yang-Ming Univ. (Taiwan); Chung-Yi Wang M.D., CHENG HSIN GENERAL HOSPITAL (Taiwan); Jyh-Der Leu, Taipei City Hospital (Taiwan); Wei R. Chen, Univ. of Central Oklahoma (United States); Yi-Jang Lee, National Yang-Ming Univ. (Taiwan)

Immunotherapy has been reported to effectively treat various cancers. In addition, scientists are dedicated in finding whether the combination of radiotherapy and immunotherapy can efficiently suppress cancer progression and recurrence. Although radiotherapy has been widely used for breast cancer, better strategies to overcome the late-stage breast cancer remains explored. The glycated chitosan (GC), a novel immunological stimulant, was demonstrated to trigger local immune response facilitating the enhancement of radiosensitivity. Our previous study also revealed that the cell mortality and invasive ability were decreased under GC treatment, but the underlying mechanism remains unclear. In this study, we used 4T1-3R-L, a derived murine breast cancer cell line from the spontaneous metastasized liver lesion. We combined ionizing radiation with GC to treat 4T1-3R-L and found the expression of DNA damage-related genes such as gamma-H2AX was more than radiation alone. In addition, the cell cycle distribution and colony forming assay showed an increased sub-G1 population and decreased cell survival rate after IR combined GC

treatment. Moreover, GC treatment triggered TNF-alpha-related immune responsive signaling cascade was revealed by ELISA. Taken together, we sought to elucidate the underlying mechanism by the investigation of DNA damage repair process when IR combined with GC, and to explore another advantage of GC to aid other cancer treatments. Based on our most updated results, the GC treatment is able to effectively increase the radiosensitivity through an immune-responsive signaling transduction, indicating that GC could be a valuable therapeutic strategy for treating against advanced breast cancers.

9324-42, Session PMon

Combination therapy of potential gene and photodynamic therapy to enhance oral cancer therapeutic effect

Chia-Hsien Yeh, Chung Yuan Christian Univ. (Taiwan); Leaf Huang, Chung Yuan Christian Univ. (Taiwan) and The Univ. of North Carolina at Chapel Hill (United States); Gang Zheng, Univ. of Toronto (Canada); Yih-Chih Hsu, Chung Yuan Christian Univ. (Taiwan)

Photodynamic therapy (PDT) can be a therapy modality for early cancer to suppress the growth of cancer. The principle is photosensitizer absorbed by cancer cells and then cell irradiated with light, the photosensitizer is converted from the ground state to active state. It causes tumor cell death by generated free radicals and singlet oxygen. The epidermal growth factor receptor (EGFR) over-regulation related to uncontrolled cell division and promotes progression in tumor. Over-expression of human epidermal growth factor receptor (EGFR) has been detected in oral cancer cells. Combination treatment of photodynamic therapy and EGFR-targeting agents are potential therapeutic modalities for treating oral cancer based on our in vitro study. Liposome nanotechnology is used to encapsulate siRNA and modified with target ligand to receptor on the surface of tumor cells. We are the first to report that the better combination of 2 modalities to treat oral cancer is to delivery EGFR siRNA after PDT with hematoporphyrin derivative (HPD) as the photosensitizer from in vitro study. Combined therapy of EGFR siRNA and PDT showed better response as compared with PDT or gene therapy alone. Combined therapy of siRNA knockdown and PDT showed better response as compared with HPD-PDT and gene therapy alone.

9324-43, Session PMon

DQE characterization of a high-energy in-line phase contrast prototype under different kVp and beam filtration

Di Wu, Molly Wong, Yuhua Li, The Univ. of Oklahoma (United States); Wei R. Chen, Univ. of Central Oklahoma (United States); Xizeng Wu, The Univ. of Alabama at Birmingham (United States); Hong Liu, The Univ. of Oklahoma (United States)

The objective of this research is to characterize the detective quantum efficiency (DQE) of a high-energy in-line phase contrast prototype operated under different x-ray exposure conditions.

First of all, an imaging prototype is demonstrated based on a high-energy in-line phase contrast system prototype. The DQE of this system is calculated through modulation transfer function (MTF), noise power spectrum (NPS) and input signal noise (q) under same absorption radiation dose, which is estimated by employing a 4-cm-thick BR12 phantom. In this research, the x-ray exposure conditions are modified by not only using different tube voltage but also different prime beam filtration. Aluminum, Molybdenum, Rhodium, Copper filters and a combined filter are selected to acquire a variety of x-ray energy compositions with 100, 110 and 120 kVp

**Conference 9324:
Biophotonics and Immune Responses X**

output exposures. The resultant curves are compared through the modes of different kVp/same filter and different filter/same kVp.

As a result, the resultant curves, obtained under same absorption radiation dose, indicate that the overall DQE decreases with increasing exposure energy under the same beam filtration, the MTF performs similar under different condition, and the NPS is majorly affected by the percentage of input photons with energies under 35 keV.

9324-20, Session 6

Photo-nano immunotherapy for breast metastatic cancer using synergistic SWNT-GC *(Invited Paper)*

Feifan Zhou, Univ. of Central Oklahoma (United States); Rebaz A. Ahmed, Kurdistan Institution for Strategic Study and Scientific Research (Iraq); Hong Liu, The Univ. of Oklahoma (United States); Wei R. Chen, Univ. of Central Oklahoma (United States)

In our previous work, we constructed a multifunction nano system SWNT-GC, which can synergize photothermal and immunological effects. To further confirm the therapy efficacy on metastatic cancer, with a breast metastatic mouse tumor model (4T1), we investigate the therapy effects and immune response by SWNT-GC, with or without laser irradiation. Laser+SWNT-GC treatment not only remove the prime tumor, but also eliminate the metastasis tumor, finally result in a significant mice survival rate, there were no long-term survivors under other treatment. It is providing a promising treatment modality for the breast metastatic cancer.

9324-21, Session 6

Multi-modal optical assessment of vascular changes induced by the immune reaction *(Invited Paper)*

Vyacheslav Kalchenko, Yuri Kuznetsov, Weizmann Institute of Science (Israel); Igor V. Meglinski, Univ. of Otago (New Zealand); Alon Harmelin, Weizmann Institute of Science (Israel)

An increased vascular permeability is one of the major hallmark of acute inflammation associated with immune response. We present a multi-modal diagnostic approach, which is based on hybrid use of fluorescent microscopy and laser speckle imaging technique. This imaging approach was specially developed for non-invasive visualization and quantitative assessment of the immune-mediated tissue response manifested as perfusion changes and increasing vascular permeability. The developed technique was applied to monitor in real time the changes in vascular permeability induced by various chemical substances suspected as pro-inflammatory and allergenic agents. Our multi-modal optical method of visualizing the vascular events mediated by the immune reaction, is cost effective and shows great potential

9324-22, Session 6

Detection of squamous carcinoma cells using EGFR-conjugated gold nanoparticles

Wei-Yun Dai, Szetsen Lee, Yih-Chih Hsu, Chung Yuan Christian Univ. (Taiwan)

Our nano-gold particles is prepared from colloidal gold because its excellent biocompatibility. The goal of this study is to use gold nanoparticles as a diagnostic agent to detect squamous carcinoma cells. Gold nanoparticles is

synthesized in chloroauric acid solution with sodium citrate as the substrate to form nano gold particle. The gold nanoparticle size is 34.3 ± 6.2 nm and zeta potential is -36.94 ± 0.40 mV. Because the over-expression of EGFR biomarkers on squamous carcinoma cells, we hypothesize that EGFR could be a feasible biomarker as the target moiety for detection. We next further modify polyclonal antibodies of epidermal growth factor receptor (EGFR) onto surface of gold nanoparticles, the gold nanoparticles size is 27.5 ± 3.5 nm, and zeta potential is -6.54 ± 0.11 mV. It showed that EGFR antibodies attached onto the surface of gold nanoparticles. Selected squamous carcinoma cells can be selectively detected using EGFR antibody modified gold nanoparticles through receptor-mediated endocytosis. Cell death was also examined for the survival status of gold nanoparticles treatments on squamous carcinoma cells for with EGFR polyclonal antibodies modification.

9324-23, Session 6

Molecular nanoprobe for cancer imaging

Jie Zheng, The Univ. of Texas at Dallas (United States)

While nanoprobe with strong signal output and multifunctionalities open up unprecedented opportunities for developing novel biomedical technologies for cancer imaging and therapy, translation of nanoprobe into clinical practices has been hampered by the potential toxicity resulted from their long-term nonspecific accumulation in healthy tissues. On the other hand, small molecular probes that are being widely used in cancer diagnosis are often renal clearable but fail to integrate multiple imaging techniques for better health management. In the past few years, we have developed a class of molecular nanoprobe that are integrated with strengths of small molecular contrast agents and nanophotonics, making it possible to address this long-term challenge in the clinical translation of nanoprobe. In this talk, I will discuss how to synthesize such molecular nanoprobe and their pharmacokinetics and biodistribution as well as their applications in the multimodality cancer imaging and therapy.

9324-25, Session 7

The effect of low level laser therapy on HIV-1 infected cells *(Invited Paper)*

Patience Mthunzi, Council for Scientific and Industrial Research (South Africa); Fakazi C. Nhachissambe, Council for Scientific and Industrial Research (South Africa) and Univ. of KwaZulu-Natal (South Africa); Thulile Khanyile, Council for Scientific and Industrial Research (South Africa) and Univ. of the Witwatersrand (South Africa)

The realisation of the benefits of low level laser therapy (LLLT) such as the reduction of pain, inflammation, and edema; promotion of wound healing, prevention of cell death, etc.; has incited a variety of related research in medicine and biology [1]. Most of the applications of LLLT specifically to cell biology focus on the manipulation and study of molecular mechanisms of healthy cells [2, 3 and 4]. In this study we investigate the effect of LLLT to human immunodeficiency type one (HIV-1) infected cells in-vitro. TZM-bl cells were infected with the ZM53 HIV-1 pseudovirus and nourished under normal growth conditions of 37°C, 5% CO₂ and 80% humidity. Then a continuous wave laser of 660nm, 100mW was used to irradiate infected cells at 2J/cm², 4J/cm², 6J/cm², 8J/cm², 10J/cm² respectively, providing the cells with different laser dosages. Cell controls were independently prepared for each irradiated cell sample as a point of reference. We observed that at 8J/cm² and 10J/cm² the infectivity decreased by 15.7% and 15.3% respectively upon comparison to non-irradiated virus controls. Following laser treatment; cell viability studies were performed to ascertain that the supplied dosages were not lethal to the samples. The viability of more than 65% in all optically treated cells was obtained. In addition, we successfully measured the infectivity of optically treated cells and we could affirm that the cells were proficiently infected and alive. Our results suggest that an in-vitro level LLLT is applicable in enhancing the decrease of HIV-1 infectivity.

References

- [1] Huang, Ying-Ying, et al. "Biphasic dose response in low level lighttherapy." *Dose-Response* 7.4 (2009): 358-383.
- [2] Hamblin, Michael R., and Tatiana N. Demidova. "Mechanisms of low level lighttherapy." *Biomedical Optics 2006*. International Society for Optics and Photonics, 2006.
- [3] Chen, Aaron CH, et al. "Low-level laser therapy activates NF- κ B via generation of reactive oxygen species in mouse embryonic fibroblasts." *PloS one* 6.7 (2011): e22453.
- [4] Chen, Chia-Hsin, et al. "Effects of Low-Level Laser Therapy on M1-Related Cytokine Expression in Monocytes via Histone Modification." *Mediators of inflammation* 2014 (2014).

9324-26, Session 7

Selective delivery of antiretroviral drugs into live HIV-1 permissive cells using pulsed laser light

Thulile Khanyile, Council for Scientific and Industrial Research (South Africa) and Univ. of the Witwatersrand (South Africa); Patience Mthunzi, Council for Scientific and Industrial Research (South Africa)

Highly active antiretroviral therapy (HAART) which is used to treat human immunodeficiency virus type-1 (HIV-1) has contributed positively to the decline of acquired immunodeficiency syndrome (AIDS) related deaths [1]. HAART is administered orally and in high concentrations, as a result, this treatment has been reported to cause unwanted side effects [2]. Literature has suggested that drug delivery systems which deposit drugs directly into infected or diseased sites can contribute to a decline in drug related toxicities [3]. In this study we used a home-built photo-translocation setup to selectively deliver antiretroviral (ARV) drugs tenofovir, nevirapine and efavirenz into live TZM-bl cells which are HIV-1 permissive. During photo-translocation, cells were exposed to the drugs for a period of 30 minutes whilst undergoing optical treatment at 10 ps, 60 mW and a 50 ms shutter opening time per shot. Successful drug delivery was thereafter assessed using a HIV-1 inhibition assay. Following this, cell viability was measured using a Cell Titer 96 Non-Radioactive cell Proliferation assay.

Our results show that minimal toxicity was observed amongst laser irradiated cells post drug delivery. For example, cell viabilities of 82% were obtained when tenofovir was photo-translocated into the cells at a drug concentration of 20 μ g/ml, 73% nevirapine (10 μ g/ml) and 126% cell viabilities obtained for efavirenz (14 μ g/ml). Contrarily, nevirapine and efavirenz showed high levels of toxicity after a prolonged exposure period of 48 hours to TZM-bl cells. From this data, we concluded that a decrease in the drug exposure time to 30 minutes while drug photo-translocations were done resulted in elevated levels of cell viability while the desired therapeutic effects were obtained. This study therefore demonstrates that laser assisted delivery enhances the viability of TZM-bl cells after treatment with otherwise toxic ARV drug concentrations.

References

- [1] SHARMA, P. & GARG, S. (2010) Pure drug and polymer based nanotechnologies for the improved solubility, stability, bioavailability and targeting of anti-HIV drugs. *Adv Drug Deliv Rev*, 62, 491-502.
- [2] ESTE, J. A. & CIHLAR, T. (2010) Current status and challenges of antiretroviral research and therapy. *Antiviral Res*, 85, 25-33.
- [3] OJOWELE, E., MACKRAY, I., NAIDOO, P. & GOVENDER, T. (2008) Exploring the use of novel drug delivery systems for antiretroviral drugs. *Eur. J. Pharm. Biopharm*, 70, 697-710.

9324-27, Session 7

Real-time monitoring of tumor response to preoperative radiochemotherapy for rectal carcinoma by nonlinear optical microscopy

Lianhuang Li, Fujian Normal Univ. (China); Zhifen Chen, Department of Colorectal Surgery, The Affiliated Union Hospital of Fujian Medical University (China); Xingfu Wang, Department of Pathology, The First Affiliated Hospital of Fujian Medical University (China); Weizhong Jiang, Guoxian Guan, Department of Colorectal Surgery, The Affiliated Union Hospital of Fujian Medical University (China); Jianxin Chen, Fujian Normal Univ. (China)

The continuing development of multiphoton microscopy (MPM) techniques has opened many new windows in biological exploration. This novel optical imaging technique is capable of high resolution, high penetration depth, three-dimensional imaging of biological tissue and has the ability to detect cellular and subcellular microstructure of tissue by excitation of intrinsic fluorescent molecules. In this work, multiphoton microscopy (MPM), based on the second harmonic generation (SHG) and two-photon excited fluorescence (TPEF) signals, was expanded to monitor tumor response to preoperative radiochemotherapy for rectal carcinoma. It was found that histopathology of the tumors changes following preoperative radiochemotherapy and MPM has the ability of direct visualization of these changes including stromal fibrosis, colloid response and residual tumors. Our results also show the capability of MPM using the quantitative analyses of images to quantify these changes. These results suggest that MPM has the potential in label-free monitoring the tumor response to preoperative radiochemotherapy, which is crucial for evaluating whether radiochemotherapy is effective or treatment dose and strategy are approximate. This work may provide the groundwork for further exploration into the application of multiphoton-based endoscopy in a clinical setting.

9324-28, Session 7

Optical coherence tomography for monitoring the process of skin cancer induced by UVB

Shulian Wu, Yuxia Wang, Hui Li, Zheng Huang, Fujian Normal Univ. (China)

The incidence of non-melanoma skin cancer, such as basal cell carcinoma and squamous cell carcinoma, is rising in the white population. It is a growing public health problem and the global incidence is increasing. The major carcinogenic factor for most skin cancers is well established as solar ultraviolet light, especially the chronic exposure to UVB (280 nm-320nm). In our study, the skin canceration processes induced by UVB were analyzed from the perspective of tissue optics and texture. Optical coherence tomography (OCT) was used for monitoring the morphologic changes during the process of skin canceration induced by UVB, and then compared with histological analysis. Meanwhile, the optical properties, including the attenuation coefficient (μ_t) between epidermis and dermis tissue of this canceration process were systematically extracted and analyzed. Moreover, characteristic textures based on the speckle were revealed from OCT images. The results are conducive to understand the process of UVB-induced skin cancer and further be able to provide a reference for medical researchers.

Conference 9325: Design and Performance Validation of Phantoms Used in Conjunction with Optical Measurement of Tissue VII

Saturday 7 February 2015

Part of Proceedings of SPIE Vol. 9325 Design and Performance Validation of Phantoms Used in Conjunction with Optical Measurement of Tissue VII

9325-2, Session 1

Dependence of optical scattering on mixing temperature and time in Intralipid-gelatin-water based hydrogel phantoms

Puxiang Lai, Washington Univ. School of Medicine in St. Louis (United States); Xiao Xu, Lihong V. Wang, Washington Univ. in St. Louis (United States)

Intralipid is a scattering agent widely used in tissue-mimicking phantoms to reproduce the optical scattering coefficient and anisotropy coefficient of real tissue. Because accurate control of Intralipid is critical in matching the optical diffusivity of phantoms to the prescribed value, factors such as the Intralipid brand and concentration have been characterized extensively. In hydrogel phantoms, however, the temperature and the time spent mixing Intralipid with hydrogel in the liquid phase, e.g., gelatin-water solution, also play important roles, yet they have been largely ignored in previous protocols, which assume no difference between hydrogel and aqueous solution phantoms. Here, for the first time to our knowledge, we explore how temperature and the time spent mixing Intralipid with gelatin-water solution influence the resulting hydrogel's reduced scattering coefficient, as measured by Oblique-Incidence Reflectometry. We found that high temperature and prolonged mixing resulted in decreased reduced scattering coefficients, caused by separation in the Intralipid-gelatin-water emulsion. We suspect that the separation resulted from irreversible changes in the Intralipid-gelatin structure, a phenomenon not seen in Intralipid-water emulsions. Therefore, to fabricate Intralipid-gelatin-water phantoms with an optical diffusivity consistent with that of Intralipid-water counterparts, it was crucial to mix the components below 37°C for no more than 2 hours. We recommend this modified protocol for making Intralipid-based hydrogel phantoms for future optical experiments.

9325-3, Session 1

Fractal phantom design for mimicking spectral and spatial scattering in tissue

Jeremy D. Rogers, Univ. of Wisconsin-Madison (United States)

Developing phantoms that simulate optical scattering from biological tissues is an important step in designing and validating many biomedical instruments. Scattering properties are increasingly used as biomarkers for disease screening including cancer. Scattering must also be accounted for when developing light based therapies, or in applications like optogenetics where unintended light distribution may adversely affect results. Tissue scattering is often best modeled using fractals, however, no phantom yet exists that provides control over scattering coefficient, anisotropy, and fractal dimension. Here, we present a method for designing such tissue phantoms with fractal scattering properties.

Optical scattering in tissue is the result of spatial variations in refractive index. Unlike clouds containing discrete particles, tissue is a continuous medium with structures spanning a wide range of length scales from nanometer-scale macromolecules to micron scale organelles to cells spanning tens of microns. This can be statistically modeled using power-law spatial correlation functions and is referred to as fractal organization due to the self-similarity over this wide range of scales. Effects of fractal organization can be observed in the spatial distribution and spectral dependence of scattering.

This work describes the design of fractal phantoms using a composite of nano- and micro-particles of both polystyrene and silica in suspension to mimic fractal tissue by matching the statistical refractive index correlation function to that used to model fractal tissue. The limits of the Rayleigh-Gans-Debye approximation will be discussed. Application examples will include measurement of spectral dependence of scattering coefficient and spatial light distribution measured with enhanced backscattering.

9325-4, Session 1

Measurement of the optical properties of solid biomedical phantoms at NIST

Paul Lemaillet, David W. Allen, Jeeseong C. Hwang, National Institute of Standards and Technology (United States)

The biomedical optics community relies on tissue-simulating phantoms for the development and calibration of medical devices, performance assessment of systems, etc... Such phantoms need referenced to NIST (National Institute of Standards and Technology) traceable standard. In this talk we will present a measurement facility being developed at NIST to provide traceability of the optical properties solid biomedical reference phantoms. The optical properties of the sample were computed from the measurements of the total reflectance and total transmittance by a double integrating sphere setup in the continuous wave domain. An inversion procedure based on an adding-doubling algorithm was developed to allow propagation of type A and type B uncertainties to the resulting absorption and scattering coefficients. Measurements on a commercially available phantom at 633 nm and 543 nm are presented and compared to results obtained by a time domain measurement technique. Measurements of the optical properties of a biomedical phantom developed by additive manufacturing are also presented.

9325-5, Session 1

Solid switchable phantom for diffuse optical imaging

Antonio Pifferi, Alessandro Torricelli, Rinaldo Cubeddu, Davide Contini, Sanathana Konugolu Venkata Sekar, Politecnico di Milano (Italy); Fabrizio Martelli, Univ. degli Studi di Firenze (Italy); Lorenzo Spinelli, Andrea Farina, Istituto di Fotonica e Nanotecnologie, CNR (Italy); Mikhail Mazurenka, Physikalisch-Technische Bundesanstalt (Germany) and Hannoversches Zentrum für Optische Technologien (Germany); Peter Pawlak, Heidrun Wabnitz, Physikalisch-Technische Bundesanstalt (Germany)

We propose a simple and reliable solid phantom for mimicking realistic localised absorption changes within a calibrated diffusive medium. The phantom is based on the Equivalence Relation stating that any realistic absorption change can be mimicked by a totally absorbing sphere of a proper volume. Monte Carlo simulations show that - within certain conditions regarding geometry - the Equivalence Relation is valid both for continuous-wave or time-domain measurements, and holds true for different geometries (source-detector arrangement, position of the inclusion, shape of the background medium), and background properties.

Conference 9325: Design and Performance Validation of Phantoms Used in Conjunction with Optical Measurement of Tissue VII

Applying this concept, we constructed a solid phantom holding a movable black inclusion embedded in a cylinder. Translating the cylinder parallel to the phantom surface, the inhomogeneity can be positioned beneath the source-detector pair (perturbed case) or far from it (unperturbed case). Also, intermediate positions can be precisely reproduced using a translating stage. Different absorption perturbations can be mimicked by changing the volume of the black object both in transmittance and reflectance configuration.

The phantom is simple, rugged, easy to handle. The optical inhomogeneities are well characterised and reproducible depending only on the volume of the black object. Dynamic changes are produced without touching the optodes, thus with minimal artefacts. Therefore, the phantom is perfectly suited for performance assessment of diffuse optics instruments, for reproducible research studies, for quality check of clinical systems, and could also be adopted in standards.

Measurements for different applications performed with different time-resolved instruments will be presented and compared to simulations.

9325-6, Session 1

Fabrication of anatomically tapered foveal pits for retinal phantoms for optical coherence tomography

Gary C. F. Lee, Gennifer T. Smith, Monica N. Agrawal, Audrey K. Ellerbee, Stanford Univ. (United States)

Optical Coherence Tomography (OCT) has become a standard tool in many ophthalmology clinics for diagnosing many retinal diseases. Nonetheless, the technical and clinical communities still lack a standardized phantom that could aid in evaluating and normalizing the many protocols and systems used for diagnosis. Existing retinal phantoms designed for OCT imaging mimic some important features of the retina: for example, one group recently demonstrated a phantom that was able to accurately mimic the thickness and relative intensities of all the retinal layers. The morphology of the foveal pit and anatomical tapering of the retinal layers underlying the surface, however, remains a challenge to replicate in current phantoms. Recent attempts at creating a realistic foveal pit include molding, ablation and laser etching. However, the tapering effect of the layers in and around the pit region that is commonly seen in actual retinas is either missing completely or only modestly demonstrated. In this work, we demonstrate a new fabrication procedure that is capable of reliably and repeatedly replicating the tapered appearance of the retinal layers near the foveal pit using a combination of spin-coating and replica molding. The use of different mold sizes and combinations of spin speeds enables us to achieve a range of tapering angles and pit widths seen in actual foveal pits. The ability to create an anatomically correct foveal pit will allow for a new phantom better suited for intra- and inter-system evaluation and for improved comparison of retinal segmentation algorithms.

9325-23, Session 1

Color accuracy and reproducibility in whole slide imaging scanners (Invited Paper)

Parthana Shrestha, Bas Hulsken, Philips Digital Pathology Solutions (Netherlands)

The whole slide imaging (WSI) scanners produce high-res images, which are easy to visualize and navigate at different magnification levels. Since color content of an image has a direct influence on the readers' performance and reliability of the clinical diagnosis, the scanner reproduced colors should be accurate and consistent. However, the same slide scanned by different scanners may appear different, even when viewed on the same display device, due to discrepancies in their color characteristics and configuration. To address the problem, we propose a work-flow for color reproduction

in WSI scanners such that the colors in the scanned images match to the actual slide color and the inter-scanner variation is minimum. We present a novel method of preparation and verification of the color phantom slide, consisting of a standard IT8-target transmissive film, which is used in color calibrating and profiling the WSI scanner. The ICC compliant techniques in color calibration/profiling and rendering intents are used for translating the scanner specific colors to the standard display (sRGB) color-space. Based on the quality of the color reproduction in histopathology slides, we recommend the matrix-based calibration/profiling and absolute colorimetric rendering approach. The main advantage of the proposed work-flow is that it is compliant to the ICC standard, applicable to color management systems in different platforms, and involves no external color measurement devices. We quantify color difference using CIE-DeltaE2000 metric, where DeltaE values below 1 is considered imperceptible. Our evaluation on 14 phantom slides, manufactured according to the proposed method, shows an average inter-slide color difference below 1 DeltaE. The proposed work-flow is implemented and evaluated in 35 Philips Ultra Fast Scanners (UFS). The color accuracy, measured as DeltaE between the scanner reproduced colors and reference colorimetric values of the phantom patches, is improved on average to 3.5 DeltaE in calibrated scanners from 10 DeltaE in uncalibrated scanners. The average inter-scanner color difference is found to be 1.2 DeltaE. The improvement in color performance upon using the proposed method is apparent on the visual color quality of the tissues scans.

9325-7, Session 2

3D printing of tissue-simulating phantoms for standardized biomedical optical imaging (Invited Paper)

Ronald X. Xu, Peng Liu, The Ohio State Univ. (United States)

Many biomedical optical imaging systems require appropriate calibration to ensure accurate and reproducible measurements of tissue optical properties. However, commonly used calibration phantoms are made of homogeneous materials with constant optical properties and cannot reflect the real characteristics of biologic tissue, such as multi-layer heterogeneities, physiologic variations, and multimodal contrasts. After calibration by these phantoms, the optical measurements and the reconstructed tissue properties may involve significant bias. In the meantime, the emerging 3D printing technique is capable of creating 3D heterogeneities by layer-by-layer deposition of the ink materials. We have developed several novel 3D printing processes for freeform fabrication of tissue-simulating phantoms with different optical properties, using different materials, and at different scales. Our preliminary experiment demonstrated the technical feasibility of freeform fabrication of multi-layer tissue simulating phantoms as a traceable standard for optimal calibration of biomedical optical spectral devices.

9325-8, Session 2

3D printed biomimetic vascular phantoms for assessment of hyperspectral imaging and diffuse reflectance systems

Jianting Wang, Anthony Melchiorri, Univ. of Maryland, College Park (United States); Jessica C. Ramella-Roman, Florida International Univ. (United States); Scott A. Mathews, The Catholic Univ. of America (United States); James Coburn, U.S. Food and Drug Administration (United States); Brian S. Sorg, National Cancer Institute (United States); Yu Chen, Univ. of Maryland, College Park (United States); T. Joshua Pfefer, U.S. Food and Drug Administration (United States)

The emerging technique of three-dimensional (3D) printing provides a

Conference 9325: Design and Performance Validation of Phantoms Used in Conjunction with Optical Measurement of Tissue VII

revolutionary way to fabricate objects with biologically realistic geometries. Previously we have performed optical and morphological characterization of basic 3D printed tissue-simulating phantoms and found them suitable for use in evaluating biophotonic imaging systems. In this study we assess the potential for printing phantoms with irregular, image-defined vascular networks that can be used to provide clinically-relevant insights into device performance. A previously acquired fundus camera image of the human retina was segmented, embedded into a 3D matrix, edited to incorporate the tubular shape of vessels and converted into a digital format suitable for printing. A polymer with biologically realistic optical properties was identified by spectrophotometer measurements of several commercially available samples. Phantoms were printed with the retinal vascular network reproduced as 0.6 mm diameter channels at a range of depths up to 2 mm. The morphology of the printed vessels was verified by volumetric imaging with micro-CT. Channels were filled with hemoglobin solutions at controlled oxygenation levels, and the phantoms were imaged by a near-infrared hyperspectral reflectance imaging (HRI) system and a visible wavelength diffuse reflectance system. The maximum detectable imaging depth and effect of vessel depth on the accuracy of hemoglobin saturation estimates was studied. Additionally, a phantom incorporating the vascular network at two depths was printed and filled with Hb at two different saturation levels. Overall, results indicated that 3D printed phantoms are useful for assessing biophotonic system performance and have the potential to form the basis of clinically-relevant standardized test methods for assessment of medical imaging modalities.

9325-9, Session 2

Characterization of new materials and methods for fabricating a 3D, disease-mimicking bladder tissue phantom

Gennifer T. Smith, Kristen L. Lurie, Audrey K. Ellerbee, Stanford Univ. (United States)

Three-dimensional (3D) organ-mimicking phantoms provide realistic imaging environments in which to test new probe designs, evaluate the diagnostic potential of new systems, and benchmark novel image processing algorithms for modalities such as optical coherence tomography (OCT). However, few currently used phantoms demonstrate the ability to mimic diseased tissue. To enable fabrication of 3D, disease-mimicking phantoms presenting with a comprehensive range of cancer and pre-cancerous states, we introduce and characterize a new material, Dragon Skin, and a new fabrication technique, spray-coating, and apply them to fabricate a 3D bladder phantom for combined OCT and white light cystoscopy, the gold standard for bladder cancer detection. Dragon Skin is a two-part polymer similar to PDMS but has a wider range of elasticity. Spray-coating, a technique often used in illustration and hobbies such as ceramics and wood staining, can be used to create thin layers on non-uniform surfaces, making it an ideal candidate for mimicking the thin layers that characterize hollow organs like the bladder. We characterize the optical tunability (i.e., range of achievable attenuation coefficients) of Dragon Skin and the range of achievable thicknesses using spray-coating. The unique elastic properties of the Dragon Skin and the conformal nature of spray-coating enable fabrication of a phantom that includes regions that mimic a wide range of bladder disease pathologies, including inflammation, pre-cancerous lesions and tumors from various stages of cancer.

9325-10, Session 2

Fabrication of a multilayer optical tissue phantom simulating human skin structure

Jihoon Park, Yonsei Univ. (Korea, Republic of); Myungjin Ha, Sung Kon Yu, Edalat Radfar, Eunkwon Jun, Nara Lee, Yonsei Univ (Korea, Republic of); Byungjo Jung, Yonsei Univ. (Korea, Republic of)

This study shows a fabrication method for multilayered optical tissue phantom simulating whole skin structure consisting epidermis, dermis and blood vessel. Epoxy and silicone were chosen as the material for phantom body, and Indian ink and titanium dioxide were used for mimicking absorption and scattering property, respectively. In order to fabricate multilayered phantom including thin layer simulating epidermis, spin coating technique was applied. Silicone tube for mimicking blood vessels and flow was inserted into a solid dermis phantom before curing. Finally epidermis phantom was coated on the surface of the dermis phantom. The fabricated phantom was characterized and evaluated from the measurement of optical and structural-functional property, in order to verify the satisfaction of the initial purpose.

9325-11, Session 2

Multilayered phantoms with tunable optical properties for a better understanding of light/tissue interactions

Blandine Roig, Anne Koenig, François Perraut, CEA-LETI (France); Olivier Piot, Matrice Extracellulaire et Dynamique Cellulaire, CNRS, Univ. de Reims Champagne-Ardenne (France); Séverine Vignoud, CEA-LETI (France); Jonathan Lavaud, Institut Albert Bonniot (France); Michel Manfait, Matrice Extracellulaire et Dynamique Cellulaire, CNRS, Univ. de Reims Champagne-Ardenne (France); Jean-Marc Dinten, CEA-LETI (France)

We developed multilayered phantoms for many reasons: firstly, for calibration of optical systems; secondly, to mimic the optical properties of biological tissues such as skin; our final objective is to better understand light/tissue interactions especially in the case of confocal Raman spectroscopy.

The phantom preparation procedure is described including the employed method to obtain a stratified object. PDMS was chosen as the bulk material. TiO₂ was used as light scattering agent. A dye and ink were adopted to mimic, respectively, oxy-hemoglobin and melanin absorption spectra. By varying the amount of the incorporated components, we created a material with tunable optical properties.

Monolayer and multilayered phantoms were designed to allow several characterization methods. Among them, we can name:

X-ray tomography for structural information;

the Inverse Adding-Doubling method and Diffuse Reflectance Spectroscopy (DRS) with a homemade fibers bundle system for optical characterization;

Raman depth profiling with a commercial confocal Raman microscope for structural information and for our final objective.

For each technique, the obtained results are presented and correlated when possible.

A few words are said on our final objective. Raman depth profiles of the multilayered phantoms are distorted by elastic scattering. The signal attenuation through each single layer is directly dependent on its own scattering property. Therefore, determining the optical properties, obtained here with DRS, is crucial to correct properly Raman depth profiles. Thus, it would be permitted to consider quantitative studies on skin for drug permeation follow-up or hydration assessment for instance.

9325-12, Session 3

Making digital phantoms with spectral and spatial light modulators for quantitative applications of hyperspectral optical medical imaging devices

Jeeseong C. Hwang, David W. Allen, Bonghwan Chon,

Conference 9325: Design and Performance Validation of Phantoms Used in Conjunction with Optical Measurement of Tissue VII

Aniruddha Ray, National Institute of Standards and Technology (United States); David M. McClatchy III, Stephen C. Kanick, Brian W. Pogue, Dartmouth College (United States)

Hyperspectral detection of light-absorbing or scattering molecules and organelles in cells and tissues enables label-free imaging in a variety of biomedical applications. However, translation is challenging due to lack of standards for the verification/validation of the imaging devices. We will discuss a digital phantom technology based on spectrally and spatially modulated light projection to develop measurement standards to accelerate the translations of hyperspectral imaging devices. We will also present potential digital phantom standards including oximetric map of single cells for early infectious disease diagnosis and scatter map of tissue-mimicking materials for tumor margin detection for quantitative optical biopsy.

9325-13, Session PSat

Wide range imaging based on dual scanning handheld OCT probe

Hyeongeun Kim, Sungwon Shin, Yubin Son, Ulsan National Institute of Science and Technology (Korea, Republic of); Pil Un Kim, Oz-tec Co., Ltd. (Korea, Republic of); Woonggyu Jung, Ulsan National Institute of Science and Technology (Korea, Republic of)

The use of artificial skin plays a crucial role to imitate the natural skin not only in the medicine but also in the cosmetics. Identifying the quantification of engineered skin structure is essential to show the accuracy in the experiment. However, there are no existing methods to monitor morphological variations of artificial skin. For this reason, optical coherence tomography (OCT) is a potential imaging modality which offers high-resolution and cross-sectional tissue structures, non-invasively. Since OCT utilizes back-scattered signal from tissue, it incorporates inherent limitation for providing deep tissue image. Recently, many researches are introduced about improvement of depth information of OCT such as full-range, contrast enhancement reagent injection, and optical clearing.

In this study, we propose dual scanning hand-held OCT probe to improve the imaging range of OCT in axial direction. This technique employs the opposite scanning configuration which images the specimen from top and bottom simultaneously. Acquired 2D image set from each sides are then reconstructed as 3D volume image by means of semi-automatic align algorithm, and the field of view of resultant image can be enhanced as double. For easy access to the specimen, our device was built as handheld probe which is composed of five metal coated prisms to separate laser beam into two ways and to guide laser beams to top and bottom of sample. In order to evaluate the imaging capability of our device, we compared the microstructure of artificial skin before and after laser irradiation, while varying the laser exposure parameters. Our results show that the stitched 3D volume enhanced imaging field of view compared to one from the single scanning configuration, and the boundary of laser hole are visualized and segmented clearly which can help to quantize wound healing process in tissue engineering research.

9325-15, Session PSat

Effects of scattering and absorbing medium in the fluorescence conversion efficiency of physical tissue models

Suresh Anand, Sujatha Narayanan Unni, Indian Institute of Technology Madras (India)

Auto-fluorescence spectroscopy based on spectral line shape and intensity has been in use as a promising technique for detecting varying degrees of tissue malignancy. Tissue is a turbid medium with multilayered structure

constituting of multiple fluorophores, absorbers and scattering molecules. Tumor progression in tissues are accompanied by varying degrees of biochemical and morphological changes. These include changes in nuclear size and density, varying amounts of epithelial thickness and increase in the hemoglobin concentration associated with changes in metabolic activity. These changes in overall tissue scattering and absorption properties in turn modulate the fluorescence spectrum emitted and derived from tissues. Estimation of fluorescence conversion efficiency in the turbid tissue needs to take into account these effects of absorption and scattering in order to be evolved as a parameter for tissue discrimination. In this study we set to investigate the factors affecting tissue fluorescence conversion efficiency by making use of physical models of the tissue. Liquid and solid tissue models were prepared with different concentrations of absorbing and scattering media to simulate biological tissues of various degrees of malignancy. The results indicate that emitted fluorescence from the tissue model is subjected to variations by multiple scattering events and absorption. The fluorescence conversion efficiency of the models were derived and correlated to the experimental results with possible diagnostic significance.

9325-14, Session 4

Diffuse reflectance based inverse Monte Carlo model for the estimation of the dependent scattering of intralipid 20% using a simplified two fiber oblique geometry set up

Michael Raju, Sujatha Narayanan Unni, Indian Institute of Technology Madras (India)

Scattering property of intralipid is widely used for calibration and simulation of turbid media especially biological tissues, in optical spectroscopic studies. The desired phantom turbidity level matching the target tissue scattering properties is vital in the right preparation of phantoms mimicking the tissue. A simplified two fiber oblique geometry set up based on iterative inverse Monte Carlo diffuse reflectance simulation is used in this paper, for estimating intralipid scattering for the wavelengths ranging from 500 -880nm. Basic Monte Carlo for Multi Layered media (MCML) code is modified to incorporate the two fiber inverse model of diffuse reflectance with oblique illumination and perpendicular collection of light from the sample. Wavelength dependent true phase function of Intralipid is incorporated in the model and a semi empirical concentration scaling methodology is used to obtain volume concentration dependence on the reduced scattering coefficient. In the inverse modelling, the modified Twersky equation for correlated scattering has been incorporated, to obtain the reduced scattering coefficient profile of intralipid-20% for its entire volume concentration ranging from 1% to 100%. The results are shown to be in good agreement with the optical characterization studies of intralipid 20% involving bulkier instrumentation for the wavelength range. The study presented in this paper promises an in vivo fiber based methodology for quantifying the variation of optical scattering during tissue malignancy with improved resolution.

9325-16, Session 4

Diffuse photon density wave measurements in comparison with the Monte Carlo simulations

Vladimir L. Kuzmin, Saint Petersburg State Univ. (Russian Federation); David Diaz, Michael T. Neidrauer, Leonid A. Zubkov, Drexel Univ. (United States)

The Diffuse Photon Density Wave (DPDW) methodology is widely used for determination of blood oxygenation in vivo. Here we present results of Monte Carlo simulations that employ an effective numerical procedure and compare them with measured data from Intralipid aqueous solutions

Conference 9325: Design and Performance Validation of Phantoms Used in Conjunction with Optical Measurement of Tissue VII

for relative small source –detector separation distances. The Monte Carlo simulations are based upon a rigorous description of radiative transfer in terms of the Bethe-Salpeter equation with account for the Fresnel reflection at the boundary.

Iterating the Bethe-Salpeter equation one presents the scattering intensity as a sum in orders of scattering events. The contribution of the fixed scattering order is calculated as a stochastic average of random values of multi-fold spatial integrals resulting from the iteration of the Bethe-Salpeter equation. These calculations simulate within a common Monte Carlo procedure a stochastic sequence or trajectory of scattering points.

In our scheme every act of scattering contributes to the signal; it makes our approach much more efficient as compared with the commonly used Monte Carlo procedure wherein one simulates the migration of a photon packet until it reaches the detector.

To verify the approach outlined we created an experimental device where the location of incident light on a phantom surface is controlled by a digital actuator that permits to obtain an unlimited amount of experimental points for comparing with numerical simulations.

The Monte Carlo simulations for intensity and phase shift of scattered light and experimental data showed very good agreement for all source – detector separation for several light modulation frequencies.

Conference 9326: Energy-based Treatment of Tissue and Assessment VIII

Sunday - Monday 8-9 February 2015

Part of Proceedings of SPIE Vol. 9326 Energy-based Treatment of Tissue and Assessment VIII

9326-1, Session 1

Practical pathology for thermal tissue applications (*Keynote Presentation*)

James E. Coad, Jeffrey Vos, West Virginia Univ. (United States); Sharon Thomsen, Consultant (United States)

The practical aspects of evaluating tissue following both hyperthermic and cryothermic therapies will be presented. The methods for preparing and evaluating thermally treated tissues will be discussed, including hematoxylin and eosin staining with and without polarized light, trichrome staining, immunohistochemical staining, and tetrazolium-based viability assays. The strengths and weaknesses of these assays and their appropriate usage will also be reviewed.

9326-2, Session 1

Coupling of physical characteristics of non-ionizing irradiation to specific mechanisms of cell death: are we there yet? (*Keynote Presentation*)

Sharon Thomsen, Consultant (United States)

The recent discovery of the various specific "triggers" and mechanisms of cell death suggest that certain non-ionizing irradiation spectra could be coupled with specific cellular "triggers" to improve diagnostic or treatment effect. Several factors can modify these effects. These factors include the 1) physical and chemical features of the irradiation, 2) the time, geometry and intensity of the irradiation dosage, 3) the immediate and delayed effects of the irradiation on the targeted cell or tissue and 4) the physiologic, genetic and anatomical characteristics of the target. Targeted lesions. Genetic, chemical and/or physical modifications of specific intrinsic and extrinsic cellular "triggers" may be major components of diagnostic and therapeutic plans to tailor a specific irradiation to maximize its effect. However, as has been shown over the years, discovery of specific "triggers" that may work well for single cells may not be effective for more complicated tissues or organs. Toxicity and collateral damage in modified tissues or organisms have frequently prevented the discovery of the "perfect cure" no matter the correctness of the scientific rationale.

9326-3, Session 1

Utility and translatability of mathematical modeling, cell culture and small and large animal models in magnetic nanoparticle hyperthermia cancer treatment research (*Keynote Presentation*)

P. Jack Hoopes, Geisel School of Medicine at Dartmouth College (United States) and Thayer School of Engineering at Dartmouth (United States); Alicia A. Petryk, Geisel School of Medicine at Dartmouth College (United States); John A. Pearce, The Univ. of Texas at Austin (United States); Thomas Ryan, FREEFALL Consulting Group LLC (United States)

For more than 50 years, hyperthermia-based cancer researchers have

utilized mathematical models, cell culture studies and small and large animal models to better understand, develop and validate potential new treatments. It has been, and remains, unclear how and to what degree these research techniques depend on, complement and ultimately translate accurately to a successful clinical treatment. In the past, when mathematical models have not proven accurate in a clinical treatment situation, the initiating quantitative scientists (engineers, mathematicians and physicists) have tended to believe a the biomedical parameters provided them were inaccurately determined or reported. In a similar manner, experienced biomedical scientist often tend to question the value of mathematical models and cell culture results since they typically lack the level of biologic and medical variability and complexity, biologists and physicians feel are essential to accurate study and predict complex diseases and treatment. Such quantitative and biomedical interdependence, variability, diversity and promise has never been greater than it is with magnetic nanoparticle hyperthermia cancer treatment. The goal of this study is use known concepts and specific examples to exemplify and meaningfully address this situation for improved clinical gain.

9326-4, Session 1

Developing an open platform for evidence-based microwave thermal ablation treatment planning and validation (*Keynote Presentation*)

Garron Deshazer, Damian E. Dupuy, Rhode Island Hospital (United States); Edward Walsh, Brown Univ. (United States); Punit Prakash, Kansas State Univ. (United States); David Glidden, Scott A. Collins, Madeleine L. Cook, Rhode Island Hospital (United States); Krishna Nand Kesheva Murthy, Brown Univ. (United States); Thomas P. Ryan, Consultant (United States); Benjamin B. Kimia, Brown Univ. (United States); Derek Merck, Rhode Island Hospital (United States)

The clinical utility of current microwave thermal ablation planning tools is severely limited by treatment variability. We discuss the development of an open platform for evidence-based thermal ablation treatment planning and validation. Improved predictive treatment modeling and consistent outcome analysis are crucial components for useful planning and guidance tools.

Preliminary work is focused on methods and models for baseline measurements of sources and effects of treatment variability. Clinical protocols standardize collection, registration, annotation, and archival for pre-, intra-, and post-treatment 3D images from lung and liver thermal ablation procedures. These data are used to train statistical models and validate physical simulations. Physical models of target and treatment regions may be 3D printed for detailed procedure review. Supplemental 4D CT and MR thermography datasets are collected from ex vivo and in vitro ablation experiments to calibrate simulations. A combination of vendor provided treatment zone specifications and generative 4D biothermal simulation models are used as a basis for characterizing treatment effect expectation. Relative treatment effect variability is then reviewed against background anatomy or the experimental platform to identify statistical correlates with the known confounders, such as vascular heat sinks and tissue heterogeneity.

60 patient data sets have been collected and annotated. Our goal is to collect 200 patient data sets over the next two years, and to publish both the data and protocols to support open data collection/review. Preliminary findings of inadequacy of vendor specifications and estimates of clinical under-treatment based on this platform have been presented.

**Conference 9326: Energy-based Treatment of
Tissue and Assessment VIII**

9326-5, Session 2

**Antimicrobial outcomes in plasma
medicine** *(Invited Paper)*

 Thomas P. Ryan, Kenneth R. Stalder, Jean Woloszko,
ArthroCare Corp. (United States) and Smith & Nephew,
Inc. (United States)

Plasma is referred to as the fourth state of matter and is generated in the environment of a strong electric field. The result consists of highly reactive species (ions and electrons), reactive molecules, and UV radiation. Plasma Medicine unites a number of fields, including Physics, Plasma Chemistry, Cell Biology, Biochemistry, and Medicine. One treatment modality utilizes Cold Atmospheric Plasma (CAP), which is able to sterilize and treat microbes in a nonthermal manner. These gas-based plasma systems operate at room temperature and atmospheric pressure, making them very practical for a range of potential treatments and are highly portable for clinical use throughout the hospital. The hypothesis is that gas based plasma kills bacteria, fungus, and viruses but spares mammalian cells. This paper will review systematic work which shows examples of systems and performance in regards to antimicrobial effects and the sparing of mammalian cells. The mechanism of action will be discussed, as well as dosing for the treatment of microbial targets, including sterilization processes, another hospital-based need. In addition, commercial systems will be overviewed and compared, along with evidence-based, patient results. The range of treatments cover wound treatment and biofilms, as well as antimicrobial treatment, with little chance for resistance and tolerance, as in drug regimens. Current clinical studies include applications in dentistry, cancer treatment, wound treatment for bacteria and fungus, and a plasma dispenser for hand surface sterilization.

9326-6, Session 2

**The differing behavior of electrosurgical
devices made of various electrode
materials operating under plasma
conditions** *(Invited Paper)*

 Kenneth R. Stalder, Thomas P. Ryan, Jonathan Gasprede,
Jean Woloszko, Smith & Nephew plc (United States)

Coblation is an electrosurgical technology which employs electrically-excited electrodes in the presence of saline solution to produce a localized and ionized plasma that can cut, ablate, and otherwise treat tissues for many different surgical needs. To improve our understanding of how Coblation plasmas develop from devices made from different electrode materials we describe several experiments designed to elucidate material effects. Initial experiments studied simple, noncommercial cylindrical electrode test devices operating in buffered isotonic saline without applied suction. The applied RF voltage, approximately 300 V RMS, was sufficient to form glow discharges around the active electrodes. The devices exhibited significantly different operating characteristics, which we ascribe to the differing oxidation tendencies and other physical properties of the electrode materials. Parameters measured include RMS voltage and current, instantaneous voltage and current, temporally-resolved light emission and optical emission spectra, and electrode mass-loss measurements. We correlate these measured properties with some of the bulk characteristics of the electrode materials such as work functions, standard reduction potentials and sputter yields.

9326-7, Session 2

**Introduction of argon beam coagulation
functionality to robotic procedures using
the ABC D-Flex probe: equivalency with an
existing laparoscopic instrument**

 Renee A. Merchel, Kelli S. Barnes, Kenneth D. Taylor,
ConMed Advanced Energy (United States)

INTRODUCTION:

The ABC D-Flex Probe utilizes Argon beam coagulation (ABC) technology to achieve rapid superficial hemostasis during minimally invasive surgery. A small handle on the probe allows for integration with robotic surgical systems and introduces ABC to the robotic toolbox. To better understand the utility of D-Flex, this study equates the performance of the 2.3mm D-Flex probe to an existing 5mm ABC Laparoscopic Probe through comparative ex-vivo tissue analysis.

METHODS:

Three D-Flex probes and three Laparoscopic probes were used for this study. Each instrument was powered by the System 7550 generator. Ex-vivo bovine liver was used as the tissue model. Each device was held a fixed distance from the tissue and activated at various power levels for a fixed duration. Thirty samples were created at each power level. The area and depth of each burn was measured using a light microscope. The resulting dimensional data was used to correlate tissue effect between the two devices.

RESULTS:

D-Flex created burns which were smaller in surface area than the Laparoscopic probe at all power levels. Additionally, D-Flex achieved thermal penetration levels equivalent to the Laparoscopic probe.

CONCLUSION:

D-Flex implements a small 7F geometry which creates a more focused beam. When used with robotic precision, quick localized superficial hemostasis can be achieved with minimal collateral damage. Additionally, D-Flex achieved equivalent thermal penetration levels at much lower power and Argon flow-rate settings than the Laparoscopic probe.

9326-8, Session 2

**Characterization and literature review of
bowel perforation injuring using argon
beam coagulation**

 Kelli S. Barnes, Renee A. Merchel, Kenneth D. Taylor,
ConMed Advanced Energy (United States)

INTRODUCTION:

Argon Beam Coagulation (ABC) technology is used in conjunction with the ConMed ABC Flex Probe to provide non-contact hemostasis, coagulation, and tissue devitalization during gastrointestinal procedures. ABC provides a superficial tissue effect; however, there is risk of bowel perforation. The likelihood depends on power, distance to the tissue, and application duration. Previous studies which characterize these settings are focused on the APC Probe (Erbe), test at distances ≥ 2 mm, and have mixed conclusions for the depth of injury. This study characterizes the effect of power and duration for ABC bowel perforation at small distances.

METHOD:

An ABC Flex Probe was tested using the System 7550. Power, distance, and duration were varied at fixed intervals and tested on ex-vivo porcine bowel. Power was varied from 30W to 80W and distance was controlled at near contact, 1mm, and 3mm. Depth of thermal injury to the serosa layer was determined using a light microscope.

RESULTS:

Conference 9326: Energy-based Treatment of Tissue and Assessment VIII

Using a power setting of 40W and near contact distance, 3 seconds of spot application was required before perforation occurred. Increasing the distance to 1mm and 3mm, increased the time until perforation to 4 and 6 seconds respectively. At a power of 80W, perforation occurred after 1.5s at near contact, 2s at 1mm, and 3s at 3mm.

CONCLUSION:

Settings that may lead to perforation using the ABC Flex Probe at typical and smaller distances to the tissue were characterized and compared to settings characterized in the literature to be safe (40-60W and less than 3 seconds).

9326-9, Session 3

Numerical model study of radio frequency vessel sealing thermodynamics (*Invited Paper*)

John A. Pearce, The Univ. of Texas at Austin (United States)

Several clinically successful clinical radio frequency vessel-sealing devices are currently available. The dominant thermodynamic principles at work involve tissue water vaporization processes. It is necessary to thermally denature both vessel collagen and elastin to achieve a successful fusion. Collagens denature at middle temperatures, between about 60 and 90 C depending on heating time and rate. Elastin is more thermally-robust, and requires temperatures in excess of the boiling point of water to thermally fuse. Rapid boiling at low apposition pressures leads to steam vacuole formation, and frequently to substantial disruption in the vessel wall, particularly in high elastin-content arteries. High apposition pressures substantially increase the equilibrium boiling point and are necessary to ensure a high probability of a successful seal. The FDM numerical models illustrate the beneficial effects of high apposition pressures.

9326-10, Session 3

The role of glycosaminoglycans in tissue adhesion during energy-based vessel sealing

Eric A. Kramer, Nicholas S. Anderson, Univ. of Colorado at Boulder (United States); Kenneth D. Taylor, ConMed Electrosurgery (United States); Virginia L. Ferguson, Mark E. Rentschler, Univ. of Colorado at Boulder (United States)

Energy-based vessel sealing remains a common alternative to traditional mechanical ligation procedures, despite considerable uncertainty as to the origin of vascular adhesion forces. Evidence of conformational changes in Collagen IA has fostered support of denatured collagen as the origin of tissue adhesion; experimental observation suggests that while pure collagen fails to adhere, remaining vascular constituents play a critical adhesive role. This study proposes a constitutive model of thermal fusion adhesion forces by determining the effects of Glycosaminoglycan (GAG) content on the bursting pressure of sealed vessels.

GAG content of porcine splenic arteries was altered via pre-fusion treatment in 0.1% Peracetic Acid (PAA), followed by fusion with the ConMed ALTRUS® thermal fusion device and subsequent strength testing. Bursting pressures of PAA-treated vessels were significantly lower than those of control vessels (317.8± 192.7 mmHg and 576.8 ± 145.3mmHg respectively, p=5.9e-05). Histology enabled qualitative visualization of the treated arterial cross-section and of the bonding interface. GAG concentrations as quantified by the Dimethylmethylene Blue assay were decreased in PAA-treated vessels at 1.147 wt% as compared with 1.455 wt% in untreated tissue. The correlation between decreased GAG content and lower seal strengths suggests that GAGs may provide heretofore unobserved adhesive interactions to adjacent cellular tissue layers during energy-based vessel sealing.

Vessel sealing allows for decreased infection rates, reduced invasiveness, improvements in surgical dexterity and reduced foreign bodies in surgical procedures. By elucidating the components which allow for energy-based vessel sealing, this study provides an important step towards understanding the chemistry underlying thermal tissue fusion and thus its potential for expansion to avascular tissues.

9326-11, Session 3

A novel parameter for predicting arterial fusion and ablation in finite element models

Douglas Fankell, Univ. of Colorado at Boulder (United States); Eric Kramer, University of Colorado (United States); Virginia L. Ferguson, Univ. of Colorado at Boulder (United States); Kenneth D. Taylor, ConMed Electrosurgery (United States); Mark E. Rentschler, Univ. of Colorado at Boulder (United States)

Tissue fusion devices apply heat and pressure to ligate or ablate blood vessels during surgery. Although this process is widely used, a predictive finite element (FE) model incorporating both structural mechanics and heat transfer has not been developed, limiting improvements to empirical evidence. This work presents the development of a novel damage parameter, which incorporates stress, water content and temperature, and demonstrates its application in a FE model.

A FE model, using the Holzapfel-Gasser-Ogden strain energy function to represent the structural mechanics and equations developed by Cezo to model water content and heat transfer, was created to simulate the fusion or ablation of a porcine splenic artery. Using state variables, the stresses, temperature and water content are recorded and combined to create a single parameter at each integration point. The parameter is then compared to a fusion threshold value and a critical value (determined through experiments). If the critical value is reached, the element loses all strength. If only the threshold value is reached, fusion is simulated. If neither value is reached, no change occurs.

Little experimental data exists for validation, but the resulting stresses, temperatures and water content fall within ranges predicted by experimental studies. Due to the lack of published data, additional experimental studies are being conducted to rigorously validate and accurately determine the critical and threshold values. Ultimately, a novel method for demonstrating tissue damage and fusion in a FE model is presented, providing the first step to in-depth FE models simulating fusion and ablation of arteries.

9326-12, Session 3

A simplified, low power system for effective vessel sealing

Allison B. Lyle, Jenifer S. Kennedy, Dale F. Schmaltz, Aaron S Kennedy, JustRight Surgical, LLC (United States)

The first bipolar vessel sealing system was developed nearly 15 years ago and has since become standard of care in surgery. These systems make use of radio frequency current that is delivered between bipolar graspers to permanently seal arteries, veins and tissue bundles. Conventional vessel sealing generators are based off traditional electrosurgery generator architecture and deliver high power (150-300 Watts) at high voltage using complex control and sense algorithms to adjust the output for vessel sealing applications. In recent years, a need for small-scale surgical vessel sealers has developed as surgeons strive to further reduce their footprint on patients. There are many technical challenges associated with miniaturization of vessel sealing devices including maintaining electrical isolation while delivering high current in a saline environment. Research into creating a small, 3mm diameter vessel sealer revealed that a highly

Conference 9326: Energy-based Treatment of Tissue and Assessment VIII

simplified generator system could be used to achieve excellent results and subsequently a low power vessel sealing system was developed. This system delivers 25 Watts constant power while limiting voltage (<80 Vrms) and current (<2 Amps) until an impedance endpoint is achieved, eliminating the use of complicated control and sensing software. The result is optimized tissue effect, where high seal strength is maintained (> 360mmHg), but seal times ($1.7 \pm 0.7s$ versus $4.1 \pm 0.7s$), thermal spread (1mm vs $\leq 2mm$) and total energy delivery are reduced, when compared to an existing high power system.

9326-13, Session 4

Tissue healing response following hyperthermic vapor ablation in the porcine longissimus muscle

John T. Grantham, Brian T. Grisez, Justin Famoso, West Virginia Univ. (United States); Michael F. Hoey, NxThera, Inc. (United States); Christopher M. Dixon, New York Medical College (United States); James E. Coad, West Virginia Univ. (United States)

As the use of thermal ablation treatments has increased, so too has the need to understand their effects. This study was designed to classify the tissue response and healing pattern following hyperthermic vapor ablation in the in vivo porcine longissimus muscle model. Each ablation was made with the NxThera Vapor Delivery System. The swine were euthanized on day 0, 3, 7, 14, 28, 45, and 90 post-treatment. Grossly, triphenyltetrazolium chloride (TTC) staining was used to identify tissue damage. Histologically, each treatment was examined for signs of acute inflammation, chronic inflammation, foreign body reaction and fibrosis. Grossly, two areas of tissue damage were identified - a central necrotic area and an outer "transition zone" consisting of a mixture of viable and non-viable cells. The area of tissue damage was largest in day 7 samples; by day 45 the lesions developed into a healed scar. Histologic tissue change, initially seen in the day 3 group, originated in the transition zone. This included a mixture of tissue necrosis and minimal acute and chronic inflammation. As time progressed, granulation tissue began to form (Day 7) and mature (Day 14). Primary collagen deposition began in the adjacent healthy tissue (Day 28). This was followed by collagen migration and remodeling (Day 45) and formation of a central fibrotic scar (Day 90). Hyperthermic vapor ablation induces formation of a central, fibrous scar surrounded by a variably cellular zone of viable and atrophic muscle cells in a web of collagen.

9326-14, Session 4

Development of an endoluminal high-intensity ultrasound applicator for image-guided thermal therapy of pancreatic tumors

Matthew Adams, Univ. of California, Berkeley (United States) and Univ. of California, San Francisco (United States); Serena J. Scott, Vasant A. Salgaonkar, Peter D. Jones, Univ. of California, San Francisco (United States); Juan C. Plata-Camargo, Stanford Univ. (United States); Graham Sommer, Stanford Univ. Medical Ctr. (United States); Chris J. Diederich, Univ. of California, San Francisco (United States) and Univ. of California, Berkeley (United States)

A theoretical evaluation of an endoluminal ultrasound applicator for thermal ablation and hyperthermia of pancreatic tumors was performed. The applicator, positioned in the stomach or duodenal lumen by endoscope, incorporates a directional transducer array with planar, curvilinear, or

tubular elements, and is surrounded by a water-cooled balloon for acoustic coupling and sparing of the luminal wall. Patient-specific 3D anatomical models were created based on CT image studies of patients with pancreatic tumors. Anatomical structures surrounding the tumors were segmented and finite element meshes were generated using Mimics Innovation Suite. The rectangular radiator method was used to generate the power deposition fields produced by each transducer configuration, and transient 3D bioheat FEM models for thermal ablation or hyperthermia of each patient anatomy were solved using COMSOL Multiphysics. The maximum tumor temperature was controlled with a PI controller to simulate treatment monitoring under MRTI or ultrasound guidance. Results indicated that >80% of the tumor volume for small pancreatic head tumors (~2 cm diameter) could be ablated ($t_{43} > 240$ eq. min.) by using 2 MHz planar or curvilinear transducers positioned in the duodenum in a 15-20 minute treatment period while mitigating damage to the luminal wall or nearby sensitive structures. Over 85% of the volume could be elevated above 40°C at steady-state for hyperthermia of the small pancreatic head tumors. For large body tumors (~5 cm diameter), >60% of the tumor volume could be ablated or raised above 40°C for hyperthermia by repositioning the applicator along the GI tract during treatment.

9326-15, Session 4

Circumferential targeted renal sympathetic nerve denervation with preservation of the renal arterial wall using intra-luminal ultrasound

Austin R. Roth, Leslie Coleman, ReCor Medical, Inc. (United States); Kenichi Sakakura, Elena Ladich, Renu Virmani, CVPath Institute (United States)

A clinical intra-luminal ultrasound catheter system (ReCor Medical's Paradise System) has been developed to provide circumferential denervation of the renal sympathetic nerves while preserving the renal arterial endothelium in order to treat hypertension. The Paradise System features a cylindrical non-focused ultrasound transducer centered within a balloon that circulates cooling fluid and that outputs a uniform circumferential energy pattern designed to ablate tissues located 1-6 mm from the arterial wall and protect tissues within 1 mm. RF power (up to 50 W) and cooling flow rate are controlled by the Paradise Generator which can energize transducers in the 8.5-9.5 MHz frequency range. Computer simulations and tissue-mimicking phantom models were used to develop the proper power, cooling flow rate and sonication duration settings to provide consistent tissue ablation for renal arteries ranging from 5-8 mm in diameter. The modulation of these three parameters allows for a great amount of control over the near-field (border of lesion closest to arterial wall) and far-field (border of lesion farthest from arterial wall, consisting of adventitial and peri-adventitial space) depths of the tissue lesion formed by the absorption of ultrasonic energy. Porcine studies have confirmed the safety (protected region within 1 mm) and effectiveness (ablation of 1-6 mm region) of the system and provided near-field and far-field depth data to correlate with bench and computer simulation models. The safety and effectiveness of the Paradise System, developed through computer model, bench and in vivo studies, has been demonstrated in human clinical studies.

9326-16, Session 4

Catheter-based high-intensity ultrasound for epicardial ablation of the left ventricle: device design and in vivo feasibility

Vasant A. Salgaonkar, Babak Nazer, Peter D. Jones, Yasuaki Tanaka, Univ. of California, San Francisco (United States); Bennett Ng, Univ. of California, San Francisco (United States) and Univ. of California, Berkeley (United States)

**Conference 9326: Energy-based Treatment of
Tissue and Assessment VIII**

States); Srikant Duggirala, Chris J. Diederich, Edward P. Gerstenfeld, Univ. of California, San Francisco (United States)

The development and in vivo testing of a high-intensity ultrasound thermal ablation catheter for epicardial ablation of the left ventricle (LV) is presented. Scar tissue can occur in the mid-myocardial and epicardial space in patients with non-ischemic cardiomyopathy and lead to ventricular tachycardia. Current ablation technology uses radiofrequency energy, which is limited epicardially by coronary vessels, phrenic nerve, and fat. Ultrasound energy can be precisely directed to deliver targeted deep epicardial ablation while sparing intervening epicardial nerve and vessels. The ultrasound applicators were designed for sub-xyphoid placement within the pericardial space through a steerable 14-Fr sheath. The catheter consists of two rectangular planar transducers for therapy (6.5 MHz) and imaging (5 MHz) mounted at the tip of a 3.5-mm flexible nylon catheter coupled and cooled by a custom shaped balloon that constrains the relative motion between the applicator and the LV. Thermal lesions ($n = 13$) were created in the LV in a swine model in vivo. The ultrasound applicator was positioned fluoroscopically. Its orientation and contact with the LV were verified using A-mode imaging and a radio-opaque marker. Ablations employed 60-s exposures at 45 - 90 W/cm² spatiotemporal average acoustic intensity. Histology indicated thermal coagulation and ablative lesions penetrating 5.5 - 10.4 mm (95% CI) into the left ventricle along the left anterior descending artery, and the posterior and lateral walls. The transducer design enabled successful sparing of ~3 mm of intervening ventricle tissue and epicardial fat. The feasibility of targeted epicardial ablation with catheter-based ultrasound was demonstrated (Funding: UCSF-RAP).

9326-17, Session 4

Design and analysis of a conformal patch antenna for a wearable breast hyperthermia treatment system

Sergio Curto, Manoshika Ramasamy, Kansas State Univ. (United States); Minyoung Suh, North Carolina State Univ. (United States); Punit Prakash, Kansas State Univ. (United States)

Current hyperthermia systems for breast cancer treatment have limited flexibility and do not conform to the breast, thereby hindering effective treatment of targeted volumes. An ergonomically shaped and wearable system, in very close proximity to the breast, would offer enhanced energy deposition, reduced power requirements and increased comfort. The objective of this work was to design and assess the feasibility of a conformal patch antenna of an array system to be integrated into a wearable hyperthermia bra.

A coupled electromagnetic-bioheat transfer solver and a hemispheric heterogeneous numerical breast phantom were used to design and optimize a 915 MHz patch antenna. The goals were device miniaturization, bandwidth, enhanced energy deposition pattern, and reduced E-field back radiation. The antenna performance was evaluated for a 32.5 mm x 17.0 mm flat groundplane configuration and a hemispheric conformal groundplane covering the water bolus around the breast. Applied power levels were restricted to 20 W.

Results indicated a stable 68 MHz ($\pm 3\%$) -10 dB return loss bandwidth for both the conformal and flat groundplane configurations. Treatment volumes ($T > 41^\circ\text{C}$) and depth were 12.4 cm³ and 26.1 mm, respectively, for the conformal groundplane configuration, and 7.24 cm³ and 23.4 mm, respectively, for the flat groundplane configuration. E-field back-radiation reduced by 90.8% for the conformal groundplane compared to the flat groundplane configuration.

In conclusion, the proposed patch antenna with conformal groundplane shows promising performance to be integrated in a clinical array system. Prototype experimental characterization is in progress and will be presented at the conference.

9326-20, Session 4

Effect of the superposition of a static magnetic field orthogonal to an alternating magnetic field in hyperthermia therapy treatments

Jose Bante-Guerra, Dianela J. Diaz-Bleis, Caridad G. Vales-Pinzón, Ivan Y. Forero-Sandoval, Juan D. Macias, Yolanda Freile-Pelegrin, Juan J. Alvarado-Gil, Ctr. de Investigación y de Estudios Avanzados del Instituto Politécnico Nacional (Mexico)

Usual procedures in cancer therapy are radiation of tissues and chemotherapy which has been improved recently by methods of controlled release of medication. However those methods exhibit undesirable collateral effects. In order to provide additional therapeutic techniques that can target specific cells, methods based on heating on nanoparticles located at the desired zones have been devised.

At the present time magnetic hyperthermia therapy involves introducing magnetic nanoparticles (MNPs) in the blood and guiding them to the area of the tumor or directly injecting them into the affected area, after that the patient is subjected to an oscillating magnetic field to raise the temperature of the tissue to kill cancer cells.

Magnetic nanoparticles dissipate heat from relaxation losses, this effect creates a localized tissue heating. Diverse studies have been performed which analyze the effect of the size of the particles, frequency and strength of the applied field, the role of the carrier fluid, among others.

However, diverse basic mechanisms responsible of the heating are not well understood, in particular those related to the structural ordering of the nanoparticles in the magnetic fluid.

In this work, phantoms of agar gel, loaded with magnetic nanoparticles were placed under the influence of an alternating magnetic field, at the same time a static magnetic field was applied, in order to create chains like structures. Specific absorption rate (SAR) was obtained as a function of the frequency and strength of the alternating magnetic field as well as the strength of the static magnetic field.

9326-21, Session 5

Similarities and differences in ablative and non-ablative iron oxide nanoparticle hyperthermia cancer treatment (*Invited Paper*)

Alicia A. Petryk, Geisel School of Medicine at Dartmouth College (United States); Adwiteeya Misra, Elliot J. Kastner, Thayer School of Engineering at Dartmouth (United States); Courtney M. Mazur, Geisel School of Medicine at Dartmouth College (United States); P. Jack Hoopes, Geisel School of Medicine at Dartmouth College (United States) and Thayer School of Engineering at Dartmouth (United States)

The use of hyperthermia to treat cancer is well studied and has utilized numerous delivery techniques, including microwaves, radio frequency, focused ultrasound, induction heating, infrared radiation, warmed perfusion liquids (combined with chemotherapy), and recently, metallic nanoparticles (NP) activated by NIR and alternating magnetic field based platforms. It has been demonstrated by many research groups that ablative temperatures and cytotoxicity can be produced with locally NP-based hyperthermia. Such ablative NP techniques have demonstrated the potential for success. Much attention has also been given to the fact that NP may be administered systemically, resulting in a broader cancer therapy approach, a lower level of tumor NP content and a different type of NP cancer therapy (most likely

**Conference 9326: Energy-based Treatment of
Tissue and Assessment VIII**

in the adjuvant setting). To use NP based hyperthermia successfully as a cancer treatment, the technique and its goal must be understood and utilized in the appropriate clinical context. The parameters include, but are not limited to, NP access to the tumor (large vs. small quantity), cancer cell-specific targeting, drug carrying capacity, potential as an ionizing radiation sensitizer, and the material properties (magnetic characteristics, size and charge). In addition to their potential for cytotoxicity, the material properties of the NP must also be optimized for imaging, detection and direction. In this paper we will discuss the differences between, and potential applications for, ablative and non-ablative magnetic nanoparticle hyperthermia.

9326-22, Session 5

Magnetic nanoparticle hyperthermia cancer treatment efficacy dependence on cellular and tissue level particle concentration and particle heating properties

Alicia A. Petryk, Geisel School of Medicine at Dartmouth College (United States); Adwiteeya Misra, Thayer School of Engineering at Dartmouth (United States); Courtney M. Mazur, James D. Petryk, P. Jack Hoopes, Geisel School of Medicine at Dartmouth College (United States)

The use of nanotechnology for the treatment of cancer affords the possibility of highly specific tumor targeting and improved treatment efficacy. Iron oxide magnetic nanoparticles (IONP) have demonstrated success as an ablative mono-therapy and targetable adjuvant therapy. However, the relative therapeutic value of intracellular vs. extracellular IONP remains unclear. Our research demonstrates that both extracellular and intracellular IONP generate cytotoxicity when combined with an alternating magnetic field (AMF). While killing individual cells via intracellular IONP heating is an attractive goal, theoretical models and experimental results suggest that this may not be possible due to limitations of cell volume, applied AMF, IONP concentration and specific absorption rate (SAR). The goal of this study was to examine the importance of tumor size (cell number), as well as the SAR of IONPs when intracellular vs. extracellular. Mouse mammary adenocarcinoma cells were incubated with IONPs, washed, spun into different pellet sizes (0.1, 0.5 and 2 million cells) and exposed to an AMF. Following AMF exposure, intracellular IONPs generated significant SAR *ex vivo* and *in vitro*. The level of heating and associated cytotoxicity depended primarily on the number of IONPs /amount Fe per cell pellet volume and the relative density of the cells. Specifically, large cell pellets achieved greater relative cytotoxicity due to greater iron amounts, close association and subsequently higher temperatures.

9326-23, Session 5

Alternating magnetic field optimization for IONP hyperthermia cancer treatment

Elliot J. Kastner, Russell Reeves, James D. Petryk, Alicia A. Petryk, Adwiteeya Misra, William Bennett, Robert V. Stigliano, P. Jack Hoopes, Dartmouth College (United States)

Iron oxide nanoparticles (IONP) have the potential to deliver a targeted and effective thermal dose to tumors when activated in an alternating magnetic field (AMF). Biological targeting and anatomically advantageous delivery techniques have the potential to significantly improve IONP treatment accuracy and efficacy. However, delivery of a safe and effective AMF at necessary tumor tissue depths remains a significant, but addressable challenge. Although the generation and risk of AMF associated eddy currents is well documented, eddy current heating specifics related to tissue

size, geometry and composition as well as coil design, power input and AMF delivery techniques in complex living tissues is not well understood. The goal of this research is to better understand and optimize AMF hardware, physics and associated pathophysiology to improve the safety and efficacy of AMF- IONP therapy via improvement in the AMF power ratio (PR = level of energy deposited into the IONP versus the non-target tissue). Using modeling, phantom testing and *in vivo* experimentation we have focused on two techniques to improve the PR : (1) reduced power deposition in non-target tissue via manipulation of fields and eddy current flow and (2) enhancement of heat removal from non-target tissue. Preliminary results suggest that controlling tissue placement, varying electrical connectivity between tissue layers, and utilizing external cooling devices can decrease non-target heating by more than 50%, thereby allowing an increased thermal dose to the tumor while decreasing the associated eddy current and heating risk to normal tissue.

9326-24, Session 5

Macroscopic and microscopic biodistribution of intravenously administered iron oxide nanoparticles

Adwiteeya Misra, Thayer School of Engineering at Dartmouth (United States); Alicia A. Petryk, Geisel School of Medicine at Dartmouth College (United States); P. Jack Hoopes, Geisel School of Medicine at Dartmouth College (United States) and Thayer School of Engineering at Dartmouth (United States)

Iron oxide nanoparticles (IONPs) are being developed for use as novel cancer treatment technique. Preliminary *in vivo* studies have demonstrated improved efficacy of this modality in conjunction with conventional chemotherapy and radiation therapy. The success of IONPs as a therapeutic tool depends on the delivery of a safe but controlled cytotoxic thermal dose to tumor tissue following activation with an alternating magnetic field (AMF). Prior to clinical approval, a sound understanding of IONP toxicity, biodistribution and physiological clearance is essential. This time-course study determines the biodistribution of 110 nm dextran-coated IONPs (iron) from mice at 48 hours, 7 days, and 30 days post systemic administration. Mice were injected with a physiologically relevant dose of 350 mg Fe/ kg mouse. Histological analysis revealed highest concentrations of iron in the reticuloendothelial system (i.e. liver, spleen, kidney and lymph nodes) at the 48 hours time point and showed diminished, near baseline concentrations by 30 days post injection. Iron accumulation was highest in the liver and spleen while the brain, heart, and lungs showed inconsequential iron accumulation for the duration of the study. In addition to quantification of iron levels within the target organs, histo-morphological findings regarding anatomical iron deposition are presented.

9326-25, Session 5

MRI guided energized-magnetic particle treatments

Stephen Barry, Emanate Biotech (United States); Michael Garwood, Univ. of Minnesota, Twin Cities (United States); Paul R. Stauffer, Thomas Jefferson Univ. (United States); Alicia A. Petryk, Dartmouth Hitchcock Medical Ctr. (United States); Bo Lu, Thomas Jefferson Univ. (United States); P. Jack Hoopes, Dartmouth Hitchcock Medical Ctr. (United States)

Magnetic Nanoparticle Heating (MNH), driven by Alternating Magnetic Fields (AMF), has the potential to bring sub-cellular precision to thermal medicine. The magnetic nanoparticles are inherently dual therapeutic-diagnostic, sometimes termed theragnostic, devices. Particularly adaptable

**Conference 9326: Energy-based Treatment of
Tissue and Assessment VIII**

to image-guided treatments, MNH can leverage magnetic resonance imaging (MRI) both for treatment planning and intra-treatment thermal monitoring. SWIFT (SWEEP Imaging with Fourier Transformation)-based MRI is a recently developed method that has demonstrated the ability to quantify the concentration of iron oxide in tissue and thus plays an integral role in image-guided therapy. With the distribution of heating particles characterized, bioheat modeling may be used to pre-plan thermal dose distributions within the tumor and margins upon AMF application of specific intensity and duration. If particle distribution is deemed inadequate based upon the MRI, the image information can be used to guide particle administration to specific tumor and tumor margin locations to achieve a desired dose distribution. Strategies for incorporating MRI thermal monitoring during treatment will also be discussed. Desired and specific adsorption rates for currently available particle, AMF system specifications, and data supporting the development of these magnetic nanoparticle-based devices will be presented. Cancers that are underserved by current regimens that may be particularly well-treated by multi-modal treatments that include energized magnetic nano-particle, and specific treatment regimens for these cancers will be discussed. Plans and progress towards the rational combination of particle heat treatments with certain immunotherapy regimens to treat cancer will also be delineated.

9326-26, Session 5
Effect of radiation energy and intracellular iron dose on iron oxide nanoparticle enhancement of radiation cytotoxicity

Courtney M. Mazur, Dartmouth College (United States) and Univ. of California, Berkeley (United States); Rendall R. Strawbridge, Dartmouth College (United States); Ella S. Thompson, Dartmouth College (United States) and Emory Univ. (United States); Alicia A. Petryk, Dartmouth College (United States); David J Gladstone, Section of Radiation Oncology, Dartmouth-Hitchcock Medical Center (United States) and Dartmouth College (United States); P. Jack Hoopes, Dartmouth College (United States) and Thayer School of Engineering (United States)

Iron oxide nanoparticles (IONPs) are one of several high-Z materials currently being investigated for their ability to enhance the cytotoxic effects of therapeutic ionizing radiation. Studies with iron oxide, silver, gold, and hafnium oxide suggest radiation dose, radiation energy, cell type, and the type and level of metallic nanoparticle are all critical factors in achieving radiation enhancement in tumor cells. Using a single 4 Gy radiation dose we compared the level of tumor cell cytotoxicity at two different intracellular iron concentrations and two different radiation energies.

Methods: IONPs were added to cell culture media at concentrations of 0.25 mg Fe/mL and 1.0 mg Fe/mL and incubated with murine breast adenocarcinoma (MTG-B) cells for 72 hours. Extracellular iron was then removed and cells were irradiated at either 662 keV or 10 MV.

Results: At the 0.25 mg Fe/mL dose (4 pg Fe/cell), radiation energy did not affect the level of cytotoxicity. However with 1.0 mg Fe/mL (9 pg Fe/cell), the higher 10 MV radiation energy resulted in 50% greater cytotoxicity as compared to cells without IONPs irradiated at this energy. These results suggest IONP radiation enhancement may require high radiation energies and a critical threshold level of intracellular iron. In addition to the IONP-based radiation enhancement demonstrated here, delivery of localized heat via an alternating magnetic field applied to these same intracellular IONPs creates an opportunity for dual use of the particles for further enhanced cytotoxicity and improved therapeutic ratio.

9326-27, Session 6
SWIFT-MRI imaging and quantitative assessment of IONPs in murine tumors following intra-tumor and systemic delivery

Russell Reeves, Alicia A. Petryk, Geisel School of Medicine at Dartmouth College (United States); Elliot J. Kastner, Thayer School of Engineering at Dartmouth (United States); Jinjin Zhang, Hattie Ring, Michael Garwood, Univ. of Minnesota, Twin Cities (United States); P. Jack Hoopes, Geisel School of Medicine at Dartmouth College (United States) and Thayer School of Engineering at Dartmouth (United States)

Although preliminary clinical trials are ongoing, successful the use of iron-oxide magnetic nanoparticles (IONP) for heat-based cancer treatments will depend on advancements in: 1) nanoparticle platforms, 2) delivery of a safe and effective alternating magnetic field (AMF) to the tumor and 3) development of non-invasive, spatially accurate IONP imaging and quantification technique. This imaging technique must be able to assess tumor and normal tissue anatomy as well as IONP levels and biodistribution. Conventional CT imaging is capable of detecting and quantifying IONPs at tissue levels above 10 mg/gram; unfortunately this level is not clinically achievable in most situations. Conventional MRI is capable of imaging IONPs at tissue levels of 0.05 mg/gm or less, however this level is considered to be below the therapeutic threshold. We present here preliminary in vivo data demonstrating the ability of a novel MRI technique, Sweep Imaging With Fourier Transformation (SWIFT), to accurately image and quantify IONPs in tumor tissue in the therapeutic concentration range (0.1-1.0 mg/gm tissue). This ultra-short T2 MRI method (Garwood) provides a positive Fe contrast enhancement with a reduced signal to noise ratio. Additional IONP signal enhancement techniques such as inversion recovery spectroscopy and variable flip angle (VFA) are also being studied for potential optimization of SWIFT IONP imaging. Our study demonstrates the use of SWIFT to assess IONP levels and biodistribution, in murine flank tumors, following intra-tumoral and systemic IONP administration. ICP-MS and quantitative histological techniques are used to validate the accuracy and sensitivity of SWIFT-based IONP imaging and quantification.

9326-28, Session 6
Evaluate high intensity focused ultrasound ablation of prostate tumor with hyperpolarized ¹³C imaging biomarkers

Jessie E. Lee, Chris J Diederich, Vasant A Salgaonkar, Robert Bok, Andrew G Taylor, John Kurhanewicz, Univ. of California, San Francisco (United States)

Real-time hyperpolarized ¹³C MR can be utilized during high-intensity focal ultrasound (HIFU) therapy to improve treatment delivery strategies, provide treatment verification, and thus reduce the need for more radical therapies in such cases. The goal is to develop imaging biomarkers specific to thermal therapies of prostate cancer using HIFU, and to predict the success of thermal coagulation and identify tissues potentially sensitized to adjuvant treatment by sub-lethal hyperthermic heat doses. Mice with 1-cm³ solid prostate tumors received HIFU treatment (5.6 MHz, 160W/cm², 60 s), and the MR imaging follow-ups were performed on a wide-bore 14T microimaging system. ¹³C-labeled pyruvate and urea were used to monitor tumor metabolism and perfusion accordingly. After treatment, the ablated tumor tissue had no metabolism (the lactate-to-pyruvate ratio was nearly zero). Urea and the dynamic contrast enhanced (DCE) imaging both showed a significant decrease in perfusion in the treated region; however, the slight recovery shown by urea 5 days after treatment was not seen in DCE. The study demonstrates that ¹³C-labeled pyruvate and urea can potentially be

**Conference 9326: Energy-based Treatment of
 Tissue and Assessment VIII**

effective indicators for HIFU ablation. It is shown that metabolism does not recover in regions of complete HIFU ablation, but slight recovery of perfusion was observed using HP 13C urea. Therefore, the use of HP 13C urea may be superior to gadolinium due to a higher sensitivity to perfusion recovery. In addition, the co-polarization of 13C-labeled urea and pyruvate enables the acquisition of both perfusion and metabolism information in a single injection, which is not achievable using traditional DCE.

9326-29, Session 6
Characterization of nanosecond pulse electrical field shock waves using advanced imaging techniques

L. Chris Mimun, The Univ. of Texas at San Antonio (United States); Caleb C. Roth, The Univ. of Texas Health Science Ctr. at San Antonio (United States); Ronald A. Barnes Jr., Dhiraj Kumar Sardar, The Univ. of Texas at San Antonio (United States); Hope T. Beier, Bennett L. Ibey, Air Force Research Lab. (United States)

Nanosecond pulsed electric fields (nsPEF) cause the formation of small pores, termed nanopores, in the membrane of cells. Current nanoporation models treat nsPEF exposure as a purely electromagnetic phenomenon, but recent publications showing pressure transients, reactive oxygen species production, temperature gradients, and pH waves suggest the stimulus may be "dirty," causing multiple biological stressors. Our research group's goal is to quantify the multiple stressors generated during nsPEF exposure and determine their relative importance to the observed cellular response. In this paper, we report the use of advanced imaging techniques to identify a possible source of nsPEF-induced acoustic shock waves. nsPEFs were delivered in an aqueous media via a pair of 125 μ m tungsten electrodes separated by 100 μ m, mirroring previous cellular exposures. To capture images of ultra-fast phenomenon, we utilized strobe imaging methodology with a nanosecond-pulsed laser source and a charge coupled devices-camera to monitor the electrode surface and medium between the electrodes before, during and after the pulse. To measure any pressure transients emanating from the electrodes or surrounding medium, we used the Schlieren imaging technique. Resulting images and measurements confirmed that mechanical pressure waves and electrode-based stresses are formed during nsPEF, resulting in a clearer understanding of the whole exposure dosimetry. Such information will be used to quantify the impact of nsPEF-induced acoustic shock waves on cells, thus providing further evidence of non-electrical-field-induced bioeffect.

9326-30, Session 6
Nonlinear imaging of lipid membrane alterations elicited by nanosecond pulsed electric fields

Erick K. Moen, The Univ. of Southern California (United States); Gary L. Thompson, Oak Ridge Institute for Science & Education (United States); Andrea M. Armani, The Univ. of Southern California (United States); Hope T. Beier, Bennett L. Ibey, Air Force Research Lab. (United States)

Second Harmonic Generation (SHG) imaging is a useful tool for examining the structure of interfaces between bulk materials. Recently, this technique was applied to detecting subtle perturbations in the structure of cellular membranes following nanosecond pulsed electric field (nsPEF) exposure. Monitoring the membrane as it is exposed to nsPEF via SHG has demonstrated that nanoporation is likely the root cause for size-specific, increased membrane permeabilization. It is still not well understood, however, whether these poration events are field-driven, caused by mechanical forces (internal or external), or an indirect response of the cell

to ion influx and stress. To help isolate the influence of each phenomenon, two different experiments were conducted. To remove the effect of the biological response to the field, as well as the secondary (but rapid) changes in the cell due to ion influx, giant unilamellar vesicles were exposed to various amplitude and duration monopolar nsPEFs. These experiments, when compared to previous exposures performed on Jurkat cells, show what portion of the observed response is indirect. The second experiment was performed using high-voltage bipolar nsPEFs, a positive-leading-edge square pulse followed by a negative-leading-edge square pulse. This change in polarity affects membrane charging, pore formation and lifetime, as well as limits any electrophoretic-induced particle motion. By using SHG imaging to directly visualize the change in the order of phospholipids within the membrane, we are able to better understand the complex response of living cells to electric pulses.

9326-31, Session 7
Multiple-antenna microwave ablation: analysis of non-parallel antenna implants

Souvick Mukherjee, Sergio Curto, Nathan Albin, Bala Natarajan, Punit Prakash, Kansas State Univ. (United States)

Microwave ablation treatment planning is typically restricted to vendor specifications of expected ablation zone volumes based on experiments in ex-vivo tissues, presuming parallel insertion of antennas. However, this assumption is limited due to restricted control of flexible antennas and presence of intervening organs. 3D-FEM electromagnetic-bioheat transfer models were implemented to analyze ablation zone profiles of a dual antenna array operating at 2.45 GHz. Treatment conditions were 10 min and 30 W/antenna. Parallel and non-parallel implants spaced 10-25 mm were simulated by deviating antenna tips or feedpoints to create converging or diverging configurations. The 60°C isotherms were evaluated and the Dice similarity coefficients (DSC) were calculated to compare ablation zone volumes for parallel and non-parallel configuration. The impact of non-parallel antenna insertions was illustrated on patient-specific images from realistic clinical treatments. Feed divergence up to 7.5 mm/antenna yielded minimal change with respect to the ablation zone volume compared to the parallel case (DSC>0.9). Tip convergence had a greater impact on ablation zone with respect to the parallel case. A tip displacement of 3 mm/antenna yielded an average DSC of 0.78. Tip displacement of 5 mm/antenna yielded a DSC of 0.78 and 0.64 for 15 mm and 20 mm antenna spacing, respectively. In conclusion, ablation volumes with non-parallel antenna implants significantly differ from the parallel configuration. Patient-specific treatment planning tools may provide 3D-ablation volumes based on actual implanted antenna configurations. Methods to compare ablation zone volumes incorporating uncertainty in antenna positions and experimental results to validate the numerical modelling will be presented.

9326-32, Session 7
Three-dimensional finite-element analyses of multiple electrode bipolar RF global endometrial ablation

Jia Hua Xiao, Cardea Medsystem Co., Ltd. (China); Tao Hu, Dept. of Mechanical Engineering (China)

RF ablation is a minimally invasive surgical procedure to thermally ablate the targeted diseased tissue. There have been many finite-element method (FEM) studies of cardiac and hepatic RFA, but hardly find any FEM study on endometrial ablation for abnormal uterine bleeding. In this paper, a FEM model was generated to analyze the temperature distribution of bipolar RF global endometrial ablation with three pairs of bipolar electrodes placed at the perimeter of the uterine cavity. COMSOL was utilized to calculate the RF electric field and temperature field by numerically solving the bio-heat equation in the triangular uterine cavity space. The 55°C isothermal

**Conference 9326: Energy-based Treatment of
Tissue and Assessment VIII**

surfaces shows the shape of the lesion dimensions (depth and width), which reasonably match the experimental results. The results shows that the proposed ablation procedure should be sufficient to treat AUB in clinical settings.

9326-33, Session 7
Finite element method (FEM) model of the mechanical stress on phospholipid membranes from shockwaves produced in nanosecond electric pulses (nsEP)

Ronald A. Barnes Jr., The Univ. of Texas at San Antonio (United States); Caleb C. Roth, The Univ. of Texas Health Science Ctr. at San Antonio (United States); Mehdi Shadaram, The Univ. of Texas at San Antonio (United States); Hope T. Beier, Bennett L. Ibey, Air Force Research Lab. (United States)

The underlying mechanism(s) responsible for nanoporation of phospholipid membranes by nanosecond pulsed electric fields (nsPEF) remains unknown. The passage of a high electric field through a conductive medium, creates two primary contributing factors that may induce poration: the electric field interaction at the membrane and the shockwave produced from electrostriction of a polar submersion medium exposed to an electric field. Previous work has focused on the electric field interaction at the cell membrane, through such models as the transport lattice method. Our objective is to model the shock wave cell membrane interaction induced from the density perturbation formed at the rising edge of a high voltage pulse in a polar liquid resulting in a shock wave propagating away from the electrode toward the cell membrane. Utilizing previous data from Schlieren camera shockwave images and cell membrane mechanical parameters, an acoustic shock wave model based on the Helmholtz equation for sound pressure was developed and coupled to a cell membrane model with finite-element modeling in COMSOL. The acoustic structure interaction model was developed to illustrate the harmonic membrane displacements and stresses resulting from shockwave and membrane interaction based on Hookes law. Poration is predicted by utilizing membrane mechanical breakdown parameters including cortical stress limits and hydrostatic pressure gradients.

9326-34, Session 7
Development of a fast 3D treatment planning platform for clinical interstitial microwave hyperthermia within free-hand obliquely implanted HDR catheters

Vasant A. Salgaonkar, Serena J. Scott, Univ. of California, San Francisco (United States); Punit Prakash, Univ. of California, San Francisco (United States) and Kansas State Univ. (United States); I-Chow Hsu, Chris J. Diederich, Univ. of California, San Francisco (United States)

A treatment planning platform for interstitial microwave hyperthermia (HT) was developed for practical, free-hand clinical implants. Such implants, consisting of non-parallel, moderately curved antennae with varying insertion depths, are encountered in HDR brachytherapy for treating locally advanced cancer.

Numerical models were developed in COMSOL Multiphysics, a finite element analysis software package, for commercially available MA251 antennae (915 MHz, BSD Medical). To expedite treatment planning, electric fields, power deposition and temperature rises were computed for a single straight antenna in 2D axisymmetric geometry. A pre-computed library of electric field and temperature solutions was created for a range of insertion depths

(5-12 cm) and blood perfusion rates (0.5-5 kg/m³/s).

A custom HT treatment planning software package was developed in MATLAB with capabilities to interface with a commercial radiation therapy planning platform (Oncontra, Nucletron), import patient and multi-catheter implant geometries, calculate insertion depths, and perform HT planning with antennae operating in asynchronous or synchronous mode. During asynchronous operation, the net power deposition and temperature rises were approximated as a superposition sum of the respective quantities for one single antenna. During synchronous excitation, a superposition of complex electrical fields was performed with appropriate phasing to compute power deposition. Electric fields and temperatures from the pre-computed single-antenna library were utilized following appropriate non-rigid coordinate transformations.

The HT planning software allowed users to select power and phasing, assess treatment plans (3D distributions: energy and temperature), and optimize treatment parameters through gradient search techniques. It was successfully tested, deployed and adopted in the clinical workflow (R01 CA122276).

9326-35, Session 7
Geometric study of treatment variability of percutaneous thermal ablation and its causes

Krishna Nand Keshava Murthy, Benjamin B. Kimia, Brown Univ. (United States); Madeleine L. Cook, Damian E. Dupuy, Scott A. Collins, Derek Merck, Rhode Island Hospital (United States)

Image guided tumor ablation is a less expensive and minimally invasive alternative to surgery and radiotherapy. However, a major challenge for ablation is high treatment variability due to heterogeneous tissue characteristics and thermal sinks. Review of clinical ablation procedures demonstrates both treatment variability across patients and deviation from predicted treatment zones provided by device vendors. Variability in treatment effect contributes to difficulties in standardizing outcome measurements. To date, no systematic geometric analysis of treatment zone variability has been performed. The goal of this study is to quantitate 3D treatment zone variability as a function of device parameters (applicator placement, power, time) and local tissue and anatomic characteristics. A key consideration in comparing observed treatment zones and vendor specifications across patients selecting the correct coordinate system. We describe a method that uses an applicator-centric cylindrical coordinate system to normalize clinical data so that treatment shape variability can be systematically reviewed. We analyzed boundary curves formed by the longitudinal cross sections of the treatment zone segmentations. We cluster related curve shapes and identified areas of significant asymmetry. We then correlated these asymmetries with the local tissue types and anatomic structures, giving us insights into the factors causing the variability of the treatment zones. 3D shape representations of the treatment zones were additionally parameterized and Eigen shape statistics were computed to identify key modes of shape variability. This will enable us in future work to generate pre-procedure probabilities on how likely a candidate procedure plan will result in a complete treatment.

9326-36, Session 8
The working mechanism of the ‘nanoknife’: hot or not?

Rudolf M. Verdaasdonk, Hester J. Scheffer, Vrije Univ. Medical Ctr. (Netherlands); Willemien van den Bos, Jantien A. Vogel, Marc G. Besselink, Academisch Medisch Centrum (Netherlands); Martijn R. Meijerink, Vrije Univ. Medical Ctr. (Netherlands); Jean J. de la Rosette, Daniel M. de Bruin,

**Conference 9326: Energy-based Treatment of
Tissue and Assessment VIII**

Academisch Medisch Centrum (Netherlands); John H. Klaessens, Vrije Univ. Medical Ctr. (Netherlands)

The 'NanoKnife' was recently introduced as new technique based on irreversible electroporation (IRE) for selective treatment of tumors. Malignant tissue is exposed to a series of 90 μ s bursts of 20-40 A between 2-6 electrode needles at 1500V/cm interelectrode distance. The action mechanism is ascribed to high voltage damaging of ion channels in the cell membrane with minimal thermal effects.

To investigate the physical mechanisms during IRE, the NanoKnife (AngioDynamics, Albany, N.Y., USA) was studied in tissue and cell-free phantoms using high speed Schlieren techniques and thermography to image instant effects and to quantify the temperature dynamics up to millisecond resolution comparing energy settings and needle configurations. The images were processed with dedicated analysis software.

High speed imaging showed instant gas formation ascribed to electrolysis most pronounced at the negative electrode supported by the color change of the metal electrodes. Thermal imaging showed substantial thermal effects 5-10 mm symmetrical around the needles (thermal source) with temperature increase over 20 degrees (highest for negative electrode) remaining for several minutes. By adapting the length of the electrode, the distance and relative angle of each needle, the temperature distribution could be controlled. The presence of metal stents had minimal effect.

Based on in vitro-studies, the working mechanism of the NanoKnife is partly ascribed to a substantial temperature increase while no evidence is found to support membrane damage. Future in-vivo studies are needed to observe the thermal effects in tissues with perfusion. The new insights will contribute to an effective selective treatment of tumors in e.g. liver, pancreas, kidney and prostate

9326-37, Session 8
External stimulation by nanosecond pulsed electric fields to enhance cellular uptake of nanoparticles

Samantha K. Franklin, Air Force Research Lab. (United States) and The Univ. of Texas at San Antonio (United States); Hope T. Beier, Bennett L. Ibey, Air Force Research Lab. (United States); Kelly L. Nash, The Univ. of Texas at San Antonio (United States)

In the past decade, research into the biological effects of nanosecond pulsed electric fields (nsPEF) has grown considerably. nsPEF exposure of cells causes a variety of biological effects that appear different than those caused by much longer pulses (μ s and ms) commonly used for electroporation. Most notably, nsPEF induce the formation of nanopores in the plasma membrane, allowing small molecules to pass through the membrane while larger molecules remain outside the cell. Additionally, increasing either the number, amplitude, or duration of exposures appears to increase the size of the nanopores in a controlled and somewhat predictive manner. This selective poration also limits the lethality of the exposure compared to longer pulses, making nsPEF-exposure a preferred method of temporarily increasing membrane permeability. Based on this phenomenon, we attempt to control the uptake of gold nanoparticles (AuNP) by controllably increasing the exposure intensity. To evaluate the impact of surface molecules, two types of AuNP were used in this study, one created within chitosan and one created using a sodium citrate reduction method. NG108 cells were grown in a 2D culture and nanoparticles were loaded into cell media prior to exposure. Using a pair of tungsten electrodes, nsPEFs were delivered to a small population of cells on the coverslip and confocal microscopy was used to visualize AuNPs uptake and localization. Cellular uptake induced by nsPEF was compared to accepted incubation methods. Our results will determine whether successful induction of rapid nanoparticle uptake by nsPEF is achievable and if it is a useful technique for studying the dynamics of membrane pores and delivery of intracellular nanosensors.

Distribution A: Approved for public release; PA # TSRL 14-0089

9326-38, Session 8
The role of PIP2 and the IP3/DAG pathway in intracellular calcium release and cell survival during nanosecond electric pulse exposures

Zachary A. Steelman, Texas A&M Univ. (United States); Bennett L. Ibey, Gleb P. Tolstykh, Larry E. Estlack, Air Force Research Lab. (United States); Caleb C. Roth, The Univ. of Texas Health Science Ctr. at San Antonio (United States)

Phosphatidylinositol4,5-biphosphate (PIP2) is a membrane phospholipid of particular importance in cell-signaling pathways. Hydrolysis of PIP2 releases inositol-1,4,5-triphosphate (IP3) from the membrane, activating IP3 receptors on the smooth endoplasmic reticulum (ER) and facilitating a release of intracellular calcium stores and activation of Protein Kinase C (PKC). Recent studies suggest that nanosecond pulsed electric fields (nsPEF) cause depletion of PIP2 in the cellular membrane, activating the IP3 signaling pathway. However, the exact mechanism(s) causing this observed depletion of PIP2 are unknown. Complicating the matter, nsPEF create nanopores in the plasma membrane, allowing calcium to enter the cell and thus causing an increase in intracellular calcium. While elevated intracellular calcium can cause activation of Phospholipase C (a known catalyst of PIP2 hydrolysis) PIP2 depletion has been shown to occur in the absence of both extracellular calcium and in a calcium depleted intracellular environment. These observations have led to the hypothesis that the high electric field itself may be playing a direct role in the hydrolysis of PIP2 from the plasma membrane. To support this hypothesis, we used edelfosine to block the IP3/DAG pathway in Chinese Hamster Ovarian (CHO) cells prior to applying nsPEF. Fluorescence microscopy was used to monitor intracellular calcium bursts during nsPEF, while MTT survivability assays were utilized to determine whether edelfosine improved cell survival during nsPEF exposure. This work is critical to refine the role of PIP2 in the cellular response to nsPEF, and also to determine the fundamental biological effects of high electric field exposures.

9326-39, Session 8
Cells exposed to nanosecond electrical pulses exhibit biomarkers of mechanical stress

Caleb C. Roth, The Univ. of Texas Health Science Ctr. at San Antonio (United States); Ronald A. Barnes Jr., The Univ. of Texas at San Antonio (United States); Bennett L. Ibey, Hope T. Beier, Air Force Research Lab. (United States); Erick K. Moen, The Univ. of Southern California (United States); Randolph D. Glickman, The Univ. of Texas Health Science Ctr. at San Antonio (United States)

Exposures of cells to very short (<1 μ s) electric pulses in the megavolt/meter range have been shown to cause disruption of the plasma membrane. This disruption is often characterized by the formation of numerous small pores (<2 nm in diameter) in the plasma membrane that last for several minutes, allowing the flow of ions into the cell. These small pores are referred to as nanopores and the resulting damage to the plasma membrane is referred to as nanoporation. Nanosecond electrical pulse (nsEP) exposures can impart many different stressors on a cell, including electrical, electrochemical, and mechanical stress. Thus, nsEP exposure is not a "clean" insult, making determination of the mechanism of nanoporation quite difficult. We hypothesize that nsEP exposure creates acoustic shock waves capable of causing nanoporation. Our data shows that cells shielded from the nsEP-induced shock waves had higher ED50 for plasma membrane disruption indicating that the electric field is not the sole cause of nanoporation. Cells shielded from the electric field but not the acoustic shock wave exhibited mechanical stress biomarkers. The idea that nanoporation is

**Conference 9326: Energy-based Treatment of
Tissue and Assessment VIII**

caused by external mechanical force from acoustic shock waves has to our knowledge not been investigated. This work will critically challenge the existing paradigm that nanoporation is caused solely by an electrical field driven event and could provide the basis for a plausible explanation for electroporation.

9326-40, Session 8

The effects of nanosecond pulse electric fields on NIH-3T3 cells grown in 2D and 3D cultures

Joshua E. Lee, North Carolina A&T State Univ. (United States); Caleb C. Roth, The Univ. of Texas Health Science Ctr. at San Antonio (United States); Hope T. Beier, Bennett L. Ibey, Air Force Research Lab. (United States)

Several studies have explored the biological effects of nanosecond pulsed electric fields (nsPEF) on both cells cultured in vitro and on tissues in vivo. Previously characterized effects of cells exposed to nsPEF and grown in vitro include nanoporation of the plasma membrane, swelling, blebbing, calcium and sodium uptake, and apoptotic and necrotic cell death. In both clinical and animal studies, nsPEF have been shown to ablate and or porate cancer cells in tumors. Comparatively, more intense exposures (more pulses and higher amplitude) are needed to kill cells in vivo than what are required in in vitro studies. In this paper, we compare the cellular response of cells grown in vitro in 2D versus 3D when exposed to nsPEF. Cells, cultured in 3D, mimic the tissues in in vivo exposures, as the cells are in a more natural tissue-like environment. Thus we hypothesized that cells grown in 3D will be more resistant to nsPEF than cells grown in 2D. To test the hypothesis, we grew mouse fibroblasts (NIH-3T3) in a polycaprolactone nanofiber extracellular matrix well plate and in a standard 2D culture. Both the 2D and 3D tissues were stained with Yo-PRO1 and propidium iodide to evaluate the nsPEF-permeabilization of the cells. Multi-photon microscopy was used to evaluate the change in dye intensity upon exposure to nsPEF delivered by a pair of tungsten electrodes placed 50 μ m above the cells. The results demonstrated a quantitative difference in sensitivity between the cells in a 3D matrix versus those grown in a single monolayer.

Conference 9327: Optical Elastography and Tissue Biomechanics II

Saturday - Sunday 7-8 February 2015

Part of Proceedings of SPIE Vol. 9327 Optical Elastography and Tissue Biomechanics II

9327-1, Session 1

MRI & mechanobiology: new science at the intersection of engineering and medicine (Keynote Presentation)

Richard L. Ehman, Mayo Clinic (United States)

Many disease processes such as cancer cause profound changes in the mechanical properties of tissues. This accounts for the efficacy of palpation for detecting abnormalities and provides motivation for developing practical methods to quantitatively image tissue elasticity. Magnetic Resonance Elastography (MRE) is an emerging MRI-based technique that can quantitatively image tissue properties such as stiffness, viscosity, attenuation, and anisotropic behavior - providing access to a new range of previously unexplored tissue imaging biomarkers highly relevant in diagnostic medicine and in the emerging field of mechanobiology.

Human studies have demonstrated that it is feasible to apply MRE to quantitatively assess skeletal muscle, brain, thyroid, breast, myocardium, kidney, liver, and skin. The first established clinical application of the technology is for detection of hepatic fibrosis, which is a growing health problem and the most important precedent to primary hepatic malignancy. Growing clinical experience indicates that MRE is at least as accurate as liver biopsy for this diagnosis, while also being safer, more comfortable, and less expensive.

Preliminary studies suggest that MRE may be helpful in differentiating between benign and malignant neoplasms. New research has also shown that MRE-assessed estimates of tumor stiffness are helpful in the preoperative assessment of patients with brain tumors such as meningiomas.

9327-2, Session 1

Noninvasive 3D elasticity mapping using phase-stabilized optical coherence elastography

Manmohan Singh, Jiasong Li, Shang Wang, Michael D. Twa, Univ. of Houston (United States); Kirill V. Larin, Univ. of Houston (United States) and Baylor College of Medicine (United States)

We demonstrate a novel method for noninvasive quantification of the Young's modulus in three dimensions using phase stabilized swept source optical coherence elastography (PhS-SSOCE). We are able to estimate the Young's modulus of tissue mimicking agar phantoms over a volume by measuring the velocity of a shear wave induced by a focused air-pulse. By calculating the velocity in all radial directions from the origin of the induced shear wave, we are able to create a volumetric map of elasticity of the sample. Due to the sub-micron spatial sensitivity of PhS-SSOCE, the induced deformation amplitude can be minimal, thus preserving the structure and function of delicate tissues such as the cornea and sclera of the eye. The results show that this noninvasive method for elasticity mapping can provide a three dimensional estimation of elasticity of the phantoms which correlates well with the results of uniaxial compression testing.

9327-3, Session 2

Ultrasound elastography: current systems, ongoing research and future potential (Invited Paper)

Jeffrey C. Bamber, The Institute of Cancer Research (United Kingdom) and The Royal Marsden NHS Foundation Trust (United Kingdom)

This review begins with an introduction to the physical principles and technology of commercially available ultrasound elastography, drawing on material in "EFSUMB Guidelines and Recommendations on the Clinical Use of Ultrasound Elastography Part 1: Basic Principles and Technology" (Ultraschall in Med 2013; 34: 169-184) and demonstrating two unifying features of current systems, (a) that a variation in shear modulus is the common underlying physical mechanism that provides tissue contrast, and (b) that the signal processing in the scanner begins with an estimate of the time-varying tissue displacement that occurs in response to an applied force. The relationship between the available technologies is also considered in terms of the different quantities displayed (displacement, strain or shear wave speed), how the force is applied (quasi-statically or dynamically, deep or at the surface), and their advantages and disadvantages. This is followed by a summary of current research in this extremely active area, where many types and positions of the mechanical load have been employed (e.g. active and passive), novel measured quantities are being investigated, robust signal processing schemes explored, reconstruction methods for quantitative imaging developed, and the range of imaged mechanical characteristics extended. Finally, a glimpse into the future demonstrates that substantial improvements can be expected in terms of image quality, ease of use, quantification and the range of tissue mechanical characteristics that can be measured and imaged.

9327-4, Session 2

Amplitude-modulated ultrasound radiation force combined with phase-sensitive optical coherence tomography for shear wave elastography

Thu-Mai Nguyen, Shaozhen Song, Bastien Arnal, Emily Y. Wong, Tueng T. Shen, Ruikang K. Wang, Matthew O'Donnell, Univ. of Washington (United States)

Tissue stiffness can be measured from the propagation speed of shear waves (SW). Acoustic radiation force (ARF) can generate SW by focusing ultrasound in tissue for $\sim 100 \mu\text{s}$. Safety considerations and electronics abilities limit ultrasound pressures. We previously presented SW elastography combining ARF and phase-sensitive optical coherence tomography (PhS-OCT) [1]. Here, we use amplitude-modulated ARF to enhance SW signal-to-noise ratio (SNR) at low pressures.

A two-layer phantom was made of 5% and 10% gelatin. ARF was applied using a single-element transducer, driven by a 7.5 MHz, 3-ms, sine wave modulated in amplitude by a linear-swept frequency (1 to 7 kHz). Pressures between 1 to 3 MPa were tested. Displacements were tracked using PhS-OCT and numerically compressed using pulse compression methods detailed in [2]. SNR was compared to that of 200- μs bursts. Stiffness maps were reconstructed using time-of-flight computations.

200- μs bursts give 7.8 dB SNR at 3 MPa and undetectable displacements at 1 MPa. Pulse compression gives 22.0 dB at 3 MPa and 15.7 dB at 1 MPa. In all cases with detectable displacements, SW speeds were 2.15 ± 0.06 and 3.13 ± 0.07 m/s respectively in the 5% and 10%-gelatin layers.

**Conference 9327:
Optical Elastography and Tissue Biomechanics II**

We implemented amplitude-modulated ARF for high SNR displacements at low pressures. Applicability to ocular tissues (cornea, intraocular lens) is under investigation.

[1] Nguyen et al. "Visualizing ultrasonically-induced shear wave propagation using phase-sensitive OCT for dynamic elastography" *Optics Letters* 39(4):838-841, 2014.

[2] Nguyen et al. "Shear wave pulse compression for dynamic elastography using phase-sensitive OCT" *J. Biomed. Opt.* 19(1):016013, 2014.

9327-5, Session 2

Localized loading to reduce artifacts in compression optical coherence elastography

Philip Wijesinghe, Brendan F. Kennedy, David D. Sampson, The Univ. of Western Australia (Australia)

A major challenge in optical coherence elastography (OCE) is in isolating the mechanical response of a single feature in the presence of multiple coupled mechanical features. In general, under uniform loading the interplay of heterogeneous tissue features leads to a non-uniform stress distribution, which makes it challenging to quantify mechanical properties. The field-of-view of OCE, especially in in-vivo studies, is commonly smaller than the region of tissue undergoing deformation. This scenario can introduce artifacts into elastograms, as deforming mechanical features outside of the field-of-view are likely to affect the mechanical behavior within the imaged region.

In this work, we propose the use of indentation-like compression to reduce the influence of mechanical heterogeneities outside the OCE field-of-view, and to reduce the effects of surface roughness. Optics-based indentation methods have been previously investigated, aimed at providing high-sensitivity point measurements of deformation and introducing depth-sectioning capability. Unlike previous methods, we aim to combine the localized stress distribution provided by indentation with imaging via phase-sensitive compression OCE. Using finite element analysis, verified with experimental results, we demonstrate the capability of indentation to localize stress, both laterally and axially, limiting the effects of external mechanical heterogeneities on local mechanical behavior, whilst maintaining a close-to-uniform stress distribution within the OCE field-of-view. We investigate the relationships of indenter geometry, contact properties and sample thicknesses on the imparted stress field. As indentation removes the requirement for a rigid back plate, this technique may facilitate the extension of compression OCE to in-vivo scenarios.

9327-6, Session 2

3D static and quasi-static elastography of biological samples using FF-OCT

Amir Nahas, Maxime Pinsard, Institut Langevin (France); Stéphane Roux, Ecole Normale Supérieure de Cachan (France); A. Claude Boccara, Institut Langevin (France)

Organ structures, tissues and cells are characterized by their intrinsic mechanical properties. Moreover, the mechanical properties of cells are related to their structure and function: changes in those properties reflect cellular healthy or pathological states. Adding this contrast to morphological images could be a powerful help for diagnosis. In this study we present two methods to add the elastographic contrast to Full-Field OCT images and our latest results on biological tissues such as ex vivo human skin tissue or ex vivo mouse ear.

The first method is a static method based on finite element 3D digital image correlation algorithm. We register a volumetric image before and after mechanical solicitation of the sample. From those two sets of images we estimate the 3D strain tensor map inside the sample. With this method we not only have access to relative stiffness information but also to mechanical

properties of the samples such as mechanical anisotropy or compressibility.

The second method is a quasi-static method based on speckle modulation. In this method the sample is submitted to a low-amplitude periodical compression (0-12 Hz), and using a phase shifting modulation method derived from the one used in classical FF-OCT imaging we are able to retrieve the local phase map modulation directly related to the local displacement. These two methods provide a relative value of the local elastic properties along the compression axis.

9327-7, Session 3

Micro-scale mapping of tissue mechanical properties using laser speckle rheology

Zeinab Hajjarian Kashany, Seemantini K. Nadkarni, Harvard Medical School (United States)

Changes in micro-scale tissue stiffness influence morphology, differentiation, and proliferation of cancer cells, and likely provide the earliest detectable sign of the disease. Laser Speckle Rheology (LSR) is a novel optical technology for micro-scale mapping of tissue viscoelastic properties. Laser speckle, formed by interference of coherent light scattered from tissue, is exquisitely sensitive to Brownian motion of scattering particles and in turn to the viscoelastic compliance of the sample. In LSR, speckle patterns are collected through the objective lens by a high-speed camera. The collimated beam is raster scanned and the correlation analysis of speckle movies provides the speckle intensity autocorrelation function, $g_2(t)$, for individual pixels. Next, the mean square displacements (MSD) of Brownian particles are deduced and substituted in the generalized Stokes-Einstein relation (GSER) to yield a 2D map of viscoelastic modulus, $G^*(\omega)$. To test the LSR capability for micro-scale mechanical mapping, we fabricated polyethylene glycol diacrylate (PEGDA) constructs with pre-determined elasticity patterns. Briefly, the precursor PEGDA solution was covered by a photo-mask and exposed to UV light. Results demonstrated that LSR can resolve mechanical features of 50 μm size. Evaluation of ductal invasive carcinoma (DIC) biopsies using LSR, bright field microscopy, and second harmonic microscopy (SHG) indicated that the regions of low stiffness corresponded to low-intensity SHG signal and adipose tissue. Moreover, stiffer regions in LSR image matched the high intensity SHG signal, generated by desmoplastic collagen accumulation. These findings demonstrate the invaluable potential of LSR for viscoelastic mapping of tumor tissue for clinical and biological research applications.

9327-8, Session 3

Micro-elastometry using resonant acoustic spectroscopy with optical displacement sensor

Ling Li, Charles R. Krebs, Alisa S. Wolberg, Amy L. Oldenburg, The Univ. of North Carolina at Chapel Hill (United States)

Elastography based on resonant acoustic spectroscopy measures the stiffness of soft tissues via the resonance frequency of propagating longitudinal acoustic waves in tissue sample of well-defined geometry. Acoustic spectroscopy is a promising detection modality given its high sensitivity, accuracy and repeatability. We present a portable micro-elastometry device capable of measuring elasticity using strains $\leq 0.1\%$. A microwell with a fixed geometry [5 mm (l) \times 5 mm (w) \times 6 mm (d)] is chosen to contain tissue specimen for study, and a chrome steel microbead (mass: 0.7 mg, diameter: 0.5 mm) on top of the tissue surface serves as the transducer, which is actuated through magnetic coupling to a magnetic field gradient from a solenoid. The induced acoustic resonance spectrum of a specimen is detected by an optical displacement sensor, of which high sensitivity to ultralow specimen deformation ensures that the sample is within the linear viscoelastic regime. The fixed geometry of the microwell and the low actuator inertia provide this device with high measurement

**Conference 9327:
Optical Elastography and Tissue Biomechanics II**

repeatability. This device requires smaller specimen volumes (150 μL) ideal for both human and animal studies relative to commercially available devices such as Thromboelastography (TEG). Additionally, we developed a semi-automated system supporting sequenced transducer location, transduction application, and statistical data analysis. We validated the device against previously published elasticity measurements of biogels of varying agarose concentrations. Finally, elasticity measurements of human blood plasma with varying dosages of heparin elucidated the future potential of the device as a coagulation monitoring tool during surgery.

9327-9, Session 3

In vivo monitoring of external pressure induced hemodynamics in skin tissue using optical coherence tomography angiography

Woo June Choi, Hequn Wang, Ruikang K. Wang, Univ. of Washington (United States)

Characterization of the relationship between external pressure and blood flow is important in the examination of pressure-induced disturbance in tissue microcirculation. Optical coherence tomography (OCT) angiography is a promising imaging technique, capable of providing the noninvasive extraction of functional vessels within the skin tissue with capillary-scale resolution. Here, we present a feasibility study of OCT angiography to monitor effect of external pressures on blood perfusion in human skin tissue in vivo. Graded external pressure is loaded normal to the surface of the nailfold tissue of a healthy human. The incremental loading is applied step by step and then followed by an immediate release. Concurrent OCT imaging of the nailfold is performed during the pre/post loading. Blood perfusion images including baseline (at pre-loading) and corresponding tissue strain maps are calculated from 3D OCT dataset obtained at the different applied pressures, allowing visualization of capillary perfusion events at stressed nailfold tissue. The results indicate that the perfusion progressively decreases with the constant increase of tissue strain. Reactive hyperemia is occurred right after the removal of the pressure corresponding to quick drop of the increased strain. The perfusion is returned to the baseline level after a few minutes. These findings suggest that OCT microangiography may have great potential for quantitatively assessing tissue microcirculation in the locally pressed tissue in vivo.

9327-10, Session 3

An endoscopic multi-exposure laser speckle contrast analysis system for vascular measurements

Maria Tziraki, Imperial College London (United Kingdom); Lipei Song, Nankai Univ. (China); Daniel S. Elson, Imperial College London (United Kingdom)

Laser speckle contrast analysis (LASCA) is an established qualitative technique for imaging relative changes in blood flows at microcirculation level with high spatiotemporal resolution. One objective of LASCA is to infer flow velocity from the observed speckle contrast, and monitoring the spatiotemporal characteristics of blood flow and tissue perfusion is crucial for studying the metabolism and assessing the oxygenation and viability of organs.

We have developed a dual wavelength endoscopic diagnostic tool based on LASCA with the aim to image tissue blood flow and perfusion during surgical procedures. We examine and assess the effects of the collection efficiency of our endoscope for accurate quantitative measurements of speckle decorrelation times and their relations with flow velocities in tissue mimicking micro channel phantoms.

By changing the exposure time over a wide range, we recorded variations

in contrast values at different flow velocities and used mathematical models from the literature to calculate decorrelation times.

We image and infer flow at phantoms samples of various scattering coefficients.

9327-11, Session 4

In vivo optical elastography: stress and strain imaging of human skin lesions

Shaghayegh Es'haghian, Peijun Gong, Kelsey M. Kennedy, Philip Wijesinghe, David D. Sampson, Robert A. McLaughlin, Brendan F. Kennedy, The Univ. of Western Australia (Australia)

Probing the mechanical properties of skin at high resolution could aid in the assessment of skin pathologies, such as detecting the extent of cancerous skin lesions and the assessment of pathology in scars. Here, we present two in vivo elastography techniques, based on optical coherence tomography (OCT), to probe the micro- to milli-scale spatial variation in the mechanical properties of human skin. In these techniques, we characterize the local spatial variation of stress and strain imparted to skin due to compressive loading. We have developed imaging probes which can apply a local and uniform compressive load to the surface of skin whilst simultaneously imaging from the same side using OCT. The first technique is an in vivo adaptation of a tactile imaging technique, optical palpation, which uses a compliant silicone layer positioned on the skin surface as a stress sensor. Using this technique, we provide two-dimensional en face stress maps of a range of skin lesions, including pathological scarred tissue, and demonstrate the ability of in vivo optical palpation to delineate the boundary of lesions and to map the mechanical contrast between lesions and surrounding normal skin. The second technique uses phase-sensitive optical coherence elastography to provide high-resolution, three-dimensional, depth-resolved elastograms of skin. We assess the potential of this technique for in vivo skin imaging and present initial results on both normal and scarred skin.

9327-12, Session 4

Estimation of elastic parameters of ovarian tissue using phase stabilized swept source optical coherence tomography

Sreyankar Nandy, Tianheng Wang, Hassan S. Salehi, Quing Zhu, Univ. of Connecticut (United States)

We have estimated the elastic properties of ovarian tissue using phase-sensitive swept source optical coherence tomography. Ovarian tissue samples were mechanically excited by periodical vibration of a PZT transducer. The displacement and strain of the tissues were estimated during loading.

Differences in stiffness and displacement were observed for different types of tumor tissue, which can be related to the collagen content and distribution. The initial results show that the phase sensitive swept source optical coherence elastography (Phs-OCE) can be an effective tool for characterization of stiffness and other micro-mechanical properties of normal and abnormal ovarian tissue.

9327-13, Session 4

Vascular wall stress during intravascular optical coherence tomography imaging

Cuiru Sun, Ryerson Univ. (Canada); Victor X. D. Yang, Ryerson Univ. (Canada) and Sunnybrook Health Sciences Ctr. (Canada) and Univ. of Toronto (Canada)

**Conference 9327:
Optical Elastography and Tissue Biomechanics II**

Catheters are used during intravascular optical coherence tomography (IVOCT) imaging. The presence of a catheter alters the flow field, pressure distribution and frictional resistance to flow in an artery. The flow velocity and profile in a catheterized porcine carotid artery has been imaged by IVOCT previously. In this paper, we study the shear and transmural stress distribution of the catheterized vessel. COMSOL (COMSOL 4.4) was used to simulate the blood flow induced deformation in a catheterized vessel. Blood is modelled as an incompressible Newtonian fluid. Stress distribution from an idealized one thick layer vascular model with centered and eccentric catheters are simulated first to evaluate the parameters of the model and study the influence of catheterization. Then blood flow velocity and blood vessel structure with an eccentric catheter obtained through IVOCT are used to build a realistic model for simulation. Stress distribution under various flow profiles imaged by OCT were input to COMSOL to compute deformation and stress distributions. Preliminary results show nonuniform stress distribution in the circumferential direction of an eccentrically catheterized vascular model. Based on our knowledge this is the first study of transmural stress distribution during catheterization. The high-resolution 3D OCT structural image provides an unprecedented clear structure of the carotid artery, thus more accurate model geometry than those based on angiography or MRI. Simulation results obtained by integrating experimental flow data display more realistic stress conditions of the vascular wall compared to theoretical analysis or numerical simulation alone. This study may provide important information for saline flushing during IVOCT and stenotic lesion studies.

9327-14, Session 4

Quantitative shear wave imaging optical coherence tomography for noncontact mechanical characterization of myocardium

Shang Wang, Baylor College of Medicine (United States) and Univ. of Houston (United States); Andrew L. Lopez III, Yuka Morikawa, Ge Tao, Baylor College of Medicine (United States); Jiasong Li, Univ. of Houston (United States); Irina V. Larina, Baylor College of Medicine (United States); James F. Martin, Baylor College of Medicine (United States) and Texas Heart Institute (United States); Kirill V. Larin, Univ. of Houston (United States) and Baylor College of Medicine (United States)

Optical coherence elastography (OCE) is an emerging low-coherence imaging technique that provides noninvasive assessment of tissue biomechanics with high spatial resolution. Among various OCE methods, the capability of quantitative measurement of tissue elasticity is of great importance for tissue characterization and pathology detection across different samples. Here we report a quantitative OCE technique, termed quantitative shear wave imaging optical coherence tomography (Q-SWI-OCT), which enables noncontact measurement of tissue Young's modulus based on the ultra-fast imaging of the shear wave propagation inside the sample. A focused air-puff device is used to interrogate the tissue with a low-pressure short-duration air stream that stimulates a localized displacement with the scale at micron level. The propagation of this tissue deformation in the form of shear wave is captured by a phase-sensitive OCT system running with the scan of the M-mode imaging over the path of the wave propagation. The temporal characteristics of the shear wave is quantified based on the cross-correlation of the tissue deformation profiles at all the measurement locations, and linear regression is utilized to fit the data plotted in the domain of time delay versus wave propagation distance. The wave group velocity is thus calculated, which results in the quantitative measurement of the Young's modulus. As the feasibility demonstration, experiments are performed on tissue-mimicking phantoms with different agar concentrations and the quantified elasticity values with Q-SWI-OCT agree well with the uniaxial compression tests. Our pilot study of this OCE technique on ex vivo mouse cardiac muscle tissues with normal and genetically-altered cardiomyocytes indicates the potential of using Q-SWI-

OCT as an essential mechanical characterization tool to assist the research in myocardium regeneration.

9327-15, Session 4

Brillouin microscopy for arterial biomechanical imaging

Giuseppe Antonacci, Ryan Pedigri, Carl Paterson, Rob Krams, Peter Török, Imperial College London (United Kingdom)

Spontaneous Brillouin scattering is an inelastic scattering process arising from inherent thermal density fluctuations, or acoustic phonons, propagating in a medium. Over the last few years, Brillouin spectroscopy has shown great potential to become a reliable non-invasive diagnostic tool due to its unique capability of retrieving viscoelastic properties of materials such as strain and stiffness.

The detection of the weak scattered light, in addition to the resolution of the Brillouin peaks (typically shifted by few GHz from the central peak) represent one of the greatest challenges in Brillouin. The recent development of high sensitivity CCD cameras has brought Brillouin spectroscopy from a point sampling technique to a new imaging modality. Furthermore, the application of Virtually Imaged Phased Array (VIPA) etalons has dramatically reduced insertion loss simultaneously allowing fast (<1s) collection of the entire spectrum.

Hitherto Brillouin microscopy has been shown the ability to provide unique stiffness maps of biological samples, such as the human lens, in a non-destructive manner. In this work, we present results obtained using our Brillouin microscope to map the stiffness variations in the walls of blood vessels in particular when atherosclerotic plaques are formed. The stiffness of the membrane that "cover" the plaques is critical in developing acute myocardial infarction yet it is not currently possible to credibly assess its stiffness due to lack of suitable methods.

9327-16, Session 4

Visualization of elastic wave propagation induced by a mechanical pulse device for physiotherapy

Rudolf M. Verdaasdonk, Ilja Reintgen, John H. Klaessens, Albert J. van der Veen, Vrije Univ. Medical Ctr. (Netherlands); Pavel Novak, Storz Medical AG (Switzerland)

Radial pressure wave therapy is being used in physiotherapy for the pain treatment of eg. tendonitis in joints. The device (Storz Medical, MP200) consists of a hand piece in which a metal bullet is accelerated in milliseconds by high pressure air (1-5 bar) hitting a probe in contact with the skin transforming kinetic energy into an 'acoustic' pressure wave travelling towards the joints.

The characteristics of various probes were studied using Background Oriented Schlieren Imaging (BOS) to visualize to propagation of pressure waves through a tissue phantom. A fine line pattern imaged through a transparent gel slab is distorted when a pressure wave is travelling through the gel. The images recorded at high speed (2000 f/s) are enhanced by digital subtraction.

The elastic wave propagation was studied in dependence of probe types (diameter 6 - 35 mm, different shapes and materials) and pressure (1-3 bar - kinetic energy 20-170 mJ). At each setting 3 impact exposures were recorded.

High speed imaging showed cavitation effects between the probe and tissue surface. There were significant differences in the elastic wave propagation as to intensity and radial distribution depending on probe shape. The propagation speed was constant (2-3 m/s) and related to the shear modulus

**Conference 9327:
Optical Elastography and Tissue Biomechanics II**

and density of the homogeneous tissue phantom. Potentially, the pressure wave system could be used to determine tissue properties with other modalities (US) to detect inhomogeneous structures in tissues.

Background Oriented Schlieren Imaging proves to be a good visualization method of elastic wave propagation to characterize devices and optimize the design and treatment settings.

9327-17, Session 5

Simultaneous optical and mechanical probes to investigate complex cellular responses to physical cues (*Invited Paper*)

Kristina Haase, Zeinab Al-Rekabi, Louise Guolla, Ryan Hickey, Univ. of Ottawa (Canada); Dominique Tremblay, University of Ottawa (Canada); Andrew E. Pelling, Univ. of Ottawa (Canada)

It is now clear that many significant and medically relevant biological processes (for example, muscle (re)generation, stem cell differentiation and cancer metastasis) can be modulated and controlled through mechanical forces arising in the microenvironment. It is also evident that the immediate response of a cell to mechanical force is complex cytoskeletal and nuclear deformation, organelle movements and focal adhesion remodelling which all takes place far upstream any other biological events. In this talk I will describe our work utilizing simultaneous laser scanning confocal microscopy, traction force microscopy and atomic force microscopy to investigate the dynamic mechanical and biochemical responses of living cells. In combination with modern molecular biology and physical/computational approaches we physically touch and mechanically stimulate living cells in order to examine the transmission of force through the cytoarchitecture (plasma membrane, cytoskeleton, focal adhesions and the nucleus). Force transduction results in complex elastic and viscoelastic three-dimensional relaxation and remodelling. Our work has demonstrated how cells display extremely complex responses to mechanical forces and often exhibit unexpected time-dependent anisotropic mechanical properties that are intimately linked to cell function. The mechanical properties of cells are distinctly controlled by time and cell type dependent mechanisms that, in turn, are governed by the mechanical properties microenvironment. The interesting physical response of cells to mechanical stimuli is not merely a side-product of biology but is a key component of a biological and physical feedback loop governing the life of a cell.

9327-18, Session 5

High-resolution Brillouin microscopy for cell biomechanics

Giuliano Scarcelli, Seok Hyun Yun, Harvard Medical School (United States)

The biomechanical component of the interaction between cells and their local microenvironment has emerged as a crucial regulator of cellular function. This has generated great interest towards understanding how cells sense the mechanical cues of the environment and transduce them into a signaling response. To investigate mechanotransduction, tools to measure forces and elasticity at the single-cell level are needed.

Here we present high-resolution Brillouin microscopy to map intracellular elasticity. Brillouin microscopy is based on the link between the frequency shift acquired by inelastically-scattered photons and the elastic modulus of a sample. In the past years, Brillouin microscopy was demonstrated as a viable elasticity probe, in vivo and in situ, at the tissue level. Transitioning to the cell level required >100x reduction in scattering volume and >10x higher elasticity sensitivity compared to tissue-level instruments. This was achieved through increased spectrometer sensitivity and extinction as well as with efficient collection of Brillouin scattering at high resolution.

Here, we show that Brillouin cellular microscopy is able to map the

longitudinal elastic modulus with sub-cellular three-dimensional spatial resolution in a non-contact and non-invasive fashion. We also validated Brillouin microscopy against gold-standard mechanical tests and known elasticity features of cells thus showing that the novel technology is sensitive to the relevant mechanical changes occurring within a cell.

9327-19, Session 5

Cellular resolution optical elastography using phase-sensitive extended depth-of-field optical coherence microscopy

Andrea Curatolo, The Univ. of Western Australia (Australia); Martin L. Villiger, Wellman Ctr. for Photomedicine (United States) and Harvard Medical School (United States) and Massachusetts General Hospital (United States); Dirk Lorenser, Alex Fritz, Brendan F. Kennedy, David D. Sampson, The Univ. of Western Australia (Australia)

Cell mechanics is pivotal in the pathogenesis and progression of many diseases, including cancer and malaria. Phase-sensitive optical coherence elastography (OCE) is a promising technique to image the local mechanical properties of tissue subjected to a mechanical load. The resolution of OCE, at best, matches that of the underlying optical coherence tomography system. Currently, OCE provides transverse and axial resolutions limited to $\sim 10\ \mu\text{m}$ and $50\text{--}100\ \mu\text{m}$, respectively, restricting its use in cell mechanics. Here, we present, for the first time, phase-sensitive OCE combined with extended depth-of-field optical coherence microscopy (xf-OCM) to achieve optical elastography at the cellular resolution level. The employed dark-field illumination enhances scattering contrast and suppresses specular reflection. The detection and illumination paths are decoupled, with a low-Fresnel number ($N=10.5$) Bessel-like illumination exhibiting high transverse resolution along an axially extended focal range. Transverse resolution of $\sim 1.5\ \mu\text{m}$ along a focal range of $100\ \mu\text{m}$ is experimentally verified. A sensitivity of $96\ \text{dB}$ for a $12\ \mu\text{s}$ exposure time was measured with $\sim 2\ \text{mW}$ sample power, provided by a broad-bandwidth supercontinuum light source offering an axial resolution of $2\ \mu\text{m}$ in air. The displacement sensitivity was measured to be $650\ \text{pm}$ between consecutive A-scans at a line rate of $50\ \text{kHz}$. We demonstrate the superior spatial resolution of elastography with xf-OCM in comparison to a conventional, lower resolution OCE system with elastograms of structured phantoms and mouse skeletal muscle, illustrating the potential of imaging the mechanical properties of cells in a three-dimensional tissue environment and, thereby, opening up new possibilities in mechano-biology.

9327-20, Session 5

Mapping dynamic mechanical remodeling in 3D tumor models via particle tracking microrheology

Dustin P. Jones, William Hanna, Gwendolyn M. Cramer, Hamid El Hamidi, Ljubica Petrovic, Jonathan P. Celli, Univ. of Massachusetts Boston (United States)

It has become well established that the mechanical properties of the extracellular matrix (ECM) play a significant role in regulating tumor growth, invasion, and therapeutic response. At the same time, the ECM itself is also dynamically remodeled during these processes, though it remains challenging to monitor both sides of this mechanoregulatory dialogue. We use longitudinal particle tracking microrheology (PTMR) studies in 3D tumor models to monitor and spatially co-register the time-dependent changes in ECM rheology with invasion events, crosstalk with stromal partners and therapeutic interventions. Here, we describe the application of PTMR in a 2-dimensional array around a developing multicellular pancreatic cancer

**Conference 9327:
Optical Elastography and Tissue Biomechanics II**

nodule as well as subsequent correlation of local tissue mechanics with contemporaneous images of invasive fronts. This method allows us to quantify changes in the mechanical microenvironment of pancreatic tumors under multiple growth conditions. A better understanding of the ECM rheology changes interrelated with tumor growth and metastasis could provide a window for novel therapeutic strategies that target either the stroma itself or stromal crosstalk.

9327-21, Session 6

Full field OCT and tissue elasticity measurements: a critical view (*Invited Paper*)

A. Claude Boccara, Amir Nahas, Institut Langevin (France)

OCT based approaches provide a valuable endogenous morphological contrast that is by itself able to replace more traditional cancer diagnosis tools. Nevertheless in order to use it as a reliable diagnosis tool in term of sensibility and specificity a complementary diagnosis would be desirable. As in MRI or in ultrasonography measuring the mechanical properties seems to be promising: indeed many groups are working in this direction using OCT. OCT, when working only with B-scans coupled to static deformations of the sample misses the recording of the full elasticity tensor. Recording 3D imaging appears to be mandatory; nevertheless volume acquisitions are long to get with OCT.

We have recorded stacks of "en face" Full Field OCT (FFOCT) images (typically hundreds slices of 1 Megapixels) before and after the deformation of the samples and have been able measure the diagonal and non diagonal elements of the elasticity tensor in order to quantify elasticity and its anisotropy. These test have been carried on polymers and tissue, both isotropic and anisotropic ones.

If static or quasi-static approaches are most of the time, measuring the speed of shear waves both with OCT and FFOCT have proved to be able to quantify the stiffness of tissue that is proportional to square root of the elasticity in tissues.

We strongly believe that such measurements would soon valuably complement diagnosis based on OCT or FFOCT imaging.

9327-22, Session 6

Characterization of the biomechanics underlying mechanical indentation of in vivo skin using optical coherence elastography

Pin-Chieh Huang, Ryan L. Shelton, Ryan M. Nolan, Adeel Ahmad, Stephen A. Boppart, Univ. of Illinois at Urbana-Champaign (United States)

Human skin tissue deformation and redness occur often in the course of daily living but the underlying biomechanical events are poorly understood. Discomfort and potential dermatological harm may arise from these indentation, and hence, a systematic evaluation and a well-defined explanation for the underlying biomechanics and vascular changes are desired. In this study, we aim to comprehensively characterize and understand the skin-marking biomechanics of in vivo human skin, including comparative differences across variables such as age, anatomical site, etc. Skin tissue behavior under mechanical compression was first investigated by using optical coherence tomography and elastography, by visualizing detailed tissue structure and dynamics on the micron-scale and in real-time.

OCT images were acquired on in vivo human skin before and after the application of an external load. Changes in optical backscatter intensity and its indenter-geometry-associated distribution pattern were observed, which we hypothesize is related to the alteration of local fluid dynamics and hemodynamics around the indented tissue sites. Mechanical properties,

such as viscoelasticity of the skin, were also revealed in the recovery kinetics of the post-deformed skin from the time-lapse OCT images. Based on the aforementioned parameters, numerical analysis was performed for quantitative comparison between the pre-indentation and the post-indentation skin. In the future, correlations will be established between the behavior of skin at different ages and/or anatomical sites under mechanical indentation.

9327-23, Session 6

High numerical aperture Brillouin microscopy (*Invited Paper*)

Peter Török, Giuseppe Antonacci, Carl Paterson, Imperial College London (United Kingdom)

Optical elastography is a technique when samples are mechanically stimulated and simultaneously optically probed which can reveal mechanical properties of the sample under test. Due to the mechanical stimulation needed, this technique requires special access to the sample and so its use in vivo has been limited. Optical Coherence Tomography has recently been applied to elastography (Optical Coherence Elastography - OCE) yielding stiffness images from appreciable depths of the sample. Nevertheless, the spatial resolution of OCE is still limited, hitherto providing little evidence for subcellular imaging capability.

Spectroscopy of light spontaneously scattered on lattice vibrations, or optical phonons, known as Brillouin spectroscopy, is an established technique to measure elastic properties of materials. A study published in 2005 described the combination of a Brillouin spectroscope and an optical microscope thus proposing the first Brillouin microscope (BM) with 20 μ m spatial resolution. Subsequent studies, mainly by Harvard University, have established BM as an alternative to OCE in optomechanical imaging.

In this talk we describe the development of a high numerical aperture (NA) Brillouin microscope that, to the best of our knowledge, for the first time is capable of subcellular imaging. The use of high NA optics in Brillouin imaging is not straightforward because it can cause significant drop in spectral resolution. In addition to the much improved spatial resolution (\sim 1 μ m), the use of high NA optics may also lead to additional advantages, such as the possibility for determining the elastic tensor of the sample without the need for rotating the sample.

9327-24, Session 6

High speed assessment of fluid viscoelasticity in flow cytometry using nonlinear Brillouin spectroscopy

Zhaokai Meng, Georgi I. Petrov, Vladislav V. Yakovlev, Texas A&M Univ. (United States)

Brillouin microspectroscopy is a powerful tool for elasticity-sensitive non-invasive optical imaging. However, current spontaneous Brillouin spectroscopy usually requires long acquisition time ($>$ 500 ms), while its spectral quality is fundamentally limited by its optical setups. On the other hand, pulsed laser sources, due to their relatively broad spectral widths, are usually inappropriate for spontaneous Brillouin applications. Kinoshita et al. [1] has introduced impulsive stimulated Brillouin spectroscopy (ISBS) for characterizing samples' sound speeds (i.e. mechanical properties). However, the angle between the pump and probe beams should strictly follow the Bragg condition, which is practically difficult for routine uses.

In this study, we followed the basic framework of Kinoshita et al. [1]. We employed a nano-second 532 nm pulsed laser as the pump. In this way, an internal grating was generated within the sample according to the photostriction effect. A 780 nm continuous-wave laser as the probe, and was diffracted by the internal grating generated by the pump. In order to ensure the diffraction efficiency, we introduced an external grating to automatically prepare the angle between the pump and the probe. In this way, the Bragg condition will be automatically satisfied, and the optical

**Conference 9327:
Optical Elastography and Tissue Biomechanics II**

set up maintenance will be greatly simplified. As a proof-of-principle, we demonstrated some applications in the field of flow cytometry.

Reference:

1. S. Kinoshita et al., J. Opt. Soc. Am. B., 10(6), 1993

9327-25, Session 7

Biomechanics of cornea and Keratoconus in vivo with Brillouin microscopy

Giuliano Scarcelli, Sebastien Besner, Harvard Medical School (United States); Seok Hyun Yun, Wellman Ctr. for Photomedicine (United States) and Harvard Medical School (United States)

Keratoconus is the most common corneal degeneration in the US. It is an ectatic disorder characterized by the progressive thinning and bulging of the cornea, which causes severe loss in visual acuity and eventually may lead to corneal transplant. Corneal biomechanics is believed to mediate a genetic predisposition to keratoconus into its clinical manifestation. In a healthy cornea, collagen fibers provide the strength to balance the intraocular pressure (IOP); if the cornea is weakened or compromised, this mechanical balance is disrupted resulting in progressive thinning and bulging. Therefore the biomechanical characterization of the cornea is crucial to understand the progression of keratoconus and thus improve its early diagnosis and management.

Recently, we have developed Brillouin microscopy, an all-optical imaging technique that allows noncontact 3D mapping of corneal modulus and measurement of corneal stiffening by corneal collagen crosslinking. Brillouin microscopy is based on Brillouin scattering that arises from the interaction between light incident on a medium of interest and spontaneous acoustic phonons within the medium. Here, we report on the ability of Brillouin microscopy to differentiate keratoconic corneas from normal corneas based on Brillouin frequency shifts.

Brillouin images show remarkable biomechanical features distinctively different between corneas of healthy subjects and keratoconic corneas. Overall, keratoconic corneas presented lower elastic modulus than healthy corneas. Importantly, Brillouin imaging showed that the mechanical loss is primarily concentrated within the area of the keratoconic cone. Outside the cone, the Brillouin shift was comparable to that of normal corneas. Our results demonstrate the potential of Brillouin microscopy for diagnosis and treatment monitoring of keratoconus.

9327-26, Session 7

Fluorescence spectroscopy of collagen crosslinking: non-invasive and in-situ evaluation of corneal stiffness

Walfre Franco, Antonio Ortega-Martinez, Hong Zhu, Wellman Ctr. for Photomedicine (United States); Ruisheng Wang, Clarkson Univ. (United States); Irene E. Kochevar, Wellman Ctr. for Photomedicine (United States)

Collagen is a long fibrous structural protein that imparts mechanical support, strength and elasticity to many tissues. The state of the tissue mechanical environment is related to tissue physiology, disease and function. In the cornea, the collagen network is responsible for its shape and clarity; disruption of this network results in degradation of visual acuity, for example in the disease keratoconus. The objective of the present study is to investigate the feasibility of using the endogenous fluorescence of collagen cross-links to evaluate variations in the mechanical state of tissue, in particular, the stiffness of cornea in response to different degrees of photo cross-linking or RGX treatment — a novel keratoconus treatment. After removing the epithelium, rabbit corneas were stained with Rose Bengal and subsequently irradiated with a 532 nm solid-state laser. Varying

the radiant exposure resulted in different levels of stiffening, as measured by tensiometry. Analysis of the excitation spectra obtained by fluorescence spectroscopy shows a correlation between the fluorescence intensity at 370/460 nm excitation/emission wavelengths and the laser treatment. In principle, it seems feasible to use the endogenous fluorescence of collagen cross-links to evaluate the mechanical stiffness of cornea non-invasively and in situ.

9327-27, Session 7

Spatial mapping of the biomechanical properties of rabbit cornea after cross-linking using optical coherence elastography

Jiasong Li, Manmohan Singh, Srilatha Vantipalli, Zhaolong Han, Michael D. Twa, Kirill V. Larin, Univ. of Houston (United States)

Keratoconus, a structural degeneration of the cornea, is often treated with UV-induced collagen cross-linking (CXL) to increase tissue resistance to further deformation and degeneration. Optimal treatments would include customization for the individual and consideration of preexisting biomechanical properties as well as the effects induced by the treatment. This requires a technique capable of noninvasive assessment of tissue properties. In this study, we demonstrate the use of phase-stabilized swept source optical coherence elastography (PhS-SSOCE) to assess the relaxation rate of deformation which was created by a focused air-pulse in tissue-mimicking gelatin phantoms of various concentration and partially cross-linked rabbit corneas. Due to the high spatial sensitivity of Ph-SSOCE, the amplitude of these deformations was only a few microns. The results show that the relaxation rate can be quantified and used to differentiate the untreated and CXL region of the cornea. The results also indicate that the CXL region have faster relaxation rates than the untreated region. Therefore, this method can be used to spatially localize the biomechanics of the cornea. This non-contact and noninvasive measurement technique utilizes minimal force for excitation (in μm scale). Thus it can be potentially used to assess the severity of ocular disease as well as monitor the outcomes of therapeutic interventions.

9327-28, Session 7

Non-invasive estimation of corneal biomechanical properties using OCT-vibrometry

Imran B. Akca, Ernest W. Chang, Wellman Ctr. for Photomedicine (United States) and Harvard Medical School (United States) and Massachusetts General Hospital (United States); Sabine Kling, Consejo Superior de Investigaciones Científicas (Spain); Giuliano Scarcelli, Wellman Ctr. for Photomedicine (United States) and Harvard Medical School (United States) and Massachusetts General Hospital (United States); Susana Marcos, Consejo Superior de Investigaciones Científicas (Spain); Seok-Hyun Yun, Wellman Ctr. for Photomedicine (United States) and Harvard Medical School (United States) and Massachusetts General Hospital (United States)

The mechanical stability of the cornea is critical for maintaining its normal shape and optical function. Measurement of the mechanical integrity is useful in various applications ranging from biomechanics-based diagnosis of progressive keratoconus and monitoring collagen crosslinking to accurate measurement of intraocular pressure. There have been considerable efforts to develop noninvasive, sensitive methods to measure corneal biomechanics

**Conference 9327:
Optical Elastography and Tissue Biomechanics II**

in the clinic. Here, we introduce a novel technique to obtain corneal biomechanical properties using the principle of vibrography and phase-sensitive optical coherence tomography. A speaker generating monotone signals is used to excite acoustic vibration in the cornea, and the frequency is scanned for a modal analysis. The magnitude of corneal deformation is in the order of μm or less which reduces discomfort to patients and probes the cornea in a nearly linear-elasticity regime. Our modal analysis indicated that the normal corneas appeared to behave similarly to a circular thin membrane described by uniform tension. The numerical finite element analysis showed good agreement with the experimental data. Further research is warranted to understand how different parameters manifest themselves in corneal resonance and, can be estimated by the modal analysis of corneal vibration of a patient. We have shown the potential for assessing the mechanical effects of collagen cross-linking by modal analysis. Early-stage keratoconus corneas may involve spatially varying degeneration of mechanical modulus which may be detectable by modal analysis.

9327-29, Session 8

Quantitative shear wave optical coherence elastography (SW-OCE) with acoustic radiation force impulses (ARFI) induced by phase array transducer

Shaozhen Song, Nhan Minh Le, Univ. of Dundee (United Kingdom); Ruikang K. Wang, Univ. of Washington (United States); Zhihong Huang, Univ. of Dundee (United Kingdom)

Optical Coherence Elastography (OCE) is a promising non-invasive testing modality that maps the mechanical property of soft tissues with high sensitivity and spatial resolution. Shear wave OCE (SW-OCE) uses the speed of propagating shear waves to provide a quantitative measurement of localized shear modulus, making it a valuable technique for the characterization of tissues such as skin and ocular tissue. One of the main challenges in shear wave elastography is the source of shear wave, most of nowadays techniques are using external vibrators which have several drawbacks such as limited wave propagation range and difficulties in non-invasive scans. Thus, we propose linear phase array ultrasound transducer as a remote wave source, combined with the high-speed, 47k frame per second wave visualization provided by phase-sensitive OCT. In this study, we observed for the first time shear waves induced by a 128 element linear array ultrasound imaging transducer, while the ultrasound and OCT images of the OCE detection range is provided simultaneously. By emitting 10 MHz tone-bursts of sub-millisecond durations, acoustic radiation force impulses are induced in ultrasound focal region. Ultrasound beam steering is achieved by phase delay programming, covering a lateral range of 10 mm and full OCT axial (depth) range. Tissue-mimicking phantoms with agar concentration of 0.5% and 1% are used in the SW-OCE measurements. The results shows an range-extended SW-OCE elasticity map, and shear wave velocities for the softer and stiffer phantoms, as well as determining the boundary of multiple stiff inclusions. This approach opens up the feasibility to combine medical ultrasound imaging and SW-OCE for high-resolution localized quantitative measurement of tissue biomechanical property.

9327-30, Session 8

Optical coherence elastography using beat-frequency acoustic radiation force

Yueqiao Qu, Univ. of California, Irvine (United States); Teng Ma, The Univ. of Southern California (United States); Rui Li, Wenjuan Qi, Jiang Zhu, Univ. of California, Irvine (United States); Qifa Zhou, Koping Kirk Shung, The Univ. of Southern California (United States); Zhongping Chen, Univ. of California, Irvine (United States)

High-resolution elasticity mapping of tissue biomechanical properties is crucial in early detection of many diseases. We have developed a method of acoustic radiation force optical coherence elastography (ARF-OCE) that utilizes a dual-ring ultrasonic transducer in order to excite a highly localized 3-D field. The single element transducer introduced previously in our ARF imaging has low depth resolution because the ARF is difficult to discriminate along the entire ultrasound propagation path. The novel dual-ring approach takes advantage of two overlapping acoustic fields and a few-hundred-Hertz difference in the signal frequencies of the two unmodulated confocal ring transducers in order to confine the acoustic stress field within a smaller volume. This frequency difference is the resulting beating frequency of the system and depends on the sample response. The acoustic field and focusing region of the transducers have been validated by comparing the ARF-OCE measurement and the hydrophone measurement using a homogeneous silicone phantom. We have also acquired promising optical coherence tomography (OCT) and OCE imaging results using a human coronary artery tissue sample with this set-up, using a beat frequency of 500 Hz. We are currently working to compare and analyze the phantom and tissue results of the previous single element focused transducer with those of this novel dual-ring beat-frequency approach. We will be performing additional experiments using cornea tissue and arterial tissue in order to further verify our approach. The beat-frequency elastography method will be applied to ophthalmology and cardiovascular applications to achieve higher depth resolution images.

9327-31, Session 8

Combined correlation estimation of axial displacement in optical coherence elastography: assessment of axial displacement sensitivity performance relative to existing methods

Alexander Grimwood, The Royal Surrey County Hospital NHS Trust (United Kingdom) and King's College London (United Kingdom); Jeffrey C. Bamber, Alessandro Messa, The Institute of Cancer Research (United Kingdom)

Common displacement estimation techniques used in optical coherence elastography are phase shift estimation and cross-correlation tracking. The former is sensitive to displacements much smaller than the source central wavelength, but limited by carrier phase ambiguity [1]. Conversely, correlation tracking of the amplitude demodulated signal is sensitive to large (multiple wavelength) displacements but not very sensitive to sub-wavelength displacements [2].

This study introduces a combined correlation method to optical coherence elastography, using complex cross-correlation of the analytical OCT signal to determine phase shift unambiguously [3]. It has the potential to combine the sensitivity of phase shift estimation with the dynamic range of correlation tracking. Relative sensitivities are compared for the combined correlation, amplitude correlation tracking and phase shift estimation methods for axial displacement estimates across M-mode image data of a test object.

Combined correlation requires sampling the correlation function at half source carrier wavelengths. For the Vivosight™, a swept source frequency domain OCT system, interpolation of the correlation function is needed. Resultant errors reduce displacement sensitivity from that expected. However, amplitude correlation tracking is susceptible to similar errors. For phase shift estimation, unwrapping may be used to overcome ambiguity, but resulting errors also reduce sensitivity for sparsely sampled phase shifts. Displacement estimates from each method are compared, giving an indication of each technique's relative sensitivities.

[1] Kirkpatrick, S.J., Wang, R.K., and Duncan, D.D., *Opt. Express* 14(24) 11585-11597, (2006).

[2] Schmitt, J., *Opt. Express* 3, 199-211 (1998).

[3] Shiina, T., Doyley, M. M., Bamber, J. C., *IEEE Ultrasonics Symposium*, 1331-1336, (1996)

9327-32, Session 8

Elasticity measurement using multi-channel optical coherence tomography estimation of shear-wave time of flight: a comparison of relative and absolute methods

Eli Elyas, The Institute of Cancer Research (United Kingdom) and The Royal Marsden NHS Foundation Trust (United Kingdom); Alexander Grimwood, The Royal Surrey County Hospital NHS Trust (United Kingdom); Janine Erler, Thomas Cox, Univ. of Copenhagen (Denmark); Daniel J. Woods, Michelson Diagnostics Ltd. (United Kingdom); Peter Clowes, The Institute of Cancer Research (United Kingdom) and The Royal Marsden NHS Foundation Trust (Uganda); Jeffrey C. Bamber, The Institute of Cancer Research (United Kingdom) and The Royal Marsden NHS Foundation Trust (United Kingdom)

This paper evaluates in gelatine phantoms the potential to adapt a commercial optical coherence tomography (OCT) device for microelastography by measuring the speed of shear waves propagating in the medium of interest. Two approaches to speed measurement were compared, one using absolute time of arrival (TOA) and another using a novel parallel data acquisition based relative TOA measurement which mimics some important features of ultrasound shear wave elastography [1].

A needle, embedded in homogeneous gelatine containing optical scatterers, was excited to create shear wave bursts which were detected using four M-mode images acquired simultaneously using a commercial four-channel swept-source OCT system (VivoSight™). Shear-wave TOA was detected for each channel at varying distances from the needle by correlation tracking of the amplitude demodulated OCT speckle signal. Shear-wave speed was calculated from inter-channel differences of TOA for a single burst (the relative method) and compared with the speed determined from positional differences of TOA for a single channel over multiple bursts (the absolute method).

Only the relative TOA method provided shear-wave speed with acceptable lateral resolution, precision and accuracy when judged against a linear dependence of shear modulus on gelatine concentration. The absolute method would be useful with improved synchronization between shear wave initiation and OCT data acquisition, which would require hardware and software modification of the commercial system. The relative multichannel approach shows promise for the eventual provision of microelastography using the current commercial OCT system.

[1] Bercoff J, Tanter M, Fink M. IEEE Trans UFFC; 51: 396-409, 2004.

9327-33, Session PSun

Mapping tissue shear modulus on Thiel soft-embalmed mouse skin with shear wave optical coherence elastography

Shaozhen Song, Joyce Joy, Univ. of Dundee (United Kingdom); Ruikang K. Wang, Univ. of Washington (United States); Zhihong Huang, Univ. of Dundee (United Kingdom)

A quantitative measurement of the mechanical properties of biological tissue is a useful assessment of its physiologic conditions, which may aid medical diagnosis and treatment of, e.g., scleroderma and skin cancer. Traditional elastography techniques such as magnetic resonance elastography and ultrasound elastography still have limited scope of application on skin due to insufficient spatial resolution. Recently, dynamic

/ transient elastography are attracting more and more applications with the advantage of non-destructive measurements, and revealing the absolute moduli values of tissue mechanical properties. Shear wave optical coherence elastography (SW-OCE) is a novel transient elastography method, which lays emphasis on the propagation of dynamic mechanical waves. In this study, high speed shear wave imaging technique was applied to a range of soft-embalmed mouse skin, where 3 kHz shear waves were launched with a piezoelectric actuator as an external excitation. The shear wave velocity were estimated from the shear wave images, and used to recover a shear modulus map in the same OCT imaging range. Results revealed significant difference in shear modulus and structure in compliance with gender, and images on fresh mouse skin are also compared. Thiel embalming technique is also proved to present the ability to furthest preserve the mechanical property of biological tissue. The experiment results suggest that SW-OCE is an effective technique for quantitative estimation of skin tissue biomechanical status.

9327-34, Session PSun

Assessment of the biomechanical properties of porcine cornea after UV cross-linking at different intraocular pressures

Jiasong Li, Manmohan Singh, Srilatha Vantipalli, Zhaolong Han, Chih Hao Liu, Michael D. Twa, Kirill V. Larin, Univ. of Houston (United States)

Biomechanical properties of the cornea determine the shape and visual acuity of the eye. These properties of the cornea are often altered by diseases, such as keratoconus. The biomechanical changes can be the basis for the early detection of such diseases. Thus, a method capable of quantifying regional biomechanical properties of cornea tissue in vivo is highly desired. In this study, we used phase-stabilized swept-source optical coherence elastography (PhS-SSOCE) to assess the biomechanical properties of porcine corneas before and after cornea collagen cross-linking (CXL) at different intraocular pressures (IOP). We measured the velocity and recovery process rate of an air-pulse induced elastic wave and the localized deformation, respectively. The results show that the corneas became stiffer after the CXL treatment, as evidenced by the increased elastic wave velocity and recovery rate. This non-contact and noninvasive measurement technique utilizes minimal force for excitation (displacement at μm scale) of the tissue and can be potentially used to study the biomechanical properties of ocular and other delicate tissues.

9327-35, Session PSun

Quantitative assessment of the biomechanical properties of tissue-mimicking phantoms by optical coherence elastography and numerical analyses

Zhaolong Han, Jiasong Li, Manmohan Singh, Chen Wu, Chih Hao Liu, Shang Wang, Narendran Sudheendran, Rita Idugboe, Michael D. Twa, Kirill V. Larin, Univ. of Houston (United States)

Optical coherence elastography (OCE) is an emerging technique that can noninvasively assess the biomechanical properties of tissues. However, the models for reconstructing the tissue elasticity from analysis of the elastic waves measured by OCE have not been fully developed. In this study, tissue-mimicking agar phantom samples with different concentrations, 1%, 1.5% and 2%, were employed to investigate the feasibility of five available methods for assessing the elasticity, typically the Young's modulus, with four of them related to the OCE measurements. Methods one and two were the typical shear wave formula and the surface acoustic wave formula, respectively.

**Conference 9327:
Optical Elastography and Tissue Biomechanics II**

In method three the lamb frequency equation was adopted. For the fourth method, finite element simulations were conducted to compare the group wave velocities. Additionally, uniaxial mechanical compressional tests were performed on these phantom samples. Through comparisons, the lamb-frequency equation and the finite element method were found capable of providing results with higher accuracy than simplified models. The present work can be regarded as a preliminary foundation for reconstructing the biomechanical properties of the tissues by the non-invasive OCE technique via the numerical methods.

9327-36, Session PSun

Full field optical coherence tomography elastography of spheroids using after an osmotic pressure jump

Charles-Edouard Leroux, A. Claude Boccara, Institut Langevin (France)

We demonstrate the use of full field optical coherence tomography to measure spatiotemporally-resolved velocity maps inside spheroids, just after inducing an osmotic pressure jump. We use a continuum mechanics modeling of the spheroid to parameterize the data analysis. Our results indicate that, after the pressure jump, the velocity decays more slowly at the center of the spheroid, which creates a radial gradient in compression 5 minutes after the pressure jump.

9327-37, Session PSun

Measurement of tissue mechanical properties using the phase singularity of dynamic laser speckles

Jing Wang, Seemantini K. Nadkarni, Wellman Ctr. for Photomedicine (United States) and Harvard Medical School (United States) and Massachusetts General Hospital (United States)

Phase singularity, or optical vortex, defined at locations of null intensities, is a feature of speckle patterns. Laser speckle fluctuations, modulated by the Brownian motion of light scattering particles, are intimately linked to the viscoelastic properties of tissue. Therefore, by tracking the movement of phase singularities of the pseudo-phase retrieved from the speckle intensity pattern, we can measure the temporal fluctuations of speckle patterns over time and recover information on microscale mechanical gradients in tissue. Here we propose a new method to rapidly measure the viscoelasticity of tissue using the phase singularity of the pseudo-phase representation of dynamic laser speckles. We first retrieve the pseudo-phase of the speckle patterns by applying the Laguerre-Gauss filter to the intensity speckles reflected from tissue. The spatial locations of the phase singularities are identified by calculating the phase change along close circuits. The phase change along a close circuit around a phase singularity is $\pm 2\pi$. We then follow the trajectories of the phase singularities with time and quantify the mean squared displacement of the phase singularities between consecutive frames of the speckle sequence to derive the viscoelastic properties of tissue. To investigate the accuracy of this method, we prepare and measure different phantoms with varying viscoelastic properties composed of polyacrylamide hydrogel. The viscoelastic properties measured via speckle phase singularities correlate well with the mechanical moduli of phantoms measured by the mechanical rheometer. Our studies similarly demonstrate a strong correlation with standard rheometry for different tissue types including fat, muscle and vascular tissue.

9327-38, Session PSun

Brillouin spectroscopy reveals changes in muscular viscoelasticity under muscular dystrophy

Zhaokai Meng, Vladislav V. Yakovlev, Texas A&M Univ. (United States)

Muscular dystrophy (MD) is a group of muscle diseases that induce weakness in skeletal muscle, defects in muscle proteins and the death of muscle cells and tissues. The microscopic muscular mechanical properties (i.e., viscoelasticity), however, have not been thorough studied with and without MD in a non-invasive manner. On the other hand, Brillouin spectroscopy (BS) provides a novel approach for probing the local sound speed within a small volume. Moreover, recent advances in background-free Brillouin spectroscopy enable investigators to imaging not only transparent samples, but also turbid ones. In this sense, the microscopic muscular viscoelasticity (associated with local sound speed) could be characterized using BS.

In this study, we employed drosophila model of dystroglycanopathies, human congenital muscular dystrophies resulting from abnormal glycosylation of alphadystroglycan-mediated pathway. The mechanical properties of their abdominal muscular tissues were measured and imaged via Brillouin spectroscopy. As a comparison, we have also examined and imaged muscular tissues dissected from wild type drosophila. Their distinct Brillouin spectra indicate the elasticity difference induced by muscular dystrophy. Here, the Brillouin spectra were obtained by a background free VIPA (virtually imaged phased array) spectrometer described in the previous report [1]. As a reference, the Raman spectra were also acquired for each pixel.

1. Meng, Z., Traverso, A. J., & Yakovlev, V. V., Optics express, 2014, 22(5), 5410-5416.

9327-39, Session PSun

Elasticity measurement of nasal cartilage as a function of temperature using optical coherence elastography

Chih Hao Liu, M. N. Skryabina, Manmohan Singh, Jiasong Li, Chen Wu, Zhaolong Han, Rita Idugboe, Thomas Hsu, Emil N. Sobol, Michael D. Twa, Kirill V. Larin, Univ. of Houston (United States)

Current clinical methods of reconstruction surgery involve laser reshaping of the nasal cartilage. The process of stress relaxation caused by laser heating is the primary method to achieve the nasal cartilage reshaping in otolaryngology and orthopedics. However, stress relaxation in cartilage is a time and critically temperature-dependent process. In order to achieve the desired changes of cartilage shape, an accurate measurement of elastic property during the temperature and time changes needs to be performed. Optical coherence elastography (OCE) is an emerging technique capable of assessing tissue biomechanical properties completely noninvasively. In this work, we have utilized an air-puff based OCE system to analyze the elastic wave propagation in the cartilage over different temperatures. The velocity of the elastic wave was used to quantify the young's modulus of the tissue. During the experiment, the temperature of nasal cartilage was heating from 20oC to 65oC using resistor-based heating bath. The results show strong but not linear dependence of cartilage elastic properties on the temperature and are in agreement with the results obtained by uniaxial mechanical compression testing. Thus, this rapid and non-destructive experimental method is promising for in vivo measurement and monitoring biomechanical properties of the cartilage during the laser reshaping process.

**Conference 9327:
Optical Elastography and Tissue Biomechanics II**

9327-40, Session PSun

Improving resolution and strain sensitivity in phase-sensitive compression optical coherence elastography

Lixin Chin, Philip Wijesinghe, Andrea Curatolo, Kelsey M. Kennedy, The Univ. of Western Australia (Australia); Martin L. Villiger, Wellman Ctr. for Photomedicine (United States) and Harvard Medical School (United States) and Massachusetts General Hospital (United States); Robert A. McLaughlin, Brendan F. Kennedy, David D. Sampson, The Univ. of Western Australia (Australia)

Accurate estimation of local strain from displacement measurements determines the quality of elastograms generated by phase-sensitive compression optical coherence elastography (OCE). This variant of OCE has shown promise in several applications, including the identification of tumors in human breast tissue and necrotic lesions in dystrophic murine muscle tissue. However, to achieve high strain sensitivity, existing techniques aggregate measurements over a large axial range, degrading the axial resolution by five to ten times compared to the underlying optical coherence tomography (OCT) data.

In this study, we analyze the impact on the strain resolution and sensitivity of the data acquisition protocol, the data processing, and the fitting models used to estimate strain. Displacement sensitivity is commonly approximated as being proportional to the inverse square-root of the OCT signal-to-noise ratio (SNR); however this is known to be inaccurate at low SNR, such as in a dark speckle. OCT scans are also affected by phase noise caused by jitter and positioning errors of the scanning mirrors. We investigate the reductions in phase noise achievable by reducing the acquisition time and lateral shift between OCT scans used to calculate sample displacement. We explore more accurate displacement sensitivity models, combined with speckle reduction techniques, to improve strain sensitivity. In addition, the use of non-linear and 3-D fitting models is examined in order to improve the resolution of strain elastograms. The findings we present are important both in optimizing the sensitivity and resolution of elastograms as well as in characterizing noise sources in OCE.

9327-41, Session PSun

Noncontact depth-resolved micro-scale corneal elastography

Shang Wang, Baylor College of Medicine (United States) and Univ. of Houston (United States); Kirill V. Larin, Univ. of Houston (United States) and Baylor College of Medicine (United States)

Noninvasive high-resolution depth-resolved measurement of corneal biomechanics is of great clinical significance for improving the diagnosis and optimizing the treatment of various degenerated ocular diseases. Here, we report a micro-scale optical coherence elastography (OCE) method that enables noncontact assessment of the depthwise elasticity distribution in the cornea. The OCE system combines a focused air-puff device with phase-sensitive optical coherence tomography (OCT). Low-pressure short-duration air stream is used to load the cornea with the localized displacement at micron level. The phase-resolved OCT detection with nano-scale sensitivity probes the induced corneal deformation at various locations within a scanning line, providing the ultra-fast imaging of the corneal lamb wave propagation. With spectral analysis, the amplitude spectra and the phase spectra are available for the estimation of the frequency range of the lamb wave and the quantification of the wave propagation, respectively. Curved propagation paths following the top and bottom corneal boundaries are selected inside the cornea for measuring the phase velocity of the lamb wave at the major frequency components over the whole depths. Our pilot experiments on ex vivo rabbit eyes indicate the distinct stiffness of

different layers in the cornea, including the epithelium, the anterior stroma, the posterior stroma, and the innermost region, which demonstrates the feasibility of this micro-scale OCE method for noncontact depth-resolved corneal elastography. Also, the quantification of the lamb wave dispersion in the cornea could lead to the measurement of the elastic modulus, suggesting the potential of this method for quantitative monitoring of the corneal biomechanics.

9327-42, Session PSun

A study on the properties of contact pressure induced by manually operated diffuse reflectance fiber optic probes

Maksimilijan Bregar, Univ. of Ljubljana (Slovenia); Blaž Cugmas, Univ of Ljubljana (Slovenia); Franjo Pernuš, Božtjan Likar, Miran Bürmen, Univ. of Ljubljana (Slovenia)

Diffuse reflectance spectroscopy is a non-invasive spectroscopic technique suitable for assessment of soft tissue optical properties. The spectra are frequently acquired by fiber optic probes, which can be conveniently used in a variety of applications. Spectra are collected by gently pressing the probe against the tissue surface, thereby improving the light coupling and the measurement repeatability. However, the applied contact pressure leads to structural changes in the skin and the underlying soft tissue, which reflect in the optical properties, and thereby in the acquired spectra. Moreover, the pressure applied during the acquisition of spectra depends on a number of factors and can substantially affect the results obtained by the computational methods. Unfortunately, there is a lack of objective studies on the properties of contact pressure induced by manually operated probes.

In this study, we systematically assess the properties of the contact pressure applied by manually operated probes as function of the operator, probe contact area, and sample stiffness. For this purpose, three different human skin-like phantoms with different well-defined mechanical properties were used. To gain relevant statistics of the contact pressure properties, the study included ten experienced probe operators that were asked to apply gentle contact pressure to the phantoms by using three different contact area probes. A novel system for rapid simultaneous acquisition of spectra and corresponding contact pressure was used to collect the relevant data. Results show that variability of the gentle contact pressure significantly depends on the probe operators, sample stiffness and probe contact area.

9327-51, Session PSun

Fast low-noise Brillouin spectroscopy measurements of elasticity for corneal crosslinking

Michael Bakshtab, Avedro, Inc. (United States); Amit S. Paranjape, Avedro, Inc. (United States); Marc D. Friedman, David F. Muller, Avedro, Inc. (United States)

Millisecond acquisition times for Brillouin spectroscopy measurements were achieved with and without spatial filtering via high coherence fiber coupled 1 MHz bandwidth 780 nm wavelength laser stabilized by Rb D2 absorption line, via polarization extinction scheme, Rayleigh scattering absorbent, stray-light enhanced VIPA spectrometer, and EMCCD camera. The Brillouin spectral shifts, ranging from 7.8 to 8.7 GHz, were observed for various pig eye specimen, corresponding to reproducible changes of 0.5 to 1.0 GHz for the cross-linked eyes versus not cross-linked ones. Post-crosslinking densitometer for noncontact confocal Brillouin scanning microscopy of spatial profiles for corneal stiffness tests along with eye tracking-fixation system is under development.

Conference 9328: Imaging, Manipulation, and Analysis of Biomolecules, Cells, and Tissues XIII

Monday - Wednesday 9-11 February 2015

Part of Proceedings of SPIE Vol. 9328 Imaging, Manipulation, and Analysis of Biomolecules, Cells, and Tissues XIII

9328-1, Session 1

Wide area fluorescent lifetime imaging of surgical specimens using two photon microscopy at MHz rates (*Invited Paper*)

Michael G. Giacomelli, Massachusetts Institute of Technology (United States); Yuri Sheykin, Beth Israel Deaconess Medical Ctr. (United States); Jeffrey Brooker, Thorlabs Imaging Systems (United States); James L. Connolly, Beth Israel Deaconess Medical Ctr. (United States); Alex E. Cable, Thorlabs, Inc. (United States); James G. Fujimoto, Massachusetts Institute of Technology (United States)

Two photon fluorescence lifetime imaging (TP-FLIM) is a modality that enables high resolution, depth-sectioned intrinsic contrast imaging of the microenvironment of cells and tissue. However, the low acquisition rate and narrow field of view of TP-FLIM limits its use in medical applications. We demonstrate the use of fast temporal sampling to perform TP-FLIM imaging of large surgical specimens at submicron resolution. High pixel rates are combined with rapid mosaicing to survey large tissue areas. The utility of TP-FLIM is assessed for the evaluation of tumor margins.

9328-2, Session 1

Raman study for drug delivery applications and tissue imaging

Symeon Papazoglou, Ioannis Theodorakos, National Technical Univ. of Athens (Greece); Maria Patitsa, Apostolos Klinakis, Biomedical Research Foundation, Academy of Athens (Greece); Ioanna Zergioti, Yannis S. Raptis, National Technical Univ. of Athens (Greece)

In recent years, drug delivery applications and especially targeted delivery of anti-cancer drugs to specific tumor sites, has been under intense study, due to the high potential health impact that they present. In this context, a drug delivery system is developed based on a nanocapsule which will consist of multi-wall carbon nanotubes as the main carrier component, magnetic nanoparticles for the magnetic navigation of the nanocapsule, a cancer drug and fluorescent molecules for the visualization of the nanocapsule movement in a microfluidic channel.

Raman spectroscopy is a powerful tool for the investigation of the structural alterations that occur in organic species. In this work, Raman spectroscopy is employed, so as to investigate the ability of the technique to distinguish healthy from cancer tissue, by exploiting the release of specific protein markers that are produced near the tumor sites. These protein markers, that are not present in healthy cells, present characteristic bands in the Raman spectra, thus enabling the recognition of cancer cells. In parallel, a Raman study on the drug loading capacity of the nanocapsule has been conducted, aiming towards the increase of the drug loading yield for more efficient tumor curing, taking into account the side effects and the toxicity of the nanocapsule components.

9328-3, Session 1

Determination of sub-diffraction-limited organelles and biomolecules using microsphere lenses in combination with fluorescence microscopy

Hui Yang, Norman Moullan, Johan Auwerx, Martin A. M. Gijs, Ecole Polytechnique Fédérale de Lausanne (Switzerland)

A conventional optical microscope has a strict limitation in spatial resolution due to the diffraction of light. A dielectric microsphere is shown to generate a 'photonic nanojet', which exits, upon illumination, from such microsphere with a waist smaller than the diffraction limit. This phenomenon is key for the microsphere-enabled high resolution imaging that goes beyond the classical diffraction limit. We image sub-cellular organelles and biomolecules by using a microsphere in combination with a conventional fluorescence microscope. The microsphere is placed on a sample that is immersed in water, collects the near-field nano-features of the sample and generates a magnified far-field image, which is recorded through a conventional water immersion objective. We investigate the imaging capability of the microsphere on different sub-cellular organelles, i.e. centrioles, mitochondria and chromosomes in the AML12 cell line. The experimental results demonstrate imaging of features of ~ 7 -size. Not only the sub-structure of the centrioles can be resolved, which is beyond the limit of imaging with a normal microscope objective, but also the distribution and complex shape of mitochondria and chromosomes can be imaged through a microsphere with diameter of 60 microns in a distortion-free area of several 10 square microns. Moreover, the subcellular locations of mitochondrial encoded proteins and nuclear encoded proteins are studied. The experimental results also show that the magnification of the image varies with the size of the microspheres and reaches a maximal value of 6 when a 6 microns microsphere is used. The variation on the magnification is due to the different light collection capabilities of different-size microspheres. The experimental results are also verified by Finite Element Method simulations.

9328-4, Session 1

Intraoperative model based identification of tissue properties based on multimodal and multiscale measurements

Daniel Claus, Petra Schumacher, Univ. Stuttgart (Germany); Marc Wilke, Universität Stuttgart (Germany); Marijo Mlikota, Ulrich Weber, Siegfried Schmauder, Univ. Stuttgart (Germany); Nicolas Schierbaum, Tilman E. Schäffer, Eberhard Karls Univ. Tübingen (Germany); Philipp Wittmüß, Tanja Teutsch, Christina Tarin, Univ. Stuttgart (Germany); Sascha Hoffmann, Sara Brucker, Johannes Mischinger, Christian Schwentner, Arnulf Stenzl, Universitätsklinikum Tübingen (Germany); Wolfgang Osten, Univ. Stuttgart (Germany)

In many applications minimally invasive surgery has replaced open surgery, since the amount of tissue, which has to be cut, is reduced, resulting in a quicker recovery of the patient combined with reduced post operational stress and aesthetical advantages. Besides all these benefits, minimally invasive surgery has restricted the working environment of the surgeon

Conference 9328: Imaging, Manipulation, and Analysis of Biomolecules, Cells, and Tissues XIII

due to the loss of two major human senses (assisting the surgeon through the operation), three dimensional vision and haptic feedback. The work described here focuses on the recovery of the latter. Our approach is based on elastography. The obtained elastographic data assists the surgeon in minimally invasive surgery by localising different types of tissue. In that manner small tumours and/or enlarged lymph nodes hidden underneath the peritoneum, which may not have been registered in the pre-operational data, can be traced. Measurements are recorded on multiple scales of resolution (cell, tissue, organ) employing multiple elastographic techniques (e.g. AFM, 2D image correlation). Results are fed into a Finite Element (FE) model to generate an accurate description with regards to the elastic behaviour of a specific organ. Different scenarios with alternating position, shape and size of a tumour within the organ are simulated (database generation). For real time classification and segmentation of tissue in the surgical environment, the highly complex FE model can be reduced while the model properties describing the geometry of the tumour are preserved. Another method is the application of principal component analysis and template matching, comparing the pre-simulated scenarios with the measured 2D displacement.

9328-5, Session 1

Multi-parametric imaging of tumor spheroids with ultra-bright and tunable nanoparticle O₂ probes

Ruslan Dmitriev, Univ. College Cork (Ireland); Sergey Borisov, Technische Univ. Graz (Austria); James Jenkins, Dmitri B. Papkovsky, Univ. College Cork (Ireland)

Multi-modal probes allow for flexible choice of detection equipment when performing quenched-phosphorescence O₂ measurements: one- or two-photon, PLIM or intensity-based ratiometric read-outs. Spectral and temporal (e.g. FLIM-PLIM) can be used to simultaneously measure O₂ with pH, Ca²⁺, mitochondrial membrane potential, cell death markers or co-localise with specific cell markers. However, the main challenge of existing multi-modal nanoparticle probes is their limited diffusion across thick (> 20-50 μm) 3D cell models such as tumor spheroids. Here, we present new class of polymer nanoparticle probes having tunable size, charge and structure of phosphorescent dyes. Being spectrally similar to recently described MM2, PA2 and other multi-modal one- and two-photon excitable intracellular O₂ probes, they are 5-10 times brighter, demonstrate improved ratiometric response and their surface structure can be easily modified. With cultures of 2D and 3D cell models (fibroblasts, PC12 aggregates, HCT116 human colon cancer spheroids) we found cell-specific staining of polymer nanoparticles. However, the efficient staining of model of interest can be tuned by changing number of positive and negative surface groups at nanoparticle, to allow most efficient loading. Ultimately, we demonstrate how real-time monitoring of oxygenation can be used for selection of best spheroid production protocol, to achieve minimal variability and desired cell viability.

9328-6, Session 1

Optical Studies of Oxidative Stress in Pulmonary Artery Endothelial Cells

Zahra Ghanian, Univ. of Wisconsin-Milwaukee (United States); Reyhaneh Sepehr, Univ of Wisconsin-Milwaukee (United States); Annie Eis, Ganesh Kondouri, Medical College of Wisconsin (United States); Mahsa Ranji, Univ. of Wisconsin-Milwaukee (United States)

Objective: This study evaluated the dynamics of oxidative stress (mainly superoxide) induced by chemical perturbations in mitochondria of fetal pulmonary artery endothelial cells (FPAEC).

Materials and methods: The PAECs were harvested from the normal lamb lungs and grown in culture. The cells were stained with Mito-SOX

after 10 minutes of time-lapse imaging (the baseline). Superoxide level was measured before and after treating the cells with chain perturbors including potassium cyanide (15mM KCN, complex IV inhibitor), and pentachlorophenol (25μM PCP, uncoupler). In order to quantify the superoxide level (and as a result the oxidative stress) of mitochondria, the slope of changes in the fluorescence intensity of images in the red channel was calculated. Moreover, the fluorescence intensity profile of cells after background subtraction was plotted over time to monitor the dynamics of superoxide level after inducing chain perturbation in mitochondria.

Results: Addition of inhibitor (KCN) doubled (1.9812 ± 0.3556) the slope of red intensity over time translated to an increase in the level of superoxide whereas an uncoupler (PCP) increased the slope of intensity eighteen (18.1116 ± 1.9) times higher, which is a result of an increase in the level of superoxide.

Conclusion: We quantified the dynamics of superoxide levels of FPAEC by perturbing mitochondrial chain and using time lapse microscopy. Our method quantifies mitochondrial dysfunction in intact cells and can be applied in future to study the effects of perturbations, such as, hypoxia, hyperoxia, and pulmonary hypertension on the regulation of superoxide levels.

9328-7, Session 1

Cholesterol efflux monitoring in macrophage form cells by using fluorescence lifetime imaging

Young Sik Song, Yonsei Univ. (Korea, Republic of); Sang Hak Lee, Yonsei University (Korea, Republic of); Soo Hyeok Kim, National Institute on Aging (United States); Won sang Hwang, Yonsei Univ (Korea, Republic of); Dug Young Kim, Yonsei Univ. (Korea, Republic of)

Heart disease is one of the most significant threats to health care systems in most developed countries in these days. Macrophages play a key role in atherosclerotic plaque destabilization and rupture, since they accumulate large amounts of lipid through the uptake of modified lipoproteins which results in foam cell formation. Low density lipoproteins (LDL) are the main source of excess cholesterol deposition in foam cells. Cholesterol efflux is the process of removing cholesterol from macrophages in the subintima of the vessel wall, and efflux mechanism in a cell is one of the critical issues for the prevention of cardiovascular diseases. High density lipoproteins (HDL) stimulate cholesterol efflux from macrophage foam cells in the arterial wall. Radioisotope-labeled cholesterol analysis method is well known conventional method for observing cholesterol efflux. The major drawback of this method is its long and complicated process. Fluorescence intensity imaging schemes are replacing the radioisotope-labeled method in recent years for cholesterol efflux monitoring. Various spectroscopic methods are also adapted for cholesterol efflux imaging. Here we present a fluorescence lifetime imaging method for more quantitative observation of cholesterol efflux process in macrophages, which enables us to observe cholesterol level changes with various conditions. We used J774 macrophage cell and 25-NBD-cholesterol which is a famous cholesterol specific dye. Our lifetime imaging results clearly show cholesterol efflux rate very effectively. We believe that fluorescence lifetime analysis is new and very powerful for cholesterol imaging or monitoring.

9328-8, Session 1

A multi-wavelength (u.v. to visible) laser system for early detection of oral cancer

Stephen P. Najda, Piotr Perlin, Mike Leszczynski, TopGaN sp. z o.o. (Poland); Thomas J. Slight, Wyn Meredith, Compound Semiconductor Technologies Global Ltd. (United Kingdom); M. Schemmann, FOCE International

Conference 9328: Imaging, Manipulation, and Analysis of Biomolecules, Cells, and Tissues XIII

Technology (Netherlands); Harry Moseley, J. Woods, R. Valentine, Peter Mossey, E. Theaker, Univ. of Dundee (United Kingdom); Gillian Mimmagh, W. Mimmagh, 2M Engineering Ltd. (Netherlands); S Kalra, University of Dundee (United Kingdom)

A multi-wavelength (360nm - 440nm), real time Photonic Cancer Detector (PCD) optical system based on GaN semiconductor laser technology is outlined.

In cancer, tissue cells tend to create many additional blood vessels to support their growth. The molecule protoporphyrin (PpIX) is generally present in blood vessels and exhibits red fluorescence when excited with UV or blue light in the 360-440 nm range. Cancer cells and pre-cancer cells are detected by observing the red fluorescence at a matching excitation wavelength. The wavelength of the laser has to be tunable as the matching wavelength depends on the person, type of illness and the presence of other chemicals.

Cancer, found in the mouth, lips or throat, is often highly curable if diagnosed and treated early. Unfortunately, in its early stages, oral cancer can easily go unnoticed as it is often not visible using conventional imaging techniques. In fact even when a lesion is visible to the naked eye, there is no way for the dentist to see the difference between a cancerous and benign lesion.

The real-time Photonic Cancer Detector (PCD) creates an image of the oral cavity (broad field white light detection) and maps within the oral cavity suspicious changes in the oral mucosa with high sensitivity. The PCD will provide not only the image of the suspicious area or lesion but also their spatial co-ordinates within the oral cavity (saved as a digital file) allowing progression of the lesion to be monitored over time.

9328-10, Session 1
Qualitative and quantitative comparison of colonic microendoscopy image features to histopathology

Sandra P. Prieto, Amy J. Powless, Univ. of Arkansas (United States); Keith Lai, Jonathan A. Laryea, Jason S. Mizell, Univ. of Arkansas for Medical Sciences (United States); Timothy J. Muldoon, Univ. of Arkansas (United States)

Colorectal cancer is the third leading cause of cancer death in the United States, affecting more than 130,000 Americans every year. Determining tumor margins prior to surgical resection is essential to providing optimal treatment and reducing recurrence rates. Colorectal cancer recurrence can occur in up to 20% of cases, commonly within three years of surgery. Since most recurrence cases result from incomplete resection, pathologists are encouraged to remove additional tissue from either end of the tumor and H&E sections are then examined for indications of disease in the ends deemed as normal tissue.

We have developed a portable fiber bundle microendoscopy imaging system for detection of abnormalities in colonic glandular structure. The system comprises a laptop, a modified fiber bundle image guide with a 1mm active area diameter and custom LabVIEW interface, and is currently part of an ongoing pilot study at the University of Arkansas for Medical Sciences for imaging surgically resected colon tissue at to evaluate its effectiveness for detection of dysplastic lesions in fresh specimens.

Microscopy images of freshly resected human colonic epithelium were superimposed to create a wide field image of architectural changes in the glands, which were then mapped to histopathology H&W slides. Qualitatively, glandular circularity and rough placement of image guide were used to map normal and dysplastic areas from microendoscopy images to H&E slides. Quantitative metrics for correlating images were obtained by analyzing glandular diameter and spatial distribution.

9328-11, Session 1
Light Shift from Ultraviolet to Near Infrared Light:
Cerenkov Luminescence with Gold Nanocluster - Near Infrared (AuNc-NIR) Conjugates

Su Woong Yoo, Hyoyoung Mun, Gyungseok Oh, Youngjae Ryu, Min-Gon Kim, Euiheon Chung, Gwangju Institute of Science and Technology (Korea, Republic of)

Cerenkov luminescence (CL) is generated when a charged particle moves faster than the speed of light in dielectric media. Recently CL imaging becomes an emerging technique with the use of radioisotopes. However, due to relatively weak blue light production and massive tissue attenuation, CL has not applied widely. Therefore, we attempt to shift the CL emission light to more near infrared (NIR) spectrum for better tissue penetration.

Gold nanocluster (AuNc)-NIR conjugated molecules (AuNc-IR820 and AuNc-ICG) have been conjugated to be activated with ultraviolet light. We found optimal conjugate concentrations of AuNc-NIR conjugates by spectroscopy system to generate maximal photon emission. When exposed by ultraviolet light, the emission of NIR light from conjugates are verified. In quantitative analysis, AuNc-NIR conjugates emit brighter light signal than pure AuNc. This result implies that NIR fluorescent dyes (both IR820 and ICG) can be excited by AuNc emission light.

Following the above baseline experiment, we mixed ¹⁸F-FDG radioisotope to the AuNc-NIR conjugates, to confirm NIR emission induced from Cerenkov radiation. Long pass filter was used to block Cerenkov luminescence and to collect the emission from AuNc-NIR conjugates. Instead of long exposure time of CCD, we used multiple frame scheme to enable the elimination of gamma radiation strike. In summary, we obtained NIR emission light from AuNc-NIR conjugated dyes that is induced from Cerenkov luminescence activation. We plan to in vivo small animal imaging with this conjugates for validate better tissue penetration.

9328-71, Session 1
Quantifying the optical properties of turbid media using polarization sensitive hyperspectral imaging (SkinSpect): two-layer optical phantom studies

Fartash Vasefi, Nicholas B. MacKinnon, SMI (United States); Rolf B. Saager, Anthony J. Durkin, Beckman Laser Institute and Medical Clinic (United States); Robert Chave, SMI (United States); Daniel L. Farkas, SMI (United States) and The Univ. of Southern California (United States)

Purpose: To determine the performance of a polarization-sensitive hyperspectral imaging system designed to quantify lesion depth in melanoma by extracting chromophore concentrations from two-layer tissue-mimicking phantoms.

Materials and methods: A hyperspectral imaging system (SkinSpect) illuminates the phantom with spectrally-programmable linearly-polarized light at 33 wavelengths between 468nm and 857 nm. Diffusely reflected photons are separated into collinear and cross-polarized image paths and images captured for each illumination wavelength. We have developed a method which combines two depth sensitive techniques: polarization, and hyperspectral imaging, to accurately determine the spatial distribution of melanin and hemoglobin oxygenation in a skin lesion. Interchangeable layers of polydimethylsiloxane-based phantoms are used to simulate dermal and epidermal tissue and evaluate the efficacy and accuracy of this depth-sensitive method. These phantoms used coffee to approximate epidermal melanin absorption in the top layer which was fabricated at multiple

Conference 9328: Imaging, Manipulation, and Analysis of Biomolecules, Cells, and Tissues XIII

thicknesses (-100-650 μm), and bovine hemoglobin in the (semi-infinite) base layer to approximate dermal absorption. Titanium dioxide was used as a scattering agent in all phantom layers

Results: Phantom properties were characterized and validated using SkinSpect and spatially modulated quantitative spectroscopy (SMoQS). Pseudo-optical density data-cubes were analyzed using a wavelength dependent linear model to extract the relative contribution of chromophores according to Beer-Lambert and determine the effect of layer thickness on absorption spectra.

Conclusion: We have built and used a polarization sensitive hyperspectral imager for quantitative tissue imaging. The acquired reflection spectra results using tissue-mimicking phantoms suggest that the system is useful for extracting and quantifying relative chromophore concentrations in tissues.

9328-12, Session 2

Software-aided automatic cell optoporation system

Hans Georg Breunig, Saarland Univ. (Germany) and JenLab GmbH (Germany); Ana Batista, Aisada Uchugonova, Saarland Univ. (Germany); Karsten König, Saarland Univ. (Germany) and JenLab GmbH (Germany)

Laser-assisted transient cell membrane perforation ("optoporation") has emerged as a powerful noninvasive and highly efficient cell-transfection technique. It is usually done by targeting individual cells manually which significantly limits number of addressable cells per time. We present an experimental setup with custom-made software control for automated cell recognition and cell-optoporation experiments. Optoporation is achieved by transiently illuminating the cell membranes with highly focused beam-shaped sub 15 fs pulses. The LabView-based software evaluates contrast edges in bright-field sample images to identify cell locations for laser illumination and controls the hardware to transiently laser-illuminate these positions. By software-controlled stitching together of several microscopic field-of-views in principle all cells in a culture dish can be targeted without further user interaction. The software-based automation allows to significantly increase the number of treatable cells per time compared to a manual approach. For a laser illumination duration of 100 ms a 7-8 cells spots can be targeted per second. We illustrate the experimental capabilities in CHO-cell optoporation experiments and discuss the influence of laser fluence on post treatment survival and optoporation efficiency rates.

9328-13, Session 2

Trapping of single extracellular vesicles in the evanescent field of an optical cavity

Edwin van der Pol, Frank A. W. Coumans, Academisch Medisch Centrum (Netherlands); John Wilke, Christopher Earhart, Brian DiPaolo, Robert Hart, Bernardo Cordovez, Optofluidics (United States); Guus Sturk, Rienk Nieuwland, Ton G. van Leeuwen, Academisch Medisch Centrum (Netherlands)

Background: Extracellular vesicles (EV) are present in all bodily fluids and play a role in intercellular communication. Therefore, EV are potential biomarkers for metastatic carcinomas. However, due to their small size (30-1000 nm), detection and characterization of single EV remains a major challenge.

Method: EV were isolated from human urine and guided through an optical trap at a flow rate of 0.5 $\mu\text{L}/\text{min}$. The trap was formed by the evanescent field of an optical cavity on an integrated photonic device (Nanotweezer, Optofluidics, USA). A 1064 nm 322 mW laser was used to excite the cavity, which had a resonance frequency of 9400/cm. The irradiance inside the

optical trap was $\sim 0.1 \text{ MW}/\text{mm}^2$. Scattering of single EV was imaged onto a CCD camera by a 0.5 NA microscope objective. To estimate the EV diameter, we analytically described the relation between the diameter, refractive index, and light scattering of polystyrene beads and EV by Mie theory.

Results: EV were optically trapped for 0.25-5 seconds, with three EV remaining trapped until the laser was turned off. The trapped EV had a diameter of $760 \pm 90 \text{ nm}$ (mean \pm standard deviation) and their light scattering intensity was on average 24-fold higher than the background intensity.

Conclusions: For the first time, we have trapped single submicron EV in the evanescent field of an optical cavity. The combination of a switchable optical trap and the high irradiance inside the trap is attractive for Raman microspectroscopy on single EV.

9328-14, Session 2

Multimodal optical phenotyping of cancer cells

Lena Kastl, Björn Budde, Michael Isbach, Christina E. Rommel, Björn Kemper, Jürgen Schneckeburger, Westfälische Wilhelms-Univ. Münster (Germany)

There is a growing interest in cell biology and clinical diagnostics in label-free, optical techniques as the interaction with the sample is minimized and substances like dyes or fixatives do not affect the investigated cells. Such techniques include digital holographic microscopy (DHM) and the optical stretching by fiber optical two beam traps. DHM enables quantitative phase contrast imaging and thereby the determination of the cellular refractive index, dry mass and the volume, whereas optical cell stretching reveals the deformability of cells.

Since optical stretching strongly depends on the optical properties and the shape of the investigated material we combined the usage of fiber optical stretching and DHM for the characterization of pancreatic tumor cells. Our results demonstrate that these tumor cells, which are from the same metastasis but vary in their level of differentiation, show significant differences in their deformability, and even cells that differ only in the expression of one certain protein can be distinguished by their mechanical properties. Additionally, the results of the DHM measurements showed differences in volume and dry mass of the cells, whereas the refractive index showed only few variations, indicating that it does not significantly influence the results of the optical cell stretching. Thus, we could identify different populations of cell lines by parameter sets, that were retrieved by combined use of these two techniques. The obtained results show a promising new approach for the phenotyping of different cell types, especially in tumor cell characterization and cancer diagnostics.

9328-15, Session 2

Bartonella henselae infects mature human erythrocytes

Gislaine Vieira-Damiani, Marilene Neves A. da Silva, Univ. Estadual de Campinas (Brazil); Marna E. Ericson, Kalpna Gupta, Univ. of Minnesota, Twin Cities (United States); Vitor B. Pelegati, André A. de Thomaz, Mariana O. Baratti, Hernandes F. Carvalho, Carlos L. Cesar, Paulo Eduardo Neves Ferreira Velho, Univ. Estadual de Campinas (Brazil)

Human Bartonella sp. infection has potentially life threatening outcome even in immunocompetent patients. We demonstrate the time course of invasion of B. henselae into mature human erythrocytes with using single photon confocal microscopy, taking advantage of the endogenous fluorescence of the bacterium.

Peripheral blood was infected with B. henselae suspension. Unstained samples of infected and uninfected blood were analyzed by single photon

Conference 9328: Imaging, Manipulation, and Analysis of Biomolecules, Cells, and Tissues XIII

confocal microscope. The inoculated blood sample was irradiated with a 488nm argon laser [Lasos, model LGN3001], ZEISS LSM 780, with 40xN.A. 1.3 oil immersion objective (EC Plan Neofluar), with 512 x 512 pixels spatial resolution, using a pixel dwell time of 12,6 μ s, with total scanning time of order of 3s (this part could be very important because. Initially we determined the emission spectra of human erythrocytes and *B. henselae* and subsequently analyzed erythrocytes, at 20-, 48- and 72-hours post inoculation with *B. henselae* by confocal fluorescence microscopy. Both the emission spectra of live suspensions of *B. henselae* and the red blood cell were detected between 502 and 685 nm. The emission peak for *B. henselae* is 554nm and 589nm for the red blood cell.

At 20 hours, individual bacteria bind to the erythrocyte membrane and then come; at 48 hours the bacteria were adhered to the membrane and at 72 hours, *B. henselae* was detected within the infected erythrocyte we observed. Using real time, single-photon confocal imaging of *B. henselae* autofluorescence we reveal a 72 hour time course for *B. henselae* to infect mature erythrocytes in vitro.

9328-16, Session 3

Quantification of direct spotting versus microcontact printing (CP) for controlled deposition of protein(s) in different experimental conditions

Kathryn F. A. Clancy, Dan V. Nicolau, McGill Univ. (Canada)

Protein microarrays are used to develop tools in various research areas including drug discovery, disease diagnosis, and protein-ligand interaction analysis. Their efficacy depends on a well-defined pattern of immobilized proteins that have retained their bioactivity. Protein microarrays are most commonly made using a robotic spotting drop method that can lead to spots having uneven protein adsorption within the spotted area. This has been shown to lead to inaccurate readings. Alternative techniques exist, including microcontact printing (CP) with a poly(dimethylsiloxane) (PDMS) stamp that produces protein patterns on surfaces, while maintaining bioactivity for a wide range of proteins.

Here we propose to quantitatively compare the distribution of deposited proteins via direct spotting versus CP in both liquid and dry conditions. Un-labeled and fluorescently labeled protein solutions will be deposited by either the drop or CP printing method onto a functionalized glass surface then distribution of the deposited proteins will be quantified via fluorescence microscopy. Variation of the protein solution and surface properties in addition to the deposition method will also be performed. The PDMS stamp used in this project will be composed of pyramid relief structures whose aspect ratios were previously optimized.

Investigation of the experimental parameters used in the CP printing method to produce an even protein adsorption pattern will enable reliable assay answers by increasing the signal to noise ratio in printed protein microarrays.

9328-17, Session 3

Lens-free imaging of cancer cell migration in diverse microenvironments

Evelien Mathieu, IMEC (Belgium); Colin D. Paul, Johns Hopkins Univ. (United States); Richard Stahl, Geert Vanmeerbeek, Veerle Reumers, Chengxun Liu, IMEC (Belgium); Konstantinos Konstantopoulos, Johns Hopkins Univ. (United States); Liesbet Lagae, IMEC (Belgium)

Time-lapse imaging of living cells is crucial to understand dynamic biological processes. However, technical challenges in combining complex

imaging systems capable of generating data at the needed temporal and spatial resolution with environments amenable to cell growth limit the use of such assays in some research and most clinical settings. To be used for live cell applications, conventional phase contrast microscopes need to be fitted with custom-built stage top incubators, motorized translation stages, and autofocus features, resulting in expensive and bulky experimental set-ups. This need for specialized equipment limits the accessibility and throughput of live cell research.

As an alternative to complex conventional microscopy set-ups, we herein present a lens-free imaging (LFI) tool. The imager is based on in-line digital holography, and objectives are replaced by mathematical calculations, with the focus depth being a digital parameter. Importantly, the LFI system combines an extensive field of view (6.4 x 4.6 mm²) with a good resolution (1.1 μ m). Evasion of expensive objectives, precisely aligned optics, stage-top incubators, motorized translation stages and autofocus features results in a compact and inexpensive time-lapse imaging tool that is 50-fold less expensive than conventional microscopy assemblies and fits inside an ordinary cell culture incubator.

Assays typically used for the study of cell migration in one-, two-, and three-dimensional microenvironments were imaged with both LFI and conventional phase contrast microscopy. The results are compared for thorough benchmarking of the new imaging tool and to demonstrate its utility and versatility for live cell imaging applications.

9328-18, Session 4

Estimating skin blood saturation by selecting a subset of hyperspectral imaging data

Maria Ewerlöf, E. Göran Salerud, Tomas Strömberg, Marcus Larsson, Linköping Univ. (Sweden)

Spatial skin blood saturation can be estimated with hyperspectral imaging (HSI) using the full spectral wavelength range of a 400-700 nm liquid crystal tunable filter (LCTF). Depending on the image size and the strategy of solving the photon transport problem, estimation of skin blood saturation is often a time consuming and computationally demanding task. Therefore, this work aims to find sets with a reduced number of wavelengths where blood saturation in skin can be evaluated at a high precision and accuracy.

To test this, we have performed Monte Carlo simulations using a two-layered skin tissue model. The model is defined by epidermal thickness (Tepi), haemoglobin concentration (Crbc), haemoglobin saturation (Srbc), melanin concentration and spectrally dependent reduced-scattering coefficient (μ_s'). At each spatial location in the field-of-view, we detect diffusively reflected spectra with saturation levels 0-100% for a range of model parameters relevant for human skin.

We use simulated backscattered intensities to calculate an intensity ratio using the values from at least two wavelengths in the range 510-590 nm. For every combination of Tepi, Crbc and μ_s' , we perform a linear regression analysis to find the intensity ratio providing the largest sensitiveness to haemoglobin saturation and least variance from the other model parameters.

The wavelengths used for the ratio with largest sensitiveness are the ones best suited to describe skin blood saturation. Fine-tuning resolution and separation between the wavelengths and adding a possibility to calibrate for the total blood concentration has potential to solve the aim and further improve blood saturation estimation.

9328-19, Session 4

A preliminary study on a dual-modality OPT / micro-CT system

Yujie Yang, Dong Di, Liangliang Shi, Jun Wang, Institute of Automation (China); Hui Hui, Xin Yang, Key Lab.

**Conference 9328: Imaging, Manipulation, and
Analysis of Biomolecules, Cells, and Tissues XIII**

of Molecular Imaging (China); Jie Tian, Institute of Automation (China)

Optical projection tomography (OPT) is a mesoscopic scale optical imaging technique for specimens between 1mm and 10mm. Although OPT is widely used for in vivo and ex vivo imaging, its applications in high intensity tissues such as bone and thick samples are limited due to the strong absorption of the light. In contrast, X-ray micro-CT is suitable for high intensity tissue imaging but its contrast of soft tissue is poor. Therefore, imaging tools with both strong penetration and high contrast are in great demand. To address this issue, we develop a dual-modality system integrating both OPT and micro-CT. In this paper, this dual-modality system is applied to dynamic imaging of a clearing process of the rats' paws. The clearing process is essential in OPT when imaging thick or intensity tissues since it can make high intensity tissues optically transparent. In our experiment, we scan a mouse paw three times with our system – before, during and after clearing. Each time we scan CT first and then the OPT. After acquisition, 3-dimensional volumes of OPT and CT are reconstructed separately. Then we use a rigid image registration algorithm to register these volumes. Finally, the volumes are merged together. The experimental results show that the intensity of the bone became lower during the optical clearing process and we find an optimal clearing time for mouse paw. Meanwhile the experiments also point that our bimodal system performs better than single OPT or CT system when processing tissues with both high intensity and soft parts.

9328-20, Session 4

Hyperspectral imaging to monitor simultaneously multiple protein subtypes and live track their spatial dynamics: a new platform to screen drugs for CNS diseases

Stephane Marcet, Photon etc. Inc. (Canada); Simon Labrecque, Institut Univ. en Santé Mentale de Quebec (Canada); Jean-Philippe Sylvestre, Francesca Mangiarini, Marc Verhaegen, Photon etc. Inc. (Canada); Paul De Koninck, Institut Univ. en Santé Mentale de Quebec (Canada); Sébastien Blais-Ouellette, Photon etc. Inc. (Canada)

In the past decade, the efficacy of existing therapies and the discovery of innovative treatments for Central Nervous System (CNS) diseases have been limited by the lack of appropriate methods to investigate complex molecular processes at the synaptic level.

In order to better understand the fundamental mechanisms that regulate diseases of the CNS, a fast fluorescence hyperspectral imaging platform was designed to track simultaneously various neurotransmitter receptors trafficking in and out of synapses.

With this hyperspectral imaging platform, it was possible to image simultaneously five different synaptic proteins, including subtypes of glutamate receptors (mGluR, NMDAR, AMPAR), post-synaptic density proteins, and signaling proteins. In particular, we show images of one recombinantly labelled intracellular protein combined with four quantum dots, each of these linked to four different membrane receptor subtypes. This new imaging platform allows video acquisitions of at least five fluorescent markers in living neurons with a high spatial resolution. In particular, using overexpression of fluorescent protein that identifies dendrites and synapses of neurons, we simultaneously monitored the membrane diffusion of glutamate receptors and a protein associated with receptors in different cellular compartments.

This technique provides an effective method to observe several synaptic proteins at the same time, thus study how drugs for CNS impact the spatial dynamics of these proteins.

9328-21, Session 4

Second harmonic generation (SHG) imaging demonstrated a strong dependence of the collagen hydrogels' structures on the types and concentrations of ions

Xuye Lang, Julia G. Lyubovitsky, Univ. of California, Riverside (United States)

Second harmonic generation (SHG) contrast emerged as a valuable label-free spectroscopic probe to detect aggregated collagen structures within three-dimensional (3D) scaffolds. With SHG contrast we examined in situ the contributions of phosphate, sulfate and chloride ions to aggregation of collagen into a fiber within 3D hydrogels. To understand the ion-mediated structural changes, we conducted our studies throughout a wide range of salt concentrations. By changing the concentration of phosphate we could control aggregated collagen fibers' lengths along with an effective pore structure of the 3D collagen hydrogels. For phosphate concentrations of 20 mM to about 160 mM, the fiber lengths increased from 1 μ m to about 45 μ m along with increasing phosphate concentration. Further increasing the phosphate concentration led to a reduction in collagen fiber widths and lengths. Adding chloride did not lengthen the collagen fibers significantly while sulfate had a similar lengthening effect. Lowering the polymerization temperature lead to a multilateral response, which depended on the type of ion employed. Our study emphasizes the importance of ions during self-assembly of collagen and other biologically derived protein scaffolds.

9328-22, Session 4

Towards early malaria diagnosis using surface enhanced Raman spectroscopy

Keren Chen, Clement Yuen, Aniweh Yaw, Peter Preiser, Quan Liu, Nanyang Technological Univ. (Singapore)

Microscopy observation on Giemsa-stained blood smear is widely used as the gold standard procedure in malaria diagnosis. It achieves a threshold of around 4-20 parasites/ μ l and a sensitivity of over 95% in samples with 100 parasites/ μ l. However, this procedure is time-consuming; moreover, special expertise is required to ensure accuracy. Surface enhanced Raman spectroscopy (SERS) has been explored to detect hemozoin, a biomarker of malaria infection. We have developed magnetic field enriched SERS for the highly sensitive detection of the spectroscopic equivalent of hemozoin, β -hematin. However, the requirement of an external magnetic field can induce additional uncertainty in readings. In this study, we evaluated SERS for hemozoin detection in human blood infected by Plasmodium falciparum using two approaches in an attempt to achieve sensitive detection and quantification of hemozoin. In the first approach, silver nanoparticles were synthesized separately and then mixed with lysed blood; while in the second silver nanoparticles were synthesized inside the parasites of Plasmodium falciparum. The first method yielded smaller variation and a more consistent calibration curve, which is preferred in the quantification of the parasitemia level. In contrast, the second method yielded higher sensitivity of parasitemia thus could be more effective in early malaria diagnosis.

9328-55, Session PMon

Ex-vivo holographic microscopy and spectroscopic analysis of head and neck cancer

Stephen Holler, Robert Wurtz, Kelsey Auyeung, Kris Auyeung, Milan Paspaley-Grbavac, Brigid Mulroe, Fordham Univ. (United States); Maximiliano R. Sobrero, Brett A.

**Conference 9328: Imaging, Manipulation, and
Analysis of Biomolecules, Cells, and Tissues XIII**

Miles, Mount Sinai School of Medicine (United States)

Optical probes to identify tumor margins *in vivo* would greatly reduce the time, effort and complexity in the surgical removal of malignant tissue in head and neck cancers. Current approaches involve visual microscopy of stained tissue samples to determine cancer margins, which results in the excision of excess of tissue to assure complete removal of the cancer. Such surgical procedures and follow-on chemotherapy can adversely affect the patient's recovery and subsequent quality of life. In order to reduce the complexity of the process and minimize adverse effects on the patient, we have been investigating *ex vivo* tissues samples (stained and unstained) using digital holographic microscopy in conjunction with spectroscopic analyses (reflectance and transmission spectroscopy) in order to determine label-free, optically identifiable characteristic features that may ultimately be used for *in vivo* processing of cancerous tissues. The tissue samples studied were squamous cell carcinomas and associated controls from patients of varying age, gender and race. Holographic microscopic imaging scans across both cancerous and non-cancerous tissue samples yielded amplitude and phase reconstructions that were correlated with spectral signatures. Though the holographic reconstructions and measured spectra indicate variations even among the same class of tissue, preliminary results indicate the existence of some discriminating features. Further analyses are presently underway to further this work and extract additional information from the imaging and spectral data that may prove useful for *in vivo* surgical identification.

9328-56, Session PMon

**Investigating the correlation between
white matter and microvasculature
changes in aging using large scale optical
coherence tomography and confocal
fluorescence imaging combined with
tissue sectioning**

Alexandre Castonguay, Ecole Polytechnique de Montréal (Canada); Pramod Avti, Mohammad Moeini, Philippe Pouliot, Ecole Polytechnique de Montréal (Canada) and Institut de Cardiologie de Montréal (Canada); Maryam S. Tabatabaei, Ecole Polytechnique de Montréal (Canada); Samuel Bélanger, Frédéric Lesage, Ecole Polytechnique de Montréal (Canada) and Institut de Cardiologie de Montréal (Canada)

A combined serial OCT/confocal scanner was designed to image large sections of biological tissues at microscopic resolution. Serial imaging of organs embedded in agarose blocks is performed by cutting through tissue using a vibratome. The vibratome sequentially cuts slices in order to reveal new tissue to image, overcoming limited light penetration encountered in microscopy. Two linear stages allow to move the tissue with respect to the microscope objective, acquiring a 2D grid of volumes (1x1x0.3 mm) with OCT and a 2D grid of images (1x1mm) with the confocal arm. After imaging a complete plane, a vertical stage rises the tissue 200µm and the vibratome removes a slice of the corresponding thickness. This process is repeated automatically, until the entire sample is imaged. Raw data is then post-processed to re-stitch each individual acquisition and obtain a reconstructed volume of the imaged tissue. This design was used to investigate correlations between white matter and microvasculature changes in aging mice. Three age groups were used in this study (4, 12, 24 months). At sacrifice, mice were transcardially perfused with a FITC containing gel. The dual imaging capability of the system allowed to reveal different contrast information: OCT imaging reveals changes in refractive indices giving contrast between white and grey matter in the mouse brain, while transcardial perfusion of a FITC shows microvasculature in the brain with confocal imaging.

9328-58, Session PMon

**Plastic fiber optics for micro-imaging of
fluorescence signals in living cells**

Takashi Sakurai, Toyohashi Univ. of Technology (Japan); Mitsuo Natsume, Denkosha Corp. (Japan); Kowa Koida, Toyohashi Univ. of Technology (Japan)

By using the fiber-coupled microscope (FCM), *in vivo* imaging is possible at the deep site in the tissues or organs where other optical techniques are difficult to reach. The optical performance of the FCM highly depends on the properties of the fiber bundle which detects an emitting light from cells. Recently, we developed a plastic type fiber optics which included more than 10000 unit fiber that has a polystyrene-based core and a acryl cradding. Each diameter of unit fiber was less than 5 µm, and the bundle composed a circular field of view of about 450 µm wide with 800 mm length. The fiber bundle was combined with a fluorescence imaging system consisting of laser, objective lens and CCD camera. The optical performance was enough for detection of significant signal changes in each living cell labeled with green fluorescent dyes for the measurement of calcium ion. The plastic type FCM successfully detected the Ca-dependent fluorescent signal from *in vitro* preparation of the rodents' cortex. These fibers can penetrate deeper than 1 mm from the surface of the brain. The potential power of the FCM will be expected to rise continuously for the analysis of a fine structure of the cells and an organization of certain functions *in vivo*.

9328-59, Session PMon

**Formation and evolution of
atherosclerosis: a multiscale study**

Natalya O. Chelnokova, Anastasiya A. Golyadkina, Irina V. Kirillova, Elena L. Kossovich, Asel V. Polienko, Dmitry A. Zayarskiy, N.G. Chernyshevsky Saratov State Univ. (Russian Federation)

In our research we studied histological, morphometric and mechanical properties of coronary artery tissues at various stages of atherosclerotic plaque evolution. Histomorphology of the vessel intima was examined with help of probing atomic-force microscopy nanolaboratory NTEGRASpectra. Biomechanical properties of the vessel tissues were estimated using the dynamical mechanical analyzer DMA Q800 and single-column tabletop testing system Instron 5944. It was discovered that there exist significant alterations in the coronary arteries wall structure depending on evolution stage of atherosclerotic lesion. Also the hemodynamics analysis of the altered vessel allows prediction of another lesion development on the wall opposite to the plaque. The current study will allow development of innovative methods for early diagnosis and prognostics of the atherosclerosis.

9328-60, Session PMon

**Complex dielectric properties of
anhydrous polycrystalline glucose in the
terahertz region**

Ping Sun, Beijing Normal Univ. (China); Wei Liu, Capital Normal Univ. (China); Yun Zou, Qiongzhen Jia, Jiayu Li, Beijing Normal Univ. (China)

THz radiation offers innovative sensing technologies that can provide information unavailable through other conventional methods. Here, we utilize THz time-domain spectroscopy (THz-TDS) to investigate the complex dielectric properties of solid polycrystalline material of anhydrous glucose (D-(+)-glucose with purity >99.9%). THz transmission spectra of samples were measured between 0.2-2.2 THz using THz time-domain spectrometer.

**Conference 9328: Imaging, Manipulation, and
Analysis of Biomolecules, Cells, and Tissues XIII**

The measurements were conducted under a nitrogen purge with a relative humidity below 3% and at 21°. The reference THz waveform was obtained via a free space measurement and the THz waveforms of anhydrous were obtained by measuring the transmission of THz radiation through the samples. All the samples were gently ground into fine particles with a pestle and mortar and then were compressed into pellets (0.362-0.985 mm in thickness and 13 mm in diameter) with a hydraulic press using 400 kg pressure. The refractive indices and the absorption coefficients were obtained with conventional method. The absorption spectra showed that the polycrystalline glucose has multiple absorption peaks at 1.10THz, 1.17 THz, 1.67 THz, 1.72 THz, 1.83 THz and 2.00 THz. We applied the Lorentz dispersion model to analyze the complex dielectric constant. The procedure consisted in fitting the experimental data for the real and imaginary parts of complex refractive indices using finite difference time domain (FDTD) method based on the multi-resonant Lorentz model. We acquired the different Lorentz parameters for samples with different thickness. The analysis results show that the interaction of THz radiation with glucose polycrystalline materials abides by the Lorentz dispersion model. Calculations on multiple glucose molecules were carried out by the gaseous state theory within the Linearity Combination of Atomic Orbital (LCAO) method. Density Functional Theory (DFT) and Hartree-Fock (HF) function were used to determine the ground-state structures and harmonic vibrational frequencies of glucose. The B3LYP and HF functions were performed with the 6-311+G(d) Gaussian type basis set and program option 'tight' convergence criteria. The theoretical calculations basically are in accordance with the experimental results. It is found that the characterized features of anhydrous glucose mainly origin from the intermolecular modes of glucose-glucose molecules. The results indicate that THz-TDS is a powerful novel tool to characterize the glucose molecules and it has potential to find extensive applications in biological and pharmaceutical research and industry.

9328-61, Session PMon

**Determination of biological activity from
fluorescence lifetime measurements in
Saccharomyces cerevisiae**

Florian Rudek, Tobias Baselt, Benjamin Lempe, Christopher Taudt, Peter Hartmann, Westsächsische Hochschule Zwickau (Germany)

The importance of fluorescence lifetime measurement as an optical analysis tool is growing. Many applications already exist in order to determine the fluorescence lifetime, but the majority of these require the use of fluorescence-active substances to enable measurements. Every usage of such foreign materials has an associated risk. This paper investigates the use of auto-fluorescing substances as a risk free alternative to fluorescence-active substance enabled measurements. The experimental setup uses a microchip laser with a pulse length of 1.7 ns. The system operates at a frequency doubling and reaches a wavelength of 532 nm with a pulse length of 1.3 ns. For further applications, a frequency tripling is also possible to achieve a wavelength of 355 nm. The excited sample emits light due to fluorescence. A fast photodiode collects the light at the output of an appropriate optical filter. The rise time of the photodiode is about 300 ps, therefore fluorescence lifetimes can be measured with nanosecond precision. Fluorescence lifetimes can be determined from the decay of the measurement signals, which in turn characterizes the individual materials and their surrounding environment. Information about the quantity of the fluorescence active substances can also be measured based on the received signal intensity. The correlation between the fluorescence lifetime and the live condition of various tissues and cell types was investigated and is presented here.

9328-62, Session PMon

**Evaluation of apoptotic and proliferation
biomarker expression in UV-exposed
human keratinocytes using sphingomyelin
treatment**

Lily H. Laiho, Andrea Argouarch, Erin Fong, Leah Dixon, Kristina Bishard, Kevin Campbell, Leo Banuelos, Kristina Cardenas, Kathleen De Guzman, California Polytechnic State Univ., San Luis Obispo (United States)

Chronic UV exposure induces photodamage that can accumulate and cause DNA mutations. DNA damage triggers biochemical pathways within a cell that leads to either cell cycle arrest, giving the cell time to repair DNA damage, or apoptosis. This work studies the use of sphingomyelin (SM) from bovine milk for UV damage prevention.

Several biomarkers were used to observe the potential rescue effects of SM on human primary epidermal keratinocytes (KRTs) from UV-induced damage. Presence of Ki67 and EdU indicated cell proliferation, p53 and p21 assessed cell damage, and Caspase-3 signaled apoptosis. Non-SM treated KRTs and KRTs treated with 0.1% SM media 24 hours prior to 40 mJ/cm² or 60 mJ/cm² of UV radiation were fixed and IF-stained at 24 and 36 hours after UV exposure. The Ki67 and EdU response showed no rescue of cell proliferation in the SM-treated cells at either UV dosage or time point. However, there were significant differences between the SM treated and non-SM treated cells at the no-UV dosage level. For the cell damage markers p21 and p53 no significant differences were observed between SM and non-SM treated cells for p21, but significant differences for p53 were observed at 40 mJ/cm² at the 24-hour time point and at 60 mJ/cm² at the 36-hour time point. Caspase-3 showed that SM treated KRTs had significantly less apoptotic cells. These findings suggest that SM treatment may not rescue cell proliferation, but the photoprotective capabilities of SM may reduce cell damage and apoptosis.

9328-63, Session PMon

**Wound collagen monitoring with low-cost
noninvasive led system**

Rui Liu, Zhengtuo Zhao, Mengyang Zhou, Univ. of Michigan-Dearborn (United States); V. N. Du Le, Qiyin Fang, McMaster Univ. (Canada); Joe Fu-jiou Lo, Univ. of Michigan-Dearborn (United States)

During wound healing, tissue composition changes throughout the various phases of healing, including collagen deposition and remodeling. Type III collagen is produced soon after closure and reaches peak at the end of the proliferation phase, to be replaced by stronger type I collagen during wound remodeling. In this study, we construct a frequency domain fluorescence lifetime measurement system to monitor this collagen change by detecting their autofluorescence lifetimes in murine wound samples (5 mm wounds) up to three weeks post-wounding.

The system is composed with LED light source, silicon avalanche photodetectors, fiber reflectance probe and dichroic filters. The samples were excited by the ultraviolet light and emitted visible light signals. The emission lights were then divided by the dichroic and filters and detected by the photodetectors at 410 and 450 nm bands to distinguish between collagen and elastin in the tissue. The phase delay between the excitation light from LED and emission light from the samples can be used distinguish lifetimes of collagen types in the wound, and allow measurement of the ratio between collagen type I and III. Tissue histology using standard picosirius staining will also be done on tissue sections, providing an accurate collagen I/III ratio to compare to.

Our results showed that tissue lifetime increased after closure and peaked 2 weeks post-wounding, as type III collagen has longer lifetime. After 3 weeks tissue lifetime returned to the same level as unwounded skin, matching the trend seen in the histological staining.

**Conference 9328: Imaging, Manipulation, and
Analysis of Biomolecules, Cells, and Tissues XIII**

9328-64, Session PMon

Tomographic reconstruction of melanin structures of optical coherence tomography via the finite-difference time-domain simulation

Shi-Hao Huang, National Taiwan Univ. (Taiwan); Shiang-Jiu Wang, Snow. H Tseng, National Taiwan Univ (Taiwan)

Optical coherence tomography (OCT) provides high resolution, cross-sectional image of internal microstructure of biological tissue. We use the Finite-Difference Time-Domain method (FDTD) to analyze the data acquired by OCT, which can help us reconstruct the refractive index of the biological tissue. We calculate the refractive index tomography and try to match the simulation with the data acquired by OCT. Specifically, we try to reconstruct the structure of melanin, which has complex refractive indices and is the key component of human pigment system. The results indicate that better reconstruction can be achieved for homogenous sample, whereas the reconstruction is degraded for samples with fine structure or with complex interface. Simulation reconstruction shows structures of the Melanin that may be useful for biomedical optics applications.

9328-66, Session PMon

Monitor RNA synthesis in live cell nuclei by using two-photon excited fluorescence lifetime imaging microscopy

Xiao Peng, Danying Lin, Shenzhen Univ. (China); Yan Wang, Shenzhen Univ. (China) and Univ. at Buffalo (United States); Jing Qi, Wei Yan, Junle Qu, Shenzhen Univ. (China)

Probing of local molecular environment in cells is of significant value in creating a fundamental understanding of cellular processes and molecular profiles of diseases, as well as studying drug cell interactions. In order to investigate the dynamically changing in subcellular environment during RNA synthesis, we applied two-photon excited fluorescence lifetime imaging microscopy (FLIM) method to monitor the green fluorescent protein (GFP) fused nuclear protein ASF/SF2 or fibrillarin. The fluorescence lifetime of fluorophore is known to be in inverse correlation with a local refractive index, and thus fluorescence lifetimes of GFP fusions provide real-time information of the molecular environment of ASF/SF2-GFP or fibrillarin-GFP. The FLIM results showed continuous and significant fluctuations of fluorescence lifetimes of both types of fluorescent protein fusions in live HeLa cells under physiological conditions. The fluctuations of fluorescence lifetime values indicated the variations of activities of RNA polymerases. Moreover, treatment with pharmacological drugs inhibiting RNA polymerase activities led to irreversible decreases of fluorescence lifetime values. In summary, our study of FLIM imaging of GFP fusion proteins has provided a sensitive and real-time method to investigate RNA synthesis in live cell nuclei.

9328-69, Session PMon

Microscopic imaging of resin-bonded dentin using Cryo-FIB/TEM system

Turki A Bakhsh, King Abdulaziz University (Saudi Arabia)

Background and Objective:

Introduction of focused ion beam (FIB) for transmission electron microscopy (TEM) preparation had enhanced the understanding of materials interaction at nanoscale. However, this technique generates localized heat that may possibly have some effect on organic/vital structures during preparation of biological tissues. Therefore, the aim of this study was to

investigate the effect of milling with Cryogenic-FIB (C-FIB) on imaging the ultramorphological features of dentin-resin interface bonded in a tooth and compares the findings to a room-temperature FIB prepared specimens.

Methods:

After cylindrical dentin cavities (3 mm diameter ? 1.5 mm depth) were prepared on the occlusal surfaces of extracted, non-carious human premolar teeth, they were restored with Filtek Silorane adhesive/composite system (3M ESPE, USA). To investigate the ultra-morphological features of resin-dentin interface, the bonded specimens were divided into 2 groups based on the preparation technique; FIB at room temperature (NC-FIB), and with cryogenic cooling (C-FIB). Later, each group was examined under TEM.

Results:

The obtained sections by NC-FIB and C-FIB allowed spotting an abundance of scattered needle-like crystals above the resin-impregnated dentin. Unlike in NC-FIB, distinct collagen structures were clearly observed with C-FIB technique that is possibly due to the minimized effect of focused beam heating on dentin organic phase.

Conclusion:

Within the limitation of this in-vitro study, it could be concluded that combining FIB with cryogenic cooling had preserved the biological organic features of dentin. The presented cryogenic technique should be considered in future FIB/TEM studies involving biological substrates. This research was supported by King Abdulaziz University.

9328-23, Session 5

Characterization of connective tissue progenitors through phase contrast and multicolor fluorescence time-lapse microscopy

Edward Kwee, Cleveland Clinic Lerner Research Institute (United States) and Case Western Reserve Univ. (United States); Kimerly Powell, The Ohio State Univ. (United States); George Muschler, Cleveland Clinic Lerner Research Institute (United States)

Connective tissue progenitors (CTPs) are defined as the heterogeneous population of tissue resident stem and progenitor cells capable of proliferating and differentiating into connective tissue phenotypes. The prevalence and variation in clonal progeny of CTPs can be characterized using a colony formation assay. However, colony assays do not directly assess the characteristics of the colony founding CTP. We developed a large field of view, time lapse microscopy system with phase contrast and fluorescence capabilities that enables tracking from seeding through colony formation.

Cells derived from the trabecular surface of bone were prepared and seeded in an Ibidi-Ph+ chamber slide. Phase contrast images of the slide were obtained every hour using a DMI6000 Leica microscope, 10X objective, and Retiga 2000R camera. Cells were stained using fluorescent antibodies for multiple markers at the time of plating to determine marker expression on seeded cells and re-stained to determine expression on their progeny. Colonies were identified and characterized using automated image processing and analysis methods for colony area and percent cell marker expression. Following colony identification, the time lapse was reversed to identify and characterize the colony founding CTP according to morphology and marker expression. As a representative example, a CD73+ and CD90- CTP resulted in a colony with an area of 211367 square microns, 24.2% CD73 percent area expression, and 22.8% CD90 percent area expression.

This method can be used to study CTPs and other stem and progenitor cell populations to benefit point-of-care methods for assay and isolation in cell based therapies.

9328-24, Session 5

Subcellular imaging of mechanical and chemical properties using Brillouin and Raman microspectroscopies

Vladislav V. Yakovlev, Texas A&M Univ. (United States)

Brillouin microspectroscopy is a powerful tool for non-invasive elasticity-sensitive optical imaging. It is a unique technique, which allows simultaneous interrogation of sample's mechanical properties and provides optical level resolution. However, current applications are confined in imaging transparent samples. Recent advances in background-free Brillouin microspectroscopy allow investigators to imaging turbid samples without drastically lowering the image quality [1]. When utilizing the high numerical aperture objectives, sub-micron resolution (< 500 nm) could be approached, enabling sub-cellular imaging applications. In this study, we applied Brillouin spectroscopy on imaging single cells, including HeLa cells and healthy / diseased Red Blood Cells (RBC). The Brillouin spectra were obtained by a background free VIPA (virtually imaged phased array) spectrometer described in the previous report [1]. The two dimensional images were acquired. Simultaneous recording of Raman spectra allowed chemical and mechanical properties to be assessed.

1. Meng, Z., Traverso, A. J., & Yakovlev, V. V., *Optics express*, 2014, 22(5), 5410-5416.

9328-25, Session 5

Novel common path interferometer design for high-throughput widefield spectral imaging

Dushan N. Wadduwage, National Univ. of Singapore (Singapore) and Singapore-MIT Alliance for Research and Technology (Singapore); Vijay Raj Singh, SMART-Singapore MIT Alliance for Research & Technology (Singapore); Heejin Choi, Zahid Yaqoob, Massachusetts Institute of Technology (United States); Paul T. Matsudaira, National Univ. of Singapore (Singapore); Peter T. C. So, Massachusetts Institute of Technology (United States)

Fourier transform spectroscopy (FTS) is a powerful method for resolving complex spectra especially from unknown endogenous biological molecules. FTS can be operated in a wide field mode allowing its use with many high throughput, high content image cytometers. In FTS, an interferometer is introduced in the detection beam path for optical path difference (OPD) scanning and the Fourier transform of the OPD scan represents the spectrum of the light for each point. There are a number of limitations in existing wide field FTS designs. Michelson designs are often phase unstable due to its sensitivity to external vibration. Alternatively, designs based on Sagnac interferometer are very stable but requires sequential scanning over a large OPD range. Here we present a novel common-path interferometer design with the aim for full-field FTS measurement with similar phase stability as the Sagnac designs and with uniform OPD allowing strategic sampling of OPD values for spectral recovery. Our design is based on transmission (Tx) gratings for beam splitting and a prism assembly for OPD scanning. Being common-path this simple setup is highly stable and effectively captures precisely controlled OPD scans over a large FOV. Then the Fourier transform of the OPD scan is taken to recover the spectrum for each pixel in the FOV. We have successfully validated our design in calibration specimens with known spectra and in biological specimens labeled with multiple fluorophores.

9328-26, Session 5

Molecular constituents of colorectal cancer metastatic to the liver by imaging infrared spectroscopy

James V. Coe, Zhaomin Chen, Ran Li, The Ohio State Univ. (United States); Steven V Nystrom, Ohio State University (United States); Ryan Butke, Barrie Miller, Charles L. Hitchcock, Heather C. Allen, Stephen P. Povoski, Edward W. M. Martin Jr., The Ohio State Univ. (United States)

Infrared (IR) imaging spectroscopy of human liver tissue slices has been used to identify and characterize liver tumors without standard staining approaches. Liver tissue, containing different types of tumors, was surgically removed from consenting patients and frozen without formalin fixation or dehydration procedures, so that lipids and water remain in the tissues. IR imaging is performed on microtome liver tissue slices which display more structure in the amide I and II band regions than fixed tissues. IR metrics have been developed which address protein changes by virtue of 2nd derivative changes in the IR spectra of individual pixels which enables study of protein changes between tumor and nontumor regions. Someday such IR metrics may guide work on IR spectroscopic diagnostics on live patients in the operating room.

9328-27, Session 5

In vivo bioluminescence tomography based on multi-view projection and 3D surface reconstruction

Shuang Zhang, Northeastern Univ. (China); Kun Wang, Institute of Automation (China); Chengcai Leng, Nanchang Hangkong Univ. (China) and Institute of Automation (China); Kexin Deng, Insitute of Automation (China); Yifang Hu, Beijing Jiaotong Univ. (China); Jie Tian, Institute of Automation (China)

Bioluminescence tomography (BLT) is a powerful optical molecular imaging modality, which enables non-invasive real-time in vivo imaging as well as 3D quantitative analysis in preclinical studies. In order to solve the inverse problem and reconstruct inner light sources accurately, the prior structural information is commonly necessary and obtained from computed tomography (CT) or magnetic resonance imaging (MRI). This strategy requires expensive hybrid imaging system, complicated operation protocol and possible involvement of ionizing radiation. The overall robustness highly depends on the fusion accuracy between the optical and structural information.

In this study we presents a pure optical bioluminescence tomographic system (POBTS) and a novel BLT method based on multi-view projection acquisition and 3D surface reconstruction. The POBTS acquired a sparse set of white light surface images and bioluminescent images of a mouse. Then the white light images were applied to an approximate surface model to generate a high quality textured 3D surface reconstruction of the mouse. After that we integrated multi-view luminescent images based on the previous reconstruction, and applied an algorithm to calibrate and quantify the surface luminescent flux in 3D. Finally, the internal bioluminescence source reconstruction was achieved with this prior information.

Hep-G2 subcutaneous and orthotopic xenograft liver tumor mouse models were used to evaluate the performance of the new system and technique. Compared with the conventional hybrid optical-CT approach using the same inverse reconstruction method, the reconstruction accuracy of this technique was improved. The distance error between the actual and reconstructed internal source was decreased by 0.184 mm and 0.189 mm, respectively

**Conference 9328: Imaging, Manipulation, and
Analysis of Biomolecules, Cells, and Tissues XIII**

9328-28, Session 5

**Raman spectroscopy and chemometric
analysis of non-penetrating peripheral
nerve damage in swine: a tool for spectral
pathology of nerve disease**

Katherine E. Cilwa, Naval Medical Research Ctr. (United States); Tiffani Slaughter, Eric Elster, Uniformed Services Univ. of the Health Sciences (United States); Jonathan Forsberg, Nicole J. Crane, Naval Medical Research Ctr. (United States)

Over 30% of combat injuries involve peripheral nerve injury compared to only 3% in civilian trauma. In fact, nerve dysfunction is the second leading cause of long-term disability in injured service members and is present in 37% of upper limb injuries with disability. Identification and assessment of non-penetrating nerve injury would improve outcome and aid in therapeutic monitoring. We report the use of Raman spectroscopy as a non-invasive, non-destructive method for detection of nerve degeneration in intact nerves due to non-penetrating trauma. Nerve trauma was induced via compression and ischemia/reperfusion injury using a combat relevant swine tourniquet model (>3 hours ischemia). Seven days post-operatively, sciatic and femoral nerves were harvested and fixed in formalin. Control animals did not undergo compression/ischemia. Raman spectra of harvested nerves were collected using a fiberoptic probe with 3 mm spot size and 785 nm excitation. Data was preprocessed, including fluorescence background subtraction, and Raman metrics were determined using custom peak fitting MATLAB® scripts. The abilities of univariate and multivariate analysis methods to predict tissue state are compared. Injured nerves exhibited changes in Raman metrics, $p < 0.01$, indicative of 45% decreased myelin content and structural damage within nerves (44% increased protein disorder). Axonal and myelin degeneration, cell death and digestion, and inflammation of tourniquet samples were confirmed via histology. This study demonstrates the noninvasive ability of Raman spectroscopy to detect nerve degeneration associated with non-penetrating injury relevant to neurapraxic and axonometric injuries; future experiments will further explore the clinical utility of Raman spectroscopy to recognize neurologic injury.

9328-29, Session 5

**Comparison of linear (hyperspectral)
and nonlinear (pump-probe) absorption
microscopy of melanin**

Jesse W. Wilson, Sanghamitra Deb, Francisco E. Robles, Christopher P. Dall, Lejla Vajzovic, Gargi Vora, Duke Univ. (United States); Rebecca C. Stacy, Massachusetts Eye and Ear Infirmary (United States) and Massachusetts General Hospital (United States); Maria A. Selim, Prithvi Mruthyunjaya, Douglas S. Tyler, Martin C. Fischer, Warren S. Warren, Duke Univ. (United States)

Effective diagnosis and treatment of early-stage melanoma depends on finding biomarkers that gauge the potential for melanocytes to migrate and invade the surrounding tissue. A particularly interesting, optically-accessible biomarker is the melanin pigment itself. Depending on the complex interplay between a melanocyte's genes, gene expression, and interaction with the surrounding tissue, melanin can vary in terms of eumelanin/pheomelanin ratio, aggregation, metal ion content, etc. These variations typically result in subtle changes to the linear absorption spectrum. However, they can exhibit striking differences in excited state photodynamics. This nonlinear contrast is leveraged by femtosecond pump-probe microscopy, and has been demonstrated for melanoma-specific imaging contrast both in excised tissue slices and for in vivo imaging.

Here, we have performed a direct comparison between the linear

absorption spectra and pump-probe response of human melanins. We imaged unstained sections from a number of pigmented lesions from human cutaneous ($n=10$) and conjunctival ($n=5$) biopsies, with both linear hyperspectral absorption microscopy and nonlinear pump-probe microscopy. Image stacks from both modalities were coregistered, and principal component analysis of the absorption spectra and pump-probe responses were compared to assess the similarities and difference. Spatial heterogeneity in pigment was observed in 80% (12/15) of the pump-probe images, but only 27% (4/15) of the linear hyperspectral images. In conclusion, pump-probe is more sensitive to variations in melanin content, but it may be worth investigating whether hyperspectral imaging of unstained tissue sections has diagnostic value.

9328-30, Session 5

**Design of high resolution FT-IR
spectroscopic imaging instruments for
improved breast cancer detection (*Invited
Paper*)**

Rohith Reddy, Massachusetts General Hospital (United States) and Harvard Medical School (United States); David Mayerich, Univ. of Illinois at Urbana-Champaign (United States); Michael J. Walsh, Univ. of Illinois at Chicago (United States); Rohit Bhargava, Univ. of Illinois at Urbana-Champaign (United States)

Fourier transform infrared (FT-IR) spectroscopic imaging provides simultaneous chemically and spatially resolved information. Recent work has demonstrated that this spatially resolved chemical information from mid-infrared wavelengths can be utilized for automated determinations of pathologic state of biological specimens, like prostate or breast cancer tissue. Here, we present an optical model for propagation of light through an FT-IR spectroscopic imaging system and use this model to improve the design of existing imaging systems. We modify an existing FT-IR spectroscopic imaging system based on insights from the model to obtain significantly higher resolution and higher image quality while simultaneously retaining chemical contrast. We obtain high quality ex-vivo breast tissue imaging data and fine details in tissue morphology which were previously inaccessible from FT-IR spectroscopic imaging have now become available. We identify previously obscured tissue types by performing histological classification on breast cancer tissue. These features and based on bio-chemically derived spectral metrics (features) and can improve cancer detection accuracy. We present image classification results where classification of high-definition imaging results in a more accurate labelling of terminal ductal lobular units (TDLUs) which are obscured when using conventional FT-IR imaging. These results are compared to results from visible-light microscopic examination of chemically stained tissue. Results indicate that high-definition FT-IR imaging can provide information typically obtained from a variety of standard, clinically and diagnostically useful chemical stains all without the need for expensive and laborious chemical staining. Automated computer algorithms for breast cancer detection using high-definition FT-IR imaging data are also discussed.

9328-31, Session 5

**High-SNR static Fourier-transform imaging
spectrometer based on differential
structure**

Peng Jin, Shuai Shuai Zhu, Yu Zhang, Jie Lin, Harbin Institute of Technology (China)

Fourier-transform imaging spectrometers are rapidly developed due to their extensive use in industrial monitoring, target detection, and chemical identification. Static Fourier-transform imaging spectrometer

Conference 9328: Imaging, Manipulation, and Analysis of Biomolecules, Cells, and Tissues XIII

(SFIS) containing a birefringent interferometer is one of the most popular directions due to its inherent robustness. However, the SFIS suffers from its low achievable signal-to-noise ratio (SNR) because of the restriction of incident angle. Meanwhile, in applications, the SNR is perhaps the most important factor to determine the usefulness of an instrument. In this paper, we report here a Static Fourier-transform imaging spectrometer based on differential structure (SFIS-DS) in the 400-800nm wavelength range with a high SNR. As in electronic system, the differential structure can double optical efficiency and strongly restrain common mode error in the SFIS-DS. And the differential structure described here is also available for any instruments containing a birefringent interferometer. However, the drawback of the SFIS-DS is that the two images obtained by the two differential channels need precise registration which can be overcome by a sub-pixel spatial registration algorithm. The experimental results indicate the SFIS-DS can increase the SNR by no less than 40%.

9328-32, Session 5

Precise monitoring of chemical changes through localization analysis of dynamic spectra

Zachary J. Smith, UC Davis Medical Ctr. (United States); Marcos E. de Oliveira, Univ. Federal Fluminense (Brazil); Che-Wei Chang, Latevi S. Lawson, Florian Knorr, Univ. of California, Davis (United States); Renato E. de Araujo, Univ. Federal de Pernambuco (Brazil); Stephen M. Lane, Sebastian Wachsmann-Hogiu, Univ. of California, Davis (United States)

As a label-free technology, Raman spectroscopy holds the promise of monitoring real-time changes in living cells with minimal change to the cell's native systems. However, often chemical changes in a cell due to a dynamic process produce only very subtle changes in a Raman spectrum. Resolving these small changes presents a challenge to the study of dynamic processes. To overcome this, we have borrowed the technique of sub-diffraction localization from the particle-tracking field and applied it to spectroscopy. In our method we acquire a time-series of spectra from a dynamic system. We then fit individual peaks within each Raman spectrum to a Gaussian or Lorentzian profile and follow the heights, positions, and widths of these peaks in time to monitor the system's dynamics. Because the technique uses a priori knowledge of general spectral peak shapes, it can accurately measure peak locations even in very noisy spectra, implying that spectra acquired with high temporal resolution (short acquisition times) can be used. This method has significant promise in the general study of dynamic systems, such as the response of cells to drugs or stimuli, by Raman spectroscopy. We have validated the performance of this method using a variety of model systems, confirming the ability of the technique to monitor spectral changes with sub-wavenumber precision and sub-second temporal resolution. In particular, we have extracted detailed information about red blood cell damage, yeast cell behavior in an optical trap, and monitoring oxidation of chemical compounds. These and continuing results will be presented.

9328-67, Session 5

Label-free live cell measurement of nanoscale cellular architecture

Scott Gladstein, S. Thompson, Luay Almassalha, Greta Bauer, John E. Chandler, Yolanda Stypula-Cyrus, Hariharan Subramanian, Igal Szleifer, Vadim Backman, Northwestern Univ. (United States)

Partial Wave Spectroscopy (PWS) is a spectroscopic, light-scattering microscopy technique previously demonstrated to be sensitive to nanoscale structural disorder in the cell. PWS has been used for early cancer detection

in fixed cells. For the first time, we are demonstrating the use of PWS in live cells. With traditional PWS, fixation procedures alter the cellular structure that we are trying to measure. Live Cell PWS not only overcomes this issue, but also opens up PWS to new possibilities, such as studying biological processes on the nanoscale in real time. The PWS system uses low spatially coherent white light that illuminates the sample. The back scattered light is spectrally filtered and imaged onto a CCD. This produces an array of images, each at a specific wavelength. PWS measures the nanoscale disorder of intracellular architecture by calculating the root mean square (RMS) of the spectrum at each pixel. Within these RMS maps, we have been able to clearly visualize the nucleus in live HeLa cells without labeling. Our current research involves the identification of the macro molecules responsible for the generation of the nuclear signal. We expect that this signal is a unique source of information for different cell processes and mechanics correlated with cancer, necrosis, apoptosis, chromatin condensation, and cell cycle. Our preliminary data also includes a study of how the structural order is altered when cells are perturbed by treatment with drugs and homeostatic conditions, such as apoptotic induction, glycolytic inhibition, transcriptional induction and repression.

9328-33, Session 6

Parallel acquisition of Raman spectra from a 2-D multifocal array using a modulated multifocal detection scheme

Lingbo Kong, James W. Chan, Univ. of California, Davis (United States)

A major limitation of spontaneous Raman scattering is its intrinsically weak signals, which makes Raman analysis or imaging of biological specimens slow and impractical for many applications. To address this, we report the development of a novel modulated multifocal detection scheme for simultaneous acquisition of full Raman spectra from a 2-D $m \times n$ multifocal array. A spatial light modulator (SLM), or a pair of galvo-mirrors, is used to generate $m \times n$ laser foci. Raman signals generated within each focus are projected simultaneously into a spectrometer and detected by a CCD camera. The system can resolve the Raman spectra with no crosstalk along the vertical pixels of the CCD camera, e.g., along the entrance slit of the spectrometer. However, there is significant overlap of the spectra in the horizontal pixel direction, e.g., along the dispersion direction. By modulating the excitation multifocal array (illumination modulation) or the emitted Raman signal array (detection modulation), the superimposed Raman spectra of different multifocal patterns are collected. The individual Raman spectrum from each focus is then retrieved from the superimposed spectra using a post-acquisition data processing algorithm. This development leads to a significant improvement in the speed of acquiring Raman spectra. We discuss the application of this detection scheme for parallel analysis of individual cells with multifocus laser tweezers Raman spectroscopy (M-LTRS) and for rapid confocal hyperspectral Raman imaging.

9328-34, Session 8

Advanced flow cytometric analysis of nanoparticle targeting to rare leukemic stem cells in peripheral human blood in a defined model system (*Invited Paper*)

Christy L. Cooper, James F. Leary, Purdue Univ. (United States)

Leukemia stem cells are both stem-like and leukemic-like. This complicates their detection as rare circulating tumor cells in the peripheral blood of leukemia patients. Detection and targeting of rare circulating cancer stem cells presents particular challenges because there are serious consequences of mis-targeting normal stem-progenitor cells. Since leukemic stem cells are also resistant to standard chemotherapeutic regimens, new therapeutic

Conference 9328: Imaging, Manipulation, and Analysis of Biomolecules, Cells, and Tissues XIII

strategies need to be designed to kill the leukemic stem cells without killing normal stem cells. In these initial targeting studies we utilized a bioinformatics approach to design an antibody- fluorescent nanoparticle conjugate for targeting to these leukemic stem cells and to minimize targeting to normal stem-progenitor cells.

Multicolor flow cytometric analyses were performed on a BD FACS Aria III. Human leukemic stem cell-like cell RS4;11 (with putative immunophenotype CD133+/CD24+/-, CD34+/-, CD38+, CD10-/Flt3+) was spiked into normal hematopoietic stem-progenitor cells obtained from a "buffy coat" prep (with putative immunophenotype CD133-/CD34+/CD38-/CD10-/Flt3-) to be used as a model human leukemia patient. To analyze the model system, digital data mixtures of the two cell types were first created and assigned classifiers in order to create truth sets. ROC (Receiver Operating Characteristic) and multidimensional cluster analyses were used to evaluate the specificity and sensitivity of the immunophenotyping panel and for automated cell population identification, respectively. Costs of misclassification (false targeting) were also accounted for by this analysis scheme. Ultimately, this analysis scheme will be applied to use of nanoparticle-antibody conjugates at therapeutic doses for targeted killing of leukemia stem cells preferentially to normal stem-progenitor cells.

9328-35, Session 8

Combined LIBS-Raman for remote detection and characterization of biological samples

Aaron S. Anderson, Harshini Mukundan, Los Alamos National Lab. (United States); Rhonda E McInroy, Los Alamos National Laboratory (United States); Samuel Clegg, Los Alamos National Lab. (United States)

Laser-Induced Breakdown Spectroscopy (LIBS) and Raman Spectroscopy have rich histories in the analysis of a wide variety of samples, with LIBS having much more prominence in stand-off detection. In this presentation, we will report recent results from the remote LIBS and Raman analysis of samples of biological interest such as amino acids, small peptides, mono- and di-saccharides, and nucleic acids. The LIBS spectra were acquired under terrestrial and extra-terrestrial conditions, giving rise to some interesting differences. A library of spectra and peaks of interest was compiled, and was used to inform the analysis of more complex systems, such as dried bacterial spores and biofilms. We will present these results as well, along with some future applications, including the assembly of a combined LIBS/Raman spectroscopic system and stand-off detection in a variety of environments.

9328-36, Session 8

Wide-band signal based photo-acoustic imaging method using band-limited transducers

Meng Cao, Chen Zhu, Nanjing University (China); Jie Yuan, Nanjing Univ. (China); Sidan Du, Nanjing Univ (China); Xiaojun Liu, Nanjing Univ. (China); Guan Xu, Xueding Wang, Paul L. Carson, Univ. of Michigan Medical School (United States)

Photoacoustic tomography (PAT) of biological tissue offers potential advantages in distinguishing different structures according to their chemical composition. Medical photoacoustic (PA) imaging is characterized with nonionizing and noninvasive, presenting good soft tissue contrast with excellent spatial resolution. After a pulse laser irradiation, PA signals, which contains rich structural, chemical and functional information about the biological tissue, will be immediately generated. The frequency of PA signals covers the 1-50 MHz range. However, current band-limited ultrasound transducers can only receive and present a limited PA frequency range

which degrades the quality of rebuilt PA images. PA signals with a 1 MHz bandwidth can only provide approximately 1 mm spatial resolution since the velocity of sound in soft tissues is about 1.5mm/us. If the bandwidth can be increased to 50 MHz, approximately 0.02mm resolution can be achieved. Furthermore, PA signals are usually of low signal-to-noise ratio (SNR), which seriously deteriorates the image quality in PAT. We found that the accurate time between the laser pulse and the beginning of the PA signals is a random value. A multi-sample based adaptive approach is proposed to rebuild the original wideband PA signal using normal band-limited ultrasound transducers. With this method, we are capable of reconstructing a better spatial resolution PA image and reducing random noise dramatically. In addition, detail information that used to be buried in the background noise can be discovered. Both ex vivo and in vivo experiments are carried out to demonstrating the satisfactory image quality realized with this method.

9328-37, Session 8

Parallel flow cytometer using radiofrequency-tagged emission

Eric D. Diebold, Brandon W. Buckley, Claire Lifan Chen, Ata Mahjoubfar, Bahram Jalali, Univ. of California, Los Angeles (United States)

The key attribute of a high content screening technology is sample throughput. Modern flow cytometers are capable of processing more than 10,000 cells/second, but sampling individual wells from a plate at high throughput (>100,000 wells/day) using flow cytometry is still an unmet challenge. Here, we address these sample throughput shortcomings by introducing a new approach to parallel flow cytometry. We present the development of a parallel flow cytometer capable of simultaneously interrogating 4 independent samples using a single photomultiplier tube detector for each measured parameter. We measure multi-color fluorescence and scatter parameters of fluorescent beads and cells with shot noise limited sensitivity from 4 unique samples simultaneously at a throughput of approximately 10,000 events per second per flow channel. This system leverages a fluorescence microscopy analog of the orthogonal frequency domain multiplexing (OFDM) approach commonly used in wireless communication systems to perform conventional flow cytometry measurements on multiple flow channels in parallel. The use of OFDM approaches in parallel cytometry provides benefits in improving dynamic range, sensitivity, and reduction of channel crosstalk. This parallel approach to high-throughput flow cytometry offers high sample throughput without sacrificing the number of analyzed cells per sample, for example, when reduced sample volumes are used in a single flow channel to increase sample throughput. Applications of this technology in rare cell detection, drug discovery, and high content screening will be discussed.

9328-39, Session 8

Quantification of cell surface receptor expression in live tissue culture media using a dual-tracer stain and rinse approach

Xiaochun Xu, Lagnojita Sinha, Aparna Singh, Cynthia S. Yang, Jialing Xiang, Kenneth M. Tichauer, Illinois Institute of Technology (United States)

The existence of differential cell surface antigen expression between cancerous and healthy cells has been known for nearly half a century and in the last few decades our understanding of how these differences influence cancer growth and response to therapy has grown prodigiously. Despite this understanding, there remain no quantitative ways of monitoring cell surface receptor expression repeatedly in tissue culture as populations multiple or respond to therapy. We have developed a dual-tracer methodology with

Conference 9328: Imaging, Manipulation, and Analysis of Biomolecules, Cells, and Tissues XIII

a repeated rinse and image protocol to acquire tracer kinetics that can be used to quantify receptor expression. The approach employs a targeted fluorescent tracer, the signal from which is normalized mathematically to the retention of a simultaneously administered "untargeted" fluorescent tracer signal used to account for nonspecific retention of the targeted tracer. To test the dual-tracer approach, 0, 104, 105, and 106 live human glioma (U251) cells were mixed in 0.6% agarose and cell media and placed into a six-well plate to create a 3D microenvironment. Equal concentrations of both imaging agents were then added to the tops of the gels and rinsed off after 1 hour. Wells were imaged on a planar fluorescence imaging system (Pearl, LI-COR Biosciences, Lincoln, NE). Ten rinse and image cycles were repeated in succession to acquire the necessary dynamics to estimate receptor concentration from kinetic models. Results from these studies demonstrated a clear correlation between dual-tracer measured concentrations of epidermal growth factor receptor (targeted cell surface receptor that is associated with many cancer types) and cell number.

9328-40, Session 8

Non-linear optical measurements using a scanned, Bessel beam *(Invited Paper)*

Bradley B. Collier, Samir Awasthi, Deborah K. Lieu, James W. Chan, Univ. of California, Davis (United States)

In both clinical diagnostic and basic research applications, flow cytometry is an essential tool for the identification and purification of cells. Currently, flow cytometry relies heavily on exogenous fluorescent labels for analyzing cells; however, the presence of these labels can cause disruption of cellular function or even cell death. This may be acceptable for certain *ex vivo* applications, but for cells that will be transplanted into the body, label-free methods are needed to eliminate these issues. This is especially true of the growing field of regenerative medicine where specialized cells are needed for treating patients. Because the differentiation of stem cells into specific cell lineages is not an efficient process, cells need to be sorted prior to their use *in vivo* to eliminate unwanted cells.

Nonlinear optical (NLO) processes have been increasingly utilized in optical microscopy for label-free biochemical imaging because of their non-invasive, non-destructive capabilities. To demonstrate NLO processes as a new modality for flow cytometry, an optical system was developed for measuring NLO signals from particles in a microfluidic channel. To improve the excitation efficiency of NLO signals, a scanned Bessel beam was utilized to create a light-sheet across the channel. The system was tested by monitoring two-photon fluorescence from microbeads of different sizes. When compared to a Gaussian beam profile, the light sheet illumination generated stronger fluorescence from the particles and allowed for better discrimination between the different sized particles. These results lay the foundation for the future development of label-free NLO flow cytometry for cell sorting.

9328-41, Session 8

Progress on an implementation of MIFlowCyt in XML

Robert C. Leif, Stephanie H. Leif, Newport Instruments (United States)

Introduction: The International Society for Advancement of Cytometry (ISAC) Data Standards Task Force (DSTF) has created a standard for the Minimum Information about a Flow Cytometry Experiment (MIFlowCyt 1.0). The CytometryML schemas are based in part upon the Digital Imaging and Communication (DICOM) standard and are being extended and adapted to include MIFlowCyt, as well as to serve as a common standard for flow and image cytometry (digital microscopy).

Methods: The MIFlowCyt data-types were created, as previously, in XML Schema Definition Language (XSD) 1.1 or reused from CytometryML. Individual major elements of the MIFlowCyt schema were translated into

XML and filled with reasonable data.

Results: The differences in the amount of detail to be recorded for 1) users of standard techniques including data analysts and 2) others, such as method and device creators, laboratory and other managers, engineers, and regulatory specialists required that separate data-types be created to describe the instrument configuration and components. A substantial part of a means to describe a staining protocol has been developed.

Conclusions: The future use of structured XML tags and web technology should facilitate searching of experimental information, its presentation, and inclusion in structured research, clinical, and regulatory documents, as well as demonstrate in publications adherence to the MIFlowCyt standard. The use of CytometryML together with XML technology should also result in the textual and numeric data being published using web technology without any change in format.

9328-42, Session 8

Measuring oxygen tension modulation, induced by a new pre-radiotherapy therapeutic, in a mammary window chamber mouse model

Rachel L. Schafer, Arthur F. Gmitro, The Univ. of Arizona (United States)

Tumor regions under hypoxic or low oxygen conditions respond less effectively to many treatment regimens, including radiation therapy. A novel investigational therapeutic, NVX-108 (NuvOx Pharma), has been developed to increase delivery of oxygen through the use of a nano-emulsion of dodecafluoropentane. By raising pO₂ levels prior to delivering radiation, treatment effectiveness may be improved. To aid in evaluating the novel drug, oxygen tension was quantitatively measured, spatially and temporally, to record the effect of administering NVX-108 in an orthotopic mammary window chamber mouse model of breast cancer. The oxygen tension was measured through the use of an oxygen-sensitive coating, comprised of phosphorescent platinum porphyrin dye embedded in a polystyrene matrix. The coating, applied to the surface of the coverslip of the window chamber through spin coating, is placed in contact with the mammary fat pad to record the oxygenation status of the surface tissue layer. Prior to implantation of the window chamber, a tumor is grown in the SCID mouse model by injection of MDA-MB-231 cells into the mammary fat pad. Two-dimensional spatial distributions of the pO₂ levels were obtained through conversion of measured maps of phosphorescent lifetime. The resulting information on the spatial and temporal variation of the induced oxygen modulation will provide insight into the optimal timing between administration of NVX-108 and radiation treatment to provide the most effective treatment outcome.

9328-43, Session 8

Label-free cardiac contractility monitoring for drug screening applications based on compact high-speed lens-free imaging

Thomas Pauwelyn, Veerle Reumers, Geert Vanmeerbeeck, Richard Stahl, IMEC (Belgium); Stefan Janssens, KU Leuven, Dept of Cardiovascular Sciences (Belgium); Liesbet Lagae, IMEC (Belgium) and KU Leuven, Solid State Physics and Magnetism Section (Belgium); Dries Braeken, Andy Lambrechts, IMEC (Belgium)

Cardiotoxicity is the major reason leading to withdrawal of drugs from the market, despite rigorous toxicity testing during the drug development process. Existing safety screening techniques, often based on electrical (impedance) or optical (fluorescent microscopy) measurements, are too limited in throughput and are offering poor predictability of toxicity to

Conference 9328: Imaging, Manipulation, and Analysis of Biomolecules, Cells, and Tissues XIII

be applied on large numbers of compounds in the early stage of drug development.

We present a compact optical system for direct (label-free) monitoring of fast cell processes that enable low cost and high throughput drug screening. Our system is based on a high-speed lens-free in-line holographic microscope. When compared to a conventional microscope, the system combines adequate imaging resolution (approx. $4\mu\text{m}$) with a very large field-of-view (67.4mm^2) and high speed (300fps) to capture physical cell motion in real-time. This combination enables registration of cardiac contractility parameters such as cell contraction frequency and duration, or even quantification of conduction velocity, which is very challenging with existing techniques. The cost of the system is further reduced as the imaging hardware features neither lenses nor high-precision mechanical components. To complement the imaging hardware we have developed image processing software that can extract all the contractility parameters directly from the raw interference images.

We have evaluated our system using verapamil (100nM), a known L-type Ca^{2+} and hERG channel blocker. We found an increase in frequency (+22%), while the contraction strength was decreased by 24%, compared to baseline conditions. The conduction velocity was decreased from 61.4mm/s to 47.6mm/s . This outcome is supported by literature reports.

9328-44, Session 9

Optical cell cleaning with NIR femtosecond laser pulses

Aisada Uchugonova, Univ. des Saarlandes (Germany); Hans Georg Breunig, Univ. des Saarlandes (Germany) and JenLab GmbH (Germany); Ana Batista, Univ. des Saarlandes (Germany); Karsten König, Univ. des Saarlandes (Germany) and JenLab GmbH (Germany)

Femtosecond laser microscopes have been used as both micro and nanosurgery tools. The optical knock-out of undesired cells in multiplex cell clusters shall be further reported on in this study.

Femtosecond laser-induced cell death is beneficial due to the reduced collateral side effects and therefore can be used to selectively destroy target cells within monolayers, as well as within 3D tissues, all the while preserving cells of interest. This being an important application in stem cell research and cancer treatment.

Non-precise damage compromises the cell viability of neighboring cells by inducing side effects such as stress to the cells surrounding the target due to the changes in the microenvironment, resulting from both the laser and laser-exposed cells.

In this study, optimum laser parameters for optical cleaning by isolating single cells and cell colonies are exploited through the use of automated software control. Physiological equilibrium and cellular responses to the laser induced damages are also investigated.

Cell death dependence on laser focus, determination and selectivity of intensity/dosage, controllable damage and cell recovery mechanisms were studied.

9328-45, Session 9

Dynamics of cell and tissue growth acquired by means of 25mm^2 to 10cm^2 lensfree imaging

Fabien Momey, CEA Grenoble (France); Jean-Guillaume Coutard, MINATEC (France); Thomas Bordy, Fabrice P. Navarro Y Garcia, CEA-LETI (France); Mathilde Menneteau, Jean-Marc Dinten, Cédric Allier, MINATEC (France)

In this paper, we discuss a new methodology based on lensfree imaging to perform wound healing assay with unprecedented statistics. Our video lensfree microscopy setup is a simple optical system featuring only a CMOS sensor and a semi coherent illumination system. Yet it is a powerful mean for the real-time monitoring of cultivated cells. It presents several key advantages, e.g. integration into standard incubator, compatibility with standard cell culture protocol, simplicity and ease of use. It can perform the follow-up in a large field of view (25mm^2) of several crucial parameters during the culture of cells i.e. their motility, their proliferation rate or their death. Consequently the setup can gather large statistics both in space and time. But in the case of tissue growth experiments, the field of view of 25mm^2 remains not sufficient and results can be biased depending on the position of the device with respect to the recipient of the cell culture. Hence, to conduct exhaustive wound healing assay, here we propose to enlarge the field of view up to 10cm^2 through two different approaches. The first method consists in performing a scan of the cell culture by moving the source/sensor couple and then stitch the stack of images. The second is to make an acquisition by scanning with a line scan camera. The two approaches are compared in term of resolution, complexity and acquisition time. Next we have performed acquisitions of wound healing assay (keratinocytes HaCaT) both in real-time (25mm^2) and in final point (10cm^2) to assess the combination of these two complementary modalities. In the future, we aim at combining directly super wide field of view acquisitions ($>10\text{cm}^2$) with real time ability inside the incubator.

9328-46, Session 9

Label-free analysis of single and multiple cells with a 2D light scattering static cytometer

Shanshan Liu, Linyan Xie, Shandong Univ. (China); Yan Yang, Shandong Univ (China); Xu Qiao, Kun Song, Shandong Univ. (China); Beihua Kong, Qilu Hospital of Shandong Univ. (China); Xuantao Su, Shandong Univ. (China)

Cytometry has wide applications in biomedicine for cell differentiation or disease monitoring. Conventionally, cells are labeled with different kinds of dyes and running through a flow chamber in a typical cytometer, fluorescence signals are then observed with a sensitive photodiode, a photo-multiplier tube, or an image sensor. The flow control and fluorescence measurements play key roles in conventional cytometry, however the hydrodynamics focusing technique and the fluorescence observation system are the main causes that current cytometers are expensive and complex to operate.

Here we report our newly developed two dimensional (2D) light scattering static cytometric technique for cell analysis. In contrast to flowing fluidics, we adopt a scanning fiber probe for single cell excitation. Laser beam from a monochromatic 532nm laser is coupled into a multimode fiber, which is inserted into a chip that is sandwiched with two glass slides to excite static cells. Two dimensional light scattering patterns are then observed with a complementary metal oxide semiconductor (CMOS) detector.

Experimental 2D light scattering patterns from static single and multiple yeast cells are obtained. Simulation of 2D light scattering patterns from cells is usually performed with finite-difference time-domain (FDTD) algorithm on supercomputers. Here we present 2D light scattering simulations from cells with our Mie theory based algorithm, which are in good agreement with the experimental ones. Our results show that the easy to operate, conveniently available, cost-less 2D light scattering static cytometry has the potential for label-free diagnostics of diseases at cellular level in clinics.

**Conference 9328: Imaging, Manipulation, and
Analysis of Biomolecules, Cells, and Tissues XIII**

9328-47, Session 9

**Microscope-on-chip: combining lens-free
microscopy with integrated photonics**

Richard Stahl, Dries Verduyck, Tom Claes, Geert Vanmeerbeeck, Vignesh Mukund, Roelof A. Jansen, Jeonghwan Song, Luis Hoffman, Xavier Rottenberg, Andy Lambrechts, Liesbet Lagae, IMEC (Belgium)

Lens-free in-line Holographic Microscopy (LHM) is a promising imaging technique for many biomedical and industrial applications. The main advantage of the technique is the simplicity of the imaging hardware, requiring no lenses nor high-precision mechanical components. Nevertheless, the LHM systems achieve high imaging performance only in combination with a high-quality and complex illumination. Furthermore, to achieve truly high-throughput imaging capabilities, many applications require a complete on-chip integration.

We demonstrate the strength, versatility and scalability of our integrated approach on two microscopes-on-chip instances that combine image sensor technologies with photonics (and micro-fluidics): a fully integrated Point-Source (PS) LHM module for in-flow cell inspection and Large Field-of-View (LFoV) microscope with on-chip photonic illumination for large-area imaging applications.

The proposed PS-LHM module consists of a photonic illumination, a micro-fluidic channel and an imager, integrated in a total volume smaller than 0.5 mm^3 . A low-loss single-mode photonic waveguide is adapted to generate a high-NA illumination spot. Experimental results show strong focusing capabilities and sufficient overall coupling efficiency. Current PS-LHM prototype reaches imaging resolution below 600nm.

Our LFoV-LHM system is extremely vertically compact as it consists of only a 1mm-thick illumination chip and a 3mm-thick imaging module. The illumination chip is based on fractal-layout phase-matched waveguides designed to generate multiple light sources that create a quasi-planar illumination wavefront over an area few square millimeter large. Current illumination prototype has active area of approximately $1.2 \times 1.2 \text{ mm}^2$. Our LFoV-LHM prototype reaches imaging resolution of 870nm using image sensor with 1.12um pixel pitch with maximum FoV of 12.2 mm^2 .

9328-48, Session 10

**System for tracking transplanted limbal
epithelial stem cells in the treatment of
corneal stem cell deficiency**

Joseph Boadi, The Univ. of Sheffield (United Kingdom); Virender S. Sangwan, LV Prasad Eye Institute (India); Sheila MacNeil, Stephen J. Matcher, The Univ. of Sheffield (United Kingdom)

The prevailing hypothesis for the existence and healing of the avascular corneal epithelium is that this layer of cells are continually produced by stem cells in the limbus and transported onto the cornea to mature into corneal epithelium. Limbal Stem Cell Deficiency (LSCD), in which the stem cell population is depleted, can lead to blindness. LSCD can be caused by chemical and thermal burns to the eye. A popular treatment, especially in emerging economies such as India, is the transplantation of limbal stem cells onto damaged limbus with hope of repopulating the region and hence regenerating the corneal epithelium. In order to gain insights into the success rates of this treatment, new imaging technologies are needed in order to track the transplanted cells.

Optical Coherence Tomography (OCT) is well known for its high resolution in vivo images of the retina. A custom OCT system has been built to image the corneal surface, to investigate the fate of transplanted limbal stem cells. We evaluate two methods to label and track transplanted cells: melanin labelling and magneto-labelling. To evaluate melanin labelling, stem cells are loaded with melanin and then transplanted onto a rabbit cornea denuded of

its epithelium. The melanin displays strongly enhanced backscatter relative to normal cells. To evaluate magneto-labelling the stem cells are loaded with magnetic nanoparticles (20-30nm in size) and then imaged with a custom-built, magneto-motive OCT system.

9328-49, Session 10

**Human oral mucosal epithelial cell sheets
imaging with high-resolution phase-
diversity homodyne OCT**

Naoko Senda, Kentaro Osawa, Hitachi, Ltd. (Japan)

There is a growing need for quality evaluation techniques of stem cells and regenerative tissues for development of regenerative medicine, which enable the stable supply of constant quality products. Conventionally, quality of regenerative tissues such as cell sheets is evaluated with invasive tests such as a histological stain of samples for examination, and there is a need for development of non-invasive tests to evaluate regenerative tissues for transplantation.

We demonstrated non-invasive imaging inside a living cell sheet of human oral mucosal epithelial cells, thickness of which is about 30-50 μm corresponding to 3-5 multilayered cells, by phase-diversity homodyne optical coherence tomography (OCT). The new method OCT developed in Hitachi enables cell imaging because of high resolution (axial resolution; $\sim 2.6 \mu\text{m}$, lateral resolution; $\sim 1 \mu\text{m}$, in the air), whereas conventional OCT was not used for cell imaging because of low resolution (10-20 μm). To achieve high resolution, we constructed a free-space interferometer including a phase-diversity detection system and high numerical aperture objective.

Nuclei inside a cell sheet were imaged with sufficient spatial resolution to identify each cell. The image showed good correlation with laser confocal microscopy observation of the cell sheet after fluorescence staining of the nuclei. The cell sheet was constructed by cell layers, and the size of cells depended on the layer, which varies according to degree of differentiation. Therefore, the imaging inside a cell sheet enabled evaluation of layered structure and differentiation. It suggested that the new method OCT could be useful for non-invasive cell sheet evaluation test.

9328-50, Session 11

**Using neural networks for high-speed
blood cell classification in a holographic-
microscopy flow-cytometry system**

Bendix Schneider, Univ. Gent (Belgium); Geert Vanmeerbeeck, Liesbet Lagae, Richard Stahl, IMEC (Belgium); Peter Bienstman, Univ. Gent (Belgium)

High-throughput cell sorting with flow cytometers is an important tool in modern clinical cell studies. Most cytometers use biomarkers that selectively bind to the cell, but induce significant changes in morphology and inner cell processes leading sometimes to its death. This makes label-based cell sorting schemes unsuitable for further investigation.

We propose a label-free technique that uses a digital inline holographic microscopy (DIHM) for cell imaging and an integrated, optical neural network for classification. Cells are flowing through a microfluidic channel and are illuminated by a laser point source (pinhole) from the top. The forward beam and the scattered light interfere at the channel's backplane where a detector array (CCD/gratings) is placed. A jet of steam bubbles controls the microfluidic channel's outlets. Each detector element forms an input node of the subsequent neural network. We use a feed-forward architecture consisting of one input, one hidden, and one output layer.

DIHM usually employs an image reconstruction algorithm before classification is carried out. Typically however, this reconstruction algorithm becomes the predominating time-limiting factor. As in our approach the neural network operates directly on the interference pattern, this

**Conference 9328: Imaging, Manipulation, and
Analysis of Biomolecules, Cells, and Tissues XIII**

reconstruction step is left out. The perspective of dense integration, together with a time-saving decision step makes our approach attractive for ultrafast, large-scale cell sorting. We tested our neural network on a binary classification task using real data. Monocytes and granulocytes were separated with more than 95% accuracy.

9328-51, Session 11

**High throughput cellular time-stretch
imaging on a spinning planar platform**

Anson H. L. Tang, Antony C. S. Chan, Yeung P., Belle S. M. Kwok, Barbara P. Chan, Edmund Y. Lam, Kenneth K. Y. Wong, Kevin K. Tsia, The Univ. of Hong Kong (Hong Kong, China)

Optical time-stretch imaging has recently emerged as a new imaging modality enabling ultrafast frame rate (>MHz) and is thus appealing to cellular assay applications which continually have the pressing need for scaling the measurement throughput. For example, it is proven to be an effective tool for single-cell suspension assay (e.g. imaging flow cytometry) at an unprecedented imaging throughput. However, time-stretch imaging is intrinsically incompatible with fluorescence detection, the retrieved data from individual cells typically lack the chemical-specific information, which is otherwise obtained through fluorescence labeling – a gold standard used in bioassays.

We report a new generation of time-stretch imaging, called asymmetric-detection time-stretch optical microscopy (ATOM) integrated with a rapid-spinning planar assay platform, based on a modified digital versatile disc (DVD), for high-throughput image-based cellular assays with the capability of direct ATOM read-out of chemical-specific information. Specifically, ATOM here captures high-resolution and high-contrast images of the selectively captured microparticles/cells on the spinning DVD (at ~ 3000 rpm, or the linear speed 3 – 18 m/s), which is functionalized for chemical-specific cell binding. As the targeted cell groups are selectively fixed at predefined spatial locations within the large-area functionalized DVD, chemical-specific information is directly obtained by ATOM without using fluorescence-labeling at an ultrahigh speed – a unique specification absent in time-stretch imaging flow cytometry. As a proof-of-concept demonstration, we employ this ultrafast technology, running at an ATOM line-scan rate of 20 MHz, to image the 3T3 fibroblast cells cultured directly on the DVD, and the streptavidin-linked beads which are selectively fixed on the DVD.

9328-52, Session 11

On tracking spinal disc cells

Katherine P. Dempsey, Ka Po Lam, James B. Richardson, Sharon Owen, Keele Univ. (United Kingdom)

This paper proposes combining the mean shift algorithm and advanced texture-based analysis to facilitate cells tracking in in vitro, time-lapsed microscopy over an extended time period. The effectiveness of this technique was examined in the context of unlabelled, phase contrast (PC) imaging with the goal to investigate the life cycle of back disc cells. Computationally, the typically low contrast PC image adds to the challenges of cell tracking, which is often compounded by the highly varying cell morphology. To accurately determine cell locations in successive time frames, the algorithm uniquely identified each cell by computing six textural features including contrast, smoothness and entropy. More significantly, such features were also used to estimate the number of vesicles detected within each cell by means of an unsupervised learning procedure. Preliminary results were compared to the Ground Truth (manually) constructed to facilitate benchmarking against existing tracking algorithms that were developed using the mean shift procedure. More importantly, our study took advantage of the 4-D spatiotemporal data captured in the experiments, enabling detailed examination of the phenotype of the vesicle containing cells with quantitative measurements of adherence, motility and

morphology. Crucially, this would facilitate characterisation of cell behaviour and thus perform enhance our understanding of the underlying cell biology.

9328-53, Session 11

**Fast and robust identification of single
bacteria in environmental matrices by
Raman spectroscopy**

Jean-Charles Baritoux, CEA-LETI (France); Emmanuelle Schultz, MINATEC (France); Anne-Catherine Simon, Anne-Gaelle Bourdat, Isabelle Espagnon, Patricia Laurent, Jean-Marc Dinten, Commissariat à l'Énergie Atomique (France)

We report on our recent results on robust identification of single bacterial cells by Spontaneous Raman Scattering. We investigated the robustness of identification with respect to growth conditions and environmental matrix. *B. Subtilis* and *E. Coli* were cultured either in Luria Broth or Trypticase Soy Broth at a Temperature of either 30°C or 37°C. The bacteria were then resuspended at concentrations ranging from 10^3 to 10^6 cells/uL in river water (Seine River), and water contaminated with airborne particles. The measurement system developed in our lab combines Lensfree imaging with Raman Spectroscopy. Lensfree imaging allowed fast detection of bacteria over a large Field-Of-View in the presence of contaminants. The beam of a 25mW Laser was then focused on single detected cells, and Raman scattered light was integrated for 10s by the high-throughput spectrometer of our instrument. This resulted in collected Raman spectra with a Signal-to-Noise-Ratio (defined as the ratio of standard deviation of the Raman peak at 1445cm^{-1} , to the standard deviation of the signal in the peak free region $1850\text{--}2500\text{cm}^{-1}$) of at least 10. A total of 720 spectra were acquired on contaminated samples, and 320 spectra were acquired in ideal conditions for reference. In 88.6% of the cases, a Support Vector Machine classifier robustly identified the bacteria measured in environmental matrices with the same species grown in ideal conditions. These results suggest that Spontaneous Raman Scattering is suitable for micro-organisms monitoring in difficult the conditions encountered during field operation.

9328-54, Session 11

**Effects of cholesterol depletion on
membrane nanostructure in MCF-7 cells by
atomic force microscopy**

Yuhua Wang, Ningcheng Jiang, Fujian Normal Univ. (China)

The cell membrane is composed of phospholipids, glycolipid, cholesterol and proteins that are dynamic and heterogeneous distributed in the bilayer structure and many researches have showed that the plasma membrane in eukaryotic cells contains microdomains termed "lipid raft" in which cholesterol, sphingolipid and specific membrane proteins are enriched. Cholesterol extraction induced lipid raft disruption is one of the most widely used methods for lipid raft research and M?CD is a type of solvent to extract the cholesterol from the cell membrane. In this study, the effect of M?CD treatment on the membrane nanostructure in MCF-7 living cells was investigated by atomic force microscopy. Different concentrations of M?CD were selected to deplete cholesterol and the morphology and nanostructure of the cell membrane were detected. The results show that different concentration of M?CD can all induce the alteration of the cell morphology. Even at low concentration (1.0 mg/ml) of M?CD, the roughness of membrane surface decrease significantly. This may indicate that the microdomains of the cell membrane disappear and the cell membrane appears more smoothly. Cholesterol can affect nanostructure and inhomogeneity of the plasma membrane in living cells.

9328-70, Session 11

**Frequency-domain fluorescence lifetime
imaging system (pco.flim) based on a in-
pixel dual tap control CMOS image sensor**

Robert Franke, Gerhard A Holst, PCO AG (Germany)

The luminescence lifetime as a beneficial analytical parameter is known for many years and well described by a large variety of publications. Many instruments including 2D measuring systems with cameras have been developed and applied in the past years. However, since the instrumentation to perform either time- or frequency-domain lifetime measurements is rather complex, new developments in CMOS image sensor technology achieved to create new image sensors, which can efficiently be used to create easier to handle for luminescence lifetime measuring systems. The principle of these modulatable CMOS image sensors, while initially designed for distance measurements, shows a clear analogy to frequency-domain FLIM measurements, which has been proven by researchers[1,2]. Based on this principle a new CMOS image sensor has been developed, integrated into a camera system and has been investigated within a research project.

The image sensor has a resolution of 1024 x 1024 pixels with a 5.6 μm pitch and can be modulated up to 50 MHz. The first measurements show an effective dynamic range of better than 1 : 1024 (corresponding to 10 bit dynamic). The frame rate is in the range of 90 double frames/s, which results in an effective frame rate for measurements of appr. 22 frames/s. The camera system pco.flim, which incorporates the sensor, generates all required modulation signals from 1 kHz to 50 MHz (sinusoidal and rectangular). It does all pixel correction to generate linear and high quality images, while the basic image processing is done in the computer. The modulation frequency can be freely adjusted and frequency sweep operation will be possible with up to 16 selectable frequencies.

The characteristics of the camera systems are presented, and first results are discussed with the help of the phasor approach[3], that has been established to provide a more global view to pixel-wise fluorescence lifetime data and compare time- and frequency-domain results. Based on these results and the experiences of the on-going tests, it can be expected, that the pco.flim will ease the introduction of luminescence lifetime imaging systems to broader applications. As supplement a modulatable laser diode has been developed, which is optimized to be used with the pco.flim camera system.

The work was supported by grants of the German Federal Ministry for Education and Research (BMBF) for the project "FLI-Cam" in the Biophotonik III program and the project "FLENDOS" in the Biophotonik IV program.

References: [1] H. Heß, et al., Proceedings Opto 2002, P7 (2002). [2] A. Esposito, et al., Optics Express, 13 (2005) 9812. [3] Michelle A. Digman, et al., Biophysical Journal: Biophysical Letters (2007) L14.

Conference 9329: Multiphoton Microscopy in the Biomedical Sciences XV

Sunday - Tuesday 8-10 February 2015

Part of Proceedings of SPIE Vol. 9329 Multiphoton Microscopy in the Biomedical Sciences XV

9329-1, Session 1

Some new directions for multiphoton processes and their biomedical applications (*Keynote Presentation*)

Paras N. Prasad, Univ. at Buffalo (United States)

No Abstract Available

9329-2, Session 1

Multiphoton microscopy in brain imaging (*Keynote Presentation*)

Anna Letizia Allegra Mascaro, Ludovico Silvestri, European Lab. for Non-linear Spectroscopy (Italy) and Natl. Inst. of Optics, Natl. Res. Council (INO-CNR) (Italy); Irene Costantini, European Lab. for Non-linear Spectroscopy (Italy); Leonardo Sacconi, European Lab. for Non-linear Spectroscopy (Italy) and Natl. Inst. of Optics, Natl. Res. Council (INO-CNR) (Italy); Bohumil Maco, Graham W Knott, Ecole Polytechnique Federale de Lausanne (Switzerland); Francesco S. Pavone, European Lab. for Non-linear Spectroscopy (Italy)

Brain Imaging is becoming an important field in the frame of the neurophotonics in correlations with other medical ones in neuroscience studying functional and morphological aspects.

In this presentation an overview on multi photon imaging of the brain will be presented, together with innovative aspects related to big area imaging and correlative microscopy approaches.

Multiphoton imaging applications will be described together with methods to improve the penetration depth and obtain large area detection, or correlating functional aspects in vivo on single neuron with large area, even on whole brain, morphological aspects. Connecting super resolution features at the nanometer level with micro, meso and macroscopic architectures is in fact one of the challenging aspects to understand brain functioning.

9329-3, Session 1

Fluorescence lifetime imaging: techniques and applications (*Keynote Presentation*)

Wolfgang Becker, Becker & Hickl GmbH (Germany)

The paper gives an overview on the commonly used FLIM techniques and their application to life sciences. Fluorescence lifetime imaging (FLIM) uses the fact that the fluorescence lifetime of a fluorophore depends on its molecular environment but not on its concentration. Molecular effects in biological systems can therefore be investigated independently of the variable, and usually unknown concentration of the fluorophore. FLIM techniques can be classified into time-domain and frequency-domain techniques, photon counting and analog techniques, and point-scanning and wide-field imaging techniques. It also matters whether a technique acquires the signal waveform in a few time gates or in a large number of time channels, and whether this happens simultaneously or sequentially. Virtually all these combinations are in use, leading to a wide variety of instrumental principles. Different principles differ in the number of photons required for a given lifetime accuracy, the acquisition time required to record

these photons, the photon flux they can be used at, their time resolution, their ability to resolve the parameters of multi-exponential decay functions, multi-wavelength capability, optical sectioning capability, and compatibility with different imaging and microscopy techniques. Typical applications of FLIM are protein interaction experiments by FRET, ion concentration measurements, and measurements of metabolic activity via the fluorescence decay parameters of NADH and FAD.

9329-4, Session 2

Fluorescence polarization and fluctuation analysis (FPFA): a method for simultaneously measuring fluorescence lifetime, time-resolved anisotropy, fluorophore concentration, molecular brightness, and lateral diffusion times (*Invited Paper*)

Tuan A. Nguyen, Jithesh V. Veetil, Pabak Sarkar, Steven S. Vogel, National Institutes of Health (United States)

Both Förster resonance energy transfer (FRET) and fluorescence correlation spectroscopy (FCS) can be used to study protein interactions and protein-complex conformational changes in living cells. FRET can detect the proximity between two fluorophores on a 1-10 nm scale. It can be measured by monitoring a change in the fluorescence lifetime of a FRET donor for Hetero-FRET, or by monitoring fluorescence anisotropy for Homo-FRET between two or more identical fluorophores. FCS can measure the concentration of a fluorophore in solution, molecular brightness (the number of fluorophores associated with a complex in solution), and the correlation time (an attribute sensitive to the mass and shape of a protein complex). We have developed a hybrid single-molecule method that simultaneously measures fluorescence lifetime (for Hetero-FRET measurements), time-resolved anisotropy (for Homo-FRET and rotational diffusion time measurements), and FCS (for measuring fluorophore concentration, molecular brightness, and lateral diffusion time measurements). This new form of spectroscopy is named Fluorescence Polarization and Fluctuation Analysis (FPFA). We will review how FPFA can be used to: 1) monitor protein-protein interactions, 2) detect conformational changes in a protein complex, 3) screen for mutations affecting protein complex assembly, and 4) monitor two independent FRET reactions simultaneously.

9329-5, Session 2

Recent advances in pattern matching based multi-species FLIM analysis (*Invited Paper*)

Benedikt Krämer, PicoQuant GmbH (Germany); Thomas Niehörster, Anna Löscherberger, Julius-Maximilians-Univ. Würzburg (Germany); Marcelle König, Paja Reisch, Matthias Patting, Felix Koberling, PicoQuant GmbH (Germany); Ingo Gregor, Georg-August-Univ. Göttingen (Germany); Markus Sauer, Julius-Maximilians-Univ. Würzburg (Germany); Rainer Erdmann, PicoQuant GmbH (Germany)

We already showed that the well established approach to separate different species in confocal microscopy by spectral deconvolution can be

**Conference 9329:
Multiphoton Microscopy in the Biomedical Sciences XV**

successfully transferred to fluorescence decays as an alternative to multi-exponential decay fitting and to the phasor analysis approach.

A quantitative decomposition of multicomponent FLIM data with a multi-exponential fitting approach can be time consuming and prone to errors if the lifetime decay patterns are complex (multi-exponential). We describe the complex single pixel decay with a linear combination of reference decays (patterns), which can be highly multi-exponential and do not have to be described itself mathematically. In a two step process we calculate analytically the individual amplitudes for the reference patterns followed by a re-iteration with MLE fitting. The low number of fitting parameters results finally in a faster analysis and a better signal to noise ratio in the analyzed images.

This procedure is now further sped up by a purely analytical vector projection based method.

We will compare the different approaches for multi-species FLIM analysis and present latest application examples also combining spectral and lifetime information for a multidimensional fluorescence pattern analysis.

9329-6, Session 2

Application of quantitative fluorescence imaging techniques for investigating intracellular interactions and dynamics of HIV-1 proteins

Yves Mely, Halina Anton, Nedal Taha, Marianna Sholokh, Salah El Meshri, Univ. de Strasbourg (France); Pascal Didier, Univ. of Strasbourg (France); Emmanuel Boutant, Ludovic Richert, Eleonore Real, Univ. de Strasbourg (France); Hugues de Rocquigny, Univ. of Strasbourg (France)

Quantitative imaging techniques, such as Fluorescence Lifetime Imaging Microscopy (FLIM), fluorescence recovery after photobleaching (FRAP), fluorescence correlation and cross-correlation spectroscopy (FCS and FCCS), and raster imaging correlation spectroscopy (RICS) are powerful tools to monitor the dynamics and interactions of proteins in live cells. We used these tools to monitor the intracellular fate of the nucleocapsid proteins (NCp7) of the Human immunodeficiency virus type 1 (HIV-1) that are likely released in the late steps of reverse transcription. We found that NCp7 localizes mainly in the cytoplasm and the nucleoli, where it binds and diffuses with ribosomal RNAs. The binding of NCp7 to ribosomes was further evidenced by the intracellular co-diffusion of NCp7 with a protein of the large ribosomal subunit. Moreover, micro-injection of NCp7 labeled by an environment sensitive probe together with the use of FLIM allowed us to confirm the nature of its cellular partners. We also investigated the assembly of the HIV-1 Gag polyproteins, which are the key proteins involved in the formation of new viral particles at the plasma membrane. Using fluorescently labeled Gag polyproteins, we have been able to monitor by FRET/FLIM techniques and time-laps microscopy the assembly process of Gag in cells. Oligomerisation of Gag molecules was found to be initiated in the cytoplasm. The dependence of the assembly process on the time and the Gag sequence was also investigated, which allowed us to draw a dynamic picture of Gag assembly in cells.

9329-7, Session 2

New dimensions in TCSPC FLIM: recording transient lifetime effects, spatial mosaics, simultaneous FLIM/PLIM

Hauke Studier, Wolfgang Becker, Becker & Hickl GmbH (Germany)

Time correlated single photon counting fluorescence lifetime imaging

(TCSPC FLIM) is based on the recording of multi-dimensional information of photons. These fluorescence photons are characterized by their times within the laser pulse period, and the coordinates of the laser spot in the scanning area in the moment when a photon was detected. A FLIM image is an array of pixels, each containing a full fluorescence decay curve in a large number of time bins [1]. In 64-bit environment, FLIM data can be measured with unprecedented numbers of pixels and time channels. More important, the FLIM data can be extended by additional dimensions without compromising the pixel numbers. These can be the wavelength of the fluorescence photons, or the wavelength of the laser pulse that excited the photon, the time from a stimulation of the sample, a time in the period of an additional modulation of the laser, or the distance along the Z axis [2]. We demonstrate the performance of 64-bit FLIM for imaging of transient fluorescence-lifetime phenomena, for Z stack FLIM, for multi-wavelength FLIM, and for simultaneous recording of FLIM and phosphorescence lifetime imaging (PLIM) [3].

1. W. Becker, The bh TCSPC Handbook. Becker & Hickl GmbH (2012), available on www.becker-hickl.com
2. H. Studier, W. Becker, Megapixel FLIM. Proc. SPIE 8948 (2014)
3. Wolfgang Becker, Bertram Su, Axel Bergmann, Klaus Weisshart, Oliver Holub, Simultaneous fluorescence and phosphorescence lifetime imaging. Proc. SPIE 7903 (2011)

9329-8, Session 2

Fiber-optic two-photon endomicroscopic fluorescence lifetime and fluorescence correlation spectroscopy imaging

Wenxuan Liang, Johns Hopkins Univ. (United States); Guanghan Meng, Shanghai Jiao Tong Univ. (China); Gunnsteinn Hall, Johns Hopkins Univ. (United States); Ming-Jun Li, Corning Incorporated (United States); Xingde Li, Johns Hopkins Univ. (United States)

Fluorescence lifetime imaging (FLIM) and fluorescence correlation spectroscopy (FCS) are valuable analytical tools for fundamental biomedical research as extensions to conventional intensity-based fluorescence microscopy. Translating these tools to in vivo animal model and clinical studies is largely limited due to the lack of access to internal organs by a standard microscope. An endomicroscopic implementation of these modalities is thus highly desirable. Herein we report the development of a versatile fiber-optic two-photon endomicroscopic system that is capable of performing both fluorescence lifetime and FCS imaging. With a series of technological innovations, the endomicroscope achieves high collection efficiency and low background noise, both of which are critical for accurate FLIM and FCS measurements. Initial experiments demonstrated that our system could evaluate fluorescence lifetime with subcellular resolution and a frame rate of ~3fps, on both stained and unstained biological tissues. Especially, through phasor lifetime analysis of NADH autofluorescence, in vivo cellular metabolic status can be potentially assessed; via measuring the change of donor fluorescence lifetime, Förster resonance energy transfer (FRET) can be realized to resolve molecular interactions. Furthermore, with imaging guidance, FCS measurement can be performed on any spots of interest. Initial FCS experiments using fluorescent beads solution showed that, through either single-point or scanning FCS approaches, our system could capture and differentiate an extended range of macroscopic flow rates in addition to the diffusion property of the beads, and these results reveal promising future applications for monitoring flow speed inside small vessels or renal microtubules.

**Conference 9329:
Multiphoton Microscopy in the Biomedical Sciences XV**

9329-9, Session 2

Observing conformational dynamics of single membrane transporters in a fast anti-Brownian electrokinetic trap

Bertram Su, Thomas Heitkamp, Universitätsklinikum Jena (Germany); Monika G. Düser, Nawid Zarrabi, Univ. Stuttgart (Germany); Michael Börsch, Friedrich-Schiller-Univ. Jena (Germany) and Abbe Ctr. of Photonics Jena (Germany)

To monitor conformational changes of individual membrane transporters in liposomes in real time, we attach two fluorophores to selected domains of a protein. Sequential distance changes between the dyes are recorded and analyzed by Förster resonance energy transfer (FRET). Using freely diffusing membrane proteins reconstituted in liposomes, observation times are limited by Brownian motion through the confocal detection volume. A. E. Cohen and W. E. Moerner have invented and built microfluidic devices to actively counteract Brownian motion of single nanoparticles in electrokinetic traps (ABELtrap). Here we present a version of an ABELtrap with a laser focus pattern generated by electro-optical beam deflectors and controlled by a programmable FPGA chip. This ABELtrap could hold single fluorescent nanobeads for more than 10 seconds, increasing the observation times of a single particle by a factor of 1000. Conformational changes of single FRET labeled membrane transporters (FoF1-ATP synthase) in the ABELtrap are presented.

9329-97, Session 2

Imaging of oxygenation in 3D tissue models with multi-modal phosphorescent probes

Dmitri B. Papkovsky, Ruslan Dmitriev, Univ. College Cork (Ireland); Sergey Borisov, Graz University of Technology (Austria)

Recently we have developed several new cell-penetrating phosphorescent probes - small molecule and nanoparticle based structures - which allow real-time, high-resolution imaging of O₂ concentration in respiring cells and tissues and detailed physiological studies with 3D tissue models. The probes can be used on standard imaging platforms and in different detection modalities, with preference to PLIM (Phosphorescence Lifetime Imaging) under one or two-photon excitation [1,2]. Their performance and utility of the O₂ imaging method have been demonstrated with 2D cell cultures, multi-cellular spheroids (from primary neurons and cancer cells), tissue slices and live animals. In the talk we will present the different probe structures and their use in imaging biological studies performed with several different in vitro and ex-vivo tissue models [2]. Examples include multi-parametric and functional imaging of cell cultures, multi-cellular spheroid samples and tissue slices, effects of hypoxic environment, drug action and metabolic stimulation on cell and tissue function, performed by one-photon confocal FLIM and by two-photon ratiometric intensity imaging.

1. Kondrashina AV et al, A phosphorescent nanoparticle based probe for sensing and imaging of (intra)cellular oxygen in multiple detection modalities, *Adv. Funct. Mater.*, 2012 Dec 5, 22(23), 4931-4939.
2. Dmitriev RI et al, Imaging oxygen in neural cell and tissue models by means of anionic cell-permeable phosphorescent nanoparticles *Cell. Mol. Life Sci.*, 2014, DOI 10.1007/s00018-014-1673-5

9329-10, Session 3

Cell metabolism, FLIM and PLIM and applications (Invited Paper)

Angelika C. Rueck, Sviatlana Kalinina, Univ. Ulm (Germany)

Cell metabolism, in detail energy metabolism of living cells and organisms is determined by the chemical reactions that provide energy for vital processes. Mainly two reactions, glycolysis and oxidative phosphorylation (OXPHOS) are the key players. It is well accepted that both reactions are correlated with the fluorescence lifetimes of NADH and FAD, which change in dependence on the relative contribution of glycolysis versus OXPHOS. The time resolved fluorescence characteristics of NADH and FAD are therefore achieving increased interest in fluorescence guided diagnosis of various diseases. However, as observed in a variety of investigations, the situation is complex and the result is influenced by other parameters like oxidative stress or tissue architecture. Thus fluorescence lifetime imaging (FLIM) of NADH and FAD does not always correlate with cell metabolism. Observation of a "negative" Warburg effect is just one example. Moreover, oxygen consumption has to be taken into account in order to understand the underlying mechanisms. Phosphorescence lifetime imaging (PLIM) is a new method to observe oxygen consumption.

Within this presentation the basic mechanisms and relations of FLIM, PLIM and cell metabolism will be discussed and clinically relevant applications will be demonstrated. This includes investigations on Alzheimers related disease, tumour diagnosis as well as Sepsis control.

9329-11, Session 3

Flavin fluorescence lifetime imaging of living peripheral blood mononuclear cells on micro and nano-structured surfaces

Tibor Teplicky, International Laser Ctr. (Slovakia) and Univ. of Ss. Cyril and Methodius (Slovakia); Julia Horilova, International Laser Ctr. (Slovakia) and Pavol Jozef Safarik Univ. (Slovakia); Jaroslav Bruncko, International Laser Ctr. (Slovakia); Cecile Gladine, Unité de Nutrition Humaine, Clermont Univ., Univ. d'Auvergne (France); Ingrid Lajdova, Slovak Medical Univ. (Slovakia); Anton Mateasik, Dusan Chorvat Jr., Alzbeta Marcek Chorvatova, International Laser Ctr. (Slovakia)

Fabricated micro and nano-structured surfaces were evaluated for use with living cells. Metabolic state of living peripheral blood mononuclear cells (PBMC) was tested by means of endogenous flavin fluorescence. PBMC were positioned on a coverslip, non-covered, or covered with micro or nano-structured surfaces (polymer coating, or ZnO layers). Polymer coating was achieved by 2-photon photopolymerisation of OrmoComp (Micro Resist Technology GmbH by laser microFAB workstation by Newport with Spirit ultrafast amplified laser, 520nm). Different micro-structures created by 3D photopolymerisation were tested. The ZnO layer, in the form of densely arranged and uniformly distributed nanocolumnar crystals, was fabricated on the half of the coverslip by pulsed laser deposition (Pulsed Nd:YAG laser Quanta Ray at 355 nm, 10 Hz repetition frequency, 20 ns pulse length, laser fluence 2.8 J.cm⁻²; a sintered ZnO target was ablated in the reaction chamber at 5 Pa of O₂ for 20 minutes; the thickness of ZnO layer was approx. 300 nm). Confocal microscopy (LSM 510 META, Zeiss, excitation at 488nm) and Fluorescence Lifetime Imaging Microscopy (FLIM, HPM 100-40 detector, BDL-475 laser and SPC-830 TCSPC board, Becker & Hickl) were employed to gather images of flavin fluorescence of living PBMC on micro or nano-structured surfaces. We recorded for the first time flavin fluorescence lifetime images of PBMC in control conditions. Gathered data are the first step towards monitoring of the interaction of different micro/nano-surfaces and/or micro/nano-structures with living cells and thus evaluation of their potential applicability in the biomedical field. Supported by LASERLAB-EUROPE III 7FP grant n°284464, ERDF OPRD project Competence Center for SMART Techn. for Electr. and Inform. Systems and Services, ITMS 26240220072, APVV-0242-11 and APVV SK-FR-2013-0020.

**Conference 9329:
Multiphoton Microscopy in the Biomedical Sciences XV**

9329-12, Session 3

Characterization of porcine eyes based on autofluorescence lifetime imaging

Ana Batista, Univ. de Coimbra (Portugal) and Saarland Univ. (Germany); Hans Georg Breunig, Univ. des Saarlandes (Germany) and JenLab GmbH (Germany); Aisada Uchugonova, Univ. des Saarlandes (Germany); António Miguel Morgado, Univ. de Coimbra (Portugal); Karsten König, Univ. des Saarlandes (Germany) and JenLab GmbH (Germany)

Multiphoton microscopy is of high interest in ophthalmology. Its feasibility has already been demonstrated ex-vivo, in the human cornea, and in-vivo, in the retina of small animals. We aim to image and characterize ex-vivo the porcine cornea, lens, and retina, based on their autofluorescence, using two-photon excitation laser systems.

Freshly enucleated porcine eyes were obtained from the local slaughterhouse. The cornea, lens, and retina were dissected and placed on glass bottom petri dishes. Live cell imaging solution was used to keep the samples hydrated during image acquisition. Samples were imaged using a laser-scanning microscope, consisting of a broadband sub-15fs NIR laser with a 16-channel PMT detector for signal collection, and the commercially available tomograph, MPTflex (JenLab GmbH, Jena, Germany). For a better discrimination of tissues' intrinsic fluorophores with 16-channel PMT detection, the reconstructed spectra of NADH, FAD, and Collagen type I, obtained using the amount of photons detected in each channel, was compared with the fluorescence spectra acquired with a spectrometer.

Two-photon excitation allows ex-vivo imaging of porcine cornea, lens, and retina at multiple depths. Anatomical differences were observed in autofluorescence intensity images. Different autofluorescence lifetime distributions were measured between cornea, lens, and retina and between different structures of the same tissue.

9329-13, Session 3

Time-resolved anisotropy imaging with a single detector

Vladislav I. Shcheslavskiy, Wolfgang Becker, Becker & Hickl GmbH (Germany)

Time-resolved anisotropy measurements play a key role in investigations of the protein-protein interactions, receptor-ligand binding, microviscosity in liquids and polymers. Time-resolved measurements of anisotropy are in general difficult because the differences between intensity of the different polarization components are small compared to the absolute values of these components itself. Since parallel and perpendicular components are detected with different efficiencies, normal anisotropy measurements require calibration of the efficiency in two detection channels. Moreover, often a different IRF of both channels has to be taken into account. In this paper, we investigate a new configuration for time-resolved anisotropy measurements. Instead of using analyzers in front of the detectors, we modulate the polarization of the beam incident on the sample with liquid crystal polarization rotator. The recording of the decay curves is synchronized with the modulation, so that the measured curves correspond to different rotation angles. Synchronization is achieved by using a digital angle signal from the rotator as a routing signal. For analysis of the anisotropy decay curves we have implemented an approach based on moments. This approach has not been used so far for analysis of time-resolved anisotropy experiments. In addition to fast calculation of the curves, it has an advantage, that it is not limited to exponential anisotropy decays. This simple and cheap experimental configuration based on Becker & Hickl DCS-120 confocal scanner does not require neither the measurement of the relative efficiencies, nor IRF since the measurements are done with a single detector and anisotropy decay analysis is performed by moments method.

9329-14, Session 3

Time-resolved spectral imaging: better photon economy, higher accuracy

Farzad Fereidouni, Univ. of California, Davis (United States); Keimpe Reitsma, Micro-Key BV (Netherlands); Gerhard A. Blab, Hans C. Gerritsen, Utrecht Univ. (Netherlands)

Lifetime and spectral imaging are complementary techniques that offer a noninvasive solution for monitoring metabolic processes, identifying biochemical compounds, and characterizing their interactions in biological tissues, among other tasks. Newly developed instruments that perform time-resolved spectral imaging can provide even more information and reach higher sensitivity than either modality alone. Here we report a multispectral lifetime imaging system based on a field-programmable gate array (FPGA), capable of operating at high photon count rates (12 MHz) per spectral detection channel, and with time resolution of 200 ps. We performed error analyses to investigate the effect of gate width and spectral-channel width on the accuracy of estimated lifetimes and spectral width.

Temporal and spectral phasors were used for analysis of recorded data, and we demonstrated blind un-mixing of the fluorescent components using information from both modalities. Fractional intensities, spectra, and decay curves of components were extracted without need for prior information. We further tested this approach with fluorescently doubly-labeled DNA, and demonstrated its suitability for accurately estimating FRET efficiency in the presence of either non-interacting or interacting donor molecules.

9329-15, Session 3

TCSPC FLIM for clinical applications: technical solutions and first results

Alexander Jelzow, Wolfgang Becker, Becker & Hickl GmbH (Germany); Yoshihiko Katayama, Heidelberg Engineering GmbH (Germany); Karsten König, Univ. des Saarlandes (Germany); Dietrich Schweitzer, Friedrich-Schiller-Univ. Jena (Germany)

Clinical imaging by fluorescence techniques is an established tool of clinical diagnosis and research. Clinical imaging is usually restricted to the use of endogenous fluorophores present in the tissue. The excitation and emission spectra of these fluorophores are overlapping and poorly defined. Moreover, the apparent spectra are changed by variation in the relative concentration of fluorophores and by absorbers present in the tissue. Intensity images, even those with spectral resolution, therefore deliver very limited information on the state of the tissue.

A considerable improvement is obtained by recording fluorescence lifetime images (FLIM). The fluorescence lifetime measured by TCSPC is independent of the concentration, and independent of possible changes in the absorption in superficial tissue layers. Moreover, it delivers direct information on the configuration of endogenous fluorophores, on binding to proteins or lipids, on the redox state, and on other metabolic parameters.

We will describe the technical problems of clinical FLIM and their solutions, demonstrate the performance of existing systems for dermatology, ophthalmology and endoscopy, and present first results.

9329-16, Session 4

Smart 2PE (Invited Paper)

Alberto Diaspro, Istituto Italiano di Tecnologia (Italy) and Univ. degli Studi di Genova (Italy) and Nikon Imaging Ctr. at Fondazione Istituto Italiano di Tecnologia (Italy); Paolo

**Conference 9329:
Multiphoton Microscopy in the Biomedical Sciences XV**

Bianchini, Francesca Cella Zancchi, Marti Duocastella, Luca L. Lanzanò, Giuseppe Vicidomini, Istituto Italiano di Tecnologia (Italy)

A variety of unimaginable biological studies from a single cell to the tissue level, and even to whole animals were performed since the advent of 2PE microscopy. More recently, super-resolution microscopy approaches, coming up with unlimited spatial resolution, opened further possibilities in the observation and study of cellular processes. The coupling with 2PE microscopy provides an extraordinary extension of mutual possibilities. We will report about this in terms of both targeted and stochastic readout methods. The main value being in the access to 4D (x,y,z,t) information including the achievement of super-resolution within thick biological objects. Individual molecule localization (IML) implemented within selective plane illumination microscopy (SPIM) will be addressed on the way to 3D super resolution imaging in thick biological samples, exploiting non-linear photo-activation. The utilization of a single wavelength (SW) both for 2PE and fluorescence depletion will be considered. In order to further reduce the impact of the investigating beam on biological structures, gated 2PE-STED will be outlined. As well, a method for rapid access to 3D information, based on liquid lenses, will be treated. Within the variety of architectures presented, the coupling with atomic force microscopy (AFM) and nanoscale lithography will be touched on, too. So, 2PE becomes "smart" due to the high level of flexibility and adaptation to new experimental demands. As a conclusive comment, we believe that "smart" 2PE and related techniques can be considered as a mainstay of the modern nano-bio-photonics research milieu and a bright perspective in optical microscopy.

9329-17, Session 4

Deep two-photon microscopic imaging through brain tissue using the second singlet state from fluorescent agent
(Invited Paper)

Lingyan Shi, The City College of New York (United States)

In biological and biomedical studies, most of the events or functions occur in a complex tissue environment and ultimately need to be studied in preparations as intact as possible. Especially in brain research, optical imaging technique is still the only way to study neural tissues with sub-micrometer spatial resolution. Two photon (2P) microscopy has the advantages of deep tissue penetration and less photo-damage when compared with conventional microscope. To reach the highest tissue penetration depth in brain, both the pumping and emission wavelengths are desired to fall in the "tissue optical window" (650-950nm). Traditional 2P technique with first singlet (S1) excitation only allow the pumping wavelength lies in that range while the emission does not. The present study employed second singlet (S2) with 2P to achieve deep brain tissue penetration with both the emission and excitation falling in the therapeutic window. We imaged Chlorophyll ? (Chl ?) in a spinach leaf covered by fresh rat brain slices with wide band filter of 685±40nm and 525±35nm respectively. Our study shows that under 2P S2 excitation wavelength 800nm, strong emission peak of 685 nm of Chl ? under was obtained, and the imaging could reach as deep as 450 μm brain slices. This is the new study that applied 2P and S2 state technique with both the excitation and emission wavelengths fall in Therapeutic Window to investigate imaging depth on rat brain slices. It will be used for better quality images in future study on brain vasculature and neural tissue in vivo.

9329-18, Session 4

Next generation laser sources for non-linear imaging

Darryl McCoy, Coherent Scotland Ltd. (United Kingdom); Marco Arrigoni, Nigel Gallaher, Coherent, Inc. (United States)

The increasing diversity of applications and multi photon microscope configurations demands an equally adaptive ultrafast laser portfolio to meet the requirements for differing power, wavelength and peak power regimes.

Modern techniques in the neurosciences demand both higher performance, especially for imaging of calcium indicators such as GCaMP3, and also a second, simultaneous wavelength for photoactivation of opsins for optogenetics methods. New product developments from Coherent are presented which address these needs in both tuneable and fixed wavelength platforms.

Modern intravital techniques, such as for cancer research and embryology, additionally demand versatility and performance to not only enable excitation of both popular fluorescent markers, but also to empower label free techniques such as SHG, THG, CARS and endogenous fluorescence. Again we explore how flexibility can be attained through multiple tuneable wavelength outputs with add-on capabilities.

The end-game for many non-linear techniques is to not only explore complex biological problems, but to possibly deploy the methods into a clinical or preclinical setting for the wider benefit of society. We discuss the current challenges a laser company faces in targeting a set of laser parameters to successfully address these needs.

9329-19, Session 4

Latest advances in ultra-fast laser sources for multi photon microscopy

Phil Smith, Newport Corp. (United States)

The advent of compact, fully automated, and widely wavelength-tunable ultrafast oscillators has triggered an explosive growth in their use in a broad array of multiphoton imaging techniques. Over the past decade laser manufacturers have constantly improved the performance characteristics of these sources to meet the requirements of the user community. We will review the latest advances at Newport / Spectra-Physics in this field and discuss new ways of optimizing key parameters for efficient deep-tissue fluorescence generation, including turn-key, automated second order dispersion compensation that allows for optimization of the pulse width at the sample over a wide wavelength range, without compromising beam pointing and other critical beam parameters.

9329-20, Session 4

Two-photon excited fluorescence microendoscopic imaging using a GRIN lens

Wei Yan, Xiao Peng, Shenzhen Univ. (China); Danying Lin, Shenzhen Univ (China); Qi Wang, Jian Gao, Jie Zhou, Bing Yu, Junle Qu, Shenzhen Univ. (China); Hanben Niu, Shenzhen Univ (China)

With the rapid development of life science, there is an increasing demand for in vital fluorescence imaging for small animals. However, owing to the large size of objective lenses in traditional fluorescence microscopes have limited their applications mostly to superficial tissues. To overcome this disadvantage, the graded-index (GRIN) probes with small diameters can expand the capabilities of conventional microscopes to minimally invasive imaging of internal organs. Here, we presented the development of a fluorescence endoscopic imaging system using a graded-index (GRIN) lens of 1.15mm diameter and 7.65mm length. We also applied a pair of galvo mirrors to accomplish quick 2D scanning of the laser beam, and used a CCD camera to acquire the images. After calibration with fluorescent beads, the system has been applied to image intravital tumor as well as other biological samples. In conclusion, our system has provided a convenient method for in vital small animal imaging.

**Conference 9329:
Multiphoton Microscopy in the Biomedical Sciences XV**

9329-21, Session 4

Two-photon excited fluorescence emission from hemoglobin

Qiqi Sun, Yan Zeng, Wei Zhang, Hong Kong Univ. of Science and Technology (Hong Kong, China); Wei Zheng, Shenzhen Institute of Advanced Technology (China); Yi Luo, Univ. of Science and Technology of China (China); Jianan Qu, Hong Kong Univ. of Science and Technology (Hong Kong, China)

Hemoglobin, one of the most important proteins in blood, consisting of heme and globin in the red blood cell is responsible for oxygen transportation in all vertebrates. Recently, we discovered two-photon excited hemoglobin fluorescence and achieved label-free micro-vascular imaging based on the hemoglobin fluorescence. However, the mechanism of its fluorescence emission still remains unknown. In this work, we studied the two-photon excited fluorescence properties of heme/hemin (iron(II)/(III) protoporphyrin IX) and globin. We found that the hemoglobin fluorescence emission was mainly from heme while methemoglobin fluorescence was from both heme and globin. In details, we verified that fluorescence intensity of heme and hemoglobin was both quadratic dependent on the excitation power, which proved that the Soret band fluorescence of them were results of two photon excitation process. We further compared fluorescence properties of heme and hemoglobin, including two-photon action cross-section, spectrum and fluorescence lifetime. The similar spectral and temporal characteristics of heme and hemoglobin fluorescence provide strong evidence that heme is the dominant fluorophore in hemoglobin. Then we studied the fluorescence properties of heme, globin and methemoglobin, and found that the heme and globin had joint effect on the methemoglobin fluorescence. The results explain that fluorescence properties of heme and heme, hemoglobin and methemoglobin are very different with each other, which provide an opportunity to discriminate them. Finally, since heme is centrosymmetric molecule, the reason why Soret band fluorescence of heme and hemoglobin were not observed in single photon process in previous study could be due to the parity selection rule, meaning that the g-g transition allowed in two-photon process was forbidden in single photon process. The discovery of heme two-photon excited fluorescence may open a new window for heme biology research, since heme as a cofactor of hemoprotein has many functions including diatomic gases transportation, electron transfer and chemical catalysis.

9329-22, Session 4

In vivo pump-probe microscopy of melanoma: characterizing shifts in excited state photodynamics with respect to invasiveness

Jesse W. Wilson, Simone Degan, Christina S. Gainey, Christopher P. Dall, Sanghamitra Deb, Yasmine Tameze, Jennifer Zhang, Warren S. Warren, Duke Univ. (United States)

We report on the use of in vivo pump-probe microscopy to observe alterations in melanoma production associated with proliferation, invasiveness, and response to chemotherapy. We used a genetically-modified (BRAFV600E) mouse model of melanoma to assess whether the in vivo pump-probe response is altered in pigmented lesions that lack a functional copy of the tumor suppressor gene PTEN. We also compare the response of subpopulations of round and dendritic cells in these lesions. When comparing non-invasive (PTEN-competent) with invasive (PTEN-deficient) tumor models, we find that the pump-probe signature shifts in the same direction as when comparing dendritic and round cell morphology. In addition, we find that treatment with chemotherapeutics momentarily shifts the pump-probe signal to a less invasive signature. Our observations are consistent with a previous study's findings that within melanoma, the more

motile (invasive) cells tend to be more round and less dendritic.

The various factors that affect the pump-probe response of melanin, such as eumelanin/pheomelanin content, aggregation, metal ion content, and oxidation will be discussed. In addition, we will consider the optical intensity-dependence of melanin, and how the increased power required for episcopic detection (compared to transmission-mode imaging of thin tissue sections) affects interpretation of the pump-probe responses.

9329-73, Session PSun

Super resolution brain imaging by using a two-photon fluorescence microscopy with harmonic modulation

Szu-Yu Lee, National Taiwan Univ. (Taiwan); Chi-Kuang Sun, National Taiwan Univ. (Taiwan) and Academia Sinica (Taiwan) and Molecular Imaging Ctr. (Taiwan)

Discoveries in brain science progress fast thanks to the contributions of two-photon fluorescence microscopy (2PFM). However, 2PFM has the inferiority in spatial resolution due to the use of long-wavelength excitation laser when compared to confocal microscopy. To improve the diffraction-limited resolution of 2PFM without down-shifting excitation windows, we propose a novel super resolution 2PFM (s-2PFM), which imitates the cubic nature of three-photon fluorescence microscopy (3PFM) through the combination of saturated fluorescence excitation with 2PFM. From Taylor expansion, the power dependency of the saturated 2P fluorescence could be expanded into infinite polynomial terms. Higher order nonlinear terms mean the slimmer point spread functions in space, indicating improved resolution. By temporally setting a pure sinusoidal modulation (at ω) on the excitation laser and demodulate fluorescence signal at high harmonics ($2\omega, 3\omega, \dots$), we thus extract different orders of nonlinearity. Here we focus on the electronic third harmonic, which is equivalent to the 3P excitation effect. From the power dependency test with an exogenous dye, the measured slope of the electronic third harmonic is 3.19, consistent with our theoretical expectation. Thus the resulted super-resolution is also experimentally proved through imaging nanoparticles. Super resolution brain imaging by using this s-2PFM is first demonstrated ex vivo with cerebral vasculatures and neurons in a mouse brain up to a penetration depth of 340 μ m. Unlimited resolution improvement is possible based on even higher order demodulation. This technique could also be applied to any specimen with endogenous or exogenous contrast agents.

9329-74, Session PSun

Fiber based ultra-short pulse delivery for nonlinear spectroscopy and microscopy using high energy solitons

Sarah Saint-Jalm, Esben R. Andresen, Institut Fresnel (France); Abdelkrim Bendahmane, PhLAM (France); Alexandre Kudlinski, Lab. de Physique des Lasers, Atomes et Molécules (France); Hervé Rigneault, Institut Fresnel (France)

We present an approach to fiber-delivery of tunable femtosecond pulses for nonlinear spectroscopy and microscopy. The nonlinear signals we wish to detect require high peak powers in the focal volume, therefore the pulses should be Fourier-transform-limited (FTL). Most of the existing fiber delivery techniques rely on complex pre-compensation systems to counteract the dispersion and the nonlinearities of the fiber that distort and temporally broaden the pulse.

In our setup, we generate a high-energy soliton by launching an 800 nm pulse from a Ti:Sapphire laser into a custom-built solid-core photonic bandgap fiber. The soliton is intrinsically FTL at the fiber output due to the balance between anomalous dispersion and Kerr nonlinearity responsible for

**Conference 9329:
Multiphoton Microscopy in the Biomedical Sciences XV**

soliton dynamics. Moreover, the properties of the soliton allow us to tune its wavelength and delay by changing the power at the input of the fiber.

We implemented our fiber-delivery system in the most prevalent nonlinear microscopy modalities: two-photon excitation fluorescence (TPEF), second-harmonic generation (SHG), coherent anti-Stokes scattering (CARS), stimulated Raman scattering (SRS), and pump-probe. We first took advantage of the short duration of the solitons to realize TPEF and SHG images of biological samples. By controlling the delay of the soliton, we then performed pump-probe experiments on absorbing samples such as ink and melanin. Finally, we used the wavelength tunability of the soliton to generate the Stokes beam in a coherent Raman scattering setup using the spectral focusing technique. We demonstrate the abilities of this scheme by performing CARS and SRS microspectroscopy to monitor a chemical equilibrium in aqueous solutions.

9329-75, Session PSun

Interferometric second harmonic generation imaging of biological tissues

Charles-André Couture, Maxime Rivard, Institut National de la Recherche Scientifique (Canada); Konstantin Popov, Univ. of Ottawa (Canada); Mathieu Laliberté, Anthony Bertrand-Grenier, Institut National de la Recherche Scientifique (Canada); Amir Miri, McGill Univ. (Canada); François Martin, Henri Pépin, Institut National de la Recherche Scientifique (Canada); Luc Mongeau, McGill Univ. (Canada); Christian Pfeffer, Ludwig-Maximilians-Univ. (Germany); Cameron Brown, Univ. of Oxford (United Kingdom); Lora Ramunno, Univ. of Ottawa (Canada); François Légaré, Institut National de la Recherche Scientifique (Canada)

Second harmonic generation (SHG) microscopy is used to image non-centrosymmetric structures. Some biological tissues, particularly those made of collagen, possess this property. Because this is a coherent technique, the structure of the studied sample influences greatly the generated signal strength. Hence, general alignment and organization of a sample can be evaluated. However, the phase of the signal, which contains additional structural information, is lost in the measurement.

In interferometric SHG (I-SHG) microscopy, second harmonic is generated a first time out of the microscope. This signal is then directed towards the imaging setup where it interferes with the second harmonic generated in the sample. By varying the phase relationship between the two second harmonic signals that are interfering, the relative phase of the second-order susceptibility in the tissue can be retrieved pixel by pixel or equivalently the relative orientation of the second harmonic emitters. In the case of biological tissues, this measurement can help to better understand the structure of the imaged tissues at the hundred microns level and relate it to its function and its evolution relative to disease and ageing.

We have used this technique to image myosin filaments in muscles, tendon and cartilage. In particular, the macroscopic structure of tendon, formed at the nanoscale of highly aligned type I collagen, will be compared with the macroscopic structure of cartilage, which is composed at the fibrillar level of a quasi random matrix of type II collagen.

9329-76, Session PSun

FRAP (fluorescence recovery after photobleaching) imaging using SLM-controlled doughnut spots

Yi Xue, Christopher J. Rowlands, Peter T. C. So, Massachusetts Institute of Technology (United States)

FRAP (Fluorescence Recovery After Photobleaching) is an important

method to measure protein lateral diffusion in single cells. We use a doughnut shape spot, familiar from STED super-resolution imaging, to photobleach a circular area outside a sub-diffraction limited center spot (<250nm). After photobleaching, the rate of enlargement of the center spot is related to the diffusing speed of proteins. Diffusers with smaller hydrodynamic radii or higher diffusion coefficients will lead to more rapid change of intensity. Super-resolution allows better characterization of slower diffusers and better quantification of spatial heterogeneity. Spatial-temporal correlation provides information on intercellular transport anisotropy and barrier. It is also possible to measure multiple locations in a cell using doughnut spots array. This parallel scanning combined with super-resolution technique yields a diffusion mapping system with quiet high throughput. The setup is simple using only one laser source and one phase-only SLM. The SLM works as a combination of vortex 0-2pi phase plate and phase grating, located conjugate to the back focal plane of the objective. In the focal plane, the phase grating decides the position of each focal spot and the vortex 0-2pi phase plate modulates every spot to doughnut shape. The use of SLM-based method further allows facile positioning of these doughnut spots in real time.

9329-77, Session PSun

New insights and system designs for temporally-focused multiphoton optogenetics

Tom Mayblum, Adi Schejter, Technion-Israel Institute of Technology (Israel); Hod Dana, Janelia Farm Research Campus, Howard Hughes Medical Institute (United States); Shy Shoham, Technion-Israel Institute of Technology (Israel)

It is widely accepted that cellular resolution optical stimulation and recording in three-dimensional, scattering tissue is highly challenging and can currently only be achieved using multiphoton optogenetics. However, this approach still faces fundamental challenges, in particular, in the attempt to achieve effective multiphoton excitation of large membrane patches while maintaining adequate optical-sectioning; Temporal focusing (TF) is often used as a powerful solution to this challenge. Here, we address two fundamental aspects in the design of TF multiphoton optogenetics systems: the design of TF systems with specific optical sectioning, and a solution for how to obtain TF in a flexible three-dimensional pattern.

First, to better understand the relation between the optical sectioning of a TF system and its design parameters, we comparatively examine different published approaches (analytical and numerical) and find their inter-relations and how to apply them in practice. Next, we introduce a powerful solution for three-dimensional TF, employing simultaneous spatio-temporal focusing (SSTF) in a unique optical system design. In our approach, SSTF is used to shape a focal spot that approximately fits the size of a target nerve cell in both the lateral and axial dimensions. Importantly, this new design can be seamlessly integrated into the optical path before essentially any multiphoton imaging or stimulation system, thus allowing easy switching between imaging and cell-targeted stimulation, as well as simultaneous holographic multi-spot stimulation.

9329-78, Session PSun

Effects of anesthesia on the cerebral capillary blood flow in young and old mice

Mohammad Moeini, Ecole Polytechnique de Montréal (Canada) and Montréal Heart Institute (Canada); Maryam S. Tabatabaei, Ecole Polytechnique de Montréal (Canada) and Montreal Heart Institute (Canada); Samuel Bélanger, Pramod Avti, Alexandre Castonguay, Philippe Pouliot, Frédéric Lesage, Ecole Polytechnique de Montréal

**Conference 9329:
Multiphoton Microscopy in the Biomedical Sciences XV**

(Canada) and Montréal Heart Institute (Canada)

Despite the possible role of age-related cerebral microvasculature changes in cognition decline, to our knowledge previous studies of capillary flow in aging are scarce and limited to anesthetized conditions. However, anesthesia can have different effects in young and old animals. To investigate this confounding effect in aging studies, we imaged the left barrel cortex of 4- and 24-month old ($n=3$, each) C57Bl/6 mice under anaesthetized (0.75% isoflurane) and awake conditions using two-photon microscopy. Animals received dextran-FITC injections through the tail vein and their head was restrained using an implanted head-plate. Excitation was achieved by a MaiTai-BB laser oscillator ($\lambda_{\text{ext}}=800\text{nm}$, 80MHz, 150fs) and the fluorescence was detected at 520nm using a photomultiplier tube. Randomly selected capillaries (Young-Awake: $n=45$, Young-Anesthetized: $n=52$, Old-Awake: $n=32$ and Old-Anesthetized: $n=33$) were scanned perpendicularly (to measure the capillary diameter) and longitudinally (to measure the red blood cell (RBC) speed and flux). Hematocrit was calculated from the RBC flux, speed and capillary diameter. In the young animals, capillary diameter increased from 3.73 ± 0.09 to $3.94\pm 0.07\mu\text{m}$ (close to significant, $p=0.068$), hematocrit decreased from 35.0 ± 2.7 to $29.0\pm 1.6\%$ ($p=0.048$) and RBC speed showed a decreasing trend from 0.94 ± 0.10 to $0.82\pm 0.07\text{mm/s}$ with anesthesia. On the other hand, in the old animals the capillary diameter (4.08 ± 0.11 (awake) and $4.06\pm 0.10\mu\text{m}$ (anesthetized)) and RBC speed (1.04 ± 0.15 (awake) and $1.03\pm 0.09\text{mm/s}$ (anesthetized)) remained unchanged with these animal numbers and hematocrit showed only a trend of decrease from 27.3 ± 2.7 to $25.4\pm 1.8\%$ with anesthesia. In both young and old animals, RBC flux tended to increase slightly with anesthesia.

9329-79, Session PSun

Determination of the spectral dependence of reduced scattering and quantitative SHG imaging for detection of fibrillar changes in ovarian cancer

Kirby R. Campbell, Karissa B. Tilbury, Paul J. Campagnola, Univ. of Wisconsin-Madison (United States)

Here, we examine ovarian cancer extracellular matrix (ECM) modification by measuring the wavelength dependence of optical scattering measurements and quantitative second-harmonic generation (SHG) imaging metrics in the range of 800-1100 nm in order to determine fibrillar changes in ex vivo normal ovary, type I, and type II ovarian cancers. Mass fractals of the collagen fiber structure is analyzed based on a power law correlation function using spectral dependence measurements of the reduced scattering coefficient μ_s' where the mass fractal dimension is related to the power. Values of μ_s' are measured using independent methods of determining the values of μ_s and g by on-axis attenuation measurements using the Beer-Lambert Law and by fitting the angular distribution of scattering to the Henyey-Greenstein phase function, respectively. Quantitative spectral SHG imaging on the same tissues determines FSHG/BSHG creation ratios related to size and harmophore distributions. Both techniques probe fibril packing order, but the optical scattering probes structures of sizes from about 50-2000 nm where SHG imaging—although only able to resolve individual fibers—builds contrast from the assembly of fibrils. Our findings suggest that type I ovarian tumor structure has the most ordered collagen fibers followed by normal ovary then type II tumors showing the least order.

9329-80, Session PSun

Quantitative metabolic imaging captures cellular heterogeneity in head and neck cancer organoids

Amy T. Shah, Alex J. Walsh, Melissa C. Skala, Vanderbilt Univ. (United States)

About 650,000 cases of head and neck squamous cell carcinoma (HNSCC) are diagnosed each year worldwide. Drug therapies include the antibody cetuximab and the chemotherapy cisplatin, but 40% of patients do not respond to treatments. New oncology drugs are being approved, and the identification of optimal drug regimens for individual patients could improve patient outcomes. Tumor tissue can be excised, digested, and grown in culture (organoids), and these organoids mimic in vivo microenvironment conditions. Anti-cancer drugs often affect cellular metabolism, including the autofluorescent metabolic cofactors NADH and FAD. The optical redox ratio (fluorescence intensity of NADH divided by FAD) reflects relative rates of glycolysis and oxidative phosphorylation. The fluorescence lifetime reports on protein-binding of NADH and FAD. Additionally, high-resolution two-photon microscopy enables cellular-level analysis, which can be used to visualize changes in cellular heterogeneity after treatment.

This study measures the autofluorescence intensities and lifetimes from NADH and FAD in HNSCC organoids after treatment with cetuximab, cisplatin, and their combination. Preliminary results indicate shifts in the redox ratio and protein-binding of FAD in organoids after two days of treatment ($p<0.05$), agreeing with tumor size decreases after nine days of treatment ($p<0.05$). Although the protein-binding of NADH does not change after two days of cetuximab treatment, the distribution of cells shows shifts in two distinct cellular sub-populations. The visualization of changes in cellular heterogeneity after treatment could identify treatment-resistant cell subpopulations and aid in treatment planning. Overall, optical metabolic imaging combined with HNSCC organoids could predict optimal treatment regimens for HNSCC patients.

9329-81, Session PSun

A modular two-photon microscope for simultaneous imaging of distant cortical areas in vivo

Fabian F. Voigt, Jerry L. Chen, Roland Krueppel, Fritjof Helmchen, Univ. Zürich (Switzerland)

Within the past decades, two-photon microscopy has been established as a powerful method to study neuronal morphology and activity in vivo. The spatial scale of calcium imaging with cellular resolution is, however, still limited to field-of-views (FOV) typically less than 0.5 mm across. As a first step to extend the spatial reach of two-photon microscopy beyond activity patterns in local circuits, we have designed and built a modular two-photon microscope for imaging multiple cortical areas in awake, behaving mice with a maximum FOV of 2 mm. Within this FOV, the user can select smaller sub-areas (two in the current configuration) for fast imaging which can be positioned independently in x and y. Additionally, each sub-area can be focused individually by an electrically tunable lens over a z-range of up to 550 μm . The scan system consists of a single pair of galvanometric mirrors and positioning systems, which send multiple laser beams onto the scan mirrors, each directed at one sub-area. To discriminate the fluorescence signal from each sub-area we use a spatiotemporal multiplexing approach. The microscope allows simultaneous activity measurements in layer 2/3 of the barrel field in primary somatosensory cortex (S1) and secondary somatosensory cortex (S2) in mice performing a texture discrimination task. The ability to record activity with cellular resolution in two reciprocally connected cortical areas across much larger spatial scales than previously possible should help to decipher the behavior-dependent flow of information within the neocortex.

9329-82, Session PSun

Fluorescence lifetime imaging in the near-infrared region

Wolfgang Becker, Vladislav I. Shcheslavskiy, Becker & Hickl GmbH (Germany)

**Conference 9329:
Multiphoton Microscopy in the Biomedical Sciences XV**

Fluorophores emitting in the near-infrared region are used as markers in diffuse optical tomography and small-animal imaging. For these applications, it is important to know how the fluorescence lifetime depends on the binding target and on the local molecular environment on the cell level.

Moreover, lifetime variation due to variable local molecular environment may be exploitable as a probe function [7, 8]. Another advantage of NIR probes is that there is no contamination from autofluorescence. Moreover, light propagation through biological tissue at infrared wavelengths is less impaired by scattering and absorption than in the visible range. We have recently shown that even one-photon excitation and confocal detection in the NIR yields surprisingly clear images from tissue layers up to 50 μ m deep. It can be expected that the penetration depth is further enhanced by two-photon excitation and non-descanned detection. For the experiments described here we used a Zeiss LSM 7MP with OPO excitation [9] and a bh Simple Tau 150 TCSPC FLIM system. To obtain sensitivity in a wavelength range up to 900 nm the HPM-100-40 GaAsP hybrid detector of the FLIM system was replaced with an HPM-100-50 GaAs hybrid detector. The detector was attached to the NDD port of the microscope via a Zeiss T adapter. To be able to detect fluorescence up to 900 nm we replaced the standard two-photon beamsplitter in the beam path at the back of the objective lens with a 980 nm dichroic mirror. The beamsplitter is not critical, an 80/20 wideband beamsplitter can be used as well. The standard 700 nm short pass (laser blocking) filter in the T adapter was replaced with a 980 nm short pass filter. The microscope objective lens was an x20/1.0 DIC VIS-IR Plan-Apochromate for water immersion.

9329-83, Session PSun

False positives in SRS imaging of lipid droplets: identification and reduction

Xuesong Li, Wen Jiun Lam, Yan Hao, Qiqi Sun, Sicong He, Yan Zeng, Ho Yi Mak, Jianan Qu, Hong Kong Univ. of Science and Technology (Hong Kong, China)

Lipid droplets (LDs), the hubs of lipid metabolism, are highly conserved organelles where fat storage and metabolism are regulated. Quantitative measurement of LDs' distribution and content are critical for understanding how cellular fat storage is regulated under physiological and pathological conditions, including obesity and related metabolic diseases. Stimulated Raman scattering (SRS) microscopy is a promising tool to produce the unique information on cellular lipids without exogenous labels. However, the common SRS technique lacks spectral resolution. As a result, the chemical specificity cannot be ensured and false LDs features appear in SRS image. In this study, we investigated LDs at the subcellular level in *C. elegans* using multimodal nonlinear optical (NLO) microscopy techniques. Specifically, we developed a unique NLO microscope system for LDs characterization. The system can sequentially excite and probe the stimulated Raman scattering-induced CH₃ stretching of proteins/lipids information (2950 cm⁻¹), third harmonic generation (THG) signals from regions of optical heterogeneity, two-photon excited fluorescence (TPEF) of tryptophan from the proteins and TPEF signal of GFP. We examined the SRS, THG and TPEF signals in live *C. elegans* where LDs were marked by a GFP fusion protein. We found that THG reveals cellular LDs which are densely packed, leading to strong third-order susceptibilities. In addition, the tryptophan fluorescence signal was used for identifying the protein-rich granules that produced false LDs-like features in the SRS image. Combining time-resolved two-photon fluorescence technique, GFP and autofluorescent lysosome-related organelles (LROs) could be distinguished accurately and GFP signals were used to positively identify the LDs. Integration of all information from our multimodal system allowed us to identify true LDs in *C. elegans* and reject false positives. Our results indicate that THG and tryptophan fluorescence provides important morphological and biochemical information to improve the chemical specificity of SRS.

9329-84, Session PSun

Classification and recognition of texture collagen obtaining by multiphoton microscope with neural network analysis tool

Shulian Wu, Hui Li, Xiaoman Zhang, Fujian Normal Univ. (China); Yudian Huang, Pathology Department of the Fuzhou First Hospital Affiliated to Fujian Medical University (China)

Second harmonic generation microscopy (SHGM) was used to monitor the process of chronological aging skin in vivo. The collagen structures of mice model with different ages were obtained using SHGM. Then, texture feature with contrast, correlation and entropy were extracted and analyzed using the gray level co-occurrence matrix. This analysis aims to detect the object hidden in the collagen texture in aging skin. At last, the neural network tool of Matlab was applied to train the texture of collagen in different statuses during the aging process. And the simulation of mice collagen texture was carried out. The results indicated that the classification accuracy reach 90%. Results demonstrated that the proposed approach effectively detected the target object in the collagen texture image during the chronological aging process and the analysis tool based on neural network applied the skin of classification and feature extraction method is feasible.

9329-85, Session PSun

Improvement of the spatial resolution in multiphoton microscopy by saturated excitation of fluorescence

Anh Dung Nguyen, François Duport, Univ. Libre de Bruxelles (Belgium); Frédérique Vanholsbeeck, The Univ. of Auckland (New Zealand); Philippe Emplit, Serge Goldman, Simon-Pierre Gorza, Univ. Libre de Bruxelles (Belgium)

Over the last decades, various techniques have been proposed to improve the spatial resolution and break the diffraction barrier in optical microscope systems. In this context, we demonstrate, for the first time to the best of our knowledge, a significant resolution improvement in multiphoton microscopy using saturated excitation of fluorescence.

At high excitation intensity, saturation of the two-photon excitation probability of the fluorophore occurs and induces a strong nonlinear fluorescence response. Images can thus be produced by temporally modulating the excitation laser-intensity and demodulating high-order harmonics from the saturated fluorescence signal. The high-order harmonic frequencies, generated by the saturation of the fluorescence, appear at the peak of the laser excitation and thus carry structural information from a region smaller than the non-saturated excitation point spread function. Contrary to saturated excitation fluorescence in confocal microscopy, resolution improvement arises at the third order harmonic when the excitation comes from two-photon absorption.

We tested the technique on 200 nm fluorescent microspheres (Bangslabs, Dragon Green Microspheres (480,520)) by modulating a femtosecond laser (82 MHz repetition rate) at 17 kHz and demodulating the fluorescence signal at the fundamental, the second and the third order harmonics. Comparison of the images produced confirms the improvement of the spatial resolution when demodulating at the third harmonic. We also demonstrate that even better results are obtained when the appropriate linear combination of the signals at the first, second and third harmonic is used. Observations of biological samples are planned.

**Conference 9329:
Multiphoton Microscopy in the Biomedical Sciences XV**

9329-86, Session PSun

Quantitative 3D molecular cutaneous absorption in human skin using label free nonlinear microscopy

Xueqin Chen, Institut Fresnel (France); Sébastien Grégoire, Florian Formanek, Jean-Baptiste Galey, L'Oréal (France); Hervé Rigneault, Institut Fresnel (France)

Understanding the penetration mechanisms of drugs into human skin is a key issue in pharmaceutical and cosmetics research. Despite intense research in recent years [1], a label free and noninvasive method to provide a quantitative picture of the molecular diffusion and distribution in complex thick tissue in 3D, potentially for in vivo biomedical application, is currently lacking. Although SRS has been recently reported to image drug delivery into ex-vivo skin, the proposed approaches were not capable of providing unbiased concentration of active compounds. One of the reasons for this is that SRS signal is attenuated with increasing depth into the skin samples that preclude its linear relationship with molecular concentration.

To address this challenge, we designed a novel framework for imaging and reconstructing molecular concentration while penetrating within human skin. Our approach combines hyper-spectral coherent anti-Stokes Raman scattering (CARS) imaging and two-photon excited native fluorescence (TPEF), to provide 3D quantitative active compounds mapping together with detailed skin morphological identification with high resolution. Pivotal to this method is (1) the use of CARS non-resonant signal as a ruler to account for the loss of optical excitation and collection efficiencies, and (2) the use of deuterated molecules, to maximize chemical selectivity and minimize background.

With this, we report quantitative 3D time-lapse mapping of cosmetic active molecules within human skin. We demonstrate both intercellular and transcellular pathways for different active compounds, together with in-depth concentration profiles reflecting the detailed skin barrier architecture. This method provides an enabling platform for establishing functional activity of topically applied products.

9329-87, Session PSun

Statistical analysis on activation and photo-bleaching of step-wise multi-photon activation fluorescence of melanin

Zetong Gu, Zhenhua Lai, Xi Zhang, Northeastern Univ. (United States); Jihao Yin, Beihang Univ. (China); Charles A. DiMarzio, Northeastern Univ. (United States)

Melanin is regarded as the most enigmatic pigments/biopolymers found in most organisms. We have shown previously that melanin goes through a step-wise multi-photon absorption process after the fluorescence has been activated with high laser intensity. No melanin step-wise multi-photon activation fluorescence (SMPAF) can be obtained without the activation process. The step-wise multi-photon activation fluorescence has been observed to require less laser power than what would be expected from a non-linear optical process. In this paper, we examined the power dependence of the activation process of melanin SMPAF at 830nm and 920nm wavelengths. We have conducted research using varying the laser power to activate the melanin in a point-scanning mode for multi-photon microscopy. We recorded the fluorescence signals and position. We compared those images of confocal reflectance and bright field images which show the location of the melanin. A sequence of experiments indicates the relationship of activation to power, energy and time so that we can optimize the power level. Also we explored regional analysis of melanin to study the spatial relationship in SMPAF and define three types of regions which exhibit differences in the activation process.

9329-88, Session PSun

Apertureless confocal scanning microscopy under temporally controlled femtosecond pulse illumination

Dhiman Das, Soumendra N. Bandyopadhyaya, Debabrata Goswami, Indian Institute of Technology Kanpur (India)

We investigate the axial point spread function and optical sectioning capability of a commercial confocal scanning microscope for different pinhole diameters and numerical apertures. We find that the axial point spread function narrows with an increase in the numerical aperture of the objective lens and with a decrease in the pinhole diameter for the 488nm argon-ion laser. For the femtosecond laser, we show that resolution can be improved by temporal control of pulses. Since, the illumination intensity will be maximum at the focal plane of the objective lens, it is expected that most of the signal will originate from the focal plane and there is no need to use the confocal pinhole to reject the out-of-focus light. Use of high numerical aperture objective lens can serve this purpose. Scanning the focal point along the optical axis at different temporal delays between two pulses in an interferometry geometry allows us to attain similar resolution as obtained in conventional confocal microscopy. Thus we demonstrate aperture-free high resolution confocal-like microscopy with femtosecond pulse train. We can also induce and control two photon fluorescence by controlling the overlap zone for the pulse pair excitation to result in multi-photon processes.

9329-89, Session PSun

Multi-photon laser scanning omnidirectional imaging with tunable frame rate

Dapeng Zhang, Jiyi Cheng, Shih-Chi Chen, The Chinese Univ. of Hong Kong (Hong Kong, China)

We present a new imaging technique, i.e. Omnidirectional Imaging, that enables a laser scanning microscope to arbitrarily program the imaging plane. This new technique is integrated with our frame-rate tunable laser scanning microscope for real-time biological studies. Current microscopes typically run at a fixed frame rate with a flat imaging plane. However, all biological subjects are "3-dimensional (3-D)" in nature and various biological events, e.g. blood flow or neuron signaling, occur at different time scales. Accordingly, a versatile microscope with capabilities of frame-rate tuning and a 3-D programmable imaging plane is highly desirable. The frame-rate tuning function is achieved by a new synchronization circuit and related software development. We achieved ultra-high frame rates, i.e. 1000 - 10,000 fps, by trading off the imaging area, and thus at any frame rate, the "pixel dwell time" of the system remains constant, keeping a low signal-to-noise ratio. 3-D programmable imaging plane is achieved by the introduction of a high-speed piezoelectric objective scanner. During the in-plane (X-Y) raster scan procedure, the objective lens can be moved to any arbitrary position in the Z axis, thus enabling the "omnidirectional scan". These new functions will be used to investigate deep regions in brain in vivo and enable new studies that cannot be realized in the past. For example, we will follow neuron axons (not in a flat plane) in a mouse brain and identify their related neural circuits and simultaneously observe their signaling processes at 1000 fps. Detailed microscope design and biological experiments will be presented.

9329-90, Session PSun

High-resolution nonlinear ellipse rotation measurements for 3D microscopy

Lino Misoguti, Maria L. Miguez, Emerson C. Barbano, Sergio C. Zilio, Univ. de São Paulo (Brazil); Jorge Augusto

**Conference 9329:
Multiphoton Microscopy in the Biomedical Sciences XV**

Coura, Univ de São Paulo (Brazil)

Nonlinear optical effects have been widely explored for microscopy due to the possibility of three-dimension (3D) image acquisition. Recently we developed a new simple and sensitive method for measuring nonlinear ellipse rotation (NER) using a dual-phase lock-in amplifier, which could be successfully applied for measuring local nonlinearity distribution on a sample and, consequently, the 3D image acquisition. The NER is a particular refractive nonlinear effect which appears when strong elliptical polarized laser beam propagates along one nonlinear material. In isotropic medium the polarization rotation is proportional to the constant $B(n^2)$. The rotation of an elliptically polarized beam can be determined as a phase change in the modulated signal which can be easily measured by a dual phase lock-in amplifier. This method allows very high precision angle change measurements. As required for 3-D nonlinear image acquisition, we have used a tightly focused laser beam where the focal region (confocal parameter vs. beam waist) determines the dot size for the image resolution. It is a similar configuration used for two-photon absorption microscopy, for example. As prove of concept, we have used a sample composed by a glass capillary inside a cuvette with acetone and a standard computer controlled xyz translational stage to move the sample and a Ti:sapphire femtosecond laser as a light source. In comparison with harmonic generation nonlinear microscopy, this method has advantage of use only one wavelength with allows easily to choose the best transmission windows of a sample, for instance.

9329-91, Session PSun

Second Harmonic Generation quantitative measurements on collagen fibrils through correlation to electron microscopy

Stéphane Bancelin, Institut National de la Recherche Scientifique (Canada); Carole Aimé, Lab. de Chimie de la Matière Condensée de Paris (France); Ivan Gusachenko, Lab. d'Optique et Biosciences, Ecole Polytechnique (France); Laura Kowalczyk, Therapeutic Innovations (France); Gaël Latour, Lab. d'Optique et Biosciences, Institut d'Électronique Fondamentale (France); Thibaud Coradin, Lab. de Chimie de la Matière Condensée de Paris (France); Marie-Claire Schanne-Klein, Lab. d'Optique et Biosciences, Ecole Polytechnique (France)

Type I collagen is a major structural protein in mammals that shows highly structured macromolecular organizations specific to each tissue. This biopolymer is synthesized as triple helices, which self-assemble into fibrils (≈ 10 -300 nm) and further form various 3D organization. In recent years Second Harmonic Generation (SHG) microscopy has emerged as a powerful technique to probe in situ the fibrillar collagenous structure in tissues. However, this optical technique cannot resolve most of the fibrils and is a coherent process, which impedes quantitative measurements of the fibril diameter.

In this study, we correlated SHG microscopy with Transmission Electron Microscopy to determine the sensitivity of SHG microscopy and to calibrate SHG signals as a function of the fibril diameter in reconstructed collagen gels. To that end, we synthesized isolated fibrils with various diameters and successfully imaged the very same fibrils with both techniques, down to 30 nm diameter. We observed that SHG signals scaled as the fourth power of the fibril diameter, as expected from analytical and numerical calculations. This calibration was then applied to diabetic rat cornea in which we successfully recovered the diameter of hyperglycemia-induced fibrils in the Descemet's membrane without having to resolve them. Finally we derived the first hyperpolarizability from a single collagen triple helix which validates the bottom-up approach used to calculate the non-linear response at the fibrillar scale and denotes a parallel alignment of triple helices within the fibrils. These results represent a major step towards quantitative SHG imaging of nm-sized collagen fibrils.

9329-92, Session PSun

2D simultaneous spatial and temporal focusing multiphoton microscopy for fast volume imaging with improved sectioning ability

Qiyuan Song, Keio Univ. (Japan) and RIKEN (Japan); Keisuke Isobe, RIKEN (Japan); Kenichi Hirosawa, Keio Univ. (Japan); Katsumi Midorikawa, RIKEN (Japan); Fumihiko Kannari, Keio Univ. (Japan)

Simultaneous spatial and temporal focusing (SSTF) multiphoton microscopy offers us widefield imaging with sectioning ability. As extending the idea to 2D SSTF, people can utilize a 2D spectral disperser. In this study, we use a 2D spectral disperser via a virtually-imaged phased-array (VIPA) and a diffraction grating to fulfill the back aperture of objective lens with a spectrum matrix. This offers us an axial resolution enhanced around 1.7 times compared to SSTF microscopy. Furthermore, the small free spectral range (FSR) of VIPA will reduce the temporal self-imaging effect around out-of-focus region and thus reduce the out-of-focus multiphoton excited fluorescence (MPEF) signal of 2D SSTF microscopy. We experimentally show that inside a sample with dense MPEF, the contrast of the sectioning image is increased for our 2D SSTF microscope compared with SSTF microscope. In our microscope, we use a 1 kHz chirped amplification laser, a piezo stage and a sCMOS camera integrated with 2D SSTF to realize high speed volume imaging at a speed of 50 volumes per second as well as improved sectioning ability. Volume imaging of Brownian motions of fluorescent beads as small as 1 μ m has been demonstrated. Not only the lateral motion but also the axial motion could be traced.

9329-93, Session PSun

Optimizing laser and probe molecules for multi-photon microscopy

Mary J. Potasek, Gene Parilov, Karl Beeson, Simphotek Inc. (United States)

Multiple fluorescent probes (multi-dyes) and single or multi-laser configurations can significantly extend the applications and accuracy of microscopy. Multiple fluorescent probes enable the user to identify more than one target, but difficulties can arise due to overlapping spectral emissions of the different probes. In particular, spectral overlapping of fluorescent and/or phosphorescent emission signals can lead to incorrect analysis. We present a method to numerically calculate overlapping spectra. An accurate modeling tool would be valuable to predict the best laser-probes combinations for selection and screening stages.

We use a numerical method that simulates both time and space so that we can calculate on a near-instantaneous basis the absorption of laser light and electron populations. We can then calculate the intensity of the emitted signal and determine the overlap of the spectra. This is something that cannot be done using linear algebra.

9329-94, Session PSun

Motionless polarization-resolved second harmonic generation imaging of corneal collagen

Hans Georg Breunig, Ana Batista, Aisada Uchugonova, Univ. des Saarlandes (Germany); Karsten König, Univ. des Saarlandes (Germany) and JenLab GmbH (Germany)

There is a lack of imaging techniques which provide structural information on the corneal stroma in vivo. Second harmonic generation (SHG)

**Conference 9329:
Multiphoton Microscopy in the Biomedical Sciences XV**

microscopy makes that information available. However, structural features are generally only resolved in forward direction which is not accessible to in vivo imaging. We performed SHG microscopy to investigate the collagen domain orientation of ex vivo human cornea samples in forward and backward direction following an approach described by Latour et al. (Biomed. Opt. Exp. 3, 1 (2010)), which is based on a polarization resolved excitation. The ex vivo SHG imaging of human cornea samples is performed with motion-free polarization control employing a liquid-crystal retarder and sub-15 fs laser pulses. The suitability of the liquid-crystal retarder setup even for broadband fs pulses which allow for efficient low mean power application of only a few mW as a preparation for in vivo imaging is discussed.

9329-95, Session PSun

In vivo visualization of collagen fiber produced by cultured osteoblasts using sensitive second-harmonic-generation microscopy equipped with a 10-fs mode-locked Ti:sapphire laser

Eiji Hase, Katsuya Sato, Takeshi Yasui, Univ. of Tokushima (Japan)

Second-harmonic-generation (SHG) microscopy is a new tool for observing the collagen fiber in tissue in vivo. Although conventional SHG microscopy has been used in combination with a 100-fs pulse laser, it can not visualize low-order-structured, immature collagen fiber at high contrast (for example, collagen fiber produced by cultured cell) because of low nonlinear susceptibility $\chi^{(2)}$. One possible method to enhance the image contrast is use of a higher-power fs laser because the SHG light intensity indicates quadratic dependence on the average power of laser light; however, increase of the average power easily induces the photo-damage to the sample. To enhance the image contrast while avoiding the sample damage, one should increase a peak power of the laser light while maintaining the same average power as the 100-fs laser. In this paper, we constructed sensitive SHG microscopy equipped with a 10-fs Ti:Sapphire laser and applied it for in vivo visualization of collagen fiber produced by cultured osteoblasts. Since the pulse duration of the 10-fs laser is easily broadened by passing through optical components in the microscopy, we precisely compensated the group delay dispersion of them with a combination of negative-chirped mirror pair and a positive-chirped wedge prism pair. As a result, we achieved the pulse duration of 20 fs at the focal point of an objective lens. Furthermore, we succeeded to visualize collagen fibers produced by the cultured osteoblasts in vivo. Such sensitive SHG microscopy will be a powerful tool for investigating the quality of the cultured and/or regenerated tissues in bone tissue engineering.

9329-96, Session PSun

Modeling acousto-optic two-photon ophthalmoscopy in pseudophakic patients

Akos Kusnyerik, Semmelweis Univ. (Hungary); Balazs J. Rozsa, Institute of Experimental Medicine (Hungary); Pál Maák, Budapest Univ. of Technology and Economics (Hungary)

Our research group performs acousto-optic two-photon microscopy experiments in brain tissue in vivo in rodents. We transformed the optical models used for development of the custom acousto-optic microscope with world record parameters to simulate the acousto-optic device intended to investigate the human eye. In our previous publications we demonstrated the design of a coupling lens that together with the special acousto-optic scanning and focusing capabilities of the device allow the adaption to different eyes and astigmatism compensation.

In this paper we present the modeling results of operation of the acousto-

optic device in combination with pseudophakic eyes. The core of the modeling is an advanced optical eye model, where we replaced the crystalline lens with different type of IOLs. Importance of this approach is in the fact that functional retina investigation is often necessary in pseudophakic patients. Moreover the parameters of the IOLs are well known and can be more precisely implemented in the model. This way the accuracy of the established model can be further improved by comparison with measurement results performed on eyes comprising known artificial lenses.

We recognized that two-photon microscopy has the potential to verify visual acuity of the pseudophakic patient. This verification is possible because of the subcellular optical resolution of the instrument-eye combination. The modeling results demonstrate that this method is also suitable to characterize the performance of multifocal IOLs. Over 30 kHz sampling rate combined with the acousto-optic driving flexibility avoids the motion artifacts and the need for adaptive optics.

9329-98, Session PSun

A freely triggerable 766nm laser with optimized performance for STED applications

Thomas Schönau, Dietmar Klemme, Marcelle König, Benedikt Krämer, Felix Koberling, Kristian Lauritsen, Rainer Erdmann, PicoQuant GmbH (Germany)

Efficient depletion in Stimulated Emission Depletion (STED) microscopy is a key factor for achieving highest resolutions. At the same time the intensity should be limited to minimize photobleaching or other destructive effects. Typical excitation laser pulses with a pulse width below 100 ps are temporally overlapped by the depletion pulse with a longer wavelength. This requires precise synchronization and matching pulse shapes. It has been shown, that the ideal depletion pulse has a pulse width in the order of a few hundreds of picoseconds up to one nanosecond.

We present an optimized 766 nm pulsed laser source based on gain-switching of a laser diode and generating sub-ns pulses. The freely triggerable seed laser is amplified in a two stage Erbium-doped fiber amplifier and subsequently frequency doubled in single pass configuration in periodically poled lithium niobate. The output beam quality is $M^2 < 1.1$ and linearly polarized with a PER > 20dB.

We will show first results based on a confocal microscope which was upgraded with an EASYDONut phaseplate to convert this STED laser beam into the required donut-shaped focal spot while leaving the co-aligned excitation beam unaffected. On the way towards suitable imaging conditions, various experimental modalities to minimize irreversible photobleaching and to improve photon statistics will be discussed. Different analysis methods based upon the photon arrival times are also compared in order to sharpen the images and to suppress unwanted contributions in addition to spectral filtering. Finally we present first FLIM-STED results which open the door towards multilabel STED.

9329-99, Session PSun

Sarcomere-length variations during sarcomeric assembly and maturation

Zhonghai Wang, Siyu Ma, Huaxiao Yang, Clemson Univ. (United States); Thomas K. Borg, The Medical Univ. of South Carolina (United States); Bruce Z. Gao, Clemson Univ. (United States)

Sarcomere is the fundamental contractile unit of cardiomyocytes. Sarcomeric length is an important determinant of the cardiac mechanical function. Results from many researches have shown that sarcomeric length in neonatal cardiomyocytes was slightly longer than that in adult cardiomyocytes. However, when and how the important change takes place during cardiomyocyte maturation remains elusive. Here we report the

**Conference 9329:
Multiphoton Microscopy in the Biomedical Sciences XV**

observation of sarcomere-length variations during sarcomeric assembly and maturation in an in-vitro neonatal rat ventricular cardiomyocyte (NVCM) culture model. NRVMs were dissociated from ventricles of three-day-old neonatal Sprague-Dawley rats using a two-day protocol and cultured on a patterned glass-bottom dish. Real time images were captured with our lab-built two photon excitation fluorescence (TPEF) and second harmonic generation (SHG) microscope. A 16X pulse splitter was introduced to the microscope to reduce photodamage and increase cell viability during imaging. Rapid scanning for single myofibril enabled dynamic observation of sarcomeric lengths during continuous cardiomyocyte beating. Images were processed with ImageJ software and sarcomeric lengths were measured with a self-developed semi-automatic Matlab program. Observation of cell morphology and sarcomeric structure development was achieved within the period of sarcomeric assembly and maturation. Results showed sarcomeric length in early stage of cell culture varied but stabilized significantly with shortened sarcomeric length in latter stage. These results exhibited a structural and functional development of sarcomeres during sarcomeric assembly and maturation, which might shed light on the mechanism of sarcomerogenesis and development of sarcomere related diseases.

9329-100, Session PSun

Adaptation of commercial microscopes for advanced imaging applications

Craig Brideau, Univ. of Calgary (Canada); Kelvin Poon, University of Calgary (Canada); Peter Stys, Univ. of Calgary (Canada)

Today's commercially available microscopes offer a wide array of options to accommodate common imaging experiments. Occasionally, an experimental goal will require an unusual light source, filter, or even irregular sample that is not compatible with existing equipment. In these situations the ability to modify an existing microscopy platform with custom accessories can greatly extend its utility and allow for experiments not possible with stock equipment. Light source conditioning/manipulation such as polarization, beam diameter or even custom source filtering can easily be added with bulk components. Custom and after-market detectors can be added to external ports using optical construction hardware and adapters. This paper will present various examples of modifications carried out on commercial microscopes to address both atypical imaging modalities and research needs. Violet and near-ultraviolet source adaptation, custom detection filtering, and laser beam conditioning and control modifications will be demonstrated. The availability of basic 'building block' parts will be discussed with respect to user safety, construction strategies, and ease of use.

9329-101, Session PSun

All fiber based, multi-color two photon excitation microscopy with an amplified laser diode

Sebastian Karpf, Matthias Eibl, Ludwig-Maximilians- Univ. München (Germany); Robert A. Huber, Ludwig-Maximilians- Univ. (Germany) and Univ. zu Lübeck (Germany)

We present a robust all fiber based laser source in the extended near infrared for two photon microscopy. The laser is based on a master oscillator fiber power amplifier (MOPA). The output of a narrowband CW 1064 nm laser diode is modulated with a 12 GHz electro-optic amplitude modulator. Sub-nanosecond pulses are generated and amplified up to kW of peak powers in an ytterbium doped fiber amplifier (YDFA). By Raman shifting the 1064 nm light in the fiber using a second 1122 nm laser diode for seeding, the output can be switched to 1122 nm and to 1186 nm. The shifting process is fully electronically controllable and allows for fast switching

between the excitation wavelengths while the initial pulse length and spectral width are maintained. The pulse length and modulation pattern can be chosen arbitrarily and through synchronized, time gated detection the signals can be multiplexed in time. On the one hand, this reduces noise from background light and on the other hand, it enables the straight forward implementation of multi-modal imaging modalities with a simple and reliable system. We show the characteristics of this excitation laser and present two photon excitation fluorescence (TPEF) images of plant leaves and algae acquired in epi-direction. This robust fiber laser makes it a good excitation source for future inexpensive non-linear microscopes and nonlinear imaging endoscopes.

9329-102, Session PSun

Laser scanning stereomicroscopy for fast volume imaging with two-photon excitation and scanned Bessel beams

Yanlong Yang, Xi'an Institute of Optics and Precision Mechanics (China); Runze Li, Xi'an Institute of Optics and Precision Mechanics?Chinese Academy of Sciences (China); Xing Zhou, Xi'an Institute of Optics and Precision Mechanics (China); Mark Van Horn, Department of Radiology and Radiological Science, Medical University of South Carolina (United States); Tong Peng, Di Wu, Xi'an Institute of Optics and Precision Mechanics?Chinese Academy of Sciences (China); Xun Chen, Clemson Univ (United States); Ming Lei, Baoli Yao, Xi'an Institute of Optics and Precision Mechanics?Chinese Academy of Sciences (China); Tong Ye, Clemson Univ. (United States)

Bessel beams have been used in many applications due to their unique optical properties of maintaining their intensity profiles unchanged during propagation; so Bessel beams are sometimes called "nondiffracting" beams. In imaging applications, Bessel beams have been successfully used to provide extended focuses for volume imaging and uniform thin illumination areas in lightsheet microscopy. Coupled with two-photon excitation, Bessel beams have been demonstrated in realizing fluorescence volume imaging either experimentally or in numerical simulations. One drawback in volume imaging applications was the loss of depth information due to the extended point spread functions brought by Bessel beams. To solve this problem, we demonstrated previously a novel volume imaging method—two-photon fluorescence stereomicroscopy (TPFSM)—that uses tilted Bessel beams to generate stereoscopic images on a laser scanning two-photon fluorescence microscope; upon post image processing we could successfully provide 3D perception of acquired volume images by wearing anaglyph 3D glasses. However, tilted Bessel beams were generated by shifting either an axicon or an objective laterally; the slow imaging speed and severe aberrations made it hard to use in real-time volume imaging. In this report, we will describe a new design of the setup for realizing tilted Bessel beams in laser scanning microscopy without shifting either the axicon or the objective with improved focusing qualities and imaging speed. With these critical improvements, we have demonstrated that TPFSM can be performed in real-time to provide 3D visualization in scattering media without post image processing.

9329-103, Session PSun

Applied 3D printing for microscopy in health science research

Craig Brideau, Kourosh Zareinia, Peter Stys, Univ. of Calgary (Canada)

The rapid prototyping capability offered by 3D printing is considered advantageous for commercial applications. However, the ability to quickly

**Conference 9329:
Multiphoton Microscopy in the Biomedical Sciences XV**

produce precision custom devices is highly beneficial in the research laboratory setting as well. Biological laboratories require the manipulation and analysis of delicate living samples, thus the ability to create custom holders, support equipment, and adapters allow the extension of existing laboratory machines. Applications include camera adapters and stage sample holders for microscopes, surgical guides for tissue preparation, and small precision tools customized to unique specifications. Where high precision is needed, especially the reproduction of fine features, a printer with a high resolution is needed. However, the introduction of cheaper, lower resolution commercial printers have been shown to be more than adequate for less demanding projects. For direct manipulation of delicate samples, biocompatible raw materials are often required, complicating the printing process. This paper will examine some examples of 3D-printed objects for laboratory use, and provide an overview of the requirements for 3D printing for this application. Materials, printing resolution, production, and ease of use will all be reviewed with an eye to producing better printers and techniques for laboratory applications. Specific case studies will highlight applications for 3D-printed devices in live animal imaging for both microscopy and Magnetic Resonance Imaging.

9329-104, Session PSun

Two photon microscopy of native fluorophores spatial location in cancer and non-cancer cell lines

Lin Zhang, Lingyan Shi, Robert R. Alfano, The City College of New York (United States)

The fluorescence spatial spectroscopy is a useful tool to characterize the metastasis ability of cancer cells. The key fluorophores in cells including tryptophan, reduced nicotinamide adenine dinucleotide hydrate (NADH), flavin (FAD). The object of this study is to observe two major fluorophores, NADH and flavins intensity and distribution difference among breast cancer cells lines and non-cancer cells lines.

The spatial distribution and intensity of fluorophores NADH and flavins were investigated by two photon excitation using 700nm and 900nm excitation on single three different cell lines, aggressive breast cancer cell (MDA-MB-231), non-aggressive breast cancer cell (MCF-7) and non-cancer cells (MCF-10).

The results show that NADH emission intensity is higher in aggressive cancer cells than non-aggressive or non-cancer cells, while the flavin emission intensity is a little higher in cancer cells than non-cancer cells. We observed that there are more NADH gathering around the nuclei in cancer cells as compared with that in non-cancer cells and shows one side bias in non-uniform distribution. One side of nuclei has more NADH emission than that in the other side. The NADH in non-cancer cells are more uniformly distributed inside and outside nuclei. The flavins distribution shows similar results that a higher distribution outside the nuclei and one side bias in aggressive cancer cells.

The preliminary analysis of fluorescence spatial intensity and distribution of cancer and non-cancer cells reveals that the local content changes of these key components and indicates the cell metastasis ability.

9329-105, Session PSun

TICO Raman: time encoded Raman spectroscopy and microscopy with rapidly wavelength swept lasers

Sebastian Karpf, Ludwig-Maximilians-Univ. München (Germany); Matthias Eibl, Ludwig-Maximilians-Univ. München (Germany) and Univ. zu Lübeck (Germany); Wolfgang Wieser, Ludwig-Maximilians-Univ. München (Germany); Thomas Klein, Ludwig-Maximilians-Univ. München (Germany); Robert A. Huber, Ludwig-

Maximilians-Univ. München (Germany) and Univ. zu Lübeck (Germany)

We present a radically new system for stimulated Raman spectroscopy and microscopy. We employ a rapidly wavelength swept CW laser in combination with an actively modulated pump laser to create time encoded Raman (TICO - Raman) signals. A Fourier domain mode locked (FDML) laser is used as the probe laser. It provides a periodic wavelength sweep over a broad bandwidth of ~150 nm around a center wavelength of 1300 nm or 1550 nm. The pump laser is a master oscillator power amplifier based on a fiber amplified laser diode and a Raman shifter. The all fiber based setup delivers nanosecond pulses at 1064 nm and 1122 nm wavelength, with kW's of peak power. By controlled variation of the relative timing between probe and pump laser with an arbitrary waveform generator, the Raman signals are encoded in time and they are directly acquired with a synchronized, fast analog-to-digital converter. The inherently low noise of the FDML laser and an advanced two stage referencing scheme enable shot noise limited sensitivity. We present reference quality spectra of different chemicals over a comprehensive coverage from 750 cm⁻¹ to 3200 cm⁻¹ and high spectral resolution of better than 0.5 cm⁻¹. Furthermore, we show hyperspectral images of a plant stem slice in the Raman fingerprint region around 1600 cm⁻¹ with contrast of lignin and a lipid representative. We believe that this inexpensive, robust, and very flexible all fiber based Raman setup will pave the way for new biomedical sensing devices like stimulated Raman endoscopes.

9329-106, Session PSun

Imaging how the proteome respond under cell stress by stimulated Raman scattering microscopy

Lu Wei, Wei Min, Columbia Univ. (United States)

The ability to maintain protein homeostasis is essential for cells to perform normal functions. However, when cells are under stress conditions such as impaired ubiquitin-proteasome system, autophagy impairment, oxidative stress, and expression of aggregation-prone disease proteins, a substantial proportion of cellular proteins tend to aggregate due to the imbalance of protein homeostasis and impairment of protein quality control. Indeed, protein aggregation is often observed in a wide variety of aging-associated diseases, such as Huntington's disease, Alzheimer's disease and Parkinson's disease. Therefore, it is pivotal to understand how the cellular protein responds under various stress conditions. The conventional strategy to study this problem is largely based on labeling a disease-related protein-of-interest and then imaging its aggregation formation under cellular stress. Despite the useful information extractable from this approach, it is limited to the proteins with known identities, and offers no information about the global behavior of the involved cellular proteome. To this end, stimulated Raman scattering (SRS) imaging of the metabolic incorporation of deuterated amino acids, which was originally developed to image protein synthesis, is well suited to address this problem at the global proteome level. Herein we demonstrate SRS imaging of proteome response, including degradation and aggregation, under various stress conditions. Our study unveils previously unknown observation of distinct and defined subcellular compartments of misfolded/aggregated proteome, offering new biological insight as to how cells manage homeostasis spatially in a global level.

9329-107, Session PSun

Monitoring metabolic enzyme activity in cells with fluorescence lifetime imaging of NAD(P)H

Joe T. Sharick, Melissa C. Skala, Vanderbilt Univ. (United States)

The fluorescence lifetime of the metabolic co-enzyme NAD(P)H provides

a non-invasive measure of cellular metabolism. NAD(P)H has a two-exponential lifetime decay due to the free and protein-bound forms of the molecule, which have a short and long lifetime, respectively. However, the biochemical significance of changes in the bound lifetime of NAD(P)H remains unclear. In order to address this issue, the lifetime of NADH bound to specific enzymes were measured in solutions and cells using two-photon microscopy and time-correlated single photon counting. Measurements in solution demonstrated that the fluorescence lifetime of NAD(P)H bound to these specific enzymes can be robustly determined. Our hypothesis that the bound fluorescence lifetime is influenced by preferred protein binding was supported by measuring the NAD(P)H lifetime in BT474 human breast cancer cells that were treated with FX11, a competitive inhibitor of NADH binding to lactate dehydrogenase A. FX11 caused a significant decrease in the long lifetime of NAD(P)H in the cell cytoplasm versus untreated controls ($p < 0.05$). Treatment with epigallocatechin gallate (EGCG), an inhibitor of glutamate dehydrogenase, also caused a significant decrease in the long lifetime of NAD(P)H in BT474 cells ($p < 0.05$). Dichloroacetate, a small molecule activator of pyruvate dehydrogenase, caused a significant increase in the long lifetime of NAD(P)H in these cells ($p < 0.05$). These results confirm that changes in the protein-bound lifetime of NAD(P)H may be attributed to changes in the activity levels of enzymes that bind NAD(P)H, and that measuring bound NAD(P)H lifetime is a non-invasive method for probing changes in metabolic activity.

9329-109, Session PSun

Detecting the collagen-based hydrogels degradation by multiphoton microscopy (MPM)

Xuye Lang, Matthew J. Spousta, Julia G. Lyubovitsky, Univ. of California, Riverside (United States)

Collagen is widely used in tissue engineering applications because of its biocompatibility and biodegradability. Detecting collagen microstructure can help to accelerate its applications in tissue engineering. In this study, we followed the changes in microstructure of collagen hydrogels that were digested with collagenase by MPM using Second Harmonic Generation (SHG) and Two photon Fluorescence (TPF) Signals. The collagen hydrogels were modified by genipin, EDC or EDC+NHS.

For unmodified collagen hydrogels, SHG images showed degradation was underway by about 20 min. For collagen hydrogels modified with EDC or EDC+NHS, preliminary data did not indicate obvious degradation after 22 hours. Modification with genipin induced new fibers that had TPF centered at about 490 nm and 600 nm. The SHG signals were weaker in genipin modified collagen hydrogels. TPF images illustrated that the degradation of the newly induced fluorescent fibers at the surface of the materials was underway after about 2 hours.

9329-110, Session PSun

Parallel multiplexed FLIM-FRET imaging in deep tissue of live embryos

Ming Zhao, College of Optical Sciences, The Univ. of Arizona (United States); XiaoYang Wan, Univ. of Michigan (United States); Yu Li, College of Optical Sciences, The Univ. of Arizona (United States); Weibin Zhou, Univ. of Michigan (United States); Leilei Peng, College of Optical Sciences, The Univ. of Arizona (United States)

Fluorescence lifetime microscopy (FLIM) is a powerful tool for functional imaging of biochemical processes and molecular interactions in biological specimens. Currently, the most popular FLIM techniques are based on either gated cameras or time-correlated single photon counting detection. These traditional FLIM techniques have difficulty to monitor multiple fluorophores simultaneously. Furthermore, both methods are very difficult if not

impossible to be modified to study whole organisms. By combining Fourier multiplexed fluorescence lifetime imaging (FmFLIM) [1] and scanning laser optical projection tomography (SLOT) [2], we developed a novel technique that allows multiplexed FLIM-FRET imaging at the whole animal level. In our approach, lifetime images at multiple excitation-emission channels are collected simultaneously as 2D projections. Rotating the sample at multiple angles allows the tomographic reconstruction of multi-channel 3D lifetime images at isotropic spatial resolution.

Using zebrafish expressing FRET sensors as a model system, we demonstrated that this technique is well suited to study complex biochemical processes within live organisms. In transgenic zebrafish embryos that specifically expressing cAMP FRET sensors in kidney tubules, we observed donor lifetime variation at different locations. Treatment that increases cAMP levels leads to donor lifetime increase across the whole tubule, which is consistent with results obtained from live cell studies. In double transgenic zebrafish embryos expressing both cAMP and Calcium FRET sensors, the technique allowed us to readout both FRET sensors simultaneously and observe changes due to treatments. The FmFLIM based deep tissue multiplexed FRET technique provided brand new opportunities to interrogate sophisticated biological processes during development or diseases.

[1] Ming Zhao, Yu Li, Leilei Peng. Optics Express. 22, 10221 (2014).

[2] R. A. Lorbeer, et al., Optics Express. 19, 5419. (2011)

9329-111, Session PSun

In vivo non-invasive multiphoton tomography of human skin with subcellular spatial and picosecond time resolution to detect bio- and chemohazards

Karsten König, Univ. des Saarlandes (Germany) and JenLab GmbH (Germany)

High resolution non-invasive 3D imaging devices are required to detect pathogenic microorganisms such as Anthrax spores, bacteria, viruses, fungi and chemical agents entering biological tissues such as epidermis. Due to the low light penetration depth and the biodamage potential, ultraviolet light sources can not be employed to realize intratissue imaging of bio- and chemohazards.

We report on the near infrared laser technology multiphoton tomography for non-invasive detection of intratissue agents and their influence on cellular metabolism based on multiphoton autofluorescence imaging (MAI) and second harmonic generation (SHG). Femtosecond laser pulses in the spectral range of 750 nm to 850 nm have been used to image in vivo human skin with subcellular spatial and picosecond temporal resolution. The non-linear induced autofluorescence of both, skin tissues and microorganisms, originates mainly from naturally endogenous fluorophores/protein structures like NAD(P)H, flavins, keratin, collagen, elastin, porphyrins and melanin. Bacteria emit in the blue/green spectral range due to NAD(P)H and flavoproteins and, in certain cases, in the red spectral range due to the biosynthesis of Zn-porphyrins, coproporphyrin and protoporphyrin. Collagen and exogenous non-centrosymmetric molecules can be detected by SHG signals.

The system consists of a wavelength-tunable compact 80/90 MHz Ti:sapphire laser, an imaging head with galvo scan mirrors, piezo-driven objective, fast photon detector and time-resolved single photon counting unit. It can be used to perform optical sectioning and 3D autofluorescence lifetime imaging (?-mapping) with 1 μ m spatial resolution and 270 ps temporal resolution. The parameter fluorescence lifetime depends on the type of fluorophore and its microenvironment and can be used to distinguish bio- and chemohazards from cellular background and to provide information for pathogen identification. The novel in vivo non-invasive imaging system offers the possibility to detect and localize CB agents in tissues and to gain information on their impact on respiratory chain activity, cell division and metabolism. The system can also be used to detect food and water contamination.

**Conference 9329:
Multiphoton Microscopy in the Biomedical Sciences XV**

9329-112, Session PSun

Two-photon photoacoustic optical imaging using femtosecond pulses

Ben E. Urban Jr., Northwestern Univ. (United States)

We aligned an amplified Ti:Sapphire femtosecond laser (pulse width 80-fs, rep. rate 1000-Hz) with a microscopy body to investigate the nonlinear photoacoustic (PA) effect for the purpose of bioimaging. The expected quadratic dependence of photoluminescence (PL) and (PA) signal intensity to incident laser fluence was confirmed in a phantom sample using Rhodamine B fluorescent dye. We further verified the nonlinear dependence using temporal delay to show the nonlinear behavior. The PL and PA signals were then used to image a quartz capillary tube, filled with Rhodamine B fluorescent dye, in highly scattering medium, to reproduce conditions similar to a biological sample. Our results show a higher attenuation of the PL as compared to PA signal, suggesting the advantage of nonlinear PA imaging in biological specimens. We further showed, for the first time, the three dimensional TP-PA imaging of the capability in highly scattering media to axial resolutions greater than standard PA microscopy can achieve.

9329-113, Session PSun

Non-invasive discrimination between pancreatic islets and exocrine cells using multiphoton microscopy

Binlin Wu, Ge Li, Mingming Hao, Shuibing Chen, Sushmita Mukherjee, Weill Cornell Medical College (United States)

Islet transplantation is one of the most promising therapies for diabetes. The first step of this procedure is to isolate pancreatic islets. Although purer islets would be quite beneficial for islet transplantation, the current gradient centrifugation based method could only achieve ~60% purity. It has long been demonstrated that beta cells within the islets, compared to exocrine cells, have higher autofluorescence than other cells due to higher metabolism. The previous studies, however, were based on single cells, hence less relevant to islet isolation which is based on whole islets. Here we propose a non-invasive method to distinguish islets from exocrine cell clusters using multiphoton (MP) imaging. An Olympus FV1000MPE multiphoton microscope is used in this study. The excitation wavelength is varied to provide multiple-wavelength near-infrared excitation. The images acquired by three detectors in successive wavelength bands are used for analysis. The detection bandwidth covers a range of 420 nm - 650 nm, which is mainly contributed by intrinsic fluorophores such as reduced nicotinamide adenine dinucleotide (NADH) and flavin adenine dinucleotide (FAD). Multivariate analysis algorithms are used to analyze the images. Relative concentration of NADH or redox ratio is estimated to represent the level of metabolism. The results show that MP imaging can distinguish islet cells from exocrine cell cluster non-invasively using relative concentrations of the intrinsic fluorophores particularly NADH and FAD. Therefore, this method has a huge potential of facilitating clinical islet isolation.

9329-114, Session PSun

Imaging cardiomyocytes in intact tissue with a remote focusing microscope

Alexander D. Corbett, Rebecca A. B. Burton, Gil Bub, Tony Wilson, Univ. of Oxford (United Kingdom)

In cardiac imaging, the spacing between sub-cellular sarcomere structures is of great importance to physiologists in constructing models of cell function. Making accurate measurements of the sarcomere length (SL) presents a significant imaging challenge owing to the size of the SL (~2µm) and its naturally low variability (<6%), requiring a high level of precision to determine subtle changes between heart disease models. Moreover,

measurements of SL from traditional two-photon imaging have so far been ambiguous to within a factor of $\cos(\theta)$, where θ is the inclination of the tissue with respect to the focal plane.

By remotely focussing a customised two-photon microscope, it is possible to image heart cells at two oblique angles within 200ms. The oblique images uniquely resolve the tissue inclination ambiguity and reduce the variance of SL measures by as much as 23%. This improved precision is crucial in discerning between pathological models of chronic hypertension. As well as improving measurement precision, the distribution of θ across the field of view provides additional structural information which can be related to disease morphology. To validate this new imaging protocol, the value of θ calculated from the oblique planes provided the input to a rigid model cell which was used to predict the appearance of the cell in the conventional focal plane. The comparison of the model to the image data provided a confidence metric for our measurements. Finally, by considering the optical transfer function, the range of cell orientations for which the method is valid could be calculated.

9329-115, Session PSun

In vivo high-speed imaging of blood cells and tissues in mouse ear skin using multimodal nonlinear optical microscopy

Eung Jang Lee, Daeyeon Kim, Bo Ram Kim, Sung-Ho Lee, Seung-Han Park, Yonsei Univ. (Korea, Republic of)

We have developed video-rate multimodal microscope by integrating the two-photon excited fluorescence (TPEF) and the second & third harmonic generation (SHG and THG) microscopies. TPEF and SHG/THG images of subcutaneous cellular components and peripheral nerve fibers, together with the collagen fiber, in the mouse ear pinna, can be simultaneously obtained by the multimodal microscope. In addition, flow of red blood cells and dynamic change of diameter of the arteriole-like blood vessel can be visualized by THG with femtosecond laser pulses of 1036 nm. We have also observed that it is possible to distinguish the blood vessel type, i.e. arteriole-like or venule and capillary-like through the visualization of the blood vessel wall.

9329-141, Session PSun

Investigating cell membrane structure and dynamics with TCSPC-FLIM

Alix Le Marois, Dylan M. Owen, Klaus Suhling, King's College London (United Kingdom)

We report the use of Time-Correlated Single-Photon Counting (TCSPC) in a polarization-resolved Fluorescence Lifetime Imaging (FLIM) setup for the investigation of cell membrane structural and dynamic properties. This technique allows us to study the orientation and mobility of fluorescent membrane dyes, such as di-4-ANEPPDHQ and DiO, in model bilayers (GUVs, Giant Unilamellar Vesicles) of different lipid compositions. These parameters can be correlated to structural properties of membranes, i.e. viscosity, order parameters and topology. In living cells, understanding the membrane structure provides crucial information on its functional properties, such as exo- and endocytosis, cell mobility and signal transduction. In particular, we are interested in using this imaging technique to identify the processes involved at the immunological synapse during T-cell activation.

Moreover, polarisation-resolved fluorescence uniquely enables the detection of homo-FRET, i.e. non-radiative coupling between identical neighbour fluorophores. Our present target is to quantify the clustering behaviour and regionalisation of a membrane protein, I-selectin, during lymphocyte migration through the vascular endothelium. Different levels of clustering are detected when induced by immuno-targeting of I-selectin-GFP fusions, hence opening the way for in-situ studies.

**Conference 9329:
 Multiphoton Microscopy in the Biomedical Sciences XV**

9329-142, Session PSun

Microsecond wide-field TCSPC microscopy based on an ultra-fast CMOS camera

Liisa M. Hirvonen, King's College London (United Kingdom); Zdenek Petrasek, Max Planck Institute of Biochemistry (Germany); Andrew Beeby, Durham Univ. (United Kingdom); Klaus Suhling, King's College London (United Kingdom)

Ultra-fast frame rate CMOS cameras, combined with a photon counting image intensifier, can be used for microsecond resolution wide-field time-correlated single photon counting (TCSPC) microscopy. A sequence of frames is recorded after each excitation pulse, and the number and location of photons in each frame is determined. This process is repeated until enough photons are recorded for a photon arrival time histogram (decay) for each pixel of the image. This approach combines low, nanowatt excitation power with single-photon detection sensitivity, short acquisition times and allows lifetime mapping with a time resolution of ~1 microsecond. Moreover, we also show that the phosphor decay can be exploited to time the photon arrival well below the exposure time of the camera. This approach yields better timing and larger images than direct imaging of photon events.

We show that the both methods are ideal for lifetime imaging of transition metal compounds in living cells within a few seconds.

9329-143, Session PSun

Comprehensive quantitative evaluation of FLIM-FRET image data using intensity-based analysis tools

Horst K. Wallrabe, Ammasi Periasamy, Univ. of Virginia (United States)

Traditionally, FLIM-FRET data is analyzed by processing the lifetime for a limited number of complete cells or numbers of single pixels to arrive at an average E% value. The major advantage of this methodology lies in its ability to confirm that FRET has actually occurred, being independent of fluorophore concentrations and no concern about spectral bleedthrough phenomena. Average lifetimes between the bi-exponential double-label specimen and a mono-exponential single donor sample serves as a basis for the calculation of energy transfer efficiency (E%). While this semi-quantitative approach is valuable for many research projects, it does not fully explore cellular functions, such as those predicated on endosomal pH differences, specific morphological features, exploring sub-populations and the like. As proof of principle, we compared the traditional FLIM-FRET analysis method with a quantitative Region of Interest (ROI)-based method in live cells expressing dimerized C/EBP β -bZip in living cell nucleus using TCSPC FLIM-FRET microscopy. C/EBP β -bZip was tagged with either Cerulean (C) or Venus (V). Average lifetimes and E% are virtually the same, with the ROI method providing a more comprehensive distribution information. Taking the same approach exploiting the autofluorescent properties of tryptophan and NAD(P)H revealed clear differences between Normal Human Prostate cells and LNCaP cancer cells. This method can be extended to investigating specific ROIs generated via specific cellular markers (mitochondria, lysosomes, nucleus etc) to investigate discrete changes occurring in cellular micro-environments.

9329-144, Session PSun

Development of confocal immunofluorescence FRET microscopy to Investigate eNOS and GSNOR localization and interaction in pulmonary endothelial cells

Shagufta Rehman, Univ. of Virginia (United States); Lisa Palmer, Univ. of Virginia School of Medicine (United States); Ammasi Periasamy, Univ. of Virginia (United States)

Confocal FRET microscopy is a widely used technique for studying protein-protein interactions in live or fixed cells. Endothelial nitric oxide synthase (eNOS) and S-nitrosoglutathione reductase (GSNOR) are enzymes involved in regulating the bioavailability of S-nitrosothiols (SNOs) in the pulmonary endothelium and have roles in the development of pulmonary arterial hypertension. Labeling of endogenous proteins to better understand a disease process can be challenging. We have used immunofluorescence to detect endogenous eNOS and GSNOR in primary pulmonary endothelial cells and finding the right immunofluorescence labeling condition to co-localize these proteins and to study their interaction by FRET has been a challenge. We had to deal with a number of issues in selecting the right antibody, the right blocking reagent, the right FRET pair and the cross-reactivity issue. We have used Alexa 488 and Alexa 568 as a FRET pair. After a series of optimizations the data from Confocal Laser Scanning Microscopy (CLSM) demonstrate co-localization of eNOS and GSNOR in the perinuclear region of the endothelial cell primarily within the cis-Golgi with lower levels of co-localization seen within the trans-Golgi and endosome. FRET studies demonstrate, for the first time, interaction between eNOS and GSNOR in both human and bovine endothelial cells. Further characterization of eNOS-GSNOR interaction and the subcellular location of this interaction will provide mechanistic insight into the importance of S-nitrosothiol signaling in pulmonary biology, physiology and pathology.

9329-23, Session 5

**Multiphoton tomography on astronauts
 (Invited Paper)**

Karsten König, JenLab GmbH (Germany) and Univ. des Saarlandes (Germany); Martin Weinigel, JenLab GmbH (Germany); Nicole Gerlach, Ulrike Heinrich, DermaTronnier GmbH & Co. KG (Germany)

High resolution multiphoton tomography was employed to evaluate skin effects in astronauts who are working for a half year on the International Space Station (ISS). Label-free multiphoton skin biopsies were taken non-invasively with submicron spatial and picosecond temporal resolution. Skin problems such as itchiness, loss of elasticity, thinner skin and slow healing rate are the most commonly described negative impacts on astronauts' health during space flights. Besides the lack of gravity, astronauts face a significant amount of exposure to (i) extraterrestrial radiation, and (ii) bioparticles from their own skin tissue as well as that from other crew members. Scientists involved with European Space Agency Project Skin B hope to answer the question of how astronauts' skin regeneration is affected. The skin will age faster than on Earth, but astronauts may develop more efficient cell regeneration and healing rates upon arriving back home. For future interplanetary travel, multiphoton tomography including functional imaging may help to understand better the effects of cosmic rays, biocontamination and microgravity on a subcellular level.

**Conference 9329:
Multiphoton Microscopy in the Biomedical Sciences XV**

9329-24, Session 5

Targeted illumination in 3D for excitation and stimulation

Elijah Y. Yew, Peter T. C. So, Massachusetts Institute of Technology (United States)

The current state-of-art for optical imaging and stimulation of the brain utilizes acousto-optic modulators to steer a foci to an arbitrary spot within a three-dimensional space (Random Access Multiphoton Microscope). More recently, patterned illumination was demonstrated using temporally focused wide-field two-photon excitation using generalized phase contrast approach. While the RAMP microscope allows for rapid addressing of random points in a 3D space, it is done sequentially although at a very fast rate. On the other hand, patterned illumination where multiple spots are addressed simultaneously may be done using generalized phase contrast and this has a high efficiency of. The disadvantage of the previously mentioned techniques is that it is limited to a 2D plane. We present a technique of extending the generalized phase contrast into the third dimension thereby opening up a potentially advantageous way of addressing multiple arbitrary positioned spots in 3D simultaneously.

9329-25, Session 5

Breast cancer staging through nonlinear endomicroscopy

Gunnsteinn Hall, Wenxuan Liang, Lu Jiang, Kristine Glunde, Xingde Li, Johns Hopkins Univ. (United States)

Breast cancer causes over 40,000 deaths annually. Metastatic spread from the primary tumor is responsible for most of these fatalities. Early identification of metastasis risk is a major challenge. Current staging systems rely on evaluating the lymph node status through an invasive biopsy procedure. About 25% of patients undergoing sentinel lymph node biopsy suffer from adverse effects following the procedure with the effects ranging from mild to severe. Improved methodology is required to remove the need for such invasive procedures and improve the staging systems. Second harmonic generation (SHG) microscopy allows high-resolution imaging of the collagen fibers of the extracellular matrix and has shown potential for cancer detection. SHG endomicroscopy is a miniaturization of this technology, which can potentially be translated to clinical use by passing through the biopsy needle for assessing metastatic risk during core biopsy. In order to evaluate the feasibility of this technology for breast cancer staging, we imaged biopsy cores from human subjects *ex vivo*. A total number of 20 cores were imaged, including normal tissue, and stages I - IV. We found that more advanced cancers had reduced collagen signal content than early stages of cancer and normal tissue. Furthermore, we compared lymph node negative (LN-) and positive cases (LN+) and found that the LN+ cases had significantly lower collagen signal content ($p = 0.018$). Lymph node status prediction could be an important advance for breast cancer patients as the highly invasive lymph node removal procedure could be avoided.

9329-26, Session 5

Study of acetowhitening mechanisms in live mammalian cells with label-free subcellular-level multimodal nonlinear optical microscopy

Jian Lin, Sengkhon Teh, Wei Zheng, Zi Wang, Zhiwei Huang, National Univ. of Singapore (Singapore)

The tissue acetowhitening effect in acetic acid instillation procedure is a simple and economic method for neoplasia detection and has been clinically

utilized since 1925. It is suspected that the optical property (e.g. scattering) change in acetowhitening is due to coagulation of intracellular proteins, but no experimental proof has been reported yet. In this work, we use third-harmonic generation (THG) and two-photon excited fluorescence (TPEF) to investigate the acetowhitening phenomenon induced by acetic acid in live mammalian cells without labeling. We studied the acetowhitening effect with different acetic acid concentrations and the co-localized TPEF and THG imaging on tryptophan and NADH at subcellular-level reveals that the acetowhitening phenomenon is highly related with proteins involved in metabolic pathways in the nucleus and cytoplasm in live cells.

9329-27, Session 6

Optical reprogramming with ultrashort femtosecond laser pulses (*Invited Paper*)

Aisada Uchugonova, Univ. des Saarlandes (Germany); Hans Georg Breunig, Univ. des Saarlandes (Germany) and JenLab GmbH (Germany); Ana Batista, Karsten König, Univ. des Saarlandes (Germany)

The use of sub-15 femtosecond laser pulses in stem cell research is explored, with particular emphasis on the reprogramming of somatic cells.

The reprogramming of somatic cells into induced pluripotent stem (iPS) cells can be induced through the ectopic expression of defined transcription factors (Takahashi and Yamanaka, 2006, Takahashi et al., 2007, Yu et al., 2007). Conventional approaches utilize retro/lenti-viruses to deliver those genes as well as to facilitate the integration of transcription factors into that of the host genome. However, the use of viruses may result in insertional mutations caused by the random integration of genes and as a result, this may limit the use within clinical applications due to the risk of the formation of cancer (Okita et al., 2007).

In this study, a new approach is demonstrated in realizing non-viral reprogramming through the use of ultrashort laser pulses, to introduce transcription factors into the cell so as to generate iPS cells.

9329-28, Session 6

Compact fixed wavelength femtosecond oscillators for multi-photon imaging

Tommi Hakulinen, Spectra Physics (Austria); Ruben Zadayan, Tommaso Baldacchini, Newport Corp. (United States); Tilman Franke, FEI Munich GmbH (Germany)

In recent years technical development of Yb fs-oscillators has been resulting in air-cooled, compact laser systems with high output powers of 1.5 W at a wavelength of 1045 nm with a pulse duration of < 250 fs. The footprint of such lasers can be as small as about 200 mm by 200 mm including an optional second harmonic generation (SHG) for 522 nm output.

The 1045nm laser proved to be very efficient in exciting two-photon fluorescence from yellow fluorescent proteins (YFP), red fluorescent proteins (RFP) and dyes. Also SHG signals in the visible wavelength range could be created very efficiently from muscle tissue and collagen.

With this work we demonstrate that air-cooled, small-footprint fixed-wavelength lasers can present an appealing light source in multi-photon applications, where longer excitation wavelengths and pulse durations are adequate. The design of the laser allows for cost-effective, compact, and easy-to-use realization compared to traditional femtosecond lasers. The approach opens up a new market for wider audience of researchers.

**Conference 9329:
Multiphoton Microscopy in the Biomedical Sciences XV**

9329-29, Session 6

Novel applications of melanin pump-probe imaging: correlating structural and chemical variation with MC1R gene expression and the onset of Parkinson's disease

Sanghamitra Deb, Christopher P. Dall, Francisco E. Robles, Christina S. Gainey, Jesse W. Wilson, Warren S. Warren, Duke Univ. (United States); Nicole A. Kukutsch, Leiden Univ. Medical Ctr. (Netherlands)

We report on two novel applications of melanin pump-probe imaging which correlate structural and chemical morphology with clinical concerns. In the first application, we examine tissue samples from individuals with melanocortin 1 receptor (MC1R) genetic variants, who are at an increased risk of developing melanoma because of a decrease in eumelanin (black-brown melanin pigment) relative to potentially carcinogenic pheomelanin (reddish brown melanin pigment). Clinically, these MC1R variations are associated with red hair, fair skin, poor tanning ability and higher risk of cutaneous melanoma. Pump-probe microscopy can differentiate between eumelanin and pheomelanin according to their spectroscopic response. Using this technique, we correlate the pump-probe signature of melanin with melanoma diagnosis and the number of MC1R variants, and obtain molecular contrast from melanin that cannot be obtained from other multiphoton methods. The nature of melanin changes with the number of MC1R variants and stage of the melanoma, which is reflected in the pump-probe response.

Another unique application of pump-probe imaging is to characterize neuromelanins, which play an important role in brain functionality. The pigment has been implicated in Parkinson's disease where the targeted cell death of neuromelanin-containing neurons is a critical pathology of the disease. Neuromelanin may play a major role in the neurodegeneration due to its potential to catalyze oxidative damage and trigger inflammation. Our goal is to characterize the pigment changes that occur in Parkinson's disease. We see significant heterogeneity in the pump-probe response, and will discuss how this information might be useful in understanding disease progression.

9329-30, Session 6

Femtosecond pulse shaping enables molecular imaging using optical Kerr-effect dynamics

Francisco E. Robles, Martin C. Fischer, Warren S. Warren, Duke Univ. (United States)

Nonlinear techniques have proven immensely useful in the field of biology and medicine since they are inherently cross-sectional, provide molecular contrast, and are robust to scattering. Most of these techniques rely on light experiencing amplitude changes, but interactions that result in phase changes (i.e., nonlinear refractive index, n_2) remain largely unexplored. Such methods hold the promise of providing similar information to linear phase methods (e.g., DIC), but with the added aforementioned benefits of nonlinear techniques. Unfortunately, methods that measure n_2 are too slow for biological imaging or lack molecular specificity. Here, we bridge this gap by applying femtosecond pulse shaping to directly access a material's time-varying n_2 and thus determine time-resolved optical Kerr-effect (OKE) dynamics at sufficient speeds for biological imaging. Note that the OKE dynamics depend on a molecule's structure and surrounding environment, which provide unique molecular information.

The method combines a pump-probe system with femtosecond pulse shaping to generate three, equally spaced fields (i.e., pulse train) with carefully controlled phase, and employs Fourier-domain detection. Pump induced changes on a sample's n_2 produces a unique interference pattern

on the probe pulse train that is background free, and thus allows for fast (single shot) detection with sufficient sensitivity for imaging.

This novel form of molecular contrast could lead to exciting applications in cell biology and medicine, for example identifying early signs of cancer that affect molecular diffusion and intracellular reorientation due to increased chromatin. A description of the theory, experimental method, and molecular images of cells in-vitro will be presented.

9329-31, Session 6

Integration of femtosecond fiber laser and endoscopy

Huda Yousif, Hussein E. Kotb, Majid Naji, Univ. of Ottawa (Canada); Mohamed A. Abdelalim, Univ. of Ottawa (Canada) and Electronics Research Institute (Egypt); Sangeeta Murugkar, Carleton Univ. (Canada); Hanan Anis, Univ. of Ottawa (Canada)

We demonstrate the integration of a compact, low cost, and portable all-fiber femtosecond laser with a portable multimodal nonlinear optical imaging endoscope. A home-built portable, all-fiber single femtosecond laser is used as a light source and is based on all-normal dispersion fiber design. The center wavelength of the fiber laser is at 1030 nm with the output average power of 100 mW obtained after the hollow core photonic crystal fiber used for pulse compression. The pulse repetition rate is at 23 MHz and the pulse width is measured to be 170 fs. The portable multimodal nonlinear imaging miniaturized microscope combines coherent anti-Stokes Raman scattering (CARS), second harmonic generation (SHG) and two-photon excitation fluorescence (TPEF) modalities. Its design is based on a biaxial scanning micro-electro-mechanical system (MEMS) mirror and custom miniaturized optics to allow photon collection in the epi-direction. High resolution, distortion-free TPEF images obtained from fluorescent microspheres and biological samples, successfully demonstrate proof of concept. The availability of a portable miniaturized nonlinear imaging probe that is integrated with a low-cost, portable fiber-based light source could pave the path towards future clinical applications.

9329-32, Session 6

Multiphoton light-sheet microscopy using wavelength mixing: fast multicolor imaging of the beating Zebrafish heart with low photobleaching

Pierre Mahou, Lab. d'Optique et Biosciences, Ecole Polytechnique (France) and Univ. of Cambridge (United Kingdom); Julien Vermot, Univ. de Strasbourg (France); Emmanuel Beaurepaire, Lab. d'Optique et Biosciences, Ecole Polytechnique (France); Willy Supatto, Lab. d'Optique et Biosciences, Ecole Polytechnique (France)

Multicolor imaging approaches are increasingly used in biology but their application to investigate fast biological processes in complex and live tissues remains challenging. In particular, while two-photon laser scanning microscopy (2P-LSM) has become a standard to map thick and live tissues its application for fast and multicolor imaging remains challenging. To extend the multicolor capability of 2P-LSM, we recently introduced a new strategy based on wavelength mixing, resulting in optimal and simultaneous two-photon excitation of three chromophores with distinct absorption spectra[1]. This configuration has proven valuable to image live and thick multicolor tissues but is inherently slow in point-scanning imaging (i.e. imaging frame rate limited to a few hertz).

To address this issue, we extended our prior work by implementing mixed wavelength excitation in a two-photon light-sheet microscope (2P-SPIM)

**Conference 9329:
Multiphoton Microscopy in the Biomedical Sciences XV**

[2,3]. Due to the parallelization of both the illumination and signal collection we demonstrate this strategy permits fast multicolor two-photon imaging of live tissues, while dramatically reducing photobleaching compared to 2P-LSM[3] and providing improved imaging depth compared to 1-photon SPIM[2]. Finally, to illustrate the potential of this technique we present sustained multicolor two-photon movies of the beating heart in zebrafish embryos with negligible photobleaching and up to 85fps and 28million pixels/s acquisition speed. In particular, we compute 3D reconstructions of the heart periodic motion from time series recorded at successive depths with sufficient spatio-temporal resolution to track in 3D myocardial cells moving at up to 620 μ m/s.

[1] Mahou, Nature Methods (2012).

[2] Truong, Nature Methods (2011).

[3] Mahou, Nature Methods (2014).

9329-33, Session 7

Combined wavelength dependent 3D SHG imaging, optical scattering and texture analysis to characterize changes collagen architecture and development of a classification system in human ovarian cancer (*Invited Paper*)

Paul J. Campagnola, Karissa B. Tilbury, Kirby R. Campbell, Bruce L. Wen, Kevin W. Eliceiri, Vikas Singh, Manish Patankar, Univ. of Wisconsin-Madison (United States)

Five year survival rates of ovarian cancer remain poor (~30%), where this arises in part due to a poor understanding of the extracellular matrix (ECM). Thus it is important to understand the changes that occur in the ECM and how these evolve between early stage and advanced disease and also differ between disease grades. To meet this need, we interrogated the collagen fibrillar architecture in ovarian cancer using wavelength dependent SHG and optical scattering probes, separately and in conjunction. This integrated approach provides detailed structural information across different length scales of fibrillar size and organization from sub-resolution sizes (~50-100 nm) through several microns by measurement of the SHG creation ratio FSHG/BSHG and the optical spectral slope. We compared remodeling across a spectrum of ovarian cancers, where we used the current convention of type 1 (low-grade, borderline, endometrioid) and type 2 (high grade serous) tumor types. Measurement of the optical scattering spectral slope (~400-1200 nm) and SHG emission directionality (400-600 nm) differentiated type 1 and type 2 and normal tissues. Specifically, we found lower grade tumors have more organized collagen than either high grade tumors or normal ovarian stroma, and latter two are also distinct. These differences are consistent with the tumors having different etiology and genetic profiles. A classification system based on the SHG and optical scattering measurements of collagen is being developed. Additionally, a texture analysis platform using "textons", or repetitive image features provide further classification across disease grade, where the library can be used to identify unknown ovarian tumors.

9329-34, Session 7

Two- and three-photon excited fluorescence microscopy of erythrocytes using sub-50fs Ti:sapphire and Yb lasers

Marcos M. Dantus, Ilyas Saytashev, Michigan State Univ. (United States)

Multiphoton excited fluorescence imaging of red-blood cells using sub-14 fs pulses at 800 nm and sub-50 fs pulses at 1060 nm is reported. Short pulses prevent heat damage and enhance two-photon and especially

three-photon excited fluorescence (3PEF). Erythrocytes, or red blood cells (RBC) are typically observed as shadows in nonlinear optical microscopy due to the large absorption cross section and very poor fluorescence yield of hemoglobin. Using shorter pulses, however, we have found RBC's to fluoresce and permit imaging. Our findings involve TPEF based on a sub-14 fs Ti:sapphire at 800 nm and a new Yb-fiber oscillator delivering sub-50 fs pulses at 1060 nm used for third-harmonic generation (THG) and 3PEF microscopy. Both lasers are compressed to their transform limited duration at the focal plane using MIIPS. Images as well as video-rate imaging of flowing blood from both of these modalities are compared. We also report that fluorescence is enhanced as a function of time especially when using Ti:sapphire. Results exploring the loss of iron as a primary cause for enhanced fluorescence of hemoglobin will be presented. The implications of this work on studies involving blood flow and testing the viability of stored blood will be discussed.

9329-35, Session 7

Combining wide-field assessment with nonlinear optical microscopy: possibilities for multimodal imaging in epithelial (pre) cancer

Rahul Pal, Jinping Yang, Gracie Vargas, The Univ. of Texas Medical Branch (United States)

Survival rate of oral cancer patients largely depend on the time of diagnosis, which has not improved significantly over the past few decades. Recent development and characterization of nonlinear optical microscopy (NLOM) for living biological specimens have provided new avenues for deep tissue imaging at high resolution, which can be helpful in early diagnosis of a number of diseases including oral cancer and pre-cancer. However limitations in size of image areas limit applications in large area surveillance or diagnostics.

We have utilized a combination of NLOM and wide-field fluorescence (WFF) imaging in hamster models of oral inflammation/ carcinogenesis for noninvasive identification of various degrees of neoplasia and inflammation. WFF imaging with a light active glucose analog indicates areas of high glucose uptake rate while subsequent microscopy revealed abnormalities in tissue microstructure such as cellular atypia and extracellular matrix (ECM) remodeling. Quantitative analysis indicates clear separation of neoplasia from normal using combined metrics from WFF and NLOM modalities. Initial results indicate inflammation shares similarities to neoplasia in metabolic WFF assessment but lacks specific microscopic features of neoplasia. This combination of large area and microscopic imaging modalities could offer an avenue by which NLOM could be developed for clinical translation for epithelial cancer diagnostics.

Our results are encouraging in terms of identifying features associated with dysplasia and inflammation utilizing noninvasive NLOM. Multimodal imaging approach of this kind provides tissue surveillance at multiple scales over time and is expected to improve patient care in near future.

9329-36, Session 7

Four-wave mixing microscopy: a high potential nonlinear imaging method

Tobias Ehmke, Andreas Knebl, Friedrich-Schiller-Univ. Jena (Germany); Alexander Heisterkamp, Leibniz Univ. Hannover (Germany)

In the field of multiphoton microscopy the combination of several nonlinear signals like two-photon fluorescence, second harmonic generation (SHG) and third harmonic generation (THG) allows imaging of highly ordered biological tissue due to spectral separation. Additional to these signals we demonstrate the possibility to generate a signal based on frequency mixing of photons with different wavelengths. Laser light was provided by a fs-laser

**Conference 9329:
Multiphoton Microscopy in the Biomedical Sciences XV**

pumping an optical parametric oscillator and a delay line was used in order to achieve temporal overlap of the different laser pulses in the sample plane. Spatial overlap of the pulses was ensured by using a chromatically corrected objective lens. The four wave mixing (FWM) process is very sensitive to several media and provides a new contrast mechanism in the field of multiphoton microscopy. In our work, the polarization of the fields involved in the process was investigated in different media. The linear polarization of one of the two laser beams was rotated and its influence on the signal was studied. Theoretical calculations regarding the polarization support our experimental data. Furthermore, the signal efficiency of FWM microscopy in comparison with two-photon fluorescence microscopy was evaluated. A two-photon process scales with the squared pump intensity whereas in FWM microscopy an additional factor from the second interacting laser beam is existent. Thus, the signal efficiency in FWM microscopy is drastically higher than in two-photon fluorescence microscopy. Scattering processes in dense tissue also allow a detection of the FWM signal in backward direction. This is attractive for in-vivo applications.

9329-145, Session 7

Revealing starch denaturation with SHG microscopy

Nirmal Mazumder, Fu-Jen Kao, National Yang-Ming Univ. (Taiwan)

Starch is a major energy source in food products in our daily life. Starch plays a crucial role in textural modification via a process called 'gelatinization'. Starch gelatinization is influenced by a number of parameters, including temperature, water content, the break up and partial dissolution of the starch granule upon heating in the presence of water. Detail understanding of gelatinization process is required to optimize the starch-based foods.

We used SHG imaging to investigate the distribution of double helical amylopectin within starch granules during gelatinization. The aim of this work is to investigate the amylopectin crystallinity pattern on the interaction between starch and water during gelatinization. Since the interactions between starch and water also influence the starch functionality, a better understanding of those interactions could provide a basis for modifying starch functional properties as well as improving quality of starch-based food. In the present paper we briefly consider the effect of water on the fiber patterns obtained from the periphery of potato granules. The combination of SHG microscopy and Stokes polarimeter hence makes a powerful tool to investigate the structural order of starch granules.

9329-38, Session 8

Label-free second order susceptibility imaging of collagen (*Invited Paper*)

Chen-Yuan Dong, Chiu-Mei Hsueh, Ya-Der Huang, Hsuan-Shu Lee, National Taiwan Univ. (Taiwan)

The ability to image and identify different tissue constituents without extrinsic labeling would expedite tissue-based diagnosis and contribute to understanding tissue genesis. In this work, we describe the use of second order susceptibility as an alternative contrast mechanism in imaging and discriminating collagen fibers. By rotating polarization of excitation beam and analyze angular dependence of second harmonic generation intensity, different types of fibrillar collagen can be differentiated. With additional development, this technique may find potential applications in tissue engineering.

9329-39, Session 8

Influence of pulse width on photodamage and inflammation during intravital autofluorescence 2-photon microscopy of murine intestinal mucosa

Gereon Hüttmann, Lisa Krapf, Regina Orzekowsky-Schroeder, Norbert Koop, Alfred Vogel, Antje Klinger, Univ. zu Lübeck (Germany)

Ultrashort pulses with pulse widths below 10 fs have extended spectral bandwidth and should be ideal for excitation of multiple fluorophores simultaneously which occur in vital tissue. The inverse relationship between fluorescence intensity and laser pulse duration should additionally improve of signal strength. Autofluorescence 2-photon (A2P) microscopy was applied to image living gut mucosa using a 200 fs Ti:Sa laser in comparison to a 10 fs laser. Basically, the same cellular structures were visible with 10 fs pulses at a 2 to 4 times reduced excitation flux. Only one scan was needed to excite NADH, the red shifted fluorescence in lysosomes and dendritic cells, and SHG. Nonlinear photodamage, which was noticeable as hyperfluorescence and functional and structural alteration of the tissue, occurred after repeated scanning irradiation with both lasers but at different thresholds. Immigration of polymorphonuclear leucocytes into the epithelium, a sign of inflammation, occurred after a few minutes of laser irradiation with 10 fs laser pulses, but usually not after exposure with 200 fs laser pulses.

9329-40, Session 8

Yb-fiber laser for multimodal imaging

Ilyas Saytashev, Michigan State Univ. (United States); Bingwei Xu, Marcos M. Dantus, Biophotonic Solutions, Inc. (United States)

We report on multimodal depth-resolved imaging of unstained living *Drosophila Melanogaster* larva and other mammalian tissues including skin using sub-50 fs pulses centered at 1060 nm wavelength from a Yb-fiber laser oscillator. The images are obtained using a new Yb fiber oscillator, designed as a convenient ultrashort pulse source for clinical use that includes an automated pulse shaper using MIIPS and a microscope detection unit to measure and compresses the output pulses (primarily second, third and fourth order) at the focal plane. Bright images based on second and third-harmonic generation (SHG and THG) as well as two-/three-photon excited fluorescence (TPEF/3PEF) contrast, are obtained. Two-photon modalities are inversely proportional to the pulse duration while three-photon modalities are proportional to the pulse duration squared. The laser is used to image different samples including fluorescently stained slides of mouse kidney and intestine sections with standard fluorescent labels (such as DAPI and Alexa Fluor 355, 488, and 568), unstained living whole *Drosophila Melanogaster* larva, and other mammalian unstained tissues such as skin. The efficient three-photon excitation at an equivalent wavelength of 353 nm eliminates the need for a tunable femtosecond laser capable of tuning to 720 nm for efficient two-photon excitation of NAHD, DAPI and Alexa Fluor 355. Images generated by different modalities such as TPEF, 3PEF, SHG and THG are compared. Depth scans and reconstructed 3D images will be shown.

9329-41, Session 8

Label-free multi-photon imaging of Barrett esophagus

Seyed Soroush Mehravar, College of Optical Sciences, The Univ. of Arizona (United States); Philip Usera, Hemant Chatrath, Nasser Peyghambarian, College of Optical

**Conference 9329:
Multiphoton Microscopy in the Biomedical Sciences XV**

Sciences, The Univ. of Arizona (United States); Bhaskar Banerjee, The Univ. of Arizona College of Medicine (United States); Khanh Q. Kieu, College of Optical Sciences, The Univ. of Arizona (United States)

Barrett's esophagus (BE) is typical of pre-cancerous disorders where neoplastic changes are invisible to the naked eye and the practice of random biopsy is hampered by large sampling error. There is a clear need to develop in-vivo point-of-care diagnostics that can identify the histological features of neoplasia without traditional histology. Multi-photon microscopy (MPM) has emerged as an alternative solution for fast and label-free study of structures, in vivo. The inherent optical sectioning in addition to high spatial resolution of MPM enables label-free imaging of sub-cellular organelles to be imaged with sub-micron accuracy in 3-dimensions. Moreover, the multi-photon imaging (MPI) on specimens, does not affect their cellular compositions during the image acquisition.

We developed a small, portable, inexpensive MPM to explore mucosal biopsies of BE. Specimens were illuminated by a compact mode-locked fiber laser operating at a telecommunication wavelength at 1550nm and their back scattered second- and third-harmonic generation signals were investigated. THG and SHG images were compared to standard H&E microscopy. THG images displayed cell nuclei shape and distribution with sufficient resolution and contrast to identify the established features of normal and dysplastic mucosa. Furthermore, SHG images revealed the distribution and characteristics of collagen that is not seen under H&E- which changed with dysplasia.

The combination of THG and SHG images appear to generate images of cell nuclei and collagen that can lead to label-free diagnosis in Barrett's, using a small, portable MPM.

9329-42, Session 8

Non-linear imaging and characterization of atherosclerotic arterial tissue using combined SHG and FLIM microscopy

Riccardo Cicchi, Istituto Nazionale di Ottica (Italy) and European Lab. for Non-linear Spectroscopy (Italy); Christian Matthaeus, Leibniz-Institut für Photonische Technologien e.V. (Germany); Enrico Baria, Univ. degli Studi di Firenze (Italy); Marta Lange, European Lab. for Non-linear Spectroscopy (Italy); Tobias Meyer, Leibniz-Institut für Photonische Technologien e.V. (Germany); Annika Lattermann, Universitätsklinikum Jena (Germany); Benjamin Dietzek, Leibniz-Institut für Photonische Technologien e.V. (Germany) and Abbe Ctr. of Photonics Jena (Germany) and Friedrich-Schiller-Univ. Jena (Germany); Bernhard R. Brehm, Katholische Klinikum Koblenz (Germany); Juergen Popp, Leibniz-Institut für Photonische Technologien e.V. (Germany) and Abbe Ctr. of Photonics Jena (Germany) and Friedrich-Schiller-Univ. Jena (Germany); Francesco S. Pavone, European Lab. for Non-linear Spectroscopy (Italy) and Univ. degli Studi di Firenze (Italy)

Atherosclerosis is among the most widespread cardiovascular diseases and one of the leading cause of death in the Western World. Characterization of arterial tissue in atherosclerotic condition is extremely interesting from the diagnostic point of view, especially for what is concerning collagen content and organization because collagen plays a crucial role in plaque vulnerability. Routinely used diagnostic methods, such as histopathological examination, are limited to morphological analysis of the examined tissues, whereas an exhaustive characterization requires immune-histochemical examination and a morpho-functional approach. Non-linear microscopy techniques offer the potential for providing morpho-functional information

on the examined tissues in a label-free way. In this study, we employed combined SHG and FLIM microscopy for characterizing collagen organization in both normal arterial wall and within atherosclerotic plaques. Image pattern analysis of SHG images allowed characterizing collagen organization in different tissue regions. In addition, the analysis of collagen fluorescence decay contributed to the characterization of the samples on the basis of collagen fluorescence lifetime. Different values of collagen fiber mean size, collagen distribution, collagen anisotropy and collagen fluorescence lifetime were found in normal arterial wall and within plaque depositions, prospectively allowing for automated classification of atherosclerotic lesions and plaque vulnerability. The presented method represents a promising diagnostic tool for evaluating atherosclerotic tissue and has the potential to find a stable place in clinical setting as well as to be applied in vivo in the near future.

9329-43, Session 8

Biomaterial discrimination using wavelength-dependent SHG excitation efficiency

Stephen J. Matcher, Nicola H. Green, Robin M. Delaine-Smith, Gwendolen C. Reilly, Hannah Askew, Xuesong Hu, The Univ. of Sheffield (United Kingdom)

Tissue engineering is a new discipline at the interface between materials science and medicine. A major paradigm is to seed collagen-producing cells onto a synthetic polymer scaffold and then stimulate these cells to produce a new collagen-based extracellular matrix. SHG microscopy, offering label-free collagen detection, is thus a powerful tool to elucidate tissue engineering. Here we ask instead whether tissue engineering can help to elucidate SHG microscopy.

Whether the wavelength-dependence of SHG excitation efficiency carries any sample-dependent information for biomaterials is contentious. Disagreement even exists concerning whether SHG emission from collagen falls monotonically with increasing excitation wavelength. System-dependent calibration issues and light scattering effects complicate such measurements.

By seeding fibroblasts onto an electrospun polycaprolactone (PCL) fiber scaffold, we produce a sample in which two distinct species of SHG harmonophore, PCL fibers and fibroblast-derived collagen, are co-localized at the micron scale. We measure the relative epi-detected SHG signal from both materials vs excitation wavelength and find that the SHG from PCL fibers is intense at 840 nm but vanishes at 940 nm, whereas SHG from collagen is not observed at 840 nm but is distinct at 940 nm.

We formulate a model in which a wavelength-scan is considered as a momentum-space mapping of the second-order non-linear structure factor. For backward-generated SHG the range of momentum-space that is traversed is nearly two orders of magnitude higher than for forward-generated SHG. We show that forward-generated SHG will usually show a monotonic fall with wavelength but backward-generated SHG can show more complicated behaviour.

9329-44, Session 8

Discontinuous sampling in beam-scanning microscopy

Ryan D. Muir, Paul D. Schmitt, Emma L. DeWalt, Shane Z. Sullivan, Ximeng You, Garth J. Simpson, Purdue Univ. (United States)

Discontinuous sampling is demonstrated for video-rate beam-scanning microscopy with lock-in amplification (LIA) of multiple simultaneous harmonics on multiple parallel channels and for high frame rate fluorescence lifetime imaging microscopy (FLIM). In the first application, second harmonic generation (SHG) microscopy is performed with 8 MHz

**Conference 9329:
Multiphoton Microscopy in the Biomedical Sciences XV**

polarization modulation. Polarization analysis allows assessment of local structure from laboratory frame measurements. Digital lock-in amplification was performed at both the fundamental and second harmonic of the modulation frequency for three parallel channels of data acquisition. Since a complete set of polarization-dependent data could not be acquired within a single focal volume in a single line-trace of a resonant fast-scan mirror, data from the trace and retrace were combined for discontinuous LIA analysis. In this manner, data for full polarization analysis was acquired on each line in the image every 125 μ s for video-rate imaging, substantially reducing 1/f noise in polarization-dependent SHG microscopy. This same discontinuous sampling strategy was used for FLIM to perform interleaved detection for improved temporal resolution by defining a beat pattern between the laser repetition rate and the mirror period, which precisely rephased every 10 consecutive periods of the mirror. Considering both trace and retrace allowed binning with a temporal resolution of 500 ps to extract lifetime images continuously with frame rates as fast as 15 Hz. The relative simplicity of the instrumentation required to perform the analysis combined with the signal to noise advantages afforded both by the reduction in 1/f noise and through the use of higher beam intensities suggest discontinuous sampling may be particularly well suited for nonlinear optical and multi-photon imaging approaches using pulsed laser sources.

9329-45, Session 8

Second harmonic generation imaging in tissue engineering and cartilage pathologies

Magnus B. Lilledahl, Norwegian Univ. of Science and Technology (Norway); Magnus Ø. Olderøy, Norwegian Ctr. for Stem Cell Research (Norway); Andreas Finnøy, Norwegian Univ. of Science and Technology (Norway); Kristin Olstad, Norwegian Univ. of Life Sciences (Norway); Jan E. Brinchman, Norwegian Ctr. for Stem Cell Research (Norway)

The second harmonic generation from collagen is highly sensitive to what extent collagen molecules are ordered into fibrils as the SHG signal is approximately proportional to the square of the fibril thickness. This can be problematic when interpreting SHG images as thick fibers are much brighter than thinner fibers such that quantification of the amount of collagen present is difficult. On the other hand SHG is therefore also a very sensitive probe to determine whether collagen have assembled into fibrils or are still dissolved as individual collagen molecules. This information is not available from standard histology or immunohistochemical techniques. The degree for fibrillation is an essential component for proper tissue function. We will present the usefulness of SHG imaging in tissue engineering of cartilage as well as cartilage related pathologies. When engineering cartilage it is essential to have to appropriate culturing conditions which cause the collagen molecules assemble into fibrils. By employing SHG imaging we have studied how cell seeding densities affect the fibrillation of collagen molecules. Furthermore we have used SHG to study pathologies in developing cartilage in a porcine model. SHG images reveals details which can not be seen by conventional methods. In both cases SHG reveals information which is not visible in conventional histology or immunohistochemistry.

9329-46, Session 9

Stimulated Raman scattering microscopy of chemical tags in live cells (*Invited Paper*)

YanYi Huang, Xing Chen, Peking Univ. (China)

Simulated Raman scattering (SRS) microscopy offers enhanced sensitivity over the spontaneous Raman scattering. Furthermore, the intensity of the SRS signal is proportional to the analyte concentration, enabling quantitative

imaging. These advantageous features of SRS microscopy prompted us to explore its use for bioorthogonal Raman imaging. Label-free SRS detects vibrational signals from the intrinsic chemical bonds of biomolecules, and thus suffers from poor molecular specificity, because many chemical bonds are shared by different types of biomolecules. We envisioned that coupling SRS technology with the bioorthogonal Raman reporters such as the alkyne would enable live imaging of biomolecules with both high sensitivity and molecular specificity. We demonstrate SRS imaging of four major classes of biomolecules including nucleic acids, proteins, glycans, and lipids in live cells using the alkyne as the bioorthogonal Raman reporter. Through this approach we have visualized various chemical tags in live cells. The alkyne, which is small, non-perturbative, and possesses a Raman signal in the silent region, functioned as a bioorthogonal Raman reporter. Lipids, nucleic acids, proteins, and glycans were metabolically labeled with the alkyne, which enables live-cell SRS imaging with molecular specificity. In addition to an alkyne, the carbon-deuterium (C-D) bond also processes a Raman resonance within the silent region and isotopic substitution with deuterium has been explored for cellular imaging of lipids, proteins, and small molecule drugs. While the C-D bond requires only isotopic substitution and thus is more biocompatible, the alkyne offers a greater Raman cross-section. Notably, there are some alkyne-bearing drugs that are in current clinical use and our SRS imaging method will be valuable for the pharmacological studies. Furthermore, many other functional groups fulfill the criteria of the bioorthogonal Raman reporters such as azide and nitrile, and isotopic substitution with deuterium, carbon-13, or nitrogen-15 can further expand the "color palette". The bioorthogonal SRS imaging methodology complements the fluorescence and label-free microscopies by offering a new imaging modality that combines some advantageous features from both. With further improvements on the detection sensitivity, it will become achievable to specifically image the low abundant biomolecules in live cells with SRS microscopy.

9329-47, Session 9

Bioorthogonal vibrational imaging of dynamic metabolism of living systems (*Invited Paper*)

Wei Min, Columbia Univ. (United States)

Here we report a bioorthogonal vibrational imaging platform to probe dynamic metabolism of living systems with superb sensitivity, specificity and biocompatibility. To do so, we couple stimulated Raman scattering (SRS) microscopy, an emerging nonlinear Raman imaging technique, with the small, vibrant and bioorthogonal tags including stable isotopes (including deuterium and ^{13}C) and triple bonds (i.e., alkynes). Physical principle of the underlying optical spectroscopy will be presented, illustrated by emerging biomedical applications such as imaging lipid metabolism, protein synthesis, DNA replication, RNA synthesis, glucose uptake, drug tracking and multicolor imaging.

9329-48, Session 9

Visualization and quantification of peripheral myelin degeneration in amyotrophic lateral sclerosis (ALS) mouse model (SOD1G93A) and patients with stimulated Raman scattering (SRS)

Wenlong Yang, Feng Tian, Harvard Univ. (United States); Daniel Mordes, Harvard Univ. (United States) and Massachusetts General Hospital (United States); Naoki Suzuki, Satomi Suzuki, Kevin Eggan, Xiaoliang S. Xie, Harvard Univ. (United States)

Stimulated Raman Scattering (SRS) microscopy was used to study myelin

**Conference 9329:
Multiphoton Microscopy in the Biomedical Sciences XV**

degeneration in ALS mouse model (SOD1G93A) and human patients. The imaging was performed on an Olympus BX61WI upright microscope with FV300 scanning unit. The objective used in the experiment was the IR version Olympus UPLSAPO 60X water immersion objective. The laser source employed was picoEMERALD from A. P. E Berlin. Stimulated Raman loss signal at 2850 cm^{-1} , which corresponds to CH₂ symmetric stretching vibration in lipids, was probed in the imaging. An imageJ macro program was written to quantify the lipid ovoids in the nerve tissues. The program calculates spatial correlation coefficient of pre-selected templates and SRS image. Numbers of areas with correlation coefficient higher than chosen threshold values was counted as numbers of lipid ovoids. Ex vivo and in vivo 3-dimensional (3-D) SRS imaging of sciatic nerves from SOD1G93A mice from 5 weeks to 4 months old were quantified. The quantification showed progressive increase in lipid ovoids counting, which signifies degeneration of myelin. It is found that such degeneration preceded outward motor symptom onset. To enable serial observation of peripheral myelin in vivo, we developed a minimally invasive imaging procedure. Using this approach, we found significant degeneration of peripheral myelin was coincident with the earliest detectable signs of muscle denervation and preceded physiological decline in motor nerve function. For human patients, a different set of templates were used in the quantification. Significant increase in lipid ovoids counting is also observed in the ALS patients compared with control.

9329-49, Session 9

Probing myelin morphology and organization with label-free microscopy

Alicja Gasecka, Institut Univ. en Santé Mentale de Quebec, Univ. Laval (Canada) and Institut Fresnel (Canada); Pierre Gravel, Institut Univ. en Santé Mentale de Quebec, Univ. Laval (Canada) and Univ. du Québec (Canada); Raphael Turcotte, Wellman Ctr. for Photomedicine (United States); Steve Begin, Daniel Cote, Ctr. de Recherche de l'Univ. Laval Robert-Giffard (Canada) and Institut Univ. en Santé Mentale de Quebec, Univ. Laval (Canada)

Understanding the causes of neurodegenerative diseases, developing effective diagnostic strategies and comparing treatment methods often require the investigation of nervous system cells morphology (i.e. number, myelination, and size of axons in a nerve). Coherent anti-Stokes Raman Scattering (CARS) microscopy has been demonstrated to be a useful tool in neurobiology providing label-free imaging of myelin sheath in nervous system. While there is a continued interest to observe myelin structure, quantitative morphometric analysis of nerve fibres remains a challenge. In particular, in brain tissue where fibres exhibits small diameter ($\sim 1\text{-}3\mu\text{m}$) and varying local orientation. In this work, we developed an automated myelin identification and analysis method that is capable of providing a complete picture of axons myelination and morphology at microscopic scale in structurally complex samples. This so-called anisotropy-segmentation-algorithm (ASA) performs three main procedures – extract molecular anisotropy of membrane phospholipids using CARS images recorded for a large number of excitation polarization states, then identifies and classifies regions of different molecular organization using Gaussian mixture, and finally calculate myelin thickness, axon diameters and area for segmented regions. We applied this method to monitor lesions of a commonly used animal model of multiple sclerosis (MS), experimental autoimmune encephalomyelitis (EAE) in order to quantify the degree of organization/disorganization in the myelin structure. Next, we analyzed the local organization and structure of myelinated axons in the splenium of human corpus colosum. We demonstrate that ASA method provides more accurate description of the nerve fibers and allows the identification of subtle differences in myelin organization.

9329-50, Session 9

Visualizing murine meibomian glands physiology and pathology using coherent anti-stokes Raman scattering (CARS) microscopy and multi-photon microscopy (MPM)

Joachim Pruessner, Univ. zu Lübeck (Germany) and Wellman Ctr. for Photomedicine (United States); Reginald Birngruber, Univ. zu Lübeck (Germany); Conor L. Evans, Wellman Ctr. for Photomedicine (United States)

Evaporative dry eye disease is an ailment that affects approximately 21 million people in the United States alone. In most cases, a dry eye condition is caused by dysfunction of the meibomian glands (MGD) in the eyelid, which leads to a rapid evaporation of the tear film causing dryness and burning. Despite the high prevalence and the need for a better treatment, the fundamental pathogenesis remains unclear, treatments remain palliative, and diagnostic tools are limited in their number and capability. To carry out detailed examination of intact meibomian gland physiology, function, and pathology, we have employed a suite of label-free image technologies including two-photon excited fluorescence (TPEF), second-harmonic generation (SHG) and Coherent anti-Stokes Raman Scattering (CARS) microscopy. CARS microscopy, in particular, was capable of revealing the subcellular, cellular, and whole-gland level features in the lipid-rich meibomian glands. To evaluate potential alterations in eyelid tissue due to the presence of body fat or gene knockouts, we made use of mouse models. The eyelids and meibomian glands of melanocortin-4-receptor (Mc4r) mutated mice (C57BL/6 Mc4r^{e/e}, Tyr^{+/+}, loxTB Mc4r) were compared to those of wild type (C57BL/6 Mc4r^{e/e}, Tyr^{+/+}) redhead mice by acquiring and analyzing multi-channel, multi-area mosaic images as well as CARS spectral data. This study showed that a combination of non-invasive, non-linear imaging modalities could serve as a diagnostic toolkit in the evaluation of meibomian gland dysfunction and subsequent therapeutic monitoring.

9329-51, Session 9

Local organization of lipids in myelinated axons probed by polarization resolved coherent anti-stokes Raman scattering nonlinear microscopy

Paulina Gasecka, Naveen K. Balla, Julien Duboisset, Patrick Ferrand, Hervé Rigneault, Sophie Brasselet, Institut Fresnel (France)

Polarization resolved Coherent Anti-Stokes Raman Scattering (CARS) microscopy is a powerful technique to image structural information in biomolecular assemblies. While several studies have been so far performed in this field to image molecular organization of lipids in artificial membranes, only very few analyzes exist in real biological tissues. We have developed a polarization resolved CARS method capable of revealing molecular order in complex lipid assemblies, even in the absence of knowledge of the exact lipid composition, conformation and membrane morphology [1]. This method is applied to the analysis of the orientational behavior of lipids in myelin sheaths in the mice spinal cord tissue, in the context of experimental autoimmune encephalomyelitis disease (EAE). Analyzing the CARS signal modulation originating from the tuning of the incident linear polarizations leads to a direct read-out of order parameters related to the symmetry properties of the lipids angular distribution function. The data indicate the presence of high disorder as compared to artificial membranes, which can be due to the large amount of angular freedom of lipids, as well as morphology heterogeneities in myelin. Analyzing local regions shows moreover an even more significant loss of order in regions exhibiting local disruption of the myelin membranes, as a consequence of demyelination. Our results provide detailed quantitative information on local molecular

**Conference 9329:
Multiphoton Microscopy in the Biomedical Sciences XV**

arrangements, making this method a valuable tool in the structural study of the consequence of neurodegenerative diseases.

[1] F.-Z. Bioud, P. Gasecka, P. Ferrand, H. Rigneault, J. Duboisset, and S. Brasselet, *Phys. Rev. A* 89, 013836 (2014)

9329-52, Session 9

Monitoring lipid accumulation in the green microalga *botryococcus braunii* with frequency-modulated stimulated Raman scattering

Chun-Chin Wang, Dayananda Chandrappa, Nicholas Smirnoff, Julian Moger, Univ. of Exeter (United Kingdom)

The potential of microalgae as a source of renewable energy has received considerable interest because they can produce lipids (fatty acids and isoprenoids) that can be readily converted into biofuels. However, significant research in this area is required to increase yields to make this a viable renewable source of energy. An analytical tool that could provide quantitative in situ spectroscopic analysis of lipids synthesis in individual microalgae would significantly enhance our capability to understand the synthesis process at the cellular level and lead to the development of strategies for increasing yield. Stimulated Raman scattering (SRS) microscopy has great potential in this area however, the pump-probe signal from two-color two-photon absorption of pigments (chlorophyll and carotenoids) overwhelm the SRS signal and prevent its application. Clearly, the development of a background suppression technique is of significant value for this important research area.

To overcome the limitation of SRS in pigmented specimens, we establish a frequency-modulated stimulated Raman scattering (FM-SRS) microscopy that eliminates the non-Raman background by rapidly toggling on-and-off the targeted Raman resonance. Moreover, we perform the background-free imaging and analysis of intracellular lipid droplets and extracellular hydrocarbons in a green microalga with FM-SRS microscopy. We believe that FM-SRS microscopy demonstrates the potential for many applications in pigmented cells and provides the opportunity for improved selective visualization of the chemical composition of algae and plants.

9329-53, Session 10

Label-free functional imaging of membrane potential by stimulated Raman scattering microscopy (*Invited Paper*)

Bin Liu, Key Lab. of Science and Technology on Tunable Laser, Harbin Institute of Technology (China); Hyeon Jeong Lee, Interdisciplinary Life Science Program, Purdue Univ. (United States); Delong Zhang, ChienSheng Liao, Purdue Univ. (United States); Yuanqin Xia, Key Lab. of Science and Technology on Tunable Laser, Harbin Institute of Technology (China); Ji-Xin Cheng, Purdue Univ. (United States)

Measurement of membrane potential is important because changes in cellular membrane potential are used to code and transmit information between different cells. Commonly used optical methods for monitoring membrane potential, including second harmonic generation and two-photon excitation fluorescence, are based on detecting signal from voltage-sensitive dyes which may alter the properties of cellular membrane. Label-free optical recording of membrane potential with high spatiotemporal resolution is highly desired. Here, using erythrocyte ghost as a model, we demonstrate label-free imaging of membrane potential through detecting the vibrational spectrum of single membrane by hyperspectral stimulated Raman scattering (SRS) microscopy. A significant change of SRS spectral profile with respect

to the transmembrane potential was observed. Quantitative correlation between the membrane potential and the SRS spectral profile change was investigated. Specifically, the ratio of SRS signal intensity at 2930 cm⁻¹ to that at 2850 cm⁻¹ (I2930/I2850) increased by ~1.5 times when the potential across the erythrocyte ghost membrane varied from 10 mV to -10 mV. Our results show the promise of employing hyperspectral SRS imaging to measure membrane voltage in live neurons in a label-free manner.

9329-54, Session 10

Detection of human brain tumors with SRS microscopy

Daniel A. Orringer, Univ. of Michigan Health System (United States); Minbiao Ji, Harvard Univ. (United States); Spencer Lewis, Sandra Camelo-Piragua, Univ. of Michigan Health System (United States); Xiaoliang S. Xie, Harvard Univ. (United States)

Surgery is the cornerstone for the treatment of brain tumors. However, achieving optimal surgical outcomes in brain tumor surgery remains a challenge. We have previously suggested that stimulated Raman scattering (SRS) microscopy may be incorporated into the surgical workflow to improve outcomes by helping delineate tumor from adjacent normal brain. Here we describe a comprehensive series of 21 neurosurgical cases demonstrating the ability of SRS to detect the central features of tumor-infiltrated and normal brain *ex vivo*. We demonstrate key histologic features of intrinsic (low grade gliomas, high grade gliomas) and extrinsic (metastases, meningiomas, schwannomas) brain and spinal tumors. We also report the derivation of a scoring function, based on SRS image quantification, enabling rapid binary discrimination of normal- from tumor-infiltrated brain. Our results suggest that SRS may improve surgical accuracy and, therefore, outcome for brain tumor patients.

9329-55, Session 10

Imaging human melanoma using coherent anti-stokes Raman scattering (CARS) and multiphoton microscopy (MPM)

Hequn Wang, Sam Osseiran, Elisabeth Roider, Vivien Igras, David E. Fisher, Conor L. Evans, Wellman Ctr. for Photomedicine (United States)

Skin cancer is the most common type of cancer in North America, with melanoma representing the vast majority of skin cancer deaths. One in five North Americans will develop skin cancers during their lifetime. Despite routine screening, skin cancers, especially melanoma, are typically diagnosed at late stages. Optical techniques could provide non-invasive, high-resolution morphological and biochemical analyses of suspect lesions in real time. Coherent anti-Stokes Raman scattering (CARS), a coherent Raman technology whose contrast arises from the vibrations of chemical species, is a promising technology for the early diagnosis of skin cancers, especially when used as part of a multiphoton microscope toolkit. Recent CARS studies have been focused on visualizing and quantifying biomarkers thought to be important to the early stage of melanoma formation. To capture a range of potential chemical markers, a multiphoton system incorporating CARS, two-photon excited fluorescence, second harmonic generation, and fluorescence lifetime imaging was developed based on a widely tunable Insight light source. Normal and pre-cancerous melanomas of human and murine origin were imaged and analyzed using both CARS and MPM, focusing on characterizing lipids, pigments, NADH, FAD, and collagen. Specific attention was paid to spectral signatures in the Raman spectrum that could serve as biomarkers for the detection of pre-cancerous and melanoma skin lesions across a range of skin types. Complementary siRNA cell culture studies have additionally identified novel CARS signature that may be incorporated in future melanoma imaging efforts.

**Conference 9329:
Multiphoton Microscopy in the Biomedical Sciences XV**

9329-56, Session 10

Histology in vivo: chemical contrast combined with clinical multimodal multiphoton tomography

Martin Weinigel, JenLab GmbH (Germany) and Univ. of Technology, Ilmenau (Germany); Hans Georg Breunig, Saarland Univ. (Germany) and JenLab GmbH (Germany); Karsten Koenig, JenLab GmbH (Germany) and Univ. des Saarlandes (Germany)

Label free multiphoton tomography based on two-photon autofluorescence (AF), fluorescence lifetime imaging (FLIM) and second harmonic generation (SHG) is supplemented by coherent anti-Stokes Raman scattering (CARS). Here, we present a compact, mobile and flexible clinical tomograph including a novel detector design with multiple miniaturized detectors for individual acquisition of all four contrast mechanism. The illustration of the distribution of endogenous fluorophores NAD(P)H, melanin and elastin, SHG-active collagen and as well as non-fluorescent lipids within human skin in vivo is possible, which accelerates and rivals in vivo histology.

9329-57, Session 10

Mechanically-induced protein structural changes in fibrin hydrogels using B-CARS microscopy

Sapun H. Parekh, Frederik Fleissner, Mischa Bonn, Max-Planck-Institut für Polymerforschung (Germany)

Fibrin is a protein hydrogel material responsible for stabilizing the platelet-rich blood clot over a wound in blood coagulation. Its utilitarian mechanical properties, namely being stiff or deformable as needed, result from the unique hierarchical organization of the polymer network. Experimental and theoretical studies have shown that single filament stretching, network rearrangements, and protein unfolding are responsible for this unique mechanical behavior. In this work, we investigate the biophysics of fibrin unfolding in response to uniaxial stretch in situ using coherent Raman imaging. Fibrin hydrogels are stretched to regime where unfolding transitions of β -helical structures to β -sheet occur, and spatially resolved broadband coherent anti-Stokes Raman scattering (B-CARS) spectra of fibrin gels are acquired and quantitatively analyzed. The secondary structure is inferred from peak analysis of the amide I and amide III regions, which are sensitive to subtle changes in protein structure. Experiments on gels of different polymer concentration and crosslinker density show unfolding transitions that correlate with nonlinear effects seen in shear rheology. Finally, imaging results show an inhomogeneous unfolding distribution near inert beads in the gel, suggesting that local stresses on platelets within biological clots is different from the bulk mechanical response. This demonstrates the use of hyperspectral B-CARS microscopy to measure local, mechanically-induced conformational changes in proteins.

9329-58, Session 10

Simultaneous quadruple modal nonlinear optical imaging for gastric diseases diagnosis and characterization

Zi Wang, Wei Zheng, Jian Lin, Zhiwei Huang, National Univ. of Singapore (Singapore)

We report the development of a unique quadruple nonlinear optical microscopy (i.e., stimulated Raman scattering (SRS), second-harmonic generation (SHG), third-harmonic generation (THG) and two-photon excitation fluorescence (TPEF)) platform for characterization of the gastric

diseases (e.g. intestinal metaplasia(IM), adenocarcinoma, signet ring cell carcinoma). 35 samples biopsied from 28 patients with gastric diseases were imaged by the developed technique. TPEF reveals the cell morphology and can reflect the damage inside glands caused by the diseases. THG visualizes the internal structure of nuclei with high spatial resolution, which facilitates the identification of neutrophils that are usually used as a feature of inflammation. Besides, THG intensity shows the optical heterogeneity inside nuclei, which varies among different types gastric diseases. SHG images the distribution of collagen in lamina propria and submucosa. Collagen is found to aggregate for moderate gastritis and IM. SRS highlights the goblet cells found in IM. Moreover, quantitative information enabled by the nonlinear optical imaging technique provides more information for the diagnosis of gastric diseases. This work shows that the co-registration of multimodal images can be an effective means for diagnosis and characterization of gastric diseases at the cellular and molecular levels.

9329-59, Session 11

Hyperspectral stimulated Raman scattering imaging of drug-cell and drug-drug interaction (Invited Paper)

Dan Fu, Harvard Univ. (United States); Jing Zhou, Novartis Institutes for Biomedical Research, Inc. (United States); Xiaoliang S. Xie, Harvard Univ. (United States)

Recent developments in Stimulated Raman Scattering (SRS) microscopy offers exciting new opportunities in studying biological samples with high spatial and temporal resolution based on intrinsic molecular contrasts. Many biological and biomedical applications are enabled by a simple single-band SRS imaging approach which probes prominent Raman features of the molecules of interests. To extend the use of SRS microscopy to study complicated biological samples, where Raman bands from multiple species have significant overlap, we developed hyperspectral SRS imaging. It bridges the gap between SRS, which offers high acquisition speed by low information content, and spontaneous Raman, which has high specificity but low acquisition speed.

We applied hyperspectral SRS imaging to study the intracellular uptake dynamics of tyrosine kinase inhibitors (TKIs, especially for the treatment of chronic myelogenous leukemia), a class of well-known targeted cancer drugs including imatinib and nilotinib. We discovered that these drugs were selectively enriched in the lysosomes due to the lysosomotropic property of weakly basic molecules. The enrichment factor depends on not only the acid dissociation constant (pKa) of the drugs, but also their solubility. More importantly, using hyperspectral SRS imaging, we demonstrated that chloroquine can indirectly interact with TKIs through lysosome pH adjustment, thereby increasing their drug efficacy. In contrast to the commonly proposed autophagy inhibition mechanism, this provides an alternative mechanism to explain the previously demonstrated synergistic effect of chloroquine and TKIs in a number of tumor models, which could have wide implications for the development of future generation of TKI drugs.

9329-60, Session 11

In vivo microsecond scale vibrational spectroscopy imaging by modulation multiplexed stimulated Raman scattering (Invited Paper)

ChienSheng Liao, Pu Wang, Ping Wang, Robert Oglesbee, Ji-Xin Cheng, Purdue Univ. (United States)

Raman spectroscopy has been widely used to resolve chemical composition in a label-free manner. However in vivo study is still difficult because of the low Raman cross section and inefficient collection of photons. Since conventionally spectral acquisition requires a detector array to collect

**Conference 9329:
 Multiphoton Microscopy in the Biomedical Sciences XV**

spatially dispersed photons, scattered photons are blocked by a slit in order to achieve high spectral resolution, thus prolonging the acquisition time. We address the limitations by developing a modulation multiplexed stimulated Raman scattering technique. We modulate each color of a broadband femtosecond pump beam with a distinct frequency by scanning the dispersed pump beam on a spatial pattern. Through the stimulated Raman scattering process, the vibrational spectrum of the sample is coded in the narrowband Stokes beam, and then decoded by Fourier transform analysis of detected photons. By collecting all the scattered photons, this technique potentially can improve the collection efficiency one thousand times for scattering environment. Here, within 60 ps pixel dwell time, without any anesthetizing treatment, we successfully demonstrate in vivo spectroscopy imaging of *Caenorhabditis elegans* which contain multiple layers of compartments. Two kinds of compartments, lipid droplets and lysosome related organelles, are observed based on the spectral profiles, which were all assigned to lipid droplets by single color coherent Raman techniques. Our fast spectroscopy imaging opens a new window for in vivo analysis of target molecules in a scattering environment. The reported technique also holds the potential for clinical practice, for example, intraoperative cancer margin detection or endoscopy for early diagnosis.

9329-61, Session 11

Resolution and contrast enhancement in label-free microscopy

Alicja Gasecka, Institut Univ. en Santé Mentale de Quebec, Univ. Laval (Canada) and Institut Fresnel (Canada); Amy Daradich, Harold Dehez, Institut Univ. en Santé Mentale de Quebec, Univ. Laval (Canada); Michel Piche, Univ. Laval (Canada); Daniel Cote, Ctr. de Recherche de l'Univ. Laval Robert-Giffard (Canada) and Institut Univ. en Santé Mentale de Quebec, Univ. Laval (Canada)

Coherent anti-Stokes Raman Scattering (CARS) microscopy has been used with great success to image lipid-rich structures in a broad range of tissue samples. While there is a continued interest to observe tissue on a finer scale, optical microscopy is fundamentally limited in its spatial resolution (250-350nm) by diffractive effects. This issue has been essentially addressed by fluorescence microscopy techniques where optical resolution enhancement relies on manipulating the excited-state population by photochemical switching or by selective depletion of fluorophores. Unlike fluorescence, CARS is a parametric process, whereby no energy is transferred from the excitation field to the molecule, hence the tools used in fluorescence are not applicable to CARS microscopy. In this work we propose an alternative approach for enhancing optical resolution based on the intensity difference between two images acquired using either a fundamental Gaussian laser mode or a doughnut-shaped mode. This so-called Switching LAsER Mode Coherent anti-Stokes Raman Scattering (SLAM-CARS) microscopy allows for sub-diffraction-limited imaging with lateral resolution of 0.36 μm (a 30% improvement) and significant contrast enhancement. This method is a promising technique for biological applications; is straight-forward to implement and can easily be retrofitted into conventional microscopes, high laser powers are not required and no limitations are placed on the specimen (i.e., fluorescent markers used in super-resolution techniques). We applied SLAM-CARS to image myelin sheaths in mouse brainstem and map the volume, orientation and density of myelin membranes on finer scale. This technique is compatible with other imaging modalities such as reflectance or one- and two-photon fluorescence microscopy.

9329-62, Session 11

Fast spectrum extraction from SRS spectral images by independent component analysis with image compression and post sampling

Yasuyuki Ozeki, The Univ. of Tokyo (Japan)

Recently, several groups are investigating stimulated Raman scattering (SRS) spectral imaging combined with multivariate analysis. This technique allows us to discriminate different constituents by detecting tiny difference in SRS spectra. Indeed, we have recently demonstrated multicolor, label-free imaging of tissue with high-speed SRS spectral imaging and independent component analysis (ICA). Although ICA gives repeatable results for producing multicolor images, there are still remaining issues. First, ICA including the preprocessing with principal component analysis (PCA) takes some time and it hinders real-time analysis. For example, ICA of 91 spectral images of 512 x 512 pixels with 3 components takes about ~40 s. Furthermore, spectra given by ICA is not always identical to the original spectral images. In our previous report, these issues were partially solved by setting a region of interest (ROI). This method, however, requires additional preprocessing. In this paper, we show that ICA can be very quick simply by compressing the images. For example, when the image size is decreased to 64 x 64, the processing time is less than 1 s and the results are almost identical to the case without compression. Furthermore, we can obtain the ICA spectra that are quite similar to the spectral imaging data through the post sampling of PCA spectra at the locations where the ICA intensity is high. We demonstrate the proposed techniques for the imaging of polymer beads and tissue samples.

9329-64, Session 11

Nonlinear optical microscopy and optical coherence tomography platform for label-free functional biophotonic imaging

Angelika Unterhuber, Medizinische Univ. Wien (Austria); Sunil Kumar, Weizmann Institute of Science (Israel); Tschackad Kamali, Boris Hermann, Rene Werkmeister, Medizinische Univ. Wien (Austria); Yaron Silberberg, Weizmann Institute of Science (Israel); Wolfgang Drexler, Medizinische Univ. Wien (Austria)

Combining nonlinear optical microscopy (NLOM) with OCT, we present a simple and cost-effective notch filter assisted CARS instrument with simultaneously second harmonic generation (SHG), third harmonic generation (THG) and four wave mixing (FWM) imaging, which allows for parallel acquisition of OCT data using a single ultra-broad bandwidth Ti:sapphire laser. This simple, parallel NLOM-OCT approach permits the extraction of tissue morphology down to the micrometre range at depths down to 800 μm with localized chemical specificity at cellular levels to distinguish multiple molecules from biological samples in the fingerprint region with data acquisition speeds and sensitivity suitable for fast imaging of large biological specimen. The implementation of single pulse CARS using a notch filter yields an easy straight-forward robust almost alignment-free setup employing a single beam from a single source. Molecular sensitivity of CARS permits to distinguish similarly looking tissue and can be used locally for extraction of various important bio-molecules at submicron resolution and fast image acquisition rates. SHG imaging reveals extremely valuable information about collagen providing information about orientation, crystallinity and morphology. THG provides information from interfaces and FWM as the non-resonant counterpart of CARS provides depth-resolved morphologic information depending on variation of the refractive index helping in the co-registration of the wide-field OCT. The quintuple label-free NLOM-OCT platform is tested with various biological samples (bone, rat tail, skin, ...) and has the potential to play an important role in functional tissue diagnostics. It helps to identify and study changes on a cellular and molecular level.

**Conference 9329:
Multiphoton Microscopy in the Biomedical Sciences XV**

9329-65, Session 11

CARS/FWM and scanning probe microscopy of nanostructures (*Invited Paper*)

Annika M. Enejder, Michael Stührenberg, Nisha Rani Agarwal, Mahesh Namboodiri, Juris Kiskis, Chalmers Univ. of Technology (Sweden)

In Coherent anti-Stokes Raman Scattering (CARS) microscopy - and Four Wave Mixing (FWM) microscopy in general - the resolution is limited to ~400 nm at near-infrared excitation. In order to understand the image formation when mapping objects and macromolecular assemblies of sizes below the resolution, we have compared farfield CARS/FWM images of different nanostructures with (i) Atomic Force Microscopy (AFM) images of their lateral/topographical architecture at a resolution of ~10 nm and (ii) Nearfield Scanning Probe Microscopy (NSOM) images of the excitation fields at a resolution of <300 nm using a multimodal nonlinear microscope equipped with a scanning probe setup. The experimentally collected images were used as input data for nonlinear optical Finite Difference Time Domain (FDTD) computations, allowing us to reconstruct the nearfields underlying the CARS/FWM farfield images. With access to the nonlinear nearfields, localized to length scales smaller than the resolution in CARS/FWM farfield microscopy, detailed nonlinear images of the nanostructures can be reconstructed.

9329-66, Session 12

Background-free stimulated Raman spectroscopy and microscopy (*Invited Paper*)

Hervé Rigneault, Esben Andresen, Pascal Berto, Institut Fresnel (France)

Coherent Raman scattering (CRS) microscopy is a powerful method for label free imaging. Whereas Coherent anti-Stokes Raman scattering (CARS) microscopy suffers from the presence of a non-resonant, purely electronic background signal, the recently developed Stimulated Raman scattering (SRS) microscopy has the advantage of avoiding this non-resonant background. However, SRS microscopy can be hampered by different artefacts induced by cross phase modulation, two photon absorption or thermal effects. We show that these artefacts become problematic when imaging below 1800 cm⁻¹, in the vibrational fingerprint region, because this region is composed by low-intensity peaks. Furthermore, we find that scattering properties of the sample increase the impact of the artefacts and reduce the molecular specificity. In order to reduce the influence of these artefacts and move toward a truly background-free SRS microscopy, we propose and implement a method based on a double modulation approach [1]. More precisely we use three beams whose frequency differences matches the targeted vibrational bond. Those beams are generated by a synchronously pumped OPO as the fundamental, signal and idler beams. We then modulate both of the beams with a 180° phase shift in order to have at any time two beams (acting as the pump and Stokes) falling on the sample. With this we show that cross phase modulation, two-photon absorption and thermal lensing can be cancelled in SRS microscopy. We demonstrate the potential of our method on model scattering samples and on biological tissues.

[1] P. Berto, E. R. Andresen, H. Rigneault, 'Background free stimulated Raman spectroscopy and microscopy', Phys. Rev. Lett 112, 053905 (2014)

9329-67, Session 12

Pushing the limits of coherent Raman spectroscopic imaging (*Invited Paper*)

Marcus T. Cicerone, Charles H. Camp Jr., Brandon Blakely, Young Lee, National Institute of Standards and Technology (United States)

Raman spectroscopy is a powerful technique for label-free identification of chemical species in biological and biomedical samples, but typical spectral acquisition times are too long for routine imaging. We have developed a coherent Raman imaging instrument based on broadband coherent anti-Stokes Raman scattering (BCARS) that provides an unprecedented combination of speed, sensitivity, and chemical selectivity. Using this system we are able to obtain high quality Raman spectra in the fingerprint and CH stretch regions from biological specimens at 3.5 ms. We will discuss the principles on which signal generation and imaging speed improvements have been made. We will also discuss the role of photo damage in setting ultimate speed limits, and demonstrate an instrument architecture that will allow reaching that limit.

9329-68, Session 12

Fiber-laser platform for coherent Raman scattering

Christian W. Freudiger, Invenio Imaging Inc. (United States); Wenlong Yang, Gary R. Holtom, Harvard Univ. (United States); Jay Trautman, Invenio Imaging Inc. (United States); Khanh Q. Kieu, The Univ. of Arizona (United States); Sunney Xie, Harvard Univ. (United States)

Stimulated Raman Scattering (SRS) microscopy allows label-free chemical imaging and has enabled exciting applications in biology, material science, and medicine. It provides a major advantage in imaging speed over spontaneous Raman scattering. Wider adoption of the technique has, however, been hindered by the need for a costly and environmentally sensitive tunable ultra-fast dual-wavelength source. We present the development of an optimized all-fiber laser system based on the optical synchronization of two picosecond power amplifiers. To circumvent the high-frequency laser noise intrinsic to amplified fiber laser, we have further developed a high-speed noise cancellation system based on auto-balanced detection. We demonstrate high-speed and shot-noise limited SRS imaging with our novel fiber-based SRS.

9329-69, Session 12

Optimized coherent Raman scattering microscopy with a novel tunable dual-wavelength lightsource

Ingo Rimke, APE GmbH (Germany); Gregor Hehl, Univ. Stuttgart (Germany); Marcus Beutler, Peter Volz, Edlef Büttner, APE GmbH (Germany); Andreas Volkmer, Univ. Stuttgart (Germany)

We present a novel tunable dual-wavelength 2-picosecond light source for narrow-bandwidth coherent Raman scattering (CRS) microscopy. To optimize the imaging performance, the spectra of the effective pump and Stokes pulse are matched to typical Raman line widths of 10-cm⁻¹ in condensed phase matter. Numerical simulations are performed, investigating the influence of the pulse duration and bandwidth, on dual-color CRS signal generation, assuming that both the pump and the Stokes beams are transform-limited pulses with the same spectral width.

The novel light source (picoEmerald S, APE) is designed to match optimum

**Conference 9329:
Multiphoton Microscopy in the Biomedical Sciences XV**

conditions identified in the simulations. It comprises from an amplified Yb-fiber oscillator providing 2-ps pulses at 1030 nm and a synchronously green-pumped optical parametric oscillator (OPO) generating wavelength tunable pulses of 10 cm⁻¹ bandwidth. The noise figure of the system is measured and compares to established Nd:YVO systems. Combining the 1030 nm pump and the 700 to 960nm OPO pulses results in frequency differences between the two beams tuneable over a broad range from 700 to 4500 cm⁻¹. This covers both the important fingerprint and the CH-stretch region. Optimized SRS imaging in the fingerprint region as well as the CH-stretch region is demonstrated by fast imaging living HeLa cells. It is also found that SRS spectra of polystyrene beads are in perfect agreement with their corresponding Raman spectra as calculated by our numerical simulations. Using an optimized lock-in-amplifier also video-rate imaging is demonstrated.

9329-70, Session 12

Towards low-noise fiber sources for coherent Raman microscopy

Erin S. Lamb, Hanzhang Pei, Frank W. Wise, Cornell Univ. (United States)

A compact, robust, and inexpensive fiber-based source for coherent Raman imaging would benefit both researchers and the clinical application of these imaging techniques. However, the relative intensity noise of fiber sources has precluded their use for stimulated Raman scattering (SRS) microscopy without the use of electronic noise cancellation. A recently demonstrated fiber optical parametric oscillator (OPO) was used to achieve high-quality images using coherent anti-Stokes Raman scattering microscopy, and demonstrated that the self-consistent nature of the oscillator aided low-noise frequency conversion. Thus, reducing the intensity noise on the fiber laser used to pump this device will be a critical step in creating a fiber-based source for SRS microscopy. We will report the design and construction of high-energy dissipative soliton fiber lasers as a potential source of quiet picosecond pulses at 1 μm, along with application to pumping the OPO.

9329-71, Session 12

Optimized signal-to-noise ratio with shot noise limited detection in Stimulated Raman Scattering microscopy

Miriam J. B. Moester, Freek Ariese, Johannes F. de Boer, Vrije Univ. Amsterdam (Netherlands)

We demonstrate our shot noise limited set-up for Stimulated Raman Scattering (SRS) microscopy. In SRS, two different colored laser beams are incident on a sample. If the energy difference between them matches a molecular vibration of a molecule, energy is transferred from one beam to the other. By applying amplitude modulation to one of the beams, the modulation transfer to the other beam can be measured. The efficiency of this process is a direct measure for the number of molecules of interest in the focal volume. Combined with laser scanning microscopy, this technique allows for fast and sensitive imaging with sub-micrometer resolution. Recent technological advances have shown an improvement of the sensitivity of SRS applications, but few show shot noise limited detection. We present a basic SRS set-up with mainly commercial components and a custom built transimpedance amplifier that reaches shot noise limited detection over a broad window of biologically relevant laser powers.

This set-up is used to demonstrate that the highest signal-to-noise ratio (SNR) in SRS with shot noise limited detection is achieved with a time averaged laser power ratio of 2:1 of the modulated and unmodulated beam. The dominant noise source is the shot noise of the unmodulated, detected beam, shifting the optimal SNR away from equal beam powers, where the most signal is generated. For a fixed total laser power, other power ratios decrease the SNR and increase photodamage from unnecessary exposure.

We demonstrate improved image quality and signal-to-noise ratio on polystyrene beads and C. Elegans worms.

9329-72, Session 12

Detecting polymeric nanoparticles with coherent anti-stokes Raman scattering microscopy in tissues exhibiting fixative-induced autofluorescence

Natalie L. Garrett, Univ. of Exeter (United Kingdom);
Lisa Godfrey, Univ. College London (United Kingdom);
Aikaterini Lalatsa, Univ. of Portsmouth (United Kingdom);
D. R. Serrano, Univ. Complutense de Madrid (Spain);
Ijeoma F. Uchegbu, Andreas G. Schatzlein, Univ. College London (United Kingdom); Julian Moger, Univ. of Exeter (United Kingdom)

Recent advances in pharmaceutical nanotechnology have enabled the development of nano-particulate medicines with enhanced drug performance. Although the fate of these nano-particles can be macroscopically tracked in the body (e.g. using radio-labeling techniques), there is little information about the sub-cellular scale mechanistic processes underlying the particle-tissue interactions, or how these interactions may correlate with pharmaceutical efficacy. To rationally engineer these nano-particles and thus optimize their performance, these mechanistic interactions must be fully understood.

Coherent Anti-Stokes Raman scattering (CARS) microscopy provides a label-free means for visualizing biological samples, but can suffer from a strong non-resonant background in samples that are prepared using aldehyde-based fixatives. We demonstrate how formalin fixative affects the detection of polymeric nanoparticles within kidneys following oral administration using CARS microscopy, compared with samples that were snap-frozen. These findings have implications for clinical applications of CARS for probing nanoparticle distribution in tissue biopsies.

Conference 9330: Three-Dimensional and Multidimensional Microscopy: Image Acquisition and Processing XXII

Monday - Thursday 9-12 February 2015

Part of Proceedings of SPIE Vol. 9330 Three-Dimensional and Multidimensional Microscopy: Image Acquisition and Processing XXII

9330-39, Session PMon

Auto-tracking of focal plane based on a tunable lens in digital holographic microscopy

Ju Wan Kim, Jeong Heon Han, Jonghyun Eom, Byeong Ha Lee, Gwangju Institute of Science and Technology (Korea, Republic of)

The floating cells in fluid are suffered Brownian motion, which makes the cells fluctuate in depth direction and the cell imaging difficult. To solve this problem, we propose the automatic focal point tracking system that is utilizing the digital holographic microscopy (DHM) and an electrical tunable lens. It is based on Mach-Zehnder interferometer with a HeNe laser as a coherence light source, and the tunable lens was used for the dynamic focusing element. The variation of the sample position with respect to the focusing lens is calculated by the numerical auto-focusing algorithm, widely used in DHM, at first. Then, the calculated new focal point is applied to control the focal length of the tunable lens. Therefore, the focal plane could be kept in-focused onto the floating sample position in real time, which permits an effective detection of back-scattering signal. The proposed system is expected to be applied for high throughput fluorescence imaging for floating cells.

9330-50, Session PMon

Computed tomography of refractive index by low-coherence interferometry

Yi Wang, Northeastern Univ. at Qinhuangdao (China); Zhenhe Ma, Northeastern University (China); Hongxian Zhou, Northeastern Univ. (China)

We present a fast computed tomography system for imaging of refractive index by a transmission low-coherence interferometer. The forward-scattering light through a sample across 10mm dimension interferes with reference light, and the approximated projection data of refractive indices within the sample are calculated from interference fringes. The projection data set at sufficient angular views are acquired, and the refractive index distribution of the sample is reconstructed with a filter back-projection algorithm. The proposed method is experimentally verified using a phantom.

9330-51, Session PMon

A novel method for image denoising of fluorescence molecular imaging based on fuzzy C-Means clustering

Jie Tian, Institute of Automation (China); Yu An, Jie Liu, Beijing Jiaotong Univ. (China); Chongwei Chi, Jinzuo Ye, Yamin Mao, Xin Yang, Institute of Automation (China); Shixin Jiang, The department of Biomedical Engineering, School of Computer and Information Technology, Beijing Jia (China)

As an important molecular imaging modality, fluorescence molecular

imaging (FMI) has the advantages of high sensitivity, low cost and ease of use. By labeling the regions of interest with fluorophore, FMI can noninvasively obtain the distribution of fluorophore in-vivo. However, due to the fact that the spectrum of fluorescence is in the section of the visible light spectrum, there are mass of autofluorescence on the surface of the bio-tissues, which is a major disturbing factor in FMI. Meanwhile, the high-level of dark current for charge-coupled device (CCD) camera and other influencing factor can also produce a lot of background noise. In this paper, a novel method for image denoising of FMI based on fuzzy C-Means clustering (FCM) is proposed. The method is based on the fact that the fluorescence signal is the major component of the fluorescence imaging, and the intensity of autofluorescence and other background signals is relatively lower than the fluorescence signal. First, the fluorescence image is smoothed by sliding-neighborhood operations to initially eliminate the noise. Then, the wavelet transform (WLT) is performed on the fluorescence images to obtain the major component of the fluorescence signals. After that, the FCM method is adopt to separate the major component and background of the fluorescence images. Finally, the proposed method was validated using the fluorescence data obtained by in-vivo implanted fluorophore experiment and mouse liver cancer experiment, and the results show that the proposed method can effectively obtain the fluorescence signal while eliminate the background noise, which could increase the accuracy and efficiency of reconstruction to some extent.

9330-52, Session PMon

Reversibly switchable fluorescence microscopy

Junjie Yao, Washington Univ. in St. Louis (United States); Daria M. Shcherbakova, Albert Einstein College of Medicine of Yeshiva Univ. (United States); Chiye Li, Washington Univ. in St. Louis (United States); Arie Krumholz, Ramon A. Lorca, Erin Reinl, Sarah K. England, Washington Univ. School of Medicine in St. Louis (United States); Vladislav V. Verkhusha, Albert Einstein College of Medicine of Yeshiva Univ. (United States); Lihong V. Wang, Washington Univ. in St. Louis (United States)

Confocal microscopy, with optical sectioning, has revolutionized biological studies by providing sharper images than conventional optical microscopy. Here, we introduce a fluorescence imaging method with enhanced resolution and imaging contrast, which can be implemented using a commercial confocal microscope setup. This approach, termed reversibly switchable photo-imprint microscopy (rsPIM), is based on the switching dynamics of reversibly switchable fluorophores. When the fluorophores are switched from the bright (ON) state to the dark (OFF) state, their switching rate carries information about the local excitation light intensity. In rsPIM, a polynomial function is used to fit the fluorescence signal decay during the transition. The extracted high-order coefficient highlights the signal contribution from the center of the excitation volume, and thus sharpens the resolution in all dimensions. In particular, out-of-focus signals are greatly blocked for large targets, and thus the image contrast is considerably enhanced. Notably, since the fluorophores can be cycled between the ON and OFF states, the whole imaging process can be repeated. rsPIM imaging with enhanced image contrast was demonstrated in both fixed and live cells, using a reversibly switchable synthetic dye and a genetically encoded red fluorescent protein. Since rsPIM does not require modification of commercial microscope systems, it may provide a simple and cost-effective solution for sub-diffraction imaging of live cells.

**Conference 9330: Three-Dimensional and Multidimensional Microscopy:
 Image Acquisition and Processing XXII**

9330-53, Session PMon

**Optical coherence detection with
 stimulated emission: a feasibility study**

Chun-hui Yu, Shen-Shou M. Chung, National Yang-Ming Univ. (Taiwan); Wen-Chuan Kuo, National Yang-Ming University, Institute of Biophotonics (Taiwan); Fu-Jen Kao, National Yang-Ming Univ. (Taiwan)

We have used stimulated emission to detect fluorescence through pump-probe configuration. This is implemented by converting the incoherent spontaneous fluorescence signal into the coherent stimulated one. 2D fluorescence lifetime image can then be obtained by varying the delay between the excitation and stimulated beams under raster scanning.

In this study a 635 nm, 8MHz pulsed laser (pulse width ~50ps) is used as the pump beam. The beam was modulated at 100 KHz by a function generator. A second laser, operating at 705 nm and synchronized with the pump laser, is used as the probe (stimulation) beam. The probe beam is configured to form a Michelson interferometer so that optical coherence tomography (OCT) can be implemented, to enable 3D fluorescence image with good axial resolution.

The coherent nature of stimulated emission is appropriated for OCT, an interferometric technique, using fluorescence as a viable and unique contrast in addition to the scattered light. Note that fluorescence provides labeling specificity through its unique immunocytochemistry contrast. This capacity, however, is lacking in scatter light based OCT. The judicious use of coherent stimulated emission for OCT would allow unprecedented contrast in 3D tissue imaging, with revolutionary prospects.

9330-54, Session PMon

**High-resolution imaging of biological
 tissue with full-field optical coherence
 tomography**

Yue Zhu, Wanrong Gao, Nanjing Univ. of Science and Technology (China)

A novel full-field optical coherence tomography system with low cost and high resolution has been developed for imaging of cells and tissues. Compared with other FFOCT systems illuminated with optical fiber bundle, the improved Köhler illumination arrangement with a halogen lamp was used in the proposed FFOCT system. High numerical aperture microscopic objectives were used for imaging and a piezoelectric ceramic transducer (PZT) was used for phase-shifting. En face tomographic images can be obtained by applying the five-step phase-shifting algorithm to a series of interferometric images which are recorded by a smart CCD camera. Three-dimensional images can be generated from these tomographic images. Imaging of the chip of Intel Pentium 4 processor demonstrated the ultrahigh resolution of the system (lateral resolution 0.8 μm), approaching the theoretical resolution 0.7 μm ?0.5 μm (lateral? axial). En face images of cells of onion surface and potted plant leaves cells show the excellent performance of the system for generating en face images of biological tissues. Our system is characterized by its high resolution, low cost and simple arrangement for adjustment, providing a practical method of performing FFOCT imaging.

9330-55, Session PMon

**Wide-field sectioning with the aid of
 undersampled scanning microscopy**

Yubo Duan, Nanguang Chen, National Univ. of Singapore (Singapore)

Wide-field optical microscopy is efficient and robust for imaging dynamic

real-time process, but it has no depth sectioning capability due to lack of axial high frequency components in the three-dimensional (3D) optical transfer function (OTF) (the 'missing cone' problem). Thus, a stack of wide-field images is not real 3D image but every slice contains out-of-focus background. On the other hand, scanning microscopy techniques, e.g. confocal microscopy, focal modulation microscopy (FMM) and multiphoton microscopy, have depth sectioning ability and are successful in imaging thick biological samples. However, they generally require temporal and spatial scanning which will take a long time, and thus are not very suitable for dynamic real-time imaging. Here we introduce a hybrid technique to combine the scanning microscopy and wide-field microscopy in Fourier space to balance the sectioning capability and imaging speed.

The out-of-focus and scattering photon contributions in wide-field image are usually considered as exhibiting only low frequency spatial structures. Several groups applied structured illumination to modulate the in-focus photon contribution and retrieve the image directly in Fourier space or in spatial domain by maximum likelihood approach. Here we substitute the low frequency components of wide-field images by the corresponding frequency components of undersampled FMM images to eliminate the out-of-focus and scattering photon contributions. The benefit of this hybrid technique is that we can speed up the FMM imaging process by reducing the sampling rate, and obtain the sectioning capacity for the wide-field imaging.

9330-56, Session PMon

**Development of large FOV 3D scanner
 based on confocal microscopy**

Hyeong-Jun Jeong, Dae-Gab Gweon, KAIST (Korea, Republic of); Min Kook Ko, Dentium Co., Ltd. (Korea, Republic of); Dukho Do, Jiheun Ryu, Jayul Kim, KAIST (Korea, Republic of)

Techniques for 3D scanning have numerous demands in various industries such as reverse engineering and prototyping, reconstruction and documentation of cultural artifacts, orthotics and prosthetics, and quality control/inspection system. There are many kinds of techniques for 3D scanner and each technique has their own specification; resolution, field of view and measurement speed, depends on the objects. If we want to acquire 3D information of specific target or object, therefore, we should apply an appropriate technique. However, most of techniques have limitation on their specifications. For example, the larger field of view is demanded, the worse resolution and lower imaging speed is performed. In this thesis, we tried to overcome this limitation, i.e. large field of view and high speed high resolution 3D scanner is developed. Target specification is 10 mm X 10 mm X 5 mm FOV, 20 μm resolution and within 5s imaging speed. The scanner is based on confocal microscope system using micro-lens array. We removed 2 dimensional scanning device like galvano mirror commonly used in confocal microscopy and replaced it with micro-lens array, thereby imaging speed is improved. Micro-lens array's dimension is 15 mm X 15 mm and composed of 500X500 micro-lens of which diameter is 30 μm . Pinhole array is used for the optical sectioning right behind the micro-lens array or only one pinhole can be utilized with collecting lens in descanning structure. Z-axis scanning is accomplished by using electrically tunable lens instead of mechanical moving of objectives or sample stages. So we can stabilize the system and improve imaging speed.

9330-57, Session PMon

**A software tool for STED-AFM correlative
 super-resolution microscopy**

Sami V. Koho, Takahiro Deguchi, Univ. of Turku (Finland); Madis Löhmus, Laboratory of Biophysics, University of Turku (Finland); Tuomas Näreoja, Karolinska Institutet (Finland); Pekka E. Hänninen, Univ. of Turku (Finland)

Conference 9330: Three-Dimensional and Multidimensional Microscopy: Image Acquisition and Processing XXII

Multi-modal correlative microscopy allows combining the strengths of several imaging techniques to provide unique contrast. However it is not always straightforward to setup instruments for such customized experiments, as most microscope manufacturers use their own proprietary software, with limited or no capability to interface with other instruments – this makes correlation of the multi-modal data extremely challenging. We introduce a new software tool for simultaneous use of a Stimulated Emission Depletion (STED) microscope with an Atomic Force Microscope (AFM).

In our experiments, a Leica TCS STED commercial super-resolution microscope, together with an Agilent 5500ilm AFM microscope was used. With our software, it is possible to synchronize the data acquisition between the STED and AFM instruments, as well as to perform automatic registration of the AFM images with the super-resolution STED images. The software was realized in LabVIEW; the registration part was also implemented as an ImageJ macro. The synchronization was realized by controlling simple trigger signals, also available in the commercial STED microscope, with a low-cost National Instruments USB-6501 digital I/O card. The registration was based on detecting the positions of the AFM tip inside the STED field-of-view, which were then used as landmarks for registration. The registration should work on any STED and tip-scanning AFM microscope combination, at nanometer-scale precision. Our method has been tested with both sub-resolution fluorescent beads, and with fixed cell samples. The software will be released under an open-source license.

9330-58, Session PMon

Swept-source phase microscopy based on acousto-optic wavelength swept laser

Soonwoo Cho, Gahee Han, Hyung Seok Lee, Hwi Don Lee, Seung Won Jun, Chang-Seok Kim, Pusan National Univ. (Korea, Republic of)

Recently, spectral domain phase microscopy (SDPM) has been studied to obtain three-dimensional (3-D) nanometer-scale image by using a broadband light source and an area CCD detector. In order to construct the X-Y-Z 3-D surface profile of SDPM, 1-D mechanical scanning (for Z-direction) is required because two axes of CCD pixels provide a spatial area information of sample (for X and Y-direction).

In this work, we propose the swept source phase microscopy (SSPM) based on acousto-optic wavelength swept laser. The depth-resolved phase information can be obtained by wavelength scanning of the swept laser (for Z-direction), and both the axes of CCD pixels provide the 2-D spatial information of the sample (for X and Y-directions). Therefore, the 3-D surface profile can be easily constructed without any mechanical scanning.

The wavelength-swept laser is mainly consist of a semiconductor optical amplifier (SOA), center wavelength of 800 nm, and an acousto-optic tunable filter (AOTF) which can be tuned electronically by modulation of acoustic wave. Since swept laser do not suffered from the mechanical constraints and vibration, image shift can be reduced.

To demonstrate stable and high speed 3-D imaging, a large area beam is illuminated to the sample and CCD has a frame rate of 128 fps.

In conclusion, we demonstrate that this SSPM system can be ideal for stable and high speed nano-scale imaging due to the absence of mechanical scanning of whole system.

9330-59, Session PMon

Tomographic STED microscopy to study bone resorption

Takahiro Deguchi, Sami V. Koho, Univ. of Turku (Finland); Tuomas Näreojä, Karolinska Institutet (Finland); Juha Peltonen, Pekka E. Hänninen, Univ. of Turku (Finland)

We present a 3D tomographic super-resolution light microscopy, based

on Stimulated Emission Depletion microscopy (STED) and its application in osteoclast bone resorption study. In order to improve axial resolution in standard STED system, the 3D tomography was realized by imaging a sample at two different angles; one conventionally from below and another from the side. The second observation is acquired via a metal-coated silicon mirror, positioned above the region of interest by a custom-built micro-positioner. The acquired two sets of 3D stacks are computationally registered and fused to produce a 3D tomogram, which has super-resolution in all three dimensions.

In the past osteoclast imaging was mainly conducted either by optical microscopy, whose 200x200x500nm resolution was insufficient to study nanoscale structures and interactions, or electron microscopy, where obtaining a dense enough staining for studying protein binding and interactions is extremely difficult. With the presented 3D tomography, we optically investigate fluorescently labeled actin cytoskeleton, through thin and smooth bone layer, particularly at ruffled borders (RB), which are directly associated with active bone resorption in osteoclasts. RB is a complex folded membrane with active exo- and endocytosis, involving specific proteins, e.g. cathepsin K, focal adhesions and integrins. We aim to visualize nanoscale structures of RB and localization of the resorption-associated proteins within RBs. The novel information would provide deeper understanding of the protein roles during the bone resorption, resorption mechanism and transcytosis of resorbed bone, that would ultimately lead to finding specific molecular inhibitor targets to modulate excessive bone resorption in osteoporosis.

9330-60, Session PMon

single-channel stereoscopic video imaging modality based on a transparent rotating deflector

Edalat Radfar, Jihoon Park, Eunkwon Jun, Myungjin Ha, Sangyeob Lee, Yonsei Univ. (Korea, Republic of); SungKon Yu, SeulGi Jang, Bio-Optics Lab., department of bio medical engineering, Yonsei University (Korea, Republic of); Byungjo Jung, Yonsei Univ. (Korea, Republic of)

An imaging system has been recently developed using single-channel and transparent rotating deflector (TRD). This system is based on Snell's law (law of refraction of light), in which two images with a desired disparity are consecutively taken and then processed. In the previous design, the TRD had been put in front of the camera lens. Since each right and left views were sequentially captured, a manual low speed active method had been used as a preliminary mode via normal active shutter glasses. Using MCU as a centralized control system, camera, motor driver and glasses were controlled through general purpose input/output (GPIO) ports.

Image disparity is a function of refractive index, effective length, and rotation angle of TRD. Bigger TRD and rotation angle result in high torque, low rotation speed and frame rate. To overcome this limitation, a microscopic lens system was designed with a certain interval for placing a small TRD inside the lens.

Image disparity was measured in both methods and the results were compared. The results showed improvements in image disparity-FOV ratio of new design. Interestingly, the image disparity of new system was also bigger than the first one at the same angle and TRD size.

In addition, color check and image quality evaluations showed significant improvements of output in the new design.

It is the first time in this project that presentation of 3D output is technically feasible in 3D conventional methods using 3D image processing.

**Conference 9330: Three-Dimensional and Multidimensional Microscopy:
 Image Acquisition and Processing XXII**

9330-61, Session PMon

Resolution analysis in compressive multidimensional microscopy

Angel D. Rodriguez, Pere Clemente Pesudo, Eva Salvador Balaguer, Esther Irlles, Enrique Tajahuerce, Fernando Soldevila Torres, Jesús Saez Lancis, Univ. Jaume I (Spain)

Despite systems that scan a single-element benefit from mature technology, they suffer from acquisition times linearly proportional to the spatial resolution. A promising option is to use a single-pixel system that benefits from data collection strategies based on compressive sampling. Single-pixel systems also offer the possibility to use dedicated sensors such as a fiber spectrometer or two photodiodes for multispectral and 3D imaging, respectively. The image is obtained by lighting the scene with microstructured masks implemented onto a programmable spatial light modulator. The masks are used as generalized measurement modes where the object information is expressed and the image is recovered through algebraic optimization.

The fundamental reason why the bucket detection strategy can outperform conventional optical array detection is the use of a single channel detector that simultaneously integrates all the photons transmitted through the patterned scene. Spatial frequencies that are not transmitted through this low quality optics are demonstrated to be present in the retrieved image.

Our work makes two specific contributions within the field of single-pixel imaging through patterned illumination. First, we demonstrate that single-pixel imaging improves resolution of conventional imaging systems overcoming the Rayleigh criterion. An analysis of resolution using a low NA microscope objective for imaging at a CCD camera shows that single-pixel cameras are not limited at all by the optical quality of the collection optics. Second, we experimentally demonstrate the capability of our technique to properly recover an image even when an optical diffuser is located in between the sample and the bucket detector.

9330-62, Session PMon

A high-precision vibrating section method for blockface imaging

Tao Jiang, Dongli Xu, Hui Gong, Huazhong Univ. of Science and Technology (China)

The large number of neurons in the brain, which connected to each other, form complex neural networks. It is the fundamental basis of brain function. Acquiring neuroanatomical architecture of the brain is of great significance to understanding brain function and disease. Optical imaging methods have submicron resolution but limited imaging depth. By combining sample preparation and sectioning technologies, high-resolution imaging of mouse brain can be achieved. We developed a robust high-precision vibratome based on leafspring-electromagnetic structure. Vibration frequency of the system is about 80 Hz and vibration amplitude is continuously adjustable within range of 0-3mm. Vertical deflection of the knife during vibration is controlled to be less than 3 μ m by adjusting specially designed knife holder and surface roughness is ensured. Mouse brains prepared by formaldehyde fixation and agarose embedding can be sectioned with minimal influence on fluorescent signal and brain morphology. Using structured illumination microscopy (SIM), high throughput 3D imaging of the blockface of the mouse brain can be performed with a voxel size of 0.33 μ m by 0.33 μ m by 2.0 μ m. By alternating the sectioning and imaging process, we can acquire three-dimensional structural data of whole mouse brain. Combining vibrating sectioning and blockface imaging using SIM, we obtained deformation-free whole mouse brain interval sampling data and high-resolution continuous data. This method will be a powerful tool to help us to obtain neuron connectivity map of the entire brain.

9330-63, Session PMon

Imaging collagen fiber axial-orientation using Brillouin spectroscopy

Zhaokai Meng, Vladislav V. Yakovlev, Texas A&M Univ. (United States)

Collagen is an important structural component in many biological tissues including bones, teeth and vascular endothelial layers. Its fibrillar arrangement can produce tissues with distinct anisotropies, which is closely linked with their biological functions. However, current techniques, including second harmonic generation spectroscopy or Raman spectroscopy, could only map in-plane orientations of the collagen fibers. Recent advances in background-free Brillouin microspectroscopy allows investigators to study the local sound speed within small volumes (< 5 μ m³), which has shown sensitivity to the collagen's local fibers out-of-plane orientations. Moreover, the background-free Brillouin microspectroscopy is advantageous in rapid imaging of turbid samples, making 3D orientation mapping of collagen fibers possible.

In this study, we employed rat-tail tendons dissected from the Sprague-Dawley rats aged 12 months. The Brillouin spectra were obtained by a background free VIPA (virtually imaged phased array) spectrometer described in the previous report [1]. The free spectral range of the Brillouin spectrometer is 33.3 GHz, sufficient to probe local sound speed up to ~6200 m/s. The 2-D image was accomplished by using a scanning procedure. By comparing the theoretical simulations (based on a Finite Difference Time Domain (FDTD) method for acoustic waves) and the experimental results, the axial orientations of the collagen fibers could be retrieved for each pixel. As a reference, the Raman spectra were obtained for each pixel, and the in-plane orientations were retrieved as well.

Reference:

1. Meng, Z., Traverso, A. J., & Yakovlev, V. V., Optics express, 2014, 22(5), 5410-5416.

9330-65, Session PMon

Fourier ptychography for multimodality imaging

Siyuan Dong, Kaikai Guo, Pariksheet Nanda, Guoan Zheng, Univ. of Connecticut (United States)

Fourier ptychography is a recently developed computational approach for high-resolution, high-throughput imaging. By combining the synthetic aperture and phase retrieval techniques, Fourier ptychography uses a unique data fusion process to expand the Fourier passband and recover the lost phase information at the same time. It transforms the general challenge of high-resolution imaging from one that is tied to physical limitation of the optics to one that is solvable through computation. In this talk, we will report our recent developments of the Fourier ptychography approach for gigapixel microscopy, quantitative phase imaging, 3D holography imaging, spectrum-multiplexing, and super-resolution imaging. We will also demonstrate this approach for various microscopy and photography imaging modalities.

9330-66, Session PMon

Dual-beam, crossed line-scanning fluorescence microscope with confocal resolution

Hyun-Woo Jeong, Hyung-Jin Kim, Korea Univ. (Korea, Republic of); Jung Eun, Seungjin Heo, Mikyoung Lim, Yong-Hoon Cho, KAIST (Korea, Republic of); Beop-Min

Conference 9330: Three-Dimensional and Multidimensional Microscopy: Image Acquisition and Processing XXII

Kim, Korea Univ. College of Health Sciences (Korea, Republic of)

Line-scanning microscopes are often used to overcome the limited scanning speed of conventional point-scanning confocal microscopes; however, line-scanning microscopes have reduced spatial resolution. In this study, we present the dual-beam fluorescence line-scanning microscope that can restore the original confocal resolution. This microscope forms two orthogonal line foci in the object plane, and with perpendicular scanning directions, these foci scan the same area and create two line-scan images. From these images, the real noise and confocal characteristics are analyzed. Based on this information, we developed an image restoration algorithm to produce a final image with spatial resolution comparable to conventional point-scanning confocal microscope. This algorithm was derived with the total variation regularization, and the critical images restoration factor within algorithm has been determined via an iterative process. Our results imply that the intrinsic resolution limit of line-scanning microscopes can be overcome without subsequent deterioration in spatial resolution and sacrifice of the imaging speed.

9330-1, Session 1

Optical coherence engineering for microscopy (*Invited Paper*)

L. Waller, H. Liu, J. Zhong, Z. Liu, L. Tian, Univ. of California, Berkeley (United States)

The measurement and control of high-resolution 4D functions for describing the spatial coherence of a 2D beam are becoming not only possible, but also practical. This talk will describe our work in coherence measurement and control for improved microscope imaging systems. We will show high-resolution 3D and phase images can be recovered from defocused intensity stacks or illumination angle scans via Fourier Ptychography. By leveraging recent advances in computational illumination, we achieve simultaneous multi-contrast imaging and gigapixel sized datasets in a fast and practical manner. In particular, we describe these advances within the framework of phase-space imaging.

9330-2, Session 1

Lensfree on-chip imaging using synthetic aperture

Wei Luo, Alon Greenbaum, Yibo Zhang, Aydogan Ozcan, Univ. of California, Los Angeles (United States)

High resolution imaging across a wide field-of-view (FOV) is critical in various applications in biomedical and physical sciences, among others. With unit magnification, lensfree on-chip imaging bypasses the traditional tradeoff between resolution and FOV and extends the space-bandwidth-product to >1 billion pixels over a large FOV that equals the active area of the image sensor chip. This achievement is realized by combining pixel-super resolution techniques with the state-of-the-art image sensors used in consumer electronics, including mobile-phones. However, the effective numerical aperture (NA) of previous lensfree on-chip imaging systems has been limited to ~0.8-0.9 due to poor signal-to-noise-ratio (SNR) at high spatial-frequencies and narrow acceptance angles of sensor pixels. Here we report lensfree imaging using synthetic aperture (LISA) where we utilize oblique illuminations across two orthogonal-axes to shift the high spatial-frequencies of the specimen to lower frequency bands, which can be detected by the image sensor with a significantly increased SNR. Using an iterative synthetic aperture algorithm, we combine all these additional bands of spatial-frequencies to reconstruct an enlarged frequency map of the specimen, achieving a resolution of 250 nm under 700 nm illumination wavelength, which constitutes the highest reported NA for a lensfree on-chip microscope (NA=1.4). The significant improvement in SNR due to synthetic aperture approach also enables robust phase retrieval, allowing us to image densely packed samples such as breast cancer tissue slides

and unstained Papanicolaou smears. Compared to other synthetic aperture systems, LISA features various advantages including much larger FOV, simplicity, compactness and cost-effectiveness.

9330-3, Session 1

Development of cellular resolution Gabor-domain optical coherence microscopy for biomedical applications

Patrice Tankam, Univ. of Rochester (United States); Jinxin Huang, Univ of Rochester (United States); Anand P. Santhanam, Univ. of California, Los Angeles (United States); Jungeun Won, Univ. of Rochester (United States); Cristina Canavesi, LighTopTech Corp. (United States); Jannick P. Rolland, Univ. of Rochester (United States)

We have developed a biomimetic cellular resolution imaging modality, Gabor-Domain Optical Coherence Microscopy, which combines high lateral resolution of confocal microscopy and high sectioning capability of optical coherence tomography to image deep layers in tissues with high-contrast and volumetric resolution of 2 μ m. A novelty of the custom microscope is the incorporation of a liquid lens, as in whales' eyes, for robust and rapid acquisition of volumetric imaging of deep layers in tissue down to 2 mm, thus overcoming the tradeoff between lateral resolution and depth of focus. The system with a handheld scanning probe now fits on a movable cart. We will report on the implementation of a parallelized Multi-Graphic Processing Units framework in the system to allow real-time visualization of the sample in 6 seconds after acquisition that may be completed in less than 1 minute. Furthermore, we will report on the capability of the system in different applications including ophthalmology and material science. The microscope has successfully revealed micro-structures within the cornea and in particular the endothelial cells micro-environment, which opens a path in understanding the mechanisms of Fuchs' dystrophy, a leading cause of the loss of corneal transparency. Quantitatively, the system is able to measure, for example, the edge-thickness of soft contact lenses, which is important for the fitting of the lens and the comfort of the patient. Overall, the imaging modality provides the capability to observe the three-dimensional features of different structures with micrometer resolution, which opens a wide range of future applications.

9330-4, Session 1

Large field of view full field optical coherence tomography for fingerprint imaging

Egidijus Auksorius, Jean-Marie Chassot, A. Claude Boccara, Institut Langevin (France)

Optical coherence tomography (OCT) appears to be a promising tool for fingerprint acquisition and discrimination of fakes. OCT is a non-contact, non-destructive optical method that virtually sections the volume of biological tissues that strongly scatter light such as fingerprints. Most of the OCT setups have to go through the acquisition of a full 3D image to isolate an "en-face" image suitable for fingerprint analysis. A few "en-face" OCT approaches have been proposed that use either a 2D scanning setup and image processing, or a full-field illumination using a camera and a spatially coherent source that induces cross-talks and degrades the image quality.

We have demonstrated that Full Field OCT (FFOCT) using a spatially incoherent source is able to provide "en-face" high quality optical sectioning of the skin and in particular of the fingerprints. This approach shows a unique spatial resolution that is able to reveal a number of morphological details of fingerprints that are not seen with competing OCT setups. In particular the cellular structure of the stratum corneum and the epidermis-dermis interface appear clearly with our high-resolution (1 micrometer, isotropic) setup.

Conference 9330: Three-Dimensional and Multidimensional Microscopy: Image Acquisition and Processing XXII

We will show our first design to get a large field of view (1 cm x 1 cm) while keeping a good sectioning ability of about 3 micrometers. We will display the results obtained using these two setups for fingerprints examination and will discuss which parameters should be of importance for distinguishing fakes from real fingerprints.

9330-5, Session 1

High brightness LED for confocal microscopy

Ali Vakili, Northeastern Univ. (United States); Daxi Xiong, Key Lab. of Medical Optics, Suzhou Institute of Biomedical Engineering and Technology (China); Milind Rajadhyaksha, Memorial Sloan-Kettering Cancer Ctr. (United States); Charles A. DiMarzio, Northeastern Univ. (United States)

In a confocal microscope, it is required to deliver optical power onto a very tiny spot. Radiance or brightness is the ability of a light source to generate photons in unit time and unit area. It represents not only the ability of the source to generate high enough power, but also its ability to focus the optical power onto a tiny spot.

Lasers as the most popular light sources for confocal microscopy, provide coherent light. Their spatial coherence leads to high radiance required for confocal imaging, but their temporal coherence produces speckle on the image. On the other hand, although incoherent light produced by an LED does not produce speckle, because of its low spatial coherence it has low radiance. Recently developed high brightness LEDs can provide high optical power from a small area, which implies higher radiance in comparison to ordinary LEDs.

In comparison to a point scanning microscope, line scanning confocal microscope needs lower radiance since multiple pixels are illuminated simultaneously. Therefore, high brightness LEDs are more suitable to be used in line scanning microscopes.

We have used both a laser diode and a high brightness LED with emission in infrared region. Preliminary results from our line scanning confocal microscope show that the high brightness LED is able to provide enough radiance to obtain a good image with resolution comparable with the same microscope utilizing the laser diode. Results suggest that high brightness LEDs with lower expense can be used instead of lasers for clinical applications.

9330-6, Session 1

Limited-angle, holographic tomography with optically controlled projection generation.

Arkadiusz Ku?, Wojciech Krauze, Malgorzata Kujawinska, Warsaw Univ. of Technology (Poland)

One of the hot topics in modern cell biology, apart from three-dimensional cell tracking, is to study dynamic changes in morphology of the cells in three dimensions (3D). Recently, researchers have provided several solutions for the 3D reconstruction of refractive index as well as absorption e.g. for fluorescent response. This is usually realized by capturing data through digital holography and reconstructing them with tomographic procedures. However, the quality of reconstruction depends mainly on the number and quality of the set of holograms acquired at different viewing angles. For static objects it is sufficient to rotate the object itself. Nevertheless, for dynamic studies it is required to rapidly capture holograms from multiple viewing directions, most often within a limited angular range. So far it has been demonstrated that altering the angle of illumination of the sample at high rate and within a limited angular span can be achieved using mechanical beam steering with prisms or galvanometric mirrors. In this paper we demonstrate optical-only, diffraction-based beam steering for tomography. Such solution is fast and more robust. The measurement

system is based on Mach-Zehnder interferometer configuration modified to serve as a digital holographic microscope with a high Numerical Aperture illumination module and a Spatial Light Modulator. Apart from providing an elegant solution to the alternating of the viewing angle, the capabilities of the holographic microscope system are also increased. Adding a high resolution SLM as an active optical element allows to improve measurement accuracy through aberration correction of the illuminating wavefront. The presented tomographic system works with a limited angular range of projections. In the paper we also present an improved procedure for reconstructing three-dimensional shape and refractive index distribution of a phase micro-object. We also present a novel, heuristic approach that utilizes compressed sensing regularization: total variation minimization in order to reconstruct samples that are not piecewise constant. These algorithms are well fitted for reconstruction of the data from a highly limited set of projections. The examples of tomographic reconstruction of selected biological micro-objects, illustrating the high functionality of the proposed system, are presented.

9330-7, Session 2

Development of a DMD-based fluorescence microscope

Nadya Chakrova, Sjoerd Stallinga, Bernd Rieger, Technische Univ. Delft (Netherlands)

A versatile fluorescence microscope can be built by complementing a conventional fluorescence microscope with a digital micro-mirror device (DMD). Arbitrary, non-uniform patterns are created on the DMD and projected into the sample. This patterned illumination can be used to improve lateral and axial resolution over the resolution of a widefield microscope, and to reduce the illumination dose. Patterns that have been mainly investigated so far include multi-spot [1] and line patterns [2]. Different illumination patterns require different reconstruction strategies and result in an image quality similar to confocal or structured illumination microscopy.

We present a DMD-based fluorescence microscope and focus on applying multi-spot and pseudo-random illumination patterns. The optical quality was estimated by comparing the theoretically calculated modulation transfer function with the experimental modulation transfer function, which was measured by assessing an edge-profile. Multi-spot scanning patterns result in a sectioned image, as around each spot a digital pinhole removes out-of-focus light. This technique is advantageous in case of densely labelled, relatively thick samples. An outlook is given on the use of pseudo-random illumination patterns for achieving both sectioning and resolution enhancement.

[1] York, A.G. et al., Nat. Methods 9, 749-754 (2012)

[2] Dan, D. et al., Sci.Rep. 3, 1116 (2013)

9330-8, Session 2

Multi-channel beam-scanning imaging at kHz frame rates by Lissajous trajectory microscopy

Justin A. Newman, Shane Z. Sullivan, Ryan D. Muir, Suhas Sreehari, Charles A. Bouman, Garth J. Simpson, Purdue Univ. (United States)

A beam-scanning microscope based on Lissajous trajectory imaging is described for achieving streaming 2D imaging with continuous frame rates up to 1.4 kHz. The microscope utilizes two fast-scan resonant mirrors to direct the optical beam on a circuitous trajectory through the field of view. By separating the full Lissajous trajectory time-domain data into sub-trajectories (partial, undersampled trajectories) effective frame-rates much higher than the repeat time of the Lissajous trajectory are achieved with a many unsampled pixels present. A model-based image reconstruction

Conference 9330: Three-Dimensional and Multidimensional Microscopy: Image Acquisition and Processing XXII

(MBIR) 3D in-painting algorithm is then used to interpolate the missing data for the unsampled pixels to recover full images. The MBIR algorithm uses a maximum a posteriori estimation with a generalized Gaussian Markov random field prior model for image interpolation. Because images are acquired using photomultiplier tubes or photodiodes, parallelization for multi-channel imaging is straightforward.

Preliminary results demonstrate experimental frame rates of 1.460 kHz for simultaneous acquisition of laser transmittance and polarization-dependent second harmonic generation (SHG). The use of a multi-channel data acquisition card allows for simultaneous acquisition of multiple data channels for multimodal imaging platforms with perfect image overlay. Image blur due to sample motion was also reduced by using higher frame rates. Incorporating a third resonant mirror for Z-scanning, multi-channel 3D volume rendering at video rates has been achieved. Preliminary results show that, combined with the MBIR in-painting algorithm, this instrument has the ability to generate video rate images across 6 total dimensions of space, time, and polarization for SHG, TPEF, and confocal reflective birefringence data.

9330-9, Session 2

Synchronous-digitization for video rate polarization modulated beam scanning second harmonic generation microscopy

Shane Z. Sullivan, Emma L. DeWalt, Paul D. Schmitt, Ryan D. Muir, Garth J. Simpson, Purdue Univ. (United States)

Fast beam-scanning non-linear optical microscopy, coupled with fast (8 MHz) polarization modulation and analytical modeling have enabled simultaneous nonlinear optical Stokes ellipsometry (NOSE) and linear Stokes ellipsometry imaging at video rate (15 Hz). NOSE enables recovery of the complex-valued Jones tensor that describes the polarization-dependent observables, in contrast to polarimetry, in which the polarization state of the exciting beam is recorded. Each data acquisition consists of 40 images (10 for each detector, with four detectors operating in parallel), each of which corresponds to polarization-dependent results. Processing of this image set by linear fitting contracts down each set of 10 images to a set of 5 parameters for each detector in second harmonic generation (SHG) and three parameters for the transmittance of the fundamental laser beam. Using these parameters, it is possible to recover the Jones tensor elements of the sample at video rate. Video rate imaging is enabled by performing synchronous digitization (SD), in which a PCIe digital oscilloscope card is synchronized to the laser (the laser is the master clock). The signal transient from each detector is flash digitized (80 million samples per second per channel of detection), producing gigabytes of data per second. Fast polarization modulation is achieved by modulating an electro-optic modulator—synchronously with the laser and digitizer—with a simple sine-wave at 1/10th the period of the laser, producing a repeating pattern of 10 polarization states. This approach was validated using Z-cut quartz, NOSE microscopy was performed for micro-crystals of both naproxen and glucose isomerase.

9330-10, Session 2

A new calibration tool to simply and quickly monitor and follow the performances of fluorescence microscopes

Arnaud Royon, Gautier Papon, Argolight (France)

Fluorescence microscopes have become ubiquitous in many laboratories in life sciences. For the past few years, the need for pursuing a quality approach has been arising, mainly driven by the search for guaranteed performances and comparable quantified results. However, this need faces a limitation, which is that fluorescence microscopes are used as “imaging tools” and not as “measurement tools”. This restriction is due to (i) the complexity of these devices, which does not allow their different

components to be calibrated altogether, (ii) a lack of reference materials in this field. For these reasons, the performances of fluorescence microscopes are not accessed and they produce results that should be handled with caution. We have developed a new process that enables the inscription of non-photo-bleachable fluorescent patterns with sub-micrometer sizes in three dimensions inside glass. In this paper, we present, based on this new process, a fluorescent multi-dimensional ruler adapted for the calibration and the alignment of fluorescence microscope (wide-field, confocal, multiphoton) components.

Non-exhaustively, this new tool enables the measurement of: The stage repositioning; The illumination and detection homogeneities; The field flatness; The detectors’ range of linearity, dynamic and limit of detection; The lateral and axial resolutions; The spectral response (spectrum, intensity and lifetime) of the system.

This device is warranted for five years, and can be stored without any particular precaution. Associated with our software “Log Book” and specific imaging protocols, it makes it simple and fast to monitor and follow the performances of a fluorescence microscope in a daily basis.

9330-11, Session 3

Full-field interferometric confocal microscopy using a VCSEL array

Brandon Redding, Yaron Bromberg, Yale Univ. (United States); Michael A. Choma, Yale School of Medicine (United States); Hui Cao, Yale Univ. (United States)

Confocal microscopy combines high-resolution with improved contrast and optical sectioning, making it an invaluable tool in developmental biology, clinical medicine, and optical metrology. However, traditional confocal microscopes rely on raster scanning, which limits image acquisition speed and increases system complexity. Parallel image acquisition is possible by combining interferometric detection with spatial coherence gating. In this case, each spatial mode acts as a virtual pinhole, since interference only occurs for light from the same spatial mode. Unlike physical pinholes, these virtual pinholes do not require physical separation to avoid cross-talk, enabling parallel acquisition of an entire en face plane in a single snapshot. However, the main advantage of parallelization—faster image acquisition—has thus far been mitigated by the lack of an appropriate light source. Traditional low-spatial coherence sources (e.g. thermal sources or LEDs) lack sufficient power per mode for high-speed imaging, and methods to reduce the spatial coherence of lasers (e.g. rotating diffusers) require relatively long integration times to achieve sufficiently low spatial coherence. In this work, we use a recently developed vertical cavity surface emitting laser (VCSEL) array which combines high power per mode with low spatial coherence to demonstrate full-field confocal image acquisition. The interferometric confocal microscope enables single-shot image acquisition with 18000 virtual pinholes in parallel and integration times as short as 100 μ sec (limited by the camera). In addition, interferometric detection provides access to phase information enabling quantitative phase measurements, enhanced contrast imaging of phase objects, or Doppler flow measurements.

9330-12, Session 3

A novel multimodal laser-scanning microscope control system

Zhenhua Lai, Zetong Gu, Stephen Karasek, James McLean, Xi Zhang, Charles A. DiMarzio, Northeastern Univ. (United States)

Traditional laser-scanning microscopes require complex control systems to synchronize image acquisition. The control system is especially cumbersome in a multimodal laser-scanning microscope. We have developed a novel multimodal laser-scanning microscope control system based on a National Instruments multifunction data acquisition device (DAQ), which serves as a data acquisition device as well as a programmable signal generator.

**Conference 9330: Three-Dimensional and Multidimensional Microscopy:
Image Acquisition and Processing XXII**

The novel control system is low-cost and easy-to-build, with all components off-the-shelf. The system has not only significantly decreased the complexity and the size of the microscope, but also increased the pixel resolution and flexibility of the microscope. We have utilized the novel control system to replace the control system of a Vivascope-based multimodal microscope and achieved improved performance. A separate multimodal microscope using the novel system has also been built to demonstrate that the system can be easily customized for various applications.

9330-13, Session 3

Resolving power in direct oblique plane imaging

Jeongmin Kim, Univ. of California, Berkeley (United States); Tongcang Li, Purdue Univ. (United States); Yuan Wang, Xiang Zhang, Univ. of California, Berkeley (United States)

Direct oblique plane microscopy (DOPM) enables two-dimensional (2D) imaging of any inclined plane of interest in a three-dimensional (3D) object. It is suitable for real-time imaging of living biological samples whose structures reorient rapidly or develop in arbitrary orientations. It also allows direct measurements of any tilted target plane in a specimen although such orientational information is inaccessible in sample preparation process.

DOPM has been implemented by a remote focusing technique with a tilted mirror. In the remote focusing, a second objective lens is relayed back-to-back with a first objective lens to form an aberration-free image in the remote space. By placing a tilted mirror at this remote, intermediate 3D image, a direct 2D imaging of the according oblique plane can be made through a microscope consisting of the second objective lens and a tube lens. The optical resolution of this imaging method, however, has only been roughly estimated.

Here, to accurately predict DOPM's resolving power, we formulate its point spread function (PSF) using the vectorial diffraction theory. We derive an analytical pupil function of DOPM affected by light clipping from the tilted mirror. We study an effect of the radially asymmetric pupil shape on the anisotropic optical resolution in DOPM for all oblique angles. We also show that the 2D PSF in DOPM is conceptually dissimilar from an inclined 2D section of the 3D PSF in conventional lateral imaging with a circular pupil. Optical transfer function (OTF) is also obtained from the Fourier transform of the vectorial PSF.

9330-14, Session 3

Multiplexed structured illumination microscopy for simultaneous, sub-diffraction resolution fluorescent and quantitative phase imaging

Shwetadwip Chowdhury, Joseph A. Izatt, Duke Univ. (United States)

In biological sciences, there is much emphasis on high resolution imaging as a means of elucidating structure and function at the nanoscale. However, many of these activities occur at size scales beyond the optical diffraction limit and are thus unresolvable using conventional microscopes. In response, recent years have seen the advent of sub-diffraction resolution techniques. Such sub-diffraction resolution imaging techniques can be roughly categorized into two classes. The first class surpasses the diffraction limit by coherently imaging a sample with tilted illuminations to shift high spatial-frequencies into the detection aperture. The second class of sub-diffraction resolution imaging is targeted towards fluorescent samples, and uses creative properties of fluorophores to attain "super-resolution." However, these two classes of sub-diffraction imaging techniques have long remained separate with little overlap. Here, we introduce a method that bridges this divide. In this work, we extend our previous work on structured illumination

diffraction phase microscopy (SI-DPM), which allows sub-diffraction resolution, quantitative phase (QP) imaging of transparent samples, specifically cells. Though QP imaging allows for imaging of cellular structure with endogenous contrast (such as refractive index or path length), QP imaging inherently lacks molecular specificity. Because the optical setup for SI-DPM is similar to that of SIM, there is potential for combining SI-DPM with SIM for dual QP/fluorescent imaging. Here, we describe a novel system that uses fundamental concepts from SI-DPM and SIM to multiplex QP and fluorescent information onto a single camera for sub-diffraction resolution, simultaneous QP and fluorescence imaging.

9330-15, Session 3

CMOS image sensor for multi-beam multi-functional confocal microscopy

Keiichiro Kagawa, Hiromi Nieda, Yuki Nishioka, Taishi Takasawa, Min-Woong Seo, Keita Yasutomi, Shoji Kawahito, Shizuoka Univ. (Japan)

A custom CMOS image sensor for multi-beam confocal microscopy, which has benefits of multi-mode observations as well as low photo-damage on biological tissues and high speed imaging, is developed. Based on our high-speed and high-efficiency charge modulation pixel technology called lateral electric field modulation (LEFM) and low-noise and high-dynamic-range column analog-to-digital converters (ADCs), functions of fluorescence lifetime imaging microscopy (FLIM) and fluorescence correlation spectroscopy (FCS) are integrated in the CMOS image sensor. Users can select one among conventional confocal fluorescent imaging, FLIM, and multi-point FCS according to their demand. A prototype CMOS image sensor with 27x27 effective pixels and 27x3 optical black pixels was fabricated in 0.11-um CMOS technology. The image sensor is equipped with 810 column ADCs that are connected to all pixels in parallel, so that the readout noise is suppressed by reducing the bandwidth of the readout circuits. Such a complete parallel architecture also provide global shutter. The pixel aperture is 3.8um sq., and the pixel pitch is 67.2um sq. A prototype microscope is developed based on the CMOS image sensor. The microscope is mainly composed of Nikon Eclipse Ti, a microlens array to generate a spot array, a single-mirror two-dimensional beam deflector, collimator and imaging lenses, and the CMOS image sensor. A reduced image of the excitation spot array is scanned on a dyed specimen in two dimensions, and its fluorescent image is captured by the CMOS image sensor. When the number of scanning positions is 32x32, the pixel count of a reproduced image is 832x832.

9330-16, Session 4

In vivo hemozoin malaria-pigment localization and distribution in red blood cell by multimodal microscopy system imaging

Nicolas Spegazzini, Rishikesh Pandey, Jeon Woong Kang, Massachusetts Institute of Technology (United States); Ishan Barman, Johns Hopkins Univ. (United States); Ramachandra R. Dasari, Peter T. C. So, Massachusetts Institute of Technology (United States)

The multimodal microscopy system developed in our laboratory incorporates confocal Raman, confocal reflectance, and quantitative phase microscopy (QPM) into a single imaging entity. This multi-modal system is used to investigate healthy and diseased blood samples. Quantitative phase microscopy and confocal reflectance show detailed morphology whereas confocal Raman microscopy provides detailed chemical information from the cell. Combining these intrinsic contrast imaging modalities makes it possible to obtain quantitative morphological and chemical information without exogenous staining. By using multivariate hyper spectral-spatial

**Conference 9330: Three-Dimensional and Multidimensional Microscopy:
Image Acquisition and Processing XXII**

modeling method, individual components can be resolved in the spectral and spatial domain. The depth of a healthy red blood cell (RBC) displays good correlation with its hemoglobin distribution. Moreover, in malaria infected RBCs, we can decompose in the spatial domain and obtain a molecular image for hemozoin (malaria pigment) distribution of inside the cell. This new methodology allows monitoring cell-drug interactions and cell development with minimal perturbation of the biological system. Chemical imaging by confocal Raman spectroscopy and morphological screening by QPM subsequent for investigating blood disorders is proposed.

9330-17, Session 4
Preliminary study for application of optical coherence elastography (OCE) to monitor wound healing processing

Guangying Guan, Chunhui Li, Yuting Ling, Fan Zhang, Ana Schor, Zhihong Huang, Univ. of Dundee (United Kingdom)

Wound healing is a complex and dynamic process of replacing devitalized and missing cellular structures and tissue layers. The classic model is divided into three or four sequential phases: hemostasis; inflammation; proliferation and remodeling. All the procedures are well studied and lots of effort on develop medicine to speed up the procedures or archive scar-less wound healing. Monitoring the microstructure change during the treatment is highly demanded. In this study, a new methodology has been explored aiming to monitor the morphological and mechanical property alteration of wounded tissue. Optical coherence elastography (OCE) equipped with an LDS V201 permanent magnet shaker to provide a vibration signal, has been used for the non-destructive monitoring. In vitro mice skin tissue block from normal ones, Diabetic ones and Diabetic treated with IGDS ones after 10days post wounding have been tested. The structure image is compared to the conventional Histology results, the results is quite promising and OCT system could provide depth information without slicing the sample. Which could be helpful for understanding the recover processing and analysis the different healing phases.

9330-18, Session 4
Pump probe microscopy of human hair

Naveen K. Balla, Patrick Ferrand, Institut Fresnel (France); Florian Formanek, L'Oréal (France); Jean-Baptiste Galey, L'Oréal Recherche et Innovation (France); Lucien Bildstein, Hervé Rigneault, Institut Fresnel (France)

Human hair gets its color from two biological pigments called eumelanin and pheomelanin. Eumelanin is the more common of the two and it is responsible for brown to black colors. Pheomelanin on the other hand is responsible for yellow to red colors. The composition, quantity and arrangement of these two types of melanin give hair its color. Yet, their relative distribution within the fibre is not fully known. Pump probe microscopy is a high resolution 3D imaging technique which can be used to differentiate eumelanin and pheomelanin. In this technique, a pump laser is used to excite the sample and a probe laser is used to study the nature of this excited state in the sample. We used this technique in a point scanning imaging modality to study red to black hair samples. Our first goal is to look for optimal pump-probe signal when changing the frequency between the two lasers. The pump wavelength was maintained at 820 nm and probe wavelength was varied from 630 nm to 740 nm. At wavelengths below 688 nm, red hair exhibits excited state absorption (ESA) and at longer wavelengths, it exhibits ground state depletion (GSD). Black hair on the other hand exhibits GSD at wavelengths greater than 650 nm. We chose 670 nm probe laser to study distribution of melanin in 11 different types of hair samples. Excited state life times of all these hair samples were measured by varying the time delay between the pump and probe beams.

9330-19, Session 4
Multi-color, real-time focal modulation microscopy for 3D imaging of blood flow in zebrafish

Shilpa Pant, Nanguang Chen, National Univ. of Singapore (Singapore)

Focal Modulation Microscopy (FMM) is an emerging single photon excitation, high resolution fluorescence technique that has deep imaging capabilities comparable to multi-photon microscopy. We have developed a line-scanning, multi-wavelength FMM system that can provide imaging speeds of up to 100 fps. The deep imaging capability of FMM in addition to the high imaging speed allowed us to rapidly scan whole zebrafish livers and obtain 3D videos of the blood flow. We have used our multi-color, real-time FMM system to study the changes that occur in the blood flow rate and anatomy of the liver in tumor models of zebrafish. The blood flow rate was measured in the liver of a transgenic zebrafish model (Tg (gata1:DsRed; fabp10a: EGFP-Lc3)) that expresses eGFP in the liver and DsRed in the erythrocytes. Blood flow was also measured in a liver tumor zebrafish model (Tg (flit:EGFP; gata1:DsRed) x TO(KrasG12V)). Preliminary studies indicate a change in the blood flow rate in the liver of the tumor model compared to the normal liver. An increase in the volume of the liver as well as an increase in the number blood vessels in the oncogene model could also be observed.

9330-20, Session 4
High-speed volumetric confocal imaging for tracking calcium dynamics in C. elegans neurons

Ki Hyun Kim, Sudip Mondal, Adela Ben-Yakar, The Univ. of Texas at Austin (United States)

We present a high-speed volumetric confocal imaging system for tracking calcium dynamics in *C. elegans* neurons. Depth-resolved imaging is required to observe individual cells in *C. elegans* ganglia with high density neuronal cells. Detection of small changes in neuronal signal is challenging in wide-field microscopy due to excessive out-of-focus signal. High-speed volumetric imaging is advantageous in observing transients such as calcium dynamics from multiple cells in *C. elegans* neuronal circuits. *C. elegans* expressed with pan-neuronal markers require a large field-of-view (FOV) with high resolution to capture the dynamics from multiple neurons present at different locations in the worm body. We first developed a high-speed confocal microscope with a large and flexible FOV which fits *C. elegans* and gives the optimal imaging speed. We demonstrate our system for two situations: (1) high resolution brain imaging with 350 μm x 50 μm FOV using a 1.3 NA, 40X, and oil immersion objective speed and (2) whole worm imaging with 630 μm x 50 μm FOV using a 0.95 NA, 20X, and water dipping objective. To use the full imaging speed of our confocal microscope, we scan the whole target continuously and save time due to axial stage motion. With the imaging speed and the continuous scanning, our volumetric confocal imaging system can image one volume of 350 μm x 50 μm x 30 μm or one volume of 630 μm x 50 μm x 40 μm every second. We will present time-lapse videos of calcium dynamics in *C. elegans* captured by our system.

9330-21, Session 5
3D information from 2D scans in a camera-based confocal microscope (Invited Paper)

Alexander Jesacher, Monika Ritsch-Marte, Medizinische Univ. Innsbruck (Austria); Rafael Piestun, Univ. of Colorado at Boulder (United States)

We present a laser scanning microscope with the ability to slightly refocus

Conference 9330: Three-Dimensional and Multidimensional Microscopy: Image Acquisition and Processing XXII

the sample after the acquisition of a single 2D scan. This is achieved by double-helix point spread function engineering in the emission path of the microscope and camera-based detection.

The method uses a focused laser to raster-scan the sample. The sample response (fluorescence) is imaged onto a sCMOS camera and an image is taken at each scan position. A double-helix phase mask is placed in a plane conjugated to the objective back aperture in the emission path. This mask turns the shape of the emitted fluorescence into two bright "lobes" whose rotational angle reveals the z-location of the emitter.

By pinholing the recorded images with synthetic "double-pinholes" of varying rotational angles, one can extract multiple 2D images of slightly different axial locations.

We present experimental images from the stained microtubules network in fixed African green monkey kidney cells and show that it is possible to refocus purely based on data post processing by about ± 200 nm with a high NA lens.

9330-22, Session 5

Rapid tracking of particles in three dimensions using a simple EPIC microscope setup without changing focus

Jiun-Yann Yu, Ramzi N. Zahreddine, Robert H. Cormack, Carol J. Cogswell, Univ. of Colorado at Boulder (United States)

No Abstract Available

9330-23, Session 5

3D microscope imaging robust to restoration artifacts introduced by optically thick specimens

Nurmohammed Patwary, Sharon V. King, Chrysanthe Preza, The Univ. of Memphis (United States)

We demonstrate 3D microscope imaging using computational optical sectioning microscopy (COSM) with an engineered point-spread function (PSF) robust to depth-induced spherical aberration (SA). Earlier we demonstrated that wavefront encoding (WFE) using the SQUBIC phase mask renders the PSF robust to SA [1] and that restoration of simulated images using a single WFE-PSF does not lead to artifacts as in the conventional case [2]. In this study we show experimental verification of our WFE COSM approach.

The WFE system used in this study is a commercial microscope with a modified side port imaging path, where a spatial light modulator (SLM) is used to project the SQUBIC phase mask on the back focal plane of the imaging objective [3]. Properties of the SLM cause a discrepancy between the simulated and experimental WFE-PSF [3]. Therefore, to improve the performance of the image restoration applied to experimental data, the effect of the SLM was modeled and incorporated in the simulated WFE-PSF used for the restoration of experimental data. Images of a test sample with 6 μm in diameter microspheres embedded in UV-cured optical cement (RI = 1.56), and cultured glioblastoma cells ($\sim 7 \mu\text{m}$ thick) fixed and mounted in Prolong[®] Gold (RI = 1.47) were captured using the engineered imaging path (side port) and the conventional imaging path (top port) of the system and a 63X/1.4 NA oil immersion objective lens. The acquired images were restored using a regularized space-invariant expectation maximization (SIEM) algorithm [4] based on Tikhonov-Miller regularization with a proper roughness penalty [5]. Our results demonstrate that, the restored images from the SQUBIC-WFE system are free from artifacts evident in corresponding images from the conventional system. In this study we quantify the improved restored image quality that results from incorporation of SLM characterization in the PSF model.

References:

- [1] A. Doblaz, S. V. King, N. Patwary et al., "Investigation of the SQUBIC phase mask design for depth-invariant widefield microscopy point-spread function engineering." 894914-894914-8 (2013).
- [2] N. Patwary, A. Doblaz, S. V. King et al., "Reducing depth induced spherical aberration in 3D widefield fluorescence microscopy by wavefront coding using the SQUBIC phase mask." 894911-894911-8 (2013).
- [3] S. V. King, A. Doblaz, N. Patwary et al., "Implementation of PSF engineering in high-resolution 3D microscopy imaging with a LCoS (reflective) SLM." 894913-894913-7 (2013).
- [4] [Computational Imaging Research Laboratory, Computational Optical Sectioning Microscopy Open Source (COSMOS) software package].
- [5] C. Preza, M. I. Miller, L. J. Thomas, Jr. et al., "Regularized linear method for reconstruction of three dimensional microscopic objects from optical sections," Journal of the Optical Society of America A-Optics Image Science and Vision, 9(2), 219-228 (1992).

9330-24, Session 5

High-throughput on-chip analysis of 3D swimming patterns of animal sperms using holographic lensfree imaging

Ting-Wei Su, Inkyum Choi, Jiawen Feng, Calvin Huang, Wei Luo, Aydogan Ozcan, Univ. of California, Los Angeles (United States)

Dynamic tracking of sperms in an aqueous environment is critical for inspecting the quality of sperm and has numerous applications in reproductive medicine and livestock industry. Earlier lens-based systems lack the throughput to provide accurate 3D tracking of large volumes of sperm. Here we report a lensfree high-throughput optical tracking technique that is based on partially-coherent digital in-line holography, adopting a dual-color and dual-angle illumination scheme. This platform enables us to track individual 3D trajectories of $>1,000$ sperms with sub-micron accuracy within a large sample volume (~ 9 microliter) at a frame rate of >140 frames per second. Using this imaging platform, we were able to collect thousands of sperm trajectories in a few hours and perform detailed statistical analysis of horse sperms' 3D swimming dynamics. This large spatio-temporal statistics of $>17,000$ horse sperm 3D swimming patterns revealed that they can be grouped into six categories: (i) irregular, (ii) linear, (iii) planar, (iv) helical, (v) ribbon, and (vi) hyperactivated, where categories (i), (iii) and (v) constitute the dominant portion ($>97\%$) of these swimming patterns in a plasma-free semen extender medium. Furthermore, hyperactivated swimming patterns can be divided into four sub-categories: hyper-progressive, hyper-planar, hyper-ribbon, and star-spin. Based on these experiments, we also found that horse seminal plasma increases the straightness of trajectories, i.e., it enhances the relative percentage of linear swimming patterns and suppresses planar swimming patterns, while minimally affecting the overall percentage of ribbon patterns.

9330-25, Session 5

Simultaneous multiplane imaging for 3D confocal microscopy using high-speed z-scanning multiplexing

Marti Duocastella, Giuseppe Viccidomini, Alberto Diaspro, Istituto Italiano di Tecnologia (Italy)

One of the key frontiers in optical imaging is to maximize the spatial information retrieved from a sample while minimizing acquisition time. Laser scanning confocal microscopy is a powerful imaging modality that allows real-time and high-resolution acquisition of two-dimensional (2D) sections. However, in order to retrieve information from three-dimensional (3D) volumes it is currently based on a stepwise process that consists of

**Conference 9330: Three-Dimensional and Multidimensional Microscopy:
Image Acquisition and Processing XXII**

acquiring multiple 2D sections from different focal planes by relatively slow z-focus translation. Here, we present a novel method that enables the capture of an entire 3D sample in a single step. Our approach is based on an acoustically-driven varifocal lens integrated in a commercial confocal system that enables axial focus scanning at speeds of 140 kHz or above. Such high-speed enables one or multiple focus sweeps on a pixel by pixel basis. By using a fast acquisition card properly synchronized with scanning, we can assign the photons detected at each pixel to their corresponding focal plane allowing simultaneous multiplane imaging. We exemplify this novel 3D confocal microscopy technique by imaging different biological fluorescent samples and comparing them with those obtained using traditional z-scanners. Based on these results, we find that image quality in this novel approach is similar to that obtained with traditional confocal methods, while speed is only limited by signal-to-noise-ratio. As the sensitivity of photodetectors increases and more efficient fluorescent labeling is developed, this novel 3D method can result in a significant reduction in acquisition time allowing the study of new fundamental processes in science.

9330-27, Session 6

Quantitative imaging of intact cardiac tissue using remote focusing microscopy

Alexander D. Corbett, Rebecca A. B. Burton, Gil Bub, Tony Wilson, Univ. of Oxford (United Kingdom)

Remote focussing microscopy offers many advantages when acquiring volumetric data from living tissue. The all-optical means of refocussing does not agitate the specimen by moving either the stage or imaging objective. Aberration-compensated imaging extends over volumes as large as $450\ \mu\text{m} \times 450\ \mu\text{m} \times 200\ \mu\text{m}$ (X, Y and Z) allowing data to be collected from hundreds of cells. The speed with which refocussing can be achieved is limited only by the mechanical movement of a small (2 mm diameter) mirror. Using a pair of oblique imaging planes to rapidly acquire (<200ms) depth information temporally freezes residual tissue motion in the arrested heart.

This paper discusses the progress of remote focussing microscopy from a novel imaging technique to a reliable tool in the life sciences. Specifically, we describe recent efforts to achieve the accurate calibration of both distance and orientation within the imaging volume. Using a laser machined fluorescent specimen it is possible to identify, with high sensitivity, small (<1%) depth-dependent magnification changes which are a linear function of axial misalignment of the imaging objective. The sensitivity of the calibration procedure limits distortion to <1 μm over the entire imaging volume. The repeatable nature of these subtle magnification changes allows data sets to be corrected in post-processing. This work finds direct application in identifying the microscopic effects of chronic disease in the living heart.

9330-28, Session 6

3D widefield light microscope image reconstruction without dyes

Sean Larkin, Lickenbrock Technologies, LLC (United States); Jeffrey Larson, Illinois Institute of Technology (United States); Charles Holmes, Lickenbrock Technologies, LLC (United States); Marcella Vaicik, Michael Turturro, Illinois Institute of Technology (United States); Alexander Jurkevich, Sunilima Sinha, Toshihiko Ezashi, Univ. of Missouri (United States); Georgia Papavasiliou, Eric Brey, Illinois Institute of Technology (United States); Tim Holmes, Lickenbrock Technologies, LLC (United States)

Multimodality and multispectral imaging, using 3D optical sectioning and 3D image reconstruction, are investigated as an approach to contrast

with imaging live samples without using exogenous contrast media. Contrast agents, such as fluorescent or absorbing dyes, can be toxic or alter cell behavior. Current modes of producing 3D image sets from a light microscope, such as 3D deconvolution algorithms and confocal microscopy, often require dyes. Phase contrast, brightfield and darkfield microscopy produce contrast without dyes. Some of these modalities have not previously benefitted from 3D image reconstruction algorithms, however. The image reconstruction algorithm is based on an underlying physical model that includes 3D distributions of scattering potential, which quantifies the sample's optical absorption and phase character. The algorithm is based upon optimizing an objective function - the I-divergence - while solving for elements of the 3D scattering potential. Unlike deconvolution algorithms, each microscope modality, such as phase contrast or darkfield, produces two output image sets instead of one. Contrast in the displayed image and 3D renderings is further enabled by treating the multispectral/multimodal data as a feature set in a mathematical formulation that uses the principal component method of statistics.

9330-29, Session 6

A block-based forward imaging model for improved sample volume representation in computational optical sectioning microscopy

Sreya Ghosh, Chrysanthe Preza, The Univ. of Memphis (United States)

Imaging thick samples (10-150 μm) with a fluorescence microscope is a challenge since microscope objectives are designed to be operated within a depth of field. Refractive Index (RI) variation between the immersion medium of the objective lens, the coverslip and the specimen causes refraction which changes the spherical wave-front of light and introduces aberration known as a spherical aberration (SA) [1, 2]. The effect of SA is dependent on the RI variation, the numerical aperture of the system and the thickness of the sample[3].

Modeling the response of the system allows the use of model-based computational methods for data processing [4] to improve resolution and contrast by mitigating the effect of SA and defocus blur. To simplify the complexity of the problem, the specimen is either assumed to be thin, or in the case of depth-variant algorithms [5] to have a constant RI. It is a well-known fact that the RI of a sample varies throughout the volume [6]. Therefore, images acquired through the sample volume are subjected to space variant (SV) imaging, i.e., variance both in the lateral and axial directions.

Light from a point source travels through stratified media, i.e., layers of different RI. Light from different point sources travel through different arrangements of imaging layers because of spatial variability of the specimen RI. Computation of image intensity using a spatially-variant model requires a different point spread function (PSF) for each pixel, which is not computationally feasible. To model the image formed in this case, we use a block based approximation. Current investigations with experimental and simulated data show promising results indicating the need of this new model.

A forward model that accounts for SV imaging based on a block-based representation is introduced and evaluated using experimental and simulated data in this paper. The block-based forward imaging model optimizes two numerical approximations of SV convolution [7] for an accurate and computationally feasible 3D SV image and extends the previously developed strata-based imaging model [4].

References:

- [1] Chew, W. C., [Waves and Fields in Inhomogeneous Media], IEEE press New York (1995).
- [2] Goodman, J. W. , "Introduction to Fourier Optics," Mac.Graw-Hill, New York (1960).
- [3] Egner, A. and Hell, S. W. , "Aberrations in confocal and multi-photon fluorescence microscopy induced by refractive index mismatch," 404-413 (2006).

**Conference 9330: Three-Dimensional and Multidimensional Microscopy:
Image Acquisition and Processing XXII**

[4] Preza, C. and Conchello, J., "Depth-variant maximum-likelihood restoration for three-dimensional fluorescence microscopy," *JOSA A* 21(9), 1593-1601 (2004).

[5] Preza, C. and Myneni, V., "Quantitative depth-variant imaging for fluorescence microscopy using the COSMOS software package," *BiOS*, International Society for Optics and Photonics, 757003-757003-8 (2010).

[6] Kam, Z., Hanser, B., Gustafsson, M. G., Agard, D. A. and Sedat, J. W., "Computational adaptive optics for live three-dimensional biological imaging," *Proc.Natl.Acad.Sci.U.S.A.* 98(7), 3790-3795 (2001).

[7] Nagy, J. G. and O'Leary, D. P., "Restoring images degraded by spatially variant blur," *SIAM Journal on Scientific Computing* 19(4), 1063-1082 (1998).

9330-30, Session 6
A robust simulation and reconstruction platform of fluorescence molecular tomography

Shixin Jiang, Jie Liu, Yu An, Beijing Jiaotong Univ. (China); Yamin Mao, Xin Yang, Chongwei Chi, Jie Tian, Institute of Automation (China)

Fluorescence molecular tomography (FMT) has many successful applications as a promising tomographic method for in vivo small animal imaging. As an important optical molecular imaging modality, FMT can three-dimensionally resolve fluorescence bio-distribution in small animals, which has been widely used for tumor detection and drug discovery. In the study of FMT, most of the methods, which are used to solve the forward model and inverse model of FMT, are carried out based on MATLAB or other separate programming tools. The operation efficiency was limited during the process of FMT reconstruction and multimodality applications. To solve this problem, a robust simulation and reconstruction platform of FMT is proposed in this paper. It was developed on Windows 32 bit operation system and Visual Studio 2010 with C++, which is used in our multi-modality molecular imaging system. The forward model was solved by finite-element method (FEM) based on diffusion equation (DE), and the inverse model was performed by iteration-shrinkage algorithm. Compared with the separate programs, which is used to solve forward model and inverse model of FMT, the proposed platform takes advantage in robust reconstruction and convenient integration with other imaging modalities. Besides, the parameters used in the proposed platform are less than the separate programs leading to accurate results. The numerical experiments were performed to validate the platform. The reconstruction results demonstrate that our FMT platform can obtain more accurate and robust results (the errors was about 0.2mm), compared with the separate programs (the errors was about 1mm). Our platform can be free downloaded on our website <http://www.3dmed.net>.

9330-31, Session 7
Computational modeling of STED microscopy through multiple biological cells under one- and two-photon excitation

Andrew E. Mark, Mitchell A. Davis, Matthew S. Starosta, Andrew K. Dunn, The Univ. of Texas at Austin (United States)

While superresolution microscopy techniques afford enhanced resolution for biological applications, they have largely been used to study structures in isolated cells or in superficial tissue. We use the finite-difference time-domain method to simulate the propagation of focused beams used for stimulated emission depletion (STED) microscopy through multiple layers of cells. We model de-excitation beams that provide axial and lateral confinement of the fluorescence emission spot and assess the point spread function (PSF) of the system as a function of focal depth. We compare

the spatial resolution using the STED technique to the resolution using traditional confocal and two-photon microscopy. Results show that the depletion beams retain a well-defined minimum up to the maximum simulated depth of 90 microns. PSF calculations suggest that, while the fluorescence emission signal degrades with imaging depth, imaging should remain possible as long as the fluorescence emission remains detectable.

9330-32, Session 7
Fast calculation of the best focus position

Vitalii V. Bezzubik, National Research Univ. of Information Technologies, Mechanics and Optics (Russian Federation); Gleb V. Vdovin, National Research Univ. of Information Technologies, Mechanics and Optics (Russian Federation) and Flexible Optical B.V. (Netherlands); Nikolai R. Belashenkov, National Research Univ. of Information Technologies, Mechanics and Optics (Russian Federation)

The new technique based on linear-scale differential analysis of digital image is proposed to find the best focus position of an imaging system in particular digital microscope. A lot of known passive methods of searching the best focus position of digital imaging systems are based on the image analysis and solve the problem of finding the extremum value of the estimation function by means of changing the position of the focal plane relative to the image sensor. To find the best focus position most of known methods need to analyze several frames captured in different positions of the focal plane. Thus this process takes relatively long time for the mechanical displacement of the movable element of imaging system. It is possible to improve its performance if the estimation function is calculated in less number of system positions. We propose a method of estimating of defocus value which need two measurements only. Using this method the value and sign of defocus may be found if the result of linear-scale differential analysis of the images is compared with pre-defined look-up table (LUT) of imaging system. It is shown that the mean values of the differential responses in regions of edges of objects decrease while the scale increases. This dependence is good fitted by exponential approximation and its decrement is determined by blur amount related to imaging system. Comparing the decrement with LUT one can calculate the defocus and find the best focus position. The method has been tested on series of images captured by digital microscope. It is shown that method is low sensitive to spatial noise and fast enough due to application of integer operations in calculations of differential responses.

9330-33, Session 7
Nonlinear optical output of atomic systems via numerical simulation of time-dependent Schrodinger equation, stimulated by laser sources in and out of resonance conditions within the non-perturbative regime

Stephen Karasek, Charles A. DiMarzio, Northeastern Univ. (United States)

Nonlinear optical effects have had a major impact on many fields in optics since their discovery. Much recent progress has been made possible by numerical simulations, built on a firm bedrock of theory and verified experimentally, but testing different parameters to observe different, and sometimes quite exciting, results. More specifically, we investigate how Time-Dependent Schrodinger Equations (TDSE) of electrons travelling within atomic and molecular potential wells, propagated with Finite Difference Methods, and excited with different types of laser sources, can show nonlinear photonic output.

In particular, here we are interested in resonance conditions of these

Conference 9330: Three-Dimensional and Multidimensional Microscopy: Image Acquisition and Processing XXII

systems. The parameters of a laser source, as well as the source type, have a substantial impact on the system's TDSE. With the right conditions, and knowledge of the system's current energy state, we can effectively choose what energy state to move the system to. We can likewise reduce the energy state by choosing conditions that are different enough from resonance conditions, i.e. the "wrong" conditions.

In this paper we will show the effects of laser source conditions both in and out of resonance, in several different atomic systems with potential wells, and resulting nonlinear photonic output for each combination of parameters.

9330-34, Session 7

A new analytical model to optimize phase-sensitive detection in photothermal optical coherence tomography systems

Maryse Lapierre-Landry, Jason M. Tucker-Schwartz, Melissa C. Skala, Vanderbilt Univ. (United States)

Photothermal optical coherence tomography (PTOCT) is a promising technique to increase molecular contrast in OCT images. The imaging capabilities of PTOCT have already been demonstrated experimentally for ex vivo and in vivo applications. However, a theoretical understanding of the PTOCT signal with respect to imaging and tissue parameters must be further developed in order to aid in system design, optimize signal processing algorithms, and improve experimental outcomes. A model of the depth-resolved PTOCT signal throughout a tissue sample has been developed using the bio-heat conduction equation as well as established OCT analytical models. The model describes the expected change in optical path length throughout the sample, and the expected signal-to-noise ratio at all depths. A detection limit is predicted by the model based on system and sample characteristics, such as imaging wavelength and sample attenuation coefficients. The model also enables a comparison with existing models and experimental results from multi-photon microscopy (MPM), a method of similar capabilities. Comparing PTOCT to MPM could facilitate the choice between imaging modalities and could allow for imaging parameter optimization based on sample properties. This work provides a practical platform to predict the most appropriate imaging approach for a particular application. By contributing to a more comprehensive understanding of PTOCT signals in tissues, this model provides improved resources for in vivo pre-clinical imaging.

9330-35, Session 7

Single frame polarimetric microscopy

Thomas G. Brown, Univ. of Rochester (United States)

A polarization dependent point spread function can, in principle, provide full polarimetric information in a single measurement. In multidimensional microscopy, this can take different forms depending on whether one is using a confocal geometry or a full-frame wide field measurement. We discuss the implementation of this class of methods for different modes of multidimensional microscopy and examine the usefulness of the method for very low light single molecule imaging.

9330-36, Session 8

Standing-wave excitation of fluorescence in a laser-scanning microscope allows precise contour mapping of the red blood cell membrane

Rumelo Amor, Univ. of Strathclyde (United Kingdom); Sumeet Mahajan, Univ. of Southampton (United Kingdom);

William B. Amos, MRC Lab. of Molecular Biology (United Kingdom); Gail McConnell, Univ. of Strathclyde (United Kingdom)

Standing-wave excitation of fluorescence is highly desirable in optical microscopy because it improves the axial resolution. We demonstrate here that multiplanar excitation of fluorescence by a standing wave can be produced in a single-spot laser scanning microscope by placing a plane reflector close to the specimen. Using a model specimen consisting of a monolayer of dye covalently attached to the surface of a planoconvex lens, we have observed concentric fluorescence fringes from excitation at the antinodes and confirmed that the fringe spacing is equal to the antinode spacing $\lambda/2n$, where λ is the excitation wavelength and n is the medium refractive index. Since the axial locations of the antinodes are joined to the lateral positions of the fringes, we obtain an accurate reconstruction of the specimen in three dimensions from a single snapshot. By reducing the detection bandwidth to 5 nm, we have observed that the standing waves close to a reflector are radially modulated in a precise way, with a frequency proportional to the Stokes shift, corresponding to a Moiré pattern between the excitation and emission standing-wave fields. We show by the use of dyes specific for the cell membrane how standing-wave excitation can be exploited to generate precise contour maps of the surface membrane of red blood cells, with an axial resolution of ~90 nm. The method, which requires only the addition of a plane mirror to a confocal laser scanning microscope, may well prove useful in studying diseases which involve the red cell membrane, such as malaria.

9330-37, Session 8

An information-theoretic approach to designing the plane spacing for multifocal plane microscopy

Amir Tahmasbi, The Univ. of Texas at Dallas (United States) and The Univ. of Texas Southwestern Medical Ctr. at Dallas (United States); Sripad Ram, Jerry Chao, Anish V. Abraham, The Univ. of Texas at Dallas (United States); E. Sally Ward, The Univ. of Texas Southwestern Medical Ctr. at Dallas (United States); Raimund J. Ober, The Univ. of Texas at Dallas (United States) and The Univ. of Texas Southwestern Medical Ctr. at Dallas (United States)

Multifocal plane microscopy (MUM) is a 3D imaging modality which enables the localization and tracking of single molecules at high spatial and temporal resolution by simultaneously imaging distinct focal planes within the sample. MUM overcomes the depth discrimination problem of conventional microscopy and allows high accuracy localization of a single molecule in 3D along the z-axis. An important question in the design of MUM experiments concerns the appropriate number of focal planes and their spacings to achieve the best possible 3D localization accuracy along the z-axis. Ideally, it is desired to obtain a 3D localization accuracy that is uniform over a large depth and has small numerical values, which guarantee that the single molecule is continuously detectable. Here, we address this concern by developing a plane spacing design strategy based on the Fisher information. In particular, we analyze the Fisher information matrix for the 3D localization problem along the z-axis and propose spacing scenarios termed the strong coupling and the weak coupling spacings, which provide appropriate 3D localization accuracies. Using these spacing scenarios, we investigate the detectability of the single molecule along the z-axis and study the effect of changing the number of focal planes on the 3D localization accuracy. We also examine the effect of a variety of other imaging parameters, such as the photon count, the emission wavelength and the magnification, on the localization accuracy and on the plane spacing. We further introduce a new software module that helps to design the plane spacings for a MUM setup.

**Conference 9330: Three-Dimensional and Multidimensional Microscopy:
Image Acquisition and Processing XXII**

9330-38, Session 8

Extending depth of field in confocal microscopy by tunable acoustic gradient-index lens

Kuo-Jen Hsu, National Taiwan Univ. (Taiwan) and National Tsing Hua Univ. (Taiwan); Kuan-Yu Li, National Taiwan Univ. (Taiwan); Yung-Hsin Shih, Hen-Yi Lin, Yen-Yin Lin, National Tsing Hua Univ. (Taiwan); Shi-Wei Chu, National Taiwan Univ. (Taiwan); Ann-Shyn Chiang, National Tsing Hua Univ. (Taiwan) and Academia Sinica (Taiwan)

Confocal microscopy was firstly proposed by Marvin Minsky in 1957. A pinhole placed in front of the photodetector at the conjugate plane of focus to eliminate signals from out-of-focus region to enhance image axial contrast and thus provides optical sectioning capability. Conventionally, increasing the size of pinhole can extend the thickness of virtual optical section but the worse image contrast would be the cost. An axial scanning setup can be an alternative to extend the depth of field with good image contrast, but the axial scanning speed would be another limitation. Recently, several methods have been proposed to provide fast axial scanning capability, such as quickly moving objective with fast piezoelectric material, shifting focus by deformable lens and freely assigning focus in 3-dimensional space by acousto-optic deflectors (AODs). Nevertheless, the axial scanning rates of the first 2 methods are lower than 1 kHz due to inertia. AODs are powerful for fast point scan but not efficient to complete a volume image. Therefore, a fast axial scanning technique is highly desirable to achieve real-time volumetric imaging. Here we demonstrate a simple concept of thick-section imaging in confocal microscopy by a tunable acoustic gradient-index (TAG) lens cascaded with the objective. TAG lens can be a gradient-index lens with a fast time-varying index distribution. We show fluorescence beads displaced by several tens of μm apart in depth being captured in a single frame. This result shows our strategy can provide large depth of field and capable of detect simultaneous events happened in 3D space.

9330-40, Session 9

Method of live cells tomography based on phase shifting lateral shearing interferometric microscopy

Gennady G. Levin, Mikhail I. Latushko, Gennady N. Vishnyakov, All-Russian Research Institute for Optical and Physical Measurement (Russian Federation)

In vivo noninvasive observations of a live cell by means of quantitative phase imaging or optical microtomography using low-coherence illumination are of particular interest in medicine today.

A prototype of the optical microtomograph for live cells is presented in this work. It is a combination of an interference shearing phase shifting microscope working in low-coherence transmitted illumination of an LED and equipped with an angle scanning system of a test specimen for obtaining different projections.

The original patented on-axis lateral shearing common-path interferometer is a 4f-optical system with an inclinable mirror and a beam splitting double Dove prism inside is used to obtain a shear interferogram of a cell.

A series of sheared interferograms is registered at a CCD with different phase shifts and processed by a phase shifting method for reconstruction of 1D derivative of the 2D optical path length map of light passed through a cell.

A test specimen is moved with a piezoelectric nanopositioner between two confocal microscope objectives within a range of formed light cone to provide different illumination angles. To provide unambiguous confrontation of a certain projection and an illumination angle the illumination system is calibrated before the measurements.

Phase images obtained at different illumination angles are considered to be a projection data for further 3D spatial refractive index distribution of live cell reconstruction using well-known tomography algorithms. We show the basic possibility of work of such an algorithm. The level of self-noise of the microscope does not exceed several nanometers due to low-coherence illumination.

9330-41, Session 9

An integrated approach to determine prior information for improved wide-field imaging models from computational interference microscopy

Md Shohag Hossain, Sharon V. King, Chrysanthe Preza, The Univ. of Memphis (United States)

Imaging thick biological samples introduces spherical aberration (SA) due to a spatially varying refractive index (RI) mismatch between the specimen and the immersion medium of the lens. SA causes the point spread function (PSF) of a wide field fluorescence microscope to change thereby making the imaging process depth-variant. Model-based restoration methods rely on the accuracy of the model they use. We have been developing models [1, 2] for depth-variant fluorescence imaging that assume constant RI for the sample. Knowledge of prior sample information (such as spatially varying RI within the sample) can improve these models enabling more accurate three-dimensional (3D) restoration.

The goal of this study is the development of an integrated approach to determine sample prior information from interference microscopy data using a computational optical sensing and imaging (COSI) paradigm. In this COSI system we are integrating a DIC microscope without a condenser-side Nomarski prism (referred to as a Koehler-DIC microscope in [3]) with a model-based computational method [4] that determines sample attributes, such as amplitude and phase. This approach provides the benefit of a simple implementation in that interference microscopy can be implemented with either a single static Nomarski prism or a liquid-crystal-based prism [5] in any wide-field imaging system.

Results from simulated and experimental data of polystyrene bead samples will be presented, which validate this approach and demonstrate the type of sample prior information it can derive. This study will also substantiate whether or not our DIC forward imaging model [6] predicts the image intensities from the simple Koehler DIC arrangement, thus making them suitable for processing with our previously developed computational algorithms in order to retrieve sample prior information.

References:

- [1] C. Preza and J.A. Conchello, "Depth-variant maximum-likelihood restoration for three-dimensional fluorescence microscopy," *JOSA A*, vol. 21, no. 9, pp. 1593-1601 (2004).
- [2] Yuan, S., and Preza, C., "3D fluorescence microscopy imaging accounting for depth-varying point-spread functions predicted by a strata interpolation method and a principal component analysis method," *Proc SPIE Vol. 7904, 79040M* (2011).
- [3] S. B. Mehta and C. J. R. Sheppard, "Partially coherent image formation in differential interference contrast (DIC) microscope," *Opt. Express* 16, 19462 (2008).
- [4] Preza, C. and O'Sullivan, J. A., "Quantitative phase and amplitude imaging using differential-interference contrast (DIC) microscopy", in *Computational Imaging VII*, Charles A. Bouman, Eric L. Miller, Ilya Pollak, eds., *Electronic Imaging, Proc. SPIE Vol. 7246, 724604* (2009).
- [5] Zahreddine, R. N., Cormack, R. H., Masterson, H., King, S. V. and Cogswell, C. J., "Real-time quantitative differential interference contrast (DIC) microscopy implemented via novel liquid crystal prisms," *Proc SPIE Vol. 8227, 822710-822710-6* (2012).
- [6] Preza, C., Snyder, D. L., and Conchello, J. A., "Theoretical development and experimental evaluation of imaging models for differential interference contrast microscopy," *JOSA A*, 16(9), 2185-2199, 1999.

**Conference 9330: Three-Dimensional and Multidimensional Microscopy:
Image Acquisition and Processing XXII**

9330-42, Session 9

Analysis of dissected tissues with digital holographic microscopy: quantification of inflammation mediated tissue alteration, influence of sample preparation, and reliability of numerical autofocussing

Björn Kemper, Philipp Lenz, Dominik Bettenworth, Westfälische Wilhelms-Univ. Münster (Germany); Philipp Krausewitz, Department of Medicine B, University of Muenster (Germany); Dirk Domagk, Steffi Ketelhut, Westfälische Wilhelms-Univ. Münster (Germany)

Quantitative phase contrast imaging with digital holographic microscopy (DHM) has been demonstrated to be a versatile tool for high resolution non-destructive analysis of surfaces and multi-modal minimally-invasive monitoring of living cell cultures in-vitro. As quantitative phase imaging with DHM is based on the detection of optical path length changes the method is label-free and only requires low light intensities for object illumination which minimizes the interaction with the sample. Also for the analysis of dissected tissues quantitative DHM phase contrast prospects application fields by stain-free imaging and the quantification of tissue density changes. We show that DHM allows imaging of different layers with high contrast in unstained tissue sections. Furthermore, our results demonstrate that alterations of the spatial refractive index distribution in murine and human tissue samples represent a reliable parameter that is related of different degrees of inflammation in experimental colitis and Crohn's disease. As the investigation of fixed samples represents a very important application field in pathology, we also analyzed the influence of the sample preparation. The retrieved data demonstrate that the quality of quantitative DHM phase images of dissected tissues depends strongly on the fixing method and common staining agents. Finally, we evaluated the automated refocussing feature of DHM for application on dissected tissues and revealed that on moderate stained samples highly reproducible holographic autofocussing can be achieved. This paves the way towards the usage of DHM in digital pathology for automated histological examinations.

9330-43, Session 9

Dual-modality wide-field photothermal quantitative phase microscopy and depletion of cell populations

Nir A. Turko, Itay Barnea, Omry Blum, Rafi Korenstein, Natan T. Shaked, Tel Aviv Univ. (Israel)

We present a new dual-modality technique for selective depletion and extermination of populations of cells based on wide-field photothermal (PT) quantitative phase imaging and simultaneous PT cell extermination. The cells are first labeled by plasmonic gold nanoparticles, which evoke local plasmonic resonance when illuminated by a light wave in a wavelength corresponding to their specific plasmonic resonance peak. This reaction creates changes of temperature, resulting in a change of phase. These changes are recorded by a quantitative phase microscope (QPM), producing specific imaging contrast and enabling bio-labeling in phase microscopy. Using this technique, we have shown discrimination of EGFR over-expressing (EGFR+) cancer cells from EGFR under-expressing (EGFR-) cancer cells. Then, we increased the excitation power in order to evoke greater temperatures, which caused specific cell death, all under real-time phase acquisition using QPM. Close to 100% of all EGFR+ cells were immediately exterminated when illuminated with the strong excitation beam, while all EGFR- cells survived. For the second experiment, in order to simulate a condition where circulating tumor cells (CTCs) are present in blood, we have mixed the EGFR+ cancer cells with white blood cells (WBCs) from a healthy donor. Here too, we have used QPM to observe and record the phase of the cells as they were excited for selective visualization and

then exterminated. The WBCs survival rate was over 95%, while the EGFR+ survival rate was less than 5%. The technique may be the basis for real-time detection and controlled treatment of CTCs.

9330-44, Session 9

Three wavelength phase shift interferometry for quantitative cell microscopy

Glenn W. Pagano, Christopher Mann, Northern Arizona Univ. (United States)

Three wavelength temporal phase shifting interferometry is used generate several micron 3D surface profiles using a red wavelength light emitting diode and bandpass filters. The low noise precision of a single wavelength is maintained by utilizing intermediate synthetic wavelengths and hierarchical optical phase unwrapping. The surface profiles between two and three wavelengths are compared. It is shown experimentally, using several samples, the noise amplified by several micron two wavelength phase shift interferometry is removed by use of a third wavelength. The single wavelength precision over several microns is demonstrated with a VSLI step height standard and cancer cells.

9330-45, Session 10

Image reconstruction for structured-illumination microscopy with low signal level

Kaiqin Chu, NSF Ctr. for Biophotonics Science and Technology (United States); Zachary J. Smith, Univ. of California, Davis (United States); Sebastian Wachsmann-Hogiu, NSF Ctr. for Biophotonics Science and Technology (United States)

Among current super-resolution microscopy techniques, structured illumination microscopy (SIM) is attractive for live cell imaging due to its wide field nature and ability to use general-purpose fluorescence labels. However just as with any fluorescence microscopy, the broad applicability of SIM suffers due to the photo-bleaching of fluorophores and photo-toxicity to living biological samples. We have significantly advanced the applicability of this technique by developing a new image reconstruction algorithm. Using a pre-filtering process to estimate experimental parameters and applying total variation as a constraint during reconstruction, we can reduce exposure times by two orders of magnitude compared to standard SIM, while preserving the resolution improvement and image quality. With reduced photon-exposure, photo-bleaching and toxicity are significantly reduced. We have demonstrated the ability to image 15 times more time points than the current standard SIM system on live HeLa cells. Additionally, the algorithm has been tested over many samples (both fixed and live cells), and across several different hardware systems with similar performance.

9330-46, Session 10

Dark-field illuminated fiber bundle endoscopy with iterative I1-min image reconstruction for honeycomb pattern removal

Xuan Liu, Lijun Zhang, Mitchell Kirby, Michigan Technological Univ. (United States); Divyaansh Raj, Livingston high school (United States); Shaohai Qi, The First Affiliated Hospital of Sun Yat-Sen Univ. (China); Feng

**Conference 9330: Three-Dimensional and Multidimensional Microscopy:
 Image Acquisition and Processing XXII**

Zhao, Michigan Technological Univ. (United States)

Coherent fiber bundle can be used as endoscopic probe in various imaging modalities to obtain microscopic images in tight space. A robust, miniature fiber bundle imaging probe is considered to have great potential for in situ cellular imaging that can potentially replace invasive tissue biopsy. However, it is challenging to obtain intrinsic-contrast images without exogenous contrast agent using a fiber bundle probe. First, light reflected from the end facets of fiber bundle can be much larger in magnitude compared to light that is back-scattered from the sample. Second, the non-uniform transmittance of fiber bundle results in a honeycomb pattern overlaid with true object and reduces the visibility of microscopic features. To provide intrinsic endoscopic imaging at cellular resolution using a fiber bundle probe, we developed a dark-field illuminated reflectance fiber-optic microscope (DRFM) along with an algorithm that promotes image sparsity through l_1 -norm minimization. To suppress specular reflection from fiber bundle facets, we adopted a dark-field configuration by blocking central rays in illumination arm and inserting a low pass spatial frequency filter in detection arm. To remove the honeycomb pattern of fiber bundle while preserve image resolution and contrast, we chose to minimize the image l_1 norm in wavelet domain using iterative shrinkage thresholding (IST) algorithm which involves matrix-vector multiplication and shrinkage/soft thresholding in each iteration. To validate the performance of the system, high resolution, intrinsic-contrast imaging was conducted on US Air Force resolution target, onion cells, cultured human mesenchymal stem cells and human umbilical vein endothelial cells.

9330-47, Session 10

**Two-dimensional compressive sensing
 in spectral domain optical coherence
 tomography**

Daguang Xu, Yong Huang, Jin U. Kang, Johns Hopkins Univ. (United States)

In the past decade, compressive sensing (CS) has emerged as an effective technique for sampling a signal with smaller number of measurements than that is required by the classical Shannon/Nyquist theory. Applications of CS on optical coherence tomography (OCT) imaging have been studied by many groups. In most previous studies, CS was applied to the under-sampled spectral measurements to reconstruct A-mode image. This process is repeated for several A-scans, which are placed laterally to form a B-scan image. Usually 40%-50% spectral data is needed to reconstruct a high-quality OCT B-scan for biological samples with complex morphology. However, this method only considers under-sampling for each A-scan and acquires the same number of A-scans as the classical method, which does not take full advantage of the sparse sampling. The size of spectral measurements required for a B-scan image can be further reduced by exploring the sparse sampling in the lateral dimension of the B-scan. In this paper, we proposed a novel two-dimensional (2D) CS OCT approach which reconstructs the B-scan image using a subset of the spectral data that is under-sampled in both axial and lateral dimensions: a fraction of the A-scans for a B-scan are acquired; for each acquired A-scan, its spectral data is under-sampled. Our method is evaluated using spectral data from an in-house developed SD OCT. Experimental results show that our approach can obtain high quality B-scan image using 20% spectral data, which takes 40% number of A-scans and acquires 50% spectral data for each selected A-scan.

9330-48, Session 10

Graphics processing unit-accelerated real-time compressive sensing spectral domain optical coherence tomography

Daguang Xu, Yong Huang, Jin U. Kang, Johns Hopkins Univ. (United States)

Recent studies on applications of compressive sensing (CS) in the spectral domain optical coherence tomography (SD OCT) have shown that high quality OCT image can be successfully reconstructed from highly under-sampled k-space data, which can potentially reduce data acquisition time and alleviate the data storage and transferring burden. However, CS SD OCT is usually solved by an iterative algorithm that requires numerous matrix-vector computations, which takes significant computation time compared to classical reconstruction methods. This hinders the practicality of CS SD OCT system for the clinical applications that typically require real-time or immediate image reconstruction. As a highly effective massively parallel processor, a graphics processing unit (GPU) has received notable success in accelerating the matrix-vector operations, which makes it the ideal computing unit for real-time CS reconstruction. In this paper, we systematically demonstrated two real-time CS SD OCT systems based on a conventional desktop computer having three GPUs. The first one takes fast Fourier transform (FFT) as the sensing technique and under-sampled linear wavenumber spectral sampling as input data, while the second one uses non-uniform fast Fourier transform (NUFFT) and under-sampled nonlinear wavenumber spectral sampling, respectively. The maximum reconstruction speed of 72k and 33.5k A-line/s were achieved for these two systems, respectively, with the A-scan size 2048. This result shows more than 100 times speed enhancement compared to the best C++ and MATLAB implementations. Finally, we present real-time dispersion compensated image reconstruction for both systems, which does not introduce obvious computation burden while significantly improves the image quality.

Conference 9331: Single Molecule Spectroscopy and Superresolution Imaging VIII

Saturday - Sunday 7-8 February 2015

Part of Proceedings of SPIE Vol. 9331 Single Molecule Spectroscopy and Superresolution Imaging VIII

9331-1, Session 1

Multifocus fluorescence correlation spectroscopy

Vit Dolezal, Lars Kreutzburg, Renate Holzhaue, Lennart Lohmann, Univ. zu Lübeck (Germany); Richard Börner, Univ. zu Lübeck (Switzerland); Christian G. Hübner, Univ. zu Lübeck (Germany)

Fluorescence correlation spectroscopy(FCS) is a well-established method for studying molecular motions, interactions, and reactions. Conventional FCS provides only limited information about drift component of a molecular motion and the determination of absolute diffusion coefficients is not exact. Inspired by the application potential of the two-focus FCS, we have designed a multi-focus FCS scheme, which is able to provide information on the direction of drift motion. We implement this by four separated detection foci, due to the spatial displacement relative to each other in respect to a single, common excitation focus. We carried out a computational simulation of the whole experiment and explored the limits of our approach. The experiments are performed on a home-built scanning confocal microscope with 488 nm and 592 nm cw lasers as the excitation sources. The laser light is focused by a water immersion objective lens into the sample cell. Fluorescence, which is collected by the same objective lens, is divided into four beams, each of which is focused by an achromatic lens through a pinhole, which is a part of the detection assembly (together with a biconvex lens and single photon counting module). The assembly is pre-aligned and can be moved in x, y, and z in order to place the detection foci at the desired positions.

First experiments on standard fluorophores demonstrates the feasibility of our method. The analysis of the correlation functions reproduces the drift component in xy-plane with reasonable accuracy. The determination of the z-component remains unresolved. The results of detailed studies of flow fields in micro capillary devices are presented. In the future, directed motion in living cells will be assessed.

9331-2, Session 1

Emission of superradiant photon pairs from dyes coupled to Ag nanoantennas

Vladimir P. Drachev, Univ. of North Texas (United States); David Lyvers, Univ. of North Texas (United States) and UES, Inc. (United States); Ricardo Lopez, Univ. of North Texas (United States)

The cooperative interaction of continuously pumped few-emitter ensembles interacting with a single damped cavity below the lasing threshold represent a new class of photon sources with non-trivial statistical properties, which can be tailored for particular type of applications [1,2]. For example, a possibility to quickly bring the two resonant quantum dots in and out of resonance with a single cavity mode would allow implementing a deterministic source of indistinguishable (superradiant) photon pairs required for quantum information processing [1]. The numerical simulations predict a giant photon bunching caused by generation of correlated photon pairs which can be observable in time-correlated single photon counting type experiments with emitters in low-quality factor cavities [2]. Here the photon statistics, quantified in terms of second-order photon correlation function, is investigated experimentally for few-emitter systems in a weak coupling regime with Ag nanoantennas. Changing the nanoantenna resonance in the photon correlations measurements allows us to adjust the plasmon cavity with dye molecules, ATTO-650. The second order correlation function was measured with a PicoQuant MicroTime200 system.

We show that an antibunching minimum at near zero correlation time for a single dye emission switch to the bunching maximum for several dyes coupled to the plasmonic nanoantennas. The physical origin of the bunching for small number of dyes can be microscopically explained by emission of superradiant photon pairs.

1. M. Hennrich, A. Kuhn, and G. Rempe, Phys. Rev.Lett. 94, 053 604 (2005).

2. V. V. Temnov and U. Woggon, Opt. Express 17, 5774 (2009).

9331-3, Session 1

H4 tail interactions revealed by fluorescent fluctuation spectroscopy

Nathan P. Nurse, Chongli Yuan, Purdue Univ. (United States)

Chromatin structure and the transcriptional state of a gene can be modulated by modifications made on H3 and H4 tails of histones. Elucidating the internucleosomal interactions of these tails is vital to understanding epigenetic regulation. Fluorescence correlation spectroscopy (FCS) and photon counting histogram (PCH) analysis were used to investigate the role of H3 and H4 tails on cis (intra-array) and trans (inter-array) interactions. Differentiation between cis and trans interactions is often difficult with conventional techniques. The distinction, however, is important because these interactions model short and long range chromatin interactions respectively. Diffusivity revealed by FCS will be affected by both cis and trans interaction while molecular brightness revealed by PCH will be affected by trans interactions only. Combining FCS and PCH analysis, we can decouple the contribution of histone tails to cis and trans effects. A Mg²⁺ gradient was employed to facilitate compaction and oligomerization of tetranucleosomes with H3 and/or H4 tail truncations. H3 tails were found to play a multifunctional role and exhibit the ability to partake in both attractive cis and trans interactions simultaneously. H4 tails partake in attractive cis and repulsive trans interactions at low [Mg²⁺]. These interactions are diminished at higher [Mg²⁺]. Simultaneous H3 and H4 tail truncation inhibited array oligomerization but maintained local array compaction.

9331-4, Session 1

Plasmonic nanoantennas for enhanced single molecule analysis at micromolar concentrations

Hervé Rigneault, Deep Punj, Jérôme Wenger, Institut Fresnel (France); Mathieu Mivelle, Niek F. Van Hulst, Maria F. Garcia-Parajo, Thomas Van Zanten, ICFO - Institut de Ciències Fotòniques (Spain)

Single-molecule fluorescence techniques are key for a number of applications, including DNA sequencing, molecular and cell biology and early diagnosis. Unfortunately, observation of single molecules by diffraction-limited optics is restricted to detection volumes in the femtolitre range and requires pico- or nanomolar concentrations, far below the micromolar range where most biological reactions occur. This limitation can be overcome using plasmonic nanostructures, which enable the confinement of light down to nanoscale volumes. Although these nanoantennas enhance fluorescence brightness, large background signals and/or unspecific binding to the metallic surface have hampered the detection of individual fluorescent molecules in solution at high concentrations. Here we introduce a novel 'antenna-in-box' platform that is based on a gap-antenna inside a

**Conference 9331: Single Molecule Spectroscopy
 and Superresolution Imaging VIII**

nanoaperture [1]. The nanoantenna is based on a dimer made of two gold half-spheres surrounded by a box aperture and is milled in a gold film by focused ion beam (FIB). Fluorescence Correlation Spectroscopy (FCS) measurements were taken for each nanoantenna to quantify the volume reduction and the fluorescence enhancement factor. Using the dominant fluorescence emission from the nanoantenna gap region, we isolated detection volumes down to 58 zL, enabling the observation of a single fluorescent molecule diffusing within a solution of concentration exceeding 10 micromolar along with a large enhancement of the single molecule fluorescence, up to 1100-fold for antennas. We demonstrate the efficiency of the designed 'antenna-in-box' for various relevant bio-molecules. Thus we believe the demonstrations revealed in this work are a prelude of a new class of nanoscale biomolecular studies that are to follow to investigate enzymatic reactions, and nanoscale composition of live cell membranes.

[1] D. Punj, M. Mivelle, S. B. Moparthy, T. S. van Zanten, H. Rigneault, N. F. van Hulst, M. F. Garcia-Parajo, J. Wenger, "A plasmonic 'antenna-in-box' platform for enhanced single-molecule analysis at micromolar concentrations" *Nature Nanotechnology* 8, 512-516 (2013)

9331-5, Session 2
Motion of chromosomal loci and the mean-squared displacement of a fractional Brownian motion in the presence of static and dynamic errors

Mikael P. Backlund, William E. Moerner, Stanford Univ. (United States)

Mean-squared displacement (MSD) analysis is one of the most prevalent tools employed in the application of single-particle tracking to biological systems. In camera-based tracking, the effects of finite localization error ("static error") and finite exposure time ("dynamic error" or "motion blur") on the MSD have been well-characterized for the case of pure Brownian motion, producing a constant offset of $2\sigma^2 - 2DtE/3$ to the straight-line MSD (where σ is the localization precision, D is the diffusion coefficient, and tE is the exposure time). However, particles tracked in cellular environments often do not undergo pure Brownian motion, but instead can for instance exhibit anomalous diffusion wherein the MSD curve obeys a power law with respect to time, $MSD = 2D^*t^\alpha$, where D^* is an effective diffusion coefficient and $0 < \alpha \leq 1$. There are a number of models that can explain anomalous diffusive behavior in different subcellular contexts. Of these models, fractional Brownian motion (FBM) has been shown to accurately describe the motion of labeled particles such as mRNA and chromosomal loci as they traverse the cytoplasm or nucleoplasm (i.e. crowded viscoelastic environments). Despite the importance of FBM in biological tracking, there has yet to be a complete treatment of the MSD in the presence of static and dynamic errors analogous to the special case of pure Brownian motion. We here present a closed-form, analytical expression of the FBM MSD in the presence of errors. We demonstrate its value using both simulated and live-cell data, applying it to the study of chromosomal locus motion in budding yeast cells.

9331-6, Session 2
Single particle tracking through highly scattering media with multiplexed two-photon excitation

Evan P. Perillo, Yen-Liang Liu, Cong Liu, Hsin-Chih Yeh, Andrew K. Dunn, The Univ. of Texas at Austin (United States)

3D single-particle tracking (SPT) has been a pivotal tool to furthering our understanding of dynamic cellular processes in complex biological systems, with a molecular localization accuracy (10-100 nm) often better than the diffraction limit of light. However, current SPT techniques utilize either CCDs or a confocal detection scheme which not only suffer from poor temporal

resolution but also limit tracking to a depth less than one scattering mean free path in the sample (typically $<15\mu\text{m}$). In this report we highlight our novel design for a spatiotemporally multiplexed two-photon microscope which is able to reach sub-diffraction-limit tracking accuracy and sub-millisecond temporal resolution, but with a dramatically extended SPT range of up to 200 μm through dense cell samples. We have validated our microscope by tracking (1) fluorescent nanoparticles in a prescribed motion inside gelatin gel (with 1% intralipid) and (2) labeled single EGFR complexes inside skin cancer spheroids (at least 8 layers of cells thick) for ~10 minutes. Furthermore we discuss future capabilities of our multiplexed two-photon microscope design, specifically to the extension of (1) simultaneous multicolor tracking (i.e. spatiotemporal co-localization analysis) and (2) FRET studies (i.e. lifetime analysis). The high resolution, high depth penetration, and multicolor features of this microscope make it well poised to study a variety of molecular scale dynamics in the cell, especially related to cellular trafficking studies with in vitro tumor models and in vivo.

9331-7, Session 2
Observing bimolecular interactions with single-molecule tracking microscopy

Cong Liu, Yen-Liang Liu, Evan P. Perillo, Quincy Zhuang, Andrew K. Dunn, Hsin-Chih Yeh, The Univ. of Texas at Austin (United States)

Molecular interactions play critical roles in all corners of biology, but current single-molecule tracking techniques do not probe molecular interactions while tracking the molecules in the 3D space. Whereas single-molecule binding/unbinding kinetics have long been observed on TIRF microscopes (based on FRET) and recently in ABEL traps, these methods are not suitable for probing molecular trafficking and dynamic processes deep inside mammalian cells. Here we show that diffusion coefficient (D) can be used in the confocal-feedback 3D molecular tracking microscopy as an indicator for molecular binding detection (i.e. D decreases when the tracked molecule binds to a partner and vice versa). In our method, only the tracked molecules need to be fluorescently labeled. The binding partners are unlabeled and thus can exist at a high concentration during detection (important for probing weak interactions). A prior knowledge of the tracking accuracy (50 nm) enables us to determine the optimal algorithm for extracting diffusion coefficients from the mean square displacement curves, approaching the theoretical limit of diffusion coefficient uncertainty. We are also able to identify diffusion coefficient change points with rigorous likelihood test without the artifacts that arise from binning and thresholding. Monte-Carlo simulations of binding/unbinding kinetics of a single DNA molecule suggest that our method is able to recover time-varying diffusion coefficients as well as the melting/hybridizing rates with high confidence.

Observing molecular association/disassociation events along the 3D trajectory, our molecular binding and tracking microscope can help researchers to map molecular interactions hotspots inside a cell.

9331-8, Session 2
Single-molecule exploration of photoprotective mechanisms in light-harvesting complexes

Hsiang-Yu Yang, Gabriela S. Schlau-Cohen, Stanford Univ. (United States); Michal Gwizdala, Vrije Univ. Amsterdam (Netherlands); Tjaart Krüger, Univ. of Pretoria (South Africa); Pengqi Xu, Roberta Croce, Rienk van Grondelle, Vrije Univ. Amsterdam (Netherlands); William E. Moerner, Stanford Univ. (United States)

Plants harvest sunlight by converting light energy to electricity through the primary events in photosynthesis. One important question is how the light harvesting machinery adapts to fluctuating sunlight intensity. As a result

**Conference 9331: Single Molecule Spectroscopy
and Superresolution Imaging VIII**

of regulation processes, efficient light harvesting and photoprotection are balanced. Some of the biological steps in the photoprotective processes have been extensively studied and physiological regulatory factors have been identified. For example, the effects of lumen pH and carotenoid composition have been explored. However, the importance of photophysical dynamics and its relation to photoprotection remain poorly understood. Conformational and excited-state dynamics of individual proteins are often difficult to study and cannot be probed by ensemble-averaged measurements. To address the problem, we use the Anti-Brownian Electrokinetic (ABEL) trap to investigate the fluorescence from individual copies of light-harvesting complex II (LHCII), the primary antenna protein in higher plants, in a solution-phase environment. Perturbative surface immobilization or encapsulation schemes are avoided, and therefore the intrinsic dynamics and heterogeneity in the fluorescence of individual proteins are revealed. We perform simultaneous measurements of fluorescence intensity, excited-state lifetime, and emission spectrum of single trapped proteins. By analyzing the correlated changes between these observables, we identify forms of LHCII with different fluorescence intensities and excited-state lifetimes. The distinct forms may be associated with different energy dissipation mechanisms in the energy transfer chain. Changes of relative populations in response to pH and carotenoid composition are observed, which may extend our understanding of the molecular mechanisms of photoprotection.

9331-9, Session 2
Dynamic carbon nanotube tracking by independent target restoration microscopy of cells

Nicolas Spegazzini, Rishikesh Pandey, Jeon Woong Kang, Massachusetts Institute of Technology (United States); Ishan Barman, Johns Hopkins Univ. (United States); Ramachandra R. Dasari, Peter T. C. So, Massachusetts Institute of Technology (United States)

Carbon nanotube-based probes have shown promise in biomedical applications such as drug and nucleic acid delivery, optical and electronic sensors. Single-walled carbon nanotubes profit from the surface area and large aspect ratio, allowing for multivalent binding sites. Previous work in our Laboratory was demonstrated using high-speed confocal Raman imaging the first temporal imaging of carbon nanotubes and the first temporal cellular uptake imaging of nanomaterials with the ability to distinguish multiple pristine carbon nanotube species. Using fast line-scanning confocal Raman imaging carbon nanotube uptake was measured in live cells. Spatiotemporal and spectral tracking of nine nanotube derived and two cell-intrinsic Raman bands was conducted simultaneously in RAW 264.7 macrophages. In superresolution imaging based on fluorescence localization microscopy as well as photo activated localization microscopy (PALM) or stochastic optical reconstruction microscopy (STORM) combine time-resolved localization and sequential activation of photoswitchable fluorophores in order to fit the point spread function (PSF) and finally construct high resolution images. In contrast with fluorescence localization microscopy this label-free technique called independent target restoration microscopy (ITRM) based on high-speed confocal Raman imaging can provide spatiotemporal, multichannel spectral resolution and decompose the chemical fingerprint information for each species considered in the study. We acquired Raman movies from nanotube-based and cell-intrinsic scattering signal. Movies resolved the cell position, background denoted by lipid and protein signals as well as aggregation states of nanotubes transiently, single species and defects. The study resolves the real-time molecular hyperspectral imaging of cells using Raman spectroscopy, providing muxing in terms of spectroscopy and photostability. Young Investigator best paper competition BO403

9331-10, Session 3
Optical nanoscopy 2.0 (Keynote Presentation)

Alberto Diaspro, Istituto Italiano di Tecnologia (Italy) and Univ. degli Studi di Genova (Italy); Paolo Bianchini, Francesca Cella Zanacchi, Giuseppe Vicidomini, Colin J. R. Sheppard, Luca L. Lanzanò, Marti Duocastella, Marta d'Amora, Gustavo De Miguel, Istituto Italiano di Tecnologia (Italy); Ranieri Bizzarri, Lab. NEST, Consiglio Nazionale delle Ricerche (Italy)

Optical microscopy, more than ever, is in the spotlight. Confocal and multi-photon microscopy allowed to improve the three-dimensional (3D) optical sectioning ability of the wide-field microscope towards 3D imaging of thick biological samples. The occurrence of "super-resolution" approaches dramatically changed the paradigm of microscopy in the direction of nanoscopy. Terms like super resolution microscopy and optical nanoscopy refer to the possibility of achieving an unlimited spatial resolution at the image formation process. The Rayleigh or Sparrow or Abbe criteria can be viewed within the information capacity theory: sub-diffraction or super resolution can be obtained by encoding information from the saturated spatial channel of the microscope system into the temporal channel and decoding after the collection. Nowadays, the optical nanoscope can image biological specimens at the 10-50 nm scale surpassing the 200 nm of the optical microscope. Nanoscopy is well consolidated today and I think that we are moving to Nanoscopy 2.0. Here, we will discuss targeted and stochastic readout methods expanded to multi-photon excitation microscopy and coupled with scanning probe microscopy systems or incorporating fluorescence correlation spectroscopy or light sheet illumination schemes. The maturity of "classical" nanoscopy approaches allows designing miniaturized devices or to apply general concepts to nanoscale lithography or other fields. Nanoscopy 2.0 can be seen as a trend en route for the integration with other devices. A variety of architectures will be outlined and further variations on the super resolution theme addressed, including coupling with atomic force microscopy (AFM) and fluorescence correlation spectroscopy (FCS).

9331-11, Session 3
Multi-color quantum dot stochastic optical reconstruction microscopy (qSTORM)

Kayvan F. Tehrani, Jianquan Xu, Peter A. Kner, The Univ. of Georgia (United States)

Although Single Molecule Localization (SML) techniques have pushed the resolution of fluorescence microscopy beyond the diffraction limit, the accuracy of SML has been limited by the brightness of the fluorophores. The introduction of Quantum Dots (QD) for SML promises to overcome this barrier, and the QD Blueing technique provides a novel approach to SML microscopy (Hoyer et al., Nano Letters 11 245, 2010). QDs have higher quantum yield making them brighter and providing a higher accuracy of localization. The blueing technique is also faster and more quantitative than other SML techniques such as dSTORM. The initial bleaching step required by dSTORM is not necessary and each QD is imaged only once as its emission spectrum moves through the blueing window in contrast to dSTORM where the same molecule might be imaged multiple times. Single color QD Blueing has been demonstrated. However in biological imaging, multi-color staining is very important for showing the features of the sample under study. Here we introduce two color super-resolution microscopy using Quantum Dot Blueing on biological samples. We demonstrate simultaneous imaging of microtubules and mitochondria in HepG2 cells with a localization accuracy of 40nm. We further show how QD Blueing can be optimized through the control of the sample mounting medium.

**Conference 9331: Single Molecule Spectroscopy
and Superresolution Imaging VIII**

9331-12, Session 3

3D-superlocalization microscopy and tracking of single membrane proteins in living bacteria

Anja Renz, Marc Renz, Universitätsklinikum Jena (Germany); Michael Börsch, Friedrich-Schiller-Univ. Jena (Germany) and Abbe Ctr. of Photonics Jena (Germany)

FoF1-ATP synthases are membrane-embedded protein machines that catalyze the synthesis of adenosinetriphosphate. Using 3D-STORM (STochastic Optical Reconstruction Microscopy) and PALM (PhotoActivated Localization Microscopy) in epi- and TIR-illumination as well as 3D-SIM (Structured Illumination Microscopy), we explore the spatial distribution and analyze the diffusion properties of bacterial FoF1-ATP synthases in living *E. coli* cells under physiological conditions. For quantitative mean square displacement (MSD) analysis, the limited size of the observation area in the membrane with a significant membrane curvature had to be considered. Because the surface coordinate system yielded different localization precision, we applied a sliding observation window approach to obtain an onedimensional diffusion coefficient of FoF1-ATP synthase in living *E. coli*.

9331-13, Session 4

Multiple-pulse pumping with time-gating for ultrasensitive detection and imaging

Joseph D. Kimball, Sangram Raut, Texas Christian Univ. (United States); Rafal Fudala, Ryan Rich, Ignacy Gryczynski, Julian Borejdo, Univ. of North Texas Health Science Ctr. (United States); Hung Doan, Texas Christian Univ. (United States); Karol Gryczynski, Badri Maliwal, Univ. of North Texas Health Science Ctr. (United States); Zygmunt Gryczynski, Texas Christian Univ. (United States)

As fluorescence sensitivity reaches the single molecule level, fluorescence detection and imaging becomes constrained by the background signal generated on a sample. A typical background signal will include direct scattering of excitation and Raman scattering of the sample as well as autofluorescence from the sample and additives. Contributions from endogenous chromophores and fixatives typically are spread over a broad wavelength range and spectrally overlap with the probe signal- becoming a major limitation for sensitive detection and quantitative imaging. Most of the background is instantaneous and short-lived (picosecond to nanosecond time scale), and using long-lived fluorescence probes combined with time-gated detection allows for significant suppression of an unwanted background. Recently, we reported a simple new approach with bursts of closely-spaced laser excitation pulses for excitation (multi-pulse excitation) that allows for many-fold increase in the intensity of a long-lived probe over the background signal. This technology can be easily implemented for biomedical diagnostics and imaging to significantly enhance the signal of long-lived probes over the background. We demonstrate that a burst of 2-10 pulses spaced 3 ns apart (corresponding to a "burst repetition rate" of 330 MHz) allows for high signal enhancement of the 20 ns probe over the sub-nanosecond/nanosecond background. As an example we present DNA detection using Ethidium Bromide (EtBr) and Ethidium Bromide Homodimer (EtBrHD) that significantly increase their fluorescence lifetimes while bound to DNA. Using multi-pulse and time-gated detection we are able to increase sensitivity of both almost 2 order of magnitudes.

9331-14, Session 4

Multidimensional fluorescence analysis: recent advances with pattern matching (Invited Paper)

Benedikt Krämer, PicoQuant GmbH (Germany); Thomas Niehörster, Anna Löschberger, Julius-Maximilians-Univ. Würzburg (Germany); Marcelle König, Paja Reisch, Matthias Patting, Felix Koberling, PicoQuant GmbH (Germany); Ingo Gregor, Georg-August-Univ. Göttingen (Germany); Markus Sauer, Julius-Maximilians-Univ. Würzburg (Germany); Rainer Erdmann, PicoQuant GmbH (Germany)

We already showed that the well established approach to separate different species in confocal microscopy by spectral deconvolution can be successfully transferred to fluorescence decays as an alternative to multi-exponential decay fitting and to the phasor analysis approach.

A quantitative decomposition of multicomponent FLIM data with a multi-exponential fitting approach can be time consuming and prone to errors if the lifetime decay patterns are complex (multi-exponential). We describe the complex single pixel decay with a linear combination of reference decays (patterns), which can be highly multi-exponential and do not have to be described itself mathematically. In a two step process we calculate analytically the individual amplitudes for the reference patterns followed by a re-iteration with MLE fitting. The low number of fitting parameters results finally in a faster analysis and a better signal to noise ratio in the analyzed images.

This procedure is now further sped up by a purely analytical vector projection based method.

We will compare the different approaches for multi-species FLIM analysis and present latest application examples also combining spectral and lifetime information for a multidimensional fluorescence pattern analysis.

9331-15, Session 4

Photothermal imaging of individual carbon nanofibers with optical microresonators

Kevin D. Heylman, Kassandra A. Knapper, Univ. of Wisconsin-Madison (United States); Erik H Horak, University of Wisconsin Madison (United States); Randall H. Goldsmith, Univ. of Wisconsin-Madison (United States)

Single-molecule spectroscopy is a powerful tool for the mechanistic investigations of chemical and biological dynamics because unsynchronized processes can be directly observed. However, the traditional reliance upon fluorescence for single-molecule measurements limits such investigations to systems where the target is fluorescent. While addition of fluorescent labels can provide additional valuable information, the determination of the time-varying absorption spectrum of individual non-fluorescent molecules is an outstanding challenge.

Ultrahigh-Q optical microresonators offer a way of eliminating the need for fluorescence by enabling additional sensitive means of interaction with individual molecules or particles. The interaction, either resonant or non-resonant, between an adsorbed target species and the propagating mode of the resonator can allow sensitive single-particle detection. We present a new two-beam experimental geometry, where the goal is not detection of individual molecules, but the measurement of optical spectra and spectral dynamics of non-fluorescent molecules of interest. Our experiment relies on ultrahigh-Q toroidal optical microresonators as platforms for photothermal spectroscopy. Transitions are optically driven in the particle or molecule of interest, while the thermalization of the excitation energy is detected by the resonator. The relevant heat flows are explored with numerical simulations. We demonstrate implementation of the concept by making measurements

**Conference 9331: Single Molecule Spectroscopy
and Superresolution Imaging VIII**

on individual carbon nanotubes and spectral evolution in gold nanoparticles. Pathways toward spectroscopy on individual non-fluorescent molecules will be described.

9331-16, Session 4

Mapping the mouse connectome: progress towards a high-throughput super-resolution nanoscope

Christopher J. Rowlands, Yi Xue, Edward S. Boyden, Peter T. C. So, Massachusetts Institute of Technology (United States)

Many researchers would like to know the 'wiring diagram' for the brain, in order to better understand consciousness, cognition, mental disorders, and so on. Mapping every neuron and synapse in even just the mouse brain is a daunting technological challenge, requiring approximately 50nm spatial resolution in 3D, throughput of approximately one gigapixel per second, and a dataset that is 47 petabytes in size. We present progress to date on construction of an instrument capable of meeting these challenges, and thereby mapping the mouse brain within a year.

The instrument is a highly parallel RESOLFT system, capable of imaging in excess of one million points in parallel, each with 3D super-resolution. Two separate interference patterns are overlapped in 3D space; one pattern provides a 3D-resolved body-centered cubic node array, and the other pattern suppresses all the out-of-plane nodes to leave a single plane of 3D-resolved spots. Top-hat beamshapers are used to ensure constant resolution across the field of view and to make optimal use of laser power. Currently, testing is being performed using sCMOS cameras in order to ensure that system specifications are well-defined before purchasing the final custom-made 1000 frames-per-second intensified CMOS cameras, which are necessary in order to hit throughput targets. Excitation and switching on of the fluorophores is achieved using two separate light-sheets for power efficiency and to avoid unnecessary photoswitching of out-of-plane fluorophores.

Data will be shown regarding the design of the instrument, super-resolution performance, throughput measurements, as well as prospects for successfully imaging the mouse brain.

9331-17, Session 4

Single-acquisition super-resolution microscopy: 40% resolution improvements at millisecond time scales

Craig Snoeyink, Texas Tech Univ. (United States)

Traditional super-resolution imaging systems such as SIM, STORM, PALM, STED, and so on rely on trading temporal resolution in exchange for impressive gains in spatial resolution. However the resulting poor temporal resolution prevents them from capturing fast cellular or biomolecular phenomena. Here we present a new super-resolution imaging modality which trades high-frequency data for low-frequency data, maintaining much of its temporal resolution. Temporal resolution is maintained in large part due to the fact that every single image acquired has improved diffraction limited resolution, a capability termed single-acquisition super-resolution (SASR) imaging. In fact, we will show that with high NA/high magnification microscope objectives common to super-resolution microscopes we can achieve a nearly 40% improvement in spatial resolution with no cost to temporal resolution. The result is a remarkably accessible and fast super-resolution imaging system capable of orders of magnitude faster data acquisition. These gains are achieved by imaging with the Bessel Beam Microscopy system which places an axicon into the imaging path of the microscope. This has the side effect of increasing the image depth of field. To counteract this we will present a unique 3D deconvolution algorithm that is capable of reconstructing simple 3D objects from a single 2D BBM image.

9331-18, Session 5

Nanohole arrays allow the measurement and correction of spatial nonuniformities and spectral effects in 3D single-molecule localization

Alexander R. von Diezmann, Matthew D. Lew, Maurice Y. Lee, Stanford Univ. (United States); Andreas Gahlmann, Univ. of Virginia (United States); William E. Moerner, Stanford Univ. (United States)

Localizing single fluorescent molecules to subdiffraction precision is the basis for single-particle-tracking and super-resolution imaging. Both techniques have been extended to three dimensions (3D) using a variety of axial ('z') position encoding methods, and have been used with multicolor detection. However, the challenge of registering multicolor 3D datasets to an accuracy on par with typical single-molecule localization precision highlights errors not commonly accounted for in single-color 3D imaging. Most 3D localization methods use fluorescent fiducials for calibration of the microscope's 3D response and/or generating control points for color channel registration, and spectral mismatch between this fiducial and the label of interest can result in significant (10s of nm) inaccuracies. Further, while nonidealities in the optics of a 3D single-molecule imaging system can cause spatially dependent variation in a single-molecule z-estimator, this is not measured when using only one or a few fiducials for calibration. We report the fabrication and use of subdiffraction Nanohole Arrays (NHAs) as fiducials to sample the 3D field of view with many finely spaced emitters of arbitrary spectrum, avoiding errors due to spectral mismatch. We use the fine spacing of the NHA to measure the spatial variation in 3D response for several imaging systems and demonstrate how accounting for this variation is necessary for accurate calibration. By this method, we demonstrate accurate 3D imaging and channel registration throughout the field of view for both single molecules in vitro and biological structures.

9331-19, Session 5

Rapid super-resolution line scanning microscopy using virtually structured detection

Rongwen Lu, Yanan Zhi, Benquan Wang, Qiuxiang Zhang, Xincheng Yao, The Univ. of Alabama at Birmingham (United States)

Structured illumination microscopy (SIM) has tremendous applications in super-resolution fluorescence imaging. However, SIM entails the wide field illumination pattern, which limits its application in the thick specimen (i.e., over 100 micrometers). In addition, SIM requires complicated mechanical operation of the grating to generate the structured illumination patterns with different phases and orientations, which is particularly challenging for the moving sample. We have recently developed a super-resolution method, termed virtually structured detection (VSD). We integrated VSD to the confocal scanning laser microscope (SLM). VSD applies structural modulation virtually and does not require manipulation of the grating, and thus is phase-artifact free. In addition, the converged single point illumination facilitates the imaging in thick tissues. However, the VSD based SLM requires a two-dimensional image for each sampling spot of the raster scanning pattern, which compromises the imaging speed rate. In this paper, we integrate VSD to line scanning microscopy (LSM) to enhance the image acquisition speed. A line instead of a single spot illumination is delivered to the sample and only one direction scanning is needed to cover the imaging field, which substantially increases the imaging speed. To achieve isotropic transverse resolution enhancement, a motorized dove prism is employed to automatically control the line illumination and the corresponding scanning direction which is perpendicular to the line illumination. Further development of the VSD based LSM promises the imaging with sub-diffraction-limit resolution of the moving sample (i.e., the human eye) or dynamics of the sample with video rate.

**Conference 9331: Single Molecule Spectroscopy
 and Superresolution Imaging VIII**

9331-21, Session 5

Effect of labeling density and time post labeling on quality of antibody-based super resolution microscopy images

Amy M. Bittel, Isaac Saldivar, Oregon Health & Science Univ. (United States); Nicholas Dolman, Thermo Fisher Scientific Inc. (United States); Andrew K. Nickerson, Li-Jung Lin, Xiaolin Nan, Summer L. Gibbs, Oregon Health & Science Univ. (United States)

Super resolution microscopy (SRM) has overcome the historic spatial resolution limit of light microscopy, enabling fluorescence visualization of intracellular structures and multi-protein complexes at the nanometer scale. Using single-molecule localization microscopy, the precise location of a stochastically activated population of photoswitchable fluorophores is determined during the collection of many images to form a single image with resolution of ~ 10 - 20 nm, an order of magnitude improvement over conventional microscopy. One of the key factors in achieving such resolution with single-molecule SRM is the photophysical properties of the photoswitchable fluorophores used, particularly the photoswitching properties including the number photons emitted per switching event and the amount of time the fluorophore is in the fluorescent state. In current work, both the intrasample and intersample heterogeneity of the fluorophore photoswitching properties was investigated. Eight commercially available fluorophores that span the visible spectrum and cover three fluorophore classes including rhodamine, cyanine, and BODIPY were characterized for their photoswitching properties and used for comparative imaging studies. All fluorophores showed extensive intrasample heterogeneity in photon output where the average photon number measured per switching event were less than 2% of the highest photon numbers measured. The intersample photon output was less diverse between imaging fields for each fluorophore, however there were distinct trends in heterogeneity with the three tested cyanine scaffolds having the highest variability. Finally microtubules were labeled with these fluorophores via antibodies and imaged to evaluate the impact of the measured heterogeneity on image resolution.

9331-57, Session 5

Image-scanning microscopy

Joerg Enderlein, Georg-August-Univ. Göttingen (Germany)

Recent years have seen an explosion in new advanced and super-resolution methods in fluorescence microscopy, which have culminated in the Nobel Prize in Chemistry for 2014. One of the early methods of these techniques was structured illumination microscopy (SIM), which combines wide-field imaging with a structured illumination for doubling the resolution of a wide-field microscope. An alternative approach is image scanning microscopy (ISM), which combines a conventional confocal laser scanning microscope with a wide-field imaging detector. Although the idea was theoretically proposed by Colin Sheppard already in 1988, its first successful realization was only achieved in 2010. Since then, a whole flood of modifications and implementations of this idea have been published, and by now, even the first commercial implementation of ISM (Airy Scan Microscope by Carl Zeiss Jena) is available. I will present the working principle of ISM and its several implementations and applications.

9331-22, Session 6

Realization of super-resolution imaging by microlens assisted laser scanning microscopy

Kuan-Yu Li, Yun-Ju Liu, Yang Tsao, National Taiwan Univ.

(Taiwan); Kung-Hsuan Lin, Academia Sinica (Taiwan); Chih-Wei Chang, Shi-Wei Chu, National Taiwan Univ. (Taiwan)

Optical microscopy is broadly applied in many research fields, especially in biomedicine, for its non-invasive characteristic. The resolution is limited to $\lambda/2$ due to diffraction limit. To overcome this limit, many efforts on super-resolution microscopy have been made in past few decades, including near-field scanning optical microscopy (NSOM), far-field photo-activated localization microscopy (PALM), and stimulated emission depletion (STED) microscopy. However, the near-field techniques require sample stability, while the far-field techniques need fluorescence and high-intensity laser illumination. Accordingly, they suffer from sample applicability and photobleach/photodamage, respectively. Recently, a new method utilizing dielectric microlenses and bright-field microscopy to achieve super-resolution was reported.

Because confocal microscopy provides better contrast than bright-field microscopy, here we combine confocal laser scanning microscopy with dielectric microlenses, and successfully achieve far-field super-resolution with at least $\lambda/4.5$ resolution. The magnification and field of view of the microlenses are determined. While the mechanism of the microlens super-resolution imaging is still in debate, we have further elucidated the underlying mechanisms by incorporating nano-positioning techniques and imaging under tunable laser illumination. In comparison with other super-resolution techniques, far-field super-resolution of the dielectric microlenses can be easily achieved without high-intensity laser illumination, fluorescence, or extra sample preparation and are ready for widespread applications.

9331-23, Session 6

Extracting information from single molecules in 3D super-resolution imaging and from dynamical processes in solution (Keynote Presentation)

William E. Moerner, Stanford Univ. (United States)

A quarter of a decade has elapsed since the first single-molecule detection and spectroscopy in condensed matter in 1989. After early explorations at low temperatures, room-temperature studies of single molecules now span multiple fields including biophysics, cellular biology, quantum optics, and materials science. When single-molecule imaging is combined with active control of the emitter concentration, enhanced spatial resolution well beyond the optical diffraction limit can be obtained for a wide array of biophysical structures in cells. Single-molecule emitters also provide precise and accurate 3D position as well as orientation when combined with a double-helix point spread function polarization microscope or with a number of additional new point spread functions with advanced capabilities. If high-resolution spatial information is not needed, a machine called the Anti-Brownian Electrokinetic trap provides real-time suppression of Brownian motion for single molecules in solution. By extracting multiple parameters from each molecule, this device has been used to explore the detailed dynamics of photosynthetic antenna proteins, multisubunit enzymes, redox enzymes, and even single fluorophores. With advanced analysis of the motion of the molecule in the trap, the diffusion coefficient and electrokinetic mobility can be estimated in real time, providing new variables for single-molecule studies. The examples provided here illustrate some of the frontiers where the power of optics applied to single-molecule spectroscopy and imaging can yield new insights into the behavior of complex systems.

**Conference 9331: Single Molecule Spectroscopy
and Superresolution Imaging VIII**

9331-24, Session 6

Image-scanning microscopy (ISM) and stochastic optical fluctuation imaging (SOFI): making it easy and user-friendly

Ingo Gregor, Dirk Haehnel, Simon C. Stein, Anja Huss, Joerg Enderlein, Georg-August-Univ. Göttingen (Germany)

Recent years have seen a tremendous increase of new and novel methods of high and superresolution fluorescence microscopy. Among them, our group has developed to powerful methods: Confocal Spinning Disc Image-Scanning Microscopy (CSDISM), and Superresolution Optical Fluctuation Imaging (SOFI). However, new microscopy techniques that provide not only enhanced image quality and resolution, but they are also simple enough for finding broad application. Here, we present embedding solutions for both CSDISM and SOFI which enable potential users to implement them in an easy and straightforward way into their existing microscopy systems. In the case of CSDISM, we have integrated the method into the environment of the widely used and popular MicroManager Open Source Imaging platform. This allows any researcher who already has a commercial Confocal Spinning Disk microscope to easily implement the image-scanning option and thus to double the spatial resolution. For SOFI, we have developed a dedicated hardware based on a Freely Programmable Gate Array (FPGA) which converts, in real time, image movies taken by high-speed CCD systems into SOFI cumulant images. Thus, all algorithmic complexities and numerical workload of SOFI calculations are taken care of.

9331-25, Session 6

A new method to achieve tens of nm axial super-localisation based on conical diffraction PSF shaping

Clément Fallet, Maxime Dubois, Stephane Oddos, Julien Caron, Bioaxial (France); Jean-Yves Tinevez, Spencer L. Shorte, Institut Pasteur (France); Gabriel Y. Sirat, Roger Persson, Bioaxial (France)

We present here a new depth estimation method based on conical diffraction, for super-localisation fluorescence imaging, permitting to obtain the axial position of a small emitter (fluorophore or dye) beyond the Rayleigh diffraction limit.

This can be achieved by passing the emitted light through a thin biaxial crystal positioned between a polarization state generator and a polarization state analyzer, and focusing on a camera. In the crystal, the light is subjected to conical diffraction leading to a spatial-axially dependent modulation of the beam. The two polarisation states are chosen in order to shape the PSF in such a way that it exhibits significant variations along z-axis. This 3D diffraction effect is then exploited to measure the position of the emitter.

In this configuration, an estimator was chosen to measure the axial position of the emitter with respect to the plane conjugated with the camera. A preliminary experiment demonstrated that we could measure the axial position with an accuracy of up to one tenth of the Rayleigh range.

This technique can lead to nanoscopy applications thanks to resolution levels of tens of nm using high NA microscope objectives. Moreover being fully compatible with 2D super-resolution imaging systems which it can easily be coupled with, this technique could result in a full 3D-super resolution microscope.

9331-26, Session 7

Extended resolution structured illumination imaging of dynamic process in living cells (*Invited Paper*)

Dong Li, Lin Shao, Eric Betzig, Howard Hughes Medical Institute (United States)

Every superresolution technique provides the theoretical capability to resolve ultra-structures beyond the diffraction barrier, but many of them encounter practical limitations when imaging nano-scale dynamics in living biological samples, especially over long-term course and large field of view. Structured illumination microscopy (SIM) stands out in the context of live imaging, since many fewer raw images and much lower light levels are required. In addition, its higher photon efficiency leads to better high frequency support in its optical transfer function (OTF). However, its well-known disadvantage is that its resolution is usually limited to ~100 nm. Here we report two approaches to extend the resolution into sub-100 nm regime, while retaining the above merits to accomplish sub-second imaging speed over scores of time points, without apparent phototoxicity. The first involves total internal reflection fluorescence SIM imaging at numerical aperture (NA) of 1.7. We attain ~80 or 90 nm resolution for 488/510 nm and 560/585 nm excitation/emission wavelength, respectively. The second is nonlinear SIM, which uses a photoswitchable fluorescent protein and NA 1.49 objective to achieve resolution down to ~45 nm, also at high speed and over multiple frames. Moreover, by combining nonlinear SIM with the lattice light sheet microscopy, we demonstrate the feasibility of improving the axial resolution by 4 fold in live 3D imaging. All of these methods permit us to observe dynamics unresolvable by conventional means, such as paired myosin head domains binding with actin filaments, the assembly as dissolution of ring-like clathrin and caveolin vesicles, etc.

9331-27, Session 7

Video-rate super-resolution fluorescence microscopy using all-optical two-photon image scanning microscopy

Ingo Gregor, Martin Spiecker, Joerg Enderlein, Georg-August-Univ. Göttingen (Germany)

Since about 20 years Abbe's resolution limit has been overcome in fluorescence microscopy by the first demonstration of STED microscopy (1). Later, methods based on single-molecule localization joined the field, such as PALM (2) and STORM (3). These methods use principles that operate beyond the diffraction of light. Increased spatial resolution can also be achieved by a class of methods exploiting excitation and detection modalities still bound to light diffraction like structured illumination microscopy (SIM) (4) and image scanning microscopy (ISM) (5). While not reaching the resolution of STED, PALM, and STORM, they do not require any special labels, sample conditions, or excitation power, and may be applied to any sample at any wavelength.

ISM was presented in a theoretical study by Sheppard (6) finding that it is able to double the resolution of a scanning confocal microscope. The first implementation needed several minutes to record one image. York et al. (7) had overcome this limitation by using a multifocal excitation scheme. We demonstrated an acquisition time of less than 1 s per image using a spinning-disk confocal microscope (CSD-ISM) (8). The drawback of these systems is that the images have to be processed after recording, so a huge amount of data has to be processed.

Here, we present an all-optical implementation of ISM based on a resonant confocal laser-scanning microscope using two-photon excitation. The all-optical implementation means that the images are recorded directly with the full resolution and no post-processing is necessary. By this one can take the full advantage of the speed of the resonant laser-scanner providing a frame-rate of about 30 fps and a live view to the sample.

**Conference 9331: Single Molecule Spectroscopy
and Superresolution Imaging VIII**

- Hell S.W. and Wichmann J. (1994) Breaking the diffraction resolution limit by stimulated emission: Stimulated-emission-depletion fluorescence microscopy. *Opt. Lett.* 19(11), 780-782.
- Betzig E. et al. (2006) Imaging intracellular fluorescent proteins at nanometer resolution. *Science* 313(5793), 1642-1645.
- Rust M.J., Bates M., and Zhuang X. (2006) Sub-diffraction-limit imaging by stochastic optical reconstruction microscopy (STORM). *Nat Methods* 3(10) 793-795.
- Gustafsson M.G. (2000) Surpassing the lateral resolution limit by a factor of two using structured illumination microscopy. *J. Microsc.* 198(Pt 2), 82-87.
- Müller C.B. and Enderlein J. (2010) Image scanning microscopy. *Phys. Rev. Lett.* 104(19), 198101.
- Sheppard C.J.R. (1988) Super-resolution in confocal imaging. *Optik (Stuttg)* 80 53-54
- York A.G. et al. (2012) Resolution doubling in live, multicellular organisms via multifocal structured illumination microscopy. *Nat. Methods* 9(7), 749-754
- Schulz O. et al (2013) Resolution doubling in fluorescence microscopy with confocal spinning-disk image scanning microscopy. *PNAS* 110(52), 21000-21005

9331-28, Session 7
Video-rate nanoscopy using sCMOS camera-specific single-molecule localization algorithms

Fang Huang, Yale School of Medicine (United States);
Tobias M. P. Hartwich, Yu Lin, Joerg Bewersdorf, Yale Univ.
(United States)

To be considered for "Young Investigator best paper competition BO403".

Single molecule localization based super resolution microscopy relies on precise and accurate localization of a large number of single molecules. However, the necessity of accumulating large numbers of localization estimates limits the time resolution to typically seconds to minutes.

Two of the major limitations are the acquisition speed and the photon budget. Replacing EMCCD cameras which are usually implemented in such experiments with recently introduced sCMOS cameras results in a leap in both acquisition speed and effective quantum efficiency [1]. However, the intrinsic pixel-dependent Gaussian noise of the sCMOS cameras introduces localization artifacts and greatly reduces the reliability of the results.

Here, we present a set of specially designed statistics-based algorithms that allows for the first time to fully characterize an sCMOS camera and perform unbiased and precise localization analysis. Using this method we demonstrate Cramer-Rao lower bound-limited single molecule localization with an sCMOS camera. Combining the novel algorithm with a recently developed multi-emitter fitting algorithm and optimized imaging condition, we show that this technique shortens the typical acquisition time for fixed samples by up to two orders of magnitude without compromising the field of view. Furthermore, we demonstrate localization-based super-resolution microscopy in live cells by monitoring dynamics of protein clusters, vesicles and organelles at reconstruction speeds from 2 to 30 frames per second [2].

The here presented method allows to take full advantages of sCMOS technology and record faster and more precise super-resolution images without compromises.

- F. Long et al. *Opt. Express* 20, 17741-17759 (2012).
- F. Huang et al. *Nat. Methods* 10(7), 653-658 (2013).

9331-29, Session 7
Stimulated emission depletion microscopy to study amyloid fibril formation

Pierre Mahou, Nathan Curry, Dorothea Pinotsi, Gabriele S. Kaminski Schierle, Clemens Kaminski, Univ. of Cambridge (United Kingdom)

Aggregation of peptides and proteins is a characteristic of many neurodegenerative disorders, such as Parkinson's, Alzheimer's and Huntington's diseases. The ability to image these aggregation processes and the corresponding structures formed in situ is a key requirement to understand the molecular mechanisms of these diseases and potentially progress in the search for therapeutic intervention. However, the characteristic length scale of these aggregates, the so-called amyloid fibrils, is of the order of several nanometres (two orders of magnitude smaller than the spatial resolution of conventional optical microscopes), which suggests that optical super-resolution microscopy techniques are the appropriate candidates to study their formation and structure in situ[1,2].

For that purpose, we report on the implementation and novel application of Stimulated Emission Depletion microscopy (STED)[3] to monitor the formation of amyloid fibrils in vitro and in cells. We investigate different labelling strategies and study quantitatively the influence of labelling density and demonstrate that an optimized density is required to avoid labelling artefacts. We also compare our results with a single-molecule localisation technique (dSTORM) and discuss the advantages/inconveniences of both techniques for this application.

Eventually, we report on the combination of STED microscopy with Atomic Force Microscopy (AFM) in correlative type of measurements for the study of amyloid fibril formation. Interestingly, STED microscopy permits the fast and specific localisation of labelled aggregates with a resolution that can be tuned while AFM provides a better resolved morphological map and mechanical properties of the aggregates.

[1] Kaminski Schierle, *J. Am. Chem. Soc.* (2011).

[2] Pinotsi, *Nano Letters* (2014).

[3] Hell, *Optics Letters* (1994).

9331-30, Session 8
Optimization of image acquisition for high-speed single molecule switching nanoscopy in live cells (Invited Paper)

Fang Huang, Yale School of Medicine (United States); Yu Lin, Joerg Bewersdorf, Yale Univ. (United States)

Single Molecule Switching Nanoscopy (SMSN) is a fluorescence microscopy technique that breaks the diffraction limit of resolution at the expense of an increased image recording time. The spatiotemporal resolution of SMSN strongly depends on localization precision, localization density and the photoswitching rate of the fluorophores. Recently, we have reported advances in improving temporal resolution down to 33 ms by combining new sCMOS camera technology, novel sCMOS-specific localization algorithms and high readout laser intensities to induce rapid fluorophore blinking for fast SMSN imaging. Here we present a study systematically optimizing of excitation laser intensity and camera frame rate to achieve both high precision and high density localizations within a limited time. We performed SMSN on microtubules (MT) of COS7 cells (immuno-labeled for β -tubulin with Alexa 647) at varying laser intensities and frame rates and measured the number of photons detected per switching cycle, the localization uncertainty and density. Our data reveals that laser intensity or exposure time have only a small effect on photon output of Alexa 647. Furthermore, we also demonstrates that imaging at 800-1,600 frames per second (fps) at intensities up to 113 kW/cm² provides nearly uncompromised localization precision and >3-fold higher localization density in a 10-second interval, than imaging at 50-100 fps at an intensity of 10 kW/cm² (used traditionally in SMSN).

**Conference 9331: Single Molecule Spectroscopy
and Superresolution Imaging VIII**

9331-31, Session 8

Fast scanning gated STED microscopy in living cells

Edward Allgeyer, Francesca Bottanelli, Yale School of Medicine (United States); Emil B. Kromann, Yale Univ. (United States); Travis J. Gould, Bates College (United States); Joerg Bewersdorf, Yale School of Medicine (United States)

Stimulated emission depletion (STED) microscopy has been established as important technique for imaging below the diffraction limit facilitating new discoveries in an array of biological systems. In STED microscopy a “donut-shaped” laser focus is super-imposed onto the diffraction-limited focus of an excitation laser. The donut-shaped beam suppresses fluorescence in the periphery of the excitation spot, reducing the effective point spread function to a sub-diffraction size. However, the application of STED microscopy in live cell imaging poses a number of challenges. Here we detail a novel fluorescence microscope with an emphasis on imaging in live cells. This instrument realizes STED in a beam scanning confocal geometry. We demonstrate the instrument’s capability using both fixed and live biological specimens demonstrating resolution below 30 nm in fixed cells and long imaging acquisitions in living cells. The constructed instrument employs fast 16 kHz resonance scanning that reduces pixel dwell times to the nanosecond regime limiting photo-damage and bleaching and gated detection for further improving the resolution. Our system achieves imaging speeds greater than video rate over a large field of view utilizing FPGA based data collection. Further, the system incorporates a spatial light modulator allowing automatic alignment of the STED doughnut and excitation spots and system aberration correction and interleaved line by line excitation and collection for simultaneous two color imaging.

9331-32, Session 8

The importance of the photon arrival times in STED microscopy

Marco Castello, Luca L. Lanzanò, Istituto Italiano di Tecnologia (Italy); Iván Coto Hernández, Istituto Italiano di Tecnologia160 (Italy) and DISI, University of Genoa (Italy); Christian Eggeling, Univ. of Oxford (United Kingdom); Alberto Diaspro, Giuseppe Vicidomini, Istituto Italiano di Tecnologia (Italy)

In a stimulated emission depletion (STED) microscope the region from which a fluorophore can spontaneously emit shrinks with continued STED beam action after its excitation event. This fact has been recently used to implement a versatile, simple and cheap STED microscope that uses a pulsed excitation beam, a STED beam running in continuous-wave (CW) and a time-gated detection: By collecting only delayed (with respect to the excitation events) fluorescence the STED beam intensity needed for obtaining a certain spatial resolution strongly reduces, which is fundamental to increase live cell imaging compatibility. This new STED microscopy implementation, namely gated CW-STED, is in essence limited (only) by the reduction of the signal associated with the time-gated detection.

Here we show the recent advances in gated CW-STED microscopy and related methods. We show that the time-gated detection can be substitute by more efficient computational methods when the arrival-times of all fluorescence photons are provided. Finally, we show the potential to combine fluorescence correlation spectroscopy (FCS) with the (gated) CW-STED implementation: this synergy offers the unique property of tuning the effective detection volume by sorting the photons in time.

9331-33, Session 8

Superresolution imaging of cells with stimulated emission depletion nonlinear structured illumination (STED-SIM)

Han Zhang, Yu Li, Ming Zhao, College of Optical Sciences, The Univ. of Arizona (United States); Leilei Peng, College of Optical Sciences, The Univ. of Arizona (United States) and The Univ. of Arizona (United States)

Nonlinear structured illumination microscopy (SIM) is a fast widefield superresolution imaging technique. The key of nonlinear SIM is a strong nonlinear optical effect. Saturated-SIM (SSIM) and photoswitchable-SIM has been previously demonstrated. We report a new approach that applies nonlinear structured illumination by combining a uniform excitation field and a patterned stimulated emission depletion (STED) field. The nature of STED effect allows fast switching response, negligible stochastic noise during switching, low overall background and theoretical unlimited resolution, and thus makes STED-SIM potentially a better alternative to SSIM and photoswitchable-SIM.

Our approach of STED-SIM utilizes two orthogonal 1D gratings to generate a 2D grid STED structured pattern, which differ from rotating the 1D structured illumination pattern as employed in previous approaches. As the 2D grid requires negligible phase shifting time, the imaging speed of our STED-SIM system is therefore only limited by the speed of camera.

STED-SIM microscope was first tested on fluorescent beads samples and achieved full field imaging over 10²10 microns at the speed of 2s/frame with 4-fold improved resolution. The technique has been applied on biological samples. Superresolution images with tubulin of U2OS cells and granules of neuron cells have been obtained. Testing of live cell imaging is underway.

9331-34, Session PSun

Dithienylethene-based fluorescence molecular photoswitches for photoswitching nanoimaging

Ming-Qiang Zhu, Huazhong Univ. of Science and Technology (China)

A series of fluorescence molecular photoswitches based on dithienylethene (DTE), naphthalimide (NI) and perylenemonoimide (PMI) dyad modified by dithienylethenes (DTEs) have been developed and screened for photoswitching nanoimaging. For PMI-DTEs, although the photochromic speed has not changed, which only depends on DTEs from the point of mechanism, the fluorescence switching speed and fluorescence on/off ratio greatly increase when the number of substituted DTEs increases from 1 to 3 due to the enhanced quenching of multiple DTEs against single PMI emission. The high sensitive fluorescence on/off switching of the trident PMI-3DTE dyad enabled recyclable fluorescence patterning, all-optical transistor and photoswitching nanoimaging. NI-DTE and PMI-3DTEs have been copolymerized with hydrophilic monomers enabling photoswitching nanoimaging in living cells. The photoswitching nanoimaging demonstrated that sub-40 nm spatial resolution was obtained. We also synthesized fluorescent molecular switches based on spiropropan (SP) and hexaarylbiimidazole (HABI) and investigated their potential application in photoswitching nanoimaging. These fluorescent molecular switches hold promising prospective in photoswitching nanoscopy, allowing photoswitching nanoimaging of polymer microstructures and live cells with sub-50 nm resolution.

**Conference 9331: Single Molecule Spectroscopy
and Superresolution Imaging VIII**

9331-35, Session PSun

Coherent structured illumination imaging method with isotropic resolution enhancement

Joo Hyun Park, Eun Seong Lee, Korea Research Institute of Standards and Science (Korea, Republic of); Sang-Won Lee, Jae Yong Lee, Korea Research Institute of Standards and Science (Korea, Republic of) and Korea Univ. of Science and Technology (Korea, Republic of)

We develop a method for improving the isotropy of 2D super-resolution in the coherent structured illumination microscopy (SIM) implemented for imaging non-fluorescent samples. To alleviate the problem of anisotropic lateral resolution in the coherent SIM employing the two-angle orthogonal illumination, we introduce a hexagonal-lattice illumination that incorporates three standing-wave fields simultaneously superimposed at the orientations equally divided in the lateral plane. A mathematical formulation worked out to describe the coherent image formation in the three-angle SIM and an explicit Fourier-domain framework derived for reconstructing an image with enhanced resolution. To investigate the validity of our proposed method, we numerically simulate a coherent SIM imaging with the 3-angle structured illumination applied to a computer-generated resolution test target. The lateral-resolution performance is evaluated by examining the reconstructed images of various test patterns on the target, compared with those in the 2-angle structured illumination scheme. The orientation-dependent degradation in the lateral resolution can be reduced in the three-angle SIM, from 27.6% to 7.7% (by a factor of approximately 3.6), while the spatial resolution in the directions allowing the best enhancement remains 0.54 times the resolution limit of coherent bright-field imaging, almost the same as that of the orthogonal SIM. The three-angle SIM is extended more isotropically than the orthogonal SIM on the 2D frequency passband. Our proposed method to improve the isotropy of spatial resolution in coherent SIM is expected to benefit a diversity of imaging applications that require high resolution beyond the diffraction limit without relying on the fluorescence contrast of samples.

9331-36, Session PSun

Enhancement of the Förster resonance energy transfer efficiency in genetically encoded tagRFP-KFP fuse protein

Maria G. Khrenova, Lomonosov Moscow State Univ. (Russian Federation) and Bach Institute of Biochemistry (Russian Federation); Tatiana V. Ivashina, Institute of Biochemistry and Physiology of Plants and Microorganisms (Russian Federation); Alexander V. Nemukhin, Lomonosov Moscow State Univ. (Russian Federation); Alexander P. Savitsky, A.N. Bach Institute of Biochemistry (Russian Federation)

Förster resonance energy transfer (FRET) is a powerful tool to investigate biochemical and biophysical processes in vitro and in vivo. FRET biosensors change their spectral properties while interacting with the target molecules: either position of the fluorescence band or fluorescence lifetime. The latter group is supposed to be more promising as fluorescence proteins (FPs) that compose FRET pairs usually have broad fluorescence band and fluorescence lifetime changes can be detected more precisely. Our FRET system is composed of fluorescent protein TagRFP as an energy donor and chromoprotein KFP as an energy acceptor. We performed combined quantum mechanics / molecular mechanics (QM/MM) calculations to characterize TagRFP and KFP. Theoretically this pair can show up to 90 % FRET efficiency, whereas efficiency of the first sensor based on these proteins is 50 % only. Therefore the aim of our study was to modify the linker structure to enhance FRET efficiency. We performed molecular

dynamic simulations for various oligopeptides mimicking linkers and analyzed their conformational dynamics. The oligopeptides of interest contain DEVD motif that is specifically recognized by caspase-3. Suggested fuse proteins were synthesized and characterized via single molecule detection approach as well as measuring properties on statistical ensemble. We suggest a series of novel linkers with FRET efficiency starting from 70 %.

9331-37, Session PSun

Direct comparing the performance of low-light cameras in super-resolution localization microscopy

Zhen-Li Huang, Shaoqun Zeng, Zhe Hu, Zeyu Zhao, Luchang Li, Britton Chance Ctr. for Biomedical Photonics (China)

Super-resolution localization microscopy, including the popular PALM and STORM, depends on imaging of thousands or even tens of thousands individual single molecules to realize a super-resolution image. On the other hand, with the rapid advance in the field of low-light detectors, a large number of commercial cameras is suitable of imaging the weak fluorescence from single molecules, thus making it important and even confusing in selecting a suitable low-light detector for super-resolution localization microscopy. Although many studies have been reported to quantify the performance of the low-light detectors in super-resolution localization microscopy, these studies are carried out in an indirect manner. As a consequence, the conclusions are vulnerable to the influence of the experimental conditions.

Here we will introduce a direct method for quantifying the performance of low-light detectors in super-resolution localization microscopy. In this method, we consider the influence of a variety of experimental factors on the quality of the performance comparison. We further select two commercial EMCCD and sCMOS cameras as representative low-light detectors and present a direct comparison. We believe that this study can provide useful information for selecting a suitable low-light detector for super-resolution localization microscopy.

9331-39, Session PSun

Autofluorescence based visualization of proteins from unstained native-PAGE

Manjunath Siddaramaiah, Bola Sadashiva S. Rao, Kapaettu Satyamoorthy, Krishna Kishore Mahato, Manipal Univ. (India)

Proteins are the most diverse and functionally active biomolecules in the living system. In order to understand their diversity and dynamic functionality, visualization in native form without altering their structural and functional properties during the separation from the complex mixtures is very much essential. In the present study, a sensitive methodology for optimal visualization of unstained or untagged proteins in native polyacrylamide gel electrophoresis (N-PAGE) has been developed where, concentration of the acrylamide and bis-acrylamide mixture, Percentage of the gel, fixing of the N-PAGE by methanol: acetic acid: water and washing of the gel in the milli-q water has been optimized for highest sensitivity using laser induced autofluorescence. The outcome with bovine serum albumin (BSA) in PAGE was found to be highest at acrylamide and bis-acrylamide concentrations of 29.2 and 0.8 respectively in 12% N-PAGE. After the electrophoresis run, washing of the N-PAGE immediately with milli-q water for 12 times and eliminating the methanol: acetic acid: water fixing of the N-PAGE yielded better sensitivity of visualization. Using the above methodology 25ng of BSA protein band in PAGE was clearly identified by the technique. The currently used staining techniques for the visualization of proteins are coomassie brilliant blue and silver staining, have the sensitivity of 100ng and 5ng respectively. The current methodology was found to

**Conference 9331: Single Molecule Spectroscopy
and Superresolution Imaging VIII**

be more sensitive as compared to coomassie staining and less sensitive compared to silver staining respectively. The added advantage of this methodology is the faster visualization of proteins without altering their structure and functional properties.

9331-40, Session PSun

High-density high-resolution label locating for 3D super-resolution microscopy

Craig Snoeyink, Texas Tech Univ. (United States)

Bessel Beam Microscopy can be used to locate fluorescent particles/molecules to better than an order of magnitude beyond the diffraction limit. However, like most 3D locating techniques it has traditionally been limited to isolated emitters. Here we present an image analysis algorithm, based on genetic programming, that extends this capability to groups of emitters at emitter-emitter spacings far below the diffraction limit. Using simulated and experimental images, we show that this new algorithm is capable of localizing two particles to 10 nm in three dimensions even at spacings on the order of 60 nm. We will also show that this new algorithm is capable of localizing particles in three dimensions at an order of higher magnitude density than previously possible, up to 5 emitters in a 200 nm x 200 nm x 200 nm box. These particles are located with an average accuracy that is an order of magnitude smaller than the diffraction limited resolution of the imaging system. This localization resolution of emitter at such close proximity helps fill a gap in capability between FRET techniques on one end and traditional localization techniques on the other.

9331-42, Session PSun

Investigating field carcinogenesis using x-ray fluorescence microscopy

Scott T. Young, Andrew J. Radosevich, Wenli Wu, Northwestern Univ. (United States); Stefan Vogt, Argonne National Lab. (United States); Luay Almossalha, Northwestern Univ. (United States); Qiaoling Jin, Si Chen, Argonne National Lab. (United States); Tatjana Paunesku, Gayle Woloschak, Vadim Backman, Northwestern Univ. (United States)

In field carcinogenesis, there are subcellular changes that occur throughout the organ that lead to the eventual formation of cancer. However, due to the diffraction limit of light, it is especially difficult to image a cell and observe what these changes are. Even super resolution methods that are able to circumvent the diffraction limit fall short due to induced artifacts from the necessary sample preparation. Recently, the development of the bionanoprobe located in the Advanced Photon Source (APS) at Argonne National Laboratories (ANL) allows us to image the cell at subdiffraction length-scales with minimal sample preparation. Utilizing the phenomenon of x-ray fluorescence, it is possible to determine the elemental distribution map throughout the cells with high spatial resolution. The use of cryofixation allows us to preserve the cell's natural structure while maintaining its structural integrity during scanning. In this study, HT29 cells were cultured onto silicon nitride membranes. Both untreated and treated with valproic acid, a known chromatin decondenser, cells were prepared for scanning. The cells were then flash frozen in liquid ethane and scanned at 100 nanometer resolution with 10 keV hard x-rays. Analysis of the elemental distribution maps revealed elemental changes in the nucleus between untreated and treated cells, suggesting that XFM is a viable method to detect changes in chromatin density.

9331-43, Session PSun

Mapping DNA-Lac repressor interaction with ultra-fast optical tweezers

Carina Monico, Univ. of Oxford (United Kingdom); Alessia Tempestini, Francesco Vanzi, Francesco S. Pavone, Marco Capitanio, Univ. degli Studi di Firenze (Italy)

The lac operon is a well known example of gene expression regulation, based on the specific interaction of Lac repressor protein (LacI) with its target DNA sequence (operator). LacI and other DNA-binding proteins bind their specific target sequences with rates higher than allowed by 3D diffusion alone. Generally accepted models predict a combination of free 3D diffusion and 1D sliding along non-specific DNA. We recently developed an ultrafast force-clamp laser trap technique capable of probing molecular interactions with sub-ms temporal resolution, under controlled pN-range forces. With this technique, we tested the interaction of LacI with different DNA constructs: a construct with two copies of the O1 operator separated by 300 bp and a construct containing the native E.coli operator sequences. Our measurements show at least two classes of LacI-DNA interactions: long (in the tens of s range) and short (tens of ms). Based on position along the DNA sequence, the observed interactions can be interpreted as specific binding to operator sequences (long events) and transient interactions with nonspecific sequences (short events). Moreover, we observe continuous sliding of the protein along DNA, passively driven by the force applied with the optical tweezers.

9331-44, Session PSun

An automated tool for 3D tracking of single molecules in living cells

Lucia Gardini, Marco Capitanio, Francesco S. Pavone, Univ. degli Studi di Firenze (Italy)

Since the behaviour of proteins and biological molecules is tightly related to cell's environment, more and more microscopy techniques are moving from in vitro to in living cells experiments. Looking at both diffusion and active transportation processes inside a cell requires three-dimensional localization over a few microns range, high SNR images and high temporal resolution. Since protein dynamics inside a cell involve all three dimensions, we developed an automated routine for 3D tracking of single fluorescent molecules inside living cells with nanometer accuracy, by exploiting the properties of the point-spread-function of out-of-focus quantum dots bound to the protein of interest.

9331-48, Session PSun

A new detector approach for time-resolved widefield microscopy

Yury Prokazov, Werner Zuschratter, Leibniz Institute for Neurobiology Magdeburg (Germany); Claus A. M. Seidel, Heinrich-Heine-Univ. Düsseldorf (Germany); Sebastian Tannert, PicoQuant GmbH (Germany); Ottmar Jagutzki, RoentDek Handels GmbH (Germany); Bernhard H. Mueller, ProxiVision GmbH (Germany); Rainer Erdmann, PicoQuant GmbH (Germany); Michael Beeck, Best Systeme GmbH (Germany); Suren Felekyan, Ralf Kuehnemuth, Heinrich-Heine-Univ. Düsseldorf (Germany); Evgeny Turbin, Leibniz Institute for Neurobiology Magdeburg (Germany)

Picosecond time-resolved fluorescence microscopy detection has gained a significant interest for biological applications to study not only structures but to analyze also functionality. Upto date mainly confocal laser scanning

Conference 9331: Single Molecule Spectroscopy and Superresolution Imaging VIII

microscopes are used for these measurements. Here we present a new approach based on a widefield fluorescence microscope equipped with a newly developed detector head based on time and spatial resolved single photon counting. This detector can record for each event the picosecond timing, the spatial information as well as the macroscopic arrival time. The detector is based on a two stage MCP equipped with either a delay line or a charge sensitive anode. The time resolution is <100ps which fits to all used label and allows beside normal fluorescence lifetime analysis als time-resolved FRET studies.

The complete system is mainly used for multi-parametric fluorescence detection. In this poster we show basic technical parameters of the detector head and first microscopic measurement examples. Since the system is free of scanning parts it can be used also for low light level monitoring of long term dynamics in living cells.

This research has been performed by a joint German research cooperation funded by the ministry of education and research (BMBF, project code 13N12672, tCam4Life)

9331-58, Session PSun

Enhanced molecular rotor for single molecule detection

Hana Jaafari, Texas Christian Univ. (United States); Ryan M. Rich, Univ. of North Texas Health Science Ctr. at Fort Worth (United States); Sangram Raut, Joseph D. Kimball, Texas Christian Univ. (United States); Rafal Fudala, Ignacy Gryczynski, Univ. of North Texas Health Science Ctr. at Fort Worth (United States); Hung Doan, Texas Christian Univ. (United States); Julian Borejdo, Univ. of North Texas Health Science Ctr. at Fort Worth (United States); Nicholas Smith, Texas Christian Univ. (United States); Ilkay Bora, Texas Christian Univ. (United States) and Univ. of Copenhagen (Denmark); Bo W. Laursen, Univ. of Copenhagen (Denmark); Sergei Dzyuba, Texas Christian Univ. (United States); Zygmunt Karol Gryczynski, Texas Christian Univ. (United States) and Univ. of North Texas Health Science Ctr. at Fort Worth (United States)

We present single molecule fluorescence studies of symmetrical BODIPY dyad and triad. We characterized the steady-state intensities and time-resolved intensity decays in various media. The photophysical properties of these molecular rotors demonstrated a good correlation with the local solvent viscosity. Thus, these dyes are viable reporters on the viscosity of molecular solvents and cellular environments. We discuss the photophysical and chemical properties of these fluorescent rotors and highlight their advantages in applications as they relate to single-molecule studies. The goal is to develop bright, easily accessible, small-molecule probes to be used for sensitive detection in various physiological systems.

Conference 9332: Optical Diagnostics and Sensing XV: Toward Point-of-Care Diagnostics

Monday - Thursday 9-12 February 2015

Part of Proceedings of SPIE Vol. 9332 Optical Diagnostics and Sensing XV: Toward Point-of-Care Diagnostics

9332-30, Session PMon

Sample to answer visualization pipeline for low-cost point-of-care blood cell counting

Suzanne Smith, Council for Scientific and Industrial Research (South Africa); Thegaran Naidoo, Commonwealth Scientific and Industrial Research Organisation (South Africa); Emlyn Davies, Louis Fourie, Zandile Nxumalo, Hein Swart, Philip Marais, Kevin Land, Pieter Roux, Council for Scientific and Industrial Research (South Africa)

We present a visualization pipeline from sample to answer for point-of-care blood cell counting applications. Effective and low-cost point-of-care medical diagnostic tests provide developing countries and rural communities with accessible healthcare solutions [1], and can be particularly beneficial for blood cell count tests, which are often the starting point in the process of diagnosing a patient [2].

The initial focus of this work is on total white and red blood cell counts, using a microfluidic cartridge (previously reported in [3]) for sample processing. Analysis of the processed samples has been implemented by means of two main optical visualization systems developed in-house: 1) a fluidic operation analysis system using high speed video data to determine volumes, mixing efficiency and flow rates, and 2) a microscopy analysis system to investigate homogeneity and concentration of blood cells. Fluidic parameters were derived from the optical flow [4] as well as color-based segmentation of the different fluids using a hue, saturation and value (HSV) color space. Cell count estimates were obtained using automated microscopy analysis and were compared to gold standard manual methods for cell counting using a haemocytometer.

The results using the first iteration microfluidic device [3] showed that the most simple - and thus low-cost - approach for microfluidic component implementation was not adequate as compared to gold standard techniques. An improved microfluidic design has been developed to incorporate enhanced mixing and metering components, which together with this work provides the foundation on which to successfully implement automated, rapid and low-cost blood cell counting tests.

References:

1. "Nano/Microfluidics for diagnosis of infectious diseases in developing countries", W. G. Lee, Y.-G. Kim, B. G. Chung, U. Demirci and A. Khademhosseini, *Advanced Drug Delivery Reviews*, 62, 449 (2010).
2. "Point-of-care estimation of haemoglobin concentration in neonates and infants", E. Schapkaitz, J.N. Mahlangu and M. Letsoalo, *South African Journal of Child Health*, 6, 10-11 (2012).
3. "Characterization of microfluidic components for low-cost point-of-care devices", S. Hugo, K. Land and H. Becker, *Proceedings of the 17th International Conference on Miniaturized Systems for Chemistry and Life Sciences*, 27 - 31 October 2013, Freiburg, Germany, 461-463 (2013).
4. "Two-frame motion estimation based on polynomial expansion," G. Farneback, *Lecture Notes in Computer Science* 2749, 363-370 (2003).

9332-31, Session PMon

Hyperspectral imaging for detection of cholesterol in human skin

Matija Milanic, Norwegian Univ. of Science and Technology (Norway); Asgeir Bjorgan, Norwegian Univ of Science and Technology (Norway); Marcus Larsson, Department of

Biomedical Engineering. Linköping University (Sweden); Paolo Marraccini M.D., CNR - Istituto di fisiologia clinica (Italy); Tomas Strömberg, Department of Biomedical Engineering. Linköping University (Sweden); Lise L. Randeberg, Norwegian Univ. of Science and Technology (Norway)

Hypercholesterolemia is characterized by high levels of cholesterol in the blood and is associated with an increased risk of atherosclerosis and coronary heart disease. Early detection of hypercholesterolemia is necessary to prevent onset and progress of cardiovascular disease.

Optical imaging techniques might have a potential for early diagnosis and monitoring of hypercholesterolemia. In this study hyperspectral imaging was investigated for this application. The main aim of the study was to identify spectral and spatial characteristics that can aid identification of hypercholesterolemia in facial skin.

The first part of the study involved a numerical simulation of human skin affected by hypercholesterolemia. A literature survey was performed to identify characteristic morphological and physiological parameters. Realistic numerical models were prepared and Monte Carlo simulations were performed to obtain hyperspectral images. Based on the simulations optimal wavelength regions for differentiation between normal and cholesterol rich skin were identified.

In the second part of the study, the simulations were verified by a clinical study involving volunteers with elevated and normal levels of cholesterol. The faces of the volunteers were scanned by two hyperspectral cameras covering the spectral range between 400 nm and 2500 nm, and characteristic spectral features of the affected skin were identified. Processing of the images was done after noise reduction and masking of the images. The identified features were compared to the known cholesterol levels of the subjects.

The results of this study demonstrate that hyperspectral imaging can be a promising, rapid modality for detection of hypercholesterolemia.

9332-32, Session PMon

Phase resolved Doppler OCT for microvascular anastomosis surgical evaluation and prediction

Yong Huang, Johns Hopkins Univ. (United States); Dedi Tong, Johns Hopkins Univ. (United States) and Beijing Jishuitan Hospital (China); Shan Zhu, Lehao Wu, Qi Mao, Zuhaib Ibrahim, W. P. Andree Lee, Gerald Brandacher, Jin U. Kang, Johns Hopkins Univ. (United States)

Evolution and improvements in microsurgical techniques and tools have paved the way for super-microsurgical anastomoses with vessel diameters often approaching below 0.8 mm in the clinical realm and even smaller (0.2-0.3 mm) in murine models. Several imaging and monitoring devices have been introduced for post-operative monitoring but intra-operative guidance, assessment and predictability have remained limited to binocular optical microscope and surgeon's experience. In this work we evaluated high-resolution real time 3D phase resolved Doppler optical coherence tomography (PRDOCT) for intra-operative evaluation of luminal narrowing, thrombus formation and flow alterations. 22 mouse femoral artery anastomoses and 17 mouse venous anastomoses were performed and evaluated with PRDOCT. Flow status, vessel inner lumen 3D structure, and early thrombus detection were analyzed based on PRDOCT imaging results. Initial PRDOCT based predictions were correlated with actual long term surgical outcomes. Eventually two cases of mouse orthotopic limb

Conference 9332: Optical Diagnostics and Sensing XV: Toward Point-of-Care Diagnostics

transplantation were carried out and PRDOCT predicted long term success rates were confirmed by actual results. PRDOCT was able to provide high-resolution 3D visualization of the vessel flow status and vessel inner lumen. The assessments based on PRDOCT visualization shows a 92% sensitivity and 90% specificity for arterial anastomoses and 90% sensitivity and 86% specificity for venous anastomoses. PRDOCT appears to be an effective evaluation tool for microvascular anastomosis. It can predict the long term vessel patency with high sensitivity and specificity.

9332-33, Session PMon

Determination of in vivo skin moisture level by near-infrared reflectance spectroscopy

Inga Saknite, Janis Spigulis, Univ. of Latvia (Latvia)

In this study, near-infrared (NIR) spectroscopy was used to noninvasively determine skin moisture level by diffuse reflectance spectrum of skin in vivo in the spectral range 900-1700 nm. Skin dryness is dependent mostly on water concentration in epidermis and dermis, thus noninvasive determination of skin moisture level is possible by diffuse reflectance spectroscopy. Water has 3 absorption peaks in the spectral range 900-1700 nm: 976 nm, 1196 nm, and 1453 nm.

Experimental setup consisted of halogen lamp light source, InGaAs sensor NIR camera in the spectral range 900-1700 nm (Artray, ARTCAM-031TNIR), spectrometer in the spectral range 900-1700 nm (OceanOptics, NirQuest512), and NIR bandpass filters. NIR camera was used for imaging of a larger skin area, and NIR spectrometer was used for spectra comparison at point measurements. Cross polarization effect was used to reduce instantly reflected light by using NIR polarizers.

Experiment was performed on 20 healthy volunteers with different skin types. Small area of skin (approximately 1x1 cm) was covered with skin moisturizer. 3 different moisturizers were tested for comparison. NIR images and diffuse reflectance spectra were acquired at different times after the moisturizer was inflicted. As skin thickness and thus light scattering properties change depending on the location in the body, experiment was done on different parts of the body.

Results show that NIR diffuse reflectance spectroscopy can be used to noninvasively determine skin moisture level. Comparison of diffuse reflectance spectra at different body sites is given, as well as comparison of the effect of different moisturizers.

9332-34, Session PMon

Refractive index measurement using an optical cavity based biosensor with a differential detection

SaiHim Cho, Cody Joy, Joshua Brake, Seunghyun Kim, LeTourneau Univ. (United States)

We report a low cost optical cavity based biosensor using differential detection for point-of-care diagnostics. Three collimated lasers at different wavelengths pass through the optical cavity and come into the CMOS array detector that measures the change of the three lasers' intensities while a sample fluid is flowing inside the cavity. We employ differential detection which calculates the differential values by dividing the difference of normalized intensity values from two different wavelength sources by the sum of them. In our simulation, we designed our cavity structure so that two wavelengths for the differential value calculation change in opposite directions upon sensing layer thickness increase which leads to greater responsivity than monitoring the intensity of an individual laser. Responsivity, defined as the change of the measurable quantity for a certain condition change, is proportional to the sensitivity of the device. The noise introduced along the light path for all three lasers is expected to be canceled out due to the differential value calculation. Therefore, differential

detection sensing mechanism enhances the sensitivity through higher responsivity and noise cancelation. To reduce noise further, especially due to unstable laser diode output, we choose a reference pixel value in each CMOS image frame and subtract it from all other pixels. The three laser diode system enhances the fabrication tolerance to three times larger than the case when only two laser diodes are used. In this presentation, we will demonstrate the benefits of the differential detection method and discuss simulation results, the fabrication process, and preliminary measurement results.

9332-35, Session PMon

Paper-based surface enhanced Raman spectroscopy of phenobarbital sodium for point-of-care therapeutic drug monitoring

Moe Yokoyama, Takahiro Nishimura, Kenji Yamada, Michiko Kido, Hieyong Jeong, Yuko Ohno, Osaka Univ. (Japan)

We propose a drug concentration measurement method based on Raman spectroscopy of tear fluids with paper substrates. This method aims at point-of-care drug testing for therapeutic drug monitoring (TDM). We focus on tear fluids as good alternative specimens to blood for on-site TDM. Its drug concentrations have correlation with those in plasma. Tear collection is easy compared with blood sampling. In our method, we use paper substrates as tear collection tool and measurement substrate. By inserting the end of paper substrate into the conjunctival sac, tear fluids can be easily collected on the paper by capillary action. Raman spectroscopy is an optical technique that has some advantages including less sample volumes, no need for pretreatment, and measurability regardless of the sample state, even if it is liquid sample absorbed on paper. This technique enables a rapid and simple drug measurement with paper substrate. In addition, the sensitivity can be improved by surface enhanced Raman spectroscopy (SERS). In this paper, we confirm that various therapeutic drugs whose concentration has correlation between in tear and in plasma including anti-epileptic agents can be detected by Raman spectroscopy with paper substrate. Our proposal method does not require blood sampling, complex treatment, or much time. Therefore it can be applied to rapid, safe and simple TDM. It enables point-of-care TDM not only in hospital but also in nursing home and home care. We also attempt manufacturing of disposable SERS substrate with filter paper for high sensitive and inexpensive drug measurement.

9332-36, Session PMon

Biomedical applications of laser-induced breakdown spectroscopy (LIBS)

Unnikrishnan V. K., Rajesh Nayak, Sujatha Bhat, Stanley Mathew, VaseDEVAN B. Kartha, Santhosh Chidangil, Manipal Univ. (India)

In recent years, LIBS has been shown to be a versatile elemental analysis tool attracting increased attention because of the broad range of applications. LIBS can be used for analysis of both environmental samples and physiological samples (tissue and body fluids). Conventional spectroscopy techniques like inductively coupled plasma-mass spectroscopy (ICP-MS), and atomic absorption spectroscopy (AAS) are good in analytical performance, but their sample preparation method is destructive and environmentally hazardous. All these methods are capable of analysing only one element at a time. Compared to these methods, LIBS has numerous potential advantages such as simplicity in the experimental setup, less sample preparation, less destructive analysis of sample etc. In this paper, we report some of the biomedical applications of LIBS. From the experiments carried out on clinical samples (calcified tissues or teeth and gall stones) for trace elemental mapping and detection, it was found that LIBS is a robust tool for such applications. It is seen that the presence and relative concentrations of major elements (calcium, phosphorus and magnesium)

Conference 9332: Optical Diagnostics and Sensing XV: Toward Point-of-Care Diagnostics

in human calcified tissue (tooth) can be easily determined using LIBS technique. The importance of this study comes in anthropology where tooth and bone are main samples from which reliable data can be easily retrieved. Similarly, elemental composition of bile juice and gall stone collected from the same subject using LIBS was found to be similar. The results show interesting prospects for LIBS to study cholelithiasis (the presence of stones in the gall bladder, is a common disease of the gastrointestinal tract) better.

9332-37, Session PMon

Multivariate optical computing for fluorochrome discrimination

Ryan J. Priore, Joseph A. Swanstrom, CIRTEMO (United States)

The success of a commercial fluorescent diagnostic assay is dependent on the selection of a fluorescent biomarker; due to the broad nature of fluorescence biomarker emission profiles, only a small number of fluorescence biomarkers may be discriminated from each other as a function of excitation source. Multivariate Optical Elements (MOEs) are thin-film devices that encode a broad band, spectroscopic pattern allowing a simple broadband detector to generate a highly sensitive and specific detection for a target analyte. MOEs have historically been matched 1:1 to a discrete analyte or class prediction; however, MOE filter sets are capable of sensing projections of the original sparse spectroscopic space enabling a small set of MOEs to discriminate a multitude of target analytes. This optical regression can offer real-time measurements with relatively high signal-to-noise ratio that realize the advantages of multiplexed detection and pattern recognition in a simple optical instrument. The specificity advantage of MOE-based sensors allows fluorescent biomarkers that were once incapable of discrimination from one another via optical band pass filters to be employed in a common assay panel. A simplified MOE-based sensor may ultimately reduce the requirement for highly trained operators as well as move certain life science applications like disease prognostication from the laboratory to the point of care. This presentation will summarize the design and fabrication of compressed detection MOE filter sets for detecting multiple fluorescent biomarkers simultaneously with strong spectroscopic interference as well as comparing the detection performance of the MOE sensor with traditional optical band pass filter methodologies.

9332-38, Session PMon

Measurement of contrast of phantom and in vivo subsurface blood vessels using two near-infrared imaging systems

Jeremy Hebden, Aysha Alkhaja, Univ. College London (United Kingdom); Laure Mahe, Univ. Claude Bernard Lyon 1 (France); Samuel Powell, Nicholas L. Everdell, Univ. College London (United Kingdom)

A quantitative comparison has been performed between two commercial near-infrared (NIR) vein-viewing systems which are designed to supplement the clinician's traditional skills in locating veins by means of visualisation and palpation. The AccuVein AV300 and Novarix IV-eye real-time imaging systems employ very different imaging geometries; the former generates an image from reflected NIR light produced by a beam scanned across the surface, while the latter illuminates the viewed region at four points on the periphery and records the resulting distribution of diffusely transmitted light. The comparison involved measuring the contrast produced by absorbing rods (simulated blood vessels) in a cylindrical phantom with tissue-like optical properties, and the contrast of superficial blood vessels in the arms of healthy volunteers. The locations and sizes of the blood vessels were independently verified using a clinical ultrasound imaging system. The phantom measurements suggested that the AV300 displays the most superficial vessels with greater contrast, but the IV-eye is able to detect vessels when they are at a depth up to 2 mm greater than the limit observed

for the AV300. The results for thirty healthy volunteers also indicated that the AV300 typically displays vessels with higher overall contrast, but the effectiveness of the IV-eye at visualising deeper vessels was even more pronounced, with a maximum depth several millimetres greater than that achieved by the AV300, and more than ten times as many vessels observed at depths below 4 mm.

9332-1, Session 1

Attenuated total reflection Fourier transform infrared (ATR-FTIR) spectroscopy as a bedside diagnostic tool for detecting renal disease biomarkers in fresh urine samples

Katherine V. Oliver, Univ. College London (United Kingdom); Faith Matjiu, Cameron Davey, Shabbir Moochhala, Robert J. Unwin, The Royal Free Hospital (United Kingdom); Peter R. Rich, Univ. College London (United Kingdom)

Attenuated total reflection (ATR)-FTIR spectroscopy is a convenient technique for analysing biomedical samples due to its sensitivity to subtle compositional changes, speed of data acquisition and ease of sample preparation. We have applied the technology to the detection of disease biomarkers in urine and investigated the translation of these diagnostic methods to simple bench-top spectrometers.

To demonstrate the use of ATR-FTIR spectroscopy as a diagnostic tool we previously developed a rapid and reagent-free method to diagnose the kidney stone disease, cystinuria, by quantitation of urinary cystine. We were able to detect cystine to clinically relevant levels and analysis of urine from 33 cystinuric patients showed that cystine could be quantitated from spectra with accuracy comparable to the current clinical gold standard.

In order to establish whether such diagnostic techniques could be translated to the clinic, we have installed a room-temperature bench-top infrared spectrometer in the renal unit at the Royal Free Hospital, London. Spectra of urine from patients with a range of conditions, including diabetes, kidney disease, stone disease and urinary tract infections, were recorded by a nurse and the data were correlated to medical conditions to assess the diagnostic capabilities of the system and to identify potential spectral patterns associated with disease. 206 spectra have been recorded to date; these show it is possible to detect urea, creatinine, protein, lipids, sugars and other minor metabolites, including potential disease biomarkers. Several spectral peaks of potential diagnostic interest were identified that show variations between normal and diseased samples.

9332-2, Session 1

Time-resolved fluorescence detection enables dramatical reduction of tracer concentrations for renal function monitoring

Felix Koberling, Volker Buschmann, PicoQuant GmbH (Germany); Cathleen Fichtner, Ruprecht-Karls-Univ. Heidelberg (Germany); Deborah Herdt, Daniel Schock-Kusch, Hochschule Mannheim (Germany); Sabine Neudecker, Anatoli Shmarlouski, Yury Shulhevich, Dzmitry Stsepankou, Norbert Gretz, Jürgen Hesser, Ruprecht-Karls-Univ. Heidelberg (Germany); Matthias Raedle, Hochschule Mannheim (Germany); Rainer Erdmann, PicoQuant GmbH (Germany)

Preclinical measurements of renal function using the glomerulus filtration

Conference 9332: Optical Diagnostics and Sensing XV: Toward Point-of-Care Diagnostics

rate (GFR) as indicator are of high relevance when measuring toxicity of newly developed drugs. Recent developments using fluorescent markers (FITC-Sinistrin) have shown that they achieve highly accurate and reliable values using percutaneous measurement with intelligent patches [1, 2]. However, the high cost of marker substance demands for a more sensitive technology. We developed a new system based on pulsed laser excitation combined with time-correlated single photon counting (TCSPC) that records a continuous photon stream that allows for extracting the fluorescent decay pattern information. This strategy is able to distinguish between background (that is mainly characterized by autofluorescence) and marker signal by applying statistical unmixing of given decay curves. Since awake animals are measured, a lightweight measurement head that is connected via an optical fiber both to a laser light source and a photo multiplier is required to minimize motion artifacts. Remaining artifacts in the signal are removed by a pattern recognition approach [3].

The new system has demonstrated three-orders of magnitude higher sensitivity compared to the intelligent patch and is able to completely eliminate artifacts and background.

1) A. Schreiber et al., American Journal of Physiology - Renal Physiology, Vol. 303, F783-F788 (2012)

2) Schock-Kusch D, et al., Kidney international, Vol. 79, No 11, 1254-1258 (2010)

3) A. Shmarlouski et al., Biomedical Signal Processing and Control, Vol. 14, 30-41 (2014)

9332-3, Session 1

Biomarkers of chronic kidney disease in the urine of diabetic/hypertensive patients by means of Raman spectroscopy

Elzo E. S. Vieira, Jeyse A. M. Bispo, Adriana B. Fernandes, Landulfo Silveira Jr., Univ. Camilo Castelo Branco (Brazil)

Diabetes mellitus (DM) and arterial hypertension (AH) are common diseases that, if untreated, predispose the patient to renal failure. This study aimed to evaluate possible biomarkers in the urine of patients with DM and AH capable to predict the chronic renal disease, by means of Raman spectroscopy. Urines were obtained from patients with DM and AH, and separated into four groups: no symptoms of diseases related to DM and AH (G1), with low clinical complications (G2), with severe clinical complications (G3), and with chronic kidney disease (G4) arising from DM and AH. It has been used a dispersive Raman spectrometer (830nm, 250mW, 20s accumulation). In the spectra of urine it was identified Raman peaks at 680cm⁻¹ (creatinine), 1004cm⁻¹ (urea) and 1128cm⁻¹ (glucose). The results revealed that G2, G3 and G4 presented the creatinine peak with lower intensity than G1 (p<0.001). It was observed that G2, G3 and G4 showed lower intensity of the urea peak compared to G1 (p<0.001) and G4 showed lower intensity compared to G2 and G3 (p<0.001). Despite not significant, the glucose peak showed lower intensity in G1 when compared to the other groups. A model for classification of groups according to clinical criteria, using Sparse Multinomial Logistic Regression, taking as inputs the intensities of creatine, urea and glucose peaks allowed correct classification of 88.9% for G1, 36.8% for G2, 43.8% for G3 and 84.2% for G4. These results demonstrated the possibility of obtaining diagnostic information for complications of kidney disease associated to DM and AH.

9332-4, Session 1

Rapid urinary tract infection diagnosis and antibiogram, directly from urine samples, using surface enhanced Raman spectroscopy

Katerina Hadjigeorgiou, Univ. of Cyprus (Cyprus); Evdokia Kastanos, Univ. of Nicosia (Cyprus); Costas Pitris, Univ. of

Cyprus (Cyprus)

Bacterial resistance to antibiotics is a major health care problem mostly caused by the inappropriate use of antibiotics. At the root of the problem lies the current method for determination of bacterial susceptibility to antibiotics which requires overnight cultures leading physicians, suspecting a bacterial infection, to prescribe an antibiotic without waiting for the antibiogram results. In this work, a rapid method of diagnosis and antibiogram for a Urinary Tract Infection, directly from urine, was developed using filtering, silver nanoparticles, and Surface Enhanced Raman Spectroscopy (SERS). Initially, SERS was used to determine the concentration of bacteria in urine thus providing a diagnosis of UTI. SERS spectra of several concentrations of various gram negative bacteria (namely *Escherichia coli*, *Proteus* spp., *Klebsiella* spp., *Enterobacter* spp., and *Citrobacter* spp) ranging from 10³ to 10⁸ cells/ml showed a linear correlation between high-wave spectral intensity and concentration. For antibiotic sensitivity testing, SERS spectra of the five species of gram negative bacteria were obtained after a 2.5 hour exposure to the antibiotics: amoxicillin, amoxicillin/clavulanic acid, ciprofloxacin, cefaclor, cefuroxime, ceftriaxone, cefazoline, amikacin and gentamycin. Spectral analysis revealed clear separation between bacterial samples exposed to antibiotics to which they were sensitive and samples exposed to antibiotics to which they were resistant. With the enhancement provided by SERS and the application of the technique directly on urine or blood samples, bypassing the need for overnight cultures, this technology can become the basis for the development of rapid methods of diagnosis and antibiogram for a variety of bacterial infections.

9332-5, Session 1

Sensitivity advantage of mid-infrared spectroscopy using a wavelength-tunable external cavity-laser relative to an FTIR instrument

Stephen J. Matcher, David T. D. Childs, Dmitry G. Revin, Ihtesham U. Rehman, Richard A. Hogg, John W. Cockburn, The Univ. of Sheffield (United Kingdom)

Mid-infrared spectroscopy is one of the most promising technologies for monitoring analyte concentrations in bio-fluids. The spectral region beyond 3 microns is rich in molecular absorption bands which provide much greater chemical specificity than the UV, visible and near-infrared. For over 60 years the method of choice to perform mid-infrared spectroscopy has been Fourier Transform Infrared Spectroscopy (FTIR). Introduced by Fellgett in 1951, this method multiplexes all wavenumbers from a broad-band infrared source onto a single element photodetector simultaneously, thus overcoming the strong optical losses associated with a monochromator. Only within the last few years has FTIR's position as the method of choice begun to be challenged, by the development of the external cavity tunable quantum cascade laser. Early QCL's had very narrow linewidths and tuning ranges: ideal for gas sensing but poorly matched to solid and liquid phase materials. Recent research however has produced EC-QCL's with many 100's of cm⁻¹ of tuning.

We analyse the theoretical sensitivity of FTIR versus EC-QCL spectroscopy. In particular, an analogy with near-infrared optical coherence tomography (OCT) emphasises an important point. When acquiring an N-point mid-infrared spectrum, EC-QCL spectroscopy is predicted to generate the same spectral SNR as FTIR in a time $\frac{1}{N}$ shorter, using identical detected flux and receiver noise levels. Hence EC-QCL spectroscopy could potentially operate $\frac{1}{N}$ faster with no loss of spectral SNR.

We report results from a high-speed external cavity laser which points to spectral acquisition rates of over 100 kHz being achievable.

**Conference 9332: Optical Diagnostics and
Sensing XV: Toward Point-of-Care Diagnostics**

9332-6, Session 1

Gold sputtered Blu-Ray disks as novel and cost effective sensors for surface enhanced Raman spectroscopy

Michel K. Nieuwoudt, Auckland UniServices Ltd. (New Zealand); Jake W. Martin, Xindi Wang, Nina I. Novikova, Jenny Malmstrom, Cather M. Simpson, David E. Williams, The Univ. of Auckland (New Zealand)

Surface Enhanced Raman spectroscopy (SERS) offers sensitive and non-invasive detection of a variety of compounds as well as unparalleled information for establishing molecular the identity of both inorganic and organic compounds, not only in biological fluids but in all other aqueous and non-aqueous media. The localized hotspots produced through SERS at the solution/nanostructure interface of clustered gold or silver nanoparticles enable detection levels of parts per trillion. Recent developments in advanced fabrication methods have enabled the manufacture of SERS substrates with repeatable surface nanostructures which provide reproducible quantitative analysis, historically a weakness of the SERS technique. In this paper we describe the novel use of gold sputtered Blu-Ray surfaces as SERS substrates. Blu-Ray disks provide ideal surfaces for SERS substrates with their repeatable and regular nano-gratings. We show that the unique surface features and composition of the recording surface enables the formation of gold nano-islands with nanogaps, simply through gold sputtering, and relate this to a 500 fold signal increase of the melamine Raman signal in aqueous solutions and detection to 68 ppb. Melamine is a triazine compound and appears not only as environmental contaminant in environmental groundwater but also as an adulterant in foods due to its high nitrogen content. We have shown significant SERS signal enhancements for spectra of melamine using gold-sputtered Blu-Ray disk surfaces, with reproducibility of 12%. Blu-Ray disks have a unique combination of design, surface features and composition of the recording surface which makes them ideal for preparation of SERS substrates by gold sputter-coating.

9332-7, Session 2

Long term response of a Concanavalin A based fluorescence glucose sensor

Andrea K. Locke, Texas A&M Univ. (United States); Brian M. Cummins, North Carolina State Univ. (United States); Alexander A. Abraham, Gerard L. Coté, Texas A&M Univ. (United States)

Competitive binding assays comprised of the protein Concanavalin A (ConA) have been shown to have the potential for use in designing continuous glucose monitoring devices. However, due to its time dependent thermal instability, the lifetime of these ConA based assays has been short-lived. In an attempt to design sensors with longer in vivo lifetimes, different groups have immobilized the protein to various surfaces [1,2]. For example, Ballerstadt et al. have shown that by immobilizing ConA on the interior of a micro-dialysis membrane and allowing dextran to be freely suspended within solution, allowed for successful in vivo glucose sensing up to 16 days [3]. However in an attempt to maximize the binding rate and utilize all of ConA's binding sites, both assay components will need to be freely suspended in solution. Therefore, to increase the in vivo sensing lifetime without immobilization, this work explores the glucose response of an assay comprised of modified ConA and a single fluorescently labeled competing ligand in free solution. The behavior of this assay in the presence of varying glucose concentrations is monitored via fluorescence polarization over a 30 day period under physiological conditions.

References

- (1) Schultz, J. S.; Mansouri, S.; Goldstein, I. J. *Diabetes Care* 1982, 5, 245.
- (2) Aloraefy, M.; Pfefer, J.; Ramella-Roman, J.; Sapsford, K. 2012; *Proc. SPIE* Vol. 8367.

(3) Ballerstadt, R.; Evans, C.; McNichols, R.; Gowda, A. *Biosens. & Bioelectron.* 2006, 22, 275.

9332-8, Session 2

Ex-vivo glucose sensors using micro-dialysis: importance of on-line recovery rate determination by multi-analyte infrared spectrometry

Herbert M. Heise, Fachhochschule Südwestfalen (Germany); Thorsten Vahlsing, Fachhochschule Südwestfalen (Germany) and RWTH Aachen (Germany); Sven Delbeck, Janpeter Budde, Lars Cocchieri, Fachhochschule Südwestfalen (Germany); Steffen Leonhardt, RWTH Aachen (Germany); Dieter Ihrig, Fachhochschule Südwestfalen (Germany)

Micro-dialysis has often been used in the clinical environment for continuously harvesting body fluids in a minimal-invasive manner, but a drawback of this process are variable recovery rates. By using multivariate infrared spectroscopy and its inherent multi-analyte capability for whole blood, interstitial fluid or dialysate measurements, the application of acetate or mannitol containing perfusates has been investigated. The latter marker substance is suggested especially for application with single external cavity tuneable quantum cascade lasers, which render only a limited wavenumber interval compared with FTIR-spectrometers, but can be much smaller in device size. However, as severe spectral overlap exists for mannitol and glucose, studies for the simultaneous quantification of both monosaccharides were carried out with impressive selectivity. In-vitro recovery rate experiments were carried out on aqueous glucose or serum samples. By investigating simultaneously the depletion of the concentration of the marker substances from the perfusate using different micro-dialysis catheters for subcutaneous skin implantation or a dialysis system with a planar membrane for whole blood application, micro-dialysis recovery rates were determined by infrared spectrometry. Results confirmed the theoretical nonlinear relationship between the relative dialysate marker concentration and the recovery rates of glucose as predicted from the diffusion constants of the analytes of interest. By using a recovery-corrected determination of glucose levels, excellent agreement with glucose reference measurements can be achieved for micro-dialysis coupled infrared sensors.

9332-9, Session 2

Low-cost high performance readout system for fiber-optic biosensors

Dag R. Hjelme, Sør-Trøndelag Univ. College (Norway) and Norwegian Univ. of Science and Technology (Norway); Håkon Strømstad, Sør-Trøndelag Univ. College (Norway)

Background: Fiber-optic biosensors based on interferometric measurement of dimensional change in stimuli-responsive hydrogel immobilized on an optical fiber end-face is an emerging sensor technology with many interesting applications in medicine. We have earlier demonstrated nanometer length resolution from hydrogel sensors using readout instrumentation based on superfluorescent Er fiber source and a tunable optical filter and PC based data acquisition. As a step toward developing a low-cost compact design, we have designed and tested a stand-alone instrument. Initial test demonstrates that this instrument is capable of replacing the traditional instrumentation system.

Methods: The new instrument consists of a fiber coupled superfluorescent light emitting diode at 830nm and standard low-cost grating spectrometer. All signal conditioning and processing is performed in an onboard microprocessor (ARM Cortex). The instrument report absolute length and length changes. We have tested the new instrument with a glucose sensitive

Conference 9332: Optical Diagnostics and Sensing XV: Toward Point-of-Care Diagnostics

hydrogel sensor (from GlucoSet AS) using two different LEDs. The sensor lengths were around 55 μ m.

Results: The rms noise on the length measurement is better than 3 nm, whereas the length change resolution is better than 0.25 nm. This is an order of magnitude better than old instrument. To study the potential for further cost saving we evaluated the effect of reduced spectrometer and LED specification to be able to optimize the instrument to different application requirements.

Conclusions: Our results demonstrate that nanometer length change resolution is feasible using a compact low cost design. This opens for exploring new applications of the hydrogel biosensor technology.

9332-10, Session 2

SERS based sensing of glycated albumin in serum samples

Rishikesh Pandey, Nicolas Spegazzini, Jeon Woong Kang, Massachusetts Institute of Technology (United States); Ishan Barman, Johns Hopkins Univ. (United States); Gary Horowitz, Harvard Medical School (United States); Ramachandra R. Dasari, Peter T. C. So, Massachusetts Institute of Technology (United States)

Glycated albumin (GA) is an important marker, which provides retrospective index of integrated blood glucose values over extended periods of time, with intrinsic half-life of ca. 60-90 days. Unlike HbA_{1c}, GA is unaffected by reduced erythrocyte survival or an increase in young erythrocytes and shows a strong correlation with the development of serious diabetes complications including nephropathy and retinopathy. At present, there is no existing "gold standard" for fructosamine measurement because of the lack of suitability of existing approaches for routine clinical laboratory application. As a consequence, there is critical, unmet need for sensitive and selective methodology for determination of this "underestimated marker of diabetes" preferably in a reagent-free, facile manner.

Here, we present the first demonstration of surface enhancement Raman spectroscopy (SERS) based sensing approach to detect and potentially quantify glycated albumin in both commercial albumin samples and measurement of fructosamine in serum samples acquired from diabetic patients and normal subjects. We also evaluate the efficacy of SERS especially in view of predicative power and reproducibility in the determination of this important analyte. We believe that this sensing approach can provide a uniquely powerful tool for determination of glycated albumin in routine clinical diagnostics in the future.

9332-11, Session 3

Comparing multiple nanoparticles with SERS

Brian Walton, Gerard L. Coté, Texas A&M Univ. (United States)

Surface Enhanced Raman Spectroscopy (SERS) is one potential means of monitoring analytes at low concentrations. Toward a continuing effort to use SERS for point of care (POC) biosensing, a fundamental study that compared spherical gold colloid, nanocages and nanoshells was performed. Gold nanoparticles have been most commonly used in SERS. Since their extinction coefficient is in the visible wavelength range, which interferes with endogenous fluorophores in biological media, they can be problematic for POC sensing. To overcome this concern, in the past gold particle aggregates were formed typically using salt to extend the extinction range into the near infrared (NIR) region. However, this aggregation process is time dependent, causing the particle aggregates to fall out of solution, and generally does not provide good reproducibility. Thus, in this work, nanocages and nanoshells, tuned to have their extinction coefficients in the NIR range without the necessity for aggregation, were analyzed and

compared as an alternative to using gold colloid for quantifiable SERS signaling. Scanning electron microscope (SEM) and transverse electron microscope (TEM) images were collected for each material along with their extinction coefficients, aggregation properties, and SERS spectrum. Overall, all three particles produced strong SERS signals but the gold nanoparticles with salt and larger nanoshells fall out of solution while the nanocages were shown to be more stable over time and hence have the potential to be a more reproducible substrate for SERS biosensing.

9332-12, Session 3

Mannan modified polyethylene sinter bodies for the rapid diagnosis of borreliosis in diagnostic pipette tip

Mohammed A. Alasel, Michael Keusgen, Philipps-Univ. Marburg (Germany)

Development of powerful assays for the detection of clinically relevant biomarkers is of major concern for many researchers. Three main requirements for a point of care assay are: i) high sensitivity, ii) low cost and iii) short time for analysis. Many methods have been developed for serological diagnosis, for example enzyme-linked immunosorbent assay (ELISA), lateral flow tests (LFA) and western blot. However no method meets all the mentioned requirements at the same time. In our work we are developing a new type of serological assay having the advantages of low cost, high sensitivity and rapid result (10 min), in addition to the enrichment of the analyte from large sample volumes. The new assay format is based on the integration of 3-dimensional polyethylene sinter body loaded with antigens or antibodies placed in a pipette tip using ABICAP technology (Antibody Binding Column for Analytical Purpose). Binding of the biomarker can be detected using nanoparticles based on bovine serum albumin (BSA) and sudan IV which is conjugated with streptavidin and horseradish peroxidase (HRP). Streptavidin will bind to a biotinylated secondary antibody and a red color comes from sudan IV. Applying HRP substrate solution to the assay, the red color of sudan IV will turn into violet or blue leading to an increase in the sensitivity of the photometric read out.

9332-13, Session 3

Label-free, multiplexed, molecular sensing and imaging by stamping SERS

Greggy Santos, Univ of Houston (United States); Ming Li, Univ. of Houston (United States); Jianbo Zeng, Fusheng Zhao, Univ of Houston (United States); Wei-Chuan Shih, Univ. of Houston (United States)

Surface-enhanced Raman spectroscopy (SERS) is a spectroscopic technique, where Raman scattering is boosted primarily by enhanced electric field due to localized surface plasmon resonance (LSPR). With advances in nanofabrication techniques, SERS has attracted great attention for label-free molecular sensing and imaging. However, the practical use of SERS has often encountered an inherent issues regarding a molecule transfer step where target molecules need to be within the close proximity of a SERS-active surface by either mixing with nanoparticles or coating onto surface-bound nanostructures. To address this issue, we have developed stamping surface-enhanced Raman spectroscopy (S-SERS) for label-free, multiplexed, molecular sensing and large-area, high-resolution molecular imaging on a flexible, non-plasmonic surface without solution-phase molecule transfer. In this technique, a polydimethylsiloxane (PDMS) thin film and nanoporous gold disk SERS substrate play the roles as molecule carrier and Raman signal enhancer, respectively. After stamping the SERS substrate onto the PDMS film, SERS measurements can be directly taken from the "sandwiched" target molecules. The performance of S-SERS is evaluated by the detection of Rhodamine 6G (R6G), urea, and its mixture with acetaminophen (APAP), in physiologically relevant concentration range, along with corresponding SERS spectroscopic maps. S-SERS features

Conference 9332: Optical Diagnostics and Sensing XV: Toward Point-of-Care Diagnostics

simple sample preparation, low cost, and high reproducibility, which could lead to SERS-based sensing and imaging for point-of-care and forensics applications.

Ming Li, Jing Lu, Ji Qi, Fusheng Zhao, Jianbo Zeng, Jorn Chi-Chung Yu, and Wei-Chuan Shih, "Stamping surface-enhanced Raman spectroscopy for label-free, multiplexed, molecular sensing and imaging," *Journal of Biomedical Optics* 19(5): 050501, 2014.

9332-14, Session 3

Direct measurement of hemoglobin concentration of erythrocytes using photothermal angular light scattering

Ui-Han Kim, Dong-Hak Lee, Hun Kim, Su-Ho Ryu, Soocheol Kim, Chulmin Joo, Yonsei Univ. (Korea, Republic of)

Mass concentration of hemoglobin ([Hb]) provides a measure of the oxygen-carrying capacity of blood, and thus is used as an important indicator to diagnose blood disorders such as anemia.

Conventional hematology analyzers provide accurate determination of [Hb], but they are bulky, expensive to operate, and time-consuming. The cyanide methemoglobin method, commonly employed in portable [Hb] detectors, requires chemicals for destroying the lipid bilayers of erythrocytes and for subsequent Hb cyanization. Yet, the chemicals such as potassium cyanide and dimethylaurylamine oxide are toxic and involve extra cost.

Here, we demonstrate a novel chemicals-free and direct [Hb] detection method, based on photothermal (PT) angular scattering spectroscopy. A small volume of blood sample (~20 nL) is loaded in a microcapillary tube, which is illuminated by a 632-nm probe light. The light is then scattered by the tube to form a distinct pattern, which varies with refractive index and diameter of the tube. A photothermal light at 532-nm is then directed to the tube. The Hb absorbs the PT light energy and produces heat due to photothermal effect, which in turn alters the refractive index of blood. Highly sensitive [Hb] measurement of blood samples can be made by monitoring the resultant change in the angularly-dispersed scattering pattern. Our prototype system could measure [Hb] with a detection limit of <0.1 g/dL and exhibited a great correlation with a hematology system ($r > 0.92$).

In this presentation, we will describe operating principle and implementation of our device, along with experimental results with clinical samples.

9332-15, Session 3

Gold-nanoshells as surface plasmon resonance (SPR) sensors

Sathiyamoorthy Krishnan, Michael C. Kolios, Ryerson Univ. (Canada)

Surface plasmon (SP) is an oscillation of group of electrons at metal surface. The excitation of SP depends on properties of dielectric medium adjacent to metal surface and it varies with change in dielectric properties. SP resonance (SPR) has applications in medicine and biology; such metals have been used as contrast agents in PA imaging, and as sensors for biological agents. The present study is on investigation of plasmonic properties of the core-shell (CS) for surface plasmon resonance sensor (SPR) application. Here the core is a polystyrene sphere and shell is an Au layer. The size of the core is 1 μ m and the shell thickness is 45 nm. CS particles were prepared by a chemical method and characterised by TEM and optical spectroscopy. Optical absorption studies showed that CS particles exhibit plasmonic peaks at 745 nm and 836 nm. We choose the two peaks because blood exhibit significant absorption variation at 750 nm and 850 nm respectively depends on its oxy or deoxy state. The oxyhemoglobin has significantly lower absorption at 660 nm wavelength than deoxyhemoglobin, while at 940 nm deoxyhemoglobin exhibits absorption slightly higher than oxyhemoglobin. Blood of various concentrations and CS particles of

identical concentration were taken for all studies. Three concentrations of blood (with hematocrit levels 1.6%, 0.8%, and 0.4%) were prepared in PBS solution. Optical spectroscopy studies of CS showed decrease in absorption, and shift in plasmonic peak with increase in blood concentration. Plasmonic peak at 750 nm showed 4.11 ± 0.26 nm wavelength shift per percent dilution of hematocrit. Preliminary optical spectroscopy studies show that CS can be employed to monitoring oxygen saturation of RBC and a whole blood Immunoassay. As CS offers better absorption than many other molecular species, CS can be employed novel class of contrast agent for photoacoustic based imaging. It can also find applications in scattering-based acoustic and optical imaging methodologies which offer a new approach to non-invasive point-of-care detection, diagnosis, and monitoring.

9332-16, Session 4

Non-invasive in vivo monitoring of circulating amphotericin b using multi-wavelength photoplethysmography

Pratik Adhikari, Louisiana Tech Univ. (United States); Wakako M. Eklund, Pediatrix Medical Group of Tennessee, P.C. (United States); Patrick D. O'Neal, Louisiana Tech Univ. (United States)

A multi-wavelength photoplethysmograph designed to sense the in vivo concentration of the antifungal amphotericin b (delivered intravenously as Abelcet[®]) is presented. This technology was previously reported to quantify the blood concentration of optically absorptive therapeutic agents such as nanoparticles or quinine. Amphotericin b is widely used in the clinical setting to treat severe mycosis for a wide spectrum of the population. Although amphotericin b is a main line pharmacologic, the treatment is dose-limited due to nephrotoxicity. This report presents a prototype used to assess the real time bioavailability of intravenously delivered amphotericin b which has absorption peaks between 325-500 nm. The algorithm has been adapted to quantify the concentration based on the extinction at three wavelengths (~400 nm, 660 and 940 nm). The prototype estimates the concentration of amphotericin b in the pulsatile blood via a mathematical estimation of the tissue optical properties and penetration depth for wavelengths relevant to the compound. This prototype has potential for use in a clinical setting for dose verification, peak serum level estimation, and monitoring of clearance and bioavailability in the bloodstream. Our initial examination presents the suitability of the device to sense both experimental and clinical (5 mg/kg) concentrations of the drug.

9332-17, Session 4

Venous pooling and drainage affects photoplethysmographic signals at different vertical hand positions

Michelle Hickey, Justin Phillips, Panicos Kyriacou, City Univ. London (United Kingdom)

The aim of the current work is to investigate the possibility of augmenting pulse oximetry algorithms to enable the estimation of venous parameters in peripheral tissues. In order to further understand the contribution of venous blood to the photoplethysmographic (PPG) signal, recordings were made from six healthy volunteer subjects during an exercise in which the right hand was placed in various positions above and below heart level. The left hand was kept at heart level as a control while the right hand was moved. A custom-made two-channel dual wavelength PPG instrumentation system was used to obtain the red and infrared plethysmographic signals from both the right and left index fingers simultaneously using identical sensors. Laser Doppler flowmetry signals were also recorded from an adjacent fingertip on the right hand. Analysis of all acquired PPG signals indicated changes in both ac and dc amplitude of the right hand when the position was changed, while those obtained from the left (control) hand remained relatively

Conference 9332: Optical Diagnostics and Sensing XV: Toward Point-of-Care Diagnostics

constant. Most clearly, in the change from heart level to 50cm below heart level there is a substantial decrease in both dc and ac amplitudes. This decrease in dc amplitude most likely corresponds to increased venous pooling, and hence increased absorption of light. It is speculated that the decrease in ac PPG amplitude is due to reduced arterial emptying during diastole due to increased downstream resistance due to venous pooling.

9332-18, Session 4

Novel multi wavelength sensor concept to detect total hemoglobin concentration, methemoglobin and oxygen saturation

Ulrich Timm, Helge Gewiss, Jens Kraitl, Univ. Rostock (Germany); Kirstin Stuepmann, German Red Cross (Germany); Michael Hinz, Sebastian Koball, University of Rostock (Germany); Hartmut Ewald, Univ. Rostock (Germany)

The existing Hb monitoring system [1] was enhanced to allow the measurement of the hemoglobin derivate methemoglobin(MetHb). MetHb is one of main hemoglobin derivatives besides oxyhemoglobin (O2Hb), deoxyhemoglobin(RHb) and carboxyhemoglobin (COHb). MetHb is not able to bind oxygen unlike O2Hb. Standard pulse oximeter can only measure two derivatives, namely O2Hb and RHb but the presence of other derivative in the blood can distort the readings. High MetHb concentrations can be caused by local anesthesia, several medications or drugs. By using an artificial blood flow model the concentration of each derivate could be varied separate and the optical properties were monitored by spectrometers. Based on the results an LED based Sensor system was developed. The paper will describe a novel multi-wavelength photometric method to measure the MetHb concentration non-invasively. Clinic trials (also under hypoxia) are done to prove and demonstrate the performance of the sensor system. The results are compared to the gold standard, the BGA measurement, and other POC devices which are invasive and non-invasive.

[1] DOI: 10.1117/12.2038202 In proceeding of: SPIE 8951, Volume: Optical Diagnostics and Sensing XIV: Toward Point-of-Care Diagnostics

9332-19, Session 4

Laser speckle imaging device for the assessment of peripheral microcirculation

Bruce Yang, Tyler B. Rice, Sean White, Laser Associated Sciences, LLC (United States)

Laser speckle imaging (LSI) as a technology has previously demonstrated great potential as a tool within medical diagnostics. The ability to measure blood flow is a key component in the diagnosis and monitoring of such medical conditions as peripheral vascular disease, hypovolemic shock, sleep apnea, and diabetes. LSI has often been utilized to monitor blood flow; however, the form factor of its previous embodiments and the need for trained personnel prevented its practical applications within medicine.

As a critical life-sustaining element, blood flow monitoring throughout the body has been the key focus of many LSI studies. These studies often utilized intricate positioning devices, numerous precautions to prevent against motion artifact, and oftentimes direct line of site access to the region of interest.

The FlowMet is a blood flow monitoring device developed to circumvent all the aforementioned shortcomings of traditional LSI, thereby allowing the technology to be utilized in a point of care setting. Designed to resemble the commonly utilized pulse oximeter, the FlowMet is equally simple to operate while providing detailed information on microvascular blood flow in the periphery. The FlowMet is comprised of a compact laser diode and photodetector that clips onto the finger or toe. This novel design and application of transmission LSI does not require trained personnel for

use, minimizes motion artifact due to fixation to the finger, and allows for accurate blood flow measurement through the entire volume of the digit.

9332-20, Session 4

Optical diagnosis of acute scrotum in children

Babak Shadgan, Andrew J. Macnab, Mark Nigro, Lynn Stothers, The Univ. of British Columbia (Canada); A. M. Kajbafzadeh, Tehran Univ. of Medical Sciences (Iran, Islamic Republic of)

The acute scrotum is a critical urological condition defined as scrotal pain, swelling, and redness of acute onset. Early diagnosis and treatment is necessary in preserving testicular vitality and function. The patient history and clinical symptoms are key to the diagnosis and proper treatment planning, something that is not readily applicable in children where a reliable history and changes in sensation are lacking. The most common causes of acute scrotum in children include testicular torsion, torsion of the appendix testis, and epididymitis. These acute conditions are different in nature and pathology and therefore in treatment, which make an early and exact differential diagnosis critical.

We report a novel optical method for rapid differential diagnosis of acute scrotum by measuring and comparing tissue oxygen saturation index (TSI%) on affected and non-affected testes using a noninvasive and wireless near infrared spectroscopy device in spatially resolved configuration (SR-NIRS).

Five children with acute scrotum were studied by SR-NIRS as well as standard practice of diagnosis including physical examination, lab tests, color Doppler ultrasonography of testis and surgical exploration when necessary.

SR-NIRS could successfully differentiate between conditions by showing a higher TSI% in 2 cases of epididymitis, lower TSI% in 2 cases of testicular torsion and normal TSI% in 1 case of torsion of the appendix testis.

This observation suggests that SR-NIRS monitoring of testis appears feasible as a non-invasive, bedside and quick optical method to identify and differential diagnosis of acute scrotum conditions in children.

9332-21, Session 5

Google glass based immunochromatographic diagnostic test analysis

Steve W. Feng, Romain Caire, Bingen Cortazar, Mehmet Turan, Andrew Wong, Aydogan Ozcan, Univ. of California, Los Angeles (United States)

Integration of optical imagers and sensors into recently emerging wearable computational devices allows for simpler and more intuitive methods of integrating biomedical imaging and medical diagnostics tasks into existing infrastructures. Here we demonstrate the ability of one such device, the Google Glass, to perform qualitative and quantitative analysis of immunochromatographic rapid diagnostic tests (RDTs) using a voice-commandable hands-free software-only interface, as an alternative to larger and more bulky desktop or handheld units. Using the built-in camera of Glass to image one or more RDTs (labeled with Quick Response (QR) codes), our Glass software application uploads the captured image and related information (e.g., user name, GPS, etc.) to our servers for remote analysis and storage. After digital analysis of the RDT images, the results are transmitted back to the originating Glass device, and made available through a website in geospatial and tabular representations. We tested this system on qualitative human immunodeficiency virus (HIV) and quantitative prostate-specific antigen (PSA) RDTs. For qualitative HIV tests, we demonstrate successful detection and labeling (i.e., yes/no decisions) for up to 6x dilution of HIV samples. For quantitative measurements, we

Conference 9332: Optical Diagnostics and Sensing XV: Toward Point-of-Care Diagnostics

activated and imaged PSA concentrations ranging from 0 to 200 ng/mL and generated calibration curves relating the RDT line intensity values to PSA concentration. By providing automated digitization of both qualitative and quantitative test results, this wearable colorimetric diagnostic test reader platform on Google Glass can reduce operator errors caused by poor training, provide real-time spatiotemporal epidemic awareness, and assist with remote monitoring of various biomedical conditions.

9332-22, Session 5
Integrated elastic microscope device

Steve Lee, David Wright, The Australian National Univ. (Australia)

The emerging trends in mobile microscope is to take advantage of inexpensive high resolution CMOS sensors in smartphones. The pursuit of a low cost, durable but high power mobile microscope system of small form factor is pivotal in a myriad practices in medicine, agriculture, geology, ecology, education and marine biology. Here, we created a unique integrated hybrid soft lens-microscope frame using a combination of 3D printing technology and droplet lens fabrication techniques. Our "soft-material" approach delivers both high flexibility, durable and integrability beyond any conventional microscope fabrication technique. In this talk, we shall elaborate on the design, fabrication, integration and flexibility of our microscope frame. In addition, we will present the performance and integration of this microscope system to smartphone platform for mHealth applications.

9332-23, Session 5
Development of a mobile phone microscope image processing app for the Android OS

Kermit Sikindi, Karin M. Ennsner, Swansea Univ. (United Kingdom)

Several endeavors have been carried out in mobile phone microscopy. Their main motivation is to harness the relatively cheap and pervasive multifunctional mobile devices and create inexpensive yet powerful tools for microscopy. These tools are aimed at rural and developing areas where due to prohibitive costs, the proper medical analysis equipment is largely unavailable. However, these efforts have largely been focused on hardware and attempting to engineer the camera on the device to attain magnified images at a level akin to microscopes.

This study proposes to complement this microscopic functionality by developing software that enhance the images obtained using these devices. The research carried out in this paper aims to design and implement relatively easy to use digital image processing software that is sufficient for straightforward image enhancement functions. The software is inspired by ImageJ and run on the Android operating system. Note that ImageJ is not supported yet by the Android operating system that drives most mobile phones. To address this gap, a microscope image processing App for the Android OS is developed with several functionalities including image sharpening, finding edges, and image smoothing and contrast enhancement.

The comparison of the developed application with imageJ shows good qualitative agreement. The efforts detailed in this project have demonstrated the employment of software in enhancing digital images obtained using a mobile phone. Viewed in conjunction with the ubiquity of mobile phones, especially in the developing world, the application gains substantial potential relevance to the problem of disease diagnosis and screening in remote areas of the world.

9332-24, Session 5
Raman system for rapid, label-free early disease signature detection

Meiye Wu, Ryan W. Davis, Sandia National Labs. (United States)

In the early stages of infection, patients develop non-specific symptoms or no symptoms at all. While waiting for identification of the infectious agent, precious window of opportunity for early intervention is lost. The standard diagnostic methods require affinity reagents such as antibodies or Polymerase Chain Reaction (PCR) probes, and also require sufficient pathogen titers to reach the limit of detection. In the event of a disease outbreak, triaging the at-risk population rapidly and reliably for quarantine and medical intervention is more important than waiting for the identification of the pathogen by name. To address the need for a label-free, portable optical diagnostic system that can provide warning and inform rapid and effective response to infectious disease outbreak, we will utilize advancements in Raman spectrometry to analyze dendritic cell subsets in whole blood. Plasmacytoid dendritic cells (pDCs) only respond to virus within hours of initial infection, and myeloid dendritic cells (mDCs) respond specifically to bacterial pathogens in the same timescale, examining the activity of these two dendritic cell subtypes will rapidly distinguish infected from non-infected, and bacterial from viral infection, for the purpose of triage during an emergency outbreak. We present Raman spectroscopy results showing label-free detection of early disease signatures in innate immune cells, with the ultimate purpose of designing a low-cost, high-throughput miniaturized Raman diagnostic system meeting requirements for low-resource settings.

9332-25, Session 5
Raman spectroscopic studies of dengue and malaria infection in human blood

Saleem Muhammad, Bilal Muhammad, National Institute of Lasers and Optronics (Pakistan); Tayyaba Ijaz, Mayo Hospital Lahore (Pakistan); Samina T. Amanat, Huma A. Shakoore, PAEC General Hospital (Pakistan)

Raman spectroscopy has been employed to develop an optical diagnostic tool for prediction of malaria and dengue virus infection in human sera/plasma samples. Raman spectra were obtained from 100 healthy and diseased samples using diode laser at 532 nm as an excitation source. It was found 10 distinct Raman spectral peaks at 837, 1172, 1226, 1339, 1357, 1393, 1552, 1586, 1603 and 1673 cm^{-1} , appeared only in malaria infected samples and at 845, 1066, 1123, and 1732 cm^{-1} , only in the dengue infected ones. These Raman lines are signatures of biochemical and morphological changes associated with the malarial plasmodium Vivax and dengue virus infection and can therefore be used as biomarkers for disease recognition. Raman spectroscopy addresses the change in blood chemistry at molecular level; therefore, it may be helpful for clinical treatment of disease. In addition, a multivariate regression model was developed that utilized Raman spectra of diseased and healthy samples and partial least square (PLS) regression engine in the Mat-Lab environment. Model utilized Raman spectra of 13 malaria infected, 06 dengue virus infected, 10 non-malaria and 10 healthy samples as the trainee data set. The code was scrutinized with leave-one-sample-out cross validation methodology. Cross validation calculates the prediction accuracy, which is known as correlation coefficient r^2 between the predicted and clinical results. The value of r^2 yielded by the model is 0.98 that is accepted clinically. The model was tested for 61 unknown plasma/sera samples and was found more than 90 % accurate in accordance with the clinical results.

**Conference 9332: Optical Diagnostics and
Sensing XV: Toward Point-of-Care Diagnostics**

9332-26, Session 6

Design and validation of a diffuse reflectance and spectroscopic microendoscope with poly(dimethylsiloxane)-based phantoms

Gage J. Greening, Amy J. Powless, Joshua A. Hutchesson, Sandra P. Prieto, Aneeka A. Majid, Timothy J. Muldoon, Univ. of Arkansas (United States)

Epithelial cancers, including colorectal, esophageal, and oral cancer, account for over 80% of all cancers. Despite their prevalence, many cancers arise in basal layers of tissue and are initially undetected by conventional fiber bundle microendoscopy techniques, which are limited to visualization of surface morphology. We have designed a bench-top, fiber-bundle microendoscope to overcome this limitation by interrogating deeper into tissue to provide depth-sensitive information. Using a custom fiber optic probe consisting of a central 1 mm image guide fiber and five surrounding 200-micron delivery/collection fibers, this multi-modal technique acquires data on fluorescence, bulk tissue diffuse reflectance, and diffuse spectroscopy. Fluorescence image data was acquired by using topical proflavine (0.01% w/v in saline) as a vital dye. Excitation for proflavine was provided via the image guide fiber coupled to a blue LED (455 nm). Additionally, bulk tissue diffuse reflectance was acquired by delivering near infrared radiation (635 nm) through a delivery fiber and imaging the reflected light via the image guide fiber. This diffuse reflectance pattern is compared to a Monte Carlo model of photon propagation in tissue; spatial heterogeneities could be used to indicate sub-epithelial disease. Finally, diffuse spectral measurements were taken at increasing source-detector separations (374, 729, and 1051 μm) to gather depth-sensitive data using broadband white light illumination (300-2600 nm) from a tungsten-halogen lamp. All modalities, acquired in less than three seconds, were controlled with a custom LabVIEW interface. Validation experiments were performed to determine depth-sensitivity in poly(dimethylsiloxane)-based tissue-simulating phantoms, cell-based three-dimensional tissue-simulating phantoms, and fresh animal tissue.

9332-27, Session 6

Assessing dysplasia of a bronchial biopsy with FTIR spectroscopic imaging

Liberty Foreman, Univ. College London (United Kingdom); James A. Kimber, Imperial College London (United Kingdom); Katherine V Oliver, University College London (United Kingdom); James M Brown, Samuel M Janes, Lungs for Living Research Centre (United Kingdom); Thomas Fearn, Univ. College London (United Kingdom); Sergei G. Kazarian, Imperial College London (United Kingdom); Peter R. Rich, Univ. College London (United Kingdom)

Barrett's oesophagus is a condition where squamous epithelium cells metastasize to columnar epithelial cells in response to chronic gastric oesophageal reflux. These patients have a 30 fold increased chance of developing oesophageal adenocarcinoma (OAC). Histology is the current gold standard for staging the dysplasia of Barrett's oesophagus. It is a lengthy process with a variable ($\kappa = 0.21-0.47$) inter-observer agreement. Here we explore the use of attenuated total reflectance Fourier transform infrared (ATR-FTIR) spectroscopy as a bedside diagnostic tool.

To date, simple single element ATR-FTIR spectroscopy has not been employed as a clinical diagnostic tool for fresh biopsies. One major inherent issue is the variable tissue type present when in contact with the prism surface. By comparing FPA-FTIR imaged unstained 8 μm tissue sections to histologically assessed H&E tissue sections it was possible to accurately describe specific FTIR features of squamous epithelium, columnar

epithelium, and lamina propria. These features were used to aid the analysis of single element ATR-FTIR spectra of 731 fresh biopsies from 133 patients. Using a combination of clustering and regression analysis with a leave one patient out cross-validation, a diagnostic model was built to classify Barrett's biopsies into three categories: healthy, non dysplastic Barrett's oesophagus and high grade dysplasia (HGD) / OAC. These grouping were compared to their assignments from histological assessment. A HGD sensitivity of 95%, the minimum requirement for clinical translation, can be achieved. This would result in a reduction by 50% of Barrett's biopsies sent to for histological grading and enable immediate treatment for those patients with a high cancer risk.

9332-28, Session 6

Investigation on digital staining based on Mueller matrix imaging

Wenfeng Wang, Quan Liu, Nanyang Technological Univ. (Singapore); Supriya Srivastava, National Univ. of Singapore (Singapore)

Digital staining based on Mueller matrix measurements or their derivatives was investigated. Mueller matrix imaging was performed on thin unstained gastric tissue sections, in which tissue regions in various pathological stages were marked, such as cancer, dysplasia, intestinal metaplasia and normal glands. Each imaging measurement was restricted to one single pathological stage. The full Mueller matrices for all these samples were reconstructed using recorded images, followed by the extraction of polarization parameters. It was observed that pixel classification based on Mueller matrix elements or their principal components among various pathological stages yield higher diagnostic accuracy than that based on polarization parameters. Moreover, Mueller matrix images with a lower spatial resolution generate higher diagnostic accuracy while those with a higher spatial resolution provide more details on morphological changes.

9332-29, Session 6

Exploiting Raman spectroscopy potential in middle ear surgery

Rishikesh Pandey, Nicolas Spegazzini, Massachusetts Institute of Technology (United States); Tulio A. Valdez, Connecticut Children's Medical Ctr. (United States); Jeon Woong Kang, Massachusetts Institute of Technology (United States); Ishan Barman, Johns Hopkins Univ. (United States); Ramachandra R. Dasari, Peter T. C. So, Massachusetts Institute of Technology (United States)

Exploiting the endogenous molecular contrast may provide sufficient information to aid the process of middle ear disease diagnosis and guidance for excision of cholesteatoma. Cholesteatoma is an expansive and destructive lesion characterized by migration of keratinized hyperproliferative squamous epithelium with a fibrous stroma that can occur in the middle ear and mastoid cavity. Surgical management of cholesteatoma can be one of the most challenging operations in otolaryngology. Consequently, it is imperative to develop new tools that can provide real-time, reliable and objective diagnosis of cholesteatoma and facilitate its complete removal during surgery. To this end, Raman spectroscopy owing to its unique chemical fingerprinting and multiplexing capabilities can be employed as a highly specific probe in the middle ear disease diagnosis and guidance for excision of cholesteatoma.

In this paper we demonstrate the potential of Raman spectroscopy in distinguishing the cholesteatoma from morphologically similar but biochemically different lesions (in ex-vivo) based on the unique spectral markers. The design and performance of newly developed clinical instrument would be discussed. This work represents the first attempt to explore the potential of spectroscopic imaging techniques for middle ear

Conference 9332: Optical Diagnostics and Sensing XV: Toward Point-of-Care Diagnostics

and mastoid lesions. This successful proof-of-concept demonstration now constitutes a critical milestone towards the ultimate goal of its use as a real-time diagnostic tool for intraoperative cholesteatoma identification. Research is underway to develop a multimodal system by adding diffuse reflectance and intrinsic fluorescence spectroscopic modalities to the Raman system, which would be finally integrated inside a traditional otoscope.

Conference 9333: Biomedical Applications of Light Scattering IX

Saturday - Sunday 7-8 February 2015

Part of Proceedings of SPIE Vol. 9333 Biomedical Applications of Light Scattering IX

9333-1, Session 1

Backscattering of coherent polarized light from turbid tissue-like scattering medium with rough surface

Alexander Doronin, Univ. of Otago (New Zealand);
Lioudmila Tchvialeva, Igor Markhvida, Tim K. Lee,
Vancouver Coastal Health Research Institute (Canada);
Igor V. Meglinski, Univ. of Otago (New Zealand)

The last decade has seen growing interest to the propagation of coherent polarized light in turbid tissue-like scattering media. We investigate the depolarization of coherent polarized light backscattered from the turbid tissue-like scattering media with rough surfaces. In particular, we consider laser speckle patterns formation and the role of surface roughness in the depolarization of linearly polarized light backscattered from the media which optical properties which are in the order of human skin lesions. We present the results of computational studies based on the unified electric field Monte Carlo model. The introduced computational model is a part of generalized Monte Carlo code and utilizes the implementation of parallel computing on the NVIDIA Graphics Processing Units (GPUs) using Compute Unified Device Architecture (CUDA). The results of simulation of the backscattering of coherent linearly polarized light from rough surfaces of the turbid tissue-like scattering media are presented in comparison with the results of experimental studies and are well agreed to each other.

9333-2, Session 1

Robust estimation of vessel misfocus and real-time misfocus correction in laser speckle contrast imaging

Dene Ringuette, Iliya Sigal, Ofer Levi, Univ. of Toronto (Canada)

Laser Speckle Contrast Imaging (LSCI) is a flexible, non-invasive, label-free technique to measure relative blood flow speeds in-vivo. Near IR illumination allows deep tissue penetration due to low tissue absorption in that wavelength range. However, the low absorption leads to a reduced observed image contrast between tissue and blood vessels. This leads to a challenge in determining and automatically adjusting the best focus location in-vivo. Traditional autofocus algorithms that are based on either intensity contrast or frequency domain analysis do not work well during flow imaging with the LSCI technique, due to increased speckle and low contrast in the image. Using the LSCI-derived contrast ratio K directly, over a vessel of interest, provides a better metric for determining the location of imaging system focal plane, but the method is not robust as it possesses low signal-to-noise ratio (SNR) within a single frame. In this work we use a different metric, kurtosis of the flow profile cross-section, to estimate the degree of misfocus (axial deviation of imaging system focal plane from the imaged blood vessel) and provide a feedback mechanism for robust autofocusing during blood flow imaging in a rat's brain. We demonstrate via flow imaging simulations, imaging of flow in microfluidic capillaries, and in-vivo imaging of blood flow in brains of anesthetized rats that this metric allows for the determination of the location of best focus and assessing the degree of misfocus.

9333-3, Session 1

Optical thromboelastography (OTEG) and blood coagulation (*Invited Paper*)

Seemantini K. Nadkarni, Harvard Medical School (United States) and Massachusetts General Hospital (United States) and Wellman Ctr. for Photomedicine (United States)

Impaired blood coagulation results from several conditions associated with severe trauma, surgery or illness, and can cause life-threatening bleeding or thrombotic disorders. Deficient coagulation can lead to 'hypocoagulable' states resulting in uncontrolled bleeding that may cause severe anemia, shock and multiple organ failure. In other cases, coagulation defects may manifest as 'hypercoagulable' states, causing increased clotting that can result in potentially fatal complications such as deep vein thrombosis and pulmonary embolism. During surgery, trauma care and chronic disease management, clinicians often encounter the challenging task of maintaining a precarious balance between bleeding and coagulation. In order to achieve optimal outcome, the early detection of coagulation defects and coagulation monitoring during therapy is therefore essential. Here, we discuss a novel coagulation sensing technology termed Optical Thromboelastography (OTEG) that addresses the unmet clinical need to comprehensively assess a patient's coagulation status within minutes at the point-of-care. The technique involves placing a drop of blood in a small cartridge. A laser source illuminates the sample and a CMOS camera images temporal intensity fluctuations of laser speckle patterns reflected from the sample over time. By measuring the speckle intensity autocorrelation function and quantifying the mean square displacements of scattering particles during clotting, we can recover information about multiple coagulation metrics related to clot stiffness, clotting time, platelet function and fibrinolysis, critical to hemostasis. Our clinical studies demonstrate the potential of OTEG to rapidly identify patients at high risk of hemorrhage or thrombosis so that treatment may be tailored to address individual coagulation deficits.

9333-4, Session 2

Detection of early seizures by diffuse optical tomography

Tao Zhang, Mohammad Reza Hajihashemi, Junli Zhou, Paul R. Carney, Huabei Jiang, Univ. of Florida (United States)

In epilepsy it has been challenging to detect early changes in brain activity that occurs prior to seizure onset and to map their origin and evolution for possible intervention. Besides, preclinical seizure experiments need to be conducted in awake animals with images reconstructed and displayed in real-time.

In this report we demonstrate using a rat model of generalized epilepsy that diffuse optical tomography (DOT) provides a unique functional neuroimaging modality for noninvasively and continuously tracking such brain activities with high spatiotemporal resolution. We developed methods to conduct seizure experiments in fully awake rats using a subject-specific helmet and a restraining mechanism. Graphic processing units (GPU) based parallel code was implemented and tested with significant acceleration that allows real-time online monitoring of the pre-seizure state.

For the first time, we detected early hemodynamic responses with heterogeneous patterns, along with intracranial electroencephalogram gamma power changes, several minutes preceding the electroencephalographic seizure onset, supporting the presence of a "pre-seizure" state both in anesthetized and awake rats. Using a novel time-series analysis of scattering images, we show that the analysis of scattered

**Conference 9333:
Biomedical Applications of Light Scattering IX**

diffuse light is a sensitive and reliable modality for detecting changes in neural activity associated with generalized seizure and other CNS disorders with the additional benefit of providing access to physiological parameters that other modalities cannot access. We also observed the decoupling between local hemodynamic and neural activities. We found widespread hemodynamic changes evolving from local regions of the bilateral cortex and thalamus to the entire brain, indicating that the onset of generalized seizures may originate locally rather than diffusely. Together, these findings suggest DOT represents a powerful tool for mapping early seizure onset and propagation pathways.

9333-5, Session 2

Therapeutic efficacy testing in 3D biopsies using biodynamic imaging

Daniel A. Merrill, Purdue Univ. (United States); Ran An, Animated Dynamics, Inc. (United States); Michael Childress, Purdue Univ. (United States); Daniela E. Matei, Indiana Univ.-Purdue Univ. Indianapolis (United States); John J. Turek, David D. Nolte, Purdue Univ. (United States)

Biologically accurate tissue models are critical to chemotherapy drug development for predicting patient response. Different models may respond differently based on changes in the cellular microenvironment. Biodynamic Imaging (BDI) is a label-free, non-invasive technology that uses short-coherence dynamic light scattering and digital holography to probe intracellular motions of cells in their native microenvironment. Previously, BDI has been used to measure the drug response of *in vitro* living tissue models. Here, we present results from recent studies of chemotherapeutic efficacy in 3D *ex vivo* biopsied tissues using BDI. We show that human ovarian tumors grown in immunologically deficient mice displayed an unexpectedly greater sensitivity to platinum-based therapeutics relative to multicellular tumor spheroids grown *in vitro* from the same cell line. With the increasing reliance on tumor spheroid 3D tissue culture in drug discovery, this finding may highlight limitations of 3D culture versus more biologically relevant tissue biopsies. The success of animal model experiments has led to the first application of BDI in preclinical trials of canine multicentric lymphoma responding to doxorubicin. The 3D imaging capability of BDI enabled the measurement of tumor heterogeneity in response to the therapy. The clinical patient outcome was predicted by BDI with 90% accuracy within 24 hours of biopsy, while the clinical follow-up took one to several months. Biodynamic imaging is a fundamentally different approach to the prediction of therapeutic efficacy for personalized medicine with higher accuracy and more biological relevance than standard cell-based assays.

9333-6, Session 2

Towards quantitative laser speckle contrast imaging: the influence of multiple scattering on velocity determination

Annemarie Nadort, Koen Kalkman, Ton G. van Leeuwen, Dirk J. Faber, Univ. van Amsterdam (Netherlands)

Laser Speckle Contrast Imaging (LSCI) derives the temporal decorrelation time τ_C of dynamic speckle patterns from measurements of local spatial speckle contrast $K(T)$ where T is the exposure time of the acquisition. The τ_C , which characterizes the electric field temporal autocorrelation function $g_1(\tau)$, is related to velocity of moving scatterers by $1/\tau_C = \beta V$ where β is a proportionality constant that depends on geometry and tissue properties. In most studies, single scattering is assumed in modelling $g_1(\tau)$. In this contribution we investigate the influence of multiple scattering on τ_C in a darkfield LSCI configuration (that is capable of independent measurement of V by particle tracking) in a flow phantom by varying size and concentration of flowing scatterers. We find that in the multiple scattering regime, our results are reasonably well described by $g_1(\tau)$ as

proposed by Bonner (AO 20(12) 1981) where the multiple scattering scaling factor m is given by the reduced number of scattering events $N' = 1.4\mu_s(1-g)d$ where μ_s , g are the scattering coefficient and anisotropy factor and d is the vessel thickness; the setup specific factor 1.4 is derived from Monte Carlo simulations. N' is used rather than the actual number of scattering events $N = \mu_s d$. These results are in accordance with (multiple scattering) Diffusive Wave Spectroscopy. Our results further indicate that the regime of least scattered photons requires further investigation.

9333-7, Session 2

Correction of particle size variations in laser speckle rheology applications

Zeinab Hajjarian Kashany, Seemantini K. Nadkarni, Harvard Medical School (United States)

Laser speckle rheology (LSR) is a novel optical tool for evaluating the viscoelastic properties of fluids. In LSR, the specimen is illuminated by coherent light and speckle intensity fluctuations are quantified by cross-correlation analysis over the speckle time series to obtain the speckle intensity auto-correlation curve, $g_2(t)$. The mean square displacement (MSD) of Brownian particles is estimated from the $g_2(t)$ curve, and the complex viscoelastic modulus of medium, $G^*(\omega)$, is derived from the MSD via the generalized Stokes-Einstein equation (GSER). The accurate quantification of $G^*(\omega)$ from $g_2(t)$ curve is however complicated because $g_2(t)$ is not only modulated by the viscoelastic compliance, but also by the scattering particle size distribution of the medium.

Therefore, we utilize an elegant approach that may be readily incorporated in the LSR system without the need for additional instrumentation for evaluating the mean scattering particle size directly from speckle patterns. Specifically, we show that the parallel-polarized diffuse reflectance profile (DRP), calculated from time-averaged speckle images, exhibits certain azimuth angle dependence related to the average scattering particle size that can be used to correct for residual speckle modulations caused by particle size variations in the sample. Our studies conducted using dairy products, fat emulsions and biofluids with unknown particle size distribution, demonstrate that LSR can accurately quantify $G^*(\omega)$ of the samples by incorporating information on azimuthal angle dependence of the measured DRP. Comparison with standard reference rheometry showed close correspondence with LSR results in all cases.

9333-8, Session 3

Phase function corrected diffusion approximation (Invited Paper)

Lev T. Perelman, Edward Vitkin, Le Qiu, Vladimir M. Turzhitsky, Irving Itzkan, Harvard Univ. (United States)

From astronomy to cell biology, the manner in which light propagates in turbid media has been of central importance for many decades.

The diffusion approximation is a first order approximation to the equation of radiative transfer in a sense that scattering in the diffusion approximation is assumed to be either isotropic or near isotropic. However, in the majority of biomedical light scattering applications the phase function, which describes the angular distribution for a single scattering event, is predominantly forward directed. Nevertheless, the transport of light at large distances is still accurately described by the diffusion approximation, because the effects of anisotropic scattering become averaged out over many scattering events. This makes the diffusion approximation a powerful tool for many biomedical applications.

However, a large number of biomedical applications require the prediction of radiance near the source or the point-of-entry (POE). Here a more rigorous solution of the radiative transfer equation is needed, either computational (e.g. the Monte Carlo simulation) or analytical. In recent years, several types of perturbation analysis have been introduced in attempt to improve the performance of the diffusion approximation for biological media near the

**Conference 9333:
Biomedical Applications of Light Scattering IX**

POE. Each of these methods includes higher order terms of the scattering phase function in addition to the terms that are normally included in the diffusion approximation.

We report a straightforward and accurate method that overcomes this longstanding, unsolved problem in radiative transport. Our theory properly treats anisotropic photon scattering events and takes the specific form of the phase function into account. As a result, our method correctly predicts the spatially dependent diffuse reflectance of light near the POE for any arbitrary phase function.

9333-9, Session 3

Three dimensional modelling of broadband optical imaging systems using an electromagnetic description of light

Peter R. T. Munro, Sahan Amaratunge, Andrea Curatolo, David D. Sampson, The Univ. of Western Australia (Australia)

Full wave modelling of optical imaging and sensing of macroscopic volumes of tissue has, till now, been unfeasible. Improvements in desktop computers and numerical electromagnetic scattering solvers, make an important class of simulations tractable: the rigorous simulation of image formation of macroscopic volumes of tissue, possessing microscopic scattering features. We have developed the first such rigorous, three-dimensional, model of image formation and applied it to optical coherence tomography (OCT).

This new model minimizes both computer memory requirements and computational complexity. The pseudospectral time-domain (PSTD) method calculates light scattering, for broadband illumination, in a single simulation. This required the development of a method of modelling focused illumination using the PSTD method. A computationally efficient method of calculating the image of scattered light, for each wavelength of interest, integrated within the PSTD simulation was also developed.

This model can be used either for directly simulating image formation in OCT, or for calculating parameters such as the scattering coefficient and anisotropy factor of particular refractive index distributions, the generation of which remains an important problem to be solved with the help of this model.

We will present the key components of our model and show examples of simulated OCT images for both numerical phantoms and a refractive index model of the epidermis that we are currently developing. We will also show examples of how our model can be applied to comprehensively compare the OCT imaging properties of Bessel and Gaussian beams in the presence of specimen induced aberration.

9333-10, Session 3

Spectroscopic microscopy characterization of subdiffractive surface roughness with FDTD validation

Di Zhang, Northwestern Univ. (United States); Ilker R. Capoglu, Halliburton Co. (United States); Lusik Cherkezyan, Hariharan Subramanian, Allen Taflove, Vadim Backman, Northwestern Univ. (United States)

Despite the fundamental diffraction limit of optical microscopy, we had previously established that three-dimensional subdiffractive refractive-index(RI) fluctuations of a linear, label-free dielectric medium can be sensed in the far zone with spectroscopic microscopy. However, the air-media interface was assumed to be flat. To expand the capabilities of this technique to characterizing RI fluctuations of rough dielectric media, we investigated the spectral signature of a far-zone microscope image of samples with nanoscale surface roughness. Although light scattering from rough surfaces has been well investigated, the spectral characteristics

of reflectance intensity have not been clearly described and validated. In this investigation, the general expression for spectral component of a microscope image from rough surface($I_s(k)$) was derived to quantify the statistics of nanoscale surface fluctuations. Assuming an exponential spatial correlation of height, we created numerical models of homogenous dielectric media with random surfaces. Using the proposed models, the expression was further validated with finite difference time domain (FDTD) method. Far-zone bright-field microscope image were both numerically synthesized from the expression and obtained from FDTD simulation. $I_s(k)$ calculated from the proposed theory agreed with that from FDTD simulation. Furthermore, we showed that by analyzing $I_s(k)$ we can quantify the statistics of nanoscale surface roughness of a homogenous dielectric medium. This study has significant impact in understanding and quantifying internal RI fluctuations in dielectric media (such as in biological cells) with subdiffractive surface roughness as well as in quantifying the changes in nanoscale surface roughness of biological cells during pathophysiological conditions such as in cancer.

9333-11, Session 3

Monte Carlo estimators of absorption for radiative transport in turbid media: theory and analysis (Invited Paper)

Carole K. Hayakawa, Univ. of California, Irvine (United States) and Beckman Laser Institute and Medical Clinic (United States); Jerome Spanier, Beckman Laser Institute and Medical Clinic (United States); Vasan Venugopalan, Univ. of California, Irvine (United States) and Beckman Laser Institute and Medical Clinic (United States)

Monte Carlo solutions to the Radiative Transport Equation (RTE) are used broadly in biomedical optics for their ability to accommodate any tissue geometry and absorption and scattering properties. Within these simulations, optical absorption is accounted for through the use of different estimators or random variables. We provide a rigorous derivation of commonly used estimators that account for absorption differently within a stochastic model that is equivalent to the RTE. We provide a comparative analysis of these estimators to identify the optical property and spatial regimes under which these estimators provide superior performance, in terms of error and computational efficiency.

9333-12, Session 4

Propagation of coherent polarized light in turbid tissue-like scattering medium (Invited Paper)

Igor V. Meglinski, Alexander Doronin, Callum M. Macdonald, Univ. of Otago (New Zealand)

Coherence and polarization of light are fundamental properties of laser radiation that have been attracting great attention during the last decade. This is due to both a diversity of beautiful physical phenomena associated with multiple scattering of light, and a potential to use these phenomena for diagnostic purpose in various applications in modern medicine. In current presentation, we discuss a recent progress in modeling of coherent polarized light propagation in highly scattering turbid media, such as biological tissues. The developed modeling approach is used for imitation of major phenomena of multiple scattering of light, such as the universal decay of the temporal correlation function (TCF) and the enhancement of coherent back-scattering (CBS). The temporal coherence of light, linear and circular polarization, interference, and the helicity flip of circularly polarized light due to reflection at the medium boundary and/or scattering are taken into account. The results of simulation for coherent linearly and circularly polarized light are presented in comparison with the results of known theoretical solutions and the results of alternative models.

**Conference 9333:
 Biomedical Applications of Light Scattering IX**

9333-13, Session 4

On the photon diffusion coefficient: the role of the absorption and persistence length

H. Günhan Akarçay, Martin Frenz, Jaroslav Ricka, Univ. Bern (Switzerland)

Indubitably, in most biomedical applications where knowledge on the light propagation is paramount, the diffusion approximation has become an unavoidable model, given its relative simplicity. Yet, an essential parameter to the diffusion approximation is the so-called “photon diffusion coefficient” (D_p), the definition of which has, over the past decades, been subject to numerous discussions as to whether the absorption of the medium in which the light propagates should be taken into account or not. Absorption dependence of D_p follows from an approximation of the equation of the radiative transfer, but this seems to contradict the phenomenological intuition based on the Fick’s law.

An alternative approach consists in retrieving the diffusion model from a more physical/microscopic point of view, by using the concept of random walks. In this contribution, we use the latter and combine the statistical random walk model with concepts in line with polymer physics to determine D_p . We emphasize here the meaning of the “mean free transport path”, or “persistence length”, which unequivocally depends on the absorption properties of the material. Empirical support is provided with time of flight simulations on various sample types.

9333-14, Session 4

Investigation of the best model to characterize diffuse correlation spectroscopy measurements acquired directly on the brain

Kyle Verdecchia, Lawson Health Research Institute (Canada); Mamadou Diop, Keith St. Lawrence, Lawson Health Research Institute (Canada) and The Univ. of Western Ontario (Canada)

Diffuse correlation spectroscopy (DCS) is a non-invasive optical technique capable of monitoring tissue perfusion changes, particularly in the brain. The normalized temporal intensity autocorrelation function generated by DCS is typically characterized by assuming that the movement of erythrocytes can be modeled as a Brownian diffusion-like process instead of the expected random flow model. Carp et al. [Biomedical Optics Express, 2011] proposed a hybrid model, referred to as the hydrodynamic diffusion model, to capture both the ballistic and diffusive nature of erythrocyte motion. The purpose of this study was to compare how well the Brownian diffusion and the hydrodynamic diffusion models characterized DCS data acquired directly on the brain, avoiding the confounding effects of scalp and skull. Data were acquired from four pigs during normocapnia (39.8 ± 0.8 mmHg) and hypocapnia (22.1 ± 1.0 mmHg) with the DCS fibers placed 7 mm apart, directly on the cerebral cortex. The hydrodynamic diffusion model was found to provide a consistently better fit to the autocorrelation functions compared to the Brownian diffusion model and was less sensitive to the chosen start and end time points used in the fitting. However, the decrease in cerebral blood flow from normocapnia to hypocapnia determined was similar for the two models (-44.1 ± 5.6 % for the Brownian model and -43.5 ± 6.8 % for the hydrodynamic model), suggesting that the latter is reasonable for monitoring flow changes.

9333-15, Session 4

Modeling scattering in turbid media using the Gegenbauer phase function

Katherine W. Calabro, William Cassarly, Synopsys, Inc. (United States)

The choice of scattering phase function is critically important in the modeling of photon propagation in turbid media, particularly when the scattering path within the material is on the order of several mean free path lengths. For tissue applications, the single parameter Henyey-Greenstein (HG) phase function is known to underestimate the contribution of backscattering, while phase functions based on Mie theory can be more complex than necessary due to the multitude of parameter inputs. In this work, the two term Gegenbauer phase function is highlighted as an effective compromise between HG and Mie, as demonstrated when fitting the various phase function to measured data from phantom materials. Further comparison against the Modified Henyey-Greenstein (MHG) phase function, another two term function, demonstrates that the Gegenbauer function provides better control of the higher order phase function moments, and hence allows for a wider range of values for the similarity parameter, g . Wavelength dependence of the Gegenbauer parameters is also investigated using a range of theoretical particle distributions. Finally, extraction of the scattering properties of solid turbid samples from angularly resolved transmission measurements is performed using an iterative Monte Carlo optimization technique. Fitting results using Gegenbauer, HG, MHG, and Mie phase functions are compared.

9333-16, Session 5

Multiple imaging modalities applied via digital Fourier microscopy to assess apoptosis in living cells

Vincent M. Rossi, Oregon State Univ. (United States) and Oregon Health & Science Univ. (United States); Steven L. Jacques, Oregon Health & Science Univ. (United States)

Digital Fourier Microscopy is used in transmission mode in order to collect the Fourier transform of scattered light from samples. A Mach-Zehnder interferometer is used to introduce a reference arm, which recombines with the sample arm in order to create an interference pattern at the CCD. This interference pattern is used in order to regain phase information from the sample and thereby create a hologram of the sample. Upon regaining the sample’s phase information, multiple imaging modalities are applied and compared in order to assess scattering and morphological properties within the sample. Numerical refocusing techniques for Digital Holography are used in order to create a 3D projection of the sample. Quantitative Phase Imaging is also used in order to map the sample phase back to its 3D structure, thereby gaining sub-resolution structural information. In addition, spatial filtering is applied digitally to the collected Fourier transform prior to recreating the sample via an inverse Fourier transform. This method allows for a digital application of Optical Scatter Imaging in order to gain sub-resolution information about sources of scattering within the sample. Optical Scatter Imaging results can then be mapped back to 3D structure from the numerical refocusing technique. Samples investigated include calibration standards, polystyrene microspheres embedded in epoxy and living cells in culture. In order to assess the ability of these multiple modalities to detect morphological changes within cells at the sub-resolution scale, cells are imaged prior to and post induction of apoptosis, specifically looking for mitochondrial swelling as a result.

**Conference 9333:
Biomedical Applications of Light Scattering IX**

9333-17, Session 5

Determining the optimal system parameters to detect organelle size changes in individual cells using angular domain elastic scattering

Ashley E. Cannaday, Dustin W. Shipp, Janet Sorrells, Andrew J. Berger, Univ. of Rochester (United States)

Determining the optimal system parameters to detect organelle size changes in individual cells using angular domain elastic scattering

This project's goal is to monitor non-nuclear organelle size distributions in individual cells using angular-domain, forward-directed elastic scattering. Here, using simulated data from Mie theory, we investigate how the choices of angular range and minimum angle influence the uncertainty in estimated organelle size parameters, e.g. means and standard deviations. Additionally, we examine how the finite number of mitochondria in single cells can reduce the information about sizes that can be extracted. Based upon these simulations, we suggest how to optimize an angular-domain cell-monitoring system within a given set of optical constraints.

9333-18, Session 5

Differentiation of tissue type ultrastructure using wide field imaging of sub-diffuse scattering parameters (*Invited Paper*)

Stephen C. Kanick, David M. McClatchy III, Venkataramanan Krishnaswamy, Jonathan T. Elliott, Keith D. Paulsen, Brian W. Pogue, Thayer School of Engineering at Dartmouth (United States)

This study will present a novel approach to use high frequency structured light to image quantitative maps of scattering parameters in turbid media that are relevant to anisotropic transport in the sub-diffusion regime. Monte Carlo simulated data are used to develop a mathematical model of demodulated reflectance intensity in terms of reduced scattering coefficient, a metric of the higher moments of the scattering phase function termed gamma, and the sampled spatial frequency. A model-based inversion approach is developed that uses reflectance measured at multiple spatial frequencies to break the similarity relationship between the parameters that define scattering frequency and directionality. The approach is experimentally validated in Intralipid-based tissue phantoms with a range of lipid percentages (0.6-1.8 % lipid) returning accurate spectral images of both reduced scattering coefficient (over 0.4-1.8 mm⁻¹) and gamma (1.4-1.75). The approach is used prospectively to differentiate between tissue types and revealing contrast that is not readily observable by diffuse imaging. This optical imaging approach has the potential to provide wide-field tissue contrast based on sub-microscopic tissue structures.

9333-19, Session 6

Depth-sensitive measurements of oral epithelial tissue with oblique polarized reflectance spectroscopy

Maria J. Bailey, The Univ. of Texas at Austin (United States); Sylvia F. Lam, Catherine F. Poh, The BC Cancer Agency Research Ctr. (Canada); Adam R. Gardner, Vasan Venugopalan, Univ. of California, Irvine (United States); Konstantin V. Sokolov, The Univ. of Texas M.D. Anderson Cancer Ctr. (United States)

Early detection can dramatically reduce morbidity rates for cancer in the oral

cavity but screening techniques are limited by the non-specific symptoms associated with oral cancer progression. Benign inflammatory conditions appear very similar to premalignant and malignant lesions. Additionally, cancer in the oral cavity can be especially challenging to identify due the highly variable thickness of the epithelium and an overwhelming presence of keratinization. Optical spectroscopic methods have shown immense potential in detecting epithelial precancers by extracting alterations in optical properties in human tissues. Unfortunately, the concurrent, depth-dependent morphological and biochemical changes that occur in superficial tissue layers with precancer complicate the interpretation of spectroscopic signals as collected spectra are typically a mixture of signals from a range of depths. Furthermore, while the epithelium is thin and optically transparent, the stroma underneath is thick and turbid causing spectroscopic signals to be dominated by the scattering and hemoglobin absorption of the stromal tissue. Our group has developed oblique polarized reflectance spectroscopy (OPRS) to accommodate variations in epithelial thickness while effectively discriminating scattering signals from different tissue layers by combining polarization gating, oblique collection geometry, and multiple beveled fibers. We demonstrate the clinical relevance of OPRS by identifying pronounced spectral differences between various diagnostic categories in oral cancer patients. We report promising clinical results from an OPRS probe that have instantaneously collected polarized reflectance signals from multiple depths in epithelial tissue. Additionally, to obtain absolute reflectance, a novel two-step calibration procedure was performed using tissue-mimicking calibration phantoms.

9333-21, Session 6

Quantifying the effect of age on foveal form birefringence

Joel A. Papay, Ann E. Elsner, Indiana Univ. (United States)

Polarimetric imaging reveals structures in the eye that cannot otherwise be seen with standard scattered light imaging. It is useful for quantifying changes that occur in the birefringent tissues of the eye, including but not limited to the cornea and Henle fiber layer. The axons of the cone photoreceptors are displaced radially and outward from the foveal center in the central macula. The systematic interaction of the form birefringence from these axons and the cornea leads to a characteristic pattern called the macular bow-tie. Changes in these structures can be indicative of disease. Using a confocal polarimeter (GDx), we took foveal centered scans with 20 different polarization states for 120 normal subjects, 20 per decade, aged 20-80 yr., with equal numbers of males and females in each age group. Using Matlab, we calculated the phase retardation differences among groups over a 7.5 degree field of view. Phase data were weighted pixel by pixel by the amplitude at that location, for the crossed and parallel detectors separately. The coefficient of variation of each diametric measurement, along cone axon paths, was computed. The mean of the coefficient of variation (0.15-0.26) for all of the diametric measurements for a given eye for the crossed detector did not change systematically as a function of age. This is in contrast with previous work with $p < 0.0002$ for diabetics vs. controls. Therefore the diabetic data do not represent premature aging nor are aging norms essential for these measurements.

9333-22, Session 6

Deep spectroscopic imaging of burns in human skin using multiply scattered light

Adam Wax, Jason R. Maher, Duke Univ. (United States); Jina Kim, Howard Levinson, Duke Univ. Medical Ctr. (United States); William J. Brown, Duke Univ. (United States)

Scattering can limit the penetration depth of many optical imaging techniques. Several optical techniques in development offer potential for deeper tissue imaging but can present their own limitations. In particular, scattering based contrast can provide information on tissue health instead of relying on fluorescence or absorption makers. We have developed a

**Conference 9333:
Biomedical Applications of Light Scattering IX**

new method for deep imaging of tissue properties based on spectroscopic analysis of multiply scattered light. The technique, multispectral multiple scattering low coherence interferometry (ms²/LCI), uses coherence and spatial gating to produce images of tissue optical properties up to 9 mm deep, with millimeter scale resolution. We have demonstrated imaging in tissue properties in phantoms and shown the ability to discriminate burned tissues using ms²/LCI. Assessment of burns is an unmet clinical problem with millions of burns reported each year yet clinical judgment of burn depth is only 70% accurate. In ongoing studies, the capabilities of ms²/LCI for characterizing burn severity have been more carefully defined using progressive burns in ex vivo human skin samples, with controlled thicknesses and composition. These results will help evaluate how ms²/LCI can be used to assess burn depth and progression in the clinic.

9333-23, Session 7

Determination of the reduced scattering coefficient from 3D imaging of thick tissues by second harmonic generation microscopy *(Invited Paper)*

Paul J. Campagnola, Gunnsteinn Hall, Kevin W. Eliceiri, Univ. of Wisconsin-Madison (United States)

Both optical scattering measurements and Second Harmonic Generation (SHG) microscopy have shown great promise for disease characterization and diagnostics by probing structural aspects of collagen organization. For example, the spectral slope of reduced scattering coefficient μ_s' is related to scatterer size and organization. Similarly, initially emitted SHG radiation directionality (e. forward-backward ratio) is related to sub-resolution fibril size and distribution. Here we present a new method to determine both these parameters on a SHG microscope, where by two parameter fitting, both can be simultaneously obtained from the best fits between 3D experimental data and Monte Carlo simulations. The improved simulation framework accounts for collection apertures for the detected forward and backward components. For validation, we applied the new simulation framework to mouse tail tendon and show that the obtained spectral slope of μ_s' obtained is the similar as from bulk optical measurements and that the (FSHG/BSHG) creation values are similar to previous results from our lab. We also apply the measurements and analysis to human ovarian cancers and compare the results to bulk measurements. The overall applicability of the approach to different tissues types is also discussed. As both the spectral slope of μ_s' and (FSHG/BSHG) creation have been linked to the underlying tissue structure which can differ in diseased tissues, simultaneously obtaining these parameters on a microscope platform from the same tissue from a single measurement provides a powerful method for tissue characterization, without the need for bulk measurements.

9333-24, Session 7

Video-rate dual polarization multispectral endoscopic imaging

Anne Pigula, Neil T. Clancy, Shobhit Arya, George B. Hanna, Daniel S. Elson, Imperial College London (United Kingdom)

Linear polarization imaging often uses light polarized in a fixed direction, which provides limited information about anisotropy. Here is presented a multispectral polarization endoscope with dual illumination polarizations to identify vascular and structural changes in tissue physiology.

A stereo endoscope with dual illumination channels was fitted with a custom polarizing filter so the illumination channels were linearly polarized orthogonally to each other while an optical chopper switched between the illumination sources at a maximum frequency of 45 Hz. A pair of high-speed cameras simultaneously recorded both co- and cross-polarized (CO and CR) images synchronized with the two illumination polarization states, and a triple bandpass filter with peaks at 470, 535, and 635 nm isolated spectral

bands in the blue, green, and red regions respectively. A single acquisition cycle produced four images, which were registered with an intensity-based feature recognition algorithm. The degree of linear polarization (DoLP) isolated the signal from superficially-reflected, polarization-maintaining photons and provided a measure of depolarization.

Validation experiments were conducted on targets with known optical properties, including diffuse and specular reflectors, linear polarizers, birefringent materials, absorbing and scattering phantoms, and in vivo on superficial blood vessels in the skin and in porcine abdomens. Comparisons between wavelength bands highlighted the superficial vasculature in various porcine organs. With DoLP measurements, the system was able to identify isotropic depolarization, and by comparing DoLP responses for the two illumination polarization states, it was possible to identify anisotropic responses in both ex vivo and in vivo models.

9333-25, Session 7

Monte Carlo based investigation of berry phase for depth resolved characterization of biomedical scattering samples

Justin S. Baba, Oak Ridge National Lab. (United States); Vijay Koju, Dwayne John, The Univ. of Tennessee Knoxville (United States)

The propagation of light in turbid media is an active area of research with relevance to numerous investigational fields' e.g. biomedical diagnostics and therapeutics. The statistical random-walk nature of photon propagation through turbid media is ideal for computational based modeling and simulation. Ready access to super computing resources provide a means for attaining brute force solutions to stochastic light-matter interactions entailing scattering by facilitating timely propagation of sufficient (1 million or more) photons while tracking characteristic parameters based on the incorporated physics of the problem. One such model that works well for isotropic scattering but fails for anisotropic scatter, which is the case for many biomedical sample scattering problems, is the diffusion approximation. In this report, we address this by utilizing Berry phase evolution as a means for capturing anisotropic scattering characteristics of samples for the preceding depth where the diffusion approximation fails. We extend the polarization sensitive Monte Carlo method of Ramella-Roman, et al., to include the computationally intensive tracking of photon trajectory in addition to polarization state at every scattering event. To speed-up the computations, which entail the appropriate rotations of reference frames, the code was parallelized using openmp. The results presented reveal that Berry phase is strongly correlated to the photon penetration depth, thus potentiating the possibility of polarimetric depth resolved characterization of highly scattering samples, e.g. biological tissues.

9333-26, Session 7

Nanophotonic force microscopy: measuring particle-surface interactions using near-field photonics

Perry Schein, Pilgyu Kang, David Erickson, Cornell Univ. (United States)

Here we present a technique for measuring and characterizing interactions between colloidal particles and surfaces using the distribution of intensities of the scattered light as they interact with the evanescent field at the interface between a photonic device and a liquid medium. Particle-surface interactions play an important role in dictating the stability of colloidal suspensions, which can be critical in the quality control of many pharmaceutical products. The challenge in characterizing these interactions involving particles with sizes on the order of tens to hundreds of nanometers is that the forces involved are small, often on the order of single piconewtons and below.

**Conference 9333:
Biomedical Applications of Light Scattering IX**

Our technique works by using a microfluidic channel to flow target particles over a photonic crystal resonator. The particle undergoes Brownian motion about the equilibrium position between the optical gradient force and the surface forces. As it moves up and down in the evanescent field, the particle scatters more light when it is closer to the surface. Using the Boltzmann distribution, we relate the scattered light intensity to the relative potential energy as a function of height, and take the derivative of this to measure the force. We can subtract the known optical gradient force that we apply, giving a direct measurement of the particle-surface force as a function of separation distance. The highly localized optical intensity provided by the resonator enables us to measure much smaller particles than other light-scattering techniques. We report measurements of sub-pN forces on sub-100 nm particles in solutions of varying salt concentration.

9333-27, Session 7

Characterizing protein aggregation by observing confined Brownian fluctuations in a near-field optical trap

Dakota O'Dell, Perry Schein, Pilgyu Kang, David Erickson, Cornell Univ. (United States)

Aggregation of misfolded proteins is a critical challenge facing the development of novel protein therapeutics, as protein aggregates have been shown to reduce drug efficacy and lead to dangerous immune responses. Unfortunately, the causes of aggregation are not fully understood, and the ability for regulators to screen for and detect nanoscale protein aggregates is currently limited. Here, we present a novel technique for detecting and characterizing protein aggregates in free solution using near-field light scattering from a nanophotonic waveguide.

This technique works by analyzing the interaction of aggregates in a protein solution with a silicon nitride optical waveguide in a microfluidic channel. When a protein aggregate enters the evanescent field of the waveguide, an optical gradient force will attract the aggregate and hold it stably above the waveguide surface. This optical force will be proportional to the aggregate's volume and polarizability. By localizing the light scattered by the aggregate and tracking position fluctuations in the scattered light over time, we can determine the spring constant of the confined Brownian motion, and use a model of the optical force to determine the volume of the trapped aggregate. Because we take a series of high-throughput single particle measurements, this method is more suitable for highly polydisperse protein samples than ensemble dynamic light scattering measurements. In addition, we are also able to trap and detect protein aggregates as small as tens of nanometers because of the high optical power density in the waveguide relative to light-sheet methods.

9333-28, Session 7

Novel techniques for refractive index determination of single nanoparticles in suspension

Edwin van der Pol, Frank A. W. Coumans, Anita N. Böing, Academisch Medisch Centrum (Netherlands); Auguste Sturk, Rienk Nieuwland, Univ. van Amsterdam (Netherlands); Ton G. van Leeuwen, Academisch Medisch Centrum (Netherlands)

Background: The refractive index (RI) of nanoparticles (<500 nm) is an indispensable property in a wide range of applications. The RI relates light scattering to the size, shape, and chemical composition of nanoparticles. However, currently no method is capable of determining the RI of single nanoparticles in suspension.

Method: We have developed three novel methods to determine the RI of single nanoparticles in suspension. We measured the diameter and light scattering of nanoparticles by (1) dark-field microscopy, (2) multi-angle flow

cytometry, and (3) resistive pulse sensing combined with backscattering microscopy. For each method, we quantified light scattering using beads of known properties and solved the inverse light scattering problem by Mie theory. The method was validated on a mixture of 200 nm, and a mixture of 400 nm polystyrene (RI=1.63) and silica beads (RI=1.45). We applied each method to derive the RI of human cell-derived vesicles.

Results: Based on the RI, we have distinguished 200 nm and 400 nm silica beads from similar-sized polystyrene beads. The RI of silica and polystyrene beads were in agreement with the specifications and had an uncertainty <3%. The mean RI of human urinary vesicles was 1.37 at 405 nm.

Conclusions: We have demonstrated the use of dark-field microscopy, multi-angle flow cytometry, and resistive pulse sensing to determine the RI of single nanoparticles in suspension, such as cell-derived vesicles. The RI of vesicles is essential to data interpretation and standardization and may be utilized to distinguish vesicles from similar-sized particles in body fluids.

9333-29, Session 8

Wavelet transform a/LCI analysis of ex vivo tissue for detection of cervical dysplasia

Derek Ho, Tyler K. Drake, Adam Wax, Duke Univ. (United States)

Angle-resolved low coherence interferometry (a/LCI) is an optical biopsy technique that obtains depth resolved angular profiles of scattered light to determine nuclear morphology, and offers a promising approach for detection of epithelial cancers. Previously, we have described a size determination algorithm using the continuous wavelet transform (CWT) of the a/LCI angular scattering profile. Experimental size determination was demonstrated with polystyrene beads and cells with significant improvement in computation speed compared to the Mie theory based algorithm that is currently used.

We now present the application of a/LCI in the detection cervical dysplasia on ex vivo tissue biopsies from patients undergoing cervical cone biopsy and validate the wavelet transform size determination algorithm on clinical samples. Twenty-three biopsy sites were analyzed at the basal layer 200 μm deep within the tissue. Both Mie theory and CWT-based nuclear sizing algorithms are used to determine the nucleus diameter in the tissue, and the results are compared to establish the sizing accuracy of the CWT based algorithm. In addition, morphological results are co-registered to histopathological diagnosis of the same sample. Using Mie theory based sizing, the nuclear diameter was determined to be significantly larger for dysplastic tissue compared to healthy tissue ($p=0.002$). These biopsies were classified retrospectively using the determined nuclear diameter with 100% sensitivity (3/3), 90% specificity (18/20), and an overall accuracy of 91.3% (21/23).

9333-30, Session 8

Speckle formation in optical coherence tomography: computational study and experiment

Valentin Demidov, Univ. of Toronto (Canada); Alexander Doronin, Univ. of Otago (New Zealand); I. Alex Vitkin, Univ. of Toronto (Canada); Igor V. Meglinski, Univ. of Otago (New Zealand)

Optical Coherence Tomography (OCT) is well established imaging modality capable of acquiring cross-sectional images of turbid media, including biological tissues, utilizing back scattered low coherent light. The obtained OCT images include characteristic repetitive patterns known as speckles. Currently, there is a growing interest to the OCT speckle patterns due to their potential application for quantitative analysis of optical properties of

**Conference 9333:
 Biomedical Applications of Light Scattering IX**

probing scattering medium. In current report we consider the mechanism of OCT speckle patterns formation for the time-domain and swept source OCT approaches and introduce a new Monte Carlo based model for simulation of OCT signals and images. The Monte Carlo model takes into account polarization and coherent properties of light, mutual interference of back-scattering waves and their interference with the reference waves. The developed model is employed for simulation of OCT image, analysis of OCT speckle formation and interpretation of the experimental results.

9333-31, Session 8

OCT signal model for discrete random media

Mitra Almasian, Nienke Bosschaart, Ton G. van Leeuwen, Dirk J. Faber, Academisch Medisch Centrum (Netherlands)

BACKGROUND: When healthy tissue becomes malignant, it undergoes morphological changes, which result in a change of the scattering properties. With OCT, these scattering properties are quantified by obtaining the attenuation-coefficient through curve fitting. Commonly, a higher attenuation-coefficient is correlated with malignant tissue. However, the relation between scattering properties and sample properties, e.g. size and organization, is not well understood. Our goal is to find expressions for the OCT-signal in terms of sample properties.

METHOD: The OCT-signal (Santec InnerVision 1000 OCT system, 1300 nm) from monodisperse Silica beads with a mean diameter of 0.5, 0.8, 1.0 and 1.5 μm suspended in water for a dilution series ranging from 0.02 to 0.2 volume fraction is recorded. The attenuation-coefficient and backscatter-coefficient are derived from the data by, respectively, a single decay fit and speckle variance measurements. The OCT-signal of these samples is modelled using Mie-theory combined with the Percus-Yevick formalism to account for dependent scattering, which originates from the organization of the scatterers. The Extended Huygens-Fresnel model is used to describe the contribution of multiple scattering.

RESULTS: Experiment and simulation for the monodisperse samples are in excellent agreement. We will continue the validation of our work using poly-disperse samples. Results will be presented at the conference.

CONCLUSION: Mie theory combined with Percus-Yevick formalism and the Extended Huygens-Fresnel model is a valid model for samples of discrete random media. The organization of the scatterers has a significant influence on the OCT signal and is well described by our model.

9333-32, Session 8

Efficient signal processing in spectroscopic optical coherence tomography

Maciej Kraszewski, Michal Trojanowski, Marcin R. Strakowski, Gdansk Univ. of Technology (Poland)

Spectroscopic optical coherence tomography (SOCT) is an extension of a standard OCT technique, which allows to obtain depth-resolved, spectroscopic information on the examined sample. It can be used a source of additional contrast in OCT images e.g. by encoding certain features of the light spectrum into the hue of the image pixels. However, SOCT is based on time-frequency analysis of the interferometric signal. The most popular SOCT signal processing method – the short time Fourier transform (STFT) require calculation of hundreds of Fourier transform for each OCT A-scan. This makes generation of SOCT image very time-consuming. Computation time of an SOCT image can be over ten times slower than computation time of the standard OCT image, which may not allow for real-time imaging. Here, we present algorithm for an efficient signal processing in SOCT. The algorithm is based on the fact that the spectroscopic contrast can be obtained directly from the time-domain OCT scan without the need for computing the STFT or any other time-frequency distribution. Additional

speed-up is obtained using the recursive processing of subsequent parts of the OCT scan. The presented results show that over tenfold reduction of computation time can be obtained. This makes proposed algorithm a good solution for real-time spectral imaging using the OCT method.

9333-33, Session PSun

Analysis of water spread dynamics in human skin with near-infrared imaging

Hideobu Arimoto, National Institute of Advanced Industrial Science and Technology (Japan); Mariko Egawa, Shiseido Research Ctr. (Japan)

We investigate the dynamic water spread in human skin by near-infrared microscopic imaging using an originally developed microscope system. Water spread dynamics in the skin is important factor to evaluate the cosmetic products in its use and individual skin properties. For the quantitative evaluation of the water spread in the skin, both the time-lapse water spread dynamics and microscopic structure of the skin surface have to be measured simultaneously. To measure the time-lapse water spread, we acquire the microscopic water images sequentially at the wavelength of strong water absorption such as 1920 nm and discriminate water area from other tissue area by an image processing algorithm focusing on the absorption difference. The skin surface structure, on the other hand, is analyzed from the same image sequence acquired with the originally designed illumination which enables high-contrast skin surface structure imaging. With the help of light penetration depth estimation which is obtained from the Monte Carlo light transport simulation, we analyze the water spread dynamics in the skin taking account of the depth profile.

9333-34, Session PSun

Stokes vs. Jones: comparing two independent polarized Monte Carlo programs

H. Günhan Akarçay, Univ. Bern (Switzerland); Ansgar Hohmann, Alwin Kienle, Univ. Ulm (Germany); Martin Frenz, Jaroslav Ricka, Univ. Bern (Switzerland)

This study aims at investigating the similarities and differences between the Jones and Stokes-Mueller formalisms when modeling polarized light propagation with numerical simulations of the Monte Carlo (MC) type, which have gained significant importance for the development of medical diagnostics tools. We consider light propagation/detection of both pure and partially/totally unpolarized states. The latter case involving fluctuations, or “depolarizing effects”, is of special interest here: Jones and Stokes-Mueller are equally apt to model such effects.

We present simulation results yielded by two independent MC programs: one developed in Bern with the Jones formalism and the other implemented in Ulm with the Stokes notation. The simulated polarimetric experiments involve suspensions of polystyrene spheres with varying size, taking reflection and refraction at the sample/air interfaces into account. The simulated dataset will be made available online, for we deem it to constitute a valuable reference for other groups developing MC programs. Both programs yield identical results when propagating pure polarization states; yet, with unpolarized illumination, second order statistical differences appear, thereby highlighting the pre-averaged nature of the Stokes parameters. This study not only clarifies the misleading belief according to which “Jones cannot treat depolarizing effects”, but also serves as a validation for the two programs.

Indeed, the verification of such programs is a rather laborious task, mainly because of: (i) the lack of a golden standard, (ii) the difficulty to quantitatively compare simulations to experiments, (iii) and the complexity/diversity of definitions and conventions employed. The suitability of either model to different purposes is also discussed.

**Conference 9333:
Biomedical Applications of Light Scattering IX**

9333-35, Session PSun

A sub-diffuse tomography algorithm for blood vessels detection during brain biopsy needle using Monte Carlo computed photon path lengths

Julien Pichette, Andr anne Goyette, Marie-Andr e Tremblay, Ecole Polytechnique de Montr al (Canada); Gilles Soulez, Ctr. Hospitalier de l'Univ. de Montr al (Canada); Fr d ric Leblond, Ecole Polytechnique de Montr al (Canada)

One of the main risks associated with brain needle biopsies is hemorrhaging due to clipping blood vessels during tissue extraction. This procedure is necessary in order to determine the pathological nature of lesions (e.g. brain tumors) in order to inform the choice of treatment, possibly including surgical resection. In order to improve safety, we present a new optical spectroscopy technique using multiple diffuse reflectance signals to detect blood vessels based a 360-degrees reconstruction of the tissue surrounding the needle in terms of the optical contrast associated with hemoglobin absorption.

Monte Carlo Simulations (MCS) are performed to evaluate the sensitivity of the algorithm and to optimize the imaging geometry. Full tomographic data are obtained by simulating the different laser injection points with their respective detection points, with appropriate pre-defined source and detector sizes and numerical apertures. The optical needle geometry is modeled by a tetrahedral mesh and simulations are performed using Mesh-based Monte Carlo (MMC). Different cases (12, 24, 32 fibers) are studied. Their performance is evaluated with MMC for realistic blood vessel distributions using 3D computed tomography images of pig brains. Blood vessel detection is achieved via a novel approach exploiting rescalable MCS to recover the absorption based on computed photon path lengths. A least mean square approach for non-linear systems is used to minimize the discrepancy between measured and computed sinograms. The method can recover the absorption coefficients as well as the concentration of oxygenated and deoxygenated haemoglobin using multispectral data.

9333-36, Session PSun

Computational hair quality categorization in lower magnifications

Barmak Heshmat, Hayato Ikoma, Ik Hyun Lee, MIT Media Lab. (United States); Krishna Rastogi, MIT Media Lab. (United States) and PES Institute of Technology (India); Ramesh Raskar, MIT Media Lab. (United States)

Human scalp hair quality can be detected with industrial polarimetry techniques, SEM, and different spectroscopic techniques. The hair quality can be classified thoroughly by extensive spectroscopy and analysis of the essential components in hair down to molecular level. The current instruments for analyzing hair quality, however, are rather bulky and relatively expensive. Unfortunately the variations in the mechanical features of cuticles of healthy and damaged hairs are rather small (submicron). Therefore, strong objectives with large numerical apertures are necessary to fully resolve these features; moreover the images should be visually inspected with a trained eye to categorize the hair.

We take advantage of hair specific geometry to visualize sparse submicron cuticle peelings with tip-side highly oblique illumination. We experimentally demonstrate that the statistics of the scattering peaks from these features can directly estimate the hair quality in much lower magnifications (down to 20X) when the features themselves are below the system resolution.

After signifying these sparse features with optics we use a feature extraction method (blob detection in this case) and then calculate the density quality and area ratio of these features. We show that multiplication of these two

parameters gives the "Damage level" parameter that can estimate the hair quality.

The technique was applied to sample sets of healthy and damaged (96 hour UV exposed) hairs with different colors. Our computational categorization of black, blond, and grey hair samples is successful in all cases. Therefore, this technique has strong potential for lower cost, portable, and autonomous hair diagnostic apparatuses.

9333-37, Session PSun

Accuracy of experimental data and Monte Carlo simulation lookup table-based inverse models for assessment of turbid media optical properties with diffuse reflectance spectroscopy

Peter Naglic, Maksimilijan Bregar, Miran B rmen, Bo?tjan Likar, Franjo Pernu?, Univ. of Ljubljana (Slovenia)

Diffuse reflectance spectroscopy (DRS) is a popular method for non-invasive assessment of optical properties in turbid media (e.g. biological tissue). The optical properties are extracted from the acquired DRS spectra using various quantitative models. Light propagation in turbid media is often described by the diffusion approximation of the Boltzmann transport equation. While the diffusion approximation offers analytical solutions for simple geometries, it is sufficiently accurate only under quite restrictive assumptions. More accurate results, independent of the underlying geometry and medium optical properties, can be obtained by the Monte Carlo simulation of photon migration in turbid media. A lookup table based model, relying solely on a set of training DRS spectra collected from a set of phantoms with well-defined optical properties, is becoming increasingly popular. Although the individual quantitative models have been extensively studied, there is a significant lack of objective inter-model comparison in the field of biomedical optics.

In this study, we objectively compare the accuracy of the optical properties estimated by the three above listed quantitative models for DRS spectra acquired by fiber optic probes. For this purpose, two sets of turbid homogeneous phantoms with exactly defined optical properties are prepared. The first phantom set is used for calibration of the analytical or numerical models and for the creation of the look-up table. Subsequently, the second phantom set is used to test the inverse models and quantitatively compare the extracted optical properties. Finally, the inverse models are also tested on biological tissue samples.

9333-38, Session PSun

Parallel Monte Carlo code for simulation of propagation of light in segmented 3D structures of adult human head obtained by MRI

Stanislaw Wojtkiewicz, Adam Liebert, Institute of Biocybernetics and Biomedical Engineering (Poland)

We have developed an effective parallel Monte Carlo (MC) code for simulation of light propagation in structures obtained by MRI. The code is designed to execute parallel threads on a Linux-based cluster of computers equipped with multiple graphical processing units (GPU) utilizing NVIDIA CUDA technology. The cluster consists of two computers equipped with three GPUs each and is fully scalable. The memory size of the GPUs allows us to discretize an adult human head with voxels of 0.3mm in size (about 140e6 voxels).

In series of MC simulations we obtained 3D distributions of the sensitivities of statistical moments of distributions of time of flight of photons (DTOF) obtained at the surface of the head model to changes in the absorption

**Conference 9333:
Biomedical Applications of Light Scattering IX**

coefficient occurring in different voxels of the structure. Calculations of time-resolved light propagation in the MRI structure of the head (consisting of segmented substructures: skin, skull, CSF, gray matter and white matter) for evenly spaced (20mm) 52 sources and 61 detectors at the head model surface is performed with a speed of 1.2e6 photon packets per second.

The developed MC code allows us to: (i) calculate DTOFs and distributions of time of arrival of fluorescence photons detected at the surface of the head model, (ii) estimate distributions of visiting probabilities of light at excitation wavelength and (iii) distributions of generation probabilities of fluorescence photons, (iv) effectively calculate series of the above parameters to simulate different inflow and washout of a fluorescence dye for each of the head substructures.

9333-39, Session PSun

Scatterers shape effect on speckle patterns

Valentin Denisenkov, Vadim V. Kiyko, A. M. Prokhorov
General Physics Institute (Russian Federation) and
National Research Univ. of Information Technologies,
Mechanics and Optics (Russian Federation); Gleb V.
Vdovin, Technische Univ. Delft (Netherlands) and National
Research Univ. of Information Technologies, Mechanics
and Optics (Russian Federation)

Laser speckle analysis is a very powerful method with various existing applications, including biomedical diagnostics. The majority of the speckle applications are based on analysis of light scattered only by surface or transmitted through a layer of the sample. Speckle-based analysis usually makes use of dependence of scattered light intensity distribution from sizes of the scatterers. We propose a numerical model of multiple-layer scattering media in one-dimension which shows that properties of the scattered light are strongly dependent on the form of the scatterers. In particular, the dependence of number of speckles from the size of the scatterers was investigated for the light reflected from the surface with varying roughness; the single roughness on the surface was assumed to have the form of one-dimensional 'pyramid' with the sides having either linear or parabolic descent from the top of the 'pyramid' to the bottom. It was found that for the linear roughness, number of speckles decreased with increase of the roughness size, whereas for the parabolic roughness the number of speckles increased. Results of numerical simulation were compared with experiment investigations of roughness samples (0.5-20 μm) made of glass and copper. Due to different production processes, the glass samples have the parabolic roughness and copper samples have the linear roughness. Experiments show that the dependences of number of speckles also have different slopes as in numerical simulation. These findings can lead to new analytical methods capable of determining not only the size distribution of roughness (or scatterers) but also the shape.

9333-40, Session PSun

Numerical modeling of photon migration in the cerebral cortex of the living rat using the radiative transport equation

Hiroyuki Fujii, Hokkaido Univ. (Japan); Shinpei Okawa,
National Defense Medical College (Japan); Ken Nadamoto,
Eiji Okada, Keio Univ. (Japan); Yukio Yamada, The Univ. of
Electro-Communications (Japan); Yoko Hoshi, The Tokyo
Metropolitan Institute of Medical Science (Japan); Masao
Watanabe, Hokkaido Univ. (Japan)

A determination of the optical properties in biological tissues is one of the fundamental tasks for bio-optical imaging such as diffuse optical tomography. The determination desirably is obtained by using the

technique of inverse problem based on the radiative transport equation (RTE). However, a numerical solution of the RTE requires tremendous computational loads. Thus, this study constructs accurate and efficient modeling and calculation in biological tissues based on the three-dimensional time-dependent RTE. Then, the delta-Eddington approximation for the scattering phase function is employed to reduce computational load.

In our previous study, the cerebral cortex (ca 2mm thick) in the living rats has been measured at the source-detector spacing of 1.25mm by using near-infrared time-resolved spectroscopy. Also, the optical properties of the rat cerebral cortex have been determined by using a look-up table method based on a Monte Carlo simulation of photon migration on the assumption that the cerebral cortex is a homogeneous object. These measured profiles by experiments and optical properties are used to examine the validity of the present model.

The time-resolved profiles of the detected light intensity calculated by the constructed model are shown to agree well with the profiles experimentally obtained. It is also shown that the delta-Eddington treatment is valid for highly forward-directed scattering. The number of discrete ordinates is appropriately reduced to the half of the calculation without the treatment.

9333-41, Session PSun

Advanced Monte Carlo simulator of the polarization-sensitive optical coherence tomography systems

Maciej Kraszewski, Michal Trojanowski, Jerzy Plucinski,
Marcin R. Strakowski, Gdansk Univ. of Technology (Poland)

Simulating the optical coherence tomography (OCT) systems using the Monte Carlo method is a widely explored research area. However, there are several difficulties that need to be overcome in order to properly model the OCT imaging with the Monte Carlo algorithm. First of all the temporal and the spatial coherence of the scattered light need to be considered, since OCT is based on the interference phenomenon. For the same reason, the polarization state of the scattered light need to be calculated. Moreover, the OCT systems use the light beam that can be described by the Gaussian beam model. However, such beams cannot be directly simulated using the standard Monte Carlo algorithm. Different research groups have developed simulators dealing with some of these problems but the Monte Carlo simulator which considers all of them has not been published yet. Here we present the Monte Carlo program allowing to simulate OCT images of heterogeneous light scattering structures. The presented program considers all of the listed problems and allows to model complex sample geometries with layer boundaries described by a set of polygons. To our knowledge, it is the most advanced OCT simulator that was ever published.

9333-42, Session PSun

Biodynamic imaging of pharmacodynamics and time-dependent effects in 3D tissue

Hao Sun, Purdue Univ. (United States)

Biodynamic imaging uses coherence-gated digital holography to explore biodynamics and biomechanics in living 3D tissues by measuring intracellular motions inside their natural microenvironments. The information content of biodynamic imaging is displayed through tissue dynamics spectroscopy (TDS), which captures and displays changes in Doppler signatures from intracellular constituents in response to applied therapeutics. The affected dynamic intracellular mechanisms include organelle transport, membrane undulations, cytoskeletal restructuring, strain at cellular adhesions, cytokinesis, mitosis, exo- and endo-cytosis among others. In this paper, biodynamic imaging is applied to study pharmacokinetics/pharmacodynamics (PK/PD) which predicts and monitors the effect and efficacy of drug doses over time. The PK/PD of multicellular tumor spheroids have not previously been studied in three dimensions. Tumor spheroids have become important in early drug discovery because

Conference 9333:
Biomedical Applications of Light Scattering IX

they recapitulate in vitro many of the three-dimensional characteristics of in vivo tissues and their response to applied therapeutics. For instance, tumor spheroids have spatial heterogeneity due to the avascular growth that produces the spatial structure of a proliferating shell surrounding a hypoxic or necrotic core. Numerical simulations predict the time dependent response of the core relative to the shell of moderate-sized spheroids in which hypoxic stress in the core predisposes the core tissue to stronger PD responses, especially to cytotoxic compounds. A time-dependent study using biodynamic imaging of the physical processes that affect drug distribution and physiological effects in 3D spheroids captures time-series drug responses that depend on dose and cell line as well as on the initial conditions of the heterogeneous spheroid tissue.

9333-43, Session PSun

Electric field Monte Carlo study of coherent complex light in turbid media

Xiuwei Zhu, Xiaolei Lin, Zili Cao, Bixin Zeng, Wenzhou Medical Univ. (China); Min Xu, Fairfield Univ. (United States)

Complex light such as Bessel beam carries orbital angular momentum (OAM) and is diffractionless. Due to these properties, complex light has been widely applied in various fields, such as manipulation of microscopic objects, microscopy, and optical tweezers. In particular, Bessel beam has been shown to achieve significantly higher penetration depth in light-sheet microscopy.

In this presentation, we present here the numeric study of the propagation of polarized coherent Bessel beam in highly scattering turbid media with Electric field Monte Carlo (EMC) approach. EMC is one unique Monte Carlo method suitable for simulating coherent phenomenon of multiple scattering light. EMC has been extended to explicitly incorporate the complex incident wave front of coherent complex light and account for the mutual interference in Monte Carlo simulations. We applied EMC to investigate the interaction of coherent complex light with highly scattering turbid media such as biological tissue. The dependence of the decay of the beam intensity and the loss of the phase singularity over the penetration depth on the orbital angular momentum of the complex light and the scattering properties of a turbid medium will be reported. The performance of Bessel beam will be compared to that of a Gaussian beam. The potential application of complex light in imaging turbid media will also be discussed.

Conference 9334: Optical Methods in Developmental Biology III

Saturday - Sunday 7-8 February 2015

Part of Proceedings of SPIE Vol. 9334 Optical Methods in Developmental Biology III

9334-1, Session 1

Visualizing dynamic neuro-vascular interactions during vertebrate development (*Invited Paper*)

Paul M. Kulesa, Mary C. McKinney, Stowers Institute for Medical Research (United States)

Embryonic cell migration and cell sorting are dynamic properties utilized to shape neuro-vascular structures during vertebrate development. Unfortunately, limitations in cell labeling and molecular interrogation of two distinct cell populations simultaneously within the embryo has proved challenging. Here, we use the neural crest and endothelial cell interplay to study embryonic neuro-vascular patterning. We combine state-of-the-art dynamic in vivo imaging and 3D gene profiling in transgenic quail embryos that allow us to collect multi-scale data in the same embryo. We have discovered that neural crest and endothelial cells share common migratory pathways in the head and interact to sort into distinct structures. We hypothesize that there is a dynamic interplay between endothelial and neural crest cells that includes a role for distinct molecular signals to shape the neuro-vascular anatomy during vertebrate craniofacial morphogenesis. We will discuss examples of the complex cell behavioral and molecular analyses.

9334-2, Session 1

Mapping conduction velocity of early embryonic hearts with robust fitting algorithms

Shi Gu, Yves T. Wang, Pei Ma, Case Western Reserve Univ. (United States); Andreas A. Werdich, Brigham and Women's Hospital (United States); Andrew M. Rollins, Michael W. Jenkins, Case Western Reserve Univ. (United States)

Cardiac conduction maturation is an integral component of heart development. Optical mapping with voltage sensitive dyes allows sensitive measurements of these electrophysiological properties. However, traditional image processing methods are unsatisfactory in obtaining quantitative conduction velocity measurements from early embryonic hearts, due to the low signal-to-noise (SNR) ratios. Here, we present a novel image processing method based on least squares optimizations, without the need for temporal/spatial filtering or averaging. First, an action potential trace at each pixel is fit to a curve consisting of two cumulative normal distribution functions. The activation time is determined based on the fit, and the spatial-activation time gradient is determined with a 2D linear fit over a square-shaped area. The size of the area is adaptively enlarged until the fit parameters can be determined within a preset precision range. Finally, the conduction velocity is calculated based on the activation time gradient, averaged over several consecutive heartbeats, and further corrected for 3D geometry that can be obtained by optical coherence tomography imaging. We validated the approach against published activation potential traces with artificially generated noise, to simulate different SNR conditions on a tubular shaped digital phantom that resembled the tubular heart. This method proved to be robust, even at very low SNR (SNR=2-5) conditions. We also established an empirical equation to estimate the maximum conduction velocity that can be accurately measured under different conditions (e.g. temporal sampling rate, SNR, and pixel size). Finally, we demonstrated consistent high-resolution conduction velocity maps of quail embryonic hearts at a stage of looping.

9334-3, Session 1

Optical stimulation and inhibition in cardiac development

Yves T. Wang, Matthew T. McPheeters, Case Western Reserve Univ. (United States); Stephanie Ford, Case Western Reserve Univ. (United States) and Univ. Hospitals Case Medical Ctr. (United States); Shi Gu, Michiko Watanabe, Andrew M. Rollins, Michael W. Jenkins, Case Western Reserve Univ. (United States)

Optical control techniques are a promising new technology that enables both stimulation and inhibition, using pulsed infrared light to apply heat with high spatial precision. We can use optical control to both pace and stop early embryonic hearts without contact or genetic manipulation in in vivo and ex vivo preparations.

Optical control was applied with either a multi-mode laser with a 600- μm core fiber and lens or a single-mode laser focused to 12 μm . Optical stimulation enabled increased heart rates in vivo by 1:1 pacing, resulting in increased cardiac output, decreased stroke volume to a lesser degree, increased regurgitant flow, and altered shear stress. Further, when 2-day quail embryos were paced for 9 cycles of alternating 10 minutes of pacing at 1.25 Hz above the sinus rate and resting at the sinus rate, cardiac and body morphology defects develop by the next day, similar to those observed in fetal alcohol syndrome and neural crest cell ablation models.

Optical inhibition was demonstrated to be feasible in both in vivo and ex vivo 2-day quail embryos. Inhibition was induced with spatial specificity, enabling block of either initiation at the atrium or propagation through the ventricle. This would allow induction of cardiac arrest, which could be useful for imaging a still heart, and heart block, which would alter hemodynamics and may be useful as a model.

Optical control is a promising technology for controlling heart rate, enabling studies of the effects of hemodynamics and cardiac imaging in vivo.

9334-4, Session 1

Longitudinal optical coherence microscopy reveals the functional role of a circadian gene, cryptochrome, in drosophila heart development

Aneesh Alex, Lehigh Univ. (United States); Airong Li, Massachussetts General Hospital (United States); Xianxu Zeng, Zhan Zhang, The 3rd Affiliated Hospital of Zhengzhou Univ. (China); Rudolph E. Tanzi, Massachussetts General Hospital (United States); Chao Zhou, Lehigh Univ. (United States)

Circadian rhythms have been related to cardiovascular function and pathology. However, to date there has been no report on the role of circadian rhythm genes in heart development and function in a whole animal throughout its lifecycle in vivo. In this study, we used *Drosophila melanogaster* as the model organism to investigate the functional role of a circadian gene, cryptochrome, in heart development. *Drosophila* cryptochrome (dCry) encodes for a component of the circadian clocks dedicated to the resetting of circadian rhythms. We have developed an ultrahigh resolution optical coherence microscopy (OCM) system, which was capable of providing M-mode images of *Drosophila* heart at a frame rate of 128 Hz with axial and transverse resolutions of 1.5 μm and 4 μm ,

**Conference 9334:
Optical Methods in Developmental Biology III**

respectively. This OCM system was used for longitudinal analysis of both functional and morphological changes in the *Drosophila* heart in the same specimen throughout its post-embryonic lifecycle. Notably, heart rate (HR) and duty cycle showed significant variations during the pupa stage, while heart remodeling took place. We silenced dCry by RNAi in the *Drosophila* heart and mesoderm, and quantitatively determined the functional effect of dCry in heart throughout its development. Silencing of dCry resulted in slower HR, reduced heart duty cycles, smaller heart chamber sizes, pupal lethality and phenotypes related to segment polarity. Collectively, our studies using OCM have provided novel evidence that the circadian clock gene, dCry, plays an essential role in heart morphogenesis and function.

9334-5, Session 1

Structural and functional measurements of the embryonic heart after cardiac neural crest ablation

Pei Ma, Shi Gu, Leina Lunasco, Michael W. Jenkins, Michiko Watanabe, Andrew M. Rollins, Case Western Reserve Univ. (United States)

Cardiac neural crest cells (CNCC) play a critical role in the pathogenesis of various congenital heart diseases in human, such as DeGeorge, CHARGE, and Fetal Alcohol Syndrome. Although the exact mechanism is not fully understood, early changes in hemodynamics have been proposed as a potential mechanism. Ablation of premigratory CNCC in avian embryos has created reliable models for CNCC-related diseases, reproducing symptoms such as persistent truncus arteriosus (PTA), double outlet right ventricle and other great artery defects. Previous studies using video microscopy, ultrasound or histology lacked necessary resolution, contrast or 3D information therefore failed to provide accurate or comprehensive measurements, especially for early tubular hearts, or small structures (such as the valves) in the four-chambered hearts. Optical coherence tomography (OCT) is well suited for these applications due to its high resolution, adequate penetration range (can be further extended with optical clearing), noninvasiveness and functional imaging capability (Doppler OCT). We laser-ablated the CNCC of quail embryos at stage HH8-9 and later imaged the heart both structurally and functionally at either late looping stages (stage HH19-20) or four-chambered heart stages (stage HH34-35). At late looping stages, CNCC-ablated embryos exhibited increased retrograde blood flow, abnormal pulsed-Doppler trace pattern, abnormal looping morphology and cushion structure (including defective atrioventricular cushion closure, and reduced outflow tract cushion coverage), and abnormal body flexure. We also observed PTA and great artery defects at the four-chambered stage as expected, with additional defects in the shape, size and position of cardiac valves that were not reported by previous studies.

9334-6, Session 2

In vivo wide-field imaging reveals unexpected mechanisms of organ formation (*Invited Paper*)

Charles D. Little, The Univ. of Kansas (United States); Brenda Rongish, Andras Czirok, The Univ. of Kansas Medical Ctr. (United States); Michael B. Filla, Univ. of Kansas Medical Ctr. (United States); Rusty Lansford, Children's Hospital Los Angeles (United States)

Primitive animals that do not form tissues or organs have the same number of genes as humans; i.e., the two genomes are about the same size. If the information needed to make organs and tissues is not directly encoded in DNA where does it reside?

We hypothesize that tissue and organ formation is largely an emergent process and that the "missing" information resides in a complex biomechanical code. Our data point to emergent mechanisms that rely on 1)

tissue-scale movements, plus 2) modulation of the biomechanical properties of embryonic tissues.

To test our hypothesis, we use experimental perturbations, time-lapse imaging and computational approaches to examine live quail embryos. We record de novo tissue and organ morphogenesis using fluorescent markers of cells and ECM fibers — we then analyze the motion of both cells and ECM. By comparing the trajectories of ECM fibers to cell displacements we can quantify cell "migration" versus tissue motion (cells+ECM). Particle image velocimetry of fluorescent markers (ECM and Cells) is an unbiased method of measuring pixel drift of each component and whether the values differ. Based on thousands of recordings and computational analyses of tissue formation 75-85% of morphogenetic motion in early bird embryos is not by individual cell homing, but by tissue displacements (cells+ECM). Further, the data show that the morphogenetic displacements occur at tissue-level length scales (> 0.1mm to 5.0mm).

These empirical data support our hypothesis that much of morphogenesis is not genetically hard-wired, but is an, emergent, collective activity — similar to the building of a hornet's nest.

9334-7, Session 2

Using SPIM to track the development of the focal power of the zebrafish lens

Laura Young, Miguel Jarrin, Christopher D. Saunter, Roy Quinlan, John M. Girkin, Durham Univ. (United Kingdom)

The zebrafish is a useful model organism for 3D imaging; it is transparent and develops quickly. It is therefore ideal for tracking developmental changes in vivo, such as the formation of the eye lens, which typically occurs within four days post fertilisation (Greiling and Clark 2009).

Selective plane illumination microscopy (SPIM) is a 3D imaging using a sheet of light to optically section the sample in vivo. (Huisken, Swoger, Del Bene, Wittbrodt, and Stelzer 2004). A cylindrical lens focuses collimated light in one dimension, producing a sheet that is relayed to the sample via an objective lens.

Any optical power within the sample will additionally refract the light sheet passing through it. This could cause undesirable effects such as broadening or bending of the sheet and can create shadows in the image. In this paper we use this effect to our advantage, harnessing it to measure the optical power of the eye lens in vivo. In the non-focusing dimension of the sheet the eye lens itself focuses sheet at a distance of one focal length. This focusing is observed through the fluorescence it excites in the tissue behind the eye. We use this phenomenon to track the development of the optical power of the zebrafish lens.

Huisken, J. et al. (2004). *Science* 305(86), 1007-1009.

Greiling, T. M. and J. I. Clark (2009). *Dev Dyn.* 238 (9), 2254-65.

9334-8, Session 2

Dynamic imaging of preimplantation embryos in the murine oviduct

Jason C. Burton, Shang Wang, Irina V. Larina, Baylor College of Medicine (United States)

Studying dynamic events involved in early preimplantation embryo development and their transport from the ovary to the uterus is of great significance to improve the understanding of infertility and eventually to help reduce the infertility rate. The mouse is a widely used mammalian model in reproductive biology, however, dynamic imaging studies of mouse preimplantation embryos have been very limited due to the lack of proper imaging tools for such analysis. We introduce an innovative approach for three-dimensional imaging and tracking of murine oocytes with optical coherence tomography (OCT) as they exit the ovary and migrate through the oviduct to the uterus. The imaging is performed with spectral-domain OCT system operating at 70 kHz A-scan rate. The resolution of the

**Conference 9334:
Optical Methods in Developmental Biology III**

OCT system is measured to be around 5 microns. We performed three-dimensional tracking of the oocytes through the oviduct during different stages of the estrous cycle with volume acquisition rate at hertz level. The movement of the embryo can be clearly visualized and the velocity vectors can be quantified based on direct mapping of the trajectories. Because cilia movement in the lumen of the oviduct is a major factor in oocyte transport to the uterus, we performed quantitative analysis of the motile cilia activity. To the best of our knowledge, this is the first demonstration of using OCT for dynamic imaging and tracking of the oocytes in the oviduct. Results from our experiments indicate that OCT has great capabilities for dynamic imaging of the oviduct and oocyte tracking, which provides the foundation for future investigations to understand dynamic events during preimplantation stages in normal development as well as in mouse models with impaired cilia activity linked to infertility.

9334-9, Session 2

Monitoring morphology and vibration of zebrafish inner ear for hearing development by swept-source phase-sensitive optical coherence tomography

Jesung Park, Esteban F. Carbajal, Brian E. Applegate, Texas A&M Univ. (United States)

The zebrafish is an attractive model for studying the development of the hearing organ because of its relative transparency and the fact that it has analogous structures to the mammalian middle and inner ear but lacks the active gain of the outer hair cells that distinguish mammalian hearing. Phase-sensitive OCT is an emerging tool for morphological and functional imaging of the hearing organ which we have previously applied to in vivo imaging of the intact mouse cochlea. In the mouse we were able to measure picometer scale vibrations in the organ of Corti. The imaging system is based around a highly phase stable swept-source laser system incorporated into a Mach-Zehnder type interferometer that allows for near shot-noise limited phase measurements. Here we report on the application of this technology to imaging the zebrafish ear. In preliminary ex vivo work we have recorded the first volumetric OCT images of the zebrafish ear which clearly resolve important features including the swim bladder, Weberian ossicles, lagena and saccule. Moving forward we will apply this technology to in vivo imaging of the zebrafish ear characterizing both the morphology and vibratory response to tonal stimulation.

9334-10, Session 2

Quantifying cilia driven fluid flow in animal models of neonatal and pediatric respiratory disease

Ute A. Gamm, Brendan K. Huang, Mansoor Syed, Vineet Bhandari, Mustafa Khoka, Michael A. Choma, Yale School of Medicine (United States)

Premature infants are at high risk for respiratory diseases due to an underdeveloped respiratory system that is very susceptible to infection and inflammation. One critical aspect of respiratory health is the state of the ciliated respiratory epithelium that lines the trachea and bronchi. The ciliated epithelium is responsible for trapping and removing pathogens and pollutants from the lungs and an impairment of ciliary functionality can lead to recurring respiratory infections and subsequent lung damage. Trachea in critically ill premature infants are exposed to a wide range of potential modulators of cilia-driven fluid flow, including pH, infection, and foreign bodies (e.g. endotracheal tubes). As the potential impact of exogenous modulators are incompletely understood, our research aims to close this critical knowledge gap. We are using optical coherence tomography (OCT) to visualize ciliary fluid flow in the tracheae of mice and quantify flow velocities through particle tracking velocimetry (PTV) to

understand the influence of temperature and hyperoxia on the performance of cilia-driven fluid flow. We performed our measurements ex vivo on tracheae of adolescent mice under temperature controlled conditions. Preliminary experiments on 10 mice suggest an effect of temperature on the speed of ciliary fluid-flow; a maximum of ciliary flow was observed at body temperature while lower and higher temperatures showed a decrease (n=10). We are currently testing the influence of hyperoxia on ciliary functionality by exposing live mice to hyperoxia for 21 h (until now n=6) and 65 h (until now n=3) before harvesting the trachea.

9334-11, Session 3

An imaging and analysis toolset for the study of *Caenorhabditis elegans* neurodevelopment (*Invited Paper*)

Ryan P. Christensen, Alexandra Bokinsky, National Institutes of Health (United States); Anthony Santella, Memorial Sloan Kettering Cancer Center (United States); Yicong Wu, National Institutes of Health (United States); Javier Marquina, Yale Univ. (United States); Ismar Kovacevic, Memorial Sloan-Kettering Cancer Ctr. (United States); Abhishek Kumar, National Institutes of Health (United States) and Yale Univ. (United States); Peter Winter, Evan McCree, National Institutes of Health (United States); William Mohler, University of Connecticut Health Center (United States); Zhirong Bao, Memorial Sloan-Kettering Cancer Ctr. (United States); Daniel Colón-Ramos, Yale Univ. (United States); Hari Shroff, National Institutes of Health (United States)

How the complete nervous system develops remains mysterious. The *Caenorhabditis elegans* embryo possesses an invariant cell lineage and simple nervous system of ~200 cells, suggesting that the development of each and every neuron can be followed. However, use of *C. elegans* as a neurodevelopmental model has been limited because of its sensitivity to photobleaching and photodamage, fast embryonic movements leading to motion blur, and complex, twisted shape which makes measurement and comparison among different embryos difficult. To examine neurodevelopment in nematode embryos, we have developed a light sheet microscope capable of generating overlapping light sheets from two orthogonal objectives. The high speed and low photobleaching/photodamage offered by this microscope obviates embryo motion and allows us to image nematode embryonic development from the first cell division until hatching, approximately 14 hours. Additionally, the two volume views captured by the microscope can be computationally fused, enabling imaging with 350 nm isotropic resolution. To deal with complex embryonic shapes, we have developed computer algorithms that apply a user-defined lattice marking the nose, tail, and edges of the worm, thereby allowing us to computationally straighten the volume. Straightened volumes can be registered, facilitating comparison and combination of data obtained from different embryos. We will use our microscope and image analysis tools to create an atlas defining the position and morphology of all neurons in the developing embryo, thus providing a first look at the development of an entire nervous system.

9334-12, Session 3

Quantitative analyses for elucidating mechanisms of cell fate commitment in the mouse blastocyst (*Invited Paper*)

Nestor Saiz, Minjung Kang, Memorial Sloan-Kettering Cancer Ctr. (United States); Alberto Puliafito, Candiolo Cancer Institute (Italy); Nadine Schrode, Panagiotis

**Conference 9334:
Optical Methods in Developmental Biology III**

Xenopoulos, Xinghua Lou, Memorial Sloan-Kettering Cancer Ctr. (United States); Stefano Di Talia, Duke University Medical Center (United States); Anna-Katerina Hadjantonakis, Memorial Sloan-Kettering Cancer Ctr. (United States)

Cells of the inner cell mass (ICM) of the mouse blastocyst differentiate into the pluripotent epiblast (EPI) or the primitive endoderm (PrE), marked by the transcription factors NANOG and GATA6, respectively. To investigate the mechanistic regulation of this process, we are applying an unbiased, quantitative, single-cell resolution image analysis pipeline, to analyze embryos lacking or exhibiting reduced levels of these factors. We can infer nuclear concentrations of proteins, as well as levels, and dynamics, of transcription using reporter strains of mice. Our results provide a framework for quantitative analyses of mammalian embryos, reveal the kinetics of cell fate choice, and establish nodal points in the gene regulatory network driving ICM lineage specification.

9334-13, Session 3

Hybrid selective-plane illumination optical and optoacoustic microscopy

Amy Lin, Andrei Chekkoury, Murad Omar, Helmholtz Zentrum München GmbH (Germany); Tobias Schmitt-Manderbach, Timo Mappes, Carl Zeiss AG (Germany); Hernán López-Schier, Daniel Razansky, Vasilis Ntziachristos, Helmholtz Zentrum München GmbH (Germany)

Intravital imaging of large specimens is challenging in essence for postembryonic studies. Selective-plane illumination microscopy (SPIM) has been introduced to volumetrically visualize organisms employed in developmental biology and experimental genetics, it is ideally suited for imaging of transparent samples and can offer fast frame-rate imaging at optical microscopy resolutions with low phototoxicity, but its performance quickly deteriorates when applied to opaque tissues. To overcome this limitation, and due to the inherent robust nature of acoustic propagation against scattering, optoacoustic (photoacoustic) imaging was merged to a custom SPIM system.

Central to the implementation of a hybrid SPIM/MSOM system was a common light-sheet illumination system available to both modalities, generated from a nanosecond pulsed laser tunable in the visible spectrum. A camera was placed orthogonal to the light-sheet for fluorescence imaging, and a high frequency (24MHz) linear ultrasound array transducer with 128 elements, combined with a 125 MSamples/s data acquisition system (DAQ) was used for acoustic detection. The transducer is aligned to the plane of illumination, and by translating the sample through the light-sheet, simultaneous capturing of optical and optoacoustic readouts is possible.

The performance of this hybrid imaging system was characterized in various phantoms. Interrogation of highly scattering juvenile zebrafish revealed the enhanced capacity of this system for high-resolution imaging over extended depths and scattering content, compared to conventional SPIM. We demonstrate an approach enabling the visualization of organisms throughout their entire development, at regimes in which the tissue may become opaque.

9334-14, Session 3

New strategies for multicolor two-photon imaging of developing tissues

Willy Supatto, Pierre Mahou, Ecole Polytechnique (France) and Lab. d'Optique et Biosciences, CNRS (France); Julien Vermot, Institut de Génétique et de Biologie Moléculaire et Cellulaire, CNRS, Univ. de Strasbourg (France);

Karine Loulier, Institut de la Vision, CNRS (France); Nelly Vuillemin, Ecole Polytechnique (France) and Lab. d'Optique et Biosciences, CNRS (France); Katherine S. Matho, Institut de la Vision, CNRS (France); Xavier Morin, Ecole Normale Supérieure (France) and Institut de Biologie, CNRS (France); Jean Livet, Institut de la Vision, CNRS (France); Emmanuel Beaurepaire, Ecole Polytechnique (France) and Lab. d'Optique et Biosciences, CNRS (France)

Multicolor labeling and imaging approaches are increasingly used in developmental biology for a variety of purposes, including tracking cell migration, reconstructing cell lineage and anatomy, or performing both structural and functional investigations. A major challenge is to translate these approaches to the fast imaging of large volumes deep into intact embryonic tissues. Indeed, while point-scanning two-photon microscopy is the most effective approach for deep-tissue fluorescence imaging, its application to high-throughput or high-content imaging is hampered by low pixel rates, challenging multicolor excitation, and potential cumulative photodamage. To overcome these limitations, we report on new strategies to perform high information content imaging and analysis of tissue development based on multiphoton microscopy. We show the combination of new "Brainbow" labeling and analysis strategy with two-photon excitation of several chromophores using wavelength mixing allows investigating the clonal structure of developing central nervous system tissues [1-2]. In addition, we report on the implementation light-sheet illumination with mixed wavelength excitation to perform fast multicolor two-photon imaging with negligible photo-bleaching compared to conventional point-scanning two-photon microscopy [3]. This approach enables us to image the multi-labeled beating heart of a zebrafish embryo at high pixel rate and to reconstruct three-dimensional cell movements with sufficient spatial and temporal resolution to track individual cells during a cardiac cycle.

[1] Mahou et al., Nature Methods 9, 815-818 (2012). [2] Loulier et al., Neuron 81, 505-520 (2014). [3] Mahou et al., Nature Methods 11, 600-601 (2014).

9334-15, Session 4

The immune response in four dimensions *(Invited Paper)*

Matthew F. Krummel, Univ. of California, San Francisco (United States)

No Abstract Available

9334-16, Session 4

Applications of FF-OCT to early embryonic development *(Invited Paper)*

Audrey K. Ellerbee, Stanford Univ. (United States)

No Abstract Available

9334-17, Session 4

Multiplexed FLIM-fret imaging in deep tissue during embryo development

Ming Zhao, College of Optical Sciences, The Univ. of Arizona (United States); XiaoYang Wan, Univ. of Michigan (United States); Yu Li, College of Optical Sciences, The Univ. of Arizona (United States); Weibin Zhou, Univ. of

**Conference 9334:
Optical Methods in Developmental Biology III**

Michigan (United States); Leilei L. Peng, College of Optical Sciences, The Univ. of Arizona (United States)

Recent advances in deep tissue imaging have provided unprecedented tools to study development and diseases within live organisms. However, simple intensity mapping of fluorescent labels are prevalent in such studies, which greatly limits the types of biochemical processes that can be interrogated. Here we present a deep tissue multiplexed functional microscopy technique which combines Fourier multiplexed fluorescence lifetime imaging (FmFLIM) [1] and scanning laser optical projection tomography (SLOT) [2]. This technique simultaneously collects lifetime images of multiple excitation-emission channels as 2D projections at multiple angles. After tomographic reconstruction, 3D fluorescence intensity and lifetime images of multiple fluorophores in live zebrafish embryos are produced at isotropic spatial resolution. Using zebrafish expressing FRET sensors as a model system, we monitored lifetimes of various FRET sensors during zebrafish development and chemical treatment.

In transgenic zebrafish embryos Tg(ENPEP:rtTA Teton:Epac) expressing cAMP FRET biosensor in kidney tubules, spatial lifetime variation of donor lifetime was observed. Upon treatment with cAMP stimulus chemicals, donor lifetime within the whole kidney tubule increased as the result of increased cAMP binding. In transgenic zebrafish embryos expressing both cAMP and Calcium FRET sensors within kidney tubules, we were able to follow the lifetime changes of individual FRET sensor in real time. This technique opens new doors to investigate sophisticated biochemical machineries within the native environment of whole live organisms.

[1] Ming Zhao, Yu Li, Leilei Peng. Optics Express. 22, 10221 (2014).

[2] R. A. Lorbeer, et al., Optics Express. 19, 5419. (2011)

9334-18, Session 4

Comparison of optical projection tomography and optical coherence tomography for assessment of murine embryonic development

Manmohan Singh, Univ. of Houston (United States); Tegya J. Vadakkan, Victor Piazza, Ryan Udan, Baylor College of Medicine (United States); Michael V. Frazier, Trevor Janecek, Univ. of Houston (United States); Mary E. Dickinson, Baylor College of Medicine (United States); Kirill V. Larin, Univ. of Houston (United States) and Baylor College of Medicine (United States)

The murine model is a common model for studying cardiac development in mammals. In this study, we compare the performance of the relatively new method of Optical Projection Tomography (OPT) to Optical Coherence Tomography (OCT) to assess murine embryonic development. OPT can provide full three dimensional structural maps based on autofluorescence or can combine structural images with other fluorescence labeled targets to generate three dimensional function maps. In addition, OPT can provide superior imaging depth compared to OCT. However, OPT requires samples to be fixed, placed in an imaging media such as agar, and then cleared before imaging. OCT does not have this limitation. In this study, we compare the measured sizes of structures such as pericardial wall thickness in embryos from OPT images, OCT images, and ex vivo murine embryos. The data demonstrate the superior capability of OPT for imaging fine structures with high resolution in optically-cleared embryos while only OCT can provide structural and functional imaging of live embryos ex vivo and in utero with a resolution of 8-10 μm .

9334-19, Session 4

Optical clearing of uterus for deep imaging of mouse embryo

Chen Wu, Narendran Sudheendran, Univ. of Houston (United States); Valery V. Tuchin, N.G. Chernyshevsky Saratov State Univ. (Russian Federation); Kirill V. Larin, Univ. of Houston (United States)

Mouse embryo is considered a preferred model for the study of mammalian congenital diseases. Currently, optical coherence tomography (OCT) has become a viable tool to perform the embryonic analysis, with the advantages of high resolution and the capability of in vivo imaging. However, the major challenge of OCT technique for in utero imaging is the penetration depth. The light scattering and absorption within the uterus tissue will lead to the strong attenuation and impose limitation on imaging deep tissues. Tissue clearing is an emerging method for improving the imaging depth. In this study, the uterus horn was dissected out of the female mouse and immersed into saline solution, and then the embryo was kept imaging with OCT every three minutes for half an hour to set the baseline. Saline solution was replaced with the optical clearing agent, and embryo was imaged for another two hours. The OCT images before and after the optical clearing of uterus are compared for the investigation of influence of clearing effect. The result has demonstrated that the use of optical clearing agent can effectively improve the imaging quality and depth.

9334-20, Session 5

Reverse engineering morphogenesis in embryonic epithelia: time-lapse confocal microscopy, laser microsurgery, and force inference from cell shape (*Invited Paper*)

M. Shane Hutson, Holley E. Lynch, Sarah M. Crews, David N. Mashburn, Vanderbilt Univ. (United States); Jim Veldhuis, G. Wayne Brodland, Univ. of Waterloo (Canada)

During fruit fly embryogenesis, the morphogenetic process of germband retraction unwraps two U-shaped epithelia – the amnioserosa and germband – as cells in these tissues undergo complementary cell shape changes. We will discuss methods for assessing whether these cell shape changes are mechanically autonomous or follow the mechanical stresses applied by adjacent cells. These methods include time-lapse confocal microscopy of developing embryos labeled with E-cadherin-GFP, segmentation of these images to determine dynamic cell shapes, and laser-microsurgery to determine the extent and anisotropy with which wounds open. This information is then analyzed by two different approaches to reverse engineer the set of mechanical conditions that would yield the observed cell shapes. In one approach, the details of observed cell and/or wound shapes are quantitatively compared to forward finite element models. These models simulate small patches of epithelia subjected to a wide range of anisotropic external stress and having cells with potentially anisotropic internal cell-edge tensions. The best matches between experiments and models are used to delineate matching combinations of these anisotropies. In the second approach, segmented images of these epithelia are analyzed using the Cellular Force Inference Toolkit (CellFIT) to directly infer the tensions along each cell-cell interface and the in-plane stress within each cell. The combination of these two approaches enables a thorough description of the cellular mechanics that drive cell- and tissue-level morphogenesis during germband retraction.

**Conference 9334:
Optical Methods in Developmental Biology III**

9334-21, Session 5

Optical control of excitable cells (*Invited Paper*)

Michael W. Jenkins, Case Western Reserve Univ. (United States)

Optical control uses pulsed infrared laser light to stimulate or inhibit excitable cells without the need for contact or genetic modification. Optical control has been demonstrated in the peripheral and central nervous systems, the auditory system, and the heart.

Optical stimulation provides many advantages over traditional electrical stimulation. It has higher spatial precision, enabling stimulation of specific locations in the brain and pacing at specific sites on an early embryonic heart. It doesn't produce an artifact from current injection, allowing recordings of electrical activity proximal to the stimulation site using electrodes or optical mapping. Furthermore, it does not require contact, reducing the chance of physical damage. In embryos, optical stimulation allows controlled pacing of the heart, which results in changes in the cardiac output, the stroke volume, the retrograde flow, and the shear stress. These changes result in altered heart and body morphology, similar to those found in ethanol exposure and cardiac neural crest cell ablation models.

Optical inhibition has recently been demonstrated in the nervous and cardiac systems. In nerves, optical inhibition applies to smaller fibers before larger fibers, contrary to electrical inhibition, which allows blocking of sensory neurons before motor neurons. In the embryonic heart, optical inhibition can be used to produce either cardiac arrest or heart block, enabling additional ways to modify hemodynamics and imaging of a temporarily stilled heart.

Optical control is a new technology providing important advantages over other stimulation and inhibition techniques. Its use enables new studies in the neural and cardiovascular systems.

9334-22, Session 5

Lattice light sheet microscopy: imaging molecules, cells, and embryos at high spatiotemporal resolution (*Invited Paper*)

Wesley R. Legant, Howard Hughes Medical Institute - Janelia Farm Research Campus (United States); Bi-Chang Chen, Academia Sinica (Taiwan); Kai Wang, Lin Shao, Eric Betzig, Howard Hughes Medical Institute - Janelia Farm Research Campus (United States)

By definition, living specimens are animate. Therefore, a full understanding of dynamic biological systems will only be obtained by observing them with enough 4D spatio-temporal resolution, and for a sufficient duration, to capture the phenomena of interest. Furthermore, many physiologic behaviors are altered or lost completely when cells are removed from their native in situ multicellular environments and cultured on glass coverslips. Unfortunately, conventional widefield or confocal microscopes are either too slow, lack the spatial resolution, or induce too much photodamage to capture many biological processes, especially when imaging into non-planar specimens such as developing embryos.

To address these limitations, we have developed a new approach for sub-cellular light-sheet microscopy capable of imaging fast three-dimensional (3D) dynamic processes in vivo at signal to noise levels typically obtained only in total internal reflection fluorescence (TIRF) illumination. By utilizing a 2D optical lattice of non-diffracting beams to generate a thin (~400nm full width half maximum) plane of light coincident with the focus of a high NA detection objective, we demonstrate substantial advantages in speed, sensitivity and reduced phototoxicity compared to conventional point scanning and spinning disc microscopes as well as light-sheet microscopes utilizing single Gaussian or Bessel beams. We leverage these advantages to quantitatively image samples ranging over three orders of magnitude in

length scale from single molecules to whole embryos. Specific examples to be presented include: 3D single molecule tracking of fluorescently tagged transcription factors in densely labeled embryonic stem cell spheroids, quantification of 3D microtubule growth dynamics throughout the course of cell division, 3D protein localization throughout the course of dorsal closure in *Drosophila* and in the first cell divisions of *C. elegans* embryos, and 3D super-resolution localization microscopy in Zebrafish.

9334-23, Session 5

Cellular connectivity in the developing embryo: what can we learn from the zebrafish model? (*Invited Paper*)

Andreas A. Werdich, Brigham and Women's Hospital (United States) and Harvard Medical School (United States); Daniela Panakova, Marie Swinarski, Max-Delbrück-Ctr. für Molekulare Medizin Berlin-Buch (Germany); Steven M. Jay, Univ. of Maryland, College Park (United States); M. K. Sabeh, Gabriel Musso, Richard T. Lee, Calum A. MacRae, Brigham and Women's Hospital (United States) and Harvard Medical School (United States)

INTRODUCTION: Understanding the complex logic behind cell-to-cell interaction is a key problem in developmental biology. While the mechanisms that contribute to major cell fate decisions have been extensively studied, the processes that require mechanical, chemical and electrical inputs from neighboring cells to generate a specific functional phenotype have rarely been approached. Heart development is particularly informative for investigating such connectivity because of the complex electrical patterns that are set-up to produce a coordinated contractile response. Studying how these physiological patterns are established in development will provide insights into the mechanisms of arrhythmogenesis and parallel events that occur in other tissues, such as the central nervous system.

METHODS: We used the zebrafish embryo and combined it with fluorescence imaging of transmembrane potentials and calcium concentrations to study the electrophysiological patterning of the developing heart, from the first beat into early adulthood.

RESULTS: We identified significant heterogeneities in electrical impulse propagation in developing myocardium that emerge during chamber formation. While conduction velocity gradients are controlled by wnt-11 signals via a calcium-dependent mechanism, the directionality of electrical propagation relies on endocardial signals. Loss of function of neuregulin-1, a growth factor released from endocardial cells prevented isotropy gradients across the developing chambers and caused unidirectional conduction. Ablation of endothelium reproduced this phenotype suggesting that the endocardium is responsible for the development of conduction isotropy. Our data demonstrate that complex physiological heterogeneities are established within a single epithelial monolayer of developing cardiac myocytes and that they are essential for the normal function of the organ.

9334-24, Session 6

Systematic analysis of structural and functional defects in embryonic lethal mouse mutants (*Invited Paper*)

Mary E. Dickinson, Baylor College of Medicine (United States)

Identifying genes necessary for the normal structural and functional development of the embryo is important not only to develop a deeper understanding of how development is orchestrated but is also fundamental to the identification of genetic and environmental causes of congenital birth defects. As part of the NIH-funded mouse knock out project (KOMP) we are

**Conference 9334:
Optical Methods in Developmental Biology III**

developing a group of 3D and 4D strategies to identify specific structural and functional defects found in a mutants generated in this systematic screen. Utilizing these approaches we have been able to define new phenotypes in both known and novel genes.

9334-25, Session 6

Altered cardiac function: a contributing factor in ethanol-induced congenital heart defects?

Ganga Karunamuni, Shi Gu, Yong Qiu Doughman, Lindsay M. Peterson, Case Western Reserve Univ. (United States); Kersti K. Linask, Univ. of South Florida (United States); Michael W. Jenkins, Andrew M. Rollins, Michiko Watanabe, Case Western Reserve Univ. (United States)

Over 500,000 American women per year report drinking alcohol during pregnancy, with 1 in 5 who binge drink. As high as 54% of live-born children with Fetal Alcohol Syndrome (FAS) can present with congenital heart defects (CHDs). Currently, most studies fail to consider the role of altered cardiac function in producing CHDs, although changes in hemodynamics can profoundly affect cardiac development. We hypothesized that acute ethanol exposure creates early hemodynamic anomalies that contribute significantly to cardiac structural and functional defects. Previously, we employed optical coherence tomography (OCT), a non-destructive imaging modality capable of real-time, micrometer-scale resolution imaging, to analyze early-stage ethanol-exposed embryos that exhibited abnormalities in body flexure, blood flow, shear stress and cardiac cushions during heart looping stages. OCT also allowed for the rapid identification of CHDs in late-stage ethanol-exposed embryos, including ventriculoseptal and conotruncal defects. In addition, we measured luminal diameters which were significantly reduced in three of the five major branching arteries. Outflow and atrioventricular valves were also segmented and were found to significantly decrease in volume after ethanol exposure. To summarize, our findings correlated early cardiac dysfunction with late-stage CHDs. Furthermore, in preliminary rescue trials, the administration of nutritional supplements (choline) improved survival rates in late-stage ethanol-exposed embryos and led to a reduction in structural defects of the head/body. We thus demonstrated that functional analyses using our novel technologies can act as early, accurate gauges of cardiac normalcy and abnormalities, and may provide a platform for the testing of new therapeutic strategies.

9334-26, Session 6

Characterizing the effects of high fat diet on heart development in wild-type and CLOCK mutant drosophila melanogaster using optical coherence microscopy

Xianxu Zeng, The 3rd Affiliated Hospital of Zhengzhou Univ. (China); Airong Li, Massachussetts General Hospital (United States); Aneesh Alex, Fengqiang Li, Lehigh Univ. (United States); Zhan Zhang, The 3rd Affiliated Hospital of Zhengzhou Univ. (China); Rudolph E. Tanzi, Massachussetts General Hospital (United States); Chao Zhou, Lehigh Univ. (United States)

High fat diet (HFD)-induced obesity is a major contributor to diabetes and cardiovascular diseases. We employed an ultra-high resolution optical coherence microscopy (OCM) system to quantitatively analyze the effects of high fat diet on heart development in wild-type (WT) and CLOCK mutant Drosophila. Drosophila melanogaster has been widely adopted as a useful myocardial model for investigating cardiovascular disease mechanisms and relevant gene functions. Using OCM, non-invasive, high-speed, three-dimensional and M-mode images of Drosophila heart was obtained in vivo.

In wild-type Drosophila, we have observed significant decrease in heart rate(HR), end diastolic area (EDA) and end systolic area (ESA) in flies fed with HFD compared to those fed with normal food (NF) for 10 days. CLOCK gene is the first identified mammalian circadian gene and CLOCK mutant mice have a greatly attenuated diurnal feeding rhythm, hyperphagic and obese, and develop a metabolic syndrome of hyperleptinemia, hyperlipidemia, hepatic steatosis and hyperglycemia. To understand the functional role of CLOCK gene in the heart of HFD-fed Drosophila, we also compare the cardiac structural and functional parameters in the control and CLOCK mutant groups fed with NF and HFD. These studies demonstrate the capability of OCM imaging to non-invasively characterize cardiac changes in Drosophila at different developmental stages and to identify functional pathways involved in obesity-related cardiovascular diseases.

9334-27, Session 6

Live dynamic imaging and analysis of developmental cardiac defects in mouse models with optical coherence tomography

Andrew L. Lopez III, Shang Wang, Monica D. Garcia, Christian Valladolid, Baylor College of Medicine (United States); Kirill V. Larin, Univ. of Houston (United States); Irina V. Larina, Baylor College of Medicine (United States)

Understanding mouse embryonic development is an invaluable resource for our interpretation of human embryology. Our research is focused on developing methods for live imaging and dynamic characterization of early embryonic cardiovascular development in mouse models of human diseases and using these methods to study congenital defects in humans through multidisciplinary approaches, which include optical coherence tomography (OCT), live mouse embryo manipulations and static embryo culture, molecular biology, advanced image processing and computational modeling. We have developed an OCT based approach, which can be used for imaging of live early mouse embryos (E7.5 - E10) cultured on the imaging stage and visualizing developmental events with spatial resolution of a few micrometers (less than a size of individual cells) and a frame rate of up to hundreds of frames per second. Doppler OCT and Speckle Variance OCT analyses allows us to visualize microcirculation and analyse blood flow profiles from the earliest stages of circulation. We have successfully used this approach to visualize the structure of the whole embryos, analyze blood flow profiles and reconstruct cardiodynamics in 4D (3D+time). We are now using these methods to study how specific embryonic lethal mutations affect cardiac morphology and function during early development.

9334-28, Session 6

Measuring embryonic aortic arch pulsatile blood flow and shear stress with Doppler OCT

Lindsay M. Peterson, Shi Gu, Ganga Karunamuni, Michiko Watanabe, Michael W. Jenkins, Andrew M. Rollins, Case Western Reserve Univ. (United States)

The morphogenesis of the embryonic aortic arches into the mature great vessels is a complex process of cell migration, remodeling, and regression. During development, the great vessels evolve from six major pairs of aortic arches which sequentially emerge and are selectively reduced and remodeled. These dynamic events are vulnerable to perturbations that may result in congenital heart defects. Hemodynamic forces are known to play a significant role in the dynamic process of aortic arch remodeling. Doppler OCT is a non-contact imaging modality well suited for embryonic imaging due to its high spatial and temporal resolution. We have previously demonstrated that Doppler OCT is capable of measuring absolute blood flow from individual cross sectional images using two-beam scanning.

**Conference 9334:
Optical Methods in Developmental Biology III**

This technique allows for rapid flow measurements over the duration of a heartbeat. Absolute blood flow can then be used to calculate the shear stress along the lumen wall. We have previously established a model of ethanol exposure which has been shown to result in great vessel abnormalities. Here, to investigate the role hemodynamics may play in these abnormalities, we measure blood flow and shear stress in the 3rd aortic arch of control and ethanol exposed embryos. Pulsed Doppler traces are also acquired to measure the percentage of retrograde blood flow. We observed increases in blood flow, shear stress and percentage of retrograde blood flow in the ethanol exposed embryos compared to the control embryos. We believe these increased hemodynamic forces may be the result of a compensatory response to the ethanol exposure.

9334-29, Session PSun

Breathing laser as inertia-free swept source for time-stretch imaging modality

Xiaoming Wei, Jingjiang Xu, Yiqing Xu, Luoqin Yu, Jianbing Xu, Bowen Li, Andy K. S. Lau, Xie Wang, Chi Zhang, Kevin K. Tsia, Kenneth K. Y. Wong, The Univ. of Hong Kong (Hong Kong, China)

Wavelength-swept light source, or simply swept source, gains its popularity in a wide range of biomedical applications, primarily bioimaging. The sweep rate, however, is usually limited by the speed of the mechanical moving parts, typically 10's-100's kHz. We here demonstrate a 11.5-MHz all-fiber breathing laser as inertia-free swept source (BLISS), with an ultra-compact design, for the newly-emerged ultrafast imaging modalities, specially the time-stretch microscopy and optical coherence tomography (OCT). An all-fiber ring configuration composes of only a 0.55x5.5-cm multifunctional optical integrated module, performing the stretched-pulse additive pulse mode-locking with a bandwidth of ~60 nm. The pulse train shows an outstanding temporal stability, e.g., a shot-to-shot intensity variation of 2.1% and power fluctuation of 0.08 dB over 27 hours. The inertia-free wavelength-swept mechanism, via group-velocity dispersion, enables a sweep rate of ~700000000 nm/s—orders-of-magnitude faster than the existing swept sources. For time-stretch microscopy, no averaging is required owing to the stable temporal performance, and real-time high-quality image of the lung tissue is obtained at a frame rate of 11.5 MHz. For OCT application, it exhibits a superior roll-off slope of 4.4-mm/dB, ~38 times better than that of its Fourier-domain mode locking (FDML) counterpart. As a consequence, in vivo time-stretch OCT imaging of biological tissue is demonstrated at an A-scan rate of 11.5 MHz. With a compact configuration and stable performance, the applications of this all-fiber inertia-free laser is not only limited to the time-stretch microscopy and OCT, but also other established research areas, such as real-time single-shot digitizer and time-encoded stimulated Raman microscopy.

9334-30, Session PSun

Approach to quantify two-dimensional strain of chick embryonic heart in early stage based on spectral domain optical coherence tomography

Yuqian Zhao, Shidan Dou, Northeastern Univ. at Qinhuangdao (China); Wenlong Zhu, Qinhuangdao City Harbor Hospital (China); Yi Wang, Northeastern Univ. at Qinhuangdao (China); Tao Xu, Shenzhen Academy of Metrology and Quality Inspection (China); Fengwen Wang, Zhenhe Ma, Northeastern Univ. at Qinhuangdao (China)

The heart undergoes remarkable changes during embryonic development due to genetic programming and epigenetic influences, in which mechanical loads is a key factor. As embryonic research development, an important

goal is to develop mathematical models that describe the influence of mechanics on embryonic heart development. However, basic parameters for the modeling are difficult to acquire since the embryonic heart is tiny and beating fast in the early stages. Optical coherence tomography (OCT) technique provides depth-resolved image with high resolution and high acquisition speed in a noninvasive manner. In this paper, we performed 4D[(x,y,z) + t] scan on the outflow tract (OFT) of the chick embryonic heart at stage of HH18 (~3 days of incubation) in vivo using spectral domain OCT (SDOCT). Parameters such as displacement and geometrical size of the OFT were extracted from the structural images of the SDOCT. Two-dimensional strain vector were solved using strain-displacement relations in curvilinear cylindrical coordinates based on kinetic theory of elasticity. Based on the geometrical size and other initial conditions, two-dimensional elasticity finite element model of the OFT myocardial wall deformation were established and then solved by direct frequency response method. Comparison between experimental data and simulation result shows the utility of the finite element models. Our results demonstrate that mathematical modeling based on parameters provided by SDOCT is a useful approach for studying cardiac development in early stage.

9334-31, Session PSun

Measurement of wall shear stress in chick embryonic heart using optical coherence tomography

Zhenhe Ma, Shidan Dou, Yuqian Zhao, Yi Wang, Northeastern Univ. at Qinhuangdao (China); Tao Xu, Shenzhen Academy of Metrology and Quality Inspection (China); Guangyuan Si, Fengwen Wang, Northeastern Univ. at Qinhuangdao (China)

The cardiac development is a complicated process affected by genetic and environmental factors. Wall shear stress (WSS) is one of the components which have been proved to influence the morphogenesis during early stages of cardiac development. To study the mechanism, WSS measurement is a step with significant importance. WSS is caused by blood flow imposed on the inner surface of the heart wall and it can be determined by calculating velocity gradients of blood flow in a direction perpendicular to the wall. However, the WSS of the early stage embryonic heart is difficult to measure since the embryonic heart is tiny and beating fast. Optical coherence tomography (OCT) is a non-invasive imaging modality with high spatial and temporal resolution, which is uniquely suitable for the study of early stage embryonic heart development. In this paper, we introduce a method to measure the WSS of early stage chick embryonic heart based on high speed spectral domain optical coherence tomography (SDOCT). 4D (x,y,z,t) scan was performed on the outflow tract (OFT) of HH18 (~3 days of incubation) chick embryonic heart. After phase synchronization, OFT boundary segmentation, and OFT center line calculation, Doppler angle of the blood flow in the OFT can be achieved (This method has been described in previous publications). Combining with the Doppler OCT results, we calculate absolute blood flow velocity distribution in the OFT. The boundary of the OFT was segmented at each cross-sectional structural image, then geometrical center of the OFT can be calculated. Thus, the gradients of blood flow in radial direction can be calculated. This velocity gradient near the wall is termed wall shear rate and the WSS value is proportional to the wall shear rate. Based on this method, the WSS at different heart beating phase are compare. The result demonstrates that OCT is capable of early stage chicken embryonic heart WSS study.

9334-32, Session PSun

Improved resolution of optical coherence tomography for imaging of microstructures

Kai Shen, Hui Lu, Michael R. Wang, Univ. of Miami (United States)

Optical coherence tomography (OCT) is a well-known cross-sectional imaging technique that has been increasingly used in the medical and biomedical fields. OCT is attractive due to its advantages in non-invasive imaging and fast image acquisition and processing. When examining fine tissue structures or 3D microstructures, there is a trade-off between OCT lateral image resolution and A-scan depth. Tight focusing can achieve a high lateral image resolution but at the expense of reducing the OCT A-scan depth due to larger beam divergence after focusing. On the other hand, to achieve a greater imaging depth without significant beam divergence the focusing spot size must be somewhat larger, which would result in relatively poorer lateral resolution. The desired high lateral resolution and long OCT imaging depth cannot be attained at the same time because of the Gaussian beam focusing limitation.

We report herein our investigation of OCT image lateral resolution improvement through the use of superresolution technique along with the use of point spread function and deconvolution techniques. By doing so, the focused measurement beam spot size can be kept larger to meet the requirement of minimal divergence during the A-scan measurement. The lateral resolution is improved through the analysis of multiple B-scan images. This is a computational based image quality improvement without relying on hardware improvement on the OCT system. The presented superresolution imaging technique has been applied to examine several microstructure samples and tissues showing its advantages and benefits. The superresolution technique should help expand the applications of OCT imaging systems.

Conference 9335: Adaptive Optics and Wavefront Control for Biological Systems

Saturday - Monday 7-9 February 2015

Part of Proceedings of SPIE Vol. 9335 Adaptive Optics and Wavefront Control for Biological Systems

9335-1, Session 1

Transmissive liquid crystal device correcting the spherical aberrations in laser scanning microscopy

Ayano Tanabe, Hokkaido Univ. (Japan) and Citizen Holdings Co., Ltd. (Japan); Terumasa Hibi, Hokkaido Univ. (Japan); Kenji Matsumoto, Masafumi Yokoyama, Makoto Kurihara, Citizen Holdings Co., Ltd. (Japan); Sari Ipponjima, Hokkaido Univ. (Japan); Nobuyuki Hashimoto, Citizen Holdings Co., Ltd. (Japan); Tomomi Nemoto, Hokkaido Univ. (Japan)

Two-photon excitation laser scanning microscopy has enabled us to visualize deep regions within a biospecimen such as a living mouse brain. However, spherical aberrations induced by refractive-index-mismatch in the optical path degrade fluorescent intensities and spatial resolutions. These aberrations constitute a barrier to observing much deeper regions.

Recently, we developed transmissive liquid crystal devices correcting spherical aberrations without changing the basic design of optical path in a conventional laser scanning microscope. The device inserted in front of the objective lens was applied with an appropriate voltage according to specimen depth to correct spherical aberrations. While the device actually enhanced the axial resolution and the intensity of fluorescent beads at deep regions, those effects were not enough for practical use. In this paper, we simulated more precisely imaging performance through the device and the objective lens, and modified the design of the device. First, in order to evaluate this modification, fluorescent beads were observed by a single-photon excitation laser scanning microscope. The modified device recovered the fluorescence intensity that had reduced down to 60 percent by weak aberrations to 90 percent. Furthermore, even in the case of existing strong aberrations, that had reduced the intensity down to 30 percent, it recovered the fluorescence intensity up to 70 percent. Finally, we introduced the modified device to a two-photon excitation laser scanning microscopy and succeeded in enhancing fluorescent intensities at deep regions of a specimen. Therefore, our device is expected to be useful for observing much deeper regions within biospecimens.

9335-2, Session 1

Controlling the propagation of light in turbid media by polarization modulation

Jongchan Park, Jung-Hoon Park, HyeonSeung Yu, YongKeun Park, KAIST (Korea, Republic of)

The propagation of waves in turbid media results in random speckle patterns due to multiple scattering events which look like stochastic random processes, however since this phenomena is deterministic, it has been shown that the propagation of waves in disordered media can be effectively controlled by wavefront shaping [1]; the spatial phase or amplitude of the incident wavefront can be controlled by employing spatial light modulator or digital micromirror devices, respectively in order to generate desired transmitted wavefronts [2, 3]. Recent advance in wavefront shaping techniques offer many opportunities to exploit the high degree of freedom that is brought on by randomness. However, although those techniques can be used to utilize the randomness of turbid media for functional advantages in research field, the high price of such devices limits the potential applications in industry.

In this work, we demonstrate that polarization modulation of input wavefront can effectively control the spatial profile of the light transmitted

from turbid media. As turbid media completely mix the optical parameters of transmitted waves, polarization states can be effectively used to control the propagation of light through turbid media [4]. The focusing efficiency beyond turbid media were experimentally measured by modulating the polarization states of incident waves with a commercial in-plane switching liquid-crystal display, which is much economical compared to phase-only spatial light modulators. Computer based numerical simulations were also performed, providing well-matched results with experimental results. Due to the high degrees of freedom inherent in turbid media, arbitrary output wavefronts can be generated by our polarization modulation method.

{[1] I. Vellekoop, A. Lagendijk, and A. Mosk, "Exploiting disorder for perfect focusing," *Nature Photonics*, 4(5), 320-322 (2010).

[2] I. M. Vellekoop, and A. Mosk, "Focusing coherent light through opaque strongly scattering media," *Optics letters*, 32(16), 2309-2311 (2007).

[3] D. Akbulut, T. J. Huisman, E. G. van Putten et al., "Focusing light through random photonic media by binary amplitude modulation," *Optics express*, 19(5), 4017-4029 (2011).

[4] J.-H. Park, C. Park, H. Yu et al., "Dynamic active wave plate using random nanoparticles," *Optics Express*, 20(15), 17010-17016 (2012).

9335-3, Session 2

Holographic fluorescence microscopy with incoherent digital holographic adaptive optics (*Invited Paper*)

Changwon Jang, Jonghyun Kim, Seoul National Univ. (Korea, Republic of); David C. Clark, Univ. of South Florida (United States); ByoungHo Lee, Seoul National Univ. (Korea, Republic of); Myung K. Kim, Univ. of South Florida (United States)

Introduction of adaptive optics technology into astronomy and ophthalmology has made great contributions in these fields, allowing one to obtain recover images blurred by atmospheric turbulence or aberrations of the eye. Similar adaptive optics improvement in microscopic imaging is also of interest to researchers using various techniques. Current technology of adaptive optics typically contains three key elements: wavefront sensor, wavefront corrector and controller. These hardware elements tend to be bulky, expensive, and limited in resolution, involving, e.g., lenslet arrays for sensing or multi-actuator deformable mirrors for correcting. We have previously introduced an alternate approach to adaptive optics based on unique capabilities of digital holography, namely direct access to the phase profile of an optical field and the ability to numerically manipulate the phase profile. We have also demonstrated that direct access and compensation of the phase profile is possible not only with the conventional coherent type of digital holography, but also with a new type of digital holography using incoherent light: self-interference incoherent digital holography (SIDH). The SIDH generates complex - i.e. amplitude plus phase - hologram from one or several interferograms acquired with incoherent light, such as LEDs, lamps, sunlight, or fluorescence. The complex point spread function can be measured using a guide star illumination and it allows deterministic deconvolution of the full-field image. We present experimental demonstration of aberration compensation in holographic fluorescence microscopy using SIDH. The adaptive optics by SIDH provides new tools for improved cellular fluorescence microscopy through intact tissue layers or other types of aberrant media.

**Conference 9335: Adaptive Optics and
Wavefront Control for Biological Systems**

9335-4, Session 2

**Computational adaptive optics for
broadband optical interferometric
tomography of biological tissue** *(Invited
Paper)*

 Stephen A. Boppart, Univ. of Illinois at Urbana-Champaign
(United States)

High-resolution real-time microtomography of scattering tissues is important for many areas of biology and medicine. However, the effects of system and sample aberrations, the compromise between transverse resolution and depth-of-field, and low sensitivity deep in tissue continue to impede progress towards cellular-level volumetric tomography. Computed optical imaging techniques have the potential to solve these long-standing limitations. Computational adaptive optics (CAO) and Interferometric synthetic aperture microscopy (ISAM) are computed imaging techniques that enable high-resolution volumetric tomography with aberration-corrected imaging and spatially-invariant resolution, respectively. In CAO, aberration correction is demonstrated in a tomogram, rather than the optical beam of a broadband optical interferometry system. Based on Fourier optics principles, aberrational correction is performed on a virtual pupil using Zernike polynomials. In ISAM, three-dimensional Fourier-domain resampling, in combination with high-speed broadband OCT, is used to achieve high-resolution in vivo tomography with enhanced depth sensitivity over a depth-of-field extended by more than an order of magnitude, in real-time. CAO has the potential to augment or even replace complicated and expensive adaptive optics hardware with algorithms implemented on a standard desktop computer. When used in conjunction with ISAM, this CAO approach offers object reconstruction (within the single scattering limit) with ideal focal-plane resolution at all depths. Interferometric tomography reconstructions are characterized with tissue phantoms containing sub-resolution scattering particles, and in both ex vivo and in vivo biological tissue. Collectively, this work establishes the foundation for high-speed volumetric cellular-level tomography in living tissues.

9335-5, Session 2

**Aberration correction and imaging using
optical eigenmodes** *(Invited Paper)*

 Michael Mazilu, Kishan Dholakia, Univ. of St. Andrews
(United Kingdom)

Optical eigenmodes define a natural representation of the electromagnetic fields. These eigenmodes can be calculated for simple optical systems and importantly they can be experimentally determined and used for adaptive aberration correction and non-redundant imaging. We discuss here the theory behind these modes and how this approach can be used for single bucket imaging, coherent excitation, Raman hyper spectral imaging and aberration correction for turbid media and multimode fibres.

9335-6, Session 2

**GPU accelerated holography for
multimode fiber applications**

 Martin Ploschner, Tomáš Pátek, Univ. of Dundee (United
Kingdom)

We have recently demonstrated a GPU accelerated holographic system for real-time beam-shaping in multimode fibers [Optics Express, Vol. 22, Issue 3, pp. 2933-2947 (2014)]. The system was capable of displaying on-demand oriented cube at the distal end of the fiber at the refresh rate of 50 Hz. However, the key element of the system was an Acousto-Optic Deflector (AOD) that produced points at the distal end of the fiber in time-discrete

intervals thus cancelling the effect of interference between neighbouring points. This removed the interference but also significantly increased system complexity due to the presence of an AOD.

Here, we present an improved system without the added AOD complexity. We remove the undesired interference effects computationally using the GPU implemented Gerchberg-Saxton algorithm. The GPU implementation is two orders of magnitude faster than the CPU implementation allowing video-rate image control at the distal end of the fiber virtually free of interference effects. We discuss the GPU implementation in detail and demonstrate the functionality by displaying, on demand and at the video-rate, images created using several thousands output points.

9335-7, Session 2

**Using speckle to build compact, high-
resolution spectrometers** *(Invited Paper)*

Brandon Redding, Hui Cao, Yale Univ. (United States)

Traditional spectrometers use a grating to disperse light, and the spectral resolution scales with the optical pathlength, imposing a trade-off between device size and resolution. To develop a compact spectrometer without sacrificing resolution we turn to a multimode fiber, where a long pathlength is achieved in a small footprint by coiling the fiber. We use the wavelength-dependent speckle patterns formed by interference between the guided modes of a multimode fiber as a fingerprint to identify the input spectra. The spectral resolution is then determined by the change in wavelength required to produce an uncorrelated speckle pattern, which scales inversely with the length of the fiber. Using a 100 meter long fiber, we resolved two lines separated by 1 pm near $\lambda=1500$ nm. We also achieved broad-band operation (400–750 nm) with a 4 cm fiber with 1 nm resolution. Since the fiber can be coiled into a small volume, the entire device remains compact, lightweight, and low-cost. We applied the same approach of using wavelength-dependent speckle patterns to build an on-chip spectrometer where the device size is particularly limited. In this case, we introduced multiple scattering in a disordered structure by etching holes in a silicon membrane to increase the effective optical pathlength in a fixed footprint. We achieved 0.75 nm resolution at $\lambda=1500$ nm in a 25 μ m radius spectrometer. Such a high-resolution on-chip spectrometer could enable compact, low-cost spectroscopy for portable sensing or increasing lab-on-a-chip functionality.

9335-8, Session 2

**Analysis of the angular span of the optical
phase conjugation phenomenon**

Chia-Ta Tseng, National Taiwan Univ. (Taiwan)

Optical Phase Conjugation (OPC) is a physical phenomenon that may enable propagation of light in reversed directions. We analyze the OPC phenomenon for light propagation through scattering medium. Here we model a light source embedded within a scattering medium emitting a CW light through the scattering medium. The pseudospectral time-domain (PSTD) simulation technique is employed to obtain numerical solutions of Maxwell's equations. Amplitude and phase of the outgoing light is recorded and later used to generate phase-conjugated light which back-propagates through the scattering medium. By changing the angular span of the region of phase-conjugated light, we can analyze back-propagation of light for different angular spans. The simulation results may help determine the optimal angular span for practical back-propagation of light.

**Conference 9335: Adaptive Optics and
Wavefront Control for Biological Systems**

9335-9, Session 3

**Novel real time wavefront sensor in a
SPIM microscope and active tracking of
aberrations in a living animal (*Invited
Paper*)**

 Jonathan M. Taylor, Univ. of Glasgow (United Kingdom);
Christopher D. Saunter, Cyril J. Bourgenot, Gordon D. Love,
John M. Girkin, Durham Univ. (United Kingdom)

Adaptive optics (AO) can potentially allow high resolution imaging deep inside living tissue, mitigating against the loss of resolution due to aberrations caused by overlying tissue. Closed-loop AO correction is particularly attractive for moving tissue and spatially varying aberrations, but this requires wavefront sensing, which in turn requires suitable "guide stars" for use as wavefront references. A number of approaches to this problem have been presented in the literature, but generally approaches are limited to particular applications.

We will present a novel method for generating an orthogonally illuminated guide star suitable for direct wavefront sensing in a wide range of fluorescent biological structures, and present results demonstrating its use for measuring time-varying aberrations, in vivo. By adapting a Selective Plane Illumination Microscope (SPIM) we are able to generate a spatially localized guide star with properties suitable for wavefront sensing. Our technique is applicable in biological tissue with almost arbitrary fluorescent labelling: the only requirement is that there needs to be a minimal separation, of around 10 microns, between fluorescent structures in the sample in at least one dimension, and access for oblique illumination of the target area.

9335-10, Session 3

**Adaptive optimisation of illumination
beam profiles in fluorescence microscopy**

 Thomas J. Mitchell, Christopher D. Saunter, Gordon D.
Love, John M. Girkin, Durham Univ. (United Kingdom)

Optically sectioning fluorescence microscopy techniques have equipped modern developmental biology with an observation toolkit boasting high spatial and temporal resolution. The precision-engineered intensity profiles of the illumination beams required for these imaging methods can unfortunately be heavily distorted by optical mis-alignment and aberrations caused by refractive index mis-matches within the sample and mounting media. Thus the situation arises where optimum performance of the instrument requires the analysis and subsequent adjustment of the illumination beam profile. Though adaptive optics techniques have been used to optimise the illumination beam in confocal fluorescence microscopy, a similar approach has not yet been used for wide-field optically sectioning illumination techniques, such as that used in a single-plane illumination microscope (SPIM). We have investigated the benefits of using adaptive optical elements to alter and optimise the illumination beam shape of a SPIM; the inclusion of a directly addressable optical element that can alter phase or intensity in the illumination beam widens the potential uses of a single microscope system. The corresponding altered illumination beam profiles were recorded using a custom-made high dynamic range beam profiling device that we developed for beam analysis in fluorescence microscopy. We present the results of our investigation and describe the development of the beam profiling device.

9335-11, Session 3

**Adaptive optics STED microscopy in thick
biological tissue**

Mary Grace M. Velasco, Yale Univ. (United States); Edward

 S. Allgeyer, Yale School of Medicine (United States);
Emil B. Kromann, Yale Univ. (United States); Travis J.
Gould, Bates College (United States); Daniel Burke,
Martin J. Booth, Univ. of Oxford (United Kingdom); Joerg
Bewersdorf, Yale School of Medicine (United States)

Super-resolution microscopy techniques have realized sub-diffraction limit resolution on the order of tens of nanometers. For thick samples such as tissue sections, stimulated emission depletion (STED) microscopy is the preferred super-resolution method due to its basis on a confocal laser scanning geometry that provides optical sectioning. To achieve super-resolution, STED microscopy incorporates a high-intensity "donut-shaped" laser focus into a conventional confocal setup. If this focus is super-imposed onto the diffraction-limited focus of the excitation laser, fluorophores at the periphery of the excitation focus will be quenched via STED while those in the center can still fluoresce. In this way, the effective point-spread function is engineered to a sub-diffraction size.

The quality of the donut is critical to achieving super-resolution via STED. If the intensity in the donut center is non-negligible, fluorescence will be suppressed in that region as well, thus negating any resolution enhancement. This is of particular concern when attempting 3D STED in thick tissue sections since sample-induced aberrations compromise the quality of the donut shape and impose a practical limit on the maximum depth to which one can image. To overcome this constraint, we employ adaptive optics to correct specimen-induced aberrations. Using spatial light modulators and a novel image quality feedback metric, we demonstrate on-the-fly correction of the random aberrations introduced by a thick tissue sample. This implementation of adaptive optics can be modified for use in in vivo neuroimaging via STED, which has to date been limited to the superficial layers of the mouse cortex.

9335-12, Session 3

**Closed-loop optimized phase masks
for extended-depth-of-field light-sheet
microscopy**

 Omar Palillero-Sandoval, ICFO - Instituto de Ciencias
Fotónicas (Spain) and Instituto Nacional de Astrofísica,
Óptica y Electrónica (Mexico); Omar E. Olarte, Jordi
Andilla, ICFO - Institut de Ciències Fotòniques (Spain);
Luis Raúl Berriel-Valdos, J. Félix Aguilar, Instituto Nacional
de Astrofísica, Óptica y Electrónica (Mexico); David
Artigas-García, Pablo Loza-Alvarez, ICFO - Institut de
Ciències Fotòniques (Spain)

Most of the more relevant problems in biological sciences require fast three-dimensional (3D) imaging of living samples. Some advanced optical methods, such as spinning-disk confocal microscopy and Light-sheet fluorescence microscopy (LSFM), have been used to capture images upto a few volumes-per-second (vps). This is not enough for some biological experiments, such as the imaging of heart beating dynamics, or, the propagation of a calcium wave in a living organism, that require imaging at volumetric videorate (30 vps). Intrinsic optical sectioning and scanless operation make LSFM an ideal platform for volumetric videorate imaging, except for the fact that volumes are captured by speed-limiting motor-based sample translations. An interesting passive alternative for fast 3D imaging is the use of wavefront coding to extend the depth-of-field (DOF) of the collection arm of a light-sheet microscope. By doing this, the light-sheet can be rapidly swept within the extended DOF capturing the 3D features of the sample at volumetric videorates. In this approach, the DOF is extended by coding the pupil function of the imaging lens by using a custom-designed phase mask. A posterior restoration step is required to decode the information of the captured images based on the applied coding mask. This hybrid optical-digital approach is known as wavefront coding. In this work we present the use of adaptive optics tools to generate and characterize a set of different wavefront coding masks suitable for our modified LSFM. Furthermore, we present a systematic comparison of the

**Conference 9335: Adaptive Optics and
Wavefront Control for Biological Systems**

imaging performance of the designed phase masks and some encouraging results on biological samples.

9335-13, Session 4

In vivo deep tissue optical imaging via wavefront compensation *(Invited Paper)*

Meng Cui, Howard Hughes Medical Institute (United States)

Multiphoton microscopy has been widely adopted in biological studies for its advantages in deep tissue imaging at sub-cellular resolutions. However, the aberration and scattering in the sample often lead to distorted laser focus and reduced focus intensity, limiting the achievable resolution and imaging depth. Measuring and compensating the wavefront distortion hold great promise to in vivo high-resolution imaging. We have developed the Iterative MultiPhoton Adaptive Compensation Technique (IMPACT), which takes advantages of the inherent nonlinearity in the multiphoton signals to ensure rapid convergence of the wavefront measurements. Different from conventional adaptive optics, IMPACT can handle not only the low order aberration modes, but also the high order modes due to random scattering. Our recent experiments show that IMPACT can work to improve the imaging inside and through intact adult mouse skull. Interestingly, IMPACT measurement even works on blood flow. Here, we discuss the latest in vivo results enabled by IMPACT, which would be very difficult if not impossible for conventional methods.

9335-14, Session 4

High-speed in vivo volumetric deep tissue imaging by remote focusing and wavefront compensation *(Invited Paper)*

Lingjie Kong, Meng Cui, Howard Hughes Medical Institute (United States)

High-speed in vivo volumetric deep tissue imaging is highly desirable in biological and medical research, such as neuroscience and immunology, to study the signaling dynamics and the cell-cell interactions in large cell populations at high spatial and temporal resolutions. However, the aberration and random scattering resulting from the inhomogeneous refractive index distribution in biological tissue causes deteriorated point spread function and limits the maximum imaging depth. We have developed the Iterative MultiPhoton Adaptive Compensation Technique (IMPACT) to rapidly measure and compensate the wavefront distortion for deep-tissue imaging. Now we integrate IMPACT with our newly developed high-speed remote-focusing-based volumetric imaging system. Here we discuss its applications in neuroscience and immunology research.

9335-15, Session 4

Wavefront sensing and analysis for underwater laser propagation

Sergio R. Restaino, U.S. Naval Research Lab. (United States)

A series of experimental tests have been conducted to evaluate the benefit of using some form of Adaptive Optics to shape a laser beam that is propagating under water. The experiments were carried out at the NRL laboratory facility in Stennis, MS, where a large Plexiglas tank of water is equipped with heating and cooling plates that allow for a well measured thermal gradient that in turn generates different degrees of turbulence that can distort a propagating laser beam. In this paper we present an analysis of the wavefront measured in various conditions and derive statistical parameters from it.

9335-16, Session 5

Fibre-based imaging: new challenges *(Invited Paper)*

Martin Ploschner, Univ. of Dundee (United Kingdom); Branislav Straka, Brno Univ. of Technology (Czech Republic); Kishan Dholakia, Univ. of St. Andrews (United Kingdom); Tomá? ?i?már, Univ. of Dundee (United Kingdom)

Small, fiber-based endoscopes have already improved our ability to image deep within the human body. Current fiber-based devices consist of bundles of fibers in which individual fibers represent single pixels in the transmitted image. A novel approach introduced recently utilized disordered light within a standard multimode optical fibre for lensless imaging. The two most important limitations of this exciting technology are (i) the lack of bending flexibility (transformation matrix is only valid as long as the fibre remains stationary) and (ii) high demands on computational power, making the performance of such systems slow.

We discuss possible routes to allow additional flexibility of such endoscopes by broader understanding of light transport processes within. We show that typical fibers retain highly ordered propagation of light over remarkably larger distances, which allows correction operators to be introduced in imaging geometries to maintain high-quality performance in such flexible micro-endoscopes.

Separately, we introduce a GPU toolbox to make these techniques faster and more accessible to researchers. The toolbox optimizes the acquisition time of the transformation matrix of the fibre by synchronous operation of CCD and SLM. Further, it uses the acquired transformation matrix retained within the GPU memory to design, in real-time, the desired holographic mask for on-the-fly modulation of the output light fields. We demonstrate the functionality of the toolbox by acquiring the transformation matrix at the maximum possible refresh rate, and using it to display an on-demand oriented cube, at the distal end of the fibre with refresh-rate of 20ms.

9335-17, Session 5

Complex pattern projection through a multimode fiber

Damien Loterie, Salma Farahi, Demetri Psaltis, Christophe Moser, Ecole Polytechnique Fédérale de Lausanne (Switzerland)

Wavefront shaping through multimode fibers has many interesting applications such as micromanipulation and endoscopy, where the small diameter of fibers advantageous for miniaturization. Recent works presented imaging techniques through multimode fibers based on digital phase conjugation or on transmission matrices. The wavefront is either controlled for the sample excitation (as fluorescence scanning endomicroscopy) or decoded on the collection path with an uncontrolled emission.

Many free-space imaging techniques could be adapted to multimode fibers in a reflection configuration, if the wavefront propagating through them can be well controlled for the illumination of a sample and well decoded on the way back.

Pattern projection using a transmission matrix approach has been shown before, however there were limitations to make continuous shapes due to destructive interference. These interferences can originate e.g. from incomplete control over the input wavefront during illumination or phase drifts during the interferometric measurement of output wavefronts during calibration.

Here, we experimentally demonstrate accurate wavefront control at the output of a multimode fiber with a transmission matrix approach. Using a spatial light modulator and off-axis holography, we measure the transmission matrix of the fiber in a Fourier basis. A simple and novel phase

Conference 9335: Adaptive Optics and Wavefront Control for Biological Systems

correction scheme ensures the accuracy of the measurement. Using this matrix, we can generate patterns in both amplitude and phase with good contrast, accuracy and resolution, and without deleterious interference effects. We reach correlations over 90% between experimental and desired wavefronts. The same data is used to decode wavefronts travelling back through the fiber.

9335-18, Session 5

Delivery of an ultrashort spatially focused pulse to the other end of a multimode fiber using digital phase conjugation

Edgar E. Morales Delgado, Ioannis N. Papadopoulos, Salma Farahi, Demetri Psaltis, Christophe Moser, Ecole Polytechnique Fédérale de Lausanne (Switzerland)

Multimode optical fibers potentially allow the transmission of larger amounts of information than their single mode counterparts because of their high number of supported modes. However, propagation of a light pulse through a multimode optical fiber suffers from spatial distortions due to superposition of the various exited modes and from time broadening due to modal dispersion.

We present a method based on digital phase conjugation to selectively excite specific optical fiber modes in a multimode fiber that follow similar optical paths as they travel through the fiber. In this way, they can interfere constructively at the fiber output generating an ultrashort spatially focused pulse. The excitation of a limited number of modes following similar optical paths limits modal dispersion, allowing the transmission of the ultrashort pulse. Digital scanning of the spatially focused pulse without movable elements is shown.

We also investigate if the intensity of the pulse delivered as a focused spot on the other end of the fiber is enough to excite two-photon fluorescence of a fluorescent dye whose spectral absorption peak occurs at half the wavelength of the delivered pulse.

We have experimentally demonstrated the delivery of a focused pulse through a 30 cm, 200 micrometer core multimode fiber with a duration of approximately 500 fs. This study contributes towards adding two-photon imaging capability for endoscopy using commercial multimode fibers.

9335-19, Session 6

Direct wavefront sensing for optimal resolution recovery over large fields of view (*Invited Paper*)

Kai Wang, Wenzhi Sun, Na Ji, Eric Betzig, Howard Hughes Medical Institute (United States)

When imaging deep into biological samples, the phase and amplitude of imaging light field will be altered due to refractive index heterogeneity and absorption. Because phase plays a critical role in image formation, correction of wavefront distortion can dramatically improve imaging quality and recover nearly diffraction limited resolution. Biological tissue is so complex that complete wavefront compensation can require hundreds of measurements and corresponding corrective elements, and even then, such complex corrections improve imaging quality only over very limited fields of view. To simplify the measurement and extend the field of view, we instead measure an averaged aberration over a volume. This averaged aberration contains wavefront distortions shared over that volume and makes both measuring and correcting such aberration more practical. Depending on the characteristics of the biological sample, the size of the averaging volume can be adjusted flexibly to optimize both the correction improvement and field of view. We employ direct wavefront sensing, more specifically the Shack-Hartman (SH) sensor, in our adaptive optical (AO) microscope to take its advantages of high speed and simplicity. To work with the sensor, a fluorescent guide star is generated inside the biological sample using

nonlinear excitation. The averaged aberration can be directly obtained by scanning guide star excitation, integrating the de-scanned fluorescence over a volume. After compensating the aberration, we demonstrate high resolution in vivo imaging over large volumes in the brains of zebrafish, the fruit fly, and the mouse.

9335-20, Session 6

Wavefront correction using machine learning methods for single molecule localization microscopy

Kayvan F. Tehrani, Jianquan Xu, Peter A. Kner, The Univ. of Georgia (United States)

Optical Aberrations are a major challenge in imaging biological samples. In particular, in single molecule localization (SML) microscopy techniques (STORM, PALM, etc.) a high Strehl ratio point spread function (PSF) is necessary to achieve sub-diffraction resolution. Distortions in the PSF shape directly reduce the resolution of SML microscopy. The system aberrations caused by the imperfections in the optics and instruments can be compensated using Adaptive Optics (AO) techniques prior to imaging, however, aberration caused by the biological sample, both static and dynamic, have to be dealt with in real time. A challenge for wavefront correction in SML microscopy is a robust optimization metric, since image intensity cannot be used due to the naturally high fluctuations in photon emission by single molecules. Here we evaluate different intensity-independent metrics and compare different machine learning methods for AO wavefront optimization. We compare image processing methods such as Run-length, Edge detection, FWHM, and wavelet as wavefront correction metrics and show their relative intensity independence for different machine learning methods. We further compare the performance of different machine learning algorithms such as the genetic and particle swarm algorithms. We show that the particle swarm algorithm converges faster than the genetic algorithm for bright fluorophores.

9335-21, Session 6

Wavefront shaping optical coherence tomography for enhancing penetration depth (*Invited Paper*)

YongKeun Park, KAIST (Korea, Republic of)

Optical coherence tomography (OCT) is a non-invasive optical technique based on coherence gating. The penetration depth of OCT is limited up to a few millimeters, and can be further reduced when imaging highly turbid sample such as skin tissues. The limitation of the penetration depth in OCT is mainly resulted from multiple scattering. In OCT, only single back-scattered light is regarded as signal which exponentially decays as the penetration depth increases (1).

To address this issue, we showed that complex wavefront shaping in OCT can suppress multiple scattering and demonstrated the enhancement of the penetration depth and signal-to-noise ratio (2, 3). The back-scattered coherence-gated light is utilized as the feedback to find the optimal incident wavefront, which maximizes the light delivery to a target depth. We achieved a high-speed synchronization between the wavefront shaping control using a dynamic micromirror device. We measured depth-enhanced 2-D OCT images with various tissue phantoms in which transport mean free paths are systematically varied. The enhancements of the penetration depth up to 92% were achieved.

**Conference 9335: Adaptive Optics and
Wavefront Control for Biological Systems**

9335-22, Session 6

**Performance of a combined optical
coherence tomography and scanning laser
ophthalmoscope with adaptive optics for
human retinal imaging applications**

Elaine M. Wells-Gray, The Ohio State Univ. (United States); Robert J. Zawadzki, Univ. of California, Davis (United States); Susanna C. Finn, Univ. of Massachusetts Lowell (United States); Cherry Greiner, InfraReDx, Inc. (United States); John S. Werner, Univ. of California, Davis (United States); Stacey S. Choi, Nathan Doble, The Ohio State Univ. (United States)

We describe the design and performance of a recently implemented retinal imaging system for the human retina that combines adaptive optics (AO) with spectral domain optical coherence tomography (OCT) and scanning laser ophthalmoscopy (SLO). This AO-OCT-SLO system simultaneously acquires SLO frames and OCT B-scans at 60 Hz with an OCT volume acquisition scan rate of 0.24 Hz. The SLO images are used to correct for eye motion during the registration of OCT B-scans. Key optical design considerations are discussed including: minimizing system aberrations through the use of off-axis relay telescopes; choice of telescope magnification based on pupil plane requirements and restrictions; and the use of dichroic beam splitters to separate and re-combine OCT and SLO beams around the non-shared horizontal scanning mirrors. We include an analysis of closed-loop AO correction on a model eye and compare these findings with system performance in vivo. The 2D and 3D OCT scans included in this work demonstrate the ability of this system to laterally and axially resolve individual cone photoreceptors, while the corresponding SLO images show the en face mosaic at the photoreceptor layer. Images from control subjects and those with retinitis pigmentosa are presented and compared.

9335-23, Session 6

**Adaptive optics for single molecule
switching and STED nanoscopy (*Invited
Paper*)**

Brian R. Patton, Robert Vrees, Daniel Burke, Univ. of Oxford (United Kingdom); Travis J. Gould, Joerg Bewersdorf, Yale Univ. (United States); Martin J. Booth, Univ. of Oxford (United Kingdom)

Superresolution microscopes have been able to resolve features on the scale of tens of nanometers and lower. These microscopes - including scanning methods (STED, RESOLFT, etc.) and stochastic wide field methods (PALM, STORM, GSDIM, etc.) - all suffer from the effects of aberrations that compromise resolution, signal and consequently image quality. Adaptive optics has been demonstrated in a range of diffraction-limited resolution microscope modalities to compensate for system and specimen-induced aberrations. However, the use of adaptive optics in superresolution microscopes presents new challenges. We investigate how aberrations affect the properties of superresolution microscopes and develop new adaptive optics schemes to measure and correct the aberrations. In particular we show how the commonly-used 2D STED configuration is robust to aberrations, whereas the 3D STED configuration is particularly sensitive. We show how this sensitivity can be utilised during the STED system construction and alignment and demonstrate the necessary enhancements to the aberration correction methodology required by 3D STED imaging in thick samples. We will demonstrate how we have performed three-dimensionally resolved superresolution imaging through thick (~10 to 50 micrometre) specimens. Significant improvements in resolution and image intensity are achieved. The adaptive correction of specimen-induced

aberrations in this manner will be an essential step to the wider use of superresolution methods in a wider range of biologically relevant specimens.

9335-24, Session 7

**Indirect wavefront sensing in adaptive
optics (*Invited Paper*)**

Na Ji, Howard Hughes Medical Institute (United States)

In adaptive optics, wavefront measurement methods can be divided into two classes: direct methods where wavefront sensors are used to measure the wavefront phase slopes directly, and indirect wavefront sensing where the performance of the imaging system in response to manipulations of the imaging light field is monitored and used to derive the wavefront aberration. Although generally slower, indirect wavefront-sensing methods work for both transparent and scattering samples. In this talk, I will compare different indirect wavefront-sensing methods and discuss some general principles on their application.

9335-25, Session 7

Wavefront coding with adaptive optics

Gleb V. Vdovin, Flexible Optical B.V. (Netherlands) and Technische Univ. Delft (Netherlands) and National Research Univ. of Information Technologies, Mechanics and Optics (Russian Federation); Oleg Soloviev, Flexible Optical B.V. (Netherlands); Vitalii V. Bezzubik, National Research Univ. of Information Technologies, Mechanics and Optics (Russian Federation); Vsevolod Patlan, Flexible Optical B.V. (Netherlands); Michel Verhaegen, Temitope E Agbana, Delft University of Technology (Netherlands)

Microscopy with high numerical aperture and large magnification suffers from limited depth of field. Multiframe image fusion, multi-exposure imaging and wavefront coding belong to the set of tools to address the problem.

In our experiments we have implemented wavefront coding with a micromachined membrane deformable mirror (MMDM). Computer post-processing of encoded images has been used to increase the depth of field of an optical microscope.

9335-26, Session 7

**Measurement of the time-resolved
reflection matrix for enhancing imaging
depth and light energy delivery (*Invited
Paper*)**

Wonshik Choi, Sungsam Kang, Seungwon Jeong, Pilsung Kang, Hakseok Ko, Yonghyeon Jo, Korea Univ. (Korea, Republic of); Youngwoon Choi, Zahid Yaqoob, Massachusetts Institute of Technology (United States)

Multiple light scattering occurring in a turbid medium undermines imaging targets embedded in the medium and attenuates the intensity of propagating waves. Here, we propose methods to enhance imaging depth and to efficiently deliver light energy into a scattering medium. We measure the time-resolved reflection matrix of a scattering medium using wide-field and time-gated detection. From this matrix, we reconstruct target objects embedded in a scattering medium. We also derive and experimentally implement an incident wave pattern that optimizes the detected signal corresponding to a specific arrival time. These lead to enhanced imaging depth and light delivery. The proposed method will lay a foundation for deep-tissue in vivo imaging and efficient phototherapy in the near future.

**Conference 9335: Adaptive Optics and
Wavefront Control for Biological Systems**

9335-41, Session 7

**Phase retrieval method for simple
aberration determination in PALM/STORM
and SPT**

 Corey Butler, Imagine Optic SA (France) and
Interdisciplinary Institute for Neuroscience, Univ. of
Bordeaux (France); François Le, Grégory Clouvel, Imagine
Optic SA (France)

Single molecule localization methods, like photoactivation localization microscopy (PALM), stochastic optical reconstruction microscopy (STORM) and single particle tracking (SPT) enable us to locate fluorescent molecules with nanometric precision. The quality of the point spread function (PSF) strongly influences the accuracy of detections in these methods, therefore it is highly important to correct for aberrations induced by the optical elements and the biological sample. While these aberrations can be successfully corrected with adaptive optics, for example deformable mirrors, the process of aberration determination remains a complicated task. Currently available image-based iterative algorithms, such as genetic, 3N etc [1, 2] typically require 30-100 images to be taken, which takes a significant amount of time and bleaches the sample. Also the quality of correction in this case frequently depends on the user's personal judgment. Here we adapted the phase retrieval method, described in [3], for single molecule localization microscopy. For the complete determination of present aberrations, this method requires only three images of the point source (i.e. 200nm fluorescent bead) to be taken at different focal positions and does not require any specific knowledge from the user. The parameters, stability and performance of the phase retrieval method for single molecule localization microscopy will be discussed.

[1] Débarre et al (2009) Opt. Lett., 34, 2495-2497.

[2] Facomprez et al (2012) Opt. Express, 20, 2598-2612.

[3] Hanser et al (2003) Opt. Lett., 28, 801-803.

9335-27, Session 8

**Transmission matrix correlations in
anisotropically scattering media (*Invited
Paper*)**

 Benjamin Judkewitz, Charité Universitätsmedizin Berlin
(Germany)

The classical (tilt/tilt) memory effect has received considerable attention over the last decades. However, due to the requirement for thin samples and a screen at a distance it is believed to be inapplicable to biological tissues. Here, we express the memory effect in terms of transmission matrix features to predict and experimentally validate another type of correlation that exists in biological media. These shift/shift correlations do not require samples to be thin, as long as scattering is anisotropic and the mapping between input and output wavefronts preserves some level of directionality. Furthermore, we showed that the extent of correlations can be directly determined from the spatial speckle autocorrelation function during plane-wave illumination.

9335-28, Session 8

**New algorithms for binary wavefront
optimization**

 Xiaolong Zhang, Peter A. Kner, The Univ. of Georgia
(United States)

Binary amplitude modulation promises to allow rapid focusing through strongly scattering media with a large number of segments due to the faster update rates of digital micromirror devices (DMDs) compared to spatial

light modulators (SLMs). While binary amplitude modulation has a lower theoretical enhancement than phase modulation, the faster update rate should more than compensate for the difference – a factor of $\pi^2/2$. Here we present two new algorithms, a genetic algorithm and a transmission matrix algorithm, for optimizing the focus with binary amplitude modulation that achieve enhancements close to the theoretical maximum. Genetic algorithms have been shown to work well in noisy environments and we show that the genetic algorithm performs better than a stepwise algorithm. Transmission matrix algorithms allow complete characterization and control of the medium but require phase control either at the input or output. Here we introduce a transmission matrix algorithm that works with only binary amplitude control and intensity measurements. We apply these algorithms to binary amplitude modulation using a Texas Instruments Digital Micromirror Device and a Spatial Light Modulator. Here we report an enhancement of 105 with 1024 segments (10.25% of the theoretical maximum) using a genetic algorithm with binary amplitude modulation and an enhancement of 123 with 1024 segments (12.0% of the theoretical maximum) using an intensity-only transmission matrix algorithm.

9335-29, Session 8

**Structured illumination enables image
transmission through scattering media**

 Vicente Durán-Bosch, Pere Clemente Pseudo, Esther Irles,
Fernando Soldevila Torres, Enrique Tajahuerce-Romera,
Univ. Jaume I (Spain); Ángel David Rodríguez Jimenez,
Universitat Jaume I (UJI) (Spain); Pedro Andrés Bou, Univ.
de València (Spain); Jesús Lancis, Univ. Jaume I (Spain)

Precise control of light propagation through highly scattering media is a much desired goal with major technological implications. Since interaction of light with turbid media results in partial or complete depletion of ballistic photons, it is in principle impossible to transmit images through distances longer than the extinction length. In biomedical optics, scattering is the dominant light extinction process accounting almost exclusively for the limited imaging depth range. In addition, most scattering media of interest are dynamic in the sense that the scatter centers continuously change their positions with time.

In this work, we employed a single-pixel system, which overcomes the fundamental limitation imposed by multiple scattering even in the dynamically varying case. A sequence of microstructured light patterns codified onto a programmable spatial light modulator was used to sample an object and measurements were captured with a single-pixel detector. Acquisition time was reduced by using compressive sensing techniques. The patterns are used as generalized measurement modes where the object information is expressed. Contrary to the techniques based on the transmission matrix, our approach does not require any a-priori calibration process. The presence of a scattering medium between the object and the detector scrambles the light and mixes the information from all the regions of the sample. However, the object information that can be retrieved from the generalized modes is not destroyed. Our implementation is a first step to tackle the general problem of imaging objects completely embedded in a scattering medium.

9335-30, Session 8

**Non-invasive imaging through opaque
scattering layers (*Invited Paper*)**

 Jacopo Bertolotti, Univ. of Exeter (United Kingdom);
Elbert G. van Putten, Christian Blum, Ad Lagendijk, Willem
L. Vos, Allard P. Mosk, Univ. Twente (Netherlands)

Non-invasive imaging requires the ability to form sharp pictures even when a strongly scattering material acts as a screen between the object and the detector. Light scattering scrambles the optical signal, blurring the picture

**Conference 9335: Adaptive Optics and
Wavefront Control for Biological Systems**

and making direct imaging impossible. Several approaches, each with their own range of applicability, advantages and limitations, were proposed and demonstrated in the past. Ranging from adaptive optics, to optical coherence tomography, to diffuse tomography, to wavefront-shaping techniques.

We have recently demonstrated a novel reference-free imaging method that can retrieve the image of a fluorescent object behind a thin layer that scatters all incident light. The incident laser light is scrambled by a diffuser which transmits negligible ballistic light. The speckles that hit the object excite fluorescence, that appear as a diffused blob on the front side of the diffuser. However the optical memory effect allows deterministic scanning of this overlap when the scattering layer has a physical thickness that is small compared to the distance to the object. By varying the incident angle, an angle-dependent intensity is measured from which the autocorrelation of the object can be extracted. Subsequently the shape of the object can be retrieved from the autocorrelation.

9335-31, Session 8

Extreme wavefront control for imaging in complex media (*Invited Paper*)

Antonio M. Caravaca-Aguirre, Donald B. Conkey, Eyal Niv, Jacob D. Dove, Todd W. Murray, Rafael Piestun, Univ. of Colorado at Boulder (United States)

We address two critical problems in wavefront control through complex media: high-speed feedback for real time adaptive focusing and imaging non-invasively without use of the memory effect.

We demonstrate a system capable of measuring the transmission matrix of a multimode fiber or scattering medium by projecting binary-amplitude computer generated holograms using a digital micromirror device (DMD) and a field programmable gate array controller (FPGA). This system is capable of focusing light through a complex medium in a few tens of milliseconds, one order of magnitude faster than demonstrated in previous reports. In one application, the focus spot can be preserved during bending of an optical multimode fiber, opening opportunities for endoscopic imaging and energy delivery applications.

In a second system, a photoacoustic signal provides feedback for optical focusing through a scattering medium. Optimizing the photoacoustic response using the spatially non-uniform sensitivity of the ultrasound transducer results in the enhancement of a speckle grain creating a sub-acoustic optical focus. The optical focus is used to reconstruct sub-acoustic resolution images behind a diffusing wall.

9335-32, Session 8

Wavefront shaping, adaptive optics, and everything in between (*Invited Paper*)

Ivo M. Vellekoop, Univ. Twente (Netherlands)

The instruments for wavefront shaping and adaptive optics are remarkably similar. However, where adaptive optics is concerned about improving the performance of an existing imaging system, in wavefront shaping there is no imaging system to start with at all.

So far, the research communities for adaptive optics and wavefront shaping have been largely separated. The research fields have different theoretical backgrounds with their corresponding jargon. To add to the confusion, the two fields make different basic assumptions about the optical system and these assumptions are not always expressed explicitly.

I will try to bring these research fields closer together by explicitly comparing their starting points, assumptions, theoretical background, algorithms, and instruments. In many ways, the two fields are extreme cases of a continuum, and we will have a peek at what lies in between.

9335-33, Session 9

Speckle-scale optical focusing in turbid media with photoacoustically guided wavefront shaping (PAWS) (*Invited Paper*)

Lihong V. Wang, Puxiang Lai, Lidai Wang, Jian Wei Tay, Washington Univ. in St. Louis (United States)

Optical methods play increasingly important roles in biomedical imaging and therapy. Many of these methods rely on the ability to deliver light tightly to the investigation sites. The resolution, however, declines precipitously as light travels beyond ~ 10 mean free paths into tissue (~ 1 mm for human skin), due to strong scattering (think about how a flashlight beam diffuses through your palm). Efficient focused delivery of light beyond this limit has long been one of the greatest challenges in biomedical optics. Recently, ultrasonically guided phase conjugation and wavefront shaping approaches have been developed to tackle this limitation. However, most of these implementations provide only acoustic diffraction-limited optical focusing. Here, we present a new modality called photoacoustically guided wavefront shaping (PAWS), which uses nonlinear photoacoustic (PA) signals generated from the Grueneisen relaxation effect as feedback to guide iterative wavefront optimization. We show that by maximizing the strength of the nonlinear PA signals, completely diffuse light can be focused to a single optical speckle grain. In experiments, we obtained a bright focal spot on the scale of $5\text{--}7\ \mu\text{m}$, much smaller than the $65\ \mu\text{m}$ acoustic focus, with an enhancement of peak fluence by ~ 6000 times. Once it has been engineered to respond much faster, nonlinear PAWS will pave the way for many high-resolution optical applications, including imaging, sensing, therapy, and manipulation, that require highly confined intense optical focusing inside highly scattering biological tissue.

9335-34, Session 9

Time-reversed ultrasonically encoded (TRUE) optical focusing in vivo

Puxiang Lai, Yan Liu, Cheng Ma, Xiao Xu, Washington Univ. in St. Louis (United States); Alexander A. Grabar, Uzhgorod National Univ. (Ukraine); Lihong V. Wang, Washington Univ. in St. Louis (United States)

Light is highly scattered in deep biological tissue by wavelength-scale refractive index inhomogeneities of the medium. As a result, ballistic and quasi-ballistic photons that are not scattered or scattered once can survive only within depths of ~ 10 mean free paths (corresponding to ~ 1 mm in human skin). Beyond that, light is scattered randomly, preventing the formation of an optical focus or sharp image using lenses. The feasibility of overcoming this limit has recently been proved by using internal-guide-star-based wavefront shaping and time-reversed ultrasonically encoded (TRUE) optical focusing techniques. Most of the implementations so far, however, yield operation speeds no faster than 1 Hz, preventing them from being applied in living tissue, where the observed optical speckles decorrelate fast (on the order of ms) due to physiological motions, such as blood flow and aspiration. Here, we report our latest explorations of TRUE optical focusing in living tissue, using two relatively fast responding photorefractive crystals (SPS:Te and BSO) as the phase conjugation mirrors to generate the time-reversed light. With shortened durations of hologram writing and reading, we have successfully limited the operation cycle of TRUE optical focusing to within 10 ms, approaching the decorrelation time of typical living tissue. Through experiments, we showed that the new TRUE scheme was able to focus diffuse light deep inside living biological tissue, with resolution determined by the focal size of the ultrasonic transducer. With further improvement, in vivo applications with TRUE optical focusing are on the horizon.

**Conference 9335: Adaptive Optics and
 Wavefront Control for Biological Systems**

9335-35, Session 9

**Time-reversed adapted-perturbation
 (TRAP) optical focusing inside scattering
 media**

Cheng Ma, Xiao Xu, Yan Liu, Lihong V. Wang, Washington Univ. in St. Louis (United States)

Multiple scattering is a major impediment to optical imaging, sensing and manipulation. The fundamental problem is to focus light in a regime where multiple scattering becomes dominant while the residual ballistic component is negligible. In such diffusive regimes, the only feasible strategy for creating foci is to shape the input wave front based on feedback from implanted or virtual guide stars. However, the introduction of the guide stars must either be invasive or by physical contact, limiting the scope of their application. Here, we explore the possibility of focusing light inside scattering media by employing intrinsic dynamics as guide stars. In this technology, the perturbation of the electromagnetic field due to spontaneous permittivity variations is remotely detected. A virtual field is then synthesized which adapts to the detected perturbation. The generated field is a time reversed copy of the differential field associated with the embedded novelty. The field reverses the forward scattering process and converges to the origin of the perturbation. With this technology, we can dynamically focus light onto a moving target, as well as onto an extended volume with constant permittivity fluctuations. Subsequently, a time-variant object obscured by highly scattering media can be non-invasively imaged via speckle scanning microscopy. Because this method probes the permittivity variation remotely and non-resonantly, it is completely non-invasive, non-contacting, and passive. Potential applications include tracking vehicles in still fogs, imaging and photoablation of angiogenic vessels in tumors, and studying dynamics in tissue.

9335-36, Session 9

**Fast scanning of the time-reversed
 ultrasonically encoded focus by frequency-
 chirped wavefront recording**

Yuta Suzuki, Lihong V. Wang, Washington Univ. in St. Louis (United States)

Focusing light deep into biological tissue is desirable for biomedical applications such as optical imaging, diagnostics, manipulation, and therapy. However, due to scattering, optical focusing using an ordinary lens is limited to depths of one transport mean free path (approximately 1 mm in human breast tissue). To overcome this limit, time-reversed ultrasonically encoded (TRUE) focusing was previously demonstrated, in which an ultrasound beam modulates (or encodes) the light travelling inside the turbid medium. By recording and then reading out the wavefront of the ultrasonically encoded light, an optical focus can be generated inside the tissue. TRUE focusing has been implemented using both analog and digital devices. A digital implementation of TRUE focusing is highly attractive for therapeutic applications because a focus with high energy can be generated. However, its operation is time consuming, due to the long integration times required to overcome the low signal-to-noise ratio during recording. Here, we propose a multiplexed wavefront recording technique by frequency-chirping the ultrasound and light, thereby speeding up the generation of multiple TRUE foci. As a result, the time taken was reduced by more than 10-fold. We then demonstrate accelerated fluorescent imaging deep inside a thick turbid medium, to confirm the improved resolution and the imaging capability of our proposed method.

9335-37, Session 9

**Noninvasive imaging through scattering
 media (*Invited Paper*)**

Ori Katz, Institut Langevin (France) and Ecole Supérieure de Physique et de Chimie Industrielles de la Ville de Paris (France)

Multiple scattering of light in complex samples such as biological tissues renders most samples opaque to conventional imaging techniques, a problem of great practical importance. However, although random, scattering is a deterministic process, and it can be undone, controlled, and even exploited by carefully shaping the input wavefront, forming the basis for the emerging field of optical wavefront-shaping^{1,2}, and opening the path to imaging through visually opaque samples³ and to the control of scattered ultrashort pulses⁴. Unfortunately, many demonstration of all-optical wavefront-shaping¹⁻⁴ require a localized feedback signal from the target, and thus an invasive implantation of an optical probe.

I will present a few of our recent efforts in addressing this challenge⁵⁻⁷. These include the use of the photoacoustic effect to focus and control light non-invasively inside a scattering medium⁵, and the use of optical nonlinearities to focus light noninvasively through scattering samples⁶. I will also show how the inherent correlations of scattered light allow one to “see through” opaque samples and ‘around corners’ without wavefront-shaping and using nothing but a conventional camera⁷, challenging the common view on diffuse scattered light as an information-less halo.

References

- [1] Mosk et al., Nature Photonics 6, 283 (2012).
- [2] Wiersma, Nature Photonics 7, 188 (2013).
- [3] Katz et al., Nature Photonics 6, 549 (2012).
- [4] Katz et al., Nature Photonics 5, 372 (2011).
- [5] Chaigne, Katz et al. Nature Photonics 8, 58 (2014).
- [6] Katz et al., arXiv:1405.4826 (to appear in Optica, 2014)
- [7] Katz, et al., arXiv:1403.3316 (to appear in Nature Photonics, 2014).

9335-42, Session PMon

**Comparison of a novel adaptive lens with
 deformable mirrors and its application in
 high-resolution in-vivo OCT imaging**

Stefano Bonora, Institute for Photonics and Nanotechnology, CNR (Italy) and Institute of Physics of the ASCR, v.v.i. (Czech Republic); Yifan Jian, Simon Fraser Univ. (Canada); Luca Rizzotto, Institute for Photonics and Nanotechnology, CNR (Italy); Pengfei Zhang, Azhar Zam, Edward N. Pugh Jr., Univ. of California, Davis (United States); F. Mammano, Istituto di Biologia Cellulare e Neurobiologia, CNR (Italy); Robert J. Zawadzki, Univ. of California, Davis (United States); Marinko V. Sarunic, Simon Fraser Univ. (Canada)

We present a novel adaptive lens that can correct high order aberrations, and which has the potential to increase the diffusion of adaptive optics to many new applications by simplifying the integration of a wavefront corrector inside existing systems. The adaptive lens design that we present can correct for Zernike wavefront aberrations up to the 4th order. The adaptive lens performance are compared with the one of a membrane and bimorph deformable mirrors used together in a wide field microscope setup, using a Shack-Hartmann wavefront sensor for closed loop control.

The adaptive lens was also integrated with Fourier Domain Optical Coherence Tomography for in-vivo imaging of mouse retinal structures using an image based wavefront sensorless control.

9335-43, Session PMon

Focusing on moving target in scattering media

Haojiang Zhou, California Institute of Technology (United States)

Focusing light onto hidden targets through complex media such as biological tissue has many important applications in biology and medicine, but to achieve this, photons would have to be launched into the scattering tissue just right so the end up in the correct place. Theoretically, wavefront shaping or phase conjugation can realize its implementation. While, in practice, a noninvasive and efficient reference guide star, remains an important challenge. Here, we show optical time-reversal focusing using a new technique termed Time Reversal by Analysis of Changing wavefronts from Kinetic targets (TRACK). By taking the difference of fields between time-varying scattering caused by a moving object and applying optical time reversal, light can be focused back to the location previously occupied by the object. We demonstrate this approach with discretely moved objects as well as with particles in an aqueous flow, and obtain a focus with peak strength of 204 to the background. We further demonstrate that the generated focus can be used to noninvasively count particles in a flow-cytometry configuration—even when the particles are hidden behind a strong diffuser. By achieving optical time reversal and focusing noninvasively without any external guide stars, using just the intrinsic characteristics of the sample, this work paves the way to a range of scattering media imaging applications, including underwater and atmospheric focusing as well as noninvasive in vivo flow cytometry. This work may also lead the way towards diagnosis without blood drawing.

Conference 9336: Quantitative Phase Imaging

Saturday - Tuesday 7-10 February 2015

Part of Proceedings of SPIE Vol. 9336 Quantitative Phase Imaging

9336-1, Session 1

New developments in oblique-back-illumination microscopy for phase imaging in thick tissue (*Invited Paper*)

Jerome Mertz, Boston Univ. (United States)

Historically, phase contrast imaging has been one of the most prevalent applications of widefield microscopy. The most common techniques are Zernike phase contrast and Normarski differential interference contrast (DIC). As successful as these techniques have been in the lab, they suffer a drawback in the clinic, namely they only work in the transmission direction. This limits their application to thin samples only, such as cell monolayers or thin tissue slices. We have developed a technique called Oblique Back-illumination Microscopy (OBM) that provides DIC-like contrast in arbitrarily thick tissue. Illumination is delivered into the sample via two diametrically opposed off-axis light sources. The illumination undergoes scattering within the tissue, and a portion is collected on axis by the objective, ultimately to be imaged by the camera. Because the light sources are situated off axis this collected illumination traverses the focal plane in an oblique manner, thus leading to phase gradient contrast. The advantage of using two light sources instead of a single source is that it allows the acquisition of two images with opposing illumination obliquities, which in turn enables the separation of phase contrast from amplitude contrast.

I will present some new results on OBM, including a scanning variation of OBM based on the principle of reciprocity that can be implemented as a simple add-on to any laser scanning microscope. Examples will be shown where scanning OBM is combined with two-photon and CARS microscopes, conferring an additional capacity of simultaneous phase imaging that is automatically co-registered.

9336-2, Session 1

Path-length stabilized low-coherent reflection-type quantitative phase microscope for nanometer-resolution profiling of plasma membrane

Toyohiko Yamauchi, Hidenao Iwai, Kentaro Goto, Shu Homma, Yutaka Yamashita, Hamamatsu Photonics K.K. (Japan)

We have developed a transportable and user-friendly prototype of low-coherent reflection-type quantitative phase microscope (QPM). Our setup is based on a full-field Linnik type phase-shifting interference microscope and is optimized for the surface profiling of live cell's membrane. Unlike commonly available transmission-type quantitative phase microscopes which tell optical thickness, our reflection-type setup is able to obtain the geometrical thickness (real shape) of the sample, decoupled with the refractive index. The coherence length of our imaging lightsource (halogen lamp) was around 1 micrometer so that we can selectively obtain the interference of the light reflected from the cell membrane, whose reflectivity in culture medium is only the order of 0.1%. Moreover, our setup has a feedback controlled path-length stabilization circuit so that users can implement an accurate phase shifting interferometry with 1 nanometer of reproducibility. The stabilization circuit made it possible to install our setup even in a noisy environment such as biology labs without optical bench. In the presentation, we will also show our recent biomedical application studies, including video-rate imaging of cell plasma membrane, phase-resolved 3D tomography of live cells and visualization of filopodial extension.

9336-3, Session 1

Spectral modulation interferometry (SMI) for quantitative phase imaging

Ruibao Shang, Shichao Chen, Yizheng Zhu, Virginia Polytechnic Institute and State Univ. (United States)

Optical phase is perhaps the most important intrinsic contrast mechanism for stain-free imaging of biological samples. Conventional techniques, such as phase contrast microscopy and differential interference contrast microscopy, are qualitative in nature in that optical phase is converted into intensity nonlinearly and hence hard to be quantified. In recent years, various quantitative phase microscopy (QPM) techniques have been developed capable of quantifying both the phase and amplitude of a sample. Mostly interferometric approaches, these techniques can provide sensitive phase measurement at nanometer/sub-nanometer scale. Nevertheless, there has been a continuing need for improvement in QPM's speed and sensitivity for a growing list of applications in live cell imaging and surface metrology.

In this presentation, we introduce a novel spectral-domain interferometric technique, termed spectral modulation interferometry (SMI), and demonstrate its application for high-sensitivity, high-speed and speckle-free quantitative phase imaging. Spectral-domain low coherence interferometry is known for its high sensitivity in optical phase determination. Here, SMI modulates phase and amplitude information of a sample onto a carrier wave in spectral domain to achieve high phase sensitivity and maintain high acquisition speed at the same time. Additionally, SMI eliminates speckle interference through its line-scanning and spectrum-spreading implementation. Such performance is promising to reveal finer structures at higher speed that can be used to better understand biophysical dynamics of a sample. We will introduce the principles of SMI and discuss its application for dynamic characterization of biological specimens.

9336-4, Session 1

Super-resolution interference microscopy for 3D nanometrology

Pavel S. Ignatyev, Andrey V. Pravdivtsev, Alexander B. Zenzinov, Konstantin V. Indukaev, Pavel A. Osipov, AMPHORA Labs Co., Ltd. (Russian Federation)

The technology of Modulation Interference Microscopy (MIM) brings together design, optical, methodical and algorithmic solutions to develop super-resolution microscopes for 3D imaging and metrology. Three generations of microscopes based on the MIM technology have been developed so far for biomed studies, material science, as well as for optical and semiconductor industry [1,2].

In this study we demonstrate essential principles of the MIM technology, as well as new methods for optical scheme optimization. Resolution of MIM based microscopes (0.1 nm vertical and 10-100 nm lateral) was demonstrated in the course of experiments in HOPG structures and in targets developed for lateral resolution tests. We cover metrological aspects of the MIM system uncertainty determination. With linear uncertainty $\leq 3\%$ of 56nm and vertical in the range of 0.1-4 nm (depending on measurement sub-range), MIM is considered a promising tool for measuring varied micro- and nano-scale structures.

MIM application in semiconductor industry demonstrated a number of advantages compared to optical profilometers and confocal microscopes. A new MIM system with super-flat long travel coordinate table was developed for measuring 300mm wafers. We demonstrate some results of MIM application for Critical dimension (CD) measurement of various semiconductor structures.

The results of MIM applications in the biomed area, particularly, for studying nanoparticles, blood cells, cancer cells and viruses indicate that it has serious potential for use in clinical diagnostics [3].

[1] Loparev A. V., Ignat'ev P. S., Indukaev K. V., Osipov, P. A., Mazalov I. N., Kozyrev A. V., "A high-speed modulation interference microscope for biomedical studies," *Measurement Techniques*, 52(11), 1229-1235 (2009)

[2] Andreev A. G., Grigoriev S. N., Romash E. V., Bushuev S. V. and Ignatiev P. S., "Modulation interference microscope as a tool for measuring the linear dimensions of nanostructures," *Measurement Techniques*, 55(5), 542-545(2012)

[3] Ignatyev P. S., Indukaev K. V., Osipov P. A., Sergeev I. K., "Laser Interference Microscopy for Nanobiotechnologies," Translated from *Meditsinskaya Tekhnika*, 47(1), 27-30 (2013)

9336-5, Session 1

Wave fronts vs. phase-imaging interference

Victor M. Muzafarov, Vladimir A. Andreev, Konstantin V. Indukaev, Pavel A. Osipov, AMPHORA Labs Co., Ltd. (Russian Federation)

There are different areas of applying phase-imaging interference methods for studying both macro- and micro-objects. Discrete data of the CCD measurements are obtained as an intermediate set of information to recover characteristics we are interested in the study of these objects. In this investigation, our main concern is the study of a general-purpose problem of reconstructing and further analyzing wave fronts corresponding to the object under consideration.

In particular, as to the problems of phase-imaging interference microscopy, the greatest challenge has been in the 2D phase unwrapping to construct the so-called phase image of the object. There has been a plethora of algorithms for phase unwrapping, and these algorithms share the common property that the phase unwrapping is effected by pointing out some preferential taking the discrete one-dimensional path (by pixel-to-pixel, for the measured discrete two-dimensional CDD data) to resolve the well-known ($\lambda/2$)-problem and construct the continuous phase image of the object.

We propose the new approach to solve the problem of the 2D phase unwrapping. The key feature of our approach is that, by the measured two-dimensional discrete CDD data, we reconstruct the holomorphic wave front amplitude $A(x,y,z)$ (WFA). In the momentum representation, the WFA singularities (poles and corresponding residues, as well as cuts and jumps across these cuts) contain the whole information about the object. In this way we need further to attract powerful topological tools (see e.g. [1] and refs. therein) to study and classify the WFA singularities. The problem of the 2D phase unwrapping therewith amounts to the well-known topological problem of "combing of the hedgehog" for $\text{Ln } A(x,y,z)$.

[1] V. I. Arnold, *Singularities of functions, wave fronts, caustics and multidimensional integrals*, Cambridge Scientific Publishers (2012)

9336-6, Session 1

Quantitative phase imaging unit

KyeoReh Lee, YongKeun Park, KAIST (Korea, Republic of)

Conventional bio-imaging techniques employing interference, such as phase contrast (PC), and differential interference contrast (DIC) microscopy, are mainly focused on viewing the cells, tissues, and membranes with higher contrast. However, recently developed holography based quantitative phase imaging (QPI) techniques enable various physical studies of biological samples by imaging due to their quantitative capability, including mechanical properties of red blood cell membrane [1], optical dry mass measurement [2], 3D refractive index tomography [3], and single-cell light scattering [4].

However, despite the advantages of QPIs, the translation of the QPI techniques into biological and clinical laboratories is still lagged mainly due to the cost-heavy features and frequent maintenance requirement originated from complicated optical instrument, and incompatibility with existing microscopes.

Here we report simple and low-cost QPI microscopy that also compatible with the conventional microscope – quantitative phase imaging unit (QPIU) [5]. QPIU consists of only three optical components – two polarizer (or one polarizer and one waveplate), and polarizing prism. We imaged QPI of microspheres, and various blood cells (discocyte, echinocyte, and lymphocyte) with fine quality using QPIU. Moreover, since QPIU is inherently common-path interferometry, low phase background noise can be also achieved. We measured red blood cell membrane fluctuation with 5 mrad background phase noise, which corresponds to 9 nm.

References:

[1] Y. Park, C. A. Best, T. Auth et al., "Metabolic remodeling of the human red blood cell membrane," *Proceedings of the National Academy of Sciences*, 107(4), 1289-1294 (2010).

[2] G. Popescu, Y. Park, N. Lue et al., "Optical imaging of cell mass and growth dynamics," *American Journal of Physiology-Cell Physiology*, 295(2), C538-C544 (2008).

[3] Y. Park, M. Diez-Silva, G. Popescu et al., "Refractive index maps and membrane dynamics of human red blood cells parasitized by *Plasmodium falciparum*," *Proceedings of the National Academy of Sciences*, 105(37), 13730-13735 (2008).

[4] H. Ding, Z. Wang, F. Nguyen et al., "Fourier transform light scattering of inhomogeneous and dynamic structures," *Physical review letters*, 101(23), 238102 (2008).

[5] K. Lee, and Y. Park, "Quantitative phase imaging unit."

9336-7, Session 1

Fast quantitative birefringence imaging of biological samples using quadri wave interferometry

Sherazade Aknoun, Institut Fresnel (France) and Aix-Marseille Univ. (France); Pierre Bon, Institut d'Optique Graduate School (France) and Bordeaux Univ. (France); Julien Savatier, Institut Fresnel (France) and Aix-Marseille Univ. (France); Benoit F. Wattellier, PHASICS S.A. (France); Serge Monneret, Institut Fresnel (France) and Aix-Marseille Univ. (France)

Quantitative phase imaging techniques [1-4] are now conventionally used in microscopy for measuring specific properties of semi-transparent samples. The strength of those techniques is their non-invasive and fast approach. However, it is hard to obtain specific organelle imaging inside a given sample as the contrast only comes from the local optical path difference of the object.

To overcome this limitation, we propose to use quantitative anisotropy imaging. Indeed, anisotropy has been used to reveal ordered fibrous structures in biological samples without any staining or labelling with polarized light microscopy [5-7]. Recent studies have shown polarimetry as a potential diagnostic tool for various dermatological diseases on thick tissue samples [8]. Particularly, specific collagen fibers spatial distribution has been demonstrated to be a signature for the optical diagnosis and prognosis of cancer in tissues [9].

In this paper, we describe a technical improvement of our technique based on high-resolution quadri-wave lateral shearing interferometry (QWLSI) to perform quantitative linear birefringence measurements on biological samples. The system combines a set of quantitative phase images with different excitation polarizations to create birefringence images. These give information about the local retardance and structure of dynamic biological anisotropic components such as actin fibers.

We propose using a commercial QWLSI [10] (SID4Bio, Phasics SA, Palaiseau, France) directly plugged onto a lateral video port of an inverted microscope (TE2000-U, Nikon, Japan). By introducing a liquid crystal retarder to rotate the incident polarization, we are able to take a retardance image in less than 1 second.

Results on living cells will be presented showing some quantitative measurements on actin filaments and vesicles.

References

- [1] E. Cuche, F. Bevilacqua, and C. Depeursinge, "Digital holography for quantitative phase-contrast imaging," *Opt. Lett.*, vol. 24, pp. 291-293, Mar 1999.
- [2] B. Kemper and G. von Bally, "Digital holographic microscopy for live cell applications and technical inspection," *Appl. Opt.*, vol. 47, pp. A52-A61, Feb 2008.
- [3] G. Popescu, T. Ikeda, R. R. Dasari, and M. S. Feld, "Diffraction phase microscopy for quantifying cell structure and dynamics," *Opt. Lett.*, vol. 31, pp. 775-777, Mar 2006.
- [4] P. Bon, J. Savatier, M. Merlin, B. Wattellier, and S. Monneret, "Optical detection and measurement of living cell morphometric features with single-shot quantitative phase microscopy," *Journal of Biomedical Optics*, vol. 17, no. 7, pp. 076004-1-076004-7, 2012.
- [5] R. Oldenbourg, E. Salmon, and P. Tran, "Birefringence of single and bundled microtubules," *Biophysical Journal*, vol. 74, no. 1, pp. 645 - 654, 1998.
- [6] F. Massoumian, R. Juskaitis, M. A. A. Neil, and T. Wilson, "Quantitative polarized light microscopy," *Journal of Microscopy*, vol. 209, no. 1, pp. 13-22, 2003.
- [7] S. Sugita and T. Matsumoto, "Quantitative measurement of the distribution and alignment of collagen fibers in unfixed aortic tissues," *Journal of Biomechanics*, vol. 46, pp. 1403-1407, Apr. 2013.
- [8] A. Pierangelo, A. Benali, M.-R. Antonelli, T. Novikova, P. Validire, B. Gayet, and A. D. Martino, "Ex vivo characterization of human colon cancer by mueller polarimetric imaging," *Opt. Express*, vol. 19, pp. 1582-1593, Jan 2011.
- [9] M. W. Conklin, J. C. Eickhoff, K. M. Ricking, C. A. Pehlke, K. W. Eliceiri, P. P. Provenzano, A. Friedl, and P. J. Keely, "Aligned collagen is a prognostic signature for survival.
- [10] P. Bon, G. Maucort, B. Wattellier, and S. Monneret, "Quadriwave lateral shearing interferometry for quantitative phase microscopy of living cells," *Opt. Express*, vol. 17, pp. 13080-13094, Jul 2009.

9336-8, Session 1

Differential fluorescence holography

David C. Clark, Myung K. Kim, Univ. of South Florida (United States)

Digital holography provides complete 3D information of optical field, including both its amplitude and phase profiles, which is the basis of a host of powerful imaging and processing techniques. For example, in differential holography, one can obtain background-free 3D complex profile of the optical field. Recently, we have used differential holography to study the deflection of microfibers by swimming cells. The method proved to be highly effective for background-free imaging, highlighting the time-varying parts of the 3D object scene. High-precision spatial and temporal tracking of the cells and fibers has been demonstrated. We extend similar background-free differential imaging technique to a new type of holography of incoherent light: self-interference incoherent digital holography (SIDH). The SIDH generates complex - i.e. amplitude plus phase - hologram from one or several interferograms acquired with incoherent light, such as LEDs, lamps, sunlight, or fluorescence. Differential SIDH is used for 3D tracking of time-dependent fluorescence images. The time-dependency may arise from temporal variation of fluorescence signals or motion of fluorescent structures. The background subtraction is in both the amplitude and phase of the optical field. It can be a sensitive means of tracking subtle variations in the object volume, even when the amplitude variation may be too weak to detect. The background subtraction also leads to significant improvement

in sensitivity and contrast. The object scene becomes more sparse and the hologram has much higher dynamic range for a given camera bit depth.

9336-9, Session 1

Quantitative phase recovery from asymmetric illumination on an LED array microscope

Lei Tian, Laura Waller, Univ. of California, Berkeley (United States)

The LED array microscope is a new computational illumination platform which can flexibly provide multiple contrast modes, including quantitative phase. Phase contrast is introduced by any complex transfer function, created by using asymmetric illumination patterns. In the differential phase contrast (DPC) method, one captures two images from a complementary pair of asymmetric illuminations. From this data, quantitative phase can be reconstructed by inversion algorithms. The DPC method can be easily implemented on the LED array microscope by simply taking one image with one half of brightfield LEDs on, and one with the other half. The first derivative of the phase along the axis of asymmetry is extracted by taking the difference between the two images. Distinct from commercial phase contrast methods such as Zernike phase contrast, DIC and Hoffman modulation contrast, DPC does not mix any absorption information into the phase derivative information. Thus, the DPC image can be numerically integrated to obtain quantitative phase. Direct integration from single axis DPC suffers from low frequency artifacts, which can be alleviated by multi-axis DPC measurements. For better reconstruction accuracy, we model the phase transfer function from the asymmetric illumination with explicit consideration of the discrete source distribution caused by the LED array. We then study reconstruction methods for quantitative phase recovery from multiple DPC measurements under varying illumination conditions.

9336-10, Session 2

Multiplexed off-axis interferometric phase microscopy for dynamic cell measurements (*Invited Paper*)

Natan T. Shaked, Pinhas Girshovitz, Irena Frenklach, Tel Aviv Univ. (Israel)

We present a new approach of optically multiplexing several off-axis interferograms on the same digital camera, each of which encodes a different field of view of the sample. Since the fringes of these interferograms are in different directions, as obtained experimentally by the optical system, we are able to double or even triple the amount of information that can be acquired in a single camera exposure, with the same number of camera pixels, while sharing the camera dynamic range. We present two optical implementations, an external-interferometry module attached to an existing imaging system, and a multiplexing module attached to an existing off-axis interferometric system. We also show that this method can partially solve the problem of limited off-axis interferometric field of view due to low-coherence illumination. Our experimental demonstrations include quantitative phase imaging of microscopic diatom shells, fast swimming sperm cells and microorganisms, and contracting cardiomyocytes.

9336-11, Session 2
Using electrochemistry - total internal reflection imaging ellipsometry to monitor biochemical oxygen demand on the surface tethered polyelectrolyte modified electrode

Wei Liu, Gang Jin, Institute of Mechanics (China); YanYan Chen, Bei'er Lv, Hongwei Ma, Suzhou Institute of Nano-Tech and Nano-Bionics, Chinese Academy of Science (China)

Biochemical oxygen demand (BOD) is the amount of dissolved oxygen consumption of aerobic biological organism in water to degrade organic material in a given water sample at certain temperature over a specific time period. It is widely used as an indication of the organic pollution of water. Traditionally, it will take 5 days to get the BOD value. To develop a rapid BOD detection, a microbial membrane is covered at the top of Clark electrode. Since the electrode measures the dissolved oxygen consumption of the microbial membrane, the measurement time can be reduced from days to hours. However, the signal drift of the electrode would make the results less reliable.

Total internal reflection imaging ellipsometry (TIRIE) has been proven as a powerful tool to study redox reactions on the electrode surface, for it enjoys high interface sensitivity in the ellipsometric phase. By integrating the electrochemistry and TIRE (EC-TIRIE), we could monitor dissolved oxygen reduction on the surface of Clark electrode synchronously.

To amplify the TIRE signal, a surface tethered weak polyelectrolyte, carboxylated poly(OEGMA-*r*-HEMA) has been intruded on the sensing surface, for it will swell when the surrounding pH increases because of the dissolved oxygen reduction on the electrode surface. The results has shown that the system could detect BOD value from 3 mg/L to 25 mg/L. For two given water samples, the deviation of the detection is less than 10% compared with the conventional BOD₅ value. The consistent efficiency of the both electrical signal and the optical signal is less than 10%.

9336-12, Session 2
Phase-shifting interference with pumping noise-to-signal

Victor M. Muzafarov, AMPHORA Labs Co., Ltd. (Russian Federation)

In this investigation we have taken the new line of attack for the phase-shifting interference microscopy which is based upon the idea that both object signals and attendant noises---measured as mixed signals by the matrix receiver---are considered as physical observables on equal terms.

Reasoning from this idea we show that the phase-shifting interference with a windowed *n*-step algorithm may be essentially generalized to formulate a successive procedure of reconstructing the object wave front amplitude via the data measured, so that the object signals level of by attendant noises---the approach named as the phase-shifting interference with linking the noise-to-signal. Both the signal sought and the unknown values of attendant noises appear in mathematical equations of the proposed procedure in an equivalent manner.

This procedure is realized as a linear system of equations of order *n*. It is shown that the case *n*=7 be of an especial interest for the phase-shifting interference microscopy since the system of our equations be over-defined (*n*>7) or undefined (*n*<7) otherwise.

The features peculiar to the proposed procedure is, in particular, that for a given phase-shifting interference with *n*-step algorithm (*n*>3), one can write (*n*-3) model independent sum rules for intensities measured by CCD (by pixel-to-pixel) with different phase shifts. Both pre- and post-evaluating of CCD data by our procedure may be performed to select the most 'noisy' pixels.

9336-13, Session 2
Towards an incoherent off-axis digital holographic microscope

Zahra Monemhaghdoost, Ecole Polytechnique Fédérale de Lausanne (Switzerland); Frédéric Montfort, Lyncée Tec SA (Switzerland); Philippe Degol, Ecole Polytechnique Fédérale de Lausanne (Switzerland); Yves Emery, Lyncée Tec SA (Switzerland); Christian D. Depeursinge, CDep engineering Sàrl (Switzerland); Christophe Moser, Ecole Polytechnique Fédérale de Lausanne (Switzerland)

We propose and experimentally demonstrate an off-axis digital holographic microscope which uses a broadband illumination source. Thanks to the off-axis geometry, only a single full field interferogram is needed to reconstruct phase and amplitude of the sample and coherence noise is removed thanks to the broad bandwidth of the illuminating source. This is the first time to our knowledge that off-axis digital holographic microscopy is pushed to the incoherent regime. This is realized thanks to a combination of a thick transmission volume grating recorded holographically into thick glass and thin transmission phase gratings recorded into thin photopolymers, that filters the beam containing the sample information in two dimensions through diffraction. The filtered beam creates the reference arm of the interferometer. The undiffracted transmitted beam creates the sample arm of the interferometer. Spatial filtering, which works based on the high angular selectivity of thick volume gratings, reduces the alignment spatial sensitivity which is an advantage over the conventional spatial filtering done with pinholes. By using a second thin grating, we introduce a desired coherence plane tilt in the reference beam which is sufficient to create high-visibility interference over the entire field of view in off-axis configuration. The full-field off-axis interferograms are created from which the amplitude and phase can be reconstructed.

9336-14, Session 2
Fast control of temporal and spatial coherence properties of microscope illumination using DLP projector

Jose A. Rodrigo Martin Romo, Tatiana Alieva, Univ. Complutense de Madrid (Spain)

Recently, cost-effective DLP projectors have found alternative applications in metrology, lithography and optical microscopy. The provided fast programmable color controlled image formation makes them attractive for microscope illumination schemes. It has been shown that different microscopic wide-field modalities such as bright field, dark field, oblique and structured illumination can be easily obtained and rapidly changed using a DLP projector.

Here we propose to use the DLP projector technology for fast and programmable control of temporal and spatial coherence of microscope illumination. This control is required for introducing the coherence parameters in the algorithms used for quantitative imaging with partially coherent light, which does not suffer from undesirable effects of fully coherent light, or for appropriate visualization of complex specimens where non traditional field correlation is needed. According to the Van Cittert-Zernike theorem the mutual intensity of the illumination beam at the sample plane is related to the image projected to the back focal plane of the Kohler condenser through the Fourier transform. Thus the form and the shape of the projected images, which play the role of condenser aperture, control the spatial coherence properties of illumination. Temporal coherence is controlled by choosing the appropriate color spectrum of the projected image.

Image formation for different types of coherence illumination conditions, produced by images of different forms and colors is experimentally analysed. Quantitative phase imaging for different illumination coherence states is experimentally demonstrated.

9336-15, Session 2

Experimental setup combining digital holographic microscopy (DHM) and fluorescence imaging to study gold nanoparticle mediated laser manipulation

Georgios C. Antonopoulos, Mirko Rakoski, Laser Zentrum Hannover e.V. (Germany); Benjamin Steltner, Laser Zentrum Hannover eV (Germany); Stefan Kalies, Tammo Ripken, Heiko Meyer, Laser Zentrum Hannover e.V. (Germany)

Our research combines Digital Holographic Microscopy (DHM) and fluorescence microscopy to study the basic mechanisms of gold nanoparticle mediated laser manipulation. This talk will focus on the technical aspects of the setup and holographic image reconstruction. Results pertaining to cell volume change and calcium response of cells in laser transfection will be shown as an application.

For the reconstruction of phase images from fringe image data, a phase unwrapping algorithm will be presented that can cope with the vast amount of data that was captured. This algorithm is a hybrid between a block unwrapping technique and a path following unwrapper. It combines the robustness of a path following algorithm and a parallelizable block unwrapping preprocessing step.

The setup enables simultaneous acquisition of fluorescence and phase images. For cell manipulation, a picosecond laser was coupled into the setup and weakly focused on cells incubated with gold nanoparticles. To study the cell volume change in the first minute after irradiation, phase images were captured with a frame rate of 30fps. Analysis of cell volume data with double exponential least square fits suggests that volume change is effected by different transport mechanisms depending on the exposure time and the radiant intensity of the transfection laser. Fluorescence images yielded the calcium signal of the cells. The setup is suitable to study fast cell changes simultaneously in phase and fluorescence for different laser based cell manipulation scenarios as well.

9336-16, Session 2

Subwavelength light focusing and imaging via wavefront shaping and measurement in complex media

Jung-Hoon Park, Chunghyun Park, Yong-Hoon Cho, YongKeun Park, KAIST (Korea, Republic of)

We demonstrate that multiple scattering can be controlled via wavefront shaping in order to obtain a sub-diffraction limited focus at an arbitrary position (1) and the full-field dynamic sub-wavelength imaging (2). Due to the random structure of the highly scattering media there are no restrictions on the physical position of the focus giving the system a high degree of freedom. We first demonstrate that the multiple scattering can be used to steer and focus sub-diffraction limited light spots with arbitrary polarization (3) or wavelength (4) within its inhomogeneous structure.

We also present that the full-field dynamic sub-wavelength imaging can be obtained by transferring the optical near-field into propagating far-field components by multiple light scattering from disordered nanoparticles, which was previously demonstrated in microwave regime (5). We achieve sub-wavelength light focusing by far-field wavefront control or imaging from a single-shot measurement of a speckle field. This new concept can be regarded as aperture-less scan-free near-field nanoscopy. Two-dimensional imaging can also be readily obtained by scanning the near-field focus or employing the concept of the transmission matrix (6, 7). This technique can also be utilized for reflection-type optical tomography of biological tissue based on optical coherence tomography (8) or digital phase conjugation technique for suppressing multiple light scattering (9).

9336-17, Session 2

Telecentric digital holography microscopy: perturbation free quantitative phase imaging

Ana Doblas, Emilio Sánchez-Ortiga, Genaro Saavedra, Manuel Martínez-Corral, Univ. de València (Spain); Jorge Ivan Garcia-Sucerquia, Univ. Nacional de Colombia Sede Medellín (Colombia)

In this contribution, the sketch of an off-axis digital holographic microscope (DHM) is performed. It is known that quantitative phase measurements are perturbed by the insertion of a spherical phase wavefront due to the utilization of a microscope objective (MO). Different approaches have been investigated to compensate this wavefront, both numerically and physically. Inspired by the properties of telecentric imaging systems, the use of an afocal-telecentric DHM was reported to delete this phase perturbation by the imaging system. In this study, we present an overview of telecentric DHMs. Firstly, we have compared the reconstructed quantitative phase images (QPIs) obtained from telecentric setups and regular configuration in which numerical post-processing is required. From these results, we see that accurate measurements are also provided for the telecentric performance. Moreover, we have shown that the spherical phase factor also has a strong impact in amplitude-contrast imaging. In fact, the size of the Fourier transform of the image is spreaded depending on the radius of curvature of the spherical factor. This spreading can produce an overlapping between the different terms in the Fourier space and, consequently, a reduction of the resolution limit. In order to preserve the resolution, we provide a recipe to achieve diffraction-limited DHMs. To sum up our study, we present a configuration of a DHM in which accurate QPIs are provided without losing lateral resolution, this configuration is implemented by using an afocal-telecentric DHM limited by diffraction.

9336-18, Session 2

Quantitative polarization microscopy using interferometric spectral multiplexing

Chengshuai Li, Yizheng Zhu, Virginia Polytechnic Institute and State Univ. (United States)

Optical birefringence occurs naturally in many biological specimens with unique structural and molecular organizations, such as cytoskeleton and mitotic spindles. Quantitative imaging of birefringence can reveal important biophysical and biochemical information, by determining of the orientation of optical axes and the magnitude of the relative phase retardation between the two polarizations. Conventionally, multiple images with specific phase and polarization settings are required for extracting the values of these parameters, usually achieved by rotating polarizers and/or waveplates. The performance of such approaches is often limited by the accuracy and repeatability of these adjustments.

In this presentation, we introduce a novel spectral-domain interferometry technique for fast, sensitive imaging of birefringence. This technique takes advantage of the spectral multiplexing capability of spectral-domain low coherence interferometry to modulate phase information from both polarizations into the spectral interferogram for simultaneous detection. Consequently, the orientation and magnitude of sample birefringence can be extracted without the need for rotating optics. The spectral-domain interferometry approach also offers to isolate sample signals from out-of-band shot noise, hence promising in achieving better measurement sensitivity. The principle of the technique and its demonstration using various samples will be presented and discussed.

9336-19, Session 2
Coherence-controlled holographic microscopy for live-cell quantitative phase imaging

Tomás Slabý, Brno Univ. of Technology (Czech Republic) and TESCANA, a.s. (Czech Republic); Aneta Krisová, CEITEC Brno Univ. of Technology (Czech Republic) and TESCANA, a.s. (Czech Republic); Martin Lostak, Brno Univ. of Technology (Czech Republic) and TESCANA, a.s. (Czech Republic); Jana Colláková, CEITEC Brno Univ. of Technology (Czech Republic); Veronika Juzová, TESCANA, a.s. (Czech Republic); Pavel Veselý, Radim Chmelík, CEITEC Brno Univ. of Technology (Czech Republic)

In this paper we present coherence-controlled holographic microscopy (CCHM) and various examples of observations of living cells including combination of CCHM with fluorescence microscopy.

CCHM is a novel technique of quantitative phase imaging (QPI). It is based on grating off-axis interferometer, which is fully adapted for the use of incoherent illumination. This enables high-quality QPI free from speckles and parasitic interferences and lateral resolution of classical widefield microscopes. Label-free nature of QPI makes CCHM a useful tool for long-term observations of living cells. Moreover, coherence-gating effect induced by the use of incoherent illumination enables QPI of cells even in scattering media. Combination of CCHM with common imaging techniques brings the possibility to exploit advantages of QPI while simultaneously identifying the observed structures or processes by well-established imaging methods.

We used CCHM for investigation of general parameters of cell life cycles and for research of cells reactions to different treatment. Cells were also visualized in 3D collagen gel with the use of CCHM. It was found that both the cell activity and movement of the collagen fibers can be registered. The method of CCHM in combination with fluorescence microscopy was used in order to obtain complementary information about cell morphology and identify typical morphological changes associated with different types of cell death. This combination of CCHM with common imaging technique has a potential to provide new knowledge about various processes and simultaneously their confirmation by comparison with known imaging method.

9336-20, Session 3
Super-resolution, complex field imaging microscope via Fourier ptychography

Xiaoze Ou, California Institute of Technology (United States); Guoan Zheng, Univ. of Connecticut (United States); Changhui Yang, California Institute of Technology (United States)

Fourier ptychography is a newly developed super-resolution technique, which employs angularly varying illuminations to acquire high spatial frequency components of the sample that exceed the pass-band of the microscope system, and a phase retrieval algorithm to synthesize these components, resulting in a resolution surpassed the diffraction limit of the objective lens. In the paper, we illustrated the principle of Fourier ptychography, and we demonstrated that by introducing an LED matrix and a CCD camera to a conventional microscope system, the potential power of this conventional microscope can be fully explored: The achievable resolution is no longer limited by the intrinsic numerical aperture (NA) of the objective lens, but the summation of objective NA and illumination NA. Quantitative phase information can be reconstructed along with intensity information by merely using intensity measurement. Moreover, the aberration of the microscope system can be characterized and eliminated from the reconstructed image without extra measurement. We believe that this conversion from a conventional microscope to a high-resolution, large

field-of-view, aberration free Fourier ptychographic microscope can bring dramatic benefits to biological and clinical application such as cell culture monitoring, digital pathology, hematology analysis and etc.

9336-21, Session 3
Speckle correlation reflection phase microscopy

Youngwoon Choi, Poorya Hosseini, Massachusetts Institute of Technology (United States); Wonshik Choi, Korea Univ. (Korea, Republic of); Ramachandra R. Dasari, Peter T. C. So, Zahid Yaqoob, Massachusetts Institute of Technology (United States)

Speckle wave fields, generated by illuminating random media with coherent light, are an interesting subject due to the intriguing optical properties and unique advantage for holographic imaging. In general, speckle waves have been considered an obstacle for imaging in astronomy and life sciences, but many studies have proved that either static or dynamic speckle waves can be used to improve imaging performance by reducing diffraction noise. The short spatial coherence length of dynamic speckle waves enables to reject the interference caused by unwanted reflection. The short autocorrelation length, axial as well as lateral, can also provide depth sectioning (similar to confocal and low-coherence methods) and lead to improved spatial resolution. Here we present a reflection phase microscopic technique featured with single-shot and wide-field capability using time-varying speckle-field as an illumination source. By introducing an identical dynamic speckle-field on two different arms of the interferometer, a correlation process is automatically generated through the interferometric measurements. The decorrelation nature of 3-dimensional speckle-field allows the system to achieve confocal equivalent depth selectivity as well as improved lateral resolution. The proposed technique will facilitate the measurement of fast dynamics associated with the motion of cell membranes.

9336-22, Session 3
Halo-free quantitative phase imaging with partially coherent light

Tan H. Nguyen, Hassaan Majeed, Christopher A. Edwards, Minh N. Do, Lynford L. Goddard, Gabriel Popescu, Univ. of Illinois at Urbana-Champaign (United States)

Quantitative Phase Imaging (QPI) has recently become a valuable tool for extracting information on the refractive index and morphology of transparent specimens. Most interferometry-based QPI systems use fully coherent illumination, which have coherence areas that are larger than the field of view. These systems have low depth sectioning capability and low lateral resolution. The lateral resolution for these cases are limited by the numerical aperture (NA) of the objective instead of from both the objective and the condenser. In contrast, partially coherent QPI methods illuminate specimens with a higher solid angle. Higher lateral resolution and better depth sectioning are obtained as a result. However, since the coherence area may be smaller than the object size, previously reported partially coherent methods have under-estimated phase values, low phase contrast, and the well-known halo effect. In this paper, we formulate a model for interferometry-based QPI for both the traditional and common-path regimes. Our model predicts that traditional methods give correct phase values without halo irrespective of the illumination's coherence area while the common-path ones gives lower phase values due to the intrinsic halo effect. Since common-path methods have higher stability to measurement noise than traditional methods, they have become increasingly popular. Therefore, an algorithm to fix the measurements and generate correct phase values is needed. In this paper, we propose an iterative method to solve the inverse problem using our model. We show that halo-free quantitatively correct phase images can be obtained using a typical 40X objective with the condenser $NA \leq 0.09$.

9336-23, Session 3
Partially coherent phase imaging with source shape estimation

Jingshan Zhong, Nanyang Technological Univ. (Singapore); Lei Tian, Univ. of California, Berkeley (United States); Justin Dauwels, Nanyang Technological Univ. (Singapore); Laura Waller, Univ. of California, Berkeley (United States)

Phase recovery from a stack of defocused intensity images can be viewed as a nonlinear inverse problem, since the phase is transferred into intensity by wave diffraction. For the case of coherent illumination, the Kalman filtering approach used here provides a theoretically near-optimal phase recovery from the defocused intensity stack. This work extends the method to the case of an arbitrary source shape creating partially coherent illumination at the sample.

Many imaging systems (e.g. bright field microscope) have partially coherent (Köhlher) illumination, which is in the Fourier plane of the sample. The Van Cittert-Zernike theory shows the coherence can be modeled with a much simpler 2D function than a 4D function of a general case. The measured defocused intensity can be modeled as a convolution between the intensity that would have been measured with coherent illumination and a scaled source shape. We formulate a state-space model for the Kalman filter, with intensity measurement as observation of the unknown state. We also derive a sparse Kalman filter for the partially coherent phase retrieval algorithm. By adding an extra optimization step, we show that it is possible to estimate the source shape also from the intensity images. The estimation of source shape provides convenience for situations where the measurement or a priori knowledge of the source is difficult or impossible to obtain. We validate our algorithms in a Nikon TE300 microscope with various condenser apertures. We expect the partially coherent phase recovery will find use in biological phase imaging microscope, X-ray, and transmission electron microscope imaging.

9336-24, Session 3
Quantitative phase-shifting DIC using programmable spatial light modulators

Tan H. Nguyen, Christopher A. Edwards, Gabriel Popescu, Univ. of Illinois at Urbana-Champaign (United States)

Compared to Phase Contrast, Differential Interference Contrast (DIC) has been known to give higher depth specificity as well as a halo-free modality to image transparent specimens. However, since DIC uses very low coherence illumination, the phase information is only defined locally, within the coherence area, which is typically comparable to the diffraction spot. Although high resolution, high contrast images are obtained by DIC, it typically only provides qualitative information. In this paper, we introduce a common-path phase-shifting DIC system building from a 4-f system using two SLMs. One of them will be the modulation component while the other will serve as a compensator. The two SLM block functions as a zero-order wave retarder. In this setup, we shift the phase of one of two fields to 4 values $0, \pi/2, \pi$ and $3\pi/2$. The interferograms are recorded for each phase-shift values and an algorithm is further applied to reconstruct the phase gradient. Our system can be used as an add-on module to any commercial DIC microscope. It provides halo-free, high throughput quantitative phase information about the sample with low temporal, spatial noise and good depth sectioning. A Fourier optics analysis is also added to study the behavior of the system. Experimental results are shown for standard control samples (e.g. polystyrene beads) and live cells.

9336-25, Session 3
Confocal based quantitative reflection phase microscopy system development

Vijay Raj Singh, Singapore-MIT Alliance (Singapore); Peter T. C. So, Massachusetts Institute of Technology (United States)

Phase contrast microscopic imaging techniques are most commonly used in visualizing transparent samples e.g. biological cells. The existing transmission based quantitative phase measurement methods provide the average index of refraction of the cells and this is inherently limited for not able to provide imaging capability in 3D. In this work, we present a multiple-aperture based confocal reflection phase microscopy system development by utilizing a digital micromirror device (DMD, from Texas Instruments). An array of confocal pinhole is generated by using the 'ON' state of micro-mirrors of DMD. The phase information of foci is detected by using a common-path based interferometer system. The programmable raster scanning of pinhole array provides the high speed optically sectioned quantitative tomographic phase imaging capability. Compare to existing system, the proposed system provides the 3D distribution of refractive index variation in reflected light mode with excellent axial depth sectioning capability. The proposed system is aimed for imaging the dynamics of biological cells and able to provide the capability to distinguish the quantitative phase information of cell membrane and cell nucleus.

9336-26, Session 3
Fourier ptychography for multimodal imaging (Invited Paper)

Guoan Zheng, Siyuan Dong, Kaikai Guo, Univ. of Connecticut (United States); Xiaoze Ou, California Institute of Technology (United States)

Fourier ptychography (FP) is a recently developed imaging modality that uses angularly varying illumination to extend a system's performance beyond the limit defined by the employed objective. Here we will report the applications of FP for multimodal imaging, including phase microscopy, gigapixel microscopy, 3D holographic imaging, super-resolution fluorescence imaging, and incoherent photographic imaging. The FP innovation may provide new insights for the development of high-resolution, high-throughput imaging platforms using photon, X-ray and electron.

9336-27, Session 3
CINCH (confocal incoherent correlation holography) high spatial resolution super resolution fluorescence microscopy based upon FINCH (Fresnel incoherent correlation holography) (Invited Paper)

Gary Brooker, Nisan Siegel, Johns Hopkins Univ. (United States)

FINCH is a single path incoherent holographic technique that now can produce super resolved microscopic images that have higher transverse resolution than those from the focused plane of a widefield microscope using high NA objectives. However extended depth of focus is afforded by FINCH since it is a holographic process. As part of an ongoing effort to improve the image quality of FINCH, we have investigated the application of confocal excitation/emission to FINCH. The resulting hybrid technique between FINCH and confocal microscopy is called CINCH. FINCH by itself has been shown to produce images that exceed the Rayleigh limit. We applied a Nipkow spinning disk to an intermediate image plane in FINCH

to present FINCH with a single plane in an attempt to harness the power of holography to extract more information from single confocal image planes. CINCH demonstrates what is possible with FINCH when the light from different object planes is disambiguated. In initial experiments with biological samples, CINCH images were as good or better than those from confocal microscopy. It should be noted that the spinning disk confocal method is only one of a number of confocal methods that may be employed for this purpose. Other means of disambiguation are possible and include laser scanning confocal microscopy, combining FINCH with a single image plane, such as from two-photon confocal microscopy, light sheet microscopy or other means to present single image planes to FINCH. Results from CINCH will be presented.

9336-28, Session 3

Quantitative phase imaging through scattering media

Vera Kollárová, Jana Colláková, Zbynek Dostál, CEITEC Brno Univ. of Technology (Czech Republic); Tomas Slabý, Brno Univ. of Technology (Czech Republic); Pavel Veselý, Radim Chmelík, CEITEC Brno Univ. of Technology (Czech Republic)

Coherence-controlled holographic microscope (CCHM) is an off-axis holographic system. It enables observation of a sample and its quantitative phase imaging with coherent as well as with incoherent illumination. The spatial and temporal coherence can be modified and thus also the quality and type of the image information. The coherent illumination provides numerical refocusing in wide depth range similarly to a classic coherent-light digital holographic microscopy (HM). Incoherent-light HM is characterized by a high quality, coherence-noise-free imaging with up to twice higher resolution compared to coherent illumination. Owing to an independent, free of sample reference arm of the CCHM the low spatial light coherence induces coherence-gating effect. This makes possible to observe specimen also through scattering media.

We have described theoretically and simulated numerically imaging of a two dimensional object through a scattering layer by CCHM using the linear systems theory. We have investigated both strongly and weakly scattering media characterized by different amount of ballistic and diffuse light. The influence of a scattering layer on the quality of amplitude as well as phase signal is discussed for both types of the scattering media. A strong dependence of the imaging process on the light coherence is demonstrated.

The theoretical calculations and numerical simulations are supported by experimental data gained with model samples, as well as real biologic objects, particularly then by time-lapse observations of live cells reactions to substances producing optically turbid emulsion.

9336-29, Session 3

Hyperspectral quantitative phase microscopy

Jae Hwang Jung, KAIST (Korea, Republic of); Jaeduck Jang, Samsung Advanced Institute of Technology (Korea, Republic of); YongKeun Park, KAIST (Korea, Republic of)

Quantitative phase imaging (QPI) has become a prospective technique to study biological samples. High precision and sensitivity of QPI enable various biological applications such as measuring membrane fluctuations of RBCs. Recently, spectroscopic QPI techniques, which are QPI with multiple wavelengths, have been developed. Measuring optical dispersion from spectroscopic field information is one of the promising properties to enhance the molecular specificity of QPI techniques. Several ideas, such as utilizing band-pass filters, multiple lasers, and spatial light modulator, have been demonstrated spectroscopic QPI. Despite considerable advances, previous spectroscopic QPI techniques have technical limitations, including

a limited number of wavelengths, restricted field-of-view, low spectral resolution and bandwidth.

In this work, we demonstrate the swept-source diffraction phase microscopy (ssDPM) to measure full-field spectroscopic quantitative phase image of individual microscopic samples in visible spectrum (450-750 nm) with spectral resolution less than 8 nm. This system, ssDPM, consists of the custom-built swept-source and diffraction phase microscopy (DPM). DPM, which is the common-path interferometric QPI technique, can measure optical fields with high stability. The custom-built swept-source mainly consists of a white-light source, a diffraction grating, a rotating mirror, and a pinhole. While white light is dispersed by the grating, the spectral band that passes the pinhole is controlled by angle of rotating mirror. To verify this technique, we measured refractive indices of polystyrene beads and bovine serum albumin solution.

9336-31, Session 4

Integral functions of the phase image of biological microobjects: an algorithm and the role in cell morphology and physiology

Vladimir P. Tychinsky, Tatiana V. Vyshenskaya, Alexander V. Kretushev, Vladislav D. Zverzhkhovskiy, Moscow State Institute of Radiotechnics, Electronics and Automation (Russian Federation); Alexander A. Shtil, N.N. Blokhin Russian Cancer Research Ctr. (Russian Federation) and National Research Nuclear Univ. MEPhI (Russian Federation)

The entirety of parameters obtained in phase imaging of bacterial and eukaryotic cells ('phase portrait'; Tychinsky et al., 2013) provides a valuable tool for description of structural and functional characteristics of microobjects. This analysis is based on differential optical parameters of individual subcellular compartments. The integral functions of the phase image are the dependence of the area and phase volume of the image's portion (within the isolines) on the isoline's phase height. We developed an algorithm for identification of the boundaries of subcellular compartments. The characteristic straight lines are drawn to the phase volume function in the areas where this curve (i.e., changes of optical parameters) is monotonous. These characteristic lines represent a first degree polynomial approximation of the part of the integral function. The abscisses of the intersection points of these lines correspond to the values of the heights of isolines that limit the subcellular compartments in the phase image. These points may serve as descriptors of the physical parameters of organelles. Besides these characteristic points the functional state of the cell can be described by the angle of characteristic lines to the phase volume function at the area that corresponds to an organelle (e.g., mitochondria). If the object's geometric shape is known, the integral functions allow for calculation of average radial profile of refractivity or refractive index. We discuss the significance of integral functions of the phase image for understanding cellular response to stress stimuli including anticancer drugs and metabolic poisons.

We dedicate this study to the memory of late Professor V.P.Tychinsky, an eminent scholar of coherent phase microscopy.

9336-32, Session 4

Fast processing of quantitative phase profiles from off-axis interferograms for real-time applications

Pinhas Girshovitz, Natan T. Shaked, Tel Aviv Univ. (Israel)

The reconstruction of quantitative phase profiles of dynamic microscopic samples captured using digital off-axis interferometry typically involves off-line post-processing. The processing speed for extracting the

unwrapped quantitative phase profile from the captured interferograms is performed in approximately two frames-per-second (fps) for 1 megapixel interferograms on a conventional computer, which does not suit many real-time applications. Here, we present improved algorithms that significantly decrease the extraction time of the sample quantitative phase profile. In previous work, we presented algorithms that are capable of reaching processing frame-rates of more than 30 fps for one megapixel interferograms. Here, we present new, improved algorithms that significantly decrease the extraction time of the sample wave-front in off-axis interferometry. This is done by further improving the performance of the different stages of the conventional off-axis reconstruction algorithm and removing unnecessary operations in the reconstruction procedure. While using a simple single-core processing unit on a standard personal computer, without using advanced hardware to enable parallelization of the image data processing, the new algorithms are capable of reaching processing frame rates of 45 fps for one megapixel interferograms in a general case, where an unwrapped phase profile is needed, and frame rates of up to 150 fps for one mega pixel interferograms when the phase unwrapping procedure is not required. Using the new approach, we can reach real-time processing and visualization on standard processors. The new algorithms are demonstrated experimentally for quantitative visualization of rapidly-changing biological samples.

9336-33, Session 4

Quantitative phase retrieval using nonlinear propagation

Jen-Tang Lu, Chien-Hung Lu, Jason W. Fleischer, Princeton Univ. (United States)

Quantitative phase retrieval is growing in importance, in fields ranging from wavefront sensing to biomedical imaging. Consequently, there have been many methods devised to measure the phase of a wave. As electronic devices only record time-averaged intensity, and most illumination sources are not coherent, noninterferometric methods have become increasingly popular. These approaches take two (or more) intensity measurements and use a numerical algorithm to reconstruct the phase. The paradigm method is the Gerchberg-Saxton (GS) algorithm, where phase is iteratively reconstructed with two measured intensity distributions at two different measurement planes (typically near field and far field). However, linear propagation algorithms are "black box" methods that do not provide an independent measure of the phase being retrieved. This makes linear methods susceptible to noise, conjugate solutions, and local minima in phase space. There are also no guidelines for the boundary conditions, as initial phase guesses are random and no phase reference is available for stopping the iterations.

In nonlinear systems, intensity-induced index changes upon propagation also contribute to phase evolution, making nonlinear systems much more sensitive to phase inputs. At the same time, noise can be reduced, as phase-matching conditions (conservation of wave energy and momentum) effectively act as a nonlinear filter. Here, we show that nonlinear feedback leads to a remarkable convergence property in the iteration algorithm, and that the reconstructed phase error can be minimized by tuning the nonlinearity.

9336-34, Session 4

PRoCAST: a quantitative phase imaging tool for prostate cancer recurrence prediction

Shamira Sridharan, Univ. of Illinois at Urbana-Champaign (United States); Virgilia Macias, Univ. of Illinois at Chicago (United States); Krishnarao V. Tangella, Presence Covenant Medical Ctr. (United States); Andre Kajdacsy-Balla, Univ. of Illinois at Chicago (United States); Gabriel Popescu, Univ.

of Illinois at Urbana-Champaign (United States)

Among individuals who undergo radical prostatectomy, the risk for prostate cancer recurrence is 25% whereas the risk for death due to cancer is 7-12%. Identifying individuals at risk for recurrence is very important. We developed PRoCAST: Predicting Recurrence of Cancer using the Anisotropy of Scattering by Tissue, a method that identifies recurrent cases using the anisotropy of light scattering in the stroma immediately adjoining glands as a marker. For our study, we used prostatectomy samples from 89 individuals with recurrence and 91 without recurrence. 89 cases in each group were matched based on age at prostatectomy, Gleason grade and pTNM stage. PRoCAST predicted recurrence with 77% sensitivity and 62% specificity (AUC 0.72) which was significantly better than the widely used clinical tool CAPRA-S (AUC 0.54) tested on the same population. A lower anisotropy value corresponded to a higher chance of recurrence, which means that the stroma adjoining glands of individuals with recurrence had a more fractionated morphology. The cases used in our study were also the ones in which current methods fail. We expect even higher discrimination ability by PRoCAST in a general population of individuals who undergo prostatectomy.

9336-35, Session 4

C++ software integration for a high-throughput slim platform

Mikhail E. Kandel, Zelun Luo, Kevin Han, Gabriel Popescu, Univ. of Illinois at Urbana-Champaign (United States)

As a new technique, the lack of ready-made commercial hardware and software tools limits QPI systems to propose built platforms beyond the reach of those outside the optics community. The scripts and modules designed for experiments are often purpose built and limited due to the abstractions found in higher-level programming languages, resulting in a palpable chasm between promised and realized hardware performance. Instrumentation difficulties are further compounded by the general unfamiliarity with intricacies such as background calibration, objective lens attenuation, and spatial light modular alignment, make successful measurement difficult for the uninitiated or inattentive. This poses an immediate challenge for moving our techniques to biological oriented collaborators and clinical practitioners.

Further, the multi-shot approach in SLIM requires reliable, synchronous, and parallel operation of three independent hardware devices – not meeting these challenges results in degraded phase and slow acquisition speeds, forcing a compromise between magnification and detail, narrowing applications to holistic statements about complex phenomena.

To meet the problems of performance and accessibility we describe our shift to the C++ software stack and explain our motivations, design and vision for the next generation of Quantitative Phase Imaging system. We emphasize computational techniques such as threading for hardware automation, in addition to methods for users interaction, visualization, and archival storage. Overall, these improvements have resulted in orders of magnitude increase in throughput enabling large scale studies of cell growth and rapid digitization of clinically relevant specimen.

9336-36, Session 4

Phase correction in low coherence diffraction phase microscopy using the optical transfer function

Christopher A. Edwards, Gabriel Popescu, Lynford L. Goddard, Univ. of Illinois at Urbana-Champaign (United States)

Quantitative phase imaging (QPI) techniques using white light have demonstrated lower noise than their laser-based counterparts. This is due to reduced speckle noise, a byproduct of the lower spatial coherence.

Unfortunately, insufficient spatial coherence has also been proven to cause a high-pass filtering effect, which reduces the measured phase and produces object-dependent artifacts, such as the well-known halo effect. These artifacts can be removed experimentally, but only by excessive filtering of the source which results in extended exposure times and limited dynamic measurement capabilities.

Diffraction phase microscopy (DPM) is a particular QPI technique that combines the common-path and off-axis geometries by using a diffraction grating, 4f system, spatial filter, and CCD. This allows for low noise, single-shot imaging, where the interferogram produced at the CCD is used to obtain the phase information and reconstruct the surface topography with sub-nanometer accuracy. Recently, a reflection-based DPM system using partially coherent white-light illumination (epi-wDPM) was developed for applications in materials science. We seek a simple method for obtaining proper height measurements while maintaining strong illumination.

In this work, we present a method for measuring the transfer function of the epi-wDPM system which shows the missing low frequencies below kONAcon due to the limited spatial coherence and the missing high frequency above kONAobj, due to the limited objective numerical aperture. Using this transfer function as a model, we performed deconvolution to remove the halo and obtain proper quantitative phase measurements. This allows us to obtain proper topography and halo-free imaging at much faster acquisition speeds.

9336-37, Session 5

Incoherent quantitative phase imaging for label-free cytoskeleton single-shot imaging and organelle trafficking

Pierre Bon, Ctr. National de la Recherche Scientifique (France) and Institut d'Optique Graduate School (France); Sandrine Lécart, Univ. Paris-Sud 11 (France); Emmanuel Fort, Institut Langevin (France); Sandrine Lévêque-Fort, Ctr. National de la Recherche Scientifique (France) and Institut des Sciences Moléculaires d'Orsay (France)

Quantitative phase imaging (QPI) is a powerful method to visualize a semi-transparent sample in a quantitative manner. Several techniques have been released to achieve QPI in the last decade and the majority of them need spatially coherent illumination. However, coherent illumination leads to noisy, poor resolution imaging and diffraction rings around the structures that limit the use of QPI for intracellular compounds imaging.

We propose to use spatially incoherent illumination to achieve single-shot QPI with increased resolution and sensitivity. We have shown that quadri-wave lateral shearing interferometry (QWLSI) is one of the few techniques able to retrieve QPI under non spatially coherent illumination [1,2]. Single-shot incoherent QPI is achieved without any microscope modification: the microscope Köhler illumination is used and a QWLSI is used a conventional camera. In our case, the frame rate of acquisition is 50Hz with 600x600 measurement points.

We will show that label-free cytoskeleton imaging using incoherent QPI is possible within fixed or living cells (CHO cells) with a very good signal/noise ratio [3]. We will present a way to discriminate microtubules from actin using the quantitative value obtained with QPI and simulation tools. This will compare our approach with fluorescence labelling showing the discrimination capability of incoherent QPI. We will then discuss label-free vesicle and mitochondrion trafficking on the cytoskeleton at high frame-rate and 3D resolution.

[1] Bon, Maucort, Wattellier, and Monneret, "Quadriwave lateral shearing interferometry for quantitative phase microscopy of living cells," *Opt. Express* 17, 13080-13094 (2009)

[2] Bon, Aknoun, Monneret, Wattellier, "Enhanced 3D spatial resolution in quantitative phase microscopy using spatially incoherent illumination", *Opt. Express*, 22(7), 8654-8671 (2014)

[3] Bon, Lécart, Fort, Lévêque-Fort, "Fast Label-Free Cytoskeletal Network Imaging in Living Mammalian Cells", *Biophysical J.*, 106, 1588 - 1595 (2014)

9336-38, Session 5

Holographic quantitative imaging of sample hidden by turbid medium or occluding objects

Vittorio Bianco, Lisa Miccio, Francesco Merola, Istituto Nazionale di Ottica (Italy); Pasquale Memmolo, Istituto Nazionale di Ottica (Italy) and Ctr. for Advanced Biomaterials for Health Care, Istituto Italiano di Tecnologia (Italy); Oriella Gennari, Melania Paturzo, Istituto Nazionale di Ottica (Italy); Paolo A. Netti, Ctr. for Advanced Biomaterials for Health Care, Istituto Italiano di Tecnologia (Italy); Pietro Ferraro, Istituto Nazionale di Ottica (Italy)

Lab-on-chips (LoCs) are complex systems that integrate electronics, microfluidics and imaging and typically are able to manipulate very few quantities of liquids with dimensions of tens to hundreds of microns. In the recent years big effort in developing LoCs devices have been spent due to the great potentialities of miniaturization. Among the future application there are: diagnostics, point-of-care medical analysis and chemical synthesis, just to name a few.

Our investigation concerns the developing of quantitative imaging technique to be integrated in microfluidic LoCs devices for biological applications. Many techniques are commonly used for imaging cells, such as confocal and fluorescence microscopy, as well as atomic force microscopy and tomography. However, the scattering processes can severely affect the imaging capabilities in LoC platforms whenever a turbid medium flows inside the channel or when the channel walls are optically rough.

Here, we demonstrate that by exploiting the properties of Digital Holography in microscopy it's possible to get quantitative and non-invasive imaging of biological samples through turbid media and/or scattering walls. Different numerical procedures have been provided depending on the ratio $R = DO/DT$ between the size of the occluding objects, DO, i.e. the dimension of the smaller element of the scattering medium, and the dimensions of the target to be imaged and/or detected, DT. In particular, it will be shown that both amplitude imaging and phase-contrast mapping of cells hidden behind a flow of Red Blood Cells can be obtained.

9336-39, Session 5

Comparative biophysical study of red blood cells from mother and fetal cord blood using diffraction optical micro-tomography

Hyunjoo Park, KAIST (Korea, Republic of); SungHun Na, Kangwon National Univ. Hospital (Korea, Republic of); YongKeun Park, KAIST (Korea, Republic of)

To understand aging process of red blood cells (RBCs), characterizations of biophysical properties of RBCs at various stages in life span are essential. Especially, fetal cord blood has distinctive functions and biophysical properties for fast growing and development of fetus in a short period. In order to investigate biophysical characteristics of individual RBCs in cord blood, here we perform the comparative study of individual RBCs from mother and fetal blood using a common-path diffraction optical micro-tomography (cDOT). cDOT, a label-free and noninvasive laser holographic microscopy, measures the quantitative phase images at the various incident illumination beams. From the measured phase images, 3-D refractive index (RI) map of individual RBCs is reconstructed using diffraction tomographic algorithm. From 3-D RI map, the morphological and biochemical parameters of individual RBCs including of the cellular volume, surface area, sphericity index, the cellular hemoglobin concentration, and the cellular dry mass are quantitatively characterized. In addition, cDOT simultaneously measures the dynamics membrane fluctuation, which manifest the deformability of

RBCs with nanometer sensitivity. Through profiling of individual RBCs in three groups of a non-pregnant women, maternal, and fetal cord blood, we present unique biophysical characteristics of cord blood; the large cellular volume, more disk-like morphology and similar level of fluctuation despite increased membrane curvature in a dimple. These results lead us to new biological insight for RBCs under various physiological condition related to ageing via exploiting a quantitative phase imaging technique.

9336-40, Session 5

Differentiating neutrophils using the optical coulter counter

Ethan F. Schonbrun, Giuseppe Di Caprio, Harvard Univ. (United States)

We present an optical measurement system that quantifies cell volume and nuclear morphology of neutrophils in high-throughput. Neutrophils are the most common type of white blood cells in the body and are the first responders of the immune system. While current clinical hematology analyzers can differentiate neutrophils from a blood sample, they do not give other quantitative information beyond their count. Specifically, a better understanding of the age distribution of a neutrophil population could be used as an early indicator of infection or the general load on the immune system.

Both cell volume and nuclear morphology are suspected to change in neutrophils as they age in the blood stream. Neutrophils shrink in size as they progress through their natural lineage and consequently cell volume should correlate inversely to cell age. In addition, as they age, the shape of their nuclei progress from elliptical, to banded, to fully segmented into two, three, or more lobes.

Recently we have developed an optical coulter counter that quantifies the volume of cells as they flow through a microfluidic channel. Unlike other optical methods for measuring cell volume, the optical coulter counter is independent of the cell's refractive index and does not require decoupling from a phase or scattering signal. We combine this with fluorescence imaging of the nucleus and machine vision analysis to quantify nuclear morphology. By correlating these two metrics that quantify cell age, the health of the immune system can now be studied in greater detail.

9336-41, Session 5

Quantitative phase imaging with a 3D resolution equivalent to fluorescence: application to label-free biological tissue reconstruction

Pierre Bon, Institut d'Optique Graduate School (France) and Ctr. National de la Recherche Scientifique (France); Sherazade Aknoun, PHASICS S.A. (France) and Institut Fresnel (France); Serge Monneret, Institut Fresnel (France) and Ctr. National de la Recherche Scientifique (France); Brahim Lounis, Univ. of Bordeaux (France); Benoit F. Wattellier, PHASICS S.A. (France); Laurent Cognet, Institut d'Optique Graduate School (France) and Ctr. National de la Recherche Scientifique (France) and Univ. Bordeaux 1 (France)

Quantitative phase imaging (QPI) is a powerful method to visualize a semi-transparent sample in a quantitative manner. Several techniques have been released to achieve QPI in the last decade and the majority of them need spatially coherent illumination. Coherent illumination bears however several disadvantages since it leads to noisy, poor resolution imaging (especially in the axial direction), limiting thus the use of QPI for biological tissue imaging. Using a spatially incoherent illumination rather than a coherent one would

present multiple advantages: (i) axial sectioning is achieved with a doubled lateral resolution compared to coherent QPI; (ii) a 3D reconstruction of the sample can be obtained simply by scanning it in the axial direction; and (iii) this approach can also be applied to highly scattering samples, usually not compatible with QPI because of the coherence loss.

We propose here to use spatially incoherent illumination combined with axial scanning of the sample (z-scan) and a numerical 3D deconvolution to achieve QPI and obtain the same 3D resolution as in fluorescence imaging. Indeed, we have shown that quadri-wave lateral shearing interferometry (QWLSI) is one of the few techniques able to retrieve QPI under spatially incoherent illumination [1,2]. Moreover, incoherent QPI is performed without any major microscope customization since QWLSI can be directly plugged onto the microscope camera port under regular Köhler illumination.

We provide quantitative 3D reconstruction of complex structures (such as brain tissue) and discuss the applications of this technique combined with regular fluorescence imaging.

[1] Bon, Maucort, Wattellier, and Monneret, "Quadriwave lateral shearing interferometry for quantitative phase microscopy of living cells," Opt. Express 17, 13080-13094 (2009)

[2] Bon, Aknoun, Monneret, Wattellier, "Enhanced 3D spatial resolution in quantitative phase microscopy using spatially incoherent illumination", Opt. Express, 22(7), 8654-8671 (2014)

9336-42, Session 5

Bright-field quantitative phase microscopy (BFQPM) for accurate phase imaging using conventional microscopy hardware

Micah H. Jenkins, Thomas K. Gaylord, Georgia Institute of Technology (United States)

Most quantitative phase microscopy methods require the use of custom-built or modified microscopic configurations which are not typically available to most bio/pathologists. There are, however, phase retrieval algorithms which utilize defocused bright-field images as input data and are therefore implementable in existing laboratory environments. Among these, deterministic methods such as those based on inverting the transport-of-intensity equation (TIE) or a phase contrast transfer function (PCTF) are particularly attractive due to their compatibility with Köhler illuminated systems and numerical simplicity. Recently, a new method has been proposed, called multi-filter phase imaging with partially coherent light (MFPI-PC), which alleviates the inherent noise/resolution trade-off in solving the TIE by utilizing a large number of defocused bright-field images spaced equally about the focal plane. Despite greatly improving the state-of-the-art, the method has many shortcomings including the impracticality of high-speed acquisition, inefficient sampling, and attenuated response at high frequencies due to aperture effects. In this report, we present a new method, called bright-field quantitative phase microscopy (BFQPM), which efficiently utilizes a small number of defocused bright-field images and recovers frequencies out to the partially coherent diffraction limit. The method is based on a noise-minimized inversion of a PCTF derived for each finite defocus distance. We present simulation results which indicate nanoscale optical path length sensitivity and improved performance over MFPI-PC. We also provide experimental results imaging live bovine mesenchymal stem cells at sub-second temporal resolution. In all, BFQPM enables fast and accurate phase imaging with unprecedented spatial resolution using widely available bright-field microscopy hardware.

9336-43, Session 5

Multimodal label-free growth and morphology characterization of different cell types in a single culture with quantitative digital holographic phase microscopy *(Invited Paper)*

Björn Kemper, Jana Wibbeling, Lena Kastl, Jürgen Schnekenburger, Steffi Ketelhut, Westfälische Wilhelms- Univ. Münster (Germany)

For the analysis of the impact of pharmaceuticals or pathogens on different cellular phenotypes under identical measurement conditions and to analyze interactions between different cellular specimens a minimally-invasive quantitative observation of different cell types in a single culture is of particular interest. Digital holographic microscopy (DHM), a variant of quantitative phase microscopy (QPM), provides high resolution detection of optical path length changes that is suitable for stain-free minimally-invasive live cell analysis. Due to low light intensities for object illumination, QPM minimizes the interaction with the sample and has been demonstrated in particular to be suitable for long-term time-lapse investigations, e.g., for the detection of cell morphology alterations due to drugs and toxins. Furthermore, QPM has been demonstrated to be a versatile tool for the quantification of cellular growth and motility. Thus, we studied the feasibility of QPM for the analysis of mixed cell cultures and explored if quantitative phase images provide sufficient information to distinguish between different cell types and to extract cell specific parameters. For the experiments quantitative phase imaging with DHM was utilized. Mixed cell cultures with different cell types were observed with quantitative DHM phase contrast up to 80 h. The obtained series of quantitative phase images were evaluated by adapted algorithms for image segmentation. From the segmented images the area covered by the cells, the cellular dry mass and the mean cell thickness were calculated and used in the further analysis as parameters to quantify the reliability the measurement principle. The obtained results demonstrate that it is possible to characterize the growth of cell types with different morphology features separately in a single culture.

9336-44, Session 5

Quantifying the effects of micro-environments on breast cancer cell proliferation using quantitative phase imaging

Mustafa A. Mir, Univ. of California, Berkeley (United States); Tiina Jokela, Mark A. LaBarge, Lawrence Berkeley National Lab. (United States); Lydia L. Sohn, Univ. of California, Berkeley (United States)

Like many other cell functions, metastases and cancer-cell differentiation are directed by complex interactions with the specific microenvironmental niche a cell inhabits. To investigate these interactions, LaBarge et al. (Stem Cell Rev., 2007) have developed a parallel microenvironment microarray (MEArray) platform, which allows one to investigate distinct components of the microenvironment (e.g. Collagen, TGF- β , and IGF1) in a combinatorial manner. Currently, measurements on MEArrays have been limited to endpoint immunofluorescence measurements or time-lapse measurements using qualitative techniques such as phase-contrast. Here, we demonstrate that we are able to perform label-free quantitative time-lapse studies of cells cultured on MEArrays through Diffraction Phase Microscopy (DPM), a common-path, off-axis, quantitative phase-imaging modality. In particular, we measured the effects of a combinatorial array of microenvironments (Collagen1, TGF- β , IGF1, and TenascinC) that have been known to induce an epithelial-mesenchymal transition (EMT) in MCF-7 breast-cancer cells. We show that we are able to detect significant differences in the proliferation dynamics of cells grown in different environments using DPM. Our findings

suggest that quantitative phase-imaging measurements can be used to identify EMT, a process associated with metastasis, in a label-free manner. Furthermore, such quantitative, multi-parametric, time-lapse measurements can offer a unique insight into the role of the microenvironment in cancer progression.

9336-45, Session 5

Prostate cancer diagnosis using quantitative phase imaging and machine learning algorithms

Tan H. Nguyen, Shamira Sridharan, Univ. of Illinois at Urbana-Champaign (United States); Virgilia Macias, Andre K. Balla, Univ. of Illinois at Chicago (United States); Minh N. Do, Gabriel Popescu, Univ. of Illinois at Urbana-Champaign (United States)

Recent works have shown that refractive index measurements from QPI can offer very competitive medical diagnosis results compared to those from H&E stained images. This paper demonstrates, for the first time to our knowledge, the use of QPI images obtained from the Spatial Light Interferometry Microscopy (SLIM) to do prostatic cancer diagnosis. From a dataset of 240 patients with verified outcomes from Department of Pathology at University of Chicago, we build a machine learning algorithm to segment different regions of the biopsies (e.g. gland, stroma and lumen) based on the tissue's textural behavior with the accuracy for all grades of at least 80%. Based on this labeled map, another automated diagnosis step is applied to determine the outcome of the patients. First, a subsequent weak-classifier determines whether the patient is benign or malignant based on local information surround segmented glands. This fact is based on an underlying hypothesis that existence of basal cell layers will generate different textural behavior in QPI images. Then, morphological information of the segmented gland and stroma will be used to further grade the biopsy in each group using a final classifier. Our method is superior to those using H&E image in the sense that it requires less time for sample preparation, high throughput. Furthermore, the image contrast is intrinsically better for stromal region of QPI images. This information is especially important to produce the true Gleason grade of high-grade cancerous samples.

9336-46, Session 5

Quantitative phase imaging to verify non-proliferation in quiescent and senescent cells

Basanta Bhaduri, Arindam Chakraborty, Mikhail E. Kandel, Supriya G. Prasanth, Gabriel Popescu, Univ. of Illinois at Urbana-Champaign (United States)

Cell proliferation depends on the presence of growth factors, typically supplied as serum. When growth factors are withdrawn, the cells cannot pass a restriction point in the late G1 phase, and they stably but reversibly arrest growth in G0 which is called quiescence. However, when growth factors are restored, quiescent cells initiate DNA synthesis after a lag that exceeds the duration of G1. Mitotic cells can also enter an essentially irreversible growth-arrested state termed senescence. A significant difference between quiescent and senescent cells is their response to growth factors. In both cases, growth factors induce the expression of a common set of genes. However, whereas quiescent cells resume proliferation, senescent cells remain arrested with a G1 DNA content.

It was never shown quantitatively whether quiescent and senescent cells are non-proliferating and whether there is any difference between them in terms of cellular dry mass change in the long run. Spatial light interference microscopy (SLIM) is a special type of quantitative phase imaging (QPI) technique for cellular dry mass measurement with high resolution and sensitivity. In this work we have used SLIM to measure

cellular dry mass of quiescent and senescent cells every 15 minutes for 24 hours by quantitatively imaging the phase. WI38 human primary fibroblasts were obtained, cultured, and assessed for quiescence or senescence. Unstimulated asynchronous cells were used as a control. Further we'll also show the difference in mass transport in these cells by phase imaging at 10 Hz and using dispersion-relation phase spectroscopy (DPS).

9336-47, Session 6

Wavelength-scanning phase imaging

Poorya Hosseini, Yongjin Sung, Youngwoon Choi, Peter T. C. So, Zahid Yaqoob, Massachusetts Institute of Technology (United States)

Conventional wide-field quantitative phase imaging (QPI) permits label-free measurement of object's optical properties that may be exploited in a range of biological studies such as single cell volume measurements in erythrocytes (1), cell growth dynamics (2), and dynamics of pathogen infection (3). Furthermore, quantitative phase measurements at multiple wavelengths has created an opportunity for exploring new avenues in phase microscopy such as enhancing imaging-depth (4) or measuring hemoglobin concentrations in erythrocytes (5). To this end, QPI has been demonstrated both at few selected spectral points as well as with high spectral resolution (7,8). Recently, we have set out to develop a stable quantitative dispersion phase microscope based on near-common-path geometry allowing low-noise measurements in a wide spectral range (400 - 750 nm). The feasibility of the approach is initially demonstrated in measuring dispersion curves of various fluorescent bead samples. In this meeting, we will present a theoretical framework and some primary results on how this spectral phase measurement capability may be used in providing structural and functional imaging of biological cells.

References:

1. Curl CL, Bellair C, Harris P, Allman BE, Roberts A, Nugent KA, et al. Single cell volume measurement by quantitative phase microscopy (QPM): a case study of erythrocyte morphology. *Cell Physiol Biochem*. 2006;17(5-6):193-200.
2. Mir M, Wang Z, Shen Z, Bednarz M, Bashir R, Golding I, et al. Optical measurement of cycle-dependent cell growth. *Proc Natl Acad Sci*. 2011;108(32):13124-9.
3. Lee S, Kim YR, Lee JY, Rhee JH, Park C-S, Kim DY. Dynamic analysis of pathogen-infected host cells using quantitative phase microscopy. *J Biomed Opt*. 2011;16(3):036004-036004.
4. Mann CJ, Bingham PR, Paquit VC, Tobin KW. Quantitative phase imaging by three-wavelength digital holography. *Opt Express*. 2008;16(13):9753-64.
5. Park Y, Yamauchi T, Choi W, Dasari R, Feld MS. Spectroscopic phase microscopy for quantifying hemoglobin concentrations in intact red blood cells. *Opt Lett*. 2009;34(23):3668-70.
6. Lue N, Kang JW, Hillman TR, Dasari RR, Yaqoob Z. Single-shot quantitative dispersion phase microscopy. *Appl Phys Lett*. 2012;101(8):084101.
7. Jung J-H, Jang J, Park Y. Spectro-refractometry of individual microscopic objects using swept-source quantitative phase imaging. *Anal Chem*. 2013;85(21):10519-25.
8. Rinehart M, Zhu Y, Wax A. Quantitative phase spectroscopy. *Biomed Opt Express*. 2012;3(5):958-65.

9336-48, Session 6

Lensless phase contrast microscopy and imaging through a multimode fiber

Dirk E. Boonzajer Flaes, Daniel W. E. Noom, Elias Labordus, Kjeld S. E. Eikema, Johannes F. de Boer, Stefan M. Witte, Vrije Univ. Amsterdam (Netherlands)

Lensless microscopes provide exciting new applications in medicine and research. As most optical components are replaced by computer algorithms, they allow visualization at otherwise inaccessible locations using miniaturized devices.

The setup is highly compact, consisting of an RGB-detector illuminated by one single-mode fiber, transmitting red, green and blue laser light. The sample is placed between the fiber and the RGB-detector. From the Fresnel diffraction patterns at different wavelengths it is possible to retrieve both amplitude and phase information of the sample with high accuracy [1]. This information is obtained from a single exposure of the RGB-detector, enabling imaging of moving objects. The numerically retrieved phase information provides real-time phase- and amplitude videos where the focal plane can be decided afterwards. We captured real-time images of moving beads in a flow cell at different focal distances and living, freely moving *C. elegans* with $<2 \mu\text{m}$ resolution [2]. This system provides a first step towards lensless imaging flow cytometry with quantitative phase contrast.

To access more remote locations, this robust lensless imaging technique could also be employed to make small endoscopes, using a multimode fiber to guide the light to the sample and the image back to the sensor. However, light propagating through the fiber is scrambled. Using a 2D spatial light modulator, the fiber scattering properties can be characterized and compensated, enabling imaging through optical fibers. The ability to perform wide-field phase contrast microscopy at the end of a fiber would be a powerful new tool for clinical and industrial applications.

[1] Noom, D. W. E., Eikema, K. S. E. & Witte, S. Lensless phase contrast microscopy based on multiwavelength Fresnel diffraction. *Opt. Lett.* 39, 193-196 (2014).

[2] Noom, D. W. E., Boonzajer Flaes, D. E., Labordus, E., Eikema, K. S. E. & Witte, S. Manuscript in preparation.

9336-49, Session 6

Simple optical tomography measurements using quantitative phase imaging unit

Kyoohyun Kim, KyeoReh Lee, KAIST (Korea, Republic of); Zahid Yaqoob, Peter T. C. So, Massachusetts Institute of Technology (United States); YongKeun Park, KAIST (Korea, Republic of)

Three-dimensional (3-D) refractive index (RI) distribution of biological samples is an intrinsic optical property which is sensitive to chemical composition and morphology inside cells. Measuring 3-D RI distribution of samples provides useful information related to pathophysiological conditions of live biological samples as RI values correspond to the concentrations of proteins inside cells and tissues. Among several tools, optical tomography is commonly used for acquiring 3-D RI tomograms, which measures multiple 2-D optical fields with various illumination angles via interferometry and reconstructs tomograms using appropriate algorithms. However, despite of the advantages of the label-free RI measurements of biological cells, most studies using optical tomographic imaging are merely conducted in biological laboratories since optical tomographic microscopy requires complicated and costly optical setups which are not compatible with conventional microscopes.

Here, we present a quantitative phase imaging unit tomography (QPIUT) system measuring 3-D RI distribution of biological cells which utilizes a simple optical setup that can serve as an add-on for conventional microscopes. QPIUT uses a common-path self-reference interferometry utilizing only three optical components (one Rochon polarizer placed between two polarizers) to measure optical fields from various illumination angles, and reconstructs 3-D RI distribution of samples using optical diffraction tomography algorithm. We investigate chemical and morphological parameters of red blood cells and eukaryotic cells from 3-D RI distribution with high phase stability using QPIUT attached to a conventional microscope.

9336-50, Session 6

Thermal nano-imaging using quantitative phase microscopy

Jaeduck Jang, Soohwan Sul, Taeho Shin, Changhoon Jung, Eui-Seong Moon, Samsung Advanced Institute of Technology (Korea, Republic of)

Quantitative phase microscopy (QPM) has been developed for label-free quantitative optical imaging of biological systems. QPM visualizes physical and chemical properties of biological cells by measuring optical path differences (OPD) determined by their refractive index (RI) and thickness. In addition to biological applications, QPM has been recently utilized for nanomaterial characterization such as defect identification in semiconductors and non-invasive thermal imaging of nanostructures. Probing the spatial variation of temperature is of fundamental interest in biological and material applications, in particular, drug delivery, nanochemistry, and thermoelectrics. Conventional microscopic techniques as a temperature probe include nano-tip-coupled thermal microscopy, infrared spectroscopy, and fluorescence-based optical techniques. These specialized techniques, however, are applicable only under particular experimental conditions. QPM that features non-invasive, quantitative, fast real-time imaging at ambient conditions has been recently used for thermal imaging with high thermal sensitivity of less than one Kelvin. A high-cost commercial wavefront analyzer (WFA) was employed for phase imaging. Although the WFA simplifies the experimental scheme for phase image detection, the state-of-art WFA still suffer from low acquisition rate and pixel resolution, compared to current QPM techniques. In this study, we have developed a thermal nano-imaging technique using diffraction phase microscopy without resorting to the WFA. Our thermal imaging microscope is based on the common-path type of QPM, where temperature difference induces changes in RI and, in turn, phase delay.

9336-51, Session 6

Quantitative phase imaging with programmable illumination

Taewoo Kim, Christopher A. Edwards, Lynford L. Goddard, Gabriel Popescu, Univ. of Illinois at Urbana-Champaign (United States)

Even with the recent rapid advances in the field of microscopy, non-laser light sources used for light microscopy have not been developing significantly. Most current optical microscopy systems use halogen bulbs as their light sources to provide a white-light illumination. Due to the confined shapes and finite filament size of the bulbs, only little room is available for modification in the light source, which prevents further advances in microscopy.

By contrast, commercial projectors provide a high power output that is comparable to the halogen lamps while allowing for great flexibility in patterning the illumination. In addition to their high brightness, the illumination can be patterned to have arbitrary spatial and spectral distributions. Therefore, commercial projectors can be adopted as a flexible light source to an optical microscope by careful alignment to the existing optical path.

In this study, we employed a commercial projector source to a quantitative phase imaging system called spatial light interference microscopy (SLIM), which is an outside module for an existing phase contrast (PC) microscope. By replacing the ring illumination of PC with a ring-shaped pattern projected onto the condenser plane, we were able to recover the same result as the original SLIM. Furthermore, the ring illumination is replaced with multiple dots aligned along the same ring to minimize the overlap between the scattered and unscattered fields. This new method minimized the halo artifact of the imaging system, which allows for a halo-free high-resolution quantitative phase microscopy system.

This research is supported by NSF STC CBET 0939511 Emergent Behavior of

Integrated Cellular Systems (GP) and Beckman Graduate Fellowship (TK). For more information, please visit <http://light.ece.illinois.edu/>.

9336-133, Session 6

Optical diffraction tomography for 3-D tracking of optically trapped colloidal particles

Kyoohyun Kim, Jonghee Yoon, YongKeun Park, KAIST (Korea, Republic of)

We propose and experimentally demonstrate 3-D tracking of optically trapped particles using optical diffraction tomography (ODT). Colloidal particles are optically trapped by a holographic optical tweezers system, and ODT reconstructs 3-D refractive index (RI) distribution of the samples with high lateral and axial resolution. We first validate the proposed method for 3-D tracking of 2- μ m silica beads on the vertices of a 6- μ m side rotating cube. We compare the results with volumetric fields reconstructed by conventional Rayleigh-Sommerfeld back-propagation method. The proposed method is also exploited for tracking 3-D positions of a colloidal particle at the vicinity of biological cells.

9336-52, Session 7

Temperature microscopy using quantitative phase imaging

Guillaume Baffou, Julien Savatier, Serge Monneret, Institut Fresnel (France)

We recently developed a thermal microscopy technique based on quadriwave lateral shearing interferometry [1]. This label-free technique is able to quantitatively map at the submicrometric scale the temperature in three dimensions and the heat source density (power per unit area) on a sample surface. We illustrated the capabilities of this technique on gold nanoparticles illuminated at their plasmonics resonance to turn them into ideal nanosources of heat, an effect at the basis of a fast growing research area named thermal plasmonics [2].

In this presentation, we will introduce the principle of this thermal microscopy technique and illustrate its capabilities by presenting recent associated studies of thermal induced processes at the microscale in hydrodynamics [3], nanochemistry[4] and thermal biology at the single cell level [5,6].

[1] Baffou et al. ACS Nano 6, 2452 (2012)

[2] Baffou et al. Lasers & Photon. Rev. 7, 171 (2013)

[3] Baffou et al. J. Phys. Chem. C 118, 4890 (2014)

[4] Baffou et al. Chem. Soc. Rev. 43, 3898 (2014)

[5] Zhu et al. ACS Nano 6, 7227 (2012)

[6] Baffou et al. Nature Methods, accepted (2014)

9336-53, Session 7

Semiconductor defect metrology using laser-based quantitative phase imaging

Renjie Zhou, Christopher A. Edwards, Gabriel Popescu, Lynford Goddard, Univ. of Illinois at Urbana-Champaign (United States)

In-line detection of sub-10 nm killer defects in patterned wafers is a grand challenge, especially as the semiconductor industry moves beyond the 11 nm node, according to the 2013 International Technology Roadmap for Semiconductors report on metrology. Over the past three years, we have

developed a highly sensitive defect inspection metrology tool based on a laser reflection quantitative phase imaging system, called epi-illumination diffraction phase microscopy (epi-DPM). This system has been used for detecting 20 nm defects in 32 nm node, 22 nm node, and 9 nm node patterned wafers. The first version of this system used a 532 nm solid state laser. During the imaging, we scanned the wafer in plane and captured an image stack. Using the phase and amplitude images retrieved from the system and a comprehensive image post-processing method, we were able to detect different types of defects with sizes down to 20 nm by 100 nm in a 22 nm node wafer. This wafer has 22 nm wide, 120 nm or 260 nm long, and 110 nm high line patterns. To address the inspection need in 9 nm node densely patterned wafers, we further improved the sensitivity and resolution by using a 10x more power stable (quantified with phase noise) 405 nm diode laser with a Faraday rotator based isolator. This update enabled detection of 15 nm by 90 nm defects in a 9 nm node wafer.

9336-54, Session 7

Holographic techniques for high pressure studies

Filippo Saglimbeni, Silvio Bianchi, Univ. degli Studi di Roma La Sapienza (Italy); Richard W. Bowman, Queens' College Cambridge (United Kingdom); Graham M. Gibson, Miles J. Padgett, Univ. of Glasgow (United Kingdom); Roberto Di Leonardo, Univ. degli Studi di Roma La Sapienza (Italy)

Diamond anvil cells allow the behavior of materials to be studied at pressures up to hundreds of gigaPascals in a small and convenient instrument. However, physical access to the sample is impossible once it is pressurized. We show that holographic techniques open the way to unprecedented dynamical measurements of colloidal dynamics inside diamond anvil cells. Using a modified holographic optical tweezers geometry, we can optically trap through a long working distance lens, overcoming the constraints imposed by the limited angular acceptance of the anvil cell.

On the other hand, using coherent light for illumination, we can record in-line holograms of trapped particles and use Lorenz-Mie scattering theory for 3D tracking and sizing with nanometer resolution. Accurate bead sizing is crucial for reliable viscosity measurements and provides a convenient optical tool for the determination of the bulk modulus of individual colloidal particles. This method could be used to investigate the effect of high pressure to the complex rheology of soft materials or to the biomechanics of cells and single biological molecules.

9336-55, Session 7

In-situ measurements of nanoscale phenomena using diffraction phase microscopy

Christopher A. Edwards, Steven J. McKeown, SukWon Hwang, Paul Froeter, Xiuling Li, John A. Rogers, Gabriel Popescu, Lynford L. Goddard, Univ. of Illinois at Urbana-Champaign (United States)

Quantitative phase imaging (QPI) provides highly accurate topographical and/or refractive index data by capturing both the amplitude and phase of the imaging field. When the field from the source interacts with the specimen, a fingerprint of its structure is encoded upon the phase front of the imaging field. Although typical CCDs and detectors only respond to intensity, by capturing the phase, we can reconstruct a map of the sample's surface at the nanoscale. Diffraction phase microscopy (DPM) is a particular QPI technique that combines the off-axis and common-path configurations allowing for single-shot, high-speed dynamics with sub-nanometer noise levels.

In this work, we present recent results on several novel applications. The first application includes in-situ measurements of the dissolution of biodegradable materials proposed for use in biodegradable electronic implants. The materials are stored in both PBS and Bovine serum at 37° C in order to mimic conditions within the human body. Here, we are able to track small nanometer reductions in the height over the course of several weeks as the material is dissolved. The second application is monitoring the self-assembly of nanotubes. A strained bilayer of Si₃N₄ was deposited onto <111> Si and etched anisotropically with KOH. The solution etches underneath the bilayer which then rolls up and self-assembles due to strain. Finally, we present results on the expansion and deformation of palladium structures for use in hydrogen sensing applications. The hydrogen induced lattice expansion of palladium is optically monitored to show nanoscale changes in the structures.

9336-76, Session PMon

Wavevector space calculations in the focal region: optical trapping, lens focusing, and the Gouy phase

Renjie Zhou, Taewoo Kim, Lynford L. Goddard, Gabriel Popescu, Univ. of Illinois at Urbana-Champaign (United States)

We use the wavevector space method to calculate several optical problems that involve solving scattered fields around the focal region. The first problem is optical trapping where light is focused by a lens and used to manipulate small particles such as cells around the focal region. Although the scattering force and the gradient force are used to explain this phenomena, the physical origin of these forces are still not well understood. Here, we provide the trapping force calculation based on the momentum of the scattered field from the particle, thus, avoiding the scattering force and gradient force confusion. Our calculation assumes a spherical wave, instead of Gaussian beam, interacting with a spherical particle with arbitrary size (not limited to the Rayleigh regime). The second problem is calculating light focusing by a lens as a result of interference due to diffraction. By modeling the lens shape with ball functions, we obtain the scattering potential of different thin lenses and calculate the scattered field. Adding the reference beam, the field distribution around the focus is calculated. The third optical problem is calculating the Gouy phase, due to the confinement of the light field around the focus. The field confinement is related to the transverse wavevector second order momentum that can be naturally calculated using the wavevector space field solution. The Gouy phase also relates to the phase imaging, and optical resolution through the uncertainty principle.

9336-77, Session PMon

An efficient autofocusing scheme for quantitative phase imaging

Mikhail E. Kandel, Basanta Bhaduri, Gabriel Popescu, Univ. of Illinois at Urbana-Champaign (United States)

Acquiring a time-lapsed quantitative phase image over a wide field of view remains a challenging and time consuming endeavor due to natural sample and environmental variation. While, these challenges are intrinsic to imaging biologically active or clinically prepared specimen, they are especially well pronounced when acquiring large fields of view at sizes where manual focusing is unsustainable.

Failure to correctly determine the best focus results in a significant loss of spatial frequencies (blurry) and may invalidate comparison between experiments or even among cells on the same plate.

Overzealous autofocusing schemes can greatly increase acquisition times, and a misjudgment on the part of the operator leads to overexposure and death of the specimen - invariably adding phototoxicity as a source of experimental error. These same effects are enhanced when acquiring 4D

data of cells attached to substrates, where the subject often occupies only a fraction of the acquisition volume. When improperly managed, such data sets become large and unwieldy, containing vast swaths of empty space.

We find in QPI high SNR and repeatability, enabling us to drastically reduce light intensity while maintaining precise localization. We present our experiences with designing a depth scanning autofocusing system backed by a 3D mesh that interpolates onto the specimen and is adjusted during the acquisition process. To speed up operation, a low magnification pre-scan is performed to narrow the search window and identify the sample. Further, by acquiring full field images we are able to compensate for factors that would result in counterintuitive best-focus pictures, in particular robust handling of dividing cells in confluent cultures.

9336-80, Session PMon

Optimization and automatization of the Fourier filtering for phase quantification in microtomography

Freddy A. Monroy-Ramirez, Univ. Nacional de Colombia Sede Medellín (Colombia); Edgar M. Torres, Univ. Nacional de Colombia Sede Bogotá (Colombia)

The microtomography is a noninvasive technique that results from the union of digital off-axis holography and tomography. The difference maps calculated from the holographic recordings translucent microscopic sample in different angular positions, phase is taken as input to the tomography technique, which in turn allows calculation of 3D maps shape and refractive index of the samples under study. To calculate the phase difference maps necessary filter in Fourier space of zero order and select the order of interest; typically this filtering process was performed manually using digital masks of different shapes and sizes, which makes it a slow process and not reproducible. This results in a decrease in the lateral resolution of the reconstructed optical field. In this work we show a numerical optimization strategy and process automation Fourier filtering to obtain phase maps to be used in the microtomography technique, which improves the reproducibility, computation time and lateral resolution. The strategy is implemented to calculate the 3D maps refractive index of pollen grains.

9336-81, Session PMon

Incoherent common-path diffraction optical tomography (icDOT)

KyeoReh Lee, Seungwoo Shin, KAIST (Korea, Republic of); Youngcan Kim, Imperial College London (United Kingdom); Kyoohyun Kim, HyunJoo Park, YongKeun Park, KAIST (Korea, Republic of)

Common-path diffraction optical tomography (cDOT) is a non-invasive and label-free optical holographic technique for measuring both the three-dimensional refractive index (RI) tomograms and the two-dimensional dynamic phase images of a sample. By means of common-path geometry of cDOT, extremely high phase sensitivity is achieved and subtle cell membrane motions can be measured. This useful tomographic technique, however, is restricted by speckle noise. Due to the nature of coherent light, methods of quantitative phase imaging (QPI) suffer from speckle noise. This noise decreases spatial phase sensitivity of QPI images. To overcome this speckle noise problem, several researches used partially coherent illuminating light sources such as light emitting diode (LED) or light passed through rotating ground glass.

In this work, we present an improved optical tomographic technique, being referred as incoherent common-path diffraction optical tomography (icDOT) using Ti-sapphire pulsed laser. Because of temporally incoherent character of the pulsed laser, speckle noise is reduced and spatial phase sensitivity of QPI image is improved. We demonstrate this improved tomographic technique by comparing the measured field images of the individual bead

and red blood cell. With the ability of icDOT technique, fine measurement of cell morphology and membrane motion can be realized.

9336-82, Session PMon

3D optical study of melittin associated red blood cells using a common-path diffraction optical tomography

YongKeun Park, Joonseok Hur, HyunJoo Park, SangYoon Lee, KAIST (Korea, Republic of)

In this study, three-dimensional morphologies and physical quantities of red blood cells (RBCs) of which membranes are perforated by melittin binding are measured quantitatively and noninvasively by common-path diffraction optical tomogram (cDOT). This is a novel quantitative imaging technique and superior to measure red cell indices at the individual cell level. Melittin from bee venom is well-known antimicrobial peptide, which induces small pores in membranes. The sizes of these pores vary depending on the associated melittin concentration that these pores allow leakage of atomic ions as well as molecules with tens of kilodaltons. Firstly, we observed that the action of melittin on RBCs changes the morphologies from discocyte to echinocyte and spherocyte using cDOT, which measures three-dimensional refractive-index map of RBCs employing cytoplasmic hemoglobin as a scatter. In addition, the alteration in structural details and biophysical properties of melittin bound RBCs such as volume, surface area, hemoglobin concentration and cellular mass are quantitatively measured. Also, the mechanical property is quantified through dynamic membrane fluctuation, which was measured with nanometer sensitivity. As first in-depth investigation into the effects of melittin on RBC, the results are expected to provide insights about both the action of melittin and unique characteristic of RBC membrane.

9336-83, Session PMon

Spectro-angular light scattering of individual microscopic samples

Jae Hwang Jung, YongKeun Park, KAIST (Korea, Republic of)

Light scattering measurement provides optically and chemically valuable information such as size, shape, refractive index and light absorption. Angle-resolved light scattering (ARLS) signals are utilized to obtain structural information, and spectroscopic light scattering signals are utilized to study chemical properties. Although ARLS and spectroscopic light scattering techniques have been utilized for long time, there are only limited number of techniques that can measure spectro-angular light scattering measurement. In addition, simultaneous measurements of both spectroscopic and angle-resolved light scattering have not been demonstrated yet.

In this work, we present a light scattering measurement technique, referred to as swept-source Fourier transform light scattering (ssFTLS) that can measure angle-resolved light scattering at multiple wavelengths in visible spectrum. Employing spectroscopic quantitative phase microscopy and Fourier transform light scattering technique, spectro-angular light scattering of individual microscopic objects is measured in angular range within $\pm 70^\circ$ in visible spectrum (450-750 nm) at a few seconds. The angular and spectral resolution of ssFTLS is less than 10 mrad and 8 nm, respectively. The results of ssFTLS for individual microscopic polystyrene beads immersed in phosphate buffered saline and bovine serum albumin solutions are in good agreement with Mie theoretical results. Low standard deviation of experimental results implies high stability and repeatability of this system.

9336-84, Session PMon

Observation of spectral shift induced by light scattering of individual microscopic objects

Jae Hwang Jung, YongKeun Park, KAIST (Korea, Republic of)

Spectral shifts, also referred as Wolf shifts, have been studied since Wolf verified the spectrum of partially coherent light could be changed during propagation even in the free space. The origin of these spectral shifts is coherency, which implies correlation of waves, rather than relativistic or Doppler effects. Without knowledge that spectrum could be changed during propagation, focusing, diffraction, or scattering, one may misinterpret observations to wrong conclusions. Although many theoretical studies introduced cases for the generation of spectral shifts, however, most observational research is limited to macroscopic system, such as aperture, slits, and multiple scatters.

In this paper, we present the experimental observation of the spectral shifts of light scattering from individual microscopic-sized spheres for the first time. To measure spectroscopic angle-resolved light scattering spectrum, we utilized spectroscopic quantitative phase microscopy and Fourier transform light scattering technique, which is a numerical field propagation method. The light scattering spectrum along the scattering angles are investigated for different illumination bandwidths, size of spheres, and refractive index of spheres. The illumination bandwidth, the size of spheres, and refractive index of spheres affect the magnitude, the period, and the phase of the spectral shifts, respectively. The direct measurements of spectral shifts and Mie theoretical analysis indicates that these shifts are explained as the result of interference of the light.

9336-85, Session PMon

Spectroscopic diffraction optical tomography

Jae Hwang Jung, YongKeun Park, KAIST (Korea, Republic of)

Recently, diffraction optical tomography (DOT) based on quantitative phase imaging (QPI) technique has been developed for measuring three-dimensional (3-D) distribution of refractive index (RI) of a sample. 3-D RI distribution is reconstructed from multiple quantitative optical fields obtained via QPI at various illumination angles. While typical QPI with normal illumination provides axially projected RI information that is coupled with thickness of the sample, DOT enable to determine 3-D RI distribution which provides better contrast for subcellular structures even without any staining and labeling.

In this work, we present spectroscopic DOT (SDOT) which enables to measure 3D distribution of the RI as well as local optical dispersion. Common-path interferometry based DOT has been utilized with a custom-built wavelength swept-source to reconstruct RI distribution at multiple wavelengths in visible spectrum. The RI distributions of microscopic polystyrene spheres and healthy human red blood cells are reconstructed at thirteen wavelengths and compared with previously reported values. Since 4D RI distribution, three for spatial and one for spectral dimension, is measured via SDOT, the local RI dispersion is investigated. As a preliminary demonstration of the RI dispersion measurement, the distinctive RI dispersion of hemoglobin in the red blood cell is investigated. We expect that SDOT is a promising technique for identifying subcellular organelles via absolute RI distribution and local RI dispersion.

9336-86, Session PMon

In vitro study of hydrostatic pressure effects on human erythrocytes

SangYun Lee, Joon Young Koh, Hyunjoo Park, YongKeun Park, KAIST (Korea, Republic of)

The highly elevated blood pressure level due to the chronic hypertension continuously damages to human blood vessels and causes heart malfunctions. However, the effects of hydrostatic pressures itself on human erythrocytes have not been yet investigated due to lack of abilities in measuring precise morphological and biomechanical properties of live cells without disturbing physiological conditions.

Here, we measure the morphological and biomechanical properties of human red blood cells under various hydrostatic pressure levels in vitro by employing common-path diffraction optical tomography (cDOT) [1]. cDOT enables simultaneously measuring 3-D distributions of refractive index map and out-of-membrane fluctuation of individual red blood cells with small phase noises [2]. Hence, the biophysical property changes of a particular red blood cell induced by different experimental conditions can be successively and precisely traced. In experiments, the hydrostatic pressure was exerted on diluted bloods in a micro-fluidic channel using a syringe pump and then cDOT was performed. In addition, the mechanical properties of membranes cortex such as shear modulus, bending rigidity, and area compression modulus were quantified from the measured membrane fluctuation by applying to theoretical model based on fluctuation-dissipation theorem [3].

Reference

- [1] G. Popescu, Y. Park, W. Choi, R. R. Dasari, M. S. Feld and K. Badizadegan, "Imaging red blood cell dynamics by quantitative phase microscopy," *Blood Cells, Molecules, and Diseases* 41(1), 10-16 (2008)
- [2] Y. Park, C. A. Best, K. Badizadegan, R. R. Dasari, M. S. Feld, T. Kuriabova, M. L. Henle, A. J. Levine and G. Popescu, "Measurement of red blood cell mechanics during morphological changes," *Proceedings of the National Academy of Sciences* 107(15), 6731-6736 (2010)
- [3] Y. Kim, H. Shim, K. Kim, H. Park, J. H. Heo, J. Yoon, C. Choi, S. Jang and Y. Park, "Common-path diffraction optical tomography for investigation of three-dimensional structures and dynamics of biological cells," *Optics Express* 22(9), 10398-10407 (2014)

9336-87, Session PMon

LCD panel characterization by measuring spatially resolved full Jones matrix of individual pixels

Jongchan Park, HyeonSeung Yu, Jung-Hoon Park, YongKeun Park, KAIST (Korea, Republic of)

With the large variety of liquid-crystal display (LCD) techniques, the optical characterization of LCD panel is crucial for developing and testing of LCDs. The most popular ways to characterize LCDs are based on intensity measurements since the transmittance of light after propagating through a polarizer and an analyzer is the easily accessible figure of merit for LCD performance characterization [1]. However, the optical responses of LCDs can only be fully described in the manner of polarization states, which reflects the working principle of LCDs. Previously, polarization sensitive LCD characterizations using the Stokes parameters have been reported, however it cannot directly describe the complex nature of electric field [2]. Recently, there was an attempt to measure Jones matrix component of LCDs, however spatially resolved full Jones matrix has never been addressed [3].

In this work, we present a method to characterize individual pixels in liquid-crystal display (LCD) by measuring spatially resolved full Jones matrix components. Employing polarization-sensitive digital holographic microscopy based on off-axis Mach-Zehnder interferometry, 2D spatial maps of complex amplitudes of the light passing through LCD panel were

quantitatively and precisely measured. The sequential measurements with four different bases of polarization states of incident and outgoing waves at a given applied bias on individual LCD pixel resolves full Jones matrix components, which enable to characterize the complex optical responses of LCD panel with respect to arbitrary polarization states of incident light [4]. Due to the generality of our approach, the presented method can be applied to measure complex optical response of other various types of LCD.

{[1] D. H. Brainard, D. G. Pelli, and T. Robson, "Display characterization," Encyclopedia of imaging science and technology, (2002).

[2] A. Márquez, I. Moreno, C. Lemmi et al., "Mueller-Stokes characterization and optimization of a liquid crystal on silicon display showing depolarization," Optics express, 16(3), 1669-1685 (2008).

[3] I. Moreno, P. Velásquez, C. Fernández-Pousa et al., "Jones matrix method for predicting and optimizing the optical modulation properties of a liquid-crystal display," Journal of applied physics, 94(6), 3697-3702 (2003).

[4] Y. Kim, J. Jeong, J. Jang et al., "Polarization holographic microscopy for extracting spatio-temporally resolved Jones matrix," Optics express, 20(9), 9948-9955 (2012).

9336-88, Session PMon

Method for observing phase objects without halos and directional shadows

Yoshimasa Suzuki, Kazuo Kajitani, Hisashi Ohde, Olympus Corp. (Japan)

A new phase contrast method for visualizing phase objects without halos which causes a spurious bright area at the edge of the phase object and directional shadows is proposed. The key optical element is an annular aperture at the front focal plane of a condenser with a larger diameter than those used in standard phase microscopy. The annular aperture is concentric with the pupil of an objective. The light flux passing through the annular aperture is changed by the specimen's surface profile, and then a shift of the image of the annular aperture occurs at the objective pupil. Therefore, the light flux passing through the objective is changed and contributes to form the image.

We compared images of induced pluripotent stem (iPS) cells using our approach to those of standard phase microscopy to identify difference between the two techniques. The outline of the iPS cells is clearly visible with our method, whereas it is not visible due to halos in the phase contrast method. Additionally, we can focus on the outlines of the cells very easily thanks to the halo-less images and can obtain height information of the cells by following the changes in outline as the focus is shifted. Such height information is potentially useful for investigating the cell viability and will be an essential evaluation index for live cells in the future.

9336-89, Session PMon

Common-path diffraction optical tomography revealing 3D structures and dynamics of biological cells

Kyoohyun Kim, KAIST (Korea, Republic of); Youngchan Kim, KAIST (Korea, Republic of) and Imperial College London (United Kingdom); Hyoeun Shim, Univ. of Ulsan (Korea, Republic of) and Seegene Medical Foundation (Korea, Republic of); Hyunjoon Park, Ji Han Heo, Jonghee Yoon, Chulhee Choi, KAIST (Korea, Republic of); Seongsoo Jang, Univ. of Ulsan (Korea, Republic of); YongKeun Park, KAIST (Korea, Republic of)

Quantitative phase imaging (QPI) techniques have been developed for measuring quantitative structural and chemical information about biological samples. Two-dimensional (2-D) QPI based on a common-

path interferometry can precisely reveal temporal axial fluctuation of cell membranes within the range of few milliradians. 3-D QPI implements off-axis Mach-Zehnder interferometry to measure multiple 2-D optical fields with various illumination angles, and reconstructs 3-D refractive index (RI) distribution of biological samples, which is an intrinsic optical parameter that is sensitive to chemical compositions and structures of samples. However, none of the existing techniques can measure both 2-D dynamics and 3-D structures of biological samples within single optical setup. Common-path interferometry for 2-D QPI is misaligned when an illumination beam is tilted for tomographic imaging, while Mach-Zehnder interferometry for 3-D QPI suffers from phase noise, which limits stable phase measurements.

Here, we present a common-path tomographic imaging technique, referred as common-path diffraction optical tomography (cDOT) to measure both 2-D dynamics and 3-D structures of biological samples within a single optical setup. Samples are illuminated with various illumination angles, and diffracted beams collected by an objective lens are de-scanned by a galvanomirror to ensure common-path interferometry. We demonstrate the capability of cDOT by measuring chemical and morphological parameters of individual red blood cells from 3-D RI tomograms as well as mechanical parameters from 2-D dynamic phase images. Furthermore, we also measure 3-D RI tomograms of eukaryotic cells like hepatocytes.

9336-90, Session PMon

Lipid droplets label-free imaging using optical diffraction tomography

Kyoohyun Kim, SeoEun Lee, KyeoReh Lee, Ji Han Heo, Jonghee Yoon, Mina Kim, Jae Hwang Jung, Hyunjoon Park, Jennifer H. Shin, Chulhee Choi, YongKeun Park, KAIST (Korea, Republic of)

Lipid droplet (LD), composed of a neutral lipid core and surrounding phospholipid monolayer, is a cellular organelle for main storage of neutral lipids. Since LDs are implicated in lipid homeostasis and metabolic disease, the studies of LDs have begun to be highlighted in recent years. The morphology and dynamics of LDs are essential for studying of their cell biology and regulation mechanism, and the labeling of LDs with specific organic dyes or fluorescent tagged proteins are the typical methods for LD imaging. Such fluorescence imaging is powerful in specificity, however, it cannot be used for long-time measurements due to photobleaching of fluorophores. Recently, researchers have developed tomographic imaging techniques which measure label-free three-dimensional (3-D) refractive index (RI) distribution of samples, an intrinsic optical property providing chemical and morphological information of biological cells.

Here, we employ optical diffraction tomography to investigate structural and chemical parameters of LDs inside hepatocytes. Optical diffraction tomography measures multiple 2-D optical fields of biological samples with different illumination angles, and reconstructs label-free three-dimensional (3-D) refractive index (RI) distribution of samples via Fourier diffraction theorem. From RI tomograms, we obtain concentration, contents and volume of individual LDs inside hepatocytes. We expose hepatocytes in oleic acid solution, and it clearly shows that total contents and concentration of LDs inside hepatocytes are significantly increased by three times as oleic acid promotes LD formation of cells. We also track individual LDs for 96 seconds, and studies non-Brownian motion of LDs induced by cytoskeleton.

9336-91, Session PMon

3D refractive index map of intraerythrocytic parasite-babesia microti invaded RBCs using diffraction phase micro-tomography

Hyunjoon Park, KAIST (Korea, Republic of); Sung-Hee Hong,

Sang-Eun Lee, Korea National Institute of Health (Korea, Republic of) and Korea Ctrs. for Disease Control and Prevention (Korea, Republic of); YongKeun Park, KAIST (Korea, Republic of)

We present 3-D refractive index (RI) distribution of individual RBCs from a mouse infected with *Babesia microti*, causing fatal human babesiosis, by employing a label-free and noninvasive optical holographic micro-tomography. We first measure a precise location, volume and RI of invaded individual parasite vacuoles inside live RBCs. Since this quantitative optical technique allows simultaneous measurement of 3D structure as well as surface dynamics of host RBCs, the change in the morphological, chemical, and mechanical properties of RBCs by parasite infection are quantified at the single-cell level.

We found that the cellular volume and total dry mass of individual RBCs infected with *B. microti* increase, while the mass concentration of them was similar as healthy. In addition, the morphological and biochemical alternation in RBCs occurs similarly regardless of whether RBCs adapt *B. microti*-parasite vacuoles or not. This micro-tomographic optical approach provides better understanding of the distinctive characteristics of RBCs infected with *B. microti* parasite for biological studies and medical diagnostic purposes.

9336-92, Session PMon

Quantitative phase imaging of cellular and subcellular structures for non-invasive screening diagnostics of socially significant diseases

Irina Vasilenko, Maimonides State Classical Academy (Russian Federation) and Russian Medical Academy of Postgraduate Education (Russian Federation); Vladislav Metelin, Maimonides State Classical Academy (Russian Federation); Marat Nasyrov, Russian Medical Academy of Postgraduate Education (Russian Federation); Alexander B. Kuznetsov, Evgenii Sukhenko, Pirogov Russian National Research Medical Univ. (Russian Federation); Vladimir Belyakov, Russian Medical Academy of Postgraduate Education (Russian Federation)

Contemporary non-invasive computerized technologies become more important in verifying and differential diagnostics of a number of socially significant diseases. In this context, the measurements performed on separate cells are quite perspective. The novel laser-optic technologies of cellular imaging provide a quantitative analysis of the parameters of cellular structure and function without its contrasting and fixation. The objective of the present study is to increase the quality of the early diagnosis using cytological differential-diagnostic criteria for reactive changes in the nuclear structures of the immunocompetent cells.

Mononuclear cells were determined using computer phase-interference microscope (Westtrade LTD, Moscow, Russia): height accuracy 0,5 nm, coordinate accuracy 10 nm, image area 256x256 pixels, optical magnification 1000, acquisition time 4-12 sec. The complex algorithm included the definition of optic and geometrical characteristics of living cells, statistical analysis of data and creation of medical documents.

In experiments in vitro, the dynamics of indices membrane and interphase nucleus were studied after induction of proliferative and apoptosis processes. In vivo 200 volunteers, 53 patients with multiple sclerosis, and 127 recipients of the renal grafts were investigated. The main attention is paid to determining of cellular functional state based on nuclear structural characteristics which include nucleolus organizer areas reflecting metabolic and proliferative cellular activity and being markers of cell transformation. It is felt that complex and detailed investigation of the proliferation and apoptosis processes would enable obtaining new knowledge to solve the problem on the modern level - improving diagnostics and tactics of management and treatment of patients.

9336-93, Session PMon

A new approach for phase image analysis of asymmetrical microobjects

Vladislav D. Zverzhkhovskiy, Tatiana V. Vyshenskaya, Moscow State Institute of Radiotechnics, Electronics and Automation (Russian Federation); Alexander V. Kretushev, Institute of Radio Engineering and Electronics (Russian Federation); Alexander A. Shtil, N.N. Blokhin Russian Cancer Research Ctr. (Russian Federation) and Institute of Radio Engineering and Electronics (Russian Federation) and National Research Nuclear Univ. MEPhI (Russian Federation); Vladimir P. Tychinsky, Anatoly A. Evdokimov, Institute of Radio Engineering and Electronics (Russian Federation)

We provide a novel approach for the analysis of mammalian cells that lack central symmetry (in particular, human tumor cells). The method is based on our studies (...?????) in which the impact of an individual organelle into the integral phase image of an asymmetric cell is analyzed. Essentially, we highlight an organelle containing area in the cell topogram. If the cell is flattened the curve of the area (due to the nucleus or mitochondria) is negligibly small, and this portion of the cell can be generally considered a part of a wedge. Subtraction of the area's trend allows to determine the organelle's impact and the parameters of its 'phase portrait'. Using this approach one can analyze a number of organelles simultaneously; also, each individual compartment can be described. The method is especially applicable to local cellular processes whose impacts into the integral phase image are low. Importantly, we demonstrate quantitative dynamic changes of chromatin structure and function in the nuclei of H16 colon carcinoma cells treated with the transcriptional inhibitor actinomycin D. Finally, the optical characteristics of compartments at the cell periphery can be identified whereas this analysis might be problematic in other methods of phase imaging.

9336-94, Session PMon

Multi-mode microscopy in real-time with LED array illumination

Ziji Liu, Univ. of Electronic Science and Technology of China (China) and Univ. of California, Berkeley (United States); Lei Tian, Laura Waller, Univ. of California, Berkeley (United States)

Bright-field, dark-field and phase contrast are three of the most popular imaging modalities in biological microscopy, each provide useful information about different sample properties. However, these complementary contrast modes typically rely on different optical configurations. Thus, one must insert hardware add-ons or otherwise change the physical setup for the microscope in order to switch between these modes. We demonstrate here a single-camera imaging configuration that can simultaneously acquire bright-field, dark-field and phase contrast images at 50Hz frame rates. Our method uses an LED array illuminator, which has recently been demonstrated to provide flexible illumination patterns for various imaging modes, without physically switching the optical components. In earlier reports of this method, samples were static because the hardware speed was not fast enough to meet real-time acquisition and processing requirements. We demonstrate our latest work on the experimental system developed to realize multi-contrast modes including bright-field, dark-field, and 3D differential phase-contrast (DPC) microscopy in real-time to follow the dynamic biological process. This microscope is equipped with a specially designed LED array as the illumination source and a synchronized high-speed camera. Fast LED pattern switching and a real-time processing algorithm are realized with TDM (time divide multiplexing) method. Furthermore, the equipment achieves performance metrics of 50Hz with

2560?2160. With available hardware modifications, this system could potentially operate at hundreds of image stacks per second.

9336-95, Session PMon

Single-bacterial identification based on holographic machine learning

YoungJu Jo, Jae Hwang Jung, Hyunjoo Park, YongKeun Park, KAIST (Korea, Republic of)

Despite the importance of rapid identification of bacterial species in medicine and food hygiene, the conventional techniques require long procedural time due to their culture-based and biochemical nature. A number of biomolecular or optical approaches, such as direct sequencing, angle-resolved light scattering, and Raman spectroscopy, have been tried for decades to solve this problem. However, most of these techniques are either still time-consuming, require careful labeling, or have limited measurement sensitivity.

Here, we present a rapid and label-free identification of bacterial species at the single-bacterium level. Quantitative phase imaging (QPI) of an individual bacterium holographically extracts the information about cellular structure and biochemical compositions. The optical field map obtained by a single-shot measurement is propagated to the far-field by Fourier transform light scattering (FTLS) to obtain the high-quality angular scattering map. After collecting the FTLS maps of individual bacteria belonging to similarly shaped but different species, we apply a series of techniques in supervised machine learning to classify the FTLS patterns. For systematic construction of the criteria of each bacterial species, species-specific components of the patterns are employed while the differences induced by bacterial growth and division are abandoned. The accuracy of species identification was ~95% when the final classification model was tested via cross-validation.

As the proposed methodology enables single-shot identification of unlabeled individual bacteria, simply combining the microfluidic technologies will dramatically shorten the time required for bacterial identification, from days to minutes. Employment of various QPI modalities will further enhance the sensitivity and generality of our method.

9336-97, Session PMon

Combined effect of complex wavefront shaping and optical clearing agent on the suppression of multiple light scattering in optical coherence tomography

HyeonSeung Yu, YoungJu Jo, YongKeun Park, KAIST (Korea, Republic of)

In optical coherence tomography, the multiple light scattering strongly degrades the imaging signal, resulting in limited penetration depth. Optical clearing agents has long been studied as a tool for reducing scattering in the biological tissue, by matching the refractive index between the cells and surrounding medium. By treating various optical clearing agents, several studies showed the successful depth increments in-vivo imaging in OCT. More recently, another approach to manipulate the multiple light scattering has been proposed: modulation of the incident light field instead of manipulating the scattering sample itself. Our group has incorporated this wavefront shaping technique into the spectral domain optical coherence tomography (SD-OCT), where the complex field impinging onto the sample is controlled via high speed the digital micro-mirror device (DMD). It produces 2-D OCT images with the 92% enhancement of the penetration depth at its optimal condition.

In this work, both complex wavefront shaping and the optical clearing agent are simultaneously applied to increase the penetration depth OCT system. While the DMD provides the depth enhanced 2D imaging in SD-OCT, the tissue phantoms are treated with the optical clearing agents, such as glycerol and PEG. The penetration depth increments for the various

conditions of optical clearing agents and wavefront modulations are studied, which will give an insight into the maximum controllability on multiple scattering in OCT system.

9336-98, Session PMon

White-light interferometric microscopy for wafer defect inspection

Renjie Zhou, Christopher A. Edwards, Casey Bryniarski, Marjorie Dallmann, Gabriel Popescu, Lynford L. Goddard, Univ. of Illinois at Urbana-Champaign (United States)

Laser quantitative phase imaging (QPI) has been widely used in the past for biological and material science imaging. However, the laser-speckle has hindered laser QPI for highly sensitive imaging applications, such as in in-line inspection of integrated circuit (IC) device fabrication beyond the 9 nm node. Over the past year, we have developed a white-light light emitting diode (LED) based QPI technique to address the future needs in defect inspection metrology. The system is based on the principle of epillumination white-light diffraction phase microscopy, called epi-wDPM. In addition to phase imaging, we also added automated XYZ scanning of the wafer, enabling pixel level wafer translation during the imaging. In-plane and vertical through focus wafer scans are made possible with a LabVIEW interface that also integrates the image retrieval processing and thus enables real-time defect inspection. Before completing the interferometric inspection system, we first performed bright-field inspection of a 9 nm node wafer with XYZ scanning, and the results showed that we can clearly detect 15 nm by 90 nm defects. Recently, we finished building and testing the 3D scanning real-time epi-wDPM system. This system has a spatial coherence area of about the diffraction spot, which is sufficient for inspecting densely patterned wafers. There are several issues, relating to polarization and image contrast, which will be discussed at the conference along with our latest results.

9336-99, Session PMon

Optical parameters of living vs. fixed lymphocytes detectable by coherent phase microscopy

Tatiana V. Vyshenskaya, Vladimir P. Tychinsky, Ivan V. Klemayshov, Moscow State Institute of Radiotechnics, Electronics and Automation (Russian Federation); Yuriy B. Matveev, Pirogov Russian National Research Medical Univ. (Russian Federation); Vladislav D. Zverzhkhovskiy, Moscow State Institute of Radiotechnics, Electronics and Automation (Russian Federation); Alexander A. Shtil, N.N. Blokhin Russian Cancer Research Ctr. (Russian Federation); Alexander B. Kuznetsov, Pirogov Russian National Research Medical Univ. (Russian Federation)

Coherent phase microscopy (CPM) allows for quantitative real time assessment of key parameters of the living bacterial and eukaryotic cells. We generated an optical model of a symmetrical (elliptic) lymphocyte in which the cell is divided into concentric layers termed zones. The four zones comprised the peripheral (organelle-free) cytoplasm, the dense cytoplasm with organelles, the nucleus, and the nucleoli [Tychinsky V.P. et al. J. Biomed. Opt. 2012]. We developed an algorithm of measurement of the area, phase volume and refractivity index of each zone. An advantage of CPM is the work with non-fixed cells; however, experimental conditions might hamper the analysis of fresh cells. We therefore compared the optical parameters generated by CPM of living vs fixed (4% formaldehyde in a physiological buffer) lymphocytes using an Airyscan microscope designed in Moscow Institute of Radioengineering, Electronics and Automation. Using the algorithm [1] we demonstrated that, for each zone, average values of

area, phase volumes and refractivity indices were similar for live and fixed cells whereas at the zone boundaries these parameters differed. In contrast to freshly isolated cells, the phase profiles of fixed counterparts were less sharp, supposedly due to down-regulation of trans-membrane transport and electric potential. Interestingly, formaldehyde, unlike methanol [Wang Y. et al., 2013], preserved general cellular structure and did not alter the nuclear refractivity index, a parameter important in cancer diagnosis [Bista R. et al., 2012].

9336-100, Session PMon

Dynamics of neuronal filopodia measured using SLIM

Taewoo Kim, Anika Jain, Rajiv Iyer, Martha U. Gillette, Gabriel Popescu, Univ. of Illinois at Urbana-Champaign (United States)

Neuronal networks play a central role in animal activities including cognitive functions, movements, and intellectual functions. Therefore, it is important to understand how they are formed and what affects the connectivity of a network. In forming the networks, axonal or dendritic filopodia play a central role by acting as “fingers” that look for the connection sites through active spatial scanning. Thus, understanding the dynamics of filopodia has a potential to explain the active formation of neuronal networks. Dendritic filopodia are dynamic protrusions that occur during early postnatal development. These structures are typically 200-300 nm wide and 2-20 μ m long, thus, require a high-resolution microscopy technique to be observed.

Spatial light interference microscopy (SLIM) is a quantitative phase imaging (QPI) technique based on the phase-shifting interferometry. Built as an external module for a commercial phase contrast microscope, SLIM has a diffraction limited resolution and sub-nanometer temporal and spatial sensitivity. Using this technique, quantitative phase images of rat hippocampal dendrites are obtained. Two different preparations have been used for the sample, one without any external cues and the other with semaphorin3A, which selectively promotes dendrite growth. Furthermore, filopodia at the tip of a dendrite and filopodia on the shaft of a dendrite have been analyzed separately. The dry mass measurement and dispersion-relation phase spectroscopy (DPS) data shows that filopodia at the tip of a dendrite are much more dynamic than those on the shaft. Also, semaphorin3A-treated samples showed more deterministic transport compared to untreated samples, which dominantly shows random behavior.

Supported by NSF STC CBET 0939511 Emergent Behavior of Integrated Cellular Systems (GP, MUG), NIH MH101655 (MUG), and Beckman Graduate Fellowship (TK). For more information, please visit <http://light.ece.illinois.edu/>.

9336-101, Session PMon

Effect of substrate stiffness on melanoma cell behavior studied by QPI

Shamira Sridharan, Yanfen Li, Mikhail E. Kandel, Kristopher A. Kilian, Gabriel Popescu, Univ. of Illinois at Urbana-Champaign (United States)

Melanoma is a sub-type of skin cancer that is observed in 2% of all skin cancer cases but accounts for a majority of skin cancer-related deaths. In our project, we aim at understanding how the behavior of melanoma cells is influenced by the stiffness of the substrate. The different stiffnesses are selected to mimic the microenvironment the cells might encounter in the body. The substrates used are polyacrylamide gels with fibronectin, a connective tissue component, stamped on the gel. B16 melanoma cells of metastatic and non-metastatic sub-type attach to the fibronectin on the polyacrylamide gels of stiffnesses 1kPa, 40kPa and 100kPa. The cell growth and movement are measured from the quantitative phase images obtained using Spatial Light Interference Microscopy (SLIM) for 24 hours. Preliminary results indicate that 40kPa substrate is optimal for the growth rate of both

metastatic and non-metastatic cells. We also observed that the while the metastatic cell line showed higher motility, the non-metastatic cells had a higher growth rate.

9336-102, Session PMon

Quantification of glial cell dynamics under vasoactive intestinal peptide treatment

Taewoo Kim, Samuel Irving, Martha U. Gillette, Gabriel Popescu, Univ. of Illinois at Urbana-Champaign (United States)

Glial cells have numerous supportive functions, including structural, chemical and metabolic support, to the neurons in the central nervous system (CNS). More specifically, astrocytes, which are the most common type of glial cells in the brain, are the primary support for neurons. More recently, the signaling capabilities of astrocytes have also been discovered, suggesting that astrocytes are not only the support, but also an essential element in the CNS. Studies have shown that the interaction between neurons and astrocytes is mediated by vasoactive intestinal peptide (VIP), which is released by neurons and affects glial functions. VIP is known to stimulate the mitotic activities in astrocytes. However, other possible effects of VIP on astrocytes have not yet been thoroughly understood.

In this study, the effects of VIP on astrocytes have been studied using a quantitative phase imaging technique, called spatial light interference microscopy (SLIM). SLIM, with its label-free imaging, high resolution and sub-nanometer sensitivity, can measure the dry mass of the cell at 0.5 Hz. Fast measurements on a glial culture before and after the treatment has been conducted to show the difference in cell dynamics caused by VIP. Furthermore, the morphology change caused by the peptide is also quantified by analyzing the power spectrum, or the data in the spatial frequency domain. A more thorough understanding and quantification of the effect of VIP on astrocytes will be provided through this experiment.

This research is supported by NSF STC CBET 0939511 Emergent Behavior of Integrated Cellular Systems (MUG, GP), NSF IOS 1354913 (MUG), and a Beckman Graduate Fellowship (TK). For more information, please visit <http://light.ece.illinois.edu/>.

9336-103, Session PMon

Emergent patterns in cellular growth as studied by QPI

Mikhail E. Kandel, Jon Liang, Gabriel Popescu, Univ. of Illinois at Urbana-Champaign (United States)

Spatial analysis of cellular growth in adherent cultures has, formerly, required manual calculation of morphological surface areas, per-pixel analysis of the image statistics within a selected region, or intensity of fluorescent signals attributed to tagged organelles. Such features are often strongly biased by the microscope and users, often requiring orders of magnitude increases in data and human labor.

With SLIM we are able to acquire cellular statistics with unambiguous meaning (cell mass) without compromising on magnification and details, enabling the decomposition of complex phenomena into individual actors. For this purpose, we developed a new software tool that integrates SLIM operation with programmable stage scanning, which allows us, for example, to image microscope well plates. We present our preliminary work on studying the behavior of cellular cultures at the single cell level in terms of dry mass change. In particular, we present early work on a method that seeks to quantify spatial inhomogeneity in cellular growth rates, in an effort to understanding the interplay between cell confluence and growth on a local scale. We hope that this technique can be used to augment conventional cell cycle phase analysis, in particular enabling insight into the changes in cellular mass that are coincident with mitosis.

9336-56, Session 8

Label-free measurements of membrane tether thickness using optical tweezers combined with SLIM

Mohammad Sarshar, Winson Wong, Bahman Anvari, Univ. of California, Riverside (United States)

Various cellular activities such as motility, division, and endocytosis involve a change in the cell shape. The mechanical interactions between the cell membrane and cytoskeleton play an important role in regulating changes in the cell shape. Tether formation from cellular membranes provides a technique to characterize the mechanical properties of cell membranes and membrane-cytoskeleton interactions. Accurate measurement of the nano-scale tether diameter is relevant to quantification of membrane tension, bending modulus, and adhesion energy of the membrane-cytoskeleton structure. We have integrated optical tweezers with quantitative phase imaging, based on spatial light interference microscopy (SLIM), to simultaneously form tethers from HEK-293 cells and measure their diameters. Tether thickness along the illumination axis is measured using the quantitative phase map of the sample and the refractive index (RI) mismatch between the sample and the surrounding media. The RI of the tethers ranged from 1.354 to 1.368 (cell culture medium RI=1.337). Our SLIM imaging system provided a 38 nm resolution in tether thickness measurements. Tether diameter fluctuations of <100 nm were resolved on tethers that ranged between 600–900 nm in diameter. Our integrated platform also provides the ability to simultaneously manipulate and image cell organelles in a non-contact and marker-free manner at nanometer spatial resolution.

9336-57, Session 8

Quantitative phase imaging of cell division in ecoli using digital holographic microscopy

Vimal Prabhu Pandiyan, Hanu Phani Ram G., Renu John, Indian Institute of Technology Hyderabad (India)

— Digital holographic microscope (DHM) is an emerging quantitative phase imaging technique with unique imaging scales and resolutions leading to multitude of applications. The unique imaging speeds offered by this technique comprise a novel investigational and applied tool for cellular imaging, studying the morphology and real time dynamics of cells and a number of related applications. Furthermore, the numerical propagation and digital optics offers to DHM unique tools able to increase the depth of focus, compensate for aberrations and image distortion. The aim of this work is to develop and characterize a DHM platform for imaging dynamics of cell division in Ecoli. This involves setting up an interferometric microscope based on a Mach Zehnder interferometer and characterizing the system in terms of sensitivity and resolution. This involves 3-D and depth imaging as well as reconstruction of phase profiles of Ecoli. In this work we recorded the hologram of Ecoli and reconstructed the recorded hologram with Fresnel propagation algorithm. We also used the aberration correction algorithm for correcting the aberration which is introduced by the Microscope objective in the object path using linear square fitting techniques. This work also explores results from our system with importance to its clinical feasibility and pathological significance.

9336-58, Session 8

Complex refractive index change measurement of photoactive yellow protein (PYP) upon light irradiation using ssFTLS

KyeoReh Lee, Youngmin Kim, Hyotcherl Ihee, YongKeun Park, KAIST (Korea, Republic of)

Complex refractive index (RI), related to the electric permittivity, is the value that describes the overall light-interacting property of materials. Although either the real or imaginary part of complex RI is used in various practical fields: biology, chemistry, food industry, agriculture, pharmaceutical industry, and even gemology, the whole information of complex RI as a function of wavelength, has not been fully utilized.

We present the measurements of complex RI of photoactive yellow protein (PYP) in various wavelengths using swept-source Fourier transform light scattering (ssFTLS) technique [1]. PYP is one of the small bacterial photo-receptor. When PYP molecules absorb blue light, they become excited state, and about 0.2 seconds later, they relax down to the original ground state [2].

We found significant RI difference between ground and excited state of PYP upon excitation with blue light. Interestingly, it is not only imaginary, but also real part of the complex RI changes significantly. Since the two states are composed of exactly same compounds, this difference should be originated by the structural change of the protein. This result cannot be explained by the theory that the real RI of protein can be solely determined by their amino acid compositions [3]. Applying Kramer-Kronig relations, we also found the causality of our results, and discussed the origin of real RI of proteins.

References:

- [1] J. Jung, and Y. Park, "Spectro-angular light scattering measurements of individual microscopic objects," *Optics express*, 22(4), 4108-4114 (2014).
- [2] M. Kumauchi, M. T. Hara, P. Stalcup et al., "Identification of Six New Photoactive Yellow Proteins—Diversity and Structure-Function Relationships in a Bacterial Blue Light Photoreceptor," *Photochemistry and photobiology*, 84(4), 956-969 (2008).
- [3] H. Zhao, P. H. Brown, and P. Schuck, "On the distribution of protein refractive index increments," *Biophysical journal*, 100(9), 2309-2317 (2011).

9336-59, Session 8

Digital holography microscopy as a tool to screen for diabetes

Ana Doblas, Univ. de València (Spain); Jaime Esteve, Enrique Roche, Univ. Miguel Hernández de Elche (Spain); Francisco Javier Ampudia-Blasco, Genaro Saavedra, Manuel Martínez-Corral, Univ. de València (Spain); Jorge Ivan Garcia-Sucerquia, Univ. Nacional de Colombia Sede Medellín (Colombia)

In this contribution, an off-axis digital holographic microscope (DHM) is used to provide quantitative phase imaging (QPI) of red blood cells (RBCs) samples. The DHM has been setup in an afocal-telecentric mode to provide QPIs free of phase perturbations introduced by the imaging system. These QPIs, which are obtained from a single shot and with no numerical post-processing, can be used to screen from diabetes as it has been done with polarizing-interference microscopy. With our telecentric-DHM we have measured the phase maps of the RBC samples of patients suffering from diabetes mellitus type 1 (DM1) and of a control group of people; the experimental results shown that the measured phase values are significantly different for both groups. Furthermore, because the phase values of each group are not overlap, this measurement is a good parameter to screen for DM1 diabetes. We also show that these phase measurements are strongly

correlated with the glycated hemoglobin (HbA1C) and the blood glucose values as they are measured using high performance liquid chromatography (HPLC) and a regular glu-cometer, respectively.

9336-61, Session 8

Diagnosis of breast cancer biopsies using quantitative phase imaging

Hassaan Majeed, Mikhail E. Kandel, Kevin Han, Zelun Luo, Univ. of Illinois at Urbana-Champaign (United States); Virgilia Macias, Univ. of Illinois at Chicago (United States); Krishnarao V. Tangella, Christie Clinic (United States) and Univ. of Illinois at Urbana-Champaign (United States); Andre K. Balla, Univ. of Illinois at Chicago (United States); Gabriel Popescu, Univ. of Illinois at Urbana-Champaign (United States)

The standard practice in the histopathology of breast cancers is to examine a hematoxylin and eosin (H&E) stained tissue biopsy under a microscope. The pathologist looks at certain morphological features, visible under the stain, to diagnose the presence of tumors and assigns a grade to each tumor. This determination is made based on a qualitative inspection making it subject to investigator bias. A quantitative method for detection of these morphological features from images of tissue biopsies is, hence, highly desirable as it would lead to earlier and more accurate detection and grading of breast cancers. We present here a method of distinguishing between cancerous and noncancerous regions as well as between high grade and low grade tumor regions in breast tissue biopsies using quantitative phase imaging. We generated optical path length maps of unstained breast tissue biopsies using Spatial Light Interference Microscopy (SLIM) and extracted different spatial distribution parameters (variance, power spectrum decay length etc.) as well as optical scattering parameters (mean scattering length, anisotropy factor, etc.) from these optical path length maps. Comparisons of these parameters between cancerous and noncancerous regions allowed us to differentiate between the two regions. Furthermore, we also compared the variations of these parameters between the stromal and between the epithelial regions of low grade and high grade cancers in order to form a basis for discriminating between the two grades. Due to its quantitative nature our method is potentially automatable, opening up the possibility of automated high throughput and early screening of biopsies for better health outcomes.

9336-62, Session 8

Challenging strategies for adapting coherent imaging and diagnostics to bio-microfluidics (*Invited Paper*)

Pietro Ferraro, Lisa Miccio, Francesco Merola, Pasquale Memmolo, Istituto Nazionale di Ottica, CNR (Italy)

Quantitative three-dimensional (3D) imaging and diagnostics purposes at Lab on Chip scale require the scaling-down and simplification of microscopy tools. While diagnostics tools still need to be quantitative, label-free and, as much as possible, accurate strong efforts are needed for finding new, smart and effective solution for adapting the optical microscopy on this small scale. Furthermore the access to the sample can be complicated by the architecture of the microfluidic chip thus encountering difficulties in practical applications. Novel strategies for adapting and integrating the conventional systems will be presented at the aim to show that coherent imaging tool can provide versatile and full-diagnostics in microfluidic channels. At same time recent achievements in high-throughput modality for diagnostic purposes will be illustrated by exploiting the quantitative feature of the interference microscopy techniques.

9336-63, Session 8

The study of fast membrane dynamics in red blood cells

SangYun Lee, Hyunjoo Park, YongKeun Park, KAIST (Korea, Republic of)

In this study, we present frequency-dependent non-equilibrium nature of membrane fluctuations in red blood cells (RBCs). The dynamic membrane fluctuation was measured employing diffraction phase microscopy (DPM) equipped with a high-speed camera. We performed the systematic investigation on fast membrane dynamics in RBCs and the effects of ATP.

ATP plays important roles in RBC membrane morphology and dynamics. The first approach employing point dark field microscopy revealed that membrane fluctuations of RBCs decrease when ATPs was washing out [1]. Whereas others found the radial fluctuating membrane was less affected by ATP concentration changes, especially in a high temporal-frequency regime [2, 3]. The recent study of membrane fluctuation using quantitative phase imaging techniques showed that the out-of-membrane fluctuation exhibits strong non-Gaussian properties driven by ATP [4]. Here, to investigate the effect of ATP, we measured the dynamic fluctuation of RBCs from healthy, metabolically ATP-depleted, chemically ATP-depleted group. In addition, to fully utilize the high frame rate, an incoherent deep red (wavelength = 650 nm) LED was used as a light source for DPM. The power spectral densities of the height displacements are analyzed to address that the characteristics of RBC fluctuations is far from the thermal equilibrium and hence belongs to the regime of non-equilibrium dynamics.

Reference

- [1] S. Levin and R. Korenstein, "Membrane fluctuations in erythrocytes are linked to MgATP-dependent dynamic assembly of the membrane skeleton," *Biophysical journal* 60(3), 733-737 (1991)
- [2] J. Evans, W. Gratzer, N. Mohandas, K. Parker and J. Sleep, "Fluctuations of the red blood cell membrane: relation to mechanical properties and lack of ATP dependence," *Biophysical journal* 94(10), 4134-4144 (2008)
- [3] T. Betz, M. Lenz, J.-F. Joanny and C. Sykes, "ATP-dependent mechanics of red blood cells," *Proceedings of the National Academy of Sciences* 106(36), 15320-15325 (2009)
- [4] Y. Park, C. A. Best, T. Auth, N. S. Gov, S. A. Safran, G. Popescu, S. Suresh and M. S. Feld, "Metabolic remodeling of the human red blood cell membrane," *Proceedings of the National Academy of Sciences* 107(4), 1289-1294 (2010)

9336-64, Session 8

QPI for prostate cancer diagnosis: quantitative separation of Gleason grades 3 and 4

Shamira Sridharan, Univ. of Illinois at Urbana-Champaign (United States); Virgilia Macias, Univ. of Illinois at Chicago (United States); Krishnarao V. Tangella, Presence Covenant Medical Ctr. (United States); Andre Kajdacsy-Balla, Univ. of Illinois at Chicago (United States); Gabriel Popescu, Univ. of Illinois at Urbana-Champaign (United States)

1 in 7 men receive a diagnosis of prostate cancer in their lifetime. The aggressiveness of the treatment plan adopted by the patient is strongly influenced by Gleason grade. Gleason grade is determined by the pathologist based on the level of glandular formation and complexity seen in the patient's biopsy. However, studies have shown that the disagreement rate between pathologists on Gleason grades 3 and 4 is high and this affects treatment options. We used quantitative phase imaging to develop an objective method for Gleason grading. Using the glandular solidity, which is the ratio of the area of the gland to a convex hull fit around it, and anisotropy of light scattered from the stroma immediately adjoining the

gland, we were able to quantitatively separate Gleason grades 3 and 4 with 78% accuracy in 43 cases marked as difficult by pathologists.

9336-65, Session 8

3D quantitative phase imaging of neural networks using WDT

Taewoo Kim, S. Chris Liu, Martha U. Gillette, Gabriel Popescu, Univ. of Illinois at Urbana-Champaign (United States)

White-light diffraction tomography (WDT) is a recently developed 3D imaging technique based on a quantitative phase imaging system called spatial light interference microscopy (SLIM). The technique has achieved a sub-micron resolution in all three directions with high sensitivity granted by the low-coherence of a white-light source. Demonstrations of the technique on single cell imaging have been presented previously; however, imaging on any larger sample, including a cluster of cells, has not been demonstrated using the technique.

Neurons in an animal body form a highly complex and spatially organized 3D structure, which can be characterized by neuronal networks or circuits. Currently, the most common method of studying the 3D structure of neuron networks is by using a confocal fluorescence microscope, which requires fluorescence tagging with either transient membrane dyes or after fixation of the cells. Therefore, studies on neurons are often limited to samples that are chemically treated and/or dead.

WDT presents a solution for imaging live neuron networks with a high spatial and temporal resolution, because it is a 3D imaging method that is label-free and non-invasive. Using this method, a mouse or rat hippocampal neuron culture and a mouse dorsal root ganglion (DRG) neuron culture have been imaged in order to see the extension of processes between the cells in 3D. Furthermore, the tomogram is compared with a confocal fluorescence image in order to investigate the 3D structure at synapses.

This research is supported by NSF STC CBET 0939511 Emergent Behavior of Integrated Cellular Systems (MUG, GP), IGERT 0903622 NeuroEngineering (SCL) and Beckman Graduate Fellowship (TK). For more information, please visit <http://light.ece.illinois.edu/>.

9336-132, Session 8

Nuclear dynamics in metastatic cells studied by quantitative phase imaging

Silvia P. Ceballos, Univ. of Illinois at Urbana-Champaign (United States) and National Univ. of Colombia (Colombia); Mikhail E. Kandel, Shamira Sridharan, Univ. of Illinois at Urbana-Champaign (United States); Freddy Alberto Monroy-Ramirez, Univ. Nacional de Colombia Sede Medellín (Colombia); Gabriel Popescu, Univ. of Illinois at Urbana-Champaign (United States)

We used a new quantitative high spatiotemporal resolution phase imaging tool to explore the nuclear structure and dynamics of individual cells. We used a novel analysis tool to quantify the diffusion of nucleoli inside live cells and compared the nuclear dynamics in metastatic and non metastatic cells.

9336-66, Session 9

Profiling individual human red blood cells using holographic optical tomography (*Invited Paper*)

YongKeun Park, Youngchan Kim, KAIST (Korea, Republic

of); Hyeon Shim, Seongsoo Jang, College of Medicine and Asan Medical Ctr. (Korea, Republic of)

Due to its strong correlation with the pathophysiology of many diseases, information about human red blood cells (RBCs) has a crucial function in hematology. Therefore, measuring and understanding the morphological, chemical, and mechanical properties of individual RBCs is a key to unlocking the secrets of a number of RBC-related diseases, as well as to opening up new possibilities for diagnosing diseases in their earlier stages. In this study, a precise and sensitive optical holographic technique, referred to as Common-path diffraction optical tomography (cDOT) was presented that is well suited for the study of RBC pathophysiology as well as the diagnosis of RBC-related diseases (1, 2). The primary advantage of cDOT is its ability to analyze single cell profiling. cDOT can provide not only routine red cell indices but also additional indices such as sphericity, surface area, and membrane fluctuation. The structural, chemical, and mechanical information for RBCs are important for hemodiagnosis, and cDOT simultaneously measures these parameters at the individual cell level. Furthermore, secondary parameters such as RDW can also be directly obtained from these measurements. The correlations between the indices at the single cell level can be analyzed quantitatively for better understanding of the pathophysiological mechanism behind human diseases.

9336-67, Session 9

Using digital inline holographic microscopy and quantitative phase contrast imaging to assess viability of cultured mammalian cells

Sergey Missan, 4Deep Inwater Imaging (Canada); Olga Hrytsenko, Dept. of Biology, Dalhousie Univ. (Canada)

We have used digital inline holographic microscopy to record holograms of mammalian cells (HEK 293, E0771, and B16) in culture. The holograms have been reconstructed using Octopus software (4Deep Inwater Imaging), and phase shift maps unwrapped using the FFT-based phase unwrapping algorithm. The unwrapped phase shifts were used to determine the optical thickness of the cells. Addition of 0.5 mM H₂O₂ to cell media produced rapid rounding of cultured cells, followed by cell membrane rupture. The cell morphology changes and cell membrane ruptures were detected in real time and were apparent in the unwrapped phase shift images. The results indicate that quantitative phase contrast imagery produced by the digital inline holographic microscopes can be used for the label-free real time automated determination of cell viability and confluence in the mammalian cell cultures.

9336-68, Session 9

High throughput analysis of blood smears using diffraction phase microscopy

Hassaan Majeed, Mikhail E. Kandel, Basanta Bhaduri, Univ. of Illinois at Urbana-Champaign (United States); Krishnarao V. Tangella, Christie Clinic (United States); Gabriel Popescu, Univ. of Illinois at Urbana-Champaign (United States)

In spite of the recent advances in automated blood analyzer technologies such as flow cytometers and impedance analyzers, blood smear analysis remains an indispensable technique for diagnosis of several hematological disorders. The reason is that these blood analyzers do not provide information on individual cell morphology which needs to be obtained through a blood smear test. Blood smear tests are carried out in pathology labs by chemically staining a smear of blood on a glass slide and observing the shape and morphology of each cell in order to aid in the diagnosis of diseases such as malaria, anemia and leukemia among others. The diagnosis

relies on information that is qualitative and hence subjective. We report here on a quantitative label-free method for obtaining the optical path length image of an entire blood smear at 100x magnification by using diffraction phase microscopy. Using a slide scanning and mosaic stitching software platform developed in-house we are able to obtain the quantitative phase image of the entire smear at high throughput. This image is then used to extract different cellular shape parameters such as cell volume, surface area, sphericity etc. providing a quantitative morphological picture to a pathologist in all three spatial dimensions that is a marked improvement on the qualitative information available in a conventional smear test. Since the optical path length map of a cell is a function of the refractive index variation within it, our images also allow the detection of the infection of parasites within cells based on the refractive index contrast within them, in a label-free manner.

9336-69, Session 9

Diagnosis of colorectal cancer using quantitative phase imaging

Shamira Sridharan, Jon Liang, Univ. of Illinois at Urbana-Champaign (United States); Virgilia Macias, Anish Shah, Roshan Patel, Univ. of Illinois at Chicago (United States); Krishnarao V. Tangella, Presence Covenant Medical Ctr. (United States); Grace Guzman, Andre Kajdacsy-Balla, Univ. of Illinois at Chicago (United States); Gabriel Popescu, Univ. of Illinois at Urbana-Champaign (United States)

Colorectal cancer screening is important because it results in detection of cancer in early stages while also recognizing pre-malignant lesions in tissue that can eventually turn cancerous. Pathologists make the diagnosis of benign or cancerous colon from hematoxylin and eosin (H&E) stained colon biopsies. Other methods of examining slides could bring additional information on the nature of the lesions and serve as an adjunct to diagnosis, especially for more difficult cases of differential diagnosis. In our study, we used unstained tissue samples of all 4 conditions, namely, normal, hyperplasia, dysplasia and cancer, and imaged it using a quantitative phase imaging method, Spatial Light Interference Microscopy (SLIM). We used the phase distribution to make the diagnoses using a machine learning algorithm, support vector machine (SVM). Using the data from the 98 cases in the testing set, we studied the robustness of our method on another 97 cases. 96% of the benign cases and 92% of the cancerous cases were accurately classified. We are currently in the process of classifying the benign samples as normal, hyperplasia and dysplasia. Our preliminary results show the potential for quantitative phase imaging to be a valuable tool for pathologists for colorectal cancer screening.

9336-70, Session 9

Label-free quantitative analysis of phagocytosis using quantitative phase imaging techniques

Jonghee Yoon, Kyoohyun Kim, Jae Hwang Jung, YongKeun Park, KAIST (Korea, Republic of)

Phagocytosis plays essential roles in host defense against microbial pathogens and in clearance of impaired cells such as apoptotic cells. Phagocytic cells such as macrophages express pattern recognition proteins such as Toll-like receptors, then they detect foreign pathogens and ingest them via membrane movements. Ingested foreign materials are eliminated by interacting various intracellular organelles. Although many studies have reported physiology and function of phagocytosis, there are still limitations to observe phagocytic process quantitatively. Electron microscopy has been used to obtain high spatial resolution images of intracellular structures of phagocytic cells, however, it has limitations in live-cell analysis. Fluorescent

proteins are also used to study phagocytosis by labeling plasma membrane or pathogens, but they are not suitable for long-term observation because of photobleaching, phototoxicity, and photodamage.

In this work, we demonstrate three-dimensional (3-D) quantitative analysis of phagocytosis by macrophage using quantitative phase imaging techniques. 3-D refractive index (RI) tomograms are reconstructed from multiple two-dimensional holograms with various angles of illumination. 3-D tomograms distinguish intracellular vacuoles and phagosomes in macrophages through RI difference. Label-free imaging technique enables live-cell phagosome tracking in time-lapse sequences. Through this demonstration, we propose that quantitative phase imaging techniques is invaluable tool for 3-D quantitative analysis of phagocytosis without labeling.

9336-71, Session 9

Digital holographic microscopy applied to cell biology *(Invited Paper)*

Christian D. Depeursinge, Ecole Polytechnique Fédérale de Lausanne (Switzerland) and King Abdullah Univ. of Science and Technology (Saudi Arabia); Pierre P. Marquet, Kaspar Rothenfusser, Benjamin Rappaz, Pascal Jourdain, Ecole Polytechnique Fédérale de Lausanne (Switzerland); Pierre J. Magistretti, Ecole Polytechnique Fédérale de Lausanne (Switzerland) and King Abdullah Univ. of Science and Technology (Saudi Arabia)

Digital holographic microscopy (DHM) has recently emerged as a powerful quantitative phase technique particularly in the field of cell imaging allowing to non-invasively explore the cell structure and dynamics with a nanometric axial sensitivity. In this talk, the main advantages of quantitative phase digital holographic microscopy (QP-DHM), resulting in particular from the possibility to propagate the whole object wave (amplitude and phase) diffracted by the observed specimen during the numerical reconstruction of the digitally recorded holograms, will be explained. In addition, it will also present through different illustrative applications related to various fields of cell biology, how the quantitative phase signal, representing a very powerful intrinsic contrast, allows, by providing various relevant biophysical cell parameters, to study important cell processes. Finally a special attention will be drawn to issues related to cell neuroscience including especially the development of a synthetic aperture approach allowing a significant improvement of resolution facilitating the observation of both the local neuronal network activity and the dendritic spine dynamics. Full DHM based tomography also provides quantitative phase data and consequently, an invaluable insight in cell dynamics studies.

9336-72, Session 9

Noninvasive characterization and comparison of yeasts populations by dry mass and morphological parameters measurements with quadri wave lateral shearing interferometry

Sherazade Aknoun, Institut Fresnel (France) and Aix-Marseille Univ. (France); Pierre Bon, Institut d'Optique Graduate School (France) and Bordeaux Univ. (France); Julien Savatier, Institut Fresnel (France) and Aix-Marseille Univ. (France); Benoit F. Wattellier, PHASICS S.A. (France); Serge Monneret, Institut Fresnel (France) and Aix-Marseille Univ. (France)

We study the use of quadri wave lateral shearing interferometry to measure cell dry mass and make comparisons among individuals and between

different yeast populations. The measurement is based on single-shot quantitative phase imaging that can be implemented like a camera on any kind of conventional microscope using a standard illumination source [1].

During the life of a cell, its dry mass (i.e. the mass of all cellular content except water, usually expressed in pg), is deeply modified. We know that it also involves all the metabolic and structural functions of the cell and its study can reveal important information on cells. In the last decade it has been used for yeast cell cycle [2], mammalian cells [3] or stem cells colonies [4] studies.

Cell cycle is often studied with fluorescent labeling but in 1952 Barer [5] showed that the phase integrated over the entire cell is proportional to the dry mass. Determination of cell dry mass by quantitative phase imaging can be done by several means, all being noninvasive and label-free. This eliminates any bias, introduced for instance by fluorescent probes.

We will show that the high contrast brought by QWLSI and artifacts free imaging allows a precise cellular segmentation from which we can deduce different morphological parameters of interest. First, we will focus on the metrology aspects of our technique: noise level, repeatability and robustness against different samples and imaging conditions (including magnification). Then, we will present dry mass follow-ups for growth rate determination. Measurements over an entire yeast population enable discriminating between different genotypes. The different cell cycle stages are identified within the whole population thanks to classification methods, either supervised or non-supervised.

References

- [1]. P. Bon, G. Maucort, B. Wattellier, and S. Monneret, "Quadriwave lateral shearing interferometry for quantitative phase microscopy of living cells," *Opt. Express*, vol. 17, pp. 13080-13094, Jul 2009.
- [2] B. Rappaz, E. Cano, T. Colomb, V. S. Jonas Kühn, P. J. Magistretti, P. Marquet, and C. Depeursinge, "Noninvasive characterization of the fission yeast cell cycle by monitoring dry mass with digital holographic microscopy," *J. Biomed. Opt.*, vol. 14, no. 1083-3668, p. 034049, 2009.
- [3] P. Girshovitz and N. T. Shaked, "Generalized cell morphological parameters based on interferometric phase microscopy and their application to cell life cycle characterization," *Biomed. Opt. Express*, vol. 3, no. 8, pp. 1757-1773, 2012.
- [4] T. A. Zangle, J. Chun, J. Zhang, J. Reed, and M. A. Teitell, "Quantification of biomass and cell motion in human pluripotent stem cell colonies," *Biophys J*, vol. 105, pp. 593-601, Aug. 2013.
- [5] R. Barer, "Interference microscopy and mass determination," *Nature*, vol. 169, pp. 366-367, Mar. 1952.

9336-73, Session 9

Label-free quantification of emergent behaviors in human neuron network

Taewoo Kim, Mustafa A. Mir, Univ. of Illinois at Urbana-Champaign (United States); Anirban Majumder, Steven Stice, The Univ. of Georgia (United States); Gabriel Popescu, Univ. of Illinois at Urbana-Champaign (United States)

The growth and formation of neural networks is a highly dynamic and complex process. Even though it is very important to understand this process, there is only a shallow understanding. Fluorescence microscopy is the mostly widely used method for this process. However, this technique requires fixation of the sample, in addition to fluorescence labeling, which ultimately disturbs the sample.

Spatial light interference microscopy (SLIM) is a quantitative phase imaging modality that measures the optical path length distribution through a specimen that is transparent under the visible spectrum. The method has been used to measure the dry mass distribution of a sample, since the optical path length directly relates to the dry mass density.

Using this technique, we have obtained quantitative phase images of a differentiated human neuron culture over 24 hours. Furthermore, for

validation of the technique and analysis, a control culture and a neuron culture treated, reduced in the neurite growth by adding 15 mM lithium chloride, is imaged in the same manner.

We characterized the development of the neural network at both the single cell level and the population level, by analyzing the dry mass growth, cellular dynamics and spatial organization of the cells. These results showed a shift from the active growth of neural processes to the transport between cells, and indicated clear phase-dependent changes in the process of neuron network formation.

This research is supported by NSF STC CBET 0939511 Emergent Behavior of Integrated Cellular Systems (GP, SS), NSF CAREER 08-46660 (GP), CBET-1030361 MRI (GP) and Beckman Graduate Fellowship (TK). For more information, please visit <http://light.ece.illinois.edu/>.

9336-74, Session 9

Multiparametric characterization of red blood cells using quantitative phase spectroscopy and microfluidic devices

Han Sang Park, Matthew T. Rinehart, Adam Wax, Duke Univ. (United States)

Quantitative phase spectroscopy (QPS) has been previously used to study spectral and temporal characteristics of individual cells in vitro. While automatic discrimination of cell type and pathology remains elusive, many metrics have been defined to investigate structural mechanics, molecular content, and dynamic responses to a wide range of stimuli. Here, we present phase-based multiparametric characterization of individual blood cells that allow population identification and quantification. We use holographic interference microscopy to examine spectral and temporal behavior of static and flowing cells including their responses to mechanical stresses during flow through microfluidic devices. The off-axis Mach-Zehnder spectroscopic interferometer illuminates samples with a supercontinuum source (450-750nm) and operates in 2 modes to capture spectral signatures and temporal dynamics. When using the high-spectral resolution imaging modality, the illumination scheme can select an arbitrary center wavelength in <1ms with a rapidly-tunable custom filter. The spectral bandwidth of the system is <1nm and allows accurate measurement of wavelength-dependent properties, such as refractive index increment and spectroscopic dispersion, of varying cell populations. Using the high-speed (>2kHz) imaging mode of the interferometer, nanoscale motions of the red blood cells can be quantified at a single wavelength with parameters such as mean square displacement and changes in optical volume. Furthermore, we evaluate physical changes in cell properties due to mechanical deformation through imaging within microfluidic channels. By determining spectral and temporal metrics of red blood cells using QPS, we present a method to differentiate cells by their disease state and potentially selectively discriminate cell populations using microfluidic devices.

9336-75, Session 9

Lab on chip optical imaging of biological sample by quantitative phase microscopy

Lisa Miccio, Istituto Nazionale di Ottica (Italy); Pasquale Memmolo, Istituto Nazionale di Ottica (Italy) and Ctr. for Advanced Biomaterials for Health Care, Istituto Italiano di Tecnologia (Italy); Francesco Merola, Istituto Nazionale di Ottica (Italy); Paolo A. Netti, Ctr. for Advanced Biomaterials for Health Care, Istituto Italiano di Tecnologia (Italy); Pietro Ferraro, Istituto Nazionale di Ottica (Italy)

Quantitative imaging and three dimensional (3D) morphometric analysis of flowing and not-adherent cells is an important aspect for diagnostic purposes at Lab on Chip scale. Diagnostics tools need to be quantitative,

Conference 9336: Quantitative Phase Imaging

label-free and, as much as possible, accurate. In recent years digital holography (DH) has been improved to be considered as suitable diagnostic method in several research field. In this paper we demonstrate that DH can be used for retrieving 3D morphometric data for sorting and diagnosis aims. Several techniques exist for 3D morphological study as optical coherent tomography and confocal microscopy, but they are not the best choice in case of dynamic events as flowing samples. Recently, a DH approach, based on shape from silhouette algorithm (SFS), has been developed for 3D shape display and calculation of cells biovolume. Such approach, adopted in combination with holographic optical tweezers (HOT) was successfully applied to cells with convex shape. Unfortunately, it's limited to cells with convex surface as sperm cells or diatoms. Here, we demonstrate an improvement of such procedure. By decoupling thickness information from refractive index ones and combining this with SFS analysis, 3D shape of concave cells is obtained. Specifically, the topography contour map is computed and used to adjust the 3D shape retrieved by the SFS algorithm. We prove the new procedure for healthy red blood cells having a concave surface in their central region. Experimental results are compared with theoretical model and we also show the method suitability to classify, in terms of morphology, different RBC shapes.

Conference 9337: Nanoscale Imaging, Sensing, and Actuation for Biomedical Applications XII

Monday - Thursday 9-12 February 2015

Part of Proceedings of SPIE Vol. 9337 Nanoscale Imaging, Sensing, and Actuation for Biomedical Applications XII

9337-15, Session PMon

Persistent luminescence in nanophosphors for long term in-vivo bio-imaging (*Invited Paper*)

Bruno Viana, Ecole Nationale Supérieure de Chimie de Paris (France); Aurelie Bessiere, Sunchinder Sharma, Didier Gourier, Laurent Binet, IRCP Chimie Paris (France); N. Basavaraju, K. R. Priolkar, Goa Univ. (India); Thomas Maldiney, Elliot Teston, Cyrille Richard, Univ. Paris Descartes (France); Daniel Scherman, Univ. Paris Descartes (France) and Chimie-ParisTech (France)

Optical imaging constantly demands more sensitive tools intended for biomedical research and medical applications. Near-infrared persistent luminescence nanoparticles have recently been introduced to enable highly sensitive in vivo optical detection and complete avoidance of tissue autofluorescence [1, 2]. However, the first generation of persistent luminescence nanoparticles had to be excited ex vivo, prior to systemic administration, which prevented long-term imaging in living animal [1]. We presently introduce a novel generation of optical nanoprobles, based on chromium-doped zinc gallate [2], whose persistent luminescence can be activated in vivo through living tissues using highly penetrating low energy photons from the red region of the visible spectrum [4,5]. Surface functionalization of this photonic probe can be adjusted to favour multiple challenging biomedical applications. In addition others compounds in the spinel family (namely AB₂O₄ A=Zn, Mg and B=Ga, Al...) can be used either to tune the emission wavelengths by chromium crystal field variation or to adjust the traps depth in order to better control the release of the traps through photo stimulation [6].

9337-19, Session PMon

Performance evaluation for different sensing surface of BICELLS bio-transducers for dry eye biomarkers

María-Fe Laguna, Miguel Holgado Bolaños, Univ. Politécnica de Madrid (Spain); Beatriz Santamaría, Univ. Politécnica de Madrid (Spain); Ana L. Hernández, Univ. Politécnica de Madrid (Spain); María Victoria Maigler, Univ. Politécnica de Madrid (Spain) and Bio Optical Detection S.L. (Spain); Álvaro Lavín, Jesús de Vicente, Univ. Politécnica de Madrid (Spain); Javier Soria, Tatiana Suarez, Bioftalmik S.L. (Spain); Carlota Barcina, Mónica Jara, Antibody Bcn (Spain); Francisco J. Sanza, Univ. Politécnica de Madrid (Spain) and Bio Optical Detection S.L. (Spain); Rafael Casquel del Campo, Univ. Politécnica de Madrid (Spain); Álvaro Otón, Univ. Politécnica de Madrid (Spain) and Bio Optical Detection S.L. (Spain); Teresa Riesgo, Univ. Politécnica de Madrid (Spain)

We have recently proved an efficient methodology for label-free biosensing by using Biophotonic Sensing Cells (BICELLS) for dry eye diseases where a single drop of tear is needed for this test. The Limit of detection mainly depends on the transducers sensitivity, resolution of the optical reader and the performance of the immunoassay. This later plays and important role in

the final response of the sensing system as a whole, and the immobilization process is probably the most critical step during the biosensor fabrication.

For the case of dry eye disease, different proteins have been validated as biomarkers such as: S100A6, CST4, MMP9, PRDX5, ANXA1, ANXA11, PLAA. For this work different antibodies were tested aiming to use those one presenting the best response. Furthermore, different sensing surfaces were tested in order to demonstrate the best conditions for detecting for recognizing the above-mention proteins.

The reader employed was recently tested for infectious diseases, and in this work an adaptation of this novel platform have been used. The results found during the experiments show the capability of this technology to be used as a Point of Care device. Finally, the Limits of Detections achieved are in the order of ng/mL ensuring the validation for real applications.

9337-20, Session PMon

Characterisation of orientation distribution of gold nanorods using high-order image correlation spectroscopy

Timothy T. Y. Chow, James W. M. Chon, Swinburne Univ. of Technology (Australia)

Image Correlation Spectroscopy (ICS) can be used to analyse plasmonic nanoparticles dispersed randomly in dielectric medium, but is yet to be applied in characterising orientation of anisotropic nanoparticles. Here we propose using high-order ICS (HICS) to characterise the orientation distribution of plasmonic gold nanorods in random media, which will provide much faster and easier characterization method to conventional polarization methods.

The proposed HICS method is to use the sensitivity of HICS on variation of quantum yield of emitting particles. Generally, ICS is sensitive to the density of one species (i.e. fixed quantum yield). If the sample consists of nanorods of random orientation, their scattering or emission quantum yield will be varied according to the excitation light polarization direction, and therefore the precision will be reduced. However, HICS has the ability to compute the density of multiple species with varying quantum yield in one image. To study the practicality on characterising static distribution of orientation of plasmonic nanorods-embedded samples, confocal laser scattering images of random nanorods with various orientation distributions, concentrations and other conditions are simulated. These images are analysed by HICS, and the results show that HICS could be used to indicate the statistic distribution model of the orientation of the embedded rods. In this paper we present the degree of tolerance of this method, with testing conditions of noise background, concentration, point spread function variation and defocused images.

9337-21, Session PMon

Super-resolution fluorescence imaging of C2C12 cell differentiation

Jing Qi, Xiao Peng, Junle Qu, Shenzhen Univ. (China)

Actin and tubulin play important roles in a variety of cellular processes, such as muscle contraction, cell motility, cell division and vesicle movement, etc. The importance of actin and tubulin has also been indicated in myogenic differentiation. Till now, a lot of research has been focused on the structure of these proteins and the regulatory mechanisms of their dynamics. However, their organization during myogenic differentiation still needs further clarification. The resolution of the conventional fluorescence

**Conference 9337: Nanoscale Imaging, Sensing,
and Actuation for Biomedical Applications XII**

microscopy can only achieve around 200 nm, leading to the development of super-resolution microscopy. In this study, we have applied stochastic optical reconstruction microscopy (STORM) method to investigate the structure of actin and tubulin in the differentiation process of C2C12 myoblasts. STORM is one of the novel super-resolution techniques that are based on accuracy localization of photoswitchable fluorophores. By using STORM technique, we achieved an imaging resolution of ~30 nm in C2C12 cells under differentiation conditions. Moreover, we treated C2C12 cells with drug influencing their normal development for functional study of actin and tubulin proteins during the process. Taken together, our results have provided better understanding of muscle development via regulations of cytoskeleton proteins.

9337-22, Session PMon

Plasmon based super-resolution microscopy: break the diffraction limits

HeeSang Ahn, SeonHee Hwang, Tae Lim Yoon, Sang Mok Kim, Kyujung Kim, Pusan National Univ. (Korea, Republic of)

Super-resolution imaging below a diffraction limit has considerable interests to analyze tiny molecular interactions. Evanescent fields based total internal reflection fluorescence (TIRF) microscopy is widely used in order to achieve extremely high depth resolution around 100 nm. However, TIRF microscopy is not possible to obtain high spatial resolution under the diffraction limit. Thus, there have been lots of investigations to increase spatial resolution with nanostructures. The nanostructures on surface are able to redistribute uniform evanescent fields and localize fields smaller than 100 nm with a precise structure design. In this research, various shaped nanostructures which can localize evanescent fields are fabricated by electron beam lithography and a thermal annealing method. The localization of near-field distribution that is associated with localized surface plasmon on the nanostructures was analyzed theoretically and experimentally. For experimental confirmation, we used cancer cells stained with Alexa Fluor 488. The results suggest the imaging resolution can be obtained down to 100 nm with optimized plasmonic nanostructures. A calculated data proves the formation of localized fields can be clearly identified on the surface. Fluorescence images of cancer cell taken on the nanostructures were compared with the images taken on the non-patterned films. Consequently, resolution-enhanced images of cancer cells were achieved by taking the images on the periodic nanostructures and random nanopatterns. Those image data support the feasibility of obtaining extremely enhanced image resolution, thus the diffraction limits can be easily broken by applying nanostructures to conventional TIRFM.

9337-23, Session PMon

Imaging highly-absorbing nanoparticles using photothermal microscopy

Simon-Alexandre Lussier, Hamid Moradi, Alain Price, Maxime Daneau, Sangeeta Murugkar, Carleton Univ. (Canada)

Gold nanoparticles (NPs) have tremendous potential in biomedicine. They can be used as absorbing labels inside living cells for the purpose of biomedical imaging, biosensing as well as for photothermal therapy. We demonstrate photothermal imaging of highly-absorbing particles using a pump-probe setup. The photothermal signal is recovered by heterodyne detection, where the excitation pump laser is at 532 nm and the probe laser is at 638 nm. Proof of concept images of red polystyrene microspheres and gold nanoparticles are obtained with this home-built multimodal microscope. The increase in temperature at the surface of the gold NPs, due to the pump laser beam, can be directly measured by means of this photothermal microscope and then compared with the results from theoretical predictions. This technique will be useful for characterization of

nanoparticles of different shapes, sizes and materials that are used in cancer diagnosis and therapy.

9337-24, Session PMon

Systematic study and quantification of optical forces on porous silicon nanoparticles

Fook-Chiong Cheong, Thorlabs, Inc. (United States); Jeremy W. Mares, Vanderbilt Univ. (United States); Tobias Paprotta, Jens Schumacher, Thorlabs, Inc. (United States); Sharon M. Weiss, Vanderbilt Univ. (United States); Alex E. Cable, Thorlabs, Inc. (United States)

In this work, we report using an optical tweezers system to study the light-matter interaction and gradient optical forces of porous silicon nanoparticles. The particles are fabricated by first electrochemically etching a multi-layer porous film into a silicon wafer and then breaking up the film using ultra-sonication. The particles have pore sizes ranging from 20-30nm. The particle diameters are approximately 100-300nm and can be size-sorted by centrifugation. A commercially available optical tweezers system is used to systematically study the optical forces interacting with these nanoparticles. This work opens new strategic approaches to enhance optical forces and optical sensitivity to mechanical motion that could be the basis for future biophotonics applications.

9337-1, Session 1

Confocal Raman microscopy and hyperspectral dark field microscopy imaging of chemical and biological systems (Invited Paper)

Henrique E. Toma, Univ. de São Paulo (Brazil); Jorge da Silva Shinohara, Daniel Grasseschi, Univ. de Sao Paulo (Brazil)

Hyperspectral imaging coupled with optical microscopy can provide accurate information on the distribution of the chemical species in materials and biological samples, based on the analysis of their electronic and vibrational profiles. As a matter of fact, confocal Raman microscopy is one of the best ways to access the chemical distribution of molecules, especially under resonance Raman or SERS conditions. On the other hand, enhanced dark field optical microscopy can be employed for hyperspectral imaging in the visible, while extending the optical resolution up to the nanoscale dimension. It allows the detection of gold or silver single nanoparticles, as well as their spectral monitoring from their characteristic surface plasmon bands. These two hyperspectral microscopies can be conveniently combined to provide electronic and vibrational information of the chemical species in a wide variety of systems at the nanoscale. Several examples, focusing on the chemical interface of dye solar cells [1], nickel and palladium nanowires [2], and dye coated gold nanoparticles [3], and Hella cells will be discussed in this presentation. Another interesting association involves the use of spectroelectrochemical techniques with hyperspectral imaging (Fig. 1). This line of investigation is particularly rewarding for monitoring electrochemically active species at several applied potentials, by confocal Raman and dark field optical microscopy. (FAPESP Grant 2013/24725-4)

9337-2, Session 1

Scanning localized magnetic fields in microfluidic system using single spin in diamond nanocrystal.

Kangmook Lim, Univ. of Maryland, College Park (United States)

The ability to measure weak local magnetic fields with high spatial resolution and high sensitivity is valuable for the study of biological systems and critical for understanding magnetic properties of molecules and solids. Nitrogen vacancy (NV) color centers in diamond have demonstrated highly sensitive optical detection of magnetic fields. Effective integration of these magnetic field probes into microfluidic systems enables the study of magnetic properties of isolated chemical and biological samples in a fluid environment. Here we demonstrate a method to perform localized nano-precise magnetometry using a single NV center in a microfluidic device. We manipulate a magnetic particle within a liquid environment using a combination of flow control and magnetic actuation above a diamond nanocrystal with a single NV center. We map out the magnetic field distribution of the magnetic particle by varying its position relative to the NV center and performing an optically resolved electron spin resonance (ESR) measurement. We attain a magnetic particle spatial resolution of 48 nm and DC magnetic field sensitivity of 17.5 microTesla/Hz^{1/2}. These results open up the possibility for studying local magnetic properties of biological and chemical systems with high sensitivity in an integrated microfluidic platform.

9337-3, Session 1

Atomic force microscopy (AFM), Raman microspectroscopy (RM) and gene chip monitoring of porcine trophoblast derived cells differentiation

Qifei Li, Sierra Heywood, Lifu Xiao, Mingjie Tang, Anhong Zhou, S. Clay Isom, Utah State Univ. (United States)

As an interesting model for stem-like cell research, porcine trophoblast derived cells have the regenerative properties, indefinite passage, and foreign DNA receptivity. Currently, traditional identification of stem cells differentiation has limitations: time-consuming, lengthy and invasive approaches. Here, atomic force microscopy (AFM) and Raman microspectroscopy (RM)—both considered as label-free, non-invasive and comparatively fast techniques—are applied to detect the biophysical and biochemical properties of trophoblast derived stem-like cells under conditions designed to induce differentiation over 15 and 30 days. It was found that the diameter of undifferentiated cells changed slightly comparing to that of differentiated cells over time, and the diameter of undifferentiated cells was less than that of differentiated cells. Meantime, the Young's modulus of undifferentiated cells was found to be less than that of differentiated cells over 30 days of differentiation. In addition, the intensities of characteristic Raman peaks of protein and nucleic acids decreased over time for differentiated cells, while these intensities of undifferentiated cells have no significant change. Furthermore, the Raman spectra of differentiated cells were successfully separated from undifferentiated cells by principal component analysis (PCA). Gene chip was also applied to analyze gene expression of the same cells after AFM and RM which indicated the changes of some marker genes for cell function of these stem-like cells over the time. Our results demonstrated the potential application of combination of three instrument techniques in study biophysics of embryonic cell differentiation.

9337-4, Session 1

Super-resolution optical microscopy using solid-immersion of high-index microspheres

Arash Darafsheh, Consuelo Guardiola Salmeron, Averie Palovcak, Jarod C. Finlay, Alejandro Carabe-Fernandez, The Univ. of Pennsylvania Health System (United States)

Optical microscopy is one of the oldest and most important imaging techniques in life sciences; however, its spatial resolution is limited to $\sim \lambda/2$, where λ is the wavelength of light, due to the diffraction effects. Optical super-resolution imaging would have a profound impact on many interdisciplinary areas, such as imaging of biological structures, inspection of semiconductor devices, microfluidics, and nanophotonics. We demonstrate that super-resolution imaging of specimens containing sub-diffraction-limited features is achievable through high-index microspheres embedded in a transparent thin film covering the specimen. By using barium titanate glass microspheres with ~ 2 - $100 \mu\text{m}$ diameters and index of refraction ~ 1.9 - 2.1 embedded in a transparent thin film on top of a specimen, we clearly discerned sub-diffraction-limited features through a conventional optical microscope. The achieved improvement in imaging resolution was calculated based on measuring the imaging system's effective point-spread function through image deconvolution. Each microsphere acts as an auxiliary lens that collects high spatial frequencies and projects them to the far field with magnification enabling visualization of features on the order of $\sim \lambda/7$. We demonstrate feasibility of microsphere-assisted imaging technique for biological microscopy for observation of double-strand DNA breaks in U87 glioblastoma cells irradiated by a clinical proton beam.

9337-5, Session 1

Single and multiprobe apertureless nanothermal imaging of electromagnetic excitation over a wide range of wavelengths from the near to mid-infrared (*Invited Paper*)

Aaron Lewis, The Hebrew Univ. of Jerusalem (Israel); Rimma Dekhter, Sophia Kokotov, Patricia Hamra, Boaz Fleischman, Hesham Taha, Nanonics Imaging Ltd. (Israel)

Near-field optical effects have generally been detected using photodetectors. There are no reports on the use of the temperature changes caused by electromagnetic radiation using thermal sensing probes for scanned probe microscopy. In this paper we apply our development of such probes to monitor the effects of electromagnetic radiation at a number of different wavelengths using the heating caused in a sample by specific wavelengths and their propagation. The paper will catalogue effects over a wide spectrum of wavelengths from the near to mid infrared. The method has been applied from devices to molecules. The thermal sensing probes are based on glass nanopipettes that have metal wires that make a contact at the very tip of a tapered glass structure. These probes are cantilevered and use normal force tuning fork methodology to bring them either into contact or near-contact since this feedback method has no jump to contact instability associated with it. Data will be shown that defines the resolution of such thermal sensing to at least the 32 nm level. In addition the probes have the important attribute of having a highly exposed tip that allows for either optical sensing methodologies with a lens either from directly above or below or heat sensing with a single or additional probe in a multiprobe scanning probe system. With such a system it will be shown that apertureless infrared excitation and detection can be affected and results will be shown on a variety of systems including devices and a suspended carbon nanotube. The approach described in this paper has considerable advantages over purely optical methods for both excitation and detection to which it can be directly compared.

**Conference 9337: Nanoscale Imaging, Sensing,
and Actuation for Biomedical Applications XII**

9337-6, Session 1

**Hyperlens arrays for subwavelength
imaging and microscopy (*Invited Paper*)**

Alexander N. Cartwright, Tania Moein, Jingbo Sun, Univ. at Buffalo (United States); Xiaoming Liu, Ji Zhou, Tsinghua Univ. (China); Natalia M. Litchinitser, Univ. at Buffalo (United States)

No Abstract Available

9337-7, Session 1

**Quantitative analysis of confocal images
to characterize structural disorder in
biological cells: a novel method to analyze
cancerous and noncancerous cells**

Peeyush Sahay, Hemendra M. Ghimire, Huda Almagbadi, Vibha Tripathi, Jahangir Alam, Lauren Thompson, Omar Skalli, Prabhakar Pradhan, The Univ. of Memphis (United States)

Several evidences show that structural changes in a wide range of length scales in biological cells are associated with progress in carcinogenesis. Therefore, measuring and quantifying the structural changes progressing inside a cell could be a potential biomarker for cancer diagnostics. However, there is no as such robust technique to measure the degree of structural disorders inside the cells and the structural changes at different length scales has not been well studied. We performed a novel study to quantify the degree of structural disorders developing within the cells by combining confocal microscopy imaging, and techniques used in condensed matter physics for analyzing disordered systems, namely Inverse Participation Ratio (IPR) method. The experiments were conducted to study 1024 × 1024 pixel resolution confocal images of MCF-10A and MCF-7 breast control and cancer cell lines, respectively. The results show a significant increased sub-micron scales degree of structural disorders in correlation with the degree of carcinogenesis. In particular, the MCF-7 cells exhibited higher structural disorder than MCF-10A cells at all the length scales examined (0.2 – 1 μm). This study is first of its kind where the structural disorder of cells have been quantified and analysed using confocal microscopy images, with structural disorders characterized in terms of IPR values. The preliminary results are quite encouraging in terms of providing new insight towards diagnostic processes, and the method has potential to add new dimension to biological and medical research fields, especially in cancer detection and prevention.

9337-8, Session 1

**Nano-imaging collagen by atomic force,
near-field microscope and nonlinear
microscope**

Ken Choong Lim, Nanyang Technological Univ. (Singapore); Jin Kai Tang, Singapore Institute of Manufacturing Technology (Singapore) and Nanyang Technological University (Singapore); Hao Li, Boon Ping Ng, Shaw Wei Kok, Singapore Institute of Manufacturing Technology (Singapore); Qi Jie Wang, Nanyang Technological Univ. (Singapore); Ying Zhang, Singapore Institute of Manufacturing Technology (Singapore)

As most abundant protein in human body, collagen has very important role in vast numbers of bio-medical applications. Especially the unique second order nonlinear properties of fibrillar collagen make it can be used a very

important index in nonlinear optical imaging based disease diagnosis on brain, skin, liver, colon, kidney, bone, heart and other human organs. The second-order nonlinear susceptibility of collagen has been explored at the macroscopic level and was explained as volume-averaged molecular hyperpolarizability. However, the details of the origin of optical second harmonic signal from collagen fiber at the molecular level are still not very clear. Such information is very important for interpolating bio-information from the optical images obtained by polarization-dependent SHG method. The later has shown great potential on control the cell-collagen interaction for tissue engineering applications. In this paper, we report our works on using atomic force microscope (AFM) and nonlinear near field scanning microscope (SHG-SNOM) to study nanostructure of collagen and pro-collagen fibers and its effect on SHG anisotropy.

9337-9, Session 1

**Extraordinary transmission-based
super-resolved axial imaging using
subwavelength metallic nanoaperture
arrays**

Wonju Lee, Youngjin Oh, Yonsei Univ. (Korea, Republic of); Jong-Ryul Choi, Daegu-Gyeongbuk Medical Innovation Foundation (Korea, Republic of); Kyujung Kim, Pusan National Univ. (Korea, Republic of); Donghyun Kim, Yonsei Univ. (Korea, Republic of)

Super-resolution techniques have been widely investigated to analyze characteristics of various cells and biomolecules. For sub-diffraction-limited resolution, several microscopies were developed based on stimulated emission depletion, structured light illumination, single molecule localization, etc. Here, we explored use of plasmonic localization-based metallic nanopatterns to break the diffraction limit for biomolecular imaging. Target fluorescence was excited for nanoscale sampling by highly localized plasmon fields created by aperture arrays under total internal reflection (TIR). Most of these techniques have been used to address enhancement of lateral imaging resolution rather than axial resolution in fluorescence microscopy, whereas axial resolution was generally limited on a scale of a few hundreds of nanometers. Also, it is often desired to observe phenomena in the deeper region than is typically allowed within the TIR range of 100 nm from surface while maintaining super-resolution. In this presentation, a super-resolved axial imaging technique was investigated using metallic nanoaperture arrays. Extraordinary transmission (EOT) of light can be induced through subwavelength nanoaperture arrays at thick metal film by plasmonic coupling. The feasibility of EOT field is explored for super-resolved axial imaging of biological targets. Penetration depth of EOT is much longer than that of evanescent waves under TIR and can be controlled by modulating the nanoapertures. Deeper axial information may be available from fluorescence signals detected on EOT fields. By experimental measurements, axial characteristics of gliding movements of bacteria as well as axial distribution of ganglioside in cells were analyzed and compared with conventional microscopy techniques. The results confirm sub-diffraction-limited axial resolution.

9337-10, Session 2

**Nanoscale dynamics in live cells studied by
quantitative phase imaging (QPI) (*Keynote
Presentation*)**

Gabriel Popescu, Univ. of Illinois at Urbana-Champaign (United States)

Most living cells do not absorb or scatter light significantly, i.e. they are essentially transparent, or phase objects. Quantifying cell-induced shifts in the optical path-length permits nanometer scale measurements of structures and motions in a non-contact, label-free manner. Spatial Light

**Conference 9337: Nanoscale Imaging, Sensing,
and Actuation for Biomedical Applications XII**

Interference microscopy (SLIM) is a highly sensitive QPI method developed in our laboratory. Due to its sub-nanometer pathlength sensitivity, SLIM enables interesting structure and dynamics studies over broad spatial (nanometers-centimeters) and temporal (milliseconds-weeks) scales.

I will review our recent results on applying SLIM to basic cell dynamics studies: neuroprogenitor cell differentiation and neural network formation, red blood cell membrane fluctuations of banked blood, and time-resolved cell tomography for 3D intracellular transport studies.

9337-11, Session 2

Portable plasmonic interferometer sensor for rapid and label-free diagnosis of cancer markers *(Invited Paper)*

Qiaoqiang Gan, Univ. at Buffalo (United States); Yun Wu, Univ. of Buffalo (United States); Xie Zeng, Univ. at Buffalo (United States)

No Abstract Available

9337-12, Session 2

Label-free monitoring of individual DNA hybridization using SERS

Ji Qi, Jianbo Zeng, Fusheng Zhao, Univ. of Houston (United States); Gregg Santos, Univ of Houston (United States); Steven Lin, MD Anderson Cancer Center (United States); Balakrishnan Raja, Ulrich Strych, Richard Willson, Univ of Houston (United States); Wei-Chuan Shih, Univ. of Houston (United States)

Sequence-specific detection of DNA hybridization at the single-molecule level has been instrumental and gradually become a ubiquitous tool in a wide variety of biological and biomedical applications such as clinical diagnostics, biosensors, and drug development. Label-free and amplification-free schemes are of particular interest because they could potentially provide in situ monitoring of individual hybridization events, which may lead to techniques for discriminating subtle variations due to single-base modification without stringency control or repetitive thermal cycling. Surface-enhanced Raman spectroscopy (SERS) has been widely used for molecular detection and identification by exploiting the localized surface plasmon resonance effect when the target molecules are near gold or silver nanostructures. However, effective and robust SERS assays have yet become a reality for trace detection. Recently, we have developed a SERS substrate by shaping nanoporous gold thin films into monolithic submicron disks, called nanoporous gold disks (NPGD). Here we demonstrate in situ monitoring of the same immobilized ssDNA molecules and their individual hybridization events over more than an hour. A microfluidic environment prevents sample drying, allows small sample volume, and permits agile fluid manipulation. We show time-lapsed monitoring of DNA hybridization with 20 pM target concentration. The surface density of the immobilized probes was controlled to be at 2 molecules/ μm^2 , suggesting single molecule detection has been achieved.

Ji Qi, Jianbo Zeng, Fusheng Zhao, Steven Hsesheng Lin, Balakrishnan Raja, Ulrich Strych, Richard C. Willson, and Wei-Chuan Shih**, "Label-free, in situ SERS monitoring of individual DNA hybridization in microfluidics," *Nanoscale* 6(15), 8521-8526, 2014, DOI: 10.1039/C4NR01951B.

9337-13, Session 2

Determination of thickness and density of a wet multilayer polymer system with sub-nanometer resolution by means of a dual polarization silicon-on-insulator microring

Jan-Willem Hoste, Univ. Gent (Belgium) and IMEC (Belgium); Bruno G. De Geest, Univ. Gent (Belgium); Peter Bienstman, Univ. Gent (Belgium) and IMEC (Belgium)

Determination of both thickness and refractive index of a thin biomolecular or polymer layer in wet conditions is a task not easily performed. Available tools such as XPS, AFM, ellipsometry and integrated photonic sensors often have difficulties with the native wet condition of said agents—under-test, perform poorly in the sub-5 nm regime or do not determine both characteristics in an absolute simultaneous way. The thickness of a multilayer system is often determined by averaging over a large amount of layers, obscuring details of the individual layers. Even more, the interesting behavior of the first bound layers can be covered in noise or assumptions might be made on either thickness or refractive index in order to determine the other.

As a way around these problems, a silicon-on-insulator (SOI) microring is used to study the adsorption of a bilayer polymer system on the silicon surface of the ring. To achieve this, the microring is excited with TE and TM polarized light simultaneously and by tracking the shifts of both resonant wavelengths, both the refractive index and the thickness of the adsorbed layer can be determined with a resolution on thickness smaller than 50 pm and a resolution on refractive index smaller than 0.01 RIU. An adhesive polyethyleneimine (PEI) layer is adsorbed to the surface, followed by cycling layer-by-layer adsorption of poly(sodium-4-styrene sulfonate) (PSS) and poly(allylamine) hydrochloride (PAH). This high-resolution performance in wet conditions with the added benefits of the SOI microring platform such as low cost and multiplexability make for a powerful tool to analyze thin layer systems, which is promising to research binding conformation of proteins as well.

9337-16, Session 2

Tunable vapor-condensed nanolenses for label-free nanoscale imaging and sensing *(Invited Paper)*

Euan McLeod, Chau Nguyen, Patrick Huang, Wei Luo, Muhammed Veli, Aydogan Ozcan, Univ. of California, Los Angeles (United States)

Label-free optical detection and imaging of individual nanoparticles such as viruses can be challenging due to their small optical scattering cross-sections. Here we use a combination of lensfree holographic imaging and self-assembled vapor-condensed nanolenses to significantly enhance the scattering signatures of these nanoparticles, enabling the detection of individual spherical particles smaller than $D=40$ nm in diameter, and individual rod-shaped particles smaller than 20 nm in diameter, over an ultra-large field of view >20 mm². Whereas typical nanoparticle imaging systems rely on scattered intensity, which scales as $1/D^6$ for Rayleigh-regime particles, holographic imaging captures an interference pattern, whose signal is proportional to the field amplitude (i.e., proportional to $1/D^3$). This reduction in scaling exponent is commensurate with a significant enhancement in optical signal.

The use of tunable vapor-condensed nanolenses provides even greater sensitivity, and further reduces the scaling exponent. The nanolenses are formed by exposing the substrate with adsorbed nanoparticles to polyethylene glycol (PEG) vapor for a few minutes. The PEG vapor condenses as a liquid film on the substrate, and small menisci, or nanolenses, form adjacent to the adsorbed particles. The height and shape of the nanolenses can be tuned via the exposure time and PEG vapor

**Conference 9337: Nanoscale Imaging, Sensing,
and Actuation for Biomedical Applications XII**

temperature. We demonstrate compatibility with a variety of different nanoparticles, and with functionalized surface capture for specific particle detection. The enhancement factors provided by self-assembled nanolenses quantitatively agree with our models of the evolution of the lens shape and resulting optical scattering fields.

9337-17, Session 2

**Persistence length of actin filaments
on surfaces patterned with various
concentrations of myosin**

Dan V. Nicolau, McGill Univ. (Canada)

No Abstract Available

9337-18, Session 2

**Super absorbing mid-IR metasurface for
surface enhanced infrared absorption
spectroscopy**

Borui Chen, Dengxin Ji, Qiaoqiang Gan, Alexander N.
Cartwright, Univ. at Buffalo (United States)

No Abstract Available

Conference 9338: Colloidal Nanoparticles for Biomedical Applications X

Saturday - Monday 7-9 February 2015

Part of Proceedings of SPIE Vol. 9338 Colloidal Nanoparticles for Biomedical Applications X

9338-1, Session 1

Design and optimization of polymer nanoshuttles for nanomedicine (*Invited Paper*)

Daniela Guarnieri, Enza Torino, Raffaele Vecchione, Istituto Italiano di Tecnologia (Italy); Paolo A. Netti, Univ. degli Studi di Napoli Federico II (Italy)

Current advances in nanotechnology hold the promises to greatly impact on current medical practice. Since nanometric materials interact with cells, tissue and organs at a molecular level, they may be used as probes for ultrasensitive molecular sensing and diagnostic imaging or carriers for drug and gene delivery. However, along with the excitement that has driven the development of novel nanocarriers, there have been increasing concerns regarding the risks these materials may generate. As these nanostructures are intentionally engineered to target specific cells or tissues, it is imperative to ensure their safety. The optimal design of safe and functional nanocarriers for medicine requires a better understanding of the interaction between the physical-chemistry properties of the nanoparticle surface with the complex protein machinery existing at the cell membrane. In particular the effect of the particles properties (charge, shape, protein coating) on the the mechanism of cellular uptake is highly relevant both to assess the real biological risks coupled with the use of nanomaterial (nanopathology and nanotoxicology) and to engineer carriers able to improve the medical practice. The nanometric size and the surface molecular decoration may activate mechanisms of cellular uptake different from those commonly used by cells these open the possibility to activated/modulated the membrane crossing by tuning chemical-physical properties of nanometric materials. In this lecture, the design and production of novel degradable polymeric nanocavities via layer-by-layer and temperature induced phase separations technology will be presented along with a detailed characterization of their in vitro and in vivo performances. Furthermore, possible mechanisms of cellular uptake will be discussed and critically presented. The effect of size, shape surface charges, surface bioconjugation on cell membrane crossing will be exploited and elucidated. Particular attention will be devoted to surface molecular decoration able to guide the nanoparticle throughout the cytosol.

9338-2, Session 1

Multifunctional metal rattle-type nanocarriers for MRI-guided photothermal cancer therapy

Yuran Huang, National Ctr. for Nanoscience and Technology of China (China)

In the past decade, enormous species of nanomaterials have been developed for biomedical application, especially cancer therapy. Realizing visualized therapy is highly promising now because of the potential accurate, localized treatment. In this work, we firstly synthesized metal nanorattles (MNRs), which utilized porous gold shells to carry multiple MR imaging contrast agents - superparamagnetic iron oxide nanoparticles (SPIONs) inside. A fragile wormpores-like silica layer was manipulated to encapsulate 8 nm oleylamine- SPIONs and mediate the in-situ growth of porous gold shell, and was finally etched by alkaline solution to obtain the rattle-type nanostructure. As shown in results, this nanostructure with unique morphology could absorb near-infrared light, convert to heat to kill cells, inhibit tumor growth. As carrier for multiple SPIONs, it also revealed well function for T2-weighted MR imaging in tumor site. Moreover, the rest inner space of gold shell could also introduce the potential ability as

nanocarriers for other cargos such as chemotherapeutic drugs, which is still under investigation. This metal rattle-type nanocarrier may pave the way of novel platforms for cancer therapy in the future.

9338-3, Session 1

Stem cell/nanoparticle hybrids for targeted cancer therapy (*Invited Paper*)

Jacob M. Berlin, Karen S. Aboody, Rachael Mooney, City of Hope Beckman Research Institute (United States)

Targeted drug delivery is a long-standing goal for cancer therapy. Nanoparticles have shown promise as platforms for targeted drug delivery, but major challenges remain for controlling the distribution of nanoparticles within tumors. Neural Stem Cells (NSCs) are appealing candidates for use as carriers for nanoparticles in order to overcome these biodistribution challenges. NSCs have demonstrated inherent tumor tropic properties in invasive and metastatic tumor models, migrating selectively to invasive tumor foci, penetrating hypoxic tumor regions, and even traversing through the blood-brain barrier to access intracranial tumor foci following intravenous administration. NSCs do not intrinsically have any anti-tumor efficacy; they must be modified in some way to exploit their tumor targeting abilities. My collaborator, Dr. Karen Aboody, is a pioneer in genetically altering NSCs to express an enzyme that will convert a prodrug into the active compound. This approach was recently evaluated in a first-in-human safety/feasibility clinical trial using modified NSCs to treat recurrent gliomas.

As NSC-based therapy moves into the clinic, there is an opportunity to develop complementary techniques to enable NSCs to destroy tumors. The combination of NSCs and nanoparticles offers the potential of a general drug targeting system. We have demonstrated that NSCs can either be modified to bear nanoparticles on their surface or can internalize them. The nanoparticles can release drugs or used for photothermal ablation. In all cases, the NSCs remained viable and targeted the delivery of the nanoparticles to tumors in vivo, enhancing the therapeutic efficacy of the nanoparticles.

9338-4, Session 1

Gold based hybrid nanosystems as potential agents for diagnostic and therapy

Frederic Lerouge, Ecole Normale Supérieure de Lyon (France) and Univ. Claude Bernard Lyon 1 (France); Julien R. G. Navarro, Ecole Normale Supérieure de Lyon (France) and Ecole Normale Supérieure de Cachan (France); Guillaume Micouin, Ecole Normale Supérieure de Lyon (France); Patrice L. Baldeck, Ecole Normale Supérieure de Lyon (France) and Univ. Joseph Fourier (France); Chantal Andrau, Cryille Monnereau, Ecole Normale Supérieure de Lyon (France); Stéphane Parola, Ecole Normale Supérieure de Lyon (France) and Univ. Claude Bernard Lyon 1 (France); Arnaud Favier, Marie Thérèse Charreyre, Ecole Normale Supérieure de Lyon (France)

In this communication we describe the synthesis and characterization of nanomaterials combining gold nanoparticles of different shape and size (spheres, bipyramids...etc) with chromophores. The synthesis of the nanoparticles will first be described together with their photophysical

**Conference 9338:
Colloidal Nanoparticles for Biomedical Applications X**

properties¹. Then, a complete study of bio compatible polymer functionalized gold nanoparticles such as bipyramidal-like nanostructures will be presented, dark-field microscopy shows that the biocompatible gold nanoparticles are internalized after incubation with cancer cells² (see image). The study will then be deepened with the preparation of luminescent hybrid nanoparticles, using a multifunctional polymer grafted on the particles making these object very efficient agents for imaging and therapy of cancer³. Finally, the study on these hybrid nanostructures will show very interesting chromophore-particle interactions⁴.

[1] "Synthesis, electron tomography and single-particle optical response of twisted gold nano-bipyramids" Navarro, JRG; Manchon, D; Lerouge, F; et al. *Nanotechnology*, 23, 145707, 2012.

[2] "Synthesis of PEGylated gold nanostars and bipyramids for intracellular uptake" Navarro, JRG; Manchon, D; Lerouge F; et al. *Nanotechnology*, 23, 465602, 2012.

[3] "Nanocarriers with ultrahigh chromophore loading for fluorescence bio-imaging and photodynamic therapy" Navarro, JRG; Lerouge, F; Cefruga, C; et al. *Biomaterials*, 34, 8344, 2013.

[4] "Plasmonic bipyramids for fluorescence enhancement and protection against photobleaching" Navarro, JRG; Lerouge, F; Micoin G; et al. *Nanoscale*, 6, 5138, 2014.

9338-5, Session 1

Nanoarchitected electrochemical biosensors for sensitive and selective detection of leukemia cells and cell-associated biomarkers *(Invited Paper)*

Junjie Zhu, Nanjing Univ. (China)

Leukemia is one of the most common fatal cancers that affect the bone marrow, the blood cells, and other parts of the lymphatic system. Electrochemical cytosensing has emerged as an extremely attractive method that can be readily implemented into quantitative bioassays for high-throughput clinical applications. In this work, we have developed a series of robust, nanobiotechnology-based electrochemical biosensing approaches with high sensitivity, selectivity, and reproducibility toward the simultaneous multiplex detection and classification of both acute myeloid leukemia and acute lymphocytic leukemia cells, quantitative evaluation of DR4/DR5 expression on leukemia cell surface as well as dual-channel detection of matrixmetalloproteinase-2 (MMP-2) in human serum. The optimization of electron transfer and cell capture processes at specifically tailored nanobiointerfaces and the incorporation of multiple functions into rationally designed nanoprobe provide unique opportunities of integrating high specificity and signal amplification on one electrochemical biosensor. These versatile electrochemical biosensing platforms hold great promise as new point-of-care diagnostic tools for early detections and believed to be of great clinical value for the evaluation of therapeutic effects on leukemia patients after radiation therapy or drug treatment.

9338-6, Session 2

Detection and in vivo imaging of quorum-sensing pyocyanin in bacterial biofilms by SERS

Gustavo Bodelon, Vanesa Lopez, Veronica Montes, Sergio Rodal-Cedeira, Celina Costas, Isabel Pastoriza-Santos, Jorge Perez-Juste, Univ. de Vigo (Spain); Luis M. Liz-Marzan, Univ. de Vigo (Spain) and CIC biomaGUNE (Spain)

All cellular organisms, including bacteria, use chemical molecules as signals to sense and interact with other cells. In nature most bacteria exist in biofilms or groups of bacterial populations enclosed in an extracellular polymeric matrix regulated by a cell-to-cell communication system termed

quorum sensing (QS). Bacterial biofilms form in biotic and abiotic surfaces, they are highly resilient to antimicrobials, and thereby they represent a threat for human health. To date there is no efficient drug that specifically targets bacteria in biofilms. Therefore, an understanding of these complex bacterial systems is important for developing new therapeutic strategies. The opportunistic bacterial pathogen *Pseudomonas aeruginosa* releases small metabolites termed pyocyanins that act as virulence factors and as intercellular signals for regulating biofilm formation. Surface-enhanced Raman scattering (SERS) spectroscopy can be used as a powerful analytical technique for the spectroscopic characterization of molecules. However, a direct and label-free SERS identification of biomolecules in complex systems represents a formidable challenge. Herein we report the use of SERS for imaging and monitoring pyocyanin production within bacterial populations in colony biofilms from *P. aeruginosa*. To this end we generated plasmonic hybrid materials as SERS-active substrates to allow simultaneous bacterial growth and detection of pyocyanin produced within bacterial populations and colony biofilms from *P. aeruginosa*. This study gives insight into direct, label-free in situ SERS detection and imaging of a cellular metabolite in the context of a complex biological system such as a bacterial biofilm.

9338-7, Session 2

Au@pNIPAM nanoparticles as surface-enhanced resonance Raman spectroscopy (SERRS) tags for cell immunophenotyping *(Invited Paper)*

Gustavo Bodelón, Veronica Montes, Cristina Fernandez-Lopez, Celina Costas, Univ. de Vigo (Spain); Luis M. Liz-Marzán, Univ. de Vigo (Spain) and CIC biomaGUNE (Spain); Isabel Pastoriza-Santos, Jorge Pérez-Juste, Univ. de Vigo (Spain)

A rapid surface-enhanced resonance Raman spectroscopy (SERRS) method has been developed for the detection and differentiated of growth factor receptors (GFR) on cells. SERRS tag labels were prepared by conjugating polyisopropylamide (pNIPAM) coated gold nanoparticles with commercial antibodies and dye molecules. After incubation with the immunogold labels, cell lines that over express GFR could easily be measured and differentiated by Raman spectroscopy. The immunogold were prepared by coating gold nanoparticles with a porous thermoresponsive polymer shell (pNIPAM) which allows the diffusion of the dye molecules (Astra blue, Nile Blue A and Malachite green), followed by coating with polyacrylic acid through the layer by layer technique. Finally, the SERRS tags were bioconjugated with the antibodies. Raman maps were collected across fixed and labelled cells lines, and the maps were used to determine specificities and organism coverages. The research presented here demonstrates the feasibility of utilizing SERRS labelling for sensitive differentiation strategies.

9338-8, Session 2

Label-free detection of the interaction between the quorum sensing receptor LasR and its acyl-homoserine-lactone ligand by surface-enhanced Raman scattering spectroscopy

Celina Costas, Vanesa Lopez, Gustavo Bodelón, Isabel Pastoriza-Santos, Jorge Perez-Juste, Univ. de Vigo (Spain); Luis M. Liz-Marzán, Univ. de Vigo (Spain) and CIC biomaGUNE (Spain) and IKERBASQUE. Basque Foundation for Science (Spain)

All unicellular organisms, including bacteria, use chemical molecules as

**Conference 9338:
Colloidal Nanoparticles for Biomedical Applications X**

signals to sense and interact with other cells. Quorum sensing (QS) is a widespread phenomenon that enables bacteria to establish cell-to-cell communication and to regulate the expression of specific genes involved in bacterial virulence. Signaling via N-acyl homoserine lactones (AHLs) is the paradigm for QS and is particularly well characterized in the opportunistic human pathogen *Pseudomonas aeruginosa*. It has been shown that AHLs diffuse from one bacterium to another where they bind to a protein termed LasR in a 1:1 molar ratio. Subsequently, this complex binds to regulatory regions in the DNA and triggers the expression of more than 150 target genes. It is believed that upon lactone binding, LasR gets activated by modifying its structural conformation. However, to date there are no direct molecular evidences to proof this. Herein we report the use of surface-enhanced Raman scattering (SERS) spectroscopy for investigating the conformational changes in the structure of LasR upon interaction with its AHL ligand (3-oxo-C12-HSL). To this end, we obtained SERS substrates consisting in Au nanoparticles thin films and we genetically modified LasR with a C-terminal cysteine in order to direct an oriented deposition of the purified protein onto the Au nanoparticles surface. Our results show that the addition of AHL ligand induces changes in the SERS spectra of LasR, providing a direct evidence of structural activation in this important QS signal receptor. Finally, this study suggests that Raman spectroscopy could be used for screening inhibitors of the LasR-AHL interaction, relevant to anti-QS therapeutic development.

9338-9, Session 2

The limits of field enhancement in nanoplasmonic optical sensing (*Invited Paper*)

Francisco Javier García de Abajo, ICFO - Institut de Ciències Fotòniques (Spain)

We explore the limits in the field enhancement that can be achieved in narrow particle gaps and near sharp corners and tips. In particular, we study the role of nonlocal effects, the spill out of the conduction electron gas outside the metal surface, and purely geometrical effects. The implications for the maximum sensitivity of molecular sensing techniques, such as SEIRA and SERS, are also discussed.

9338-10, Session 3

Bio-functional silicon quantum dots prepared by one step green strategy for in vivo applications (*Invited Paper*)

Romuald Intartaglia, Istituto Italiano di Tecnologia (Italy)

Nanomaterials for in vivo applications present a growing interest as delivery vehicles, gene detection systems, labeling and therapeutic agents. In particular, many efforts have been reported in the synthesis of inorganic nanoparticles, such as heavy metal quantum dots (QDs), for long-term, real-time cell labeling applications. However, these QDs endanger several health issues due to their chemical composition, artificial ligand and/or the employed solution routes. Therefore, other alternatives, taking into account the nanoparticles fabrication strategy and the minimum toxicity of the carrier itself, are crucial for potential success of nanomaterials in the clinical setting. Owing to its biocompatibility and biodegradability, silicon nanoparticles (Si-NPs) are ideal candidates for in vivo applications. [1] Recently, pulsed laser ablation in liquids (PLAL), that fulfills the twelve principles of green chemistry, has emerged as an alternative approach to generate highly pure semiconductor NPs [2-7]. This presentation will summarize our work over the past four years on the synthesis of silicon QDs prepared by ultra-fast (fs, ps) laser ablation of silicon target in non-contaminated aqueous solution. Size-control and optical properties study of laser-generated NPs in deionized water will be presented. Furthermore, we will report on the systematic bioconjugation of Si-NPs fabricated by the PLAL, resulting in functional Si-NPs bioconjugates (DNA, Protein) with an

example of their use in imaging of human fibroblast cell. In the perspective to achieve high production yield of NPs by PLAL, results on the productivity based on ablation/photofragmentation model and an outlook towards the gram scale synthesis of Si-NPs will be discussed.

- [1] Ji-Ho Park et al, *Nature Materials* 8, 331 (2009).
- [2] R. Intartaglia et al, *J. Phys. Chem. C*, 115, 5102 (2011).
- [3] R. Intartaglia et al, *Opt. Mater. Express*, 2, 510, (2012).
- [4] R. Intartaglia et al, *Nanoscale*, 4, 1271 (2012).
- [5] R. Intartaglia et al, *Phys Chem Chem Phys*, 14, 15406 (2012).
- [6] K. Bagga et al, *Laser Phys. Lett.* 10, 065603 (2013).
- [7] R. Intartaglia et al, *Opt. Express*, 22, 3117 (2014).

9338-11, Session 3

Laser synthesis and characterization of bioconjugated hydroxyapatite nanocrystals for biomedical applications

Marina Rodio, Alberto Diaspro, Romuald Intartaglia, Istituto Italiano di Tecnologia (Italy)

Hydroxyapatite particles are promising biomaterials for bone tissue regeneration, cell proliferation and as plasmid DNA delivery vector, because they bear outstanding properties such as chemical similarity to the human mineral constituent, bioactivity, and are fairly easily bioconjugated [1,2]. Recently, protein conjugated particles (200 nm in size) have been shown to be efficient platform for bone regenerative therapy with high bone cells proliferation also in conjunction with proteins [3]. Further, hydroxyapatite nanostructures with size less than 50 nm are known to enhance bioactivity properties. However, ultra small conjugated HaP-NPs are difficult to synthesize colloiddally, which is attributed to the requirement of high temperature process for their crystallization [2]. The conventional multi-step chemicals routes are less effective and may cause health issues. In this context the current work aims to explore the approach of in situ conjugation during laser ablation in liquid [4-6] for the design of ultra-small, highly crystalline and conjugated HA-NPs, using Serum Albumin as model protein. Successful conjugation and integrity of the protein is proved by various methods such as UV-Vis, infrared spectrometry, and electron microscopy, whereas nanoparticles size-quenching is clearly observed varying the protein concentration. Crystallinity and stoichiometric ratio of HaP-NPs is assessed by HRTEM, XRD and EDX combined with ICP analysis, respectively. Introducing 0.1 mM protein, the conjugation efficiency of 17% and ? potential of -36 mV is reached, resulting in 4 nm average sized highly crystalline HaP bioconjugates.

- [1] M. Sadat-Shojai et al., *Acta BioMater.*, 9, 7591 (2013)
- [2] F. Vazquez-Hernandez et al, *Mater. Sci. Eng. B*, 174, 290 (2010)
- [3] C. M. Curtin et al, *Adv. Mater.*, 24(6), 749 (2012)
- [4] R. Intartaglia et al, *Opt. Mater. Express*, 2, 510, (2012).
- [5] R. Intartaglia et al, *Nanoscale*, 4, 1271 (2012).
- [6] K. Bagga et al, *Laser Phys. Lett.* 10, 065603 (2013).

9338-12, Session 3

Programming nanoparticle assembly

Amelie Heuer-Jungemann, Antonios G. Kanaras, Univ. of Southampton (United Kingdom)

New tools to control the assembly of inorganic nanocrystals is of great interest in order to allow a systematic investigation of their physical properties (e.g., plasmon resonance and electron spin) and for the fabrication of mesoscale materials with tunable functions. Several approaches have so far been used to control self-assembly, mainly utilizing strategies based on prefabricated templates, small-molecule and

**Conference 9338:
Colloidal Nanoparticles for Biomedical Applications X**

electrostatic interactions, novel solution-deposition methods, nanowelding, and biomolecular tools. Each of these methods offers alternative pathways towards the self-assembly and creation of mesoscale structures of different sizes, shapes, and architectures. The applications of such arrays range from scaffolds for biological systems to the fabrication of new drugs.

In this presentation we discuss our recent achievements to nanoparticle self-organization using various chemical tools. We will particularly highlight how the appropriate selection of ligands and the intrinsic properties of nanoparticle function can influence their organization.

9338-13, Session 3

Core-shell AgSiO₂-protoporphyrin IX nanoparticle: effect of the Ag core on reactive oxygen species generation

Marjorie Lismont, Carlos Pàez-Martinez, Dreesen Laurent, Univ. de Liège (Belgium)

Photodynamic therapy (PDT) for cancer treatment is based on the use of a light sensitive molecule to produce, under specific irradiation, toxic reactive oxygen species (ROS). A way to improve the therapy efficiency is to increase the amount of produced ROS near cancer cells. This aim can be achieved by using a metal enhanced (ME) process arising when an optically active molecule is located near a metallic nanostructure. A commonly used photosensitizer to treat skin cancers is protoporphyrin IX (PpIX), which one presents an intense absorption band around 400 nm. Because of silver nanoparticles (Ag NPs) exhibit a strong localized surface plasmon resonance (LSPR) around the same wavelength, ME ROS phenomenon is expected when PpIX is in closed proximity to AgNPs.

Here we study the effect of the coupling between AgNPs and PpIX molecule on the ROS production efficiency. By applying a silica growth Stöber process on AgNPs, we are able first, to encapsulate the PpIX into the silica-shell, and second, to graft the PpIX molecule onto the silica surface. We report the distance-dependent aspect of ROS production when PpIX is loaded into and onto the silica capping shell. We investigate the behaviour of this coupling effect for 60 nm sized Ag NPs coated with silica shell thickness from 7 to 25 nm.

9338-14, Session 3

Engineering the streptavidins for nanoparticles assembly (Invited Paper)

Cheng-An J. Lin, Wei-Ling Hung, Ting-En Lin, Hsin-An Chen, Walter H. Chang, Chung Yuan Christian Univ. (Taiwan)

Wild-type streptavidin, which contains four biotin binding sites, have been used for nanoparticles bioconjugation. We introduced a new method how to engineer the wild-type streptavidins and characterize through polymer-coated gold nanoparticles. Electrophoretic method was great for separating mono-functional nanoparticles and the complexity of nanoparticles assembly with biotin-avidin system. Nanoparticles with defined number of biotin or streptavidin can be optimized by EDC chemistry and can be mass-produced through gel electrophoresis. The assembly of nanoparticles was also presented in this study. (This research was supported by Ministry of Science and Technology (Taiwan) - MOST 101-2628-E-033-001-MY3, 102-2622-E-033-010-CC3, 103-2221-E-033-014-MY3)

9338-15, Session 4

Nanoparticle-assisted stimulated-emission-depletion nanoscopy (NP-STED) (Invited Paper)

Emiliano Cortes, Stefan A. Maier, Imperial College London (United Kingdom)

In traditional optical microscopy resolution is always diffraction-limited except for fluorescence microscopy where the localization of single emitters allows going well beyond that limit. The very first idea of either sequentially or stochastically fluorescence switching between on and off states in single molecules followed by their spatial localization had allowed the development of new nanoscopes with unprecedented resolution for optical imaging techniques [1].

In this context, stimulated-emission-depletion (STED) nanoscopy remains as the fastest and the most suitable technique for tracking the dynamics of small organisms. This technique uses stimulated emission to turn off the capability of emitters to emit spontaneously. In a typical STED nanoscope, a focused excitation beam is spatially overlapped with a doughnut-shaped beam that de-excites emitters to the ground state everywhere except for within the centre of the doughnut providing diffraction-unlimited resolution in the transverse plane. By increasing the power of the doughnut beam the emission region can be reduced up to a point thus allowing theoretically subnanometer resolution and even intramolecular imaging possibilities. Even though, in practise, other parallel phenomenon appears when high power lasers are employed such as photostability of the dyes and/or photobleaching process and also increasing the cost of the set-up.

In this talk we show for first time the possibility to locally enhance the power of the depletion beam by coupling it with the plasmon resonance of metallic nanoparticles [2]. Employing small fluorescent-label metallic nanoparticles we achieve high depletion intensities with low laser powers by exploiting the near-field enhancement occurring near the nanoparticles. We also show improvement in resolution and photostability by tuning the nanoparticle size and shape.

[1]- Hell, S. W.; Wichmann, J. Breaking the Diffraction Resolution Limit. *Opt. Lett.* 1994, 19, 780-782.

[2]- Sivan, Y.; Sonnefraud, Y.; Kéna-Cohen, S.;Pendry, J.B.;Maier, S.A. Nanoparticle-Assisted Stimulated-Emission-Depletion Nanoscopy. *ACS Nano* 2012, 6, 5291-5296.

9338-16, Session 4

Evidence of energy transfer in nanoparticle-porphyrins conjugates for radiation therapy enhancement (Invited Paper)

Konstantin Kudinov, The Univ. of Southern California (United States); Daniel Cooper, Pooja Pyagi, McGill Univ. (Canada); Devesh Bekah, McGill University (Canada); Dhritiman Bhattacharyya, Colin Hill, Jonathan K. Ha, Stephen E. Bradforth, The Univ. of Southern California (United States); Jay L. Nadeau, McGill Univ. (Canada)

We report progress towards combining radiation therapy (RT) and photodynamic therapy (PDT) using scintillating nanoparticle (NP)-photosensitizer conjugates. In this approach, scintillating NPs are excited by clinically relevant ionizing radiation sources and subsequently transfer energy to conjugated photosensitizers via FRET, acting as an energy mediator between ionizing radiation and photosensitizer molecules. The excited photosensitizers generate reactive oxygen species that can induce local damage and immune response. Advantages of the scheme include:

1) Compared with traditional radiation therapy, a possible decrease of the total radiation dose needed to eliminate the lesion ;

**Conference 9338:
Colloidal Nanoparticles for Biomedical Applications X**

- 2) Compared with traditional PDT, the ability to target deeper and more highly pigmented lesions;
- 3) The possibility of additional photosensitizing effects due to the scintillation of the nanoparticles.

In this work, the photosensitizer molecule chlorin e6 was covalently bound to the surface of LaF₃:Ce NPs. After conjugation, the photoluminescence intensity of NPs decreased, suggesting FRET. Observation of a change in the rise time of porphyrin stimulated emission compared to free porphyrin molecules was sought to confirm this. In addition, scintillation spectra of different sizes and shapes of nanoparticles were measured using clinical radiation sources. Preliminary calculations suggest that the observed scintillation efficiencies are sufficient to enhance RT. *in vitro* cancer cell studies suggest scintillating nanoparticles showed low toxicity, but also a low degree of uptake. Conjugation of photosensitizers to the particles improved cell binding, with conjugates localized primarily in membranes. Survival curves with radiation exposure suggest that the particles alone cause some radiosensitization, comparable to that seen with gold nanoparticles.

9338-17, Session 4

Bifunctional luminescent magnetic nanowires for intracellular rheology studies (*Invited Paper*)

Gaëlle Charron, Jean-François Berret, Univ. Paris 7-Denis Diderot (France)

In the last ten years, mechanical properties of cells have attracted attention as biomarkers of the cell state[1]. For instance, several authors have shown that the stiffness of invasive metastatic cells is noticeably weaker than that of their non invasive counterparts, a phenomenon that is thought to facilitate the process of vascular invasion [1,2] However, the cellular mechanisms responsible for the cell viscoelastic properties are still poorly understood.

In the last few years, Berret et al. have reported the use of magnetic nanowires as passive micro-rheometers to probe intracellular viscoelastic properties [3,4]. The study of their dynamics under a rotating magnetic field also demonstrated their potential as active rheometer [5]. These nanowires were fabricated by controlled complexation of superparamagnetic iron oxide nanoparticles and polyelectrolytes [6].

In order to gain insights into the relationship between the observed mechanical properties and the structural state of the cell, there is a need to couple the visualisation of the micro-rheometers to conventional fluorescence markers of cell compartments. To this end, we present here the fabrication of bifunctional luminescent magnetic nanowires designed to investigate the rheological properties of intracellular medium under confocal fluorescence microscopy. These luminescent magnetic nanowires are derived from the first generation of magnetic nanowires and incorporate a ternary mixture of magnetic nanoparticles, quantum dots and polycationic polymer. Depending on the ternary composition, the length, stiffness and brightness of the nanowires can be tuned. In particular, the optimisation of the composition for intracellular visualisation will be discussed.

1. Carlo, D. D. A Mechanical Biomarker of Cell State in Medicine. *J. Lab. Autom.* 17, 32–42 (2012).
2. Swaminathan, V. et al. Mechanical stiffness grades metastatic potential in patient tumor cells and in cancer cell lines. *Cancer Res.* canres.0247.2011 (2011). doi:10.1158/0008-5472.CAN-11-0247
3. Chevry, L., Colin, R., Abou, B. & Berret, J.-F. Intracellular micro-rheology probed by micron-sized wires. *Biomaterials* 34, 6299–6305 (2013).
4. Colin, R., Yan, M., Chevry, L., Berret, J.-F. & Abou, B. 3D rotational diffusion of micrometric wires using 2D video microscopy. *EPL Europhys. Lett.* 97, 30008 (2012).
5. Frka-Petesic, B. et al. Dynamics of paramagnetic nanostructured rods under rotating field. *J. Magn. Mater.* 323, 1309–1313 (2011).
6. Yan, M., Fresnais, J., Sekar, S., Chapel, J.-P. & Berret, J.-F. Magnetic

Nanowires Generated via the Waterborne Desalting Transition Pathway. *ACS Appl. Mater. Interfaces* 3, 1049–1054 (2011).

9338-18, Session 4

Influence of surface chemistry on the colloidal properties and photoluminescence of upconversion nanoparticles and measurement of absolute quantum yields (*Invited Paper*)

Ute Resch-Genger, Bundesanstalt für Materialforschung und -prüfung (Germany)

Lanthanide-doped up-converting nanoparticles (UCNPs) gained much attention as novel labels and probes in bioanalytical and theranostic applications. Advantageous compared to organic dyes and other nanocrystalline materials are their excitability in the near infrared (NIR), commonly at 976 nm, providing almost background-free signals, the multitude of characteristic narrow emission bands in the visible (vis) and NIR ideal for multiplexing applications, their excellent photostability, and their long luminescence lifetimes in the μ s range suitable for time-gated emission and homogeneous time-resolved FRET assays. Due to the up-converting nature of their photoluminescence and the multi-photon absorption processes, the quantum yield (QY) of these particles becomes, however, excitation power density-dependent and can be measured only absolutely. The application of UCNPs requires synthetic routes and surface modification protocols for the preparation of large quantities of monodisperse particles of pure crystallinity and exact stoichiometric composition which are water dispersible and carry surface groups for subsequent (bio)functionalization. Moreover, to assess their performance, methods are needed for the challenging determination of their excitation power density-dependent QY.

For a systematic study of the influence of surface chemistry on the up-conversion emission of $\text{?NaYF}_4(\text{Yb}^{3+}/\text{Er}^{3+})$, we developed a luminescence-controlled large scale synthesis of monodisperse oleate-capped UCNPs and modified the surface of these initially hydrophobic particles with nine different coatings to render them water-dispersible [5]. In parallel, we designed a custom-built integrating sphere setup [6] for the absolute determination of power density-dependent QY. Here, we present a luminescence-based classification of our surface modifications into two groups, i.e., (1) additional (amphiphilic) layer coatings and (2) ligand exchange strategies, demonstrate the influence of surface chemistry on the non-radiative deactivation of UCNPs, and show methods for the determination of saturation QY.

9338-19, Session 4

Doped semiconductor nanocrystals (*Invited Paper*)

Andreas Riedinger, David J. Norris, Maximilian Fischer, ETH Zürich (Switzerland)

In general, nanocrystals are particles roughly 5 nm in diameter that are produced by wet chemistry. They are crystalline, uniform in size, and can exhibit very strong, stable, and tunable fluorescence. Thus, they have been investigated for use in bio-imaging. The incorporation of impurities (also called dopants) in these nanocrystals can lead to very interesting photophysical properties. The optical as well as electronic properties of doped semiconductor nanocrystals may change dramatically, dependent on the type of impurity and its precise location in the crystal lattice. If the dopant is, for instance present as an interstitial impurity it may act as a donor, while at substitutional site it could act as an acceptor. At the Optical Materials Engineering Laboratory, we are interested in the synthesis of new classes of doped nanocrystals. Here, especially new strategies for incorporation of unusual impurities are under study. We then evaluate

**Conference 9338:
Colloidal Nanoparticles for Biomedical Applications X**

of such doped nanocrystals by means of optical spectroscopy, electron microscopy and other suitable techniques to pin down the position of the dopant within the nanocrystals and investigate its influence on the optical properties. In this talk I will present strategies for the incorporation of such impurities, how to control its location in the crystal lattice and discuss the overall observed changes in the optical and crystallographic properties. These findings are interesting for various purposes such as bio-imaging as well as optoelectronic applications.

9338-20, Session 5

Mechanisms of cell penetration and cytotoxicity of ultrasmall Au nanoparticles conjugated to doxorubicin and/or targeting peptides (*Invited Paper*)

Jay L. Nadeau, Xuan Zhang, McGill Univ. (Canada)

Nano-gold has shown considerable promise as a drug carrier. Despite a large body of literature, the ideal size and surface chemistry of gold nanoparticles for drug delivery has not been well established. Most studies have focused on 20-50 nm diameter particles with long circulation times (days). However, smaller particles are potentially better for two reasons: they can be cleared by the kidneys, facilitating regulatory approval for human use; and they can enter cell nuclei, important for certain therapeutic applications. We previously showed that ultra-small (diameter 2.7 nm) gold nanoparticles conjugated to doxorubicin (Au-Dox) reduce the EC50 of doxorubicin in resistant murine B16 melanoma cells by a factor of nearly 20, and in more sensitive human SK-MEL-28 melanoma cells by a factor of 2. Au-Dox is less toxic to normal, doxorubicin-sensitive cells than Dox alone. Here we investigate the mechanisms of this surprising result using a variety of techniques. Uptake of stably conjugated Au-Dox into cell nuclei is visualized using a combination of confocal, electron, and fluorescence lifetime imaging microscopies. The mechanisms of cell entry are evaluated using a panel of blockers, establishing that the particles enter by endocytosis as well as non-endocytic mechanisms. Finally, a genome-wide screen is used to identify candidate genes that confer resistance to Au-Dox. All together, these results indicate that Au-Dox enters B16 cells more rapidly and more efficiently than Dox alone, and that its expulsion from the cells by resistance genes is suppressed. This has implications for design of nanoparticle carriers to target drug-resistant cells.

9338-21, Session 5

Fluorescent nanoparticle interactions with biological systems: what have we learned so far? (*Invited Paper*)

Shang Li, Gerd Ulrich Nienhaus, Karlsruher Institut für Technologie (Germany)

With the rapid advancement of nanotechnology, a wide range of intrinsically fluorescent nanomaterials have become available as probes, including semiconductor quantum dots (QDs), metal nanoclusters (NCs), up-converting NPs and nanodiamonds. Fluorescent NPs frequently exhibit excellent photophysical properties, color tunability and facile bioconjugation, making them promising as probes for fluorescence-related applications, especially in the biological and biomedical areas. Still, relatively little is known about how fluorescent NPs behave in the complex biological environment, which is actually of essential importance for their use in biological applications [1]. Recently, our group has quantified interactions of QDs and metal (i.e., Au and Ag) NCs with serum proteins and living cells by the combined use of different spectroscopic and microscopic techniques. Our studies showed that: (1) interactions with proteins may significantly alter the photophysical properties of the NPs as well as the responses of cell internalizing them [2]; (2) the protein surface charge distributions play an important role in the interactions of NPs with proteins and cells [3]; (3) ultrasmall NPs (diameter less than 10 nm) showed a cellular internalization

behavior distinctly different from the one observed with larger particles (diameter ~100 nm) [4]. These studies provide an important foundation for the design and development of fluorescent NPs for future cancer therapy, drug delivery, and bioimaging applications.

Acknowledgments

We acknowledge support by the Deutsche Forschungsgemeinschaft (DFG) through the Center for Functional Nanostructures (CFN), the Priority Program SPP1313 and the KIT in the context of the Helmholtz STN program. L. S. acknowledges support by the Carl Zeiss Foundation.

References

1. L. Shang and G.U. Nienhaus, *Mater. Today*, 2013, 16, 58-66.
2. L. Shang, S. Brandholt, F. Stockmar, V. Trouillet, M. Bruns and G.U. Nienhaus, *Small*, 2012, 8, 661-665; L. Shang, F. Stockmar, N. Azadfar and G.U. Nienhaus, *Angew. Chem. Int. Ed.*, 2013, 52, 11154-11157.
3. P. Maffre, F. Amin, W.J. Parak, K. Nienhaus and G.U. Nienhaus, *Beilstein J. Nanotechnol.*, 2011, 2, 374-383; L. Shang, L.X. Yang, J. Seiter, M. Heine, G. Brenner-Weiss, D. Gerhsen and G.U. Nienhaus, *Adv. Mater. Interfaces* 2014, 1, 1300079; L. Treuel, S. Brandholt, P. Maffre, S. Wiegele, L. Shang and G.U. Nienhaus, *ACS Nano*, 2014, 8, 503-513.
4. X. Jiang, C. Röcker, M. Hafner and G.U. Nienhaus, *ACS Nano*, 2010, 4, 6787-6797; L.X. Yang, L. Shang and G.U. Nienhaus, *Nanoscale*, 2013, 5, 1537-1543.

9338-22, Session 5

Understanding the redox coupling between quantum dots and the neurotransmitter dopamine in hybrid self-assemblies

Xin Ji, Florida State Univ. (United States); Nikolay S. Makarov, Los Alamos National Lab. (United States); Wentao Wang, Goutam Palui, Florida State Univ. (United States); Istvan Robel, Los Alamos National Lab. (United States); Hedi Mattoussi, Florida State Univ. (United States)

Interactions between luminescent quantum dots and redox active molecules involve complex charge transfer processes, and have great ramifications in biology. The redox active neurotransmitter dopamine is involved in a range of brain activities. We used steady-state and time-resolved fluorescence along with transient absorption bleach measurements, to probe the effects of changing the QD size and valence on the rate of photoluminescence quenching in QD-dopamine conjugates, when the pH of the medium was varied. In particular, we measured substantially larger quenching efficiencies, combined with more pronounced shortening in the PL lifetime decay when smaller size QDs and/or alkaline pH were used. Moreover, we found that changes in the QD size alter both the electron and hole relaxation for red- and green-emitting QDs but with very different extents. For instance, a more pronounced change in the hole relaxation was recorded in alkaline buffers and for green-emitting QDs compared to their red-emitting counterparts. We attribute these results to the more favorable electron transfer pathway from the reduced form of the complex to the valence band of the QD. This process benefits from the combination of lower oxidation potential and larger energy mismatch in alkaline buffers and for green-emitting QDs. In comparison, the effects of pH changes on the rate of electron transfer from excited QDs to dopamine are less affected by QD size. These findings provide new insights into the mechanisms that drive the quenching of QD emission in these assemblies.

**Conference 9338:
Colloidal Nanoparticles for Biomedical Applications X**

9338-23, Session 5

Polyelectrolyte multilayer microcapsules as smart carriers for controlled drug delivery (*Invited Paper*)

Alfredo Ambrosone, Istituto di Cibernetica Eduardo Caianiello (Italy); Susana Carregal-Romero, Philipps-Univ. Marburg (Germany); Valentina Marchesano, Daniela Intartaglia, Istituto di Cibernetica Eduardo Caianiello (Italy); Wolfgang J. Parak, Philipps-Univ. Marburg (Germany); Claudia Tortiglione, Istituto di Cibernetica Eduardo Caianiello (Italy)

Nanomedicine aims to develop smart therapeutic tools and strategies for human health. In this context, polyelectrolyte multilayer microcapsules (PEM) may serve as excellent carriers for drug delivery. Herein, we describe the synthesis, the functionalization and the bioactivity of optical-responsive PEMs engineered to achieve spatio-temporal control of a specific cell signalling pathway controlling animal development. PEMs, made by layer-by-layer assembly of non-degradable polymers, were filled with bioactive molecules and tested in vivo by using the freshwater polyp *Hydra vulgaris* as a simple invertebrate model. Immediately after uptake, the capsules were opened on demand by light into the animal cells. Phenotypical, cellular and molecular analysis of irradiated animals demonstrated the activation of the desired cell signalling. In conclusion, our outstanding approach paves the way for upcoming therapies based on remote control of drug delivery.

9338-24, Session 5

Antibacterial activities of CdO-ZnO nanocomposite synthesized by microwave-assisted method

Sivasubramanian Dhanuskodi, Bharathidasan Univ. (India)

CdO-ZnO nanocomposite was prepared by microwave-assisted method with cadmium chloride, zinc chloride and ammonium hydroxide as starting materials and characterized by XRD, SEM and FT-IR. It exhibits hexagonal cubic structure with an average crystallite size of 22 nm. The surface morphological image displays a irregular shaped stone like structure. The UV - Vis spectra reveals the bandgap as 2.92 eV. The fluorescence spectrum shows a near band edge emission at 422 nm. The significant antimicrobial activities were studied against gram negative (*Escherichia coli*, *Pseudomonas aeruginosa*, *Proteus vulgaris*, *Klebsiella-pneumonia*) and gram positive (*Staphylococcus aureus*, *Enterococcus faecalis*, *Enterococci spp*, *Bacillus spp*) bacteria. The zone of inhibition is found to be more for gram positive bacteria than gram negative bacteria. This study indicates that zone of inhibition of 37 mm has high antibacterial activity towards the gram positive bacterium *Staphylococcus aureus*.

References:

1. Edgar Mosequera, Ignacio del pozo, Mauricio Morel, J. Solid State Chem. 206 (2013) 265-271.
2. D. V. Satish, Ch. Rama Krishna, Ch. Venkata Reddy, U S. Udayachandran Thampy, R. V. S. S. N. Ravikumar, Phys. Scripta. 86 (2012) 035708 (1- 6).
3. T. Logeshwaran, M. Parthibavarman, T. Arunkumar, NanoVision, 3 (2013) 44-52
4. D. V. Satish, Ch. Rama Krishna, Ch. Venkata Reddy, T. Raghavendra Rao, P. S. Rao, R. V. S. S. N. Ravikumar, J.Molec. Struc.1034 (2013) 57-61.

9338-25, Session 5

Nanoparticles for cell imaging and activations (*Invited Paper*)

Junwoo Cheon, Yonsei Univ. (Korea, Republic of)

One of the important trends of next-generation nanomedicine is theranostics that is defined by the combination of therapeutics and diagnostics on a single platform. Magnetic nanoparticles are among one of the most essential platforms for targeted imaging, therapy, and simultaneous monitoring of therapeutic efficacy. In this talk, I will discuss magnetic nanoparticles as a core platform material for theranostics and add a variety of functionalities such as drug, targeting moiety, and gene to enhance their performance. Their unique utilization in highly accurate dual-modal MR imaging, therapeutic hyperthermia of cancer cells, controlled drug release, gene delivery, and molecular level cell signaling and cell fate control will be discussed.

9338-26, Session 6

Multifunctional perfluorocarbon nanoemulsions for cancer therapy and imaging

Donald A. Fernandes, Ryerson Univ. (Canada); Dennis D. Fernandes, Univ. of Toronto Mississauga (Canada); Yan J. Wang, Ryerson Univ. (Canada); Yuchong C. Li, Claudiu C. Gradinaru, Univ. of Toronto Mississauga (Canada); Derick Rousseau, Michael C. Kolios, Ryerson Univ. (Canada)

There is interest for the use of nanoemulsions as therapeutic agents, particularly Perfluorocarbon (PFC) droplets, whose amphiphilic shell protects drugs against physico-chemical and enzymatic degradation. When delivered to their target sites, these PFC droplets can vaporize upon laser excitation, efficiently releasing their drug payload and/or imaging tracers. Due to the optical properties of gold, coupling PFC droplets with gold nanoparticles significantly reduces the energy required for vaporization.

In this work, nanoemulsions with a perfluorohexane core and Zonyl FSP surfactant shell were produced using an oil-in-water technique. Droplets were characterized in terms of size and morphology using high resolution fluorescence techniques (i.e. Total Internal Reflection Fluorescence Microscopy, TIRFM, and Fluorescence Correlation Spectroscopy, FCS), electron microscopy, and light scattering techniques (i.e. Dynamic Light Scattering, DLS). The ability of PFC droplets to vaporize are demonstrated using Photoacoustic Microscopy (PAM).

Our emulsion synthesis technique has given a reproducible, unimodal size distribution of PFC droplets corresponding to an average hydrodynamic diameter of 53.5 ± 3.8 nm, from DLS and FCS, with long-term stability at physiological conditions. Their size and stability makes them cost effective drug delivery vehicles suitable for efficient internalization within cancer cell lines. To vaporize the nanoemulsions, silica coated gold nanoparticles (scAuNPs) were used and excited with a 532 nm laser. Taken together, TIRFM, dual-colour FCS, and PAM show that scAuNPs are within the same diffraction-limited spot of these PFC droplets before vaporization.

9338-27, Session 6

Shape responses of ultrathin hydrogel microcapsules (*Invited Paper*)

Eugenia Kharlampieva, The Univ. of Alabama at Birmingham (United States)

The dynamic control over materials shape plays a key role in the complex biological environment and has attracted considerable attention in science, engineering, and medicine. This talk will focus on synthesis, shape

**Conference 9338:
Colloidal Nanoparticles for Biomedical Applications X**

responses, and cellular uptake of shape-specific hydrogel microcapsules of poly(methacrylic acid) (PMAA). The PMAA capsules of cubical, discoidal, and spherical shapes are obtained as hollow replicas of inorganic templates through chemical cross-linking of hydrogen-bonded layer-by-layer films. These hydrogels are capable of keeping the shape of the templates despite the ultrathin capsule wall and the highly hydrated state of the PMAA network. We show that pH-induced volume transitions in those systems are strongly influenced by capsule wall thickness, composition, and crosslink density. Single-component cubic capsules bulged into a spherical shape when pH was changed from acidic to neutral, while capsule size remained virtually unchanged. In contrast, the dual-component PMAA/poly(vinylpyrrolidone) capsules retained their cubic shapes while increasing in size at pH=7.4. These shape responses are rationalized by a difference in hydrogel rigidity expressed as the ratio of the polymer contour length between neighboring cross-links to the persistence polymer length. Shape-dependent cellular uptake will be discussed by comparing internalization of shaped and spherical capsules using J774A.1 macrophage, HMVEC endothelial, and 4T1 breast cancer cells. Our work illustrates that shaped hydrogel capsules are versatile platforms for developing polymer microstructures with a broad range of pH-controlled shapes and sizes to be potentially utilized in controlled drug delivery.

9338-28, Session 6

Binding of cationic porphyrins to zeolite nanoparticles

Anna G. Gyulkhandanyan, Institute of Biochemistry (Armenia); Robert K. Ghazaryan, Yerevan State Medical Univ. (Armenia); Anna Zakoyan, Hakob O. Sargsyan, Aram G. Gyulkhandanyan, Institute of Biochemistry (Armenia); Marina H. Paronyan, Science and Production Ctr. "Armbiotechnology" (Armenia); Grigor V. Gyulkhandanyan, Institute of Biochemistry (Armenia)

In photodynamic therapy of tumors and photodynamic inactivation of bacteria nanoparticles of zeolites are widely used to enhance the effectiveness and targeted delivery of photosensitizers. The first attempts to combining of zeolites with porphyrins showed that porphyrins are associated with outer surface of zeolites better than encapsulates at the internal pores. Further studies showed that cationic porphyrins well encapsulates in the inner region of zeolites by ion exchange mechanism, whereas anionic porphyrins are not embedded, and the neutral only in a trace amounts. We have investigated the binding of nanoparticles of zeolite (clinoptilolite) with a number of cationic porphyrins. For study of the mechanism of binding the zeolite nanoparticles with porphyrins we selected 5 types of cationic porphyrins so that they differed by hydrophobicity (with the various peripheral groups), by the presence of hydroxyl groups (for studying the possible hydrogen-bond with the surface of the zeolite), by various central metal atoms (Zn and Ag), by various provisions of the lateral functional group (third or fourth position in the pyridyl ring). To study the ionic bond the zeolite with porphyrins we investigated the interaction of nanoparticles with neutral photosensitizer (Al-phthalocyanine) and with anionic porphyrin (chlorin e6). Binding studies of these 7 porphyrins gives grounds for assuming that the main mechanism of binding zeolite nanoparticles with porphyrins is an ionic bond. We investigated the binding of the zeolite nanoparticles to Gram (+) microorganisms (*St. aureus*) and was shown that the efficiency of such nanocomposites is higher compared with a free porphyrins.

9338-29, Session 6

Biomimetic silica nanospheres: a versatile nanotool for protein immobilization (Invited Paper)

Erienne Jackson, Mariana Ferrari, Univ. ORT Uruguay

(Uruguay); Maria Valeria Grazú Bonavía, Univ. de Zaragoza (Spain); Jesus Martinez de la Fuente, Spanish Research Council (Spain); Lorena Betancor, Univ. ORT Uruguay (Uruguay)

Traditional methods for the synthesis of silica nanoparticles often require use of organic solvents and/or surfactants, high temperatures and harsh sol-gel processing conditions. These may be considered as inherent limitations when studying the integration of biological molecules on silica spheres. Biomimetic silica particles can be synthesized as a nanosized material within seconds in a process mimicked from living organisms such as diatoms and sponges. The benign reaction conditions associated with biomimetic silica formation *in vitro* are compatible with integrity and biological activity of proteins and DNA as it only requires a hydrolyzed tetramethoxysilane aqueous buffered solution at pH 8.0, room temperature and polyamine molecule to catalyze the silica nanospheres deposition (300-500 nm). Moreover, the reaction occurs within seconds and any molecule present in the synthetic reaction mixture become entrapped as a network of fused silica nanospheres rapidly forms. Although this type of material has been previously used for enzyme entrapment by our group and many others, the potential of biomimetic silica has not yet been fully explored. We have focused our investigations in size and polydispersity modification of the particles to improve their potential as protein carrier. The use of an inert protein template (BSA) enabled the rapid synthesis of positively charged disperse 200-400 nm particles that behaved as ionic exchanger with a range of proteins. Absence of BSA during synthesis produced aggregates and an increase polydispersity of the final spheres. The incorporation of BSA during the synthesis develops porosity inside the nanoparticles, accessible for nitrogen sensing (pore size 4.5 nm). Characterization of different batches of nanoparticles demonstrated the reproducibility of the synthetic strategy. The silica nanospheres were tested as support for immobilization of lipases from three different sources: *Rhizomucor miehei* (RML), *Thermomyces lanuginosus* (TLL) and *Bacillus thermocatenolatus* (BTL). We have tested the potential of preformed silica nanospheres as immobilization support by functionalizing the particle surface with glutaraldehyde and covalently linking the enzyme on it. We have also prepared nanoimmobilized using laccase from *Trametes versicolor*, horseradish peroxidase and GFP. Comparative studies were performed in which the enzymes were both entrapped or attached to the surface of the particles either through covalent linkage or ionic adsorption. The percentage of enzyme immobilization was always above 80%. Enzyme stability experiments demonstrated that both strategies provided enzymatic stabilization against heat and organic solvents (ie for lipases against methanol, ethanol, tert butanol). Increases in stabilization factors against temperature were as high as 24 and 28 times compared to the soluble enzyme for silica entrapped and silica glutaraldehyde immobilized respectively for RML. The nanoimmobilized proved successful in their reutilization which added to their ease of preparation and cost-effective synthesis represents a remarkable advantage in its use as a nanosupport for surface integration of biomolecules. Evidence show the versatility of biomimetic silica nanoparticles as protein carrier which opens up a range of possible investigative lines related to immobilized enzymes: direct enzyme pro-drug activation, synthesis of high added value products through nanobiocatalysis, enzymatic sensing, etc.

9338-30, Session 7

Disease specific protein corona (Invited Paper)

Morteza Mahmoudi, Masoud Rahman, Tehran Univ. of Medical Sciences (Iran, Islamic Republic of)

It is now well accepted that upon their entrance into the biological environments, the surface of nanomaterials would be covered by various biomacromolecules (e.g. proteins and lipids). The absorption of these biomolecules, so called 'protein corona', onto biomaterials confers them a new 'biological identity'. Although the formation of protein coronas on the surface of nanoparticles has been widely investigated, there are few reports on the effect of various diseases on the biological identity of nanoparticles. As the type of diseases may tremendously change the composition of the

protein source (e.g., human plasma/serum), one can expect that amount and composition of associated proteins in the corona composition may be varied in disease type manner. To test this hypothesis, various types of nanoparticles were incubated with plasma from human subjects with different diseases and medical conditions (e.g., breast cancer, diabetes, hypercholesterolemia, rheumatism, favism, smoking, hemodialysis, thalassemia, hemophilia A and B, pregnancy, common cold and hypofibrinogenemia). The obtained protein coronas were analyzed and the effect cellular responses to these different corona coated nanoparticles were probed. Our results demonstrate that the type of disease has a crucial role in the protein corona composition and the cellular responses (e.g. uptake and toxicity) to the nanoparticles. The results of these disease specific protein corona could provide a novel approach for applying nanomedicine to personalized medicine, improving diagnosis and treatment of different diseases tailored to the specific conditions and circumstances.

9338-32, Session 7

Dendronized iron oxide colloids for imaging the sentinel node (*Invited Paper*)

Geneviève Pourroy, Julien C. Jouhannaud, Antonio Garofalo, Delphine Felder-Flesch, Univ. de Strasbourg (France)

Nanoparticles combining optical and magnetic signals are promising for the detection of sentinel nodes by hand-held probes in cancer surgery. Now, radioactive colloids (RuS labelled with 99mTc) or/and Vital Blue dye are injected around the primary tumour and detected by nuclear probe or the eye respectively. The aim of our work is to replace the radioactive colloids by magnetic colloids. Thus, we have developed and optimized dendronized iron oxide nanoparticles. The nanoparticles were produced in an aqueous basic media and sorted by varying the ionic force, temperature and magnetic field parameters. The dendrons are either of first or second generation and bear a Patent Blue dye and/or a fluorescent dye. The suspensions have been characterized for size, magnetic susceptibility and the amount of incorporated Patent Blue/fluorescent dye. We show that the structure and the composition of the aggregates strongly impact the optical and magnetic properties of the suspensions and therefore are critical for optimizing their detection sensitivity. Major attention was given to the effect of the dendron length, the grafting ratios, as well as to the electrostatic interactions between the dendron and the dye. Finally, in-vivo experiments on rats have been performed to determine the biodistribution and to assess the detection sensitivity of these markers using the hand-held probe designed by Eurorad.

Acknowledgments

This work was supported by the European Union in the framework of the program «Nano@matrix» INTERREG IV Upper Rhine Valley.

9338-79, Session 7

Efficient delivery of quantum dots in live cells by gold nanoparticle mediated photoporation

Ranhua Xiong, Freya Joris, Ine De Cock, Jo Demeester, Stefaan C. De Smedt, Andre G. Skirtach, Kevin Braeckmans, Univ. Gent (Belgium)

QDs have been successful in imaging of fixed and permeated cells, but intracellular delivery of QDs into live cells remains a major challenge of QDs for living cellular imaging. Recently, gold nanoparticle (AuNP) mediated photoporation shows an efficient, non-toxicity approach for delivery of macromolecules from tens of kDa to hundreds of kDa to live cells with high throughput. By a pulse laser (< 10 ns) exciting AuNPs attached the cell membrane, it could heat of AuNPs at low laser intensity. While using laser pulses of sufficiently high intensity, the temperature AuNPs can increase to

several hundred degrees due to which the water surrounding the AuNP in tissue evaporates, resulting in an instantaneous water vapour nanobubble (VNB) that emerges around the AuNP. The size of a VNB can be tuned from ten to several hundred nanometres (nm) depending on the laser intensity. When the thermal energy of the AuNP is consumed, the VNB violently collapses and causes local damage by high-pressure shock waves. Due to the extremely short lifetime of VNBs (<1 μ s), the diffusion of heat from the AuNP into the environment is negligible so that almost all energy of the irradiated AuNP is converted to mechanical energy (expansion of the VNB) without heating of the environment. Here, we found a high efficiency and low toxicity of intracellular delivery of QDs into cells by this VNB induced photoporation. We found the positive QDs cells is more than 80% and mean fluorescent intensity of cells is more than three folders of controlled samples at a optimized experimental situations. Meanwhile, the percentage of live cells is as high as ~85%. From these results, we can see the QDs can be efficiently delivered into live cells with very low toxicity by this VNB inducing photoporation.

9338-34, Session 8

Metal doping in NIR fluorescent gold nanoclusters and their biological applications (*Invited Paper*)

Eunkeu Oh, Lauren D. Field, James B. Delehanty III, Ramasis Goswami, Alan L. Huston, Igor L. Medintz, U.S. Naval Research Lab. (United States)

Impurity doping in nanoparticles (NPs) is a process in which specific atoms are intentionally added during synthesis to provide either extra electrons or extra holes. Even after decades of research focused on optimizing the properties of colloidal metal NPs, little progress has been made on this process for small fluorescent metal nanoclusters (NCs). Similar to semiconductor quantum dots, NC-materials exhibit unique quantum confinement effects which lead to size-dependent optical spectra and fluorescence emission which can span the ultra violet, visible to near-infrared. Such NCs are useful in solar cells and solid-state lighting or, alternatively, cellular delivery, imaging and sensing for biological applications. Here, we synthesized ultrasmall fluorescent gold nanoclusters (AuNCs) doped with different metal including Ag, Cu, Pt, Zn and Cd. For synthesis, the metal-doped AuNCs were directly reduced in the presence of bidentate-poly (ethylene glycol) PEG dithiolane ligands that terminated in either a methoxy, amine, carboxy or azide group in water at room temperature. We systematically altered the doping ratio of metal per AuNC and examined the optical properties changes. We noted that even one or two impurities (i.e., atoms) per NC caused a dramatic enhancement in the fluorescence efficiency. The emission peak was observed at around 800 - 820 nm and quantum yields were in the 10-12% range, which represents a 40% improvement from without metal doping. Biological utility was prototyped by direct cellular microinjection or bioconjugating the AuNCs with Ag dopant to cell penetrating peptides (CPPs) which allowed for their subsequent endocytic uptake and imaging in COS-1 cells. We also show that the AuNCs maintain high photostability under direct illumination while eliciting minimal cytotoxicity.

9338-36, Session 8

Brightness-equalized quantum dots (*Invited Paper*)

Andrew M. Smith, Sung Jun Lim, Univ. of Illinois at Urbana-Champaign (United States)

Quantum dots are semiconductor nanocrystals that absorb and emit light at wavelengths tunable by the size of the crystal. Size-tuning provides access to a broad range of optical spectra, however it is fundamentally problematic for many applications because it leads to a large mismatch in absorption cross-section and fluorescence brightness across a series of colors. Here

**Conference 9338:
Colloidal Nanoparticles for Biomedical Applications X**

we present a new series of colloidal based on multi-domain core/shell structures for which the fluorescence brightness is matched across a broad range of emission colors and excitation wavelengths. We use alloyed cores with composition-tunable bandgaps and finely adjust the domain size and electronic properties of the shell to precisely match both absorption cross-section and quantum yield. This equalization process reduces the green-to-red disparity in fluorescence brightness from 30-fold to <1.1-fold and enables access to a wider spectral range with a compact size. We show that the equalized optical properties translate from the ensemble level down to the single-molecule level, in both one- and two-photon excitation modes, and even to the complex microenvironments of tumor tissue. These results are expected to lead to a new generation of quantitative, multicolor bioimaging probes with tunable photon emission rates independent of wavelength, a feature currently not available from any other type of colloidal material.

9338-37, Session 8

Understanding the protein-nanoparticles interactions using spectroscopy (*Invited Paper*)

Amitava Patra, Indian Association for the Cultivation of Science (India)

The research in bio-conjugated nanoparticles has been paid a great attention because of their promising applications. During the interactions of nanoparticles with proteins, that may alter protein conformation, expose novel epitopes on the protein surface, or perturb the normal protein function, which could induce unexpected biological reactions and lead to toxicity. Our motivation is to study the protein- Au nanoparticle interactions using steady state and time resolved spectroscopy to identify the specific binding site of protein with nanoparticles by using surface energy transfer. Again we will discuss the interactions between mycobacterium tuberculosis derived protein MPT63 and gold nanocluster (Au NC). Two single cysteine mutants of MPT63, namely G20C and G75C have been used to study the position dependence of cysteine residues on nanocluster-protein interactions. In the presence of MPT63, the enhancement of fluorescence intensity and the decay time of Au nanocluster confirm the binding of MPT63 to Au NC. It reveals that both electrostatics and other factors play crucial roles to define the complexity of protein-Au NC interactions.

References

1. T.Sen, and A. Patra, J. Phys. Chem. C 2012, 116, 17307-17317 (Invited Feature Article).
2. T. Sen, S. Mandal, S. Haldar, K. Chattopadhyay, and A. Patra, J. Phys. Chem. C, 2011, 115, 24037-24044.
3. T.Sen, K. K. Haldar and A. Patra, J. Phys. Chem. C, 2008, 112, 17945-17951.
4. B. Paramanik, S.Bhattacharyya, and A. Patra, J. Lumin, 2013, 134, 401-407.
5. B. Paramanik, A. Kundu, K. Chattopadhyay and A. Patra, RSC Adv. (2014).

9338-38, Session 8

Three dimensional time-gated tracking of non-blinking quantum dots in live cells (*Invited Paper*)

James H. Werner, Matt DeVore, Aaron M. Keller, Dominik Stich, Jennifer A. Hollingsworth, Mary E. Phipps, Los Alamos National Lab. (United States); Bridget S. Wilson, Diane S. Lidke, The Univ. of New Mexico (United States); Michael H. Stewart, U.S. Naval Research Lab. (United States); Yagnaseni Ghosh, Los Alamos National Lab. (United States)

Single particle tracking has provided a wealth of information about biophysical processes such as motor protein transport and diffusion in cell

membranes. Probes employed for these studies include fluorescent dyes, fluorescent proteins, colloidal gold, and quantum dots (QDs). Quantum dots, in particular, provide a good compromise between size and photo-stability requirements for tracking biological motion for long time periods in a minimally perturbative fashion. However, QD blinking (or motion of the QD out of the image plane of an epi-fluorescence microscope) generally limits observation times to several seconds. Here, we overcome these limitations by using novel non-blinking quantum dots as probes and employing a custom 3D tracking microscope to actively follow motion in 3D in live cells. In addition, while it is well recognized that the large Stokes shift of QD makes them useful probes to minimize auto-fluorescence background for live cell imaging, here we also exploit another feature of QDs (their long, >10 ns fluorescence lifetimes) to enhance signal to noise. Here, signal to noise is improved in the cellular milieu through the use of pulsed excitation and time-gated detection.

9338-39, Session 8

A folic acid labelled carbon quantum dot - protoporphyrin IX conjugate for use in folate receptor targeted two-photon excited photodynamic therapy (*Invited Paper*)

Dean Nicholas, Univ. of Ulster (United Kingdom); C. Fowley, A. P. McHale, Univ. of Ulster (Ireland); Sukanta Kamila, Jason Sheng, Jordan Atchison, Univ. of Ulster (United Kingdom); John F. Callan, Univ. of Ulster (Ireland)

Photodynamic therapy (PDT) requires the simultaneous combination of a photosensitising drug (PS), molecular oxygen and light of a specific wavelength, to generate singlet oxygen and other reactive oxygen species which are potent intracellular cytotoxins [1]. While approved for the treatment of non-melanoma skin cancer, PDT has also been trialled for use in other cancers such as head and neck, oesophageal, prostate, and bladder cancer. There are however, several limitations that prevent PDT obtaining wider spread clinical appeal. For example, currently approved PS drugs absorb light in the visible region of the electromagnetic spectrum limiting its penetration through human tissue restricting its use to superficial lesions. Secondly, PS molecules also tend to be hydrophobic and can aggregate in aqueous solution, leading to a reduction in singlet oxygen production [2]. Our work seeks to take advantage of the beneficial photophysical properties of Quantum Dots (QDs) to address some of the difficulties currently faced with the use of conventional PS drugs in PDT. QD-PS conjugates were synthesised that enable indirect excitation of the PS by energy transfer (FRET) from the QD using two-photon excitation wavelengths in the phototherapeutic window (750-900nm) [3]. The ability of these conjugates to produce singlet oxygen was assessed in cell free systems using chromogenic and fluorogenic traps. In addition, the cytotoxicity of the conjugates against cancer cell lines was also determined in vitro and in vivo. The results demonstrate QD-PS conjugates are promising candidates for use in two-photon excitation PDT.

9338-78, Session 8

Short-wavelength infrared (SWIR) quantum dots for high speed imaging of physiology in freely moving mice

Oliver T. Bruns, Thomas S. Bischof, Daniel K. Harris, Yanxiang Shi, Massachusetts Institute of Technology (United States); Lars Riedemann, Thomas Reiberger, Massachusetts General Hospital (United States); Klavs F. Jensen, Massachusetts Institute of Technology (United States); Rakesh K. Jain, Massachusetts General Hospital

(United States); Mounji G. Bawendi, Massachusetts Institute of Technology (United States)

In vivo optical imaging has the unique advantage of combining high-resolution with fast acquisition speeds. Fluorescent labels can be detected in this setting with very high sensitivity, ultimately allowing the detection and tracking of single labeled biological entities. Compared to other imaging modalities, this allows studying fast biological processes in great detail.

Imaging deep in tissue or a whole animal is limited by tissue autofluorescence, tissue and blood absorbance, and scattering. Imaging in the short-wavelength infrared (SWIR) (1000-2000nm) addresses these challenges simultaneously as there is minimal autofluorescence, significantly reduced light absorptions from blood and other structures and scattering is strongly diminished.

Here we introduce high quality SWIR emitting core shell quantum dots as versatile labels for this window. These dots exhibit a dramatically higher QY (up to 30%) compared to previous SWIR labels.

Applying this new technology for SWIR imaging allows us to perform biological imaging on a new level. Due to their tunable emission and small size we can perform color SWIR imaging of metabolic processes at video rate, demonstrating the impressive benefits of the SWIR band and the potential of designing experiments with multi colors similar to the visible. The emission signal is strong enough to detect and track single aggregate particles while combining high resolution with high penetration depth and high speed. We used this to generate detailed three dimensional quantitative flow maps of brain vasculature in only a few minutes while still resolving the smallest capillaries. We clearly image the drastic differences between healthy brain tissue and a tumor in the brain.

Applying our novel QD technology in the SWIR band allows us to bring optical imaging to a new level by imaging very fast physiological processes, for example enabling visualization of the heart rate in awake and freely moving mice. The combination of speed, penetration depth, and sensitivity of this new technology will enable studies which could only be done in smaller animals like fly or zebra fish larvae to be performed in mice, a mammalian model more relevant to humans.

9338-77, Session PSun

Single nanoparticle Raman spectroscopy and nanoparticle surface analysis using waveguides

Bernardo Cordovez, Robert Hart, Christopher Earhart, Brian DiPaolo, Abbey Weith, Ian Adam, Optofluidics (United States)

We present a nanophotonic waveguide based analytical system that enables single submicrometer particle Raman spectroscopy and individual nanoparticle surface characterization. In this talk we will discuss the underlying physics of the system as well its analytical capabilities. The system's core technology exploits the high optical field gradients generated in the evanescent field on nanophotonic waveguides to optically excite micro and nanoparticles very efficiently. The core technology is a microfluidic flow cell with nanophotonic waveguides running through the bottom of the flow channel. As particles in solution are delivered microfluidically to the analysis waveguides (which guide single mode near IR or IR light), once they penetrate the guide's evanescent field, near-field light is transformed to far field light. The light scattering signature for each particle is analyzed in two ways: 1) For single sub micrometer particle chemical identification, the light is filtered and routed to a Raman spectrometer, where spectroscopic signatures from the particles can be resolved in a few seconds. 2) For single particle surface coating characterization (e.g. understanding surface functionalization success on single particles, conformality of coating on a nanoparticle, chemical state of the surface, etc.) proprietary algorithms are used which evaluate the interaction of the particle with the waveguide. Applications to both applications include biopharm quality control, contaminants analysis in forensics, nanomedicine, and nanotoxicity.

9338-40, Session 9

Size dependence of gold nanorod stability: the need for customized surface chemistry

Elliott SoRelle, Stanford Univ. School of Medicine (United States); Orly Liba, Zeshan Hussain, Milan Gambhir, Stanford Univ. (United States); Adam de la Zerda, Stanford Univ. School of Medicine (United States)

Nanoparticles can be synthesized in a wide array of shapes and sizes to suit specific biomedical applications in therapy and imaging. Prerequisite to such applications is the ability to conjugate a particle's surface with targeting biological moieties (such as antibodies) and to be non-toxic and stable in biological environments. Here we report significant flaws in the common methods used to functionalize the surface of gold nanorods (GNRs) of larger-than-usual sizes. We find that while GNRs of sizes smaller than 50 x 15 nm can be effectively stabilized by polyethylene glycol (PEG)-based methods, larger GNRs form major aggregates and crash under similar functionalization conditions. In this study, GNRs of sizes up to 90 x 30 nm were synthesized using two different published methods. Particle morphology and size distributions were characterized using Transmission Electron Microscopy (TEM), and optical spectra were measured by Vis-NIR Spectrometry. The colloidal stability of each GNR was assayed at various stages of functionalization using Zeta Potential and Vis-NIR measurements. The results of these experiments indicate that large GNRs functionalized with PEG undergo irreversible aggregation after minimal washing by centrifugation. The serum stability of large GNRs was assessed, as well as the ability of large GNRs to be adapted for biological applications. Finally, the photoacoustic signal of large vs. small GNRs was compared. Our observations underscore that the biomedical advantages of novel nanoparticle synthesis methods may not be realized without concurrent customized surface functionalization methods. More generally, materially-identical nanoparticles (i.e. GNRs) exhibit varying stability as a function of particle size.

9338-41, Session 9

Functionalization of carbon nano-onions for biomedical applications (Invited Paper)

Silvia Giordani, Istituto Italiano di Tecnologia (Italy)

Nano-platforms capable of carrying therapeutic agents which demonstrate recognition capability for specific targeting and which can produce an optical output for imaging hold great potential in the treatment of cancer and/or various types of infections, such as HIV. Despite much interest in different carbon-based nano-materials, multi-shell fullerenes, known as carbon nano-onions (CNOs), as functional constructs for intracellular transport have not yet been explored. However, given their size, homogeneity and purity (compared with carbon nanotubes), they could in principle add an important new avenue for the transport of therapeutic agents.

CNOs discovered in 1992, are structured by concentric shells of carbon atoms.1 They display several unique properties, such as a large surface area to volume ratio, a low density and a graphitic multilayer morphology. Analogous to carbon nanotubes, CNOs display poor solubility in both aqueous and organic solvents.2

In my research group we have developed a versatile and robust approach for the functionalisation of CNOs, involving the facile introduction of a number of simple functionalities onto their surface by treatment with in-situ generated diazonium compounds.3 Our recent results have shown that chemical functionalization of the CNOs dramatically enhance their solubility and attenuate their inflammatory properties.4

Recently, we have developed a synthetic multi-functionalisation strategy for the introduction of different functionalities (receptor targeting unit and imaging unit) onto the surface of the CNO. We are now investigating the ability of these nanoconstructs to act as imaging agents5 and drug delivery systems.6

**Conference 9338:
Colloidal Nanoparticles for Biomedical Applications X**

References

[1] Ugarte, D. Nature 1992, 359, 707. [2] Bartelmess, J.; Giordani, S. Beilstein J. Nanotechnol., 2014, submitted. [3] Flavin, K.; Chaur, M. N.; Echegoyen, L.; Giordani, S. Org. Lett. 2010, 12, 840. [4] Yang, M.; Flavin, K.; Kopf, I.; Radics, G.; Hearnden, C. H. A.; McManus, G. J.; Moran, B.; Villalta-Cerdas, A.; Echegoyen L. A.; Giordani, S.; Lavelle, E. C. Small, 2013, DOI: 10.1002/sml.201300481. [5] Giordani, S.; Bartelmess, J.; Biondi, I.; Cheung, S.; Grossi, M.; Wu, D.; Echegoyen, L.; O'Shea, D. J. Mat. Chem.B, 2014, submitted. [6] manuscript in preparation

9338-42, Session 9
Multifunctional iron oxide nanoparticles for biomedical applications

Maarten Bloemen, Carla Denis, Thomas Van Stappen, Katholieke Univ. Leuven (Belgium); Luc De Meester, KU Leuven (Belgium); Nick Geukens, Ann Gils, Thierry Verbiest, Katholieke Univ. Leuven (Belgium)

Multifunctional nanoparticles have attracted a lot of attention since they can combine interesting properties like magnetism, fluorescence or plasmonic effects. As a core material, iron oxide nanoparticles have been the subject of intensive research. These cost-effective and non-toxic particles are used nowadays in many applications. We developed a hetero bifunctional PEG ligand that can be used to introduce functional groups (carboxylic acids) onto the surface of the NP. Via click chemistry, a siloxane functionality was added to this ligand, for a subsequent covalent ligand exchange reaction. The functionalized NP have an excellent colloidal stability in complex environments like buffers and serum or plasma. Antibodies were coupled to the introduced carboxylic acids and these NP-antibody bioconjugates were brought into contact with Legionella pneumophila bacteria for magnetic separation experiments.

9338-43, Session 9
Design of "smart" multifunctional MOF nanocarriers for controlled and targeted drug delivery (Invited Paper)

Stefan Wuttke, Andreas Zimpel, Ludwig-Maximilians-Univ. München (Germany)

The development and study of novel functionalized nanoparticles as drug delivery systems is the goal of our research. The central idea is to design hybrid nanomaterials based on metal-organic frameworks (MOFs), which could offer a new platform for biomedical applications. These materials are expected to display novel and enhanced properties compared to more established nanomaterials such as polymers, gold nanoparticles, iron oxide nanoparticles, liposomes and mesoporous silica. MOFs are crystalline materials and have regular pores, with a large pore surface area, and a highly designable framework that permit tuning the pore shape, pore size, and internal and external surface functionality. As a result, MOF nanoparticles with well-defined and tuneable structures can be realized. Our research is focus on the design of MOF nanoparticles with inner pore functionalization for controlled interaction with biologically active molecules, as well as outer functionality for target cell uptake, triggered drug release, and with surface shielding against unwanted interactions inside the physiological environment. Here we describe the synthesis, characterization and internal as well as external surface functionalization of two different MOF nanoparticles intending their use as drug delivery vehicle. First we report the loading capacity and their reproducibility of the two types of MOF nanoparticles compared with other nanocarriers. Second focus will be the surface functionalization of the MOF particles with different polymers (Polymer@MOF) and the formation of a lipid bilayer shell around the MOF nanoparticles (Lipid@MOF). Last but not least cytotoxic and anti-proliferative effects of the multifunctional MOF nanocarriers on different cells will be discussed.

9338-44, Session 9
Amphitropic liquid crystal phases from polyhydroxy sugar surfactants: Fundamental studies

Rauzah Hashim, Univ. of Malaya (Malaysia); Osama K. Abou-Zied, Sultan Qaboos Univ. (Oman); Bakir A. Timimi, Univ. of Southampton (United Kingdom)

The self-assembly phenomena on a special class of poly-hydroxy sugar surfactant have been studied extensively. This class of material are classified as amphitropic liquid crystals since they exhibit both thermotropic and lyotropic liquid crystalline properties. Hence the potential applications of these non-ionic surfactants are more versatile than those from the conventional lyotropic liquid crystals including from thermotropic phases, but the latter is yet to be realized. Unfortunately, due to the lack of interest (or even awareness), fundamental studies in thermotropic glycolipids are scanty to support application development, and any tangible progress is often mired by the complexity of the sugar stereochemistry. However, some applications may be pursued from these materials taking advantage of the sugar chirality and the tilted structure of the lipid organization which implies ferroelectric behavior. Here, we presented our studies on the stereochemical diversity of the sugar units in glycosides that form the thermotropic/lyotropic phases. The structure to property relationship compares different chain designs and other popular polyhydroxy compounds, such as monooleins and alkylpolyglucosides. Different structural properties of these glycosides are discussed with respect to their self-assembly organization and potential applications, such as delivery systems and membrane mimetic study.

9338-45, Session 9
Surface modification of inorganic nanoparticles for biomedical applications

Mahmoud G. Soliman, Beatriz Pelaz, Philipps-Univ. Marburg (Germany); Pablo del Pino, CIC BiomaGUNE (Spain); Wolfgang J. Parak, Philipps-Univ. Marburg (Germany)

Nanoparticles surface is one of the most important parameters to define their biological fate. Thus, providing different sizes and/or materials nanoparticles with an equivalent organic surface will allow to evaluate the impact of the core nature or the size in an individual manner. The polymer coating technique has been used during years for coating of nanoparticles, which as synthesized originally, are only dispersible in organic media. The nanoparticles obtained using this methodology are highly stable in physiological media. Aiming to use this technique in water soluble nanoparticles, a new round-trip process was developed using a phase transfer step before the polymer coating. This new phase transfer protocol allows for phase transfer of NPs made of different materials (Au and Ag), sizes (up to 100 nm) and shapes (spheres, rods and flat-triangular prisms), which can be then coated with an amphiphilic polymer. The colloidal stability of surface modified colloids was assayed against different biological media via UV/Vis spectroscopy and dynamic light scattering. Toxicity of these particles was tested in cancer and non-cancer cells showing no-toxicity.

9338-46, Session 9
Quantifying the density of surface capping ligands on semiconductor quantum dots (Invited Paper)

Naiqian Zhan, Goutam Palui, Florida State Univ. (United States); Jan-Philip Merkl, Florida State Univ. (United States)

States) and Univ. Hamburg (Germany); Hedi Mattoussi, Florida State Univ. (United States)

We have previously shown that bidentate ligands made of borohydride-reduced lipoic acid appended with a short polyethylene glycol (LA-PEG) yields hydrophilic QDs with great colloidal stability. More recently we showed that combined with a mild photochemically-driven ligation this strategy provides nanocrystals that can be easily functionalized with groups that are greatly important in biology; those groups are altered by sodium borohydride.

We have combined the design of an aldehyde-appended LA-PEG (LA-PEG-CHO) with the above photoligation strategy to prepare QDs with good control over the fraction of intact CHO groups per nanocrystal. We then applied the extremely efficient hydrazone coupling ligation to react the QD with hydrozopyridine. This reaction produces a well-defined absorption feature at 354 nm ascribed to the hydrazone chromophore. We exploited this unique optical signature to accurately measure the number of aldehyde groups per QD when the fraction of LA-PEG-CHO per nanocrystal was varied, by comparing the optical signature at 354 with the molar extinction coefficient of the chromophore. This allowed us to extract an estimate for the number of LA-PEG ligand per QDs for a few distinct size nanocrystals. We further complemented these findings with the use of NMR spectroscopy to estimate of the ligand density using well defined signatures of the terminal protons of the ligands, and found a good agreement between the two techniques. We anticipate that this strategy could be applied other nanoparticles such as those of Au and metals and semiconductor nanocrystals.

9338-47, Session 10

Plasmonic nanoengineering in metal nanostructures: from solid nanocubes to complex hollow multi-walled nanoboxes (Invited Paper)

Aziz Genç, Institut de Ciència de Materials de Barcelona (Spain); Javier Patarroyo, Institut Català de Nanotecnologia (Spain); Raul Arenal, Univ. de Zaragoza (Spain); Luc Henrard, Univ. of Namur (Belgium); Edgar Gonzalez, Univ. Javeriana (Colombia); Neus G. Bastus, Victor F. Puntes, Institut Català de Nanotecnologia (Spain); Jordi Arbiol, Consejo Superior de Investigaciones Científicas (Spain)

Complex metal nanoparticles offer a great playground for plasmonic nanoengineering, where it is possible to cover plasmon resonances from ultraviolet to near infrared by modifying the morphologies from solid nanocubes to nanoframes and multiwalled hollow nanoboxes. We experimentally show that structural modifications, i.e. void size and final morphology, are the dominant determinants for the final plasmonic properties, while compositional variations allow us to get a fine tuning. EELS mappings of localized surface plasmon resonances (LSPRs) reveal an enhanced plasmon energy and intensity field inside the voids of hollow AuAg nanostructures along with the enhanced extend of plasmon intensities around the nanostructures. Simulations by discrete dipole approximation (DDA) also reveal the effects of structural nanoengineering on plasmonic properties of hollow metal nanostructures. Possibility of tuning the LSPR properties of hollow metal nanostructures in a wide range of energy by modifying the void size/shell thickness is shown by Mie scattering theory calculations, which reveals that void size is the dominant factor for tuning the LSPRs. As a proof of concept for enhanced plasmonic properties, we show effective label free sensing of bovine serum albumin (BSA) with the single walled AuAg nanoboxes.

9338-48, Session 10

SERS active colloidal nanoparticles for the detection of small blood biomarkers using aptamers

Haley L. Marks, Texas A&M Univ. (United States); Samuel Mabbott, University of Strathclyde (United Kingdom); George W. Jackson, BioTex, Inc. (United States) and Base Pair Biotechnologies (United States); Duncan Graham, Univ. of Strathclyde (United Kingdom); Gerard L. Cote, Texas A&M Univ. (United States)

Functionalized colloidal nanoparticles for SERS serve as a promising multifunctional assay component for blood biomarker detection. Proper design of these nanoprobe through conjugation to spectral tags, protective polymers, and sensing ligands can provide experimental control over the sensitivity, range, reproducibility, particle stability, and integration with biorecognition assays. Additionally, the optical properties and degree of electromagnetic SERS signal enhancement can be tuned by altering the nanoparticle shape, size, and material so that the colloid's local surface plasmon resonance (LSPR) aligns where maximal enhancements occur, specifically at 532 ± 120 nm for the excitation laser used in this work. Aptamers, synthetic affinity ligands derived from nucleic acids, provide a number of advantages for biorecognition of small molecules with low immunogenicity. They are simpler and more economical to produce, are capable of greater specificity and affinity than antibodies, are easily tailored to specific functional groups, and their intrinsic negative charge can be utilized for additional particle stability[1,2,3]. In this work, a competitive binding assay involving SERS active nanoparticles that are functionalized using a mixed self-assembled monolayer consisting of thiolated Raman reporter molecules and aptamers is presented. These particles were bound to a derivative of the analyte of interest, which was immobilized on a magnetic nanoparticle. The pre-bound aptamer/nanoparticle conjugates were exposed to varying concentrations of the target analyte down to the picomolar range, and the SERS nanoprobe displaced by competitive binding were collected and their SERS signals analyzed.

1. J. K. Immunology, Vol. 3rd. (W.H. Freeman, New York; 1997).
2. Moghaddam, A., Løbersli, I., Gebhardt, K., Braunagel, M. & Marvik, O.J. Selection and characterisation of recombinant single-chain antibodies to the hapten Aflatoxin-B1 from naive recombinant antibody libraries. Journal of Immunological Methods 254, 169-181 (2001).
3. Jayasena, S.D. Aptamers: An emerging class of molecules that rival antibodies in diagnostics. Clinical Chemistry 45, 1628-1650 (1999).

9338-49, Session 10

Degradable plasmon resonant liposomes for controlled drug delivery

Shellie Knights-Mitchell, Joshua D. Williams, Marek Romanowski, The Univ. of Arizona (United States)

Nanotechnology use in drug delivery promotes a reduction in systemic toxicity, improved pharmacokinetics, and better drug bioavailability. Liposomes continue to be extensively researched as drug delivery systems (DDS) with formulations such as Doxil® and Ambisome® approved by FDA and successfully marketed in the US. However, the limited ability to precisely control release of active ingredients from these vesicles continues to challenge the broad implementation of this technology. Moreover, the full potential of the carrier to sequester drugs until it can reach its intended target has yet to be realized. Here, we describe a liposomal DDS that releases therapeutic doses of an anticancer drug in response to external stimulus. Earlier, we introduced degradable plasmon resonant liposomes (Troutman et al., Adv. Mater. 2008, 20, 2604). These constructs, obtained by reducing gold on the liposome surface, facilitate spatial and temporal release of drugs upon laser light illumination. Utilizing this concept, we

**Conference 9338:
Colloidal Nanoparticles for Biomedical Applications X**

report on drug encapsulation stability, and demonstrate controlled release of contents by external stimuli. Degradable plasmon resonant liposomes have been developed to stably encapsulate and retain doxorubicin at physiological conditions represented by isotonic saline at 37 °C and pH 7.4. Subsequently, they are stimulated to release contents either by a 5 °C increase in temperature or by laser illumination (760 nm and 70 mW/cm² power density). Successful development of degradable plasmon resonant liposomes responsive to near-infrared light or mild hyperthermia can provide a new delivery method for multiple lipophilic and hydrophilic drugs with pharmacokinetic profiles that limit clinical utility.

9338-50, Session 10

Synthesis and modelling of optical properties of gold-silver alloy nanoparticles

David Rioux, Michel Meunier, Ecole Polytechnique de Montréal (Canada)

Gold silver alloy nanoparticles (NPs) are promising for chromatic labeling of biological material because of their composition-dependent plasmon resonance. Compared to the conventionally used fluorophores and quantum dots, plasmonic NPs offer the advantage of being highly stable as they do not photobleach nor blink. For example, alloy NPs with various compositions, which have a plasmon resonance at different wavelengths, can be used to target specific cells to help biomedical imaging and diagnosis. In this case, it is desirable to use large NPs (~60nm) that scatter light efficiently. However, synthesis of alloy NPs with controlled size has never been achieved for sizes larger than about 20-30 nm, where light scattering is far too weak for practical imaging applications.

We report on a new size and composition-controlled synthesis of monodispersed AuAg alloy NPs up to 100+ nm based on a seeded growth approach where alloy NPs are grown on small gold seeds [1]. We compare this approach to standard chemical reduction techniques as well as laser synthesis of alloy NPs. In addition, we have introduced a new model of the dielectric function of these alloy NPs based on the band structures of gold and silver for interband transitions and the Drude model for intraband contributions [2]. Using Mie theory with this dielectric function, the optical absorption and scattering spectra of the NPs as well as the near field amplification can be predicted. We will also discuss on the size distribution, as well as the alloy composition profile inside the particle as obtained by transmission electron microscopy and their influence on the optical properties.

1 D. Rioux and M. Meunier, (In preparation).

2 D. Rioux, S. Vallières, S. Besner, P. Muñoz, E. Mazur, and M. Meunier, *Adv. Opt. Mater.* 2, 176 (2014).

9338-51, Session 11

Magnetic microcapsule as a MRI-visible multifunctional theranostic platform for remote cancer therapy with synergistic antitumor effect (Invited Paper)

Niveen M. Khashab, King Abdullah Univ. of Science and Technology (Saudi Arabia)

Multifunctional theranostic platform, with properties of cell imaging and remote cancer therapy, are extensively studied in the development of new cancer therapy approaches. Superparamagnetic iron oxide nanoparticles (SPIO NPs)-based nanocomposites, have shown excellent promise not only to enhance the sensitivity of magnetic resonance imaging (MRI), but also can be controlled by a magnetic field. In this work, we develop a multifunctional drug delivery system by using SPIO NPs as a layer, assembled with two polyelectrolyte, poly(allylamine hydrochloride) (PAH)

and poly(4-styrene sulfonate Sodium) (PSS). In this system, the PSS and PAH are pH-responsive, which is benefit for the drug release in tumor environment. The SPIO layer is useful for controlled drug delivery, magnetic hyperthermia, MRI contrast as well as its internalization by cells, showing a synergistic antitumor effect together with chemotherapeutic efficacy. After addition of the SPIOs layer, the system exhibits low toxicity to cells. Our work encourages further exploration of SPIO-based microsystems for cancer combination therapy.

9338-52, Session 11

RF heating of nano-clusters for cancer therapy

Renat R. Letfullin, Alla R. Letfullin, Rose-Hulman Institute of Technology (United States); Thomas F. George, Univ. of Missouri-St. Louis (United States)

Nanodrugs selectively delivered to a tumor site can be activated by radiation for drug release, or nanoparticles (NPs) can be used as a drug themselves by producing biological damage in cancer cells through thermal, mechanical ablations or charged particle emission. Radio-frequency (RF) waves have an excellent ability to penetrate into the human body without causing healthy tissue damage, which provides a great opportunity to activate/heat NPs delivered inside the body as a contrast agent for diagnosis and treatment purposes. However the heating of NPs in the RF range of the spectrum is controversial in the research community because of the low power load of RF waves and low absorption of NPs in the RF range. To resolve these weaknesses in the RF activation of NPs and dramatically increase absorption of contrast agents in tumor, we suggest aggregating the nano-clusters inside or on the surface of the cancer cells. Nano-clusters have much higher absorption efficiency than single NPs, making activation of NPs by RF radiation feasible. Thus, this paper analyzes the absorption efficiency of nano-clusters in the RF range of the spectrum in order to establish whether it is possible to heat the nano-cluster to the temperatures enough to ablate the cells. Using a phenomenological approach by taking data from available experiments on RF heating of NPs, we are able to simulate temperature changes in metal and dielectric nano-clusters, which in return allowed us to estimate their absorption efficiency in the RF range.

9338-53, Session 11

Monitoring biological responses driven by magnetic hyperthermia in vitro and in vivo

Alfredo Ambrosone, Istituto di Cibernetica Eduardo Caianiello (Italy); Grazyna Stepień, Maria Moros, Univ. de Zaragoza (Spain); Federica Fabozzi, Valentina Marchesano, Istituto di Cibernetica Eduardo Caianiello (Italy); Sara Rivera, Jesus M. de la Fuente, Univ. de Zaragoza (Spain); Claudia Tortiglione, Istituto di Cibernetica Eduardo Caianiello (Italy)

Iron-based magnetic nanoparticles (MNP) generate intracellular heat offering undeniable advantages for biomedical hyperthermia. Despite the promising potential of these approaches, cellular and molecular mechanisms associated to MNP-mediated heat generation and transfer remain marginally understood. Herein, we present a comprehensive description of early biological responses activated by magnetic hyperthermia in vitro (murine melanoma cell line B16-F10) and in vivo (the invertebrate aquatic model *Hydra vulgaris*). Following MNP internalization, alternating magnetic fields were applied to MNP-treated cells and animals in order to stimulate NP heating. The local heating effects on tissues and cells were immediately monitored by a multitude of approaches: i) in vivo through optical microscopy ii) ex vivo on isolated cells using apoptotic/necrosis cell markers as well as proliferation, and iii) at molecular level, by assessment of heat shock gene expression via qRT-PCR. Surprisingly, even in absence of cell

**Conference 9338:
Colloidal Nanoparticles for Biomedical Applications X**

damages, MNP heating triggers the activation of molecular pathways, which may serve as biomolecular thermometers to estimate intracellular-confined temperature increases.

9338-54, Session 12

Cancer cell uptake behavior of Au nanoring and its localized surface plasmon resonance induced cell inactivation efficiency

Che-Kuan Chu, Yi-Chou Tu, Chih-Ken Chu, Yu-Wei Chang, Shih-Yang Chen, Ting-Ta Chi, Ming-Jyun Li, Yean-Woei Kiang, Chih-Chung Yang, National Taiwan Univ. (Taiwan)

Au nanorings (NRIs), which have the LSP resonance wavelength around 1058 nm, either with linked antibody or without antibody, are applied to SAS oral cancer cell solution for cell inactivation through the localized surface plasmon-induced photothermal effect when it is illuminated by a laser of 1065 nm in wavelength. Various incubation times after the application of Au NRIs to cell solutions are considered for observing the variations of cell uptake of Au NRI and hence the threshold laser intensity for cancer cell inactivation. In each case of incubation time, the cell solution is washed for evaluating the Au NRI number per cell adsorbed and internalized by the cells. Also, the Au NRIs adsorbed (remaining on cell membrane) are etching with KI/I₂ to evaluate the Au NRI number per cell internalized by the cells. The threshold laser intensities before washout, after washout, and after KI/I₂ etching are calibrated from the circular area sizes of inactivated cells around the illuminated laser spot center under the illuminations of various laser power levels. The adsorbed and internalized Au NRIs per cell are obtained from inductively coupled plasma mass spectrometry measurements of the flushed solution in the KI/I₂ etching process and the remaining cell solution, respectively. The adsorbed Au NRI number per cell reaches a maximum at 12 hrs in incubation time. By comparing the variation of threshold laser intensity for cell inactivation, it is found that the adsorbed NRIs can cause more effective cancer cell inactivation, when compared with the internalized NRIs.

9338-55, Session 12

Laser-induced vapor nanobubbles for efficient delivery of macromolecules in live cells (*Invited Paper*)

Ranhua Xiong, Koen Raemdonck, Karen Peynshaert, Ine Lentacker, Ine De Cock, Joseph Demeester, Stefaan C. De Smedt, Andre G. Skirtach, Kevin Braeckmans, Univ. Gent (Belgium)

There is a great interest in delivering macromolecular agents into living cells for therapeutic purposes, such as siRNA for gene silencing. Although substantial effort has gone into designing non-viral nanocarriers for delivering macromolecules into cells, translocation of the therapeutic molecules from the endosomes after endocytosis into the cytoplasm remains a major bottleneck. Laser-induced photoporation, especially in combination with gold nanoparticles, is an alternative physical method that is receiving increasing attention for delivering macromolecules in cells. By allowing gold nanoparticles to bind to the cell membrane, nanosized membrane pores can be created upon pulsed laser illumination. Depending on the laser energy, pores are created through either direct heating of the AuNPs or by vapour nanobubbles (VNBs) that can emerge around the AuNPs. Macromolecules in the surrounding cell medium can then diffuse through the pores directly into the cytoplasm. Here we present a systematic evaluation of both photoporation mechanisms in terms of cytotoxicity, cell loading, and siRNA transfection efficiency. We find that under conditions of VNBs are much more efficient than direct photothermal disturbance of the plasma membrane without any noticeable cytotoxic effect. Interestingly, by

tuning the laser energy the pore size could be changed, allowing control of the amount and size of molecules that are delivered in the cytoplasm. As only a single nanosecond laser pulse is required, we conclude that VNBs are an interesting photoporation mechanism that may prove very useful for efficient high-throughput macromolecular delivery in live cells.

9338-56, Session 12

Analysis of bacteria-derived outer membrane vesicles using tunable resistive pulse sensing

Evgeny Bogomolny, Jiwon Hong, Cherie Blenkiron, The Univ. of Auckland (New Zealand); Denis Simonov, The Univ. of Auckland (New Zealand); Priscila Dauros, The Univ. of Auckland (New Zealand); Simon Swift, Department of Molecular Medicine and Pathology (New Zealand); Anthony Phillips, The Univ. of Auckland (New Zealand); Geoff Willmott, The Univ. of Auckland (New Zealand) and The MacDiarmid Institute for Advanced Materials and Nanotechnology (New Zealand)

Accurate characterization of submicron particles within biological fluids presents a major challenge for a wide range of biomedical research. Detection, characterization and classification are difficult due to the presence of particles and debris ranging from single molecules up to particles slightly smaller than cells. Especial interest arises from extracellular vesicles (EVs) which are known to play a pivotal role in cell-signaling in multicellular organisms. Tunable resistive pulse sensing (TRPS) is increasingly proving to be a useful tool for high throughput particle-by-particle analysis of EVs and other submicron particles. This study examines the capability of TRPS for characterization of EVs derived from bacteria, also called outer membrane vesicles (OMVs). Measurement of a size distribution (124 ± 3 nm modal diameter) and concentration (lower bound 7.4 × 10⁹ mL⁻¹) are demonstrated using OMVs derived from uropathogenic Escherichia coli. Important aspects of measurement are discussed, including sample preparation and size selection. Application of TRPS to study EVs could assist the development of these particles in clinical diagnostics and therapeutics.

9338-57, Session 12

Penetration of spherical and rod-like gold nanoparticles into intact and barrier-disrupted human skin

(*Invited Paper*)

Christina M. Graf, Daniel Nordmeyer, Freie Univ. Berlin (Germany); Sebastian Ahlberg, Charité Universitätsmedizin Berlin (Germany); Joerg Raabe, Swiss Light Source (Switzerland); Annika Vogt, Juergen M. Lademann, Fiorenza Rancan, Charité Universitätsmedizin Berlin (Germany); Eckart Ruehl, Freie Univ. Berlin (Germany)

Recent results on the uptake of nanoparticles and drugs into cells and skin are presented, as probed by microscopy and spectromicroscopy approaches. Nanoparticles are prepared in narrow size distributions by colloidal chemistry. They are functionalized by organic ligands so that their electrostatic stabilization and aggregation in biological media can be controlled. Particle uptake into cells and skin is determined by fluorescence microscopy, as well as X-ray microscopy and tomography. These studies allow us to identify with high spatial resolution, where nanoparticles are penetrating into biological matter. Especially, particle size effects are of interest in this context as well as cell type dependent uptake properties of nanoparticles. For skin the importance of the barrier provided by the

**Conference 9338:
Colloidal Nanoparticles for Biomedical Applications X**

upper horny layer, the stratum corneum, for particle uptake is investigated. This includes mechanically and chemically-induced barrier damage. Results on barrier damage induced by tape stripping, oxazolone-induced allergic contact dermatitis, and mechanical impact (pricking) are shown. Furthermore, the uptake of drug nanocarriers and antiinflammatory drugs into skin is reported. Label-free approaches of spectromicroscopy are applied, such as X-ray microscopy. Perspectives for complimentary approaches, such as optical near-field microscopy are highlighted. Finally, the use of the reported results regarding novel concepts of drug delivery in topical therapy of inflammatory skin diseases by using drug nanocarriers is discussed.

9338-58, Session 12

Optically generated hybridoma using bispecific gold nanoparticles

Daniella Yeheskely-Hayon, Limor Minai, Dvir Yelin, Technion-Israel Institute of Technology (Israel)

Cell-cell fusion, i.e. the process during which two individual cells merge to form a single hybrid cellular entity, is a common event in many naturally occurring biological processes. For many applications in biomedicine and biotechnology, artificial induction of cell fusion is a critical step for obtaining cellular entities with a desired set of properties that cannot be found in nature. An important example for such applications is the formation of immortalized hybrid splenic-myeloma cells for the production of monoclonal antibodies that are widely used in biomedical research, clinical diagnosis and cancer therapy. In this work, we utilize the localized plasmonic interaction between bispecific gold nanoparticles and intense ultrashort laser pulses to form hybridoma cells via selective induction of fusion between specific cells. Our bispecific nanoparticles, coated by two different molecules having high affinity to immortal myeloma cells and to mouse splenocytes, play a dual role in promoting fusion: first, their affinity to two both cell types effectively couples these cells together; second, their unique optical properties allow the laser pulses to locally compromise the cells' membranes, which result in a highly selective fusion process.

Compared to the other methods for cell fusion, our approach for plasmonic cell fusion does not require intensive and time-consuming cell sorting, operates on large cell populations, and has low toxicity and high specificity.

9338-59, Session 12

Quantification of nanoparticle uptake by cells and its correlation to basic physicochemical parameters

Wolfgang J. Parak, Philipps-Univ. Marburg (Germany)

No Abstract Available

9338-61, Session 12

Membrane-targeting peptides for nanoparticle-facilitated cellular imaging and analysis (*Invited Paper*)

Joyce Breger, James B. Delehanty III, Kelly Boeneman Gemmill, Lauren D. Field, U.S. Naval Research Lab. (United States); Juan B. Blanco-Canosa, Philip E. Dawson, The Scripps Research Institute (United States); Alan L. Huston, Igor L. Medintz, U.S. Naval Research Lab. (United States)

The controlled delivery of nanomaterials to the plasma membrane is critical for the development of nanoscale probes that can eventually enable

cellular imaging and analysis of membrane processes. Chief among the requisite criteria are delivery/targeting modalities that result in the long-term residence (e.g., days) of the nanoparticles on the plasma membrane while simultaneously not interfering with regular cellular physiology and homeostasis. Our laboratory has developed a suite of peptidyl motifs that target semiconductor nanocrystals (quantum dots (QDs)) to the plasma membrane where they remain resident for up to three days. Notably, only small a percentage of the QDs are endocytosed over this time course and cellular viability is maintained. This talk will highlight the utility of these peptide-QD constructs for cellular imaging and analysis.

9338-62, Session 12

Inhibition of bacterial growth by iron oxide nanoparticles with and without attached drug: Have we conquered the antibiotic resistance problem in cystic fibrosis lung infections?

Leisha M. Armijo, Annaka Westphal, Priyanka Jain, Angelina Malagodi, Franye Fornelli, Allison Hayat, Michael French, The Univ. of New Mexico (United States); Hugh D. C. Smyth, The Univ. of Texas at Austin (United States); Marek Osifski, The Univ. of New Mexico (United States)

No Abstract Available

Conference 9339: Reporters, Markers, Dyes, Nanoparticles, and Molecular Probes for Biomedical Applications VII

Sunday - Tuesday 8-10 February 2015

Part of Proceedings of SPIE Vol. 9339 Reporters, Markers, Dyes, Nanoparticles, and Molecular Probes for Biomedical Applications VII

9339-26, Session PSun

Phospholipid liposomes functionalized by protein

Olga E. Glukhova, Olga A. Grishina, Georgy V. Savostyanov, N.G. Chernyshevsky Saratov State Univ. (Russian Federation)

Finding new ways to deliver neurotrophic drugs to the brain in newborns is one of the contemporary problems of medicine and pharmaceutical industry. Modern researches in this field indicate the promising prospects of supramolecular transport systems for targeted drug delivery to the brain which can overcome the blood-brain barrier (BBB). Thus, the solution of this problem is actual not only for medicine, but also for society as a whole because it determines the health of future generations.

Phospholipid liposomes due to combination of lipo- and hydrophilic properties are considered as the main future objects in medicine for drug delivery through the BBB as well as increasing their bioavailability and toxicity. Liposomes functionalized by various proteins were used as transport systems for ease of liposomes use. Designing of modification oligosaccharide of liposome surface is promising in the last decade because it enables the delivery of liposomes to specific receptor of human cells by selecting ligand and it is widely used in pharmacology for the treatment of several diseases.

The purpose of this work is creation of a coarse-grained model of bilayer of phospholipid liposomes, functionalized by specific to the structural elements of the BBB proteins, as well as prediction of the most favorable orientation and position of the molecules in the generated complex by methods of molecular docking for the formation of the structure. Investigation of activity of the ligand molecule to protein receptor of human cells by the methods of molecular dynamics was carried out.

9339-27, Session PSun

Impact of magnetite nanoparticle incorporation on the eigenfrequencies of nanocomposite microcapsules

Olga E. Glukhova, N.G. Chernyshevsky Saratov State Univ. (Russian Federation); Olga A. Grishina, N.G. Chernyshevsky Saratov State Univ. (Russian Federation)

Modern researches showed that nanocomposite films with magnetite nanoparticle incorporation have good perspectives for applications in electronics to create antireflective coatings and also for biomedical applications to create coatings with remote control of physical properties using alternative magnetic field or microwave radiation, which is very important for fabrication of new generation substrates in tissue engineering and advanced drug delivery systems. In particular, the unique properties of advanced nanocomposite microcapsules allowed developing of the supramolecular system of targeted drug delivery. A study of the behavior of the nanocomposite shell of microcapsules, which consists of alternate layers of negatively charged iron oxide nanoparticles and cationic polyallylamine hydrochloride molecules, was carried out.

The aim of the present study was to investigate the effect of the number of nanoparticle layers on magnetic properties of polyelectrolyte/nanoparticles nanocomposite microcapsules prepared via layer-by-layer technique using iron oxide colloids.

In result of numerical simulation using ANSYS Workbench software the behavior of the nanocomposite shell of microcapsules depending on the concentration of magnetite particles in it was investigated. Modal and harmonic analysis of behavior of the microcapsules shell was conducted in water at a temperature of 37 °. As a result of numerical experiment the eigenfrequencies and mode shape were first time defined for any modifications of the nanocomposite microcapsules. It has been established that the magnetic permeability value depends on the number of iron oxide nanoparticle layers in a nanocomposite microcapsule.

9339-28, Session PSun

Emitting terahertz frequency wave by charged fullerene C36 inside carbon nanotube under electric field

Olga E. Glukhova, Anna S. Kolesnikova, Mikhail M. Slepchenkov, N.G. Chernyshevsky Saratov State Univ. (Russian Federation)

First it is introduced a new method of producing terahertz waves based on carbon nanotubes with several encapsulated fullerene C60 and charged C36 fullerene was proposed. C60 fullerenes were connected by chemical bonds between themselves and with the wall (10,10) nanotube by tight-binding molecular dynamic (MDTB) method. Charged +1e fullerene C36 is located in a potential well near a chain of C60. Potential well formed by van der Waals interactions between the charged fullerene and fullerene chain. Charged fullerene C36 can not escape from the potential well without an external driving force, but can range controlled by an external electric field. The theoretical possibility of generating radiation terahertz range free charged fullerene C36 has been proven in this report. Free fullerene fluctuates in the potential well created by the atomic framework nanotubes and several fullerenes polymerized with its walls and each other. Physical conditions, under which terahertz range may operate at frequency of 0.7 THz, was found. The field strength 106 V / cm and the charge +5e fullerene are necessary conditions under which the generation of terahertz frequency ranges is implemented.

The proposed model nanoemitter is a new model. Additional heating magnetic field, the alternating field is not used in this model. Principle of operation of the proposed model is based on the carbon peapod in a constant electric field.

9339-29, Session PSun

A control of phospholipid motion on graphene layer under external electric field

Olga E. Glukhova, Anna S. Kolesnikova, Mikhail M. Slepchenkov, N.G. Chernyshevsky Saratov State Univ. (Russian Federation); Dmitriy S. Shmygin, N.G. Chernyshevsky Saratov State Univ. (Russian Federation)

To create complex lipid structures we need to transport the phospholipids into the place of assembling. Lipid structures, include membranes, consist of phospholipid molecules. We select the external electric field to control the motion of phospholipid and have simulated motion of phospholipid on graphene layer in electric field. We used method AMBER for calculations. Calculations for different values of electric field strength were held. Also,

Conference 9339: Reporters, Markers, Dyes, Nanoparticles, and Molecular Probes for Biomedical Applications VII

we studied situation when there were no external electric field at all: there were uncontrolled motion and the modes of control of motion were not found. Thereby we had to use additional molecules to control phospholipid motion. For that purpose we used molecule of fullerene C_{36} (bonded with phospholipid by Van-der-Vaals interaction) because it's known that motion of fullerene C_{36} can be controlled by external electric field. But we found, that heavy phospholipid molecule can't be controlled by light molecule of small fullerene and then we used different number of C_{36} and then C_{60} to find out the optimal mode of control. Both fullerenes C_{36} and C_{60} were charged to $+1e$. Value of electric field strength varied from 105 to 107 V/m. We found that motion of phospholipid molecule can be controlled by three charged $+1e$ fullerene C_{60} in external electric field with strength 106 V/m.

9339-30, Session PSun

Stability of composites based on graphene layers and carbon nanotubes

Olga E. Glukhova, Anna S. Kolesnikova, Georgy V. Savostyanov, N.G. Chernyshevsky Saratov State Univ. (Russian Federation); Dmitriy S. Shmygin, N.G. Chernyshevsky Saratov State Univ. (Russian Federation); Mikhail M. Slepchenkov, N.G. Chernyshevsky Saratov State Univ. (Russian Federation)

A series of calculations of enthalpy of composites based on graphene layers and nanotubes was held. The stability study was received by molecular mechanics method REBO (reactive empirical bond order).

First, we studied the simple structure, made of one nanotube (zigzag or armchair) and two graphene layer, bonded with tube by chemical interaction. Calculations of enthalpy from different geometric properties (length, diameter of nanotubes) were held. And then enthalpy of complex structure of many layers and tubes was investigated. Additionally dependence of enthalpy from distance between tubes in structure was studied. Length and diameter of CNT in simple structures were varied. Sizes of graphene sheets were the same for all simple structures.

It's possible to say, that all composite with armchair CNTs are stable, but ones with biggest diameter of CNT are more stable than other. Length influences slight to the stability: notable increasing of length gives a little rise in enthalpy. The value of enthalpy for one large composite (made of big 7 graphene sheets and 45 CNTs of biggest diameter): -0.446 eV/atom, shows that enlarged composite is more stable than smaller ones. The dependence of enthalpy from distance between nanotubes in structure is certain: stable descends with increasing of distance.

9339-31, Session PSun

Prediction of stability for carbon nanotori

Olga E. Glukhova, Anna S. Kolesnikova, Georgy V. Savostyanov, Mikhail M. Slepchenkov, N.G. Chernyshevsky Saratov State Univ. (Russian Federation)

At the present time carbon nanostructures are the main functional material for the development of electronic devices of broad applications. Optoelectronic devices, ultra-flat flexible displays, various types of high-performance biosensors are already constructed based on carbon materials. One of the most perspective for practical application forms of carbon nanostructures are nanotori. To successfully apply nanotori in bio- and nano-electronics is necessary that the structure of this type had a high stability. This paper presents the results of prediction the stability of toroidal structures using computer modeling methods. Objects of a study were nanotori with chirality indexes (10,10), (13,0) and (13,6). Atomic structure of these objects was obtained by folding of carbon nanotubes with relevant chirality type and size. The stability of carbon nanotori are determined by scanning of the local stresses map. Identify of the fragments with maximum stresses in the atomic structure allows to predict the location

of possible defects as well as to establish the effect of curvature of the atomic framework on the properties of nanotori. Calculation of the local stress was carried out using an original method. Also, for each of the studied toroidal structures we calculated an enthalpy of the nanotori formation reaction. Obtained results showed that the highest stability is characterized for carbon nanotori (13, 0) formed by the folding of a carbon nanotube with the zigzag configuration of the atomic framework. These nanotori are characterized by the lowest enthalpy of structure formation (101 eV).

9339-32, Session PSun

Theoretical study of the behavior of cryptand with different ion metal inside carbon nanotube

Olga E. Glukhova, Anna S. Kolesnikova, Denis A. Melnikov, Mikhail M. Slepchenkov, Vladislav V. Shunaev, N.G. Chernyshevsky Saratov State Univ. (Russian Federation)

Crown ethers and their complexes are widely used as molecular containers in technical fields, and in the fields of medicine and agriculture. Three-dimensional analog of crown ethers having the property of natural ionophores is cryptand. Encapsulation of metal ions into the cryptand increases the cation selectivity of the molecule - the "guest" and led to increase of their ionophore-like transport properties. Cryptand ability to act as a system "guest" - "host" led to its application in electronics as optical biosensors and in medicine as a drug to combat diseases caused by excess heavy metals in the body. In this paper we study the behavior of [2.2.2] cryptand with various metal ions (Na, K, Eu, Fe) inside the carbon nanotube of armchair type. Atomic structure of the cryptand is optimized by semi-empirical method PM6. Stability of the studied complexes is determined by calculation the enthalpy of the formation reaction. To identify regularities of behavior for cryptand inside a carbon nanotube we carried out a series of numerical experiments in molecular dynamics using Amber force field at different temperatures and under the influence of external electric fields of different strength. We have established the dependence of the oscillation frequency of the cryptand inside a carbon nanotube. On the basis of the established effect of fluctuations for cryptand inside the nanotube is predicted that such complexes can be used as miniature radiating systems.

9339-33, Session PSun

Manipulation of fullerene molecules on graphene

Olga E. Glukhova, Vadim V. Mitrofanov, Vladislav V. Shunaev, Mikhail M. Slepchenkov, N.G. Chernyshevsky Saratov State Univ. (Russian Federation)

Due to the increasing demand for functionalization of graphene and its application as a functional element of real electronic and / or mechanical devices, as well as due to its unique adhesive and sensory abilities the actual problem is the use of graphene as a substrate on which the assembly of supramolecular structures. Elements of such structures can be different molecules driven by external factors, and can be easily transported on graphene. These molecules primarily include miniature spheroidal fullerenes easy to navigate on the surface of graphene, in particular icosahedral C_{60} . The aim of this work was to find an effective method of manipulation of fullerene C_{60} on graphene. As such method we proposed to introduce in graphene sheet structural defect of the atomic framework namely defect Stone-Wales (pentagon-heptagon pairs). Another structural defect studied in this paper is adsorbed on the Stone-Wales defect hydrogen atom. Molecular dynamics and tight binding method were applied to calculate the location of the molecule C_{60} on graphene sheet and its movement. To identify regularities of behavior of fullerene on graphene sheet we carried out a series of numerical experiments at different temperatures. In this paper we calculated the energy profile of interaction between fullerene and graphene sheet. Obtained results showed that forming on the surface of the

**Conference 9339: Reporters, Markers, Dyes, Nanoparticles,
and Molecular Probes for Biomedical Applications VII**

graphene sheet defects in a certain way, one can control the trajectory of molecules on graphene. .

9339-34, Session PSun

Simulation of the formation for molecular compounds of nanotubes with different chirality indexes to create new molecular devices on their basis

Olga E. Glukhova, Anna S. Kolesnikova, Georgy V. Savostyanov, Mikhail M. Slepchenkov, N.G. Chernyshevsky Saratov State Univ. (Russian Federation)

The main property of carbon nanotubes that determinates their wide application in electronics is a change of the chirality for ideal structure of a nanotube at implementing of structural Stone-Wales defect (pentagon-heptagon pairs) to its atomic framework. This property allows us to create nanotube-based different electronic devices (diodes, transistors, resistors), similar to traditional silicon devices. Nanotube with incorporated defect can be considered as a metal-semiconductor heterojunction. On the basis of this heterojunction semiconductor elements of very small size can be implemented, less than the current silicon elements. To create devices based on metal-semiconductor heterojunction is necessary to know the mechanisms of formation of the molecular compounds of nanotubes with different chirality. The aim of this work is a theoretical study of the formation of the molecular compounds of nanotubes with different chirality leading to the appearance of the metal-semiconductor heterojunction using molecular modeling methods. The object of investigation is a heterojunction formed by the compound of nanotubes with chirality indices (13,10) and (14, 10). To identify regularities of change in the electronic structure of the compound nanotubes we calculated the density of electronic states (DOS) for the heterojunction, and for each of its constituent chiral tubes. Also, we carried out a numerical evaluation of the reaction enthalpy of formation of the heterojunction. Based on these results it can be concluded that the investigated molecular compounds can be used to create highly sensitive sensors.

9339-35, Session PSun

Structure and properties of composites based chitosan and carbon nanostructures: atomistic and coarse-grained simulation

Olga E. Glukhova, Anna S. Kolesnikova, Olga A. Grishina, Mikhail M. Slepchenkov, N.G. Chernyshevsky Saratov State Univ. (Russian Federation)

At the present time actual task of the modern materials is the creation of biodegradable biocompatible composite materials possessing high strength properties for medical purposes. One of the most promising biomaterials from a position of creation on their basis super strong nanofibres is chitosan. The aim of this work is a theoretical study of the structural features and physico-mechanical properties of biocomposite materials based on chitosan and carbon nanostructures. As matrix nanocomposite we considered various carbon nano-objects, namely carbon nanotubes and graphene.

Using the developed original software complex «KVAZAR» we built atomistic and coarse-grained models of the biocomposite material. To identify regularities of influence of the configuration of the carbon matrix on the mechanical and electronic properties of biocomposite we carried out a series of numerical experiments using a classical algorithm of molecular dynamics and semi-empirical methods. Quantitative estimation of the elastic modulus of the composite biomaterial was performed. The regularities of the electron density distribution for created biocomposite are established.

The obtained results allow us to suggest that the generated biocomposite based on chitosan and carbon nanostructures has high stability and strength

characteristics. Such materials can be used for example in biomedicine as a base material for creating of artificial limbs.

9339-36, Session PSun

**Development of new turn-on fluorescent probes for prostate cancer imaging
(Invited Paper)**

Takao Yogo, Keitaro Umezawa, Mako Kamiya, Yasuteru Urano, The Univ. of Tokyo (Japan)

Prostate cancer is one of the most common malignant tumors among adult men, and incidence rates of prostate cancer have dramatically increased. Radical prostatectomy is known as a standard operative remedy for prostate cancer, because naked-eye discrimination of small prostate cancer during surgery is severely limited. However, resecting entire prostate gland and surrounding tissue, including nerves in some cases, would carry a risk of erectile dysfunction. Nowadays, fluorescence visualization of tumors is highly expected as a powerful tool for image-guided surgery. Therefore, we aimed at developing a new fluorogenic probe for prostate cancer, which can enable complete removal of tiny tumors without injuring nerves.

Previously, we developed a highly sensitive fluorescent probe targeted to gamma-glutamyltransferase (GGT) based on Hydroxymethyl-Rhodamine Green (HMRG), and succeeded in visualizing GGT-overexpressing tiny tumors.[1] In order to develop a probe of our aim, here we focused on hepsin, a protease which is over-expressed on the cell membrane of prostate cancer cells. By incorporating hepsin-specific peptides (Ac-KQLR, Ac-QRR) to HMRG scaffold, we designed and synthesized new fluorescent probes targeted to hepsin (Ac-KQLR-HMRG and Ac-QRR-HMRG).

The developed probes could sensitively and quickly react with hepsin in vitro to yield the fluorescent increase up to 50 fold. Furthermore, live-cell imaging using tumor/normal cells revealed that significant fluorescence increase was observed only in case of prostate cancer cell lines. Consequently, we succeeded in developing prostate-cancer-specific fluorescent probes, and further applications (in vivo imaging and clinical sample) are now under investigation.

[1] Y. Urano et al. Sci. Transl. Med. 3, 110ra119(2011)

9339-37, Session PSun

Biomedical applications involving multiphoton probes

Mary J. Potasek, Karl Beeson, Evgueni Parilov, Simphotek Inc. (United States)

Many techniques in biological and clinical science use multiphoton absorbers for fluorescence. The applications include medical imaging for living cells, diagnostic techniques for disease and spectroscopy. The intrinsic value of the multiphoton absorber coefficients is therefore of the utmost importance. Additionally, the laser intensity at which the absorber saturates can determine which absorber, dye or protein is useful for a particular application.

Yet, experimental methods for determining the optical coefficients often yield different results. Furthermore many traditional investigations of saturation in multiphoton absorbers use an approximate analytical formula that assumes a steady-state approximation. Using a numerical simulation for Maxwell's equations and coupled electron population dynamics, we show how to analyze the different methods used to measure multiphoton absorbers and; also, show that the commonly used analytical formula for determining saturation in multiphoton absorbers is often not correct. We fit experimental data and obtain values for multiphoton absorbers that accurately reflect their intrinsic values. We also present the optical properties of a large number of multiphoton materials used in biology.

**Conference 9339: Reporters, Markers, Dyes, Nanoparticles,
and Molecular Probes for Biomedical Applications VII**

9339-1, Session 1

Cytotoxic mechanism of silica-phthalocyanine-based near infrared photoimmunotherapy *(Invited Paper)*

Hisataka Kobayashi, National Cancer Institute (United States)

Near infrared (NIR) photoimmunotherapy (PIT) is a newly developed, molecularly-targeted cancer photo-therapy based on conjugating a near infrared silica-phthalocyanine dye, IR700, to a monoclonal antibody (MAb) thereby targeting cancer-specific cell-surface molecules. When exposed to NIR light, the conjugate induces a highly-selective necrotic cell death only in receptor-positive MAb-IR700-bound cancer cells. Necrosis occurs as early as 1 minute after exposure to NIR light and results in irreversible morphologic changes on target-expressing cells including cellular swelling, bleb formation, and rupture of vesicles due to membrane damage. Meanwhile, immediately adjacent receptor-negative cells are unharmed. We have investigated NIRPIT-induced membrane damages from the physical, chemical and biochemical perspective. Three-dimensional dynamic observation of tumor cells undergoing PIT along with quantitative phase contrast microscopy showed rapidly swelling in treated cells immediately after light exposure suggesting rapid water influx into cells. Using a hyperosmolar culture with high dextran concentration, cells did not expand, but rather decreased in size. Even after maximally damaging the cell membrane, minimal oxidative changes were found in phosphatidylcholine by a high sensitivity lipid mass spectroscopy. However, by exposing the cell to NIR light, the silica-phthalocyanine dye ligated and released a side chain containing sulfonic acid that converted IR700 from highly hydrophilic to strongly hydrophobic. The photo-induced ligand exchange reaction led to aggregation of the conjugate along with all directly associated proteins leading to a compromise in the membrane pressure and an imbalance in the osmotic pressure between inside and outside of cells. This theory could explain the high cellular specificity of NIRPIT-induced cytotoxicity.

9339-2, Session 1

NIR fluorescent silica nanoparticles as reporting labels in bioanalytical applications *(Invited Paper)*

Gabor Patonay, Maged Henary, Gala Chapman, Georgia State Univ. (United States)

The use of the NIR spectral region (650-900 nm) is advantageous due to the inherently lower background interference in biological matrices and the high molar absorptivities of NIR chromophores. NIR carbocyanines are increasingly used in analytical, bioanalytical and medical applications. These dyes can be used as reporter labels for sensitive bioanalytical use, such as immunochemistry. Due to their sensitivity for polarity changes in the microenvironment fluorescence quantum yield can vary dependent on the environment. NIR dyes typically have relatively low fluorescent quantum yield as compared to visible fluorophores, especially in aqueous buffer but the lower quantum yield is compensated by much higher molar absorptivities. The fluorescence intensity of NIR reporting labels can significantly be increased by enclosing several dye molecules in silica nanoparticles. The use of NIR dyes in silica nanoparticles creates a unique challenge as the dyes can be unstable under certain conditions. Self quenching may also become a problem for carbocyanines at higher concentrations that typically found in silica nanoparticles. Dyes possessing high Stokes' shift can significantly decrease this problem. NIR dyes are uniquely positioned for achieving this goal by substituting meso position halogens in NIR fluorescent carbocyanines with a linker containing amino moiety, which also serves as a linker to covalently attach the dye molecule to the nanoparticle backbone. The resulting silica nanoparticle can contain a large number of NIR dyes dependent on the size. For example some NIR fluorescent silica nanoparticle labels developed in our laboratory has an average radius around 15 nm, containing 16-20 covalently attached dye

molecules inside of the nanoparticle. The primary applications of these particles are for bright fluorescent labels that can be used in applications such as immunochemistry, flow cytometry, etc.

9339-3, Session 1

Multi-molecular imaging of cancer cells and leukocytes is critical for accurate micrometastasis monitoring using activatable probes

Bryan Q. Spring, Akilan Palanisami, Tayyaba Hasan, Harvard Medical School (United States) and Massachusetts General Hospital (United States)

Molecular-targeted, activatable probes are emerging for optical biopsy of cancer. An underexplored potential clinical use of this approach is to monitor and treat residual cancer micrometastases that escape surgery and chemotherapy. We recently reported a platform for activatable photoimmunotherapy and in vivo microendoscopy of residual metastases that enables high-fidelity imaging and treatment of cancer cells. This talk will discuss non-specific uptake of activatable probes by leukocytes, or white blood cells, residing in non-tumor tissues as well as micrometastatic lesions, and methods to overcome this challenge to accurate tumor recognition.

9339-4, Session 1

Results of the first-in-human clinical trial for MB-102, a novel fluorescent tracer agent for real-time measurement of glomerular filtration rate

Richard B. Dorshow, Martin P Debreczeny, MediBeacon, LLC (United States); Thomas C Dowling, Ferris State University (United States)

The fluorescent tracer agent 2,5-bis[N-(1-carboxy-2-hydroxy)]carbamoyl-3,6-diaminopyrazine, designated MB-102, has been developed with properties and attributes necessary for use as a direct measure of glomerular filtration rate (GFR). Comparison to known standard exogenous GFR agents in animal models has demonstrated an excellent correlation. A clinical trial to demonstrate this same correlation in humans is in progress. This clinical trial is the first in a series of trials necessary to obtain regulatory clearance from the FDA. We report herein the comparison of plasma pharmacokinetics between MB-102 and the known standard exogenous GFR agent Iohexol in human subjects recruited to have normal renal function. In addition, a prototype noninvasive fluorescence detection device was employed to simultaneously measure the transdermal fluorescence from MB-102 in these same subjects. Blood samples over a period of 12 hours were collected from each subject to assess pharmacokinetic parameters including half-life, area under the curve, and clearance. Urine samples were collected over this same period to assess percent injected dose recovered in the urine. Transdermal fluorescence was measured for over 4 hours post administration of the agent to assess correlation with the plasma pharmacokinetics. Results indicate MB-102 is a GFR agent in humans from the comparison to the standard agent, and yield a strong correlation between the plasma and fluorescence pharmacokinetics.

**Conference 9339: Reporters, Markers, Dyes, Nanoparticles,
and Molecular Probes for Biomedical Applications VII**
9339-5, Session 1
**Ratiometric cellular sensor based on
J-aggregate trapping in liposomes (*Invited
Paper*)**

Albert Lee, The Univ. of Texas at Austin (United States) and The Univ. of Texas M.D. Anderson Cancer Ctr. (United States); Geoffrey P. Luke, Stanislav Y. Emelianov, The Univ. of Texas at Austin (United States); Konstantin V. Sokolov, The Univ. of Texas at Austin (United States) and The Univ. of Texas M.D. Anderson Cancer Ctr. (United States)

We present a ratiometric cellular sensor based on highly-concentrated indocyanine green (ICG) dye entrapped inside liposomes. ICG molecules are known for their ability to form J-aggregates at high concentrations which exhibit two pronounced absorbance peaks at ca. 780 and ca. 890 nm. Upon dissociation of J-aggregates the ICG spectrum undergoes a blue shift and is characterized by a strong peak at 800 nm and a shoulder at ca. 740 nm. These spectral changes provide an opportunity to develop a ratiometric sensor. Our strategy is to trap ICG molecules at a high concentration inside liposomes thus preserving J-aggregates. Antibody conjugation to ICG-loaded liposomes can render their molecular specificity. Molecular interactions between targeted ICG-loaded liposomes and cells would result in release of ICG molecules and spectral changes that are associated with dissociation of J-aggregates can be detected using spectroscopic photoacoustic imaging deep inside tissue in vivo. We have successfully synthesized sub-200 nm ICG-loaded liposomes and demonstrated formation of J-aggregates. Disruption of liposomes using Triton detergent leads to dissociation of J-aggregates and spectral changes from peaks at 780 and 890nm to 740 and 800nm along with a large increase in optical density. Furthermore, interactions between ICG-loaded liposomes and macrophages (J774A.1) results in an onset of ICG fluorescence that is co-localized with the cells indicating intracellular release of the dye. Therefore, unique optical properties of ICG molecules can be used in development of liposome based ratiometric cellular sensors for photoacoustic and fluorescent imaging modalities.

9339-6, Session 1
**Spectroscopic characterization of the
binding mechanism of fluorescein and
carboxyfluorescein in human serum
albumin**

Saba A. J. Sulaiman, Sultan Qaboos Univ. (Oman); H. Udani Kulathunga, Sultan Qaboos Univ (Oman); Osama K. Abou-Zied, Sultan Qaboos Univ. (Oman)

Fluorescein (FL) has been used as a fluorescent tracer in medical applications due to its high quantum yield of fluorescence in physiological conditions. It is used as a probe to measure the permeability of the human blood-ocular barriers. However a rapid metabolic mechanism to a weakly fluorescent conjugate (FL-monoglucuronide) was reported. In order to minimize the metabolic effect on FL, the molecule was used as a tracer after binding to human serum albumin (HSA). But when FL is administered systemically to study its rate of penetration through the blood-ocular barrier, the degree of its binding to albumin may affect the observed results. In this regard, a detailed characterization of the binding between FL and HSA is beneficial. In the present work, we characterize the binding properties of the HSA-FL complex using steady-state and time-resolved fluorescence measurements. Binding of FL in HSA causes partial quenching of the intensity and a reduction in the lifetime of the fluorescence of W214 (the sole tryptophan in HSA) which is located in subdomain IIA binding site (Site I). We estimated the distance between FL and W214 to be 2.42 nm using Förster's resonance energy transfer theory. The close proximity of FL to W214, along with the calculated quenching rate constant (k_q

= $5.13 \times 10^{12} \text{ M}^{-1} \text{ s}^{-1}$) using the Stern-Volmer equation, indicates that FL binds in Site I of HSA. By carrying out a site-competitive experiment, we determined the location of FL in Site I to be similar to that of the binding of the anticoagulant drug warfarin. Changing the concentration of FL and HSA enabled the calculation of the binding constant between FL and W214 using the signal change in the fluorescence of HSA and the absorbance of FL. The calculated value ($K = 10,000 \text{ M}^{-1}$) points to a moderate binding strength. The local environment around the FL molecule in the binding site is close to some of the properties of water and a polar, aprotic solvent such as DMSO. Our results indicate that FL is chemically stable inside HSA, and that the moderate binding strength of the FL-HSA complex should not affect the FL release to the target when used as a probe. Finally, molecular dynamics simulations show that the warfarin binding site has a large degree of flexibility and heterogeneity which explain the high affinity of the site for binding versatile molecular structures including several drugs.

9339-7, Session 2
**Energy transfer between host and dopant
in lanthanide-based nanoparticles for
imaging and photodynamic therapy**

Brian G. Yust, The Univ. of Texas-Pan American (United States); Francisco J. Pedraza, Dhiraj Kumar Sardar, The Univ. of Texas at San Antonio (United States)

Recently, there has been a great deal of interest in fluorescent and upconverting lanthanide-based nanoparticles for biomedical imaging and photodynamic therapy applications. In most cases, these nanoparticles are singly or doubly doped, and the dopants are directly excited at real energy levels to provide emission that can be used for cellular imaging or activation of photodynamic compounds. For example, the well known erbium-ytterbium codopant system is often excited at 980 nm where both dopants have an energy level. Since ytterbium does not have any higher energy levels to be excited, the energy is transferred to the erbium or thulium to allow for another excited state absorption which results in visible fluorescence, known as upconversion. Some of the most commonly studied dopant ratios in nanocrystals are very low, between 1 and 20 percent, where the quantum yield is known to be somewhat high. However, very little work has been done exploring emitting ions doped into nanocrystals comprised of lanthanides which can contribute to excited state absorption or Stokes emission through direct energy transfer. Herein, the visible and near-infrared spectroscopy and energy transfer efficiency between lanthanide ions in the host crystal and emitting dopants for a number of different nanoparticles will be explored, such as erbium and thulium doped into KYb2F7, NdF3, and YbF3. The upconversion, Stokes emission, and quantum yield will be compared with well-known systems such as NaYF4: ErYb, and the benefits of each will be discussed. Furthermore, the cytotoxicity and cellular uptake will be discussed.

9339-8, Session 2
**Effects of nanoparticle surface chemistry
on optical properties and cellular
interaction**

Francisco J. Pedraza III, The Univ. of Texas at San Antonio (United States); Brian G. Yust, The Univ. of Texas-Pan American (United States); Ivan Beeks, Andrew Tsin, Dhiraj Kumar Sardar, The Univ. of Texas at San Antonio (United States)

Fluorescent nanoparticles such as KYb2F7:Tm³⁺ nanoparticles have shown potential in biological applications due to their ability to absorb and emit within the biological window. Aside from the nanoparticle's properties, one of the biggest factors in determining their ability to perform in a biological setting is the surface chemistry. When nanoparticles are hydrophobic it

**Conference 9339: Reporters, Markers, Dyes, Nanoparticles,
and Molecular Probes for Biomedical Applications VII**

is common the use biocompatible polymers such as polyethylene glycol (PEG) and polyvinylpyrrolidone (PVP), which offer several advantages including ease of functionalization, hydrophilicity, and nullification of potential toxicity. Other coatings used include pluronic acid and folic acid, which ensure hydrophilicity and prevent nanoparticle aggregation, allowing better dispersion and cellular uptake. Folic acid is also used in photodynamic therapy for targeting since cancerous cells overexpress folate receptors. In order to study the effects of the nanoparticle surface chemistry, KYb2F7:Tm³⁺ nanoparticles were synthesized using PEG, PVP, pluronic acid, and folic acid leaving a coating following the synthesis. The changes in optical properties were examined by collecting absorption and emission spectra as well as the calculation of the absolute quantum yield. To study the effects on the cell viability Rhesus Monkey Retinal Endothelial cells (RHREC) treated with KYb2F7:Tm³ then counted following a 24 hours uptake period. The cellular uptake was studied by incubating RHREC in media containing nanoparticles and imaged live under a Zeiss 710 Live Cell confocal microscope. The effects of the surface modification on optical properties, cytotoxicity, and cellular uptake of various biocompatible coatings on KYb2F7:Tm³⁺ will be discussed.

9339-9, Session 2

Molecule-specific darkfield and multiphoton imaging using gold nanocages

Amy J. Powless, Samir V. Jenkins, Mary Lee McKay, Jingyi Chen, Timothy J. Muldoon, Univ. of Arkansas (United States)

Gold nanostructures have been demonstrated in a variety of biomedical imaging applications to complement currently used contrast agents due to their robust optical properties, biological inertness, and ready conjugation of molecule-specific targeting moieties to the surface.

Gold nanocages (AuNCs), in particular, are hollow, cubic nanoparticles made by galvanic replacement reaction of silver nanoparticles with gold salts. The optical properties are readily controlled by adjusting the quantity of gold used. Therefore, these AuNCs are highly tunable to scatter or absorb at wavelengths that can be tailored to a specific application, for instance, the near infrared region to increase optical depth penetration in bulk tissue.

We have bioconjugated anti-epidermal growth factor receptor (anti-EGFR) antibodies to AuNCs, tuned to preferentially scatter at 700nm, as an optical contrast agent. Following a two-step method, AuNCs (edge length of 53.8nm ± 7.8 nm) were PEGylated using O-pyridyl disulfide-poly(ethylene glycol)-succinimyl valeric acid-activated ester (OPSS-PEG-SVA) by incubating on ice for 4 hours, then bioconjugated to anti-EGFR overnight at 4°C. A human breast adenocarcinoma cell line, MDA-MB-468, which strongly overexpresses EGFR, was successfully immunolabeled with the bioconjugated AuNCs. For comparison, three negative controls were evaluated, unlabeled cells, cells labeled with bare AuNCs, and cells labeled with PEGylated AuNCs. Darkfield images of unlabeled and labeled cells were quantitatively compared to conventional immunofluorescence for validation. Additionally, a time series of multiphoton images were acquired to observe uptake of AuNCs in live cells.

We have demonstrated a method for using tunable gold nanocages for molecular-specific imaging in darkfield and multiphoton microscopy.

9339-10, Session 3

Activatable thermo-sensitive ICG encapsulated pluronic nanocapsules for temperature sensitive fluorescence tomography

Tiffany C. Kwong, Farouk Nouzi, Univ. of California, Irvine (United States); Uma Sampathkumaran, Yue Zhu, Maksudul

M. Alam, InnoSense LLC (United States); Gultekin Gulsen, Univ. of California, Irvine (United States)

Fluorescent tomography has been hindered by poor tissue penetration and weak signal which results in poor spatial resolution and quantification accuracy. Recently, activatable temperature responsive fluorescent probes which respond to focused ultrasound heating have been reported. This has led to our new imaging modality, "Temperature-modulated fluorescent tomography" that provides higher resolution fluorescent tomography in deep tissue with more accurate quantification. This technique relies on activatable thermo-sensitive fluorescent nanocapsules whose fluorescence quantum efficiency is temperature dependent. Within a 4–5°C temperature range, the fluorescent signal increases more than 10-fold and this process is reversible. These thermo-reversible Pluronic micelle encapsulates ICG inside its core and we have further functionalized them with polyethylene glycol (PEG) for in vivo tumor targeting in a carcinogen-induced rat tumor model. Here we show the temperature sensitive response of the probes ex vivo, and report on the feasibility of these temperature sensitive nanocapsules for in vivo applications by studying their pharmacokinetics and toxicity effects in vitro and in vivo.

9339-11, Session 3

Enhancing immunotherapy with magneto-plasmonic nanoparticles

Konstantin V. Sokolov, Chun-Hsien Wu, Figen Beceren-Braun, M. Anna Zal, Tomasz Zal, The Univ. of Texas M.D. Anderson Cancer Ctr. (United States)

Significant progress was made recently on the front of tumor immunotherapy, known as adoptive cell therapy (ACT). However, this highly promising cancer treatment faces two fundamental challenges: (i) inadequate trafficking of infused T cells to tumor sites, and (ii) the inability to readily assess the presence and distribution of T cell subsets in tumor. Here, we describe a novel strategy to addressing these challenges. It is based on dual-function magneto-plasmonic nanoparticles (MPNs) which consist of primary 6 nm iron oxide core-gold shell particles that form highly uniform spherical assemblies with sizes from ca. 70 to 180 nm. Due to the superparamagnetic iron oxide core, the nanoparticles can transduce a mechanical force in response to a magnetic field gradient, thereby allowing magnetically-guided cell steering and deposition, whereas the gold coating endows the particles with strong plasmonic resonances in the near infra-red (NIR) range that can be used for deep tissue photoacoustic (PA) imaging. We demonstrated that MPNs conjugated with anti-CD8 antibodies which are specific for cytotoxic T cells used in ATC label CD8⁺ T cells with high specificity ex vivo and in vivo. Flow cytometry showed high viability of labeled CD8⁺ T cells. Labeled T cells can be easily manipulated by a small ca. 2 mm neodymium magnet in suspension and under flow conditions. Furthermore, MPNs generate high contrast in MRI with the potential to detect few cells per imaging voxel. This study could establish image guided magnetic field-mediated T cell trafficking as a novel approach for enhancing anti-solid tumor immunotherapies.

9339-12, Session 3

Lanthanide (Ln³⁺)-doped calcium molybdate nanoparticle (CaMoO₄:Ln³⁺, Ln=Eu, Tb) based SERS-fluorescence bimodal imaging probes for detection and imaging of fatty acid responsive GPR120 and CD36 receptors

Lifu Xiao, Abdul K. Parchur, Han Xu, Qifei Li, Timothy A. Gilbertson, Anhong Zhou, Utah State Univ. (United States)

Mechanisms of the chemoreception of fatty acids in fat-responsive

**Conference 9339: Reporters, Markers, Dyes, Nanoparticles,
and Molecular Probes for Biomedical Applications VII**

tissues are of great importance to the study of fat intake and treatment of obesity. However, the roles of the cognate receptors in this process remain unclear. To investigate the roles of two receptors (GPR120 and CD36) in fatty acid signaling pathways, we designed a novel approach to detection of GPR120 and CD36 and their distribution in chemosensory cells, based on bi-functional composite nanoparticles that integrate the Surface-enhanced Raman scattering (SERS) and fluorescence functions. This kind of nanoparticle consists of two components: 1) the Lanthanide (Ln³⁺)-doped Calcium Molybdate nanoparticle (CaMoO₄:Ln³⁺, Ln=Eu, Tb), which has intense optical emission in visible light range; 2) the 5 nm gold nanosphere (Au), which is functional for surfaced-enhanced Raman scattering (SERS). The two components were bound together to form a composite nanoparticle (CaMoO₄:Ln@Au). The composite nanoparticle can be conjugated with antibodies to GPR120 and CD36, respectively, for specific targeting. As a model to demonstrate the SERS-Fluorescence bi-functional imaging, we used a HEK293 cell line transfected with cDNA sequences encoding mature peptides of GPR120 and CD36, respectively and simultaneously. Our preliminary data include (1) the structural characterization of the CaMoO₄:Ln@Au (Ln=Eu, Tb) composite nanoparticles; (2) the specificity tests of GPR120 and CD36 antibodies; and (3) SERS and fluorescence images of HEK293 cells expressing GPR120 and CD36. Applications of this SERS-fluorescence bimodal probe in detection of the potential interaction between the two receptors and fatty acid is undergoing.

9339-13, Session 3
**Intracellular delivery of a survivin-specific
theranostic agent by pmma nanoparticles
and carbon nanotubes**

Francesco Baldini, Barbara Adinolfi, Istituto di Fisica Applicata Nello Carrara (Italy); Claudio Domenici, Istituto di Fisiologia Clinica (Italy); Giuliano Giambastiani, Istituto di Chimica dei Composti OrganoMetallici (Italy); Ambra Giannetti, Istituto di Fisica Applicata Nello Carrara (Italy); Mario Pellegrino, Univ. di Pisa (Italy); Giovanna Sotgiu, Istituto per la Sintesi Organica e la Fotoreattività (Italy); Sara Tombelli, Cosimo Trono, Istituto di Fisica Applicata Nello Carrara (Italy); Giulia Tuci, Istituto di Chimica dei Composti OrganoMetallici (Italy); Greta Varchi, Istituto per la Sintesi Organica e la Fotoreattività (Italy)

Theranostic agents coupled to nanoparticles and nanotubes are highly promising and fascinating tools for the intracellular detection and silencing of specific mRNA molecules. The use of an antisense oligonucleotide which acts as molecular beacon (MB) and able to generate a fluorescent signal when it hybridizes with the target mRNA, may represent an innovative strategy that conjugates the ability of sensing specific mRNA with the pharmacological silencing activity preventing the overexpression of proteins associated to pathologic conditions. The mRNA specific for survivin was chosen as target in this work, being survivin overexpressed in cancer cells and at very low levels in most healthy tissues. The MB was characterised in vitro and its functionality was verified in solution and after adsorption onto polymethylmethacrylate (PMMA) fluorescent nanoparticles (NPs) and carbon nanotubes (CNTs). PMMA NPs, CNTs and MB-adsorbed onto these delivery agents were then tested on human lung carcinoma A549 cells and on human dermal fibroblasts (HDFa) as negative controls, in terms of cell vitality and internalization. These experiments provided a clear evidence of the subcellular distribution of nanoparticles and nanotubes in living cells and of their ability to promote the MB internalization.

9339-14, Session 3
**Regulatory section: chemistry
requirements for marketing imaging
agents**

Ramesh Raghavachari, U.S. Food and Drug Administration
(United States)

No Abstract Available

9339-15, Session 4
**Water-soluble polymer photoswitch based
on dithienylethene-naphthalimide dyad as
lysosensor for super-resolution bioimaging**

Ming-Qiang Zhu, Huazhong Univ. of Science and
Technology (China)

A novel photoswitchable fluorescent monomer (DTE-NI), in which a dithienylethene (DTE) unit was used as the photoswitchable quencher against a highly-emissive and pH sensitive naphthalimide (NI) unit, in conjunction with a polymerisable vinyl group was synthesized. Copolymerization of DTE-NI with N-isopropylacrylamide (NIPAM) gave water-soluble photoswitchable fluorescent polymer Poly[NIPAM-co-(DTE-NI)] (polymer 1). Compared with the corresponding DTE-NI small molecule that is limited in functionalizable modification, the polymer that integrates controllable hydrophilic NIPAM units and pre-designed fluorescent switching units exhibits good aqueous solubility and biocompatibility. We have utilized polymer 1 as a fluorescent probe in cellular imaging. It is noteworthy that the fluorescence of polymer 1 is pH sensitive which is beneficial for intracellular target recognition in acidic microenvironment structures like lysosome. The localization-based super-resolution fluorescence imaging demonstrated that sub-40nm spatial resolution was obtained. It is concluded that dithienylethene-containing photoswitchable fluorescent polymer is promising as new-generation imaging agents and would enhance the development of photoswitchable fluorescent macromolecules for super-resolution fluorescence bioimaging.

9339-16, Session 4
**Development of bright green, maturation
improved, reversibly switchable
fluorescent proteins based on EGFP**

Sam Duwé, Elke De Zitter, Benjamien Moeyaert, Vincent
Gielen, Johan Hofkens, Peter Dedecker, Katholieke Univ.
Leuven (Belgium)

Recent developments in fluorescent protein (FP) technology have made FPs essential as 'smart labels' for biosensing and advanced fluorescence imaging. Photoswitchable and photoconvertible FPs for example play a crucial role in superresolution microscopy, but still require optimization to access the entire potential. The recently developed EGFP-based reversibly switchable (RS) FP, rsEGFP, has outstanding properties in terms of photoswitching speed and stability, but has low brightness when expressed in vitro at 30-37 °C, due to reduced maturation and folding. We aimed to develop a new RSFP with improved brightness and similarly good photoswitching behavior.

The gene encoding rsEGFP was fused to a bait-peptide sequence, that interferes with the folding/maturation, and subjected to mutagenesis. A homebuilt E. coli colony screening-system was used to select a 20-fold brighter FP with slightly slower off-switching and reduced contrast. A single backmutation sufficed to increase the switching speed and contrast, but decreased the brightness to 10 times that of rsEGFP. Further random

**Conference 9339: Reporters, Markers, Dyes, Nanoparticles,
and Molecular Probes for Biomedical Applications VII**

mutagenesis resulted in a series of RSFPs up to 30 times brighter than rsEGFP with similar or improved photoswitching speed and stability, and enhanced contrast. In vitro protein expression revealed greatly enhanced maturation kinetics for all created RSFPs compared to rsEGFP, while all FP's exhibited similar quantum yield, extinction coefficient and pKa values. Improvements to photoswitching and brightness were explained with structural information from x-ray crystallography. All mutants were shown to localize perfectly in several fusion constructs and were used for superresolution microscopy using pcSOFI, which makes optimal use of the reversible photoswitching.

9339-17, Session 4

In vivo detection of cancer cells with immunoconjugated fluorescent probes by macro zoom microscopy and two-photon microscopy

Shigehiro Koga, Yusuke Oshima, Atsuhiko Hikita, Ehime Univ. (Japan); Koichi Sato M.D., Motohira Yoshida M.D., Yuji Yamamoto M.D., Tadahiro Iimura D.D.S., Ehime University (Japan); Yuji Watanabe, Takeshi Imamura, Ehime Univ. (Japan)

Main advantages of the optical imaging technique include achieving high spatiotemporal resolution without radiation exposure, and low cost as compared with conventional clinical imaging techniques such as CT, MRI and PET. Although a large number of research have been reported as regards fluorescence imaging with immunoconjugated probes for cancer detection, it is difficult to distinguish cancer-specific fluorescent signal and background noise including nonspecific signal from the fluorescent probe and intrinsic autofluorescence under wide-field fluorescence microscopy. In this study, to apply fluorescence imaging techniques for clinical settings, we prepared near infrared (NIR) fluorophore-conjugated anti-CEA antibody for mice bearing tumor of CEA expressing cells. CEA expressing cancer cells were inoculated subcutaneously into nude mice. One week after the inoculation, tumor mass was exposed and observed by a fluorescence macro/zoom microscope and a two-photon microscope 24 hours after injection of the NIR fluorophore-conjugated anti-CEA antibody via the tail vein. In the result, tumors of CEA expressing cancer cells were specifically detected in vivo on the macro/zoom fluorescence microscope. Furthermore, cancer-specific fluorescent signal of CEA expressing cancer cells was captured in vivo by a two-photon microscope. In addition, we generated spontaneous lymph node metastasis model mice for micro-lesions in the early phases of cancer. The lymph node metastasis was successfully visualized only by two-photon microscopy. These results suggest that two-photon excitation microscopy in conjunction with an immunoconjugated probe could be widely adapted to detection of cancer-specific molecular targets in clinical applications of fluorescence imaging technique.

9339-18, Session 4

In vitro and in vivo investigation of pH tumor status using genetically encoded sensors and fluorescence imaging

Elena V. Zagaynova, Marina V. Shirmanova, Irina N. Druzhkova, Maria Lukina, Ludmila B. Snopova, Natalia N. Prodanetz, Nizhny Novgorod State Medical Academy (Russian Federation); Vsevolod V. Belousov, Sergey A. Lukyanov, M. M. Shemyakin and Yu. A. Ovchinnikov Institute of Bioorganic Chemistry (Russian Federation) and Nizhny Novgorod State Medical Academy (Russian Federation)

Introduction. The increased glycolytic activity in tumors there is formed a reverse gradient of pH. Intracellular pH of tumor cells is more alkaline compared to normal cells of the organism, and extracellular pH of a tumor is more acidic. The intracellular pH plays the main role in regulation of activity of glycolic enzymes and formation of the effect of multi-drug resistance. Materials and methods. To analyze intracellular pH there were used cancer cell lines stably expressing a genetically encoded sensor of cytosolic localization. The sensor has two excitation peaks of fluorescence (at about 420 and 500 nm) which allows ratiometrically calculate pH value. In alkaline medium there is a proportional decrease of the peak at 420 nm and an increase of the peak at 500 nm. Ratiometric assessment of a sensor signal was performed by fluorescence microscopy and macroimaging. There were developed methods of assessment of intracellular pH level in tumor cells culture, spheroids and animal's tumors. Results. In the in vitro system have been shown, that in more alkaline conditions excitation maxima of genetically encoded sensor at 420 nm decreased and at 500 nm increased, resulting in increase of the I500/I420 ratio. The cells were injected subcutaneously to nude mice to generate tumors, and whole body fluorescence imaging was performed in vivo to visualize the indicator emission at 520 nm. Calculation of the I500/I430 ratio showed that the signal of the sensor in HeLa tumor is highly heterogeneous, which indicates differences in pHi value in a tumor tissue. The data of the fluorescence imaging were confirmed by histopathological investigation and hypoxia analysis on the tumor tissue sections.

9339-19, Session 5

Fluorescence characterization of water-driven self-assembled lipids and their temperature-induced phase transitions

N. Idayu Zahid, Univ. of Malaya (Malaysia); Osama K. Abou-Zied, Sultan Qaboos Univ. (Oman); Rauzah Hashim, Univ. of Malaya (Malaysia)

Water-driven self-assembly of lipids displays a variety of liquid crystalline phases that are crucial for membrane functions. In this work, we characterized the temperature-induced phase transitions in aqueous self-assembly systems using steady-state and time-resolved fluorescence measurements. The phase transitions were investigated using tryptophan (Trp) and two of its ester derivatives (Trp-C4 and Trp-C8) to probe the polar head group region and pyrene to probe the hydrophobic tail region. We estimated the polarity of the head group region to be close to that of simple alcohols for all phases. We detected a basic medium that is equivalent to an aqueous solution of pH \approx 10.0 in the polar head group region for the inverse cubic phase of a Guerbet glycolipid. The basic effect is attributed to the restricted motion of water in the nanochannels (diameter of 2.3 nm) in which water molecules are situated very close to the OH groups of the sugar units. The very small channels also force the tryptophan moiety to be very close to the sugar units and the water molecules in which the local environment is mostly basic. The pyrene fluorescence indicates that the pyrene molecules are dispersed among the tails of the hydrophobic region, yet remain in close proximity to the polar head groups. The ratio of the vibronic peak intensities of pyrene (I1/I3) is used as a benchmark to determine the relative polarity of the hydrophobic region in the different phases. All the studied lipid compositions show completely reversible temperature-induced phase transitions, reflecting the thermodynamic equilibrium structures of their mesophases. Probing both regions of the different lipid phases reveals a large degree of heterogeneity and flexibility of the lipid self-assembly. These properties are crucial for carrying out different biological functions such as the ability to accommodate various molecular sizes.

**Conference 9339: Reporters, Markers, Dyes, Nanoparticles,
and Molecular Probes for Biomedical Applications VII**

9339-20, Session 5

Imaging small biomolecules in live cells and animals by stimulated Raman scattering of alkyne vibrational tags

Lu Wei, Fanghao Hu, Yihui Shen, Zhixing Chen, Columbia Univ. (United States); Yong Yu, Chih-Chun Lin, Meng C. Wang, Baylor College of Medicine (United States); Wei Min, Columbia Univ. (United States)

Innovations in optical microscopy have tremendously expanded our knowledge at the microscopic level. Fluorescence microscopy, in particular, with the advent of versatile fluorescent tags, enables imaging molecules of interest with high specificity and sensitivity. However, common fluorescent tags are relatively bulky and thus perturbative when used to tag small biomolecules, such as nucleosides, amino acids, choline, fatty acids and drugs. Herein, we report an effective and novel chemical imaging platform, apart from fluorescence microscopy, to image a broad spectrum of small biomolecules in live cells by the coupling of alkyne moieties (i.e., C≡C) as nonlinear vibrational tags with stimulated Raman scattering (SRS) microscopy. Alkynes, as tags, are small (only two atoms), exogenous (nearly non-existent inside cells) and bioorthogonal (inert to reactions with endogenous biomolecules). In addition, alkynes exhibit a distinctly strong Raman peak in the cell-silent Raman region. SRS microscopy, a nonlinear vibrational imaging technique, offers distinctive advantages such as Raman amplification, bond-selectivity, background-free and biocompatibility. Thus, the coupling of alkyne tags with SRS microscopy offers sensitivity, specificity and biocompatibility for probing small biomolecules in living systems with minimum perturbation. We have demonstrated this technique by tracking alkyne-bearing drugs in mouse tissues and visualizing de novo synthesis of DNA, RNA, proteins, phospholipids and triglycerides through metabolic incorporation of alkyne-tagged small precursors (nucleosides, amino acids, choline, fatty acids) in live cells. Hence, SRS imaging of alkynes may do for small biomolecules what fluorescence imaging of fluorophores has done for larger species. Wei L et al. *Nat. Methods*, 11, 410 (2014)

9339-21, Session 5

A bi-functional contrast agent for simultaneous optical and magnetic resonance imaging in vivo

Alex T. Luk, Gultekin Gulsen, Univ. of California, Irvine (United States); Mehmet B. Unlu, Bogaziçi Üniv. (Turkey); Melissa Ali-Santosa, Cindy R. M. Rodas, Joey E. Pazzi, Univ. of California, Irvine (United States)

Diffuse optical tomography (DOT) has the ability to non-invasively provide functional and molecular information, but is limited by its low spatial resolution and quantitative accuracy due to the highly scattering nature of biological tissue. Multi-modality techniques have been developed to overcome the inherent limitations of optical imaging by utilizing anatomical information as a priori to improve the optical imaging reconstruction process. However, intrinsic optical and MR signals do not necessarily overlap fully, which is especially true for tumors. In contrast, a bi-functional contrast agent can provide a perfect platform for multi-modality studies by providing both optical and MR contrast simultaneously. We report the results of a novel polymer based bi-functional MRI-optical contrast agent (Gd-DTPA-polylysine-IR800) designed specifically for simultaneous MR and optical imaging by our industrial collaborators from GE Global Research. This multi-modal probe combines gadolinium, which is an FDA approved MRI contrast agent with optical contrast agent IR800 to cross validate DOT dynamic reconstruction results with DCE-MRI images. In vivo studies of this bi-functional agent were performed on rats bearing R3220 breast cancer model through the tail vein injection. The pharmacokinetics of the agent was monitored in the tumor and bladder by a hybrid MRI-DOT system. Diffuse optical tomography reconstruction results of this bifunctional contrast agent

with and without a priori MR anatomical information have been compared and cross-validated with the DCE-MRI results.

9339-22, Session 5

Radionuclide mediated x-ray and optical signal amplification for quantitative imaging of infection and cancer

Michael A. McDonald, Johns Hopkins Medicine (United States)

A model system is presented that utilizes radionuclide mediated secondary X-ray fluorescence via photoelectron absorption in nonradioactive dye-tagged molecules for single photon emission computed tomography (SPECT) signal amplification. Secondary fluorescence is demonstrated in a CZT detector-based SPECT imaging system and tissue-equivalent phantoms incorporating low concentrations of Iodine-125 or Iodine-123 as well as nonradioactive Barium at relatively higher concentration. Spatiotemporal correlation is made with X-ray induced visible fluorescence using resonance energy transfer pairs. Data is presented demonstrating significantly increased signal intensity at lower administered radionuclide dose than typically utilized for diagnostic studies. Quantification and detection of Barium at orders of magnitude lower concentration than currently used for X-ray contrast is demonstrated. It is envisioned that this method of signal amplification via secondary ionizations-- which can occur tens of microns away from the site of primary radionuclide excitation-- can be manipulated to enhance the signal from precancerous breast tissue such as ductal carcinoma in situ (DCIS) subsequent to radionuclide targeting and incorporation of nonradioactive molecules shown to have increased uptake in DCIS (e.g., gadolinium, trace elements, etc.). Preliminary work demonstrating signal amplification in vitro in breast cancer cell lines and tuberculosis culture is presented, including initial attempts at using the ionophore Beauvericin to enhance intracellular accumulation of Barium.

9339-23, Session 5

Quantum dots targeted to VEGFR2 as a contrast agent for OCT/LIF dual-modality imaging of colorectal cancer in a mouse model

Jordan L. Carbary, Jennifer K. Barton, Urs Utzinger, The Univ. of Arizona (United States)

Optical Coherence Tomography/Laser Induced Fluorescence (OCT/LIF) dual-modality imaging allows for minimally invasive, non-destructive endoscopic visualization of colorectal cancer in mice. This technology allows for the longitudinal tracking of morphological (OCT) and biochemical (fluorescence) changes simultaneously as colorectal cancer forms, compared to current methods of colorectal cancer screening in humans which rely on morphological changes alone. Ideally, the contrast agent used for this system should not compete with autofluorescence of the tissue or with the OCT wavelength range. NIR quantum dots (QD) have great potential as contrast agents for this dual-modality approach. We have shown that QDot655 targeted to vascular endothelial growth factor receptor 2 (VEGFR2) (QD655-VEGFR2) can be applied to the colon of carcinogen treated mice in vivo and provide significantly increased contrast between the diseased and undiseased tissue with high sensitivity and specificity. In this study, QD655-VEGFR2 was used in a longitudinal in vivo study on the ability to correlate early fluorescence signal to tumor development over time. QD655-VEGFR2 was applied to the colon of AOM or saline treated mice in vivo via lavage. OCT/LIF images of the distal colon were taken at five consecutive time points 3, 6, 9, 12 and 15 weeks post AOM injection. Tumors in the OCT images were then compared to the fluorescence intensity maps of the QDot655 signal to determine when VEGFR2 expression begins in the disease process. Fluorescence signal correlated with developing

**Conference 9339: Reporters, Markers, Dyes, Nanoparticles,
 and Molecular Probes for Biomedical Applications VII**

morphological changes in the OCT images, providing early indication of disease and biochemical information on the tumors.

9339-40, Session Plen

**Bridging molecular and cellular biology
 with optics**

Gabriel Popescu, Univ. of Illinois at Urbana-Champaign
 (United States)

No Abstract Available

9339-24, Session 6

**Silica nanoparticles containing
 therapeutics for attenuation of oxidative
 stress in neurons (*Invited Paper*)**

Desiree White-Schenk, Riyi Shi, James F. Leary, Purdue
 Univ. (United States)

Oxidative stress plays a major role in many disease pathologies, notably in the central nervous system (CNS). For instance, after initial spinal cord injury, the injury site tends to increase during a secondary chemical injury process based on oxidative stress from necrotic cells and the inflammatory response. Prevention of this secondary chemical injury would represent a major advance in the treatment of people with spinal cord injuries.

Few therapeutics are useful in combating such stress in the CNS due to side effects, low efficacy, or half-life. Mesoporous silica nanoparticles show promise for delivering therapeutics based on the formation of a porous network during synthesis. Ideally, they increase the circulation time of loaded therapeutics to increase the half-life while reducing overall concentrations to avoid side effects. The current study explored the use of silica nanoparticles for therapeutic delivery of anti-oxidants, in particular, the neutralization of acrolein which can lead to extensive tissue damage due to its ability to generate more and more copies of itself when it interacts with normal tissue.

Both an FDA-approved therapeutic, hydralazine, and natural product, epigallocatechin gallate, were explored as anti-oxidants for acrolein with nanoparticles for increased efficacy and stability in neuronal cell cultures. Not only were the nanoparticles explored in neuronal cells, but also in a co-cultured in vitro model with microglial cells to study potential immune responses to near-infrared (NIRF)-labeled nanoparticles and uptake. Studies included nanoparticle toxicity, uptake, and therapeutic response using fluorescence-based techniques with both dormant and activated immune microglia co-cultured with neuronal cells.

9339-25, Session 7

**New method to detect organic
 nanoparticles in live tissue (*Invited Paper*)**

Dror Fixler, Inbar Yariv, Bar-Ilan Univ. (Israel)

In recent years, infiltrating materials into the human body has become a great challenge many researches are facing. Recently nanoparticles (NPs) are being evaluated for use, in many fields. It is well known that when the particle size decreases, the proportion of the surface area increases, which predicts greater biological activity per given mass compared to larger particles. By using NPs it will be possible to infiltrate materials to the patient's body without the need for injection, but by transdermal delivery only. For this purpose we fabricated NPs and developed a technique that can detect them within tissues. The technique used in this work for forming organic NPs (ONPs) is the application of sonic waves to a solution, known as sonochemistry. In the present study, we present for the first time the fabrication of Vitamin B12 and Penicillin NPs by the sonochemistry technique and the enhanced activity of Vitamin B12, Penicillin and MB in comparison to the bulk form. In this work is a new optical technique for extracting the reduce scattering confidence (μ_s) which based on an optical iterative method for phase retrieval known as the Gerchberg-Saxton (G-S) algorithm. The objective of this work is to bring us closer to determining the penetration depth of NPs within tissues, through a new technique combining an experimental setup and iterative G-S algorithm.

Conference 9340: Plasmonics in Biology and Medicine XII

Saturday - Sunday 7-8 February 2015

Part of Proceedings of SPIE Vol. 9340 Plasmonics in Biology and Medicine XII

9340-2, Session 1

DNA origami based assembly of gold nanoparticle dimers for surface enhanced Raman scattering

Vivek Thacker, Lars O. Herrmann, Daniel O. Sigle, Univ. of Cambridge (United Kingdom); Tao Zhang, Tim Liedl, Ludwig-Maximilians-Univ. München (Germany); Jeremy J. Baumberg, Ulrich F. Keyser, Univ. of Cambridge (United Kingdom)

Plasmonic sensors are extremely promising candidates for label-free single molecule analysis but require exquisite control over the physical arrangement of metallic nanostructures. We employ self-assembly based on the DNA origami technique [1] for accurate positioning of individual gold nanoparticles. Our innovative design leads to strong plasmonic coupling between two 40 nm gold nanoparticles reproducibly held with gaps of 3.3 ± 1 nm. This is confirmed through far field scattering measurements on individual dimers which reveal a significant red shift in the plasmonic resonance peaks, consistent with the high dielectric environment due to the surrounding DNA. We use surface enhanced Raman scattering (SERS) [2] to demonstrate local field enhancements of several orders of magnitude through detection of a small number of dye molecules as well as short single-stranded DNA oligonucleotides. This demonstrates that DNA origami is a powerful tool for the high-yield creation of SERS-active nanoparticle assemblies with reliable sub-5 nm gap sizes and has great potential application for a wide variety of biosensing and single-molecule applications.

References

[1] Rothemund, P. W. K. Folding DNA to create nanoscale shapes and patterns. *Nature*, 440(7082), 297-302, (2006).

[2] Nie, S. Probing Single Molecules and Single Nanoparticles by Surface-Enhanced Raman Scattering. *Science*, 275(5303), 1102-1106, (1997).

[3] Thacker, V.V., Herrmann, L.O., Sigle D.O., Zhang T., Liedl T., Baumberg J.J., and Keyser U.F. DNA origami based self-assembly of gold nanoparticle dimers for surface enhanced Raman scattering. *Nature Communications*, 5(3448), (2014).

9340-3, Session 1

Amplifying the SERS signal of DNA bases via the chemical resonance

Lindsay M. Freeman, Lin Pang, Yeshaiahu Fainman, Univ. of California, San Diego (United States)

Label-free detection methods of DNA bases using surface-enhanced Raman spectroscopy (SERS) have yet to be successfully utilized due to inconsistent signal readouts. We have identified the primary reason for the discrepancies in the SERS signals of nucleic acids as being caused by the charge-transfer chemical resonance of the base silver system which is dependent on excitation wavelength.

Time-dependent density functional theory (TD-DFT) methods to calculate the electronic transitions and resonance Raman spectra of base silver complexes are performed, and the optimal excitation wavelength for the charge-transfer electronic transition is found for each base silver complex. The enhancement caused by the chemical resonance is then experimentally measured for adenine, cytosine, guanine and thymine at multiple excitation wavelengths. The dependence of the Raman intensity on excitation wavelength shows good agreement with the TD-DFT calculations.

In order to fully achieve the maximum Raman intensity, both the electromagnetic and chemical resonance must be enhanced by the appropriate wavelength selection. Based on the optimal chemical resonance Raman wavelength, we design a SERS substrate which has an electromagnetic maximum wavelength that matches the chemical resonance wavelength. By aligning both resonances, the highest Raman intensity can be found for each base silver system.

We have proven that the variance in DNA bases' Raman intensities are caused by chemical enhancement. By incorporating the chemical resonance and optimizing both the chemical and electromagnetic resonances, we believe a label-free DNA SERS based detection method can be realized.

9340-38, Session 1

Stamping SERS for creatinine sensing

Ming Li, Wei-Chuan Shih, Univ. of Houston (United States)

Urine can be obtained easily, readily and non-invasively. The analysis of urine can provide metabolic information of the body and the condition of renal function. Creatinine is one of the major components of human urine associated with muscle metabolism. Since the content of creatinine excreted into urine is relatively constant, it is used as an internal standard to normalize water variations. Moreover, the detection of creatinine concentration in urine is important for the renal clearance test, which can monitor the filtration function of kidney and health status. In more details, kidney failure can be imminent when the creatinine concentration in urine is high. A simple device and protocol for creatinine sensing in urine samples can be valuable for point-of-care applications. We reported quantitative analysis of creatinine in urine samples by using stamping surface enhanced Raman scattering (S-SERS) technique with nanoporous gold disk (NPGD) based SERS substrate. S-SERS technique enables label-free and multiplexed molecular sensing under dry condition, while NPGD provides a robust, controllable, and high-sensitivity SERS substrate. The performance of S-SERS with NPGDs is evaluated by the detection and quantification of pure creatinine, mixture of creatinine and urea, and creatinine in artificial urine within physiologically relevant concentration ranges. Moreover, the potential application of our method has been evaluated using urine samples collected from diseased mice models.

REFERENCES:

Ming Li, Jing Lu, Ji Qi, Fusheng Zhao, Jianbo Zeng, Jorn Chi-Chung Yu, and Wei-Chuan Shih, "Stamping surface-enhanced Raman spectroscopy for label-free, multiplexed, molecular sensing and imaging," *Journal of Biomedical Optics* 19(5): 050501, 2014.

9340-4, Session 2

Optimization of gold nanorod arrays for SERS enumeration of CTCs

Jonathan Calderón, Daniel Hill, Maria Isabel Gomez, Univ. de València (Spain)

The enumeration of circulating tumor cells (CTCs) is a promising approach for early cancer detection and frequent monitoring of treatment response. Through the engineering of nanostructured substrates on which targeted CTCs can be directly identified using Surface-Enhanced Raman Spectroscopy (SERS), the unreliability and time consumption of other approaches are avoided. Specifically, when gold is conveniently nanostructured, field enhancements large enough to overcome the low molecular Raman cross-section of adsorbed molecules, such as CTC biomarkers and even single molecules, enable their detection.

**Conference 9340:
Plasmonics in Biology and Medicine XII**

Here, we report on the modelling of gold nanorod array substrates for the enumeration of CTCs by SERS. From the finite element method (FEM), the Localized Surface Plasmon Resonance (LSPR) characteristics of the arrays are calculated, in order to investigate their potential as SERS substrates. Averaging the electric field in a volume around each nanoparticle, an estimation of its suitability for SERS can be obtained. An optimization of the geometrical parameters of the nanostructures (size, aspect ratio and pitch distances) were optimized for an excitation wavelength of 785 nm (a common line in Near IR Raman spectroscopy) and SERS enhancement factors of around 10⁷ were calculated. Based on these results several arrays of Au nanorods were fabricated using electron beam lithography and the 'lift off' process, and we compare LSPR properties from transmittance measurements with theoretical results. Finally we demonstrate the suitability of the structures as SERS substrates by using organic compounds generally used to check SERS activity (crystal violet and Rhodamine 6G) as well as CTCs.

9340-5, Session 2

Silica-coated gold nanostars for surface-enhanced resonance Raman spectroscopy mapping of integrins in breast cancer cells

Michael B. Fenn Jr., Nikša Roki, Chris Bashur, Florida Institute of Technology (United States)

Surface-Enhanced Resonance Raman Spectroscopy (SERRS) has been increasingly demonstrated as a valuable tool for cancer research and diagnosis. Targeted silica-coated gold nanostars (Si@AuNS) were synthesized for high-sensitivity SERRS-based detection and localization of breast cancer cell integrins using high-speed Raman mapping. We tuned the size and morphology of the Si@AuNS to achieve a maximum plasmon resonance matching the 785nm Raman laser-light source. To realize maximum SERRS enhancement, batches of Si@AuNS were coated with one of six different Raman reporter molecules (e.g. rhodamine B isothiocyanate, malachite green isothiocyanate, IR-783) onto the gold surface prior to silica coating. Each reporter molecule exhibited significant Raman scattering enhancement, and spectrally distinct fingerprints potentially allowing a high degree of targeted multiplexing. The Si@AuNS combined with IR-783 Dye provided the greatest SERRS enhancement of all reporters investigated. Nanostars of 60-70nm diameter were coated with an 8-10nm thick silane coating (TEOS/APTES) providing reactive amine groups on the particle surface. Subsequent surface modification was performed using carboximide chemistry. The silane surface was then coated with a combination of mPEG-acid for improved dispersion, and PEG-diacid for conjugation of the targeting biomolecules. Cyclo-RGDf/k peptide was used for targeting integrins of breast cancer cells in-vitro having known high-level integrin expression (e.g. BT549). 2-D and 3-D Raman maps were collected from the cells cultured on collagen and fibronectin-coated MgF2 substrates, and high intensity SERRS signals detected were used to localize integrins. This method could greatly improve the understanding of integrin distribution and expression related to extracellular matrix composition and breast cancer invasiveness.

9340-6, Session 2

DNA-guided assembly of three-dimensional nanostructures for surface-enhanced Raman spectroscopy

Li-An Wu, National Yang-Ming Univ. (Taiwan); Yu-Ting Lin, National Cheng Kung Univ. (Taiwan); Yih-Fan Chen, National Yang-Ming Univ. (Taiwan)

Surface enhancement Raman spectroscopy (SERS) has drawn much attention in recent years because its ability to greatly enhance Raman signals to allow for the detection of molecules at low concentration. When using metallic nanoparticles as SERS substrates, many studies have shown

that the size of the interparticle gap significantly affects the enhancement of the Raman signals. Given that the optimal interparticle gap is as small as a few nanometers, fabricating sensitive, uniform, and reproducible SERS substrates remains challenging. Here we report a three-dimensional SERS substrate created through the assembly of core-shell nanoparticles using DNA. By using DNA of appropriate sequence and length, DNA-functionalized nanoparticles were assembled into ordered and highly packed nanostructures. The interparticle distance was precisely controlled by adjusting the design of the DNA and the thickness of the silver shell coated on the gold nanoparticles. Compared with randomly aggregated nanoparticles, the interparticle distance in the synthesized nanostructures can be more uniform and better controlled. In addition, the DNA-guided assembly process allows us to create precise nanostructures without using complex and expensive fabrication methods. The study demonstrates that the synthesized nanostructures can be used as effective SERS substrates to successfully measure the Raman signals of malachite green, a toxic compound that is sometimes illegally used on fish, as well as Fluorescein isothiocyanate (FITC) at low concentrations.

9340-7, Session 2

Plasmonics-active SERS nanoprobe for biomedical sensing

Andrew M. Fales, Hsin-Neng Wang, Hoan Thanh Ngo, Tuan Vo-Dinh, Duke Univ. (United States)

No Abstract Available

9340-9, Session 3

Surface-enhanced Raman imaging of tissue sections for metabolic analysis

Megumi Shiota, Shogo Yamazoe, FUJIFILM Corp. (Japan) and Keio Univ. School of Medicine (Japan); Masayuki Naya, FUJIFILM Corp. (Japan); Mitsuyo Ohmura, Mayumi Kajimura, Makoto Suematsu, Keio Univ. School of Medicine (Japan) and Japan Science and Technology Agency (Japan)

We present the surface-enhanced Raman spectroscopy (SERS) imaging of tissue metabolites by using our novel SERS substrate composed of self-assembled unique structure.

SERS is a promising technology for label-free detection of molecule characterized by its high-sensitivity and fingerprint nature. Various SERS devices have been developed but it has been difficult to fabricate the device with high uniformity over a large area.

We, therefore, developed a new SERS substrate which provides small variability of signal intensities over a large area. It has utilized a self-assembled nanostructure of boehmite that is easily achieved by a hydrothermal preparation of aluminum as a template for subsequent gold deposition. The transparent nature of boehmite enables measurement of Raman scattering from the back-side of the substrate. It enables conducting a SERS sensing and imaging without any obstruction by the sample.

By using this device, we conducted tissue imaging of the mouse ischemic brain[1] and the mouse tumor-bearing liver on the SERS substrates. The results showed that the specific distributions of some metabolites correlated with the distributions of ischemic region and tumor region. In this study, we succeeded in imaging of urea which is difficult to detect by matrix-assisted laser desorption ionization/imaging mass spectrometry (MALDI/IMS). The result suggests that this SERS substrate has a great potential as a metabolic analysis tool.

[1] Yamazoe et al. ACS Nano, 8, 6 (2014)

**Conference 9340:
Plasmonics in Biology and Medicine XII**

9340-11, Session 3

A multimodal imaging agent for intrinsic surface enhanced Raman scattering of biological tissue

Christoph B. Pohling, Jos Campbell, Timothy A. Larson, Sanjiv S. Gambhir, Stanford Univ. (United States)

As an optical method, Raman imaging has great potential for medical applications due to chemo-selective image contrast, microscopic resolution and multiplexing capabilities. However, it suffers from weak signals resulting in acquisition times of up to several hours, preventing its frequent use in clinical practice. In order to overcome this limitation, Surface Enhanced Raman Scattering (SERS) has been developed where metallic nanostructures provide Surface Plasmon Resonance Effects (SPRE), enhancing signals of nearby molecules. The range of SERS is usually limited to a few nm and therefore direct coating of gold nanospheres with Raman marker molecules led to bright contrast agents in the recent past. This, however, limits SERS to the coating material and does not provide the versatile intrinsic information of arbitrary sample molecules. We hereby address this issue by the development of a multimodal plasmonic nanoparticle-based imaging agent for intrinsic Raman spectroscopy. The concept of SERS active gold nanospheres, passivated by an ultrathin layer of silica, has been transferred to a core shell particle of hematite and gold that provides superior SPRE. The usability for Raman imaging was evaluated by simulation and experimental studies on COS and U87 cell lines. By taking advantage of its iron oxide core, magnetic alignment of the nanoparticle was performed in order to increase its SERS efficiency for excitation by polarized light. Finally, we demonstrate additional signal contrast in Magnetic Resonance Imaging (MRI) and Photo Acoustic Tomography (PAT), illustrating multimodality and promising transferability of this concept towards clinical applications.

9340-12, Session 3

Monolithic nanoporous gold disks with large surface area and high-density plasmonic hot-spots

Fusheng Zhao, Jianbo Zeng, Univ. of Houston (United States); Masud Arnob, Gregg Santos, Univ of Houston (United States); Wei-Chuan Shih, Univ. of Houston (United States)

Plasmonic metal nanostructures have shown great potential in sensing, photovoltaics, imaging and biomedicine, principally due to enhancement of the local electric field by light-excited surface plasmons, the collective oscillation of conduction band electrons. Thin films of nanoporous gold have received a great deal of interest due to the unique 3-dimensional bicontinuous nanostructures with high specific surface area. However, in the form of semi-infinite thin films, nanoporous gold exhibits weak plasmonic extinction and little tunability in the plasmon resonance, because the pore size is much smaller than the wavelength of light. Here we show that by making nanoporous gold in the form of disks of sub-wavelength diameter and sub-100 nm thickness, these limitations can be overcome. Nanoporous gold disks (NPGDs) not only possess large specific surface area but also high-density, internal plasmonic "hot-spots" with impressive electric field enhancement, which greatly promotes plasmon-matter interaction as evidenced by spectral shifts in the surface plasmon resonance. In addition, the plasmonic resonance of NPGD can be easily tuned from 900 to 1850 nm by changing the disk diameter from 300 to 700 nm. The coupling between external and internal nano-architecture provides a potential design dimension for plasmonic engineering. The synergy of large specific surface area, high-density hot spots, and tunable plasmonics would profoundly impact applications where plasmonic nanoparticles and non-plasmonic mesoporous nanoparticles are currently employed, e.g., in in-vitro and in-vivo biosensing, molecular imaging, photothermal contrast agents, and

molecular cargos.

REFERENCES:

Fusheng Zhao, Jianbo Zeng, Md Masud Parvez Arnob, Po Sun, Ji Qi, Pratik Motwani, Mufaddal Gheewala, Chien-Hung Li, Andrew Paterson, Uli Strych, Balakrishnan Raja, Richard C. Willson, John C. Wolfe, T. Randall Lee, and Wei-Chuan Shih, "Monolithic NPG nanoparticles with large surface area, tunable plasmonics, and high-density internal hot-spots," *Nanoscale* 6, 8199-8207, 2014.

9340-13, Session 4

Nanostructuring for sensitivity enhancement of biosensors based on surface plasmon resonance and surface-enhanced Raman scattering

Jean-François Bryche, Institut d'Électronique Fondamentale (France) and Lab. Charles Fabry (France); Grégory Barbillon, Institut d'Électronique Fondamentale (France); Anne-Lise Coutrot, Lab. Charles Fabry (France); Frédéric Hamouda, Institut d'Électronique Fondamentale (France); Mitradeep Sarkar, Lab. Charles Fabry (France); Raymond Gillibert, HORIBA Scientific (France) and Univ. Paris 13 (France); Aurore Olivéro, Lab. Charles Fabry (France) and HORIBA Scientific (France); Julien Moreau, Lab. Charles Fabry (France); Marc Lamy de la Chapelle, Univ. Paris 13 (France); Bernard Bartenlian, Institut d'Électronique Fondamentale (France); Michael T. Canva, Lab. Charles Fabry (France)

Surface Plasmon Resonance Imaging (SPRI) sensors and Surface Enhanced Raman Scattering (SERS) sensors have a wide range of application such as medical diagnostics, food safety or drug discovery. We aim to combine both techniques in one unique biosensor system to take advantage of both of them: SPRI sensors allow real-time and parallel detection of biomolecular interactions but its specificity relying solely on the chip surface functionalization while SERS can identify target molecules by their vibrational modes

Most SPR systems are based on the use of conventional flat metallic biochips with propagating surface plasmons. Nano-structures are known for their ability to enhance local electrical field, pushing back the detection limit to trace molecules. Indeed, SPR and SERS sensitivities are linked to the intensity of the electrical field and its square, respectively.

In this contribution, we present numerical and experimental results on a novel sample consisting in an array of gold nano-structures above a continuous gold film deposited on glass substrate. We have studied several shapes, diameters and periods such as nanodisks with diameters between 40 nm to 300 nm and periods between 80 nm and 500 nm. We demonstrated that the coupling between the array of nano-structures and the continuous film leads to higher enhancement factor in SERS and SPR experiment than with an array of gold nanostructures alone. Nanostructures were fabricated by Electron Beam Lithography and by soft UV Nanoimprint Lithography (UV-NIL), which is well-adapted for a large scale production of biosensors for industrial applications.

9340-14, Session 4

Effect of transformation on plasmonic chiral nanostructures for the detection of alpha-helical monomers and proteins

Eng Huat Khoo, A*STAR Institute of High Performance Computing (Singapore)

**Conference 9340:
Plasmonics in Biology and Medicine XII**

In this paper, we introduce transformations to the chiral nanostructures to investigate its effects on the optical rotational properties and sensitivity detection of biomolecules. Transformation such as rotations and reflection affect the overall dissymmetry properties of electromagnetic fields. This in turn affects the chiral fields and the attractive force on the biomolecules surrounding the chiral nanostructures. We obtain the circular dichroism (CD) spectra of the nanostructures under different transformations in simulation. CD resulted from the differential absorption of left and right circular polarized light. The simulation results show that some CD modes change their polarity, resonance wavelength or amplitude at certain transformations. The nanostructures are then fabricated using e-beam lithography and lift-off process. The experiments are performed using broad band optical microscopy with quarter waveplate to generate left and right polarized light. The CD spectra for both simulation and experimental results match very well. Subsequently, the transformed nanostructures are submerged in a solution of alpha-helical monomers and proteins. Some unique results such as reduction in CD amplitude, no wavelength shift at resonance and the appearance of other CD modes in the spectra is observed. At some rotation angle, the wavelength shift is larger than the un-rotated nanostructures while at others, there is no effect. The transformed nanostructures has different dissymmetries at different angles, which affect the ability to interact with the biomolecules and hence, the sensitivity. We believe that these results is important for the detection of protein with various alpha-helical contents, and determination of various protein structures.

9340-15, Session 4

A computer model for the prediction of sensitivity in SPR sensing platforms

Kristel D. Izquierdo, Instituto Tecnológico y de Estudios Superiores de Monterrey (Mexico); Arnoldo Salazar, Univ. of California, Irvine (United States); Adrian Losoya-Leal, Sergio O. Martinez-Chapa, Instituto Tecnológico y de Estudios Superiores de Monterrey (Mexico)

Surface Plasmon Resonance (SPR) biosensors have become increasingly popular in clinical diagnostics for in-site detection of low concentrations of biological analytes, given that they offer advantages such as real-time and label-free monitoring, simplicity, high sensitivity and fast-response compared to other conventional methods such as enzyme immunoassays (ELISA, EMIT) and chromatographic techniques (LC-MS, HPLC). In general, SPR biosensors relate the changes in refractive index immediate to a metal-dielectric interface, product of the changes in analyte concentration, to the changes in the intensity of the reflected light at the SPR interface. There are multiple interrelated parameters in these sensors that affect their sensitivity performance; therefore, the analysis of their behavior is of great importance when optimizing the design of SPR sensing platforms. A computer model for the prediction of sensitivity in SPR biosensors is presented in this paper. The model uses the analytical solution of the kinetic equations of mass transport to correlate changes in concentration to changes in refractive index. These results are connected with simulations that relate changes in refractive index to shifts in both the SPR resonance angle and the response curves. Finally we analyze these relations and numerically optimize the parameters involved for the best sensing performance. This work will aid in the optimization of both design and performance parameters for the construction of highly-sensitive SPR platforms in the laboratory.

9340-16, Session 4

SPR-MS: from identifying adsorbed molecules to image tissues

Jean-François Masson, Julien Breault-Turcot, Simon Forest, Pierre Chaurand, Univ. de Montréal (Canada)

SPR sensors have become valuable analytical sensors for biomolecule detection. While SPR is heralded with high sensitivity, label-free and

real-time detection, nonspecific adsorption and detection of ultralow concentrations remains issues. Nonspecific adsorption can be minimized using adequate surface chemistry. For example, we have employed peptide monolayers to reduce nonspecific adsorption of crude serum or cell lysate. It is important to uncover the nature of molecules nonspecifically adsorbing to surfaces in these biofluids, to further improve understanding of the nonspecific adsorption processes. Mass spectrometry (MS) provides a complementary tool to SPR to identify biomolecule adsorbed to surface. Trypsin digestion of the proteins adsorbed to surfaces led to identification of characteristic peptides from the proteins involved in nonspecific adsorption. While albumin dominates nonspecific adsorption as expected, proteins of far lesser concentration were also involved in nonspecific adsorption such as complement C3. MS analysis of the peptide fragment was also used to obtain a better understanding of the orientation of albumin nonspecifically adsorbed on the SPR sensors. Nonspecific adsorption in crude cell lysate results mainly from lipids, as confirmed with SPR and MS. Thus, hydrophobic peptides must be employed to minimize nonspecific adsorption. We also recently demonstrated that imaging SPR can be used in combination to imaging MS to image tissue sections. Thin sections of mouse liver were inserted in the fluidic chamber of a SPRi instrument. The biomolecules of the tissue were transferred with a transfer buffer to the SPRi chip for quantification. The SPR chip was then imaged using MALDI-MS imaging to identify the biomolecules that were transferred to the SPRi chip. This technique of imaging SPR-MS provides quantitative and qualitative information about the composition of tissues

9340-17, Session 4

Matching plasmon resonances to the C=C and C-H bonds in estradiol

Ifeoma G. Mbomson, Nigel P. Johnson, Univ. of Glasgow (United Kingdom); Scott McMeekin, Glasgow Caledonian Univ. (United Kingdom); Richard De La Rue, Univ. of Glasgow (United Kingdom)

We tune nanoantennas to resonate within mid-infrared wavelengths to match the vibrational resonances of C=C and C-H of the hormone estradiol. Modelling and fabrication of the nanoantennas produce plasmon resonances between 2 μ m to 7 μ m. The hormone estradiol was dissolved in ethanol and evaporated, leaving thickness of a few hundreds of nanometres on top of gold asymmetric split H-like shaped on a fused silica substrate. The reflectance was measured and a red-shift is recorded from the resonators plasmonic peaks. Fourier transform infrared spectroscopy is use to observe enhanced spectra of the stretching modes for the analyte which belongs to alkenyl biochemical group.

9340-1, Session 5

Understanding the TERS effect with on-line tunneling and force feedback using multiprobe AFM/NSOM with Raman integration (Invited Paper)

Aaron Lewis, The Hebrew Univ. of Jerusalem (Israel); Rimma Dekhter, Patricia Hamra, Yossi Bar-David, Hesham Taha, Nanonics Imaging Ltd. (Israel)

Tip enhanced Raman scattering (TERS) has evolved in several directions over the past years. The data from this variety of methodologies has now accumulated to the point that there is a reasonable possibility of evolving an understanding of the underlying cause of the resulting effects that could be the origin of the various TERS enhancement processes. The objective of this presentation is to use the results thus far with atomic force microscopy (AFM) probes with noble metal coating, etching, transparent gold nanoparticles with and without a second nanoparticle [Wang and Schultz, ANALYST 138, 3150 (2013)] and tunneling feedback probes [R. Zhang et. al.,

**Conference 9340:
Plasmonics in Biology and Medicine XII**

NATURE 498, 82 (2013)]. We attempt at understanding this complex of results with multiprobe techniques of two gold nanoparticles with controlled separation. This complex quantum system enters, in the near-field, into a regime of extreme non-locality. This produces a highly confined and broadband plasmon field with all k vectors for effective excitation. Normal force tuning fork feedback with exposed tip probes provides an excellent means to investigate these effects with TERS probes that we have shown can circumvent the vexing problem of jump to contact and permit on-line switching between tunneling and AFM feedback modes of operation. [Discussion with Zachary Schultz are acknowledged]

9340-18, Session 5

Plasmonic lenses and bioparticle separation

Ahmet A. Yanik, Xiangchao Zhang, Univ. of California, Santa Cruz (United States)

No Abstract Available

9340-19, Session 5

Effect of tip geometry on two photon excited luminescence of single gold nanorods

Arif M. Siddiquee, Swinburne Univ. of Technology (Australia)

Gold nanorods have emerged as attractive bio-labelling agents, with their efficient and stable scattering and two-photon luminescence (TPL) mediated by surface plasmons. Due to their chemically inert, blinking/bleaching-free, non-linear behaviour makes them particularly useful for targeted cancer cell imaging. The lightning-rod effect which concentrates electrostatic fields at tips or protrusions along with surface plasmon resonance effect plays a crucial role in the TPL emission process. These phenomena can be explored by fixing the aspect ratio and varying the tip geometry of the nanorods as sharply curved tips would produce stronger field enhancement. However, the volume of the tip that is involved in the local enhancement region will be smaller for a sharper tip, therefore reducing the number of atoms that are involved in luminescence process.

In this paper, we investigated such balancing effects by using gold nanorods of three different tip geometries. We measured TPL brightness of individual particles by calculating their TPL action cross section (TPACS). The TPACS value per unit volume of bipyramids was found almost two times higher than the nanorods and dumbbells which can be attributed to the effect of sharper tip radius of curvature of bipyramidal shaped nanorods than the others. The measured average TPACS value of our bipyramids was about $2e4$ GM while for nanorods and dumbbells it was $6e3$ GM. To explore the effect of local field enhancement of these different tip geometries, we performed numerical calculation which matches nicely with our experimental findings which confirm the effect of local electric field in the TPL emission.

9340-20, Session 5

Photo-thermal effects in DNA/gold nanorods complexes

Luciano De Sio, BEAM Engineering for Advanced Measurements Co. (United States) and Univ. della Calabria (Italy); Giulio Caracciolo, Univ. degli Studi di Roma La Sapienza (Italy); Ferdinanda Annesi, Istituto per i Processi Chimico-Fisici (Italy); Tiziana Placido, Univ. degli Studi di Bari Aldo Moro (Italy); Daniela Pozzi, Univ. degli Studi di

Roma La Sapienza (Italy); Roberto Comparelli, Alfredo Pane, M. Lucia Curri, Istituto per i Processi Chimico-Fisici (Italy); Nelson V. Tabiryan, BEAM Engineering for Advanced Measurements Co. (United States); Roberto Bartolino, Univ. della Calabria (Italy)

Biocompatible gold nanoparticles (GNPs) have gained considerable attention in recent years for potential applications in medicine due to their size dependent electronic, optical and chemical properties. Gold nanorods (GNRs) are an attractive class of GNPs and are considered excellent candidates for biological sensing applications due to the plasmon absorbance band sensitivity to the refractive index of the surrounding material, which allow for an extremely accurate sensing. In addition, GNRs present two distinct plasmon absorption bands, namely transversal and longitudinal ones, which can be tuned up to near-infrared (NIR). Such NIR absorption peaks can be excited by a laser at specific absorption wavelength to induce a local heating, potentially allowing for the selective thermal destruction of cancerous tissues. DNA is the fundamental genetic component of living matter and represents the "key element" of any biological system. In this framework, we have studied the electrostatic interaction between an aqueous solution of positively charged GNRs dispersed in a negatively charged short DNA solution. A comprehensive investigation as a function of GNRs concentration has been performed, based on zeta-potential, dynamic light scattering, gel electrophoresis and morphological analysis. Moreover, by considering DNA as an ad-hoc "bio-environment", we have investigated the effect of the localized (photo-thermal heating) and delocalized temperature variation on the DNA melting. Finally, we have performed a thermographic analysis in order to show the difference between localized and delocalized temperature variation. These results offer novel opportunities for designing original plasmonic assisted biomedical therapies.

9340-21, Session 5

UV plasmonics with magnetic spin-polarized nanoparticles

Vladimir P. Drachev, Hari Bhatta, Soumya Nag, Univ. of North Texas (United States); Arrigo Calzolari, Univ. of North Texas (United States) and Istituto Nanoscienze (Italy); Marco Buongiorno Nardelli, Univ. of North Texas (United States)

Various technological applications of magnetic nanoparticles include high-density recording, magnetic processing, and biomedicine[1]. The plasmon resonance of magnetic nanoparticles such as Co is in the ultraviolet spectral range, which is the range for bio-molecules resonances and attractive for the two-photon absorption in the visible. A long lasting search for plasmonic materials in the ultraviolet spectral range does not consider Co as a promising candidate [2]. Moreover, it is common belief that the quality of the plasmon resonance of Co is quite low, which follows, in particular, from the experimental data for permittivity of bulk cobalt [3]. Here we show that Co nanoparticles with high quality crystal structure and spin polarization support an excellent plasmon resonance at about 275 nm, which is comparable with the noble metal. We involve magnetic properties of Co and find that single domain nanoparticles show high-quality plasmon resonance due to effect of the spin polarization on the density of states of d-band and, as a consequence, on the Co nanoparticle permittivity. Colloidal magnetic cobalt nanoparticles were fabricated by the reduction of cobalt salt using trioctylphosphine as a surfactant and oleic acid as a stabilizer. Our experiments and density functional theory simulations show that Co nanoparticle can play a similar role for ultraviolet plasmonics as Ag or Au mean for the visible range.

1. Hafeli, U., Schutt, W., Teller, J. & Zborowski, M. (eds) Scientific and Clinical Applications of Magnetic Materials (Plenum, New York, 1997).
2. McMahon, J. M., Schatz, G. C., Gray, S. K. Phys. Chem. Chem. Phys. 15, 5415 (2013).
3. Johnson, P. B., and Christy, R. W. Phys. Rev. 9, 5056 (1974).

**Conference 9340:
Plasmonics in Biology and Medicine XII**

9340-22, Session 6

Hyperspectral backscattering imaging of cells using gold-silver alloy nanoparticles as chromatic biomarkers

Sergiy Patskovsky, David Rioux, Éric Bergeron, Michel Meunier, Ecole Polytechnique de Montréal (Canada)

Hyperspectral imaging is a powerful technique for multiplexed analysis of cells tagged by chromatic biomarkers. Gold silver alloy nanoparticles (NPs) are promising for chromatic labeling of biological material because of their composition-dependent plasmon resonance. For example, alloy NPs with various compositions can be used to target specific cells. Hyperspectral imaging of these cells can be used to spatially localize NPs on cells and extract the scattering spectrum of each NP to identify its composition [1]. We report on a new backscattering approach and instrumentation for fast wide-field hyperspectral imaging of NPs in cellular environment. This approach is more sensitive and, due to the use of high numerical aperture objectives, provides better spatial resolution than standard transmission darkfield [2]. It is also faster than hyperspectral confocal imaging because it does not require rastering of light beam on the sample. It is also important to understand and predict beforehand the optical properties of the alloy NPs in order to optimize them for multiplexed imaging. We use an analytic model for the dielectric function of gold silver alloys [3] along with Mie theory to predict the optical properties of alloy NPs and compare these with experimental alloy NPs. We namely study the influence of NPs size and composition on their extinction and scattering spectra as well as the electric field distribution around the nanostructures. The backscattering technique was also used to obtain a real time 3 dimensional distribution of plasmonic NPs over the cells [4].

- 1 S. Patskovsky, E. Bergeron, and M. Meunier, J. Biophotonics 6, 1 (2013).
- 2 S. Patskovsky, E. Bergeron, D. Rioux, M. Simard, and M. Meunier, Analyst (2014).
- 3 D. Rioux, S. Vallières, S. Besner, P. Muñoz, E. Mazur, and M. Meunier, Adv. Opt. Mater. 2, 176 (2014).
- 4 S. Patskovsky, E. Bergeron, D. Rioux, and M. Meunier, J. Biophotonics (2014).

9340-23, Session 6

Biologically active plasmonic devices: fusing direct-write lithography with molecular self-assembly to create hybrid nano-sensor surfaces

Alasdair W. Clark, Jonathan M. Cooper, Univ. of Glasgow (United Kingdom)

In this paper, we show the integration of direct-write lithography with molecular self-assembly to create novel, biologically activate nano-plasmonic systems and sensors with tuneable plasmonic properties dictated by the local biomolecular environment. By combining complex metallic nanostructures with DNA and protein nanopatterning, we demonstrate hybrid nano-sensor surfaces and devices for high-sensitivity colorimetric detection and enhanced Raman spectroscopy.

Acting as antennae for light radiation, the plasmonic resonances inherent to metallic nanoparticles allow for photonic manipulation beyond the diffraction limit, bridging the gap between far-field optics and nanoscale electrical signals. Key to the advancement of plasmonic systems are reliable strategies for high-resolution assembly of particles into functional devices. Although molecular assembly is perhaps the most promising of these strategies, directing the assembly of nanoparticle networks on surfaces, and their interaction with existing surface features, is sufficiently challenging that its use has been limited.

Our approach combines electron-beam-lithography, dip-pen-nanolithography, and molecular self-assembly to create hybrid nano-optical

surfaces whose optical and plasmonic properties can be altered through single nanoparticle binding. By precise alignment of surface nanostructures (typically Au and Ag bowtie, diamond and cross shapes) to DNA and protein nanopatterns, we are able to dictate, with better than 10nm control, the binding location of individual nanoparticles. As a result, we can precisely engineer the final geometry and plasmonic response of the devices after biomolecular binding; controlling the hotspot number, location and frequency, along with the scattering response of each structure. We use this control to create colorimetric and enhanced-Raman sensors with single event sensitivity.

9340-24, Session 6

Enhanced performance of plasmonic biosensors using high field confinement around metallic nanostructures due to the coupling of propagating plasmons of a thin metallic film

Mitradeep Sarkar, Mondher Besbes, Julien Moreau, Jean-François Bryche, Aurore Olivéro, Lab. Charles Fabry (France); Grégory Barbillon, Institut d'Électronique Fondamentale (France); Anne-Lise Coutrot, Lab. Charles Fabry (France); Bernard Bartenlian, Institut d'Électronique Fondamentale (France); Michael T. Canva, Lab. Charles Fabry (France)

Metallic nanostructures have the ability to confine electromagnetic field in their vicinity, which has been widely used in Surface Plasmon Resonance (SPR) detection and Surface Enhanced Raman Scattering (SERS). These processes strongly depend on the field intensity confined around nanostructures. Our aim is to enhance the local field intensity in nanostructured biochips for trace concentration biosensing.

We have extensively studied 3D arrays of metallic nanocylinders which can sustain the Localized Surface Plasmons (LSP). However, the excitation wavelengths of LSP are not tunable due to their limited dispersion. We have shown that by adding a thin metallic film below the array we can enhance the field intensity around the cylinders. The Propagating Surface Plasmon (PSP) excited in such a metallic film can be harmonically coupled to the Bragg waves that exist owing to the periodicity of the structure to give rise to the Hybrid Lattice Plasmon (HLP) mode. This mode can be tuned over wide ranges of excitation wavelength and also have high field confinement in the structure.

In order to evaluate biosensors we introduce convenient parameters such as Sensitivity Enhancement Factor (SEF) and Sensitivity Figure of Merit (SFOM), which takes into account the concentration of target molecules required for the analysis, as well as the unavoidable index drift of the surrounding medium. We have shown by numerical simulations and also by experimental results that the hybrid modes in the nanostructured biochip can help to enhance the detection capabilities of processes such as SERS and SPR detection.

9340-25, Session 6

Plasmonic cell manipulation for biomedical and screening applications

Dag Heinemann, Markus Schomaker, Stefan Kalies, Merve Sinram, Patrick Heeger, Laser Zentrum Hannover e.V. (Germany); Hugo Murua Escobar, Univ. Rostock (Germany); Heiko Meyer, Laser Zentrum Hannover e.V. (Germany) and Medizinische Hochschule Hannover (Germany); Tammo Ripken, Laser Zentrum Hannover e.V. (Germany)

**Conference 9340:
Plasmonics in Biology and Medicine XII**

Modulation of the cell membrane permeability by the plasmonic interaction of gold nanoparticles and short laser pulses for cell manipulation or destruction has been the objective of several recent studies. Gold nanoparticles in close vicinity to the cellular membrane are irradiated to evoke a nanoscale membrane perforation, enabling extracellular molecules to enter the cell. However, besides several basic studies no real translation from proof of concept experiments to routine usage of this approach was achieved so far.

In order to provide a reproducible and easy-to-use platform for gold nanoparticle mediated (GNOME) laser manipulation, we established an automated and encased laser setup. We demonstrate its feasibility for high-throughput cell manipulation. In particular, protein delivery into canine cancer cells is shown. The biofunctional modification of cells was investigated using the caspase 3 protein, which represents a central effector molecule in the apoptotic signaling cascade. An efficient and temporally well-defined induction of apoptosis was observed with an early onset 2 h after protein delivery by GNOME laser manipulation. Besides protein delivery, modulation of gene function using GNOME laser transfection of antisense molecules was demonstrated, showing the potential of this technique for basic science and screening purposes.

Concluding, we established GNOME laser manipulation of cells as a routine method, which can be utilized reliably for the efficient delivery of biomolecules. Its intrinsic features, being low impairment of the cell viability, high delivery efficiency and universal applicability, render this method well suited for a large variety of biomedical application.

9340-26, Session 6

Investigation of Electron Beam Irradiation Effect on Pore Formation

For Single Molecule Bio-Sensor Fabrication

Seong Soo Choi, Myoung Jin Park, Sun Moon Univ. (Korea, Republic of); Chul Hee Han, Sun Moon Univ (Korea, Republic of); Sung In Kim, Jung Ho Yoo, Kyung Jin Park, National Nanofab Ctr. (Korea, Republic of); Namkyou Park, Seoul National Univ. (Korea, Republic of)

The Au pores on pyramidal array were fabricated. The 0.5 keV energy electron beam irradiation was applied for nanomembrane. ~ 3.5 nm diameter Au pore was drilled using 200 keV STEM. The fabricated nanopore can utilized as optical nanobio sensor for ultrafast single molecule sensor.

9340-8, Session PSun

Bidimensional assemblies of nonspherical gold nanoparticles for SERS analysis of biomolecules

Paolo Matteini, Marella de Angelis, Istituto di Fisica Applicata Nello Carrara (Italy); Lorenzo Ulivi, Istituto dei Sistemi Complessi (Italy); Sonia Centi, Univ. degli Studi di Firenze (Italy); Roberto Pini, Istituto di Fisica Applicata Nello Carrara (Italy)

To date, direct SERS analysis of proteins has been mainly devoted to the characterization of short peptide fragments or to the prosthetic group of metallo-proteins due to their strong SERS response. Nonetheless, this perspective restricts the investigation to very limited peptide sequences and appears of scarce interest for a thorough characterization of the protein. In other studies, the protein is modified with specific aminoacid motifs (e.g. the hexahistidine tag), which has assured a successful binding of the biomolecule to the metal surface and thus the possibility to gain insights into its spectroscopic characterization, although at the expense of a

sustainable practice.

We tried to overcome the limitations depicted above by setting-up an effective platform for the structural SERS detection of proteins. Our proposal escapes the needs of a preliminary modification of the biomolecule and confers rapidity and reproducibility to the analysis. Optimal results are achieved by the use of nonspherical tipped metallic nanostructures with controlled architectural parameters and their assembly into organized bidimensional arrays including a regular distribution of hot spots for protein entrapment and detection. The nanoscale distribution of the electric-field enhancement was simulated with a finite element method. The simulation evidenced that two main sites can be responsible for substantial SERS activity corresponding to the contact points between the corners of the nanoparticles and the nanoscale areas at the interface between nanoparticles.

9340-27, Session PSun

Enhancing the sensitivity of localized surface plasmon resonance (LSPR) biosensors using nanorods and DNA aptamers

Po-Chun Chuang, National Yang-Ming Univ. (Taiwan); Pei-Chen Liao, National Cheng Kung Univ. (Taiwan); Yih-Fan Chen, National Yang-Ming Univ. (Taiwan)

Localized surface plasmon resonance (LSPR) biosensors have drawn much attention for their promising application in point-of-care diagnostics. While surface plasmon resonance (SPR) biosensing systems have been well developed, LSPR systems have the advantages of simpler and more compact setups. The LSPR peak shifts caused by the binding of molecules to the LSPR substrates, however, are usually smaller than 1 nm if no signal amplification mechanism is used. When using nanoparticles to enhance the sensitivity of LSPR biosensors, because of the short field penetration depth, the nanoparticles should be very close to the LSPR substrate to induce significant shifts in the LSPR peak position. In this study, we used DNA aptamers and gold nanorods to significantly increase the change in the LSPR peak position with the concentration of the target molecules. The dynamic range of the measurement could be tuned by adjusting the amount of gold nanorods. We have successfully used the proposed mechanism to detect 10 pM interferon-gamma (IFN- γ), a biomarker related to the diagnosis of latent tuberculosis infection. The calibration curves obtained in pure buffers and serum-containing buffers show that accurate detection can be achieved even when the sample is from complex biological fluids such as serum. Because of the enhancement in the sensitivity by the proposed sensing scheme, it is possible to use a low-cost spectrometer to build a LSPR biosensing system.

9340-28, Session PSun

Analysis of transmission through multiple slit and grooves structures for biosensors

Bikash Nakarmi, Yong Hyub Won, Bong Ho Kim, KAIST (Korea, Republic of)

Surface Plasmon resonance have been of great concern in present research of biosensors due to its compactness and high sensitivity on sensing different analyte. Various structures such as slit only, slit and groove and groove slit groove have been proposed and analyzed to obtain the optimum optical transmission through the structure. However the multiple slit and groove structure and detail analysis of slit/slits structures have not been done. Hence, we analyze the transmission through slit only, slit and groove, groove-slit-groove, and multi-slit and grooves structure on the silver metal to obtain the efficient optical transmission through the structure. Also we have analyze the effect of refractive index change of the analyte on the transmission properties that is flowing through the structure. The change

**Conference 9340:
Plasmonics in Biology and Medicine XII**

in transmission properties at the output can be used for biosensors to measure the glucose amount, chemical sensors to measure the different amount of hydrogen peroxide and others. The main principle involved in sensing is the change in the transmission intensity and wavelength shift of at the output with different refractive index analyte flowing on the structures. Plane wave with the wavelength of 400 nm to 800 nm are used to see the effect of change in refractive index with different amount of analyte on the transmission parameters such as transmitted intensity, wavelength shift and others. The sensitivity of the structure with the change in the refractive index is also measured which will decide its usage on various types of sensing application including chemical sensors and biosensors.

9340-29, Session PSun

Numerical investigation of plasmonic properties of gold nanoshells

Sathiyamoorthy Krishnan, Michael C. Kolios, Ryerson Univ. (Canada)

Gold nanoshell (Au) exhibits plasmon excitation at the near-infrared regime where optical transmission through tissue is optimal. The peak absorption wavelength of the gold nanoshell can be tuned by varying size and thickness of the core and shell of the core-shell (CS) particles. CS particles can be used in numerous biomedical applications. It also provides optical enhancement required for other modalities such as reflectance confocal microscopy and OCT in the IR regime

Understanding how the plasmon excitation is modified when changing the shell thickness or composition, or the core material of the CS, is important for the optimization of the particle design. We numerically investigated the plasmonic properties of CS using a finite element model (COMSOL, Burlington, MA, USA.). We studied optical properties of core-shell containing polystyrene as core and Au as shell in water. The core size was 300nm and the thickness of the shell was optimized for maximum SP excitation by increasing the shell thickness in steps of 10 nm from 10 nm to 50 nm. A shell thickness in the range between 20 to 30 nm exhibits the maximum SP excitation. Two plasmonic modes, one at 600 nm corresponding to core-shell interface (outer mode) and the other at 670 nm corresponding to shell-surrounding dielectric interface (inner mode) were observed. Efficient plasmonic coupling between the two modes occurs when the size of the Au shell is between 20 to 30 nm. When the thickness of the Au shell is less than the skin depth of excited plasmon, only one prominent plasmonic mode is observed. At a thickness greater than 30nm, two well separated plasmonic modes are observed. The outer plasmonic mode is broadened than the inner mode confirmed that the inner plasmonic mode is confined at the core-shell interface. One of the CS applications for SPR sensors is investigated by simulating CS particle in various refractive index media with refractive indices that varied from 1.33 (water) to 1.61. A red shift in wavelength and an increase in amplitude of absorption peak are observed. The wavelength shift of outer (670 nm) mode is investigated for SPR sensor applications. The studies showed that the outer mode exhibits wavelength shift ($d\lambda/dn$) of 764 ± 13 (nm/RIU) is comparable to most commonly used prism (970 (nm/RIU)) and grating (309 (nm/RIU)) based surface plasmon resonance techniques.

9340-32, Session PSun

Theoretical approach to surface plasmon scattering microscopy for single nanoparticle detection in near infrared region

Taehwang Son, Donghyun Kim, Yonsei Univ. (Korea, Republic of)

We present a theoretical approach to single nanoparticle detection using surface plasmon scattering microscopy in near infrared wavelength.

Rigorous coupled wave analysis (RCWA) was performed to obtain a near-field image on the reflection plane. 814-nm wavelength light was assumed to be incident under total internal reflection condition on a BK7 glass substrate coated with 45-nm gold thin film. A 200-nm polystyrene sphere and a 50-nm gold nanoparticle were utilized as targets attached to the gold film. Surface plasmon polariton (SPP) which is induced by near-infrared light on the gold film is perturbed so that parabola-shaped surface waves are observed on the reflection plane. The wave cannot be represented with high harmonic frequency due to computational memory limitation. Although inherent periodicity of RCWA adds interference, parabola-shaped waves are clearly distinguishable. The polystyrene and the gold nanoparticle show an opposite phase with the wave, in which the intensity at the center of polystyrene tends to be high while that of gold is low. The parabola-shaped wave was also derived with an analytical solution. A polystyrene sphere and a gold nanoparticle are regarded as refractive index defect, which is defined using delta function without considering their volume. The effective wave vector of SPP shows a heart-patterned graph, which elucidates how a parabola-shaped wave appears. By changing the phase of the analytical solution from 0 to 180 degree, the center of wave becomes darker. This implies that the refractive index difference of polystyrene and gold causes a 180 degree phase shift of SPP.

9340-33, Session PSun

Optical near-field response of plasmonic nanostructures for ultrashort light pulses

Hongki Lee, Donghyun Kim, Yonsei Univ. (Korea, Republic of)

Electromagnetically amplified local field or hot-spots are created by surface nanostructures when they are coupled with the incident light. These localized near-fields have drawn significant interests for their ability to reduce the size of amplified light field below diffraction-limited volume. For the applications with pulsed light incidence, we have investigated the temporal dynamics of electromagnetic waves using various nanostructures. Electromagnetic fields excited and localized on the two-dimensional array of nanostructures as well as incident light absorption were numerically calculated by finite difference time domain method. The calculation was performed by varying the conditions which can affect the excitation of the localized near-fields on the nanostructures, which include light wavelength and geometrical parameters such as shape, size, height, and period. The two-dimensional models include arrayed posts and apertures that are circular, triangular and square in shape. The posts and apertures were placed on the metallic film with varying periods from 100 nm to 900 nm and varying diameters from 100 nm to 500 nm in the case of the circular shape. The height of the nanostructure was varied to the point where the evanescent field of a metallic film exists. The results have confirmed localization of fields, although the degree of localization depends on specific parameters. For circular nanostructures, those with 200-nm diameter showed the highest localization at 532-nm wavelength. At 850-nm wavelength, the localization was the highest for nanostructures of 100-nm diameter, in which case the localized field enhancement was as high as 961 times over the incident light. More extensive results including the influence on the field distribution and enhancement and the temporal dynamics of localized near-fields at and near nanostructures are to be discussed.

9340-34, Session PSun

Silver nanoislands based SERS-active substrates for DNAs detection

Hyerin Song, Seunghun Lee, Taeyoung Kang, Kyujung Kim, Pusan National Univ. (Korea, Republic of)

Conventional Raman spectroscopy is a useful tool for qualitative analysis. As conventional Raman spectroscopy does not provide distinctive spectra since the intensities of the signal are weak, many researchers are eager to overcome the limitation. SERS is one of the powerful advanced

**Conference 9340:
Plasmonics in Biology and Medicine XII**

Raman spectroscopy. Our research is based on SERS and enhances signal intensities by applying nanoisland structures. Nanoislands structure localizes electromagnetic fields by surface plasmon phenomena and it enhances intensity of Raman signal. To observe the correlation between the amount of enhanced signal intensities and the sizes of the nanoisland structures, diverse sizes of silver nanoisland structures were fabricated by a thermal annealing method from the 10 nm, 20 nm and 30 nm thickness of silver films for SERS-active substrates. Annealing temperature was 200 °C and the process was done for 10 minutes. To confirm enhancing effects, we measured Raman spectra of gold nanoparticles attached DNAs on the nanoisland structures. Consequently, we obtained distinct enhanced Raman spectra, and found the correlations between sizes of nanoislands which depend on thickness of initial silver films and enhancement factors. This silver nanoisland structured SERS-active substrate can be easily fabricated by a hotplate and we verified the efficiency of the substrates. The result suggests that nanoislands substrates can be used as an efficient SERS-active substrate for detecting low concentrations of tiny biomolecules.

9340-35, Session PSun

Surface-plasmon enhanced Brillouin scattering from gold nano-structures

Zhaokai Meng, Vladislav V. Yakovlev, Texas A&M Univ. (United States)

Brillouin spectroscopy is a powerful tool for elasticity-sensitive non-invasive optical imaging. However, its relatively weak signal strength usually results long acquisition time and poor spectral quality. In this study, enhancements of Brillouin scattering at 532 nm was observed from various acoustic modes on glass coated with periodic arrays of gold nanodisks. The similar enhancements were also observed from the bulk phonons within various liquids (including methanol and water) covered on the gold nanodisks. This enhancement is considered to be attributed by the surface plasmons generated by the nanostructures, and is found to be dependent on their geometries (i.e., aspect ratio and diameter) of the golden nanodisks. When employing the recent advances in virtually imaged phased array (VIPA) based background-free Brillouin spectrometers, the acquisition time could even be further optimized [1]. The results of this study suggest that nanodisk arrays can provide a platform for surface-enhanced Brillouin scattering analogous to other surface-enhanced spectroscopies, and suggest an approach for further reduce the integration time for Brillouin spectroscopy.

Reference:

1. Meng, Z., Traverso, A. J., & Yakovlev, V. V., *Optics express*, 2014, 22(5), 5410-5416.

9340-36, Session PSun

Optical properties of plasmon-resonant gold nanoparticles with different morphologies

Olga Bibikova, Univ. of Oulu (Finland) and Saratov State Univ. (Russian Federation); Alexey Popov, Alexander Bykov, Prateek Singh, Univ. of Oulu (Finland); Elizaveta Panfilova, Institute of Biochemistry and Physiology of Plants and Microorganisms (Russian Federation); Vitaly Khanadeev, Institute of Biochemistry and Physiology of Plants and Microorganisms (Russian Federation) and Saratov State Univ. (Russian Federation); Ilya Skovorodkin, Univ. of Oulu (Finland); Boris Khlebtsov, Institute of Biochemistry and Physiology of Plants and Microorganisms (Russian Federation) and Saratov State Univ. (Russian Federation); Matti Kinnunen, Seppo

Vainio, Krisztian Kordas, Univ. of Oulu (Finland); Vladimir Bogatyrev, Nikolai Khlebtsov, Institute of Biochemistry and Physiology of Plants and Microorganisms (Russian Federation) and Saratov State Univ. (Russian Federation); Valery V. Tuchin, N.G. Chernyshevsky Saratov State Univ. (Russian Federation) and Univ. of Oulu (Finland)

Plasmon-resonant gold nanoparticles (PRNPs) have been widely used in various biomedical applications, which are based on two principles: (1) unique optical properties, which are determined by PRNPs size, morphology, structure; (2) functionalization of the PRNPs surface.

In this work, we estimated the ratio between scattering and absorption coefficients of PRNPs (naked or encapsulated in silica shells) with different morphologies. A silica shell around a nanoparticle was prepared as described elsewhere [1]. We compared the backscattering of nanospheres synthesized by Frens method [2] and nanostars prepared as described by Yuan et al [3] in tissue-mimicking phantoms by the confocal microscopy. The nanospheres have higher scattering ability in comparison with the nanostars of a comparable size.

Scattering properties of PRNPs and silica-gold nanocomposites were investigated using optical coherence tomography (OCT) by imaging of nanoparticle suspensions in glass capillary. The most intensive signal was registered from the nanocomposites suspensions.

The as-prepared and functionalized PRNPs of different morphology were used for cell optoporation. The cells were irradiated by a laser in the presence of PRNPs for enhanced cell membrane permeabilization and more efficient penetration of targetes into cells.

References:

1. Khlebtsov B., Panfilova E., Khanadeev V., Bibikova O., Terentyuk G., Ivanov A., Rumyantseva V., Shilov I., Ryabova A., Loshchenov V., Khlebtsov N. *ACS Nano* 9, 7077–7089 (2011).
2. Frens G. *Nature: Phys. Sci.* 241, 20-22 (1973).
3. Yuan, H., Khoury, C. G., Hwang, H., Wilson, Ch. M., Grant, G. A., Vo-Dinh, T. *Nanotechnology* 23(7), 075102 (2012).

9340-37, Session PSun

Dynamic plasmonic trapping and manipulation of metallic particles for SERS application

Yuquan Zhang, Nankai Univ. (China)

We introduce a novel plasmonic tweezers for trapping and manipulating metallic particles and its application on Surface-enhanced Raman scattering (SERS). In the first part, we discuss the interaction mechanism between metallic particles and surface plasmons (SPs) in the plasmonic tweezers excited by a focused radially polarized beam. We show that metallic particles of nanometer to micrometer sizes can be attracted and trapped in such plasmonic tweezers instead of being repulsed by a conventional optical tweezers due to high scattering force. Through numerical analysis, we find that the resultant total force in the plasmonic tweezers is the result not of a stronger gradient force dominating an opposing scattering force, but instead of a dominant gradient force assisted by a weak scattering force acting in the same direction. Then we consider manipulating the metallic particles by modifying the incident beam properties in the plasmonic tweezers. The optical vortices (OV) are chosen to excite the plasmonic vortices and rotate particles in the plasmonic tweezers. We show that metallic particles in plasmonic vortices can be trapped and rotated in a certain radius according to OV's topological charge, due to the optical force provided by the orbital angular momentum (OAM). Finally, we introduce the application of the plasmonic tweezers in SERS. By trapping and dragging a single gold nanoparticle with the plasmonic tweezers, we demonstrated a dynamic single-particle-film SERS system, which produces a SERS enhancement factor of $\sim 10^9$, and therefore provides a promising approach to controllable SERS detection and imaging.

Conference 9341: Bioinspired, Biointegrated, Bioengineered Photonic Devices III

Saturday - Sunday 7 -8 February 2015

Part of Proceedings of SPIE Vol. 9341 Bioinspired, Biointegrated, Bioengineered Photonic Devices III

9341-1, Session 1

DNA probe based multiplexing and super-resolution imaging (*Keynote Presentation*)

Peng Yin, Harvard Univ. (United States)

Super-resolution fluorescence microscopy is a powerful tool for biological research, but obtaining multiplexed images for a large number of distinct target species remains challenging. Here we use the transient binding of short fluorescently labeled oligonucleotides (DNA-PAINT, a variation of point accumulation for imaging in nanoscale topography) for simple and easy-to-implement multiplexed super-resolution imaging that achieves sub-10-nm spatial resolution in vitro on synthetic DNA structures. We also report a multiplexing approach (Exchange-PAINT) that allows sequential imaging of multiple targets using only a single dye and a single laser source. We experimentally demonstrate ten-color super-resolution imaging in vitro on synthetic DNA structures as well as four-color two-dimensional (2D) imaging and three-color 3D imaging of proteins in fixed cells.

9341-2, Session 2

Bioinspired stimuli-responsive color-tunable photonic fibers

Mathias Kolle, Joseph D. Sandt, Massachusetts Institute of Technology (United States); James Hardin, Harvard Univ. (United States); Christian D. Argenti, Massachusetts Institute of Technology (United States); Jennifer A. Lewis, Joanna Aizenberg, Harvard Univ. (United States)

Biological materials have evolved in countless cases to satisfy a diverse range of sophisticated optical, mechanical, or chemical requirements imposed by stringent boundary conditions on the respective organisms' survival. Multifunctional biological materials perform well in harsh environments and outcompete many man-made material solutions. 21st century materials and technology innovation would benefit from a much more systematic biological approach to materials design. Our research is focused on identifying universal material and system design rules at the origin of nature's most unique light manipulation strategies, and on implementing key concepts in artificial optical material development scenarios. Here, this strategy is exemplified in the study of a recently invented bio-inspired photonic fiber material. The mechano-sensitive color-tunable photonic fibers consist of an elastic core and an elastomer-based multilayer cladding. Light interference in the curved, concentrically arranged, layered nano-scale cladding architecture is responsible for the macroscopically emerging bright, vivid coloration. Fibers with claddings composed of between 30 and 250 bilayers can be manufactured at room temperature. The fibers exhibit a reflectivity of up to 95% and narrow reflection bandwidths. Being exclusively composed of elastic materials, the fibers can be reversibly deformed up to a strain of 150%, which results in a simultaneous, predictable variation of the fibers' optical appearance. Inspired by a biological photonic material, the soft photonic fiber system provides a rich platform for investigating the interplay of composition and morphology at multiple length scales, which is frequently exploited by natural organisms to tailor a material's functionality, and can be exploited in human applications.

9341-3, Session 2

Bioinspired artificial light collectors for enhancement of imaging in dim environments

Hewei Liu, Yinggang Huang, Chi-Chieh Huang, Hongrui Jiang, Univ. of Wisconsin-Madison (United States)

Owing to the structural and fabrication technological limitations, the light sensitivity of the artificial imaging sensors such as charge-coupled device (CCD) cannot be compared to the sensitivity of the natural visual systems. Therefore, it is difficult to capture clear images for manmade observing devices in dim environments. In nature, elephantnose fish (*Gnathonemus petersii*) has evolved a special visual system to detect objects in dim and turbid water. A group of sandglass-shaped micro-cups are arranged in front of the photoreceptors, and the inner reflecting surface of the cups can collect light into the bottom where the photoreceptors are located. Inspired by this functional retina structure, we developed an artificial light collector array to improve the imaging ability of sensors in dim environments. Each collector acts as a parabolic mirror in micrometer-scale which reflects the incoming light from a large input to a small output, increasing the light intensity for several times. With the light collectors, the imaging sensors can get images in very dim environments. The fabrication of the light collectors was realized by a series of techniques based on femtosecond laser 3D micromachining. The light collectors were transferred onto a PDMS hemispherical shell, which is more closed to the structure of the fish retina. By scanning the device and image processing techniques such as super-resolution image reconstruction, high-resolution images can be achieved.

9341-4, Session 2

Design and microfabrication of an artificial compound eye inspired by vision mechanism of *Xenos peckii*

Dongmin Keum, Inchang Choi, Min H. Kim, Ki-Hun Jeong, KAIST (Korea, Republic of)

Xenos Peckii, which is an endoparasite of paper wasps has an unusual visual system. The eyes of the male *Xenos Peckii* have a small number of optical units with a large convex lens and multiple photoreceptor cells. Each optical unit, called eyelet, can capture part of the total field of view (FOV), and the whole image is completed by assembling the partial images from each eyelet. This optical scheme results in higher resolution and better sensitivity than conventional compound eyes. Here, we present an artificial compound eye (ACE) inspired by the vision mechanism of *Xenos Peckii*. A single channel of the ACE consists of a post with slanted top surface to refract the incident light, and a microlens to focus the light from the post structure. The post arrays were fabricated by pressing a spin-coated photoresist using a ball lens during softbaking process and illuminating UV light from backside of the glass substrate with a prepatterned metal mask. The microlens arrays were developed using a resist reflow and a microimprinting method. Each channel detects a part of the whole FOV, and the images are stitched in the following image processing step. A conventional image sensor can be directly integrated with the device due to the flat image plane. The proposed method provides technical solutions for miniaturized wide FOV and high resolution compound eye camera, which can be combined with commercialized image sensors.

**Conference 9341: Bioinspired, Biointegrated,
Bioengineered Photonic Devices III**

9341-5, Session 2

Biomimetic photonic structures and sensors *(Invited Paper)*

Rajesh R. Naik, Air Force Research Lab. (United States)

Biomimetics is an interdisciplinary effort aimed at understanding biological principles and then applying those principles to improve existing technology. Nature has been able to achieve some incredible performance properties using a limited materials palette through a hierarchy of organization that spans from the molecular to the macroscopic to create optical structures and sensors. In my talk, I will describe our research efforts in the area of biomimetics to develop materials and sensors. Our research efforts have been directed at not only understanding how biological organisms create optical structures, but also how this process can be replicated to create sensor materials. We also explore the use of plasmonics as tool to probe biomolecular structure and interfacial interactions with nanomaterial surfaces. I will also cover some of our recent work towards developing low-cost, devices using localized surface plasmon resonance (LSPR) spectroscopy of metallic nanoparticles for chemical and biological sensing.

9341-6, Session 3

Organic ultrathin-film photonic and electronic devices on 1 μm thick ultra-flexible substrate *(Invited Paper)*

Tomoyuki Yokota, The Univ. of Tokyo (Japan); Tsuyoshi Sekitani, The Univ. of Tokyo (Japan) and Osaka Univ. (Japan); Martin Kaltenbrunner, Univ. of Tokyo (Japan) and Johannes Kepler Univ. Linz (Austria); Siegfried G. Bauer, Johannes Kepler Univ. Linz (Austria); Takao Someya, The Univ. of Tokyo (Japan)

We report recent progress of organic ultrathin-film photonic and electronic devices that are manufactured on 1- μm -thick polymeric films. First, the polymer-based organic solar cells were fabricated on the 1.2- μm polyethylene naphthalate (PEN) foils. These devices are as low as 4 g/m² with efficiency of 4.2%, which is comparable to that on glass substrate. The specific weight is evaluated to be 10 W/g, which is the largest reported for any solar cell technology including inorganic devices. These devices also show large, reversible quasi-linear compression ratios over 70%. In this development, we used PEDOT:PSS as a transparent electrode, instead of ITO. The change in resistance of PEDOT:PSS on the 1.2- μm PEN film was negligibly small (<1%) after 100 cycles of application of 50% compression. By making full use of such mechanical flexibility, the organic solar cells were laminated with pre-stretched rubber substrate to make flexible devices to be stretchable. Second, the OLED devices were manufactured on 1.4 μm polyethylene terephthalate (PET) by using highly flexible conducting polymers, semiconducting polymers, and thin metal layers. They are shown to be extremely flexible, with the radii of curvature below 10 μm , with luminance of 100 cd/m². Third, we have fabricated the 2-V operational organic thin-film transistors which have very thin gate dielectric layers comprising 20-nm thick aluminum oxide layer and self-assembled monolayer (SAMs). The transistors exhibit the mobility of 1.6 cm²/Vs and large on-off ratio (>10⁸).

9341-7, Session 3

A wearable, conformal, optical sensor bandage for the non-invasive, two-dimensional mapping of cutaneous oxygenation

Zongxi Li, Emmanuel Roussakis, Wellman Ctr. for Photomedicine, Harvard Medical School (United States); Pieter L. Koolen, Ahmed M. S. Ibrahim, Kuyulhee Kim, Beth Israel Deaconess Medical Ctr., Harvard Medical School (United States); Lloyd F. Rose, Jesse Wu, U.S. Army Institute of Surgical Research (United States); Alexander J. Nichols, Wellman Ctr. for Photomedicine, Harvard Medical School (United States); Yunjung Baek, KAIST (Korea, Republic of); Reginald Birngruber, Univ. zu Lübeck (Germany); Gabriela Apiou-Sbirlea, Wellman Ctr. for Photomedicine, Harvard Medical School (United States); Robina Matyal, Thomas Huang, Beth Israel Deaconess Medical Ctr., Harvard Medical School (United States); Rodney Chan, U.S. Army Institute of Surgical Research (United States); Samuel J. Lin, Beth Israel Deaconess Medical Ctr., Harvard Medical School (United States); Conor L. Evans, Wellman Ctr. for Photomedicine, Harvard Medical School (United States)

Clinical monitoring of wound oxygenation with high spatiotemporal resolution poses a considerable challenge, due to the complex surface topology and soft mechanics of the skin. Current clinical oxygen sensing techniques are often limited to point measurements, or rely on bulky and expensive optical systems. Here, using a rapid-drying, liquid bandage containing oxygen-sensing molecules, we created a wearable sensor bandage that conforms the surface geometry of skin and wounds, and provides two-dimensional maps of cutaneous oxygenation in a non-disruptive fashion. By embedding both an oxygen-sensing porphyrin-dendrimer phosphor and a reference dye in a biocompatible liquid bandage matrix, the phosphorescence intensity and lifetime of the sensor bandage captured by a camera-based imaging device can be used to quantify and map both the pO₂ and oxygen consumption of the underlying tissue. The transparent bandage gives visual access to the underlying tissue while providing long-term wound protection. Proof-of-principle studies have been performed on several clinically-relevant animal models to demonstrate the sensor's ability to monitor tissue ischemia, burn progression, as well as skin graft integration.

9341-8, Session 3

Optical design and modelling of tissue for application as wearable optoelectronic sensors

Olena Kulyk, Ashu K. Bansal, Shuoben Hou, Eric M. Bowman, Ifor D. W. Samuel, Univ. of St. Andrews (United Kingdom)

Studying light-tissue interactions enables the development of novel non-invasive sensing methods, which introduce improvements to current conventional diagnostic techniques and allow chronic ambulatory monitoring. In this work we explore the anisotropic optical properties of muscle, and design an optical model for complex tissue containing: the skin, adipose tissue, and muscle. We have developed optical designs of wearable sensors which detect backscattered light from tissue and simulated the operation to optimize the performance of prototype devices. In this work, we will demonstrate wearable sensors for tissue oxygenation, and isotonic/isometric muscle contraction sensing. These wearable sensors

**Conference 9341: Bioinspired, Biointegrated,
Bioengineered Photonic Devices III**

have been made using organic semiconductors, which in addition to being non-invasive, introduce benefits such as flexibility, low weight, wavelength tunability, easy fabrication and the possibility to make large uniform areas for both sources and detectors. We will present a proof of concept application for the muscle contraction sensor, actuating a robotic arm using the signals coming from a volunteer's biceps and deltoid muscles and we will discuss the potential for improving the functionality of current active prosthetics.

9341-9, Session 3
OLED microdisplays as biophotonic platform for optogenetics

Anja Steude, Malte C. Gather, Univ. of St. Andrews (United Kingdom)

Organic light-emitting diode (OLEDs) microdisplays are novel optoelectronic devices which are already applied in electronic viewfinders, video cameras, or personal video players integrated in wearable glasses. They typically comprise of a silicon chip containing the electronics to address $> 10^5$ individual top-emitting OLED pixels deposited directly on the chip and covered only by a micrometer thin barrier layer. Here, we discuss the prospect of using OLED microdisplays as platform for advanced cell biology and optical cell manipulation. The displays have a size of a few millimeters and each pixel has dimensions in the range of several micrometers; small enough to resolve, address and interface parts of individual live cells. As a first proof-of-principle, we investigated the biophysics of light-controlled locomotion (phototaxis) of the green alga *Chlamydomonas reinhardtii*. Besides being a famous model organism for cellular movement, photosynthesis, light-perception, and cell-cell-recognition, this unicellular alga is the natural source for photoreceptors that established the fast-growing novel research field of optogenetics, i.e. the combination of optics and genetics to observe and control cells or tissue. Using OLED microdisplays, we propose to perform optogenetics with high spatial and temporal resolution to investigate processes like neuronal activity or cell signalling.

9341-10, Session 4
MicroLED probes for optogenetic control of cortical circuits (Invited Paper)

Keith Mathieson, Robert Scharf, Niall McAlinden, Erdan Gu, Shuzo Sakata, Martin D. Dawson, Univ. of Strathclyde (United Kingdom)

Many interesting regions of the brain lie deep below the surface making it challenging to deliver light in a spatially precise fashion using wavefront correction imaging techniques. An alternative method is to use waveguides or fibres. However, scaling up to many optical sites using these techniques can lead to an invasive probe that damages the neural circuitry under study. One solution is to microfabricate cellular-scale LEDs on a minimally invasive probe allowing the delivery light to deep areas of the brain with high spatiotemporal accuracy [1,2]. Here we report on gallium nitride on silicon probes with multiple LEDs per shank. The probes are 80 μ m wide, 30 μ m thin and cover ~1mm of cortex with LEDs that can be as small as 10 μ m in diameter. Each LED provides an irradiance up to 500mW/mm² at the surface. We have studied the light output of these devices, the volume of tissue illuminated and the thermal characteristics of the probes. We show that the microLED devices can operate at pulse widths and frequencies relevant to optogenetic studies without increasing the temperature of nearby neurons by more than 0.5 $^{\circ}$ C. The probes have shown site-specific activation of cortical neurons in vivo in mice expressing channelrhodopsin-2. This provides an optical interface for controlling neural activity in targeted neural circuits aimed at furthering our understanding of cortical processes.

[1] McAlinden et al. OPTICS LETTERS, Vol. 38, No. 6, March 2013

[2] Kim et al. SCIENCE, Vol. 340, No. 211, April 2013

9341-11, Session 4
Femtosecond pumped biological laser

Mark Mackenzie, Heriot-Watt Univ. (United Kingdom); Hamilton Charlotte, Heriot-Watt Univ. (United Kingdom) and The Univ. of Edinburgh (United Kingdom); Kirsty J. Martin, Rebecca S. Saleeb, Rory R. Duncan, Lynn Paterson, Ajoy K. Kar, Heriot-Watt Univ. (United Kingdom)

A biological laser was created using Human Embryonic Kidney cells containing the fluorescent dye Calcein AM. The cells were placed in a laser cavity formed from two high reflectivity dielectric plane mirrors with a separation of 9 μ m, defined using microspheres, and aligned using plastic screws pressing on one of the mirrors. The alignment was measured by reflecting the beam of a HeNe laser off the two cavity mirrors and observing the interference fringes created by the two overlapping reflections. The cells were pumped using the output of an OPO frequency doubled twice in BBO crystals to give 474nm femtosecond pulses and focused through a 16x objective (0.25 NA). Single cells were observed to lase on multiple longitudinal and transverse modes with lasing lasting up to 50s, for an input pulse energy of 1.25 nJ at 1 kHz repetition rate. The above results will be presented as well as an investigation of alternative gain media and the potential applications of biological lasers which we aim to demonstrate in future work.

9341-12, Session 4
Demonstration of cell lasers made from common cell types and different fluorescent dyes

Matjaz Humar, Wellman Ctr. for Photomedicine (United States) and Harvard Medical School (United States) and Jožef Stefan Institute (Slovenia); Seok Hyun Yun, Wellman Ctr. for Photomedicine (United States) and Harvard Medical School (United States)

Lasers made from biological materials are a very promising technology, which can pave the way to biocompatible light sources, more efficient sensing, flow cytometry and imaging. Here we present a novel method for transforming single cells to laser sources using simple well known procedures, materials and cells. The cells are placed in between two highly reflective dielectric mirrors used as the laser resonator. Fluorescent stains commonly used for cell staining were employed as the laser gain. Depending on the specific dye molecule, the dye was present either only in the interior of the cell or only in the exterior medium or both. The cells in between mirrors were pumped by an external laser and the spectrum as well as the light distribution were measured using a spectrometer and a camera. The cells have higher refractive index than the surrounding medium and act as lenses making the laser cavity stable and insensitive to misalignments. We have demonstrated lasing in range of wavelengths from green to red, dependent on the dye and mirrors used. The lasing of individual cell is stable in time and the lifetime of the laser exceeds 10,000 pulses at 10 Hz repetition rate. Each cell presents a multitude of different transversal lasing modes, which are dependent upon the shape and refractive index distribution inside the cell. As a proof of concept we show how the transversal modes change as we change the osmolarity of the medium. The cell laser modes could be used for cell characterization and sensing.

**Conference 9341: Bioinspired, Biointegrated,
Bioengineered Photonic Devices III**

9341-13, Session 4

Photodynamic therapy using internal molecular resonance energy transfer source

Seonghoon Kim, Yi Rang Kim, HyeongChan Jo, Mijeong Jeon, KAIST (Korea, Republic of); Seok Hyun Yun, Wellman Ctr. for Photomedicine (United States) and Massachusetts General Hospital (United States) and KAIST (Korea, Republic of)

Conventional photodynamic therapy (PDT) uses external light irradiation to excite photosensitizers and produce selective cytotoxicity on target tissues. A common challenge in this technique has been a shallow light penetration depth of <1 cm in tissue, which has limited the clinical applications of PDT to the diseases localized in superficial tissues, such as the skin, retina, or epithelial layers of hollow organs that can be accessed by fiber-optic catheters. We have demonstrated a novel approach using bioluminescence as an internal energy source that can excite photosensitizers at the cell membrane via Förster resonance energy transfer. Previously, we have used quantum dot-assisted bioluminescence sources and delivered them separately from photosensitizers. Here, we report a chemical conjugate of Renilla luciferase 8.6 and rose bengal to maximize the FRET efficiency. We found that the amount of reactive oxygen species generated by the conjugates was enough to kill cancer cells in vitro as confirmed by an MTT assay. The cytotoxicity level was actually higher than that of conventional PDT at a laser intensity of a few mW. The results suggest a novel therapeutic strategy to treat diseases beyond the reach of current PDT procedures, potentially in combination with other treatment modalities, such as chemotherapy.

9341-14, Session 4

Micro-patterning colloidal quantum dots based light sources for cellular array imaging (Invited Paper)

Gauri Behave, The University of Texas at Austin (United States); Elaine Ng, Stanford University (United States); Youngkyu Lee, The University of Texas at Austin (United States); Xiaojing Zhang, Dartmouth College (United States)

We have developed a colloidal quantum dot (QD) - based multicolor excitation light source array designed for high throughput lab-on-a-chip cell screening and imaging. We have demonstrated preliminary measurements of fluorescence excitation that is suitable for the arrayed fluorescence immunoassay. Ex vivo transmission microscopy and fluorescence imaging of cultured cancer cells (MDA-MB 231 and SKBr3) were performed to demonstrate the efficacy of the QD-based light source. Our low-cost light source array is highly compatible with commercially available fluorescence microscopes and fluorescent markers commonly used for biomedical imaging and screening.

9341-15, Session 5

Analysis of quasi-periodic pore structure of centric marine diatom frustules

Gregory A. Cohoon, Univ. of Arizona (United States); Christine E. Alvarez, Keith Meyers, The Univ. of Arizona (United States); Dimitri D. Deheyn, Mark Hildebrand, Scripps Institution of Oceanography (United States); Khanh Q. Kieu, The Univ. of Arizona (United States);

Robert A. Norwood, Scripps Institution of Oceanography (United States)

Diatoms are a common type of phytoplankton characterized by their silica skeleton called a frustule. The diatom frustule is composed of two valves and a series of connecting girdle bands. Diatom frustules have a unique shape and valves in particular species display an intricate pattern of pores resembling a photonic crystal structure. The diatoms analyzed are from the cylindrical shaped Coscinodiscophyceae order. Our work focuses on two diatom species in particular Coscinodiscus wailiesii and Coscinodiscus radiatus. These diatoms are chosen for their large size and previous work on the optical filtering properties of the frustule. We use various numerical techniques to analyze the periodic and quasi-periodic valve pore structure on diatoms using MATLAB's image processing and graph libraries. The process consists of analyzing scanning electron microscope images of the diatom valve to find pore locations and then generating a spatial graph connecting each pore to its nearest neighbors. With this approach we can analyze the graph to find pores with regular and irregular connections. We quantitatively identify defect locations and pore spacing information in the valve and use this information to better understand the optical and biological properties of the diatom.

9341-16, Session 5

Effect of ICG concentration on the fluorescence characteristics of erythrocyte-derived optical vectors

Jack Tang, Danielle Bacon, Univ. of California, Riverside (United States); Victor Sun, Wangcun Jia, John S. Nelson, Univ. of California, Irvine (United States); Bahman Anvari, Univ. of California, Riverside (United States)

Indocyanine green (ICG) is the only near-infrared (NIR) dye approved by the FDA for specific imaging applications such as choroidal angiography, and assessment of cardiac and hepatic function. Despite its long history of clinical use, the potential of ICG as a chromophore for broader imaging and phototherapeutic applications has been limited due to its short circulation half-life, and nearly exclusive uptake by the liver. Encapsulation of ICG has been investigated as an approach to prolong its circulation time. We have utilized erythrocytes as a platform for ICG encapsulation and delivery. We refer to these constructs as NIR erythrocyte-mimicking transducers (NETs) as they are capable of transducing the NIR light into heat or fluorescence emission. To utilize NETs as effective probes for fluorescence imaging, we aim to maximize their fluorescence quantum yield by changing the ICG loading concentration between 40–320 μM during the fabrication process.

Our results indicate that the relative fluorescence quantum yield of NETs is increased by $\approx 10\%$ when doubling the loading concentration of ICG from 40 μM to 80 μM . However, further increasing the ICG loading concentration from 80 μM to 160 μM reduces the fluorescence quantum yield by $\approx 50\%$ due to self-quenching. Thus, there is an optimal ICG loading concentration that maximizes the fluorescence quantum yield of NETs. These findings serve as the basis for the engineering of NETs with potential for in-vivo imaging.

9341-17, Session 5

Bioinspired biomedical devices: analysis of the labrum of aedes aegypti mosquitoes via Raman and Brillouin microspectroscopy

Vladislav V. Yakovlev, Texas A&M Univ. (United States)

Mosquitoes demand recognition in the field of biofluidics by reason of a flexible, minimally-invasive microneedle, the labrum, which is utilized for painless insertion into tissue and extraction of biological fluid. Mimicry of the female mosquito labrum for use as a biomedical device is no trivial task

Conference 9341: Bioinspired, Biointegrated, Bioengineered Photonic Devices III

as a complete understanding of morphology, and chemical composition is required. Previous literature has analyzed the physical structure of the labrum and employed it as a template for microneedle design, but this literature fails to address the chemical architecture and local mechanical properties from which the labrum acquires its utility. This work proposes that through quantification of the chemical architecture and mechanical properties a more complete understanding of the unique utility of the mosquito labrum may be formulated. A powerful combination of Raman and Brillouin microspectroscopies was used to assess for chemical composition and elastic properties of the labrum. Implications of the data herein are fabrication of a more robust microneedle device suitable for applications in the field of medicine in the areas of therapeutic drug delivery and pain mitigation during biofluid collection.

9341-18, Session 5

Natural production of biological optical systems

Seung Ho Choi, Young L. Kim, Purdue Univ. (United States)

Synthesis and production in nature often provide ideas to design and fabricate advanced biomimetic photonic materials and structures, leading to excellent physical properties and enhanced performance. In addition, the recognition and utilization of natural or biological substances have been typical routes to develop biocompatible and biodegradable materials for medical applications. In this respect, biological lasers utilizing such biomaterials and biostructures have been received considerable attention, given a variety of implications and potentials for bioimaging, biosensing, implantation, and therapy. However, without relying on industrial facilities, eco-friendly massive production of such optical components or systems has not yet been investigated. We show examples of bioproduction of biological lasers using agriculture and fisheries. We anticipate that such approaches will open new possibilities for scalable eco-friendly 'green' production of biological photonics components and systems.

9341-19, Session 5

Untwisting the polarization properties of light reflected by scarab beetles

Luke McDonald, Ewan D. Finlayson, Peter Vukusic, Univ. of Exeter (United Kingdom)

Despite previously published work describing aspects of circularly polarised (CP) reflection in biological systems [1-4], there is a scientific appetite for enhanced understanding of how the structure of some beetles' exoskeletons manipulate polarisation states of reflected light. To this end, we set out to quantify the bidirectional reflectance distribution function (BRDF) directly associated with the CP properties of several broadband reflecting beetles.

We use the experimental technique of imaging scatterometry (ISM), whereby scattered light is recorded concurrently as a function of incident angle and wavelength [5, 6]. By incorporating circularly polarising filters, we have measured the CP response of several species of broadband reflecting beetle belonging to the genus *Chrysina*.

The handedness of polarised light reflected from many Scarabs is left-handed [1-3]. Some species, however, such as *C. resplendens* are also observed to reflect right-handed light. In addition to the polarisation signature of the reflected light, the reflected hue and intensity are also determined by the structure of the outer region of the beetles' exoskeleton. In conjunction with experimental optical measurements, we have used modelling to extract key structural and optical parameters from the exoskeletal nano-architecture, using a model based on a twisted, birefringent, lamella structure revealed by transmission electron micrographs.

This work elucidates for the first time the full BRDF associated with circular polarisation and highlights the subtle differences in structural makeup that influence the variations in complete optical signatures of the *Chrysina* genus.

[1] S. A. Jewell, P. Vukusic, N. W. Roberts, N. J. Physics. 9, 99 (2007)

[2] V. Sharma et al., Science, 325, 449-51 (2009)

[3] H. Arwin et al., Philosophical Magazine, 92, 1583-99 (2012)

[4] T. Chiou et al., Current Biology, 18, 429-34 (2008)

[5] D. Stavenga et al., Optics express, 17, 193-202 (2009)

[6] P. Vukusic, D. Stavenga, J. R. Soc. Interface, 6, 133-48 (2009)

9341-20, Session 5

Progress towards elucidating the structure-function relationships of a natural nanoscale photonic device in cuttlefish chromatophores (*Invited Paper*)

Leila Deravi, The Univ. of New Hampshire (United States); Andrew P. Magyar, Sean Sheehy, Harvard Univ. (United States); George Bell, Lydia Mathger, Alan Kuzirian, Roger T. Hanlon, Marine Biological Lab. (United States); Evelyn L. Hu, Kevin Kit Parker, Harvard Univ. (United States)

Cuttlefish, *Sepia officinalis*, possess neurally controlled, pigmented chromatophores that allow rapid changes in skin patterning and coloration in response to visual cues. This process of adaptive coloration is enabled by the 500% change in chromatophore surface area during actuation. We report three adaptations that help explain how color intensity is maintained in a fully expanded chromatophore when the pigment granules are distributed maximally: (i) a tether system that presumably helps distribute individual granules to the periphery, (ii) pigment layers as thin as three granules that are optically effective, and (iii) the presence of high-refractive-index proteins - reflectin and crystallin - in granules. The latter discovery, combined with our finding that isolated chromatophore pigment granules fluoresce between 650-720 nm, refutes the prevailing hypothesis that cephalopod chromatophores are exclusively pigmentary organs composed solely of omochromes. Perturbations to granular architecture alter optical properties, illustrating a role for nanostructure in the agile, optical responses of chromatophores. Our results suggest that chromatophore pigment granules are more complex than homogeneous clusters of chromogenic pigments. They are luminescent protein nanostructures that facilitate the rapid and sophisticated changes exhibited in dermal pigmentation.

9341-21, Session 6

Biocompatible step-index optical fibers made of hydrogels

Myunghwan Choi, Harvard Medical School (United States); Matjas Humar, Harvard Medical School (United States) and Massachusetts General Hospital (United States) and Jožef Stefan Institute (Slovenia); Xiangwei Zhao, Southeast Univ. (China); Seok-Hyun Yun, Harvard Medical School (United States)

The limited penetration of light in biological tissue poses a serious challenge for many applications of light in vivo. Optical fibers or endoscopes have been widely used to deliver light into the body, but the materials, such as glass and plastic, that are commonly used in the light-guiding devices are not biocompatible and must be removed after use. To overcome this limitation, we fabricated a step-indexed optical fiber using biocompatible hydrogels. Flexible hydrogels may be implanted in tissue. By optimizing chemical compositions, we attained efficient light guiding at clinical scale with 1/e attenuation length greater than 10 cm. In addition to conventional applications in optical sensing, the permeable nature of hydrogels allowed in situ doping of chemicals to the fibers. Doping of laser dyes allowed light amplification, generation of amplified spontaneous emission, and whispering-gallery-mode lasing. We envision that hydrogel optical fibers may be useful for optical health monitoring and light-based therapy in vivo.

**Conference 9341: Bioinspired, Biointegrated,
Bioengineered Photonic Devices III**

9341-22, Session 6

Towards a multi-functional disposable microneedle based probe

Clement Yuen, Quan Liu, Nanyang Technological Univ. (Singapore)

Recently, we showed the advantage of using the silver-coated stainless steel microneedle to act as a probe for intradermal surface enhanced Raman scattering (SERS) measurements in a skin-mimicking phantom to: 1) provide more specific chemical information of the endogenous biomolecules than other techniques, such as fluorescence, 2) offer augmented signal and improved penetration depth in contrast to the ordinary Raman spectroscopy, and 3) eliminate the need for skillful needle administration and the subcutaneous injection of SERS-active nanoparticles in the typical SERS in vivo measurements. However, these stainless steel microneedles, and other metal microneedles, or hypodermic needles pose several issues in: 1) sharp waste production, 2) contamination due to reuse of microneedle, and 3) bio-incompatibility if breakage occurs. Although a dissolvable microneedle can solve these aforesaid issues, bodily fluid sampling and drug delivery are difficult to be realized in a dissolved needle. Moreover, the fabrication of dissolved needles requires expensive techniques and stringent requirements, e.g. photolithography, and clean room.

In this paper, we investigate a cost-effective alternative to realize a microneedle made of agarose for SERS measurements in a skin-mimicking phantom. We also study the shape-changing capability of the microneedle after usage to avoid reuse and prevent sharp waste production. The feasibility of using the microneedle to draw and dispense fluid is also investigated, which is analogous to the delivery of drug and sampling of bodily fluid, showing that the device is promising to function: 1) as a measurement probe, 2) for drug delivery, and 3) for bodily fluid sampling, in biomedical applications.

9341-23, Session 6

An optical microneedle for antimicrobial blue light therapy

Jeesoo An, Wellman Ctr. for Photomedicine, Massachusetts General Hospital (United States) and Harvard Medical School (United States); Caio M. Guimaraes, Univ. de Pernambuco (Brazil); Matjaz Humar, Wellman Ctr. for Photomedicine, Massachusetts General Hospital (United States) and Harvard Medical School (United States) and Jožef Stefan Institute (Slovenia); Moonseok Kim, Wellman Ctr. for Photomedicine, Massachusetts General Hospital (United States) and Harvard Medical School (United States); Myunghwan Choi, Wellman Ctr. for Photomedicine (United States) and Harvard Medical School (United States); Tianhong Dai, Wellman Ctr. for Photomedicine (United States) and Massachusetts General Hospital (United States); Seok-Hyun Yun, Wellman Ctr. for Photomedicine, Massachusetts General Hospital (United States) and Harvard Medical School (United States) and Harvard-MIT Health Sciences and Technology (United States)

Antimicrobial blue light therapy is a promising treatment option for multi-drug resistant microbial skin and soft tissue infections. However, limited light penetration in the tissue is considered one of the main hurdles limiting its therapeutic effect. To overcome this, we developed an optical light-delivering waveguide array. The biocompatible fractional micro-needle allows the therapeutic light to penetrate the superficial skin layer and biofilm to enable more effective treatment of infections. The design parameters, such as the needle length, diameter and interspacing, of the

device were determined considering the depth of infection, the penetration depth of blue light and the risk of tissue damage. The results of a feasibility study in a mouse model of burn infections will be presented.

9341-24, Session 6

High-resolution endomicroscopy using a graded-index lens coated by scattering layers

Changhyeong Yoon, Jungho Moon, Hakseok Ko, Pilsung Kang, Yonghyeon Jo, Wonshik Choi, Korea Univ. (Korea, Republic of)

In biomedical optics, label-free imaging of biological tissues is essential in vivo applications. But biological cells are transparent and colorless, which makes the reflected signal very low and the image contrast extremely poor. Recently, studies were reported in which the differential interference contrast (DIC) - like images were obtained by oblique illumination method in reflection geometry.

In this study, we combined this idea with our transmission matrix method to improve both the contrast and resolution of endoscopic imaging. We used a gradient-index (GRIN) lens as an optical probe. Especially, we coated the GRIN lens' input part with a turbid medium. Due to the multiple light scattering in the turbid medium, even the angular spectrum whose spatial frequency is larger than the passband set by the numerical aperture (NA) of the GRIN lens can be captured. By measuring the transmission matrix of the GRIN lens with scattering layers, we achieved endoscopic imaging with spatial resolution beyond the diffraction limit of the bare GRIN lens.

In addition to the resolution enhancement, we attached two multimode fibers at the side of GRIN lens to provide oblique illumination to the target specimen. We switched beam path to each multimode fiber and acquired high-resolution object images for the two opposite oblique illuminations. By subtracting the two images, we obtained high-contrast DIC-like images.

Our advanced endomicroscope featured with enhanced contrast and high spatial resolution will help interrogating biological tissues in great detail.

9341-25, Session 6

Biointegrated micro-cavities for single cell force-mapping (*Invited Paper*)

Nils Kronenberg, Univ. of St. Andrews (United Kingdom); Philipp Liehm, Univ. of St. Andrews (United Kingdom); Anja Steude, Malte C. Gather, Univ. of St. Andrews (United Kingdom)

Monitoring the mechanical properties of single cells is considered a key factor to the understanding of a range of fundamental biological processes. Until recently, it was assumed that vertical forces can be neglected in the analysis of cell mechanics. However, it has now been shown that the out-of-plane and in-plane forces exerted by cells are of the same order of magnitude.

Here, we present a completely new approach to measure out-of-plane cellular forces which overcomes the limitations of Traction Force Microscopy (TFM), currently the most widely-used method to investigate cellular forces. Our approach is based on interferometrically detecting deformations of an elastic probe, rather than on tracking bead displacement. The centerpiece of our innovation is a novel optical micro-cavity sensor that is directly integrated with the live cells. The sensor enables fast force mapping across a large field of view by analysing changes in resonance wavelength. Our approach avoids any phototoxic effects and therefore allows the measurement of cellular forces at high frame rates over hours or days.

Being based on wide-field imaging, the method yields information on the deformation at each point of the image simultaneously and with diffraction limited lateral resolution. Vertical displacements are detected with accuracy

**Conference 9341: Bioinspired, Biointegrated,
Bioengineered Photonic Devices III**

of 5 nm or better. Force maps can be recorded without the need for zero-force images, thus increasing throughput, eliminating the need to detach non-migrating cells after force mapping and enabling measurements of multiple cells on one substrate.

9341-26, Session PSun

**Biocompatible optical needle array for
antibacterial blue light therapy**

Caio M. Guimarães, Univ. de Pernambuco (Brazil); Jeeseo An, Wellman Ctr. for Photomedicine, Massachusetts General Hospital (United States) and Harvard Medical School (United States); Matjaz Humar, Wellman Ctr. for Photomedicine, Massachusetts General Hospital (United States) and Harvard Medical School (United States) and Jožef Stefan Institute (Slovenia); Will A. Goth, The Univ. of Texas at Austin (United States); Seok-Hyun Yun, Harvard Medical School (United States) and Wellman Ctr. for Photomedicine (United States) and Massachusetts General Hospital (United States)

Biocompatible Optical Needle Array (BONA) can be a powerful tool complementing the novel antibacterial blue light therapy. To prove the efficacy of light delivery of BONA and optimize the design, we fabricated an experimental model. Light transmittance curve was plotted using a skin phantom. The micro-needle significantly increased transmittance of the light and allowed the light to reach deeper layer in a skin phantom. Photobleaching test on a dye-infused skin phantom showed us light delivery pattern around needles. Regarding to mechanical properties of BONA, effective skin penetration of needles with minimal skin damage was our main concern. Needle resistance were determined using one axis of a custom biaxial tensile strain device. BONA is able to deliver light to deeper skin tissue layers successfully as shown in experiments. There is still room for improvements regarding tip sharpness and manufacturing time and cost, which would be solved with the enhanced fabrication method proposed.